Fundão Tailings Dam Review Panel

Report on the Immediate Causes of the Failure of the Fundão Dam

Panel:
Norbert R. Morgenstern (Chair)
Steven G. Vick
Cássio B. Viotti
Bryan D. Watts

August 25, 2016

EXECUTIVE SUMMARY

The Fundão Tailings Dam failed on November 5, 2015 in a liquefaction flowslide that initiated at the dam's left abutment. This Investigation was performed to determine its cause.

In structuring its investigation process, the Panel systematically identified and evaluated multiple causation hypotheses. It further imposed hypothesis testing by means of the following three questions that the candidate failure mechanism should be able to explain:

1. Why did a flowslide occur?
2. Why did the flowslide occur where it did?
3. Why did the flowslide occur when it did?

Forensic methods adopted by the Panel integrated multiple lines of evidence: observations from eyewitness accounts; data and imagery in geographic information system (GIS) format; field evidence from subsurface exploration by the Panel and others; advanced laboratory testing; and sophisticated computer modeling. Responding to the above three questions for hypothesis testing demanded a high level of quantification and exhaustive detail in each of these aspects of the Investigation's evidence-based approach.

To understand the failure first requires understanding the materials the dam contained and their properties. There were two types of tailings, both produced in slurry form and delivered in separate pipelines to the Fundão impoundment. *Sand tailings,* or simply *sands,* are a mixture of sand-sized and finer silt particles. The sands are relatively free-draining, but when loose and saturated are susceptible to *liquefaction*, a process whereby the material loses nearly all of its strength and flows as a fluid. The *slimes*, on the other hand, are much finer and clay-like in nature—soft and compressible with low permeability. How these two materials interacted is key to understanding the failure.

Another central aspect is how their deposition was influenced by a series of unplanned occurrences during the dam's construction and operation. Together, these incidents established the conditions that allowed the failure to take place. These included: (1) damage to the original Starter Dam that resulted in increased saturation; (2) deposition of slimes in areas where this was not intended; and (3) structural problems with a concrete conduit that caused the dam to be raised over the slimes.

It was originally planned to deposit sands behind a compacted earthfill Starter Dam, then raise it by the upstream method to increase progressively its capacity. These sands, in turn, would retain slimes deposited behind them such that the two materials would not intermingle. To preserve the free-draining characteristics of the sands, a 200 m beach width was required to prevent water-borne slimes from being deposited near the dam crest where they would impede drainage. A high-capacity drainage system at the base of the Starter Dam would allow water to drain from the sands, reducing saturation.

The first incident occurred in 2009 shortly after the Starter Dam was completed. Due to construction defects in the base drain, the dam was so badly damaged that the original concept could no longer be implemented. Instead, a revised design substituted a new drainage blanket at a higher elevation.

Together with the revised design there was a fundamental change in the design concept whereby more widespread saturation was allowed and accepted. This increase in the extent of saturation introduced the potential for sand liquefaction.

The second incident associated with slimes and water management occurred over an extended period of time in 2011 and 2012 while the new design was being constructed. During operation, the 200 m beach width criterion was often not met, with water encroaching to as little as 60 m from the crest. This allowed slimes to settle out in areas where they were not intended to exist.

Another incident occurred in late 2012 when a large concrete conduit beneath the dam's left abutment, the Secondary Gallery, was found to be structurally deficient and unable to support further loading. This meant that the dam could not be raised over it until it had been abandoned and filled with concrete. In order to maintain operations in the interim, the alignment of the dam at the left abutment was set back from its former position. This placed the embankment directly over the previously-deposited slimes. With this, all of the necessary conditions for liquefaction triggering were in place.

As dam raising continued, surface seepage began to appear on the left abutment setback at various elevations and times during 2013. The saturated mass of tailings sands was growing, and by August, 2014 the replacement blanket drain intended to control this saturation reached its maximum capacity. Meanwhile, the slimes beneath the embankment were responding to the increasing load being placed on them by the rising embankment. The manner in which they did so, and the consequent effect on the sands, is what ultimately caused the sands to liquefy.

As the softer slimes were loaded, they compressed. At the same time, they also deformed laterally, squeezing out like toothpaste from a tube in a process known as *lateral extrusion*. The sands immediately above, forced to conform to this movement, experienced a reduction in the horizontal stress that confined them. This allowed the sands to, in effect, be pulled apart and in the process become looser.

To replicate this process in the laboratory, the Panel applied these stress changes to the Fundão sand. The saturated specimen completely and abruptly collapsed, losing nearly all its strength—a laboratory demonstration of liquefaction. The Panel then undertook a program of numerical modeling to determine whether stress changes similar to those imposed in the laboratory would have also occurred in the field. Using computer simulation of how the slimes deformed during embankment construction, and tracking the corresponding response of the sands, comparable stress conditions that caused the sands to liquefy in the laboratory were reproduced computationally. Simply put, what is known to have occurred during the failure was replicated in the laboratory, and what occurred in the laboratory is shown to have occurred at the left abutment of the dam.

A related aspect of the failure was the series of three small seismic shocks that occurred about 90 minutes earlier. By then the left abutment of the dam had reached a precarious state of stability. Computer modeling showed that the earthquake forces produced an additional increment of horizontal movement in the slimes that correspondingly affected the overlying sands. Although the movements are quite small and the associated uncertainties large, this additional movement is likely to have accelerated the failure process that was already well advanced.

Hence the failure of the Fundão Tailings Dam by liquefaction flowsliding was the consequence of a chain of events and conditions. A change in design brought about an increase in saturation which introduced the potential for liquefaction. As a result of various developments, soft slimes encroached into unintended areas on the left abutment of the dam and the embankment alignment was set back from its originally-planned location. As a result of this setback, slimes existed beneath the embankment and were subjected to the loading its raising imposed. This initiated a mechanism of extrusion of the slimes and pulling apart of the sands as the embankment height increased. With only a small additional increment of loading produced by the earthquakes, the triggering of liquefaction was accelerated and the flowslide initiated.

Immediately following this Executive Summary is an inventory of structures and their locations to help the reader become oriented to the various features associated with the site.

INVENTORY OF STRUCTURES

Term	Figure Reference
Alegria Mine	1
Auxiliary Foundation (Base) Drain	2
Conveyor	1
Dike 1	1
Dike 1A (a.k.a. Old Dike 1A)	2
Dike 2	1
El. 826 m Blanket Drain	2
Fabrica Nova Waste Pile	1
Fundão Dam	1
Germano Buttress	1
Germano Main Dam	1
Grota da Vale	1
Kananets®	2
Left Abutment (LA)	2
Main Gallery	2
Overflow Channel	2
Plateau	2
Principal Foundation (Base) Drain	2
Reinforcement (Equilibrium) Berm	2
Right Abutment (RA)	2
Santarem Dam	1
Secondary Gallery	2

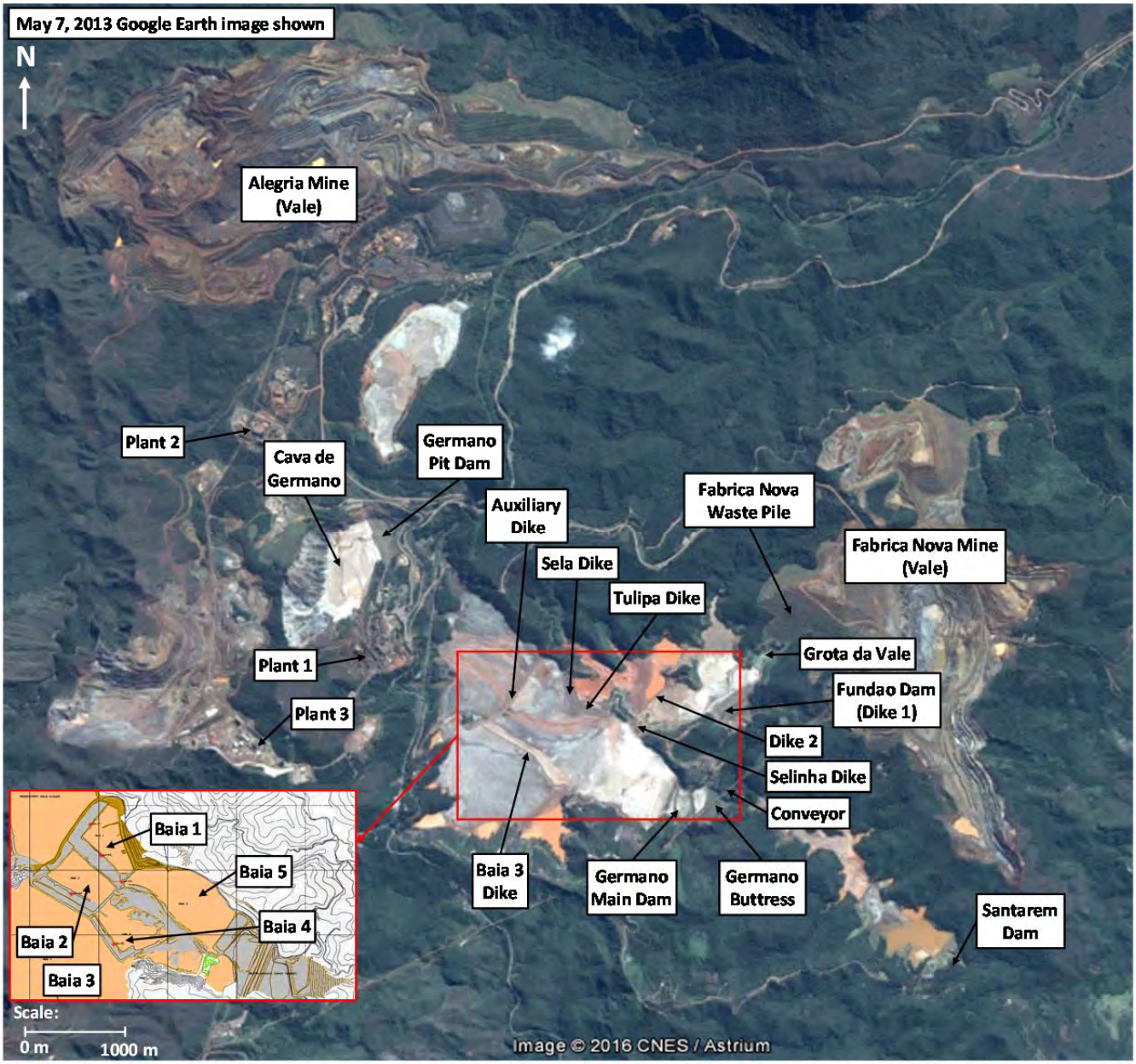

Figure 1 Inventory of structures – Samarco Site

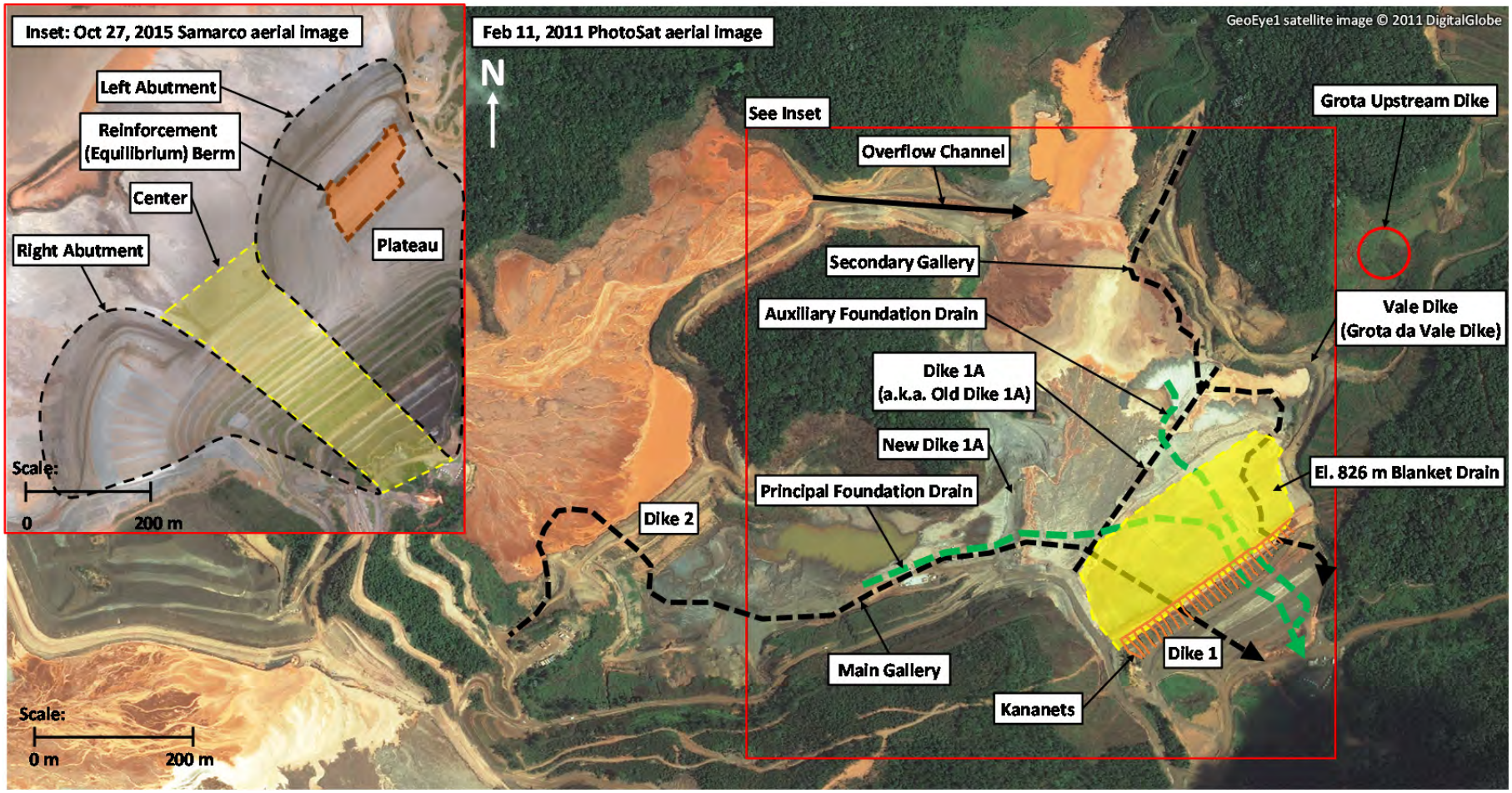

Figure 2 Inventory of structures – Fundão Dam

TABLE OF CONTENTS

TABLE OF CONTENTS
(continued)

List of Tables

List of Figures

TABLE OF CONTENTS

(continued)

TABLE OF CONTENTS

(continued)

List of Appendices

TABLE OF CONTENTS

(continued)

1 INTRODUCTION

1.1 The Failure

On the afternoon of November 5, 2015, the Fundão Tailings Dam in Minas Gerais collapsed. Its crest had reached El. 900 m, making the dam 110 m high. Several dozen people were working on or near the dam at the time. Some were hauling and spreading tailings for raising the dam, others were constructing gravel blanket drains in anticipation of the next stage of construction, and still others were engaged in the daily activities required to operate and maintain the tailings system.

Sometime after about 2:00PM[1] many in the Germano plant complex felt a tremor lasting several seconds. Although windows rattled and objects fell from tables, there did not appear to be any serious damage. Work resumed.

At 3:45PM shouts came over radio that the dam was collapsing. A cloud of dust had formed over the left abutment[2], and those closest to the area designated the "setback" could see cracks forming at the recently-constructed drainage blanket. The slope above them was beginning to undulate "like a wave" as if it were "melting," bringing the dam crest down after it. The tailings that had been solid ground just minutes before transformed into a roiling river, overtopping but not breaching the downstream Santarem Dam, then entering the town of Bento Rodriguez shortly thereafter enroute to its ultimate destination in the sea.

Eyewitness descriptions and videos definitively establish several things. The first is that the Fundão failure initiated at the dam's left abutment, not at the right side or its downstream toe. The second is that the failure occurred due to flow liquefaction of the tailings, a process whereby water pressures in the interstitial voids between the tailings particles increased to such an extent that the mass of material lost strength and flowed like a liquid. And third is that this transformation from solid to liquid was complete and abrupt, leaving a fluid of apparent viscosity and hydraulic behavior little different from water in just seconds.

The question remains as to what triggered liquefaction and what factors promoted its occurrence. That is the focus of this report.

1.2 The Investigation

This Investigation of the Fundão Tailings Dam failure was commissioned by BHP Billiton Brasil Ltda., Vale S.A. and Samarco Mineração S.A. The firm of Cleary Gottlieb Steen & Hamilton LLP (CGSH) was engaged to conduct the Investigation with the assistance of a panel of experts. The Fundão Tailings Dam Review Panel (Panel) includes four members, all specialist geotechnical engineers in water and tailings dams: Norbert R. Morgenstern (Chair), Steven G. Vick, Cássio B. Viotti, and Bryan D. Watts.

[1] All times in this report refer to local Brazilian time.
[2] The conventions *left* and *right* indicate direction, location, or orientation as seen by an observer looking downstream. The left and right *abutments* are where the constructed dam meets the respective valley sides.

The Panel's Terms of Reference defined the scope of its activities. Specifically, the Panel was instructed to provide its independent and unbiased professional judgment and expertise in determining the immediate cause(s) of the incident.

In accomplishing this purpose, the Panel could examine any or all of the following:

- geotechnical designs of the Fundão Tailings Dam and structures associated with the dam, including both intact and breached embankments, and including both the original design and all lifts of the embankment structure;
- interpretation of results of geotechnical investigations and associated laboratory testing of the Fundão Tailings Dam;
- patterns, trends, and relationships in instrumentation behavior of the Fundão Tailings Dam;
- interpretation of instrumentation and performance data in relation to the Fundão Dam's behavior;
- materials, methods, procedures, and quality assurance/quality control practices for the construction and modification of the Fundão Dam;
- water balance and water quality as they relate to the incident;
- seismic activity in the region on the day of the incident;
- operational procedures and planning for tailings deposition and water management at the Fundão Dam;
- inspection and surveillance procedures and implementation, including reports issued by the Independent Tailings Review Board (ITRB) and other outside auditors;
- the Engineer of Record's field reviews;
- issues identified by the National Department of Mineral Production (DNPM) and the Brazilian federal and state environmental agencies in the course of their oversight;
- the design and structure of other similar tailings dams in the vicinity; and
- other matters the Panel deems appropriate to be examined.

Seismologists Gail Atkinson and Ivan Wong provided the Panel with input in their field of expertise. The firm of Klohn Crippen Berger provided analytical, field, and laboratory support, and the firm of TÜV SÜD provided local assistance in Brazil.

The Panel was provided with available information and witnesses necessary to achieving its purpose. The Panel was asked not to assign fault or responsibility to any person or party, or to evaluate environmental or other downstream effects or damages. None of the Panel members had performed previous work for Samarco or was currently engaged in any other assignment for BHP Billiton Brasil or Vale during the conduct of the Investigation.

During the course of the Investigation, the Panel conducted the following activities:

- site inspection and meetings;
- meetings with eyewitnesses and technical personnel;
- compilation and review of project documents;
- assembly of GIS data and imagery;
- reconstruction of tailings stratigraphy;
- compilation and assembly of pre-failure subsurface and laboratory data;
- subsurface investigations at the site and laboratory testing;
- compilation and interpretation of instrumentation data;
- analytical studies:
  - seepage modeling;
  - consolidation modeling;
  - stability analysis;
  - deformation analysis; and
  - dynamic response analysis.
- geologic assessment;
- fault tree analysis; and
- preparation of this report.

2 HISTORY

This section provides a compilation of historical facts and circumstances considered by the Panel to be most relevant to understanding the failure, with particular emphasis on the left abutment where the failure is known to have initiated. The complete history is much more extensive, and no attempt is made here to review it in its entirety.

2.1 The Concept (2004-2007)

Beneficiation of iron ore at Samarco's Germano Complex results in two distinct kinds of tailings produced and transported in slurry form as separate streams. *Sands*, or sand tailings, are actually composed of both sand and silt-sized particles in roughly equal proportion. During deposition, they form a gently-sloping beach through which transport water drains fairly rapidly. *Slimes,* on the other hand, are fine-grained and clayey in nature. The clay-sized particles remain suspended and eventually settle in standing water to produce a softer material of lower permeability.

At Germano, a way was devised to use these two types of tailings and their different characteristics to best advantage. The sands were deposited to form a buttress or "stack" that retained the slimes discharged separately behind it. The sands, in turn, were retained by an earthfill or rockfill *starter dam* at the downstream toe of the stack, as illustrated on Figure 2-1 for Samarco's Germano Buttress structure. Over time, the Germano Starter Dam was raised according to the *upstream method* or *upstream construction*. With this procedure, the dam crest moves progressively upstream over previously-deposited tailings as the dam is raised.

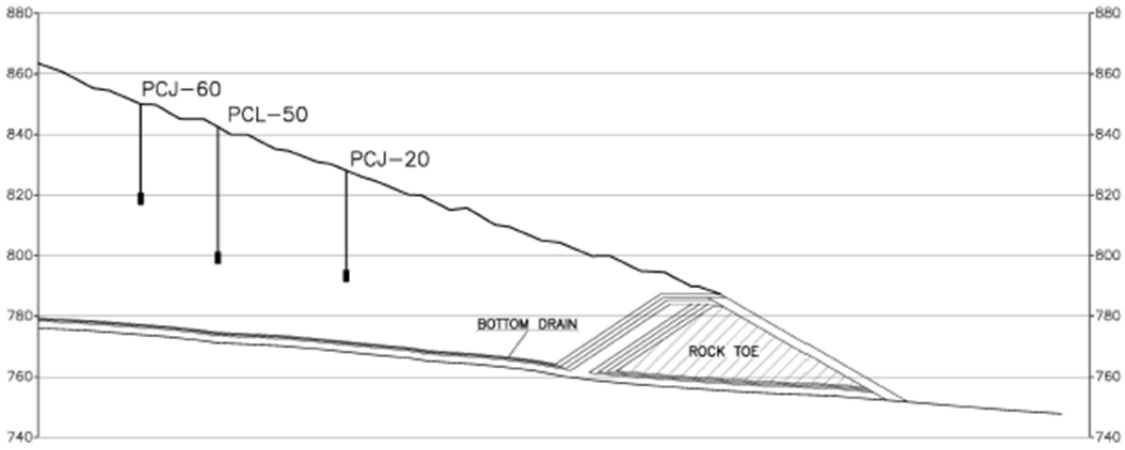

Figure 2-1 Germano Buttress (Pimenta de Ávila 2011)

Adequate drainage of the sands was the key to this concept. Figure 2-1 shows that drainage was promoted by highly-pervious bottom drains underlying the sand and extending beneath the Starter Dam to prevent water from accumulating and saturating the deposit. The absence of any significant water pressure was to be confirmed with the piezometers shown in the figure. Provided that no

slimes were present to impede downward drainage and that the sands remained unsaturated, resistance to liquefaction—a well-known vulnerability of upstream construction—could be assured.

By 2005, the existing tailings facilities at Samarco's Germano operation were nearing capacity, and a new third pellet plant would increase production of both sand and slimes. The adjacent Fundão Valley was chosen as a new tailings site. In the layout that emerged, the sands and slimes would initially be physically separated, with sands deposited behind Dike 1 and slimes behind Dike 2, as represented on Figure 2-2. Retention of the slimes required that the sands deposited between the two dikes always remain at a higher elevation throughout the raising process. This was a matter of reservoir geometry, and the dikes in Figure 2-2 had been strategically positioned for sands and slimes in 70% and 30% proportion of the total received from all plants.

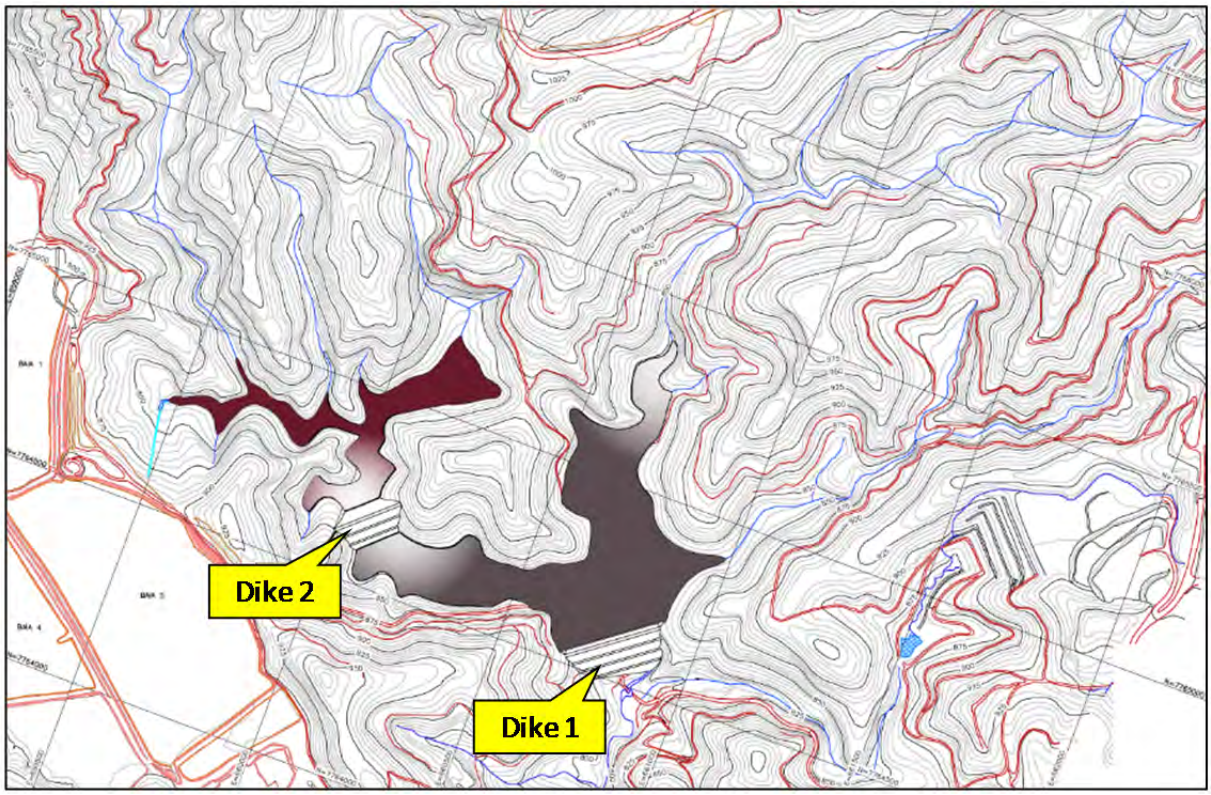

Figure 2-2 Fundão Dikes 1 and 2

Two alternative methods were considered for raising Dike 1 after filling the space between the two dikes with sand. One was *centerline* raising depicted on Figure 2-3 using compacted sand tailings in the downstream slope. This alternative was not selected, with the drained stack concept shown on Figure 2-4 adopted instead. The Dike 1 Starter Dam would be a conventional earthfill structure constructed of compacted saprolite soils to crest El. 830 m, with subsequent upstream raising with sand tailings to El. 920 m.

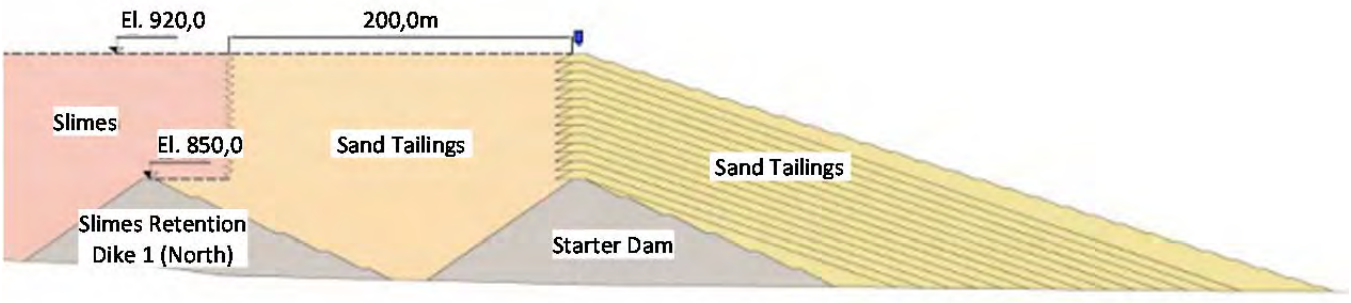

Figure 2-3 Centerline raising of Dike 1 considered but not implemented

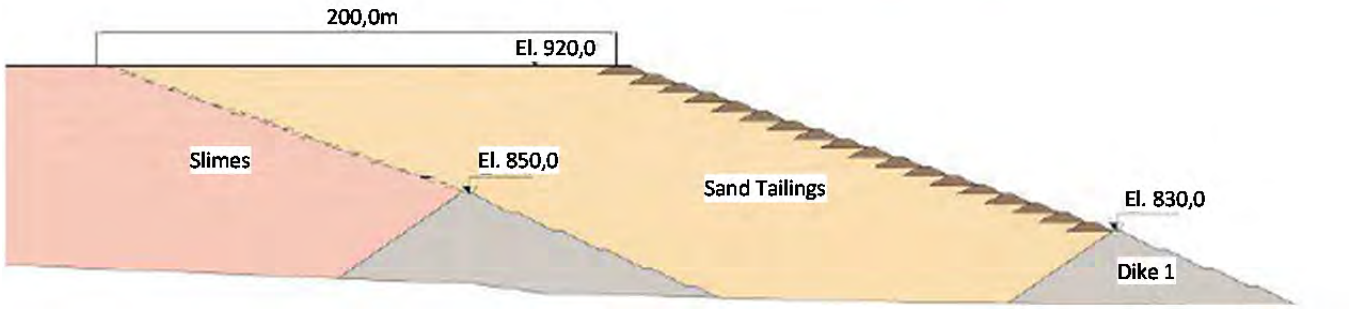

Figure 2-4 Upstream raising of Dike 1 by the "drained stack" concept

Thus, the Germano Buttress structure became the prototype for Fundão. Like its predecessor, the Dike 1 Starter Dam for Fundão would be underlain by a high-capacity base drain of gravel and rock. This would connect to another drain on the Starter Dam's upstream face, along with other complimentary drainage features—all to minimize saturation in the sand deposit behind it.

A remaining design consideration was how to evacuate surface water inflows from ordinary precipitation, floods, and discharged tailings slurry. This would be accomplished by two concrete galleries, 2 m diameter decant conduits of reinforced concrete extending beneath the tailings deposit and Dike 1 itself. The Main Gallery would be beneath the right abutment and the Secondary Gallery beneath the left as indicated on Figure 2-5.

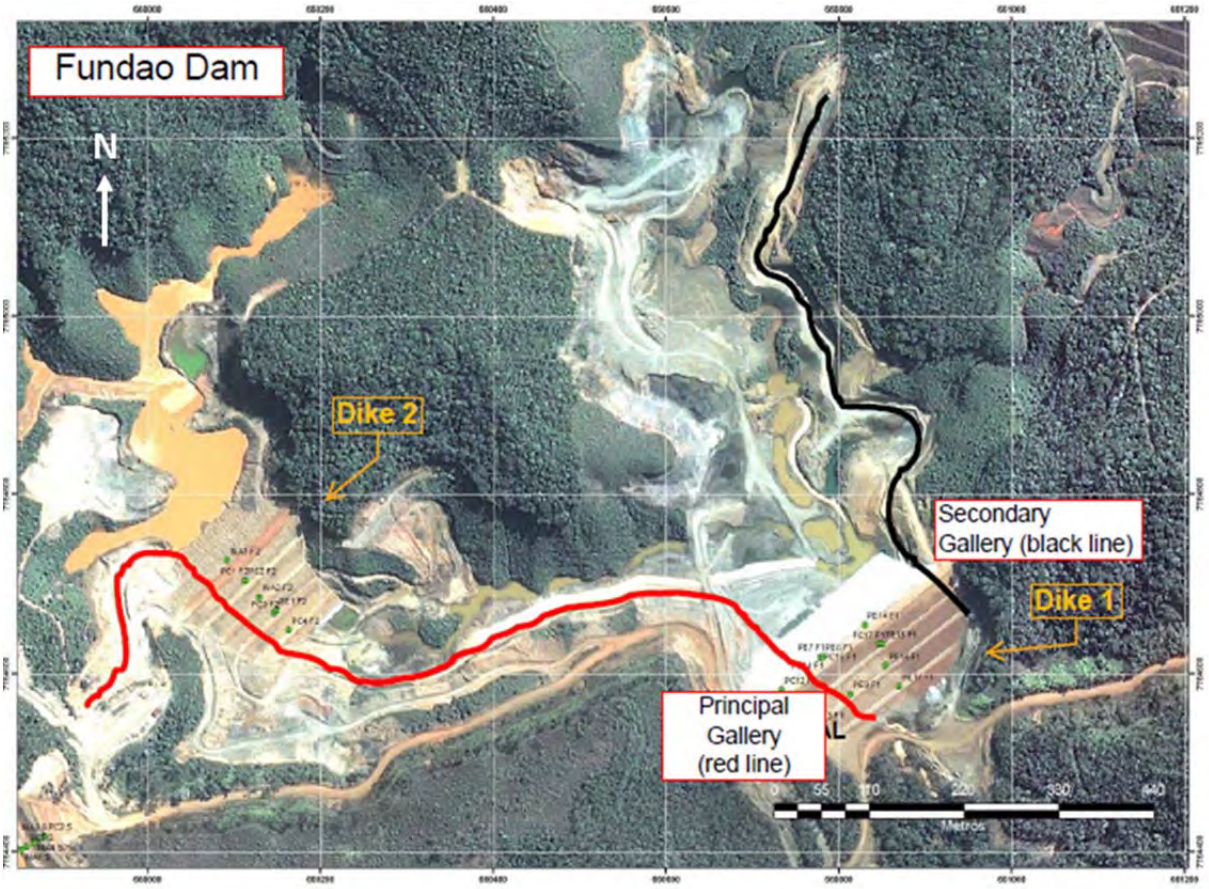

Figure 2-5 Main (Principal) and Secondary Galleries

In the Panel's estimation, this design concept for Fundão offered several advantages. With the dam located in a narrow valley constriction, the site was efficient, requiring a modest amount of dam fill for the storage volume achieved. Once above the valley floor, the reservoir expanded to provide large capacity relative to the area it occupied. But the concept also had certain vulnerabilities. The design was not adaptable to variation in the proportion of sands and slimes received. And most importantly, it depended on achieving adequate drainage of the sands.

2.2 The Piping Incident (2009–2010)

Construction of the Dike 1 Starter Dam, with its requisite drains and galleries, was completed in October, 2008. Shortly after full-scale discharge of sand tailings began on April 13, 2009, large seepage flows carrying fines appeared on the downstream slope above the main underdrain as shown on Figure 2-6, conditions symptomatic of the process of *piping* or *internal erosion*.

Figure 2-6 Internal erosion effects on downstream slope of Dike 1

An Emergency Action Plan in place for the dam at that time was immediately implemented. The reservoir was lowered, a berm was constructed over the affected portion of the dam slope, and provisions were made for holding the reservoir's remaining contents in the downstream Santarem Dam should failure occur. Engineering investigations later revealed serious construction flaws in the base drain and its filters, including a portion of the drain's outlet that had never been completed. This allowed water pressure within it to build until causing the slope to erode and slump.

As these investigations continued, the impending rainy season made it too late to fully restore the drainage features to their original condition, making it impossible to repair the damage. Instead, all of the drains were sealed. With this, the most important element of the original design concept became inoperative.

Additionally, the balance between sands and slimes crucial to the dam raising plan was changed. Filling of Dike 2 had begun earlier than anticipated, making its slimes level higher, not lower, than the projected sands in Dike 1. At the same time, reduction in pellet production reduced the amount of sand available while delivery of slimes continued. This required construction of yet a third dike between Dikes 1 and 2, designated Dike 1A, to provide additional slimes capacity. It was November 2010 before all of the measures made necessary by the piping incident were finally completed.

It remained to devise a new design concept to replace the old one.

2.3 The Recovery (2011–2012)

A revised design for raising Dike 1 to El. 920 m was first described in the 2011 Operations Manual, then updated in the 2012 version when the dam had reached crest El. 845 m. The central feature was the addition of a blanket drain on the surface of the tailings to replace the inoperative base drain below them. As shown on Figure 2-7, the new blanket drain was at El. 826 m just below the Starter Dam crest. Figure 2-8 depicts how the blanket drain would become embedded within the tailings during raising of the dam, intercepting seepage that could otherwise emerge on the slope and reduce its stability. In order to augment capacity for discharging the collected seepage flows, the blanket drain also contained slotted pipes called "Kananets®".

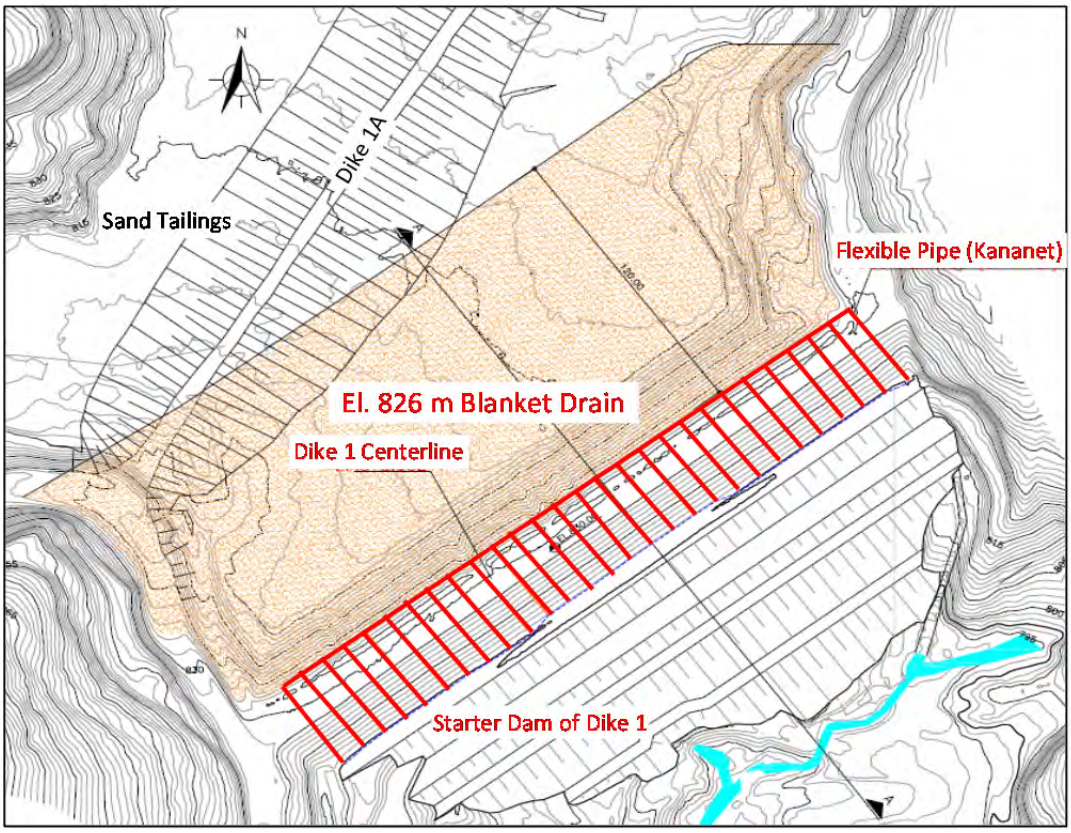

Figure 2-7 Blanket drain (plan view) on tailings surface at El. 826 m

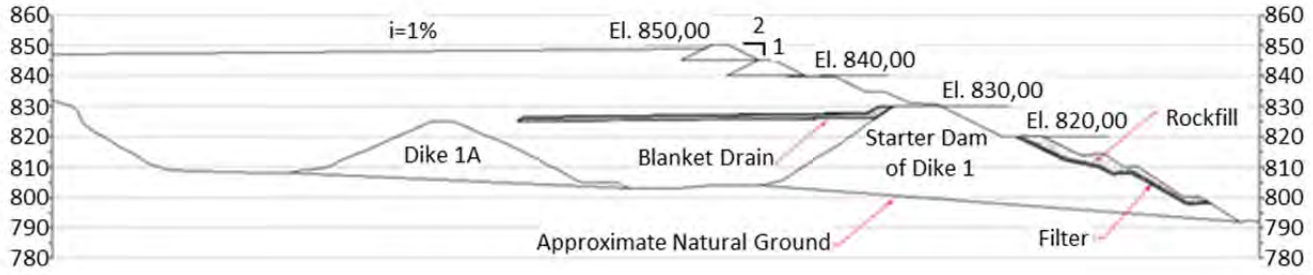

Figure 2-8 El. 826 m blanket drain (section) showing extent behind Dike 1

Comparing Figure 2-8 to Figure 2-1, it can be seen that the new blanket drain represented an attempt to replicate the drained-stack concept by providing drainage for the overlying tailings. But the sands below this drain would remain saturated, as would much of the tailings behind it. Once the base drain became inoperative, the control of saturation embodied in the original design concept could not be restored.

A requirement common to both the original and revised designs was that the sands be free-draining. To ensure that low-permeability slimes would not be deposited where they could impede this drainage, water containing the slimes had to be restricted from the area of sand deposition. To do so, a 200 m minimum beach width had been specified in the original 2007 Operations Manual, a provision retained in the 2011 and 2012 versions.

But as operation proceeded, this beach-width criterion was not consistently achieved. As explained in greater detail in Section 5.1.3, a new Overflow Channel was conveying water and slimes from Dike 2 to the rear of the Dike 1 reservoir, making beach management more difficult. No longer were the sands and slimes physically separated; the interface between them could only be controlled by adjusting the amount of sand spigotted from the dam crest in relation to the amount of slimes-laden water being introduced. As plotted on Figure 2-9 and documented in Appendix B, during much of 2011 and 2012, beach widths violated the 200 m minimum more often than not, at times encroaching to as little as 60 m from the crest.

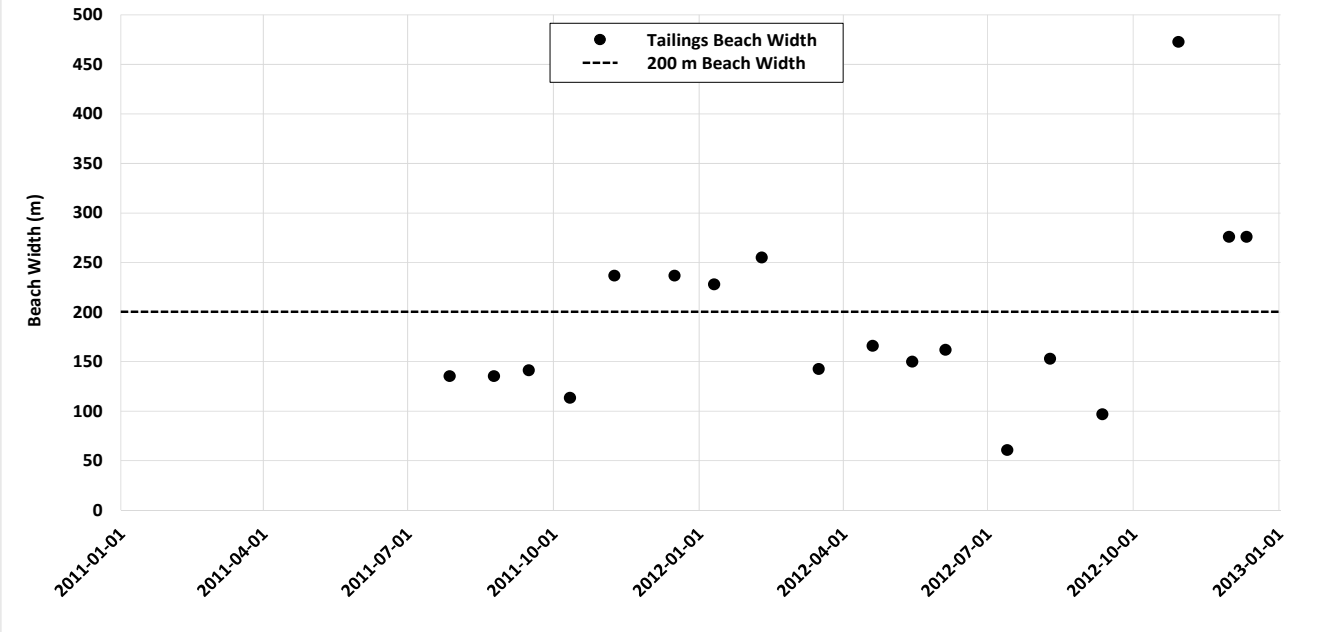

Figure 2-9 Monthly beach width measurements by Samarco, 2011-2012

2.4 The Setback (2012–2014)

Even as recovery from the 2009 Starter Dam piping incident remained underway, new conditions were developing that would directly affect the left abutment. The galleries shown on Figure 2-5 that evacuated water from the Fundão impoundment were found to be structurally deficient. This first

became evident for the Main Gallery at the right abutment when in July, 2010 a vortex appeared in the reservoir above it, showing that tailings and water were entering. Inspections revealed cracking and structural damage from foundation settlement and construction defects. Were either of the galleries to collapse, uncontrolled release of tailings from the reservoir or failure of the dam would be possible. So in January, 2011 a program of jet grouting was initiated to repair the Main Gallery and return it to service.

Similar conditions were discovered for the Secondary Gallery, and jet grouting was undertaken there as well. But by July, 2012, it was apparent that jet grouting had not cured these problems. After a sinkhole appeared in the tailings overlying the Secondary Gallery in November, 2012, repair efforts were abandoned. Instead, plans were made to plug both galleries by filling them with concrete from their outlets to a point beneath the projected crest of the 920 raise in order to prevent their collapse. Moreover, it was discovered from structural analyses that the Secondary Gallery could not support tailings higher than El. 845 m, some 10 m lower than the tailings already were at that time.

Because the height of tailings at the left abutment already exceeded the load capacity of the Secondary Gallery, the dam could not be raised any further over this area until the plugging operation was completed. As a temporary solution, it was decided to realign the dam at the left abutment by moving it back behind the portion of the gallery to be filled with concrete so that embankment raising could continue. This realignment shown on Figure 2-10 became the “setback”.

The setback would move the crest closer to the reservoir water and the slimes it contained, but it was anticipated that the dam would be quickly returned to its original alignment as soon as the plugging operations were done. At the same time, as will be explained more fully in Section 5, moving the crest back from its original alignment would also place it closer to, if not over, areas where beach encroachment and slimes deposition had already occurred.

Filling of the Secondary Gallery was completed on August 22, 2013. Meanwhile, dam raising had continued, with seeps that began to appear at the left abutment as early as June 26, 2012, at El. 845 m. In February, 2013, three-dimensional seepage modeling of the 920 raise showed that additional drains would be needed at the abutments if seepage breakout were to be prevented. This analysis was borne out when seepage, saturation, and cracking began appearing at several locations at the left abutment during 2013. The first such incident occurred in March at El. 855 m, followed by another seep in June at El. 855 m. Both were treated by constructing a drain. A third seep on November 15 appeared at El. 860 m and was accompanied by slumping of the slope shown on Figure 2-11. Another drain was provided to address this condition. On December 26, seepage occurred at El. 860 m and there was cracking on the left abutment crest at El. 875 m.

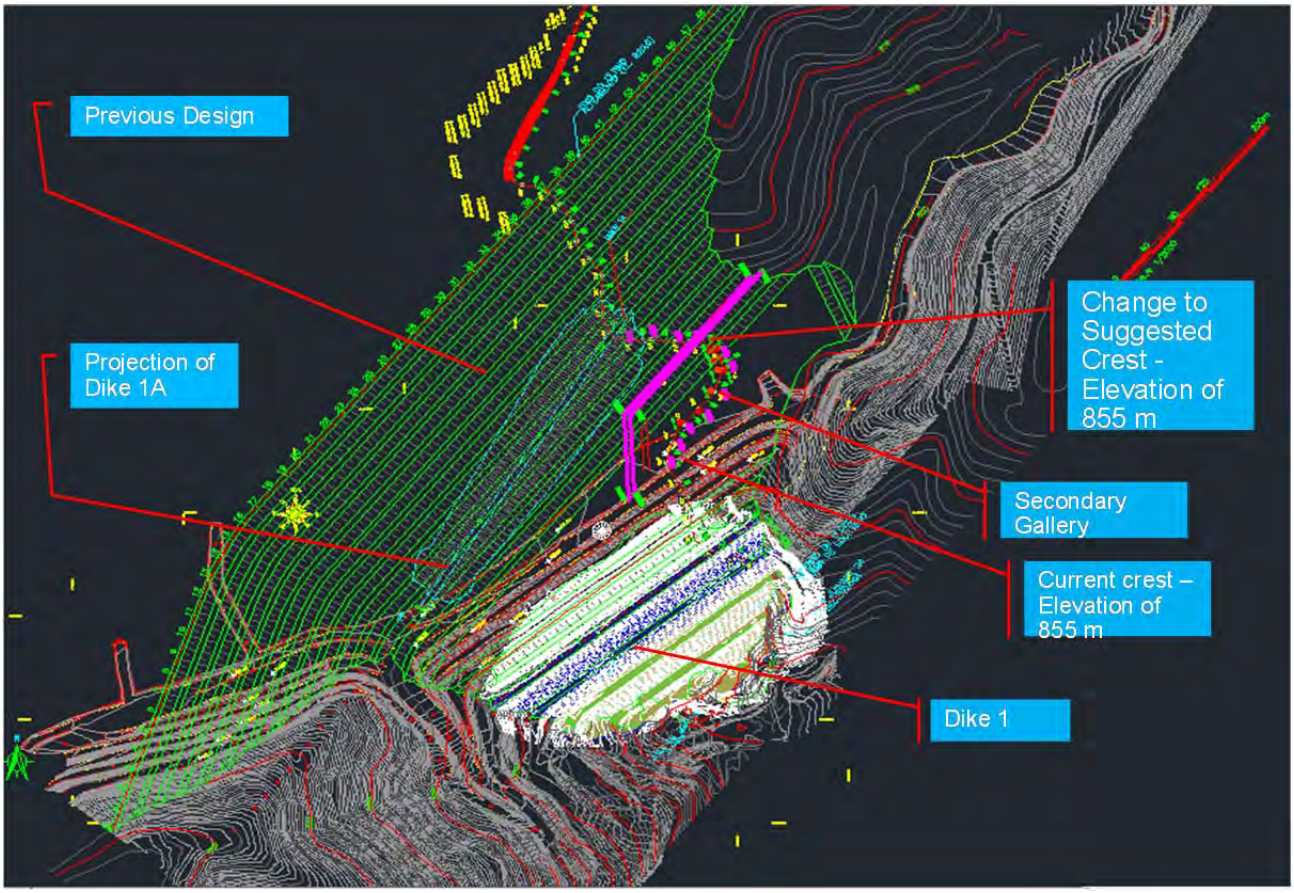

Figure 2-10 Left abutment setback proposed in June, 2012

Figure 2-11 November, 2013 seepage, cracking, and slumping at left abutment El. 860 m

Following these 2013 episodes of seepage and cracking, it had become apparent by January, 2014 that the El. 826 m blanket drain was no longer sufficient and that additional drains would be needed at the left abutment. This coincided with plans for an entirely new project for future raising of the dam by an additional 20 m from its then-planned maximum elevation of 920 m. Not only would this new El. 940 m raise add needed drainage features to the left abutment; it would eventually integrate them with an independent drainage system entering from the adjacent Grota da Vale and Fabrica Nova waste pile. As shown on Figure 2-12, the result would be what the Panel considers to be a complex and elaborate drainage system.

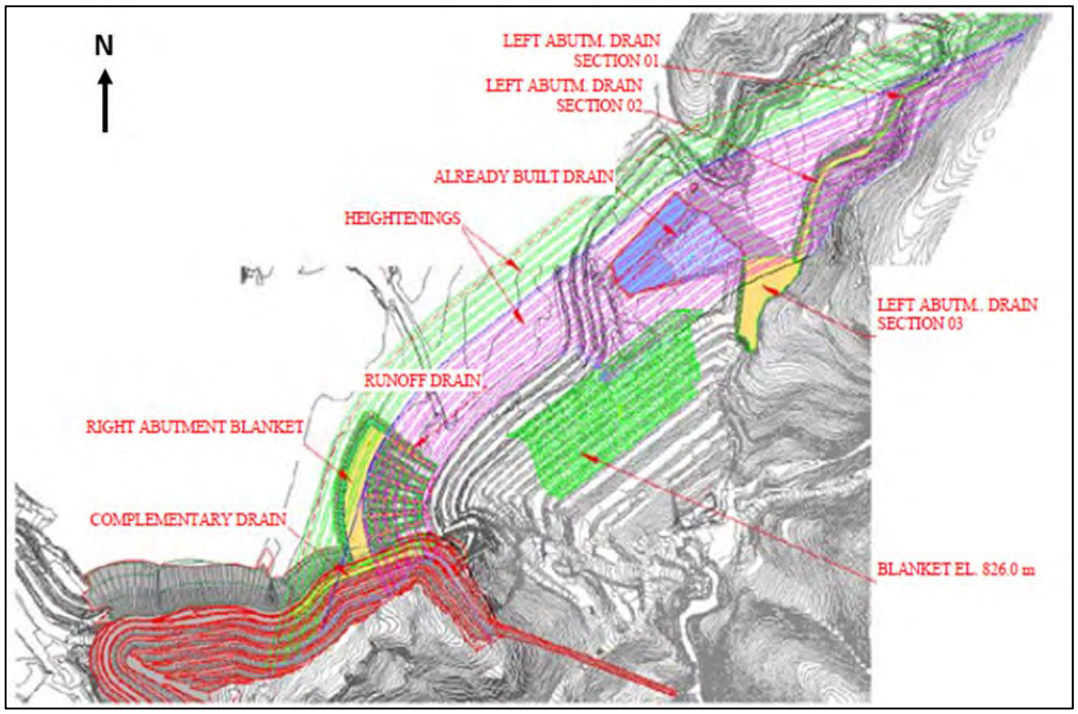

Figure 2-12 Proposed drainage scheme for 940 raise

The more immediate effect was that construction of additional drains in the left abutment area would require the setback to be maintained until they were completed. This entailed further delay in restoring the original alignment. As a result, the setback had risen at an average rate of 18 m/yr during 2013 and 3.0 m in September, a monthly record. In the 18 months since the setback decision had been made, the dam had grown by more than 20 m, and by January 2014 the Fundão Dam looked like Figure 2-13.

Figure 2-13 Fundão Dam in January, 2014 showing left abutment setback and adjacent Grota da Vale

2.5 The Slope Incident (August 2014)

Just after sunrise on August 27, 2014 a series of cracks much more extensive than anything that had occurred the previous year were discovered that extended behind the dam crest, emerged at the toe, and encompassed most of the slope as shown on Figure 2-14. Accompanying the cracking was shallow saturation at the toe, as shown on Figure 2-15.

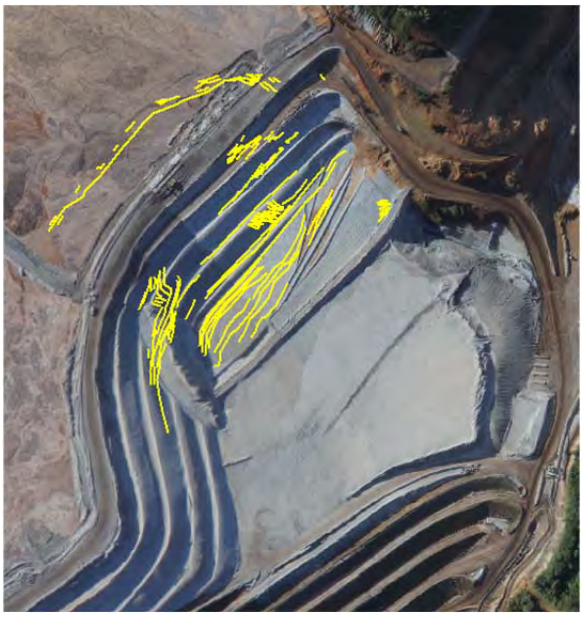

Figure 2-14 August 27, 2014 cracking at left abutment setback

Figure 2-15 Cracks on dam crest and saturation at toe of slope, August 27, 2014

Stabilizing the slope became paramount, and construction was quickly mobilized to do so. Within two weeks, the reinforcement or "equilibrium" berm shown on Figure 2-16 was completed.

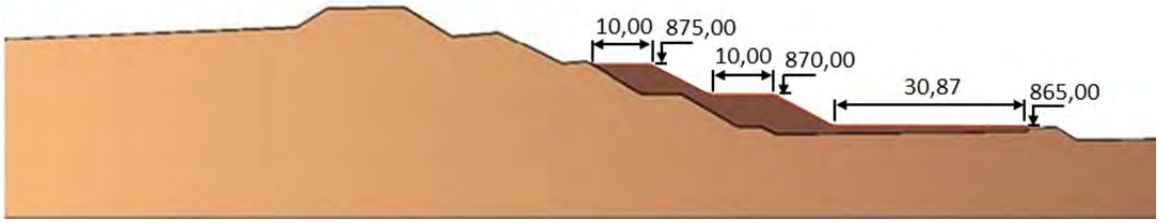

Figure 2-16 Reinforcement berm for left abutment setback, August, 2014

Construction of the left abutment drain was still ongoing, and it was not until a year later, August, 2015, that the drain was completed and fill placement over the area it covered could resume.

October, 2015 was a period of intense activity on the left abutment. The dam crest was being raised to El. 900 m, preparations were being made for cyclone sand placement on the El. 875 m bench, while at the same time the reinforcing berm was being extended by raising the El. 875 m and El. 895 m benches. The net result was that the monthly increase in crest height of 2.9 m—an annualized rate of rise of 35 m/yr—rivaled the record of 3.0 m set in 2013.

2.6 The Earthquakes (November 5, 2015)

Explosions are detonated every day at mines throughout the region, so the small-magnitude seismic events they produce are not unusual. At the same time, while larger earthquakes are rare in Brazil, small earthquakes in Minas Gerais are relatively common. Either way, the tremor on the afternoon of November 5, 2015 was not unprecedented.

According to felt reports at the plant about 2 km from Fundão, shaking was strong enough to cause a computer to fall from a tabletop, but not so strong as to produce structural damage other than minor cracking.

Detailed analysis of instrumentally-recorded events and mine records show that on November 5, 2015, two blasts occurred at a nearby mine within seconds of each other just after 1PM. This was almost three hours before the failure. Later at around 2:15PM a series of three small-magnitude earthquakes occurred over a period of four minutes on the afternoon of November 5, 2015. They preceded the failure by some 90 minutes with the time sequence shown in Table 2-1 below and occurred almost directly beneath the Fundão deposit.

Table 2-1 Pre-failure earthquakes and mine blasts on November 5, 2015 (E.g., Atkinson 2016)

Local time	Moment Magnitude M_w	Distance from Fundão	Identification
1:01:49PM	2.1	2.6 km	mine blast
1:06:06PM	2.3	2.6 km	mine blast
2:12:15PM	2.2	< 2 km	earthquake (foreshock)
2:13:51PM	2.6	< 2 km	earthquake (main shock)
2:16:03PM	1.8	< 2 km	earthquake (aftershock)
3:45PM			*Dam failure*

The implications of the earthquakes will be discussed in Section 6.

2.7 The Collapse (November 5, 2015)

On the afternoon of November 5, 2015, most activity was on or near the right abutment where drains were being constructed, placing several workers in a position to see along the length of the dam crest. On the left abutment, fill was being placed on the El. 875 m bench of the setback in preparation for start-up of cyclone sand placement. Figure 2-17 shows the locations of eyewitnesses engaged in these and other activities at the time of failure.

Figure 2-17 Eyewitness locations on the afternoon of November 5, 2015

The first thing noticed by many workers on the dam, including those at locations 4 and 6, was a cloud of dust drifting up from the left side heralding the failure. A worker at 4 watched as waves developed in the central portion of the reservoir, accompanied by cracks forming on the left side and blocks of sand moving up and down on the left abutment setback. Another worker at 5 saw a crack open up along the crest of the left abutment setback then propagate in both directions, beginning closer to the left abutment, reaching it, then progressing to the right. And at location 9 at the toe of the dam, witnesses experienced an avalanche of mud-like tailings cascading down from the left abutment, but no movement of the starter dike itself.

These observations establish that failure originated at the left abutment setback and that the Starter Dam did not participate in the failure mechanism. However, these workers on the dam crest had been unable to see precisely how and where the failure began, and by the time they made these observations the first stages of failure were already well advanced.

Other observers at the left abutment had a closer view of the developing failure sequence. Workers at locations 1 and 2 were the first to see the failure initiate near the left abutment drain where they were standing, placing the time at 3:45PM. Here, a sudden jet of dirty water “exploded” out of the drain. The first movement and cracking was also reported at the exposed drain and along the adjacent edge of the plateau, placing the exit of the rupture surface at or around El. 857 m. A worker at 1, who was standing on the plateau, felt it begin to move beneath him and crack around him, detaching from the setback slope and moving downstream.

Next to move was the lower slope of the setback. Eyewitnesses at 2, 3, and 5 describe slope movement having propagated “from the bottom up” on the lower benches, not from the crest down, placing the seat of movement at lower elevations. A worker at 3 observed a small bulldozer on the El. 875 m bench moving or being pushed outward, placing the head of the incipient failure at or above this elevation. At first, the lower slope progressed slowly forward “like a snake.” Remaining intact and moving as a unit, it then bulged, becoming grossly distorted as movement accelerated, coming down “like a wave,” or as if it were “melting”. Subsequently, a witness at 3 characterized the violent turbulence of the fluidized mass as “going in somersaults” downstream.

Taken together, these eyewitness observations can be synthesized into the sequence of events at failure initiation portrayed on Figure 2-18.

Figure 2-18 Failure initiation sequence

By the time the events on Figure 2-18 had occurred, the growing failure would have become apparent to the observers on the crest at locations 4, 5, and 6 as it progressed back behind the crest and into the reservoir. Only then did the central and right sides of the dam begin to disintegrate.

A conveyor crossing the Fundão stream channel about 1300 m downstream from the offset crest stopped functioning at 3:49PM, four minutes after failure is reported to have begun at 3:45PM. From this, it is ascertained that the flowslide was moving at about 11 m/s by the time it reached the conveyor. It is calculated that 32 million m^3 of tailings was lost, representing 61% of the impoundment contents—an unusually high proportion in relation to tailings dam failure statistics. In a matter of hours, the Fundão Dam was gone, and what once had been Figure 2-19(a) became Figure 2-19(b).

Figure 2-19 Fundão damsite and reservoir (a) before, (b) after failure

3 WHAT DID THE PANEL DO?

3.1 Diagnostic Strategy

The methodologies adopted and activities conducted during the Panel's Investigation were important to its outcome. The instruction to the Panel in its Terms of Reference was to determine the immediate cause or causes of the breach of the Fundão Tailings Dam on November 5, 2015. This is fundamentally a diagnostic exercise as reflected in the overall framework adopted by the Panel. The Panel's diagnostic strategy consisted of three parts:

1. *Hypothesis formulation.* Candidate failure modes were identified based on known causes of tailings dam failures as they pertain to specific conditions of the Fundão Dam.
2. *Hypothesis screening.* The candidate failure modes were screened using a process of elimination to arrive at one or more that were most consistent with the evidence.
3. *Hypothesis testing.* The surviving failure modes were tested for their ability to predict conditions that occurred at times and locations other than those on November 5, 2015 at the left abutment.

With regard to the third item of hypothesis testing, the Panel developed criteria that its causation conclusion should meet. These took the form of three questions:

1. **Why did a flowslide occur?** That the failure occurred by flowsliding is self-evident but not by itself informative. Any explanation of the failure must go beyond this to determining the events, conditions, and mechanisms that allowed flowsliding to occur.
2. **Why did the flowslide occur where it did?** In principle, there were many places on the Fundão Dam where failure might have occurred. The failure hypothesis must explain what was different about the left abutment that caused the failure to occur there and not at some other location.
3. **Why did the flowslide occur when it did?** Failure occurred when the embankment at the left abutment reached El. 898 m following a series of small earthquakes. The failure explanation must establish why failure did not occur at some previous time at lower elevation and the relationship, if any, between the failure and the earthquakes. The hypothesis must also explain why flowsliding did not occur in association with the cracking incident of August, 2014.

As the tests of the Panel's hypothesis, these three questions constitute the central topics of the remainder of this report and the framework around which it is built.

3.2 Investigation Methodology

The Panel also followed a systematic structure in its investigative efforts. The elements of the Investigation and the tasks that comprised them are described below, with reference to the related appendices.

- **Reconstruction of the dam and its properties.** Most if not all of the key physical evidence was destroyed when the dam washed downstream with the failure. A virtual representation of the dam and its internal composition therefore had to be reconstructed through a lengthy and painstaking process consisting of:
  - *Compilation of digital topographic data and imagery in GIS format*. This allowed the progression of dam raising and tailings deposition to be tracked over time. The methodology adopted is described in Appendix A.
  - *Reconstruction of design, construction, and operational history*. This was done through assembly and interpretation of documents, photographs, and aerial imagery, as described in Appendix B.
  - *Subsurface exploration and laboratory testing*. This incorporated both pre-failure data and independent Panel field investigations at surrogate locations. It allowed estimation of pre-failure engineering properties of dam materials, as contained in Appendices C and D.
- **Compilation of instrumentation data.** The dam contained a large number of instruments that measured internal water pressures, flows, and movements. Together, this data provides a record of the dam's engineering behavior, allowing trends and changes to be tracked throughout its life. Instrumentation data is contained in Appendix E.
- **Synthesis of eyewitness interviews.** The Fundão failure was witnessed by a large number of people at different locations on and near the dam. Their accounts are of content and value unusual for dam failure investigations of this kind and provide insight into the processes that were taking place during the hours and minutes leading up to the failure.
- **Analytical studies.** With the reconstructed dam, instrumentation data, and eyewitness accounts in place, the Panel was able to simulate the operation of potential failure mechanisms and related processes through a variety of numerical modeling techniques:
  - *Consolidation modeling.* This was to evaluate the effects of loading rate on pore pressure development and is described in Appendix F.
  - *Seepage modeling.* This provided information on internal flow and pressure conditions at times and locations where measured instrumentation data was not available. Seepage modeling is described in Appendix G.
  - *Stability analysis.* This provided the calculated degree of embankment stability under various conditions at various times and is found in Appendix H.
  - *Deformation analysis.* Closely linked to stability, deformation modeling provides further insight into failure-related processes and mechanisms as contained in Appendix I. The deformation analysis is central to identifying the causative liquefaction trigger mechanism, and the concluding section of this report is devoted to the development of this topic.
  - *Dynamic response analysis.* This numerically simulates earthquake shaking and is found in Appendix J.
- **Seismological studies.** Conducted independently from the Panel's Investigation, seismological studies provided key input that is contained in a separate report.

3.3 Potential Failure Modes and Triggers

The Panel considers that the evolutionary character of its design and operation makes the Fundão Dam extraordinarily complex. This is reflected in the large number of potential failure modes, which in turn makes a structured process for their evaluation mandatory. Appendix K details how the approach to hypothesis formulation and screening of Section 3.1 was implemented. First, the following potential failure modes were considered:

1. overtopping;
2. internal erosion;
3. Starter Dam foundation or embankment sliding; and
4. liquefaction.

All but liquefaction were ruled out as being inconsistent with physical evidence and/or eyewitness accounts.

Amplifying on liquefaction as the cause of flowsliding, the second stage was to evaluate liquefaction triggering mechanisms, again adopting the same hypothesis formulation and screening process. Here, the Panel used fault trees to structure the assessment in real time, modifying them as the Investigation unfolded. Applied as a heuristic aid rather than a reliability application, formal fault tree symbology was not necessary or adopted. The Panel's final fault tree for liquefaction triggering is shown on Figure 3-1.

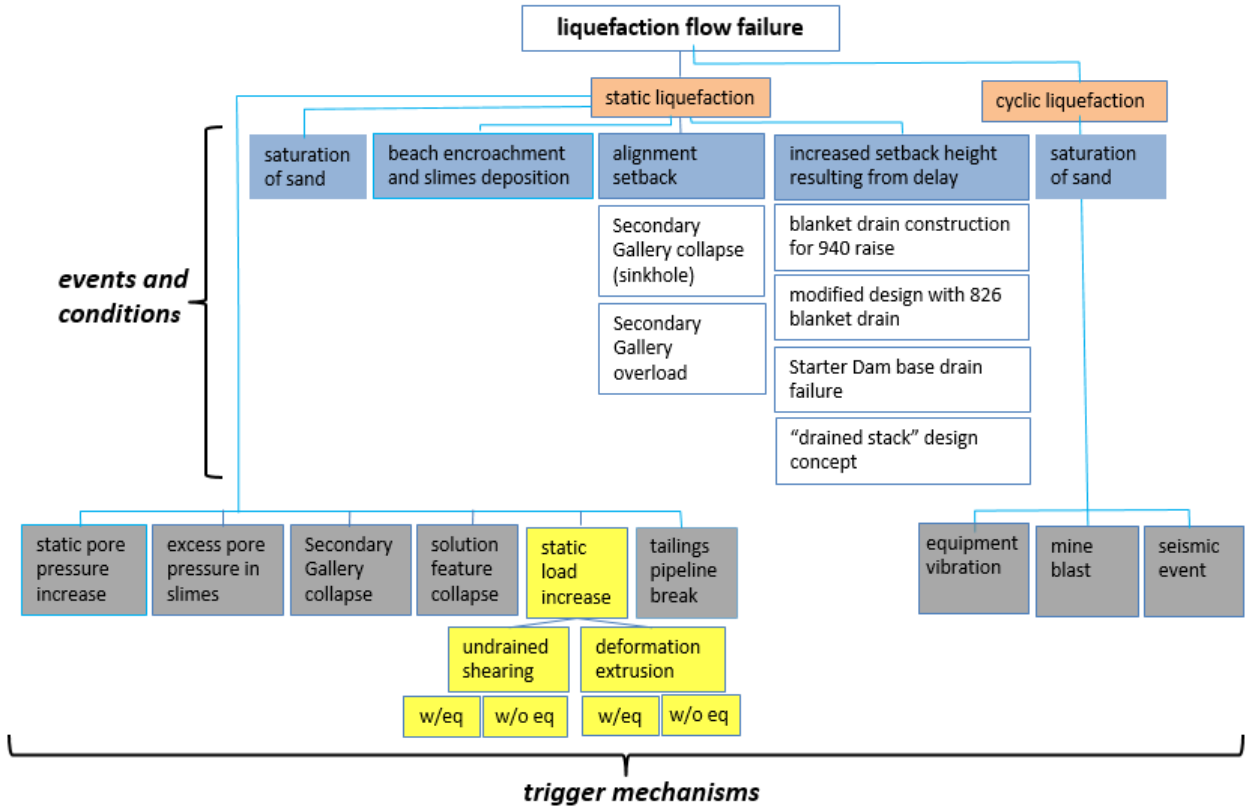

Figure 3-1 Fault tree for liquefaction triggering

The top event on Figure 3-1 is liquefaction flow failure. The next tier of events represents the two fundamental liquefaction processes: static and cyclic, either of which might have been operative. In this representation, cyclic-induced liquefaction flow failure is distinct from cyclic pore pressure contribution to static liquefaction.

The bottom tier of candidate initiating events represent liquefaction trigger mechanisms, and those shaded in grey were ruled out for reasons developed in Appendix K. These are:

- cyclic liquefaction:
  - equipment vibration;
  - mine blasting; and
  - seismic-induced.
- static liquefaction:
  - static pore pressure increase;
  - excess pore pressure in slimes;
  - Secondary Gallery collapse;
  - solution feature collapse; and
  - tailings pipeline break.

The surviving liquefaction trigger mechanism is static load increase, shown in yellow on Figure 3-1 with its two subsidiary processes: undrained shearing and deformation-related extrusion. Both of these might be operative either with or without cyclic pore pressure contribution from the November 5, 2015 earthquake series.

Also important on Figure 3-1 are the antecedent events and conditions shaded in blue that allowed or promoted static liquefaction at the left abutment. These are: (1) saturation of the sand; (2) water encroachment that allowed slimes deposition on the tailings beach; (3) the alignment setback; and (4) the increased height of the setback resulting from continued raising of the dam.

These four factors are central elements of the following sections of this report.

4 WHY DID A FLOWSLIDE OCCUR?

Determining why a flowslide occurred necessarily involves considering the conditions required for liquefaction, the first of which is saturation. In this regard, Section 2 presented the original "drained stack" design concept, that in the view of the Panel was not in principle amenable to liquefaction, and explained design changes that brought about an extent of saturation not anticipated in that concept. The new design allowed saturated conditions within the tailings, as evidenced by the extensive system of piezometers intended to measure it and limiting criteria established to evaluate it.

Another requirement for liquefaction concerns the properties of the materials involved, in this case sand tailings. This section shows how their void ratio—a measure of their propensity to expand or contract during shearing—influenced their susceptibility to liquefaction during the kind of rapid failure that occurred. Along with this is a related requirement for liquefaction: a reduction in strength during rapid shearing that produces flow behavior.

The Panel found no credible pre-failure assessment of liquefaction for the Fundão Dam in any of the documents it reviewed. Nor did it find any boring or cone penetration test (CPT) penetrating the full depth of the tailings that would have made such an assessment possible. For these reasons, the Panel has relied on its own analyses to determine why a flowslide occurred, the first test it has imposed on its explanation of the failure.

4.1 Strength Behavior

When load is applied to soil particles as a shear stress, *shearing* is said to occur. If these particles are in a tightly-packed arrangement—such as dense sands or stiff clays—the soil particles must first move apart to order to move past each other during shearing. This produces an increase in volume of the soil mass, and such soils are said to be *dilatant*. Generally speaking, dilatant soils are strong, which is why mechanical compaction is commonly used to achieve this condition.

By contrast, when shearing a loose particle arrangement—for example, loose sands or soft clays—the opposite occurs. The particles move together and the soil mass compresses. Soils displaying this tendency for volume decrease are called *contractive*. Hydraulically-placed and uncompacted materials such as tailings are often contractive.

When the soil mass is saturated, the spaces between the particles, or *voids*, are filled with water. If the soil is contractive and shearing occurs, the water may inhibit the particles from moving together so that the water itself carries part of the load. This produces pressure in the water, or *pore pressure.* But since water has no strength, the strength of the saturated soil mass can be reduced. Whether or not this occurs depends on whether or not the water escapes from the voids. And this, in turn, depends on yet another necessary condition for flowsliding—the rate of shearing.

Shearing a contractive, saturated soil slowly enough for pore pressure to dissipate as fast as it is generated produces a *drained* condition. Pore pressure does not develop and the soil retains its strength. On the other hand, if shearing occurs too rapidly for pore pressure to dissipate, *undrained* shearing is said to occur. In the case of Fundão, the failure developed within minutes and clearly occurred under undrained conditions. But in addition, the undrained strength of contractive sands

decreases markedly under the large strains imposed during flowsliding. It is this characteristic that gives flowslides their speed and mobility.

4.2 Tailings Volume Change, Undrained Strength, and Liquefaction

Different loading conditions can induce static liquefaction. Figure 4-1 provides stress paths for test data on Fundão sand tailings, where p´ is mean effective confining stress and q is shear stress. Stress paths for two tests are shown, both consolidated to the same stress at the start of shearing.

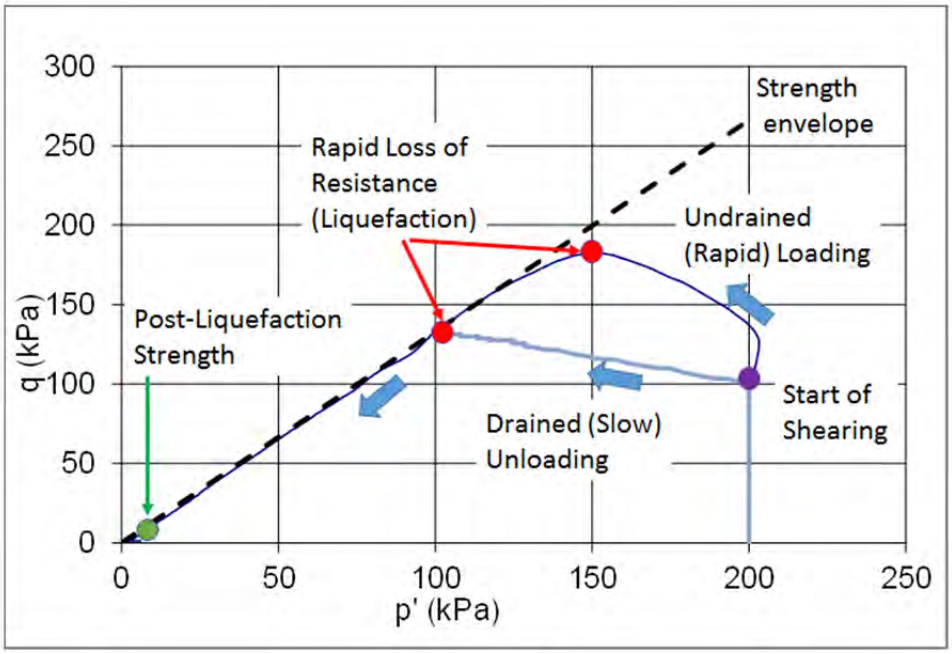

Figure 4-1 Stress paths for undrained loading and drained unloading of sand, Fundão test data

In the first test, conventional undrained loading is applied to simulate rapid shearing. When the stress path reaches the strength envelope it reaches a condition of liquefaction. As shearing resistance reduces due to changes in pore pressure, it progresses downward along the envelope and strength rapidly diminishes until arriving at a very low *post-liquefaction* strength.

The second test represents a different stress path central to understanding the Fundão failure. Instead of being loaded, the sample is laterally unloaded to simulate horizontal spreading. In addition, the unloading process is conducted slowly under drained conditions. As seen on Figure 4-1, the behavior on reaching the strength envelope is the same as before: liquefaction occurs, strength rapidly decreases, and the same post-liquefaction value results. In both tests, the loss of strength accompanying liquefaction is dramatic and nearly instantaneous, so much so that this behavior is sometimes referred to as *collapse*. The parallels between this kind of behavior in the laboratory and that which occurred during the Fundão failure are evident.

Thus, if the necessary conditions are present, liquefaction can occur under either slowly-imposed or rapidly-imposed changes in stress that can be produced by either loading or unloading. The essential

point is that it is the rate of shearing, not necessarily the rate of loading, that controls liquefaction of contractive materials, and the change in shear resistance derives from the intrinsic properties of the soil.

The most important such property is the tendency for volume change during shearing. This depends on two factors: first, how loose or dense the soil is, as characterized by its *void ratio*; and second, the level of stress it experiences. Figure 4-2 plots void ratio e versus effective stress p´. At any given effective stress, there exists some void ratio at which there is no tendency for either increase or decrease in volume during shearing. The *critical state line* (CSL) is the locus of these points and delineates the boundary between dilatant (volume increase) and contractive (volume decrease) conditions.

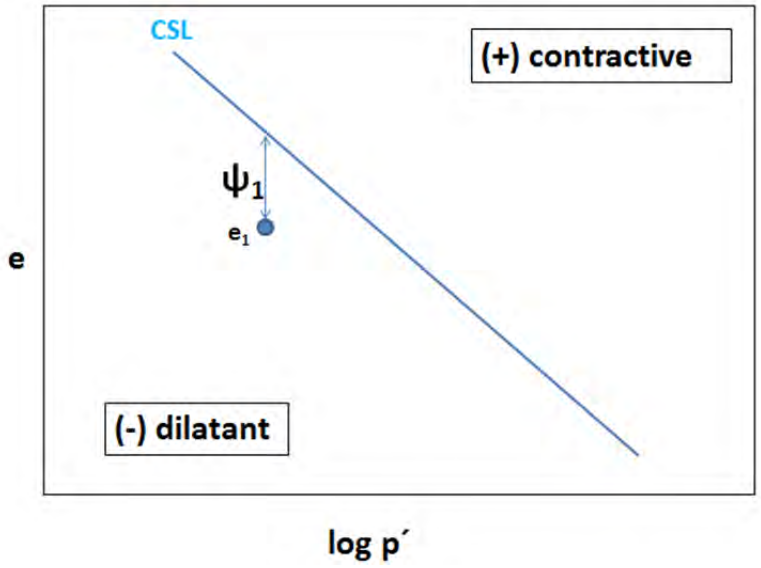

Figure 4-2 Definition of state parameter

The degree of contractiveness or dilatancy can be characterized by the *state parameter* ψ, shown on Figure 4-2 for some existing void ratio e_1. State parameter is defined as the difference in void ratio between e_1 and the void ratio on the CSL at the same mean effective stress. The magnitude of ψ, or the vertical distance of e_1 from the CSL, expresses the degree of contractiveness or dilatancy at that void ratio, with a negative sign convention for dilatancy and positive for contractiveness.

The relationships shown on Figure 4-2 are for constant stress. Figure 4-3 shows what happens when stress increases, for example when loading from embankment raising is imposed.

At the initial void ratio e_1 the tailings are dilatant with negative ψ_1, meaning that they act like a dense sand from an undrained strength standpoint. Under imposed loading and effective stress increase, compression occurs and e_1 reduces to e_2 in Figure 4-3. Now e_2 lies on the other side of the CSL and state parameter ψ_2 has positive sign. Thus, a material that initially had the dilatant behavior of a dense sand takes on the contractive characteristics of a loose sand as a result of the increased stress it now experiences.

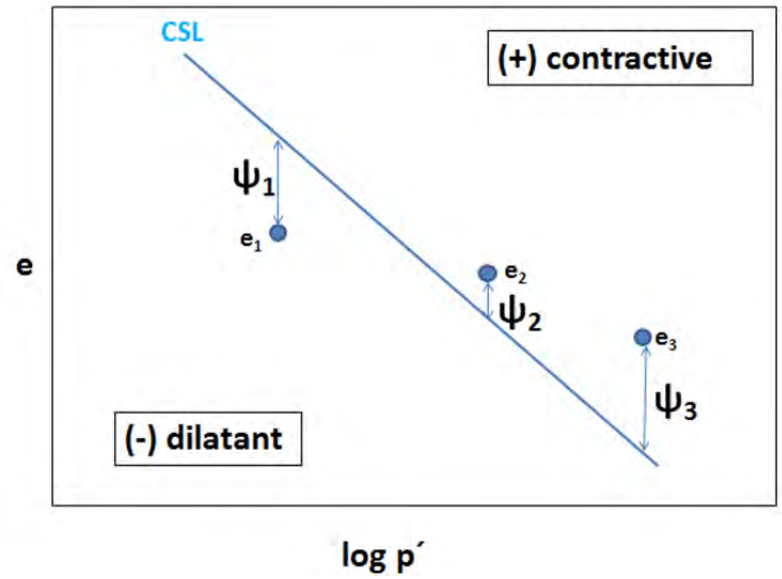

Figure 4-3 Change in state parameter for increasing stress

As loading continues and effective stress increases still more, e_2 reduces to e_3 as the result of further compression, and the magnitude of ψ_2 increases to ψ_3. Thus, not only can continued loading transform a dilatant material into a contractive one, it can also increase its degree of contractiveness.

These principles are applied to the Fundão tailings sand on Figure 4-4 that provides a statistical summary from Appendix C of CPT data on sand tailings obtained by Samarco prior to the failure in early 2015. The five CPTs were located along two transects on the Fundão tailings beach, one behind the left abutment setback and another in the central portion. While in theory contractive materials are those having $\psi > 0$, in practice $\psi > -0.05$ is often adopted as the boundary (Shuttle and Cunning 2007).

Shaded areas on Figure 4-4 indicate relative proportions of contractive material. Upper and lower histograms are for the left abutment and central transects, respectively, at locations given in Appendix C.

On this basis, approximately 70% to 80% of the sand tailings within 75 m of the dam crest are indicated to have been contractive, and 95% or more at greater distance up to 180 m. This demonstrates that the majority of hydraulically-discharged Fundão sand tailings satisfied the contractiveness requirement for liquefaction flowsliding. This is confirmed by CPT-based liquefaction criteria developed by Robertson (2010) on Figure 4-5 that supplements state parameter with liquefaction field case histories. These include flow liquefaction of the Nerlerk offshore berm for the encircled point labeled 19, 20, and 21, a case that figures prominently in the Fundão assessment as subsequently explained in Section 6.

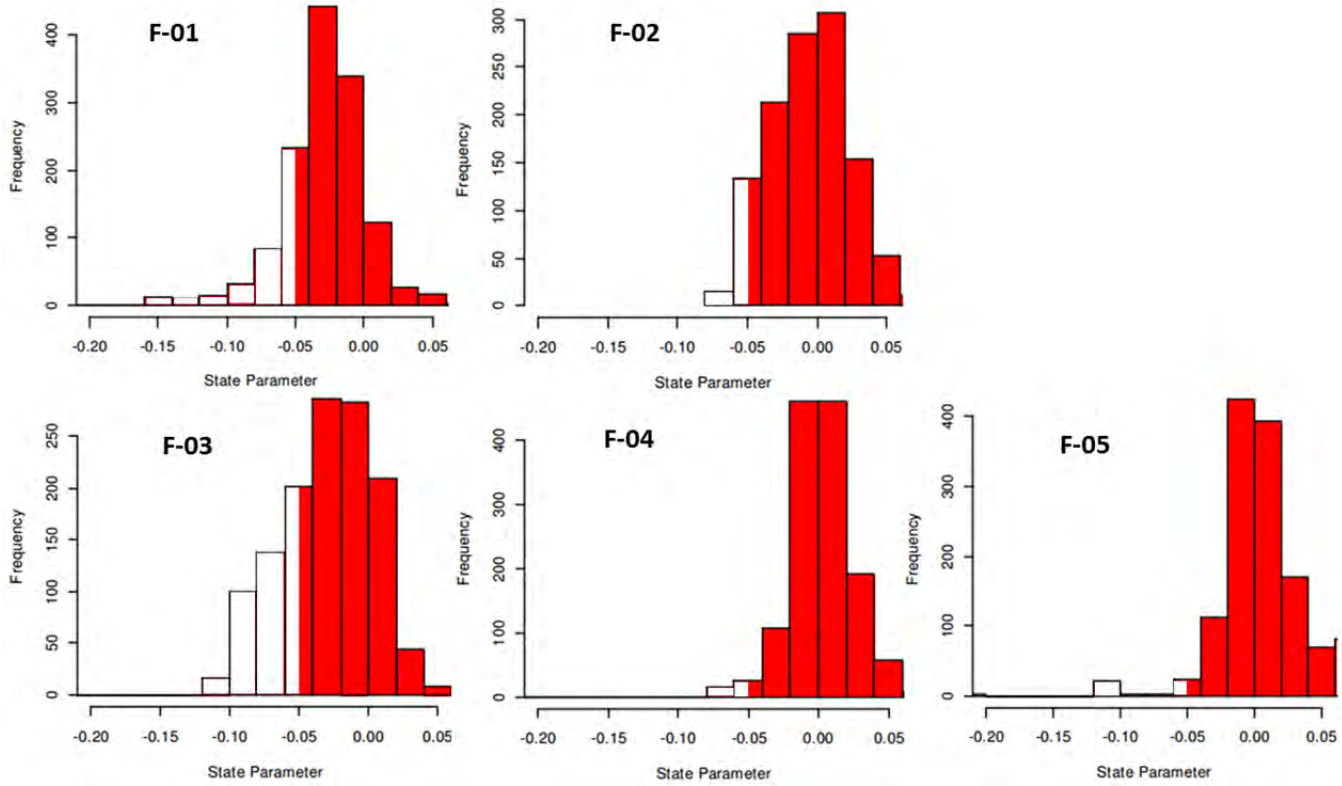

Figure 4-4 Histograms of state parameter for Fundão sand tailings

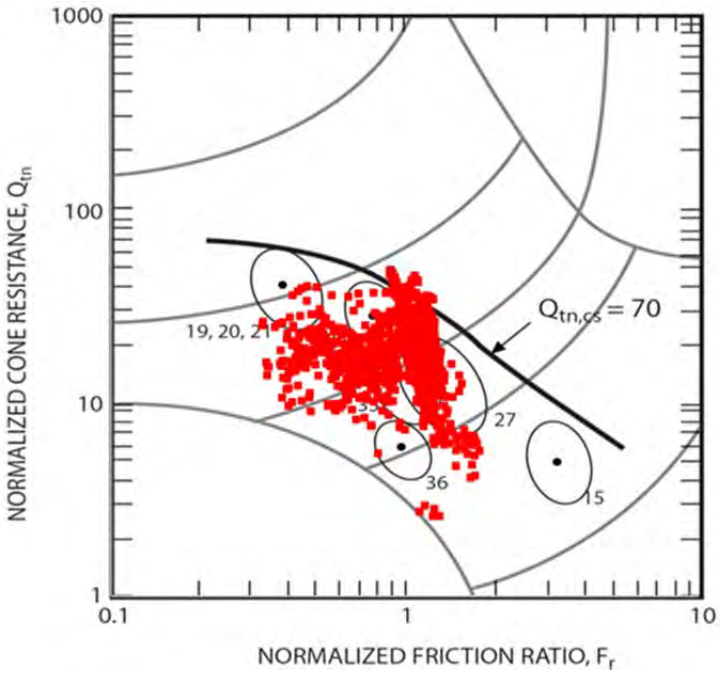

Figure 4-5 Robertson (2010) liquefaction criterion for Fundão CPT F-02 data

The 2015 Fundão CPT data also demonstrate the propensity for reduction in undrained strength of the sand tailings subject to the large deformations that accompany flowsliding. This can be shown by comparing undrained yield (peak) strength to critical (also known as residual or post-liquefaction) undrained strength. Figure 4-6 applies the CPT correlations of Sadrekarimi (2014) for undrained yield strength in simple shear and critical undrained strength.

Figure 4-6 shows that mean undrained strength ratio dropped from 0.21 before the flowslide to 0.07 during it, demonstrating that the Fundão sand tailings were susceptible to significant loss of strength.

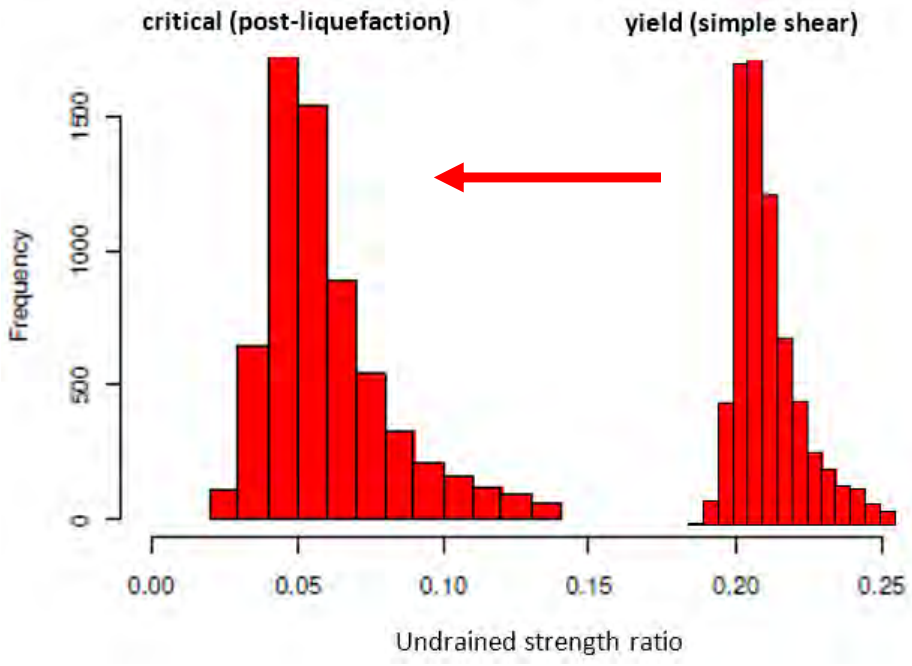

Figure 4-6 Yield (pre-flowslide) and critical (post-flowslide) undrained strengths for aggregated 2015 Fundão CPT data

4.3 Saturation

Saturation is another necessary condition for liquefaction flowsliding. It is useful to chart how saturation conditions of the Fundão Dam changed over time in response to events during the dam's evolution. To begin with, and as explained previously in Section 2.1, the "drained stack" concept of the Germano Buttress provided the model for the original Fundão design. With its high-capacity base drain extending beneath the dam and the sand tailings behind it, the aim was to reduce saturation and the accompanying effects on stability.

The original concept became inoperative after the damage sustained to the Starter Dam in the 2009 piping incident. The revised design that emerged relied instead on a blanket drain at El. 826 m near the top of the sand that had nearly filled the Starter Dam by that time. The El. 826 m blanket drain, which included the Kananet® pipes, was called upon to carry nearly all of the seepage as the dam grew higher and the impoundment larger with time. It became increasingly unable to do so, resulting in expanding volumes of saturated tailings.

The progression of conditions that promoted saturation is best illustrated by the following series of figures that integrates this information. Figure 4-7 shows the blanket drain in July, 2011, shortly after its completion the previous November. At that time the drain spanned the entire width of the Starter Dam. In this early configuration—which most closely resembled the original drained-stack concept—the impoundment size was limited and the drain was beneath the discharged tailings where it could intercept downward drainage to maximum effect.

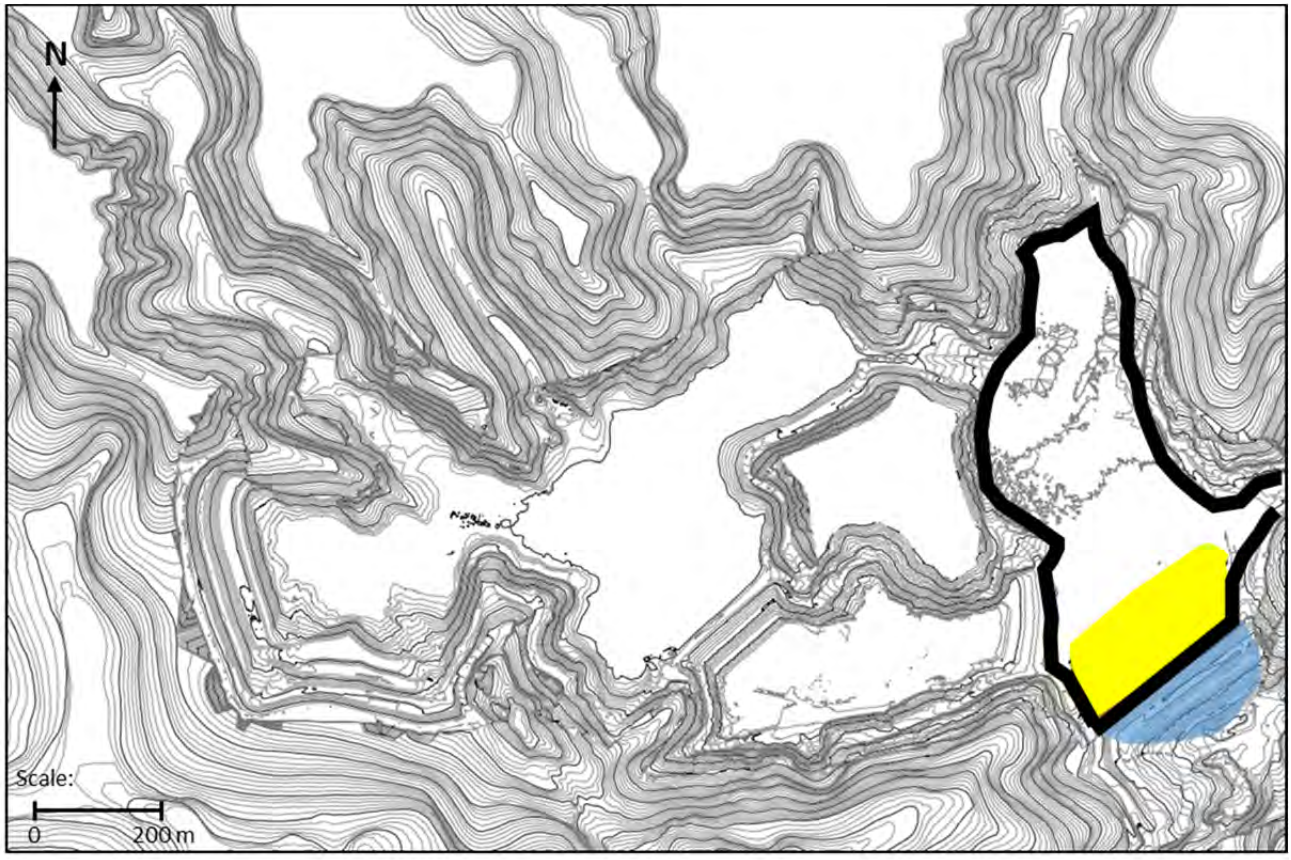

Figure 4-7 July, 2011 configuration showing El. 826 m blanket drain (yellow), Starter Dam embankment (blue) and impoundment outline

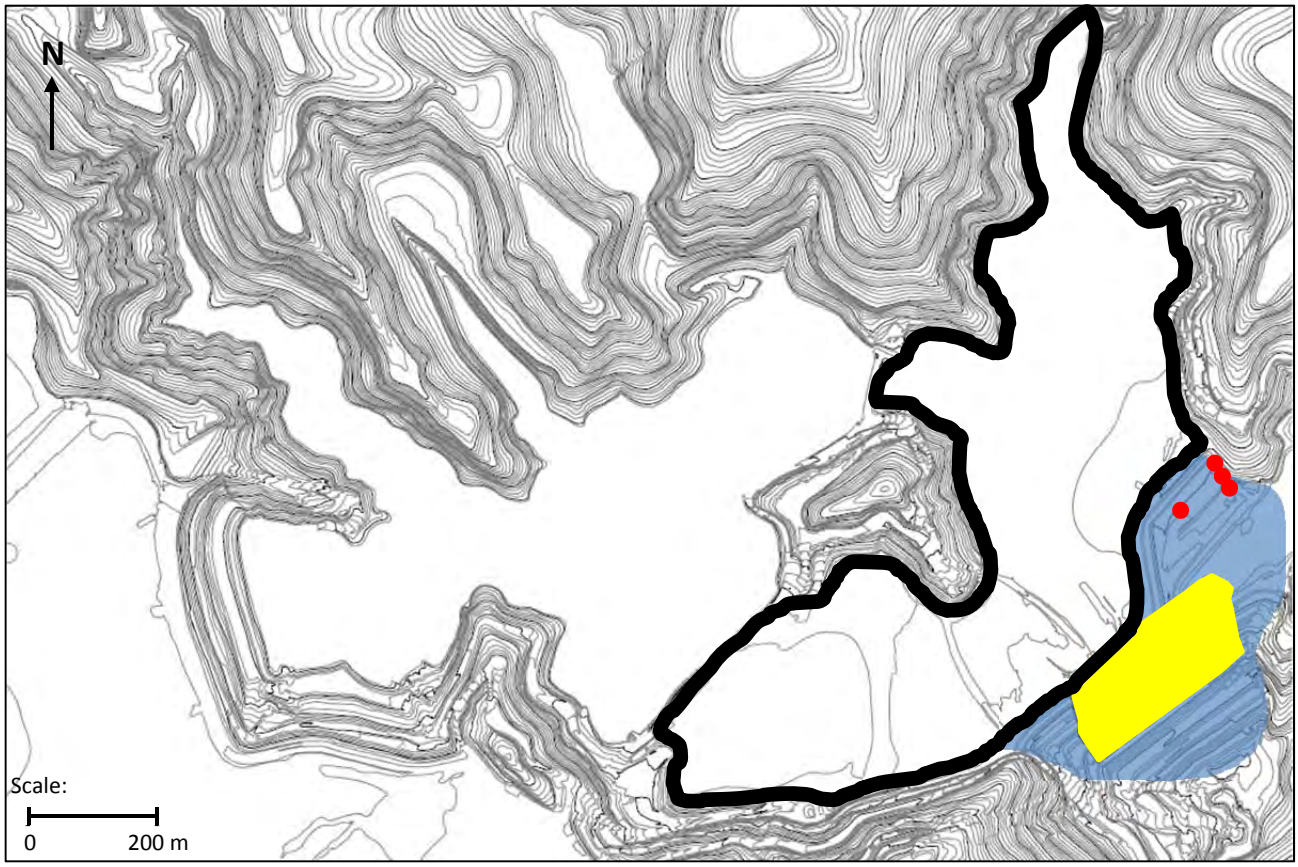

Figure 4-8 August, 2013 configuration showing El. 826 m blanket drain, raised dam, impoundment outline, and left abutment seeps (red dots)

Figure 4-8 shows that by August, 2013 both the embankment and impoundment had widened considerably as the dam grew higher, expanding beyond the limits of the drain on both sides. This had the effect of funneling seepage flow into the much narrower drain, and in the process raising the saturation level in the tailings. At the same time, the impoundment was moving upstream and becoming more distant from the drain as upstream dam raising progressed, also increasing the volume of saturated tailings.

With the left abutment setback by then in place, seeps appeared at El. 855 m in March and June, 2013 as the rising saturation reached the tailings surface, and again in November and December at El. 860 m. This shows that the saturation level at the surface of the left abutment rose some 5 m in elevation during the course of 2013. Localized drains constructed to treat these seeps had mostly near-surface effects, preventing further seepage breakout on the embankment face but not significantly reducing saturation in the tailings mass behind them.

Figure 4-9 shows that by August, 2014 the impoundment had nearly doubled in size, principally on the right side. With this enlargement came a seep on the right abutment at El. 855 m in July, followed by another in January the next year. As upstream raising continued, the impoundment became even further removed from the drain, expanding the volume of saturated tailings behind it still further.

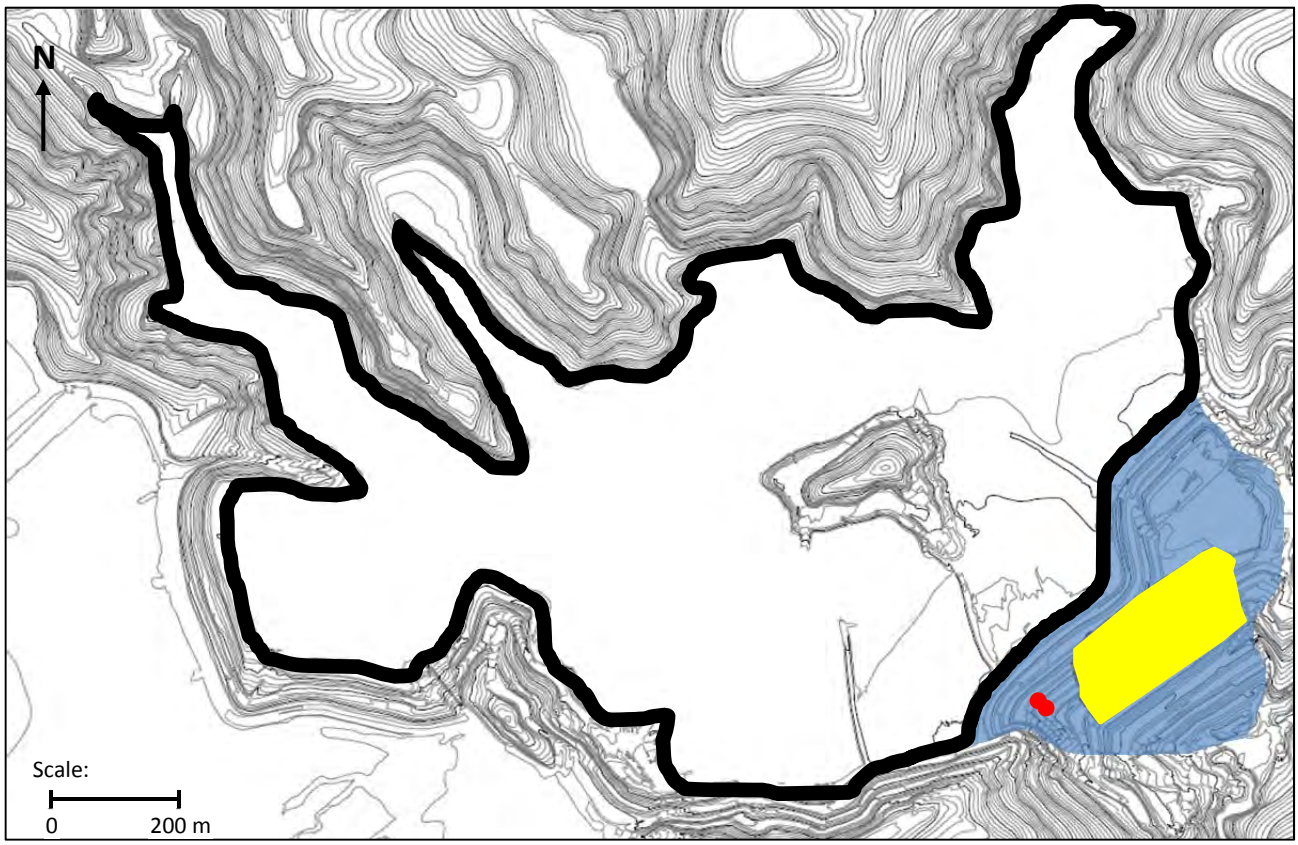

Figure 4-9 August, 2014 configuration showing El. 826 m blanket drain, raised dam, impoundment outline, and right abutment seeps (red dots)

Besides these incremental effects, a more fundamental change occurred on or about August, 2014 when three things happened simultaneously. As shown on Figure 4-10, flow from the El. 826 m blanket drain stopped increasing, then dropped briefly, partially recovered, and remained essentially unchanged thereafter. Also, flows from the Starter Dam base drain (a remnant of the original base drain salvaged after the 2009 piping incident) stopped diminishing and began increasing. In addition, artesian flow appeared at the toe of the Starter Dam.

An explanation consistent with these events is that the El. 826 m blanket drain with its Kananet® outlet pipes reached its maximum capacity. With the drain unable to divert additional seepage, saturation on the right abutment increased, breaking out in July at El. 855 m. At the same time, the diminished effectiveness of the blanket drain caused base drain flow to reverse its previous trend and begin increasing, while related increase in flow into the foundation caused artesian conditions to appear at the Starter Dam toe. And, as discussed subsequently in detail, all of these things were accompanied by the shallow saturation and unprecedented cracking of the left abutment that also occurred in August, 2014.

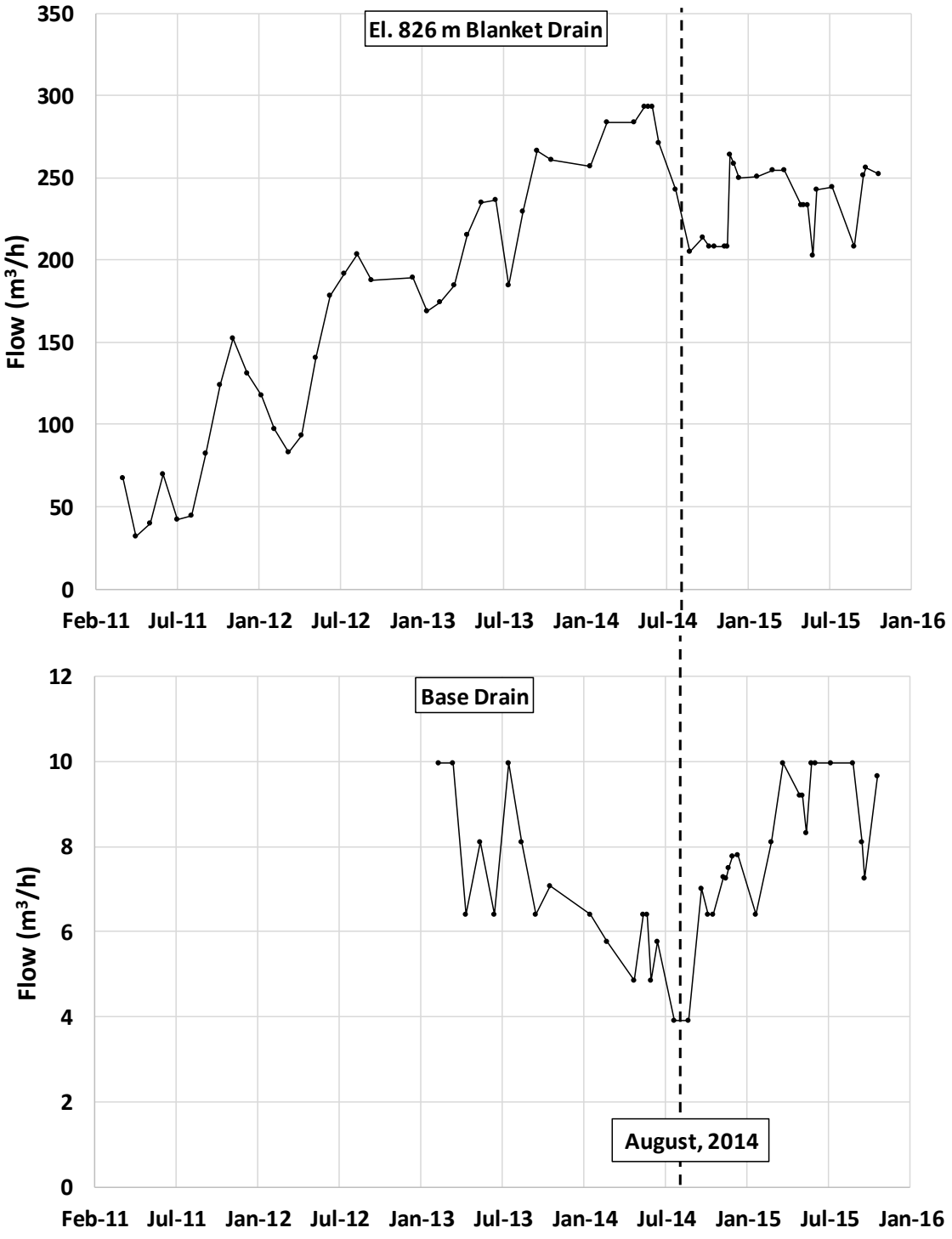

Figure 4-10 Measured flows from El. 826 m blanket drain and Starter Dam base drain

Figure 4-11 shows the drain configuration in November, 2015 with the ever-expanding impoundment. In preparation for the new 940 raise, the new blanket drain at El. 860 m had been completed at the left abutment setback and a companion drain at the right abutment was under construction. Had failure not intervened and had the dam alignment been restored, both of these new drains would have underlain the tailings much as the El. 826 m blanket drain once did. But as it was, neither had any effect on the tailings saturation that had already developed.

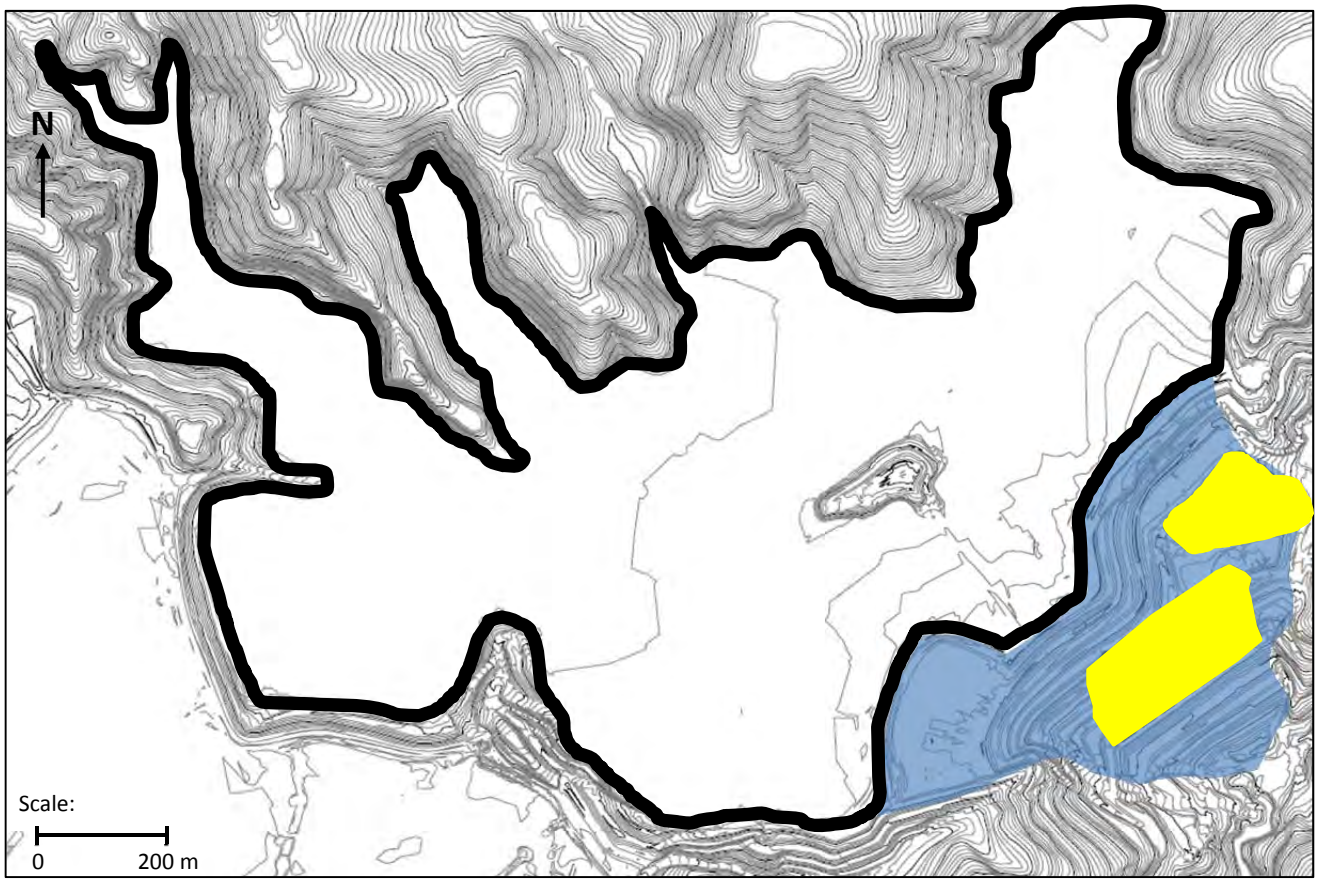

Figure 4-11 November, 2015 configuration showing El. 826 m and El. 860 m blanket drains, raised dam, and impoundment outline

Figure 4-12 summarizes the time-sequence of these impoundment drainage provisions. As upstream raising continued and the impoundment expanded, the El. 826 m blanket drain became increasingly more distant from the tailings it was intended to drain and eventually could no longer keep pace with rising saturation levels. With this, the saturated conditions necessary for liquefaction flowsliding were satisfied.

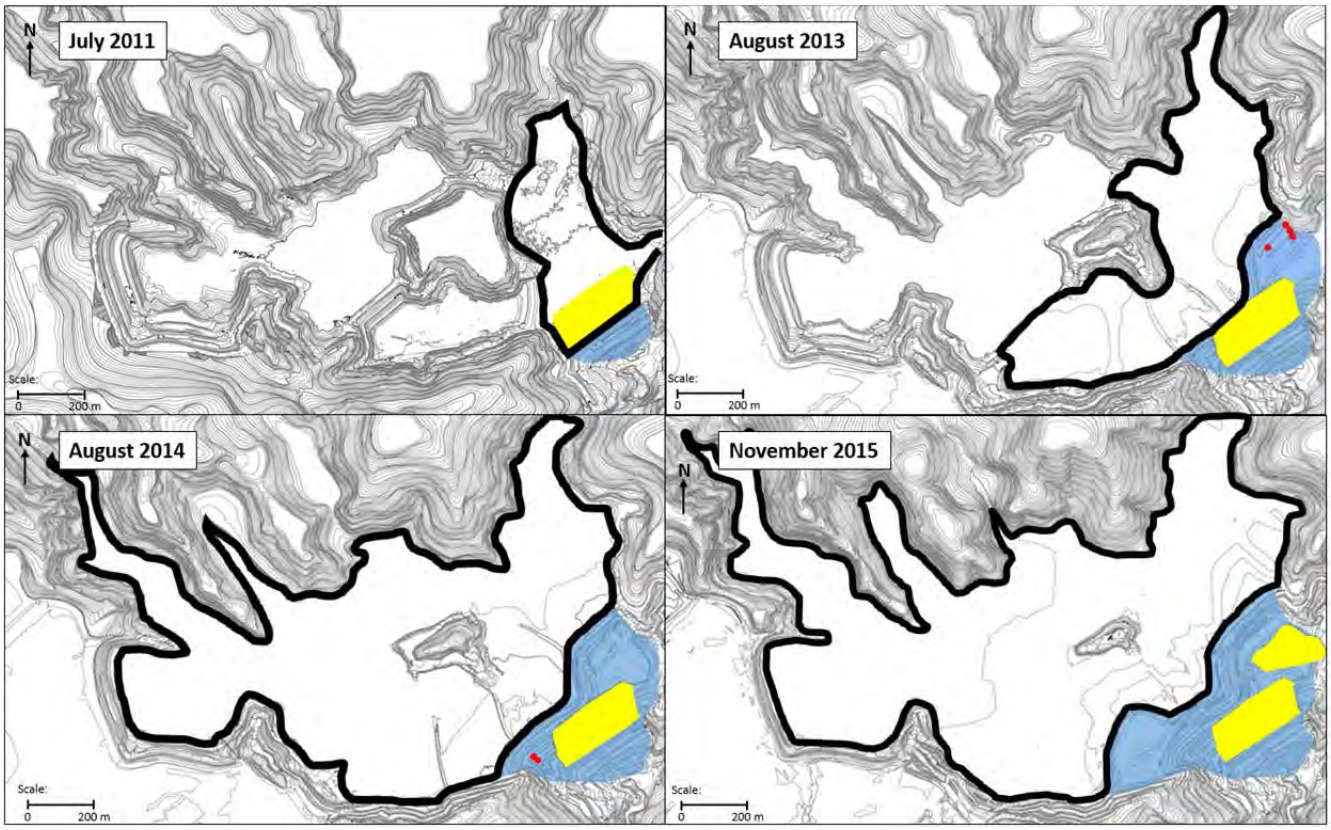

Figure 4-12 Progression of impoundment and drainage provisions with time

The beginning of this section posed the question: Why did a flowslide occur? In response, it has been shown that all of the necessary conditions were present. The sand tailings were contractive, they were saturated, and they were susceptible to severe loss of strength during the rapid failure that developed.

But an important factor has yet to be addressed. And that concerns the slimes.

5 WHY DID THE FLOWSLIDE OCCUR WHERE IT OCCURRED?

The eyewitness accounts summarized in Section 2.7 show that the flowslide of November 5, 2015 initiated on the left abutment where the dam had been set back from its former alignment. Section 4 has established why the flowslide occurred. It remains to explain why the flowslide initiated at the left abutment and not at some other location.

To do so requires identifying features or properties unique to the left abutment. In this respect, the defining feature of the left abutment setback was the presence of slimes beneath the embankment slope. The following discussions explain the characteristics of the slimes, where they were deposited, and how the setback influenced their effect on the embankment. Comparing these factors at the left and right abutments shows why the failure initiated at the former and not the latter.

5.1 The Slimes

5.1.1 Slimes Characteristics

Two types of tailings, *sands* and *slimes* were produced in the plants and conveyed in separate slurry pipelines to the Fundão and Germano impoundments. The sands are cohesionless and the slimes cohesive in character. As indicated on Figure 5-1, the two materials are readily distinguished by their color, the sands being gray and the slimes variously described as red, brown, or chocolate color.

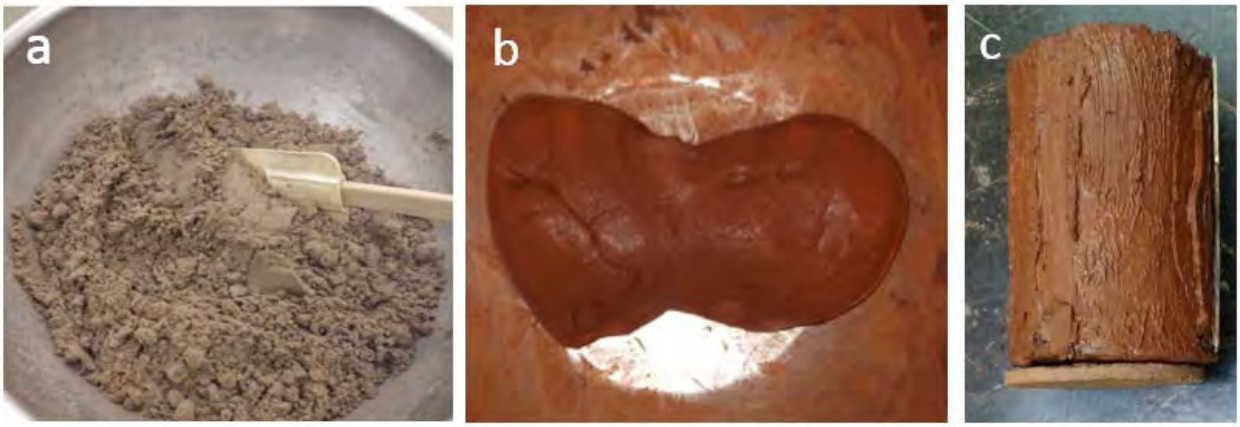

Figure 5-1 Sand and slimes tailings. (a) sand; (b) remolded slimes; (c) intact slimes specimen

The gradations of the two materials are compared on Figure 5-2, which shows that the sands contain approximately 40% silt, while the slimes are comprised entirely of silt and clay-sized particles.

The slimes contain only a small proportion of conventional clay minerals illite and kaolinite, the majority being hematite and goethite with some quartz. X-ray diffraction analysis of mineral composition is shown on Table 5-1.

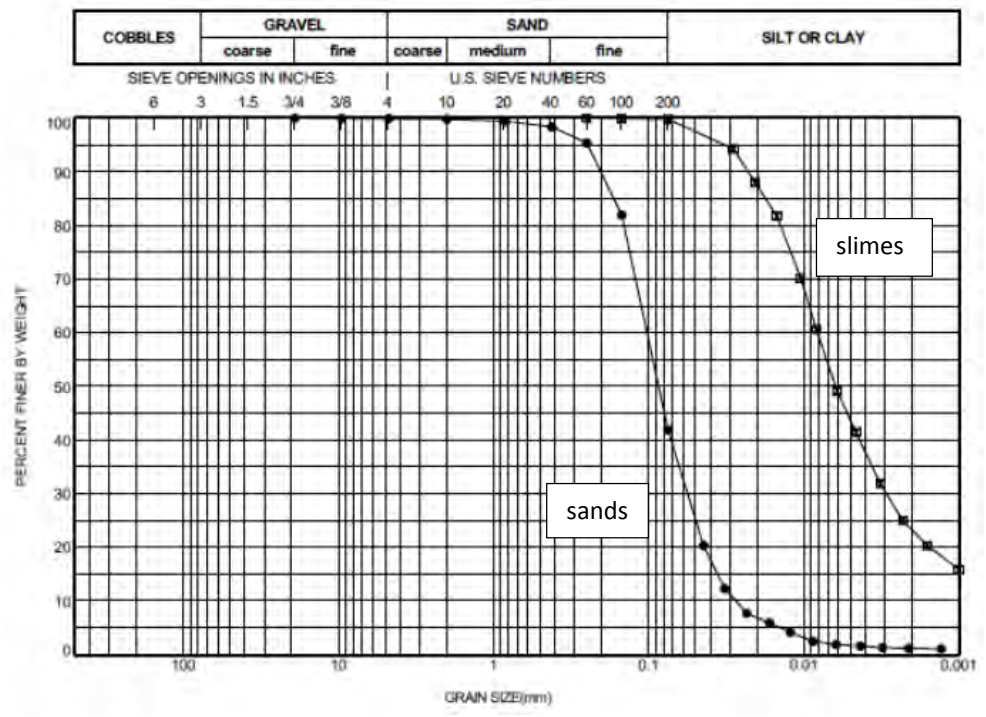

Figure 5-2 Sands and slimes gradation

Table 5-1 Slimes mineralogy

Mineral	Ideal Formula	#1 Slimes
Chalcopyrite ?	$CuFeS_2$	< 0.1
Goethite	α-$Fe^{3+}O(OH)$	30.9
Hematite	α-Fe_2O_3	42.9
Illite-Muscovite	$KAl_2AlSi_3O_{10}(OH)_2$	1.4
Kaolinite	$Al_2Si_2O_5(OH)_4$	4.4
Plagioclase	$NaAlSi_3O_8 – CaAl_2Si_2O_8$	1.1
Quartz	SiO2	19.2
Total		100.0

The concentration of iron-derived minerals in the slimes gives them a high specific gravity of nearly 4.0 that distinguishes them from the lighter sands. Where laboratory testing was available, the Panel was able to use specific gravity as a marker to distinguish the relative proportion of sands and slimes in tested samples. Despite the near-absence of clay minerals, the slimes classify as low-plasticity clay from Atterberg limits, with corresponding low permeability. Index properties of the slimes are given on Table 5-2, along with those for sands for comparison.

Table 5-2 Index properties

Property	Sands	Slimes
percent minus 0.074 mm	40-45	98-100
percent minus 0.002 mm	<2	20-25
specific gravity	2.8-2.9	3.9-4.0
plasticity index	non plastic	7-11
permeability	$3x10^{-4}$ cm/s	$< 10^{-6}$ cm/s

While the two materials in unadulterated form are easily distinguishable based on these measured properties, they are often mixed in various proportions in the field. Without laboratory testing, slimes can be difficult to identify from ordinary soil classification techniques, making their signature color their distinguishing characteristic in the field.

From the standpoint of the behavior of the Fundão Dam, the most important engineering property of the slimes that distinguishes them from sands is deformability. The slimes are softer and more compressible, as indicated by the compression curves on Figure 5-3. It will be shown in the following section that deformability of the slimes was a central factor in triggering liquefaction in the sands.

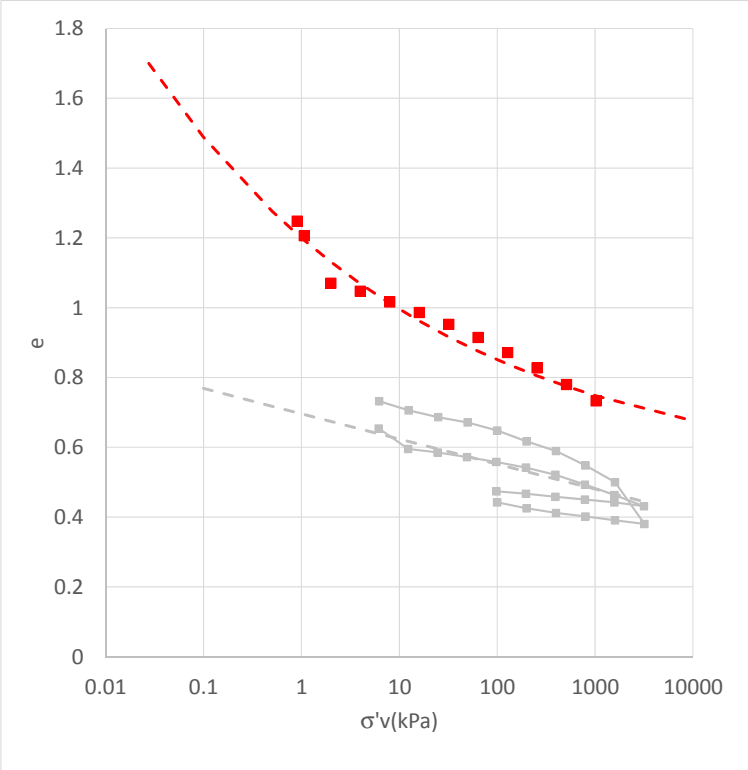

Figure 5-3 e log p curves for sand (grey) and slimes (red) from laboratory and field data; dashed lines used in modeling

5.1.2 Slimes Deposition and Identification

The tailings deposition process governs how sands and slimes are distributed areally and with depth. Figure 5-4 depicts this process in an idealized way when sands are discharged onto an above-water beach and from there into ponded water containing suspended slimes. Spigotting deposits exclusively sand tailings on the beach, while predominantly slimes sediment from the ponded water at greater distance. Between these two areas is an intermediate zone where intermixing of sands and slimes occurs at times when sands are being discharged. When sand discharge is temporarily suspended or relocated elsewhere, slimes layers are deposited that become embedded in and interlayered with the intermixed materials.

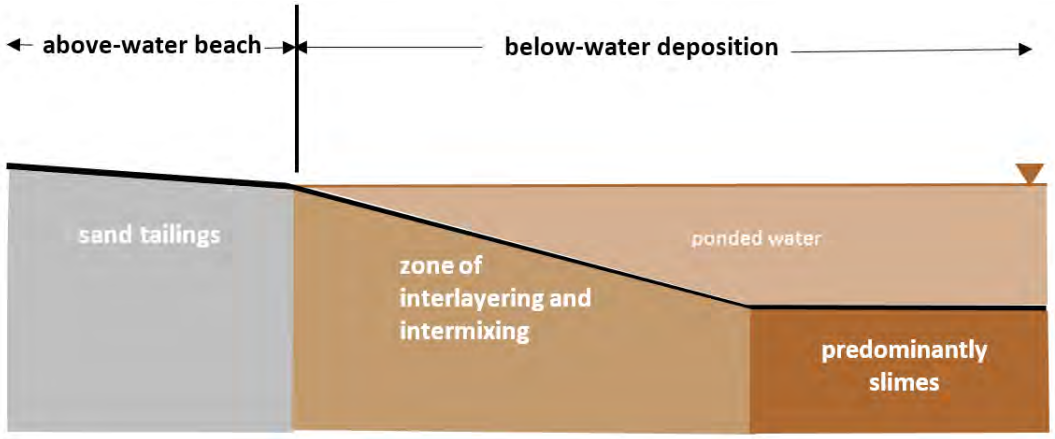

Figure 5-4 Idealized process of sands and slimes deposition

Figure 5-4 represents conditions at a particular moment in time, but the actual process is dynamic and constantly changing. The location of the interface between the beach and ponded water depends on both the depth of water—which varies according to precipitation inflows and water release—and the amount of tailings reaching that location from the sand discharge pipeline—which is regularly relocated. Thus, the dimensions of the three zones are always shifting. For the same reasons, they change with depth as the deposit accretes.

Figure 5-4 constitutes the conceptual basis for reconstructing tailings stratigraphy during the Investigation. The slimes-laden ponded water can be readily identified by its red color. Imagery from a variety of sources and related records provide snapshots of ponded water location and configuration that, when assembled and tracked over time, produce a three-dimensional representation of sands and slimes. The procedures used to create this tailings deposition model are described in Appendix A, and key findings are presented in Appendix B.

The Panel's development of the tailings deposition history involved review and distillation of hundreds of documents and records, most importantly: (1) publically-available satellite photographs; (2) drone photographs and post-2012 topography; (3) monthly Samarco instrumentation reports; (4) weekly construction reports; (5) consultant reports; and (6) interviews with Samarco engineering staff. The consultant reports were the primary source of drill holes, cone penetration tests and

laboratory data on the tailings sands and slimes. The engineering data from these reports are summarized in Appendices C and D.

Topographic information was assembled in Civil 3D using 40 different sets of basin-wide topographic surfaces at successive dam heights from 2009 to November, 2015. The quality of that topographic information increased considerably after Samarco initiated its drone program in early 2013. With the drone aerial photographs and topography, it was possible to input stripped ground topographic surfaces into Civil 3D to model the as-constructed base of Dike 1. This was especially useful because the abutments were stripped as the dam was raised. Some 15 different stripped surfaces were stitched into Civil 3D.

All information was assembled in a geographic information system (GIS) which enabled data to be queried and displayed in multiple views in real time. The Civil 3D model and the GIS system became the common source of the topography, stratigraphy and groundwater data used in the suite of analyses for this work.

5.1.3 Slimes Mapping

It can be recalled from Section 2.1 that the original design concept for Fundão was predicated on free-draining conditions in the sand tailings comprising the embankment. Achieving this required that drainage not be impeded by deposition of lower-permeability slimes. This was to have been assured by physically separating and separately discharging of the sand and slimes tailings behind Dikes 1 and 2, respectively.

Section 2.2 described how this concept was abandoned after the Dike 1 Starter Dam was seriously damaged by piping and internal erosion. In addition, subsequent structural problems with the Main and Secondary Galleries made it necessary to re-route water and slimes from the Dike 2 impoundment into Dike 1. These problems happened during 2011 and 2012 when tailings that would later underlie the left abutment setback were being deposited. The aerial image in Figure 5-5 shows that an Overflow Channel was constructed from the Dike 2 slimes reservoir to the Dike 1 reservoir from January, 2011 to July, 2012. This Overflow Channel introduced slimes into the Dike 1 reservoir.

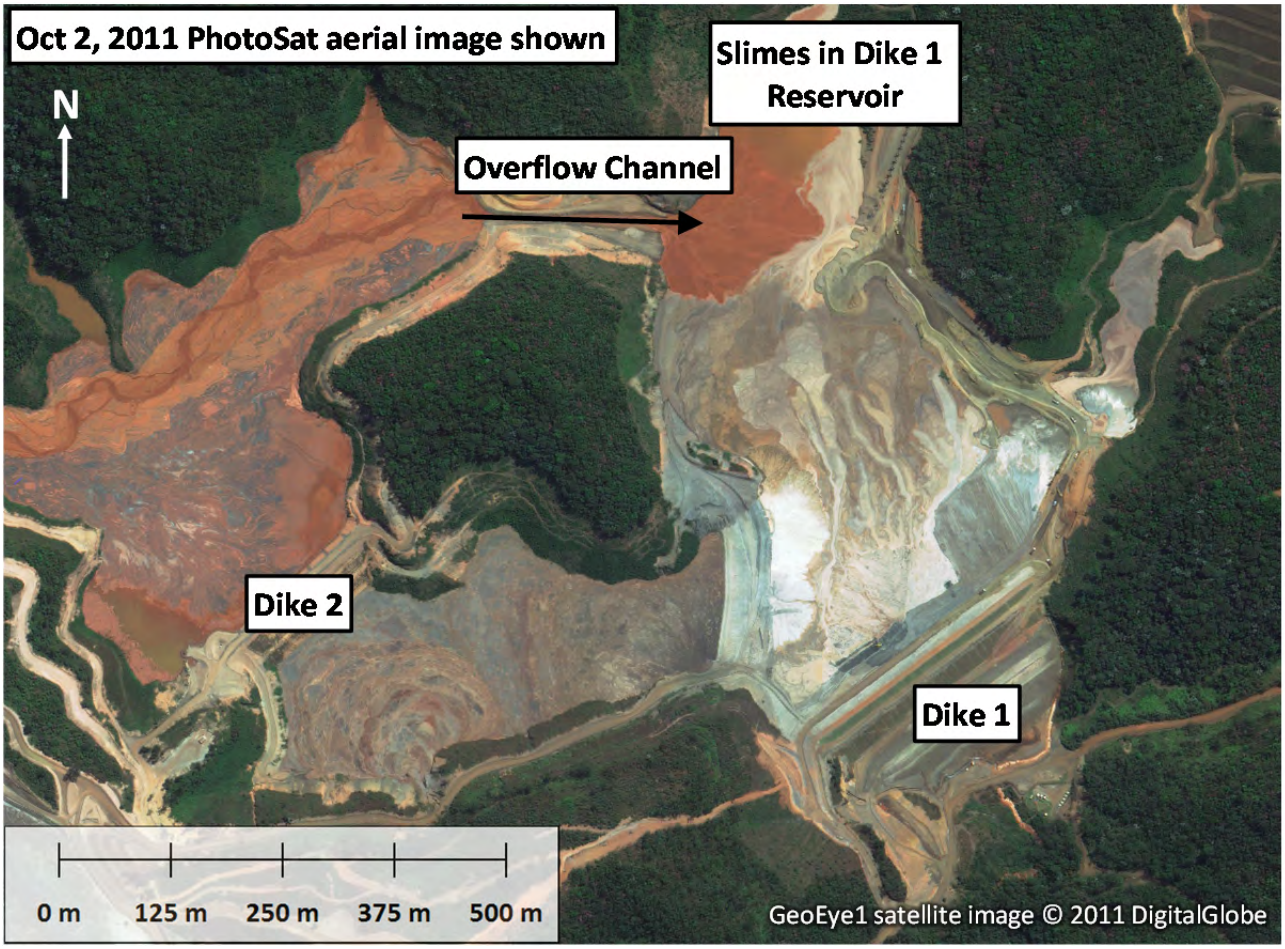

Figure 5-5 Slimes Overflow Channel from Dike 2 reservoir to Dike 1 reservoir

The Overflow Channel was closed in August, 2012 but not before slimes were deposited between El. 824 m and El. 850 m. Operation of the Overflow Channel and resulting slimes deposition is illustrated by imagery at selected dates during late 2011 and early 2012 on Figure 5-6.

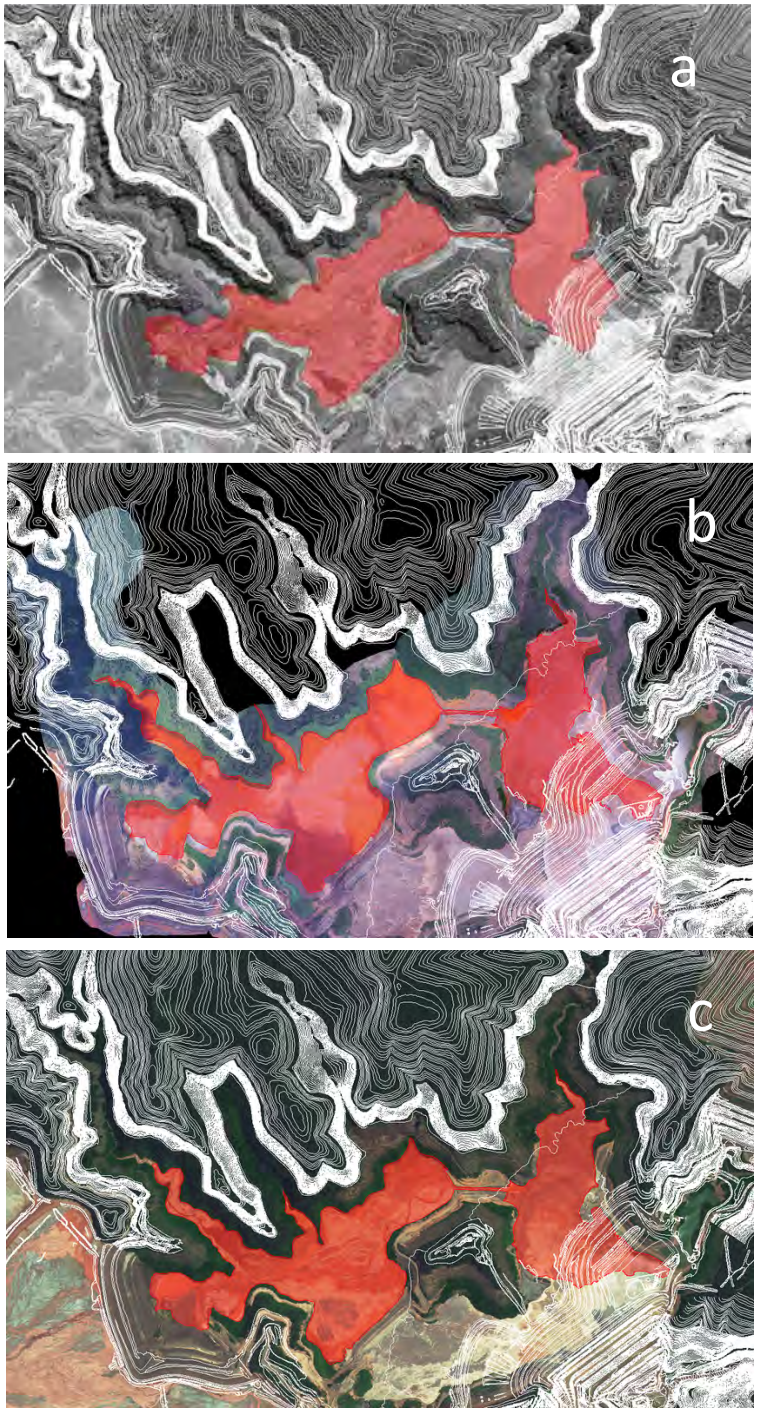

Figure 5-6 Slimes deposition (a) September 20, 2011; (b) January 21, 2012; (c) March 3, 2012. Slimes highlighted in red; final embankment contours in white

5.1.4 Drill Hole Information

The locations of slimes inferred from mapping can be compared to logs of drill holes through the left abutment tailings. Figure 5-7 shows borings and CPTs that penetrated a target interval of El. 830 m to El. 850 m. These holes were drilled at different times and surface elevations, but for reference they are superimposed on imagery from January, 2012. Also on Figure 5-7 for comparison are the outlines of slimes mapped at El. 841 m on that date that also appear on Figure 5-6b.

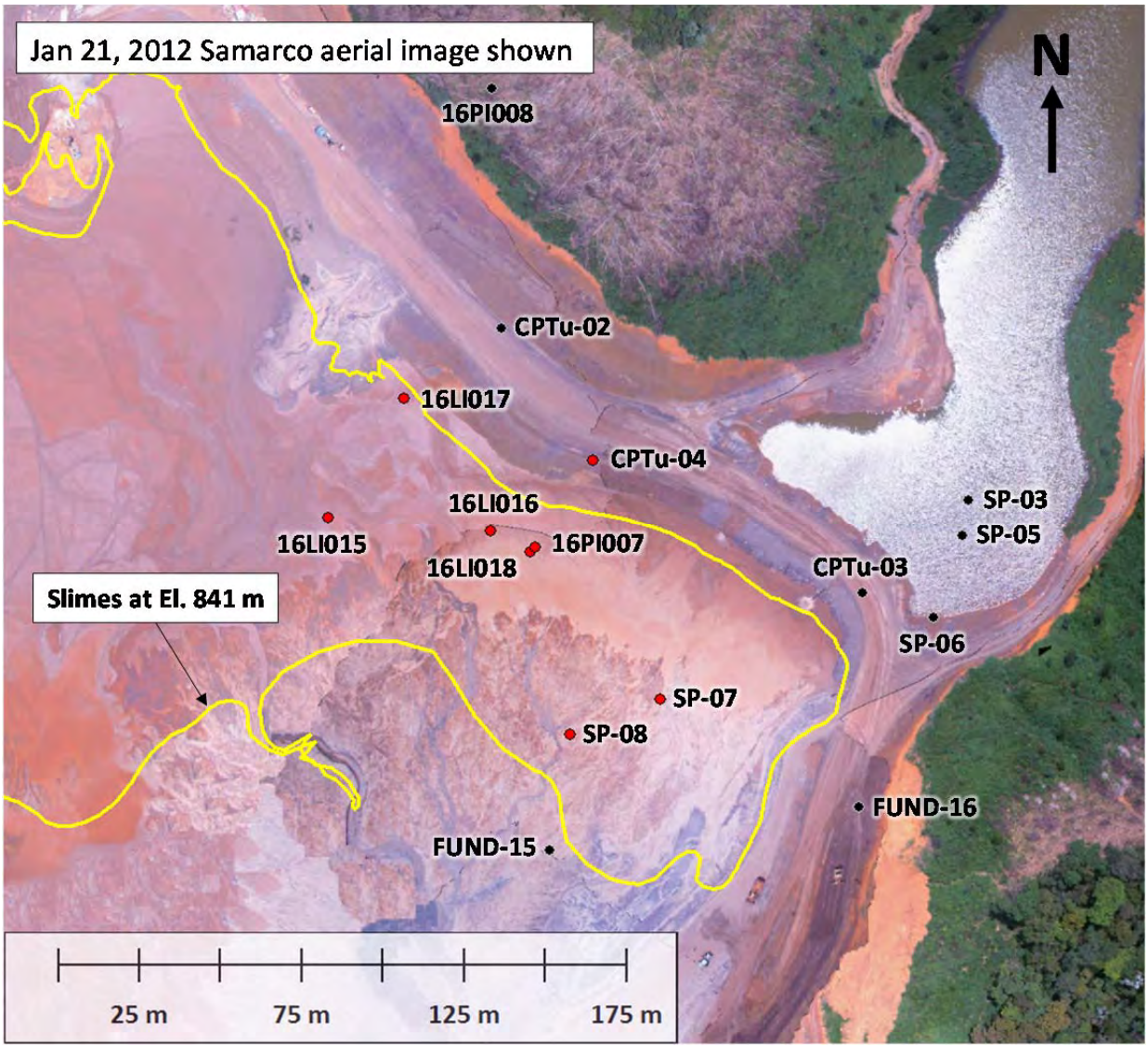

Figure 5-7 Left Abutment Drill Holes. Red circles indicate slimes within target interval of El. 830 m to El. 850 m.

No laboratory testing was conducted on recovered samples from any of the borings, so sample descriptions on the logs rely on visual classification alone with associated uncertainties as discussed in Section 5.1.1. For purposes of this assessment, slimes were taken as material logged as red or

brown in color, as opposed to grey for sands, often noting the presence of clay in varying amounts. Slimes were taken in CPTs as materials having apparent fines content of 100% that are not associated with road fill or other introduced materials. On this basis, Figure 5-7 shows holes indicating the presence of slimes within the target elevation interval in red and holes with no such indications in black. It can be seen that the drill hole information corresponds to the area of mapped slimes. A number of other holes not shown on Figure 5-7 were drilled over the Secondary Gallery for purposes of investigating its foundation conditions. With a surface elevation at or near El. 835 m, they mostly penetrated tailings below the target interval.

Within those holes where slimes were identified, their distribution is more difficult to determine because the tailings were not continuously sampled. However, SP-07 is notable in having distinguished two discrete clay layers corresponding to slimes: a 2 m thick layer at El. 836.36 m and a deeper 2 m layer at El. 828.36 m. Also, CPTu-04 penetrated slimes layers up to several centimeters thick. It is reasonable then from the drill holes to categorize discrete layers of slimes as ranging from a few centimeters to a few meters in thickness, with the remainder of the slimes material intermixed with sand in varying proportions. This characterization is consistent with the zone of interlayering and intermixing portrayed on Figure 5-4.

5.1.5 Slimes Mass Balance

The distribution of slimes estimated from drill hole information can be supplemented on a broader level using a mass balance approach. To this end, slimes production records were compared with the potential slimes volumes between El. 840 m and El. 850 m. A mass balance was derived by assuming a dry unit weight of the slimes taken from measurements of recently-deposited slimes sampled in Germano as part of this Investigation. The mass balance assumptions and calculations are given in Appendix B.

The mass balance provides a measure of the volumetric proportion of constituent slimes and slimes layers within a specified zone. Figure 5-8 portrays the results in cross section. Here, the region designated *predominantly slimes* is nearly 100% slimes, *interbedded slimes* is estimated to contain 20% or more slimes overall, and the zone of *isolated slimes* less than this amount. Although distinct boundaries are shown between these regions, actual conditions are transitional in character.

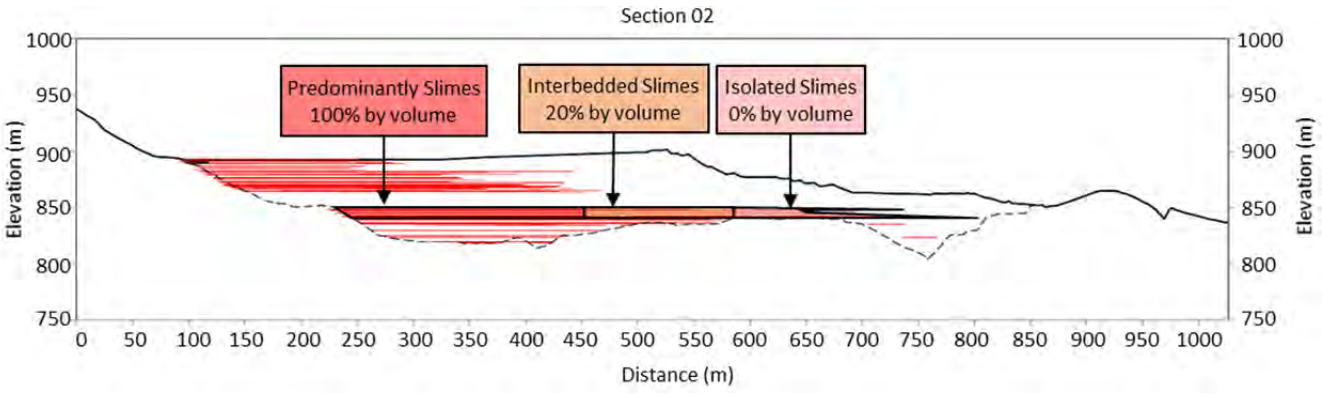

Figure 5-8 Distribution of slimes at left abutment

The preceding discussions have shown that slimes were present at the left abutment, in particular between El. 830 m and El. 850 m, and that their concentration increased with distance behind the dam. How these conditions influenced the embankment requires accounting for the setback.

5.2 The Left Abutment Setback

5.2.1 Events and Circumstances

Circumstances surrounding the modification of the dam alignment that resulted in the setback have been reviewed in Section 2.4. Due to structural problems and construction defects, the dam could not continue to be raised over the Secondary Gallery until repairs had been made. But when these repairs proved unsuccessful, the Secondary Gallery had to be abandoned and filled with concrete. To accommodate tailings storage requirements during these periods, beginning in October, 2012 the dam alignment at the left abutment was shifted back from its former location as shown on Figure 5-9. This created what is called here the *setback*, with the vacant area in front of it the *plateau* or *platform*.

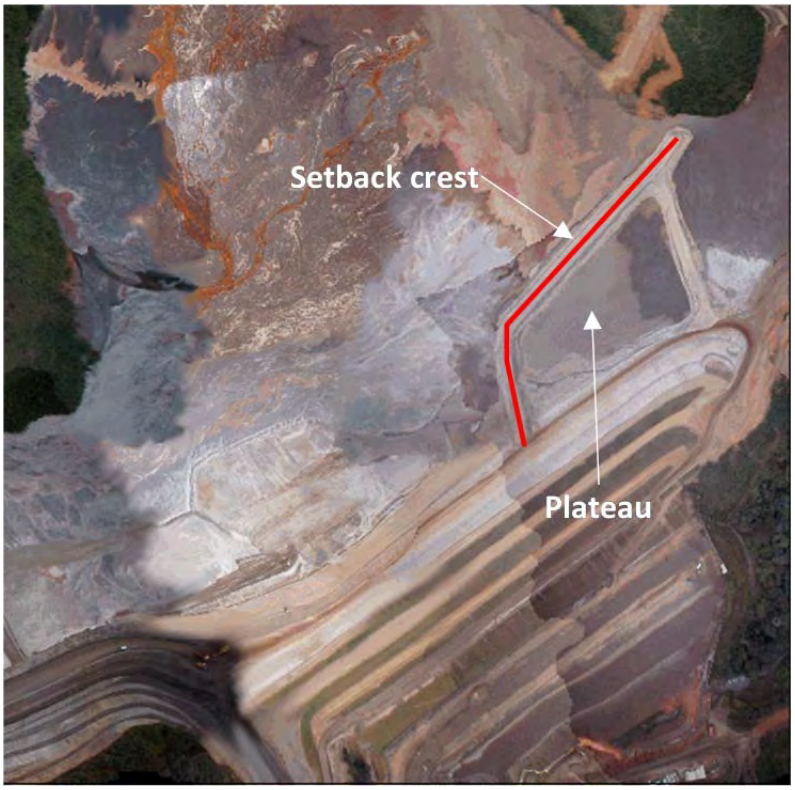

Figure 5-9 Aerial photograph of the setback alignment in October, 2012

The setback was initiated when the plateau was at approximately El. 855 m. By the end of 2013, the crest had risen to El. 877 m, or about 22 m high.

Starting in August, 2013, the first compacted fill was placed to rebuild the setback portion of the embankment and return it to its former alignment while dam raising continued. This occurred until August, 2014 when the slope showed serious signs of distress as reviewed in Section 2.5. The setback was immediately buttressed with a tailings sand berm. By then, the crest had reached El. 885 m, or 30 m high.

Infilling of the setback was further delayed by requirements for the proposed raise of the Fundão Dam to a crest elevation of 940 m. Design analyses concluded that more drainage would be needed to reduce the phreatic surface on both abutments, including a large blanket drain at the left abutment to be constructed in four stages. The first stage was a blanket drain at El. 860 m on the setback plateau. Construction began in November, 2014 and did not conclude until August, 2015 when setback infilling was resumed.

The setback had significant effects. Moving the embankment back toward the impoundment caused it to be raised over the slimes deposited in 2011 and 2012. In addition to influencing foundation conditions, these slimes also changed the seepage regime, elevating the phreatic surface on the left abutment.

5.2.2 Slimes Configuration

The combined effect of the slimes deposition described in Section 5.1 and the setback is best shown by a series of illustrations representing various points in time. The extent of newly-added tailings since the previous time step is indicated on the sections and in plan view on the insets to Figure 5-10. Compacted tailings that were mechanically placed during embankment raise construction are distinguished from the hydraulically-discharged sands by lines separating the two on the cross sections.

Figure 5-10 shows that the alignment setback caused all or most of the embankment to be constructed over slimes. In addition, as the embankment became higher and its crest moved upstream, more of the embankment slope became underlain by the higher proportion of slimes in the interbedded region.

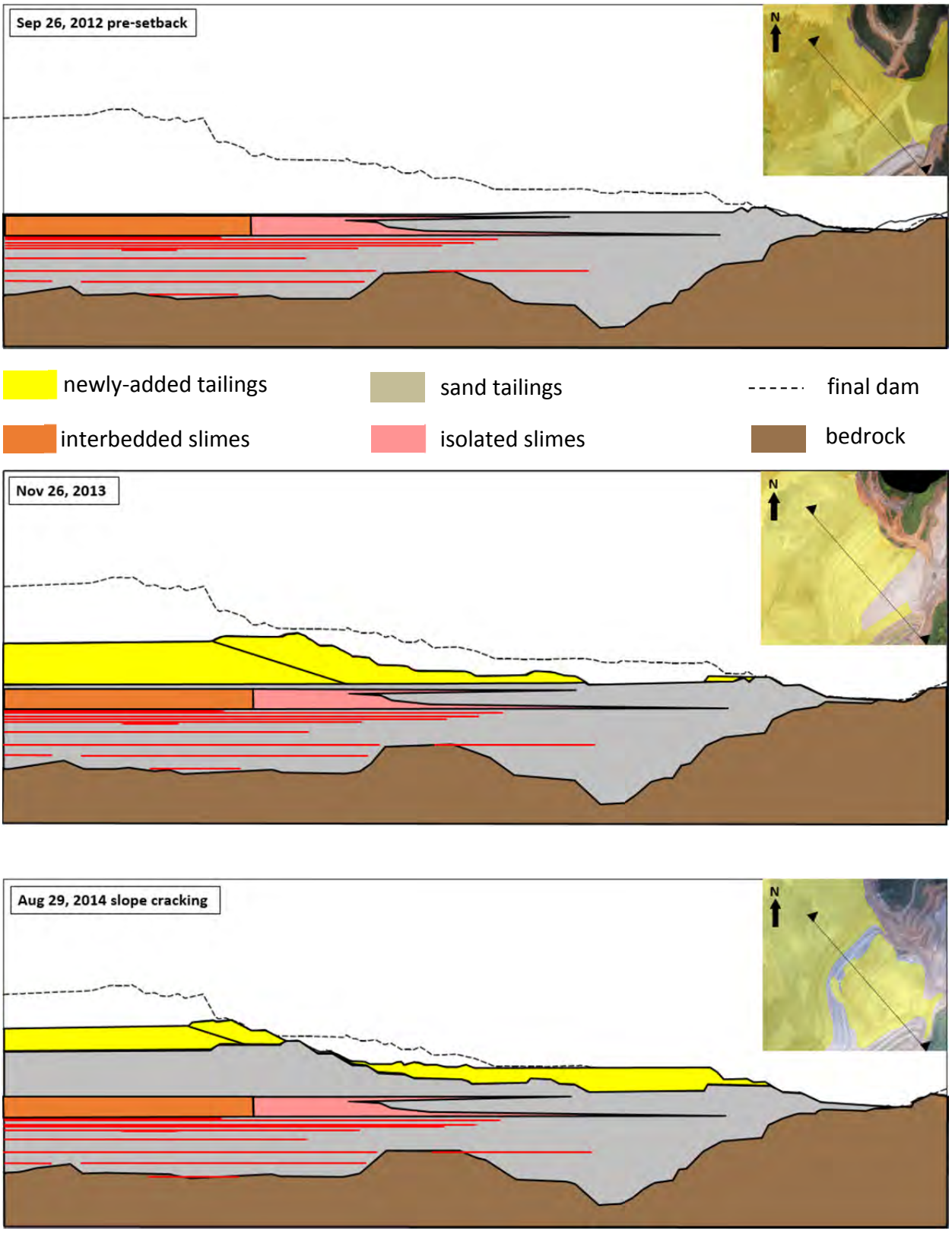
Sep 26, 2012 pre-setback
N
newly-added tailings
sand tailings
final dam
interbedded slimes
isolated slimes
bedrock
Nov 26, 2013
N
Aug 29, 2014 slope cracking
N

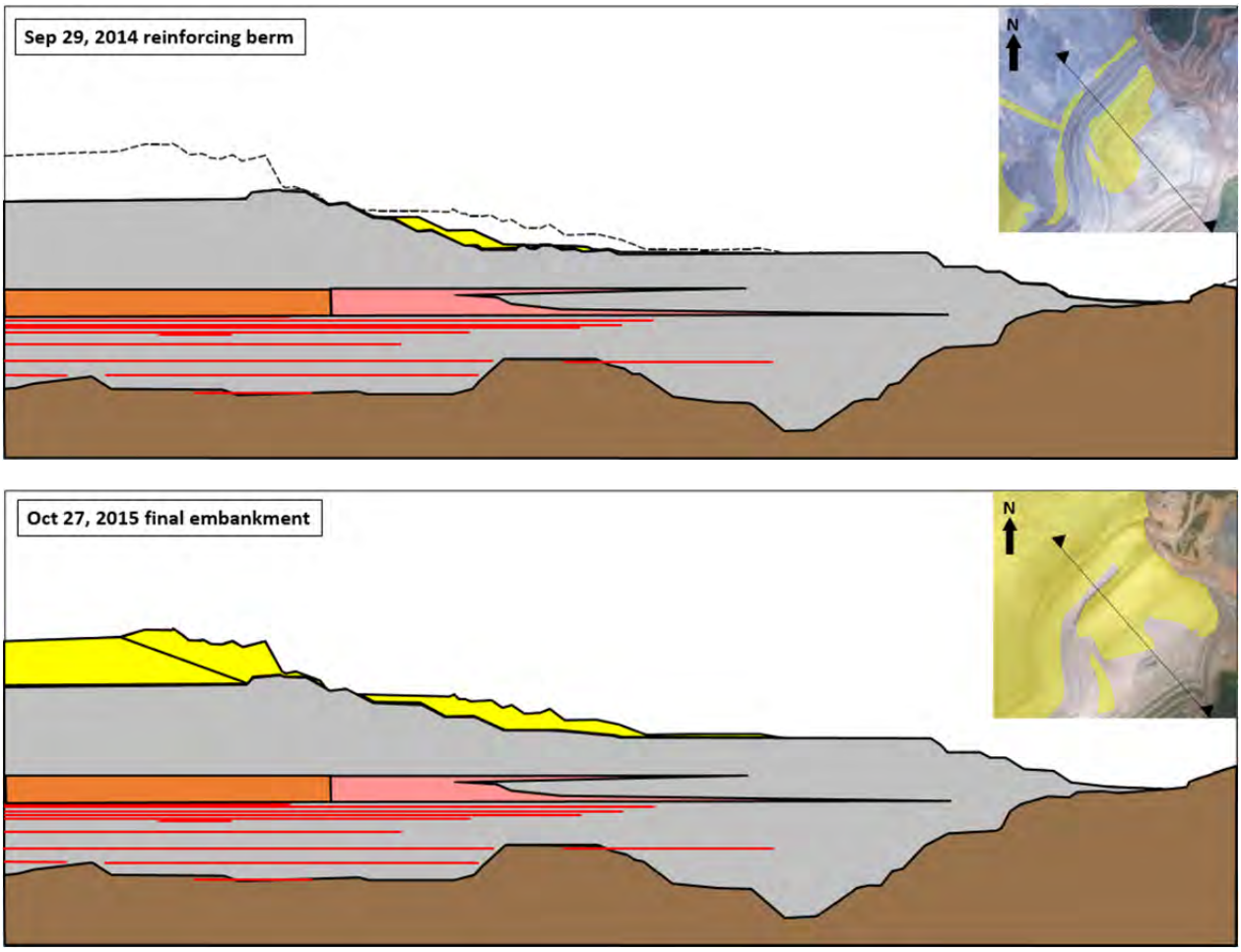

Figure 5-10 Sequential raising of setback embankment over slimes

The areal extent of the slimes depicted on Figure 5-10 deposited in 2011 and 2012 beneath the left abutment setback is shown on Figure 5-11, where again it can be seen that by the time the embankment reached its final height, slimes would be present beneath the entire setback slope and much of the plateau area.

Figure 5-11 Slimes beneath final embankment: (a) September 20, 2011; (b) January 21, 2012; (c) March 3, 2012. Slimes highlighted in red; final embankment contours in white

5.2.3 Rate of Rise

As indicated on Figure 5-12, the rate of rise of the dam crest at the left abutment varied during the life of the setback. The average 1.3 m/mo during 2015, or an annualized rate of 15.7 m/yr, was intermediate between rates experienced during 2013 and 2014. Also during 2015 in the months immediately prior to failure, raising accelerated from as low as 0.4 m to 2.9 m. The small negative rate of rise in September, 2014 was produced by regrading related to construction of the reinforcing berm and is not consequential to the overall trend.

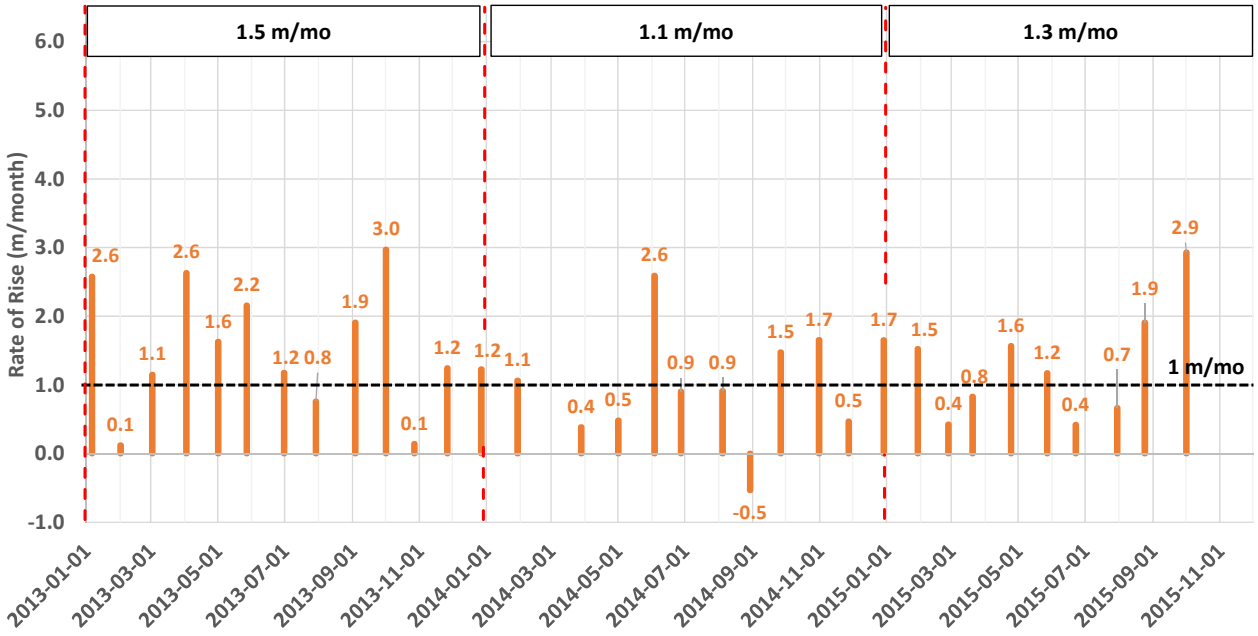

Figure 5-12 Rate of dam crest rise at left abutment setback

5.3 Comparison of Left and Right Abutments

Thus far, it has been established that slimes existed beneath the embankment slope at the left abutment as a consequence of their earlier deposition together with the setback of the dam alignment. To explain why failure initiated here and not elsewhere, it is useful to compare conditions at the left abutment to those at the right, where failure resulted from and was preceded by flowsliding on the left. The question then becomes why failure initiated at the left abutment and not the right. This requires comparing conditions at the two locations.

5.3.1 Right Abutment Conditions

Figure 5-13 shows Section AA at the right abutment and its internal composition based on mapping as described in Section 5.1.3. The distinguishing feature of the right abutment compared to the left is the nearly complete absence of slimes beneath the embankment slope. The only region of slimes lies below El. 825 m where it is confined both upstream and downstream by natural ground. This is in sharp contrast to the left abutment on Figure 5-8 where slimes can be seen to extend beneath virtually the entire length of the slope.

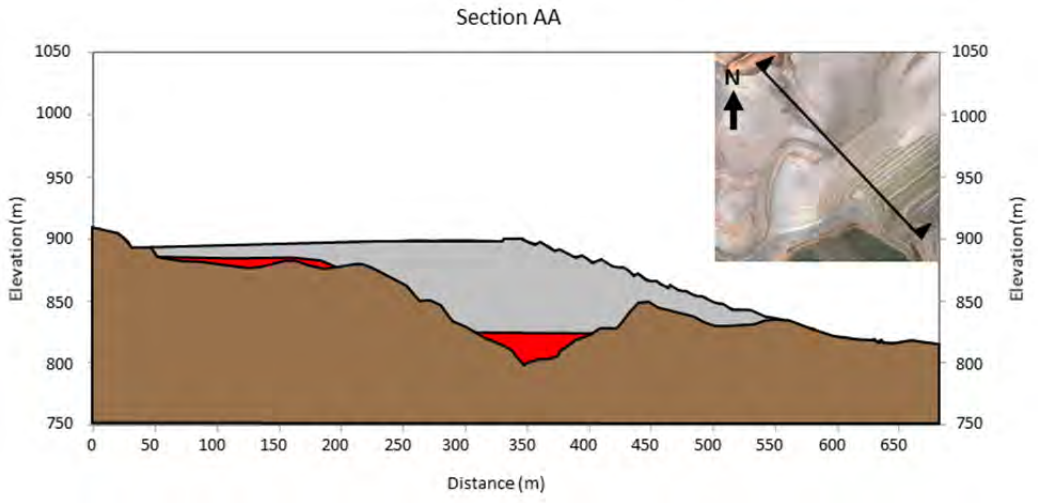

Figure 5-13 Slimes at right abutment Section AA

The left and right abutments can be compared more directly by overlaying the respective sections. Figure 5-14 provides an overlay of Section 01 at the left abutment and right abutment Section AA, coincident at the respective dam crests. Geometrically, the greater overall steepness and extended length of the 3.0H:1.0V right abutment slope stands out.

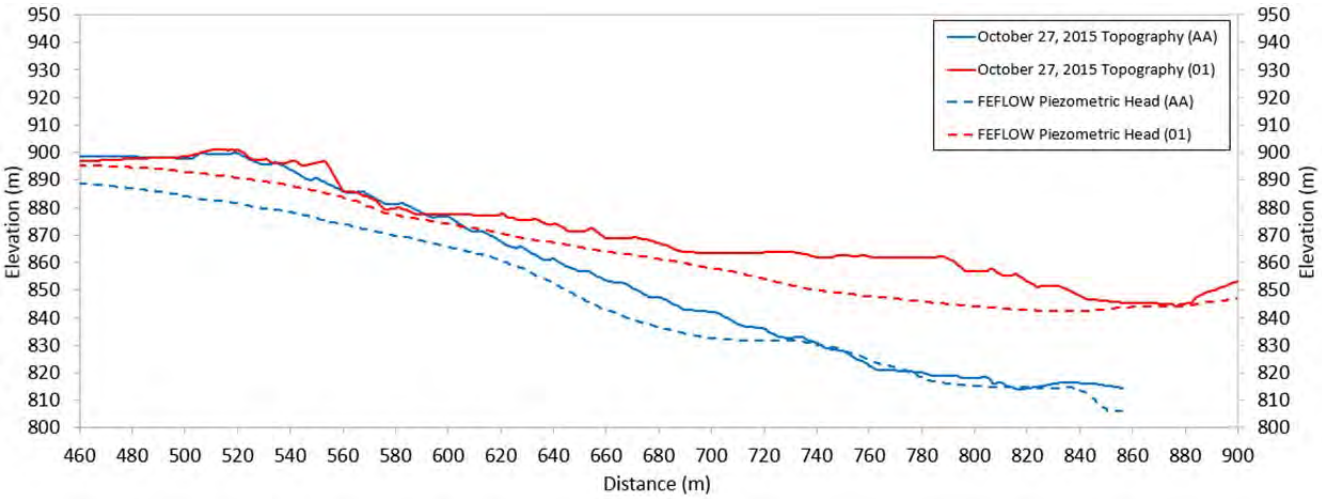

Figure 5-14 Geometry and piezometric comparison of left and right abutments

Also depicted on Figure 5-14 is the difference between the piezometric surface at the two locations, with generally higher conditions on the left that reflect the influence of slimes. This is illustrated in more detail on Figure 5-15.

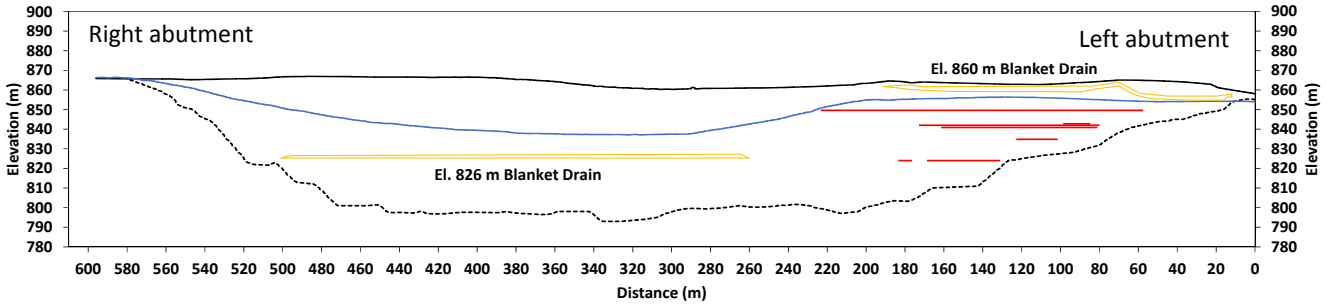

Figure 5-15 Longitudinal section from FEFLOW, view looking upstream. Phreatic surface shown in blue, El. 826 m blanket drain in yellow, slimes in red.

Figure 5-15 is based on results of a 3D steady state and transient seepage analysis of the tailings impoundment performed as part of the Investigation and described in Appendix G. The estimated phreatic surface from this modeling is shown on the longitudinal section. On the left abutment, inflows from Grota da Vale together with the slimes maintain the phreatic surface at a higher elevation. In contrast to the right abutment, the slimes on the left extend outward toward the El. 826 m blanket drain and limit the lateral extent of its influence.

The rate of rise of the embankment crest at the right abutment is shown on Figure 5-16, which can be compared to conditions at the left from Figure 5-12. Average annual rates are generally similar except during 2015 when the right abutment was raised at a higher rate of 1.6 m/mo compared to 1.3 m/mo on the left. The right abutment experienced an unusually high rate of rise of 5.4 m/mo in August, 2015 on a newly-initiated realignment of the crest that was set back from the former location to allow for drain construction depicted on Figure 2-12.

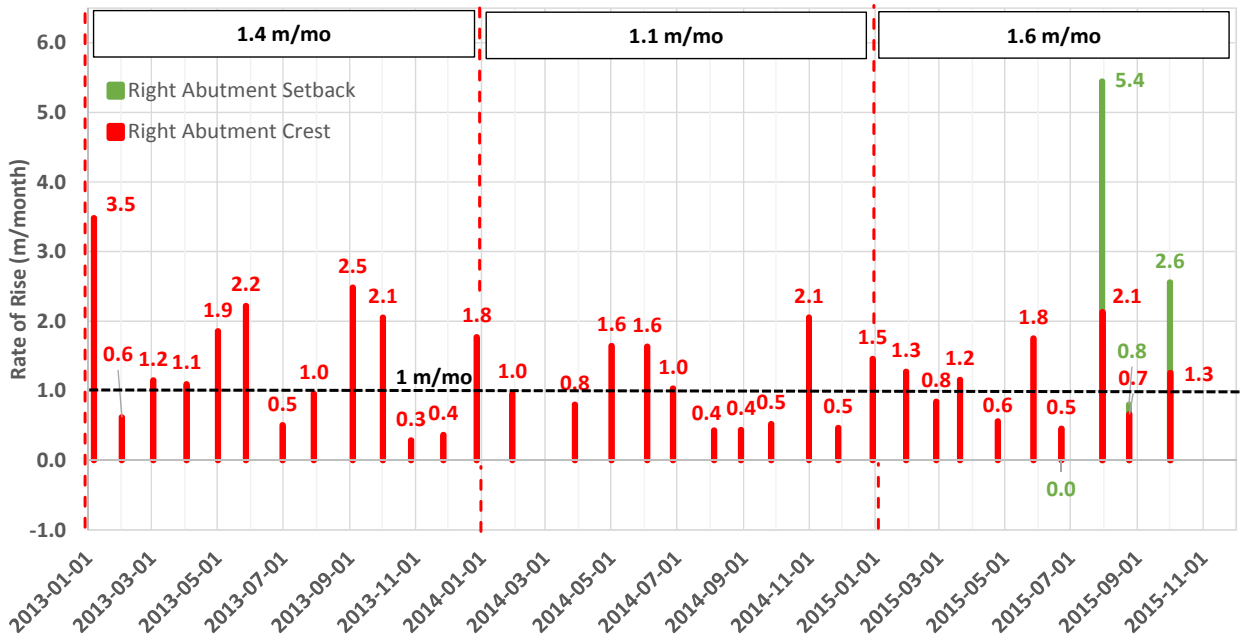

Figure 5-16 Rate of rise at right abutment

Conditions conducive to failure at the right abutment therefore include greater slope steepness and higher rate of rise than the left abutment, although these are mitigated somewhat by the lower piezometric conditions. The net effect can be evaluated by means of stability analysis.

5.3.2 Right Abutment Stability

Section 4.1 reviewed the aspects of soil behavior that give rise to flowsliding in saturated, contractive materials. Shearing that occurs slowly enough to allow pore pressures to dissipate is said to occur under *drained* conditions, while *undrained* conditions pertain to rapid shearing associated with flowsliding.

Stability analyses for these two conditions adopt corresponding strength parameters. *Effective-stress analysis*, or ESA, uses friction angle and cohesion to represent drained shearing, while *undrained strength analysis*, or USA, for undrained shearing uses undrained strength typically expressed as a ratio to the effective vertical overburden stress.

Stability analyses for the right abutment Section AA on November 5, 2015 are shown on Figure 5-17 for both ESA and USA, where a calculated factor of safety (FS) less than 1.0 indicates failure. The ESA adopts a friction angle of 35 degrees and 5 kPa for compacted tailings fill and 33 degrees and zero kPa for hydraulically-discharged tailings, while the USA uses an undrained strength ratio in compression of 0.25 for tailings below the piezometric surface.

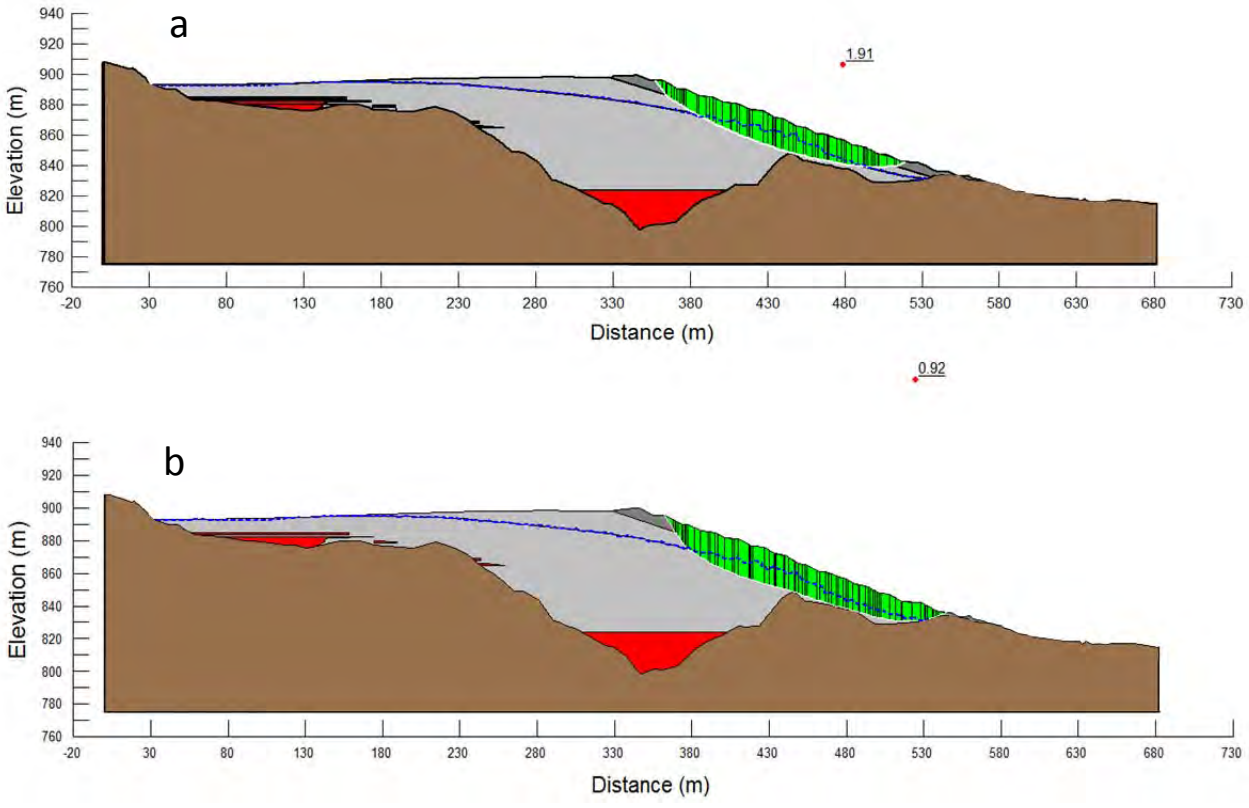

Figure 5-17 Stability analyses at right abutment Section AA; (a) effective stress (ESA); (b) undrained strength (USA)

Figure 5-17 shows FS = 1.91 for ESA conditions and FS = 0.92 for USA. Hence, with a USA factor of safety less than 1.0, rapid failure and associated flowsliding should have initiated at the right abutment if undrained conditions had been operative. The fact that failure did not initiate there means that undrained strength was not fully mobilized and that drained conditions represented by the ESA prevailed at the right abutment. It is equally apparent that the rate of embankment rise at the right abutment was not itself sufficient to mobilize undrained strength in the sand tailings.

5.4 Flowslide Occurrence at the Left Abutment

The conditions discussed in this section make it possible to answer the question of why failure initiated at the left abutment rather than at the right. Two main factors were operative. First, compared to the right abutment, the left abutment had higher and more adverse piezometric conditions. But most importantly, the embankment slope was underlain by slimes at the left abutment causing undrained strength to be mobilized, conditions that did not exist at the right abutment. Undrained shearing and subsequent reduction in undrained strength—the phenomenon of static liquefaction—resulted in the left abutment flowslide. The triggering mechanism for static liquefaction, and the role of the slimes in producing this mechanism, are explained in the following section.

6 WHY DID THE FLOWSLIDE OCCUR WHEN IT OCCURRED?

6.1 Triggering Mechanisms

Section 4 of this report outlined the conditions required for liquefaction flowsliding. These are: the presence of loose, contractant tailings; the existence of saturated conditions; and rapid failure producing undrained conditions with accompanying reduction in undrained strength. The Fundão flowslide occurred because all of these necessary conditions were present.

Section 5 considered why the flowslide occurred at the left abutment. It was shown that softer, more compressible slimes were deposited in areas intended to be exclusively sand beach, and that the setback of the dam alignment resulted in these materials being present beneath the embankment slope as it was further raised upstream. By contrast to the left abutment, undrained strength was not mobilized at the right abutment, which was not underlain by slimes, and neither were high rates of construction sufficient to induce liquefaction there. The reason that the flowslide occurred at the left abutment is that the presence of slimes-enriched tailings inhibited drainage, enhanced saturation, and promoted undrained shearing.

This section considers what caused liquefaction flowsliding to occur as it did on November 5, 2015. As part of its assessment, the Panel noted that the failure did not occur earlier in the left abutment construction sequence when conditions such as those in the August, 2014 cracking incident were manifested, but that it did occur shortly after the earthquake sequence earlier that day. The timing of the failure event, and the operative conditions at this and other times, goes to the question of liquefaction triggering. Clearly, the softer slimes at the left abutment—and in particular how they responded to increased stress during dam raising—must play a prominent role in any theory of causation.

Drawing on their own experiences and those of others, Martin and McRoberts (1999) have emphasized the need for a physical trigger to initiate rapid shearing, and they catalog numerous potential triggers:

1. Oversteepening at the toe due to erosion, localized initially-drained slumps and construction activities such as excavation.
2. Loading due to rapid rate of impoundment raising, steepening at the crest, and construction activities at the crest.
3. Changes in pore pressure due to increased pond levels, accelerated rates of construction, movements, and other processes.
4. Overtopping due to severe storms, failure of diversion facilities, seismic deformation resulting in loss of freeboard.
5. Vibrational loading due to earthquakes, construction traffic, blasting.

These and other physical trigger mechanisms unique to the Fundão Dam have been considered in Appendix K. It is evident from the above that when contractant tailings are present in the structural portion of a tailings dam, the evaluation of liquefaction triggering is a formidable task.

Of particular interest was static liquefaction initiated by a rise in phreatic surface alone. In the early deliberations of the Panel, this ranked highly as a potential cause. As discussed in Appendix K, the levelling-off of piezometric pressures in the months prior to the failure provides evidence against it. Cyclic liquefaction also received attention, but had it been the sole triggering mechanism, the right abutment would have failed before the left, as discussed in Appendix K.

As summarized on Figure 3-1, the surviving candidate liquefaction triggering mechanisms are static load increases generated directly by either undrained shearing of the slimes or by deformations at the base of the sand leading to collapse. Either trigger mechanism might be augmented by earthquake effects if shown to be consequential. While their end result is similar, their stress paths differ. In the case of undrained shearing, the question arises whether the load due to embankment construction, coupled with the deformation of the underlying slimes-enriched material, can directly induce pore pressures in the loose sand sequence that would lead to undrained failure.

The shearing mechanism is based on undrained shear in the underlying slimes material together with mobilized frictional resistance in the overlying sands. Liquefaction in the overlying sands would be induced by uncontrolled deformation of a sliding mechanism with a factor of safety of unity. An example of a tailings dam that exhibited this failure mechanism is the Los Frailes dam in Spain. In a later portion of this section and in Appendix I, the relationship between undrained strength in the underlying slimes and factor of safety will be presented, as will the sliding developed in the slimes associated with the factors of safety. It will be shown that sliding in the slimes would induce failure associated with a deformation mechanism prior to the initiation of shear failure. In addition, the shear failure mechanism as presently analyzed does not take into account additional three dimensional resistance, which will be substantial. Moreover, shear failure mechanisms are often accompanied by the development of a down-drop block, or graben, at the initiation of the movement, and eyewitness reports do not provide any evidence of such a feature. For both the analytical results to be discussed and the additional items mentioned above, the Panel favors the deformation mechanism as the basis for initiating the failure when it occurred.

The alternative deformation-related trigger mechanism is termed here *lateral extrusion*, with reference to horizontal spreading of the softer slimes due to loading that induces a corollary elongation effect in the overlying sands. The mechanism of lateral extrusion is somewhat more indirect. It asks whether stress changes in the sand above the slimes-enriched layer, as it is undergoing deformation, result in a stress path that leads to collapse and static liquefaction.

Although not included on the list of Martin and McRoberts (1999), lateral extrusion as a static liquefaction trigger mechanism is not new or without precedent. It has been identified by Jefferies and Been (2016) in their discussion of the static liquefaction of the Nerlerk berm, where they state that:

> "The dangerous nature of declining mean-stress paths in terms of liquefaction behavior, caused by basal extrusion, was not understood in 1983."

Much of the subsequent content of this section is devoted to the lateral (basal) extrusion mechanism, incorporating developments much more recent than those referred to above.

The case of static liquefaction of sands associated with the 1938 failure of the Fort Peck Dam has some similarity to the Nerlerk case in that it has been interpreted to have been caused by shear failure of a weak shale foundation. The difference resides in the basal straining mechanism but the net result in creating stress changes in the saturated sand above is similar.

An important case of static liquefaction occurred at the Germano Complex itself in 2005. As shown in Figure 6-1, a low dike being raised over interlayered and intermixed slimes in the Baia 4 area experienced a sudden, high-mobility failure that moved rapidly over a distance of 80 m. The Baia 4 failure was attributed to liquefaction.

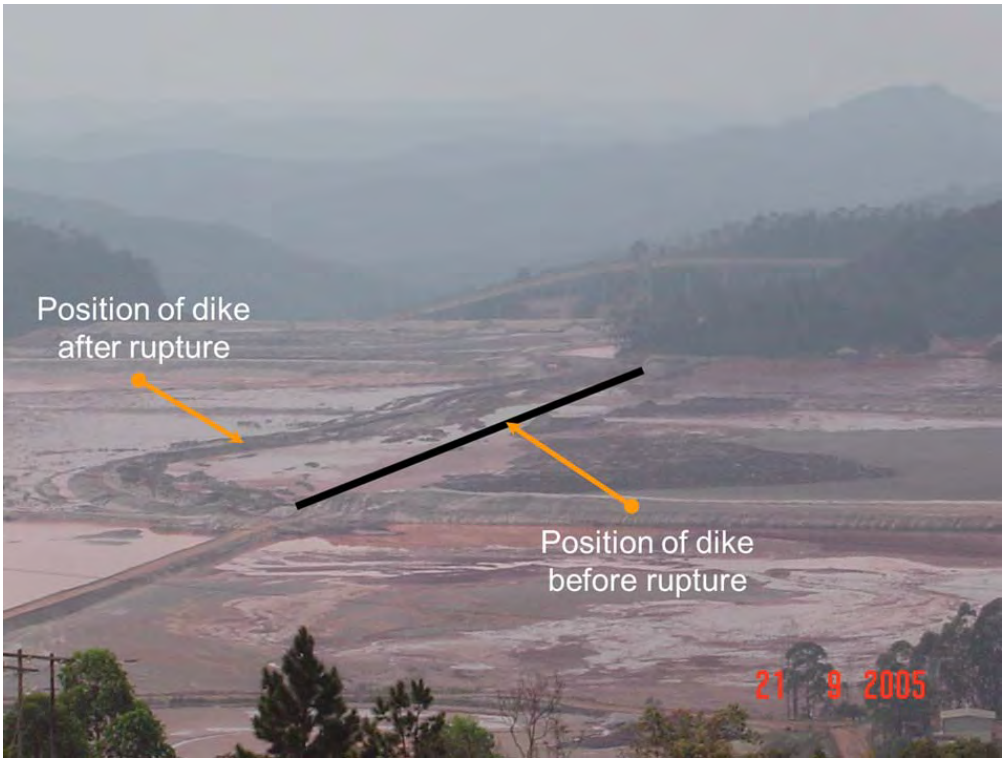

Figure 6-1 2005 Baia 4 static liquefaction failure

The Baia 4 failure provided the basis for determining parameters for slimes-rich layers used in modeling of the Fundão failure. Specifically, parameters relating to the peak undrained shear strength of these layers and the reduction in strength at large deformations were derived by back calculation from pre-failure and post-failure conditions. In these respects, the Baia 4 failure provided an important link between the theoretical studies conducted by the Panel and actual experience at the Germano Complex itself (see Appendix C for details).

Numerical simulations were also grounded in other field experience from the Germano Complex. As explained in Appendix I, field loading trials in 2008 and 2013 provided deformation response and consolidation properties for the slimes-rich layers.

6.2 Loading Conditions

As discussed in Section 4, the ability for rapid loading to result in rapid failure, and hence liquefaction of loose saturated sands, is well understood. However, this is not the case with slower loading.

Sasitharan et al. (1993) demonstrated that a loose granular deposit can collapse as a result of slow loading, as well as during rapid loading, mobilizing a resistance that is much less than the ultimate frictional resistance.

Skopek et al. (1994) demonstrated the mechanics of collapse by following the loading paths utilized above with dry sand and found a sudden volume decrease at essentially the same stress condition, consistent with the data noted above. These two sets of experiments demonstrate the value of the collapse testing to find a yield surface separating collapsing from non-collapsing states in loose, contractive soils like tailings.

Testing is also of value in understanding the role of cyclic loading from earthquakes leading to liquefaction. This is illustrated on Figure 6-2.

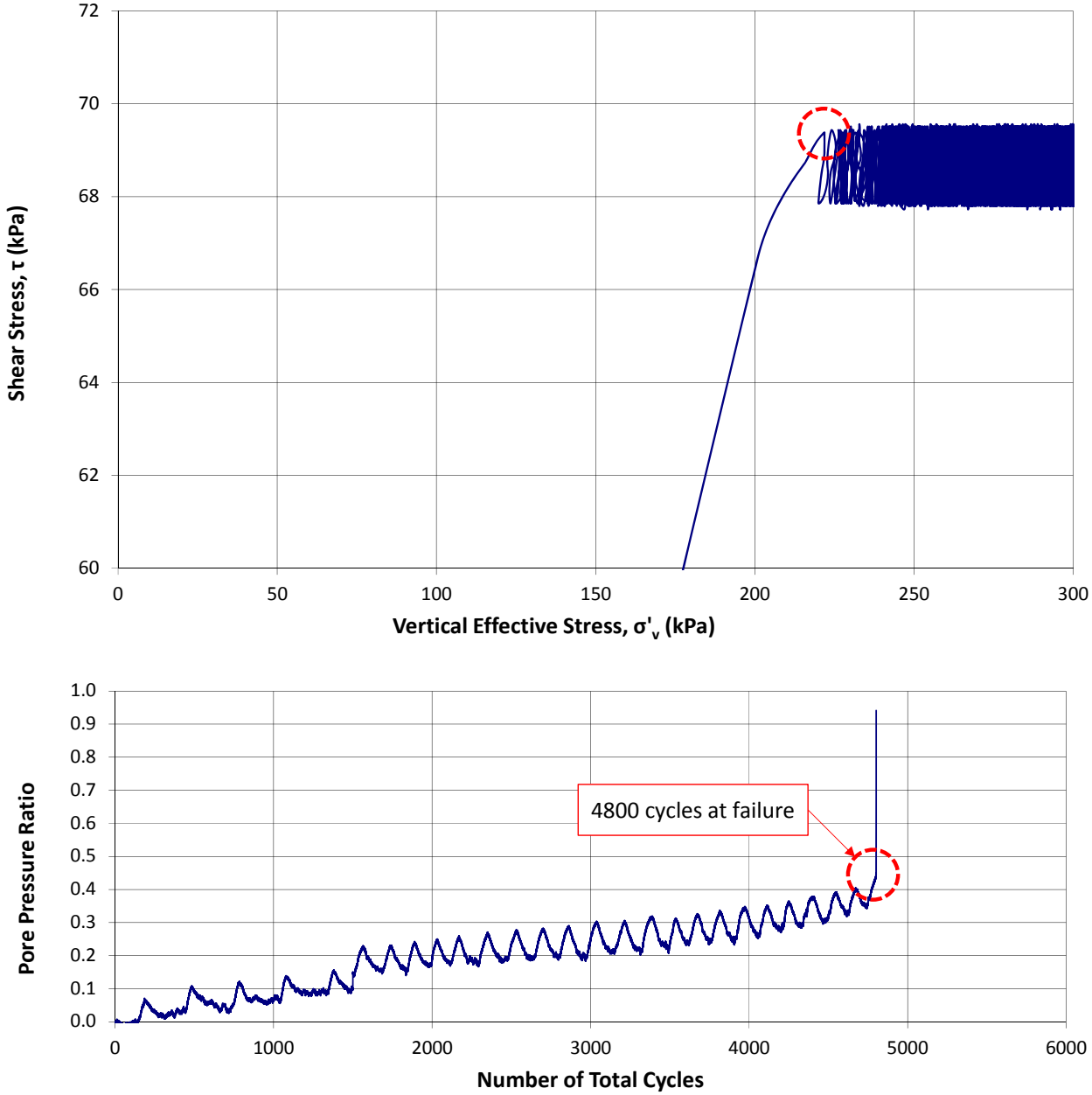

Figure 6-2 Stress path during cyclic loading

During cyclic loading shear stresses vary with time, and this can induce an increase in pore pressure resulting in a reduction of p'. As shown, the stress path migrates to the yield surface and, upon intersection, liquefaction under the applied static stresses results. The sensitivity to cyclic loading depends upon the magnitude of the cyclic shear stress, the duration of dynamic loading, the existing static stresses, and the state of the tailing sands. This topic is discussed in more detail in Section 6.5,

where cyclic tests representing the specific earthquake loading for the Fundão Dam will be presented.

In addition to the stresses applied, the loading due to embankment raising must also be considered. This was based on actual survey data, as illustrated in Appendix B. As previously shown on Figure 5-12, the rate of rise at the left abutment reached a value of 2.9 m/month. There is no evidence that this rate had a material effect on the sands, but it could certainly induce an increment of undrained loading on the underlying slimes.

6.3 Ground Conditions

The assessment of ground conditions that influence the formulation of the trigger mechanisms relies on piezometric data prior to the failure and CPT profiles to determine the contractive/dilative behavior of the deposit in the vicinity of the left abutment.

With respect to the piezometric data, Appendix E contains the plots of piezometers in the vicinity of the left abutment up to the time of the failure. Seepage simulation, summarized in Appendix G, extrapolates this data and its trends. The significance of this data in assessing potential trigger mechanisms is also discussed in Appendix K of this report.

With respect to the CPT profiles, the Panel has utilized the Robertson (2010) procedure previously shown on Figure 4-5 for evaluating the contractant/dilatant behavior of the deposits, primarily because it incorporates liquefaction failures of tailings dams and other deposits for immediate comparison. All CPT interpretations are available in Appendix C.

There have been three campaigns of CPT testing in the vicinity of the left abutment where failure was initiated. They also have a bearing on the slumps that developed in 2014; see Section 2 of the Report:

1. April, 2014;
2. September, 2014 – March, 2015; and
3. June, 2015.

The first campaign was limited in scope and reliability but does provide some information in the vicinity of the large-scale cracking that developed in August, 2014. This CPT data does not indicate contractive behavior, but rather dilatant or close to the contractant/dilatant boundary. This is consistent with the absence of any significant mobility of the affected material and the observation that none of the small slumps that preceded it in 2013 propagated by undrained retrogression. There is some indication of densified layering within the profiles, suggesting that the mass of tailings adjacent to the slope may have benefitted from densification associated with construction traffic on the beach.

The second campaign from September, 2014 to March, 2015 has the most data in the region of interest. CPTs F-01 to F-05, which explore from El. 854 m to El. 889 m, all reveal contractant characteristics of beach material, consistent with the existence of potential collapse behavior. Relevant data has previously been summarized on Figure 4-4.

The third campaign, conducted in June, 2015, provided less insight into conditions at the left abutment because it covered a substantial area, even outside of Fundão. Sounding FUND-06 encountered dilatant sand over an isolated loose layer between El. 862 m and El. 864 m. Sounding FUND-07 encountered dilatant sand from El. 895 m to El. 886 m, followed by soft phyllite to a depth of El. 865 m.

6.4 The Lateral Extrusion Mechanism

6.4.1 Detailed Description

The lateral extrusion mechanism is predicated on the presence of saturated, loose sands overlying soft slimes, with confinement of the slimes that varies according to the constructed profile.

As the structure increases in height, the slimes are loaded vertically but tend to extrude or spread laterally, rather like squeezing toothpaste from a tube. In doing so, the overlying sands tend to move with the slimes but lack ductility. As a result, stress changes arise that tend to reduce lateral confinement of the sands. This induces collapse of saturated sand or development of cracks in unsaturated material.

This mechanism, without liquefaction, is well known to designers of embankments on soft clays. Under these conditions the lateral deformation of the foundation often results in vertical tensile cracking of the overlying embankment fill. At failure, the shear strength of the fill cannot be relied upon because of the absence of shear resistance along the open cracks that it sustains.

6.4.2 Extrusion and Collapse of Saturated Loose Sand

The Panel has experimentally demonstrated the lateral extrusion mechanism leading to collapse by conducting drained triaxial compression tests that adopt a specially-designed stress path. Designated *extrusion collapse* tests, they simulate the reduction in horizontal stress in the sand due to slimes extrusion while keeping the vertical stresses constant. Details of the test procedures and data obtained are provided in Appendix D, which includes the results from the tests that were performed. The results of two tests are shown on Figure 6-3, one on a contractive specimen with an initial state parameter $\Psi = +0.01$ and another with $\Psi = +0.04$. These values are on the contractive side of CPT data previously shown on Figure 4-4 and as such tend to bracket the characteristic state in the field. In both cases, as the shear stress along this loading path approaches the ultimate friction line, collapse occurs in an abrupt and sudden manner after only small deformations in the sand. This testing provides both a qualitative demonstration and a quantitative reference for collapse of Fundão sand associated with the extrusion mechanism.

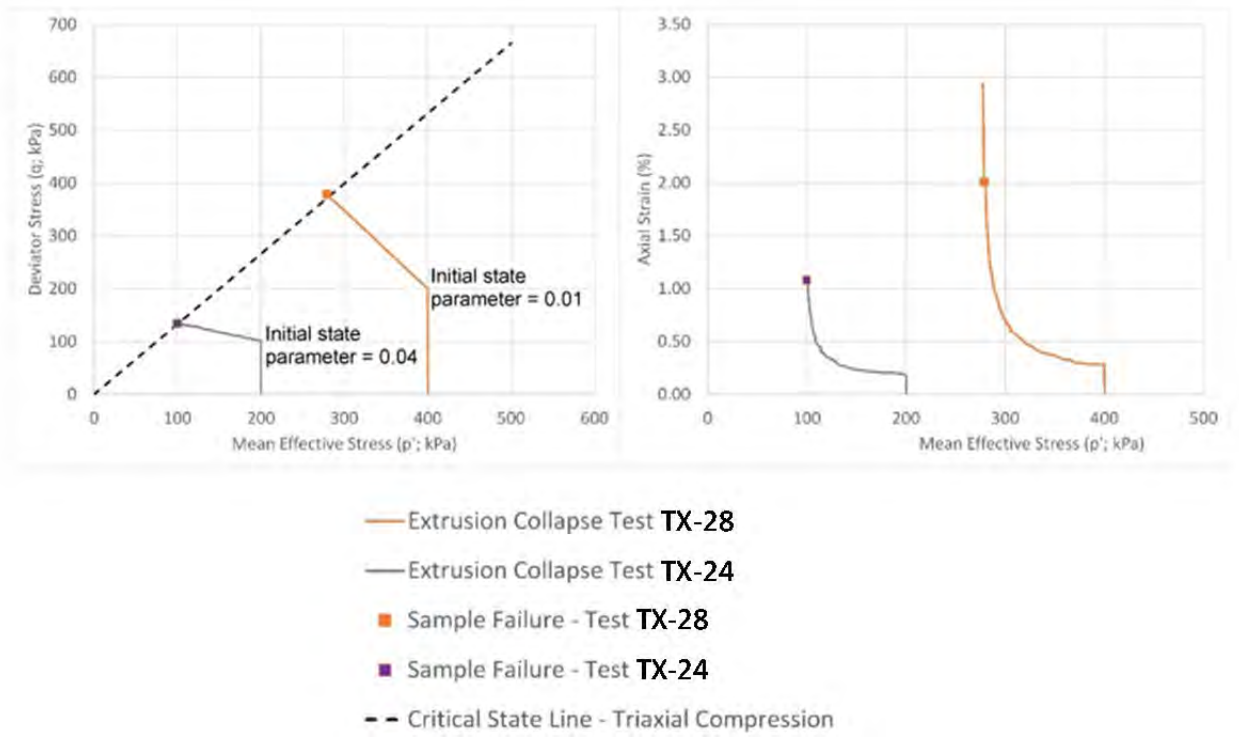

Figure 6-3 Extrusion collapse tests on Fundão sand

6.4.3 Numerical Simulation - Formulation

In order to analyze the lateral extrusion mechanism and resulting collapse, the Panel has undertaken numerical simulation of the construction of the Fundão Dam left abutment section. This analysis follows the history of construction, the evolution of piezometric pressures, the deformation within the slimes and sands, and the spatial variation of the state parameter. An important output from the analysis will be the demonstration of stress paths to failure comparable to those utilized in Section 6.4.2 for quantifying collapse behavior.

The cross-section adopted for the analysis is based on Section 01, at the left abutment provided in Appendix B. Materials within the cross-section have been grouped into the following material types:

1. Bedrock: All materials below the “stripped ground” survey were assigned to this material type;
2. Uncompacted tailings sand not intermixed or interbedded with slimes;
3. Slimes/sand deposits in varying proportions, designated as:
   - predominantly slimes;
   - mixed sand and slimes;
   - interbedded slimes; or
   - isolated slimes; and
4. Compacted sand.

The embankment configuration was modeled at four-month time intervals throughout the majority of the construction history, starting at the end of 2011. For the final six months (June to November, 2015), this time interval was reduced to monthly in order to gain additional resolution of model response close to the time of failure. Details of the modeling process and its formulation are presented in Appendix I.

The geotechnical properties for each of the materials listed above constitute a fundamental input to the modeling. Formulations of increasing complexity were adopted in an iterative manner to provide a check on model performance. This gave confidence in the results from analyses based on the most complex formulation for loose sand behavior, the critical state model NorSand presented by Jefferies and Been (2016). Parameter sensitivity analyses were completed for the critical state model to assess variations of the influence of the strength and continuity of the slimes layer.

Elastic properties for the sand were based on shear wave velocity measurement in Appendix C converted to an approximate large strain modulus. The elastic properties for the slimes were based on one-dimensional consolidation test data calibrated to a 2008 field loading trial by Samarco described in Appendix F.

The shear strength for beached sand was set at a frictional angle of $\phi' = 33°$, based on tests conducted by the Panel in Appendix D. The compacted tailings sand was modelled with a friction angle of $\phi' = 35°$ and 5 kPa cohesion, in accordance with the values used by others during designs.

The slimes were given a peak shear strength of $\phi_p = 12.4°$, equivalent to an undrained strength ratio of 0.22. This reduced linearly to one-third of the initial value at a plastic strain of 20%, reflecting a modest sensitivity. Support for this formulation is provided in Appendix C from back-calculation of the Baia 4 failure described in Section 6.1.

Critical state parameters assigned to the uncompacted tailings sand were derived from triaxial compression laboratory tests provided in Appendix D. One parameter needed for the critical state formulation was derived from modeling single-element response (equivalent to a laboratory test) as discussed in detail in Appendix I. In addition, it was necessary to declare an initial state parameter to seed the analysis. Following recommendations of Jefferies and Been (2016) and utilizing CPT data from the 2015 field campaign, this seed value was set at $\Psi = -0.02$.

It is also necessary to characterize the various sand-slimes mixtures listed above. Here, no direct experimental information is available, hence judgment is needed to establish both elastic and strength properties. Both elastic and strength properties of the slimes described above were blended with those of the sand in accordance with estimated proportions of those materials within the cross-sections. “Predominantly Slimes” were treated as pure slimes and “Isolated Slimes” were considered as pure sands. “Mixed Sand and Slimes” were a 50:50 mixture and “Interbedded Slimes” were taken to be 80% sand. The resulting properties are summarized in Appendix I.

The formulation of the behavior of the sand/slimes mixtures and their relative proportions is the greatest source of uncertainty in the analysis. As a result, sensitivity analyses have been conducted to explore how variations in assumed sand/slimes behavior influence the model results.

One final element in the formulation of the analysis is the treatment of the pore-water pressures. The pore-water pressures were assigned by setting the phreatic surface based on the integration of piezometric response provided by the hydrogeologic model summarized in Appendix G. As such, no stress-induced pore pressures are considered.

As shown in Appendix F, the slimes appear to fully consolidate on average over the loading history from 2011 to failure. However, in the model it is assumed that increments of loading generate an undrained response. The pore pressures developed are assumed to dissipate prior to the next load increment and do not accumulate over time.

6.4.4 Numerical Simulation - Results

An important check on any complex numerical model is to replicate the experimental information that constitutes the building blocks of the comprehensive constitutive relationship needed to undertake more complex analysis. Figure 6-4 and Figure 6-5 show the results of a simulation of a drained triaxial compression test and an undrained stress-controlled triaxial compression test. The latter follows a stress path simulating the effect of the extrusion mechanism in the slimes on the overlying sand developed in Section 6.4.2 above. The correspondence between numerical simulation and experiment is encouraging. The model strength result is about 3% less than the experimental value and it will be used as a reference to assess proximity of the simulation to collapse.

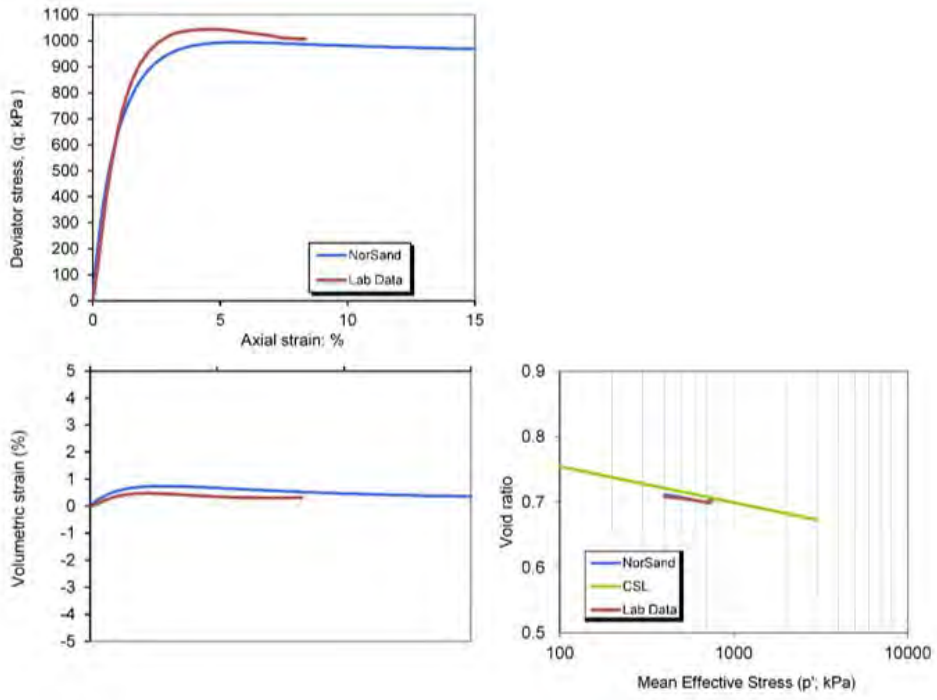

Figure 6-4 Simulated drained triaxial compression test (Test ID TX-12)

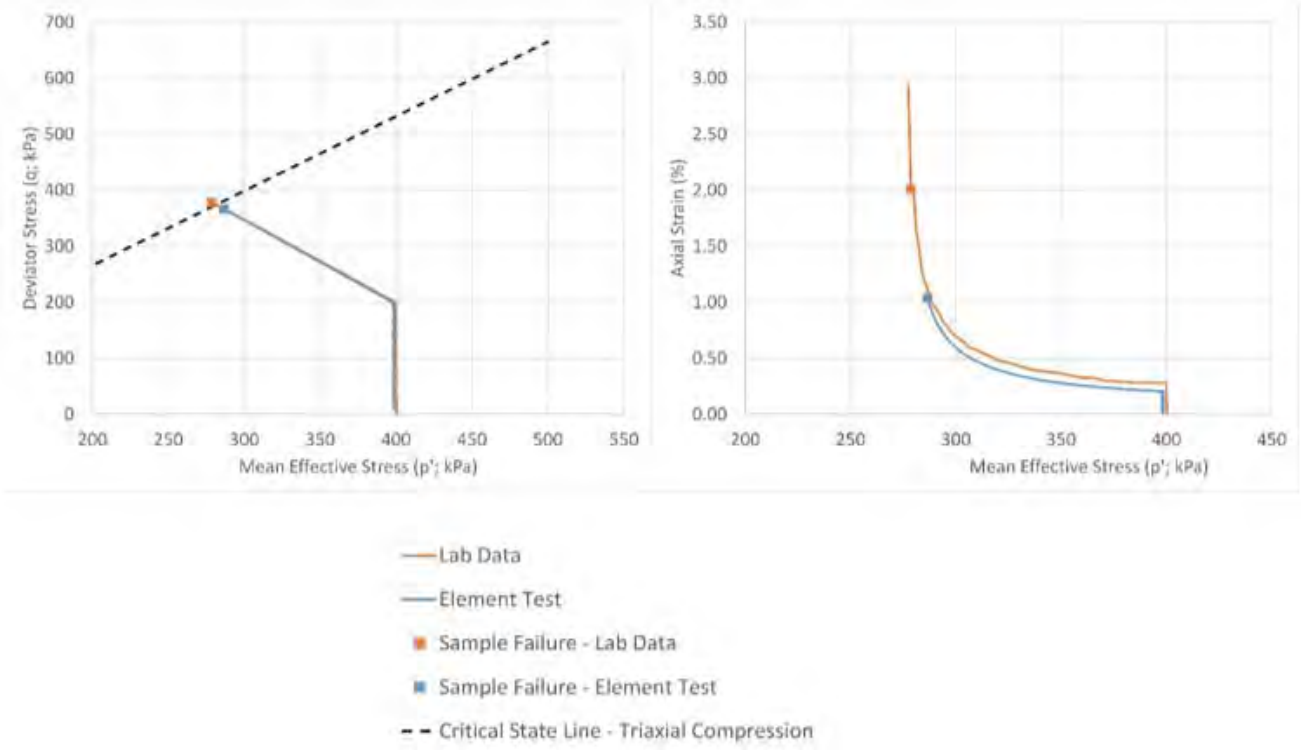

Figure 6-5 Simulated extrusion collapse test (Test ID TX-28)

Appendix I presents the results and general conclusions from a variety of simulations intended to explore the sensitivity to assumptions with respect to the distribution of slimes-enriched deposits and to their assumed geotechnical properties. In the view of the Panel, the case that best represents the evolution of collapse in the saturated loose sands overlying the slimes rich deposits is presented on Figure 6-6.

The Mobilized Instability Ratio (MIR) is a criterion for the triggering of collapse. It is defined as the ratio of the deviator stress and mean effective stress to the ratio at the onset of collapse. The color zonation represents the MIR related to the collapse strength determined from laboratory tests. The maximum value computed is 80%. Numerical convergence limitations inhibit the modeling from progressing further. However, the information available from the simulation provides compelling support for the hypothesis that collapse was triggered by lateral extrusion of the slimes-rich deposits.

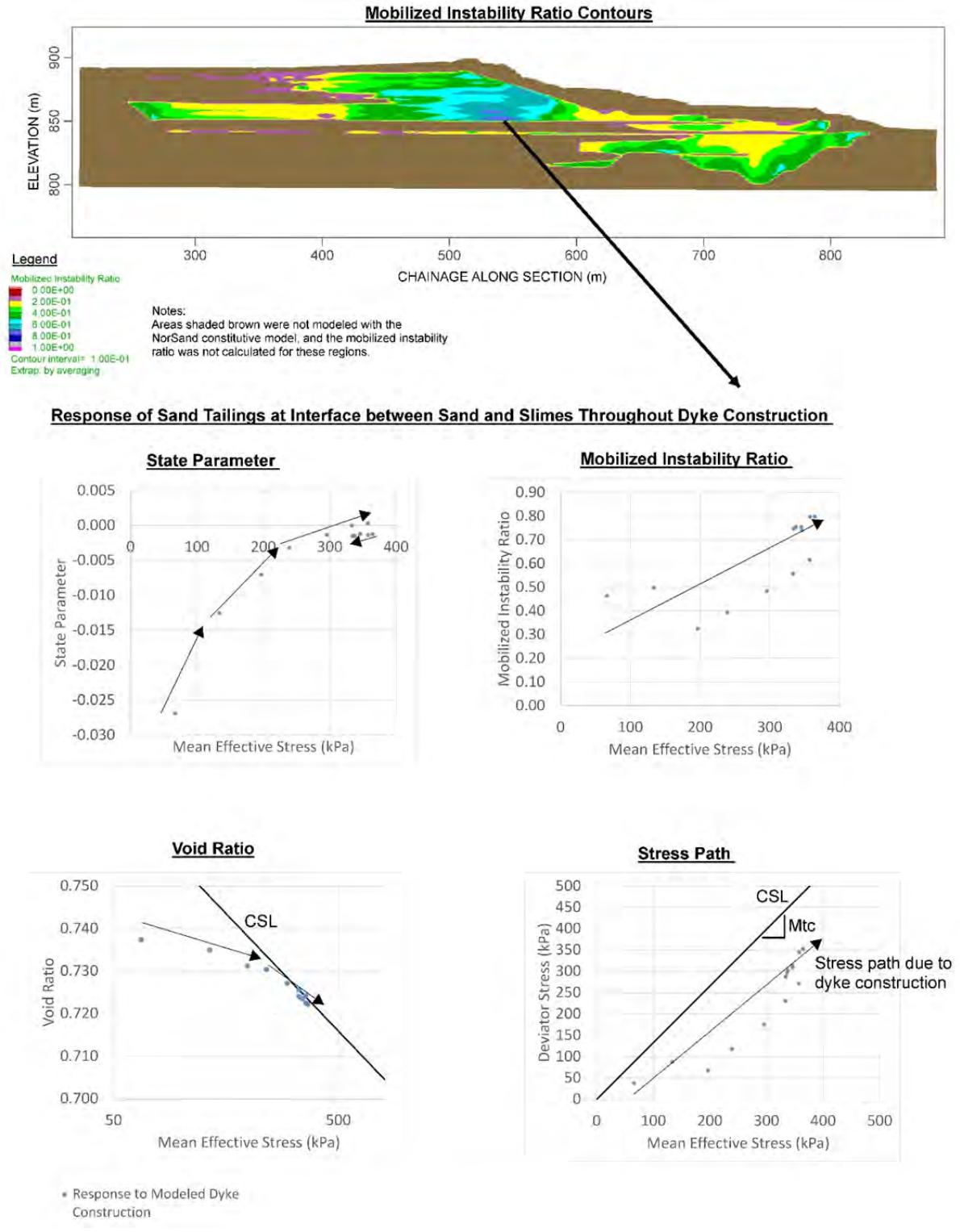

Figure 6-6 Mobilized Instability Ratio

Figure 6-6 also plots the stress path calculated throughout construction of the Fundão Dam. Operation of the lateral extrusion mechanism is cumulative during construction as reflected by the results plotted. The stress path has been calculated at the base of the sand which is the location where collapse would be initiated. The calculation indicates that 80% of the available collapse resistance has been mobilized with the strength as prescribed in the analysis and determined by laboratory tests. Numerical instability, from a computational perspective, precluded advancing the calculations further.

Figure 6-7 provides a comparison of laboratory data from Figure 6-5 with the simulated field stress path on Figure 6-6. It shows that the field stress path displays similarity to the controlled laboratory stress path and is migrating towards the ultimate strength line. As noted above, numerical convergence limitations preclude completing the analysis.

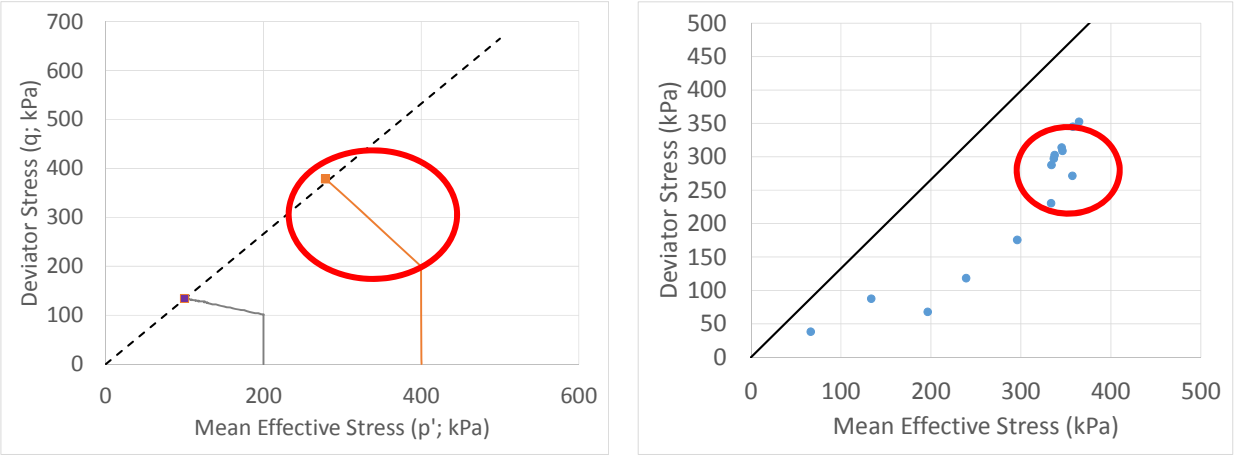

Figure 6-7 Comparison of laboratory and simulated field stress path

Figure 6-8 plots horizontal deformations along the slimes/sand interface at various stages of construction of the Fundão Dam. It illustrates that the largest lateral movements occur beneath the slope and downstream of the crest. This implies compressive straining in the downstream direction and extension straining in the upstream direction. Extension strains result in a reduction of horizontal confinement consistent with the lateral extrusion hypothesis.

It is also of interest to note that the maximum horizontal displacements beneath the lower part of the slope coincide with eyewitness reports of slope movement having initiated on the lower benches, as described in Section 2.7.

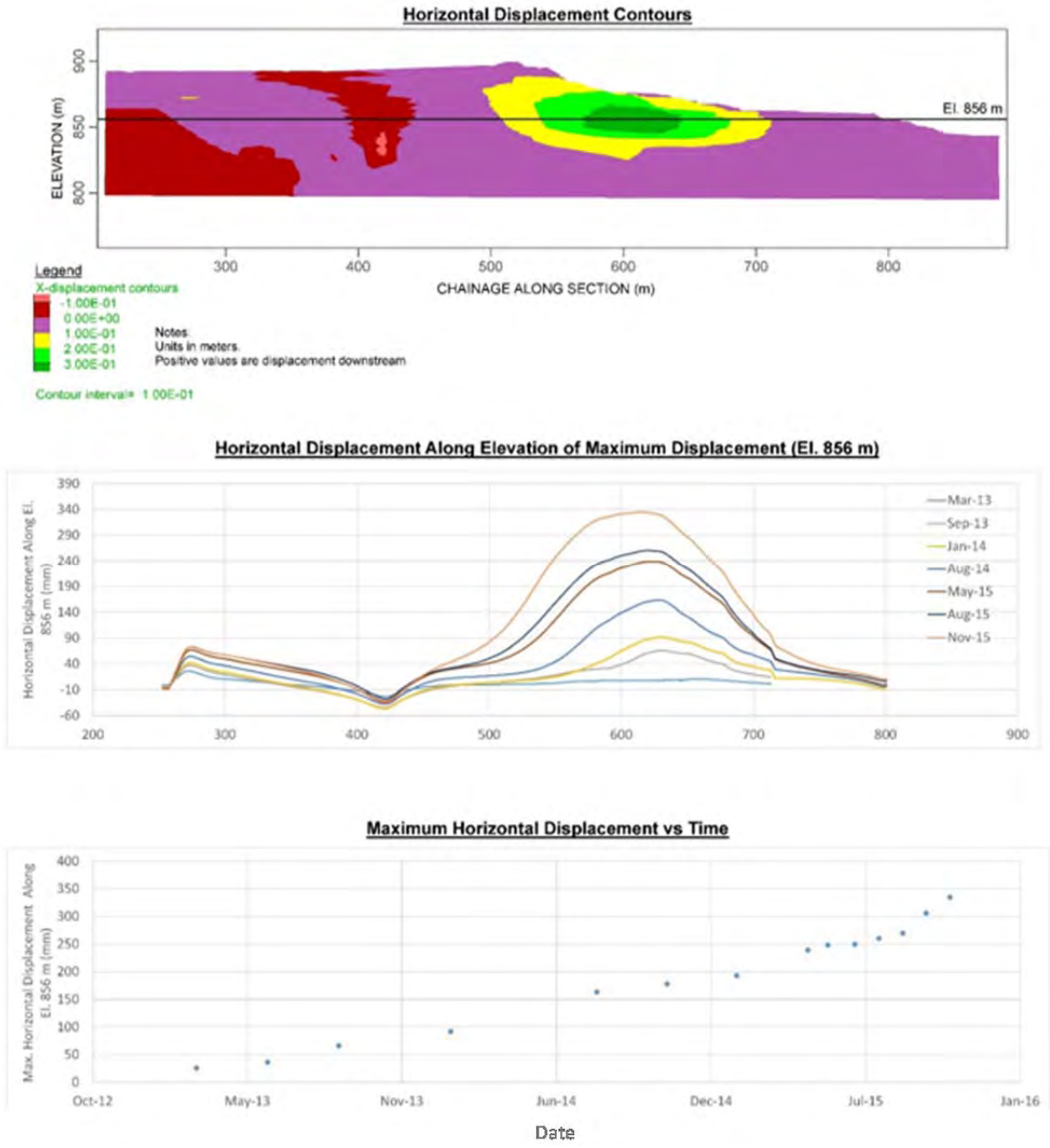

Figure 6-8 Horizontal displacements at sand/slimes interface

6.5 Displacements to Trigger Liquefaction by Lateral Extrusion

In order to determine the sliding deformation that would overcome the limitations of numerical convergence issues and meet a MIR of unity, the numerical analysis has departed from following the loading history and now imposes a specified slip to calculate the MIR response. As shown in Appendix I, a sliding displacement of 600 mm is required for an MIR of unity. By extrapolation, from

past values relating MIR and mobilized shear strength it is found that the sliding displacement of 600 mm would be calculated if the undrained strength ratio were equal to 0.14. This value is consistent with the sensitivity of the slimes.

6.6 Comparison Between Shearing Mechanism and Lateral Extrusion

In order to use this critical sliding displacement to evaluate the relative likelihood of the lateral extrusion mechanism triggering liquefaction versus other mechanisms, it is necessary to compare the 600 mm value with slip associated with a shearing mechanism that could develop due to the mobilization of low strengths in the slimes-rich layers. The shearing mechanism is a sequence involving undrained yielding of the slimes-rich layer leading to a general shear failure throughout the dam slope, which in turn results in an acceleration of displacements that triggers liquefaction. In order to evaluate which of these mechanisms was the more probable liquefaction trigger, the Mohr-Coulomb model discussed in Section 6.4.3 was used to estimate the magnitude of deformations that would develop at the onset of general shear failure due to yielding in the slimes-rich layer. Details are presented in Appendix I.

The pattern of displacements resulting in November, 2015 if a factor of safety of unity was approached is shown on Figure 6-9. The pattern of displacements is similar to that shown previously for the NorSand model analyses.

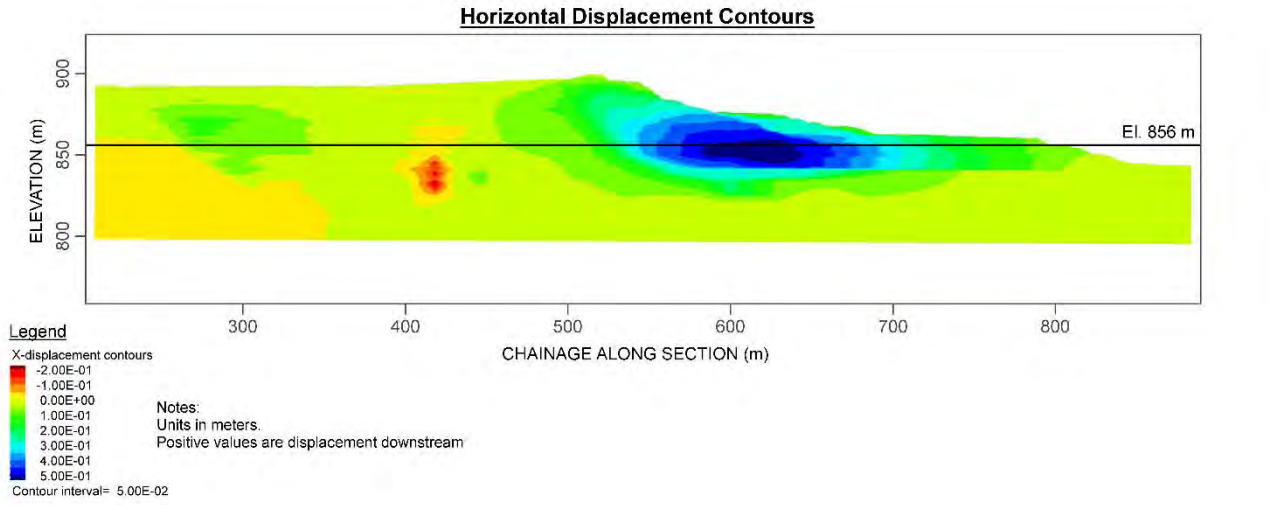

Figure 6-9 Horizontal displacements resulting from Mohr-Coulomb analysis approaching a factor of safety of unity

The deformation model used for failure analysis is equivalent to limit equilibrium analysis and hence provides a linkage between sliding displacement at failure and factor of safety. As discussed earlier in this section, a factor of safety of unity represents a trigger for the onset of liquefaction. The deformations associated with the onset of liquefaction with the shearing mechanism are much greater than those associated with the lateral extrusion mechanism. Therefore, liquefaction would be initiated by lateral extrusion prior to the development of shear failure.

The Panel regards the results from the numerical simulation as providing compelling support for the lateral extrusion mechanism accounting for the occurrence of the flowslide on November 5, 2015.

6.7 The Role of Earthquakes

6.7.1 Earthquake Loads

The Panel has relied on the Atkinson Report (2016) for evaluating the seismic history at the damsite and for recommending ground motions to be considered in response analyses (Atkinson 2016). The seismology report summarizes the regional seismicity and the instrumental records that were obtained from the earthquakes that occurred just prior to the collapse of the dam. It concludes that the site experienced natural earthquakes, as summarized in Table 2-1, with a Moment Magnitude, M_w, of up to 2.5 and epicenters close to the dam. As reviewed in Appendix K, earthquake loading from such small shocks would not usually be considered consequential to structures with robust design and operation. However, as discussed in detail above, the dam was in a very fragile state at the time of the earthquakes and the question arises whether the earthquakes hastened its collapse. Hence, a more detailed evaluation was warranted.

Understandably, there is considerable uncertainty in the determination of ground motions, and the Panel requested that the seismologists provide a range of ground motions and associated estimates of likelihood. These records form the basis of the dynamic response analysis needed to calculate the magnitude of stresses in the dam induced by the earthquake and the duration of earthquake loading. Both the median and 84th percentile (mean plus one standard deviation) ground motions were used for the dynamic response analyses.

6.7.2 Dynamic Response Analysis

Details of the dynamic response analyses are presented in Appendix J, and the soil properties used in these analyses are summarized in Appendices C and D.

Prior to calculating the dynamic response of the dam to the prescribed earthquake loading, the dynamic response was calculated at the site where the earthquake was experienced and where the subjective intensity characterization was first assembled. The intent of the calibration was to confirm that, within the bounds of the uncertainty associated with these analyses, the calculated ground motions were reasonable. Calculations were conducted by means of an industry standard method called SHAKE. The seismological advisors concurred that the calculated response was acceptable.

The recommended median and 84th percentile ground motions were then used to calculate the cyclic stresses and number of significant cycles to be considered in assessing the dynamic response of the dam. These ground motions are used to calculate both potential pore pressure development in saturated sand above the slimes as well as potential displacements in the slimes-rich deposits.

Cyclic Loading and Pore Pressure Response

It was the intent to apply the cyclic loading discussed above to a test specimen of sand on the brink of collapse, having been brought to that state by reducing horizontal stresses following the path associated with the lateral extrusion mechanism. However, it was not practical to apply the small

stresses calculated, and significantly larger stresses were applied during testing. Figure 6-2 illustrates the type of response that would indicate that the imposed earthquakes could have a significant effect on failure of the dam. In specific tests undertaken on the fragile test specimen, many more cycles (>1000) were applied than the 4-5 indicated by the calculations. Details of the testing are summarized in Appendix D. Collapse occurred only after more than 1200 cycles at stresses significantly larger than indicated by the analysis to have been produced by the earthquakes and no specific excess pore pressures were generated.

The Panel concludes that no cyclic induced pore pressures resulted from the assumed earthquake loading.

Cyclic Loading and Sliding in Slimes

Another potential result of the imposed earthquake loading is to induce deformations in the slimes-rich deposits as a result of the cyclic stresses discussed above. These deformations are calculated by adopting the earthquake motions computed at the top of the slimes and imposing them directly into analysis to calculate the seismic induced slip using a classical method entitled Newmark-type analysis and using a well-accepted computer program called SLAMMER. Details of these calculations are presented in Appendix J.

Reflecting the uncertainty in the prescribed ground motions, six time histories were selected from those recommended by Atkinson (2016). Those selected reflected the upper-bound of the range evaluated in the seismic study. The average calculated displacement was 5 mm. This can be compared with the rate of displacement calculated by the deformation analyses prior to failure. Estimates of rate of displacement from both NorSand and Mohr-Coulomb analyses indicate rates of approximately 1 mm per day. Hence, the displacements calculated from the SLAMMER analyses are of limited significance when compared with the rates of displacements associated with static loading alone. Nevertheless, given the proximity of the dam to collapse due to prior construction loading, this likely accelerated the failure process that was already well-advanced

6.8 Timing of the Failure

The introductory portions of this section posed the following three questions, which are answered below.

Why did flowsliding not occur on August, 2014 cracking incident?

The August, 2014 cracking incident did not display the mobility associated with flowsliding indicating that liquefaction did not occur. Figure 4-3 previously explained in principle how increased loading can cause a formerly dilatant material to become contractant. This effect is displayed in the NorSand model of conditions prevailing on or about August of 2014. As shown on Figure 6-10 on August, 2014 the sand is on or close to the CSL, which is a boundary between contractant and dilatant behavior. At this point the sand became loose enough to exhibit volume change and associated cracking but was not sufficiently loose to exhibit liquefaction. Also, Section 4.3 explained that a fundamental change in seepage patterns happened on or about the same time. Together these two changes, one in sand behavior and the other in saturation, produced the observed effects.

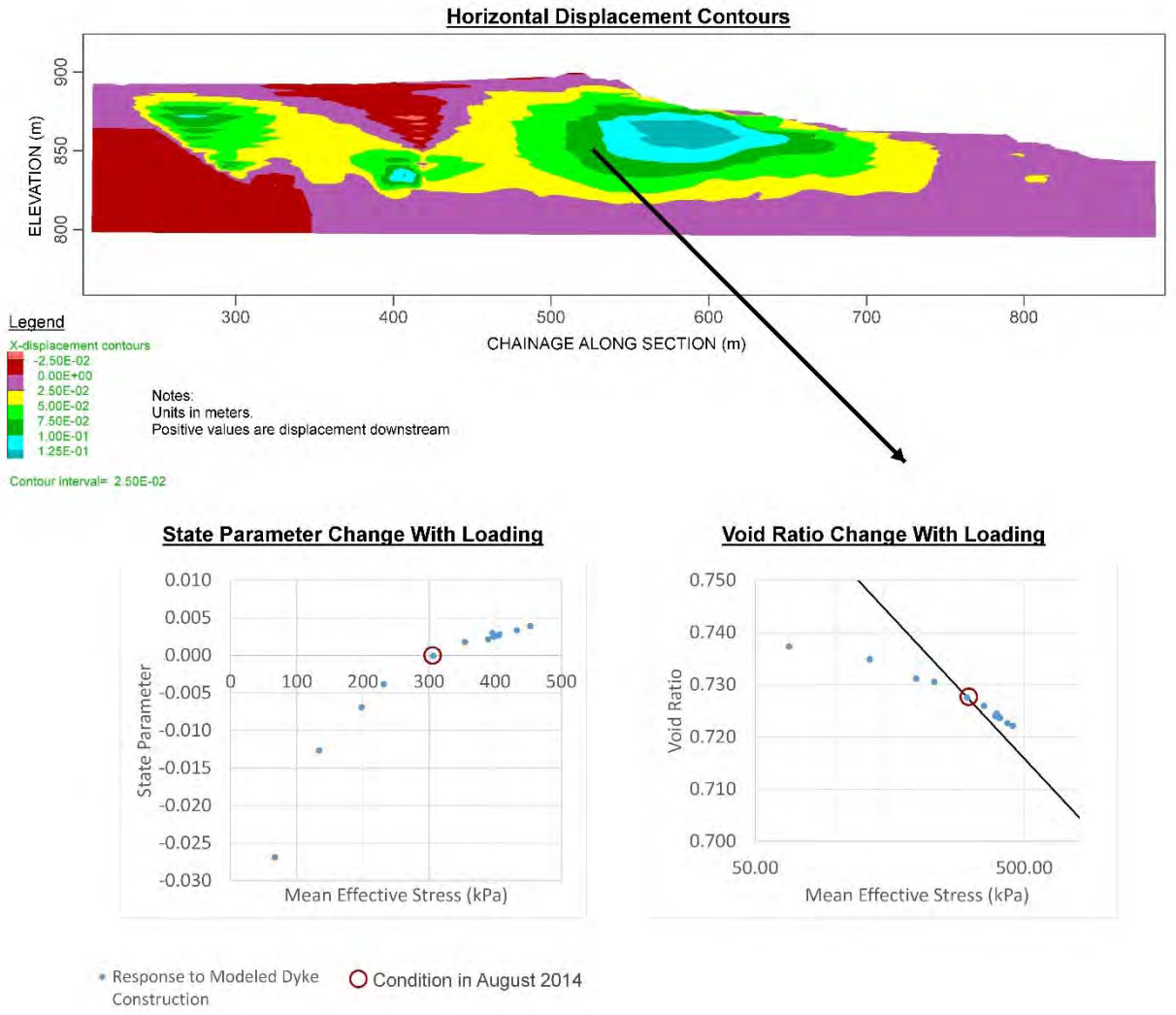

Figure 6-10 Example NorSand model output

Why did flowsliding occur under the conditions that prevailed on November 5, 2015?

The Panel concludes that the flowslide that occurred on November 5, 2015 was instigated by a lateral extrusion mechanism seated in the slimes-rich deposit at depth in the embankment that resulted in a reduction of lateral confinement of the overlying contractant and saturated sand. The extrusion mechanism created sufficient sliding displacement to generate a MIR of unity which is the criterion for triggering collapse.

Why did flowsliding occur following the earthquakes?

The earthquakes were small and would normally not be regarded as consequential for an ordinary dam. The Fundão Dam was subjected to lateral extrusion in the slimes-rich deposits beneath the left abutment and stress readjustment associated with this mechanism was leading it to collapse and liquefaction.

The prescribed earthquake motions have two potential effects on the dam. One is cyclic stresses that induce pore pressures in the sand and the other is cyclic stresses that induce deformations in the slimes-rich deposits. Experiments conducted on samples of sand representative of the stresses prior to collapse did not develop any pore pressure response due to the applied earthquake motions. However, the same earthquake motions applied to the behavior of the slimes-rich deposits indicated sliding displacements in the range of several millimeters. These displacements are of limited significance when compared with the displacements associated with static loading alone. Given the proximity of the dam to collapse due to prior construction loading, these earthquake induced displacements likely accelerated the failure process that was already well-advanced.

7 CONCLUSIONS

The mandate to the Panel was to conduct an investigation into the cause(s) of the breach of the Fundão Tailings Dam on November 5, 2015. To fulfill this mandate, the Panel was expected to provide its independent and unbiased professional judgement and expertise in determining the immediate cause(s) of the Incident and that this report would identify these immediate cause(s).

The Panel has responded to its mandate by framing three questions with accompanying answers. These questions and a summary of the responses, presented below, identify the immediate causes.

Question 1: Why Did a Flowslide Occur?

The original design concept for the Fundão Dam employed an unsaturated sand zone to support the weak slimes zone. Unsaturated sand is not amenable to liquefaction and hence the original design was robust in this regard. However, difficulties were encountered in executing the design and a modified design was put forward and adopted. As part of this modification, a change in the design concept was also adopted and saturated conditions were permitted to develop in the sand.

The flowslide required three conditions to develop: (1) saturation of the sand; (2) loose uncompacted sand; and (3) a trigger mechanism. Depositing sand tailings by hydraulic means resulted in loose conditions. The growth in the saturated conditions is well-documented. Hence, all the conditions prevailed for liquefaction to develop resulting in a flowslide, provided it was triggered. Triggering is discussed in the response to Question 3.

Question 2: Why Did the Flowslide Occur Where It Occurred?

Eyewitness accounts revealed that the flowslide initiated on the left abutment, where the dam had been set back from its former alignment. Studies of the depositional history associated with the growth of the Fundão Dam revealed that slimes encroached into the area preserved for sand deposition alone. The design incorporated a 200 m zone separating the two deposits but historical information reveals that slimes had encroached into the area on a number of occasions. The presence of slimes introduces a barrier to downward drainage and a zone of potential weakness that might affect stability. Deposition in the area of the right abutment was almost slimes free.

The setback was implemented to accommodate repairs to a deficient conduit at the base of the impoundment as well as the construction of additional horizontal blanket drains to facilitate subsequent dike-raising. This change in geometry resulted in substantial embankment loading over slimes-rich deposits. This distinguishes the left abutment area from the right and accounts for the location of flowslide initiation.

Question 3: Why Did the Flowslide Occur When It Occurred?

The initiation of a flowslide requires not only the presence of saturated contractant tailings but also a trigger mechanism to initiate the process that mobilizes undrained shearing and hence flowsliding. Following an evaluation of potential trigger mechanisms, the Panel concluded that lateral extrusion initiated the failure.

The lateral extrusion mechanism develops as the dam increases in height, loading the slimes-rich zone vertically which tends to extrude or spread laterally, rather like squeezing toothpaste from a tube. This results in stress changes in the overlying sands which reduce their confinement, leading to collapse.

This mechanism for collapse was modelled by tests in the laboratory and by computational modeling that predicted to an acceptable degree that collapse should have occurred about the time that the dam was raised to the height that was attained on November 5, 2015.

The role of the earthquakes that occurred just prior to collapse was also investigated quantitatively. Calculations with recommended design motions reveal that about 5 mm of displacement may have been induced in the slimes. Given the proximity of the dam to collapse due to prior construction loading, this likely accelerated the failure process that was already well-advanced.

ACKNOWLEDGEMENTS

We would like to express our appreciation to Klohn Crippen Berger, which provided indispensable engineering and organizational assistance. We especially wish to recognize the efforts of Cindy Wang, without whose creative skill and determination in synthesizing reams of information and data our efforts could never have proceeded far. In addition, we wish to recognize the contribution of Joe Quinn not only for his leadership and analytical modeling but also his role in the field and laboratory studies. The contribution of Chris Dickinson and his colleagues resulted in an important synthesis of all seepage related issues.

Most of all, the Panel wishes to acknowledge the sacrifices of the victims, their loved ones, and those left homeless. We can only hope that our work may in some small measure help to prevent such occurrences from ever happening again.

REFERENCES

Atkinson, G. 2016. *Analysis of Ground Motions from Nov. 5, 2015 Earthquake Sequence near Fundão Dam, Brazil.* Report to CGSH on July 20, 2016.

Jefferies, M. and K. Been. 2016. *Soil Liquefaction: A Critical State Approach.* 2nd ed. London: Taylor & Francis.

Martin, T.E. and E.C. McRoberts. 1999. "Some Considerations in the Stability Analysis of Upstream Tailings Dams," in *Tailings and Mine Waste '99: Proceedings of the 6th International Conference on Tailings and Mine Waste, January 24 to 27, 1999.* Rotterdam, Netherlands: A.A. Balkema.

Pimenta de Ávila, J. 2011. "The Drained Stacking of Granular Tailings: A Disposal Method for a Low Degree of Saturation of the Tailings Mass," in *Proceedings of the Tailings and Mine Waste Conference, Vancouver, BC, November 6 to 9 2011.* Vancouver: University of British Columbia.

Robertson, P.K. 2010. "Evaluation of Flow Liquefaction and Liquefied Strength Using the Cone Penetration Test." *Journal of Geotechnical and Geoenvironmental Engineering.* 136(6): 842-853.

Sadrekarimi, A. 2014. "Effect of the Mode of Shear on Static Liquefaction Analysis." *Journal of Geotechnical and Geoenvironmental Engineering.* 140(12): 04014069-1-04014069-12.

Sasitharan, S., P.K. Robertson, D.D. Sego and N.R. Morgenstern. 1993. "Collapse Behaviour of Sand." *Canadian Geotechnical Journal.* 30(4): 569-577.

Shuttle, D.A. and J. Cunning. 2007. "Liquefaction Potential of Silts from CPTu." *Canadian Geotechnical Journal.* 44(1): 1-19.

Skopek, P., N.R. Morgenstern, P.K. Robertson and D.C. Sego. 1994. "Collapse of Dry Sand." *Canadian Geotechnical Journal.* 31(6): 1008-1014.

GUIDE TO THE APPENDICES

Guide to the Appendices

INTRODUCTION

This guide describes the contents of the appendices and presents the associated references. There are 11 appendices as follows:

- **Appendix A: GIS/Imagery Methodology**
  - Describes the tools and data sources used to develop a computer model of the Fundão Dam and basin.
- **Appendix B: GIS/Imagery Outputs**
  - Describes the outputs from the data compilation and synthesis using GIS.
- **Appendix C: Field Geotechnical Data and Interpretation**
  - Summarizes the pre-failure geotechnical investigation data available and describes the Panel's 2016 geotechnical data obtained from its field program.
- **Appendix D: Laboratory Geotechnical Data and Interpretation**
  - Describes the pre-failure laboratory data on the tailings and the subsequent laboratory programs prescribed by the Panel to determine engineering properties.
- **Appendix E: Samarco Field Monitoring Data**
  - Presents the Samarco field monitoring data reviewed by the Panel. The instrument types reviewed include Casagrande and vibrating wire piezometers, water level indicators, survey monuments, and flow monitoring stations.
- **Appendix F: Consolidation Modeling**
  - Evaluates the one-dimensional consolidation behavior of the slimes at the left abutment as Dike 1 is raised.
- **Appendix G: Seepage Modeling**
  - Presents the results of steady state and transient three-dimensional seepage modeling completed in order to provide pore pressure conditions for stability and deformation modeling.
- **Appendix H: Limit Equilibrium Analysis of Dike 1 Abutments Prior to Failure**
  - Summarizes results of drained and undrained static slope stability analysis undertaken on the right and left abutments for various conditions prior to failure.
- **Appendix I: Deformation Analysis of the Left Abutment**
  - Describes the assessment of the influence of deformations within the slimes layers on the stress state of the overlying tailings sand at the left abutment.

- **Appendix J: Dynamic Response Analysis**
  - Presents results of dynamic responses analyses of the November 5, 2015 earthquakes at Samarco.
- **Appendix K: Potential Failure Modes and Triggers**
  - Description of failure mode and trigger screening process leading to remaining failure mode and trigger mechanisms examined in detail in the main report.

APPENDIX NUMBERING CONVENTION

This section presents the numbering convention used for sections, figures, and tables in the appendices and accompanying attachments. Appendix B has been used as an example.

- Appendices:
  - Appendix B: second appendix
  - Section B5: fifth section of Appendix B
  - Figure/Table B5-1: first figure/table in the fifth section of Appendix B
- Attachments:
  - Attachment B2: second attachment in Appendix B
  - Section B.B2-1: first section of the second attachment in Appendix B
  - Figure/Table B.B2-1: first figure/table in the second attachment in Appendix B

APPENDIX REFERENCES

General

The references cited in the appendices are both public and project documents. Public documents refer to those that are readily available to the public, whether free or at a cost, including academic papers and standards. Project documents are those received from CGSH throughout the course of the Investigation which are not publicly available.

Appendix A includes a list of documents, public and project, that are not included in the reference list presented in this section. These were separated as they typically do not require in-text citations such as AutoCAD drawings, satellite aerial images and recurring monitoring reports and records. The full list of project files excluded from the reference list is given in Appendix A, and include:

- Software;
- Topography and aerial images;
- As-built and design surveys;
- Recurring Samarco reports and specific records;

- Photographs;
- Consulting and engineering reports related to geotechnical investigations;
- Engineering audit reports; and
- Interviews and eyewitness accounts.

Public documents are cited in-text using (Author Date) format. Public references are listed below under the Public Documents Section.

Project documents are listed numerically in the order that they are encountered in the appendices. In-text citations are depicted using superscript text and/or square brackets. Project references are listed below under the Project Documents Section.

Public Documents

Anderson, M.P. and W.W. Woessner. 1991. *Applied Groundwater Modeling: Simulation of Flow and Advective Transport*. 2nd ed. London: Elsevier Inc.

ASTM D4767-11. 2011. "Standard Test Method for Consolidated Undrained Triaxial Compression Test for Cohesive Soils." Annual Book of ASTM Standards, Vol.04.08.

ASTM D6913-04(2009)e1. 2009. "Standard Test Methods for Particle-Size Distribution (Gradation) of Soils Using Sieve Analysis." Annual Book of ASTM Standards, Vol.04.09.

ASTM D7181-11. 2011. "Standard Test Method for Consolidated Drained Triaxial Compression Test for Soils." Annual Book of ASTM Standards, Vol.04.09.

ASTM D1125-14. 2014. "Standard Test Methods for Electrical Conductivity and Resistivity of Water." Annual Book of ASTM Standards, Vol.11.01.

ASTM D4972-13. 2013. "Standard Test Method for pH of Soils." Annual Book of ASTM Standards, Vol.04.08.

ASTM D4253–16. 2016. "Standard Test Methods for Maximum Index Density and Unit Weight of Soils Using a Vibratory Table." Annual Book of ASTM Standards, Vol.04.08.

ASTM D4254-16. 2016. "Standard Test Methods for Minimum Index Density and Unit Weight of Soils and Calculation of Relative Density." Annual Book of ASTM Standards, Vol.04.08.

ASTM D698-12e. 2012. "Standard Test Methods for Laboratory Compaction Characteristics of Soil Using Standard Effort." Annual Book of ASTM Standards, Vol.04.08.

ASTM D4318-10e. 2010. "Standard Test Methods for Liquid Limit, Plastic Limit, and Plasticity Index of Soils." Annual Book of ASTM Standards, Vol.04.08.

ASTM D2216-10. 2010. "Standard Test Methods for Laboratory Determination of Water (Moisture) Content of Soil and Rock by Mass." Annual Book of ASTM Standards, Vol.04.08.

ASTM D1140-14. 2014. “Standard Test Methods for Determining the Amount of Material Finer than 75-µm (No. 200) Sieve in Soils by Washing.” Annual Book of ASTM Standards, Vol.04.08.

ASTM D422-14. 2014. “Test Method for Particle Size Analysis of Soils - ADJD0422.” Adjunct to D422 Test Method for Particle-Size Analysis of Soils.

ASTM D5311-13. 2013. “Standard Test Method for Load Controlled Cyclic Triaxial Strength of Soil.” Annual Book of ASTM Standards, Vol.04.08.

ASTM D2435/D2435M-11. 2011. “Standard Test Methods for One-Dimensional Consolidation Properties of Soils Using Incremental Loading.” Annual Book of ASTM Standards, Vol.04.08.

ASTM D3080/D3080M-11. 2011. “Standard Test Method for Direct Shear Test of Soils Under Consolidated Drained Conditions.” Annual Book of ASTM Standards, Vol.04.08.

ASTM D6528-07. 2007. “Standard Test Method for Consolidated Undrained Direct Simple Shear Testing of Cohesive Soils (Withdrawn 2016).” Annual Book of ASTM Standards, Vol.04.08.

ASTM D854-14. 2014. “Standard Test Methods for Specific Gravity of Soil Solids by Water Pycnometer.” Annual Book of ASTM Standards, Vol.04.08.

Atkinson, G. 2016. *Analysis of Ground Motions from Nov. 5, 2015 Earthquake Sequence near Fundão Dam, Brazil.* Report to CGSH on July 20, 2016.

Boulanger, R.W. and I.M. Idriss. 2016. "CPT-Based Liquefaction Triggering Procedure." *Journal of Geotechnical and Geoenvironmental Engineering, ASCE*. 142(2):0415077-1-0415077-14.

Cedergren, H.R. 1972. “Seepage Control in Earth Dams,” in *Embankment Dam Engineering, Casagrande Volume*. Malabar, FL: Krieger Publishing Company.

Conlin, B.H. 1987. “A Review of the Performance of Mine Tailings Impoundments under Earthquake Loading Conditions,” in *Earthquake Geotechnique: 2nd Vancouver Geotechnical Society Symposium*. Vancouver: Vancouver Geotechnical Society.

Eckersley, J.D. 1990. “Instrumented Laboratory Flowslides.” *Géotechnique*. 40(3): 489-502.

Fell, R., P. MacGregor, D. Stapledon and G. Gell. 2005. *Geotechnical Engineering of Dams*. Leiden, Netherlands: A.A. Balkema.

Gajo, A. 2004. “The Influence of System Compliance on Collapse of Triaxial Sand Samples.” *Canadian Geotechnical Journal*. 41(2): 257-273.

Greening, P.D. and D.F.T. Nash. 2004. “Frequency Domain Determination of G0 using Bender Elements.” *Geotechnical Testing Journal*. 27(3): 288-294.

Head, K.H. and R.J. Epps. 2014. *Manual of Soil Laboratory Testing, Volume 3 - Effective Stress Tests*. 3rd ed. Dunbeath, Scotland: Whittles Publishing.

Idriss, I.M. and R.W. Boulanger. 2008. *Soil Liquefaction During Earthquakes*. Oakland, CA: Earthquake Engineering Research Institute.

International Code Council. 2015. *2015 International Building Code*. Country Club Hills, IL: Author.

Jefferies, M. and K. Been. 2016. *Soil Liquefaction: A Critical State Approach.* 2nd ed. London, England: Taylor & Francis.

Junaideen, S.M., L.G. Tham, K.T. Law, F.C. Dai and C.F. Lee. 2010. "Behaviour of Recompacted Residual Soils in a Constant Shear Stress Path." *Canadian Geotechnical Journal*. 47(6): 648-661.

Ladd, R. S. 1978. "Preparing Test Specimens Using Undercompaction." *Geotechnical Testing Journal.* 1(1): 16-23.

Lo, R.C., E.J. Klohn and W.D.L. Finn. 1988. "Stability of Hydraulic Sandfill Tailings Dams." *ASCE Geotechnical Special Publication No. 21*. 549-572.

Mavko, G. 2005. "Parameters that Influence Seismic Velocity: Conceptual Overview of Rock and Fluid Factors that Impact Seismic Velocity and Impedance." *Stanford Rock Physics Laboratory*. Accessed July 29, 2016. https://pangea.stanford.edu/courses/gp262/Notes/8.SeismicVelocity.pdf

Olson, S. and T.D. Stark. 2002. "Liquefied Strength Ratio from Liquefaction Flow Failure Case Histories." *Canadian Geotechnical Journal*. 39(3): 629-647.

Plewes, H.D., M.P. Davies and M.G. Jefferies. 1992. "CPT Based Screening Procedure for Evaluating Liquefaction Susceptibility," in *Proceedings of the 49th Canadian Geotechnical Society Conference*. Toronto: Canadian Geotechnical Society.

Robertson, P.K. 2009. "Interpretation of Cone Penetration Tests – a Unified Approach." *Canadian Geotechnical Journal.* 46: 1337–1355.

Robertson, P.K. 2010a. "Evaluation of Flow Liquefaction and Liquefied Strength Using the Cone Penetration Test." *Journal of Geotechnical and Geoenvironmental Engineering*. 136(6): 842-853.[1]

Robertson, P.K. 2010b. "Soil Behaviour Type from the CPT: An Update." *2nd International Symposium on Cone Penetration Testing, CPT'10.* Huntington Beach, CA.

Robertson, P.K. and C.E. Wride. 1998. "Evaluating Cyclic Liquefaction Potential Using the Cone Penetration Test." *Canadian Geotechnical Journal.* 35(3): 442-459.

Salamatpoor, S. and S. Salamatpoor. 2014. "Evaluation of Babolsar Sand Behaviour by Using Static Triaxial Tests and Comparison with Case History." *Open Journal of Engineering*. 4: 181-197.

Sasitharan, S., P.K. Robertson, D.D. Sego and N.R. Morgenstern. 1993. "Collapse Behaviour of Sand." *Canadian Geotechnical Journal.* 30(4): 569 - 577.

Silva, W.J., N. Abrahamson, G. Toro and C. Constantino. 1997. *Description and Validation of the Stochastic Ground Motion Model.* Report submitted to Brookhaven National Laboratory, Associated Universities, Inc., New York, NY.

[1] This paper is referenced as Robertson (2010) on CPT plots in Appendix C.

Skopek, P., N.R. Morgenstern, P.K. Robertson and D.C. Sego. 1994. "Collapse of Dry Sand." *Canadian Geotechnical Journal.* 31: 1008-1014.

Styler, M.A. 2014. *Investigations Into the Use of Continuous Shear Wave Measurements in Geotechnical Engineering*. (Electronic Theses and Dissertations (ETDs) 2008+. T, University of British Columbia) Accessed July 29, 2016: http://dx.doi.org/10.14288/1.0135594.

Terzaghi, K., R.B. Peck and G. Mesri. 1996. *Soil Mechanics in Engineering Practice*. New York, NY: John Wiley & Sons.

University of British Columbia (UBC). 2016. "Electron Microbeam / X-Ray Diffraction Facility." Accessed February 24, 2016. https://www.eoas.ubc.ca/research/infrastructure/emxdf.html.

Vaid, Y.P. and S. Sivathayalan. 1996. "Errors in Estimates of Void Ratio of Laboratory Sand Specimens." *Canadian Geotechnical Journal*. 33(6), 1017-1020.

Vaughan, P.R. 1994. "Assumption, Prediction and Reality in Geotechnical Engineering." *Géotechnique.* 44(4): 573-609.

Vucetic, M. and R. Dobry. 1991. "Effect of Soil Plasticity on Cyclic Response." *Journal of Geotechnical Engineering, ASCE.* 117(1): 89-107.

Weber, J.P. 2015. *Engineering Evaluation of Post-Liquefaction Strength*. (PhD diss., University of California, Berkeley) Accessed July 29, 2016. http://escholarship.org/uc/item/20n2x8q5.

Winckler, C., R. Davidson, L. Yenne, and J. Pilz. 2014. "CPTu-Based State Characterization of Tailings Liquefaction Susceptibility," in *Proceedings of the 34th Annual USSD Conference on Dams and Extreme Events, 7 to 11 April 2014.* San Francisco: U.S. Society on Dams.

Yamashita, S., T. Kawaguchi, Y. Nakata, T. Mikami, T. Fujiwara and S. Shibuya. 2009. "Interpretation of International Parallel Test on the Measurement of G_{max} using Bender Elements." *Soils and Foundations*. 49(4): 631-650.

Project Documents

A list of specific private documents relied upon by the Panel has been omitted to avoid any inference of fault or responsibility to any person or party.

ATTACHMENT A1

Data Sources

Appendix A: Attachment A1
Data Sources

TABLE OF CONTENTS

List of Tables

Table A.A1-1 List of software references

Software Name	Reference
Global Mapper	Blue Marble Geographics. 2016. *Global Mapper v17.2* [computer software].
	Blue Marble Geographics. 2016. *Global Mapper v17.1* [computer software].
	Blue Marble Geographics. 2015. *Global Mapper v16.2* [computer software].
Muck3D	MineBridge Software Inc. 2013. *Muck3D Version 3.1.1* [computer software].
	MineBridge Software Inc. 2013. *Muck3D Version 3.0.1* [computer software].
Civil 3D	Autodesk Inc. 2013. *AutoCAD Civil 3D 2014* [computer software].
ArcGIS	Esri Inc. 2014. *ArcGIS 10.2.2 for Desktop* [computer software].
MAPGEO2010	Instituto Brasileiro de Geografía e Estatistica (IBGE). 2010. *MAPGEO 2010* [computer software].

Table A.A1-2 List of topography and aerial images

Source	Topography	Aerial Image	Samarco Document Number (File Name)	Survey Date (Drawing Date)	Survey Method
See Note 1		x	See Note 1	Unknown	Unknown
	x	x		2011-04-14	Drone
	x			Unknown (2011-10-24)	LiDAR
	x			**2011-07-01**	Unknown
	x	x		2012-01-21	Drone
	x	x		2012-09-02	Drone
	x	x		2012-09-26	Drone
	x	x		2013-01-01	Drone
	x	x		2013-02-01	Drone
	x	x		2013-03-02	Drone
	x	x		2013-04-02	Drone
	x	x		2013-05-01	Drone
	x	x		2013-05-27	Drone
	x	x		2013-06-30	Drone
	x	x		2013-07-29	Drone

Source	Topography	Aerial Image	Samarco Document Number (File Name)	Survey Date (Drawing Date)	Survey Method
See Note 1	x	x	See Note 1	2013-09-03	Drone
	x	x		2013-10-01	Drone
	x	x		2013-10-27	Drone
	x	x		2013-11-26	Drone
	x	x		2013-12-27	Drone
	x	x		2014-01-29	Drone
	x	x		2014-02-27[3]	Drone
	x	x		2014-03-28	Drone
	x	x		2014-05-01	Drone
	x	x		2014-06-03	Drone
	x	x		2014-06-27	Drone
	x	x		2014-08-04	Drone
	x	x		2014-08-29	Drone
	x	x		2014-09-26	Drone
	x	x		2014-10-31	Drone
	x	x		2014-11-27	Drone
	x	x		2014-12-29	Drone
	x	x		2015-01-29	Drone
	x	x		2015-02-26	Drone
	x	x		2015-03-20	Drone
	x	x		2015-04-24	Drone
	x	x		2015-05-27	Drone
	x	x		2015-06-22	Drone
	x	x		2015-07-27	Drone
	x	x		2015-08-24	Drone
	x	x		2015-10-01	Drone
	x	x		2015-10-27	Drone
	x	x		2015-10-27	Drone
	x	x		2015-11-06	Drone
	x	x		2016-05-27	Drone
	x	x		2011-12-13	Drone
	x	x		2012-09-26	Drone
	x	x		2013-01-06	Drone
	x	x		2013-05-02	Drone
	x	x		2013-08-21	Drone
	x	x		2014-09-05	Drone

Source	Topography	Aerial Image	Samarco Document Number (File Name)	Survey Date (Drawing Date)	Survey Method
See Note 1	x	x	See Note 1	2014-12-14	Drone
		x		2015-07-16	Drone
	x			**2012-04-01**	LiDAR or other photogrammetry
	x	x		**1974**	Unknown
PhotoSat		x	(fundao_dam_wo3705a_rapideye_2009apr18)	2009-04-18	Satellite
PhotoSat		x	(fundao_dam_wo3705a_rapideye_2009aug18)	2009-08-18	Satellite
PhotoSat	x	x	(fundao_dam_wo3705b_prism_avnir_2009nov15_shifted)	2009-11-15	Satellite Stereo Pair
PhotoSat		x	(fundao_dam_wo3705a_rapideye_2010jan17)	2010-01-17	Satellite
PhotoSat		x	(fundao_dam_wo3705a_rapideye_2010feb22)	2010-02-22	Satellite
PhotoSat		x	(fundao_dam_wo3705a_rapideye_2010apr27)	2010-04-27	Satellite
PhotoSat		x	(fundao_dam_wo3705a_rapideye_2010jun19)	2010-06-19	Satellite
PhotoSat		x	(fundao_dam_wo3705a_rapideye_2010aug07)	2010-08-07	Satellite
PhotoSat		x	(fundao_dam_wo3705a_rapideye_2010oct29)	2010-10-29	Satellite
PhotoSat		x	(fundao_dam_wo3705a_rapideye_2010dec22)	2010-12-22	Satellite
PhotoSat		x	(fundao_dam_wo3705a_geoeye1_2011feb11)	2011-02-11	Satellite
PhotoSat		x	(fundao_dam_wo3705a_rapideye_2011apr09)	2011-04-09	Satellite
PhotoSat		x	(fundao_dam_wo3705a_rapideye_2011aug17)	2011-08-17	Satellite
PhotoSat	x	x	(fundao_dam_wo3682b_wv1_2011sep21_shifted)	2011-09-21	Satellite Stereo Pair
PhotoSat		x	(fundao_dam_wo3682b_ge1_2011oct02_shifted)	2011-10-02	Satellite
PhotoSat	x	x	(fundao_dam_wo3682c_wv2_2012mar03_shifted)	2012-03-03	Satellite Stereo Pair
PhotoSat	x	x	(fundao_dam_wo3682d_pleiades_2013may08_shifted)	2013-05-08	Satellite Stereo Pair
PhotoSat	x	x	(fundao_dam_wo3682a_wv1_2014aug02_shifted)	2014-08-02	Satellite Stereo Pair
PhotoSat		x	(fundao_dam_wo3682a_ge1_2014aug10_shifted)	2014-08-10	Satellite
PhotoSat	x	x	(fundao_dam_wo3679a_wv2_2015jun24_shifted)	2015-06-24	Satellite Stereo Pair
PhotoSat		x	(fundao_dam_wo3679a_wv2_2015jul10_shifted)	2015-07-10	Satellite
PhotoSat		x	(fundao_dam_wv2_2015jul21_shifted)	2015-07-21	Satellite
PhotoSat	x	x	(fundao_dam_wv2_2015nov10_shifted)	2015-11-10	Satellite Stereo Pair
PhotoSat		x	(fundao_dam_wv2_2015nov12_shifted)	2015-11-12	Satellite
Google Earth		x	-	2005-04-07	Satellite
Google Earth		x	-	2008-05-24	Satellite

Source	Topography	Aerial Image	Samarco Document Number (File Name)	Survey Date (Drawing Date)	Survey Method
Google Earth		x	-	2011-05-25	Satellite
Google Earth		x	-	2011-09-24	Satellite
Google Earth		x	-	2011-10-01	Satellite
Google Earth		x	-	2013-05-07	Satellite
Google Earth		x	-	2014-08-10	Satellite
Google Earth		x	-	2013-08-10	Satellite
Google Earth		x	-	2015-07-20	Satellite
Google Earth		x	-	2015-11-09	Satellite

1. A list of specific private documents relied upon by the Panel has been omitted to avoid any inference of fault or responsibility to any person or party.
2. **Bolded** entries denote unknown survey dates. Where the month and year are given, the survey is assumed to have occurred on the first of the month.
3. The drone survey conducted on February 27, 2014 was received late in the Investigation and was not included in the rate of rise calculation or pond and slimes mapping data set.

Table A.A1-3 List of raw drone photos reviewed by Panel

Survey Date	Survey Program	Purpose of Review
2015-10-27	Recurring Fundão surveys	To understand the surface drainage system at the left setback
2016-04-12	Post-failure Secondary Gallery survey	To locate the exposed remnants of the Secondary Gallery along the as-built alignment and to determine the thickness of cover remaining on top of the Secondary Gallery
2016-05-27	Post-failure Secondary Gallery survey	To determine the change in thickness of cover remaining on top of the Secondary Gallery since the April 12, 2016 survey for viability of excavation to investigate the possibility of a Gallery collapse
2015-11-06	Post-failure Fundão survey	To understand site conditions post-failure
2015-11-09	Post-failure Fundão survey	
2015-11-11	Post-failure Fundão survey	
2015-11-14	Post-failure Fundão survey	
2015-11-20	Post-failure Fundão survey	
2015-11-15	Post-failure Germano survey	To look for presence of sand boils in post-failure images
2015-12-06	Post-failure Germano survey	
2015-07-04	Recurring Germano surveys	To look for presence of sand boils in pre-failure images
2015-07-17	Recurring Germano surveys	

Table A.A1-4 List of as-built and design surveys

A list of specific private documents relied upon by the Panel has been omitted to avoid any inference of fault or responsibility to any person or party.

Table A.A1-5 List of Samarco reports

A list of specific private documents relied upon by the Panel has been omitted to avoid any inference of fault or responsibility to any person or party.

Table A.A1-6 List of Samarco records

A list of specific private documents relied upon by the Panel has been omitted to avoid any inference of fault or responsibility to any person or party.

Table A.A1-7 List of photographs

A list of specific private documents relied upon by the Panel has been omitted to avoid any inference of fault or responsibility to any person or party.

Table A.A1-8 List of engineering audit reports

A list of specific private documents relied upon by the Panel has been omitted to avoid any inference of fault or responsibility to any person or party.

Table A.A1-9 List of interviews and eyewitness accounts

A list of specific private documents relied upon by the Panel has been omitted to avoid any inference of fault or responsibility to any person or party.

ATTACHMENT A2

Stripped Ground Compilation

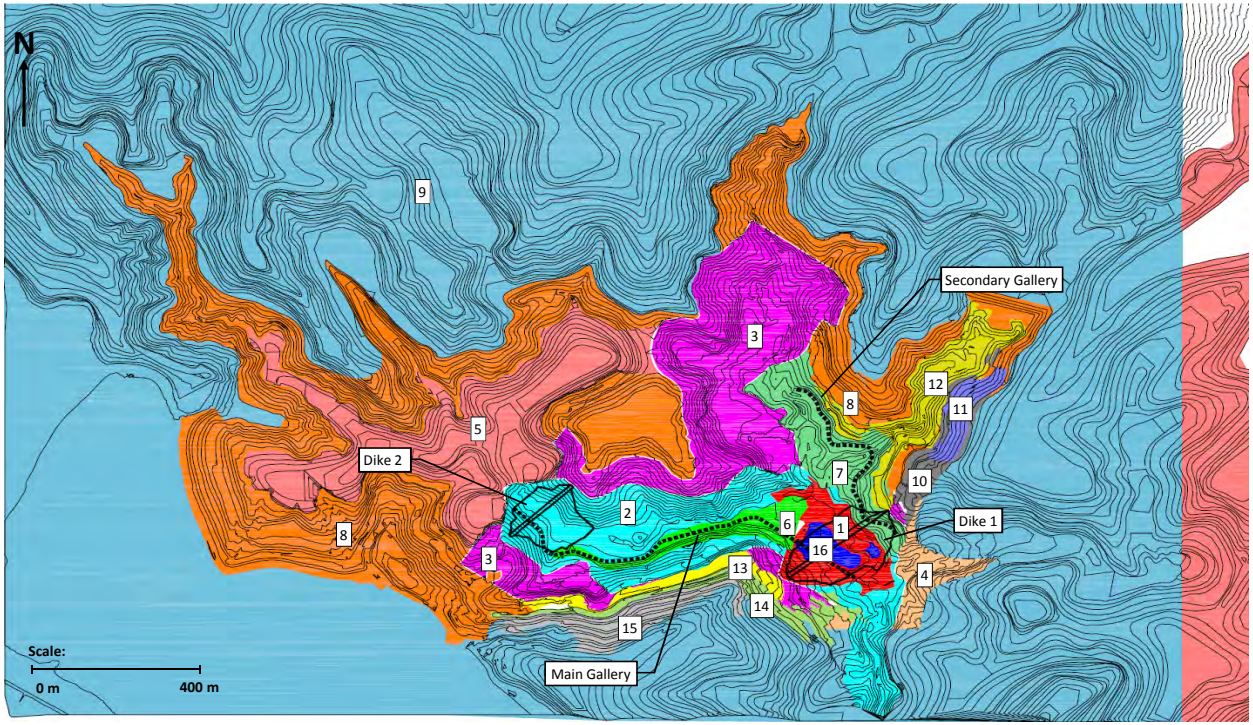

Legend:

No.	Topography Source Drawing	Survey Date (Latest Drawing Date)
1	A list of specific private documents relied upon by the Panel has been omitted to avoid any inference of fault or responsibility to any person or party.	- (2007-11-12)
2		- (2010-09-27)
3		- (2009-10-##)
4		2010-08-10 (2011-02-11)
5		1974-##-##
6		- (2010-10-14)
7		- (2010-10-14)
8		2012-01-21
9		2013-12-27
10		2014-08-04
11		2015-04-24
12		- (2010-11-29)
13		2013-01-01
14		2014-01-26
15		2014-03-28
16	Topography modified to reflect the as-built surface under Dike 1.	

Note: "##" denotes unknown date.

APPENDIX A

GIS/Imagery Methodology

Appendix A
GIS/Imagery Methodology

TABLE OF CONTENTS

List of Tables

TABLE OF CONTENTS

(continued)

List of Figures

List of Attachments

A1 INTRODUCTION

This appendix describes the tools and data sources used to develop a computer model of the Fundão Dam and basin. This was necessary because much of the tailings evacuated the impoundment during the dike failure leaving no opportunity to conduct site investigations to determine stratigraphy after the fact. Large amounts of data were available from Samarco. A geographic information system (GIS) program was used to organize this data.

A major consideration in the compilation of this data was to understand the slimes deposition history because site records of deposition prior to 2012 were not kept. Multiple sources of data from within Samarco's database were used to develop that depositional history. Where needed, external sources of data were used to fill the gaps in the Samarco records.

This appendix describes the techniques used to compile the data, and Appendix B describes the output.

A2 TOOLS

A2.1 Geographic Information Systems

A2.1.1 Global Mapper

The compilation of data required a central repository where information could be catalogued, viewed and manipulated in 2D and 3D when necessary. Global Mapper was used for this purpose. This software allowed the Panel to:

- view topography, aerial images, as-built and design surveys;
- plot drill hole locations in plan;
- overlay any combination of the above data sources for purposes of the Investigation; and
- generate 3D surfaces for viewing and cutting of sections/profiles.

The complete reference and versions of the software used are listed in Attachment A1.

A2.1.2 ArcGIS

ArcGIS was used to perform the same function as Global Mapper, but primarily to process the outputs from the seepage model for presentation purposes. The complete reference and versions of the software used are listed in Attachment A1.

A2.2 AutoCAD Civil 3D

AutoCAD Civil 3D (Civil 3D) was used to process and manipulate 3D topographic and as-built information for inputs to the stability and seepage models. True scale sections for presentation were also created using Civil 3D.

The complete reference and versions of the software used are listed in Attachment A1.

A2.3 Muck3D

Muck3D is a modeling and visualization tool used for geotechnical and mining applications. It was developed to support tailings deposition modeling but can be used for a variety of generic 3D modeling applications. Muck3D was used to visualize and reconstruct, where necessary, elements of the facility for which there was no as-built survey or 3D information. This software allowed the Panel to:

- import and view the topographic data in 3D;
- build the structures in a 3D environment;
- export the structures for seepage or stability analyses; and
- view the internal components of the facility in 3D.

The complete reference and versions of the software used are listed in Attachment A1.

A3 DATA SOURCES

A3.1 General

The large volume of records and data available from Samarco had to be filtered to develop a tailings deposition history without the direct input of Samarco staff and consultants, except through interviews. Documents were collected from Samarco, and were translated for the Panel by others. From this laborious process, sufficient data was collected to reconstruct the tailings deposition history with limitations as described in various sections of this report. The completeness of the data varies considerably from the start of tailings deposition in 2009 to failure in November, 2015.

The primary sources of data used to reconstruct the Fundão facility are listed on Figure A3-1 and discussed in the following sections. The most valuable data sources are topographic surveys and aerial images which show the physical state of the facility at the time of survey. As Figure A3-1 shows, there is a significant data gap prior to 2013. It was necessary to fill these gaps with supporting data sources including:

- as-built and design surveys;
- Samarco reports and records;
- photographs;
- consulting and engineering reports;
- engineering audit reports; and
- interviews and eyewitness accounts.

The consulting and engineering reports as well as interviews conducted post-failure filled in details on past incidents and clarified observations from the aforementioned data sources. They did not necessarily contribute directly to the reconstruction of the facility.

The data sources are listed in detail in Attachment A1.

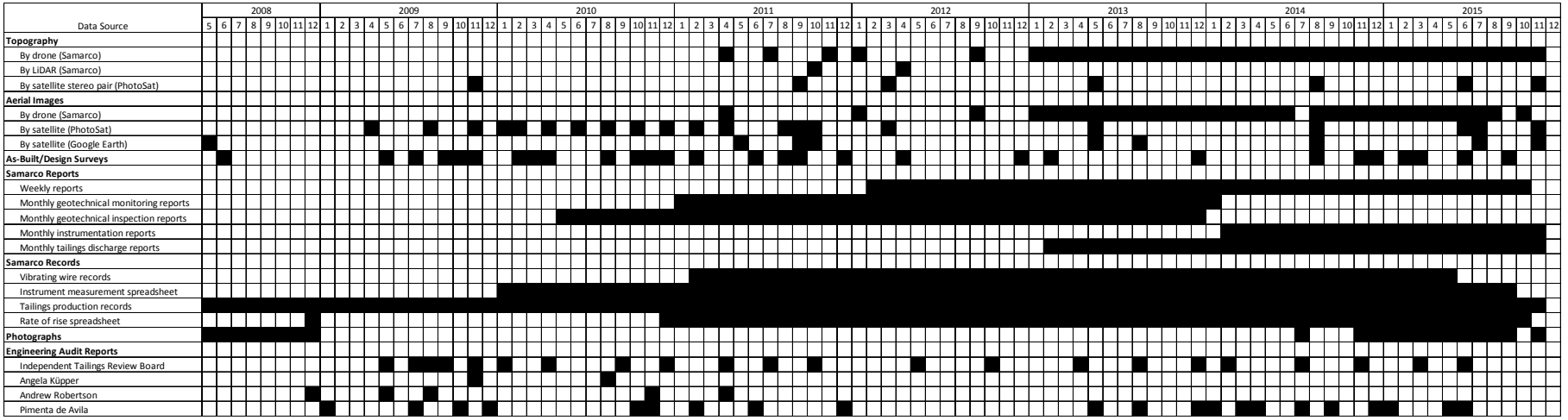

Notes: 1. Dates shown are in monthly increments.
2. Multiple references can be indicated within each month.
3. Consulting and engineering reports, interviews and eyewitness accounts are not included in this summary.

Figure A3-1 Summary of data sources used for tailings deposition history

A3.2 Topography and Aerial Images

A3.2.1 General

Topography and aerial images form the basis for the modeling of the tailings deposition. There are two distinct periods of record:

- pre-2013 when sporadic surveys were done; and
- post-2013 when the drone program was implemented on a monthly basis.

Prior to 2013, surveys were done to support activities such as the jet grouting program for the Main and Secondary Galleries. They do not appear to have been done for the purposes of monitoring tailings deposition. Therefore, the surveys were not only sporadic; they often covered a small area from the toe of Dike 1 to a limited portion upstream of the dike crest. The method of survey is not known for all surveys.

The drone survey program was undertaken by a drone survey company and became continuous on a monthly basis starting January, 2013. Prior to this time, only three full-basin drone surveys were completed, all in 2012. In addition to the topography and aerial images, raw drone photos were made available to the Panel. Where needed, these drone photos were reviewed for greater detail in areas of interest such as the left abutment setback.

In total, 42 topographic surveys and 40 aerial images from Samarco were used in the reconstruction of the Fundão facility. These surveys, in addition to the raw drone photos utilized, are listed in Attachment A1.

A3.2.2 Drone Program

The surveys from the drone program were provided by a survey company that was contracted by Samarco from 2011 onward. These surveys were also the first Samarco topographic data set made available to the Panel. The surveys were provided to the Panel as AutoCAD drawings with contouring at intervals of 1 m, typically. The contouring was software-generated and at times did not follow accepted contouring standards. Patching at times left stranded contours.

As described by the drone survey company, the survey data was collected in the following manner:

1. A Global Positioning System (GPS) device and camera are attached to a small remote controlled plane (a.k.a. the drone).
2. The drone is launched over the Fundão facility. Photos, coordinates and *ellipsoidal*[1] elevations are collected.

[1] *Ellipsoidal* refers to the elevation collected by the GPS device based on an assumed ellipsoid shape for the surface of the Earth. This is a reference elevation depending on the ellipsoid model used by the GPS device.

3. The data is downloaded and coordinates are adjusted using the closest survey monument to the flight area. The elevation data is converted from ellipsoidal to *orthometric*[2] using the software MAPGEO2010. Samarco has historically reported orthometric elevations.

4. Due to battery limitations on the drone, the surveys were usually conducted over several days, up to a maximum of 7 days. The survey dates presented herein are the dates on the last day of survey.

The projection and datum of the drone program data set are presented in Table A3-1. Given that this was the first and most consistent topographic data set made available, the Panel project workspace was set to those listed below.

Table A3-1 Projection and datum summary

Item	
Projection	Universal Transverse Mercator (UTM)
Zone	23K
Horizontal Datum	Córrego Alegre
Vertical Datum	SIRGAS2000(1)

1. Orthometric[2] elevations reported.

A3.2.3 Limitations

The surveys done prior to the drone program have the following limitations:

1. No aerial images accompanied the topographic surveys which made it difficult to determine the surface conditions.
2. The resolution is often more coarse (i.e., greater contour intervals) than the drone surveys.

The drone topographic data set has the following limitations:

1. Aerial images and topography were patched in areas deemed to have minimal change since the previous survey. The patching at times stretched over multiple survey periods which made it difficult to determine the surface conditions based on aerial image alone. In these cases, supporting data sources were used to confirm observations based on aerial image or topography alone. Typically, these areas included:
   a. The Dike 2 reservoir at the toe of Sela and Tulipa Dike.
   b. Grota da Vale.
   c. The Dike 1 reservoir upstream of the trafficked beach extent.
   d. The left abutment setback following completion of the El. 860 m blanket drain.

[2] *Orthometric* refers to the elevation above mean sea level at a given x-y position based on a geoid (non-ellipsoid) shape for the surface of the Earth.

2. Point survey errors were noted on the downstream slope of Dike 1 and on the Island in a few surveys. These anomalies are minimal and limited to the aforementioned areas. They do not affect the subsequent analyses.

A3.3 Supporting Data Sources

A3.3.1 Additional Topography and Aerial Images

A3.3.1.1 ERG Engenharia

ERG Engenharia (ERG) is a consulting engineering company based in Belo Horizonte specializing in mining and infrastructure projects. They provided survey services to Samarco over the operating period for Fundão. Surveys on record cover 2007 to 2015 which overlap the drone survey program. For overlapping periods, the ERG surveys were reviewed, but most did not contain information that was required for reconstruction in addition to the drone surveys. For this reason, they were not generally used.

The limited ERG surveys that were used are listed in Attachment A1.

A3.3.1.2 PhotoSat

The availability of topographic data at the onset of the Investigation was unknown. So the Panel approached PhotoSat, a satellite company, to obtain aerial images and topography at various dates throughout the operating period for Fundão. PhotoSat obtained satellite images and used *stereo pairs*[3] to generate elevation data. This data set was received prior to the drone surveys.

The PhotoSat data was compared to the data from the drone survey program once the latter became available for review. An elevation difference was noted between the PhotoSat and Samarco data set of up to 15 m within the tailings impoundment. However, this elevation difference was generally around 3 m to 5 m.

Following the discovery of this elevation discrepancy, the PhotoSat data was adjusted to the Córrego Alegre horizontal datum and vertically fit to the Samarco data using areas outside of the changing tailings impoundment. The elevation difference was reduced to ~1 m which, when coupled with the 0.5 m to 1 m accuracy of the PhotoSat data, accumulates to ~2 m vertical error. With this error band, it was not possible to use the PhotoSat data set to determine dike crest or pond elevations; however, the accompanying aerial images were coupled with the closest Samarco survey to estimate pond extent and elevations. This is discussed in more detail in Appendix B.

The PhotoSat projection and datum details are given in Table A3-2. Figure A3-2 shows the pre- and post-control fit comparison of a PhotoSat elevation grid and the common Samarco drone topography.

[3] *Stereo pairs* are two or more images taken at known angles with respect to each other. Knowing the angles allows the calculation of relative elevation for objects on the ground.

Table A3-2 PhotoSat projection and datum summary

Item	Original Delivery	Following Control Fit
Projection	Universal Transverse Mercator (UTM)	Universal Transverse Mercator (UTM)
Zone	23K	23K
Horizontal Datum	WGS84, re-projected to Córrego Alegre	Córrego Alegre
Vertical Datum	EGM2008(1)	Fit to Samarco drone survey

1. Orthometric[2] elevations reported.

For the purposes of seepage modeling, the PhotoSat data set error was within the layer thickness (2.5 m) limitations of the model and therefore could be used without adjustments.

In total, 7 PhotoSat elevation grids and 24 PhotoSat aerial images were used in the reconstruction of the Fundão facility. These surveys are listed in Attachment A1.

A3.3.1.3 Google Earth

Google Earth images were used to fill aerial image gaps where needed. In total, 10 aerial images were used in the reconstruction of the Fundão facility. These are listed in Attachment A1.

A3.3.2 As-Built and Design Surveys

Drawings from Samarco and various consultants were used as the basis for the as-built condition of the structures at Fundão. Preference was given to as-built surveys, and where needed, design drawings were used to fill gaps in the data set. The value of this data set is the ability to incorporate internal features that cannot be captured by aerial images or topographic surveys.

In total, 127 surveys were used in the reconstruction of the Fundão facility. These surveys are listed in Attachment A1.

A3.3.3 Samarco Reports and Records

A3.3.3.1 Recurring Reports

Reports and records from Samarco were used to:

- identify incidents, including location, date and other relevant details;
- fill gaps in the topography and aerial image data set;
- obtain instrumentation and flow monitoring readings; and
- provide supporting evidence of activities in the form of photos and descriptions.

Five types of reports were used in the reconstruction of the Fundão facility as listed in Table A3-3. All of the reports originated from Samarco's dam geotechnical management group.

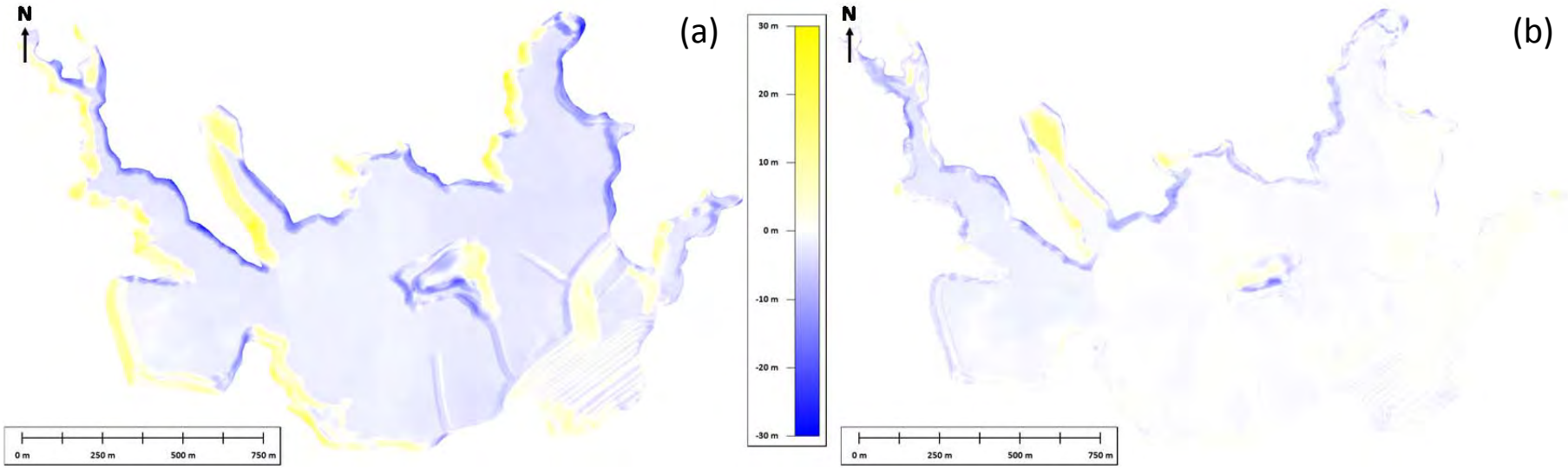

1. Elevation differences between Samarco topography (surveyed August 4, 2014) and PhotoSat topography (surveyed August 2, 2014) are shown as isopachs.
2. Yellow denotes areas where the Samarco survey is higher than the PhotoSat survey.
   Blue denotes areas where the Samarco survey is lower than the PhotoSat survey.
   White denotes areas where the Samarco and PhotoSat surveys are similar in elevation.

Figure A3-2 Comparison of PhotoSat elevation grid and Samarco drone topography – pre- (a) and post- (b) control fit

Table A3-3 Summary of Samarco reports used

Report Type	Period on Record	Data Extracted from Report
Weekly reports	February 2012 – November 2015	Photos, tailings deposition location (sporadic) records, flow monitoring data, description of ongoing activities
Monthly geotechnical monitoring reports	January 2011 – January 2014	Beach widths, pond elevations, piezometer readings
Monthly geotechnical inspection reports	May 2010 – October 2015	Photos and record of action items logged for left abutment
Monthly instrumentation reports	February 2014 – May 2014	Piezometer readings, rainfall
	June 2014 – November 2015	Piezometer readings, rainfall until end of October 2015(1), drain flows, survey monument data at left abutment
Monthly tailings discharge reports	February 2013 – November 2015	Beach widths, dike and pond elevations

1. Rainfall records from November 1, 2015 to December 2, 2015 were provided separate from the instrumentation reports. See Attachment A1 TableA.A1-6.

A3.3.3.2 Other Records

Daily, monthly and annual tailings production records from Samarco and Vale's neighboring Alegria Mine were reviewed. The most useful records are the daily production records followed by the monthly. This allows for comparison of production records against topographic isopachs. However, the multiple data sources have inconsistent record intervals and values. Therefore, a combination of data sources was required to compile a comprehensive tailings production history. The data sources are listed in Attachment A1 and the results of this compilation discussed in Appendix B.

Samarco provided Dike 1 crest elevations, rates of rise, beach width measurements, pond elevations and freeboard in a rate of rise spreadsheet. This data source is listed in Attachment A1 and the uses discussed in Appendix B.

A3.3.4 Photographs

In addition to photographs included in the weekly reports described in Section A3.3.3.1, photographs from various parties were sourced for supporting evidence of noted incidents and construction activities. These photographs were made available to the Panel, but not necessarily discussed or presented in formal documentation such as reports or drawings. Photographs were typically taken during:

- construction monitoring activities;
- regular inspection site visits; and
- incident-driven inspections.

A3.3.5 Consulting and Engineering Reports

A number of consulting and engineering reports from Samarco and other parties were reviewed. The main type was investigation reports which included the location of drill holes. This information was

extracted and input to GIS for compilation and synthesis. The referenced reports are summarized in Appendix C.

A3.3.6 Engineering Audit Reports

Audits were performed by various parties throughout the operating period for Fundão. Auditing parties produced reports that covered:

- recurring site visits;
- design reviews on an as-needed basis;
- incident-driven inspections; and
- Failure Modes and Effects Assessment (FMEA) workshops.

These parties and associated audit periods on record are summarized in Table A3-4.

Table A3-4 Summary of engineering auditor reports

Auditor	Operating Period	Number of Audits
Independent Tailings Review Board (ITRB)	May 2009 – November 2015	22
Andrew Robertson	January 2007 – April 2011	8(1)
Angela Küpper	November 2009 – August 2010	2
Pimenta de Ávila	April 2001 – November 2015	42(2)

1. Includes one report by Peter M. Byrne referenced as part of Andrew Robertson's January, 2007 report.
2. Includes design reviews and audits completed before and after Fundão.

A list of reports reviewed by the Panel is given in Attachment A1.

A3.3.7 Interviews and Eyewitness Accounts

CGSH conducted a series of interviews with key engineering staff and eye witnesses from the failure. These interviews served the following purpose:

- clarify issues and conflicting information extracted from the data sets;
- qualitatively describe and link gaps in understanding from the quantitative data sets described above; and
- construct the failure mode on the left abutment.

A list of interviews and eyewitness accounts reviewed by the Panel is given in Attachment A1.

A4 DATA COMPILATION AND SYNTHESIS

A4.1 Fundão and Germano Facilities

The data sources discussed above describe the physical state of the Fundão and Germano facilities over time. From this, the key points of interest discussed in Appendix B can be derived, including:

- structures and dike components;
- historic water routing;
- raising history;
- slimes depositional history;
- tailings production;
- incident history; and
- sand boil history at Germano.

A4.2 Stripped Ground for Fundão

As the Fundão facility developed, the surrounding natural ground was stripped where needed to create access roads or form the foundation for the raising of the dam. The evolution of the changing stripped ground under the dam was not tracked by any one survey from Samarco. Therefore, it was necessary to stitch together a stripped ground survey using multiple Samarco surveys to capture the changes over time.

The compiled stripped ground and associated data sources are given in Attachment A2.

A5 RELIABILITY/UNCERTAINTY/GAPS

The record keeping by Samarco was typical for large tailings dams in many parts of the world. As is customary for a data set consisting of multiple sources, inconsistencies were noted during data collections. These were resolved as presented in Appendix B, based on the Panel's best interpretation of the documents. Where conflicts existed, different data sources were compared in an effort to reduce the inconsistencies. Although the data set sampling was limited due to time and volume, the compiled information was sufficient for the reconstruction of the Fundão facility for purposes of analyses.

The following data gaps were noted:

1. The lack of drill holes or CPTs in Dike 1 from the crest to bedrock. This would have clarified the stratigraphy of tailings behind Dike 1.
2. No annual tailings deposition plans and no records of tailings discharge locations were on the dam with time. The tailings pipeline alignments were shown in one 2014 drawing (see Appendix B Attachment B7), but the spigot locations were tracked through sporadic site photos in weekly reports. The spigot locations on November 5, 2015 were provided by Samarco (see Appendix B Attachment B7).
3. No staff gauge in the pond to consistently determine the pond elevation over time. Instead, the Panel used topographic surveys to estimate the extent and elevation of the pond.

APPENDIX B

GIS/Imagery Outputs

Appendix B
GIS/Imagery Outputs

TABLE OF CONTENTS

TABLE OF CONTENTS
(continued)

TABLE OF CONTENTS

(continued)

List of Tables

TABLE OF CONTENTS

(continued)

List of Figures

TABLE OF CONTENTS

(continued)

List of Attachments

B1 INTRODUCTION

This appendix describes the outputs from the data compilation and synthesis using the geographic information system (GIS) as described in Appendix A. This appendix is a listing of specific tasks undertaken by the Panel to provide background in support of various failure hypotheses. All of our work was based solely on the extensive documentation made available to us. In some cases, the Panel used interviews to clarify issues identified in the documentation. Our work on each task was only taken far enough to pursue or eliminate various failure hypotheses.

This appendix starts with a description of the basic components of the tailings impoundment in Section B2 to provide context for the sections that follow.

Section B3 describes the historic water routing in the tailings impoundment. Routing of the tailings water was complex because of the adjustments that needed to be made to respond to the failed underdrains and decant facilities, as described in Section 2 of the main report. A basic understanding of the tailings pond routing and decanting was necessary to trace the distribution of slimes with time.

Section B4 describes the infilling and drainage features at Grota da Vale which drains into the left abutment where the failure initiated. Grota da Vale receives seepage and surface runoff from the Fabrica Nova Waste Pile. Tailings were also deposited in this area. Various drainage measures were implemented there which impacted the drainage of the left abutment. Thus, it was necessary to understand the history so that phreatic conditions on the left abutment at the time of failure could be modeled properly.

Section B5 describes the raising history of the impoundment, particularly the last six months before failure at the left abutment. This was especially important at the left abutment where infilling of the setback was always planned but delayed.

Section B6 describes the techniques used to clarify the slimes spatial distribution and depositional history. Section B7 describes the tailings production history, which was also a necessary input to understand the slimes distribution.

Section B8 describes the history of incidents such as seepage breakouts and slope movements at Dike 1 prior to failure. Section B9 summarizes the results of an aerial image review done for the Germano facility to determine whether any sand boils could be linked to the seismic activity on November 5, 2015.

B2 STRUCTURES AND DIKE COMPONENTS

B2.1 General

The details for various structures and dike components for the Fundão facility were compiled using data sources given in Appendix A. This facilitated the following:

- identification of historic and internal structures that would otherwise have not been apparent from topographic surveys alone;

- consistency across different analyses and models created during the course of the Investigation; and
- context for the noted incidents and events at Fundão.

The structures are separated into dikes, drainage, and decant types, and are described in the following sections.

B2.2 Dikes

A summary of the dikes that are part of the Fundão facility is given in Table B2-1. Refer to Figure B.B1-1 in Attachment B1 for locations. Details of each dike are given in Attachment B1.

Table B2-1 Summary of dikes at Fundão

Name	Description	Purpose	Operating Period
Dike 1	Saprolite starter dike, upstream raised sand embankment. Dike separated into left abutment, center, and right abutment.	Impound sand tailings deposited in Dike 1 reservoir	September 2008 to November 2015
Dike 2	Saprolite starter dike, centerline raised embankment	Impound slimes deposited in Dike 2 reservoir until Dike 1 sand embankment was sufficiently raised to contain the slimes	September 2008 to February 2014
Old Dike 1A (a.k.a. Dike 1A)	Local fill and tailings dike upstream of Dike 1	Impound sand and slimes deposited in Dike 1 reservoir until Dike 1 remediation works were complete	December 2009 to January 2011
New Dike 1A	Local fill and tailings dike upstream of Old Dike 1A and downstream of Dike 2	Keep sand from inundating the jet grouting platform where repairs were on-going for the Main Gallery	January 2011 to February 2012
Grota Upstream Dike	Dike downstream of Fabrica Nova Waste Pile	Contain the fines from seepage and surface runoff from the Fabrica Nova Waste Pile	May 2010 to September 2011
Vale Dike (Grota da Vale Dike)	Local fill starter dike, continuously raised with fill and tailings as needed to maintain access	Separate the water accumulated in Grota da Vale from the left abutment of Dike 1, maintain access to the Secondary Gallery from the left abutment	November 2010 to November 2015
PDE Dike (Pilha de Estéril União (Vale))	Local fill dike	Keep the water flowing in from Grota da Vale away from the area of sand deposition between Old Dike 1A and Dike 1 during construction of the Vale Dike	March 2010 to May 2010

B2.3 Drainage Features

A summary of the drainage features at Fundão is given in Table B2-2. Refer to Figure B.B1-2 for locations. Details for each feature are given in Attachment B1.

Table B2-2 Summary of drainage features at Fundão

Name	Area	Description	Purpose	Operating Period
Principal Foundation Drain	Dike 1	Trapezoidal rockfill drain	Drain the sand tailings in Dike 1 reservoir	September 2008 to April 2009
Auxiliary Foundation Drain	Dike 1	Trapezoidal rockfill drain	Drain the sand tailings in Dike 1 reservoir	September 2008 to April 2009
Vertical Chimney Drain	Dike 1	"Future ore" chimney drain	Intercept seepage through starter dike	September 2008 to November 2015
Horizontal Foundation Drain	Dike 1	"Future ore" drainage blanket	Convey water from Vertical Chimney Drain to Foundation Drains	September 2008 to November 2015
Upstream Drainage Blanket	Dike 1	Rockfill drainage blanket	Drain the sand tailings in Dike 1 reservoir	September 2008 to April 2009
Grota Thalweg Drain	Dike 1	Rockfill finger drain	Convey water from Grota da Vale under Secondary Gallery platform to Dike 1 reservoir	April 2008 to November 2015
Contingency Drains	Dike 1	Rockfill finger drains	Additional drainage capacity on top of Foundation Drains on left and right abutments of Starter Dam	Decommissioned prior to operation
El. 826 m Blanket Drain	Dike 1	Rockfill drainage blanket	Replacement drain for Foundation Drains, drain the sand tailings in Dike 1 reservoir	December 2010 to November 2015
Kananets®	Dike 1	27 pipes embedded within the El. 826 m blanket drain	Convey water from El. 826 m blanket drain to downstream face of Dike 1	December 2010 to November 2015
Vale Toe Drain	Fabrica Nova Waste Pile	Rockfill drain at toe of Fabrica Nova Waste Pile draining to a solid pipe along Grota da Vale	Collect and convey seepage from Fabrica Nova Waste Pile to area downstream of Dike 1	June 2014 to November 2015
El. 855 m Buried Drain	Dike 1	Sand and rockfill finger drain wrapped in geotextile	Treatment for seepage, collect water at contact of left abutment with stripped slope	July 2013 to November 2015
El. 860 m Buried Drain	Dike 1	Sand and rockfill slope drain wrapped in geotextile	Treatment for seepage, collect water at contact of left abutment with stripped slope	November 2013 to November 2015
Left Abutment Rockfill Trench	Dike 1	Rockfill trench wrapped in geotextile	Convey water collected from El. 855 m and El. 860 m Buried Drains across setback platform	June 2013 to November 2015
Left Abutment Open Channel	Dike 1	Geotextile lined open channel, an extension of the Left Abutment Rockfill Trench as the setback platform was raised		January 2014 to January 2015
El. 860 m Blanket Drain (Stage 1)	Dike 1	Rockfill drainage blanket	Drain the sand tailings in Dike 1 reservoir above El. 860 m	August 2015 to November 2015
Vale El. 940 m Toe Drain (Stage 2)	Grota da Vale	Rockfill finger drain	Drain the sand tailings in Dike 1 reservoir above El. 860 m along the contact with Grota da Vale	Construction not completed prior to failure
El. 855 m Inverted Drain	Dike 1	Rockfill applied to downstream slope	Collect seepage breakout at El. 855 m of the right abutment and mitigate piping	July 2014 to November 2015
El. 860 m Inverted Drain	Dike 1	Rockfill applied to downstream slope	Collect seepage breakout at El. 860 m of the right abutment and mitigate piping	January 2015 to November 2015

Name	Area	Description	Purpose	Operating Period
Right Abutment El. 940 m Drain	Dike 1	Series of rockfill finger drains	Drain the sand tailings in Dike 1 reservoir above El. 855 m	Construction not completed prior to failure

B2.4 Decant Structures

A summary of the decant structures at Fundão is given in Table B2-3. Refer to Figure B.B1-3 for locations. Details for each feature are given in Attachment B1.

Table B2-3 Summary of decant structures at Fundão

Name	Description	Purpose	Operating Period(s)
Main Gallery	Concrete gallery, 1207 m long, 2 m diameter	Decant for Dike 2 reservoir	September 2008 to July 2010 July 2011 to October 2013
Secondary Gallery	Concrete gallery, 811 m long, 2 m diameter	Decant for Dike 1 reservoir	September 2008 to October 2010 November 2010 to December 2011 March 2012 to August 2012 October 2012 to June 2013
Auxiliary Spillway	2x 1.2 m dia. HDPE pipes, vertical riser intakes	Decant for Dike 1 and Dike 2 reservoirs	February 2013 to November 2015
4th Spillway	3x 1.2 m dia. HDPE pipes, vertical riser intakes	Decant for Dike 1 and Dike 2 reservoirs	November 2014 to November 2015
Grota da Vale Overflow (Grota Overflow)	Buried pipe outlet from Grota da Vale to left abutment concrete channel	Decant for water ponded in Grota da Vale	August 2015 to November 2015
Overflow Channel	Excavated open channel north of the Island between Dike 1 and Dike 2 reservoirs	Inter-basin decant for Dike 2 reservoir to Dike 1 reservoir	February 2011 to August 2012 July 2013 to January 2014
Auxiliary Spillway Island Canal	Excavated open channel in tailings from east side of Island to south side	Intra-basin decant in Dike 1 reservoir for water to be directed away from Secondary Gallery and to the Auxiliary/4th Spillway	July 2013 to November 2013

B2.5 Stability Berms

Two stability berms were installed at Fundão as given in Table B2-4. Refer to Figure B.B1-4 for locations. Details for each feature is given in Attachment B1.

Table B2-4 Summary of stability berms at Fundão

Name	Description	Purpose	Operating Period
Stability Berm	Rockfill berm placed on downstream face of Dike 1	Required for stability of Dike 1 Starter Dam following April 2009 piping incident	July 2010 to November 2015
Reinforcement Berm	Sand berm placed on downstream face of left abutment setback	Required for stability of setback following August 2014 incident	September 2014 to November 2015

B3 HISTORIC WATER ROUTING AND TIMELINE

B3.1 General

The distribution of slimes within the tailings impoundment was governed by the pond location. Therefore, it was necessary to know the position/location of the Dike 1 and Dike 2 decants over time. There were four main decants for Fundão over its operating life:

- Main Gallery (draining Dike 2 reservoir);
- Secondary Gallery (draining Dike 1 reservoir);
- Auxiliary Spillway (draining Dike 1 and Dike 2 reservoirs once Dike 2 was deliberately overtopped); and
- 4th Spillway (draining Dike 1 and Dike 2 reservoirs once Dike 2 was deliberately overtopped).

Construction defects in the Main and Secondary Galleries were identified during operation. Out of necessity, the Auxiliary and 4th Spillways were constructed as replacements. The construction sequence associated with remediating the Galleries and installing the replacement decants resulted in opportunity for water to move between the two reservoirs prior to the overtopping of Dike 2 by:

- flow through the Overflow Channel north of the island;
- pumping between the two reservoirs; and
- flow through the Dike 2 breach.

The following were also identified in relation to the items above:

- the periods when the Dike 1 and Dike 2 reservoirs were connected or separated; and
- the periods when tailings were diverted from Fundão altogether.

B3.2 Data Sources and Methodology

The following steps were taken to generate a timeline of water routing and basin configuration:

1. Review available topography and aerial images to determine the working decant, pond location and direction of surface water flow within the facility.
2. Identify key dates for the operation, repair, and closure of decants using Samarco reports and engineering audit reports.
3. Overlay the above information in a chronological manner and derive periods when slimes had opportunity to access the Dike 1 reservoir.

B3.3 Summary of Findings

The Fundão timeline by decant configuration is shown in Attachment B2.

B4 GROTA DA VALE TIMELINE

B4.1 General

Grota da Vale refers to the area impounded between the Fabrica Nova Waste Pile and the left abutment of Dike 1. This was a natural tributary to Fundão Creek prior to the development of both the waste pile and Fundão. As described in Section B2, a pond developed in this area over time due to the construction of the Vale Dike, and later, the raising of the left abutment of Dike 1.

The contribution of hydraulic head from Grota da Vale to the left abutment of Dike 1 is a key part of the seepage and stability model. Although the influence of the pond is inherently "built into" the piezometric readings, the presence of a pond is considered a boundary condition and source of water for the seepage model. In order to track the movement of water out of Grota da Vale over time, a timeline separate from the decant version presented in Section B3 was developed.

B4.2 Data Sources and Methodology

The following steps were taken to generate a tailings deposition, construction and water routing history for Grota da Vale:

1. Review available topography and aerial images to determine the working decant, pond location and direction of surface water flow within the facility.
2. Identify key dates for the operation, repair, and closure of decants using Samarco reports and engineering audit reports.
3. Overlay the above information in a chronological manner and track the movement of water out of Grota da Vale.

B4.3 Summary of Findings

The Grota da Vale timeline is shown in Attachment B2.

B5 RAISING HISTORY

B5.1 Dike 1 Crest

B5.1.1 General

This section presents the Dike 1 crest elevation and rate of rise over the operating life of the Fundão facility. The objectives of this exercise include:

- verify the rate of rise graphs provided by Samarco in the rate of rise spreadsheet using topographic surveys;
- compare the dike crest elevations presented in the Samarco monthly geotechnical monitoring reports with the topographic surveys; and

- determine the crest elevation and rate of rise at the left and right setbacks in comparison with the central section of Dike 1.

Samarco's rate of rise spreadsheet is listed as a reference in Appendix A Attachment A1.

B5.1.2 Data Sources and Limitations

Multiple sources documenting the dike crest elevation over time were reviewed as listed in Table B5-1.

B5.1.3 Methodology

B5.1.3.1 Central Section of Dike 1 and Left Setback

The Samarco surveys were processed using AutoCAD Civil 3D (Civil 3D) and sections were cut through each instrumentation section (AA to NN, 01 to 03). The crest elevation for each section was then picked from the Civil 3D surface created from the surveys. The minimum and maximum elevations across the dike were plotted to check for areas of large differences which may indicate times of uneven raising (see Section B5.1.4). The elevations were then averaged across the dike to obtain an average dike crest elevation at the time of survey as shown on Figure B.B3-1 in Attachment B3.

The layout for the section lines is shown on Figure B5-1.

Table B5-1 Dike crest elevation data sources, limitations, and utility

Originator	Source	Date Range	Limitations *Impact on Interpretation of Data*	Utility
Samarco	Topography (includes as-built surveys)	2008 to 2015	Some surveys noted in Appendix A Attachment A1 have unconfirmed survey dates, and therefore, were assumed to have been conducted on the first of the month of the drawing date. *These elevations may be plotted earlier than when the survey was conducted.*	Used
Samarco	Monthly instrumentation reports	2014 to 2015	The location of measurements is unknown, and the data shows large steps in time which were not observed in the other data sets. *The steps are investigated in Section B5.2.3.3 as part of the pond elevation.*	Not used
Samarco	Monthly geotechnical monitoring reports	2011 to 2014	The method for choosing the point survey location along the dike crest is unknown. *These elevations may not consistently reflect the minimum, maximum or average elevation of the dike crest.*	Used
Samarco	Rate of rise spreadsheet	2008 to 2015	Plot of crest elevation over time is simplified. Only values approximately every 5 m in elevation are shown. *Although the overall rate of rise may be applicable, elevations between plotted data points should be considered approximations only.*	Not used

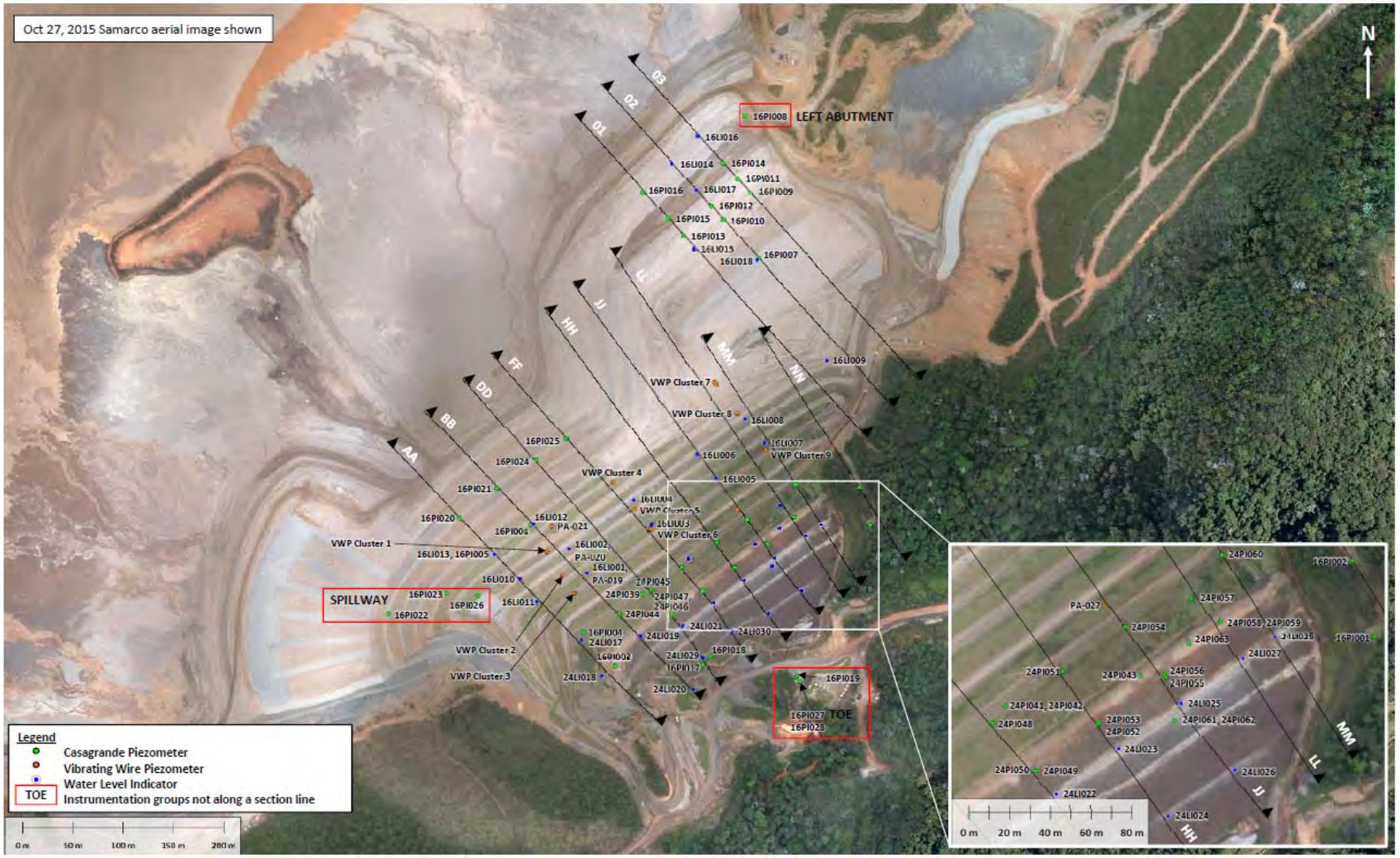

Figure B5-1 Dike 1 piezometer plan and instrumentation sections

B5.1.3.2 Right Setback

The setback near the right abutment was also examined. Construction began in June, 2015 and is first seen in the June 22, 2015 survey. The right setback crest was continuously raised up to time of failure. A drain was being constructed at the platform of the setback in preparation for the planned dam raise to El. 940 m. Once the right setback crest was established, the non-setback portion of the crest was excavated to facilitate the construction of the drain.

A section different from the instrumentation sections was used to determine the elevations of the right setback crest. This was necessary to intersect the setback crest. The section orientation is shown on Figure B5-2.

Figure B5-2 Plan showing section through right setback

B5.1.3.3 Rate of Rise

The average monthly rate of rise for Dike 1 was calculated using the average crest elevation for the central section of Dike 1, the left setback and the right setback. The elevation from an earlier survey was subtracted from the next chronological survey and plotted at the earlier survey date assuming 30 days per month.

B5.1.3.4 Samarco Rate of Rise

Samarco's plot of dike crest over time was copied as-is from the rate of rise spreadsheet.

B5.1.3.5 Samarco Monthly Monitoring Reports

The crest elevations from the monthly reports were extracted in combination with the given survey dates.

B5.1.4 Variations across the Dike Crest

The central section of Dike 1 and the left setback minimum, maximum and average elevations for the sections sampled at different times are shown in Attachment B3. This was not done for the right setback as the height of the setback is much less than at the left setback. For the central section of Dike 1 and the left setback, the variations are generally less than 1 m which supports the use of the average dike crest elevation when referring to rate of rise.

Five instances in time were noted to show a variation greater than 2 m in elevation across the crest and are listed in Table B5-2. A threshold value of 2 m was chosen assuming the rate of rise could be up to 1 m/mo and the surveys could have been conducted before the completion of one raise while the start of the next had begun on different parts of the dam.

Table B5-2 Surveys with dam crest variations greater than 2 m

Area	Survey Date	Minimum Sampled Crest Elevation (m)	Maximum Sampled Crest Elevation (m)	Difference (m)	Comments
Central section of Dike 1	April, 2012[(1)]	845.0	847.5	2.5	Little change on dam crest elevation at Sections AA and BB from the previous survey on January 21, 2012. This is possibly due to delayed raising of the crest in this area. The remainder of the crest was raised by approximately 2.5 m.
	2012-09-20	855.0	857.3	2.2	Dam crest at Sections AA, BB and DD is higher than the rest of the crest. This is likely due to the earlier raising in this area as part of access road construction for the Auxiliary Spillway installation at the right abutment.
	2013-01-06	861.0	859.0	2.0	Dam crest at Section AA is 2 m lower than the crest at Section HH which is close to where the setback begins. This may be due to uneven raising while focus is placed on moving material to the setback crest and the central section of Dike 1 crest area closest to the setback.
Left setback	2013-01-06	859.4	857.4	2.0	This is in the early stages of construction of the setback. The area closest to the central section of Dike 1 crest (Section 01) appears to have been raised earlier than areas farther from the central section of Dike 1 crest (Section 03).
	2013-04-02	860.4	863.5	3.1	The area closest to the central section of Dike 1 crest (Section 01) appears to have been raised earlier than areas farther from the central section of Dike 1 crest (Section 03).

1. Exact survey date not given, assumed to have taken place on the 1st.

B5.1.5 Summary of Findings

The average crest elevation over time for the central section of Dike 1 and the left and right setback are shown in Attachment B3. Samarco's elevations from the rate of rise spreadsheet as well as the monthly monitoring reports are shown on the same plot.

Using topography and values from Samarco's monthly reports, the average dike crest elevation and rates of rise are shown on Figure B5-3 to Figure B5-6 below.

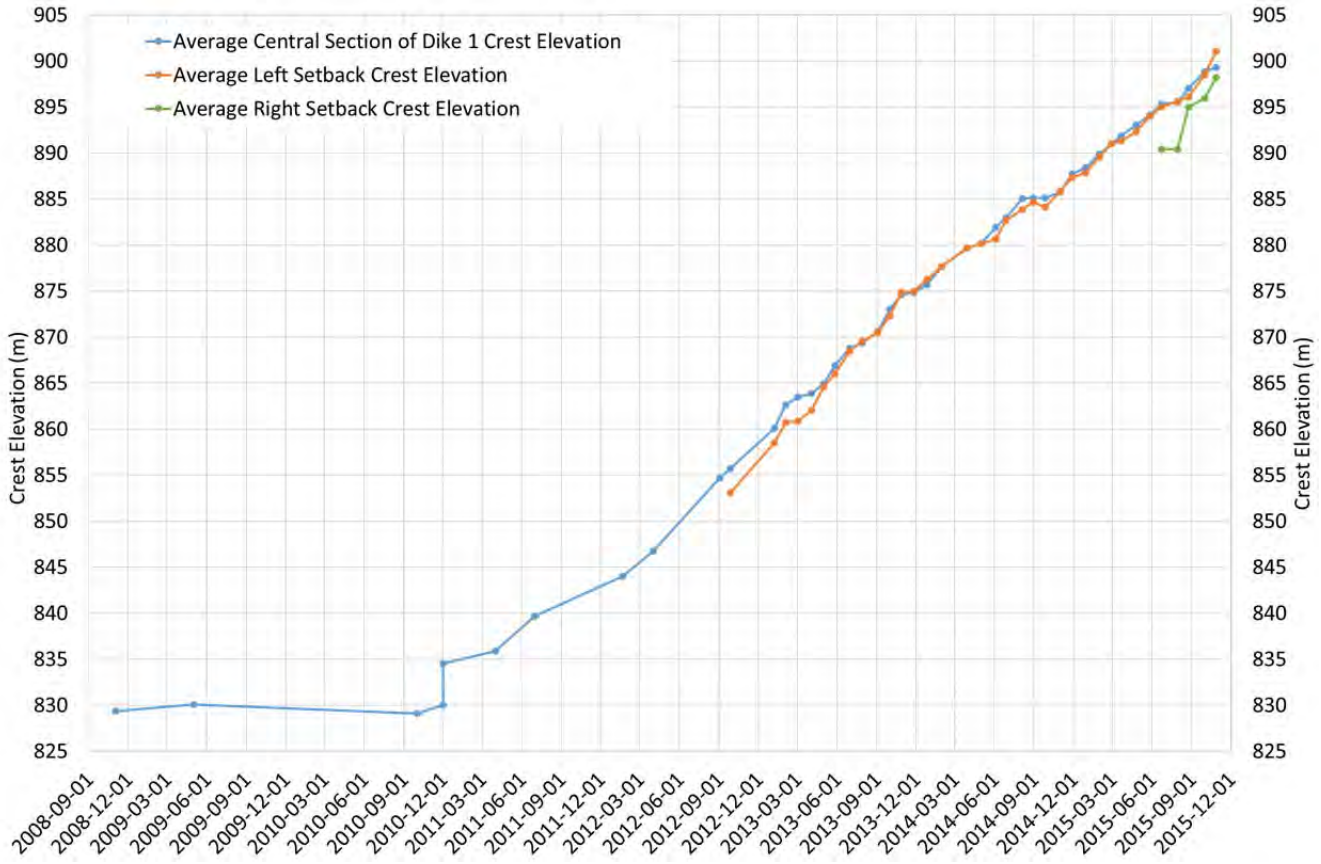

Figure B5-3 Average dike crest elevation over time

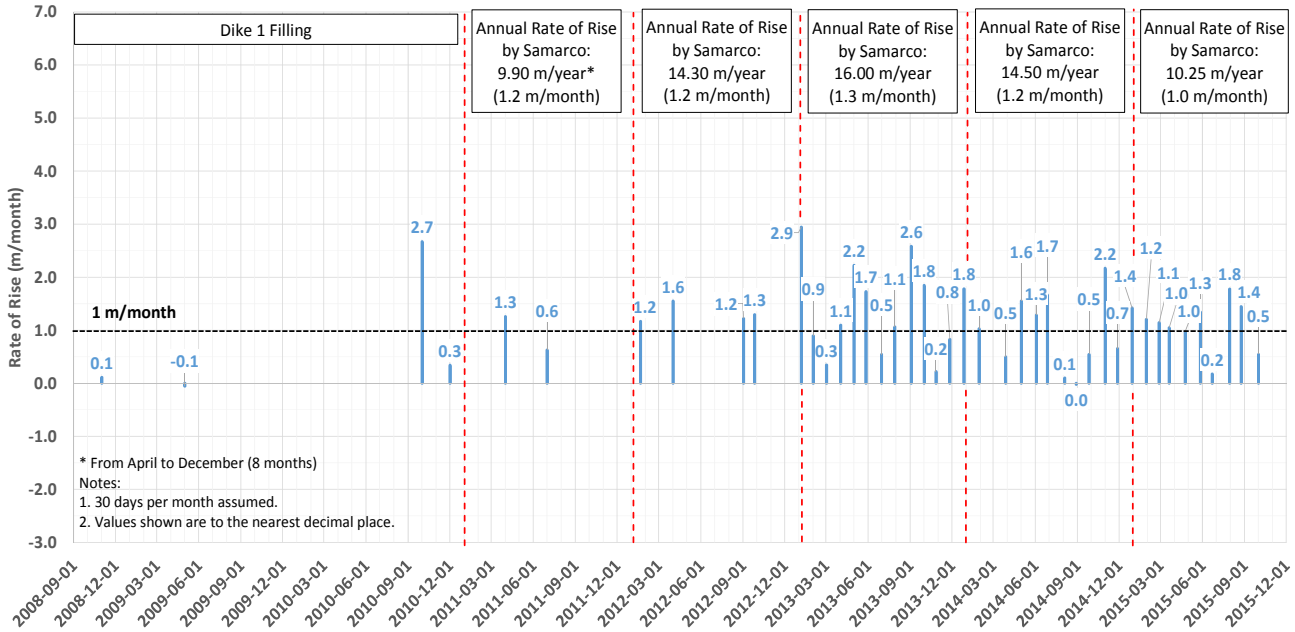

Figure B5-4 Central section of Dike 1 rate of rise

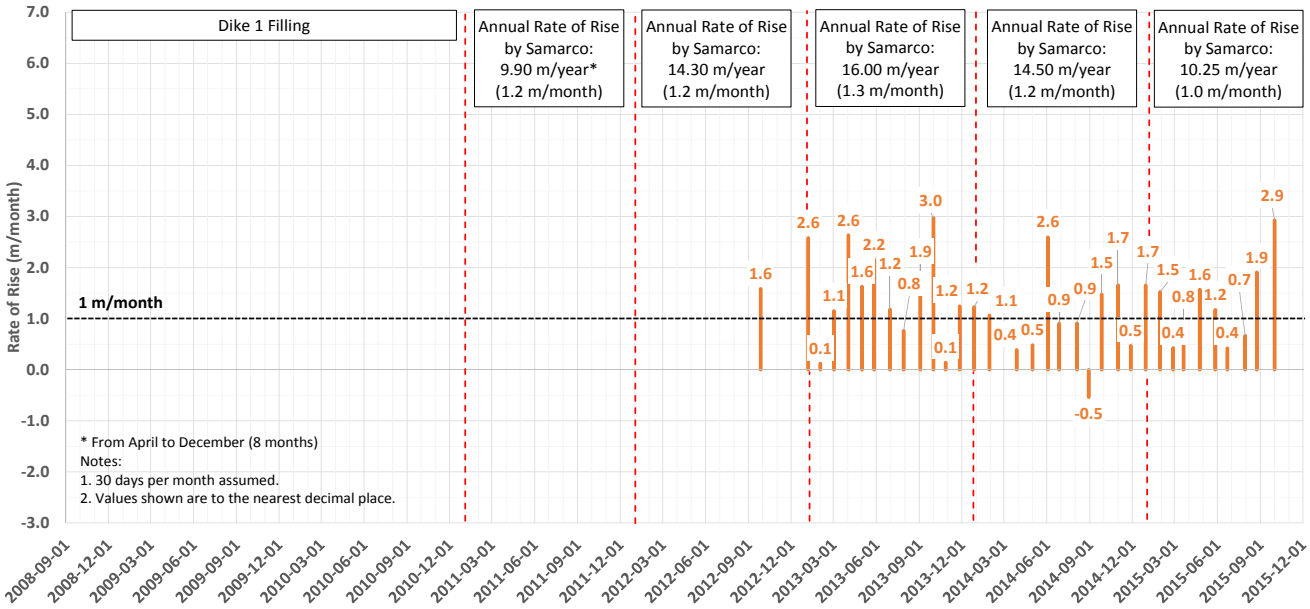

Figure B5-5 Left abutment setback rate of rise

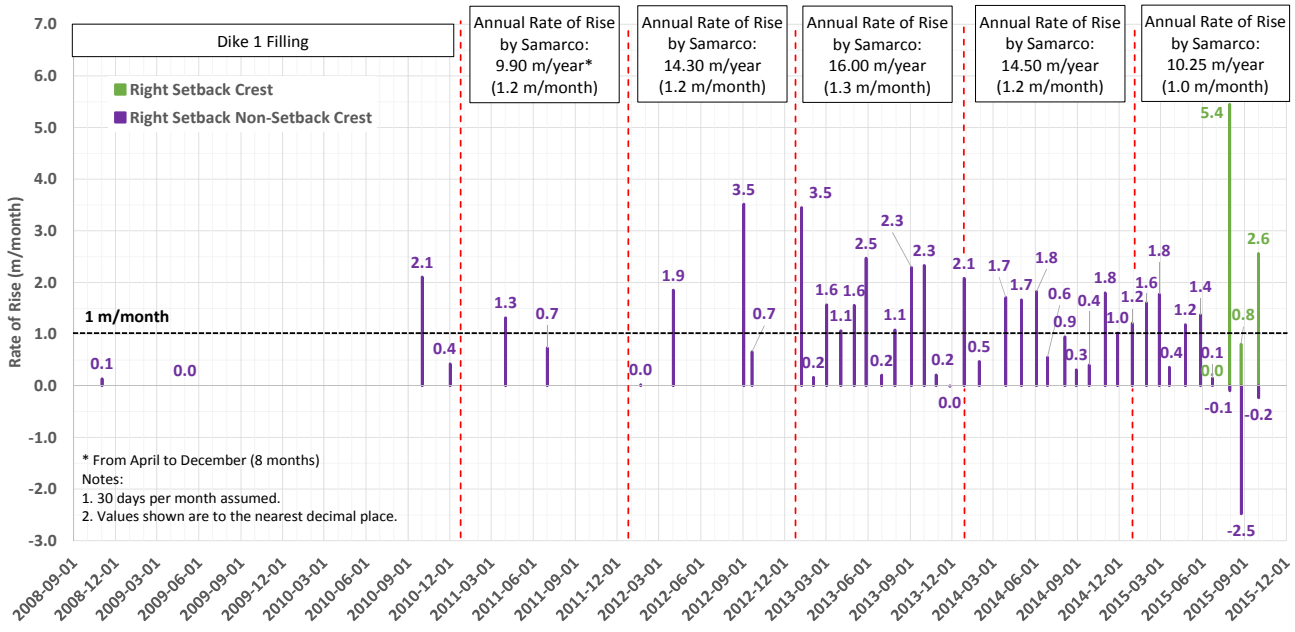

Figure B5-6 Right abutment setback rate of rise

In summary:

1. Variations across the central section of Dike 1 and left setback crest at any given time were generally less than 1 m, which supports the use of the average dike crest elevation when referring to the rate of rise.
2. The left setback crest elevation at times was 3 m lower than the central section of Dike 1 crest elevation before the setback was well established by May, 2013.
3. The rates of rise for the central section of Dike 1 ranged from 0.1 m/mo to 2.9 m/mo. The majority of the highest rates of rise occurred in 2013:
   - The negative rate of rise (-0.1 m/mo) shown on May, 2009 is small enough to be caused by survey limitations. This was also the time when remediation works were on-going for Dike 1, which may have resulted in minor changes to the crest elevation.
4. The rates of rise for the setback ranged from 0.1 m/mo to 3.0 m/mo. Similar to the central section of Dike 1, the majority of the high rates of rise occurred in 2013. However, in the last two months leading up to failure, the rates of rise were close to the all-time high at 1.9 m/mo and 2.9 m/mo, respectively.
   - The negative rate of rise (-0.5 m/mo) shown on August 29, 2014 was due to grading of the crest (downstream to upstream) as part of remediation works after the August, 2014 incident.
5. The rate of rise at the right setback (2.6 m/mo) was comparable to the rate of rise at the left setback (2.9 m/mo) in the month leading up to failure. However, the height of the right

setback at time of failure was approximately 5 m whereas the height of the left setback was approximately 36 m.

- The negative rate of rise for the non-setback crest intersecting the right setback section line on August 24, 2015 was due to excavation for placement of drain material in preparation for the El. 940 m raise. About 3 m of material was removed. By this time, the right setback crest had taken over as the right abutment crest.

B5.2 Pond Elevation

B5.2.1 General

This section presents the methodology and assumptions in mapping pond extent and elevation at different times during the life of the Fundão facility. The objectives of this exercise include:

- determine the pond elevation in the Fundão impoundment and Grota da Vale over time;
- verify the pond elevations provided by Samarco in the rate of rise spreadsheet using Samarco topographic surveys;
- investigate the possible reasons for the step-like behavior shown in the pond elevation data series from the Samarco monthly instrumentation reports; and
- map the pond extent in 3D as an input to seepage and stability analyses.

There are five ponds within the Fundão facility:

- Dike 1 pond;
- Dike 2 pond;
- New Dike 1A pond;
- Grota Upstream Dike pond; and
- Grota da Vale pond.

The elevation of the New Dike 1A pond was not tracked over time as it stayed relatively static in order to facilitate the jet grouting repairs of the Main Gallery. The locations are illustrated on Figure B5-7.

B5.2.2 Data Sources and Limitations

Multiple sources documented the pond rate of rise over time and are listed in Table B5-3. The tailings beach survey appeared to have been updated monthly. Topography from aerial images was used as secondary support to the monthly pond elevations.

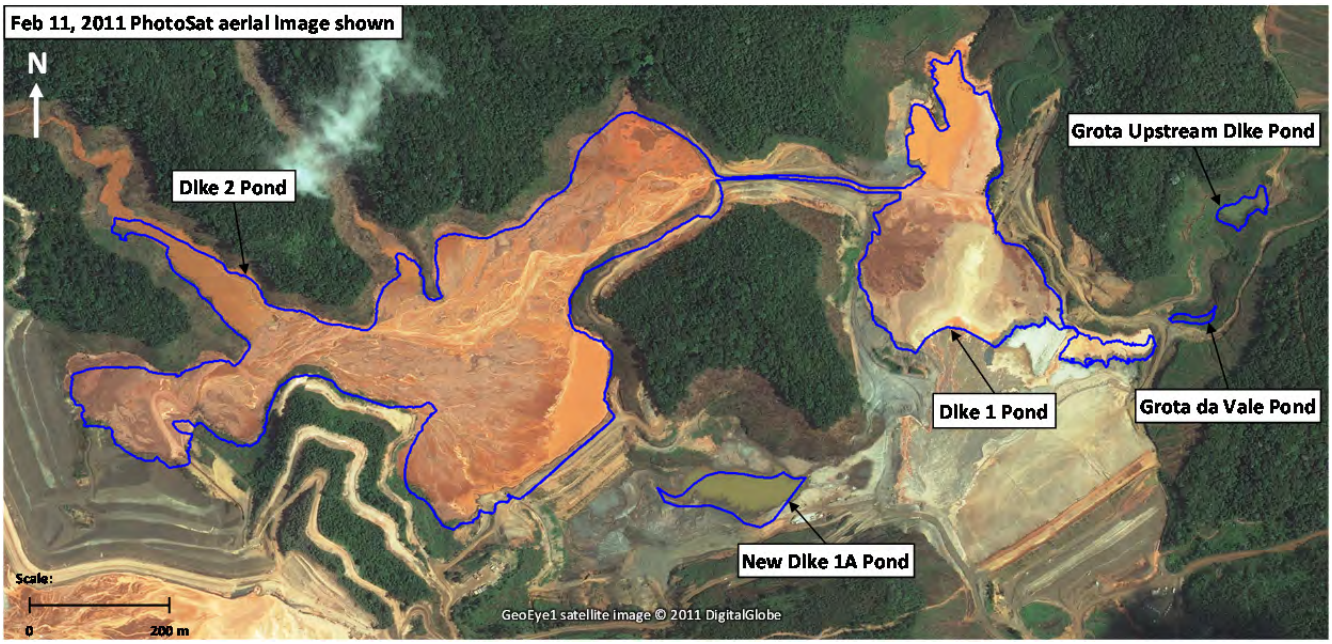

Figure B5-7 Location of ponds in Fundão

Table B5-3 Pond elevation and beach width data sources

Originator	Source	Data Type	Date Range	Area	Limitations *Impact on Interpretation of Data*	Utility
Samarco	Topography	Pond elevation, beach width	2008 to 2015	Dike 1, Dike 2, Grota Upstream Dike, Grota da Vale	Some surveys have unconfirmed survey dates, and therefore, were assumed to have been conducted on the first of the month of the drawing date. *These elevations may be plotted earlier than when the survey was conducted.*	Used
Samarco	Monthly instrumentation reports	Pond elevation	2014 to 2015	Dike 1	The location of measurements is unknown, and the data shows large steps in time which were not observed in the other data sets. *The steps are investigated in Section B5.2.3.3.*	Not used
Samarco	Monthly geotechnical monitoring reports	Pond elevation, beach width	2011 to 2014	Dike 1	The method for choosing the point survey location along the tailings beach is unknown. *These elevations may not consistently reflect the minimum, maximum or average elevation of the pond.* The measured beach widths shown in plan were at times measured diagonally. Actual beach widths may be smaller. *The minimum beach width was not consistently measured.*	Used
Samarco	Rate of rise spreadsheet	Pond elevation, beach width	2011 to 2015	Dike 1	The location of measurements is unknown. The plot of dike crest and reservoir elevation over time shows the pond data series labeled as "tailings solids elevation" as opposed to pond elevation. *The elevations were assumed to be consistently surveyed in the Dike 1 reservoir as they were plotted against the dike crest elevation and used to calculate freeboard. The title of the plot and heading of the data table both denote the elevations plotted as being those of the pond, not the tailings beach. Assume legend entry was erroneous.*	Not used
Samarco	Monthly tailings discharge reports	Beach width	2013 to 2015	Dike 1	The measured beach widths shown in plan were at times measured diagonally. Actual beach widths may be smaller. *The minimum beach width was not consistently measured.*	Not used

B5.2.3 Methodology

B5.2.3.1 Pond Mapping

The assumptions for the pond mapping exercise are presented in Table B5-4.

Table B5-4 Assumptions for mapping of pond extent and elevation

File Type	Reason	Assumptions
Samarco topography	Gives indication of tailings pond and beach locations Provides pond elevations	Ponding occurs at the lowest elevation in the Dike 1 and Dike 2 reservoirs
Vale topography		
PhotoSat topography	Gives indication of tailings pond and beach locations Serves as secondary check on Samarco topography	Due to limitations of the PhotoSat surveys, the PhotoSat topography is only being used to estimate the beach shape while the elevations are picked off the Samarco topography
Samarco aerial images	Provides visual guide on location of pond	Light-colored swirls are indicative of the foam layer which is present on the tailings pond where sand meets slimes
PhotoSat aerial images		
Google Earth aerial images(1)		
Monthly point surveys of Dike 1 tailings beach(2)	Gives a starting point from which a minimum beach offset can be delineated	Samarco survey shows the minimum beach width. The Dike 1 crest line is offset by the minimum beach width to obtain the maximum pond extent
Site or field photos during inspections, construction activities	Supports the elevations picked off of topography especially in early years when full-basin surveys are not available	The observed tailings elevation and pond/slimes locations seen in photos can be used in combination with the closest topography date to estimate the tailings/pond elevation

1. Given how close in time the Google Earth images were to Samarco or PhotoSat images, they were not used to delineate pond boundaries.
2. From monthly geotechnical monitoring reports.

B5.2.3.2 Monthly Geotechnical Monitoring Reports

From July, 2011 to January, 2014, Samarco included point surveys of the Dike 1 crest, tailings beach and Secondary Gallery intake in the monthly geotechnical monitoring reports. The exact dates of these surveys are given in each monthly report.

In order to approximate the ponds for these months, the beach widths were assumed to represent the minimum at that point in time. The pond boundaries were then drawn parallel to the Dike 1 crest and tied into the basin contours from the closest preceding topographic survey. The point surveys and estimated pond boundaries are shown in the image timeline in Attachment B4.

The pond elevation over time is compared to those extracted from topography on Figure B5-8. In general, the monthly monitoring report pond elevations fall between the minimum and maximum elevations obtained from topography. Therefore, these pond elevations and boundaries were used to fill gaps in the topography data set.

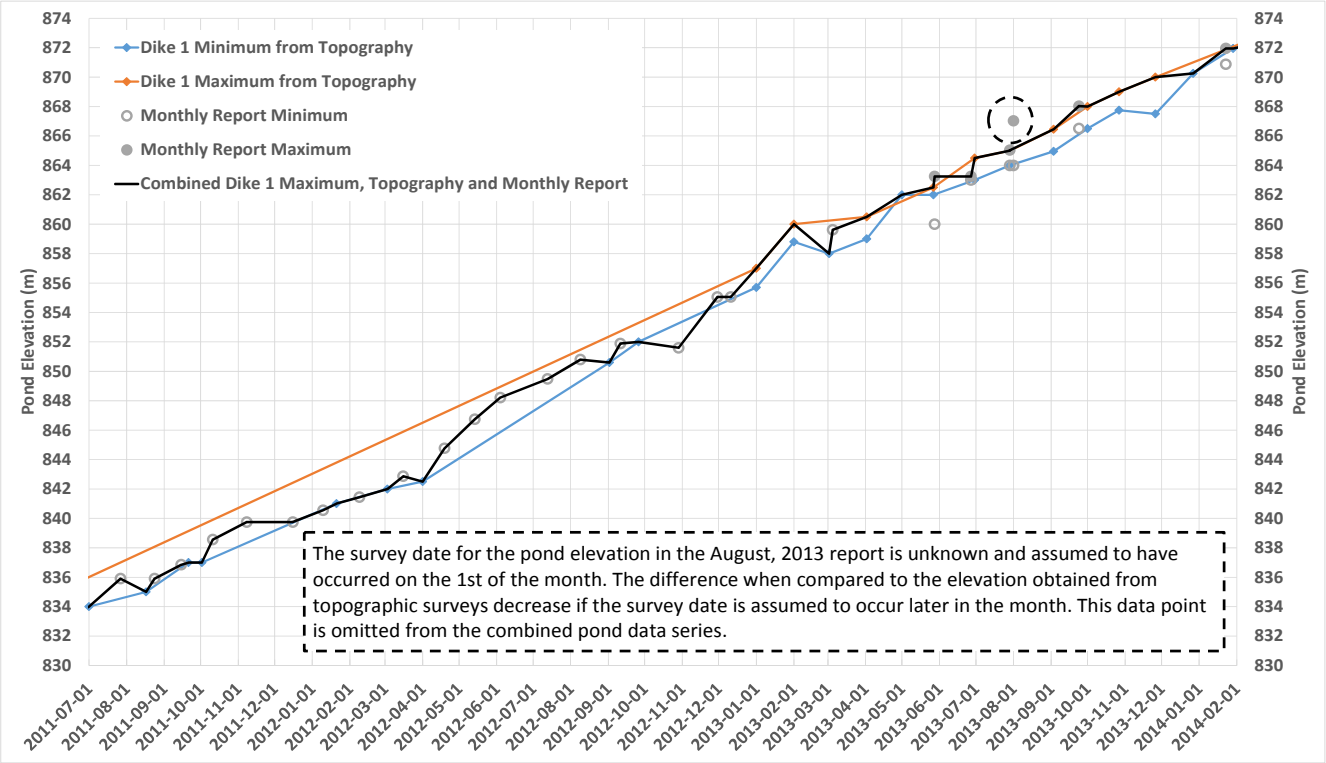

Figure B5-8 Comparison of pond elevations from monthly geotechnical monitoring reports and topographic surveys

B5.2.3.3 Monthly Instrumentation Reports and Rate of Rise Spreadsheet

The pond elevations in the November, 2015 instrumentation report and rate of rise spreadsheet were plotted against the combined Dike 1 pond elevation data series from Section B5.2.3.2. The following were noted:

- As seen on Figure B5-9, several steps up to 5 m in elevation at a time were noted in the instrumentation report data series.
  - A review of weekly reports shows most corresponded with activities at the intakes of the Secondary Gallery or Auxiliary Spillway. These include construction of temporary coffer dams and use of stoplogs to improve water quality downstream at Santarem.
- The instrumentation report data series shows periods of constant pond elevation prior to a step in the data series.
  - The constant pond elevation is not consistent with the dike being continuously raised. The pond elevation was likely not updated regularly in the instrumentation reports.
- The rate of rise data series generally follows the trend from the combined topography and monthly geotechnical monitoring reports series. However, the location and method of survey are not known.

For the reasons discussed above, neither data set was used to represent the pond elevation over time.

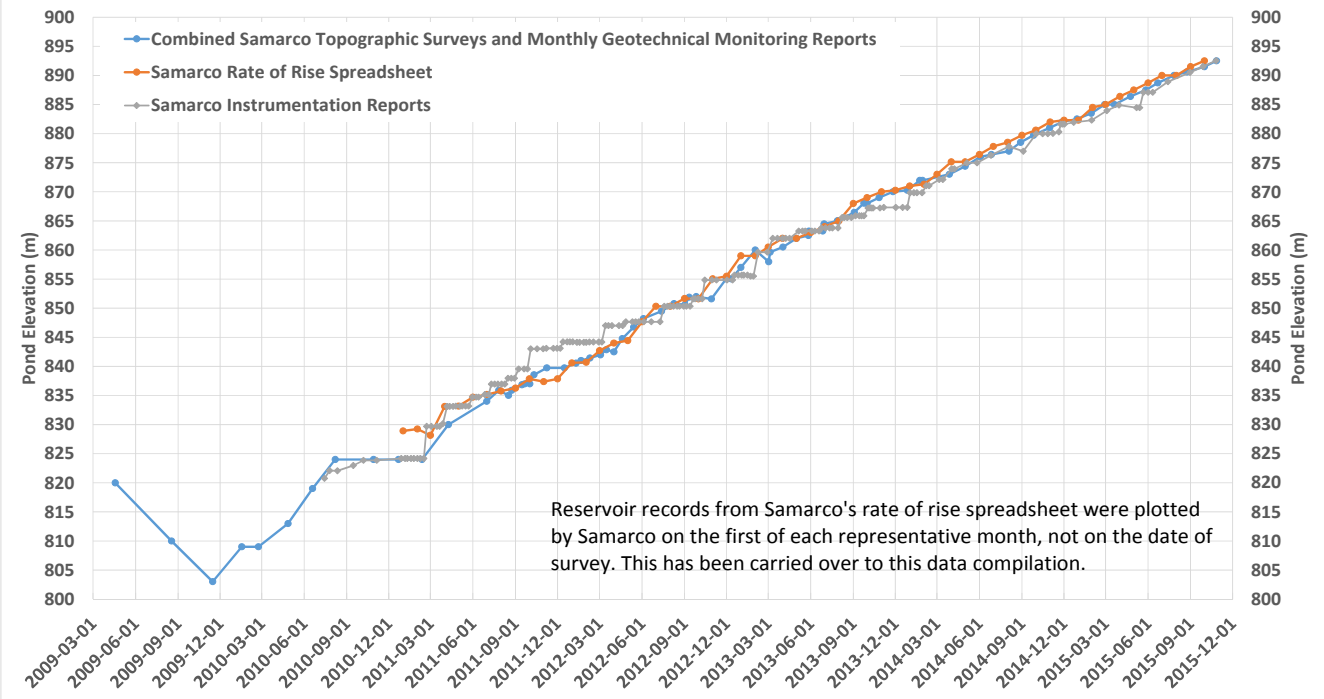

Figure B5-9 Comparison of pond elevations from monthly instrumentation reports, rate of rise spreadsheet and topographic surveys

B5.2.4 Beach Width

The four sources of beach width data, as listed in Section B5.2.2, are compared on Figure B5-10. The following were noted:

- The monthly tailings discharge reports estimate beach widths using the monthly drone topographic surveys.
  - In general, the values from the monthly tailings discharge reports match those obtained from topographic surveys. Therefore, this data set is not needed to fill a gap and has been excluded from the consolidated data series.
- The location and method of data collection for the values given in the rate of rise spreadsheet are unknown. They also cover a similar period as the topographic surveys.
  - The rate of rise values are excluded from the consolidated data series.
- For overlapping periods, the beach widths from the monthly geotechnical monitoring reports and topographic surveys are not consistent. Often, the topographic surveys show shorter beach widths, particularly at the left abutment.

- The minimum beach width between the two data sets is used for the consolidated beach width data series.

The minimum design beach width for Fundão was supposed to be 200 m[1]. The consolidated beach width data set over time is shown on Figure B5-11. The operational requirement was not consistently met at both the left and right abutments as shown on Figure B5-12. The ingress of the pond to the dike crest occurred more frequently at the left abutment compared to the right during the critical period between El. 840 m and El. 850 m where the beach below water (and slimes incursion) lies below the embankment slope by November, 2015. This is shown on Figure B5-13.

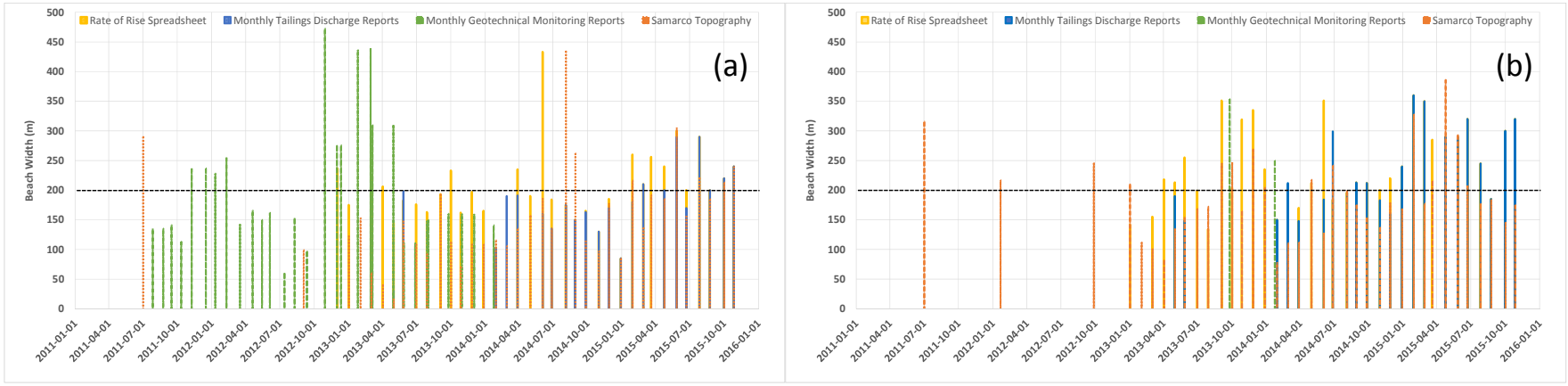

Figure B5-10 Comparison of beach width data sources – left (a) and right (b) abutment

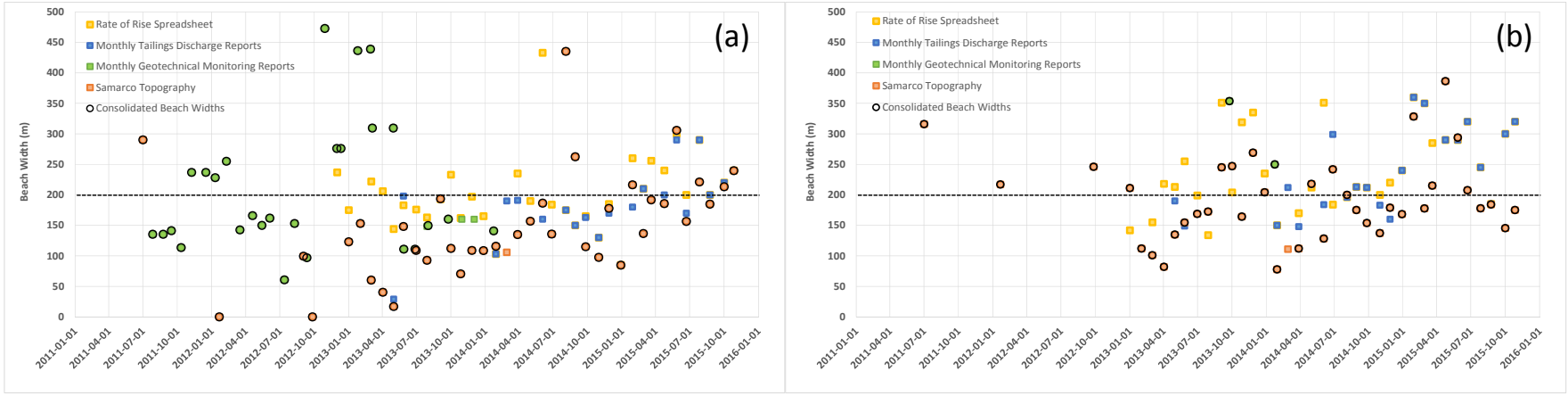

Figure B5-11 Beach width over time – left (a) and right (b) abutment

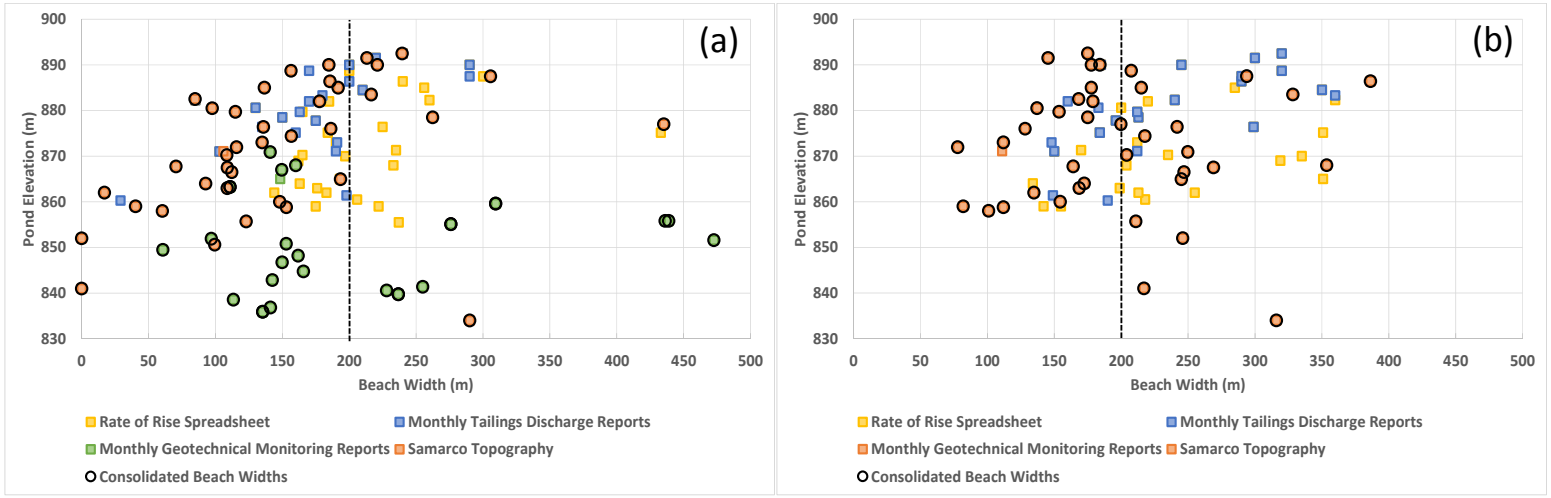

Figure B5-12 Beach width vs. pond elevation – left (a) and right (b) abutment

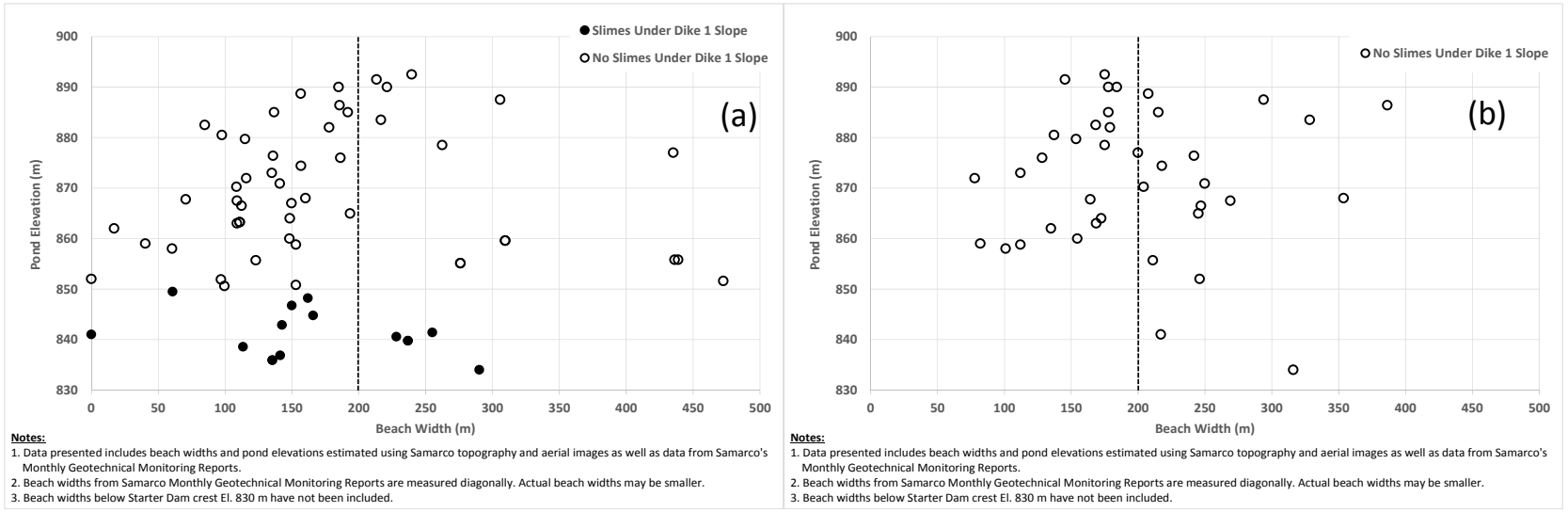

Figure B5-13 Beach width vs. pond elevation at left (a) and right (b) abutment – consolidated beach widths

B5.2.5 Summary of Findings

The pond elevation data series over time is shown on Figure B5-14 below.

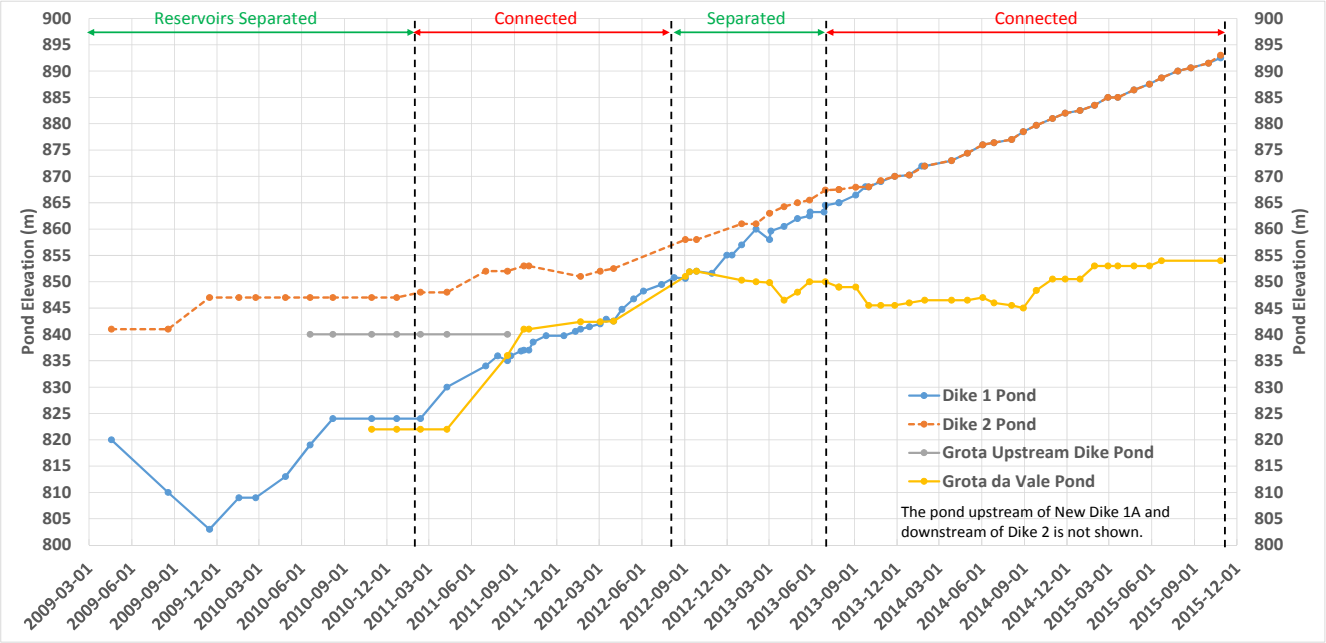

Figure B5-14 Pond elevation over time

Key findings are as follows:

1. There are differences within the beach width data set. The values from the monthly geotechnical monitoring reports were used to fill the data gaps from topography.
2. More often than not, the beach widths did not meet the operational minimum of 200 m.
3. The consolidated beach width over time data series shows there were more instances of beach incursions in the critical El. 840 m to El. 850 m elevation range at the left abutment compared to the right abutment.
4. The pond elevations from the monthly geotechnical monitoring reports generally fall between the minimum and maximum pond elevations delineated using topography. Therefore, these values were used to fill in the data gaps from the topography to create one combined pond elevation data series over time.
5. In general, the pond elevations from Samarco's rate of rise spreadsheet follow a similar trend as the combined pond series. However, given that the location of these measurements are unknown, they are removed from the data set in favor of the combined data series.
6. The pond elevations in the instrumentation report show several jumps in the reservoir level that range from 2 m to 5 m. Most jumps corresponded with activities at the intakes of the

Secondary Gallery or Auxiliary Spillway. These include construction of temporary coffer dams and use of stoplogs to improve water quality downstream at Santarem.

7. Given the finding above and the suspicious constant pond elevations, the data from the instrumentation reports was not used.
8. The Dike 2 pond merges, as expected, with the Dike 1 pond after Dike 2 is overtopped.
9. The Grota da Vale pond is more or less a constant presence over the life of the facility. In the months leading up to failure, the pond was at approximately El. 855 m.

B5.3 Left Abutment Geometric Changes

B5.3.1 General

This section describes the geometric changes at the left setback of Dike 1 from May, 2015 to November, 2015. During these months, the El. 860 m blanket drain was being constructed as part of the El. 940 m raise. In addition, the setback was being prepared for deposition of cyclone tailings to facilitate a quicker infilling of the setback and return to the original dike crest alignment.

Monthly topographic surveys and aerial images were the primary sources for identification of geometric changes. These changes were compared to construction reports and photos for confirmation where possible. This was done to supplement the dike crest rate of rise documented in Section B5.1 and identify the areas other than the dike crest where loading was substantial prior to failure.

B5.3.2 Data Sources and Limitations

The primary source of information is the drone surveys which provide both topography and aerial images. Patching of aerial images was noted for the setback platform following the completion of the El. 860 m blanket drain in August, 2015. This, in addition to the limited resolution of the aerial images, necessitated the review of additional data sources as listed in Table B5-5.

Table B5-5 Summary of data sources and limitations for left abutment geometric changes review

Originator	Data Source	Content Relevant to Review	Limitations
Samarco	Drone topography and aerial images	Geometry of left abutment, visual confirmation of on-going activities	Aerial images were patched following completion of the El. 860 m blanket drain, potential point survey errors noted on downstream slope of left setback
Samarco	Raw drone aerial images	Additional photos at different angles	Photos at different zoom scales, sometimes difficult to locate in plan
Samarco	Monthly geotechnical inspection reports	Description of on-going activities, site photographs	Photos can be lower resolution and difficult to locate in plan
Samarco	Weekly reports		
Samarco	Construction photos	Photos of construction of El. 860 m blanket drain	Exact date of photo is not always provided
VOGBR	July 2015 inspection photos	Inspection observations, photos	Exact date of photo is not always provided

B5.3.3 Methodology

The topography was used to create Digital Elevation Models (DEMs) with the GIS program Global Mapper. The DEMs were cropped to the area of interest at the left abutment. Isopachs were created using the cropped DEMs by overlaying one survey on top of the previous survey. The isopachs were used as a visualization tool to identify cut or fill areas. Focus areas are shown on Figure B5-15.

Areas that showed significant elevation changes were flagged and compared to construction reports and photos. The objective was to determine if the elevation changes seen in the DEMs could be confirmed by field observations.

The details of the left abutment geometric changes are given in Attachment B5, which includes:

- cross sections;
- cross sections with time;
- aerial images;
- DEMs;
- isopachs;
- summary of loading changes; and
- site photographs.

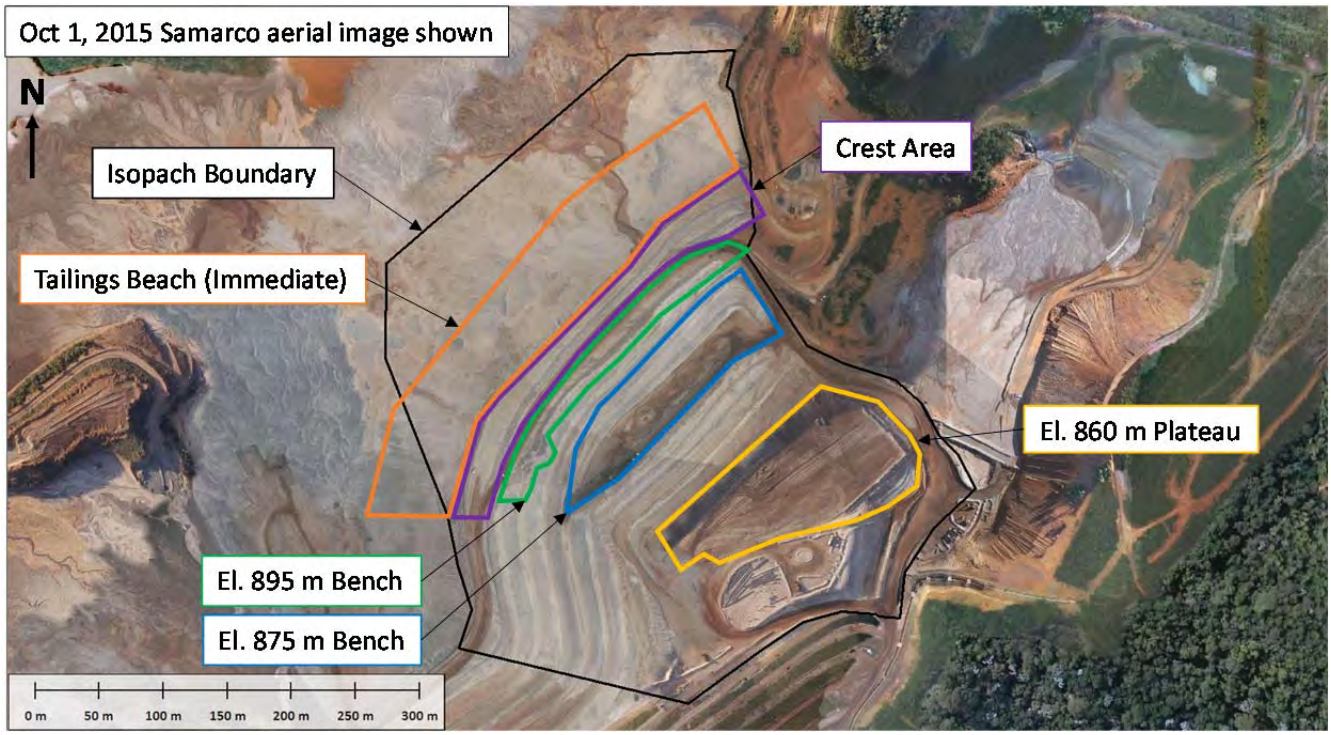

Figure B5-15 Left abutment areas of interest

B5.3.4 Left Abutment Drainage

The surface drainage system at the left abutment setback was documented for the months leading up to failure to investigate how surface/groundwater was managed. Ponded water was observed at the toe of the El. 860 m blanket drain in many of the site photos (see dashed blue lines on site photos in Attachment B5). The first instance was noted in construction photos from the week of June 29, 2015. Ponded water is also visible on photos from the morning of November 5, 2015, prior to the failure.

The surface water pathway and outlet for this ponded water is as shown on Figure B5-16. The history of water routing on the setback platform is expanded further in Section B8 as part of the documentation of drains installed at the setback in response to seepage incidents. From this review, there appears to be a surface drainage system in place to convey water away from the left abutment setback.

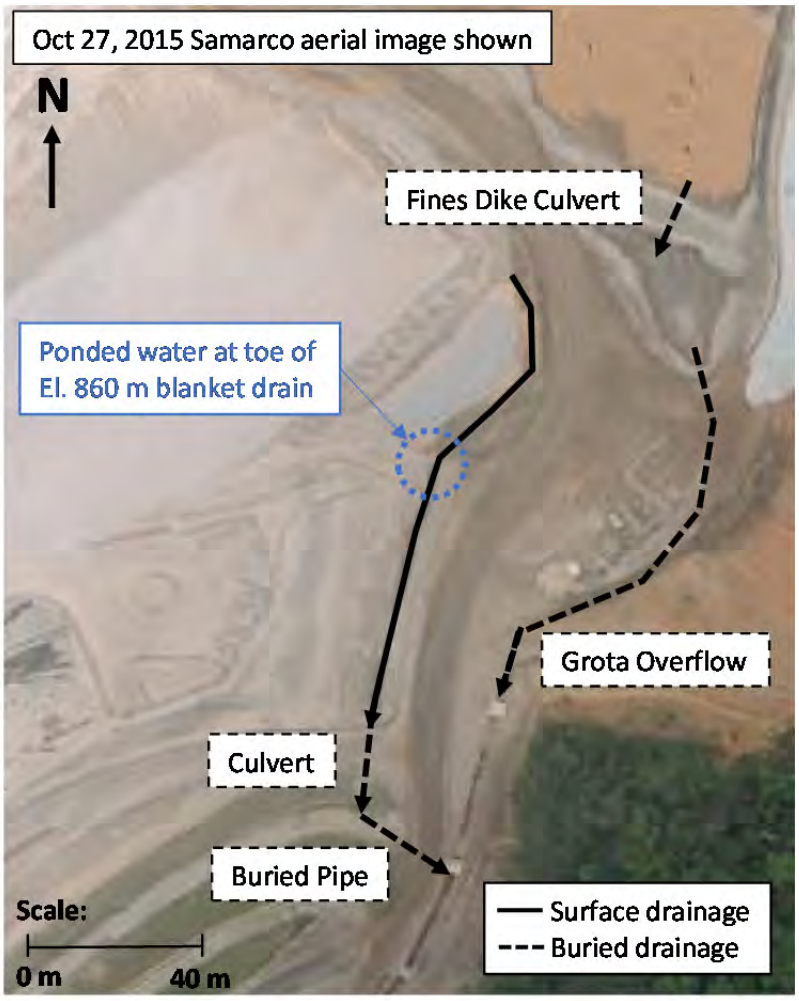

Figure B5-16 Drainage at left setback prior to failure

B5.3.5 Historical Access Roads and Post-Failure Remnant

B5.3.5.1 Observations

Photos from a drone flight in the area of the left abutment on April 12, 2016 show remnants of the left abutment. When overlaid with contours from January, 2012 and 2014, it appears the post-failure surface coincides with a historical access road under the tailings in two locations: one under the remnants of the left abutment and another several meters below the remnants on a lower bench. This is shown on Figure B5-17.

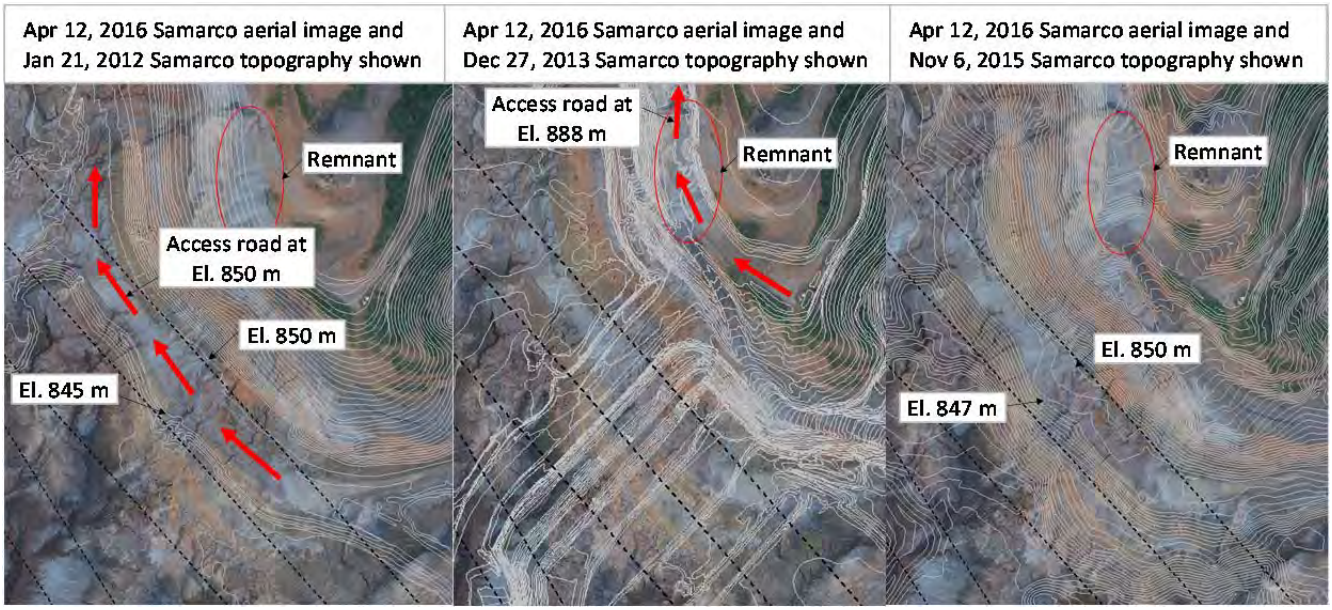

Figure B5-17 April 12, 2016 aerial image with January, 2012, January, 2014 and immediate post-failure topography

A review of topographic surveys, weekly reports and photographs was undertaken to assess the likelihood of historic access roads acting as preferential seepage pathways under the embankment.

From past topographic surveys and aerial images, it appears the access road at El. 850 m was constructed starting February, 2011 and was first captured in its entirety in the January, 2012 survey. The road upon which the left abutment remnant is sitting was constructed in April, 2013 and was best captured in the December, 2013 survey.

B5.3.5.2 Access Road Construction

A review of weekly reports show the following:

- It is unknown if the natural ground was consistently stripped back to phyllite during periods of access road construction. Figure B5-18 shows what looks like colluvium remaining on the stripped slopes in the area of the access road at El. 850 m.
- Oversized material was placed on the access roads in other locations around the facility for traffic purposes, as seen on Figure B5-19.
- Figure B5-20 shows one instance when, the ground against which the left abutment was being raised was stripped to remove loose material prior to raising. In addition, the oversized material on the roads was removed and the area smoothed in preparation for the raise. However, it is unknown whether this practice was consistently applied or extended further upstream to access roads underlying the non-compacted tailings. Figure B5-20 shows the stripped slope to consist of a mix of phyllite and colluvium.

Figure B5-18 Photos of access to the Secondary Gallery tulipas from weekly reports on week of April 9-15, 2012 (left) and April 30-May 6, 2012 (right)

Figure B5-19 Photo of access between Selinha Dike and Dike 1 on right abutment from weekly report dated March 19-25, 2012

Figure B5-20 Photos of ground preparation prior to upstream raise from weekly report dated May 21-27, 2012

B5.3.5.3 Drill Hole Log Review

Ten of the standard penetration test (SPT) logs from the installation of the piezometers on the setback were reviewed to see if oversized material was encountered. These locations were chosen given their proximity to the road at El. 850 m. The review showed:

- Of the ten, two encountered schist at the elevations shown on Figure B5-21 and did not encounter oversized material.
- Most of the holes were not deep enough to reach the road at El. 850 m and did not encounter oversized material.

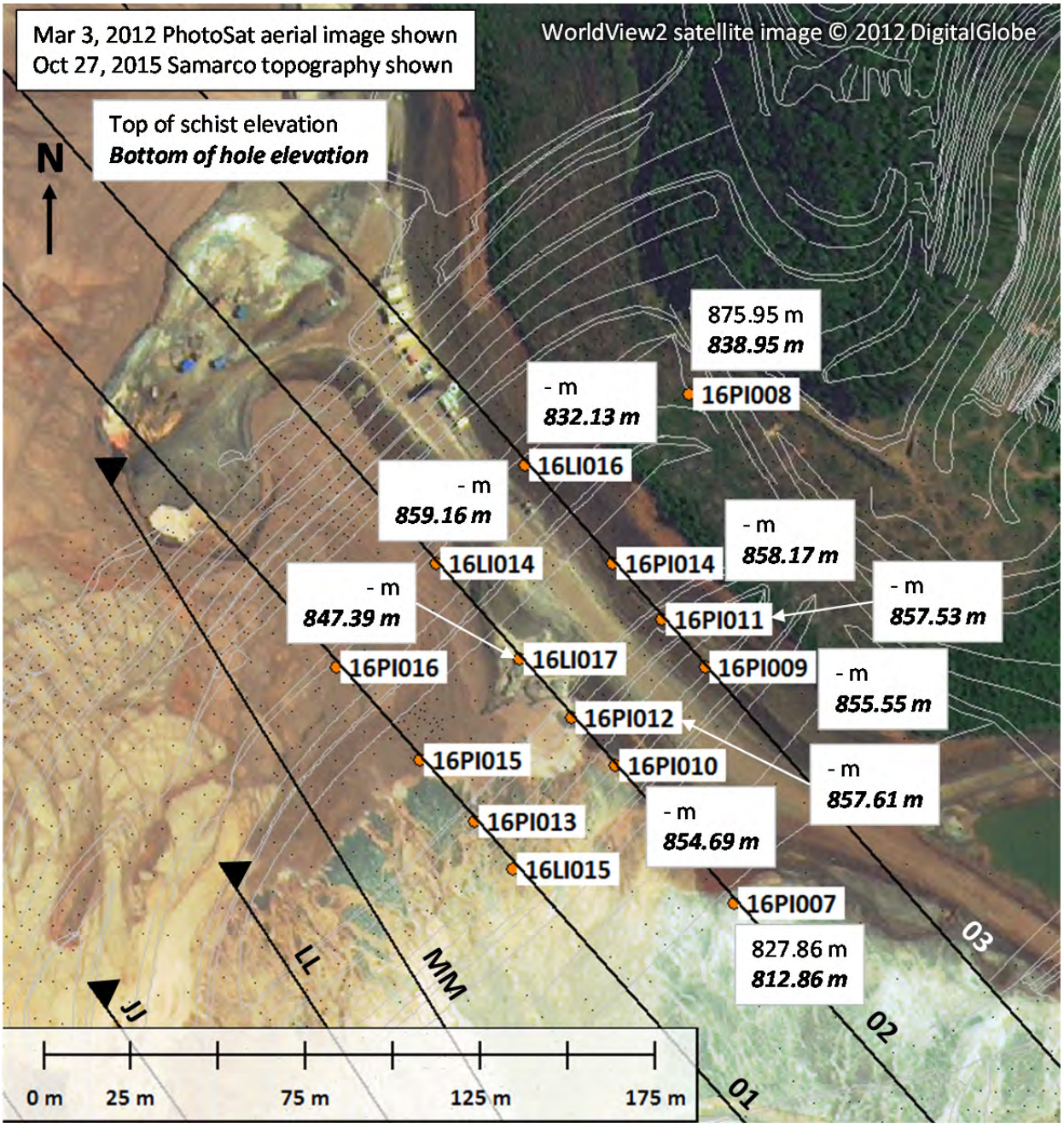

Figure B5-21 Left abutment drill hole review for oversized material

B5.3.5.4 Implication on Observations and Analyses

The possibility of historical access roads acting as a seepage conduit due to oversized material or insufficient stripping prior to placement of tailings was considered. The above review showed that in practice, both were addressed in the area of the upstream raise. Stripping for access road construction was done to remove loose material. This appears to have been sufficient to expose stable materials given its strong correlation with the post-failure surface.

This review exercise revealed the importance of incorporating the access road construction over time into the stripped ground survey used in seepage and stability analyses. The cuts were as deep as 15 m for the road at El. 850 m and in the exact location of Section 03 on the setback. The details of the stitched stripped ground survey are presented in Appendix A.

B5.3.6 Summary of Findings

Table B5-6 summarizes loading increases estimated using sections for the tailings beach and isopachs for all other noted areas. The crest area covers a portion upstream and downstream of the immediate crest centerline and therefore reports lower values than those presented in Section B5.1.

Key observations are as follows:

1. The elevation of the tailings beach increased 1 m to 2 m between surveys, with local areas raised up to 5.7 m at a time.
2. The crest area was raised an average of 1 m to 2 m between surveys, with one local area raised up to 5 m at a time.
3. Drain construction took place in June, July, and August, with an average of 1.3 m of material placed between surveys.
4. The downstream side of the 875 m bench was raised an average of 1.5 m between surveys during July.
5. Localized areas of the 895 m bench were loaded with up to 5.9 m of fill during October between surveys.

Table B5-6 Summary of loading changes at the left abutment

Period	El. 860 m Plateau	El. 875 m Bench	El. 895 m Bench	Crest Area	Tailings Beach
April 24 to May 27	-	-	-	Max: 5 m ① Avg: 1.9 m	Max: 4.2 m ① Avg: 1.3 m
May 27 to June 22	Max: 5 m ⑤ Avg: 1.3 m ④	Max: 3 m Avg: 0.7 m ⑥	Max: 2.5 m Avg: 0.7 m	Max: 4 m ③ Avg: 1 m	Max 2.5 m Avg. 0.4 m
June 22 to July 27	Max: 3.1 m ⑩ Avg: 1.4 m	Max: 3.4 m ⑨ Avg: 1.5 m	-	Max: 2.7 m ⑧ Avg: 1.2 m	Max: 5.2 m ⑧ Avg: 1 m
July 27 to August 24	Max: 3.9 m ⑭ Avg: 1.4 m	-	-	Max: 5.6 m ⑬ Avg: 1.5 m	Max: 4 m Avg: 1.3 m
August 24 to October 1	Max: 5.3 m ⑰ Avg: 1.2 m	-	Max: 7.7 m ⑯ Avg: 2.1 m	Max: 3.6 m Ave: 1.5 m	Max: 4.4 m Avg: 1.2 m
October 1 to October 27	- ⑲	- ⑲	Max: 5.9 m ⑳ Avg[3]: 0.9 m	Max: 4.8 m Avg: 2.3 m	Max: 5.7 m Avg: 1.9 m

1. Average values estimated as a weighted average in each specified area. The tailings beach average rise was visually estimated for the distance 40 m upstream of the dike crest using the cross sections with time (see Attachment B5).
2. Numbers in circles indicate event number from Attachment B5 Section B.B5-7.
3. See isopach – area has both cut and fill.

In addition to the geometric changes, the following were noted:

- There was ponded water at the toe of the El. 860 m blanket drain from June, 2015 to November, 2015. A review of raw drone photos and topography indicates the presence of an open channel and culvert through the road fill to convey the water away from the left abutment setback plateau.
- The area where the dike was raised against the left abutment was stripped to phyllite prior to placement of material. Historical access roads in the immediate vicinity of the dam raise were also stripped of oversized material (used for trafficable surface) and graded prior to placement of material. Therefore, the likelihood of historical access roads acting as seepage conduits appears to be low.

B6 SLIMES DEPOSITIONAL HISTORY AND SPATIAL RECONSTRUCTION

B6.1 General

This section presents the methodology and assumptions in delineating slimes boundaries at different times during the life of the Fundão facility. The design basis for the Fundão tailings facility was to maintain separation between the sand and slimes tailings. Sand tailings was to be placed upstream of Dike 1 and slimes upstream of Dike 2 as shown on Figure B6-1.

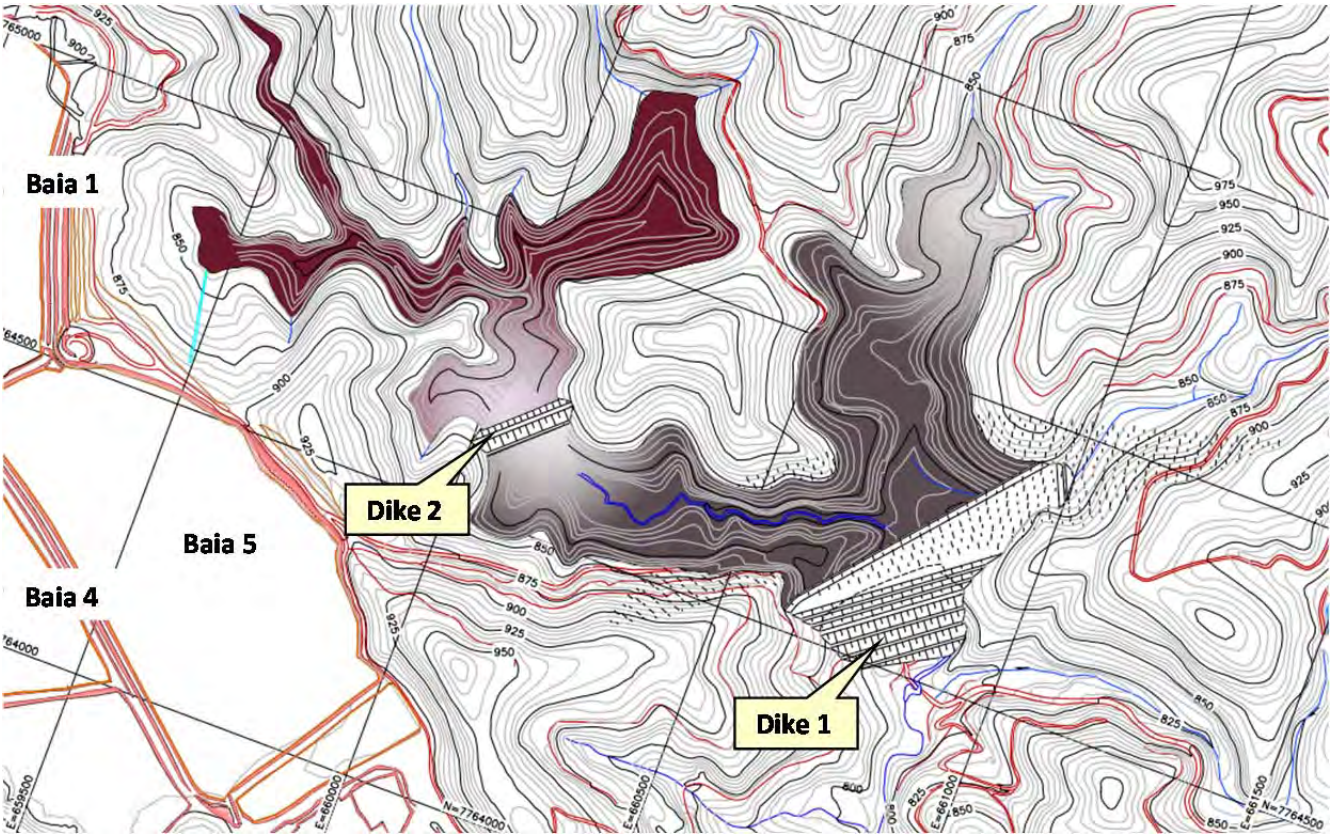

Figure B6-1 Pimenta de Ávila design drawing[2] for Fundão at El. 850 m

In April, 2009, Dike 1 experienced a piping incident which resulted in the construction of Old Dike 1A, then referred to as Dike 1A, to allow tailings deposition to continue during remediation works for Dike 1. Following the completion of Old Dike 1A, slimes were pumped over Dike 2 into the Old Dike 1A reservoir. This was the first instance of slimes incursion in the Dike 1 reservoir.

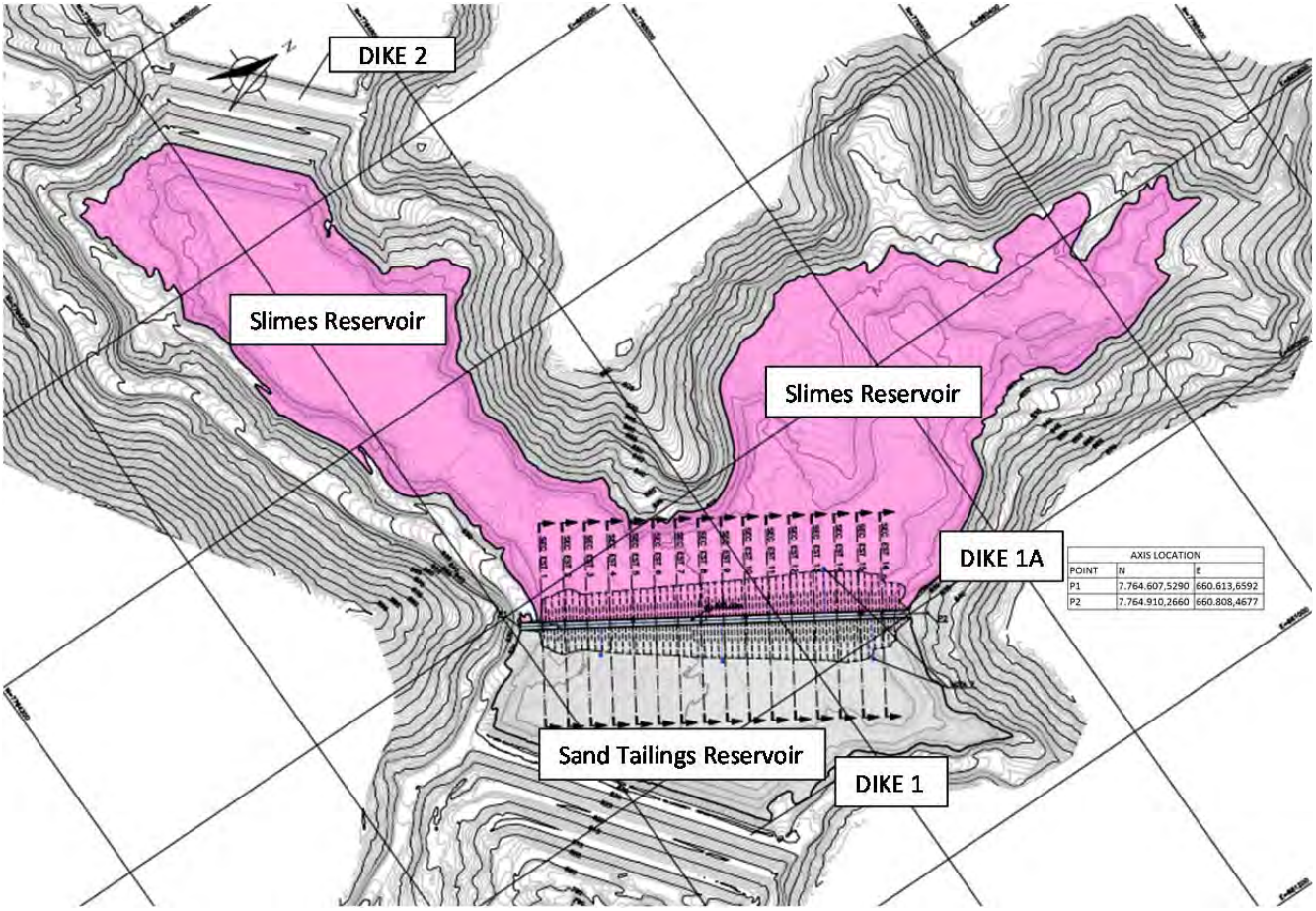

Figure B6-2 Pimenta de Ávila design drawing[3] for Old Dike 1A

As shown in the Fundão timeline by decant (see Section B3), slimes had other opportunities to reach the Dike 1 reservoir including the Overflow Channel north of the Island, through inter-basin pumping, and with breaching and eventual deliberate overtopping of Dike 2.

B6.2 Data Sources and Methodology

B6.2.1 Assumptions and Procedure

In order to estimate the extent of slimes, a combination of the data sources in Table B6-1 were used. It is important to note that in the Dike 1 reservoir, the slimes boundaries are meant to represent areas where slimes layers *could* be present from ingress of the pond water over the sloping sand deposit. The connected slimes layers then form a region of slimes layers that is much closer to a stratified deposit than a continuous deposit of slimes. The exception is in the instances when slimes were deposited in the Dike 1 reservoir directly.

Table B6-1 Data sources and assumptions for delineation of slimes boundaries

Data Type	Reason for Use	Assumptions
Samarco topography	Gives indication of tailings pond and beach locations. Provides pond/slimes elevations.	Slimes are fluid so will flow to a nearly horizontal surface.
Vale topography		
PhotoSat topography	Gives indication of tailings pond and beach locations. Serves as secondary check on Samarco topography.	Due to limitations of the PhotoSat surveys, the PhotoSat topography is only being used to estimate the beach shape while the elevations are picked off the Samarco topography.
Samarco aerial images	Provides visual guide on location of sand and slimes tailings by color	Slimes are red, sand is grey, and light-colored swirls are indicative of the foam layer which is present on the tailings pond where sand meets slimes
PhotoSat aerial images		
Google Earth aerial images[1]		
Monthly point surveys of Dike 1 tailings beach[2]	Gives a starting point with which a minimum beach offset can be delineated	Samarco survey shows the minimum beach width. The Dike 1 crest line is offset by the minimum beach width to obtain the maximum pond (and slimes) extent.
Site or field photos during inspections, construction activities	Supports the elevations picked off of topography especially in early years when full-basin surveys are not available	The observed tailings elevation and pond/slimes locations seen in photos can be used in combination with the closest topography date to estimate the tailings/pond elevation.

1. Given how close in time the Google Earth images were to Samarco or PhotoSat images, they were not used to delineate slimes boundaries.
2. From monthly geotechnical monitoring reports.

The pond boundaries delineated as described in Section B5.2 were used to represent the slimes boundaries for periods when slimes had access to the Dike 1 and Dike 2 reservoirs. The point surveys and estimated slimes boundaries are shown in the image timeline in Attachment B6.

B6.2.2 Connecting the Slimes Layers

The slimes layers are connected where a continuous slimes layer could feasibly exist. Breaks in the continuity result in a sand layer separating two slimes layers. For example, the opening and closing of the Overflow Channel north of the Island can result in a sand layer separating two slimes layers.

The beach fluctuations within each month are not captured in the topography which is surveyed monthly. There are likely many instances of interlayering within the connected slimes layers.

B6.3 Mapped Slimes Extent

An image timeline of the slimes is given in Attachment B6. In section, the slimes extent are as shown on Figure B6-3 and connected as described in Section B6.2.2.

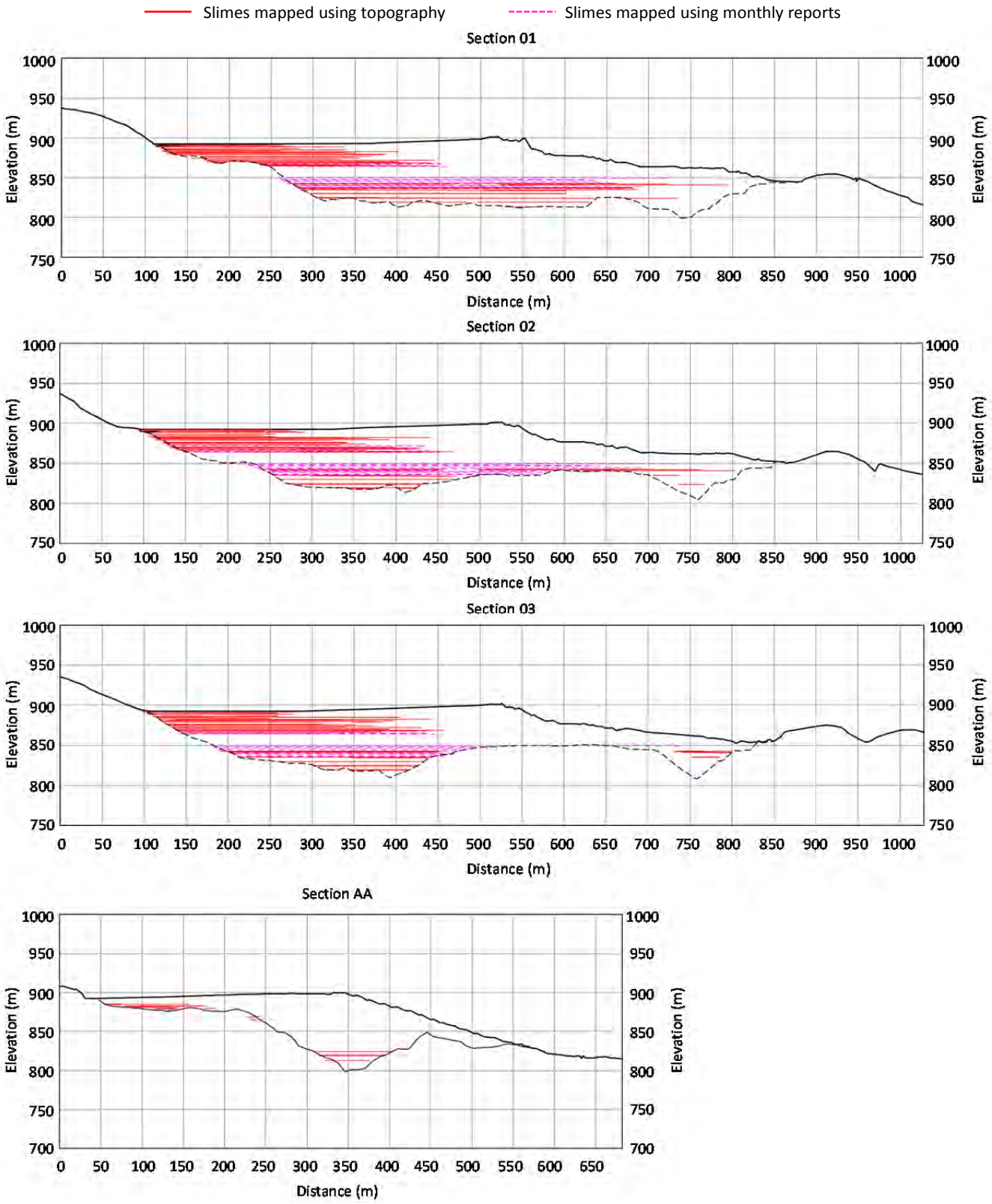

Figure B6-3 Sections 01, 02, 03 and AA with mapped slimes layers

B6.4 Slimes Access to Dike 1 Reservoir

Table B6-2 below summarizes the period during which slimes had access to the Dike 1 reservoir, as distilled from Section B3, and identifies the periods when slimes had access to the Dike 1 reservoir.

Table B6-2 Slimes access to Dike 1 reservoir

Operating Period	Fundão Basin Configuration	Slimes to Dike 1 via	Slimes Elevation Range
April, 2010 to January, 2011	Separated, Old Dike 1A completed	Pumping over Dike 2	813 m to 824 m
February, 2011 to July, 2012	Connected	Overflow Channel north of Island	824 m to 849.5 m
July, 2013 to December, 2013	Connected	Overflow Channel north of Island	863 m to 870 m
January, 2014 to February, 2014	Connected	Dike 2 breach	870 m to 872 m
March, 2014 to November, 2015	Connected	Overtopped Dike 2	872 m to 892.5 m

From April, 2010 to January, 2011, slimes were pumped over the crest to the toe of Dike 2. Although not anticipated in the original design of the Fundão facility, the redesign in 2009, which included Old Dike 1A, permitted storage of sand and slimes in the Dike 1 reservoir while the El. 826 m blanket drain was implemented.

From February, 2011 to July, 2012, the Overflow Channel north of the Island was opened to allow water from the Dike 2 reservoir to exit the facility via the Secondary Gallery while the Main Gallery was being repaired.

From July, 2013 to December, 2013, the Overflow Channel was reopened following completion of the Secondary Gallery plugging. This was anticipated in the design of the facility as the sand and slimes reservoirs were supposed to have merged beyond El. 850 m which was the starter Dike 2 crest elevation.

From January, 2014 to February, 2014, slimes had access to the right side of the Dike 1 reservoir via a breach on the left abutment of Dike 2. Shortly after, Dike 2 was overtopped in March, 2014 and the two reservoirs became one until the time of failure.

B6.5 Vertical Distribution of Slimes

The Fundão timeline (Section B3) showed different points in time when the Dike 1 and Dike 2 reservoirs were connected. It is important to consider the difference in control of the sand beach in order to minimize slimes ingress to the Dike 1 reservoir at these times.

For example, the construction of the Overflow Channel north of the Island allowed uncontrolled discharge of slimes toward the Secondary Gallery and also towards Dike 1. In later years, sand dikes were pushed out onto the sand beach upstream of Dike 1 in order to limit encroachment of the pond (and slimes) to the dike crest.

According to a Samarco employee, the beach construction methodology included significant track-packing, and control of the pond ingress with the use of dikes. Also, personnel working on the dam noted the lack of slimes. Equipment was also described as having ventured out nominally 100 m from the dike crest to borrow material for the upstream raise. The above points to decreased potential for the pond/slimes to encroach on the Dike 1 crest compared to earlier years when the push-up dikes were not observed in aerial images.

In the Dike 2 reservoir, the vertical distribution of slimes is virtually 100% with the exception of occasional deposition of contaminated sand tailings and sopão at the toe of the Sela Dike. In the Dike 1 reservoir, there are varying vertical distributions of slimes due to different types of operational beach control, as summarized in Table B6-3.

Table B6-3 Vertical distribution of slimes in Dike 1 reservoir

Operating Period	Access to Dike 1 Reservoir	Beach Control	Vertical Distribution of Slimes	Slimes Elevation Range
April, 2010 to January, 2011	Old Dike 1A	Provided by Old Dike 1A	Sand co-deposited at toe of Dike 2, slimes thoroughly mixed with sand	813 m to 824 m
February, 2011 to July, 2012	Overflow Channel north of Island	Provided by deposition of sand tailings off the crest of Dike 1	Stratified deposit upstream of Dike 1 due to beach fluctuations, likely many instances of interlayering within the connected slimes layers	824 m to 849.5 m
July, 2013 to December, 2013	Overflow Channel north of Island	Provided by deposition of sand tailings off the crest of Dike 1	Diluted as water wraps around the island and travels to the Auxiliary Spillway via the Auxiliary Spillway island canal	863 m to 870 m
January, 2014 to February, 2014	Dike 2 breach	Provided by push-up dikes and deposition of sand tailings off the crest of Dike 1	Diluted as water travels north of the Island through the Dike 2 reservoir to reach the Auxiliary/4th Spillway	870 m to 872 m
March, 2014 to November, 2015	Overtopped Dike 2	Provided by push-up dikes and deposition of sand tailings off the crest of Dike 1	Diluted as water travels north of the Island through the Dike 2 reservoir to reach the Auxiliary/4th Spillway	872 m to 892.5 m

The highest elevation of slimes mapped that underlie the left abutment setback slope is El. 849.5 m as shown on Figure B6-3. In order to better understand the stratification of slimes, a mass balance was completed for the El. 840 m to El. 850 m layer. The beach fluctuations show a relatively tight grouping of pond extents during this time.

B6.6 Slimes Mass Balance

B6.6.1 Partitioning of Reservoir by Slimes Stratigraphy

A mass balance was done for the El. 840 m to El. 850 m layer of slimes to better understand the stratigraphy of slimes in this zone of mixing and interlayering. The transition from predominantly slimes to interbedded slimes to isolated slimes is expected to be gradual from the northernmost part of the Dike 1 reservoir to the crest. For the purposes of the mass balance, this layer of slimes was divided into three zones in plan as summarized in Table B6-4 and shown on Figure B6-4.

Table B6-4 Graduation of slimes stratigraphy

Slimes Stratigraphy	Area	Reason	Mass Balance Assumption
Predominantly slimes, no sand	Dike 2 reservoir, northern part of Dike 1 reservoir extended south to the Secondary Gallery intake	Greater likelihood of slimes being present along the flow path within the Dike 1 reservoir when the outlet is set at the Secondary Gallery intake	100% slimes
Interbedded slimes, some sand in between the fingers of slimes	Dike 1 reservoir between the area of predominantly slimes and the area of isolated slimes	Continued pond presence allows more time for slimes particle to travel into this area and deposit	Percentage of slimes estimated through mass balance calculation
Isolated slimes, more sand than slimes	Dike 1 reservoir between the dike crest and some distance upstream of the measured beach widths	These fingers of pond/slimes incursion were likely too far and too varied for significant slimes particle transport and deposition	0% slimes

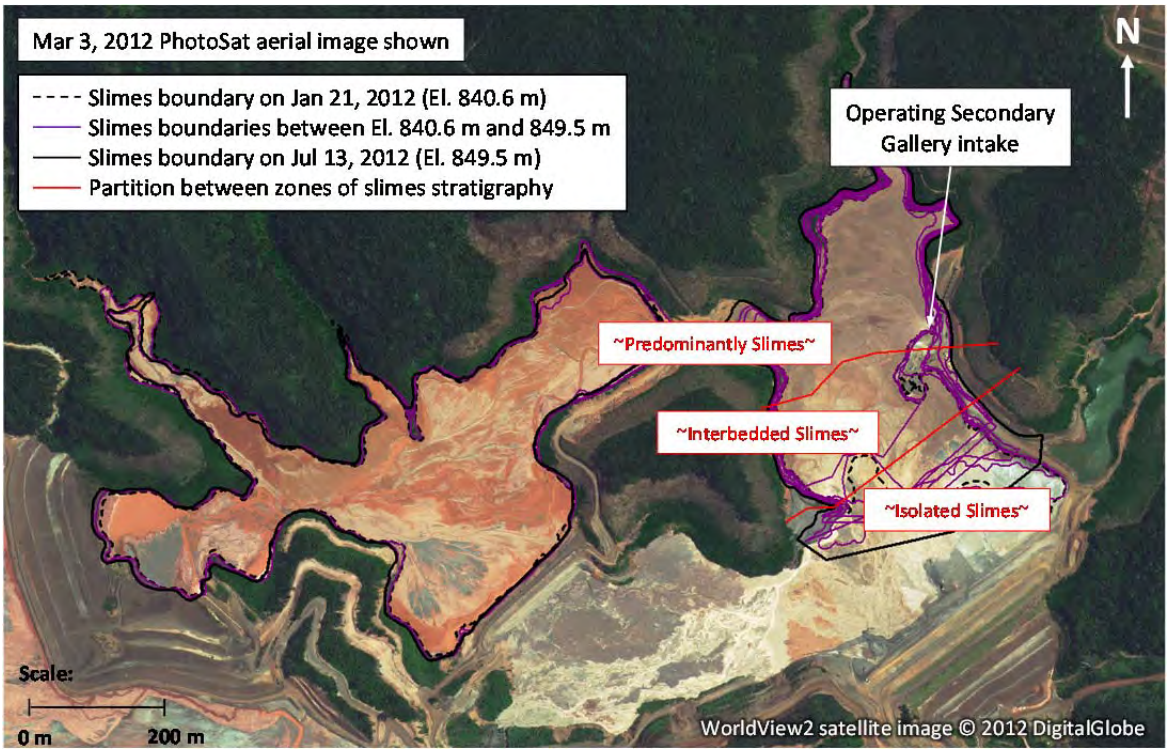

Figure B6-4 Zones of slimes stratigraphy

B6.6.2 Mass Balance Inputs and Assumptions

The sand weight and tailings volume were not needed for the slimes mass balance. The approach adopted is shown on Figure B6-5 below. The volume of slimes deposited between t_0 (January 21, 2012) when slimes were deposited at El. 840 m and t_f (July 13, 2012) when slimes were deposited at El. 850 m was partitioned into the three zones of slimes stratigraphy. The boundary between the zone of interbedded and isolated slimes was estimated from the historic tailings water cover. The slimes production in dry metric tonnes (Section B7) was converted to total slimes volume including

water using material parameters obtained during the Panel field investigation program at GSSAM16-02, a location in the south corner of Baia 3 where the deposit is predominantly slimes.

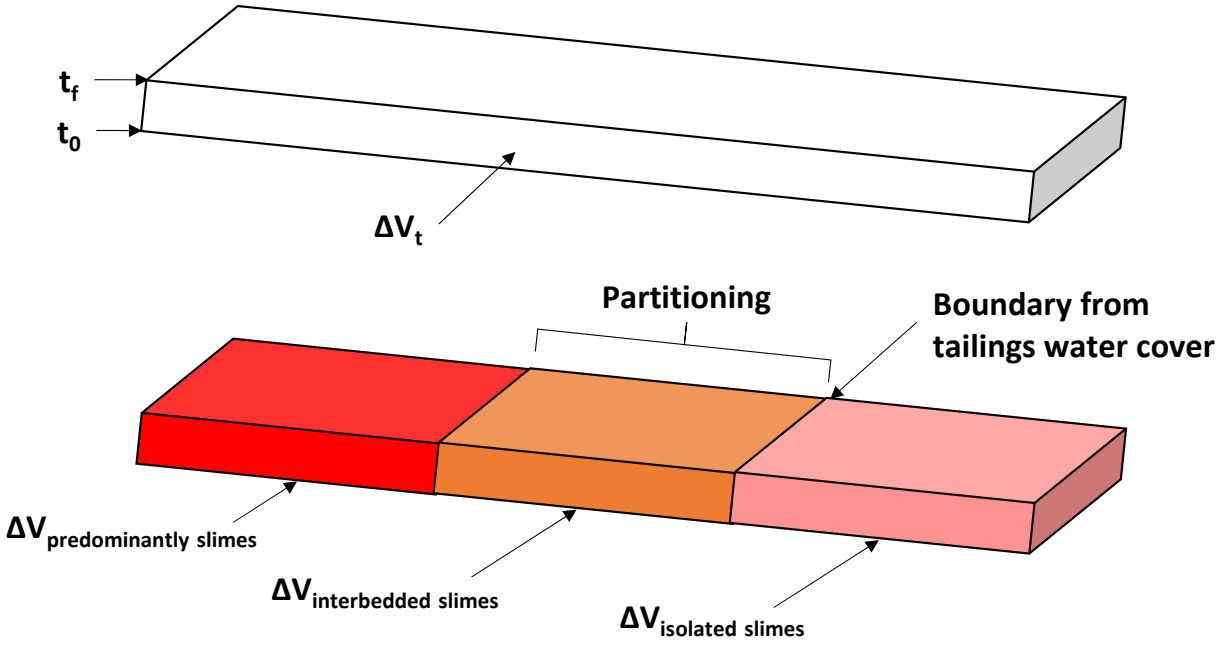

$\Delta V_{predominantly\ slimes}$ → 100% slimes, 0% sand tailings

$\Delta V_{isolated\ slimes}$ → 0% slimes, 100% sand tailings

$\Delta V_{interbedded\ slimes} = \Delta V_t - \Delta V_{predominantly\ slimes}$

Figure B6-5 Mass balance block diagram

Key assumptions include:

- The average slimes density at GSSAM16-02 in Germano is representative of slimes properties at Fundão shortly (less than 1 year) after deposition.
- All of the slimes produced at Samarco and Vale were sent to Fundão at this time.
- The loss of slimes through the Secondary Gallery is negligible.
  - Slimes are seen in aerial images at the intake of the Secondary Gallery in Dike 1. Furthermore, site photographs show slimes entering the Secondary Gallery and this had been noted by ITRB previously (Figure B6-6). However, there is no quantitative method to track the amount of slimes lost through the Gallery, and has been excluded from the mass balance.

Photo 3 – Secondary Gallery intake without grillage to prevent debris entry or provide personnel safety

Photo 4 - Intake (from prior inspection) showing debris entry

Figure B6-6 Secondary Gallery intake showing presence of slimes, photo from October, 2011 ITRB report

B6.6.3 Percent Slimes in Interbedded Zone

Table B6-5 summarizes the inputs and results for the percent of slimes by volume within the interbedded zone. Approximately 20% of the layer between El. 840 m and 850 m within the interbedded zone is slimes by volume, meaning the remaining 80% is sand. The results are shown in section on Figure B6-7.

Table B6-5 Summary of inputs and results for slimes mass balance

Item	Unit	Value
Predominantly slimes zone		
Samarco tailings production	dry metric tonne	2,109,939
Dry unit weight	kN/m^3	16.45
Specific gravity	-	3.806
Unit weight of water	kN/m^3	9.807
Void ratio	-	1.268
Weight of tailings	dry metric tonne	1,972,287
Isopach fill volume(1)	m^3	1,175,511
Slimes volume	m^3	1,175,511
Percent slimes	%	100
Interbedded slimes zone		
Dry unit weight	kN/m^3	16.45
Specific gravity	-	3.806
Unit weight of water	kN/m^3	9.807
Void ratio	-	1.268
Weight of tailings	dry metric tonne	137,652
Isopach fill volume(1)	m^3	461,876
Slimes volume	m^3	82,043
Percent slimes	%	**18**

1. Isopach fill volumes estimated using Global Mapper.

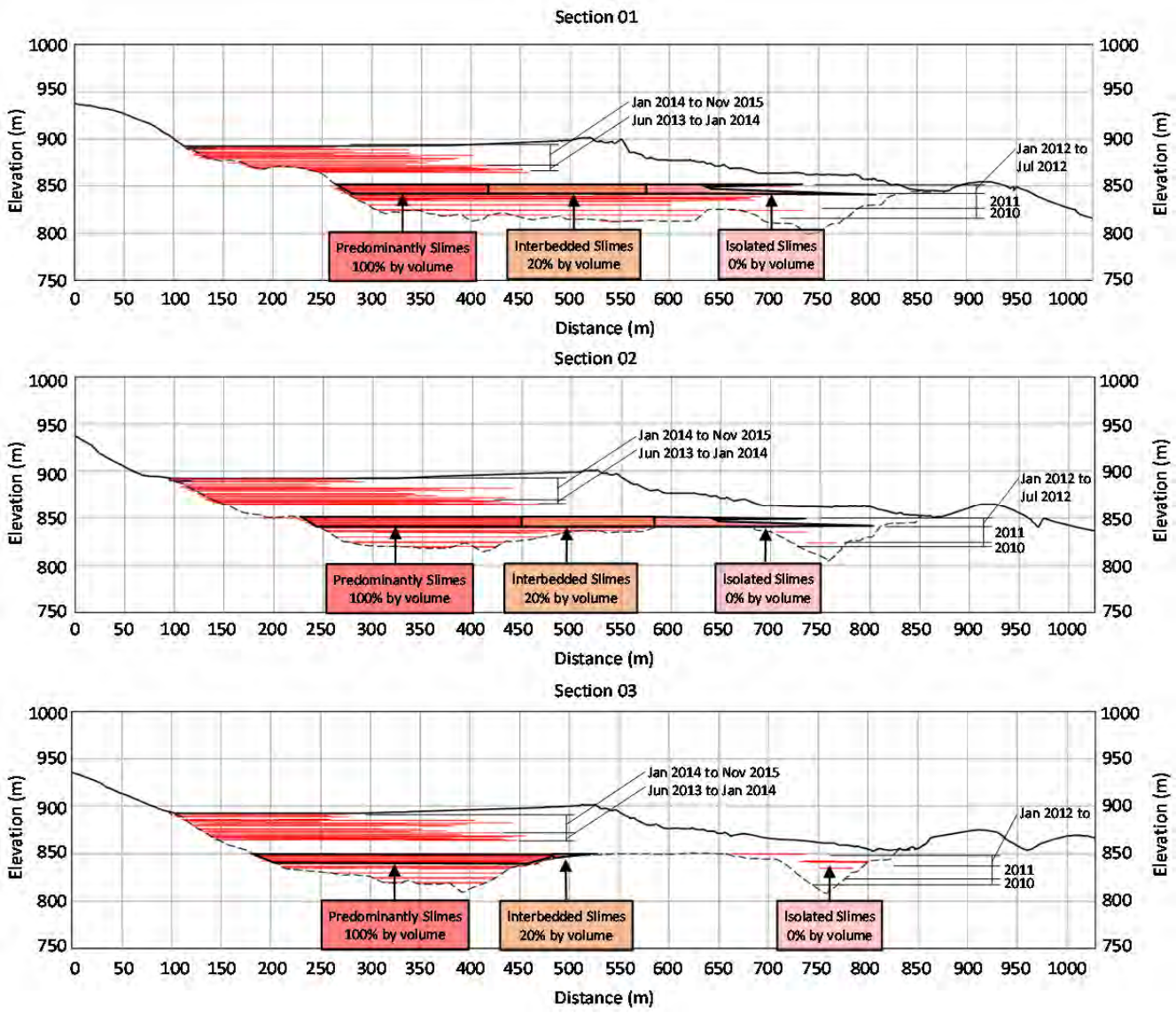

Figure B6-7 Percent slimes by volume in Section 01, 02 and 03

B6.6.4 Sensitivity Analysis

Sensitivities to the inputs were checked and are presented on Figure B6-8. The inputs varied include:

- slimes dry unit weight;
- location of boundary between the predominantly slimes and interbedded slimes zones;
- tailings production in dry metric tonnes between El. 840 m and El. 850 m; and
- location of boundary between the interbedded slimes and isolated slimes zones.

The percent slimes is most sensitive to the slimes dry unit weight. A 5% increase in the slimes dry unit weight results in the percent slimes by volume dropping from 18% to 5%. Conversely, a 5% decrease in the slimes dry unit weight results in the percent slimes by volume increasing from 18% to 32%.

As expected, the percent slimes is also sensitive to the location of the boundary between predominantly slimes and interbedded slimes. A 3% increase in the plan area of the predominantly slimes zone drops the percent slimes by volume from 18% to 3%.

The high level of sensitivity of the percent slimes by volume to these input parameters further highlights the uncertainty associated with the calculation.

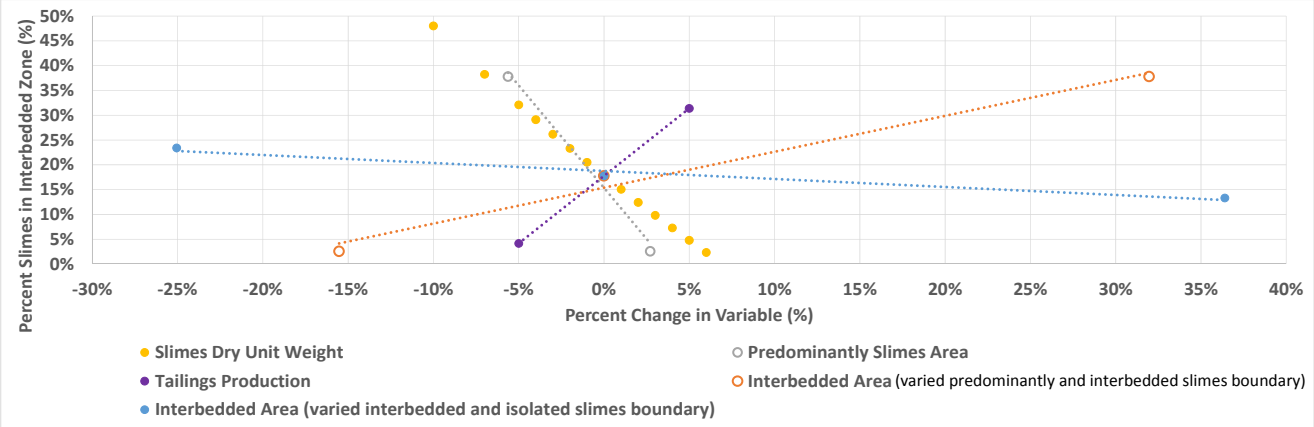

Figure B6-8 Sensitivity analyses for calculation of percent slimes in interbedded zone

B6.7 Supporting Evidence for Presence of Slimes at the Left Abutment

B6.7.1 Drill Hole Review

A review of available drill hole data at the left abutment was conducted to search for presence of slimes from El. 840 m to El. 850 m. A similar review by others of drill holes was undertaken as part of the New Dike 1A raise design. The results are discussed in Appendix C, Section C2.2.1. A summary of the drill hole types reviewed, and the criteria for determining whether the layer is slimes is given in Table B6-6.

Table B6-6 Drill hole criteria for determining presence of slimes

Drill Hole Type	Criteria for Slimes
Cone penetration test (CPT)	Material index > 2.7, increase in pore pressure, reduced tip resistance, fines content > 50% - 100%
Standard penetration test (SPT)	Material description including: ▪ Clay/clayey/little clay ▪ Brown ▪ Red ▪ Mottled[(1)]

1. Translation given as “variegated” in logs, assumed to mean “mottled”.

Of the 110 drill holes reviewed at the left abutment, 17 contained data between El. 840 m and El. 850 m, of which 8 encountered slimes as per the criteria set out in Table B6-6. These 8 drill holes are in the immediate vicinity of the left abutment (Figure B6-9) and encounter material that underlies the November, 2015 embankment slope (Figure B6-10). A summary table of drill holes is given in Table B6-7.

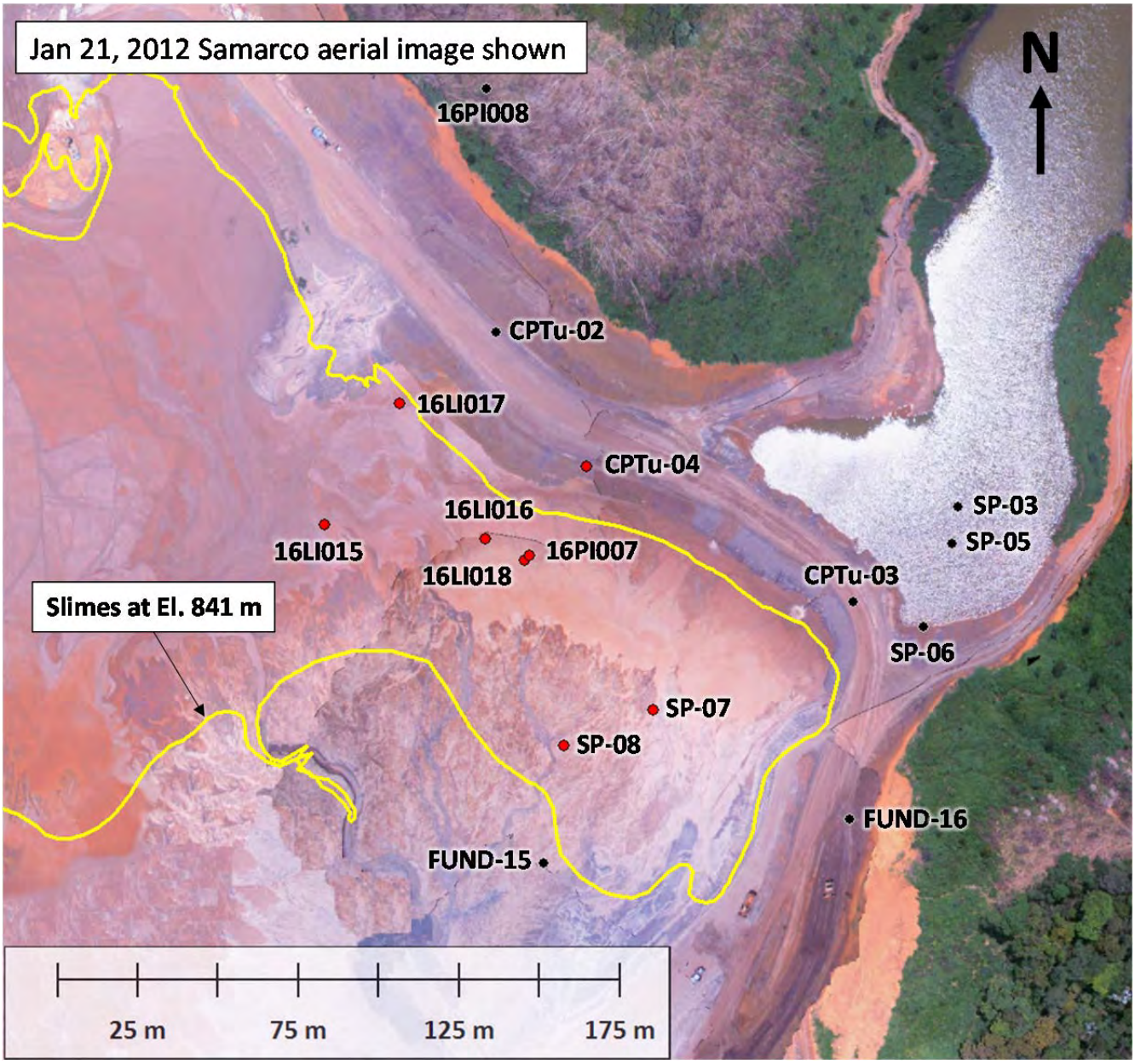

Black dots indicate drill holes with data in elevation range 840 m to 850 m that do not indicate presence of slimes. Red dots indicate drill holes with data in elevation range 840 m to 850 m that do indicate presence of slimes.

Figure B6-9 Drill hole review for slimes at left abutment

Table B6-7 Summary of drill holes reviewed for presence of slimes

Name	Easting[1]	Northing[1]	Top of Hole (m)	Depth of Hole (m)	Bottom of Hole (m)	Test Type	Data between El. 840 m and El. 850 m	Material Description				Slimes?
								Clay/Clayey/ Little Clay	Brown	Red	Variegated[2]	
SP-03	660988.8	7764918.5	850.0	27.0	823.0	SPT	Y	x			x	N[3]
SP-05	660986.8	7764907.1	850.5	34.0	816.5	SPT	Y	x			x	N[3]
SP-06	660977.9	7764881.2	851.4	24.4	827.0	SPT	Y		x		x	N[3]
SP-07	660893.8	7764855.1	862.4	60.5	801.9	SPT	Y	x	x	x		Y
SP-08	660866.2	7764844.0	862.1	61.0	801.1	SPT	Y	x	x		x	Y
16PI007	660855.3	7764903.4	862.9	50.0	812.9	SPT	Y	x	x		x	Y
16PI008	660842.2	7765049.0	879.5	40.5	839.0	SPT	Y					N
16LI015	660791.7	7764913.1	865.0	26.5	838.5	SPT	Y	x	x		x	Y
16LI017	660815.2	7764950.7	864.4	17.0	847.4	SPT	Y	x	x		x	Y
16LI016	660841.6	7764908.6	862.6	30.5	832.1	SPT	Y	x	x			Y
16LI018	660854.0	7764902.0	858.7	23.5	835.2	SPT	Y	x	x			Y
CPTu-02	660845.0	7764973.0	861.0	12.8	848.2	CPT	Y	N/A, based on CPT criteria for slimes[4]				N
CPTu-03	660956.0	7764889.0	851.5	21.7	829.8	CPT	Y					N
CPTu-04	660873.0	7764931.0	855.0	14.8	840.2	CPT	Y					Y
FUND-15	660859.8	7764807.5	861.6	23.3	838.4	SPT	Y					N
FUND-16	660955.8	7764824.1	854.7	15.3	839.5	SPT	Y					N
FUND-16	660955.0	7764821.0	854.6	12.3	842.3	CPT	Y	N/A, based on CPT criteria for slimes[4]				N

1. Coordinates are in UTM Zone 23K Córrego Alegre.
2. Translation given as “variegated” in logs, assumed to mean “mottled”.
3. Drill holes are located in Grota da Vale, not in the immediate vicinity of the left abutment.
4. See Table B6-6.

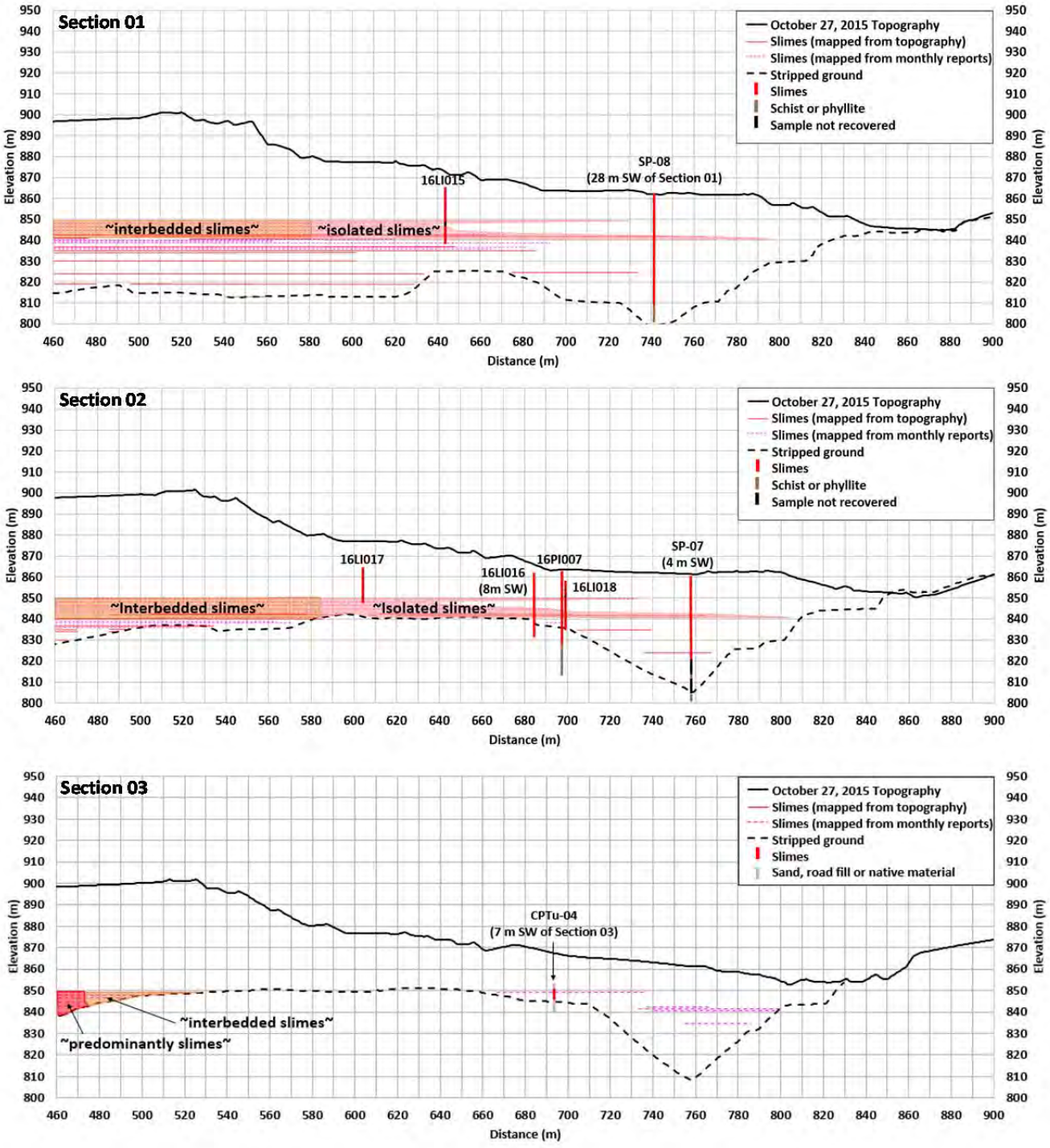

Figure B6-10 Drill hole lithology shown on Sections 01, 02, 03

Within the eight holes where slimes were identified, their distribution is more difficult to determine because the tailings were not continuously sampled. However, SP-07 is notable in having distinguished two discrete clay layers corresponding to slimes: a 2 m thick layer at El. 836.36 m and a

deeper 2 m layer at El. 828.36 m. Also, CPTu-04 penetrated slimes layers up to several centimeters thick. It is reasonable then from the drill holes to categorize discrete layers of slimes as ranging from a few centimeters to a few meters in thickness, with the remainder of the slimes material intermixed with sand in varying proportions.

The drill hole logs for the holes shown on Figure B6-10 and Table B6-7 are given in Appendix C.

B6.7.2 Phreatic Surface from Left Abutment to Right Abutment

The presence of a pond in Grota da Vale implies there should be a hydraulic gradient from the pond to the El. 826 m blanket drain. The El. 860 m blanket drain is too high to have an effect on this gradient which, in the absence of any impermeable layers, should follow the slope of the stripped ground under the dike. In order to check this, a longitudinal section was cut along the El. 860 m bench from the left to the right abutment as shown on Figure B6-11.

Due to the lack of piezometers along the longitudinal section alignment, the phreatic surface output from the calibrated seepage model (discussed in Appendix G) was plotted. The section is shown on Figure B6-12.

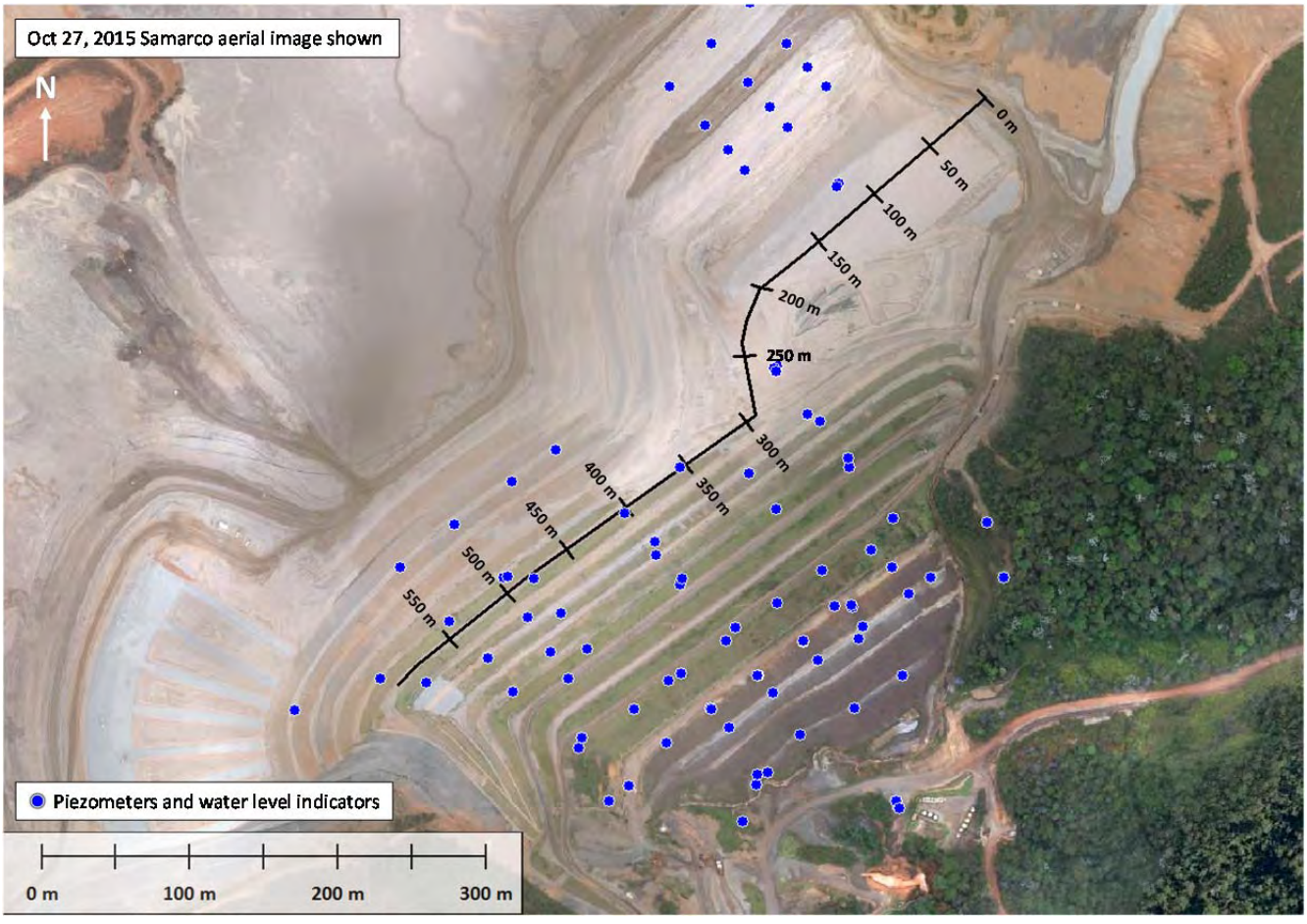

Figure B6-11 Alignment of longitudinal section from left to right abutment

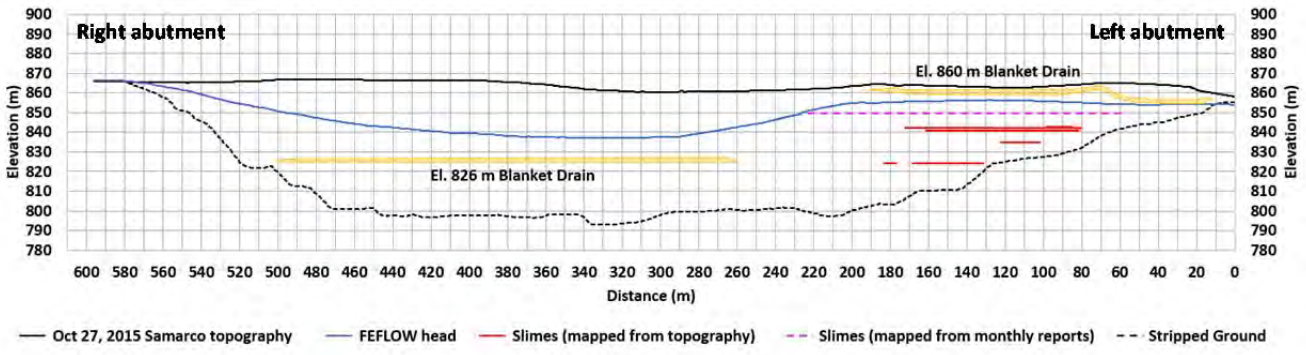

Figure B6-12 Longitudinal section from left to right abutment

There appears to be a perched water table in the left abutment area. The piezometric readings from the piezometers at the left setback are presented in the following section.

B6.7.3 Phreatic Surface at Left Setback

Due to the lack of piezometers along the El. 860 m bench from the left to right abutment, the stripped ground and piezometric readings for the nine piezometers on the left setback have been shown in plan on Figure B6-13 and Figure B6-14. The former figure shows the last available piezometric record prior to the failure on November 5, 2015. The latter figure shows the last available reading from 16LI015 before it was damaged.

Despite a steeply sloped stripped ground surface moving away from the left abutment, the piezometric records denote a relatively flat water table. This again implies there is an impedance to downward drainage to the El. 826 m blanket drain below the left setback. The presence of an elevated phreatic surface at the left abutment supports the presence of slimes below the dike fill, resulting in a waterfall effect at the end of the slimes extents. It is also noted in Appendix G that flow from Grota da Vale elevates the piezometric surface on the left abutment.

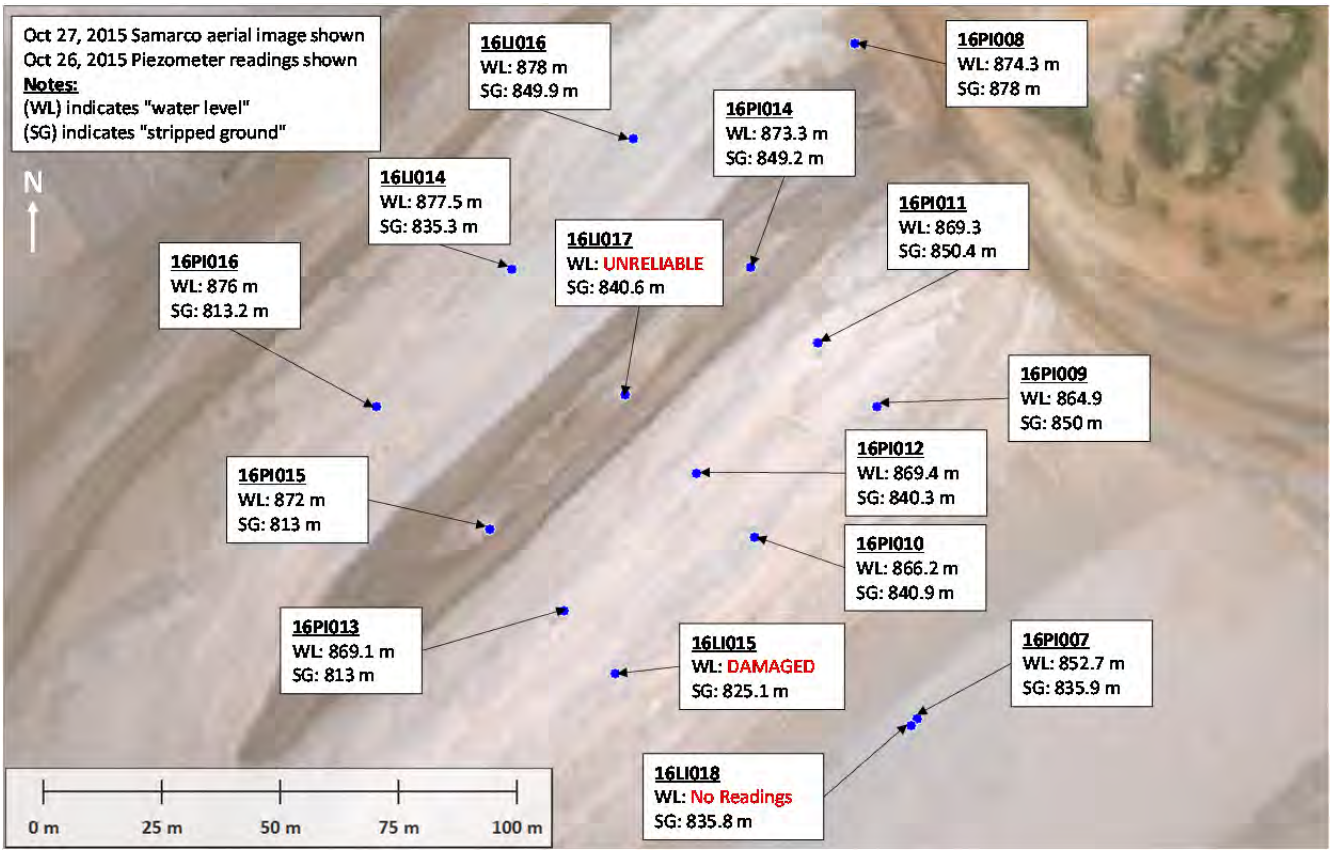

Figure B6-13 Piezometric readings and stripped ground elevation at setback in October, 2015

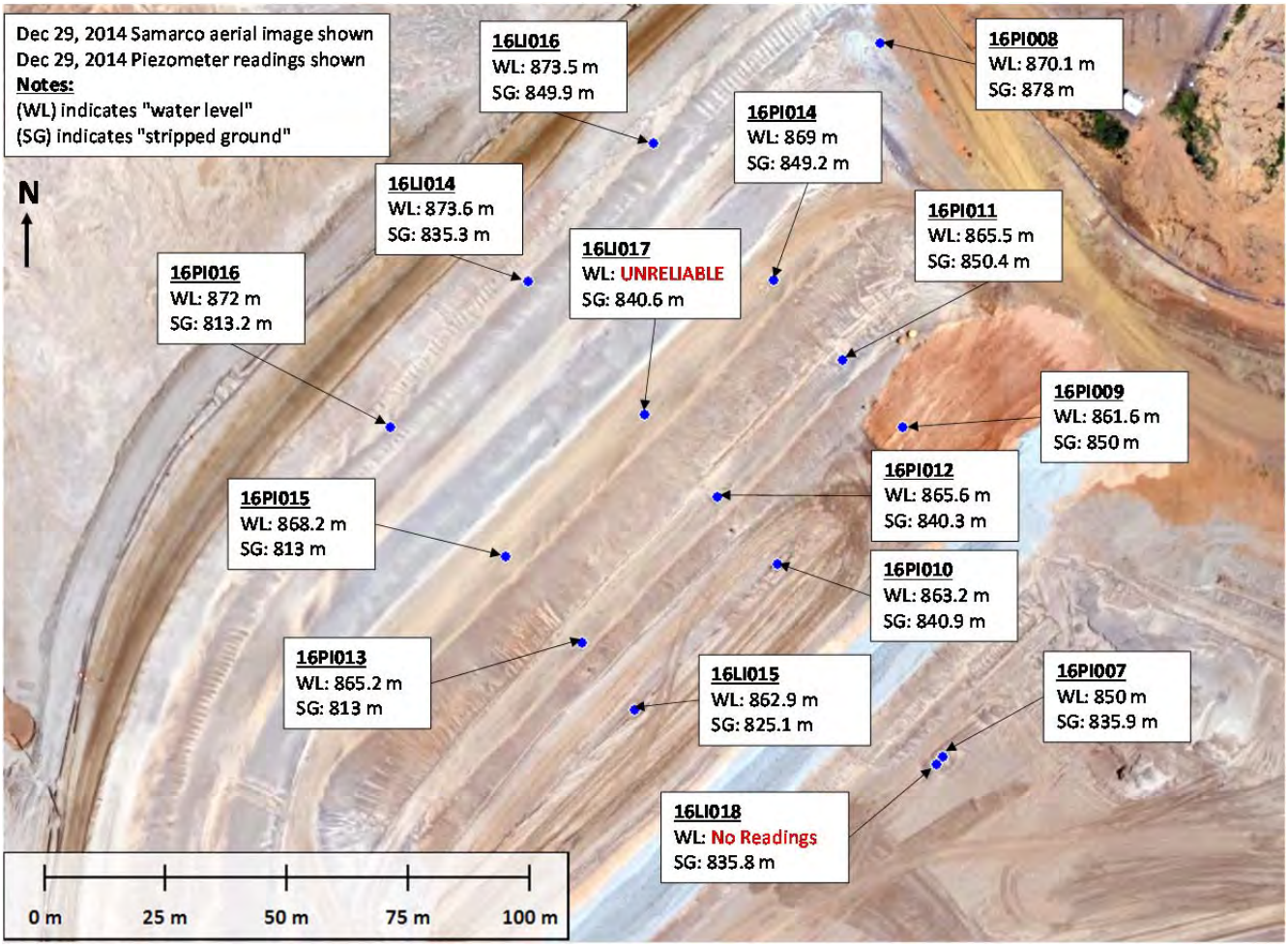

Figure B6-14 Piezometric readings and stripped ground elevation at setback in December, 2014

B6.8 Summary of Findings

From the available information, 72 slimes boundaries were delineated. An image timeline of the individual slimes boundaries are presented in Attachment B6. Also included in Attachment B6 is a summary of slimes information in tabular format.

A summary of findings is as follows:

1. Slimes incursion into the Dike 1 reservoir was planned below El. 825 m with the construction of Old Dike 1A. It was also anticipated above El. 850 m when the sand and slimes reservoirs were supposed to have merged with the deliberate overtopping of the starter Dike 2 crest.
2. The opening of the Overflow Channel north of the Island allowed slimes into Dike 1 from El. 825 m to El. 850 m. Beach control during this time was difficult given the location of the Secondary Gallery intake and the need to route water through said intake. In addition, the left abutment setback began during this time, further pushing the dike crest close to the Secondary Gallery intake and tailings pond.

3. The slimes boundaries mapped using a combination of aerial images, topography and beach width measurements do not indicate the absolute presence of slimes.
4. The different ways slimes had access to the Dike 1 reservoir resulted in different types of slimes deposits including:
   a. Mixed with sand below El. 824 m.
   b. Stratified/mixed from El. 824 m to El. 850 m.
   c. Diluted from El. 850 m to El. 893 m.
5. A mass balance on the critical slimes layer below the left abutment setback slope from El. 840 m to El. 850 m shows the slimes occupy approximately 20% by volume, with the remainder 80% occupied by sand.
6. There are eight drill holes in the vicinity of the left abutment that encountered slimes between El. 840 m and El. 850 m.
7. The elevated phreatic surface with a lack of gradient while moving away from the steeply sloped left abutment stripped ground indicates the presence of impermeable layers under the setback dike fill.

B7 TAILINGS PRODUCTION

B7.1 General

The tailings production record over the life of the Fundão facility was compiled as part of the Investigation. The key outputs from this exercise are as follows:

- Check the amount of sand and slimes produced against the design criteria of 70% sand, 30% slimes.
- Estimate the amount of slimes produced and deposited in Fundão between the key slimes elevations of El. 840 m and El. 850 m, as described in Section B6.6.
- Quantify the contribution of slimes from the neighboring Vale Alegria Mine to Fundão.
- Identify the locations of spigots at Dike 1 in the months leading up to the failure to approximate zones of beach saturation for input to seepage modeling.
- Determine whether there was a correlation between changes in tailings production rate and incidents at Fundão.

B7.2 Plant Operating History

There are three plants at Samarco that produced tailings during the operation of Fundão which began in 2008:

- Plant 1: operational from January 1, 2008 to November 5, 2015, produces sand, slimes and sopão.
- Plant 2: operational from January 1, 2008 to November 5, 2015, produces sand and slimes.

- Plant 3: operational from April 8, 2014 to November 5, 2015, produces sand and slimes.

In addition, the neighboring Vale mine (Alegria) produces both sand and slimes with a portion of the slimes being deposited at the Samarco site. During an interview with a Samarco specialist engineer, it was stated that Vale did not deposit any sand tailings at Samarco. Invoices from Samarco to Vale for the disposal of slimes from Alegria Mine go as far back as August, 2000. Slimes deposition in Fundão continued up to the time of failure.

B7.3 Types of Tailings

Tailings were classified as either slimes tailings (slimes) or sand tailings (sand). Generally, Fundão slimes are clays, with some brown or red, while Fundão sand tailings are fine sands, generally grey. Additional deposition constituents in Fundão were sopão and contaminated sand tailings. Sopão is a unique output from Plant 1 comprised of material washed off the plant floors. This material is dark grey. Contaminated sand tailings are those with excessively high fines content which is not suitable for use as upstream raise material.

The properties of the tailings are described in Appendix D. Samarco's geotechnical department documented the tailings properties in order to convert production in dry metric tonnes to production in cubic meters. These properties are given in Table B7-1.

Table B7-1 Samarco tailings material parameters from Samarco's geotechnical department

	Actual Density of Particles	Specific Mass	Specific Dry Mass	Content of Solids (mass)	Moisture - Process Engineering	Saturation	Moisture Content - Soil Mechanics	Void Ratio
	G $\left(\frac{\gamma_s}{\gamma_w}\right)$	ρ $\left(\frac{W_t}{V_t}\right)$ (t/m^3)	ρ_d $\left(\frac{W_s}{V_t}\right)$ (t/m^3)	P $\left(\frac{W_s}{W_t}\right)$ (%)	w_t $\left(\frac{W_w}{W_t}\right)$ (%)	Sr $\left(\frac{V_w}{V_v}\right)$ (%)	w $\left(\frac{W_w}{W_s}\right)$ (%)	$\left(\frac{V_v}{V_s}\right)$
	1	2	3	4	5		6	7
			(4/100) * 2					
PLANT 1, 2 and 3								
Sandy tailings	2.890	-						
Discharge (Mud)		1.500	0.780	52.0	49		94	2.7
Deposits		1.713	1.537	89.7	10	38	11	0.88
Mud	3.450							
Discharge (Mud)		1.350	0.473	35.0	64		183	6.3
Deposits		1.980	1.380	69.7	30	100	43	1.50
VALE Mud								
Mud	4.410	-						
Discharge (Mud)		1.337	0.436	32.6	67		207	9.12
Deposits		2.03	1.336	65.7	34		52	2.30
SOPÃO - SAME QUANTITY ADOPTED AS FOR SANDY TAILINGS OF PLANT 1								
Sandy tailings	3.250	-						
Discharge (Mud)		1.500	0.780	52.0	51		97	3.17
Deposits		1.90	1.300	68.4	32	100	46	1.50

KEY

Quantities informed by the process - Plant 1 and Plant 2

Quantities adopted — Reference Quantities

Quantities calculated

B7.4 Review of Production Records

B7.4.1 Data Sources

Production records were available from Samarco's geotechnical and processing departments for different periods and at different recording frequencies. The sources reviewed are summarized in Table B7-2 and also documented in Appendix A. For discussion purposes, they have been numbered Data Set 1 through 3 in this appendix.

Table B7-2 Tailings production records data sources

Data Set No.	File Name	Originator	Data Frequency	Data Availability			
				Fundão Sand	Fundão Slimes	Fundão Sopão	Vale Slimes
1	2015_12_22_Disp. de Rejeito Curto_Medio_Longo Prazo	Samarco, Geotechnical Department	Monthly	Projected[1] (2014 – 2032) Measured (January 2014 – October 2015)			
2	Massas concentradores 2008 a 2015 SAMARCO	Samarco, Processing Department	Daily	Measured (January 1, 2008 – November 5, 2015)		Not included	
3	Balanço de Massas_ SAMARCO_Vale_rev17dez	Samarco, Processing and Geotechnical Department	Annual	Measured by Geotechnical Dept. (2008 – October 2015) Measured by Processing Dept. (January 1, 2008 – November 5, 2015)		Not included	Measured by Geotechnical Dept. (2008 – October 2015)

1. The measured values replace the projected values when data is available.

The data sources for tailings production are summarized as follows:

- Sopão production quantities are available on a monthly basis from Data Set 1 from 2014 onward only.
- Vale slimes quantities are available on a monthly (Data Set 1, 2014 to 2015) and annual (Data Set 3, 2008 to 2015) basis.
- Sand and slimes produced by Samarco are available on a daily (Data Set 2, 2008 to 2015), monthly (Data Set 1, 2014 to 2015) and annual (Data Set 3, 2008 to 2015) basis.
- Data Set 3 includes annual production quantities from both the geotechnical and processing departments at Samarco.

B7.4.2 Comparison of Records

B7.4.2.1 Geotechnical and Processing Department

Both the geotechnical and processing departments at Samarco tracked the production of sand and slimes tailings. Only the geotechnical department tracked the incoming quantity of Vale slimes. Table B7-3 shows a comparison of overlapping records for the two departments. According to a Samarco specialist engineer, the percent of sand vs. slimes differs as both departments have different ways of quantifying the tailings. However, the annual totals are similar.

The percent difference for slimes produced as documented by the two departments varies from 8% to 71%. The reason for this difference is unknown, but is covered in the sensitivity analysis as part of the mass balance discussed in Section B6.6.4.

The most complete data set for tailings production over the life of Fundão is from Samarco's processing department. Given the small difference in annual totals from the two departments, the values from the processing department in Data Set 2 are carried forward for subsequent analyses.

B7.4.2.2 Data Sets 1, 2, 3

Table B7-4 compares annual tailings production from each of these data sets. The following observations were noted:

- The total annual tailings production between all three data sets are the same when sopão and Vale slimes are excluded.
- Sopão production data is unique to Data Set 1. Based on records for 2014 and 2015, 500,000 dry metric tonnes of sopão are produced each year, which is approximately 2% of total tailings production.

Table B7-3 Comparison of geotechnical and processing department tailings production records

Year	Tailings Type	Geotechnical Department		Relative Percent Difference[1]	Processing Department		Relative Percent Difference[1]	Relative Percent Difference between Geotechnical and Processing
		Data Set 1	Data Set 3		Data Set 2	Data Set 3		
2008	Sand	N/A	9,709,391	N/A	9,990,617	9,990,617	0%	-3%
	Slimes (w/o Vale)		1,916,449		1,535,468	1,535,468	0%	25%
	Total		11,625,840		11,526,085	11,526,085	0%	1%
2009	Sand		11,021,885		11,611,779	11,611,779	0%	-5%
	Slimes (w/o Vale)		2,691,285		2,101,391	2,101,391	0%	28%
	Total		13,713,170		13,713,170	13,713,170	0%	0%
2010	Sand		12,411,142		13,768,530	13,768,530	0%	-10%
	Slimes (w/o Vale)		3,947,447		2,590,059	2,590,059	0%	52%
	Total		16,358,589		16,358,589	16,358,589	0%	0%
2011	Sand		11,133,575		13,082,527	13,082,527	0%	-15%
	Slimes (w/o Vale)		4,522,911		2,642,605	2,642,605	0%	71%
	Total		15,656,486		15,725,132	15,725,132	0%	0%
2012	Sand		12,195,013		13,369,510	13,369,510	0%	-9%
	Slimes (w/o Vale)		4,499,651		3,325,154	3,325,154	0%	35%
	Total		16,694,664		16,694,664	16,694,664	0%	0%
2013	Sand		12,627,852		13,117,521	13,117,521	0%	-4%
	Slimes (w/o Vale)		3,914,960		3,425,291	3,425,291	0%	14%
	Total		16,542,812		16,542,812	16,542,812	0%	0%
2014	Sand	16,381,397	16,381,397	0%	17,002,354	17,002,354	0%	-4%
	Slimes (w/o Vale)	5,098,153	5,098,153	0%	4,536,301	4,536,301	0%	12%
	Total	21,479,550	21,479,550	0%	21,538,655	21,538,655	0%	0%
	Percent Sand	76%	76%	N/A	79%	79%	N/A	-3%
	Percent Slimes	24%	24%	N/A	21%	21%	N/A	13%
2015	Sand	17,493,753	17,109,178	2%	17,928,346	17,928,346	0%	-5%
	Slimes (w/o Vale)	4,959,593	4,864,445	2%	4,525,000	4,525,000	0%	8%
	Total	22,453,346	21,973,623	2%	22,453,346	22,453,346	0%	-2%
	Percent Sand	78%	78%	N/A	80%	80%	N/A	-2%
	Percent Slimes	22%	22%	N/A	20%	20%	N/A	10%

1. Relative percent difference shown is between data sets.
2. Sand cells shown in grey. Slimes cells shown in orange.
3. w/o = without

Table B7-4 Comparison of annual tailings production between data sets

Year	Data Set Number[1]	Samarco			Vale	Total		Percent Difference Relative to Data Set #2		
		Sand	Slimes	Sopão	Slimes	Without Vale Slimes	With Vale Slimes	Sand	Slimes Without Vale	Total[2]
2008	2	9,990,617	1,535,468	N/A	N/A	11,526,085	N/A	-	-	-
	3	9,990,617	1,535,468	N/A	326,068	11,526,085	11,852,153	0%	0%	0%
2009	2	11,611,779	2,101,391	N/A	N/A	13,713,170	N/A	-	-	-
	3	11,611,779	2,101,391	N/A	1,416,776	13,713,170	15,129,946	0%	0%	0%
2010	2	13,768,530	2,590,059	N/A	N/A	16,358,589	N/A	-	-	-
	3	13,768,530	2,590,059	N/A	1,144,967	16,358,589	17,503,556	0%	0%	0%
2011	2	13,082,527	2,642,605	N/A	N/A	15,725,132	N/A	-	-	-
	3	13,082,527	2,642,605	N/A	1,267,254	15,725,132	16,992,386	0%	0%	0%
2012	2	13,369,510	3,325,154	N/A	N/A	16,694,664	N/A	-	-	-
	3	13,369,510	3,325,154	N/A	1,188,023	16,694,664	17,882,687	0%	0%	0%
2013	2	13,117,521	3,425,291	N/A	N/A	16,542,812	N/A	-	-	-
	3	13,117,521	3,425,291	N/A	1,029,042	16,542,812	17,571,854	0%	0%	0%
2014	1	16,381,397	5,098,153	498,592	1,005,581	21,978,142	22,983,723	-4%	12%	2%
	3	17,002,354	4,536,301	N/A	1,005,581	21,538,655	22,544,236	0%	0%	0%
	2	17,002,354	4,536,301	N/A	N/A	21,538,655	N/A	-	-	-
2015	1	17,493,753	4,959,593	508,199	995,671	22,961,545	23,957,216	-2%	10%	2%
	3	17,928,346	4,525,000	N/A	995,669	22,453,346	23,449,015	0%	0%	0%
	2	17,928,346	4,525,000	N/A	N/A	22,453,346	N/A	-	-	-

1. The values from Samarco's processing department in Data Set 3 are presented in this table.
2. Data Set 2 is selected as the primary source of tailings production data and carried forward for subsequent analyses.
3. Percent difference in total tailings is calculated from the total tailings including sopão. Without sopão in 2014 and 2015, the percent difference for total tailings production is 0%.

B7.4.3 Consolidation of Records

The differences noted in Section B7.4.2.2 are small enough to not affect the overall trend in production rate. However, for the purpose of the slimes mass balance calculation, a daily production record was required. Therefore, a combined tailings production record was produced using the following:

- daily sand production from Samarco's processing department in Data Set 2;
- daily slimes production from Samarco's processing department in Data Set 2; and
- annual slimes production from Vale converted to daily assuming a constant rate from Samarco's geotechnical department in Data Set 3.

As noted in Section B7.4.2.2, sopão records were only available from January, 2014 to October, 2015. As the amount is negligible (~2%) compared to the total amount of tailings produced, these quantities were not included in the consolidated tailings production record.

The annual tailings production from the data sources listed above are summarized in Table B7-5.

The consolidated monthly production of tailings is shown on Figure B7-1 and Figure B7-2. Samarco assumed a constant solids percentage and void ratio to estimate the volume of tailings produced from the weight of tailings recorded. These values are given in Table B7-1. Using the same assumptions, the monthly incremental and cumulative tailings production over time in units of volume are shown on Figure B7-3 and Figure B7-4.

Table B7-5 Annual tailings production over the life of the Fundão facility

Year	Sand	Slimes (Samarco)	Slimes (Vale)	Without Vale Slimes			With Vale Slimes			Percentage of Vale Slimes	
				Total Tailings	Percent Sand	Percent Slimes	Total Tailings	Percent Sand	Percent Slimes	In Total Slimes	In Total Tailings
	(tms)[1]	(tms)[1]	(tms)[1]	(tms)[1]	(%)	(%)	(tms)[1]	(%)	(%)	(%)	(%)
2008	9,990,617	1,535,468	326,068	11,526,085	87%	13%	11,852,153	84%	16%	18%	3%
2009	11,611,779	2,101,391	1,416,776	13,713,170	85%	15%	15,129,946	77%	23%	40%	9%
2010	13,768,530	2,590,059	1,144,967	16,358,589	84%	16%	17,503,556	79%	21%	31%	7%
2011	13,082,527	2,642,605	1,267,254	15,725,132	83%	17%	16,992,386	77%	23%	32%	7%
2012	13,369,510	3,325,154	1,188,023	16,694,664	80%	20%	17,882,687	75%	25%	26%	7%
2013	13,117,521	3,425,291	1,029,042	16,542,812	79%	21%	17,571,854	75%	25%	23%	6%
2014	17,002,354	4,536,301	1,005,581	21,538,655	79%	21%	22,544,236	75%	25%	18%	4%
2015[2]	17,928,346	4,525,000	995,669	22,453,346	80%	20%	23,449,015	76%	24%	18%	4%

1. tms = toneladas métricas secas = dry metric tonnes.
2. 2015 records only up to November 5, 2015.

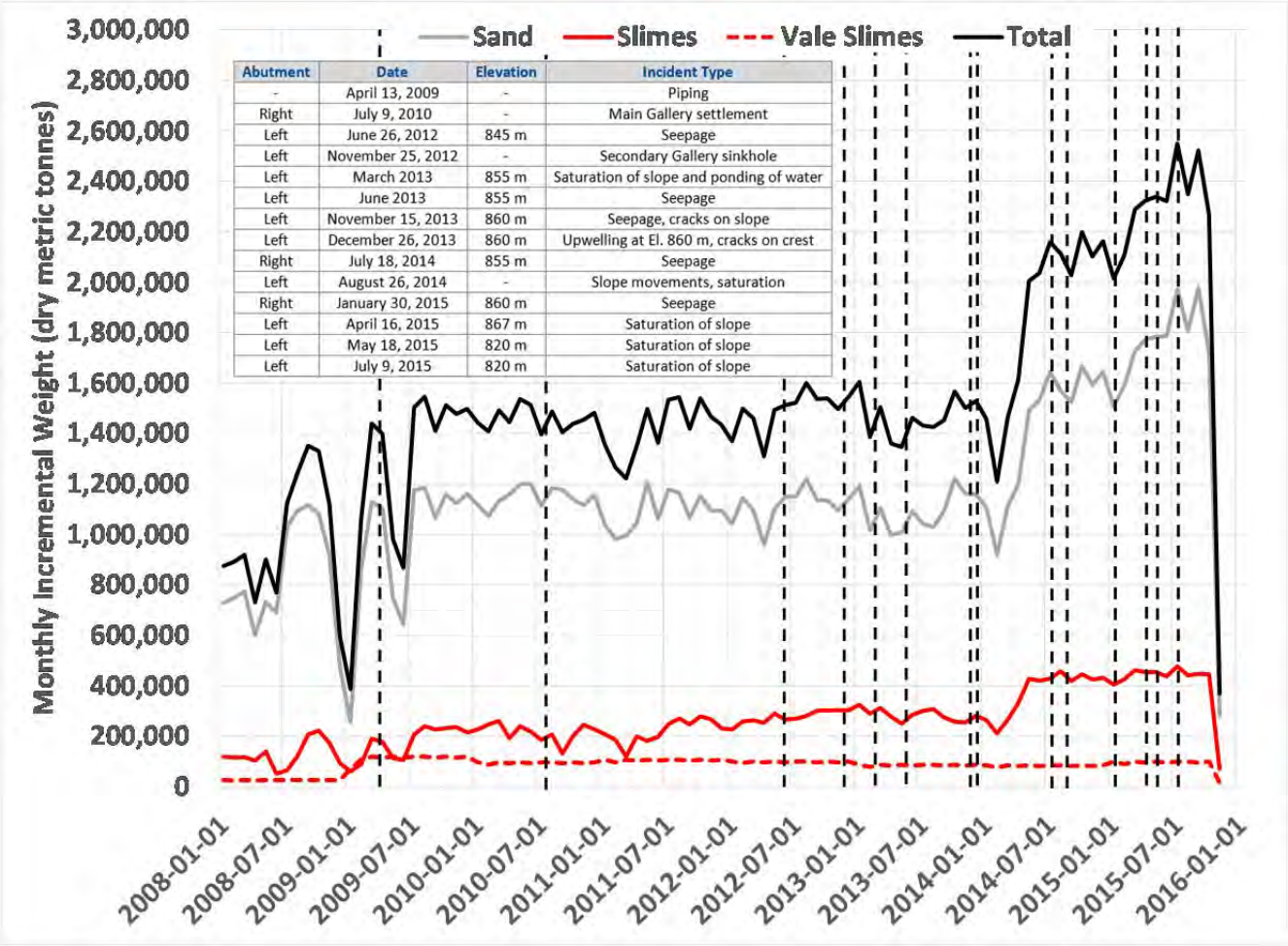

Abutment	Date	Elevation	Incident Type
-	April 13, 2009	-	Piping
Right	July 9, 2010	-	Main Gallery settlement
Left	June 26, 2012	845 m	Seepage
Left	November 25, 2012	-	Secondary Gallery sinkhole
Left	March 2013	855 m	Saturation of slope and ponding of water
Left	June 2013	855 m	Seepage
Left	November 15, 2013	860 m	Seepage, cracks on slope
Left	December 26, 2013	860 m	Upwelling at El. 860 m, cracks on crest
Right	July 18, 2014	855 m	Seepage
Left	August 26, 2014	-	Slope movements, saturation
Right	January 30, 2015	860 m	Seepage
Left	April 16, 2015	867 m	Saturation of slope
Left	May 18, 2015	820 m	Saturation of slope
Left	July 9, 2015	820 m	Saturation of slope

Figure B7-1 Monthly incremental tailings production over time by weight

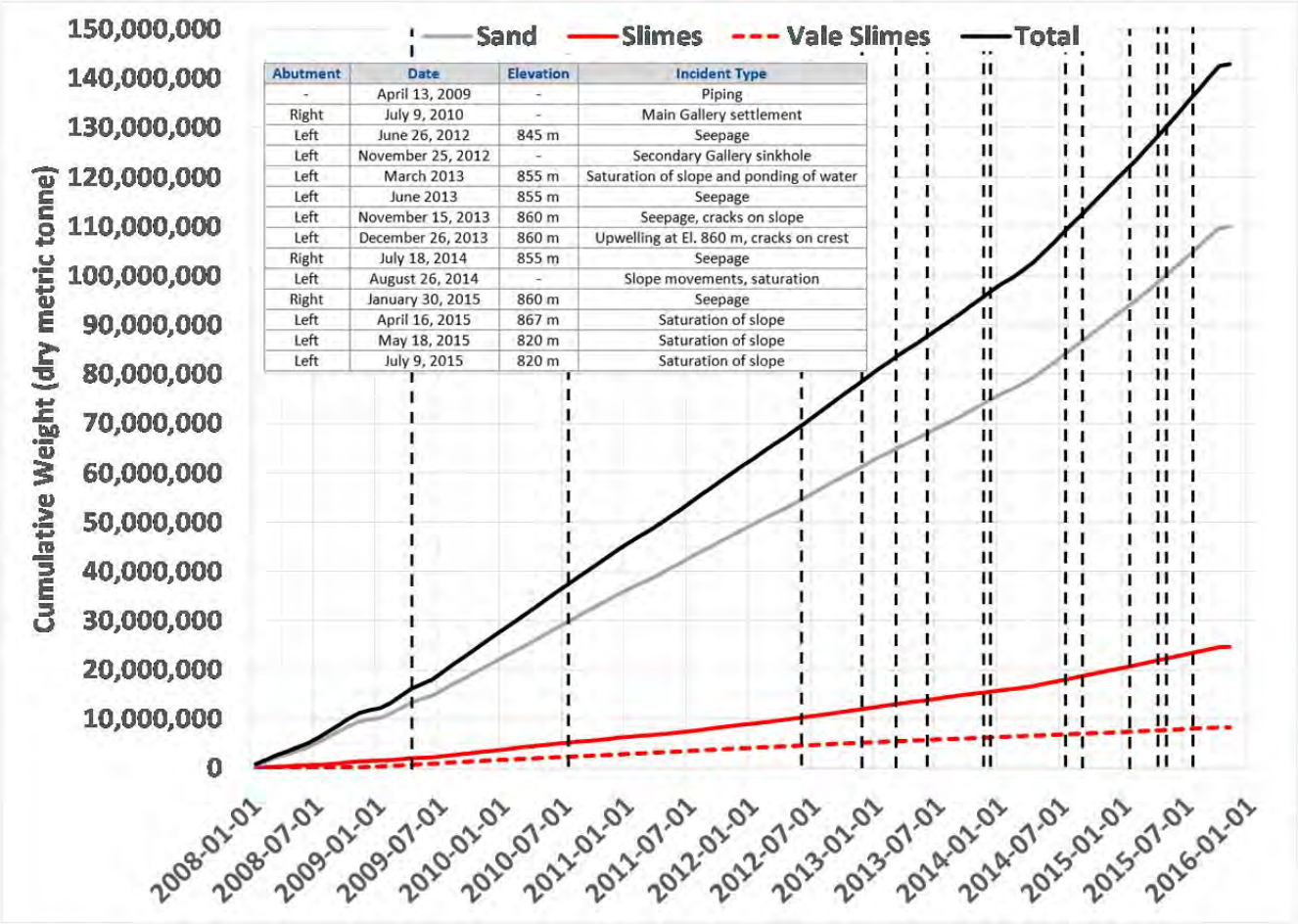

Abutment	Date	Elevation	Incident Type
-	April 13, 2009	-	Piping
Right	July 9, 2010	-	Main Gallery settlement
Left	June 26, 2012	845 m	Seepage
Left	November 25, 2012	-	Secondary Gallery sinkhole
Left	March 2013	855 m	Saturation of slope and ponding of water
Left	June 2013	855 m	Seepage
Left	November 15, 2013	860 m	Seepage, cracks on slope
Left	December 26, 2013	860 m	Upwelling at El. 860 m, cracks on crest
Right	July 18, 2014	855 m	Seepage
Left	August 26, 2014	-	Slope movements, saturation
Right	January 30, 2015	860 m	Seepage
Left	April 16, 2015	867 m	Saturation of slope
Left	May 18, 2015	820 m	Saturation of slope
Left	July 9, 2015	820 m	Saturation of slope

Figure B7-2 Cumulative tailings production over time by weight

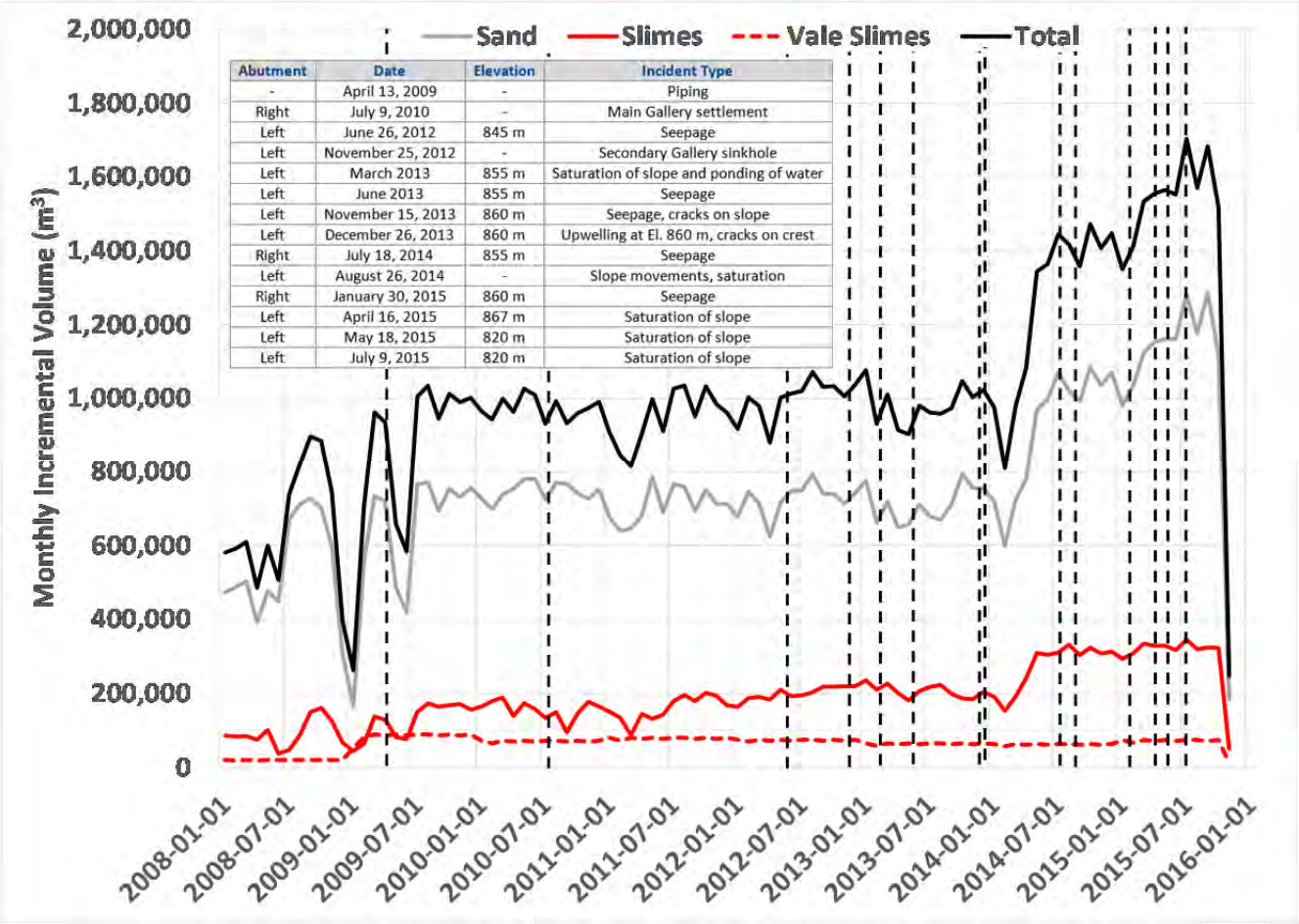

Abutment	Date	Elevation	Incident Type
-	April 13, 2009	-	Piping
Right	July 9, 2010	-	Main Gallery settlement
Left	June 26, 2012	845 m	Seepage
Left	November 25, 2012	-	Secondary Gallery sinkhole
Left	March 2013	855 m	Saturation of slope and ponding of water
Left	June 2013	855 m	Seepage
Left	November 15, 2013	860 m	Seepage, cracks on slope
Left	December 26, 2013	860 m	Upwelling at El. 860 m, cracks on crest
Right	July 18, 2014	855 m	Seepage
Left	August 26, 2014	-	Slope movements, saturation
Right	January 30, 2015	860 m	Seepage
Left	April 16, 2015	867 m	Saturation of slope
Left	May 18, 2015	820 m	Saturation of slope
Left	July 9, 2015	820 m	Saturation of slope

Figure B7-3 Monthly incremental tailings production over time by volume

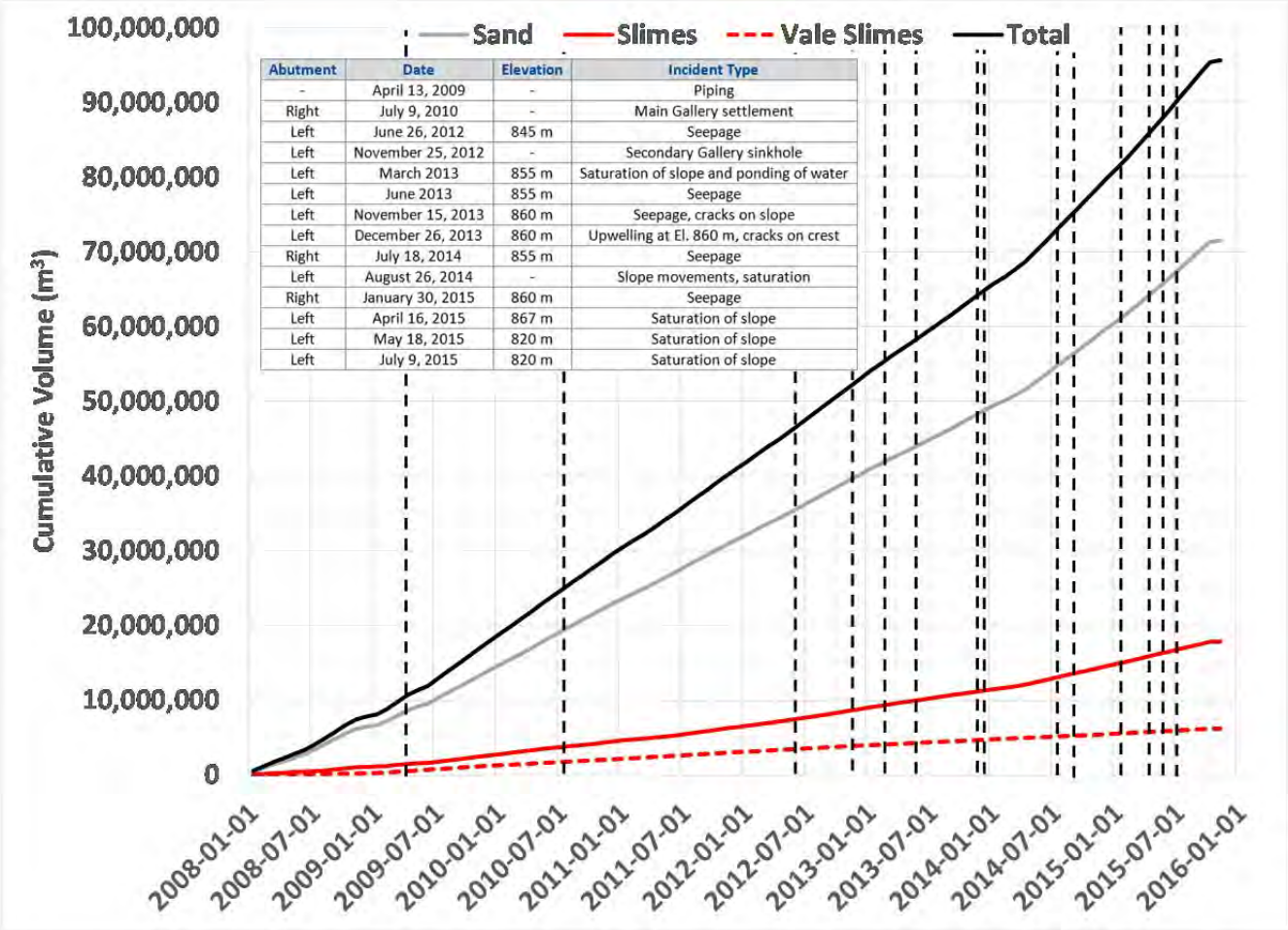

Abutment	Date	Elevation	Incident Type
-	April 13, 2009	-	Piping
Right	July 9, 2010	-	Main Gallery settlement
Left	June 26, 2012	845 m	Seepage
Left	November 25, 2012	-	Secondary Gallery sinkhole
Left	March 2013	855 m	Saturation of slope and ponding of water
Left	June 2013	855 m	Seepage
Left	November 15, 2013	860 m	Seepage, cracks on slope
Left	December 26, 2013	860 m	Upwelling at El. 860 m, cracks on crest
Right	July 18, 2014	855 m	Seepage
Left	August 26, 2014	-	Slope movements, saturation
Right	January 30, 2015	860 m	Seepage
Left	April 16, 2015	867 m	Saturation of slope
Left	May 18, 2015	820 m	Saturation of slope
Left	July 9, 2015	820 m	Saturation of slope

Figure B7-4 Cumulative tailings production over time by volume

B7.5 Spigot Locations Prior to Failure

It was only necessary to understand spigot locations in the last two months of deposition because the seepage model requires finer inputs for areas of recharge (for example, saturated beach in areas of active deposition). Therefore, a review of qualitative descriptions and site photos in weekly reports was undertaken in an effort to narrow the spigot locations down to weekly intervals, where possible.

Samarco did not track the location of spigots over time for sand and slimes deposition. However, the alignment of tailings pipelines from the plants on site, as well as from the neighboring Vale Alegria Mine, remained largely unchanged over time. The alignment at the end of 2014 is shown in a Samarco drawing in Attachment B7. The spigot locations on November 5, 2015 as noted by Samarco are also shown in Attachment B7 and confirm observations based on the October 27, 2015 aerial image.

Figure B7-5 to Figure B7-7 illustrate the location of spigots in the two months leading up to failure. Spigot locations the week of September 20, 2015 and September 27, 2015 are unknown.

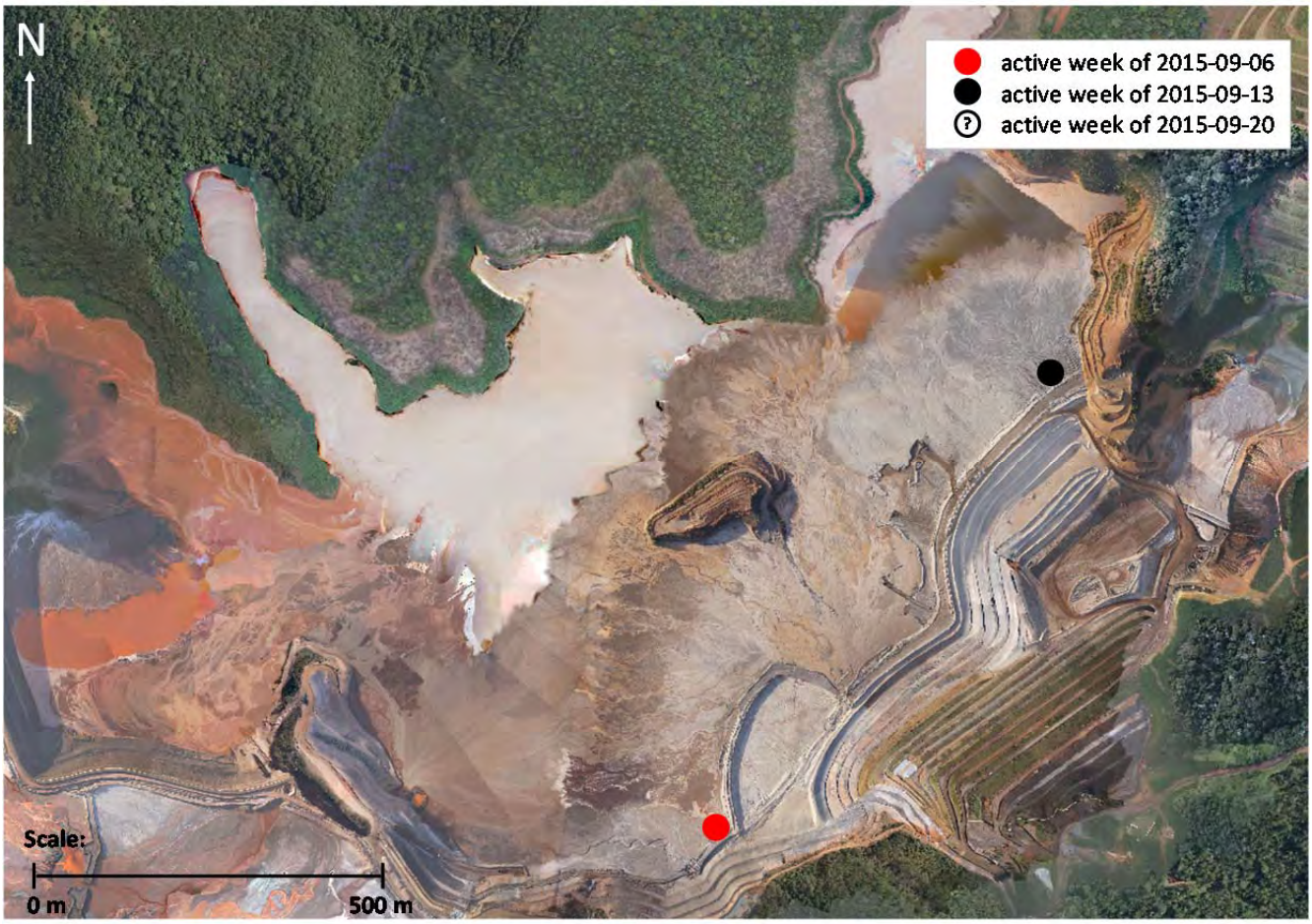

Figure B7-5 Spigot locations from September 6, 2015 to September 26, 2015, shown on the August 24, 2015 Samarco aerial image

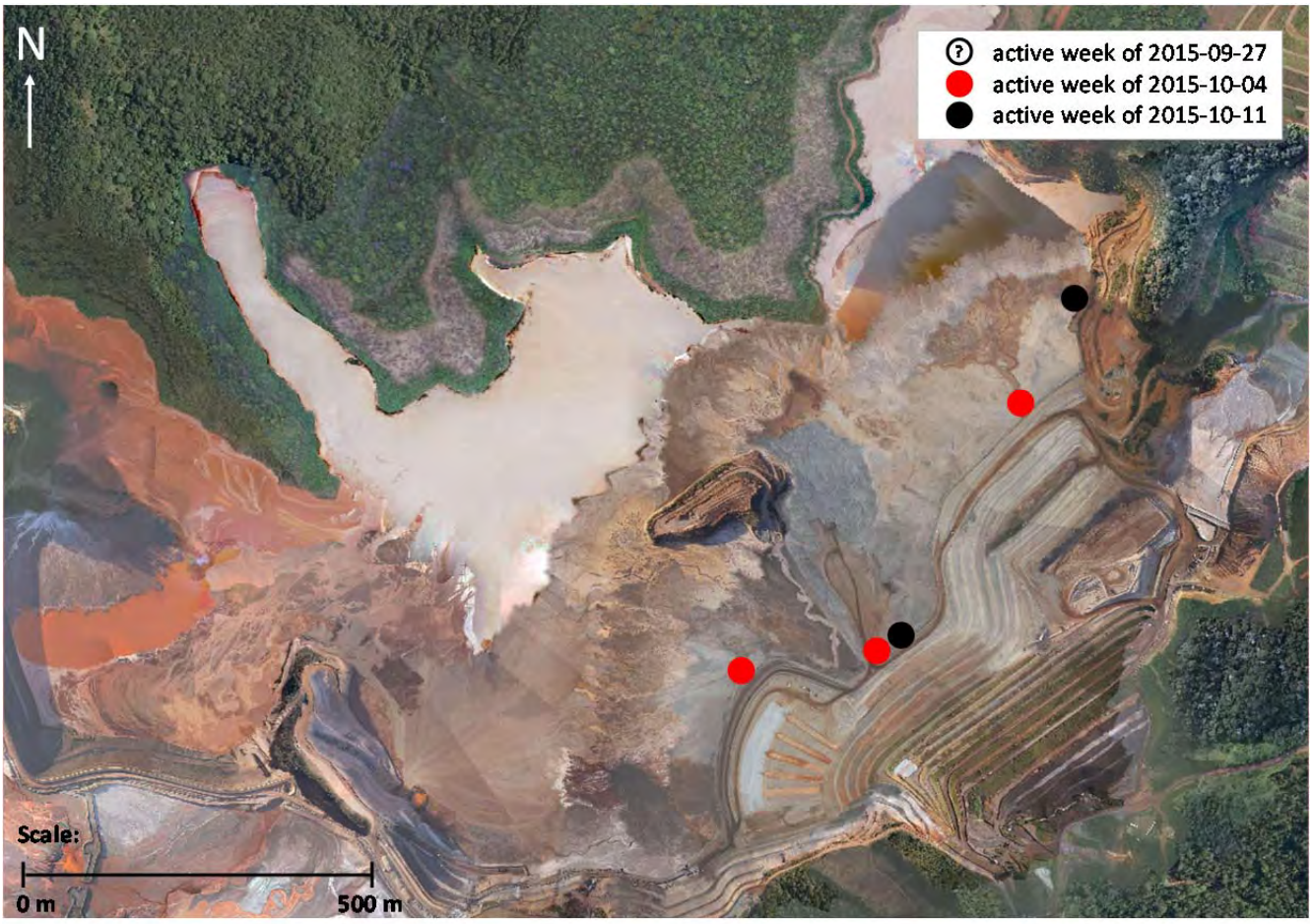

Figure B7-6 Spigot locations from September 27, 2015 to October 17, 2015, shown on the October 1, 2015 Samarco aerial image

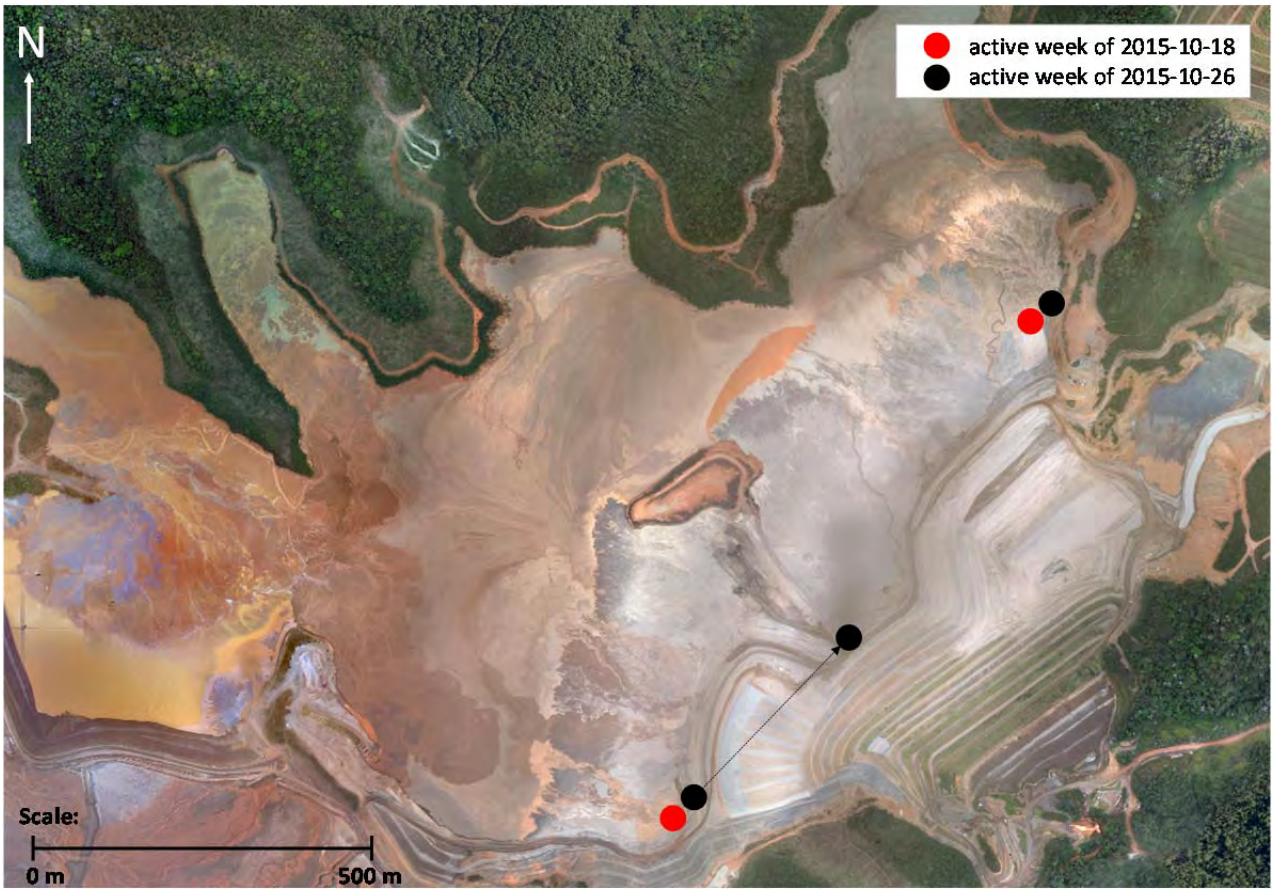

Figure B7-7 Spigot locations from October 18, 2015 to October 31, 2015, shown on the October 27, 2015 Samarco aerial image

B7.6 Summary of Findings

The key outputs from this exercise are summarized as follows:

- Determine whether there was a correlation between changes in tailings production and incidents at Fundão:
  - With the exception of the piping incident in April, 2009, the majority of the noted seepage and cracking incidents appear to occur following an increase in production in January, 2014.
- Check the amount of sand and slimes produced against the design criteria of 70% sand, 30% slimes:
  - Without accounting for slimes from Vale, the percentage of sand produced, and averaged from 2008 to 2015 is approximately 82%. Slimes occupy 18% of total production.
  - Accounting for slimes from Vale, the percentage of sand produced, and averaged from 2008 to 2015 is approximately 77%. Slimes occupy 23% of total production.

- Estimate the amount of slimes produced and deposited in Fundão between the key slimes elevations of El. 840 m and El. 850 m as described in Section B6.6:
  - From January 21, 2012 to July 13, 2012, 2,109,939 dry metric tonnes of slimes were produced and assumed to be deposited entirely in Fundão. This includes the contribution from Vale.
- Quantify the contribution of slimes from the neighboring Vale Alegria Mine to Fundão:
  - The slimes from Vale, averaged from 2008 to 2015, was approximately 25% of total slimes production. This accounts for approximately 6% of total (sand and slimes) tailings production.
  - From 2009 to 2011, Vale slimes were more than 30% of total slimes production.
- Track the location of spigots at Dike 1 in the months leading up to failure to delineate zones of recharge for input to seepage modeling:
  - Spigotting of sand tailings took place along the entire Dike 1 crest from the left abutment to the right abutment in the two months leading up to failure.

B8 INCIDENT HISTORY

B8.1 General

The integration of information from reports with GIS made it possible to provide a spatial element in addition to the chronological element. Table B8-1 summarizes the noted incidents at Fundão. Details for each incident along with the evolution of the Left Abutment Rockfill Trench are documented in fact sheets in Attachment B8.

Table B8-1 Summary of incidents at Fundão

Abutment	Date	Elevation	Incident Type
-	April 13, 2009	-	Piping
Right	July 9, 2010	-	Main Gallery settlement
Left	June 26, 2012	845 m	Seepage
Left	November 25, 2012	-	Secondary Gallery sinkhole
Left	March 2013	855 m	Saturation of slope and ponding of water
Left	June 2013	855 m	Seepage
Left	November 15, 2013	860 m	Seepage, cracks on slope
Left	December 26, 2013	860 m	Upwelling at El. 860 m, cracks on crest
Right	July 18, 2014	855 m	Seepage
Left	August 26, 2014	-	Slope movements, saturation
Right	January 30, 2015	860 m	Seepage
Left	April 16, 2015	867 m	Saturation of slope
Left	May 18, 2015	820 m	Saturation of slope
Left	July 9, 2015	820 m	Saturation of slope

Over the life of the Fundão facility, there were seven seepage incidents noted at the left abutment. Of the seven, four occurred at the setback at El. 855 m and above. The right abutment experienced two seepage incidents between mid-2014 and the beginning of 2015.

B8.2 August, 2014 Slope Movements

B8.2.1 General

Data was assembled for the August, 2014 slope movements at the left abutment setback. This was necessary to provide inputs to the stability and deformation models.

During this event, the left abutment setback cracked and displaced. As described in Attachment B8, the observations included:

- cracks at the crest, upstream tailings beach and downstream slope of the setback;
- uplift at the toe of the slope at the El. 865 m bench;
- saturation at the toe of the El. 865 m bench; and
- upwelling with artesian flow at toe of Dike 1.

B8.2.2 Data Sources

The following items were assembled as listed in Table B8-2.

Table B8-2 Data sources and processing for August, 2014 incident

Item	Purpose	Data Source	Methodology
Left setback geometry	Input to stability and deformation model	August 29, 2014 Samarco topography	Imported and processed in Civil 3D
Reinforcement Berm geometry	Input to stability and deformation model	September 26, 2014 Samarco topography	Imported and processed in Civil 3D
Location of cracks	Deformation model validation	ERG survey (G001609-K-000058_R-35) August 29, 2014 Samarco survey (G001609-K-100004)	Imported to Global Mapper and intersection with section lines plotted
Phreatic surface on August 26, 2014	Input to stability model	Left abutment piezometer records starting at different times in September 2014	Back-extrapolate piezometer readings based on rate of rise correlating to the reservoir rate of rise (see Figure B8-1). Upwelling was noted at the toe of the slope, so the piezometric surface was adjusted to reflect this field observation.
Slimes extent	Input to stability and deformation model	Slimes mapping, see Section B6.3	Imported and processed in Civil 3D
Boundary between isolated, interbedded and predominantly slimes	Input to stability and deformation model	Slimes mass balance, see Section B6.6	Imported and processed in Civil 3D

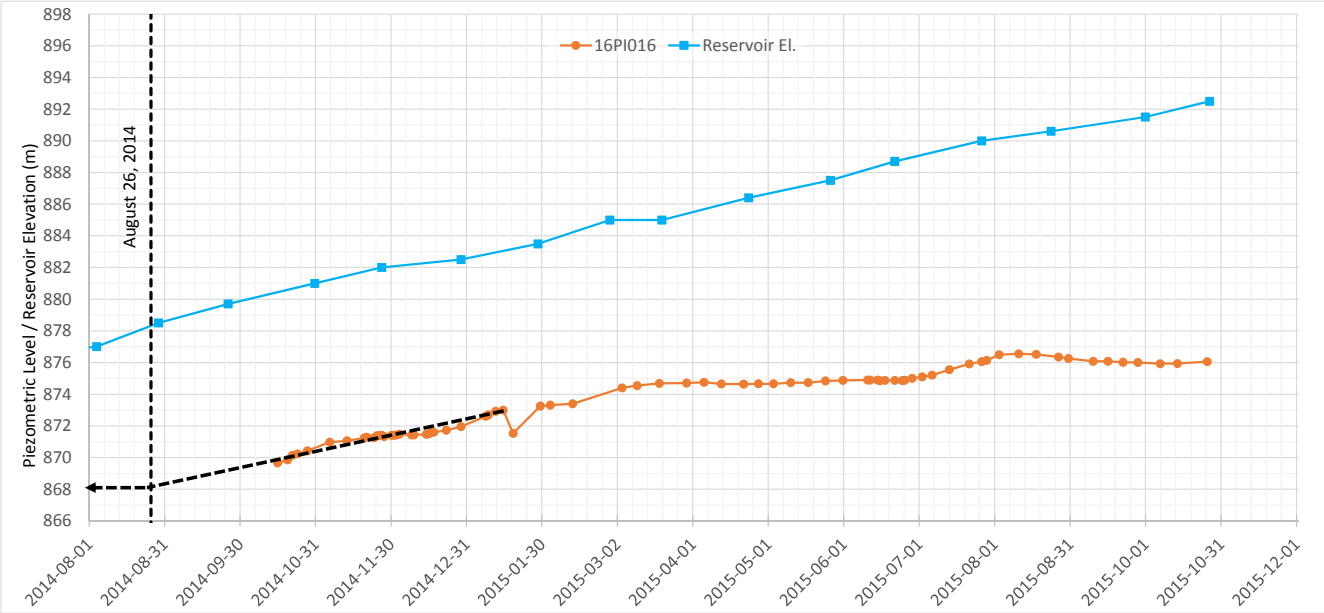

Figure B8-1 Example of back-extrapolation of piezometric record to August 26, 2014 (16PI016)

B8.2.3 Summary of Findings

The left abutment setback geometry, the back extrapolated piezometric surface and the location of cracks are shown on Figure B8-2.

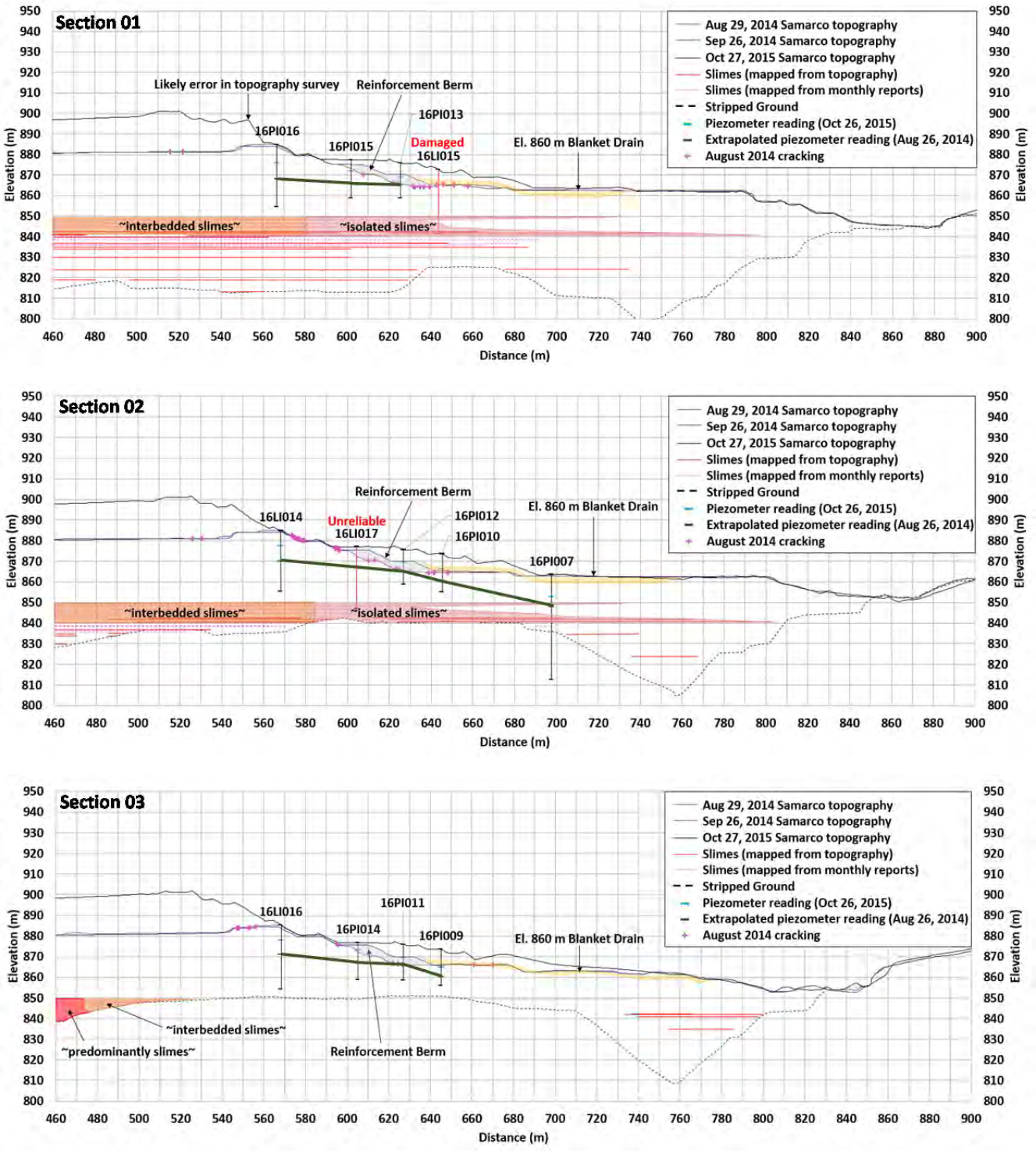

Figure B8-2 August, 2014 data compilation for Section 01, 02, 03

B9 GERMANO SAND BOIL INVESTIGATION

B9.1 General

The Panel completed a review of aerial images from the Germano facility in order to determine whether any sand boils could be linked to the seismic activity on November 5, 2015 that preceded the failure by about two hours.

Sand boils have formed in Germano routinely due to past construction activities. For instance, there was evidence of sand boils in the Germano area at the location of the 2008 test fill[4]. Features that are visible in post-failure photos may or may not be related to seismic activity.

Drone photos from Germano were compiled post-failure by a survey company at the request of the Panel. The surveys were completed on November 17, 2015 and December 6, 2015. Pre-failure photos from Germano were from the most recent drone survey prior to the failure, taken on July 4, 2015 and July 17, 2015. Further details on aerial photo sources are included in Appendix A.

Sand boils are circular in shape and have a raised or slightly conical appearance. Photos from the pre- and post-failure drone programs were reviewed for these key features.

The drone height is not consistent through all of the photos so it was not possible to accurately judge the scale of the features in many images. Many photos overlap and it was often possible to identify the same feature in multiple photos.

B9.2 Post-Failure Photos

Eighty-two “potential” sand boil locations were flagged in the Germano area from the post-failure photos. The following six figures show examples of these features. All coordinates are in UTM Zone 23K Córrego Alegre.

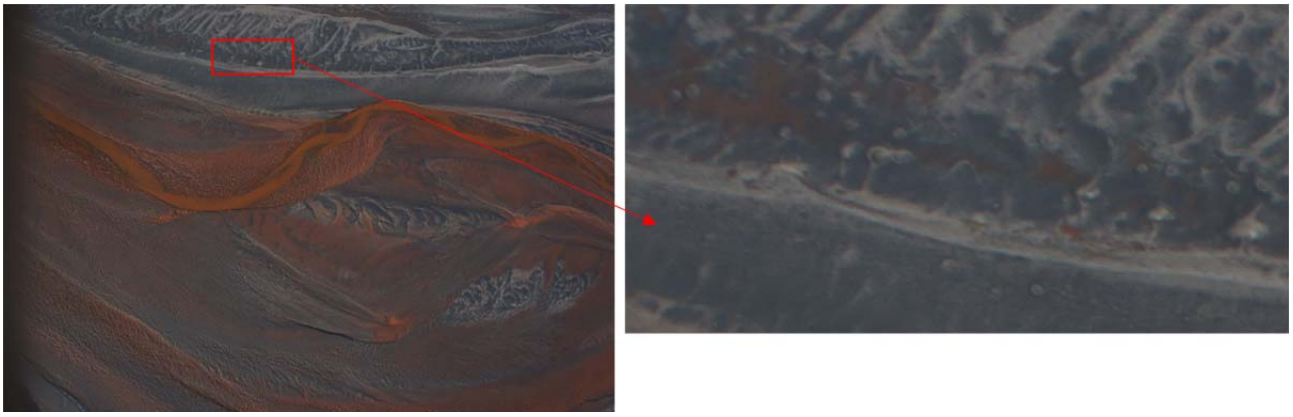

Figure B9-1 Example of features at Germano (location: 658738 m E, 7764506 m N)

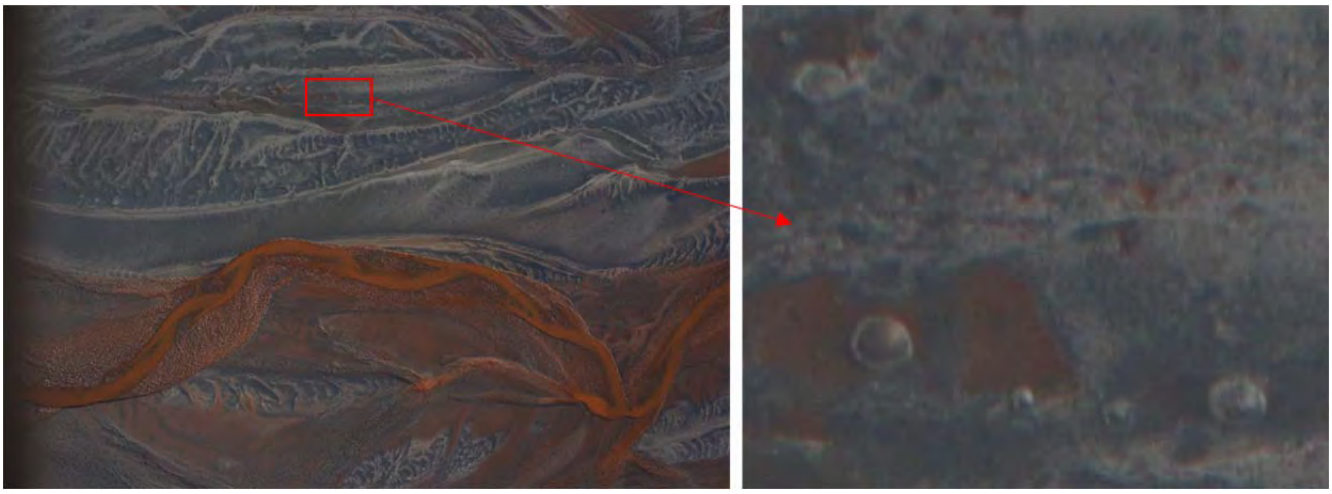

Figure B9-2 Example of features at Germano (location: 658751 m E, 7764509 m N)

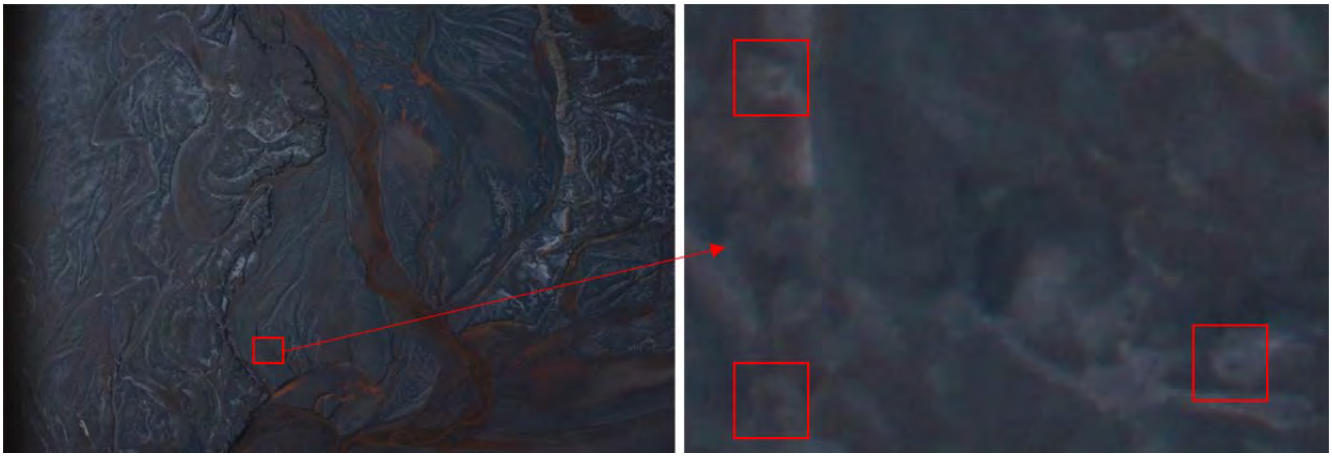

Figure B9-3 Example of features at Germano (location: 658613 m E, 7764594 m N)

Figure B9-4 Example of features at Germano (location: 659115 m E, 7764741 m N)

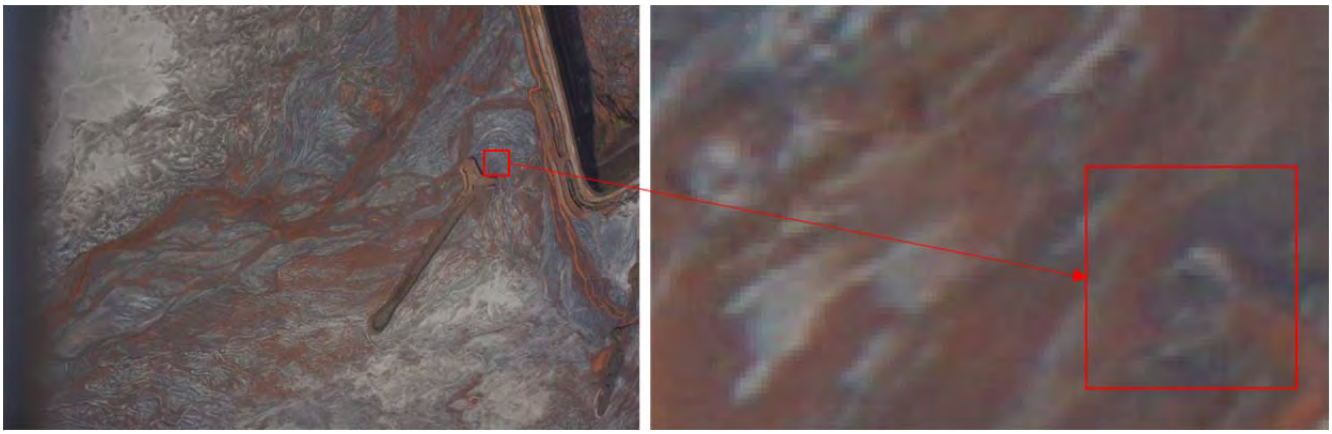

Figure B9-5 Example of features at Germano (location: 659232 m E, 7764572 m N)

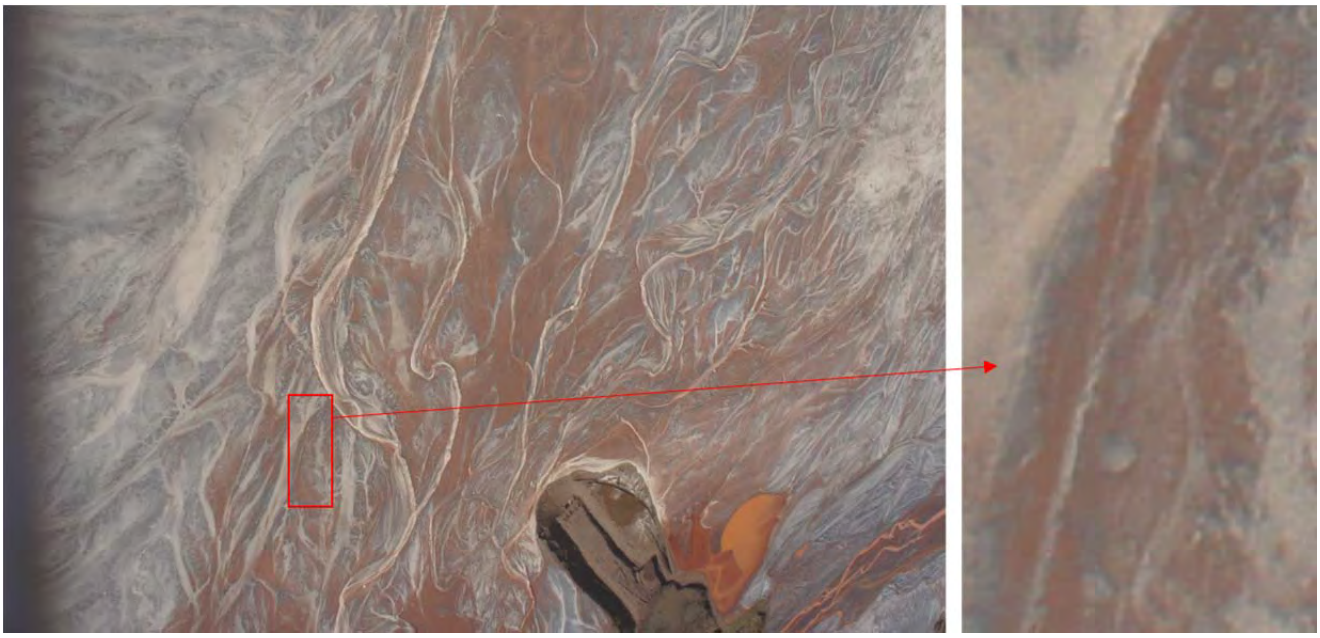

Figure B9-6 Example of features at Germano (location: 659381 m E, 7764218 m N)

The approximate ground locations of the mapped features are shown in yellow on Figure B9-7. Lineations and clusters of features were found at several locations (see Figure B9-1). As shown on Figure B9-7, the majority of features were mapped in the Auxiliary and Sela basins with some upstream of the Tulipa Dike.

The October 27, 2015 and July 16, 2015 aerial images show tailings deposition at the northwest end of the Auxiliary basin. Local erosion has formed a meandering channel that flows from the pipeline outlet across the Auxiliary basin to a breach in the Auxiliary Dike and towards the Sela Dike. As shown on Figure B9-7, the majority of the mapped features in Germano are localized around the meandering channel and near the small pond bordering the Sela Dike (see example feature on Figure B9-4). These areas have the highest degree of saturation from the tailings stream which demonstrates a correlation between formation of the features and areas of active tailings deposition.

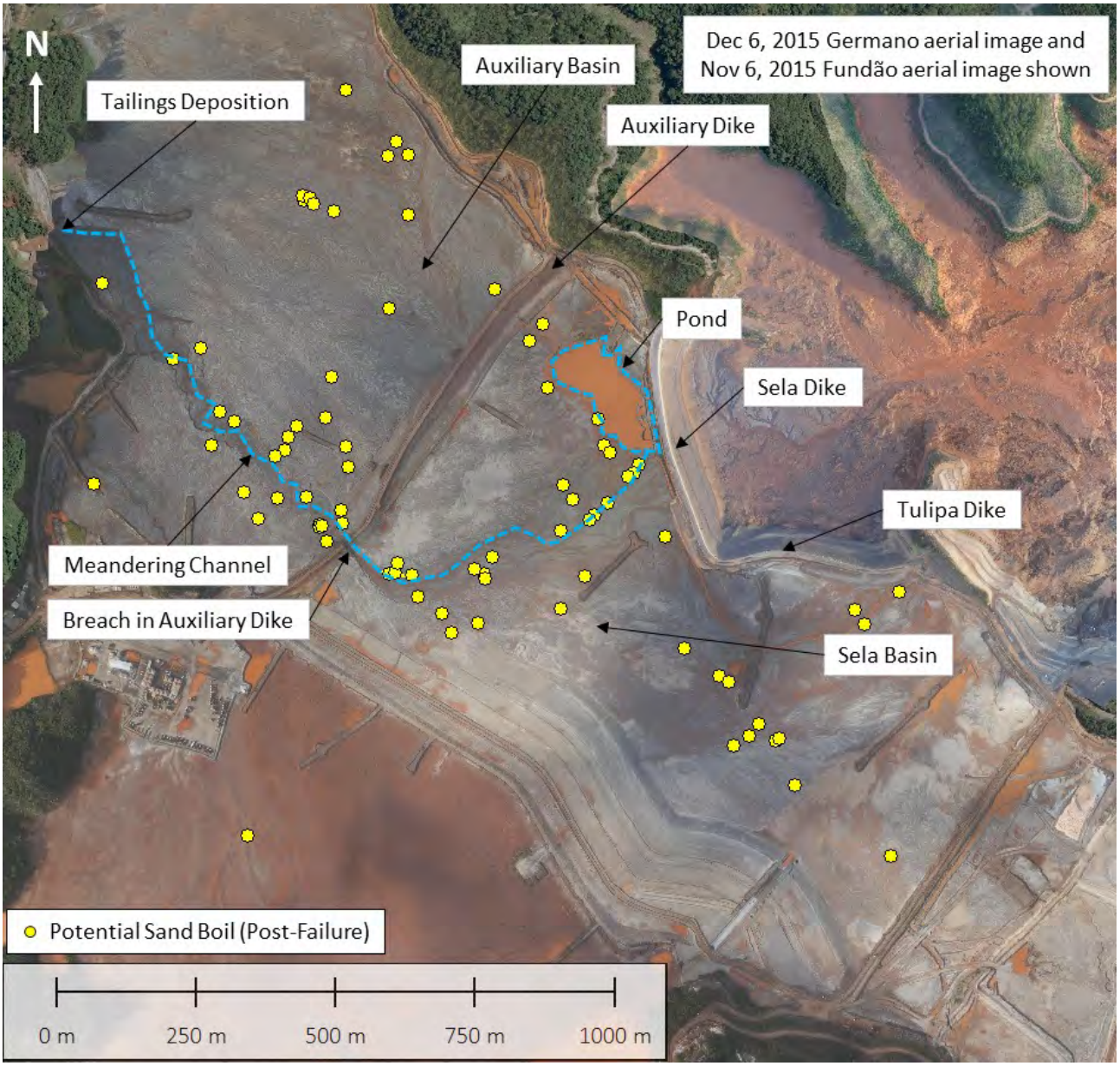

Figure B9-7 Location of features identified in the Germano facility

B9.3 Pre-Failure Photos

Drone photos from the July 4 and 17, 2015 surveys of Germano were reviewed to determine whether the features similar to the prototype sand boil were present before the seismicity on November 5, 2015. 31 photos were flagged as showing similar features to the prototype sand boil. The following two figures show example features from the pre-failure photos. Coordinates are in UTM Zone 23K Córrego Alegre.

Figure B9-8 Example of features at Germano (location: 658434 m E, 7764801 m N)

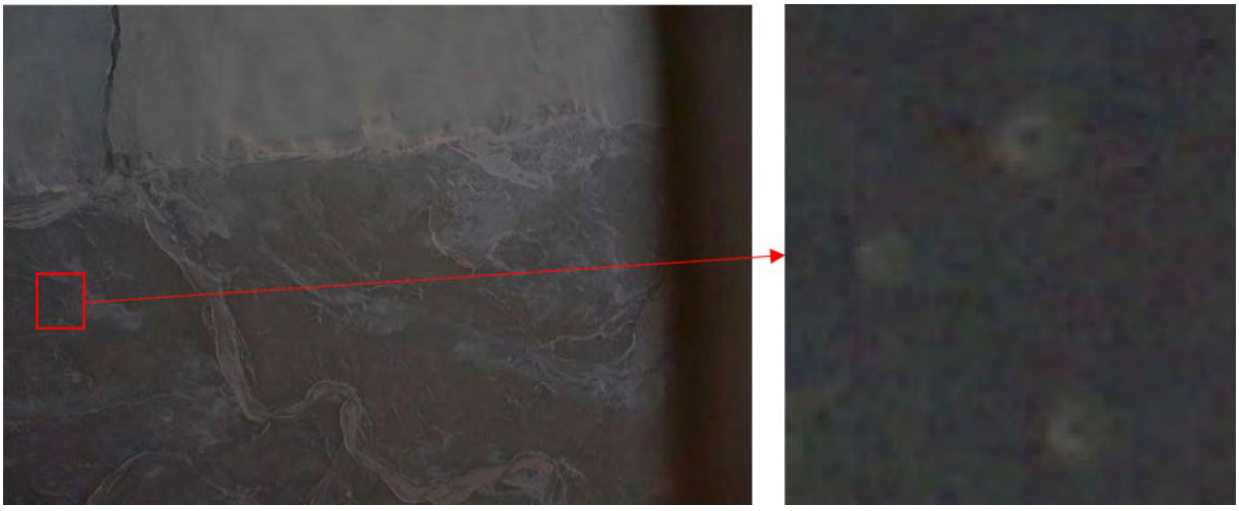

Figure B9-9 Example of features at Germano (location: 658859 m E, 7764315 m N)

The locations of these features were mapped to compare to those mapped using the post-failure photos. The results are shown on Figure B9-10.

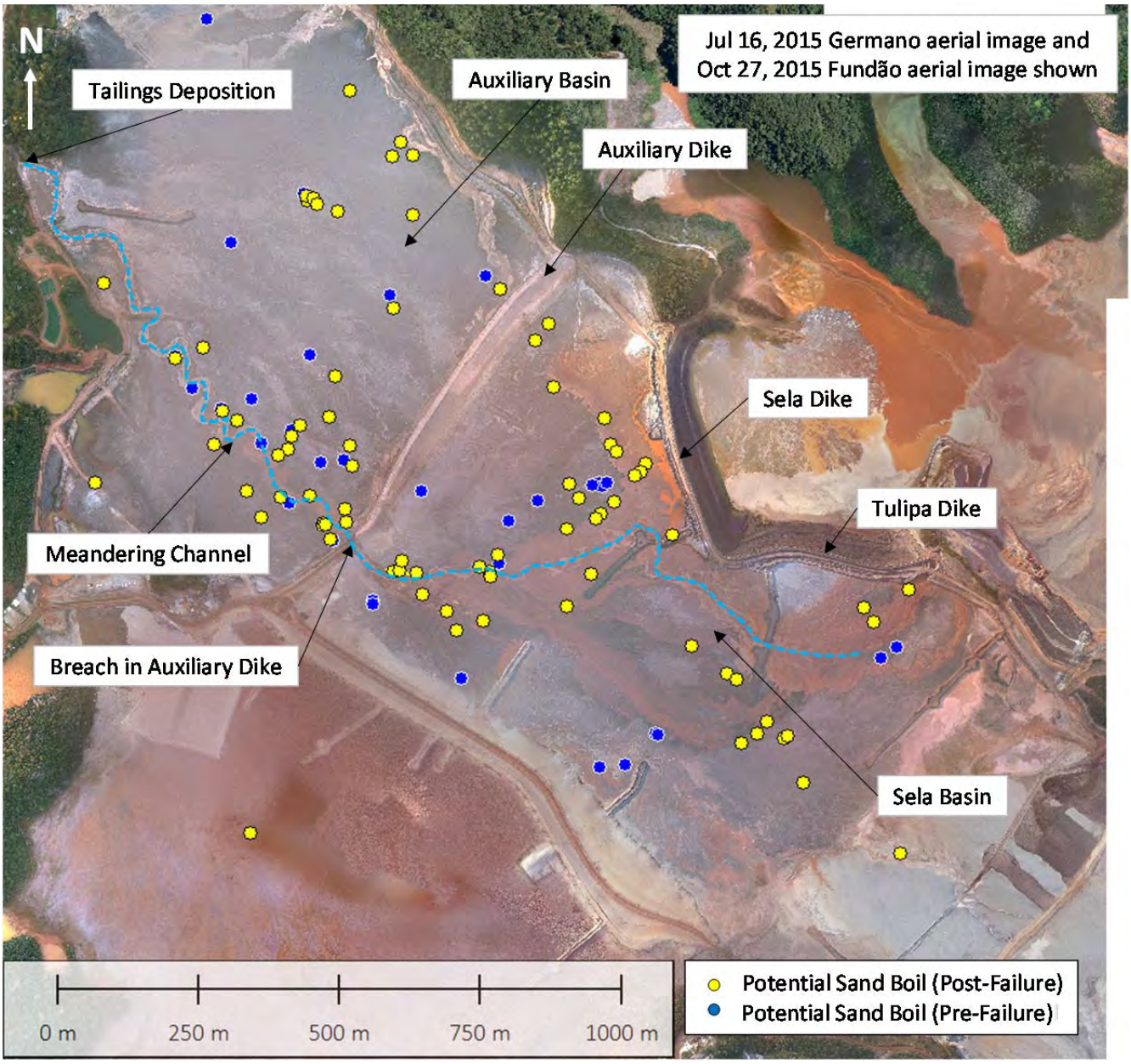

Figure B9-10 Location of features mapped pre- and post-failure

It is unlikely that any of the features seen in the pre- and post-failure images are the same given that this was an active tailings deposition area during the fall of 2015. However, Figure B9-10 shows that the pre-failure features also plot in the locally saturated areas.

B9.4 Summary of Findings

As described above, circular features were identified at a number of locations in Germano both pre- and post-failure. Due to the limitations of the aerial photo review, it is not possible to determine whether the post-failure images show sand boils or some other type of depositional feature. The similar appearance of the pre- and post-failure features gives an inconclusive result. Additionally, the drone operator who had been flying the Germano and Fundão sites for several years stated in an interview that he had not seen any sand boils at Germano after the earthquake of November 5, 2015.

ATTACHMENT B1

Structures and Dike Components

Appendix B: Attachment B1
Structures and Dike Components

TABLE OF CONTENTS

List of Figures

B.B1-1 OVERVIEW

The structures and dike components at Fundão have been classified as follows:

- Dikes (Figure B.B1-1);
- Drainage features (Figure B.B1-2);
- Decant structures (Figure B.B1-3); and
- Stability berms (Figure B.B1-4).

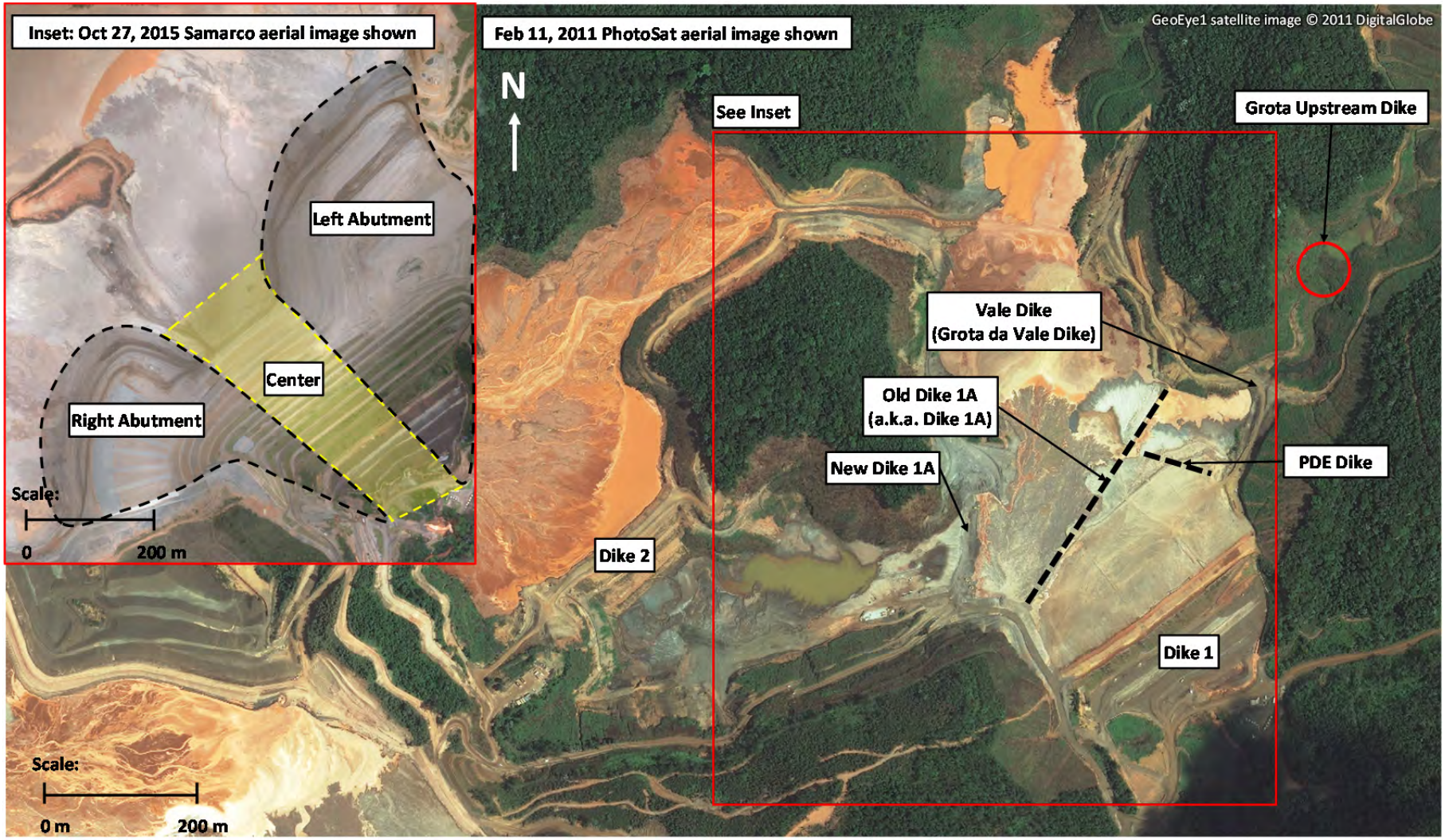

Figure B.B1-1 Dikes at Fundão

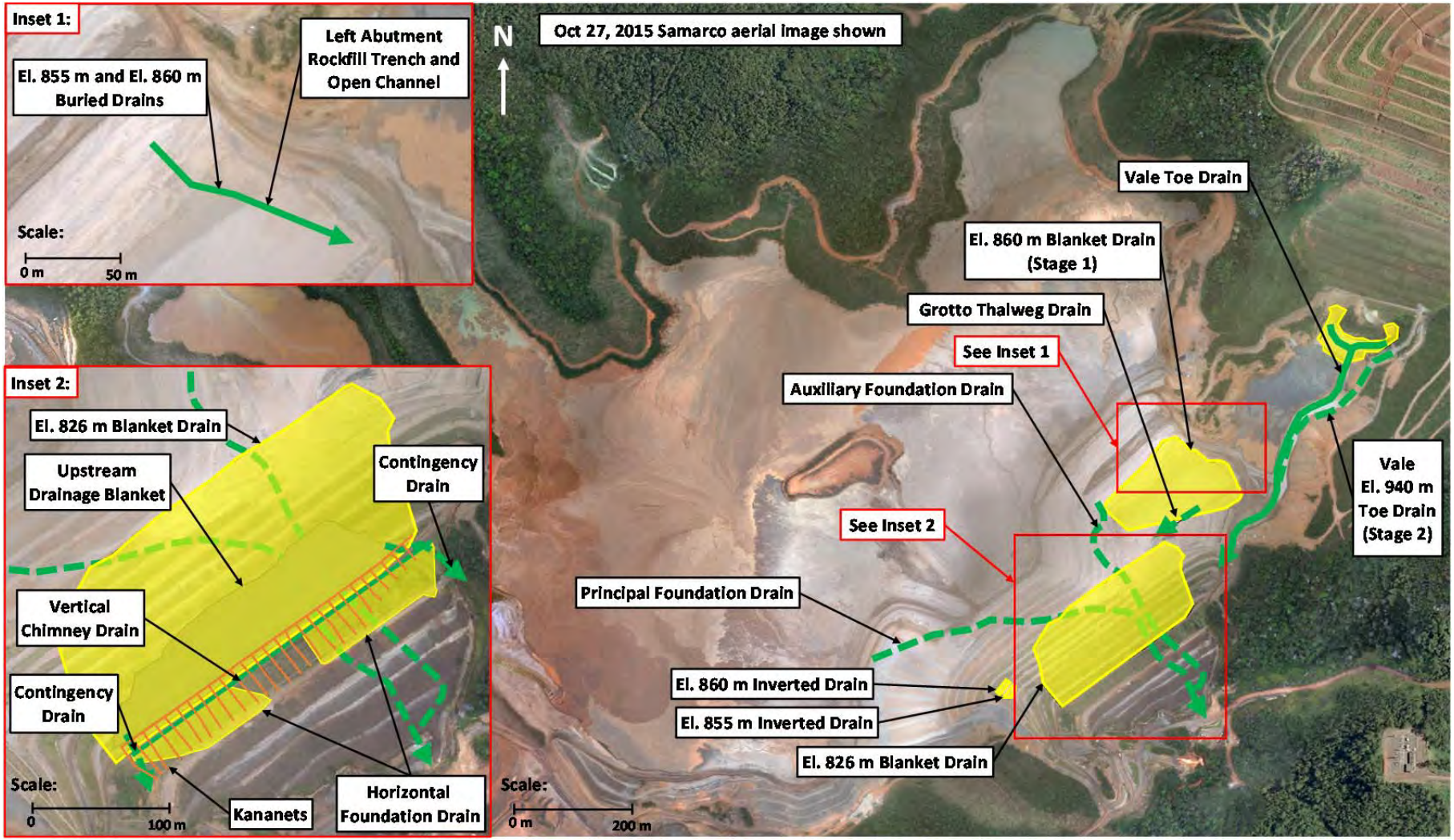

Figure B.B1-2 Drainage features at Fundão

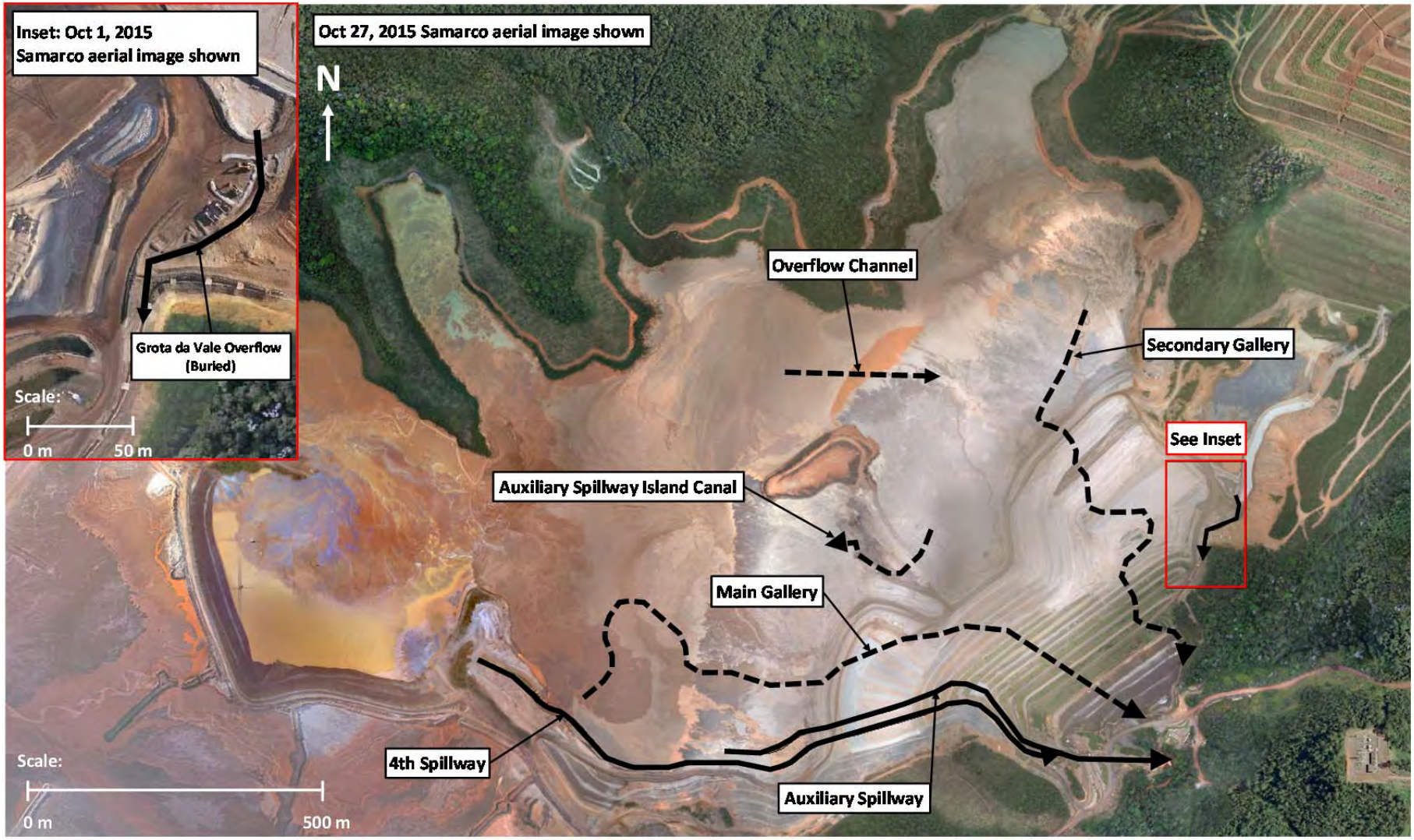

Figure B.B1-3 Decant structures at Fundão

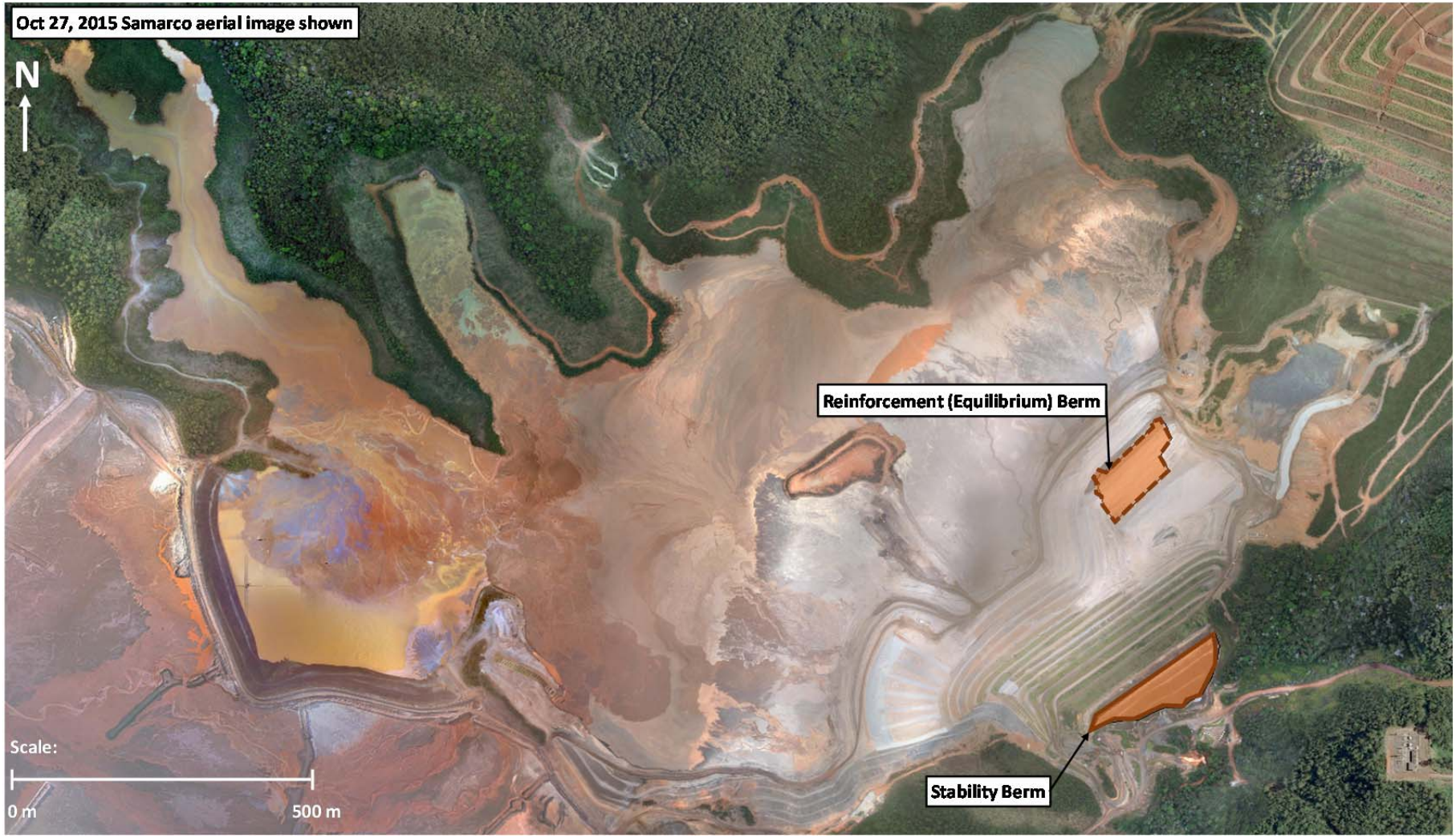

Figure B.B1-4 Stability berms at Fundão

B.B1-2 DIKES

Dike 1		
Area	Dike 1	
Purpose	Impound sand tailings deposited in Dike 1 reservoir	
Description	Saprolite starter dam, upstream raised sand embankment. Dike separated into left abutment, center, and right abutment.	
Construction period	July, 2007 to September, 2008	
Operating period	September, 2008 to November, 2015	
Photographs	 Photo 32 – Upstream face of FD 1 covered with blanket drain that has been eroded December, 2008 Andrew Robertson audit photo taken during site inspection showing the upstream drainage blanket heavily eroded to sand tailings discharge in the Dike 1 reservoir.	 Photo 2 – Initial Seepage flow – April 13, 2009 May, 2009 Andrew Robertson audit photo showing the downstream slope of Dike 1 during the April, 2009 piping incident.
Noted incidents	Erosion of upstream drainage blanket prior to tailings discharge. Piping incident in April, 2009. Multiple seepage incidents over the life of the Fundão facility. Slope movements at left setback in August 2014. Dam failure on November 5, 2015.	
Notes	-	

Dike 2		
Area	Dike 2	
Purpose	Impound slimes deposited in Dike 2 reservoir until Dike 1 sand embankment was sufficiently raised to contain the slimes	
Description	Saprolite starter dam, centerline raised embankment	
Construction period	July, 2007 to September, 2008	
Operating period	September, 2008 to February, 2014 (deliberately overtopped)	
Photographs	 Photo 22 – Funao Dam 2 with large upstream tailings and water pond. Note large pool forming in valley in background Photo from December 3, 2008 Andrew Robertson inspection.	 Photo 24 – Downstream face of FD 2: Decant gallery: Main Basedrain seen in valley leading towards pool behind FD 1. Photo from December 3, 2008 Andrew Robertson inspection.
Noted incidents	None	
Notes	-	

Old Dike 1A (a.k.a. Dike 1A)	
Area	Dike 1 reservoir
Purpose	Impound sand and slimes deposited in Dike 1 reservoir until Dike 1 remediation works were complete
Description	Local fill and tailings dike upstream of Dike 1
Construction period	November, 2009 to December, 2009
Operating period	December, 2009 to January, 2011
Photographs	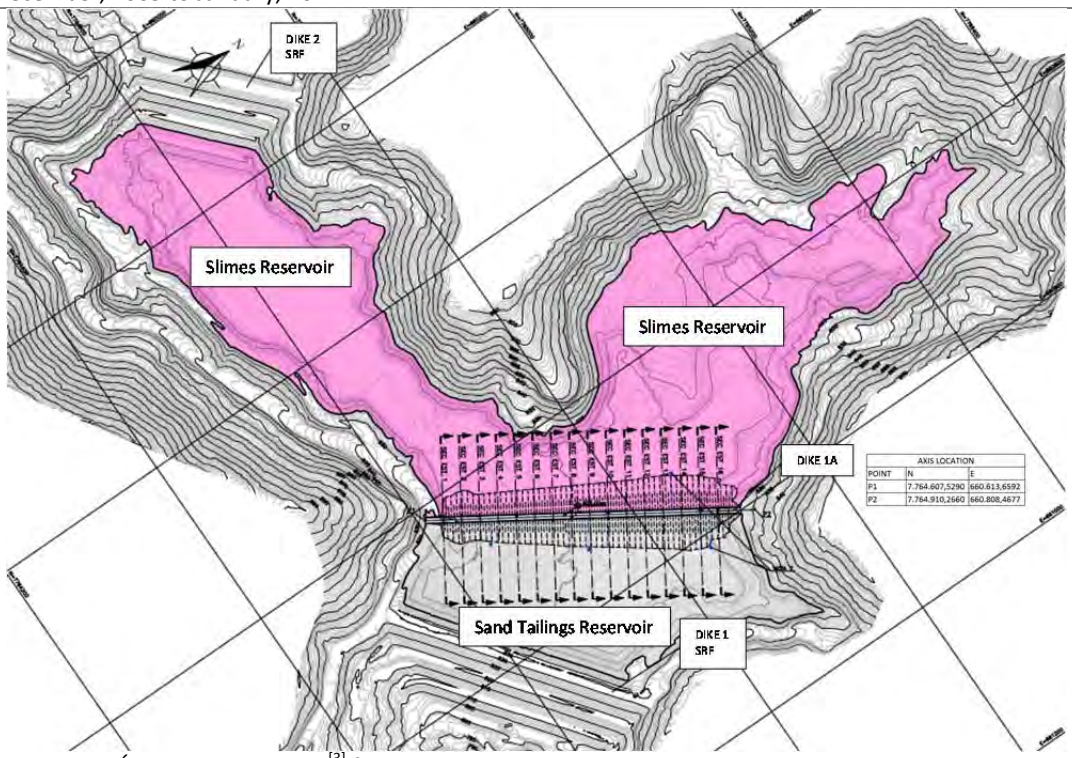 Pimenta de Ávila design drawing[3] for Old Dike 1A.  May, 2010 construction photos of Dike 1 remediation works. Photo was taken standing at the left abutment of Dike 1.
Noted incidents	None
Notes	-

New Dike 1A		
Area	Dike 1 reservoir	
Purpose	Keep sand from inundating the jet grouting platform where repairs were on-going for the Main Gallery	
Description	Local fill and tailings dike upstream of Old Dike 1A	
Construction period	August, 2010 to December, 2010	
Operating period	January, 2011 to February, 2012	
Photographs	 Photo 1 – overview of the New Dike 1A on the day of rupture January, 2011 photo from Pimenta de Ávila New Dike 1A raise calculation log[5].	 Photo 24 – Fundao Dike A1 downstream with sand seepage drain recently placed. April, 2011 Andrew Robertson inspection photo.
Noted incidents	January 27, 2011 slope failure	
Notes	-	

Grota Upstream Dike	
Area	Grota da Vale
Purpose	Contain the fines from seepage and surface runoff from the Fabrica Nova Waste Pile
Description	Dike downstream of Fabrica Nova Waste Pile
Construction period	May, 2010 (assume constructed at same time as Grota da Vale Dike)
Operating period	May, 2010 to September, 2011
Photographs	None available
Noted incidents	None
Notes	-

Vale Dike (Grota da Vale Dike)	
Area	Downstream of Fabrica Nova Waste Pile and Grota Upstream Dike
Purpose	Separate the water accumulated in Grota da Vale from the left abutment of Dike 1, maintain access to the Secondary Gallery from the left abutment
Description	Local fill starter dike, continuously raised with fill and tailings as needed to maintain access
Construction period	March, 2010 to October, 2010
Operating period	November, 2010 to November, 2015 with periodic interruptions for placement of sand tailings in Grota da Vale
Photographs	 May 2010 construction photos during Dike 1 remediation works.
	 Photo from weekly report, week of April 16, 2012, showing raising of the Grota da Vale Dike.
Noted incidents	None
Notes	-

PDE Dike (Pilha de Estéril União (Vale))	
Area	Downstream of Vale Dike within reservoir between Old Dike 1A and Dike 1
Purpose	Keep the water flowing in from Grota da Vale away from the area of sand deposition between Old Dike 1A and Dike 1 during construction of the Vale Dike
Description	Local fill dike
Construction period	February, 2010
Operating period	March, 2010 to May, 2010
Photographs	 March, 2010 construction photo during Dike 1 remediation works.
Noted incidents	None
Notes	-

B.B1-3 DRAINAGE FEATURES

Principal Foundation Drain		
Area	Dike 1 Reservoir	
Purpose	Drain the sand tailings in Dike 1 reservoir	
Description	Trapezoidal rockfill drain	
Construction period	2007 to September, 2008	
Operating period	September, 2008 to April, 2009 (decommissioned by plugging)	
Photographs	 October, 2007 construction photo of partially completed Principal Foundation Drain.	 April, 2009 photo of exposed Principal (Main) and Auxiliary (Secondary) Foundation Drains during plugging.
Noted incidents	Clogging of drain due to lack of protection over exposed drains prior to tailings placement. Other noted construction-related deficiencies.	
Notes	-	

Auxiliary Foundation Drain		
Area	Dike 1 Reservoir	
Purpose	Drain the sand tailings in Dike 1 reservoir	
Description	Trapezoidal rockfill drain	
Construction period	2007 to September, 2008	
Operating period	September, 2008 to April, 2009 (decommissioned by plugging)	
Photographs	 October, 2007 construction photo of partially completed Auxiliary Foundation Drain.	 April, 2009 photo of exposed Principal (Main) and Auxiliary (Secondary) Foundation Drains during plugging.
Noted incidents	Clogging of drain due to lack of protection over exposed drains prior to tailings placement. Other noted construction-related deficiencies.	
Notes	-	

<table>
<tr><th colspan="3">Vertical Chimney Drain</th></tr>
<tr><td>Area</td><td colspan="2">Dike 1</td></tr>
<tr><td>Purpose</td><td colspan="2">Intercept seepage through Starter Dam</td></tr>
<tr><td>Description</td><td colspan="2">“Future ore” chimney drain</td></tr>
<tr><td>Construction period</td><td colspan="2">2007 to September, 2008</td></tr>
<tr><td>Operating period</td><td colspan="2">September, 2008 to November, 2015</td></tr>
<tr><td>Photographs</td><td> 
April, 2008 construction photo of partially completed Vertical Chimney Drain.</td><td> 
January, 2008 construction photo of partially completed Vertical Chimney Drain and “future ore” material used (brown color).</td></tr>
<tr><td>Noted incidents</td><td colspan="2">From the August, 2009 Andrew Robertson engineering audit report where FD1 is Dike 1:
The chimney drain in FD1 is of questionable reliability, as it was constructed using ‘future ore’ which is of questionable grading consistency and permeability. The FD1 dam remediation should therefore assume that this drain will not function. A downstream Stabilization Berm, with a filter/drain layer at the dam interface is required to stabilize the resulting dam, as has been demonstrated by Pimenta (CL-3).</td></tr>
<tr><td>Notes</td><td colspan="2">-</td></tr>
</table>

Horizontal Foundation Drain	
Area	Dike 1
Purpose	Convey water from Vertical Chimney Drain to Foundation Drains
Description	“Future ore” drainage blanket
Construction period	October, 2007
Operating period	September, 2008 to November, 2015
Photographs	 October, 2007 construction photo of Horizontal Foundation Drain circled in red. Photo was taken looking in the direction of the Secondary Gallery and Fabrica Nova Waste Pile.
Noted incidents	No noted incidents; however, the as-built drawing appears to show an incomplete surveyed extent of the drain where the left and right extents are not connected.
Notes	-

Upstream Drainage Blanket	
Area	Dike 1
Purpose	Drain the sand tailings in Dike 1 reservoir
Description	Rockfill drainage blanket
Construction period	2008
Operating period	September, 2008 to April, 2009 (decommissioned through complete removal)
Photographs	 December, 2008 Andrew Robertson site inspection photo showing the upstream face of Dike 1 covered with eroded drainage blanket.
Noted incidents	Drainage blanket was not protected from erosion prior to placement of sand tailings. Structure was removed in its entirety during the April, 2009 remediation works.
Notes	-

Grota Thalweg Drain	
Area	Dike 1 reservoir
Purpose	Convey water from Grota da Vale under Secondary Gallery platform to Dike 1 reservoir
Description	Rockfill finger drain
Construction period	April, 2008
Operating period	April, 2008 to November, 2015
Photographs	 April, 2008 construction photo showing the Secondary Gallery platform crossing the Grota da Vale tributary with the Grota Thalweg Drain at the base. The Fabrica Nova Waste Pile is seen in the back right.
	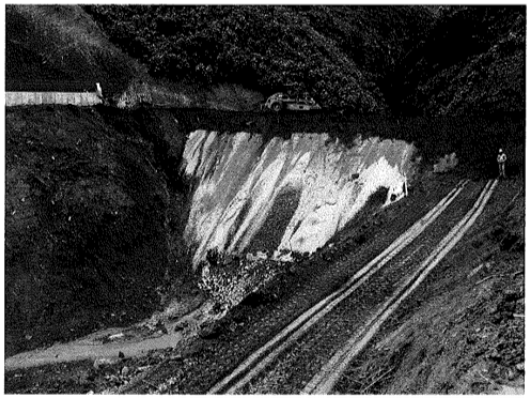 Construction photo from as-built report[6].
Noted incidents	None
Notes	-

Contingency Drains		
Area	Dike 1	
Purpose	Additional drainage capacity on top of Foundation Drains on the left and right abutments of the Starter Dam	
Description	Rockfill finger drains	
Construction period	February, 2008	
Operating period	Decommissioned prior to operation	
Photographs	 February, 2008 construction photo showing partially completed Contingency Drain at left abutment with Secondary Gallery in the background.	 Construction photo showing upstream end of Contingency Drain on right abutment during excavation in May, 2010.
Noted incidents	Questionable construction quality, plugged prior to operation as part of Dike 1 remediation works.	
Notes	-	

El. 826 m Blanket Drain	
Area	Dike 1
Purpose	Replacement drain for Foundation Drains to drain the sand tailings in Dike 1 reservoir
Description	Rockfill drainage blanket
Construction period	June, 2010 to November, 2010
Operating period	December, 2010 to November, 2015
Photographs	 November, 2010 construction photo showing placement of upper layer of sand and tailings over drain rock towards the end of blanket drain construction.  November, 2010 construction photo showing placement of tailings sand on top of completed blanket drain.
Noted incidents	None
Notes	Shown in [7].

Kananets®		
Area	Dike 1	
Purpose	Convey water from El. 826 m blanket drain to downstream face of Dike 1	
Description	27 pipes embedded within the El. 826 m blanket drain	
Construction period	November, 2010	
Operating period	December, 2010 to November, 2015	
Photographs	 October, 2010 construction photo showing installation of Kananet® pipe (1 of 27) through the Dike 1 crest.	 July, 2014 VOGBR site inspection photo showing the Kananets® discharging into a concrete channel.
Noted incidents	None	
Notes	Shown in [7].	

Vale Toe Drain		
Area	Fabrica Nova Waste Pile	
Purpose	Collect and convey seepage from Fabrica Nova Waste Pile to area downstream of Dike 1	
Description	Rockfill drain at toe of Fabrica Nova Waste Pile draining to a solid pipe along Grota da Vale	
Construction period	September, 2013 to June, 2014	
Operating period	June, 2014 to November, 2015	
Photographs	 Construction photo from week of March 24, 2014 showing the exposed drain at the toe of the Fabrica Nova Waste Pile[8].	 November, 2013 construction photo showing the installation of the drain pipe leading from the toe of the Fabrica Nova Waste Pile to the left abutment concrete channel[9].
Noted incidents	None	
Notes	-	

El. 855 m Buried Drain		
Area	Dike 1	
Purpose	Treatment for seepage, collects water at contact of left abutment with stripped slope	
Description	Sand and rockfill finger drain wrapped in geotextile	
Construction period	April, 2013 to June, 2013	
Operating period	July, 2013 to November, 2015	
Photographs	 April 22, 2013 weekly report photo showing the beginning of the drain construction. Photo was taken looking upstream towards the crest of the dike with the stripped left abutment to the right.	 April 22, 2013 weekly report photo showing the beginning of the drain construction. Photo was taken looking upstream towards the crest of the dike with the stripped left abutment to the right.
Noted incidents	None	
Notes	No drawing found. Planned alignment shown in [10].	

El. 860 m Buried Drain	
Area	Dike 1
Purpose	Treatment for seepage, collects water at contact of left abutment with stripped slope
Description	Sand and rockfill slope drain wrapped in geotextile
Construction period	November, 2013
Operating period	November, 2013 to November, 2015
Photographs	 November 18, 2013 weekly report showing the four layers of the buried drain.
Noted incidents	None
Notes	No engineering drawings or design report available. Drain was installed by the Samarco operations team to address a seepage incident in November, 2013.

Left Abutment Rockfill Trench		
Area	Dike 1	
Purpose	Conveys water collected from El. 855 m and El. 860 m Buried Drains across setback platform	
Description	Rockfill trench wrapped in geotextile	
Construction period	June, 2013	
Operating period	June, 2013 to November, 2015	
Photographs	 June 17, 2013 weekly report showing the yet unfilled rockfill trench.	 June 17, 2013 weekly report showing the beginning of the filling of the rockfill trench.
Noted incidents	None	
Notes	No engineering drawings or design report available. Trench was implemented by Samarco's operations team to convey water from the El. 855 m Buried Drain to Grota da Vale.	

Left Abutment Open Channel		
Area	Dike 1	
Purpose	Conveys water collected from El. 855 m and El. 860 m Buried Drains across setback platform	
Description	Geotextile lined open channel, an extension of the Left Abutment Rockfill Trench as the setback platform was raised	
Construction period	December, 2013	
Operating period	January, 2014 to January, 2015	
Photographs	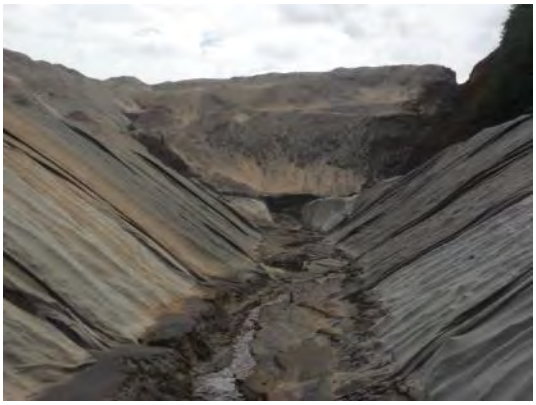 Photo looking in the direction of the left setback crest. The open channel is lined with geotextile and is receiving water from the buried drains at El. 855 m and El. 860 m[11].	 March 27, 2014 VOGBR site inspection photo showing meandering erosion channel from end of open channel to Grota da Vale.
Noted incidents	None	
Notes	No engineering drawings or design reports available. The channel was implemented by Samarco's operations team to allow continued raising of the left setback without burying the rockfill trench which served as the outlet for the buried drains at El. 855 m and El. 860 m.	

El. 860 m Blanket Drain (Stage 1)		
Area	Dike 1	
Purpose	Drain the sand tailings in Dike 1 reservoir above El. 860 m	
Description	Rockfill drainage blanket	
Construction period	November, 2014 to August, 2015	
Operating period	August, 2015 to November, 2015	
Photographs	 November 20, 2014 construction photo showing placement of drain rock on upper bench of the El. 860 m Blanket Drain.	 August, 2015 construction photo showing placement of sand tailings on top of filter layer of drain. The toe of the finished drain is exposed awaiting connection to Stage 3 of the El. 940 m drain.
Noted incidents	None	
Notes	Stage 1 refers to this blanket drain which was to connect to Stage 2 (Vale El. 940 m Toe Drain) via Stage 3 (connecting blanket drain) to drain to the left abutment concrete channel with Stage 4 (continued blanket drain).	

Vale El. 940 m Toe Drain (Stage 2)		
Area	Grota da Vale	
Purpose	Drain the sand tailings in Dike 1 reservoir above El. 860 m along the contact with Grota da Vale	
Description	Rockfill finger drain	
Construction period	November, 2015	
Operating period	Construction not completed prior to failure	
Photographs	 November, 2015 construction photo showing the partially completed Vale El. 940 m Toe Drain with the left abutment of Dike 1 to the right of the photo.	 November, 2015 construction photo showing the partially completed Vale El. 940 m Toe Drain with the Fabrica Nova Waste Pile in the background.
Noted incidents	None	
Notes	Stage 1 refers to this blanket drain which was to connect to Stage 2 (Vale El. 940 m Toe Drain) via Stage 3 (connecting blanket drain) to drain to the left abutment concrete channel with Stage 4 (continued blanket drain).	

El. 855 m Inverted Drain		
Area	Dike 1	
Purpose	Collect seepage breakout at El. 855 m at the right abutment and mitigate piping	
Description	Rockfill applied to downstream slope	
Construction period	July, 2014 (initial installation of sand and gravel by Samarco) June, 2015 (remediated drain based on VOGBR design)	
Operating period	July, 2014 to November, 2015	
Photographs	 July, 2014 VOGBR site inspection photo showing the initially placed inverted drain[12].	 July, 2015 VOGBR site inspection photo showing the remediated inverted drain[13].
Noted incidents	None	
Notes	Reported in [14]. This is at times referred to as the El. 850 m drain.	

El. 860 m Inverted Drain		
Area	Dike 1	
Purpose	Collect seepage breakout at El. 860 m at the right abutment and mitigate piping	
Description	Rockfill applied to downstream slope	
Construction period	January, 2015 (initial installation of sand and gravel by Samarco) June, 2015 (remediated drain based on VOGBR design)	
Operating period	January, 2015 to November, 2015	
Photographs	 April 17, 2015 VOGBR site inspection photo showing the pipes used to collect and measure the seepage flow from the El. 860 m Inverted Drain[12].	 July, 2015 VOGBR site inspection photo showing the remediated inverted drain on the upper bench[13].
Noted incidents	None	
Notes	Shown in [13]. This is at times referred to as the El. 855 m drain.	

Right Abutment El. 940 m Drain	
Area	Dike 1
Purpose	Drain the sand tailings in Dike 1 reservoir above El. 855 m
Description	Series of rockfill finger drains
Construction period	August, 2015 to November, 2015
Operating period	Construction not completed prior to failure
Photographs	 November, 2015 construction photo showing partially completed Right Abutment El. 940 m Drain. Photo was taken from the right abutment looking towards the left with the Fabrica Nova Waste Pile in the background.
Noted incidents	None
Notes	-

B.B1-4 DECANT STRUCTURES

Main Gallery		
Area	Dike 1 reservoir	
Purpose	Decant for Dike 2 reservoir	
Description	Concrete gallery, 1207 m long, 2 m diameter	
Construction period	July, 2007 to September, 2008	
Operating period	September, 2008 to July, 2010 July, 2011 to October, 2013 (decommissioned by plugging)	
Photographs	 November, 2007 construction of Main Gallery (bottom) and Secondary Gallery (top).	 February, 2008 construction photo showing the Main Gallery next to a partially constructed Principal Foundation Drain. Photo was taken standing on the right abutment of Dike 2 looking towards Dike 1.
Noted incidents	July, 2010 settlement which led to formation of a sinkhole at the top of the tailings. Multiple instances of cracks and operational defects.	
Notes	As-built alignment documented in multiple surveys.	

Secondary Gallery		
Area	Dike 1 reservoir	
Purpose	Decant for Dike 1 reservoir	
Description	Concrete gallery, 811 m long, 2 m diameter	
Construction period	July, 2007 to September, 2008	
Operating period	September, 2008 to October, 2010 November, 2010 to December, 2011 March, 2012 to August, 2012 October, 2012 to June, 2013 (decommissioned by plugging)	
Photographs	 November, 2007 construction of Main Gallery (bottom) and Secondary Gallery (top).	 July, 2007 construction photo of completed Secondary Gallery tulipas (vertical riser intakes).
Noted incidents	Multiple instances of cracks and operational defects. Secondary Gallery sinkhole on November 25, 2012.	
Notes	As-built alignment documented in multiple surveys.	

Auxiliary Spillway		
Area	Dike 1 reservoir	
Purpose	Decant for Dike 1 and 2 reservoirs	
Description	2x 1.2 m dia. HDPE pipes, vertical riser intakes	
Construction period	July, 2012 to January, 2013	
Operating period	February, 2013 to November, 2015	
Photographs	 December, 2012 construction photo showing the Auxiliary Spillway pipes buried with sand tailings[15].	 February, 2013 BVP construction photo from the construction summary report showing the tulipas (vertical riser intakes) of the Auxiliary Spillway[16].
Noted incidents	None	
Notes	-	

4th Spillway		
Area	Dike 1 reservoir	
Purpose	Decant for the Dike 1 and Dike 2 reservoirs as the Auxiliary Spillway capacity was insufficient	
Description	3x 1.2 m dia. HDPE pipes (2 are extensions of the Auxiliary Spillway), vertical riser intakes	
Construction period	June, 2013 to September, 2015 (capping of upstream end by September, 2015, initial flow through system in November 2014)	
Operating period	November, 2014 to November, 2015	
Photographs	 Weekly report photo from week of November 17, 2014 showing screens around the 4th Spillway tulipas to protect from entry of debris to the decant system.	 Construction photo showing the Auxiliary Spillway tulipas (2x) to the far right and the 4th Spillway tulipas (3x) from the center to the left of the photo[17].
Noted incidents	None	
Notes	-	

<table>
<tr><th colspan="3">Grota da Vale Overflow (Grota Overflow)</th></tr>
<tr><td>Area</td><td colspan="2">Grota da Vale</td></tr>
<tr><td>Purpose</td><td colspan="2">Decant for water ponded in Grota da Vale</td></tr>
<tr><td>Description</td><td colspan="2">Buried pipe outlet from Grota da Vale to left abutment concrete channel</td></tr>
<tr><td>Construction period</td><td colspan="2">Unknown</td></tr>
<tr><td>Operating period</td><td colspan="2">August, 2015 to November, 2015</td></tr>
<tr><td>Photographs</td><td> 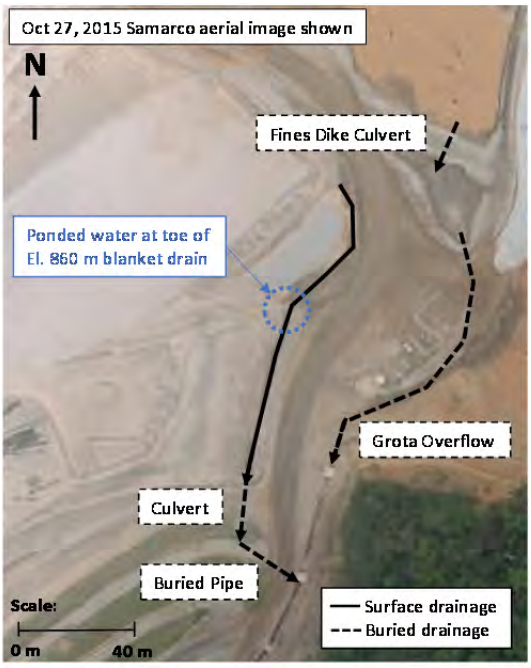
</td><td> 
November, 2015 site photo showing the inlet of the Grota da Vale Overflow looking toward the left abutment of Dike 1. The exposed toe of the El. 860 m blanket drain can be seen to the right.</td></tr>
<tr><td></td><td> 
November, 2015 site photo showing the outlet of the Grota da Vale Overflow in the left abutment concrete channel. The Fabrica Nova Waste Pile can be seen in the background.</td><td> 
November, 2015 site photo showing the outlet of the buried pipe and culvert which collect water from the toe of the El. 860 m blanket drain. The Fabrica Nova Waste Pile can be seen in the background.</td></tr>
<tr><td>Noted incidents</td><td colspan="2">None</td></tr>
<tr><td>Notes</td><td colspan="2">No drawings or design reports are available. The alignment of the overflow pipe was approximated based on site photos and aerial images.</td></tr>
</table>

Overflow Channel	
Area	Between Dike 1 and Dike 2 reservoirs
Purpose	Inter-basin decant for Dike 2 reservoir to Dike 1 reservoir
Description	Excavated open channel north of the Island between Dike 1 and Dike 2 reservoirs
Construction period	January, 2011 June, 2013
Operating period	February, 2011 to August, 2012 July 2013 to January 2014
Photographs	 First and second operational period for the Overflow Channel. Samarco aerial image from January, 2012 is shown at the top with July 2013 shown at the bottom.
	 Weekly report photo from week of July 15, 2013 showing the Overflow Channel in operation and decanting slimes from the Dike 2 reservoir into the Dike 1 reservoir.
Noted incidents	None
Notes	-

<table>
<tr><th colspan="3">Auxiliary Spillway Island Canal</th></tr>
<tr><td>Area</td><td colspan="2">Dike 1 reservoir</td></tr>
<tr><td>Purpose</td><td colspan="2">Intra-basin decant in Dike 1 reservoir for water to be directed away from Secondary Gallery and to the Auxiliary/4th Spillway</td></tr>
<tr><td>Description</td><td colspan="2">Excavated open channel in tailings from east side of Island to south side</td></tr>
<tr><td>Construction period</td><td colspan="2">June, 2013</td></tr>
<tr><td>Operating period</td><td colspan="2">July, 2013 to November, 2013</td></tr>
<tr><td rowspan="2">Photographs</td><td> 
Weekly report photo from week of July 1, 2013 showing the excavation of the Auxiliary Spillway Island Canal.</td><td> 
Weekly report photo from week of July 8, 2013 showing continued excavation of the Auxiliary Spillway Island Canal.</td></tr>
<tr><td> 
Weekly report photo from week of July 15, 2013 showing the Canal in operation. Photo was taken looking in the upstream direction toward the Dike 1 reservoir.</td><td> 
Weekly report photo from week of July 22, 2013 showing the Canal in operation. Photo was taken looking in the downstream direction toward Dike 2.</td></tr>
<tr><td>Noted incidents</td><td colspan="2">None</td></tr>
<tr><td>Notes</td><td colspan="2">No engineering drawings or design reports are available.</td></tr>
</table>

B.B1-5 STABILITY BERMS

Stability Berm	
Area	Dike 1
Purpose	Required for stability of Dike 1 Starter Dam following April, 2009 piping incident
Description	Rockfill berm placed on downstream face of Dike 1
Construction period	January, 2010 to July, 2010
Operating period	July, 2010 to November, 2015
Photographs	 February, 2010 construction photo showing initial stripping in preparation for installation of the Stability Berm.  April, 2010 construction photo showing execution of the Stability Berm on the downstream face of Dike 1.
Noted incidents	None
Notes	-

Reinforcement (Equilibrium) Berm	
Area	Dike 1
Purpose	Required for stability of setback following August, 2014 incident
Description	Sand berm placed on downstream face of left abutment setback
Construction period	August to September, 2014
Operating period	September, 2014 to November, 2015
Photographs	 Weekly report photo from week of September 8, 2014 showing completed Reinforcement Berm on left setback.
Noted incidents	None
Notes	-

ATTACHMENT B2

Timelines

Appendix B: Attachment B2
Timelines

TABLE OF CONTENTS

List of Figures

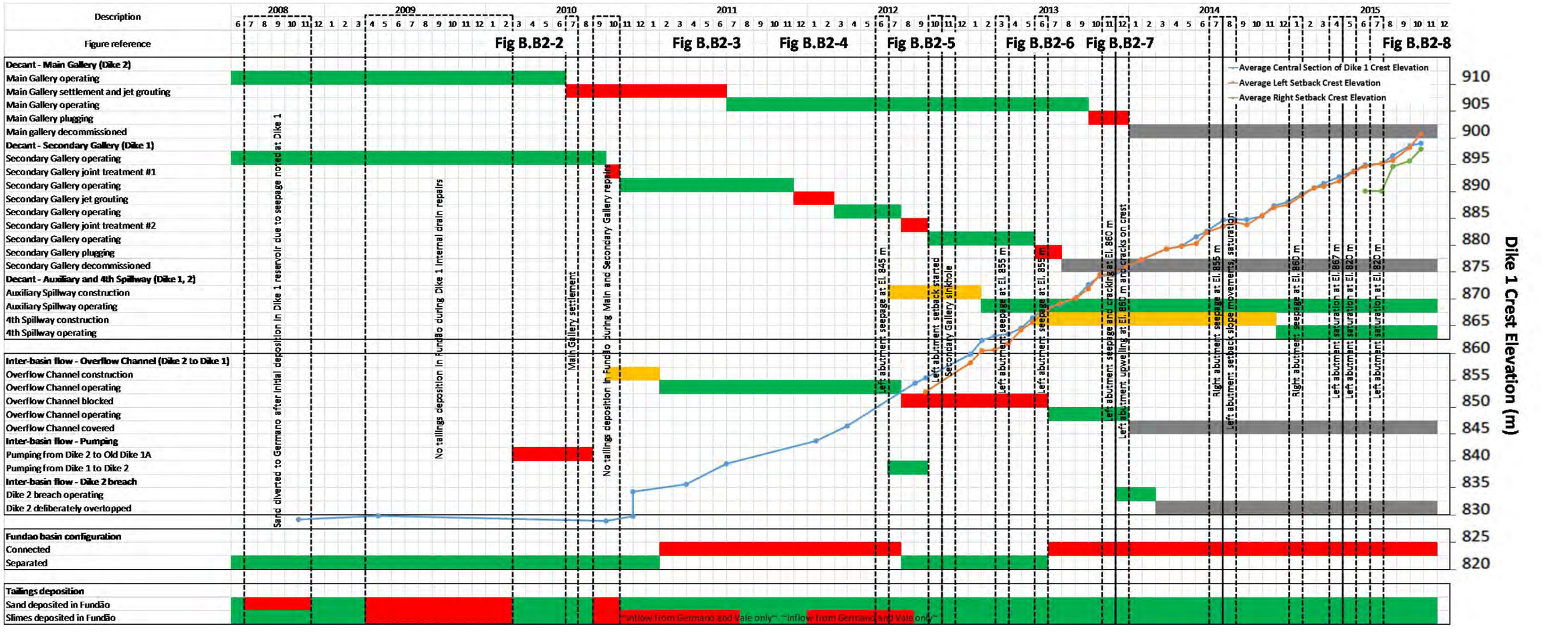

1. Tailings deposition history is based on descriptions in ITRB reports only.
2. Dike 1 crest elevation as presented in Appendix B, Section B5.1.

Figure B.B2-1 Fundão timeline by decant configuration

Photographs shown were taken during Dike 1 remediation construction work activities. Photos are ordered looking downstream from crest of Dike 2 moving to the Old Dike 1A/Dike 1 reservoir.

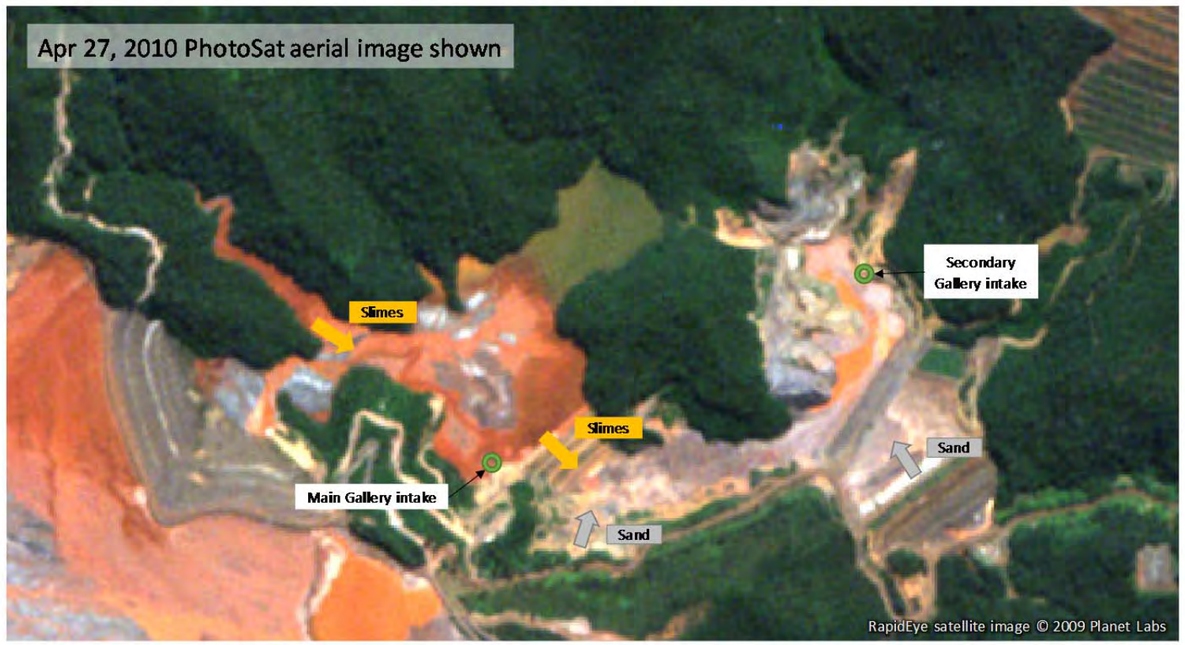

Figure B.B2-2 Fundão timeline by decant – April, 2010

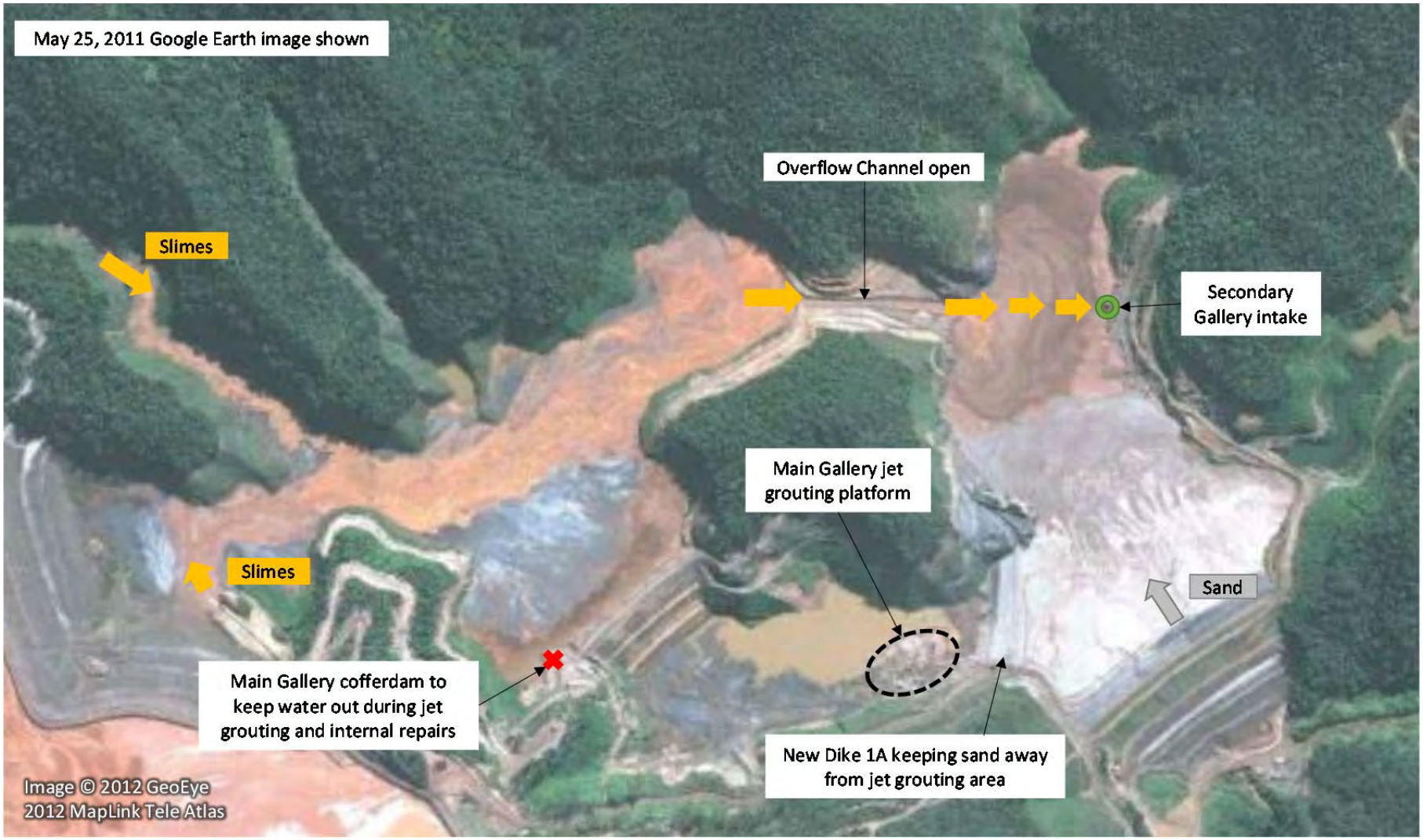

Figure B.B2-3 Fundão timeline by decant – May, 2011

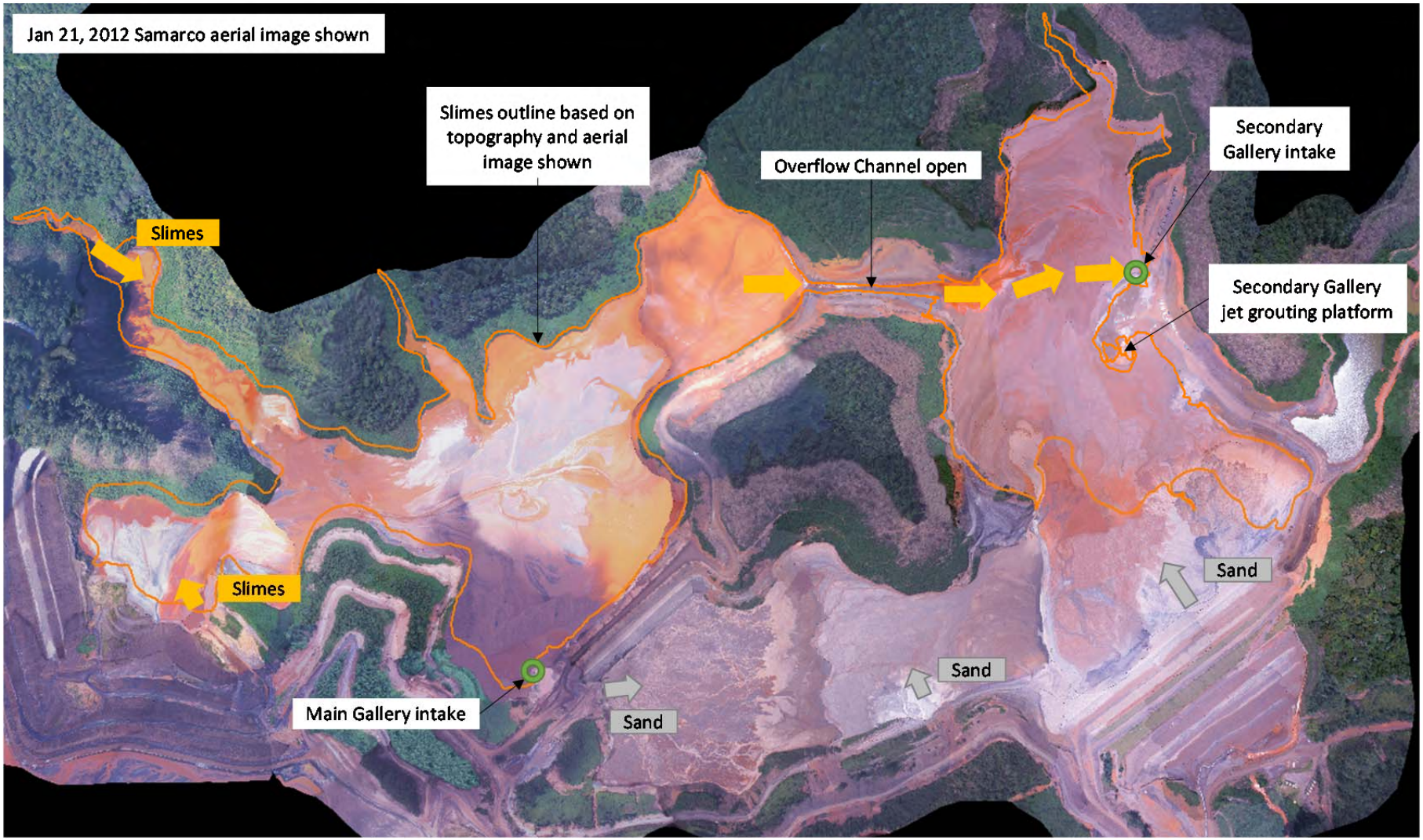

Figure B.B2-4 Fundão timeline by decant – January, 2012

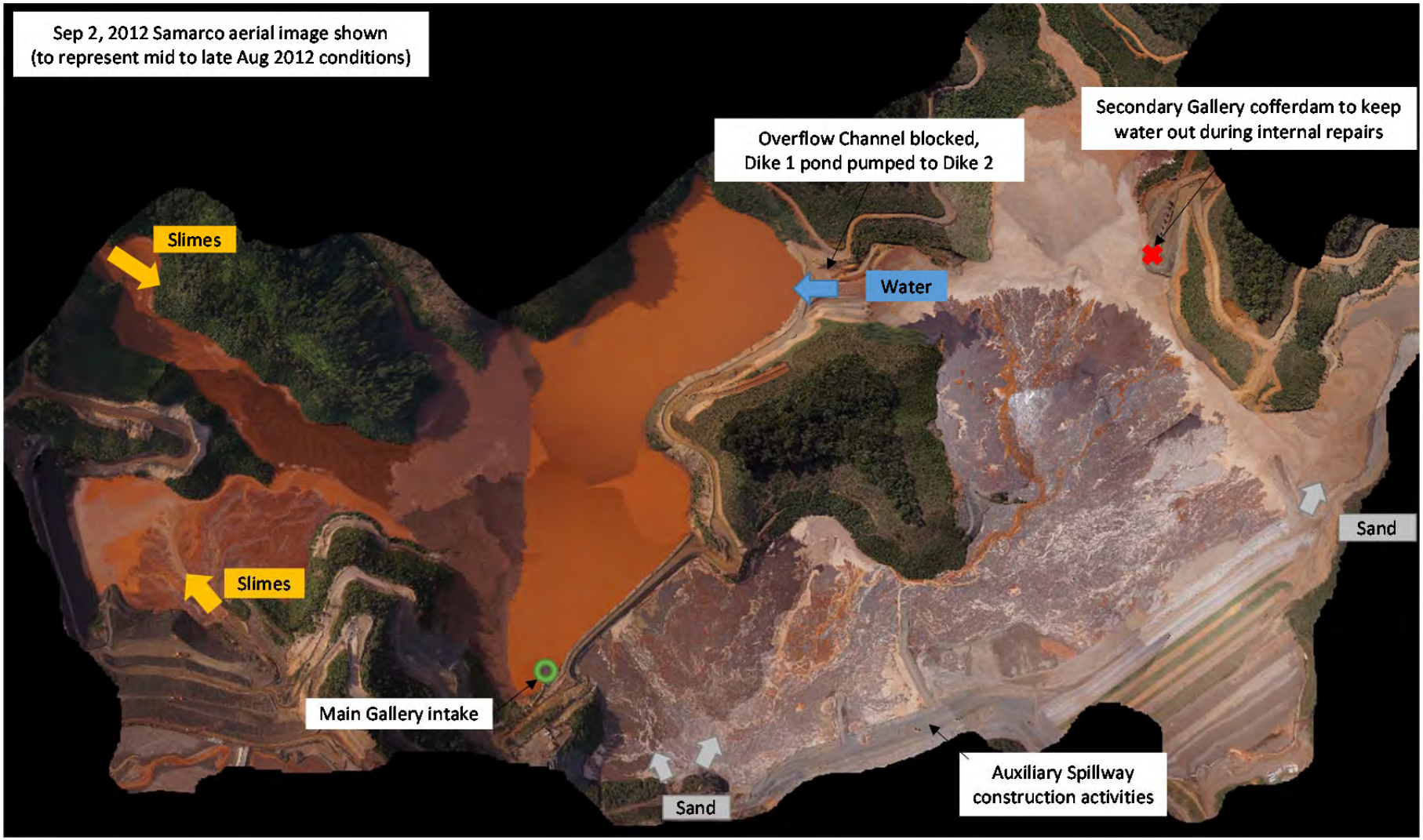

Figure B.B2-5 Fundão timeline by decant – September, 2012

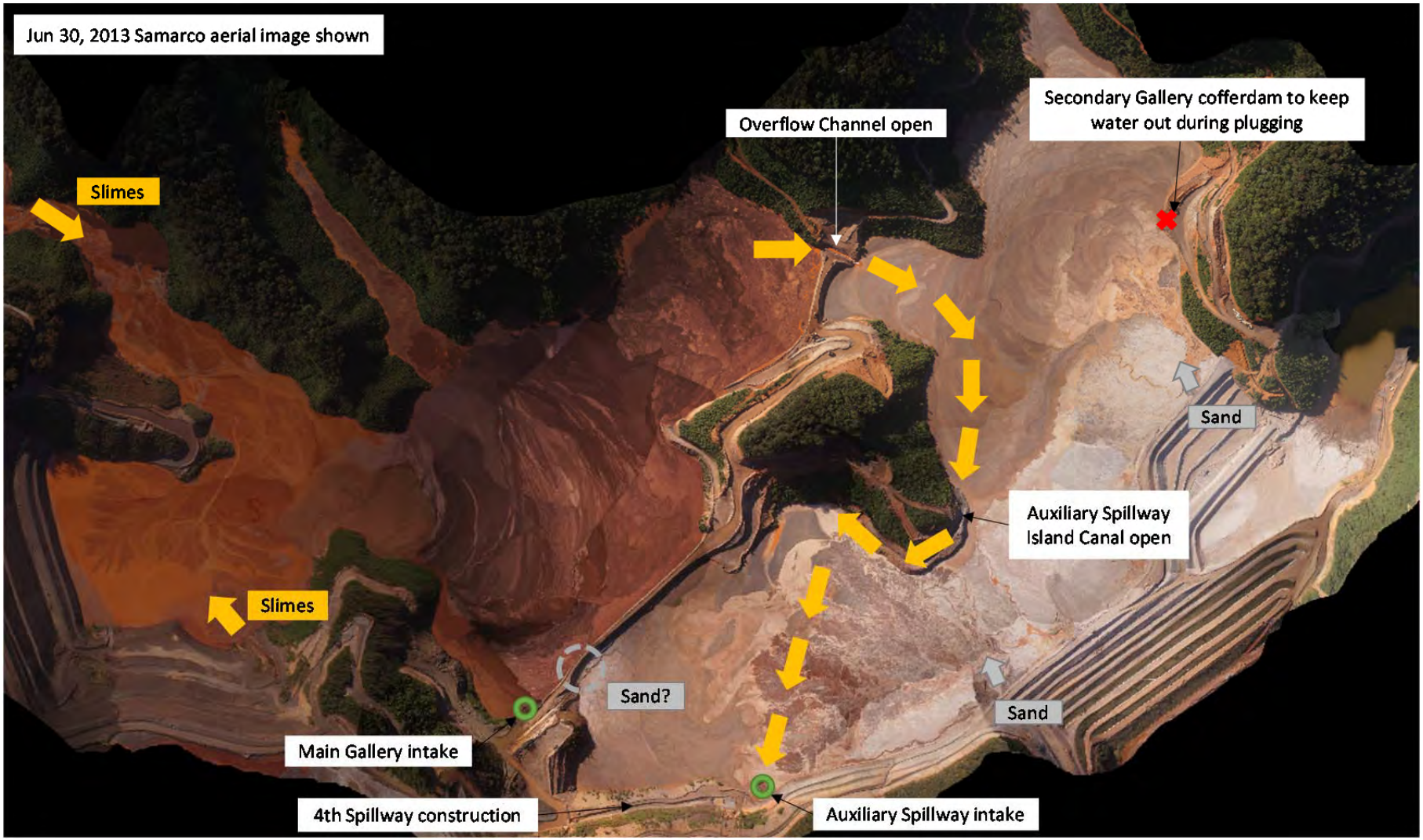

Figure B.B2-6 Fundão timeline by decant – June, 2013

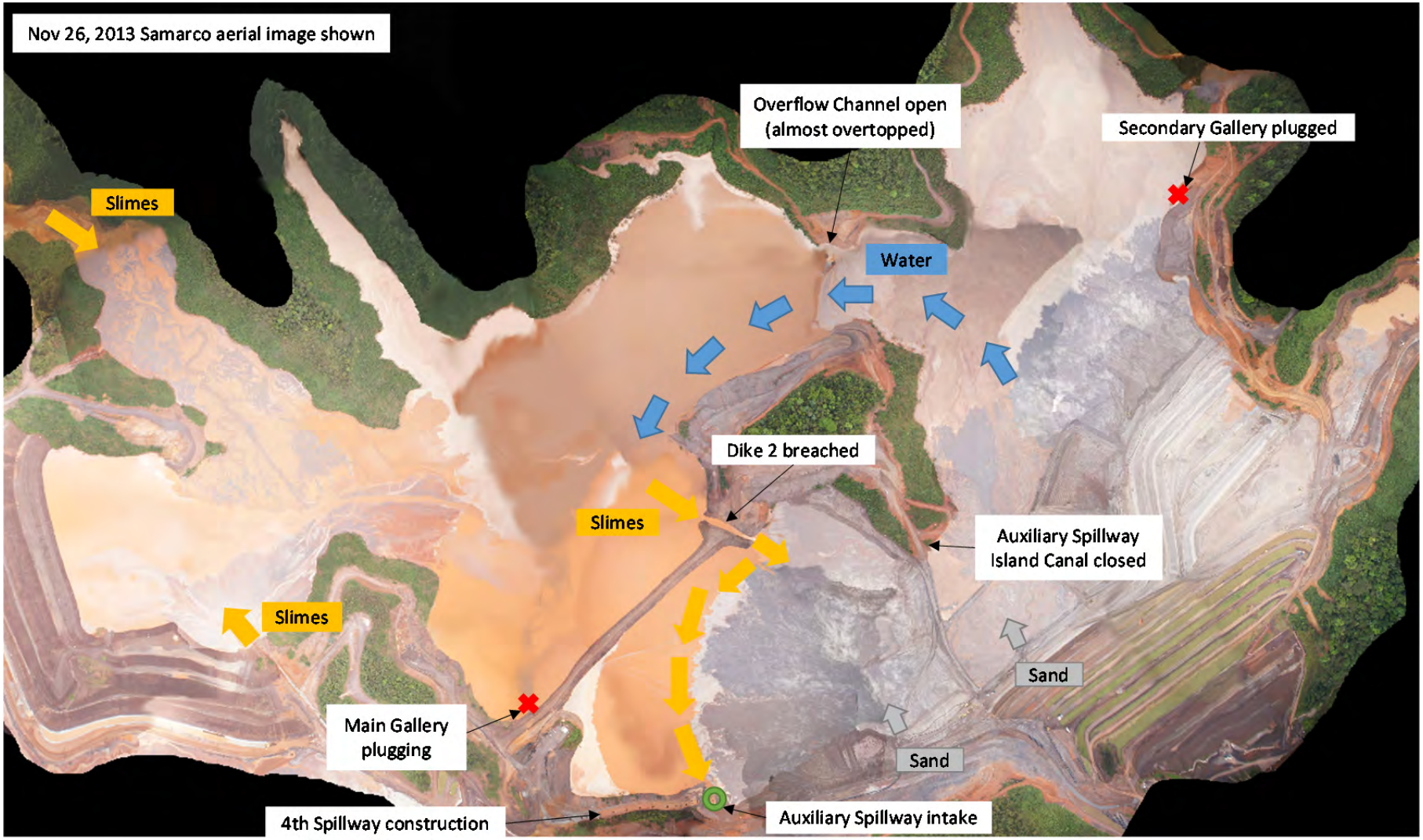

Figure B.B2-7 Fundão timeline by decant – November, 2013

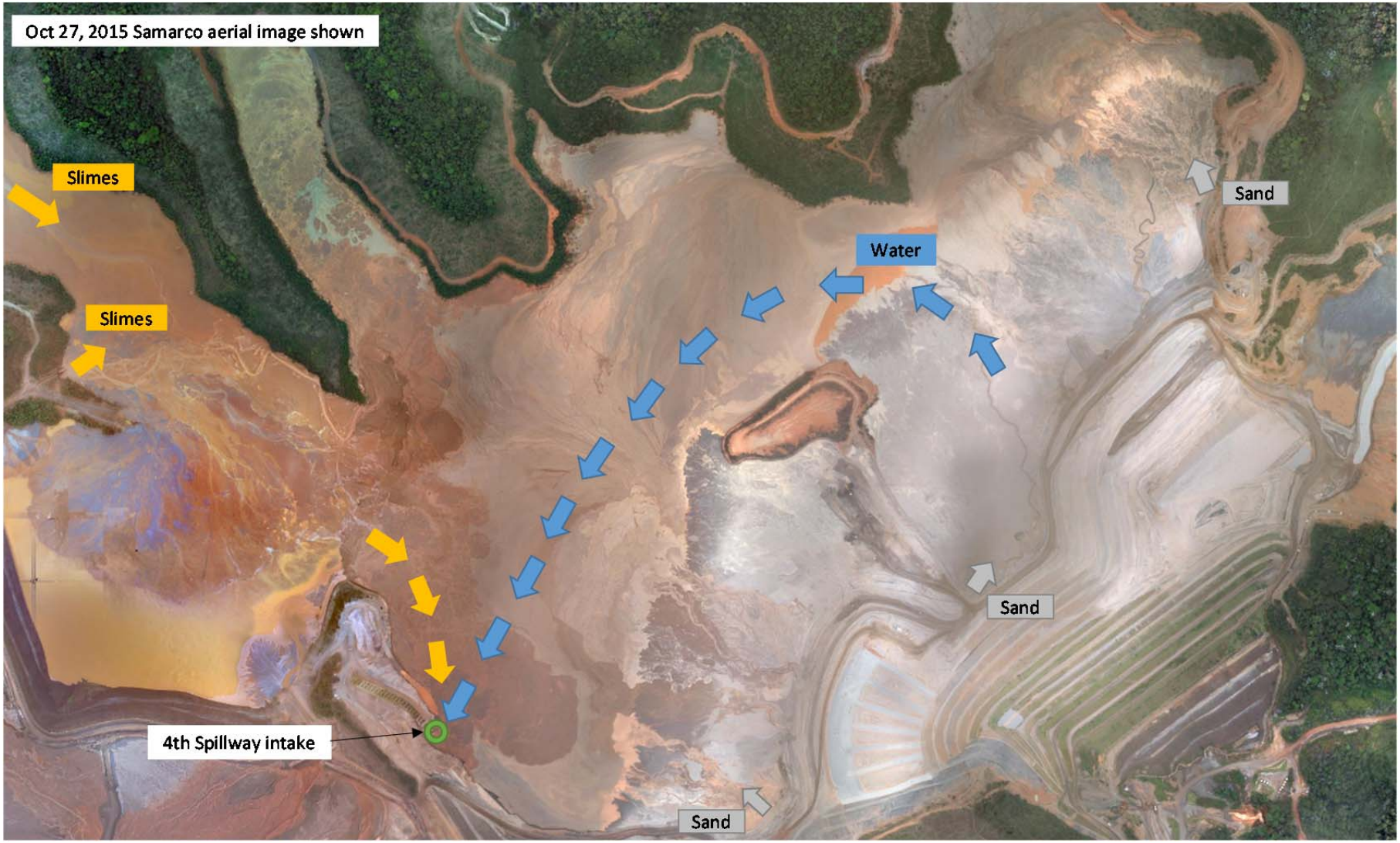

Figure B.B2-8 Fundão timeline by decant – October, 2015

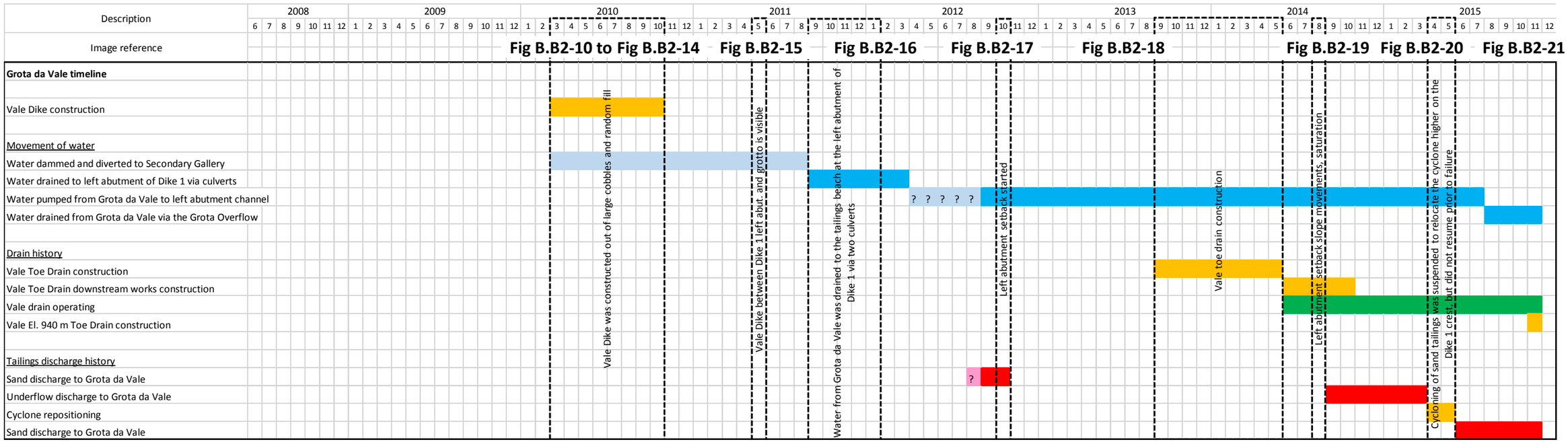

Figure B.B2-9 Grota da Vale timeline

Figure B.B2-10 Grota da Vale timeline – Vale Dike (February, 2010)

Figure B.B2-11 Grota da Vale timeline – Vale Dike (March, 2010)

Figure B.B2-12 Grota da Vale timeline – Vale Dike (May, 2010)

Figure B.B2-13 Grota da Vale timeline – Vale Dike (June, 2010)

Figure B.B2-14 Grota da Vale timeline – Vale Dike (November, 2010)

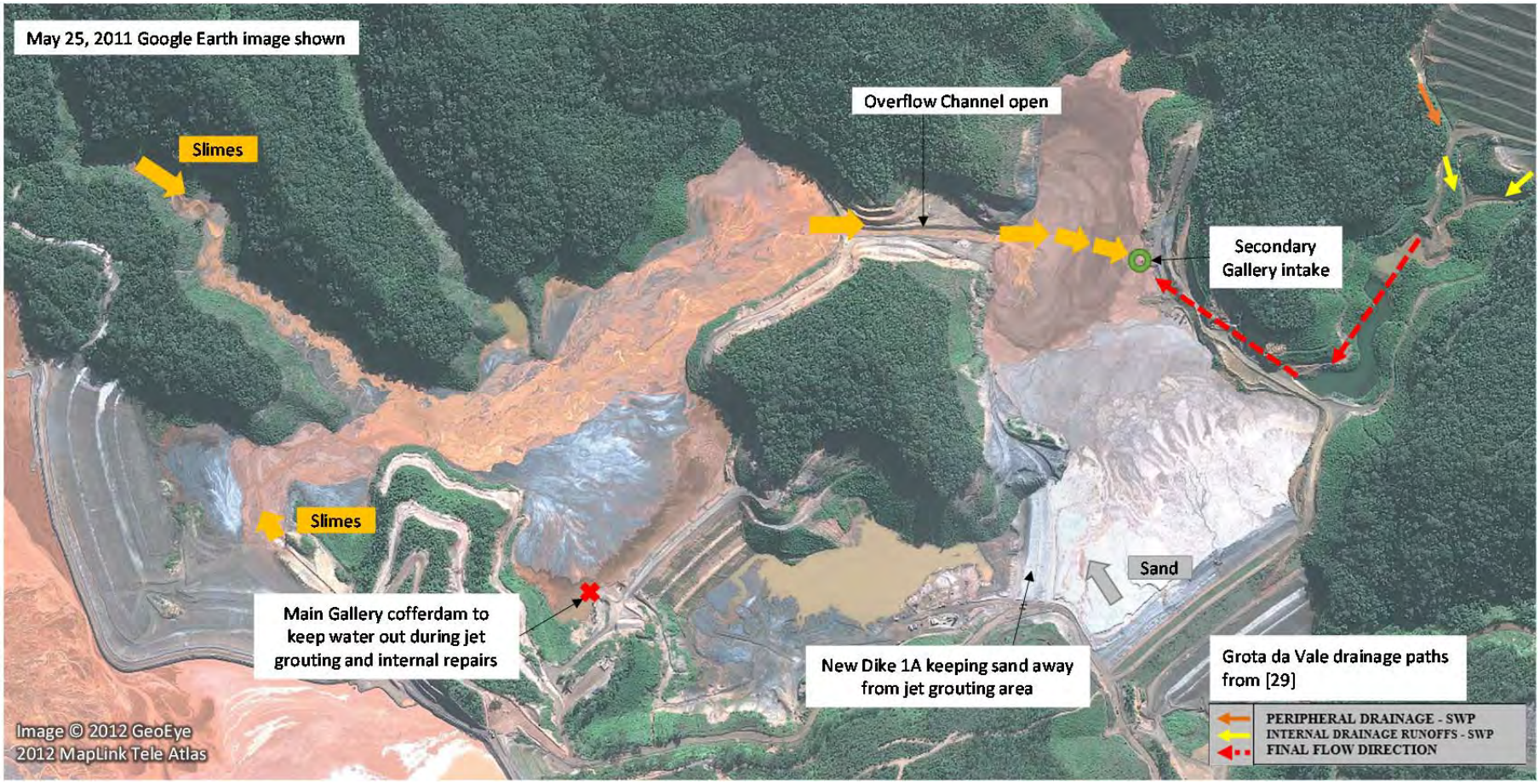

Figure B.B2-15 Grota da Vale timeline – May, 2011

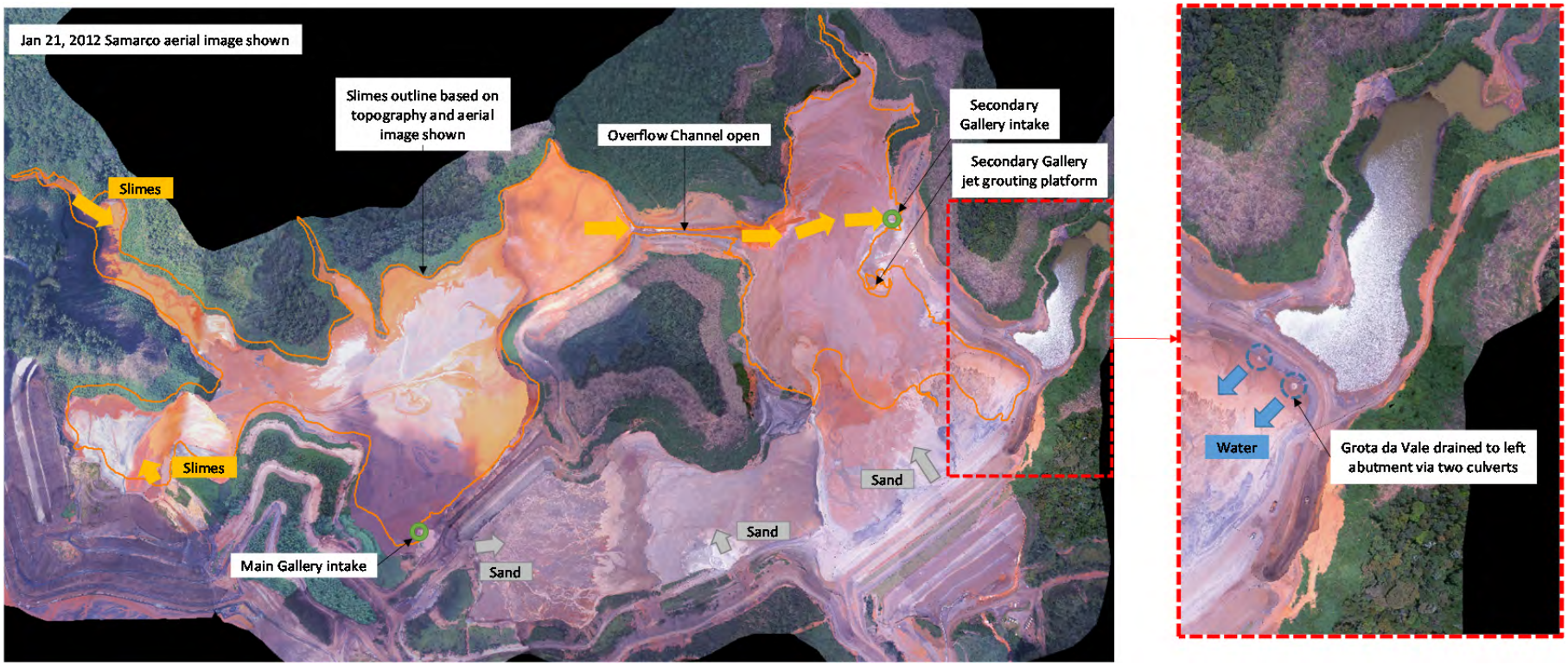

Figure B.B2-16 Grota da Vale timeline – January, 2012

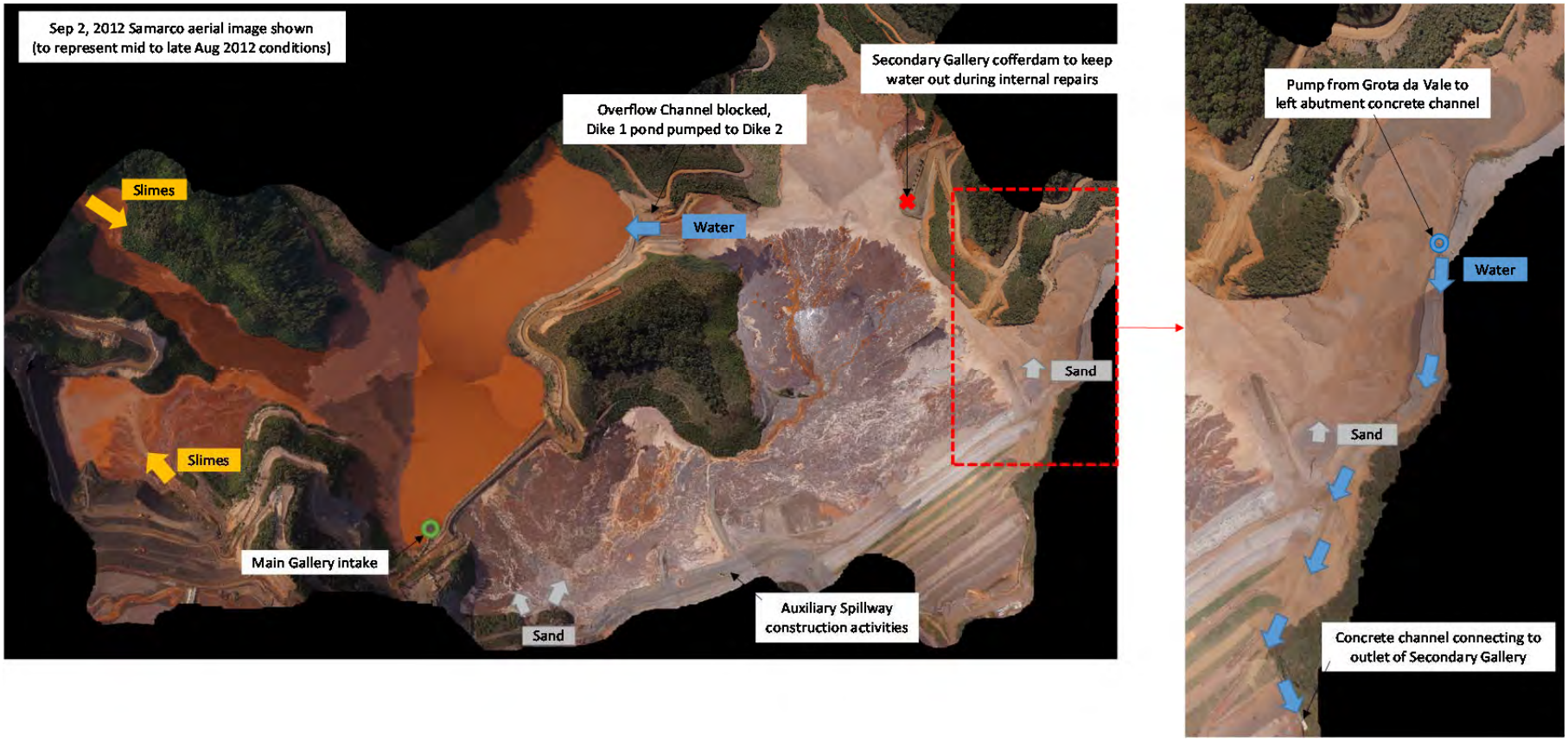

Figure B.B2-17 Grota da Vale timeline – September, 2012

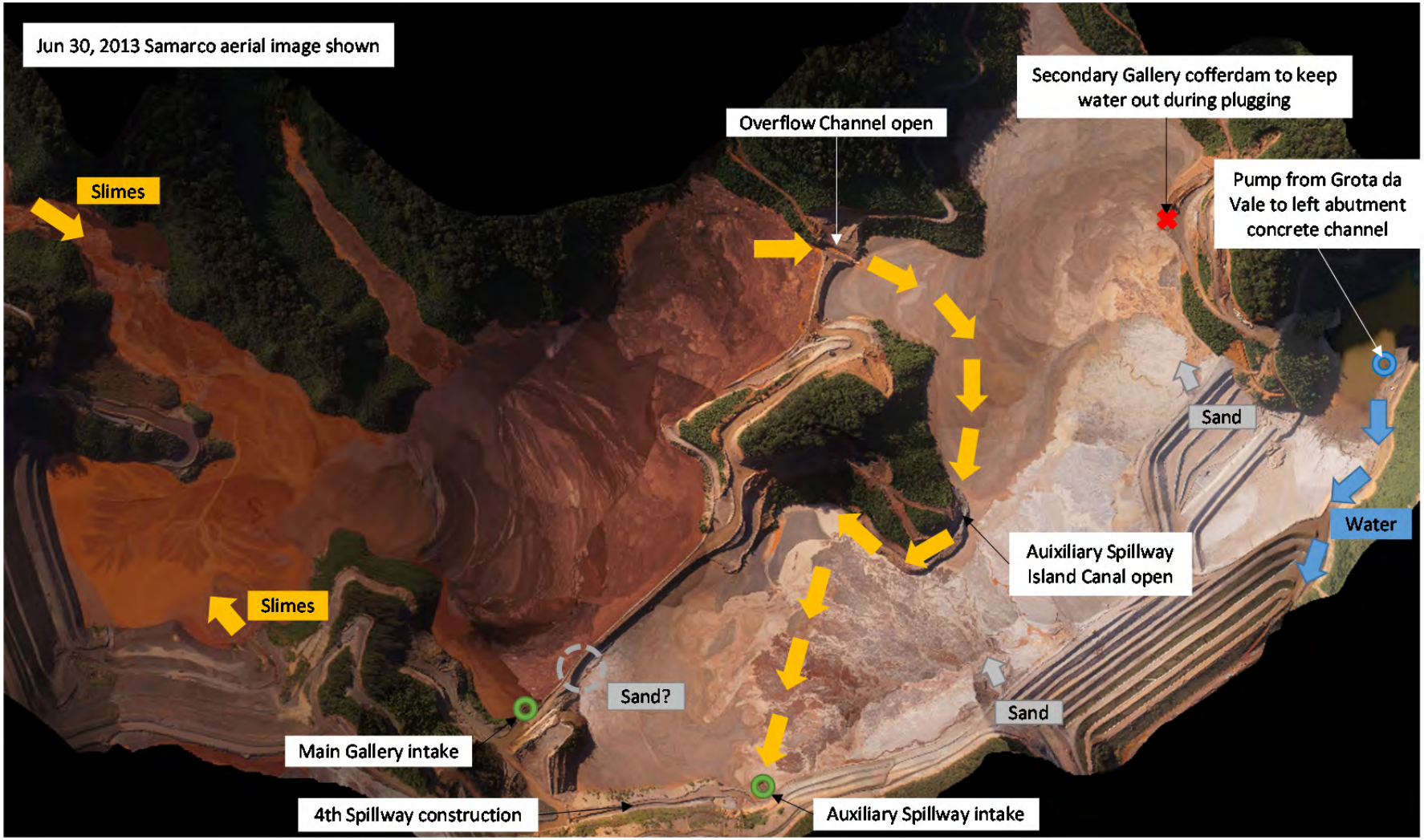

Figure B.B2-18 Grota da Vale timeline – June, 2013

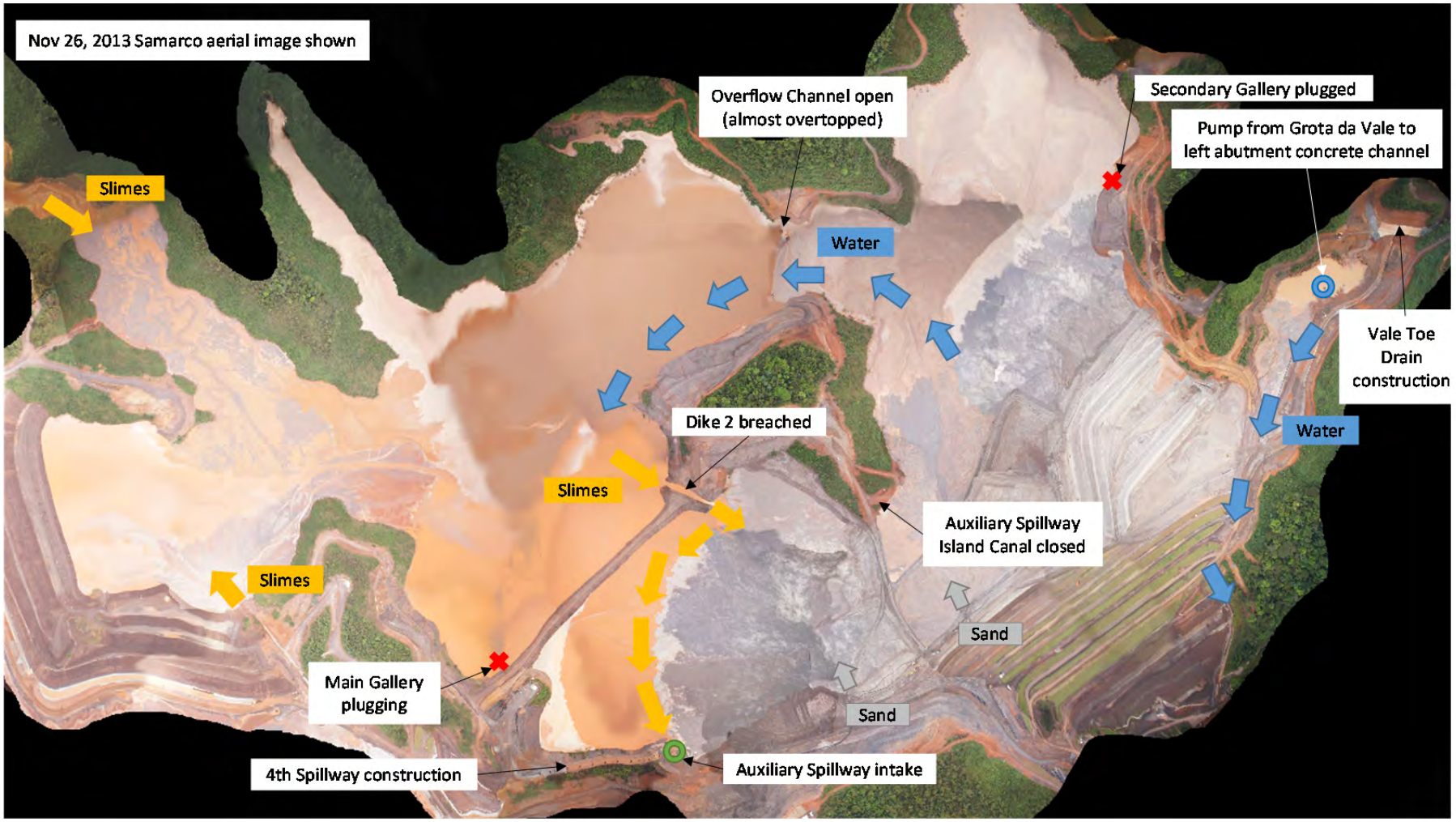

Figure B.B2-19 Grota da Vale timeline – November, 2013

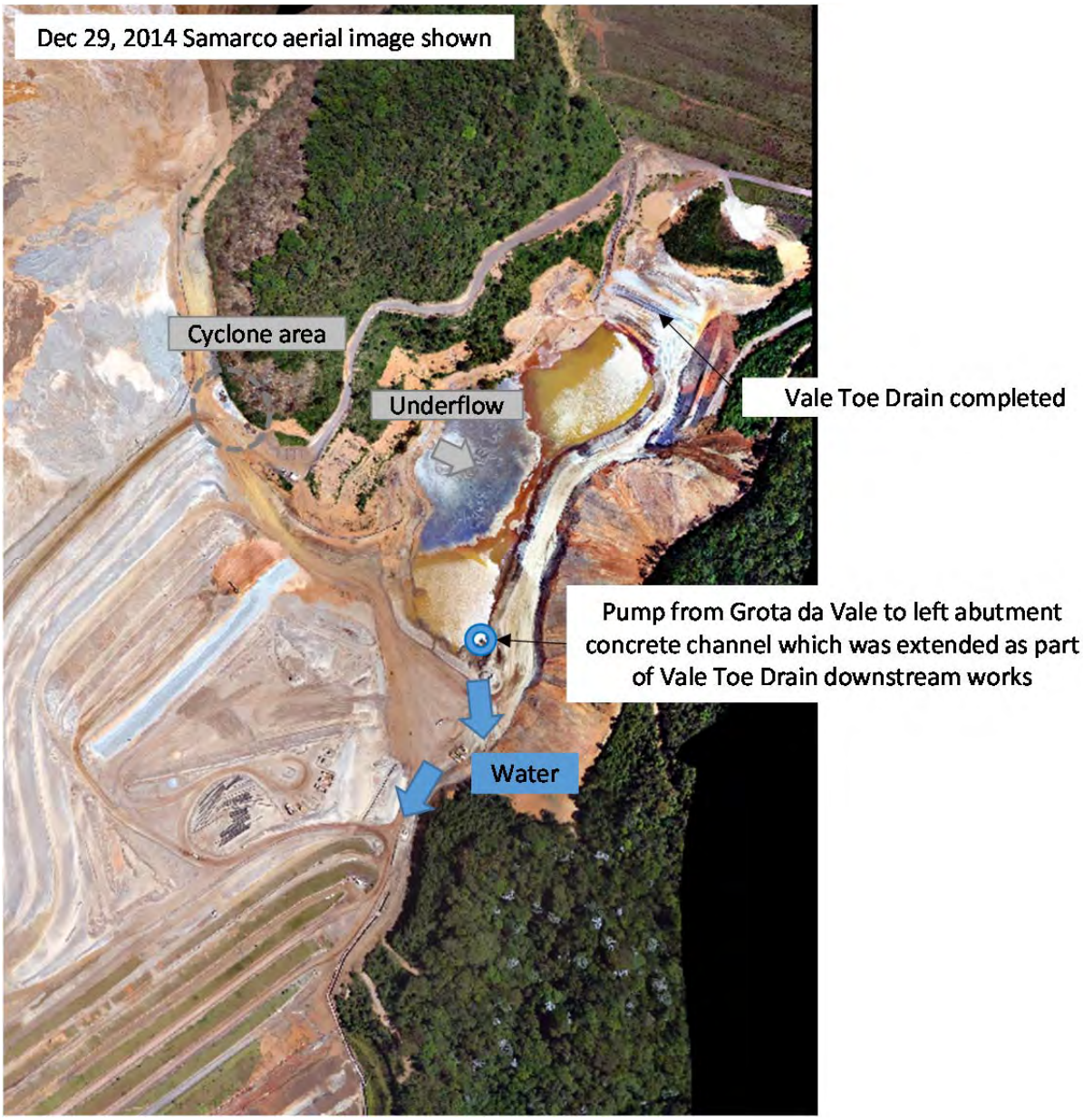

Figure B.B2-20 Grota da Vale timeline – December, 2014

Figure B.B2-21 Grota da Vale timeline – October, 2015

ATTACHMENT B3

Dike 1 Crest Elevation

Appendix B: Attachment B3
Dike 1 Crest Elevation

TABLE OF CONTENTS

List of Tables

List of Figures

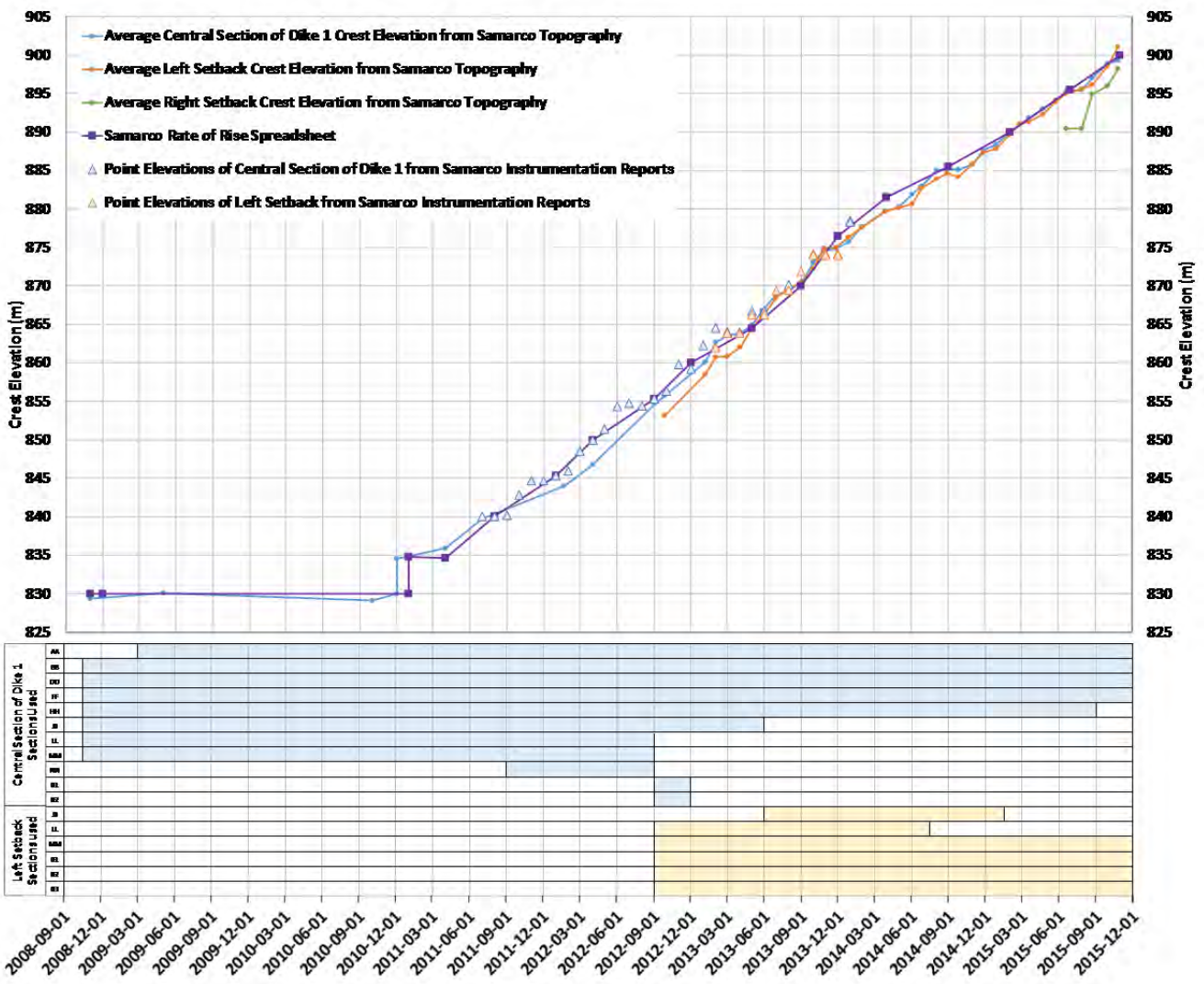

Figure B.B3-1 Comparison of data sources for Dike 1 crest elevation

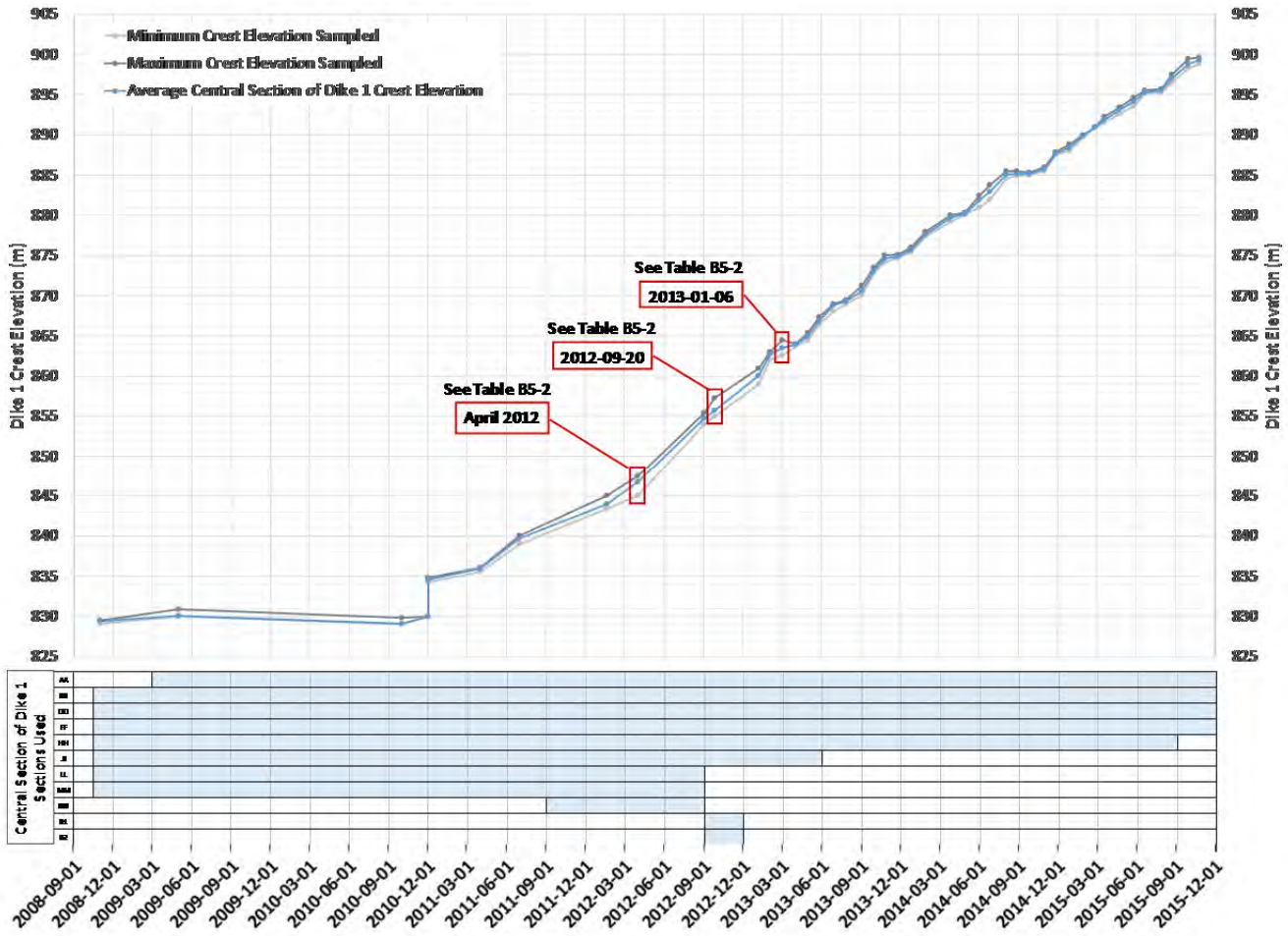

Figure B.B3-2 Minimum, maximum and average Dike 1 crest elevations from Samarco topography

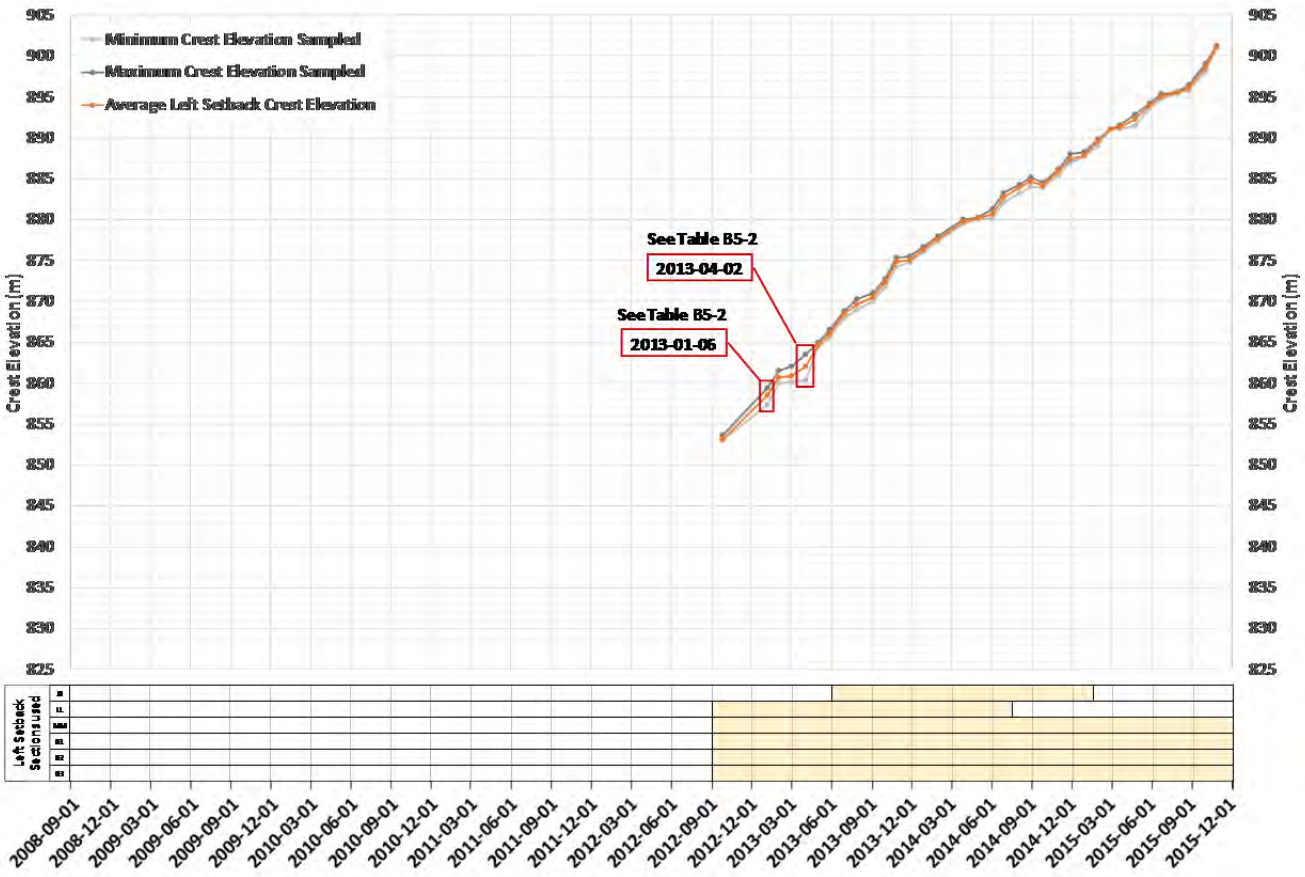

Figure B.B3-3 Minimum, maximum and average left setback crest elevations from Samarco topography

Table B.B3-1 Summary of Dike 1 crest elevation from Samarco topography

		Central Section of Dike 1												Left Setback							Right Setback		
Survey Date	Drawing Number	Section AA Crest Elevation (m)	Section BB Crest Elevation (m)	Section DD Crest Elevation (m)	Section FF Crest Elevation (m)	Section HH Crest Elevation (m)	Section JJ Crest Elevation (m)	Section LL Crest Elevation (m)	Section MM Crest Elevation (m)	Section NN Crest Elevation (m)	Section 01 Crest Elevation (m)	Section 02 Crest Elevation (m)	Average (m)	Section JJ Crest Elevation (m)	Section LL Crest Elevation (m)	Section MM Crest Elevation (m)	Section 01 Crest Elevation (m)	Section 02 Crest Elevation (m)	Section 03 Crest Elevation (m)	Average (m)	Crest Elevation (m)	Plateau Elevation (m)	Non-Setback Crest Elevation (m)
November 2008	G021600-O-130124_R03	-	829.4	829.5	829.5	829.5	829.4	829.1	829.3	-	-	-	**829.4**	-	-	-	-	-	-	-	-	-	-
May 2009	G021600-O-130415_R-01	830.9	830.0	830.0	830.0	830.0	830.0	830.0	830.0	-	-	-	**830.1**	-	-	-	-	-	-	-	-	-	-
October 2010	G011609-K-100002_R1	829.9	829.0	829.0	829.0	829.0	829.0	829.0	829.0	-	-	-	**829.1**	-	-	-	-	-	-	-	-	-	-
December 2010	G011609-K-100007_R0	834.5	834.3	834.6	834.5	834.4	834.8	834.6	834.6	-	-	-	**834.5**	-	-	-	-	-	-	-	-	-	-
2011-04-14	2011_0414_FundaoBarramento.DWG	836.0	836.0	836.0	836.0	835.8	835.5	836.0	836.0	-	-	-	**835.9**	-	-	-	-	-	-	-	-	-	-
July 2011	SA-1849_R02	839.8	840.0	840.0	840.0	840.0	840.0	839.0	839.0	-	-	-	**839.7**	-	-	-	-	-	-	-	-	-	-
2011-10-24	G001609-K-022243	840.0	840.0	840.0	840.0	840.0	840.0	840.0	840.0	840.0	-	-	**840.0**	-	-	-	-	-	-	-	-	-	-
2012-01-21	G001609-K-000024_R-00	845.0	844.6	843.7	843.4	843.6	844.0	844.2	844.1	843.4	-	-	**844.0**	-	-	-	-	-	-	-	-	-	-
April 2012	G001613-O-100064_R00	845.1	845.0	845.3	846.5	847.5	847.5	847.5	847.5	847.5	-	-	**846.8**	-	-	-	-	-	-	-	-	-	-
2012-09-02	G001609-K-000059_R0	854.5	854.4	854.5	854.4	854.6	855.4	855.3	855.3	854.7	854.9	854.0	**854.7**	-	-	-	-	-	-	-	-	-	-
2012-09-26	G001609-K-000063_R3	856.0	857.3	856.3	855.1	855.5	855.5	855.9	855.7	855.3	855.2	855.0	**855.7**	-	853.6	853.0	853.0	853.0	853.0	**853.1**	-	-	-
2013-01-06	G001609-K-000067_R0	859.0	859.6	860.3	860.8	861.0	860.0	-	-	-	-	-	**860.1**	-	859.2	859.4	858.6	858.0	857.4	**858.5**	-	-	-
2013-02-01	G001609-K-000068_R1	862.0	863.0	863.0	863.0	862.7	862.3	-	-	-	-	-	**862.7**	-	861.5	861.0	860.5	860.0	860.7	**860.8**	-	-	-
2013-03-02	G001609-K-000069_R0	862.6	863.5	863.7	863.8	864.5	863.0	-	-	-	-	-	**863.5**	-	862.0	861.0	860.7	860.5	860.2	**860.9**	-	-	-
2013-04-02	G001609-K-000070_R1	863.8	864.0	864.0	864.0	863.8	863.6	-	-	-	-	-	**863.9**	-	863.5	863.0	862.6	860.7	860.4	**862.1**	-	-	-
2013-05-01	G001609-K-000074_R1	864.9	864.8	865.2	865.4	864.5	864.8	-	-	-	-	-	**864.9**	-	865.0	864.5	864.5	864.5	864.5	**864.6**	-	-	-
2013-05-27	G001609-K-000075_R0	866.5	866.7	867.1	867.3	866.7	-	-	-	-	-	-	**866.9**	865.5	866.4	866.5	866.2	865.7	865.8	**866.0**	-	-	-
2013-06-30	G001609-K-000079_R1	869.0	869.0	869.0	869.0	868.1	-	-	-	-	-	-	**868.8**	868.0	868.5	868.5	868.5	868.5	868.8	**868.5**	-	-	-
2013-07-29	G001609-K-000081_R1	869.5	869.5	869.5	869.2	869.0	-	-	-	-	-	-	**869.3**	869.0	869.0	869.1	869.9	870.3	870.3	**869.6**	-	-	-
2013-09-03	G001609-K-000083_R0	870.6	871.3	870.7	870.5	870.0	-	-	-	-	-	-	**870.6**	870.0	870.0	870.6	871.0	871.0	870.5	**870.5**	-	-	-
2013-10-01	G001609-K-000086_R2	873.0	872.9	872.8	873.5	873.0	-	-	-	-	-	-	**873.0**	872.7	871.8	872.0	872.3	872.3	872.7	**872.3**	-	-	-
2013-10-27	G001609-K-000089_R1	874.7	874.4	874.1	874.8	875.0	-	-	-	-	-	-	**874.6**	874.8	875.0	875.3	875.1	874.8	874.2	**874.9**	-	-	-
2013-11-26	G001609-K-000090_R2	875.0	875.1	874.7	874.7	874.8	-	-	-	-	-	-	**874.8**	874.8	874.8	874.9	875.5	875.2	875.0	**875.0**	-	-	-
2013-12-27	G001609-K-000091_R2	875.4	875.4	875.9	875.8	876.0	-	-	-	-	-	-	**875.7**	876.5	876.6	876.0	876.2	876.1	876.4	**876.3**	-	-	-
2014-01-29	G001609-K-000092_R-01	877.4	877.5	877.5	878.0	878.0	-	-	-	-	-	-	**877.7**	878.0	877.5	877.5	877.6	877.9	877.4	**877.7**	-	-	-
2014-03-28	G001609-K-000101_R-00	879.2	879.5	879.5	880.1	880.0	-	-	-	-	-	-	**879.7**	879.5	879.5	879.5	879.8	880.0	880.0	**879.7**	-	-	-
2014-05-01	G001609-K-000103_R-01	880.1	880.1	880.3	880.3	880.3	-	-	-	-	-	-	**880.2**	880.2	880.0	880.2	880.0	880.3	880.2	**880.1**	-	-	-
2014-06-03	G001609-K-000103_R-01	882.0	882.4	882.5	881.8	881.0	-	-	-	-	-	-	**881.9**	880.4	880.2	880.8	880.8	880.7	881.3	**880.7**	-	-	-
2014-06-27	G001609-K-000104	883.3	883.8	883.2	882.5	882.0	-	-	-	-	-	-	**883.0**	882.1	882.5	883.0	883.3	882.7	882.8	**882.7**	-	-	-
2014-08-04	G001609-K-000105_R0	884.6	885.2	885.2	885.5	884.9	-	-	-	-	-	-	**885.1**	884.0	-	883.2	884.0	884.0	884.3	**883.9**	-	-	-
2014-08-29	G001609-K-100005	884.9	885.1	885.2	885.5	885.0	-	-	-	-	-	-	**885.1**	884.5	-	884.0	884.7	884.9	885.2	**884.7**	-	-	-
2014-09-26	G001609-K-100006_R-01	885.3	885.3	885.0	885.0	885.0	-	-	-	-	-	-	**885.1**	884.3	-	884.0	884.0	884.0	884.5	**884.2**	-	-	-
2014-10-31	G001609-K-100006_R-01	886.0	886.0	886.0	885.5	885.5	-	-	-	-	-	-	**885.8**	885.4	-	885.7	886.1	886.1	886.1	**885.9**	-	-	-
2014-11-27	G001609-K-100008	887.8	887.8	887.8	887.6	887.6	-	-	-	-	-	-	**887.7**	887.5	-	887.0	888.0	887.4	887.0	**887.4**	-	-	-
2014-12-29	G001680-K-100001_R-01	888.3	888.1	888.8	888.8	888.0	-	-	-	-	-	-	**888.4**	887.9	-	887.7	887.8	887.8	888.3	**887.9**	-	-	-
2015-01-29	G001680-K-100002_R-01	889.8	889.8	889.8	890.0	890.0	-	-	-	-	-	-	**889.9**	889.0	-	889.5	889.8	889.8	889.8	**889.6**	-	-	-
2015-02-26	G001680-K-100003_R-01	891.0	891.0	891.0	891.0	891.0	-	-	-	-	-	-	**891.0**	-	-	891.0	891.0	891.0	891.0	**891.0**	-	-	-
2015-03-20	G001680-K-100004_R-00	891.6	892.0	892.3	891.5	891.7	-	-	-	-	-	-	**891.8**	-	-	891.1	891.5	891.5	891.1	**891.3**	-	-	-
2015-04-24	G001680-K-100005_R-01	893.0	893.4	893.4	893.0	892.6	-	-	-	-	-	-	**893.1**	-	-	892.8	892.8	892.1	891.4	**892.3**	-	-	-
2015-05-27	G001680-K-100006_R-00	893.6	894.1	894.6	894.6	893.8	-	-	-	-	-	-	**894.1**	-	-	893.6	894.2	894.1	894.1	**894.0**	-	-	-
2015-06-22	G001680-K-100007_R-02	895.1	895.6	895.4	895.2	895.2	-	-	-	-	-	-	**895.3**	-	-	895.4	895.2	894.7	894.8	**895.0**	**890.4**	**891.5**	**895.2**
2015-07-30	G001680-K-100008_R-00	895.7	895.5	895.6	895.4	895.3	-	-	-	-	-	-	**895.5**	-	-	895.7	895.4	895.6	895.6	**895.6**	**890.4**	**891.5**	**895.4**
2015-08-24	G001680-K-100009_R01	897.5	897.4	896.6	896.5	897.0	-	-	-	-	-	-	**897.0**	-	-	896.3	896.4	895.8	896.0	**896.1**	**895.0**	**891.5**	**895.3**
2015-10-01	G001680-K-100010	898.3	899.5	899.1	898.4	-	-	-	-	-	-	-	**898.8**	-	-	898.0	899.0	898.3	898.7	**898.5**	**896.0**	**893.5**	**892.2**
2015-10-27	G001680-K-100011_R-00	899.4	899.7	898.8	899.4	-	-	-	-	-	-	-	**899.3**	-	-	901.0	901.0	901.0	901.2	**901.1**	**898.2**	**893.5**	**892.0**

Legend

	Exact survey date unknown, assumed to have been conducted on the first of the month.
	No drawing number available; topography is from a drone survey trial.
	No elevation sampled since the section line does not intersect the location of interest.

ATTACHMENT B4

Pond Elevation and Beach Width

Samarco Monthly Geotechnical Monitoring Reports – Beach Width Measurements
Summary of Pond Elevations
Pond Image Timeline

Samarco Monthly Geotechnical Monitoring Reports – Beach Width Measurements

July 2011

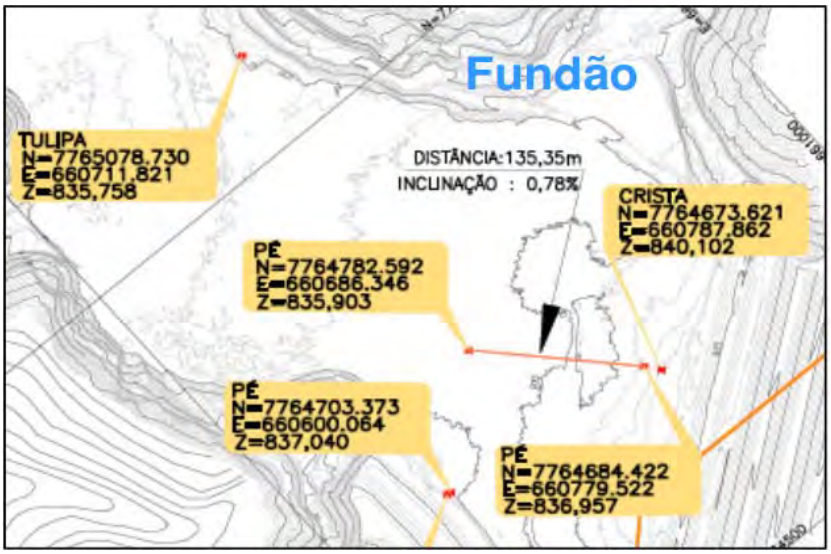

August 2011

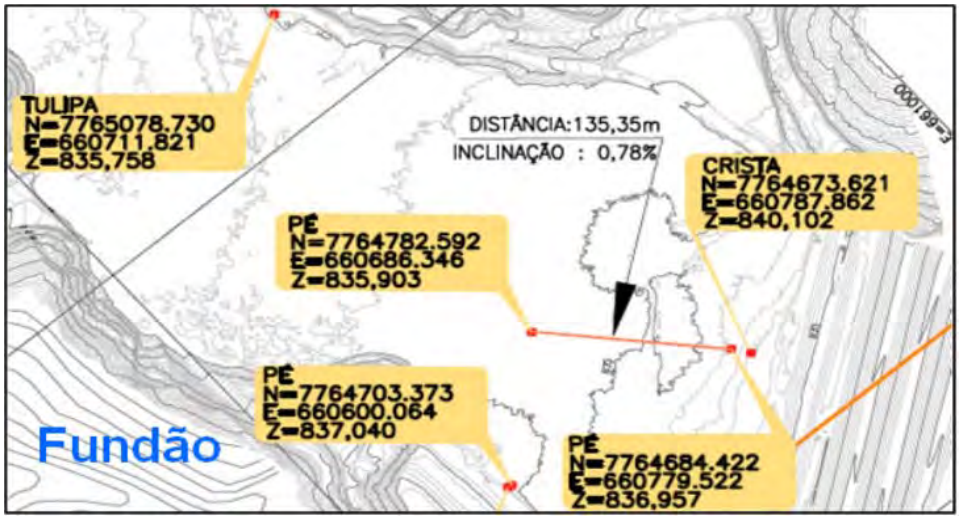

The point elevations and beach widths are the same as those presented in the previous monitoring report.

September 2011

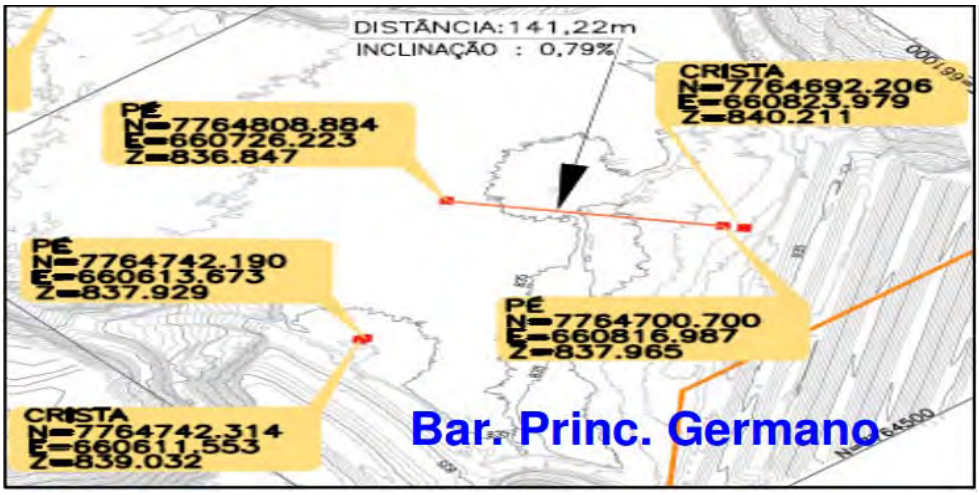

Dam was mislabeled as Germano in the September 2011 monitoring report.

October 2011

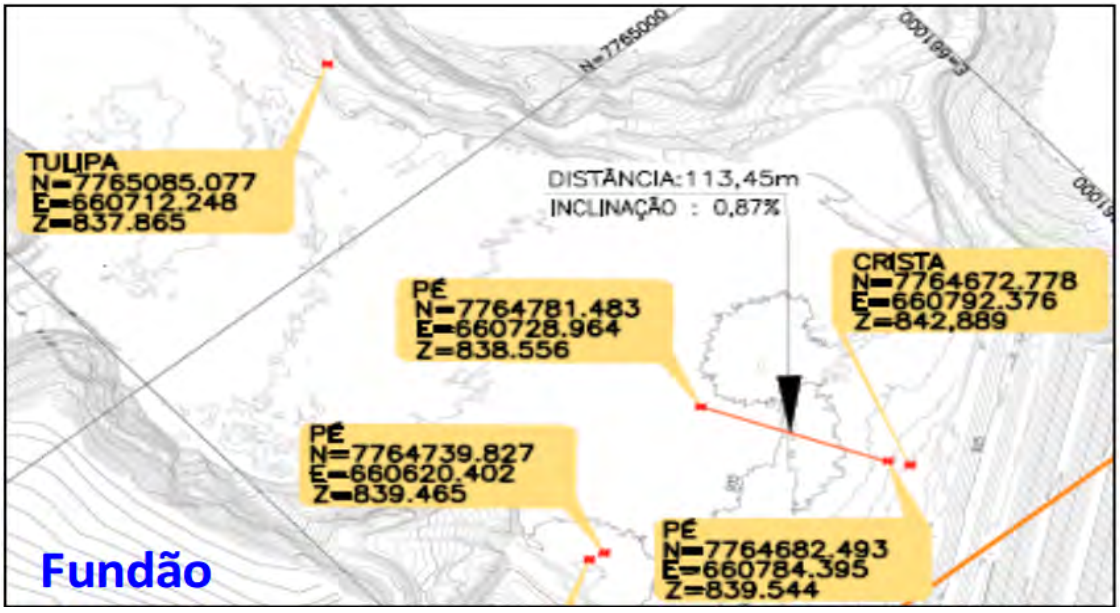

November 2011

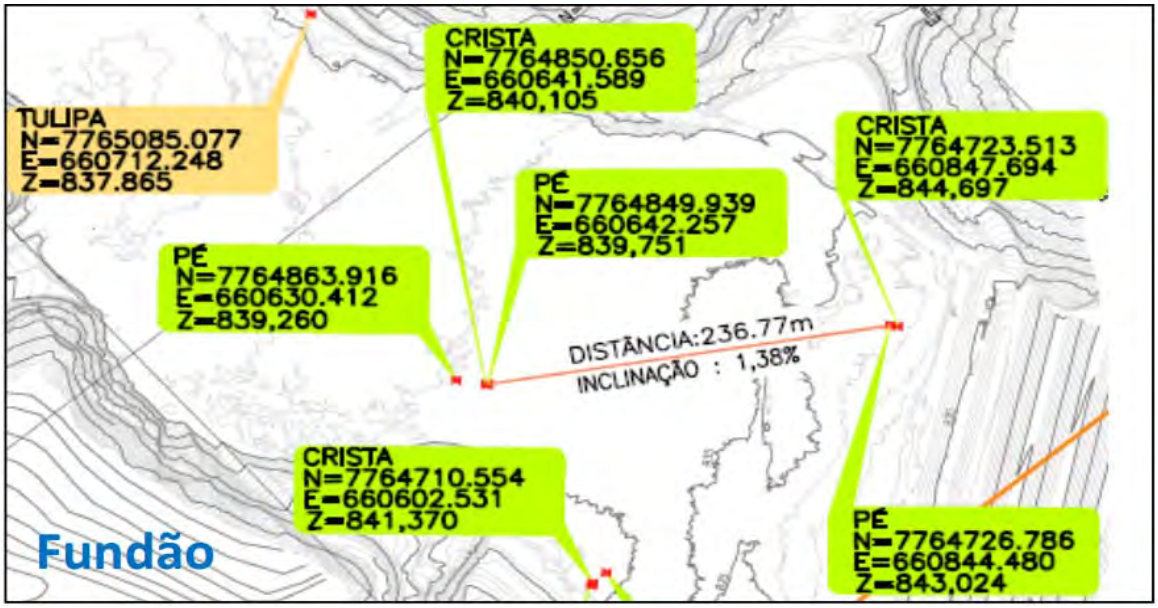

December 2011

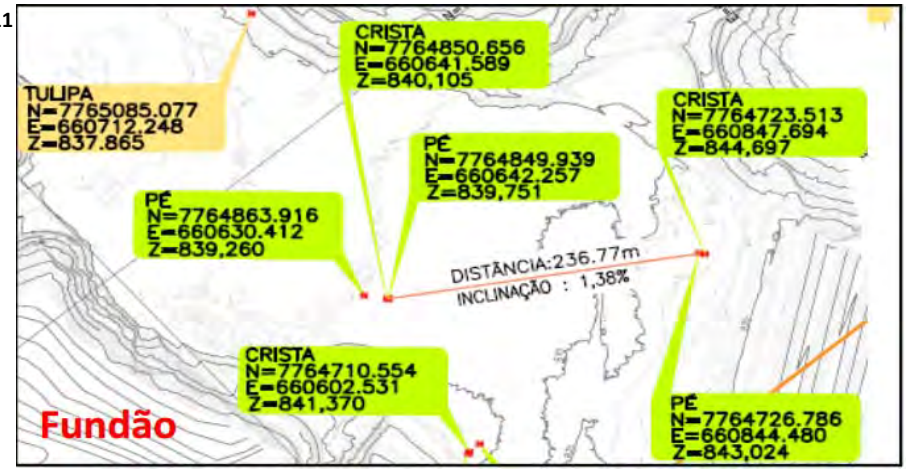

The point elevations and beach widths are the same as those presented in the previous monitoring report.

January 2012

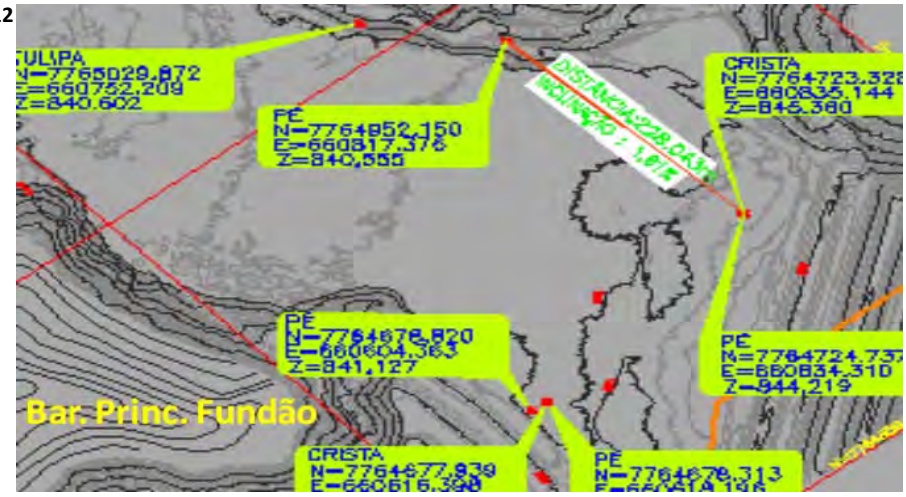

February 2012

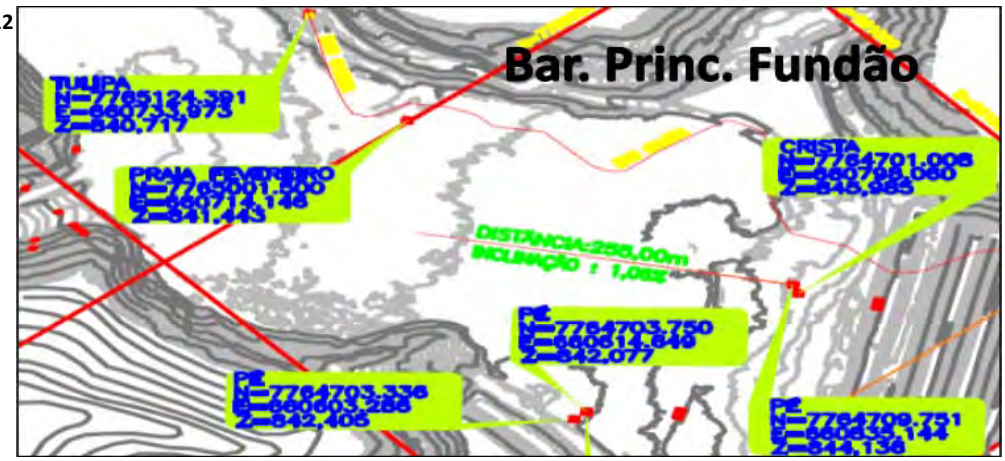

The coordinates for the upstream toe of Dike 1 do not plot where it is shown in the monitoring report. The coordinates are assumed to be erroneous.

March 2012

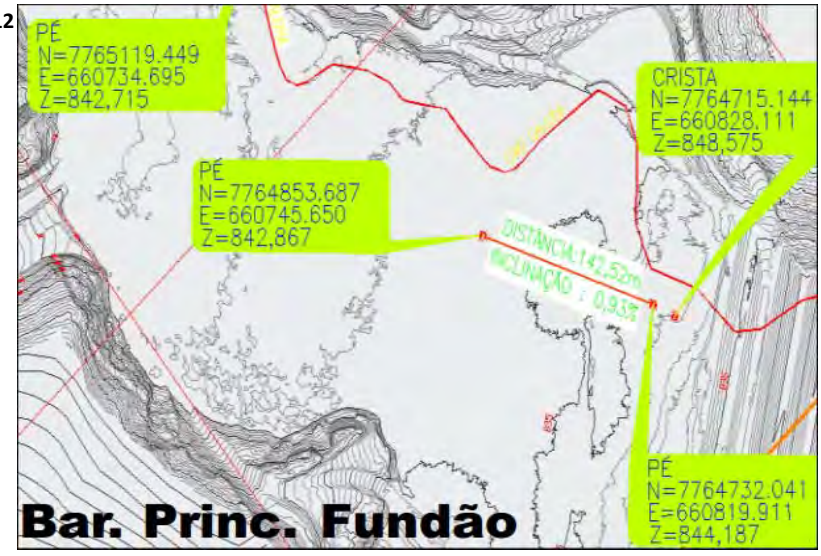

April 2012

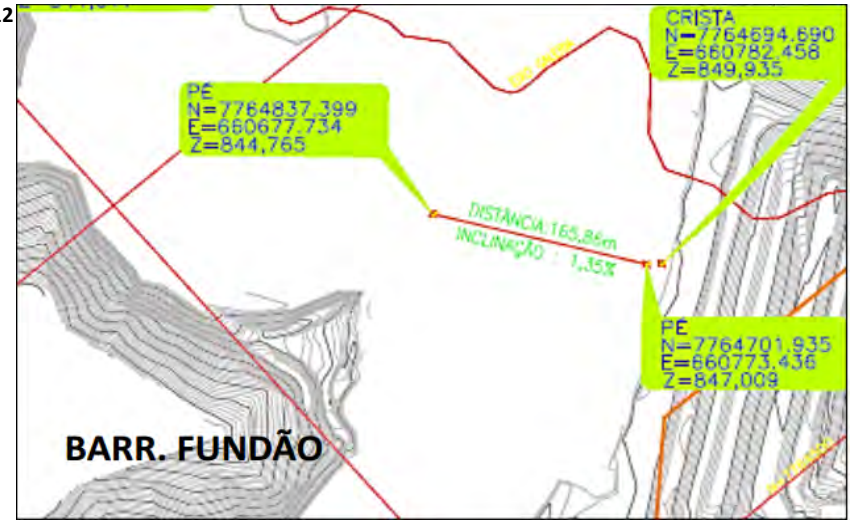

May 2012

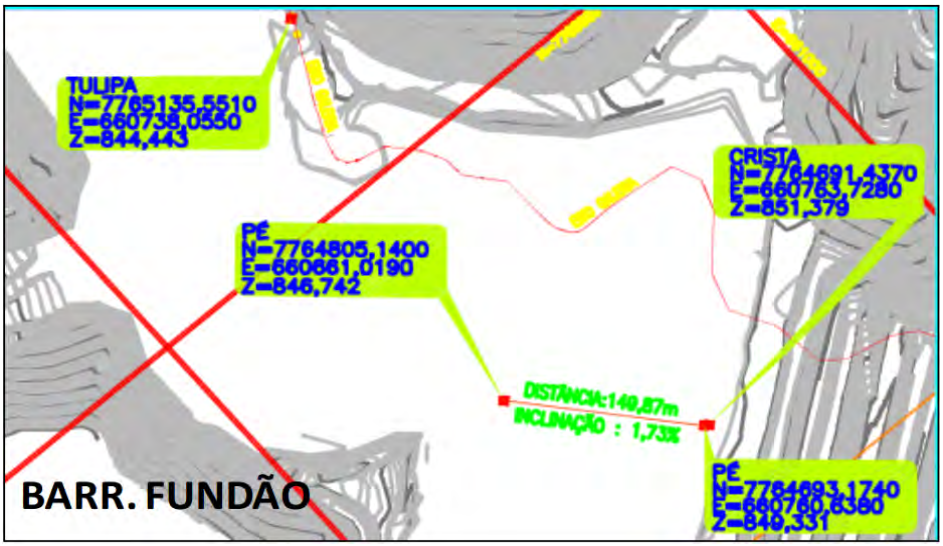

June 2012

July 2012

August 2012

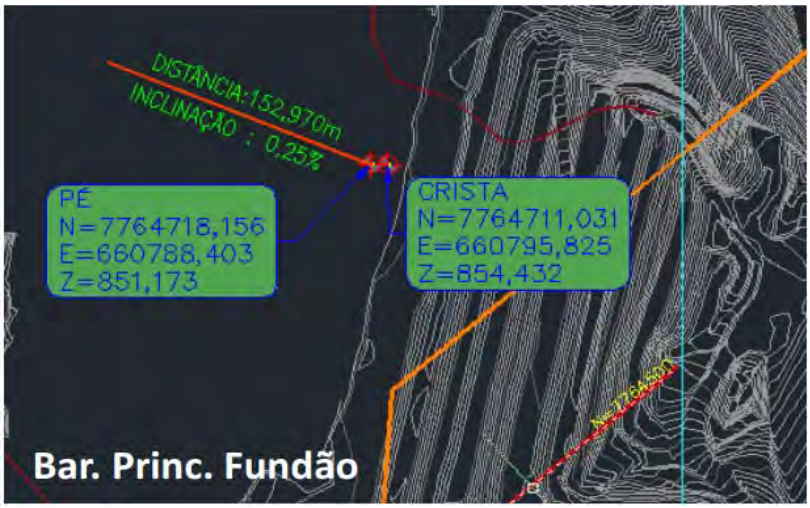

September 2012

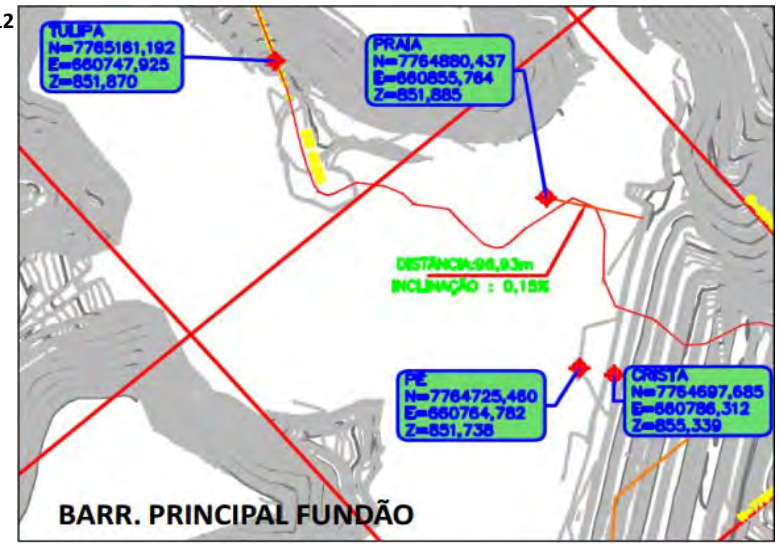

October 2012

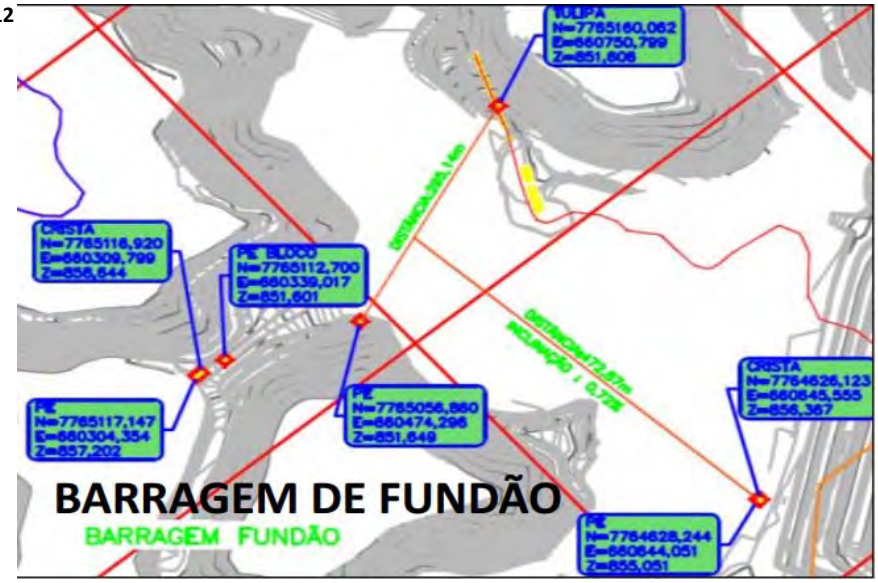

November 2012

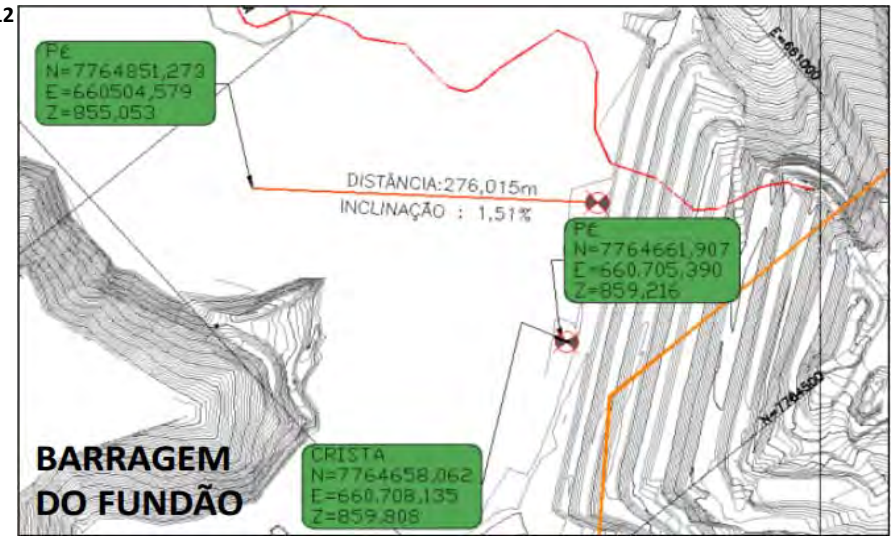

December 2012

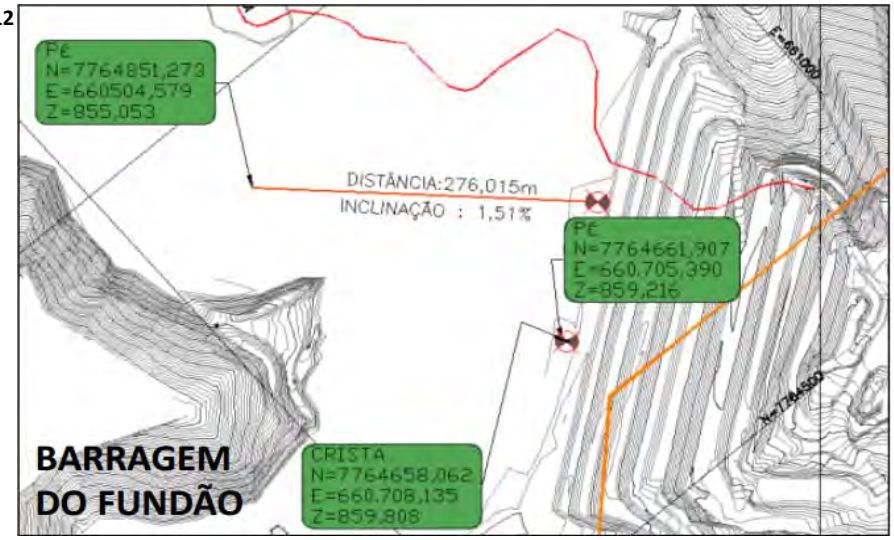

The point elevations and beach widths are the same as those presented in the previous monitoring report.

January 2013

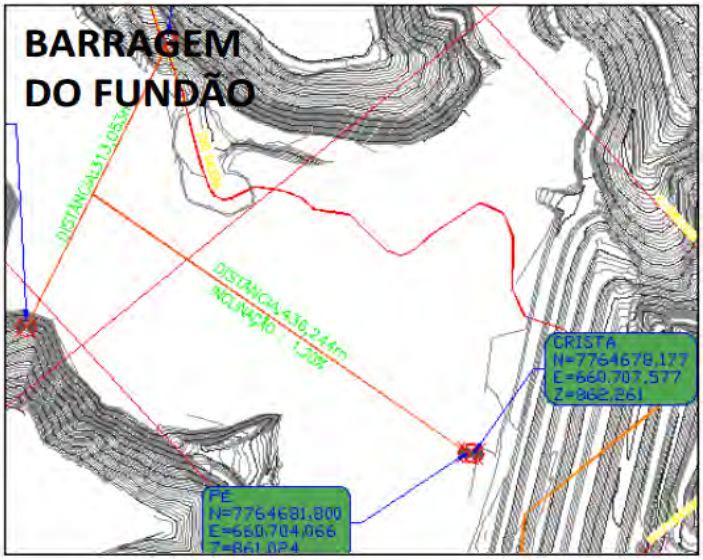

February 2013

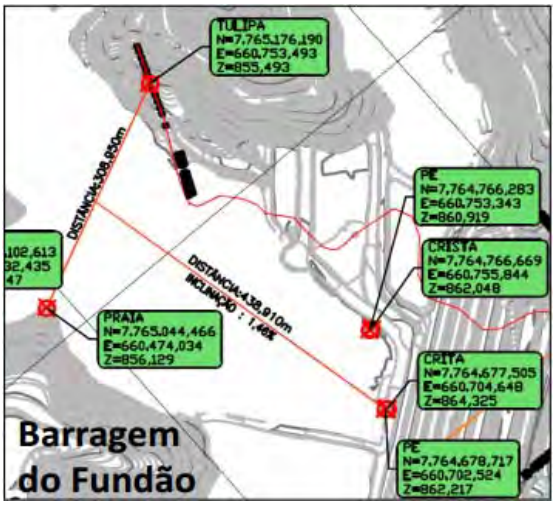

March 2013

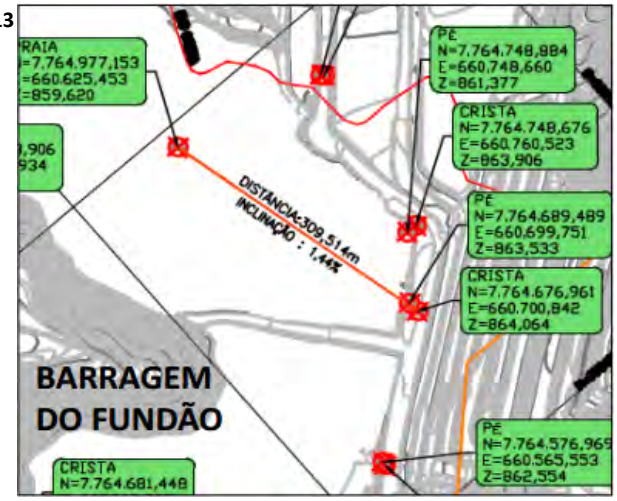

April 2013

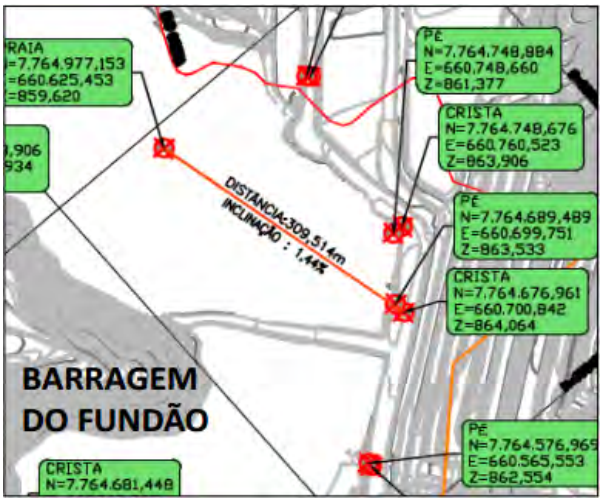

May 2013

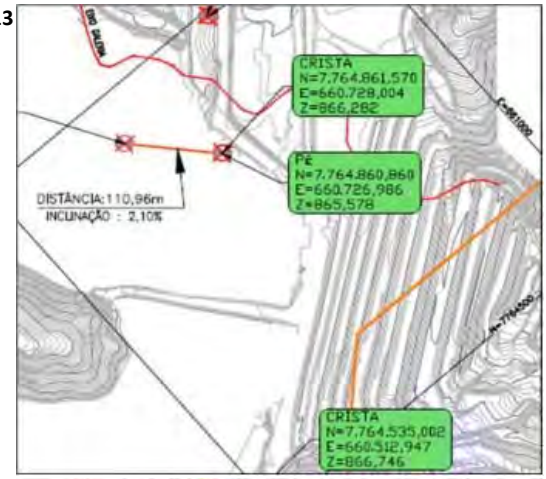

June 2013

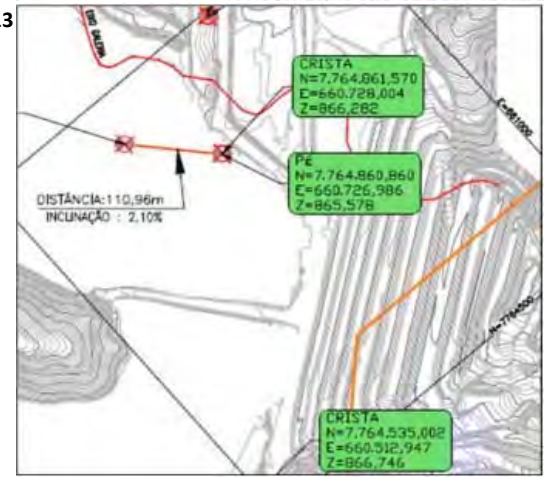

The point elevations and beach widths are the same as those presented in the previous monitoring report.

July 2013

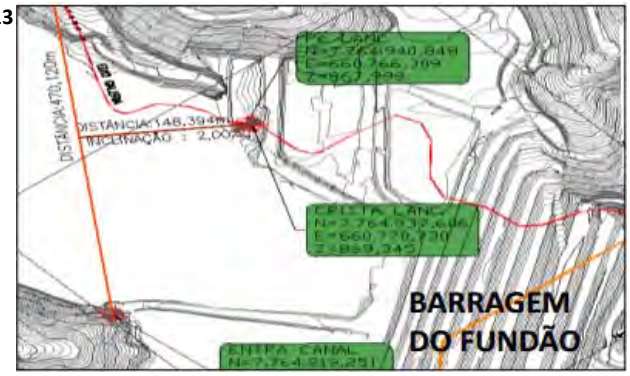

August 2013

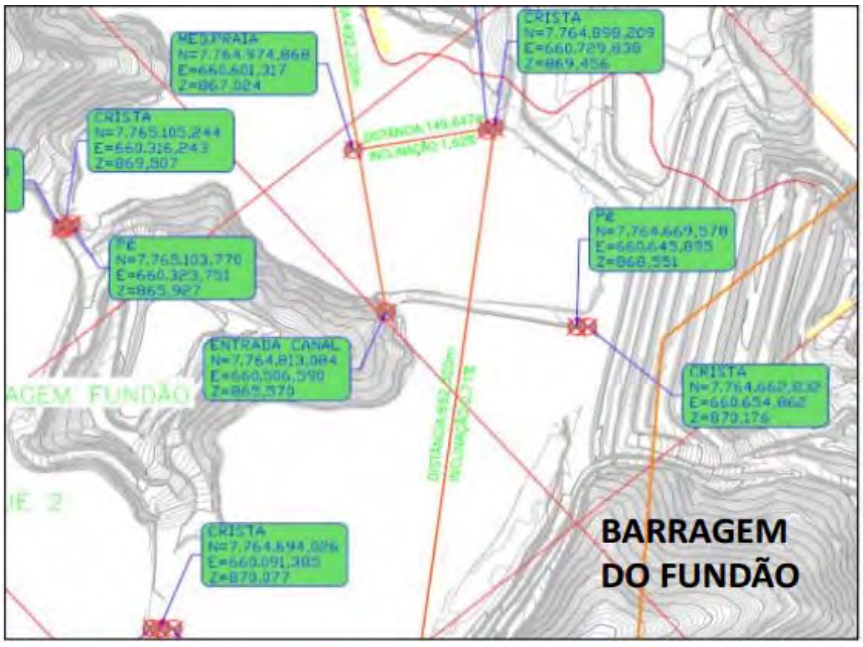

September 2013

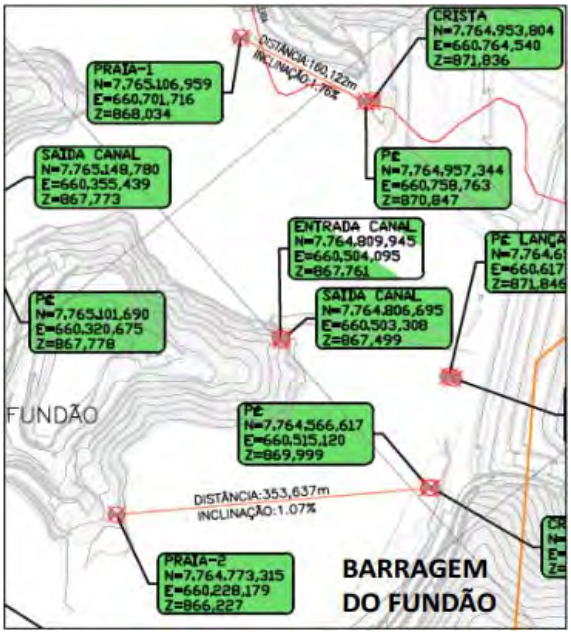

October 2013

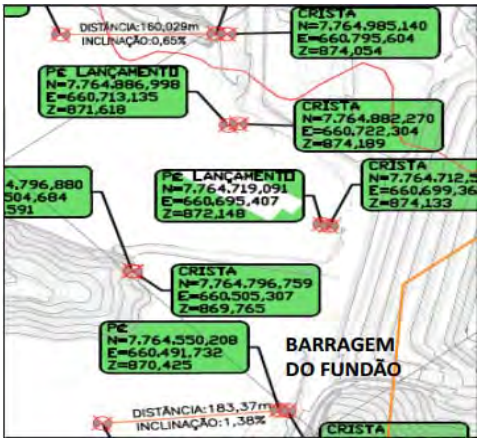

November 2013

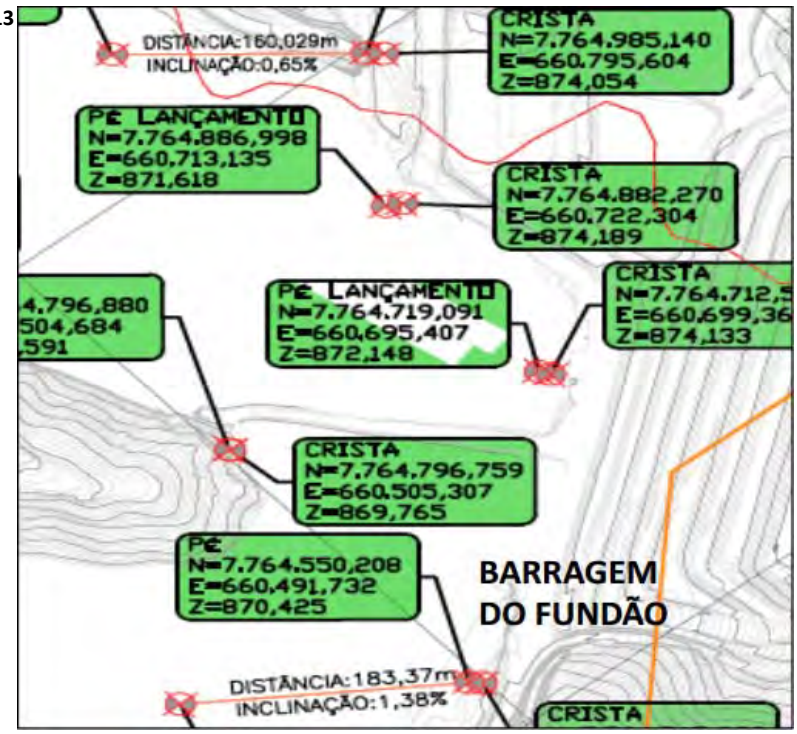

The point elevations and beach widths are the same as those presented in the previous monitoring report.

December 2013

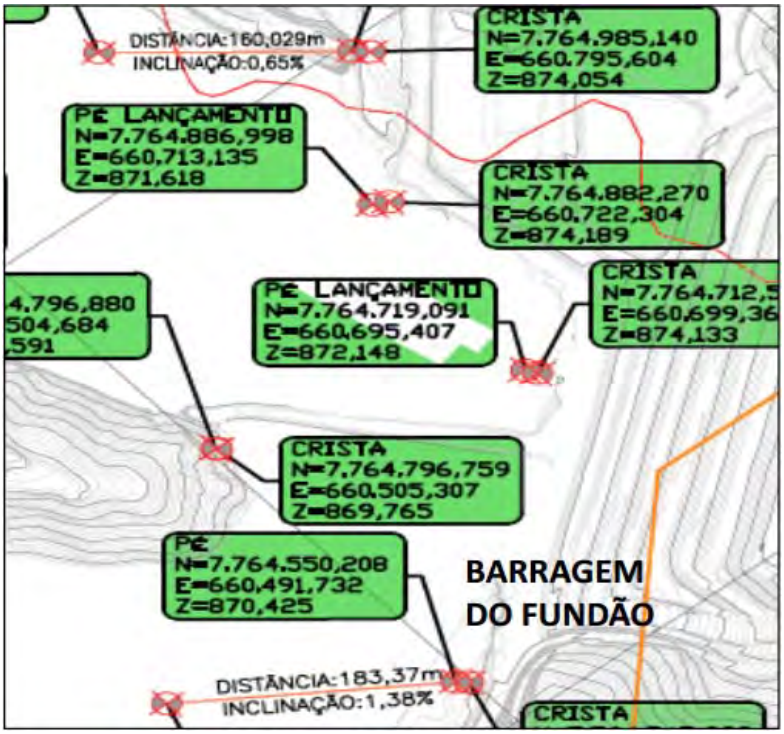

The survey date for the data shown in the December 2013 report is given as October 30, 2013 which is the same date as the one given in the October 2013 report. The measurements shown are discarded from the beach width data set.

January 2014

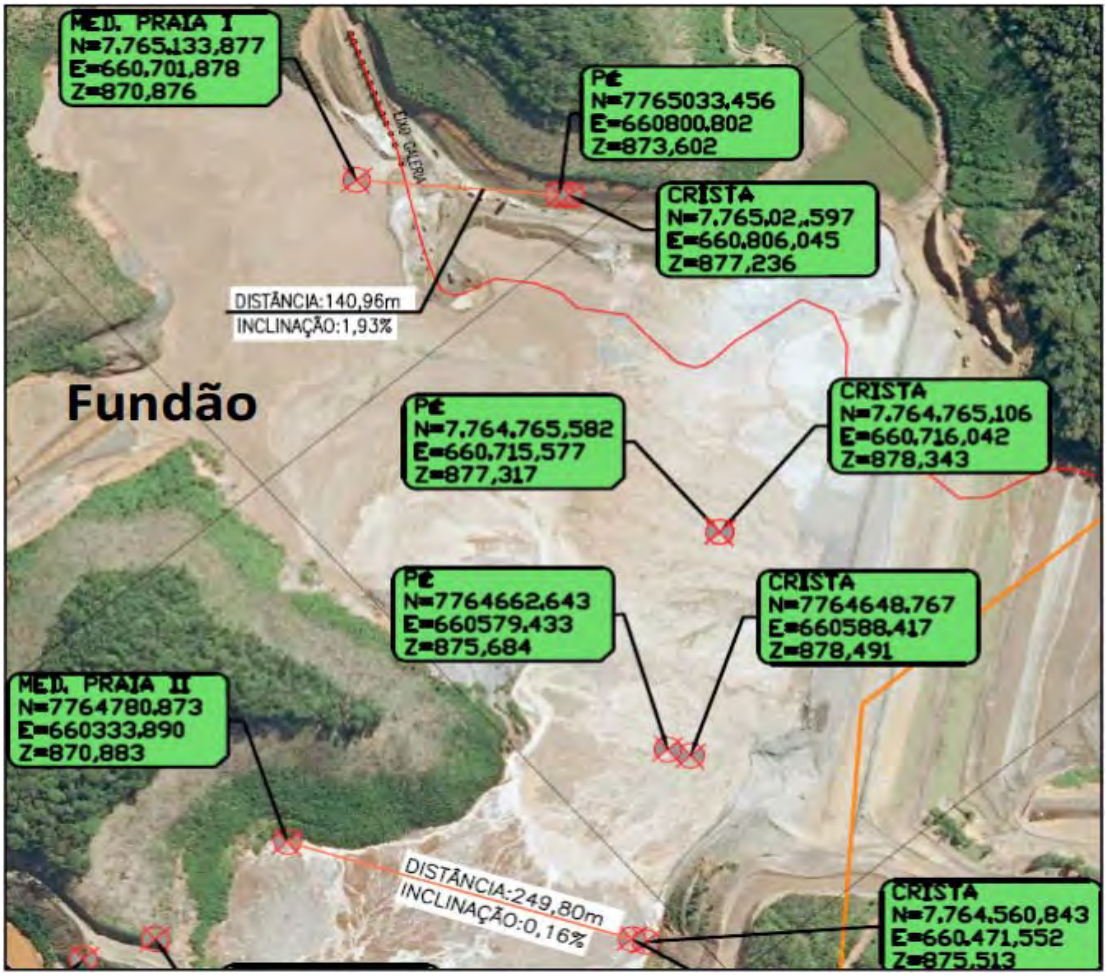

Summary of Pond Elevations

File Survey Date	Basis for Delineation	Pond Elevation (m)								Topography Source							
		Dike 2 Max.	Dike 1 Min.	Dike 1 Max.	Old Dike 1A Min.	Old Dike 1A Max.	New Dike 1A	Grota Upstream Dike	Grota da Vale Dike	Stitched Stripped Ground	G021600-O-130458_R-00 (not shown in image timeline)	G021600-O-130415_R-01	SA-1849-R02	041-A-MN-GR-09-006	G011609-K-100006	SA-1788	Monthly Samarco Survey (survey date shown)
2009-04-18	PhotoSat aerial image	841.0	820.0	-				-	-	x							
2009-08-18	PhotoSat aerial image	841.0	805.0	810.0				-	-	x							
2009-11-15	PhotoSat aerial image	847.0	-	-	803.0	808.0		-	-	x				x			
2010-01-17	PhotoSat aerial image	847.0	-	-	809.0	-		-	-	x							
2010-02-22	PhotoSat aerial image	847.0	-	-	809.0	-		-	-	x							
2010-04-27	PhotoSat aerial image	847.0	-	-	813.0	-		-	-	x		x		x			
2010-06-19	PhotoSat aerial image	847.0	-	-	819.0	-		840.0	-	x		x		x			
2010-08-07	PhotoSat aerial image	847.0	-	-	824.0	-		840.0	-	x		x		x			
2010-10-29	PhotoSat aerial image	847.0	-	-	824.0	-	820.0	840.0	822.0	x					x	x	
2010-12-22	PhotoSat aerial image	847.0	-	-	824.0	-	819.0	840.0	822.0	x						x	
2011-02-11	PhotoSat aerial image	848.0	824.0	-			822.0	840.0	822.0	x	x					x	
2011-04-09	PhotoSat aerial image	848.0	830.0	-			822.0	840.0	822.0	x	x					x	
2011-07-01	Samarco topography	852.0	834.0	-			unable to determine						x				
2011-07-27	Samarco monthly report	-	835.9	-			unable to determine						x				
2011-08-17	PhotoSat aerial image	852.0	835.0	-			823.0	840.0	836.0				x				
2011-08-24	Samarco monthly report	-	**835.9**	-			unable to determine						x				
2011-09-15	Samarco monthly report	-	836.8	-			Unable to determine - outside of monthly report coverage						x				
2011-09-21	PhotoSat aerial image	853.0	837.0	-			-	-	841.0	x			x				
2011-10-02	PhotoSat aerial image	853.0	837.0	-			-	-	841.0	x			x				
2011-10-11	Samarco monthly report	-	838.6	-			Unable to determine - outside of monthly report coverage						x				
2011-11-08	Samarco monthly report	-	839.8	-			Unable to determine - outside of monthly report coverage						x				
2011-12-16	Samarco monthly report	-	**839.8**	-			Unable to determine - outside of monthly report coverage						x				
2012-01-10	Samarco monthly report	-	840.6	-			Unable to determine - outside of monthly report coverage										2012-01-21
2012-01-21	Samarco topography	851.0	841.0	-					842.4								2012-01-21
2012-02-09	Samarco monthly report	-	841.4	-				unable to determine									2012-01-21
2012-03-03	PhotoSat aerial image	852.0	842.0	-					842.4								2012-01-21
2012-03-16	Samarco monthly report	-	842.9	-				unable to determine									2012-01-21
2012-04-01	Vale survey	852.5	842.5	-					842.5								2012-04-01 (Vale)
2012-04-19	Samarco monthly report	-	844.8	-					unable to determine								2012-04-01 (Vale)
2012-05-14	Samarco monthly report	-	846.7	-					unable to determine								2012-04-01 (Vale)
2012-06-04	Samarco monthly report	-	848.2	-					unable to determine								2012-04-01 (Vale)
2012-07-13	Samarco monthly report	-	849.5	-					unable to determine								2012-04-01 (Vale)
2012-08-09	Samarco monthly report	-	850.8	-					unable to determine								2012-04-01 (Vale)
2012-09-02	Samarco topography	858.0	850.6	-					851.0								2012-09-02
2012-09-11	Samarco monthly report	-	851.9	-					851.9								
2012-09-26	Samarco topography	858.0	852.0	-					852.0								2012-09-26
2012-10-29	Samarco monthly report	-	851.6	-					unable to determine								
2012-11-30	Samarco monthly report	-	855.1	-					unable to determine								
2012-12-11	Samarco monthly report	-	**855.1**	-					unable to determine								
2013-01-01	Samarco topography	861.0	855.7	857.0					850.3								2013-01-01
2013-01-25	Samarco monthly report	-	855.8	-					unable to determine								
2013-02-01	Samarco topography	861.0	858.8	860.0					850.0								2013-02-01
2013-02-28	Samarco monthly report	-	855.8	-													
2013-03-02	Samarco topography	863.0	858.0	-					849.9								2013-03-02
2013-03-05	Samarco monthly report	-	859.6	-					unable to determine								
2013-04-02	Samarco topography	864.3	859.0	860.5					846.5								2013-04-02
2013-04-30	Samarco monthly report	-	**859.6**	-					unable to determine								
2013-05-01	Samarco topography	865.0	862.0	-					848.0								2013-05-01
2013-05-08	PhotoSat aerial image	Excluded from dataset - date of survey and image show similar conditions to the May 1, 2013 Samarco topographic survey															
2013-05-27	Samarco topography	865.5	862.0	862.5					850.0								2013-05-27
2013-05-28	Samarco monthly report	-	860.0	863.2					unable to determine								
2013-06-27	Samarco monthly report	-	863.0	**863.2**					unable to determine								2013-06-30
2013-06-30	Samarco topography	867.4	863.0	864.5					850.0								2013-06-30
2013-07-29	Samarco topography	867.5	864.0	865.0					849.0								2013-07-29
2013-07-29	Samarco monthly report	-	864.0	865.0					unable to determine								2013-07-29

File Survey Date	Basis for Delineation	Pond Elevation (m)								Topography Source							
		Dike 2 Max.	Dike 1 Min.	Dike 1 Max.	Old Dike 1A Min.	Old Dike 1A Max.	New Dike 1A	Grota Upstream Dike	Grota da Vale Dike	Stitched Stripped Ground	G021600-O-130458_R-00 (not shown in image timeline)	G021600-O-130415_R-01	SA-1849-R02	041-A-MN-GR-09-006	G011609-K-100006	SA-1788	Monthly Samarco Survey (survey date shown)
2013-08-01	**Samarco monthly report**	-	864.0	867.0					unable to determine								2013-09-03
2013-09-03	Samarco topography	868.0	865.0	866.5					849.0								2013-09-03
2013-09-24	Samarco monthly report	-	866.5	868.0					unable to determine								2013-10-01
2013-10-01	Samarco topography	868.0	866.5	868.0					845.5								2013-10-01
2013-10-27	Samarco topography	869.2	867.8	869.0					845.5								2013-10-27
2013-10-30	Samarco monthly report	Monthly report does not provide coordinates or elevations for crest or beach - unable to estimate															
2013-11-26	Samarco topography	870.0	867.5	870.0					845.5								2013-11-26
2013-12-02	Samarco monthly report	Monthly report does not provide coordinates or elevations for crest or beach - unable to estimate															
2013-12-27	Samarco topography	870.3	870.3	-					846.0								2013-12-27
2014-01-23	Samarco monthly report	-	870.9	872.0					unable to determine								2014-01-29
2014-01-29	Samarco topography	872.0	872.0	-					846.5								2014-01-29
2014-03-28	Samarco topography	873.0	873.0	-					846.5								2014-03-28
2014-05-01	Samarco topography	874.4	874.4	-					846.5								2014-05-01
2014-06-03	Samarco topography	876.0	876.0	-					847.0								2014-06-03
2014-06-27	Samarco topography	876.4	876.4	-					846.0								2014-06-27
2014-08-04	Samarco topography	877.0	877.0	-					845.5								2014-08-04
2014-08-10	PhotoSat aerial image	Excluded from dataset - date of survey and image show similar conditions to the pre- and proceding Samarco topographic survey															
2014-08-29	Samarco topography	878.5	878.5	-					845.0								2014-08-29
2014-09-26	Samarco topography	879.7	879.7	-					848.4								2014-09-26
2014-10-31	Samarco topography	881.0	880.5	881.0					850.5								2014-10-31
2014-11-27	Samarco topography	882.0	882.0	-					850.5								2014-11-27
2014-12-29	Samarco topography	882.5	882.5	-					850.5								2014-12-29
2015-01-29	Samarco topography	883.5	883.5	-					853.0								2015-01-29
2015-02-27	Samarco topography	885.0	885.0	-					853.0								2015-02-27
2015-03-20	Samarco topography	885.0	885.0	-					853.0								2015-03-20
2015-04-24	Samarco topography	886.4	886.4	-					853.0								2015-04-24
2015-05-27	Samarco topography	887.5	887.5	-					853.0								2015-05-27
2015-06-22	Samarco topography	888.7	888.7	-					854.0								2015-06-22
2015-06-24	PhotoSat aerial image	Excluded from dataset - date of survey and image show similar conditions to the pre- and proceding Samarco topographic survey															
2015-07-10	PhotoSat aerial image																
2015-07-21	PhotoSat aerial image																
2015-07-27	Samarco topography	890.0	890.0	-					-								2015-07-27
2015-08-24	Samarco topography	890.6	890.0	890.6					-								2015-08-24
2015-10-01	Samarco topography	891.5	891.5	-					-								2015-10-01
2015-10-27	Samarco topography	893.0	892.5	-					854.0								2015-10-27

Notes:
1. Bolded text or values indicate the same date or values were given in the monthly monitoring report as the previous report.
2. Grey cells denote data not included in final pond data series.

Pond Image Timeline

2009-04-18

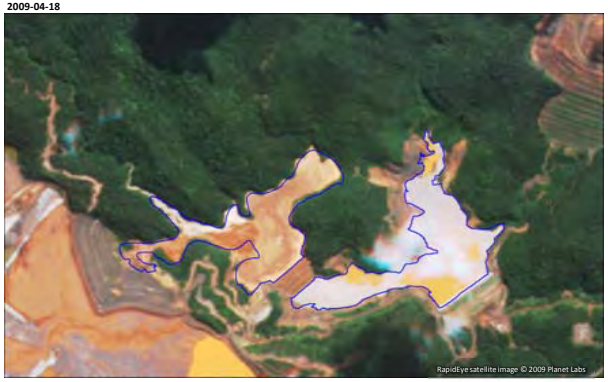

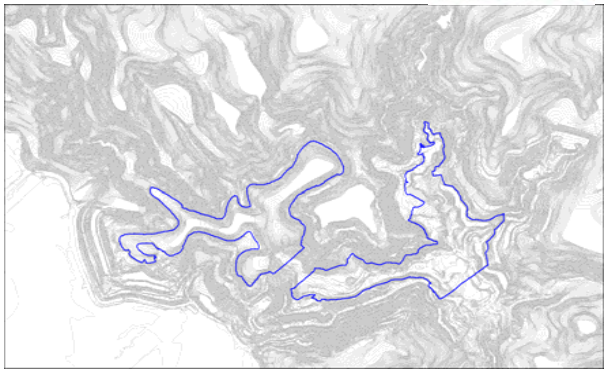

2009-08-18

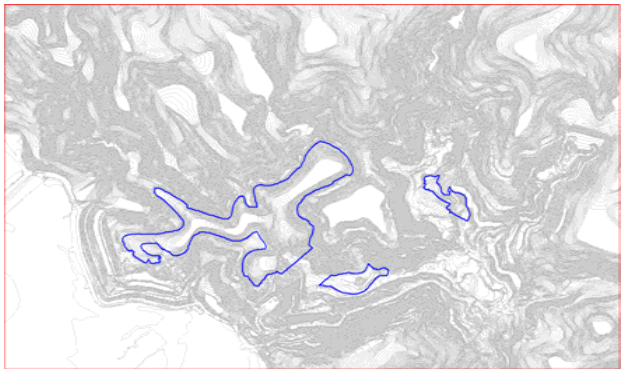

2009-11-15

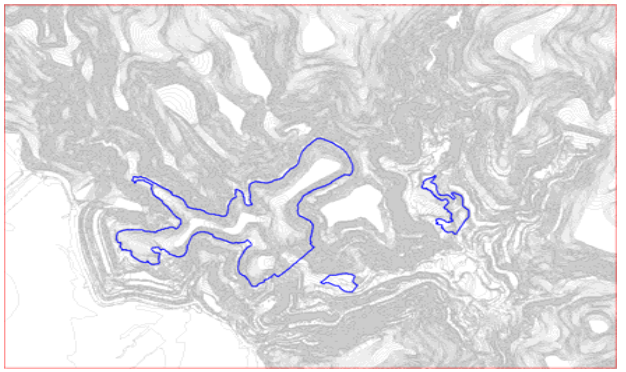

2010-01-17

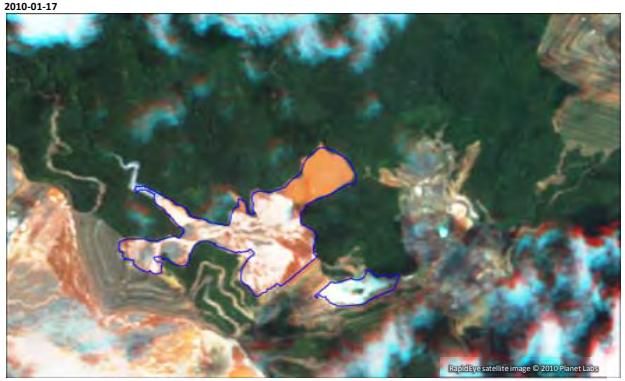

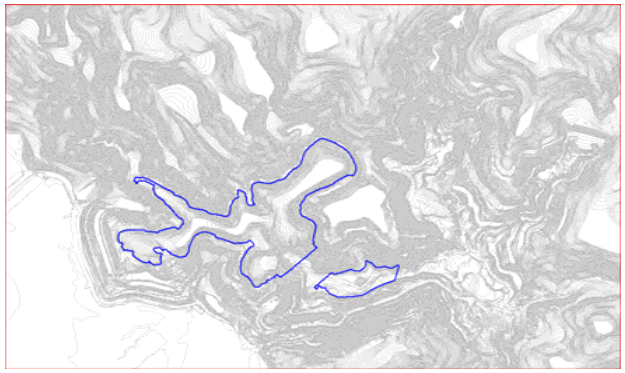

2010-02-22

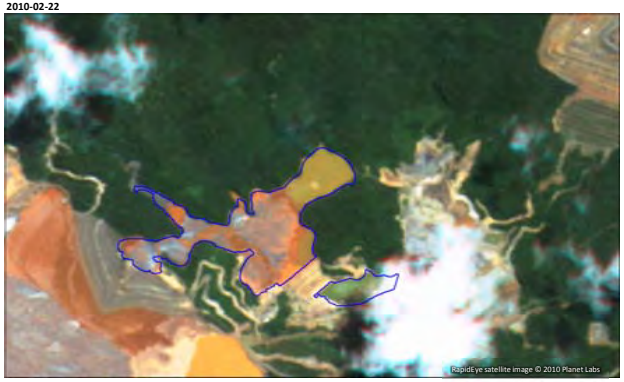

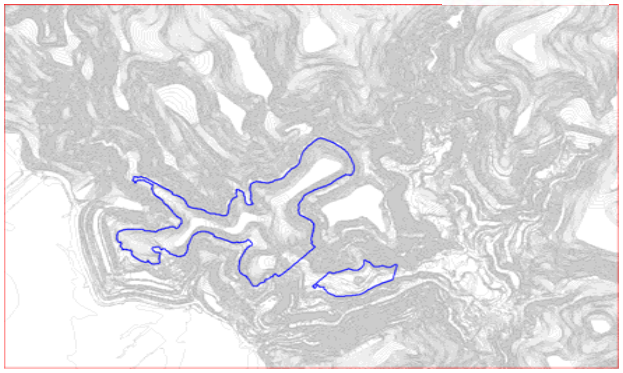

2010-04-27

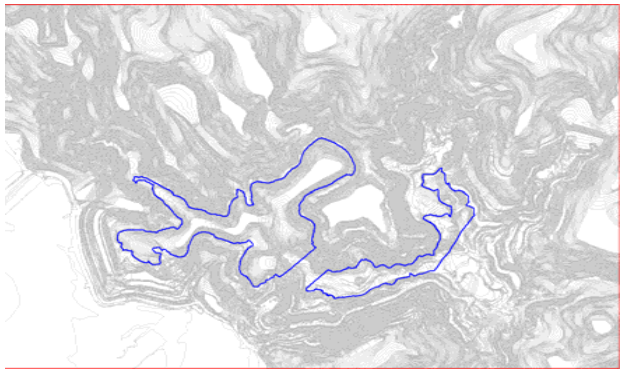

2010-06-19

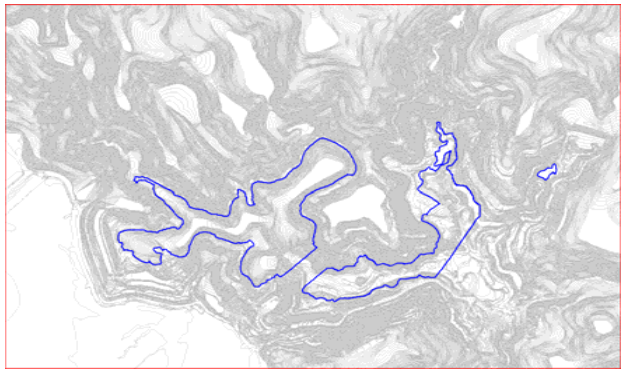

2010-08-07

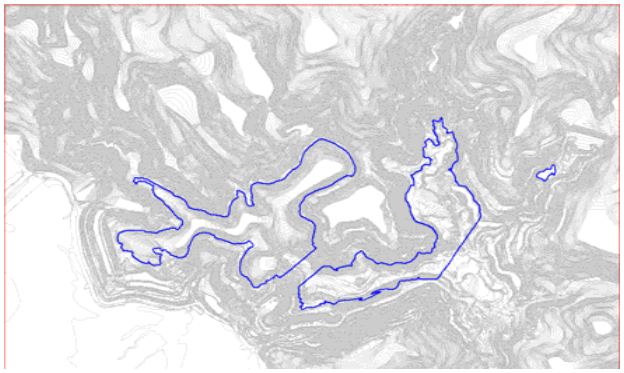

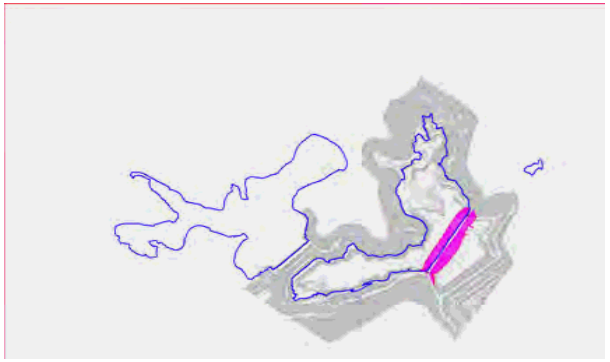

2010-10-29

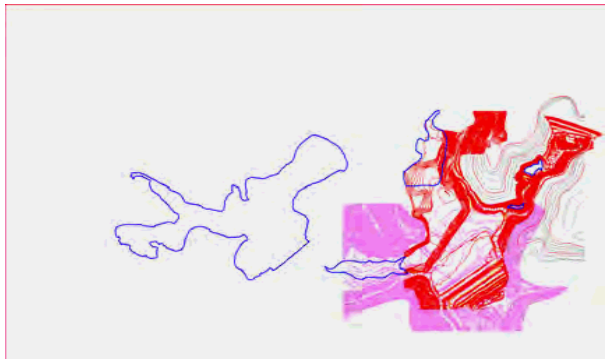

2010-12-22

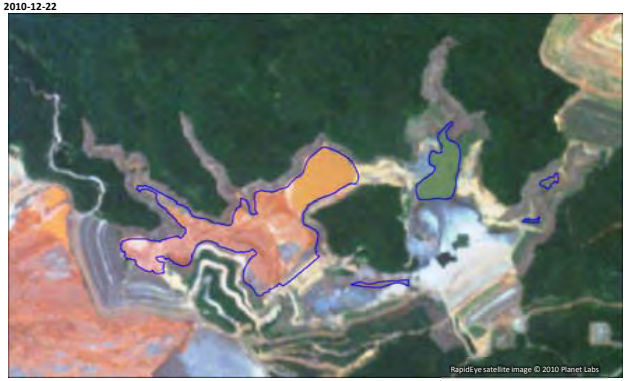

2011-02-11

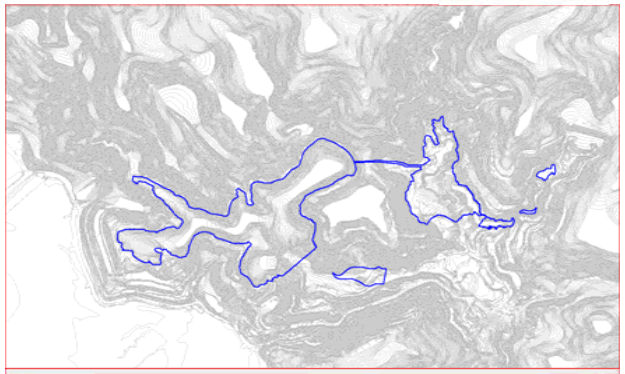

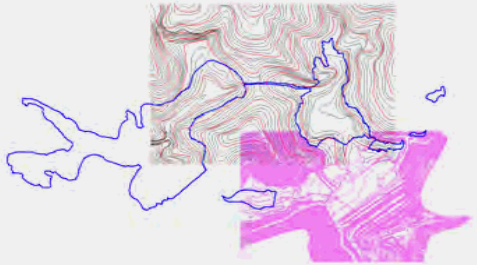

2011-04-09

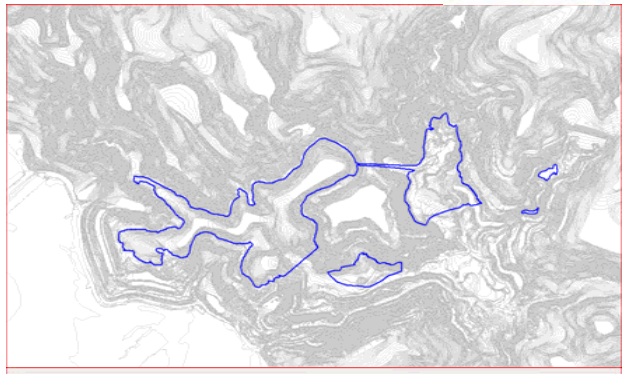

2011-07-01

2011-07-27 (Monthly Report)

2011-08-17

2011-08-24 (Monthly Report)

2011-09-15 (Monthly Report)

2011-09-21

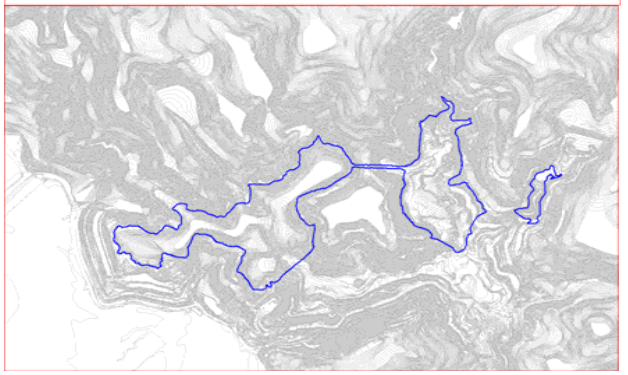

2011-10-02

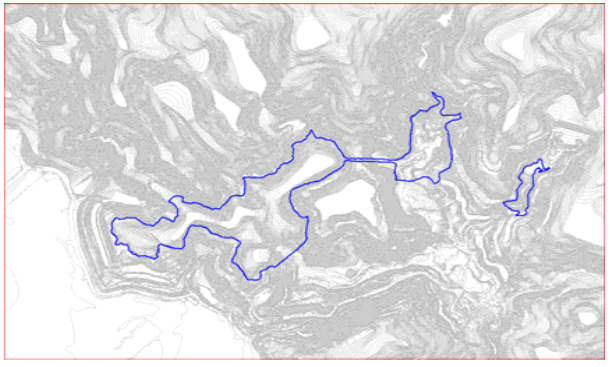

2011-10-11 (Monthly Report)

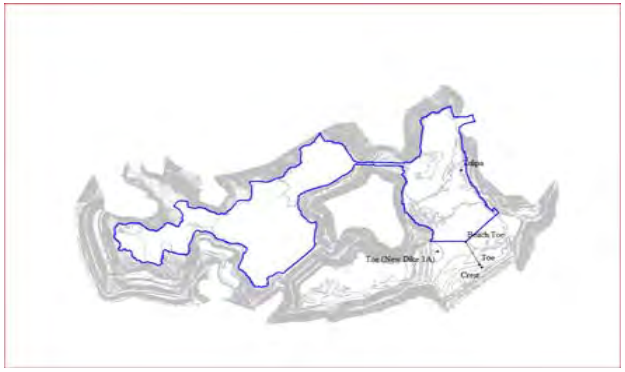

2011-11-08 (Monthly Report)

2011-12-16 (Monthly Report)

2012-01-10 (Monthly Report)

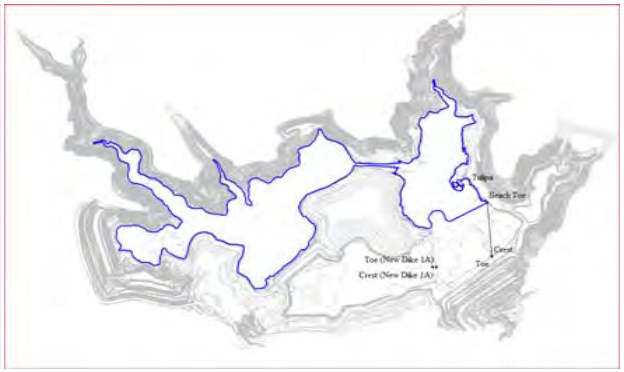

2012-01-21

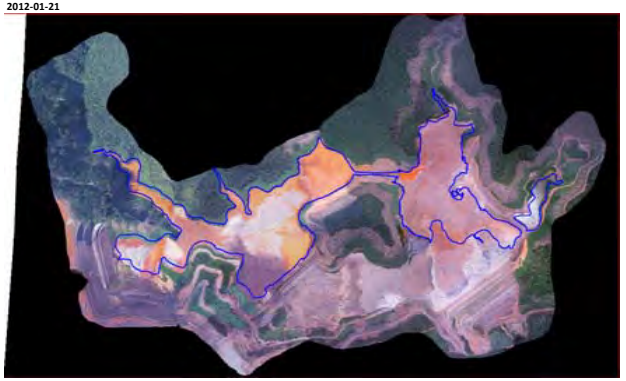

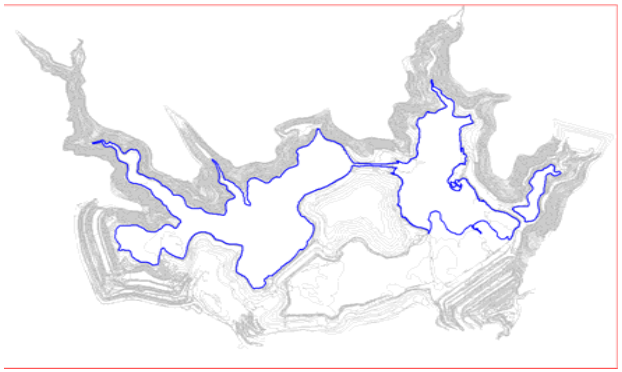

2012-02-09 (Monthly Report)

2012-03-03

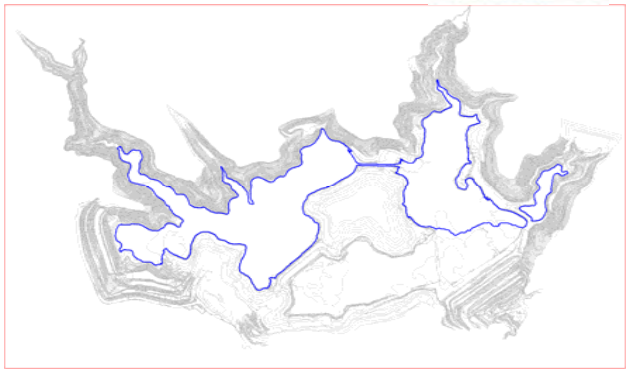

2012-03-16 (Monthly Report)

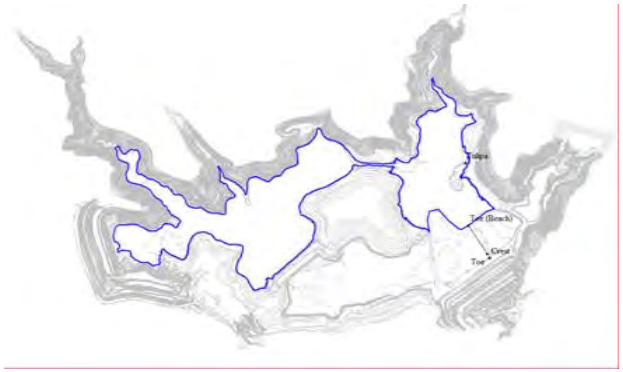

2012-04-01

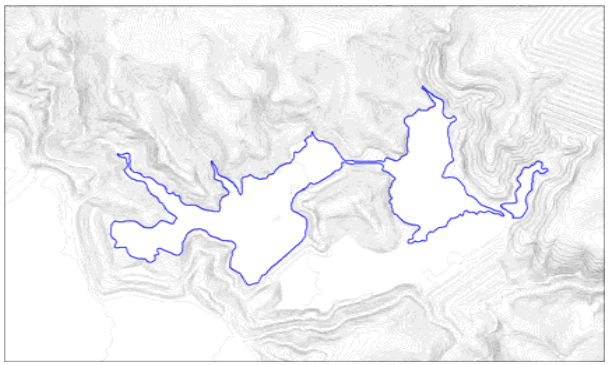

2012-04-19 (Monthly Report)

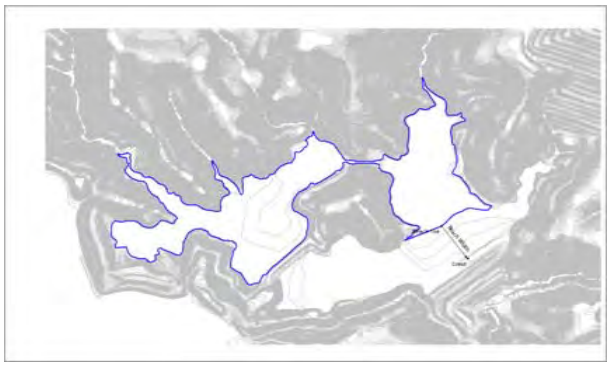

2012-05-14 (Monthly Report)

2012-06-04 (Monthly Report)

2012-07-13 (Monthly Report)

2012-08-09 (Monthly Report)

2012-09-02

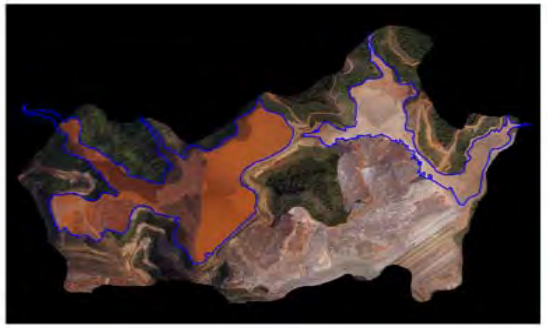

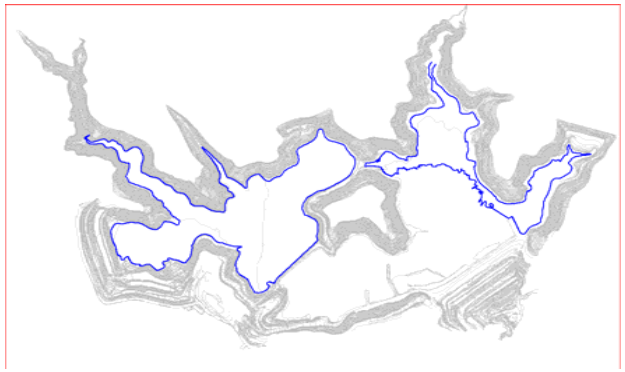

2012-09-11 (Monthly Report)

2012-09-26

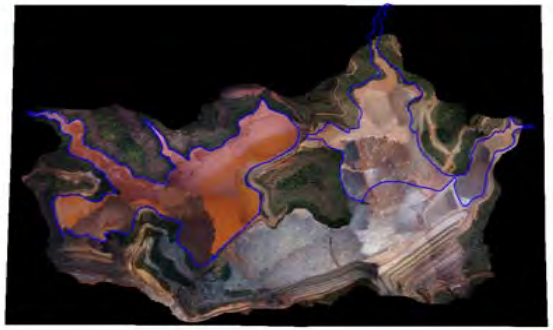

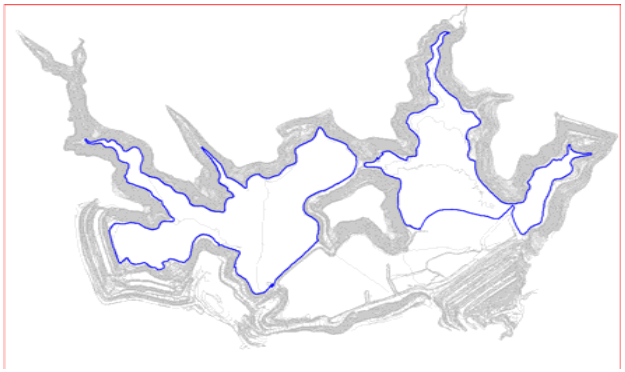

2012-10-29 (Monthly Report)

2012-11-30 (Monthly Report)

2012-12-11 (Monthly Report)

2013-01-01

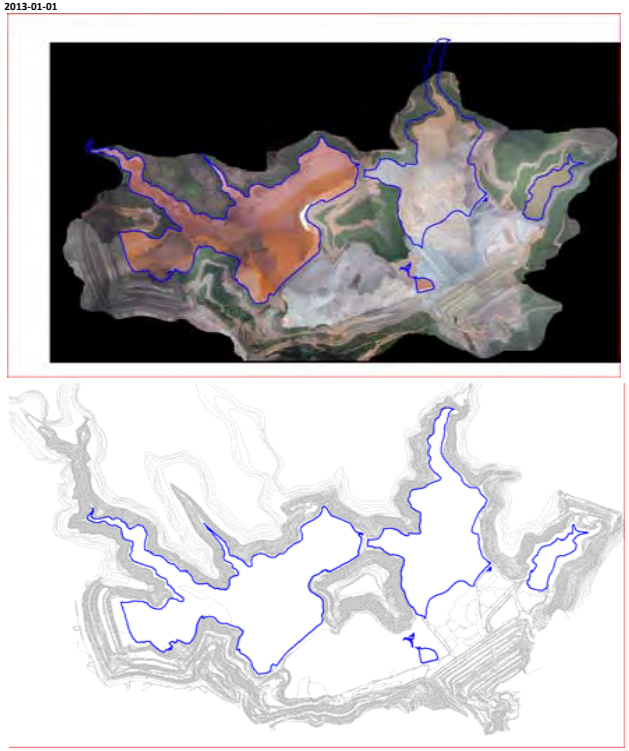

2013-02-01

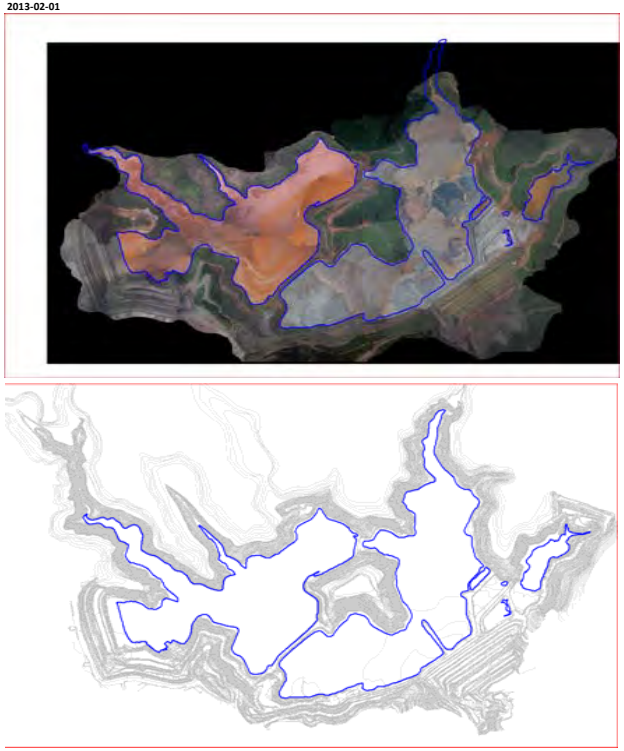

2013-03-02

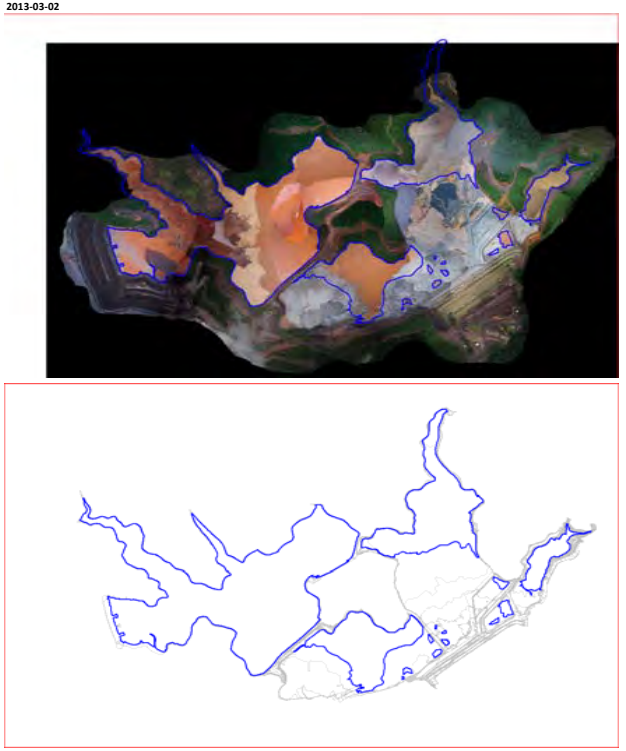

2013-03-05 (Monthly Report)

2013-04-02

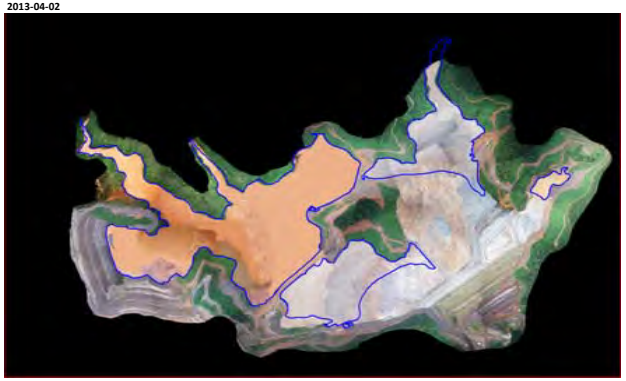

2013-05-01

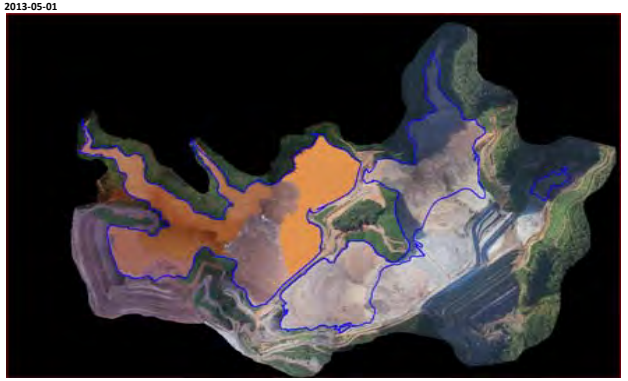

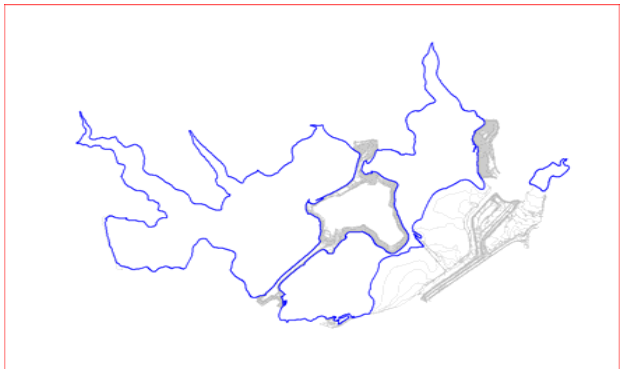

2013-05-27

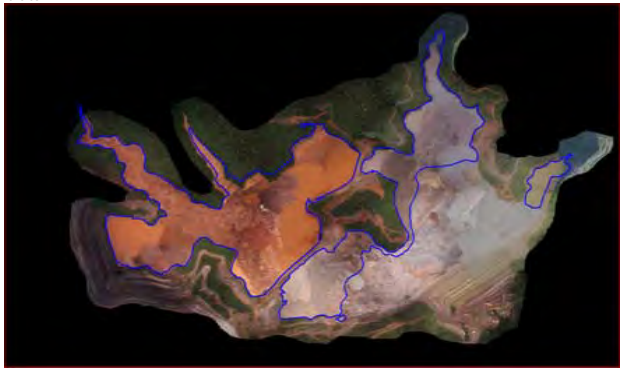

2013-05-28 (Monthly Report)

2013-06-27 (Monthly Report)

2013-06-30

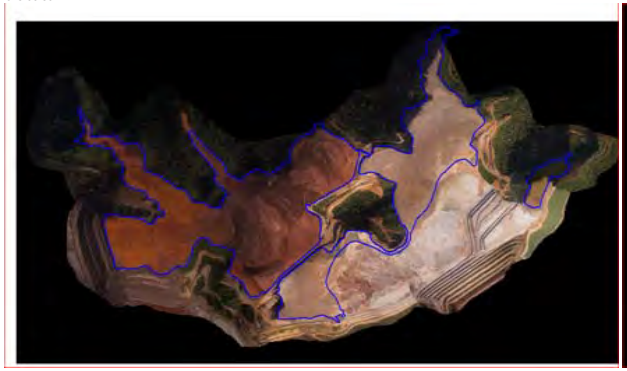

2013-07-29

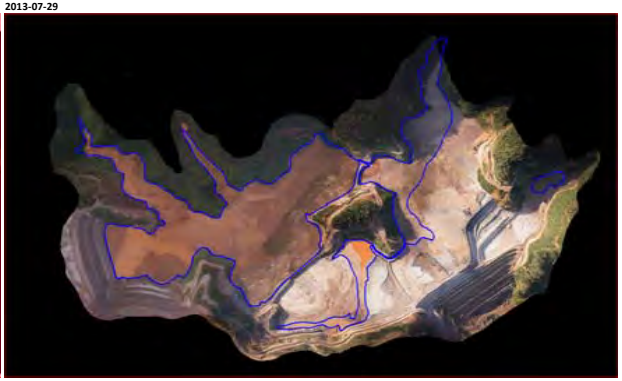

2013-07-29 (Monthly Report)

2013-08-01 (Monthly Report, survey date unknown)

2013-09-03

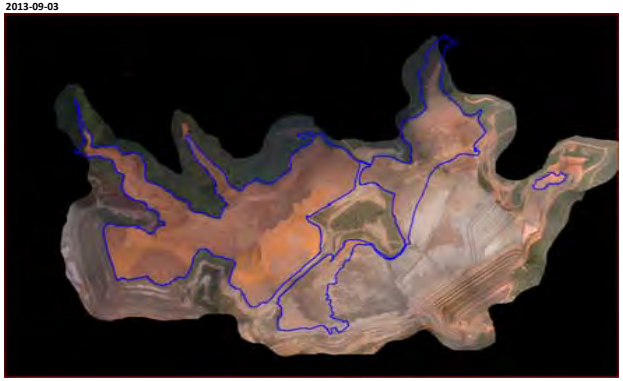

2013-09-24 (Monthly Report)

2013-10-01

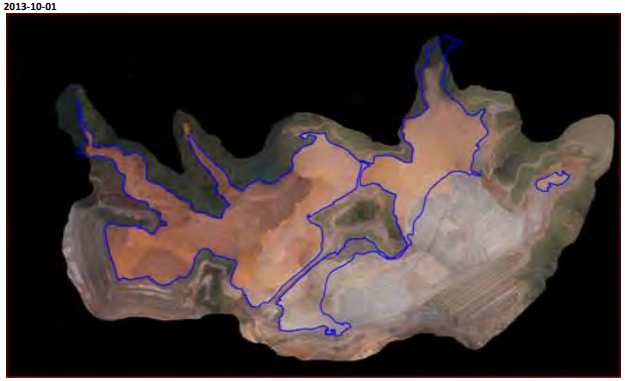

2013-10-27

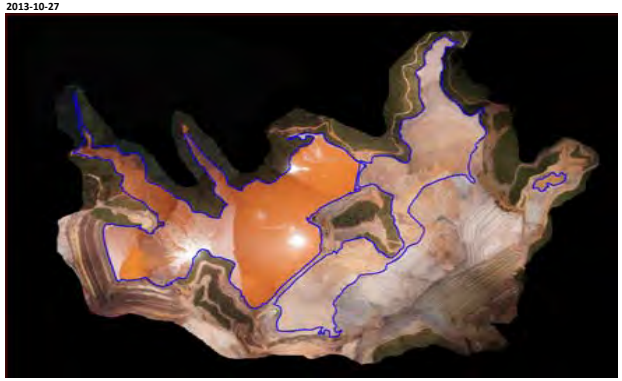

2013-11-26

2013-12-27

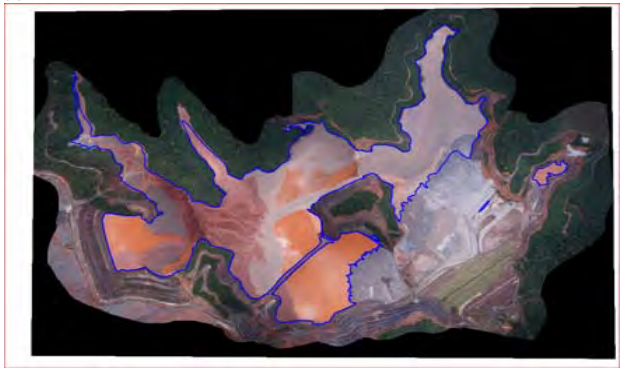

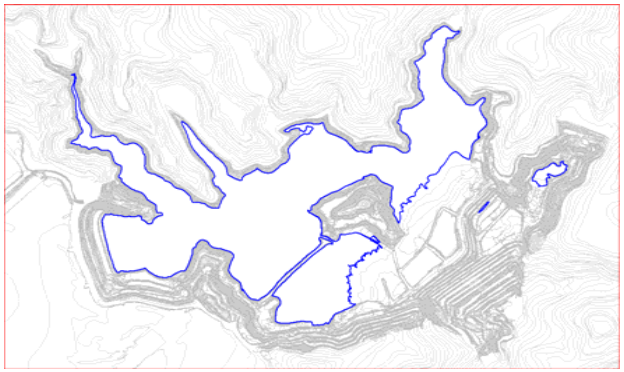

2014-01-23 (Monthly Report)

2014-01-29

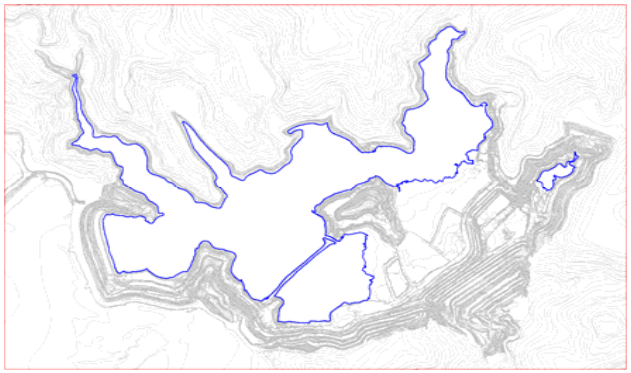

2014-03-28

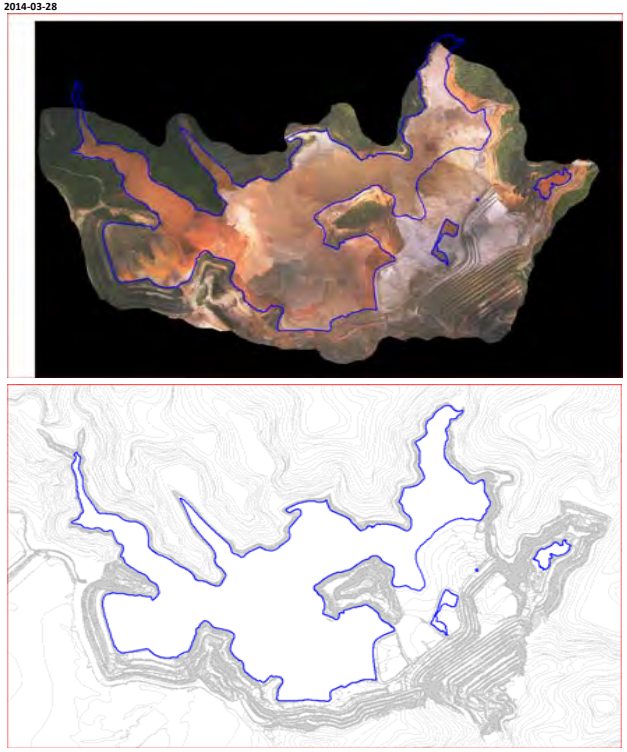

2014-05-01

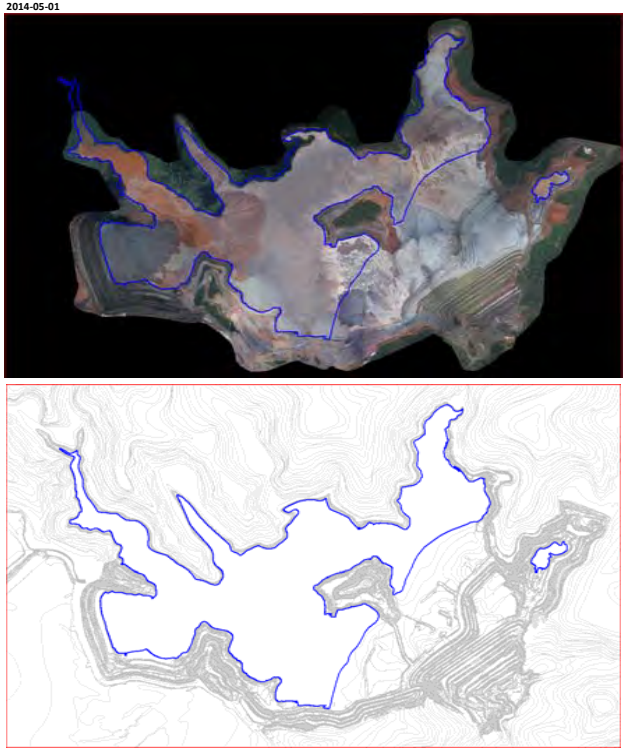

2014-06-03

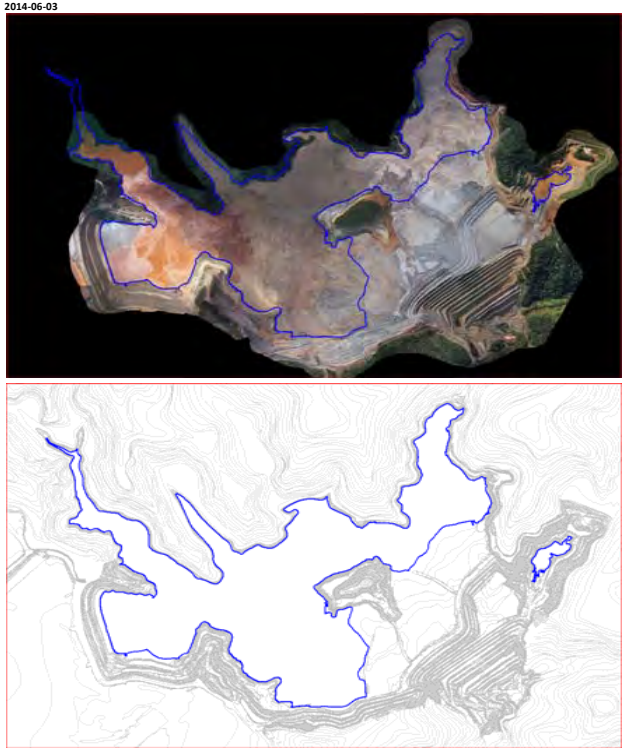

2014-06-27

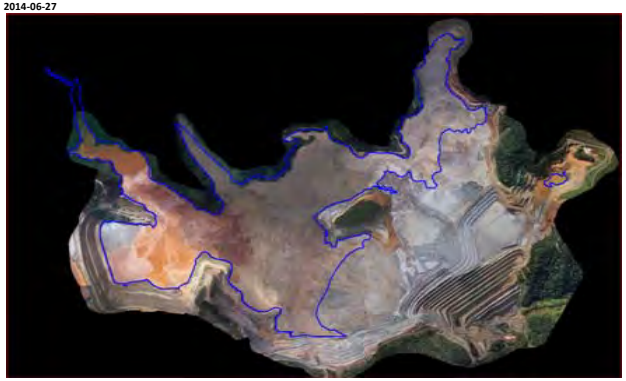

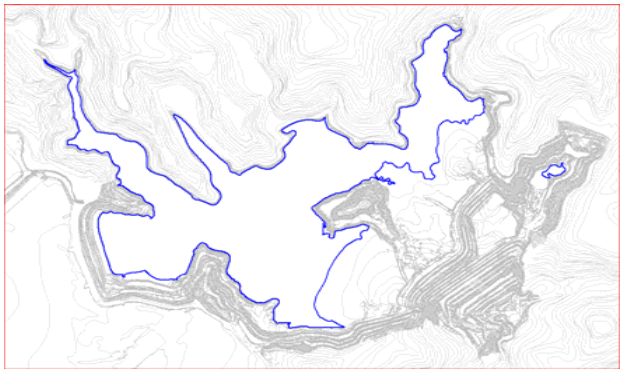

2014-08-04

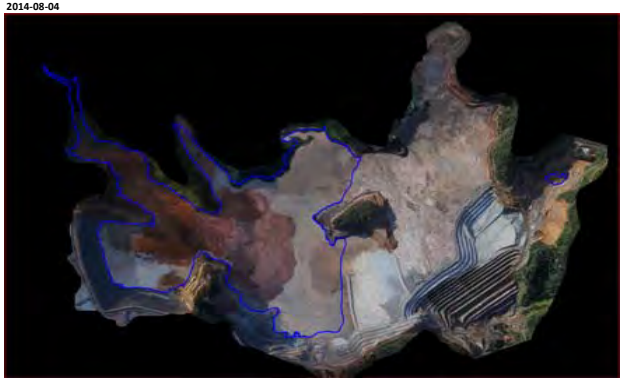

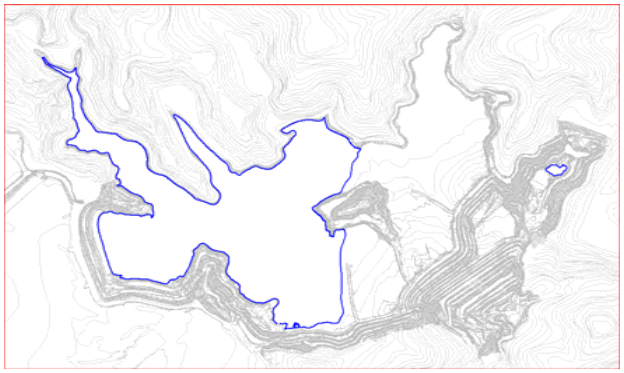

2014-08-29

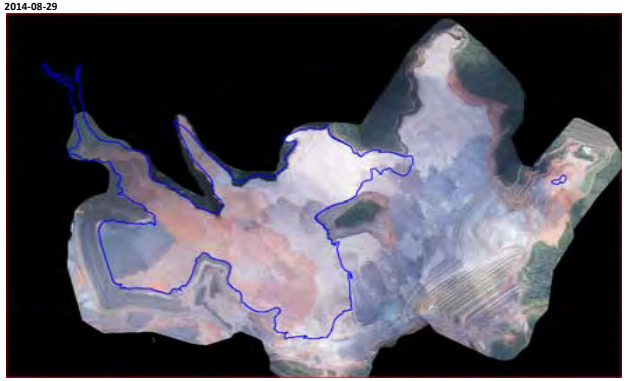

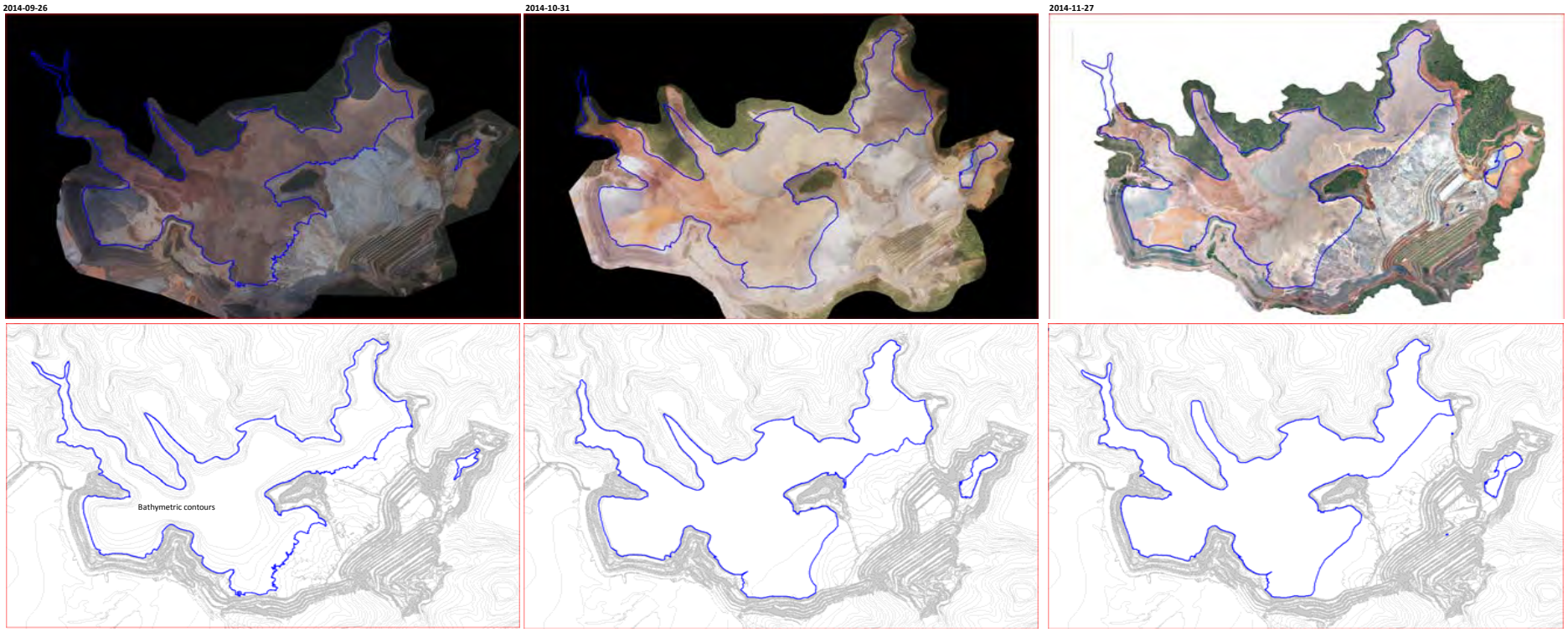
2014-09-26
2014-10-31
2014-11-27
Bathymetric contours

2014-12-29

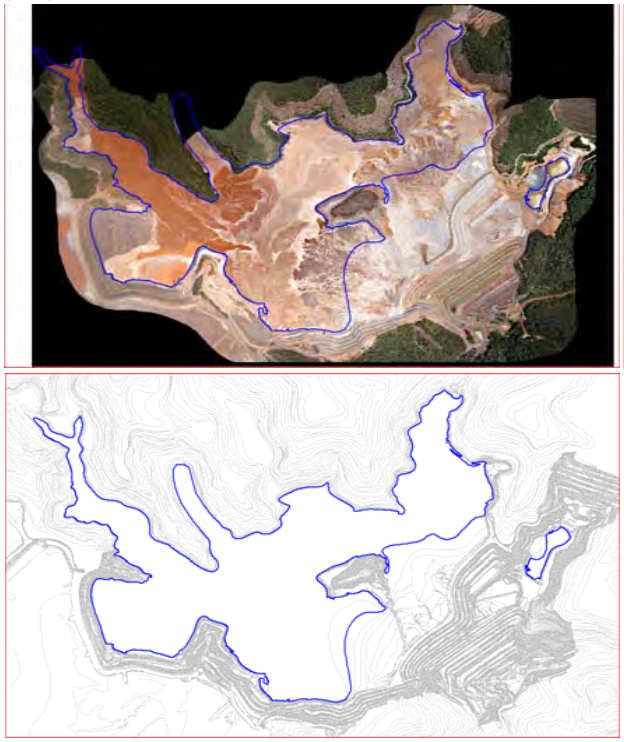

2015-01-29

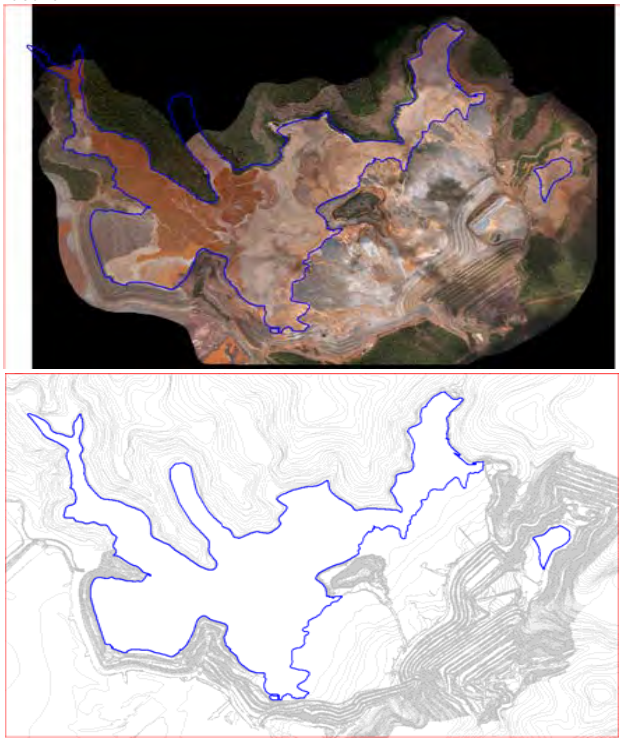

2015-02-27

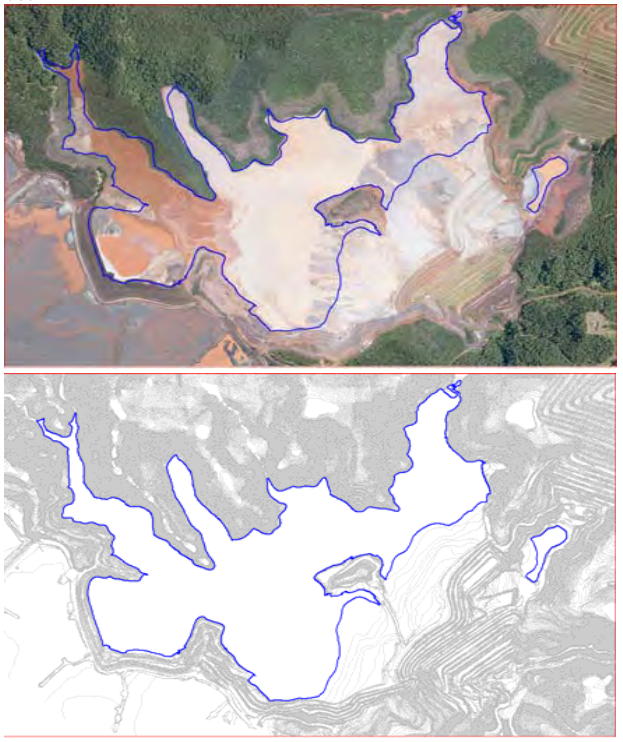

2015-03-20

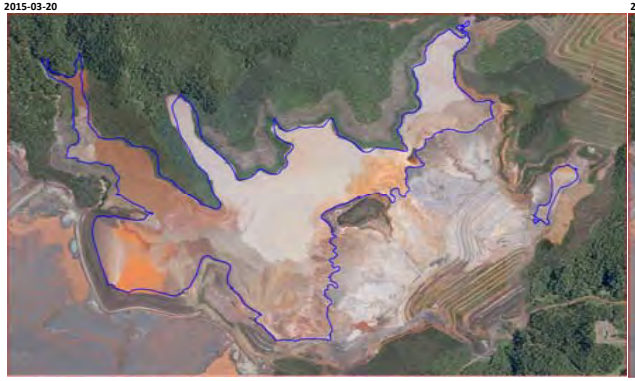

2015-04-24

2015-05-27

2015-06-22

2015-07-27

2015-08-24

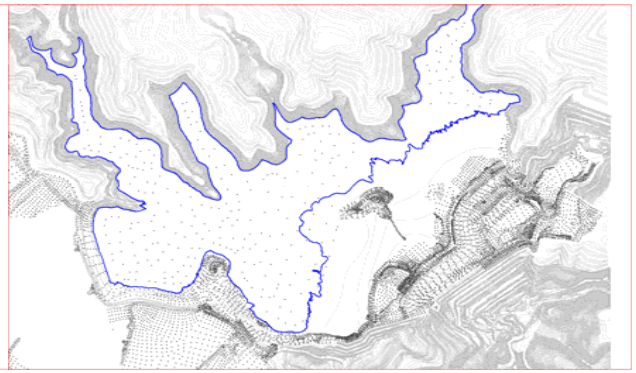

2015-10-01

2015-10-27

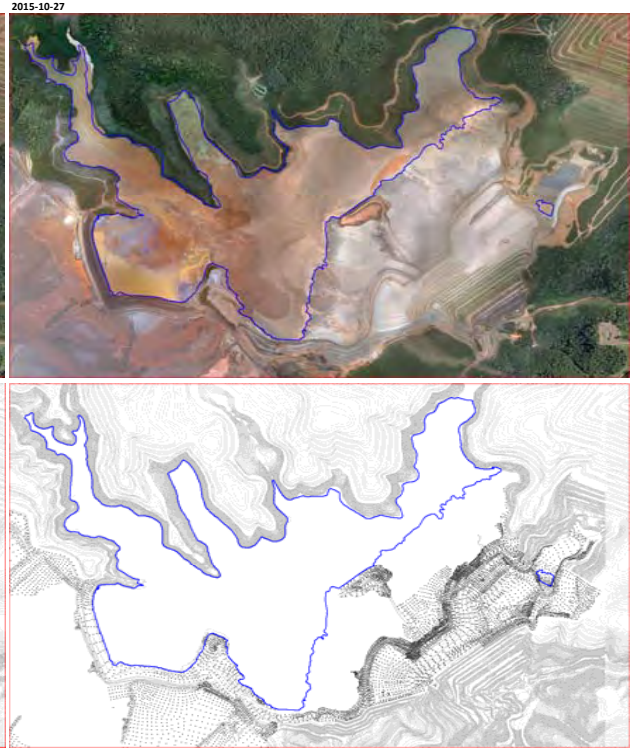

ATTACHMENT B5

Left Abutment Geometric Changes

Appendix B: Attachment B5
Left Abutment Geometric Changes

TABLE OF CONTENTS

List of Tables

List of Figures

TABLE OF CONTENTS

(continued)

B.B5-1 PLAN VIEW

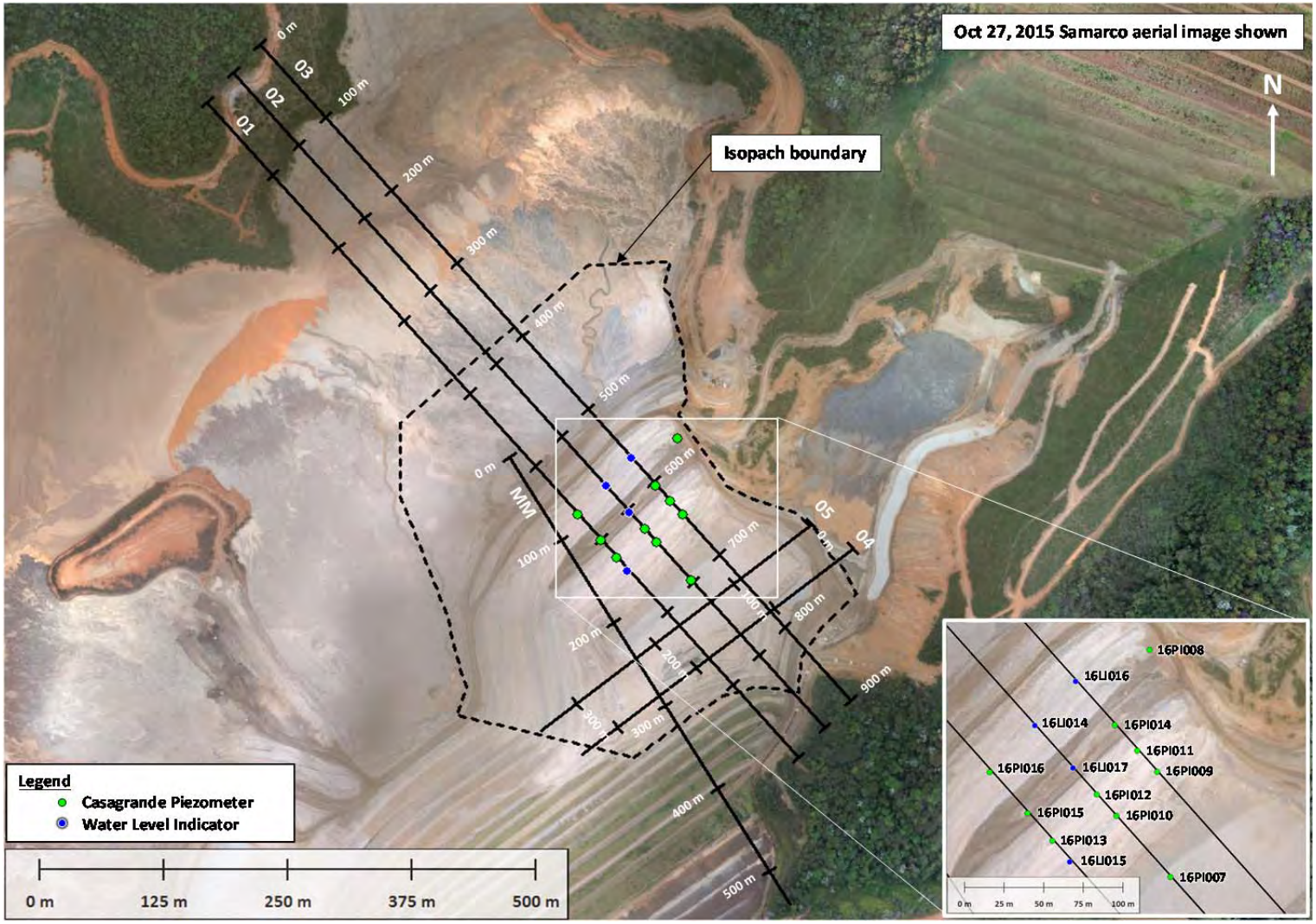

Figure B.B5-1 Left abutment plan

B.B5-2 CROSS SECTIONS

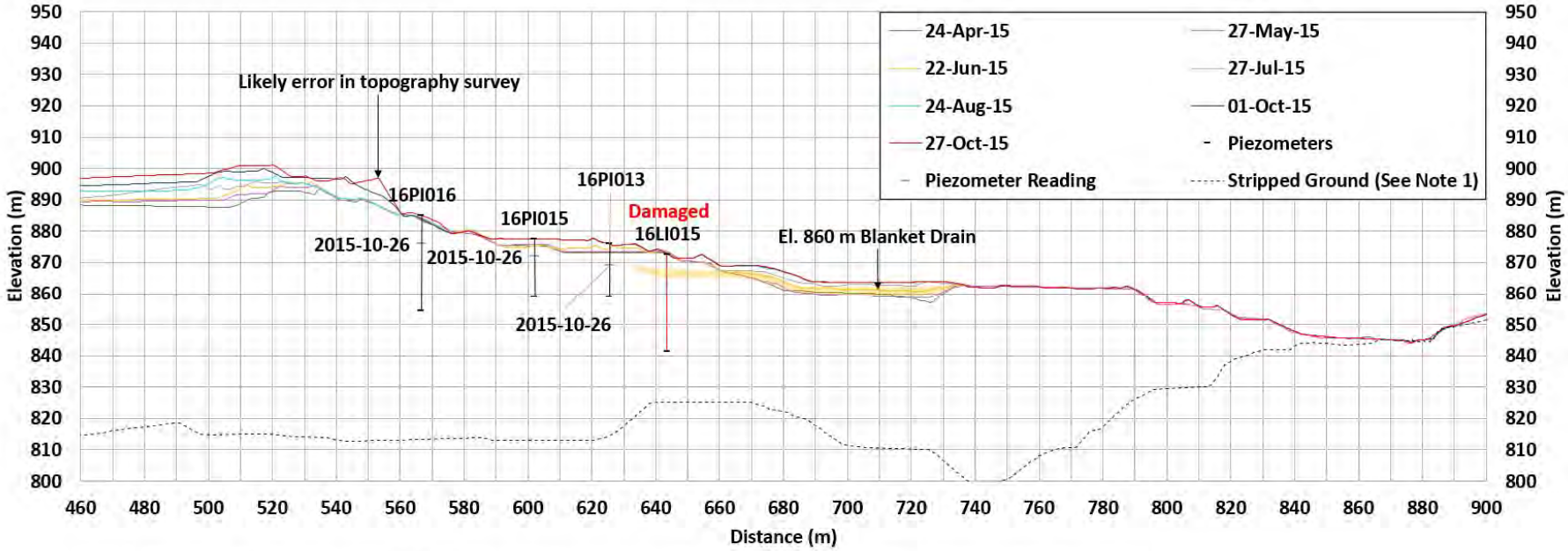

Note 1: Stripped ground shown was stitched from multiple surveys to obtain the most representative estimate of the foundation under Dike 1 and tailings.

Figure B.B5-2 Section 01

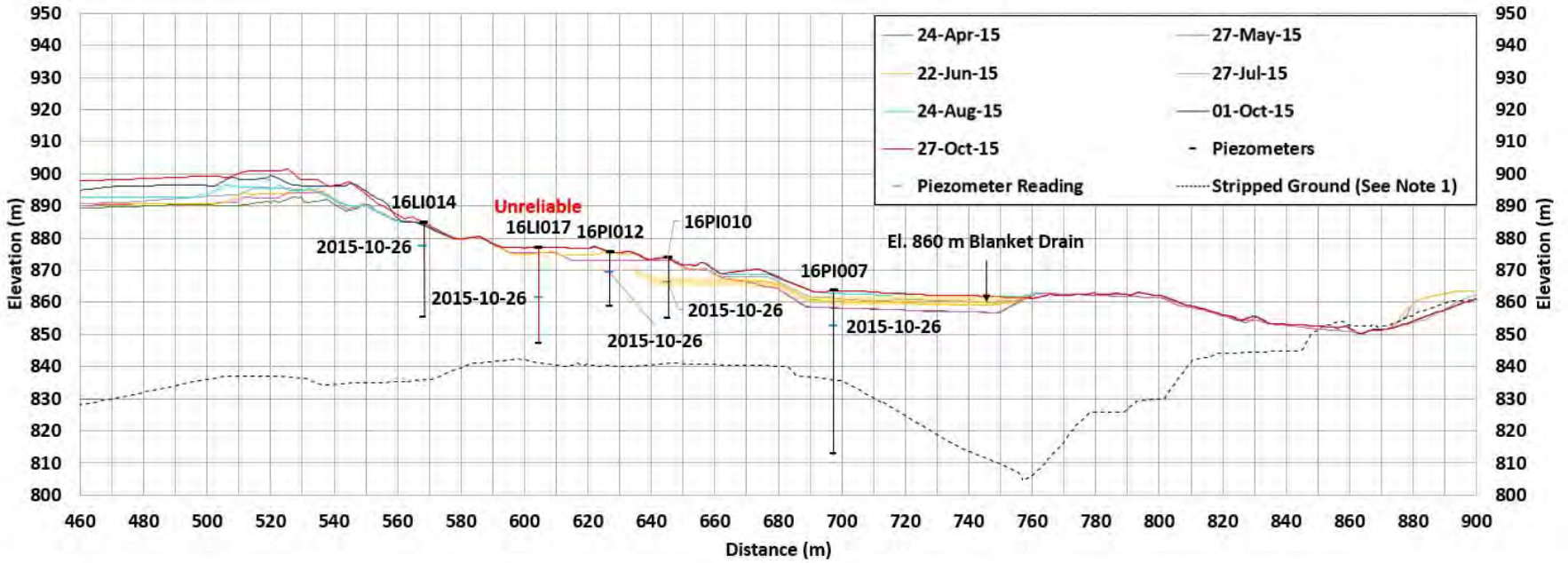

Note 1: Stripped ground shown was stitched from multiple surveys to obtain the most representative estimate of the foundation under Dike 1 and tailings.

Figure B.B5-3 Section 02

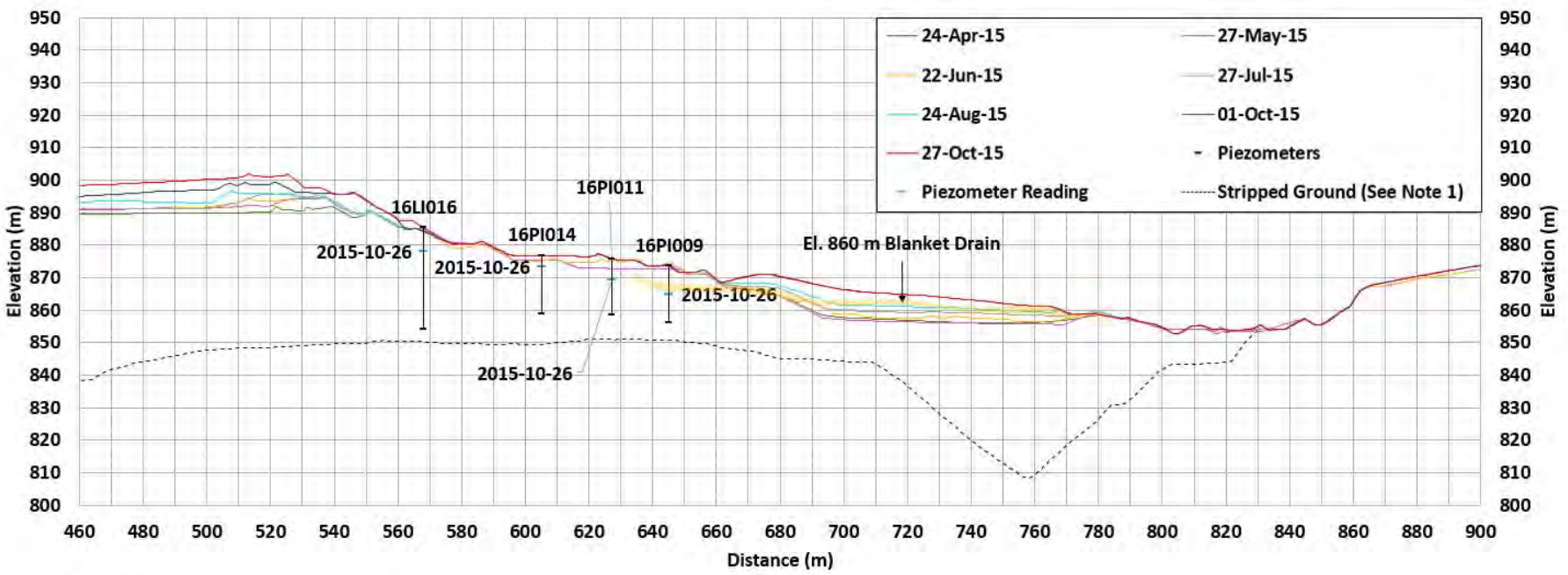

Note 1: Stripped ground shown was stitched from multiple surveys to obtain the most representative estimate of the foundation under Dike 1 and tailings.

Figure B.B5-4 Section 03

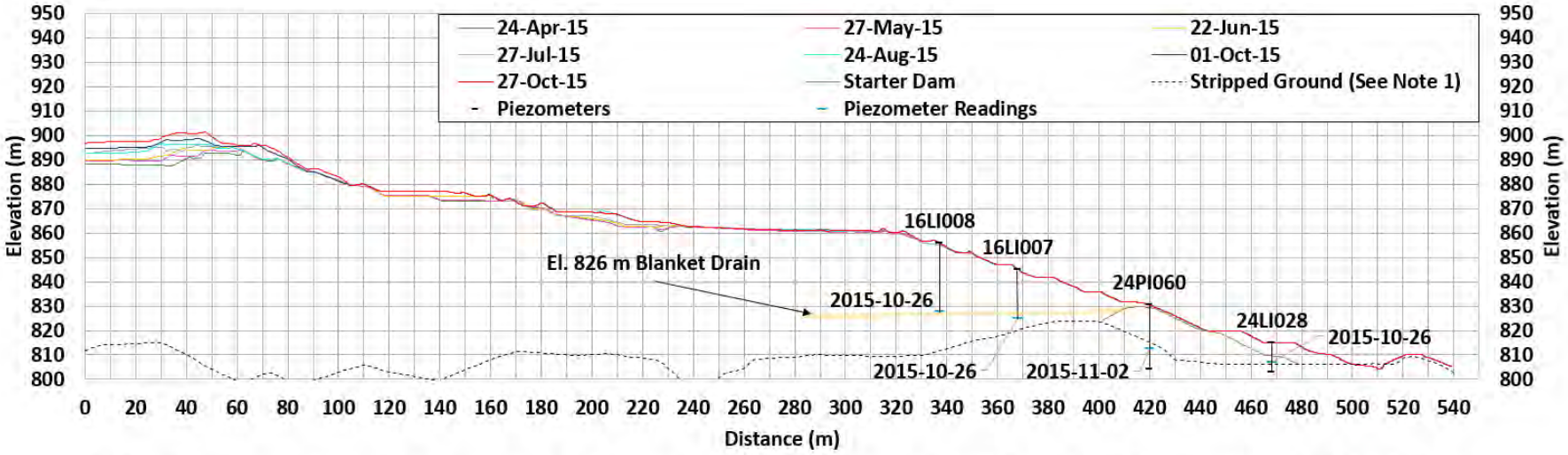

Note 1: Stripped ground shown was stitched from multiple surveys to obtain the most representative estimate of the foundation under Dike 1 and tailings.

Figure B.B5-5 Section MM

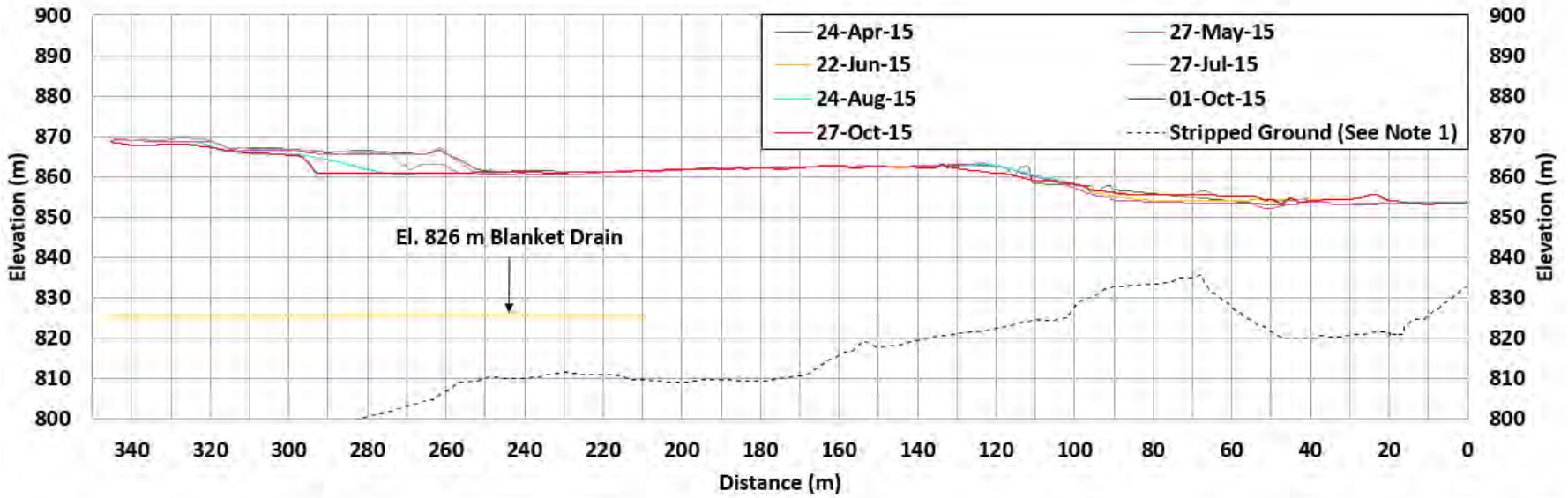

Note 1: Stripped ground shown was stitched from multiple surveys to obtain the most representative estimate of the foundation under Dike 1 and tailings.

Figure B.B5-6 Section 04

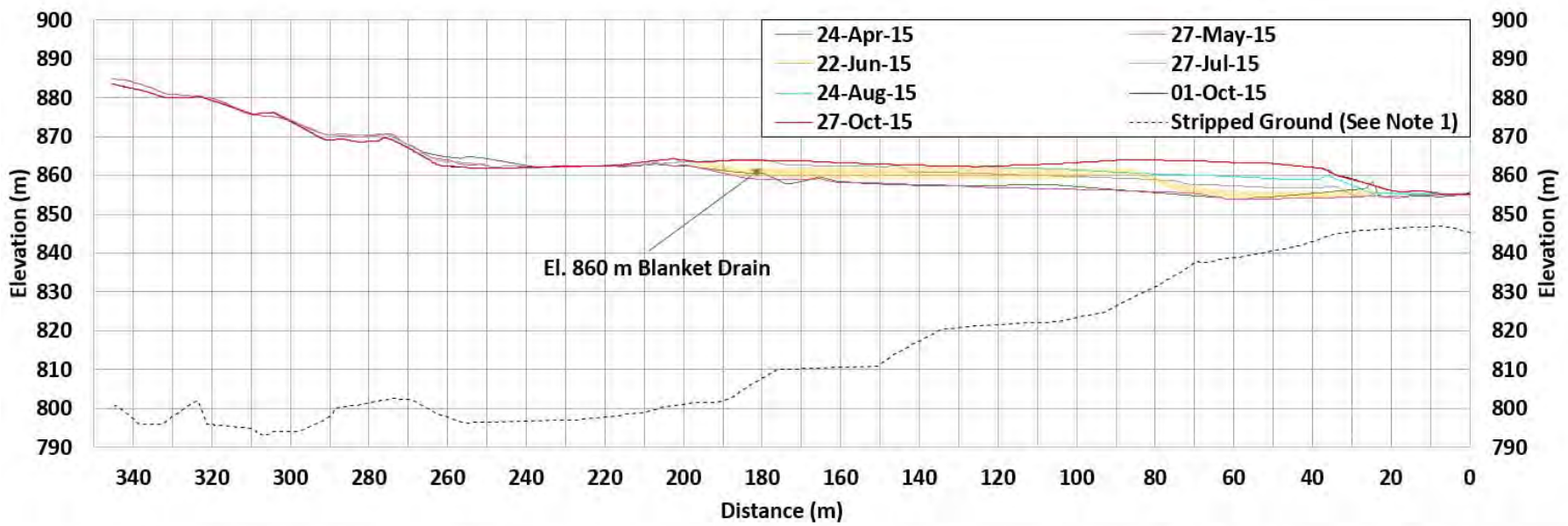

Note 1: Stripped ground shown was stitched from multiple surveys to obtain the most representative estimate of the foundation under Dike 1 and tailings.

Figure B.B5-7 Section 05

B.B5-3 CROSS SECTIONS WITH TIME

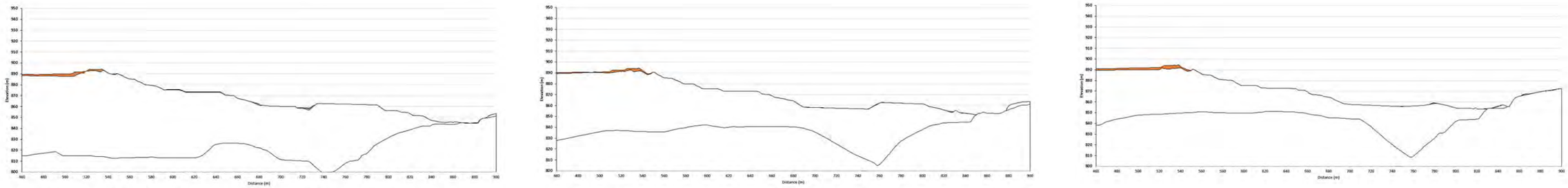

Section 01 **Section 02** **Section 03**

Figure B.B5-8 2015-04-24 to 2015-05-27

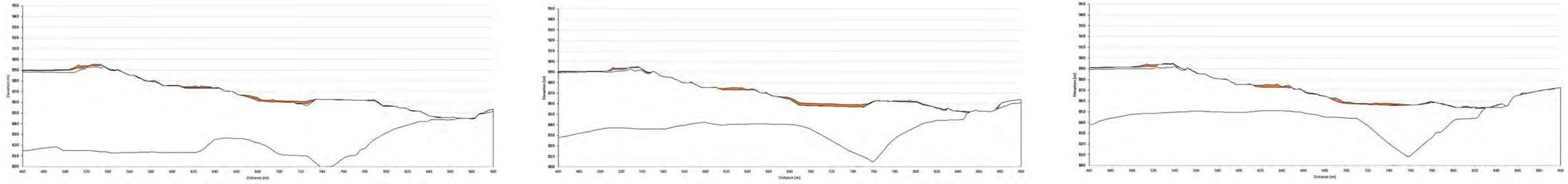

Section 01 **Section 02** **Section 03**

Figure B.B5-9 2015-05-27 to 2015-06-22

Fill Cut

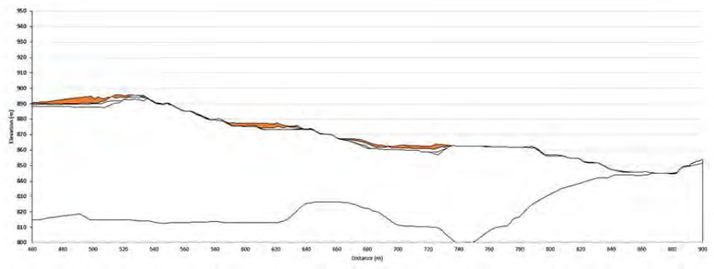

Section 01

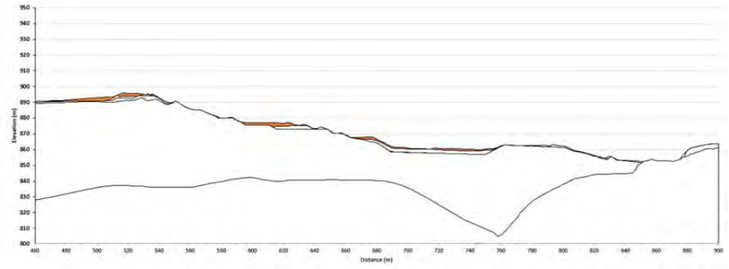

Section 02

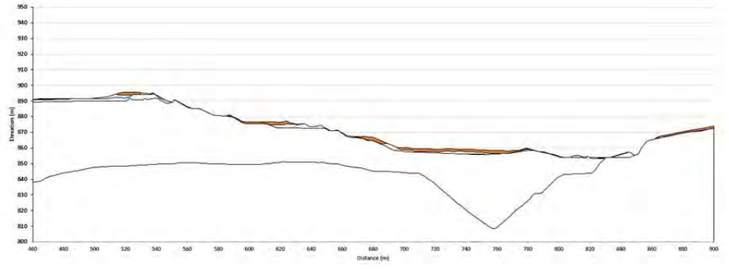

Section 03

Figure B.B5-10 2015-06-22 to 2015-07-27

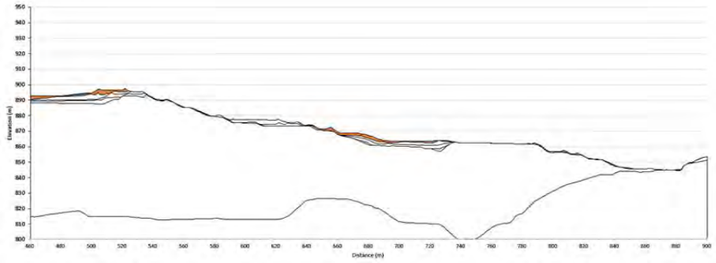

Section 01

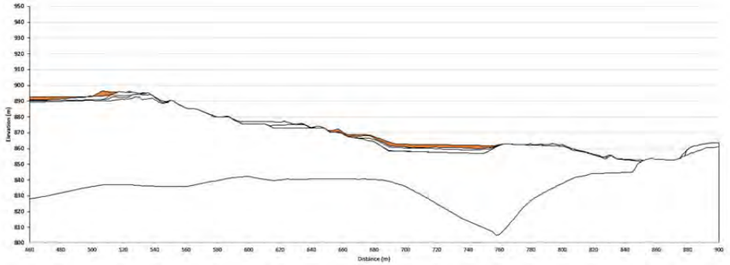

Section 02

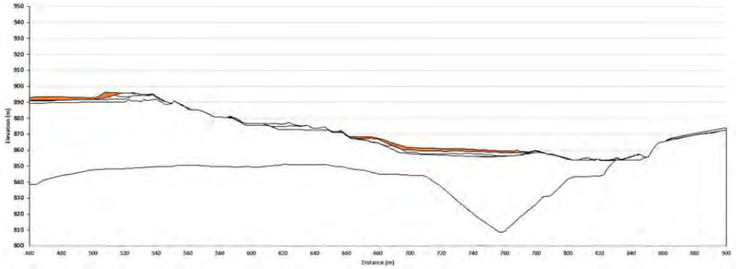

Section 03

Figure B.B5-11 2015-07-27 to 2015-08-24

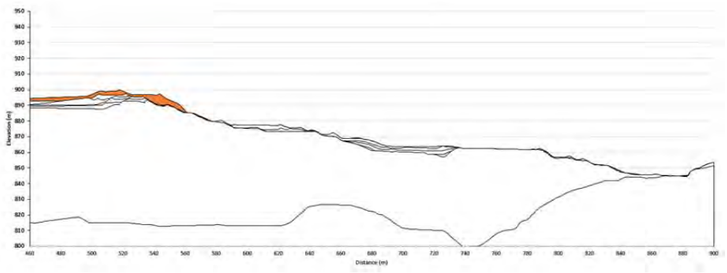

Section 01

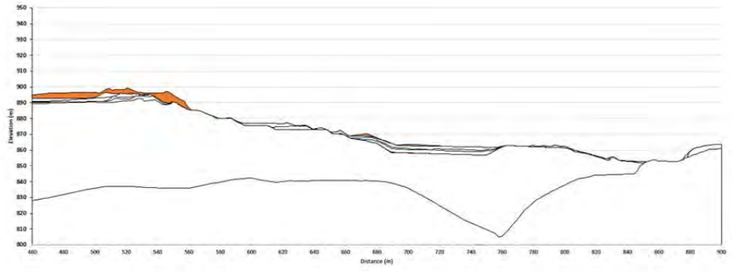

Section 02

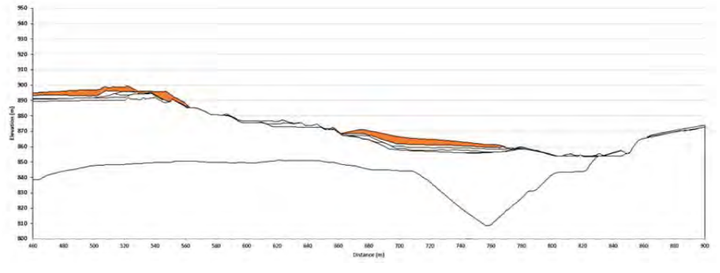

Section 03

Figure B.B5-12 2015-08-24 to 2015-10-01

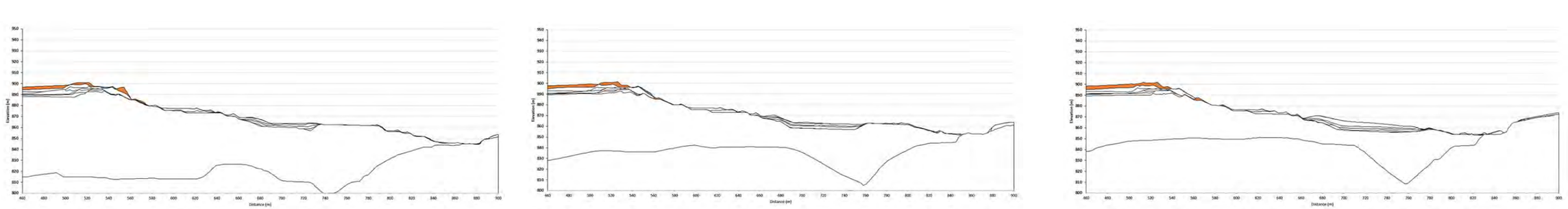

Section 01

Section 02

Section 03

Figure B.B5-13 2015-10-01 to 2015-10-27

Fill Cut

B.B5-4 AERIAL IMAGES

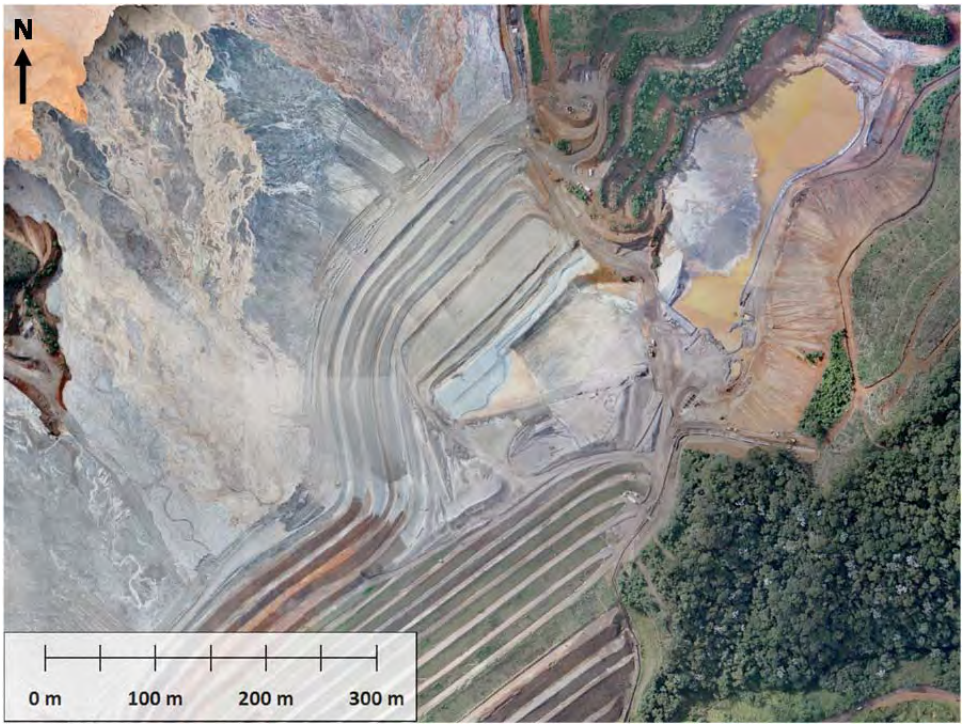

Figure B.B5-14 Aerial image 2015-04-24

Figure B.B5-15 Aerial image 2015-05-27

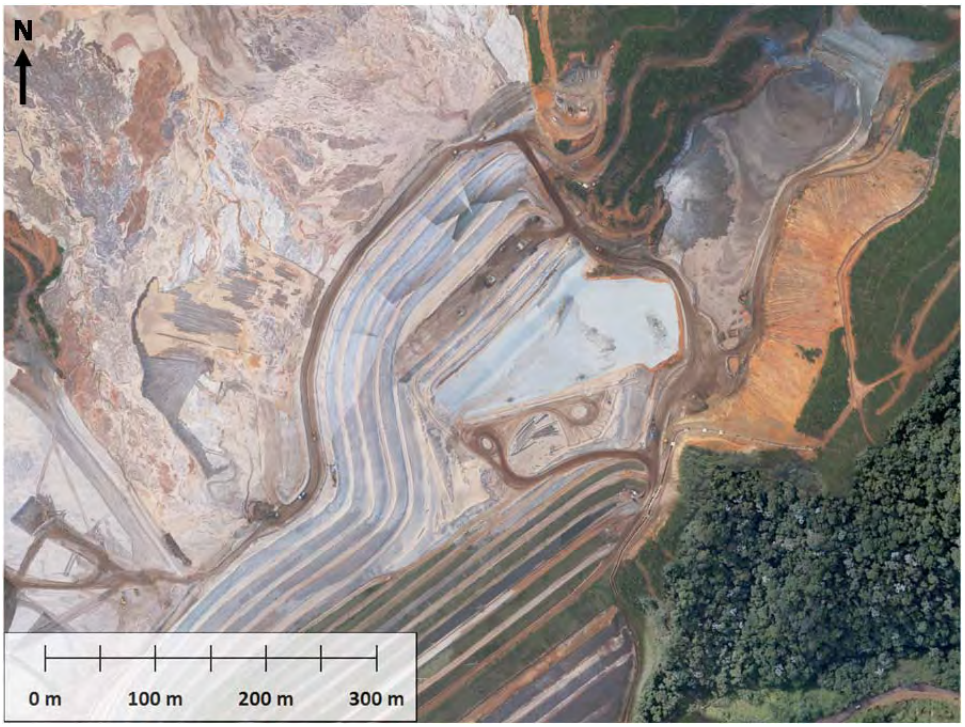

Figure B.B5-16 Aerial image 2015-06-22

Figure B.B5-17 Aerial image 2015-06-27

Figure B.B5-18 Aerial image 2015-08-24

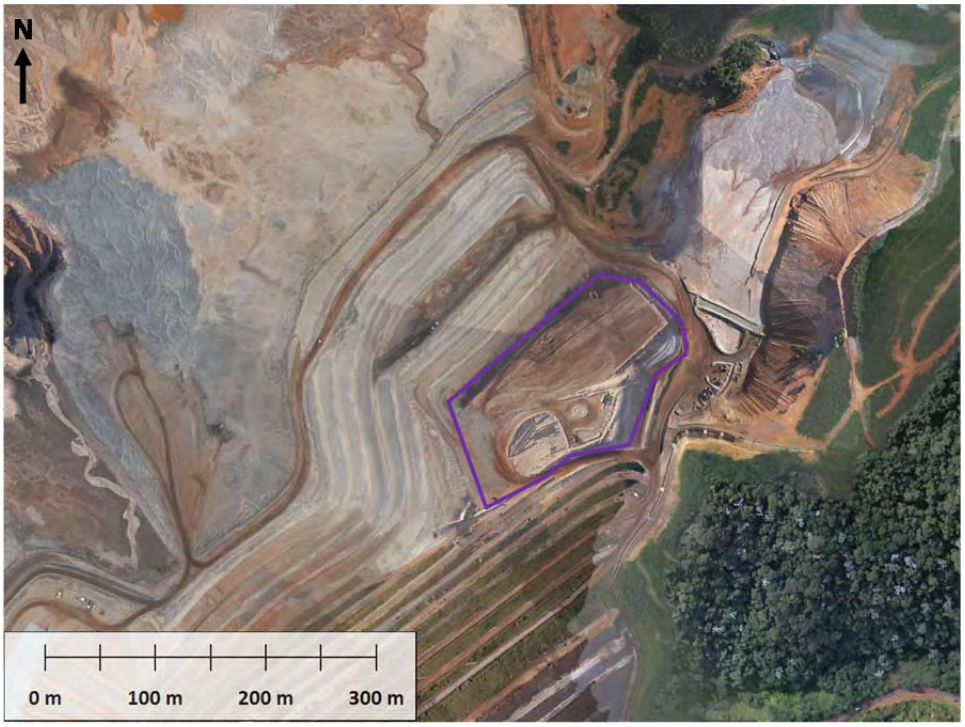

Figure B.B5-19 Aerial image 2015-10-01[1]

[1] The area outlined in purple on Figure B.B5-19 is unchanged from Figure B.B5-18. The image was likely stitched in this area.

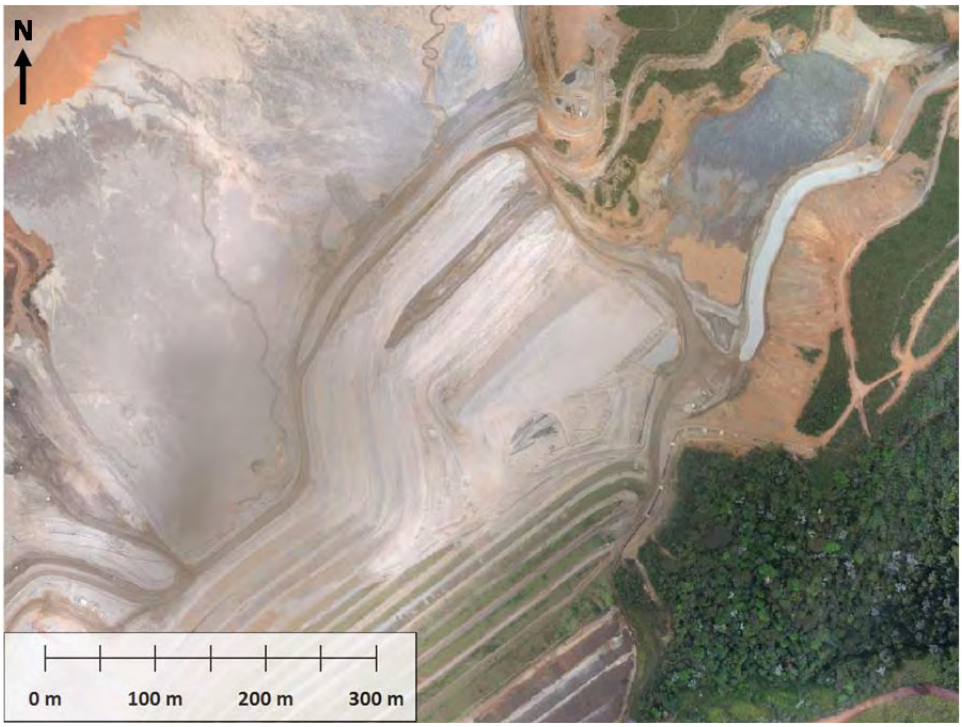

Figure B.B5-20 Aerial image 2015-10-27

B.B5-5 DIGITAL ELEVATION MODELS (DEMS)

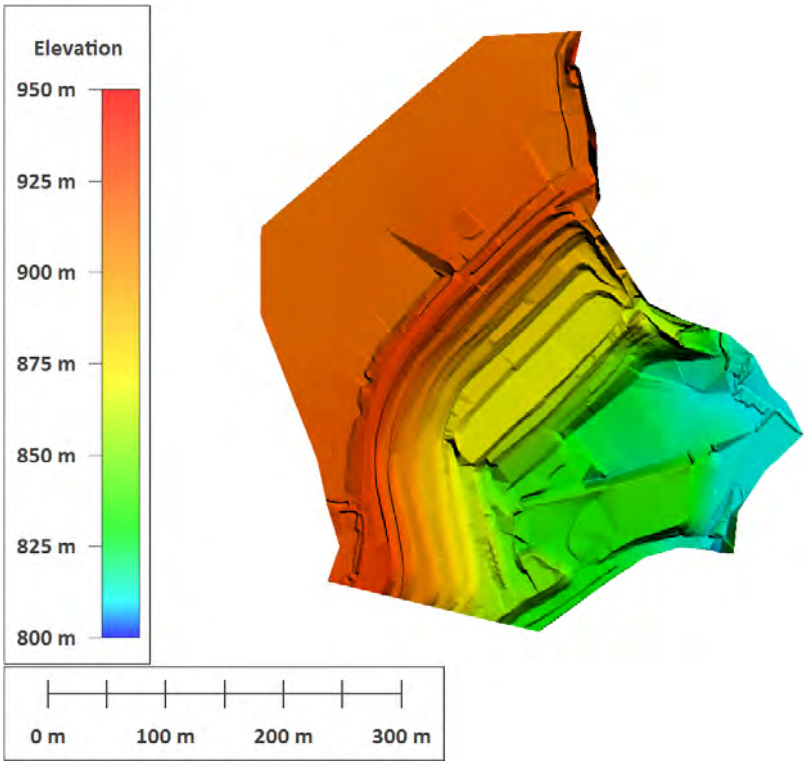

Figure B.B5-21 DEM 2015-04-24

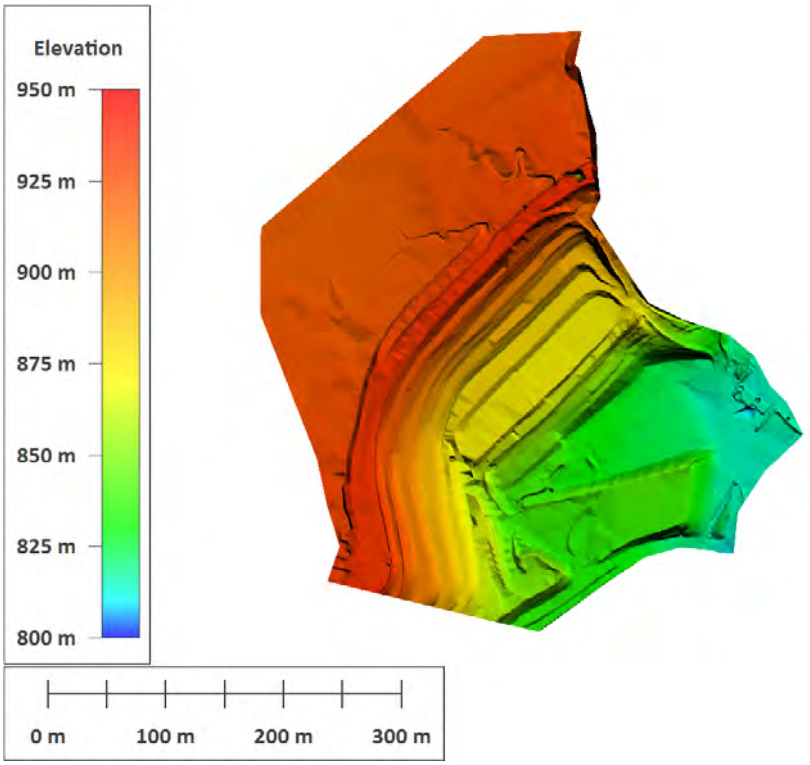

Figure B.B5-22 DEM 2015-05-27

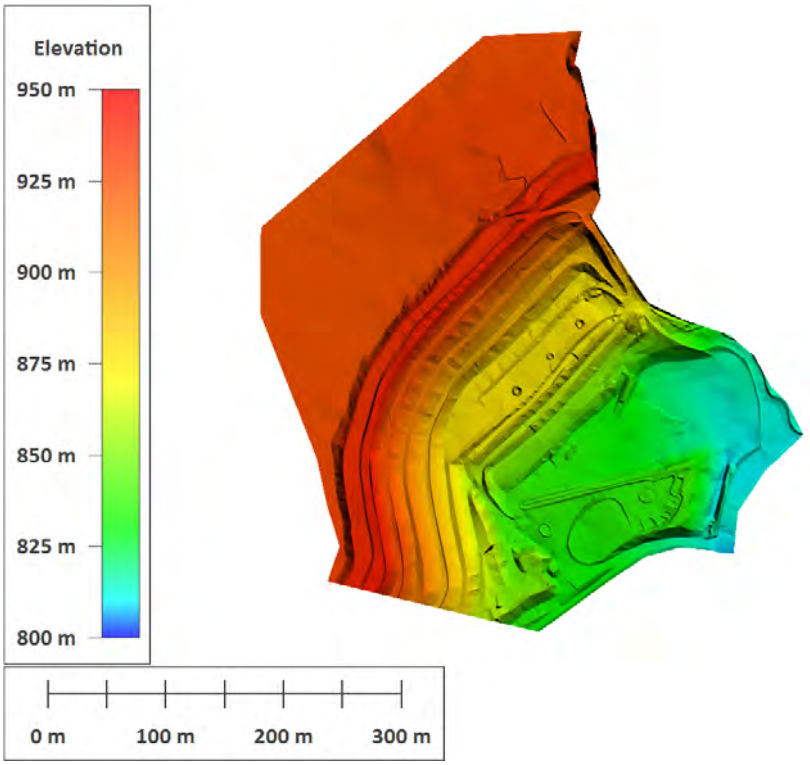

Figure B.B5-23 DEM 2015-06-22

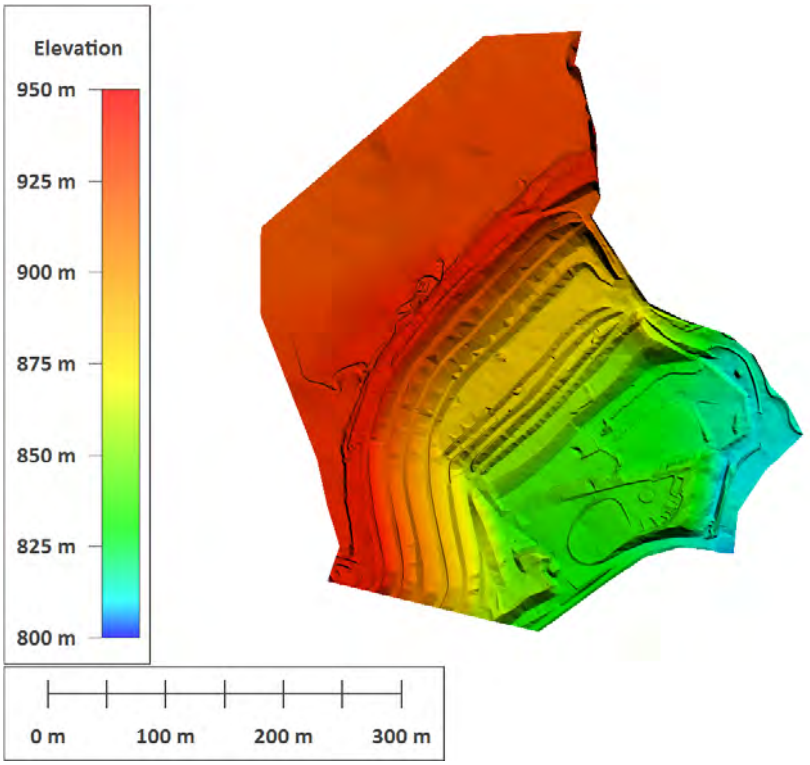

Figure B.B5-24 DEM 2015-07-27

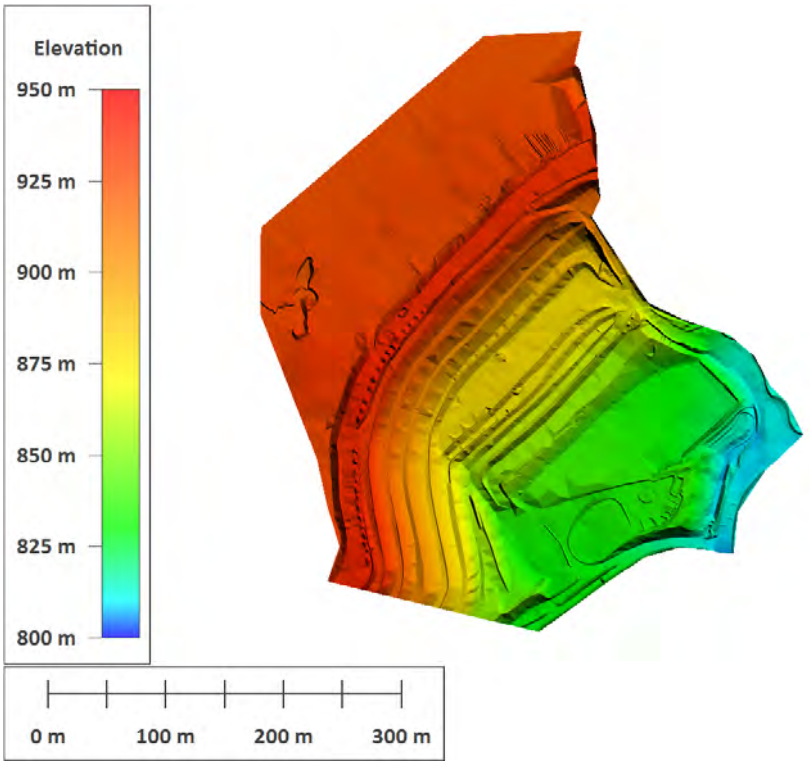

Figure B.B5-25 DEM 2015-08-24

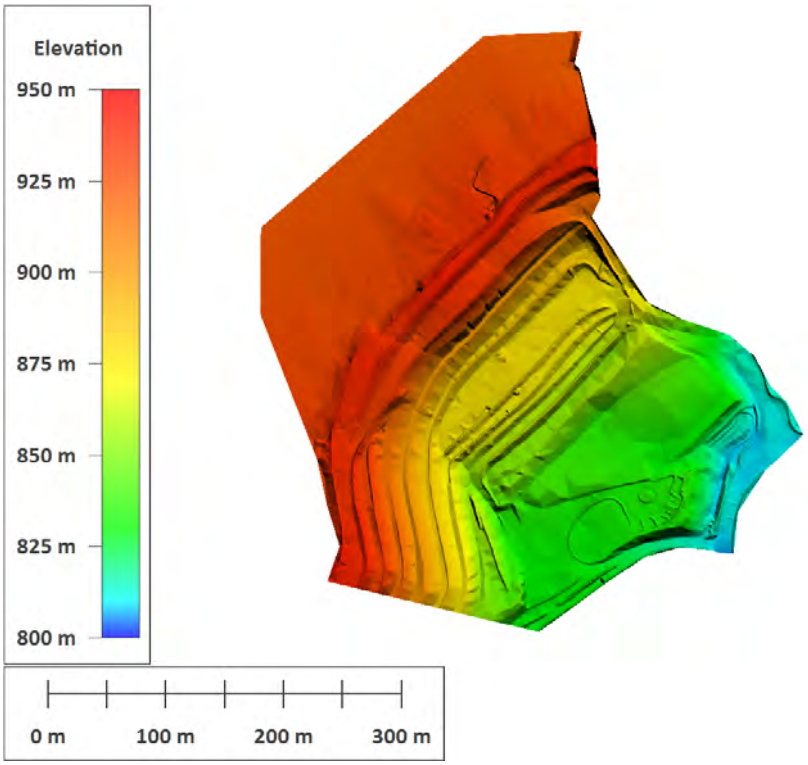

Figure B.B5-26 DEM 2015-10-01

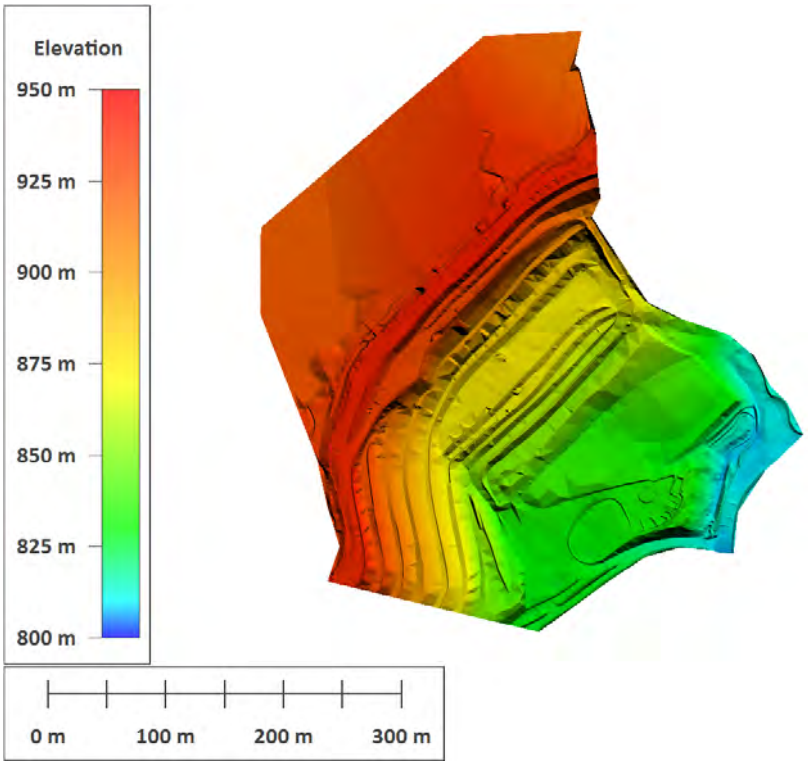

Figure B.B5-27 DEM 2015-10-27

B.B5-6 ISOPACHS

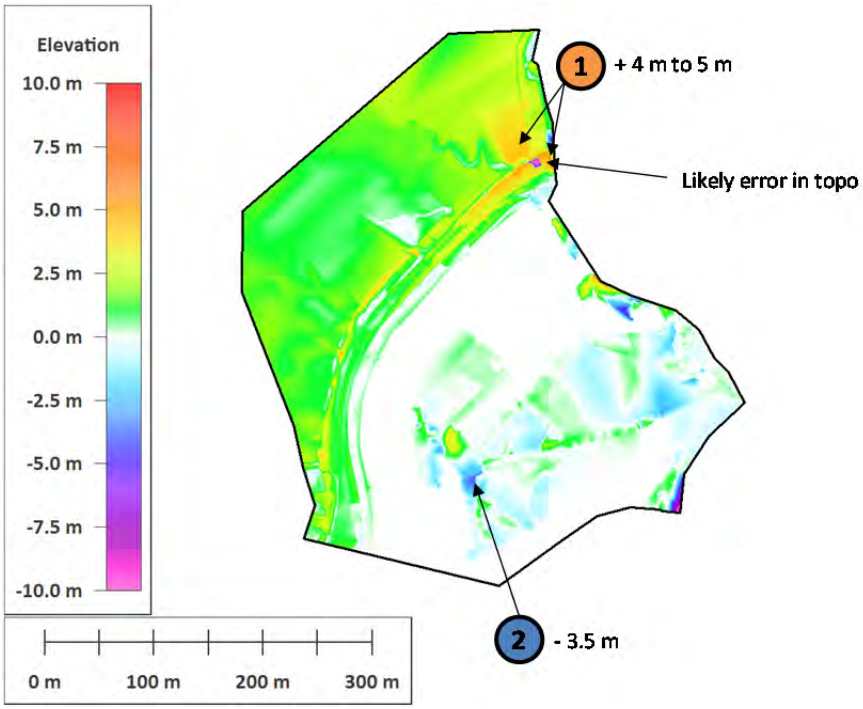

Figure B.B5-28 Isopach 2015-04-24 to 2015-05-27

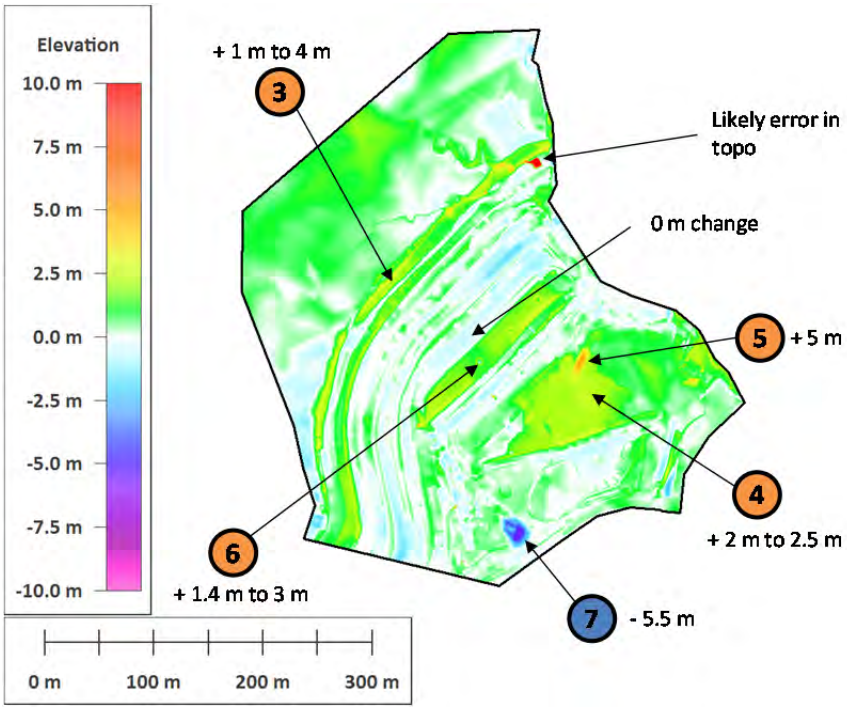

Figure B.B5-29 Isopach 2015-05-27 to 2015-06-22

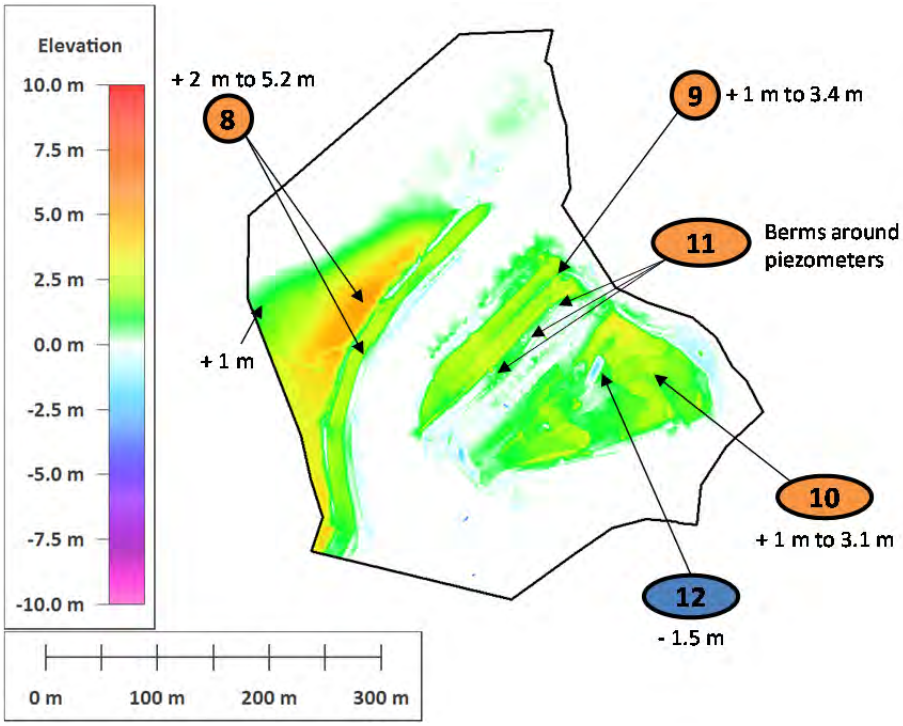

Figure B.B5-30 Isopach 2015-06-22 to 2015-07-27

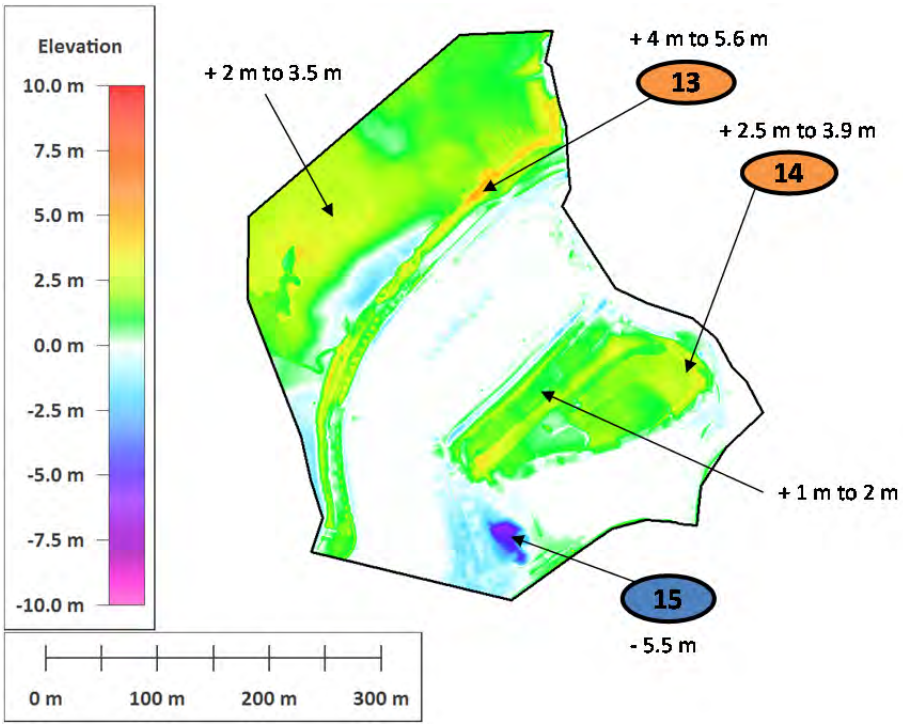

Figure B.B5-31 Isopach 2015-07-27 to 2015-08-24

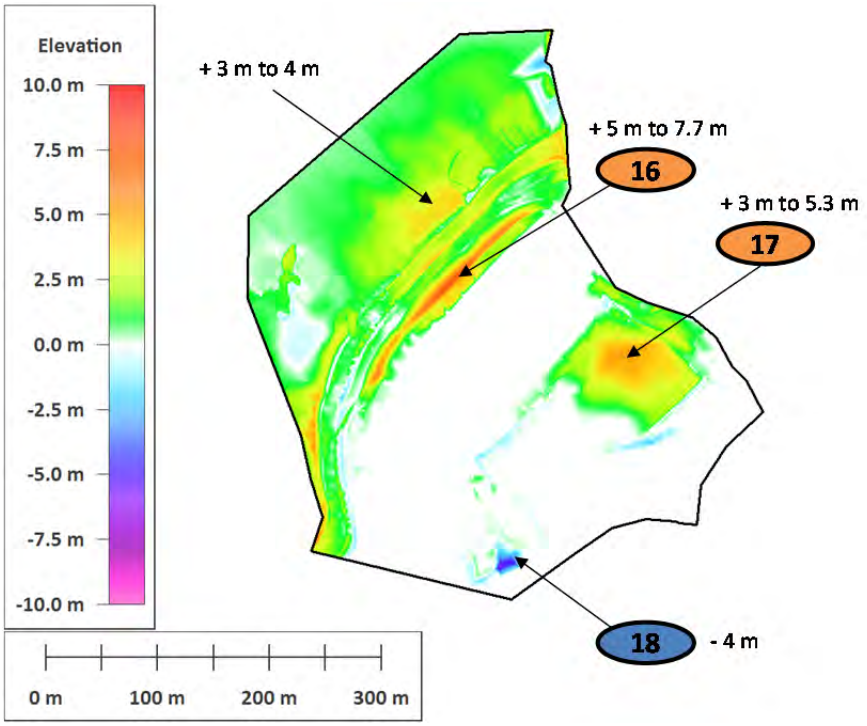

Figure B.B5-32 Isopach 2015-08-24 to 2015-10-01

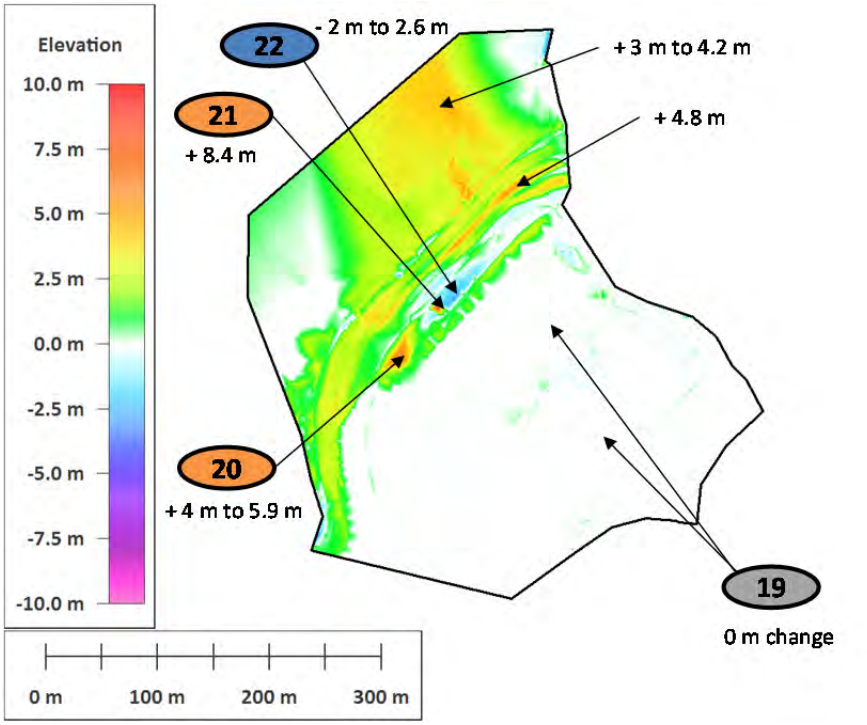

Figure B.B5-33 Isopach 2015-10-01 to 2015-10-27

B.B5-7 SUMMARY OF LOADING CHANGES

Table B.B5-1 Summary of loading changes[2]

Time Period (all in 2015)	Elevation Increase (Fill)		Elevation Decrease (Cut)	
	Observation	Comment	Observation	Comment
April 24 to May 27, 2015	1. Increase in elevation (up to +4.2 m locally) on upstream side of dam (tailings deposition) and at dam crest (up to +5 m locally) on far east side of left abutment.	1. Tailings deposition and crest raise (referred to as "Phase 4" in May 3 weekly report). Supported with aerial images.	2. Area of decreased elevation (-3.5 m) on west side of setback platform.	2. Approximately 5 m of fill material was placed to the southwest of this area in 2014. Appears to have been used as a borrow source during construction in 2015. This cut may be removal of a stockpile from the area or reshaping around the road.
May 27 to June 22, 2015	3. Increased elevation on upstream side of dam and at dam crest (+1 m to 4 m at crest). 4. Increased elevation on west side of blanket drain (+2 m to 2.5 m on west side). 5. Small area with larger elevation increase (+5 m) on drainage blanket. 6. Increased elevation at El. 875 m bench – from approximately El. 873 m to El. 875 m (+1.4 m to 3 m on downstream side of bench, 0 m change on upstream side of bench).	3. Crest raise on Dike 1 and work on the El. 890 m and El. 895 m benches described in the weekly reports. Supported with aerial images and site photos. 4. Construction of blanket drain (drain rock and gravel placement). Confirmed with site photos. 5. Not verified with site photos. Assumed to be stockpile or equipment in place at the time of survey. Material is removed in July 27 survey (see event 12). 6. Weekly report from June 7 states there was fill placement on the El. 875 m bench to El. 877 m elevation.	7. Area of decreased elevation (-5.5 m) on west side of setback platform.	7. Approximately 5 m of fill material was placed here in 2014. Appears to have been used as a borrow source during construction in 2015. Based on aerial images. This is not the same location where material was taken in May (different part of the borrow area).
June 22 to July 27, 2015	8. Increased elevation of tailings beach on west side of setback (+2 m to 5.2 m in localized area). 9. Increased elevation of El. 875 m bench – from approximately El. 875 m to El. 877 m (fill ranges from 1 m to 3.4 m). 10. Increased elevation at blanket drain (+1 m to 3.1 m). 11. Three features seen on El. 875 m bench in July topography. Small circular berms with a depression in the middle.	8. July aerial image and DEM show depression in tailings area immediately upstream of dam crest. Based on the July 27 aerial image and the DEM, it appears this area was filled in with tailings over the course of the month. The position of the tailings pipeline supports this. 9. Site photos show construction on the El. 875 m bench. The weekly report from July 7 states "Landfill over the left-side abutment drain, to the 877.0 m elevation." 10. Drain rock placement shown in site photos from this period. Photos from the end of the month and beginning of August also show sand placement. 11. These are small berms placed around the piezometers for protection. Features on DEM match piezometer locations.	12. Decrease in elevation where point (5) was in previous isopach (-1.5 m).	12. Assume stockpile or equipment present during previous survey was removed.
July 27 to August 25, 2015	13. Increase in elevation on upstream side of dam and at dam crest (+4 m to 5.6 m in localized area). 14. Increased elevation at blanket drain (up to +3.9 m on bermed areas at perimeter).	13. Completion of crest raise to El. 897.5 m referenced in weekly report. Crest raise visible in aerial images. 14. Sand placement over drain rock and gravel shown in site photos from early August. Photos from mid to late August show tailings placement over sand layer. Also visible in aerial images. Samarco's as-built section shows that the drain material should be only 2 m to 2.5 m thick. However, between the June and September survey that have placed up to 5.5 m material in some areas. Some of this is likely tailings.	15. Area of decreased elevation (-5.5 m) on west side of setback platform.	15. Approximately 5 m of fill material was placed here in 2014. Appears to have been used as a borrow source during construction in 2015. Based on aerial images.

[2] Table lists numbered "events", with an associated observation and comment for each. The event numbers correspond to the numbered markups in Section B.B5-6.

Time Period	Elevation Increase (Fill)		Elevation Decrease (Cut)	
August 24 to October 1, 2015	16. Increased elevation of El. 895 m and higher benches. There appears to be a small berm placed on the edge of the El. 895 m bench (+5 m to 7.7 m locally). 17. There is a “plateau” on the blanket drain showing increased elevation (+3 m to 5.3 m locally). The rest of the drain does not change.	16. Construction photos and records confirm bench raises at El. 890 m, El. 895 m, and El. 900 m. Construction of a berm on the El. 875 m bench is described in the weekly reports. However, the large increase in the isopach is in the area of the El. 895 m bench (not El. 875 m). The topography survey shows no increase in the level of the El. 875 m bench (it is possible that the survey was not updated here). The September 27 weekly report shows raising of the "L.S.A. drain protection berm" - this is likely the berm at El. 895 m. 17. May be explained by stockpiled material (tailings) seen in construction photos from late August. The aerial image from October 1 does not appear to have been updated in the area of the blanket drain (image was patched). The aerial image does not show the stockpiles The raw drone photos from this time period do not show the stockpiles. They were likely spread sometime during the month.	18. Area of decreased elevation (-4 m) on west side of platform of setback platform.	18. Approximately 5 m of fill material was placed here in 2014. Appears to have been used as a borrow source during construction in 2015. Based on aerial photos.
October 1 to October 27, 2015	19. No change shown in the area of the blanket drain. 20. Increased elevation in the area of the “pullout” along the El. 895 m bench (+4 m to 5.9 m). 21. Increased elevation in the “bump” to the east of the “pullout” along the El. 895 m bench (+8.4 m).	19. This makes it look like the material placed in the “plateau” area (see event 17) remained in place. The aerial images from October 1 and October 27 look very similar in this area. The weekly reports state that there was work being completed on the El. 875 bench during this period (including photos), but the topographic survey does not show any changes on the bench. The aerial image from October 27 is different in this area than the image from October 1, so we know something must have changed. It is possible that the survey was not updated in some areas. 20. Possible construction of a pullout or truck turnaround in this area. Site photos show only the side slope of this area and reshaping on the benches (See photo 20-A and far left of 19-A). The weekly report states: “3 m widening downstream, between piles 27 to 41, at the left-side abutment, for crest heightening to 900 m” (October 4) and “Heightening of the berm downstream from the left-side abutment, to ensure a safe height (5.00 m) between banks 895/900 m, allowing the heightening to proceed” (October 11). 21. This “bump” is created by one point in the survey that is approximately 10 m higher than the points around it. This is likely an error in the topography survey.	22. Area of decreased elevation along the El. 895 m bench, east of the “pullout” (-2 m to 2.6 m).	22. This is along the same bench as the “pullout”. It appears that one part of the bench got wider and the other part got narrower. We have not confirmed from site photos if or why this material was removed. This is the same area where the berm was added in the previous month (see event 16). This may have been levelled or removed.

B.B5-8 SITE PHOTOS

The numbering system used in the photo captions below corresponds to the numbering given in Table B.B5-1. For example, photo “3-A” is the first photo related to item 3 in Table B.B5-1, and photo “3-B” is the second photo related to the same item. Photos that do not correspond to a numbered event from Table B.B5-1 are labeled as MISC-A through MISC-H. Translations of photo captions from Portuguese to English have been accepted as-is with no review of the translation by the Panel.

B.B5-8.1 May, 2015

1-A: Photo from weekly report, week of May 3, 2015: "Elevation of the left-side abutment, phase 4."

MISC-A: Photo from weekly report, week of May 3, 2015: "Continued hydrocyclone assembly."

MISC-B: Photo from weekly report, week of May 17, 2015: "Construction of drainage chutes at the left-side abutment of Dike 1."

MISC-C: Photo from weekly report, week of May 24, 2015: "Continued construction of blanket drain at the left-side abutment of Dike 1."

B.B5-8.2 June, 2015

3-A: Photos from weekly report, week of May 31, 2015: "Construction begin of the 25.00 m plateau upstream at, to the 890 m elevation. At Dike 1."

3-B: Photo from weekly report, week of May 31, 2015: "Heightening along the entire crest of Dike 1, finalizing the 895.00 m bank."

3-C: Photo from weekly report, week of June 7, 2015: "Spreading and compaction of the tailings on the left-side abutment."

4-A: Photo from weekly report, week of June 14, 2015: "Construction of a drainage blanket on the left-side abutment of Dike 1."

6-A: Photo from weekly report, week of June 7, 2015: "Landfill over the left-side abutment drain, to the 877.0 m elevation."

6-B: Photo from weekly report, week of June 14, 2015: "Elevation of the axis return on the L.S.A. of Dike 1."

6-C: Photo from weekly report, week of June 14, 2015: "Surface leveling downstream of the 895.0 m bank, on Dike 1."

6-D: Photo from June 21, 2015 site visit by ITRB showing view of left abutment.

6-E: Photo from weekly report, week of June 21, 2015: "Elevation of the crest at the left-side abutment connection."

6-F: Photo from weekly report, week of June 21, 2015: "Elevation of phase 4 to allow the elevation of the 900 m bank, Dike 1."

B.B5-8.3 July, 2015

8-A: Photo from weekly report, week of June 28, 2015: "Heightening of the platform upstream from bay C, near PL1 cannon."

8-B: Photo from weekly report, week of June 28, 2015: "Opening of a new loading yard in Bay C reservoir."

8-C: Photo from weekly report, week of July 19, 2015: "Spacing marking from Bank 895 to bank 900 and elevation 895.5."

8-D: Photo from weekly report, week of July 19, 2015: "Leveling of the entire extent of the Dike 1 crest."

9-A: Photo from weekly report, week of June 28, 2015: "Heightening of the original axis return."

10-A: Photo from weekly report, week of June 28, 2015: "Construction of drain carpet on the left-side abutment of Dike 1."

10-B: VOGBR photo of dam crest on July 2, 2015[18].

10-C: VOGBR photo from July 2, 2015[18] showing drain rock placement on left setback.

9-D: Photo from weekly report, week of July 5, 2015: "Tailings discharge to recover the original axis of Dike 1."

10-E: Photo from weekly report, week of July 5, 2015: "Construction of drain blanket on the left-side abutment of Dike 1." Dashed blue line around ponded water.

10-F: Photo from weekly report, week of July 5, 2015: "Construction of drain blanket on the left-side abutment of Dike 1."

10-G: Photo from Technical Monitoring Photographic Report (2015-06-29 to 2015-07-03)[19] showing drain rock placement on the left setback.

10-H: Photo from Technical Monitoring Photographic Report (2015-06-29 to 2015-07-03)[19] showing left setback. Dashed blue line around ponded water.

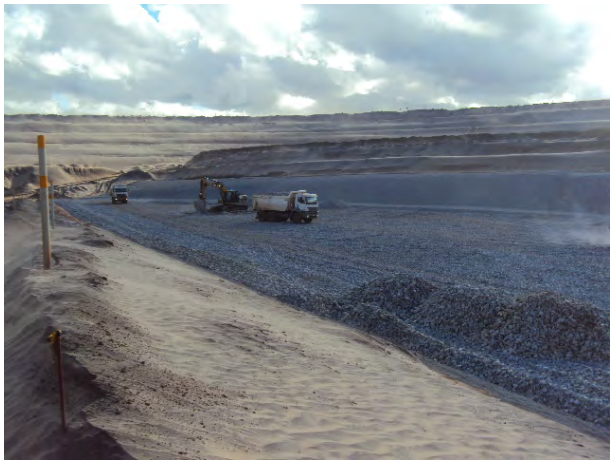

10-I: Photo from Technical Monitoring Photographic Report (2015-06-29 to 2015-07-03)[19] showing drain rock placement on left setback.

10-J: Photo from Technical Monitoring Photographic Report (2015-07-13 to 2015-07-17)[20] showing sand placement.

MISC-D: VOGBR photo from July 2, 2015[18]: "Left Abutment - Saturation in the Slope - El. 826 m."

MISC-E: Photo from weekly report, week of July 19, 2015: "Construction of the dike to contain solids at Grota da Vale completed."

MISC-F: Photo from weekly report, week of July 21, 2015: "Overflow pipes setup on the dike built at Grota da Vale."

B.B5-8.4 August, 2015

13-A, B: Photos from weekly report, week of August 2, 2015: "Heightening of the crest of Dike 1, phases 1 and 3, to the 895.50 m elevation, piles 6 to 20."

13-C: Photo from weekly report, week of August 9, 2015: "Heightening of the upstream platform, between as piling 20 to 40, to the 896.00 m elevation."

13-D: Photo from weekly report, week of August 9, 2015: "Topographic milestones between piles 10 and 20, to the 897.00 m elevation."

14-A: Photo from weekly report, week of August 9, 2015: "Construction of the drain downstream from the left-side abutment of Dike 1."

14-B Samarco construction photo from August 10, 2015 showing drain construction on the left setback.

14-C: Samarco construction photo from August 11, 2015 showing drain construction on the left setback.

14-D: Samarco construction photo from August 14, 2015 showing drain construction on the left setback. Dashed blue line around ponded water.

14-E: Photo from VOGBR report dated July 21, 2015 to August 20, 2015[21] showing left setback. Dashed blue line around ponded water.

14-F: Photo from VOGBR report dated July 21, 2015 to August 20, 2015[21]. Dashed blue line around ponded water.

14-G: Samarco construction photo from August, 2015 (exact date unknown) showing left setback. Dashed blue line around ponded water.

14-H, I: Photos from VOGBR report dated August 21, 2015 to August 28, 2105[22]. Dashed blue line around ponded water.

B.B5-8.5 September, 2015

16-A: Photo from weekly report, week of September 6, 2015: "Heightening of Dike 1's crest to the 898 m elevation."

16-B: Photo from weekly report, week of September 6, 2015: "Heightening of the 890.00 m bank."

16-C, D: Photo from weekly report, week of September 6, 2015: "Tanker truck and power grader to water and level the 898.00 m crest, near the left-side abutment channel."

16-E: Photo from weekly report, week of September 13, 2015: "Extension of the pipeline, positioning of the cannon and discharge of the Plant 3 sand tailings into Bay “C”, Dike 1, to ensure the shore width (minimum of 200 m)."

16-F: Photo from weekly report, week of September 13, 2015: "Alignment of the US 3 line on the left-side abutment of Dike 1."

16-G: Photo from weekly report, week of September 13, 2015: "890/895 m elevation leveling to allow continuity of the heightening of the return to the original axis of Dike 1, Left-side abutment"

16-H, I: Photo from weekly report, week of September 20, 2015: "Heightening of the axis return in the 890.00 m - 895.00 m bank, left-side abutment of Dike 1."

16-J: Photo from weekly report, week of September 20, 2015: "Construction of a dike to form a bay, in the 875.00 m elevation. This activity is to allow the return to the original axis, downstream from the left-side abutment, for controlled hydraulic discharge with minimum outflow."

16-K: Photo from weekly report, week of September 27, 2015: "Construction of a dike for tailings to be discharged hydraulically at the original axis, L.S.A., Dike 1."

16-L: Photo from weekly report, week of September 27, 2015: "Heightening of the L.S.A. drain protection dike, between piles 1A and 7A."

17-A: Photos from VOGBR report dated August 21, 2015 to August 28, 2105[22]. Dashed blue line around ponded water. Stockpiles could account for increased elevations seen in isopach for August 24, 2015 to October 1, 2015 surveys.

B.B5-8.6 October, 2015

19-A: Photo from weekly report, week of October 18, 2015: "875.00 m bank earthfill for axis return and crest stability."

19-B: Photo from weekly report, week of October 25, 2015: "Preparation of the axis return area for hydraulic discharge."

20-A: Photo from weekly report, week of October 4, 2015: "3 m widening downstream, between piles 27 to 41, at the left-side abutment, for crest heightening to 900 m."

20-B: Photo from weekly report, week of October 4, 2015: "Construction of a dike for tailings to be discharged hydraulically at the return of the original axis, left-side abutment of Dike 1."

20-C, D: Photo from weekly report, week of October 11, 2015: "Heightening of the berm downstream from the left-side abutment, to ensure a safe height (5.00 m) between banks 895/900 m, allowing the heightening to proceed."

20-E: Photo from weekly report, week of October 11, 2015: "Heightening of the crest, downstream, to elevation 899.00 m, left-side abutment."

20-F: Photo from weekly report, week of October 24, 2015: "Construction of a reinforcement berm downstream from the 895/900 m bank, on the left-side abutment."

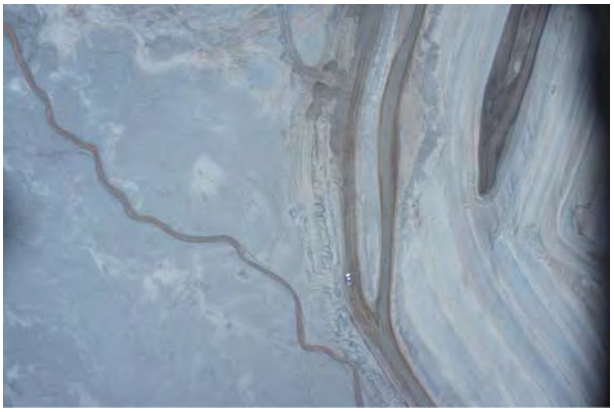

20-G: Raw drone photo showing greater detail of the “pullout” from October 28, 2015.

B.B5-8.7 November, 2015

MISC-G: Photo from morning on day of failure from eyewitness report, November 5, 2015, showing toe of El. 860 m blanket drain.

MISC-H: Photo from morning on day of failure from eyewitness report, November 5, 2015, showing toe of El. 860 m blanket drain.

ATTACHMENT B6

Slimes Depositional History and Spatial Reconstruction

Summary of Slimes Elevations
Slimes Image Timeline

Summary of Slimes Elevations

File Survey Date	Basis for Delineation	Slimes Elevation (m)		Topography Source						
		Dike 2 (Max.)	Dike 1 (Min.)	Stitched Stripped Ground	G021600-O-130458_R-00 (not shown in image timeline)	G021600-O-130415_R-01	SA-1849-R02	041-A-MN-GR-09-006	SA-1788	Monthly Samarco survey (survey date shown)
2009-04-18	PhotoSat aerial image	841.0	no slimes in Dike 1	x						
2009-08-18	PhotoSat aerial image	841.0	no slimes in Dike 1	x						
2009-11-15	PhotoSat aerial image	847.0	no slimes in Dike 1	x						
2010-01-17	PhotoSat aerial image	847.0	no slimes in Dike 1	x						
2010-02-22	PhotoSat aerial image	847.0	no slimes in Dike 1	x						
2010-04-27	PhotoSat aerial image	847.0	813.0	x		x		x		
2010-06-19	PhotoSat aerial image	847.0	819.0	x		x		x		
2010-08-07	PhotoSat aerial image	847.0	824.0	x		x		x		
2010-10-29	PhotoSat aerial image	847.0	no slimes in Dike 1	x						
2010-12-22	PhotoSat aerial image	847.0	no slimes in Dike 1	x						
2011-02-11	PhotoSat aerial image	848.0	824.0	x	x	x			x	
2011-04-09	PhotoSat aerial image	848.0	830.0	x	x	x			x	
2011-07-01	Samarco topography	852.0	834.0				x			
2011-07-27	Samarco monthly report	852.0	835.9				x			
2011-08-24	Samarco monthly report	852.0	**835.9**				x			
2011-08-17	PhotoSat aerial image	852.0	835.0				x			
2011-09-15	Samarco monthly report	852.0	836.8				x			
2011-09-21	PhotoSat aerial image	853.0	837.0				x			
2011-10-02	PhotoSat aerial image	853.0	837.0				x			
2011-10-11	Samarco monthly report	853.0	838.6				x			
2011-11-08	Samarco monthly report	852.0	839.8				x			
2011-12-16	Samarco monthly report	852.0	**839.8**				x			
2012-01-10	Samarco monthly report	852.0	840.6							2012-01-21
2012-01-21	Samarco topography	851.0	841.0							2012-01-21
2012-02-09	Samarco monthly report	852.0	841.4							2012-01-21
2012-03-16	Samarco monthly report	852.0	842.9							2012-01-21
2012-03-03	PhotoSat aerial image	852.0	842.0							2012-01-21
2012-04-01	Vale survey	852.5	842.5							2012-04-01 (Vale)
2012-04-19	Samarco monthly report	852.5	844.8							2012-04-01 (Vale)
2012-05-14	Samarco monthly report	853.0	846.7							2012-04-01 (Vale)
2012-06-04	Samarco monthly report	853.0	848.2							2012-04-01 (Vale)
2012-07-13	Samarco monthly report	853.0	849.5							2012-04-01 (Vale)
2012-08-09	Samarco monthly report	insufficient info to estimate	no slimes in Dike 1							
2012-09-02	Samarco topography	858.0	no slimes in Dike 1							2012-09-02
2012-09-11	Samarco monthly report	insufficient info to estimate	no slimes in Dike 1							
2012-09-26	Samarco topography	858.0	no slimes in Dike 1							2012-09-26
2012-10-29	Samarco monthly report	insufficient info to estimate	no slimes in Dike 1							
2012-11-30	Samarco monthly report	insufficient info to estimate	no slimes in Dike 1							
2012-12-11	Samarco monthly report	insufficient info to estimate	no slimes in Dike 1							
2013-01-01	Samarco topography	861.0	no slimes in Dike 1							2013-01-01
2013-01-25	Samarco monthly report	insufficient info to estimate	no slimes in Dike 1							
2013-02-01	Samarco topography	861.0	no slimes in Dike 1							2013-02-01
2013-02-28	Samarco monthly report	insufficient info to estimate	no slimes in Dike 1							
2013-03-02	Samarco topography	863.0	no slimes in Dike 1							2013-03-02
2013-03-05	Samarco monthly report	insufficient info to estimate	no slimes in Dike 1							
2013-04-02	Samarco topography	864.3	no slimes in Dike 1							2013-04-02
2013-04-30	Samarco monthly report	insufficient info to estimate	no slimes in Dike 1							
2013-05-01	Samarco topography	865.0	no slimes in Dike 1							2013-05-01
2013-05-08	PhotoSat aerial image	Excluded - date of survey and image show similar conditions to the May 1, 2013 Samarco survey. No slimes in Dike 1.								
2013-05-27	Samarco topography	865.5	no slimes in Dike 1							2013-05-27
2013-05-28	Samarco monthly report	insufficient info to estimate	no slimes in Dike 1							
2013-06-27	Samarco monthly report	867.4	**863.2**							2013-06-30

File Survey Date	Basis for Delineation	Slimes Elevation (m)		Topography Source						
		Dike 2 (Max.)	Dike 1 (Min.)	Stitched Stripped Ground	G021600-O-130458_R-00 (not shown in image timeline)	G021600-O-130415_R-01	SA-1849-R02	041-A-MN-GR-09-006	SA-1788	Monthly Samarco survey (survey date shown)
2013-06-30	Samarco topography	867.4	864.5							2013-06-30
2013-07-29	Samarco topography	867.5	865.0							2013-07-29
2013-07-29	Samarco monthly report (July)	insufficient info to estimate	865.0							2013-07-29
2013-08-01	**Samarco monthly report**	insufficient info to estimate	867.0							2013-09-03
2013-09-03	Samarco topography	868.0	866.5							2013-09-03
2013-09-24	Samarco monthly report	insufficient info to estimate	868.0							2013-10-01
2013-10-01	Samarco topography	868.0	868.0							2013-10-01
2013-10-27	Samarco topography	869.2	869.0							2013-10-27
2013-10-30	Samarco monthly report	Monthly report does not provide coordinates or elevations for crest or beach - unable to estimate								
2013-11-26	Samarco topography	870.0	870.0							2013-11-26
2013-12-02	Samarco monthly report	Monthly report does not provide coordinates or elevations for crest or beach - unable to estimate								
2013-12-27	Samarco topography	870.3	870.3							2013-12-27
2014-01-23	Samarco monthly report	insufficient info to estimate	870.9							2014-01-29
2014-01-29	Samarco topography	872.0	872.0							2014-01-29
2014-03-28	Samarco topography	873.0	873.0							2014-03-28
2014-05-01	Samarco topography	874.4	874.4							2014-05-01
2014-06-03	Samarco topography	876.0	876.0							2014-06-03
2014-06-27	Samarco topography	876.4	876.4							2014-06-27
2014-08-04	Samarco topography	877.0	877.0							2014-08-04
2014-08-10	PhotoSat aerial image	Excluded from dataset - date of survey and image show similar conditions to the pre- and proceding Samarco topographic survey								
2014-08-29	Samarco topography	878.5	878.5							2014-08-29
2014-09-26	Samarco topography	879.7	879.7							2014-09-26
2014-10-31	Samarco topography	881.0	881.0							2014-10-31
2014-11-27	Samarco topography	882.0	882.0							2014-11-27
2014-12-29	Samarco topography	882.5	882.5							2014-12-29
2015-01-29	Samarco topography	883.5	883.5							2015-01-29
2015-02-27	Samarco topography	885.0	885.0							2015-02-27
2015-03-20	Samarco topography	885.0	885.0							2015-03-20
2015-04-24	Samarco topography	886.4	886.4							2015-04-24
2015-05-27	Samarco topography	887.5	887.5							2015-05-27
2015-06-22	Samarco topography	888.7	888.7							2015-06-22
2015-06-24	PhotoSat aerial image	Excluded from dataset - date of survey and image show similar conditions to the pre- and proceding Samarco topographic survey								
2015-07-10	PhotoSat aerial image									
2015-07-21	PhotoSat aerial image									
2015-07-27	Samarco topography	890.0	890.0							2015-07-27
2015-08-24	Samarco topography	890.6	890.6							2015-08-24
2015-10-01	Samarco topography	891.5	891.5							2015-10-01
2015-10-27	Samarco topography	893.0	892.5							2015-10-27

Notes:

1. Bolded text or values indicate the same date or values were given in the monthly monitoring report as the previous report.
2. Grey cells denote data not included in final slimes data series.

Slimes Image Timeline

2009-04-18

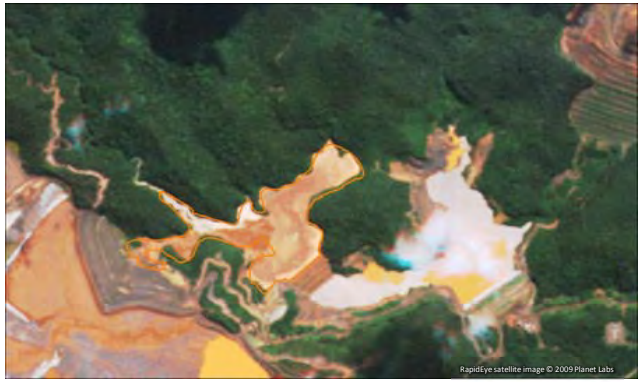

2009-08-18

2009-11-15

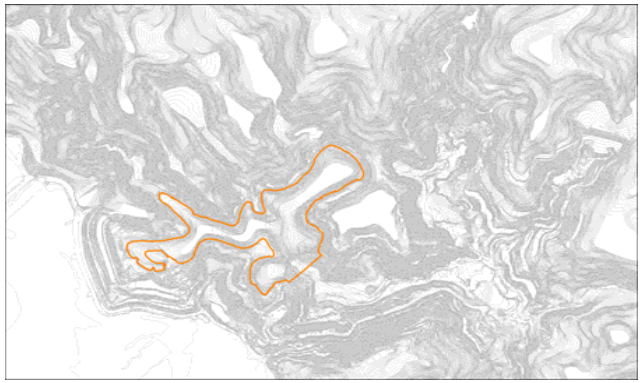

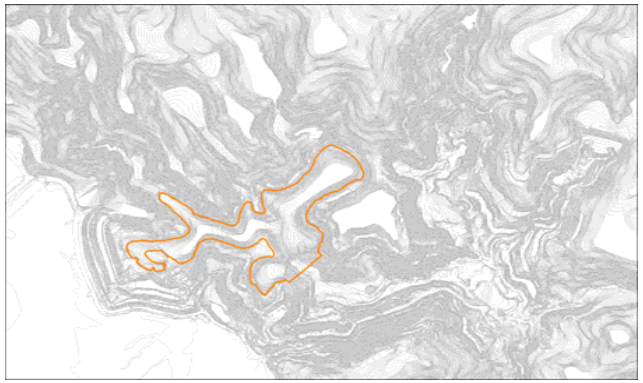

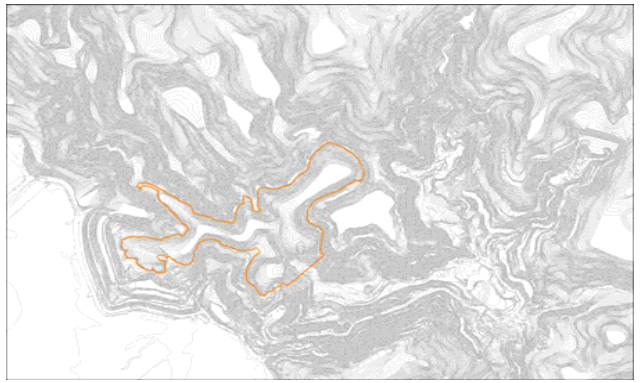

2010-01-17

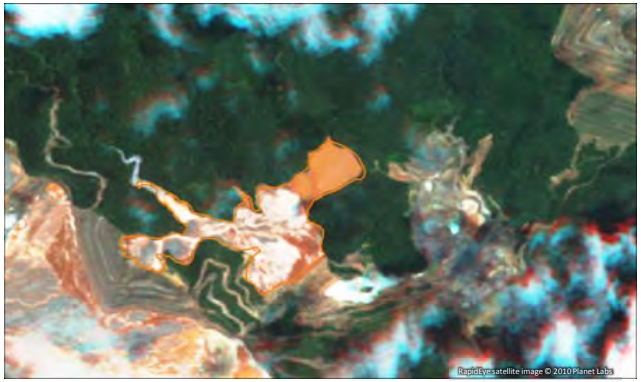

2010-02-22

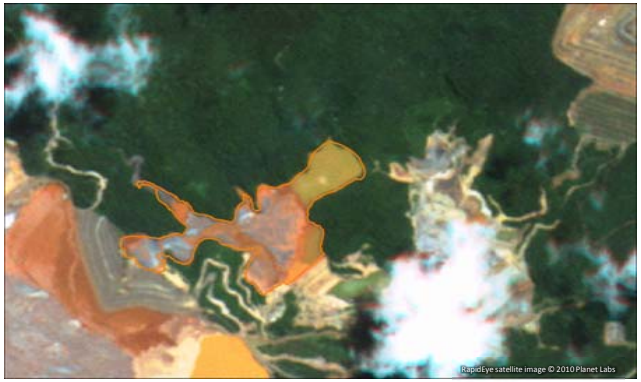

2010-04-27

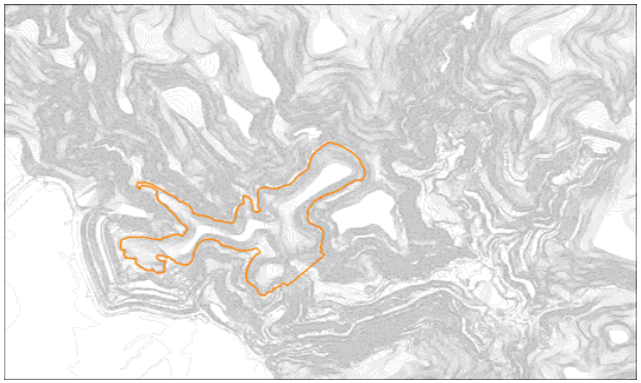

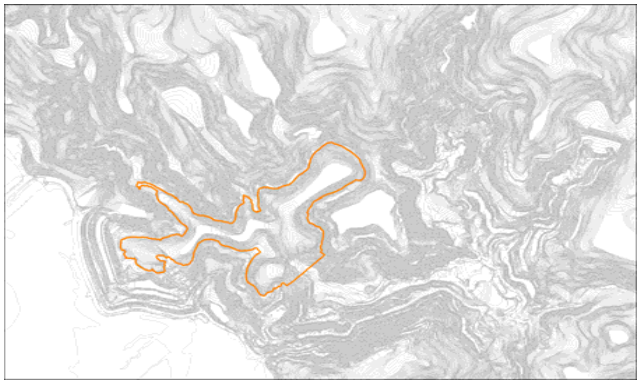

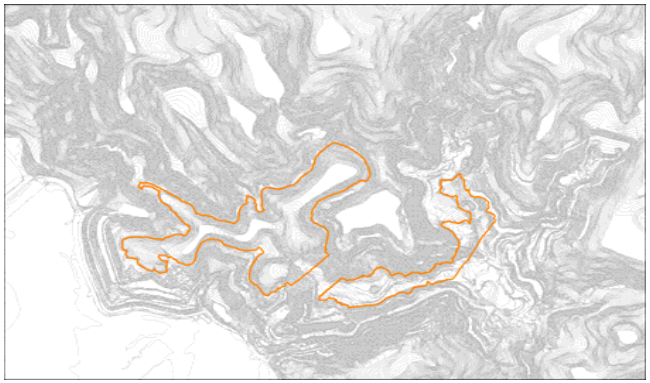

2010-06-19

2010-08-07

2010-10-29

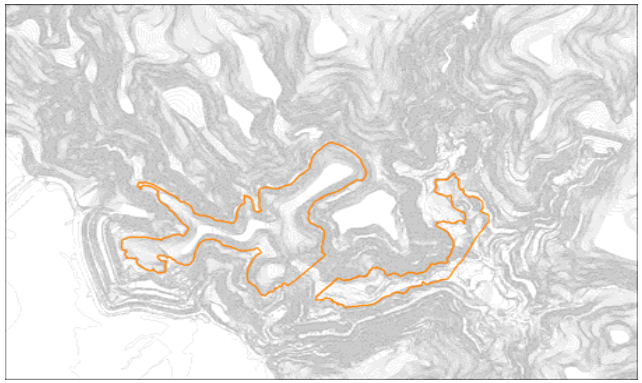

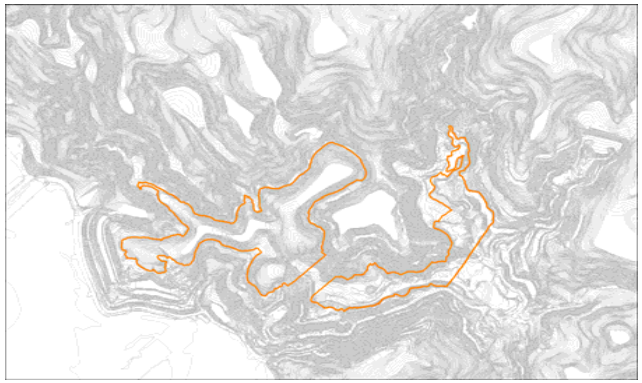

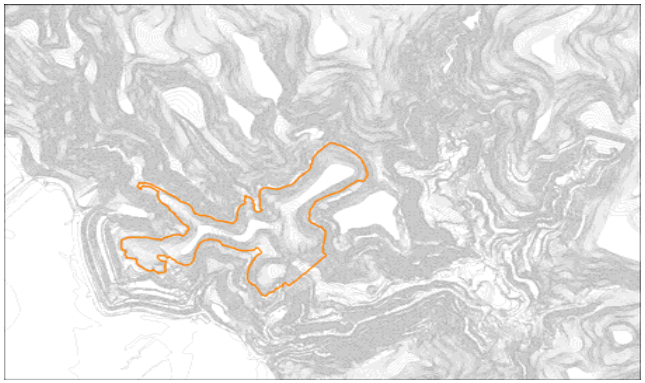

2010-12-22

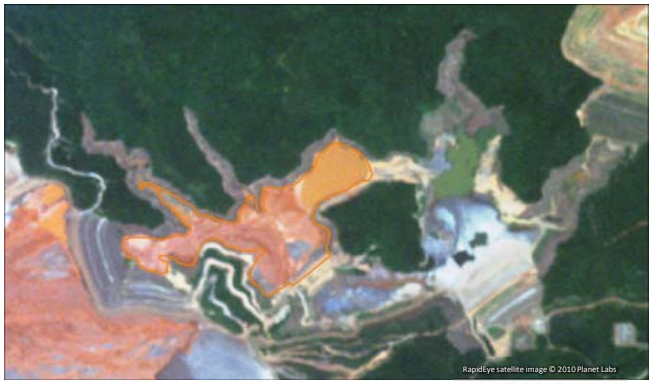

2011-02-11

2011-04-09

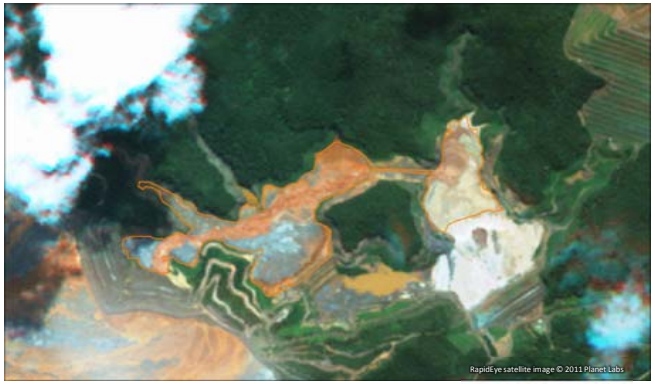

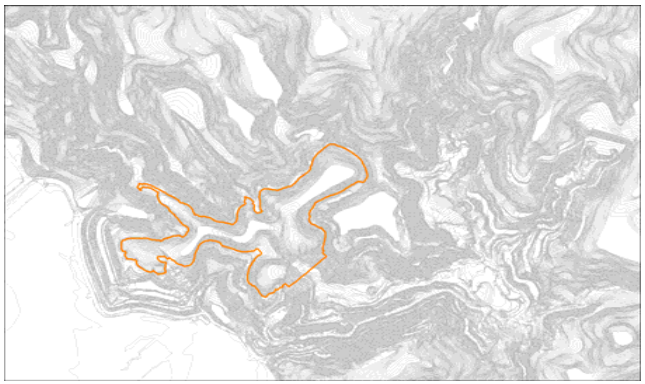

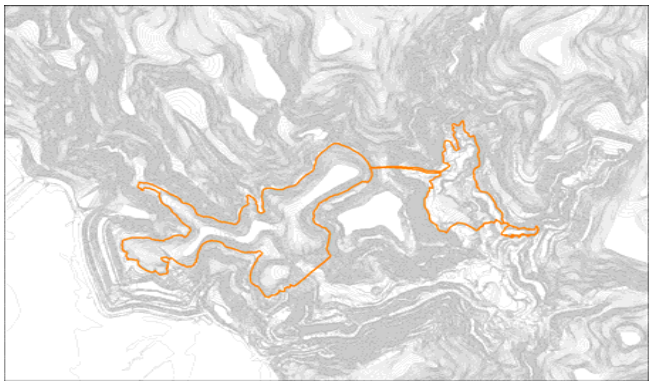

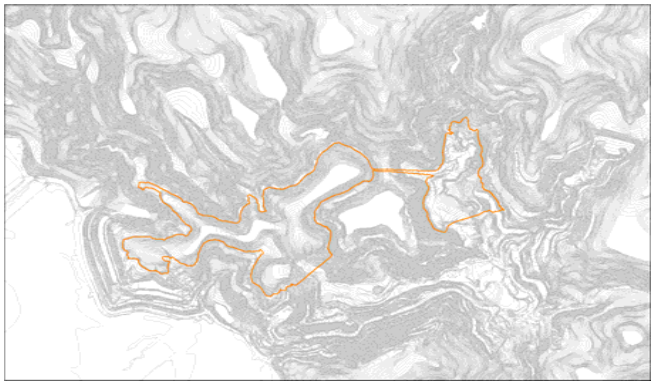

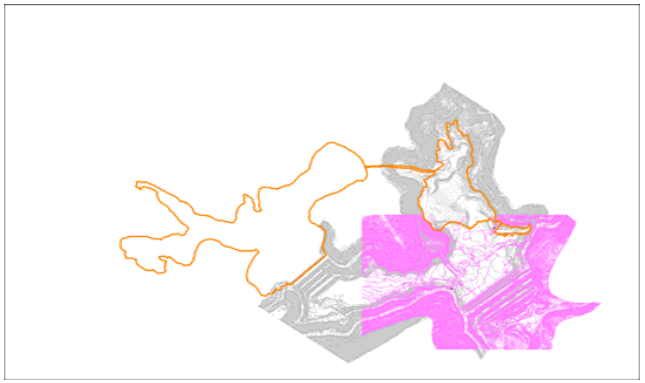

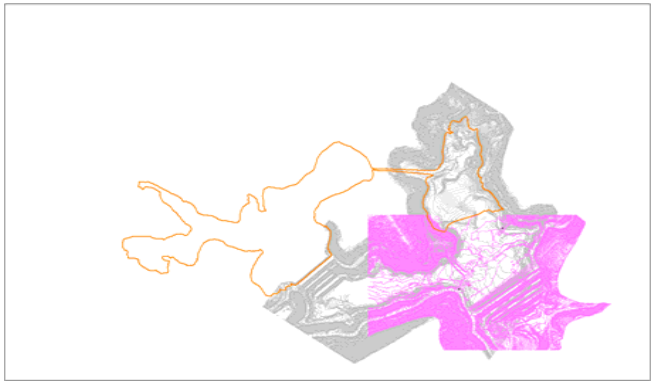

2011-07-01

2011-07-27 (Monthly Report)

2011-08-24 (Monthly Report)

2011-08-17

2011-09-15 (Monthly Report)

2011-09-21

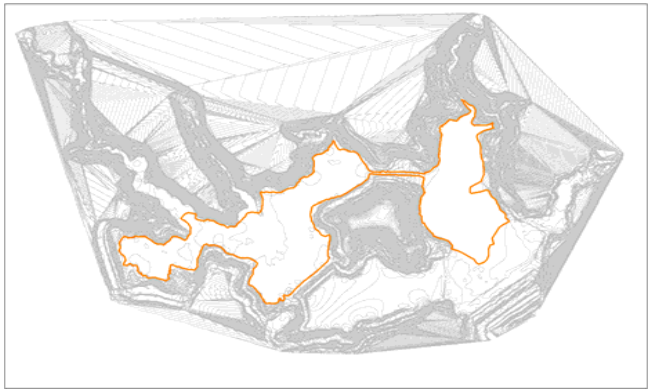

2011-10-02

2011-10-11 (Monthly Report)

2011-11-08 (Monthly Report)

2011-12-16 (Monthly Report)

2012-01-10 (Monthly Report)

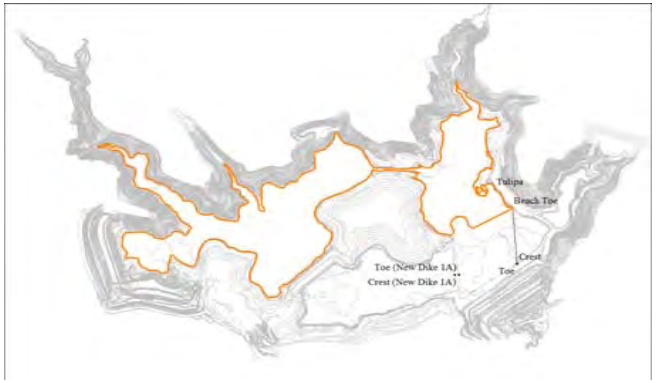

2012-01-21

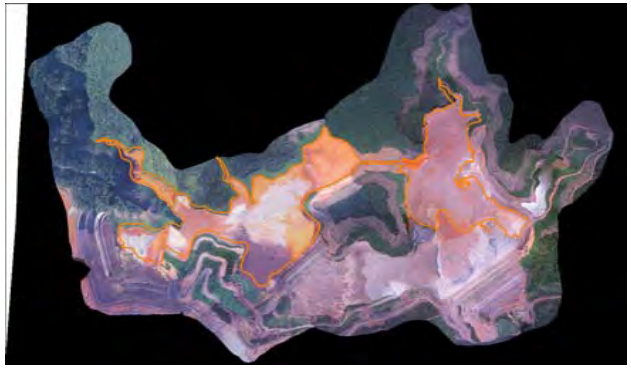

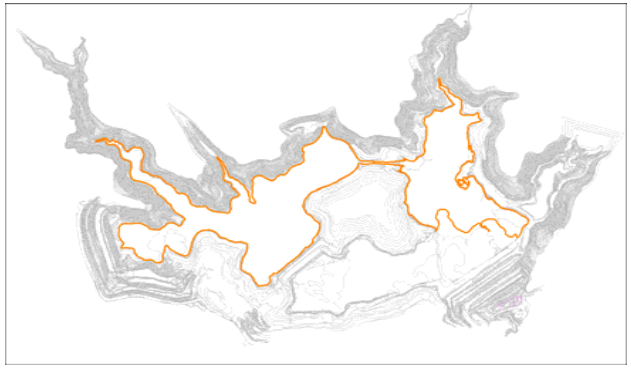

2012-02-09 (Monthly Report)

2012-03-03

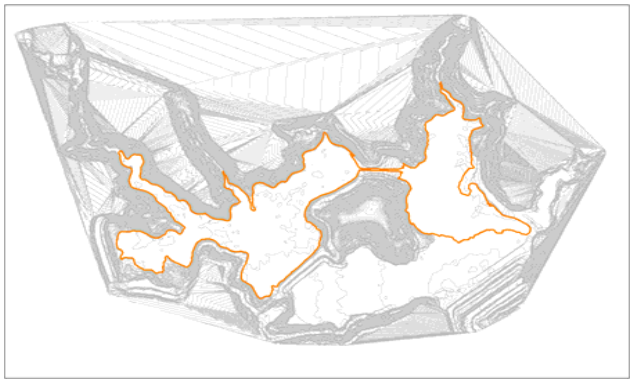

2012-03-16 (Monthly Report)

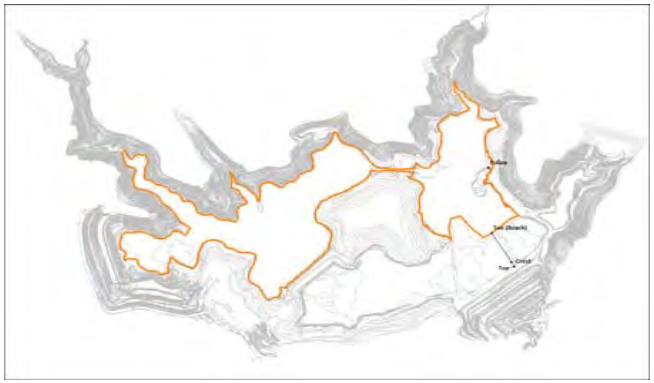

2012-04-01

2012-04-19 (Monthly Report)

2012-05-14 (Monthly Report)

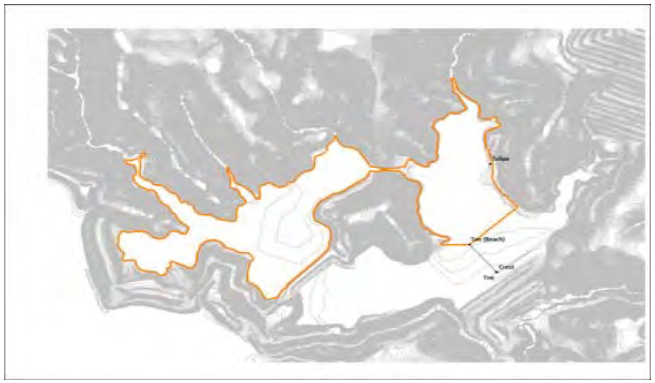

2012-06-04 (Monthly Report)

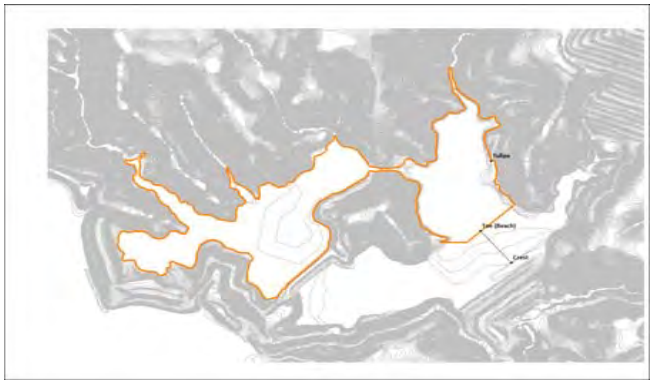

2012-07-13 (Monthly Report)

2012-09-02

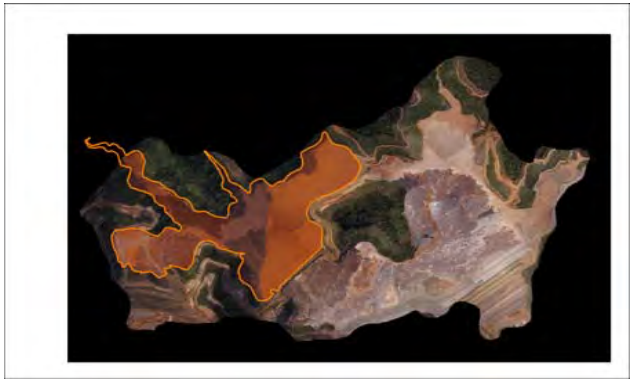

2012-09-26

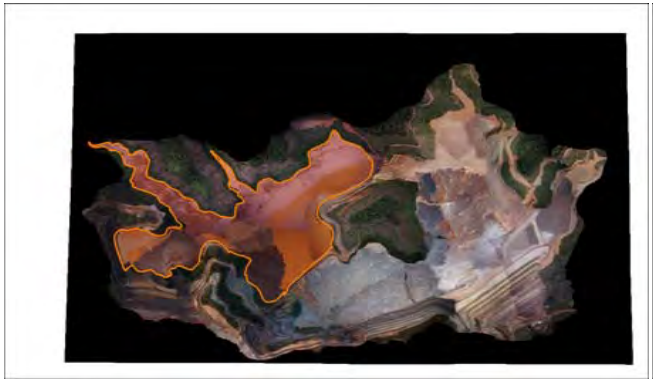

2013-01-01

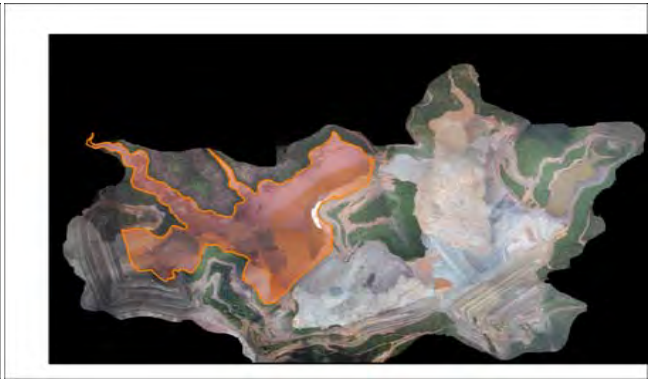

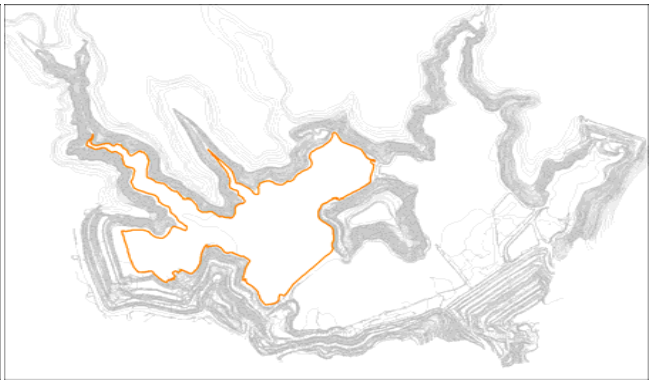

2013-02-01

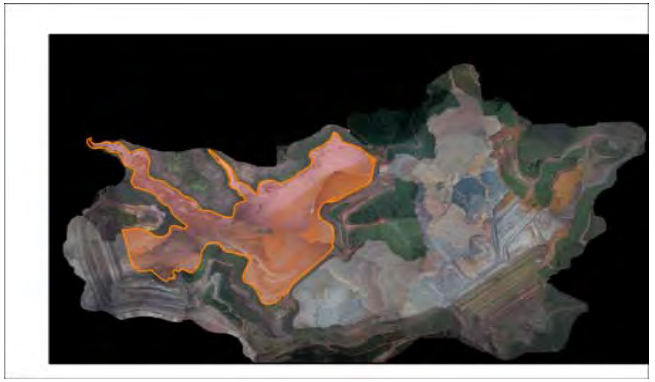

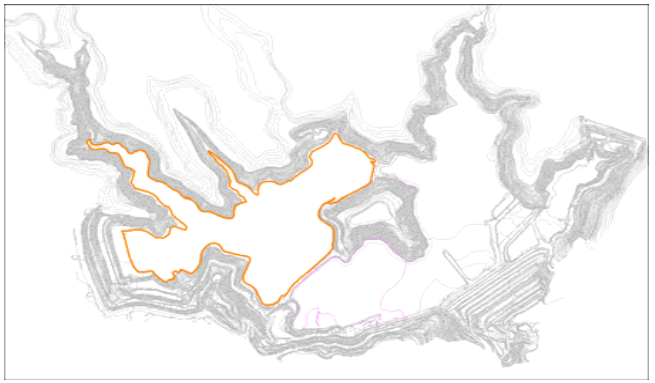

2013-03-02

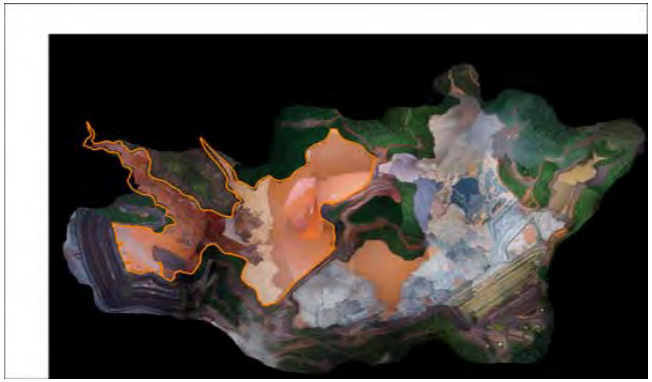

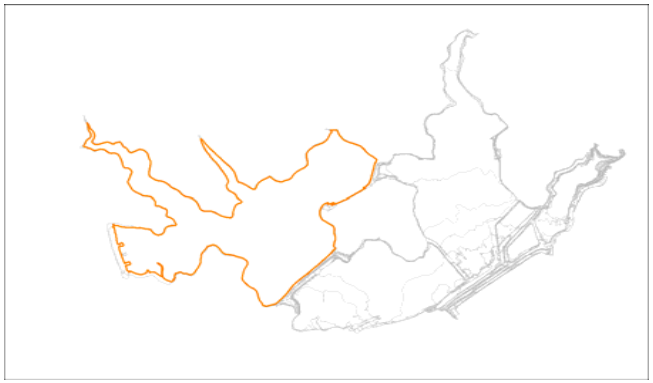

2013-04-02

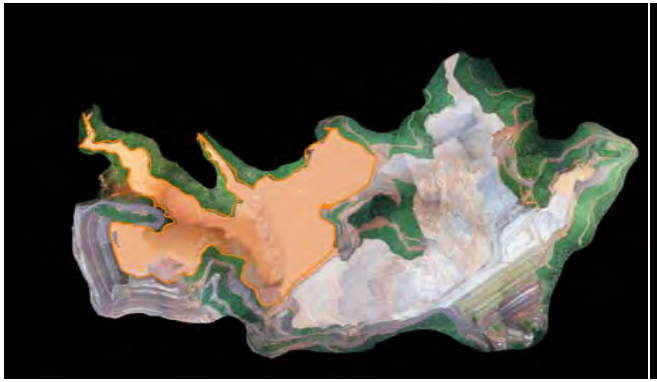

2013-05-01

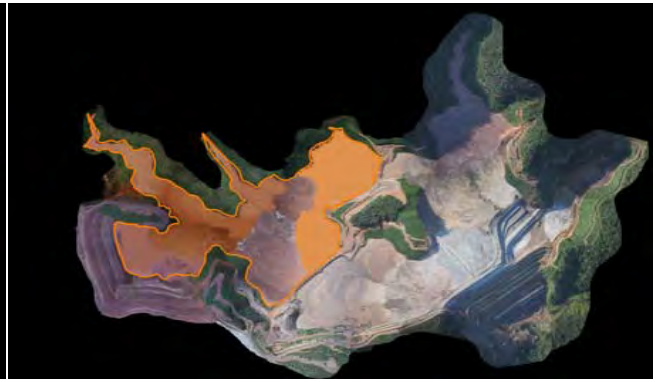

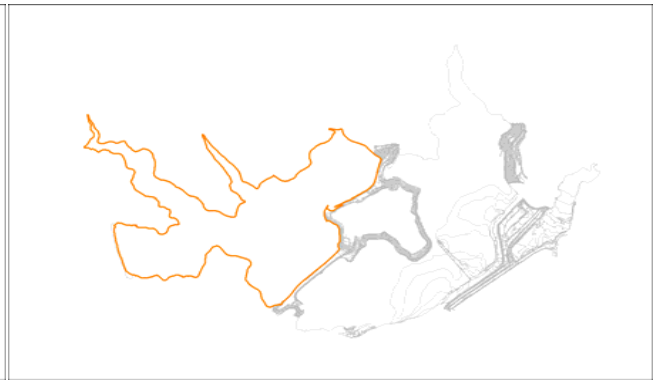

2013-05-27

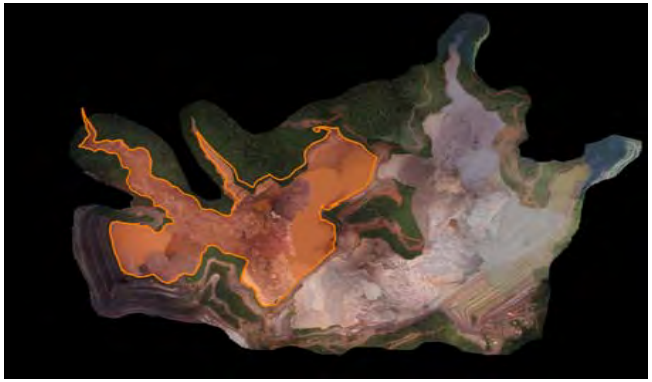

2013-06-27 (Monthly Report)

2013-06-30

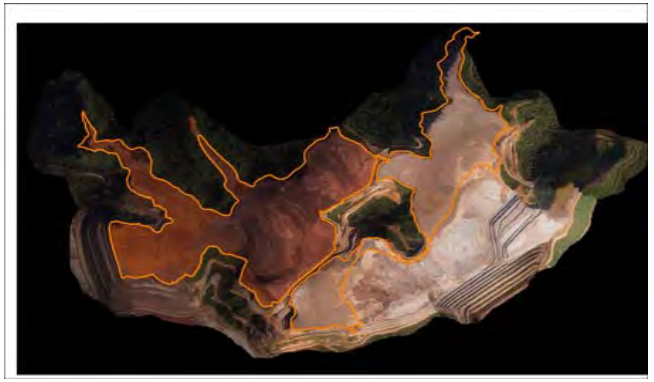

2013-07-29

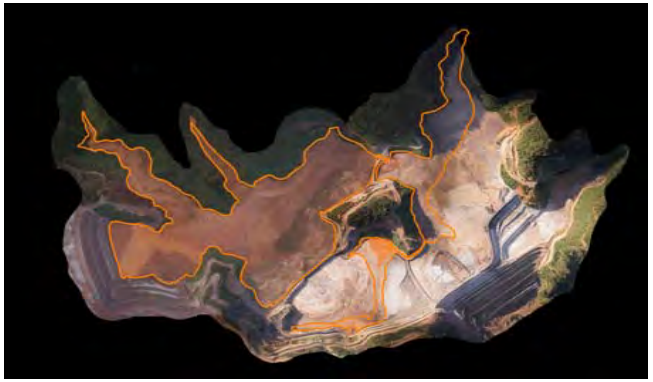

2013-07-29 (Monthly Report)

2013-08-01 (Monthly Report, survey date unknown)

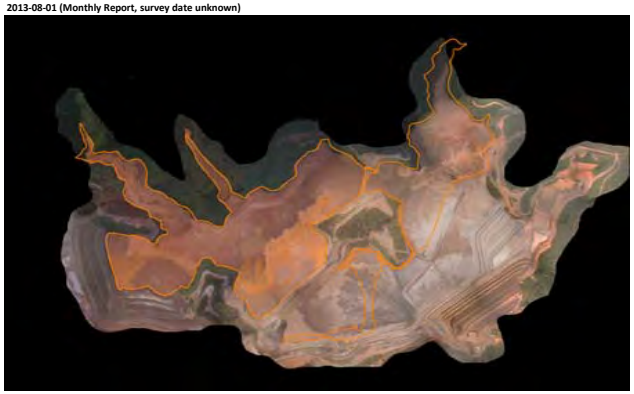

2013-09-03

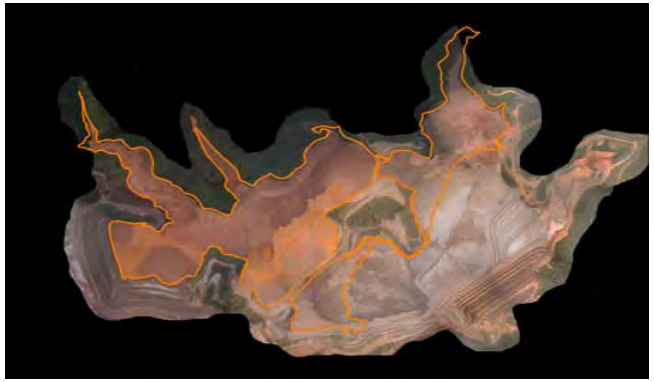

2013-09-24 (Monthly Report)

2013-10-01

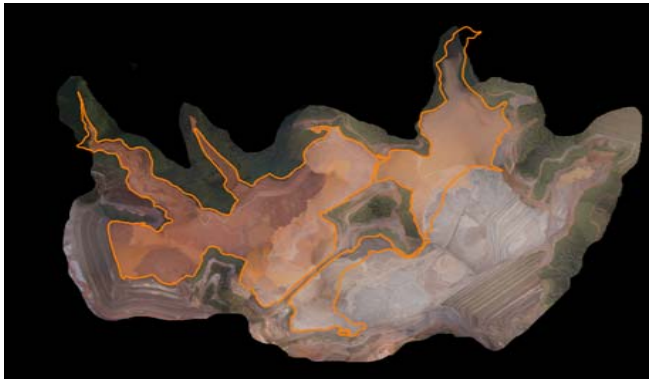

2013-10-27

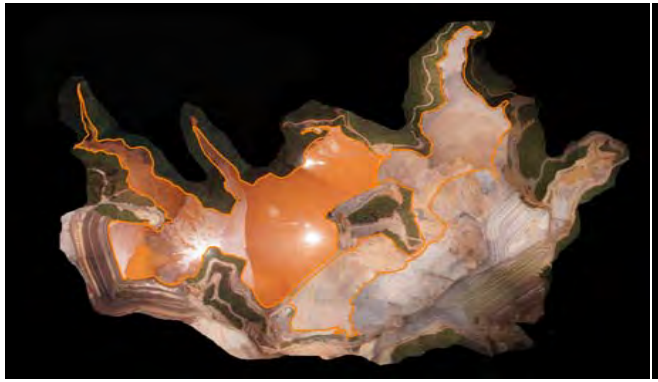

2013-11-26

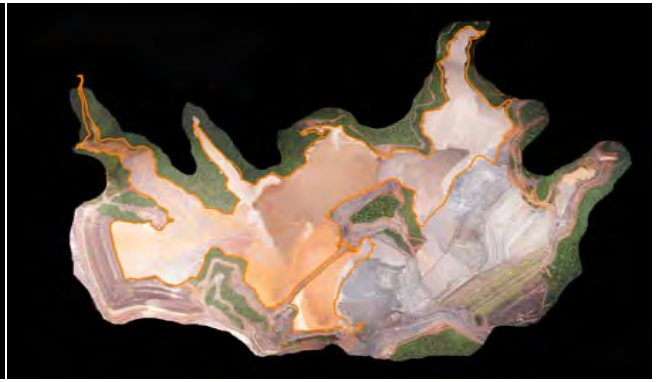

2013-12-27

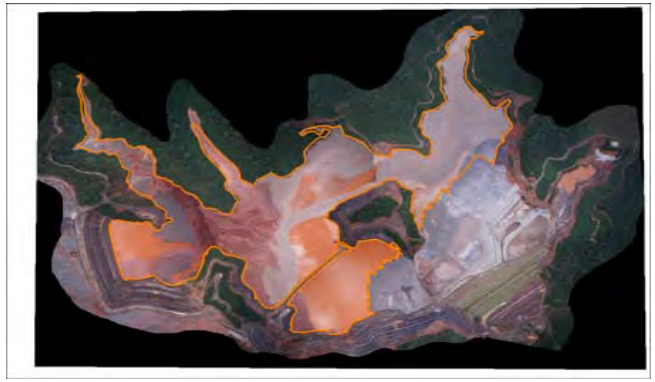

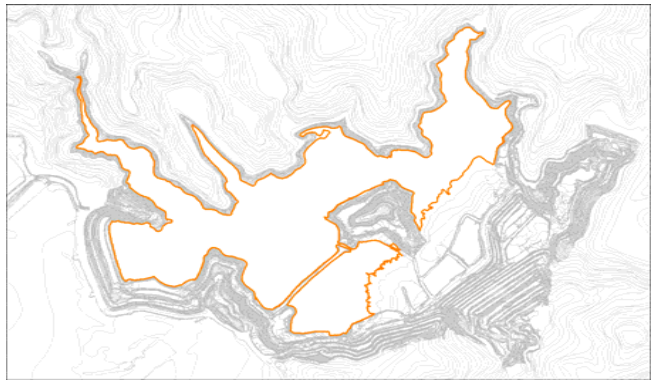

2014-01-23 (Monthly Report)

2014-01-29

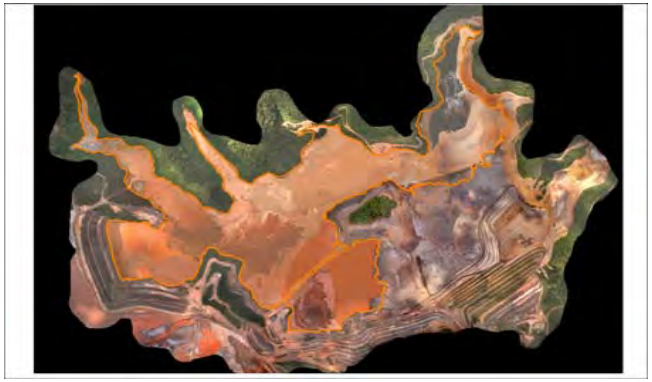

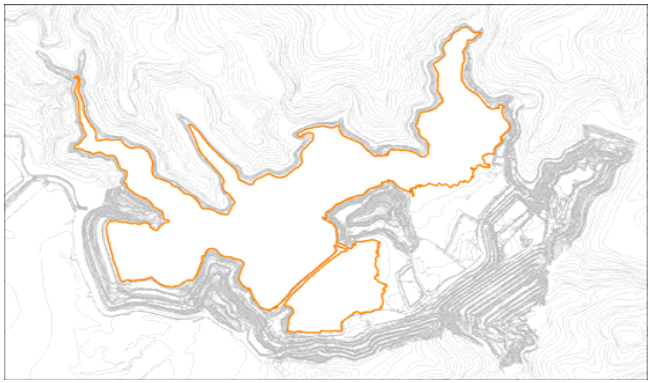

2014-03-28

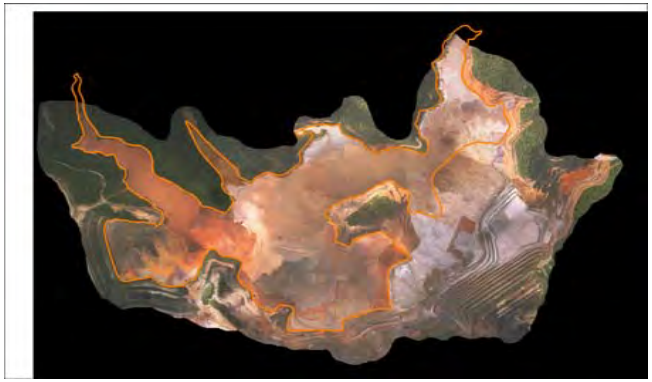

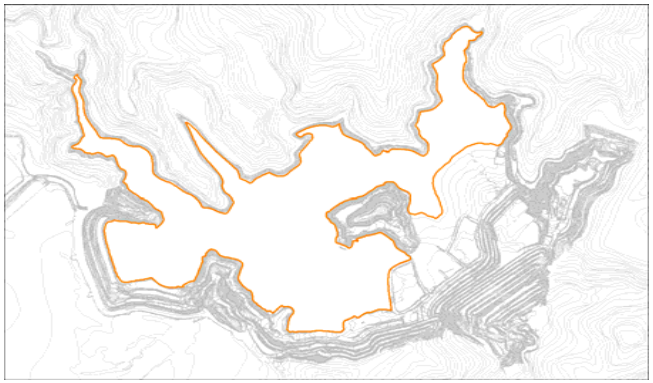

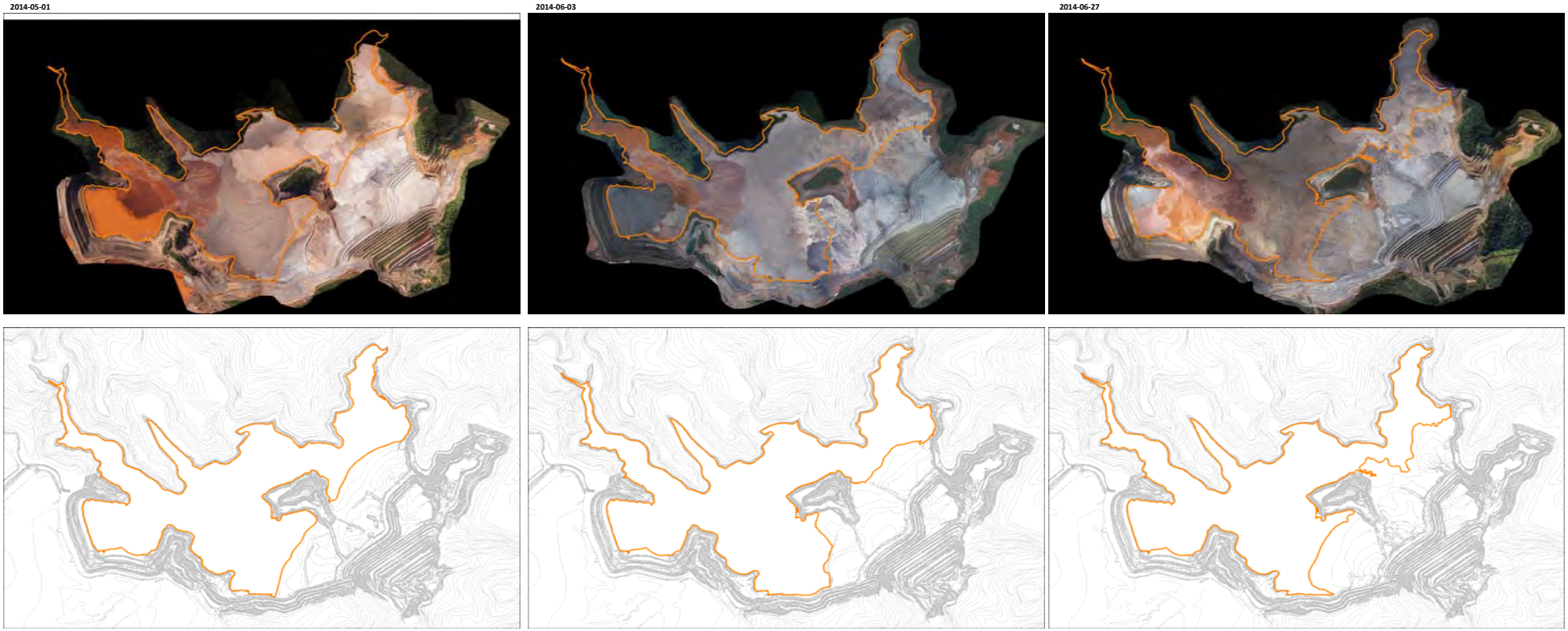
2014-05-01
2014-06-03
2014-06-27

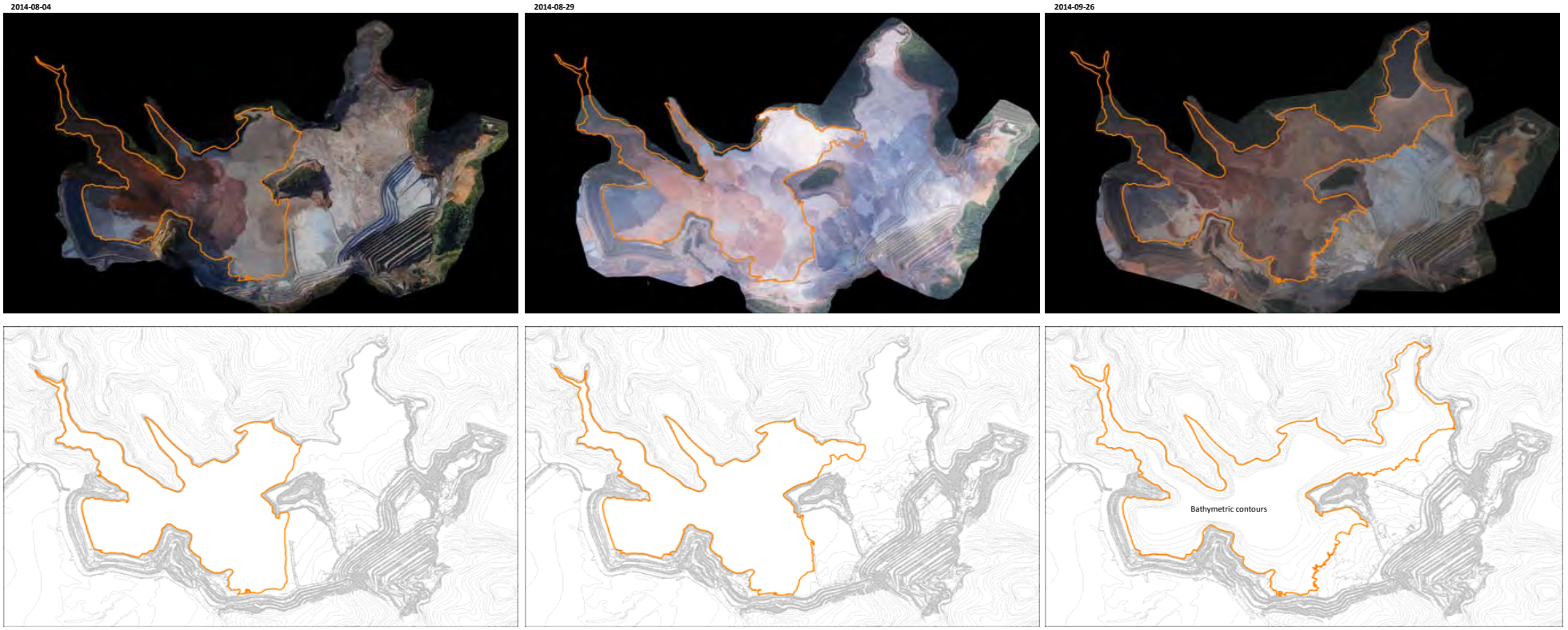
2014-08-04
2014-08-29
2014-09-26
Bathymetric contours

2014-10-31

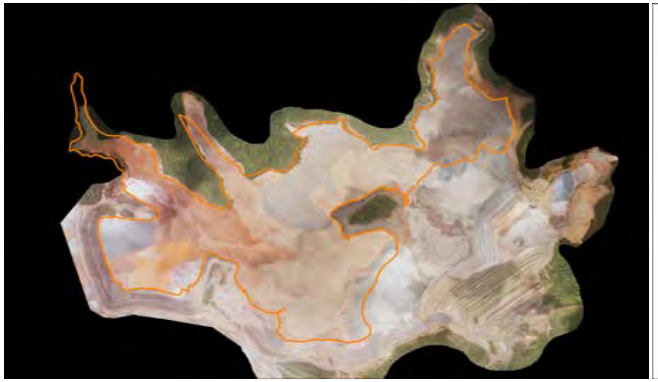

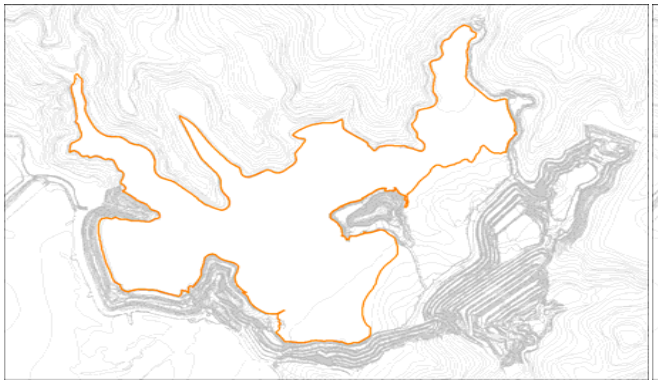

2014-11-27

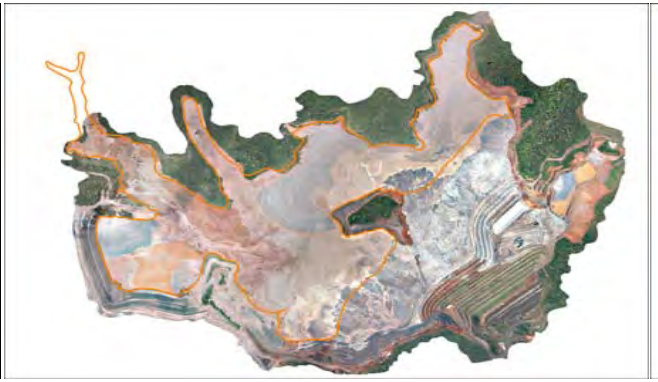

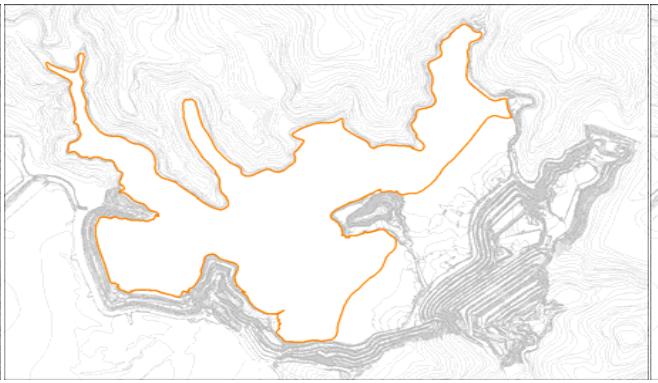

2014-12-29

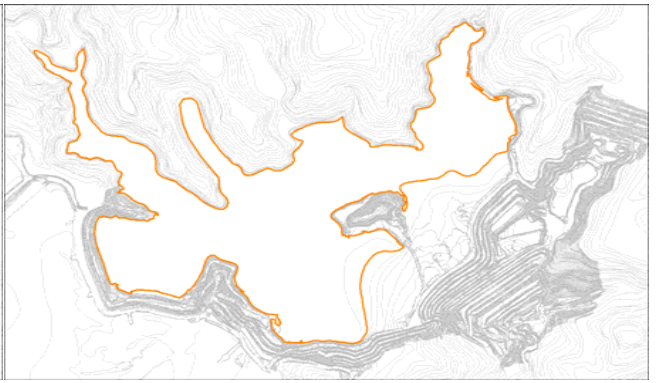

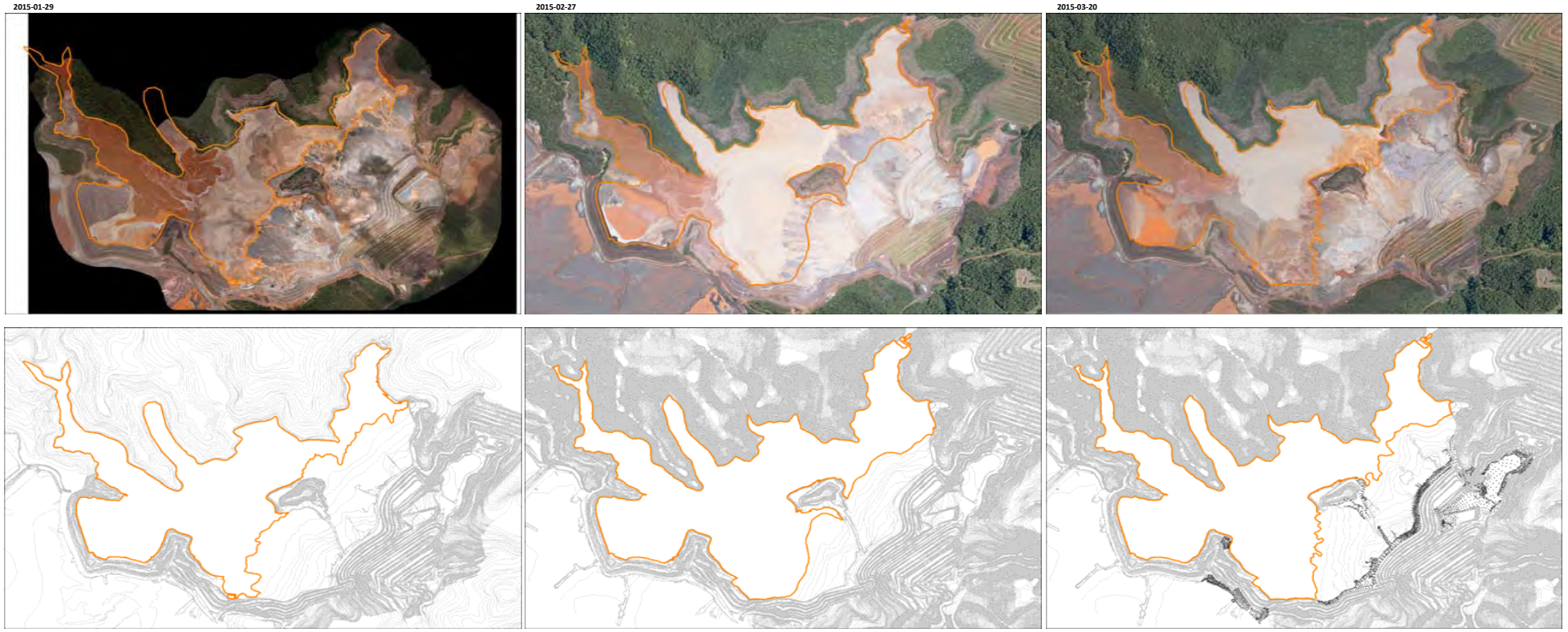
2015-01-29
2015-02-27
2015-03-20

2015-04-24

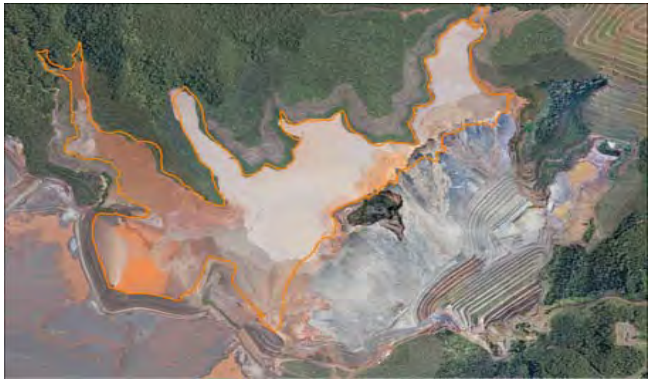

2015-05-27

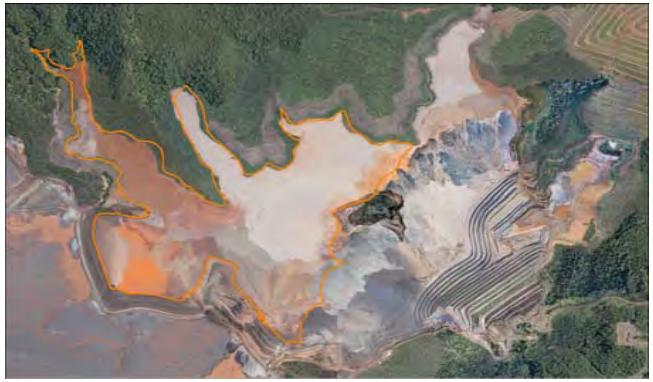

2015-06-22

2015-07-27

2015-08-24

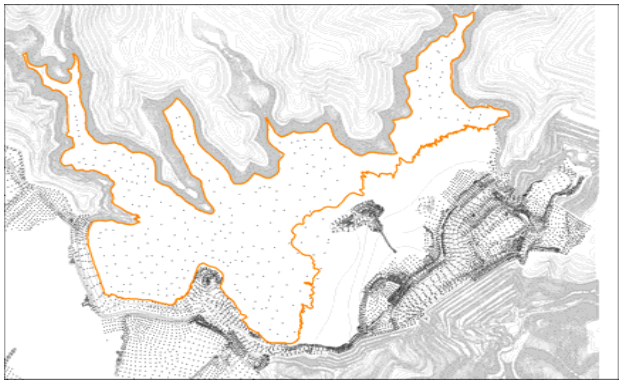

2015-10-01

2015-10-27

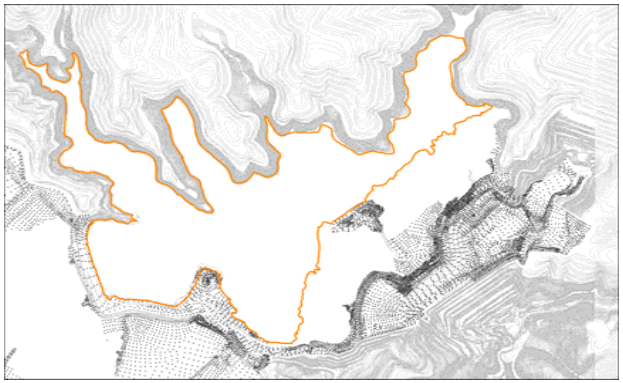

ATTACHMENT B7

Tailings Production

CONVENTIONS

PLANT I
- TAILINGS PIPE
- SLURRY PIPE
- PLANT I TAILINGS PIPE – PIT
- LOAN AREA ARM
- SOPÃO SLURRY PIPE

PLANT II
- TAILINGS PIPE – LINE I
- TAILINGS PIPE – LINE II
- TAILINGS PIPE – LINE I AND II
- SLURRY PIPE
- TAILINGS PIPE (ARM TO PIT)

PLANT III
- TAILINGS PIPE
- SLURRY PIPE

DUCTS
- SANTAREM
- GUALAXO

- LOAN AREA ARM
- VALVE

VALE
- SLURRY PIPE

NOTES

NOTE: UTM COORDINATES SYSTEM: ALEGRE STREAM, SPINDLE 23S
EQUIDISTANCE FROM THE CONTOUR LINES: 1m
UNIT OF MEASURE: METERS

REFERENCE DRAWINGS

REVISION Nº	DESCRIPTION	T.E.	DATE	DES.	VERIF.	APROV.	RELEASE
06	[illegible]	B	[illegible]	H.C.A.	–	–	–
05	UPDATED PIPING – PLANT III	B	[illegible]	A.C.M.	W.F.F.	B.L.S.	–
04	UPDATED PIPING – REGISTRY OF VALVES	B	[illegible]	A.C.M.	W.C.	B.L.S.	–
03	UPDATED PIPING	B	[illegible]	A.C.M.	W.C.	B.L.S.	–
00	INITIAL ISSUE	B	[illegible]	A.C.M.	W.C.	–	–

ERG www.ergbh.com.br

DRAWING No. 081-A-MN-GR-13-0042

T.E. – TYPES OF ISSUE
A – PRELIMINARY; B – FOR APPROVAL; C – FOR INFORMATION PURPOSES; D – P/ QUOTE; E – FOR CONSTRUCTION; F – AS PURCHASED; G – AS BUILT; H – CANCELLED; L – APPROVED

ISSUE
DES.
PROJ. –
VERIF.
APROV. –

SAMARCO MINERAÇÃO S.A.

TITLE: GERMANO – OVERALL
GERMANO DAM
UPDATED TOPOGRAPHY
REGISTRY OF PIPING PLAN

SCALE 1:7.500
SAMARCO No. G002409–T–000004
REVISION 06

A1

[Left margin:] This drawing is the property of SAMARCO MINERAÇÃO S.A and cannot be copied, reproduced or distributed to third parties without its authorization.	Samarco lines thickness. 1 – Red – 0.10mm 2 – Yellow – 0.5mm 3 – Green – 0.20mm 4 – Cyan – 0.30mm 5 – Blue – 0.15mm 6 – Magenta – 0.60mm 7 – White – 0.40mm 8 – Gray – 0.80mm	Extra line thickness adopted in this Samarco drawing 17 18 19 20 21 22 23 24 25

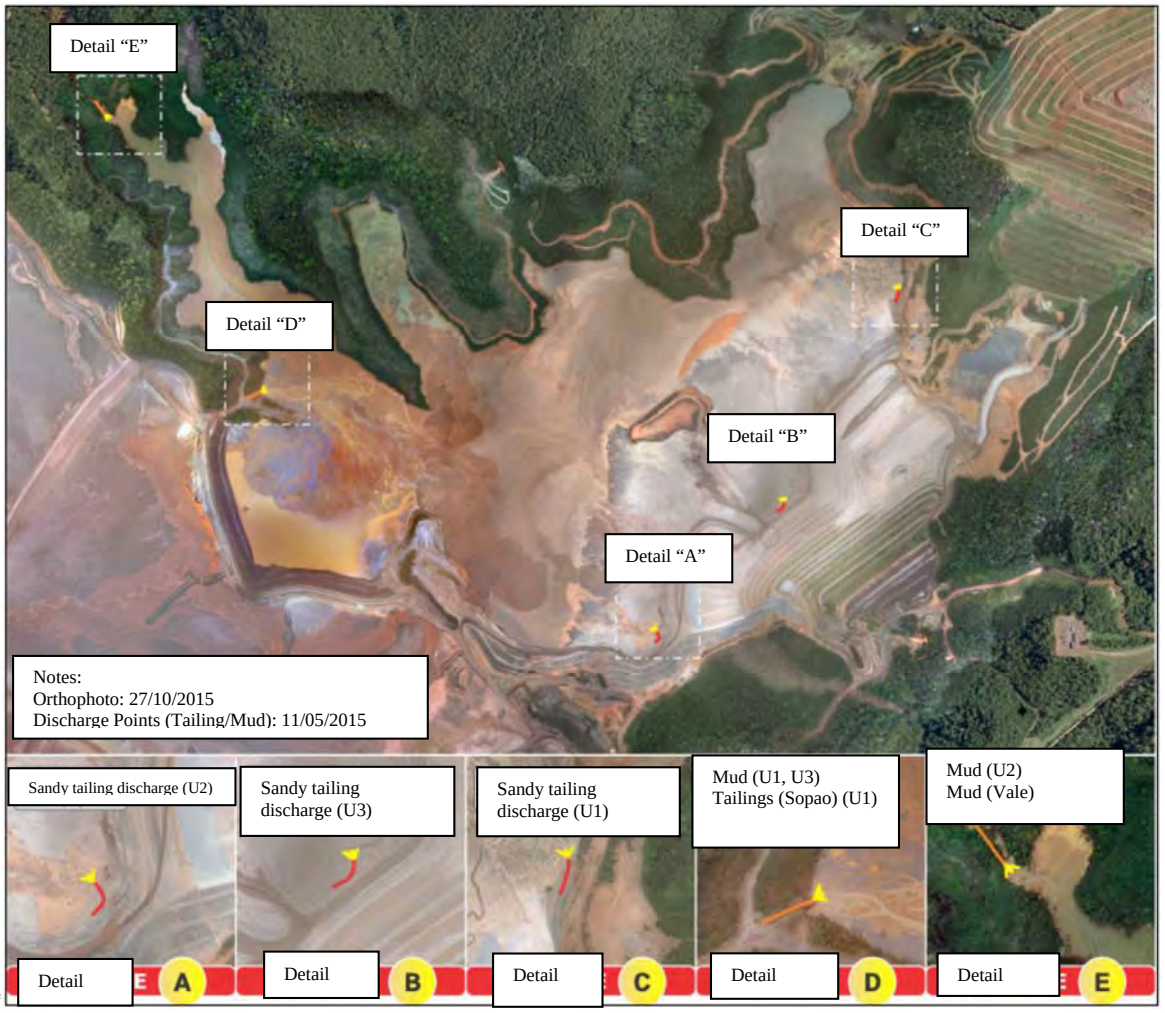

NOTES

REFERENCE DRAWINGS

Logo of hired company	Drawing number N_DES_CONTRATADA

T.E. - TYPES OF ISSUE

A – Preliminary B – For approval	C – For knowledge D – For quote	E – For construction F - As Purchased	G - As Built H – Cancelled L – Approved

ISSUE	[Logo: Samarco] SAMARCO MINERAÇÃO S.A			
DES	HC 01/20/2016	TITLE GERMANO – GENERAL FUNDÃO DAM TOPOGRAPHIC UPDATE REGISTERS PLAN DISPOSAL POINTS (TAILING/SLURRY)		
PROJ	HC 01/20/2016			
VERIF	HC 01/20/2016			
APPROV	HC 01/20/2016	SCALE Indicated	SAMARCO Nº G001600-0-200001	REVIEW 0

REVIEWS	0	Initial issue	--	01/20/2016	HC	WS	WS	WS
	Number	DESCRIPTION	T.E.	DATE	DES.	VERIF.	APPROV.	REL.

ATTACHMENT B8

Incident History

Appendix B: Attachment B8
Incident History

TABLE OF CONTENTS

List of Tables

List of Figures

B.B8-1 INTRODUCTION

The list of incidents documented over the life of the Fundão facility are given below in Table B.B8-1 and shown in plan on Figure B.B8-1. Section B.B8-2 includes the fact sheets for each incident. Section B.B8-3 includes documentation on the evolution of the left abutment open channel.

Table B.B8-1 Summary of incidents at Fundão

Abutment	Date	Elevation	Incident Type
-	April 13, 2009	-	Piping
Right	July 9, 2010	-	Main Gallery settlement
Left	June 26, 2012	845 m	Seepage
Left	November 25, 2012	-	Secondary Gallery sinkhole
Left	March, 2013	855 m	Saturation of slope and ponding of water
Left	June, 2013	855 m	Seepage
Left	November 15, 2013	860 m	Seepage, cracks on slope
Left	December 26, 2013	860 m	Upwelling at El. 860 m, cracks on crest
Right	July 18, 2014	855 m	Seepage
Left	August 26, 2014	-	Slope movements, saturation
Right	January 30, 2015	860 m	Seepage
Left	April 16, 2015	867 m	Saturation of slope
Left	May 18, 2015	820 m	Saturation of slope
Left	July 9, 2015	820 m	Saturation of slope

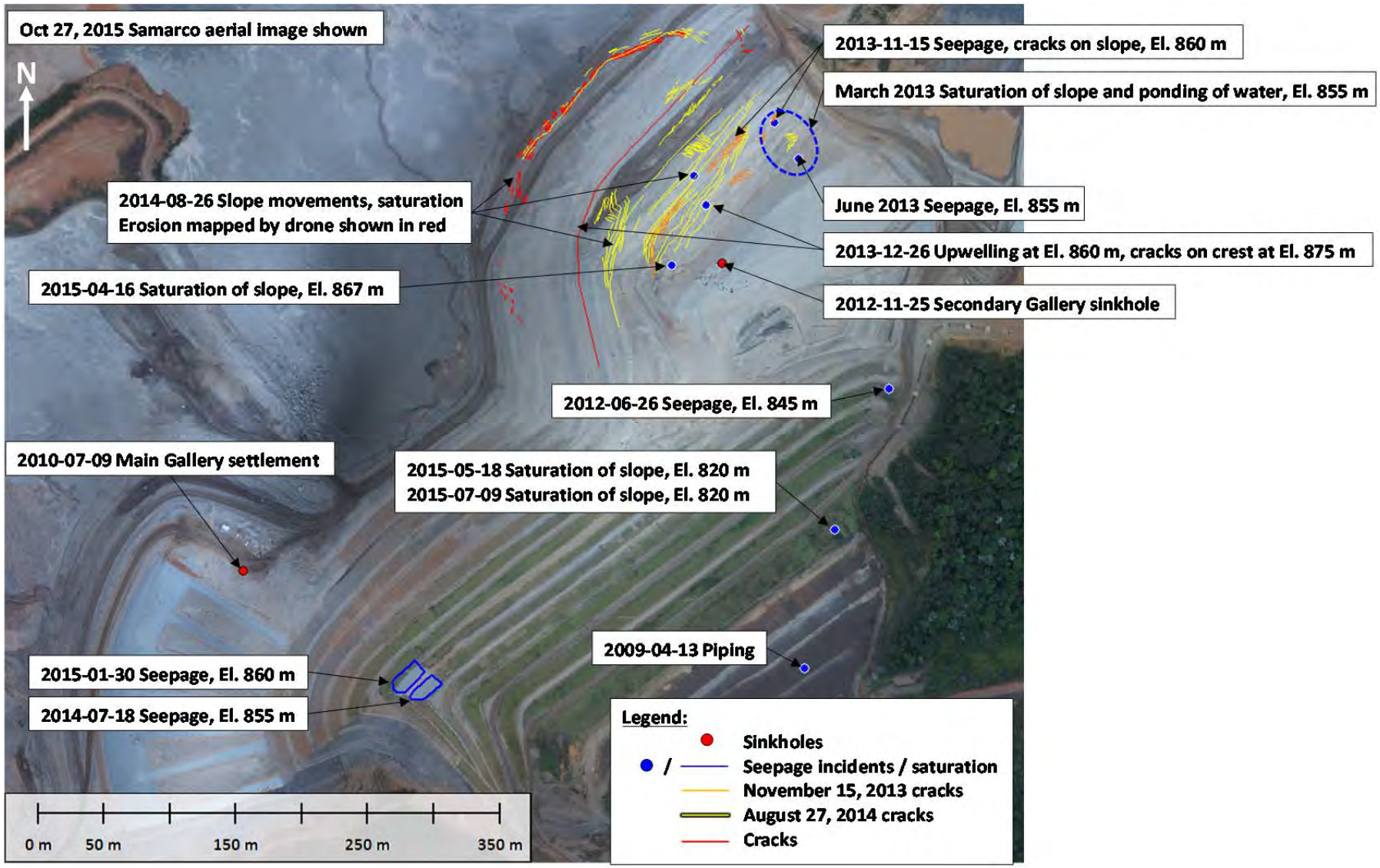

Figure B.B8-1 Incidents at Fundão shown in plan

B.B8-2 FACT SHEETS

April 13, 2009 Piping Incident

Description

- A leak on the downstream face of Dike 1 above the Principal Foundation Drain developed.
- A berm was placed immediately on top of the leak, but this did not stop the flow.
- Tailings deposition was diverted from Fundão, the Dike 1 reservoir drained, and the Principal and Auxiliary Foundation Drains excavated on the upstream and downstream side of Dike 1 for inspection. Both drains were noted to have defects such as erosion of the filter layers and clogging of drain material with fines.
- Both drains were decommissioned by plugging on the upstream side of Dike 1. The downstream remnants were extended past the Reinforcement Berm placed on the downstream slope of Dike 1.
- The base drains were replaced with one blanket drain at El. 826 m with 27 Kananet® pipes.
- Old Dike 1A was constructed to allow continued deposition of tailings in Fundão while the El. 826 m blanket drain was constructed.

Photos

April 13, 2009 site inspection photo[23] showing piping on the downstream face of Dike 1. The Principal Foundation Drain can be seen to the right of the spring.

October, 2010 construction photo showing plugging of the Auxiliary Foundation Drain to the left with the excavated Principal Foundation Drain to the right.

References	Conflicting references
ITRB and Andrew Robertson engineering audit reports and [24].	None

July 9, 2010 Main Gallery Settlement

Description

- The module between Joint 26 and 27 experienced settlement which manifested as a vortex at the surface of the tailings.
- Tailings deposition in this area was suspended and an inspection showed tailings entering the Gallery through a large crack.
- New Dike 1A was built to shield this area from tailings deposition while jet grouting was completed on the foundation of the Gallery.

Photos

July, 2010 site inspection photo[25] showing the vortex that formed at the surface of the tailings above the settlement.

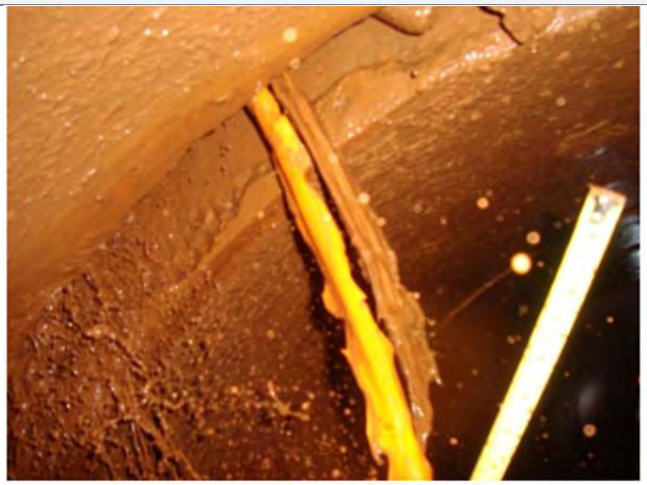

Foto 05: Junta Fungenband danificada.
Detalhe de desnível do concreto.

July, 2010 inspection photo from GMAIA[26] showing the inflow of tailings to the Gallery.

References	Conflicting references
Samarco 2010 presentation[27], Samarco 2010 presentation[28], GMAIA 2010 inspection[26]	Joint references differ between sources, the second most common being the leak having occurred between Joints 22 and 23 instead of 26 and 27. This is due to different stationing having been used on drawings over time.

June 26, 2012 Left Abutment Seepage at El. 845 m

Description

- Seepage was noted at El. 845 m on the non-setback part of the dike crest at the left abutment. VOGBR attributed this to the damming of water in the Grota da Vale which was upstream of the seepage location.
- The saturated upstream raise material was excavated and a drain installed. The drain consisted of a geotextile, granular material and coarse rockfill.
- No formal drain exit was installed until around May, 2015 in the form of a concrete channel that discharged into a buried pipe crossing the left abutment access road to the left abutment concrete channel.
- Flow records for this drain were not available.

Photos

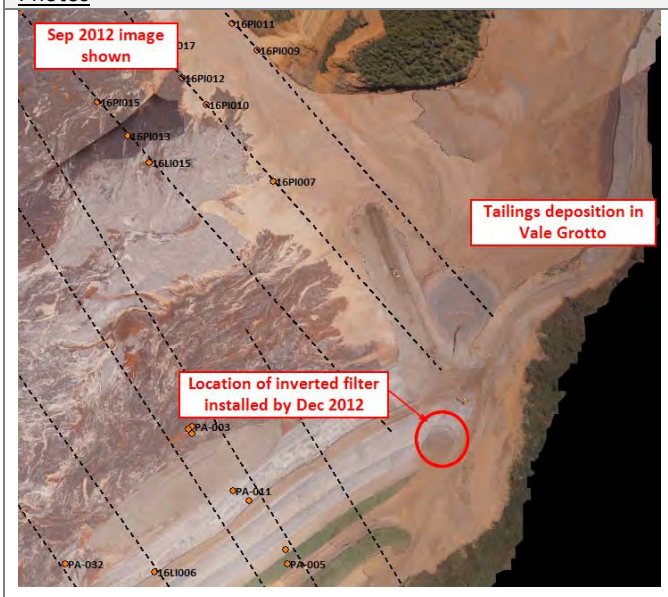

Marked up September 2, 2012 Samarco aerial image shown.

Figure·5.4·–·Performance·of·an·inverted·drain·-·Dike·1·heightening,·left·abutment.¶

Photo from VOGBR 2013 report[29].

References	Conflicting references
Samarco weekly reports, VOGBR 2013 report[29]	None

November 25, 2012 Secondary Gallery Sinkhole

Description

- Sinkhole discovered on the El. 855 m bench at the setback portion of Dike 1 at the left abutment. This sinkhole was located above the Secondary Gallery at Joint 18.
- An inspection revealed slug discharge of tailings and water from the tailings side of the Secondary Gallery.
- Joint 18 was grouted internally.

Photos

November 25, 2012 inspection photo[30] showing the sinkhole.

December 14, 2012 inspection photo[30] showing evolution of the sinkhole since November 25.

References	Conflicting references
Samarco 2012 inspection[30]	None

March 2013 Seepage at Left Abutment at El. 855 m and Ponding of Surface Water

Description

- The weekly report from the week of March 25, 2013 notes a saturated region at the left abutment.
- After a review of aerial images, part of the reason for saturation and ponding could be lack of surface drainage control on the left abutment roads above the dam. Topography shows this area to be ~El. 855 m.
- A buried drain (Drain 1) was put in, leading to a geotextile-wrapped rockfill trench (Drain 2) on the left setback. The buried drain was an inverted trapezoid, geotextile-wrapped rockfill drain.
- The geotextile-wrapped rockfill trench (Drain 2) eventually became a large open channel on the setback platform as the dam was raised around it. Details on the evolution of this drain are given on the last fact sheet of this section.

Photos

March 2, 2013 Samarco aerial image showing the Secondary Gallery sinkhole to the left and a region of saturation and ponding to the right at the dam's contact with the left abutment.

Weekly report from week of March 25, 2013.

References	Conflicting references
Weekly reports	None

June 2013 Seepage at Left Abutment at El. 855 m

Description

- There are a number of conflicting records on the elevation and date of this seepage incident:

Source	Date of Incident	Elevation of Incident
ITRB	June, 2013	845 m
Samarco[31]	June, 2013	855 m
	August, 2013	855 m
VOGBR[13]	August, 2013	855 m

- There is no mention of seepage events in the June or August, 2013 weekly reports, but drain construction activities were mentioned in the June reports. This drain (likely Drain 1 from March, 2013) was connected to the open channel wrapped in geotextile running down the left abutment (likely Drain 2). No signs of this activity can be seen in the August, 2013 aerial image. It is possible that the incident took place during end of buried drain (Drain 1) construction in June. The drains that were already going to be executed as part of the March, 2013 saturation event were used to address this new seepage event.
- No clear description or photos of this drain are available except from weekly reports that seem to show:
  - 1 m layer of sand being placed upstream of the buried drain (Drain 1); construction was started in April, 2013.
  - The sand being connected to the rockfill trench (Drain 2).

Photos

Construction photo from June 17-23, 2013 weekly report showing the geotextile and sand placement, with the beginnings of the rockfill trench to the left.

Construction photo from June 17-23, 2013 weekly report showing the beginnings of the rockfill trench.

June 2013 Seepage at Left Abutment at El. 855 m

Photos

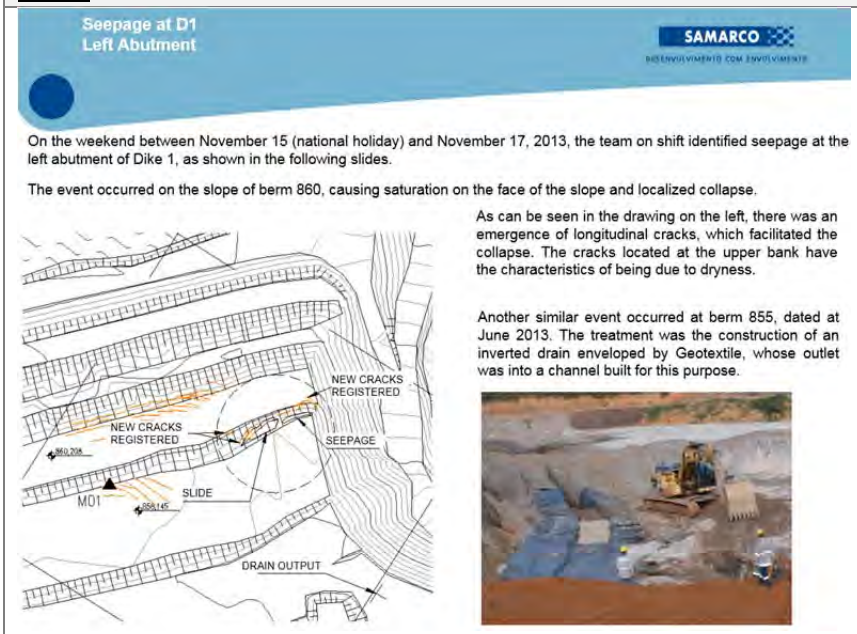

Document from Samarco[31] showing details of the November 2013 seepage event and mention of the June 2013 incident.

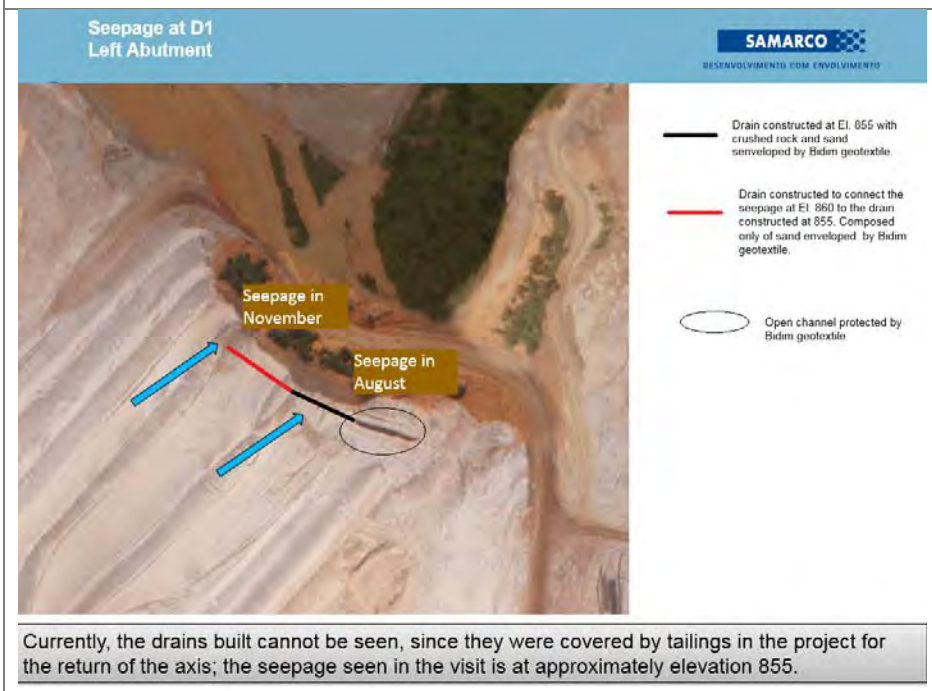

Document from Samarco[31] showing details of the drains constructed at the left abutment to address the November and August, 2013 incident. The August, 2013 incident was referred to in a previous slide as the June, 2013 incident.

References	Conflicting references
ITRB, weekly reports, Samarco 2013 document[31], VOGBR document[13]	Dates and elevation as listed in the “Description” section.

June 2013 Seepage at Left Abutment at El. 855 m

November 15, 2013 Left Abutment Seepage and Cracks at El. 860 m

Description

- There are a number of conflicting records on the elevation and date of this seepage incident:

Source	Date of Incident	Elevation of Incident
ITRB	November, 2013	855 m
Samarco[31]	Between November 15 and 17, 2013	860 m
VOGBR[13]	November, 2013	860 m

- The slope face was saturated and localized slumping was noted. Longitudinal cracks appeared. Cracks at higher elevations were dry.
- An inverted drain (Drain 3) was placed and connected to the one placed at El. 855 m (Drain 1) which was connected to the rockfill trench (Drain 2).

Photos

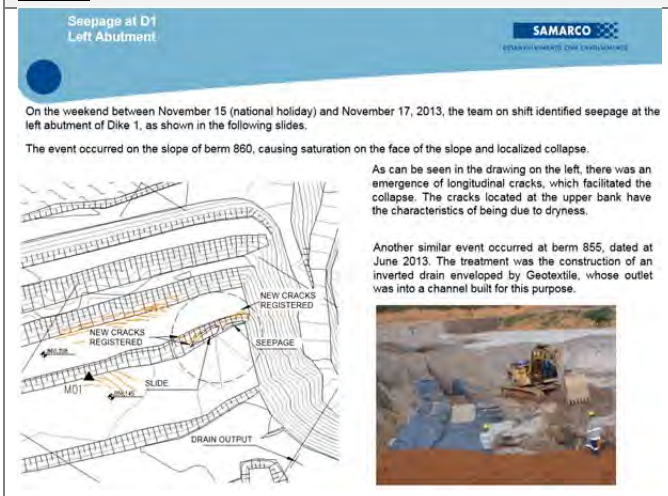

Document from Samarco[31] showing details of the November 2013 seepage event and mention of the June, 2013 incident.

Document from Samarco[31] showing details of the saturated and slumped slope in November, 2013.

References

Samarco 2013 document[31], VOGBR 2013 inspection[13]

Conflicting references

Dates and elevation as listed in the "Description" section.

December 26, 2013 Left Abutment Upwelling at El. 860 m and Cracks on Crest

Description

- Upwelling incident noted in December 23-30, 2013 Samarco weekly report and confirmed to be observed on December 26, 2013 in December 2013 Samarco monthly geotechnical inspection report.
- Cracks noted in December 30, 2013 to January 5, 2014 Samarco weekly report and confirmed to be observed on December 26, 2013 in December 2013 Samarco monthly geotechnical inspection report.
- Upwelling elevation inconsistencies between sources:
  - Weekly report states El. 855 m.
  - Aerial image taken by drone on December 27, 2013 shows sand placement at ~El. 858 m. For consistency with naming convention for other seepage incidents, this will be referred to as the El. 860 m upwelling since it is on the downstream face of the El. 860 m bench.
- 1 m of sand was placed on the slope face to retain fines. Setback was raised following the sand placement.
- Cracks were noted to be approximately 10 mm wide and 60 m long along the crest.

Photos

Photo from December 23-29, 2013 weekly report showing placement of sand over area of upwelling.

Photo from December 23-29, 2013 weekly report showing placement of sand over area of upwelling.

December 26, 2013 Left Abutment Upwelling at El. 860 m and Cracks on Crest

Photos

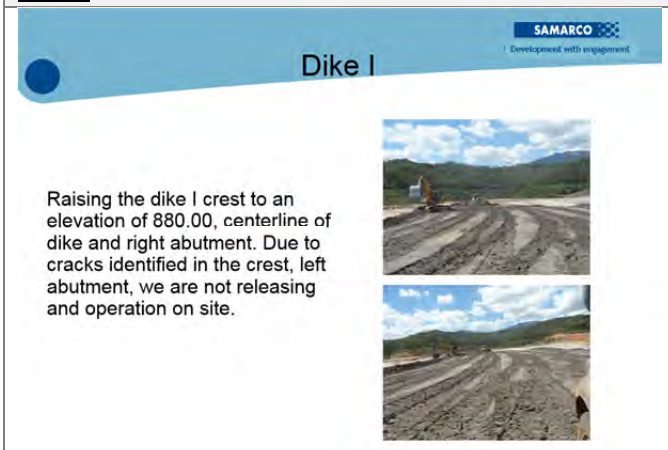

December 30, 2013 to January 1, 2014 weekly report describing temporary cessation of operation at the left abutment due to cracks.

December 26, 2013 inspection photo from Samarco geotechnical inspection report showing a crack on the crest.

References	Conflicting references
Weekly reports, geotechnical inspection report	None

July 18, 2014 Right Abutment Seepage at El. 855 m

Description

- There are a number of conflicting records on the elevation and date of this seepage incident:

Source	Date of Incident	Elevation of Incident
ITRB	Not stated	855 m
Samarco[14]	July 18, 2014	855 m
VOGBR[13]	Late 2014	950 m

- The incident was discussed in detail by Samarco[14] which concluded:
  - The interface between the soil backfill and sand tailings as part of the Auxiliary Spillway construction works has become a preferred seepage path.
  - The closest piezometer to the seepage incident is approximately 50 m away on Section AA. This piezometer (16LI011) showed the water level to be below the point of seepage.
- The saturated slope was excavated and replaced with a sand and gravel drain which can be seen in the drone aerial image taken on August 4, 2014. During a site visit in April 2015, VOGBR noted saturation of the bench downstream of the drain and recommended replacing the drain with one of VOGBR's design. This was done in May, 2015.
- Flow from this drain was regularly monitored and reported in instrumentation and weekly reports.

Photos

July, 2014 inspection photo showing seepage outbreak on the downstream face of Dike 1.

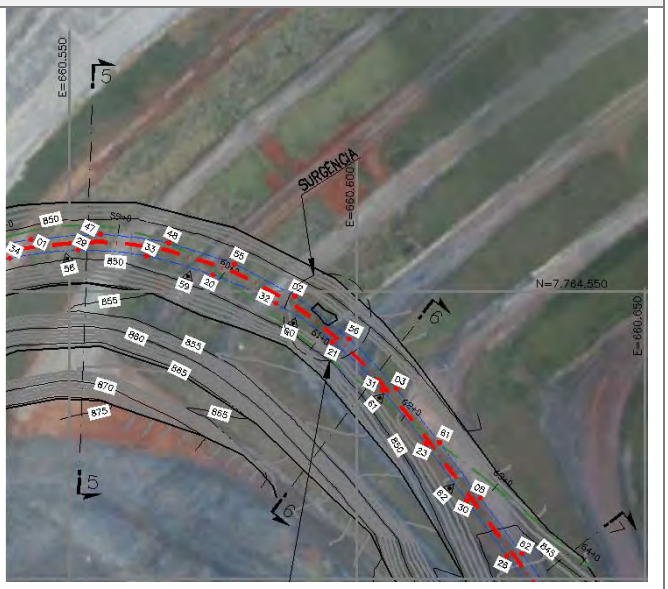

Location plan showing the seepage outbreak in relation to the earthworks extent for the Auxiliary Spillway.

July 18, 2014 Right Abutment Seepage at El. 855 m	
Photos	
 July, 2014 inspection photo showing the sand and gravel drain placed.	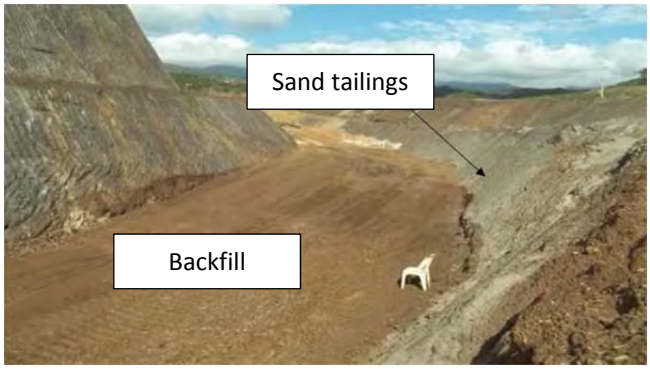 Marked up photo from the Auxiliary Spillway construction period showing the interface between the backfill and sand tailings.
References	Conflicting references
Samarco 2014 inspection[14], VOGBR[13]	Dates and elevation as listed in the “Description” section.

August 26, 2014 Left Abutment Setback Slope Movement

Description

- At 6:00 AM on August 27, 2014, cracks were observed on the upstream beach, dam crest and downstream slope of the setback. The cracks showed differential thicknesses, some on crest ~6 cm, reaching up to 3x as thick on the upstream bench.
- Uplift at the toe of the El. 865 m bench was noted by the ITRB.
- Water was not observed on the upstream beach and crest, only normal saturation of sand tailings. At the toe of the El. 865 m bench, saturation was noted.
- Samarco designed and implemented a Reinforcement Berm. Piezometers and survey monuments were also installed.

Photos

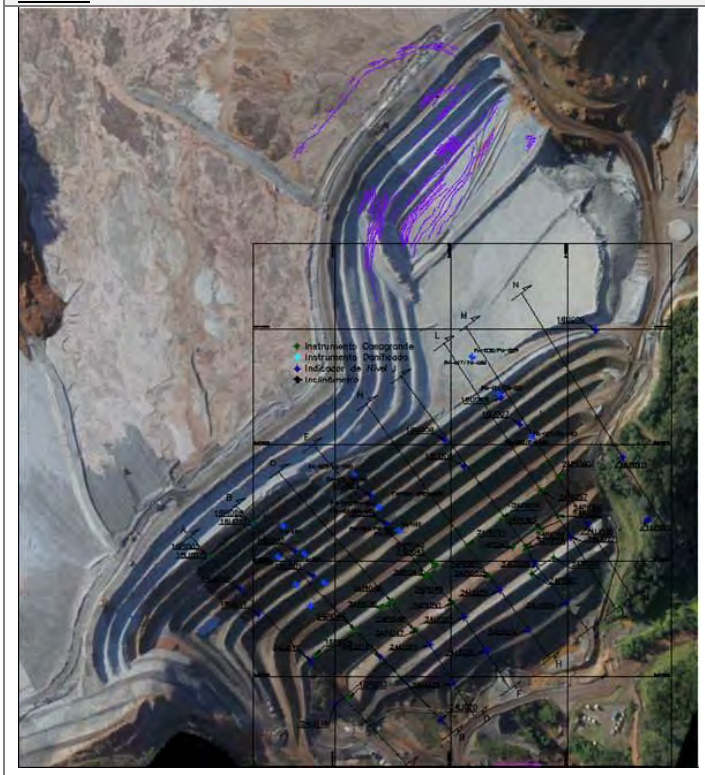

Location plan showing the mapped cracks.

September 2014 inspection photo showing saturation of material at the toe of the El 865 m bench.

References	Conflicting references
Samarco 2014 inspection[32], Samarco surveys[33, 34]	None

January 30, 2015 Right Abutment Seepage at El. 860 m

Description

- There are a number of conflicting records on the elevation and date of this seepage incident:

Source	Date of Incident	Elevation of Incident
ITRB	Not stated	855 m
Samarco[35]	January 30, 2015	855 m
VOGBR[13]	January 30, 2015	955 m

- According to topography, this incident occurred on the downstream face of the El. 860 m bench at El 858 m. This is one bench above the incident that occurred in July, 2014.
- Incident discussed in detail by Samarco[35] which concluded:
  - The interface between the soil backfill and sand tailings as part of the Auxiliary Spillway construction works has become a preferred seepage path.
  - The closest piezometer to the seepage incident is approximately 50 m away on Section AA. This piezometer (16LI010) showed the water level to be below the point of seepage.
- The saturated slope was excavated and replaced with a sand and gravel drain. During a site visit in April, 2015, VOGBR recommended replacing the drain with one of VOGBR's design. This was done in May, 2015.
- Flow from this drain was regularly monitored and reported in instrumentation and weekly reports.

Photos

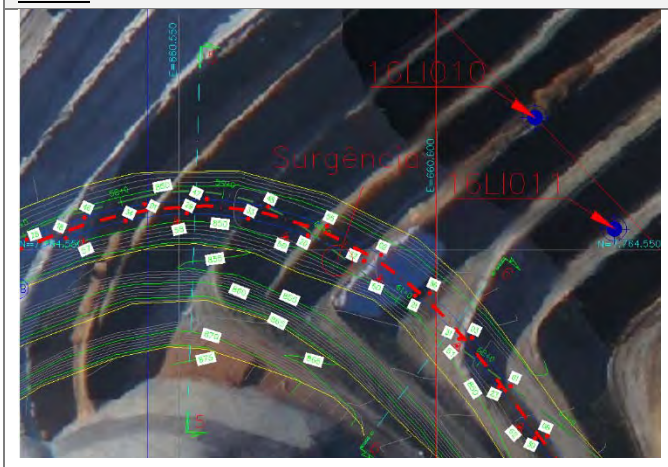

Location plan showing the seepage outbreak in relation to the earthworks extent for the Auxiliary Spillway.

January, 2015 construction photo showing the beginning of stripping for placement of drain material on the slope[35].

References	Conflicting references
Samarco 2015[35], VOGBR 2015 inspection[13], ITRB report	Dates and elevations as noted in "Description" Section.

April 16, 2015 Saturation at Left Abutment, El. 867 m

Description

- Saturation above and below the El. 860 m blanket drain was noted by Samarco in the monthly geotechnical report. A photograph shows saturation at El. 867 m just above the on-going construction of the El. 860 m blanket drain.
- Drone aerial images from February 27, 2015 to April 24, 2015 show saturation at the location of the monthly report photograph.

Photos

Photo from monthly geotechnical report showing saturation at the toe of the slope above the El. 860 m blanket drain.

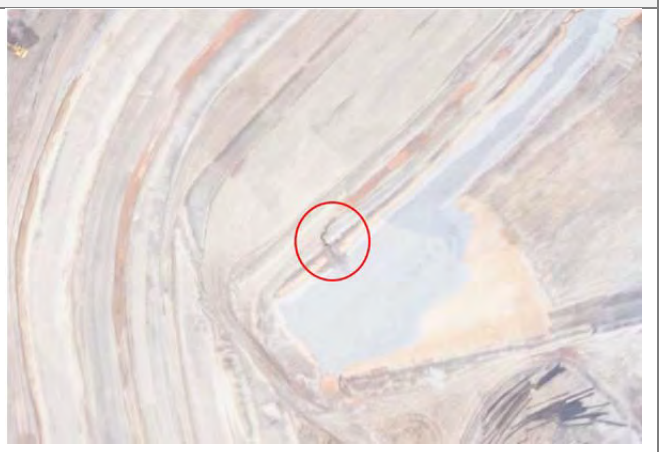

February 27, 2015 aerial image.

March 20, 2015 aerial image.

April 24, 2015 aerial image.

References	Conflicting references
Samarco 2015 inspection[36]	None

May 18, 2015 Saturation at Left Abutment, El. 820 m

Description

- Saturation of slope was noted by Samarco in the monthly geotechnical inspection report.

Photos

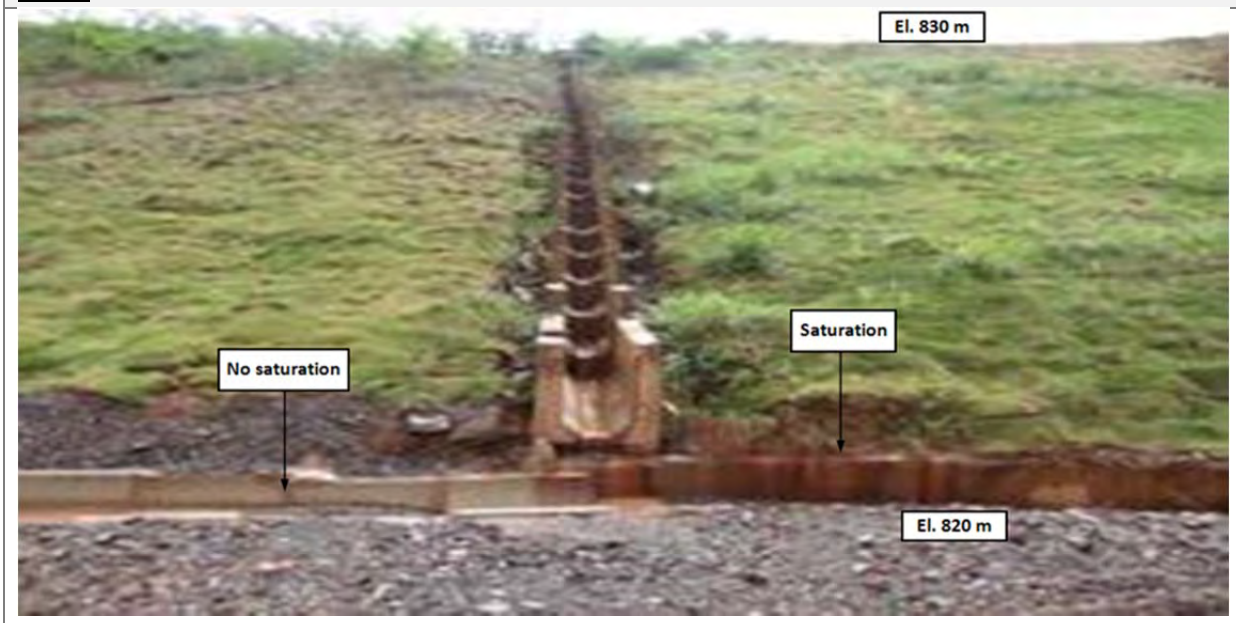

Marked up May, 2015 inspection photo from the Samarco geotechnical inspection report showing saturation of the slope left of the concrete channel.

References	Conflicting references
Samarco 2015 inspection[36]	None

July 9, 2015 Saturation at Left Abutment, El. 820 m

Description

- Saturation of the slope was noted by VOGBR during the July, 2015 site visit as part of "Regular Safety Inspections".
- This appears to be the same saturation that was noted by Samarco in May, 2015.

Photos

July, 2015 inspection photo from VOGBR showing saturated slope between El. 830 m and El. 820 m bench.

References	Conflicting references
VOGBR 2015 inspection[13]	None

B.B8-3 EVOLUTION OF THE LEFT ABUTMENT ROCKFILL TRENCH

Evolution of the Left Abutment Rockfill Trench (Drain 2)

Description

- The rockfill trench (Drain 2) was initially put in as part of June, 2013 seepage incident and receives water from the El. 855 m buried drain (Drain 1) and the El. 860 m drain (Drain 3 installed in November, 2013).
- Water from this drain was permitted to sheet flow across the setback plateau and access road to Grota da Vale.
- As the setback was raised around this trench, it became a large open channel lined with geotextile. This can be seen in the drone aerial image taken on December 27, 2013. By January 29, 2015, the aerial image shows the open channel having been buried with a light grey material. It is unclear whether this is drain rock or dry tailings sand.
- During a May interview with a Samarco employee, the buried open channel was recounted to have an outlet in the form of a buried pipe. The alignment of this pipe is unknown to the Panel, but based on site photographs and aerial images, it is likely at the exposed toe of the El. 860 m blanket drain. Ponded water is consistently noted at this location.
- VOGBR completed a drain design in May, 2014 to convey water from the buried El. 855 m drain (Drain 1) to the left abutment concrete channel. No records were found of this design having been implemented. However, as part of the design process, VOGBR conducted a site visit and took photographs of the open channel as it existed in March, 2014.

Photos

Marked up drone aerial image taken December 27, 2013.

Marked up drone aerial image taken January 29, 2015.

Evolution of the Left Abutment Rockfill Trench (Drain 2)

Photos

Marked up drone aerial image taken May 27, 2015.

Marked up drone aerial image taken June 22, 2015.

March 27, 2014 site visit photo from VOGBR showing the open channel looking down the slope of the dam toward the plateau of the left setback.

March 27, 2014 site visit photo from VOGBR showing the open channel looking upslope towards the dam crest. The erosion on the setback plateau can be seen to the right of the photo.

Evolution of the Left Abutment Rockfill Trench (Drain 2)	
Photos	
	
July 10, 2014 site visit photo from VOGBR showing a pipe conveying water from the open channel through the access road berm. The water then sheet flows across the access road to Grota da Vale which is to the right of the photo.	January 16, 2015 construction photo showing the buried open channel with light grey material.
References	Conflicting references
VOGBR 2014[11]	None

ATTACHMENT C1

Pre-Failure Field Program Data

Appendix C: Attachment C1
Pre-Failure Field Program Data

DeltaGeo (July 2011) (Section C2.2.1)

DeltaGeo (September 2012 – July 2013) (Section C2.2.2)

Fugro (April 2014) (Section C2.2.3)

Fugro (June 2014 – August 2014) (Section C2.2.4)

Fugro (June 2014 – May 2015) (Section C2.2.5)

Fugro (September 2014 – March 2015) (Section C2.2.6)

Fugro (March 2015 – July 2015) (Section C2.2.7)

Fugro/Geocontrole (June 2015) (Section C2.2.8)

July 2011
DeltaGeo
New Dike 1A
(Section C2.2.1)

Figure C.C1-1 – DeltaGeo (2011) Test Location Plan

CPTu-P1 CPT Plots
CPTu-P1 CPT Liquefaction Susceptibility and Soil Behavior Type Plots
CPTu-P2 CPT Plots
CPTu-P2 CPT Liquefaction Susceptibility and Soil Behavior Type Plots
CPTu-P3 CPT Plots
CPTu-P3 CPT Liquefaction Susceptibility and Soil Behavior Type Plots
CPTu-P4 CPT Plots
CPTu-P4 CPT Liquefaction Susceptibility and Soil Behavior Type Plots

NOTE:
1. May 25, 2011 Google Earth aerial image shown.

LEGEND:
◆ Piezocone Penetration Test (CPTu)

PROJECT
Fundão Tailings Dam Review Panel

TITLE
DeltaGeo (July 2011)
Test Location Plan

FIGURE NO.
C.C1-1

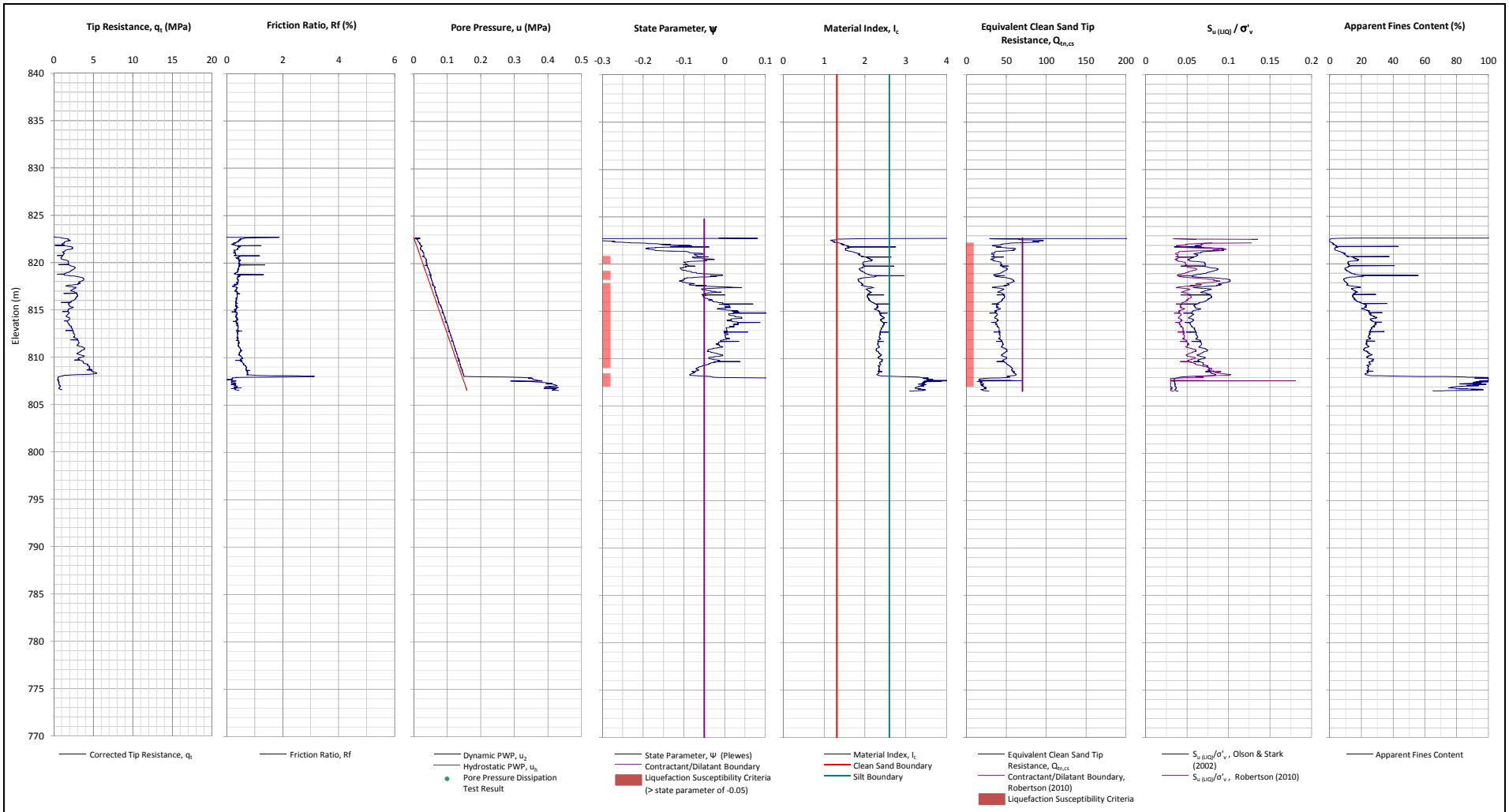

Notes:
1. This interpretation is based on the water and soil saturated unit weights γ_w=9.807 kN/m^3 and γ_{sat}=22 kN/m^3.
2. The friction ratio Rf is calculated as Rf=f_s/q_t.
3. The hydrostatic pore pressure is calculated using the ground water level (GWL) determined from CPT pore pressure dissipation tests (where available) or dynamic pore pressure.
4. Soil boundary layers (where plotted) are based on KCB interpretation.
5. The data presented have been plotted to the axis limits. Data may exist beyond the axis limits shown.
6. The Material Index (I_c) boundaries are based on Robertson and Wride (1998).
7. The $Q_{tn,cs}$ contractant/dilatant boundary=70 and is based on Robertson (2010).
8. The State Parameter (Ψ) is calculated using Plewes, et al. (1992) assuming a K0 of 0.5.
9. Coordinates are in UTM Zone 23K Córrego Alegre.

PROJECT
Fundão Tailings Dam Review Panel

TITLE
DeltaGeo (2011) - New Dike 1A
CONE PENETRATION TEST CPTu-P1
N:7764722.65m E:660585.97m 2011-01-07

Liquefaction susceptibility after Robertson (2010) "Evaluation of Flow Liquefaction and Liquefied Strength Using the Cone Penetration Test"	Liquefaction susceptibility after Olson & Stark (2003) "Yield Strength Ratio and Liquefaction Analysis of Slopes and Embankments"	State parameter approximation - Robertson (2009) "Interpretation of cone penetration tests - a unified approach"

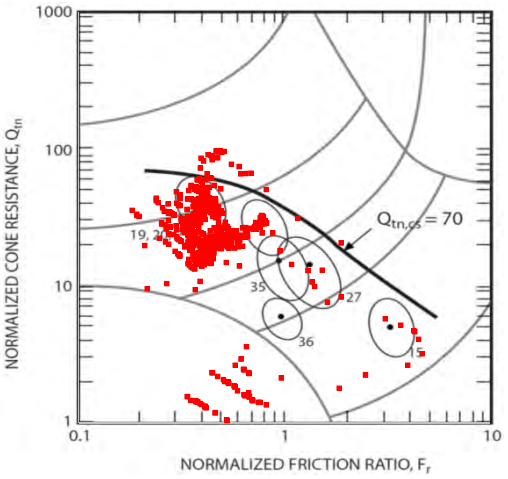

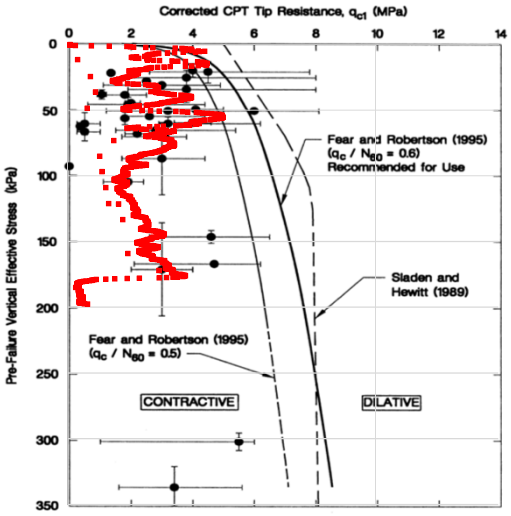

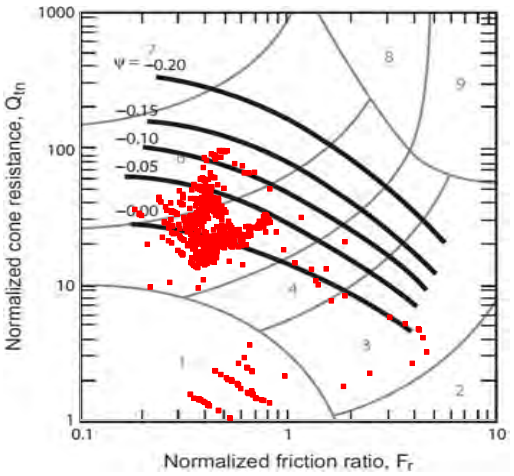

NOTE:

PROJECT

Fundão Tailings Dam Review Panel

TITLE

DeltaGeo (2011) - New Dike 1A
CPTu-P1 Liquefaction Susceptibility and Soil Behavior Type

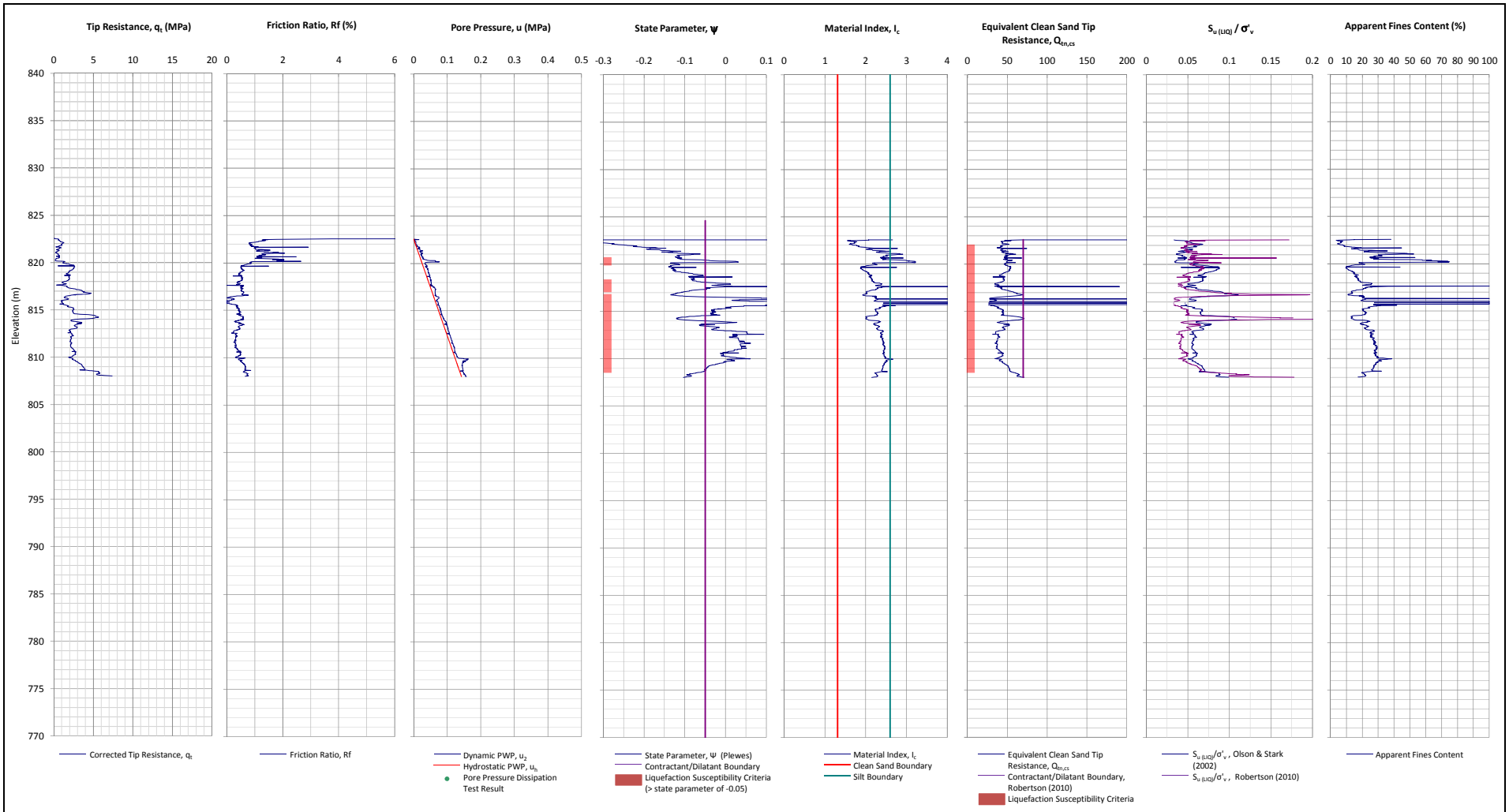

Notes:
1. This interpretation is based on the water and soil saturated unit weights γ_w=9.807 kN/m^3 and γ_{sat}=22 kN/m^3.
2. The friction ratio Rf is calculated as Rf=f_s/q_t.
3. The hydrostatic pore pressure is calculated using the ground water level (GWL) determined from CPT pore pressure dissipation tests (where available) or dynamic pore pressure.
4. Soil boundary layers (where plotted) are based on KCB interpretation.
5. The data presented have been plotted to the axis limits. Data may exist beyond the axis limits shown.
6. The Material Index (I_c) boundaries are based on Robertson and Wride (1998).
7. The $Q_{tn,cs}$ contractant/dilatant boundary=70 and is based on Robertson (2010).
8. The State Parameter (Ψ) is calculated using Plewes, et al. (1992) assuming a K0 of 0.5.
9. Coordinates are in UTM Zone 23K Córrego Alegre.

PROJECT
Fundão Tailings Dam Review Panel

TITLE
DeltaGeo (2011) - New Dike 1A
CONE PENETRATION TEST CPTu-P2
N:7764686.93m E:660568.82m 2011-01-07

Liquefaction susceptibility after Robertson (2010) "Evaluation of Flow Liquefaction and Liquefied Strength Using the Cone Penetration Test"	Liquefaction susceptibility after Olson & Stark (2003) "Yield Strength Ratio and Liquefaction Analysis of Slopes and Embankments"	State parameter approximation - Robertson (2009) "Interpretation of cone penetration tests - a unified approach"

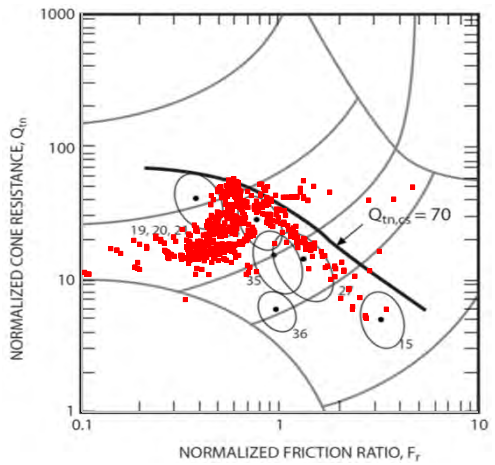

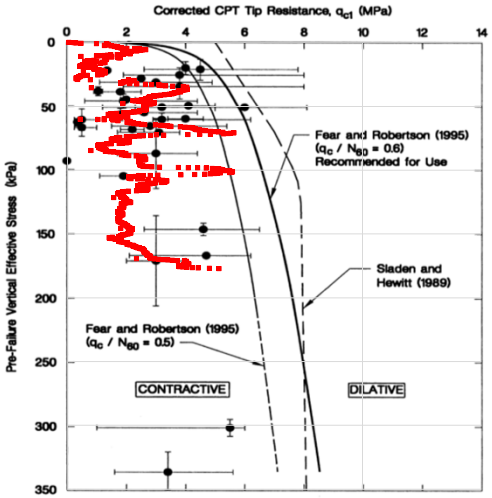

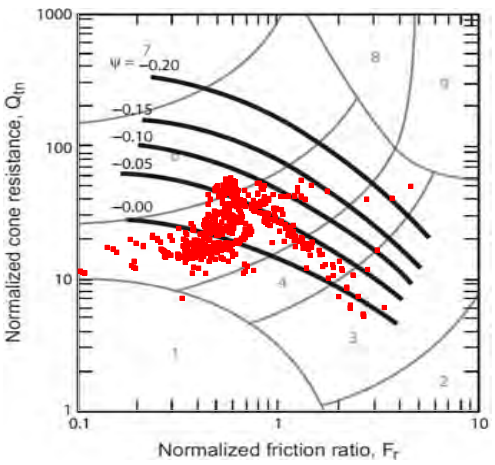

NOTE:

PROJECT

Fundão Tailings Dam Review Panel

TITLE

DeltaGeo (2011) - New Dike 1A
CPTu-P2 Liquefaction Susceptibility and Soil Behavior Type

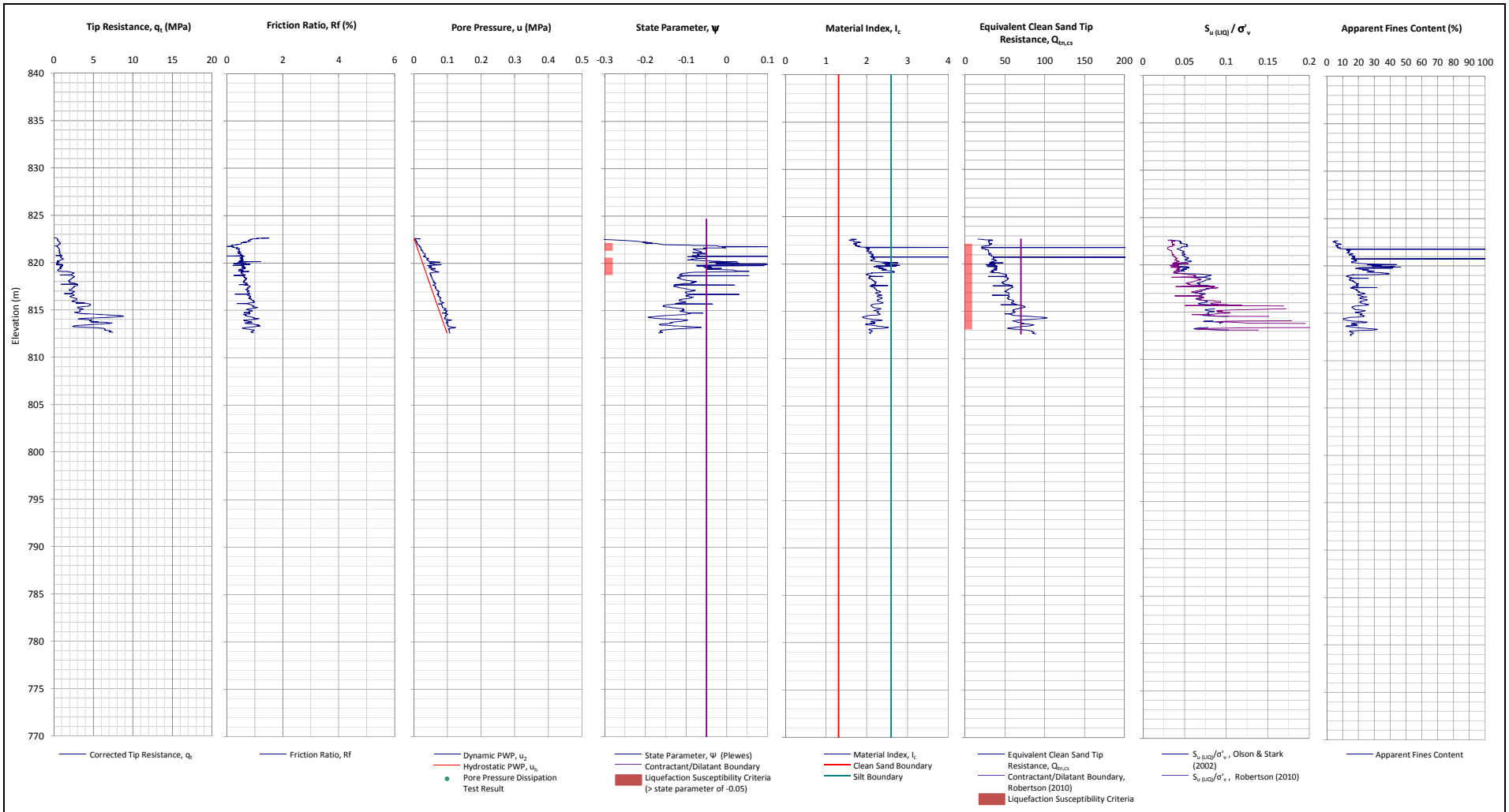

Notes:
1. This interpretation is based on the water and soil saturated unit weights γ_w=9.807 kN/m^3 and γ_{sat}=22 kN/m^3.
2. The friction ratio Rf is calculated as Rf=f_s/q_t.
3. The hydrostatic pore pressure is calculated using the ground water level (GWL) determined from CPT pore pressure dissipation tests (where available) or dynamic pore pressure.
4. Soil boundary layers (where plotted) are based on KCB interpretation.
5. The data presented have been plotted to the axis limits. Data may exist beyond the axis limits shown.
6. The Material Index (I_c) boundaries are based on Robertson and Wride (1998).
7. The $Q_{tn,cs}$ contractant/dilatant boundary=70 and is based on Robertson (2010).
8. The State Parameter (Ψ) is calculated using Plewes, et al. (1992) assuming a K0 of 0.5.
9. Coordinates are in UTM Zone 23K Córrego Alegre.

PROJECT
Fundão Tailings Dam Review Panel

TITLE
DeltaGeo (2011) - New Dike 1A
CONE PENETRATION TEST CPTu-P3
N:7764665.49m E:660568.98m 2011-01-07

Liquefaction susceptibility after Robertson (2010) "Evaluation of Flow Liquefaction and Liquefied Strength Using the Cone Penetration Test"	Liquefaction susceptibility after Olson & Stark (2003) "Yield Strength Ratio and Liquefaction Analysis of Slopes and Embankments"	State parameter approximation - Robertson (2009) "Interpretation of cone penetration tests - a unified approach"

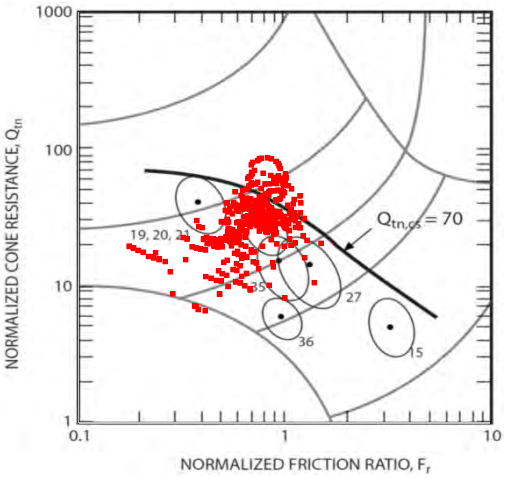

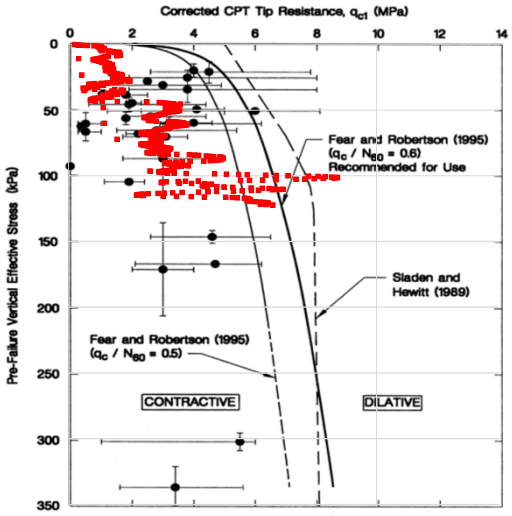

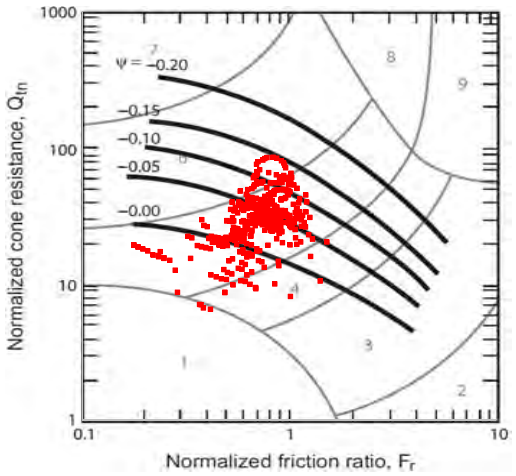

NOTE:

PROJECT

Fundão Tailings Dam Review Panel

TITLE

DeltaGeo (2011) - New Dike 1A
CPTu-P3 Liquefaction Susceptibility and Soil Behavior Type

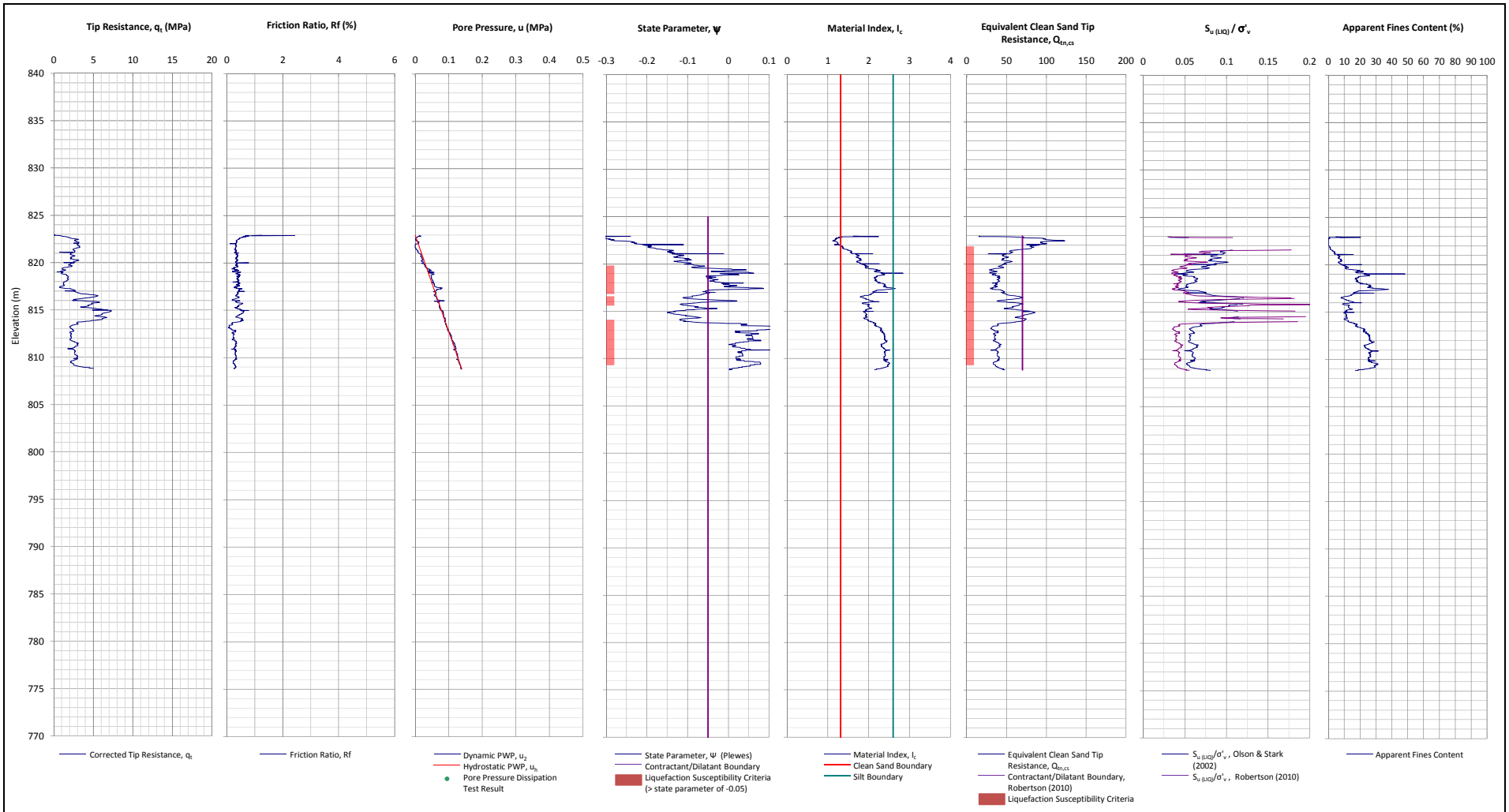

Notes:
1. This interpretation is based on the water and soil saturated unit weights γ_w=9.807 kN/m^3 and γ_{sat}=22 kN/m^3.
2. The friction ratio Rf is calculated as Rf=f_s/q_t.
3. The hydrostatic pore pressure is calculated using the ground water level (GWL) determined from CPT pore pressure dissipation tests (where available) or dynamic pore pressure.
4. Soil boundary layers (where plotted) are based on KCB interpretation.
5. The data presented have been plotted to the axis limits. Data may exist beyond the axis limits shown.
6. The Material Index (I_c) boundaries are based on Robertson and Wride (1998).
7. The $Q_{tn,cs}$ contractant/dilatant boundary=70 and is based on Robertson (2010).
8. The State Parameter (Ψ) is calculated using Plewes, et al. (1992) assuming a K0 of 0.5.
9. Coordinates are in UTM Zone 23K Córrego Alegre.

PROJECT
Fundão Tailings Dam Review Panel

TITLE
DeltaGeo (2011) - New Dike 1A
CONE PENETRATION TEST CPTu-P4
N:7764687.81m E:660590.25m 2011-01-07

Liquefaction susceptibility after Robertson (2010) "Evaluation of Flow Liquefaction and Liquefied Strength Using the Cone Penetration Test"	Liquefaction susceptibility after Olson & Stark (2003) "Yield Strength Ratio and Liquefaction Analysis of Slopes and Embankments"	State parameter approximation - Robertson (2009) "Interpretation of cone penetration tests - a unified approach"

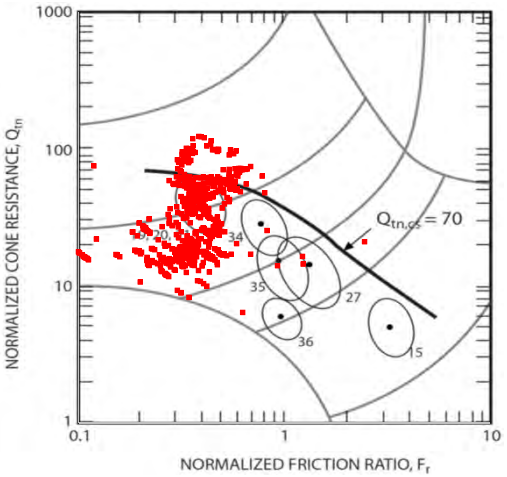

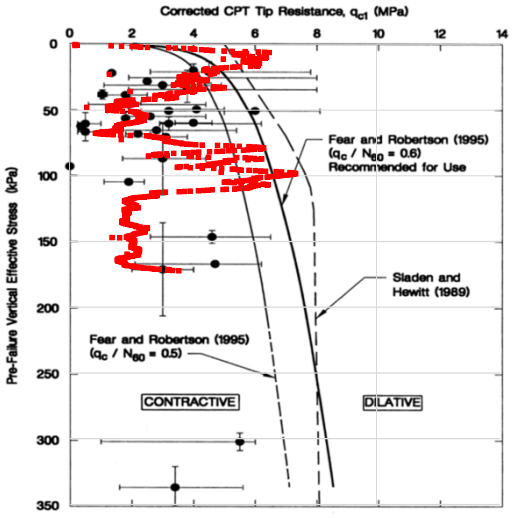

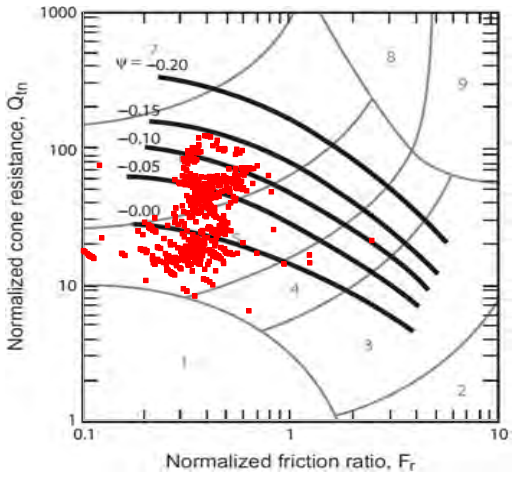

NOTE:		PROJECT Fundão Tailings Dam Review Panel
		TITLE DeltaGeo (2011) - New Dike 1A CPTu-P4 Liquefaction Susceptibility and Soil Behavior Type

September 2012 – July 2013
DeltaGeo
Dike 1
(Section C2.2.2)

Figure C.C1-2 – DeltaGeo (September 2012 – July 2013) Test Location Plan

CPTu-02 CPT Plots
CPTu-02 CPT Liquefaction Susceptibility and Soil Behavior Type Plots
CPTu-03 CPT Plots
CPTu-03 CPT Liquefaction Susceptibility and Soil Behavior Type Plots
CPTu-04 CPT Plots
CPTu-04 CPT Liquefaction Susceptibility and Soil Behavior Type Plots
CPTu-06 CPT Plots
CPTu-06 CPT Liquefaction Susceptibility and Soil Behavior Type Plots

NOTE:

1. May 1, 2013 Samarco aerial image shown.
2. Other tests in program were done on natural ground and are not relevant to the Investigation.
3. No coordinate information were available for these drill holes. All locations shown are approximate and were based on photos from the installation logs, top of hole elevations, and topography closest to the date of drill hole execution.
4. Logs for CPTu-01 and CPTu-01A are not presented due to low depth of penetration.

LEGEND:

◆ Piezocone Penetration Test (CPTu)

PROJECT

Fundão Tailings Dam Review Panel

TITLE

DeltaGeo (September 2012 - July 2013)
Test Location Plan

FIGURE NO.

C.C1-2

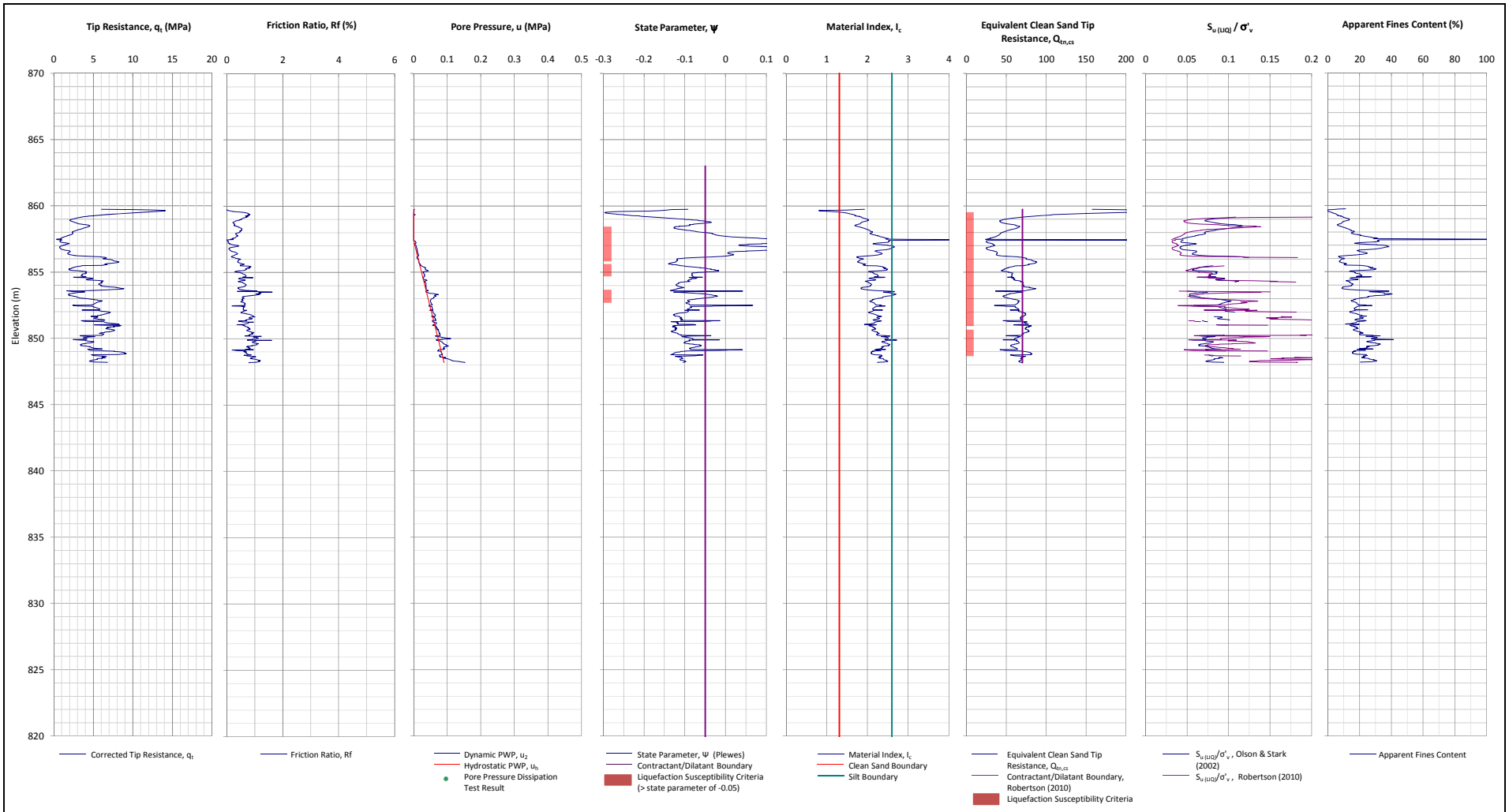

Notes:

1. This interpretation is based on the water and soil saturated unit weights γ_w=9.807 kN/m^3 and γ_{sat}=22kN/m^3.
2. The friction ratio Rf is calculated as Rf=f_s/q_t.
3. The hydrostatic pore pressure is calculated using the ground water level (GWL) determined from CPT pore pressure dissipation tests (where available) or dynamic pore pressure.
4. Soil boundary layers (where plotted) are based on KCB interpretation.
5. The data presented have been plotted to the axis limits. Data may exist beyond the axis limits shown.
6. The Material Index (I_c) boundaries are based on Robertson and Wride (1998).
7. The $Q_{tn,cs}$ contractant/dilatant boundary=70 and is based on Robertson (2010).
8. The State Parameter (Ψ) is calculated using Plewes, et al. (1992) assuming a K0 of 0.5.
9. Location data was not provided in the log. An approximate location was estimated from installation log photographs and topography.
10. Coordinates are in UTM Zone 23K Córrego Alegre.

PROJECT

Fundão Tailings Dam Review Panel

TITLE

DeltaGeo (September 2012 - July 2013) - Dike 1
CONE PENETRATION TEST CPTu-02
N:7764973m E:660845m 2013-06-18

Liquefaction susceptibility after Robertson (2010) "Evaluation of Flow Liquefaction and Liquefied Strength Using the Cone Penetration Test"	Liquefaction susceptibility after Olson & Stark (2003) "Yield Strength Ratio and Liquefaction Analysis of Slopes and Embankments"	State parameter approximation - Robertson (2009) "Interpretation of cone penetration tests - a unified approach"

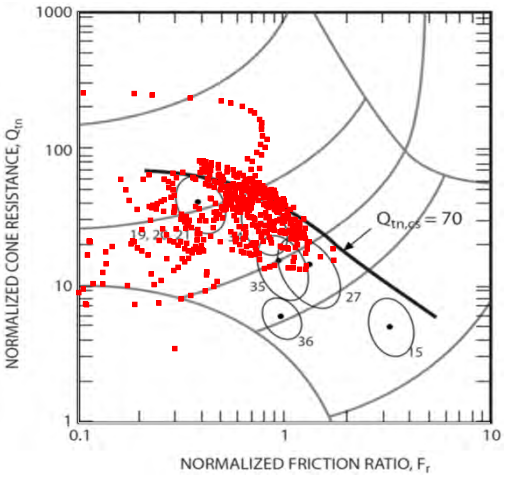

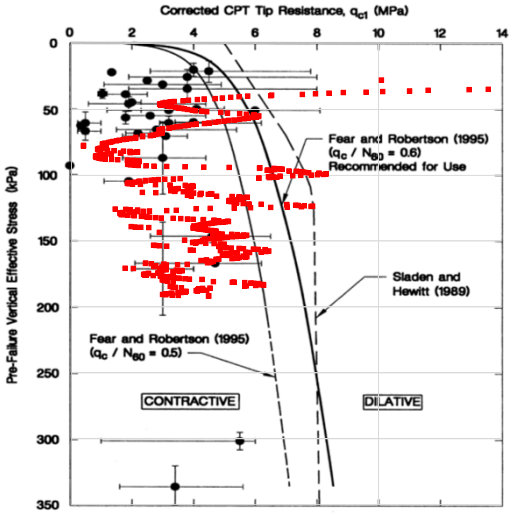

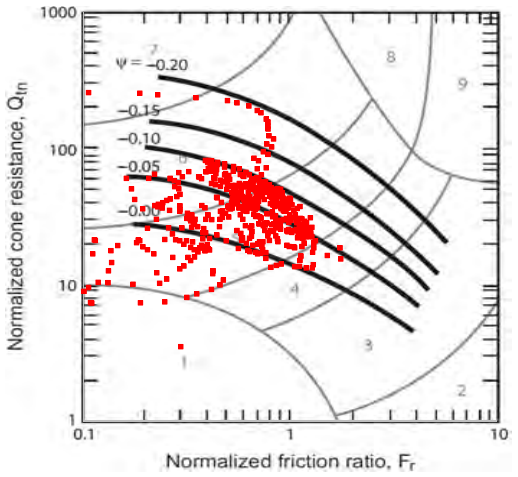

NOTE:

PROJECT

Fundão Tailings Dam Review Panel

TITLE

DeltaGeo (September 2012 - July 2013) - Dike 1
CPTu-02 Liquefaction Susceptibility and Soil Behavior Type

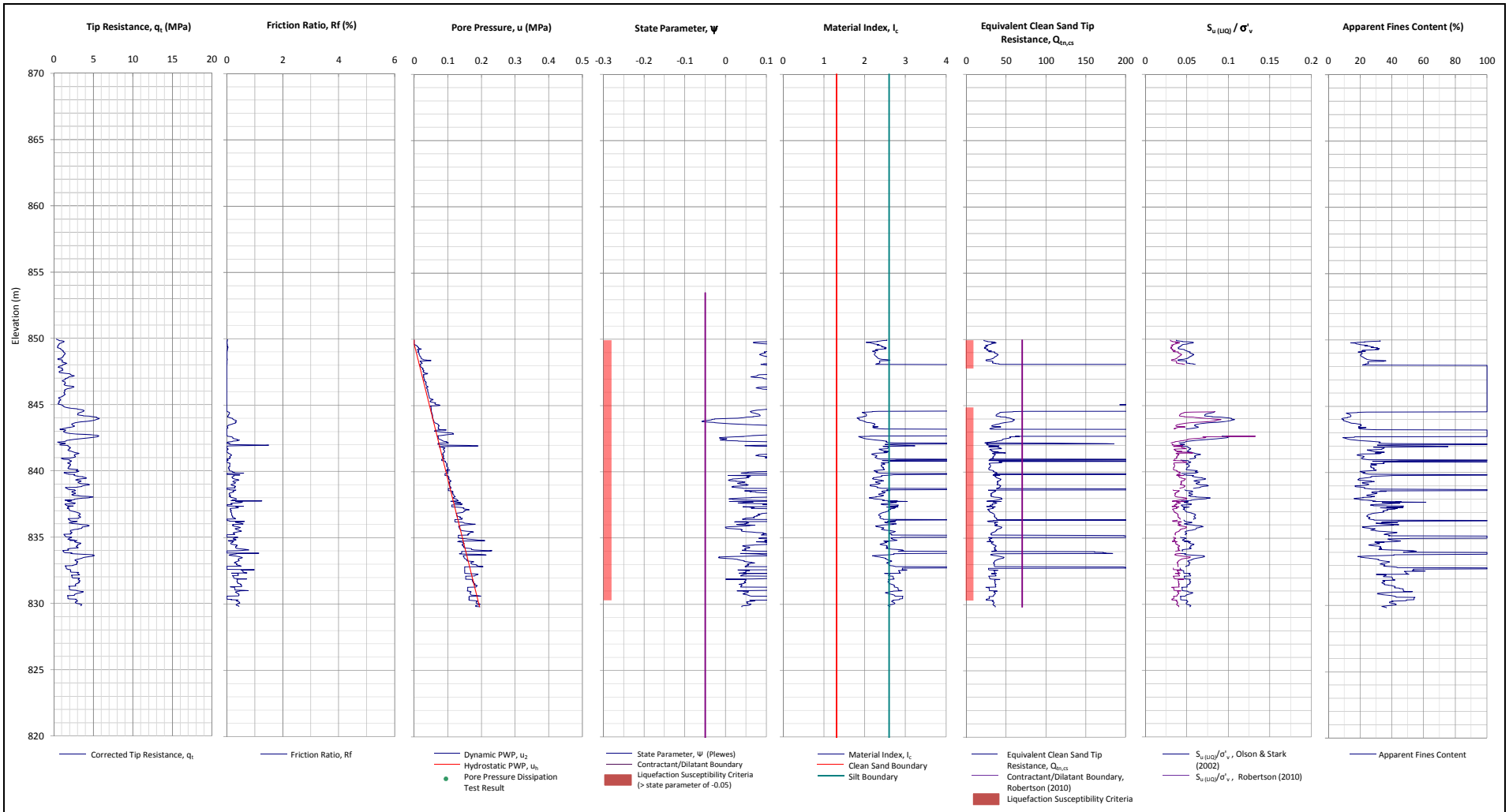

Notes:

1. This interpretation is based on the water and soil saturated unit weights γ_w=9.807 kN/m^3 and γ_{sat}=22kN/m^3.
2. The friction ratio Rf is calculated as Rf=f_s/q_t.
3. The hydrostatic pore pressure is calculated using the ground water level (GWL) determined from CPT pore pressure dissipation tests (where available) or dynamic pore pressure.
4. Soil boundary layers (where plotted) are based on KCB interpretation.
5. The data presented have been plotted to the axis limits. Data may exist beyond the axis limits shown.
6. The Material Index (I_c) boundaries are based on Robertson and Wride (1998).
7. The $Q_{tn,cs}$ contractant/dilatant boundary=70 and is based on Robertson (2010).
8. The State Parameter (Ψ) is calculated using Plewes, et al. (1992) assuming a K0 of 0.5.
9. Location data was not provided in the log. An approximate location was estimated from installation log photographs and topography.
10. Coordinates are in UTM Zone 23K Córrego Alegre.

PROJECT

Fundão Tailings Dam Review Panel

TITLE

DeltaGeo (September 2012 - July 2013) - Dike 1
CONE PENETRATION TEST CPTu-03
N:7764889m E:660956m 2013-06-19

Liquefaction susceptibility after Robertson (2010) "Evaluation of Flow Liquefaction and Liquefied Strength Using the Cone Penetration Test"	Liquefaction susceptibility after Olson & Stark (2003) "Yield Strength Ratio and Liquefaction Analysis of Slopes and Embankments"	State parameter approximation - Robertson (2009) "Interpretation of cone penetration tests - a unified approach"

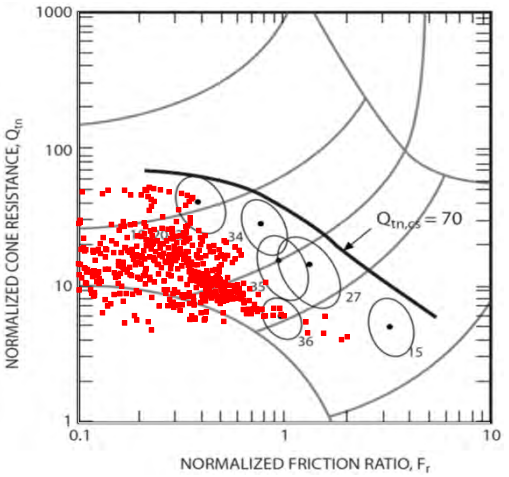

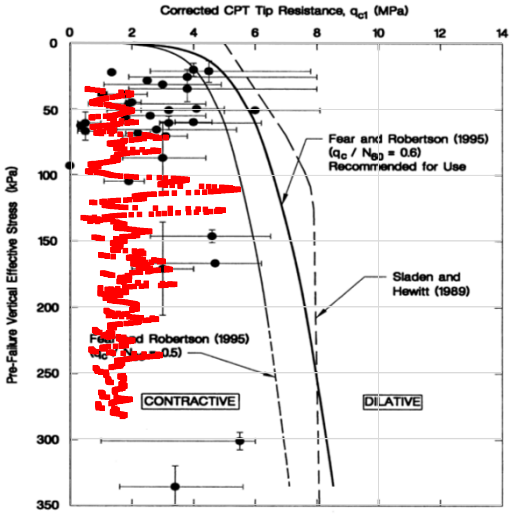

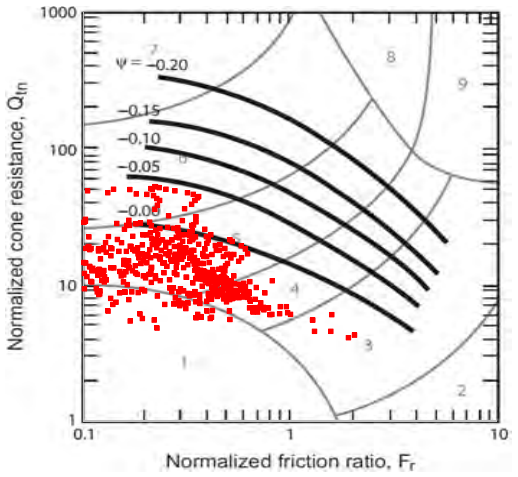

NOTE:

PROJECT

Fundão Tailings Dam Review Panel

TITLE

DeltaGeo (September 2012 - July 2013) - Dike 1
CPTu-03 Liquefaction Susceptibility and Soil Behavior Type

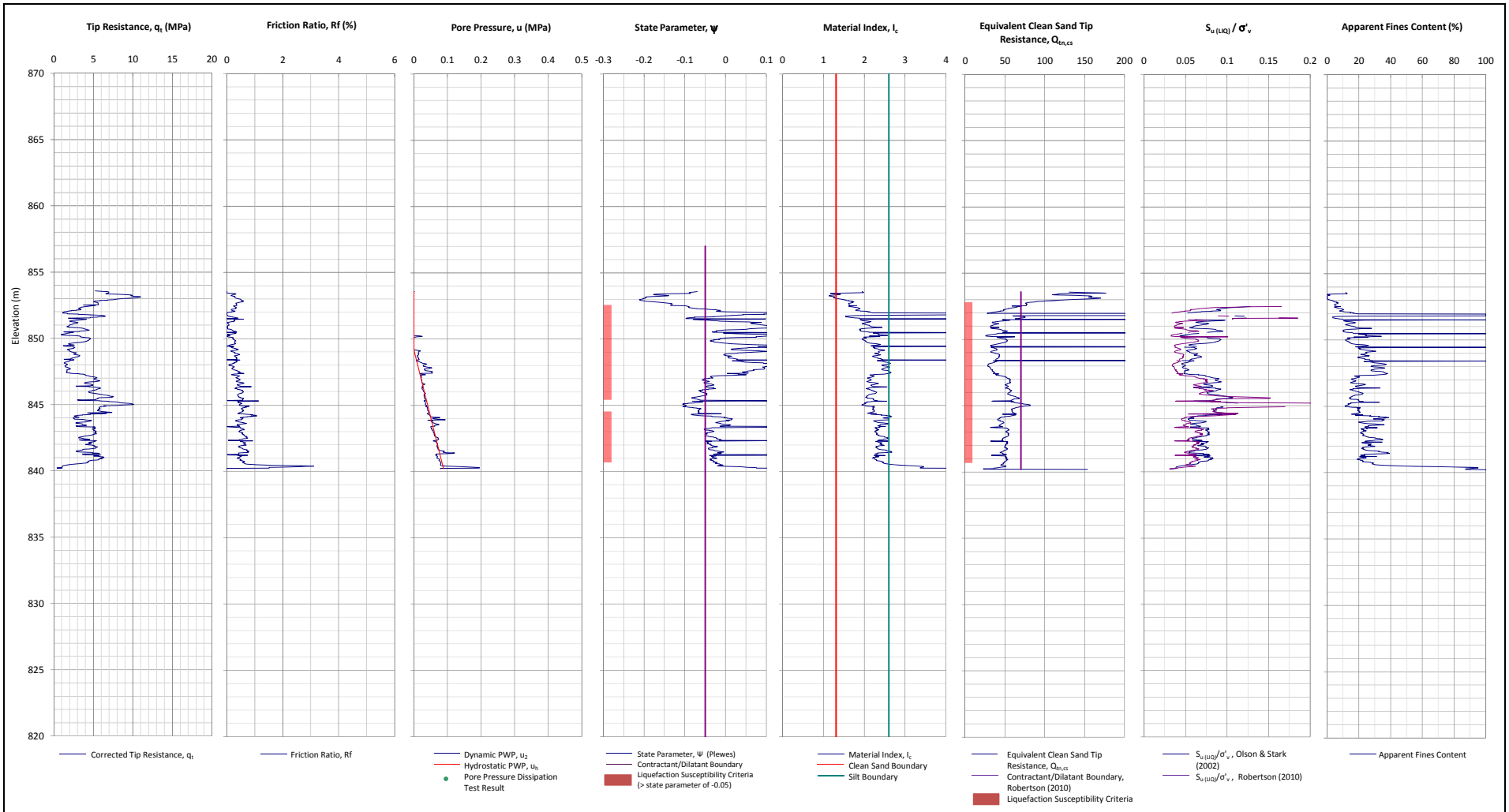

Notes:

1. This interpretation is based on the water and soil saturated unit weights γ_w=9.807 kN/m^3 and γ_{sat}=22kN/m^3.
2. The friction ratio Rf is calculated as Rf=f_s/q_t.
3. The hydrostatic pore pressure is calculated using the ground water level (GWL) determined from CPT pore pressure dissipation tests (where available) or dynamic pore pressure.
4. Soil boundary layers (where plotted) are based on KCB interpretation.
5. The data presented have been plotted to the axis limits. Data may exist beyond the axis limits shown.
6. The Material Index (I_c) boundaries are based on Robertson and Wride (1998).
7. The $Q_{tn,cs}$ contractant/dilatant boundary=70 and is based on Robertson (2010).
8. The State Parameter (Ψ) is calculated using Plewes, et al. (1992) assuming a K0 of 0.5.
9. Location data was not provided in the log. An approximate location was estimated from installation log photographs and topography.
10. Coordinates are in UTM Zone 23K Córrego Alegre.

PROJECT

Fundão Tailings Dam Review Panel

TITLE

DeltaGeo (September 2012 - July 2013) - Dike 1
CONE PENETRATION TEST CPTu-04
N:7764931m E:660873m 2013-06-27

Liquefaction susceptibility after Robertson (2010) "Evaluation of Flow Liquefaction and Liquefied Strength Using the Cone Penetration Test"	Liquefaction susceptibility after Olson & Stark (2003) "Yield Strength Ratio and Liquefaction Analysis of Slopes and Embankments"	State parameter approximation - Robertson (2009) "Interpretation of cone penetration tests - a unified approach"

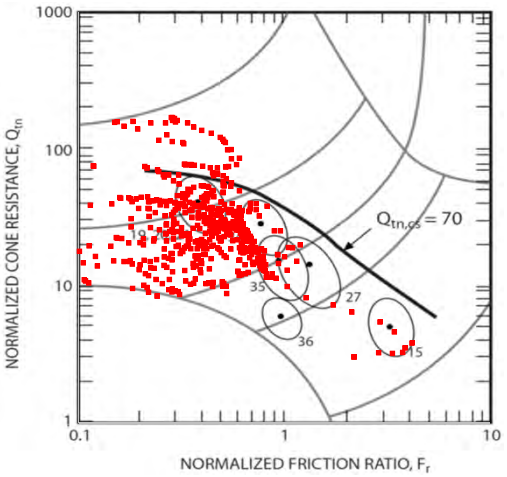

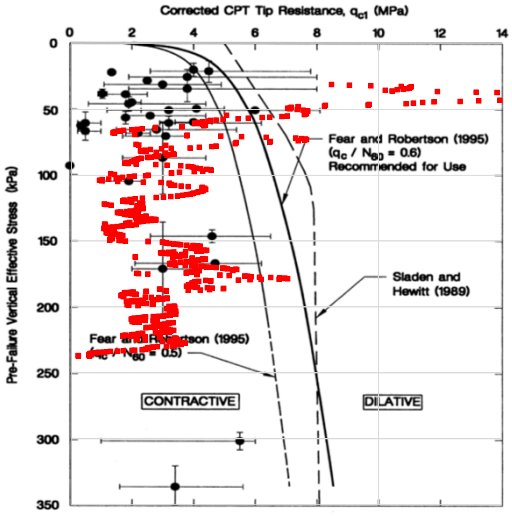

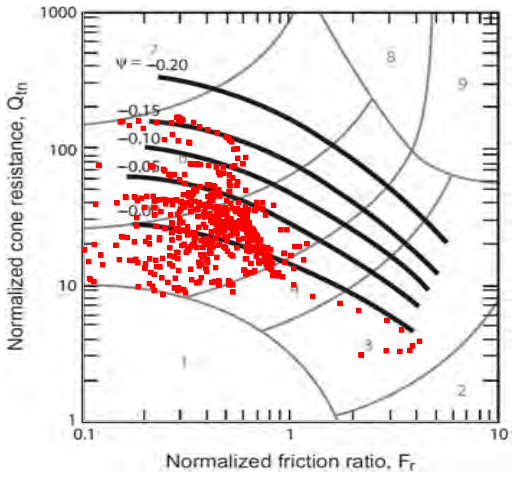

NOTE:

PROJECT

Fundão Tailings Dam Review Panel

TITLE

DeltaGeo (September 2012 - July 2013) - Dike 1
CPTu-04 Liquefaction Susceptibility and Soil Behavior Type

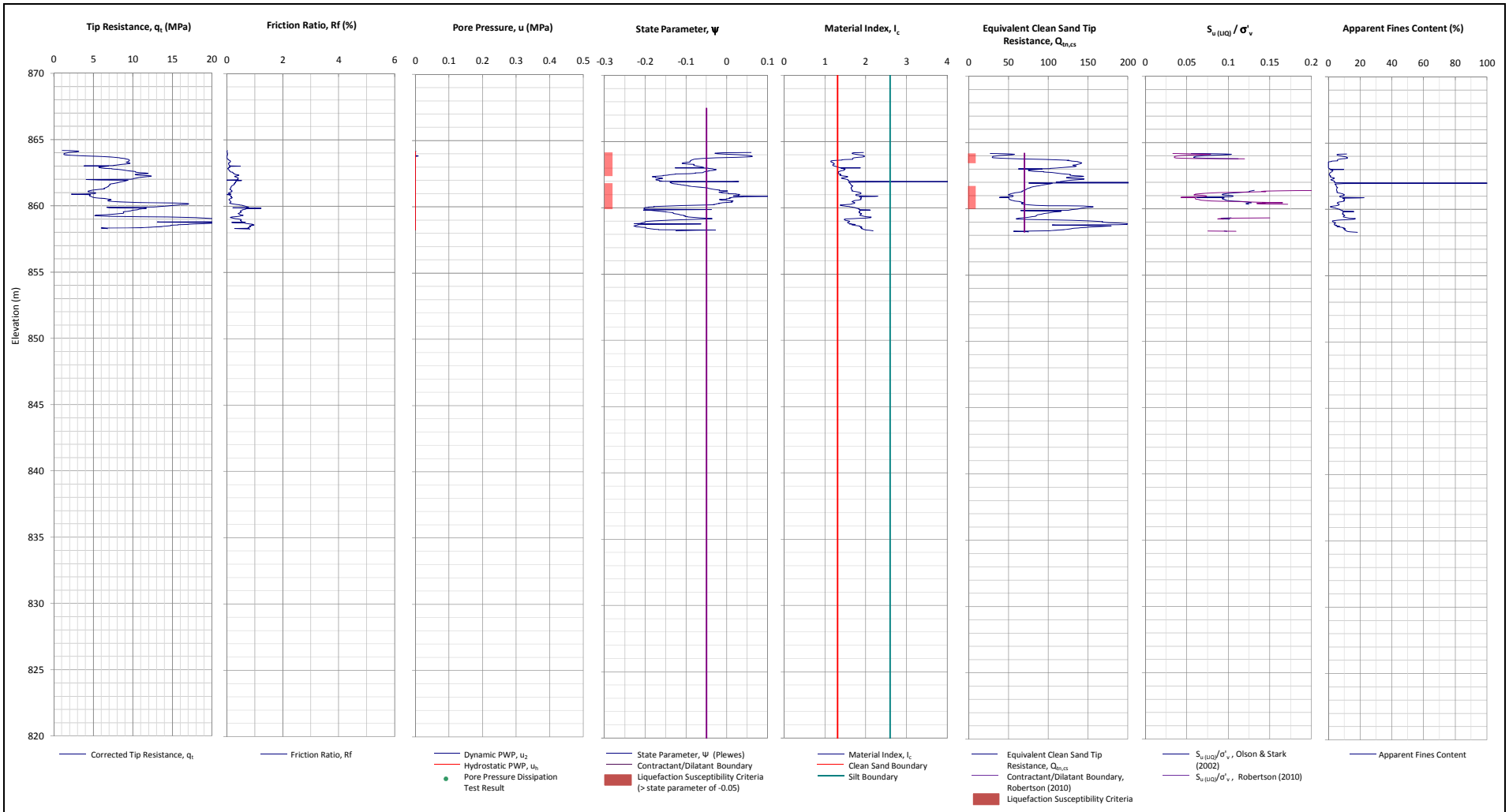

Notes:

1. This interpretation is based on the water and soil saturated unit weights γ_w=9.807 kN/m^3 and γ_{sat}=22kN/m^3.
2. The friction ratio Rf is calculated as Rf=f_s/q_t.
3. The hydrostatic pore pressure is calculated using the ground water level (GWL) determined from CPT pore pressure dissipation tests (where available) or dynamic pore pressure.
4. Soil boundary layers (where plotted) are based on KCB interpretation.
5. The data presented have been plotted to the axis limits. Data may exist beyond the axis limits shown.
6. The Material Index (I_c) boundaries are based on Robertson and Wride (1998).
7. The $Q_{tn,cs}$ contractant/dilatant boundary=70 and is based on Robertson (2010).
8. The State Parameter (Ψ) is calculated using Plewes, et al. (1992) assuming a K0 of 0.5.
9. Location data was not provided in the log. An approximate location was estimated from installation log photographs and topography.
10. Coordinates are in UTM Zone 23K Córrego Alegre.

PROJECT: Fundão Tailings Dam Review Panel

TITLE: DeltaGeo (September 2012 - July 2013) - Dike 1
CONE PENETRATION TEST CPTu-06
N:7765000m E:660831m 2013-07-09

Liquefaction susceptibility after Robertson (2010) "Evaluation of Flow Liquefaction and Liquefied Strength Using the Cone Penetration Test"	Liquefaction susceptibility after Olson & Stark (2003) "Yield Strength Ratio and Liquefaction Analysis of Slopes and Embankments"	State parameter approximation - Robertson (2009) "Interpretation of cone penetration tests - a unified approach"

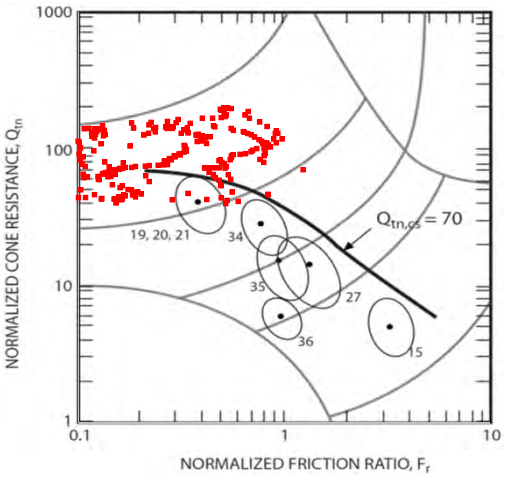

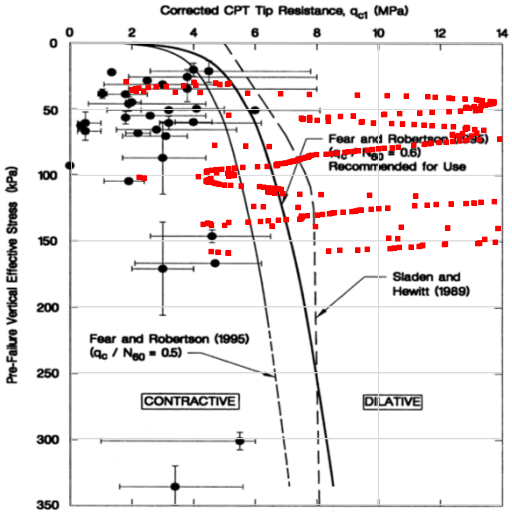

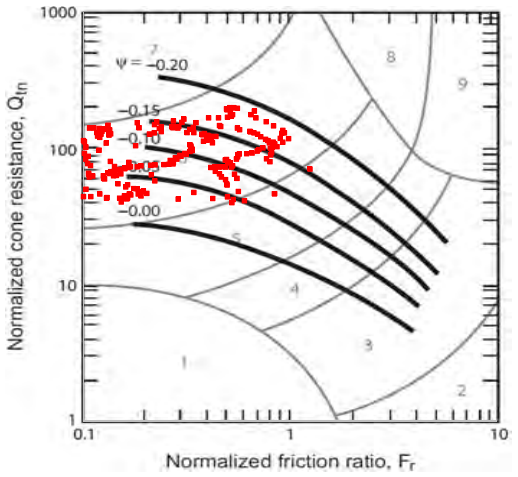

NOTE:

PROJECT

Fundão Tailings Dam Review Panel

TITLE

DeltaGeo (September 2012 - July 2013) - Dike 1
CPTu-06 Liquefaction Susceptibility and Soil Behavior Type

April 2014
Fugro
Dike 1
(Section C2.2.3)

Figure C.C1-3 – Fugro (April 2014) Test Location Plan

NA-01 CPT Plots
NA-01 CPT Liquefaction Susceptibility and Soil Behavior Type Plots
NA-02 CPT Plots
NA-02 CPT Liquefaction Susceptibility and Soil Behavior Type Plots
NA-03 CPT Plots
NA-03 CPT Liquefaction Susceptibility and Soil Behavior Type Plots
NA-04 CPT Plots
NA-04 CPT Liquefaction Susceptibility and Soil Behavior Type Plots
NA-05 CPT Plots
NA-05 CPT Liquefaction Susceptibility and Soil Behavior Type Plots
NA-06 CPT Plots
NA-06 CPT Liquefaction Susceptibility and Soil Behavior Type Plots

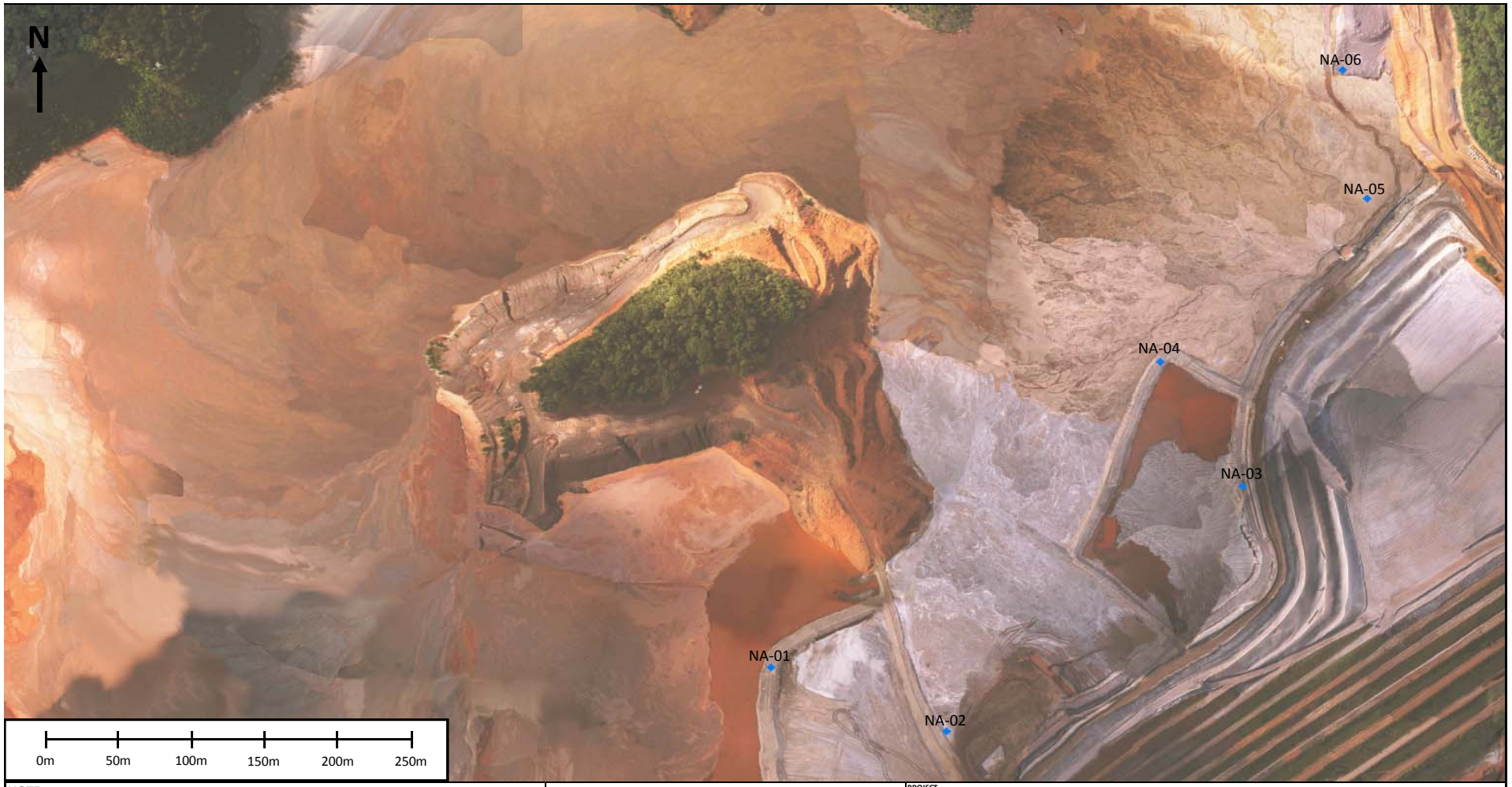

NOTE:
1. March 28, 2014 Samarco aerial image shown.

LEGEND:
◆ Cone Penetration Test (CPT)

PROJECT
Fundão Tailings Dam Review Panel

TITLE
Fugro (April 2014)
Test Location Plan

FIGURE NO.
C.C1-3

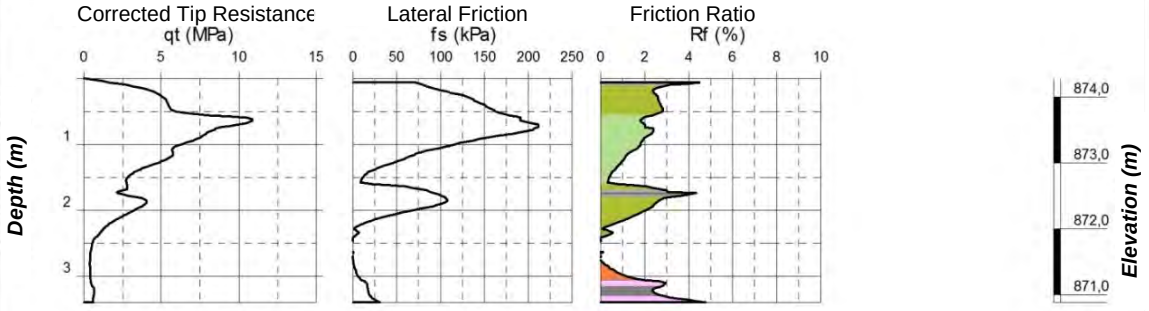

Soil Behavior – modified by Robertson et al. 1986

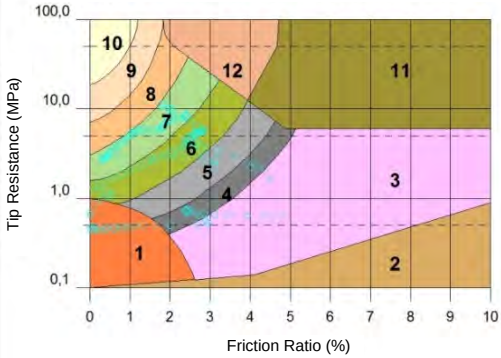

Vertical Scale 1:100

Caption: Identification of soil types from friction ratio

1 Sensitive, fine grained soil
2 Organic matter, peat
3 Clay
4 Silty clay to clay
5 Clayey silt to silty clay
6 Sandy silt to clayey silt
7 Silty sand to sandy silt
8 Sand to silty sand
9 Sand
10 Gravely sand to sand
11 Very stiff, fine grained soil
12 Sand to clayey sand

Soils type 11 and 12 are over-consolidated or sedimentary

FUGRO IN SITU GEOTECNIA	Client: SAMARCO MINERAÇÃO S.A.	
	Work/Site: FUNDAO DAM GERMANO MINE – MARIANA MG	Elevation
CPT-NA-01	Coord. E: 660373 Coord. N: 7764691 Final Depth l (m): 3,40	Cota (m): 874,28 WL (m): 1,70
Coordinator/Tech. in Charge: DANIELLA ARANHA	Fugru in Situ No. SMC-03-GRE-01	1/1
Processed by: ARON	Test date: 07/04/2014	

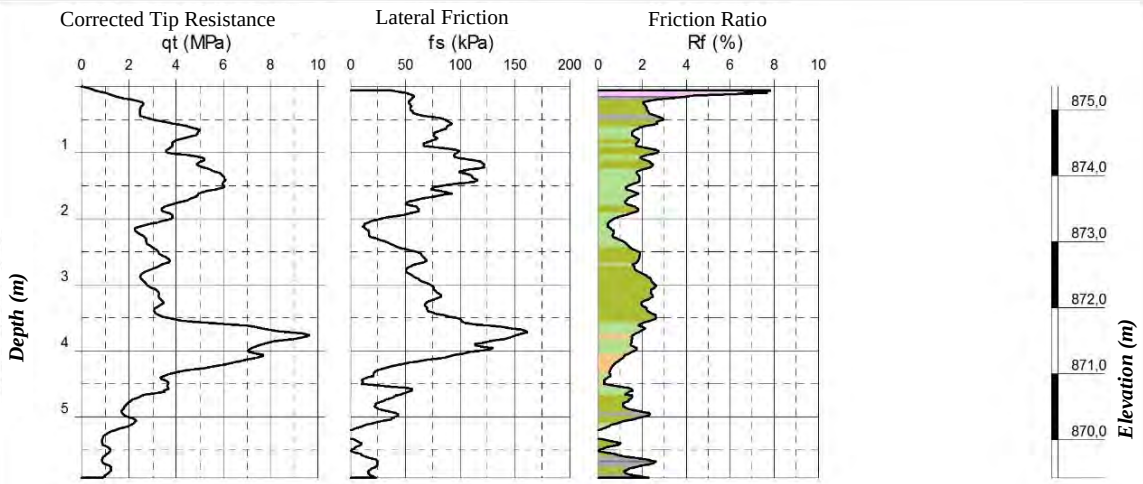

Soil Behavior – modified by Robertson et al. 1986

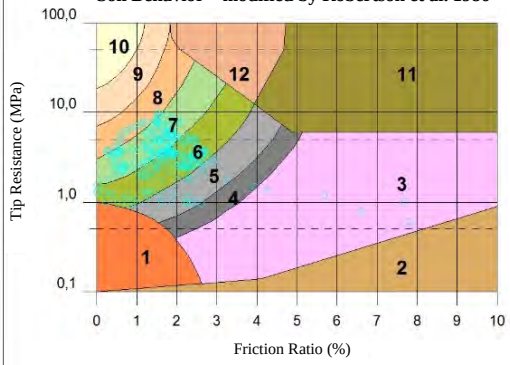

Vertical Scale 1:100

Caption: Identification of soil types from friction ratio

1 Sensitive, fine grained soil
2 Organic matter, peat
3 Clay
4 Silty clay to clay
5 Clayey silt to silty clay
6 Sandy silt to clayey silt
7 Silty sand to sandy silt
8 Sand to silty sand
9 Sand
10 Gravely sand to sand
11 Very stiff, fine grained soil
12 Sand to clayey sand

Soils type 11 and 12 are over-consolidated or sedimentary

FUGRO IN SITU GEOTECNIA

Client: SAMARCO MINERAÇÃO S.A.

Work/Site: FUNDAO DAM
GERMANO MINE – MARIANA MG

CPT-NA-02

Coord. E: 660494 Elevation (m): 875,35
Coord. N: 7764643 WL (m): 5,70
Final Depth (m): 5,92

Coordinator/Tech. in Charge: DANIELLA ARANHA

Fugru in Situ No. SMC-03-GRE-01

Processed by: ARON

Test date: 07/04/2014

1/1

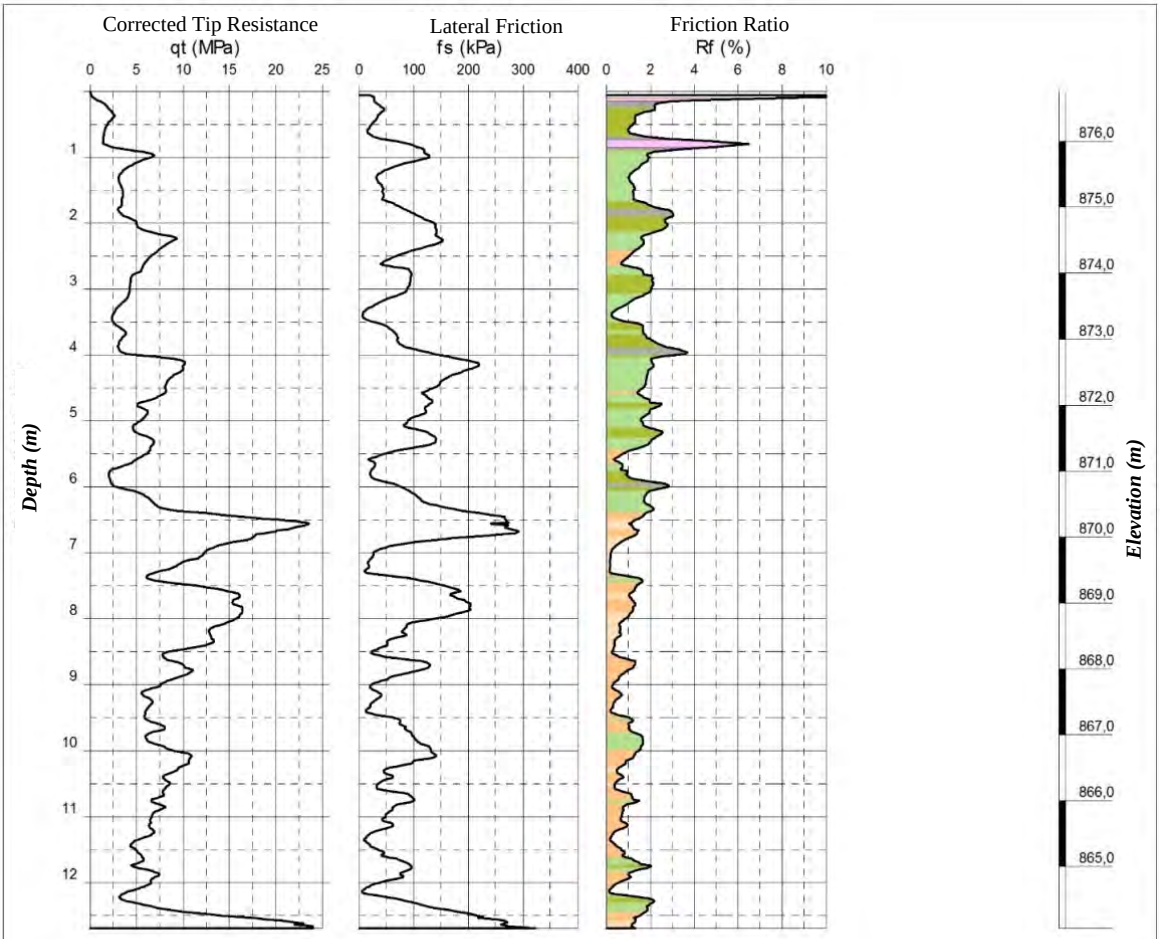

Soil Behavior – modified by Robertson et al. 1986

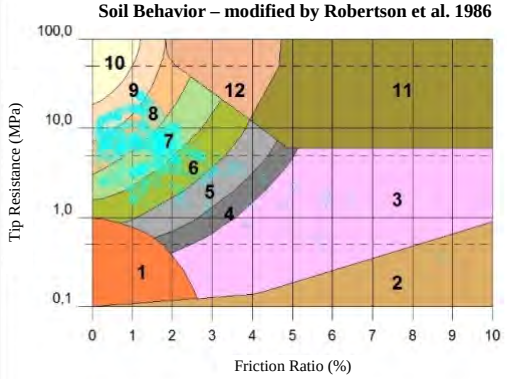

Vertical Scale 1:100

Caption: Identification of soil types from friction ratio

1 Sensitive, fine grained soil
2 Organic matter, peat
3 Clay
4 Silty clay to clay
5 Clayey silt to silty clay
6 Sandy silt to clayey silt
7 Silty sand to sandy silt
8 Sand to silty sand
9 Sand
10 Gravely sand to sand
11 Very stiff, fine grained soil
12 Sand to clayey sand

Soils type 11 and 12 are over-consolidated or sedimentary

FUGRO IN SITU GEOTECNIA

Client: SAMARCO MINERAÇÃO S.A.

Work/Site: FUNDAO DAM
GERMANO MINE – MARIANA MG

CPT-NA-03

Coord. E: 660695 Elevation (m): 876,76
Coord. N: 7764828 WL (m): DRY
Final Depth (m): 12,70

Coordinator/Tech. in Charge: DANIELLA ARANHA
Fugru in Situ No. SMC-03-GRE-01
Processed by: ARON
Test date: 07/04/2014

1/1

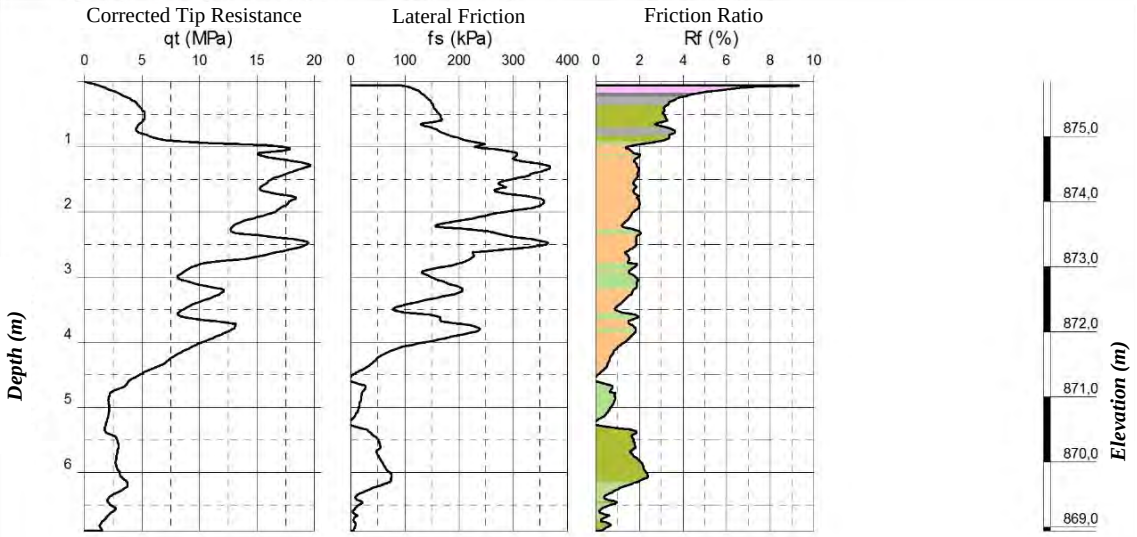

Soil Behavior – modified by Robertson et al. 1986

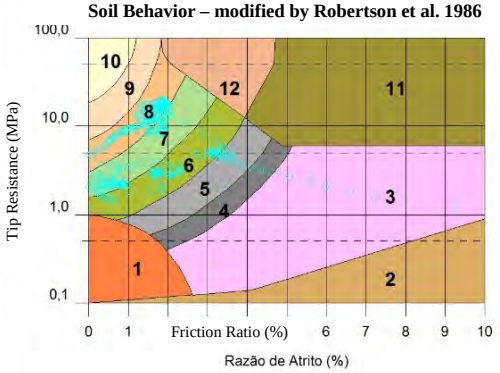

Vertical Scale 1:100

Caption: Identification of soil types from friction ratio

1 Sensitive, fine grained soil
2 Organic matter, peat
3 Clay
4 Silty clay to clay
5 Clayey silt to silty clay
6 Sandy silt to clayey silt
7 Silty sand to sandy silt
8 Sand to silty sand
9 Sand
10 Gravely sand to sand
11 Very stiff, fine grained soil
12 Sand to clayey sand

Soils type 11 and 12 are over-consolidated or sedimentary

FUGRO IN SITU GEOTECNIA

Client: SAMARCO MINERAÇÃO S.A.

Work/Site: FUNDAO DAM
GERMANO MINE – MARIANA MG

CPT-NA-04

Coord. E: 660639 Elevation (m): 875,84
Coord. N: 7764922 WL (m): 5,60
Final Depth (m): 6,90

Coordinator/Tech. in Charge: DANIELLA ARANHA

Fugru in Situ No.: SMC-03-GRE-01

Processed by: ARON

Test date: 05/04/2014

1/1

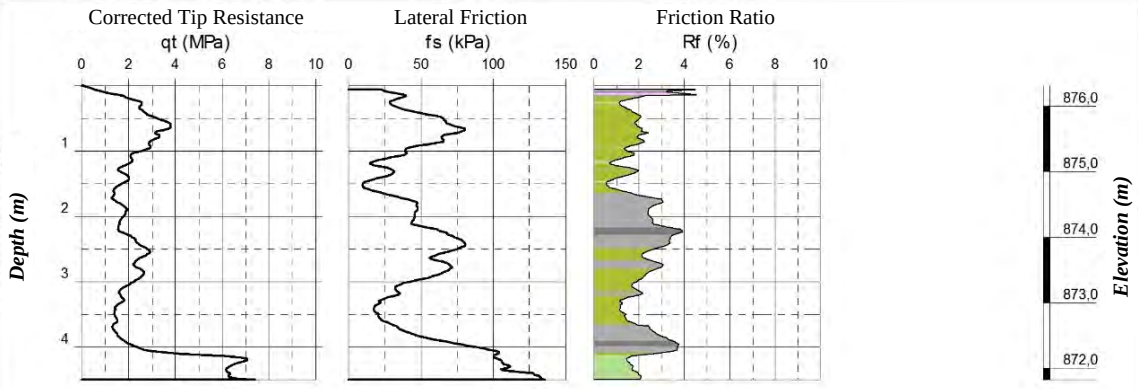

Soil Behavior – modified by Robertson et al. 1986

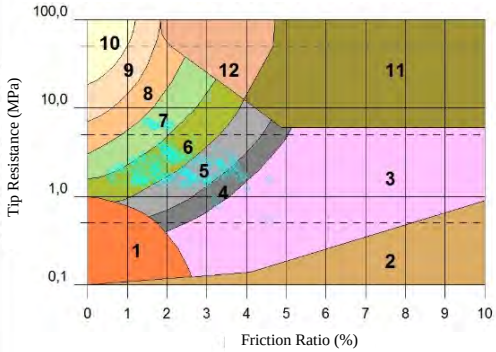

Vertical Scale 1:100

Caption: Identification of soil types from friction ratio

1	Sensitive, fine grained soil	7	Silty sand to sandy silt
2	Organic matter, peat	8	Sand to silty sand
3	Clay	9	Sand
4	Silty clay to clay	10	Gravely sand to sand
5	Clayey silt to silty clay	11	Very stiff, fine grained soil
6	Sandy silt to clayey silt	12	Sand to clayey sand

Soils type 11 and 12 are over-consolidated or sedimentary

FUGRO IN SITU GEOTECNIA

Client: SAMARCO MINERAÇÃO S.A.

Work/Site: FUNDAO DAM
GERMANO MINE – MARIANA MG

CPT-NA-05

Coord. E: 660781 Elevation (m): 876,32
Coord. N: 7765045 WL (m): 3,00
Final Depth (m): 4,50

Coordinator/Tech. in Charge: DANIELLA ARANHA

Fugru in Situ No.: SMC-03-GRE-01

Processed by: ARON

Test date: 07/04/2014

1/1

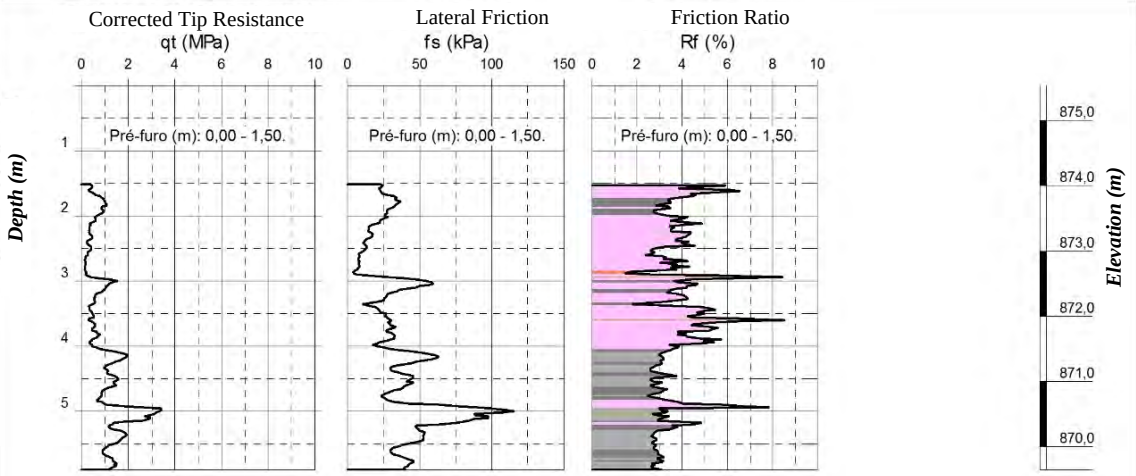

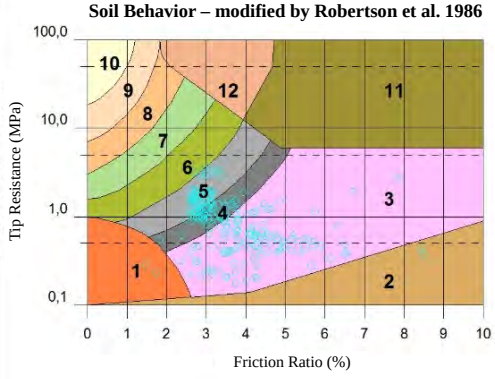

Vertical Scale 1:100

Caption: Identification of soil types from friction ratio

1	Sensitive, fine grained soil	7	Silty sand to sandy silt
2	Organic matter, peat	8	Sand to silty sand
3	Clay	9	Sand
4	Silty clay to clay	10	Gravely sand to sand
5	Clayey silt to silty clay	11	Very stiff, fine grained soil
6	Sandy silt to clayey silt	12	Sand to clayey sand

Soils type 11 and 12 are over-consolidated or sedimentary

FUGRO IN SITU GEOTECNIA

Client: SAMARCO MINERAÇÃO S.A.

Work/Site: FUNDAO DAM
GERMANO MINE – MARIANA MG

CPT-NA-06

Coord. E: 660764 Elevation (m): 875,54
Coord. N: 7765142 WL (m): 2,70
Final Depth (m): 5,90

Coordinator/Tech. in Charge: DANIELLA ARANHA

Fugru in Situ No. SMC-03-GRE-01

Processed by: ARON

Test date: : 04/04/2014

1/1

June 2014 – August 2014
Fugro
Grota da Vale
(Section C2.2.4)

Figure C.C1-4 – Fugro (June 2014 – August 2014) Test Location Plan

SPT Log SP-03
SPT Log SP-05
SPT Log SP-06
SPT Log SP-07
SPT Log SP-08

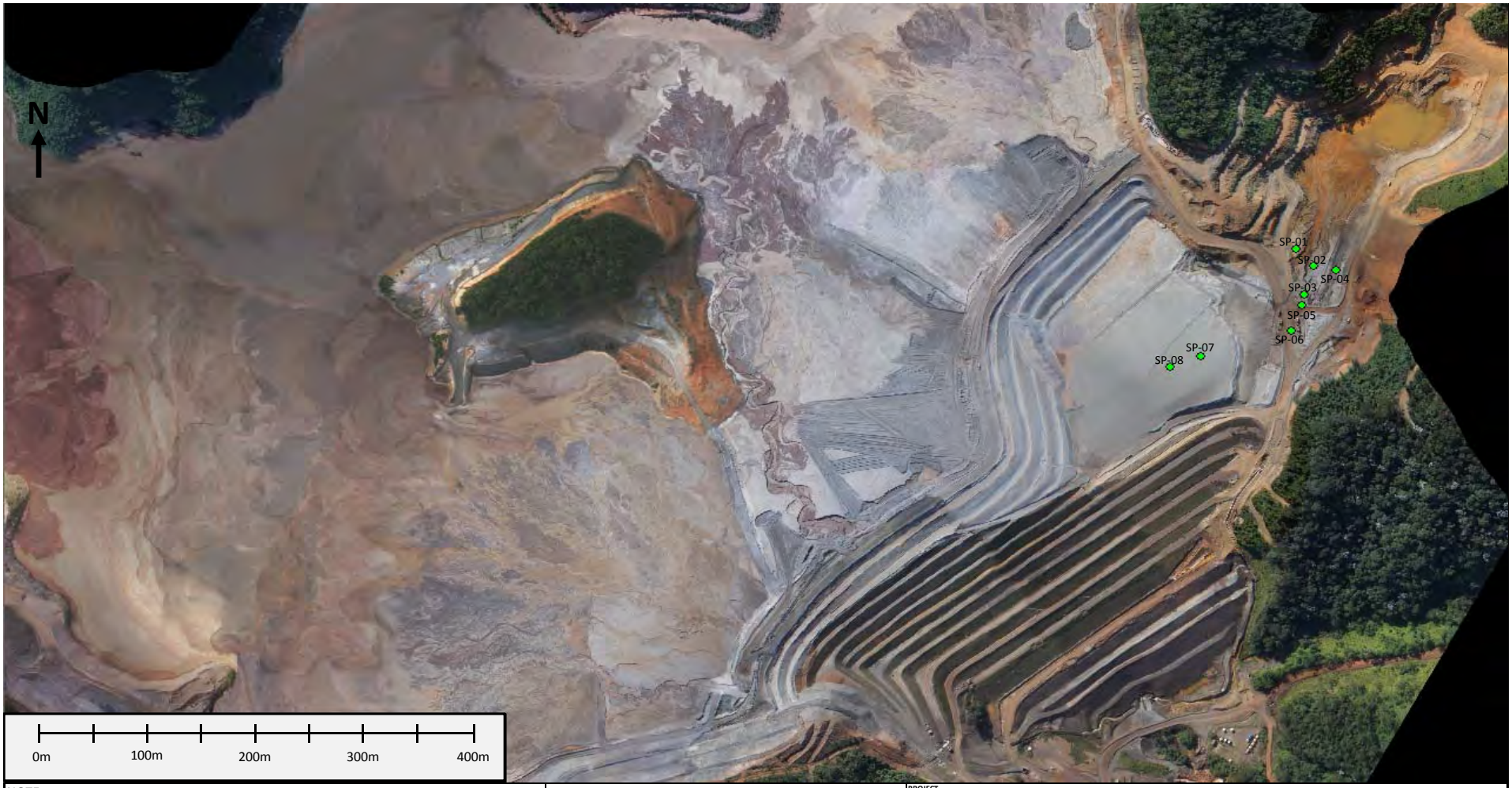

NOTE:
1. June 27, 2014 Samarco aerial image shown.
2. SPT logs for SP-03, SP-05, SP-06, SP-07 and SP-08 are presented.

LEGEND:
- Standard Penetration Test (SPT)

PROJECT
Fundão Tailings Dam Review Panel

TITLE
Fugro (June 2014 - August 2014)
Test Location Plan

FIGURE NO.
C.C1-4

Diameter of the Sounding	Water Level 24 Hrs.	Geological Profile	Elevation (m)	Blows / 30 cm Initial	Blows / 30 cm Final	Description of the Material	Geological Description
HQ	0		850			0.00 m to 3.00m - Fine to medium sand, clayey, soft and not compact, variegated grey.	Tailing's Fill / Dam
	1		849	3	4		
	2		848	3	5		
	3		847	2	2	3.00 m to 25.00 m - Sample not retrieved	
	4		846	P/60			
	5		845	P/45			
	6		844	P/50			
	7		843	P/60			
	8		842	P/65			
	9		841	P/70			
	10		840	P/60			
	11		839	P/65			
	12		838				
	13		837				
	14		836				
	15		835				
	16		834				
	17		833				
	18		832				
	19		831				
	20		830				
	21		829				
	22		828				
	23		827				
	24		826				
	25		825				

Coefficient | Degree of Weathering | Fill | Roughness | Discontinuity

Resistance to penetration index (N): 0 15 30 45 60

Recovery (%): 100 75 50 25 0

Fractures per Homogeneous Stretch. (Fractures / m): 20 15 10 5 0

Rock Quality Designation RQD: 0 25 50 75 100

Diameter of the Sounding [Drill Hole]	
	NQ - 3"
	HQ - 3,8 "
	HW - 4"

Coherence	Degree of Weathering
C1 - Coherent Rock	RS- Un-weathered or practically u-un-weathered Rock
C2 - Rock of Medium Coherence	RAD - Rock with average weathering
C3- Not very coherent rock	RAM - Very weathered Rock
C4- Non-Coherent Rock	REA - Extremely Weathered rock

FILL	ROUGHNESS		DISCONTINUITY (SPACING - CM)
D1 - Lithological contact	Profiled	I. Rough II. Smooth III. Polished	E1 - Very Spaced (>200)
D2 - Veining and veins (calcite/Silica)			E2 - Spaced (60-200)
D3 - Walls with incipient weathering	Wavy	I. Rough II. Smooth III. Polished	E3 - Average Spacing (20 - 60)
D4 - Weathered Walls	Flat	I. Rough II. Smooth III. Polished	E4 - In Proximity
D5 - Weathered walls w/fill			E5 - Very Close

WATER LEVEL MEASURMENTS

Date	Depth of Bore (m)	Water Level (m)	Depth of casing (m)
01/08/2014	27,00	CLOSED	27,00

Observations: Depth of the sounding was limited by the client.
Hole closed at 5.oo m.

FUGRO

Cliente: SAMARCO MINERAÇÃO S.A.

Obra Local: GROTA DA VALE - BARRAGEM FUNDÃO
MINA DE GERMANO - MARIANA-MG

Mixed Sounding: SP-03

Coordinates of the sounding.: E - 660989 m, N - 7764918 m

Height: 850,00

Coordinator/ Technician in Charge: DANIELLA ARANHA

Obra: 201057330-7/RJ

Drawn By: DANIELLE 1/100

Nº Fugro: SMC-03-GRE-01

Date of Execution: INÍCIO: 30/07/2014 TÉRMINO: 31/07/2014

Diameter of the Sounding	Water Level 24 Hrs.	Geological Profile	Elevation (m)	Blows / 30 cm Initial	Blows / 30 cm Final	Description of the Material	Geological Description	Coefficient	Degree of Weathering	Fill	Roughness	Discontinuity	Resistance to penetration index (N)	Recovery (%)	Fractures per Homogeneous Stretch. (Fractures / m)	Rock Quality Designation RQD
HQ	25		825			25.00 m to 27.00 m - Solid Rock, made up of quartz and hematite, silico-ferruginous. Name of rock: Itabirite	Itabirite	C2	RAD	D2	V	E3	0 15 30 45 60	100 75 50 25 0	0 5 10 15 20	0 25 50 75 100
	26		824													
	27		823					C2	RAD	D2	V	E3				
	28		822													
	29		821													
	30		820													
	31		819													
	32		818													
	33		817													
	34		816													
	35		815													
	36		814													
	37		813													
	38		812													
	39		811													
	40		810													
	41		809													
	42		808													
	43		807													
	44		806													
	45		805													
	46		804													
	47		803													
	48		802													
	49		801													
	50		800													

Diameter of the Sounding [Drill Hole]: NQ - 3" / HQ - 3,8" / HW - 4"

Coherence	Degree of Weathering
C1 - Coherent Rock	RS- Un-weathered or practically u-un-weathered Rock
C2 - Rock of Medium Coherence	RAD - Rock with average weathering
C3- Not very coherent rock	RAM - Very weathered Rock
C4- Non-Coherent Rock	REA - Extremely Weathered rock

FILL	ROUGHNESS	DISCONTINUITY (SPACING - CM)
D1 - Lithological contact	Profiled: I. Rough II. Smooth III. Polished	E1 - Very Spaced (>200)
D2 - Veining and veins (calcite/Silica)		E2 - Spaced (60-200)
D3 - Walls with incipient weathering	Wavy: I. Rough II. Smooth III. Polished	E3 - Average Spacing (20 - 60)
D4 - Weathered Walls	Flat: I. Rough II. Smooth III. Polished	E4 - In Proximity
D5 - Weathered walls w/fill		E5 - Very Close

WATER LEVEL MEASURMENTS

Date	Depth of Bore (m)	Water Level (m)	Depth of casing (m)
01/08/2014	27,00	CLOSED	27,00

Observations: Depth of the sounding was limited by the client.
Hole closed at 5.00 m.

Fugro

Client: SAMARCO MINERAÇÃO S.A.

Obra Local: BARRAGEM FUNDÃO - MINA DE GERMANO - MARIANA-MG

Mixed Sounding: SP-03

Coordinates of the sounding. Height: E - 660989 m; N - 7764918 m; 850,00

Coordinator Technician in Charge: DANIELLA ARANHA

Drawn By: DANIELLE

Scale: 1:100

Doc.: SMC-00-GRE-01

Date of Execution: INICIO: 30/07/2014 - TERMINO: 31/07/2014

Date: 201057300-7/FU

Diameter of the Sounding	Water Level 24 Hrs. (Depth, m)	Height (m)	Strokes / 30 cm Initial	Strokes / 30 cm Final	Description of the Material	Geological Description
HQ	0	850			0.00 m to 6.00 m - Fine to medium sand, Soft to medium compaction, variegated grey	Tailings Fill / Dam
	1	849	10	10		
	2	848	7	9		
	3	847	5	7		
	4	846	5	6		
	5	845	5	4		
	6	844	P/50		6.00 m to 7.00 m – Sample not retrieved	
	7	843	P/45		7.00 m to 9.00 m - Fine sand, clayey, soft, variegated grey	
	8	842	P/45			
	9	841	P/50		9.00 m to 12.00 m - Sample not retrieved	
	10	840	P/45			
	11	839	P/55			
	12	838	2	2	12.00 m to 28.00 m – Fine to medium sand, clayey, soft, moderately compact, variegated grey	
	13	837	3	4		
	14	836	5	6		
	15	835	7	9		
	16	834	10	14		
	17	833	2	2		
	18	832	5	8		
	19	831	6	8		
	20	830	2	2		
	21	829	3	4		
	22	828	8	10		
	23	827	10	16		
	24	826	5	9		
	25					

Other columns: Geological Profile; Coefficient; Degree of Weathering; Fill; Roughness; [Discontinuity; Resistance to penetration index (N) (0, 15, 30, 45, 60) / Recovery (%) (100, 75, 50, 25, 0); Fractures per Homogeneous Stretch. (Fractures / m) (20, 15, 10, 5, 0); Rock Quality Designation RQD (0, 25, 50, 75, 100)

Diameter of the Sounding [Drill Hole]: NQ - 3"; HQ - 3.5"; HW - 4"

Coherence
- C1-Cohernt Rock
- C2- Rock ofMedium Coherence
- C3-Not very coherent rock

Degree of Weathering
- RS- Un-weathered or practically un-weathered Rock
- RAD - Rock with average weathering
- RAM - Very weathered Rock
- REA - Extremely Weathered rock

FILL
- D1 - Lithological contact
- D2 - Veining and veins (calcite/Silica)
- D3 - Walls with incipient weathering
- D4 - Weathered Walls
- D5 - Weathered walls w/fill

ROUGHNESS
- Profiled: I. Rough, II. Smooth, III. Polished
- [P]rofiled: I. Rough, II. Smooth, III. Polished
- [P]rofiled: I. Rough, II. Smooth, III. Polished

DISCONTINUITY (SPACING - CM)
- E1 - Very Spaced (>200)
- E2 - Spaced (60-200)
- E3 - Average Spacing (20 - 60)
- E4 - In Proximity (6 a 20)
- E5 - Very Close (<6)

WATER LEVEL MEASURMENTS

Date	Depth of Bore (m)	Water Level (m)	Depth of casing (m)
09/08/2014	34,00	CLOSED	34,00

Observations: Depth of the sounding was limited by the client. Hole closed at 5.oo m.

FUGRO

Cliente: SAMARCO MINERAÇÃO S.A.

Obra/Local: GROTA DA VALE - BARRAGEM FUNDÃO, MINA DE GERMANO - MARIANA MG

Mixed Sounding SP-05

Coordinates of the sounding: E - 660987 m; N - 7764907 m

Elevation: 850,49

Coordinator/ Technician in Charge: DANIELLA ARANHA

Drawn By: DANIELLE

1:100

SMC-05 GRE-01

201057330-7/RJ

Date of Execution: INÍCIO: 06/08/2014 TÉRMINO: [illegible]

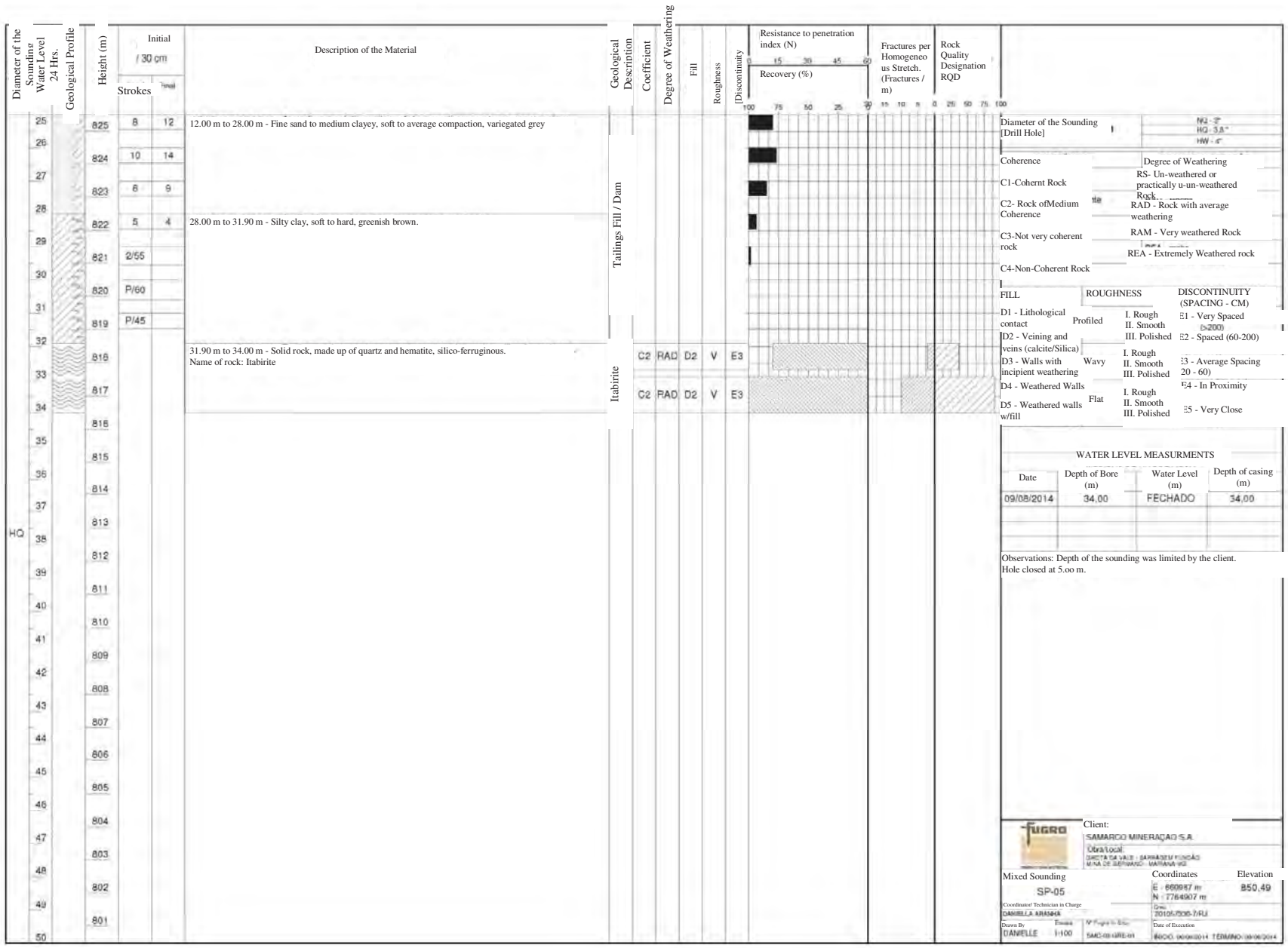
Diameter of the Sounding
Water Level 24 Hrs.
Geological Profile
Height (m)
Initial / 30 cm
Strokes
Final
Description of the Material
Geological Description
Coefficient
Degree of Weathering
Fill
Roughness
[Discontinuity
Resistance to penetration index (N)
Recovery (%)
Fractures per Homogeneous Stretch. (Fractures / m)
Rock Quality Designation RQD
HQ
12.00 m to 28.00 m - Fine sand to medium clayey, soft to average compaction, variegated grey
28.00 m to 31.90 m - Silty clay, soft to hard, greenish brown.
31.90 m to 34.00 m - Solid rock, made up of quartz and hematite, silico-ferruginous.
Name of rock: Itabirite
Tailings Fill / Dam
Itabirite
C2 RAD D2 V E3
C2 RAD D2 V E3
Diameter of the Sounding [Drill Hole]
NQ - 3"
HQ - 3,8"
HW - 4"
Coherence
C1-Coherent Rock
C2- Rock ofMedium Coherence
C3-Not very coherent rock
C4-Non-Coherent Rock
Degree of Weathering
RS- Un-weathered or practically u-un-weathered Rock
RAD - Rock with average weathering
RAM - Very weathered Rock
REA - Extremely Weathered rock
FILL
D1 - Lithological contact
D2 - Veining and veins (calcite/Silica)
D3 - Walls with incipient weathering
D4 - Weathered Walls
D5 - Weathered walls w/fill
ROUGHNESS
Profiled
Wavy
Flat
I. Rough
II. Smooth
III. Polished
DISCONTINUITY (SPACING - CM)
E1 - Very Spaced (>200)
E2 - Spaced (60-200)
E3 - Average Spacing 20 - 60)
E4 - In Proximity
E5 - Very Close
WATER LEVEL MEASURMENTS
Date
Depth of Bore (m)
Water Level (m)
Depth of casing (m)
09/08/2014
34,00
FECHADO
34,00
Observations: Depth of the sounding was limited by the client.
Hole closed at 5.oo m.
FUGRO
Client:
SAMARCO MINERAÇÃO S.A.
Obra/Local:
Mixed Sounding
SP-05
Coordinates
E - 660987 m
N - 7764907 m
Elevation
850,49
Coordinator/ Technician in Charge
DANIELLA ARAUJO
Drawn By
DANIELLE
Scale
1:100
Date of Execution
INICIO: 09/08/2014 TÉRMINO: 09/08/2014

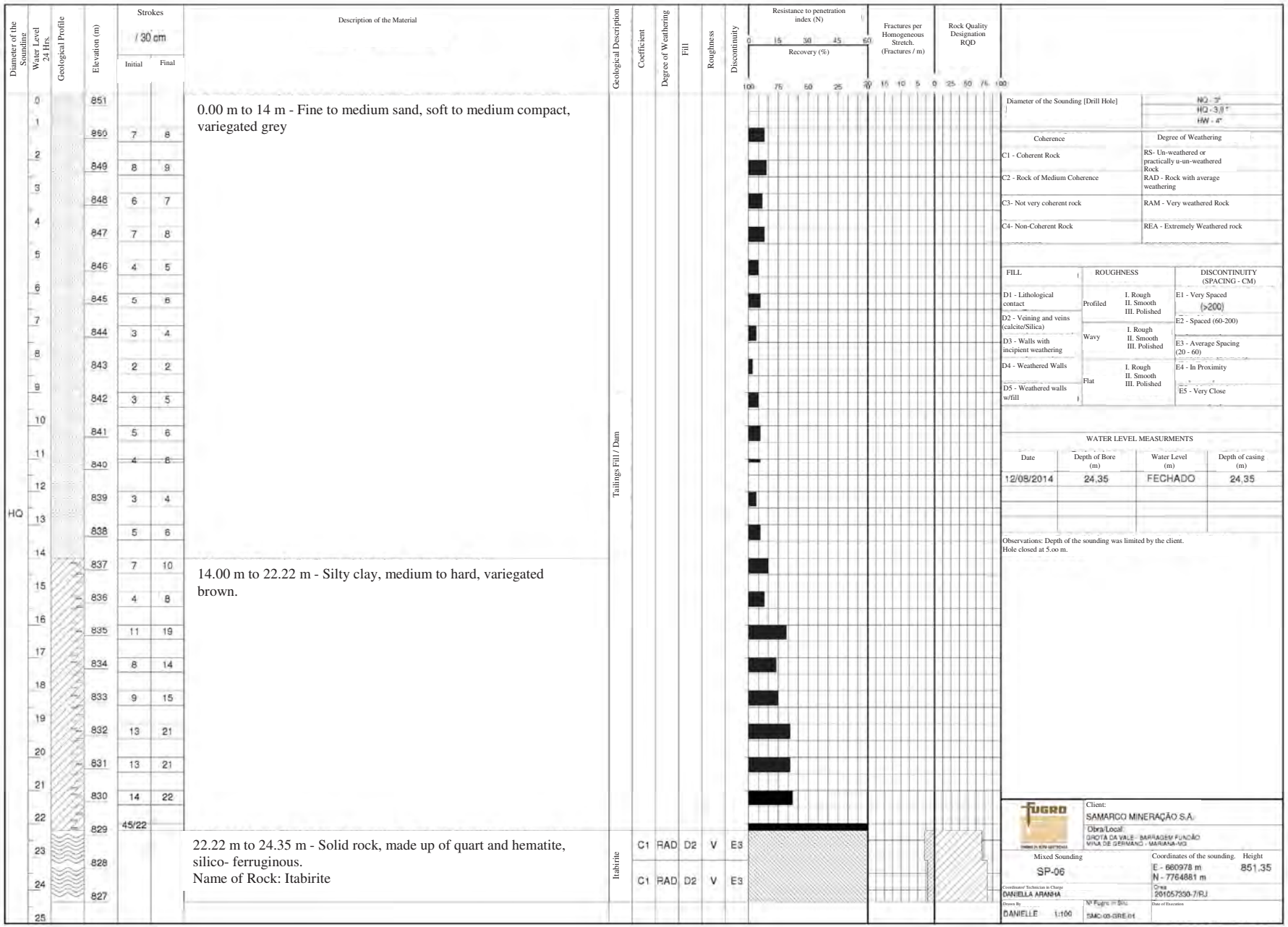
Diameter of the Sounding
Water Level 24 Hrs.
Geological Profile
Elevation (m)
Strokes / 30 cm
Initial
Final
Description of the Material
Geological Description
Coefficient
Degree of Weathering
Fill
Roughness
Discontinuity
Resistance to penetration index (N)
Recovery (%)
Fractures per Homogeneous Stretch. (Fractures / m)
Rock Quality Designation RQD
HQ
0.00 m to 14 m - Fine to medium sand, soft to medium compact, variegated grey
14.00 m to 22.22 m - Silty clay, medium to hard, variegated brown.
22.22 m to 24.35 m - Solid rock, made up of quart and hematite, silico- ferruginous.
Name of Rock: Itabirite
Tailings Fill / Dam
Itabirite
C1 RAD D2 V E3
C1 RAD D2 V E3
Diameter of the Sounding [Drill Hole]
NQ - 3"
HQ - 3,8"
HW - 4"
Coherence
C1 - Coherent Rock
C2 - Rock of Medium Coherence
C3- Not very coherent rock
C4- Non-Coherent Rock
Degree of Weathering
RS- Un-weathered or practically u-un-weathered Rock
RAD - Rock with average weathering
RAM - Very weathered Rock
REA - Extremely Weathered rock
FILL
D1 - Lithological contact
D2 – Veining and veins (calcite/Silica)
D3 - Walls with incipient weathering
D4 - Weathered Walls
D5 – Weathered walls w/fill
ROUGHNESS
Profiled
Wavy
Flat
I. Rough
II. Smooth
III. Polished
DISCONTINUITY (SPACING - CM)
E1 - Very Spaced (>200)
E2 - Spaced (60-200)
E3 - Average Spacing (20 - 60)
E4 - In Proximity
E5 - Very Close
WATER LEVEL MEASURMENTS
Date
Depth of Bore (m)
Water Level (m)
Depth of casing (m)
12/08/2014
24,35
FECHADO
24,35
Observations: Depth of the sounding was limited by the client.
Hole closed at 5.00 m.
FUGRO
Client:
SAMARCO MINERAÇÃO S.A.
Obra/Local:
GROTA DA VALE - BARRAGEM FUNDÃO
MINA DE GERMANO - MARIANA-MG
Mixed Sounding
SP-06
Coordinates of the sounding.
E - 660978 m
N - 7764881 m
Height
851,35
Coordinator/ Technician in Charge
DANIELLA ARANHA
Crea
2010573300-7/RJ
Drawn By
DANIELLE
1:100
Nº Fugro in BIU
SMC-03-SRE.01
Date of Execution

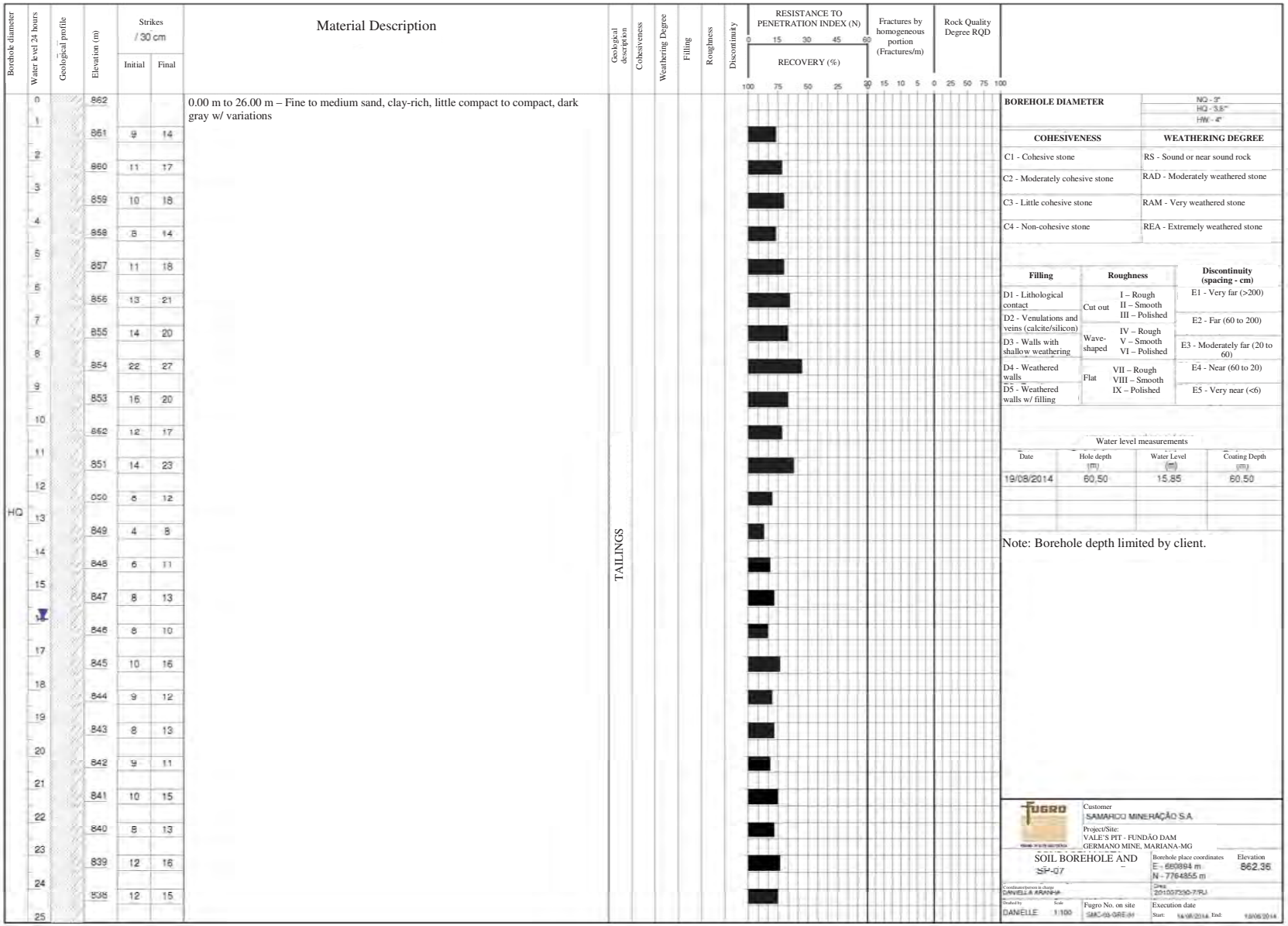
Borehole diameter
Water level 24 hours
Geological profile
Elevation (m)
Strikes / 30 cm
Initial
Final
Material Description
Geological description
Cohesiveness
Weathering Degree
Filling
Roughness
Discontinuity
RESISTANCE TO PENETRATION INDEX (N)
RECOVERY (%)
Fractures by homogeneous portion (Fractures/m)
Rock Quality Degree RQD
HQ
0.00 m to 26.00 m – Fine to medium sand, clay-rich, little compact to compact, dark gray w/ variations
TAILINGS
BOREHOLE DIAMETER
NQ - 3"
HQ - 3,8""
HW - 4"
COHESIVENESS
C1 - Cohesive stone
C2 - Moderately cohesive stone
C3 - Little cohesive stone
C4 - Non-cohesive stone
WEATHERING DEGREE
RS - Sound or near sound rock
RAD - Moderately weathered stone
RAM - Very weathered stone
REA - Extremely weathered stone
Filling
D1 - Lithological contact
D2 - Venulations and veins (calcite/silicon)
D3 - Walls with shallow weathering
D4 - Weathered walls
D5 - Weathered walls w/ filling
Roughness
Cut out
I – Rough
II – Smooth
III – Polished
Wave-shaped
IV – Rough
V – Smooth
VI – Polished
Flat
VII – Rough
VIII – Smooth
IX – Polished
Discontinuity (spacing - cm)
E1 - Very far (>200)
E2 - Far (60 to 200)
E3 - Moderately far (20 to 60)
E4 - Near (60 to 20)
E5 - Very near (<6)
Water level measurements
Date
Hole depth (m)
Water Level (m)
Coating Depth (m)
19/08/2014
60,50
15,85
60,50
Note: Borehole depth limited by client.
Customer
SAMARCO MINERAÇÃO S.A.
Project/Site:
VALE'S PIT - FUNDÃO DAM
GERMANO MINE, MARIANA-MG
SOIL BOREHOLE AND
SP-07
Borehole place coordinates
E - 660894 m
N - 7764855 m
Elevation
862,35
Drawn by
DANIELLE
Scale
1:100
Execution date
Start:
End:
19/08/2014

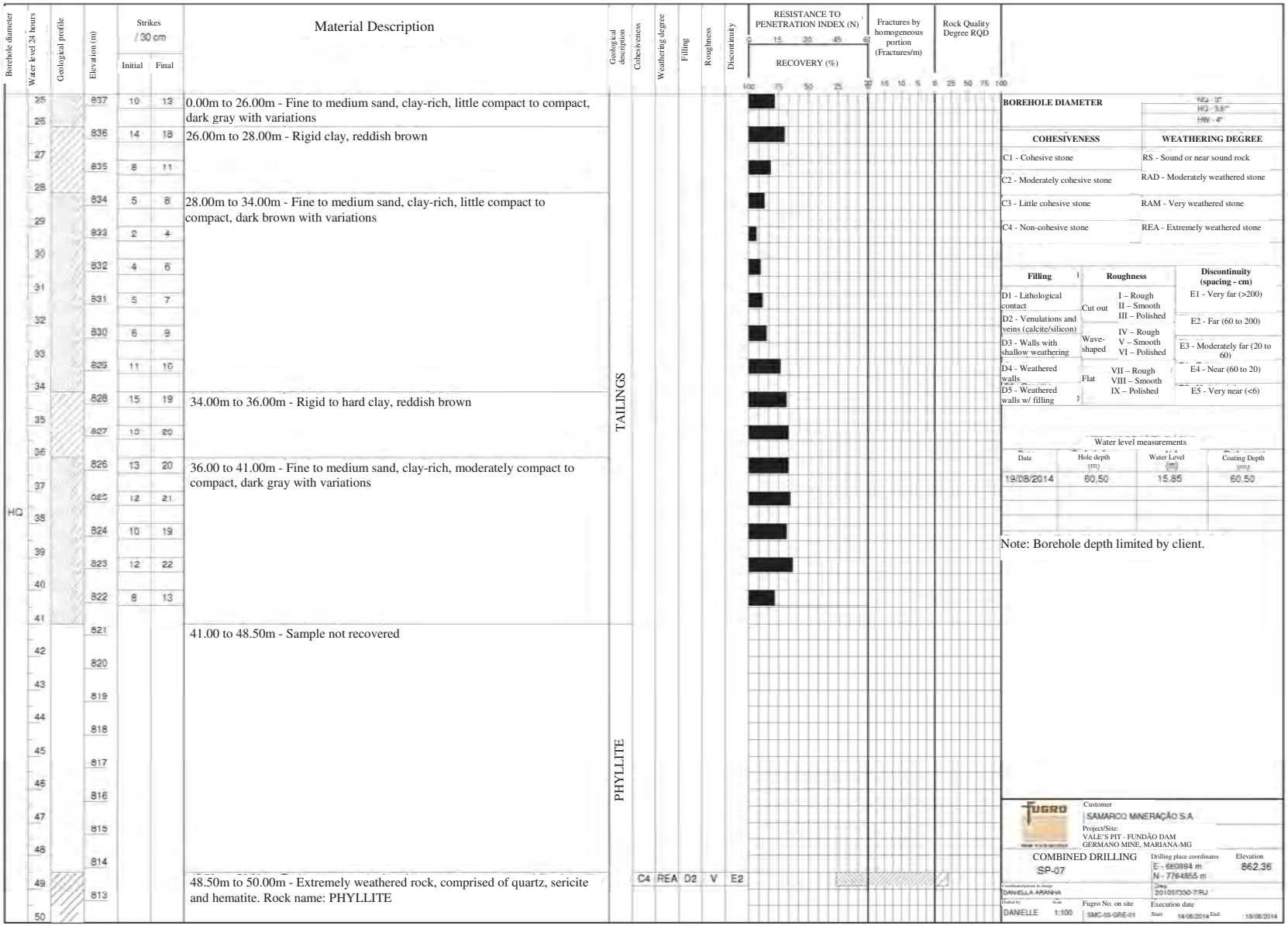
Borehole diameter
Water level 24 hours
Geological profile
Elevation (m)
Strikes / 30 cm
Initial
Final
Material Description
Geological description
Cohesiveness
Weathering degree
Filling
Roughness
Discontinuity
RESISTANCE TO PENETRATION INDEX (N)
RECOVERY (%)
Fractures by homogeneous portion (Fractures/m)
Rock Quality Degree RQD
HQ
0.00m to 26.00m - Fine to medium sand, clay-rich, little compact to compact, dark gray with variations
26.00m to 28.00m - Rigid clay, reddish brown
28.00m to 34.00m - Fine to medium sand, clay-rich, little compact to compact, dark brown with variations
34.00m to 36.00m - Rigid to hard clay, reddish brown
36.00 to 41.00m - Fine to medium sand, clay-rich, moderately compact to compact, dark gray with variations
41.00 to 48.50m - Sample not recovered
48.50m to 50.00m - Extremely weathered rock, comprised of quartz, sericite and hematite. Rock name: PHYLLITE
TAILINGS
PHYLLITE
C4 REA D2 V E2
BOREHOLE DIAMETER
HQ - 3.8"
HW - 4"
COHESIVENESS
C1 - Cohesive stone
C2 - Moderately cohesive stone
C3 - Little cohesive stone
C4 - Non-cohesive stone
WEATHERING DEGREE
RS - Sound or near sound rock
RAD - Moderately weathered stone
RAM - Very weathered stone
REA - Extremely weathered stone
Filling
D1 - Lithological contact
D2 - Venulations and veins (calcite/silicon)
D3 - Walls with shallow weathering
D4 - Weathered walls
D5 - Weathered walls w/ filling
Roughness
Cut out
I – Rough
II – Smooth
III – Polished
Wave-shaped
IV – Rough
V – Smooth
VI – Polished
Flat
VII – Rough
VIII – Smooth
IX – Polished
Discontinuity (spacing - cm)
E1 - Very far (>200)
E2 - Far (60 to 200)
E3 - Moderately far (20 to 60)
E4 - Near (60 to 20)
E5 - Very near (<6)
Water level measurements
Date
Hole depth (m)
Water Level (m)
Coating Depth (m)
19/08/2014
60,50
15,85
60,50
Note: Borehole depth limited by client.
FUGRO
Customer
SAMARCO MINERAÇÃO S.A.
Project/Site:
VALE'S PIT - FUNDÃO DAM
GERMANO MINE, MARIANA-MG
COMBINED DRILLING
SP-07
Drilling place coordinates
E - 660894 m
N - 7764855 m
Elevation
862,35
Coordinator/person in charge
DANIELLA ARANHA
Drilled by
DANIELLE
Scale
1:100
Fugro No. on site
SMC-05-GRE-01
Execution date
Start: 14/08/2014 End: 19/08/2014

Borehole diameter	Water level 24 hours	Geological profile	Elevation (m)	Strikes / 30 cm Initial	Strikes / 30 cm Final	Material Description	Geological description	Cohesiveness	Weathering degree	Filling	Roughness	Discontinuity	RESISTANCE TO PENETRATION INDEX (N) 0 15 30 45 60 / RECOVERY (%) 100 75 50 25 0	Fractures by homogeneous portion (Fractures/m) 30 15 10 5 0	Rock Quality Degree RQD 25 50 75 100
	50		812			50.00 to 58.00m - Sample not recovered	PHYLLITE								
	51		811												
	52		810												
	53		809												
	54		808												
	55		807												
	56		806												
	57		805												
	58		804			58.00 to 60.50 - Rock consisting of Quartz, sericite and hematite, aluminum-silicon rich, with fine granulation and crenulation foliation. Rock name: PHYLLITE		C1	RS	D1	V	E4			
	59		803												
	60		802					C1	RS	D1	V	E4			
	61		801												
	62		800												
HQ	63		799												
	64		798												
	65		797												
	66		796												
	67		795												
	68		794												
	69		793												
	70		792												
	71		791												
	72		790												
	73		789												
	74		788												
	75														

BOREHOLE DIAMETER	
	NQ - 3"
	HQ - 3.8 "
	HW - 4"

COHESIVENESS	WEATHERING DEGREE
C1 - Cohesive stone	RS - Sound or near sound rock
C2 - Moderately cohesive stone	RAD - Moderately weathered stone
C3 - Little cohesive stone	RAM - Very weathered stone
C4 - Non-cohesive stone	REA - Extremely weathered stone

Filling	Roughness		Discontinuity (spacing - cm)
D1 - Lithological contact	Cut out	I – Rough II – Smooth III – Polished	E1 - Very far (>200)
D2 - Venulations and veins (calcite/silicon)			E2 - Far (60 to 200)
D3 - Walls with shallow weathering	Wave-shaped	IV – Rough V – Smooth VI – Polished	E3 - Moderately far (20 to 60)
D4 - Weathered walls	Flat	VII – Rough VIII – Smooth IX – Polished	E4 - Near (60 to 20)
D5 - Weathered walls w/ filling			E5 - Very near (<6)

Water level measurements

Date	Hole depth (m)	Water Level (m)	Coating Depth (m)
19/08/2014	60,50	15,85	60,50

Note: Borehole depth limited by client.

Customer: SAMARCO MINERAÇÃO S.A.
Project/Site: VALE'S PIT - FUNDÃO DAM, GERMANO MINE, MARIANA-MG
COMBINED DRILLING
SP-07
Drilling place coordinates: E - 660894 m, N - 7764855 m
Elevation: 862,36
Coordinator/person in charge: DANIELLA ARANHA
Drawn by: DANIELLE
Scale: 1:100
Fugro No. on site: SMC-05-SPE-01
Drill: 201057300-7/RJ
Execution date: Start: 18/08/2014 End: 19/08/2014

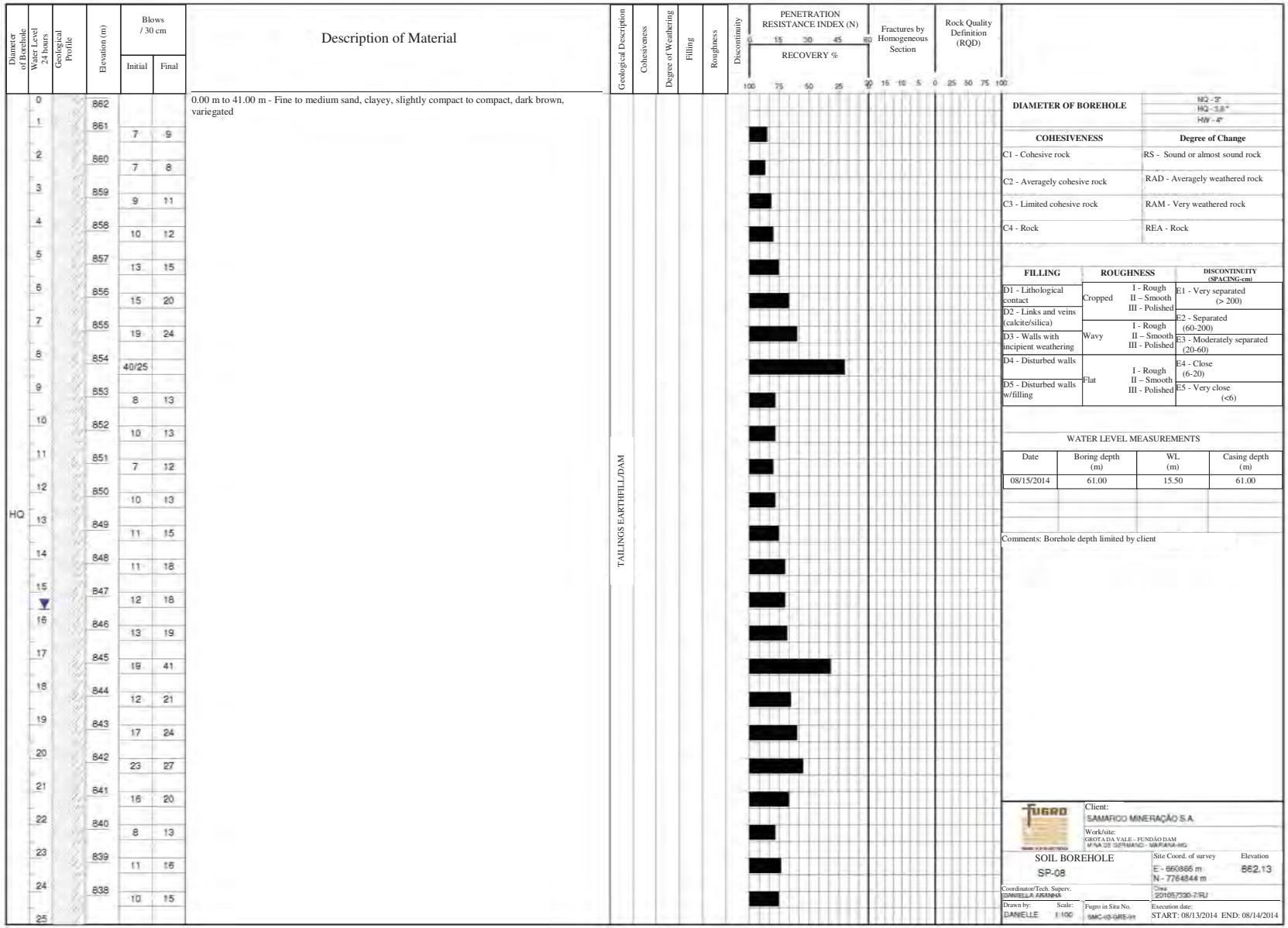
Diameter of Borehole
Water Level 24 hours
Geological Profile
Elevation (m)
Blows / 30 cm
Initial
Final
Description of Material
Geological Description
Cohesiveness
Degree of Weathering
Filling
Roughness
Discontinuity
PENETRATION RESISTANCE INDEX (N)
RECOVERY %
Fractures by Homogeneous Section
Rock Quality Definition (RQD)
0.00 m to 41.00 m - Fine to medium sand, clayey, slightly compact to compact, dark brown, variegated
TAILINGS EARTHFILL/DAM
HQ
DIAMETER OF BOREHOLE
NQ - 2"
HQ - 3.8"
HW - 4"
COHESIVENESS
Degree of Change
C1 - Cohesive rock
RS - Sound or almost sound rock
C2 - Averagely cohesive rock
RAD - Averagely weathered rock
C3 - Limited cohesive rock
RAM - Very weathered rock
C4 - Rock
REA - Rock
FILLING
ROUGHNESS
DISCONTINUITY (SPACING-cm)
D1 - Lithological contact
D2 - Links and veins (calcite/silica)
D3 - Walls with incipient weathering
D4 - Disturbed walls
D5 - Disturbed walls w/filling
Cropped
Wavy
Flat
I - Rough
II – Smooth
III - Polished
E1 - Very separated (> 200)
E2 - Separated (60-200)
E3 - Moderately separated (20-60)
E4 - Close (6-20)
E5 - Very close (<6)
WATER LEVEL MEASUREMENTS
Date
Boring depth (m)
WL (m)
Casing depth (m)
08/15/2014
61.00
15.50
61.00
Comments: Borehole depth limited by client
FUGRO
Client:
SAMARCO MINERAÇÃO S.A.
Work/site:
GROTA DA VALE - FUNDÃO DAM
MINA DE GERMANO - MARIANA-MG
SOIL BOREHOLE
SP-08
Site Coord. of survey
E - 660866 m
N - 7764844 m
Elevation
862,13
Coordinator/Tech. Superv.
DANIELLA ARANHA
Drawn by:
DANIELLE
Scale:
1:100
Fugro in Situ No.
SMC-05-GRE-01
Execution date:
START: 08/13/2014 END: 08/14/2014

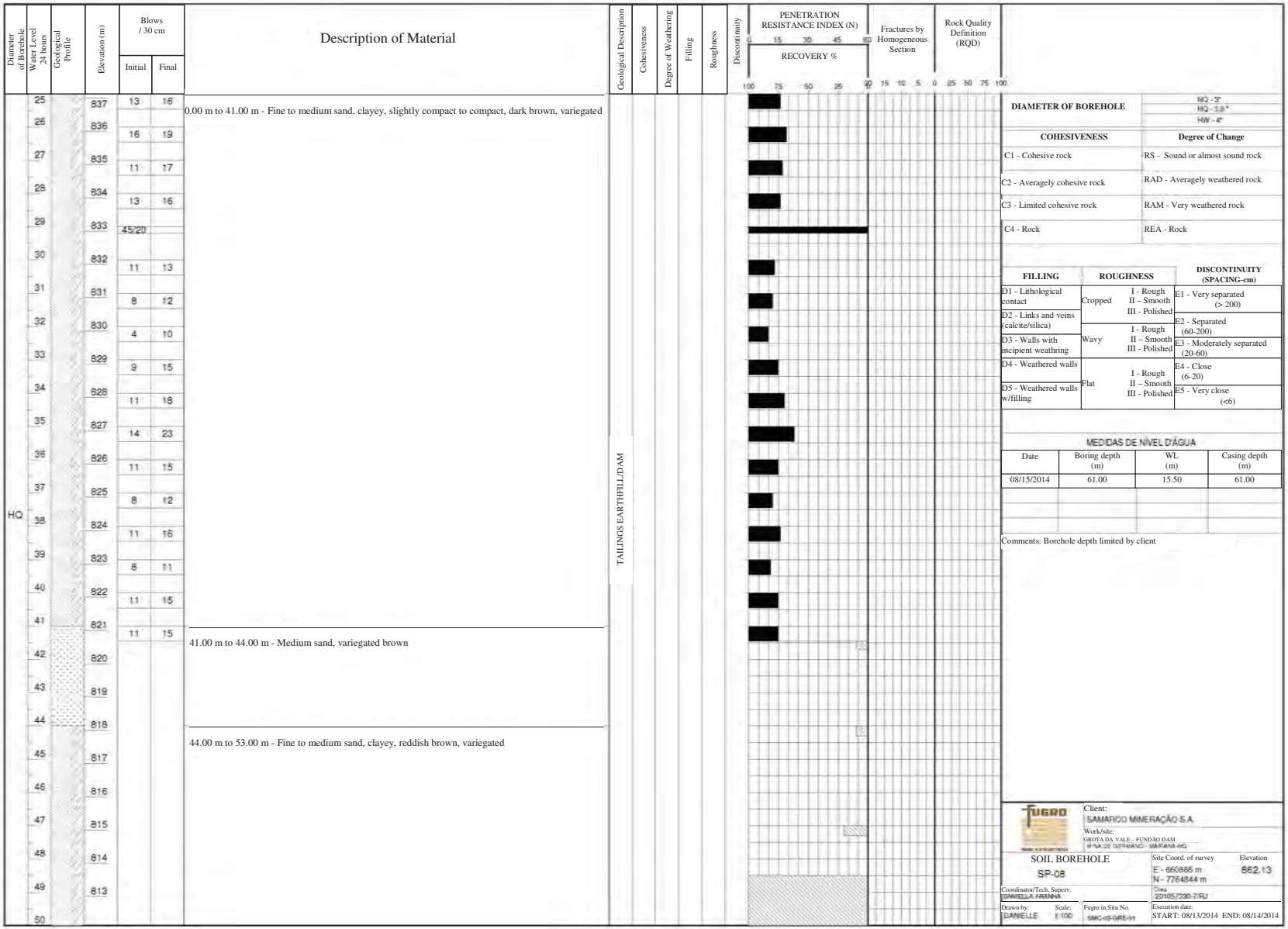
Diameter of Borehole
Water Level 24 hours
Geological Profile
Elevation (m)
Blows / 30 cm
Initial
Final
Description of Material
Geological Description
Cohesiveness
Degree of Weathering
Filling
Roughness
Discontinuity
PENETRATION RESISTANCE INDEX (N)
RECOVERY %
Fractures by Homogeneous Section
Rock Quality Definition (RQD)
HQ
0.00 m to 41.00 m - Fine to medium sand, clayey, slightly compact to compact, dark brown, variegated
41.00 m to 44.00 m - Medium sand, variegated brown
44.00 m to 53.00 m - Fine to medium sand, clayey, reddish brown, variegated
TAILINGS EARTHFILL/DAM
45/20
DIAMETER OF BOREHOLE
NQ - 3"
HQ - 3.8"
HW - 4"
COHESIVENESS
Degree of Change
C1 - Cohesive rock
RS - Sound or almost sound rock
C2 - Averagely cohesive rock
RAD - Averagely weathered rock
C3 - Limited cohesive rock
RAM - Very weathered rock
C4 - Rock
REA - Rock
FILLING
ROUGHNESS
DISCONTINUITY (SPACING-cm)
D1 - Lithological contact
D2 - Links and veins (calcite/silica)
D3 - Walls with incipient weathring
D4 - Weathered walls
D5 - Weathered walls w/filling
Cropped
Wavy
Flat
I - Rough
II – Smooth
III - Polished
E1 - Very separated (> 200)
E2 - Separated (60-200)
E3 - Moderately separated (20-60)
E4 - Close (6-20)
E5 - Very close (<6)
MEDIDAS DE NÍVEL D'ÁGUA
Date
Boring depth (m)
WL (m)
Casing depth (m)
08/15/2014
61.00
15.50
61.00
Comments: Borehole depth limited by client
FUGRO
Client:
SAMARCO MINERAÇÃO S.A.
Work/site:
SOIL BOREHOLE
SP-08
Site Coord. of survey
E - 660866 m
N - 7764844 m
Elevation
862,13
Coordinator/Tech. Superv.
DANIELLA ARANHA
Drawn by:
DANIELLE
Scale:
1:100
Fugro in Situ No.
Execution date:
START: 08/13/2014 END: 08/14/2014

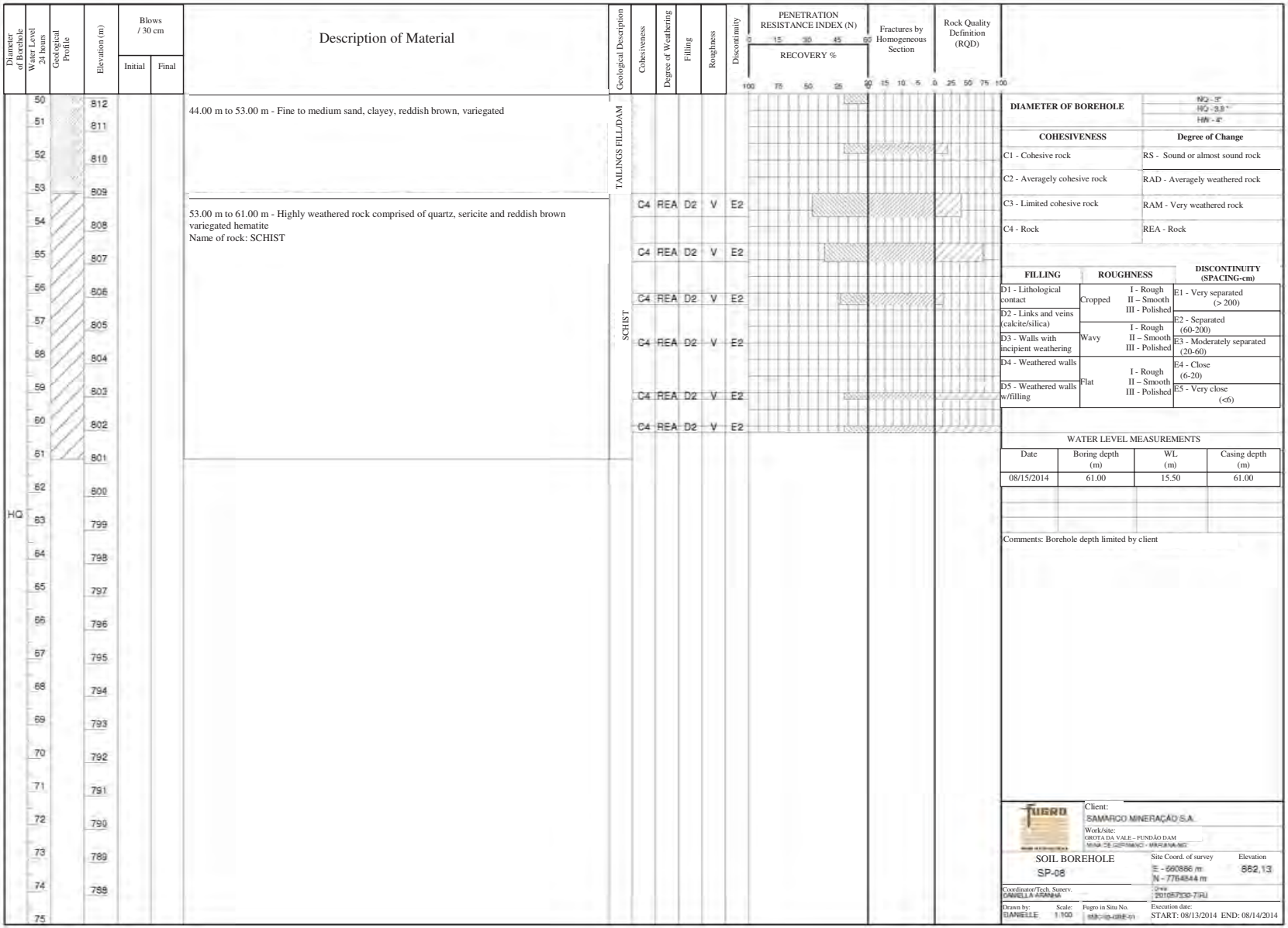
Diameter of Borehole
Water Level 24 hours
Geological Profile
Elevation (m)
Blows / 30 cm
Initial
Final
Description of Material
Geological Description
Cohesiveness
Degree of Weathering
Filling
Roughness
Discontinuity
PENETRATION RESISTANCE INDEX (N)
RECOVERY %
Fractures by Homogeneous Section
Rock Quality Definition (RQD)
HQ
50 51 52 53 54 55 56 57 58 59 60 61 62 63 64 65 66 67 68 69 70 71 72 73 74 75
812 811 810 809 808 807 806 805 804 803 802 801 800 799 798 797 796 795 794 793 792 791 790 789 788
44.00 m to 53.00 m - Fine to medium sand, clayey, reddish brown, variegated
TAILINGS FILL/DAM
53.00 m to 61.00 m - Highly weathered rock comprised of quartz, sericite and reddish brown variegated hematite
Name of rock: SCHIST
SCHIST
C4 REA D2 V E2
DIAMETER OF BOREHOLE
NQ - 3"
HQ - 3.8"
HW - 4"
COHESIVENESS
Degree of Change
C1 - Cohesive rock
RS - Sound or almost sound rock
C2 - Averagely cohesive rock
RAD - Averagely weathered rock
C3 - Limited cohesive rock
RAM - Very weathered rock
C4 - Rock
REA - Rock
FILLING
ROUGHNESS
DISCONTINUITY (SPACING-cm)
D1 - Lithological contact
D2 - Links and veins (calcite/silica)
D3 - Walls with incipient weathering
D4 - Weathered walls
D5 - Weathered walls w/filling
Cropped
Wavy
Flat
I - Rough
II – Smooth
III - Polished
E1 - Very separated (> 200)
E2 - Separated (60-200)
E3 - Moderately separated (20-60)
E4 - Close (6-20)
E5 - Very close (<6)
WATER LEVEL MEASUREMENTS
Date
Boring depth (m)
WL (m)
Casing depth (m)
08/15/2014
61.00
15.50
61.00
Comments: Borehole depth limited by client
TUGRO
Client:
SAMARCO MINERAÇÃO S.A.
Work/site:
GROTA DA VALE - FUNDÃO DAM
SOIL BOREHOLE
SP-08
Site Coord. of survey
E - 660886 m
N - 7764844 m
Elevation
862,13
Coordinator/Tech. Surserv.
DANIELLA ARANHA
Drawn by:
DANIELLE
Scale:
1:100
Fugro in Situ No.
Execution date:
START: 08/13/2014 END: 08/14/2014

June 2014 – May 2015
Fugro
Dike 1
(Section C2.2.5)

Figure C.C1-5 – Fugro (June 2014) Test Location Plan

SPT Log 16PI007
SPT Log 16PI008
SPT Log 16PI009
SPT Log 16PI010
SPT Log 16PI011
SPT Log 16PI012
SPT Log 16PI013
SPT Log 16PI014
SPT Log 16PI016
SPT Log 16LI014
SPT Log 16LI015
SPT Log 16LI016
SPT Log 16LI017
SPT Log 16LI018

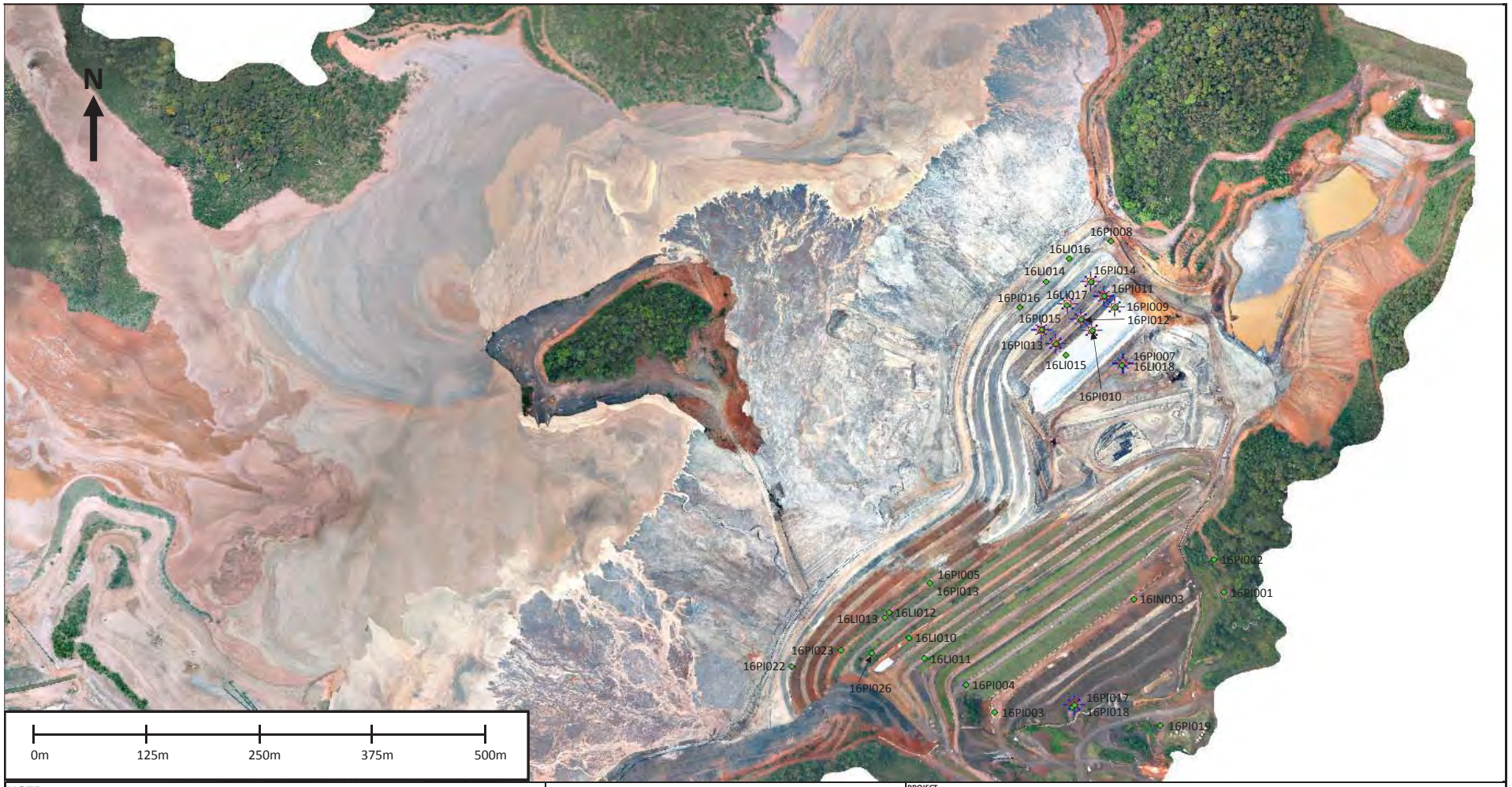

NOTE:

1. November 27, 2014 Samarco aerial image shown.
2. Only SPT logs for 16PI007, 16PI008, 16PI009, 16PI010, 16PI011, 16PI012, 16PI013, 16PI014, 16PI016, 16LI014, 16LI015, 16LI016, 16LI017, and 16LI018 are presented.

LEGEND:

- Standard Penetration Test (SPT)
- Permeability Test

PROJECT

Fundão Tailings Dam Review Panel

TITLE

Fugro (June 2014 - May 2015)
Test Location Plan

FIGURE NO.

C.C1-5

Survey Diameter	Water level 24 hours	Geological Profile	Elevation (m)	Blows /30cm Initial	Blows /30cm Final	Description of Material	Geological Description	Coherence	Degree of Alteration	Filling	Roughness	Discontinuity	RESISTANCE TO PENETRATION INDEX (N) 0 15 30 45 60 / RECOVERY (%) 100 75 50 25 0	Fractures by Homogeneous Section (fractures/m) 0 15 10 5 0	Rock quality index RQD 0 25 50 75 100
	0					0.00 m to 6.50 m - Medium clayey sand, dark brown to variegated									
	1		862												
	2		861												
	3		860												
	4		859												
	5		858												
	6		857												
	7		856			6.50 m to 11.00 m - Clay, somewhat compacted, with appearance of mining tailings, brown to variegated.									
	8		855												
	9		854												
	10		853												
	11		852												
	12		851			11.00 m to 12.50 m - , Medium clayey sand dark brown to variegated.	Tailings landfill/Dam								
HQ	13		850			12.50 m to 14.00 m - Clay, somewhat compacted, with appearance of mining tailings, brown to variegated.									
	14		849												
	15		848			14.00 m to 17.00 m - , Medium clayey sand dark brown to variegated.									
	16		847												
	17		846												
	18		845			17.00 m to 21.50 m - Clay, somewhat compacted, with appearance of mining tailings, brown to variegated.									
	19		844												
	20		843												
	21		842												
	22		841			21.50 m to 23.00 m - Medium clayey sand,dark brown to variegated.									
	23		840												
	24		839			23.00 m to 26.00 m - Clay, somewhat compacted, with appearance of mining tailings, brown to variegated.									
	25		838												

SURVEY DIAMETER

NQ - 3"
HQ - 3,8 "
HW - 4"

COHERENCE	DEGREE OF ALTERATION
C1 – Coherent rock	RS – Sound or nearly sound rock
C2 – Average coherence rock	RAD – Somewhat altered rock
C3 – Somewhat uncoherent rock	RAM – Very altered rock
C4 – Uncoherent rock	REA – Extremely altered rock

FILLING	ROUGHNESS		DISCONTINUITY (SPACING-cm)
D1 – Lithological contract	Cropped	I – Rough II – Smooth III - Polished	E1 – Very distant (> 200)
D2 – Venations and veins (calcite/silica)	undulated	IV – Rough V – Smooth VI - Polished	E2 – Distant (60 to 200)
D3 –Walls with incipient alteration	Flat	VII – Rough VIII – Smooth IX - Polished	E3 – Moderately distant (20 to 60)
D4 – Walls altered			E4 – Near (6 to 20)
D5 – Walls altered with filling			E5 – Very near (<6)

WATER LEVEL MEASUREMENTS

Date	Depth of hole (m)	W.L. (m)	Depth lining (m)
02/09/2014	50,00	13,20	50,00

Comments: CLIENT'S REQUEST TO CARRY OUT SP TEST ON SOIL STRECHES WAS NOT CARRIED OUT.
Depth of survey limited to the client.

Customer: SAMARCO MINERAÇÃO S.A.
Work/Site: FUNDÃO DAM
GERMANO MINE - MARIANA - MG

MIXED SURVEY
16PI007

Survey site coord.
E - 660855 m
N - 7764903 m

Elevation 862,86

Coordinator/Manager Technician: DANIELLE ARANHA

Crea: 2610575330-7/RJ

Reported by: DANIELLE

Scale: 1:100

Nº Page in SIG: SMC-03-GRE-01

Date conducted:
START: 28/08/2014 END: 01/09/2014

Survey Diameter	Water level 24 hours	Geological Profile	Elevation (m)	Blows /30cm Initial	Blows /30cm Final	Description of Material	Geological Description	Coherence	Degree of Alteration	Filling	Roughness	Discontinuity
	25–26		837			23.00 m to 26.00 m - Clay, somewhat compacted, with appearance of mining tailings, brown to variegated.	Tailings landfill/Dam					
	27		836			26.00 m to 27.50 m - Clayey silt, yellowish-brown	Tailings landfill/Dam					
	28–29		835, 834			27.50 m to 29.00 m - Clay, somewhat compacted, with appearance of mining tailings, brown to variegated.	Tailings landfill/Dam					
	30		833			29.00 m to 30.50 m - Clayey silt, dark brown to variegated.	Tailings landfill/Dam					
	31–35		832, 831, 830, 829, 828			30.50 m to 35.00 m - Clay, somewhat compacted, with appearance of mining tailings, brown to variegated.	Tailings landfill/Dam					
HQ	36–47		827, 826, 825, 824, 823, 822, 821, 820, 819, 818, 817, 816			35.00 m to 47.00 m - Altered rock composed of hematite lenses and acrylic lenses with quartz. Name of rock: SCHIST	XISTO	C3	RAM	D2	V	E4
								C3	RAM	D2	V	E4
								C3	RAM	D2	V	E4
								C3	RAM	D2	V	E4
								C3	RAM	D2	V	E4
								C3	RAM	D2	V	E4
								C3	RAM	D2	V	E4
								C3	RAM	D2	V	E4
	48–50		815, 814, 813			47.00 m to 50.00 m - Altered rock part composed of hematite lenses and acrylic lenses. Name of rock: SCHIST	XISTO	C2	RAD	D2	V	E3
								C2	RAD	D2	V	E3

RESISTANCE TO PENETRATION INDEX (N) 0 15 30 45 60 / RECOVERY (%) 100 75 50 25 0 — Fractures by Homogeneous Section (fractures/m) 20 15 10 5 0 — Rock quality index RQD 0 25 50 75 100

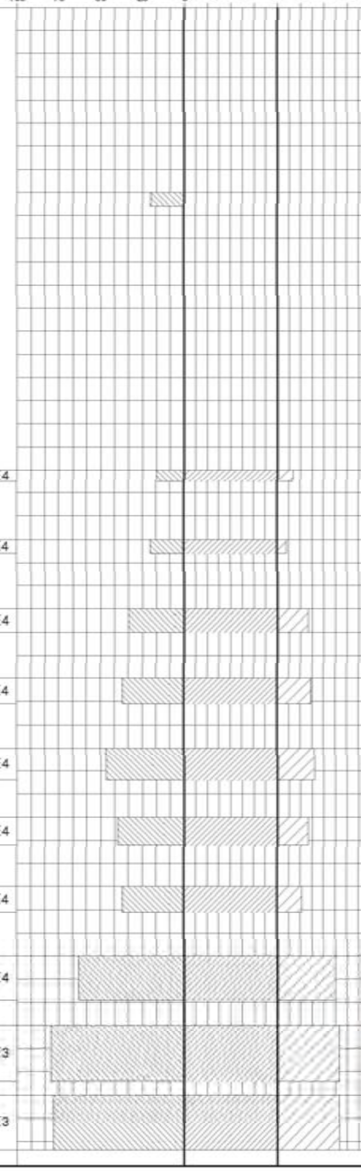

SURVEY DIAMETER	NQ - 3" HQ - 3,8" HW - 4"

COHERENCE	DEGREE OF ALTERATION
C1 – Coherent rock	RS – Sound or nearly sound rock
C2 – Average coherence rock	RAD – Somewhat altered rock
C3 – Somewhat uncoherent rock	RAM – Very altered rock
C4 – Uncoherent rock	REA – Extremely altered rock

FILLING	ROUGHNESS		DISCONTINUITY (SPACING-cm)
D1 – Lithological contract	Cropped	I – Rough II – Smooth III - Polished	E1 – Very distant (> 200)
D2 – Venations and veins (calcite/silica)			E2 – Distant (60 to 200)
D3 –Walls with incipient alteration	Wavy	IV – Rough V – Smooth VI - Polished	E3 – Moderately distant (20 to 60)
D4 –Altered walls	Flat	VII – Rough VIII – Smooth IX - Polished	E4 – Near (6 to 20)
D5 – Walls altered with filling			E5 – Very near (<6)

WATER LEVEL MEASUREMENTS			
Date	Depth of hole (m)	W.L. (m)	Depth lining (m)
02/09/2014	50,00	13,20	50,00

Comments: CLIENT REQUESTED NOT TO CARRY OUT SP TEST ON SOIL STRECHES
Depth of drilling survey limited by the client.

FUGRO	Customer: SAMARCO MINERAÇÃO S.A.	
	Work/Site: FUNDÃO DAM GERMANO MINE - MARIANA - MG	
MIXED SURVEY 16PI007	Survey site coord. E - 660855 m N - 7764903 m	Elevation 862,86
Coordinator/Manager Technician DANIELLE ARANHA	OS 201057330-7/RJ	
Reported by: DANIELLE Scale 1:100	Nº Fugro In Situ SMC-03-GRE-01	Date conducted: START: 28/08/2014 END: 01/09/2014

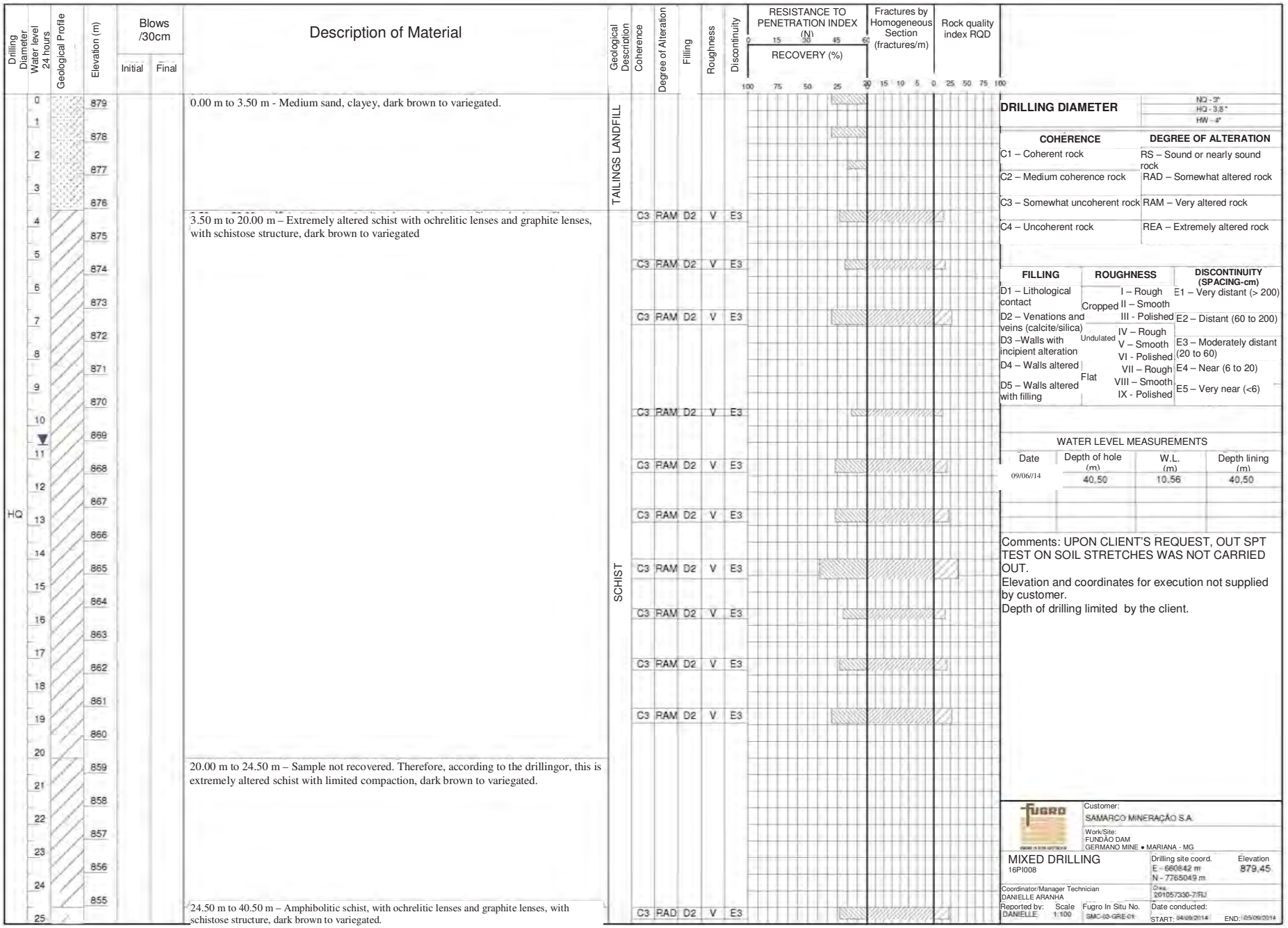
Drilling Diameter
Water level 24 hours
Geological Profile
Elevation (m)
Blows /30cm
Initial
Final
Description of Material
Geological Description
Coherence
Degree of Alteration
Filling
Roughness
Discontinuity
RESISTANCE TO PENETRATION INDEX (N)
RECOVERY (%)
Fractures by Homogeneous Section (fractures/m)
Rock quality index RQD
HQ
0.00 m to 3.50 m - Medium sand, clayey, dark brown to variegated.
TAILINGS LANDFILL
3.50 m to 20.00 m – Extremely altered schist with ochrelitic lenses and graphite lenses, with schistose structure, dark brown to variegated
C3 RAM D2 V E3
SCHIST
20.00 m to 24.50 m – Sample not recovered. Therefore, according to the drillingor, this is extremely altered schist with limited compaction, dark brown to variegated.
24.50 m to 40.50 m – Amphibolitic schist, with ochrelitic lenses and graphite lenses, with schistose structure, dark brown to variegated.
C3 RAD D2 V E3
DRILLING DIAMETER
NQ - 3"
HQ - 3,8"
HW – 4"
COHERENCE
C1 – Coherent rock
C2 – Medium coherence rock
C3 – Somewhat uncoherent rock
C4 – Uncoherent rock
DEGREE OF ALTERATION
RS – Sound or nearly sound rock
RAD – Somewhat altered rock
RAM – Very altered rock
REA – Extremely altered rock
FILLING
D1 – Lithological contact
D2 – Venations and veins (calcite/silica)
D3 –Walls with incipient alteration
D4 – Walls altered
D5 – Walls altered with filling
ROUGHNESS
Cropped
I – Rough
II – Smooth
III - Polished
Undulated
IV – Rough
V – Smooth
VI - Polished
Flat
VII – Rough
VIII – Smooth
IX - Polished
DISCONTINUITY (SPACING-cm)
E1 – Very distant (> 200)
E2 – Distant (60 to 200)
E3 – Moderately distant (20 to 60)
E4 – Near (6 to 20)
E5 – Very near (<6)
WATER LEVEL MEASUREMENTS
Date
Depth of hole (m)
W.L. (m)
Depth lining (m)
09/06//14
40,50
10,56
40,50
Comments: UPON CLIENT'S REQUEST, OUT SPT TEST ON SOIL STRETCHES WAS NOT CARRIED OUT.
Elevation and coordinates for execution not supplied by customer.
Depth of drilling limited by the client.
FUGRO
Customer:
SAMARCO MINERAÇÃO S.A.
Work/Site:
FUNDÃO DAM
GERMANO MINE • MARIANA - MG
MIXED DRILLING
16PI008
Drilling site coord.
E - 660842 m
N - 7765049 m
Elevation
879,45
Coordinator/Manager Technician
DANIELLE ARANHA
Ordem
201057330-7/RJ
Reported by:
DANIELLE
Scale
1:100
Fugro In Situ No.
SMC-03-GRE-01
Date conducted:
START: 04/09/2014
END: 05/09/2014

Drilling Diameter / Water level 24 hours / Geological Profile	Elevation (m)	Blows /30cm Initial	Blows /30cm Final	Description of Material	Geological Description	Coherence	Degree of Alteration	Filling	Roughness	Discontinuity	RESISTANCE TO PENETRATION INDEX (N) 0 15 30 45 60 / RECOVERY (%) 100 75 50 25	Fractures by Homogeneous Section (fractures/m) 30 15 10 5 0	Rock quality index RQD 0 25 50 75 100
HQ	25 854			24.50 m to 40.50 m – Amphibolitic schist, with ocrelitic lenses and graphite lenses, with schistose structure, dark brown to variegated.	SCHIST	C3	RAD	D2	V	E3			
	26												
	853												
	27												
	852					C3	RAD	D2	V	E3			
	28												
	851												
	29												
	850					C3	RAD	D2	V	E3			
	30												
	849												
	31					C3	RAD	D2	V	E3			
	848												
	32												
	847					C3	RAD	D2	V	E3			
	33												
	846												
	34					C3	RAD	D2	V	E3			
	845												
	35												
	844					C3	RAD	D2	V	E3			
	36												
	843												
	37					C3	RAD	D2	V	E4			
	842												
	38												
	841					C3	RAD	D2	V	E4			
	39												
	840												
	40					C3	RAD	D2	V	E4			
	839												
	41												
	838												
	42												
	837												
	43												
	836												
	44												
	835												
	45												
	834												
	46												
	833												
	47												
	832												
	48												
	831												
	49												
	830												
	50												

DRILLING DIAMETER

NQ - 3"
HQ - 3,8 "
HW - 4"

COHERENCE	DEGREE OF ALTERATION
C1 – Coherent rock	RS – Sound or nearly sound rock
C2 – Medium coherence rock	RAD – Somewhat altered rock
C3 – Somewhat uncoherent rock	RAM – Very altered rock
C4 – Uncoherent rock	REA – Extremely altered rock

FILLING	ROUGHNESS		DISCONTINUITY (SPACING-cm)
D1 – Lithological contact	Cropped	I – Rough II – Smooth	E1 – Very distant (> 200)
D2 – Venations and veins (calcite/silica)		III - Polished	E2 – Distant (60 to 200)
D3 –Walls with incipient alteration	Undulated	IV – Rough V – Smooth VI - Polished	E3 – Moderately distant (20 to 60)
D4 – Walls altered	Flat	VII – Rough VIII – Smooth IX - Polished	E4 – Near (6 to 20)
D5 – Walls altered with filling			E5 – Very near (<6)

WATER LEVEL MEASUREMENTS

Date	Depth of hole (m)	W.L. (m)	Depth lining (m)
09/06//14	40,50	10.56	40,50

Comments: UPON CLIENT'S REQUEST, OUT SPT TEST ON SOIL STRETCHES WAS NOT CARRIED OUT.
Elevation and coordinates for execution not supplied by customer.
Depth of drilling limited by the client.

FUGRO

Customer:
SAMARCO MINERAÇÃO S.A.

Work/Site:
FUNDÃO DAM
GERMANO MINE • MARIANA - MG

MIXED DRILLING
16PI008

Drilling site coord.
E - 660842 m
N - 7765049 m

Elevation
879,45

Coordinator/Manager Technician
DANIELLE ARANHA

Ordem
201057330-7/RJ

Reported by: DANIELLE
Scale 1:100
Fugro In Situ No. SMC-09-GRE-01
Date conducted: START: 04/06/2014 END: 05/06/2014

Drilling Diameter	Water level 24 hours	Geological Profile	Elevation (m)	Blows /30cm Initial	Blows /30cm Final	Description of Material	Geological Description	Coherence	Degree of Alteration	Filling	Roughness	Discontinuity	RESISTANCE TO PENETRATION INDEX (N) 0 15 30 45 60 / RECOVERY (%)	Fractures by Homogeneous Section (fractures/m)	Rock quality index RQD
	0		866			0.00 m to 5.00 m - Fine to medium sand, little clay, somewhat compacted to compacted, grayish brown.	TAILINGS LANDFILL/DAM								
	1		865	13	22										
	2		864	19	31										
	3		863	12	16										
	4		862	9	12										
	5		861	5	13	5.00 m to 5.45 m - Coarse sand, somewhat compacted, reddish brown.									
	6		860	7	11	5.45 m to 10.50 m - Fine to average sand, little clay, slightly compacted to compacted, grayish brown.									
	7		859	4	8										
	8		858	3	7										
	9		857	12	19										
	10		856												
	11		855												
	12		854												
	13		853												
	14		852												
	15		851												
	16		850												
	17		849												
	18		848												
	19		847												
	20		846												
	21		845												
	22		844												
	23		843												
	24		842												
	25														

DRILLING DIAMETER	NQ - 3" HQ - 3,8" HW - 4"
COHERENCE	**DEGREE OF ALTERATION**
C1 – Coherent rock	RS – Sound or nearly sound rock
C2 – Medium coherence rock	RAD – Somewhat altered rock
C3 – Somewhat uncohering rock	REA – Extremely altered rock
C4 – Uncohering rock	REA – Extremely altered rock

FILLING	ROUGHNESS		DISCONTINUITY (SPACING-cm)
D1 – Lithological contact	Cropped	I – Rough II – Smooth III - Polished	E1 – Very distant (> 200)
D2 – Venations and veins (calcite/silica)			E2 – Distant (60 to 200)
D3 –Walls with incipient alteration	Undulated	IV – Rough V – Smooth VI - Polished	E3 – Moderately distant (20 to 60)
D4 – Walls altered	Flat	VII – Rough VIII – Smooth IX - Polished	E4 – Near (6 to 20)
D5 – Walls altered with filling			E5 – Very near (≤6)

WATER LEVEL MEASUREMENTS

Date	Depth of hole (m)	W.L. (m)	Depth lining (m)
09/18/14	10,50	5,26	10,50

Comments: Depth of drilling limited by customer

Customer: SAMARCO MINERAÇÃO S.A.
Work/Site: FUNDÃO DAM
GERMANO MINE ; MARIANA - MG

MIXED DRILLING
16PI009
Drilling site coord. E - 660847 m N - 7764971 m
Elevation 866,05
Coordinator/Manager Technician: DANIELLE ARANHA
Crea 2010573307/BJ
Reported by: DANIELLE
Scale 1:100
Fugro In Situ No. SMC-03-GRE-01
Date conducted: START: 7/09/2014 END: 17/09/2014

Drilling Diameter	Water level 24 hours	Geological Profile	Elevation (m)	Blows /30cm Initial	Blows /30cm Final	Description of Material	Geological Description	Coherence	Degree of Alteration	Filling	Roughness	Discontinuity	RESISTANCE TO PENETRATION INDEX (N) 0 15 30 45 60 / RECOVERY (%)	Fractures by Homogeneous Section (fractures/m)	Rock quality index RQD
	0		865			0.00 m to 10.45 m – Fine to medium sand, clayey, little compacted to compacted, greyish brown	TAILINGS LANDFILL/DAM								
	1		864	17	25										
	2		863	18	26										
	3 ▼		862	8	19										
	4		861	11	14										
	5		860	24	43										
	6		859	40/23	20/8										
	7		858	37	29/16										
	8		857	32	32/19										
	9		856	8	12										
	10		855	5	7										
	11		854												
	12		853												
	13		852												
	14		851												
	15		850												
	16		849												
	17		848												
	18		847												
	19		846												
	20		845												
	21		844												
	22		843												
	23		842												
	24		841												
	25														

DRILLING DIAMETER

NQ - 3"
HQ - 3,8"
HW - 4"

COHERENCE	DEGREE OF ALTERATION
C1 – Coherent rock	RS – Sound or nearly sound rock
C2 – Medium coherence rock	RAD – Somewhat altered rock
C3 – Somewhat uncoherent rock	RAM – Very altered rock
C4 – Uncoherent rock	REA – Extremely altered rock

FILLING	ROUGHNESS		DISCONTINUITY (SPACING-cm)
D1 – Lithological contact	Cropped	I – Rough II – Smooth III - Polished	E1 – Very distant (> 200)
D2 – Venations and veins (calcite/silica)			E2 – Distant (60 to 200)
D3 –Walls with incipient alteration	Undulated	IV – Rough V – Smooth VI - Polished	E3 – Moderately distant (20 to 60)
D5 – Walls altered with filling	Flat	VII – Rough VIII – Smooth IX - Polished	E4 – Near (6 to 20)
D4 – Walls altered			E5 – Very near (<6)

WATER LEVEL MEASUREMENTS

Date	Depth of hole (m)	W.L. (m)	Depth lining (m)
9/18/14	10,00	3,20	10,00

Comments: Depth of survey limited by the client.

FUGRO

Customer:
SAMARCO MINERAÇÃO S.A.
Work/Site:
FUNDÃO DAM
GERMANO MINE ● MARIANA - MG

MIXED DRILLING
16PI010

Survey site coord.
E - 660821 m
N - 7764949 m

Elevation
865,19

Coordinator/Manager Technician
DANIELLA ARANHA

Ordem
201057330-7/RJ

Reported by:
DANIELLE

Scale
1:100

Fugro In Situ No.:
SMC-03-GRE-01

Date conducted:
START: 15/09/2014 END: 17/09/2014

FUGRO IN SITU GEOTECNIA

PERCUSSION SURVEY

SMC-03-GRE-01
ATTACHMENTS

CUSTOMER: SAMARCO MINERAÇÃO S.A.

WORK: FUNDÃO DAM

SITE: GERMANO MINE - MARIANA-MG

SCALE: 1:100 START: 18/09/2014 END: 18/09/2014 MANAGER: DANIELLA ARANHA CREA: 201057330-7/RJ

SURVEY: 16PI011 ELEVATION: 869,98 COORDINATES: E 660834,47 N 7764984,40

WATER LEVEL 24 h	SAMPLE	ELEVATION: (m)	/ 30 cm INITIAL	/ 30 cm FINAL	RESISTANCE TO PENETRATION INDEX (N) 0 10 20 30 40 50 60	MATERIAL CLASSIFICATION	GEOLOGICAL DESCRIPTION
0						0.00 m to 12.50 m - Fine loamy sand, somewhat compacted to very compacted, dark brown to variegated.	LANDFILL WASTE/DAM
1		869	14	19			
2		868	18	23			
3		867	24	28			
4		866	22	29			
5		865	37	28/19			
6 ▼		864	20	34/26			
7		863	15	23			
8		862	18	26			
9		861	12	18			
10		860	12	16			
11		859	10	13			
12		858	12	17			
13		857					
14		856					
15		855					
16		854					
17		853					
18		852					
19		851					
20		850					

READING INTERVAL W.L. (m)
1: 24 h -5,80
2:
3:

METHOD OF ADVANCEMENT (m)
T. SPADE: -
WASH: 0.00 - 12.50
LINER: -
USE OF BENTONITE: -
WATER LEAK: -

TIME FOR WASHING – 10 min
STARTING DEPTH (m):
PHASE 1 (cm):
PHASE 2 (cm):
PHASE 3 (cm):

COMMENTS: Depth of trial determined by customer.

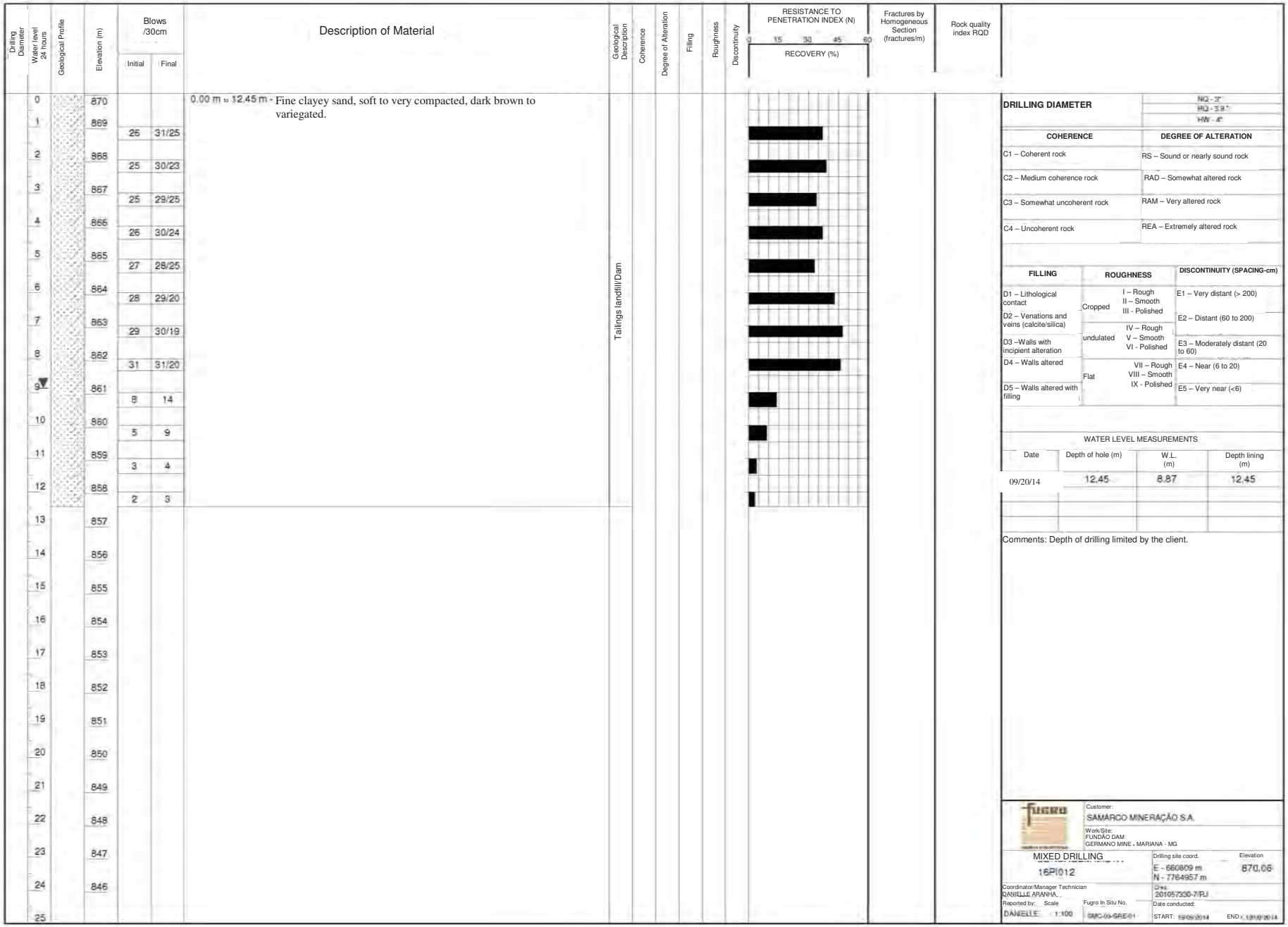
Drilling Diameter
Water level 24 hours
Geological Profile
Elevation (m)
Blows /30cm
Initial
Final
Description of Material
Geological Description
Coherence
Degree of Alteration
Filling
Roughness
Discontinuity
RESISTANCE TO PENETRATION INDEX (N)
0 15 30 45 60
RECOVERY (%)
Fractures by Homogeneous Section (fractures/m)
Rock quality index RQD
0.00 m to 12.45 m - Fine clayey sand, soft to very compacted, dark brown to variegated.
Tailings landfill/Dam
870 869 868 867 866 865 864 863 862 861 860 859 858 857 856 855 854 853 852 851 850 849 848 847 846
25 31/25
25 30/23
25 29/25
26 30/24
27 28/25
28 29/20
29 30/19
31 31/20
8 14
5 9
3 4
2 3
DRILLING DIAMETER
NQ - 3"
HQ - 3.8"
HW - 4"
COHERENCE
C1 – Coherent rock
C2 – Medium coherence rock
C3 – Somewhat uncoherent rock
C4 – Uncoherent rock
DEGREE OF ALTERATION
RS – Sound or nearly sound rock
RAD – Somewhat altered rock
RAM – Very altered rock
REA – Extremely altered rock
FILLING
D1 – Lithological contact
D2 – Venations and veins (calcite/silica)
D3 –Walls with incipient alteration
D4 – Walls altered
D5 – Walls altered with filling
ROUGHNESS
Cropped
I – Rough
II – Smooth
III - Polished
undulated
IV – Rough
V – Smooth
VI - Polished
Flat
VII – Rough
VIII – Smooth
IX - Polished
DISCONTINUITY (SPACING-cm)
E1 – Very distant (> 200)
E2 – Distant (60 to 200)
E3 – Moderately distant (20 to 60)
E4 – Near (6 to 20)
E5 – Very near (<6)
WATER LEVEL MEASUREMENTS
Date
Depth of hole (m)
W.L. (m)
Depth lining (m)
09/20/14
12.45
8.87
12.45
Comments: Depth of drilling limited by the client.
Customer:
SAMARCO MINERAÇÃO S.A.
Work/Site:
FUNDÃO DAM
GERMANO MINE - MARIANA - MG
MIXED DRILLING
16PI012
Drilling site coord.
E - 660809 m
N - 7764957 m
Elevation
870,06
Coordinator/Manager Technician
DANIELLE ARANHA
Ord.
201057330-7/PJ
Reported by:
DANIELLE
Scale
1:100
Fugro In Situ No.
SMC-09-SRE-01
Date conducted:
START: 19/09/2014
END: 19/09/2014

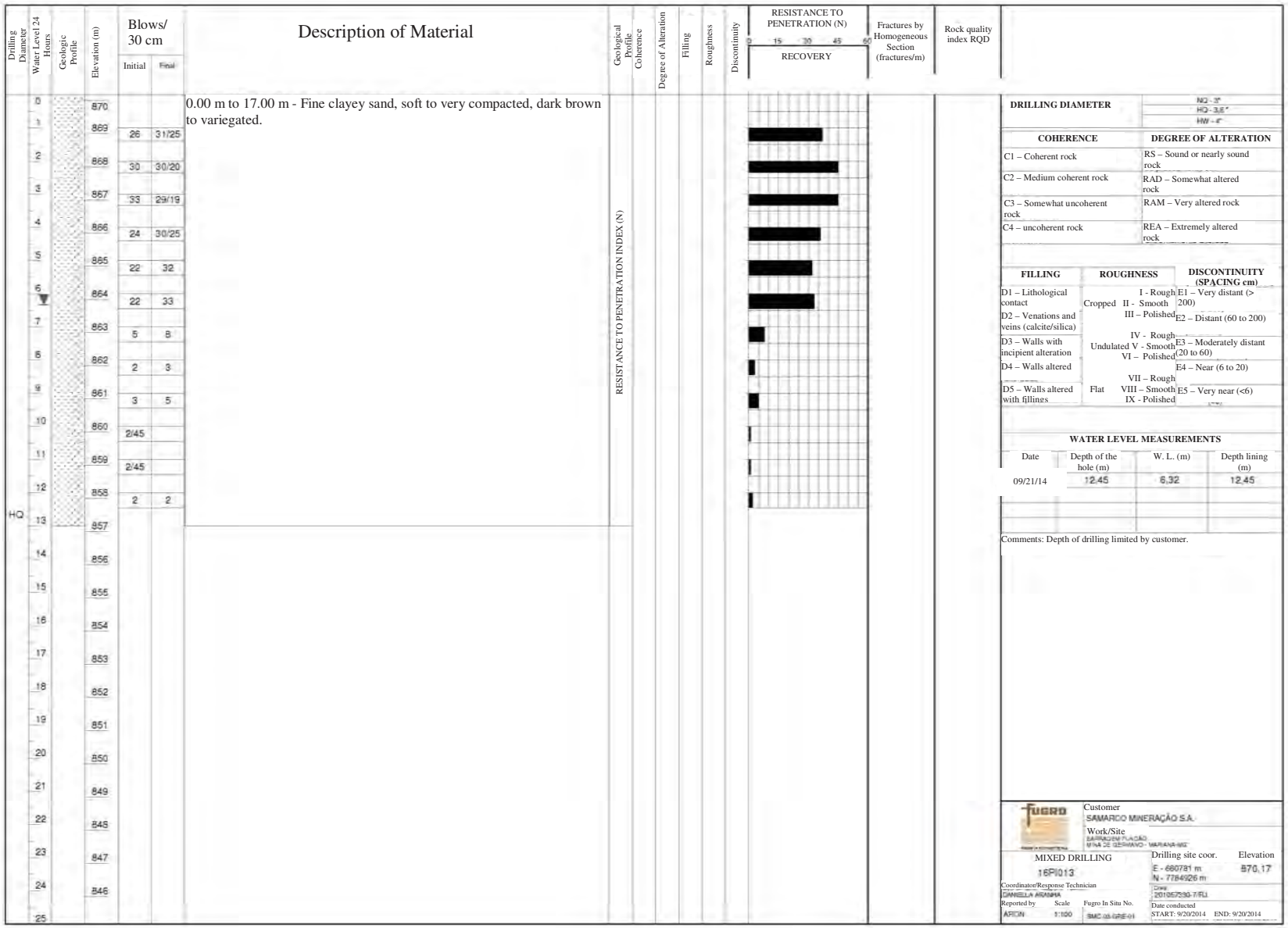
Drilling Diameter
Water Level 24 Hours
Geologic Profile
Elevation (m)
Blows/ 30 cm
Initial
Final
Description of Material
Geological Profile Coherence
Degree of Alteration
Filling
Roughness
Discontinuity
RESISTANCE TO PENETRATION (N)
0 15 30 45 60
RECOVERY
Fractures by Homogeneous Section (fractures/m)
Rock quality index RQD
0.00 m to 17.00 m - Fine clayey sand, soft to very compacted, dark brown to variegated.
RESISTANCE TO PENETRATION INDEX (N)
HQ
870
869
868
867
866
865
864
863
862
861
860
859
858
857
856
855
854
853
852
851
850
849
848
847
846
26 31/25
30 30/20
33 29/19
24 30/25
22 32
22 33
5 8
2 3
3 5
2/45
2/45
2 2
DRILLING DIAMETER
NQ - 3"
HQ - 3,8"
HW - 4"
COHERENCE
DEGREE OF ALTERATION
C1 – Coherent rock
RS – Sound or nearly sound rock
C2 – Medium coherent rock
RAD – Somewhat altered rock
C3 – Somewhat uncoherent rock
RAM – Very altered rock
C4 – uncoherent rock
REA – Extremely altered rock
FILLING
ROUGHNESS
DISCONTINUITY (SPACING cm)
D1 – Lithological contact
D2 – Venations and veins (calcite/silica)
D3 – Walls with incipient alteration
D4 – Walls altered
D5 – Walls altered with fillings
Cropped
Undulated
Flat
I - Rough
II - Smooth
III – Polished
IV - Rough
V - Smooth
VI – Polished
VII – Rough
VIII – Smooth
IX - Polished
E1 – Very distant (> 200)
E2 – Distant (60 to 200)
E3 – Moderately distant (20 to 60)
E4 – Near (6 to 20)
E5 – Very near (<6)
WATER LEVEL MEASUREMENTS
Date
Depth of the hole (m)
W. L. (m)
Depth lining (m)
09/21/14
12,45
6,32
12,45
Comments: Depth of drilling limited by customer.
FUGRO
Customer
SAMARCO MINERAÇÃO S.A.
Work/Site
BARRAGEM FUNDÃO
MINA DE GERMANO - MARIANA-MG
MIXED DRILLING
16PI013
Drilling site coor.
Elevation
E - 660781 m
N - 7784926 m
570,17
Coordinator/Response Technician
DANIELLA ARAMINA
Reported by
ARION
Scale
1:100
Fugro In Situ No.
SMC-05-SPE-01
Date conducted
START: 9/20/2014
END: 9/20/2014

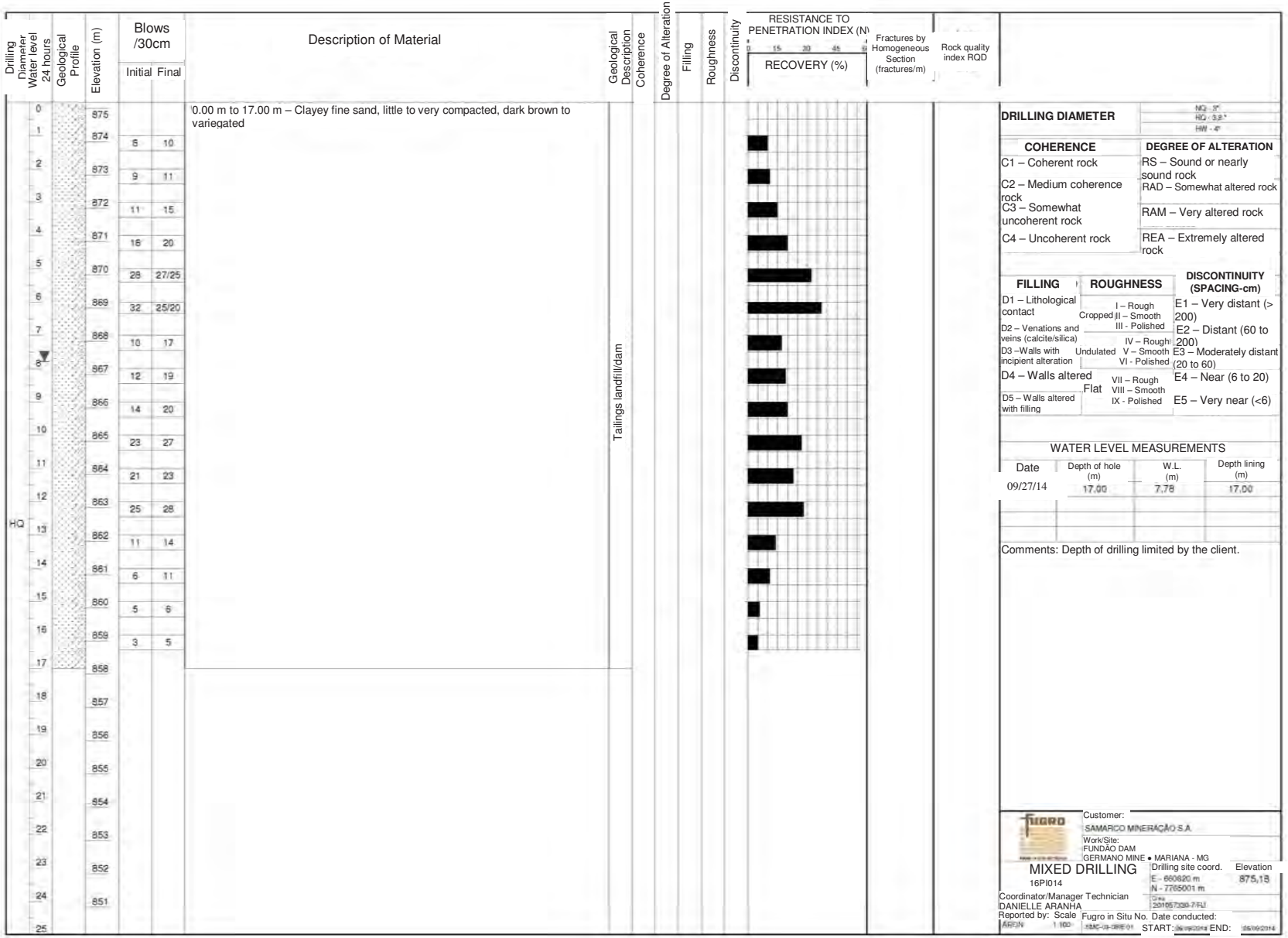
Drilling
Diameter
Water level
24 hours
Geological Profile
Elevation (m)
Blows /30cm
Initial
Final
Description of Material
Geological Description
Coherence
Degree of Alteration
Filling
Roughness
Discontinuity
RESISTANCE TO PENETRATION INDEX (N)
15
30
45
RECOVERY (%)
Fractures by Homogeneous Section (fractures/m)
Rock quality index RQD
0.00 m to 17.00 m – Clayey fine sand, little to very compacted, dark brown to variegated
Tailings landfill/dam
HQ
875
874
873
872
871
870
869
868
867
866
865
864
863
862
861
860
859
858
857
856
855
854
853
852
851
6
10
9
11
11
15
16
20
28
27/25
32
25/20
10
17
12
19
14
20
23
27
21
23
25
28
11
14
6
11
5
6
3
5
DRILLING DIAMETER
NQ - 3"
HQ - 3,8"
HW - 4"
COHERENCE
C1 – Coherent rock
C2 – Medium coherence rock
C3 – Somewhat uncoherent rock
C4 – Uncoherent rock
DEGREE OF ALTERATION
RS – Sound or nearly sound rock
RAD – Somewhat altered rock
RAM – Very altered rock
REA – Extremely altered rock
FILLING
D1 – Lithological contact
D2 – Venations and veins (calcite/silica)
D3 –Walls with incipient alteration
D4 – Walls altered
D5 – Walls altered with filling
ROUGHNESS
Cropped
Undulated
Flat
I – Rough
II – Smooth
III - Polished
IV – Rough
V – Smooth
VI - Polished
VII – Rough
VIII – Smooth
IX - Polished
DISCONTINUITY (SPACING-cm)
E1 – Very distant (> 200)
E2 – Distant (60 to 200)
E3 – Moderately distant (20 to 60)
E4 – Near (6 to 20)
E5 – Very near (<6)
WATER LEVEL MEASUREMENTS
Date
Depth of hole (m)
W.L. (m)
Depth lining (m)
09/27/14
17,00
7,78
17,00
Comments: Depth of drilling limited by the client.
Customer:
SAMARCO MINERAÇÃO S.A.
Work/Site:
FUNDÃO DAM
GERMANO MINE • MARIANA - MG
MIXED DRILLING
16PI014
Drilling site coord.
E - 660820 m
N - 7765001 m
Elevation
875,18
Coordinator/Manager Technician
DANIELLE ARANHA
Reported by: Scale
1:100
Fugro in Situ No.
Date conducted:
START:
END:

Drilling Diameter / Water Level 24 hours / Geological Profile	Elevation (m)	Blows /30cm Initial	Blows /30cm Final	Description of Material	Geological Description	Coherence	Degree of Alteration	Filling	Roughness	Discontinuity	RESISTANCE TO PENETRATION INDEX (N) / RECOVERY (%)	Fractures by Homogeneous Section (fractures/m)	Rock quality index RQD
HQ	884			0.00 m to 30.45 m – Medium to fine clayey sand, somewhat to very compacted, dark brown	TAILINGS LANDFILL/DAM								
	883	45											
	882	47											
	881	36	35/25										
	880	25	31										
	879	25	31										
	878	19	26										
	877	17	23										
	876	30	40/25										
	875	42											
	874	15	16										
	873	9	12										
	872	12	16										
	871	9	15										
	870	25	50										
	869	24	39										
	868	25	37										
	867	30	40										
	866	25	35										
	865	17	19										
	864	16	18										
	863	11	16										
	862	16	24										
	861	42											
	860	41											

DRILLING DIAMETER

NQ - 3"
HQ - 3,8"
HW - 4"

COHERENCE	DEGREE OF ALTERATION
C1 - Coherent rock	RS - Sound or nearly sound rock
C2 – Medium coherence rock	RAD - Somewhat altered rock
C3 - Somewhat uncoherence rock	RAM - Very altered rock
C4 - Uncoherence rock	REA – Extremely altered rock

FILLING	ROUGHNESS		DISCONTINUITY (SPACING-cm)
D1 - Lithological contact	Cropped	I - Rough II - Smooth III - Polished	E1 - Very distant (> 200)
D2 - Venations and veins (calcite/silica)			E2 - Distant (60 to 200)
D3 - Walls with incipient alteration	Undulating	IV - Rough V - Smooth VI - Polished	E3 - Moderately distant (20 to 60)
D4 - Walls altered			E4 - Near (6 to 20)
D5 - Walls altered with filling	Flat	VII - Rough VIII - Smooth IX - Polished	E5 - Very near (<6)

WATER LEVEL MEASUREMENTS

Date	Depth of hole (m)	Water level (m)	Depth lining (m)
10/11//2014	30,50	14,85	30,50

Comments: There was a water loss at 21.80 m
Depth of drilling limited by customer.

Customer: SAMARCO MINERAÇÃO S.A.
Work/Site: FUNDÃO DAM
GERMANO MINE – MARIANA-MG

MIXED DRILLING
16PI016

Drilling site coord.
E - 660736 m
N - 7764973 m

Elevation: 884,31

Coordinator/Manager Technician
DANIELLE ARANHA

Crea: 2010573930-7/RJ

Reported by: APOJN
Scale: 1:100
Fugro In Situ No.: SMC-09-GRE-01

Date conducted.
START: 09/10/2014 TERMINO: 10/10/2014

Drilling Diameter	Water Level 24 hours	Geological Profile	Elevation (m)	Blows /30cm Initial	Blows /30cm Final	Description of Material	Geological Description	Coherence	Degree of Alteration	Filling	Roughness	Discontinuity	RESISTANCE TO PENETRATION INDEX (N) 0 15 30 45 60 / RECOVERY (%)	Fractures by Homogeneous Section (fractures/m)	Rock quality index RQD
	25		859	30	42	0.00 m to 30.45 m – Medium to fine clayey sand, somewhat to very compacted, dark brown.	TAILINGS LANDFILL/DAM								
	26		858	12	17										
	27		857	12	17										
	28		856	10	13										
	29		855	11	16										
	30		854	12	20										
	31		853												
	32		852												
	33		851												
	34		850												
	35		849												
	36		848												
	37		847												
HQ	38		846												
	39		845												
	40		844												
	41		843												
	42		842												
	43		841												
	44		840												
	45		839												
	46		838												
	47		837												
	48		836												
	49		835												
	50														

DRILLING DIAMETER

NQ - 3"
HQ - 3,8"
HW - 4"

COHERENCE	DEGREE OF ALTERATION
C1 - Coherent rock	RS - Sound or nearly sound rock
C2 – Medium coherence rock	RAD - Somewhat altered rock
C3 - Somewhat uncoherence rock	RAM - Very altered rock
C4 - Uncoherence rock	REA – Extremely altered rock

FILLING	ROUGHNESS		DISCONTINUITY (SPACING-cm)
D1 - Lithological contact	Cropped	I - Rough II - Smooth III - Polished	E1 - Very distant (> 200)
D2 - Venations and veins (calcite/silica)			E2 - Distant (60 to 200)
D3 - Walls with incipient alteration	Undulating	IV - Rough V - Smooth VI - Polished	E3 - Moderately distant (20 to 60)
D4 - Walls altered			E4 - Near (6 to 20)
D5 - Walls altered with filling	Flat	VII - Rough VIII - Smooth IX - Polished	E5 - Very near (<6)

WATER LEVEL MEASUREMENTS

Date	Depth of hole (m)	Water level (m)	Depth lining (m)
10/11//2014	30.50	14.85	30.50

Comments: There was a water loss at 21.80 m
Depth of drilling limited by customer.

FUGRO

Customer: SAMARCO MINERAÇÃO S.A
Work/Site: FUNDÃO DAM
GERMANO MINE – MARIANA-MG

MIXED DRILLING
16PI016

Drilling site coord.: E - 660738 m N - 7764973 m
Elevation: 884,31

Coordinator/Manager Technician: DANIELLA ARANHA
Orns. 201057330-7/RJ

Reported by: ARBN
Scale: 1:100
Fugro In Situ No. SMC-03-GRE-01
Date conducted. START 09/10/2014 TÉRMINO: 10/10/2014

FUGRO IN SITU GEOTECNIA

STANDARD PENETRATION TEST

SMC-03-GRE-01
ATTACHMENTS

CLIENT: SAMARCO MINERAÇÃO S.A.
PROJECT: FUNDÃO DAM
LOCATION: GERMANO MINE – MARIANA-MG

SCALE: 1:100 START: 08/09/2014 END: 10/09/2014 RESP.: DANIELLA ARANHA CREA REG. NO:201057330- 7/RJ

BOREHOLE: 16LI014 ELEVATION: 884,61 COORDINATES: E 660776,77 N 7765009,69

WATER LEVEL 24 h	SAMPLE	ELEVATION (m)	BLOWS / 30 CM INITIAL	BLOWS / 30 CM FINAL	PENETRATION RESISTANCE INDEX (N) 0 10 20 30 40 50 60	MATERIAL CLASSIFICATION	GEOLOGICAL DESCRIPTION
0		884				0.00 m a 2.00 m - Fine sand, clayey, medium compactness, gray to variegated.	TAILINGS EMBANKMENT/ DAM
1			12	15			
2		883	23	37			
3		882	23	33		2.00 m a 5.00 m - Fine sand, compact to very compact, gray to variegated.	
4		881	30	30/20			
5		880	34	32/20			
6		879	20	35		5.00 m a 13.00 m - Fine sand, clayey, compact to very compact, gray to variegated.	
7		878	21	33			
8		877	20	33			
9		876	23	32			
10		875	24	34			
11		874	35	31/18			
12		873	36	26/19			
13		872	21	24			
14		871	6	10		13.00 m a 15.00 m - Fine to medium sand, clayey, medium compactness to compact, reddish brown to variegated.	
15		870	5	8			
16		869	6	9		15.00 m a 23.00 m - Fine to medium sand, clayey, slightly compact to moderately compact, dark gray to variegated.	
17		868	8	16			
18		867	7	15			
19		866	6	11			
20		865	4	7		NOTE:	

READING INTERVAL W.L(m)
1: 24 h -13,15
2:
3:

PROGRESS METHOD (m)
DIGGER:
WASHING: 0,00 - 25,45
LINING: 0,00
USE OF BENTONITE:
WATER LEAK:

TIME WASHING 10 min
INITIAL DEPTH (m):
STAGE 1 (cm)
STAGE 2 (cm)
STAGE 3 (cm)

OBS:

FUGRO IN SITU GEOTECNIA

STANDARD PENETRATION TEST

SMC-03-GRE-01
ATTACHMENTS

CLIENT: SAMARCO MINERAÇÃO S.A.
PROJECT: FUNDÃO DAM
LOCATION: GERMANO MINE – MARIANA-MG

SCALE: 1:100 START: 08/09/2014 END: 10/09/2014 RESP.: DANIELLA ARANHA CREA REG. NO:. 201057330- 7/RJ

BOREHOLE: 16LI014 ELEVATION: 884,61 COORDINATES: E 660776,77 N 7765009,69

WATER LEVEL 24 h	SAMPLE	ELEVATION (m)	BLOWS / 30 CM INITIAL	BLOWS / 30 CM FINAL	PENETRATION RESISTANCE INDEX (N) 0 10 20 30 40 50 60	MATERIAL CLASSIFICATION	GEOLOGICAL DESCRIPTION
		864	7	11		15.00 m a 23.00 m - Fine sand, clayey, compact to moderately compact, dark gray to variegated.	TAILINGS EMBANKMENT/DAM
		863	5	9			
		862	7	12			
		861	6	10		23.00 m a 25.45 m - Fine to medium sand, clayey, medium compactness,dark brown to variegated.	
		860	7	11			
		859					
		858					
		857					
		856					
		855					
		854					
		853					
		852					
		851					
		850					
		849					
		848					
		847					
		846					
		845					

READING INTERVAL W.L(m)
1: 24 h -13.15
2:
3:

PROGRESS METHOD (m)
DIGGER:
WASHING: 0.00 - 25.45
LINING: 0.00
USE OF BENTONITE: -
WATER LEAK:

TIME WASHING - 10 min
INITIAL DEPTH (m):
STAGE 1 (cm)
STAGE 2 (cm)
STAGE 3 (cm)

NOTE:

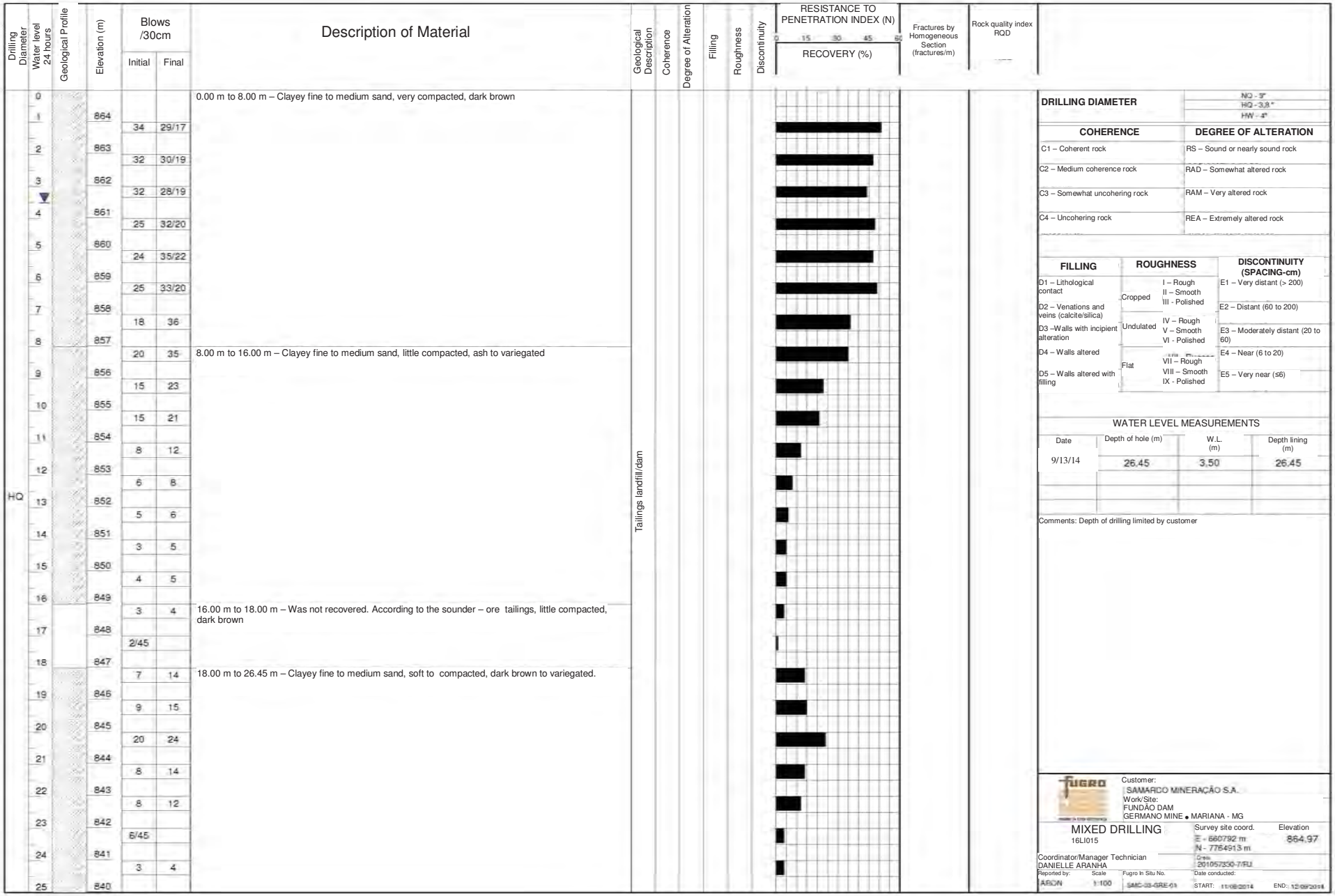
Drilling Diameter
Water level 24 hours
Geological Profile
Elevation (m)
Blows /30cm
Initial
Final
Description of Material
Geological Description
Coherence
Degree of Alteration
Filling
Roughness
Discontinuity
RESISTANCE TO PENETRATION INDEX (N)
0 15 30 45 60
RECOVERY (%)
Fractures by Homogeneous Section (fractures/m)
Rock quality index RQD
HQ
0.00 m to 8.00 m – Clayey fine to medium sand, very compacted, dark brown
8.00 m to 16.00 m – Clayey fine to medium sand, little compacted, ash to variegated
16.00 m to 18.00 m – Was not recovered. According to the sounder – ore tailings, little compacted, dark brown
18.00 m to 26.45 m – Clayey fine to medium sand, soft to compacted, dark brown to variegated.
Tailings landfill/dam
DRILLING DIAMETER
NQ - 3"
HQ - 3,8 "
HW - 4"
COHERENCE
C1 – Coherent rock
C2 – Medium coherence rock
C3 – Somewhat uncohering rock
C4 – Uncohering rock
DEGREE OF ALTERATION
RS – Sound or nearly sound rock
RAD – Somewhat altered rock
RAM – Very altered rock
REA – Extremely altered rock
FILLING
D1 – Lithological contact
D2 – Venations and veins (calcite/silica)
D3 –Walls with incipient alteration
D4 – Walls altered
D5 – Walls altered with filling
ROUGHNESS
Cropped
I – Rough
II – Smooth
III - Polished
Undulated
IV – Rough
V – Smooth
VI - Polished
Flat
VII – Rough
VIII – Smooth
IX - Polished
DISCONTINUITY (SPACING-cm)
E1 – Very distant (> 200)
E2 – Distant (60 to 200)
E3 – Moderately distant (20 to 60)
E4 – Near (6 to 20)
E5 – Very near (≤6)
WATER LEVEL MEASUREMENTS
Date
Depth of hole (m)
W.L. (m)
Depth lining (m)
9/13/14
26,45
3,50
26,45
Comments: Depth of drilling limited by customer
FUGRO
Customer:
SAMARCO MINERAÇÃO S.A.
Work/Site:
FUNDÃO DAM
GERMANO MINE • MARIANA - MG
MIXED DRILLING
16LI015
Survey site coord.
E - 660792 m
N - 7754913 m
Elevation
864,97
Coordinator/Manager Technician
DANIELLE ARANHA
Grids
201057350-7/FU
Reported by:
ARON
Scale
1:100
Fugro In Situ No.
SMC-03-GRE-01
Date conducted:
START: 11/08/2014
END: 12/09/2014

Drilling Diameter	Water level 24 hours	Geological Profile	Elevation (m)	Blows /30cm Initial	Blows /30cm Final	Description of Material	Geological Description	Coherence	Degree of Alteration	Filling	Roughness	Discontinuity	RESISTANCE TO PENETRATION INDEX (N) 0 15 30 45 60 / RECOVERY (%)	Fractures by Homogeneous Section (fractures/m)	Rock quality index RQD
HQ	25			4	5	18.00 m to 26.45 m – Clayey fine to medium sand, soft to compacted, dark brown to variegated	Tailings landfill/dam								
	26		839												
				4	5										
	27		838												
	28		837												
	29		836												
	30		835												
	31		834												
	32		833												
	33		832												
	34		831												
	35		830												
	36		829												
	37		828												
	38		827												
	39		826												
	40		825												
	41		824												
	42		823												
	43		822												
	44		821												
	45		820												
	46		819												
	47		818												
	48		817												
	49		816												
	50		815												

SURVEY DIAMETER

DIÂMETRO DA SONDAGEM	NQ - 3" HQ - 3,5" HW - 4"

COHERENCE	DEGREE OF ALTERATION
C1 – Coherent rock	RS – Sound or nearly sound rock
C2 – Medium coherence rock	RAD – Somewhat altered rock
C3 – Somewhat uncohering rock	RAM – Very altered rock
C4 – Uncohering rock	REA – Extremely altered rock

FILLING	ROUGHNESS		DISCONTINUITY (SPACING-cm)
D1 – Lithological contact	Cropped	I – Rough II – Smooth III - Polished	E1 – Very distant (> 200)
D2 – Venations and veins (calcite/silica)			E2 – Distant (60 to 200)
D3 –Walls with incipient alteration	Undulated	IV – Rough V – Smooth VI - Polished	E3 – Moderately distant (20 to 60)
D4 – Walls altered	Flat	VII – Rough VIII – Smooth IX - Polished	E4 – Near (6 to 20)
D5 – Walls altered with filling			E5 – Very near (≤6)

WATER LEVEL MEASUREMENTS

Date	Depth of hole (m)	W.L. (m)	Depth lining (m)
9/13/14	25.45	3.50	25.45

Comments: Depth of survey limited by customer

FUGRO

Customer:
SAMARCO MINERAÇÃO S.A.

Work/Site:
FUNDÃO DAM
GERMANO MINE • MARIANA - MG

MIXED DRILLING
16LI015

Survey site coord. E - 660792 m N - 7774913 m
Elevation 864.97

Coordinator/Manager Technician
DANIELLE ARANHA

Crea 2010573330-7/RJ

Reported by: ARON
Scale 1:100
Fugro In Situ No. SMC-03-GRE-01
Date conducted: START: 11/09/2014 END: 12/09/2014

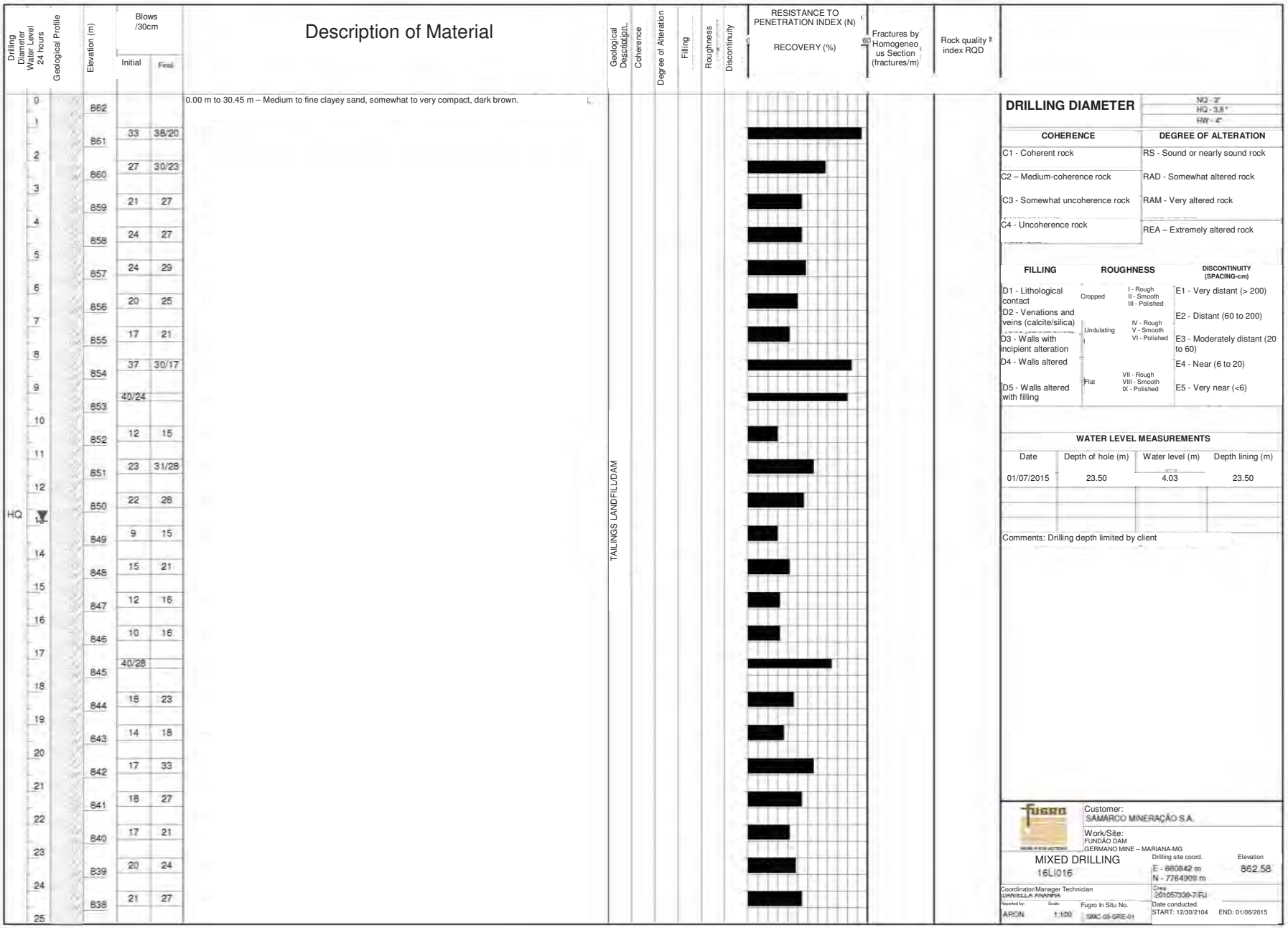
Drilling Diameter
Water Level 24 Hours
Geological Profile
Elevation (m)
Blows /30cm
Initial
Final
Description of Material
Geological Description
Coherence
Degree of Alteration
Filling
Roughness
Discontinuity
RESISTANCE TO PENETRATION INDEX (N)
RECOVERY (%)
Fractures by Homogeneous Section (fractures/m)
Rock quality index RQD
0.00 m to 30.45 m – Medium to fine clayey sand, somewhat to very compact, dark brown.
TAILINGS LANDFILL/DAM
HQ
862 33 38/20
861 27 30/23
860 21 27
859 24 27
858 24 29
857 20 25
856 17 21
855 37 30/17
854 40/24
853 12 15
852 23 31/28
851 22 28
850 9 15
849 15 21
848 12 16
847 10 16
846 40/28
845 18 23
844 14 18
843 17 33
842 18 27
841 17 21
840 20 24
839 21 27
838
DRILLING DIAMETER
NQ - 3"
HQ - 3,8 "
HW - 4"
COHERENCE
C1 - Coherent rock
C2 – Medium-coherence rock
C3 - Somewhat uncoherence rock
C4 - Uncoherence rock
DEGREE OF ALTERATION
RS - Sound or nearly sound rock
RAD - Somewhat altered rock
RAM - Very altered rock
REA – Extremely altered rock
FILLING
D1 - Lithological contact
D2 - Venations and veins (calcite/silica)
D3 - Walls with incipient alteration
D4 - Walls altered
D5 - Walls altered with filling
ROUGHNESS
Cropped
I - Rough
II - Smooth
III - Polished
Undulating
IV - Rough
V - Smooth
VI - Polished
Flat
VII - Rough
VIII - Smooth
IX - Polished
DISCONTINUITY (SPACING-cm)
E1 - Very distant (> 200)
E2 - Distant (60 to 200)
E3 - Moderately distant (20 to 60)
E4 - Near (6 to 20)
E5 - Very near (<6)
WATER LEVEL MEASUREMENTS
Date
Depth of hole (m)
Water level (m)
Depth lining (m)
01/07/2015
23.50
4.03
23.50
Comments: Drilling depth limited by client
Customer:
SAMARCO MINERAÇÃO S.A.
Work/Site:
FUNDÃO DAM
GERMANO MINE – MARIANA-MG
MIXED DRILLING
16LI016
Drilling site coord.
E - 660842 m
N - 7764909 m
Elevation
862.58
Coordinator/Manager Technician
DANIELLA ANANIAS
Reported by:
ARON
Scale:
1:100
Fugro In Situ No.
SMC-03-GRE-01
Date conducted.
START: 12/30/2104
END: 01/06/2015

Drilling Diameter	Water Level 24 hours	Geological Profile	Elevation (m)	Blows /30cm Initial	Blows /30cm Final	Description of Material	Geological Description	Coherence	Degree of Alteration	Filling	Roughness	Discontinuity	RESISTANCE TO PENETRATION INDEX (N) 0 15 30 45 60 / RECOVERY (%)	Fractures by Homogeneous Section (fractures/m)	Rock quality index RQD
HQ	25		837	22	27	0.00 m to 30.45 m – Medium to fine clayey sand, somewhat to very compact, dark brown.	TAILINGS LANDFILL/DAM								
	26														
			836	12	14										
	27														
			835	12	16										
	28														
			834	11	14										
	29														
			833	16	20										
	30														
			832	15	19										
	31		831												
	32														
			830												
	33														
			829												
	34														
			828												
	35														
			827												
	36														
			826												
	37														
			825												
	38														
			824												
	39														
			823												
	40														
			822												
	41														
			821												
	42														
			820												
	43														
			819												
	44														
			818												
	45														
			817												
	46														
			816												
	47														
			815												
	48														
			814												
	49														
			813												
	50														

DRILLING DIAMETER

NQ - 3"
HQ - 3.8"
HW - 4"

COHERENCE	DEGREE OF ALTERATION
C1 - Coherent rock	RS - Sound or nearly sound rock
C2 – Medium-coherence rock	RAD - Somewhat altered rock
C3 - Somewhat uncoherence rock	RAM - Very altered rock
C4 - Uncoherence rock	REA – Extremely altered rock

FILLING	ROUGHNESS		DISCONTINUITY (SPACING-cm)
D1 - Lithological contact	Cropped	I - Rough II - Smooth III - Polished	E1 - Very distant (> 200)
D2 - Venations and veins (calcite/silica)	Undulating	IV - Rough V - Smooth VI - Polished	E2 - Distant (60 to 200)
D3 - Walls with incipient alteration			E3 - Moderately distant (20 to 60)
D4 - Walls altered	Flat	VII - Rough VIII - Smooth IX - Polished	E4 - Near (6 to 20)
D5 - Walls altered with filling			E5 - Very near (<6)

WATER LEVEL MEASUREMENTS

Date	Depth of hole (m)	Water level (m)	Depth lining (m)
01/07/2015	23.50	4.03	23.50

Comments: Drilling depth limited by client

Customer:
SAMARCO MINERAÇÃO S.A

Work/Site:
FUNDÃO DAM
GERMANO MINE – MARIANA-MG

MIXED DRILLING
16LI016

Drilling site coord. E - 660542 m N - 7784[illegible] m
Elevation 852.56

Coordinator/Manager Technician
DANIELLA ARANHA

Crea 2[illegible]

Reported by: ARON
Scale: 1:100
SMC-GI-GRE-01

Date conducted.
START: 12/30/2104 END: 01/06/2015

Drilling Diameter	Water level 24 hours	Geological Profile	Elevation (m)	Blows /30cm Initial	Blows /30cm Final	Description of Material	Geological Description	Coherence	Degree of Alteration	Filling	Roughness	Discontinuity	RESISTANCE TO PENETRATION INDEX (N) 0 15 30 45 60 / RECOVERY (%)	Fractures by Homogeneous Section (fractures/m)	Rock quality index RQD
HQ	0		864			0.00 m a 17.00 m -Fine clayey sand, soft to very compacted, dark brown to variegated.	TAILINGS LANDFILL/DAM								
	1														
			863	14	21										
	2														
			862	18	23										
	3														
			861	22	29										
	4														
			860	23	30										
	5														
			859	40/25											
	6														
			858	20	24										
	7														
			857	8	11										
	8														
		▼	856	3	4										
	9														
			855	2	3										
	10														
			854	5	8										
	11														
			853	11	12										
	12														
			852	12	16										
	13														
			851	6	10										
	14														
			850	5	9										
	15														
			849	2	4										
	16														
			848	3	5										
	17														
			847												
	18														
			846												
	19														
			845												
	20														
			844												
	21														
			843												
	22														
			842												
	23														
			841												
	24														
			840												
	25														

DRILLING DIAMETER

NQ - 3"
HQ - 3,8"
HW - 4"

COHERENCE	DEGREE OF ALTERATION
C1 – Coherent rock	RS – Sound or nearly sound rock
C2 – Medium coherence rock	RAD – Somewhat altered rock
C3 – Somewhat uncohering rock	RAM – Very altered rock
C4 – Noncoherent rock	REA – Extremely altered rock

FILLING	ROUGHNESS		DISCONTINUITY (SPACING-cm)
D1 – Lithological contact	Cropped	I – Rough II – Smooth III - Polished	E1 – Very distant (> 200)
D2 – Venations and veins (calcite/silica)			E2 – Distant (60 to 200)
D3 –Walls with incipient alteration	Undulated	IV – Rough V – Smooth VI - Polished	E3 – Moderately distant (20 to 60)
D4 – Walls altered	Flat	VII – Rough VIII – Smooth IX - Polished	E4 – Near (6 to 20)
D5 – Walls altered with filling			E5 – Very near (<6)

WATER LEVEL MEASUREMENTS

Date	Depth of hole (m)	W.L. (m)	Depth lining (m)
09/25/2014	17,00	8,40	17,00

Comments: Depth of drilling limited by the client.

Fugro

Customer:
SAMARCO MINERAÇÃO S.A.
Work/Site:
FUNDÃO DAM
GERMANO MINE • MARIANA - MG

MIXED DRILLING
16LI017

Drilling site coord.
E - 660815 m
N - 7764951 m
Elevation
864,39

Coordinator/Manager Technician
DANIELLE ARANHA

Ordem
201057300-7/RJ

Reported by: Scale
DANIELLE 1:100

Fugro In Situ No.
SMC-03-GRE-01

Date conducted:
INÍCIO: 24/09/2014 TÉRMINO: 25/09/2014

Drilling Diameter	Water Level 24 hours	Geological Profile	Elevation (m)	Blows /30cm Initial	Blows /30cm Final	Description of Material	Geological Description	Coherence	Degree of Alteration	Filling	Roughness	Discontinuity	RESISTANCE TO PENETRATION INDEX (N) / RECOVERY (%)	Fractures by Homogeneous Section (fractures/m)	Rock quality index RQD
HQ	0		858			0.00 m to 4.00 m - Fine to medium clayey sand, dark brown.	TAILINGS LANDFILL/DAM								
	1		857												
	2		856												
	3		855												
	4 ▼		854			4.00 m to 5.00 m - Material not recovered, due to lack of compactness.									
	5		853			5.00 m to 7.00 m - Fine to medium clayey sand, dark brown.									
	6		852												
	7		851			7.00 m to 9.00 m - Material not recovered, due to lack of compactness.									
	8		850												
	9		849			9.00 m to 23.50 m - Fine to medium clayey sand, dark brown.									
	10		848												
	11		847												
	12		846												
	13		845												
	14		844												
	15		843												
	16		842												
	17		841												
	18		840												
	19		839												
	20		838												
	21		837												
	22		836												
	23		835												
	24		834												
	25														

RESISTANCE TO PENETRATION INDEX (N): 0 15 30 45 60
RECOVERY (%): 100 75 50 25 0
Fractures by Homogeneous Section (fractures/m): 20 15 10 5 0
Rock quality index RQD: 0 25 50 75 100

DRILLING DIAMETER

NQ - 3"
HQ - 3.8"
HW - 4"

COHERENCE	DEGREE OF ALTERATION
C1 - Coherent rock	RS - Sound or nearly sound rock
C2 – Medium coherence rock	RAD - Somewhat altered rock
C3 - Somewhat uncoherent rock	RAM - Very altered rock
C4 - Uncoherent rock	REA – Extremely altered rock

FILLING	ROUGHNESS		DISCONTINUITY (SPACING-cm)
D1 - Lithological contact	Cropped	I - Rough II - Smooth III - Polished	E1 - Very distant (> 200)
D2 - Venations and veins			E2 - Distant (60 to 200)
D3 - Walls with incipient alteration	Undulating	IV - Rough V - Smooth VI - Polished	E3 - Moderately distant (20 to 60)
D4 - Walls altered			E4 - Near (6 to 20)
D5 - Walls altered with filling	Flat	VII - Rough VIII - Smooth IX - Polished	E5 - Very near (<6)

WATER LEVEL MEASUREMENTS

Date	Depth of hole (m)	Water level (m)	Depth lining (m)
01/07/2015	23.50	4.03	23.50

Comments: UPON CUSTOMER'S REQUEST, SPT TEST ON SOIL STRETCHES WAS NOT CARRIED OUT.
Depth of drilling limited by customer.

FUGRO

Customer: SAMARCO MINERAÇÃO S.A.
Work/Site: FUNDÃO DAM
GERMANO MINE – MARIANA-MG

MIXED DRILLING
16LI018

Drilling site coord. E - 660854 m N - 7764902 m
Elevation 858.70

Coordinator/Manager Technician: DANIELLA ARANHA
Crew: 201057330-7-RJ

Reported by: ARON
Scale: 1:100
Fugro In Situ No.: SMC-03-DRE-01
Date conducted. START: 12/30/2104 END: 01/06/2015

September 2014 – March 2015
Fugro
Fundão, Germano
(Section C2.2.6)

Figure C.C1-6 – Fugro (September 2014 – March 2015) Test Location Plan

CPTu-F01 CPT Plots
CPTu-F01 CPT Liquefaction Susceptibility and Soil Behavior Type Plots
CPTu-F02 CPT Plots
CPTu-F02 CPT Liquefaction Susceptibility and Soil Behavior Type Plots
CPTu-F03 CPT Plots
CPTu-F03 CPT Liquefaction Susceptibility and Soil Behavior Type Plots
CPTu-F04 CPT Plots
CPTu-F04 CPT Liquefaction Susceptibility and Soil Behavior Type Plots
CPTu-F05 CPT Plots
CPTu-F05 CPT Liquefaction Susceptibility and Soil Behavior Type Plots
CPTu-F38/90 CPT Plots
CPTu-F38/90 CPT Liquefaction Susceptibility and Soil Behavior Type Plots
CPTu-F40/89 CPT Plots
CPTu-F40/89 CPT Liquefaction Susceptibility and Soil Behavior Type Plots
CPTu-F40/98 CPT Plots
CPTu-F40/98 CPT Liquefaction Susceptibility and Soil Behavior Type Plots
CPTu-F42/86 CPT Plots
CPTu-F42/86 CPT Liquefaction Susceptibility and Soil Behavior Type Plots
CPTu-F42/86A CPT Plots
CPTu-F42/86A CPT Liquefaction Susceptibility and Soil Behavior Type Plots
CPTu-F42/92 CPT Plots
CPTu-F42/92 CPT Liquefaction Susceptibility and Soil Behavior Type Plots
CPTu-F42/96 CPT Plots
CPTu-F42/96 CPT Liquefaction Susceptibility and Soil Behavior Type Plots
CPTu-F42/98 CPT Plots
CPTu-F42/98 CPT Liquefaction Susceptibility and Soil Behavior Type Plots
CPTu-F43/85 CPT Plots
CPTu-F43/85 CPT Liquefaction Susceptibility and Soil Behavior Type Plots
CPTu-F43/85A CPT Plots
CPTu-F43/85A CPT Liquefaction Susceptibility and Soil Behavior Type Plots
CPTu-F43/97 CPT Plots
CPTu-F43/9 CPT Liquefaction Susceptibility and Soil Behavior Type Plots
CPTu-F44/94 CPT Plots
CPTu-F44/94 CPT Liquefaction Susceptibility and Soil Behavior Type Plots
CPTu-F45/91 CPT Plots
CPTu-F45/91 CPT Liquefaction Susceptibility and Soil Behavior Type Plots

September 2014 – March 2015
Fugro
Fundão, Germano
(Section C2.2.6)

CPTu-F46/92 CPT Plots
CPTu-F46/92 CPT Liquefaction Susceptibility and Soil Behavior Type Plots
CPTu-F48/06 CPT Plots
CPTu-F48/06 CPT Liquefaction Susceptibility and Soil Behavior Type Plots
CPTu-F48/90 CPT Plots
CPTu-F48/90 CPT Liquefaction Susceptibility and Soil Behavior Type Plots
CPTu-F50/84 CPT Plots
CPTu-F50/84 CPT Liquefaction Susceptibility and Soil Behavior Type Plots
CPTu-F52/82 CPT Plots
CPTu-F52/82 CPT Liquefaction Susceptibility and Soil Behavior Type Plots

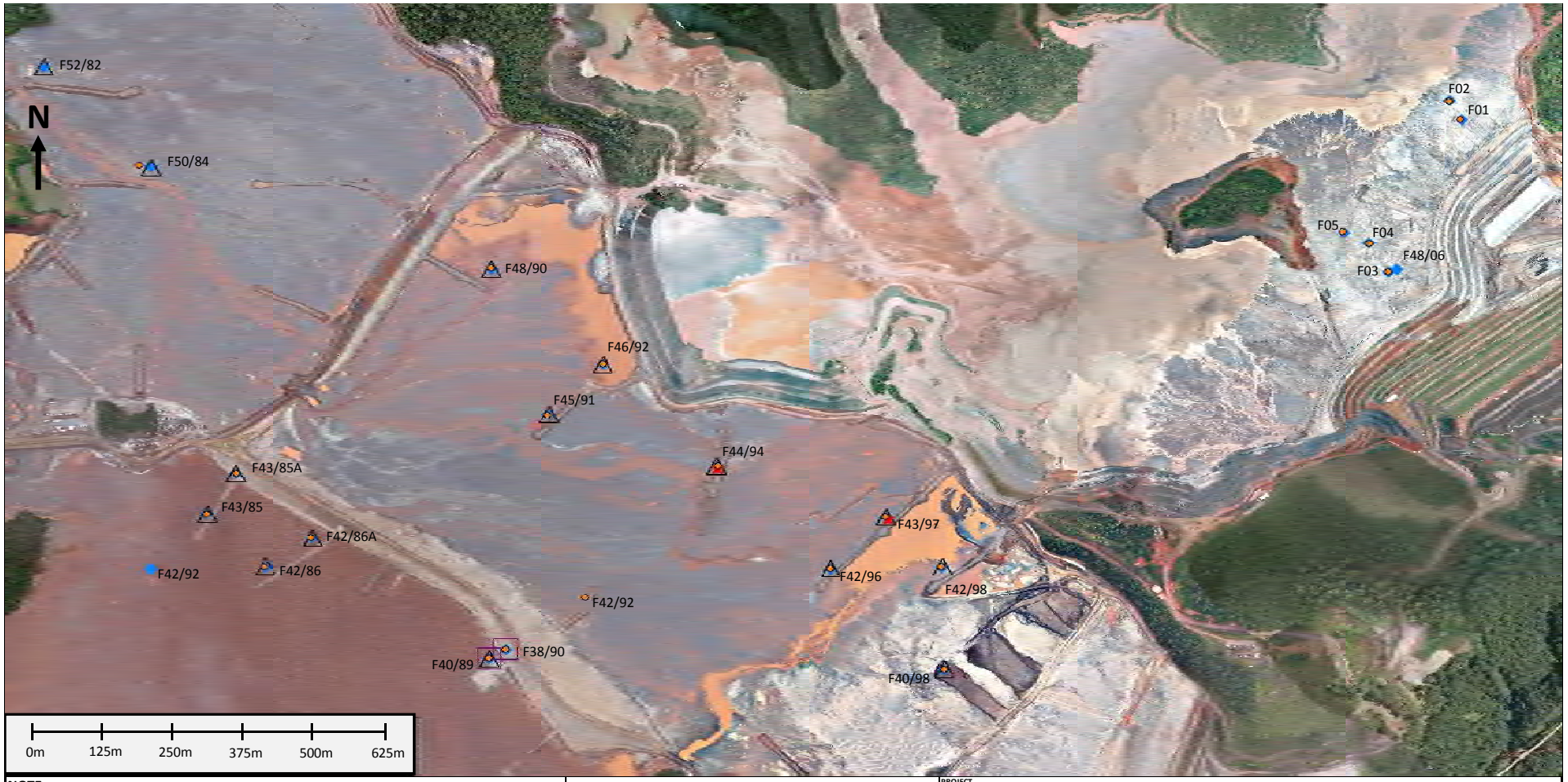

NOTE:

1. November 27, 2014 Fundão aerial image shown. December 14, 2014 Germano aerial image shown.
2. F42/92 CPT and F42/92 SCPT completed in September 2014 and December 2014 respectively at 2 separate locations.

LEGEND:

- Seismic Cone Penetration Test (SCPT)
- Piezocone Penetration Test (CPTu)
- Vane Shear Test (VST)
- Dynamic Cone Penetration Test (DCPT)
- Pressuremeter Test (PMT)

PROJECT

Fundão Tailings Dam Review Panel

TITLE

Fugro (September 2014 – March 2015)
Test Location Plan

FIGURE NO.

C.C1-6

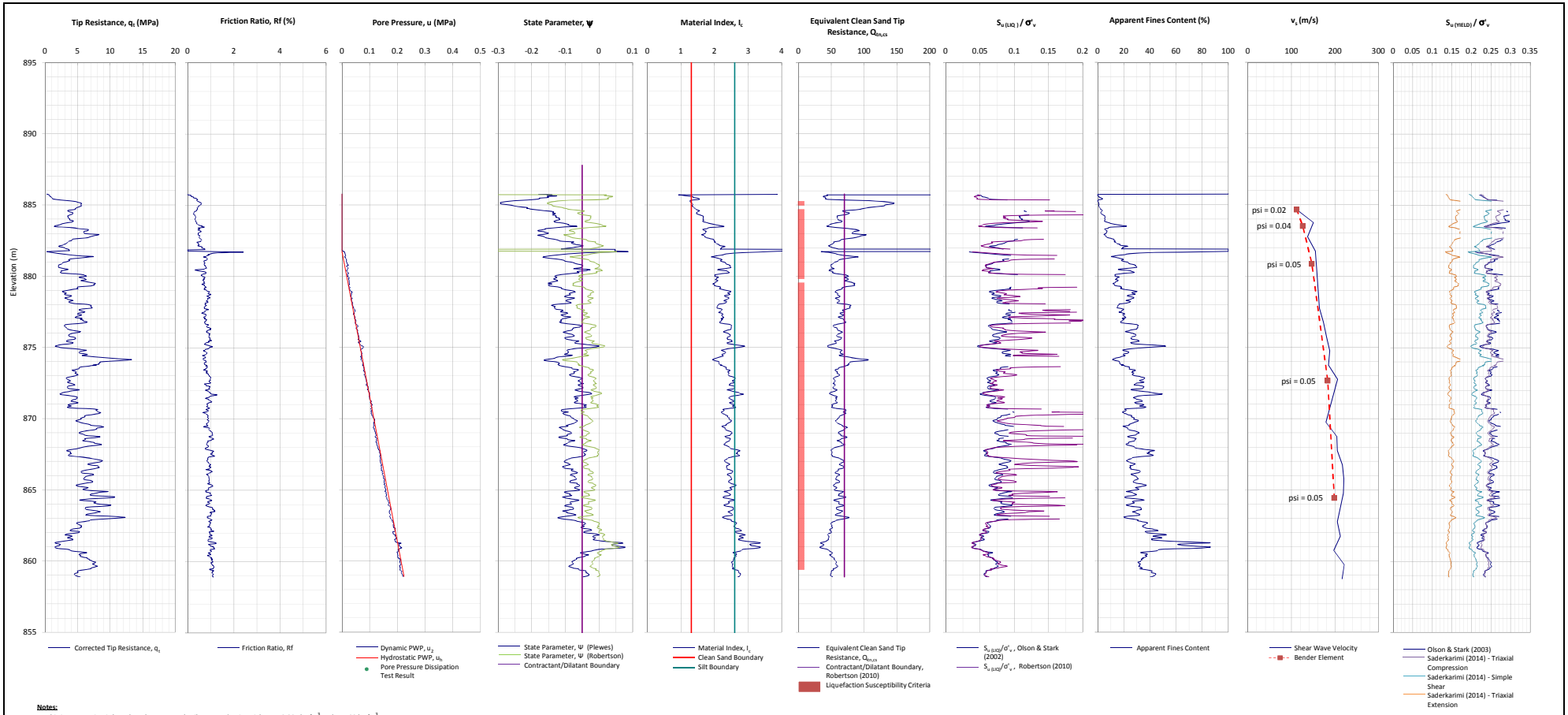

Notes:

1. This interpretation is based on the water and soil saturated unit weights γ_w=9.807 kN/m^3 and γ_{sat}=22 kN/m^3.
2. The friction ratio Rf is calculated as Rf=f_s/q_t.
3. The hydrostatic pore pressure is calculated using the ground water level (GWL) determined from CPT pore pressure dissipation tests (where available) or dynamic pore pressure.
4. Soil boundary layers (where plotted) are based on KCB interpretation.
5. The data presented have been plotted to the axis limits. Data may exist beyond the axis limits shown.
6. The Material Index (I_c) boundaries are based on Robertson and Wride (1998).
7. The $Q_{tn,cs}$ contractant/dilatant boundary=70 and is based on Robertson (2010).
8. The State Parameter (Ψ) calculated using Plewes, et al. (1992) is based on a K0 assumption of 0.5.
9. The State Parameter (Ψ) calculated using Robertson (2012) is based on the $Q_{tn,cs}$.
10. Coordinates are in UTM Zone 23K Córrego Alegre.

PROJECT

Fundão Tailings Dam Review Panel

TITLE

Fugro (September 2014 - March 2015) - Fundão
CONE PENETRATION TEST CPTu-F01
N:7765072.6m E:660716.4m 2015-01-28

Liquefaction susceptibility after Robertson (2010) "Evaluation of Flow Liquefaction and Liquefied Strength Using the Cone Penetration Test"	Liquefaction susceptibility after Olson & Stark (2003) "Yield Strength Ratio and Liquefaction Analysis of Slopes and Embankments"	State parameter approximation - Robertson (2009) "Interpretation of cone penetration tests - a unified approach"

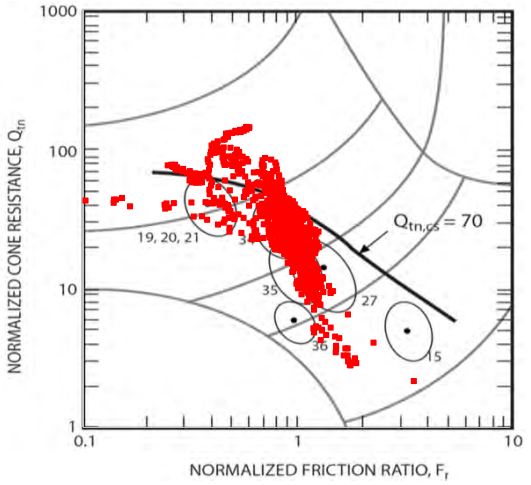

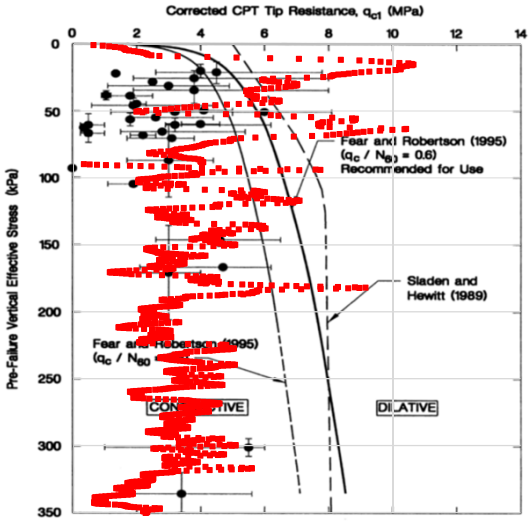

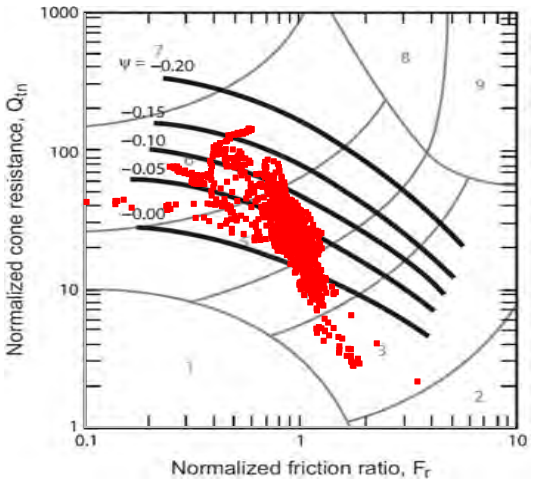

NOTE:

PROJECT

Fundão Tailings Dam Review Panel

TITLE

Fugro (September 2014 - March 2015) - Fundão
CPTu-F01 Liquefaction Susceptibility and Soil Behavior Type

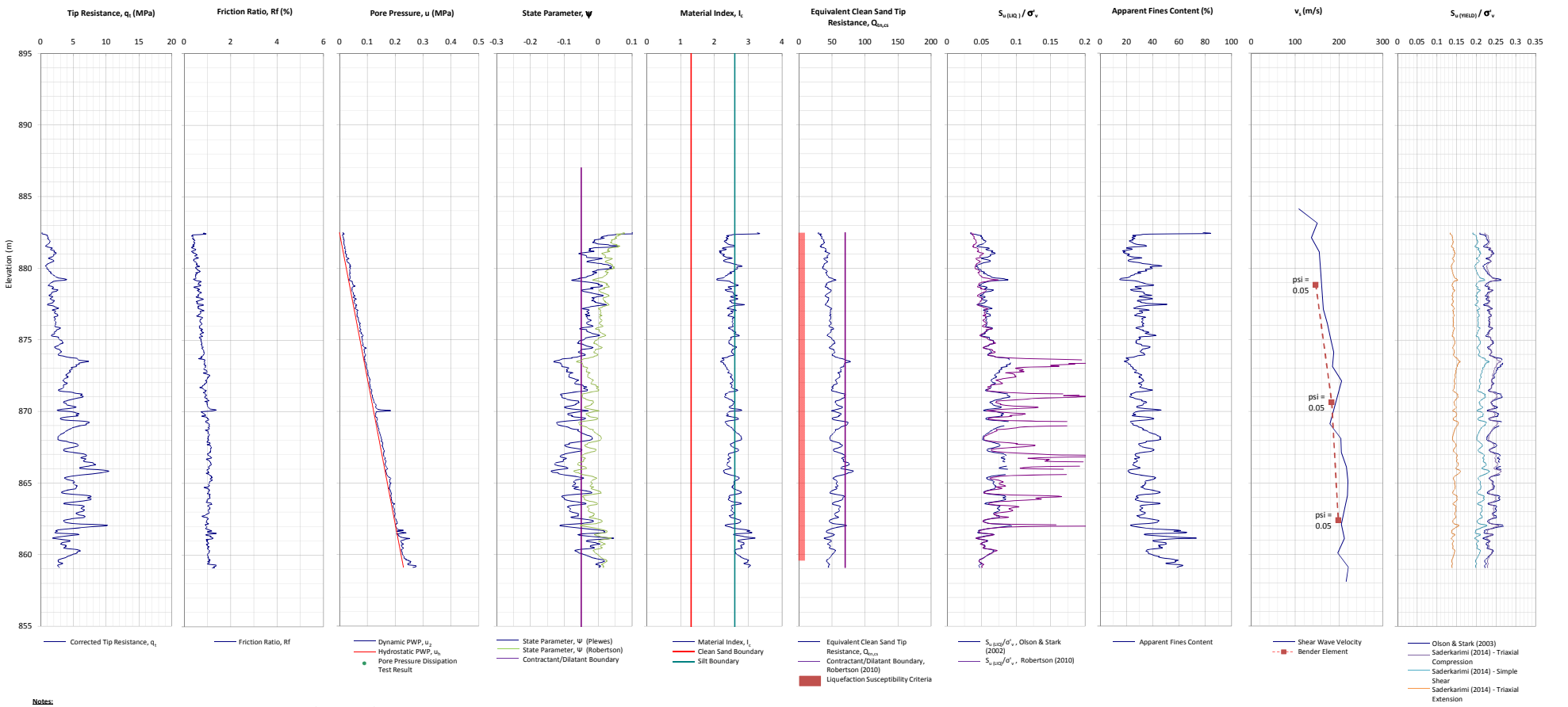

Notes:

1. This interpretation is based on the water and soil saturated unit weights γ_w=9.807 kN/m^3 and γ_{sat}=22 kN/m^3.
2. The friction ratio Rf is calculated as Rf=f_s/q_t.
3. The hydrostatic pore pressure is calculated using the ground water level (GWL) determined from CPT pore pressure dissipation tests (where available) or dynamic pore pressure.
4. Soil boundary layers (where plotted) are based on KCB interpretation.
5. The data presented have been plotted to the axis limits. Data may exist beyond the axis limits shown.
6. The Material Index (I_c) boundaries are based on Robertson and Wride (1998).
7. The $Q_{tn,cs}$ contractant/dilatant boundary=70 and is based on Robertson (2010).
8. The State Parameter (Ψ) calculated using Plewes, et al. (1992) is based on a K0 assumption of 0.5.
9. The State Parameter (Ψ) calculated using Robertson (2012) is based on the $Q_{tn,cs}$.
10. Coordinates are in UTM Zone 23K Córrego Alegre.

PROJECT

Fundão Tailings Dam Review Panel

TITLE

Fugro (September 2014 - March 2015) - Fundão
CONE PENETRATION TEST CPTu-F02
N:7765136.25m E:660690.67m 2015-02-06

Liquefaction susceptibility after Robertson (2010) "Evaluation of Flow Liquefaction and Liquefied Strength Using the Cone Penetration Test"	Liquefaction susceptibility after Olson & Stark (2003) "Yield Strength Ratio and Liquefaction Analysis of Slopes and Embankments"	State parameter approximation - Robertson (2009) "Interpretation of cone penetration tests - a unified approach"

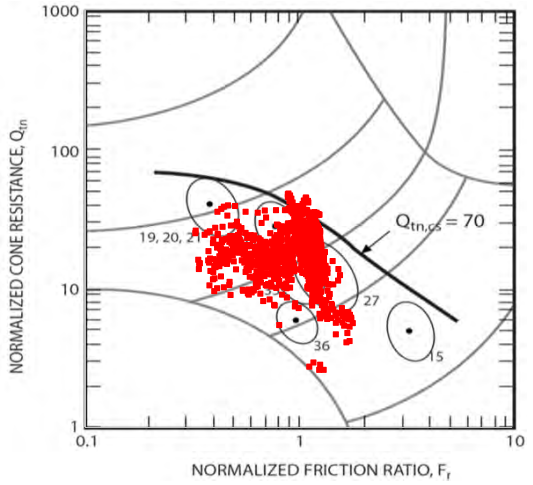

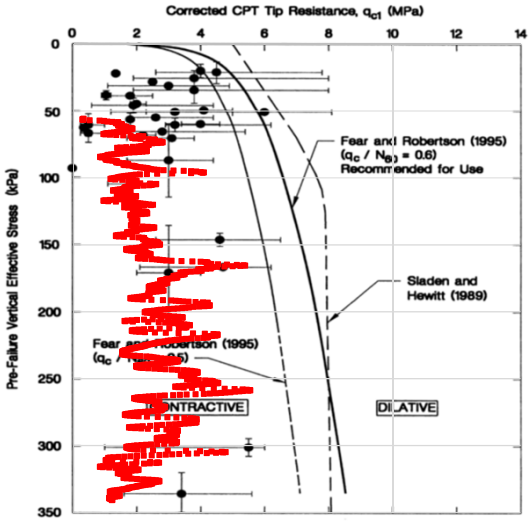

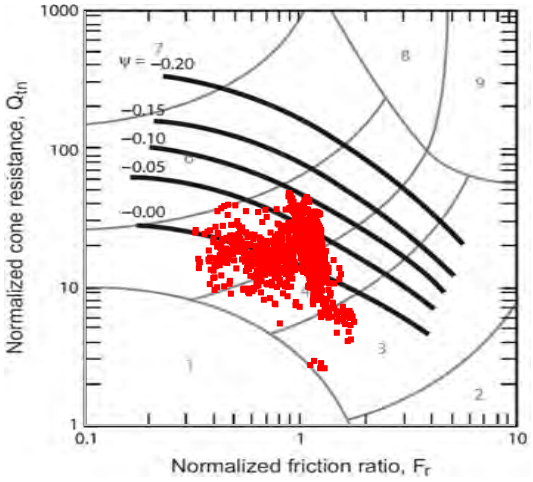

NOTE:

PROJECT

Fundão Tailings Dam Review Panel

TITLE

Fugro (September 2014 - March 2015) - Fundão
CPTu-F02 Liquefaction Susceptibility and Soil Behavior Type

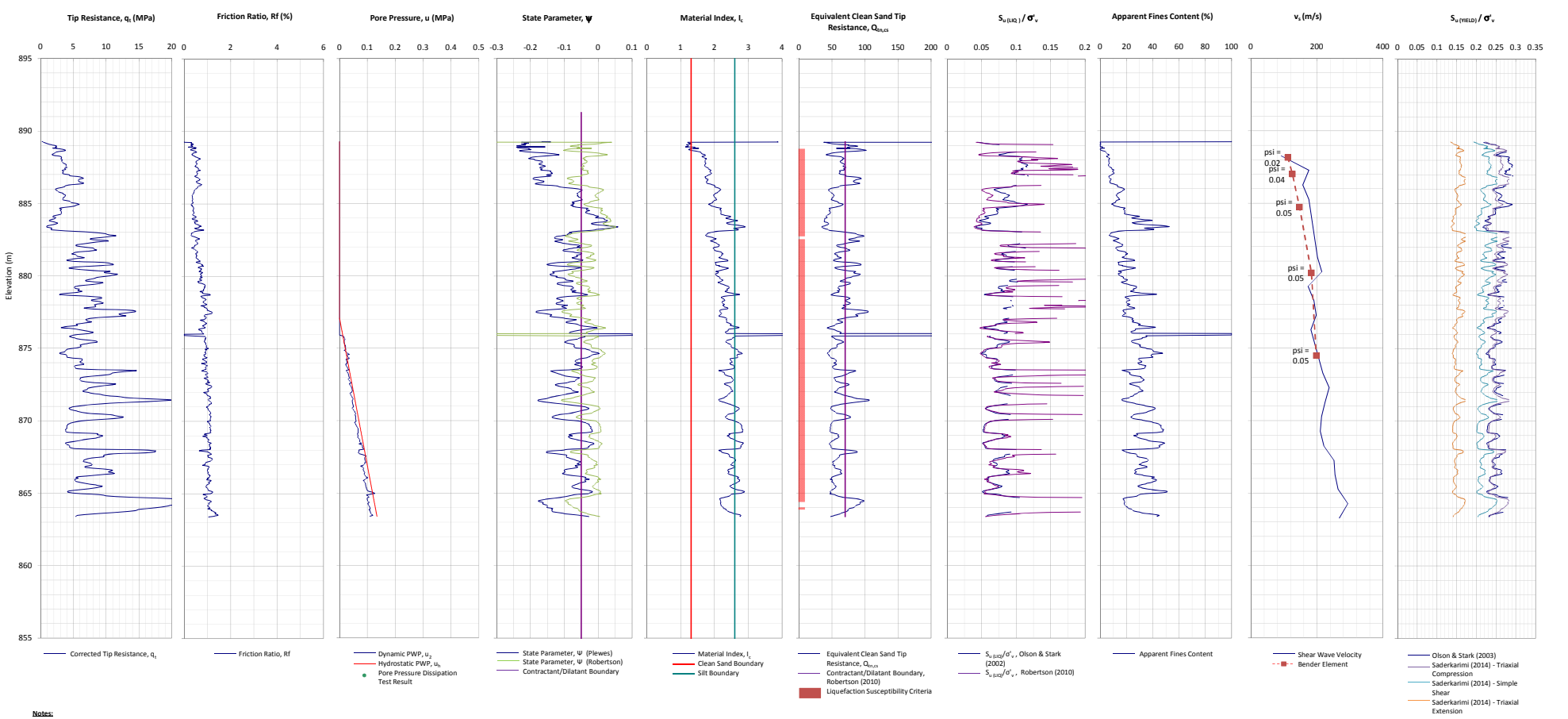

Notes:

1. This interpretation is based on the water and soil saturated unit weights γ_w=9.807 kN/m^3 and γ_{sat}=22 kN/m^3.
2. The friction ratio Rf is calculated as Rf=f_s/q_t.
3. The hydrostatic pore pressure is calculated using the ground water level (GWL) determined from CPT pore pressure dissipation tests (where available) or dynamic pore pressure.
4. Soil boundary layers (where plotted) are based on KCB interpretation.
5. The data presented have been plotted to the axis limits. Data may exist beyond the axis limits shown.
6. The Material Index (I_c) boundaries are based on Robertson and Wride (1998).
7. The $Q_{tn,cs}$ contractant/dilatant boundary=70 and is based on Robertson (2010).
8. The State Parameter (Ψ) calculated using Plewes, et al. (1992) is based on a K0 assumption of 0.5.
9. The State Parameter (Ψ) calculated using Robertson (2012) is based on the $Q_{tn,cs}$.
10. Coordinates are in UTM Zone 23K Córrego Alegre.

PROJECT
Fundão Tailings Dam Review Panel

TITLE
Fugro (September 2014 - March 2015) - Fundão
CONE PENETRATION TEST CPTu-F03
N:7764795.07m E:660584.99m 2015-03-03

Liquefaction susceptibility after Robertson (2010) "Evaluation of Flow Liquefaction and Liquefied Strength Using the Cone Penetration Test"	Liquefaction susceptibility after Olson & Stark (2003) "Yield Strength Ratio and Liquefaction Analysis of Slopes and Embankments"	State parameter approximation - Robertson (2009) "Interpretation of cone penetration tests - a unified approach"

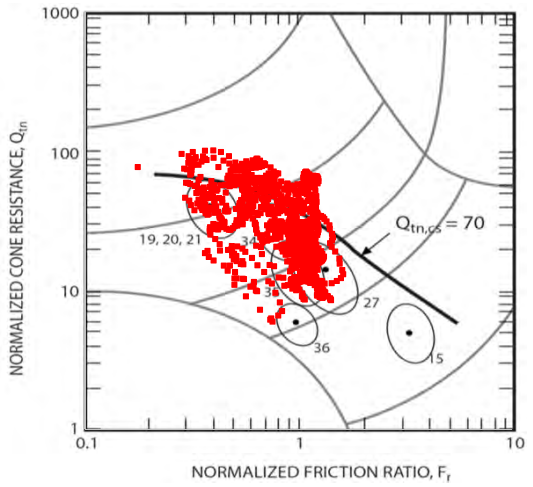

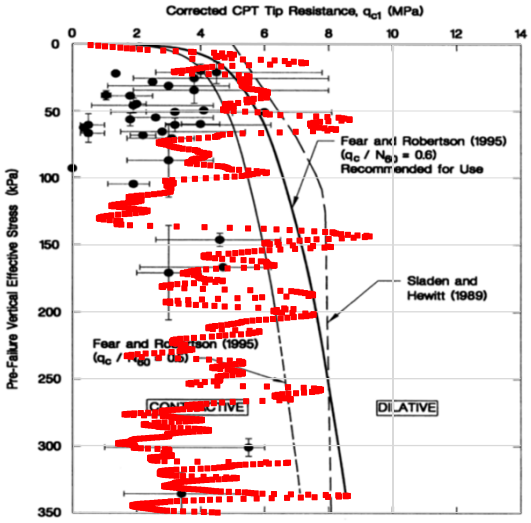

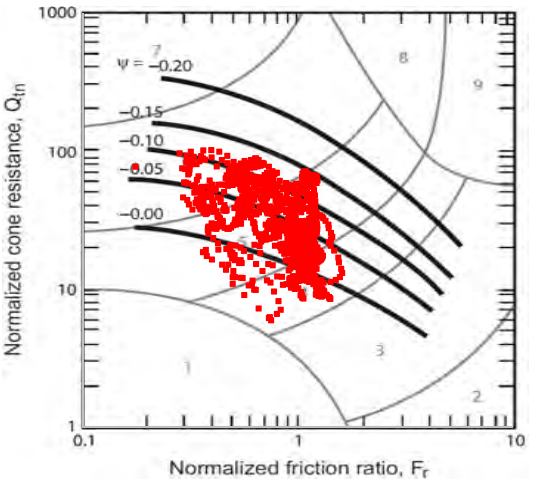

NOTE:

PROJECT

Fundão Tailings Dam Review Panel

TITLE

Fugro (September 2014 - March 2015) - Fundão
CPTu-F03 Liquefaction Susceptibility and Soil Behavior Type

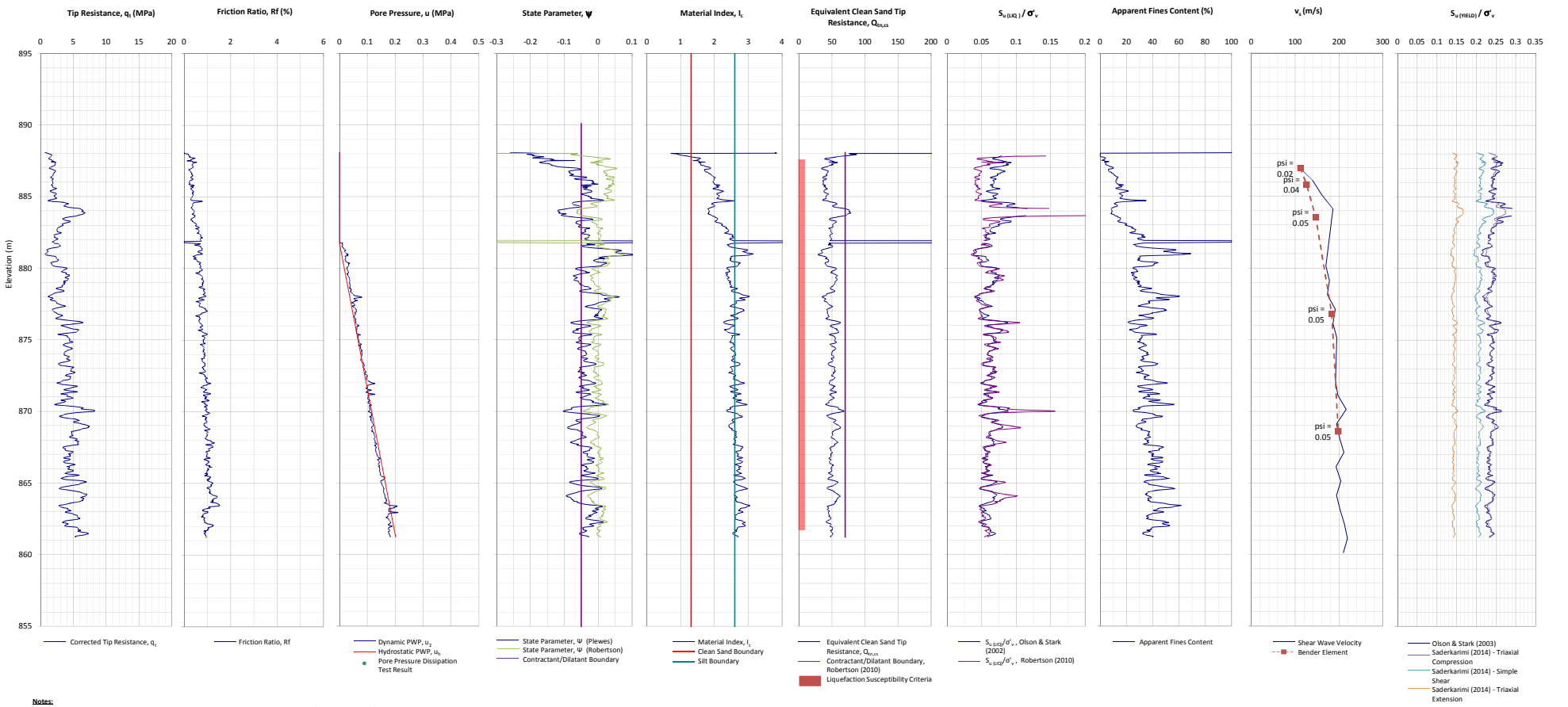

Notes:

1. This interpretation is based on the water and soil saturated unit weights γ_w=9.807 kN/m^3 and γ_{sat}=22 kN/m^3.
2. The friction ratio Rf is calculated as Rf=f_s/q_t.
3. The hydrostatic pore pressure is calculated using the ground water level (GWL) determined from CPT pore pressure dissipation tests (where available) or dynamic pore pressure.
4. Soil boundary layers (where plotted) are based on KCB interpretation.
5. The data presented have been plotted to the axis limits. Data may exist beyond the axis limits shown.
6. The Material Index (I_c) boundaries are based on Robertson and Wride (1998).
7. The $Q_{tn,cs}$ contractant/dilatant boundary=70 and is based on Robertson (2010).
8. The State Parameter (Ψ) calculated using Plewes, et al. (1992) is based on a K0 assumption of 0.5.
9. The State Parameter (Ψ) calculated using Robertson (2012) is based on the $Q_{tn,cs}$.
10. Coordinates are in UTM Zone 23K Córrego Alegre.

PROJECT

Fundão Tailings Dam Review Panel

TITLE

Fugro (September 2014 - March 2015) - Fundão
CONE PENETRATION TEST CPTu-F04
N:7764852.95m E:660548.99m 2015-03-03

Liquefaction susceptibility after Robertson (2010) "Evaluation of Flow Liquefaction and Liquefied Strength Using the Cone Penetration Test"	Liquefaction susceptibility after Olson & Stark (2003) "Yield Strength Ratio and Liquefaction Analysis of Slopes and Embankments"	State parameter approximation - Robertson (2009) "Interpretation of cone penetration tests - a unified approach"

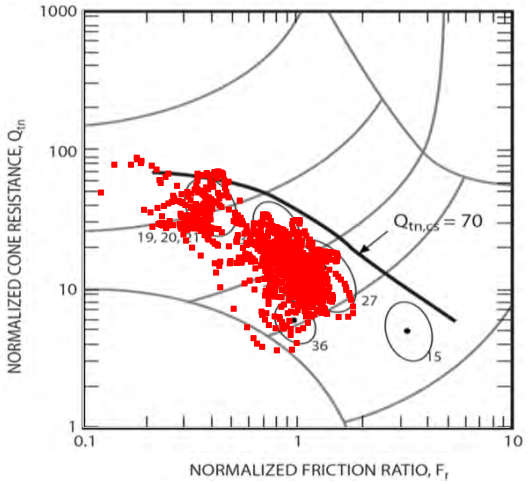

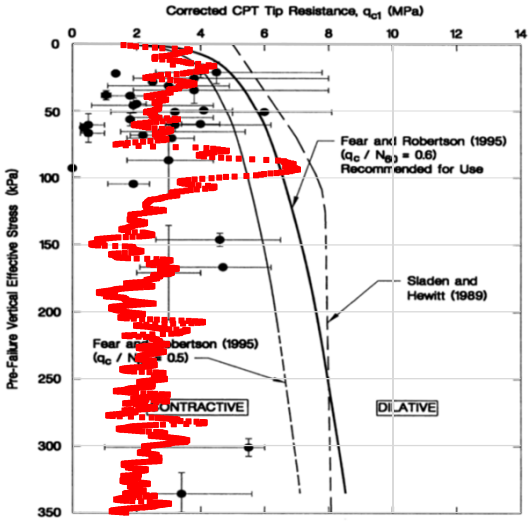

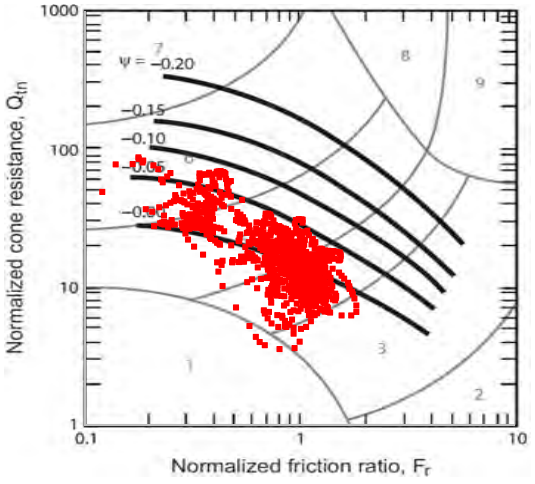

NOTE:

PROJECT

Fundão Tailings Dam Review Panel

TITLE

Fugro (September 2014 - March 2015) - Fundão
CPTu-F04 Liquefaction Susceptibility and Soil Behavior Type

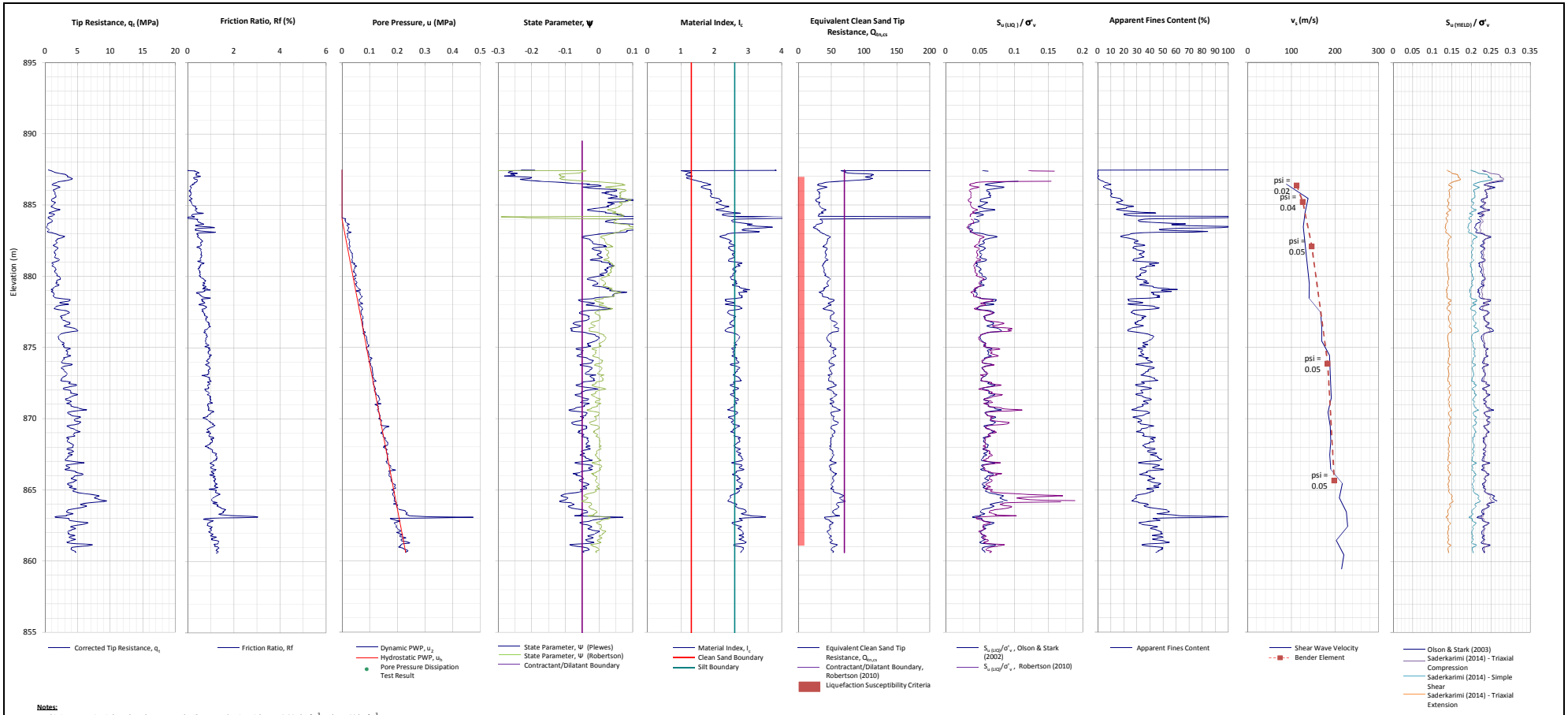

Notes:

1. This interpretation is based on the water and soil saturated unit weights γ_w=9.807 kN/m^3 and γ_{sat}=22 kN/m^3.
2. The friction ratio Rf is calculated as Rf=f_s/q_t.
3. The hydrostatic pore pressure is calculated using the ground water level (GWL) determined from CPT pore pressure dissipation tests (where available) or dynamic pore pressure.
4. Soil boundary layers (where plotted) are based on KCB interpretation.
5. The data presented have been plotted to the axis limits. Data may exist beyond the axis limits shown.
6. The Material Index (I_c) boundaries are based on Robertson and Wride (1998).
7. The $Q_{tn,cs}$ contractant/dilatant boundary=70 and is based on Robertson (2010).
8. The State Parameter (Ψ) calculated using Plewes, et al. (1992) is based on a K0 assumption of 0.5.
9. The State Parameter (Ψ) calculated using Robertson (2012) is based on the $Q_{tn,cs}$.
10. Coordinates are in UTM Zone 23K Córrego Alegre.

PROJECT

Fundão Tailings Dam Review Panel

TITLE

Fugro (September 2014 - March 2015) - Fundão
CONE PENETRATION TEST CPTu-F05
N:7764873.77m E:660505.97m 2015-03-03

Liquefaction susceptibility after Robertson (2010) "Evaluation of Flow Liquefaction and Liquefied Strength Using the Cone Penetration Test"	Liquefaction susceptibility after Olson & Stark (2003) "Yield Strength Ratio and Liquefaction Analysis of Slopes and Embankments"	State parameter approximation - Robertson (2009) "Interpretation of cone penetration tests - a unified approach"

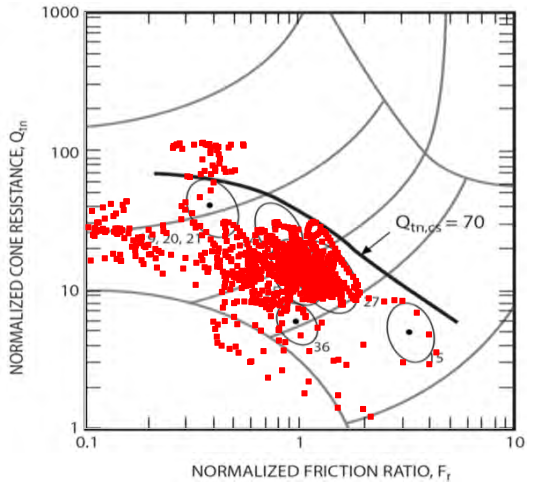

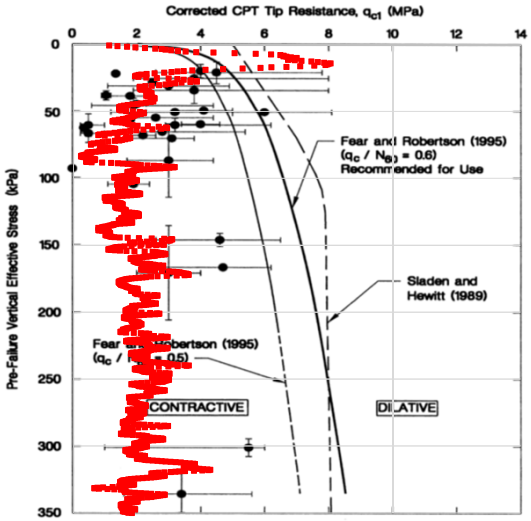

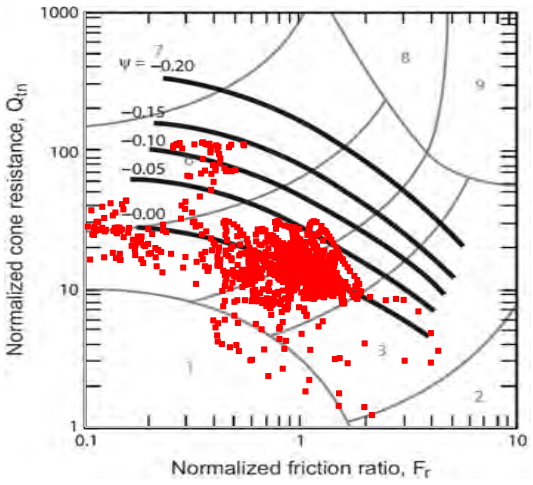

NOTE:

PROJECT

Fundão Tailings Dam Review Panel

TITLE

Fugro (September 2014 - March 2015) - Fundão
CPTu-F05 Liquefaction Susceptibility and Soil Behavior Type

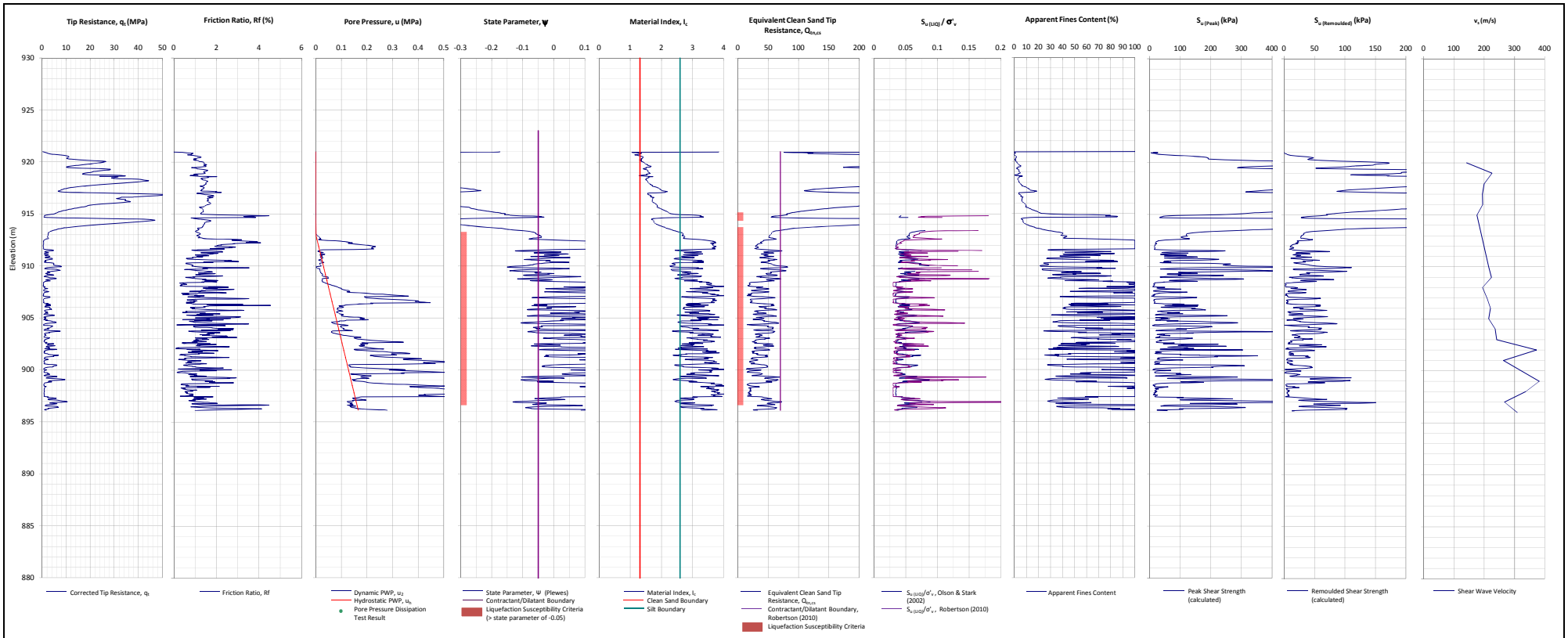

Notes:

1. This interpretation is based on the water and soil saturated unit weights γ_w=9.807 kN/m^3 and γ_{sat}=22 kN/m^3.
2. The friction ratio Rf is calculated as Rf=f_s/q_t.
3. The hydrostatic pore pressure is calculated using the ground water level (GWL) determined from CPT pore pressure dissipation tests (where available) or dynamic pore pressure.
4. Soil boundary layers (where plotted) are based on KCB interpretation.
5. The data presented have been plotted to the axis limits. Data may exist beyond the axis limits shown.
6. The Material Index (I_c) boundaries are based on Robertson and Wride (1998).
7. The $Q_{tn,cs}$ contractant/dilatant boundary=70 and is based on Robertson (2010).
8. The State Parameter (Ψ) calculated using Plewes, et al. (1992) is based on a K0 assumption of 0.5.
9. Coordinates are in UTM Zone 23K Córrego Alegre.
10. N_{kt} used in calculation of $S_{u(peak)}$ is 20.

Project: Fundão Tailings Dam Review Panel

Title: Fugro (September 2014 - March 2015) - Germano
CONE PENETRATION TEST CPTu-F38/90
N:7764039.23m E:659025.02m 2014-09-05

Liquefaction susceptibility after Robertson (2010) "Evaluation of Flow Liquefaction and Liquefied Strength Using the Cone Penetration Test"	Liquefaction susceptibility after Olson & Stark (2003) "Yield Strength Ratio and Liquefaction Analysis of Slopes and Embankments"	State parameter approximation - Robertson (2009) "Interpretation of cone penetration tests - a unified approach"

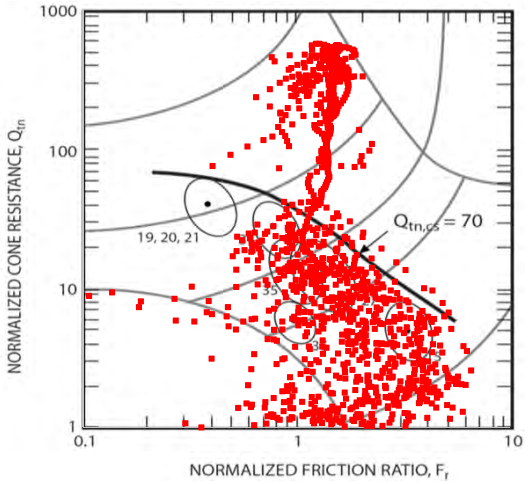

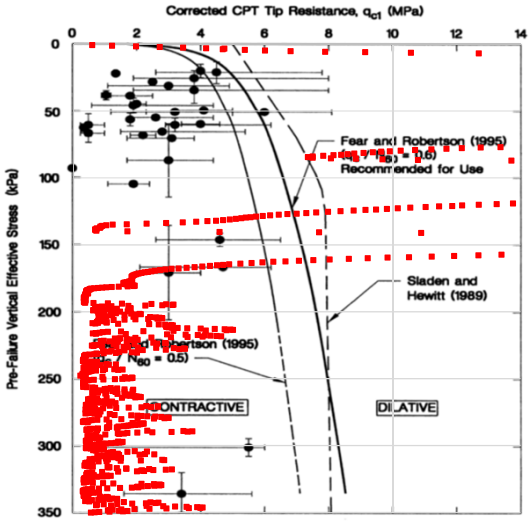

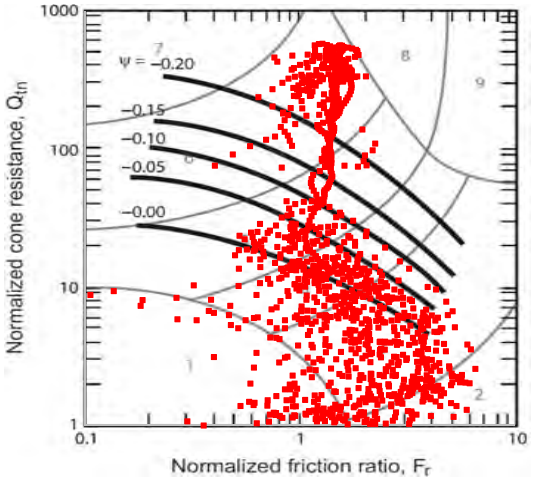

NOTE:

PROJECT

Fundão Tailings Dam Review Panel

TITLE

Fugro (September 2014 - March 2015) - Germano
CPTu-F38/90 Liquefaction Susceptibility and Soil Behavior Type

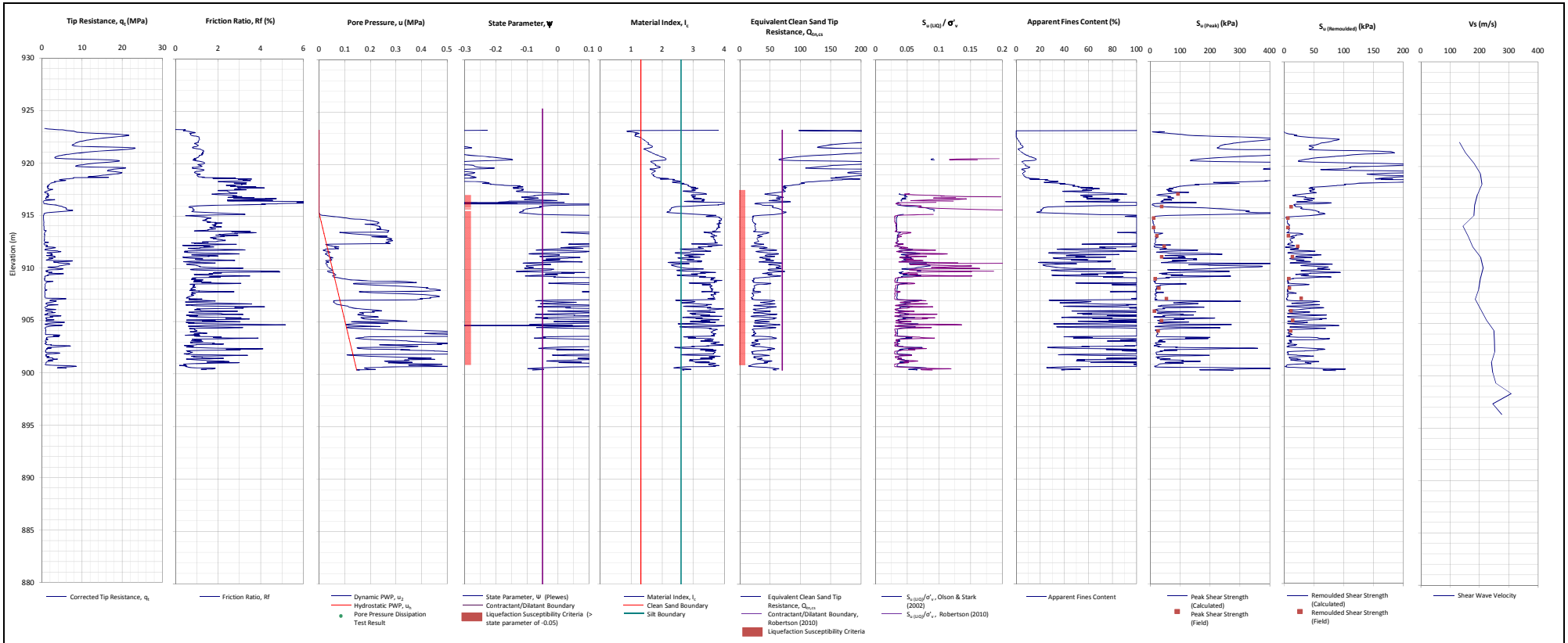

Notes:

1. This interpretation is based on the water and soil saturated unit weights γ_w=9.807 kN/m^3 and γ_{sat}=22 kN/m^3.
2. The friction ratio Rf is calculated as Rf=f_s/q_t.
3. The hydrostatic pore pressure is calculated using the ground water level (GWL) determined from CPT pore pressure dissipation tests (where available) or dynamic pore pressure.
4. Soil boundary layers (where plotted) are based on KCB interpretation.
5. The data presented have been plotted to the axis limits. Data may exist beyond the axis limits shown.
6. The Material Index (I_c) boundaries are based on Robertson and Wride (1998).
7. The $Q_{tn,cs}$ contractant/dilatant boundary=70 and is based on Robertson (2010).
8. The State Parameter (Ψ) calculated using Plewes, et al. (1992) is based on a K0 assumption of 0.5.
9. Coordinates are in UTM Zone 23K Córrego Alegre.
10. N_{kt} used in calculation of $S_{u(plot)}$ is 20.

Project: Fundão Tailings Dam Review Panel

Title: Fugro (September 2014 - March 2015) - Germano
CONE PENETRATION TEST CPTu-F40/89
N:7764950m E:659000m 2014-08-29

Liquefaction susceptibility after Robertson (2010) "Evaluation of Flow Liquefaction and Liquefied Strength Using the Cone Penetration Test"	Liquefaction susceptibility after Olson & Stark (2003) "Yield Strength Ratio and Liquefaction Analysis of Slopes and Embankments"	State parameter approximation - Robertson (2009) "Interpretation of cone penetration tests - a unified approach"

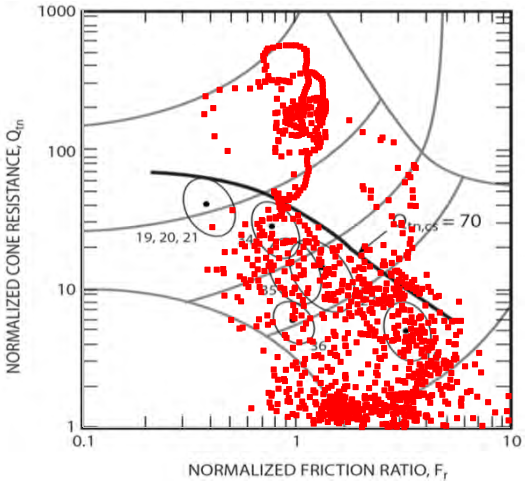

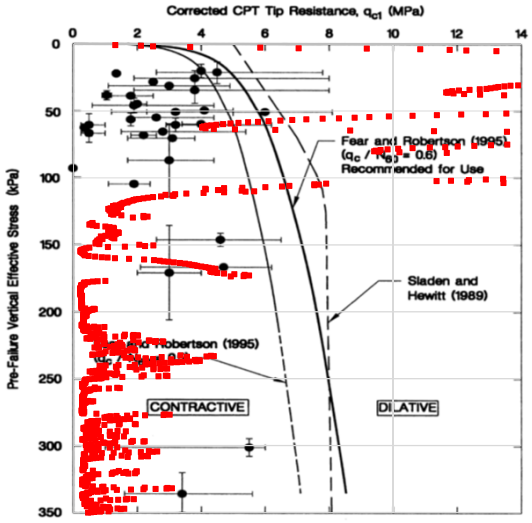

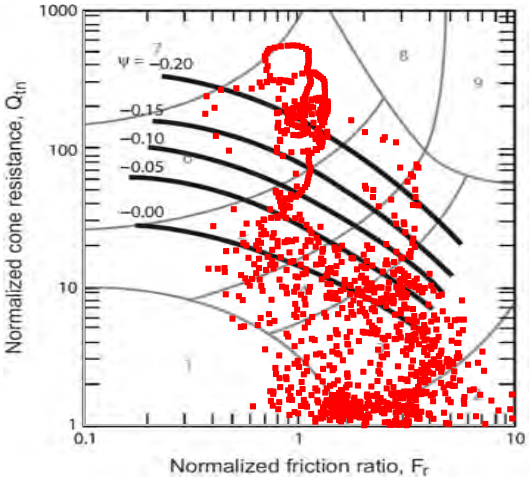

NOTE:

PROJECT

Fundão Tailings Dam Review Panel

TITLE

Fugro (September 2014 - March 2015) - Germano
CPTu-F40/89 Liquefaction Susceptibility and Soil Behavior Type

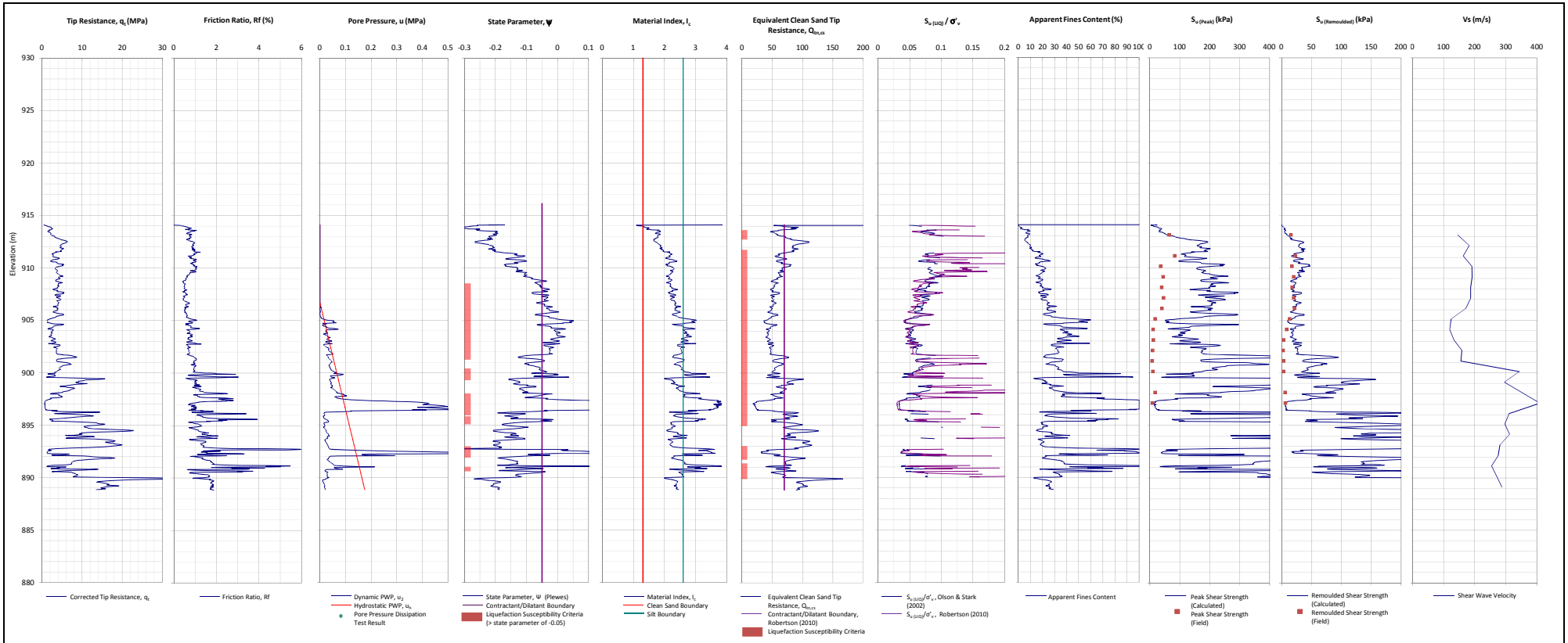

Notes:

1. This interpretation is based on the water and soil saturated unit weights γ_w=9.807 kN/m^3 and γ_{sat}=22 kN/m^3.
2. The friction ratio Rf is calculated as Rf=f_s/q_t.
3. The hydrostatic pore pressure is calculated using the ground water level (GWL) determined from CPT pore pressure dissipation tests (where available) or dynamic pore pressure.
4. Soil boundary layers (where plotted) are based on KCB interpretation.
5. The data presented have been plotted to the axis limits. Data may exist beyond the axis limits shown.
6. The Material Index (I_c) boundaries are based on Robertson and Wride (1998).
7. The $Q_{tn,cs}$ contractant/dilatant boundary=70 and is based on Robertson (2010).
8. The State Parameter (Ψ) calculated using Plewes, et al. (1992) is based on a K0 assumption of 0.5.
9. Coordinates are in UTM Zone 23K Córrego Alegre.
10. N_{kt} used in calculation of $S_{u(plot)}$ is 20.

Project: Fundão Tailings Dam Review Panel

Title: Fugro (September 2014 - March 2015) - Germano
CONE PENETRATION TEST CPTu-F40/98
N:7764000m E:659798.8m 2014-11-25

Liquefaction susceptibility after Robertson (2010) "Evaluation of Flow Liquefaction and Liquefied Strength Using the Cone Penetration Test"	Liquefaction susceptibility after Olson & Stark (2003) "Yield Strength Ratio and Liquefaction Analysis of Slopes and Embankments"	State parameter approximation - Robertson (2009) "Interpretation of cone penetration tests - a unified approach"
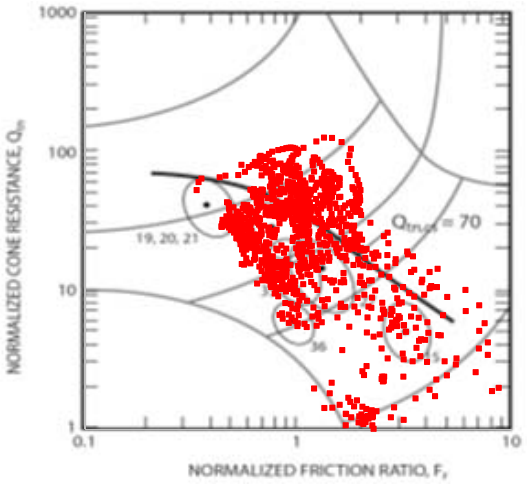	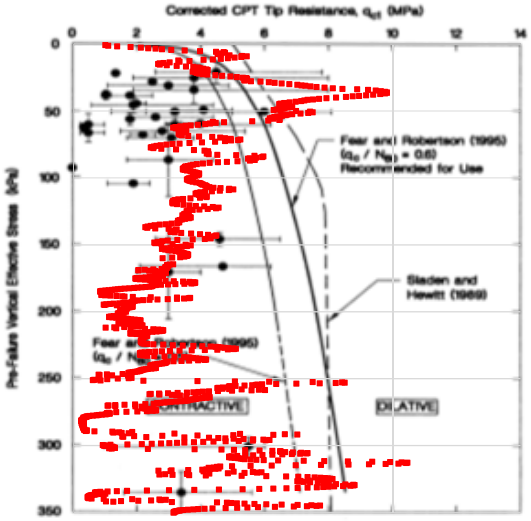	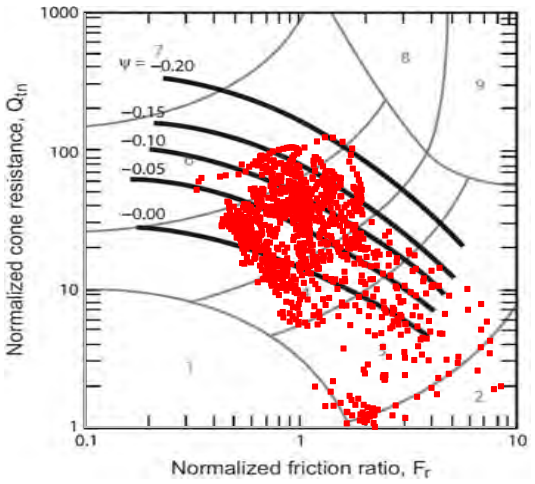

NOTE:

PROJECT

Fundão Tailings Dam Review Panel

TITLE

Fugro (September 2014 - March 2015) - Germano
CPTu-F40/98 Liquefaction Susceptibility and Soil Behavior Type

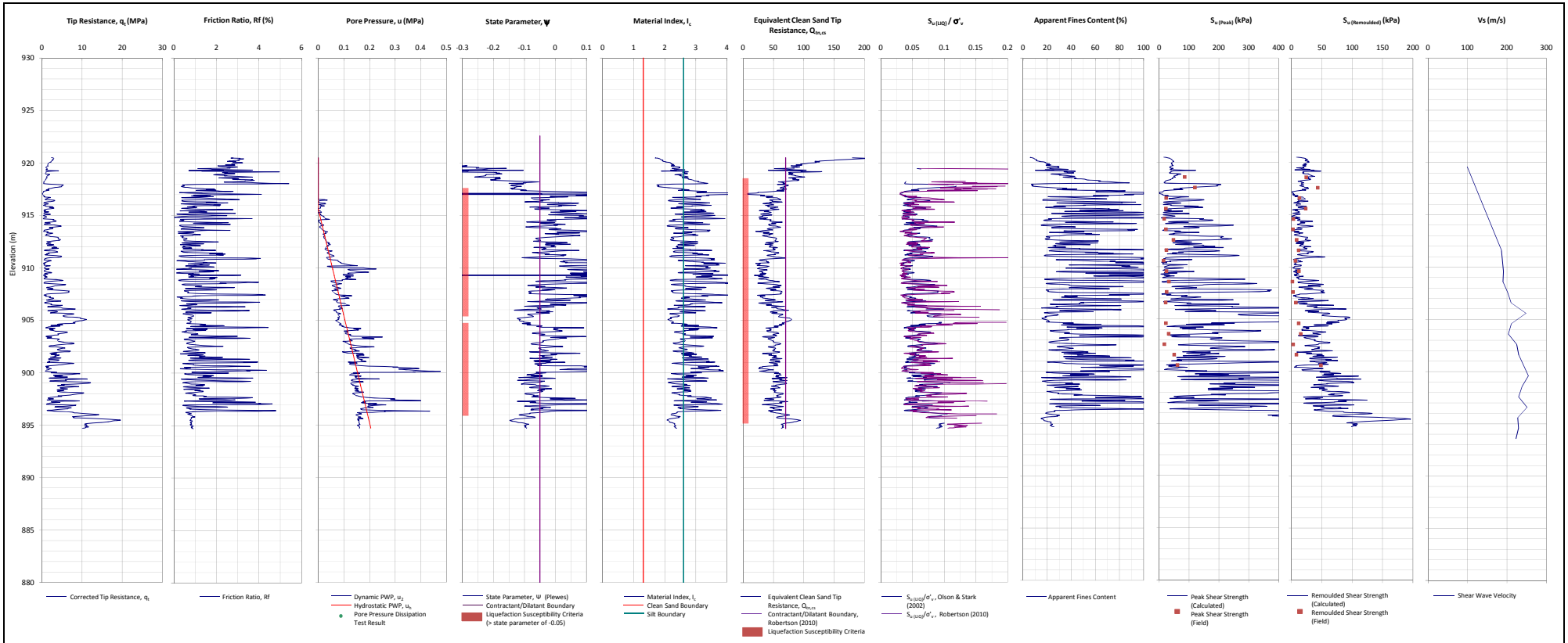

Notes:

1. This interpretation is based on the water and soil saturated unit weights γ_w=9.807 kN/m^3 and γ_{sat}=22 kN/m^3.
2. The friction ratio Rf is calculated as Rf=f_s/q_t.
3. The hydrostatic pore pressure is calculated using the ground water level (GWL) determined from CPT pore pressure dissipation tests (where available) or dynamic pore pressure.
4. Soil boundary layers (where plotted) are based on KCB interpretation.
5. The data presented have been plotted to the axis limits. Data may exist beyond the axis limits shown.
6. The Material Index (I_c) boundaries are based on Robertson and Wride (1998).
7. The $Q_{tn,cs}$ contractant/dilatant boundary=70 and is based on Robertson (2010).
8. The State Parameter (Ψ) calculated using Plewes, et al. (1992) is based on a K0 assumption of 0.5.
9. Coordinates are in UTM Zone 23K Córrego Alegre.
10. n_{ht} used in calculation of $S_{u(plot)}$ is 20.

Project: Fundão Tailings Dam Review Panel

Title: Fugro (September 2014 - March 2015) - Germano
CONE PENETRATION TEST CPTu-F42/86
N:7764204.2m E:658601.2m 2014-12-22

Liquefaction susceptibility after Robertson (2010) "Evaluation of Flow Liquefaction and Liquefied Strength Using the Cone Penetration Test"	Liquefaction susceptibility after Olson & Stark (2003) "Yield Strength Ratio and Liquefaction Analysis of Slopes and Embankments"	State parameter approximation - Robertson (2009) "Interpretation of cone penetration tests - a unified approach"

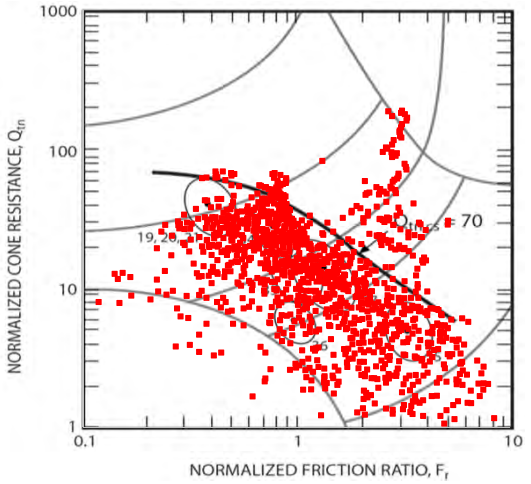

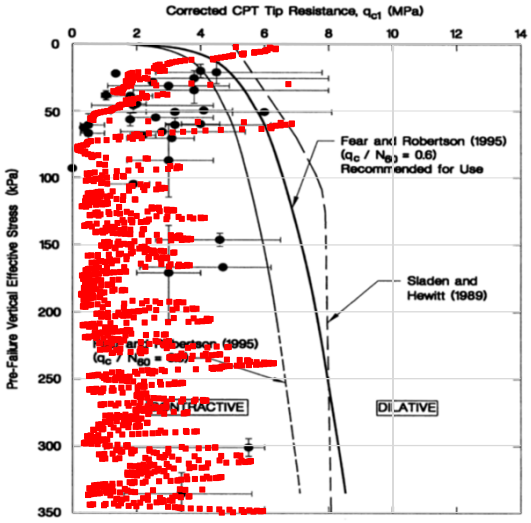

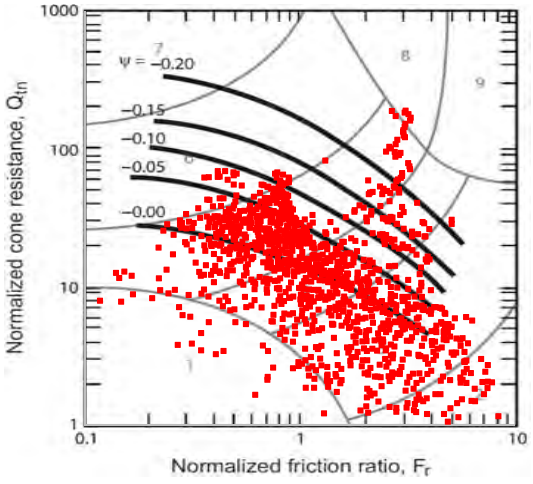

NOTE:

PROJECT

Fundão Tailings Dam Review Panel

TITLE

Fugro (September 2014 - March 2015) - Germano
CPTu-F42/86 Liquefaction Susceptibility and Soil Behavior Type

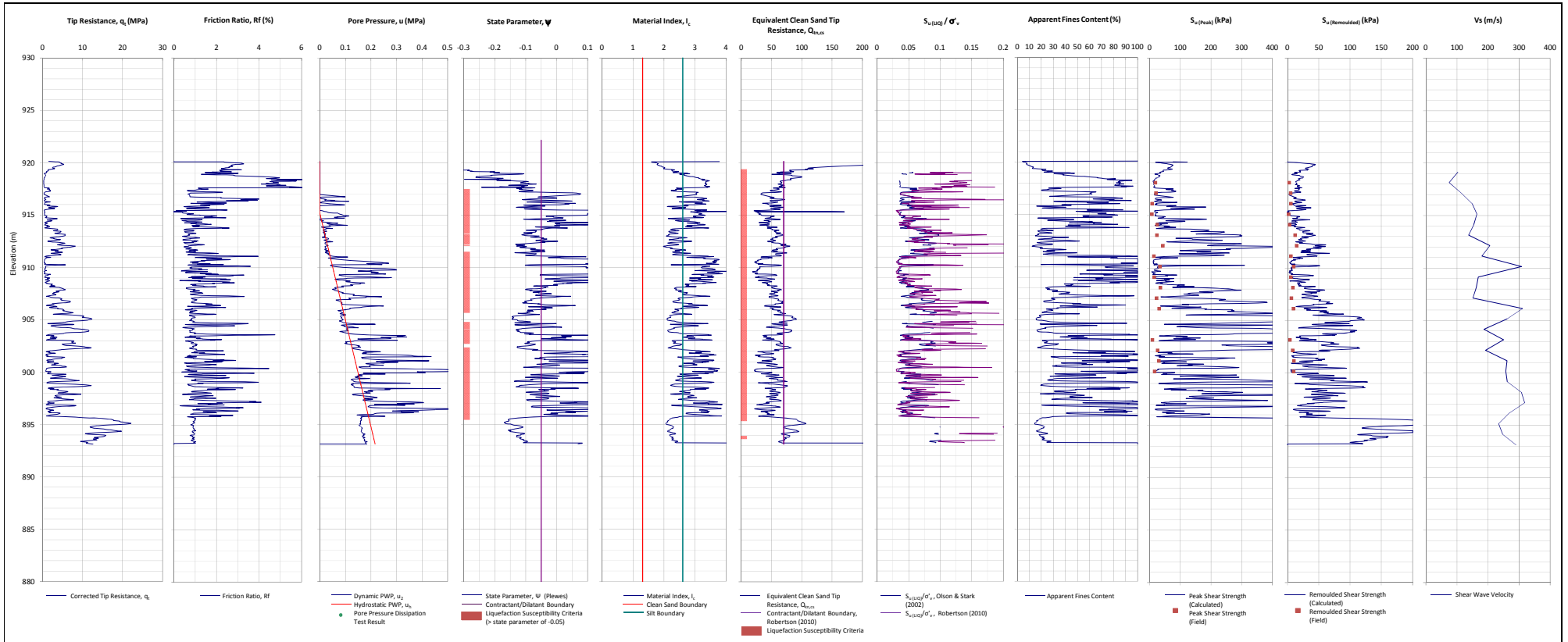

Notes:

1. This interpretation is based on the water and soil saturated unit weights γ_w=9.807 kN/m^3 and γ_{sat}=22 kN/m^3.
2. The friction ratio Rf is calculated as Rf=f_s/q_t.
3. The hydrostatic pore pressure is calculated using the ground water level (GWL) determined from CPT pore pressure dissipation tests (where available) or dynamic pore pressure.
4. Soil boundary layers (where plotted) are based on KCB interpretation.
5. The data presented have been plotted to the axis limits. Data may exist beyond the axis limits shown.
6. The Material Index (I_c) boundaries are based on Robertson and Wride (1998).
7. The $Q_{tn,cs}$ contractant/dilatant boundary=70 and is based on Robertson (2010).
8. The State Parameter (Ψ) calculated using Plewes, et al. (1992) is based on a K0 assumption of 0.5.
9. Coordinates are in UTM Zone 23K Córrego Alegre.
10. N_{kt} used in calculation of $S_{u(peak)}$ is 20.

PROJECT: Fundão Tailings Dam Review Panel

TITLE: Fugro (September 2014 - March 2015) - Germano
CONE PENETRATION TEST CPTu-F42/86A
N:7764262.3m E:658683.4m 2014-12-22

Liquefaction susceptibility after Robertson (2010) "Evaluation of Flow Liquefaction and Liquefied Strength Using the Cone Penetration Test"	Liquefaction susceptibility after Olson & Stark (2003) "Yield Strength Ratio and Liquefaction Analysis of Slopes and Embankments"	State parameter approximation - Robertson (2009) "Interpretation of cone penetration tests - a unified approach"

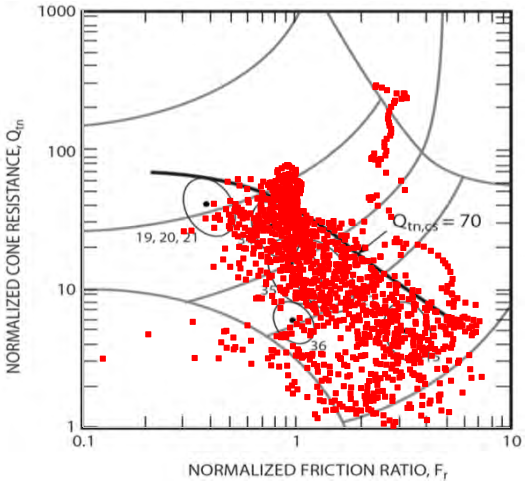

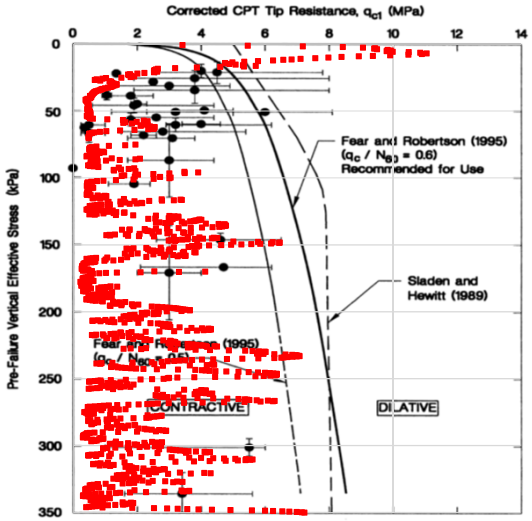

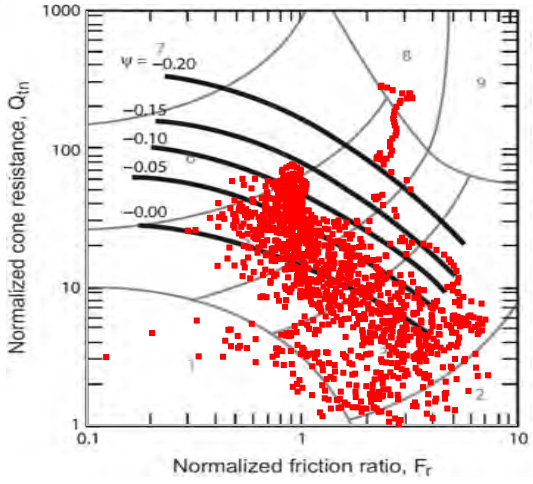

NOTE:

PROJECT

Fundão Tailings Dam Review Panel

TITLE

Fugro (September 2014 - March 2015) - Germano
CPTu-42/86A Liquefaction Susceptibility and Soil Behavior Type

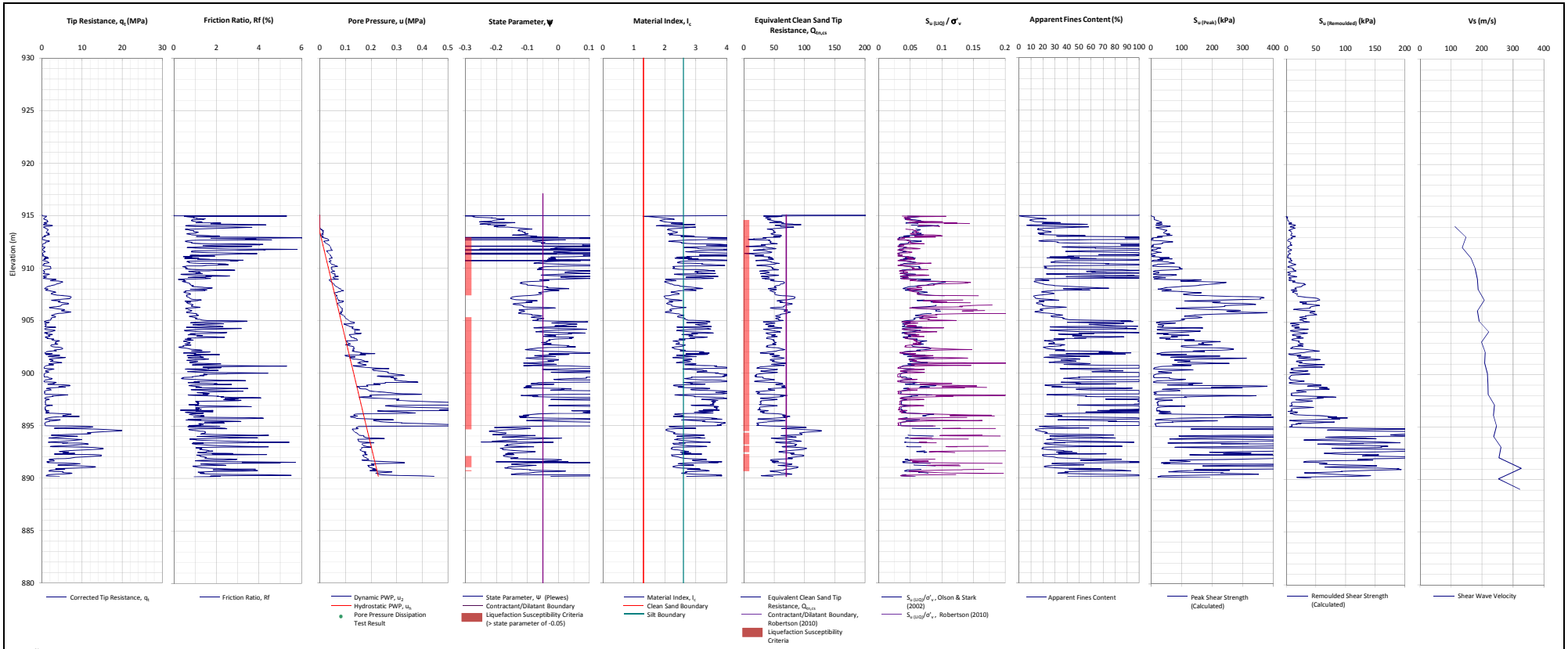

Notes:

1. This interpretation is based on the water and soil saturated unit weights γ_w=9.807 kN/m^3 and γ_{sat}=22 kN/m^3.
2. The friction ratio Rf is calculated as Rf=f_s/q_t.
3. The hydrostatic pore pressure is calculated using the ground water level (GWL) determined from CPT pore pressure dissipation tests (where available) or dynamic pore pressure.
4. Soil boundary layers (where plotted) are based on KCB interpretation.
5. The data presented have been plotted to the axis limits. Data may exist beyond the axis limits shown.
6. The Material Index (I_c) boundaries are based on Robertson and Wride (1998).
7. The $Q_{tn,cs}$ contractant/dilatant boundary=70 and is based on Robertson (2010).
8. The State Parameter (Ψ) calculated using Plewes, et al. (1992) is based on a K0 assumption of 0.5.
9. Coordinates are in UTM Zone 23K Córrego Alegre.
10. n_{ex} used in calculation of $S_{u(plot)}$ is 20.

Project: Fundão Tailings Dam Review Panel

Title: Fugro (September 2014 - March 2015) - Germano
CONE PENETRATION TEST CPTu-F42/92
N:7764200m E:656200m 2014-09-09

Liquefaction susceptibility after Robertson (2010) "Evaluation of Flow Liquefaction and Liquefied Strength Using the Cone Penetration Test"	Liquefaction susceptibility after Olson & Stark (2003) "Yield Strength Ratio and Liquefaction Analysis of Slopes and Embankments"	State parameter approximation - Robertson (2009) "Interpretation of cone penetration tests - a unified approach"

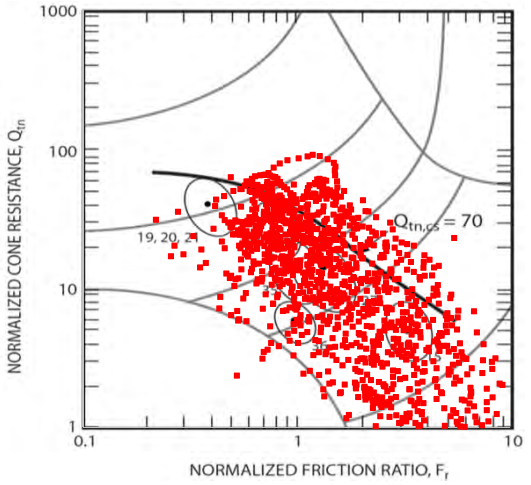

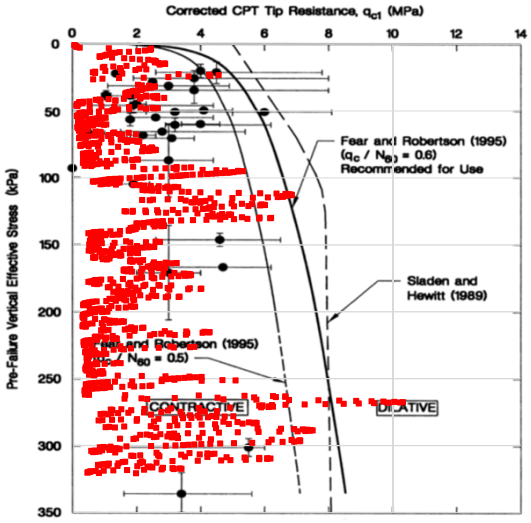

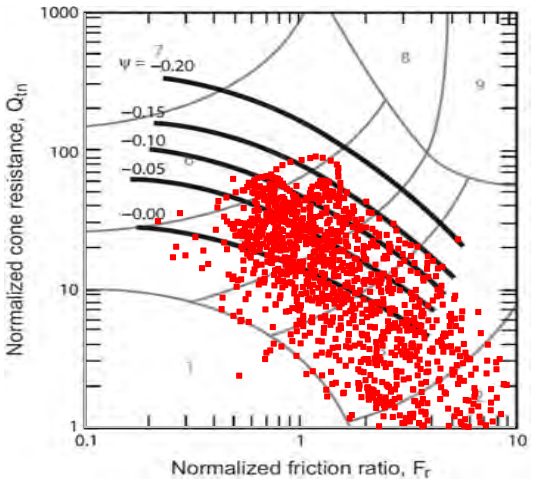

NOTE:

PROJECT

Fundão Tailings Dam Review Panel

TITLE

Fugro (September 2014 - March 2015) - Germano
CPTu-F42/92 Liquefaction Susceptibility and Soil Behavior Type

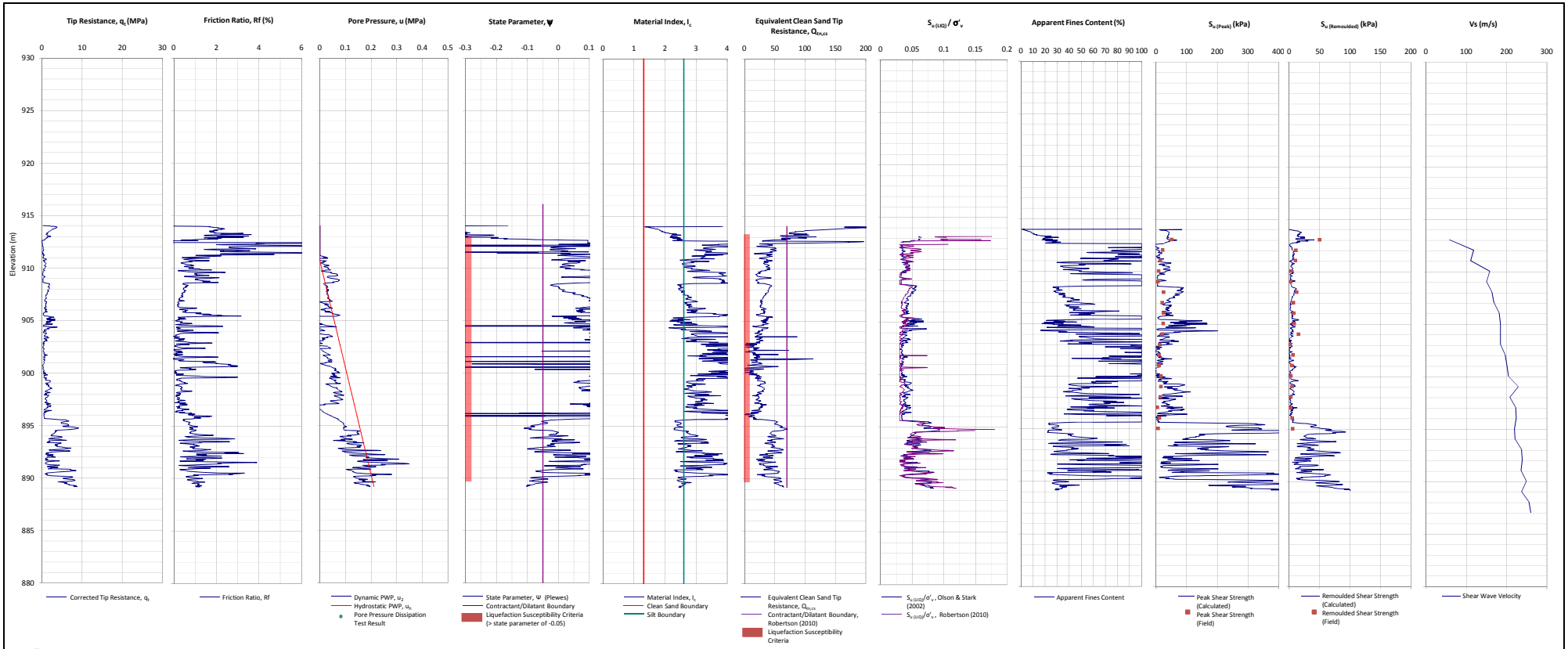

Notes:

1. This interpretation is based on the water and soil saturated unit weights γ_w=9.807 kN/m^3 and γ_{sat}=22 kN/m^3.
2. The friction ratio Rf is calculated as Rf=f_s/q_t.
3. The hydrostatic pore pressure is calculated using the ground water level (GWL) determined from CPT pore pressure dissipation tests (where available) or dynamic pore pressure.
4. Soil boundary layers (where plotted) are based on KCB interpretation.
5. The data presented have been plotted to the axis limits. Data may exist beyond the axis limits shown.
6. The Material Index (I_c) boundaries are based on Robertson and Wride (1998).
7. The $Q_{tn,cs}$ contractant/dilatant boundary=70 and is based on Robertson (2010).
8. The State Parameter (Ψ) calculated using Plewes, et al. (1992) is based on a K0 assumption of 0.5.
9. Coordinates are in UTM Zone 23K Córrego Alegre.
10. N_{kt} used in calculation of $S_{u(LIQ)}$ is 20.

Project: Fundão Tailings Dam Review Panel

Title: Fugro (September 2014 - March 2015) - Germano
CONE PENETRATION TEST CPTu-F42/96
N:7764200.1m E:659599.68m 2014-10-23

Liquefaction susceptibility after Robertson (2010) "Evaluation of Flow Liquefaction and Liquefied Strength Using the Cone Penetration Test"	Liquefaction susceptibility after Olson & Stark (2003) "Yield Strength Ratio and Liquefaction Analysis of Slopes and Embankments"	State parameter approximation - Robertson (2009) "Interpretation of cone penetration tests - a unified approach"
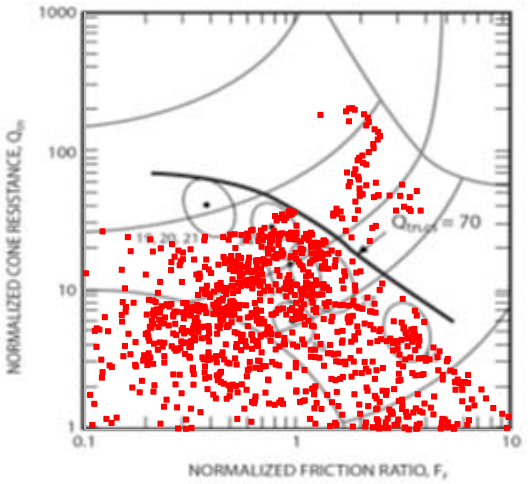	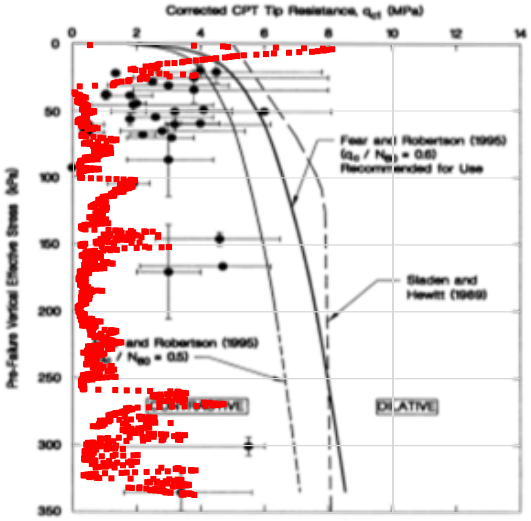	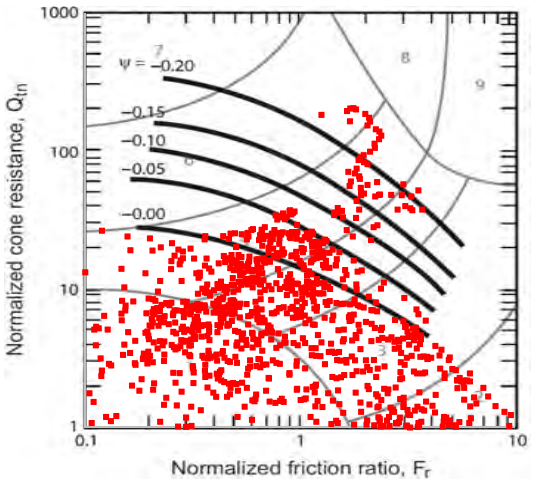

NOTE:

PROJECT

Fundão Tailings Dam Review Panel

TITLE

Fugro (September 2014 - March 2015) - Germano
CPTu-F42/96 Liquefaction Susceptibility and Soil Behavior Type

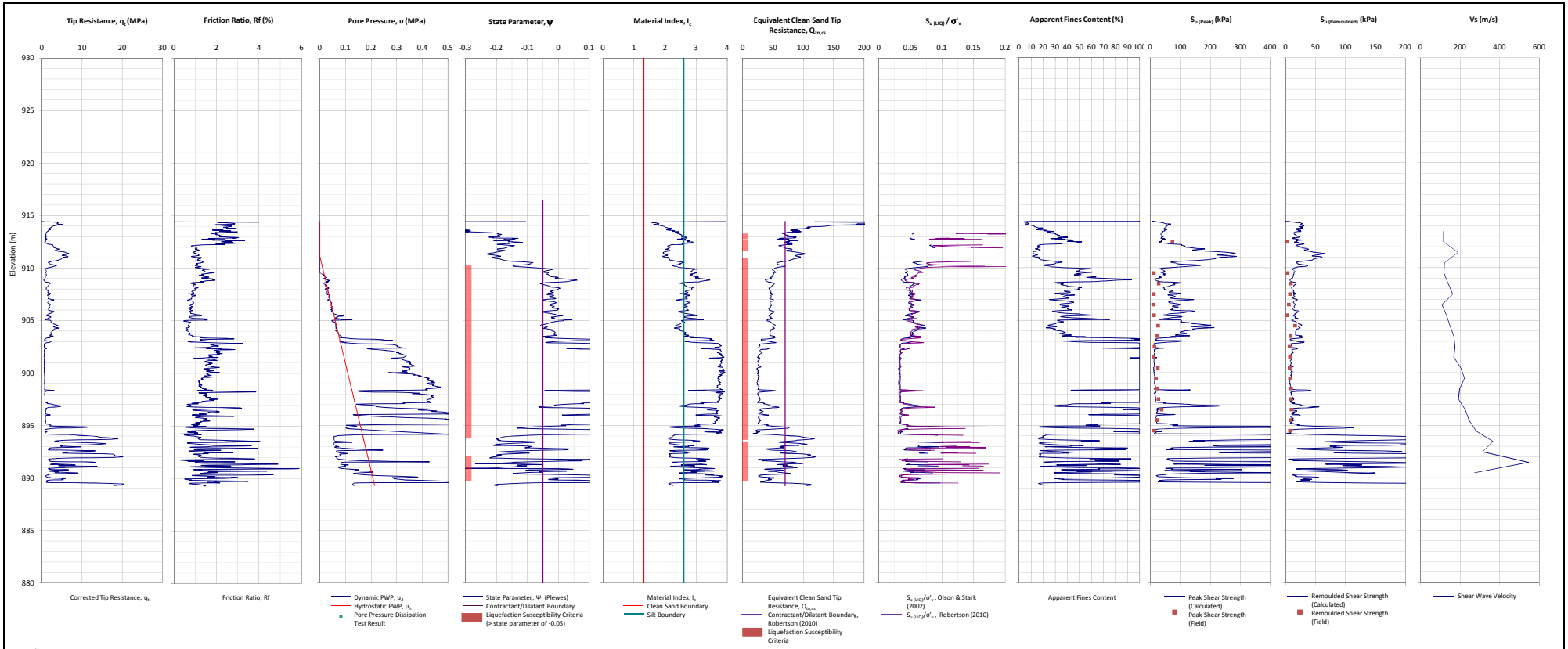

Notes:

1. This interpretation is based on the water and soil saturated unit weights γ_w=9.807 kN/m^3 and γ_{sat}=22 kN/m^3.
2. The friction ratio Rf is calculated as Rf=f_s/q_t.
3. The hydrostatic pore pressure is calculated using the ground water level (GWL) determined from CPT pore pressure dissipation tests (where available) or dynamic pore pressure.
4. Soil boundary layers (where plotted) are based on KCB interpretation.
5. The data presented have been plotted to the axis limits. Data may exist beyond the axis limits shown.
6. The Material Index (I_c) boundaries are based on Robertson and Wride (1998).
7. The $Q_{tn,cs}$ contractant/dilatant boundary=70 and is based on Robertson (2010).
8. The State Parameter (Ψ) calculated using Plewes, et al. (1992) is based on a K0 assumption of 0.5.
9. Coordinates are in UTM Zone 23K Córrego Alegre.
10. n_{ex} used in calculation of $S_{u(plot)}$ is 20.

Project: Fundão Tailings Dam Review Panel

Title: Fugro (September 2014 - March 2015) - Germano
CONE PENETRATION TEST CPTu-F42/98
N:7764203.89m E:659795.06m 2014-11-19

Liquefaction susceptibility after Robertson (2010) "Evaluation of Flow Liquefaction and Liquefied Strength Using the Cone Penetration Test"	Liquefaction susceptibility after Olson & Stark (2003) "Yield Strength Ratio and Liquefaction Analysis of Slopes and Embankments"	State parameter approximation - Robertson (2009) "Interpretation of cone penetration tests - a unified approach"

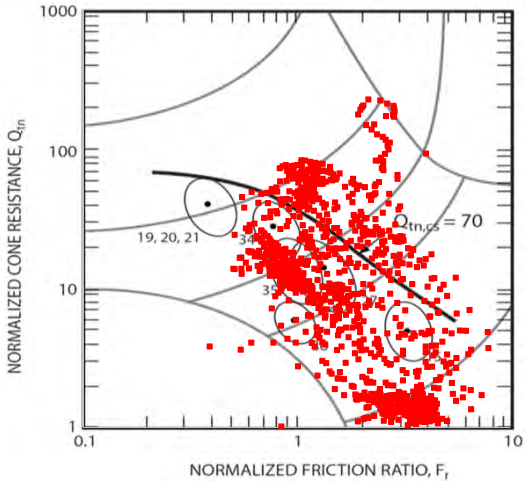

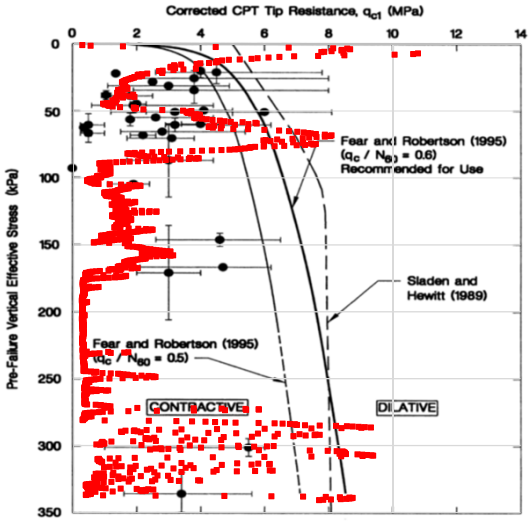

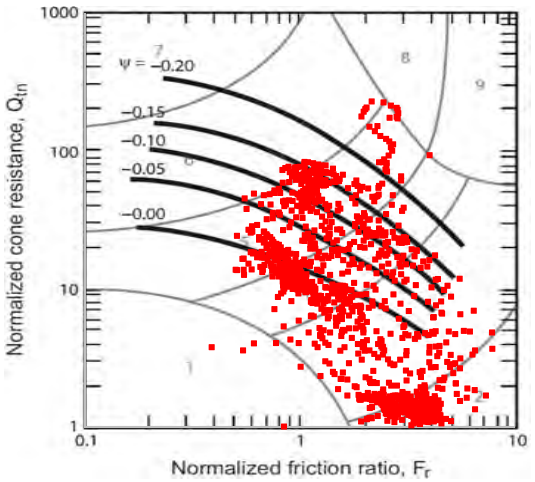

NOTE:

PROJECT

Fundão Tailings Dam Review Panel

TITLE

Fugro (September 2014 - March 2015) - Germano
CPTu-F42/98 Liquefaction Susceptibility and Soil Behavior Type

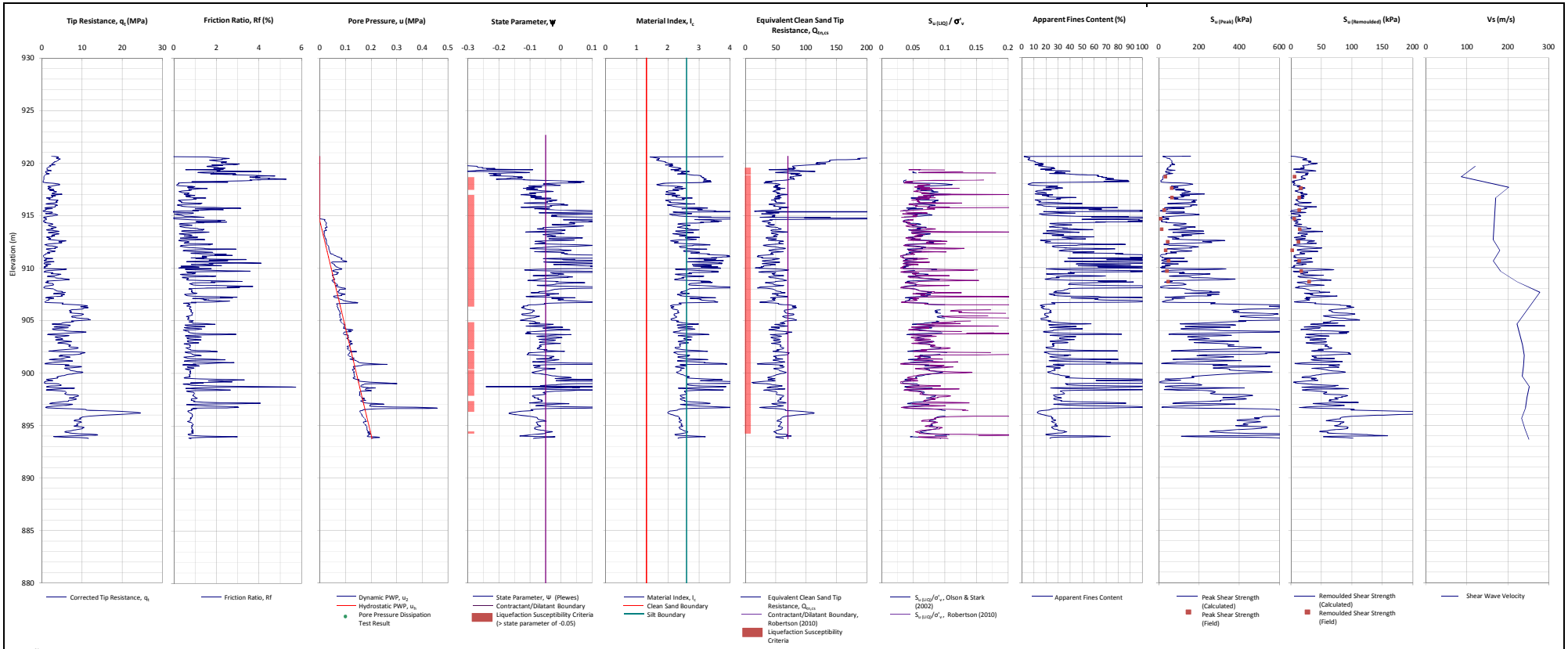

Notes:

1. This interpretation is based on the water and soil saturated unit weights γ_w=9.807 kN/m^3 and γ_{sat}=22 kN/m^3.
2. The friction ratio Rf is calculated as Rf=f_s/q_t.
3. The hydrostatic pore pressure is calculated using the ground water level (GWL) determined from CPT pore pressure dissipation tests (where available) or dynamic pore pressure.
4. Soil boundary layers (where plotted) are based on KCB interpretation.
5. The data presented have been plotted to the axis limits. Data may exist beyond the axis limits shown.
6. The Material Index (I_c) boundaries are based on Robertson and Wride (1998).
7. The $Q_{tn,cs}$ contractant/dilatant boundary=70 and is based on Robertson (2010).
8. The State Parameter (Ψ) calculated using Plewes, et al. (1992) is based on a K0 assumption of 0.5.
9. Coordinates are in UTM Zone 23K Córrego Alegre.
10. n_{ex} used in calculation of $S_{u(plots)}$ is 20.

Project: Fundão Tailings Dam Review Panel

Title: Fugro (September 2014 - March 2015) - Germano
CONE PENETRATION TEST CPTu-F43/85
N:7764309.5m E:658499.4m 2015-01-14

Liquefaction susceptibility after Robertson (2010) "Evaluation of Flow Liquefaction and Liquefied Strength Using the Cone Penetration Test"	Liquefaction susceptibility after Olson & Stark (2003) "Yield Strength Ratio and Liquefaction Analysis of Slopes and Embankments"	State parameter approximation - Robertson (2009) "Interpretation of cone penetration tests - a unified approach"

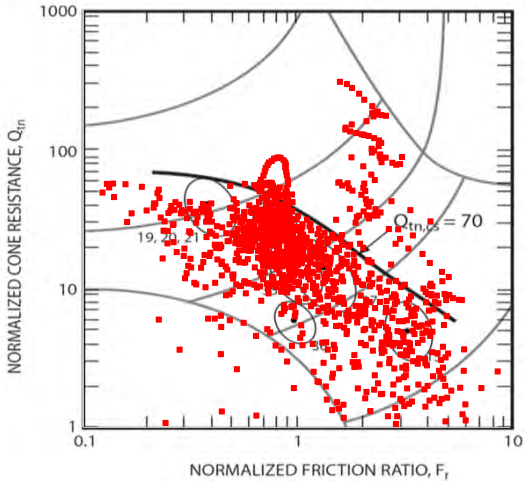

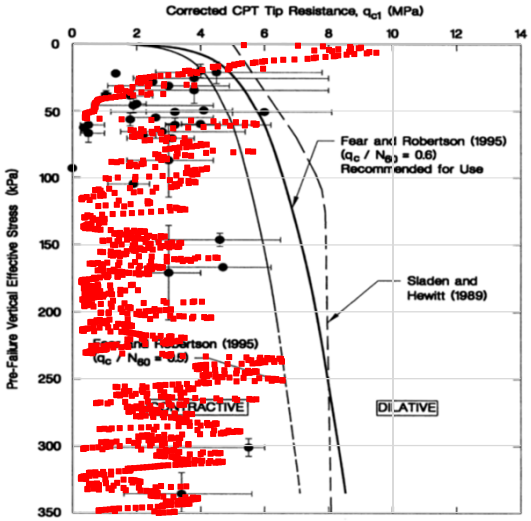

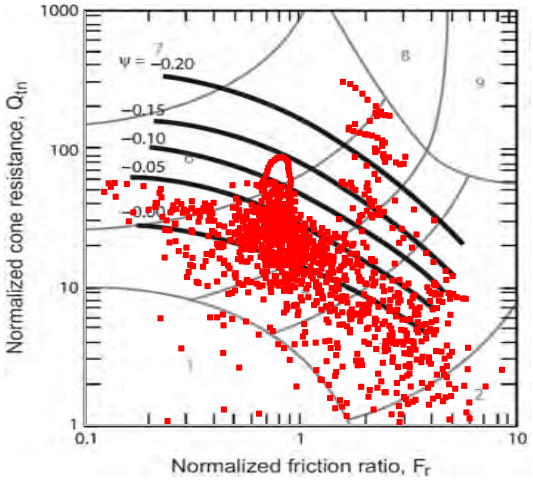

NOTE:

PROJECT

Fundão Tailings Dam Review Panel

TITLE

Fugro (September 2014 - March 2015) - Germano
CPTu-F43/85 Liquefaction Susceptibility and Soil Behavior Type

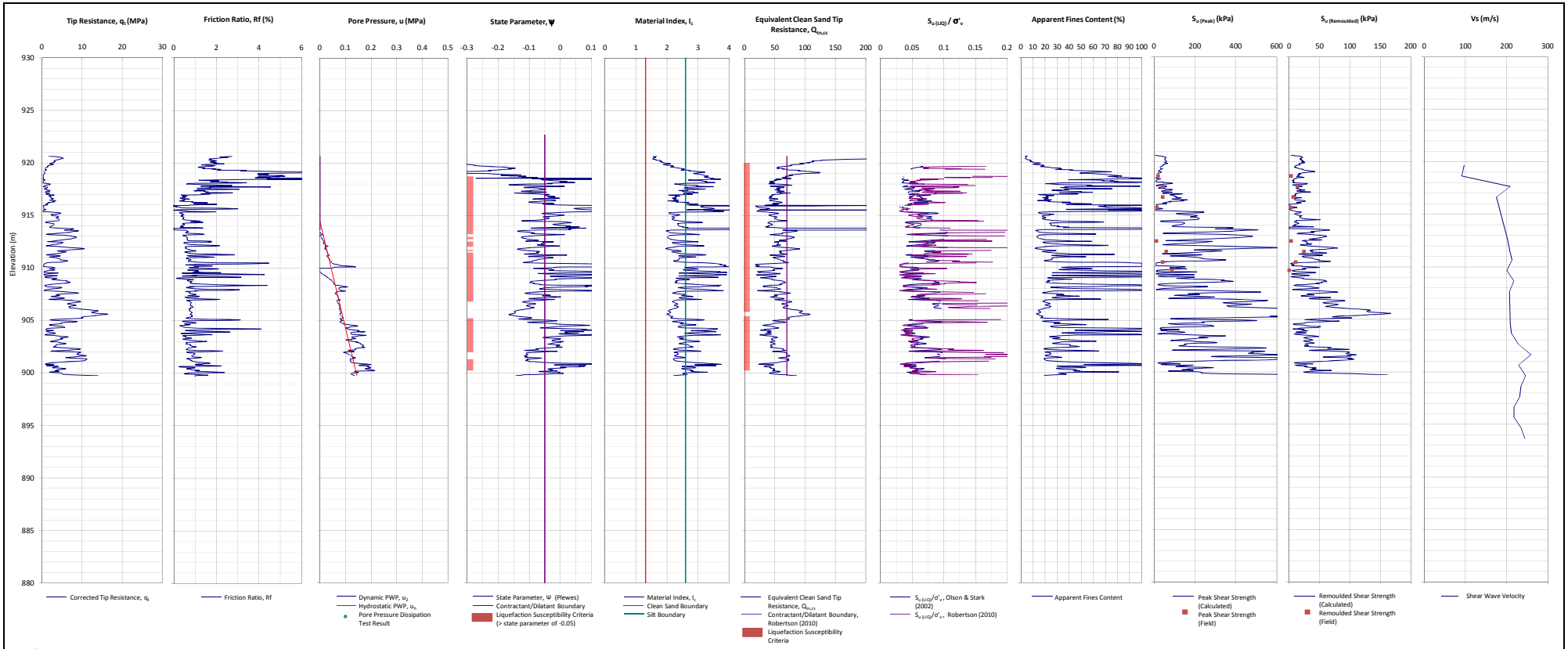

Notes:

1. This interpretation is based on the water and soil saturated unit weights γ_w=9.807 kN/m^3 and γ_{sat}=22 kN/m^3.
2. The friction ratio Rf is calculated as $Rf=f_s/q_t$.
3. The hydrostatic pore pressure is calculated using the ground water level (GWL) determined from CPT pore pressure dissipation tests (where available) or dynamic pore pressure.
4. Soil boundary layers (where plotted) are based on KCB interpretation.
5. The data presented have been plotted to the axis limits. Data may exist beyond the axis limits shown.
6. The Material Index (I_c) boundaries are based on Robertson and Wride (1998).
7. The $Q_{tn,cs}$ contractant/dilatant boundary=70 and is based on Robertson (2010).
8. The State Parameter (Ψ) calculated using Plewes, et al. (1992) is based on a K0 assumption of 0.5.
9. Coordinates are in UTM Zone 23K Córrego Alegre.
10. N_{kt} used in calculation of $S_{u(inst)}$ is 20.

Project: Fundão Tailings Dam Review Panel

Title: Fugro (September 2014 - March 2015) - Germano
CONE PENETRATION TEST CPTu-F43/85A
N:7764389.3m E:658549.2m 2015-01-13

Liquefaction susceptibility after Robertson (2010) "Evaluation of Flow Liquefaction and Liquefied Strength Using the Cone Penetration Test"	Liquefaction susceptibility after Olson & Stark (2003) "Yield Strength Ratio and Liquefaction Analysis of Slopes and Embankments"	State parameter approximation - Robertson (2009) "Interpretation of cone penetration tests - a unified approach"

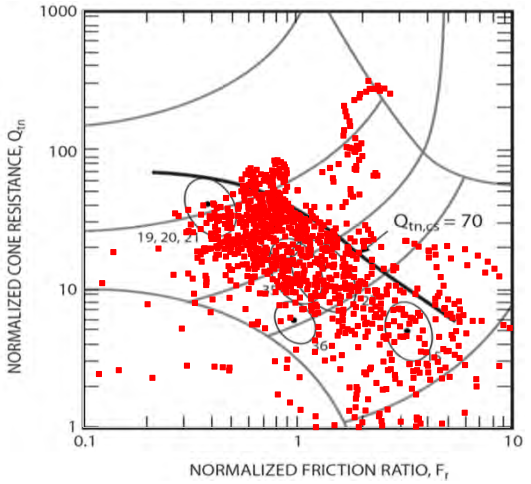

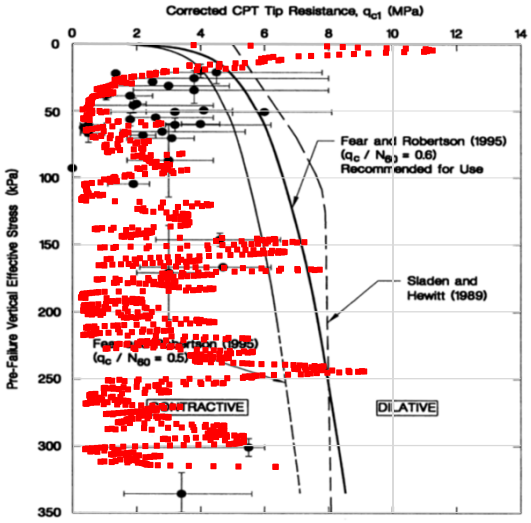

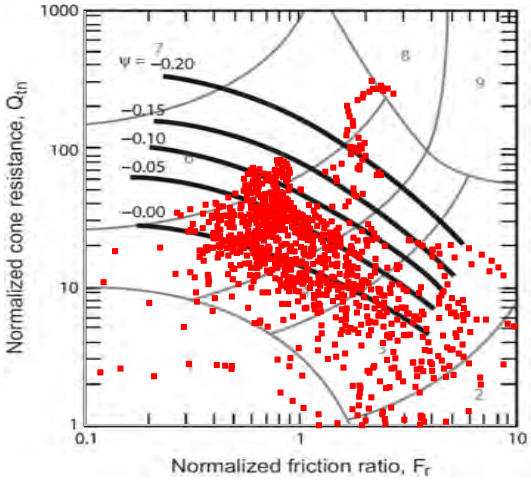

NOTE:

PROJECT

Fundão Tailings Dam Review Panel

TITLE

Fugro (September 2014 - March 2015) - Germano
CPTu-43/85A Liquefaction Susceptibility and Soil Behavior Type

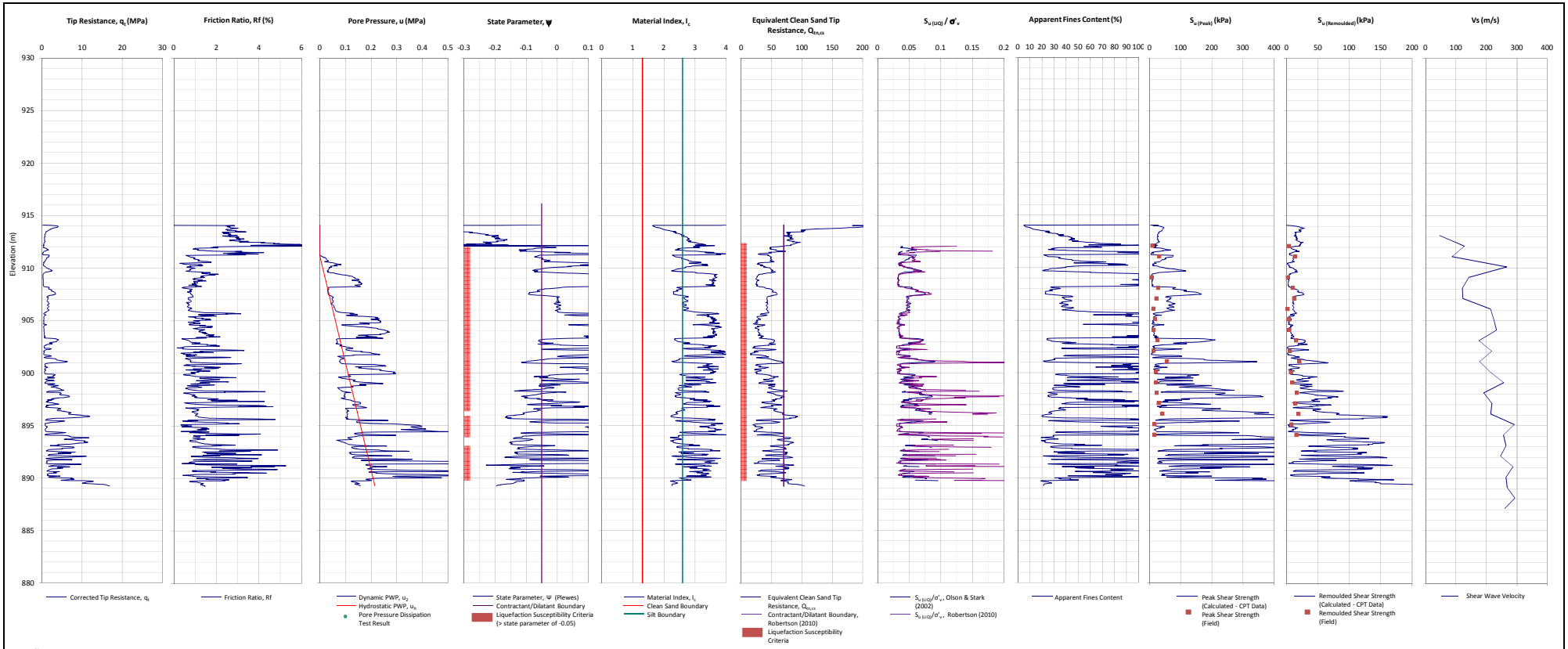

Notes:

1. This interpretation is based on the water and soil saturated unit weights γ_w=9.807 kN/m^3 and γ_{sat}=22 kN/m^3.
2. The friction ratio Rf is calculated as Rf=f_s/q_t.
3. The hydrostatic pore pressure is calculated using the ground water level (GWL) determined from CPT pore pressure dissipation tests (where available) or dynamic pore pressure.
4. Soil boundary layers (where plotted) are based on KCB interpretation.
5. The data presented have been plotted to the axis limits. Data may exist beyond the axis limits shown.
6. The Material Index (I_c) boundaries are based on Robertson and Wride (1998).
7. The $Q_{tn,cs}$ contractant/dilatant boundary=70 and is based on Robertson (2010).
8. The State Parameter (Ψ) calculated using Plewes, et al. (1992) is based on a K0 assumption of 0.5.
9. Coordinates are in UTM Zone 23K Córrego Alegre.
10. N_{kt} used in calculation of $S_{u(piezo)}$ is 20.

Project: Fundão Tailings Dam Review Panel

Title: Fugro (September 2014 - March 2015) - Germano
CONE PENETRATION TEST CPTu-F43/97
N:7764302.58m E:659697.84m 2014-10-22

Liquefaction susceptibility after Robertson (2010) "Evaluation of Flow Liquefaction and Liquefied Strength Using the Cone Penetration Test"	Liquefaction susceptibility after Olson & Stark (2003) "Yield Strength Ratio and Liquefaction Analysis of Slopes and Embankments"	State parameter approximation - Robertson (2009) "Interpretation of cone penetration tests - a unified approach"

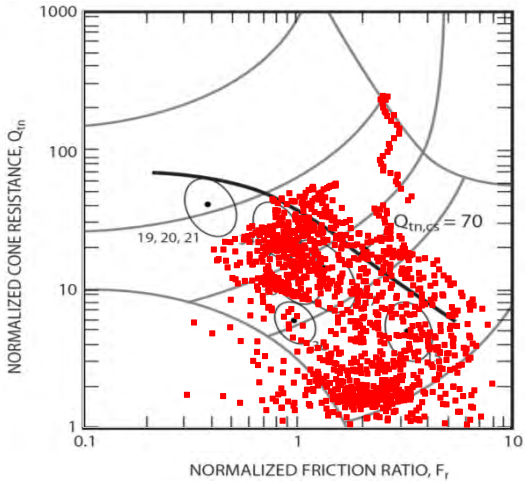

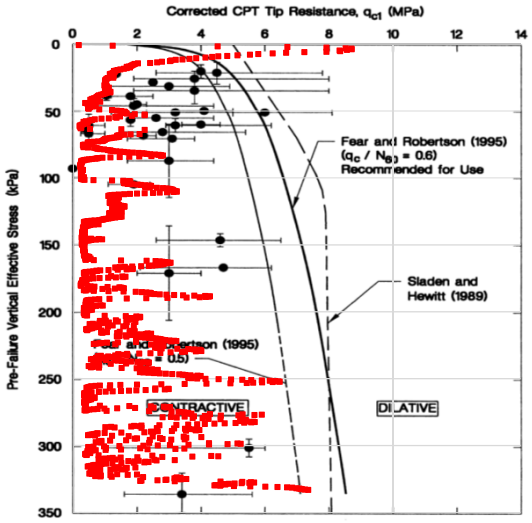

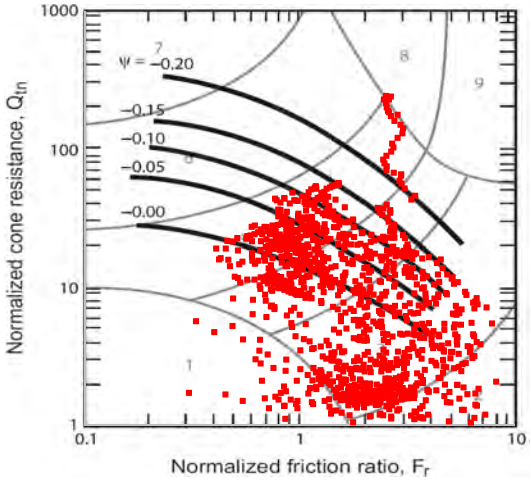

NOTE:

PROJECT

Fundão Tailings Dam Review Panel

TITLE

Fugro (September 2014 - March 2015) - Germano
CPTu-F43/97 Liquefaction Susceptibility and Soil Behavior Type

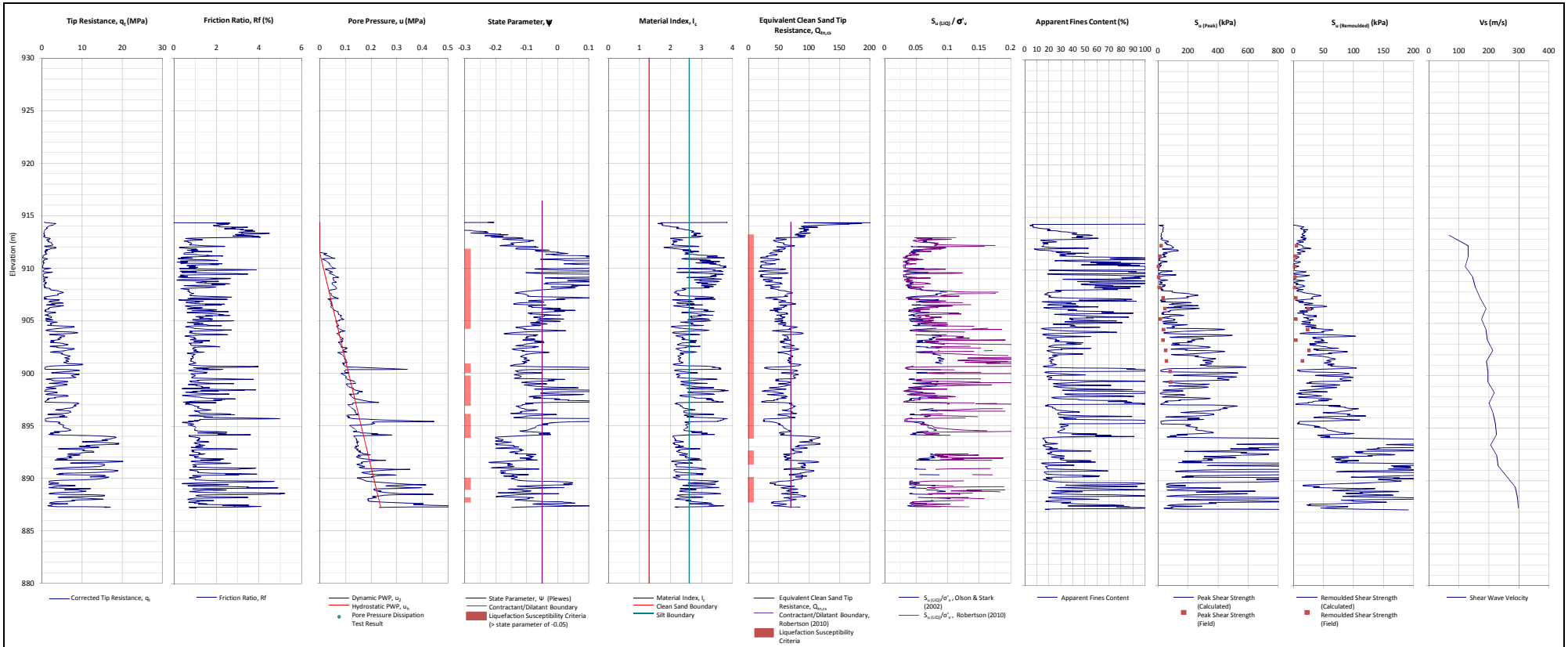

Notes:

1. This interpretation is based on the water and soil saturated unit weights γ_w=9.807 kN/m^3 and γ_{sat}=22 kN/m^3.
2. The friction ratio Rf is calculated as Rf=f_s/q_t.
3. The hydrostatic pore pressure is calculated using the ground water level (GWL) determined from CPT pore pressure dissipation tests (where available) or dynamic pore pressure.
4. Soil boundary layers (where plotted) are based on KCB interpretation.
5. The data presented have been plotted to the axis limits. Data may exist beyond the axis limits shown.
6. The Material Index (I_c) boundaries are based on Robertson and Wride (1998).
7. The $Q_{tn,cs}$ contractant/dilatant boundary=70 and is based on Robertson (2010).
8. The State Parameter (Ψ) calculated using Plewes, et al. (1992) is based on a K0 assumption of 0.5.
9. Coordinates are in UTM Zone 23K Córrego Alegre.
10. n_{Hz} used in calculation of $S_{u(plots)}$ is 20.

Project: Fundão Tailings Dam Review Panel

Title: Fugro (September 2014 - March 2015) - Germano
CONE PENETRATION TEST CPTu-F44/94
N:7764403.8m E:659398.8m 2014-11-25

Liquefaction susceptibility after Robertson (2010) "Evaluation of Flow Liquefaction and Liquefied Strength Using the Cone Penetration Test"	Liquefaction susceptibility after Olson & Stark (2003) "Yield Strength Ratio and Liquefaction Analysis of Slopes and Embankments"	State parameter approximation - Robertson (2009) "Interpretation of cone penetration tests - a unified approach"

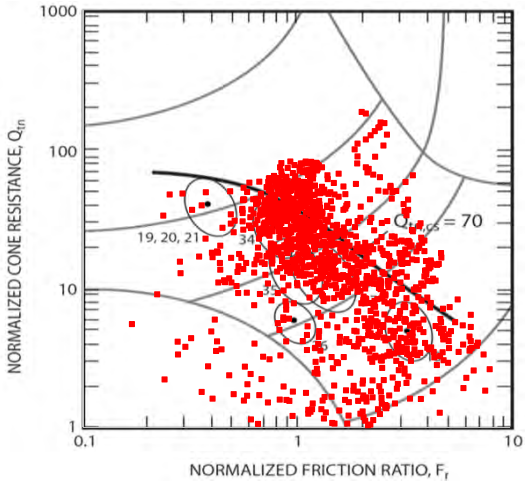

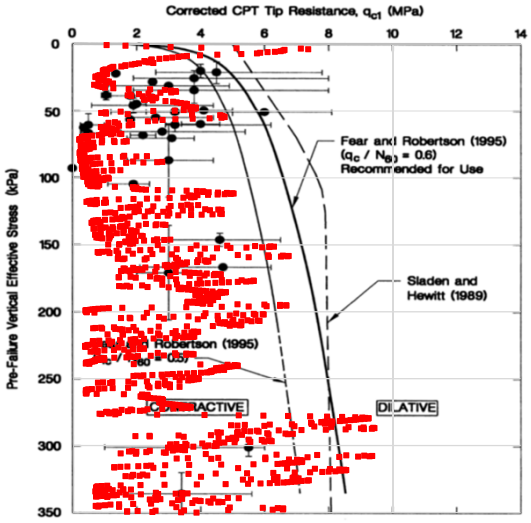

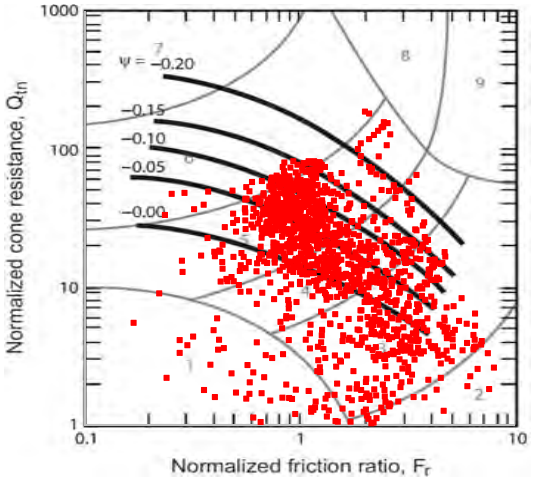

NOTE:

PROJECT

Fundão Tailings Dam Review Panel

TITLE

Fugro (September 2014 - March 2015) - Germano
CPTu-F44/94 Liquefaction Susceptibility and Soil Behavior Type

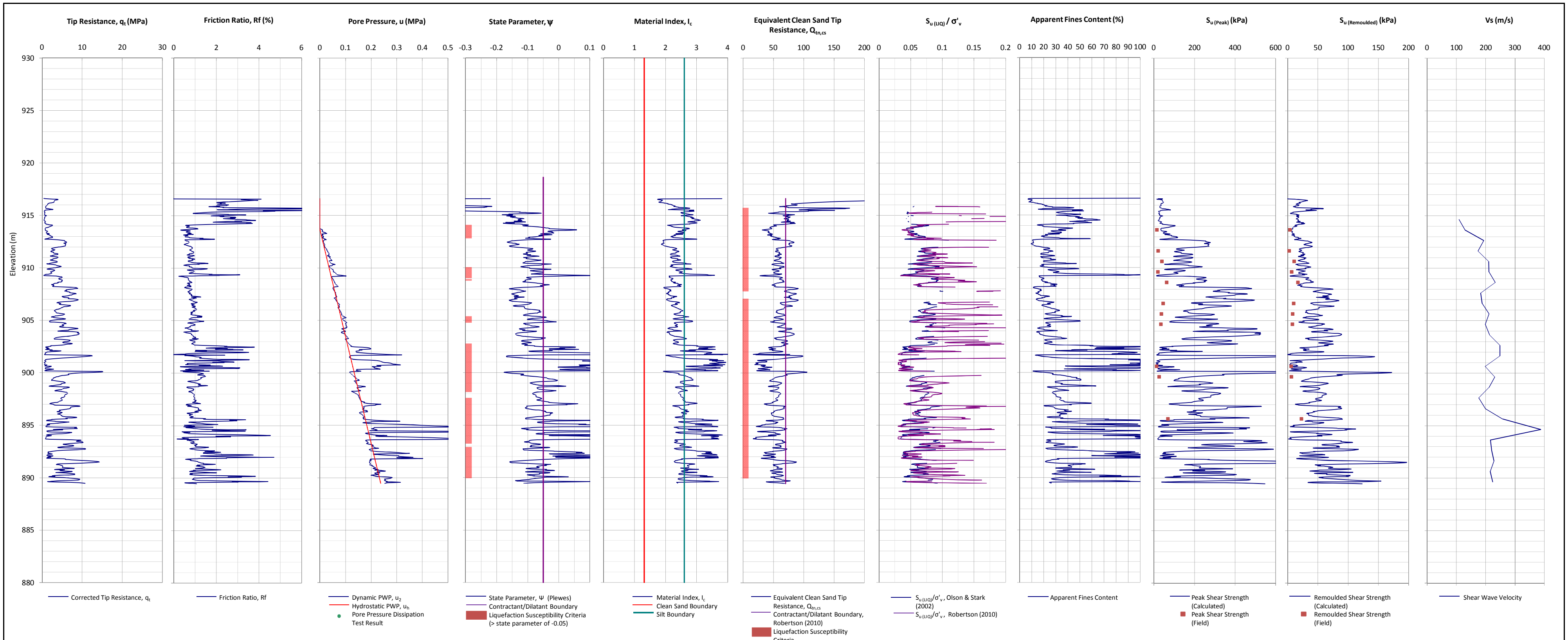

Notes:
1. This interpretation is based on the water and soil saturated unit weights γ_w=9.807 kN/m^3 and γ_{sat}=22 kN/m^3.
2. The friction ratio Rf is calculated as Rf=f_s/q_t.
3. The hydrostatic pore pressure is calculated using the ground water level (GWL) determined from CPT pore pressure dissipation tests (where available) or dynamic pore pressure.
4. Soil boundary layers (where plotted) are based on KCB interpretation.
5. The data presented have been plotted to the axis limits. Data may exist beyond the axis limits shown.
6. The Material Index (I_c) boundaries are based on Robertson and Wride (1998).
7. The $Q_{tn,cs}$ contractant/dilatant boundary=70 and is based on Robertson (2010).
8. The State Parameter (Ψ) calculated using Plewes, et al. (1992) is based on a K0 assumption of 0.5.
9. Coordinates are in UTM Zone 23K Córrego Alegre.
10. N_{kt} used in calculation of $S_{u(peak)}$ is 20.

PROJECT

Fundão Tailings Dam Review Panel

TITLE

Fugro (September 2014 - March 2015) - Germano
CONE PENETRATION TEST CPTu-F45/91
N:7764506.18m E:659100.4m 2014-11-28

Liquefaction susceptibility after Robertson (2010) "Evaluation of Flow Liquefaction and Liquefied Strength Using the Cone Penetration Test"	Liquefaction susceptibility after Olson & Stark (2003) "Yield Strength Ratio and Liquefaction Analysis of Slopes and Embankments"	State parameter approximation - Robertson (2009) "Interpretation of cone penetration tests - a unified approach"

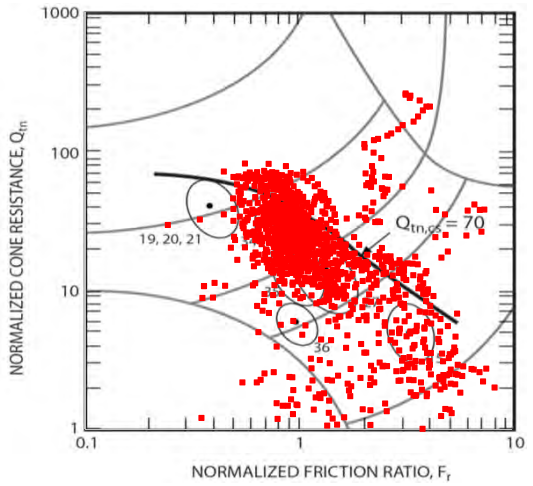

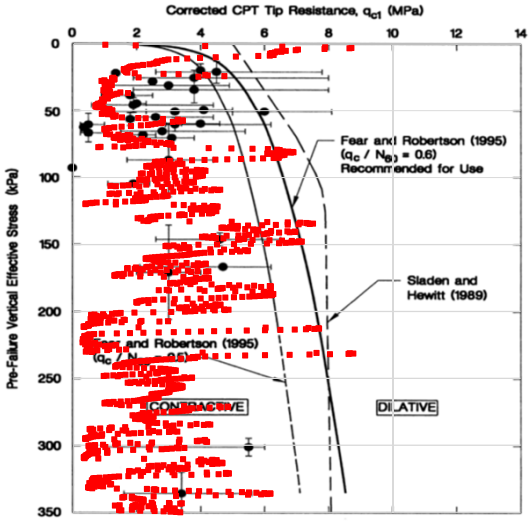

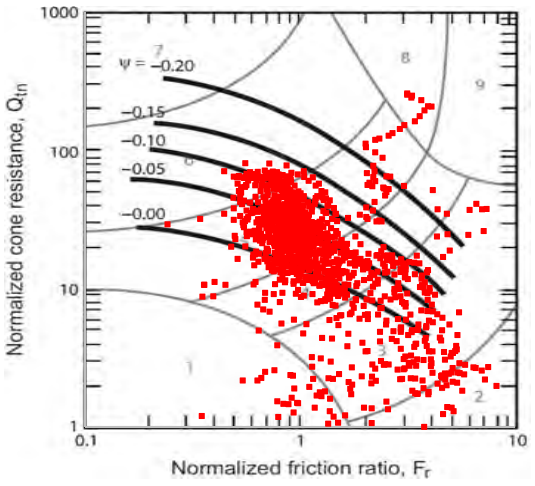

NOTE:

PROJECT

Fundão Tailings Dam Review Panel

TITLE

Fugro (September 2014 - March 2015) - Germano
CPTu-F45/91 Liquefaction Susceptibility and Soil Behavior Type

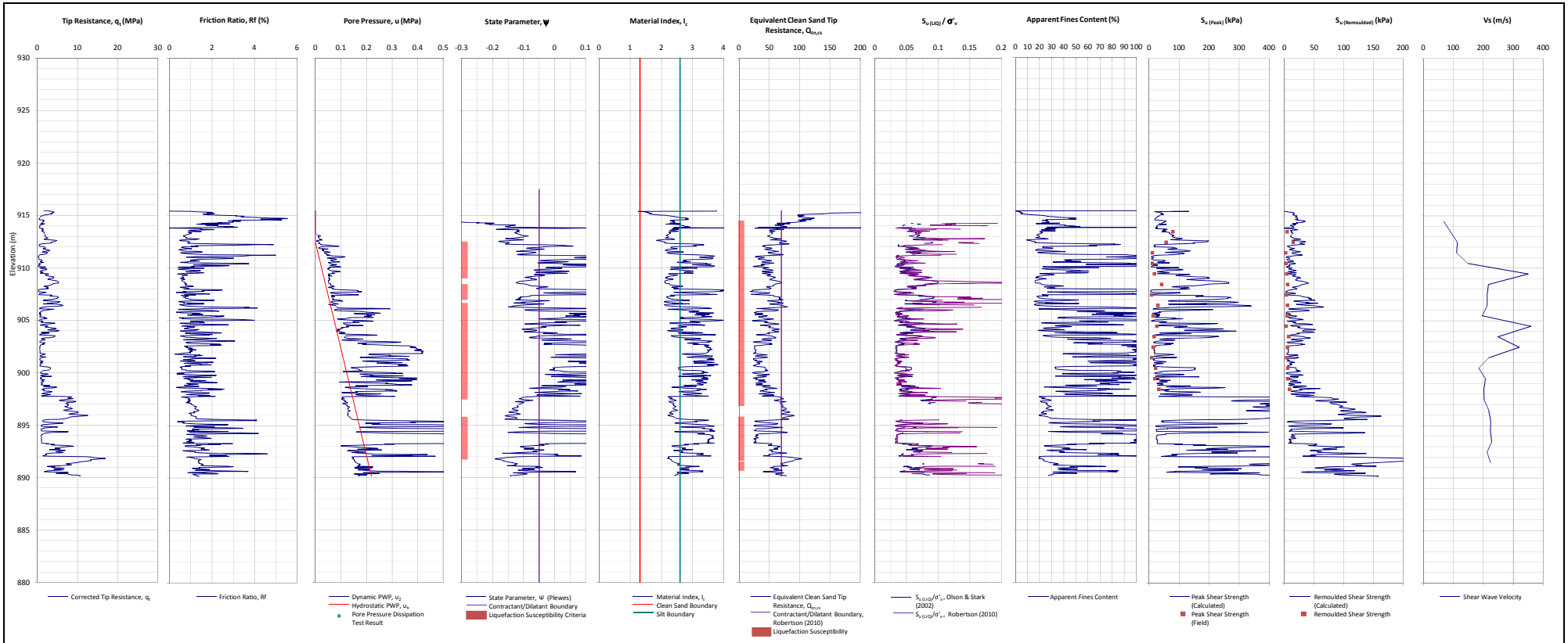

Notes:

1. This interpretation is based on the water and soil saturated unit weights γ_w=9.807 kN/m^3 and γ_{sat}=22 kN/m^3.
2. The friction ratio Rf is calculated as Rf=f_s/q_t.
3. The hydrostatic pore pressure is calculated using the ground water level (GWL) determined from CPT pore pressure dissipation tests (where available) or dynamic pore pressure.
4. Soil boundary layers (where plotted) are based on KCB interpretation.
5. The data presented have been plotted to the axis limits. Data may exist beyond the axis limits shown.
6. The Material Index (I_c) boundaries are based on Robertson and Wride (1998).
7. The $Q_{tn,cs}$ contractant/dilatant boundary=70 and is based on Robertson (2010).
8. The State Parameter (Ψ) calculated using Plewes, et al. (1992) is based on a K0 assumption of 0.5.
9. Coordinates are in UTM Zone 23K Córrego Alegre.
10. n_{ex} used in calculation of $S_{u(peak)}$ is 20.

Project: Fundão Tailings Dam Review Panel

Title: Fugro (September 2014 - March 2015) - Germano
CONE PENETRATION TEST CPTu-F46/92
N:7764605.84m E:659197.09m 2014-11-27

Liquefaction susceptibility after Robertson (2010) "Evaluation of Flow Liquefaction and Liquefied Strength Using the Cone Penetration Test"	Liquefaction susceptibility after Olson & Stark (2003) "Yield Strength Ratio and Liquefaction Analysis of Slopes and Embankments"	State parameter approximation - Robertson (2009) "Interpretation of cone penetration tests - a unified approach"

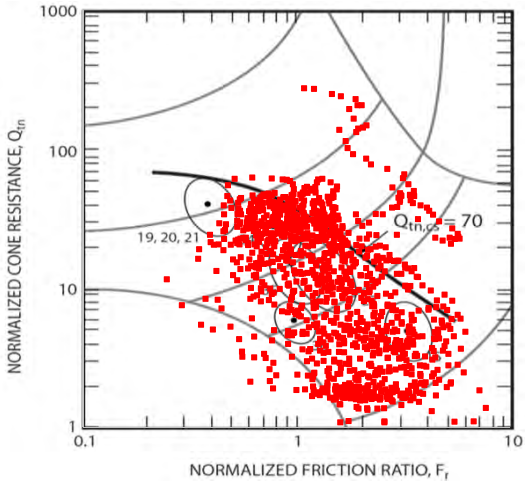

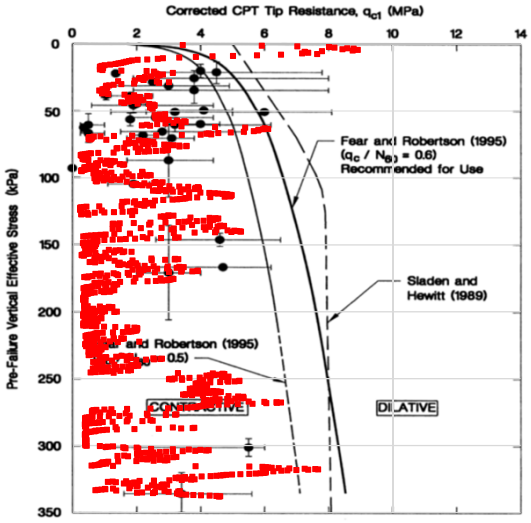

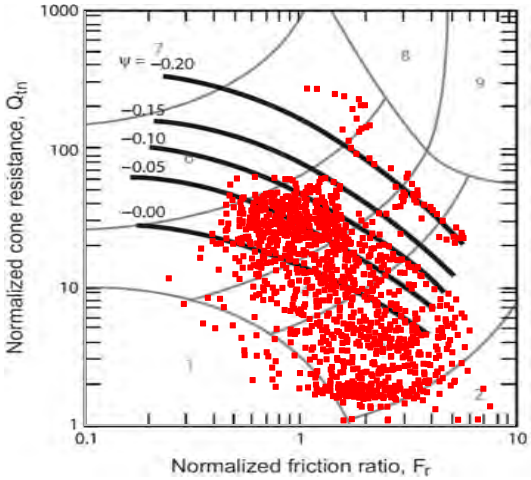

NOTE:

PROJECT

Fundão Tailings Dam Review Panel

TITLE

Fugro (September 2014 - March 2015) - Germano
CPTu-F46/92 Liquefaction Susceptibility and Soil Behavior Type

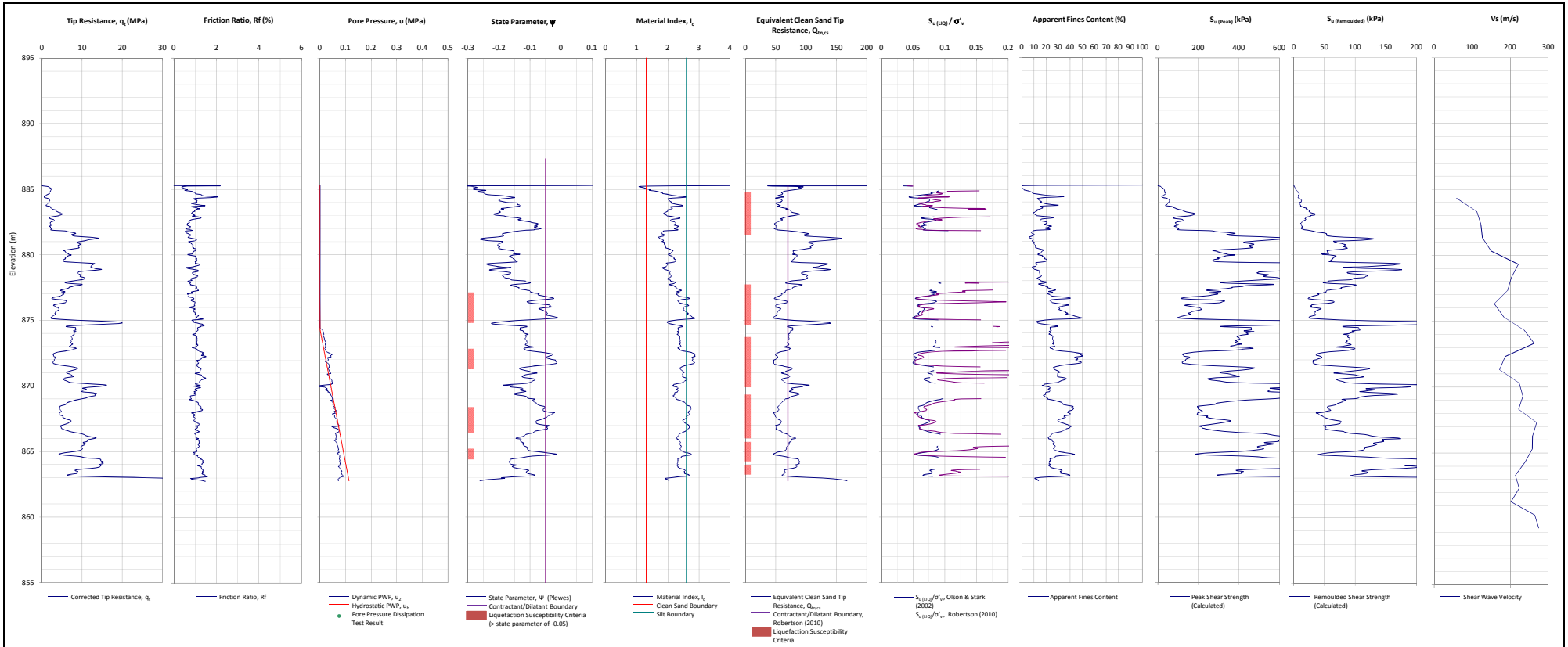

Notes:

1. This interpretation is based on the water and soil saturated unit weights γ_w=9.807 kN/m^3 and γ_{sat}=22 kN/m^3.
2. The friction ratio Rf is calculated as Rf=f_s/q_t.
3. The hydrostatic pore pressure is calculated using the ground water level (GWL) determined from CPT pore pressure dissipation tests (where available) or dynamic pore pressure.
4. Soil boundary layers (where plotted) are based on KCB interpretation.
5. The data presented have been plotted to the axis limits. Data may exist beyond the axis limits shown.
6. The Material Index (I_c) boundaries are based on Robertson and Wride (1998).
7. The $Q_{tn,cs}$ contractant/dilatant boundary=70 and is based on Robertson (2010).
8. The State Parameter (Ψ) calculated using Plewes, et al. (1992) is based on a K0 assumption of 0.5.
9. Coordinates are in UTM Zone 23K Córrego Alegre.
10. N_{kt} used in calculation of $S_{u(plot)}$ is 20.

Project: Fundão Tailings Dam Review Panel

Title: Fugro (September 2014 - March 2015) - Fundão
CONE PENETRATION TEST CPTu-F48/06
N:7764800.36m E:660599.08m 2014-11-27

Liquefaction susceptibility after Robertson (2010) "Evaluation of Flow Liquefaction and Liquefied Strength Using the Cone Penetration Test"	Liquefaction susceptibility after Olson & Stark (2003) "Yield Strength Ratio and Liquefaction Analysis of Slopes and Embankments"	State parameter approximation - Robertson (2009) "Interpretation of cone penetration tests - a unified approach"

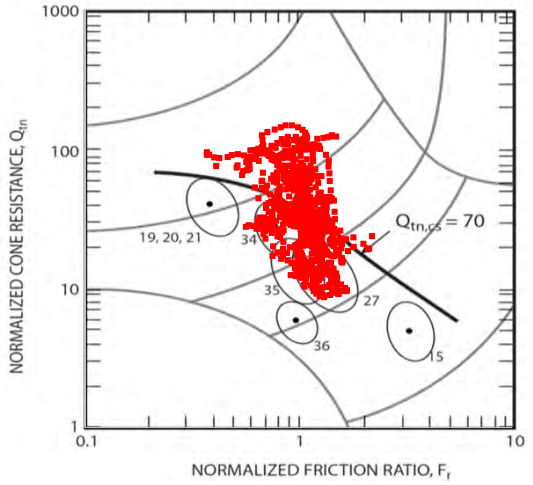

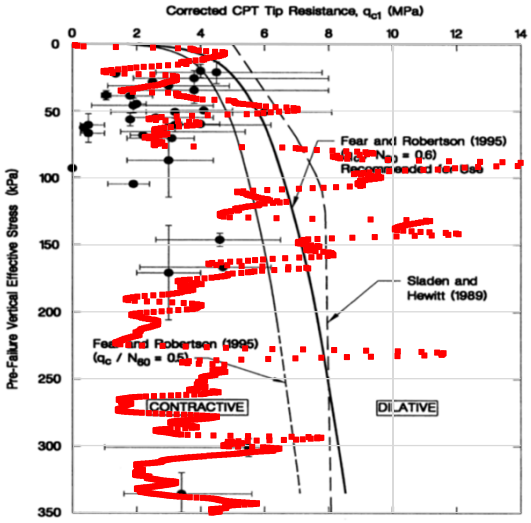

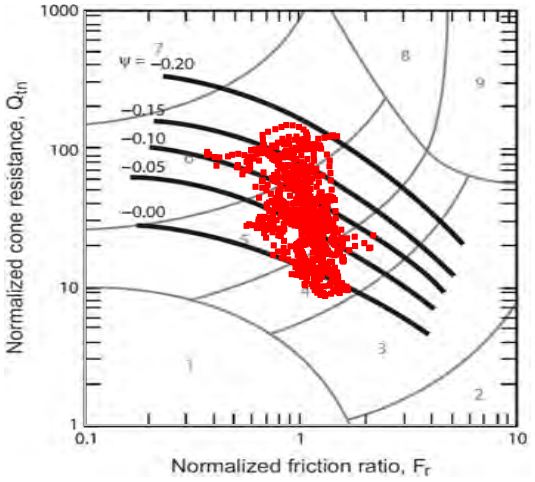

NOTE:

PROJECT

Fundão Tailings Dam Review Panel

TITLE

Fugro (September 2014 - March 2015) - Fundão
CPTu-F48/06 Liquefaction Susceptibility and Soil Behavior Type

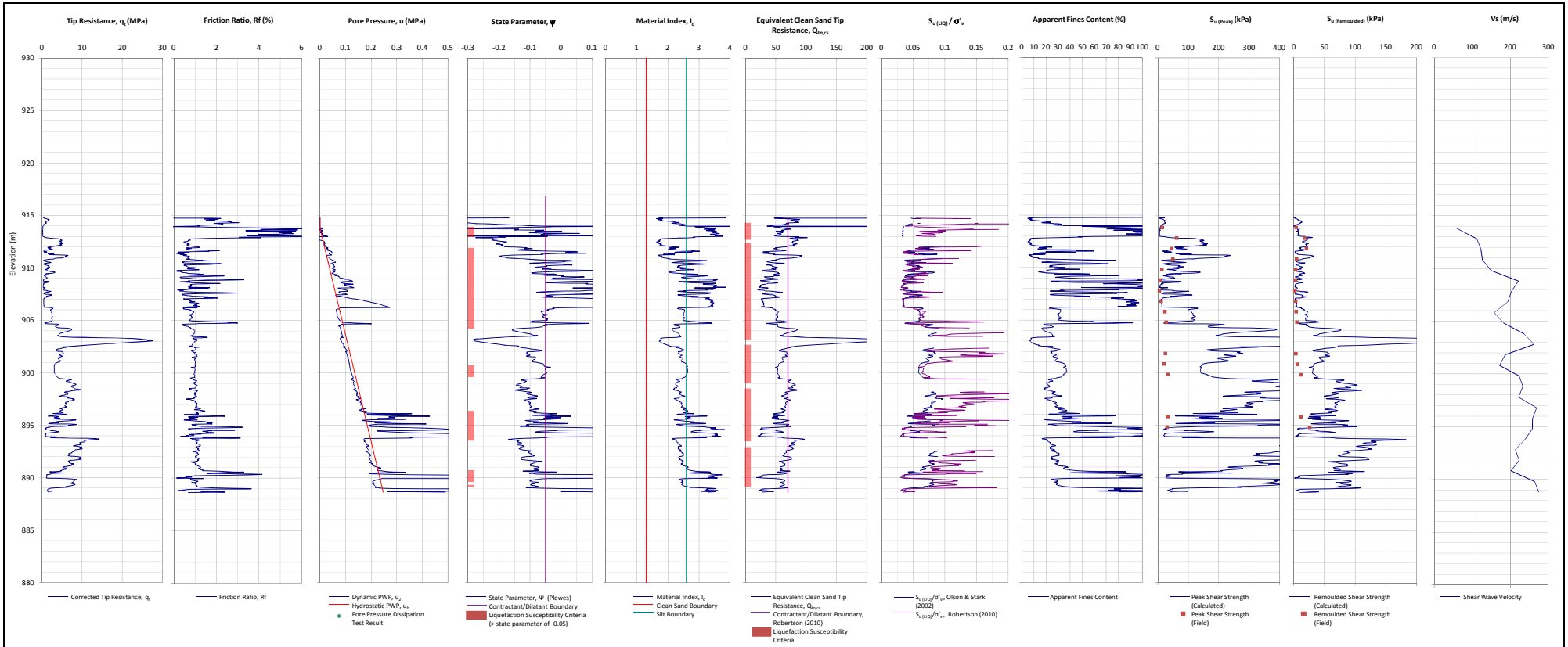

Notes:

1. This interpretation is based on the water and soil saturated unit weights γ_w=9.807 kN/m^3 and γ_{sat}=22 kN/m^3.
2. The friction ratio Rf is calculated as Rf=f_s/q_t.
3. The hydrostatic pore pressure is calculated using the ground water level (GWL) determined from CPT pore pressure dissipation tests (where available) or dynamic pore pressure.
4. Soil boundary layers (where plotted) are based on KCB interpretation.
5. The data presented have been plotted to the axis limits. Data may exist beyond the axis limits shown.
6. The Material Index (I_c) boundaries are based on Robertson and Wride (1998).
7. The $Q_{tn,cs}$ contractant/dilatant boundary=70 and is based on Robertson (2010).
8. The State Parameter (Ψ) calculated using Plewes, et al. (1992) is based on a K0 assumption of 0.5.
9. Coordinates are in UTM Zone 23K Córrego Alegre.
10. n_{ex} used in calculation of $S_{u(plots)}$ is 20.

Project: Fundão Tailings Dam Review Panel

Title: Fugro (September 2014 - March 2015) - Germano
CONE PENETRATION TEST CPTu-F48/90
N:7764795.74m E:659001.54m 2014-11-27

Liquefaction susceptibility after Robertson (2010) "Evaluation of Flow Liquefaction and Liquefied Strength Using the Cone Penetration Test"	Liquefaction susceptibility after Olson & Stark (2003) "Yield Strength Ratio and Liquefaction Analysis of Slopes and Embankments"	State parameter approximation - Robertson (2009) "Interpretation of cone penetration tests - a unified approach"

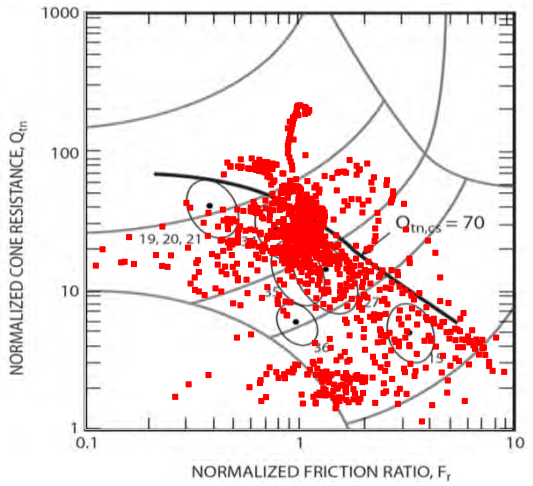

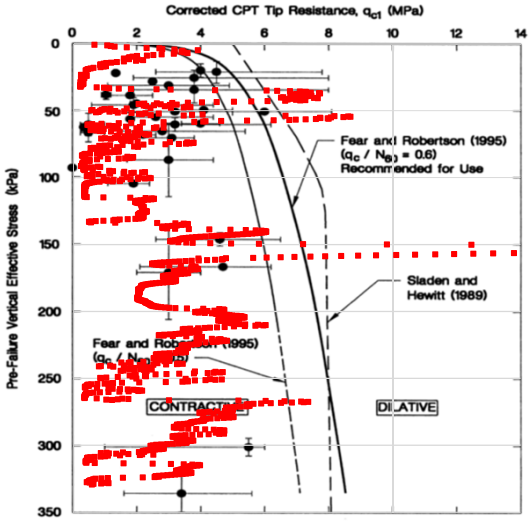

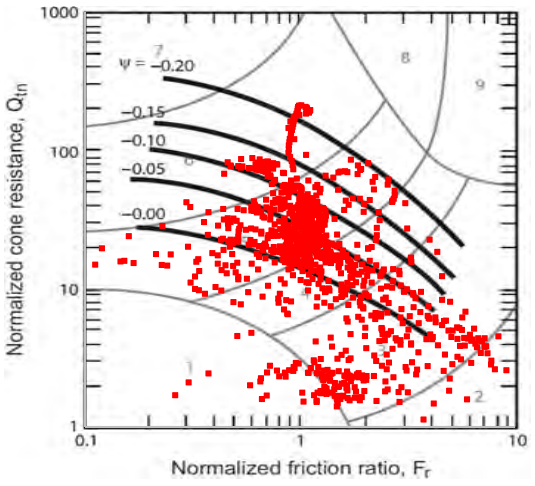

NOTE:

PROJECT

Fundão Tailings Dam Review Panel

TITLE

Fugro (September 2014 - March 2015) - Germano
CPTu-F48/90 Liquefaction Susceptibility and Soil Behavior Type

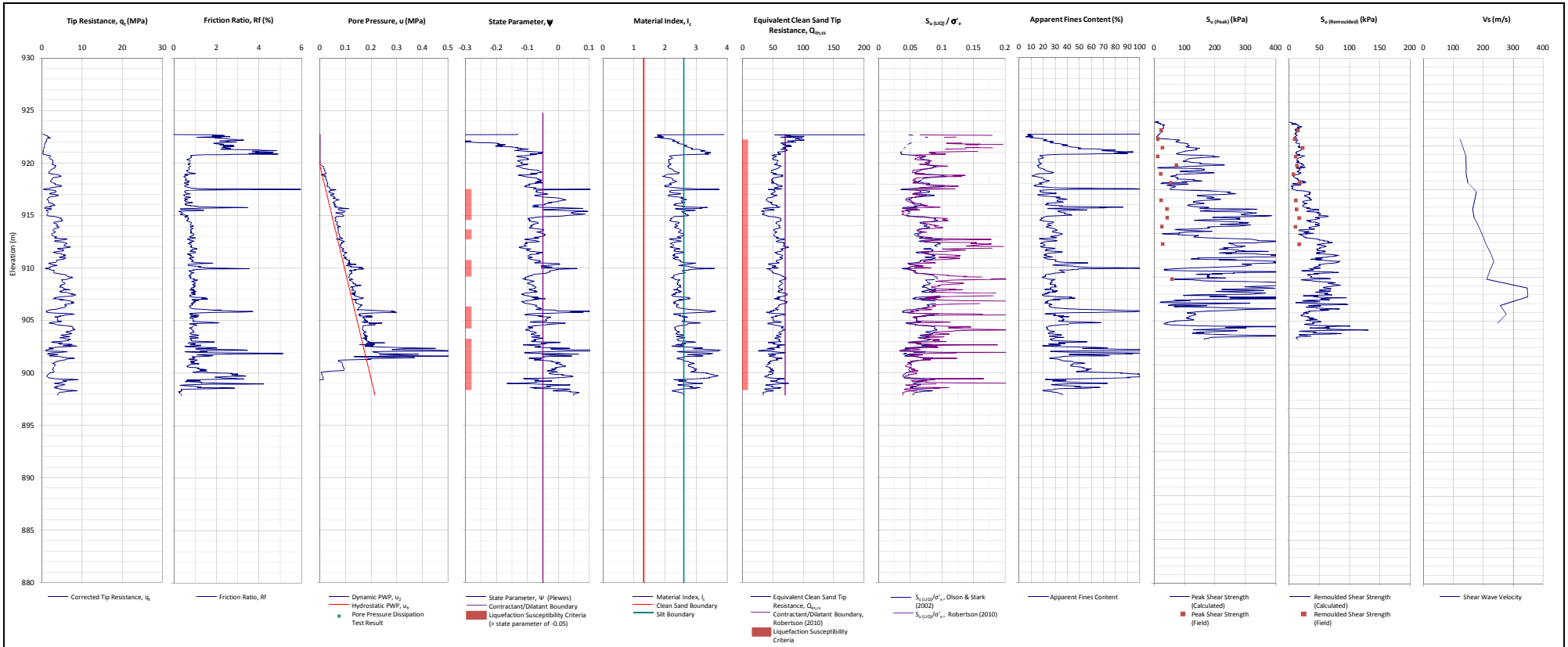

Notes:

1. This interpretation is based on the water and soil saturated unit weights γ_w=9.807 kN/m^3 and γ_{sat}=22 kN/m^3.
2. The friction ratio Rf is calculated as Rf=f_s/q_t.
3. The hydrostatic pore pressure is calculated using the ground water level (GWL) determined from CPT pore pressure dissipation tests (where available) or dynamic pore pressure.
4. Soil boundary layers (where plotted) are based on KCB interpretation.
5. The data presented have been plotted to the axis limits. Data may exist beyond the axis limits shown.
6. The Material Index (I_c) boundaries are based on Robertson and Wride (1998).
7. The $Q_{tn,cs}$ contractant/dilatant boundary=70 and is based on Robertson (2010).
8. The State Parameter (Ψ) calculated using Plewes, et al. (1992) is based on a K0 assumption of 0.5.
9. Coordinates are in UTM Zone 23K Córrego Alegre.
10. n_{ht} used in calculation of $S_{u(plot)}$ is 20.

Project: Fundão Tailings Dam Review Panel

Title: Fugro (September 2014 - March 2015) - Germano
CONE PENETRATION TEST CPTu-F50/84
N:7764998.76m E:658400.51m 2014-10-06

Liquefaction susceptibility after Robertson (2010) "Evaluation of Flow Liquefaction and Liquefied Strength Using the Cone Penetration Test"	Liquefaction susceptibility after Olson & Stark (2003) "Yield Strength Ratio and Liquefaction Analysis of Slopes and Embankments"	State parameter approximation - Robertson (2009) "Interpretation of cone penetration tests - a unified approach"

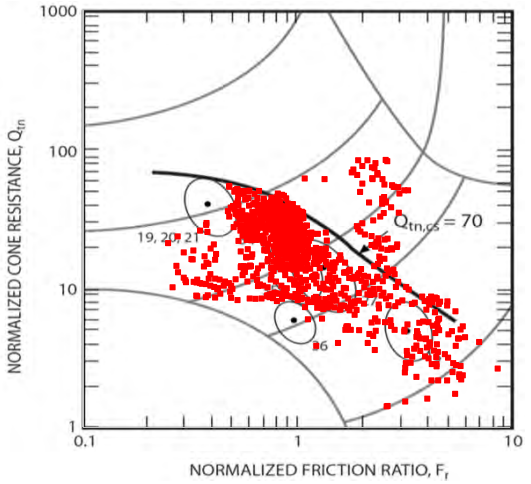

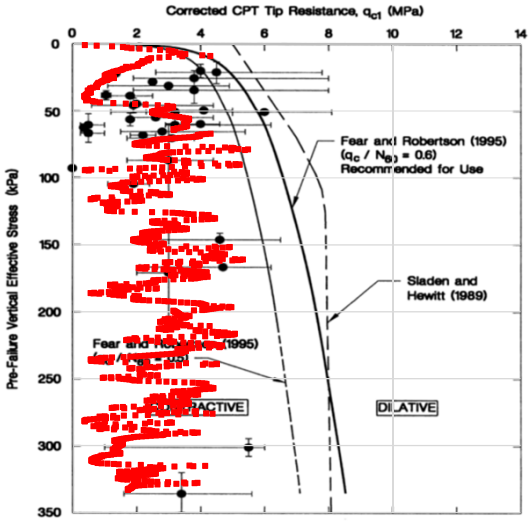

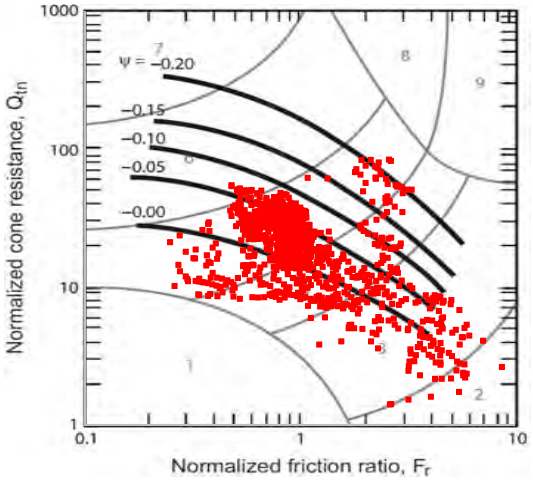

NOTE:

PROJECT

Fundão Tailings Dam Review Panel

TITLE

Fugro (September 2014 - March 2015) - Germano
CPTu-F50/84 Liquefaction Susceptibility and Soil Behavior Type

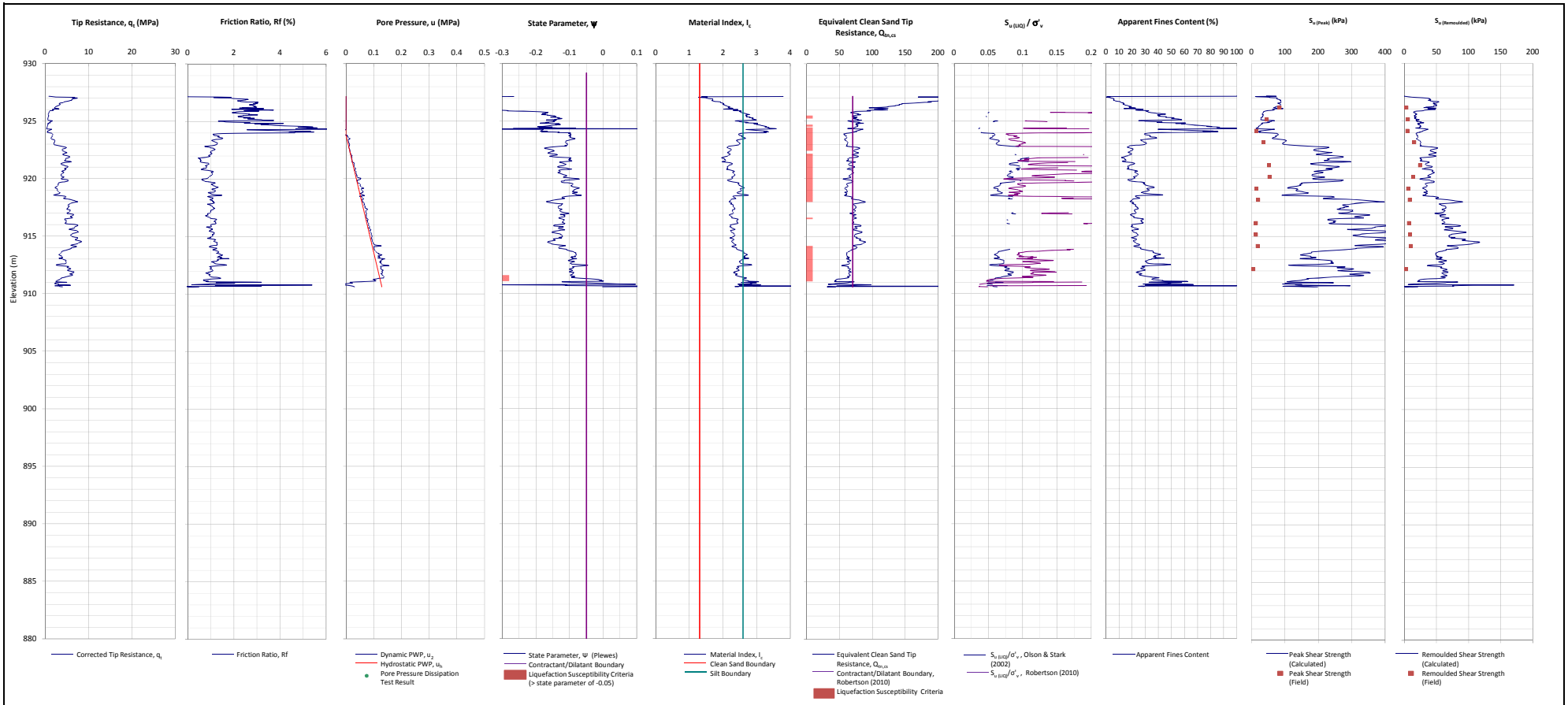

Notes:

1. This interpretation is based on the water and soil saturated unit weights γ_w=9.807 kN/m^3 and γ_{sat}=22 kN/m^3.
2. The friction ratio Rf is calculated as Rf=f_s/q_t.
3. The hydrostatic pore pressure is calculated using the ground water level (GWL) determined from CPT pore pressure dissipation tests (where available) or dynamic pore pressure.
4. Soil boundary layers (where plotted) are based on KCB interpretation.
5. The data presented have been plotted to the axis limits. Data may exist beyond the axis limits shown.
6. The Material Index (I_c) boundaries are based on Robertson and Wride (1998).
7. The $Q_{tn,cs}$ contractant/dilatant boundary=70 and is based on Robertson (2010).
8. The State Parameter (Ψ) calculated using Plewes, et al. (1992) is based on a K0 assumption of 0.5.
9. Coordinates are in UTM Zone 23K Córrego Alegre.
10. N_{kt} used in calculation of $S_{u(peak)}$ is 20.

PROJECT

Fundão Tailings Dam Review Panel

TITLE

Fugro (September 2014 - March 2015) - Germano
CONE PENETRATION TEST CPTu-F52/82
N:7765197.82m E:658210.29m 2014-10-10

Liquefaction susceptibility after Robertson (2010) "Evaluation of Flow Liquefaction and Liquefied Strength Using the Cone Penetration Test"	Liquefaction susceptibility after Olson & Stark (2003) "Yield Strength Ratio and Liquefaction Analysis of Slopes and Embankments"	State parameter approximation - Robertson (2009) "Interpretation of cone penetration tests - a unified approach"

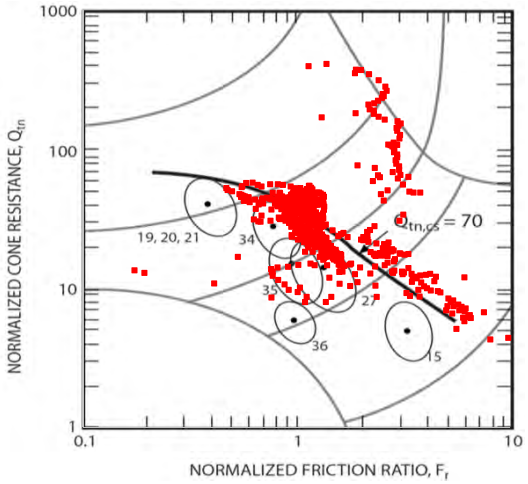

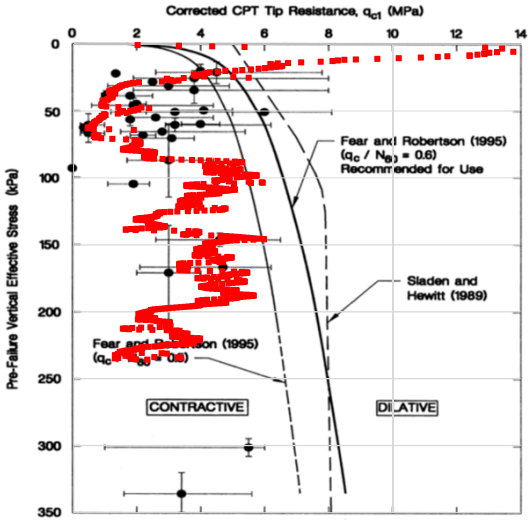

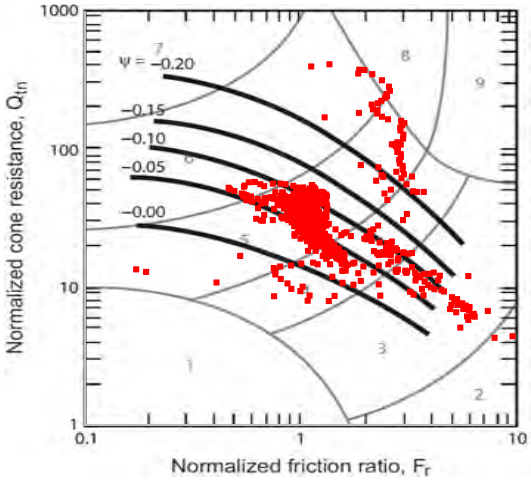

NOTE:

PROJECT

Fundão Tailings Dam Review Panel

TITLE

Fugro (September 2014 - March 2015) - Germano
CPTu-F52/82 Liquefaction Susceptibility and Soil Behavior Type

March 2015 – July 2015
Fugro
Germano Basin
(Section C2.2.7)

Figure C.C1-7 – Fugro (March 2015 – July 2015) Test Location Plan

CPTu-F03 CPT Plots
CPTu-F03 CPT Liquefaction Susceptibility and Soil Behavior Type Plots
SPT Log SP-F03
CPTu-F04 CPT Plots
CPTu-F04 CPT Liquefaction Susceptibility and Soil Behavior Type Plots
SPT Log SP-F04
CPTu-F05 CPT Plots
CPTu-F05 CPT Liquefaction Susceptibility and Soil Behavior Type Plots
SPT Log SP-F05
CPTu-F06 CPT Plots
CPTu-F06 CPT Liquefaction Susceptibility and Soil Behavior Type Plots
SPT Log SP-F06
CPTu-F07 CPT Plots
CPTu-F07 CPT Liquefaction Susceptibility and Soil Behavior Type Plots
CPTu-F10 CPT Plots
CPTu-F10 CPT Liquefaction Susceptibility and Soil Behavior Type Plots
CPTu-F11 CPT Plots
CPTu-F11 CPT Liquefaction Susceptibility and Soil Behavior Type Plots
CPTu-F14 CPT Plots
CPTu-F14 CPT Liquefaction Susceptibility and Soil Behavior Type Plots
SPT Log SP-F14
CPTu-F15 CPT Plots
CPTu-F15 CPT Liquefaction Susceptibility and Soil Behavior Type Plots
SPT Log SP-F15
CPTu-F16 CPT Plots
CPTu-F16 CPT Liquefaction Susceptibility and Soil Behavior Type Plots
CPTu-F17 CPT Plots
CPTu-F17 CPT Liquefaction Susceptibility and Soil Behavior Type Plots
SPT Log SP-F17
CPTu-F18 CPT Plots
CPTu-F18 CPT Liquefaction Susceptibility and Soil Behavior Type Plots
SPT Log SP-F18
CPTu-F19 CPT Plots
CPTu-F19 CPT Liquefaction Susceptibility and Soil Behavior Type Plots
SPT Log SP-F19

March 2015 – July 2015
Fugro
Germano Basin
(Section C2.2.7)

CPTu-F20 CPT Plots
CPTu-F20 CPT Liquefaction Susceptibility and Soil Behavior Type Plots
SPT Log SP-F20
CPTu-F21 CPT Plots
CPTu-F21 CPT Liquefaction Susceptibility and Soil Behavior Type Plots
SPT Log SP-F21
SPT Log SP-F21A
CPTu-F22 CPT Plots
CPTu-F22 CPT Liquefaction Susceptibility and Soil Behavior Type Plots
CPTu-F22A CPT Plots
CPTu-F22A CPT Liquefaction Susceptibility and Soil Behavior Type Plots
SPT Log SP-F22A
CPTu-F23 CPT Plots
CPTu-F23 CPT Liquefaction Susceptibility and Soil Behavior Type Plots
CPTu-F24 CPT Plots
CPTu-F24 CPT Liquefaction Susceptibility and Soil Behavior Type Plots
CPTu-F25 CPT Plots
CPTu-F25 CPT Liquefaction Susceptibility and Soil Behavior Type Plots
CPTu-F26 CPT Plots
CPTu-F26 CPT Liquefaction Susceptibility and Soil Behavior Type Plots
SPT Log SP-F26
CPTu-F27 CPT Plots
CPTu-F27 CPT Liquefaction Susceptibility and Soil Behavior Type Plots
CPTu-F28 CPT Plots
CPTu-F28 CPT Liquefaction Susceptibility and Soil Behavior Type Plots
CPTu-F29 CPT Plots
CPTu-F29 CPT Liquefaction Susceptibility and Soil Behavior Type Plots
CPTu-F30 CPT Plots
CPTu-F30 CPT Liquefaction Susceptibility and Soil Behavior Type Plots

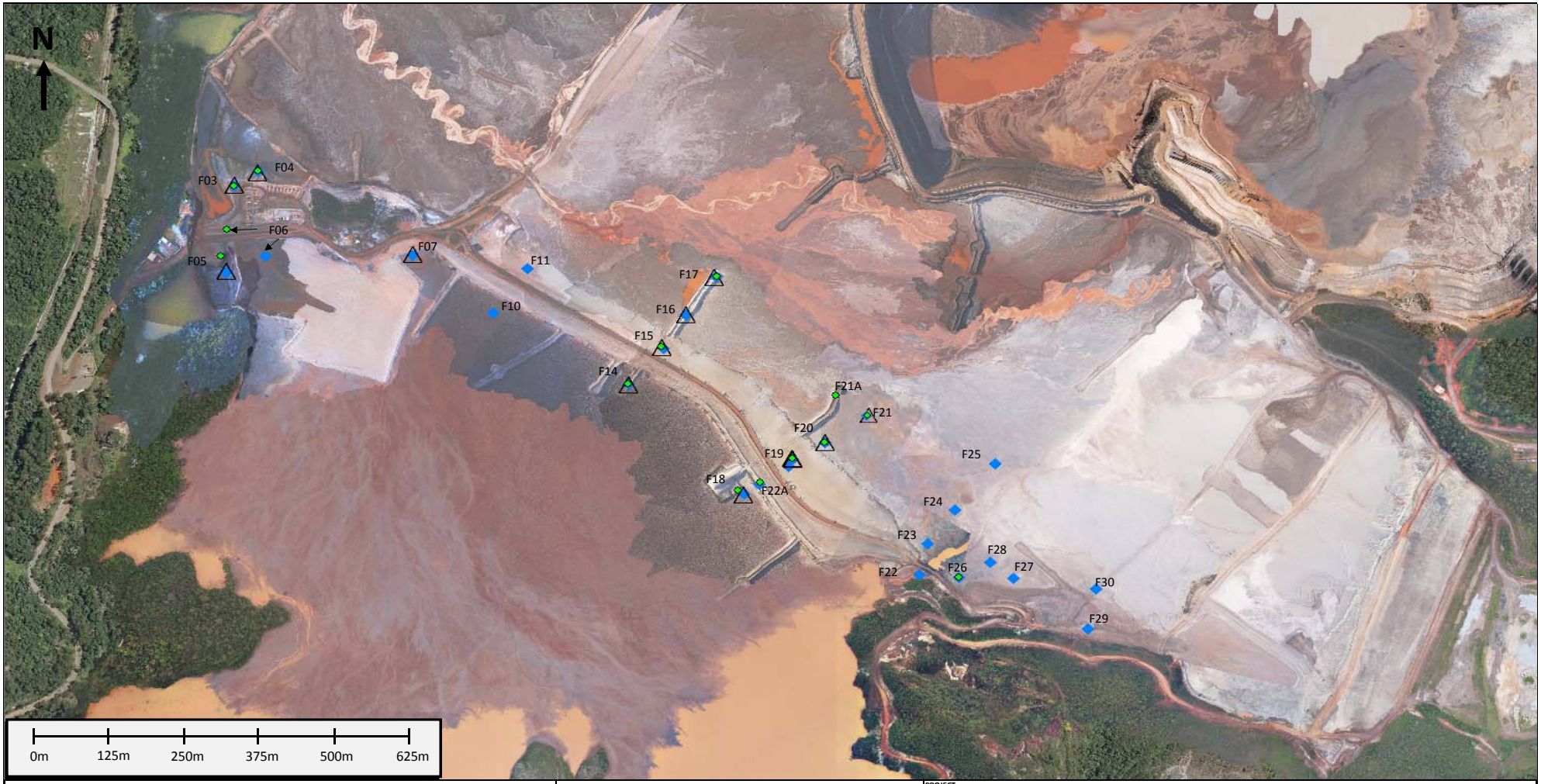

NOTE:

1. July 27, 2015 Samarco aerial image shown for Fundão. December 14, 2014 and July 16, 2015 Samarco aerial images shown for Germano.

LEGEND:

- Standard Penetration Test (SPT)
- Piezocone Penetration Test (CPTu)
- Vane Shear Test (VST)

PROJECT

Fundão Tailings Dam Review Panel

TITLE

Fugro (March 2015 – July 2015)
Test Location Plan

FIGURE NO.

C.C1-7

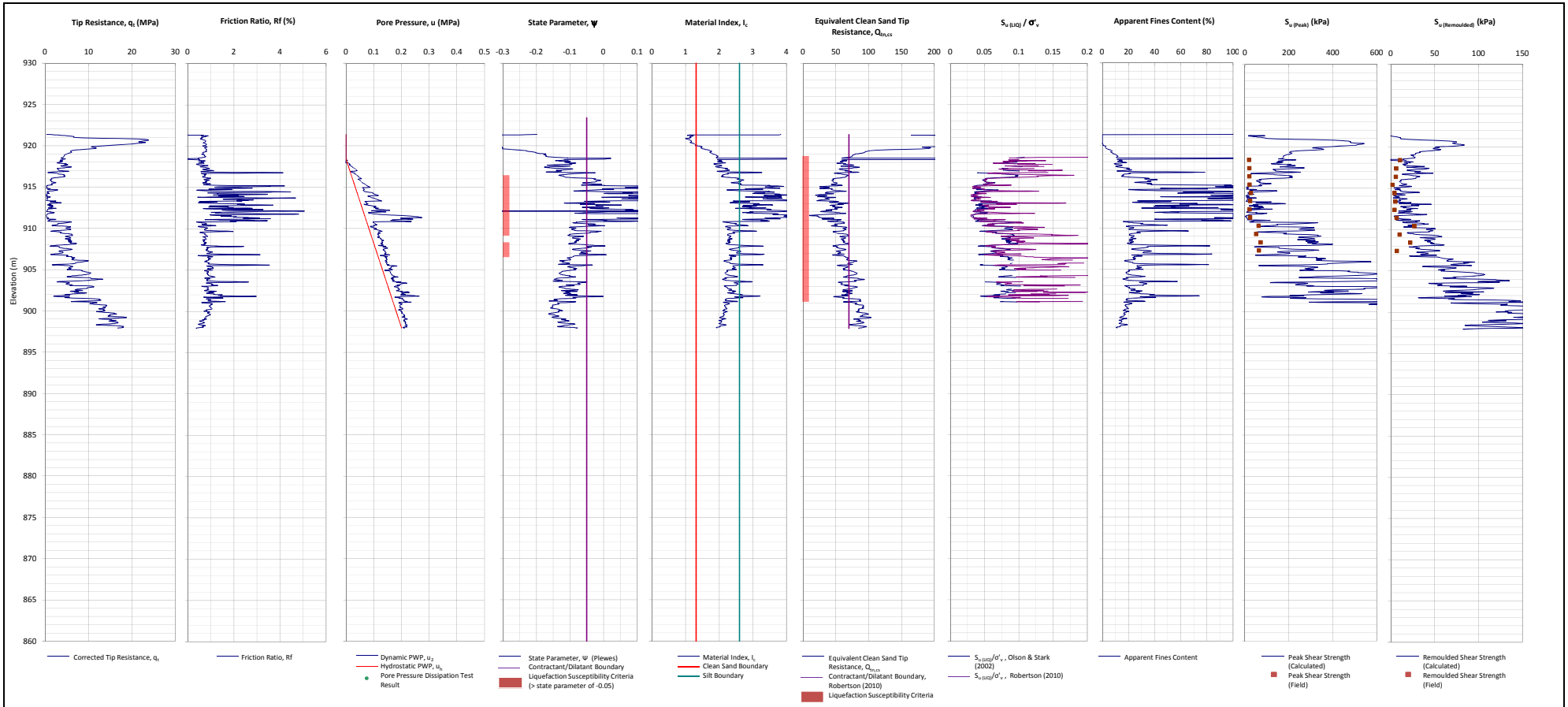

Notes:

1. This interpretation is based on the water and soil saturated unit weights γ_w=9.807 kN/m^3 and γ_{sat}=22 kN/m^3.
2. The friction ratio Rf is calculated as Rf=f_s/q_t.
3. The hydrostatic pore pressure is calculated using the ground water level (GWL) determined from CPT pore pressure dissipation tests (where available) or dynamic pore pressure.
4. Soil boundary layers (where plotted) are based on KCB interpretation.
5. The data presented have been plotted to the axis limits. Data may exist beyond the axis limits shown.
6. The Material Index (I_c) boundaries are based on Robertson and Wride (1998).
7. The $Q_{tn,cs}$ contractant/dilatant boundary=70 and is based on Robertson (2010).
8. The State Parameter (Ψ) calculated using Plewes, et al. (1992) is based on a K0 assumption of 0.5.
9. Coordinates are in UTM Zone 23K Córrego Alegre.
10. N_{kt} used in calculation of $S_{u(peak)}$ is 20.

PROJECT

Fundão Tailings Dam Review Panel

TITLE

Fugro (March - July 2015) - Germano
CONE PENETRATION TEST CPTu-F03
N:7764542m E:658175m 2015-12-28

Liquefaction susceptibility after Robertson (2010) "Evaluation of Flow Liquefaction and Liquefied Strength Using the Cone Penetration Test"	Liquefaction susceptibility after Olson & Stark (2003) "Yield Strength Ratio and Liquefaction Analysis of Slopes and Embankments"	State parameter approximation - Robertson (2009) "Interpretation of cone penetration tests - a unified approach"

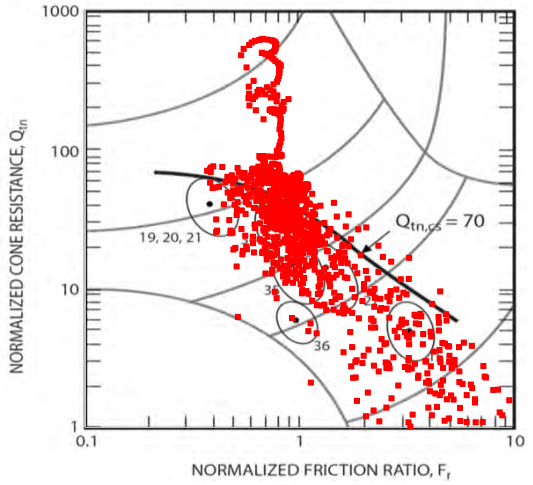

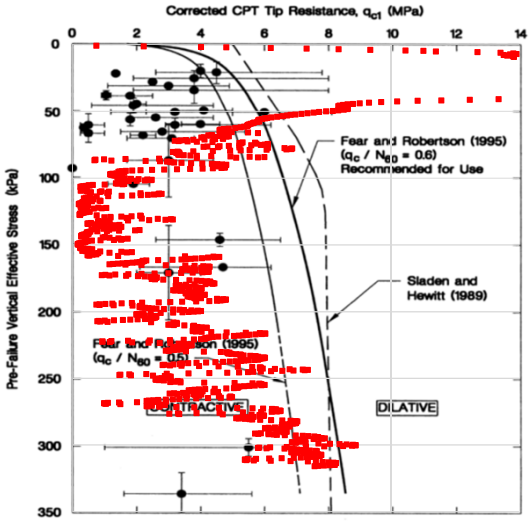

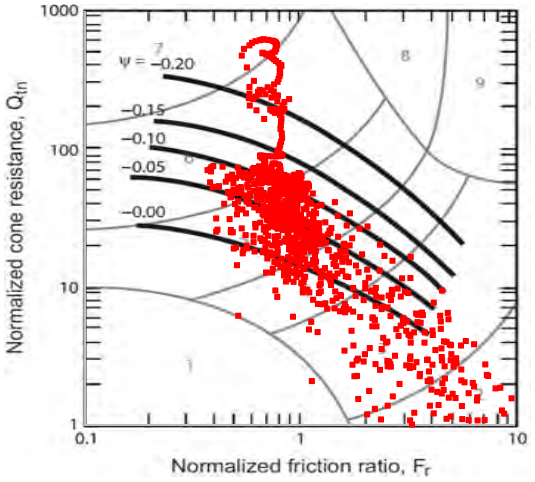

NOTE:

PROJECT

Fundão Tailings Dam Review Panel

TITLE

Fugro (March - July 2015) - Germano
CPTu-F03 Liquefaction Susceptibility and Soil Behavior Type

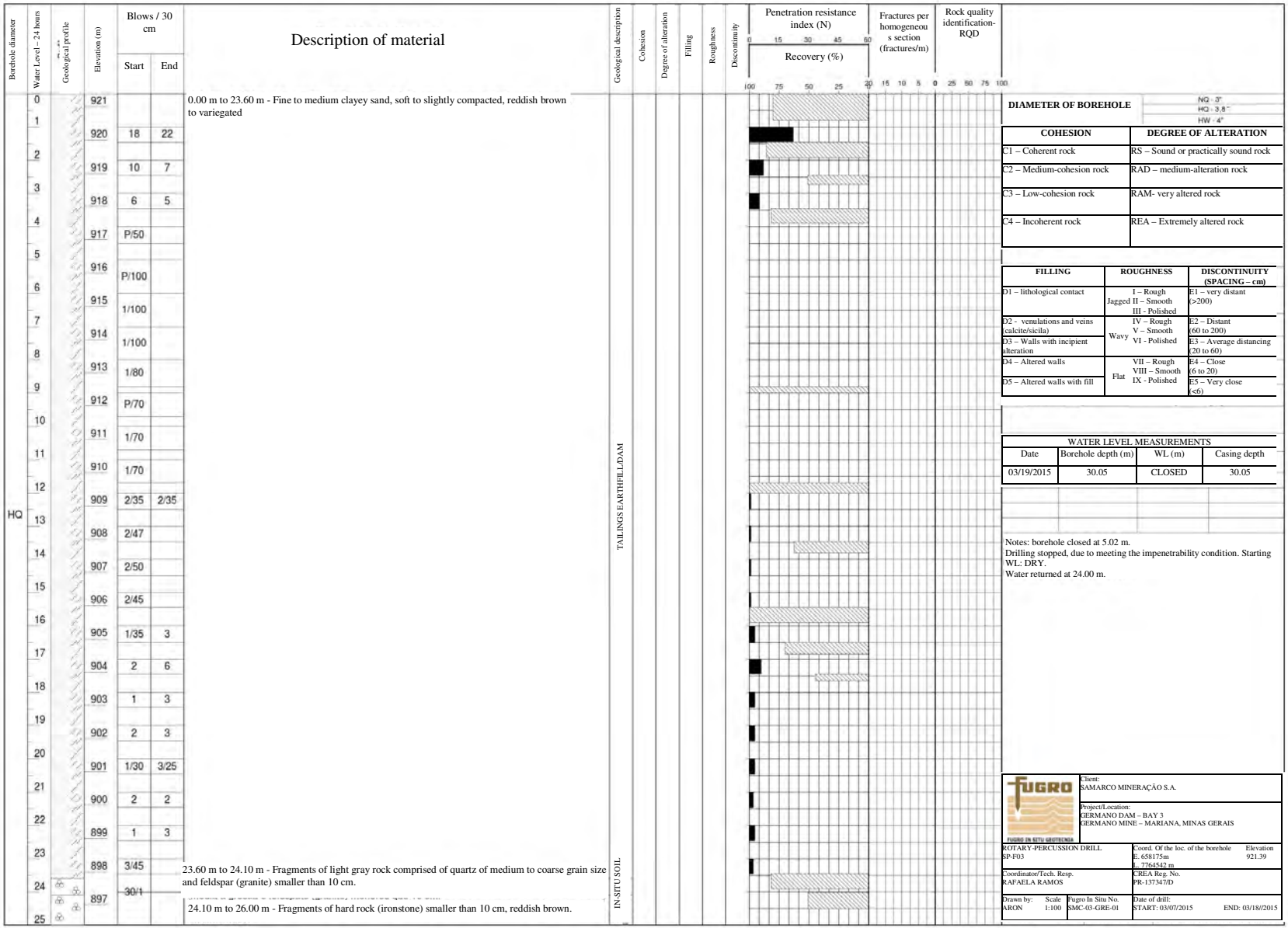

DIAMETER OF BOREHOLE

NQ - 3"
HQ - 3.8"
HW - 4"

COHESION	DEGREE OF ALTERATION
C1 – Coherent rock	RS – Sound or practically sound rock
C2 – Medium-cohesion rock	RAD – medium-alteration rock
C3 – Low-cohesion rock	RAM- very altered rock
C4 – Incoherent rock	REA – Extremely altered rock

FILLING	ROUGHNESS		DISCONTINUITY (SPACING – cm)
D1 – lithological contact	Jagged	I – Rough II – Smooth III - Polished	E1 – very distant (>200)
D2 - venulations and veins (calcite/sicila)	Wavy	IV – Rough V – Smooth VI - Polished	E2 – Distant (60 to 200)
D3 – Walls with incipient alteration			E3 – Average distancing (20 to 60)
D4 – Altered walls	Flat	VII – Rough VIII – Smooth IX - Polished	E4 – Close (6 to 20)
D5 – Altered walls with fill			E5 – Very close (<6)

WATER LEVEL MEASUREMENTS

Date	Borehole depth (m)	WL (m)	Casing depth
03/19/2015	30.05	CLOSED	30.05

Notes: borehole closed at 5.02 m.
Drilling stopped, due to meeting the impenetrability condition. Starting WL: DRY.
Water returned at 24.00 m.

Client:
SAMARCO MINERAÇÃO S.A.

Project/Location:
GERMANO DAM – BAY 3
GERMANO MINE – MARIANA, MINAS GERAIS

ROTARY-PERCUSSION DRILL
SP-F03

Coord. Of the loc. of the borehole
E. 658175m
L. 7764542 m

Elevation
921.39

Coordinator/Tech. Resp.
RAFAELA RAMOS

CREA Reg. No.
PR-137347/D

Drawn by: ARON
Scale 1:100
Fugro In Situ No. SMC-03-GRE-01
Date of drill: START: 03/07/2015 END: 03/18//2015

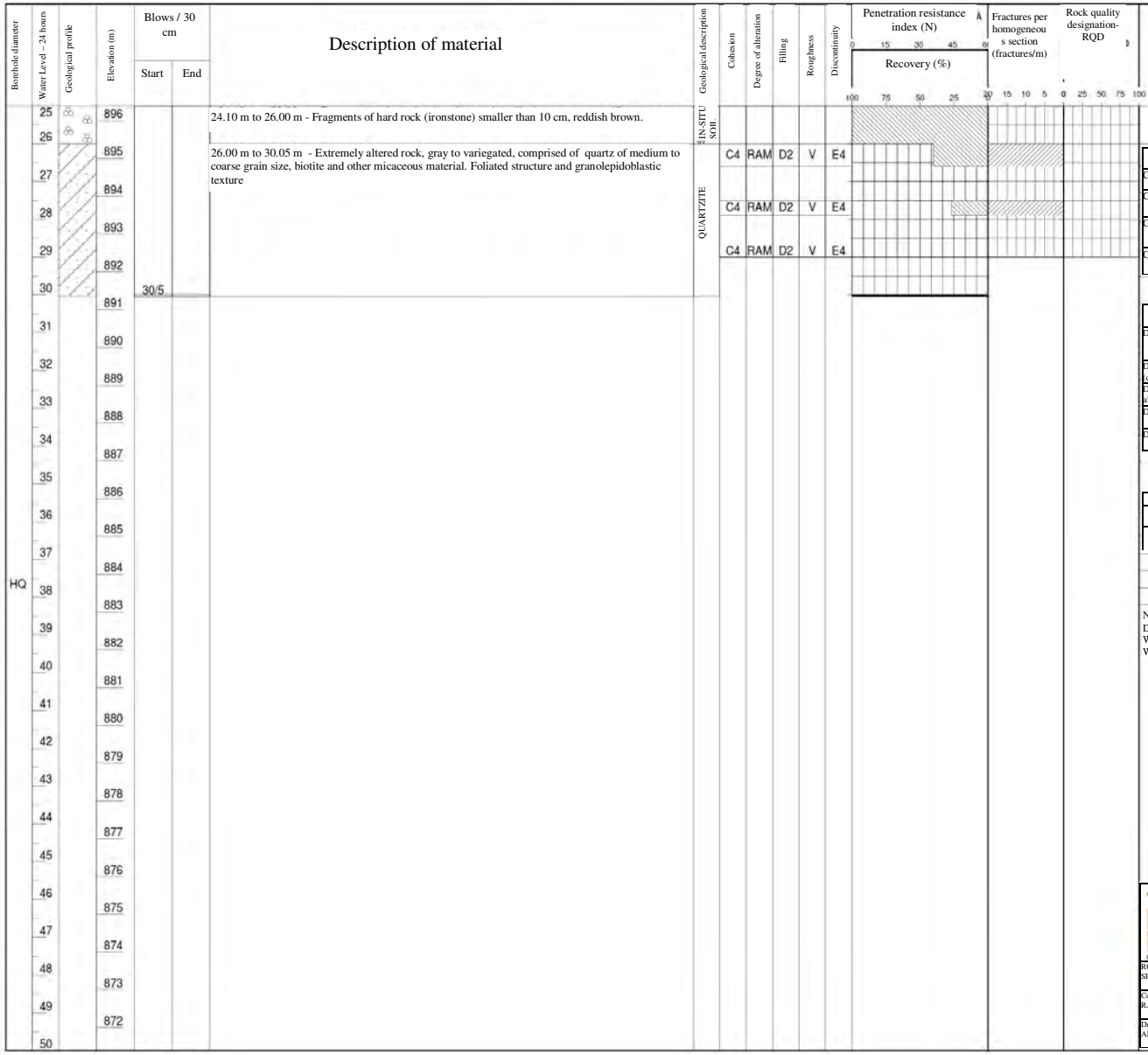

DIAMETER OF BOREHOLE

NQ - 3"
HQ - 3,8"
HW - 4"

COHESION	DEGREE OF ALTERATION
C1 – Coherent rock	RS – Sound or practically sound rock
C2 – Medium-cohesion rock	RAD – medium-alteration rock
C3 – Low-cohesion rock	RAM- very altered rock
C4 – Incoherent rock	REA – Extremely altered rock

FILLING	ROUGHNESS		DISCONTINUITY (SPACING – cm)
D1 – lithological contact		I – Rough Jagged II – Smooth III - Polished	E1 – very distant (>200)
D2 - venulations and veins (calcite/sicila)	Wavy	IV – Rough V – Smooth VI - Polished	E2 – Distant (60 to 200)
D3 – Walls with incipient alteration			E3 – Average distancing (20 to 60)
D4 – Altered walls	Flat	VII – Rough VIII – Smooth IX - Polished	E4 – Close (6 to 20)
D5 – Altered walls with fill			E5 – Very close (<6)

WATER LEVEL MEASUREMENTS

Date	Borehole depth (m)	WL (m)	Casing depth
03/19/2015	30.05	CLOSED	30.05

Notes: borehole closed at 5.02 m.
Drilling stopped, due to meeting the impenetrability condition. Starting WL: DRY.
Water returned at 24.00 m.

FUGRO IN SITU GEOTECNIA

Client:
SAMARCO MINERAÇÃO S.A.

Project/Location:
GERMANO DAM – BAY 3
GERMANO MINE – MARIANA, MINAS GERAIS

ROTARY-PERCUSSION DRILL SP-F03	Coord. Of the loc. of the borehole E. 658175m L. 7764542 m	Elevation 921.39
Coordinator/Tech. Resp. RAFAELA RAMOS	CREA Reg. No. PR-137347/D	
Drawn by: Scale ARON 1:100	Fugro In Situ No. SMC-03-GRE-01	Date of drill: START: 03/07/2015 END: 03/18/2015

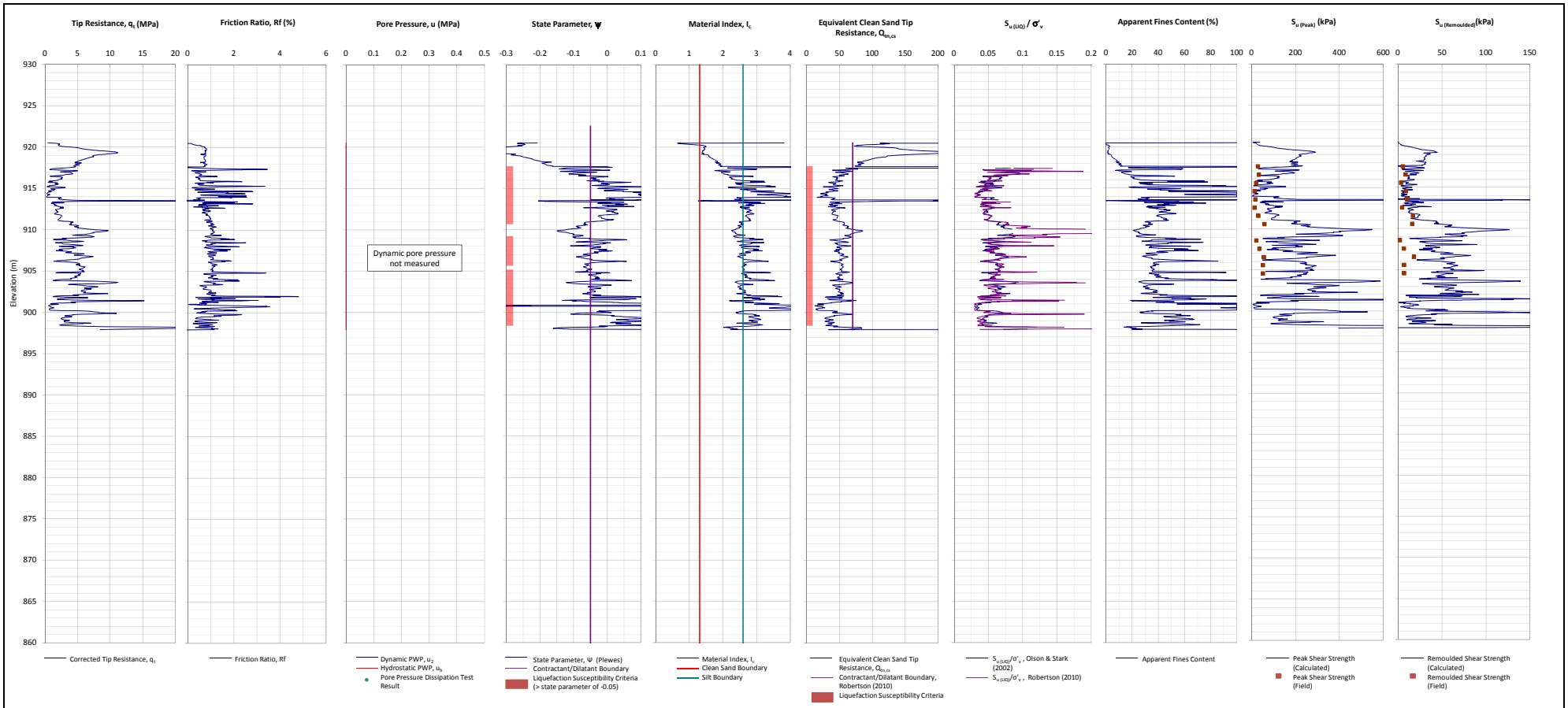

Notes:

1. This interpretation is based on the water and soil saturated unit weights γ_w=9.807 kN/m^3 and γ_{sat}=22 kN/m^3.
2. The friction ratio Rf is calculated as Rf=f_s/q_t.
3. The hydrostatic pore pressure is calculated using the ground water level (GWL) determined from CPT pore pressure dissipation tests (where available) or dynamic pore pressure.
4. Soil boundary layers (where plotted) are based on KCB interpretation.
5. The data presented have been plotted to the axis limits. Data may exist beyond the axis limits shown.
6. The Material Index (I_c) boundaries are based on Robertson and Wride (1998).
7. The $Q_{tn,cs}$ contractant/dilatant boundary=70 and is based on Robertson (2010).
8. The State Parameter (Ψ) is calculated using Plewes, et al. (1992) assuming a K0 of 0.5.
9. Coordinates are in UTM Zone 23K Córrego Alegre.
10. N_{kt} used in calculation of $S_{u(peak)}$ is 20.

PROJECT: Fundão Tailings Dam Review Panel

TITLE: Fugro (March - July 2015) - Germano
CONE PENETRATION TEST CPTu-F04
N:7764571m E:658216m 2015-03-16

Liquefaction susceptibility after Robertson (2010) "Evaluation of Flow Liquefaction and Liquefied Strength Using the Cone Penetration Test"	Liquefaction susceptibility after Olson & Stark (2003) "Yield Strength Ratio and Liquefaction Analysis of Slopes and Embankments"	State parameter approximation - Robertson (2009) "Interpretation of cone penetration tests - a unified approach"

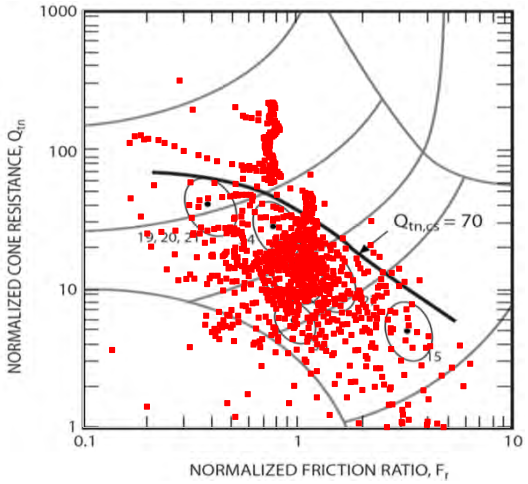

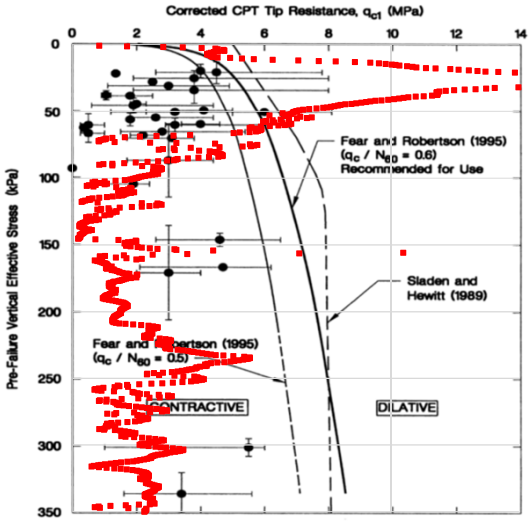

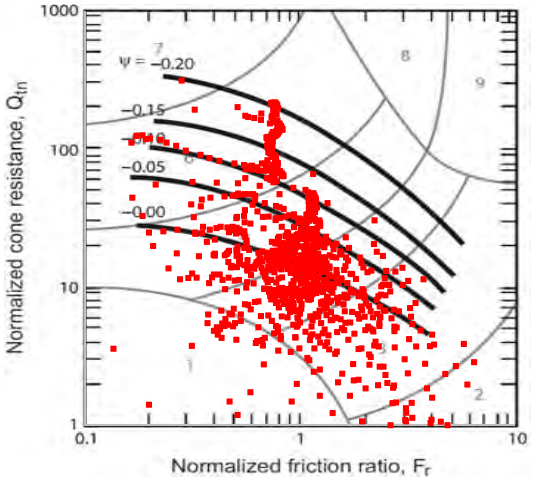

NOTE:

PROJECT	Fundão Tailings Dam Review Panel
TITLE	Fugro (March - July 2015) - Germano CPTu-F04 Liquefaction Susceptibility and Soil Behavior Type

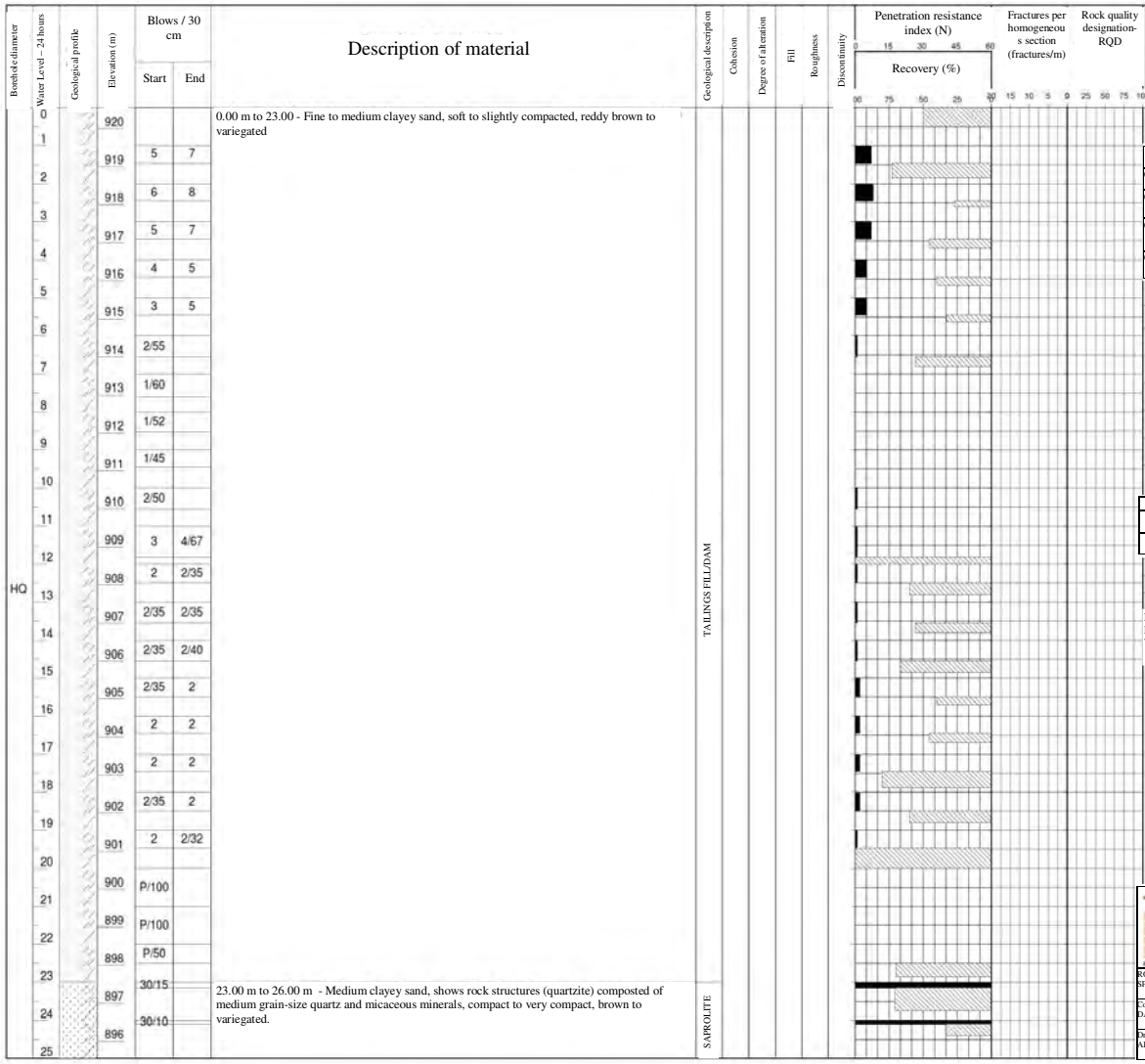

DIAMETER OF BOREHOLE

NQ - 3"
HQ - 3,8"
HW - 4"

COHESION	DEGREE OF ALTERATION
C1 – Coherent rock	RS – Sound or practically sound rock
C2 – Medium-cohesion rock	RAD – medium-alteration rock
C3 – Low-cohesion rock	RAM- very altered rock
C4 – Incoherent rock	REA – Extremely altered rock

FILL	ROUGHNESS		DISCONTINUITY (SPACING – cm)
D1 – lithological contact	Jagged	I – Rough II – Smooth III - Polished	E1 – very distant (>200)
D2 - venulations and veins (calcite/sicila)	Wavy	IV – Rough V – Smooth VI - Polished	E2 – Distant (60 to 200)
D3 – Walls with incipient alteration			E3 – Average distancing (20 to 60)
D4 – Altered walls	Flat	VII – Rough VIII – Smooth IX - Polished	E4 – Close (6 to 20)
D5 – Altered walls with fill			E5 – Very close (<6)

WATER LEVEL MEASUREMENTS			
Date	Borehole depth (m)	WL (m)	Casing depth
18/03/2015	30.50	CLOSED	30.50

Notes: borehole closed at 0.5 m.
Drilling stopped due to meeting the impenetrability condition. Initial WL: DRY.

Client: SAMARCO MINERAÇÃO S.A.	
Project/Location: GERMANO DAM – BAY 3 GERMANO MINE – MARIANA, MINAS GERAIS	
ROTARY-PERCUSSION DRILL SP-F04	Coord. Of the loc. of the borehole: E. 658216m, N. 7764571 m Elevation 920.55
Coordinator/Tech. Resp.: DANIELLA ARANHA	CREA Reg. No.: 21057330-7/RJ
Drawn by: ARON Scale 1:100 Fugro In Situ No. SMC-03-GRE-01	Date of drill: START: 16/03/2015 END: 07/03/2015

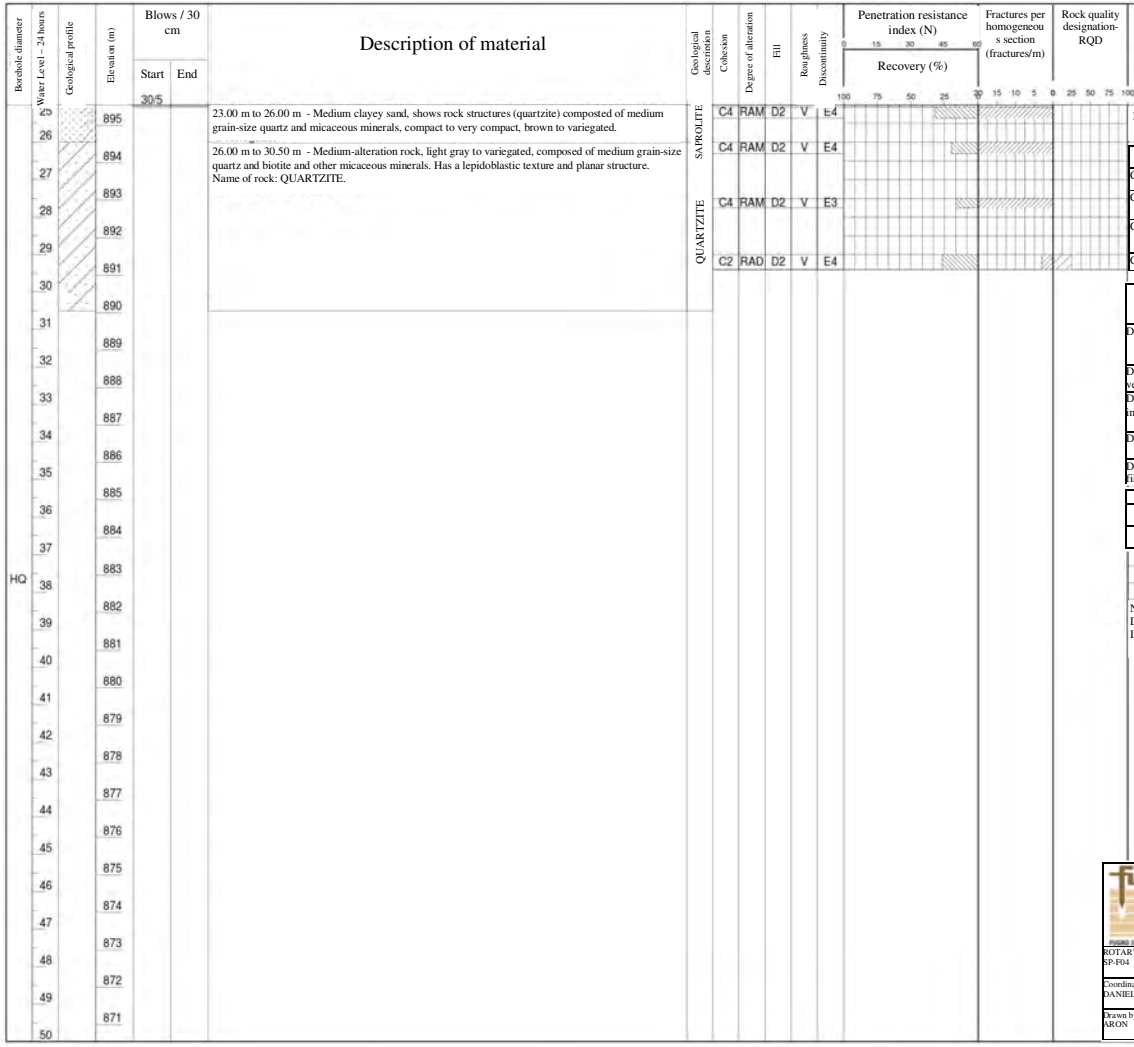

DIAMETER OF BOREHOLE

NQ - 3"
HQ - 3,8"
HW - 4"

COHESION	DEGREE OF ALTERATION
C1 – Coherent rock	RS – Sound or practically sound rock
C2 – Medium-cohesion rock	RAD – medium-alteration rock
C3 – Low-cohesion rock	RAM- very altered rock
C4 – Incoherent rock	REA – Extremely altered rock

FILL	ROUGHNESS	DISCONTINUITY (SPACING – cm)
D1 – lithological contact	I – Rough Jagged II – Smooth III - Polished	E1 – very distant (>200)
D2 - venulations and veins (calcite/sicila)	IV – Rough V – Smooth	E2 – Distant (60 to 200)
D3 – Walls with incipient alteration	Wavy VI - Polished	E3 – Average distancing (20 to 60)
D4 – Altered walls	VII – Rough Flat VIII – Smooth IX - Polished	E4 – Close (6 to 20)
D5 – Altered walls with fill		E5 – Very close (<6)

WATER LEVEL MEASUREMENTS

Date	Borehole depth (m)	WL (m)	Casing depth
18/03/2015	30.50	CLOSED	30.50

Notes: borehole closed at 0.50 m.
Drilling stopped due to meeting the impenetrability condition.
Initial WL: DRY.

FUGRO
FUGRO IN SITU GEOTECNIA

Client:
SAMARCO MINERAÇÃO S.A.

Project/Location:
GERMANO DAM – BAY 3
GERMANO MINE – MARIANA, MINAS GERAIS

ROTARY-PERCUSSION DRILL SP-F04	Coord. Of the loc. of the borehole E. 658216m N. 7764571 m	Elevation 920.55
Coordinator/Tech. Resp. DANIELLA ARANHA	CREA Reg. No. 2105733O-7-/RJ	
Drawn by: Scale ARON 1:100	Fugro In Situ No. SMC-03-GRE-01	Drawn by: Scale ARON 1:100

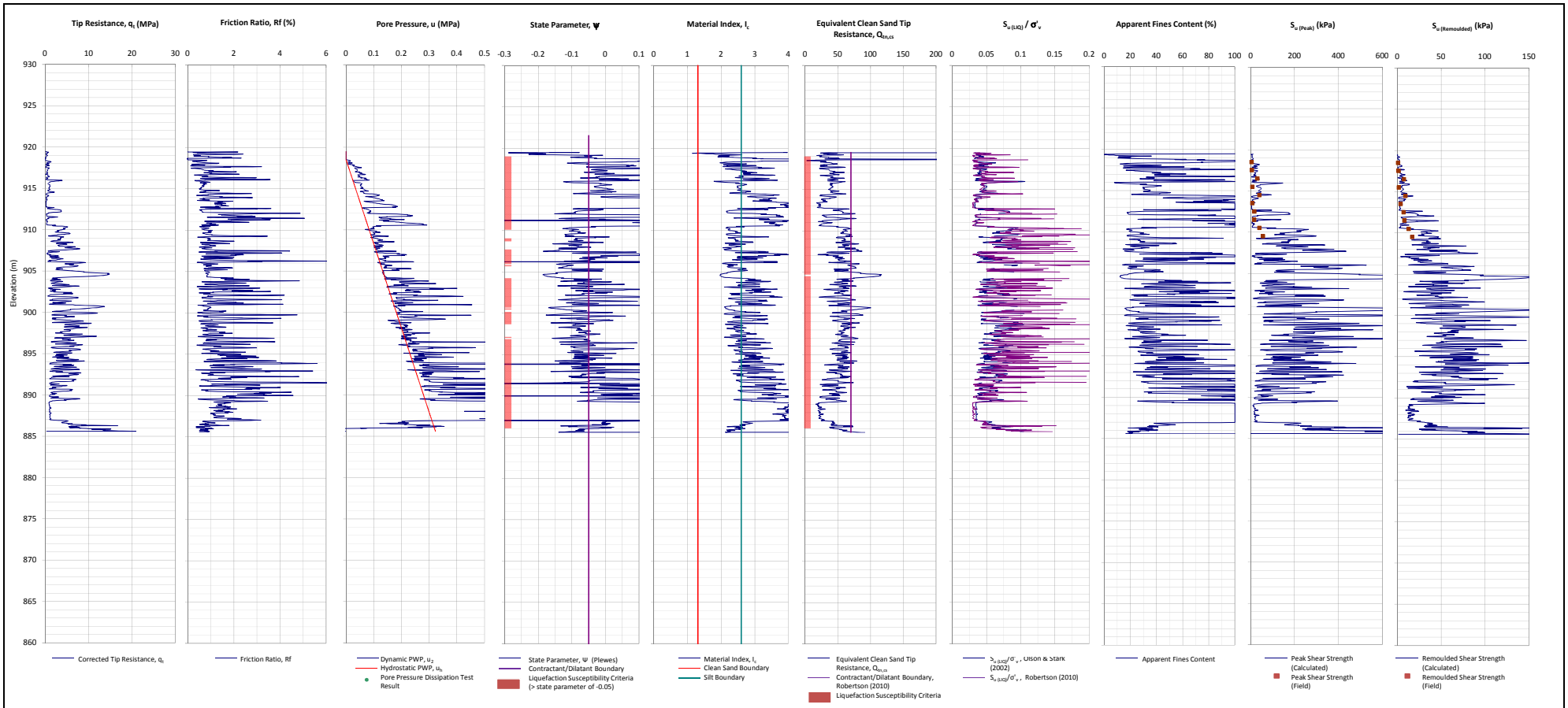

Notes:

1. This interpretation is based on the water and soil saturated unit weights γ_w=9.807 kN/m^3 and γ_{sat}=22 kN/m^3.
2. The friction ratio Rf is calculated as Rf=f_s/q_t.
3. The hydrostatic pore pressure is calculated using the ground water level (GWL) determined from CPT pore pressure dissipation tests (where available) or dynamic pore pressure.
4. Soil boundary layers (where plotted) are based on KCB interpretation.
5. The data presented have been plotted to the axis limits. Data may exist beyond the axis limits shown.
6. The Material Index (I_c) boundaries are based on Robertson and Wride (1998).
7. The $Q_{tn,cs}$ contractant/dilatant boundary=70 and is based on Robertson (2010).
8. The State Parameter (Ψ) is calculated using Plewes, et al. (1992) assuming a K0 of 0.5.
9. Coordinates are in UTM Zone 23K Córrego Alegre.
10. N_{kt} used in calculation of $S_{u(peak)}$ is 20.

PROJECT: Fundão Tailings Dam Review Panel

TITLE: Fugro (March - July 2015) - Germano
CONE PENETRATION TEST CPTu-F05
N:7764380m E:658163m 2015-03-20

Liquefaction susceptibility after Robertson (2010) "Evaluation of Flow Liquefaction and Liquefied Strength Using the Cone Penetration Test"	Liquefaction susceptibility after Olson & Stark (2003) "Yield Strength Ratio and Liquefaction Analysis of Slopes and Embankments"	State parameter approximation - Robertson (2009) "Interpretation of cone penetration tests - a unified approach"

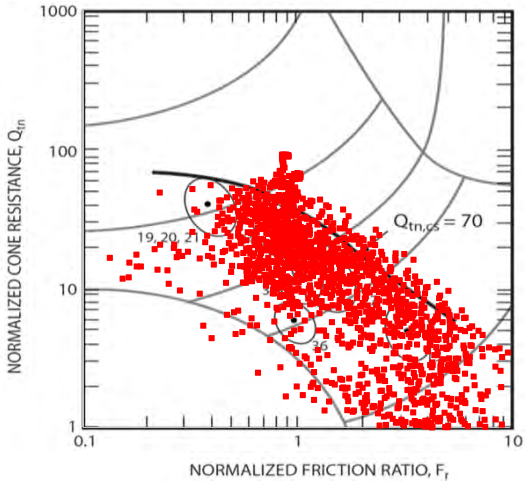

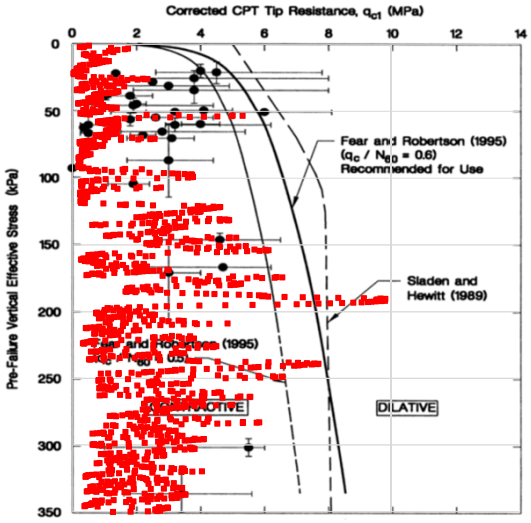

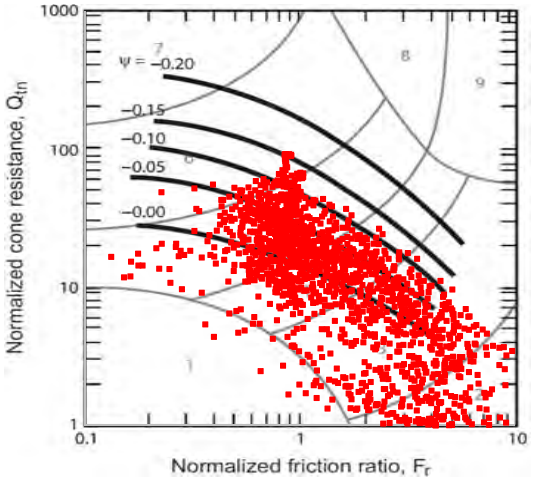

NOTE:

PROJECT	Fundão Tailings Dam Review Panel
TITLE	Fugro (March - July 2015) - Germano CPTu-F05 Liquefaction Susceptibility and Soil Behavior Type

FUGRO IN SITU GEOTECNIA

STANDARD PENETRATION TEST

SMC-03-GRE-01
ATTACHMENTS

CLIENT: SAMARCO MINERAÇÃO S.A.

PROJECT: GERMANO DAM – BAY 3

LOCATION: Germano Mine – MARIANA-MG

SCALE: 1:100 START: 17/04/2015 END: 22/04/2015 RESP.: DANIELLA CREA Reg. No. 201057330-7/RJ

BOREHOLE: SP-F05 ELEVATION: 921,25 COORDINATES: E 658153,51 N 7764411,16

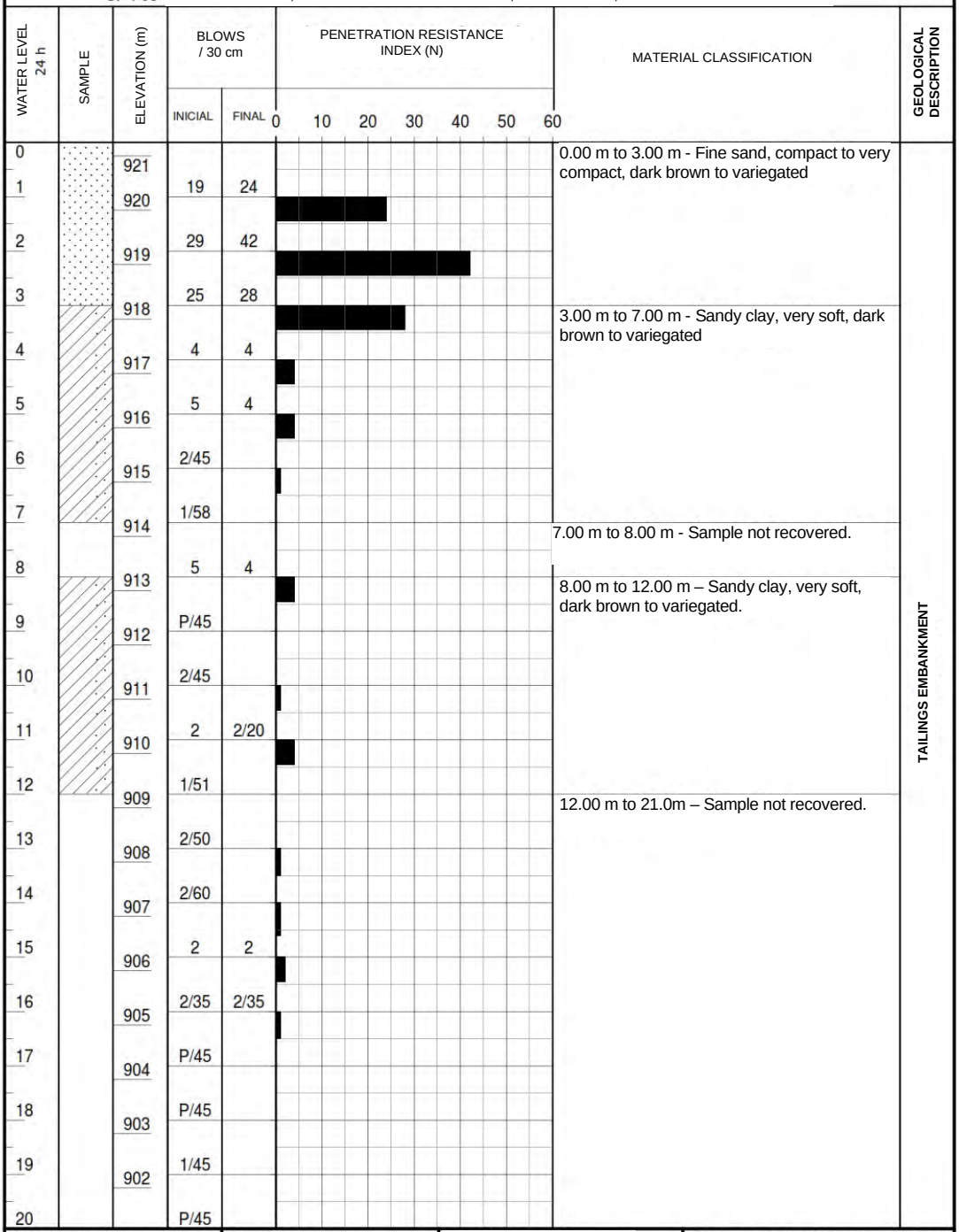

READING INTERVAL WL (m)
1: 24 h: -FECHADO
2:
3:

PROGRESS METHOD (m)
DIGGER:
WASHING: 0,00 - 29,03
LINING: 29,03
USE OF BENTONITE:
WATER LEAK:

TIME WASHING – 10 min
INITIAL DEPTH (m)
STAGE 1 (cm)
STAGE 2 (cm)
STAGE 3 (cm)

NOTE: Borehole closed at 1.20 m. Drilling stopped due to meeting the condition of impermeability. Initial WL: DRY.

FUGRO IN SITU GEOTECNIA

STANDARD PENETRATION TEST

SMC-03-GRE-01
ATTACHMENTS

CLIENT: SAMARCO MINERAÇÃO S.A.

PROJECT: GERMANO DAM – BAY 3

LOCATION: Germano Mine – MARIANA-MG

SCALE: 1:100 START: 17/04/2015 END: 22/04/2015 RESP.: DANIELLA CREA Reg. No. : 201057330-7/RJ

BOREHOLE: SP-F05 ELEVATION: 921,25 COORDINATES: E 658153,51 N 7764411,16

WATER LEVEL 24 h	SAMPLE	ELEVATION (m)	BLOWS / 30 cm INITIAL	BLOWS / 30 cm FINAL	PENETRATION RESISTANCE INDEX (N) 0 10 20 30 40 50 60	MATERIAL CLASSIFICATION	GEOLOGICAL DESCRIPTION
		901	5	11/27		12.00 m a 21.00 m - Sample not recovered.	TAILINGS EMBANKMENT
		900				21.00 m a 22.00 m - Sandy clay, hard, light brown to variegated, with fragments of hardpan smaller than 5 cm.	
		899	14	9		22.00 m a 23.00 m - Sandy clay, hard, light brown to variegated.	
		898	57			23.00 m a 25.00 m - Fine to medium sand, slightly to very compact, light brown to variegated, mineralogically composed of quartz, muscovite and garnet, originating from quartzite rock.	SAPROLITE
		897	53/22				
		896	30/8			25.00 m a 26.00 m - Sample not recovered.	
		895	30/6			26.00 m a 29.09 m - Fine to medium sand, very compact, light gray to variegated, mineralogically composed of quartz, muscovite and garnet, originating from quartzite rock.	
		894	30/3				
		893	30/4				
		892	30/3				
		891					
		890					
		889					
		888					
		887					
		886					
		885					
		884					
		883					
		882					

READING INTERVAL WL (m)
1: 24 h: CLOSED
2:
3:

PROGRESS METHOD (m)
DIGGER: -
WASHING: 0,00 - 29,03
LINING: 29,03
USE OF BENTONITE: -
WATER LEAK: -

TIME WASHING – 10 min
INITIAL DEPTH (m)
STAGE 1 (cm)
STAGE 2 (cm)
STAGE 3 (cm)

NOTE: Borehole closed at 1.20 m.
Drilling stopped due to meeting the condition of impermeability. Initial WL: DRY.

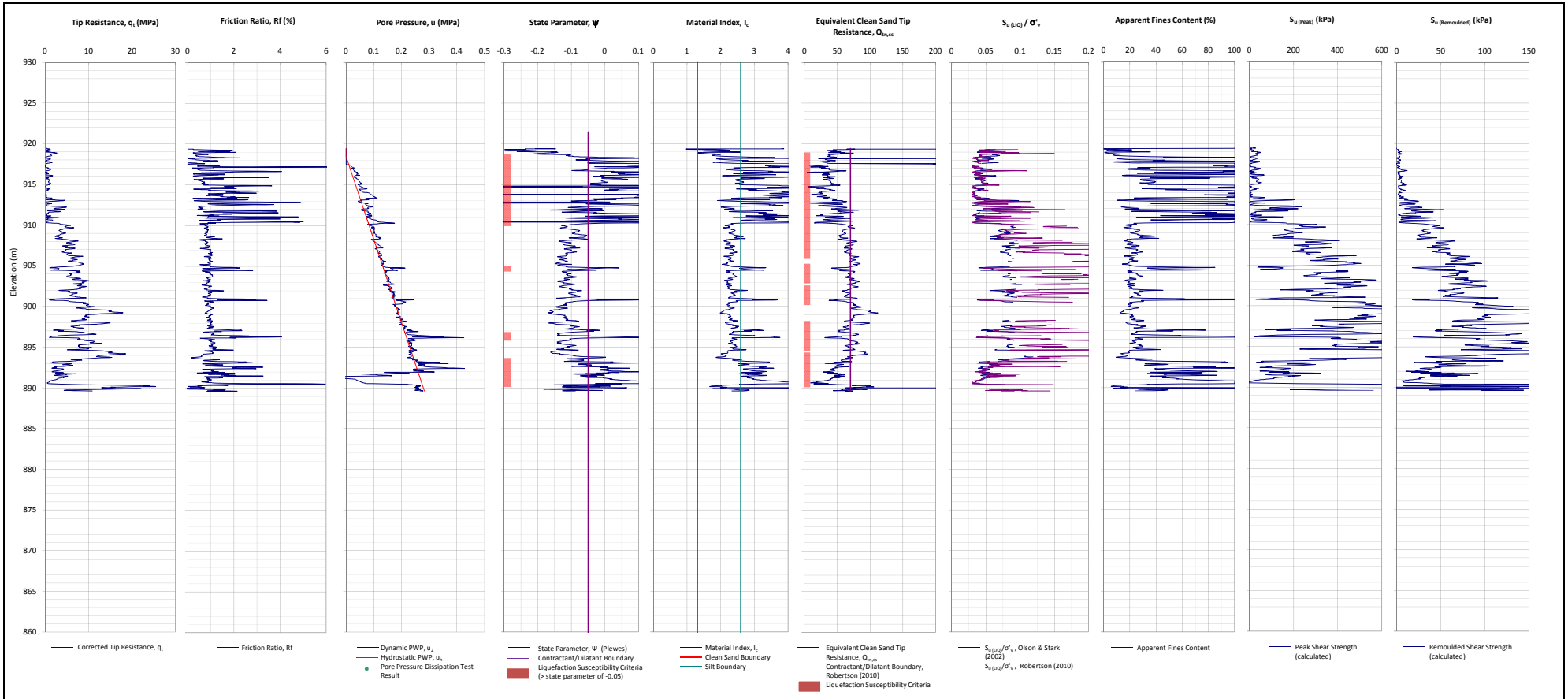

Notes:

1. This interpretation is based on the water and soil saturated unit weights γ_w=9.807 kN/m^3 and γ_{sat}=22 kN/m^3.
2. The friction ratio Rf is calculated as Rf=f_s/q_t.
3. The hydrostatic pore pressure is calculated using the ground water level (GWL) determined from CPT pore pressure dissipation tests (where available) or dynamic pore pressure.
4. Soil boundary layers (where plotted) are based on KCB interpretation.
5. The data presented have been plotted to the axis limits. Data may exist beyond the axis limits shown.
6. The Material Index (I_c) boundaries are based on Robertson and Wride (1998).
7. The $Q_{tn,cs}$ contractant/dilatant boundary=70 and is based on Robertson (2010).
8. The State Parameter (Ψ) is calculated using Plewes, et al. (1992) assuming a K0 of 0.5.
9. Coordinates are in UTM Zone 23K Córrego Alegre.
10. N_{kt} used in calculation of $S_{u(Peak)}$ is 20.

PROJECT: Fundão Tailings Dam Review Panel

TITLE: Fugro (March - July 2015) - Germano
CONE PENETRATION TEST CPTu-F06
N:7764411m E:658227m 2015-03-17

Liquefaction susceptibility after Robertson (2010) "Evaluation of Flow Liquefaction and Liquefied Strength Using the Cone Penetration Test"	Liquefaction susceptibility after Olson & Stark (2003) "Yield Strength Ratio and Liquefaction Analysis of Slopes and Embankments"	State parameter approximation - Robertson (2009) "Interpretation of cone penetration tests - a unified approach"

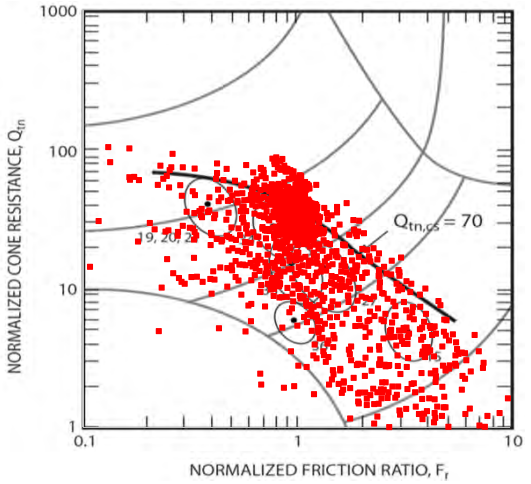

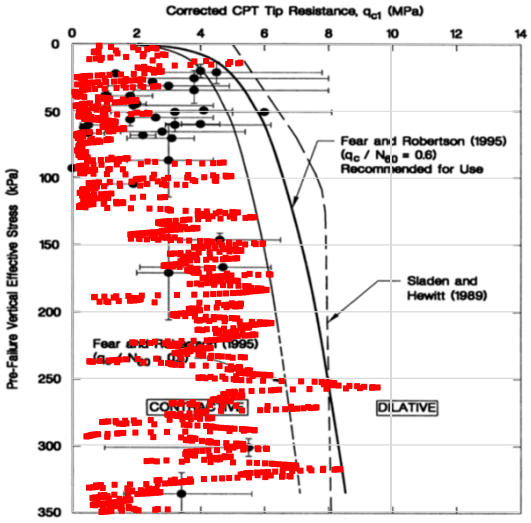

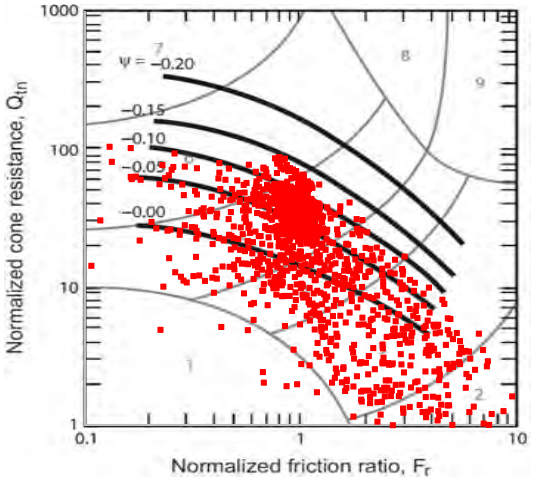

NOTE:

PROJECT	Fundão Tailings Dam Review Panel
TITLE	Fugro (March - July 2015) - Germano CPTu-F06 Liquefaction Susceptibility and Soil Behavior Type

FUGRO IN SITU GEOTECNIA

STANDARD PENETRATION TEST

SMC-03-GRE-01
ANEXOS

CLIENT: SAMARCO MINERAÇÃO S.A.

PROJECT: Fundão Dam - Bay 3

LOCATION: Germano Mine – MARIANA-MG

SCALE: 1:100 START: 22/04/2015 END: 23/04/2015 RESP.: DANIELLA ARANHA CREA: PR-137347/D

BOREHOLE: SP-F06 ELEVATION: 920,95 COORDINATES: E 658164,00 N 7764460,84

WATER LEVEL 24 h	SAMPLE	ELEVATION (m)	BLOWS / 30 cm INITIAL	BLOWS / 30 cm FINAL	PENETRATION RESISTANCE INDEX (N)	MATERIAL CLASSIFICATION	GEOLOGICAL DESCRIPTION
0							
1		920	20	22		0.00 m a 2.00 m - Fine sand, compact, light gray	TAILINGS EMBANKMENT/DAM
2		919	19	13			
▼						2.00 m a 6.00 m - Fine sand, medium compactness, fragments of rock composed of quartz and sericite smaller than 3 cm, light gray	
3		918	16	18			
4		917	20	17			
5		916	16	15			
6		915	18	17			
7		914	14	11		6.00 m a 8.00 m - Clayey fine sand, medium compactness, brown to variegated.	
8		913	1/50				
9		912	2/50			8.00 m a 10.00 m - Sample not recovered.	TAILINGS EMBANKMENT/DAM
10		911	4	6			
11		910	7	20		10.00 m a 12.00 m - Slightly sandy clay, medium to hard, dark brown to variegated.	
12		909	30/10				
13		908	26	42/27		12.00 m a 14.00 m - Medium sand, slightly clayey, very compact, reddish brown to variegated, composed or quartz and garnet originating from quartzite.	
14		907	9	18			
15		906	17	29		14.00 m a 19.09 m - Fine clayey sand, medium compactness to very compact, reddish brown to variegated, composed or quartz and garnet originating from quartzite.	SAPROLITE
16		905	30				
17		904	30/10				
18		903	30/7				
19		902	30/9				
20		901					

READING INTERVAL WL (m)
1: 24 h: -2,30
2:
3:

PROGRESS METHOD (m)
DIGGER: -
WASHING: 0,00 - 19,09
LINING: 19,09
USE OF BENTONITE: -
WATER LEAK: -

TIME WASHING – 10 min
INITIAL DEPTH (m)
STAGE 1 (cm)
STAGE 2 (cm)
STAGE 3 (cm) HQ

NOTE: Borehole closed at 13.42 m. Drilling stopped due to meeting the condition of impermeability. Initial WL: DRY

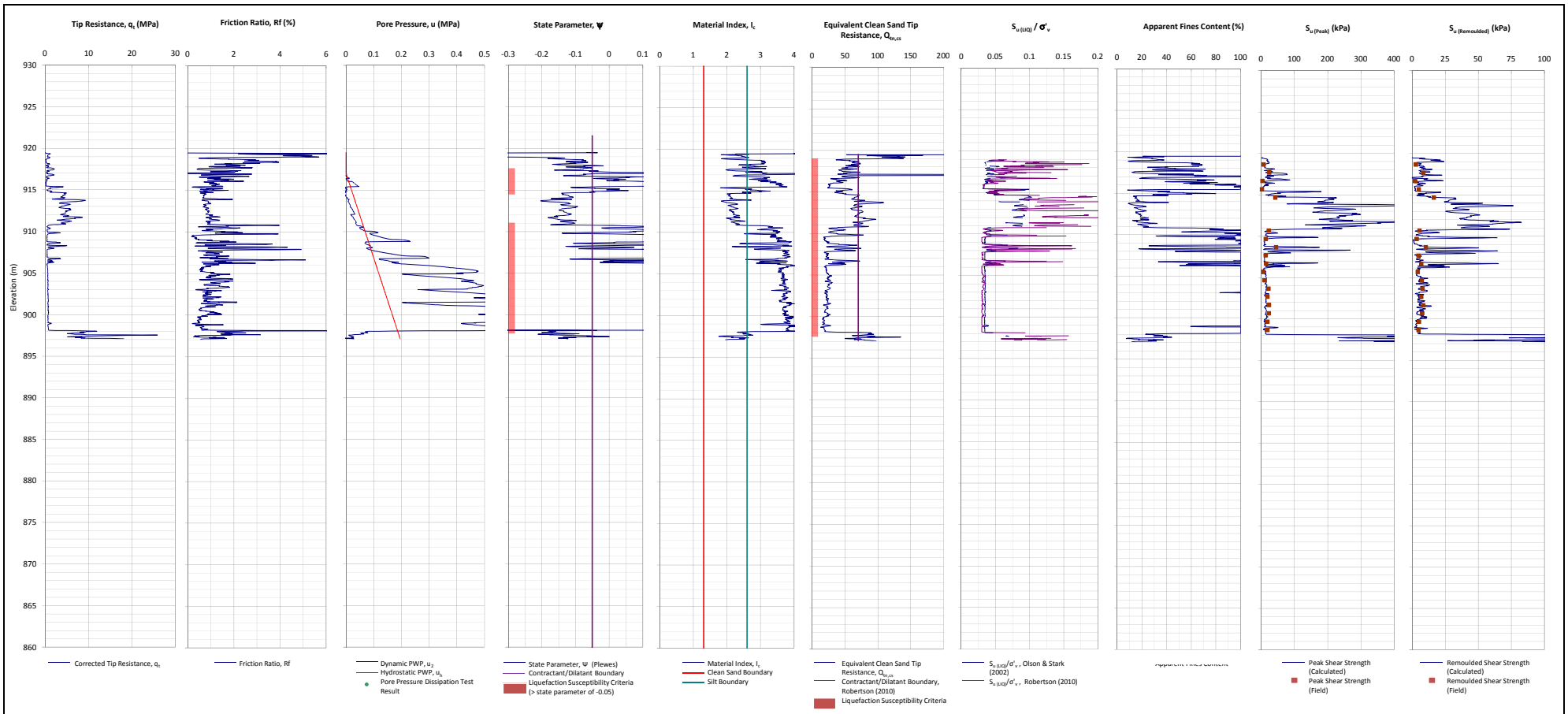

Notes:

1. This interpretation is based on the water and soil saturated unit weights γ_w=9.807 kN/m^3 and γ_{sat}=22 kN/m^3.
2. The friction ratio Rf is calculated as Rf=f_s/q_t.
3. The hydrostatic pore pressure is calculated using the ground water level (GWL) determined from CPT pore pressure dissipation tests (where available) or dynamic pore pressure.
4. Soil boundary layers (where plotted) are based on KCB interpretation.
5. The data presented have been plotted to the axis limits. Data may exist beyond the axis limits shown.
6. The Material Index (I_c) boundaries are based on Robertson and Wride (1998).
7. The $Q_{tn,cs}$ contractant/dilatant boundary=70 and is based on Robertson (2010).
8. The State Parameter (Ψ) is calculated using Plewes, et al. (1992) assuming a K0 of 0.5.
9. Coordinates are in UTM Zone 23K Córrego Alegre.
10. N_{kt} used in calculation of $S_{u(peak)}$ is 20.

PROJECT: Fundão Tailings Dam Review Panel

TITLE: Fugro (March - July 2015) - Germano
CONE PENETRATION TEST CPTu-F07
N:7764413m E:658471m 2015-03-18

Liquefaction susceptibility after Robertson (2010) "Evaluation of Flow Liquefaction and Liquefied Strength Using the Cone Penetration Test"	Liquefaction susceptibility after Olson & Stark (2003) "Yield Strength Ratio and Liquefaction Analysis of Slopes and Embankments"	State parameter approximation - Robertson (2009) "Interpretation of cone penetration tests - a unified approach"

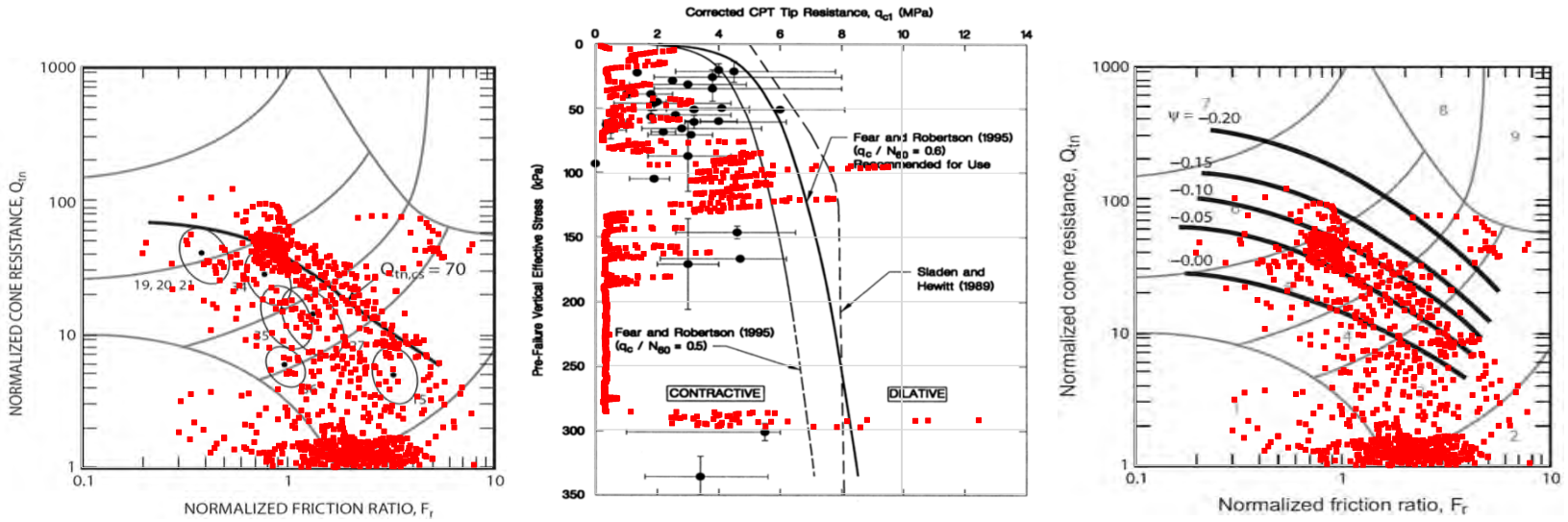

NOTE:

PROJECT

Fundão Tailings Dam Review Panel

TITLE

Fugro (March - July 2015) - Germano
CPTu-F07 Liquefaction Susceptibility and Soil Behavior Type

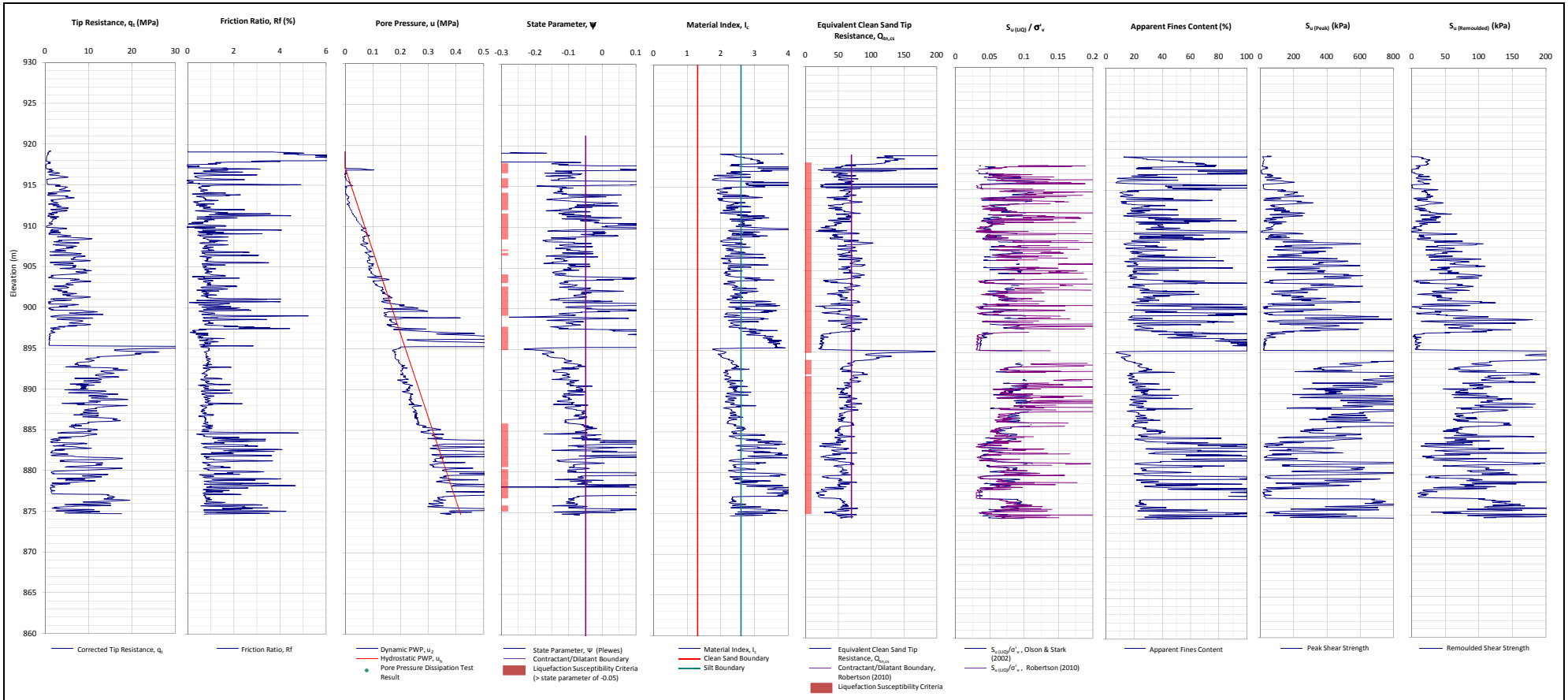

Notes:

1. This interpretation is based on the water and soil saturated unit weights γ_w=9.807 kN/m^3 and γ_{sat}=22 kN/m^3.
2. The friction ratio Rf is calculated as Rf=f_s/q_t.
3. The hydrostatic pore pressure is calculated using the ground water level (GWL) determined from CPT pore pressure dissipation tests (where available) or dynamic pore pressure.
4. Soil boundary layers (where plotted) are based on KCB interpretation.
5. The data presented have been plotted to the axis limits. Data may exist beyond the axis limits shown.
6. The Material Index (I_c) boundaries are based on Robertson and Wride (1998).
7. The $Q_{tn,cs}$ contractant/dilatant boundary=70 and is based on Robertson (2010).
8. The State Parameter (Ψ) is calculated using Plewes, et al. (1992) assuming a K0 of 0.5.
9. Coordinates are in UTM Zone 23K Córrego Alegre.
10. N_{kt} used in calculation of $S_{u(peak)}$ is 20.

PROJECT: Fundão Tailings Dam Review Panel

TITLE: Fugro (March - July 2015) - Germano
CONE PENETRATION TEST CPTu-F10
N:7764304m E:658606m 2015-03-20

Liquefaction susceptibility after Robertson (2010) "Evaluation of Flow Liquefaction and Liquefied Strength Using the Cone Penetration Test"	Liquefaction susceptibility after Olson & Stark (2003) "Yield Strength Ratio and Liquefaction Analysis of Slopes and Embankments"	State parameter approximation - Robertson (2009) "Interpretation of cone penetration tests - a unified approach"

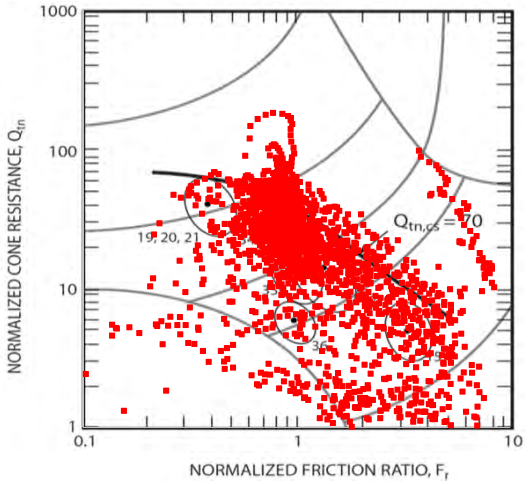

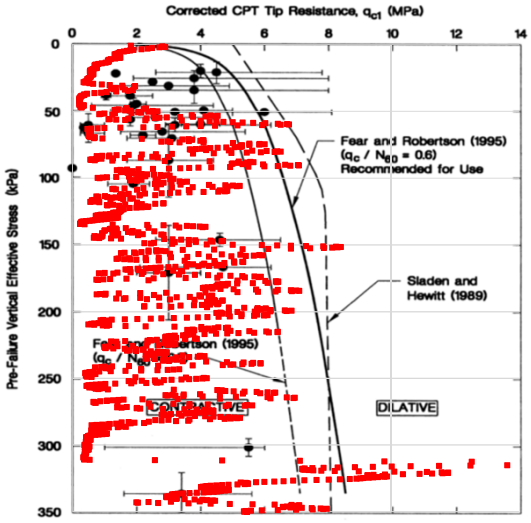

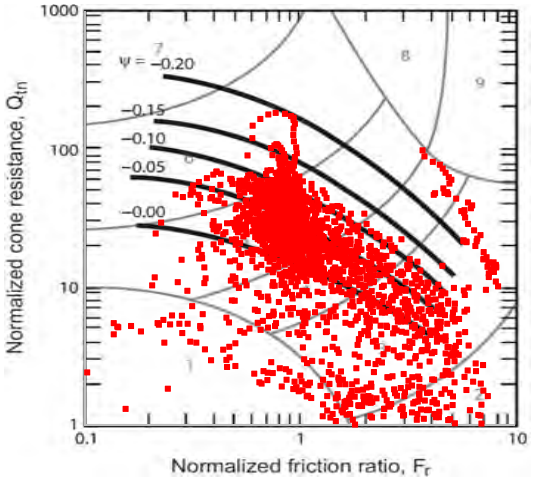

NOTE:

PROJECT	Fundão Tailings Dam Review Panel
TITLE	Fugro (March - July 2015) - Germano CPTu-F10 Liquefaction Susceptibility and Soil Behavior Type

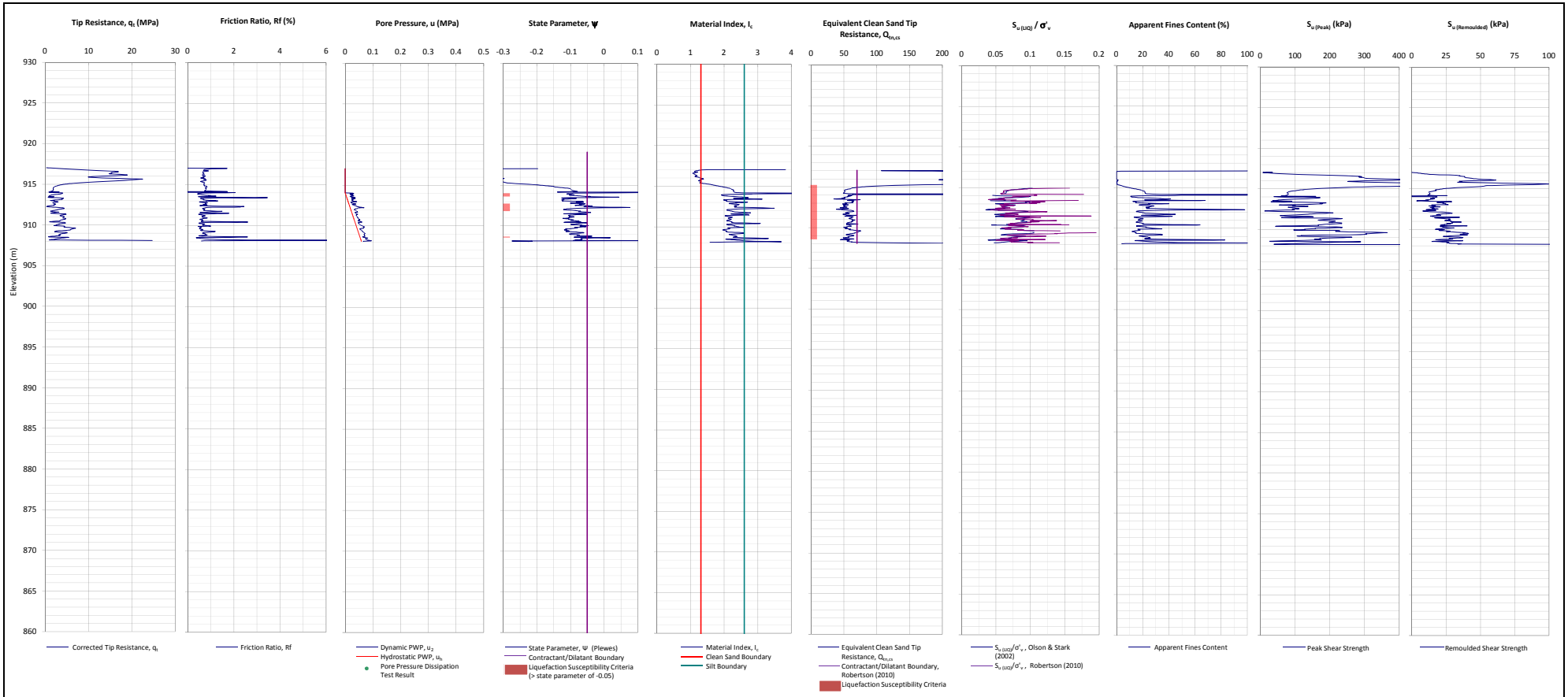

Notes:

1. This interpretation is based on the water and soil saturated unit weights γ_w=9.807 kN/m^3 and γ_{sat}=22 kN/m^3.
2. The friction ratio Rf is calculated as Rf=f_s/q_t.
3. The hydrostatic pore pressure is calculated using the ground water level (GWL) determined from CPT pore pressure dissipation tests (where available) or dynamic pore pressure.
4. Soil boundary layers (where plotted) are based on KCB interpretation.
5. The data presented have been plotted to the axis limits. Data may exist beyond the axis limits shown.
6. The Material Index (I_c) boundaries are based on Robertson and Wride (1998).
7. The $Q_{tn,cs}$ contractant/dilatant boundary=70 and is based on Robertson (2010).
8. The State Parameter (Ψ) is calculated using Plewes, et al. (1992) assuming a K0 of 0.5.
9. Coordinates are in UTM Zone 23K Córrego Alegre.
10. N_{kt} used in calculation of $S_{u(Peak)}$ is 20.

PROJECT
Fundão Tailings Dam Review Panel

TITLE
Fugro (March - July 2015) - Germano
CONE PENETRATION TEST CPTu-F11
N:7664387m E:658663m 2015-03-19

Liquefaction susceptibility after Robertson (2010) "Evaluation of Flow Liquefaction and Liquefied Strength Using the Cone Penetration Test"	Liquefaction susceptibility after Olson & Stark (2003) "Yield Strength Ratio and Liquefaction Analysis of Slopes and Embankments"	State parameter approximation - Robertson (2009) "Interpretation of cone penetration tests - a unified approach"

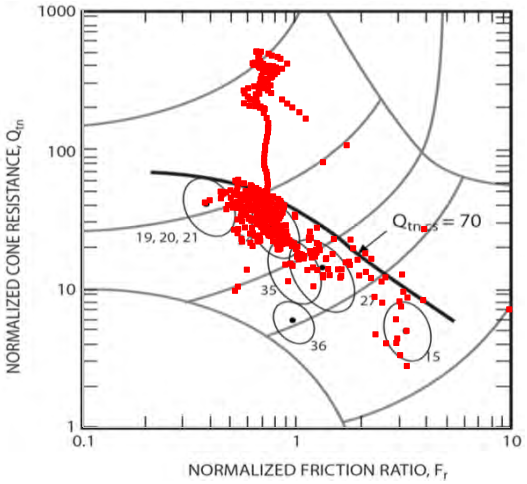

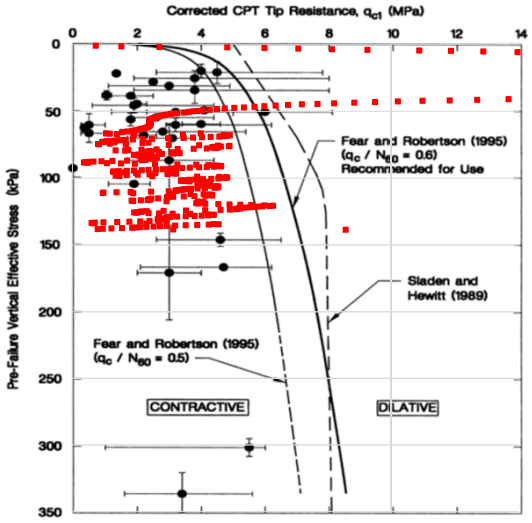

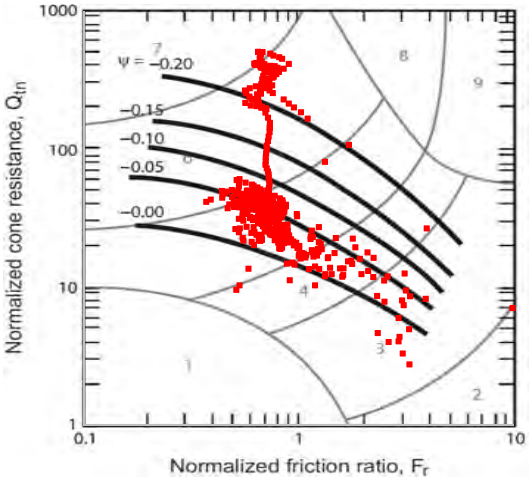

NOTE:

PROJECT

Fundão Tailings Dam Review Panel

TITLE

Fugro (March - July 2015) - Germano
CPTu-F11 Liquefaction Susceptibility and Soil Behavior Type

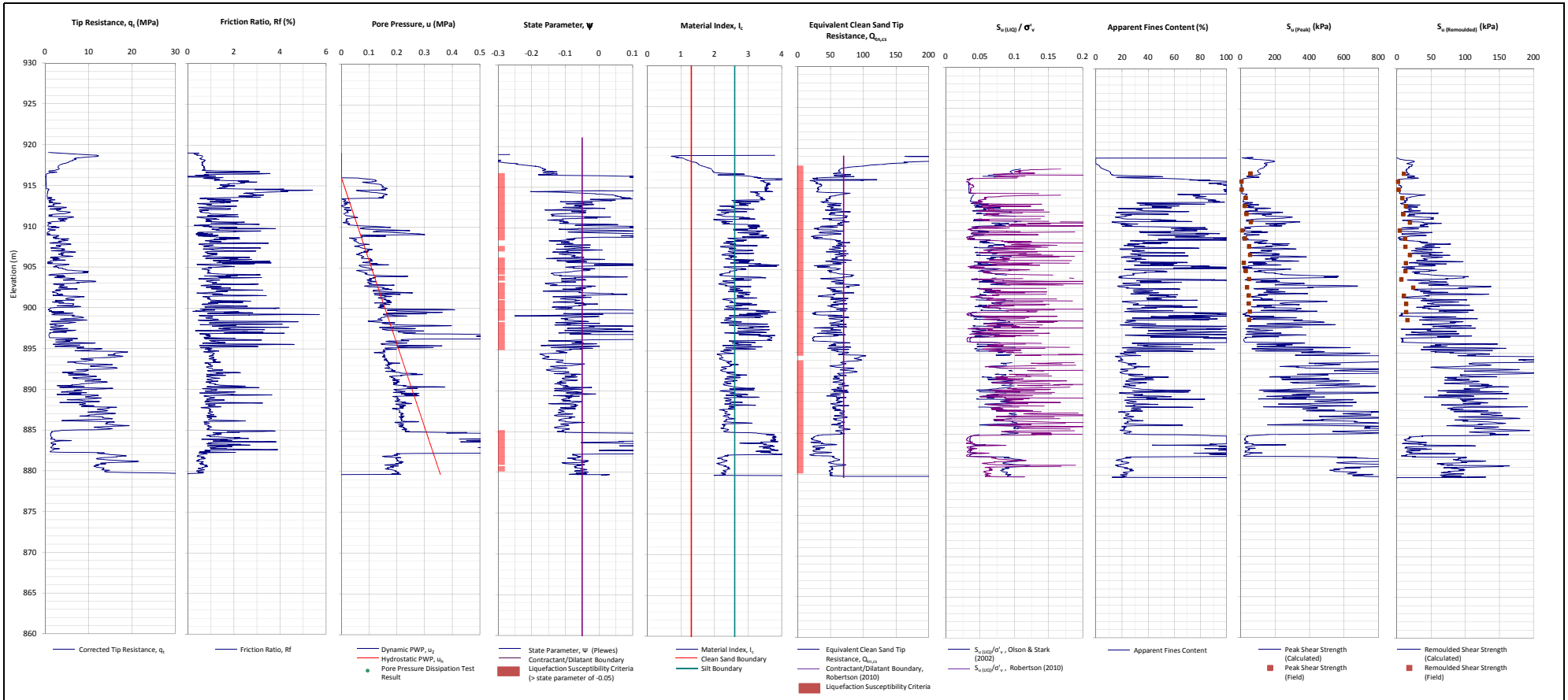

Notes:

1. This interpretation is based on the water and soil saturated unit weights γ_w=9.807 kN/m^3 and γ_{sat}=22 kN/m^3.
2. The friction ratio Rf is calculated as Rf=f$_s$/q$_t$.
3. The hydrostatic pore pressure is calculated using the ground water level (GWL) determined from CPT pore pressure dissipation tests (where available) or dynamic pore pressure.
4. Soil boundary layers (where plotted) are based on KCB interpretation.
5. The data presented have been plotted to the axis limits. Data may exist beyond the axis limits shown.
6. The Material Index (I_c) boundaries are based on Robertson and Wride (1998).
7. The $Q_{tn,cs}$ contractant/dilatant boundary=70 and is based on Robertson (2010).
8. The State Parameter (Ψ) is calculated using Plewes, et al. (1992) assuming a K0 of 0.5.
9. Coordinates are in UTM Zone 23K Córrego Alegre.
10. N_{kt} used in calculation of $S_{u(peak)}$ is 20.

PROJECT: Fundão Tailings Dam Review Panel

TITLE: Fugro (March - July 2015) - Germano
CONE PENETRATION TEST CPTu-F14
N:7764169.48m E:658829.94m 2015-05-19

Liquefaction susceptibility after Robertson (2010) "Evaluation of Flow Liquefaction and Liquefied Strength Using the Cone Penetration Test"	Liquefaction susceptibility after Olson & Stark (2003) "Yield Strength Ratio and Liquefaction Analysis of Slopes and Embankments"	State parameter approximation - Robertson (2009) "Interpretation of cone penetration tests - a unified approach"

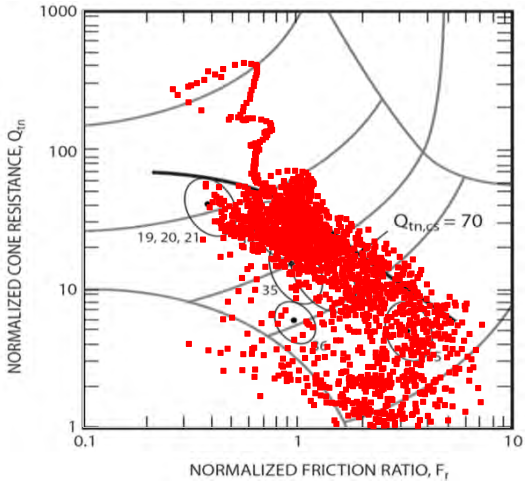

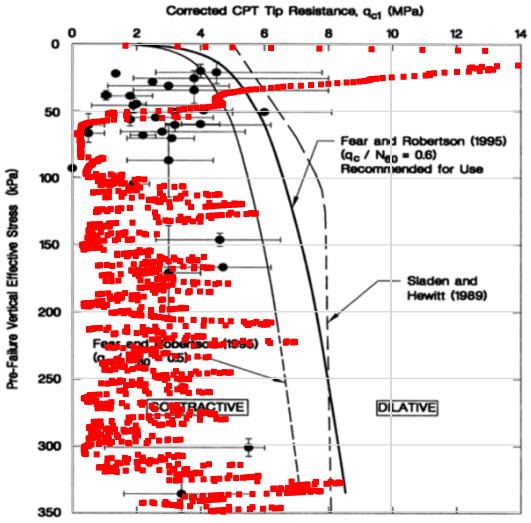

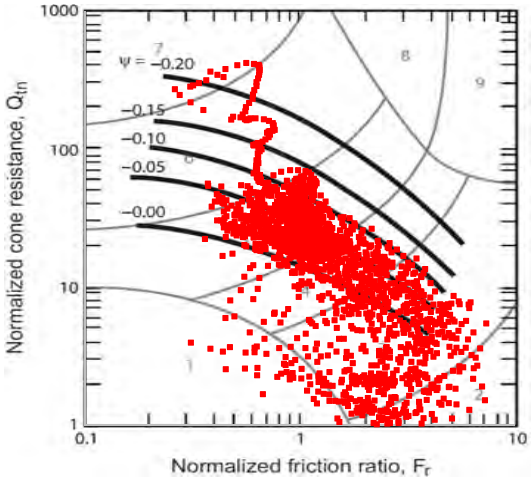

NOTE:

PROJECT

Fundão Tailings Dam Review Panel

TITLE

Fugro (March - July 2015) - Germano
CPTu-F14 Liquefaction Susceptibility and Soil Behavior Type

FUGRO IN SITU GEOTECNIA

STANDARD PENETRATION TEST

SMC-03-GRE-01
Attachments

CLIENT: SAMARCO MINERAÇÃO S.A.

PROJECT: FUNDÃO DAM

LOCATION: GERMANO MINE – MARIANA-MG

SCALE: 1:100 START: 05/07/2015 END: 07/08/2015 RESP.: DANIELLA ARANHA CREA Reg. No. 2012104580/RJ

BOREHOLE: SP-F14 ELEV. 919,06 COORDINATES: E 658829,94 N 7764169,48

Water Level 24 h	SAMPLE	ELEVATION (m)	BLOWS / 30 cm INITIAL	BLOWS / 30 cm FINAL	PENETRATION RESISTANCE INDEX (N) 0 10 20 30 40 50 60	CLASSIFICATION OF MATERIAL	Geological description
0		919				0.00 to 8.00 m- Fine clayey sand, soft to medium compactness, dark brown	TAILINGS EMBANKMENT/DAM
1		918	12	14			
2		917	12	14			
3		916	8	10			
4		915	4	4			
5		914	P/45				
6		913	10	13			
7		912	7	6			
8		911	3	4			
9		910	4	6		8.00 to 11.00 m – No recovery, material not very compact	
10		909	1/50				
11		908	6	13			
12		907	10	15		11.00m to 12.00 m – Slightly sandy clay, soft to medium, brown.	
13		906	3	6		12.00m to 13.00 m – No recovery, material not very compact.	
14		905	2/35	2/37		13.00m to 15.00m – Slightly sandy clay, soft to medium, brown.	
15		904	4	8			
16		903	5/40	2/35		15.00m to 20.00m-No recovery, material not very compact.	
17		902	P/50				
18		901	4/35	7			
19		900	12	17			
20			30	33			

READING INTEVAL W.L.(m)
1: 24 h: - CLOSED
2:
3:

HEADWAY METHOD (m)
DIGGER: -
WASHING: 0,00 - 41,04
LINING: 41,04
USE OF BENOTNITE: -
WATER LEAK:

TIME WASHING 1 - 10 min
INITIAL DEPTH
STAGE 1 (cm):
STAGE 2 (cm):
STAGE 3 (cm):

NOTE: Holle closed at 5.50m. Drilling stopped due to achievement of impenetrability conditions.
Initial WL DRY.

FUGRO IN SITU GEOTECNIA

STANDARD PENETRATION TEST

SMC-03-GRE-01
Attachments

CLIENT: SAMARCO MINERAÇÃO S.A.
PROJECT: FUNDÃO DAM
LOCATION: GERMANO MINE – MARIANA-MG

SCALE: : 1:100 START: 05/07/2015 END: 07/08/2015 RESPONSÁVEL: DANIELLA ARANHA CREA Reg. No. 2012104580/RJ

BOREHOLE: : SP-F14 ELEV. 919,06 COORDINATES: E 658829,94 N 7764169,48

Water Level 24 h	SAMPLE	ELEVATION (m)	BLOWS / 30 cm INITIAL	BLOWS / 30 cm FINAL	PENETRATION RESISTANCE INDEX (N) 0 10 20 30 40 50 60	CLASSIFICATION OF MATERIAL	Geological description
20		899				20.00m to 22.00m- Fine to medium clayey sand, compact, dark brown.	TAILINGS EMBANKMENT/DAM
21		898	27	37			
22		897	2/50			22.00m to 23.00 m – No recovery, material not very compact.	
23		896	17	14		23.00 m to 24.00m – Fine clayey sand, medium compaction, dark brown	
24		895	20	25		24.00 to 26.00 m – No recovery, material not very compact.	
25		894	30	45			
26		893	51			26.00 m to 33.00 m – Fine clayey sand, compact to very compact, dark brown	
27		892	42	52			
28		891	42	39			
29		890	32	30			
30		889	32	32			
31		888	25	36			
32		887	25	37			
33		886	25	34		33.00 m to 38.00 m – Slightly sandy clay, hard, dark brown to variegated.	
34		885	14	25			
35		884	11	29			
36		883	13	25			
37		882	50/28				
38		881	30			38.00 m to 39.00 m – No recovery, material not very compact.	SAPROLITE
39		880	52/22			39.00 m to 40.00 m – Medium to coarse sand with fragments of quartz smaller than 3 cm, very compact, light gray to variegated.	
40			50/23				

READING INTEVAL W.L.(m)
1: 24 h: - CLOSED
2:
3:

PROGRESS METHOD (m)
DIGGER: -
WASHING: 0,00 - 41,04
LINING: -
USE OF BENOTNITE: -
WATER LEAK:

TIME WASHING - 10 min
INITIAL DEPTH
STAGE 1 (cm):
STAGE 2 (cm):
STAGE 3 (cm):

NOTE: Hole closed at 5,50 m. Drilling stopped due to achievement of impenetrability conditions.
Initial WL DRY.

FUGRO IN SITU GEOTECNIA

STANDARD PENETRATION TEST

SMC-03-GRE-01
Attachments

CLIENT: : SAMARCO MINERAÇÃO S.A.
PROJECT: FUNDÃO DAM
LOCATION: GERMANO MINE – MARIANA-MG

SCALE: : 1:100 START: 05/07/2015 END: 07/08/2015 RESP.: DANIELLA ARANHA CREA Reg. No. 2012104580/RJ

BOREHOLE: SP-F14 ELEV.: 919,06 COORDINATES: : E 658829,94 N 7764169,48

Water Level 24 h	SAMPLE	ELEVATION (m)	BLOWS / 30 cm INITIAL	BLOWS / 30 cm FINAL	PENETRATION RESISTANCE INDEX (N) 0 10 20 30 40 50 60	MATERIAL CLASSIFICATION	Geological description
40		879				40.00 m to 41.00 m – Medium to coarse sand with fragments of quartz smaller than 2 cm, light gray to variegated.	SAPROLITE
41		878	30/4			41.00 m to 41.04 m – Sand originating from quartzite of a medium alteration level, composed of quartz, biotite and feldspar, very compact, light gray to variegated.	
42		877					
43		876					
44		875					
45		874					
46		873					
47		872					
48		871					
49		870					
50		869					
51		868					
52		867					
53		866					
54		865					
55		864					
56		863					
57		862					
58		861					
59		860					
60							

READING INTEVAL W.L.(m)
1: 24 h: - CLOSED
2:
3:

PROGRESS METHOD (m)
DIGGER: -
WASHING: 0,00 - 41,04
LINING: 41,04
USE OF BENOTNITE: -
WATER LEAK: -

TIME WASHING - 10 min
INITIAL DEPTH
STAGE 1 (cm):
STAGE 2 (cm):
STAGE 3 (cm):

NOTE: Hole closed at 5.50m. Drilling stopped due to achievement of impenetrability conditions.
Initial WL DRY.

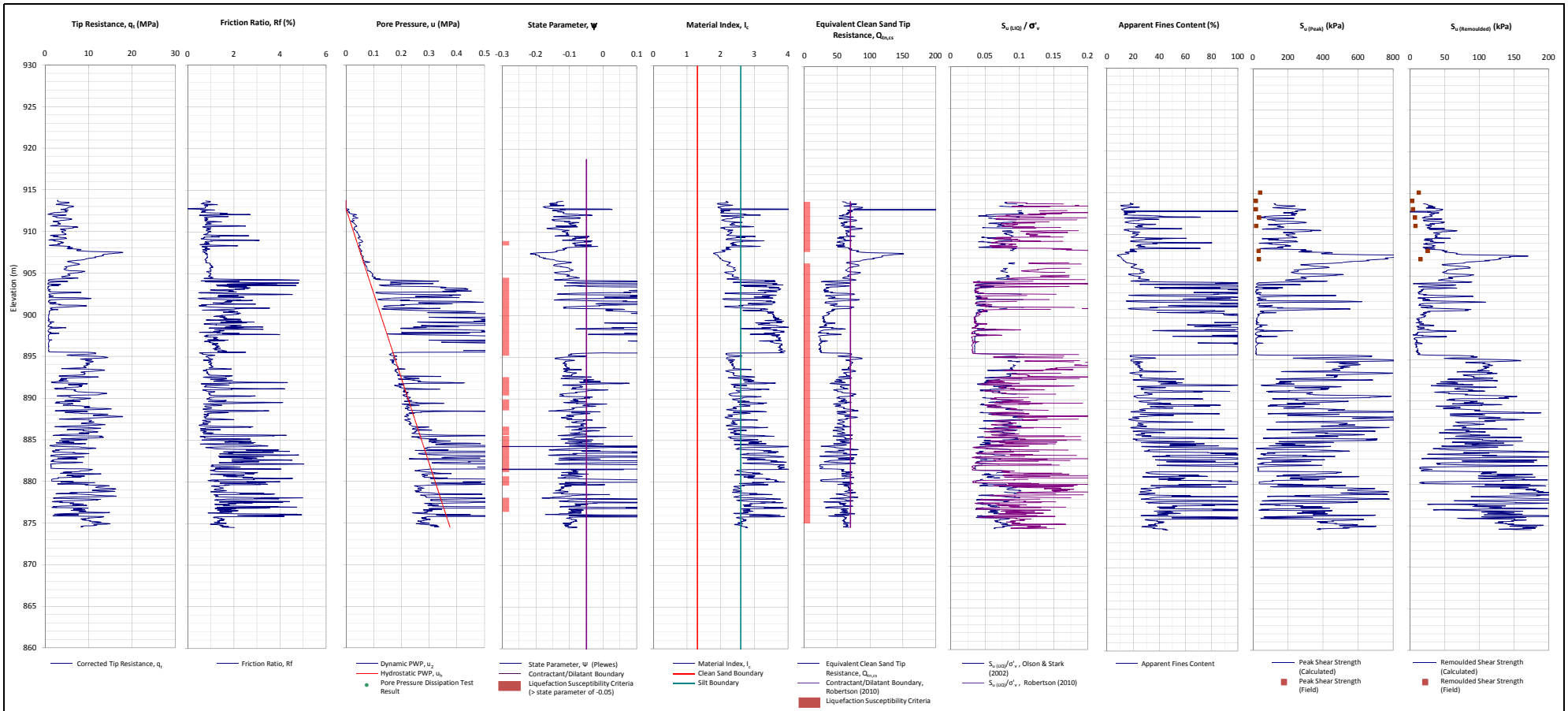

Notes:

1. This interpretation is based on the water and soil saturated unit weights γ_w=9.807 kN/m^3 and γ_{sat}=22 kN/m^3.
2. The friction ratio Rf is calculated as Rf=f_s/q_t.
3. The hydrostatic pore pressure is calculated using the ground water level (GWL) determined from CPT pore pressure dissipation tests (where available) or dynamic pore pressure.
4. Soil boundary layers (where plotted) are based on KCB interpretation.
5. The data presented have been plotted to the axis limits. Data may exist beyond the axis limits shown.
6. The Material Index (I_c) boundaries are based on Robertson and Wride (1998).
7. The $Q_{tn,cs}$ contractant/dilatant boundary=70 and is based on Robertson (2010).
8. The State Parameter (Ψ) is calculated using Plewes, et al. (1992) assuming a K0 of 0.5.
9. Coordinates are in UTM Zone 23K Córrego Alegre.
10. N_{kt} used in calculation of $S_{u(peak)}$ is 20.

PROJECT: Fundão Tailings Dam Review Panel

TITLE: Fugro (March - July 2015) - Germano
CONE PENETRATION TEST CPTu-F15
N:7764237m E:658888m 2015-05-22

Liquefaction susceptibility after Robertson (2010) "Evaluation of Flow Liquefaction and Liquefied Strength Using the Cone Penetration Test"	Liquefaction susceptibility after Olson & Stark (2003) "Yield Strength Ratio and Liquefaction Analysis of Slopes and Embankments"	State parameter approximation - Robertson (2009) "Interpretation of cone penetration tests - a unified approach"

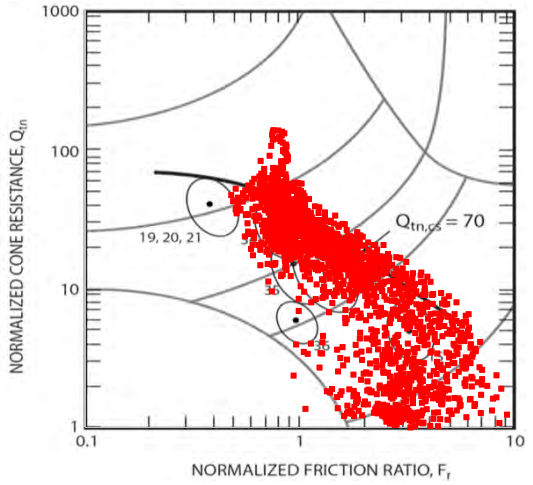

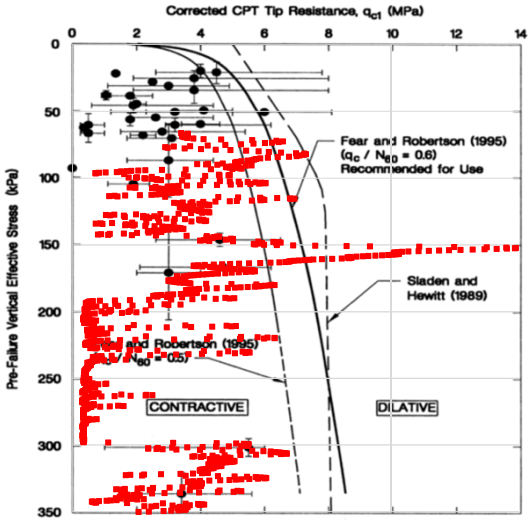

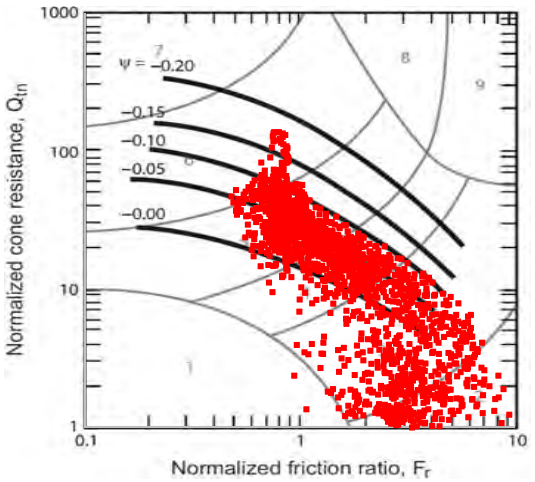

NOTE:

PROJECT

Fundão Tailings Dam Review Panel

TITLE

Fugro (March - July 2015) - Germano
CPTu-F15 Liquefaction Susceptibility and Soil Behavior Type

FUGRO IN SITU GEOTECNIA

PERCUSSION DRILLING

SMC-03-GRE-01
Attachments

CLIENT: SAMARCO MINERAÇÃO S.A.

PROJECT: **GERMANO DAM – BAY 3**

LOCATION: **MINA DE GERMANO–MARIANA-MG**

SCALE: 1:100 START: 14/05/2015 END: 15/05/2015 RESP.: DANIELLA ARANHA CREA Reg. No.: 201057330-7/RJ

BOREHOLE: SP-F15 ELEVATION: 916,60 COORDINATES: E 658885,10 N 7764239,41

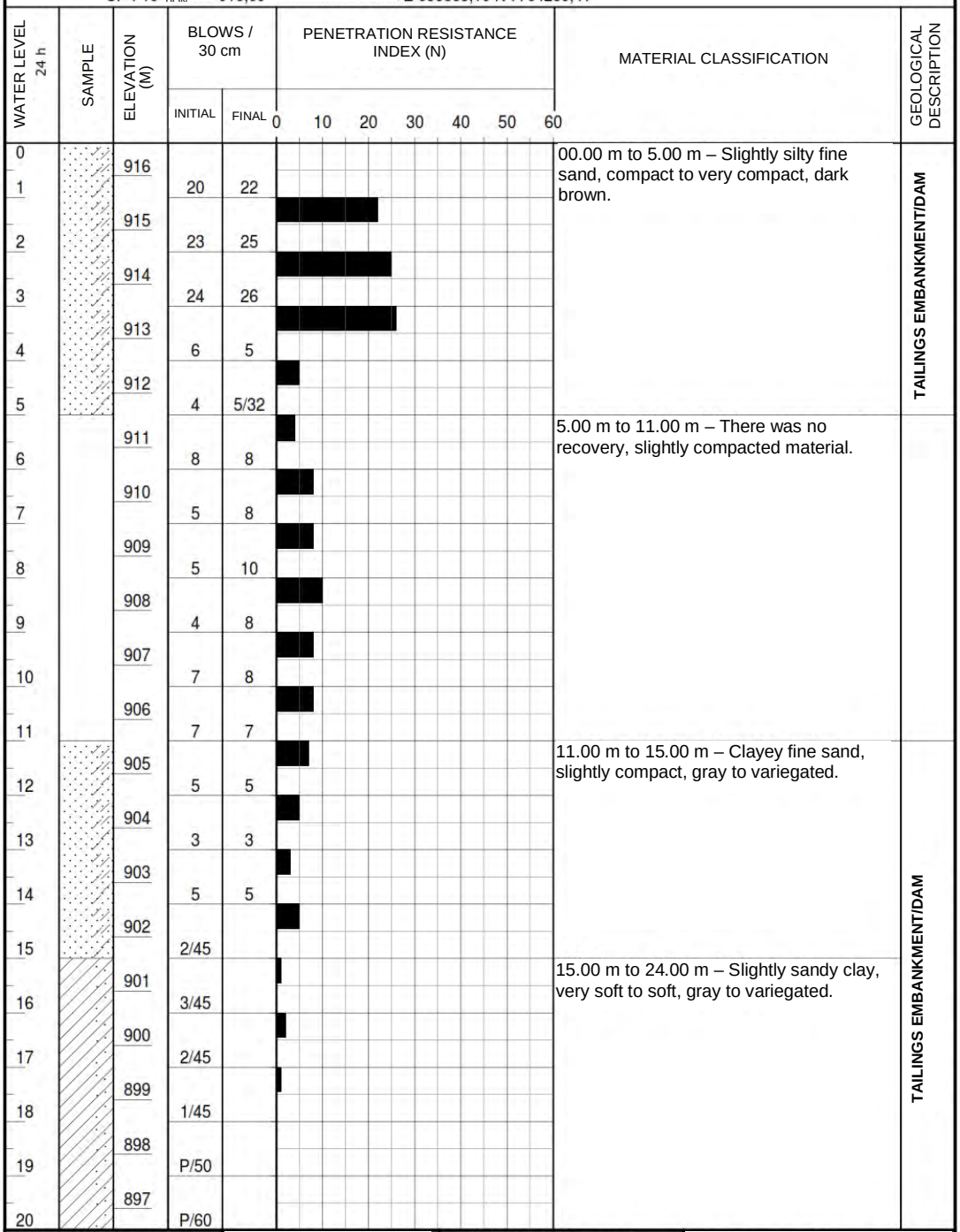

READING INTERVAL N.A(m)
1. 24 h: - CLOSED
2:
3:

PROGRESS METHOD (m)
DIGGER: -
WASHING: 0.00 – 50.06
LINING: 50.06
USE OF BENTONITE: -
WATER LEAK

TIME WASHING – 10 min
INITIAL DEPTH (m):
STAGE 1 (cm):
STAGE 2 (cm):
STAGE 3 (cm):

NOTE: Borehole closed at 3.10 m.
Drilling stopped due to meeting the condition of impermeability
Initial WL: DRY

FUGRO IN SITU GEOTECNIA

PERCUSSION DRILLING

SMC-03-GRE-01
Attachments

CLIENT: SAMARCO MINERAÇÃO S.A.

PROJECT: **GERMANO DAM – BAY 3**

LOCATION: **MINA DE GERMANO–MARIANA-MG**

SCALE: 1:100 START: 14/05/2015 END: 15/05/2015 RESP.: DANIELLA ARANHA CREA Reg. No.: 201057330-7/RJ

BOREHOLE: SP-F15 ELEVATION: 916,60 COORDINATES: E 658885,10 N 7764239,41

WATER LEVEL 24 h	SAMPLE	ELEVATION (M)	BLOWS / 30 cm INITIAL	BLOWS / 30 cm FINAL	PENETRATION RESISTANCE INDEX (N) 0 10 20 30 40 50 60	MATERIAL CLASSIFICATION	GEOLOGICAL DESCRIPTION
20		896				15.00 m to 24.00 m – Slightly sandy clay, very soft to soft, gray to variegated.	TAILINGS EMBANKMENT/DAM
21			1/70				
		895					
22			3/35	3			
		894					
23			2/40	2/35			
		893					
24			2/50				
		892				24.00 m to 29.00 m – There was no recovery, slightly compacted material.	
25			3/35	3			
		891					
26			4/34	4/34			
		890					
27			4	3			
		889					
28			10	20			
		888					
29			13	27			
		887				29.00 m to 32.00 m – Clayey fine sand, compact, dark brown to variegated.	TAILINGS EMBANKMENT/DAM
30			15	30			
		886					
31			15	23			
		885					
32			4	4			
		884				32.00 m to 33.00 m – There was no recovery, slightly compacted material.	
33			2/50				
		883				33.00 m to 37.00 m – Sandy clay, very soft to hard, reddish brown.	TAILINGS EMBANKMENT/DAM
34			3	4			
		882					
35			1/45				
		881					
36			10	11			
		880					
37			2/35	13			
		879				37.00 m to 47.00 m – There was no recovery, slightly compacted material.	
38			20	29			
		878					
39			22	32			
		877					
40			11	13			

READING INTERVAL N.A(m)
1. 24 h: - CLOSED
2:
3:

PROGRESS METHOD (m)
DIGGER: -
WASHING: 0.00 – 50.06
LINING: 50.06
USE OF BENTONITE: -
WATER LEAK

TIME WASHING – 10 min
INITIAL DEPTH (m):
STAGE 1 (cm):
STAGE 2 (cm):
STAGE 3 (cm):

NOTE: Borehole closed at 3.10 m.
Drilling stopped due to meeting the condition of impermeability
Initial WL: DRY

FUGRO IN SITU GEOTECNIA

PERCUSSION DRILLING

SMC-03-GRE-01
Attachments

CLIENT: SAMARCO MINERAÇÃO S.A.

PROJECT: **GERMANO DAM – BAY 3**

LOCATION: **MINA DE GERMANO–MARIANA-MG**

SCALE: 1:100 START: 14/05/2015 END: 15/05/2015 RESP.: DANIELLA ARANHA CREA Reg. No.: 201057330-7/RJ

BOREHOLE: SP-F15 ELEVATION: 916,60 COORDINATES: E 658885,10 N 7764239,41

WATER LEVEL 24 h	SAMPLE	ELEVATION (M)	BLOWS / 30 cm INITIAL	BLOWS / 30 cm FINAL	PENETRATION RESISTANCE INDEX (N) 0 10 20 30 40 50 60	MATERIAL CLASSIFICATION	GEOLOGICAL DESCRIPTION
40		876				37.00 m to 47.00 m - There was no recovery, slightly compacted material.	
41			9	13			
42		875	6	12			
43		874	12	14			
44		873	12	15			
45		872	11	14			
46		871	13	25			
47		870	30/12				
48		869	30/10			47.00 m to 50.00 m - Clayey sand, fine to medium, very compact, light gray to variegated.	SAPROLITE
49		868	30/10				
50		867	30/6				
51		866					
52		865					
53		864					
54		863					
55		862					
56		861					
57		860					
58		859					
59		858					
60		857					

READING INTERVAL N.A(m)
1. 24 h: - CLOSED
2:
3:

PROGRESS METHOD (m)
DIGGER: -
WASHING: 0.00 – 50.06
LINING: 50.06
USE OF BENTONITE: -
WATER LEAK

TIME WASHING – 10 min
INITIAL DEPTH (m):
STAGE 1 (cm):
STAGE 2 (cm):
STAGE 3 (cm):

NOTE: Borehole closed at 3.10 m.
Drilling stopped due to meeting the condition of impermeability
Initial WL: DRY

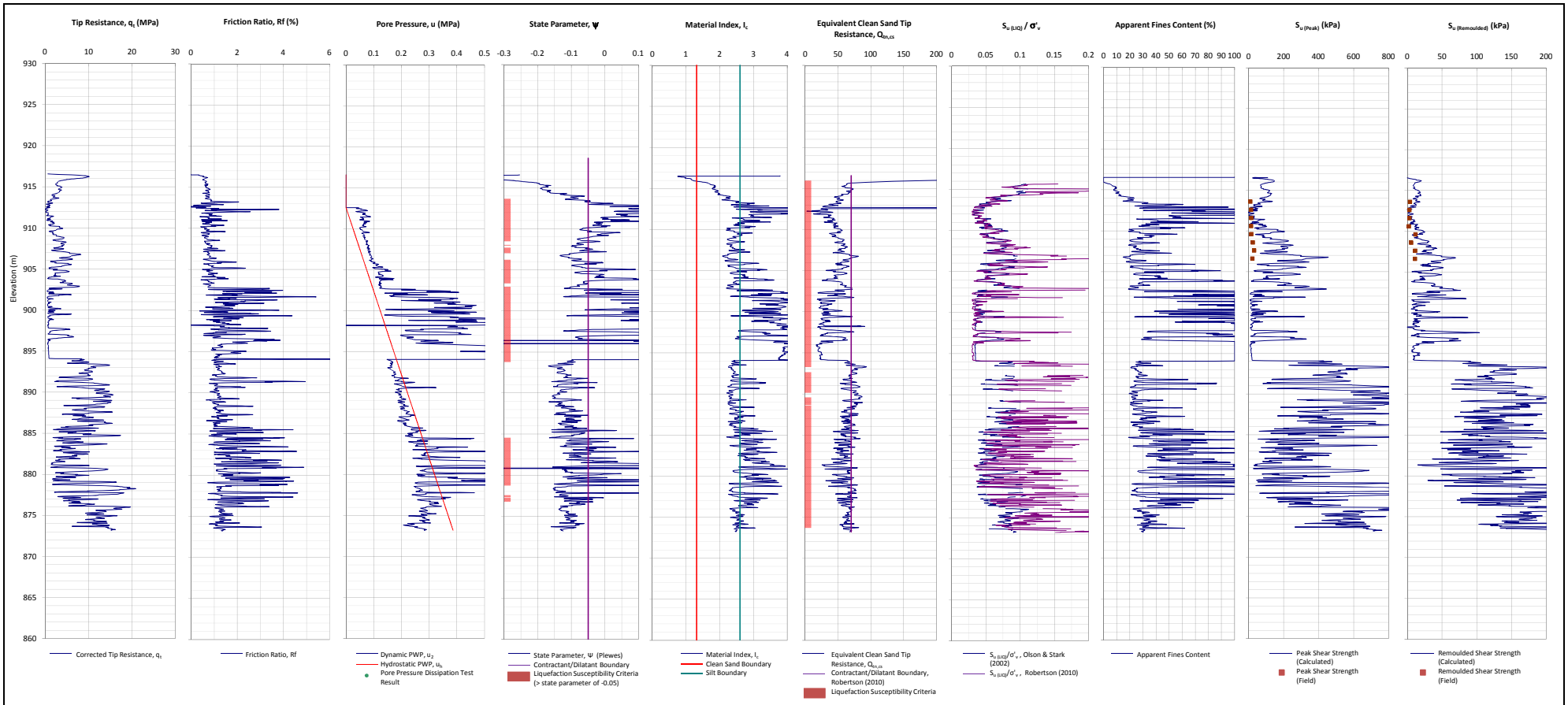

Notes:

1. This interpretation is based on the water and soil saturated unit weights γ_w=9.807 kN/m^3 and γ_{sat}=22 kN/m^3.
2. The friction ratio Rf is calculated as Rf=f_s/q_t.
3. The hydrostatic pore pressure is calculated using the ground water level (GWL) determined from CPT pore pressure dissipation tests (where available) or dynamic pore pressure.
4. Soil boundary layers (where plotted) are based on KCB interpretation.
5. The data presented have been plotted to the axis limits. Data may exist beyond the axis limits shown.
6. The Material Index (I_c) boundaries are based on Robertson and Wride (1998).
7. The $Q_{tn,cs}$ contractant/dilatant boundary=70 and is based on Robertson (2010).
8. The State Parameter (Ψ) is calculated using Plewes, et al. (1992) assuming a K0 of 0.5.
9. Coordinates are in UTM Zone 23K Córrego Alegre.
10. N_{kt} used in calculation of $S_{u(peak)}$ is 20.

Project: Fundão Tailings Dam Review Panel

Title: Fugro (March - July 2015) - Germano
CONE PENETRATION TEST CPTu-F16
N:7764300m E:658925m 2015-05-22

Liquefaction susceptibility after Robertson (2010) "Evaluation of Flow Liquefaction and Liquefied Strength Using the Cone Penetration Test"	Liquefaction susceptibility after Olson & Stark (2003) "Yield Strength Ratio and Liquefaction Analysis of Slopes and Embankments"	State parameter approximation - Robertson (2009) "Interpretation of cone penetration tests - a unified approach"

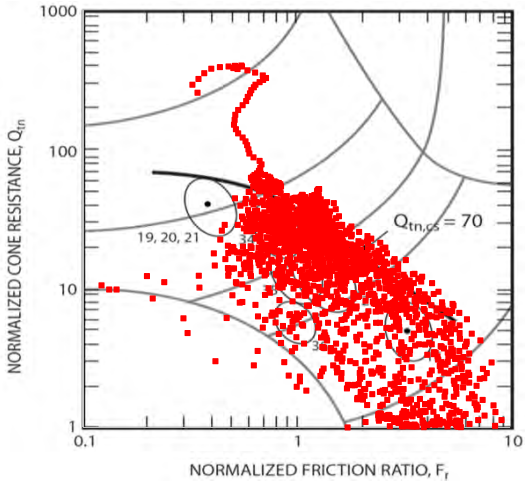

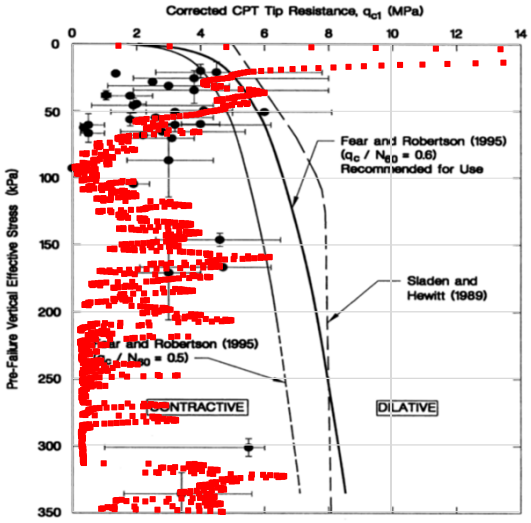

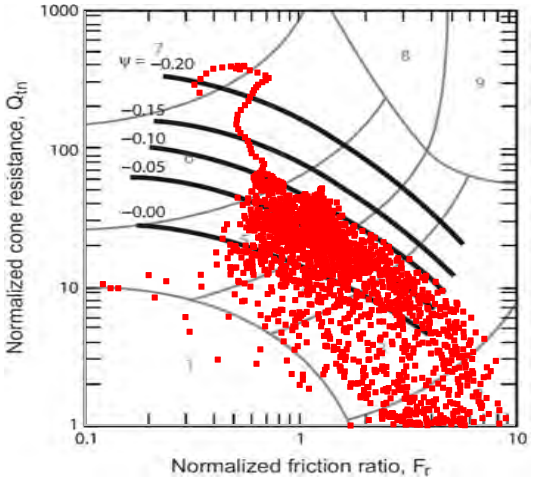

NOTE:

PROJECT

Fundão Tailings Dam Review Panel

TITLE

Fugro (March - July 2015) - Germano
CPTu-F16 Liquefaction Susceptibility and Soil Behavior Type

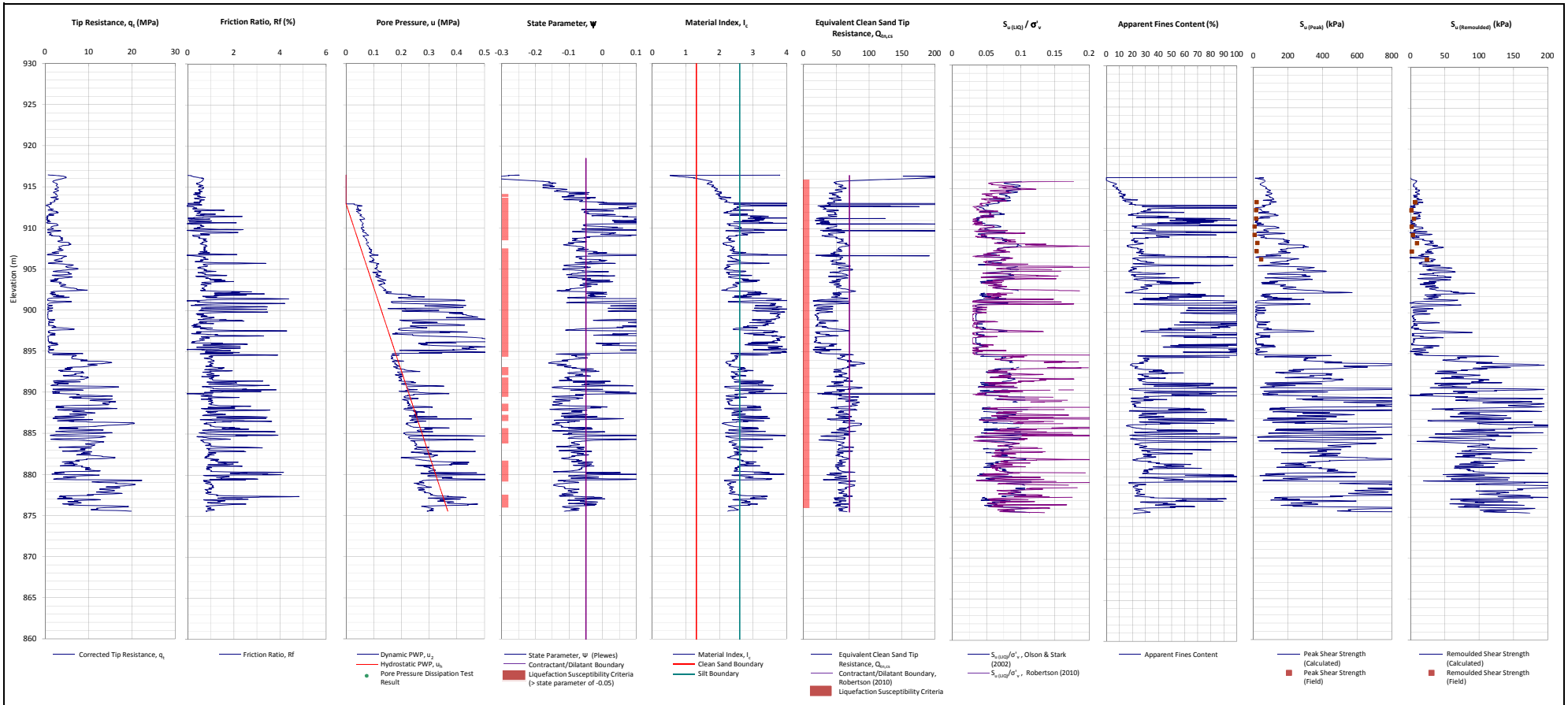

Notes:

1. This interpretation is based on the water and soil saturated unit weights γ_w=9.807 kN/m^3 and γ_{sat}=22 kN/m^3.
2. The friction ratio Rf is calculated as Rf=f_s/q_t.
3. The hydrostatic pore pressure is calculated using the ground water level (GWL) determined from CPT pore pressure dissipation tests (where available) or dynamic pore pressure.
4. Soil boundary layers (where plotted) are based on KCB interpretation.
5. The data presented have been plotted to the axis limits. Data may exist beyond the axis limits shown.
6. The Material Index (I_c) boundaries are based on Robertson and Wride (1998).
7. The $Q_{tn,cs}$ contractant/dilatant boundary=70 and is based on Robertson (2010).
8. The State Parameter (Ψ) is calculated using Plewes, et al. (1992) assuming a K0 of 0.5.
9. Coordinates are in UTM Zone 23K Córrego Alegre.
10. N_{kt} used in calculation of $S_{u(peak)}$ is 20.

PROJECT: Fundão Tailings Dam Review Panel

TITLE: Fugro (March - July 2015) - Germano
CONE PENETRATION TEST CPTu-F17
N:7764372m E:658974m 2015-06-03

Liquefaction susceptibility after Robertson (2010) "Evaluation of Flow Liquefaction and Liquefied Strength Using the Cone Penetration Test"	Liquefaction susceptibility after Olson & Stark (2003) "Yield Strength Ratio and Liquefaction Analysis of Slopes and Embankments"	State parameter approximation - Robertson (2009) "Interpretation of cone penetration tests - a unified approach"

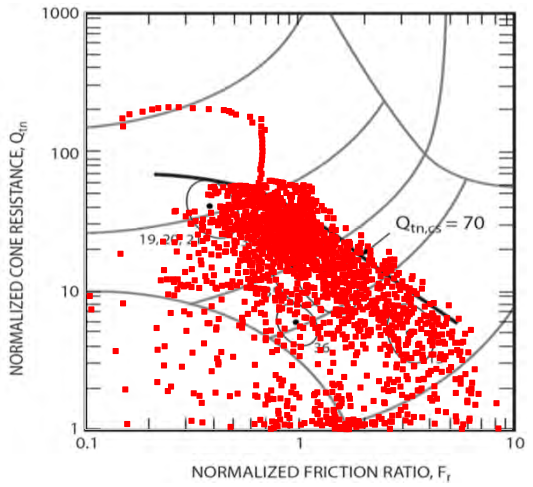

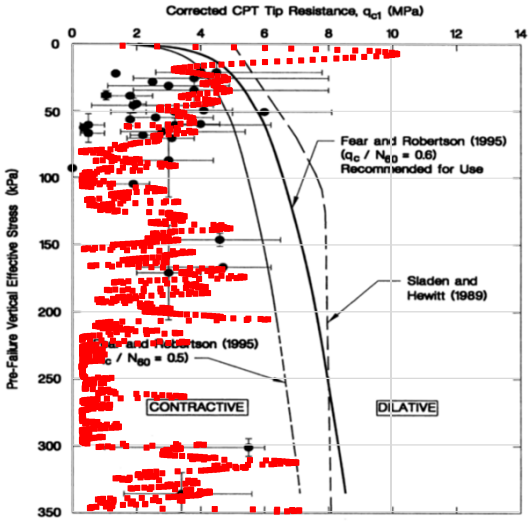

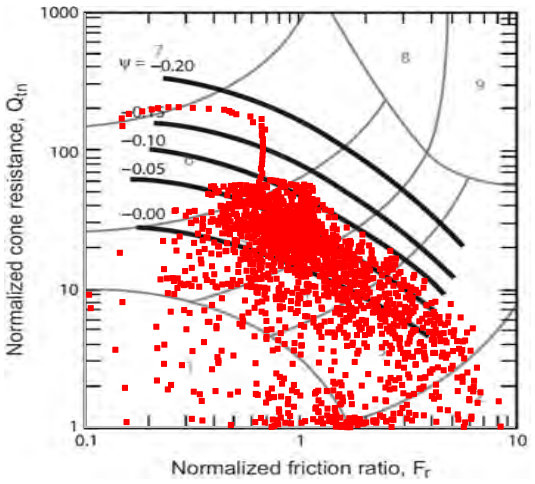

NOTE:

PROJECT

Fundão Tailings Dam Review Panel

TITLE

Fugro (March - July 2015) - Germano
CPTu-F17 Liquefaction Susceptibility and Soil Behavior Type

FUGRO IN SITU GEOTECNIA

Borehole Log

SMC-03-GRE-01
ANEXOS

CLIENT: SAMARCO MINERAÇÃO S.A.

PROJECT: GERMANO DAM BAY 3

LOCATION: MINA DE GERMANO. MARIANA.MG

SCALE: 1:100 START: 11/06/2015 END: 22/06/2015 IN CHARGE: DANIELLA ARANHA. CREA: 201057330-7/RJ

SOUNDING: SP-F17 COTA: 916,36 COORDINATES: E 658975,85 N 7764372,51

WATER LEVEL 24 h	SAMPLE	Height (m)	BLOWS / 30 cm INICIAL	BLOWS / 30 cm FINAL	PENETRATION RESISTANCE INDEX (N) 0 10 20 30 40 50 60	CLASSIFICATION OF MATERIALS	GEOLOGICAL DESCRIPTION
0		916				0.00 m to 3.00 m - Clayey fine sand, soft to low compaction, light gray to variegated coloration	EMBANKMENT OF TAILINGS / DAM
1			2	3			
		915					
2			5	6			
		914					
3			2/46				
		913				3.00 m to 14.00 m - There was no recovery, material has low compactness	
4 ▼			2/45				
		912					
5			2/48				
		911					
6			2/50				
		910					
7			2/47				
		909					
8			2/47				
		908					
9			2/48				
		907					
10			2/47				
		906					
11			7	5/35			
		905					
12			2/45				
		904					
13			2/52				
		903					
14			1/47				
		902				14.00 m to 32.00 m - Clayey fine sand, soft to compact, brown to variegated coloration	
15			2/50				
		901					
16			2/45				
		900					
17			2/57				
		899					
18			1/45				
		898					
19			3/48				
		897					
20			10/48				

READING INTERVAL WATER LEVEL (M)
1: 24 h: -4,10
2:
3:

ADVANCEMENT METHOD (m)
T. DIGGER: -
Washing:: 0,00 - 72,00
LINING: 72,00
USE OF BENTONITE: -
WATER LEAK: -

WASHING OVER TIME - 10 min
START DEPTH (M)
STAGE 1 (cm):
STAGE 2 (cm):
STAGE 3 (cm):

OBS:Borehole stopped to attend to the impenetrability condition

SMC-03-GRE-01
ANEXOS

Borehole Log

FUGRO IN SITU GEOTECNIA

CLIENT: SAMARCO MINERAÇÃO S.A.

PROJECT: GERMANO DAM BAY 3

LOCATION: MINA DE GERMANO. MARIANA.MG

SCALE: 1:100 START: 11/06/2015 END: 22/06/2015 IN CHARGE: DANIELLA ARANHA. CREA: 201057330-7/RJ

SOUNDING: SP-F17 HEIGHT: 916,36 COORDINATES: E 658975,85 N 7764372,51

WATER LEVEL 24 h	SAMPLE	Height (m)	BLOWS / 30 cm INICIAL	BLOWS / 30 cm FINAL	PENETRATION RESISTANCE INDEX (N) 0 10 20 30 40 50 60	CLASSIFICATION OF MATERIALS	GEOLOGICAL DESCRIPTION
20		896				14.00 m to 32.00 m - Clayey fine sand, soft to compact, brown to variegated coloration	EMBANKMENT OF TAILINGS / DAM
21		895	8/39	14/41			
22		894	9	14/28			
23		893	12	17/27			
24		892	13/31	14			
25		891	10	11/31			
26		890	11	15			
27		889	14	19			
28		888	35	35			
29		887	32	33			
30		886	9	10/17			
31		885	11	12/34			
32		884	14	25		32.00 m to 62.00 m - Clayey fine sand, soft to very compact, gray to variegated coloration.	
33		883	11	20			
34		882	25	35			
35		881	27	35			
36		880	6/34	7			
37		879	6/32	11			
38		878	25	28			
39		877	23	31			
40			30	44			

READING INTERVAL WATER LEVEL (M)
1: 24 h: -4,10
2:
3:

ADVANCEMENT METHOD (m)
T. DIGGER:
Washing:: 0,00 - 72,00
LINING: 72,00
USE OF BENTONITE:
WATER LEAK:

WASHING OVER TIME - 10 min
START DEPTH (M)
STAGE 1 (cm):
STAGE 2 (cm):
STAGE 3 (cm):

OBS:Borehole stopped to attend to the impenetrability condition

FUGRO IN SITU GEOTECNIA

Borehole Log

SMC-03-GRE-01
ANEXOS

CLIENT: SAMARCO MINERAÇÃO S.A.

PROJECT: GERMANO DAM BAY 3

LOCATION: MINA DE GERMANO. MARIANA.MG

SCALE: 1:100 START: 11/06/2015 END: : 22/06/2015 IN CHARGE: DANIELLA ARANHA CREA: 201057330-7/RJ

SOUNDING: I: SP-F17 HEIGHT 916,36 COORDINATES: : E 658975,85 N 7764372,51

WATER LEVEL 24 h	SAMPLE	Height (m)	BLOWS / 30 cm INICIAL	BLOWS / 30 cm FINAL	PENETRATION RESISTANCE INDEX (N) 0 10 20 30 40 50 60	CLASSIFICATION OF MATERIALS	GEOLOGICAL DESCRIPTION
40		876				32.00 m to 62.00 m - Clayey fine sand, soft to very compact, gray to variegated coloration.	EMBANKMENT OF TAILINGS / DAM
41			28	38			
		875					
42			25	32			
		874					
43			25	30			
		873					
44			19	35			
		872					
45			19	28			
		871					
46			29	35			
		870					
47			28	37			
		869					
48			26	39			
		868					
49			50/28				
		867					
50			30	39/22			
		866					
51			33	37/29			
		865					
52			9	6/27			
		864					
53			10	9/26			
		863					
54			11	23			
		862					
55			14	23			
		861					
56			30	37			
		860					
57			29	36			
		859					
58			8	15/25			
		858					
59			7	6/26			
		857					
60			3/45				

READING INTERVAL WATER LEVEL (M)
1: 24 h: -4,10
2:
3:

ADVANCEMENT METHOD (m)
T. DIGGER: -
Washing:. 0,00 - 72,00
LINING: 72,00
USE OF BENTONITE:
WATER LEAK:

WASHING OVER TIME - 10 min
START DEPTH (M)
STAGE 1 (cm):
STAGE 2 (cm):
STAGE 3 (cm):

OBS:Borehole stopped to attend to the impenetrability condition

Borehole Log

SMC-CG-GRE-01
ANEXOS

FUGRO IN SITU GEOTECNIA

CLIENT: SAMARCO MINERAÇÃO S.A.

PROJECT: GERMANO DAM BAY 3

LOCATION: MINA DE GERMANO. MARIANA.MG

SCALE: 1:100 START: 11/06/2015 END: 22/06/2015 IN CHARGE: DANIELLA ARANHA. CREA: 20105733O-7/RJ

SOUNDING: SP-F17 HEIGHT 916,36 COORDINATES: E 658975,85 N 7764372,51

WATER LEVEL 24 h	SAMPLE	Height (m)	BLOWS / 30 cm INITIAL	BLOWS / 30 cm FINAL	PENETRATION RESISTANCE INDEX (N) 0 10 20 30 40 50 60	CLASSIFICATION OF MATERIALS	GEOLOGICAL DESCRIPTION
60		856					
61			3/45			32.00 m to 62.00 m - Clayey fine sand, soft to very compact, gray to variegated coloration.	EMBANKMENT OF TAILINGS / DAM
		855					
62			11/32	11			
		854				62.00 m to 63.00 m - There was no recovery , material with low compactness.	
63			17/31	11			
		853				63.00 m to 67.00 m - Sandy clay, medium compactness, brown to variegated coloration.	
64			17/32	13			
		852					
65			9	18/29			
		851					
66			5	11/29			
		850					
67			12/31	15			
		849				67.00 m to 70.00 m - Clayey fine to medium sand, medium to high compactness, dark gray to variegated coloration.	SAPROLITE
68			14	16			
		848					
69			22	25			
		847					
70			30/6				
		846				70.00 m to 72.00 m - Clayey fine sand, saprolite from schistose rock, very compact, light gray to variegated coloration.	
71			30/2				
		845					
72							
		844					
73							
		843					
74							
		842					
75							
		841					
76							
		840					
77							
		839					
78							
		838					
79							
		837					
80							

READING INTERVAL WATER LEVEL (M)
1: 24 h: -4,10
2:
3:

ADVANCEMENT METHOD (m)
T. DIGGER:
Washing:: 0,00 - 72,00
LINING: 72,00
USE OF BENTONITE:
WATER LEAK:

WASHING OVER TIME - 10 min
START DEPTH (M)
STAGE 1 (cm):
STAGE 2 (cm):
STAGE 3 (cm):

OBS:Borehole stopped to attend to the impenetrability condition

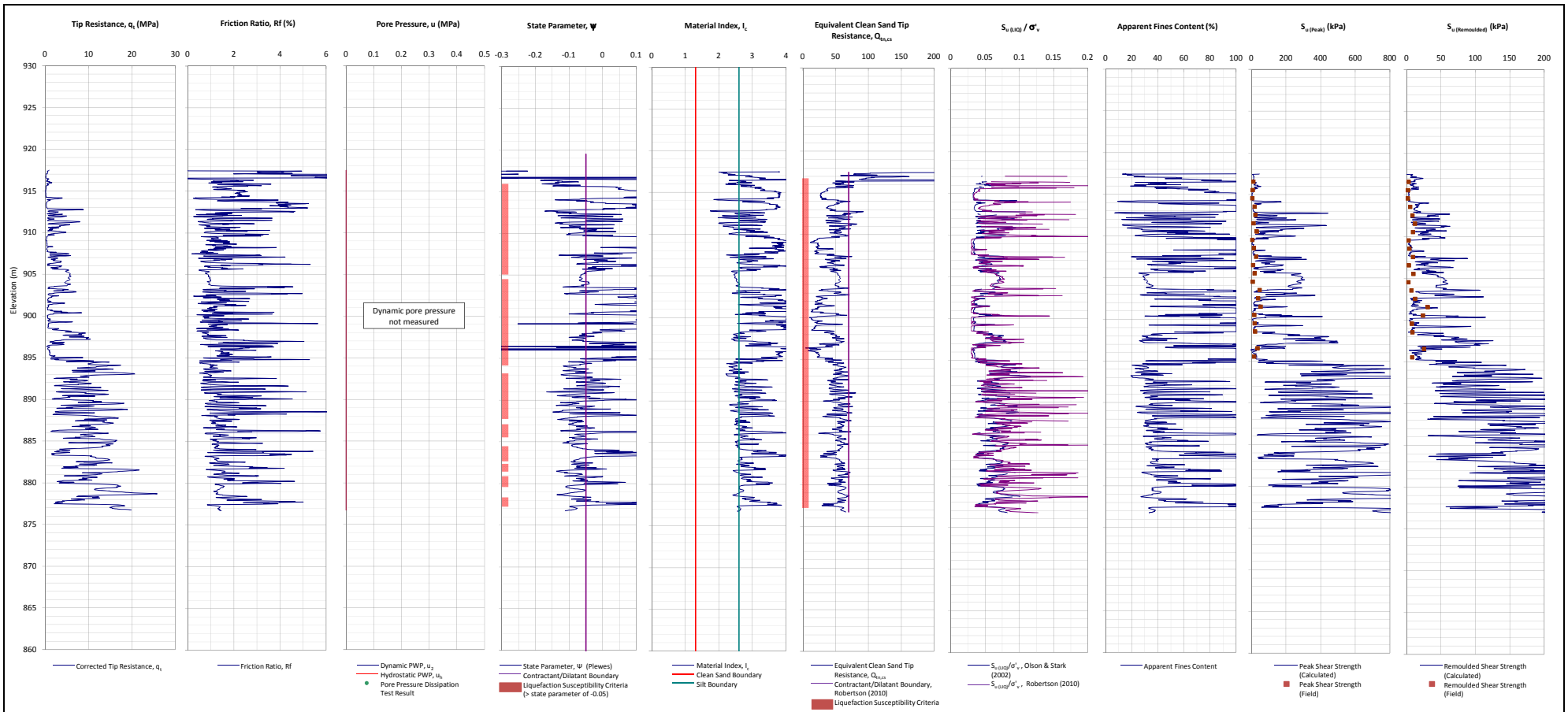

Notes:

1. This interpretation is based on the water and soil saturated unit weights γ_w=9.807 kN/m^3 and γ_{sat}=22 kN/m^3.
2. The friction ratio Rf is calculated as Rf=f_s/q_t.
3. The hydrostatic pore pressure is calculated using the ground water level (GWL) determined from CPT pore pressure dissipation tests (where available) or dynamic pore pressure.
4. Soil boundary layers (where plotted) are based on KCB interpretation.
5. The data presented have been plotted to the axis limits. Data may exist beyond the axis limits shown.
6. The Material Index (I_c) boundaries are based on Robertson and Wride (1998).
7. The $Q_{tn,cs}$ contractant/dilatant boundary=70 and is based on Robertson (2010).
8. The State Parameter (Ψ) is calculated using Plewes, et al. (1992) assuming a K0 of 0.5.
9. Coordinates are in UTM Zone 23K Córrego Alegre.
10. N_{kt} used in calculation of $S_{u(peak)}$ is 20.

PROJECT: Fundão Tailings Dam Review Panel

TITLE: Fugro (March - July 2015) - Germano
CONE PENETRATION TEST CPTu-F18
N:7763962m E:659022m 2015-03-12

Liquefaction susceptibility after Robertson (2010) "Evaluation of Flow Liquefaction and Liquefied Strength Using the Cone Penetration Test"	Liquefaction susceptibility after Olson & Stark (2003) "Yield Strength Ratio and Liquefaction Analysis of Slopes and Embankments"	State parameter approximation - Robertson (2009) "Interpretation of cone penetration tests - a unified approach"

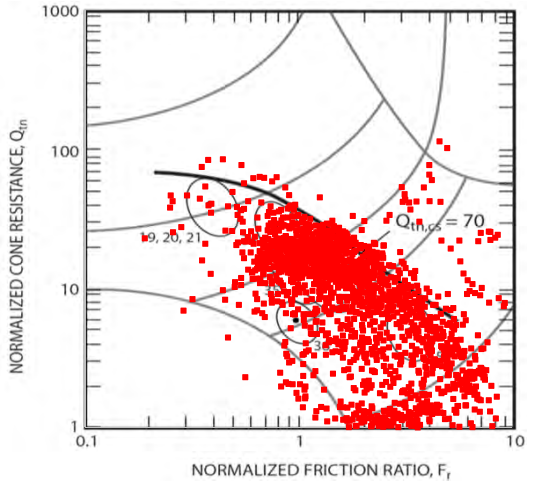

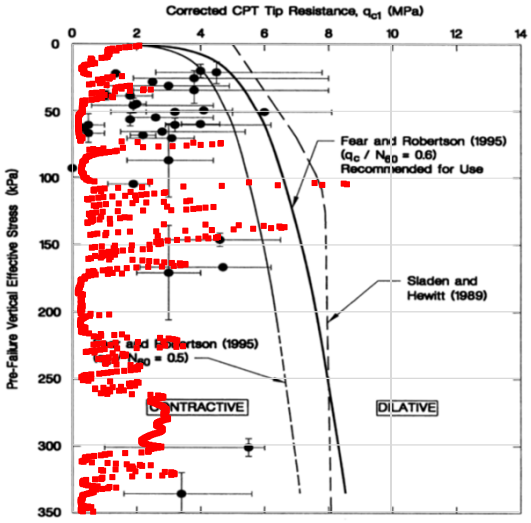

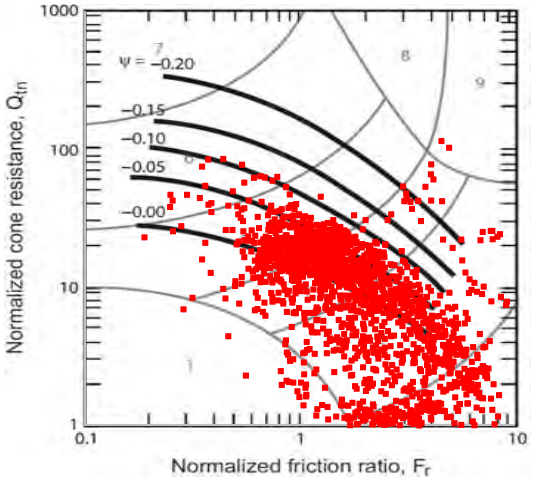

NOTE:

PROJECT

Fundão Tailings Dam Review Panel

TITLE

Fugro (March - July 2015) - Germano
CPTu-F18 Liquefaction Susceptibility and Soil Behavior Type

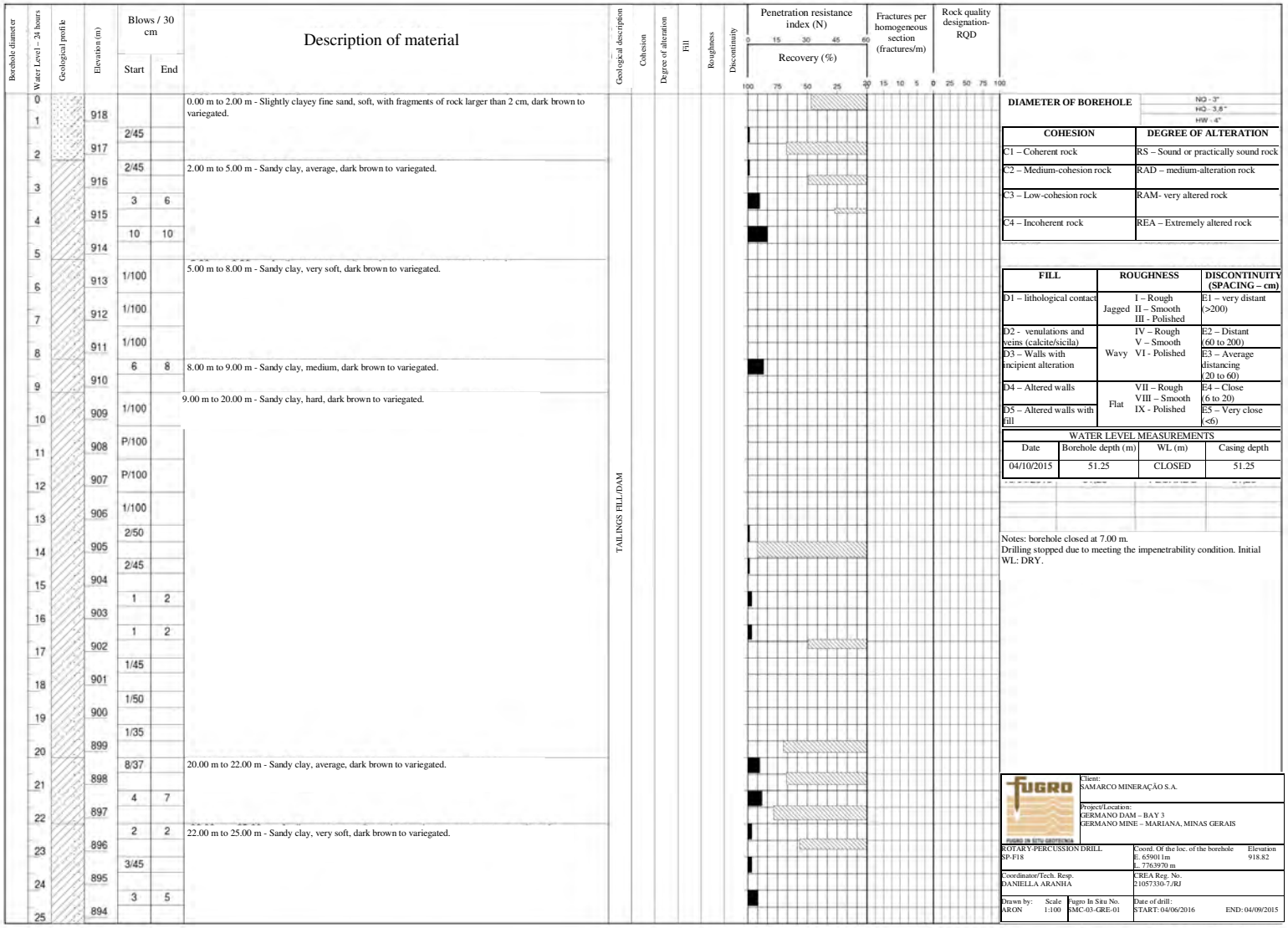

DIAMETER OF BOREHOLE

NQ - 3"
HQ - 3.8"
HW - 4"

COHESION	DEGREE OF ALTERATION
C1 – Coherent rock	RS – Sound or practically sound rock
C2 – Medium-cohesion rock	RAD – medium-alteration rock
C3 – Low-cohesion rock	RAM- very altered rock
C4 – Incoherent rock	REA – Extremely altered rock

FILL	ROUGHNESS		DISCONTINUITY (SPACING – cm)
D1 – lithological contact	Jagged	I – Rough II – Smooth III - Polished	E1 – very distant (>200)
D2 - venulations and veins (calcite/sicila)	Wavy	IV – Rough V – Smooth VI - Polished	E2 – Distant (60 to 200)
D3 – Walls with incipient alteration			E3 – Average distancing (20 to 60)
D4 – Altered walls	Flat	VII – Rough VIII – Smooth IX - Polished	E4 – Close (6 to 20)
D5 – Altered walls with fill			E5 – Very close (<6)

WATER LEVEL MEASUREMENTS

Date	Borehole depth (m)	WL (m)	Casing depth
04/10/2015	51.25	CLOSED	51.25

Notes: borehole closed at 7.00 m.
Drilling stopped due to meeting the impenetrability condition. Initial WL: DRY.

FUGRO
FUGRO IN SITU GEOTECNIA

Client:
SAMARCO MINERAÇÃO S.A.

Project/Location:
GERMANO DAM – BAY 3
GERMANO MINE – MARIANA, MINAS GERAIS

ROTARY-PERCUSSION DRILL
SP-F18

Coord. Of the loc. of the borehole
E. 659011m
L. 7763970 m

Elevation
918.82

Coordinator/Tech. Resp.
DANIELLA ARANHA

CREA Reg. No.
21057330-7/RJ

Drawn by: ARON
Scale: 1:100
Fugro In Situ No.: SMC-03-GRE-01
Date of drill: START: 04/06/2016 END: 04/09/2015

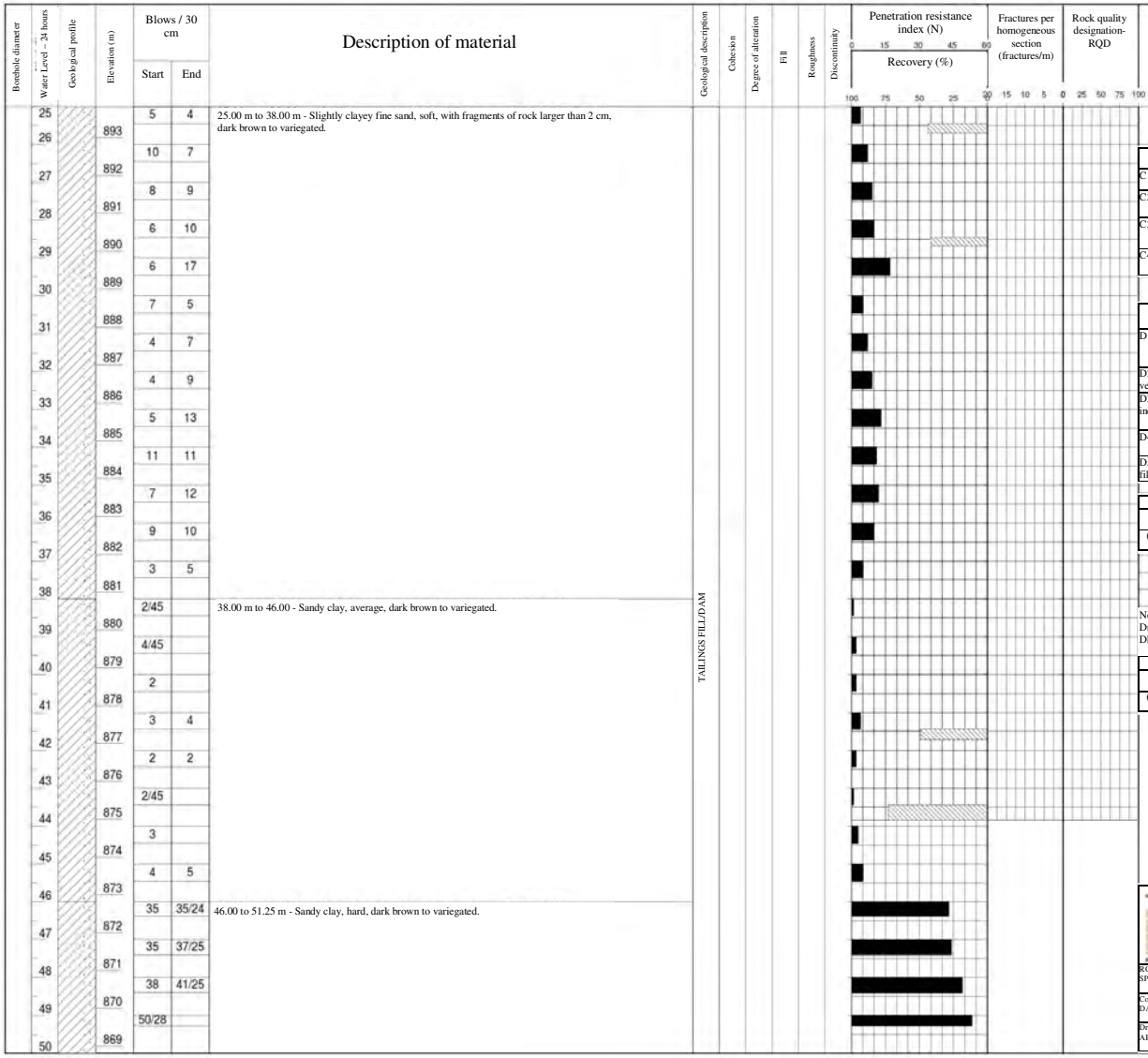

DIAMETER OF BOREHOLE

NQ - 3"
HQ - 3.8 "
HW - 4"

COHESION	DEGREE OF ALTERATION
C1 – Coherent rock	RS – Sound or practically sound rock
C2 – Medium-cohesion rock	RAD – medium-alteration rock
C3 – Low-cohesion rock	RAM- very altered rock
C4 – Incoherent rock	REA – Extremely altered rock

FILL	ROUGHNESS	DISCONTINUITY (SPACING – cm)
D1 – lithological contact	Jagged I – Rough II – Smooth III - Polished	E1 – very distant (>200)
D2 - venulations and veins (calcite/sicila)	Wavy IV – Rough V – Smooth VI - Polished	E2 – Distant (60 to 200)
D3 – Walls with incipient alteration		E3 – Average distancing (20 to 60)
D4 – Altered walls	Flat VII – Rough VIII – Smooth IX - Polished	E4 – Close (6 to 20)
D5 – Altered walls with fill		E5 – Very close (<6)

WATER LEVEL MEASUREMENTS

Date	Borehole depth (m)	WL (m)	Casing depth
04/10/2015	51.25	CLOSED	51.25

Notes: borehole closed at 7.00 m.
Drilling stopped due to meeting the impenetrability condition. Initial WL: DRY.

WATER LEVEL MEASUREMENTS

Date	Borehole depth (m)	WL (m)	Casing depth
04/10/2015	51.25	CLOSED	51.25

FUGRO

Client: SAMARCO MINERAÇÃO S.A.

Project/Location: GERMANO DAM – BAY 3
GERMANO MINE – MARIANA, MINAS GERAIS

ROTARY-PERCUSSION DRILL SP-FI8

Coord. Of the loc. of the borehole: E. 659011m, L. 7763970 m — Elevation 918.82

Coordinator/Tech. Resp.: DANIELLA ARANHA

CREA Reg. No.: 21057330-7/RJ

Drawn by: ARON — Scale 1:100

Fugro In Situ No.: SMC-03-GRE-01

Date of drill: START: 04/06/2016 END: 04/09/2015

Borehole diameter	Water Level – 24 hours	Geological profile	Elevation (m)	Blows / 30 cm Start	Blows / 30 cm End	Description of material	Geological description	Cohesion	Degree of alteration	Fill	Roughness	Discontinuity	Penetration resistance index (N) 0 15 30 45 60 / Recovery (%)	Fractures per homogeneous section (fractures/m)	Rock quality designation- RQD
	50			50/25		46.00 to 51.25 m - Sandy clay, hard, dark brown to variegated.	TAILINGS FILL/DAM								
	51		868												
				55/25											
	52		867												
	53		866												
	54		865												
	55		864												
	56		863												
	57		862												
	58		861												
	59		860												
	60		859												
	61		858												
	62		857												
	63		856												
	64		855												
	65		854												
	66		853												
	67		852												
	68		851												
	69		850												
	70		849												
	71		848												
	72		847												
	73		846												
	74		845												
	75		844												

DIAMETER OF BOREHOLE

NQ - 3"
HQ - 3.8 "
HW - 4"

COHESION	DEGREE OF ALTERATION
C1 – Coherent rock	RS – Sound or practically sound rock
C2 – Medium-cohesion rock	RAD – medium-alteration rock
C3 – Low-cohesion rock	RAM- very altered rock
C4 – Incoherent rock	REA – Extremely altered rock

FILL	ROUGHNESS		DISCONTINUITY (SPACING – cm)
D1 – lithological contact	Jagged	I – Rough II – Smooth III - Polished	E1 – very distant (>200)
D2 - venulations and veins (calcite/sicila)	Wavy	IV – Rough V – Smooth VI - Polished	E2 – Distant (60 to 200)
D3 – Walls with incipient alteration			E3 – Average distancing (20 to 60)
D4 – Altered walls	Flat	VII – Rough VIII – Smooth IX - Polished	E4 – Close (6 to 20)
D5 – Altered walls with fill			E5 – Very close (<6)

WATER LEVEL MEASUREMENTS

Date	Borehole depth (m)	WL (m)	Casing depth
04/10/2015	51.25	CLOSED	51.25

Notes: borehole closed at 7.00 m.
Drilling stopped due to meeting the impenetrability condition. Initial WL: DRY.

FUGRO
FUGRO IN SITU GEOTECNIA

Client:
SAMARCO MINERAÇÃO S.A.

Project/Location:
GERMANO DAM – BAY 3
GERMANO MINE – MARIANA, MINAS GERAIS

ROTARY-PERCUSSION DRILL SP-F18	Coord. Of the loc. of the borehole E. 659011m S. 7763970 m	Elevation 918.82
Coordinator/Tech. Resp. DANIELLA ARANHA	CREA Reg. No. 2105733O-7/RJ	
Drawn by: Scale ARON 1:100	Fugro In Situ No. SMC-03-GRE-01	Date of drill: START: 04/06/2016 END: 04/09/2015

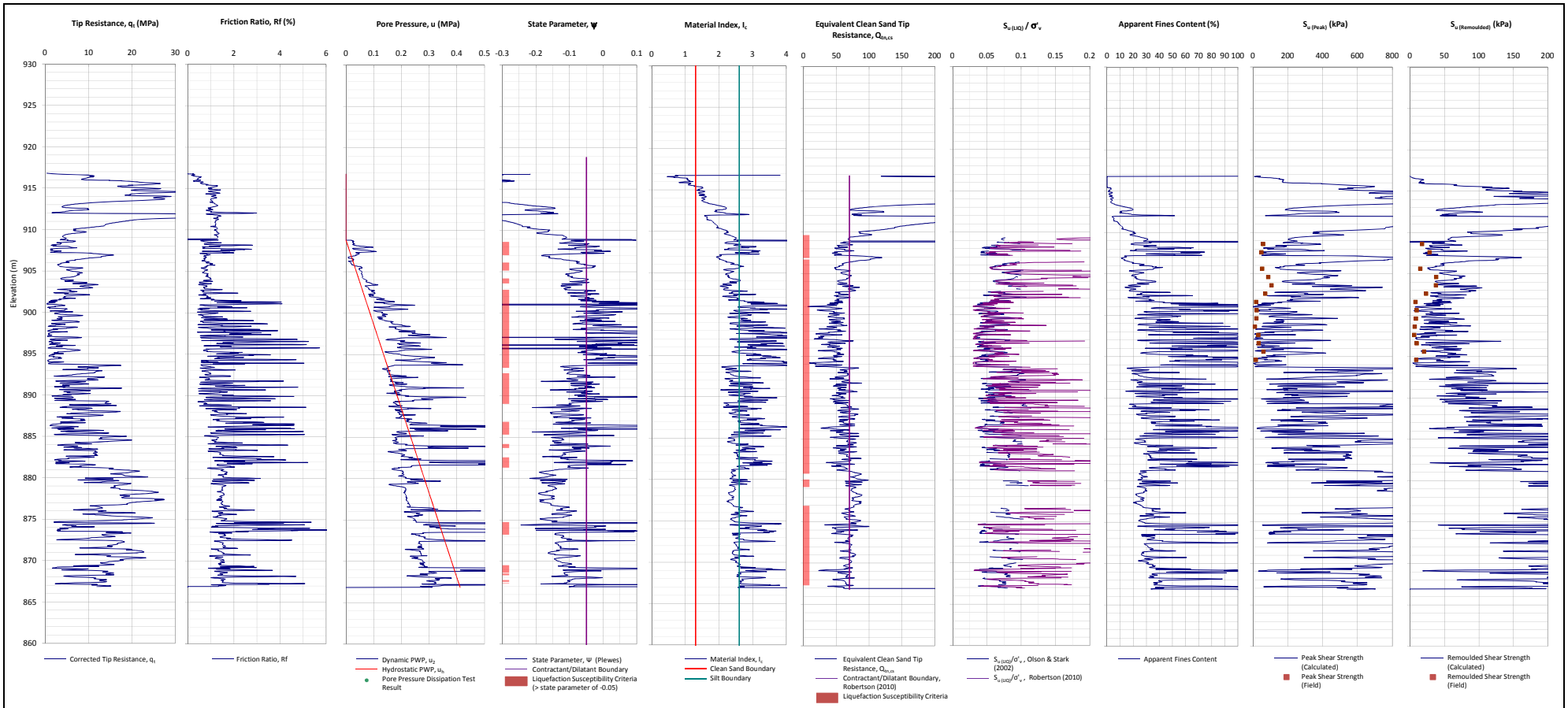

Notes:

1. This interpretation is based on the water and soil saturated unit weights γ_w=9.807 kN/m^3 and γ_{sat}=22 kN/m^3.
2. The friction ratio Rf is calculated as Rf=f_s/q_t.
3. The hydrostatic pore pressure is calculated using the ground water level (GWL) determined from CPT pore pressure dissipation tests (where available) or dynamic pore pressure.
4. Soil boundary layers (where plotted) are based on KCB interpretation.
5. The data presented have been plotted to the axis limits. Data may exist beyond the axis limits shown.
6. The Material Index (I_c) boundaries are based on Robertson and Wride (1998).
7. The $Q_{tn,cs}$ contractant/dilatant boundary=70 and is based on Robertson (2010).
8. The State Parameter (Ψ) is calculated using Plewes, et al. (1992) assuming a K0 of 0.5.
9. Coordinates are in UTM Zone 23K Córrego Alegre.
10. N_{kt} used in calculation of $S_{u(peak)}$ is 20.

PROJECT: Fundão Tailings Dam Review Panel

TITLE: Fugro (March - July 2015) - Germano
CONE PENETRATION TEST CPTu-F19
N:7764015m E:659095m 2015-03-06

Liquefaction susceptibility after Robertson (2010) "Evaluation of Flow Liquefaction and Liquefied Strength Using the Cone Penetration Test"	Liquefaction susceptibility after Olson & Stark (2003) "Yield Strength Ratio and Liquefaction Analysis of Slopes and Embankments"	State parameter approximation - Robertson (2009) "Interpretation of cone penetration tests - a unified approach"

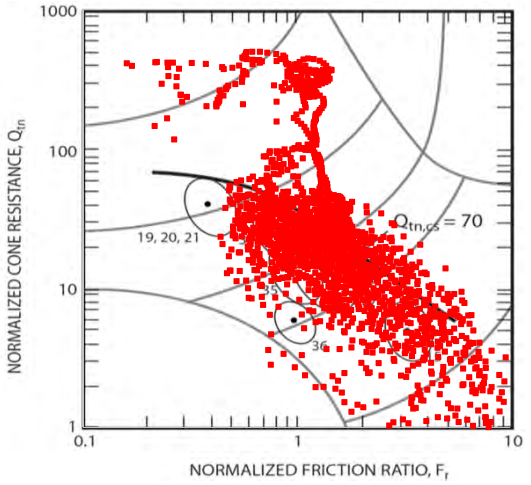

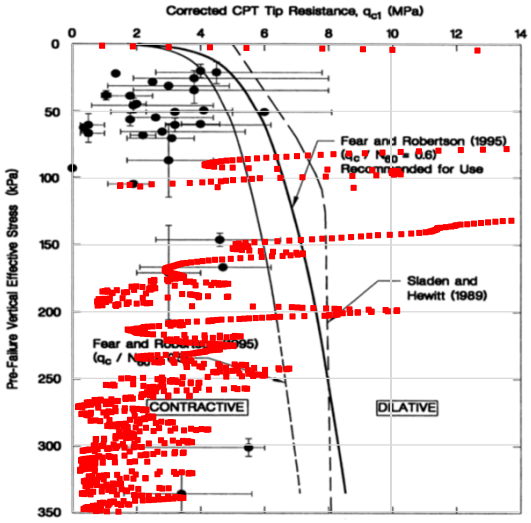

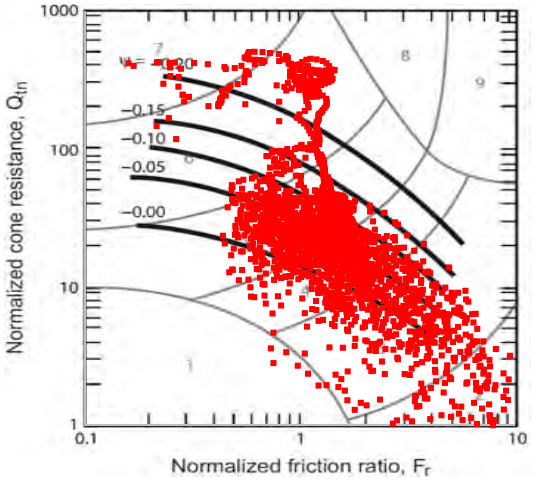

NOTE:

PROJECT

Fundão Tailings Dam Review Panel

TITLE

Fugro (March - July 2015) - Germano
CPTu-F19 Liquefaction Susceptibility and Soil Behavior Type

Borehole diameter	Water Level 24 hours	Geological profile	Elevation (m)	Blows / 30 cm Start	Blows / 30 cm End	Description of material	Geological description	Cohesion	Degree of alteration	Fill	Roughness	Discontinuity	PENETRATION RESISTANCE INDEX (N) 0 15 30 45 60	RECOVERY (%) 100 75 50 25	Fractures per homogeneous section (fractures/m) 20 15 10 5 0	Rock quality designation - RQD 0 25 50 75 100
HQ	0		916			0.00 m to 80.00 m - Fine to medium clayey sand, soft to medium compactness, dark brown to variegated Note : Since the material was soft and not very compact, there was no recovery from the following sections: i. de 13,00 a 19,00 m; ii. de 20,00 a 22,00 m; iii. de 22,00 a 24,00 m; iv. de 37,00 a 39,00 m; v. de 44,00 a 46,00 m; vi. de 58,45 a 60,50 m; vii. de 62,00 a 65,00 m; viii. de 64,50 a 74,00 m; ix. de 75,50 a 77,00 m.	TAILINGS FILL/DAM								
	1			12	13											
	2		915													
	3		914	16	17											
	4		913	15	17											
	5		912	10	8											
	6		911	10	9											
	7		910	9	8											
	8		909	10	10											
	9		908	3	4											
	10		907	5	6											
	11		906	10	10											
	12		905	9	9											
	13		904	6	5											
	14		903	2	31											
	15		902	1/45												
	16		901	1/50												
	17		900	2/45												
	18		899	P/100												
	19		898	P/100												
	20		897	P/80												
	21		896	1/48												
	22		895	1/49												
	23		894	1/48												
	24		893	1/45												
	25		892	8	9/32											

DIAMETER OF BOREHOLE	
	NQ - 3" HQ - 3,8" HW - 4"

COHESION	DEGREE OF ALTERATION
C1 – Coherent rock	RS – Sound or practically sound rock
C2 – Rock with Medium Coherence	RAD – medium-alteration rock
C3 – Rock with Low Coherence	RAM- very altered rock
C4 – Incoherent rock	REA – Extremely altered rock

FILL	ROUGHNESS		DISCONTINUITY (SPACING – cm)
D1 – lithological contact	Jagged	I – Rough II – Smooth III - Polished	E1 – very distant (>200)
D2 - venulations and veins (calcite/sicila)			E2 – Distant (60 a 200)
D3 – Walls with incipient alteration	Wavy	IV – Rough V – Smooth VI - Polished	E3 – Somehow Distant (20 a 60)
D4 – Altered walls	Flat	VII – Rough VIII – Smooth IX - Polished	E4 – Close (6 a 20)
D5 – Altered walls with fill			E5 – Very close (<6)

WATER LEVEL MEASUREMENTS

Date	Borehole depth (m)	WL (m)	Casing depth. (m)
02/09/15 - 14:00	17,45	6,40	17,45
02/10/15 - 9:38	32,45	8,60	32,45
02/12/15 - 8:17	47,45	8,50	47,45
02/23/15 - 9:30	80,00	5,69	80,00

Notes: At the client's request, the SPT test was stopped at 59.00 m, even though the SPT did not reach impenetrable material. From 59.00 to 80.00 m, the drilling was performed by rotary drill. There was a backflow of water from the start to the end of the borehole.

Client: SAMARCO MINERAÇÃO S.A.

Project/Location: GERMANO DAM – BAY 3
GERMANO MINE – MARIANA, MINAS GERAIS

ROTARY-PERCUSSION DRILL
SP-F19

Coord. Of the loc. of the borehole Elevation
E - 659101 m
N - 7764030 m
916,59

Coordinator/Tech. Resp.: RAFAELA RAMOS

CREA Reg. No.: PR-137347/D

Drawn by: FABIANO

Scale: 1:100

Fugro In Situ No.: SMC-I03-GRE-01

Date of drill: START: 02/07/2015 END: 02/13/2015

Borehole diameter	Water Level 24 hours	Geological profile	Elevation (m)	Blows / 30 cm Start	Blows / 30 cm End	Description of material	Geological description	Cohesion	Degree of alteration	Fill	Roughness	Discontinuity	PENETRATION RESISTANCE INDEX (N) 0 15 30 45 60 / RECOVERY (%) 100 75 50 25	Fractures per homogeneous section (fractures/m) 20 15 10 5 0	Rock quality designation - RQD 0 25 50 75 100
HQ	25		891	2/35	2/37	0.00 m to 80.00 m - Fine to medium clayey sand, soft to medium compactness, dark brown to variegated Note : Since the material was soft and not very compact, there was no recovery from the following sections: i. de 13,00 a 19,00 m; ii. de 20,00 a 22,00 m; iii. de 22,00 a 24,00 m; iv. de 37,00 a 39,00 m; v. de 44,00 a 46,00 m; vi. de 58,45 a 60,50 m; vii. de 62,00 a 65,00 m; viii. de 64,50 a 74,00 m; ix. de 75,50 a 77,00 m.	TAILINGS FILL/DAM								
	26														
			890	2/35	2/43										
	27														
			889	2	2/35										
	28														
			888	2/35	2/37										
	29														
			887	2/45											
	30														
			886	2	2										
	31														
			885	3	3										
	32														
			884	3	4										
	33														
			883	2	2										
	34														
			882	2/45											
	35														
			881	8	5/35										
	36														
			880	4	3										
	37														
			879	4	4/85										
	38														
			878	2	3										
	39														
			877	5	5/20										
	40														
			876	2/50											
	41														
			875	4/50											
	42														
			874	3	5										
	43														
			873	5	6										
	44														
			872	7	9										
	45														
			871	8	10										
	46														
			870	12	17										
	47														
			869	3/45											
	48														
			868	3	4										
	49														
			867	2	5										
	50														

DIAMETER OF BOREHOLE	
	NQ - 3"
	HQ - 3,8"
	HW - 4"

COHESION	DEGREE OF ALTERATION
C1 – Coherent rock	RS – Sound or practically sound rock
C2 – Rock with Medium Coherence	RAD – medium-alteration rock
C3 – Rock with Low Coherence	RAM- very altered rock
C4 – Incoherent rock	REA – Extremely altered rock

FILL	ROUGHNESS		DISCONTINUITY (SPACING – cm)
D1 – lithological contact	Jagged	I – Rough II – Smooth III - Polished	E1 – very distant (>200)
D2 - venulations and veins (calcite/sicila)			E2 – Distant (60 a 200)
D3 – Walls with incipient alteration	Wavy	IV – Rough V – Smooth VI - Polished	E3 – Somehow Distant (20 a 60)
D4 – Altered walls	Flat	VII – Rough VIII – Smooth IX - Polished	E4 – Close (6 a 20)
D5 – Altered walls with fill			E5 – Very close (<6)

WATER LEVEL MEASUREMENTS

Date	Borehole depth (m)	WL (m)	Casing depth. (m)
02/09/15 - 14:00	17,45	6,40	17,45
02/10/15 - 9:38	32,45	8,60	32,45
02/12/15 - 8:17	47,45	8,50	47,45
02/23/15 - 9:30	80,00	5,69	80,00

Notes: At the client's request, the SPT test was stopped at 59.00 m, even though the SPT did not reach impenetrable material. From 59.00 to 80.00 m, the drilling was performed by rotary drill. There was a backflow of water from the start to the end of the borehole.

FUGRO

Client: SAMARCO MINERAÇÃO S.A.

Project/Location: GERMANO DAM – BAY 3
GERMANO MINE – MARIANA, MINAS GERAIS

ROTARY-PERCUSSION DRILL
SP-F19

Coord. Of the loc. of the borehole Elevation
E - 659101 m
N - 7764030 m
916,59

Coordinator/Tech. Resp.: RAFAELA RAMOS

CREA Reg. No.: PR-137347/D

Drawn by: FABIANO | Scale: 1:100 | Fugro In Situ No.: SMC-03-GRE-01 | Date of drill: START: 02/07/2015 END: 02/13/2015

Borehole diameter	Water Level – 24 hours	Geological profile	Elevation (m)	Blows / 30 cm Start	Blows / 30 cm End	Description of material	Geological description	Cohesion	Degree of alteration	Fill	Roughness	Discontinuity	PENETRATION RESISTANCE INDEX (N) 0 15 30 45 60	RECOVERY (%) 100 75 50 25 0	Fractures per homogeneous section (fractures/m) 20 15 10 5 0	Rock quality designation - RQD 0 25 50 75 100
HQ	50		866	8	11	0.00 m to 80.00 m - Fine to medium clayey sand, soft to medium compactness, dark brown to variegated Note : Since the material was soft and not very compact, there was no recovery from the following sections: i. de 13,00 a 19,00 m; ii. de 20,00 a 22,00 m; iii. de 22,00 a 24,00 m; iv. de 37,00 a 39,00 m; v. de 44,00 a 46,00 m; vi. de 58,45 a 60,50 m; vii. de 62,00 a 65,00 m; viii. de 64,50 a 74,00 m; ix. de 75,50 a 77,00 m.	TAILINGS FILL/DAM								
	51															
			865	10	12											
	52															
			864	12	16											
	53															
			863	6	7											
	54															
			862	7	9											
	55															
			861	10	11											
	56															
			860	11	12											
	57															
			859	8	9											
	58															
			858	11	14											
	59															
	60		857													
			856													
	61		855													
	62															
			854													
	63															
			853													
	64															
			852													
	65															
			851													
	66															
			850													
	67															
			849													
	68															
			848													
	69															
			847													
	70															
			846													
	71															
			845													
	72															
			844													
	73															
			843													
	74															
			842													
	75															

DIAMETER OF BOREHOLE

NQ - 3"
HQ - 3,8"
HW - 4"

COHESION	DEGREE OF ALTERATION
C1 – Coherent rock	RS – Sound or practically sound rock
C2 –Rock with Medium Coherence	RAD – medium-alteration rock
C3 –Rock with Low coherence	RAM- very altered rock
C4 – Incoherent rock	REA – Extremely altered rock

FILL	ROUGHNESS		DISCONTINUITY (SPACING – cm)
D1 – lithological contact	Jagged	I – Rough II – Smooth III - Polished	E1 – very distant (>200)
D2 - venulations and veins (calcite/sicila)			E2 – Distant (60 a 200)
D3 – Walls with incipient alteration	Wavy	IV – Rough V – Smooth VI - Polished	E3 – Average Distancing (20 a 60)
D4 – Altered walls	Flat	VII – Rough VIII – Smooth IX - Polished	E4 – Close (6 a 20)
D5 – Altered walls with fill			E5 – Very close (<6)

WATER LEVEL MEASUREMENTS

Date	Borehole depth (m)	WL (m)	Casing depth. (m)
02/09/15 - 14:00	17,45	6,40	17,45
02/10/15 - 9:38	32,45	8,60	32,45
02/12/15 - 8:17	47,45	8,50	47,45
02/23/15 - 9:30	80,00	5,69	80,00

Notes: At the client's request, the SPT test was stopped at 59.00 m, even though the SPT did not reach impenetrable material. From 59.00 to 80.00 m, the drilling was performed by rotary drill. There was a backflow of water from the start to the end of the borehole.

FUGRO

Client: SAMARCO MINERAÇÃO S.A.

Project/Location: GERMANO DAM – BAY 3
GERMANO MINE – MARIANA, MINAS GERAIS

ROTARY-PERCUSSION DRILL
SP-F19

Coord. Of the loc. of the borehole Elevation
E - 659101 m
N - 7764030 m
916,59

Coordinator/Tech. Resp.: RAFAELA RAMOS

CREA Reg. No.: PR-137347/D

Drawn by: FABIANO

Scale: 1:100

Fugro In Situ No.: SMC-01-SPE-01

Date of drill: START: 02/07/2015 END: 02/13/2015

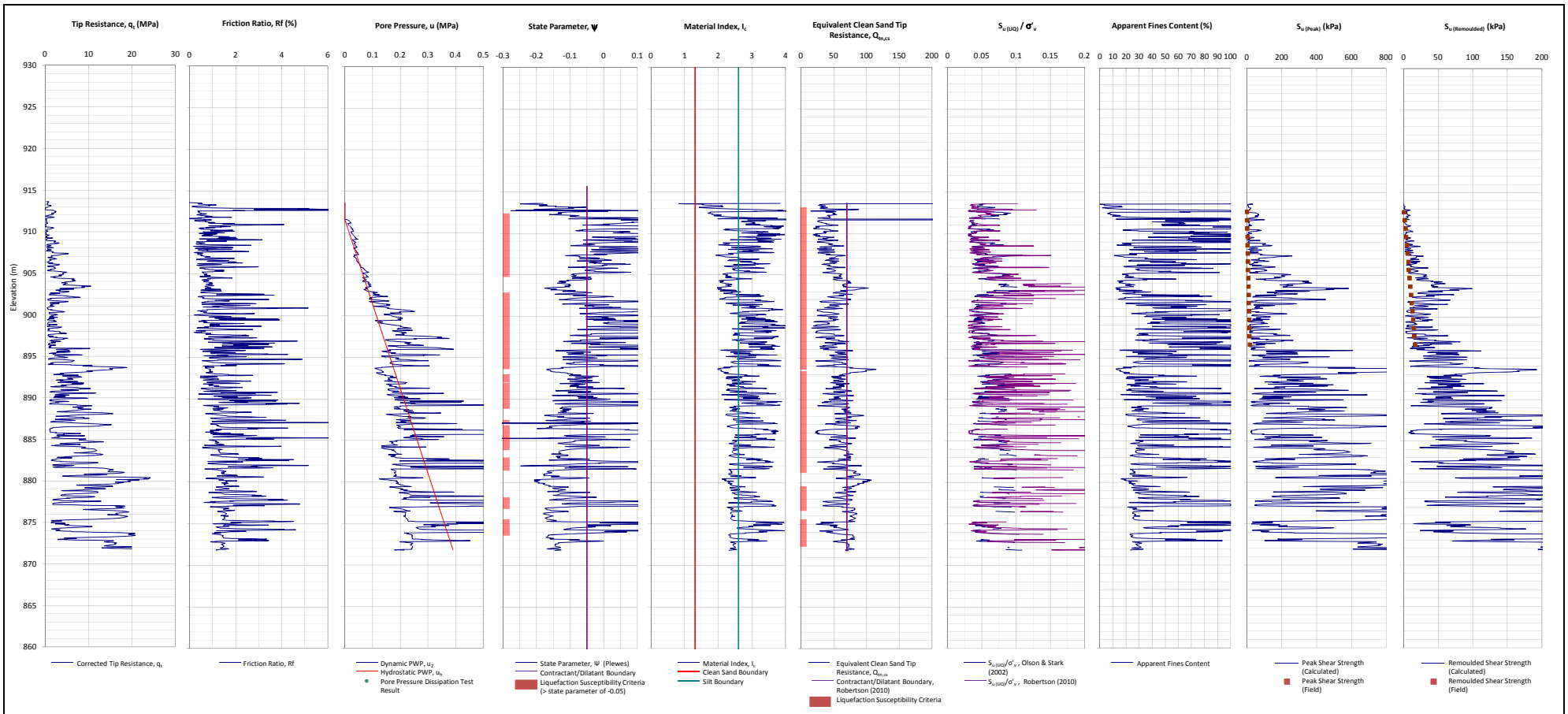

Notes:

1. This interpretation is based on the water and soil saturated unit weights γ_w=9.807 kN/m^3 and γ_{sat}=22 kN/m^3.
2. The friction ratio Rf is calculated as Rf=f_s/q_t.
3. The hydrostatic pore pressure is calculated using the ground water level (GWL) determined from CPT pore pressure dissipation tests (where available) or dynamic pore pressure.
4. Soil boundary layers (where plotted) are based on KCB interpretation.
5. The data presented have been plotted to the axis limits. Data may exist beyond the axis limits shown.
6. The Material Index (I_c) boundaries are based on Robertson and Wride (1998).
7. The $Q_{tn,cs}$ contractant/dilatant boundary=70 and is based on Robertson (2010).
8. The State Parameter (Ψ) is calculated using Plewes, et al. (1992) assuming a K0 of 0.5.
9. Coordinates are in UTM Zone 23K Córrego Alegre.
10. N_{kt} used in calculation of $S_{u(peak)}$ is 20.

PROJECT: Fundão Tailings Dam Review Panel

TITLE: Fugro (March - July 2015) - Germano
CONE PENETRATION TEST CPTu-F20
N:7764060m E:659155m 2015-03-12

Liquefaction susceptibility after Robertson (2010) "Evaluation of Flow Liquefaction and Liquefied Strength Using the Cone Penetration Test"	Liquefaction susceptibility after Olson & Stark (2003) "Yield Strength Ratio and Liquefaction Analysis of Slopes and Embankments"	State parameter approximation - Robertson (2009) "Interpretation of cone penetration tests - a unified approach"

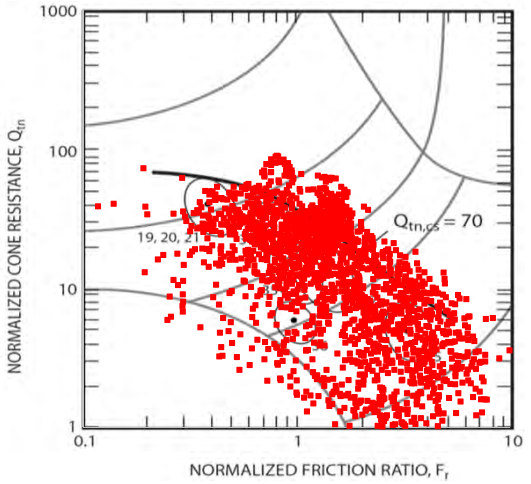

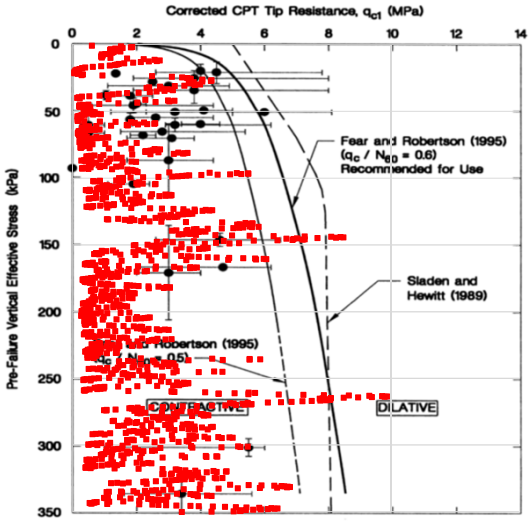

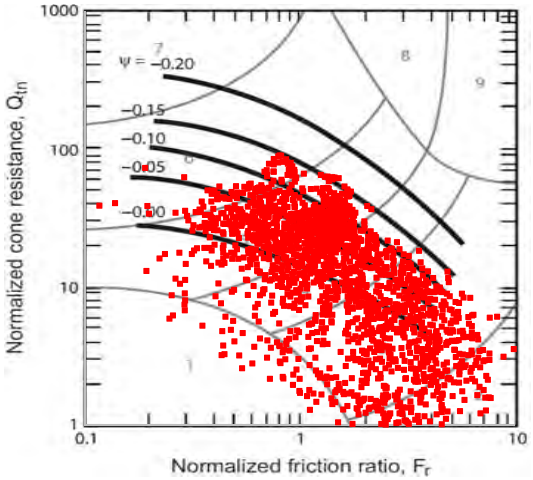

NOTE:

PROJECT

Fundão Tailings Dam Review Panel

TITLE

Fugro (March - July 2015) - Germano
CPTu-F20 Liquefaction Susceptibility and Soil Behavior Type

KCB note: The first page of the SPT log was missing from the original report.

FUGRO

STANDARD PENETRATION TEST

SMC-03-GRE-01
ATTACHMENTS

CLIENT: SAMARCO MINERAÇÃO S.A.
PROJECT: GERMANO DAM – BAY 3
LOCATION: GERMANO MINE – MARIANA, MINAS GERAIS

SCALE: 1:100 START: 4/13/2015 END: 4/16/2015 BY: DANIELLA ARANHA, CREA REG. NO.: 201057330-7/RJ

BOREHOLE: SP-F20 ELEVATION: 913.62 COORDINATES: E 659,155.13 N 7,764,058.94

WATER LEVEL 24 h	SAMPLE	ELEVATION (m)	BLOWS / 30 cm START	BLOWS / 30 cm END	PENETRATION RESISTANCE INDEX (N)	MATERIAL CLASSIFICATION	GEOLOGICAL DESCRIPTION
		893	P/100			19.00 m to 24.00 m – Not recovered.	TAILINGS FILL DAM
		892	1/80				
		891	17	17			
		890	5	3			
		889	8	15		24.00 to 29.00 m – Sandy clay, dark brown to variegated	
		888	13	20			
		887	8	15			
		886	1/80				
		885	2/55				
		884	1/50			29.00 to 30.00 m – Not recovered	
		883	19	15		30.00 m to 50.45 m – Sandy clay, soft to hard, dark brown to variegated.	
		882	20	17			
		881	15	11/32			
		880	6	9			
		879	2	8			
		878	2/35	2			
		877	9	15			
		876	14	15			
		875	12	13			
		874	10	19			

READING INTERVAL WL (m):
1.24 hr - CLOSED

ADVANCEMENT METHOD (m):
DIGGING AUGER:
WASHING: 50.45
LINING:
USE OF BENTONITE:

TIME WASHING
STARTING DEPTH
STAGE 1
STAGE 2
STAGE 3

NOTE: Borehole stopped at 2.00 m. Borehole stopped at 50 m due to difficulties encountered at SP-F19. Initial WL: DRY.

STANDARD PENETRATION TEST

SMC-03-GRE-01
ATTACHMENTS

CLIENT: SAMARCO MINERAÇÃO S.A.
PROJECT: GERMANO DAM – BAY 3
LOCATION: GERMANO MINE – MARIANA, MINAS GERAIS

SCALE: 1:100 START: 4/13/2015 END: 4/16/2015 BY: DANIELLA ARANHA, CREA REG. NO.: 201057330-7/RJ

BOREHOLE: SP-F20 ELEVATION: 913.62 COORDINATES: E 659,155.13 N 7,764,058.94

WATER LEVEL 24 h	SAMPLE	ELEVATION (m)	BLOWS / 30 cm START	BLOWS / 30 cm END	PENETRATION RESISTANCE INDEX (N) 0 10 20 30 40 50 60	MATERIAL CLASSIFICATION	GEOLOGICAL DESCRIPTION
40		873				30.00 m to 50.45 m – Sandy clay, soft to hard, dark brown to variegated.	TAILINGS FILL/DAM
41			13	15			
		872					
42			5	30			
		871					
43			22	35			
		870					
44			50/28	52			
		869					
45			19	31			
		868					
46			5	22			
		867					
47			14	24			
		866					
48			16	40			
		865					
49			19	36			
		864					
50			19	37			
		863					
51							
		862					
52							
		861					
53							
		860					
54							
		859					
55							
		858					
56							
		857					
57							
		856					
58							
		855					
59							
		854					
60							

READING INTERVAL WL (m):
1-24 h - CLOSED
2-
3-

ADVANCEMENT METHOD (m):
DIGGING AUGER:
WASHING: 0.00 50.45
LINING: 30.40
USE OF BENTONITE:

TIME WASHING 10 min
STARTING DEPTH
STAGE 1
STAGE 2
STAGE 3

NOTE: Borehole stopped at 9.00 m. Borehole stopped at 50 m due to difficulties encountered at SP-F19. Initial WL: DRY

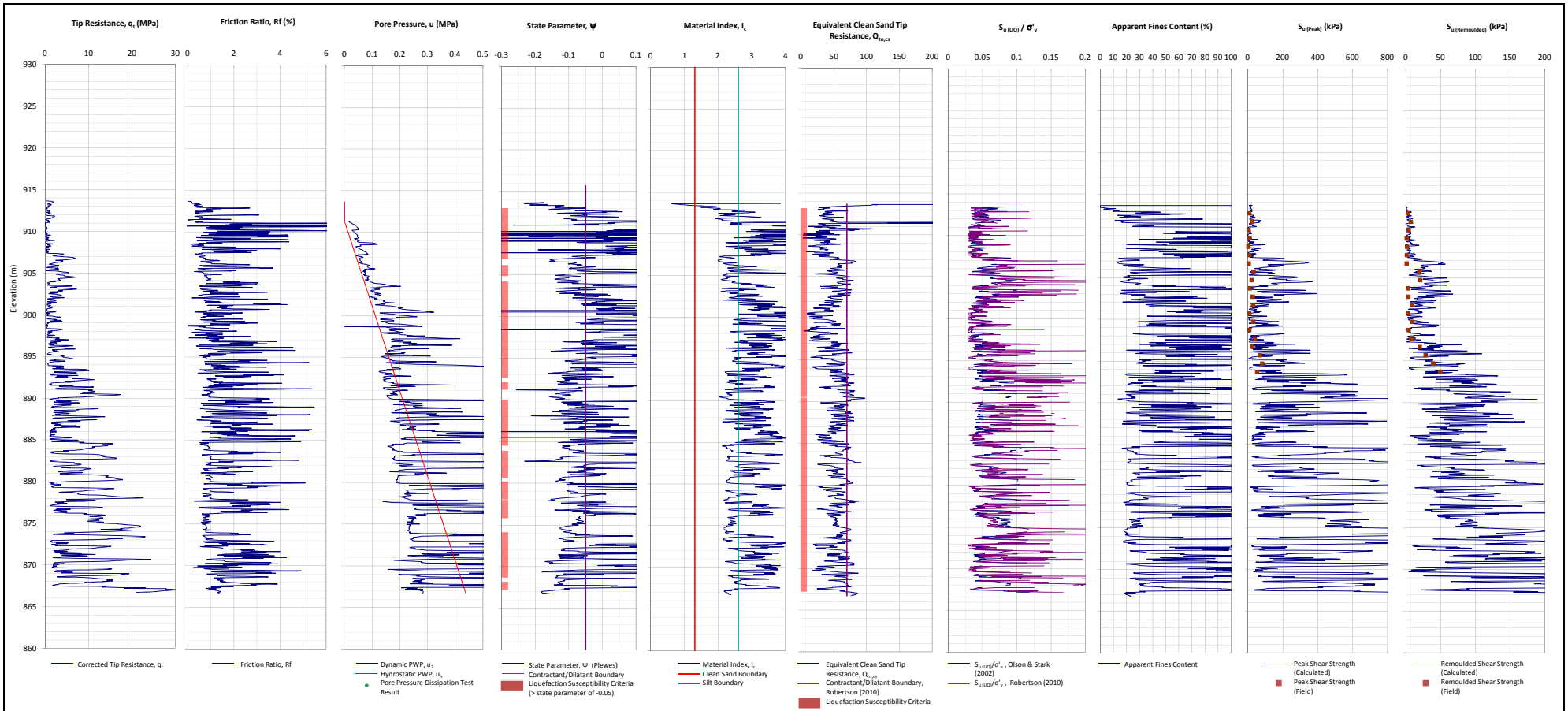

Notes:

1. This interpretation is based on the water and soil saturated unit weights γ_w=9.807 kN/m^3 and γ_{sat}=22 kN/m^3.
2. The friction ratio Rf is calculated as Rf=f_s/q_t.
3. The hydrostatic pore pressure is calculated using the ground water level (GWL) determined from CPT pore pressure dissipation tests (where available) or dynamic pore pressure.
4. Soil boundary layers (where plotted) are based on KCB interpretation.
5. The data presented have been plotted to the axis limits. Data may exist beyond the axis limits shown.
6. The Material Index (I_c) boundaries are based on Robertson and Wride (1998).
7. The $Q_{tn,cs}$ contractant/dilatant boundary=70 and is based on Robertson (2010).
8. The State Parameter (Ψ) is calculated using Plewes, et al. (1992) assuming a K0 of 0.5.
9. Coordinates are in UTM Zone 23K Córrego Alegre.
10. N_{kt} used in calculation of $S_{u(peak)}$ is 20.

PROJECT: Fundão Tailings Dam Review Panel

TITLE: Fugro (March - July 2015) - Germano
CONE PENETRATION TEST CPTu-F21
N:7764106m E:659232m 2015-03-06

Liquefaction susceptibility after Robertson (2010) "Evaluation of Flow Liquefaction and Liquefied Strength Using the Cone Penetration Test"	Liquefaction susceptibility after Olson & Stark (2003) "Yield Strength Ratio and Liquefaction Analysis of Slopes and Embankments"	State parameter approximation - Robertson (2009) "Interpretation of cone penetration tests - a unified approach"

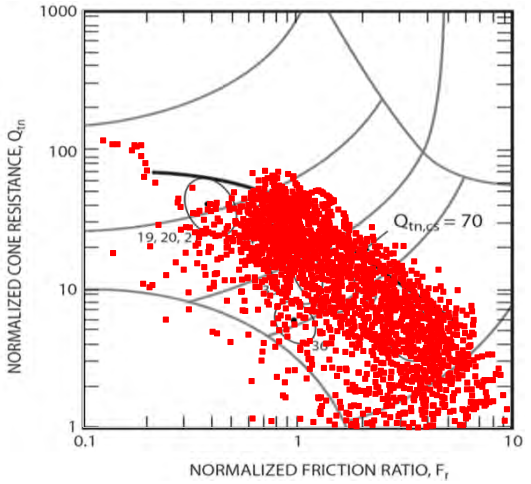

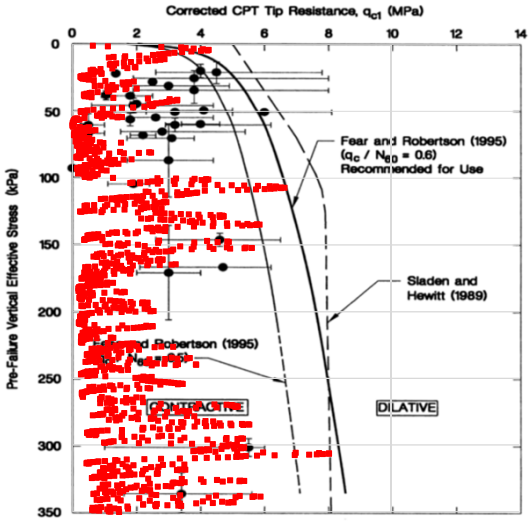

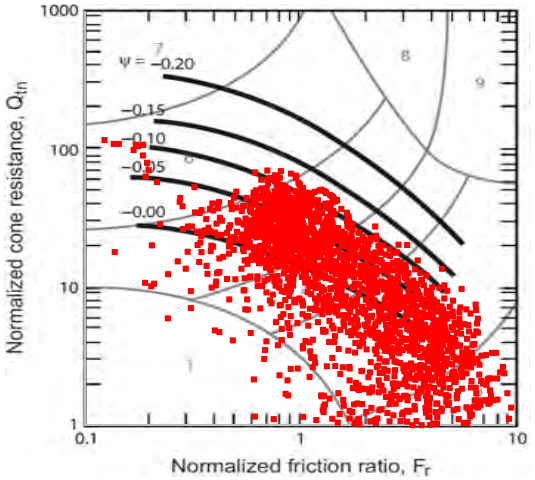

NOTE:

PROJECT

Fundão Tailings Dam Review Panel

TITLE

Fugro (March - July 2015) - Germano
CPTu-F21 Liquefaction Susceptibility and Soil Behavior Type

PERCUSSION BORING TEST

SMC-03-GRE-01
Attachments

FUGRO IN SITU GEOTECNIA

CLIENT: SAMARCO MINERAÇÃO S.A.

PROJECT: Fundão Dam - Bay 3

LOCATION: GERMANO MINE MARIANA-MG

SCALE: 1:100 START: 04/14/2015 END: 04/15/2015 RESP.: DANIELLA ARANHA CREA: 201057330-7/RJ

BOREHOLE: SP-F21 ELEVATION: 913,66 COORDINATES: E 658234,36 N 7764106,41

WATER LEVEL 24 h	SAMPLE	ELEVATION (m)	BLOWS / 30 cm INITIAL	BLOWS / 30 cm FINAL	PENETRATION RESISTANCE INDEX (N) 0 10 20 30 40 50 60	MATERIAL CLASSIFICATION	GEOLOGICAL DESCRIPTION
0						0.00 m to 2.00 m - Fine, slightly clayey sand, dark brown to variegated	TAILINGS EMBANKMENT/DAM
1		913	1/45				
2		912	8	7			
3		911	2	2		2.00 m to 23.00 m – Sandy clay, very soft to soft, dark brown to variegated	
4		910	P/45				
5		909	2/45				
6		908	1/50				
7		907	1/53				
8		906	4	7			
9		905	1				
10		904	3/45				
11		903	1/45				
12		902	P/45				
13		901	2/50				
14		900	2/45				
15		899	3/50				
16		898	1/55				
17		897	P/45				
18		896	P/45				
19		895	P/45				
20		894	1/45				

READING INTERVALh. WL(m)
1.24h CLOSED
2:
3:

PROGRESS METHOD (m)
DIGGER: -
WASHING: 0,00 - 50,45
LINING: 50,45
USE OF BENTONITE: -
WATER LEAK: -

TIME WASHING – 10 min
INITIAL DEPTH (m)
STAGE 1 (cm)
STAGE 2 (cm)
STAGE 3 (cm)

NOTE: Borehole closed at 2.50 m. Borehole closed at 50 m due to the difficulties encountered in SP-F19. Initial WL: DRY

PERCUSSION BORING TEST

SMC-03-GRE-01
Attachments

FUGRO IN SITU GEOTECNIA

CLIENT: SAMARCO MINERAÇÃO S.A.

PROJECT: Fundão Dam - Bay 3

LOCATION: GERMANO MINE MARIANA-MG

SCALE: 1:100 START:04/14/2015 END: 04/15/2015 RESP.: DANIELLA ARANHA CREA: 201057330-7/RJ

BOREHOLE: SP-F21 ELEVATION: 913,66 COORDINATES: E 658234,36 N 7764106,41

WATER LEVEL 24 h	SAMPLE	ELEVATION (m)	BLOWS / 30 cm INITIAL	BLOWS / 30 cm FINAL	PENETRATION RESISTANCE INDEX (N) 0 10 20 30 40 50 60	MATERIAL CLASSIFICATION	GEOLOGICAL DESCRIPTION
20		893				2.00 m to 23.00 m –Sandy clay, very soft to soft, dark brown to variegated	TAILINGS EMBANKMENT/DAM
21			2/45				
		892					
22			1/40				
		891					
23			18	23			
		890				23.00 m to 24.00 m - Sandy clay, hard, dark brown to variegated	
24			9	10			
		889				24.00 m to 40.00 m - Sandy clay, soft to hard, dark brown to variegated	
25			3	5			
		888					
26			5	17			
		887					
27			7	6			
		886					
28			6	14			
		885					
29			4	13			
		884					
30			5	15			
		883					
31			2	5			
		882					
32			7/45				
		881					
33			7	16			
		880					
34			6	10			
		879					
35			3	6			
		878					
36			4	7			
		877					
37			2/35	2			
		876					
38			13	18			
		875					
39			11	14			
		874					
40			10	16			

READING INTERVAL WL(m)
1: 24 h: -FECHADO
2:
3:

PROGRESS METHOD (m)
DIGGER: -
WASHING: 0,00 - 50,45
LINING: 50,45
USE OF BENTONITE: -
WATER LEAK: -

TIME WASHING – 10 min
INITIAL DEPTH (m)
STAGE 1 (cm)
STAGE 2 (cm)
STAGE 3 (cm)

NOTE: Borehole closed at 2.50 m. Borehole closed at 50 m due to the difficulties encountered in SP-F19. Initial WL: DRY

PERCUSSION BORING TEST

SMC-03-GRE-01
Attachments

FUGRO IN SITU GEOTECNIA

CLIENT: SAMARCO MINERAÇÃO S.A.

PROJECT: Fundão Dam - Bay 3

LOCATION: GERMANO MINE MARIANA-MG

SCALE: 1:100 START:04/14/2015 END: 04/15/2015 RESP.: DANIELLA ARANHA CREA: 201057330-7/RJ

BOREHOLE: SP-F21 ELEVATION: 913,66 COORDINATES: E 658234,36 N 7764106,41

WATER LEVEL 24 h	SAMPLE	ELEVATION (m)	BLOWS / 30 cm INITIAL	BLOWS / 30 cm FINAL	PENETRATION RESISTANCE INDEX (N) 0 10 20 30 40 50 60	MATERIAL CLASSIFICATION	GEOLOGICAL DESCRIPTION
40		873	6	23		40.00 m to 50.45 m - Sandy clay, medium to hard, dark brown to variegated	TAILINGS EMBANKMENT/DAM
41		872	15	25			
42		871	7	13			
43		870	5	10			
44		869	4	10			
45		868	13	30			
46		867	13	45			
47		866	25	43			
48		865	16	16			
49		864	17	16			
50		863					
51		862					
52		861					
53		860					
54		859					
55		858					
56		857					
57		856					
58		855					
59		854					
60							

READING INTERVAL WL(m)
1.24h CLOSED
2:
3:

PROGRESS METHOD (m)
DIGGER: -
WASHING: 0,00 - 50,45
LINING: 50,45
USE OF BENTONITE: -
WATER LEAK: -

TIME WASHING – 10 min
INITIAL DEPTH (m)
STAGE 1 (cm)
STAGE 2 (cm)
STAGE 3 (cm)

NOTE: Borehole closed at 2.50 m. Borehole closed at 50 m due to the difficulties encountered in SP-F19.
Initial WL: DRY

FUGRO IN SITU GEOTECNIA

SOIL BOREHOLE

SMC-03-GRE-01
Attachments

CLIENT: SAMARCO MINERAÇÃO S.A.

PROJECT: GERMANO DAM - BAY 3

LOCATION: GERMANO MINE – MARIANA-MG

SCALE: 1:100 START: 14/05/2015 END: 15/05/2015 RESP.: DANIELLA ARANHA CREA Reg. No.: 201057330-7/RJ

BOREHOLE: SP-F21A ELEVATION: 915,36 COORDINATES: E 659174,26 N 7764148,74

WATER LEVEL 24 h	SAMPLE	ELEVATION (m)	BLOWS / 30 CM INITIAL	BLOWS / 30 CM FINAL	PENETRATION RESISTANCE INDEX (N) 0 10 20 30 40 50 60	MATERIAL CLASSIFICATION	GEOLOGICAL DESCRIPTION
0		915				0.00 m and 51.00 m Destructive drilling in the tailings.	
1		914					
2		913					
3		912					
4		911					
5		910					
6		909					
7		908					
8		907					
9		906					
10		905					
11		904					
12		903					
13		902					
14		901					
15		900					
16		899					
17		898					
18		897					
19		896					
20							

READING INTERVAL WL(m)
1: 24 h: -CLOSED
2:
3:

PROGRESS METHOD (m)
DIGGER: -
WASHING: 0,00 - 60,00
LINING: 60,00
USE OF BENTONITE: -
WATER LEAK: -

TIME WASHING - 10 min
INITIAL DEPTH (m):
STAGE 1 (cm):
STAGE 2 (cm):
STAGE 3 (cm):

NOTE: Borehole closed at 7.58 m.
Drilling stopped due to meeting the condition of impermeability
Initial WL: DRY

FUGRO IN SITU GEOTECNIA

STANDARD PENETRATION TEST

SMC-03-GRE-01
Attachments

CLIENT: SAMARCO MINERAÇÃO S.A.

PROJECT: GERMANO DAM - BAY 3

LOCATION: GERMANO MINE – MARIANA-MG

SCALE: 1:100 START: 14/05/2015 END: 15/05/2015 RESP.: DANIELLA ARANHA CREA Reg. No.: 201057330-7/RJ

BOREHOLE: SP-F21A ELEVATION: 915,36 COORDINATES: E 659174,26 N 7764148,74

WATER LEVEL 24 h	SAMPLE	ELEVATION (m)	BLOWS / 30 CM INITIAL	BLOWS / 30 CM FINAL	PENETRATION RESISTANCE INDEX (N) 0 10 20 30 40 50 60	MATERIAL CLASSIFICATION	GEOLOGICAL DESCRIPTION
20		895				0.00 m and 51.00 m Destructive drilling in the tailings.	
21		894					
22		893					
23		892					
24		891					
25		890					
26		889					
27		888					
28		887					
29		886					
30		885					
31		884					
32		883					
33		882					
34		881					
35		880					
36		879					
37		878					
38		877					
39		876					
40							

READING INTERVAL WL(m)
1: 24 h: -CLOSED
2:
3:

PROGRESS METHOD (m)
DIGGER: -
WASHING: 0,00 - 60,00
LINING: 60,00
USE OF BENTONITE: -
WATER LEAK: -

TIME WASHING - 10 min
INITIAL DEPTH (m):
STAGE 1 (cm):
STAGE 2 (cm):
STAGE 3 (cm):

NOTE: Borehole closed at 7.58 m.
Drilling stopped due to meeting the condition of impermeability
Initial WL: DRY

FUGRO IN SITU GEOTECNIA

SOIL BOREHOLE

SMC-03-GRE-01
Attachments

CLIENT: SAMARCO MINERAÇÃO S.A.

PROJECT: GERMANO DAM - BAY 3

LOCATION: GERMANO MINE – MARIANA-MG

SCALE: 1:100 START: 14/05/2015 END: 15/05/2015 RESP.: DANIELLA ARANHA CREA Reg. No.: 201057330-7/RJ

BOREHOLE: SP-F21A ELEVATION: 915,36 COORDINATES: E 659174,26 N 7764148,74

WATER LEVEL 24 h	SAMPLE	ELEVATION (m)	BLOWS / 30 CM INITIAL	BLOWS / 30 CM FINAL	PENETRATION RESISTANCE INDEX (N) 0 10 20 30 40 50 60	MATERIAL CLASSIFICATION	GEOLOGICAL DESCRIPTION
40		875				0.00 m and 51.00 m Destructive drilling in the tailings.	
41		874					
42		873					
43		872					
44		871					
45		870					
46		869					
47		868					
48		867					
49		866					
50		865					
51		864	15	25		51.00 m and 58.00 m - Clayey fine sand, compact to very compact, gray to variegated.	TAILINGS EMBANKMENT/DAM
52		863	15	29			
53		862	15	35			
54		861	25	41			
55		860	42				
56		859	42/28				
57		858	50/22				
58		857	30/5			58.00 m and 60.00 m - There was no recovery, slightly compacted material.	
59		856	30/6				
60							

READING INTERVAL WL(m)
1: 24 h: -CLOSED
2:
3:

PROGRESS METHOD (m)
DIGGER: -
WASHING: 0,00 - 60,00
LINING: 60,00
USE OF BENTONITE: -
WATER LEAK: -

TIME WASHING - 10 min
INITIAL DEPTH (m):
STAGE 1 (cm):
STAGE 2 (cm):
STAGE 3 (cm):

NOTE: Borehole closed at 7.58 m.
Drilling stopped due to meeting the condition of impermeability
Initial WL: DRY

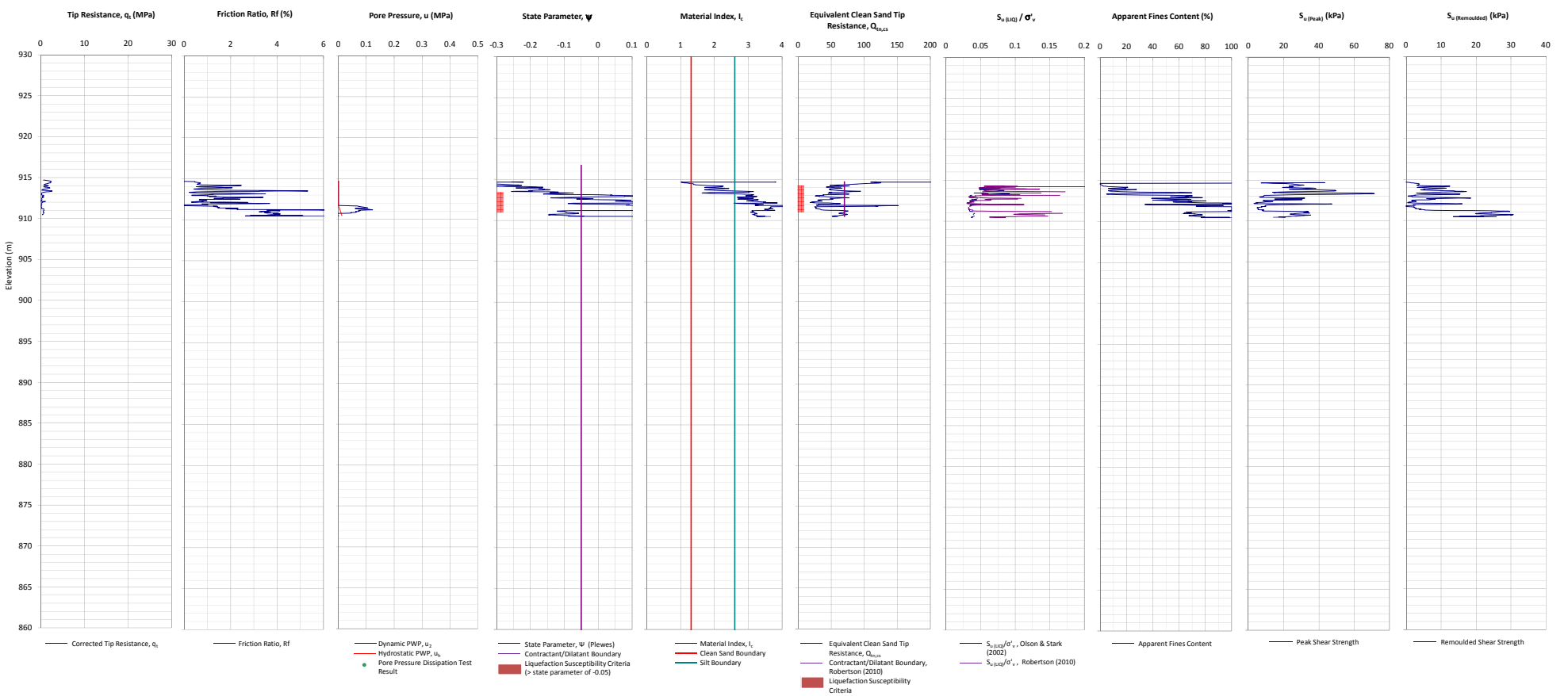

Notes:

1. This interpretation is based on the water and soil saturated unit weights γ_w=9.807 kN/m^3 and γ_{sat}=22 kN/m^3.
2. The friction ratio Rf is calculated as Rf=f_s/q_t.
3. The hydrostatic pore pressure is calculated using the ground water level (GWL) determined from CPT pore pressure dissipation tests (where available) or dynamic pore pressure.
4. Soil boundary layers (where plotted) are based on KCB interpretation.
5. The data presented have been plotted to the axis limits. Data may exist beyond the axis limits shown.
6. The Material Index (I_c) boundaries are based on Robertson and Wride (1998).
7. The $Q_{tn,cs}$ contractant/dilatant boundary=70 and is based on Robertson (2010).
8. The State Parameter (Ψ) is calculated using Plewes, et al. (1992) assuming a K0 of 0.5.
9. Coordinates are in UTM Zone 23K Córrego Alegre.
10. N_{kt} used in calculation of $S_{u(Peak)}$ is 20.

PROJECT

Fundão Tailings Dam Review Panel

TITLE

Fugro (March - July 2015) - Germano
CONE PENETRATION TEST CPTu-F22
N:7763810m E:659313m 2015-03-24

Liquefaction susceptibility after Robertson (2010) "Evaluation of Flow Liquefaction and Liquefied Strength Using the Cone Penetration Test"	Liquefaction susceptibility after Olson & Stark (2003) "Yield Strength Ratio and Liquefaction Analysis of Slopes and Embankments"	State parameter approximation - Robertson (2009) "Interpretation of cone penetration tests - a unified approach"

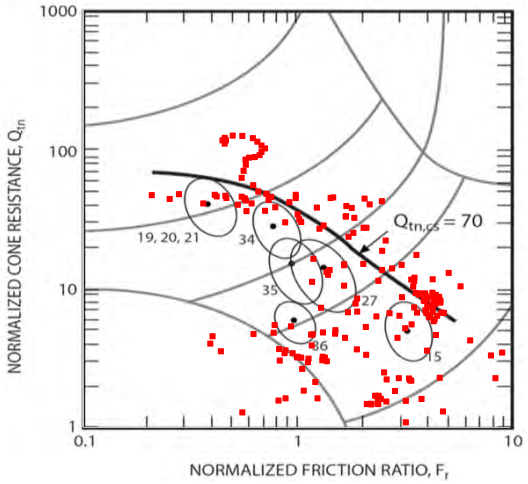

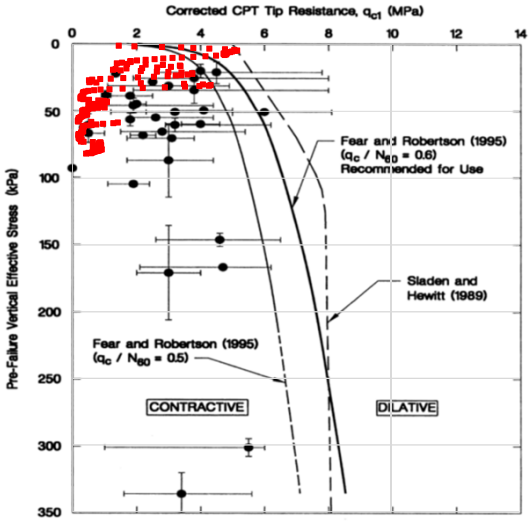

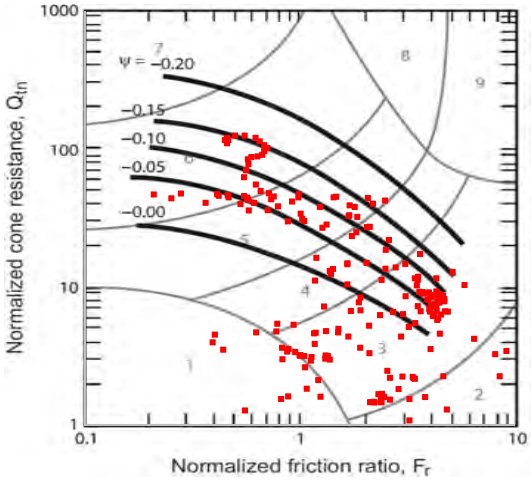

NOTE:

PROJECT

Fundão Tailings Dam Review Panel

TITLE

Fugro (March - July 2015) - Germano
CPTu-F22 Liquefaction Susceptibility and Soil Behavior Type

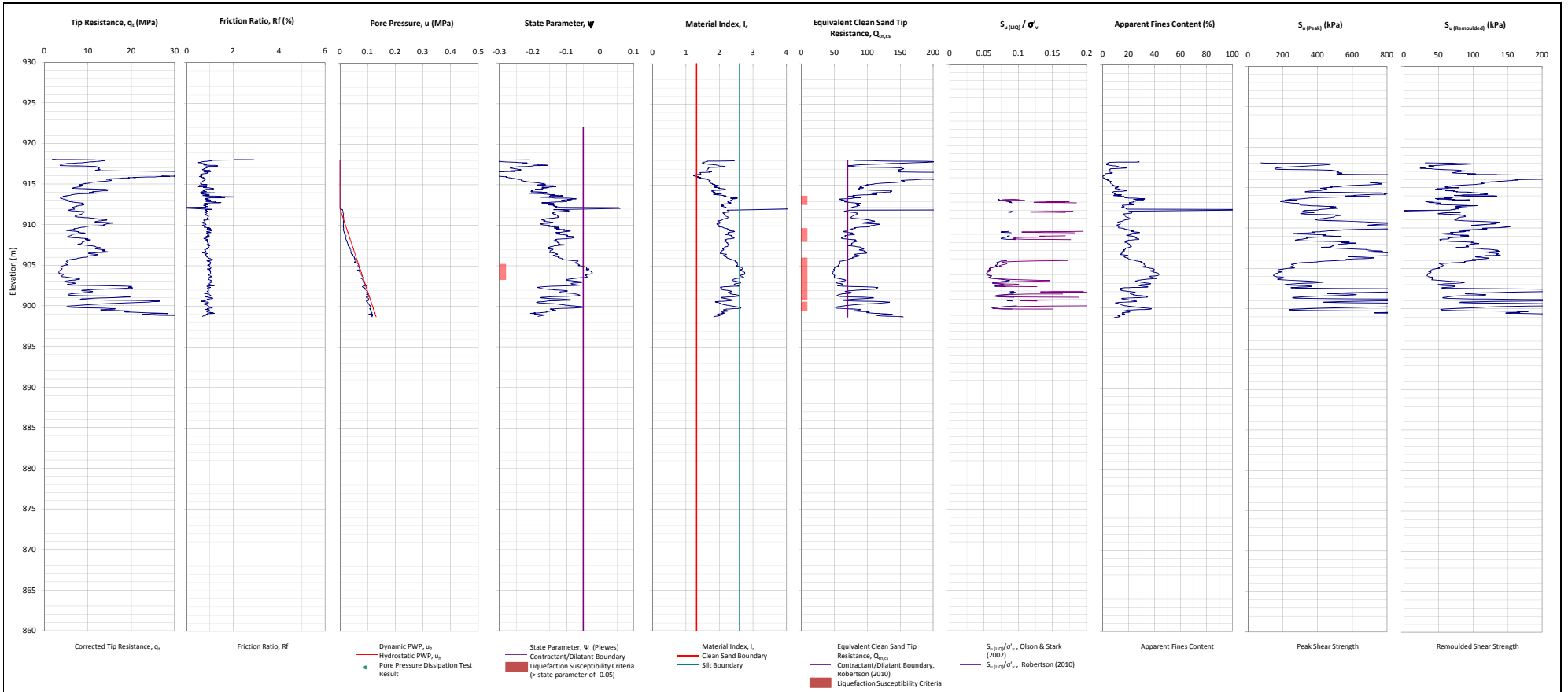

Notes:

1. This interpretation is based on the water and soil saturated unit weights γ_w=9.807 kN/m^3 and γ_{sat}=22 kN/m^3.
2. The friction ratio Rf is calculated as Rf=f_s/q_t.
3. The hydrostatic pore pressure is calculated using the ground water level (GWL) determined from CPT pore pressure dissipation tests (where available) or dynamic pore pressure.
4. Soil boundary layers (where plotted) are based on KCB interpretation.
5. The data presented have been plotted to the axis limits. Data may exist beyond the axis limits shown.
6. The Material Index (I_c) boundaries are based on Robertson and Wride (1998).
7. The $Q_{tn,cs}$ contractant/dilatant boundary=70 and is based on Robertson (2010).
8. The State Parameter (Ψ) is calculated using Plewes, et al. (1992) assuming a K0 of 0.5.
9. Coordinates are in UTM Zone 23K Córrego Alegre.
10. N_{kt} used in calculation of $S_{u(Peak)}$ is 20.

PROJECT: Fundão Tailings Dam Review Panel

TITLE: Fugro (March - July 2015) - Germano
CONE PENETRATION TEST CPTu-F22A
N:7763981m E:659047m 2015-04-08

Liquefaction susceptibility after Robertson (2010) "Evaluation of Flow Liquefaction and Liquefied Strength Using the Cone Penetration Test"	Liquefaction susceptibility after Olson & Stark (2003) "Yield Strength Ratio and Liquefaction Analysis of Slopes and Embankments"	State parameter approximation - Robertson (2009) "Interpretation of cone penetration tests - a unified approach"

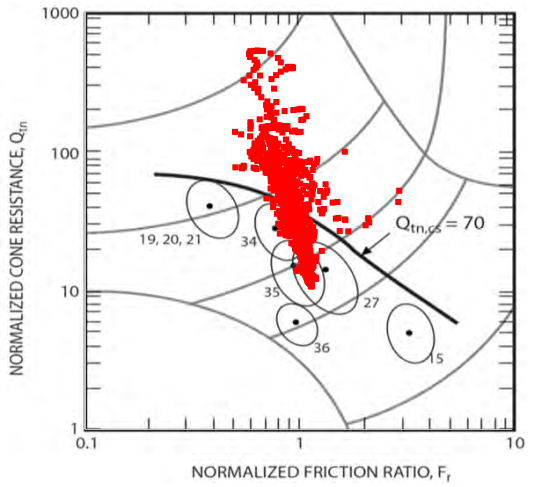

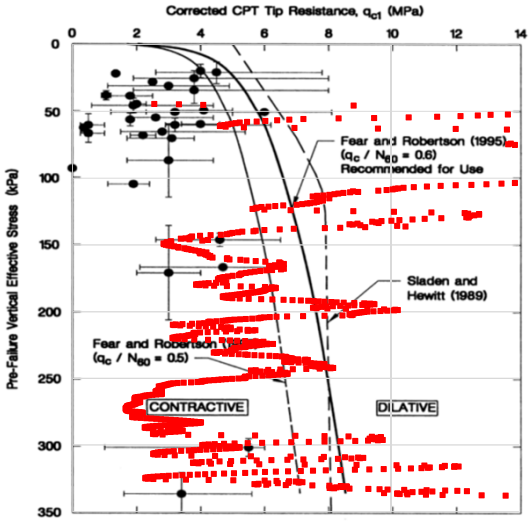

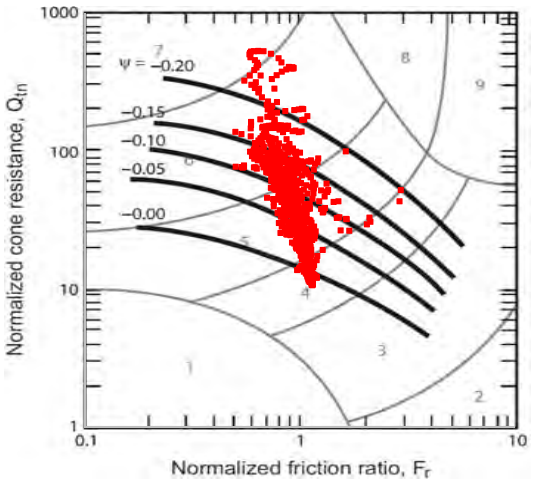

NOTE:

PROJECT

Fundão Tailings Dam Review Panel

TITLE

Fugro (March - July 2015) - Germano
CPTu-F22A Liquefaction Susceptibility and Soil Behavior Type

STANDARD PENETRATION TEST

SMC-03-GRE-01
ANEXOS

FUGRO IN SITU GEOTECNIA

CLIENT: SAMARCO MINERAÇÃO S.A.

PROJECT: GERMANO DAM – BAY 3

LOCATION: GERMANO MINE – MARIANA MG

SCALE: 1:100 BEGINNING: 4/14/2015 PERSON IN CHARGE: DANIELLA ARANHA CREA: 201057330-7/RJ

DRILLING: SP-F22A ELEVATION: 920.15 COORDINATES: E 659047.93 N 7763983.69

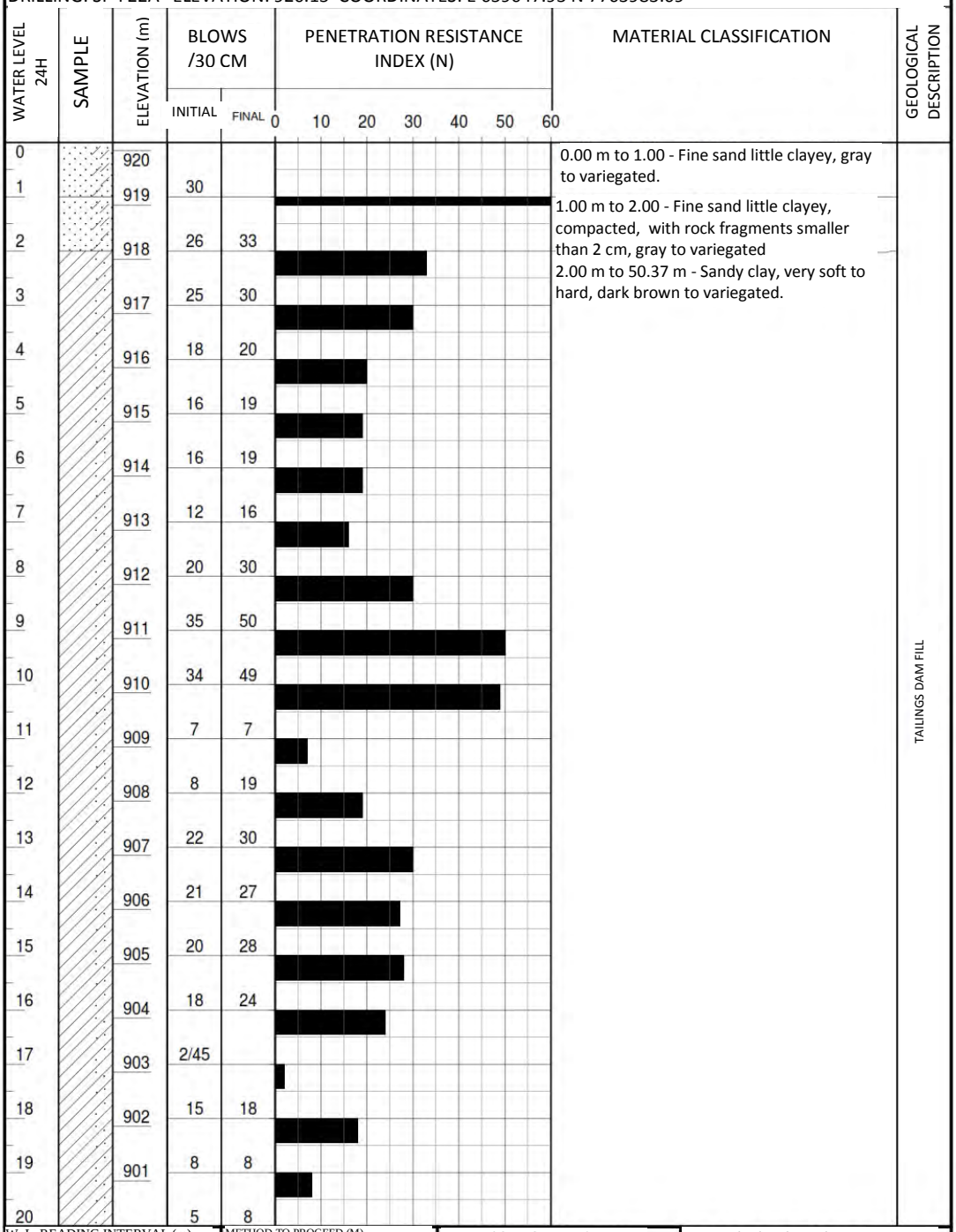

W. L. READING INTERVAL (m)
1: 24h: -CLOSED
2:
3:

METHOD TO PROCEED (M)
T-DIGGER -
WASHING 0.00 – 50.37
CASING 50.37
BENTONITE -
WATER LEAK -

TIME WASHING - 10 min
INITIAL DEPTH (m):
STAGE 1 (cm):
STAGE 2 (cm):
STAGE 3 (cm):

NOTE: hole closed at 10.80 m. Drilling depth limited by the customer.

STANDARD PENETRATION TEST

SMC-03-GRE-01
ANEXOS

FUGRO IN SITU GEOTECNIA

CLIENT: SAMARCO MINERAÇÃO S.A.
PROJECT: GERMANO DAM – BAY 3
LOCATION: GERMANO MINE – MARIANA MG

SCALE: 1:100 BEGINNING: 4/14/2015 PERSON IN CHARGE: DANIELLA ARANHA CREA: 201057330-7/RJ

DRILLING: SP-F22A ELEVATION: 920.15 COORDINATES: E 659047.93 N 7763983.69

WATER LEVEL 24H	SAMPLE	ELEVATION (m)	BLOWS /30 CM INICIAL	BLOWS /30 CM FINAL	PENETRATION RESISTANCE INDEX (N) 0 10 20 30 40 50 60	MATERIAL CLASSIFICATION	GEOLOGICAL DESCRIPTION
20		900				2.00 m to 50.37 m - Sandy clay, very soft to hard, dark brown to variegated.	TAILINGS DAM FILL
21		899	7	8			
22		898	45	35/21			
23		897	30/15				
24		896	30	42			
25		895	26	39			
26		894	26	40			
27		893	21	25			
28		892	9	10			
29		891	4	4			
30		890	11	10			
31		889	14	13			
32		888	18	20			
33		887	15	16			
34		886	27	40			
35		885	49				
36		884	50				
37		883	25	33			
38		882	8	15			
39		881	20	25			
40			13	17			

W.L. READING INTERVAL (m)
1: 24h: -CLOSED
2:
3:

METHOD TO PROCEED (M)
T-DIGGER -
WASHING 0.00 – 50.37
CASING 50.37
BENTONITE -
WATER LEAK -

TIME WASHING - 10 min
INITIAL DEPTH (m):
STAGE 1 (cm):
STAGE 2 (cm):
STAGE 3 (cm):

NOTE: hole closed at 10.80 m. Drilling depth limited by the customer.

STANDARD PENETRATION TEST

SMC-03-GRE-01
ANEXOS

FUGRO IN SITU GEOTECNIA

CLIENT: SAMARCO MINERAÇÃO S.A.
PROJECT: GERMANO DAM – BAY 3
LOCATION: GERMANO MINE – MARIANA MG

SCALE: 1:100 BEGINNING: 4/15/2015 PERSON IN CHARGE: DANIELLA ARANHA CREA: 201057330-7/RJ

DRILLING: SP-F22A ELEVATION: 920.15 COORDINATES: E 659047.93 N 7763983.69

WATER LEVEL 24H	SAMPLE	ELEVATION (m)	BLOWS /30 CM INICIAL	BLOWS /30 CM FINAL	PENETRATION RESISTANCE INDEX (N) 0 10 20 30 40 50 60	MATERIAL CLASSIFICATION	GEOLOGICAL DESCRIPTION
40		880				2.00 m to 50.37 m - Sandy clay, very soft to hard, dark brown to variegated.	TAILINGS DAM FILL
41		879	3	4			
42		878	5	5			
43		877	10	22			
44		876	19	38			
45		875	35	40/27			
46		874	29	43			
47		873	27	42			
48		872	29	44			
49		871	32	40/25			
50		870	36	45/22			
51		869					
52		868					
53		867					
54		866					
55		865					
56		864					
57		863					
58		862					
59		861					
60							

W.L. READING INTERVAL (m)
1: 24h: -CLOSED
2:
3:

METHOD TO PROCEED (M)
T-DIGGER -
WASHING 0.00 – 50.37
CASING 50.37
BENTONITE -
WATER LEAK -

TIME WASHING - 10 min
INITIAL DEPTH (m):
STAGE 1 (cm):
STAGE 2 (cm):
STAGE 3 (cm):

NOTE: hole closed at 10.80 m. Drilling depth limited by the customer.

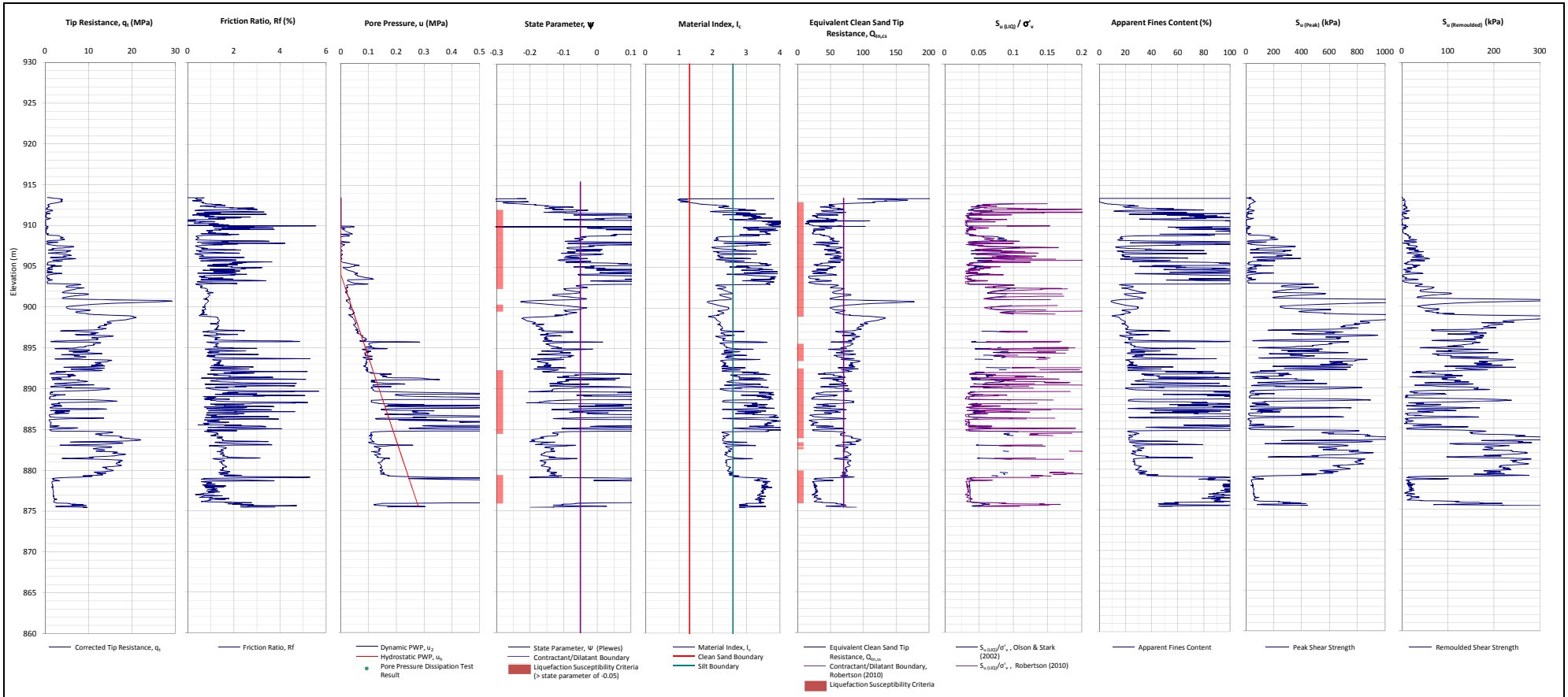

Notes:

1. This interpretation is based on the water and soil saturated unit weights γ_w=9.807 kN/m^3 and γ_{sat}=22 kN/m^3.
2. The friction ratio Rf is calculated as Rf=f_s/q_t.
3. The hydrostatic pore pressure is calculated using the ground water level (GWL) determined from CPT pore pressure dissipation tests (where available) or dynamic pore pressure.
4. Soil boundary layers (where plotted) are based on KCB interpretation.
5. The data presented have been plotted to the axis limits. Data may exist beyond the axis limits shown.
6. The Material Index (I_c) boundaries are based on Robertson and Wride (1998).
7. The $Q_{tn,cs}$ contractant/dilatant boundary=70 and is based on Robertson (2010).
8. The State Parameter (Ψ) is calculated using Plewes, et al. (1992) assuming a K0 of 0.5.
9. Coordinates are in UTM Zone 23K Córrego Alegre.
10. N_{kt} used in calculation of $S_{u(peak)}$ is 20.

PROJECT: Fundão Tailings Dam Review Panel

TITLE: Fugro (March - July 2015) - Germano
CONE PENETRATION TEST CPTu-F23
N:7763869m E:659326m 2015-03-20

Liquefaction susceptibility after Robertson (2010) "Evaluation of Flow Liquefaction and Liquefied Strength Using the Cone Penetration Test"	Liquefaction susceptibility after Olson & Stark (2003) "Yield Strength Ratio and Liquefaction Analysis of Slopes and Embankments"	State parameter approximation - Robertson (2009) "Interpretation of cone penetration tests - a unified approach"

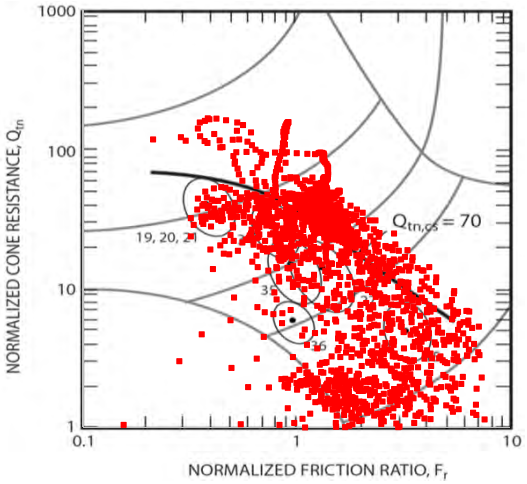

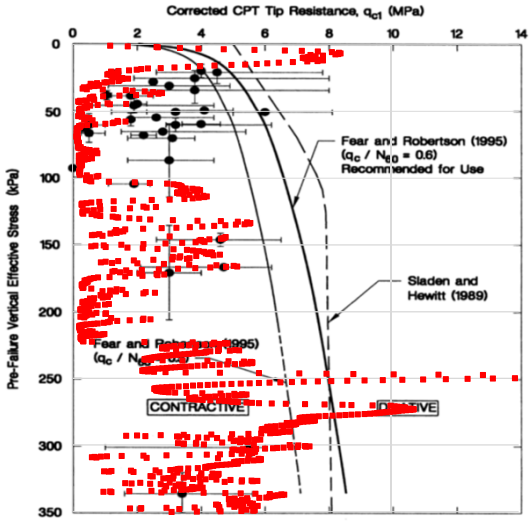

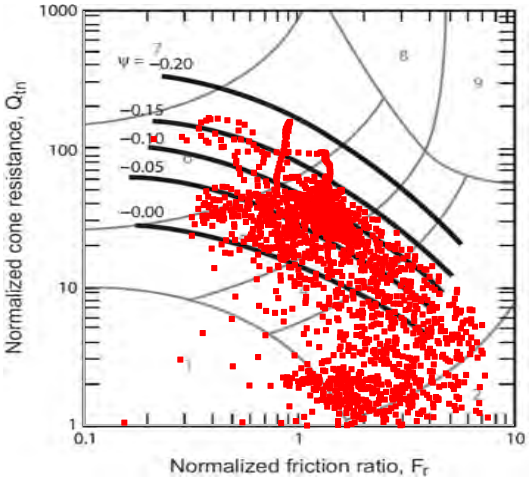

NOTE:

PROJECT

Fundão Tailings Dam Review Panel

TITLE

Fugro (March - July 2015) - Germano
CPTu-F23 Liquefaction Susceptibility and Soil Behavior Type

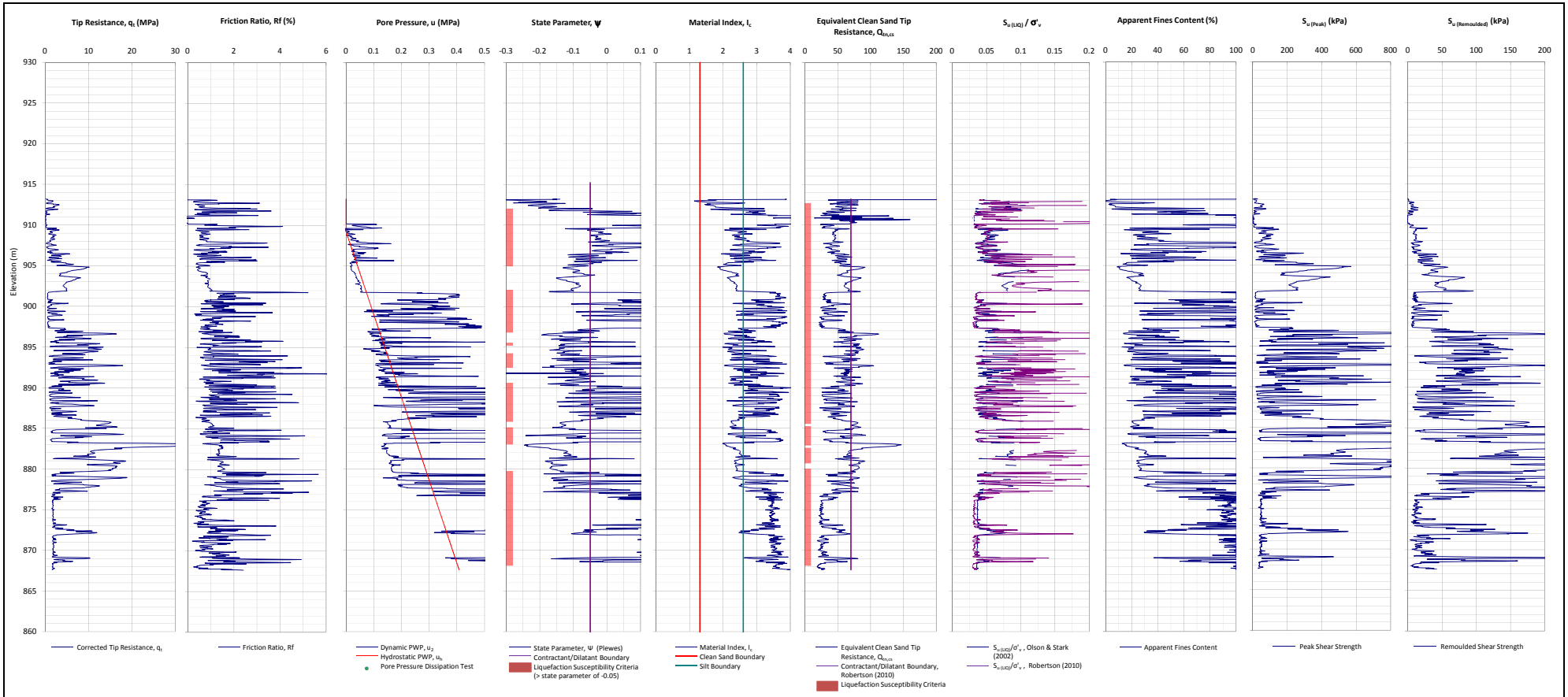

Notes:

1. This interpretation is based on the water and soil saturated unit weights γ_w=9.807 kN/m^3 and γ_{sat}=22 kN/m^3.
2. The friction ratio Rf is calculated as Rf=f_s/q_t.
3. The hydrostatic pore pressure is calculated using the ground water level (GWL) determined from CPT pore pressure dissipation tests (where available) or dynamic pore pressure.
4. Soil boundary layers (where plotted) are based on KCB interpretation.
5. The data presented have been plotted to the axis limits. Data may exist beyond the axis limits shown.
6. The Material Index (I_c) boundaries are based on Robertson and Wride (1998).
7. The $Q_{tn,cs}$ contractant/dilatant boundary=70 and is based on Robertson (2010).
8. The State Parameter (Ψ) is calculated using Plewes, et al. (1992) assuming a K0 of 0.5.
9. Coordinates are in UTM Zone 23K Córrego Alegre.
10. N_{kt} used in calculation of $S_{u(peak)}$ is 20.

PROJECT: Fundão Tailings Dam Review Panel

TITLE: Fugro (March - July 2015) - Germano
CONE PENETRATION TEST CPTu-F24
N:7763932m E:659371m 2015-03-24

Liquefaction susceptibility after Robertson (2010) "Evaluation of Flow Liquefaction and Liquefied Strength Using the Cone Penetration Test"	Liquefaction susceptibility after Olson & Stark (2003) "Yield Strength Ratio and Liquefaction Analysis of Slopes and Embankments"	State parameter approximation - Robertson (2009) "Interpretation of cone penetration tests - a unified approach"

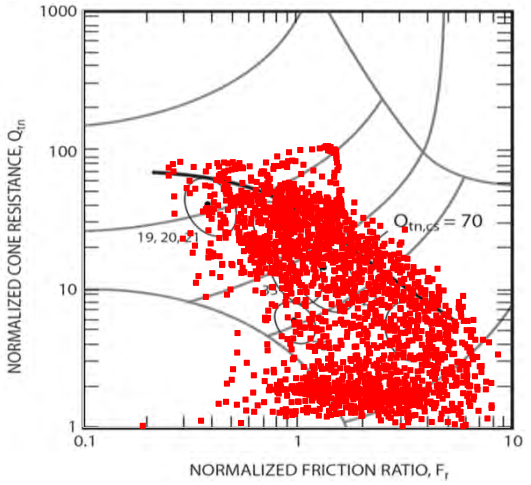

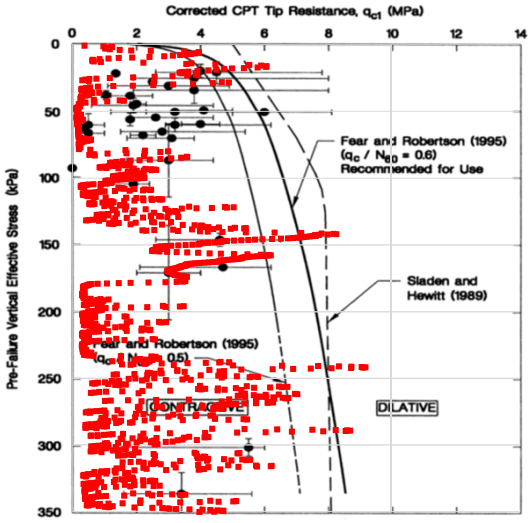

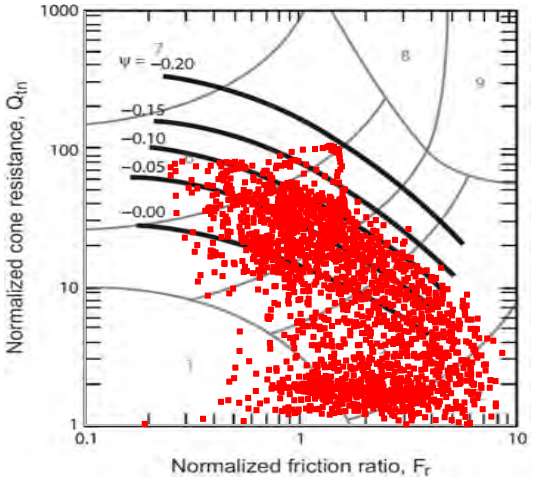

NOTE:

PROJECT

Fundão Tailings Dam Review Panel

TITLE

Fugro (March - July 2015) - Germano
CPTu-F24 Liquefaction Susceptibility and Soil Behavior Type

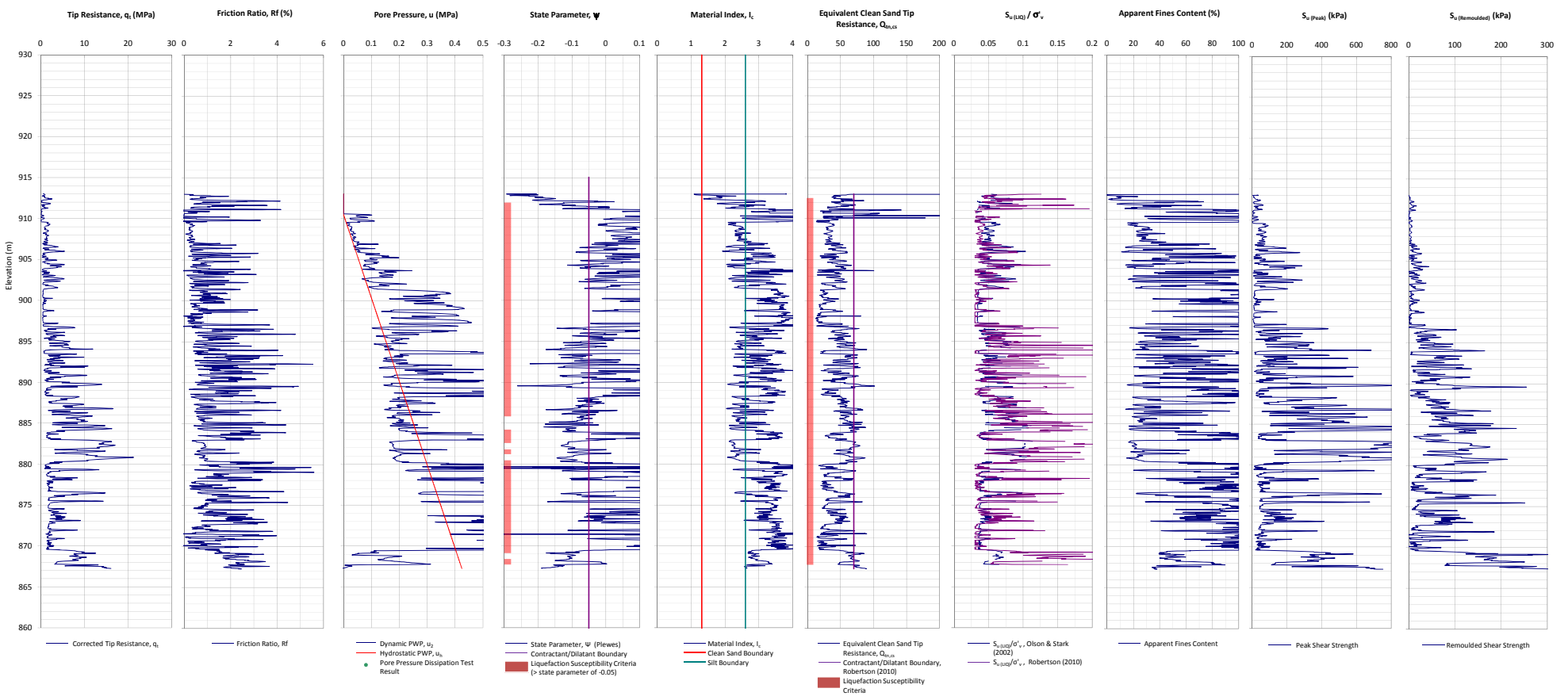

Notes:

1. This interpretation is based on the water and soil saturated unit weights γ_w=9.807 kN/m^3 and γ_{sat}=22 kN/m^3.
2. The friction ratio Rf is calculated as Rf=f_s/q_t.
3. The hydrostatic pore pressure is calculated using the ground water level (GWL) determined from CPT pore pressure dissipation tests (where available) or dynamic pore pressure.
4. Soil boundary layers (where plotted) are based on KCB interpretation.
5. The data presented have been plotted to the axis limits. Data may exist beyond the axis limits shown.
6. The Material Index (I_c) boundaries are based on Robertson and Wride (1998).
7. The $Q_{tn,cs}$ contractant/dilatant boundary=70 and is based on Robertson (2010).
8. The State Parameter (Ψ) is calculated using Plewes, et al. (1992) assuming a K0 of 0.5.
9. Coordinates are in UTM Zone 23K Córrego Alegre.
10. N_{kt} used in calculation of $S_{u(peak)}$ is 20.

PROJECT: Fundão Tailings Dam Review Panel

TITLE: Fugro (March - July 2015) - Germano
CONE PENETRATION TEST CPTu-F25
N:7764019m E:659438m 2015-03-25

Liquefaction susceptibility after Robertson (2010) "Evaluation of Flow Liquefaction and Liquefied Strength Using the Cone Penetration Test"	Liquefaction susceptibility after Olson & Stark (2003) "Yield Strength Ratio and Liquefaction Analysis of Slopes and Embankments"	State parameter approximation - Robertson (2009) "Interpretation of cone penetration tests - a unified approach"

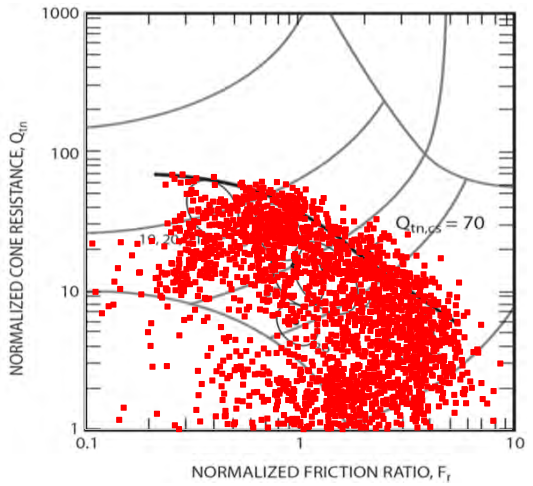

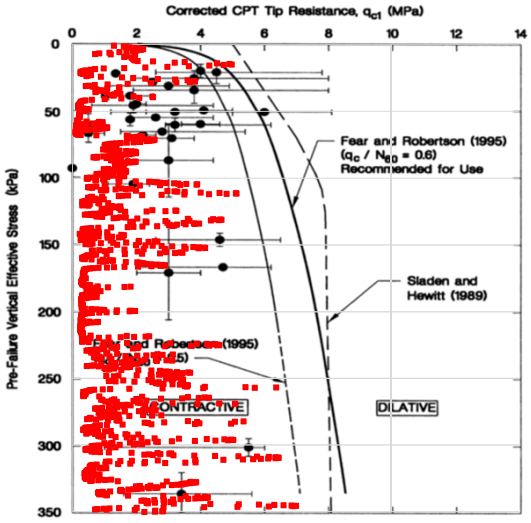

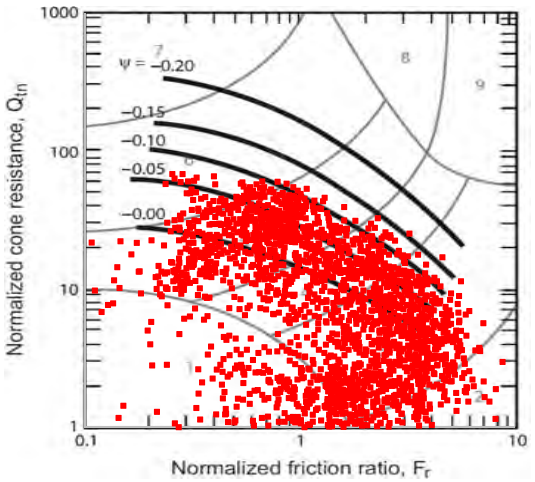

NOTE:

PROJECT

Fundão Tailings Dam Review Panel

TITLE

Fugro (March - July 2015) - Germano
CPTu-F25 Liquefaction Susceptibility and Soil Behavior Type

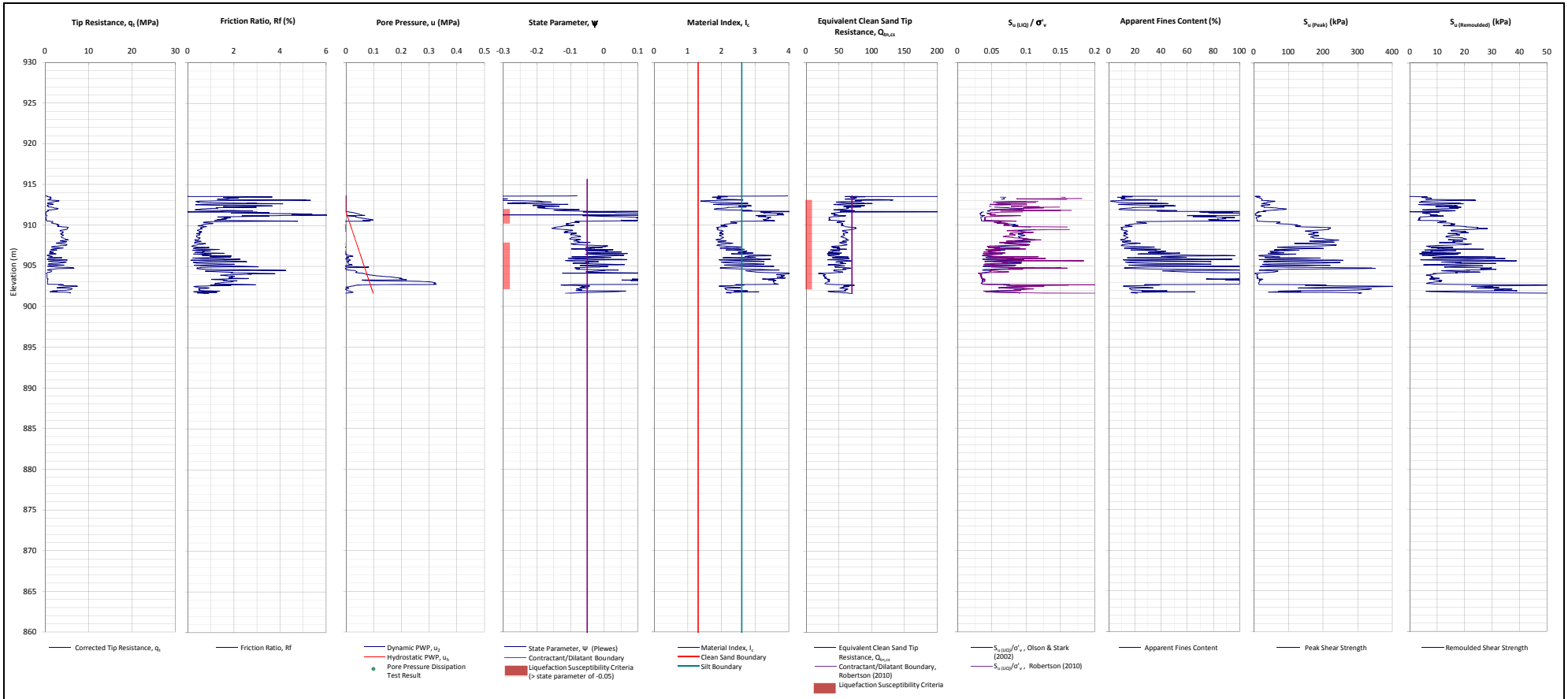

Notes:

1. This interpretation is based on the water and soil saturated unit weights γ_w=9.807 kN/m^3 and γ_{sat}=22 kN/m^3.
2. The friction ratio Rf is calculated as Rf=f_s/q_t.
3. The hydrostatic pore pressure is calculated using the ground water level (GWL) determined from CPT pore pressure dissipation tests (where available) or dynamic pore pressure.
4. Soil boundary layers (where plotted) are based on KCB interpretation.
5. The data presented have been plotted to the axis limits. Data may exist beyond the axis limits shown.
6. The Material Index (I_c) boundaries are based on Robertson and Wride (1998).
7. The $Q_{tn,cs}$ contractant/dilatant boundary=70 and is based on Robertson (2010).
8. The State Parameter (Ψ) is calculated using Plewes, et al. (1992) assuming a K0 of 0.5.
9. Coordinates are in UTM Zone 23K Córrego Alegre.
10. N_{kt} used in calculation of $S_{u(Peak)}$ is 20.

PROJECT

Fundão Tailings Dam Review Panel

TITLE

Fugro (March - July 2015) - Germano
CONE PENETRATION TEST CPTu-F26
N:7763805m E:659377m 2015-03-24

Liquefaction susceptibility after Robertson (2010) "Evaluation of Flow Liquefaction and Liquefied Strength Using the Cone Penetration Test"	Liquefaction susceptibility after Olson & Stark (2003) "Yield Strength Ratio and Liquefaction Analysis of Slopes and Embankments"	State parameter approximation - Robertson (2009) "Interpretation of cone penetration tests - a unified approach"

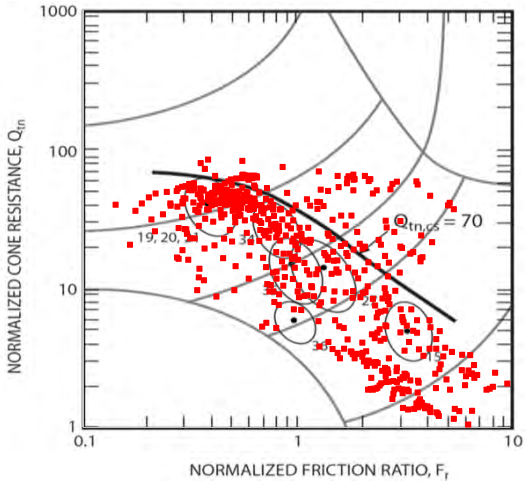

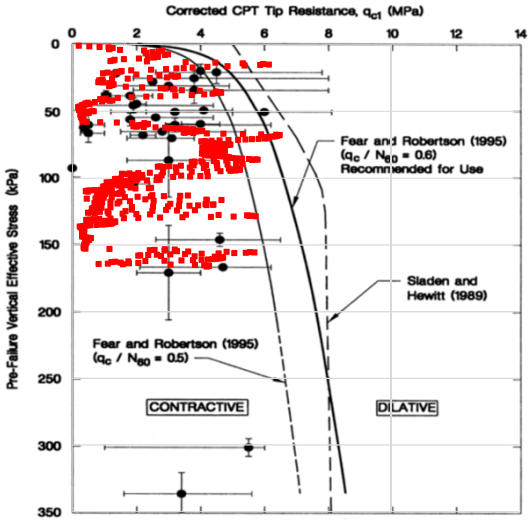

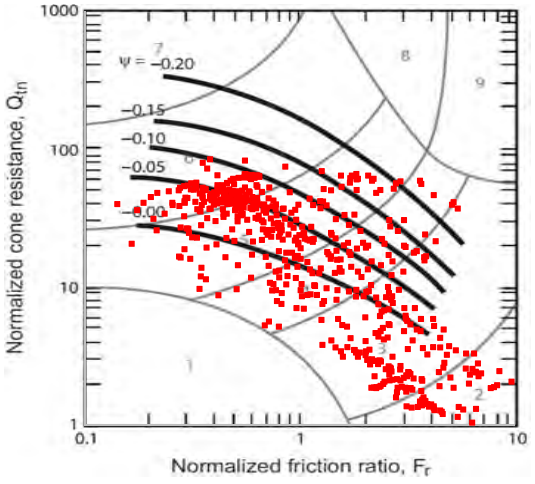

NOTE:

PROJECT

Fundão Tailings Dam Review Panel

TITLE

Fugro (March - July 2015) - Germano
CPTu-F26 Liquefaction Susceptibility and Soil Behavior Type

FUGRO IN SITU GEOTECNIA

PERCUSSION BORING TEST

SMC-03-GRE-01
ATTACHMENTS

CLIENT: SAMARCO MINERAÇÃO S.A.

PROJECT: FUNDÃO DAM

LOCATION: GERMANO MINE – MARIANA-MG

SCALE: 1:100 START: 05/12/2015 END: 05/13/2015 RESP.: DANIELLA ARANHA CREA REG. NO.: 2012104580/RJ

BOREHOLE: SP-F26 Elevation 920,03 COORDINATES: E 658885,94 N 7764194,60

WATER LEVEL 24 h	SAMPLE	ELEVATION (m)	BLOWS / 30 cm INITIAL	BLOWS / 30 cm Final	PENETRATION RESISTANCE INDEX (n) 0 10 20 30 40 50 60	MATERIAL CLASSIFICATION	GEOLOGICAL DESCRIPTION
0		920				0.00 m a 11.00 m	TAILINGS FILL/DAM
1		919	9	18		Fine to medium clayey sand, moderately to very compact, dark brown	
2		918	8	16			
3		917	32	39			
4		916	35	40/26			
5		915	40	39/23			
6		914	40	42			
7		913	17	22			
8 ▼		912	16	20			
9		911	17	24			
10		910	11	14			
11		909	13	15			
12		908	10	10		11.00 m a 13.00 m No recovery, material not very compact	
13		907	13	14			
14		906	6	7		13.00 m a 19.00 m Fine to medium clayey sand, moderately to very compact, dark brown	
15		905	8	18			
16		904	23	43			
17		903	26	51/26			
18		902	40				
19		901	15	10			
20			3	4		19.00 m a 20.00 m No recovery, material not very compact	

READING INTERVAL WL (m)
1: 24 h: -CLOSED
2:
3:

PROGRESS METHOD: (m)
DIGGER: 0,00 - 32,60
WASHING: 32,60 - 50,06
LINING: 50,06
USE OF BENTONITE: -
WATER LEAK:

TIME WASHING - 10 min
INITIAL DEPTH
STAGE 1 (cm):
STAGE 2 (cm):
STAGE 3 (cm):

NOTE: Borehole closed at 7.96 m.
Boring stopped due to achievement of impenetrability conditions.
Initial WL: DRY

FUGRO IN SITU GEOTECNIA

STANDARD PENETRATION TEST

SMO-03-GRE-01
ATTACHMENTS

CLIENT: SAMARCO MINERAÇÃO S.A.

PROJECT: FUNDÃO DAM

LOCATION: GERMANO MINE – MARIANA-MG

SCALE: 1:100 START: 05/12/2015 END: 05/13/2015 RESP.: DANIELLA ARANHA CREA REG. NO.: 2012104580/RJ

BOREHOLE: SP-F26 Elevation: 920,03 COORDINATES: E 658885,94 N 7764194,60

WATER LEVEL 24 h	SAMPLE	ELEVATION (m)	BLOWS / 30 cm INITIAL	BLOWS / 30 cm Final	PENETRATION RESISTANCE INDEX (n) 0 10 20 30 40 50 60	MATERIAL CLASSIFICATION	GEOLOGICAL DESCRIPTION
20		900				20.00 m a 34.00 m Fine to medium clayey sand, soft to moderately compact, dark brown	TAILINGS FILL/DAM
21		899	10	10			
22		898	2/45				
23		897	3/45				
24		896	1/50				
25		895	2	2			
26		894	2/35	5/32			
27		893	3	3/35			
28		892	3	5			
29		891	7	10			
30		890	6	8			
31		889	8	12			
32		888	2/60				
33		887	3	4			
34		886	12	18			
35		885	14	22		34.00 m a 35.00 m No recovery, material not very compact	
36		884	15	20		35.00 m a 38.00 m Fine clayey sand, compact, dark gray to variegated	
37		883	15	23			
38		882	5	3			
39		881	5	4		38.00 m a 39.00 m No recovery, material not very compact	
40			8	10		39.00 m a 41.00 m Slightly sandy clay, soft to moderately compact, brown to variegated	

READING INTERVAL WL (m)
1: 24 h: -CLOSED
2:
3:

PROGRESS METHOD: (m)
DIGGER:
WASHIN:G 0,00 - 32,60
LINING: 32,60 - 50,06
USE OF BENTONITE: 50,06
WATER LEAK: -

TIME WASHING - 10 min
INITIAL DEPTH
STAGE 1 (cm):
STAGE 2 (cm):
STAGE 3 (cm):

NOTE: Borehole closed at 7.96 m.
Boring stopped due to achievement of impenetrability conditions.
Initial WL: DRY

FUGRO IN SITU GEOTECNIA

STANDARD PENETRATION TEST

SMC-03-GRE-01
ATTACHMENTS

CLIENT: SAMARCO MINERAÇÃO S.A.

PROJECT: FUNDÃO DAM

LOCATION: GERMANO MINE – MARIANA-MG

SCALE: 1:100 START: 05/12/2015 END: 05/13/2015 RESP.: DANIELLA ARANHA CREA REG. NO.: 2012104580/RJ

BOREHOLE: SP-F26 Elevation: 920,03 COORDINATES: E 658885,94 N 7764194,60

WATER LEVEL 24 h	SAMPLE	ELEVATION (m)	BLOWS / 30 cm INITIAL	BLOWS / 30 cm Final	PENETRATION RESISTANCE INDEX (n) 0 10 20 30 40 50 60	MATERIAL CLASSIFICATION	GEOLOGICAL DESCRIPTION
40		880				39,00 m a 41,00 m Slightly sandy clay, soft to moderately compact, brown to variegated	TAILINGS FILL DAM
41		879	25	21			
42		878	28	30		41,00 m a 43,00 m Fine to medium sand, with fragments of rock smaller than 2 cm, compact, gray to variegated	
43		877	42				
44		876	33	38		43,00 m a 50,06 m Fine to medium silty sand. Saprolite originating from rock composed of quartz, biotite and feldspar (quartzite), moderately to very compact, gray to variegated	SAPROLITE
45		875	9/45				
46		874	27	40			
47		873	30/15				
48		872	30/10				
49		871	30/10				
50		870	30/6				
51		869					
52		868					
53		867					
54		866					
55		865					
56		864					
57		863					
58		862					
59		861					
60							

READING INTERVAL WL (m)
1: 24 h: -CLOSED
2:
3:

PROGRESS METHOD: (m)
DIGGER:
WASHING: 0,00 - 32,60
LINING: 32,60 - 50,06
USE OF BENTONITE: 50,06
WATER LEAK: -

TIME WASHING - 10 min
INITIAL DEPTH
STAGE 1 (cm):
STAGE 2 (cm):
STAGE 3 (cm):

NOTE: Borehole closed at 7.96 m.
Boring stopped due to achievement of impenetrability conditions.
Initial WL: DRY

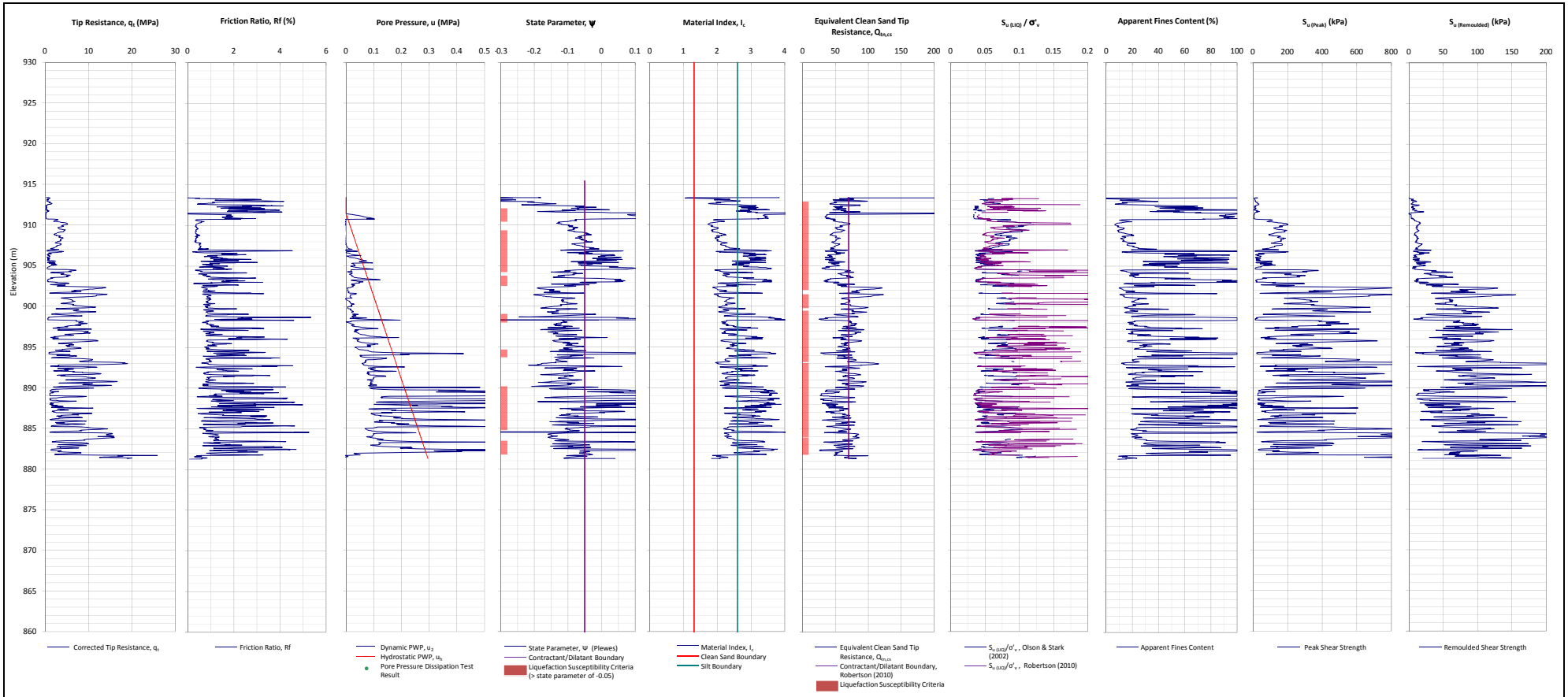

Notes:

1. This interpretation is based on the water and soil saturated unit weights γ_w=9.807 kN/m^3 and γ_{sat}=22 kN/m^3.
2. The friction ratio Rf is calculated as Rf=f_s/q_t.
3. The hydrostatic pore pressure is calculated using the ground water level (GWL) determined from CPT pore pressure dissipation tests (where available) or dynamic pore pressure.
4. Soil boundary layers (where plotted) are based on KCB interpretation.
5. The data presented have been plotted to the axis limits. Data may exist beyond the axis limits shown.
6. The Material Index (I_c) boundaries are based on Robertson and Wride (1998).
7. The $Q_{tn,cs}$ contractant/dilatant boundary=70 and is based on Robertson (2010).
8. The State Parameter (Ψ) is calculated using Plewes, et al. (1992) assuming a K0 of 0.5.
9. Coordinates are in UTM Zone 23K Córrego Alegre.
10. N_{kt} used in calculation of $S_{u(peak)}$ is 20.

PROJECT: Fundão Tailings Dam Review Panel

TITLE: Fugro (March - July 2015) - Germano
CONE PENETRATION TEST CPTu-F27
N:7763834m E:659430m 2015-03-20

Liquefaction susceptibility after Robertson (2010) "Evaluation of Flow Liquefaction and Liquefied Strength Using the Cone Penetration Test"	Liquefaction susceptibility after Olson & Stark (2003) "Yield Strength Ratio and Liquefaction Analysis of Slopes and Embankments"	State parameter approximation - Robertson (2009) "Interpretation of cone penetration tests - a unified approach"

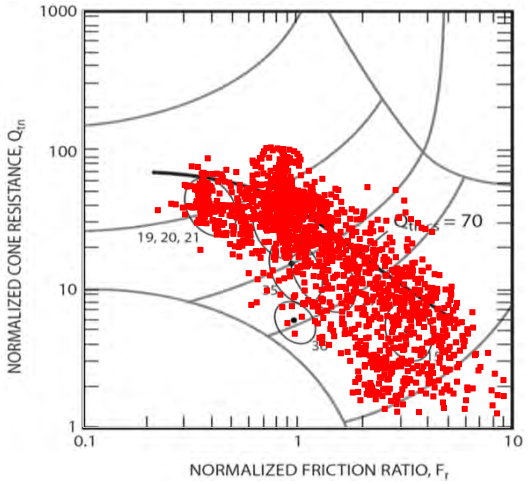

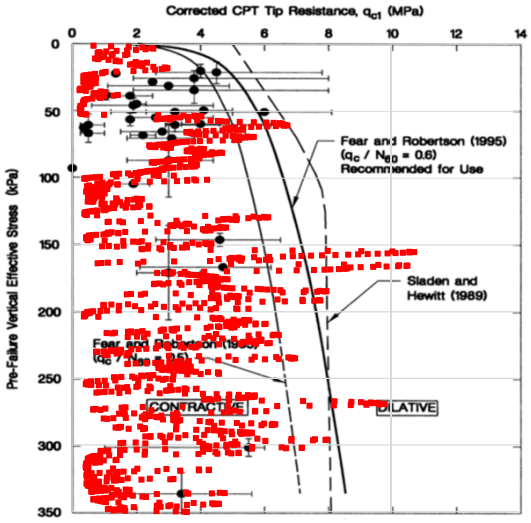

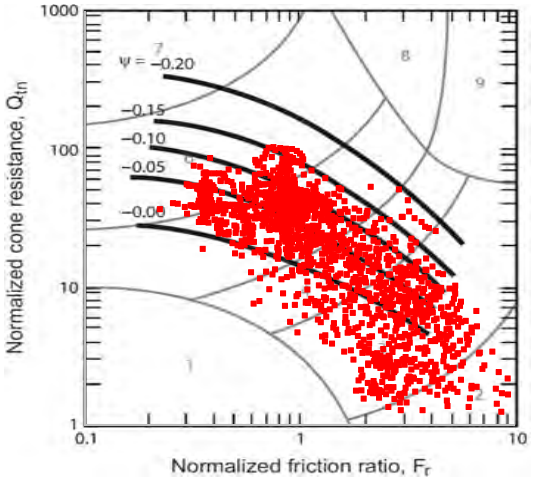

NOTE:

PROJECT

Fundão Tailings Dam Review Panel

TITLE

Fugro (March - July 2015) - Germano
CPTu-F27 Liquefaction Susceptibility and Soil Behavior Type

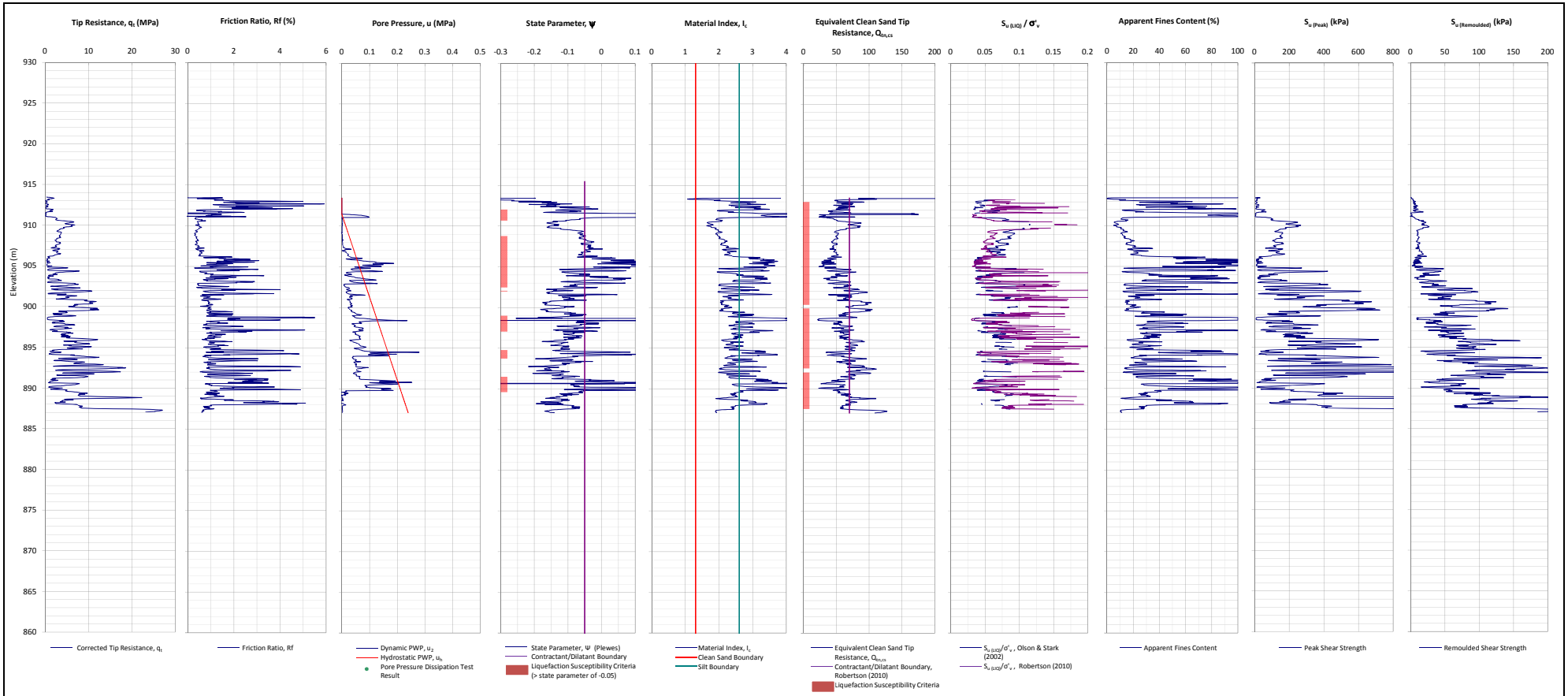

Notes:

1. This interpretation is based on the water and soil saturated unit weights γ_w=9.807 kN/m^3 and γ_{sat}=22 kN/m^3.
2. The friction ratio Rf is calculated as Rf=f_s/q_t.
3. The hydrostatic pore pressure is calculated using the ground water level (GWL) determined from CPT pore pressure dissipation tests (where available) or dynamic pore pressure.
4. Soil boundary layers (where plotted) are based on KCB interpretation.
5. The data presented have been plotted to the axis limits. Data may exist beyond the axis limits shown.
6. The Material Index (I_c) boundaries are based on Robertson and Wride (1998).
7. The $Q_{tn,cs}$ contractant/dilatant boundary=70 and is based on Robertson (2010).
8. The State Parameter (Ψ) is calculated using Plewes, et al. (1992) assuming a K0 of 0.5.
9. Coordinates are in UTM Zone 23K Córrego Alegre.
10. N_{kt} used in calculation of $S_{u(peak)}$ is 20.

PROJECT: Fundão Tailings Dam Review Panel

TITLE: Fugro (March - July 2015) - Germano
CONE PENETRATION TEST CPTu-F28
N:7763804m E:659468m 2015-03-20

Liquefaction susceptibility after Robertson (2010) "Evaluation of Flow Liquefaction and Liquefied Strength Using the Cone Penetration Test"	Liquefaction susceptibility after Olson & Stark (2003) "Yield Strength Ratio and Liquefaction Analysis of Slopes and Embankments"	State parameter approximation - Robertson (2009) "Interpretation of cone penetration tests - a unified approach"

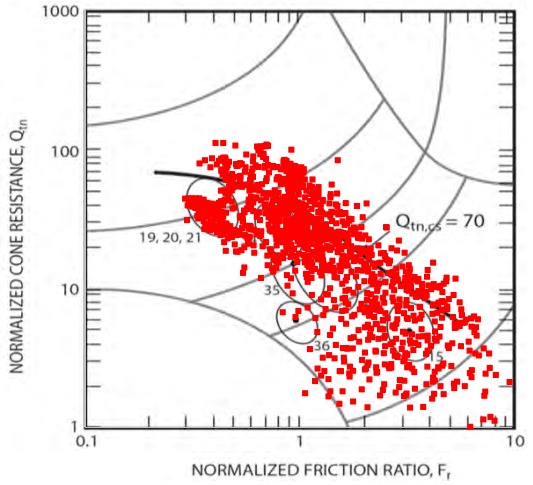

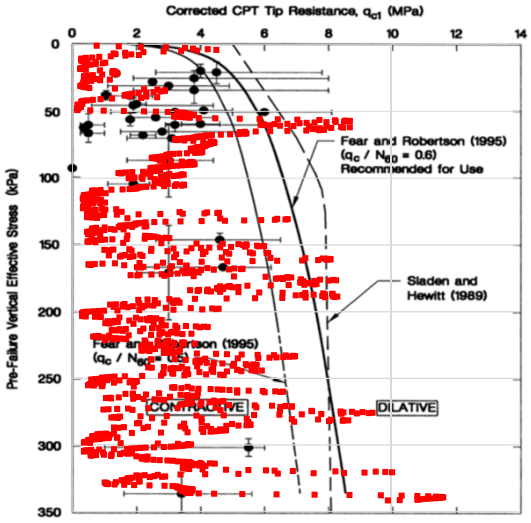

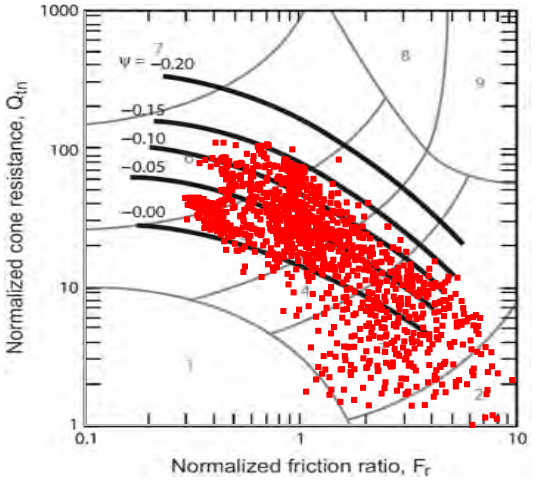

NOTE:

PROJECT	
	Fundão Tailings Dam Review Panel
TITLE	
	Fugro (March - July 2015) - Germano CPTu-F28 Liquefaction Susceptibility and Soil Behavior Type

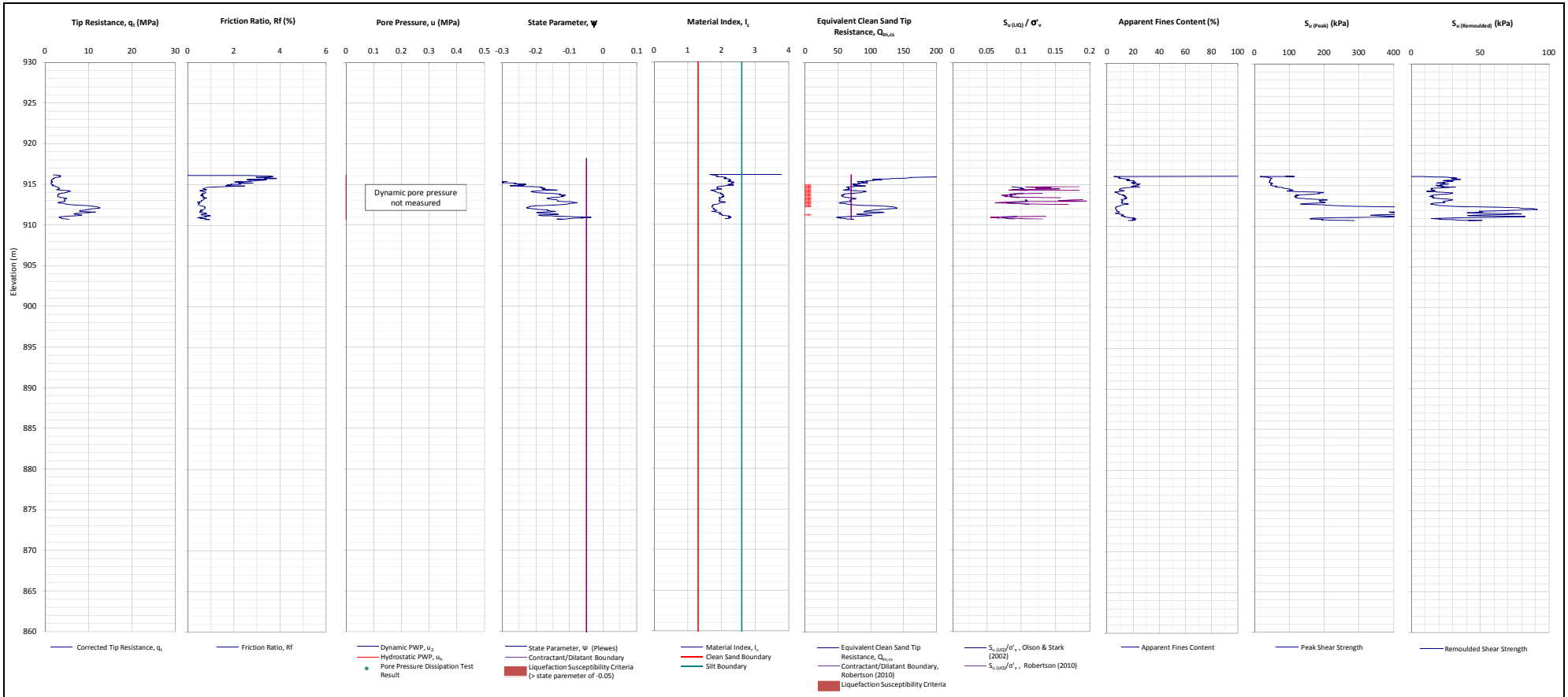

Notes:

1. This interpretation is based on the water and soil saturated unit weights γ_w=9.807 kN/m^3 and γ_{sat}=22 kN/m^3.
2. The friction ratio Rf is calculated as Rf=f_s/q_t.
3. The hydrostatic pore pressure is calculated using the ground water level (GWL) determined from CPT pore pressure dissipation tests (where available) or dynamic pore pressure.
4. Soil boundary layers (where plotted) are based on KCB interpretation.
5. The data presented have been plotted to the axis limits. Data may exist beyond the axis limits shown.
6. The Material Index (I_c) boundaries are based on Robertson and Wride (1998).
7. The $Q_{tn,cs}$ contractant/dilatant boundary=70 and is based on Robertson (2010).
8. The State Parameter (Ψ) is calculated using Plewes, et al. (1992) assuming a K0 of 0.5.
9. Coordinates are in UTM Zone 23K Córrego Alegre.
10. N_{kt} used in calculation of $S_{u(peak)}$ is 20.

PROJECT
Fundão Tailings Dam Review Panel

TITLE
Fugro (March - July 2015) - Germano
CONE PENETRATION TEST CPTu-F29
N:7763709m E:659592m 2015-03-25

Liquefaction susceptibility after Robertson (2010) "Evaluation of Flow Liquefaction and Liquefied Strength Using the Cone Penetration Test"	Liquefaction susceptibility after Olson & Stark (2003) "Yield Strength Ratio and Liquefaction Analysis of Slopes and Embankments"	State parameter approximation - Robertson (2009) "Interpretation of cone penetration tests - a unified approach"

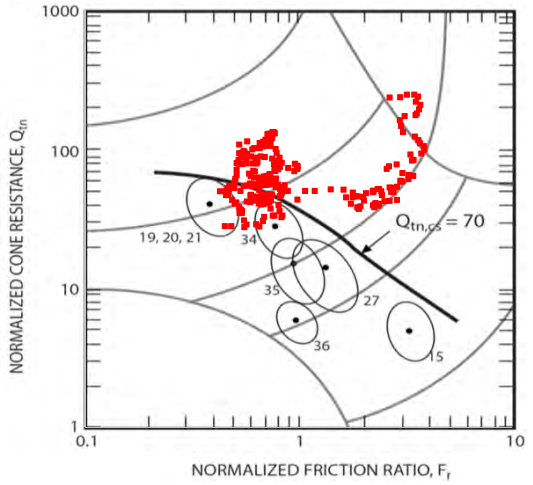

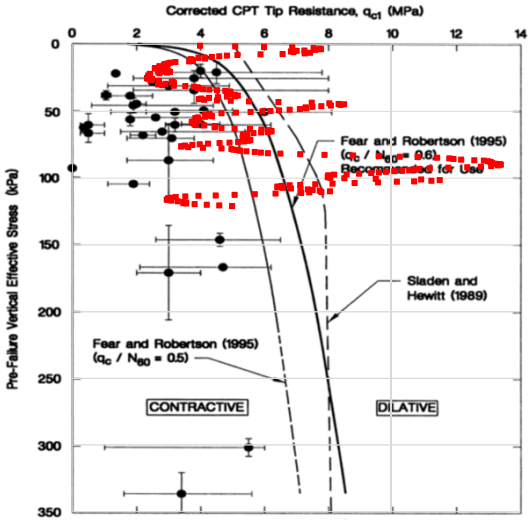

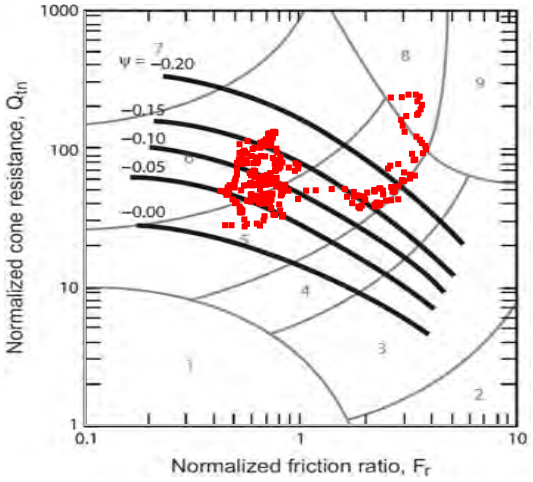

NOTE:

PROJECT

Fundão Tailings Dam Review Panel

TITLE

Fugro (March - July 2015) - Germano
CPTu-F29 Liquefaction Susceptibility and Soil Behavior Type

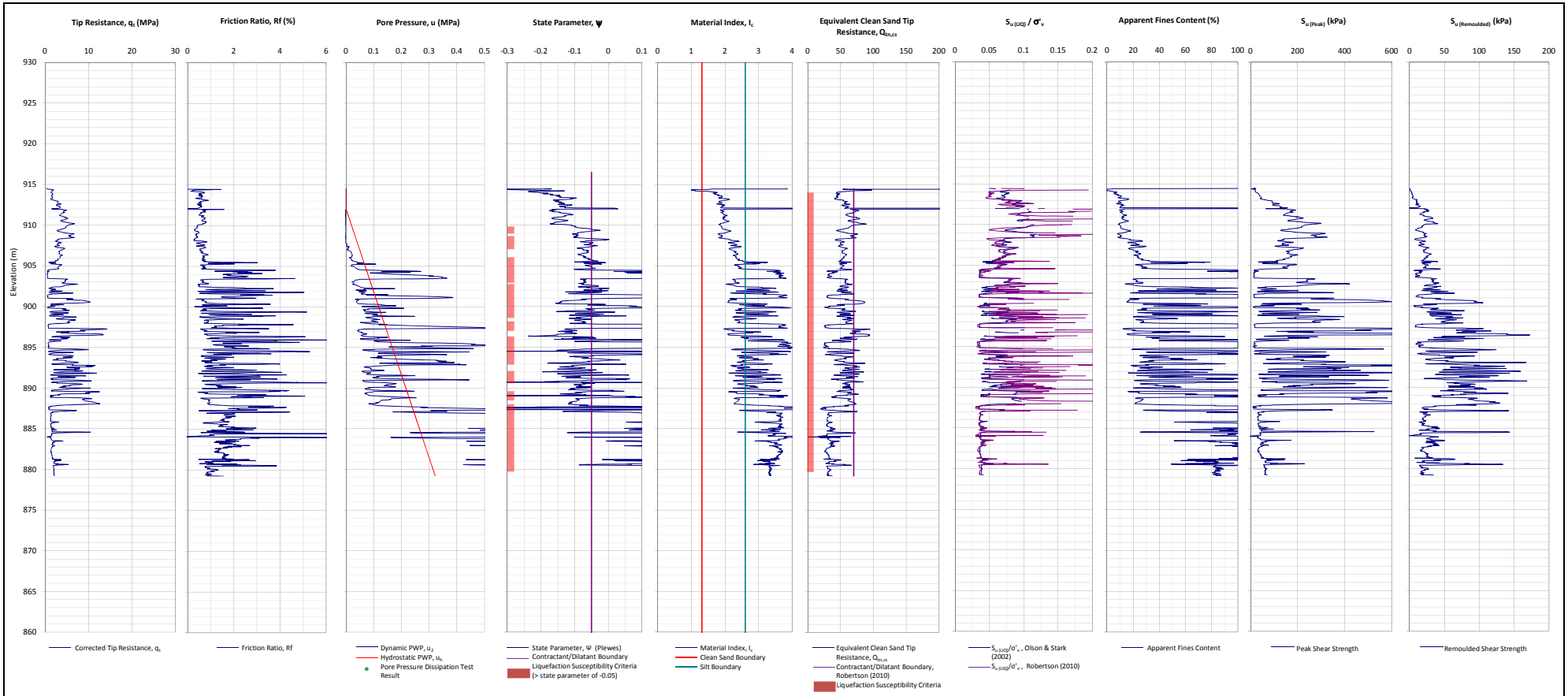

Notes:

1. This interpretation is based on the water and soil saturated unit weights γ_w=9.807 kN/m^3 and γ_{sat}=22 kN/m^3.
2. The friction ratio Rf is calculated as Rf=f_s/q_t.
3. The hydrostatic pore pressure is calculated using the ground water level (GWL) determined from CPT pore pressure dissipation tests (where available) or dynamic pore pressure.
4. Soil boundary layers (where plotted) are based on KCB interpretation.
5. The data presented have been plotted to the axis limits. Data may exist beyond the axis limits shown.
6. The Material Index (I_c) boundaries are based on Robertson and Wride (1998).
7. The $Q_{tn,cs}$ contractant/dilatant boundary=70 and is based on Robertson (2010).
8. The State Parameter (Ψ) is calculated using Plewes, et al. (1992) assuming a K0 of 0.5.
9. Coordinates are in UTM Zone 23K Córrego Alegre.
10. N_{kt} used in calculation of $S_{u(peak)}$ is 20.

PROJECT

Fundão Tailings Dam Review Panel

TITLE

Fugro (March - July 2015) - Germano
CONE PENETRATION TEST CPTu-F30
N:7763783m E:659605m 2015-03-24

Liquefaction susceptibility after Robertson (2010) "Evaluation of Flow Liquefaction and Liquefied Strength Using the Cone Penetration Test"	Liquefaction susceptibility after Olson & Stark (2003) "Yield Strength Ratio and Liquefaction Analysis of Slopes and Embankments"	State parameter approximation - Robertson (2009) "Interpretation of cone penetration tests - a unified approach"

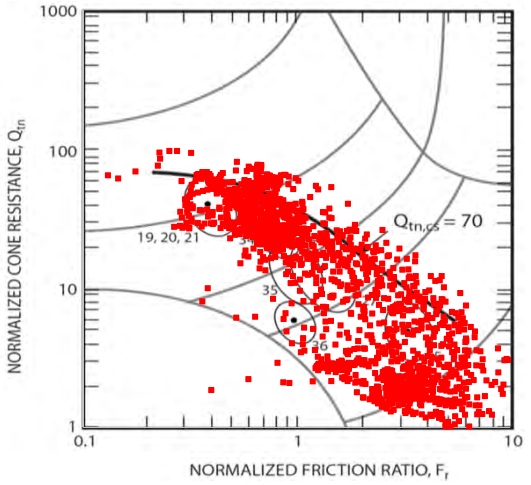

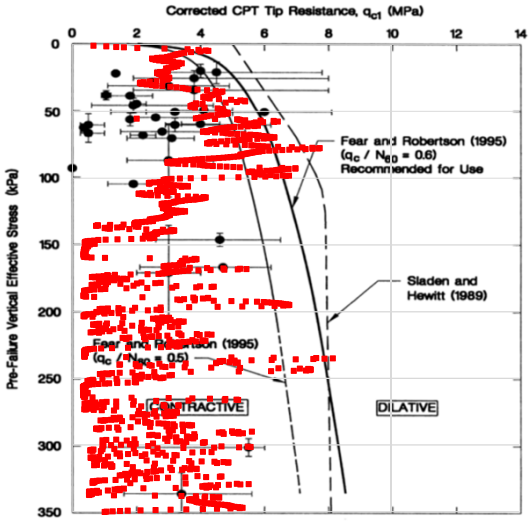

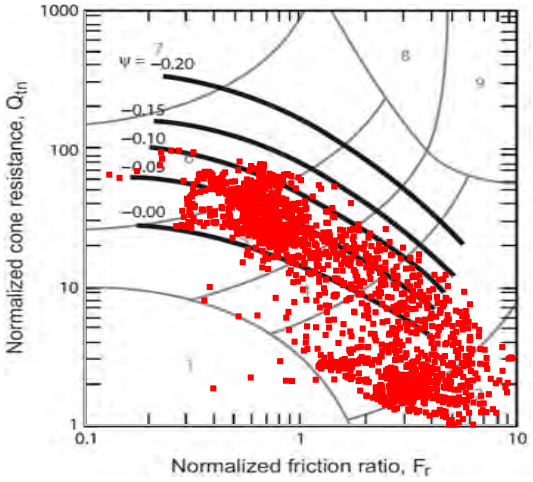

NOTE:

PROJECT	Fundão Tailings Dam Review Panel
TITLE	Fugro (March - July 2015) - Germano CPTu-F30 Liquefaction Susceptibility and Soil Behavior Type

June 2015
Fugro/Geocontrole
Dike 1
(Section C2.2.8)

Figure C.C1-8 – Fugro/Geocontrole (June 2015) Test Location Plan

FUND-01 CPT Plots
FUND-01 CPT Liquefaction Susceptibility and Soil Behavior Type Plots
FUND-02 CPT Plots
FUND-02 CPT Liquefaction Susceptibility and Soil Behavior Type Plots
SPT Log FUND-03
FUND-05 CPT Plots
FUND-05 CPT Liquefaction Susceptibility and Soil Behavior Type Plots
SPT Log FUND-05
FUND-06 CPT Plots
FUND-06 CPT Liquefaction Susceptibility and Soil Behavior Type Plots
SPT Log FUND-06
FUND-07 CPT Plots
FUND-07 CPT Liquefaction Susceptibility and Soil Behavior Type Plots
SPT Log FUND-07
FUND-15A CPT Plots
FUND-15A CPT Liquefaction Susceptibility and Soil Behavior Type Plots
SPT Log FUND-15
FUND-15B CPT Plots
FUND-15B CPT Liquefaction Susceptibility and Soil Behavior Type Plots
FUND-16 CPT Plots
FUND-16 CPT Liquefaction Susceptibility and Soil Behavior Type Plots
SPT Log FUND-16
SPT Log SP-BF-01
SPT Log SP-BF-02

NOTE:

1. June 22, 2015 Samarco aerial image shown.
2. CPT log FUND-04 is not presented due to low depth of penetration.

LEGEND:

- Piezocone Penetration Test (CPTu); performed by Fugro
- Standard Penetration Test (SPT); performed by Geocontrole

PROJECT

Fundão Tailings Dam Review Panel

TITLE

Fugro/Geocontrole (June 2015)
Test Location Plan

FIGURE NO.

C.C1-8

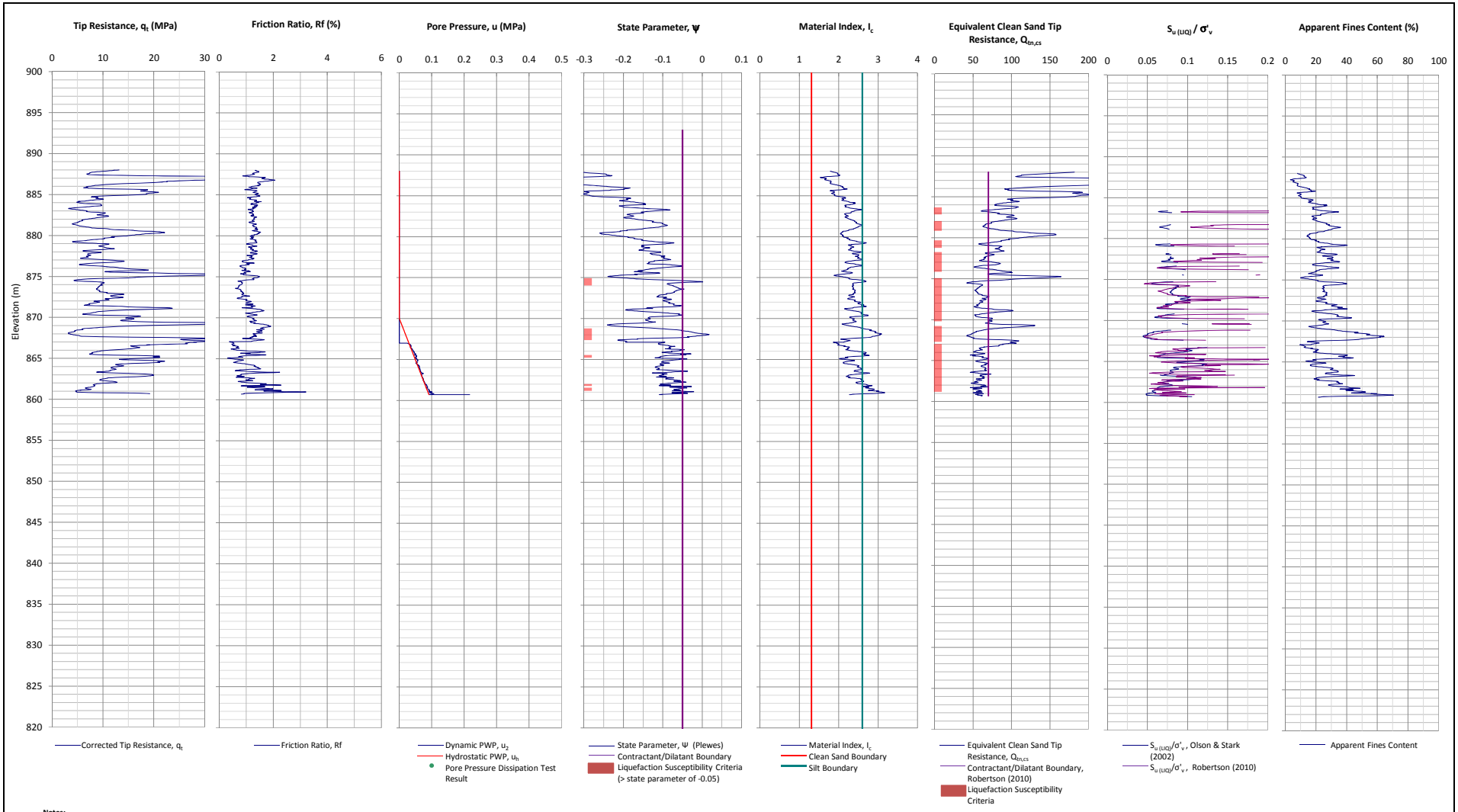

Notes:

1. This interpretation is based on the water and soil saturated unit weights γ_w=9.807 kN/m^3 and γ_{sat}=22 kN/m^3.
2. The friction ratio Rf is calculated as Rf=f_s/q_t.
3. The hydrostatic pore pressure is calculated using the ground water level (GWL) determined from CPT pore pressure dissipation tests (where available) or dynamic pore pressure.
4. Soil boundary layers (where plotted) are based on KCB interpretation.
5. The data presented have been plotted to the axis limits. Data may exist beyond the axis limits shown.
6. The Material Index (I_c) boundaries are based on Robertson and Wride (1998).
7. The $Q_{tn,cs}$ contractant/dilatant boundary=70 and is based on Robertson (2010).
8. The State Parameter (Ψ) is calculated using Plewes, et al. (1992) assuming a K0 of 0.5.
9. Coordinates are in UTM Zone 23K Córrego Alegre.

PROJECT: Fundão Tailings Dam Review Panel

TITLE: Fugro (June 2015) - Dike 1
CONE PENETRATION TEST FUND-01
N:7764596m E:660489m 2015-06-02

Liquefaction susceptibility after Robertson (2010) "Evaluation of Flow Liquefaction and Liquefied Strength Using the Cone Penetration Test"	Liquefaction susceptibility after Olson & Stark (2003) "Yield Strength Ratio and Liquefaction Analysis of Slopes and Embankments"	State parameter approximation - Robertson (2009) "Interpretation of cone penetration tests - a unified approach"

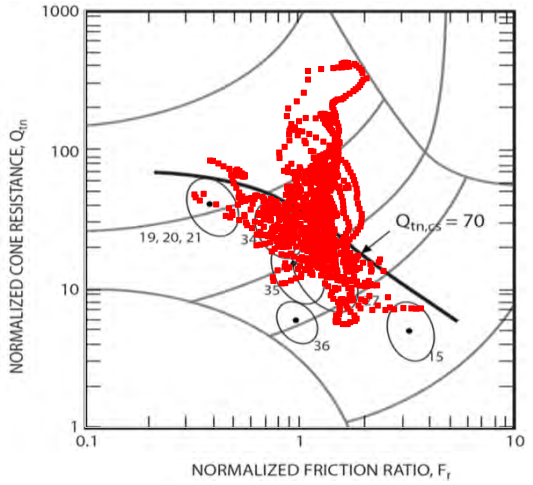

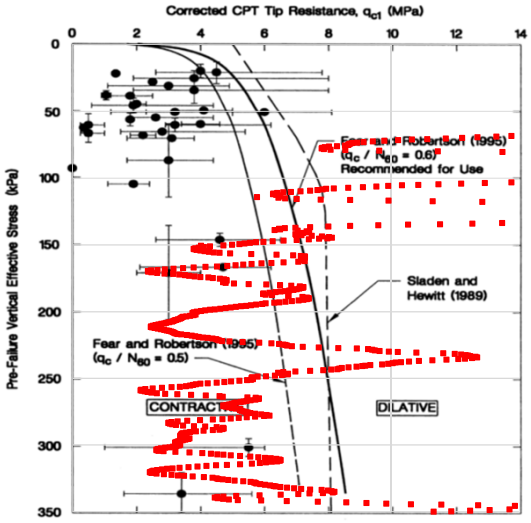

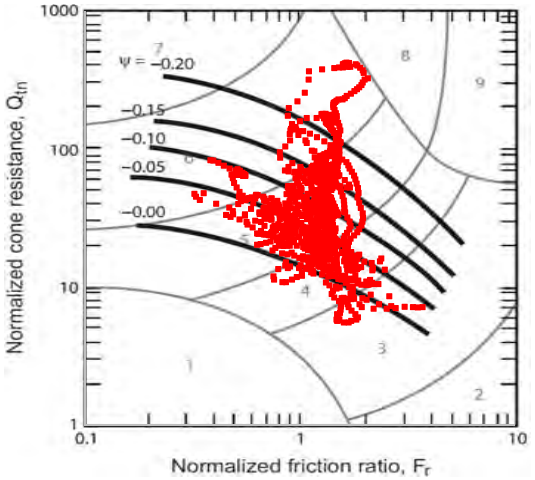

NOTE:

PROJECT

Fundão Tailings Dam Review Panel

TITLE

Fugro (June 2015) - Dike 1
FUND-01 Liquefaction Susceptibility and Soil Behavior Type

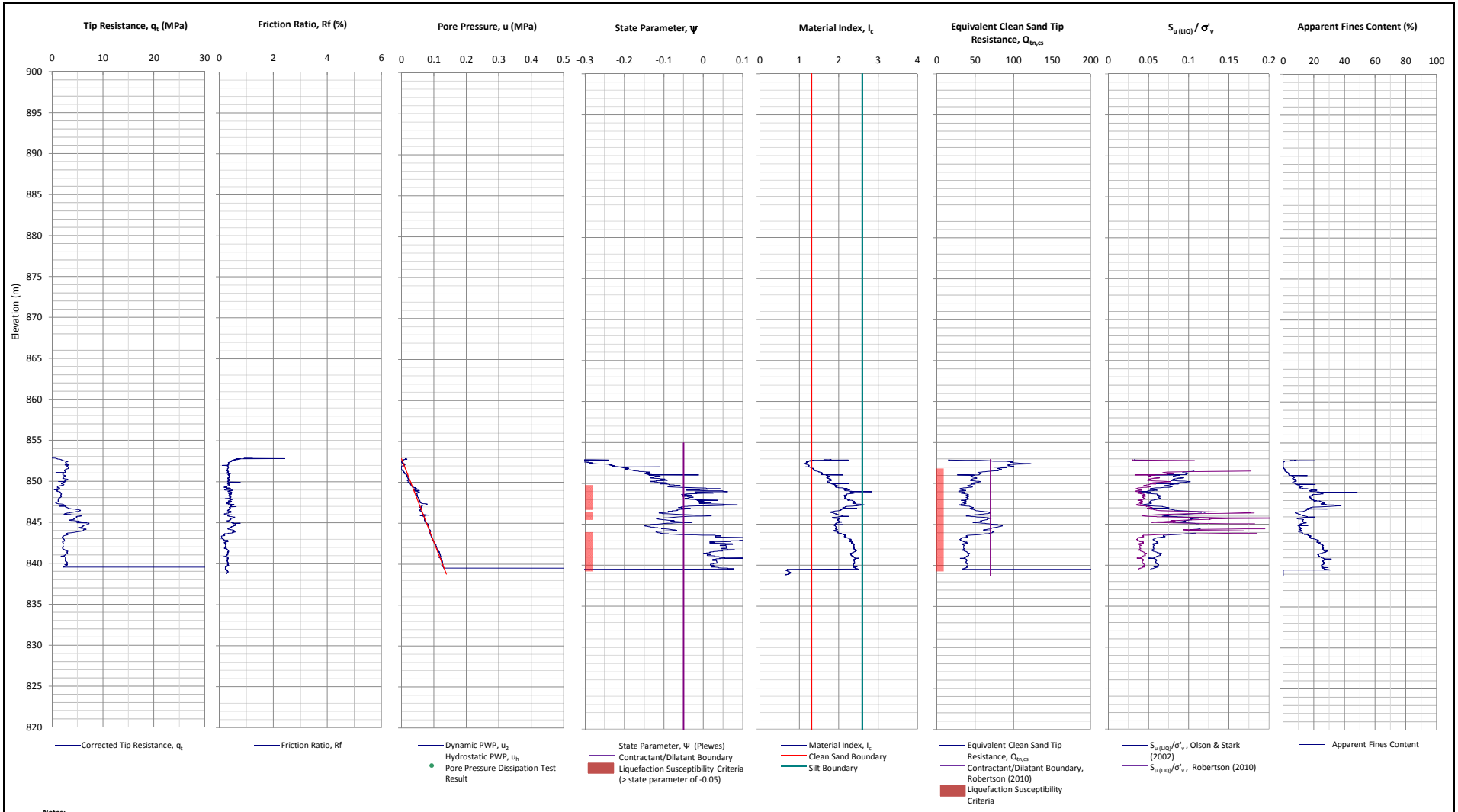

Notes:

1. This interpretation is based on the water and soil saturated unit weights γ_w=9.807 kN/m^3 and γ_{sat}=22 kN/m^3.
2. The friction ratio Rf is calculated as Rf=f_s/q_t.
3. The hydrostatic pore pressure is calculated using the ground water level (GWL) determined from CPT pore pressure dissipation tests (where available) or dynamic pore pressure.
4. Soil boundary layers (where plotted) are based on KCB interpretation.
5. The data presented have been plotted to the axis limits. Data may exist beyond the axis limits shown.
6. The Material Index (I_c) boundaries are based on Robertson and Wride (1998).
7. The $Q_{tn,cs}$ contractant/dilatant boundary=70 and is based on Robertson (2010).
8. The State Parameter (Ψ) is calculated using Plewes, et al. (1992) assuming a K0 of 0.5.
9. Coordinates are in UTM Zone 23K Córrego Alegre.

PROJECT: Fundão Tailings Dam Review Panel

TITLE:

Fugro (June 2015) - Dike 1
CONE PENETRATION TEST FUND-02
N:7764552m E:660614m 2015-06-07

Liquefaction susceptibility after Robertson (2010) "Evaluation of Flow Liquefaction and Liquefied Strength Using the Cone Penetration Test"	Liquefaction susceptibility after Olson & Stark (2003) "Yield Strength Ratio and Liquefaction Analysis of Slopes and Embankments"	State parameter approximation - Robertson (2009) "Interpretation of cone penetration tests - a unified approach"

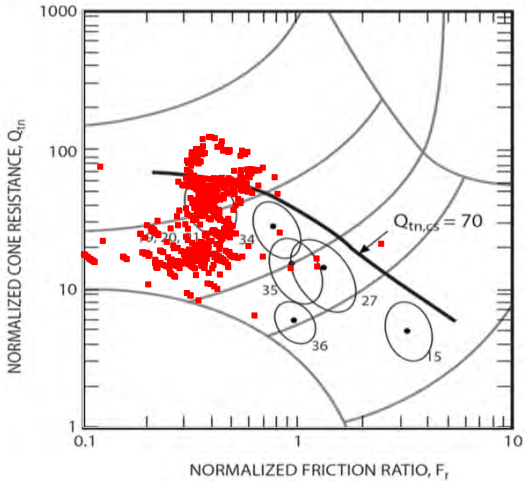

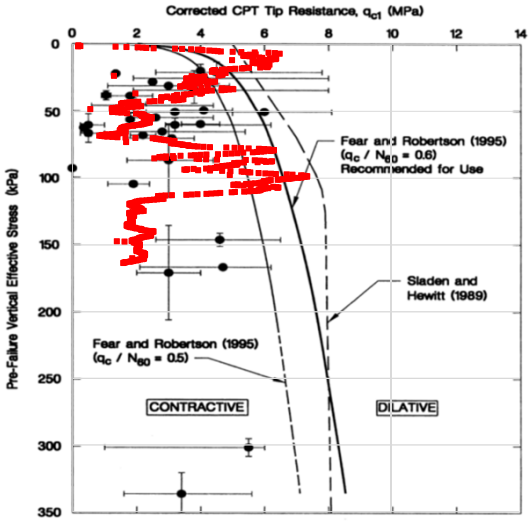

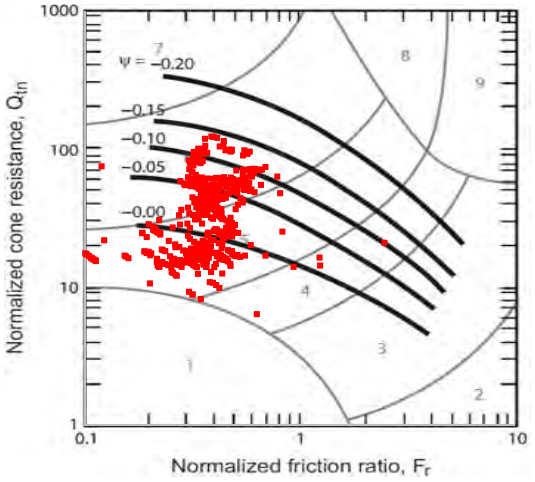

NOTE:

PROJECT

Fundão Tailings Dam Review Panel

TITLE

Fugro (June 2015) - Dike 1
FUND-02 Liquefaction Susceptibility and Soil Behavior Type

GEOTECHNICAL PROSPECTING

Geocontrole

Client: SAMARCO

Job: **Germano / Fundão EL940m - Dam Raising**

SOUNDING: **FUND-03**

Process: **11115**

Page: **1 of 2**

Start Date	Equipment	Final Depth (m)
22/6/2015	GEO106-Beretta T44	26.1

End Date	Water Table	Slope	System	Coordinates	Elevation	Sounder	Technician
23/6/2015	Dry	90°	UTM 23K	E= 660665,85 N= 7764777,09	Z= 894,84	João Paulo	Guilherme Freitas

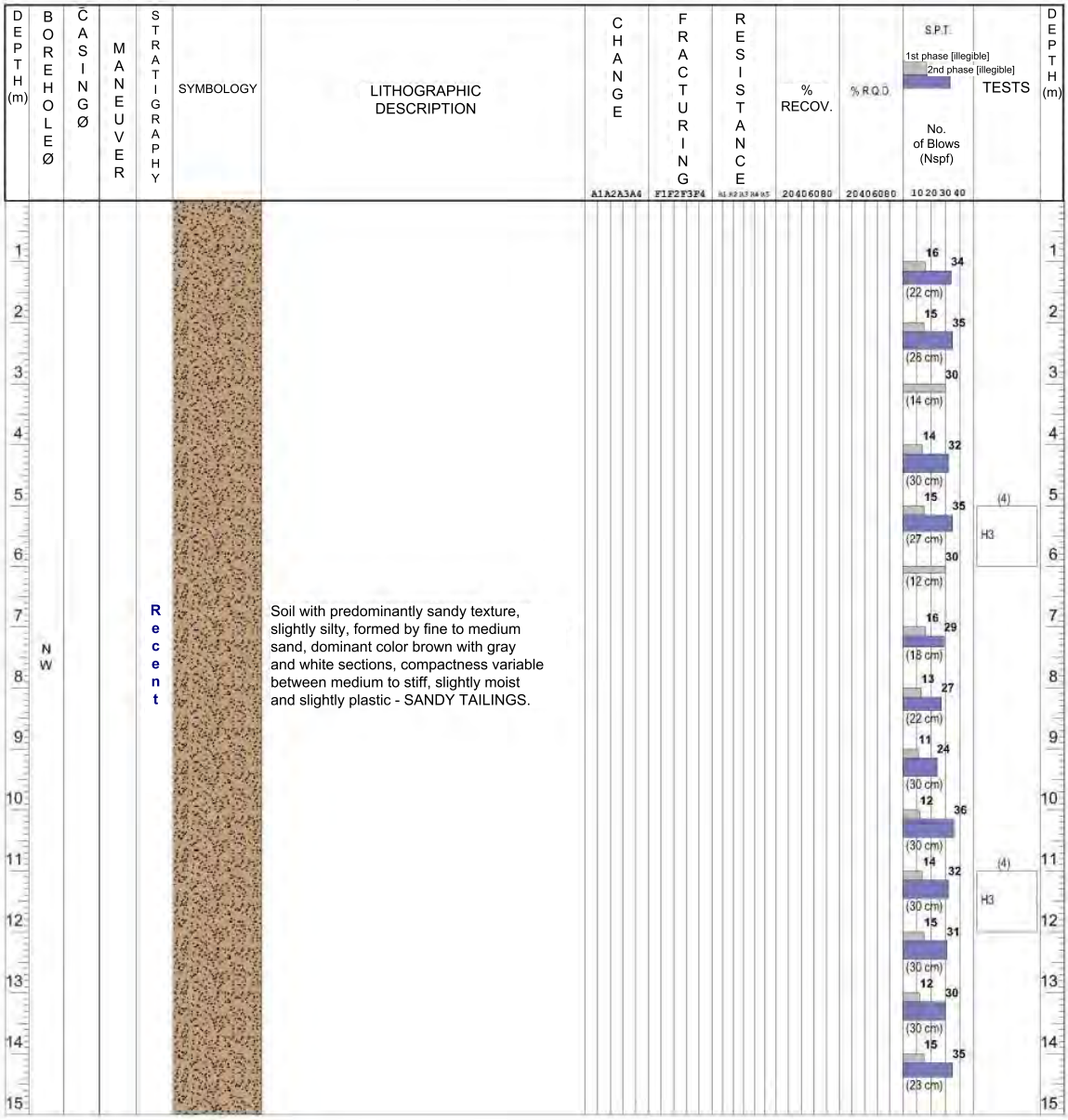

Responsible CREA Technician: Guilherme Freitas - No. 135337D

Remarks:

Legend: (4) "LEFRANC - Soil Infiltration - Permeability Test"

GEOTECHNICAL PROSPECTING

Geocontrole

Client: SAMARCO

Job: **Germano / Fundão EL940m - Dam Raising**

SOUNDING: **FUND-03**

Process: **11115**

Page: **2 of 2**

Start Date	Equipment	Final Depth (m)	End Date	Water Table	Slope	System	Coordinates	Elevation	Sounder	Technician
22/6/2015	GEO106-Beretta T44	26.1	23/6/2015	Dry	90°	UTM 23K	E= 660665,85 N= 7764777,09	Z= 894,84	João Paulo	Guilherme Freitas

DEPTH (m)	BOREHOLE Ø	CASING Ø	MANEUVER	STRATIGRAPHY	SYMBOLOGY	LITHOGRAPHIC DESCRIPTION	CHANGE A1 A2 A3 A4	FRACTURING F1 F2 F3 F4	RESISTANCE	% RECOV. 20 40 60 80	% R.Q.D. 20 40 60 80	S.P.T. 1st phase [illegible] 2nd phase [illegible] No. of Blows (Nspf) 10 20 30 40	TESTS	DEPTH (m)
16	NW			Recent		Soil with predominantly sandy texture, slightly silty, formed by fine to medium sand, dominant color brown with gray and white sections, compactness variable between medium to stiff, slightly moist and slightly plastic - SANDY TAILINGS.						13 31 (30 cm) 11 32 (30 cm) 14 36 (30 cm) 17 33 (30 cm) 17 35 (30 cm) 15 35 (30 cm) 14 35 (30 cm) 17 33 (24 cm) 18 32 (20 cm) 20 30 (14 cm) 30 (13 cm) 30	(4) H3	16
17														17
18														18
19														19
20														20
21														21
22														22
23													(4) H2	23
24														24
25														25
26						26.1m- End of Sounding						(10 cm)		26
27														27
28														28
29														29
30														30

Responsible CREA Technician: Guilherme Freitas - No. 135337D

Remarks:

Legend: (4) "LEFRANC - Soil Infiltration - Permeability Test"

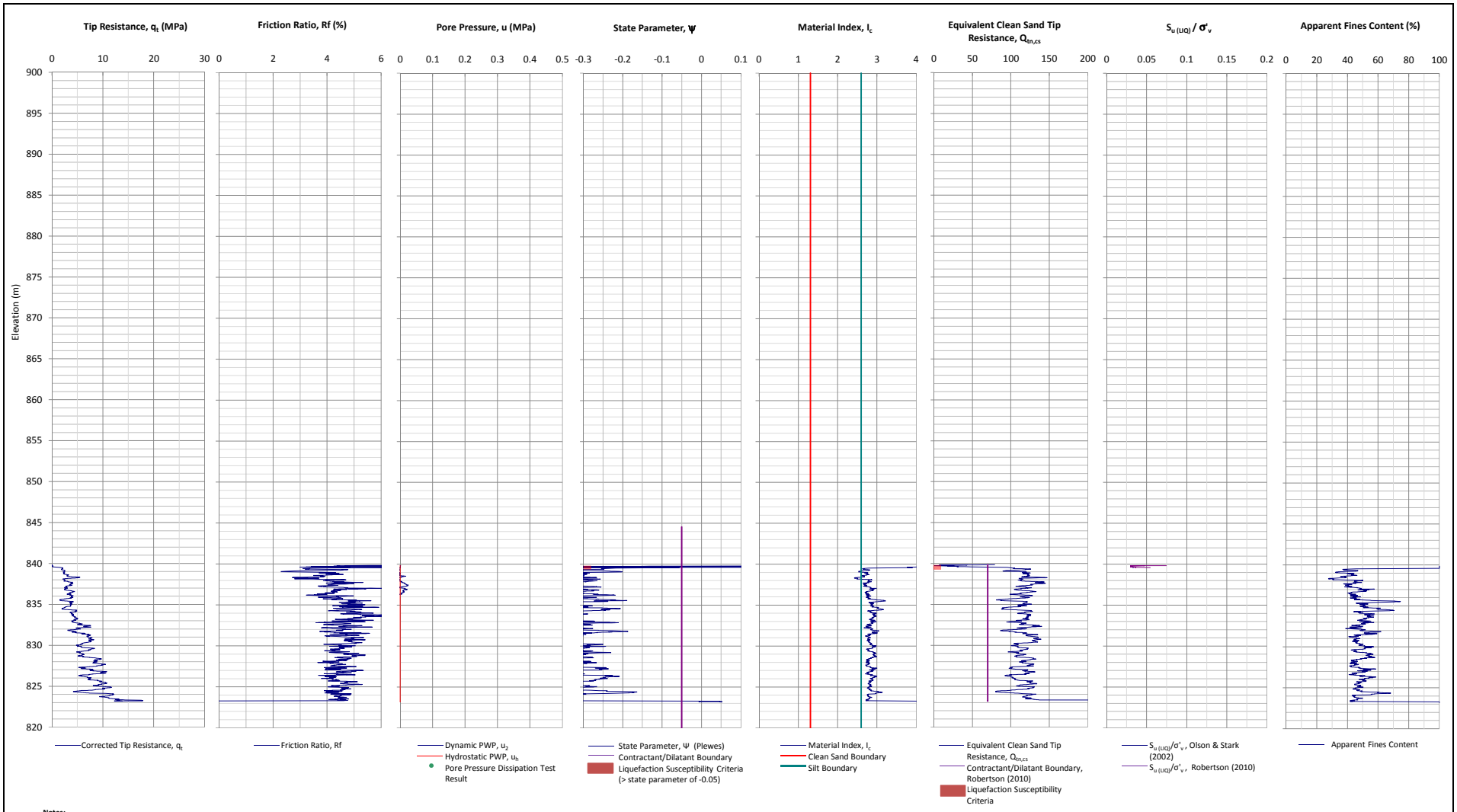

Notes:

1. This interpretation is based on the water and soil saturated unit weights γ_w=9.807 kN/m^3 and γ_{sat}=22 kN/m^3.
2. The friction ratio Rf is calculated as Rf=f_s/q_t.
3. The hydrostatic pore pressure is calculated using the ground water level (GWL) determined from CPT pore pressure dissipation tests (where available) or dynamic pore pressure.
4. Soil boundary layers (where plotted) are based on KCB interpretation.
5. The data presented have been plotted to the axis limits. Data may exist beyond the axis limits shown.
6. The Material Index (I_c) boundaries are based on Robertson and Wride (1998).
7. The $Q_{tn,cs}$ contractant/dilatant boundary=70 and is based on Robertson (2010).
8. The State Parameter (Ψ) is calculated using Plewes, et al. (1992) assuming a K0 of 0.5.
9. Coordinates are in UTM Zone 23K Córrego Alegre.

PROJECT: Fundão Tailings Dam Review Panel

TITLE:

Fugro (June 2015) - Dike 1
CONE PENETRATION TEST FUND-05
N:7764735m E:660913m 2015-06-22

Liquefaction susceptibility after Robertson (2010) "Evaluation of Flow Liquefaction and Liquefied Strength Using the Cone Penetration Test"	Liquefaction susceptibility after Olson & Stark (2003) "Yield Strength Ratio and Liquefaction Analysis of Slopes and Embankments"	State parameter approximation - Robertson (2009) "Interpretation of cone penetration tests - a unified approach"

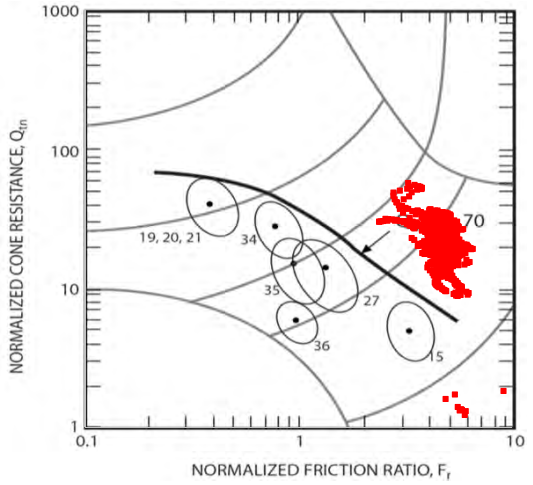

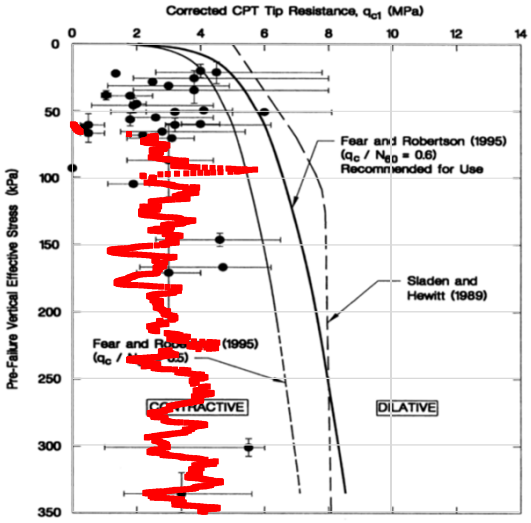

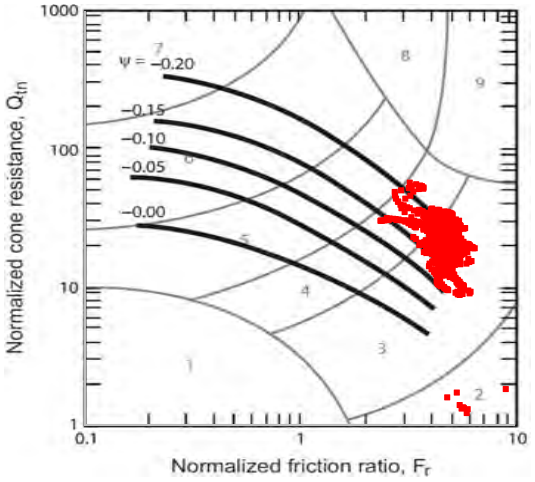

NOTE:

PROJECT

Fundão Tailings Dam Review Panel

TITLE

Fugro (2015) - Dike 1
FUND-05 Liquefaction Susceptibility and Soil Behavior Type

Geocontrole

GEOTECHNICAL PROSPECTING

SOUNDING: **FUND-05**

Process: **11115**

Client: SAMARCO

Job: **Germano / Fundão EL940m - Dam Raising**

Page: **1 of 2**

Start Date	Equipment	Final Depth (m)	End Date	Water Table	Slope	System	Coordinates	Elevation	Sounder	Technician
17/6/2015	GEO106-Beretta T44	18.07	18/6/2015	Dry	90°	UTM 23K	E= 660920,98 N= 7764733,94	Z= 841,95	João Paulo	Guilherme Freitas

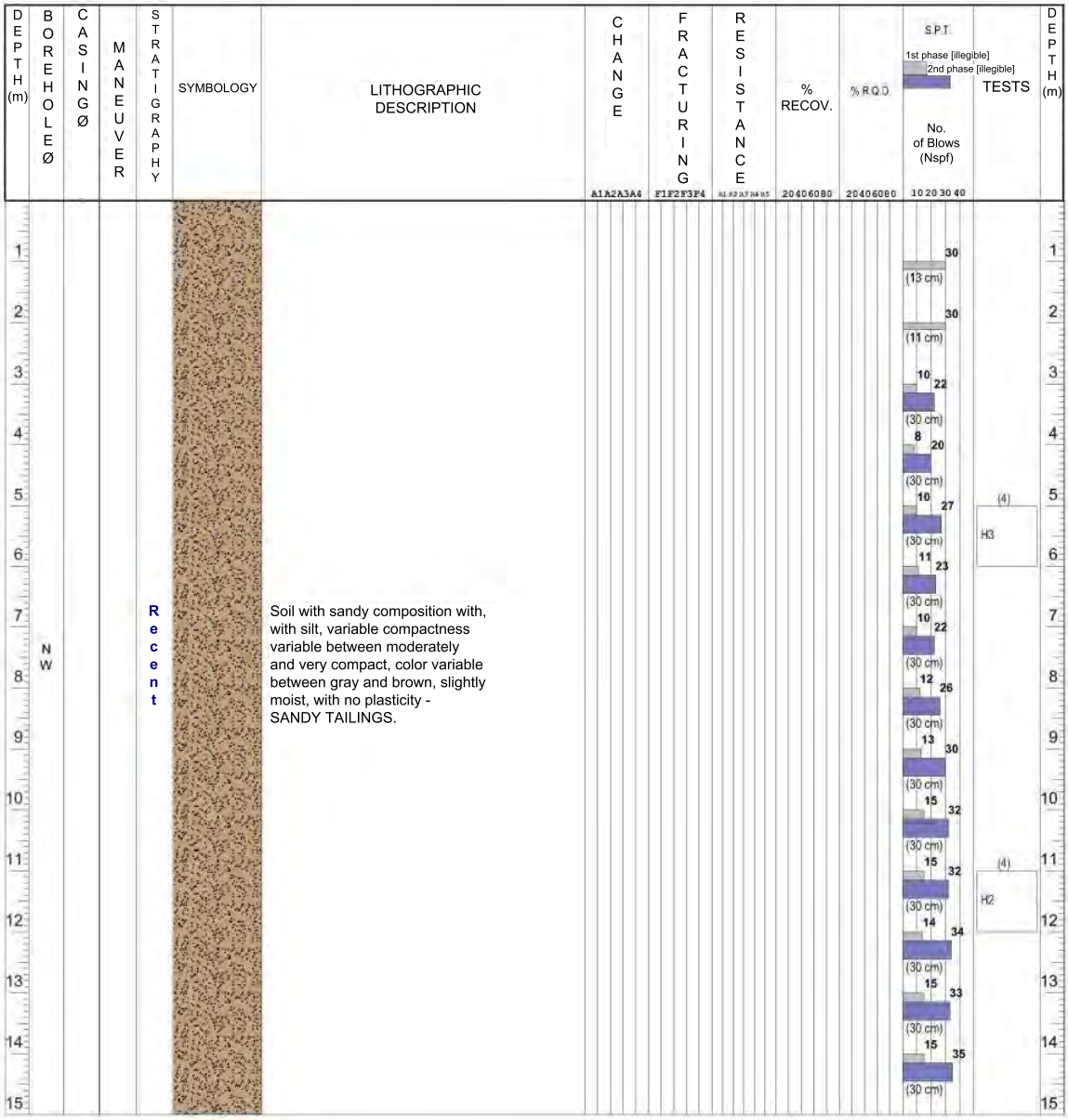

Responsible CREA Technician: Guilherme Freitas - No. 135337D

Remarks:

Legend: (4) "LEFRANC - Soil Infiltration - Permeability Test"

GEOTECHNICAL PROSPECTING

SOUNDING: FUND-05

Process: 11115

Page: 2 of 2

Client: SAMARCO

Job: Germano / Fundão EL940m - Dam Raising

Start Date	Equipment	Final Depth (m)
17/6/2015	GEO106-Beretta T44	18.07

End Date	Water Table	Slope	System	Coordinates	Elevation	Sounder	Technician
18/6/2015	Dry	90°	UTM 23K	E= 660920,98 N= 7764733,94	Z= 841,95	João Paulo	Guilherme Freitas

DEPTH (m)	BOREHOLE Ø	CASING Ø	MANEUVER	STRATIGRAPHY	SYMBOLOGY	LITHOGRAPHIC DESCRIPTION	CHANGE A1 A2 A3 A4	FRACTURING F1 F2 F3 F4	RESISTANCE	% RECOV. 20 40 60 80	% R.Q.D. 20 40 60 80	S.P.T. 1st phase [illegible] 2nd phase [illegible] No. of Blows (Nspf) 10 20 30 40	TESTS	DEPTH (m)
16												17 33 (19 cm)		16
17	NW			Recent		Soil with sandy composition with, with silt, variable compactness variable between moderately and very compact, color variable between gray and brown, slightly moist, with no plasticity - SANDY TAILINGS.						30 (13 cm) 30 (10 cm)	(4) H2	17
18						18.07m- End of Sounding						30 (7 cm)		18
19														19
20														20
21														21
22														22
23														23
24														24
25														25
26														26
27														27
28														28
29														29
30														30

Responsible CREA Technician: Guilherme Freitas - No. 135337D

Remarks:

Legend: (4) "LEFRANC - Soil Infiltration - Permeability Test"

Rua Vancouver, 66 - Jardim Canadá - 34000-000 Nova Lima Telephone: (31) 3517-9011 E-mail: mail@geocontrole.com

Sounding performed according to Standard NBR 6484/2001 - Sounding performed according to ABGE bulletin No. 3

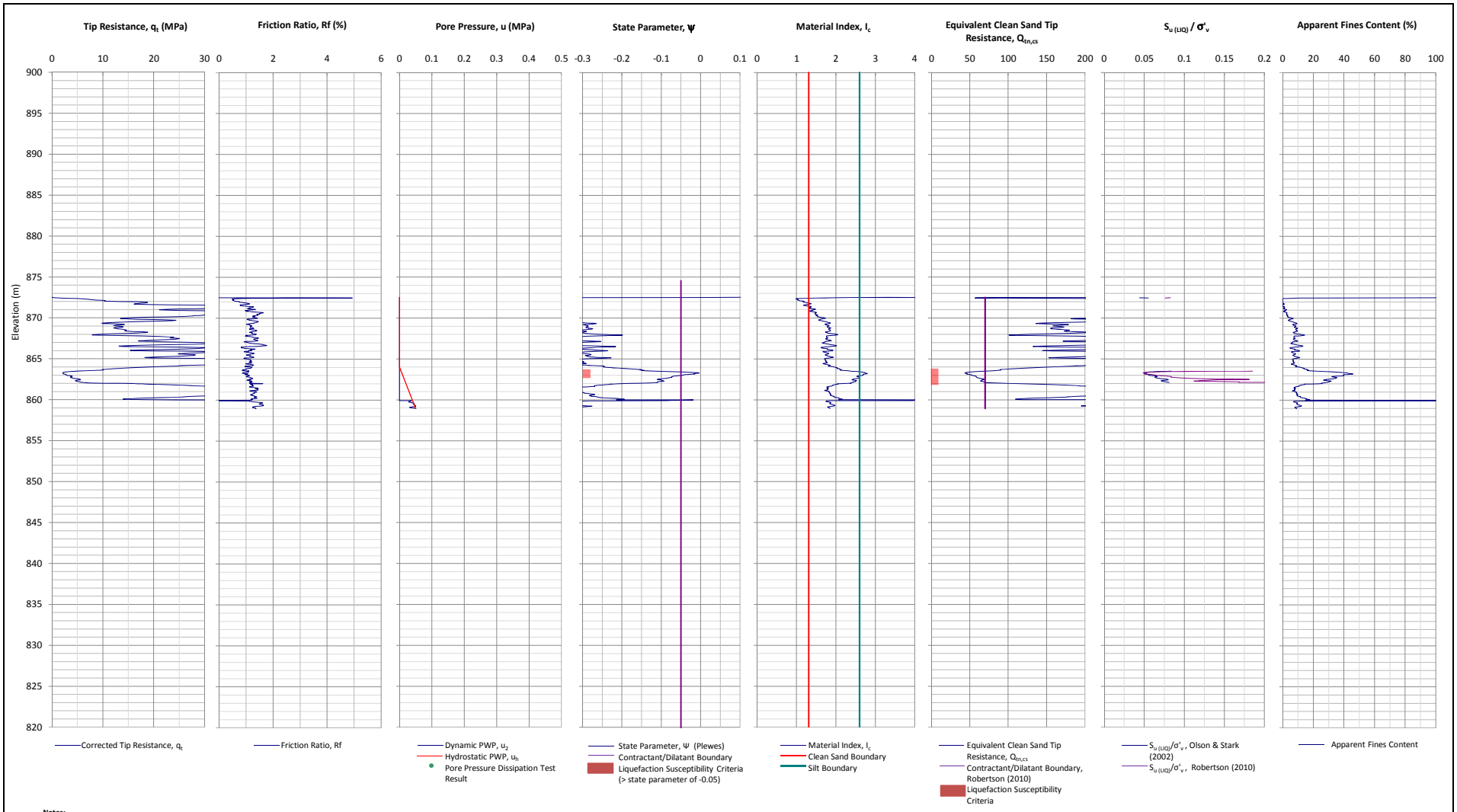

Notes:

1. This interpretation is based on the water and soil saturated unit weights γ_w=9.807 kN/m^3 and γ_{sat}=22 kN/m^3.
2. The friction ratio Rf is calculated as Rf=f_s/q_t.
3. The hydrostatic pore pressure is calculated using the ground water level (GWL) determined from CPT pore pressure dissipation tests (where available) or dynamic pore pressure.
4. Soil boundary layers (where plotted) are based on KCB interpretation.
5. The data presented have been plotted to the axis limits. Data may exist beyond the axis limits shown.
6. The Material Index (I_c) boundaries are based on Robertson and Wride (1998).
7. The $Q_{tn,cs}$ contractant/dilatant boundary=70 and is based on Robertson (2010).
8. The State Parameter (Ψ) is calculated using Plewes, et al. (1992) assuming a K0 of 0.5.
9. Coordinates are in UTM Zone 23K Córrego Alegre.

PROJECT: Fundão Tailings Dam Review Panel

TITLE:

Fugro (June 2015) - Dike 1
CONE PENETRATION TEST FUND-06
N:7764975m E:660833m 2015-06-01

Liquefaction susceptibility after Robertson (2010) "Evaluation of Flow Liquefaction and Liquefied Strength Using the Cone Penetration Test"	Liquefaction susceptibility after Olson & Stark (2003) "Yield Strength Ratio and Liquefaction Analysis of Slopes and Embankments"	State parameter approximation - Robertson (2009) "Interpretation of cone penetration tests - a unified approach"

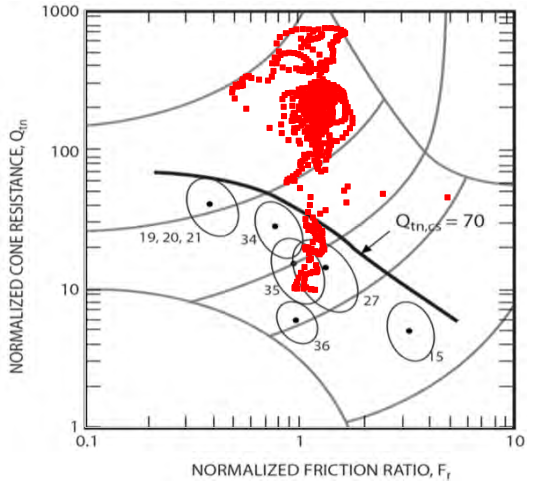

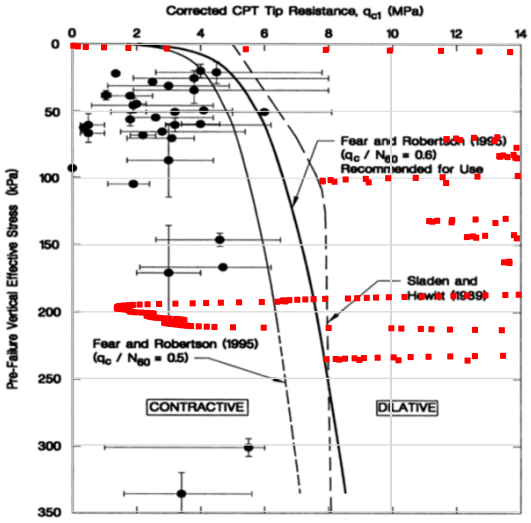

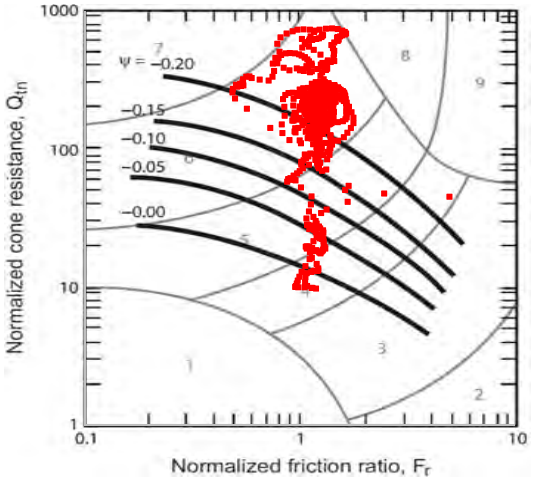

NOTE:

PROJECT

Fundão Tailings Dam Review Panel

TITLE

Fugro (June 2015) - Dike 1
FUND-06 Liquefaction Susceptibility and Soil Behavior Type

GEOTECHNICAL PROSPECTING

SOUNDING: FUND-06

Process: 11115

Page: 1 of 2

Client: SAMARCO

Job: Germano / Fundão EL940m - Dam Raising

Start Date	Equipment	Final Depth (m)	End Date	Water Table	Slope	System	Coordinates	Elevation	Sounder	Technician
16/6/2015	GEO104-Domine Futuro	19,45	18/6/2015	4,40m	90°	UTM 23K	E= 660838,77 N= 7764979,83	Z= 873,81	Ricardo Henrique	Guilherme Freitas

DEPTH (m)	BOREHOLE Ø	CASING Ø	MANEUVER	STRATIGRAPHY	SYMBOLOGY	LITHOGRAPHIC DESCRIPTION	CHANGE A1 A2 A3 A4	FRACTURING F1 F2 F3 F4	RESISTANCE	% RECOV. 20 40 60 80	% R.Q.D. 20 40 60 80	S.P.T. 1st phase [illegible] 2nd phase [illegible] No. of Blows (Nspf) 10 20 30 40	TESTS	DEPTH (m)
1–15	BW			Recent		Soil with sandy texture, composed of fine to medium quartzite sand, slightly silty, color brown with gray levels, medium compactness to very compact, slightly moist, low plasticity - SANDY TAILINGS.						8 22 (30 cm); 11 28 (30 cm); 12 35 (30 cm); 14 33 (30 cm); 13 35 (30 cm); 22 28 (17 cm); 9 21 (30 cm); 10 23 (30 cm); 10 23 (30 cm); 10 23 (30 cm); 10 26 (30 cm); 6 36 (30 cm); 8 28 (30 cm); 12 33 (30 cm)	(4) H4; (4) H3	

Responsible CREA Technician: Guilherme Freitas - No. 135337D

Remarks:

Legend: (4) "LEFRANC - Soil Infiltration - Permeability Test"

GEOTECHNICAL PROSPECTING

Geocontrole

Client: SAMARCO

Job: **Germano / Fundão EL940m - Dam Raising**

SOUNDING: **FUND-06**

Process: **11115**

Page: **2 of 2**

Start Date	Equipment	Final Depth (m)	System	Coordinates		Elevation	Sounder	Technician
16/6/2015	GEO104-Domine Futuro	19,45	UTM 23K	E= 660838,77	N= 7764979,83	Z= 873,81	Ricardo Henrique	Guilherme Freitas
End Date	Water Table	Slope						
18/6/2015	4,40m	90°						

DEPTH (m)	BOREHOLE Ø	CASING Ø	MANEUVER	STRATIGRAPHY	SYMBOLOGY	LITHOGRAPHIC DESCRIPTION	CHANGE	FRACTURING	RESISTANCE	% RECOV.	% R.Q.D.	S.P.T. 1st phase [illegible] 2nd phase [illegible] No. of Blows (Nspf)	TESTS	DEPTH (m)
16	B W			Recent		Soil with sandy texture, composed of fine to medium quartzite sand, slightly silty, color brown with gray levels, medium compactness to very compact, slightly moist, low plasticity - SANDY TAILINGS.	A1 A2 A3 A4	F1 F2 F3 F4	20 40 60 80	20 40 60 80	10 20 30 40	10 40 (30 cm) 13 37 (30 cm) 16 37 (30 cm) 14 36 (30 cm) 15 35 (30 cm)	(4) H3	16
17														17
18														18
19						19.45m- End of Sounding									19
20														20
21														21
22														22
23														23
24														24
25														25
26														26
27														27
28														28
29														29
30														30

Responsible CREA Technician: Guilherme Freitas - No. 135337D

Remarks:

Legend: (4) "LEFRANC - Soil Infiltration - Permeability Test"

Rua Vancouver, 66 - Jardim Canadá - 34000-000 Nova Lima Telephone: (31) 3517-9011 E-mail: mail@geocontrole.com

Sounding performed according to Standard NBR 6484/2001 - Sounding performed according to ABGE bulletin No. 3

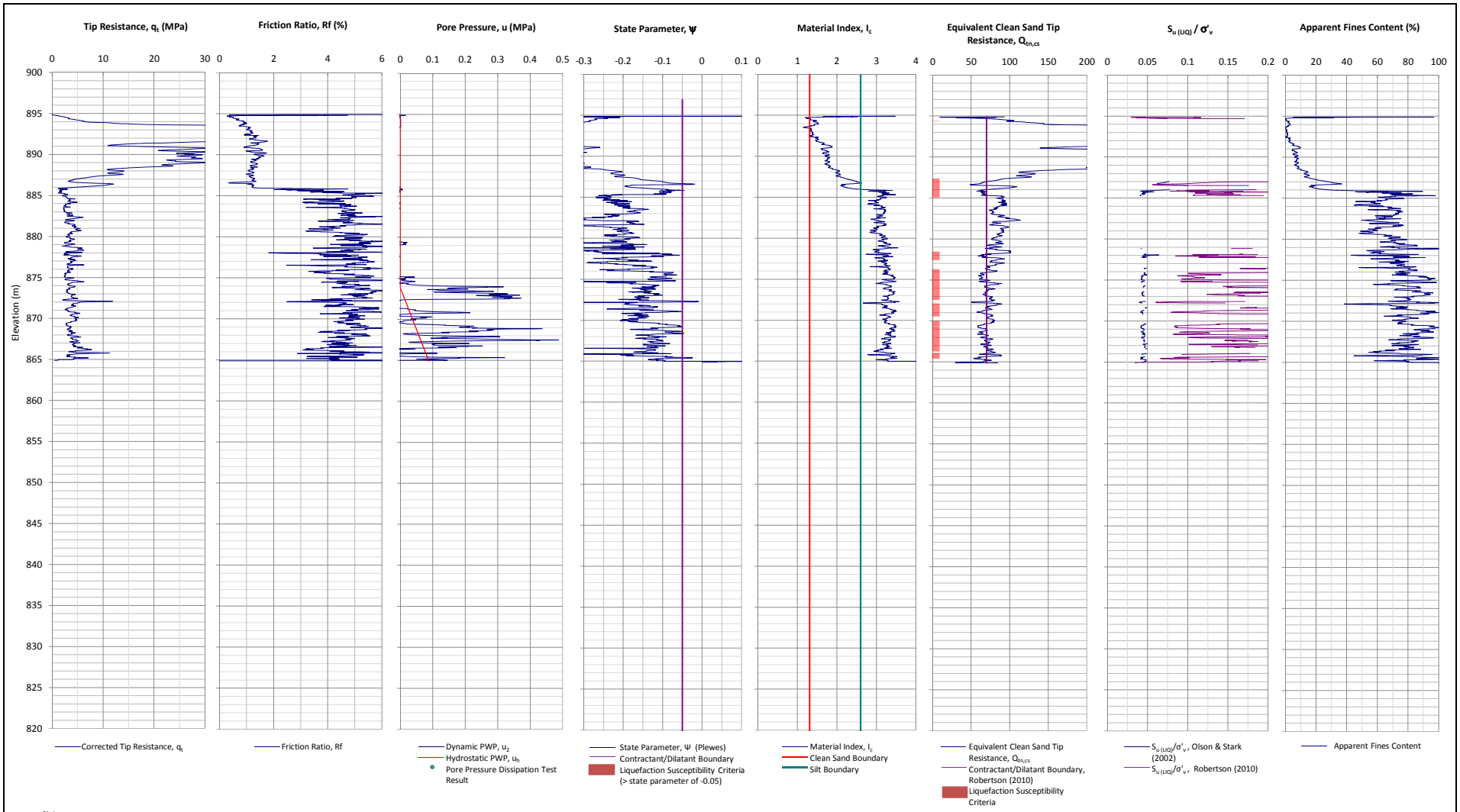

Notes:

1. This interpretation is based on the water and soil saturated unit weights γ_w=9.807 kN/m^3 and γ_{sat}=22 kN/m^3.
2. The friction ratio Rf is calculated as Rf=f_s/q_t.
3. The hydrostatic pore pressure is calculated using the ground water level (GWL) determined from CPT pore pressure dissipation tests (where available) or dynamic pore pressure.
4. Soil boundary layers (where plotted) are based on KCB interpretation.
5. The data presented have been plotted to the axis limits. Data may exist beyond the axis limits shown.
6. The Material Index (I_c) boundaries are based on Robertson and Wride (1998).
7. The $Q_{tn,cs}$ contractant/dilatant boundary=70 and is based on Robertson (2010).
8. The State Parameter (Ψ) is calculated using Plewes, et al. (1992) assuming a K0 of 0.5.
9. Coordinates are in UTM Zone 23K Córrego Alegre.

PROJECT: Fundão Tailings Dam Review Panel

TITLE:

Fugro (June 2015) - Dike 1
CONE PENETRATION TEST FUND-07
N:7765099m E:660826m 2015-06-10

Liquefaction susceptibility after Robertson (2010) "Evaluation of Flow Liquefaction and Liquefied Strength Using the Cone Penetration Test"	Liquefaction susceptibility after Olson & Stark (2003) "Yield Strength Ratio and Liquefaction Analysis of Slopes and Embankments"	State parameter approximation - Robertson (2009) "Interpretation of cone penetration tests - a unified approach"

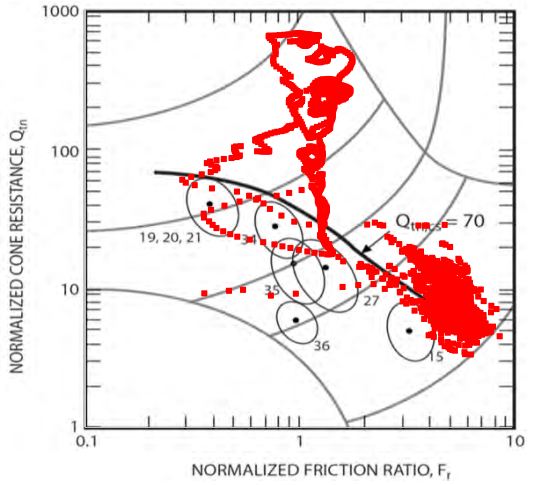

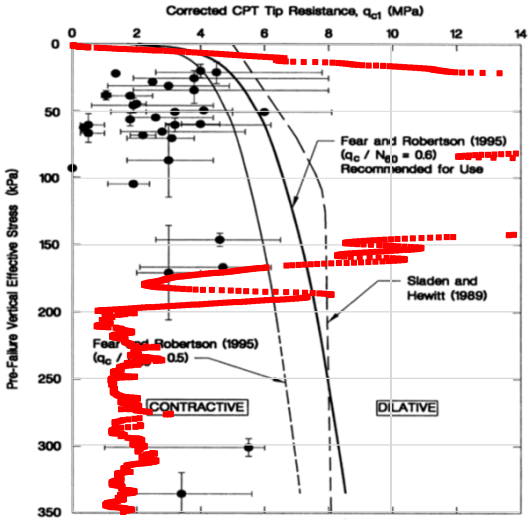

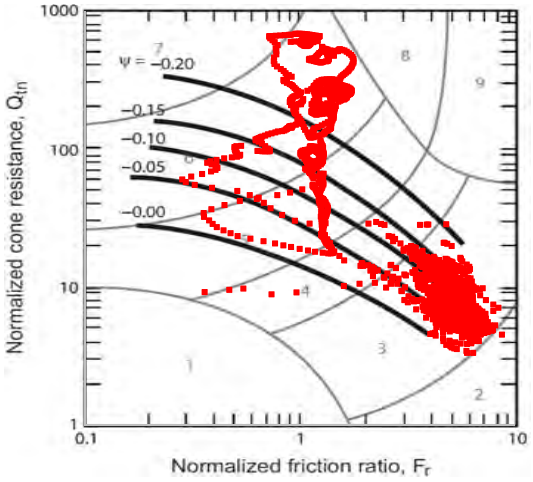

NOTE:

PROJECT

Fundão Tailings Dam Review Panel

TITLE

Fugro (June 2015) - Dike 1
FUND-07 Liquefaction Susceptibility and Soil Behavior Type

GEOTECHNICAL PROSPECTING

Geocontrole

Client: SAMARCO

Job: **Germano / Fundão EL940m - Dam Raising**

SOUNDING: **FUND-07**

Process: **11115**

Page: 1 of 2

Start Date	Equipment	Final Depth (m)	End Date	Water Table	Slope	System	Coordinates	Elevation	Sounder	Technician
25/6/2015	GEO106-Beretta T44	28.09	26/6/2015	20.70	90°	UTM 23K	E= 660824,28 N= 7765100,61	Z= 894,91	João Paulo	Guilherme Freitas

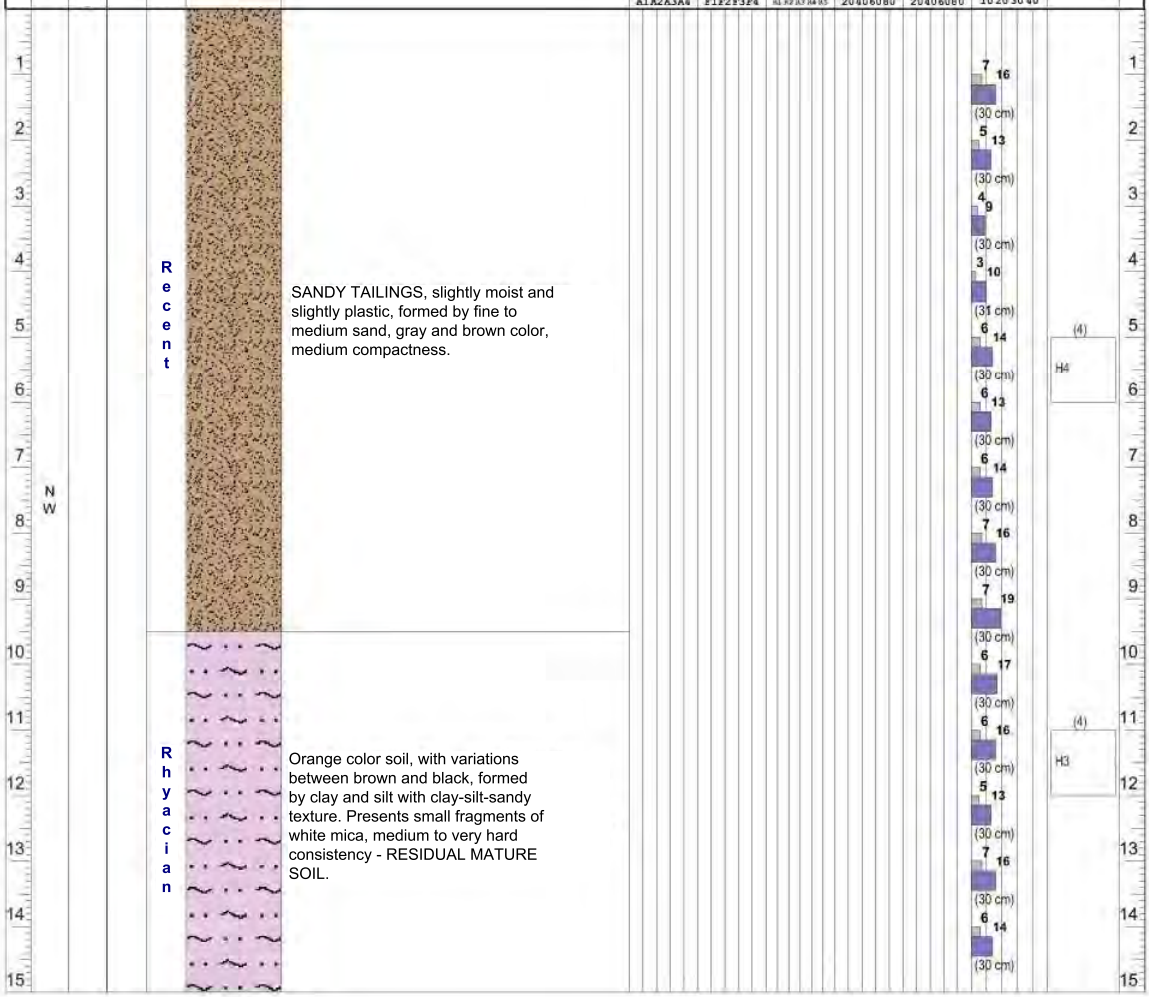

Responsible CREA Technician: Guilherme Freitas - No. 135337D

Remarks:

Legend: (4) "LEFRANC - Soil Infiltration - Permeability Test"

GEOTECHNICAL PROSPECTING

Geocontrole

Client: SAMARCO

Job: **Germano / Fundão EL940m - Dam Raising**

SOUNDING: **FUND-07**

Process: **11115**

Page: **2 of 2**

Start Date	Equipment	Final Depth (m)	End Date	Water Table	Slope	System	Coordinates	Elevation	Sounder	Technician
25/6/2015	GEO106-Beretta T44	28.09	26/6/2015	20.70	90°	UTM 23K	E= 660824,28 N= 7765100,61	Z= 894,91	João Paulo	Guilherme Freitas

DEPTH (m)	BOREHOLE Ø	CASING Ø	MANEUVER	STRATIGRAPHY	SYMBOLOGY	LITHOGRAPHIC DESCRIPTION	CHANGE	FRACTURING	RESISTANCE	% RECOV.	% R.Q.D.	S.P.T. No. of Blows (Nspf)	TESTS	DEPTH (m)
16	NW			Rhyacian		SANDY TAILINGS, slightly moist and slightly plastic, formed by fine to medium sand, gray and brown color, medium compactness.	A1 A2 A3 A4	F1 F2 F3 F4		20 40 60 80	20 40 60 80	10 20 30 40		16
17												19 (30 cm)		17
18												18 (30 cm)		18
19												19 (30 cm)	(4) H2	19
20												21 (30 cm)		20
21												26 (30 cm)		21
22												32 (30 cm)		22
23												35 (30 cm)		23
24												34 (30 cm)	(4) H2	24
25												34 (26 cm)		25
26						Extremely altered rock and extremely soft, with clay-silt matrix and relic foliation sections - SCHIST SAPROLITE.	A5					32 (24 cm)		26
27												28 (16 cm)		27
28						28.09m- End of Sounding						30 (9 cm)		28
29												(9 cm)		29
30														30

1st phase [illegible]
2nd phase [illegible]

Responsible CREA Technician: Guilherme Freitas - No. 135337D

Remarks:

Legend: (4) "LEFRANC - Soil Infiltration - Permeability Test"

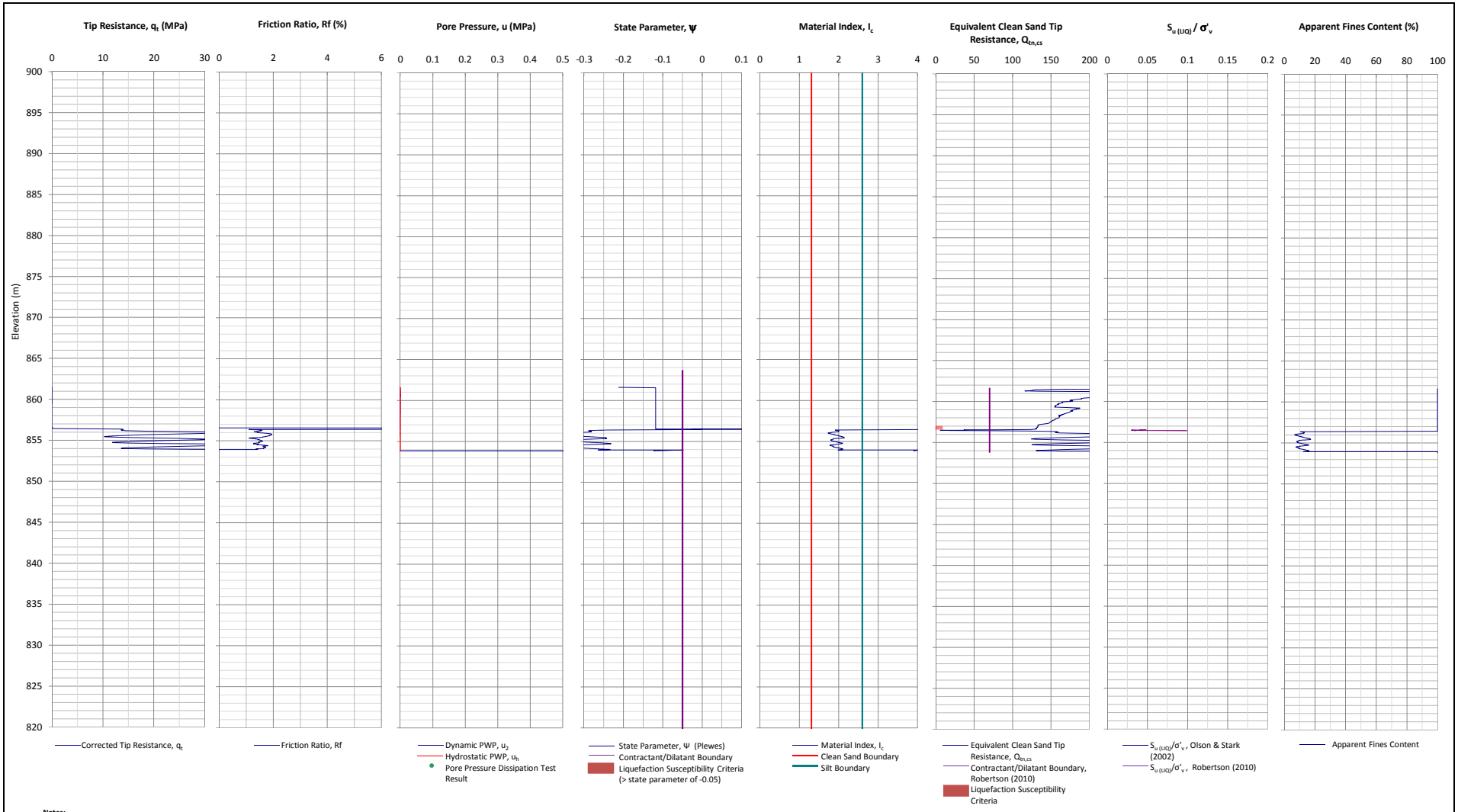

Notes:

1. This interpretation is based on the water and soil saturated unit weights γ_w=9.807 kN/m^3 and γ_{sat}=22 kN/m^3.
2. The friction ratio Rf is calculated as Rf=f_s/q_t.
3. The hydrostatic pore pressure is calculated using the ground water level (GWL) determined from CPT pore pressure dissipation tests (where available) or dynamic pore pressure.
4. Soil boundary layers (where plotted) are based on KCB interpretation.
5. The data presented have been plotted to the axis limits. Data may exist beyond the axis limits shown.
6. The Material Index (I_c) boundaries are based on Robertson and Wride (1998).
7. The $Q_{tn,cs}$ contractant/dilatant boundary=70 and is based on Robertson (2010).
8. The State Parameter (Ψ) is calculated using Plewes, et al. (1992) assuming a K0 of 0.5.
9. Coordinates are in UTM Zone 23K Córrego Alegre.

PROJECT: Fundão Tailings Dam Review Panel

TITLE: Fugro (June 2015) - Dike 1
CONE PENETRATION TEST FUND-15A
N:7764808m E:660826m 2015-06-09

Liquefaction susceptibility after Robertson (2010) "Evaluation of Flow Liquefaction and Liquefied Strength Using the Cone Penetration Test"	Liquefaction susceptibility after Olson & Stark (2003) "Yield Strength Ratio and Liquefaction Analysis of Slopes and Embankments"	State parameter approximation - Robertson (2009) "Interpretation of cone penetration tests - a unified approach"

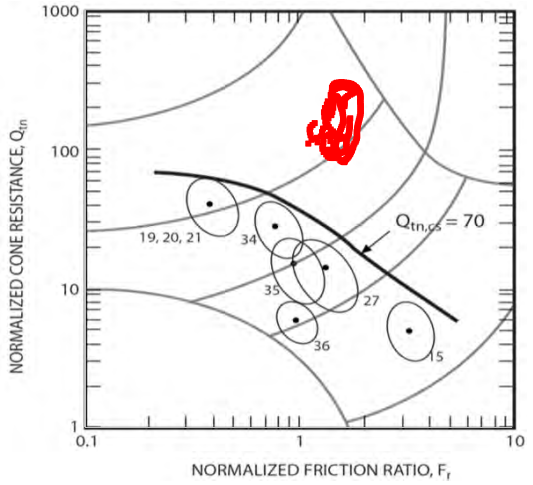

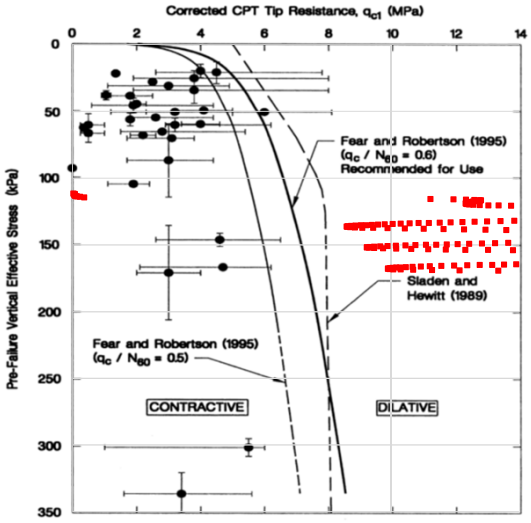

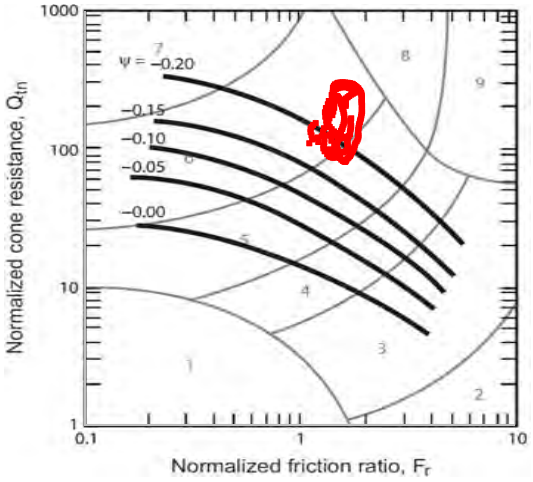

NOTE:

PROJECT

Fundão Tailings Dam Review Panel

TITLE

Fugro (June 2015) - Dike 1
FUND-15A Liquefaction Susceptibility and Soil Behavior Type

GEOTECHNICAL PROSPECTING

SOUNDING: **FUND-15**

Process: **11115**

Client: SAMARCO

Job: **Germano / Fundão EL940m - Dam Raising**

Page: 1 of 2

Start Date	Equipment	Final Depth (m)
15/6/2015	GEO106-Beretta T44	23.26

End Date	Water Table	Slope	System	Coordinates		Elevation	Sounder	Technician
16/6/2015	Dry	90°	UTM 23K	E= 660859,80	N= 7764807,52	Z= 861,62	João Paulo	Guilherme Freitas

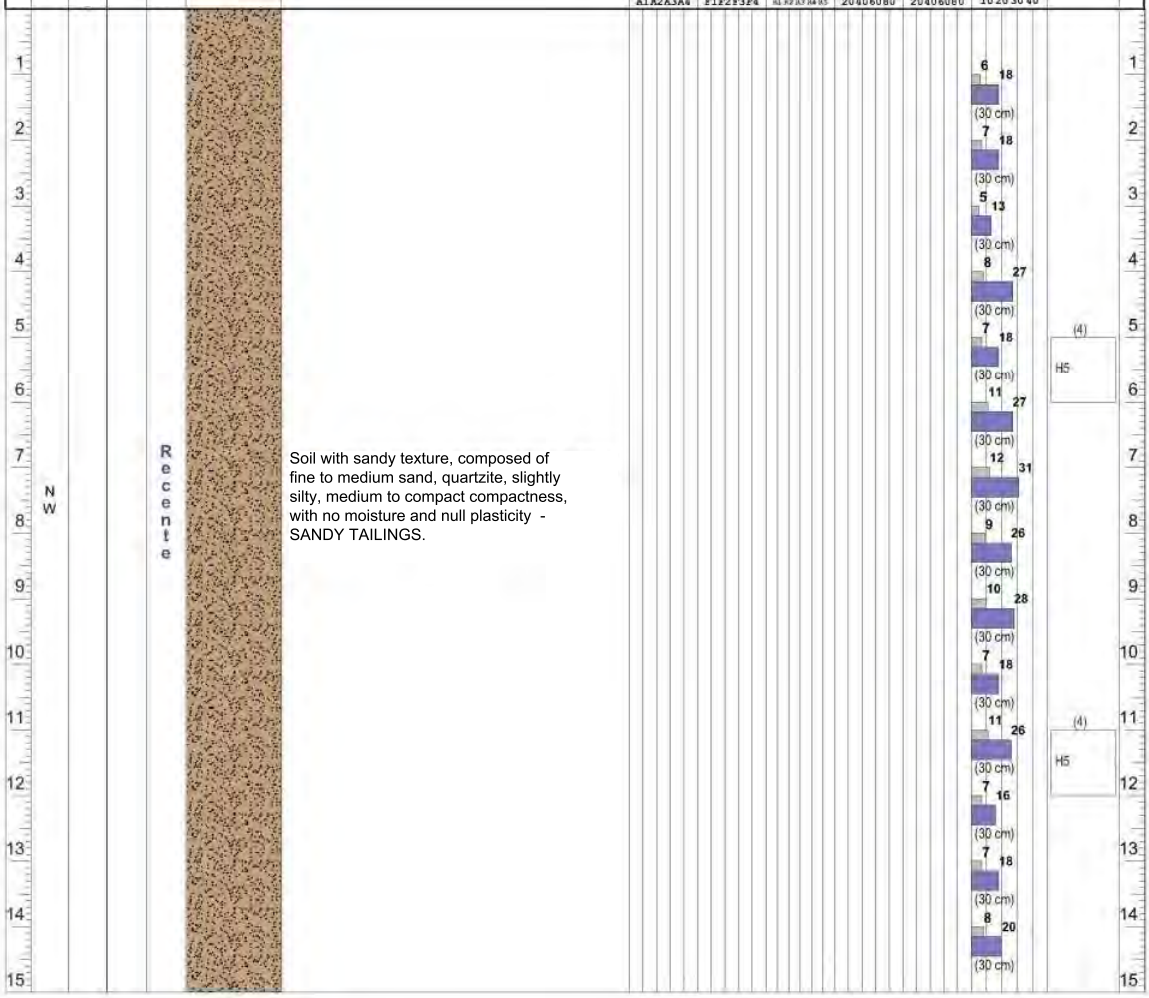

Responsible CREA Technician: Guilherme Freitas - No. 135337D

Remarks:

Legend: (4) "LEFRANC - Soil Infiltration - Permeability Test"

GEOTECHNICAL PROSPECTING

SOUNDING: FUND-15

Process: 11115

Page: 2 of 2

Client: SAMARCO

Job: Germano / Fundão EL940m - Dam Raising

Start Date	Equipment	Final Depth (m)	End Date	Water Table	Slope	System	Coordinates	Elevation	Sounder	Technician
15/6/2015	GEO106-Beretta T44	23.26	16/6/2015	Dry	90°	UTM 23K	E= 660859,80 N= 7764807,52	Z= 861,62	João Paulo	Guilherme Freitas

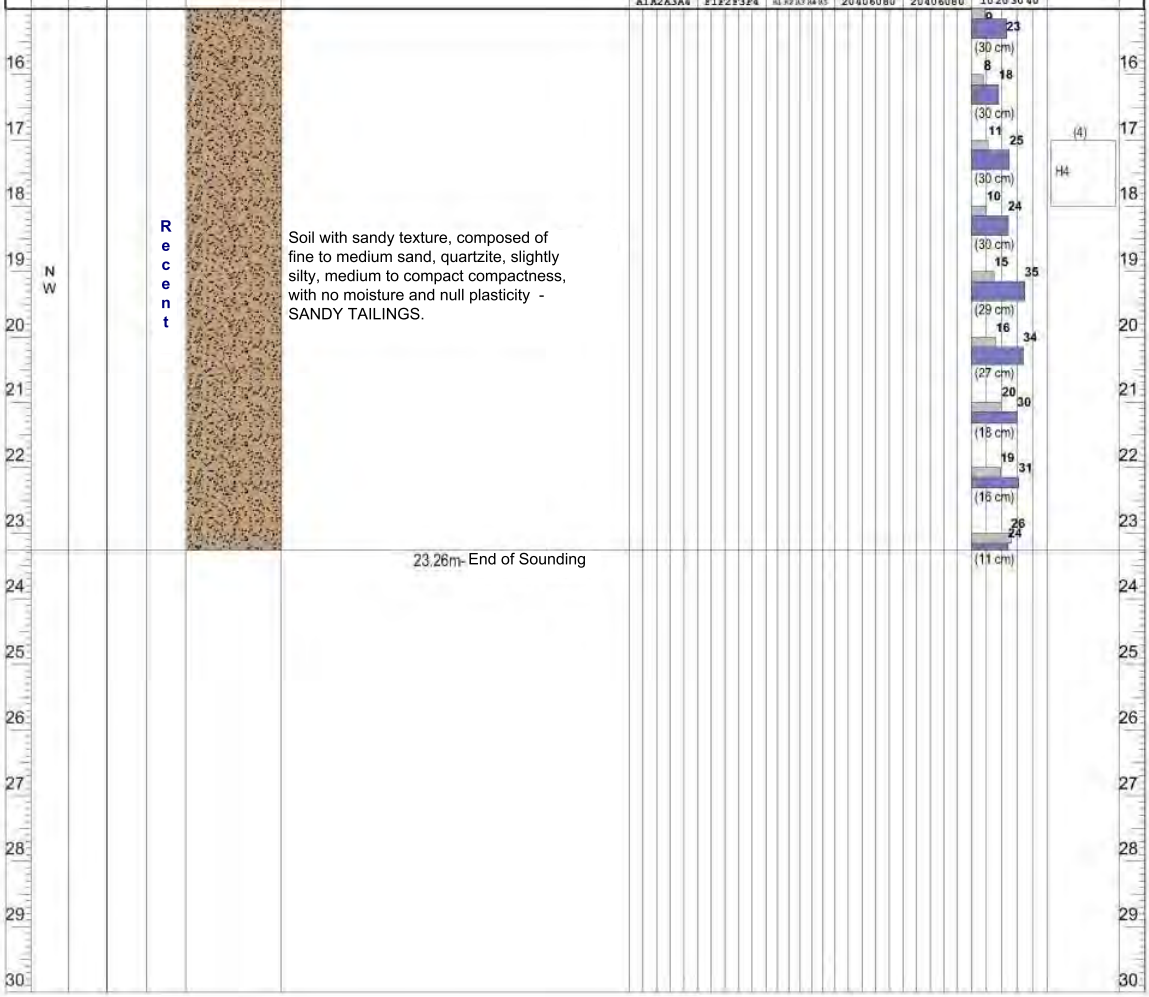

Responsible CREA Technician: Guilherme Freitas - No. 135337D

Remarks:

Legend: (4) "LEFRANC - Soil Infiltration - Permeability Test"

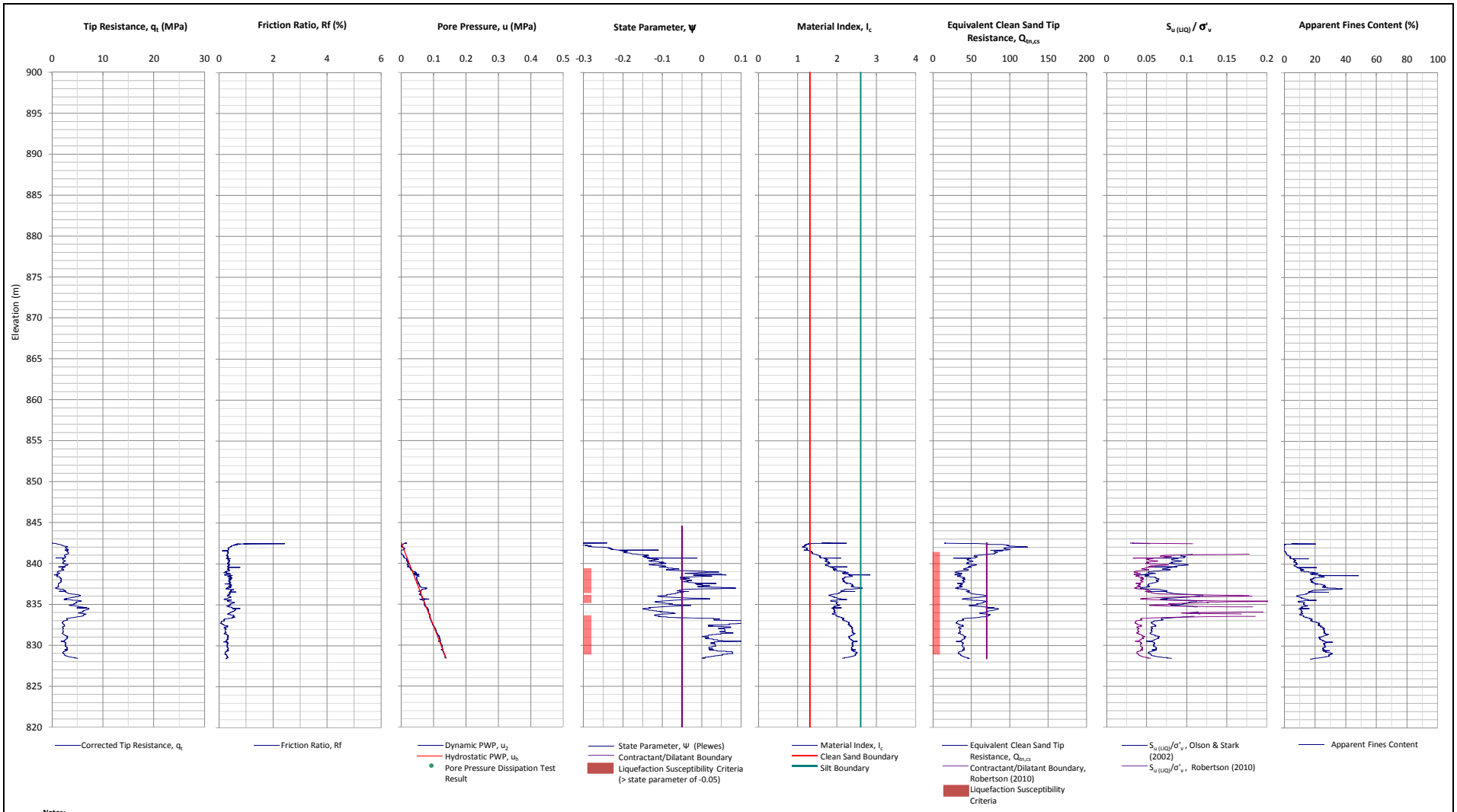

Notes:

1. This interpretation is based on the water and soil saturated unit weights γ_w=9.807 kN/m^3 and γ_{sat}=22 kN/m^3.
2. The friction ratio Rf is calculated as Rf=f_s/q_t.
3. The hydrostatic pore pressure is calculated using the ground water level (GWL) determined from CPT pore pressure dissipation tests (where available) or dynamic pore pressure.
4. Soil boundary layers (where plotted) are based on KCB interpretation.
5. The data presented have been plotted to the axis limits. Data may exist beyond the axis limits shown.
6. The Material Index (I_c) boundaries are based on Robertson and Wride (1998).
7. The $Q_{tn,cs}$ contractant/dilatant boundary=70 and is based on Robertson (2010).
8. The State Parameter (Ψ) is calculated using Plewes, et al. (1992) assuming a K0 of 0.5.
9. Coordinates are in UTM Zone 23K Córrego Alegre.

PROJECT: Fundão Tailings Dam Review Panel

TITLE: Fugro (June 2015) - Dike 1
CONE PENETRATION TEST FUND-15B
N:7764735m E:660914m 2015-06-09

Liquefaction susceptibility after Robertson (2010) "Evaluation of Flow Liquefaction and Liquefied Strength Using the Cone Penetration Test"	Liquefaction susceptibility after Olson & Stark (2003) "Yield Strength Ratio and Liquefaction Analysis of Slopes and Embankments"	State parameter approximation - Robertson (2009) "Interpretation of cone penetration tests - a unified approach"

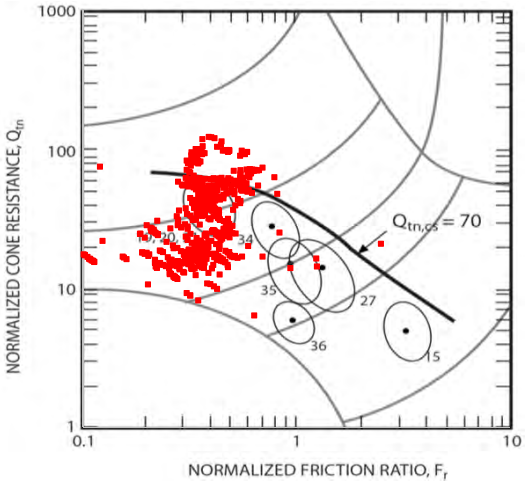

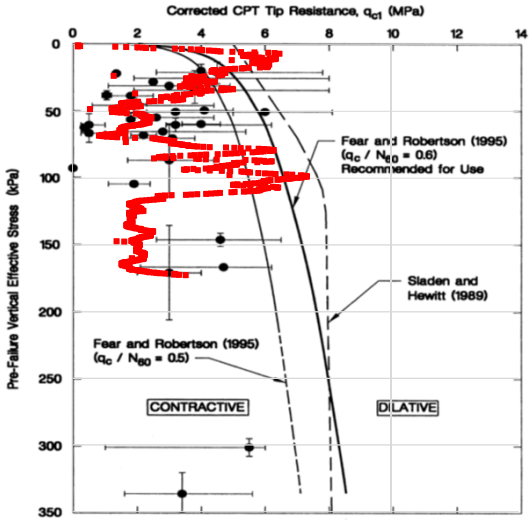

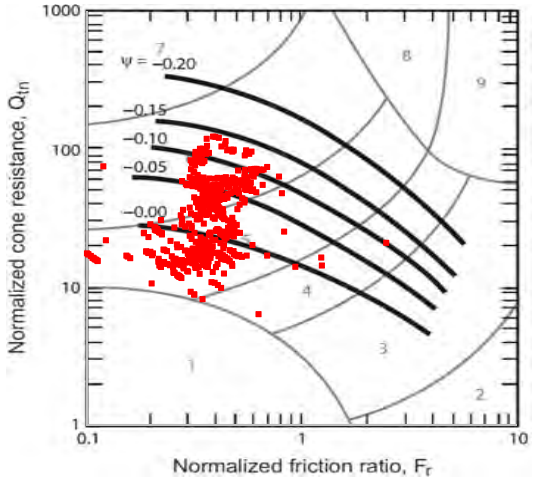

NOTE:

PROJECT

Fundão Tailings Dam Review Panel

TITLE

Fugro (June 2015) - Dike 1
FUND-15B Liquefaction Susceptibility and Soil Behavior Type

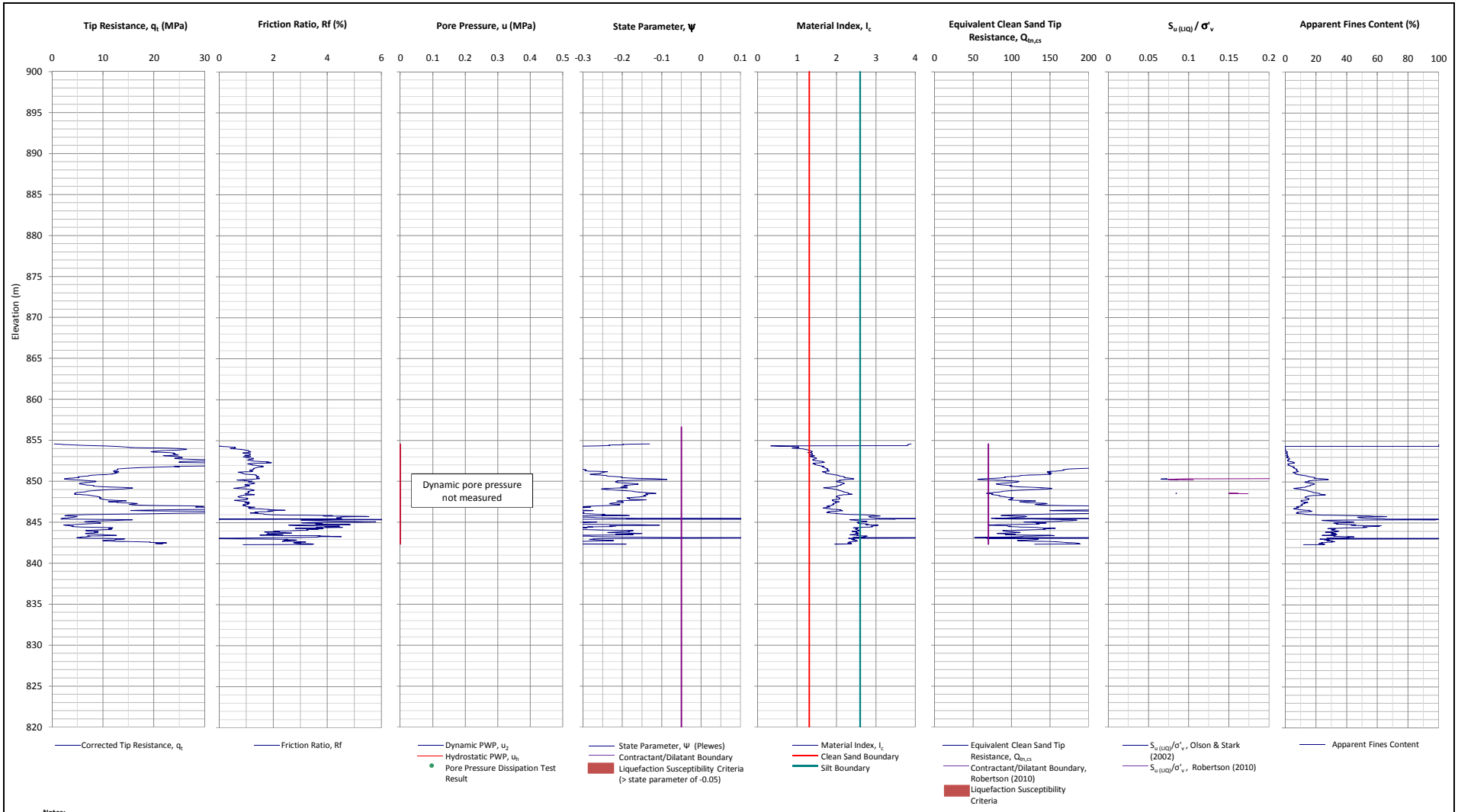

Notes:

1. This interpretation is based on the water and soil saturated unit weights γ_w=9.807 kN/m^3 and γ_{sat}=22 kN/m^3.
2. The friction ratio Rf is calculated as Rf=f_s/q_t.
3. The hydrostatic pore pressure is calculated using the ground water level (GWL) determined from CPT pore pressure dissipation tests (where available) or dynamic pore pressure.
4. Soil boundary layers (where plotted) are based on KCB interpretation.
5. The data presented have been plotted to the axis limits. Data may exist beyond the axis limits shown.
6. The Material Index (I_c) boundaries are based on Robertson and Wride (1998).
7. The $Q_{tn,cs}$ contractant/dilatant boundary=70 and is based on Robertson (2010).
8. The State Parameter (Ψ) is calculated using Plewes, et al. (1992) assuming a K0 of 0.5.
9. Coordinates are in UTM Zone 23K Córrego Alegre.

PROJECT: Fundão Tailings Dam Review Panel

TITLE: Fugro (June 2015) - Dike 1
CONE PENETRATION TEST FUND-16
N:7764821m E:660955m 2015-06-18

Liquefaction susceptibility after Robertson (2010) "Evaluation of Flow Liquefaction and Liquefied Strength Using the Cone Penetration Test"	Liquefaction susceptibility after Olson & Stark (2003) "Yield Strength Ratio and Liquefaction Analysis of Slopes and Embankments"	State parameter approximation - Robertson (2009) "Interpretation of cone penetration tests - a unified approach"

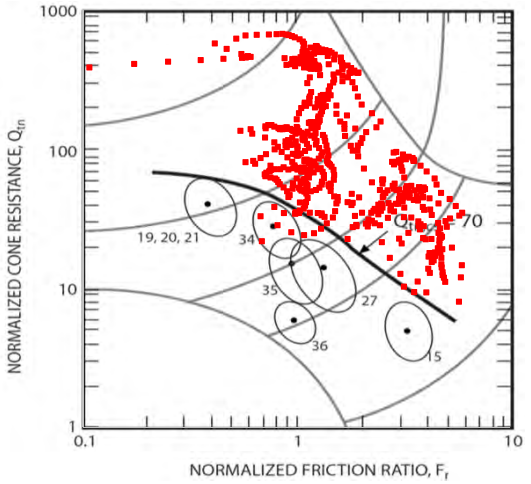

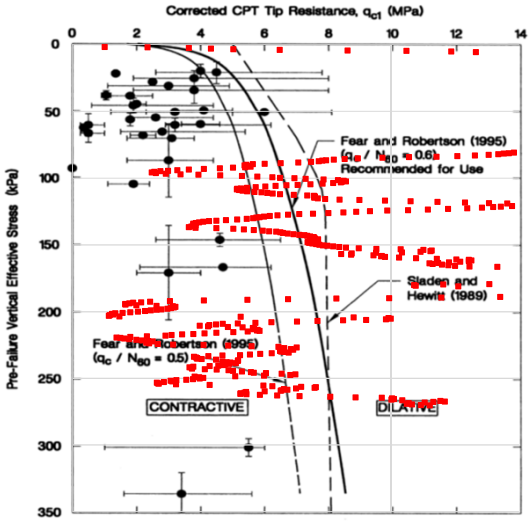

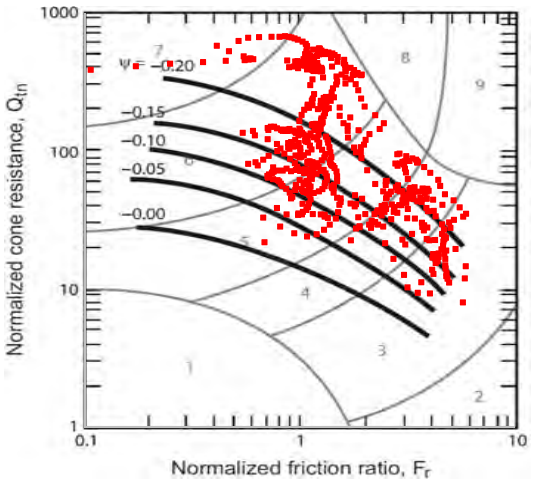

NOTE:

PROJECT

Fundão Tailings Dam Review Panel

TITLE

Fugro (June 2015) - Dike 1
FUND-16 Liquefaction Susceptibility and Soil Behavior Type

GEOTECHNICAL PROSPECTING

SOUNDING: FUND-16

Process: 11115

Page: 1 of 1

Client: SAMARCO

Job: Germano / Fundão EL940m - Dam Raising

Start Date	Equipment	Final Depth (m)
22/6/2015	GEO104-Domine Futuro	15.25

End Date	Water Table	Slope	System	Coordinates		Elevation	Sounder	Technician
23/6/2015	Dry	90°	UTM 23K	E= 660955,77	N= 7764824,06	Z= 854,70	Ricardo Henrique	Guilherme Freitas

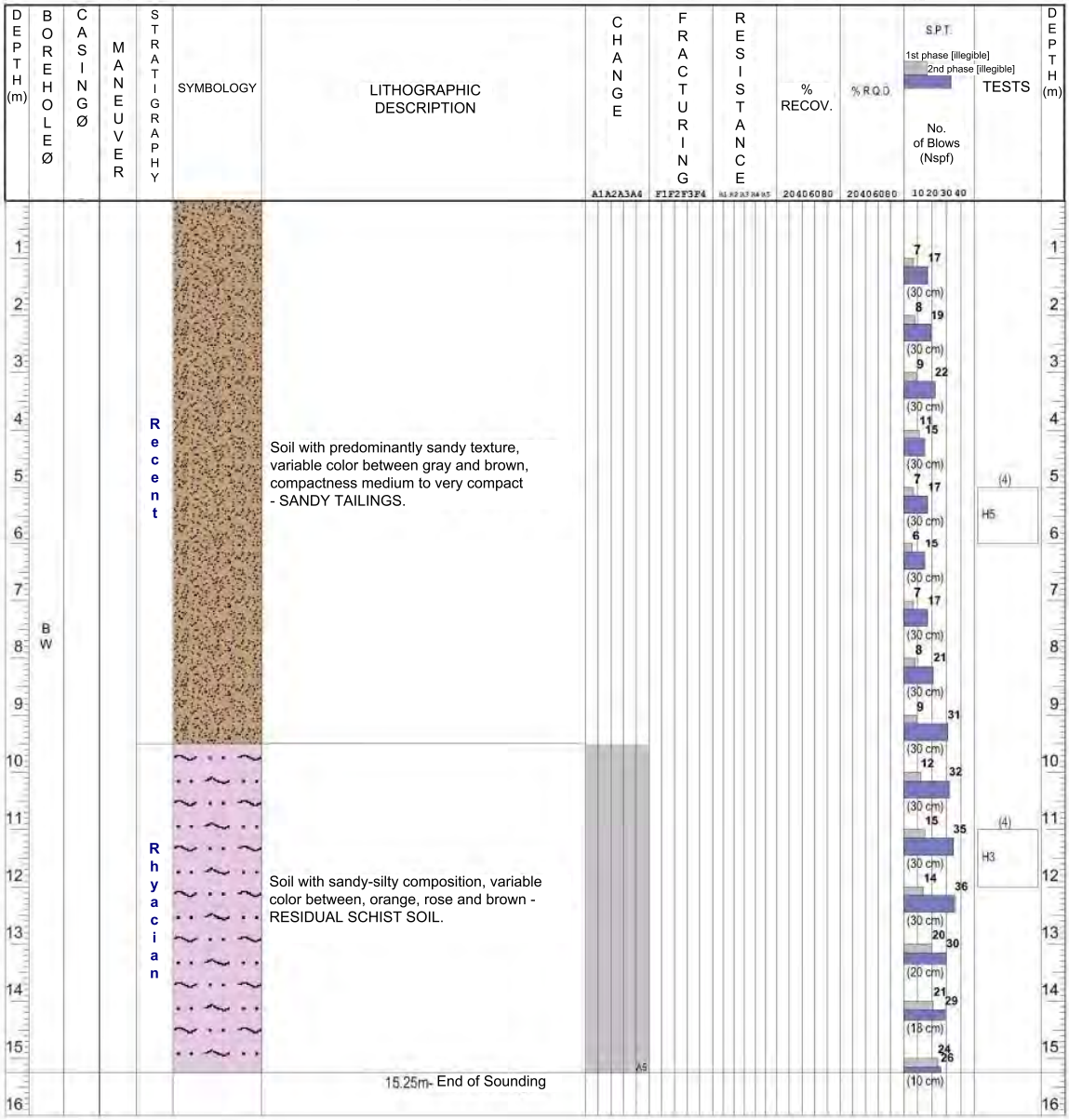

Responsible CREA Technician: Guilherme Freitas - No. 135337D

Remarks:

Legend: (4) "LEFRANC - Soil Infiltration - Permeability Test"

GEOTECHNICAL PROSPECTING

SOUNDING: SPBF01

Process: 11115

Client: SAMARCO

Job: Germano / Fundão EL940m - Dam Raising

Page: 1 of 2

Start Date	Equipment	Final Depth (m)	End Date	Water Table	Slope	System	Coordinates	Elevation	Sounder	Technician
11/6/2015	GEO104-Domine Futuro	28.1	15/6/2015	10.70m	90°	UTM 23K	E= 660769,99 N= 7764548,03	Z= 820,251	Ricardo Henrique	Guilherme Freitas

DEPTH (m)	BOREHOLE Ø	CASING Ø	MANEUVER	STRATIGRAPHY	SYMBOLOGY	LITHOGRAPHIC DESCRIPTION	CHANGE	FRACTURING	RESISTANCE	% RECOV.	% R.Q.D.	S.P.T. 1st phase [illegible] 2nd phase [illegible] No. of Blows (Nspf)	TESTS	DEPTH (m)
0							A1 A2 A3 A4	F1 F2 F3 F4		20 40 60 80	20 40 60 80	10 20 30 40		0
1				Recent		Soil with clay-silt-sandy composition, brown color, presenting limonite and quartz granules and iron formation, medium to stiff consistency - COLLUVIUM.						8 20 (30 cm)		1
2												7 19 (30 cm)		2
3												8 19 (30 cm)		3
4												9 22 (30 cm)		4
5												7 17 (30 cm)	(4) H3	5
6												8 17 (30 cm)		6
7												7 16 (30 cm)		7
8	BW											6 18 (30 cm)		8
9				Rhyacian		Soil with clay-silt composition, reddish-orange color, variable consistency between medium and stiff, medium moisture and high plasticity - MATURE RESIDUAL SOIL.						7 23 (30 cm)		9
10												9 23 (30 cm)		10
11												11 23 (30 cm)	(4) H2	11
12												9 25 (30 cm)		12
13												10 23 (30 cm)		13
14												13 31 (30 cm)		14
15														15

Responsible CREA Technician: Guilherme Freitas - No. 135337D

Remarks:

Legend: (4) "LEFRANC - Soil Infiltration - Permeability Test"

Rua Vancouver, 66 - Jardim Canadá - 34000-000 Nova Lima Telephone: (31) 3517-9011 E-mail: mail@geocontrole.com

Sounding performed according to Standard NBR 6484/2001 - Sounding performed according to ABGE bulletin No. 3

GEOTECHNICAL PROSPECTING

Geocontrole

Client: SAMARCO

Job: **Germano / Fundão EL940m - Dam Raising**

SOUNDING: **SPBF01**

Process: **11115**

Page: **2 of 2**

Start Date	Equipment	Final Depth (m)	End Date	Water Table	Slope	System	Coordinates	Elevation	Sounder	Technician
11/6/2015	GEO104-Domine Futuro	28.1	15/6/2015	10.70m	90°	UTM 23K	E= 660769,99 N= 7764548,03	Z= 820,251	Ricardo Henrique	Guilherme Freitas

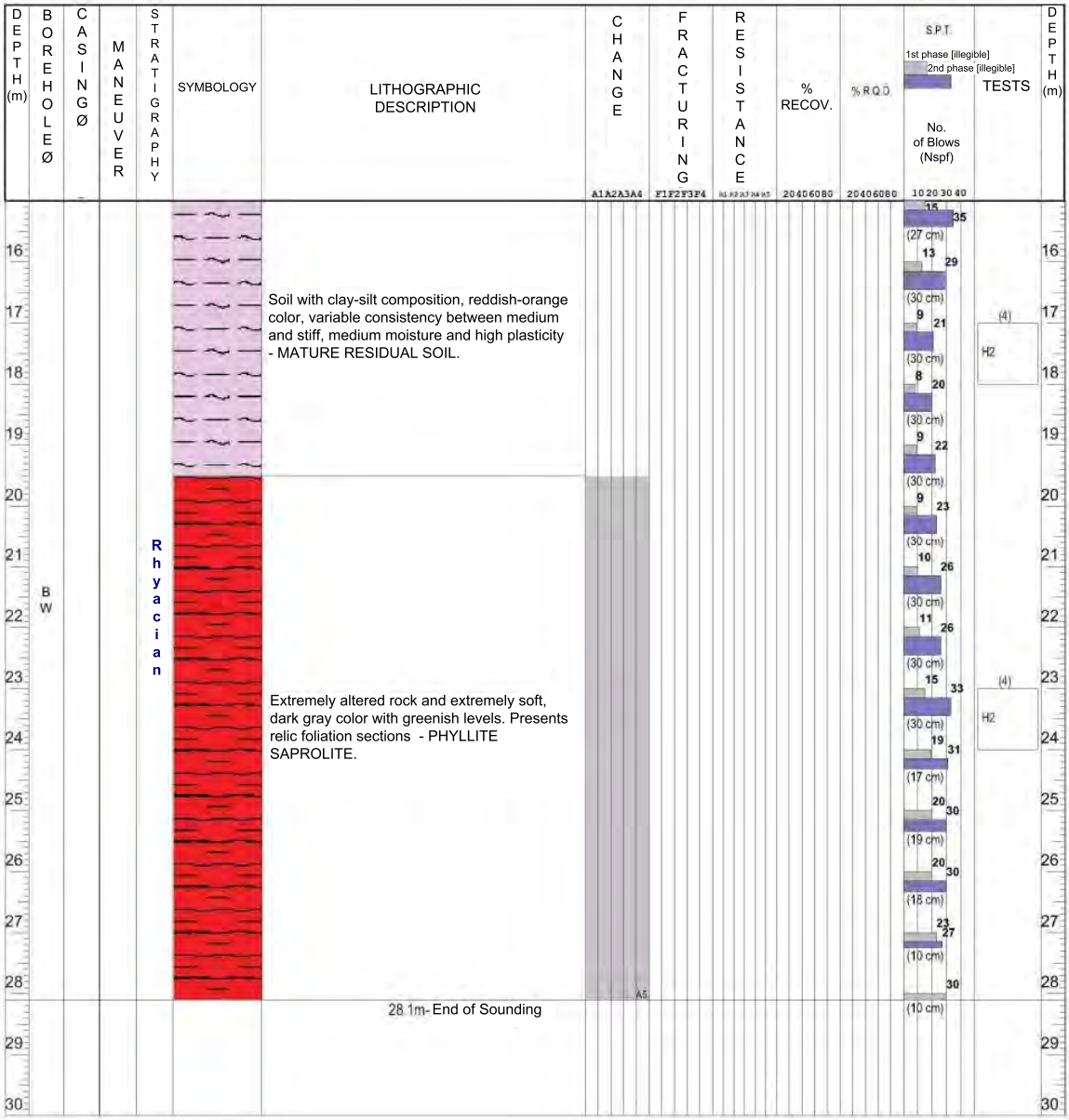

Responsible CREA Technician: Guilherme Freitas - No. 135337D

Remarks:

Legend: (4) "LEFRANC - Soil Infiltration - Permeability Test"

GEOTECHNICAL PROSPECTING

Geocontrole

Client: SAMARCO

Job: **Germano / Fundão EL940m - Dam Raising**

SOUNDING: **SPBF-02**

Process: **11115**

Page: **1 of 2**

Start Date	Equipment	Final Depth (m)	End Date	Water Table	Slope	System	Coordinates	Elevation	Sounder	Technician
10/6/2015	GEO104-Domine Futuro	16.36	11/6/2015	15.30m	90°	UTM 23K	E= 660858,18 N= 7764613,77	Z= 820,121	Ricardo Henrique	Guilherme Freitas

DEPTH (m)	BOREHOLE Ø	CASING Ø	MANEUVER	STRATIGRAPHY	SYMBOLOGY	LITHOGRAPHIC DESCRIPTION	CHANGE A1 A2 A3 A4	FRACTURING F1 F2 F3 F4	RESISTANCE	% RECOV. 20 40 60 80	% R.Q.D. 20 40 60 80	S.P.T. 1st phase [illegible] 2nd phase [illegible] No. of Blows (Nspf) 10 20 30 40	TESTS	DEPTH (m)
1	B W			Recent		Soil with clay-silt-sandy composition, variable consistency between low to compact, variable color between gray, ochre and brown tones. Presents misaligned arrangement, small fragments of phyllite and quartz granules and iron ore formation - CLAY-SILTY FILL.						6 15 (30 cm)		1
2												5 12 (30 cm)		2
3												4 10 (30 cm)		3
4												4 11 (30 cm)		4
5												6 15 (30 cm)	(4) H3	5
6												8 20 (30 cm)		6
7												8 21 (30 cm)		7
8												9 21 (30 cm)		8
9												8 22 (30 cm)		9
10												9 22 (30 cm)		10
11												12 35 (30 cm)	(4) H3	11
12												15 35 (29 cm)		12
13												14 36 (28 cm)		13
14												15 35 (30 cm)		14
15														15

Responsible CREA Technician: Guilherme Freitas - No. 135337D

Remarks:

Legend: (4) "LEFRANC - Soil Infiltration - Permeability Test"

GEOTECHNICAL PROSPECTING

SOUNDING: SPBF-02

Process: 11115

Client: SAMARCO

Job: Germano / Fundão EL940m - Dam Raising

Page: 2 of 2

Start Date	Equipment	Final Depth (m)	End Date	Water Table	Slope	System	Coordinates	Elevation	Sounder	Technician
10/6/2015	GEO104-Domine Futuro	16.36	11/6/2015	15.30m	90°	UTM 23K	E= 660858,18 N= 7764613,77	Z= 820,121	Ricardo Henrique	Guilherme Freitas

DEPTH (m)	BOREHOLE Ø	CASING Ø	MANEUVER	STRATIGRAPHY	SYMBOLOGY	LITHOGRAPHIC DESCRIPTION	CHANGE A1 A2 A3 A4	FRACTURING F1 F2 F3 F4	RESISTANCE	% RECOV. 20 40 60 80	% R.Q.D. 20 40 60 80	S.P.T. 1st phase [illegible] 2nd phase [illegible] No. of Blows (Nspf) 10 20 30 40	TESTS	DEPTH (m)
16	B W			Recent		Very compact CLAY-SILTY FILL.						10 40 (29 cm)		16
						16.36m- End of Sounding						16 34 (21 cm)		
17														17
18														18
19														19
20														20
21														21
22														22
23														23
24														24
25														25
26														26
27														27
28														28
29														29
30														30

Responsible CREA Technician: Guilherme Freitas - No. 135337D

Remarks:

Rua Vancouver, 66 - Jardim Canadá - 34000-000 Nova Lima Telephone: (31) 3517-9011 E-mail: mail@geocontrole.com

Sounding performed according to Standard NBR 6484/2001 - Sounding performed according to ABGE bulletin No. 3

ATTACHMENT C2

ConeTec Field Report

PRESENTATION OF SITE INVESTIGATION RESULTS

Samarco Mine

Prepared for:

Cleary Gottlieb Steen & Hamilton LLP (CGSH)

ConeTec Job No: 16-72004

Project Start Date: 19-APR-2016
Project End Date: 27-MAY-2016
Report Date: 16-JUN-2016

Prepared by:

ConeTec Perú S.A.C.
Av. General Córdova 313, Miraflores
Lima, Perú

Tel: +51 (1) 719-2404

Email: ConeTecSA@conetec.com
www.conetec.com
www.conetecdataservices.com

CONETEC

Introduction

The enclosed report presents the results of the site investigation program conducted by ConeTec Peru S.A.C. for Cleary Gottlieb Steen & Hamilton LLP (CGSH) at Samarco Mine near the district of Bento Rodriguez in Brazil. The program consisted of 10 resistivity seismic cone penetration test (RSCPT) locations, 1 seismic cone penetration test location (SCPT), 2 electronic vane shear test profiles, 2 sample locations and 1 standard penetration test with energy measurement (SPTe).

Project Information

Project	
Client	Cleary Gottlieb Steen & Hamilton LLP (CGSH)
Project	Samarco Mine
ConeTec project number	16-72004

A map from Google earth including the test locations is presented below.

Rig Description	Deployment System	Test Type
Portable ramset	20 ton hydraulic ramset	RSCPT, SCPT
Pagani CPT rig	15 ton rig cylinder	RSCPT, SCPT
Boart Longyear LX6		Sampling, VST, SPTe

Coordinates		
Test Type	Collection Method	EPSG Number
RSCPT, SCPT, VST, SPTe, Sampling	Consumer-grade GPS	32723

Cone Penetration Test (CPT)	
Depth reference	Depths are referenced to the existing ground surface at the time of each test.
Tip and sleeve data offset	0.1 meter This has been accounted for in the CPT data files.
Plots	Standard, resistivity, seismic and advanced CPT plots with undrained shear strength (Su-Nkt) and phi angle are provided in the release folder.

Cone Penetrometer Used for this Project						
Cone Description	Cone Number	Cross Sectional Area (cm^2)	Sleeve Area (cm^2)	Tip Capacity (bar)	Sleeve Capacity (bar)	Pore Pressure Capacity (psi)
376:T375F10U200	376	15	225	375	10	200
432:T1500F15U500	432	15	225	1500	15	500
Cone 376 and 432 were used for the RSCPT/SCPT soundings.						

Interpretation Tables	
Additional information	The Soil Behaviour Type (SBT) classification chart (Robertson et al., 1986) was used to classify the soil for this project and divide the interpretation parameters into drained and undrained classifications. At this site, materials that classified as silt (zone 6) were deemed to be undrained. A detailed set of CPT interpretations were generated and are provided in Excel format files in the release folder. The CPT interpretations are based on values of corrected tip (q_t), sleeve friction (f_s) and pore pressure averaged over a user specified interval of 20 cm. Pore pressure equilibrium profiles were used for the interpretation tables.

Adjustments to the SBT Chart (Robertson et al., 1986 presented by Lunne, Robertson and Powell, 1997)					
Original SBT Settings			Revised SBT Settings		
Zone	Unit Weight	Zone Text	Zone	Unit Weight (kN/m^3)	Zone Text
0	18.64	Undefined	0	17.50	Undefined
1	17.50	Sensitive Fines	1	17.50	Fines
2	12.50	Organic Soil	2	17.50	Fines
Additional comments		Undrained parameters have been calculated for materials that classify as undefined (Zone 0).			

Electronic Field Vane Shear Test (VST)	
Depth reference	Depths are referenced to the existing ground surface at the time of each test.
Load cell capacity	100 Nm
Additional information	Peak and remolded shear strength value are presented unless otherwise noted in the results summary. Where appropriate, residual shear strength values are also presented. Residual, or post peak strength values are somewhat subjective. They should be used in conjunction with the shear stress-rotation records.

Sampling	
Depth reference	Existing ground surface at the time of sampling.
Sampling method	Sharky

Standard Penetration Test Energy (SPTe) Measurements	
Depth reference	Depths are referenced to the existing ground surface at the time of each test.

Limitations

This report has been prepared for the exclusive use of Cleary Gottlieb Steen & Hamilton LLP (CGSH) (Client) for the project titled “Samarco Mine”. The report’s contents may not be relied upon by any other party without the express written permission of ConeTec Peru S.A.C. (ConeTec). ConeTec has provided site investigation services, prepared the factual data reporting, and provided geotechnical parameter calculations consistent with current best practices. No other warranty, expressed or implied, is made.

The information presented in the report document and the accompanying data set pertain to the specific project, site conditions and objectives described to ConeTec by the Client. In order to properly understand the factual data, assumptions and calculations, reference must be made to the documents provided and their accompanying data sets, in their entirety.

The cone penetration tests (CPTu) are conducted using an integrated electronic piezocone penetrometer and data acquisition system manufactured by Adara Systems Ltd. of Richmond, British Columbia, Canada.

ConeTec's piezocone penetrometers are compression type designs in which the tip and friction sleeve load cells are independent and have separate load capacities. The piezocones use strain gauged load cells for tip and sleeve friction and a strain gauged diaphragm type transducer for recording pore pressure. The piezocones also have a platinum resistive temperature device (RTD) for monitoring the temperature of the sensors, an accelerometer type dual axis inclinometer and a geophone sensor for recording seismic signals. All signals are amplified down hole within the cone body and the analog signals are sent to the surface through a shielded cable.

ConeTec penetrometers are manufactured with various tip, friction and pore pressure capacities in both 10 cm^2 and 15 cm^2 tip base area configurations in order to maximize signal resolution for various soil conditions. The specific piezocone used for each test is described in the CPT summary table presented in the first Appendix. The 15 cm^2 penetrometers do not require friction reducers as they have a diameter larger than the deployment rods. The 10 cm^2 piezocones use a friction reducer consisting of a rod adapter extension behind the main cone body with an enlarged cross sectional area (typically 44 mm diameter over a length of 32 mm with tapered leading and trailing edges) located at a distance of 585 mm above the cone tip.

The penetrometers are designed with equal end area friction sleeves, a net end area ratio of 0.8 and cone tips with a 60 degree apex angle.

All ConeTec piezocones can record pore pressure at various locations. Unless otherwise noted, the pore pressure filter is located directly behind the cone tip in the "u_2" position (ASTM Type 2). The filter is 6 mm thick, made of porous plastic (polyethylene) having an average pore size of 125 microns (90-160 microns). The function of the filter is to allow rapid movements of extremely small volumes of water needed to activate the pressure transducer while preventing soil ingress or blockage.

The piezocone penetrometers are manufactured with dimensions, tolerances and sensor characteristics that are in general accordance with the current ASTM D5778 standard. ConeTec's calibration criteria also meets or exceeds those of the current ASTM D5778 standard. An illustration of the piezocone penetrometer is presented in Figure CPTu.

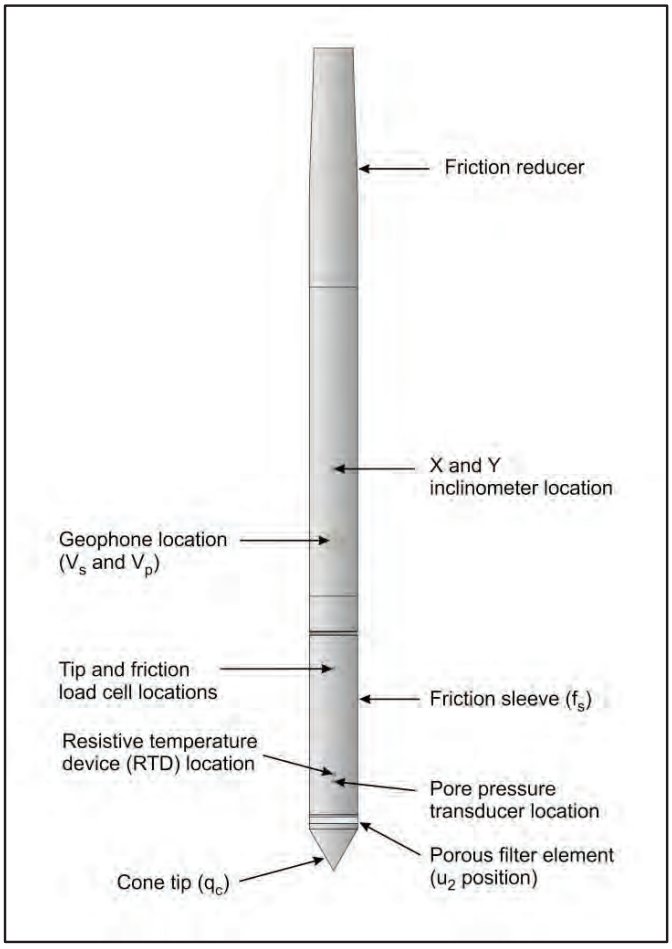

Figure CPTu. Piezocone Penetrometer (15 cm^2)

The ConeTec data acquisition systems consist of a Windows based computer and a signal conditioner and power supply interface box with a 16 bit (or greater) analog to digital (A/D) converter. The data is recorded at fixed depth increments using a depth wheel attached to the push cylinders or by using a spring loaded rubber depth wheel that is held against the cone rods. The typical recording intervals are either 2.5 cm or 5.0 cm depending on project requirements; custom recording intervals are possible. The system displays the CPTu data in real time and records the following parameters to a storage media during penetration:

- Depth
- Uncorrected tip resistance (q_c)
- Sleeve friction (f_s)
- Dynamic pore pressure (u)
- Additional sensors such as resistivity, passive gamma, ultra violet induced fluorescence, if applicable

All testing is performed in accordance to ConeTec's CPT operating procedures which are in general accordance with the current ASTM D5778 standard.

Prior to the start of a CPTu sounding a suitable cone is selected, the cone and data acquisition system are powered on, the pore pressure system is saturated with either glycerine or silicone oil and the baseline readings are recorded with the cone hanging freely in a vertical position.

The CPTu is conducted at a steady rate of 2 cm/s, within acceptable tolerances. Typically one meter length rods with an outer diameter of 1.5 inches are added to advance the cone to the sounding termination depth. After cone retraction final baselines are recorded.

Additional information pertaining to ConeTec's cone penetration testing procedures:

- Each filter is saturated in silicone oil or glycerine under vacuum pressure prior to use
- Recorded baselines are checked with an independent multi-meter
- Baseline readings are compared to previous readings
- Soundings are terminated at the client's target depth or at a depth where an obstruction is encountered, excessive rod flex occurs, excessive inclination occurs, equipment damage is likely to take place, or a dangerous working environment arises
- Differences between initial and final baselines are calculated to ensure zero load offsets have not occurred and to ensure compliance with ASTM standards

The interpretation of piezocone data for this report is based on the corrected tip resistance (q_t), sleeve friction (f_s) and pore water pressure (u). The interpretation of soil type is based on the correlations developed by Robertson (1990) and Robertson (2009). It should be noted that it is not always possible to accurately identify a soil type based on these parameters. In these situations, experience, judgment and an assessment of other parameters may be used to infer soil behaviour type.

The recorded tip resistance (q_c) is the total force acting on the piezocone tip divided by its base area. The tip resistance is corrected for pore pressure effects and termed corrected tip resistance (q_t) according to the following expression presented in Robertson et al, 1986:

$$q_t = q_c + (1\text{-}a) \bullet u_2$$

where: q_t is the corrected tip resistance
q_c is the recorded tip resistance
u_2 is the recorded dynamic pore pressure behind the tip (u_2 position)
a is the Net Area Ratio for the piezocone (0.8 for ConeTec probes)

The sleeve friction (f_s) is the frictional force on the sleeve divided by its surface area. As all ConeTec piezocones have equal end area friction sleeves, pore pressure corrections to the sleeve data are not required.

The dynamic pore pressure (u) is a measure of the pore pressures generated during cone penetration. To record equilibrium pore pressure, the penetration must be stopped to allow the dynamic pore pressures to stabilize. The rate at which this occurs is predominantly a function of the permeability of the soil and the diameter of the cone.

The friction ratio (Rf) is a calculated parameter. It is defined as the ratio of sleeve friction to the tip resistance expressed as a percentage. Generally, saturated cohesive soils have low tip resistance, high friction ratios and generate large excess pore water pressures. Cohesionless soils have higher tip resistances, lower friction ratios and do not generate significant excess pore water pressure.

A summary of the CPTu soundings along with test details and individual plots are provided in the appendices. A set of interpretation files were generated for each sounding based on published correlations and are provided in Excel format in the data release folder. Information regarding the interpretation methods used is also included in the data release folder.

For additional information on CPTu interpretations, refer to Robertson et al. (1986), Lunne et al. (1997), Robertson (2009), Mayne (2013, 2014) and Mayne and Peuchen (2012).

References

ASTM D5778-12, 2012, "Standard Test Method for Performing Electronic Friction Cone and Piezocone Penetration Testing of Soils", ASTM, West Conshohocken, US.

Lunne, T., Robertson, P.K. and Powell, J. J. M., 1997, “Cone Penetration Testing in Geotechnical Practice”, Blackie Academic and Professional.

Mayne, P.W., 2013, “Evaluating yield stress of soils from laboratory consolidation and in-situ cone penetration tests”, Sound Geotechnical Research to Practice (Holtz Volume) GSP 230, ASCE, Reston/VA: 406-420.

Mayne, P.W. and Peuchen, J., 2012, “Unit weight trends with cone resistance in soft to firm clays”, Geotechnical and Geophysical Site Characterization *4,* Vol. 1 (Proc. ISC-4, Pernambuco), CRC Press, London: 903-910.

Mayne, P.W., 2014, “Interpretation of geotechnical parameters from seismic piezocone tests”, CPT’14 Keynote Address, Las Vegas, NV, May 2014.

Robertson, P.K., Campanella, R.G., Gillespie, D. and Greig, J., 1986, “Use of Piezometer Cone Data”, Proceedings of InSitu 86, ASCE Specialty Conference, Blacksburg, Virginia.

Robertson, P.K., 1990, “Soil Classification Using the Cone Penetration Test”, Canadian Geotechnical Journal, Volume 27: 151-158.

Robertson, P.K., 2009, “Interpretation of cone penetration tests – a unified approach”, Canadian Geotechnical Journal, Volume 46: 1337-1355.

Shear wave velocity testing is performed in conjunction with the piezocone penetration test (SCPTu) in order to collect interval velocities. For some projects seismic compression wave (Vp) velocity is also determined.

ConeTec's piezocone penetrometers are manufactured with a horizontally active geophone (28 hertz) that is rigidly mounted in the body of the cone penetrometer, 0.2 meters behind the cone tip.

Shear waves are typically generated by using an impact hammer horizontally striking a beam that is held in place by a normal load. In some instances an auger source or an imbedded impulsive source maybe used for both shear waves and compression waves. The hammer and beam act as a contact trigger that triggers the recording of the seismic wave traces. For impulsive devices an accelerometer trigger may be used. The traces are recorded using an up-hole integrated digital oscilloscope which is part of the SCPTu data acquisition system. An illustration of the shear wave testing configuration is presented in Figure SCPTu-1.

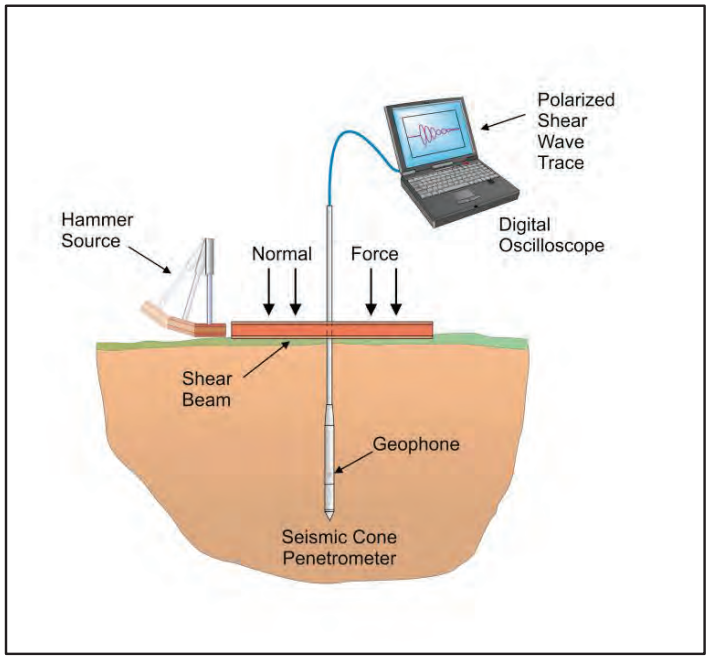

Figure SCPTu-1. Illustration of the SCPTu system

All testing is performed in accordance to ConeTec's SCPTu operating procedures.

Prior to the start of a SCPTu sounding, the procedures described in the Cone Penetration Test section are followed. In addition, the active axis of the geophone is aligned parallel to the beam (or source) and the horizontal offset between the cone and the source is measured and recorded.

Prior to recording seismic waves at each test depth, cone penetration is stopped and the rods are decoupled from the rig to avoid transmission of rig energy down the rods. Multiple wave traces are recorded for quality control purposes. After reviewing wave traces for consistency the cone is pushed to the next test depth (typically one meter intervals or as requested by the client). Figure SCPTu-2 presents an illustration of a SCPTu test.

For additional information on seismic cone penetration testing refer to Robertson et.al. (1986).

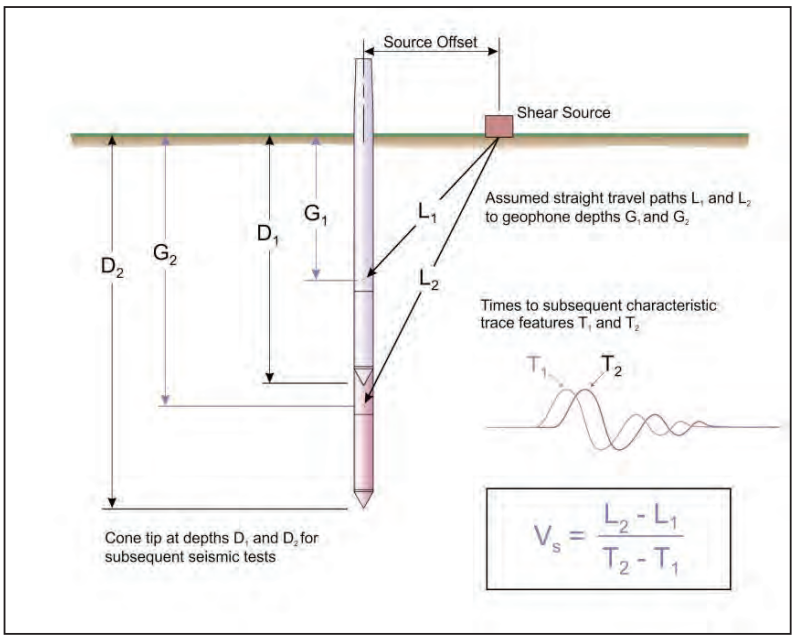

Figure SCPTu-2. Illustration of a seismic cone penetration test

Calculation of the interval velocities are performed by visually picking a common feature (e.g. the first characteristic peak, trough, or crossover) on all of the recorded wave sets and taking the difference in ray path divided by the time difference between subsequent features. Ray path is defined as the straight line distance from the seismic source to the geophone, accounting for beam offset, source depth and geophone offset from the cone tip.

The average shear wave velocity to a depth of 30 meters (V_{s30}) has been calculated and provided for all applicable soundings using an equation presented in Crow et al., 2012.

$$V_{s30} = \frac{total\ thickness\ of\ all\ layers\ (30m)}{\sum(layer\ traveltimes)}$$

The layer travel times refers to the travel times propagating in the vertical direction, not the measured travel times from an offset source.

Tabular results and SCPTu plots are presented in the relevant appendix.

References

Crow, H.L., Hunter, J.A., Bobrowsky, P.T., 2012, "National shear wave measurement guidelines for Canadian seismic site assessment", GeoManitoba 2012, Sept 30 to Oct 2, Winnipeg, Manitoba.

Robertson, P.K., Campanella, R.G., Gillespie D and Rice, A., 1986, "Seismic CPT to Measure In-Situ Shear Wave Velocity", Journal of Geotechnical Engineering ASCE, Vol. 112, No. 8: 791-803.

The cone penetration test is halted at specific depths to carry out pore pressure dissipation (PPD) tests, shown in Figure PPD-1. For each dissipation test the cone and rods are decoupled from the rig and the data acquisition system measures and records the variation of the pore pressure (u) with time (t).

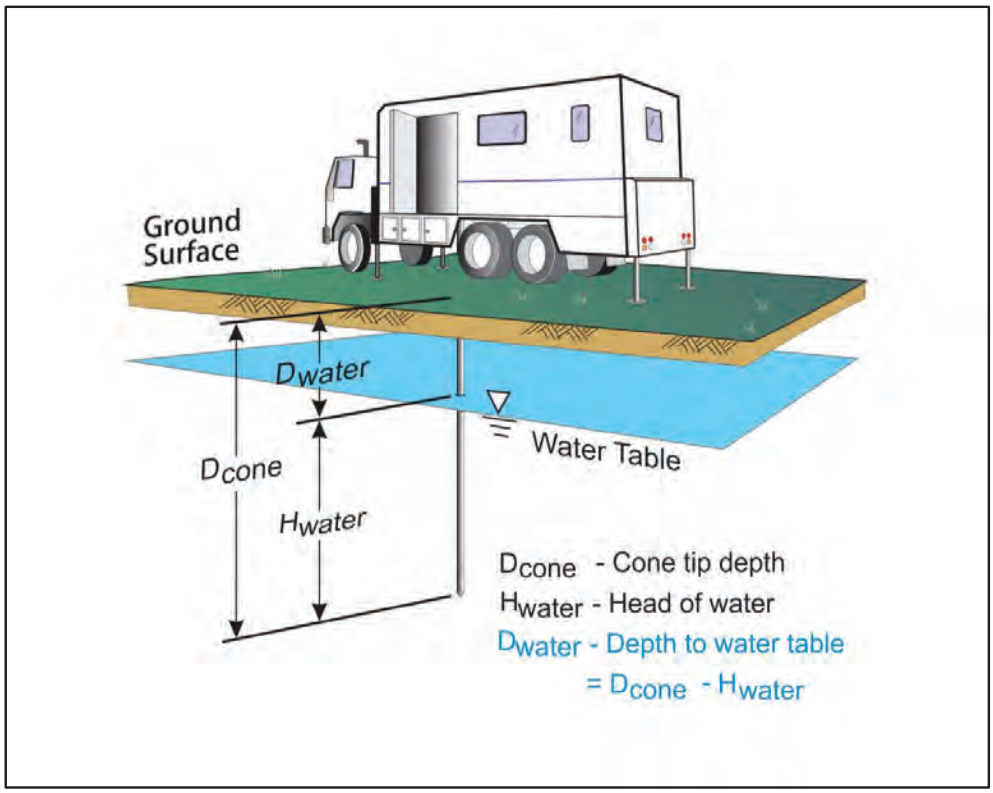

Figure PPD-1. Pore pressure dissipation test setup

Pore pressure dissipation data can be interpreted to provide estimates of ground water conditions, permeability, consolidation characteristics and soil behaviour.

The typical shapes of dissipation curves shown in Figure PPD-2 are very useful in assessing soil type, drainage, in situ pore pressure and soil properties. A flat curve that stabilizes quickly is typical of a freely draining sand. Undrained soils such as clays will typically show positive excess pore pressure and have long dissipation times. Dilative soils will often exhibit dynamic pore pressures below equilibrium that then rise over time. Overconsolidated fine-grained soils will often exhibit an initial dilatory response where there is an initial rise in pore pressure before reaching a peak and dissipating.

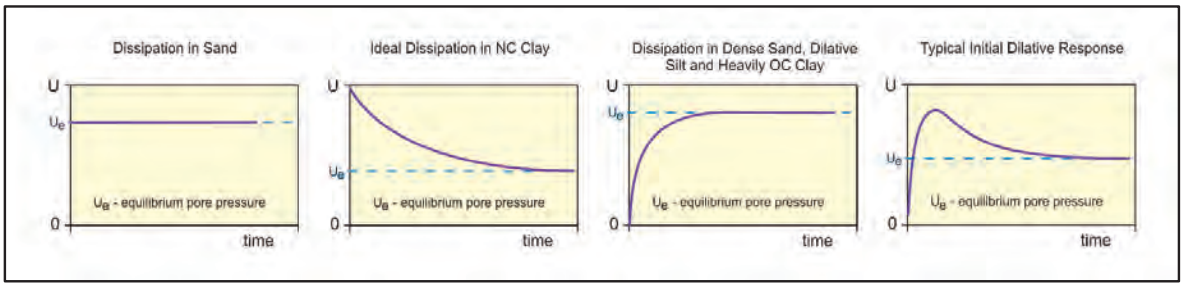

Figure PPD-2. Pore pressure dissipation curve examples

In order to interpret the equilibrium pore pressure (u_{eq}) and the apparent phreatic surface, the pore pressure should be monitored until such time as there is no variation in pore pressure with time as shown for each curve of Figure PPD-2.

In fine grained deposits the point at which 100% of the excess pore pressure has dissipated is known as t_{100}. In some cases this can take an excessive amount of time and it may be impractical to take the dissipation to t_{100}. A theoretical analysis of pore pressure dissipations by Teh and Houlsby (1991) showed that a single curve relating degree of dissipation versus theoretical time factor (T*) may be used to calculate the coefficient of consolidation (c_h) at various degrees of dissipation resulting in the expression for c_h shown below.

$$c_h = \frac{T^* \cdot a^2 \cdot \sqrt{I_r}}{t}$$

Where:

T* is the dimensionless time factor (Table Time Factor)
a is the radius of the cone
I_r is the rigidity index
t is the time at the degree of consolidation

Table Time Factor. T* versus degree of dissipation (Teh and Houlsby, 1991)

Degree of Dissipation (%)	20	30	40	50	60	70	80
T* (u_2)	0.038	0.078	0.142	0.245	0.439	0.804	1.60

The coefficient of consolidation is typically analyzed using the time (t_{50}) corresponding to a degree of dissipation of 50% (u_{50}). In order to determine t_{50}, dissipation tests must be taken to a pressure less than u_{50}. The u_{50} value is half way between the initial maximum pore pressure and the equilibrium pore pressure value, known as u_{100}. To estimate u_{50}, both the initial maximum pore pressure and u_{100} must be known or estimated. Other degrees of dissipations may be considered, particularly for extremely long dissipations.

At any specific degree of dissipation the equilibrium pore pressure (u at t_{100}) must be estimated at the depth of interest. The equilibrium value may be determined from one or more sources such as measuring the value directly (u_{100}), estimating it from other dissipations in the same profile, estimating the phreatic surface and assuming hydrostatic conditions, from nearby soundings, from client provided information, from site observations and/or past experience, or from other site instrumentation.

For calculations of c_h (Teh and Houlsby, 1991), t_{50} values are estimated from the corresponding pore pressure dissipation curve and a rigidity index (I_r) is assumed. For curves having an initial dilatory response in which an initial rise in pore pressure occurs before reaching a peak, the relative time from the peak value is used in determining t_{50}. In cases where the time to peak is excessive, t_{50} values are not calculated.

Due to possible inherent uncertainties in estimating I_r, the equilibrium pore pressure and the effect of an initial dilatory response on calculating t_{50}, other methods should be applied to confirm the results for c_h.

Additional published methods for estimating the coefficient of consolidation from a piezocone test are described in Burns and Mayne (1998, 2002), Jones and Van Zyl (1981), Robertson et al. (1992) and Sully et al. (1999).

A summary of the pore pressure dissipation tests and dissipation plots are presented in the relevant appendix.

References

Burns, S.E. and Mayne, P.W., 1998, "Monotonic and dilatory pore pressure decay during piezocone tests", Canadian Geotechnical Journal 26 (4): 1063-1073.

Burns, S.E. and Mayne, P.W., 2002, "Analytical cavity expansion-critical state model cone dissipation in fine-grained soils", Soils & Foundations, Vol. 42(2): 131-137.

Jones, G.A. and Van Zyl, D.J.A., 1981, "The piezometer probe: a useful investigation tool", Proceedings, 10th International Conference on Soil Mechanics and Foundation Engineering, Vol. 3, Stockholm: 489-495.

Robertson, P.K., Sully, J.P., Woeller, D.J., Lunne, T., Powell, J.J.M. and Gillespie, D.G., 1992, "Estimating coefficient of consolidation from piezocone tests", Canadian Geotechnical Journal, 29(4): 551-557.

Sully, J.P., Robertson, P.K., Campanella, R.G. and Woeller, D.J., 1999, "An approach to evaluation of field CPTU dissipation data in overconsolidated fine-grained soils", Canadian Geotechnical Journal, 36(2): 369-381.

Teh, C.I., and Houlsby, G.T., 1991, "An analytical study of the cone penetration test in clay", Geotechnique, 41(1): 17-34.

Resistivity testing is performed in conjunction with piezocone penetration testing with the addition of a resistivity module in order to determine the electrical resistivity of the soil.

An illustration of the piezocone penetrometer and resistivity module is presented in Figure RES-CPTu.

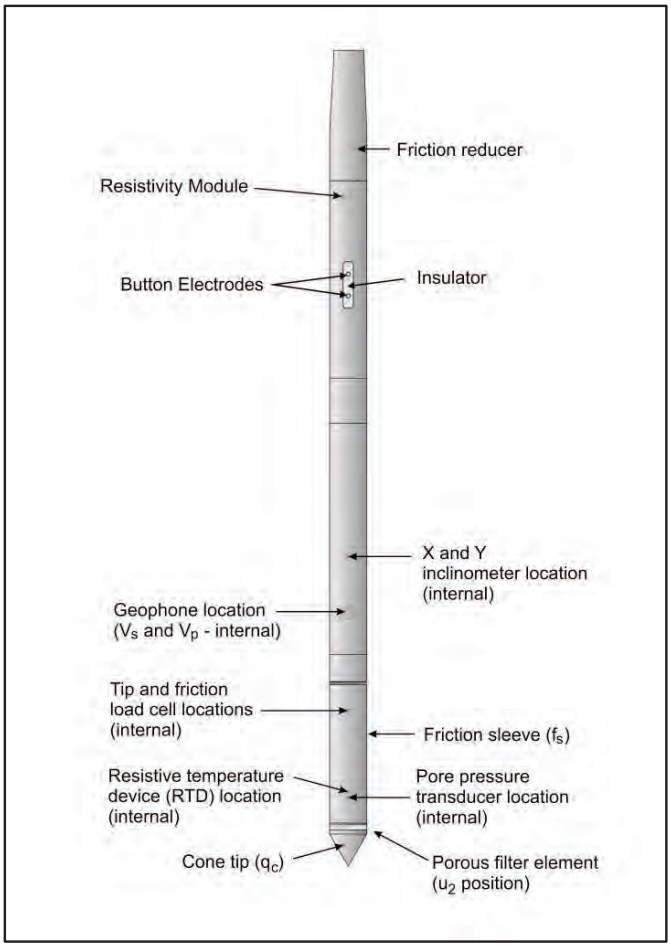

Figure RES-CPTu. Resistivity module and piezocone penetrometer

The module has two 6 mm diameter brass resistivity electrodes which are designed to be reasonably wear resistant and have high electrical conductivity. The small configuration of the electrodes provides excellent vertical resolution of resistivity changes. The insulation separating the electrodes from the cone is made of Delrin plastic.

The resistivity module measures the voltage drop across the electrodes in the soil at a given excitation current, which is proportional to the electrical resistivity of the soil. From the resultant potential difference between the electrodes a resistance is determined. A 1000 Hz source is used to avoid polarization of the electrodes. Polarization is the process where ions accumulate at the electrodes thus increasing the measured resistance.

Resistance is not a material property, it is a function of the electrode spacing and size. To convert from resistance to resistivity, a lab calibration is necessary. Resistivity modules are calibrated in a water tank

with solutions of known resistivity. The resistance across the electrodes is measured in the various solutions and a calibration curve is generated. It is necessary to assume that the calibration factors determined in the homogeneous isotropic medium do not vary significantly as the cone is advanced into the ground through soil.

Prior to the start of a test, the procedures described in the cone penetration test section are followed and the resistivity module output is verified using various resistors. The resistivity measurements are recorded on a continuous basis at the same time as the tip, friction and pore pressure measurements. Due to the vertical offset between the cone tip and the electrodes, resistivity data is not available for the last 70 cm of each profile.

The resistivity of soil is for the most part influenced by the resistivity of the pore fluid, which in turn is a measure of the groundwater chemical composition. Electrical conduction in saturated sandy soils is largely by electrolytic conduction in the pore fluid whereas for clayey soils, ion exchange contributes significantly within the soil skeleton. Resistivity measurements will increase as the saturation of the soil decreases. For additional information on resistivity cone penetration testing, refer to Campanella and Weemees, 1990.

Resistivity CPTu plots are presented in the relevant appendix.

Reference

Campanella, R.G. and Weemees, I., 1990, “Development and Use of an Electrical Resistivity Cone for Groundwater Contamination Studies”, Canadian Geotechnical Journal, Vol. 27 No. 5: 557-567.

The electronic field vane system is manufactured by ConeTec Investigations Ltd. of Richmond, British Columbia, Canada. An illustration of the vane system is presented in Figure eVST.

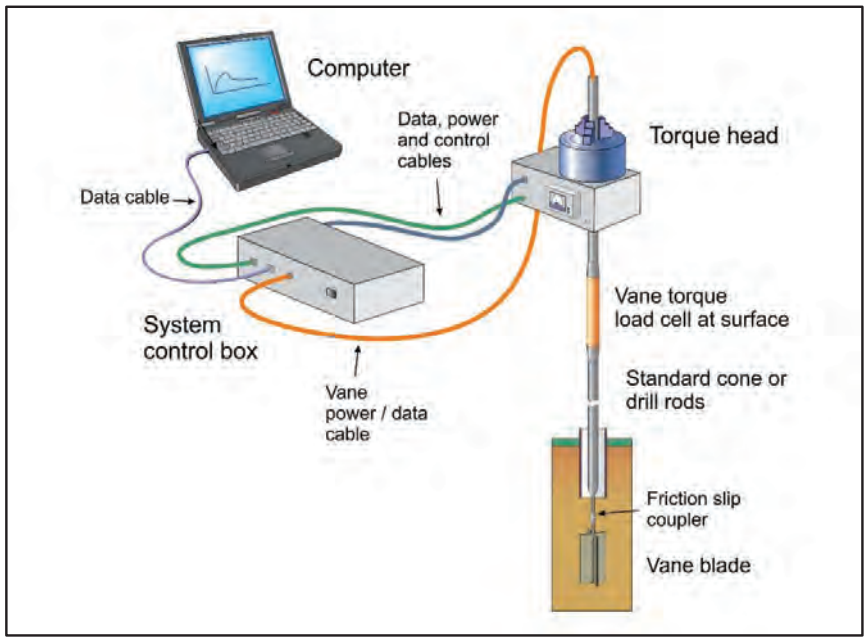

Figure eVST. Illustration of the downhole electronic field vane system

The vane system is designed with an array of strain gauges in a load cell that measure the applied torque. The torque signals are amplified and converted to digital data within the tool and are sent to the data acquisition system through a shielded cable. The system uses a friction slip coupler to permit the free slip or play of approximately fifteen degrees between the rods and the vane in order to isolate and record rod friction from the soil before rotation of the vane starts. The system is designed to use vanes of various sizes and configurations that connect to the friction slip coupler. The vanes manufactured by ConeTec have dimensions and tolerances that are in general accordance with the current ASTM D2573 standards. In very soft soil conditions and at the request of the client, ConeTec may use a large diameter vane that exceeds the ASTM D2573 size specifications in order to maximize torque resolution.

The electric motor (capable of 100 Nm of torque) is designed to clamp onto and rotate the rods and vane at a constant rate.

ConeTec's calibration criteria of the load cells are in accordance with the current ASTM D2573 standard.

The data acquisition system consists of a computer that typically records the vane data every 0.2 degrees of rotation. The system records the following parameters and saves them to a file as the test is conducted:

- Torque in newton meters
- Rotation in degrees
- Elapsed time in seconds (from the start of the test)

All testing is performed in accordance to ConeTec's field vane testing operating procedures and in general accordance with the current ASTM D2573 standard. For additional information on vane shear testing refer to Greig et. al, (1987).

Prior to the start of a vane shear test profile, a suitable sized vane is selected, the vane system is powered on and the vane load cell baseline reading is recorded with the load cell hanging freely in a vertical position.

The vane is advanced to the desired test depth through a cased hole, typically using one meter length rods with an outer diameter of 1.5 inches. Test depths are referenced to the middle of the vane. The motor rotates the vane rods at a near constant rate up to and beyond the yield stress (peak) until the load remains near constant (post peak). Following post peak readings, the vane is then rapidly rotated clockwise, typically ten times to completely remold the soil. The test procedure is repeated in order to record the remolded strength of the soil. The vane is then advanced to the next depth and the procedure is repeated or the vane is retracted to allow for drilling and vane size changes. Once the vane is retracted the final baseline is recorded and compared to previous readings as a QA/QC check.

Undrained shear strength from the field vane, $(S_u)_{fv}$, is typically calculated from torque measurements using the following general equation (ASTM D2573, 2015) taking into consideration the case of rectangular or tapered ends at the top and/or bottom of the vane.

$$(S_u)_{fv} = \frac{12 \cdot T_{max}}{\pi D^2 \left(\frac{D}{\cos(i_T)} + \frac{D}{\cos(i_B)} + 6H \right)}$$

where:

$(S_u)_{fv}$	=	undrained shear strength from the field vane
T_{max}	=	maximum value of torque
D	=	vane diameter
H	=	height of the rectangular portion of the vane
i_T	=	angle of taper at vane top (with respect to horizontal)
i_B	=	angle of taper at vane bottom (with respect to horizontal)

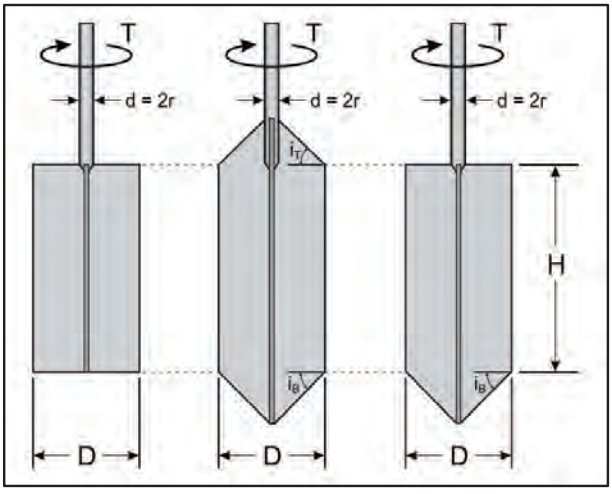

For rectangular vanes where H/D = 2, the above equation simplifies to:

$$(S_u)_{fv} = \frac{6 \cdot T_{max}}{7\pi D^3}$$

CONETEC

The recorded rod friction is subtracted from the peak and remolded torque. No correction factors are applied to the vane results to derive the mobilized shear strength ($\tau_{mobilized}$).

A summary of the vane shear tests, a table of results and individual VST plots are provided in the relevant appendices. Tabular data in Excel format is provided in the data release folder.

References

ASTM D2573 / D2573M-15, 2015, "Standard Test Method for Field Vane Shear Test in Saturated Fine-Grained Soils", ASTM International, West Conshohocken, PA.

Greig, J.W., R.G. Campanella and P.K. Robertson, 1987, "Comparison of Field Vane Results With Other In-Situ Test Results", International Symposium on Laboratory and Field Vane Shear Strength Testing, ASTM, Tampa, FL, Proceedings.

Standard penetration testing with energy measurements (SPTe) is conducted to measure the energy generated from a hammer impact that enters the drill rod string.

SPTe measurements are conducted in general accordance with the current ASTM D4633 standard.

The Pile Driving Analyzer (PDA) system manufactured by Pile Dynamics Inc. (PDI) is used to record and analyze energy measurements. The system uses the force-velocity (EFV) method to calculate SPT energy which uses both the force and velocity records to calculate the maximum transferred energy (EFV).

$$EFV = \max\left[\int F(t)v(t)dt\right]$$

The integration is performed over the time from which the energy transfer begins and terminates at the time when the energy transfer reaches a maximum value. This method is theoretically correct for all rod lengths regardless of the 2L/c stress wave travel time and the number of changes in rod cross sectional area. (L is the rod length and c is the stress wave speed in the rod.)

The Energy Transfer Ratio (ETR) is calculated by comparing the calculated energy (EFV) to the theoretical maximum potential energy (PE). The ratio is expressed as a percent of the theoretical energy of a standard SPT system which consists of a 140 lb hammer falling 30 inches. ETR is computed using the following equation:

$$ETR = \frac{EFV}{PE} x\ 100\%$$

A summary of the tests and tabular results are provided in the relevant appendix.

Reference

ASTM D4633-10, 2010, "Standard Test Method for Energy Measurement for Dynamic Penetrometers", ASTM, West Conshohocken, US.

The Sharky Sampler™ is designed to sample soils that are sensitive to sampling disturbance as the sample tube has a very low wall thickness to sample area ratio.

The sampler is comprised of a Shelby tube attached to a piston. The Shelby tube is a 30 inch thin-walled hollow aluminum tube with a three inch diameter. The bottom side of the tube is chamfered to form a cutting edge, and the top side has holes which are used to secure the tube to the piston and deployment rods.

Prior to the deployment of the sampler, the piston is extended and locked in place in so that it is flush with the leading edge of the Shelby tube. This ensures the piston remains in place and that no sample is collected prematurely.

The sampler is attached to deployment rods and is pushed into the ground to the desired depth. Inner rods are lowered through the deployment rods and attached to the piston inside the sampler. The inner rods release the piston from the leading edge of the Shelby tube.

The inner rods that are held in place while the Shelby tube is advanced into the ground, collecting a sample over the desired depth range. The sampler remains in the ground for a minimum of one minute in order for the sample to stabilize in the tube. The cohesion of the sample in the tube causes the sample to be retained as the tube is withdrawn from the hole.

Immediately after extraction from the ground, the Shelby tube ends are sealed and the tubes are labeled with the location name, sample depth, sample number and date. Each sample is logged in an Excel spreadsheet. The sample log provides information pertaining to each sample and the sample location.

The sampling is conducted in general accordance with ASTM D1587-08 (Re-approved 2012).

The sample logs are presented in the relevant appendix and the sample photos are provided in the data release folder.

References

ASTM D-1587-08 (Reapproved 2012)$^{\varepsilon 1}$, “Standard Practice for Thin-Walled Tube sampling of Soils for Geotechnical Purposes[1]”,, ASTM International, West Conshohocken, PA, US.

The appendices listed below are included in the report:

- Cone Penetration Test Summary and Standard Plots
- Advanced Cone Penetration Test Plots with Su(Nkt) and Phi Angle
- Cone Penetration Test Resistivity Plots
- Seismic Cone Penetration Test Plots
- Seismic Cone Penetration Test Tabular Results
- Pore Pressure Dissipation Summary and Pore Pressure Dissipation Plots
- Electronic Field Vane Shear Test Profile Summary and Results
- Electronic Field Vane Shear Test Plots
- Sample Summary and Sample Logs
- Standard Penetration Test with Energy Measurements (SPTe) Summary and Results

Cone Penetration Test Summary and Standard Plots

Job No:	16-72004
Client:	Cleary Gottlieb Steen & Hamilton LLP (CGSH)
Project:	Samarco, Germano Buttress
Start Date:	19-Apr-2016
End Date:	24-May-2016

CONE PENETRATION TEST SUMMARY

Sounding ID	File Name	Date	Cone	Assumed Phreatic Surface[1] (m)	Final Depth (m)	Northing[2] (m)	Easting (m)	Refer to Notation Number
GBCPT16-01	16-72004_RS01	19-Apr-2016	432:T1500F15U500		1.10	7763639	660664	3
GBCPT16-01B	16-72004_RS01B	20-Apr-2016	432:T1500F15U500		0.90	7763639	660664	3
GBCPT16-01C	16-72004_RS01C	20-Apr-2016	432:T1500F15U500		2.20	7763639	660664	3
GSCPT16-02	16-72004_RS02	21-Apr-2016	432:T1500F15U500	8.9	11.40	7764153	658559	4
GSCPT16-02B	16-72004_RS02B	24-Apr-2016	376:T375F10U200	8.9	41.65	7764155	658559	
GCCPT16-03	16-72004_RS03	26-Apr-2016	376:T375F10U200	33.2	61.65	7766164	657252	
GCCPT16-04	16-72004_RS04	2-May-2016	376:T375F10U200		35.35	7766303	657393	3
GCCPT16-04B	16-72004_RS04B	13-May-2016	432:T1500F15U500		36.35	7766300	657394	3
GSCPT16-05	16-72004_SP05	5-May-2016	376:T375F10U200	3.0	31.85	7763372	659090	5
GBCPT16-06	16-72004_RS06	16-May-2016	432:T1500F15U500	3.1	27.50	7763631	660586	
GBCPT16-06B	16-72004_RS06B	24-May-2016	432:T1500F15U500	3.1	3.35	7763631	660583	4

1. The assumed phreatic surfaces were based on pore pressure dissipation tests unless otherwise noted. Equilibrium pore pressure profile was used for the interpretation tables.
2. The coordinates were acquired using consumer-grade GPS device with datum: WGS 84/ UTM Zone 23 South.
3. Phreatic surface not detected.
4. Assumed phreatic surface based on equilibrium achieved from adjacent CPT sounding.
5. Assumed phreatic surface based on the dynamic pore pressure response.

CONETEC

CGSH

Job No: 16-72004
Date: 04:19:16 15:03
Site: Germano Buttres

Sounding: GBCPT16-01
Cone: 432:T1500F15U500

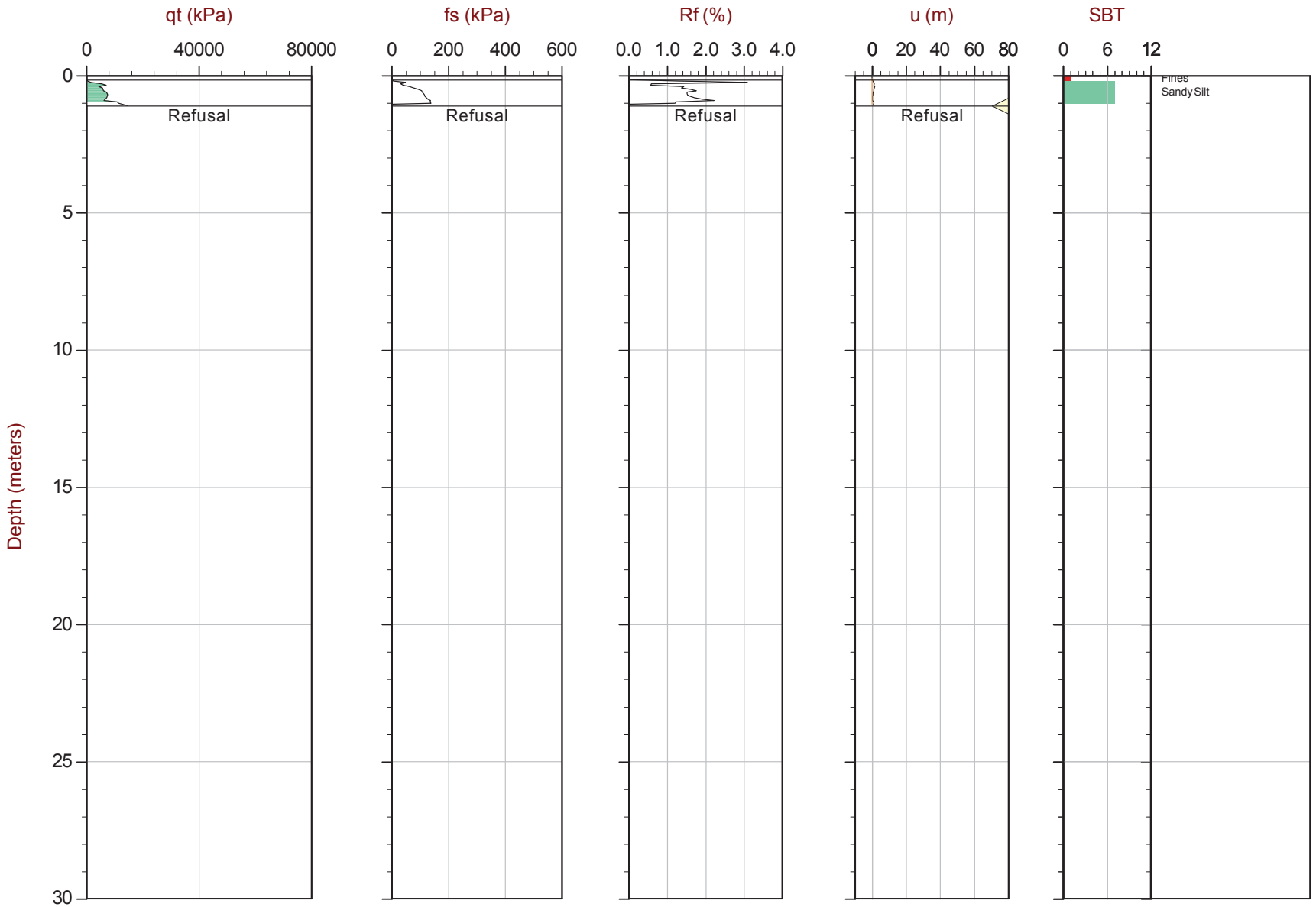

Max Depth: 1.100 m / 3.61 ft
Depth Inc: 0.050 m / 0.164 ft
Avg Int: 0.200 m
Overplot Item:

File: 16-72004_RS01.COR
Unit Wt: SBT Zones

SBT: Robertson and Campanella, 1986
Coords: UTM Zone 23 South N: 7763639m E: 660664m
Page No: 1 of 1

Assumed Ueq
Ueq
Dissipation, equilibrium achieved
Dissipation, equilibrium not achieved
Equilibrium Line

CONETEC

CGSH

Job No: 16-72004
Date: 04:20:16 12:52
Site: Germano Buttres

Sounding: GBCPT16-01B
Cone: 432:T1500F15U500

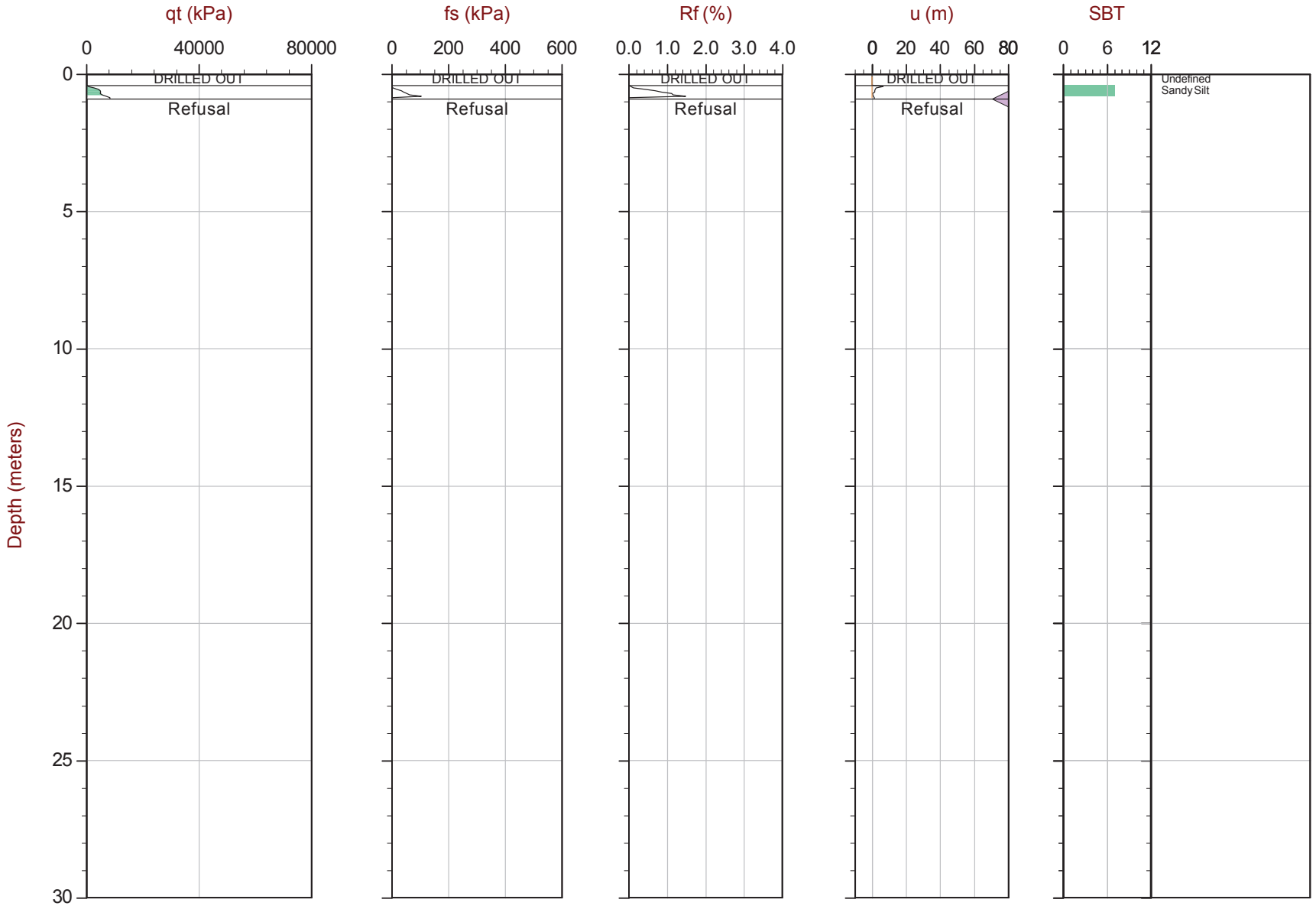

Max Depth: 0.900 m / 2.95 ft
Depth Inc: 0.050 m / 0.164 ft
Avg Int: 0.200 m
Overplot Item:

File: 16-72004_RS01B.COR
Unit Wt: SBT Zones

SBT: Robertson and Campanella, 1986
Coords: UTM Zone 23 South N: 7763639m E: 660664m
Page No: 1 of 1

Assumed Ueq
Ueq
Dissipation, equilibrium achieved
Dissipation, equilibrium not achieved
Equilibrium Line

CONETEC

CGSH

Job No: 16-72004
Date: 04:20:16 15:32
Site: Germano Buttres

Sounding: GBCPT16-01C
Cone: 432:T1500F15U500

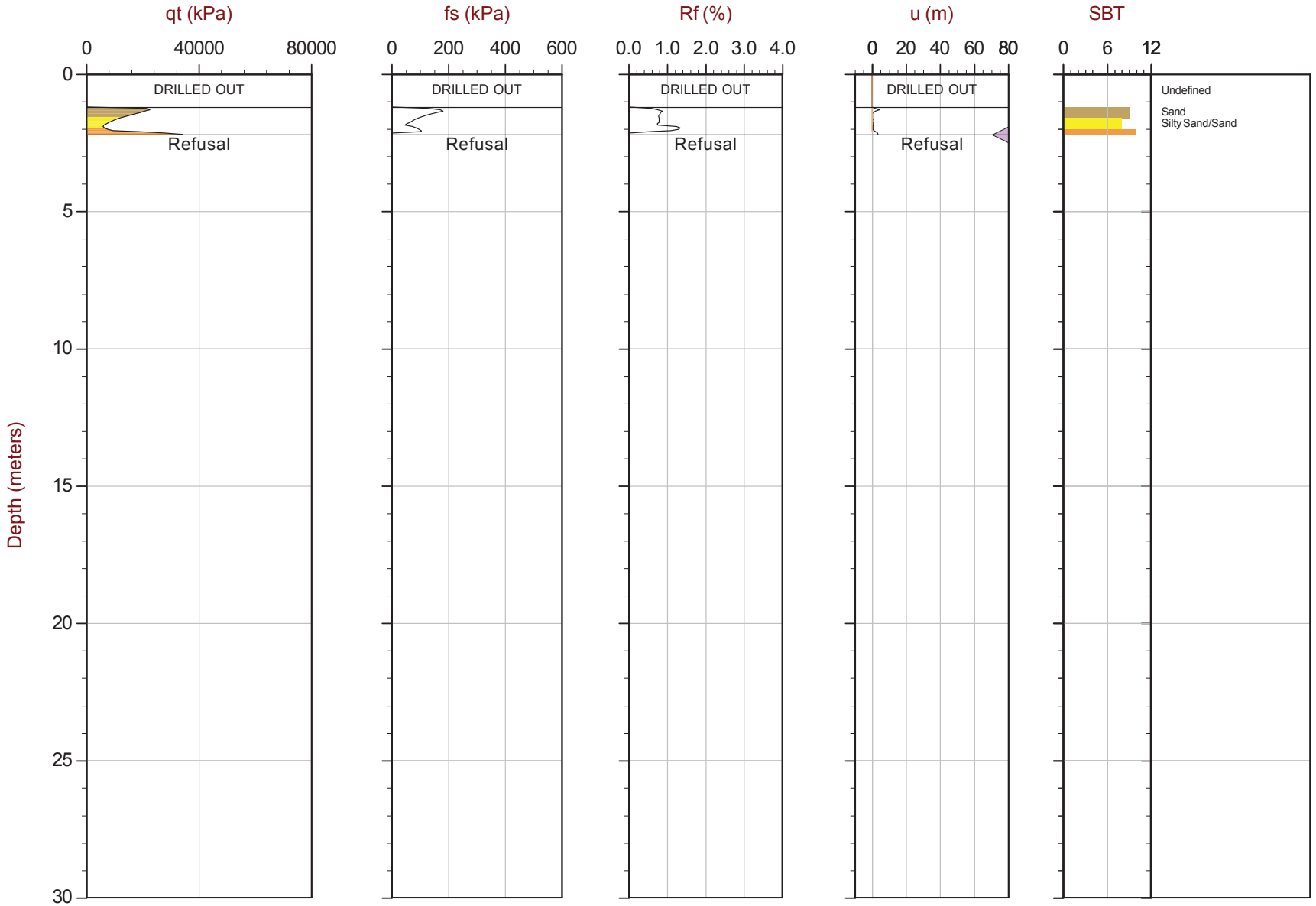

Max Depth: 2.200 m / 7.22 ft
Depth Inc: 0.050 m / 0.164 ft
Avg Int: 0.200 m
Overplot Item:

File: 16-72004_RS01C.COR
Unit Wt: SBT Zones

SBT: Robertson and Campanella, 1986
Coords: UTM Zone 23 South N: 7763639m E: 660664m
Page No: 1 of 1

Assumed Ueq
Ueq
Dissipation, equilibrium achieved
Dissipation, equilibrium not achieved
Equilibrium Line

CONETEC

CGSH

Job No: 16-72004
Date: 04:21:16 14:33
Site: Bay 3, Germano Slimes

Sounding: GSCPT16-02
Cone: 432:T1500F15U500

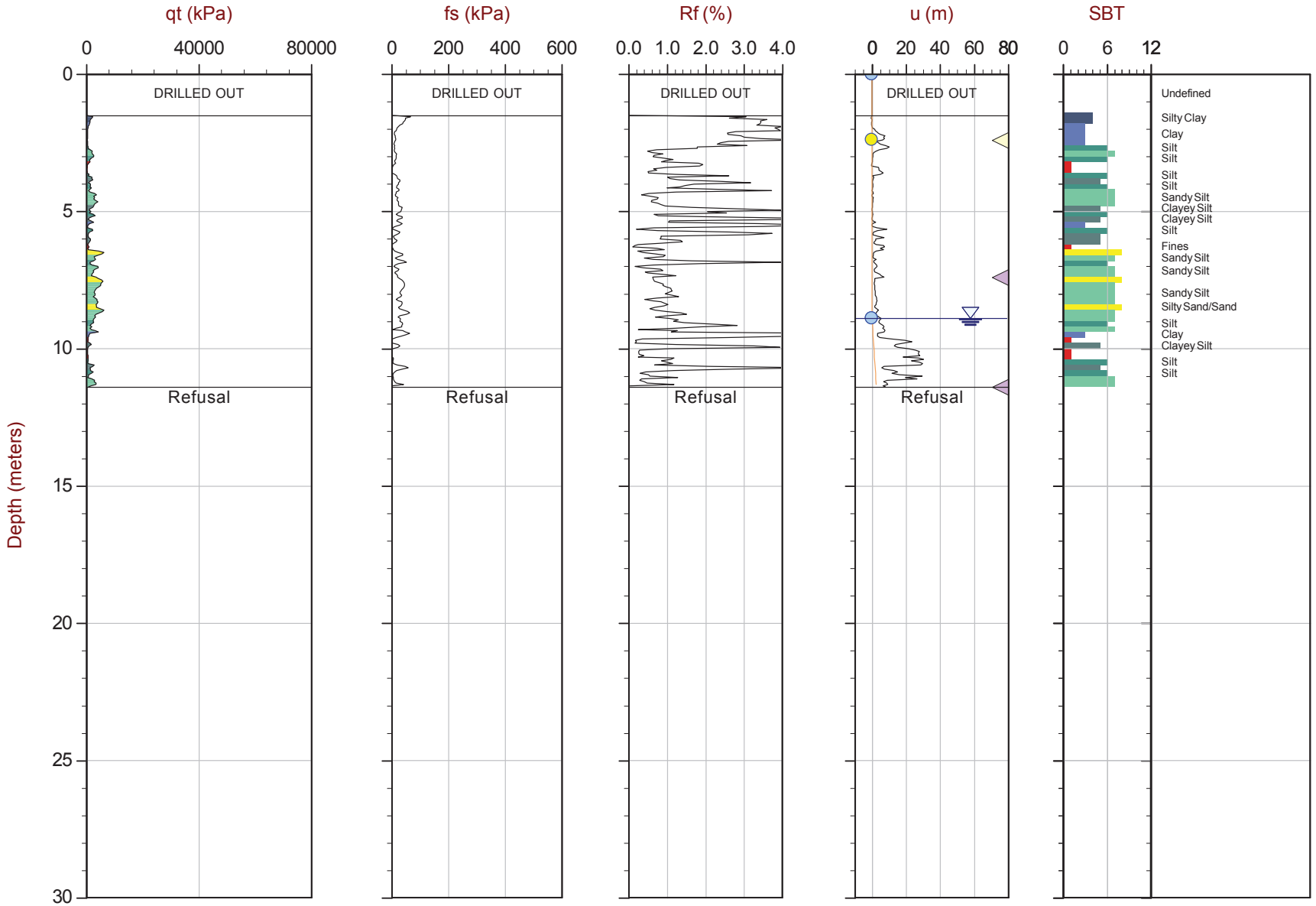

Max Depth: 11.400 m / 37.40 ft
Depth Inc: 0.050 m / 0.164 ft
Avg Int: 0.200 m
Overplot Item:

File: 16-72004_RS02.COR
Unit Wt: SBT Zones

SBT: Robertson and Campanella, 1986
Coords: UTM Zone 23 South N: 7764153m E: 658559m
Page No: 1 of 1

Assumed Ueq
Ueq
Dissipation, equilibrium achieved
Dissipation, equilibrium not achieved
Equilibrium Line

CONETEC

CGSH

Job No: 16-72004
Date: 04:24:16 11:30
Site: Bay 3, Germano Slimes

Sounding: GSCPT16-02B
Cone: 376:T375F10U200

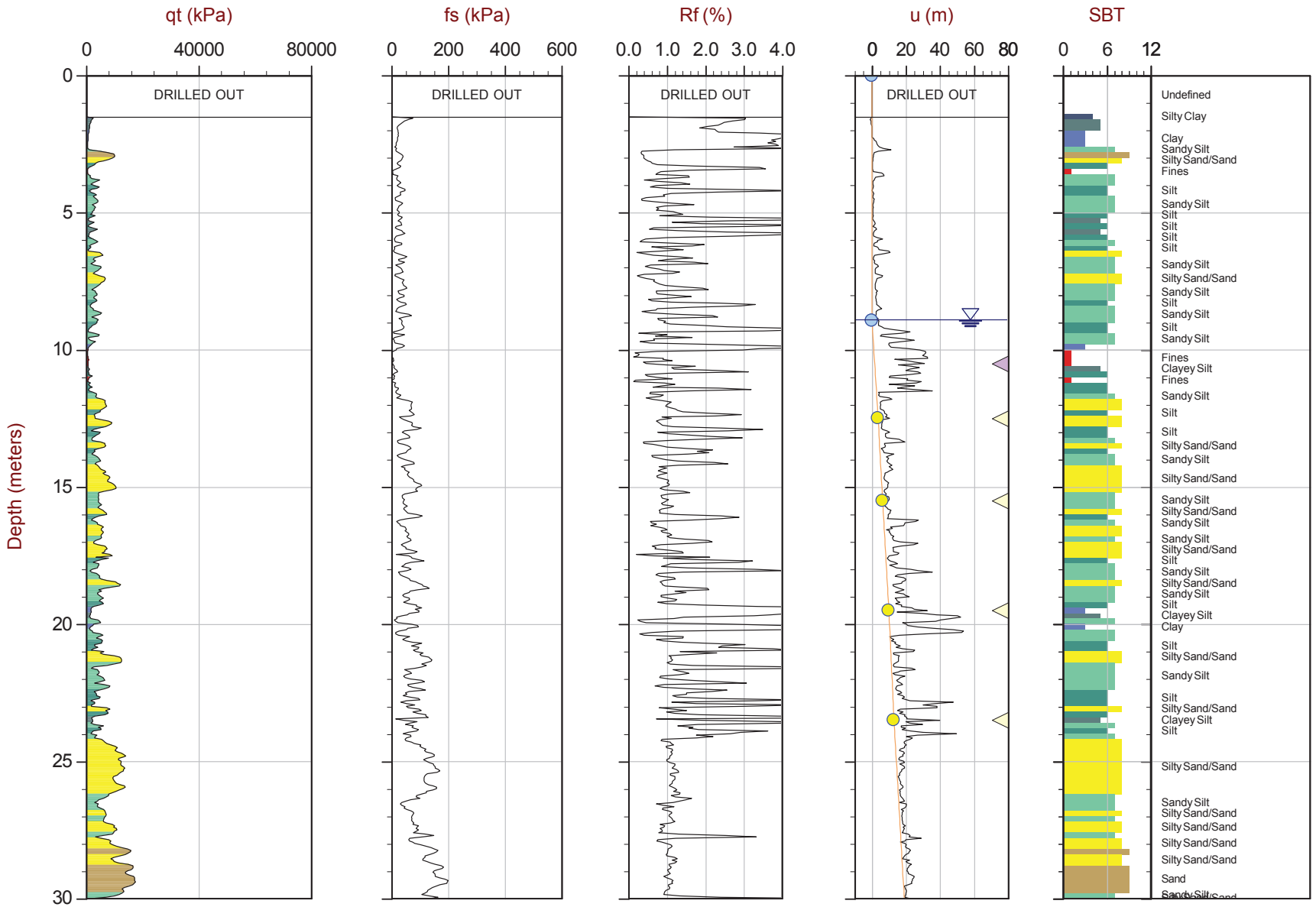

Max Depth: 41.650 m / 136.65 ft
Depth Inc: 0.050 m / 0.164 ft
Avg Int: 0.200 m
Overplot Item:

File: 16-72004_RS02B.COR
Unit Wt: SBT Zones

SBT: Robertson and Campanella, 1986
Coords: UTM Zone 23 South N: 7764155m E: 658559m
Page No: 1 of 2

Assumed Ueq
Ueq
Dissipation, equilibrium achieved
Dissipation, equilibrium not achieved
Equilibrium Line

CONETEC

CGSH

Job No: 16-72004
Date: 04:24:16 11:30
Site: Bay 3, Germano Slimes

Sounding: GSCPT16-02B
Cone: 376:T375F10U200

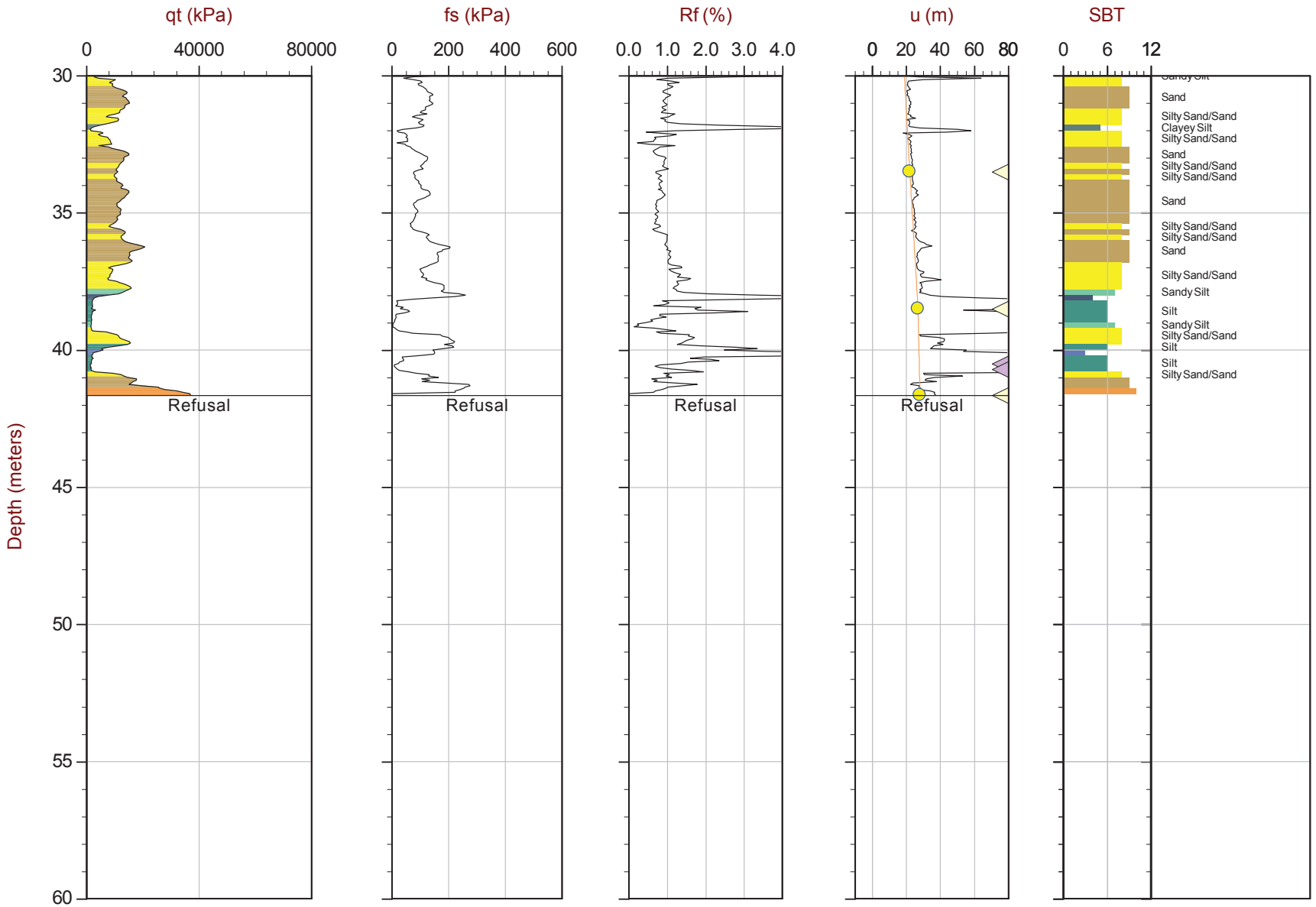

Max Depth: 41.650 m / 136.65 ft
Depth Inc: 0.050 m / 0.164 ft
Avg Int: 0.200 m
Overplot Item:

File: 16-72004_RS02B.COR
Unit Wt: SBT Zones

SBT: Robertson and Campanella, 1986
Coords: UTM Zone 23 South N: 7764155m E: 658559m
Page No: 2 of 2

Assumed Ueq
Ueq
Dissipation, equilibrium achieved
Dissipation, equilibrium not achieved
Equilibrium Line

CONETEC

CGSH

Job No: 16-72004
Date: 04:26:16 12:34
Site: Bay 3, Germano Cava

Sounding: GCCPT16-03
Cone: 376:T375F10U200

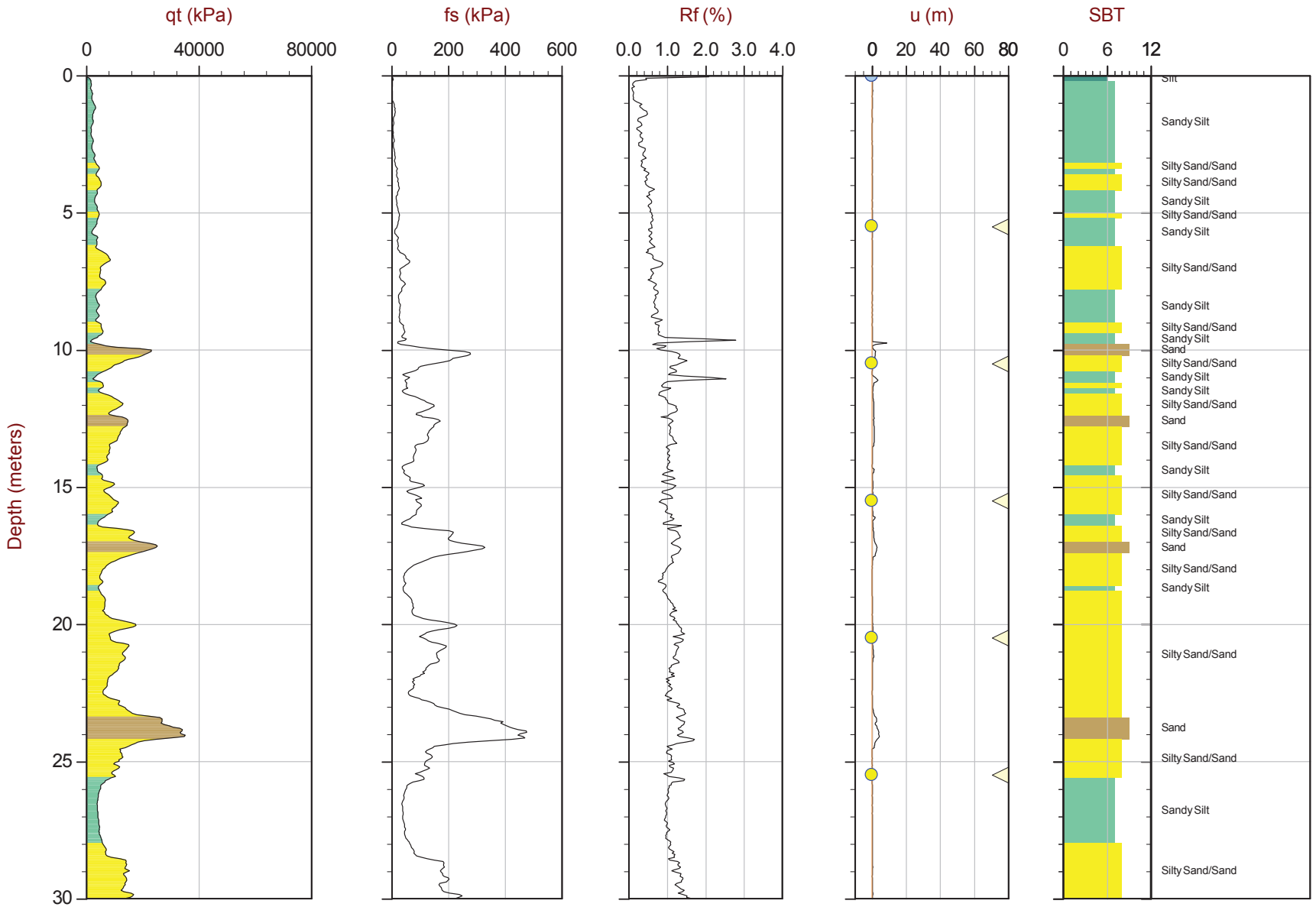

Max Depth: 61.650 m / 202.26 ft
Depth Inc: 0.050 m / 0.164 ft
Avg Int: 0.200 m
Overplot Item:

File: 16-72004_RS03.COR
Unit Wt: SBT Zones

SBT: Robertson and Campanella, 1986
Coords: UTM Zone 23 South N: 7766164m E: 657252m
Page No: 1 of 3

Assumed Ueq
Ueq
Dissipation, equilibrium achieved
Dissipation, equilibrium not achieved
Equilibrium Line

CONETEC

CGSH

Job No: 16-72004
Date: 04:26:16 12:34
Site: Bay 3, Germano Cava

Sounding: GCCPT16-03
Cone: 376:T375F10U200

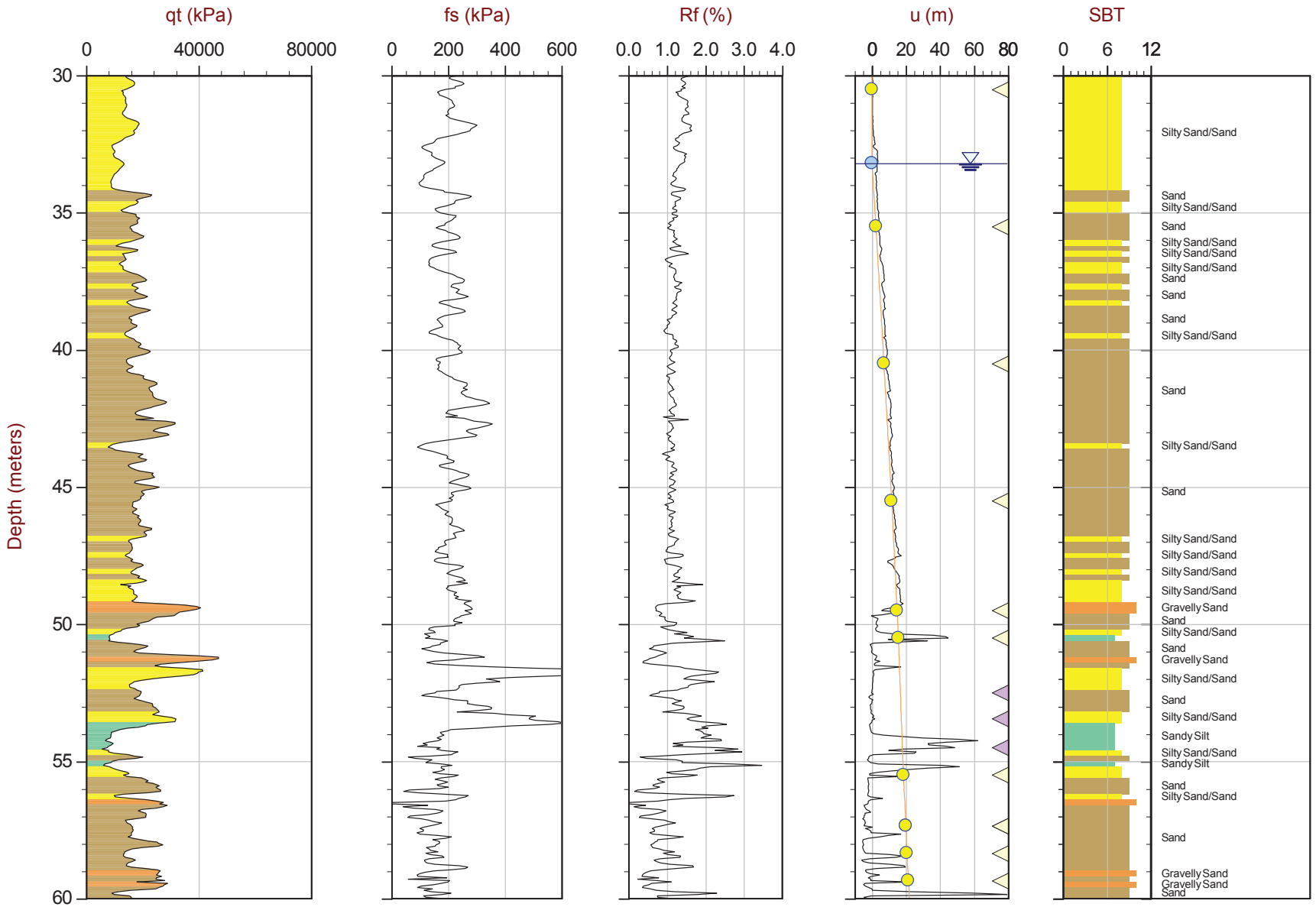

Max Depth: 61.650 m / 202.26 ft
Depth Inc: 0.050 m / 0.164 ft
Avg Int: 0.200 m

File: 16-72004_RS03.COR
Unit Wt: SBT Zones

SBT: Robertson and Campanella, 1986
Coords: UTM Zone 23 South N: 7766164m E: 657252m
Page No: 2 of 3

Overplot Item:
- Assumed Ueq
- Ueq
- Dissipation, equilibrium achieved
- Dissipation, equilibrium not achieved
- Equilibrium Line

CONETEC

CGSH

Job No: 16-72004
Date: 04:26:16 12:34
Site: Bay 3, Germano Cava

Sounding: GCCPT16-03
Cone: 376:T375F10U200

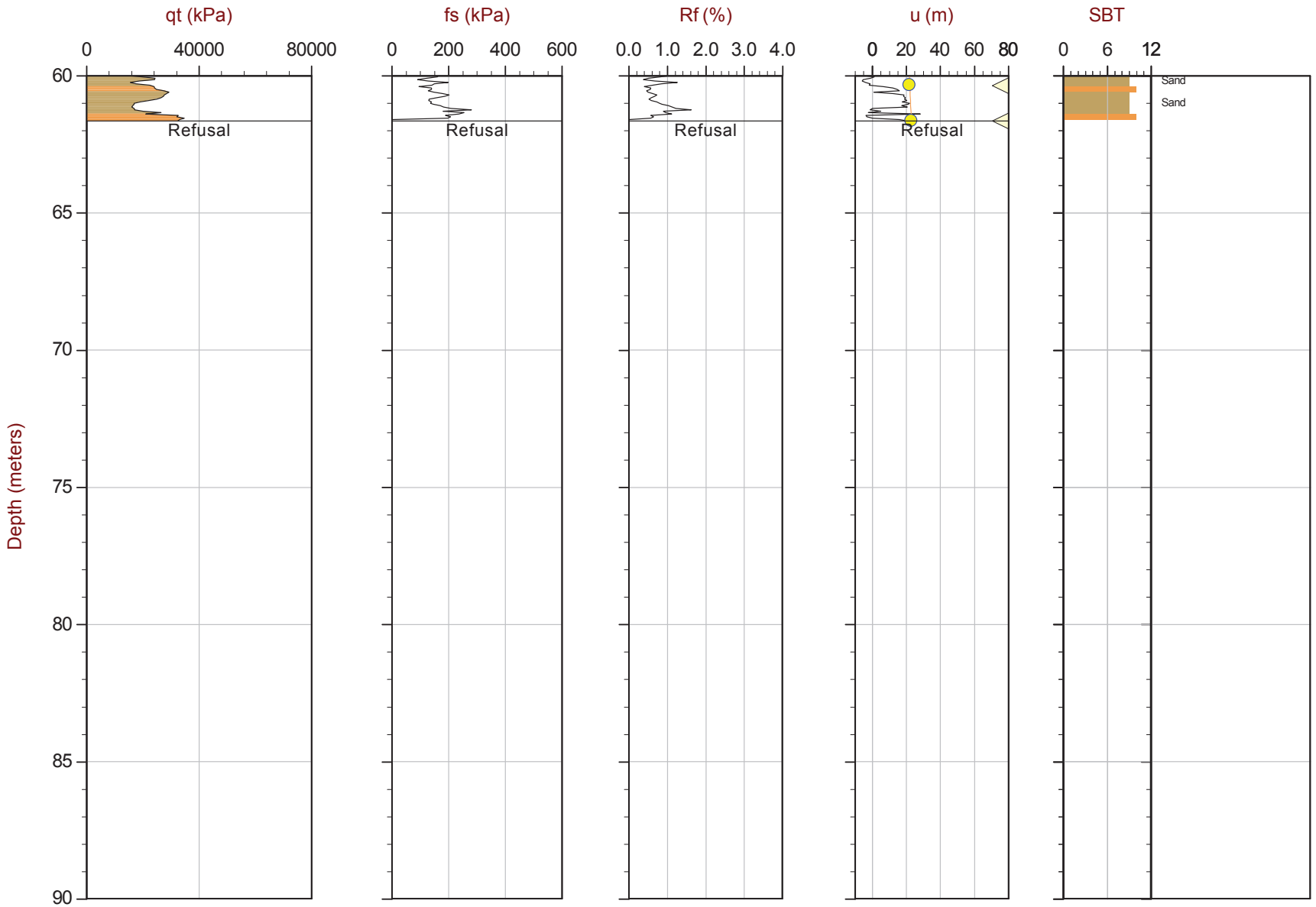

Max Depth: 61.650 m / 202.26 ft
Depth Inc: 0.050 m / 0.164 ft
Avg Int: 0.200 m

File: 16-72004_RS03.COR
Unit Wt: SBT Zones

SBT: Robertson and Campanella, 1986
Coords: UTM Zone 23 South N: 7766164m E: 657252m
Page No: 3 of 3

Overplot Item:
- Assumed Ueq
- Ueq
- Dissipation, equilibrium achieved
- Dissipation, equilibrium not achieved
- Equilibrium Line

CONETEC

CGSH

Job No: 16-72004
Date: 05:02:16 15:34
Site: Bay 3, Germano Cava

Sounding: GCCPT16-04
Cone: 376:T375F10U200

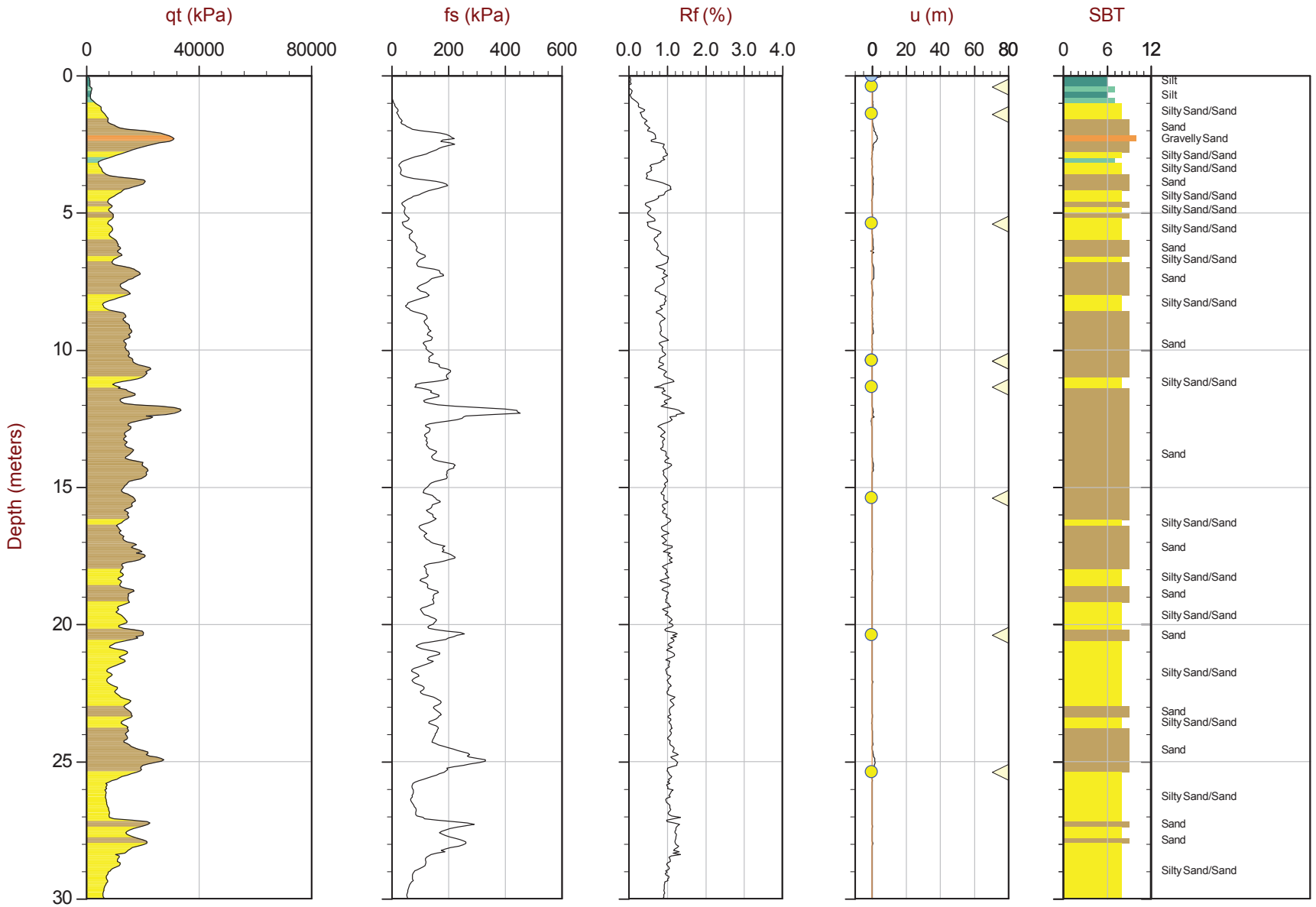

Max Depth: 35.350 m / 115.98 ft
Depth Inc: 0.050 m / 0.164 ft
Avg Int: 0.200 m
Overplot Item:

File: 16-72004_RS04.COR
Unit Wt: SBT Zones

SBT: Robertson and Campanella, 1986
Coords: UTM Zone 23 South N: 7766303m E: 657393m
Page No: 1 of 2

Assumed Ueq
Ueq
Dissipation, equilibrium achieved
Dissipation, equilibrium not achieved
Equilibrium Line

CONETEC

CGSH

Job No: 16-72004
Date: 05:02:16 15:34
Site: Bay 3, Germano Cava

Sounding: GCCPT16-04
Cone: 376:T375F10U200

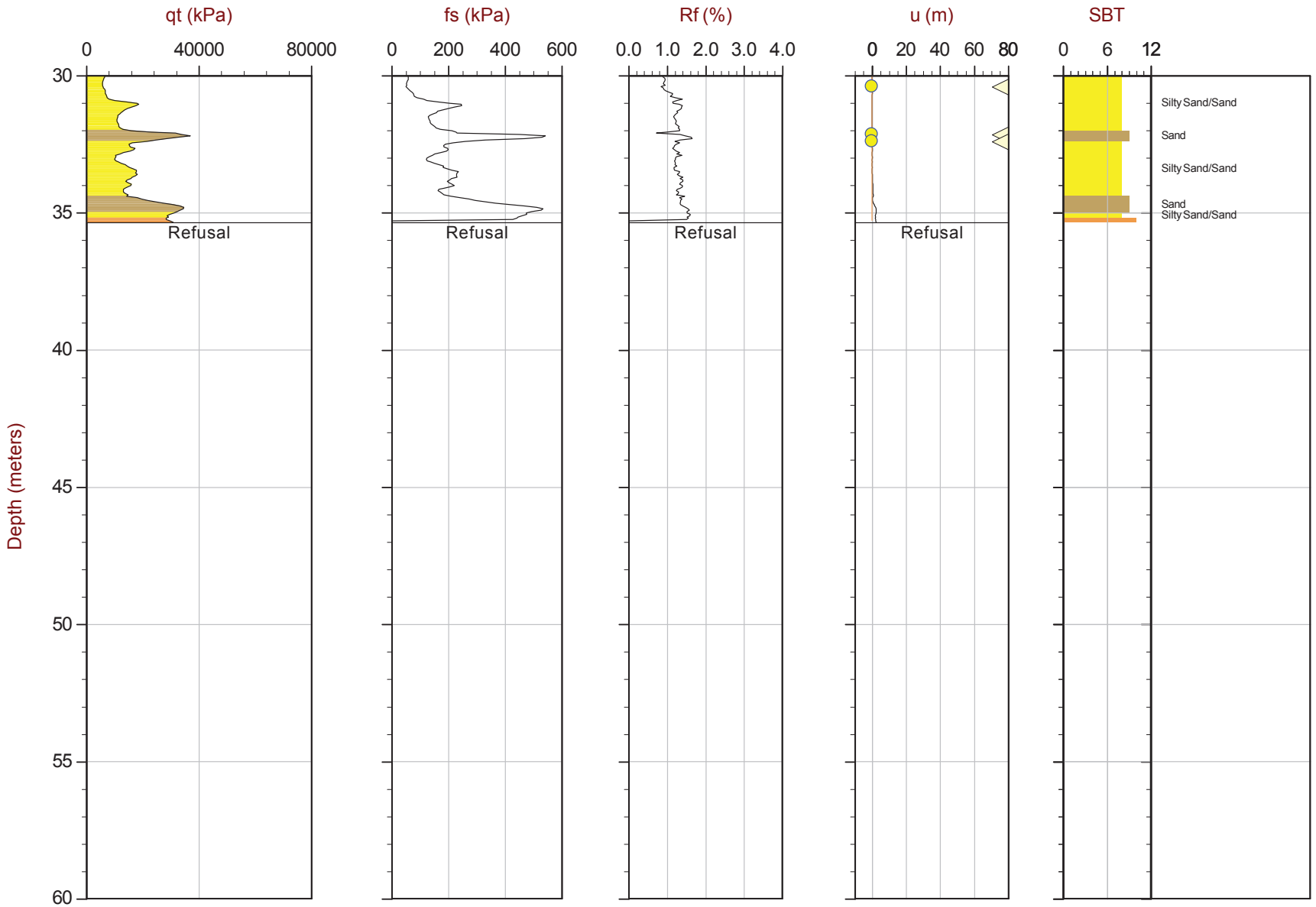

Max Depth: 35.350 m / 115.98 ft
Depth Inc: 0.050 m / 0.164 ft
Avg Int: 0.200 m
Overplot Item:

File: 16-72004_RS04.COR
Unit Wt: SBT Zones

SBT: Robertson and Campanella, 1986
Coords: UTM Zone 23 South N: 7766303m E: 657393m
Page No: 2 of 2

Assumed Ueq
Ueq
Dissipation, equilibrium achieved
Dissipation, equilibrium not achieved
Equilibrium Line

CONETEC

CGSH

Job No: 16-72004
Date: 05:13:16 13:07
Site: Germano Cava

Sounding: GCCPT16-04B
Cone: 432:T1500F15U500

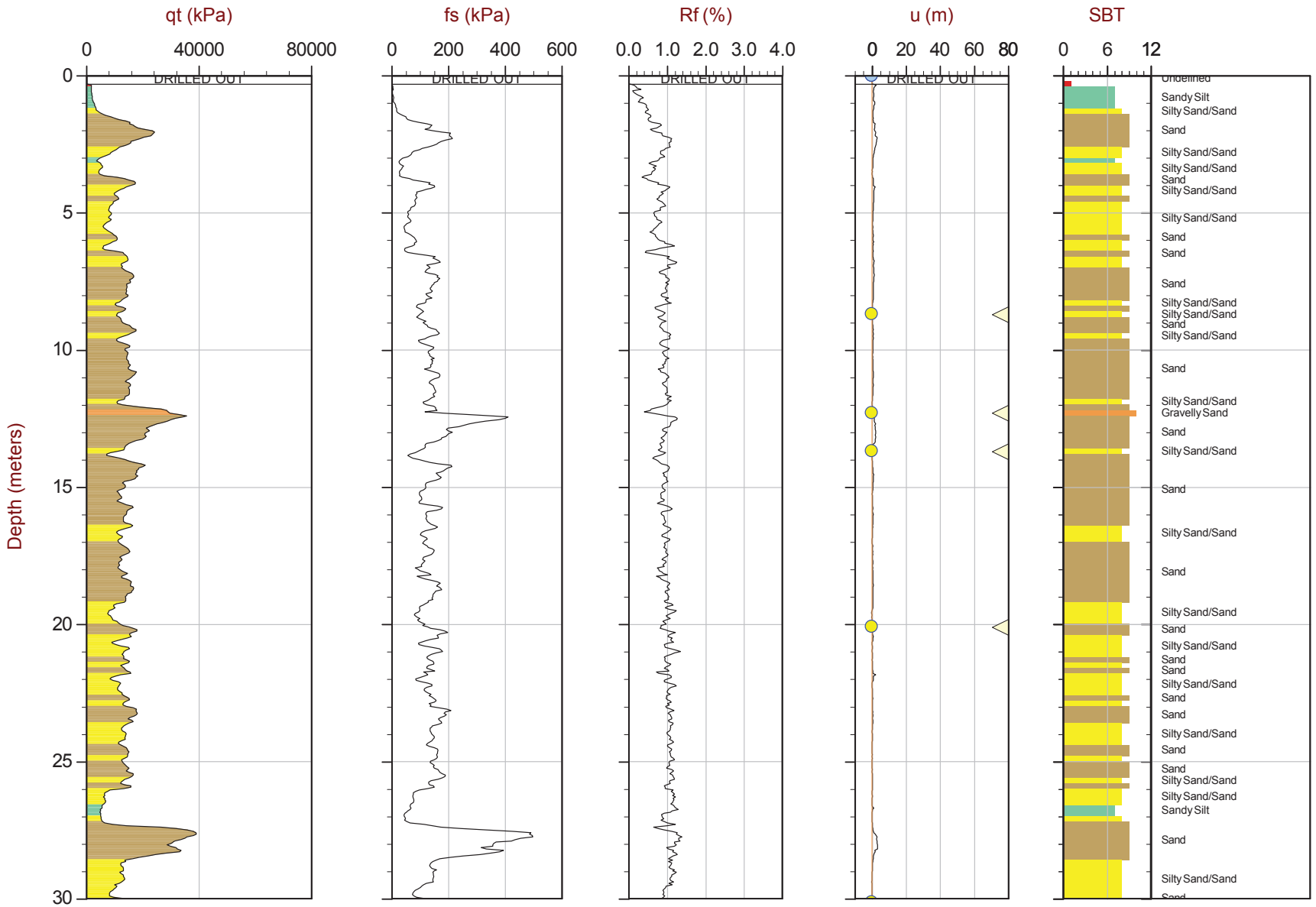

Max Depth: 36.350 m / 119.26 ft
Depth Inc: 0.050 m / 0.164 ft
Avg Int: 0.200 m
Overplot Item:

File: 16-72004_RS04B.COR
Unit Wt: SBT Zones

SBT: Robertson and Campanella, 1986
Coords: UTM Zone 23 South N: 7766300m E: 657394m
Page No: 1 of 2

Assumed Ueq
Ueq
Dissipation, equilibrium achieved
Dissipation, equilibrium not achieved
Equilibrium Line

CONETEC

CGSH

Job No: 16-72004
Date: 05:13:16 13:07
Site: Germano Cava

Sounding: GCCPT16-04B
Cone: 432:T1500F15U500

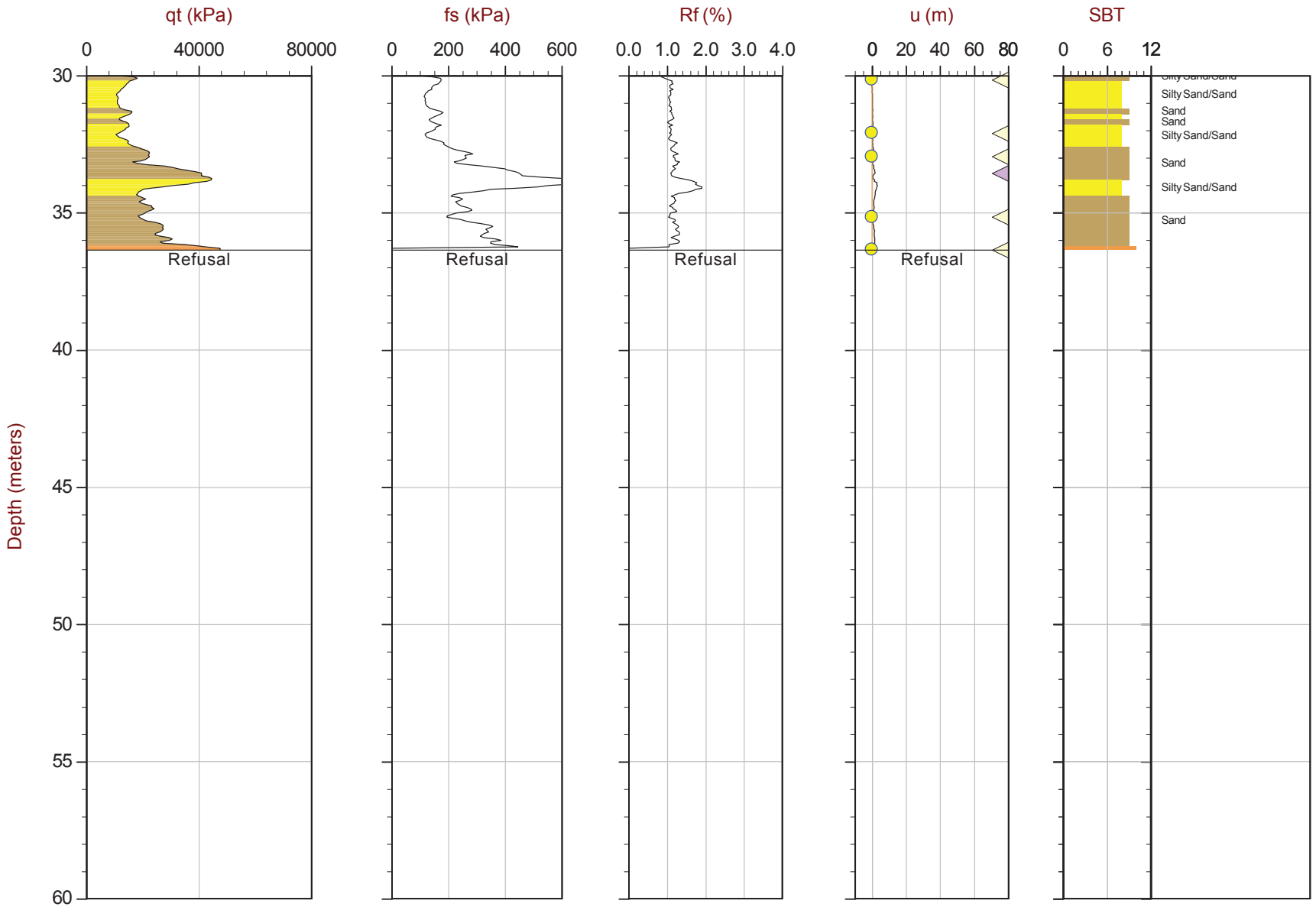

Max Depth: 36.350 m / 119.26 ft
Depth Inc: 0.050 m / 0.164 ft
Avg Int: 0.200 m

File: 16-72004_RS04B.COR
Unit Wt: SBT Zones

SBT: Robertson and Campanella, 1986
Coords: UTM Zone 23 South N: 7766300m E: 657394m
Page No: 2 of 2

Overplot Item:
- Assumed Ueq
- Ueq
- Dissipation, equilibrium achieved
- Dissipation, equilibrium not achieved
- Equilibrium Line

CONETEC

CGSH

Job No: 16-72004
Date: 05:05:16 10:41
Site: Bay 3, Germano Slimes

Sounding: GSCPT16-05
Cone: 376:T375F10U200

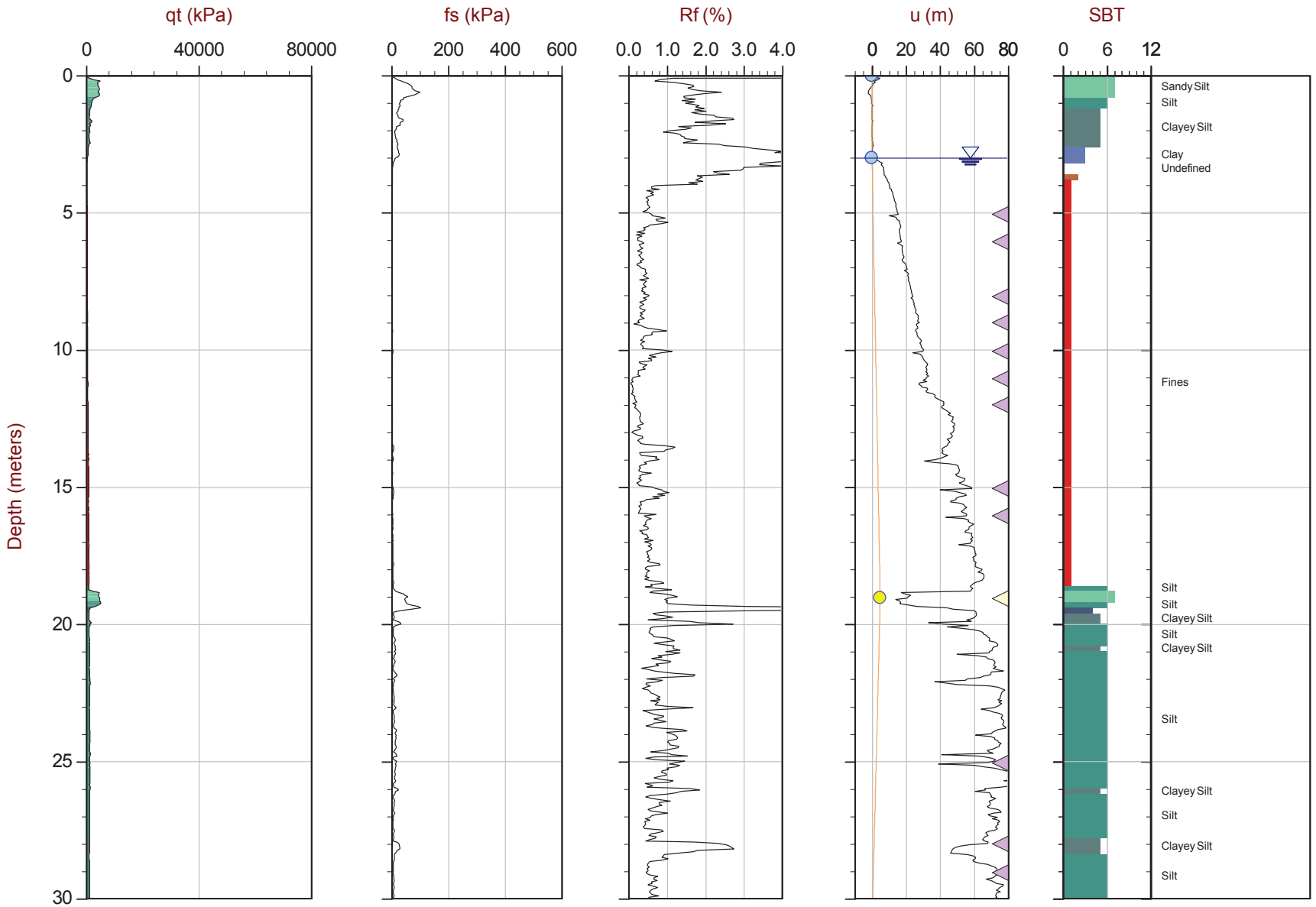

Max Depth: 31.850 m / 104.49 ft
Depth Inc: 0.050 m / 0.164 ft
Avg Int: 0.200 m
Overplot Item:

File: 16-72004_SP05.COR
Unit Wt: SBT Zones

SBT: Robertson and Campanella, 1986
Coords: UTM Zone 23 South N: 7763372m E: 659090m
Page No: 1 of 2

Assumed Ueq
Ueq
Dissipation, equilibrium achieved
Dissipation, equilibrium not achieved
Equilibrium Line

CONETEC

CGSH

Job No: 16-72004
Date: 05:05:16 10:41
Site: Bay 3, Germano Slimes

Sounding: GSCPT16-05
Cone: 376:T375F10U200

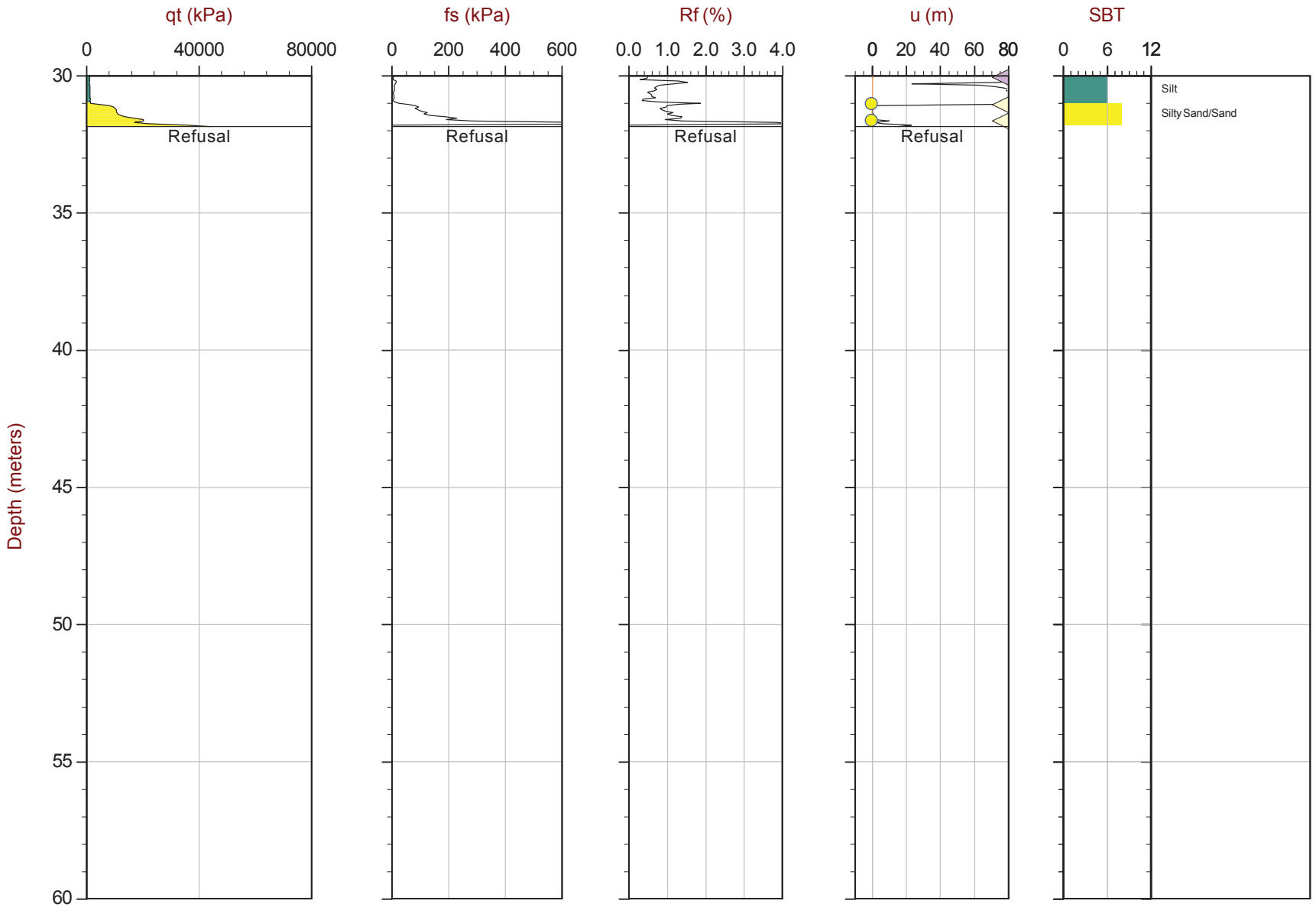

Max Depth: 31.850 m / 104.49 ft
Depth Inc: 0.050 m / 0.164 ft
Avg Int: 0.200 m
Overplot Item:

File: 16-72004_SP05.COR
Unit Wt: SBT Zones

SBT: Robertson and Campanella, 1986
Coords: UTM Zone 23 South N: 7763372m E: 659090m
Page No: 2 of 2

Assumed Ueq
Ueq
Dissipation, equilibrium achieved
Dissipation, equilibrium not achieved
Equilibrium Line

CONETEC

CGSH

Job No: 16-72004
Date: 05:16:16 13:45
Site: Germano Buttres

Sounding: GBCPT16-06
Cone: 432:T1500F15U500

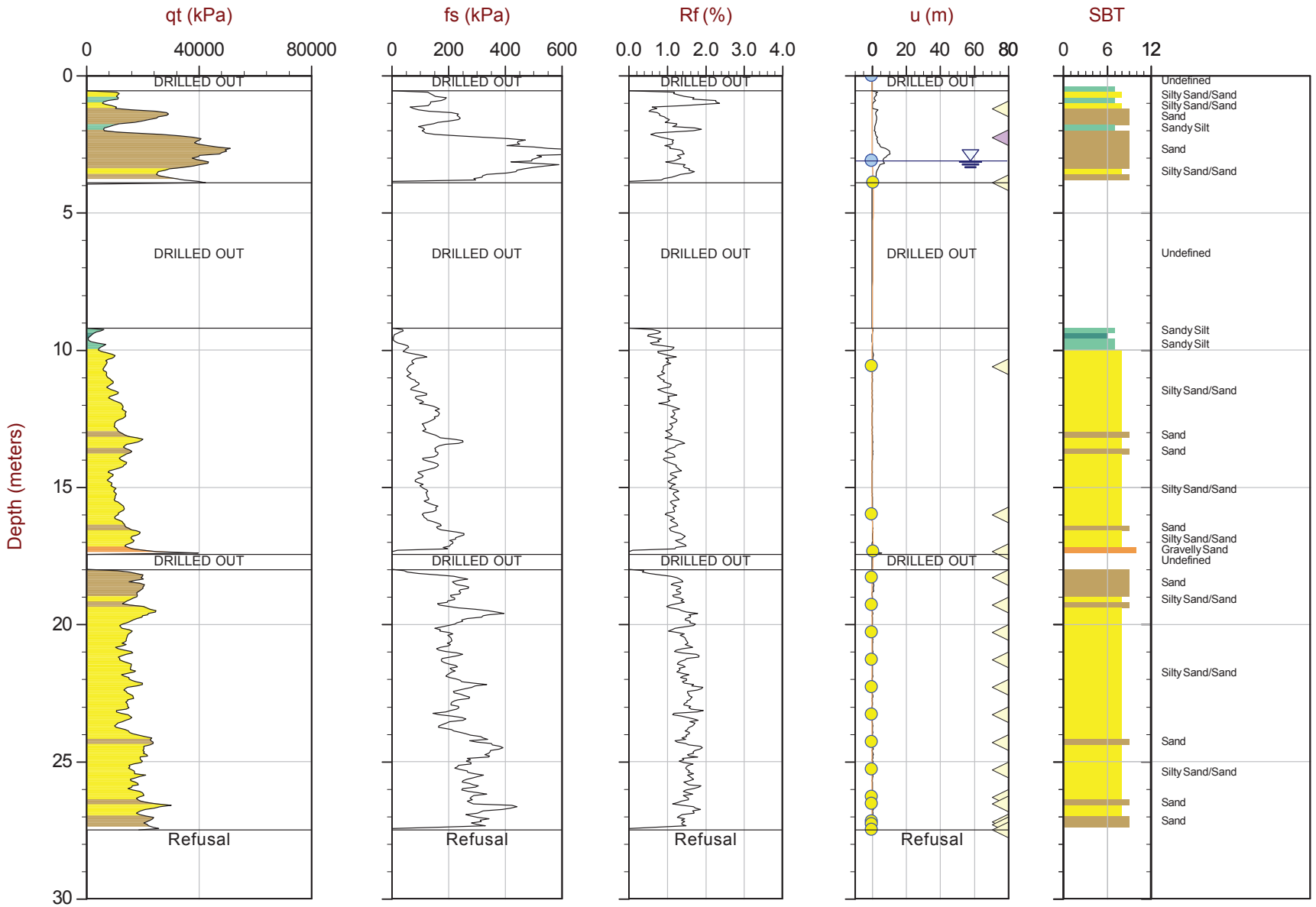

Max Depth: 27.500 m / 90.22 ft
Depth Inc: 0.050 m / 0.164 ft
Avg Int: 0.200 m

File: 16-72004_RS06.COR
Unit Wt: SBT Zones

SBT: Robertson and Campanella, 1986
Coords: UTM Zone 23 South N: 7763631 m E: 660586 m
Page No: 1 of 1

Overplot Item:
- Assumed Ueq
- Ueq
- Dissipation, equilibrium achieved
- Dissipation, equilibrium not achieved
- Equilibrium Line

CONETEC

CGSH

Job No: 16-72004
Date: 05:17:16 09:36
Site: Germano Buttres

Sounding: GBCPT16-06B
Cone: 432:T1500F15U500

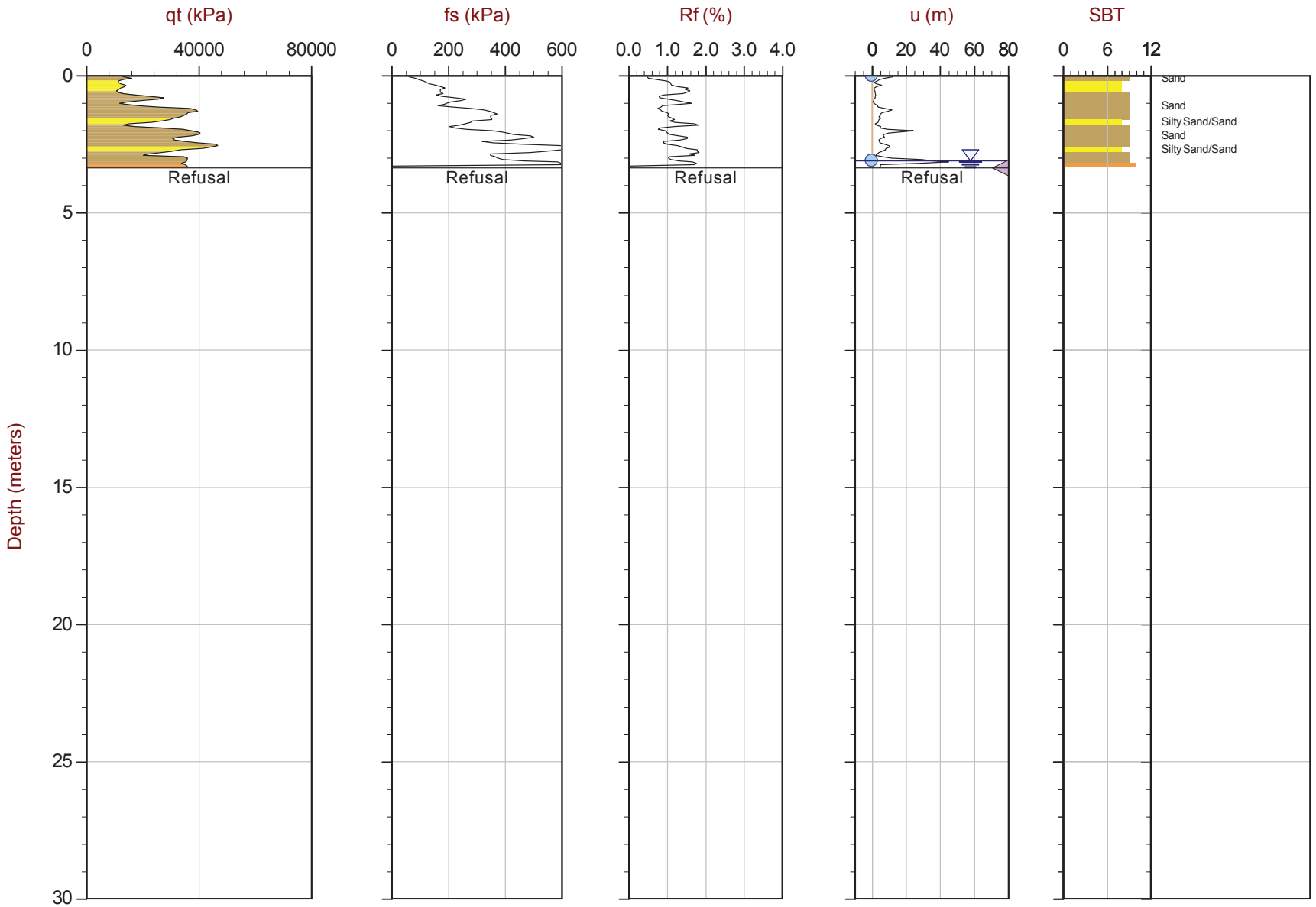

Max Depth: 3.350 m / 10.99 ft
Depth Inc: 0.050 m / 0.164 ft
Avg Int: 0.200 m

File: 16-72004_RS06B.COR
Unit Wt: SBT Zones

SBT: Robertson and Campanella, 1986
Coords: UTM Zone 23 South N: 7763631 m E: 660583m
Page No: 1 of 1

Overplot Item:
- Assumed Ueq
- Ueq
- Dissipation, equilibrium achieved
- Dissipation, equilibrium not achieved
- Equilibrium Line

Advance Cone Penetration Test Plots with Su(Nkt) and Phi Angle

CONETEC

CONETEC

CGSH

Job No: 16-72004
Date: 04:19:16 15:03
Site: Germano Buttres

Sounding: GBCPT16-01
Cone: 432:T1500F15U500

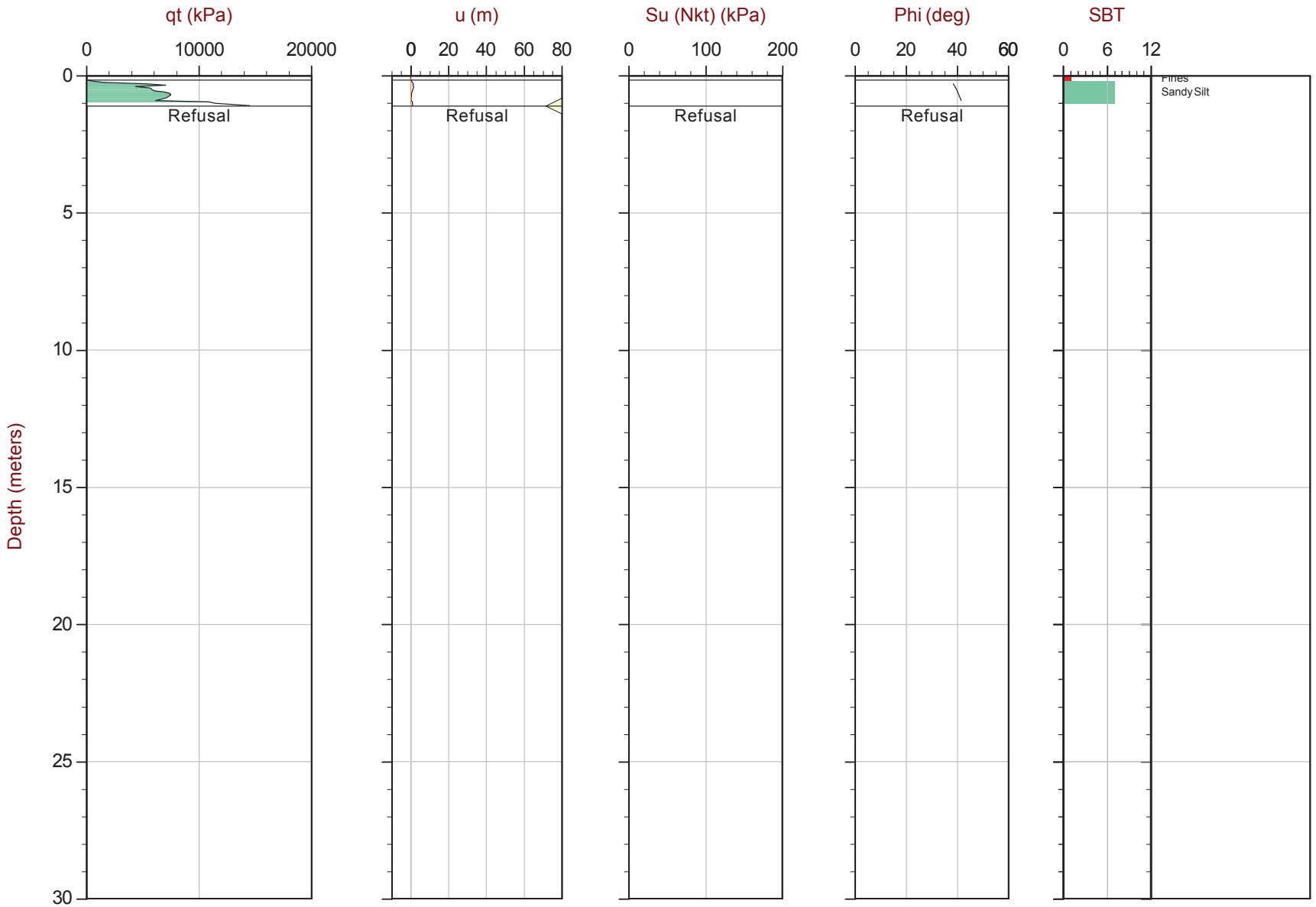

Max Depth: 1.100 m / 3.61 ft
Depth Inc: 0.050 m / 0.164 ft
Avg Int: 0.200 m
Overplot Item:
Assumed Ueq
Ueq

File: 16-72004_RS01.COR
Unit Wt: SBT Zones
Su Nkt: 15.0
Dissipation, equilibrium achieved
Dissipation, equilibrium not achieved
Equilibrium Line

SBT: Robertson and Campanella, 1986
Coords: UTM Zone 23 South N: 7763639m E: 660664m
Page No: 1 of 1

CONETEC

CGSH

Job No: 16-72004
Date: 04:20:16 12:52
Site: Germano Buttres

Sounding: GBCPT16-01B
Cone: 432:T1500F15U500

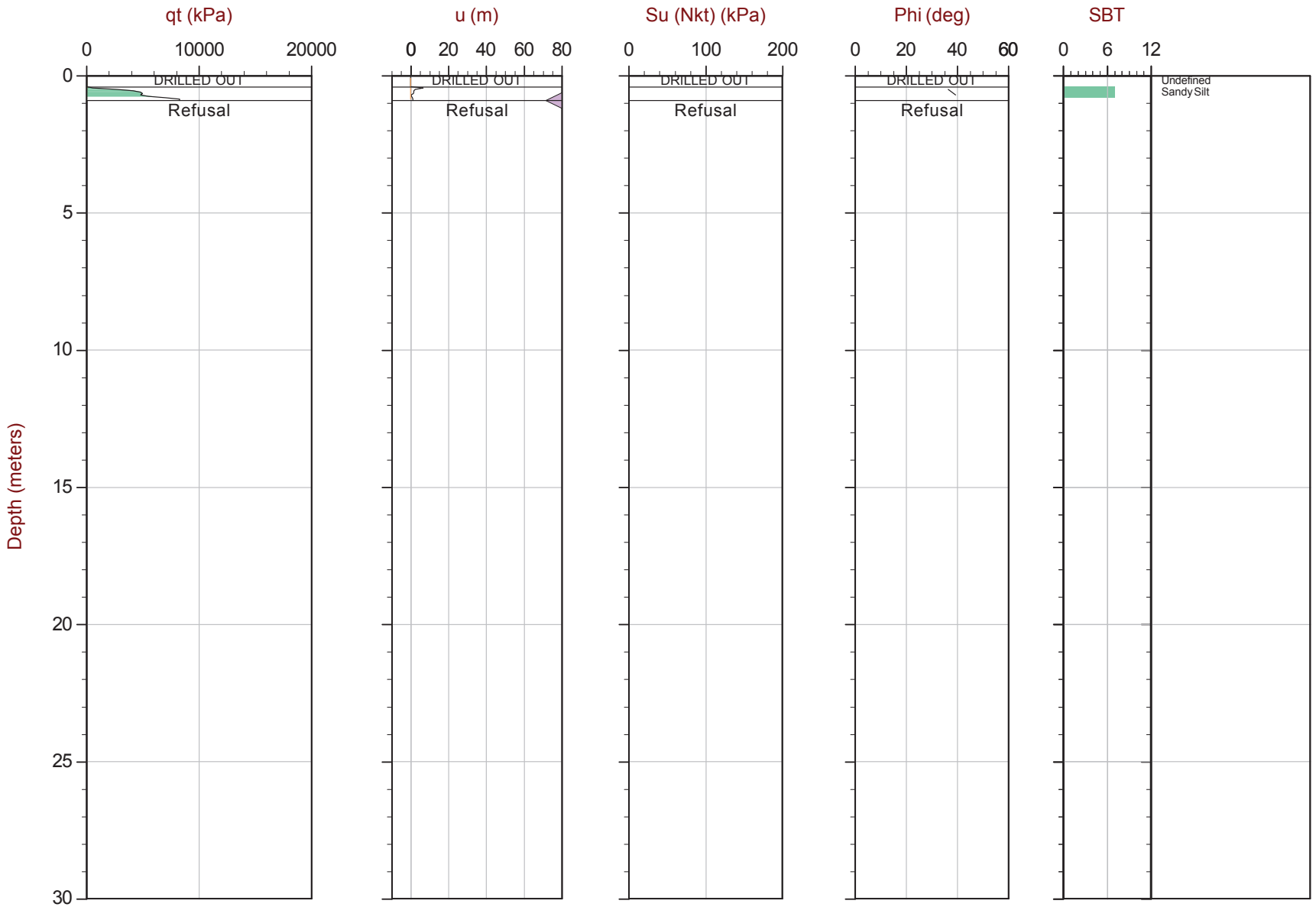

Max Depth: 0.900 m / 2.95 ft
Depth Inc: 0.050 m / 0.164 ft
Avg Int: 0.200 m
Overplot Item:
Assumed Ueq
Ueq

File: 16-72004_RS01B.COR
Unit Wt: SBT Zones
Su Nkt: 15.0
Dissipation, equilibrium achieved
Dissipation, equilibrium not achieved
Equilibrium Line

SBT: Robertson and Campanella, 1986
Coords: UTM Zone 23 South N: 7763639m E: 660664m
Page No: 1 of 1

CONETEC

CGSH

Job No: 16-72004
Date: 04:20:16 15:32
Site: Germano Buttres

Sounding: GBCPT16-01C
Cone: 432:T1500F15U500

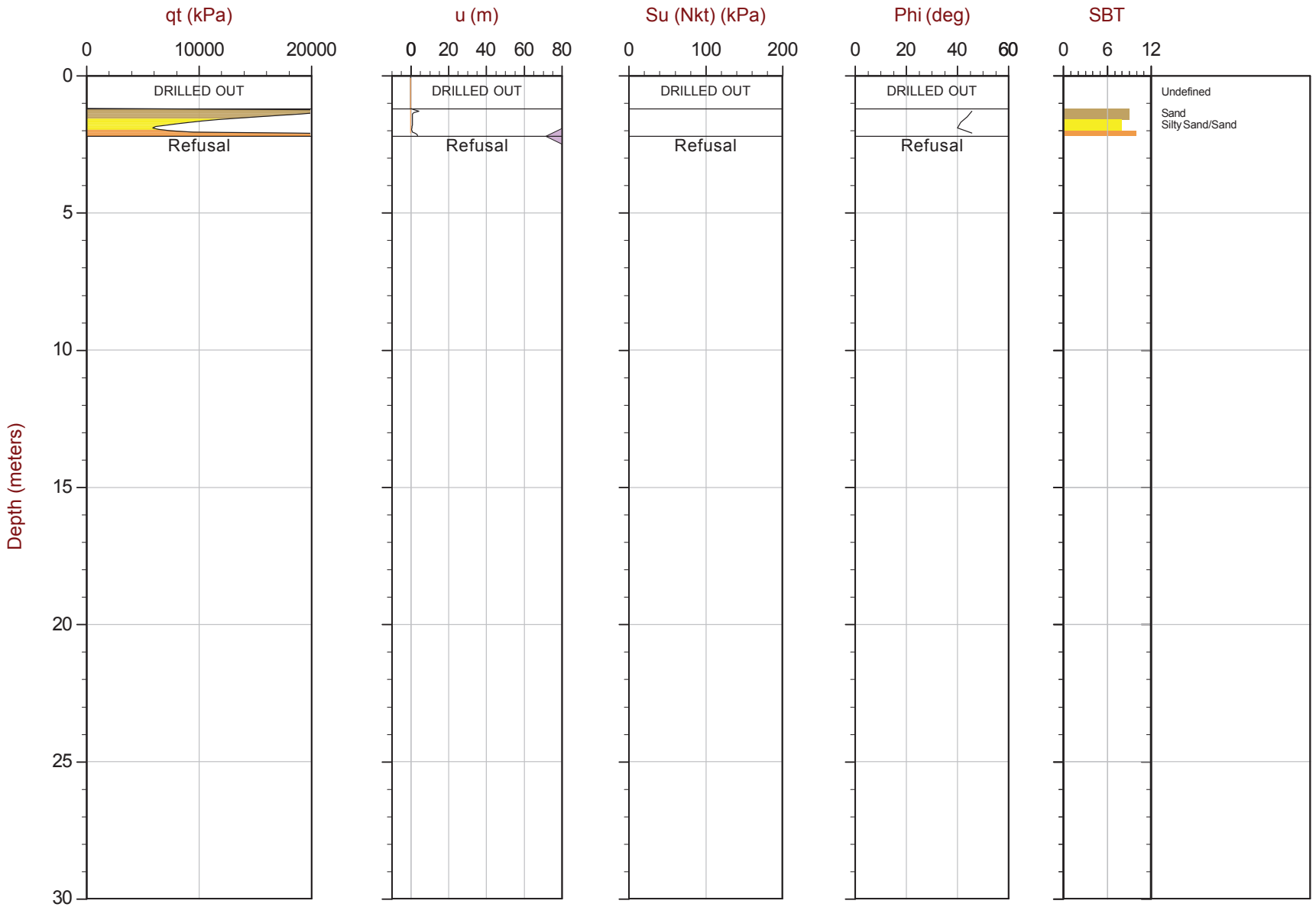

Max Depth: 2.200 m / 7.22 ft
Depth Inc: 0.050 m / 0.164 ft
Avg Int: 0.200 m
Overplot Item:
Assumed Ueq
Ueq

File: 16-72004_RS01C.COR
Unit Wt: SBT Zones
Su Nkt: 15.0
Dissipation, equilibrium achieved
Dissipation, equilibrium not achieved
Equilibrium Line

SBT: Robertson and Campanella, 1986
Coords: UTM Zone 23 South N: 7763639m E: 660664m
Page No: 1 of 1

CONETEC

CGSH

Job No: 16-72004
Date: 04:21:16 14:33
Site: Bay 3, Germano Slimes

Sounding: GSCPT16-02
Cone: 432:T1500F15U500

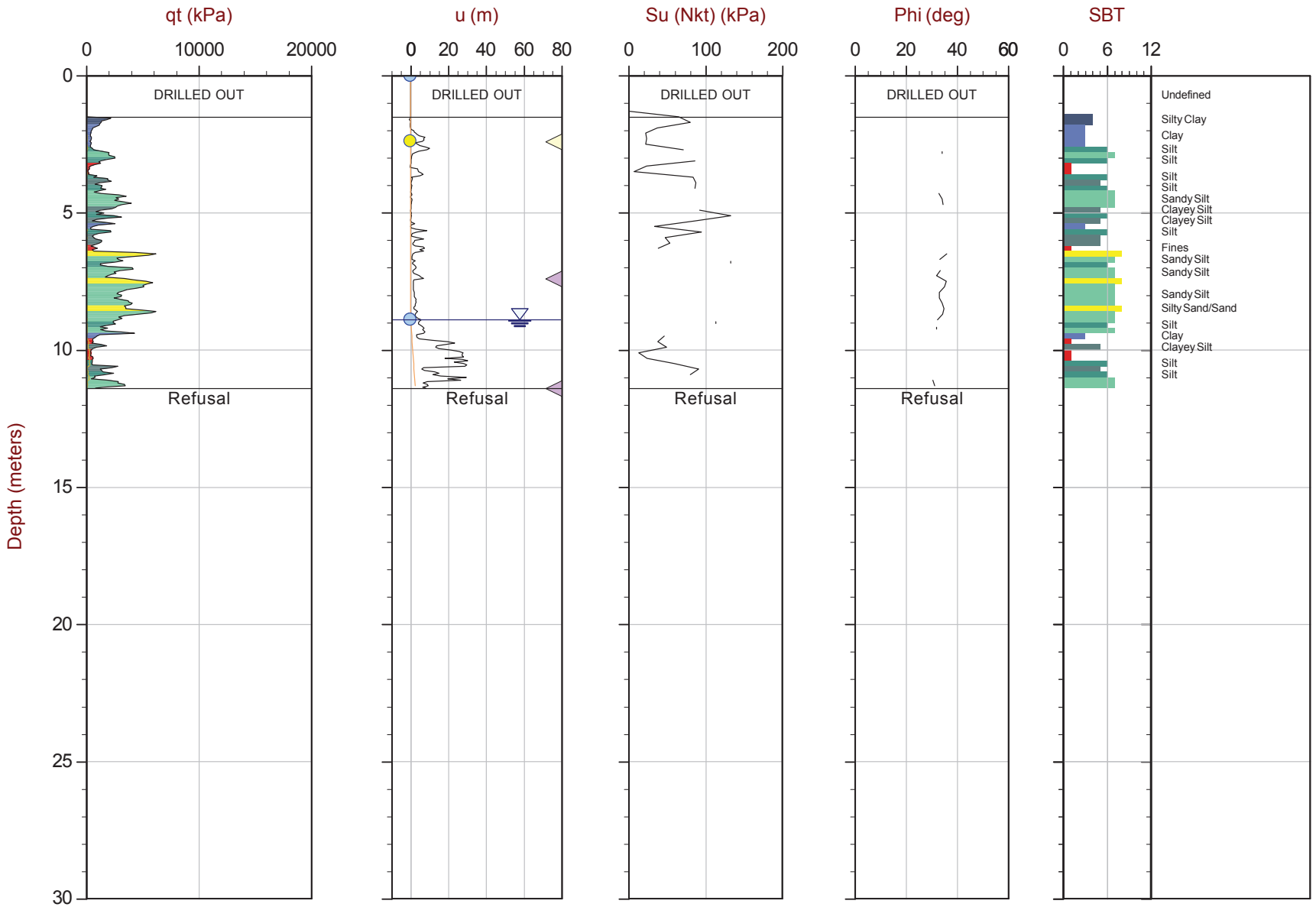

Max Depth: 11.400 m / 37.40 ft
Depth Inc: 0.050 m / 0.164 ft
Avg Int: 0.200 m
Overplot Item:
Assumed Ueq
Ueq

File: 16-72004_RS02.COR
Unit Wt: SBT Zones
Su Nkt: 15.0
Dissipation, equilibrium achieved
Dissipation, equilibrium not achieved
Equilibrium Line

SBT: Robertson and Campanella, 1986
Coords: UTM Zone 23 South N: 7764153m E: 658559m
Page No: 1 of 1

CONETEC

CGSH

Job No: 16-72004
Date: 04:24:16 11:30
Site: Bay 3, Germano Slimes

Sounding: GSCPT16-02B
Cone: 376:T375F10U200

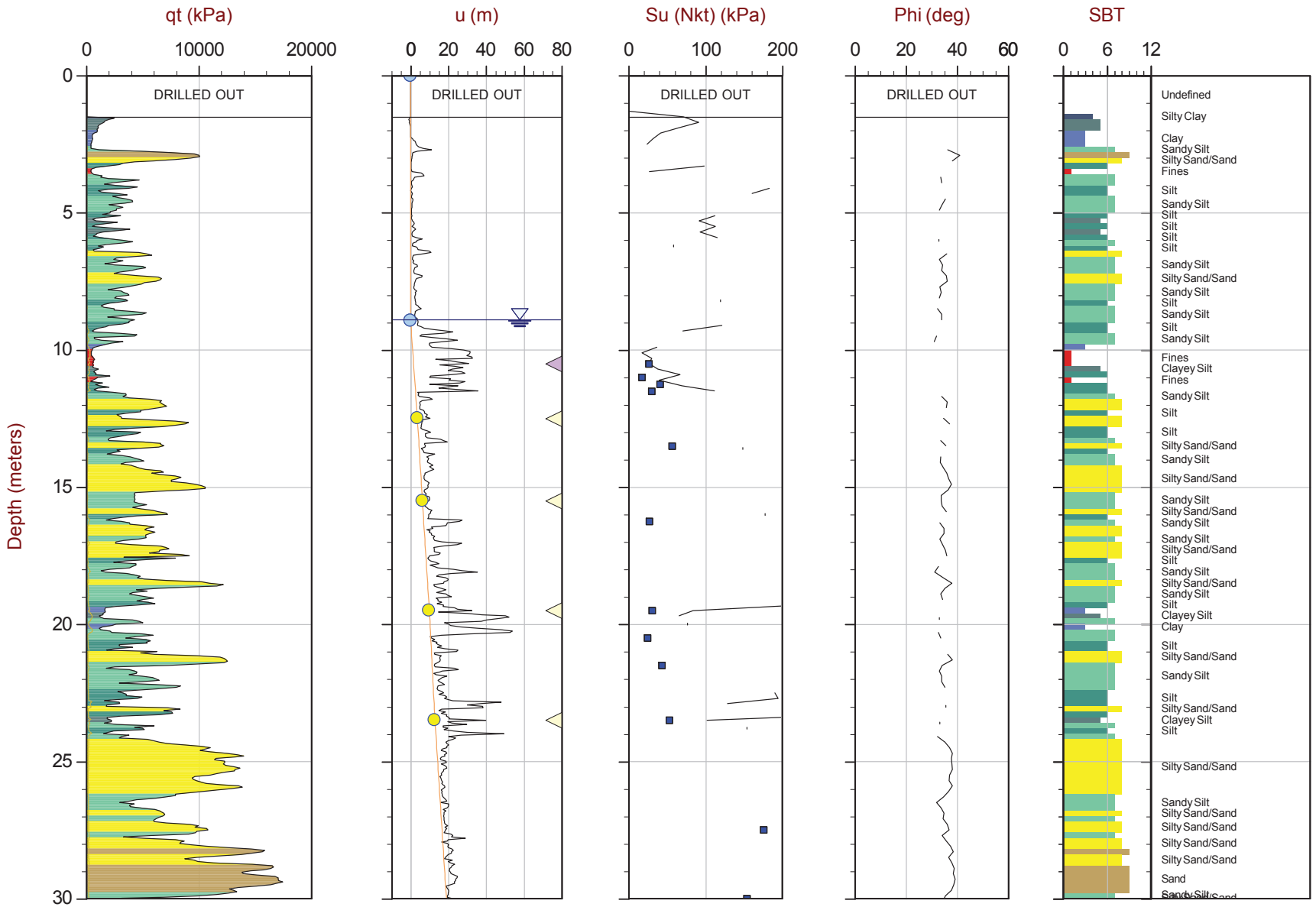

Max Depth: 41.650 m / 136.65 ft
Depth Inc: 0.050 m / 0.164 ft
Avg Int: 0.200 m
Overplot Item:
Assumed Ueq
Ueq

File: 16-72004_RS02B.COR
Unit Wt: SBT Zones
Su Nkt: 15.0
Su(VST)
Dissipation, equilibrium achieved
Dissipation, equilibrium not achieved
Equilibrium Line

SBT: Robertson and Campanella, 1986
Coords: UTM Zone 23 South N: 7764155m E: 658559m

CONETEC

CGSH

Job No: 16-72004
Date: 04:24:16 11:30
Site: Bay 3, Germano Slimes

Sounding: GSCPT16-02B
Cone: 376:T375F10U200

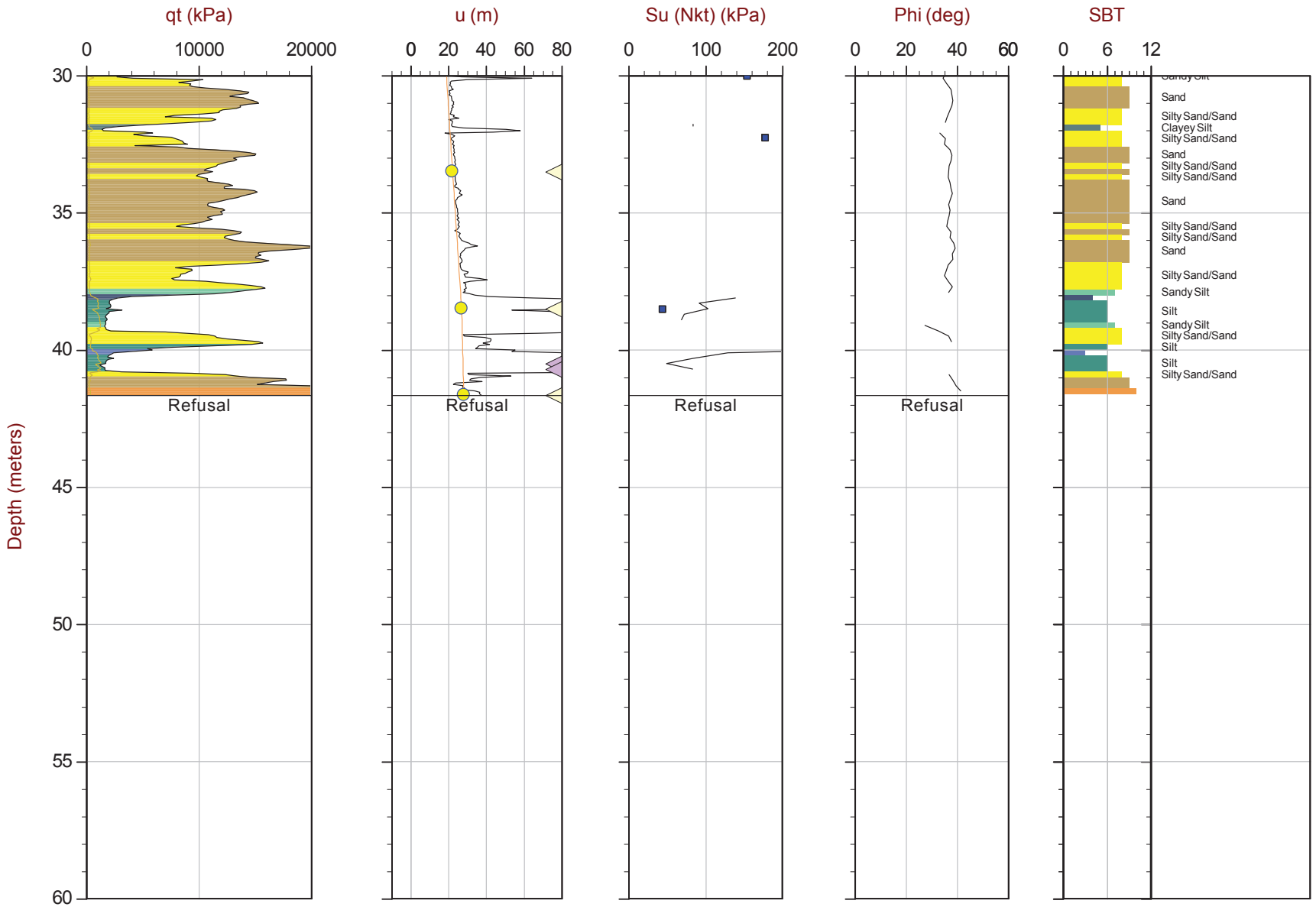

Max Depth: 41.650 m / 136.65 ft
Depth Inc: 0.050 m / 0.164 ft
Avg Int: 0.200 m
Overplot Item:
Assumed Ueq
Ueq

File: 16-72004_RS02B.COR
Unit Wt: SBT Zones
Su Nkt: 15.0
Su(VST)
Dissipation, equilibrium achieved
Dissipation, equilibrium not achieved
Equilibrium Line

SBT: Robertson and Campanella, 1986
Coords: UTM Zone 23 South N: 7764155m E: 658559m
Page No: 2 of 2

CONETEC

CGSH

Job No: 16-72004
Date: 04:26:16 12:34
Site: Bay 3, Germano Cava

Sounding: GCCPT16-03
Cone: 376:T375F10U200

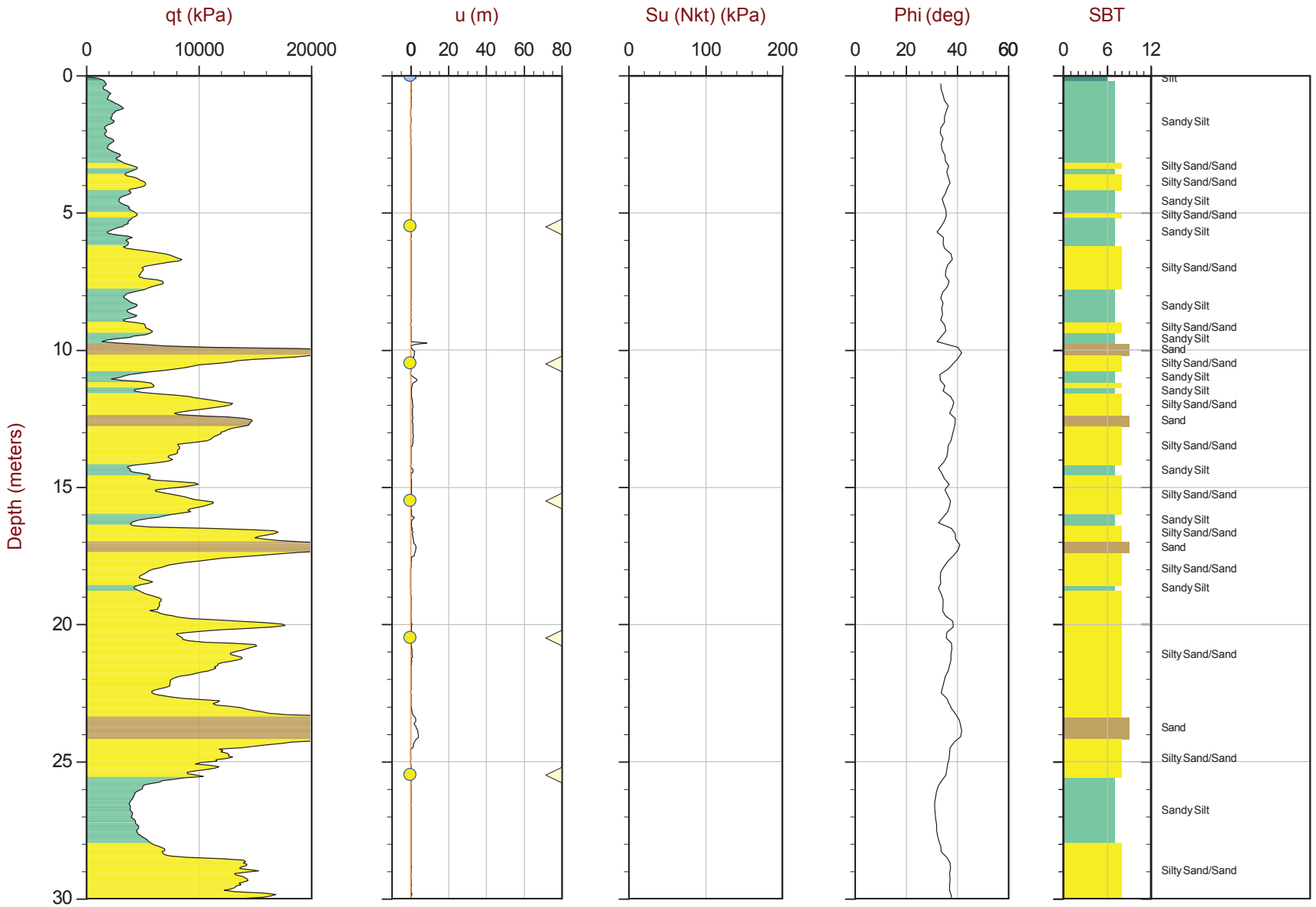

Max Depth: 61.650 m / 202.26 ft
Depth Inc: 0.050 m / 0.164 ft
Avg Int: 0.200 m
Overplot Item:
- Assumed Ueq
- Ueq

File: 16-72004_RS03.COR
Unit Wt: SBT Zones
Su Nkt: 15.0
- Dissipation, equilibrium achieved
- Dissipation, equilibrium not achieved
- Equilibrium Line

SBT: Robertson and Campanella, 1986
Coords: UTM Zone 23 South N: 7766164m E: 657252m

CONETEC

CGSH

Job No: 16-72004
Date: 04:26:16 12:34
Site: Bay 3, Germano Cava

Sounding: GCCPT16-03
Cone: 376:T375F10U200

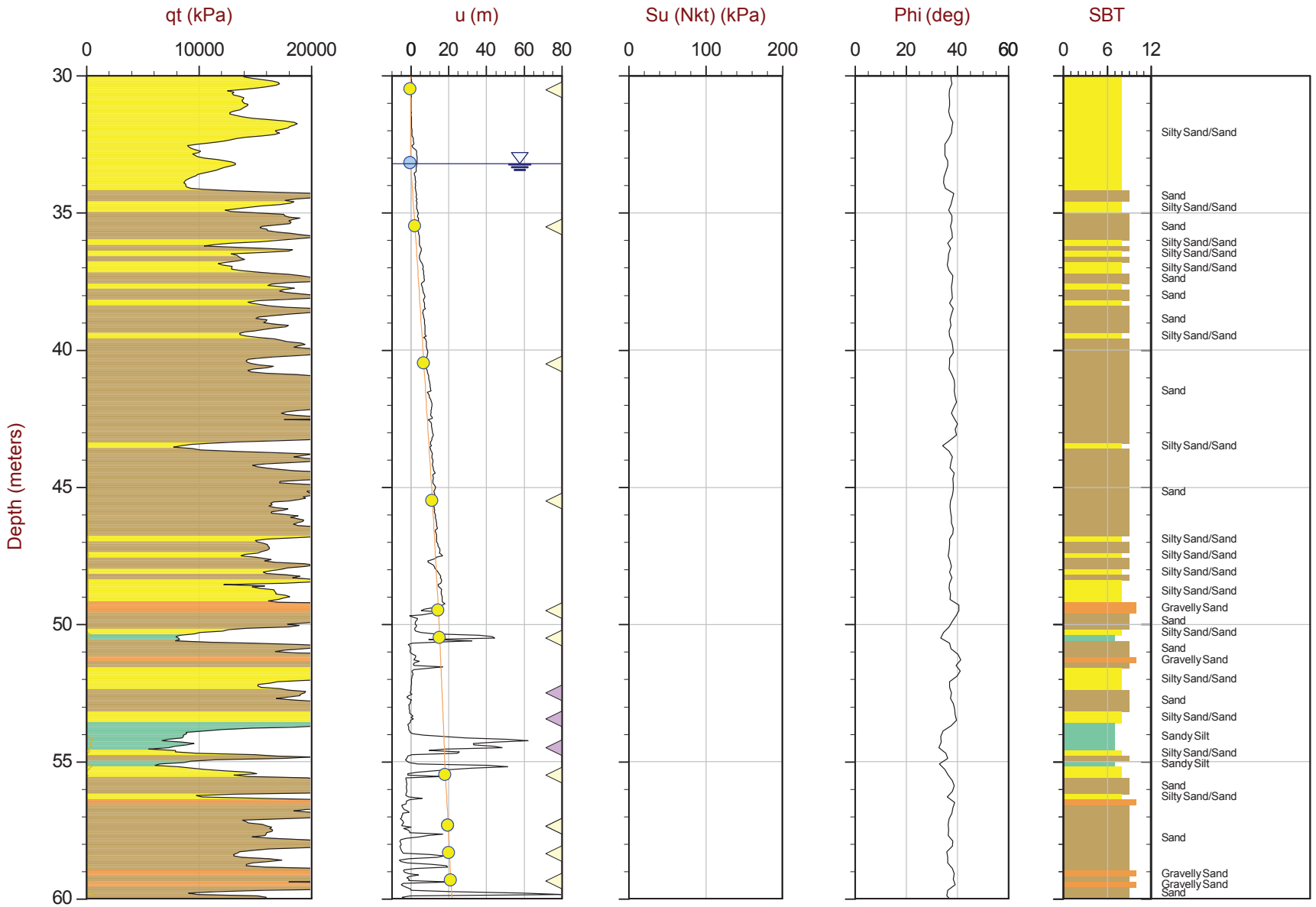

Max Depth: 61.650 m / 202.26 ft
Depth Inc: 0.050 m / 0.164 ft
Avg Int: 0.200 m
Overplot Item:
- Assumed Ueq
- Ueq

File: 16-72004_RS03.COR
Unit Wt: SBT Zones
Su Nkt: 15.0
- Dissipation, equilibrium achieved
- Dissipation, equilibrium not achieved
- Equilibrium Line

SBT: Robertson and Campanella, 1986
Coords: UTM Zone 23 South N: 7766164m E: 657252m

CONETEC

CGSH

Job No: 16-72004
Date: 04:26:16 12:34
Site: Bay 3, Germano Cava

Sounding: GCCPT16-03
Cone: 376:T375F10U200

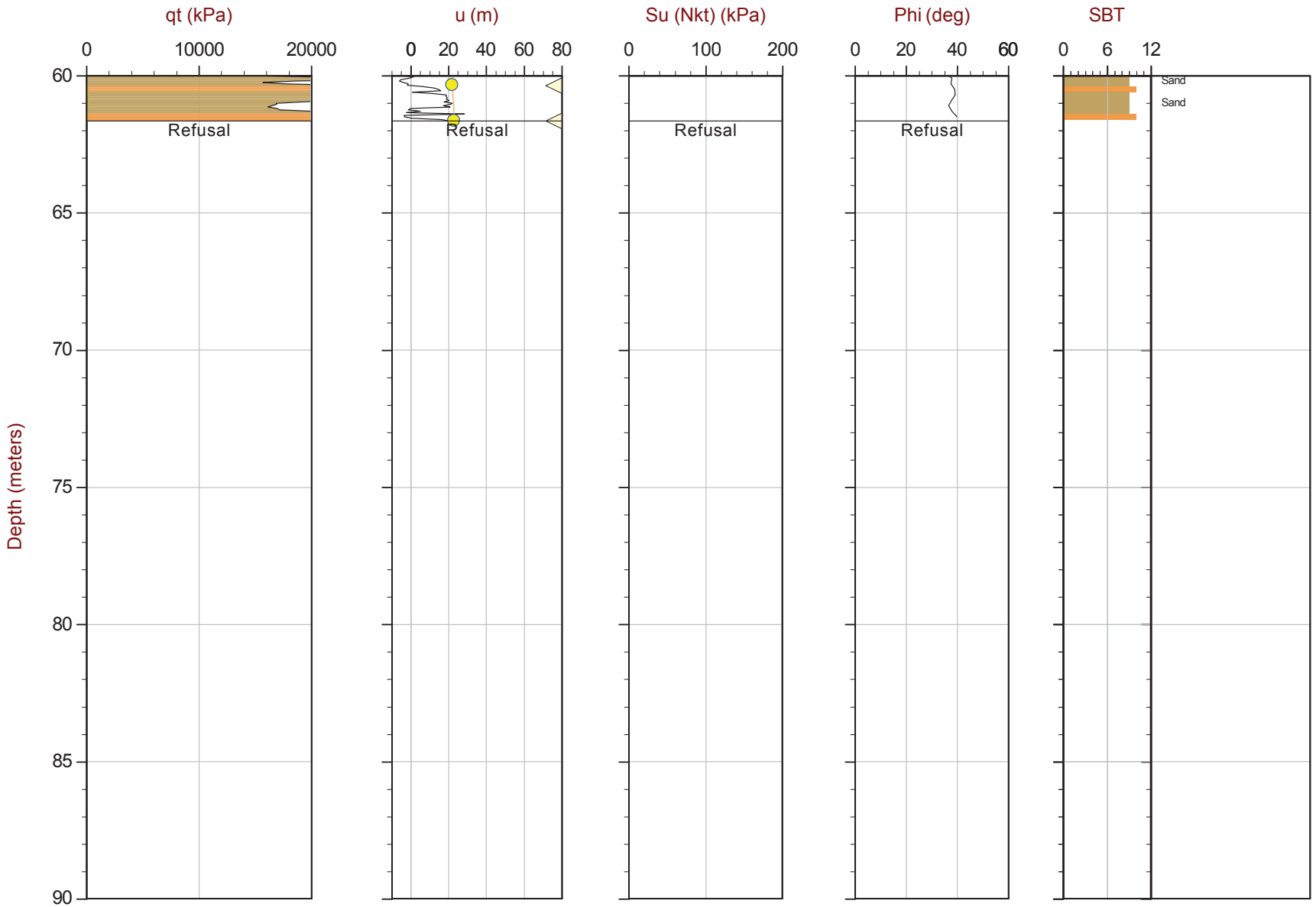

Max Depth: 61.650 m / 202.26 ft
Depth Inc: 0.050 m / 0.164 ft
Avg Int: 0.200 m
Overplot Item:
Assumed Ueq
Ueq

File: 16-72004_RS03.COR
Unit Wt: SBT Zones
Su Nkt: 15.0
Dissipation, equilibrium achieved
Dissipation, equilibrium not achieved
Equilibrium Line

SBT: Robertson and Campanella, 1986
Coords: UTM Zone 23 South N: 7766164m E: 657252m
Page No: 3 of 3

CONETEC

CGSH

Job No: 16-72004
Date: 05:02:16 15:34
Site: Bay 3, Germano Cava

Sounding: GCCPT16-04
Cone: 376:T375F10U200

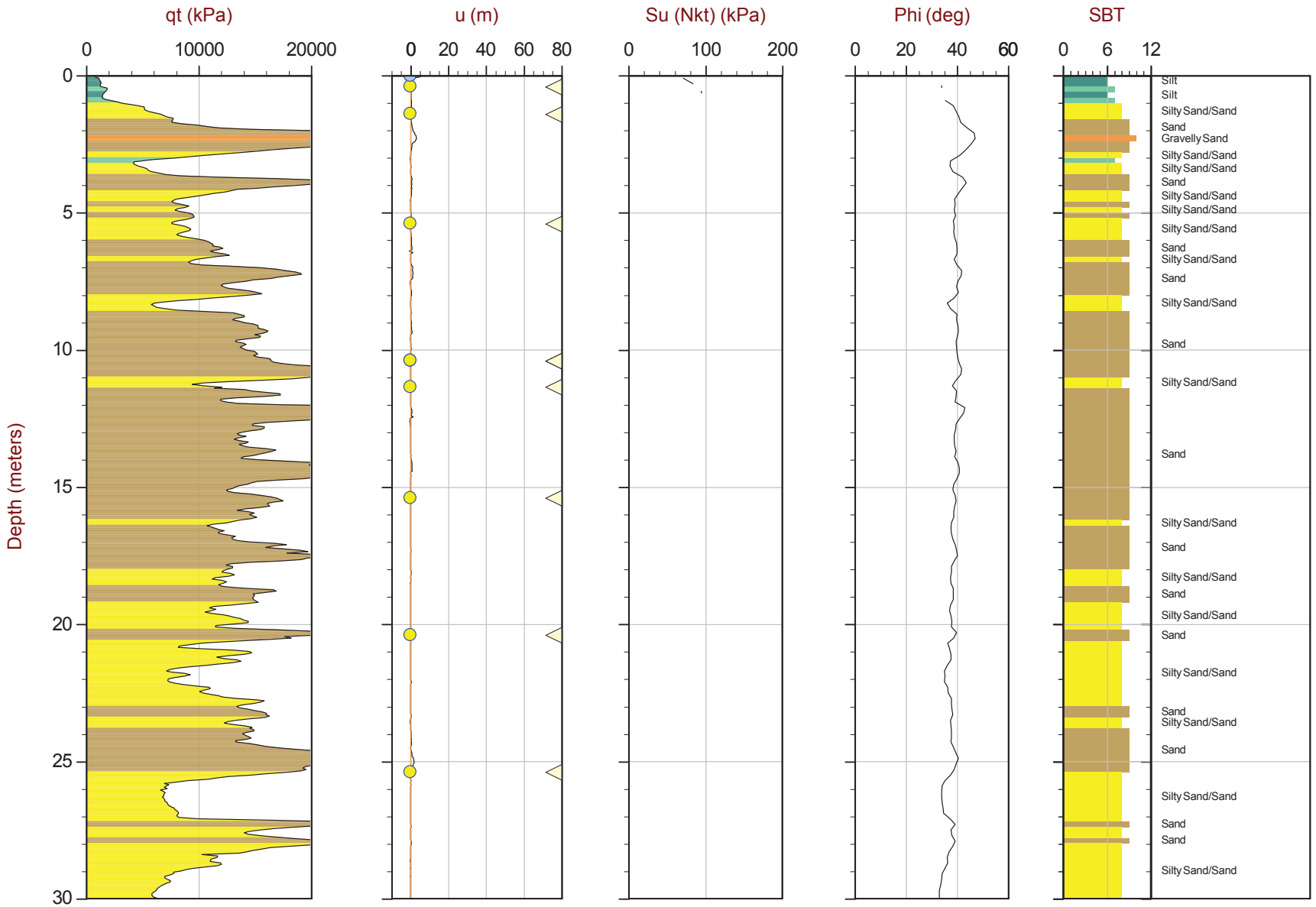

Max Depth: 35.350 m / 115.98 ft
Depth Inc: 0.050 m / 0.164 ft
Avg Int: 0.200 m
Overplot Item:
Assumed Ueq
Ueq

File: 16-72004_RS04.COR
Unit Wt: SBT Zones
Su Nkt: 15.0
Dissipation, equilibrium achieved
Dissipation, equilibrium not achieved
Equilibrium Line

SBT: Robertson and Campanella, 1986
Coords: UTM Zone 23 South N: 7766303m E: 657393m
Page No: 1 of 2

CONETEC

CGSH

Job No: 16-72004
Date: 05:02:16 15:34
Site: Bay 3, Germano Cava

Sounding: GCCPT16-04
Cone: 376:T375F10U200

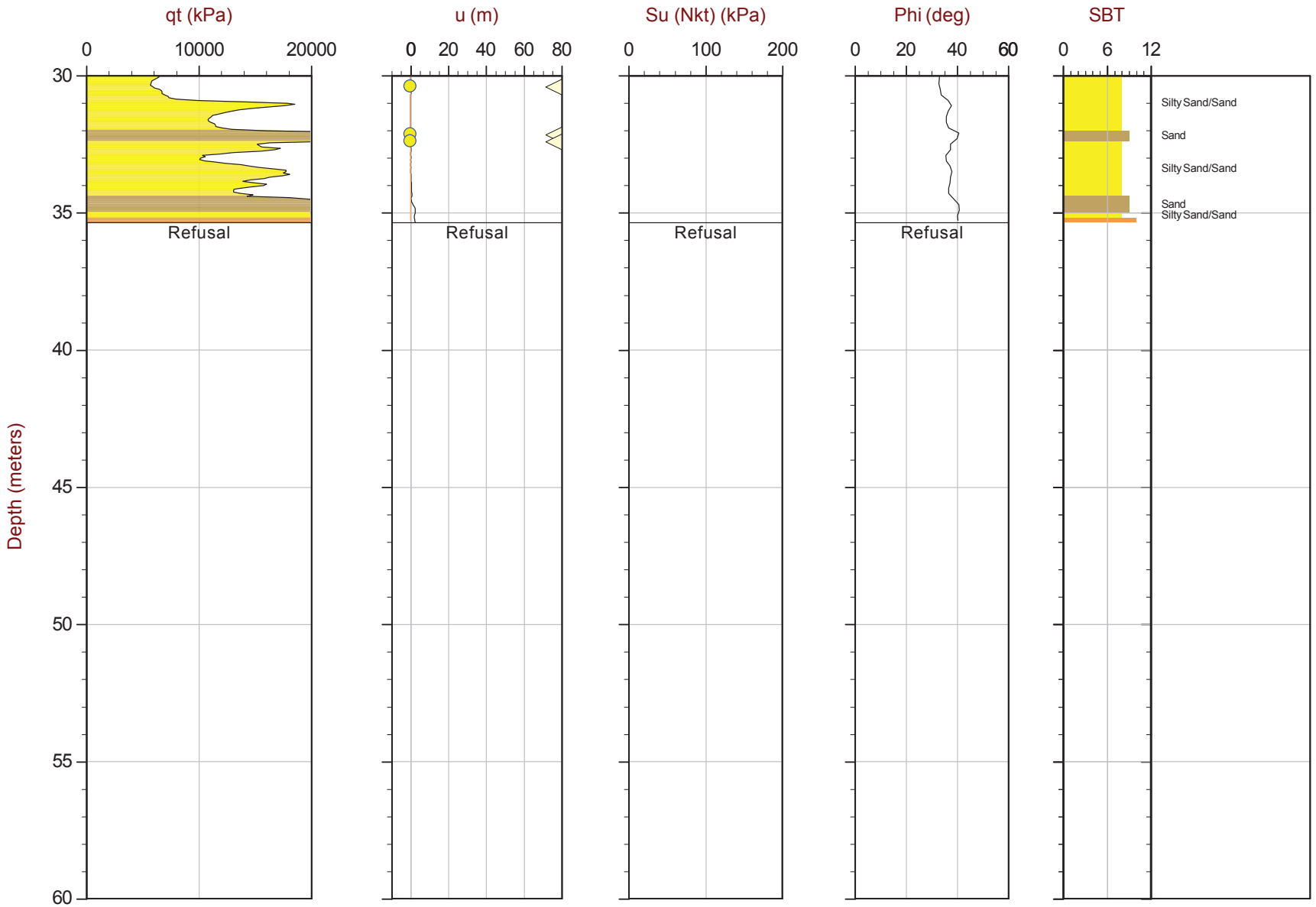

Max Depth: 35.350 m / 115.98 ft
Depth Inc: 0.050 m / 0.164 ft
Avg Int: 0.200 m
Overplot Item:
Assumed Ueq
Ueq

File: 16-72004_RS04.COR
Unit Wt: SBT Zones
Su Nkt: 15.0
Dissipation, equilibrium achieved
Dissipation, equilibrium not achieved
Equilibrium Line

SBT: Robertson and Campanella, 1986
Coords: UTM Zone 23 South N: 7766303m E: 657393m
Page No: 2 of 2

CONETEC

CGSH

Job No: 16-72004
Date: 05:13:16 13:07
Site: Germano Cava

Sounding: GCCPT16-04B
Cone: 432:T1500F15U500

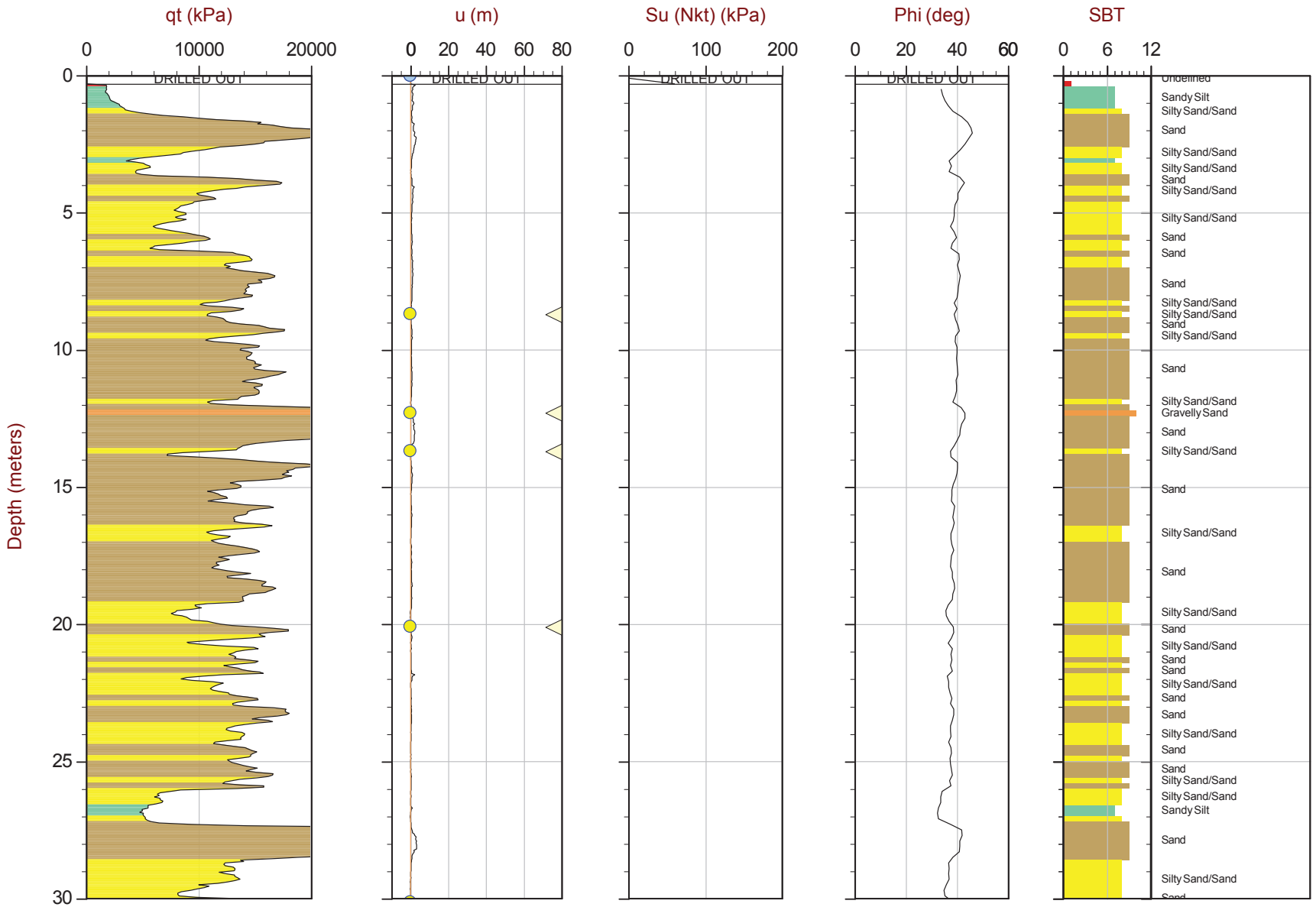

Max Depth: 36.350 m / 119.26 ft
Depth Inc: 0.050 m / 0.164 ft
Avg Int: 0.200 m
Overplot Item:
Assumed Ueq
Ueq

File: 16-72004_RS04B.COR
Unit Wt: SBT Zones
Su Nkt: 15.0
Dissipation, equilibrium achieved
Dissipation, equilibrium not achieved
Equilibrium Line

SBT: Robertson and Campanella, 1986
Coords: UTM Zone 23 South N: 7766300m E: 657394m
Page No: 1 of 2

CONETEC

CGSH

Job No: 16-72004
Date: 05:13:16 13:07
Site: Germano Cava

Sounding: GCCPT16-04B
Cone: 432:T1500F15U500

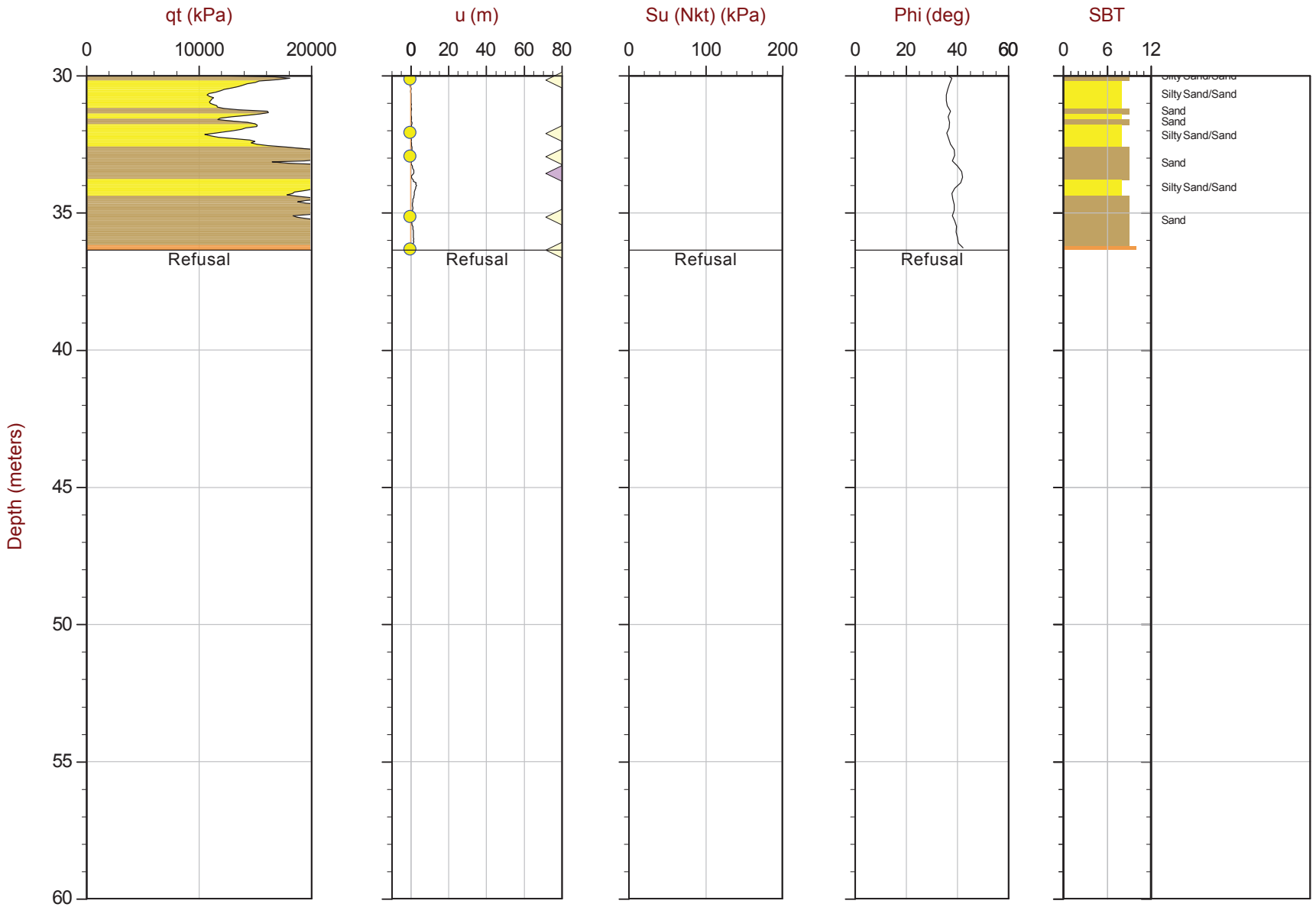

Max Depth: 36.350 m / 119.26 ft
Depth Inc: 0.050 m / 0.164 ft
Avg Int: 0.200 m
Overplot Item:
Assumed Ueq
Ueq

File: 16-72004_RS04B.COR
Unit Wt: SBT Zones
Su Nkt: 15.0
Dissipation, equilibrium achieved
Dissipation, equilibrium not achieved
Equilibrium Line

SBT: Robertson and Campanella, 1986
Coords: UTM Zone 23 South N: 7766300m E: 657394m
Page No: 2 of 2

CONETEC

CGSH

Job No: 16-72004
Date: 05:05:16 10:41
Site: Bay 3, Germano Slimes

Sounding: GSCPT16-05
Cone: 376:T375F10U200

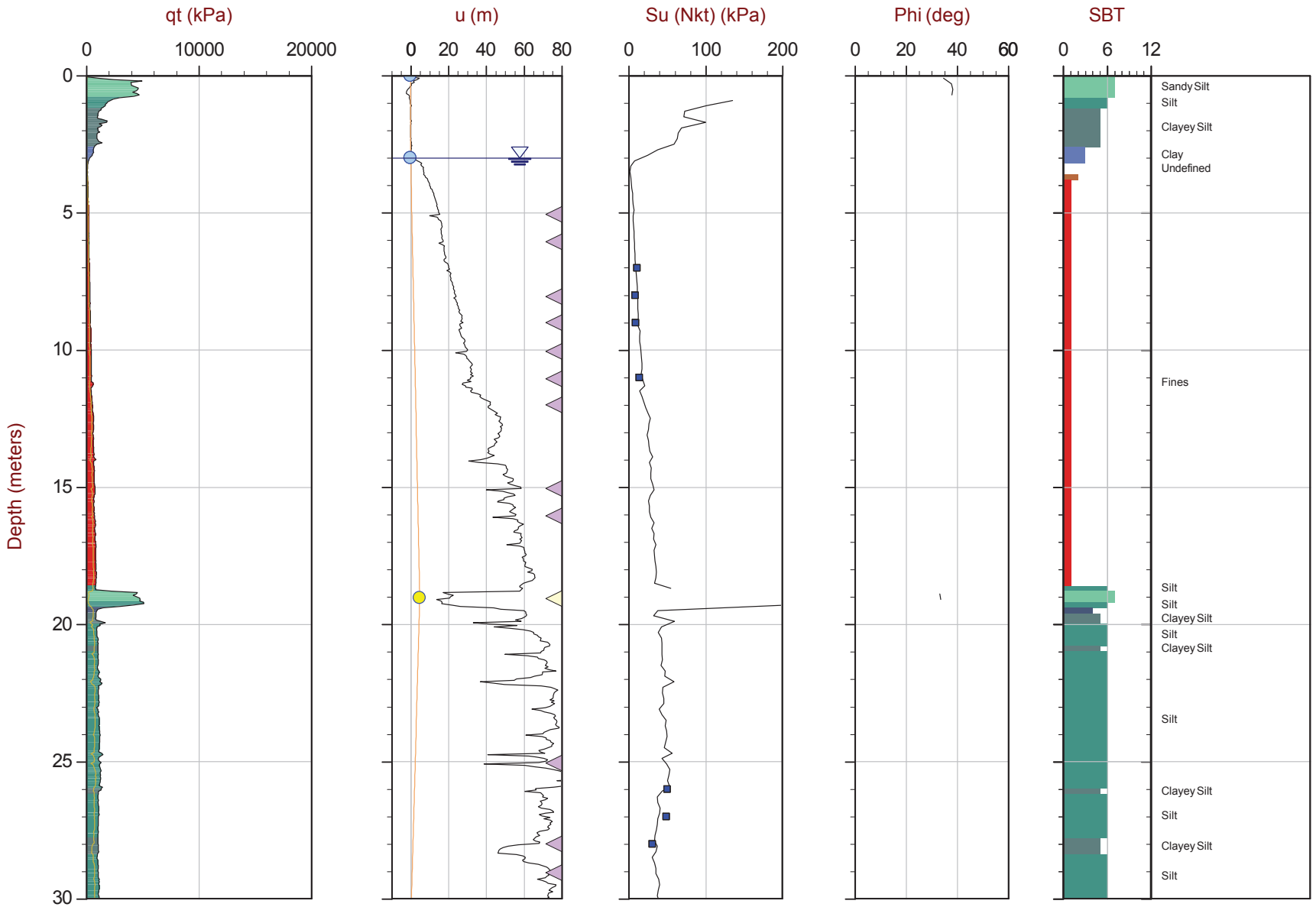

Max Depth: 31.850 m / 104.49 ft
Depth Inc: 0.050 m / 0.164 ft
Avg Int: 0.200 m
Overplot Item:
Assumed Ueq
Ueq

File: 16-72004_SP05.COR
Unit Wt: SBT Zones
Su Nkt: 15.0
Su(VST)
Dissipation, equilibrium achieved
Dissipation, equilibrium not achieved
Equilibrium Line

SBT: Robertson and Campanella, 1986
Coords: UTM Zone 23 South N: 7763372m E: 659090m
Page No: 1 of 2

CONETEC

CGSH

Job No: 16-72004
Date: 05:05:16 10:41
Site: Bay 3, Germano Slimes

Sounding: GSCPT16-05
Cone: 376:T375F10U200

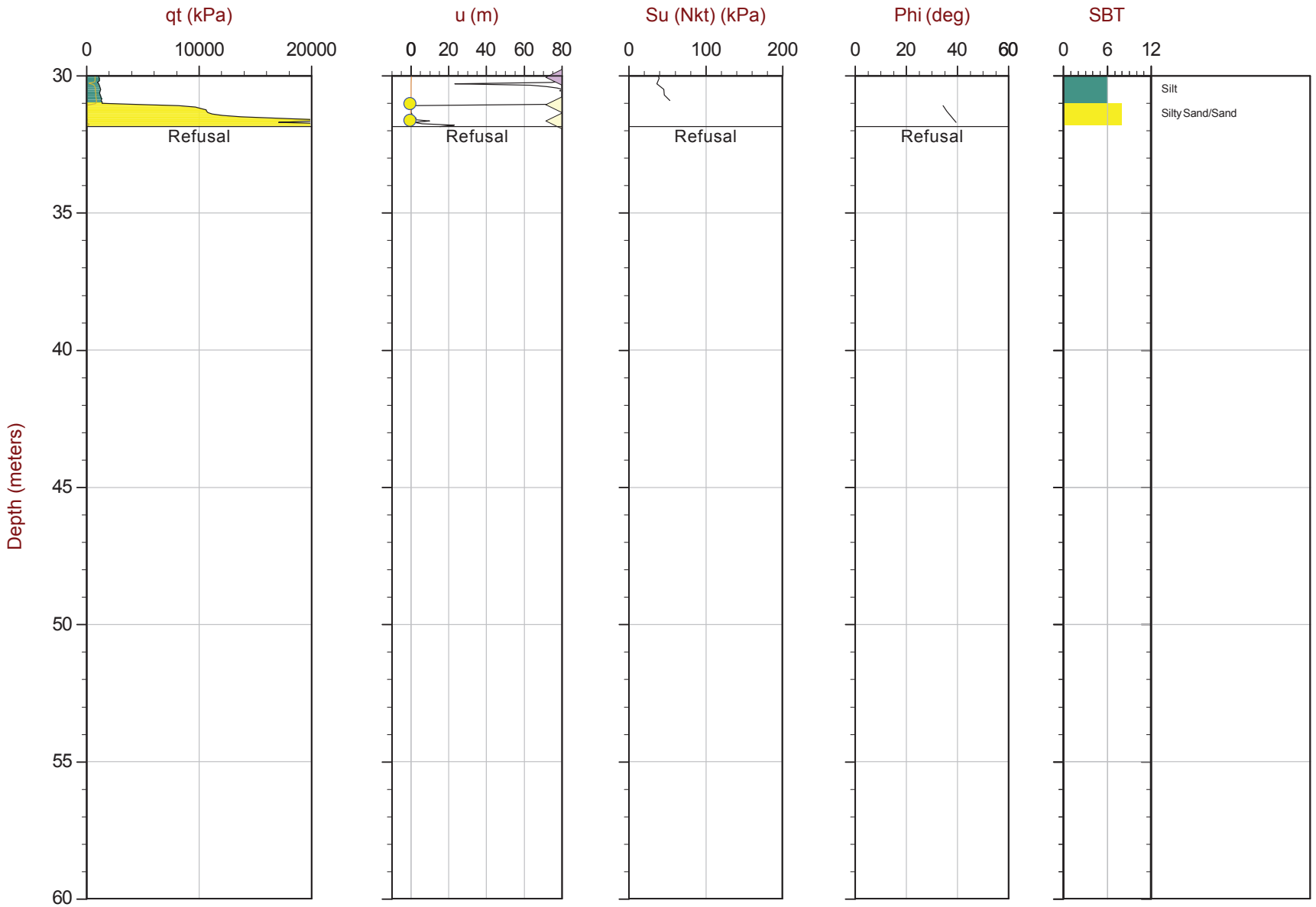

Max Depth: 31.850 m / 104.49 ft
Depth Inc: 0.050 m / 0.164 ft
Avg Int: 0.200 m
Overplot Item:
Assumed Ueq
Ueq

File: 16-72004_SP05.COR
Unit Wt: SBT Zones
Su Nkt: 15.0
Su(VST)
Dissipation, equilibrium achieved
Dissipation, equilibrium not achieved
Equilibrium Line

SBT: Robertson and Campanella, 1986
Coords: UTM Zone 23 South N: 7763372m E: 659090m
Page No: 2 of 2

CONETEC

CGSH

Job No: 16-72004
Date: 05:16:16 13:45
Site: Germano Buttres

Sounding: GBCPT16-06
Cone: 432:T1500F15U500

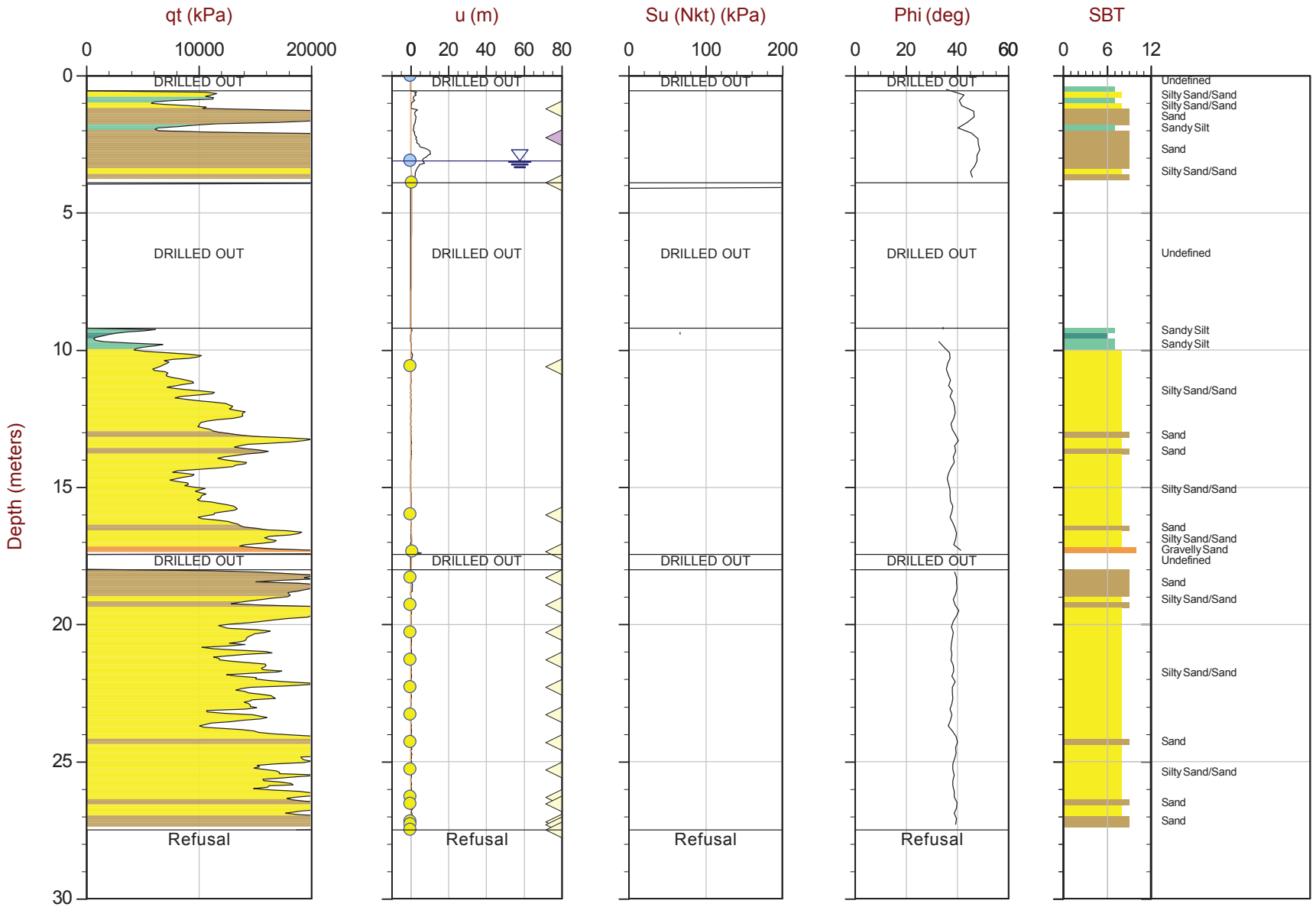

Max Depth: 27.500 m / 90.22 ft
Depth Inc: 0.050 m / 0.164 ft
Avg Int: 0.200 m
Overplot Item:
Assumed Ueq
Ueq

File: 16-72004_RS06.COR
Unit Wt: SBT Zones
Su Nkt: 15.0
Dissipation, equilibrium achieved
Dissipation, equilibrium not achieved
Equilibrium Line

SBT: Robertson and Campanella, 1986
Coords: UTM Zone 23 South N: 7763631 m E: 660586 m
Page No: 1 of 1

CONETEC

CGSH

Job No: 16-72004
Date: 05:17:16 09:36
Site: Germano Buttres

Sounding: GBCPT16-06B
Cone: 432:T1500F15U500

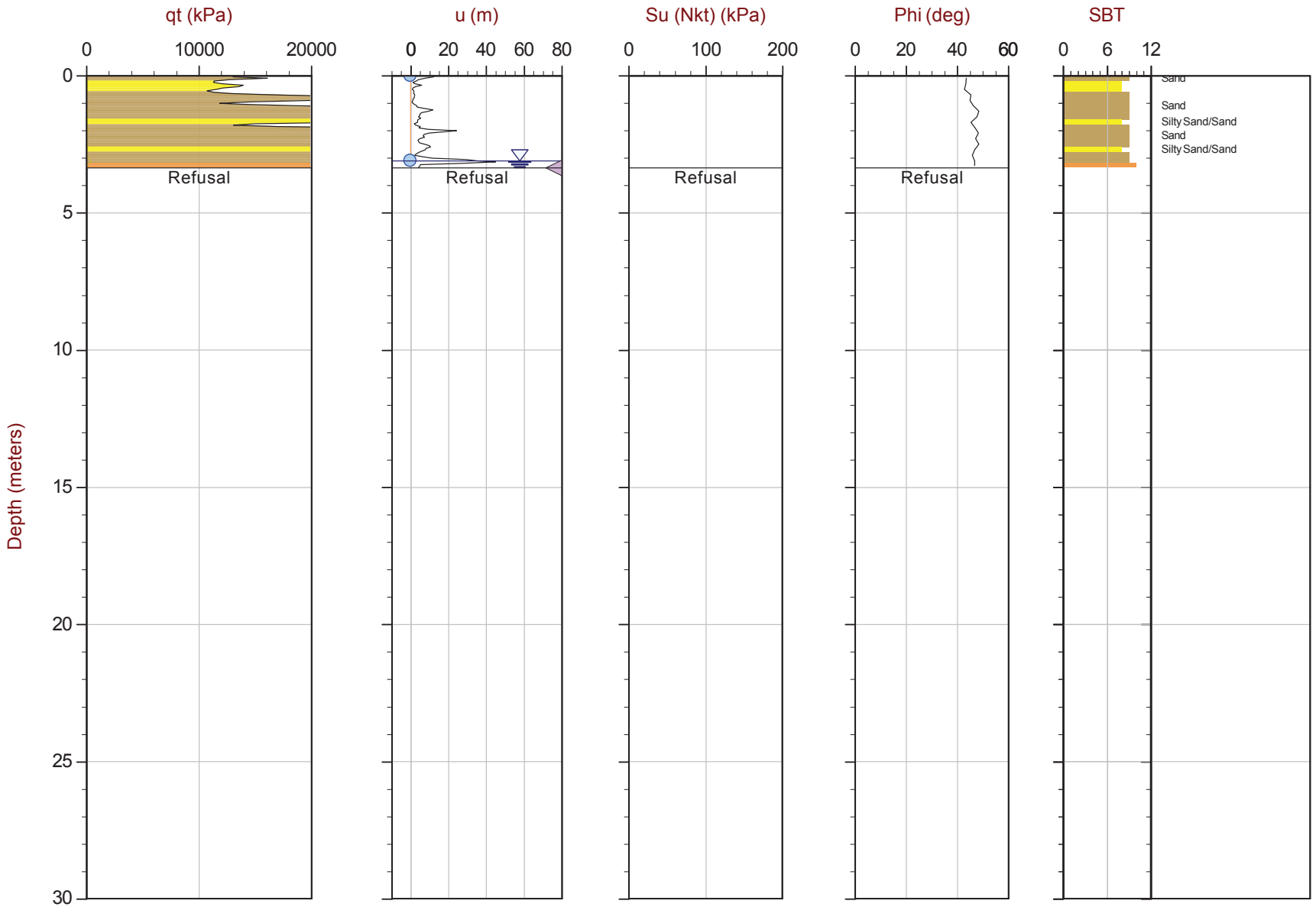

Max Depth: 3.350 m / 10.99 ft
Depth Inc: 0.050 m / 0.164 ft
Avg Int: 0.200 m
Overplot Item:
Assumed Ueq
Ueq

File: 16-72004_RS06B.COR
Unit Wt: SBT Zones
Su Nkt: 15.0
Dissipation, equilibrium achieved
Dissipation, equilibrium not achieved
Equilibrium Line

SBT: Robertson and Campanella, 1986
Coords: UTM Zone 23 South N: 7763631 m E: 660583m
Page No: 1 of 1

Cone Penetration Test Resistivity Plots

CONETEC

CONETEC

CGSH

Job No: 16-72004
Date: 04:19:16 15:03
Site: Germano Buttres

Sounding: GBCPT16-01
Cone: 432:T1500F15U500

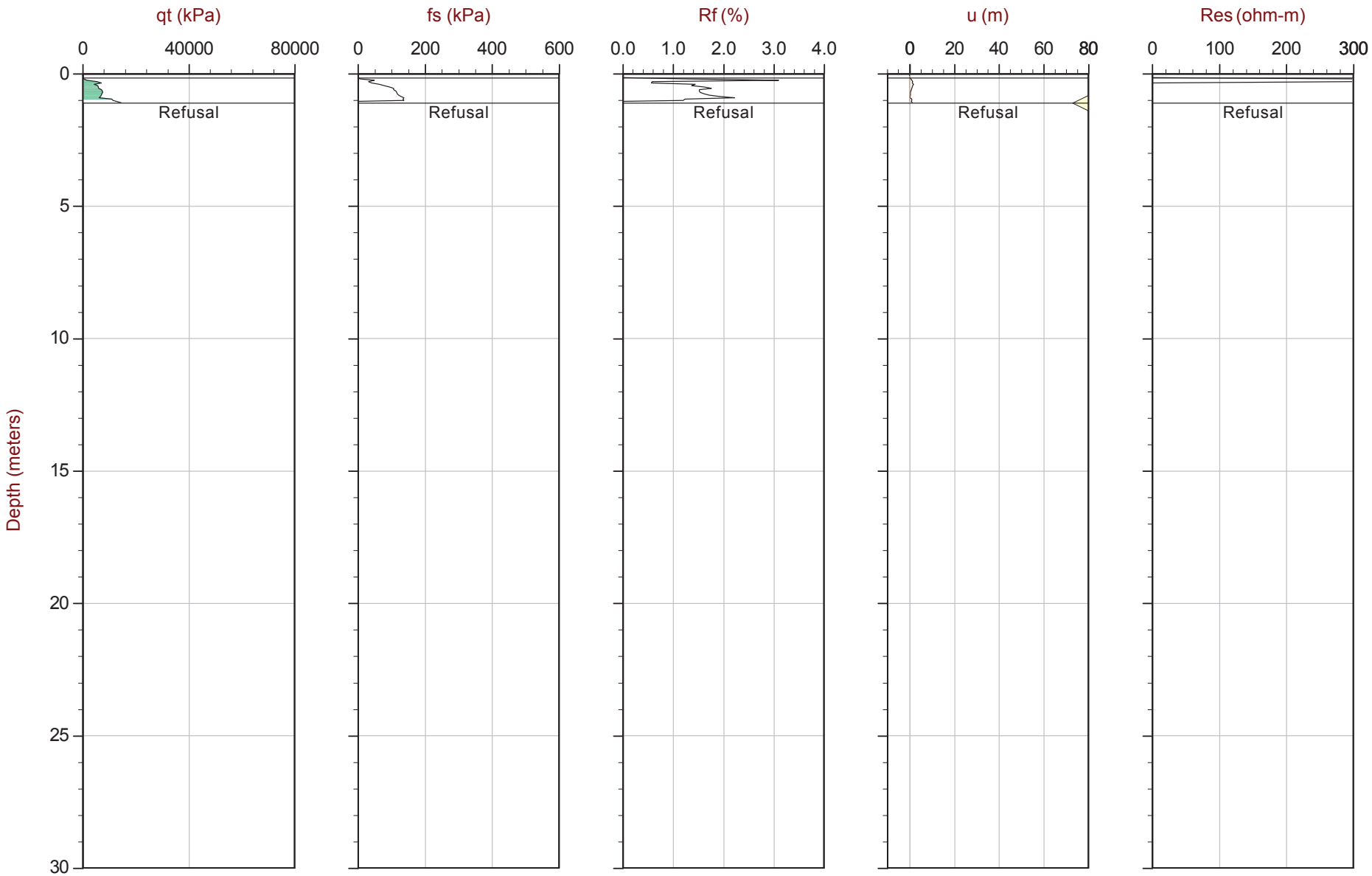

Max Depth: 1.100 m / 3.61 ft
Depth Inc: 0.050 m / 0.164 ft
Avg Int: 0.200 m
Overplot Item:

File: 16-72004_RS01.COR
Unit Wt: SBT Zones

SBT: Robertson and Campanella, 1986
Coords: UTM Zone 23 South N: 7763639m E: 660664m
Page No: 1 of 1

Assumed Ueq
Ueq
Dissipation, equilibrium achieved
Dissipation, equilibrium not achieved
Equilibrium Line

CONETEC

CGSH

Job No: 16-72004
Date: 04:20:16 12:52
Site: Germano Buttres

Sounding: GBCPT16-01B
Cone: 432:T1500F15U500

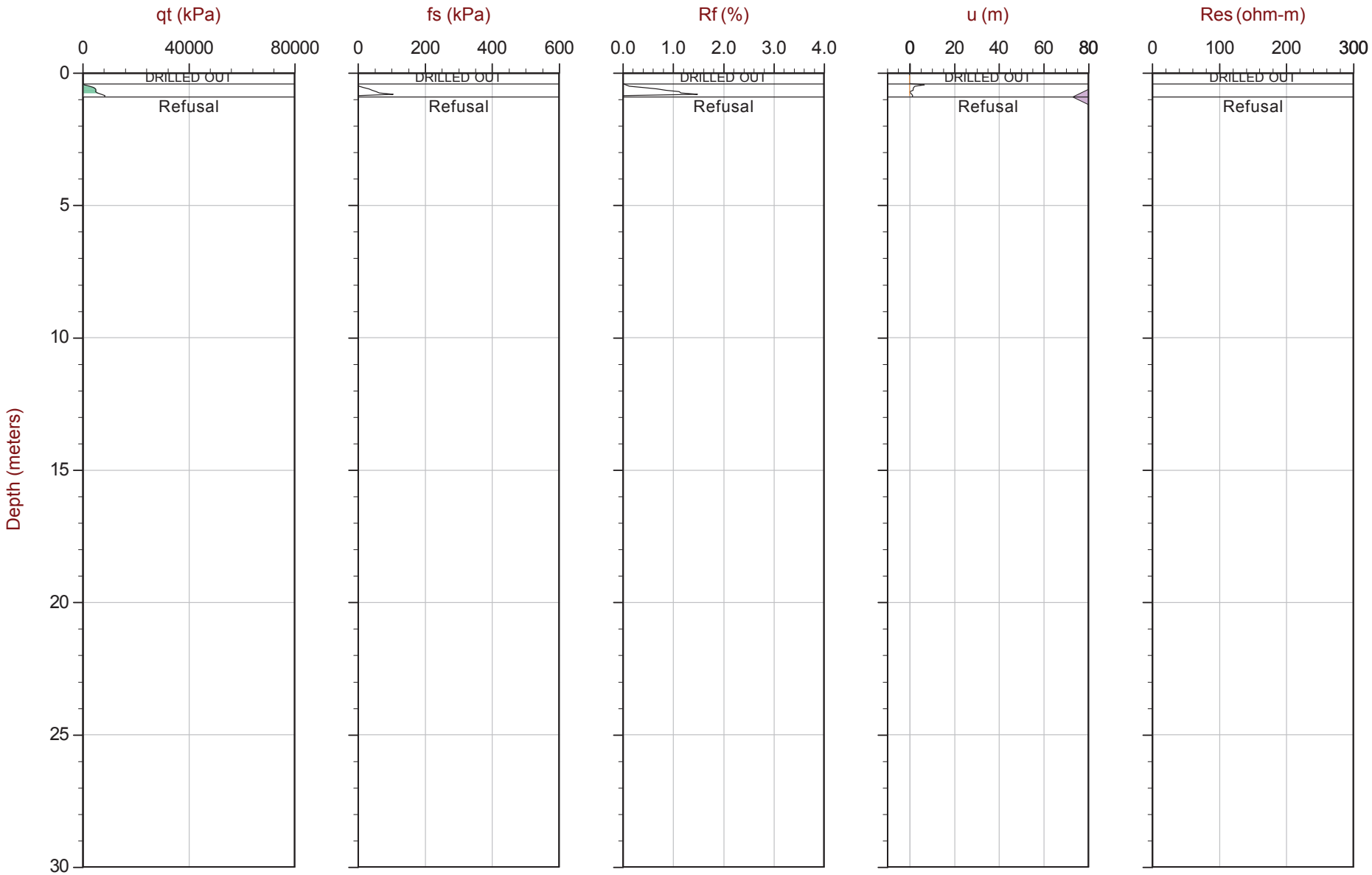

Max Depth: 0.900 m / 2.95 ft
Depth Inc: 0.050 m / 0.164 ft
Avg Int: 0.200 m
Overplot Item:

File: 16-72004_RS01B.COR
Unit Wt: SBT Zones

SBT: Robertson and Campanella, 1986
Coords: UTM Zone 23 South N: 7763639m E: 660664m
Page No: 1 of 1

Assumed Ueq
Ueq
Dissipation, equilibrium achieved
Dissipation, equilibrium not achieved
Equilibrium Line

CONETEC

CGSH

Job No: 16-72004
Date: 04:20:16 15:32
Site: Germano Buttres

Sounding: GBCPT16-01C
Cone: 432:T1500F15U500

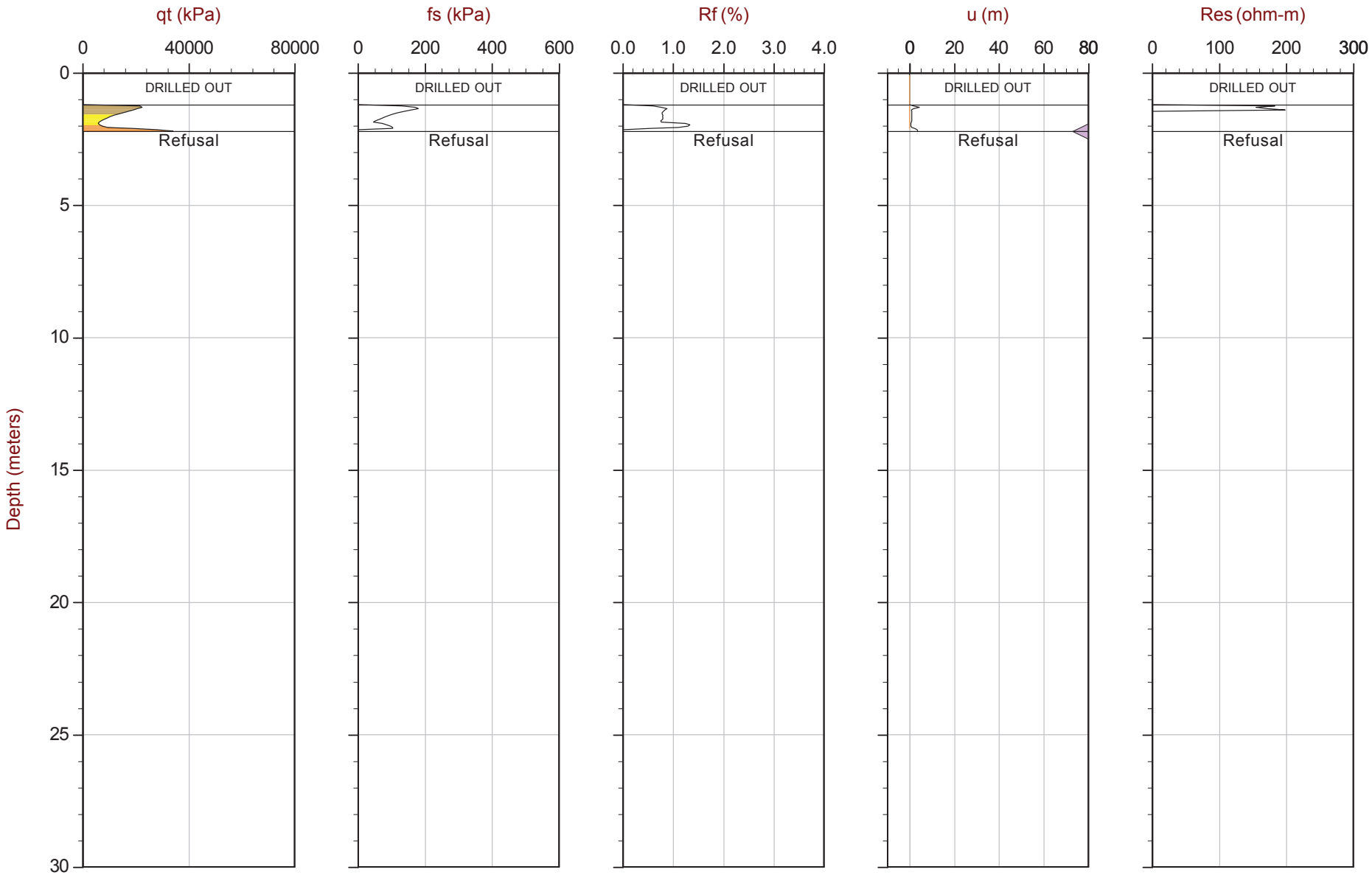

Max Depth: 2.200 m / 7.22 ft
Depth Inc: 0.050 m / 0.164 ft
Avg Int: 0.200 m
Overplot Item:

File: 16-72004_RS01C.COR
Unit Wt: SBT Zones

SBT: Robertson and Campanella, 1986
Coords: UTM Zone 23 South N: 7763639m E: 660664m
Page No: 1 of 1

Assumed Ueq
Ueq
Dissipation, equilibrium achieved
Dissipation, equilibrium not achieved
Equilibrium Line

CONETEC

CGSH

Job No: 16-72004
Date: 04:21:16 14:33
Site: Bay 3, Germano Slimes

Sounding: GSCPT16-02
Cone: 432:T1500F15U500

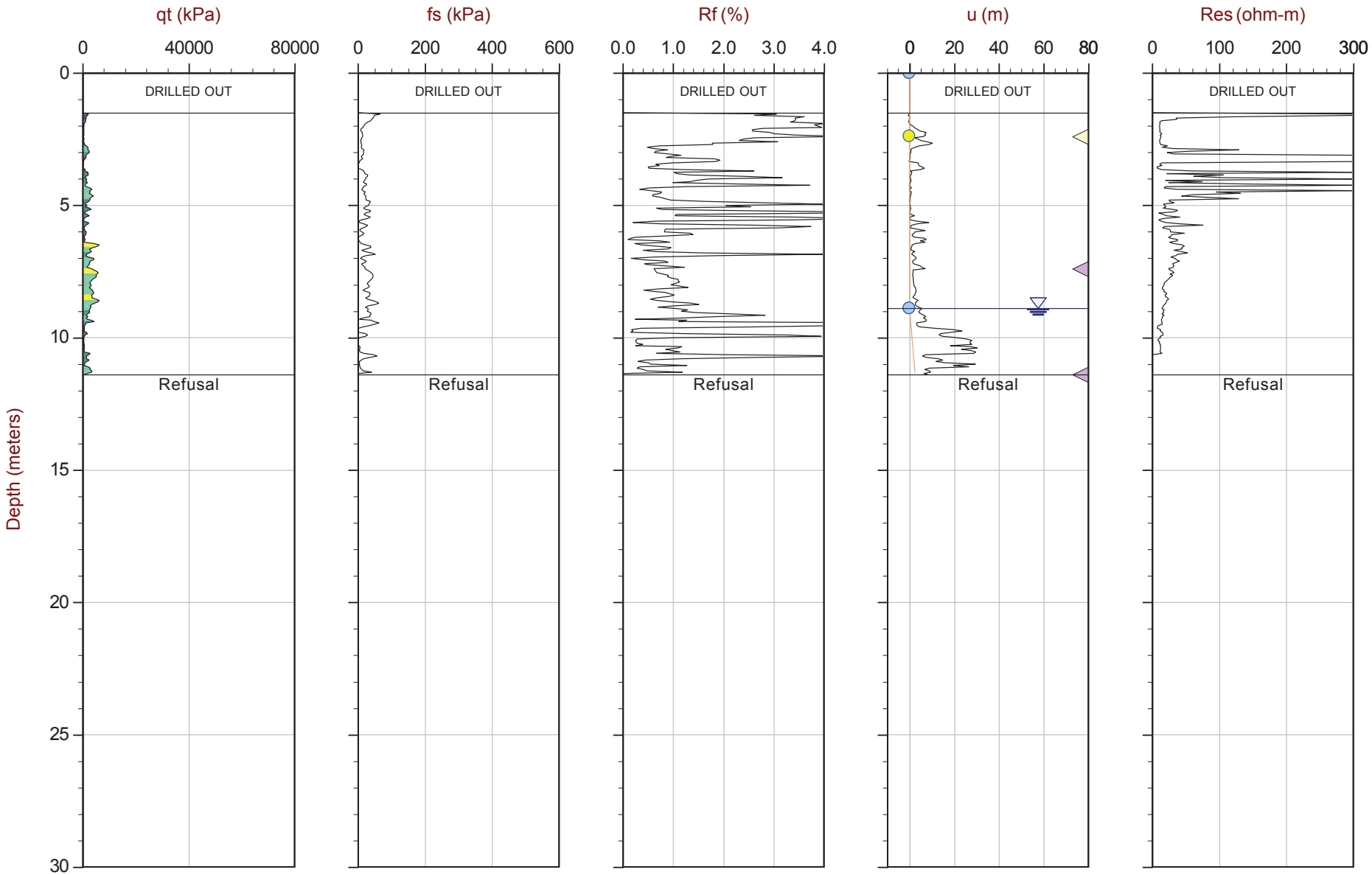

Max Depth: 11.400 m / 37.40 ft
Depth Inc: 0.050 m / 0.164 ft
Avg Int: 0.200 m
Overplot Item:

File: 16-72004_RS02.COR
Unit Wt: SBT Zones

SBT: Robertson and Campanella, 1986
Coords: UTM Zone 23 South N: 7764153m E: 658559m
Page No: 1 of 1

Assumed Ueq
Ueq
Dissipation, equilibrium achieved
Dissipation, equilibrium not achieved
Equilibrium Line

CONETEC

CGSH

Job No: 16-72004
Date: 04:24:16 11:30
Site: Bay 3, Germano Slimes

Sounding: GSCPT16-02B
Cone: 376:T375F10U200

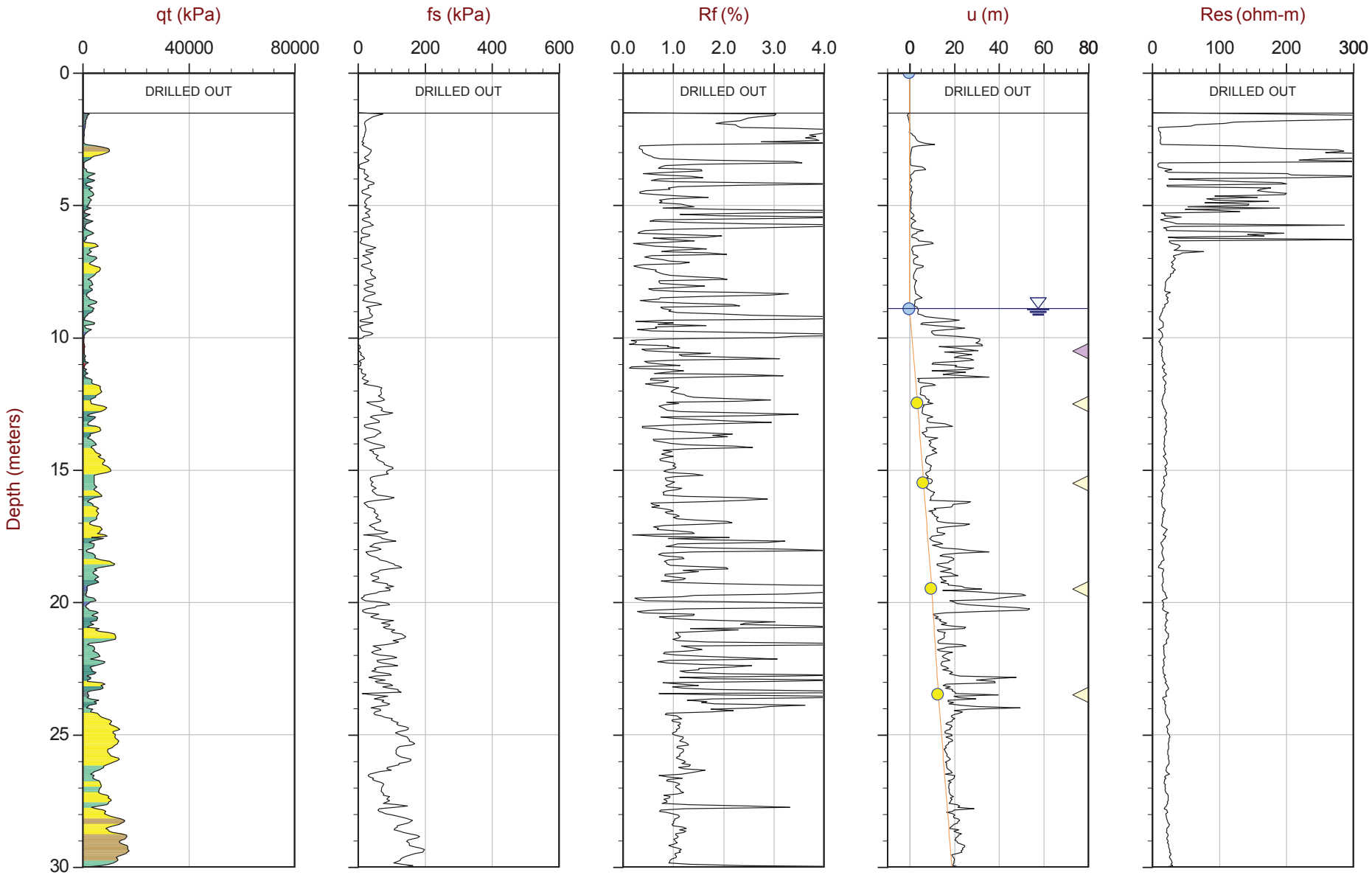

Max Depth: 41.650 m / 136.65 ft
Depth Inc: 0.050 m / 0.164 ft
Avg Int: 0.200 m
Overplot Item:

File: 16-72004_RS02B.COR
Unit Wt: SBT Zones

SBT: Robertson and Campanella, 1986
Coords: UTM Zone 23 South N: 7764155m E: 658559m
Page No: 1 of 2

Assumed Ueq
Ueq
Dissipation, equilibrium achieved
Dissipation, equilibrium not achieved
Equilibrium Line

CONETEC

CGSH

Job No: 16-72004
Date: 04:24:16 11:30
Site: Bay 3, Germano Slimes

Sounding: GSCPT16-02B
Cone: 376:T375F10U200

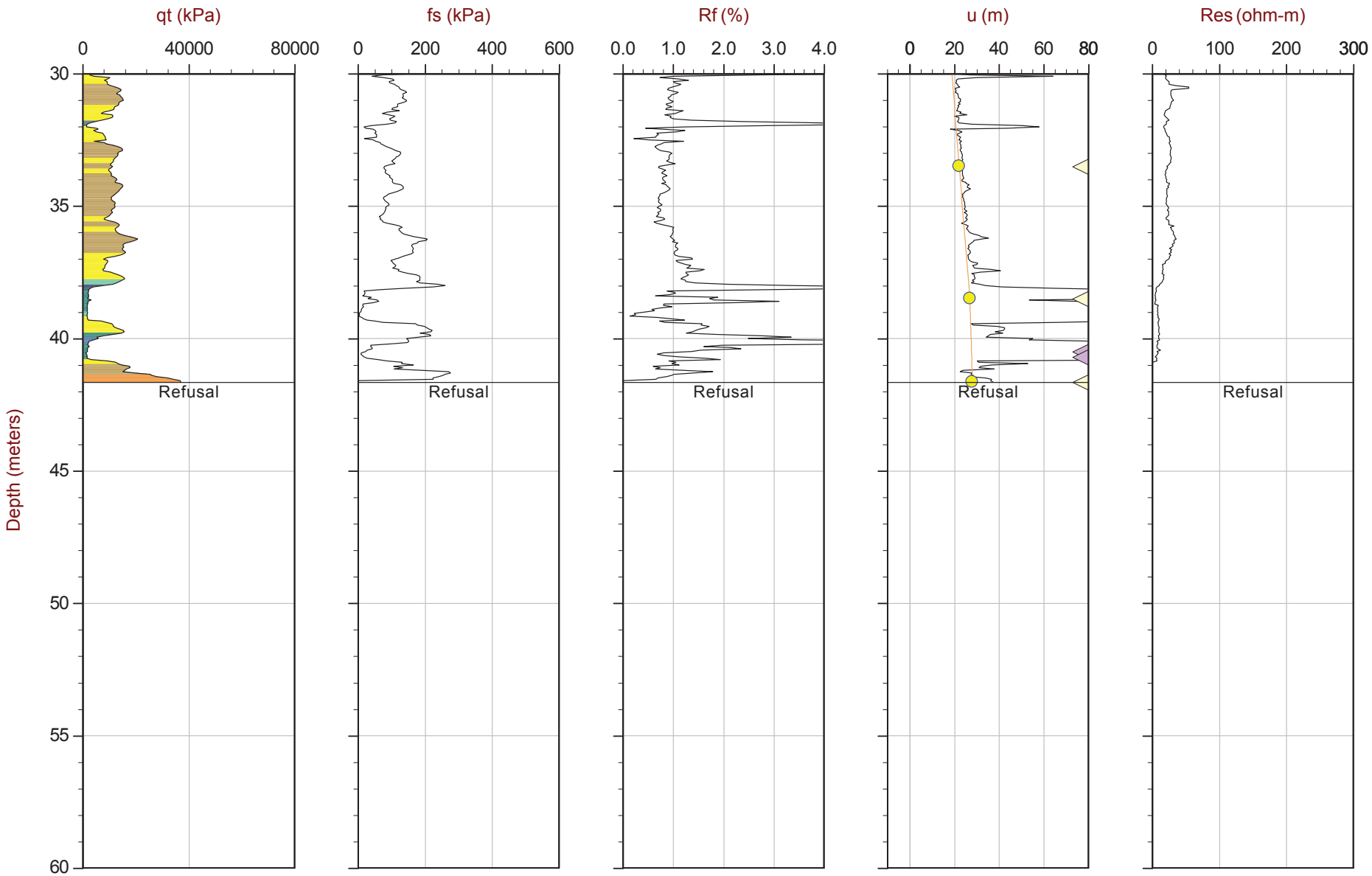

Max Depth: 41.650 m / 136.65 ft
Depth Inc: 0.050 m / 0.164 ft
Avg Int: 0.200 m

File: 16-72004_RS02B.COR
Unit Wt: SBT Zones

SBT: Robertson and Campanella, 1986
Coords: UTM Zone 23 South N: 7764155m E: 658559m
Page No: 2 of 2

Overplot Item:
- Assumed Ueq
- Ueq
- Dissipation, equilibrium achieved
- Dissipation, equilibrium not achieved
- Equilibrium Line

CONETEC

CGSH

Job No: 16-72004
Date: 04:26:16 12:34
Site: Bay 3, Germano Cava

Sounding: GCCPT16-03
Cone: 376:T375F10U200

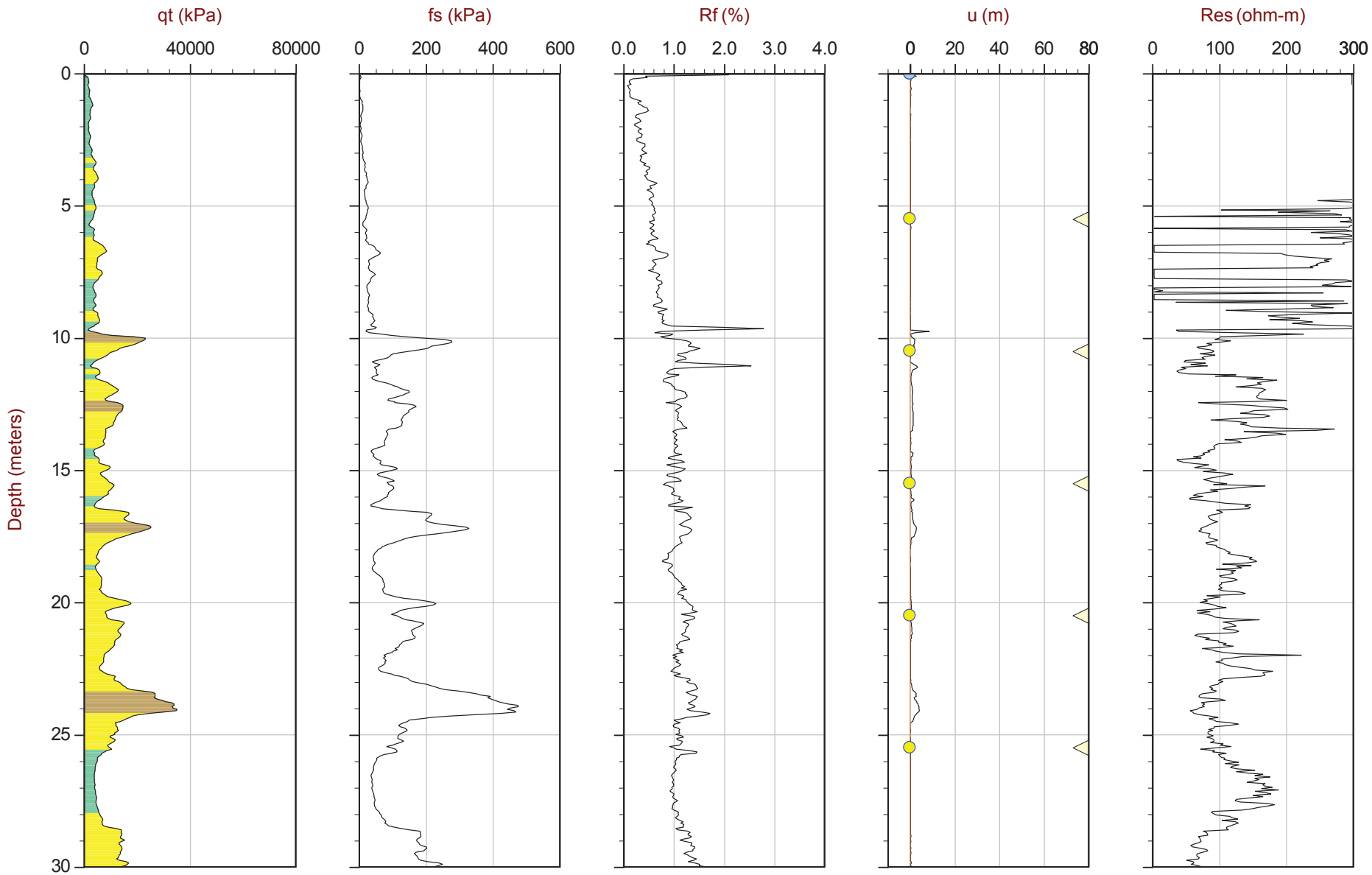

Max Depth: 61.650 m / 202.26 ft
Depth Inc: 0.050 m / 0.164 ft
Avg Int: 0.200 m
Overplot Item:

File: 16-72004_RS03.COR
Unit Wt: SBT Zones

SBT: Robertson and Campanella, 1986
Coords: UTM Zone 23 South N: 7766164m E: 657252m
Page No: 1 of 3

Assumed Ueq
Ueq
Dissipation, equilibrium achieved
Dissipation, equilibrium not achieved
Equilibrium Line

CONETEC

CGSH

Job No: 16-72004
Date: 04:26:16 12:34
Site: Bay 3, Germano Cava

Sounding: GCCPT16-03
Cone: 376:T375F10U200

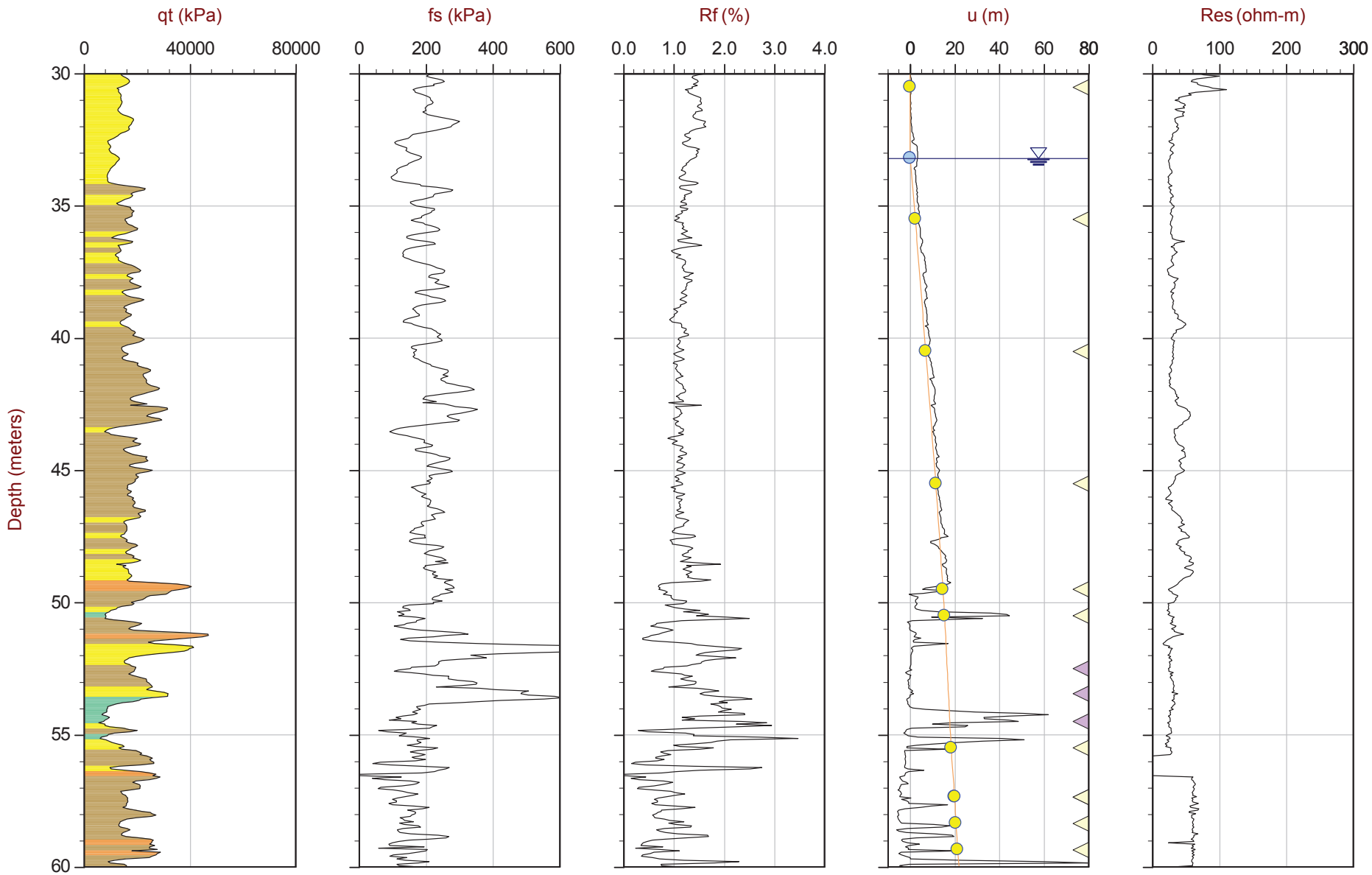

Max Depth: 61.650 m / 202.26 ft
Depth Inc: 0.050 m / 0.164 ft
Avg Int: 0.200 m
Overplot Item:

File: 16-72004_RS03.COR
Unit Wt: SBT Zones

SBT: Robertson and Campanella, 1986
Coords: UTM Zone 23 South N: 7766164m E: 657252m
Page No: 2 of 3

Assumed Ueq
Ueq
Dissipation, equilibrium achieved
Dissipation, equilibrium not achieved
Equilibrium Line

CONETEC

CGSH

Job No: 16-72004
Date: 04:26:16 12:34
Site: Bay 3, Germano Cava

Sounding: GCCPT16-03
Cone: 376:T375F10U200

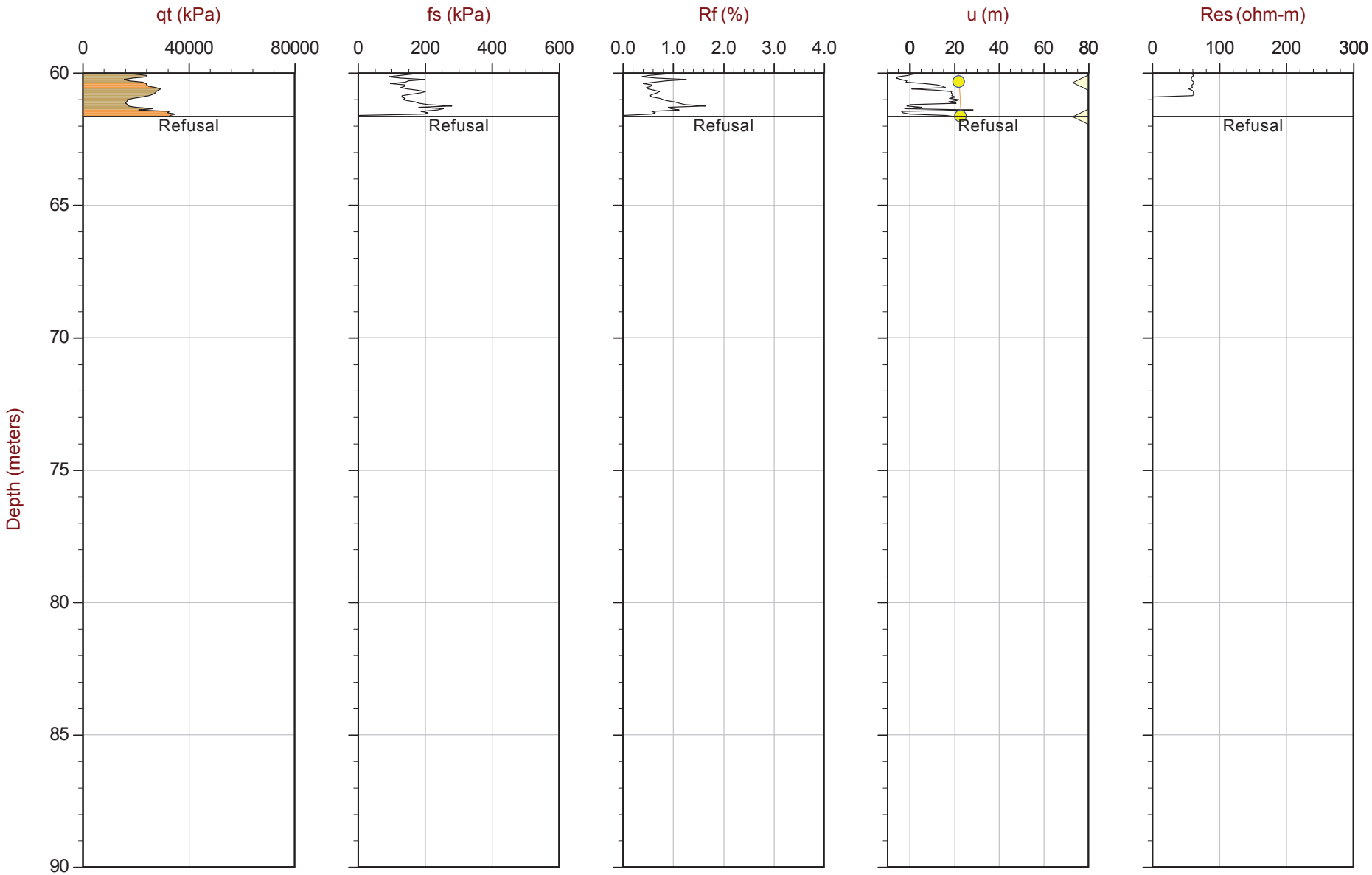

Max Depth: 61.650 m / 202.26 ft
Depth Inc: 0.050 m / 0.164 ft
Avg Int: 0.200 m

File: 16-72004_RS03.COR
Unit Wt: SBT Zones

SBT: Robertson and Campanella, 1986
Coords: UTM Zone 23 South N: 7766164m E: 657252m
Page No: 3 of 3

Overplot Item:
- Assumed Ueq
- Ueq
- Dissipation, equilibrium achieved
- Dissipation, equilibrium not achieved
- Equilibrium Line

CONETEC

CGSH

Job No: 16-72004
Date: 05:02:16 15:34
Site: Bay 3, Germano Cava

Sounding: GCCPT16-04
Cone: 376:T375F10U200

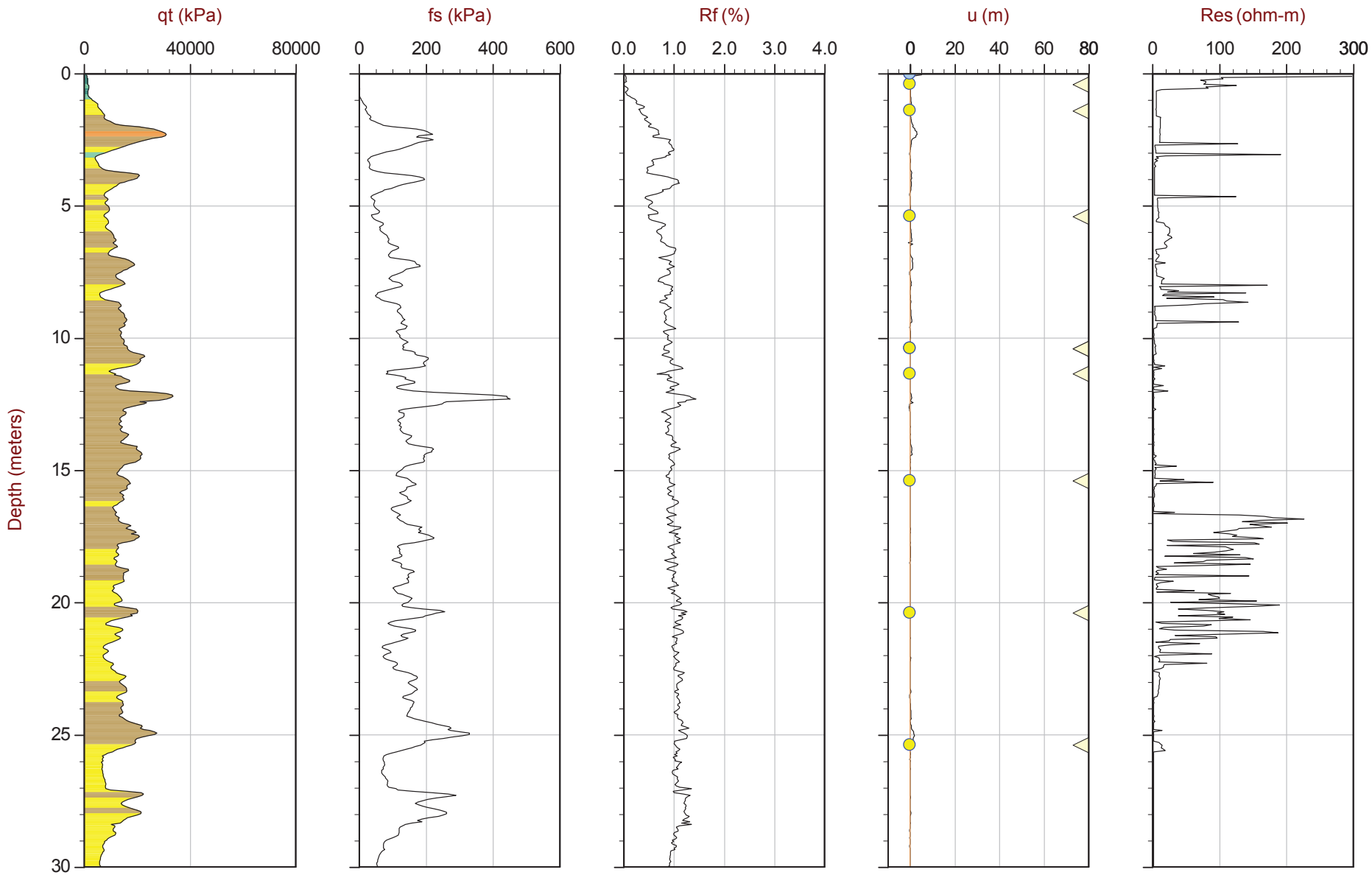

Max Depth: 35.350 m / 115.98 ft
Depth Inc: 0.050 m / 0.164 ft
Avg Int: 0.200 m
Overplot Item:

File: 16-72004_RS04.COR
Unit Wt: SBT Zones

SBT: Robertson and Campanella, 1986
Coords: UTM Zone 23 South N: 7766303m E: 657393m
Page No: 1 of 2

Assumed Ueq
Ueq
Dissipation, equilibrium achieved
Dissipation, equilibrium not achieved
Equilibrium Line

CONETEC

CGSH

Job No: 16-72004
Date: 05:02:16 15:34
Site: Bay 3, Germano Cava

Sounding: GCCPT16-04
Cone: 376:T375F10U200

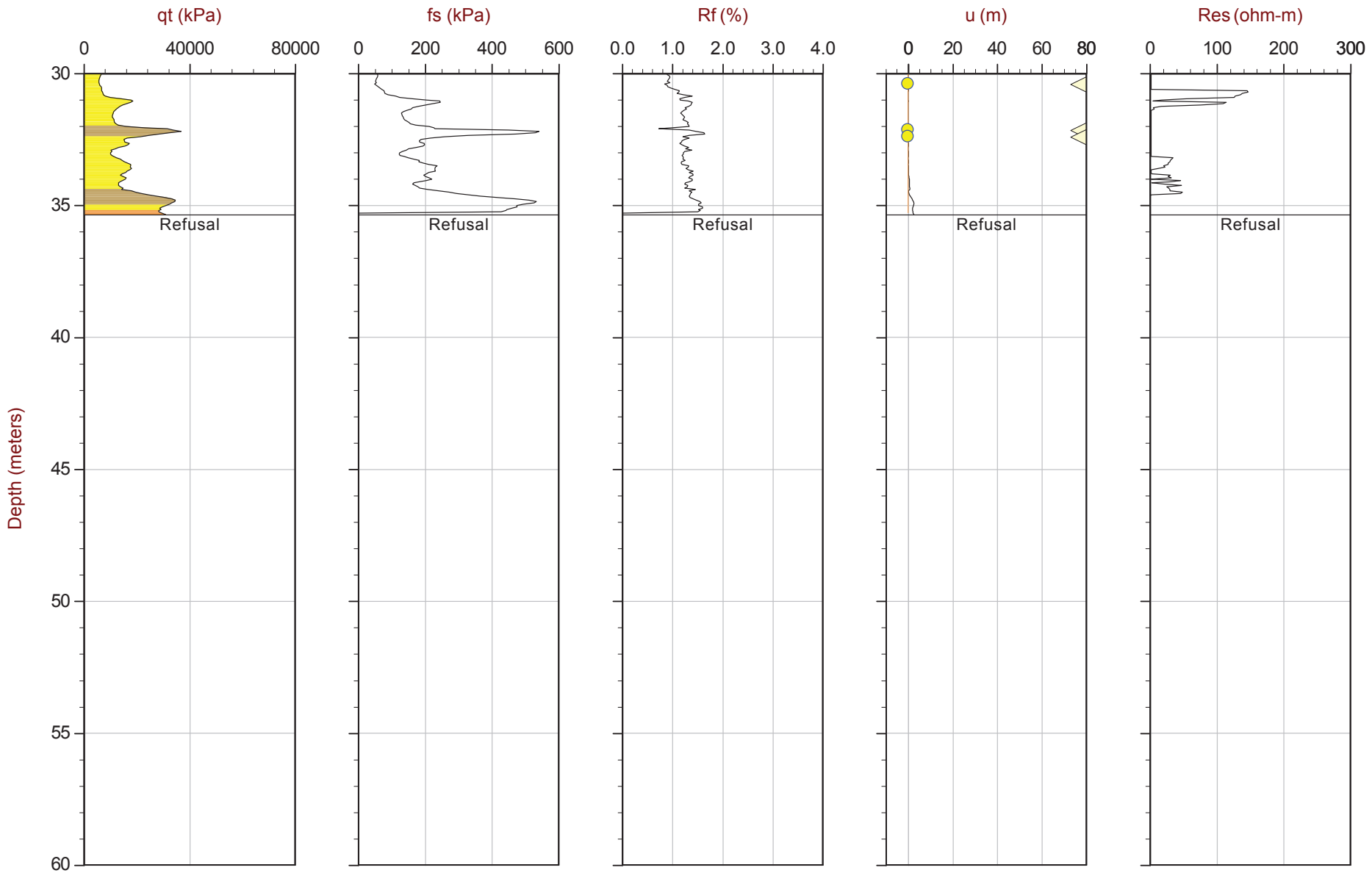

Max Depth: 35.350 m / 115.98 ft
Depth Inc: 0.050 m / 0.164 ft
Avg Int: 0.200 m
Overplot Item:

File: 16-72004_RS04.COR
Unit Wt: SBT Zones

SBT: Robertson and Campanella, 1986
Coords: UTM Zone 23 South N: 7766303m E: 657393m
Page No: 2 of 2

Assumed Ueq
Ueq
Dissipation, equilibrium achieved
Dissipation, equilibrium not achieved
Equilibrium Line

CONETEC

CGSH

Job No: 16-72004
Date: 05:13:16 13:07
Site: Germano Cava

Sounding: GCCPT16-04B
Cone: 432:T1500F15U500

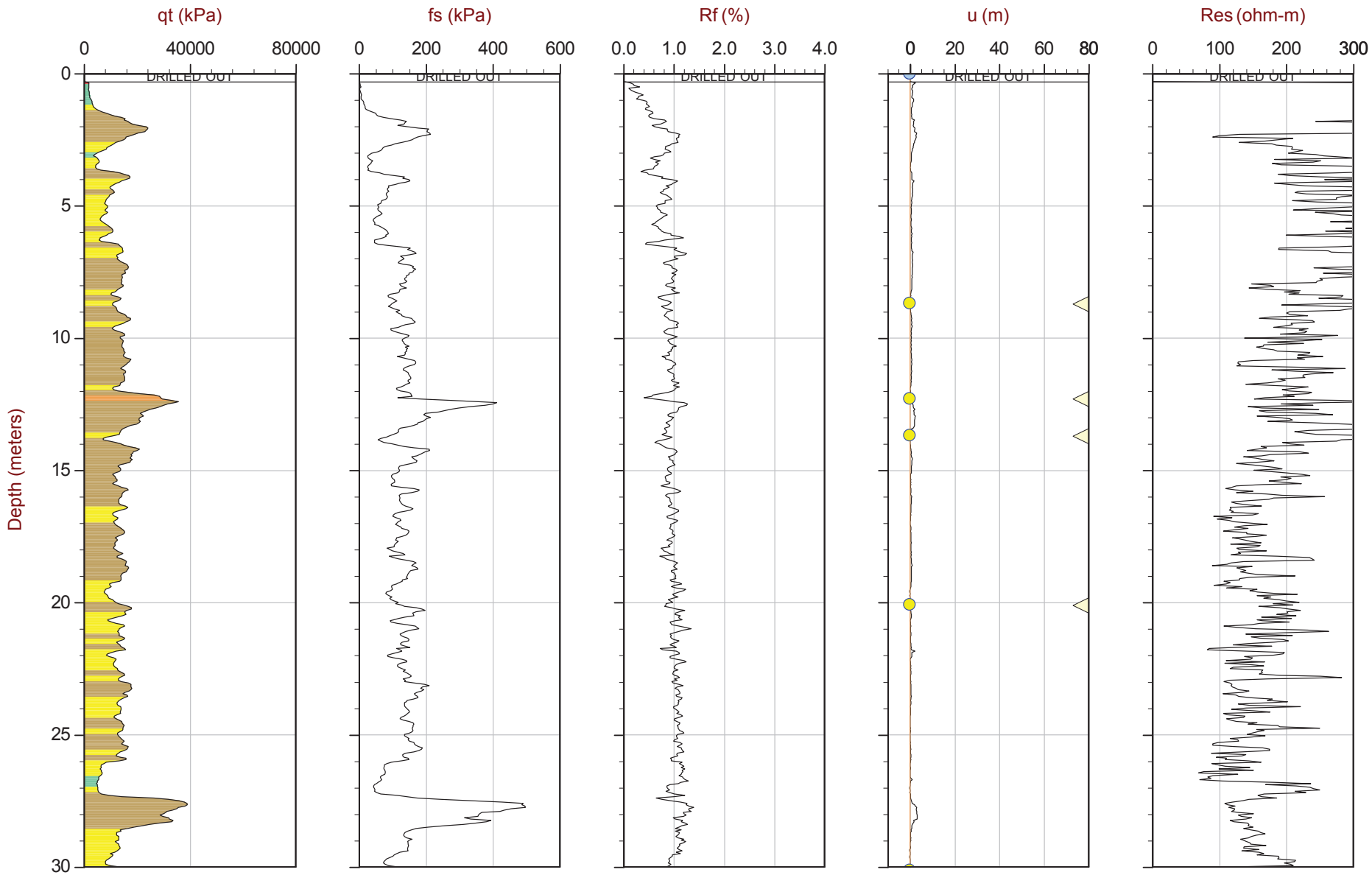

Max Depth: 36.350 m / 119.26 ft
Depth Inc: 0.050 m / 0.164 ft
Avg Int: 0.200 m
Overplot Item:

File: 16-72004_RS04B.COR
Unit Wt: SBT Zones

SBT: Robertson and Campanella, 1986
Coords: UTM Zone 23 South N: 7766300m E: 657394m
Page No: 1 of 2

Assumed Ueq
Ueq
Dissipation, equilibrium achieved
Dissipation, equilibrium not achieved
Equilibrium Line

CONETEC

CGSH

Job No: 16-72004
Date: 05:13:16 13:07
Site: Germano Cava

Sounding: GCCPT16-04B
Cone: 432:T1500F15U500

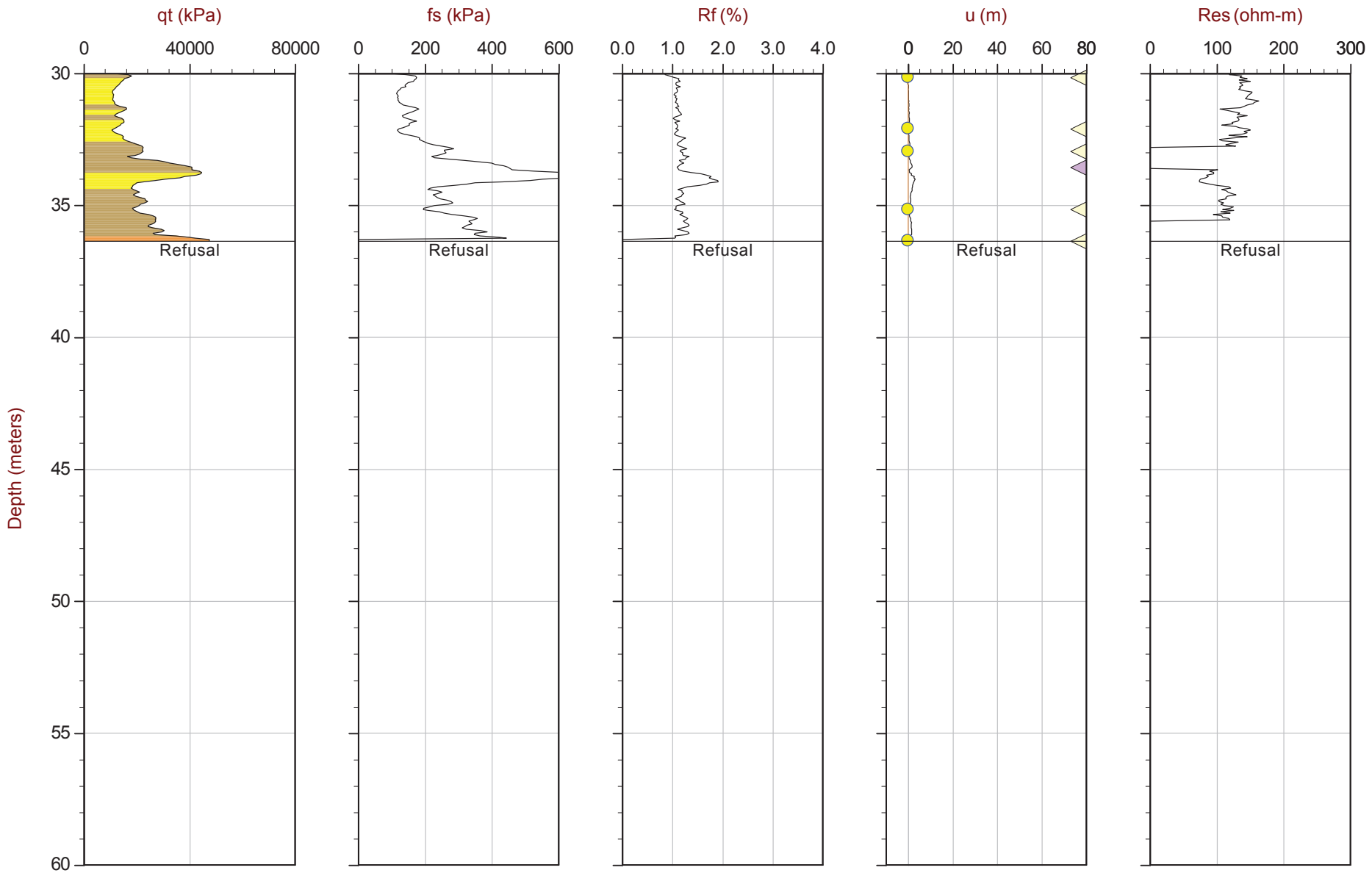

Max Depth: 36.350 m / 119.26 ft
Depth Inc: 0.050 m / 0.164 ft
Avg Int: 0.200 m
Overplot Item:

File: 16-72004_RS04B.COR
Unit Wt: SBT Zones

SBT: Robertson and Campanella, 1986
Coords: UTM Zone 23 South N: 7766300m E: 657394m
Page No: 2 of 2

Assumed Ueq
Ueq
Dissipation, equilibrium achieved
Dissipation, equilibrium not achieved
Equilibrium Line

CONETEC

CGSH

Job No: 16-72004
Date: 05:16:16 13:45
Site: Germano Buttres

Sounding: GBCPT16-06
Cone: 432:T1500F15U500

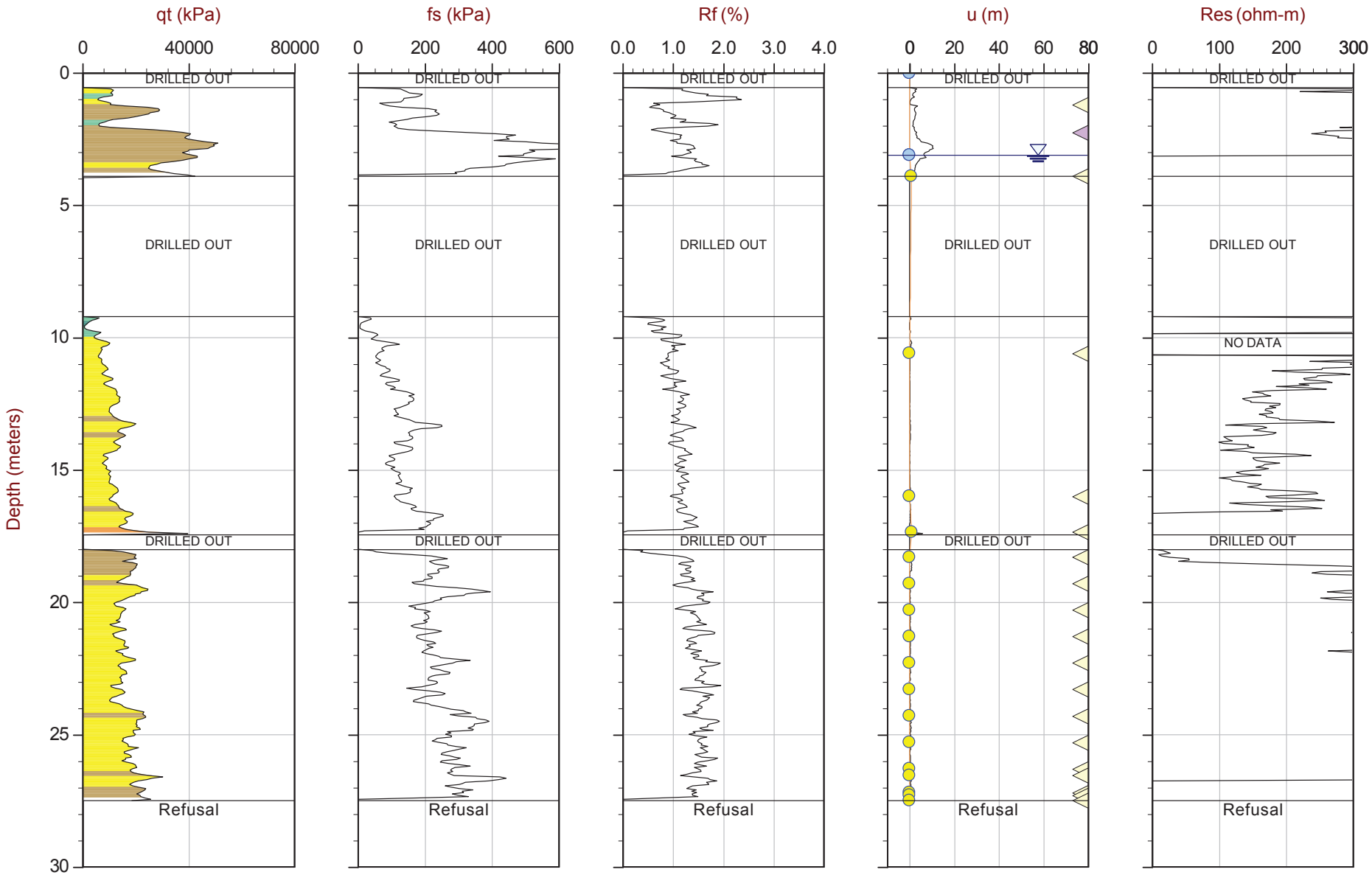

Max Depth: 27.500 m / 90.22 ft
Depth Inc: 0.050 m / 0.164 ft
Avg Int: 0.200 m
Overplot Item:

File: 16-72004_RS06.COR
Unit Wt: SBT Zones

SBT: Robertson and Campanella, 1986
Coords: UTM Zone 23 South N: 7763631 m E: 660586 m
Page No: 1 of 1

Assumed Ueq
Ueq
Dissipation, equilibrium achieved
Dissipation, equilibrium not achieved
Equilibrium Line

CONETEC

CGSH

Job No: 16-72004
Date: 05:17:16 09:36
Site: Germano Buttres

Sounding: GBCPT16-06B
Cone: 432:T1500F15U500

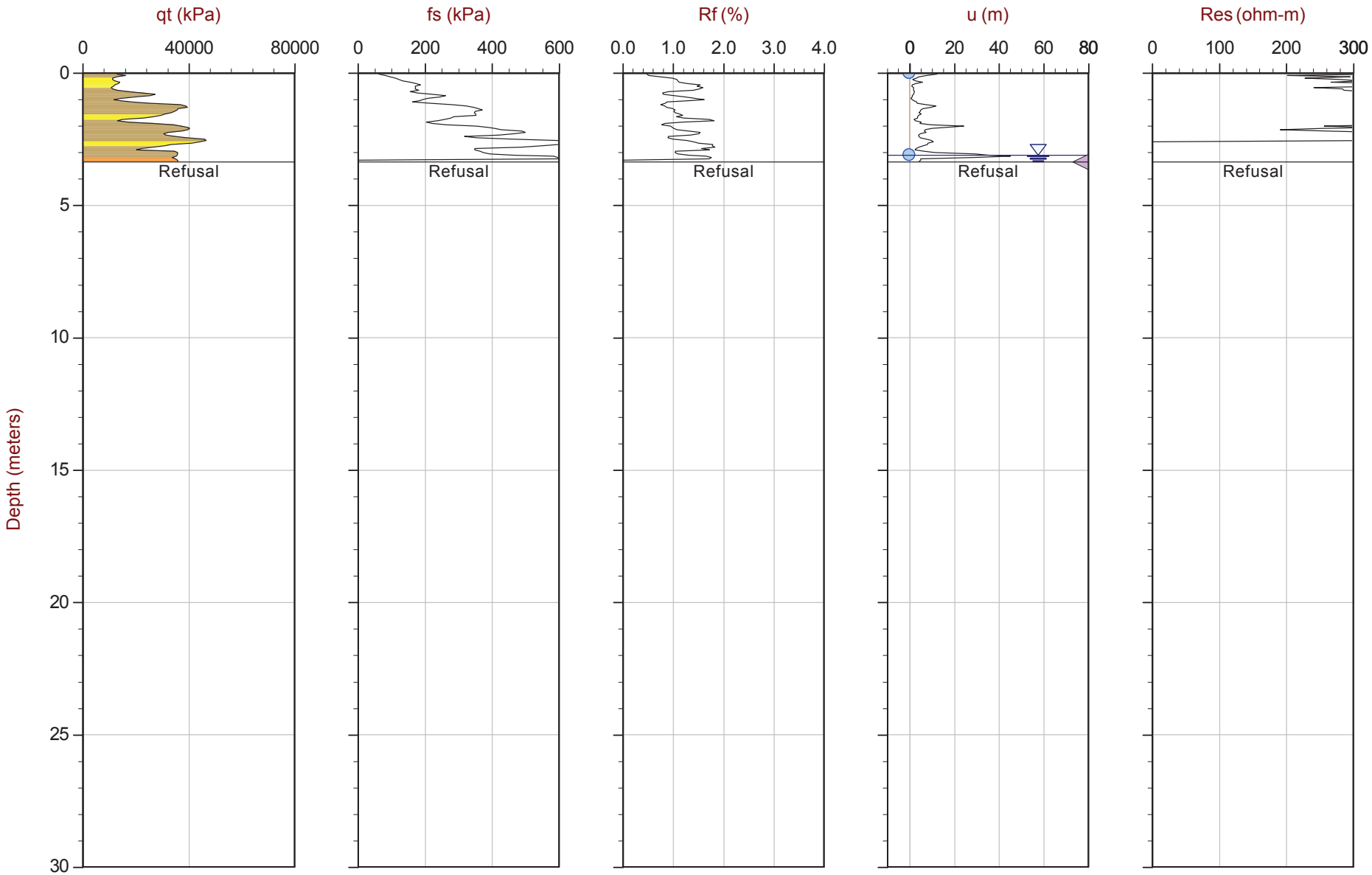

Max Depth: 3.350 m / 10.99 ft
Depth Inc: 0.050 m / 0.164 ft
Avg Int: 0.200 m

File: 16-72004_RS06B.COR
Unit Wt: SBT Zones

SBT: Robertson and Campanella, 1986
Coords: UTM Zone 23 South N: 7763631 m E: 660583 m
Page No: 1 of 1

Overplot Item:
- Assumed Ueq
- Ueq
- Dissipation, equilibrium achieved
- Dissipation, equilibrium not achieved
- Equilibrium Line

CPT Seismic Plots

CONETEC

CGSH

Job No: 16-72004
Date: 04:21:16 14:33
Site: Bay 3, Germano Slimes

Sounding: GSCPT16-02
Cone: 432:T1500F15U500

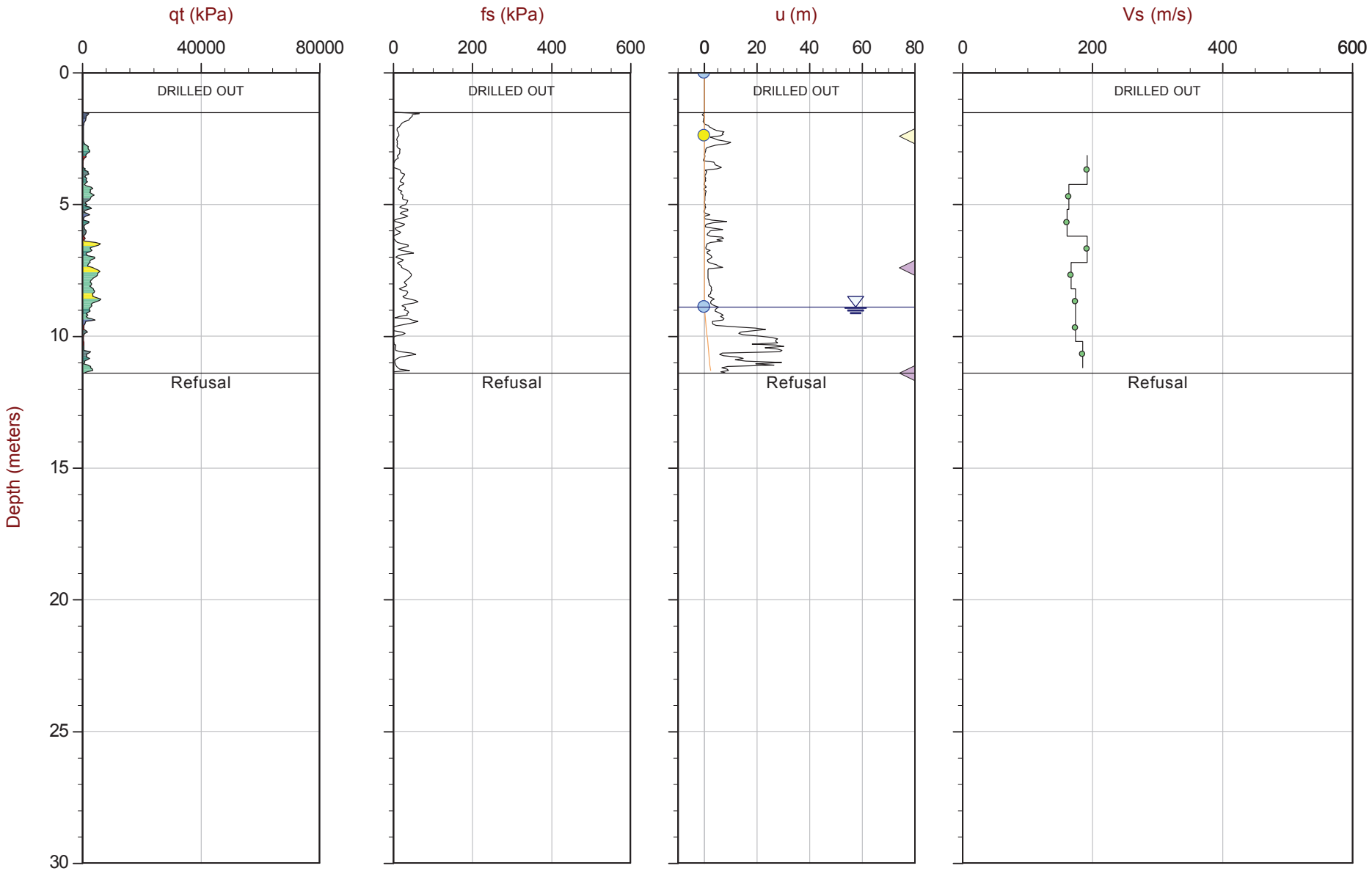

Max Depth: 11.400 m / 37.40 ft
Depth Inc: 0.050 m / 0.164 ft
Avg Int: 0.200 m

File: 16-72004_RS02.COR
Unit Wt: SBT Zones

SBT: Robertson and Campanella, 1986
Coords: UTM Zone 23 South N: 7764153m E: 658559m
Page No: 1 of 1

Overplot Item:
- Assumed Ueq
- Ueq
- Dissipation, equilibrium achieved
- Dissipation, equilibrium not achieved
- Equilibrium Line

CONETEC

CGSH

Job No: 16-72004
Date: 04:24:16 11:30
Site: Bay 3, Germano Slimes

Sounding: GSCPT16-02B
Cone: 376:T375F10U200

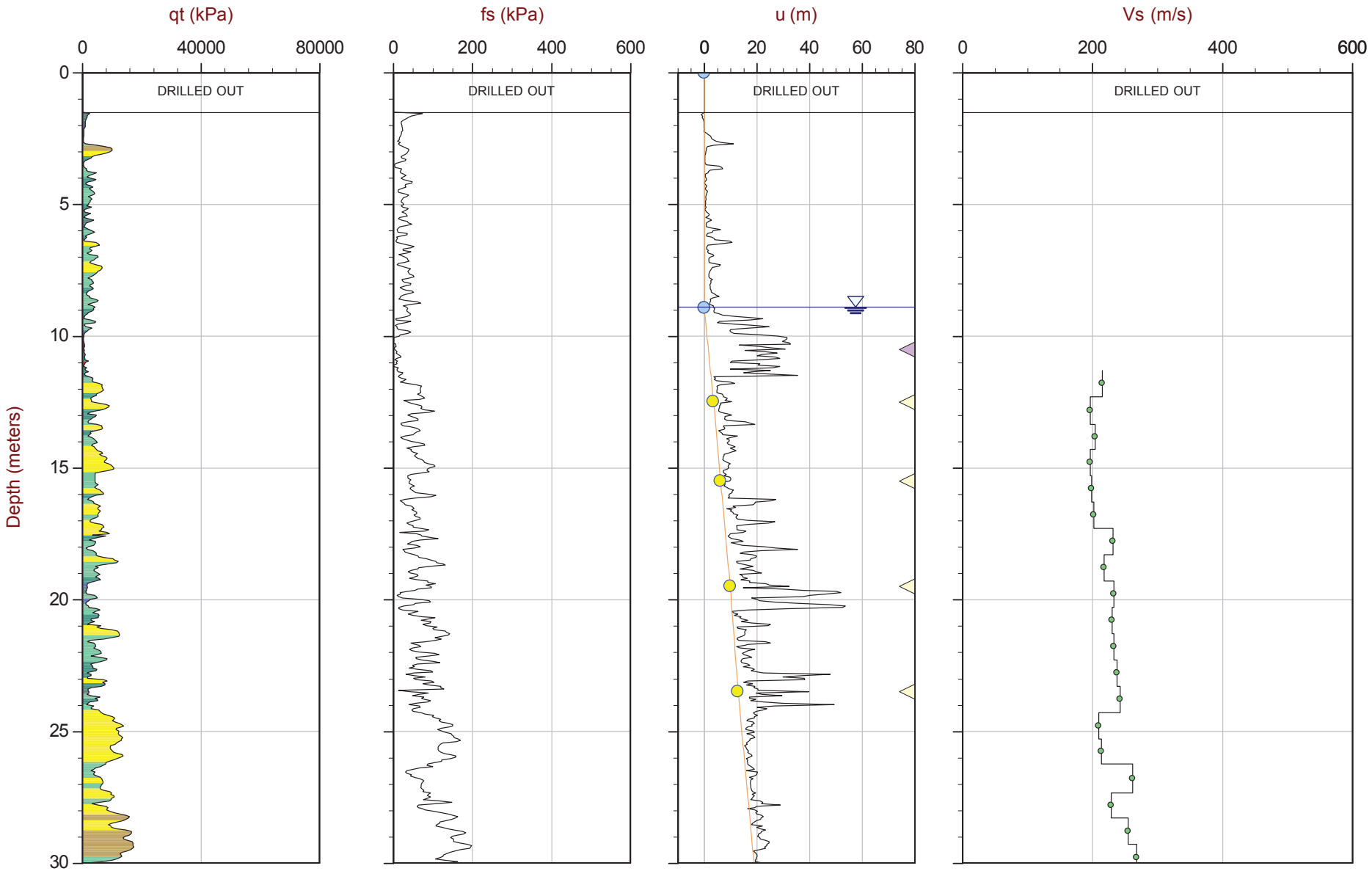

Max Depth: 41.650 m / 136.65 ft
Depth Inc: 0.050 m / 0.164 ft
Avg Int: 0.200 m

File: 16-72004_RS02B.COR
Unit Wt: SBT Zones

SBT: Robertson and Campanella, 1986
Coords: UTM Zone 23 South N: 7764155m E: 658559m
Page No: 1 of 2

Overplot Item:
- Assumed Ueq
- Ueq
- Dissipation, equilibrium achieved
- Dissipation, equilibrium not achieved
- Equilibrium Line

CONETEC

CGSH

Job No: 16-72004
Date: 04:24:16 11:30
Site: Bay 3, Germano Slimes

Sounding: GSCPT16-02B
Cone: 376:T375F10U200

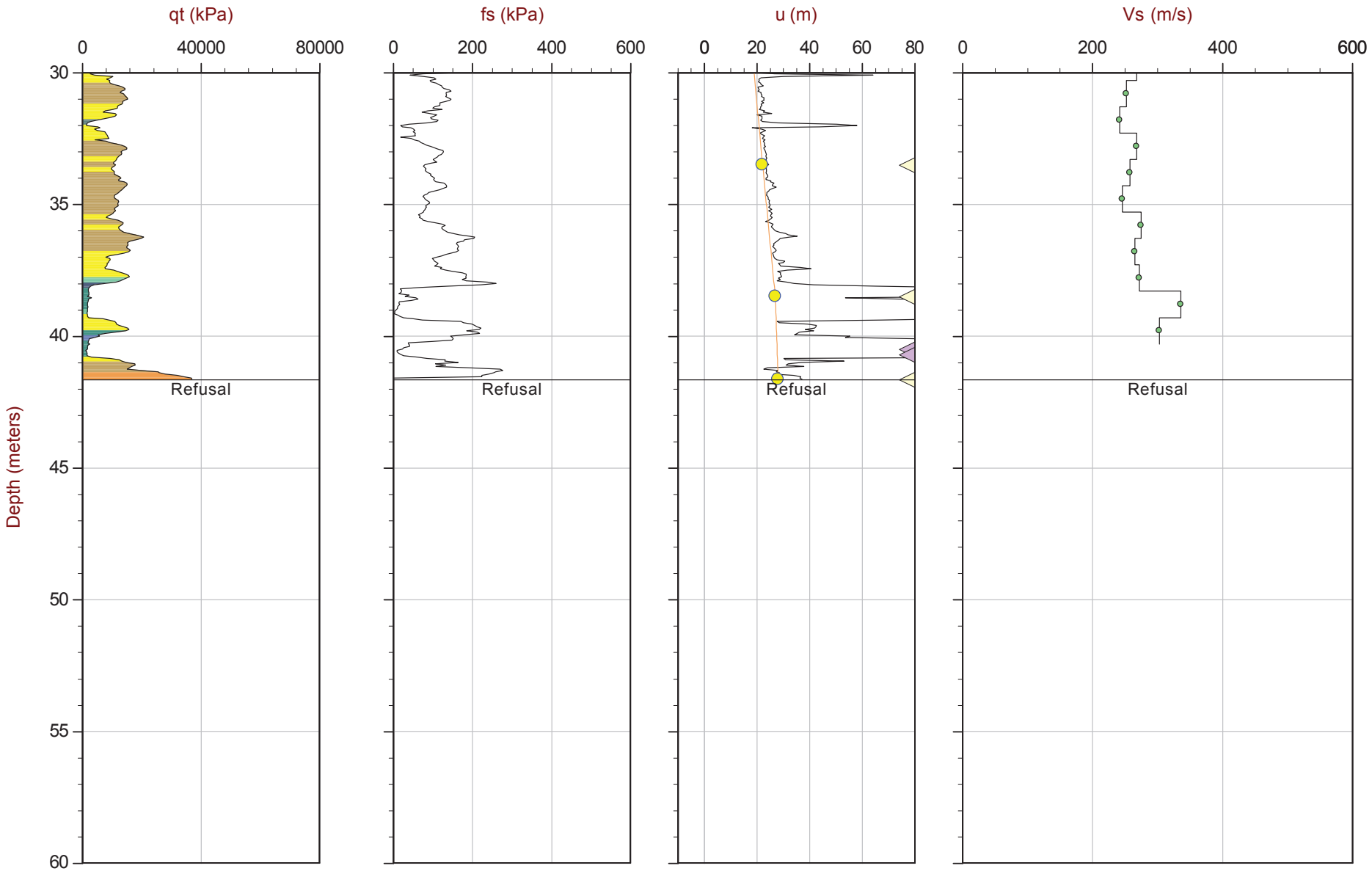

Max Depth: 41.650 m / 136.65 ft
Depth Inc: 0.050 m / 0.164 ft
Avg Int: 0.200 m

File: 16-72004_RS02B.COR
Unit Wt: SBT Zones

SBT: Robertson and Campanella, 1986
Coords: UTM Zone 23 South N: 7764155m E: 658559m
Page No: 2 of 2

Overplot Item:
- Assumed Ueq
- Ueq
- Dissipation, equilibrium achieved
- Dissipation, equilibrium not achieved
- Equilibrium Line

CONETEC

CGSH

Job No: 16-72004
Date: 04:26:16 12:34
Site: Bay 3, Germano Cava

Sounding: GCCPT16-03
Cone: 376:T375F10U200

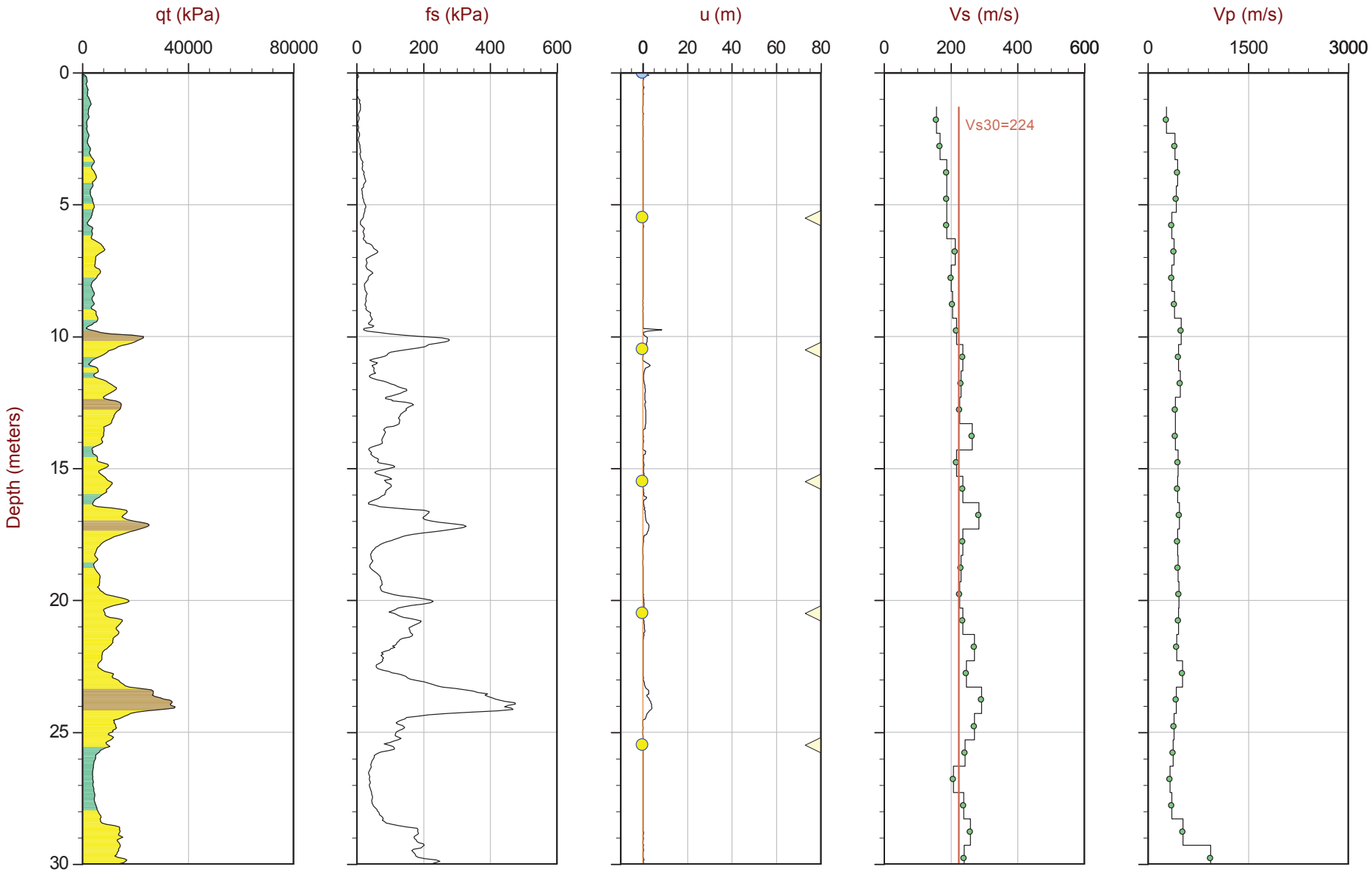

Max Depth: 61.650 m / 202.26 ft
Depth Inc: 0.050 m / 0.164 ft
Avg Int: 0.200 m
Overplot Item:

File: 16-72004_RS03.COR
Unit Wt: SBT Zones

SBT: Robertson and Campanella, 1986
Coords: UTM Zone 23 South N: 7766164m E: 657252m
Page No: 1 of 3

Assumed Ueq
Ueq
Dissipation, equilibrium achieved
Dissipation, equilibrium not achieved
Equilibrium Line

CONETEC

CGSH

Job No: 16-72004
Date: 04:26:16 12:34
Site: Bay 3, Germano Cava

Sounding: GCCPT16-03
Cone: 376:T375F10U200

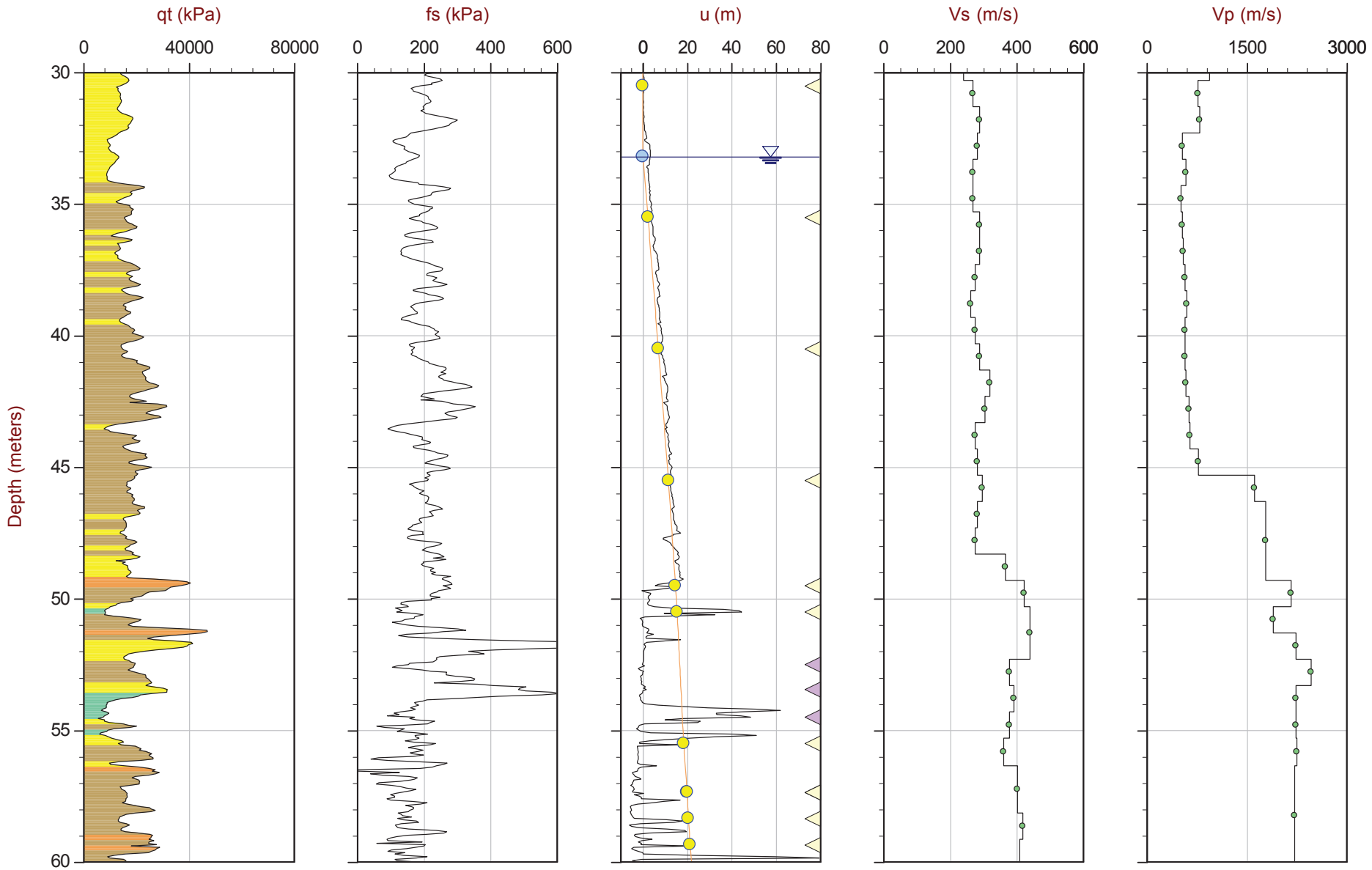

Max Depth: 61.650 m / 202.26 ft
Depth Inc: 0.050 m / 0.164 ft
Avg Int: 0.200 m
Overplot Item:

File: 16-72004_RS03.COR
Unit Wt: SBT Zones

SBT: Robertson and Campanella, 1986
Coords: UTM Zone 23 South N: 7766164m E: 657252m
Page No: 2 of 3

Assumed Ueq
Ueq
Dissipation, equilibrium achieved
Dissipation, equilibrium not achieved
Equilibrium Line

CONETEC

CGSH

Job No: 16-72004
Date: 04:26:16 12:34
Site: Bay 3, Germano Cava

Sounding: GCCPT16-03
Cone: 376:T375F10U200

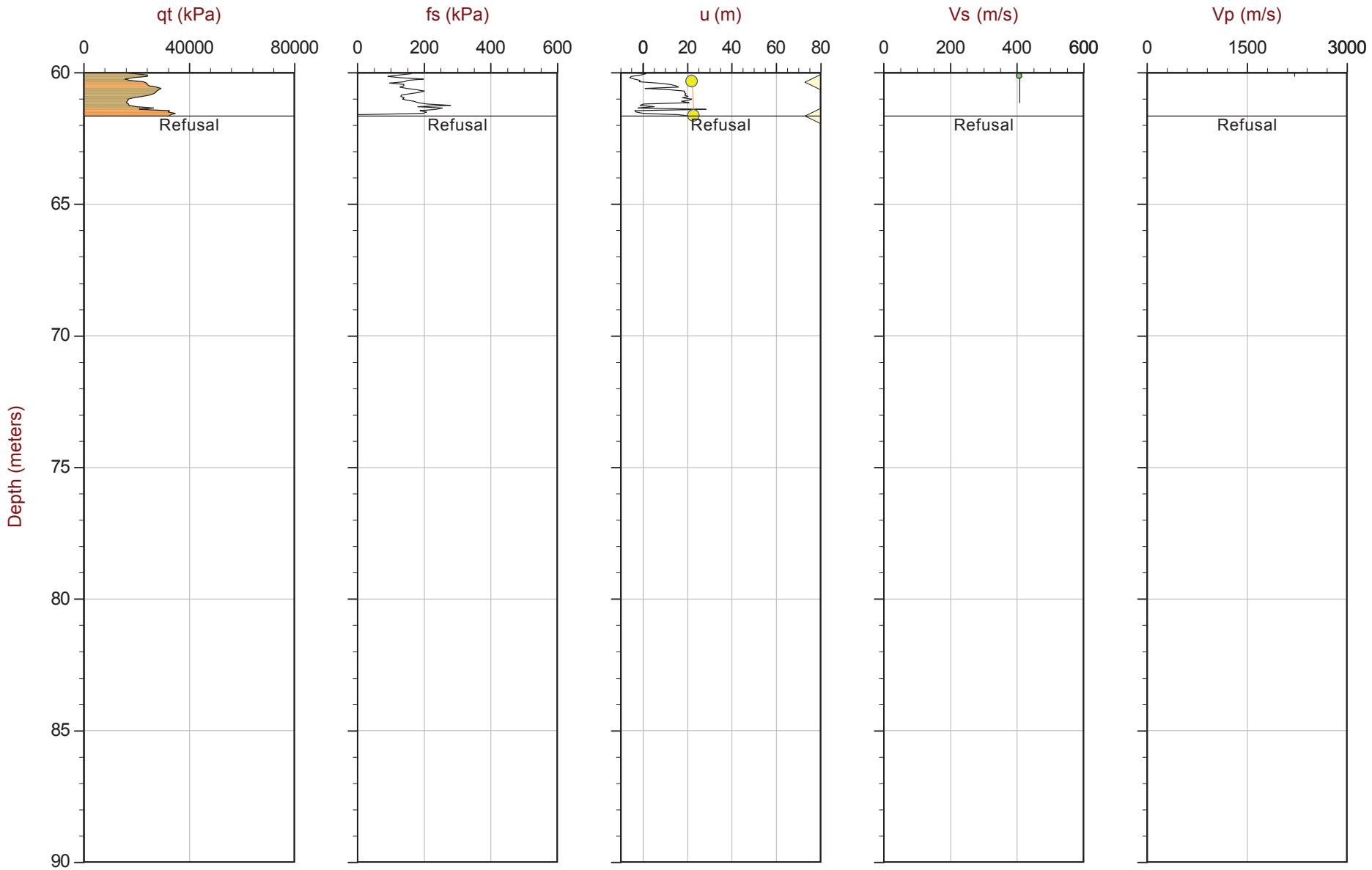

Max Depth: 61.650 m / 202.26 ft
Depth Inc: 0.050 m / 0.164 ft
Avg Int: 0.200 m

File: 16-72004_RS03.COR
Unit Wt: SBT Zones

SBT: Robertson and Campanella, 1986
Coords: UTM Zone 23 South N: 7766164m E: 657252m
Page No: 3 of 3

Overplot Item:
- Assumed Ueq
- Ueq
- Dissipation, equilibrium achieved
- Dissipation, equilibrium not achieved
- Equilibrium Line

CONETEC

CGSH

Job No: 16-72004
Date: 05:02:16 15:34
Site: Bay 3, Germano Cava

Sounding: GCCPT16-04
Cone: 376:T375F10U200

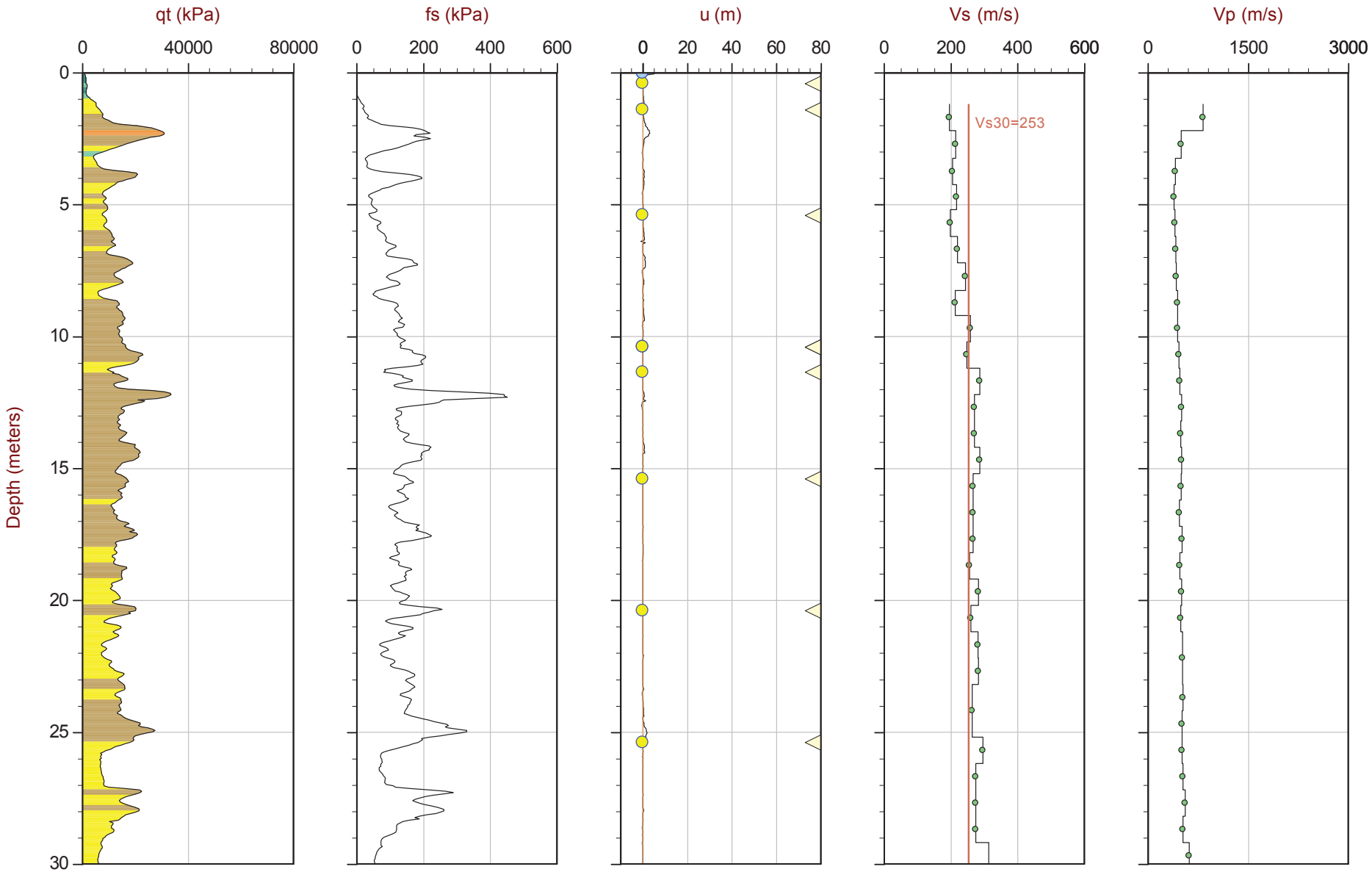

Max Depth: 35.350 m / 115.98 ft
Depth Inc: 0.050 m / 0.164 ft
Avg Int: 0.200 m
Overplot Item:

File: 16-72004_RS04.COR
Unit Wt: SBT Zones

SBT: Robertson and Campanella, 1986
Coords: UTM Zone 23 South N: 7766303m E: 657393m
Page No: 1 of 2

Assumed Ueq
Ueq
Dissipation, equilibrium achieved
Dissipation, equilibrium not achieved
Equilibrium Line

CONETEC

CGSH

Job No: 16-72004
Date: 05:02:16 15:34
Site: Bay 3, Germano Cava

Sounding: GCCPT16-04
Cone: 376:T375F10U200

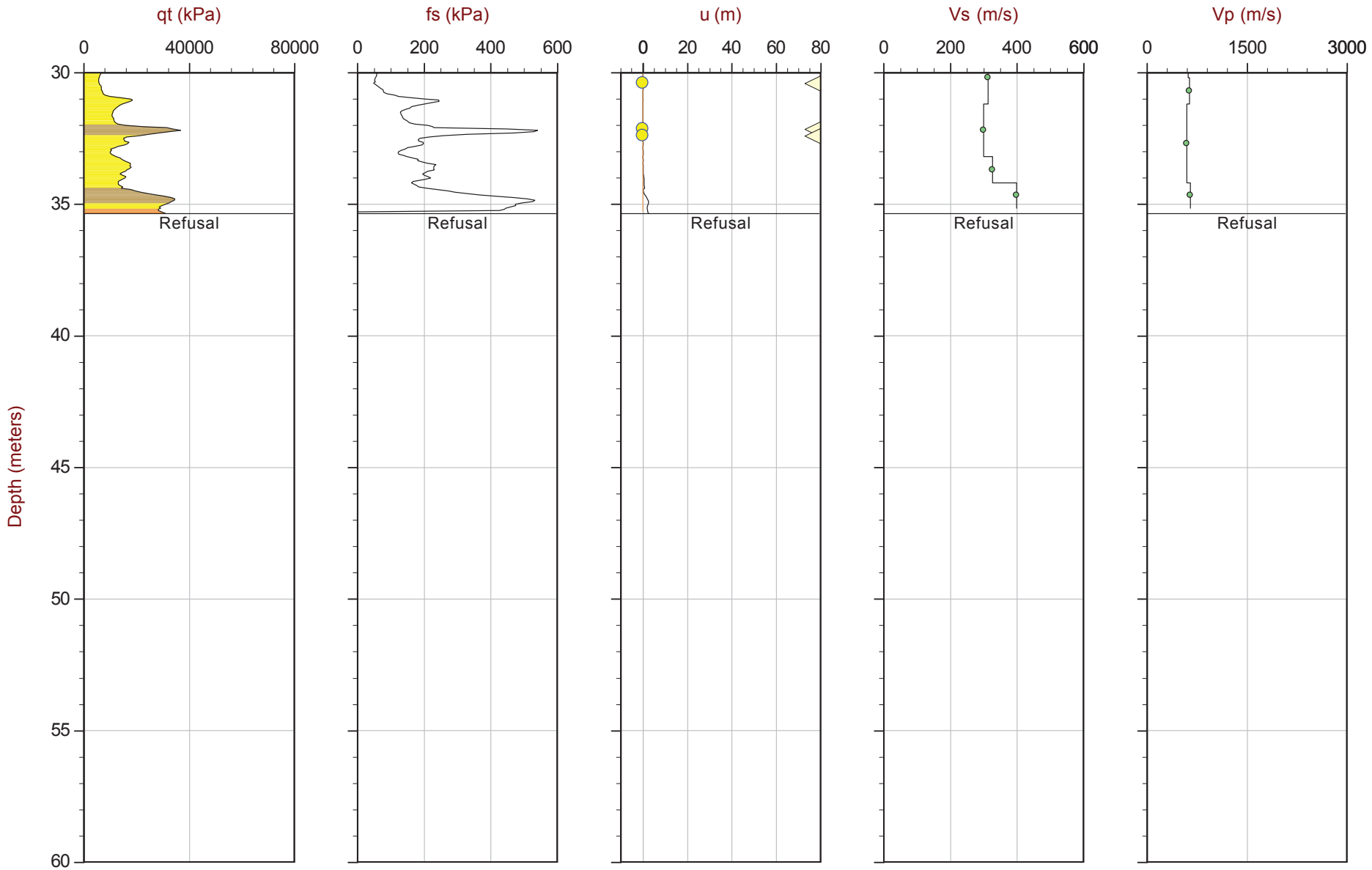

Max Depth: 35.350 m / 115.98 ft
Depth Inc: 0.050 m / 0.164 ft
Avg Int: 0.200 m
Overplot Item:

File: 16-72004_RS04.COR
Unit Wt: SBT Zones

SBT: Robertson and Campanella, 1986
Coords: UTM Zone 23 South N: 7766303m E: 657393m
Page No: 2 of 2

Assumed Ueq
Ueq
Dissipation, equilibrium achieved
Dissipation, equilibrium not achieved
Equilibrium Line

CONETEC

CGSH

Job No: 16-72004
Date: 05:13:16 13:07
Site: Germano Cava

Sounding: GCCPT16-04B
Cone: 432:T1500F15U500

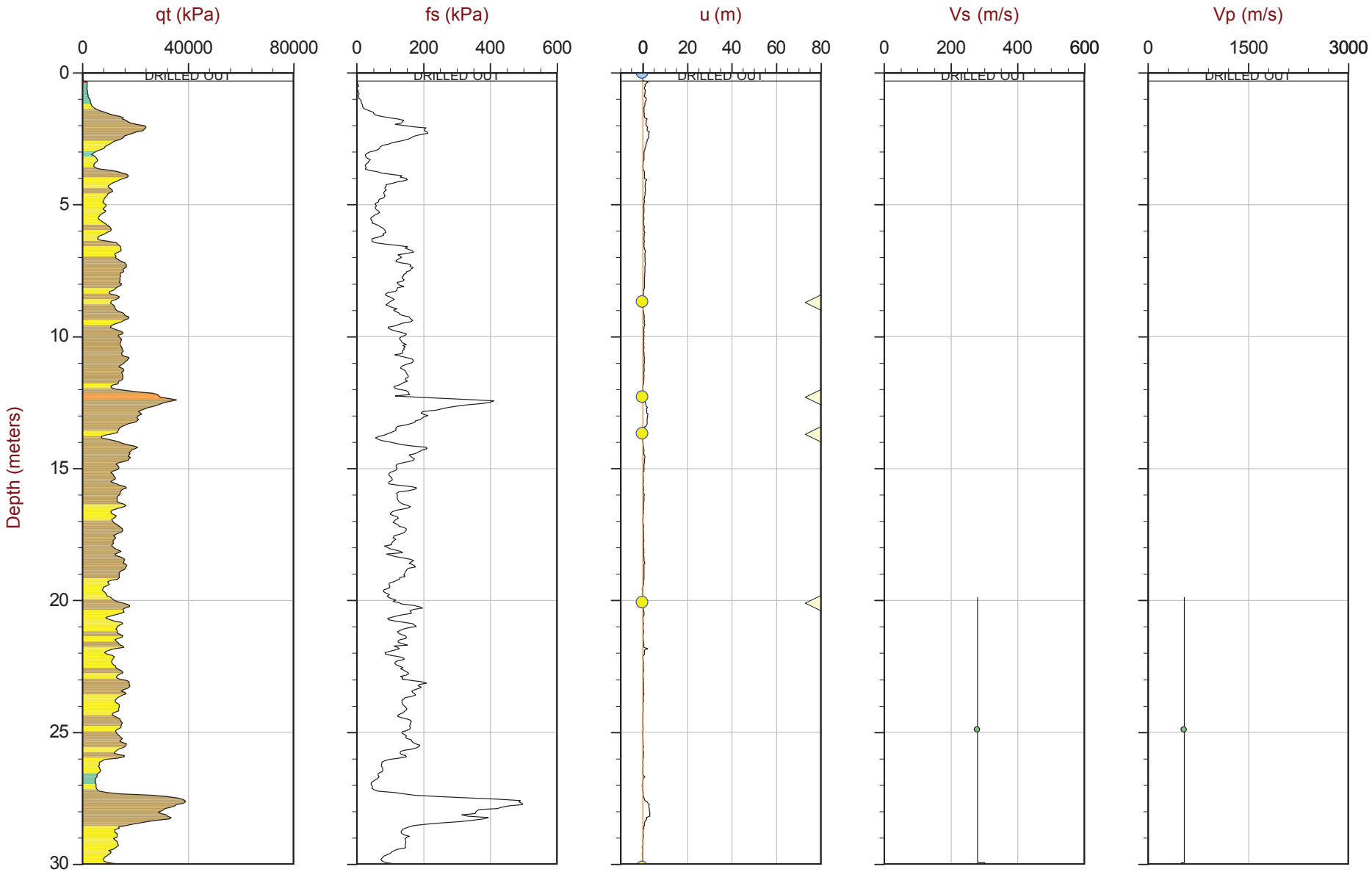

Max Depth: 36.350 m / 119.26 ft
Depth Inc: 0.050 m / 0.164 ft
Avg Int: 0.200 m

File: 16-72004_RS04B.COR
Unit Wt: SBT Zones

SBT: Robertson and Campanella, 1986
Coords: UTM Zone 23 South N: 7766300m E: 657394m
Page No: 1 of 2

Overplot Item:
- Assumed Ueq
- Ueq
- Dissipation, equilibrium achieved
- Dissipation, equilibrium not achieved
- Equilibrium Line

CONETEC

CGSH

Job No: 16-72004
Date: 05:13:16 13:07
Site: Germano Cava

Sounding: GCCPT16-04B
Cone: 432:T1500F15U500

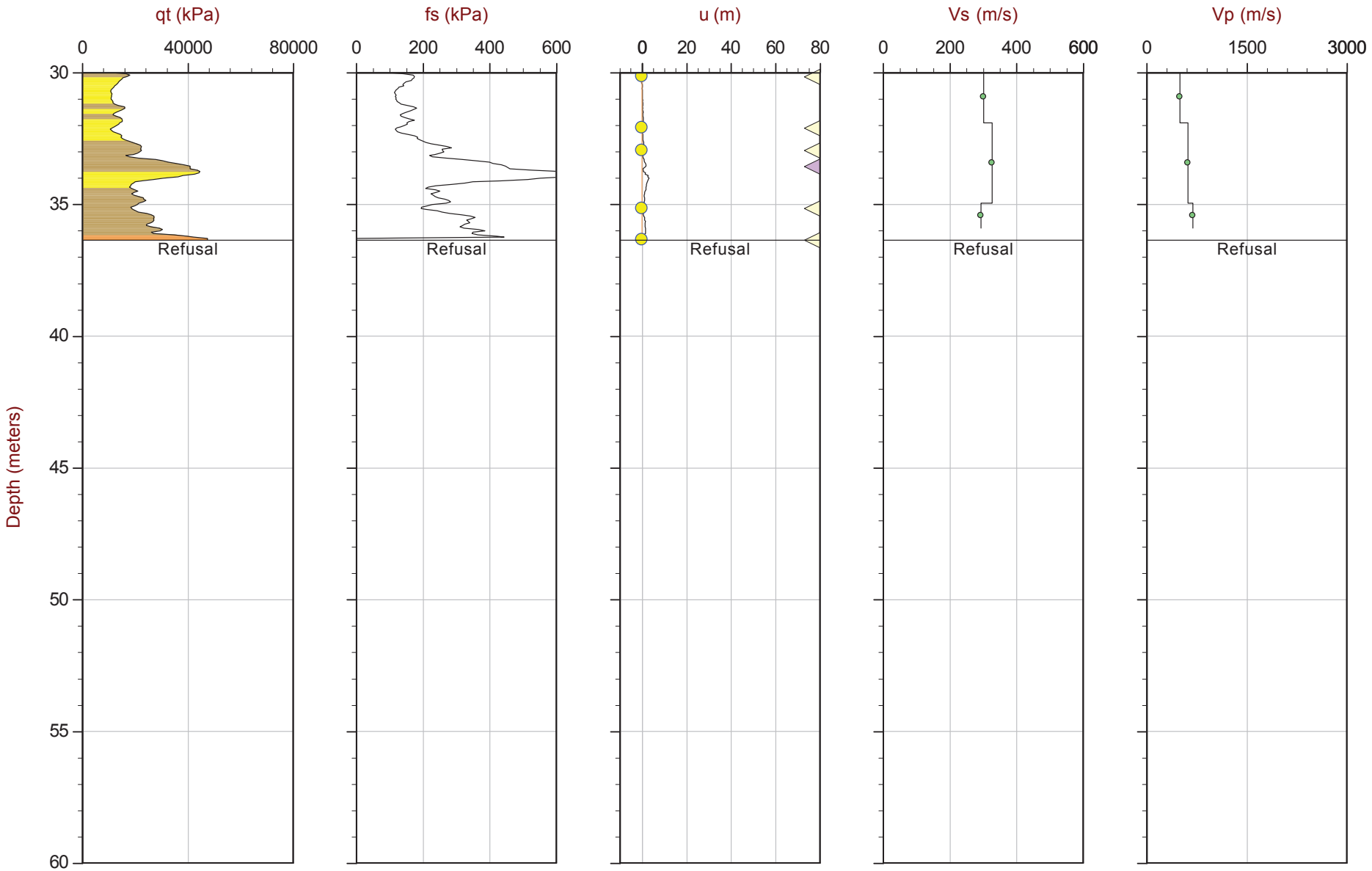

Max Depth: 36.350 m / 119.26 ft
Depth Inc: 0.050 m / 0.164 ft
Avg Int: 0.200 m
Overplot Item:

File: 16-72004_RS04B.COR
Unit Wt: SBT Zones

SBT: Robertson and Campanella, 1986
Coords: UTM Zone 23 South N: 7766300m E: 657394m
Page No: 2 of 2

Assumed Ueq
Ueq
Dissipation, equilibrium achieved
Dissipation, equilibrium not achieved
Equilibrium Line

CONETEC

CGSH

Job No: 16-72004
Date: 05:05:16 10:41
Site: Bay 3, Germano Slimes

Sounding: GSCPT16-05
Cone: 376:T375F10U200

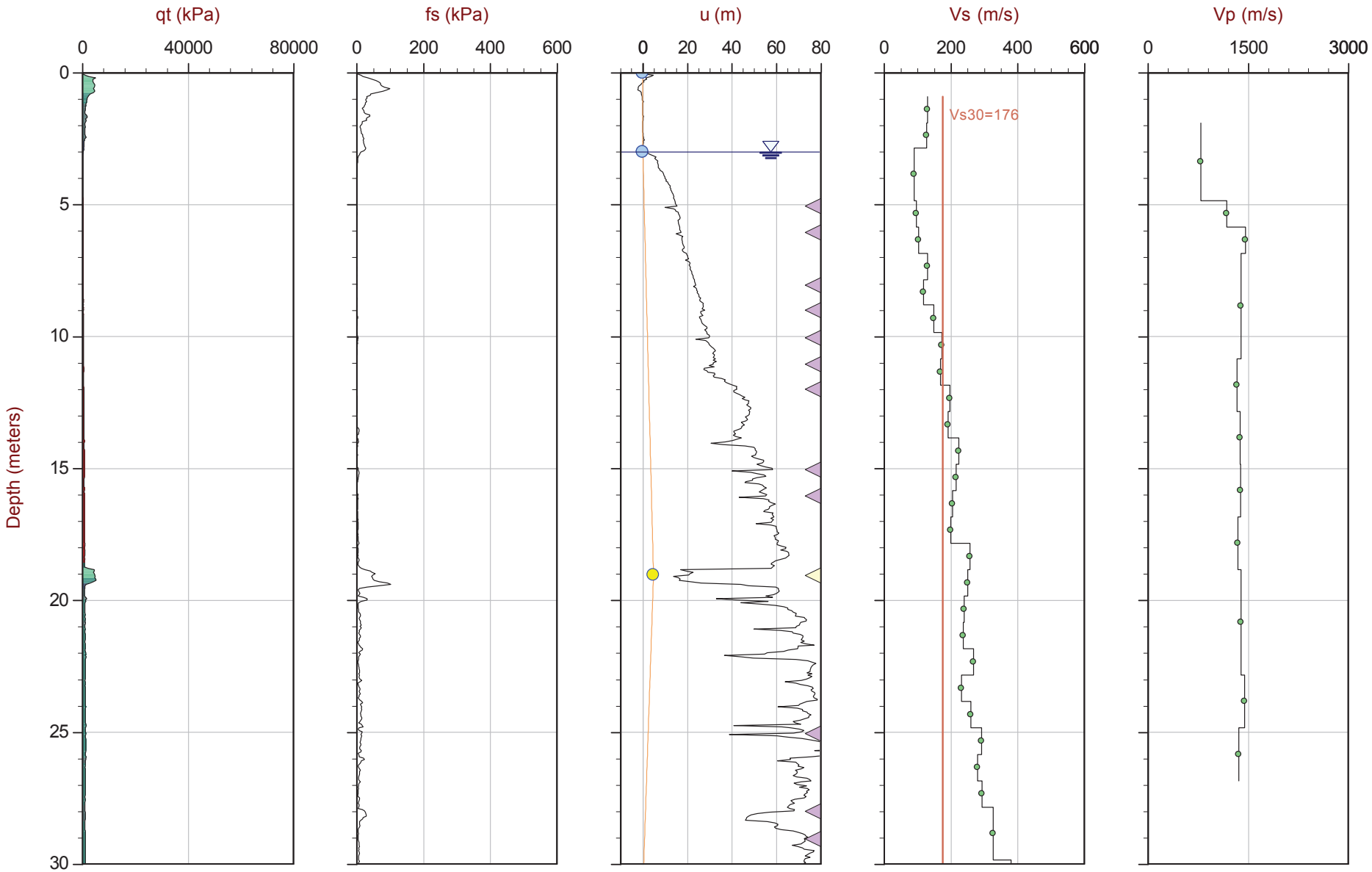

Max Depth: 31.850 m / 104.49 ft
Depth Inc: 0.050 m / 0.164 ft
Avg Int: 0.200 m
Overplot Item:

File: 16-72004_SP05.COR
Unit Wt: SBT Zones

SBT: Robertson and Campanella, 1986
Coords: UTM Zone 23 South N: 7763372m E: 659090m
Page No: 1 of 2

Assumed Ueq
Ueq
Dissipation, equilibrium achieved
Dissipation, equilibrium not achieved
Equilibrium Line

CONETEC

CGSH

Job No: 16-72004
Date: 05:05:16 10:41
Site: Bay 3, Germano Slimes

Sounding: GSCPT16-05
Cone: 376:T375F10U200

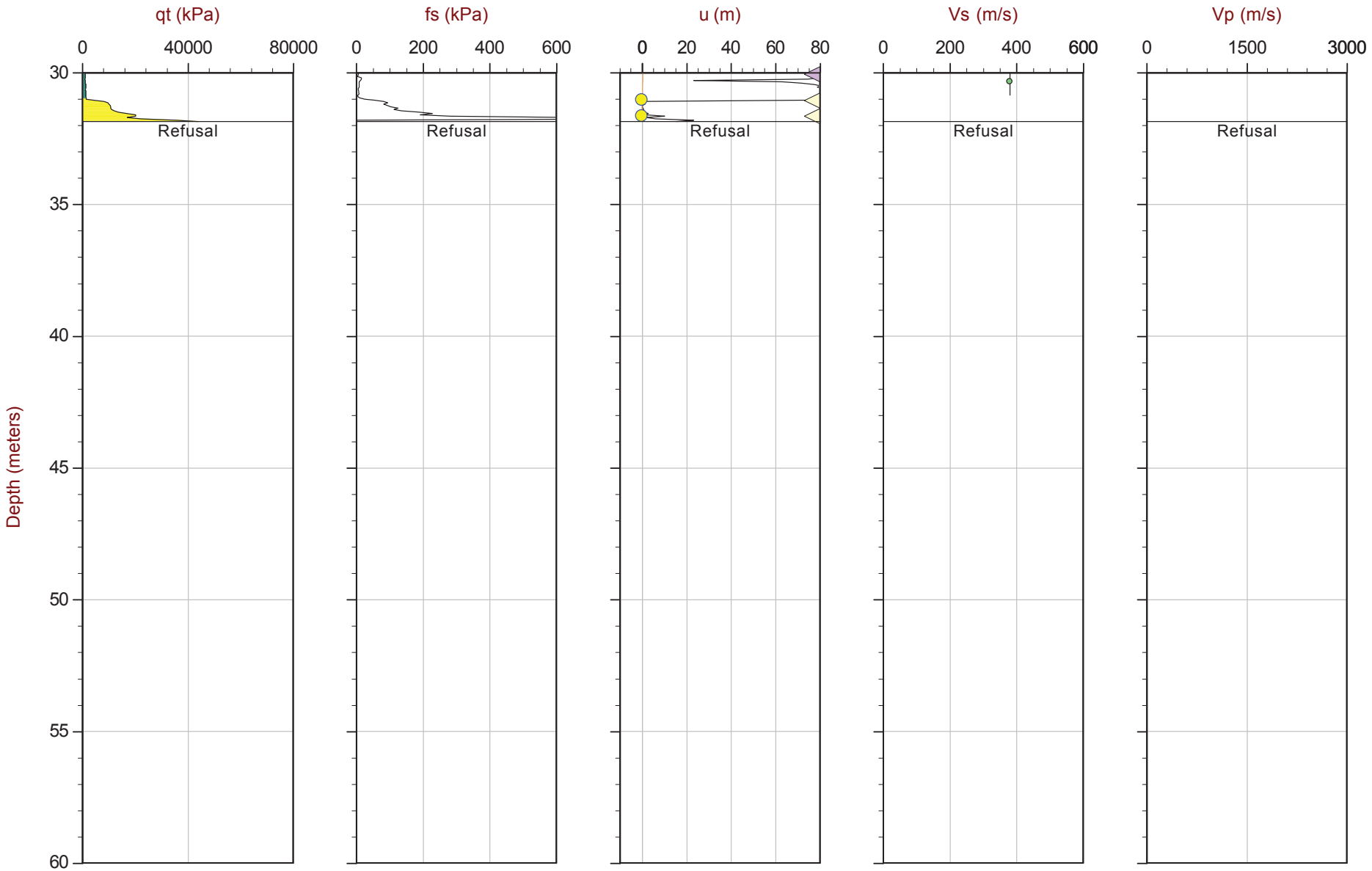

Max Depth: 31.850 m / 104.49 ft
Depth Inc: 0.050 m / 0.164 ft
Avg Int: 0.200 m
Overplot Item:

File: 16-72004_SP05.COR
Unit Wt: SBT Zones

SBT: Robertson and Campanella, 1986
Coords: UTM Zone 23 South N: 7763372m E: 659090m
Page No: 2 of 2

Assumed Ueq
Ueq
Dissipation, equilibrium achieved
Dissipation, equilibrium not achieved
Equilibrium Line

CONETEC

CGSH

Job No: 16-72004
Date: 05:16:16 13:45
Site: Germano Buttres

Sounding: GBCPT16-06
Cone: 432:T1500F15U500

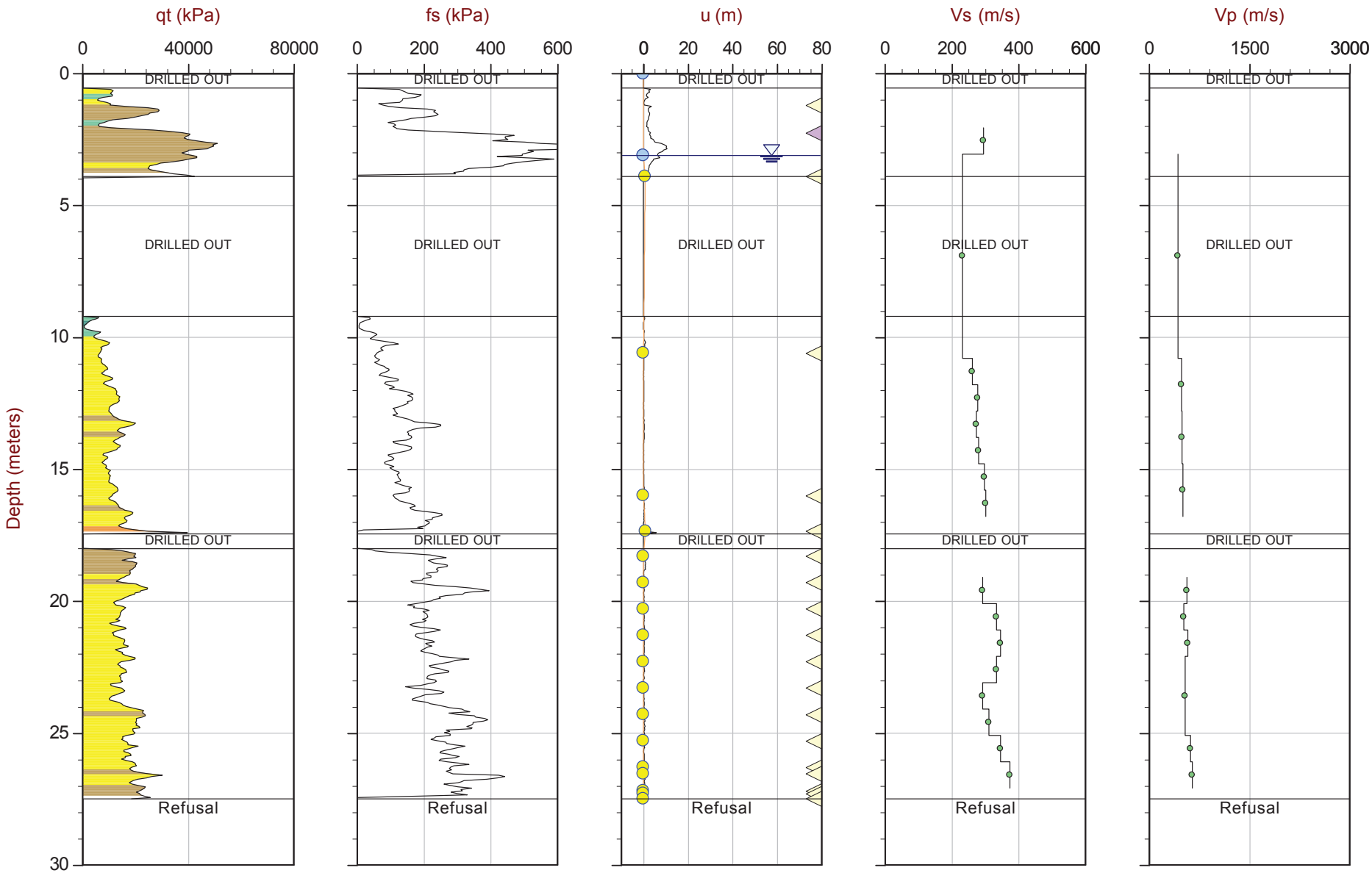

Max Depth: 27.500 m / 90.22 ft
Depth Inc: 0.050 m / 0.164 ft
Avg Int: 0.200 m
Overplot Item:

File: 16-72004_RS06.COR
Unit Wt: SBT Zones

SBT: Robertson and Campanella, 1986
Coords: UTM Zone 23 South N: 7763631 m E: 660586m
Page No: 1 of 1

Assumed Ueq
Ueq
Dissipation, equilibrium achieved
Dissipation, equilibrium not achieved
Equilibrium Line

Seismic Cone Penetration Test Tabular Results

CONETEC

Job No:	16-72004
Client:	Cleary Gottlieb Steen & Hamilton LLP (CGSH)
Project:	Samarco, Germano Buttress
Sounding ID:	GSCPT16-02
Date:	21-Apr-2016

Seismic Source:	Beam
Source Offset (m):	0.20
Source Depth (m):	0.00
Geophone Offset (m):	0.20

SCPTu SHEAR WAVE VELOCITY TEST RESULTS - Vs

Tip Depth (m)	Geophone Depth (m)	Ray Path (m)	Ray Path Difference (m)	Travel Time Interval (ms)	Interval Velocity (m/s)
3.35	3.15	3.16			
4.45	4.25	4.25	1.10	5.74	192
5.40	5.20	5.20	0.95	5.80	164
6.40	6.20	6.20	1.00	6.20	161
7.40	7.20	7.20	1.00	5.21	192
8.40	8.20	8.20	1.00	6.00	167
9.40	9.20	9.20	1.00	5.74	174
10.40	10.20	10.20	1.00	5.74	174
11.40	11.20	11.20	1.00	5.41	185

Job No:	16-72004
Client:	Cleary Gottlieb Steen & Hamilton LLP (CGSH)
Project:	Samarco, Germano Buttress
Sounding ID:	GSCPT16-02B
Date:	24-Apr-2016

Seismic Source:	Beam
Source Offset (m):	0.20
Source Depth (m):	0.00
Geophone Offset (m):	0.20

SCPTu SHEAR WAVE VELOCITY TEST RESULTS - Vs

Tip Depth (m)	Geophone Depth (m)	Ray Path (m)	Ray Path Difference (m)	Travel Time Interval (ms)	Interval Velocity (m/s)
11.50	11.30	11.30			
12.50	12.30	12.30	1.00	4.65	215
13.55	13.35	13.35	1.05	5.33	197
14.50	14.30	14.30	0.95	4.65	204
15.50	15.30	15.30	1.00	5.08	197
16.50	16.30	16.30	1.00	5.02	199
17.50	17.30	17.30	1.00	4.96	202
18.50	18.30	18.30	1.00	4.31	232
19.50	19.30	19.30	1.00	4.58	218
20.50	20.30	20.30	1.00	4.30	233
21.50	21.30	21.30	1.00	4.34	230
22.50	22.30	22.30	1.00	4.30	233
23.50	23.30	23.30	1.00	4.20	238
24.50	24.30	24.30	1.00	4.11	243
25.50	25.30	25.30	1.00	4.77	210
26.45	26.25	26.25	0.95	4.44	214
27.55	27.35	27.35	1.10	4.20	262
28.50	28.30	28.30	0.95	4.16	229
29.50	29.30	29.30	1.00	3.92	255
30.50	30.30	30.30	1.00	3.73	268
31.50	31.30	31.30	1.00	3.97	252
32.50	32.30	32.30	1.00	4.13	242
33.50	33.30	33.30	1.00	3.73	268
34.50	34.30	34.30	1.00	3.87	258
35.50	35.30	35.30	1.00	4.06	246
36.50	36.30	36.30	1.00	3.64	275
37.50	37.30	37.30	1.00	3.78	265
38.50	38.30	38.30	1.00	3.68	272
39.50	39.30	39.30	1.00	2.97	336
40.50	40.30	40.30	1.00	3.31	303

Job No:	16-72004
Client:	Cleary Gottlieb Steen & Hamilton LLP (CGSH)
Project:	Samarco, Germano Buttress
Sounding ID:	GCCPT16-03
Date:	26-Apr-2016

Seismic Source:	Beam
Source Offset (m):	0.20
Source Depth (m):	0.00
Geophone Offset (m):	0.20

SCPTu SHEAR WAVE VELOCITY TEST RESULTS - Vs

Tip Depth (m)	Geophone Depth (m)	Ray Path (m)	Ray Path Difference (m)	Travel Time Interval (ms)	Interval Velocity (m/s)
1.50	1.30	1.32			
2.50	2.30	2.31	0.99	6.30	158
3.50	3.30	3.31	1.00	5.94	168
4.50	4.30	4.30	1.00	5.31	188
5.50	5.30	5.30	1.00	5.31	188
6.50	6.30	6.30	1.00	5.31	188
7.50	7.30	7.30	1.00	4.68	213
8.50	8.30	8.30	1.00	4.95	202
9.50	9.30	9.30	1.00	4.86	206
10.50	10.30	10.30	1.00	4.59	218
11.50	11.30	11.30	1.00	4.23	236
12.50	12.30	12.30	1.00	4.32	231
13.50	13.30	13.30	1.00	4.41	227
14.50	14.30	14.30	1.00	3.78	264
15.50	15.30	15.30	1.00	4.59	218
16.50	16.30	16.30	1.00	4.23	236
17.50	17.30	17.30	1.00	3.51	285
18.50	18.30	18.30	1.00	4.23	236
19.50	19.30	19.30	1.00	4.32	231
20.50	20.30	20.30	1.00	4.41	227
21.50	21.30	21.30	1.00	4.23	236
22.50	22.30	22.30	1.00	3.69	271
23.50	23.30	23.30	1.00	4.05	247
24.50	24.30	24.30	1.00	3.42	292
25.50	25.30	25.30	1.00	3.69	271
26.50	26.30	26.30	1.00	4.12	243
27.50	27.30	27.30	1.00	4.81	208
28.50	28.30	28.30	1.00	4.19	239
29.50	29.30	29.30	1.00	3.87	259
30.50	30.30	30.30	1.00	4.14	241
31.50	31.30	31.30	1.00	3.73	268
32.50	32.30	32.30	1.00	3.46	289
33.50	33.30	33.30	1.00	3.55	282
34.50	34.30	34.30	1.00	3.73	268
35.50	35.30	35.30	1.00	3.73	268
36.50	36.30	36.30	1.00	3.46	289
37.50	37.30	37.30	1.00	3.46	289
38.50	38.30	38.30	1.00	3.64	275
39.50	39.30	39.30	1.00	3.82	262
40.50	40.30	40.30	1.00	3.64	275

Job No:	16-72004
Client:	Cleary Gottlieb Steen & Hamilton LLP (CGSH)
Project:	Samarco, Germano Buttress
Sounding ID:	GCCPT16-03
Date:	26-Apr-2016

Seismic Source:	Beam
Source Offset (m):	0.20
Source Depth (m):	0.00
Geophone Offset (m):	0.20

SCPTu SHEAR WAVE VELOCITY TEST RESULTS - Vs

Tip Depth (m)	Geophone Depth (m)	Ray Path (m)	Ray Path Difference (m)	Travel Time Interval (ms)	Interval Velocity (m/s)
41.50	41.30	41.30	1.00	3.46	289
42.50	42.30	42.30	1.00	3.13	319
43.50	43.30	43.30	1.00	3.28	305
44.50	44.30	44.30	1.00	3.64	275
45.50	45.30	45.30	1.00	3.55	282
46.50	46.30	46.30	1.00	3.37	297
47.50	47.30	47.30	1.00	3.55	282
48.50	48.30	48.30	1.00	3.64	275
49.50	49.30	49.30	1.00	2.73	366
50.50	50.30	50.30	1.00	2.37	423
52.50	52.30	52.30	2.00	4.55	440
53.50	53.30	53.30	1.00	2.64	379
54.50	54.30	54.30	1.00	2.55	392
55.50	55.30	55.30	1.00	2.64	379
56.55	56.35	56.35	1.05	2.90	361
58.35	58.15	58.15	1.80	4.47	402
59.35	59.15	59.15	1.00	2.39	418
61.35	61.15	61.15	2.00	4.89	409

Job No:	16-72004
Client:	Cleary Gottlieb Steen & Hamilton LLP (CGSH)
Project:	Samarco, Germano Buttress
Sounding ID:	GCCPT16-03
Date:	26-Apr-2016

Seismic Source:	Plate
Source Offset (m):	3.00
Source Depth (m):	0.00
Geophone Offset (m):	0.20

SCPTu COMPRESSION WAVE VELOCITY TEST RESULTS - Vp

Tip Depth (m)	Geophone Depth (m)	Ray Path (m)	Ray Path Difference (m)	Travel Time Interval (ms)	Interval Velocity (m/s)
1.50	1.30	3.27			
2.50	2.30	3.78	0.51	1.83	280
3.50	3.30	4.46	0.68	1.68	405
4.50	4.30	5.24	0.78	1.75	448
5.50	5.30	6.09	0.85	2.00	424
6.50	6.30	6.98	0.89	2.46	361
7.50	7.30	7.89	0.91	2.34	392
8.50	8.30	8.83	0.93	2.58	361
9.50	9.30	9.77	0.95	2.38	398
10.50	10.30	10.73	0.96	1.91	501
11.50	11.30	11.69	0.96	2.09	461
12.50	12.30	12.66	0.97	2.00	485
13.50	13.30	13.63	0.97	2.36	412
14.50	14.30	14.61	0.98	2.36	414
15.50	15.30	15.59	0.98	2.18	450
16.50	16.30	16.57	0.98	2.22	442
17.50	17.30	17.56	0.98	2.09	471
18.50	18.30	18.54	0.99	2.22	443
19.50	19.30	19.53	0.99	2.20	449
20.50	20.30	20.52	0.99	2.13	463
21.50	21.30	21.51	0.99	2.17	456
22.50	22.30	22.50	0.99	2.28	434
23.50	23.30	23.49	0.99	1.91	519
24.50	24.30	24.48	0.99	2.34	423
25.50	25.30	25.48	0.99	2.54	390
26.50	26.30	26.47	0.99	2.64	376
27.50	27.30	27.46	0.99	3.02	329
28.50	28.30	28.46	0.99	2.80	355
29.50	29.30	29.45	0.99	1.89	527
30.50	30.30	30.45	0.99	1.06	942
31.50	31.30	31.44	1.00	1.29	770
32.50	32.30	32.44	1.00	1.26	793
33.50	33.30	33.43	1.00	1.86	535
34.50	34.30	34.43	1.00	1.70	586
35.50	35.30	35.43	1.00	1.94	513
36.50	36.30	36.42	1.00	1.86	535
37.50	37.30	37.42	1.00	1.82	547
38.50	38.30	38.42	1.00	1.74	573
39.50	39.30	39.41	1.00	1.66	601
40.50	40.30	40.41	1.00	1.74	573

Job No:	16-72004
Client:	Cleary Gottlieb Steen & Hamilton LLP (CGSH)
Project:	Samarco, Germano Buttress
Sounding ID:	GCCPT16-03
Date:	26-Apr-2016

Seismic Source:	Plate
Source Offset (m):	3.00
Source Depth (m):	0.00
Geophone Offset (m):	0.20

SCPTu COMPRESSION WAVE VELOCITY TEST RESULTS - Vp

Tip Depth (m)	Geophone Depth (m)	Ray Path (m)	Ray Path Difference (m)	Travel Time Interval (ms)	Interval Velocity (m/s)
41.50	41.30	41.41	1.00	1.74	573
42.50	42.30	42.41	1.00	1.70	587
43.50	43.30	43.40	1.00	1.58	632
44.50	44.30	44.40	1.00	1.54	649
45.50	45.30	45.40	1.00	1.29	773
46.50	46.30	46.40	1.00	0.62	1615
49.50	49.30	49.39	2.99	1.68	1782
50.50	50.30	50.39	1.00	0.46	2166
51.50	51.30	51.39	1.00	0.53	1897
52.50	52.30	52.39	1.00	0.45	2242
53.50	53.30	53.38	1.00	0.40	2466
54.50	54.30	54.38	1.00	0.45	2242
55.50	55.30	55.38	1.00	0.45	2242
56.55	56.35	56.43	1.05	0.47	2251
60.35	60.15	60.22	3.79	1.71	2221

Job No:	16-72004
Client:	Cleary Gottlieb Steen & Hamilton LLP (CGSH)
Project:	Samarco, Germano Buttress
Sounding ID:	GCCPT16-04
Date:	02-May-2016

Seismic Source:	Beam
Source Offset (m):	0.15
Source Depth (m):	0.00
Geophone Offset (m):	0.20

SCPTu SHEAR WAVE VELOCITY TEST RESULTS - Vs

Tip Depth (m)	Geophone Depth (m)	Ray Path (m)	Ray Path Difference (m)	Travel Time Interval (ms)	Interval Velocity (m/s)
1.40	1.20	1.21			
2.40	2.20	2.21	1.00	5.09	196
3.45	3.25	3.25	1.05	4.87	215
4.45	4.25	4.25	1.00	4.86	206
5.40	5.20	5.20	0.95	4.39	217
6.40	6.20	6.20	1.00	5.01	199
7.40	7.20	7.20	1.00	4.54	220
8.45	8.25	8.25	1.05	4.28	245
9.40	9.20	9.20	0.95	4.44	214
10.40	10.20	10.20	1.00	3.86	259
11.40	11.20	11.20	1.00	4.02	249
12.40	12.20	12.20	1.00	3.48	287
13.40	13.20	13.20	1.00	3.69	271
14.40	14.20	14.20	1.00	3.69	271
15.40	15.20	15.20	1.00	3.48	287
16.40	16.20	16.20	1.00	3.74	267
17.40	17.20	17.20	1.00	3.74	267
18.40	18.20	18.20	1.00	3.74	267
19.40	19.20	19.20	1.00	3.90	256
20.40	20.20	20.20	1.00	3.53	283
21.40	21.20	21.20	1.00	3.85	260
22.40	22.20	22.20	1.00	3.54	282
23.40	23.20	23.20	1.00	3.53	283
25.40	25.20	25.20	2.00	7.54	265
26.40	26.20	26.20	1.00	3.37	296
27.40	27.20	27.20	1.00	3.64	275
28.40	28.20	28.20	1.00	3.64	275
29.40	29.20	29.20	1.00	3.64	275
31.40	31.20	31.20	2.00	6.38	314
33.40	33.20	33.20	2.00	6.65	301
34.40	34.20	34.20	1.00	3.05	327
35.35	35.15	35.15	0.95	2.37	400

Job No:	16-72004
Client:	Cleary Gottlieb Steen & Hamilton LLP (CGSH)
Project:	Samarco, Germano Buttress
Sounding ID:	GCCPT16-04
Date:	02-May-2016

Seismic Source:	Plate
Source Offset (m):	2.55
Source Depth (m):	0.00
Geophone Offset (m):	0.20

SCPTu COMPRESSION WAVE VELOCITY TEST RESULTS - Vp

Tip Depth (m)	Geophone Depth (m)	Ray Path (m)	Ray Path Difference (m)	Travel Time Interval (ms)	Interval Velocity (m/s)
1.40	1.20	2.82			
2.40	2.20	3.37	0.55	0.66	829
3.45	3.25	4.13	0.76	1.53	499
4.45	4.25	4.96	0.83	1.99	415
5.40	5.20	5.79	0.84	2.14	390
6.40	6.20	6.70	0.91	2.24	407
7.40	7.20	7.64	0.93	2.24	416
8.45	8.25	8.64	1.00	2.35	425
9.40	9.20	9.55	0.91	2.04	447
10.40	10.20	10.51	0.97	2.17	446
11.40	11.20	11.49	0.97	2.09	465
12.40	12.20	12.46	0.98	2.04	479
13.40	13.20	13.44	0.98	1.94	506
14.40	14.20	14.43	0.98	1.99	494
15.40	15.20	15.41	0.99	1.94	508
16.40	16.20	16.40	0.99	1.99	496
17.40	17.20	17.39	0.99	2.09	473
18.40	18.20	18.38	0.99	1.92	515
19.40	19.20	19.37	0.99	2.06	480
20.40	20.20	20.36	0.99	1.96	505
21.40	21.20	21.35	0.99	2.01	493
23.40	23.20	23.34	1.99	3.82	521
24.40	24.20	24.33	0.99	1.89	527
25.40	25.20	25.33	0.99	1.94	513
26.40	26.20	26.32	1.00	1.94	513
27.40	27.20	27.32	1.00	1.89	528
28.40	28.20	28.31	1.00	1.79	558
29.40	29.20	29.31	1.00	1.89	528
30.40	30.20	30.31	1.00	1.61	621
31.40	31.20	31.30	1.00	1.56	640
34.40	34.20	34.29	2.99	5.01	597
35.35	35.15	35.24	0.95	1.45	652

Job No:	16-72004
Client:	Cleary Gottlieb Steen & Hamilton LLP (CGSH)
Project:	Samarco, Germano Buttress
Sounding ID:	GSCPT16-04B
Date:	13-May-2016

Seismic Source:	Beam
Source Offset (m):	0.60
Source Depth (m):	0.00
Geophone Offset (m):	0.20

SCPTu SHEAR WAVE VELOCITY TEST RESULTS - Vs

Tip Depth (m)	Geophone Depth (m)	Ray Path (m)	Ray Path Difference (m)	Travel Time Interval (ms)	Interval Velocity (m/s)
20.10	19.90	19.91			
30.15	29.95	29.96	10.05	35.80	281
32.10	31.90	31.91	1.95	6.46	302
35.15	34.95	34.96	3.05	9.31	327
36.10	35.90	35.90	0.95	3.23	294

Job No:	16-72004
Client:	Cleary Gottlieb Steen & Hamilton LLP (CGSH)
Project:	Samarco, Germano Buttress
Sounding ID:	GSCPT16-04B
Date:	13-May-2016

Seismic Source:	Plate
Source Offset (m):	3.00
Source Depth (m):	0.00
Geophone Offset (m):	0.20

SCPTu COMPRESSION WAVE VELOCITY TEST RESULTS - Vp

Tip Depth (m)	Geophone Depth (m)	Ray Path (m)	Ray Path Difference (m)	Travel Time Interval (ms)	Interval Velocity (m/s)
20.10	19.90	20.12			
30.15	29.95	30.10	9.97	18.32	544
32.10	31.90	32.04	1.94	3.87	502
35.15	34.95	35.08	3.04	4.89	621
36.10	35.90	36.03	0.95	1.37	693

Job No:	16-72004
Client:	Cleary Gottlieb Steen & Hamilton LLP (CGSH)
Project:	Samarco, Germano Buttress
Sounding ID:	GSCPT16-05
Date:	05-May-2016

Seismic Source:	Beam
Source Offset (m):	0.20
Source Depth (m):	0.00
Geophone Offset (m):	0.20

SCPTu SHEAR WAVE VELOCITY TEST RESULTS - Vs

Tip Depth (m)	Geophone Depth (m)	Ray Path (m)	Ray Path Difference (m)	Travel Time Interval (ms)	Interval Velocity (m/s)
1.10	0.90	0.92			
2.10	1.90	1.91	0.99	7.56	131
3.05	2.85	2.86	0.95	7.42	128
5.05	4.85	4.85	2.00	21.88	91
6.05	5.85	5.85	1.00	10.28	97
7.05	6.85	6.85	1.00	9.61	104
8.05	7.85	7.85	1.00	7.63	131
9.00	8.80	8.80	0.95	8.04	118
10.05	9.85	9.85	1.05	7.05	149
11.05	10.85	10.85	1.00	5.77	173
12.05	11.85	11.85	1.00	5.90	169
13.05	12.85	12.85	1.00	5.09	197
14.05	13.85	13.85	1.00	5.21	192
15.05	14.85	14.85	1.00	4.47	224
16.05	15.85	15.85	1.00	4.62	216
17.05	16.85	16.85	1.00	4.88	205
18.05	17.85	17.85	1.00	4.99	200
19.05	18.85	18.85	1.00	3.87	258
20.05	19.85	19.85	1.00	3.98	251
21.05	20.85	20.85	1.00	4.17	240
22.05	21.85	21.85	1.00	4.21	238
23.05	22.85	22.85	1.00	3.73	268
24.05	23.85	23.85	1.00	4.31	232
25.05	24.85	24.85	1.00	3.84	260
26.05	25.85	25.85	1.00	3.41	293
27.05	26.85	26.85	1.00	3.56	281
28.05	27.85	27.85	1.00	3.40	294
30.05	29.85	29.85	2.00	6.10	328
31.05	30.85	30.85	1.00	2.62	381

Job No:	16-72004
Client:	Cleary Gottlieb Steen & Hamilton LLP (CGSH)
Project:	Samarco, Germano Buttress
Sounding ID:	GSCPT16-05
Date:	05-May-2016

Seismic Source:	Plate
Source Offset (m):	3.00
Source Depth (m):	0.00
Geophone Offset (m):	0.20

SCPTu COMPRESSION WAVE VELOCITY TEST RESULTS - Vp

Tip Depth (m)	Geophone Depth (m)	Ray Path (m)	Ray Path Difference (m)	Travel Time Interval (ms)	Interval Velocity (m/s)
2.10	1.90	3.55			
5.05	4.85	5.70	2.15	2.71	795
6.05	5.85	6.57	0.87	0.74	1179
7.05	6.85	7.48	0.90	0.62	1466
11.05	10.85	11.26	3.78	2.70	1398
13.05	12.85	13.20	1.94	1.45	1333
15.05	14.85	15.15	1.95	1.42	1380
17.05	16.85	17.11	1.96	1.42	1387
19.05	18.85	19.09	1.97	1.47	1346
23.05	22.85	23.05	3.96	2.83	1397
25.05	24.85	25.03	1.98	1.37	1451
27.05	26.85	27.02	1.99	1.46	1365

Job No:	16-72004
Client:	Cleary Gottlieb Steen & Hamilton LLP (CGSH)
Project:	Samarco, Germano Buttress
Sounding ID:	GSCPT16-06
Date:	17-May-2016

Seismic Source:	Beam
Source Offset (m):	1.00
Source Depth (m):	0.00
Geophone Offset (m):	0.20

SCPTu SHEAR WAVE VELOCITY TEST RESULTS - Vs

Tip Depth (m)	Geophone Depth (m)	Ray Path (m)	Ray Path Difference (m)	Travel Time Interval (ms)	Interval Velocity (m/s)
2.25	2.05	2.28			
3.25	3.05	3.21	0.93	3.15	295
11.00	10.80	10.85	7.64	32.71	233
12.00	11.80	11.84	1.00	3.80	262
13.00	12.80	12.84	1.00	3.58	278
14.00	13.80	13.84	1.00	3.64	274
15.00	14.80	14.83	1.00	3.55	281
16.00	15.80	15.83	1.00	3.35	298
17.00	16.80	16.83	1.00	3.30	302
19.30	19.10	19.11			
20.30	20.10	20.11	1.00	3.42	292
21.30	21.10	21.11	1.00	2.99	334
22.30	22.10	22.11	1.00	2.89	346
23.30	23.10	23.11	1.00	2.99	334
24.30	24.10	24.11	1.00	3.42	292
25.30	25.10	25.11	1.00	3.21	312
26.30	26.10	26.11	1.00	2.89	346
27.30	27.10	27.11	1.00	2.67	374

Job No:	16-72004
Client:	Cleary Gottlieb Steen & Hamilton LLP (CGSH)
Project:	Samarco, Germano Buttress
Sounding ID:	GSCPT16-06
Date:	17-May-2016

Seismic Source:	Plate
Source Offset (m):	3.00
Source Depth (m):	0.00
Geophone Offset (m):	0.20

SCPTu COMPRESSION WAVE VELOCITY TEST RESULTS - Vp

Tip Depth (m)	Geophone Depth (m)	Ray Path (m)	Ray Path Difference (m)	Travel Time Interval (ms)	Interval Velocity (m/s)
3.25	3.05	4.28			
11.00	10.80	11.21	6.93	16.02	433
13.00	12.80	13.15	1.94	3.98	487
15.00	14.80	15.10	1.95	3.98	491
17.00	16.80	17.07	1.96	3.90	503
19.30	19.10	19.33			
20.30	20.10	20.32	0.99	1.74	568
21.30	21.10	21.31	0.99	1.92	516
22.30	22.10	22.30	0.99	1.72	577
25.30	25.10	25.28	2.98	5.51	540
26.30	26.10	26.27	0.99	1.60	621
27.30	27.10	27.27	0.99	1.54	646

CPT Pore Pressure Dissipation Summary and Plots

Job No: 16-72004
Client: Cleary Gottlieb Steen & Hamilton LLP (CGSH)
Project: Samarco, Germano Buttress
Start Date: 19-Apr-2016
End Date: 24-May-2016

CPTu PORE PRESSURE DISSIPATION SUMMARY

Sounding ID	File Name	Cone Area (cm^2)	Duration (s)	Test Depth (m)	Estimated Equilibrium Pore Pressure U_{eq} (m)	Calculated Phreatic Surface (m)
GBCPT16-01	16-72004_RS01	15	1120	1.10	0.0	
GBCPT16-01B	16-72004_RS01B	15	440	0.90	Not Achieved	
GBCPT16-01C	16-72004_RS01C	15	620	2.20	Not Achieved	
GSCPT16-02	16-72004_RS02	15	600	2.40	0.0	
GSCPT16-02	16-72004_RS02	15	405	7.40	Not Achieved	
GSCPT16-02	16-72004_RS02	15	600	11.40	Not Achieved	
GSCPT16-02B	16-72004_RS02B	15	300	10.50	Not Achieved	
GSCPT16-02B	16-72004_RS02B	15	300	12.50	3.6	8.9
GSCPT16-02B	16-72004_RS02B	15	500	15.50	6.2	9.3
GSCPT16-02B	16-72004_RS02B	15	395	19.50	9.9	9.6
GSCPT16-02B	16-72004_RS02B	15	620	23.50	12.9	10.6
GSCPT16-02B	16-72004_RS02B	15	325	33.50	22.2	11.3
GSCPT16-02B	16-72004_RS02B	15	1755	38.50	27.0	11.5
GSCPT16-02B	16-72004_RS02B	15	225	40.50	Not Achieved	
GSCPT16-02B	16-72004_RS02B	15	560	40.70	Not Achieved	
GSCPT16-02B	16-72004_RS02B	15	1020	41.65	28.1	13.5
GCCPT16-03	16-72004_RS03	15	300	5.50	0.0	
GCCPT16-03	16-72004_RS03	15	300	10.50	0.0	
GCCPT16-03	16-72004_RS03	15	300	15.50	0.0	
GCCPT16-03	16-72004_RS03	15	300	20.50	0.0	
GCCPT16-03	16-72004_RS03	15	300	25.50	0.0	
GCCPT16-03	16-72004_RS03	15	305	30.50	0.0	
GCCPT16-03	16-72004_RS03	15	500	35.50	2.3	33.2
GCCPT16-03	16-72004_RS03	15	300	40.50	7.0	33.5
GCCPT16-03	16-72004_RS03	15	505	45.50	11.5	34.0
GCCPT16-03	16-72004_RS03	15	240	49.50	14.7	34.8
GCCPT16-03	16-72004_RS03	15	500	50.50	15.4	35.1
GCCPT16-03	16-72004_RS03	15	255	52.50	16.7	Not Achieved
GCCPT16-03	16-72004_RS03	15	210	53.45	17.2	Not Achieved
GCCPT16-03	16-72004_RS03	15	140	54.50	17.4	Not Achieved
GCCPT16-03	16-72004_RS03	15	900	55.50	18.4	37.1
GCCPT16-03	16-72004_RS03	15	300	57.35	20.0	37.4
GCCPT16-03	16-72004_RS03	15	285	58.35	20.5	37.9
GCCPT16-03	16-72004_RS03	15	175	59.35	21.3	38.0
GCCPT16-03	16-72004_RS03	15	500	60.35	22.2	38.2

Job No:	16-72004
Client:	Cleary Gottlieb Steen & Hamilton LLP (CGSH)
Project:	Samarco, Germano Buttress
Start Date:	19-Apr-2016
End Date:	24-May-2016

CPTu PORE PRESSURE DISSIPATION SUMMARY

Sounding ID	File Name	Cone Area (cm^2)	Duration (s)	Test Depth (m)	Estimated Equilibrium Pore Pressure U_{eq} (m)	Calculated Phreatic Surface (m)
GCCPT16-03	16-72004_RS03	15	300	61.65	23.1	38.6
GCCPT16-04	16-72004_RS04	15	375	0.40	0.0	
GCCPT16-04	16-72004_RS04	15	310	1.40	0.0	
GCCPT16-04	16-72004_RS04	15	500	5.40	0.0	
GCCPT16-04	16-72004_RS04	15	1025	10.40	0.0	
GCCPT16-04	16-72004_RS04	15	305	11.35	0.0	
GCCPT16-04	16-72004_RS04	15	700	15.40	0.0	
GCCPT16-04	16-72004_RS04	15	400	20.40	0.0	
GCCPT16-04	16-72004_RS04	15	400	25.40	0.0	
GCCPT16-04	16-72004_RS04	15	300	30.40	0.0	
GCCPT16-04	16-72004_RS04	15	1235	32.15	0.0	
GCCPT16-04	16-72004_RS04	15	440	32.40	0.0	
GCCPT16-04B	16-72004_RS04B	15	315	8.70	0.0	
GCCPT16-04B	16-72004_RS04B	15	435	12.30	0.0	
GCCPT16-04B	16-72004_RS04B	15	250	13.70	0.0	
GCCPT16-04B	16-72004_RS04B	15	355	20.10	0.0	
GCCPT16-04B	16-72004_RS04B	15	240	30.15	0.0	
GCCPT16-04B	16-72004_RS04B	15	555	32.10	0.0	
GCCPT16-04B	16-72004_RS04B	15	295	32.95	0.0	
GCCPT16-04B	16-72004_RS04B	15	545	33.55	Not Achieved	
GCCPT16-04B	16-72004_RS04B	15	490	35.15	0.0	
GCCPT16-04B	16-72004_RS04B	15	690	36.35	0.0	
GSCPT16-05	16-72004_SP05	15	6300	5.05	Not Achieved	
GSCPT16-05	16-72004_SP05	15	285	6.05	Not Achieved	
GSCPT16-05	16-72004_SP05	15	305	8.05	Not Achieved	
GSCPT16-05	16-72004_SP05	15	225	9.00	Not Achieved	
GSCPT16-05	16-72004_SP05	15	900	10.05	Not Achieved	
GSCPT16-05	16-72004_SP05	15	230	11.05	Not Achieved	
GSCPT16-05	16-72004_SP05	15	235	12.00	Not Achieved	
GSCPT16-05	16-72004_SP05	15	1100	15.05	Not Achieved	
GSCPT16-05	16-72004_SP05	15	295	16.05	Not Achieved	
GSCPT16-05	16-72004_SP05	15	1200	19.05	4.8	14.2
GSCPT16-05	16-72004_SP05	15	1300	25.05	Not Achieved	
GSCPT16-05	16-72004_SP05	15	375	28.00	Not Achieved	
GSCPT16-05	16-72004_SP05	15	280	29.05	Not Achieved	

Job No: 16-72004
Client: Cleary Gottlieb Steen & Hamilton LLP (CGSH)
Project: Samarco, Germano Buttress
Start Date: 19-Apr-2016
End Date: 24-May-2016

CPTu PORE PRESSURE DISSIPATION SUMMARY

Sounding ID	File Name	Cone Area (cm^2)	Duration (s)	Test Depth (m)	Estimated Equilibrium Pore Pressure U_{eq} (m)	Calculated Phreatic Surface (m)
GSCPT16-05	16-72004_SP05	15	5300	30.05	Not Achieved	
GSCPT16-05	16-72004_SP05	15	200	31.05	0.0	
GSCPT16-05	16-72004_SP05	15	205	31.65	0.0	
GBCPT16-06	16-72004_RS06	15	410	1.20	0.0	
GBCPT16-06	16-72004_RS06	15	230	2.25	Not Achieved	
GBCPT16-06	16-72004_RS06	15	575	3.90	0.8	3.1
GBCPT16-06	16-72004_RS06B	15	190	10.60	0.0	
GBCPT16-06	16-72004_RS06B	15	300	16.00	0.0	
GBCPT16-06	16-72004_RS06B	15	1305	17.35	0.9	16.4
GBCPT16-06	16-72004_RS06B	15	735	18.30	0.0	
GBCPT16-06	16-72004_RS06B	15	550	19.30	0.0	
GBCPT16-06	16-72004_RS06B	15	745	20.30	0.0	
GBCPT16-06	16-72004_RS06B	15	260	21.30	0.0	
GBCPT16-06	16-72004_RS06B	15	435	22.30	0.0	
GBCPT16-06	16-72004_RS06B	15	240	23.30	0.0	
GBCPT16-06	16-72004_RS06B	15	710	24.30	0.0	
GBCPT16-06	16-72004_RS06B	15	185	25.30	0.0	
GBCPT16-06	16-72004_RS06B	15	960	26.30	0.0	
GBCPT16-06	16-72004_RS06B	15	450	26.55	0.0	
GBCPT16-06	16-72004_RS06B	15	255	27.20	0.0	
GBCPT16-06	16-72004_RS06B	15	380	27.30	0.0	
GBCPT16-06	16-72004_RS06B	15	345	27.50	0.0	
GBCPT16-06B	16-72004_RS06B	15	2785	3.35	Not Achieved	

CONETEC

CGSH

Job No: 1672007
Date: 04/19/2016 15:03
Site: Germano Buttres

Sounding: GBCPT16-01
Cone: 432:T1500F15U500
Cone Area: 15 sq cm

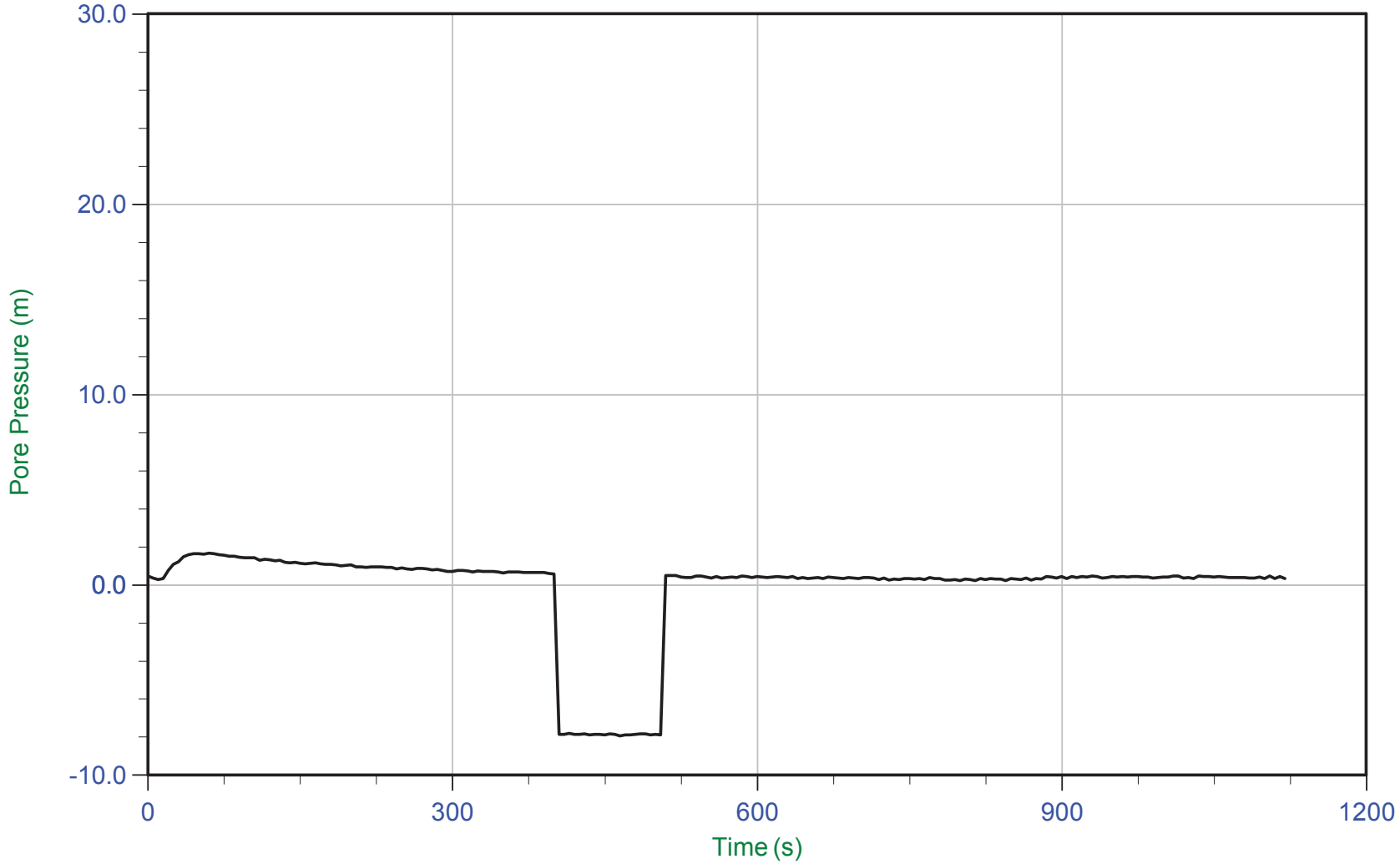

Trace Summary:

Filename: 16-72004_RS01.PPF
Depth: 1.100 m / 3.609 ft
Duration: 1120.0 s

U Min: -7.9 m
U Max: 1.7 m

WT: 0.807 m / 2.648 ft
Ueq: 0.3 m

CONETEC

CGSH

Job No: 1672007
Date: 04/20/2016 12:52
Site: Germano Buttres

Sounding: GBCPT16-01B
Cone: 432:T1500F15U500
Cone Area: 15 sq cm

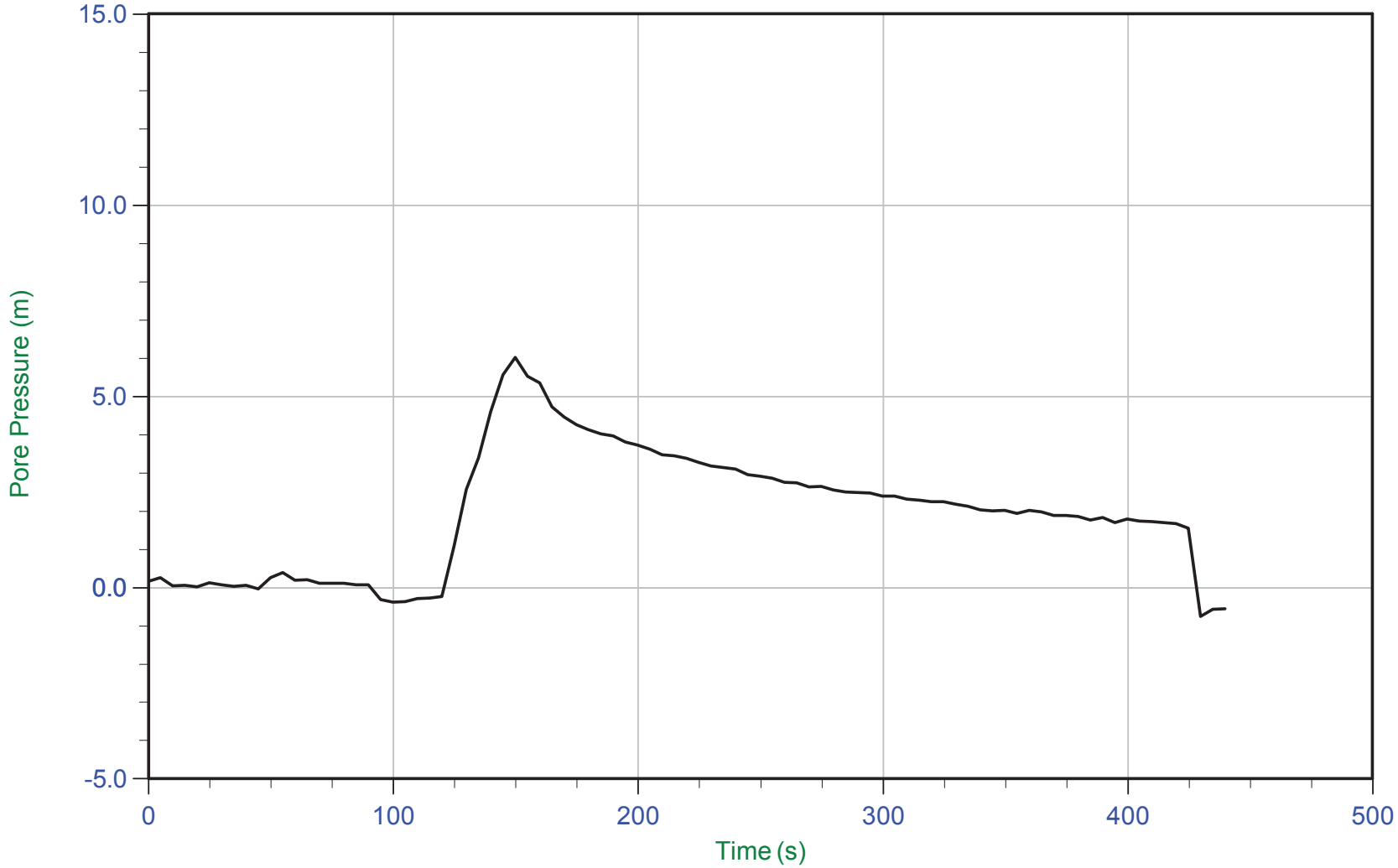

Trace Summary:

Filename: 16-72004_RS01B.PPF
Depth: 0.900 m / 2.953 ft
Duration: 440.0 s

U Min: -0.8 m
U Max: 6.0 m

CONETEC

CGSH

Job No: 1672007
Date: 04/20/2016 15:32
Site: Germano Buttres

Sounding: GBCPT16-01C
Cone: 432:T1500F15U500
Cone Area: 15 sq cm

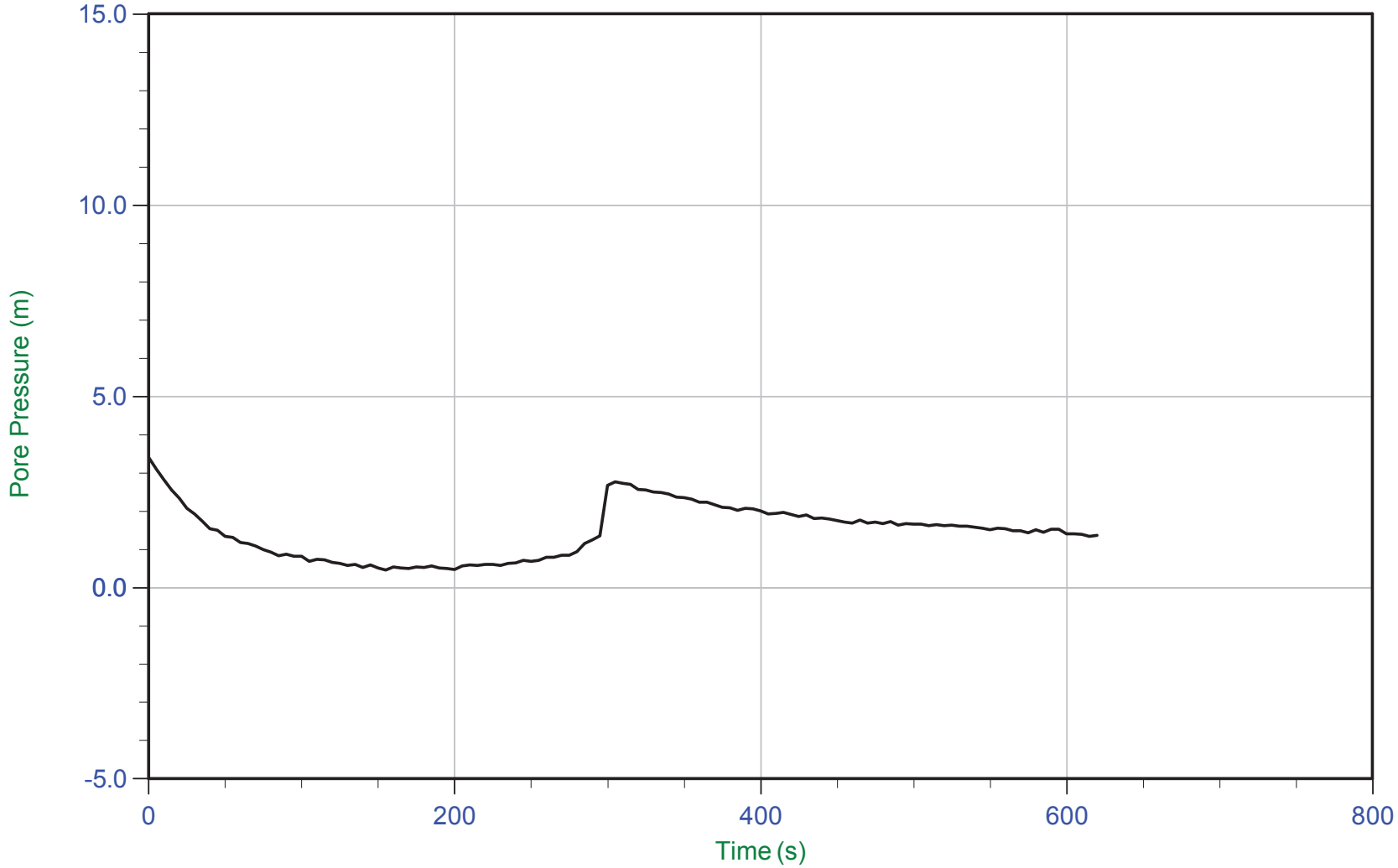

Trace Summary:

Filename: 16-72004_RS01C.PPF
Depth: 2.200 m / 7.218 ft
Duration: 620.0 s

U Min: 0.5 m
U Max: 3.4 m

CONETEC

CGSH

Job No: 1672007
Date: 04/21/2016 14:33
Site: Bay 3, Germano Slimes

Sounding: GSCPT16-02
Cone: 432:T1500F15U500
Cone Area: 15 sq cm

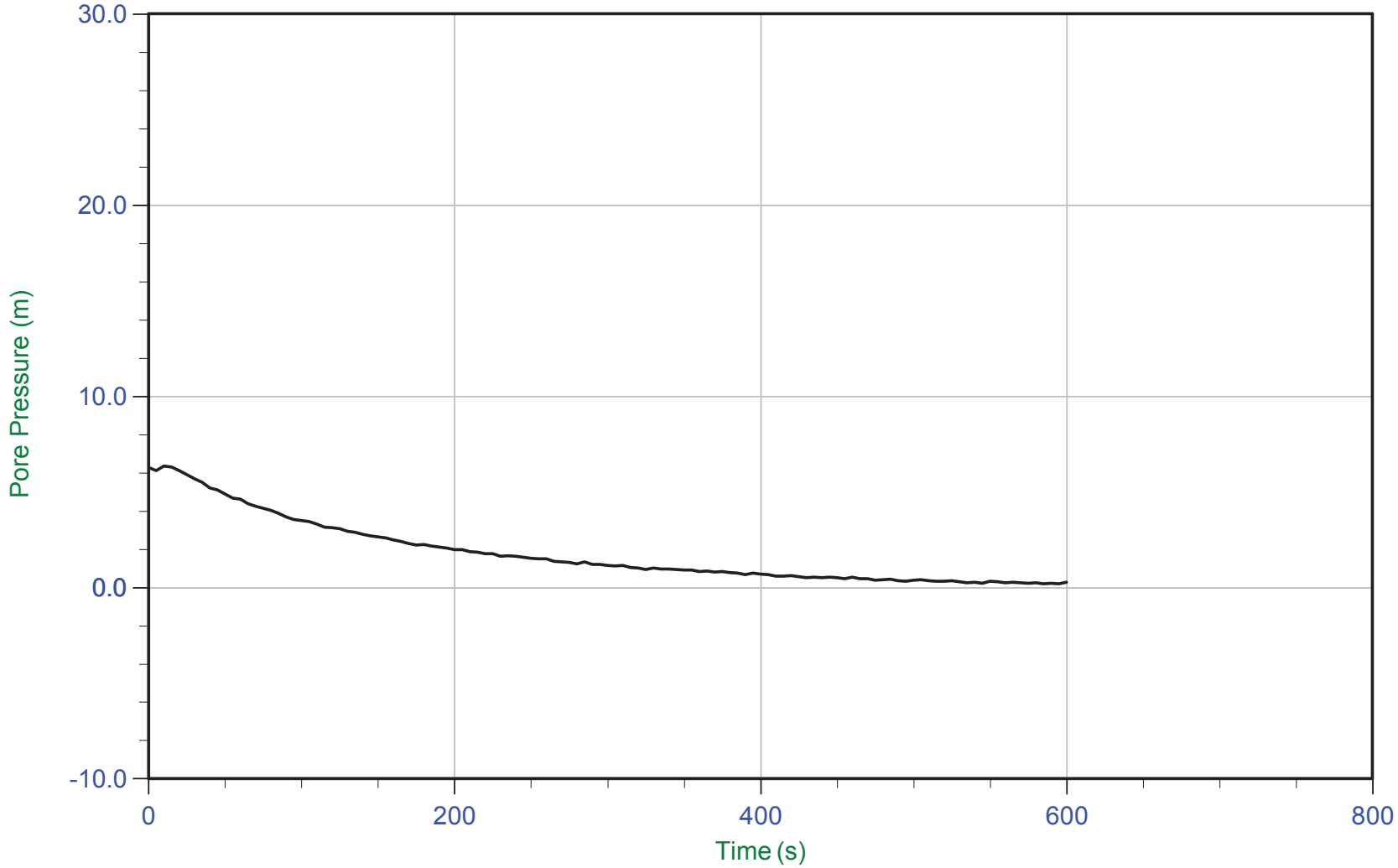

Trace Summary:

Filename: 16-72004_RS02.PPF
Depth: 2.400 m / 7.874 ft
Duration: 600.0 s

U Min: 0.2 m
U Max: 6.4 m

WT: 0.000 m / 0.000 ft
Ueq: 0.0 m

CONETEC

CGSH

Job No: 1672007
Date: 04/21/2016 14:33
Site: Bay 3, Germano Slimes

Sounding: GSCPT16-02
Cone: 432:T1500F15U500
Cone Area: 15 sq cm

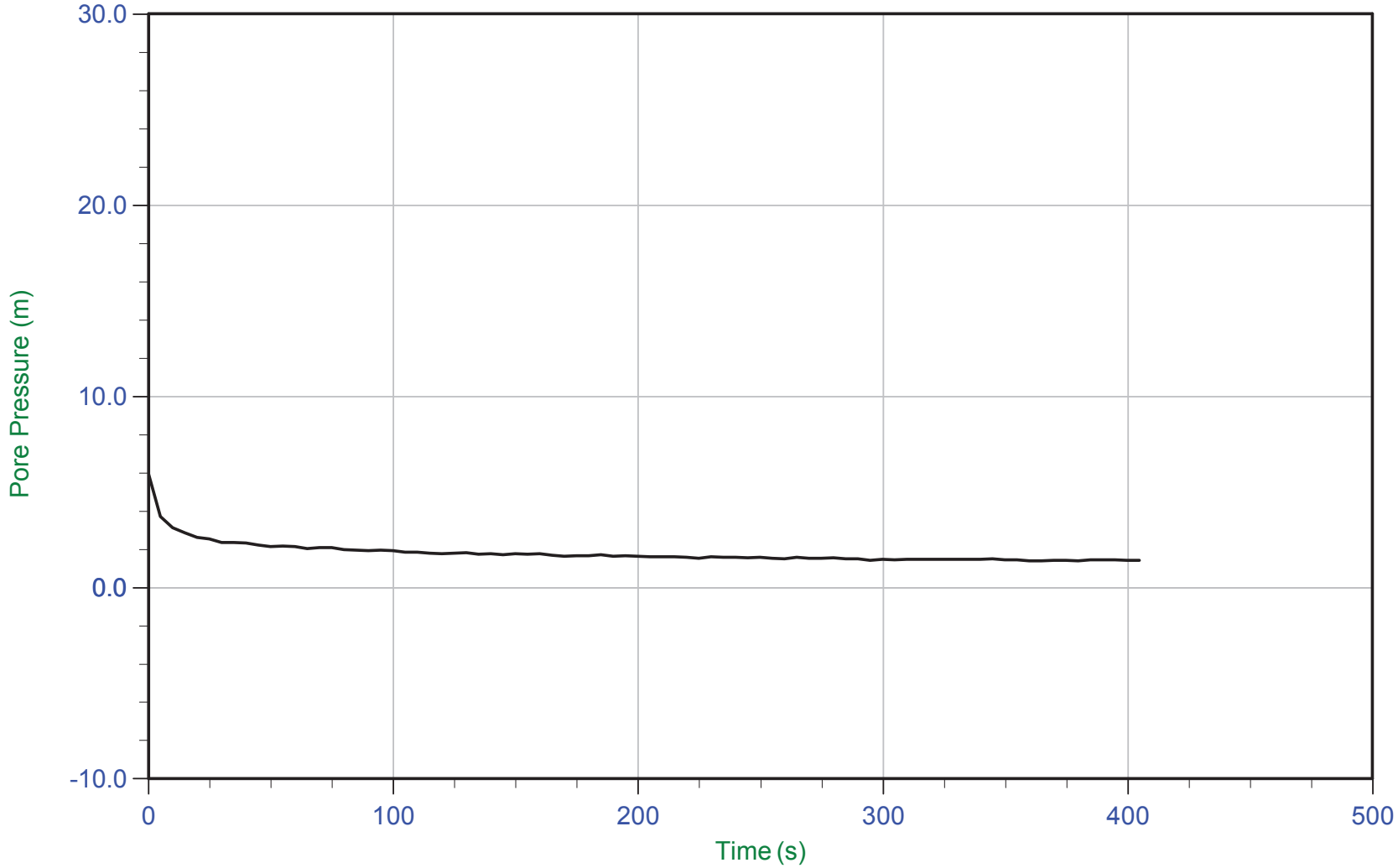

Trace Summary:

Filename: 16-72004_RS02.PPF
Depth: 7.400 m / 24.278 ft
Duration: 405.0 s

U Min: 1.4 m
U Max: 5.9 m

CONETEC

CGSH

Job No: 1672007
Date: 04/21/2016 14:33
Site: Bay 3, Germano Slimes

Sounding: GSCPT16-02
Cone: 432:T1500F15U500
Cone Area: 15 sq cm

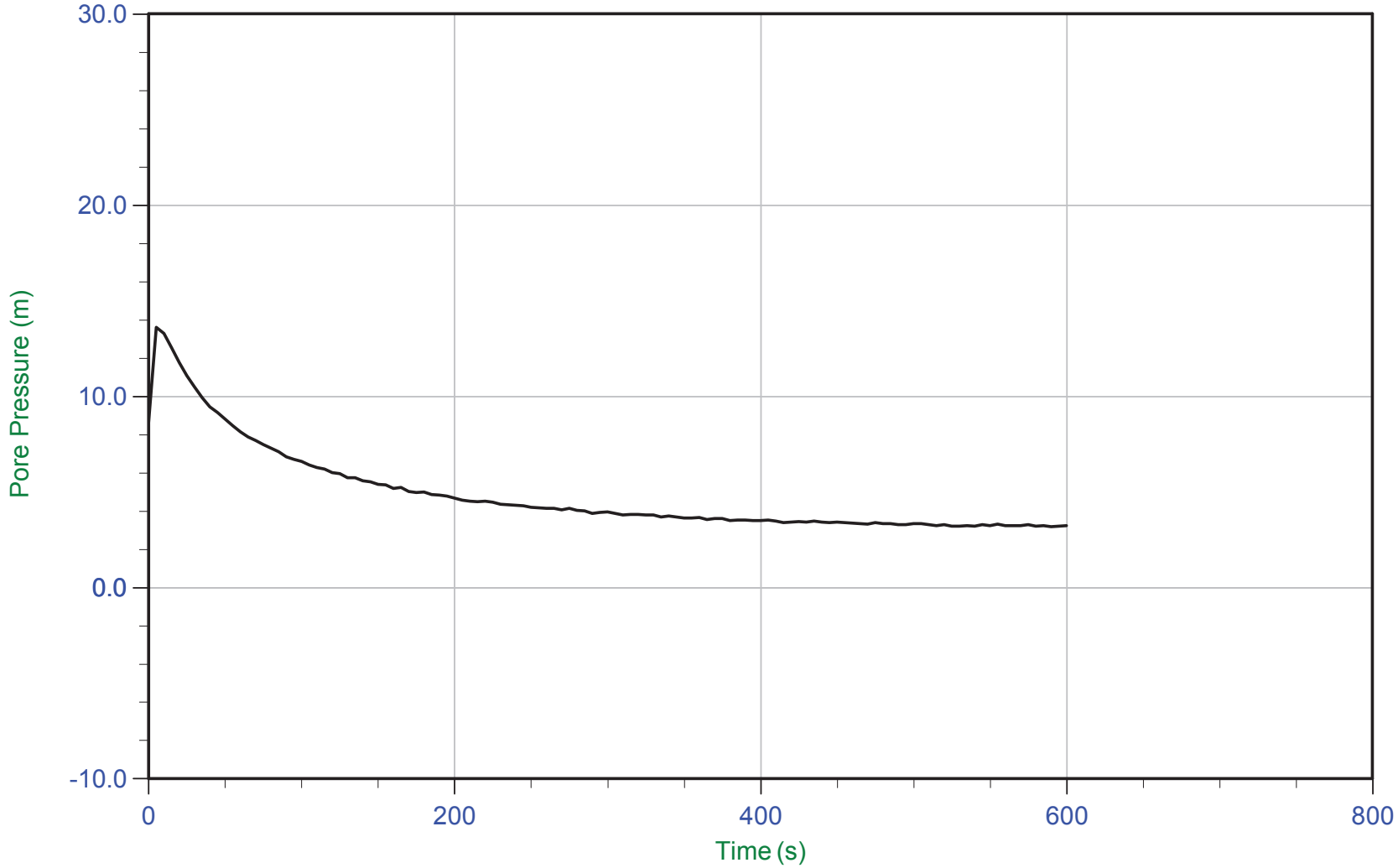

Trace Summary:

Filename: 16-72004_RS02.PPF
Depth: 11.400 m / 37.401 ft
Duration: 600.0 s

U Min: 3.2 m
U Max: 13.6 m

CONETEC

CGSH

Job No: 1672007
Date: 04/24/2016 11:30
Site: Bay 3, Germano Slimes

Sounding: GSCPT16-02B
Cone: 376:T375F10U200
Cone Area: 15 sq cm

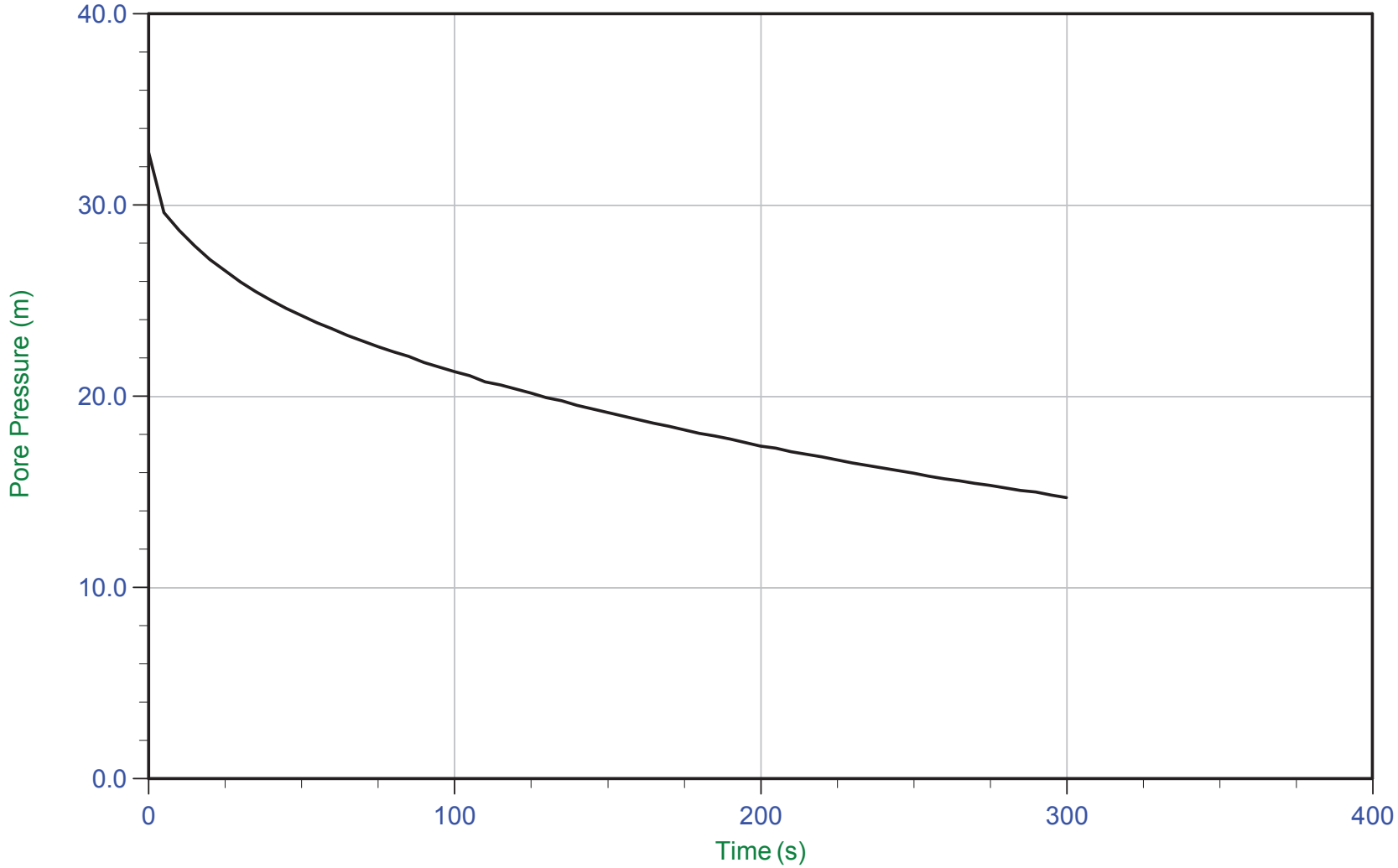

Trace Summary:

Filename: 16-72004_RS02B.PPF
Depth: 10.500 m / 34.448 ft
Duration: 300.0 s

U Min: 14.7 m
U Max: 32.8 m

CONETEC

CGSH

Job No: 1672007
Date: 04/24/2016 11:30
Site: Bay 3, Germano Slimes

Sounding: GSCPT16-02B
Cone: 376:T375F10U200
Cone Area: 15 sq cm

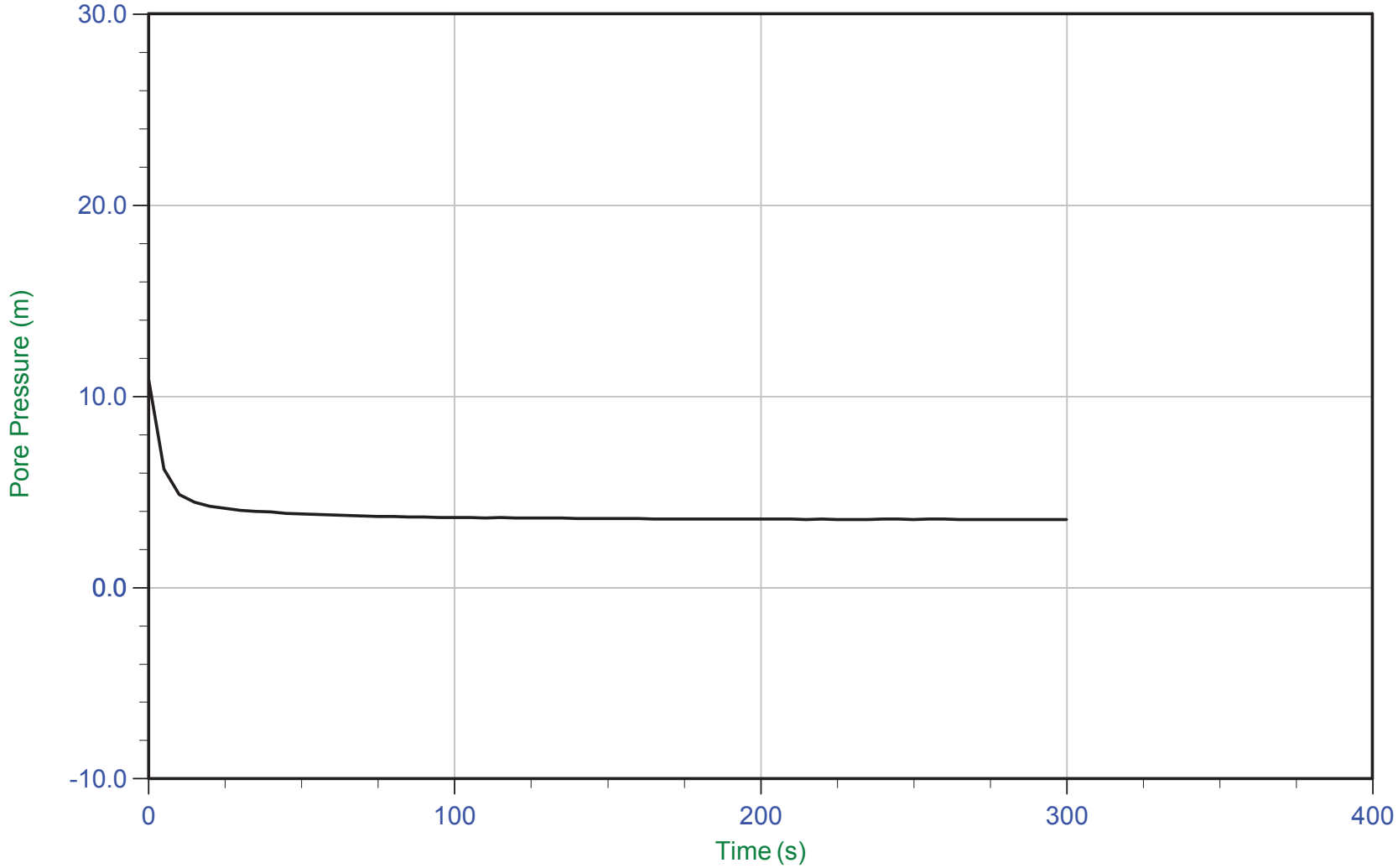

Trace Summary:

Filename: 16-72004_RS02B.PPF
Depth: 12.500 m / 41.010 ft
Duration: 300.0 s

U Min: 3.6 m
U Max: 10.9 m

WT: 8.944 m / 29.343 ft
Ueq: 3.6 m

CONETEC

CGSH

Job No: 1672007
Date: 04/24/2016 11:30
Site: Bay 3, Germano Slimes

Sounding: GSCPT16-02B
Cone: 376:T375F10U200
Cone Area: 15 sq cm

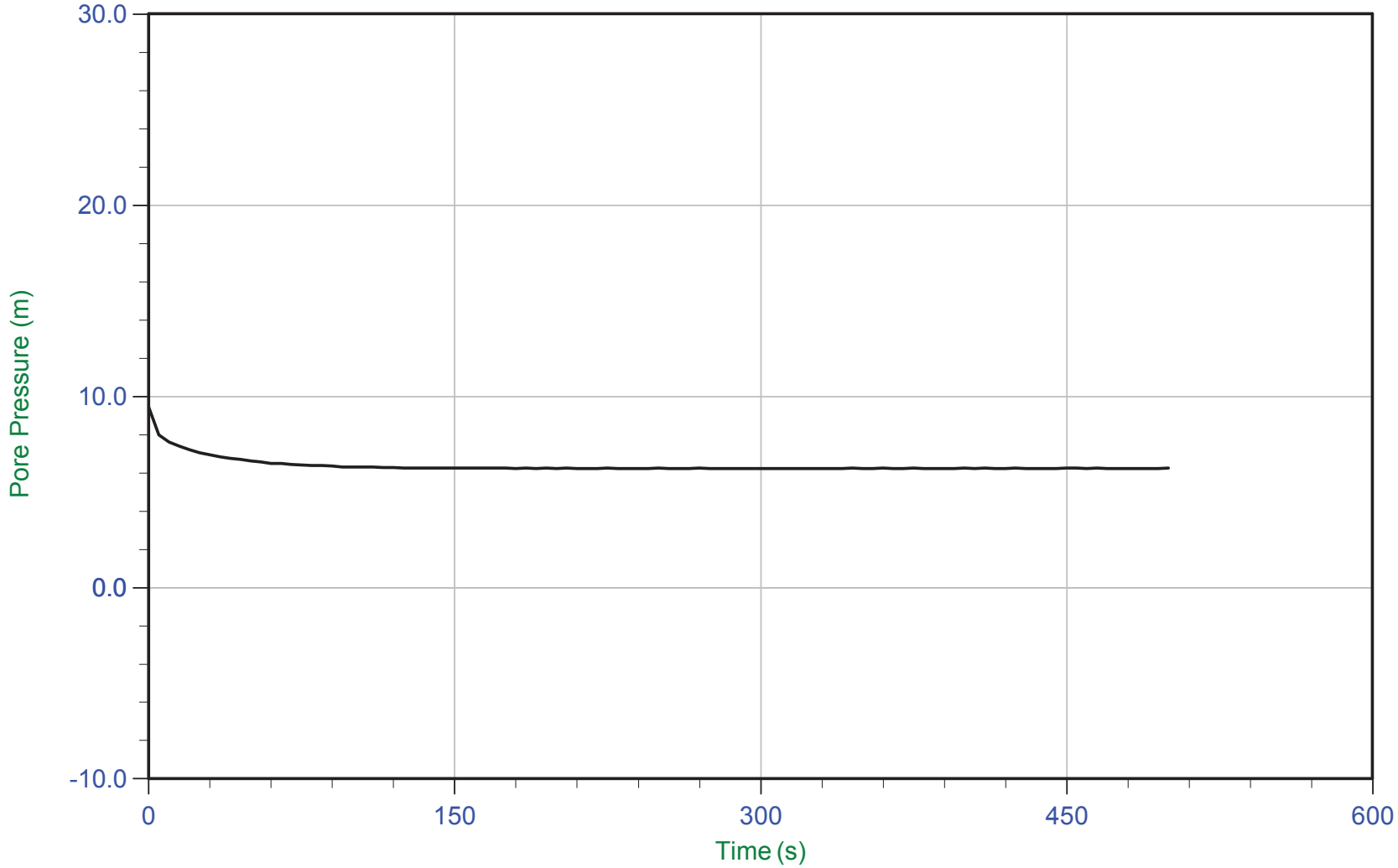

Trace Summary:

Filename: 16-72004_RS02B.PPF
Depth: 15.500 m / 50.852 ft
Duration: 500.0 s

U Min: 6.2 m
U Max: 9.5 m

WT: 9.266 m / 30.400 ft
Ueq: 6.2 m

CONETEC

CGSH

Job No: 1672007
Date: 04/24/2016 11:30
Site: Bay 3, Germano Slimes

Sounding: GSCPT16-02B
Cone: 376:T375F10U200
Cone Area: 15 sq cm

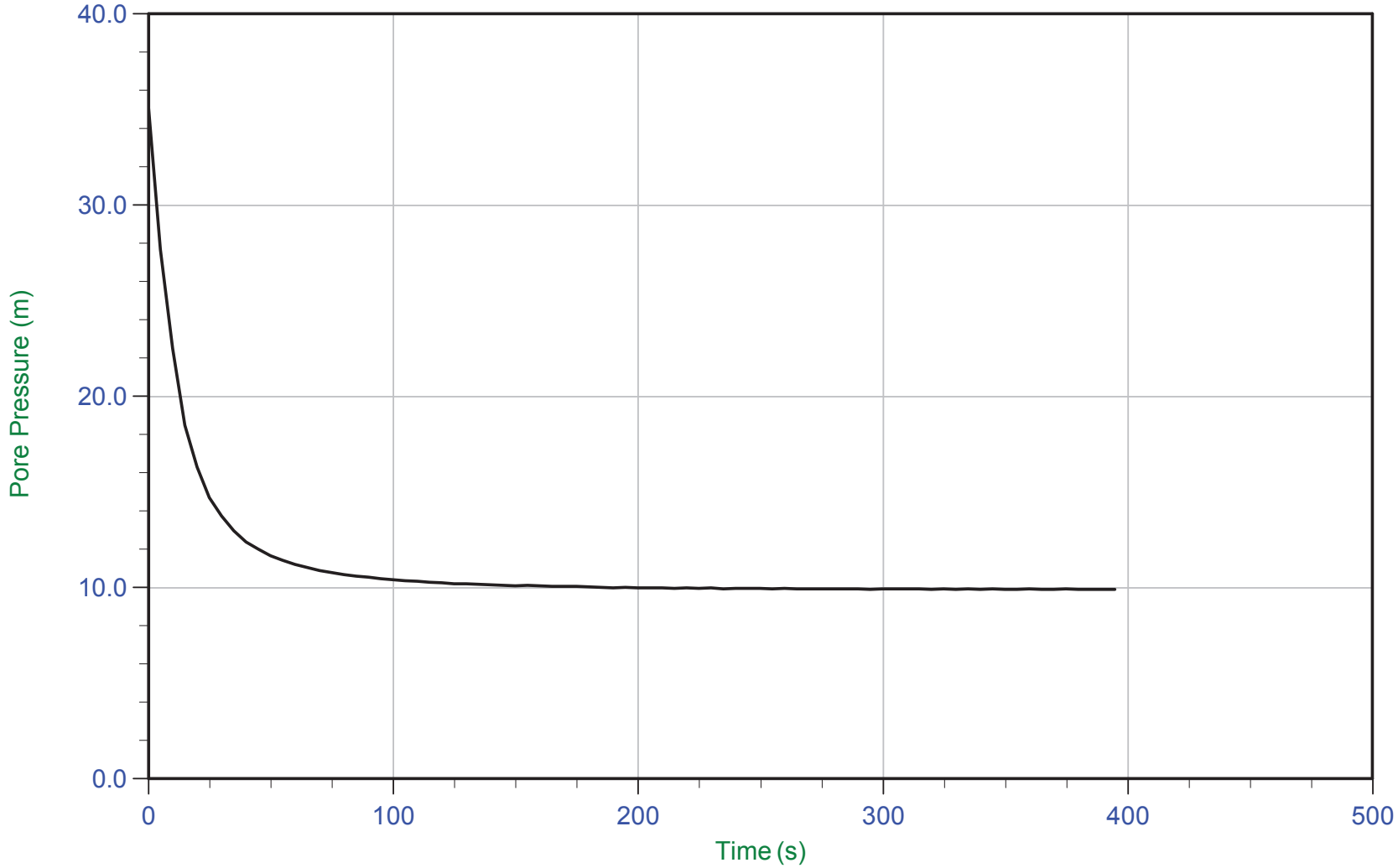

Trace Summary:

Filename: 16-72004_RS02B.PPF
Depth: 19.500 m / 63.976 ft
Duration: 395.0 s

U Min: 9.9 m
U Max: 35.0 m

WT: 9.626 m / 31.581 ft
Ueq: 9.9 m

CONETEC

CGSH

Job No: 1672007
Date: 04/24/2016 11:30
Site: Bay 3, Germano Slimes

Sounding: GSCPT16-02B
Cone: 376:T375F10U200
Cone Area: 15 sq cm

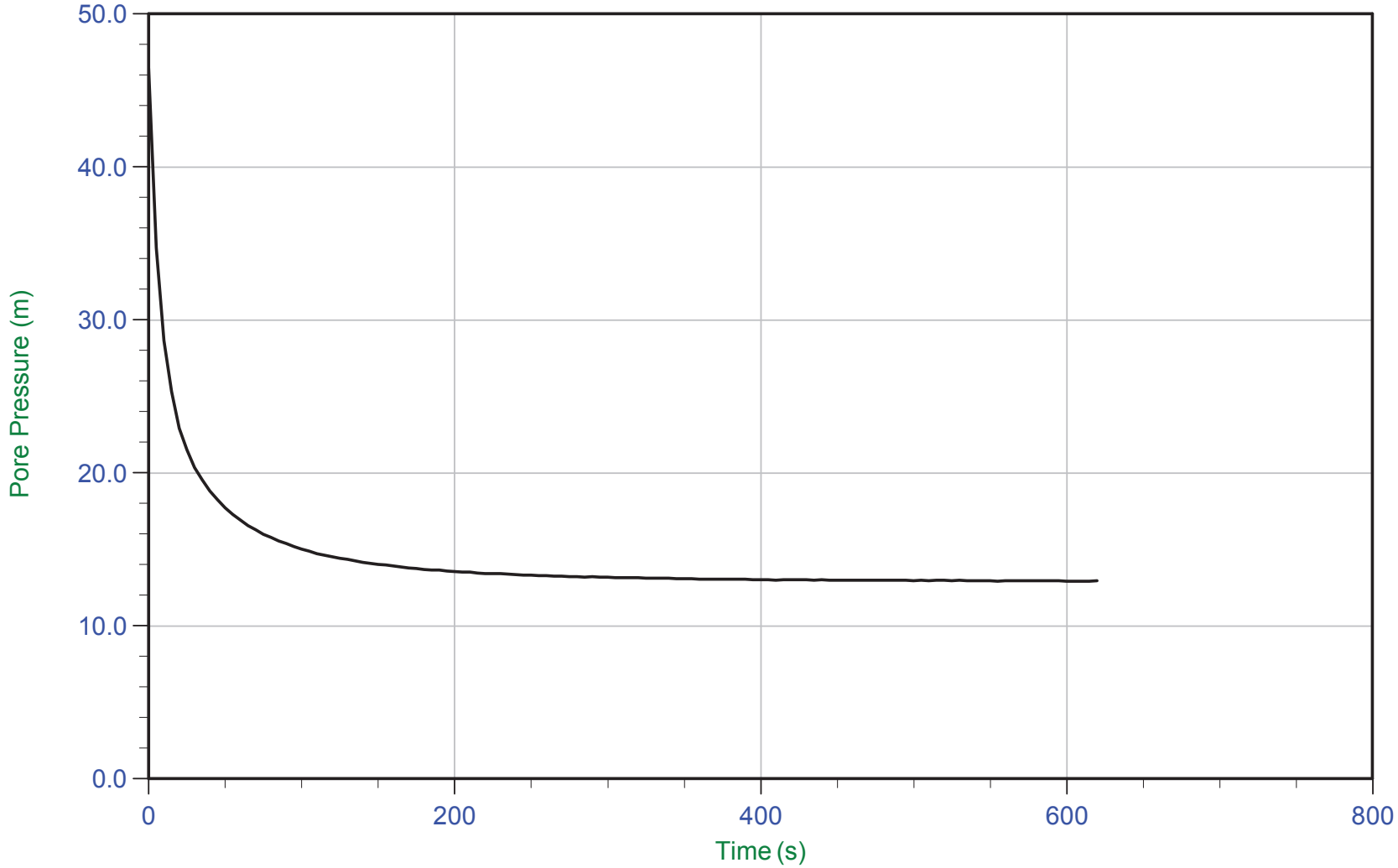

Trace Summary:

Filename: 16-72004_RS02B.PPF
Depth: 23.500 m / 77.099 ft
Duration: 620.0 s

U Min: 12.9 m
U Max: 46.5 m

WT: 10.634 m / 34.888 ft
Ueq: 12.9 m

CONETEC

CGSH

Job No: 1672007
Date: 04/24/2016 11:30
Site: Bay 3, Germano Slimes

Sounding: GSCPT16-02B
Cone: 376:T375F10U200
Cone Area: 15 sq cm

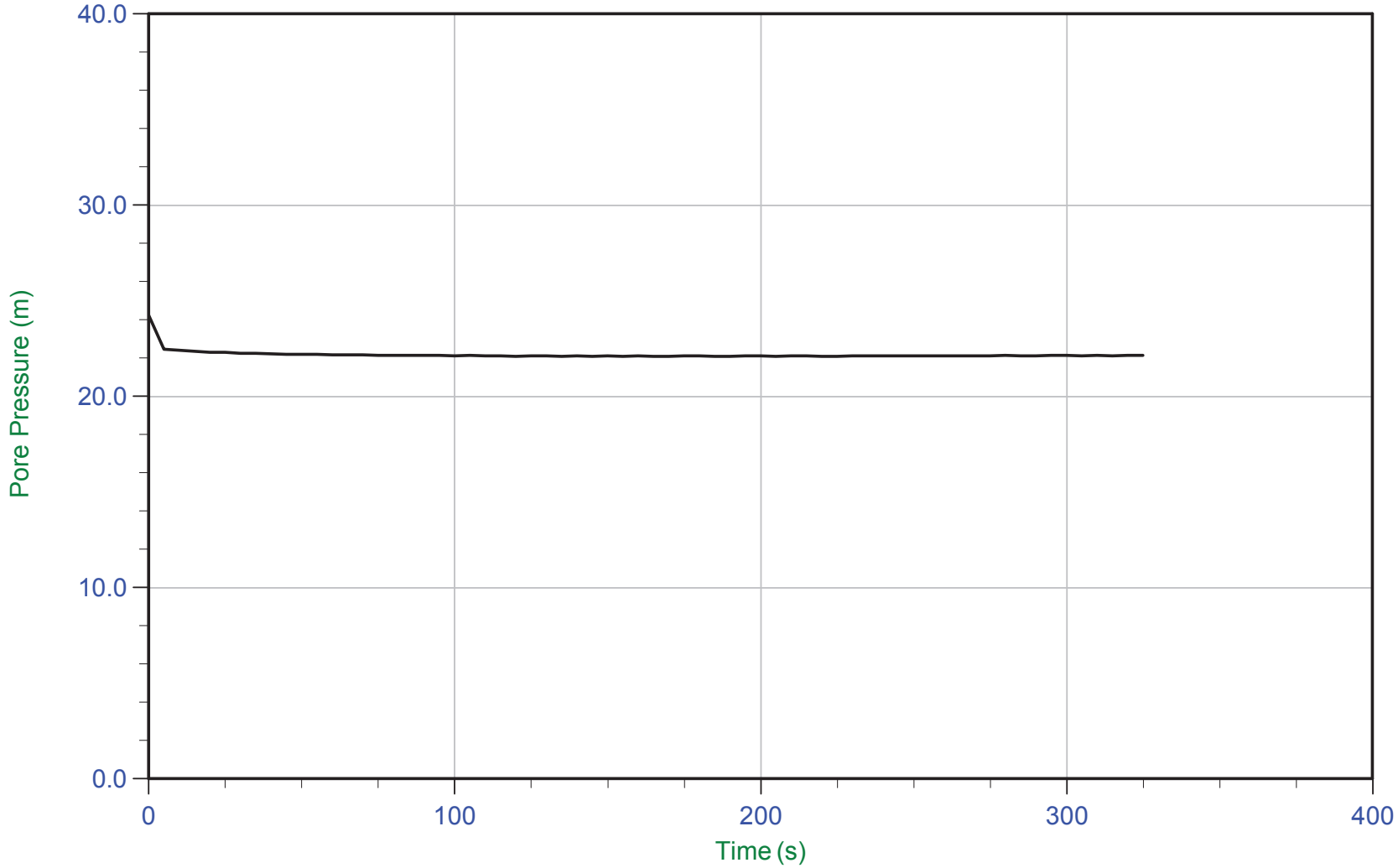

Trace Summary:

Filename: 16-72004_RS02B.PPF
Depth: 33.500 m / 109.907 ft
Duration: 325.0 s

U Min: 22.1 m
U Max: 24.3 m

WT: 11.324 m / 37.152 ft
Ueq: 22.2 m

CONETEC

CGSH

Job No: 1672007
Date: 04/24/2016 11:30
Site: Bay 3, Germano Slimes

Sounding: GSCPT16-02B
Cone: 376:T375F10U200
Cone Area: 15 sq cm

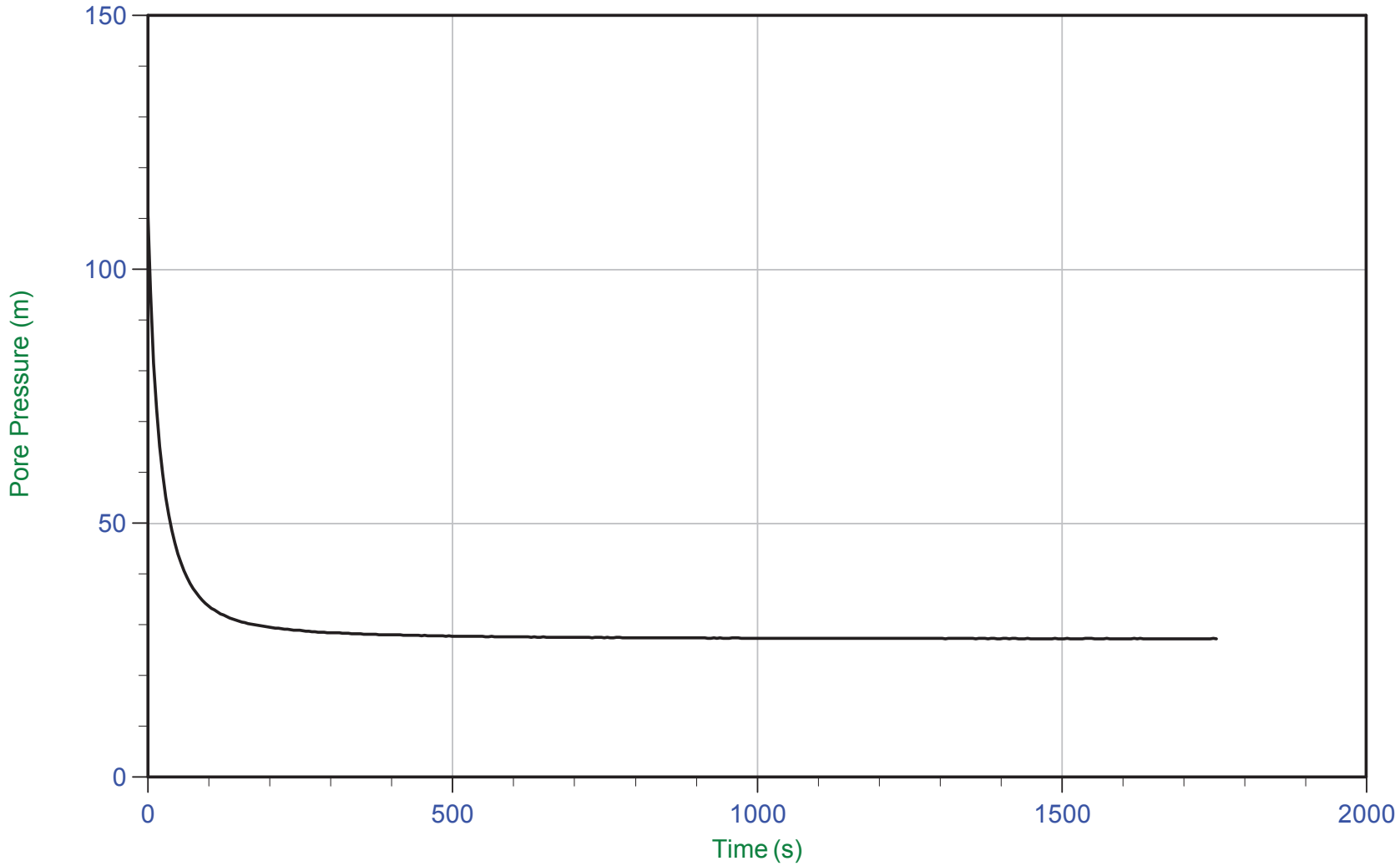

Trace Summary:

Filename: 16-72004_RS02B.PPF
Depth: 38.500 m / 126.311 ft
Duration: 1755.0 s

U Min: 27.2 m
U Max: 110.6 m

WT: 11.513 m / 37.772 ft
Ueq: 27.0 m

CONETEC

CGSH

Job No: 1672007
Date: 04/24/2016 11:30
Site: Bay 3, Germano Slimes

Sounding: GSCPT16-02B
Cone: 376:T375F10U200
Cone Area: 15 sq cm

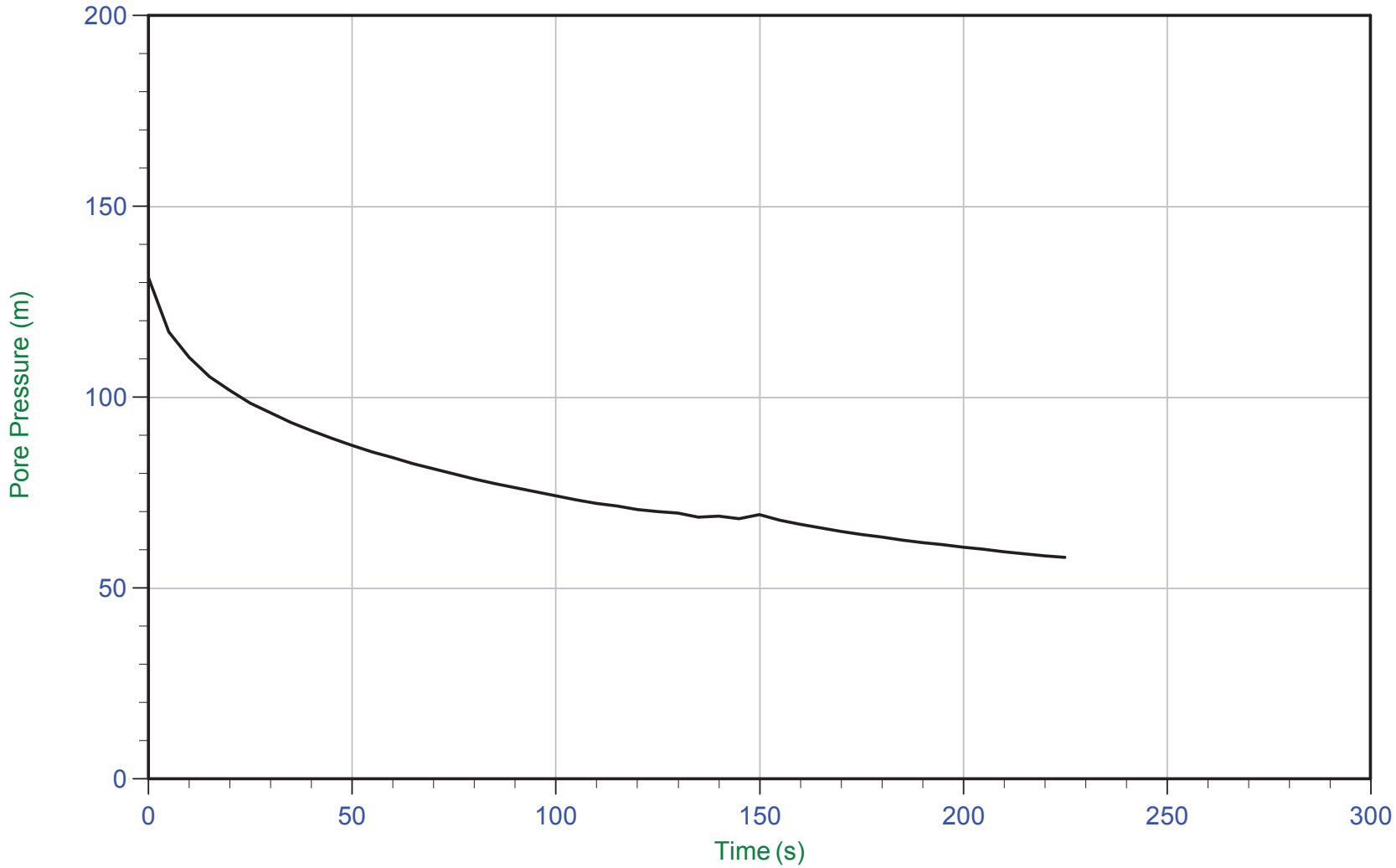

Trace Summary:

Filename: 16-72004_RS02B.PPF
Depth: 40.500 m / 132.872 ft
Duration: 225.0 s

U Min: 58.0 m
U Max: 131.4 m

CONETEC

CGSH

Job No: 1672007
Date: 04/24/2016 11:30
Site: Bay 3, Germano Slimes

Sounding: GSCPT16-02B
Cone: 376:T375F10U200
Cone Area: 15 sq cm

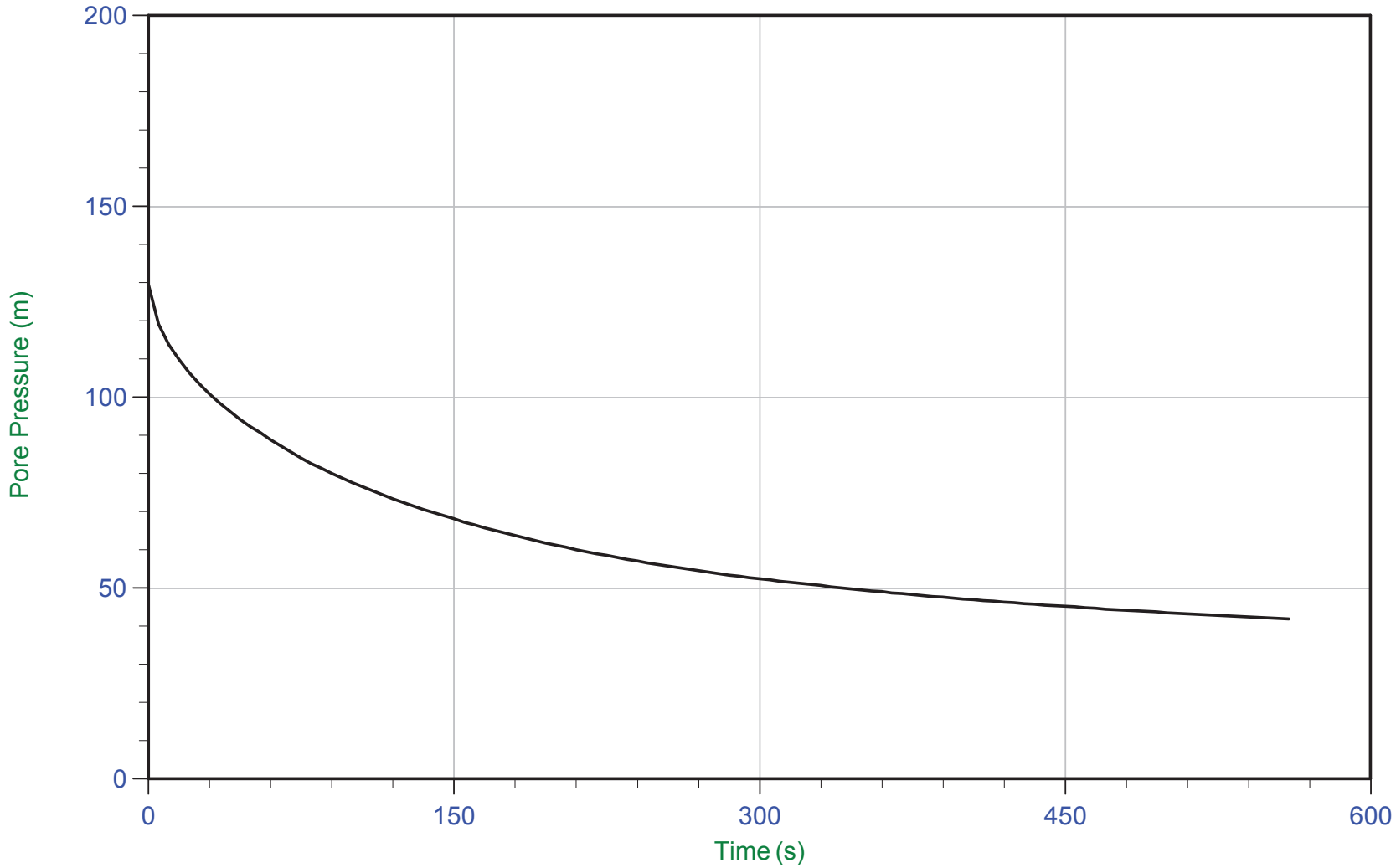

Trace Summary:

Filename: 16-72004_RS02B.PPF
Depth: 40.700 m / 133.529 ft
Duration: 560.0 s

U Min: 41.9 m
U Max: 129.5 m

CONETEC

CGSH

Job No: 1672007
Date: 04/24/2016 11:30
Site: Bay 3, Germano Slimes

Sounding: GSCPT16-02B
Cone: 376:T375F10U200
Cone Area: 15 sq cm

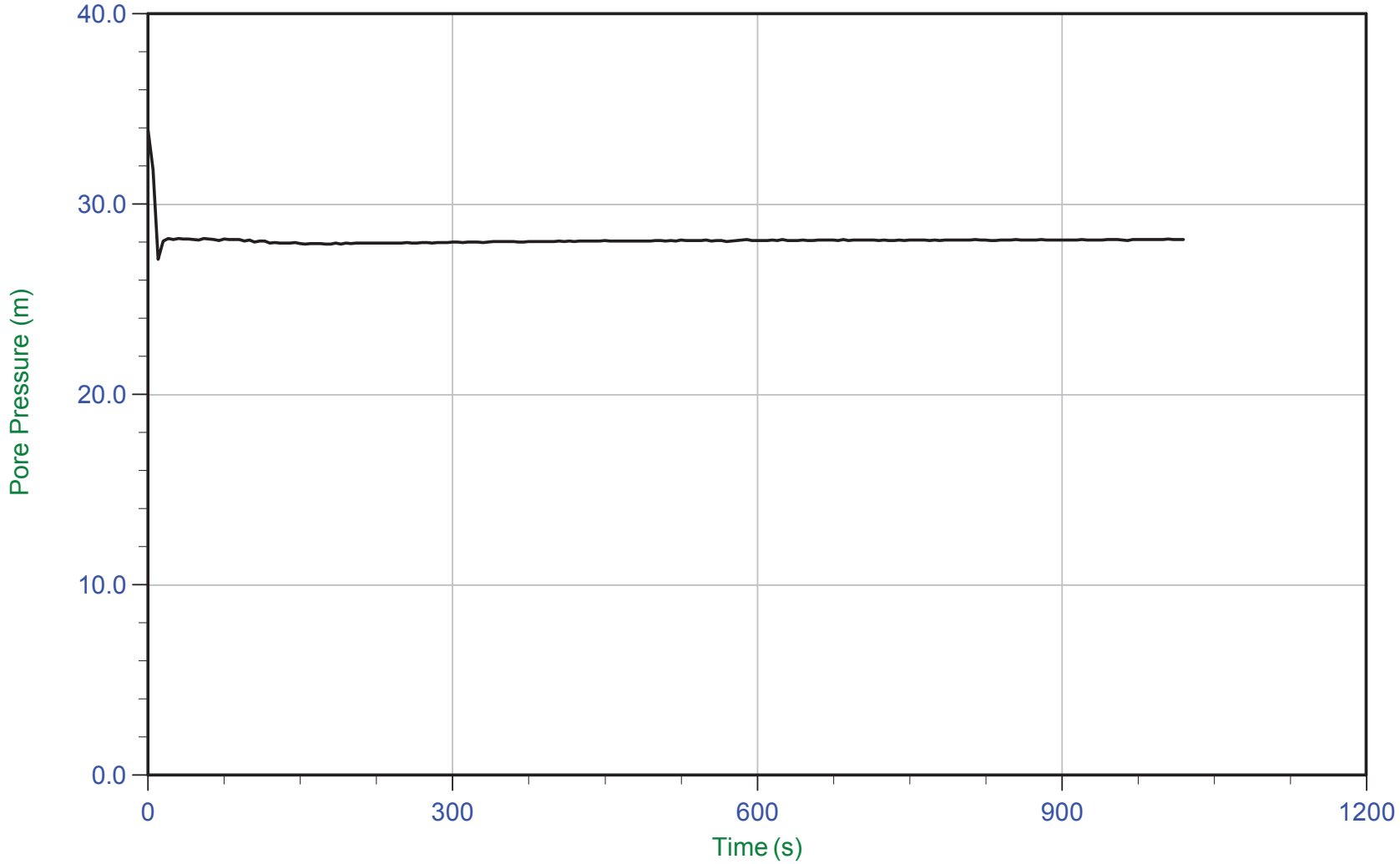

Trace Summary:

Filename: 16-72004_RS02B.PPF
Depth: 41.650 m / 136.645 ft
Duration: 1020.0 s

U Min: 27.1 m
U Max: 33.9 m

WT: 13.533 m / 44.399 ft
Ueq: 28.1 m

CONETEC

CGSH

Job No: 1672007
Date: 04/26/2016 12:34
Site: Bay 3, Germano Cava

Sounding: GCCPT16-03
Cone: 376:T375F10U200
Cone Area: 15 sq cm

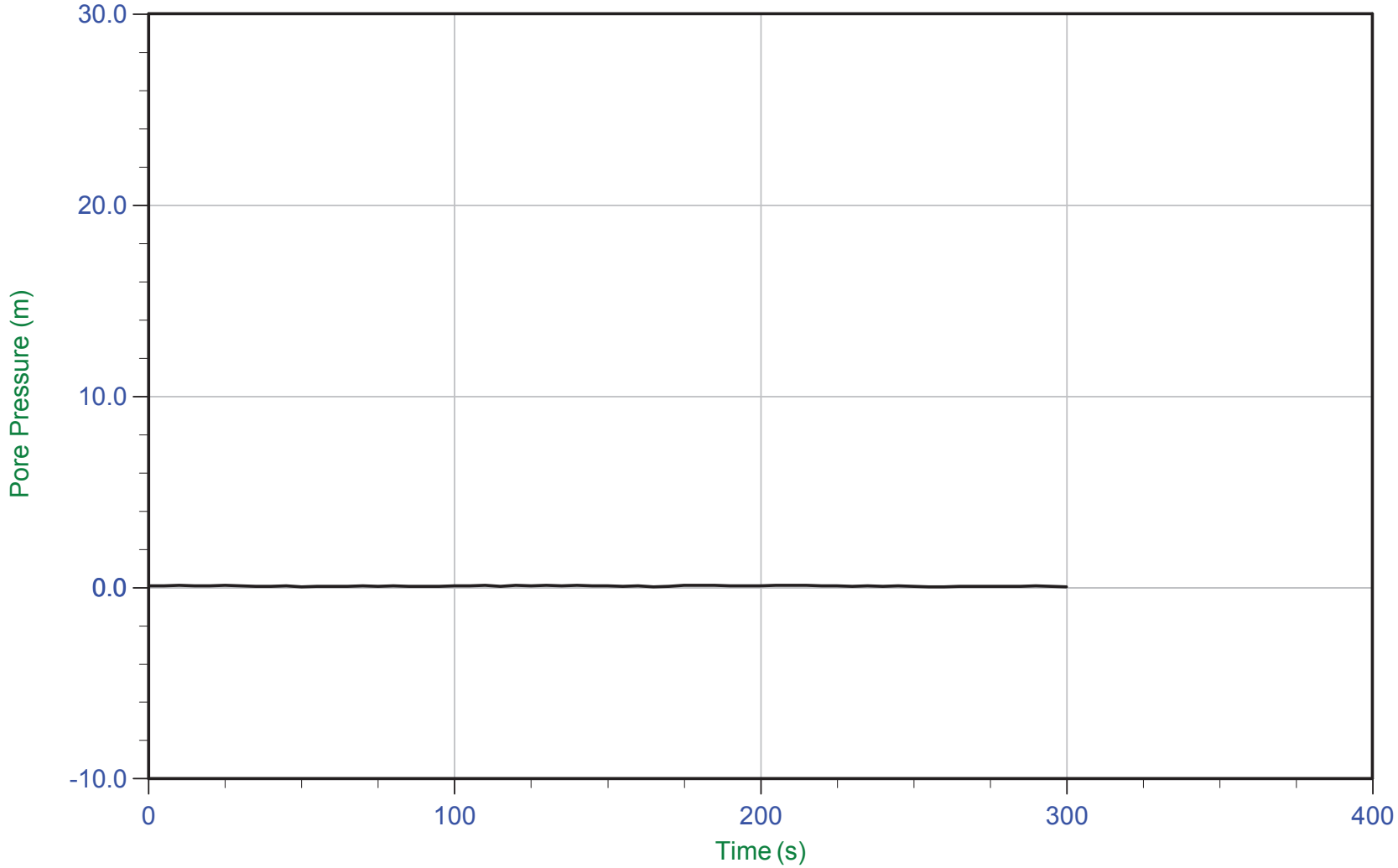

Trace Summary:

Filename: 16-72004_RS03.PPF
Depth: 5.500 m / 18.044 ft
Duration: 300.0 s

U Min: 0.0 m
U Max: 0.1 m

WT: 0.000 m / 0.000 ft
Ueq: 0.0 m

CONETEC

CGSH

Job No: 1672007
Date: 04/26/2016 12:34
Site: Bay 3, Germano Cava

Sounding: GCCPT16-03
Cone: 376:T375F10U200
Cone Area: 15 sq cm

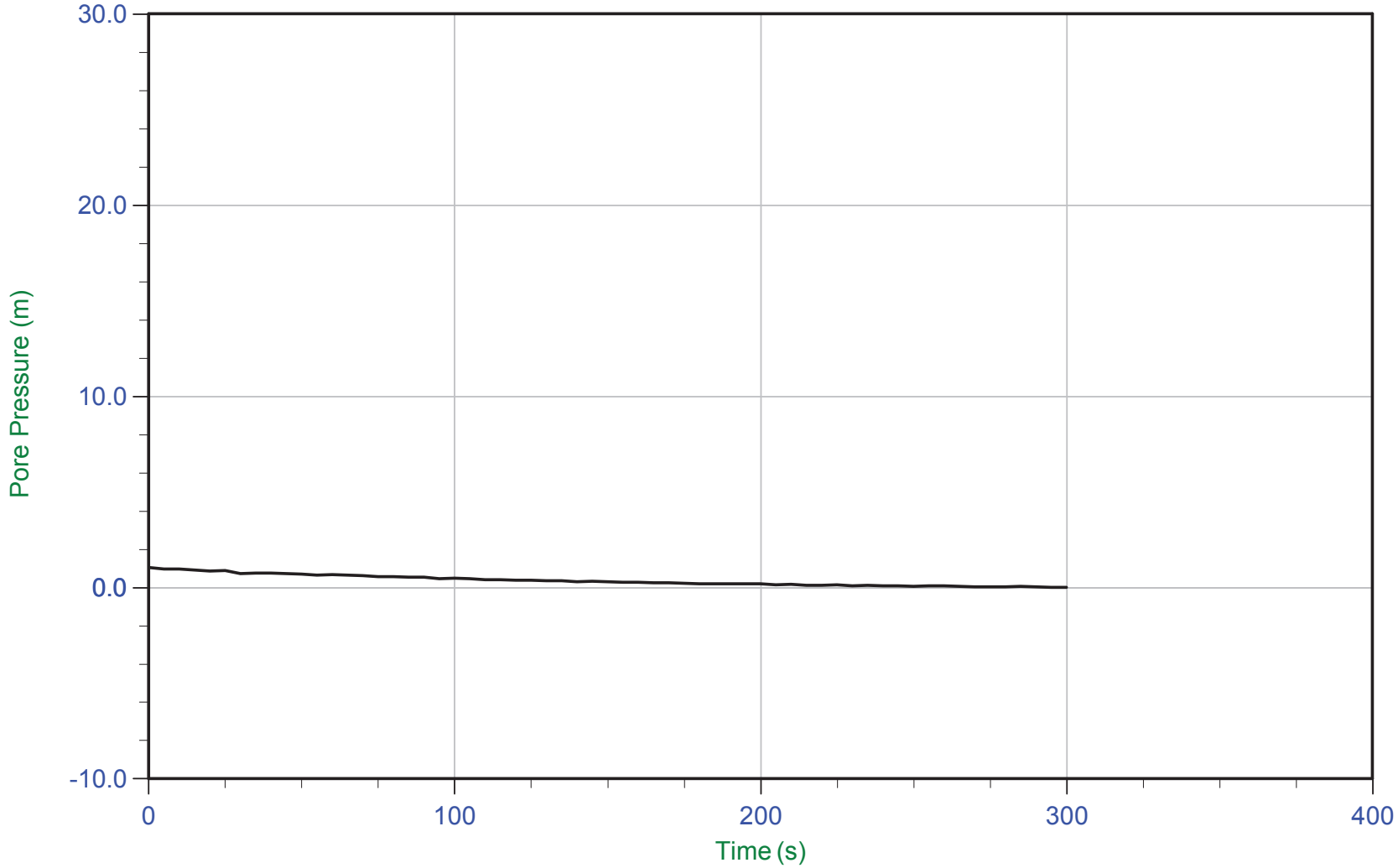

Trace Summary:

Filename: 16-72004_RS03.PPF
Depth: 10.500 m / 34.448 ft
Duration: 300.0 s

U Min: 0.0 m
U Max: 1.0 m

WT: 0.000 m / 0.000 ft
Ueq: 0.0 m

CONETEC

CGSH

Job No: 1672007
Date: 04/26/2016 12:34
Site: Bay 3, Germano Cava

Sounding: GCCPT16-03
Cone: 376:T375F10U200
Cone Area: 15 sq cm

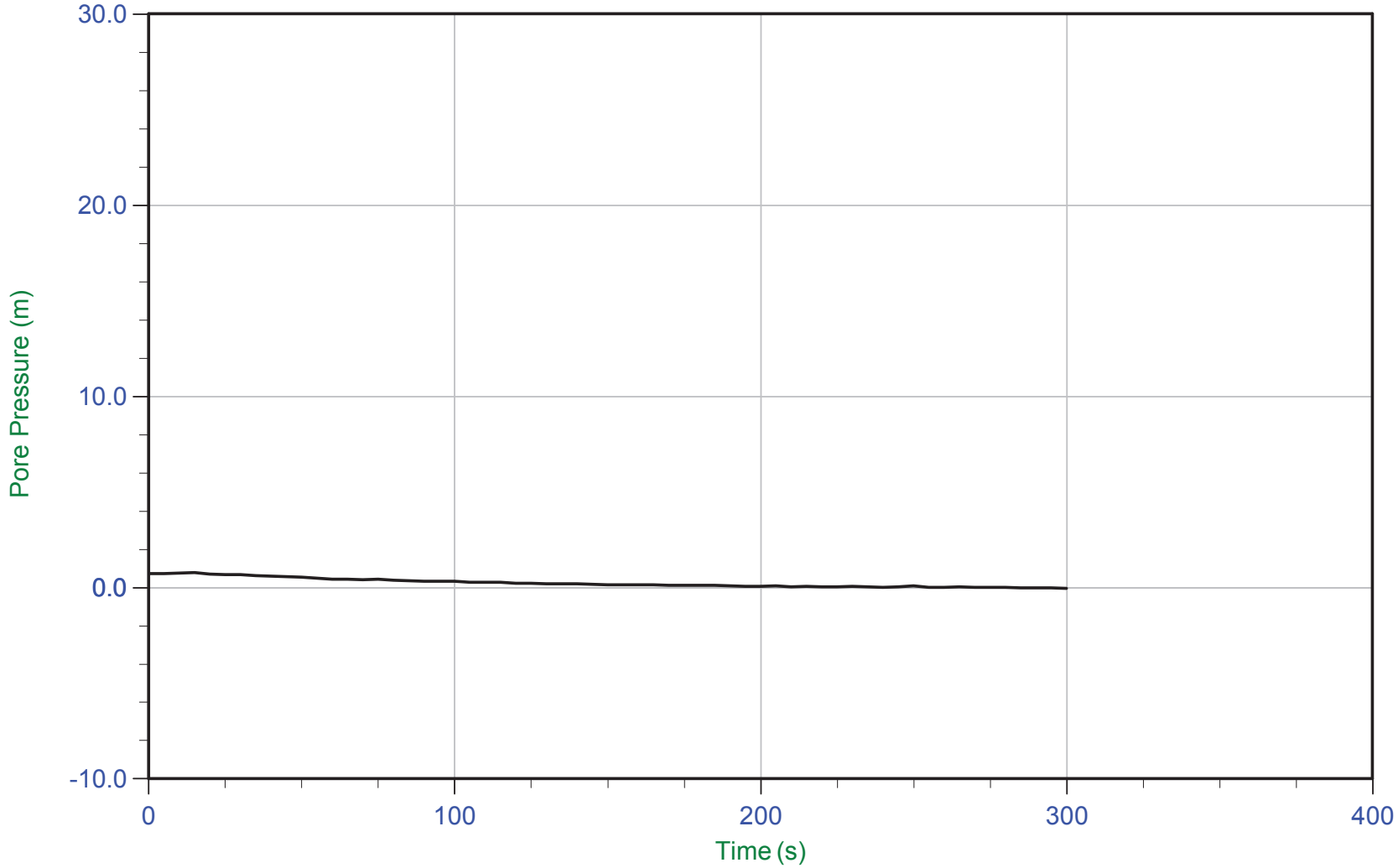

Trace Summary:

Filename: 16-72004_RS03.PPF
Depth: 15.500 m / 50.852 ft
Duration: 300.0 s

U Min: -0.0 m
U Max: 0.8 m

WT: 0.000 m / 0.000 ft
Ueq: 0.0 m

CONETEC

CGSH

Job No: 1672007
Date: 04/26/2016 12:34
Site: Bay 3, Germano Cava

Sounding: GCCPT16-03
Cone: 376:T375F10U200
Cone Area: 15 sq cm

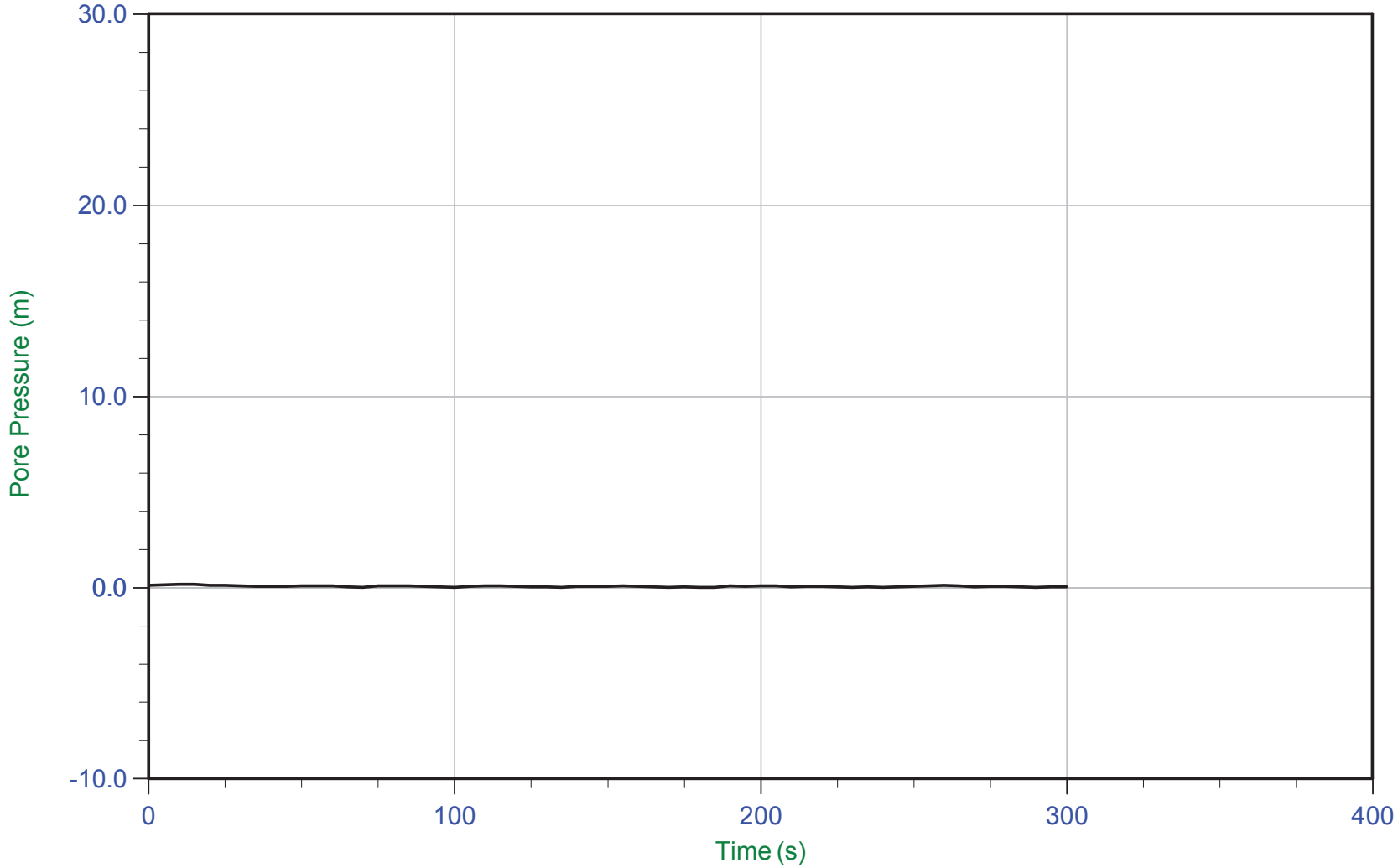

Trace Summary:

Filename: 16-72004_RS03.PPF
Depth: 20.500 m / 67.256 ft
Duration: 300.0 s

U Min: 0.0 m
U Max: 0.2 m

WT: 0.000 m / 0.000 ft
Ueq: 0.0 m

CONETEC

CGSH

Job No: 1672007
Date: 04/26/2016 12:34
Site: Bay 3, Germano Cava

Sounding: GCCPT16-03
Cone: 376:T375F10U200
Cone Area: 15 sq cm

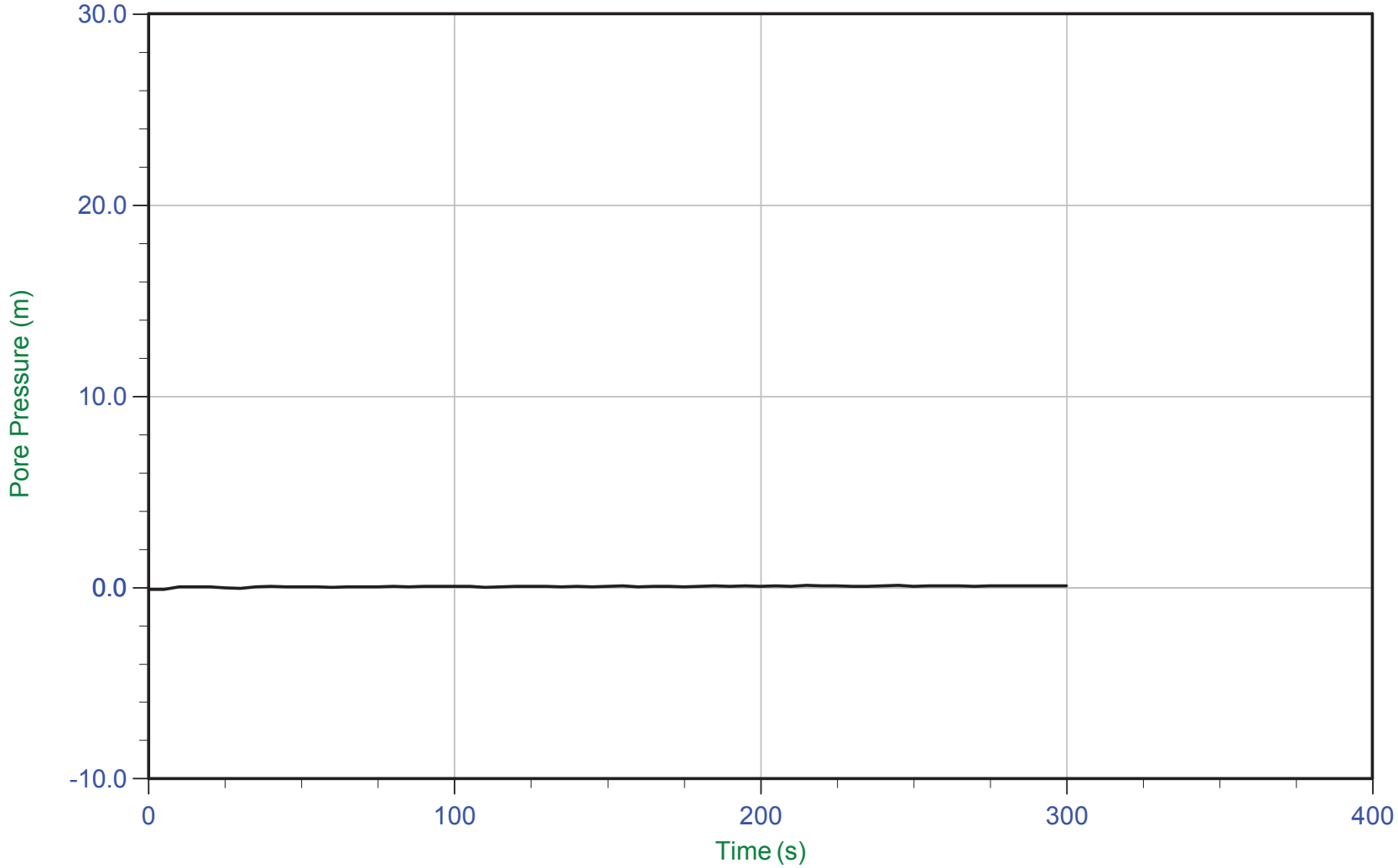

Trace Summary:

Filename: 16-72004_RS03.PPF
Depth: 25.500 m / 83.660 ft
Duration: 300.0 s

U Min: -0.1 m
U Max: 0.1 m

WT: 0.000 m / 0.000 ft
Ueq: 0.0 m

CONETEC

CGSH

Job No: 1672007
Date: 04/26/2016 12:34
Site: Bay 3, Germano Cava

Sounding: GCCPT16-03
Cone: 376:T375F10U200
Cone Area: 15 sq cm

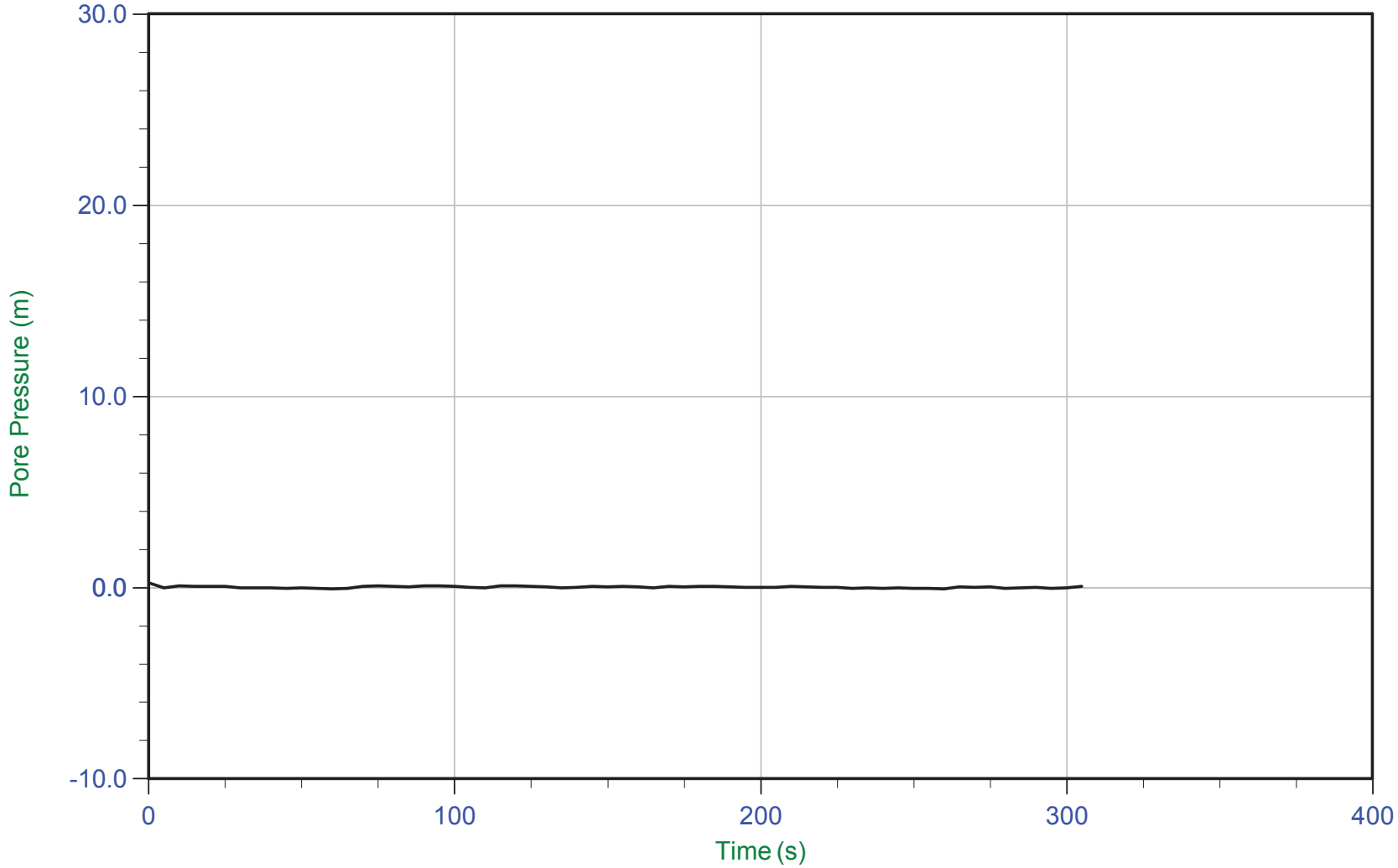

Trace Summary:

Filename: 16-72004_RS03.PPF
Depth: 30.500 m / 100.064 ft
Duration: 305.0 s

U Min: -0.1 m
U Max: 0.2 m

WT: 0.000 m / 0.000 ft
Ueq: 0.0 m

CONETEC

CGSH

Job No: 1672007
Date: 04/26/2016 12:34
Site: Bay 3, Germano Cava

Sounding: GCCPT16-03
Cone: 376:T375F10U200
Cone Area: 15 sq cm

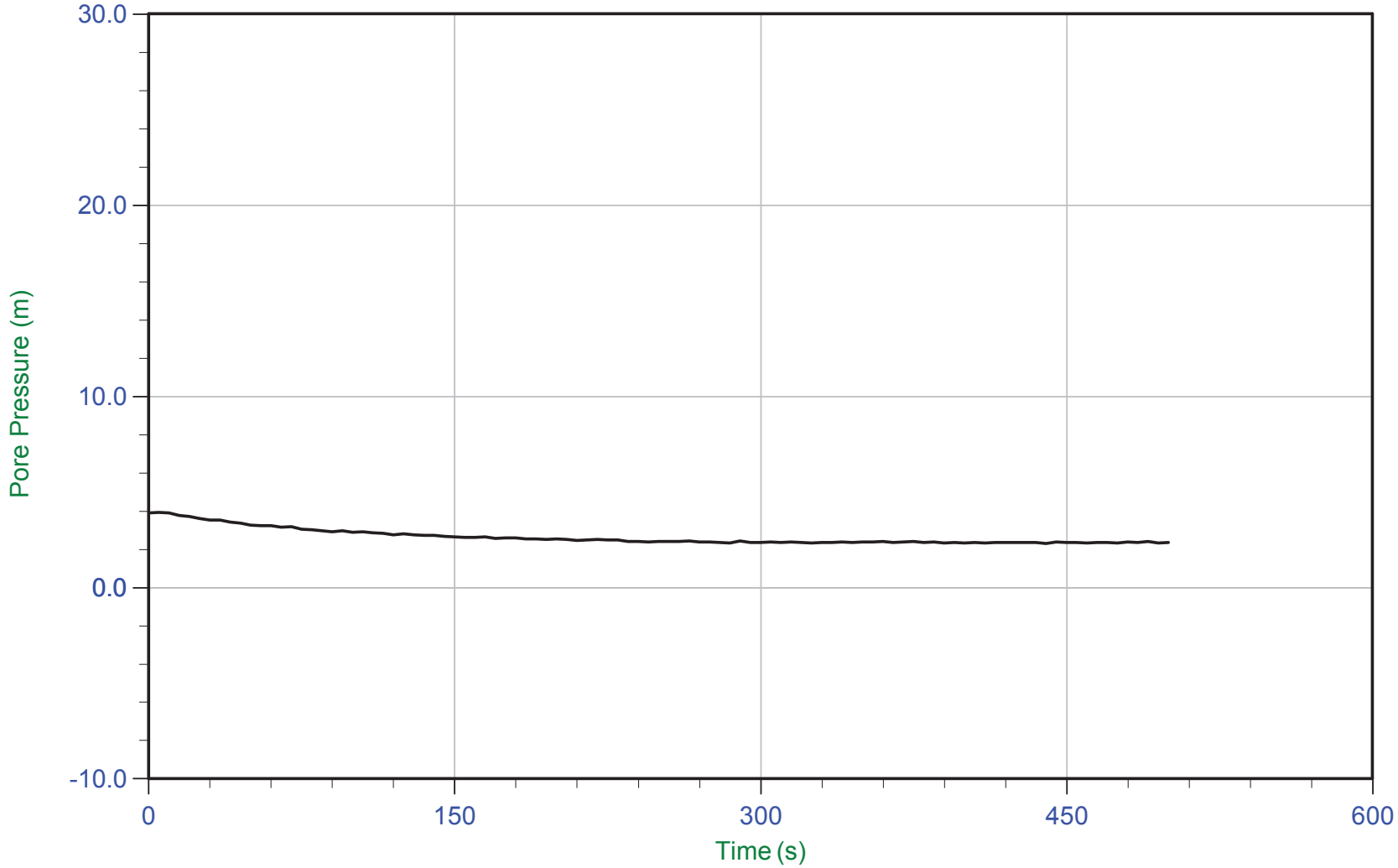

Trace Summary:

Filename: 16-72004_RS03.PPF
Depth: 35.500 m / 116.468 ft
Duration: 500.0 s

U Min: 2.3 m
U Max: 3.9 m

WT: 33.199 m / 108.919 ft
Ueq: 2.3 m

CONETEC

CGSH

Job No: 1672007
Date: 04/26/2016 12:34
Site: Bay 3, Germano Cava

Sounding: GCCPT16-03
Cone: 376:T375F10U200
Cone Area: 15 sq cm

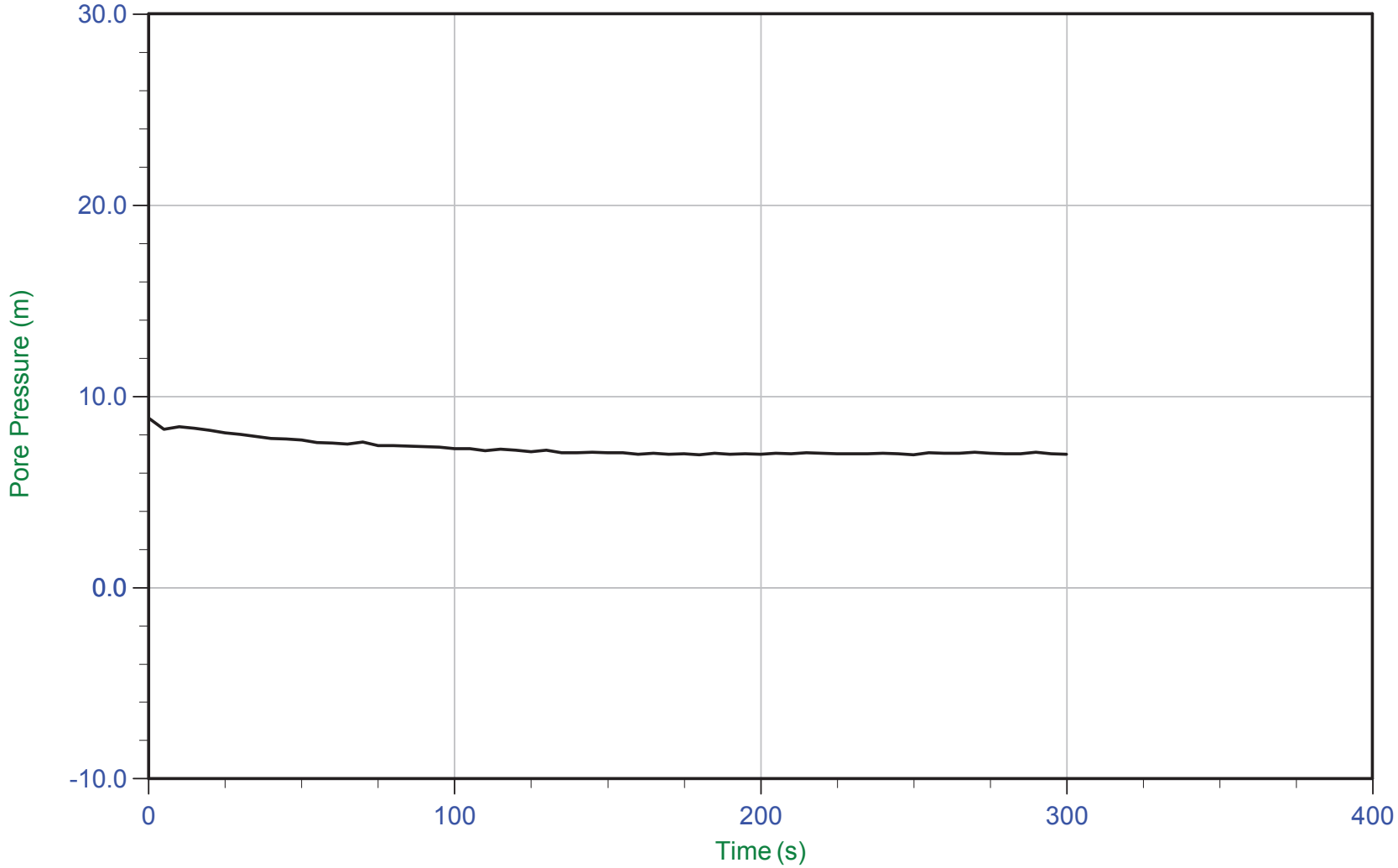

Trace Summary:

Filename: 16-72004_RS03.PPF
Depth: 40.500 m / 132.872 ft
Duration: 300.0 s

U Min: 7.0 m
U Max: 8.9 m

WT: 33.513 m / 109.949 ft
Ueq: 7.0 m

CONETEC

CGSH

Job No: 1672007
Date: 04/26/2016 12:34
Site: Bay 3, Germano Cava

Sounding: GCCPT16-03
Cone: 376:T375F10U200
Cone Area: 15 sq cm

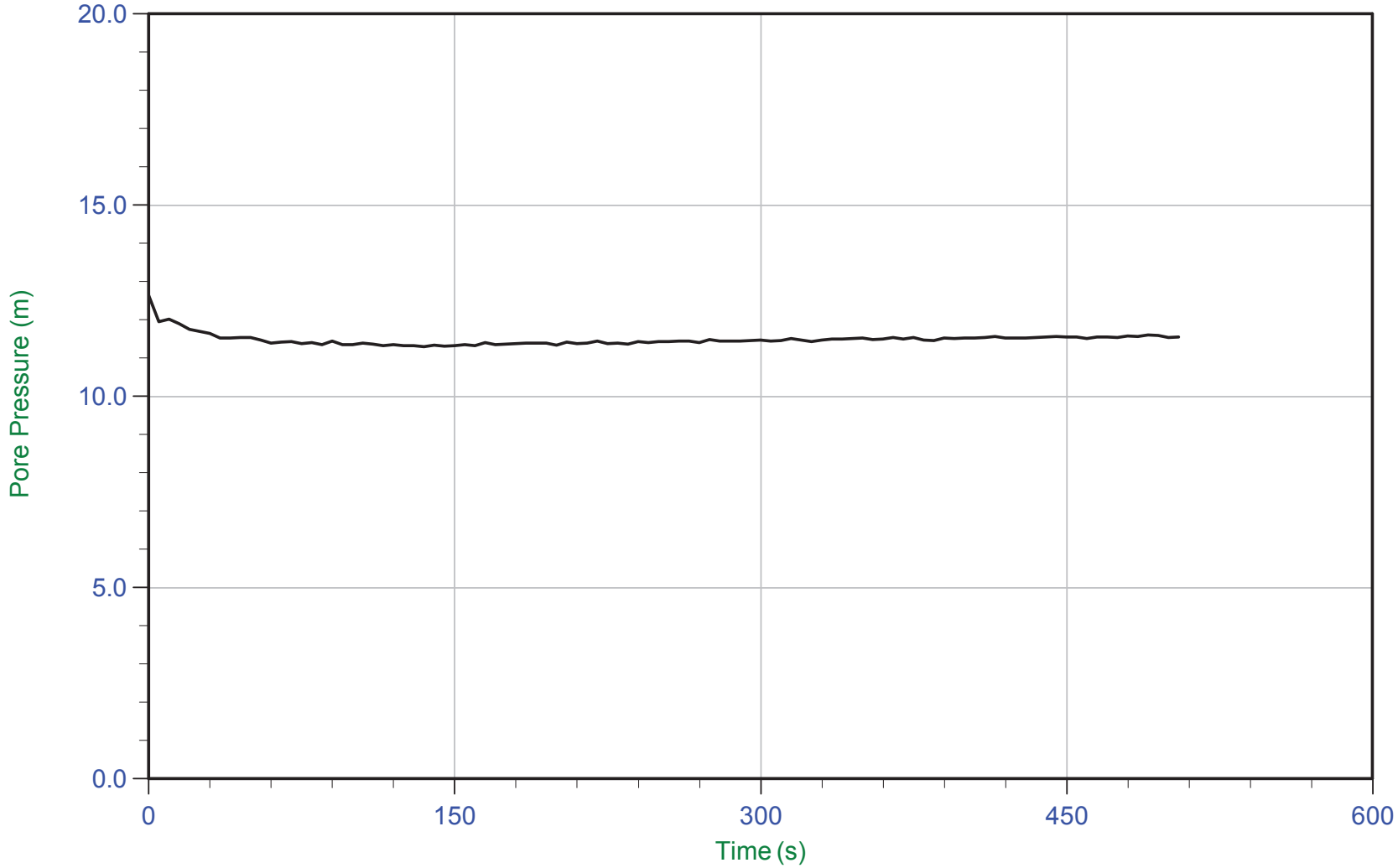

Trace Summary:

Filename: 16-72004_RS03.PPF
Depth: 45.500 m / 149.276 ft
Duration: 505.0 s

U Min: 11.3 m
U Max: 12.6 m

WT: 33.994 m / 111.528 ft
Ueq: 11.5 m

CONETEC

CGSH

Job No: 1672007
Date: 04/26/2016 12:34
Site: Bay 3, Germano Cava

Sounding: GCCPT16-03
Cone: 376:T375F10U200
Cone Area: 15 sq cm

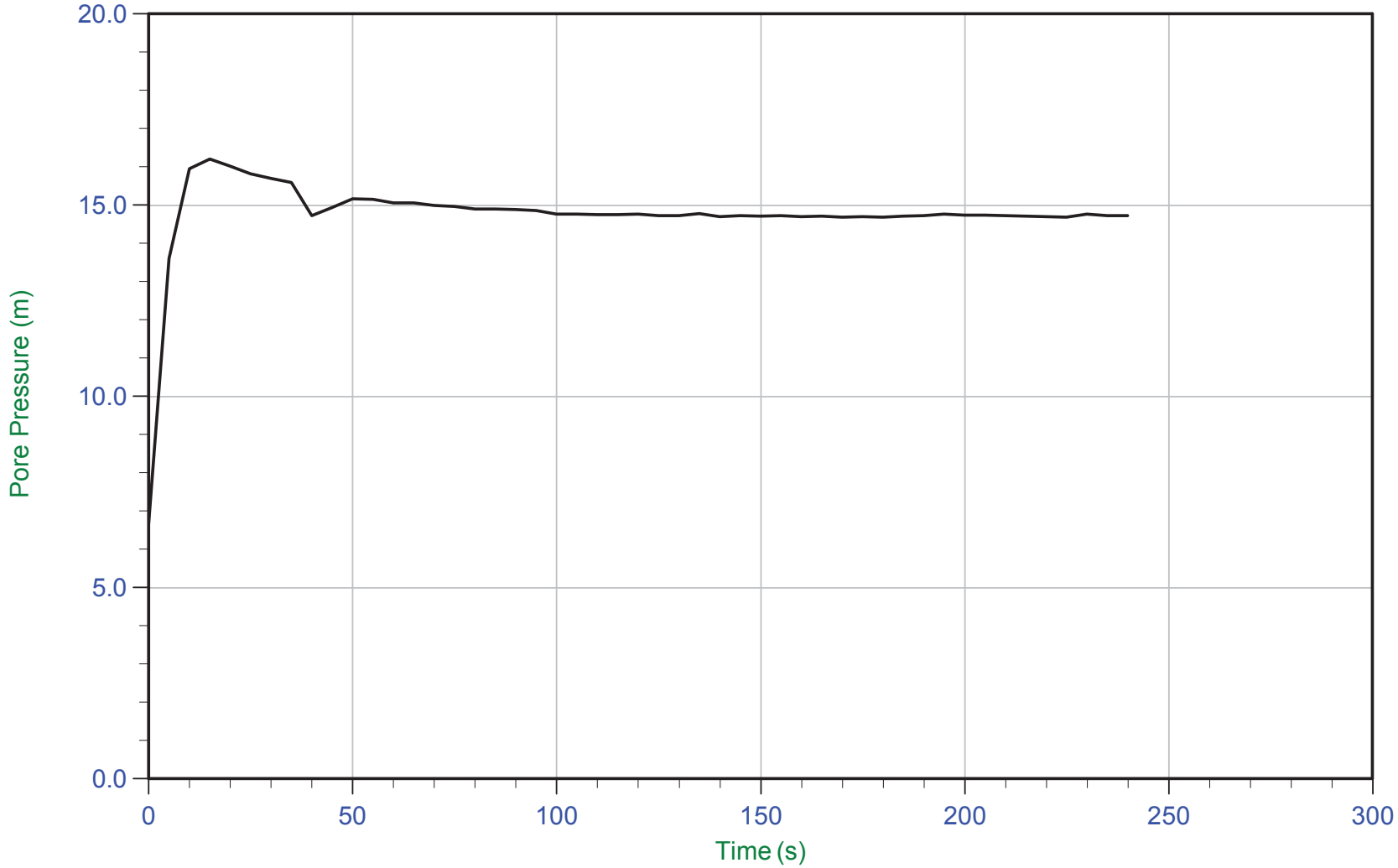

Trace Summary:

Filename: 16-72004_RS03.PPF
Depth: 49.500 m / 162.400 ft
Duration: 240.0 s

U Min: 6.7 m
U Max: 16.2 m

WT: 34.814 m / 114.218 ft
Ueq: 14.7 m

CONETEC

CGSH

Job No: 1672007
Date: 04/26/2016 12:34
Site: Bay 3, Germano Cava

Sounding: GCCPT16-03
Cone: 376:T375F10U200
Cone Area: 15 sq cm

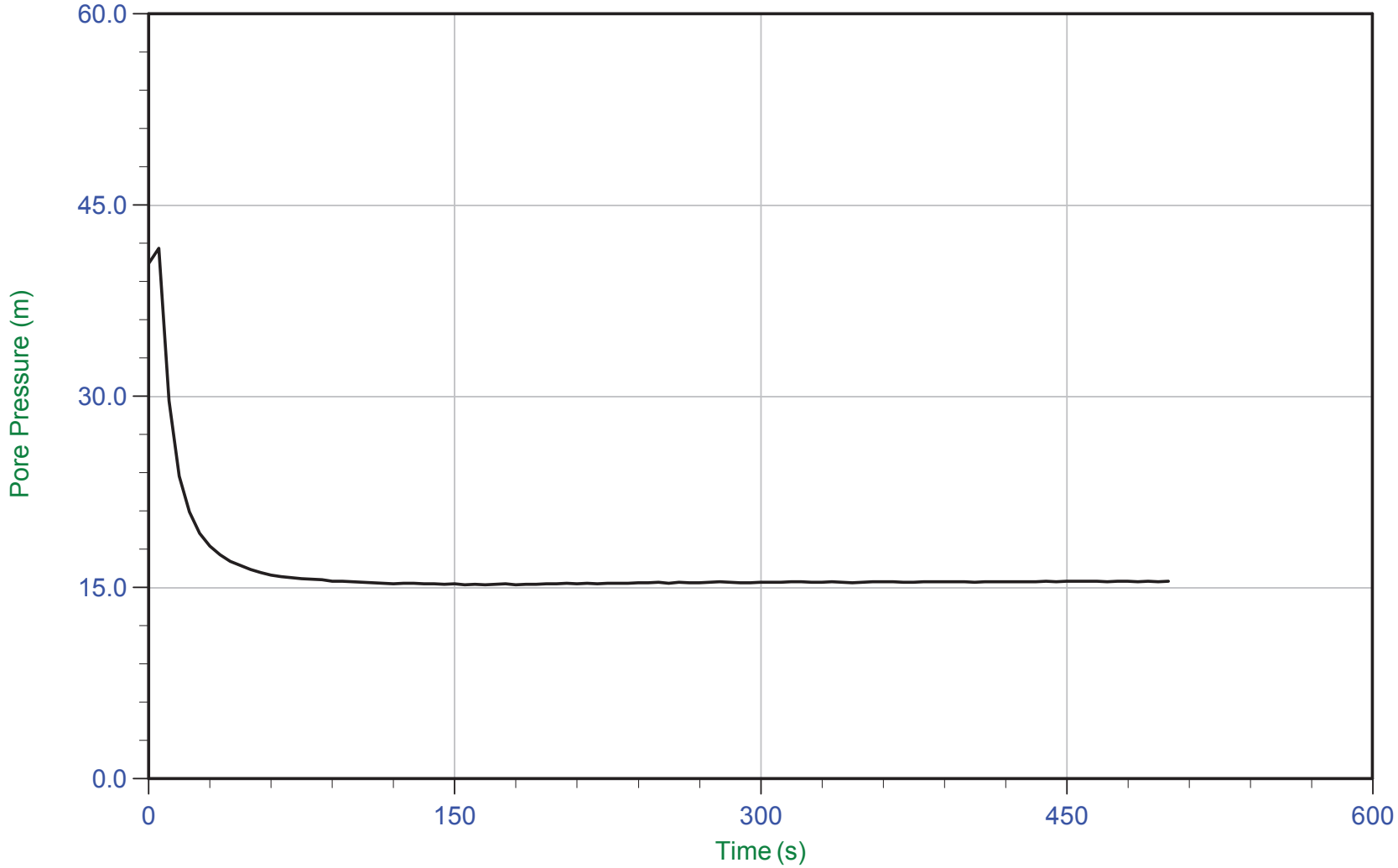

Trace Summary:

Filename: 16-72004_RS03.PPF
Depth: 50.500 m / 165.680 ft
Duration: 500.0 s

U Min: 15.2 m
U Max: 41.6 m

WT: 35.061 m / 115.028 ft
Ueq: 15.4 m

CONETEC

CGSH

Job No: 1672007
Date: 04/26/2016 12:34
Site: Bay 3, Germano Cava

Sounding: GCCPT16-03
Cone: 376:T375F10U200
Cone Area: 15 sq cm

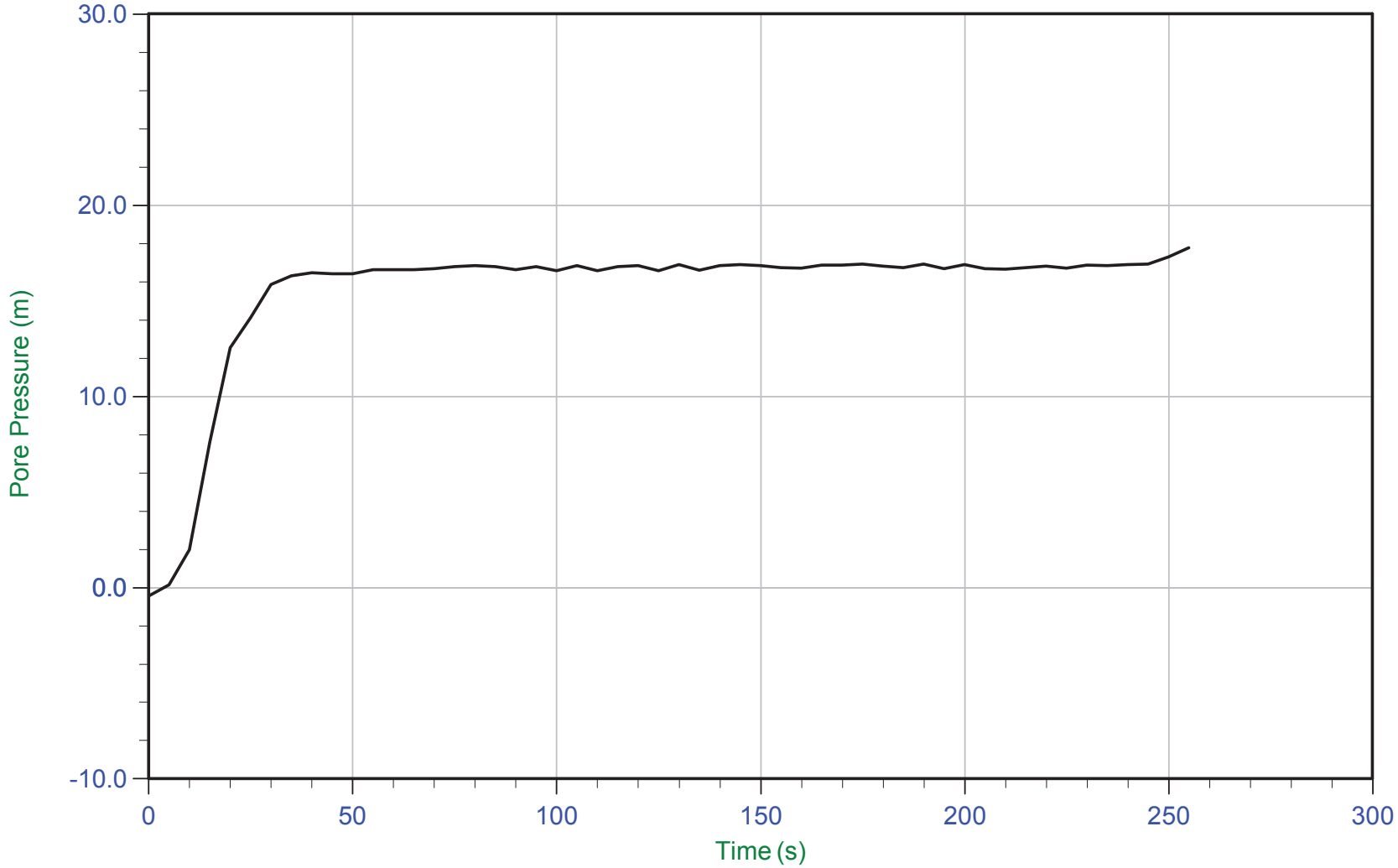

Trace Summary:

Filename: 16-72004_RS03.PPF
Depth: 52.500 m / 172.242 ft
Duration: 255.0 s

U Min: -0.4 m
U Max: 17.8 m

CONETEC

CGSH

Job No: 1672007
Date: 04/26/2016 12:34
Site: Bay 3, Germano Cava

Sounding: GCCPT16-03
Cone: 376:T375F10U200
Cone Area: 15 sq cm

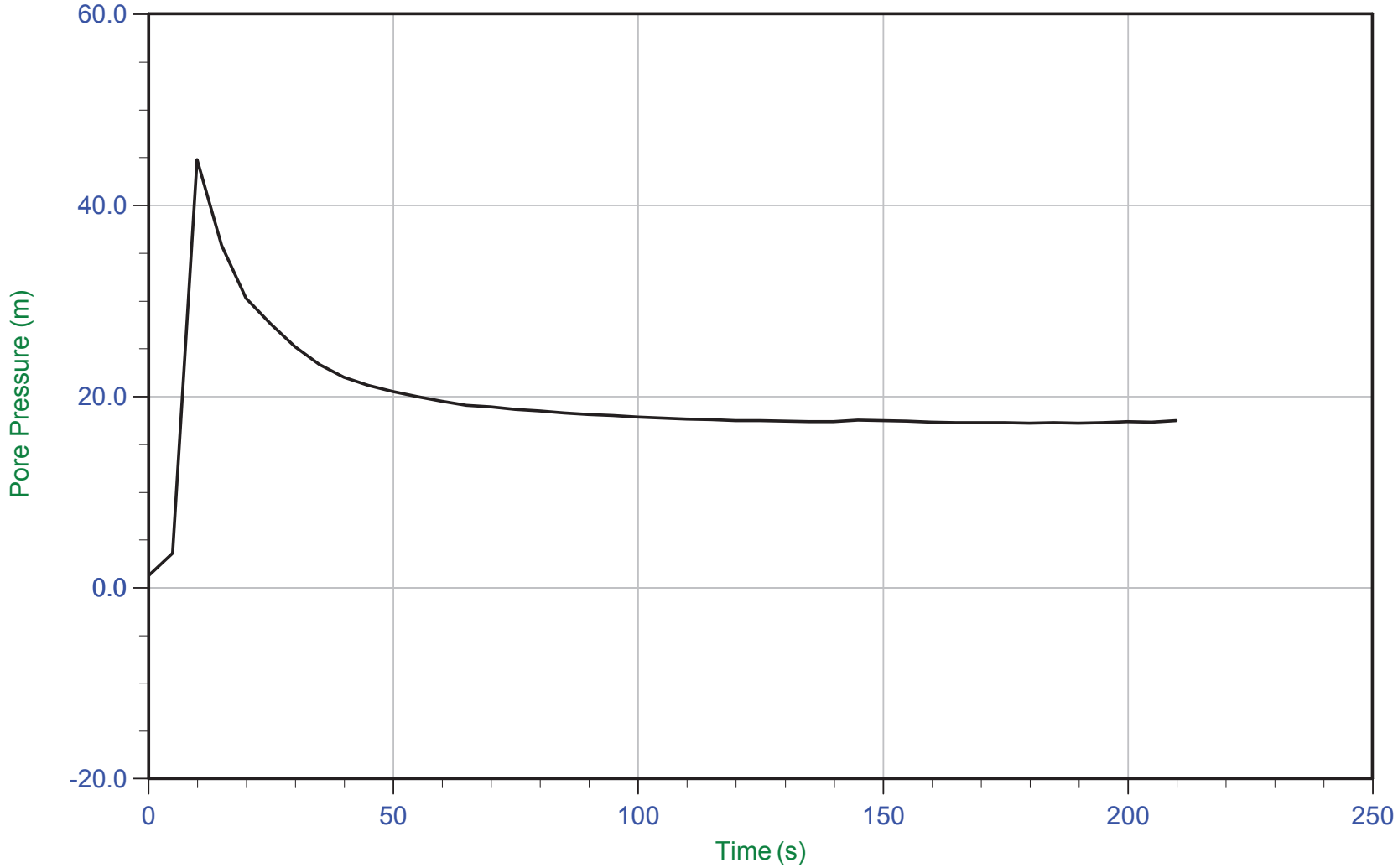

Trace Summary:

Filename: 16-72004_RS03.PPF
Depth: 53.450 m / 175.359 ft
Duration: 210.0 s

U Min: 1.3 m
U Max: 44.7 m

CONETEC

CGSH

Job No: 1672007
Date: 04/26/2016 12:34
Site: Bay 3, Germano Cava

Sounding: GCCPT16-03
Cone: 376:T375F10U200
Cone Area: 15 sq cm

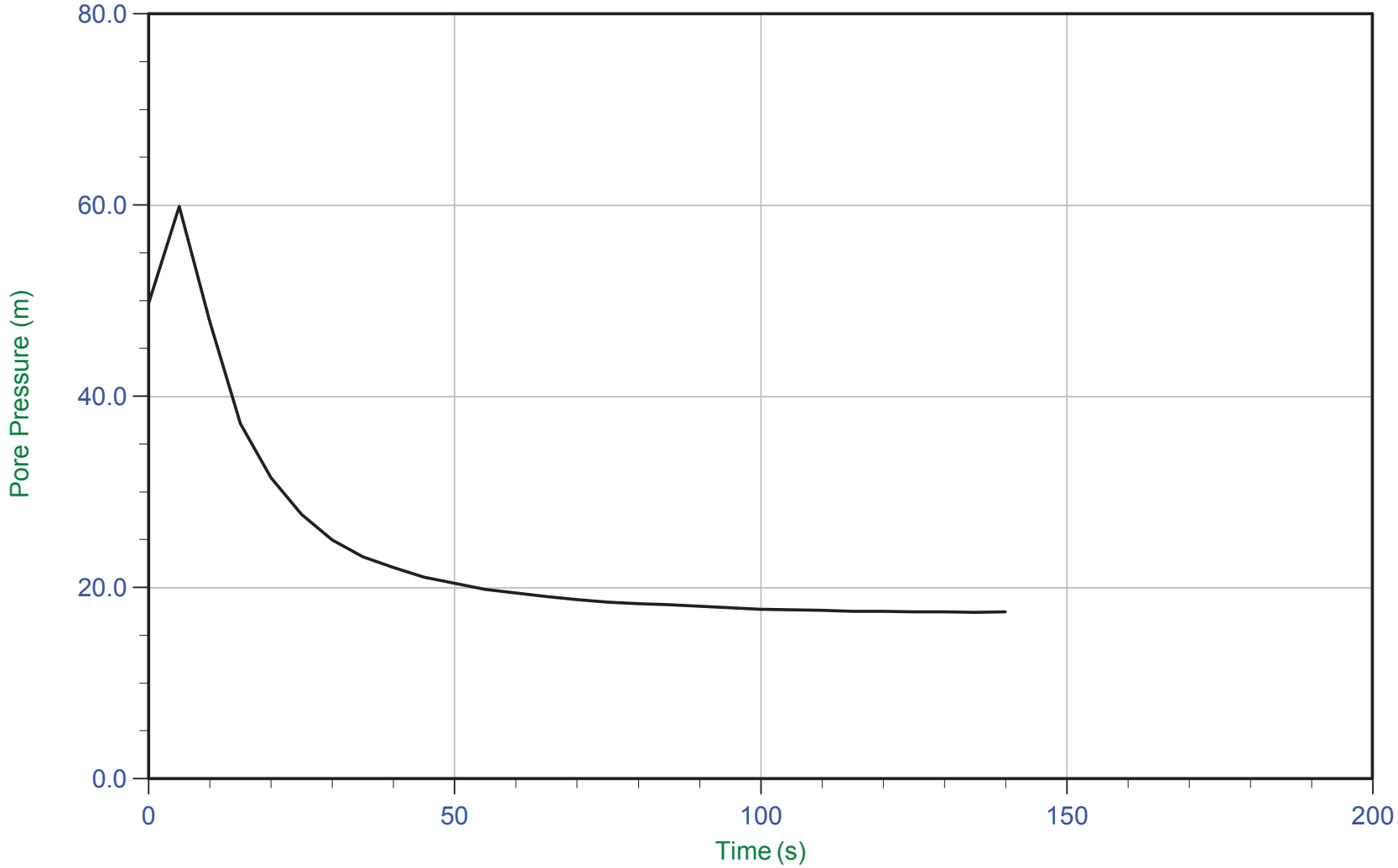

Trace Summary:

Filename: 16-72004_RS03.PPF
Depth: 54.500 m / 178.804 ft
Duration: 140.0 s

U Min: 17.4 m
U Max: 59.9 m

CONETEC

CGSH

Job No: 1672007
Date: 04/26/2016 12:34
Site: Bay 3, Germano Cava

Sounding: GCCPT16-03
Cone: 376:T375F10U200
Cone Area: 15 sq cm

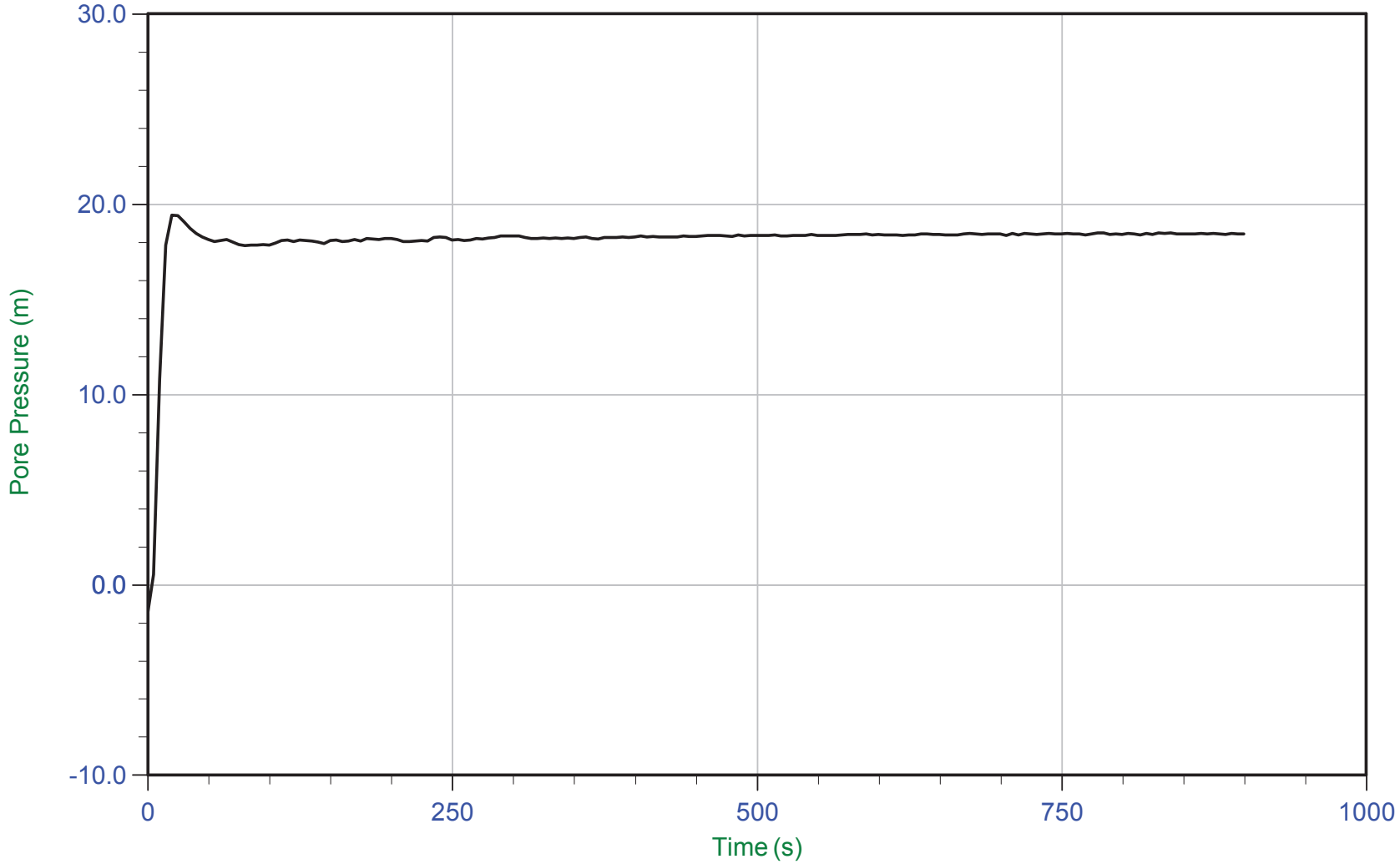

Trace Summary:

Filename: 16-72004_RS03.PPF
Depth: 55.500 m / 182.084 ft
Duration: 900.0 s

U Min: -1.4 m
U Max: 19.4 m

WT: 37.132 m / 121.823 ft
Ueq: 18.4 m

CONETEC

CGSH

Job No: 1672007
Date: 04/26/2016 12:34
Site: Bay 3, Germano Cava

Sounding: GCCPT16-03
Cone: 376:T375F10U200
Cone Area: 15 sq cm

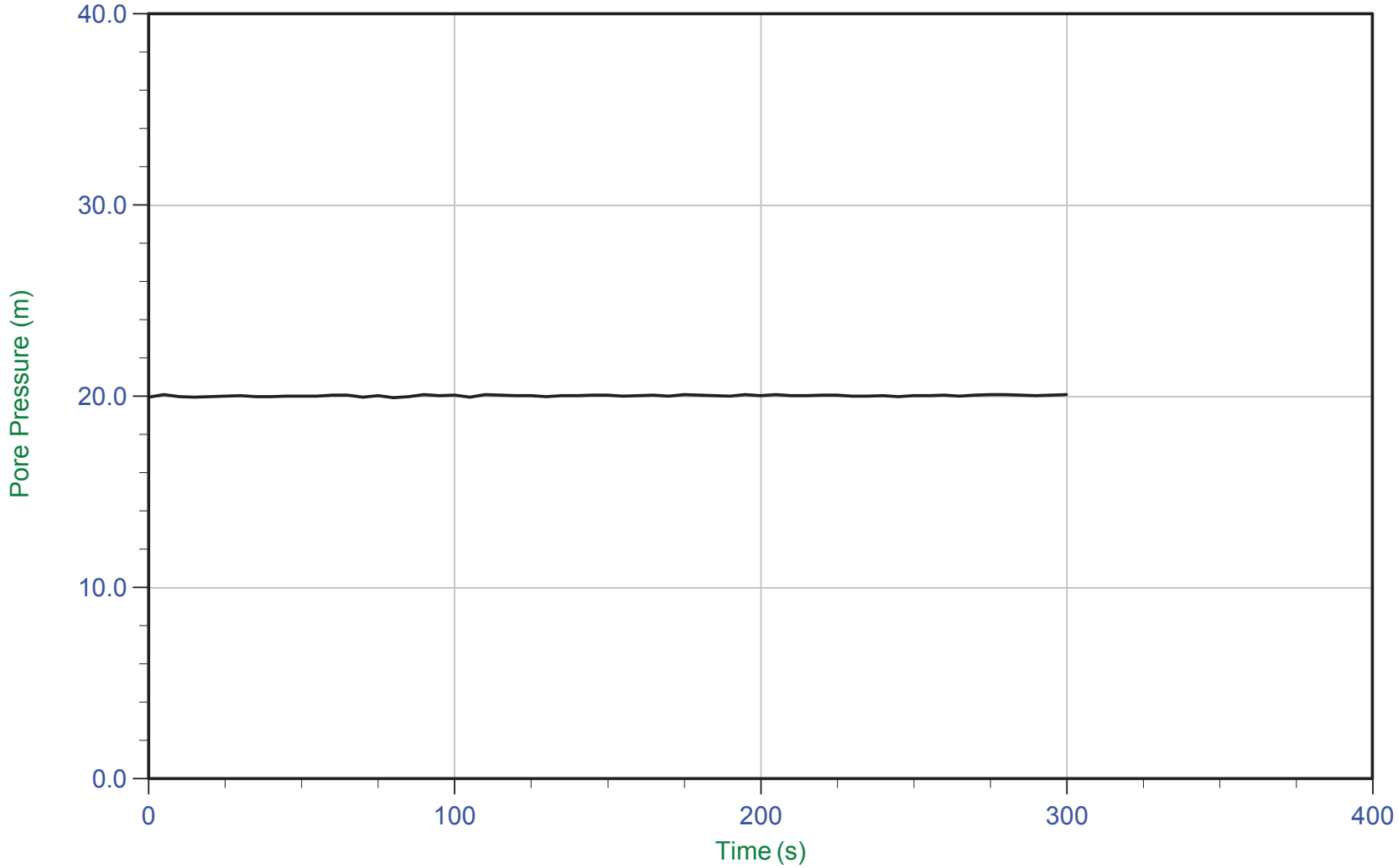

Trace Summary:

Filename: 16-72004_RS03.PPF
Depth: 57.350 m / 188.154 ft
Duration: 300.0 s

U Min: 19.9 m
U Max: 20.1 m

WT: 37.350 m / 122.538 ft
Ueq: 20.0 m

CONETEC

CGSH

Job No: 1672007
Date: 04/26/2016 12:34
Site: Bay 3, Germano Cava

Sounding: GCCPT16-03
Cone: 376:T375F10U200
Cone Area: 15 sq cm

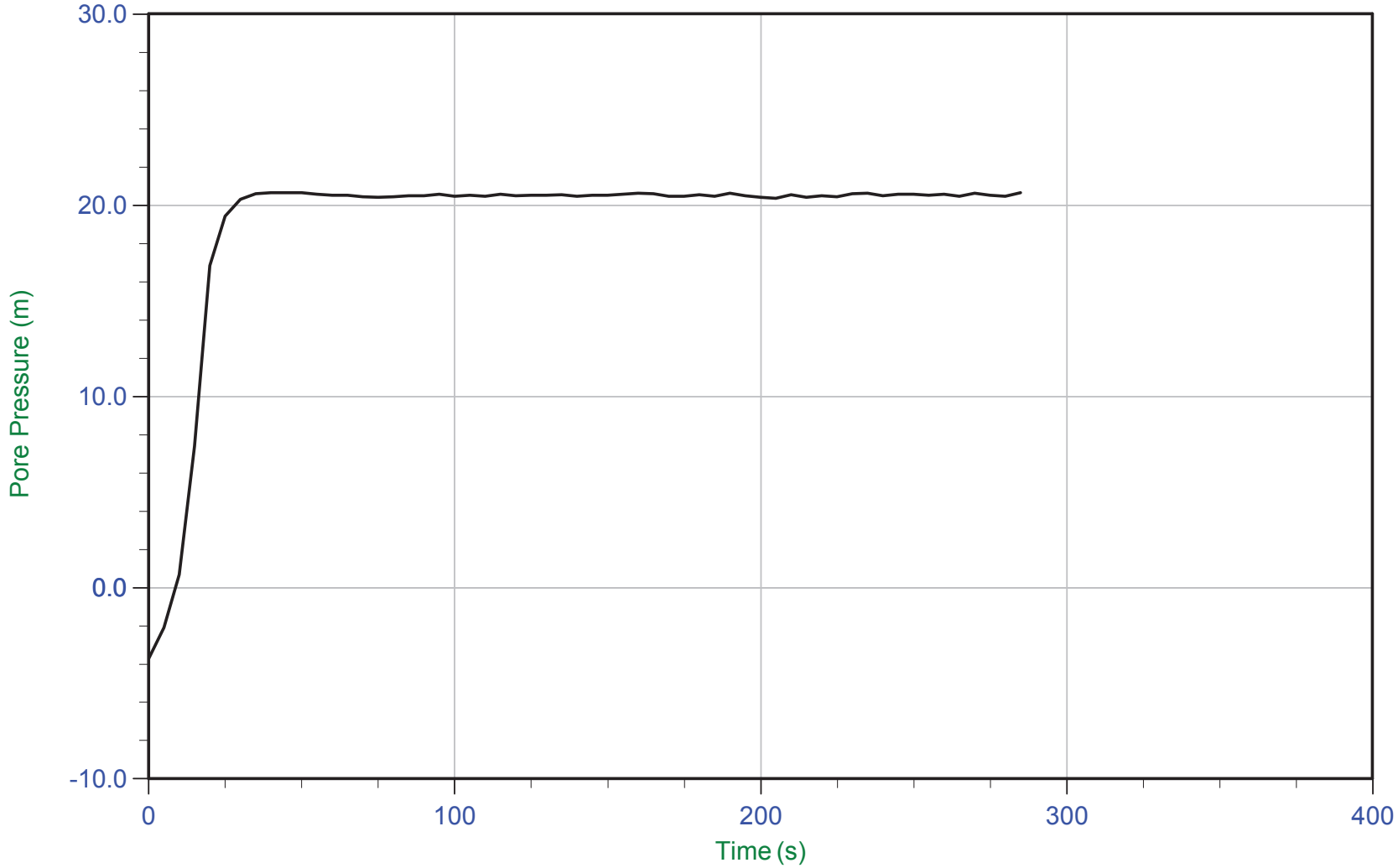

Trace Summary:

Filename: 16-72004_RS03.PPF
Depth: 58.350 m / 191.435 ft
Duration: 285.0 s

U Min: -3.7 m
U Max: 20.7 m

WT: 37.890 m / 124.310 ft
Ueq: 20.5 m

CONETEC

CGSH

Job No: 1672007
Date: 04/26/2016 12:34
Site: Bay 3, Germano Cava

Sounding: GCCPT16-03
Cone: 376:T375F10U200
Cone Area: 15 sq cm

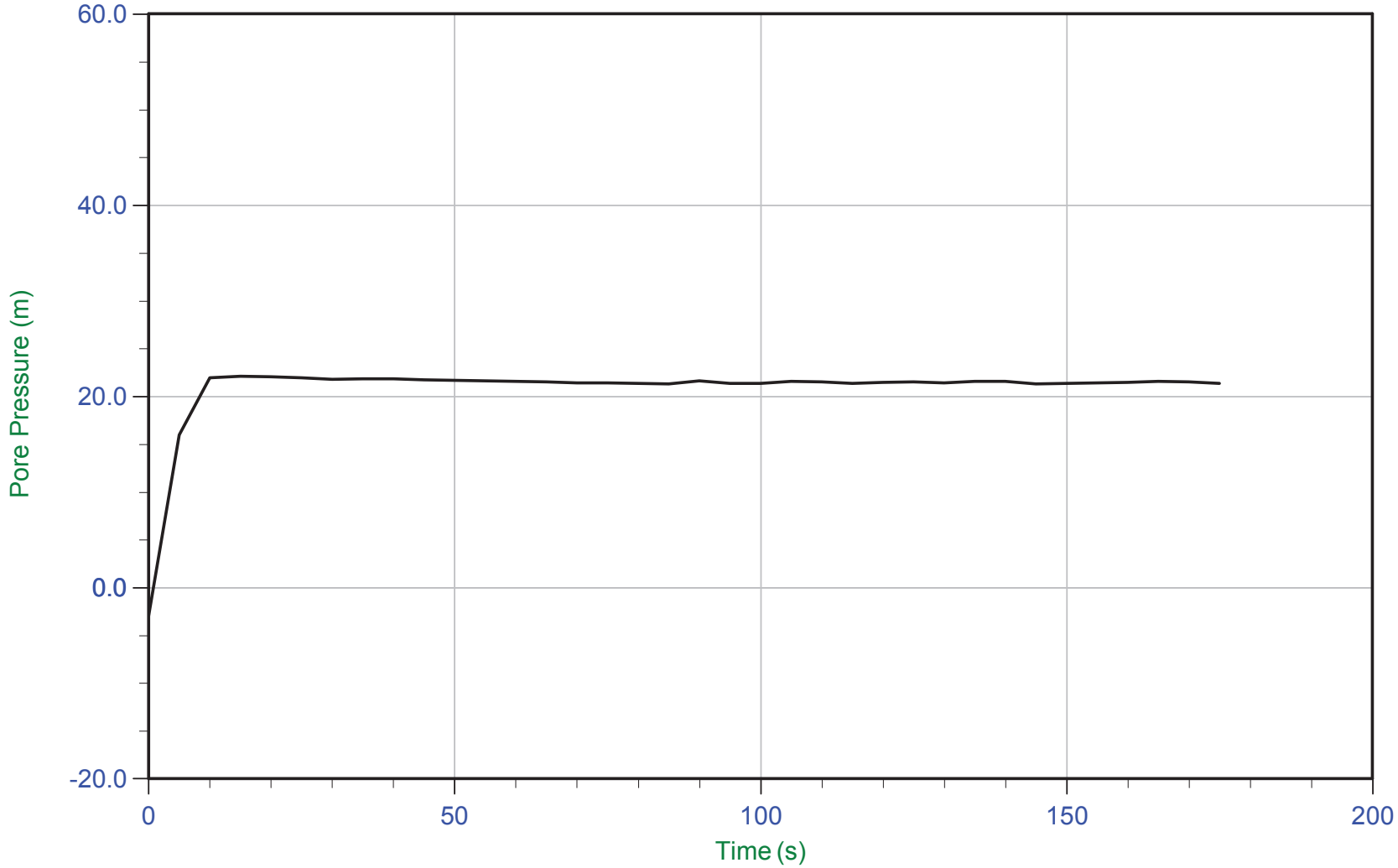

Trace Summary:

Filename: 16-72004_RS03.PPF
Depth: 59.350 m / 194.715 ft
Duration: 175.0 s

U Min: -3.0 m
U Max: 22.1 m

WT: 38.011 m / 124.706 ft
Ueq: 21.3 m

CONETEC

CGSH

Job No: 1672007
Date: 04/26/2016 12:34
Site: Bay 3, Germano Cava

Sounding: GCCPT16-03
Cone: 376:T375F10U200
Cone Area: 15 sq cm

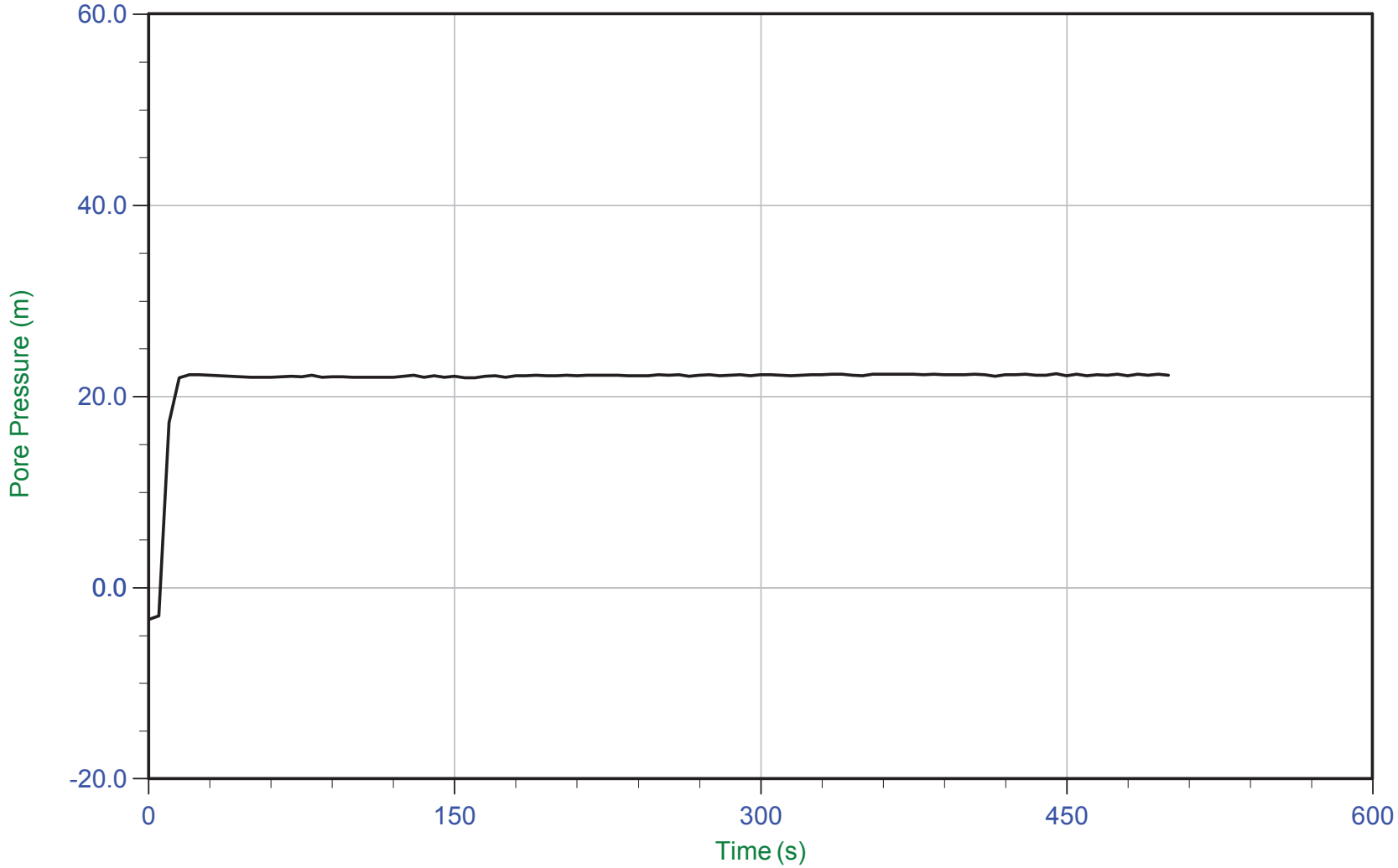

Trace Summary:

Filename: 16-72004_RS03.PPF
Depth: 60.350 m / 197.996 ft
Duration: 500.0 s

U Min: -3.4 m
U Max: 22.3 m

WT: 38.174 m / 125.241 ft
Ueq: 22.2 m

CONETEC

CGSH

Job No: 1672007
Date: 04/26/2016 12:34
Site: Bay 3, Germano Cava

Sounding: GCCPT16-03
Cone: 376:T375F10U200
Cone Area: 15 sq cm

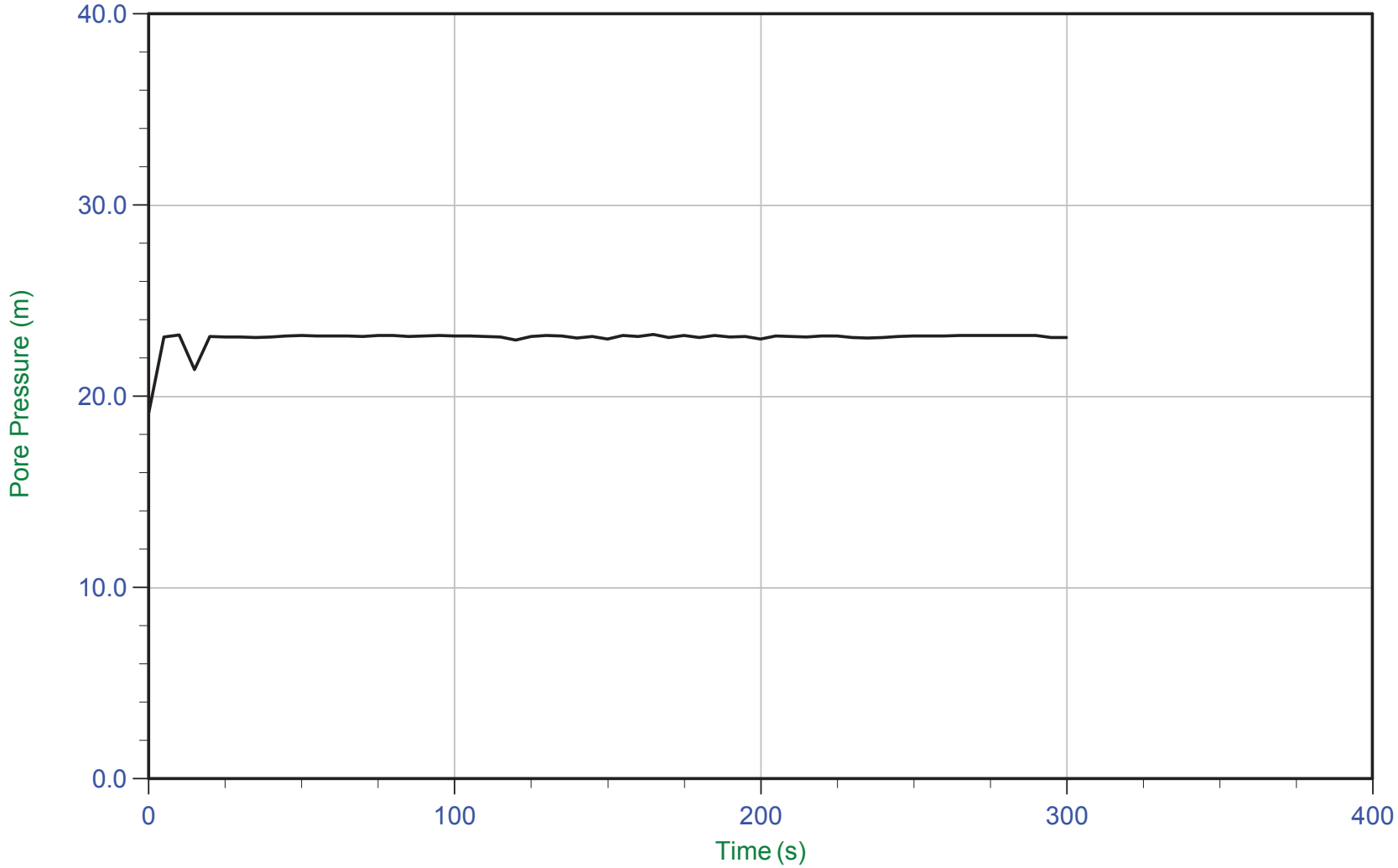

Trace Summary:

Filename: 16-72004_RS03.PPF
Depth: 61.650 m / 202.261 ft
Duration: 300.0 s

U Min: 19.1 m
U Max: 23.2 m

WT: 38.554 m / 126.488 ft
Ueq: 23.1 m

CONETEC

CGSH

Job No: 1672007
Date: 05/02/2016 15:34
Site: Bay 3, Germano Cava

Sounding: GCCPT16-04
Cone: 376:T375F10U200
Cone Area: 15 sq cm

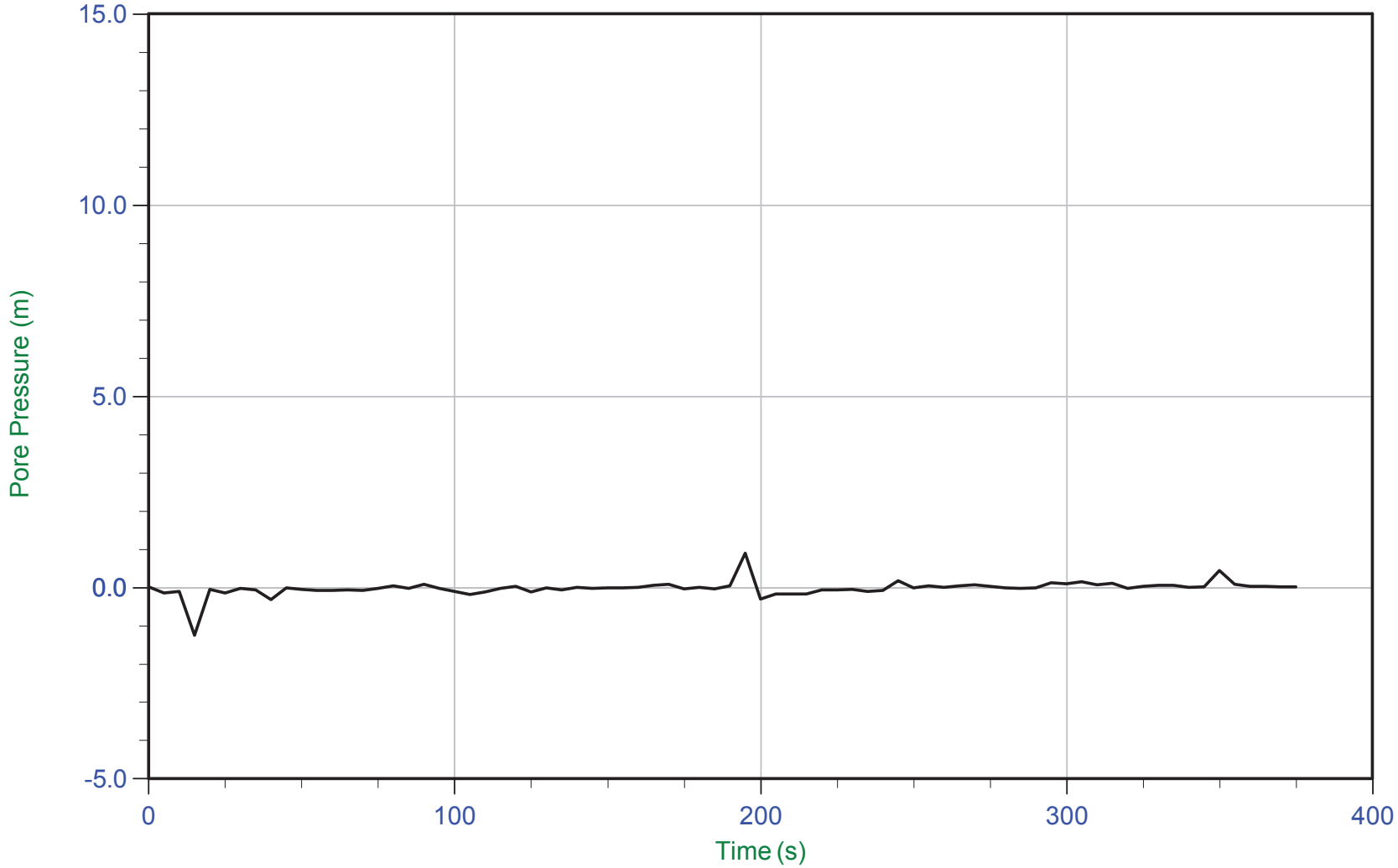

Trace Summary:

Filename: 16-72004_RS04.PPF
Depth: 0.400 m / 1.312 ft
Duration: 375.0 s

U Min: -1.2 m
U Max: 0.9 m

WT: 0.000 m / 0.000 ft
Ueq: 0.0 m

CONETEC

CGSH

Job No: 1672007
Date: 05/02/2016 15:34
Site: Bay 3, Germano Cava

Sounding: GCCPT16-04
Cone: 376:T375F10U200
Cone Area: 15 sq cm

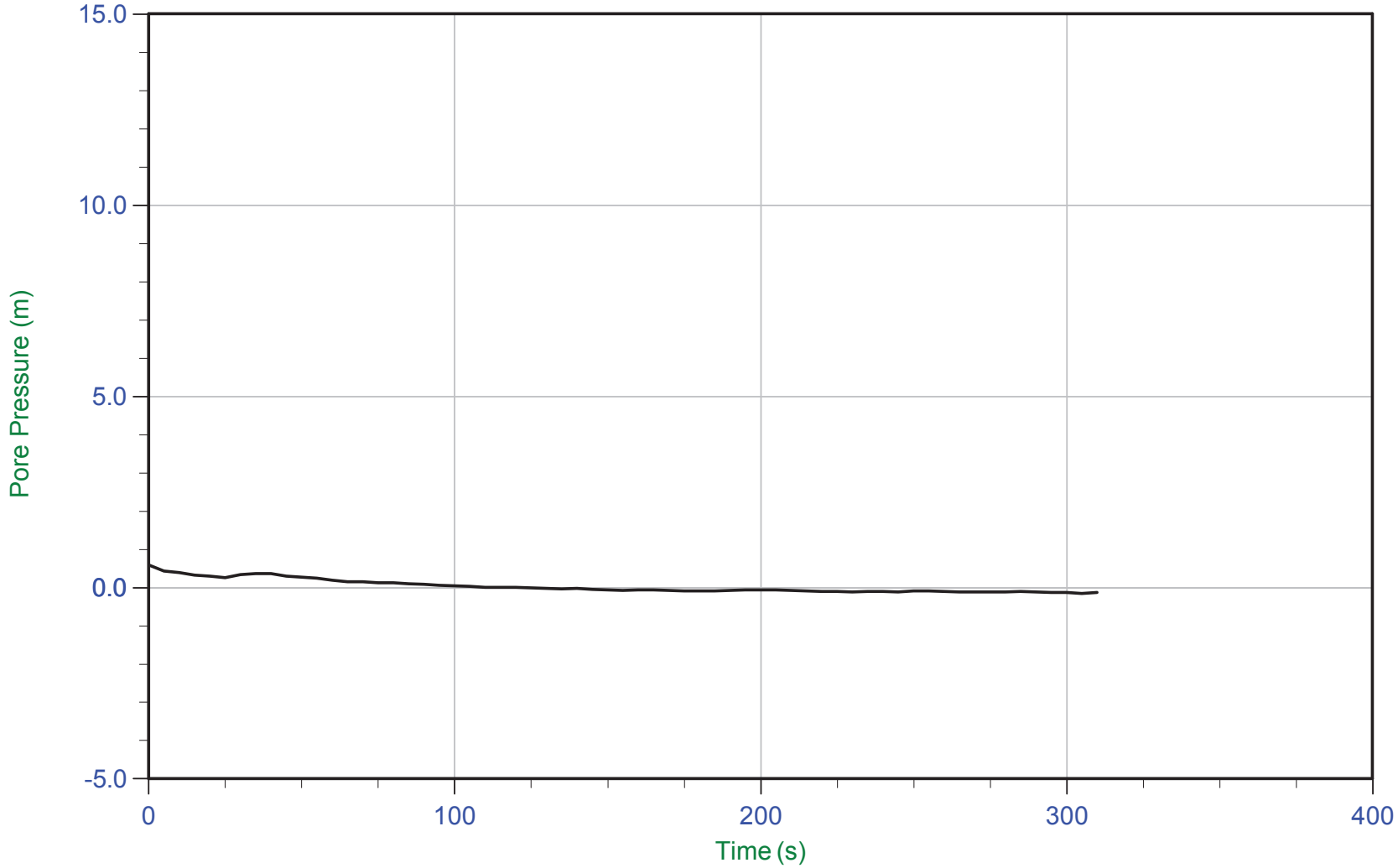

Trace Summary:

Filename: 16-72004_RS04.PPF
Depth: 1.400 m / 4.593 ft
Duration: 310.0 s

U Min: -0.1 m
U Max: 0.6 m

WT: 0.000 m / 0.000 ft
Ueq: 0.0 m

CONETEC

CGSH

Job No: 1672007
Date: 05/02/2016 15:34
Site: Bay 3, Germano Cava

Sounding: GCCPT16-04
Cone: 376:T375F10U200
Cone Area: 15 sq cm

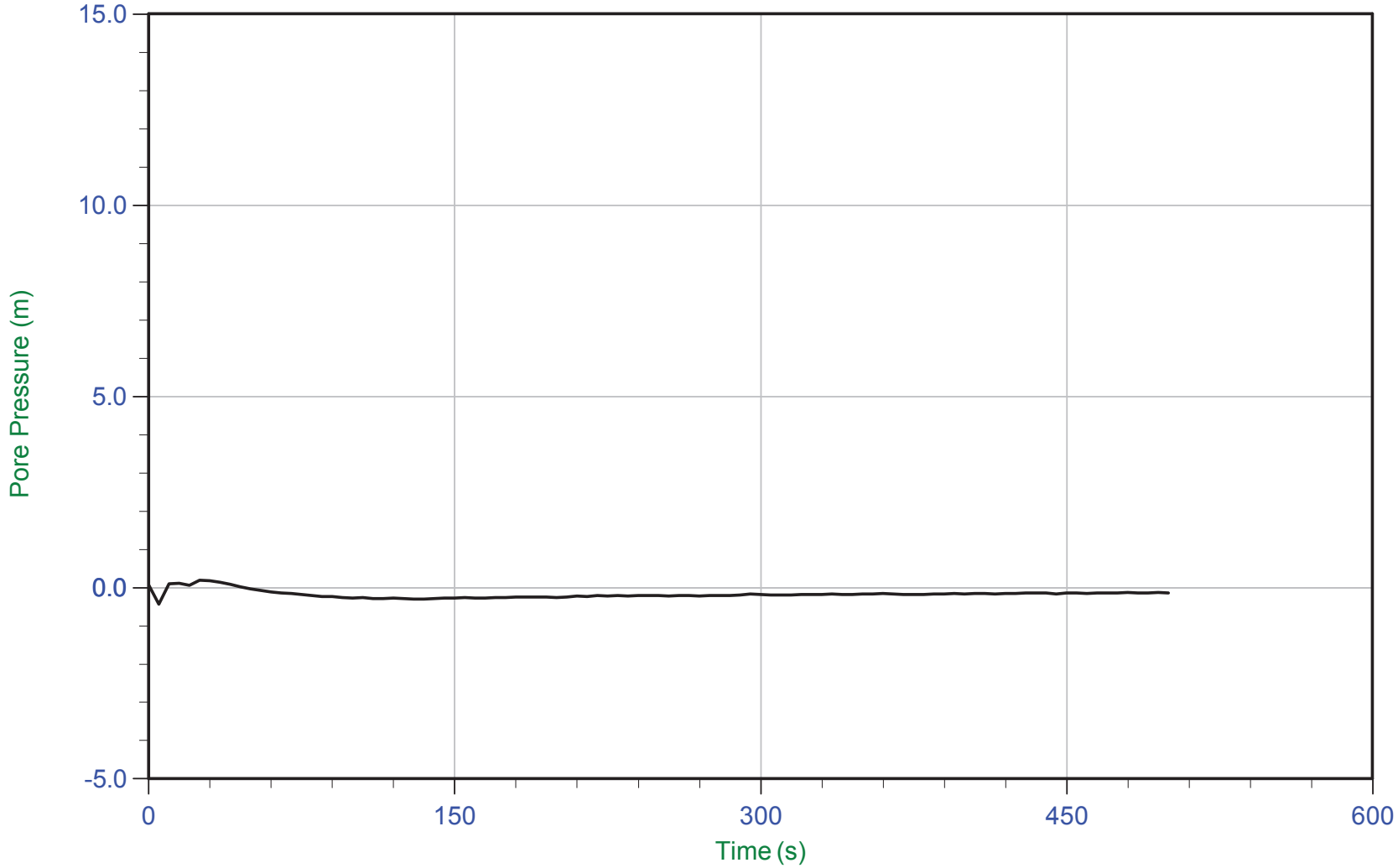

Trace Summary:

Filename: 16-72004_RS04.PPF
Depth: 5.400 m / 17.716 ft
Duration: 500.0 s

U Min: -0.4 m
U Max: 0.2 m

WT: 0.000 m / 0.000 ft
Ueq: 0.0 m

CONETEC

CGSH

Job No: 1672007
Date: 05/02/2016 15:34
Site: Bay 3, Germano Cava

Sounding: GCCPT16-04
Cone: 376:T375F10U200
Cone Area: 15 sq cm

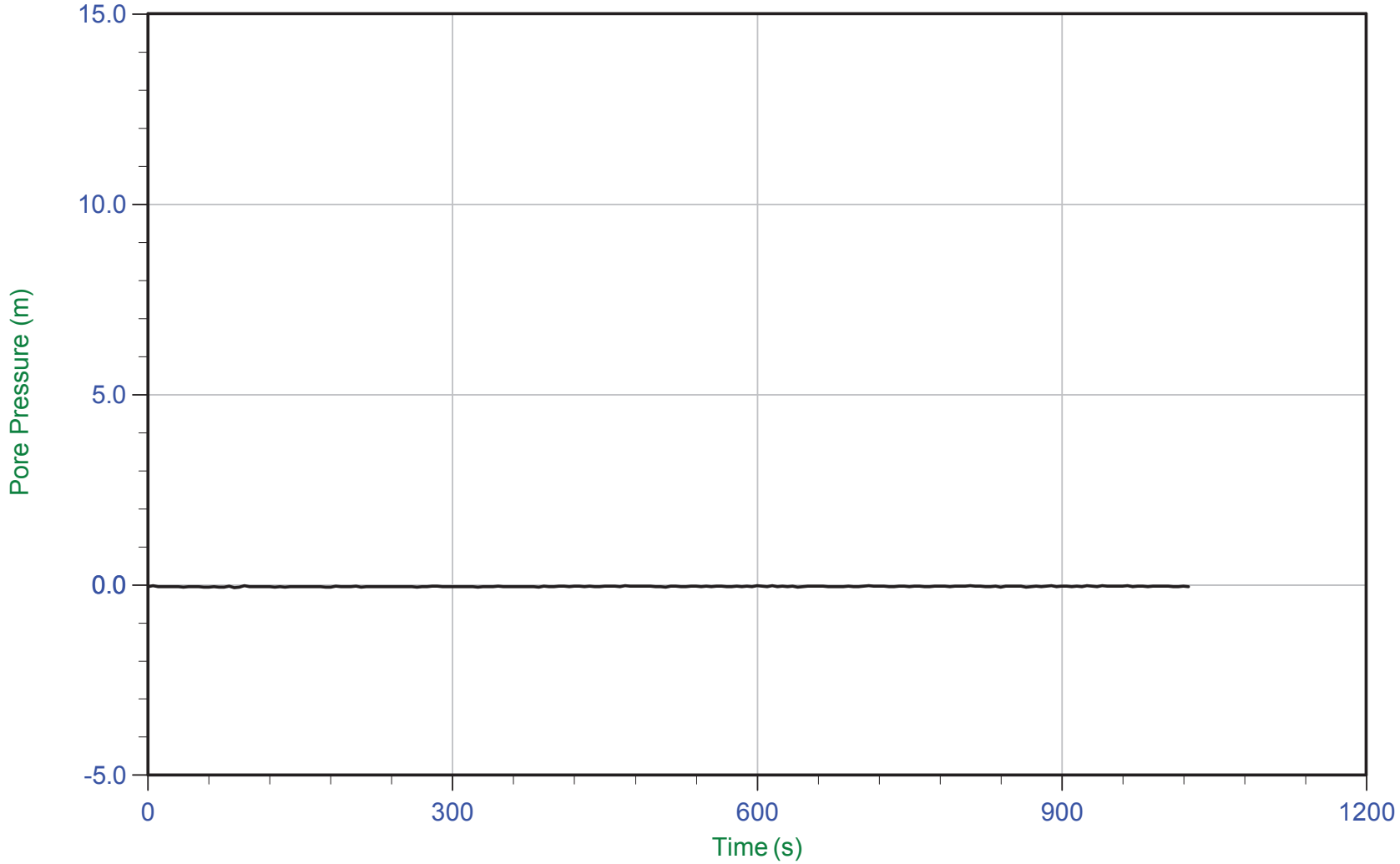

Trace Summary:

Filename: 16-72004_RS04.PPF
Depth: 10.400 m / 34.120 ft
Duration: 1025.0 s

U Min: -0.1 m
U Max: -0.0 m

WT: 0.000 m / 0.000 ft
Ueq: 0.0 m

CONETEC

CGSH

Job No: 1672007
Date: 05/02/2016 15:34
Site: Bay 3, Germano Cava

Sounding: GCCPT16-04
Cone: 376:T375F10U200
Cone Area: 15 sq cm

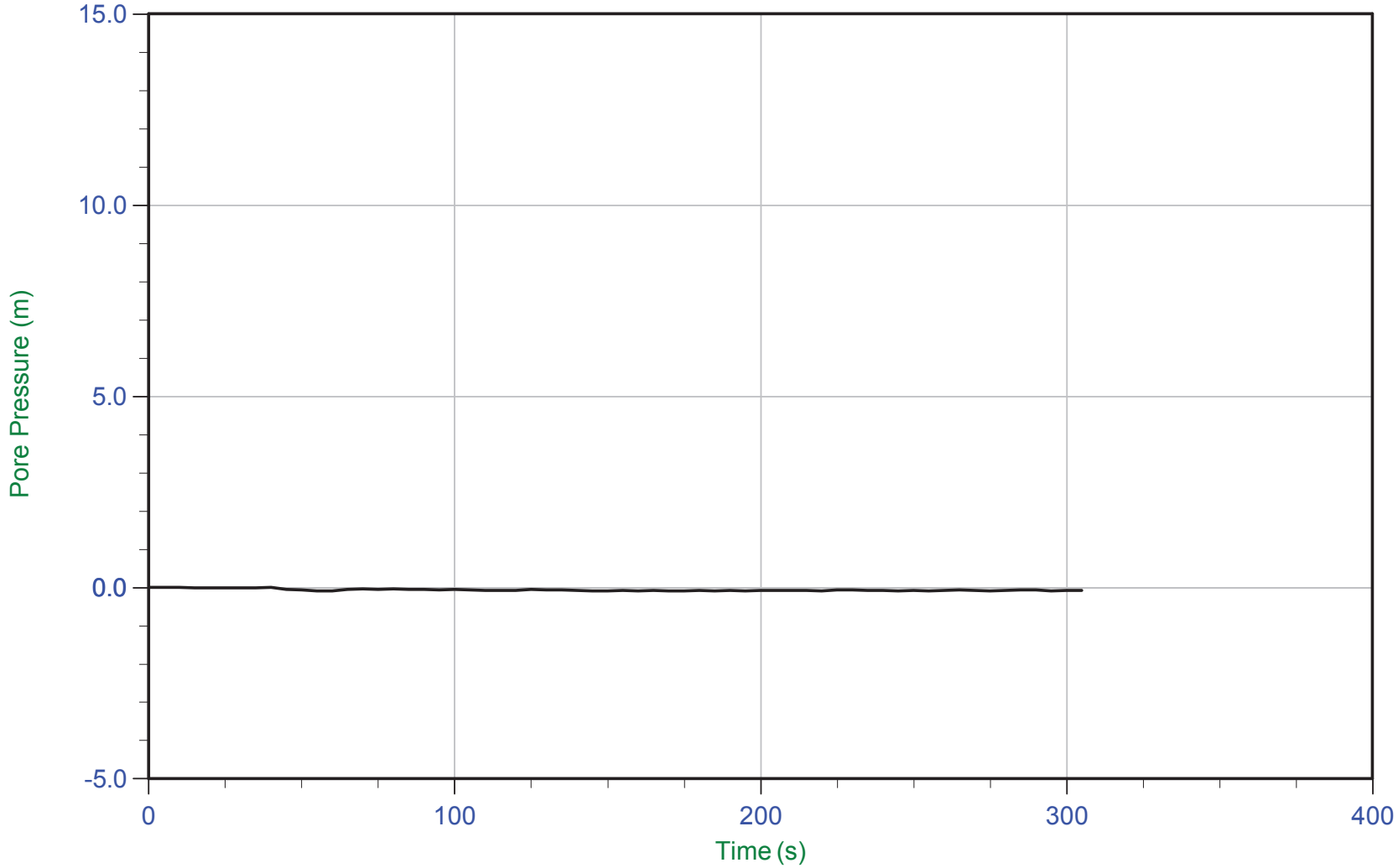

Trace Summary:

Filename: 16-72004_RS04.PPF
Depth: 11.350 m / 37.237 ft
Duration: 305.0 s

U Min: -0.1 m
U Max: 0.0 m

WT: 0.000 m / 0.000 ft
Ueq: 0.0 m

CONETEC

CGSH

Job No: 1672007
Date: 05/02/2016 15:34
Site: Bay 3, Germano Cava

Sounding: GCCPT16-04
Cone: 376:T375F10U200
Cone Area: 15 sq cm

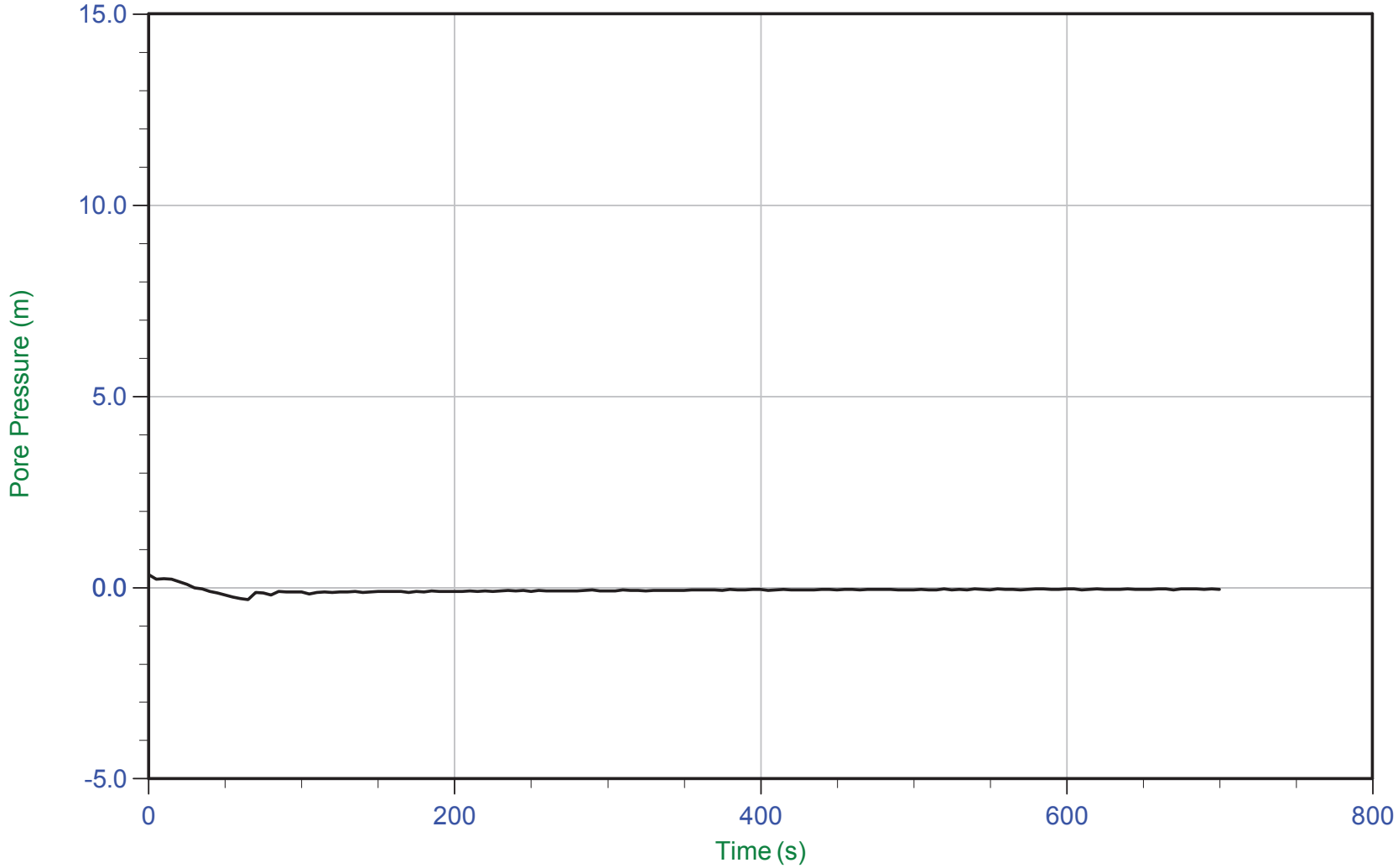

Trace Summary:

Filename: 16-72004_RS04.PPF
Depth: 15.400 m / 50.524 ft
Duration: 700.0 s

U Min: -0.3 m
U Max: 0.3 m

WT: 0.000 m / 0.000 ft
Ueq: 0.0 m

CONETEC

CGSH

Job No: 1672007
Date: 05/02/2016 15:34
Site: Bay 3, Germano Cava

Sounding: GCCPT16-04
Cone: 376:T375F10U200
Cone Area: 15 sq cm

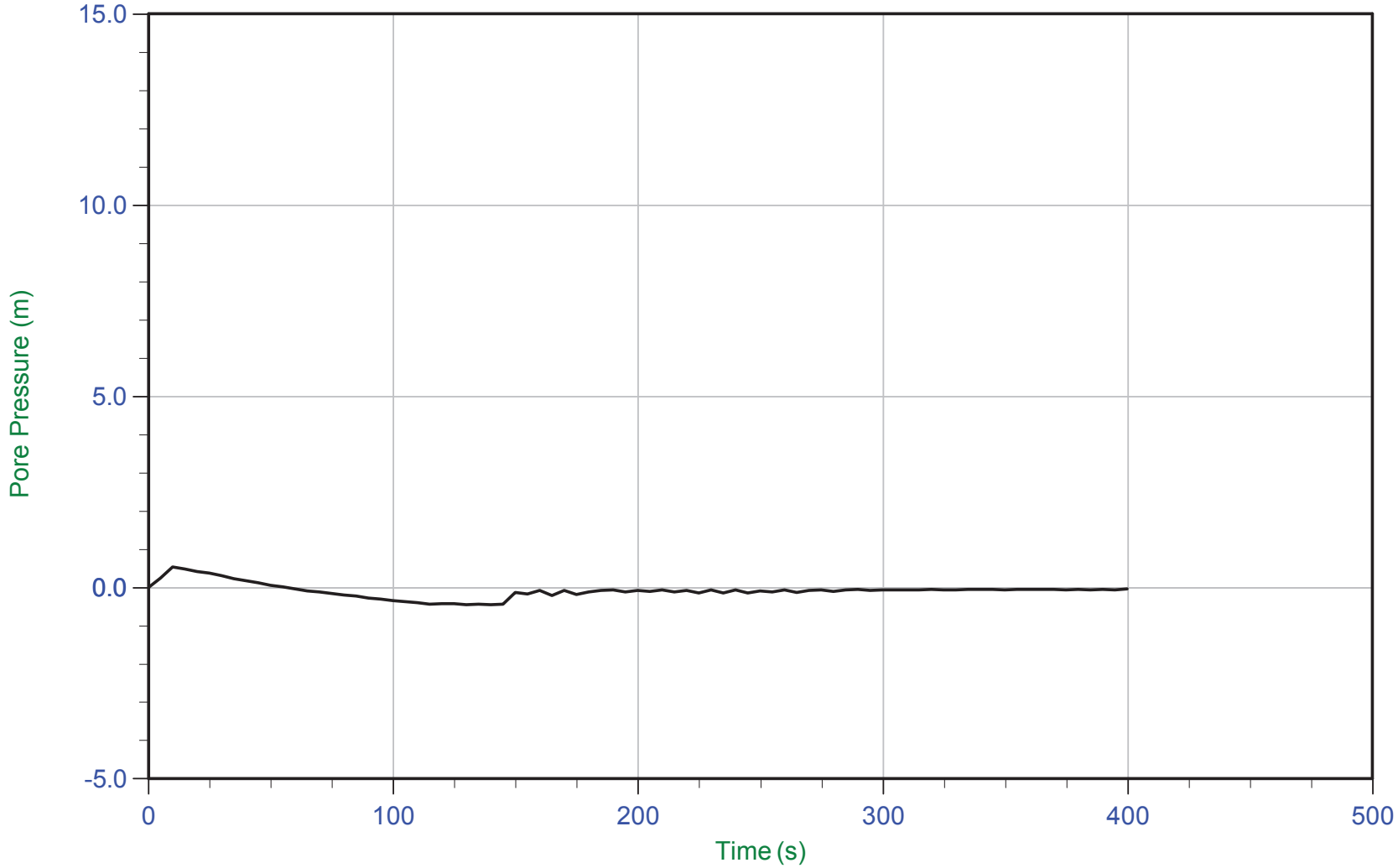

Trace Summary:

Filename: 16-72004_RS04.PPF
Depth: 20.400 m / 66.928 ft
Duration: 400.0 s

U Min: -0.5 m
U Max: 0.5 m

WT: 0.000 m / 0.000 ft
Ueq: 0.0 m

CONETEC

CGSH

Job No: 1672007
Date: 05/02/2016 15:34
Site: Bay 3, Germano Cava

Sounding: GCCPT16-04
Cone: 376:T375F10U200
Cone Area: 15 sq cm

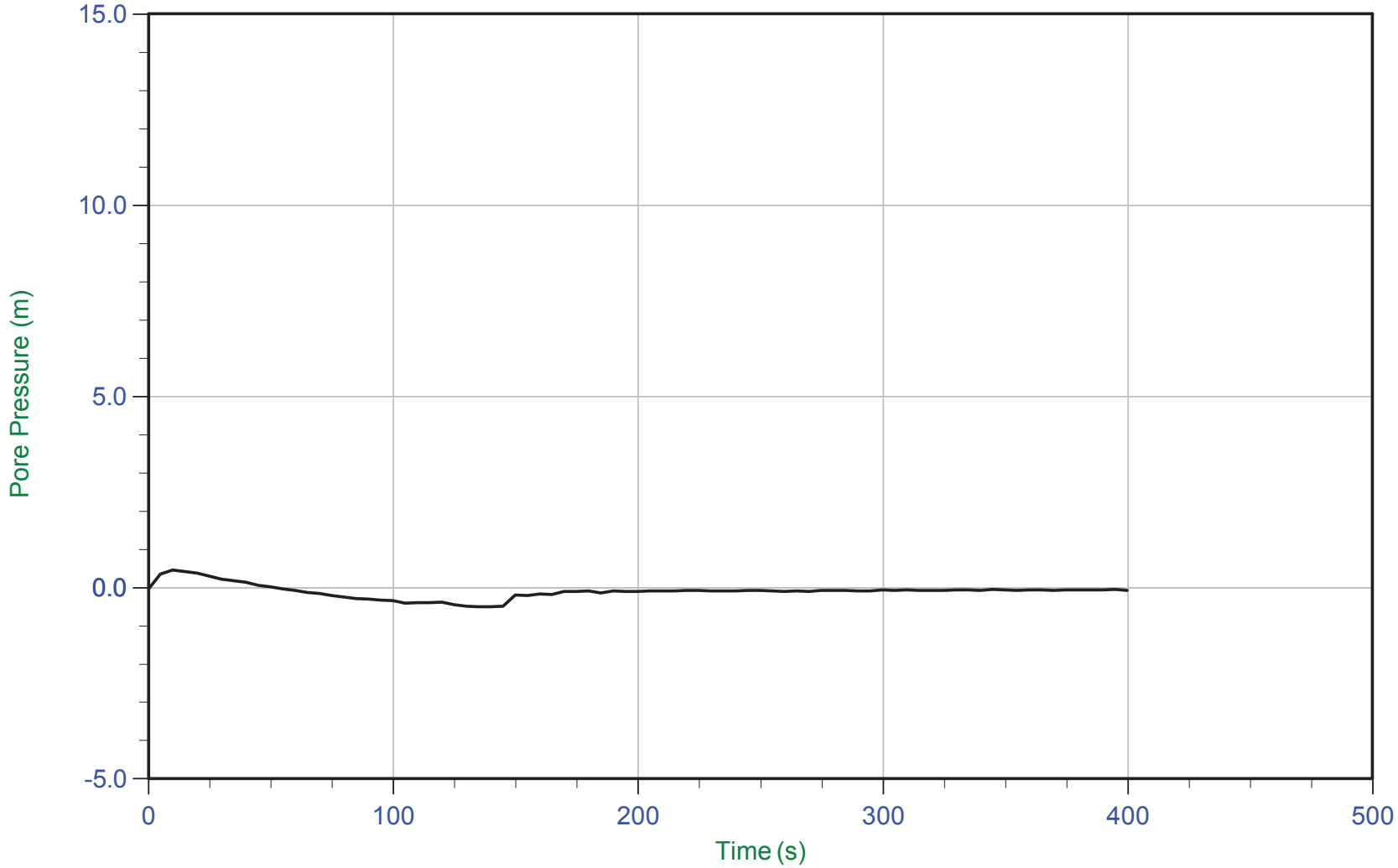

Trace Summary:

Filename: 16-72004_RS04.PPF
Depth: 25.400 m / 83.332 ft
Duration: 400.0 s

U Min: -0.5 m
U Max: 0.5 m

WT: 0.000 m / 0.000 ft
Ueq: 0.0 m

CONETEC

CGSH

Job No: 1672007
Date: 05/02/2016 15:34
Site: Bay 3, Germano Cava

Sounding: GCCPT16-04
Cone: 376:T375F10U200
Cone Area: 15 sq cm

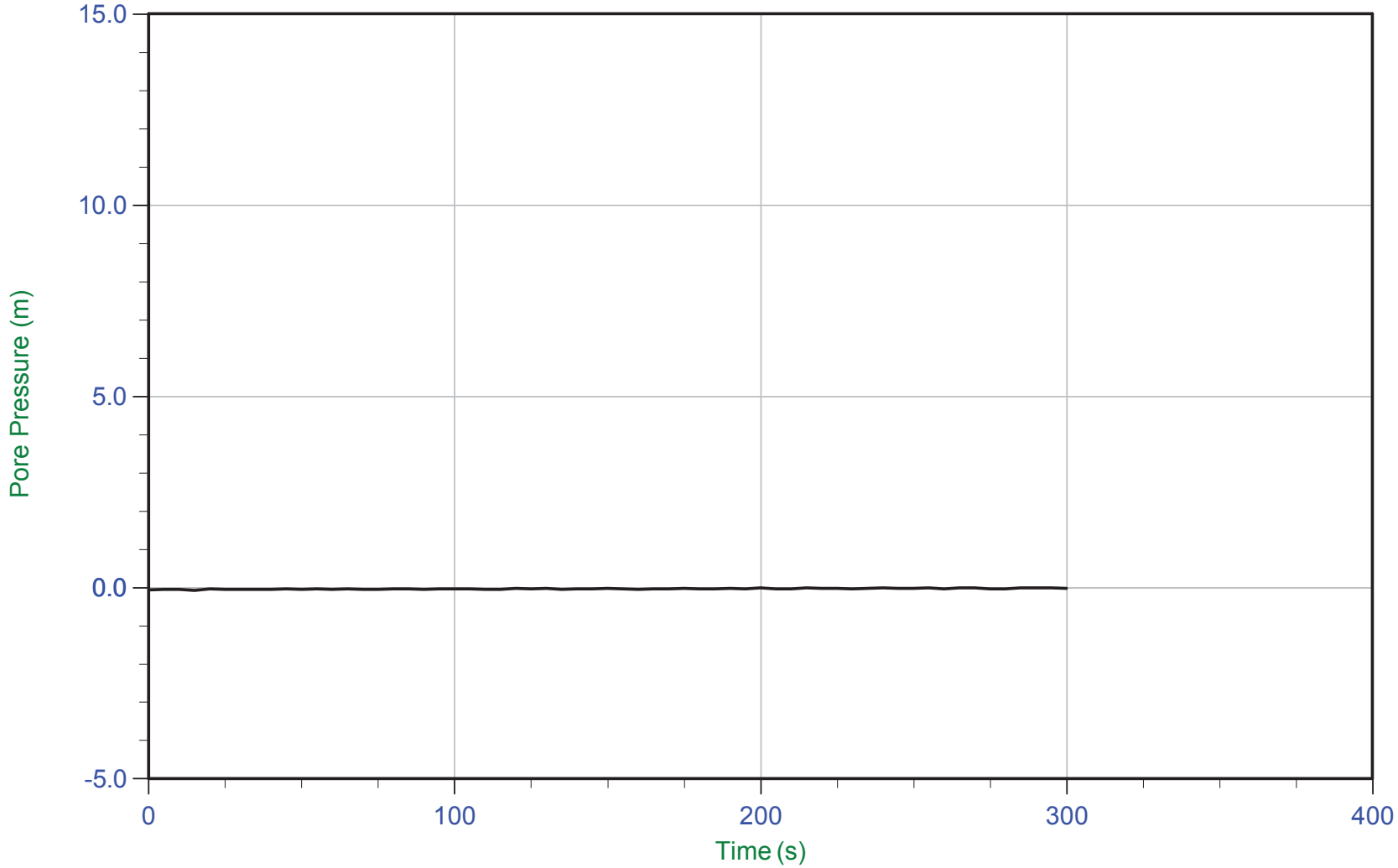

Trace Summary:

Filename: 16-72004_RS04.PPF
Depth: 30.400 m / 99.736 ft
Duration: 300.0 s

U Min: -0.1 m
U Max: -0.0 m

WT: 0.000 m / 0.000 ft
Ueq: 0.0 m

CONETEC

CGSH

Job No: 1672007
Date: 05/02/2016 15:34
Site: Bay 3, Germano Cava

Sounding: GCCPT16-04
Cone: 376:T375F10U200
Cone Area: 15 sq cm

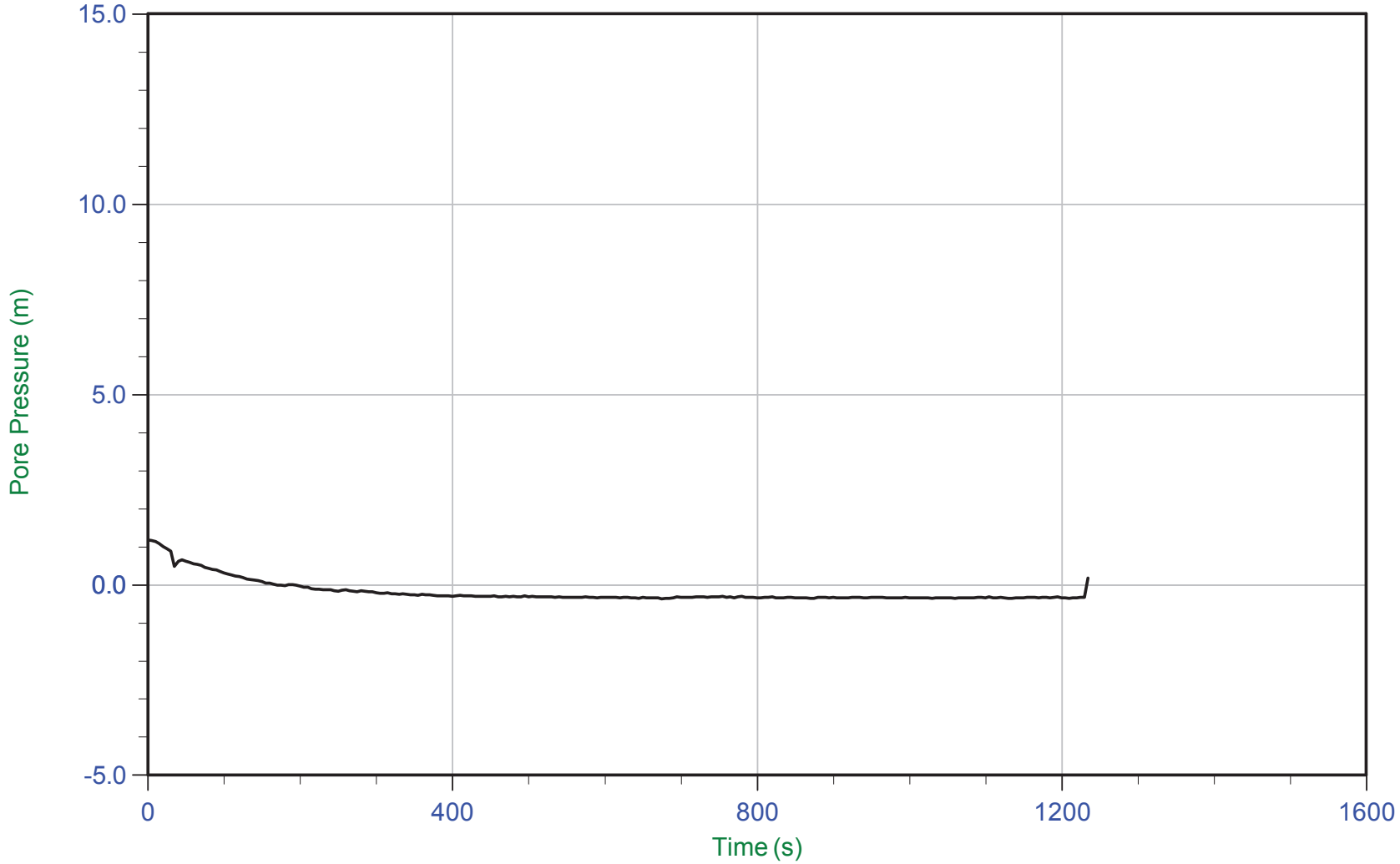

Trace Summary:

Filename: 16-72004_RS04.PPF
Depth: 32.150 m / 105.478 ft
Duration: 1235.0 s

U Min: -0.4 m
U Max: 1.2 m

WT: 0.000 m / 0.000 ft
Ueq: 0.0 m

CONETEC

CGSH

Job No: 1672007
Date: 05/02/2016 15:34
Site: Bay 3, Germano Cava

Sounding: GCCPT16-04
Cone: 376:T375F10U200
Cone Area: 15 sq cm

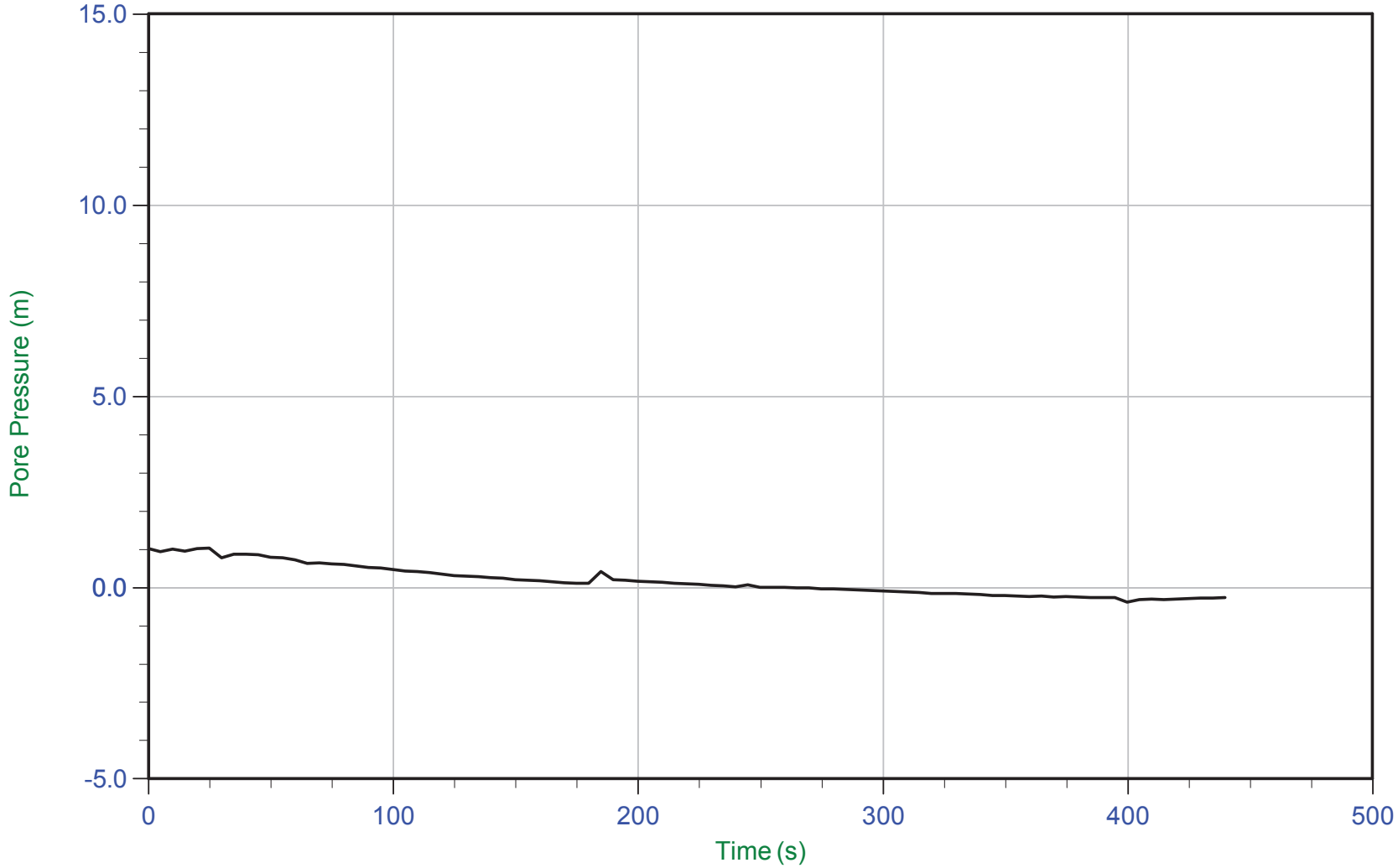

Trace Summary:

Filename: 16-72004_RS04.PPF
Depth: 32.400 m / 106.298 ft
Duration: 440.0 s

U Min: -0.4 m
U Max: 1.0 m

WT: 0.000 m / 0.000 ft
Ueq: 0.0 m

CONETEC

CGSH

Job No: 1672007
Date: 05/13/2016 13:07
Site: Germano Cava

Sounding: GCCPT16-04B
Cone: 432:T1500F15U500
Cone Area: 15 sq cm

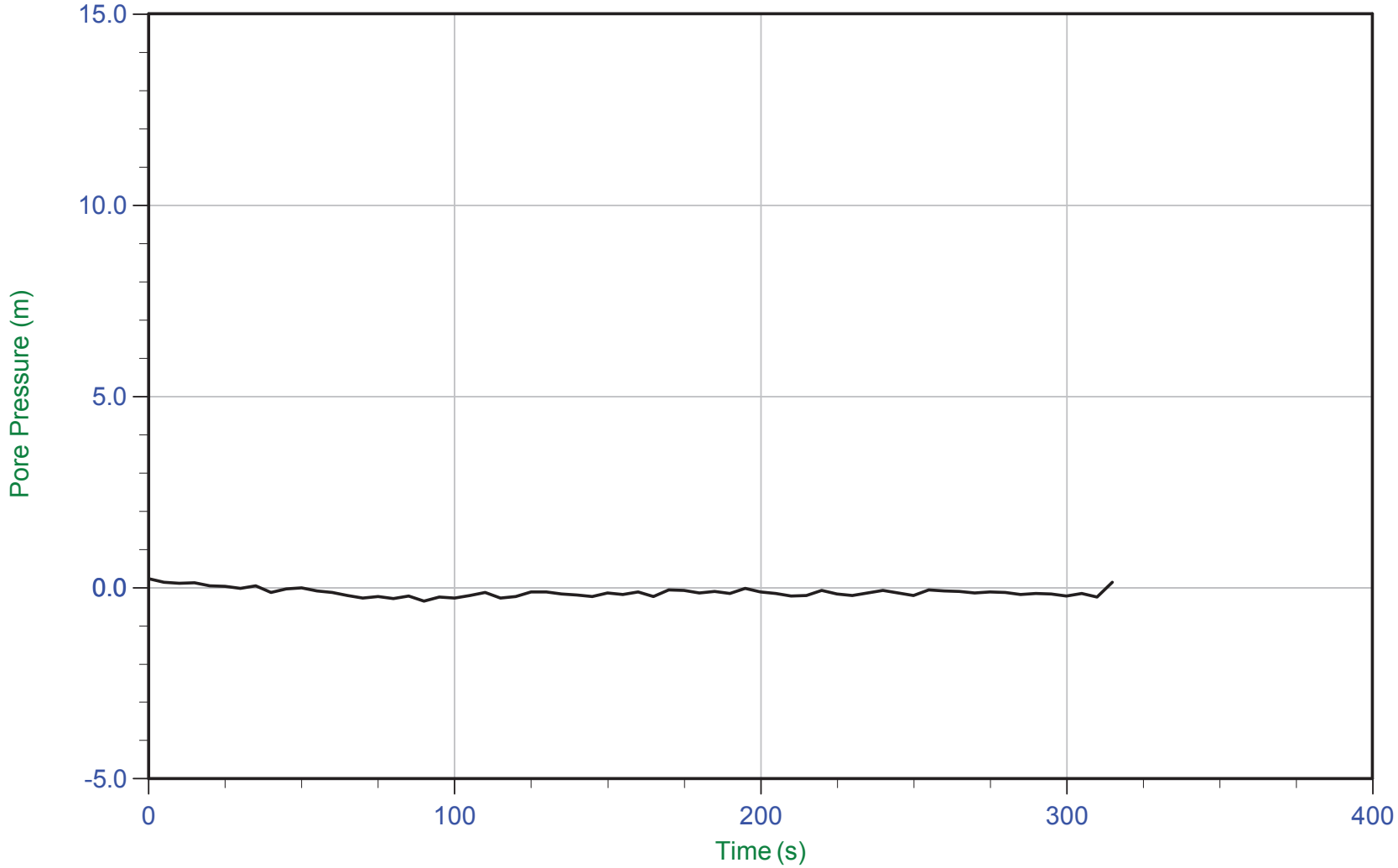

Trace Summary:

Filename: 16-72004_RS04B.PPF
Depth: 8.700 m / 28.543 ft
Duration: 315.0 s

U Min: -0.4 m
U Max: 0.2 m

WT: 0.000 m / 0.000 ft
Ueq: 0.0 m

CONETEC

CGSH

Job No: 1672007
Date: 05/13/2016 13:07
Site: Germano Cava

Sounding: GCCPT16-04B
Cone: 432:T1500F15U500
Cone Area: 15 sq cm

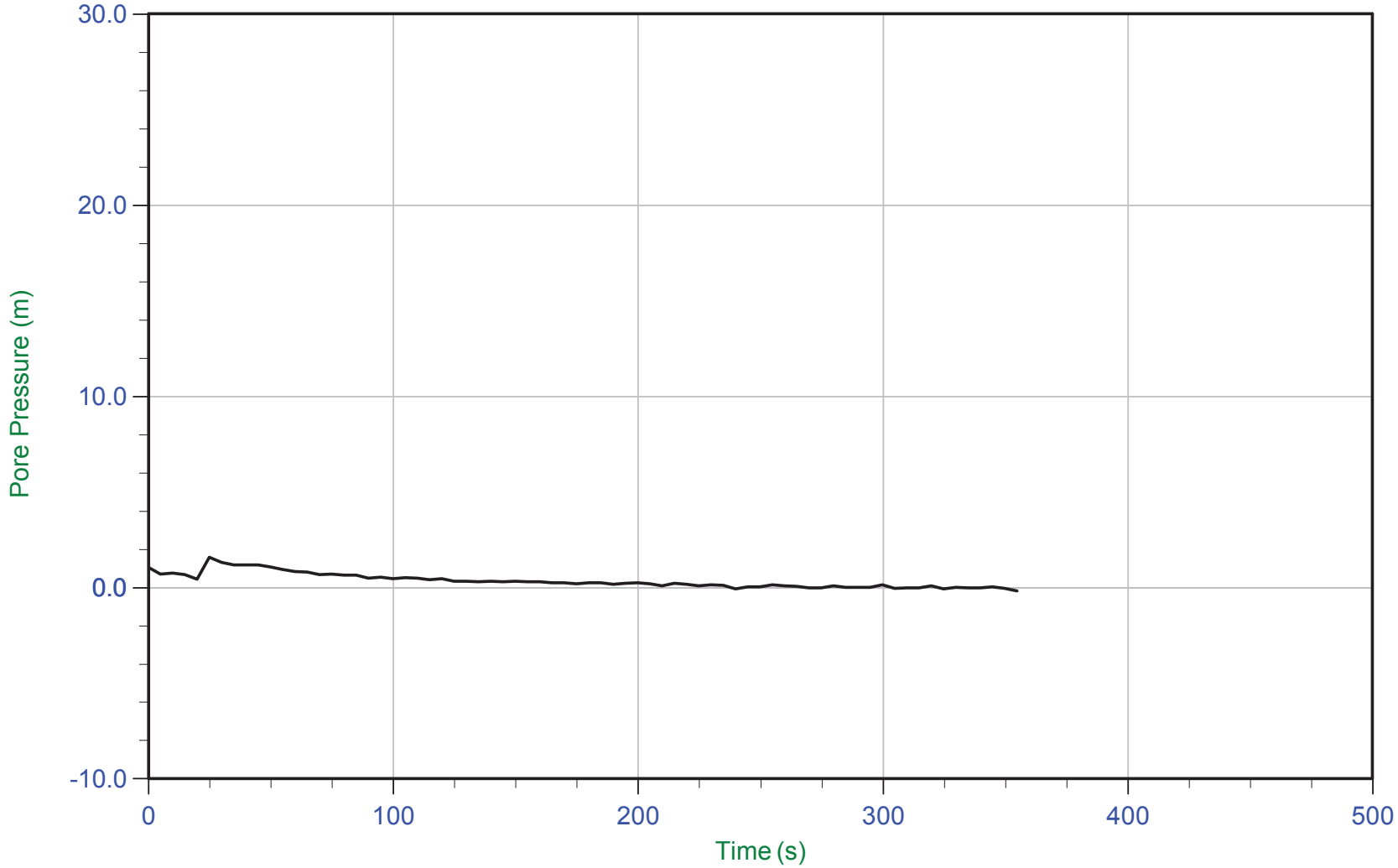

Trace Summary:

Filename: 16-72004_RS04B.PPF
Depth: 12.300 m / 40.354 ft
Duration: 355.0 s

U Min: -0.2 m
U Max: 1.6 m

WT: 0.000 m / 0.000 ft
Ueq: 0.0 m

CONETEC

CGSH

Job No: 1672007
Date: 05/13/2016 13:07
Site: Germano Cava

Sounding: GCCPT16-04B
Cone: 432:T1500F15U500
Cone Area: 15 sq cm

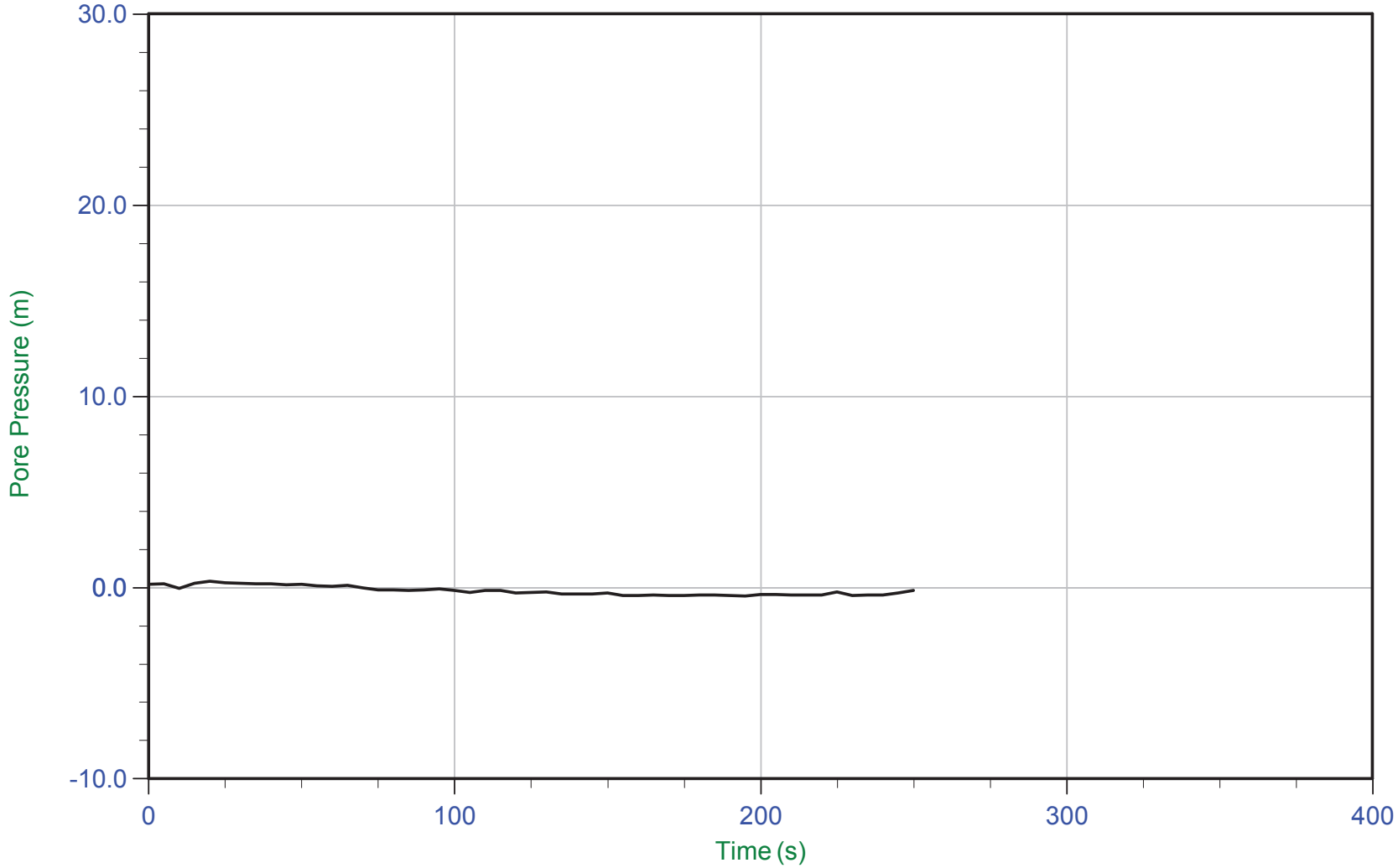

Trace Summary:

Filename: 16-72004_RS04B.PPF
Depth: 13.700 m / 44.947 ft
Duration: 250.0 s

U Min: -0.4 m
U Max: 0.3 m

WT: 0.000 m / 0.000 ft
Ueq: 0.0 m

CONETEC

CGSH

Job No: 1672007
Date: 05/13/2016 13:07
Site: Germano Cava

Sounding: GCCPT16-04B
Cone: 432:T1500F15U500
Cone Area: 15 sq cm

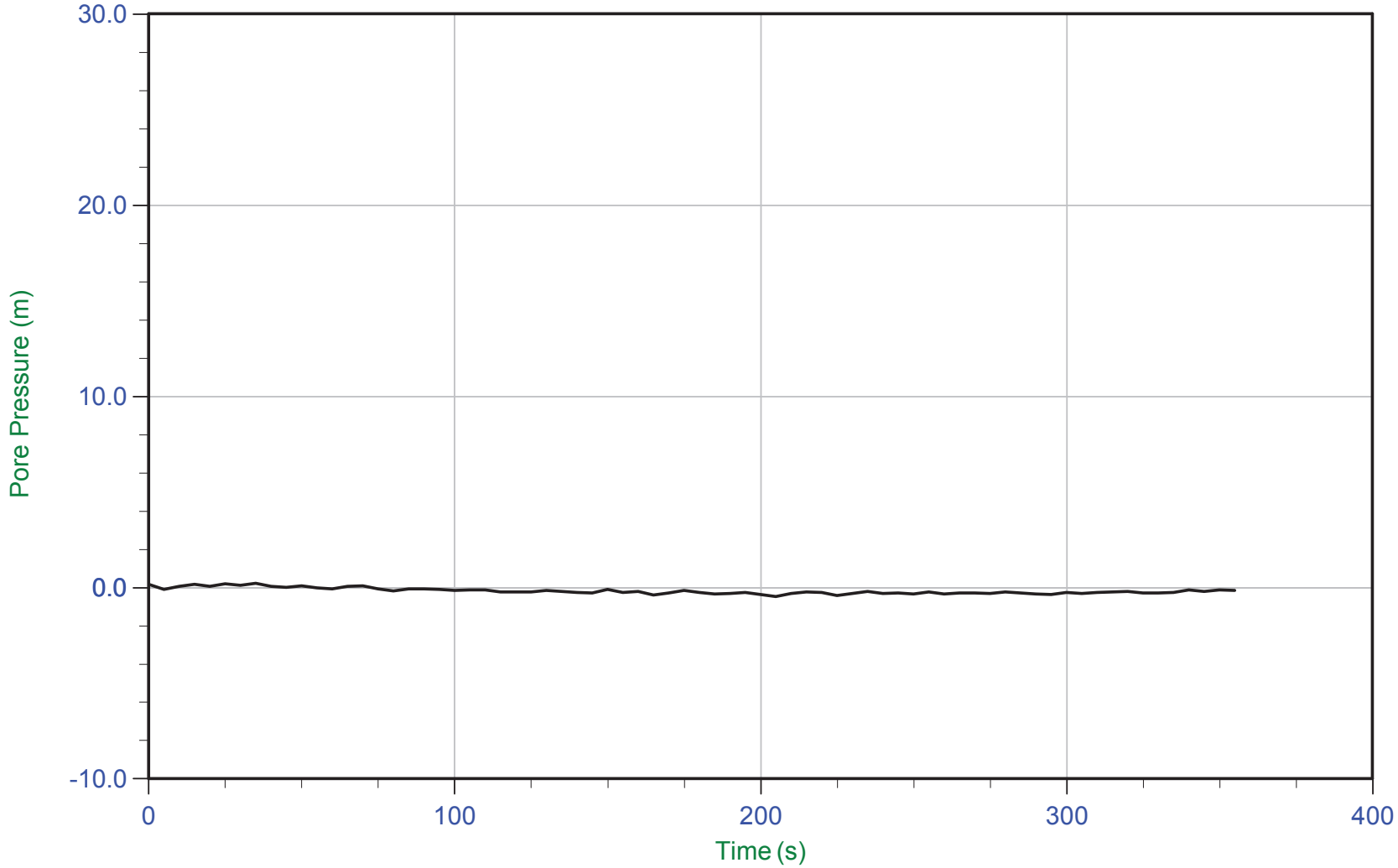

Trace Summary:

Filename: 16-72004_RS04B.PPF
Depth: 20.100 m / 65.944 ft
Duration: 355.0 s

U Min: -0.5 m
U Max: 0.2 m

WT: 0.000 m / 0.000 ft
Ueq: 0.0 m

CONETEC

CGSH

Job No: 1672007
Date: 05/13/2016 13:07
Site: Germano Cava

Sounding: GCCPT16-04B
Cone: 432:T1500F15U500
Cone Area: 15 sq cm

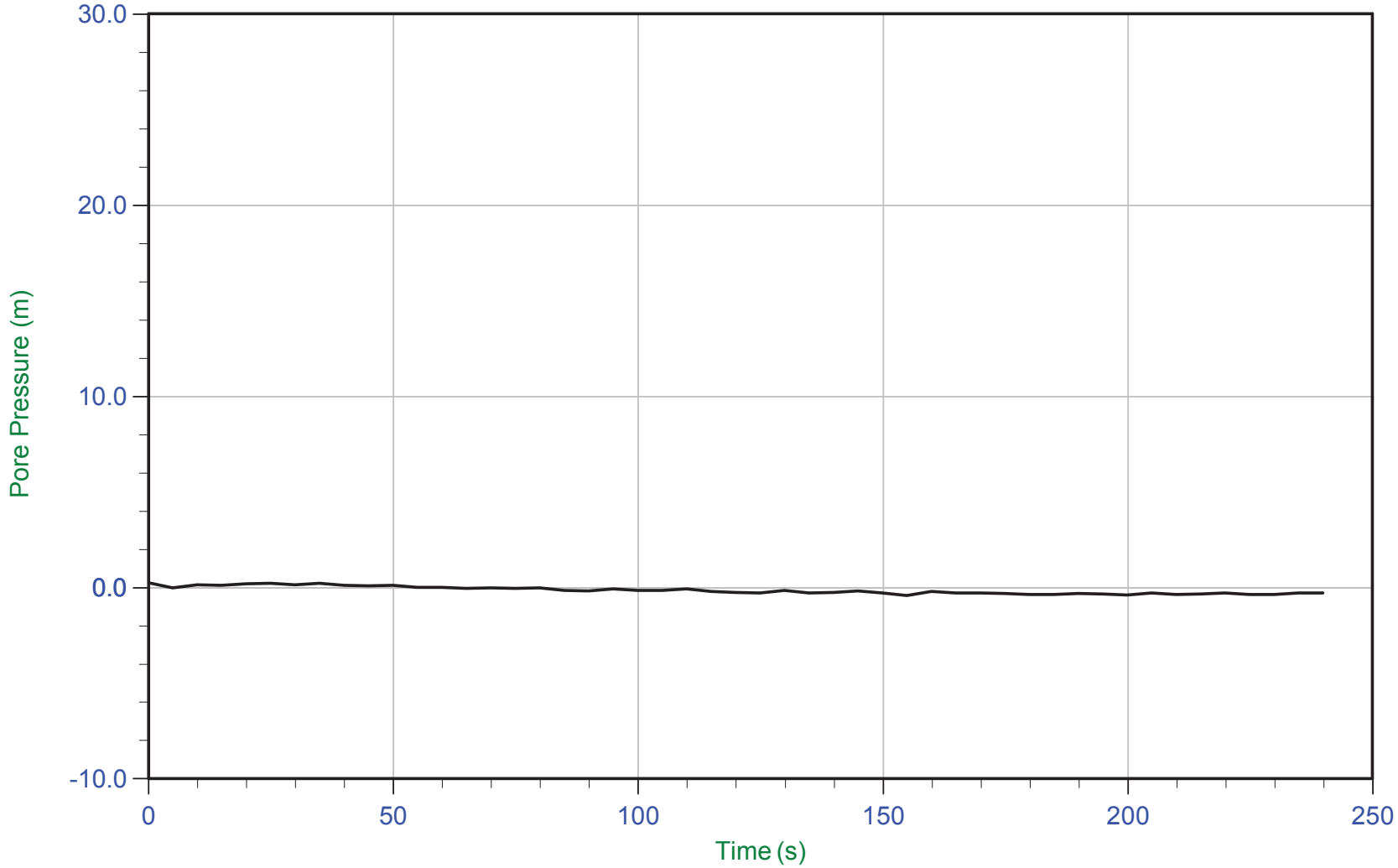

Trace Summary:

Filename: 16-72004_RS04B.PPF
Depth: 30.150 m / 98.916 ft
Duration: 240.0 s

U Min: -0.4 m
U Max: 0.3 m

WT: 0.000 m / 0.000 ft
Ueq: 0.0 m

CONETEC

CGSH

Job No: 1672007
Date: 05/13/2016 13:07
Site: Germano Cava

Sounding: GCCPT16-04B
Cone: 432:T1500F15U500
Cone Area: 15 sq cm

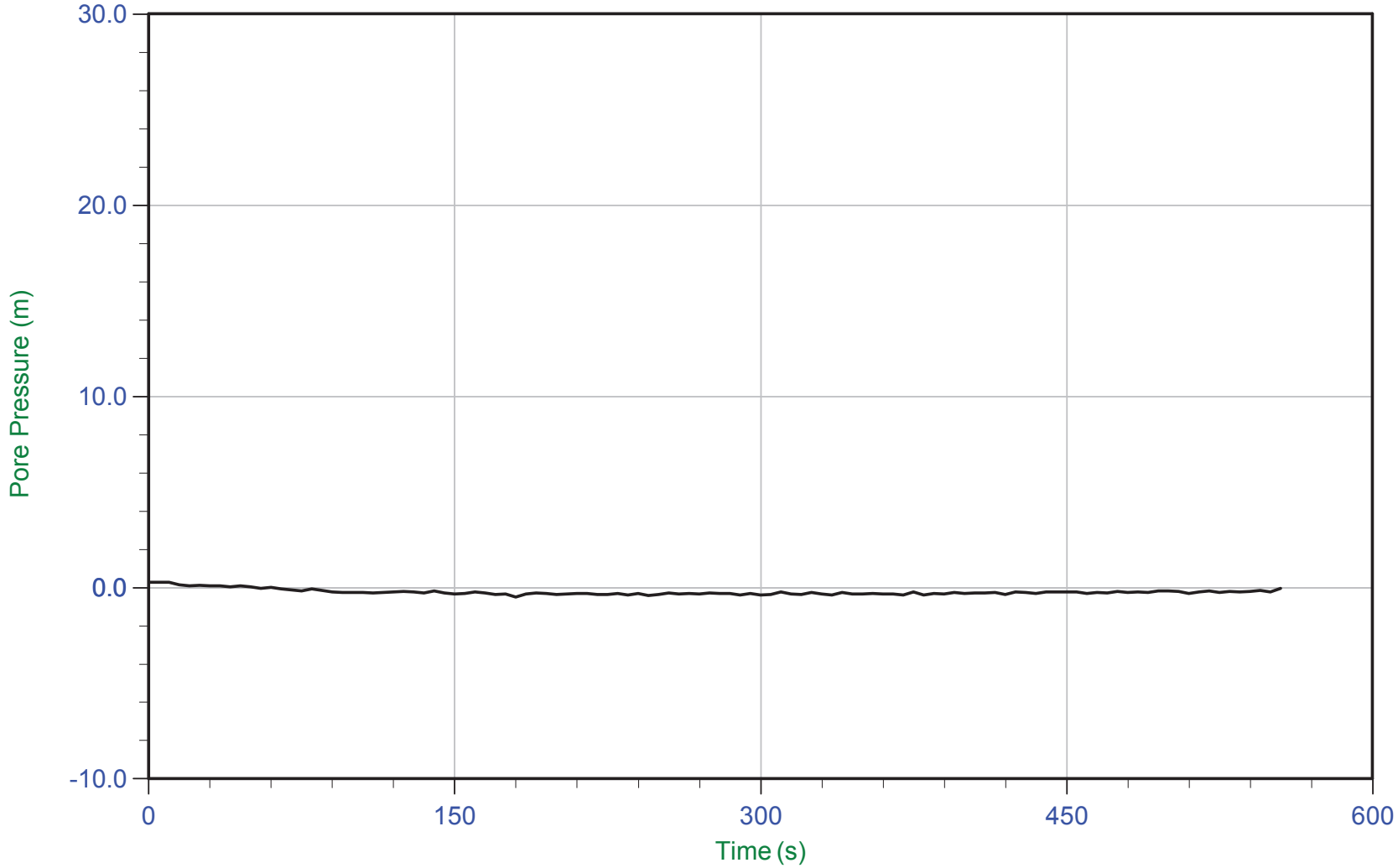

Trace Summary:

Filename: 16-72004_RS04B.PPF
Depth: 32.100 m / 105.314 ft
Duration: 555.0 s

U Min: -0.5 m
U Max: 0.3 m

WT: 0.000 m / 0.000 ft
Ueq: 0.0 m

CONETEC

CGSH

Job No: 1672007
Date: 05/13/2016 13:07
Site: Germano Cava

Sounding: GCCPT16-04B
Cone: 432:T1500F15U500
Cone Area: 15 sq cm

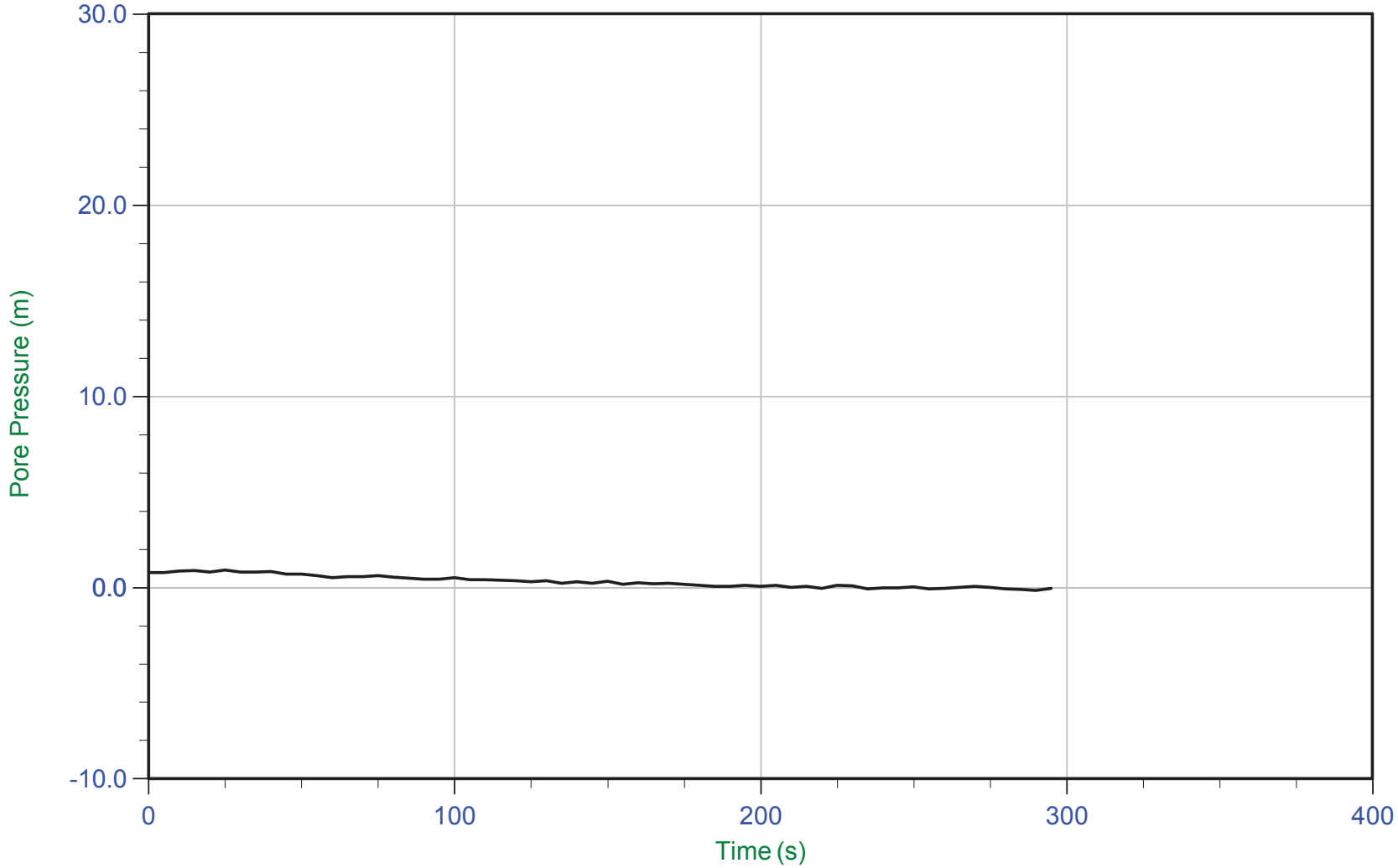

Trace Summary:

Filename: 16-72004_RS04B.PPF
Depth: 32.950 m / 108.102 ft
Duration: 295.0 s

U Min: -0.2 m
U Max: 0.9 m

WT: 0.000 m / 0.000 ft
Ueq: 0.0 m

CONETEC

CGSH

Job No: 1672007
Date: 05/13/2016 13:07
Site: Germano Cava

Sounding: GCCPT16-04B
Cone: 432:T1500F15U500
Cone Area: 15 sq cm

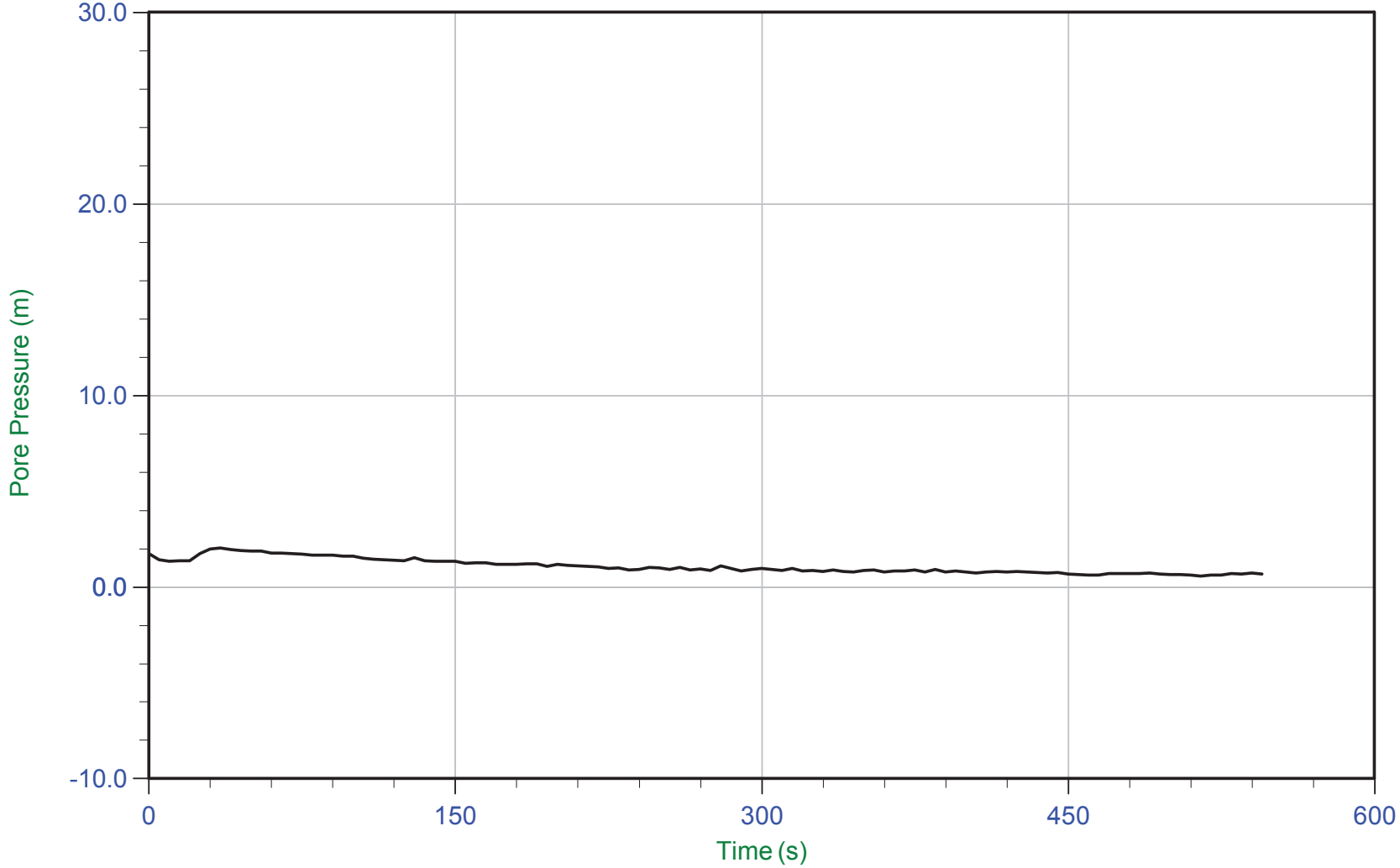

Trace Summary:

Filename: 16-72004_RS04B.PPF
Depth: 33.550 m / 110.071 ft
Duration: 545.0 s

U Min: 0.6 m
U Max: 2.0 m

CONETEC

CGSH

Job No: 1672007
Date: 05/13/2016 13:07
Site: Germano Cava

Sounding: GCCPT16-04B
Cone: 432:T1500F15U500
Cone Area: 15 sq cm

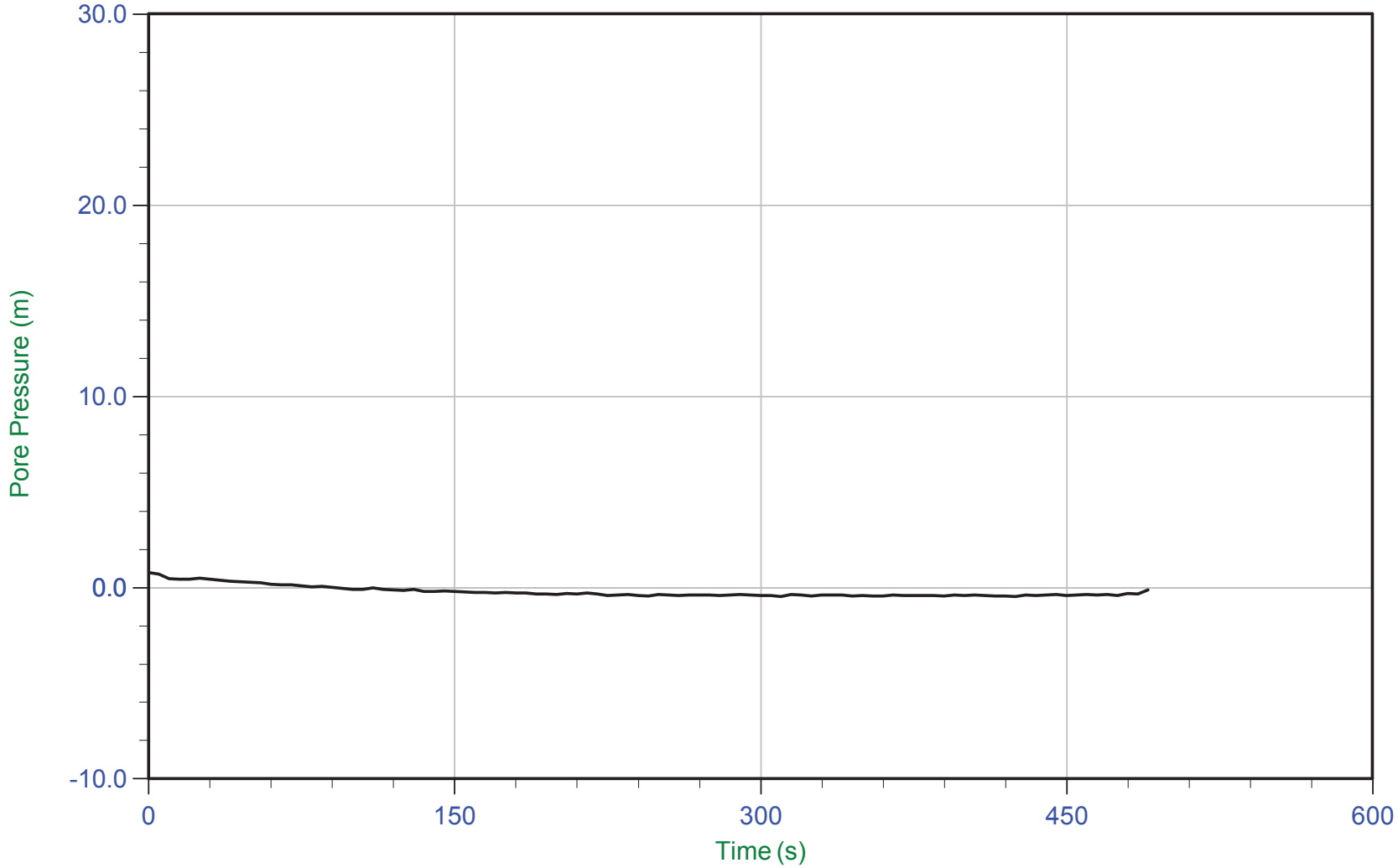

Trace Summary:

Filename: 16-72004_RS04B.PPF
Depth: 35.150 m / 115.320 ft
Duration: 490.0 s

U Min: -0.5 m
U Max: 0.8 m

WT: 0.000 m / 0.000 ft
Ueq: 0.0 m

CONETEC

CGSH

Job No: 1672007
Date: 05/13/2016 13:07
Site: Germano Cava

Sounding: GCCPT16-04B
Cone: 432:T1500F15U500
Cone Area: 15 sq cm

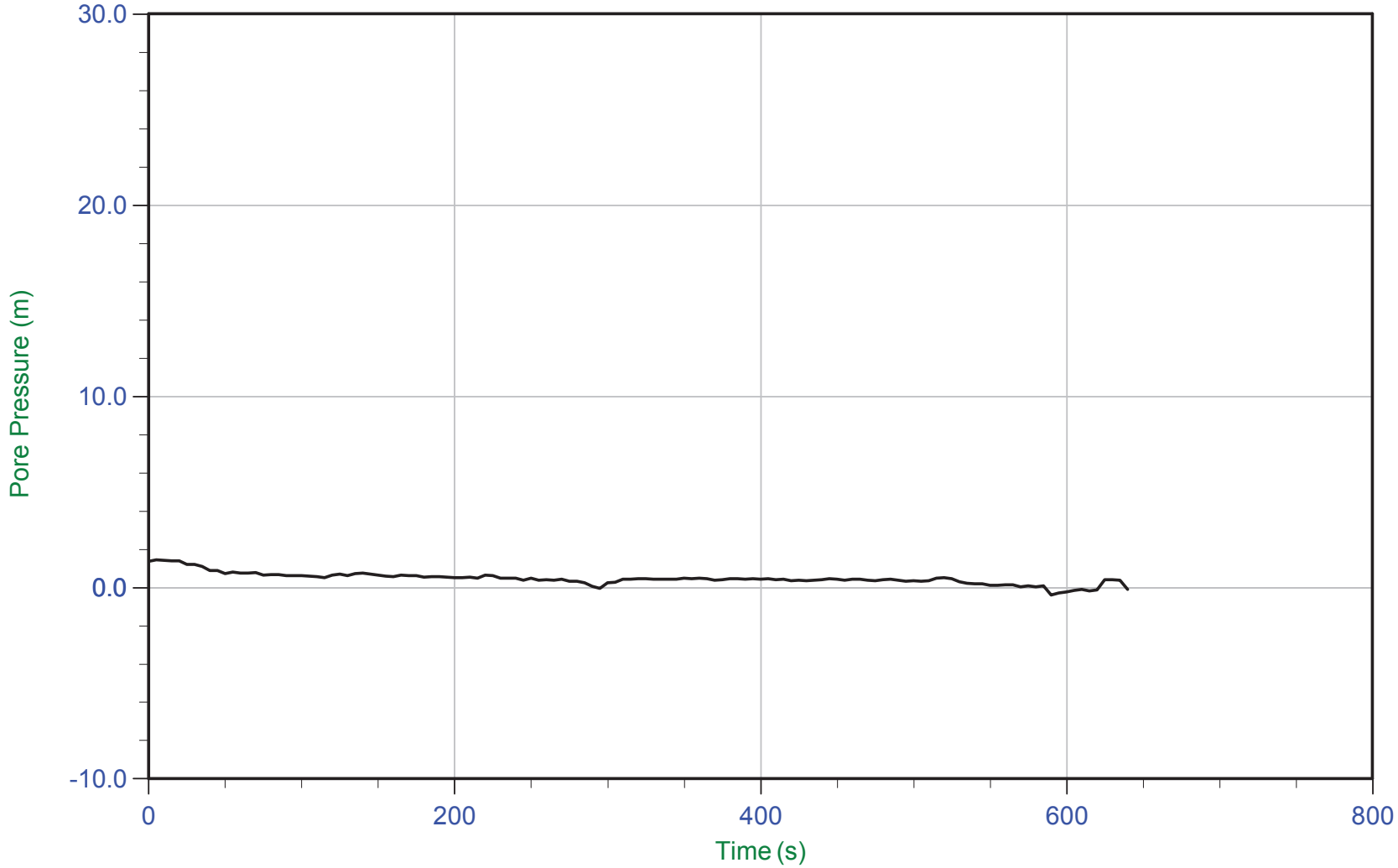

Trace Summary:

Filename: 16-72004_RS04B.PPF
Depth: 36.350 m / 119.257 ft
Duration: 640.0 s

U Min: -0.4 m
U Max: 1.4 m

WT: 36.350 m / 119.257 ft
Ueq: 0.0 m

CONETEC

CGSH

Job No: 1672007
Date: 05/05/2016 10:41
Site: Bay 3, Germano Slimes

Sounding: GSCPT16-05
Cone: 376:T375F10U200
Cone Area: 15 sq cm

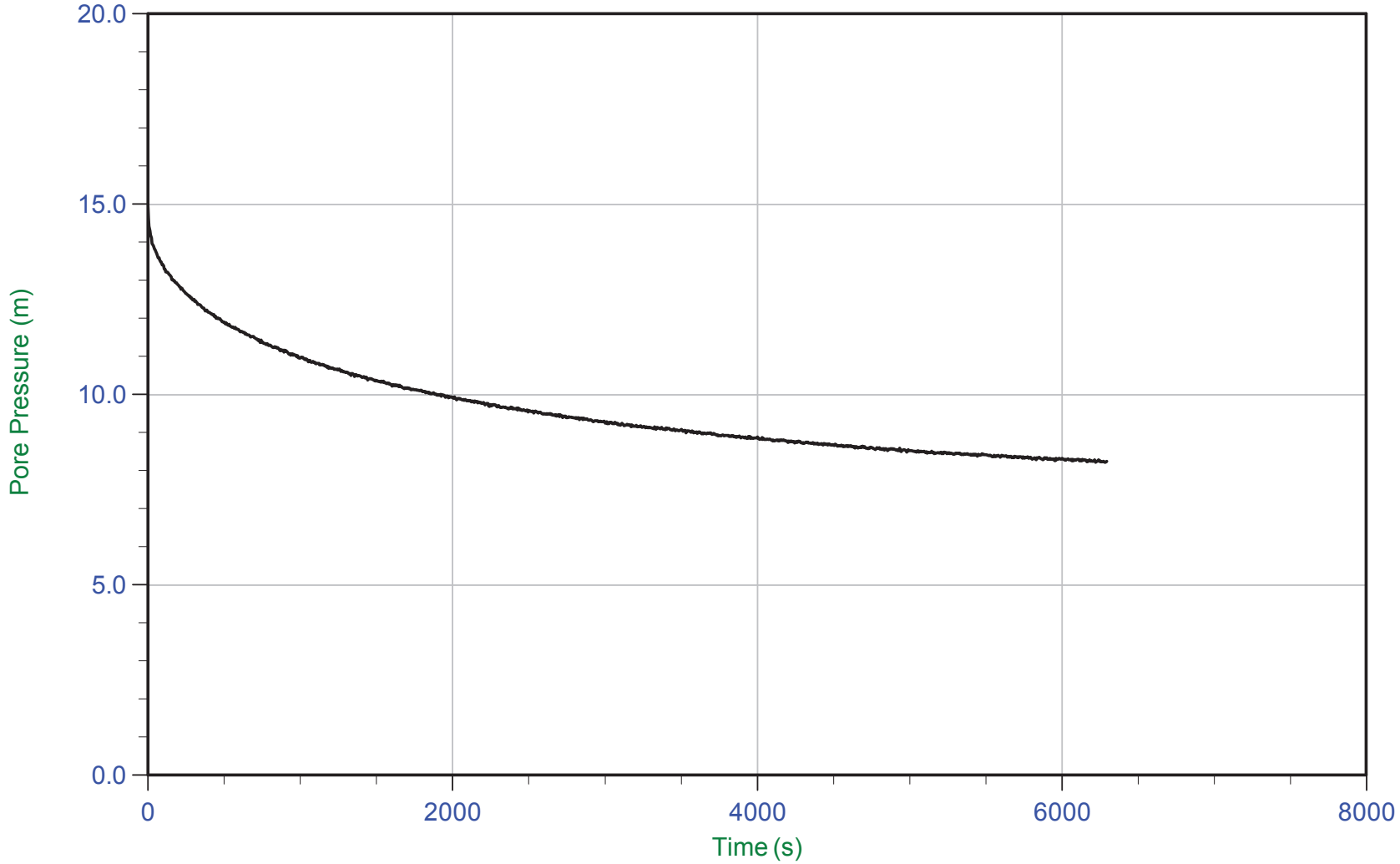

Trace Summary:

Filename: 16-72004_SP05.PPF
Depth: 5.050 m / 16.568 ft
Duration: 6300.0 s

U Min: 8.2 m
U Max: 14.9 m

CONETEC

CGSH

Job No: 1672007
Date: 05/05/2016 10:41
Site: Bay 3, Germano Slimes

Sounding: GSCPT16-05
Cone: 376:T375F10U200
Cone Area: 15 sq cm

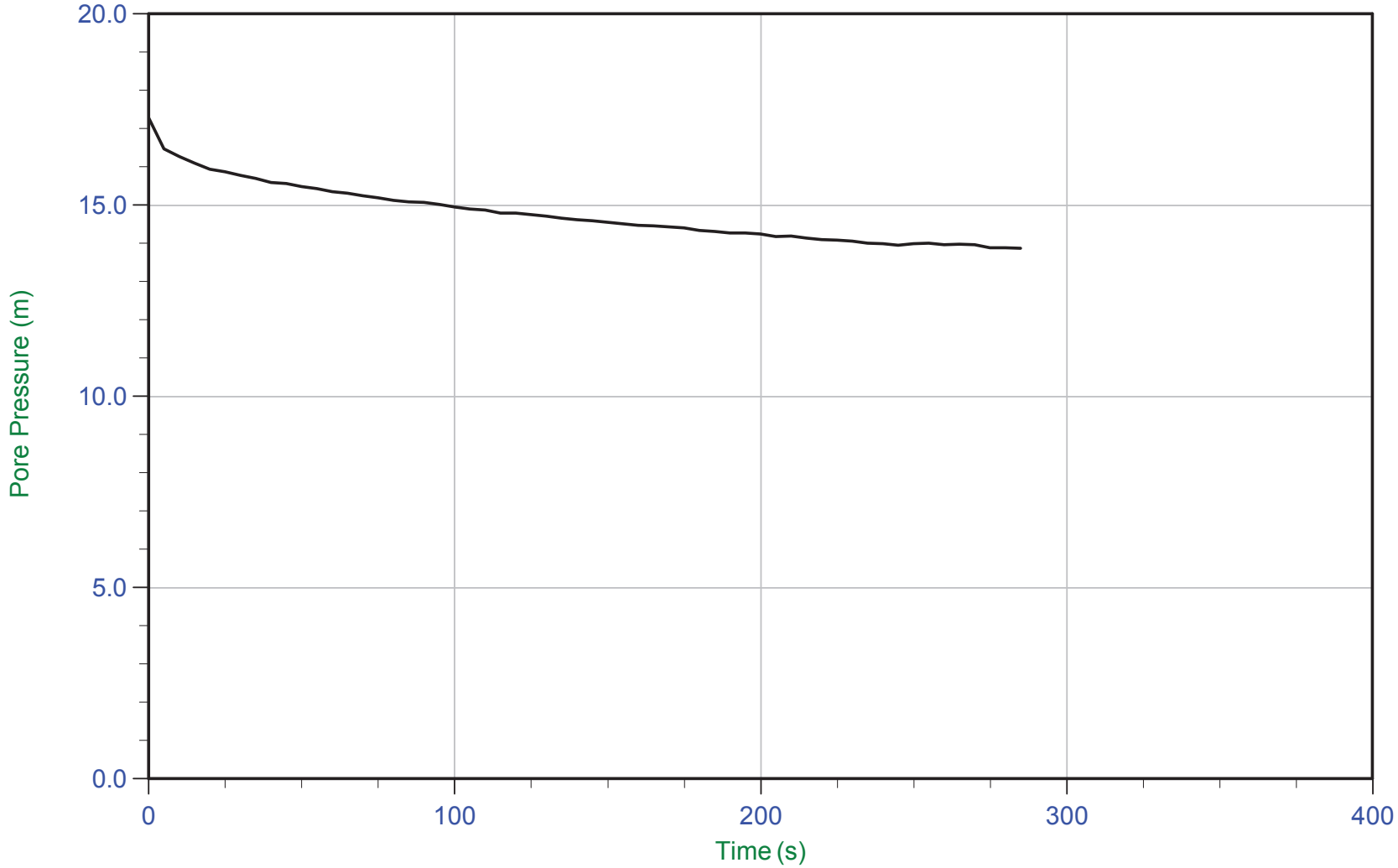

Trace Summary:

Filename: 16-72004_SP05.PPF
Depth: 6.050 m / 19.849 ft
Duration: 285.0 s

U Min: 13.9 m
U Max: 17.3 m

CONETEC

CGSH

Job No: 1672007
Date: 05/05/2016 10:41
Site: Bay 3, Germano Slimes

Sounding: GSCPT16-05
Cone: 376:T375F10U200
Cone Area: 15 sq cm

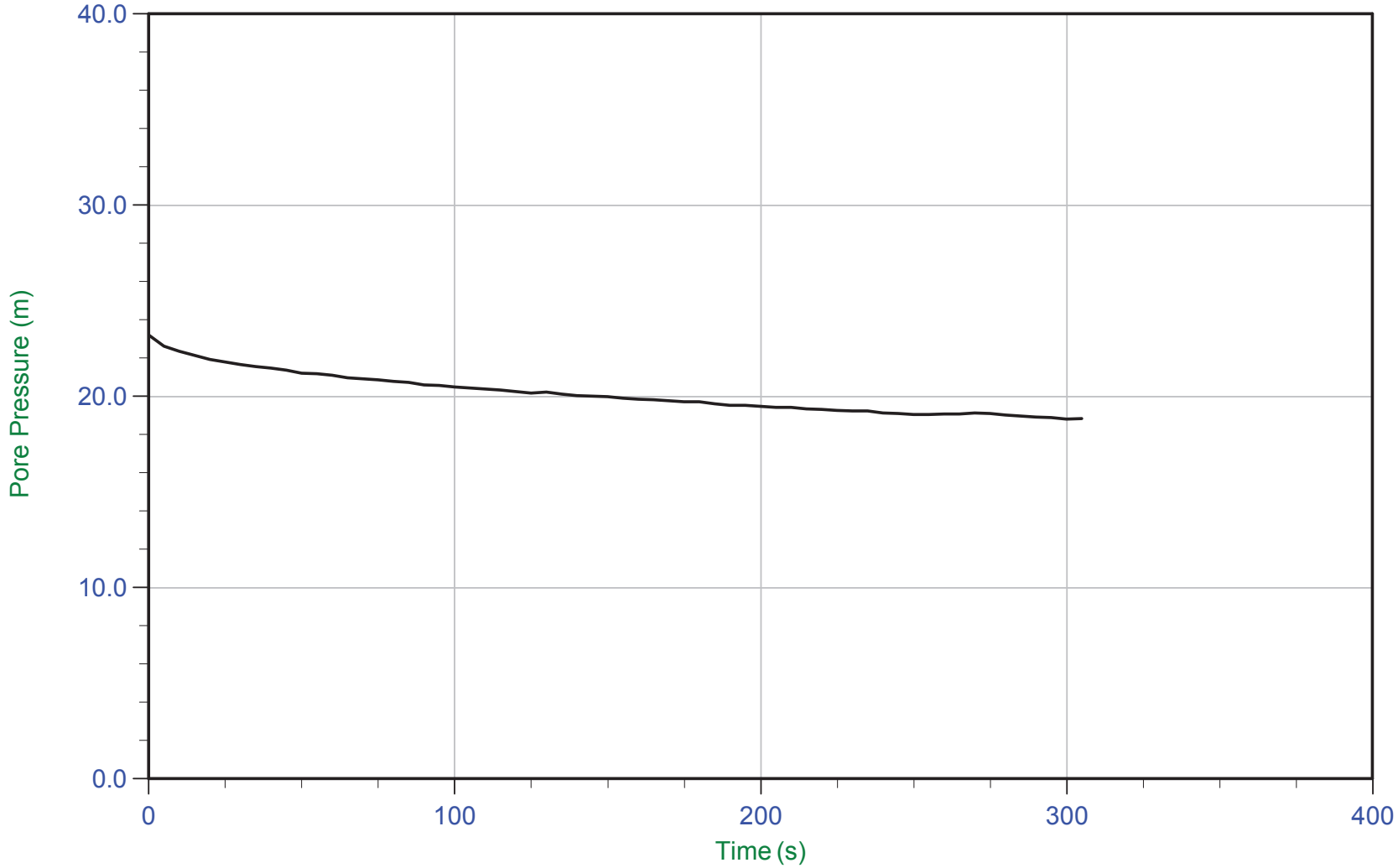

Trace Summary:

Filename: 16-72004_SP05.PPF
Depth: 8.050 m / 26.410 ft
Duration: 305.0 s

U Min: 18.8 m
U Max: 23.2 m

CONETEC

CGSH

Job No: 1672007
Date: 05/05/2016 10:41
Site: Bay 3, Germano Slimes

Sounding: GSCPT16-05
Cone: 376:T375F10U200
Cone Area: 15 sq cm

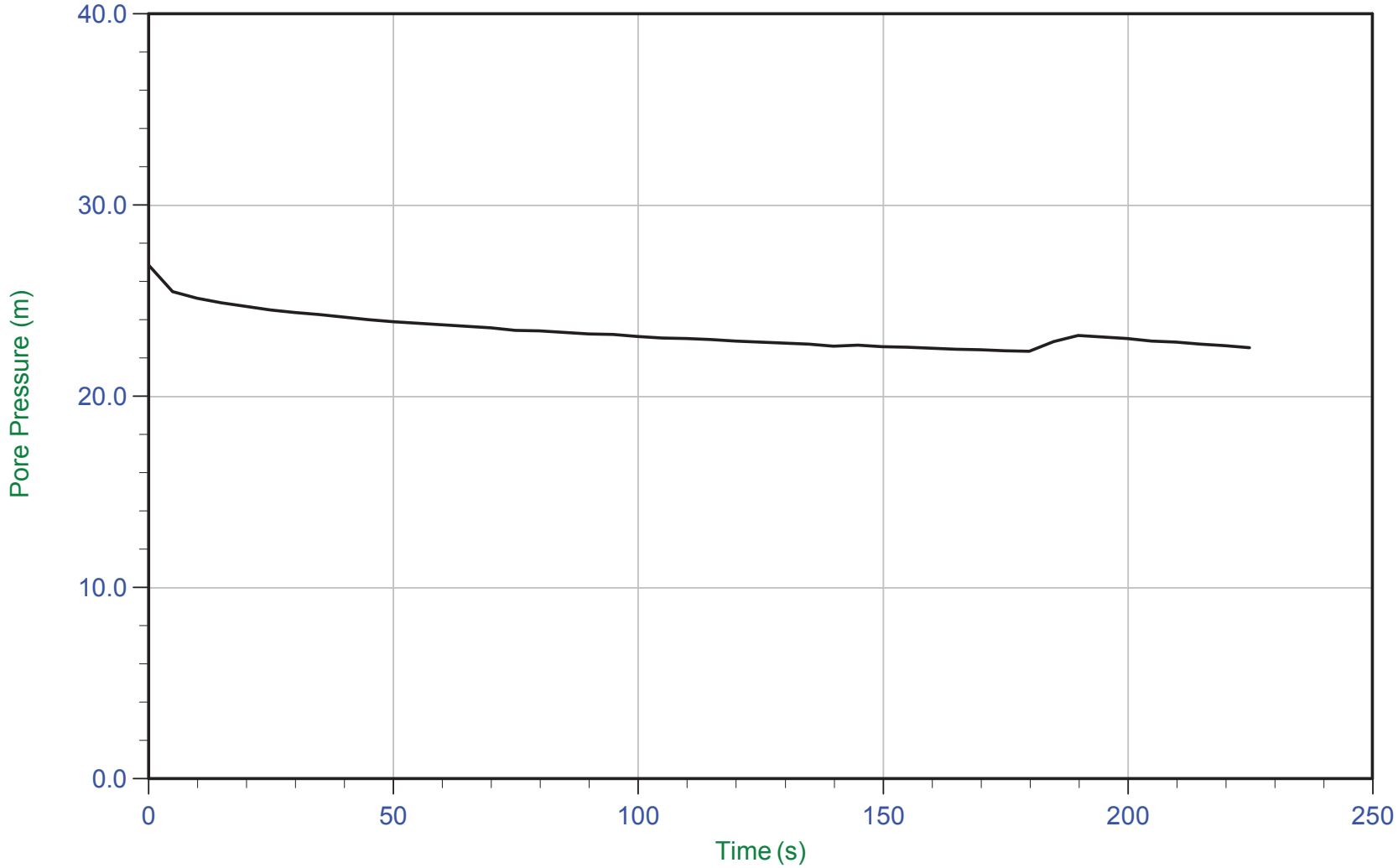

Trace Summary:

Filename: 16-72004_SP05.PPF
Depth: 9.000 m / 29.527 ft
Duration: 225.0 s

U Min: 22.4 m
U Max: 26.9 m

CONETEC

CGSH

Job No: 1672007
Date: 05/05/2016 10:41
Site: Bay 3, Germano Slimes

Sounding: GSCPT16-05
Cone: 376:T375F10U200
Cone Area: 15 sq cm

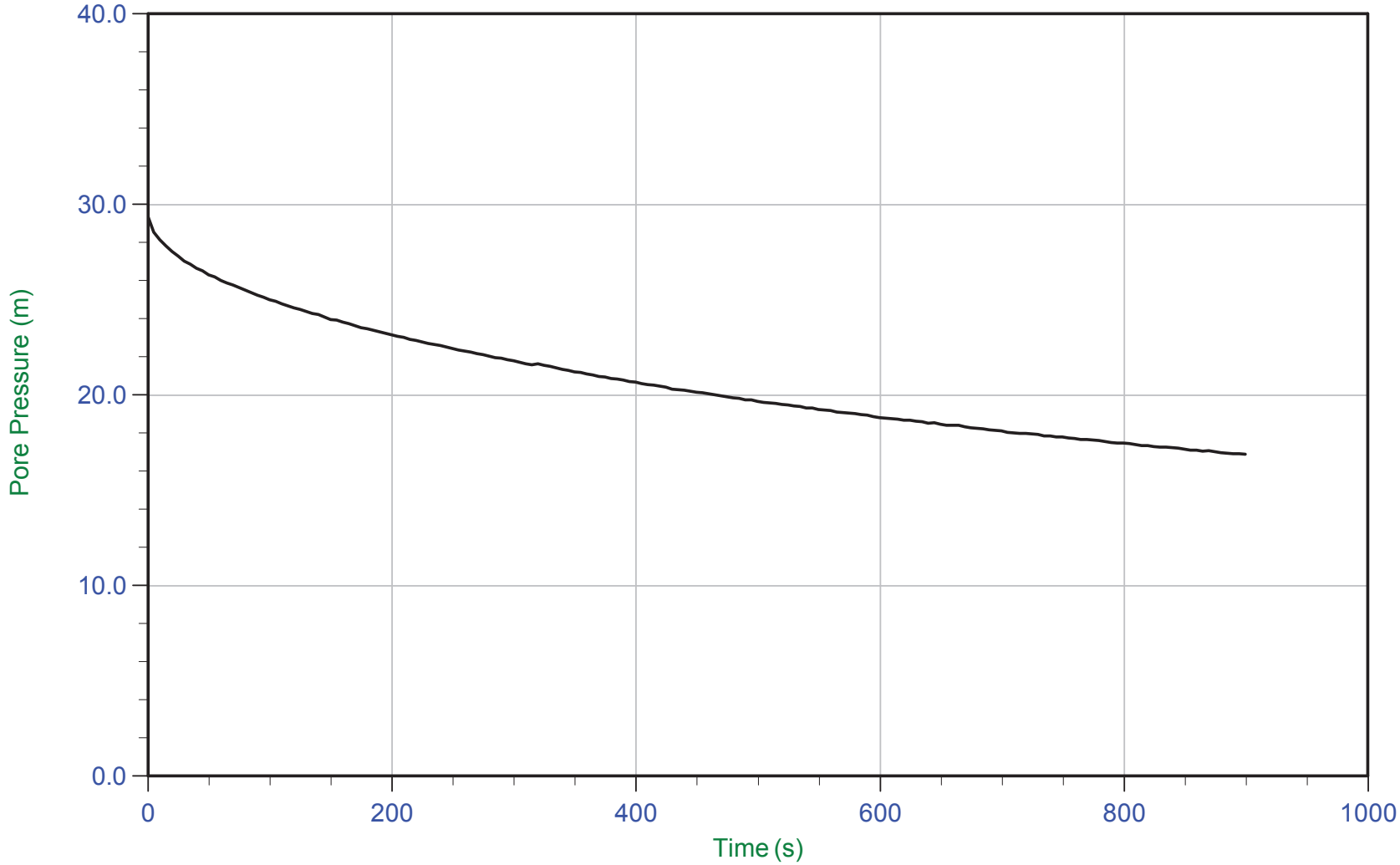

Trace Summary:

Filename: 16-72004_SP05.PPF
Depth: 10.050 m / 32.972 ft
Duration: 900.0 s

U Min: 16.9 m
U Max: 29.4 m

CONETEC

CGSH

Job No: 1672007
Date: 05/05/2016 10:41
Site: Bay 3, Germano Slimes

Sounding: GSCPT16-05
Cone: 376:T375F10U200
Cone Area: 15 sq cm

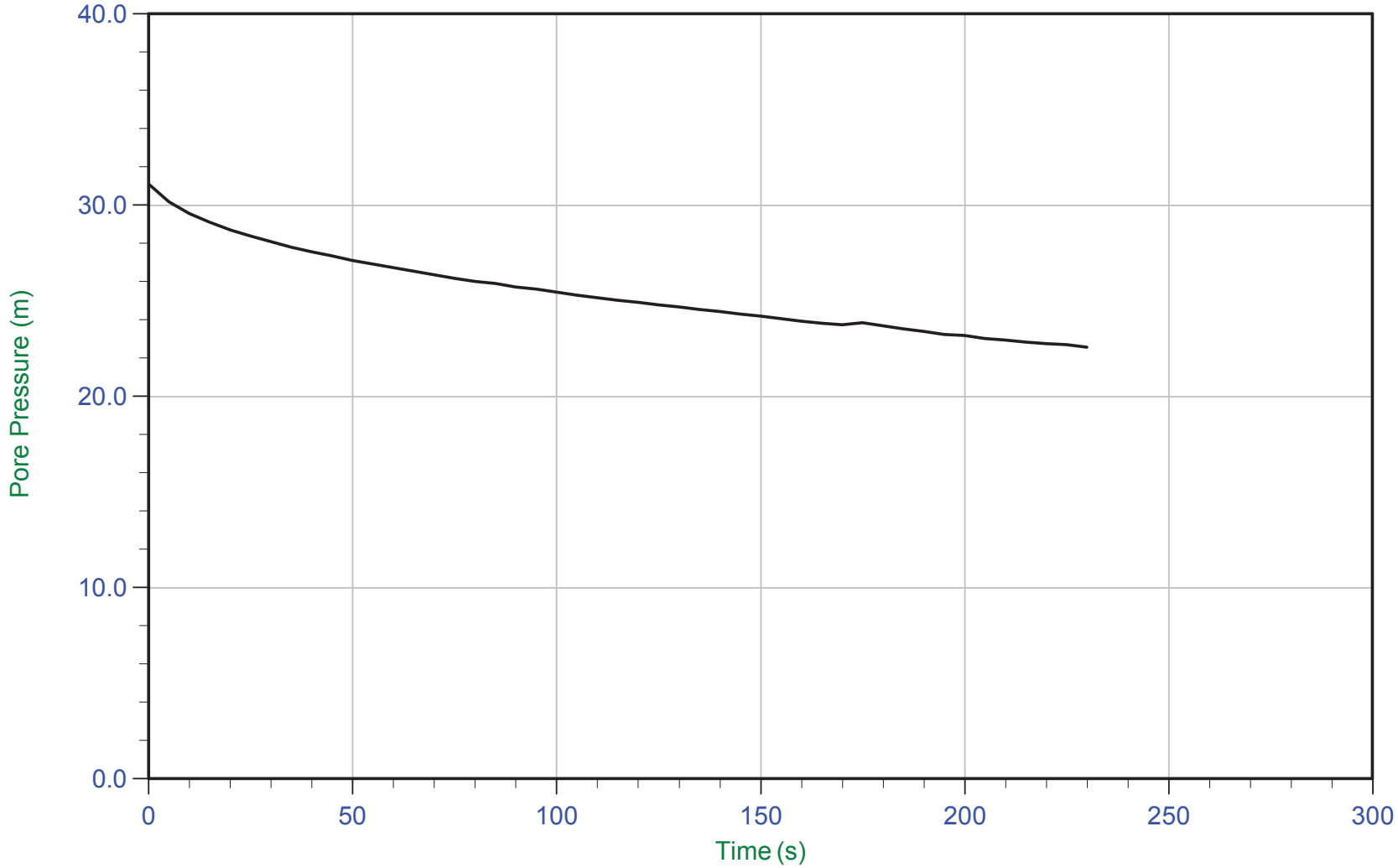

Trace Summary:

Filename: 16-72004_SP05.PPF
Depth: 11.050 m / 36.253 ft
Duration: 230.0 s

U Min: 22.6 m
U Max: 31.1 m

CONETEC

CGSH

Job No: 1672007
Date: 05/05/2016 10:41
Site: Bay 3, Germano Slimes

Sounding: GSCPT16-05
Cone: 376:T375F10U200
Cone Area: 15 sq cm

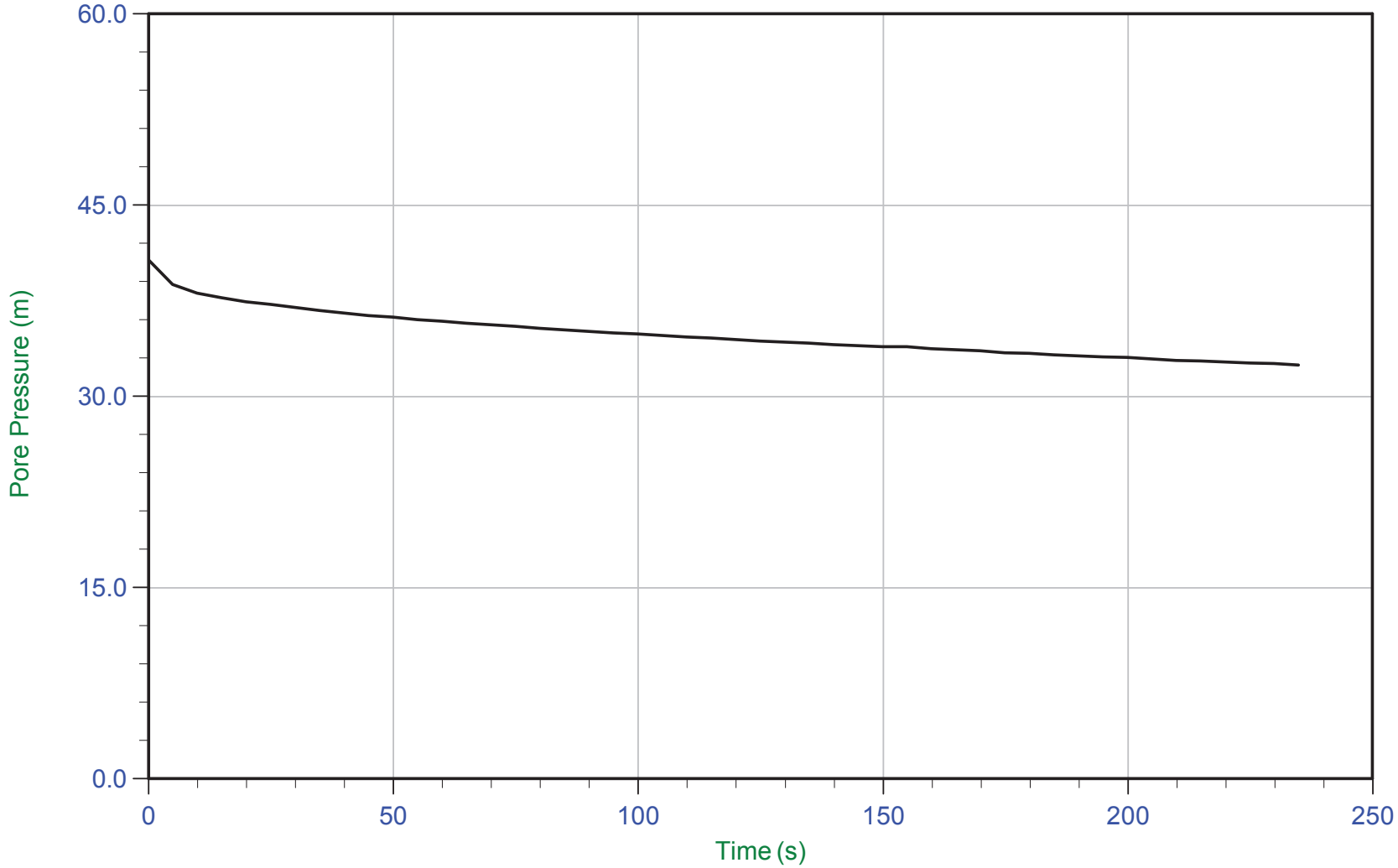

Trace Summary:

Filename: 16-72004_SP05.PPF
Depth: 12.000 m / 39.370 ft
Duration: 235.0 s

U Min: 32.5 m
U Max: 40.7 m

CONETEC

CGSH

Job No: 1672007
Date: 05/05/2016 10:41
Site: Bay 3, Germano Slimes

Sounding: GSCPT16-05
Cone: 376:T375F10U200
Cone Area: 15 sq cm

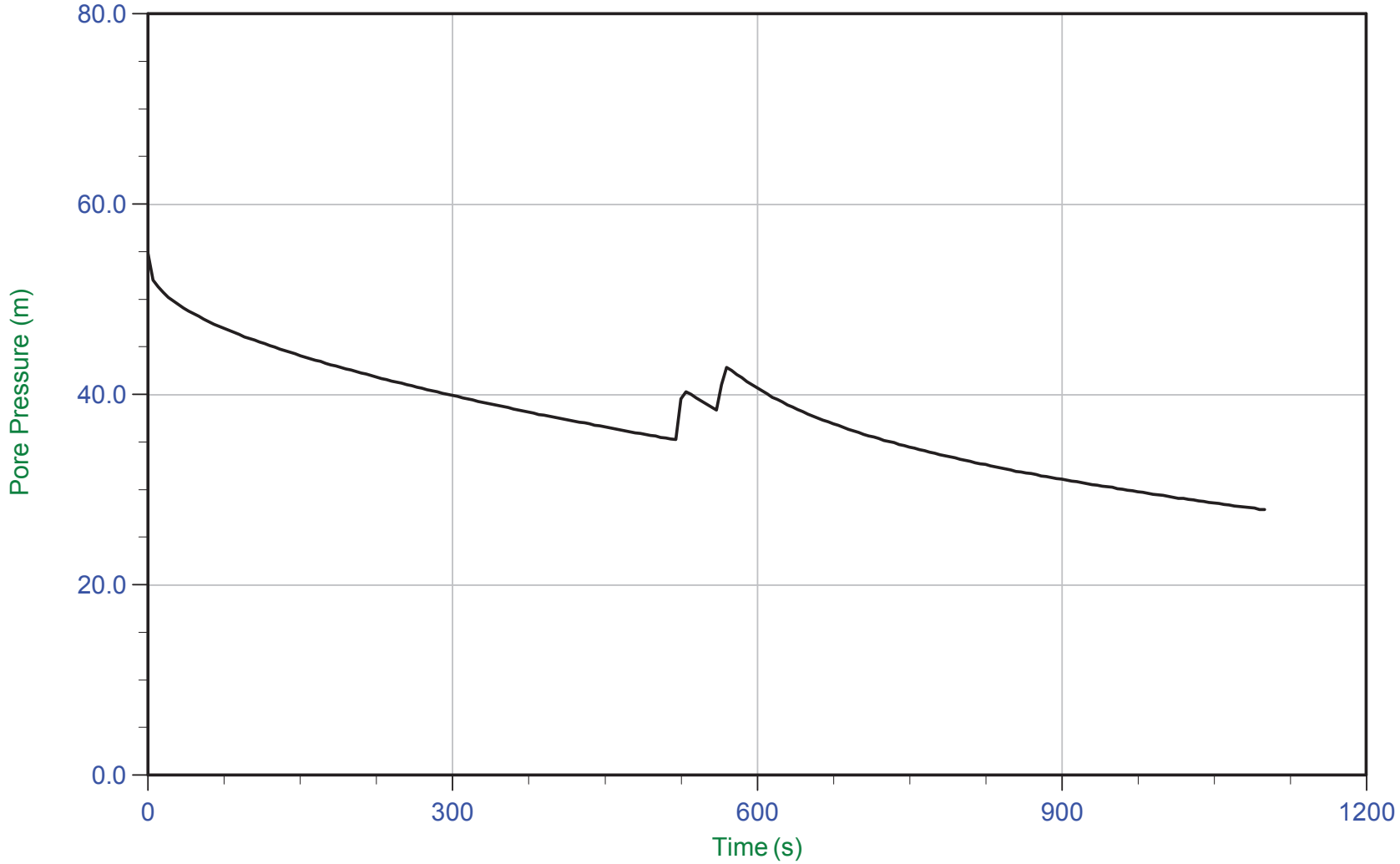

Trace Summary:

Filename: 16-72004_SP05.PPF
Depth: 15.050 m / 49.376 ft
Duration: 1100.0 s

U Min: 27.9 m
U Max: 54.8 m

CONETEC

CGSH

Job No: 1672007
Date: 05/05/2016 10:41
Site: Bay 3, Germano Slimes

Sounding: GSCPT16-05
Cone: 376:T375F10U200
Cone Area: 15 sq cm

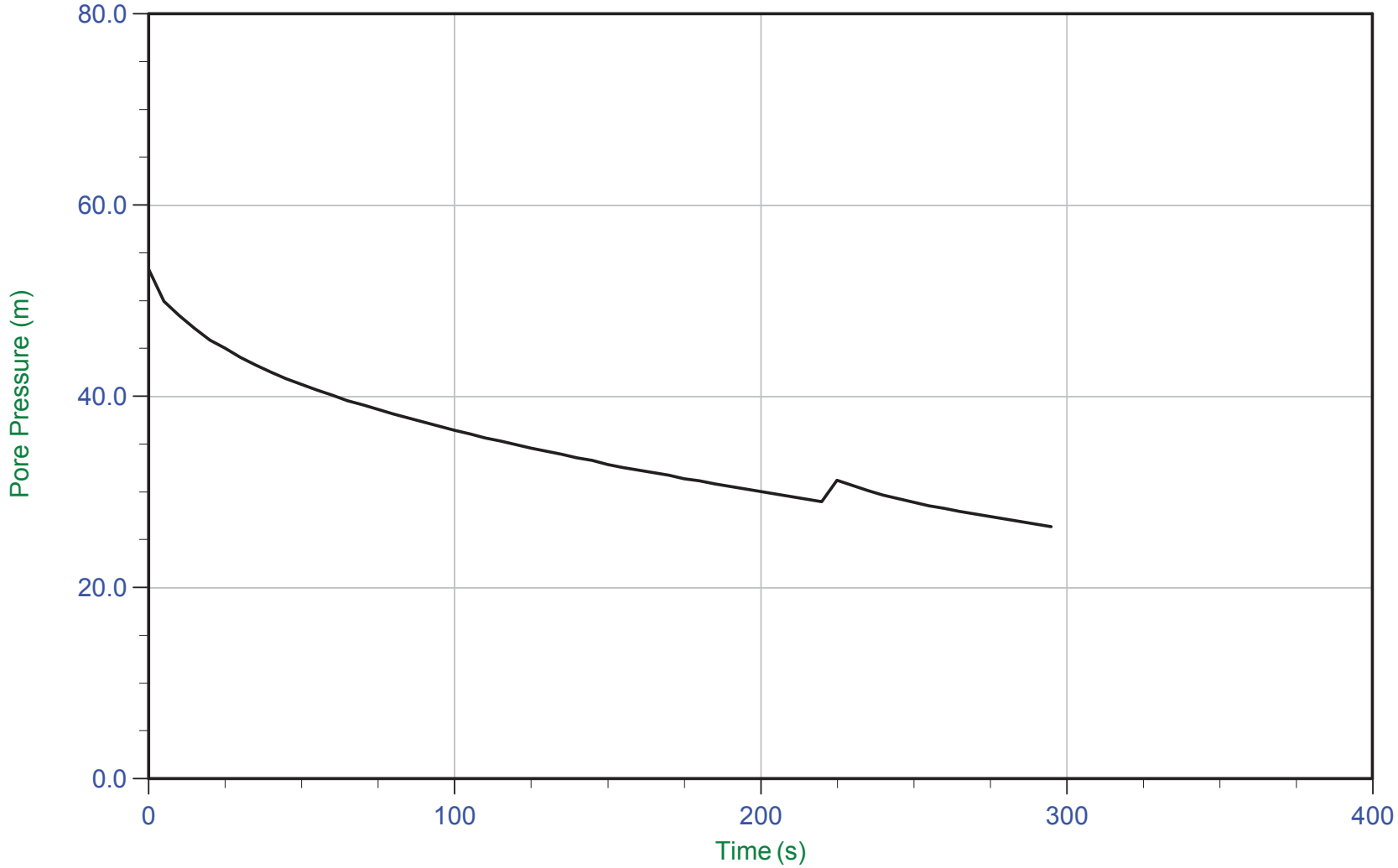

Trace Summary:

Filename: 16-72004_SP05.PPF
Depth: 16.050 m / 52.657 ft
Duration: 295.0 s

U Min: 26.4 m
U Max: 53.3 m

CONETEC

CGSH

Job No: 1672007
Date: 05/05/2016 10:41
Site: Bay 3, Germano Slimes

Sounding: GSCPT16-05
Cone: 376:T375F10U200
Cone Area: 15 sq cm

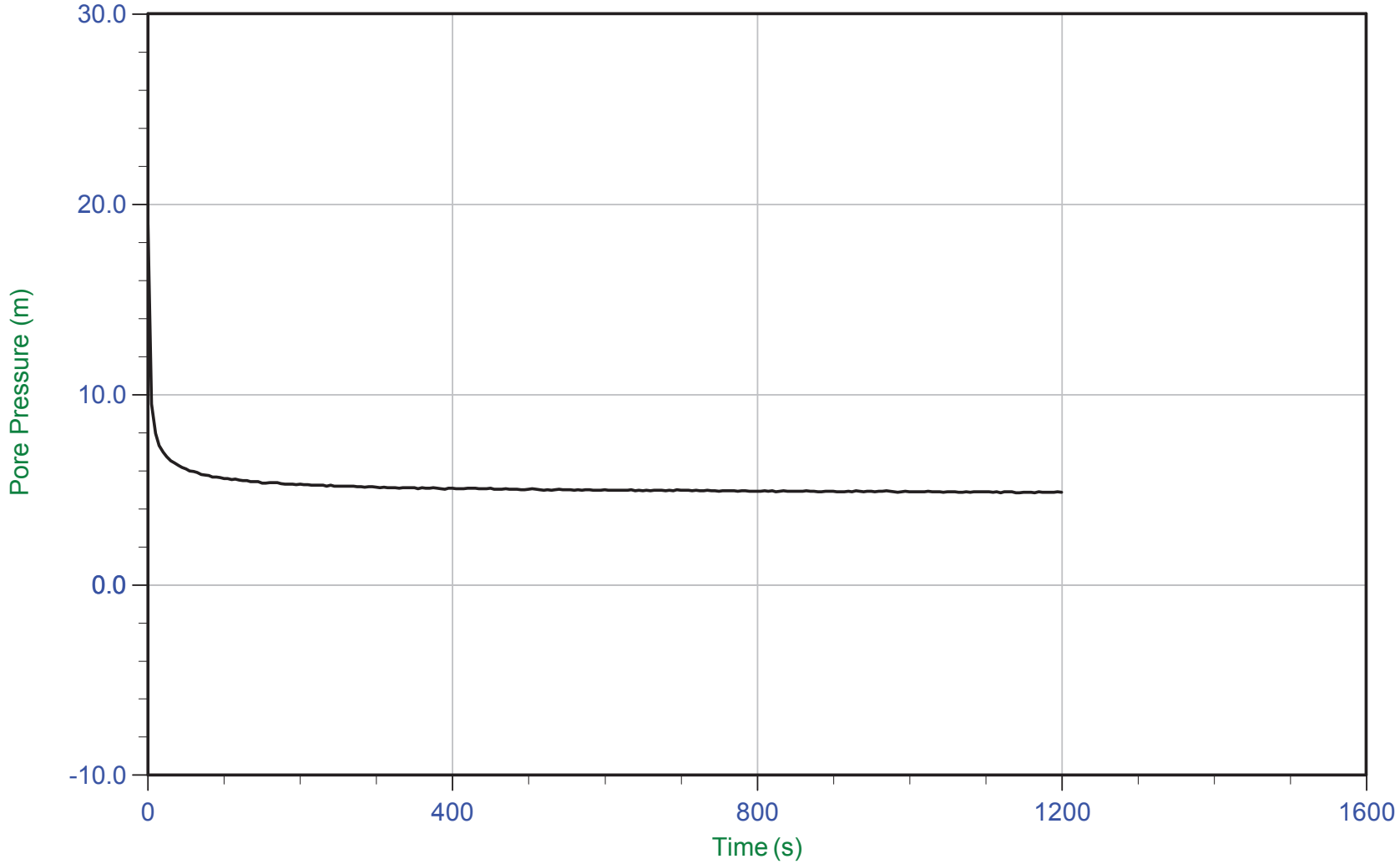

Trace Summary:

Filename: 16-72004_SP05.PPF
Depth: 19.050 m / 62.499 ft
Duration: 1200.0 s

U Min: 4.8 m
U Max: 18.9 m

WT: 14.238 m / 46.712 ft
Ueq: 4.8 m

CONETEC

CGSH

Job No: 1672007
Date: 05/05/2016 10:41
Site: Bay 3, Germano Slimes

Sounding: GSCPT16-05
Cone: 376:T375F10U200
Cone Area: 15 sq cm

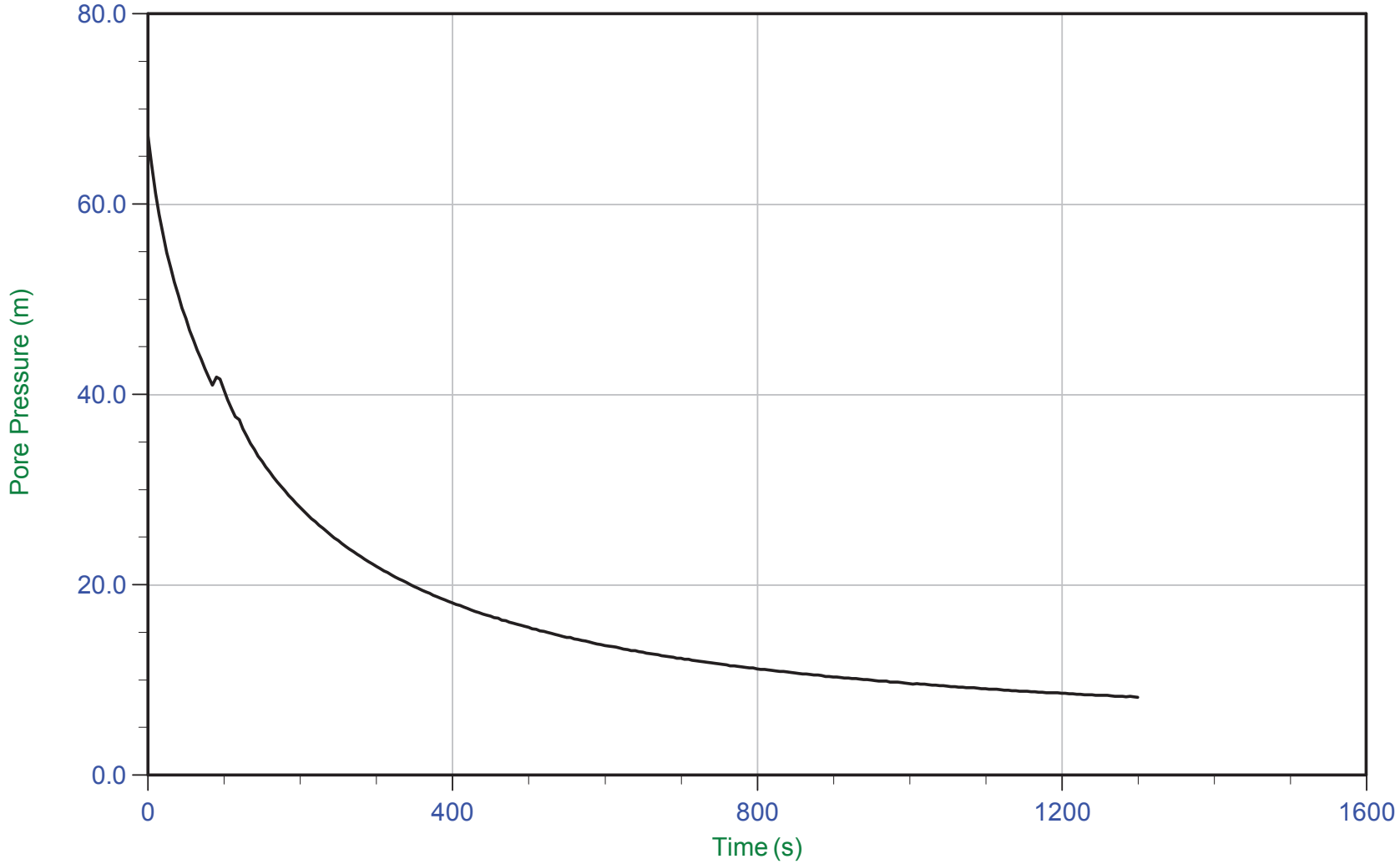

Trace Summary:

Filename: 16-72004_SP05.PPF
Depth: 25.050 m / 82.184 ft
Duration: 1300.0 s

U Min: 8.2 m
U Max: 67.2 m

CONETEC

CGSH

Job No: 1672007
Date: 05/05/2016 10:41
Site: Bay 3, Germano Slimes

Sounding: GSCPT16-05
Cone: 376:T375F10U200
Cone Area: 15 sq cm

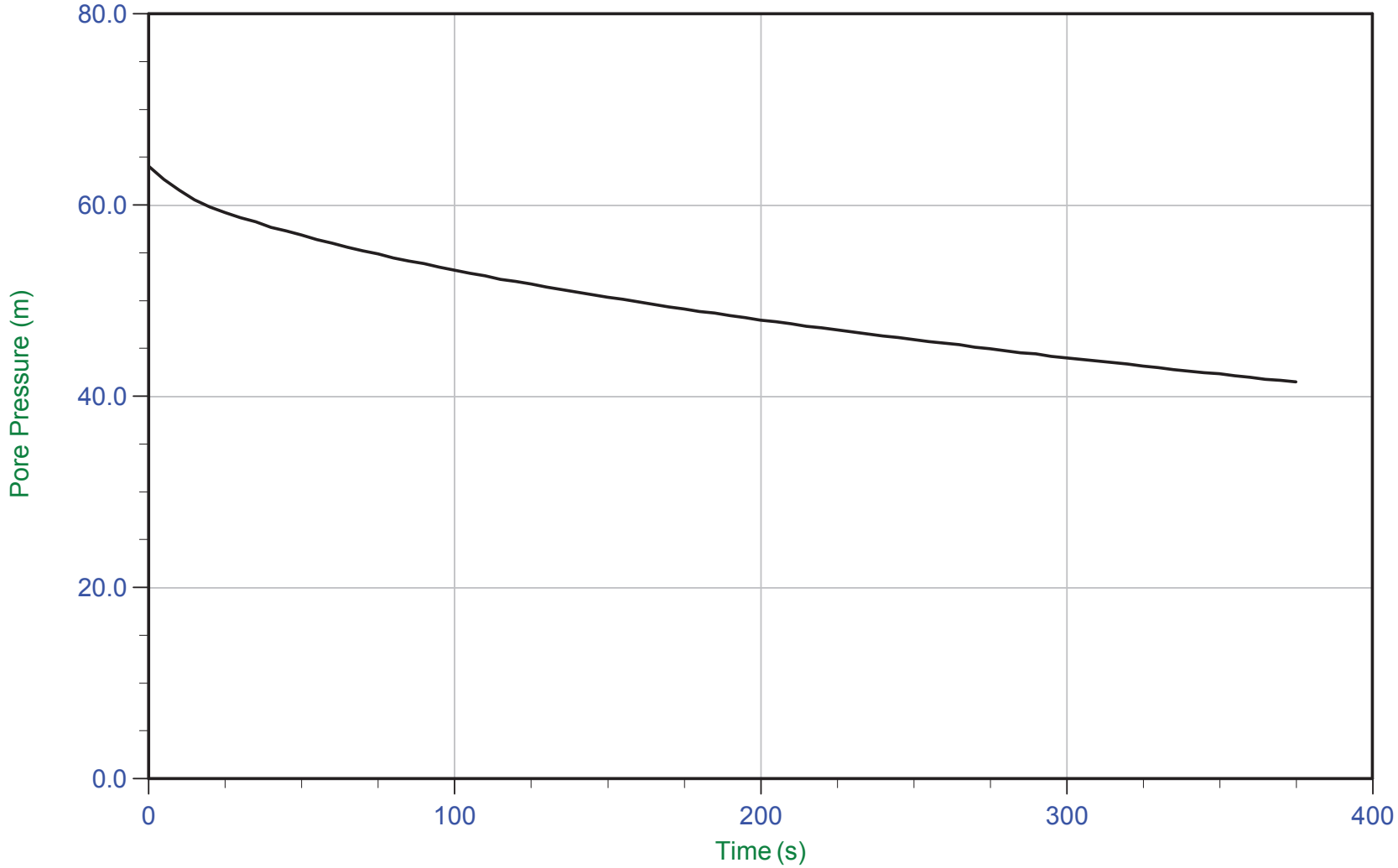

Trace Summary:

Filename: 16-72004_SP05.PPF
Depth: 28.000 m / 91.862 ft
Duration: 375.0 s

U Min: 41.5 m
U Max: 64.1 m

CONETEC

CGSH

Job No: 1672007
Date: 05/05/2016 10:41
Site: Bay 3, Germano Slimes

Sounding: GSCPT16-05
Cone: 376:T375F10U200
Cone Area: 15 sq cm

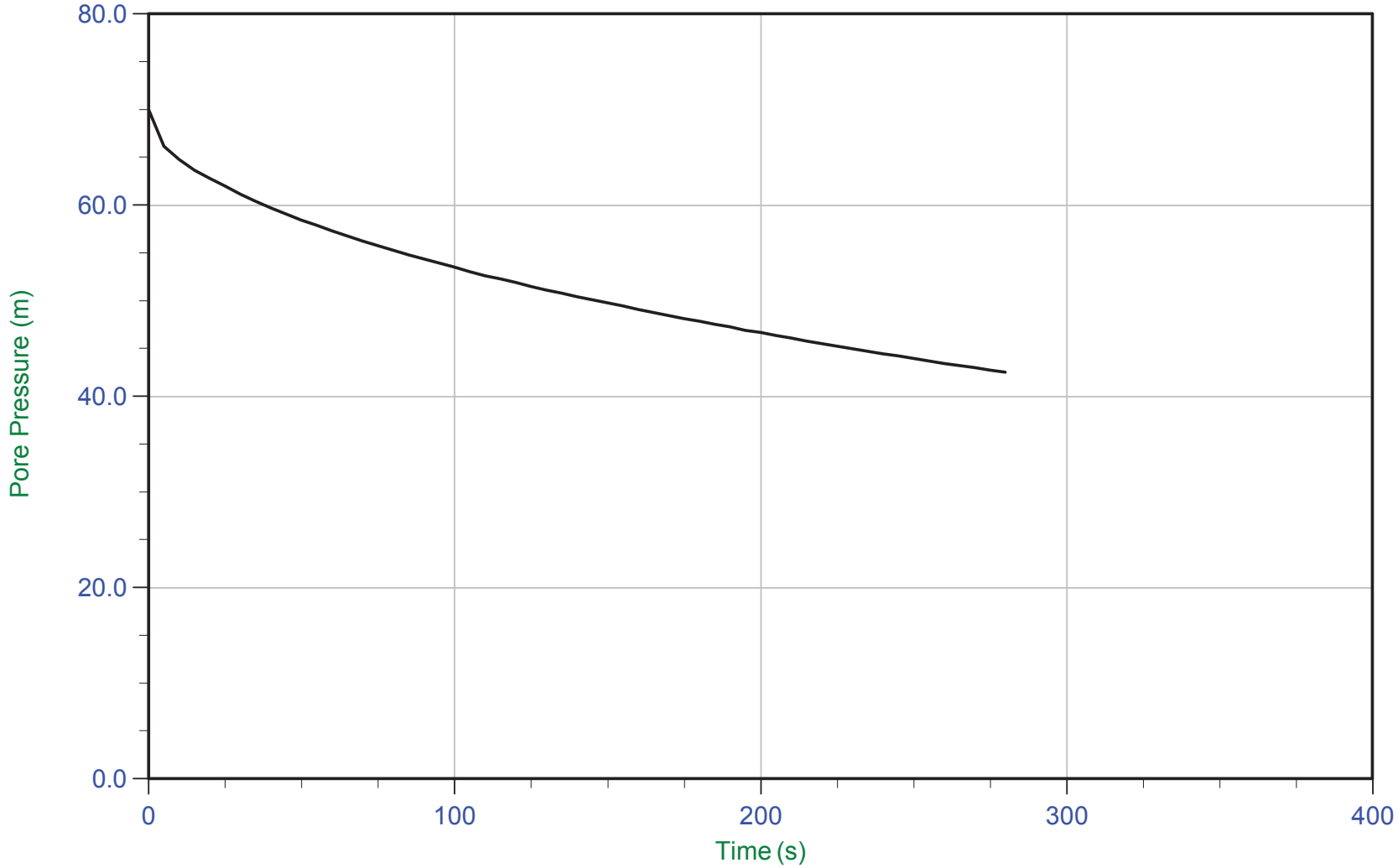

Trace Summary:

Filename: 16-72004_SP05.PPF
Depth: 29.050 m / 95.307 ft
Duration: 280.0 s

U Min: 42.5 m
U Max: 70.0 m

CONETEC

CGSH

Job No: 1672007
Date: 05/05/2016 10:41
Site: Bay 3, Germano Slimes

Sounding: GSCPT16-05
Cone: 376:T375F10U200
Cone Area: 15 sq cm

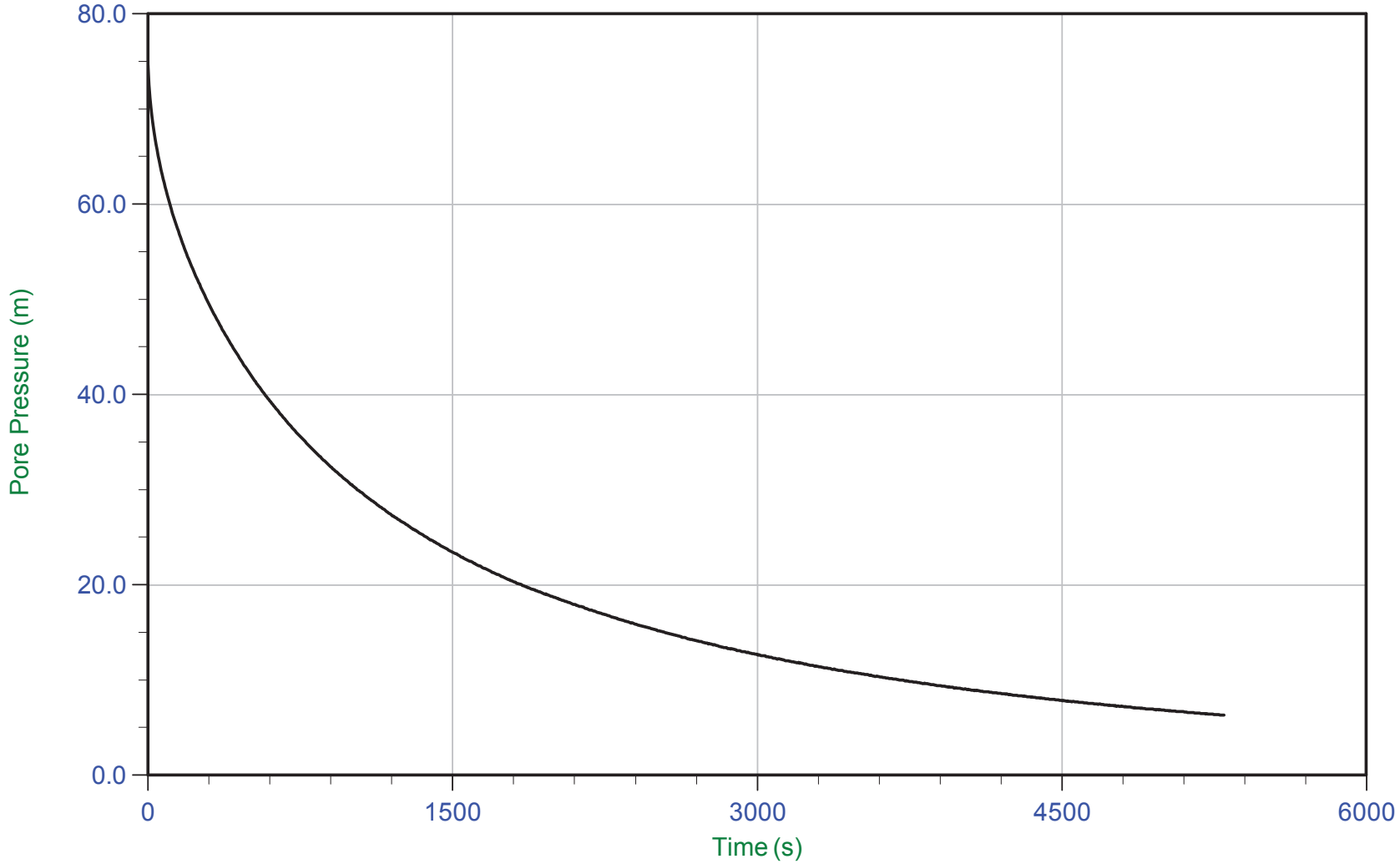

Trace Summary:

Filename: 16-72004_SP05.PPF
Depth: 30.050 m / 98.588 ft
Duration: 5300.0 s

U Min: 6.3 m
U Max: 74.7 m

CONETEC

CGSH

Job No: 1672007
Date: 05/05/2016 10:41
Site: Bay 3, Germano Slimes

Sounding: GSCPT16-05
Cone: 376:T375F10U200
Cone Area: 15 sq cm

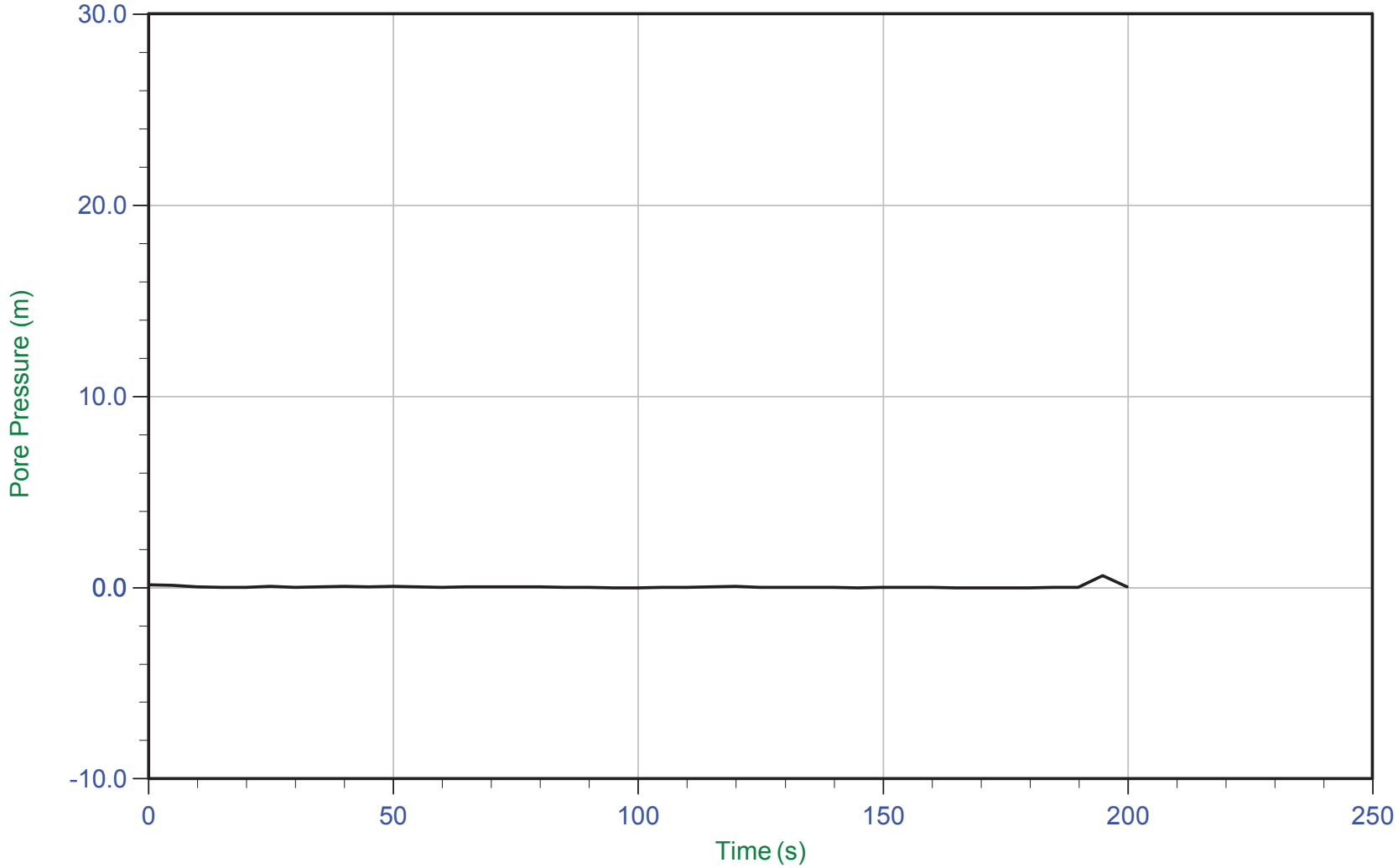

Trace Summary:

Filename: 16-72004_SP05.PPF
Depth: 31.050 m / 101.869 ft
Duration: 200.0 s

U Min: -0.0 m
U Max: 0.6 m

WT: 0.000 m / 0.000 ft
Ueq: 0.0 m

CONETEC

CGSH

Job No: 1672007
Date: 05/05/2016 10:41
Site: Bay 3, Germano Slimes

Sounding: GSCPT16-05
Cone: 376:T375F10U200
Cone Area: 15 sq cm

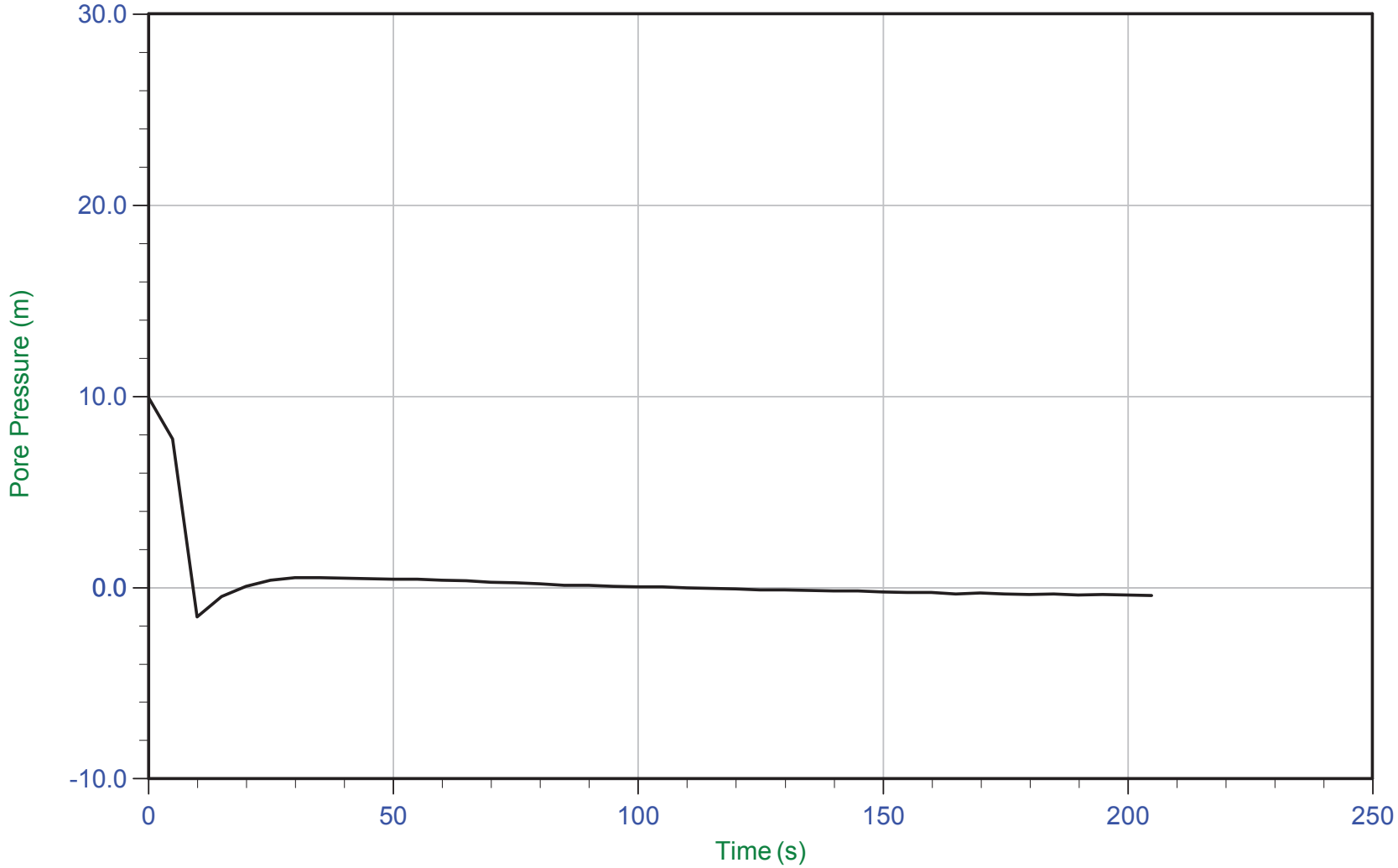

Trace Summary:

Filename: 16-72004_SP05.PPF
Depth: 31.650 m / 103.837 ft
Duration: 205.0 s

U Min: -1.5 m
U Max: 9.9 m

WT: 0.000 m / 0.000 ft
Ueq: 0.0 m

CONETEC

CGSH

Job No: 1672007
Date: 05/17/2016 09:36
Site: Germano Buttres

Sounding: GBCPT16-06B
Cone: 432:T1500F15U500
Cone Area: 15 sq cm

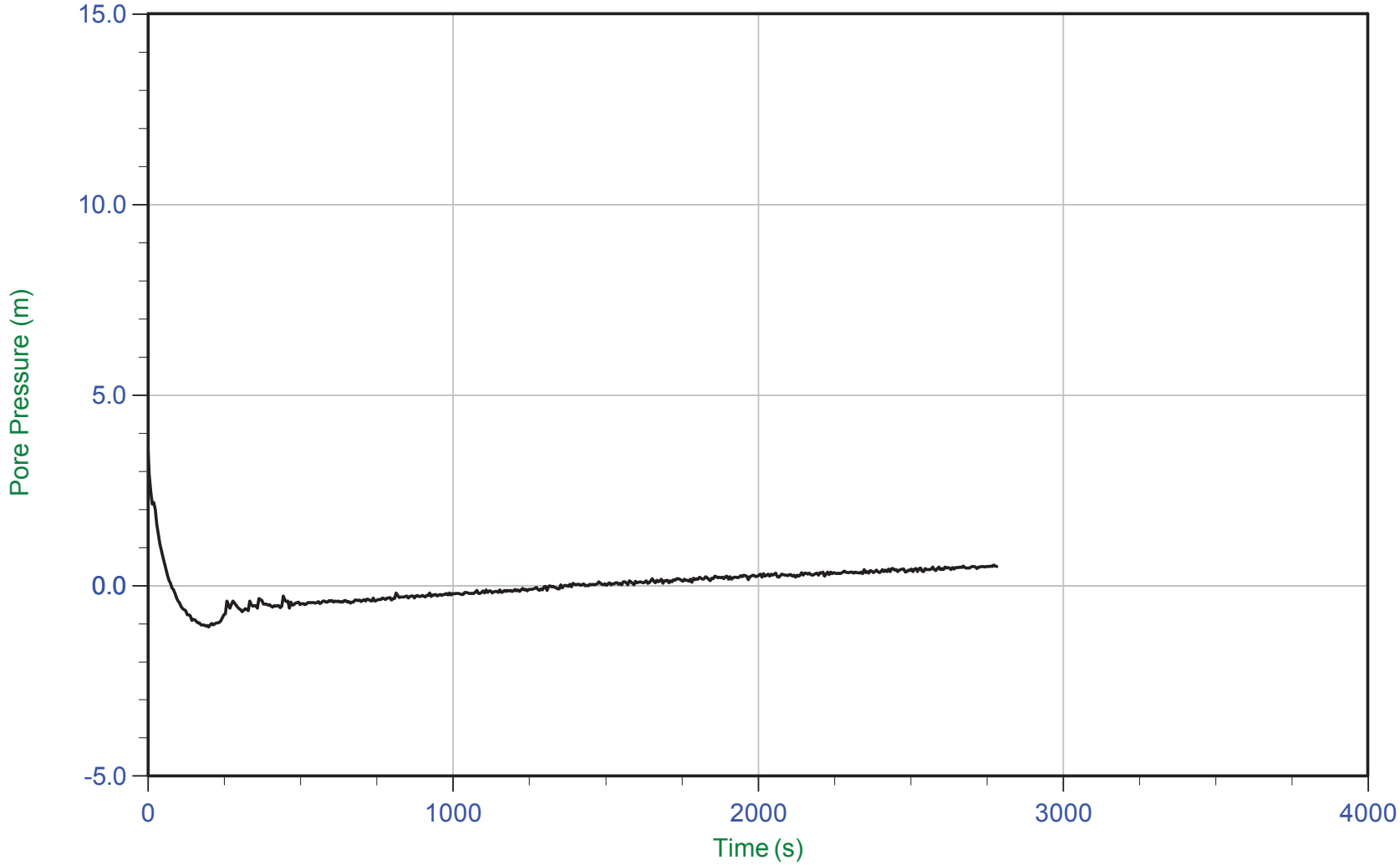

Trace Summary:

Filename: 16-72004_RS06B.PPF
Depth: 3.350 m / 10.991 ft
Duration: 2785.0 s

U Min: -1.1 m
U Max: 3.6 m

CONETEC

CGSH

Job No: 1672007
Date: 05/16/2016 13:45
Site: Germano Buttres

Sounding: GBCPT16-06
Cone: 432:T1500F15U500
Cone Area: 15 sq cm

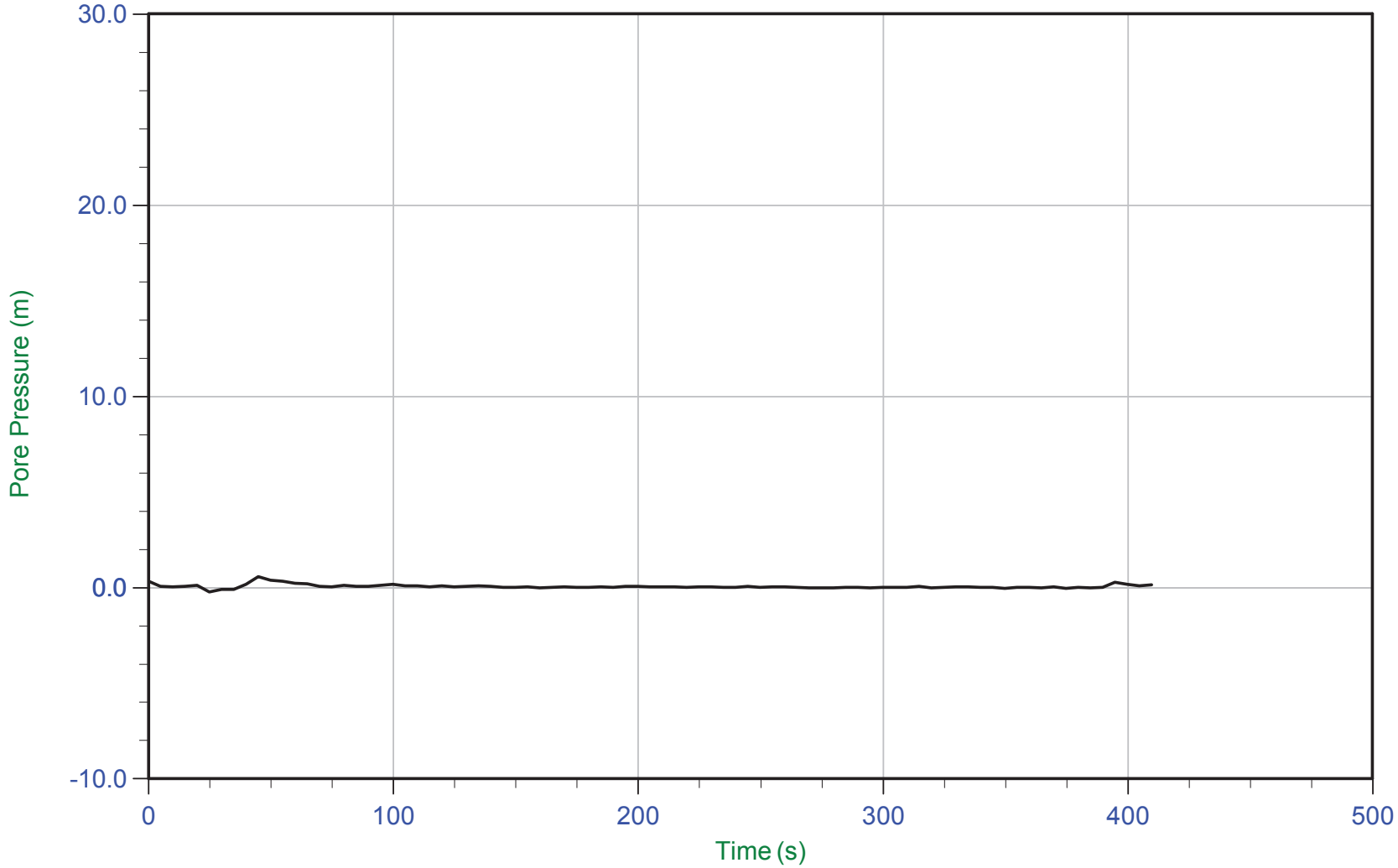

Trace Summary:

Filename: 16-72004_RS06.PPF
Depth: 1.200 m / 3.937 ft
Duration: 410.0 s

U Min: -0.2 m
U Max: 0.6 m

WT: 0.000 m / 0.000 ft
Ueq: 0.0 m

CONETEC

CGSH

Job No: 1672007
Date: 05/16/2016 13:45
Site: Germano Buttres

Sounding: GBCPT16-06
Cone: 432:T1500F15U500
Cone Area: 15 sq cm

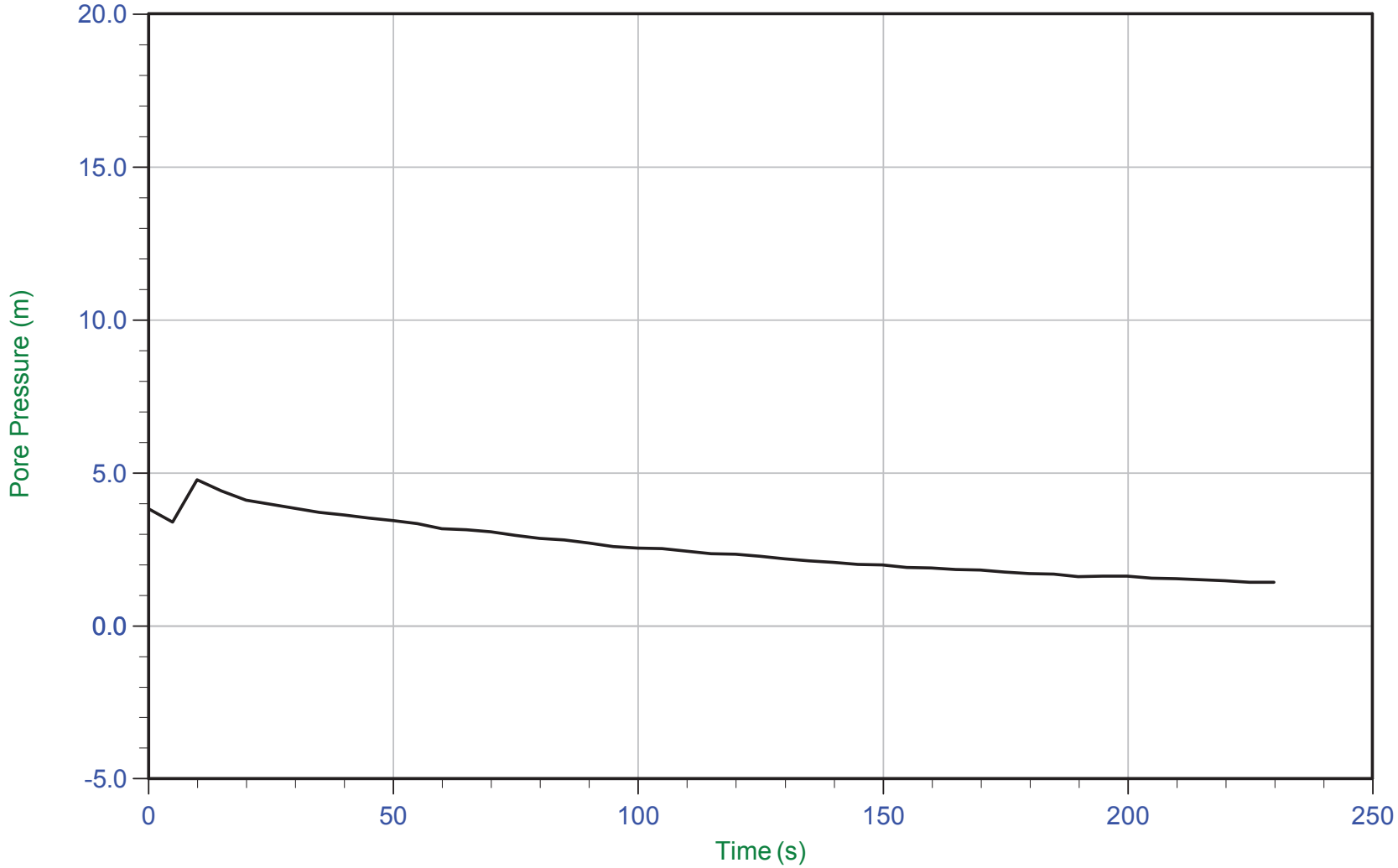

Trace Summary:

Filename: 16-72004_RS06.PPF
Depth: 2.250 m / 7.382 ft
Duration: 230.0 s

U Min: 1.4 m
U Max: 4.8 m

CONETEC

CGSH

Job No: 1672007
Date: 05/16/2016 13:45
Site: Germano Buttres

Sounding: GBCPT16-06
Cone: 432:T1500F15U500
Cone Area: 15 sq cm

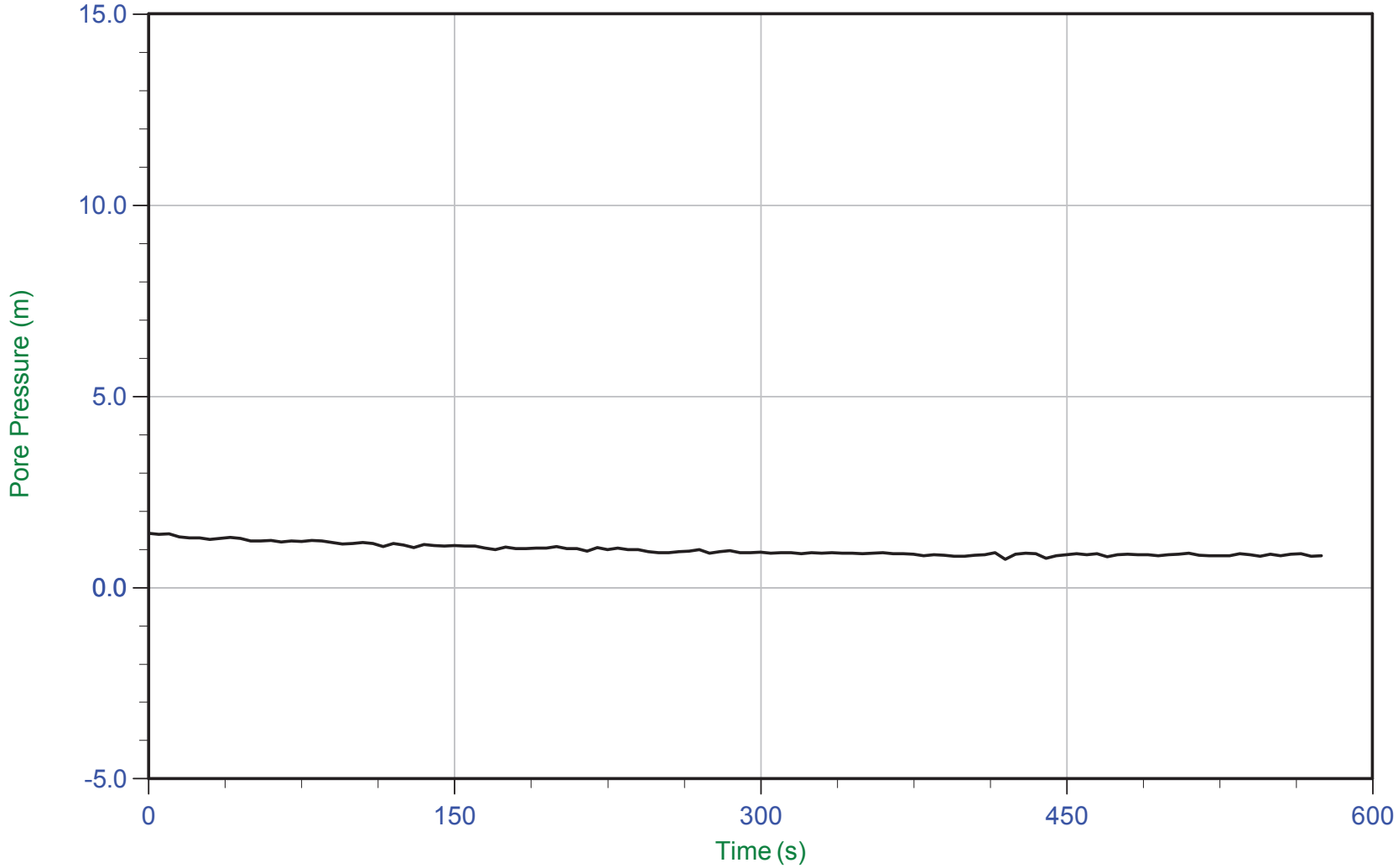

Trace Summary:

Filename: 16-72004_RS06.PPF
Depth: 3.900 m / 12.795 ft
Duration: 575.0 s

U Min: 0.7 m
U Max: 1.4 m

WT: 3.084 m / 10.118 ft
Ueq: 0.8 m

CONETEC

CGSH

Job No: 1672007
Date: 05/16/2016 13:45
Site: Germano Buttres

Sounding: GBCPT16-06
Cone: 432:T1500F15U500
Cone Area: 15 sq cm

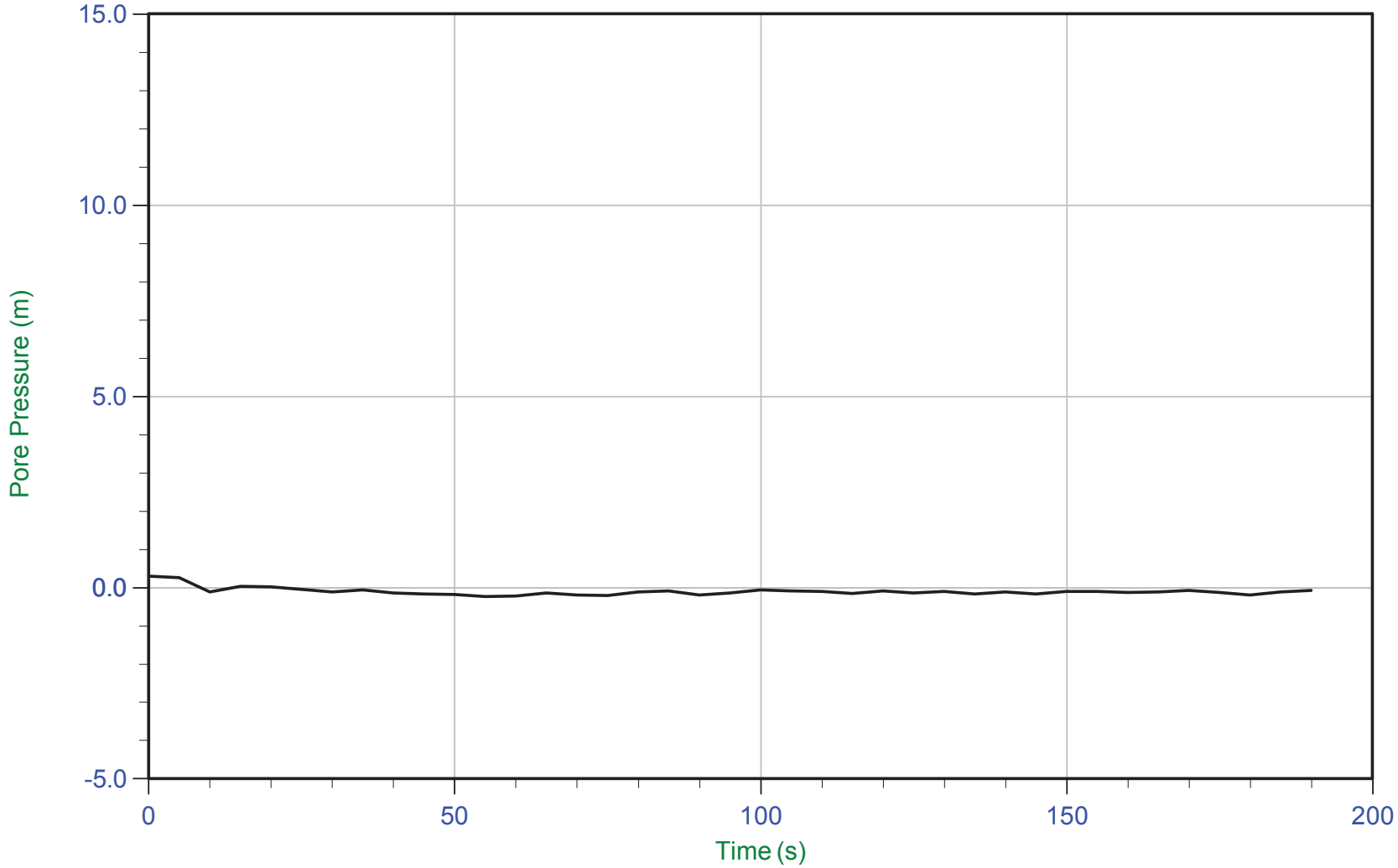

Trace Summary:

Filename: 16-72004_RS06.PPF
Depth: 10.600 m / 34.776 ft
Duration: 190.0 s

U Min: -0.2 m
U Max: 0.3 m

CONETEC

CGSH

Job No: 1672007
Date: 05/16/2016 13:45
Site: Germano Buttres

Sounding: GBCPT16-06
Cone: 432:T1500F15U500
Cone Area: 15 sq cm

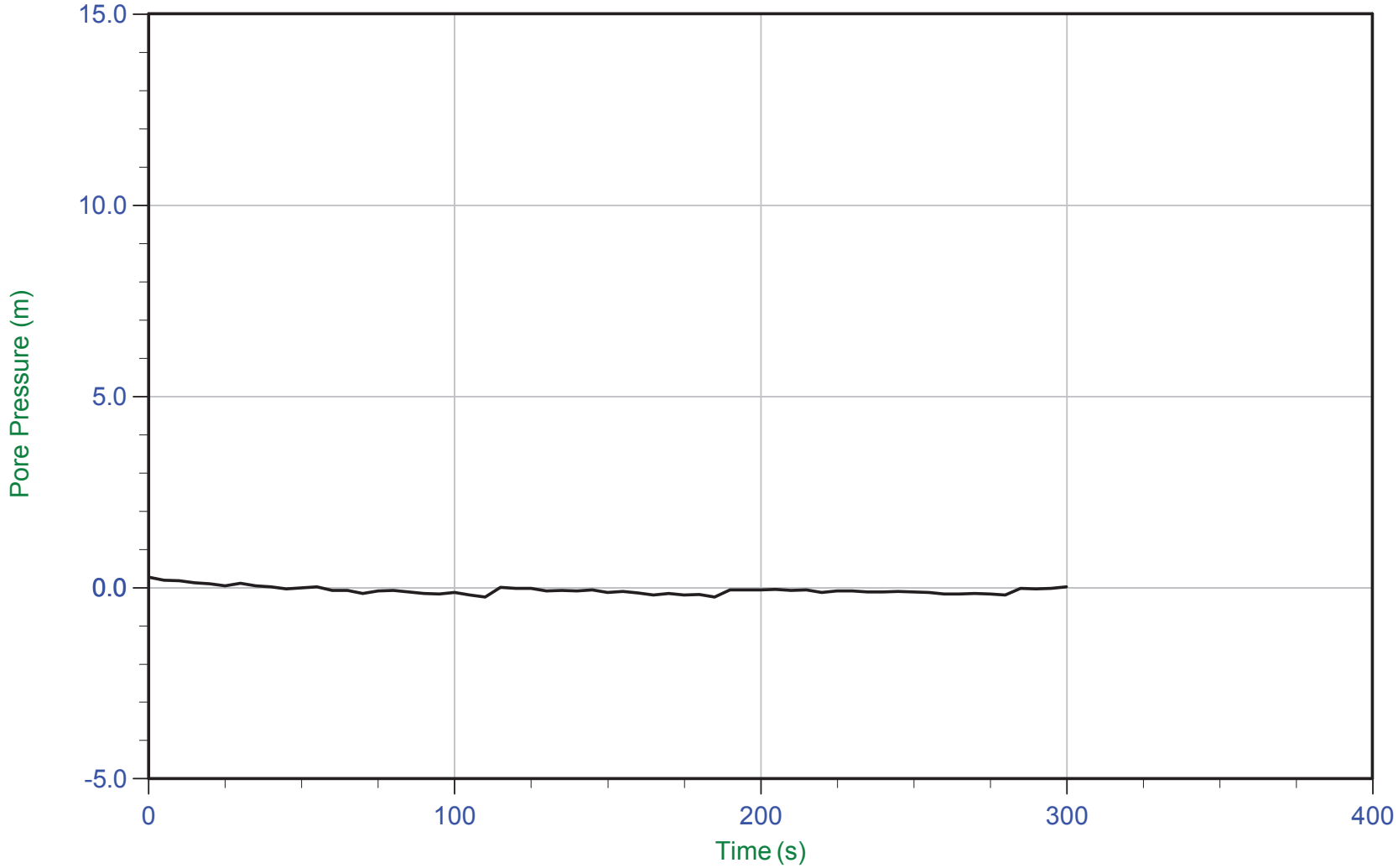

Trace Summary:

Filename: 16-72004_RS06.PPF
Depth: 16.000 m / 52.493 ft
Duration: 300.0 s

U Min: -0.3 m
U Max: 0.3 m

CONETEC

CGSH

Job No: 1672007
Date: 05/16/2016 13:45
Site: Germano Buttres

Sounding: GBCPT16-06
Cone: 432:T1500F15U500
Cone Area: 15 sq cm

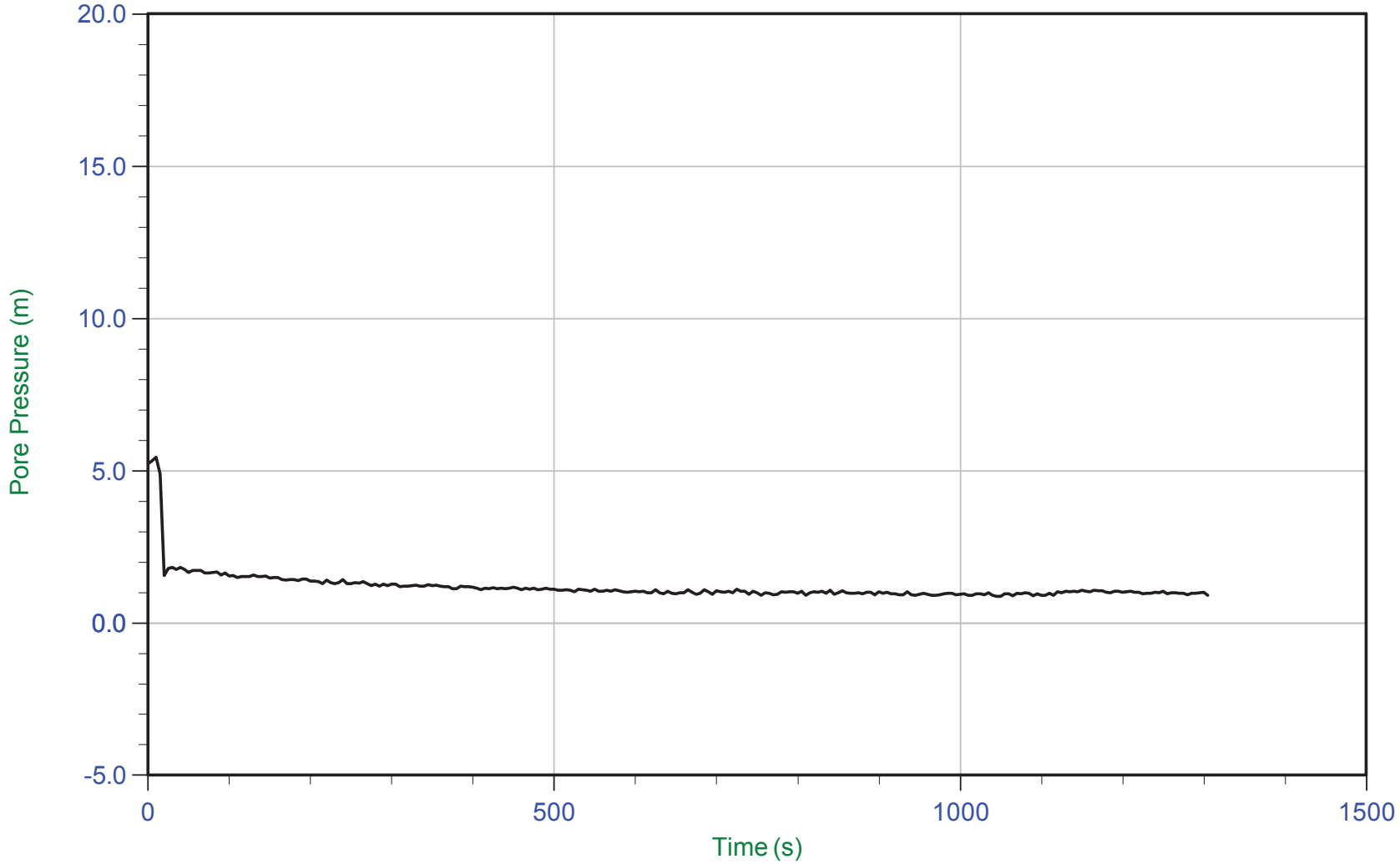

Trace Summary:

Filename: 16-72004_RS06.PPF
Depth: 17.350 m / 56.922 ft
Duration: 1305.0 s

U Min: 0.9 m
U Max: 5.4 m

WT: 16.440 m / 53.936 ft
Ueq: 0.9 m

CONETEC

CGSH

Job No: 1672007
Date: 05/16/2016 13:45
Site: Germano Buttres

Sounding: GBCPT16-06
Cone: 432:T1500F15U500
Cone Area: 15 sq cm

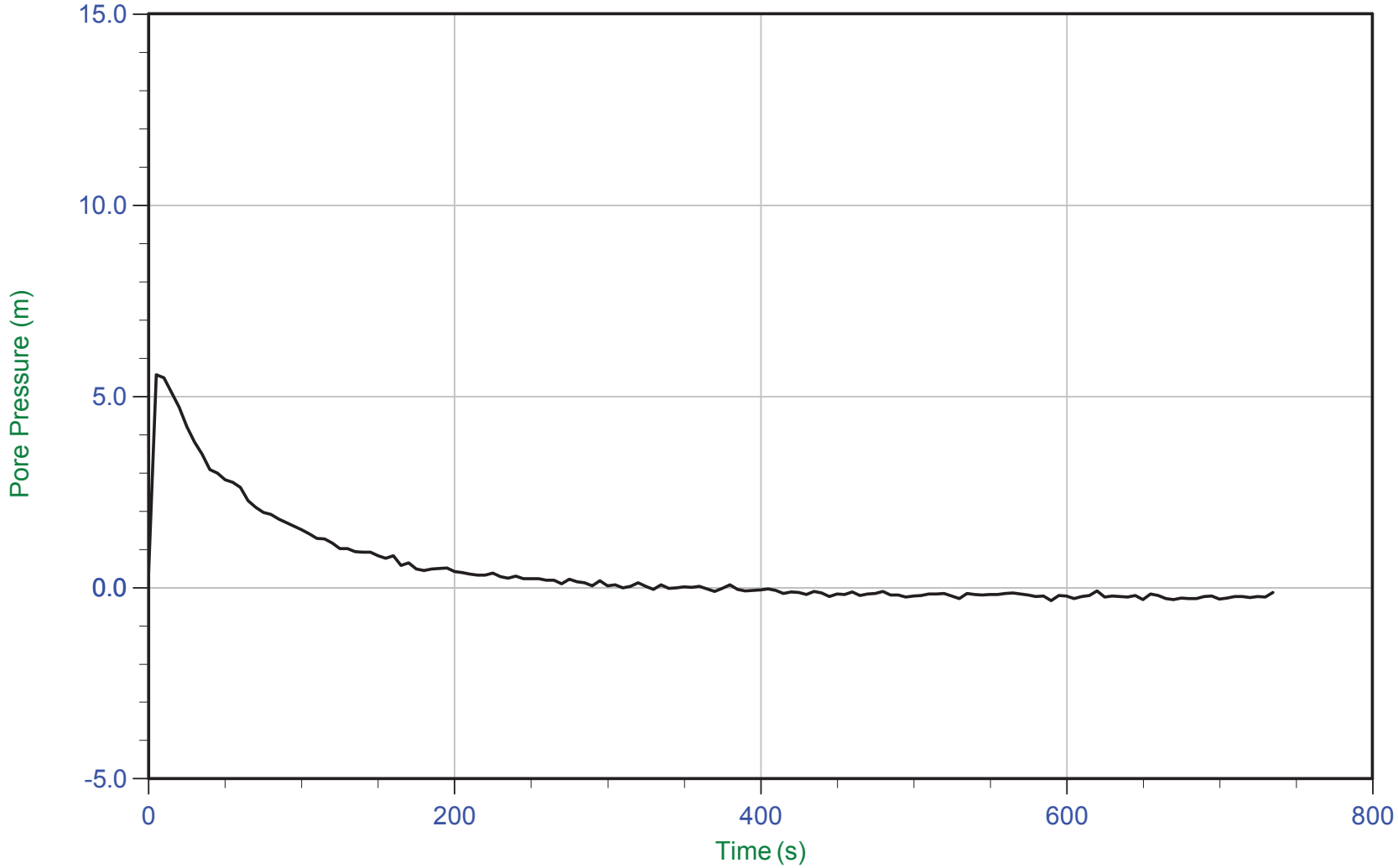

Trace Summary:

Filename: 16-72004_RS06.PPF
Depth: 18.300 m / 60.039 ft
Duration: 735.0 s

U Min: -0.3 m
U Max: 5.6 m

CONETEC

CGSH

Job No: 1672007
Date: 05/16/2016 13:45
Site: Germano Buttres

Sounding: GBCPT16-06
Cone: 432:T1500F15U500
Cone Area: 15 sq cm

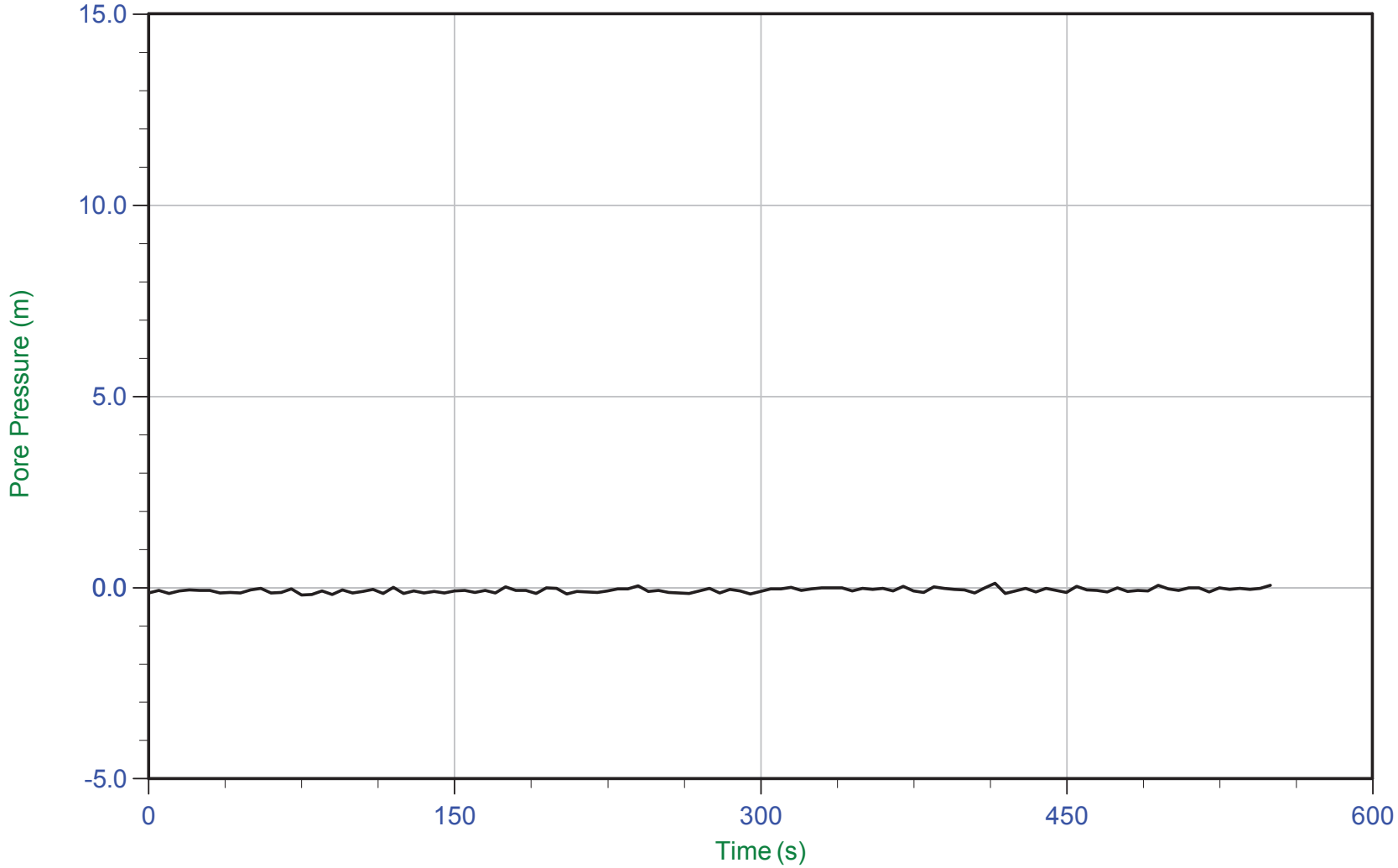

Trace Summary:

Filename: 16-72004_RS06.PPF
Depth: 19.300 m / 63.319 ft
Duration: 550.0 s

U Min: -0.2 m
U Max: 0.1 m

CONETEC

CGSH

Job No: 1672007
Date: 05/16/2016 13:45
Site: Germano Buttres

Sounding: GBCPT16-06
Cone: 432:T1500F15U500
Cone Area: 15 sq cm

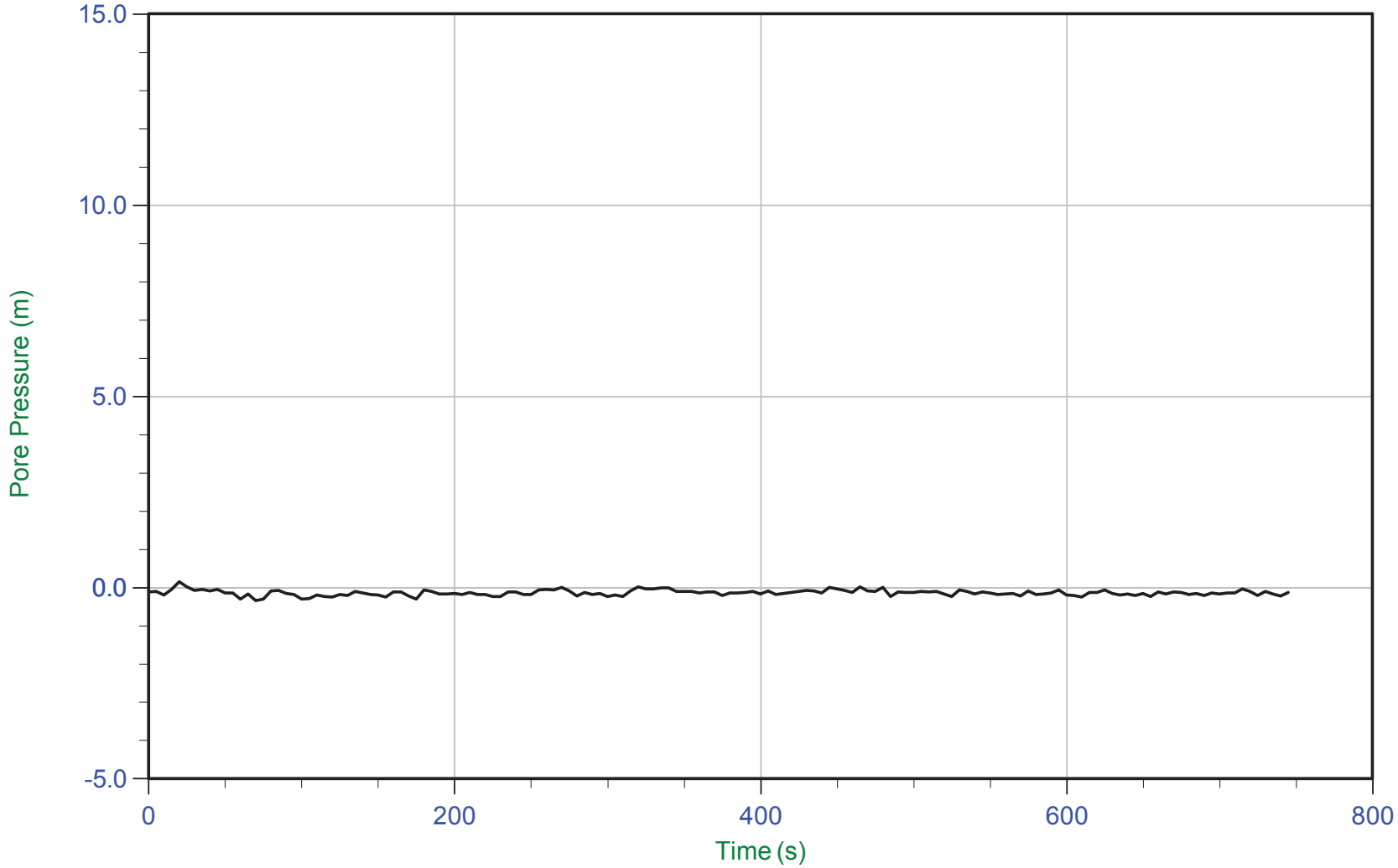

Trace Summary:

Filename: 16-72004_RS06.PPF
Depth: 20.300 m / 66.600 ft
Duration: 745.0 s

U Min: -0.3 m
U Max: 0.1 m

CONETEC

CGSH

Job No: 1672007
Date: 05/16/2016 13:45
Site: Germano Buttres

Sounding: GBCPT16-06
Cone: 432:T1500F15U500
Cone Area: 15 sq cm

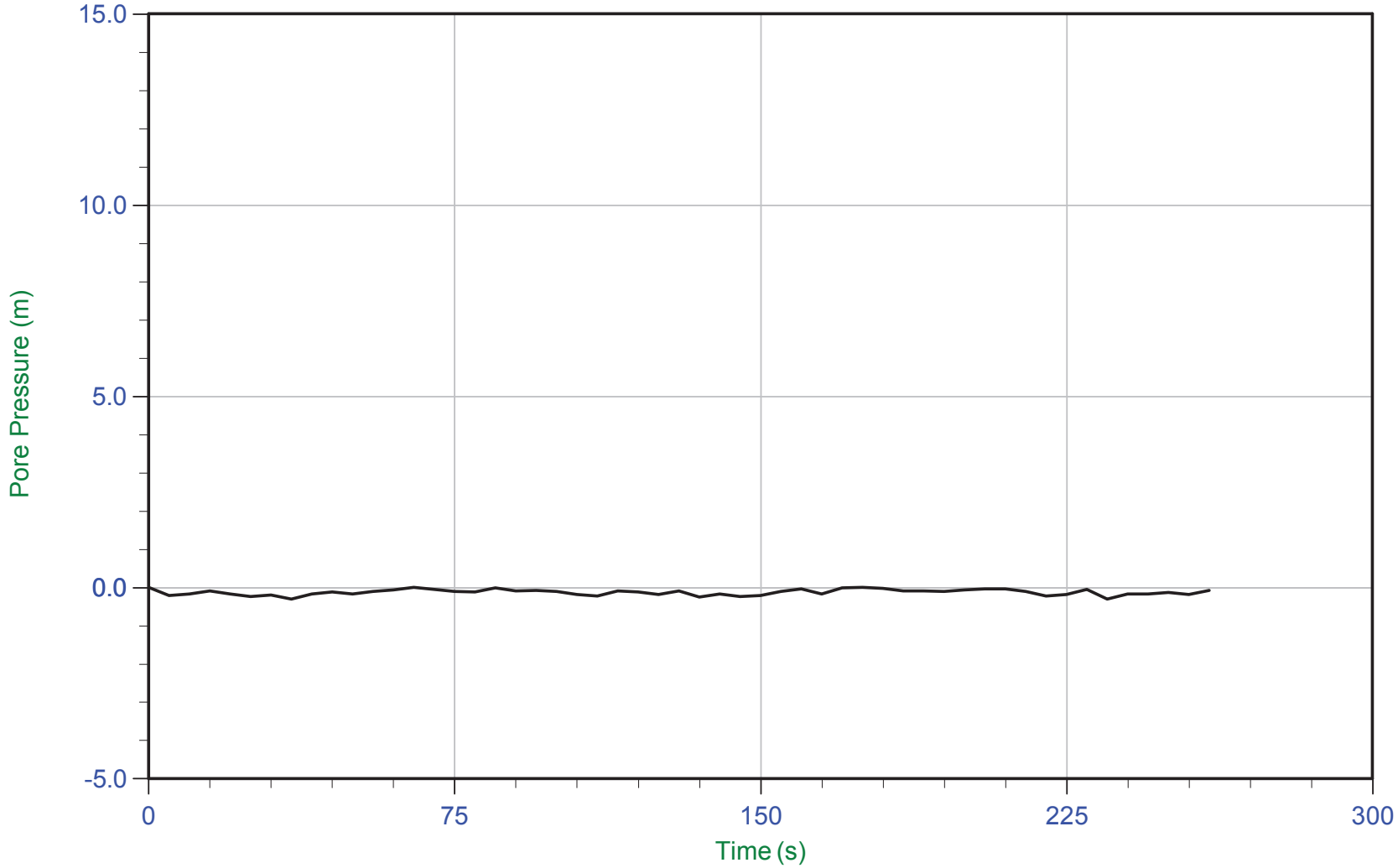

Trace Summary:

Filename: 16-72004_RS06.PPF
Depth: 21.300 m / 69.881 ft
Duration: 260.0 s

U Min: -0.3 m
U Max: 0.0 m

CONETEC

CGSH

Job No: 1672007
Date: 05/16/2016 13:45
Site: Germano Buttres

Sounding: GBCPT16-06
Cone: 432:T1500F15U500
Cone Area: 15 sq cm

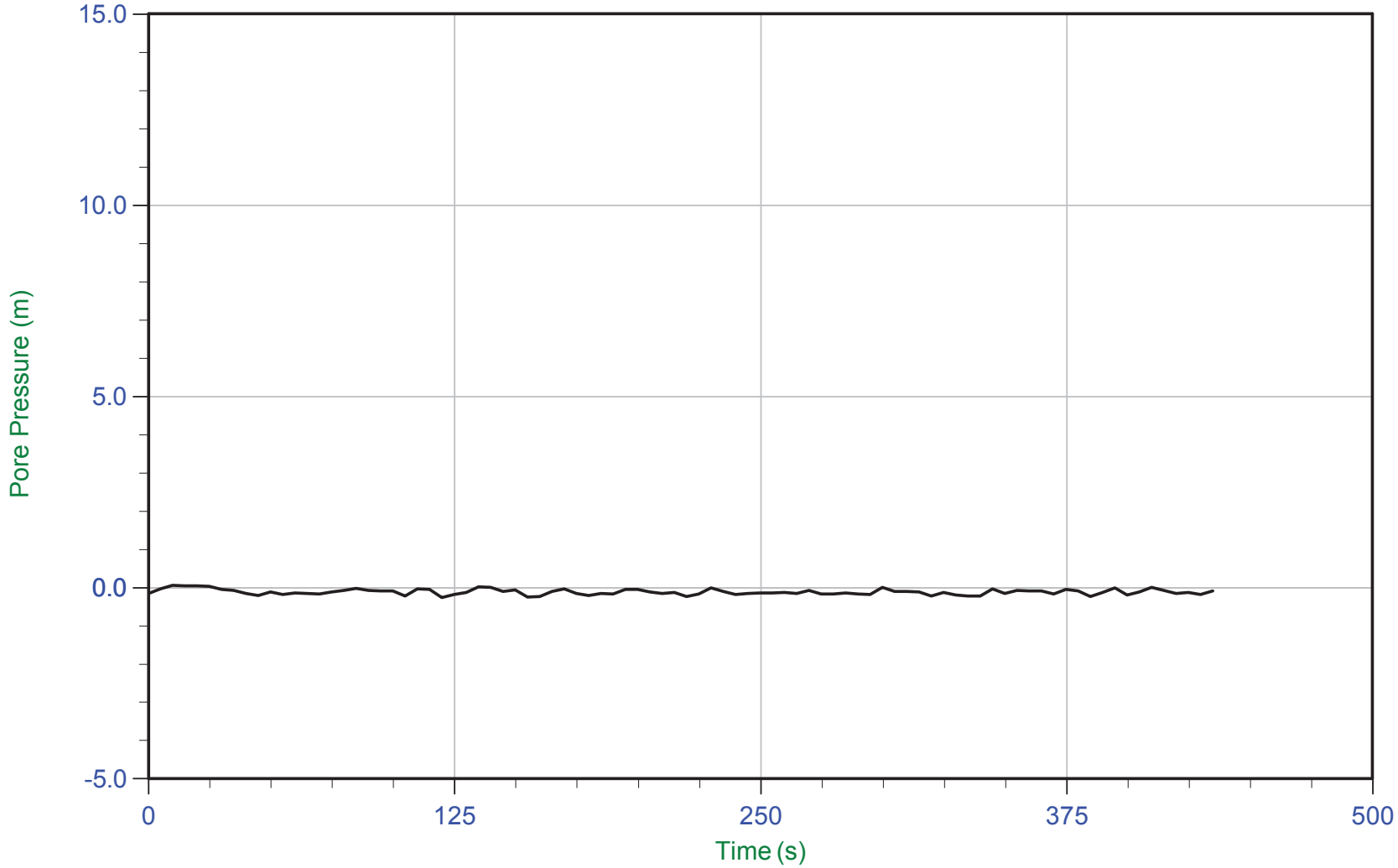

Trace Summary:

Filename: 16-72004_RS06.PPF
Depth: 22.300 m / 73.162 ft
Duration: 435.0 s

U Min: -0.3 m
U Max: 0.1 m

CONETEC

CGSH

Job No: 1672007
Date: 05/16/2016 13:45
Site: Germano Buttres

Sounding: GBCPT16-06
Cone: 432:T1500F15U500
Cone Area: 15 sq cm

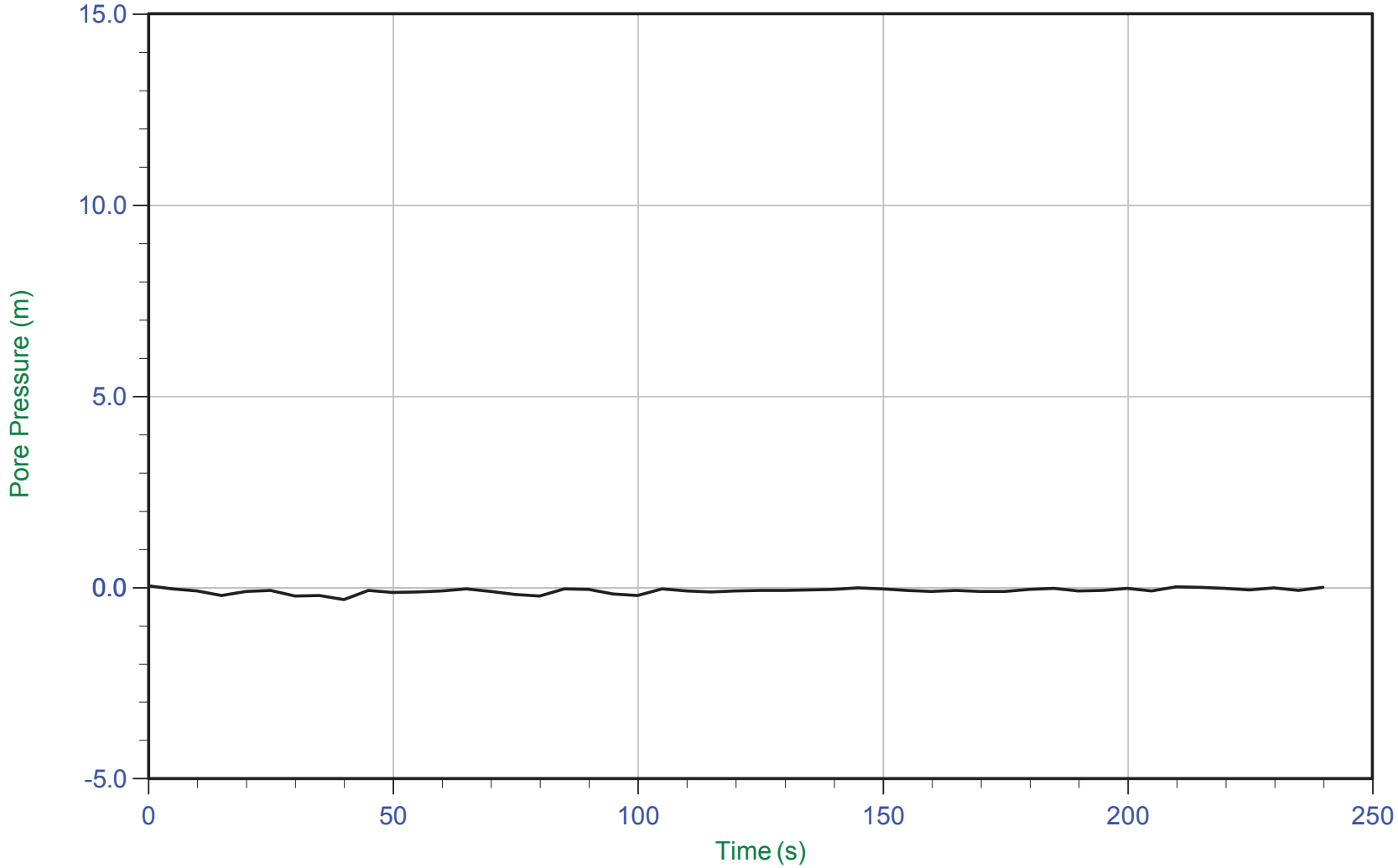

Trace Summary:

Filename: 16-72004_RS06.PPF
Depth: 23.300 m / 76.443 ft
Duration: 240.0 s

U Min: -0.3 m
U Max: 0.0 m

CONETEC

CGSH

Job No: 1672007
Date: 05/16/2016 13:45
Site: Germano Buttres

Sounding: GBCPT16-06
Cone: 432:T1500F15U500
Cone Area: 15 sq cm

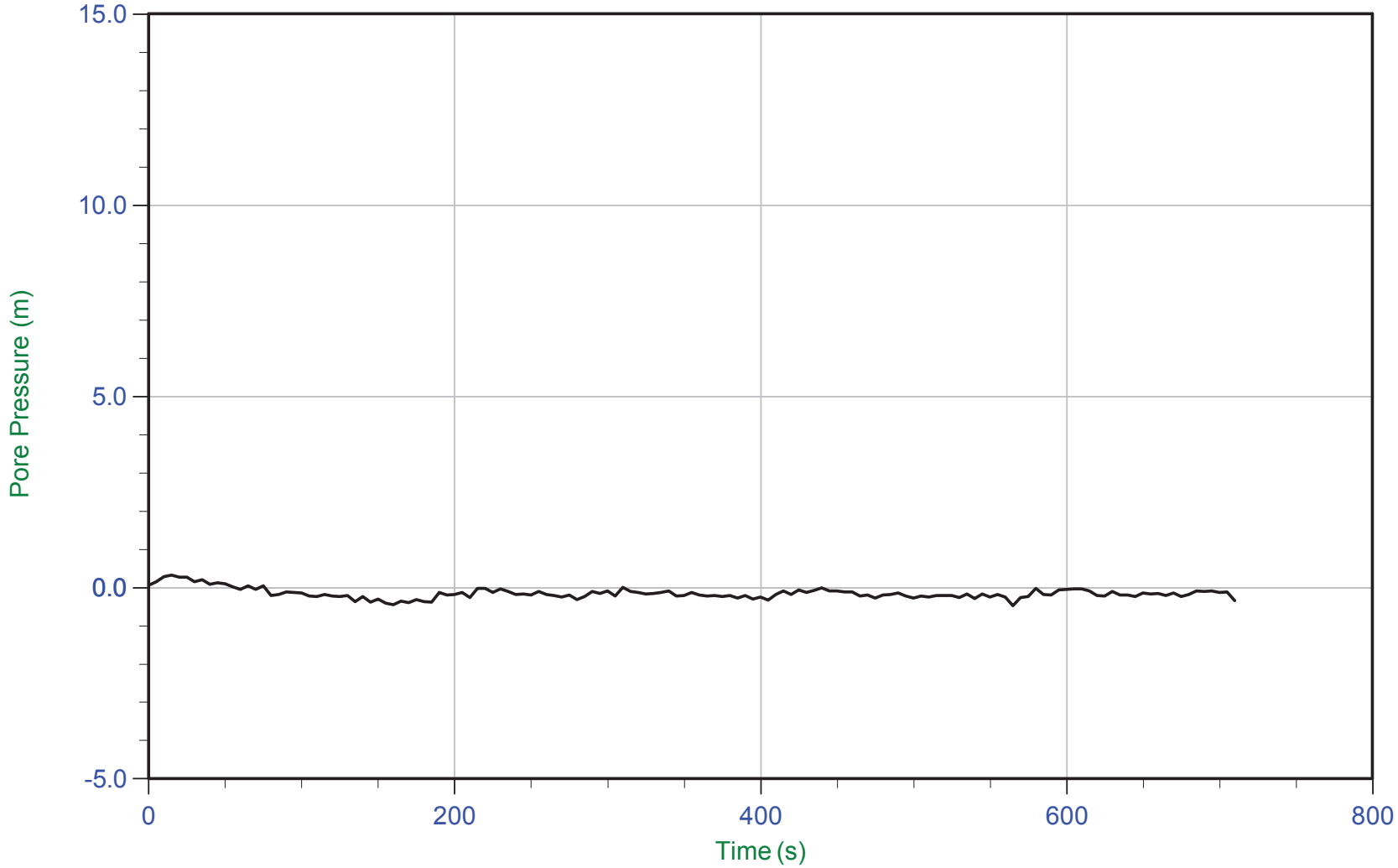

Trace Summary:

Filename: 16-72004_RS06.PPF
Depth: 24.300 m / 79.723 ft
Duration: 710.0 s

U Min: -0.5 m
U Max: 0.3 m

CONETEC

CGSH

Job No: 1672007
Date: 05/16/2016 13:45
Site: Germano Buttres

Sounding: GBCPT16-06
Cone: 432:T1500F15U500
Cone Area: 15 sq cm

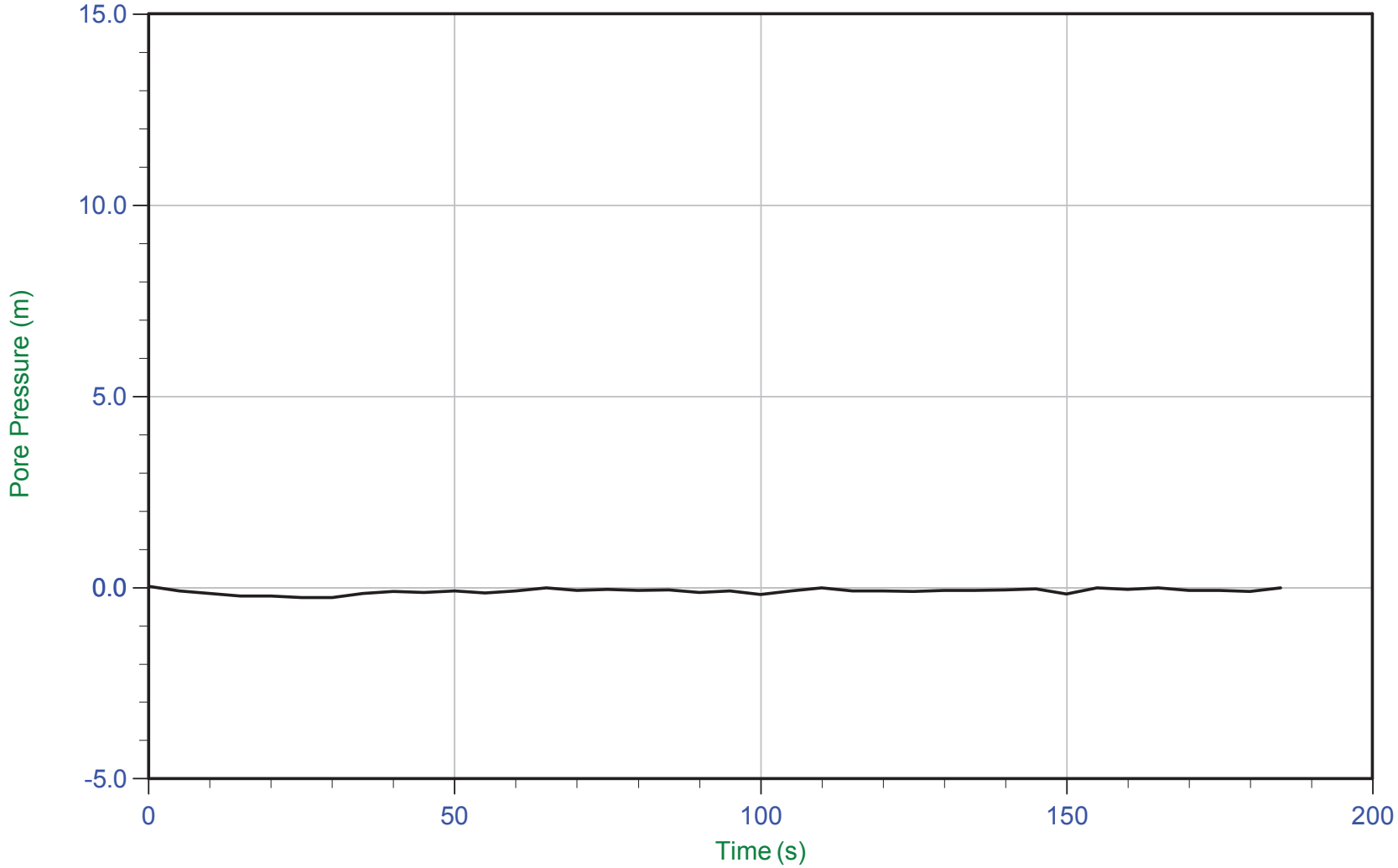

Trace Summary:

Filename: 16-72004_RS06.PPF
Depth: 25.300 m / 83.004 ft
Duration: 185.0 s

U Min: -0.3 m
U Max: 0.0 m

CONETEC

CGSH

Job No: 1672007
Date: 05/16/2016 13:45
Site: Germano Buttres

Sounding: GBCPT16-06
Cone: 432:T1500F15U500
Cone Area: 15 sq cm

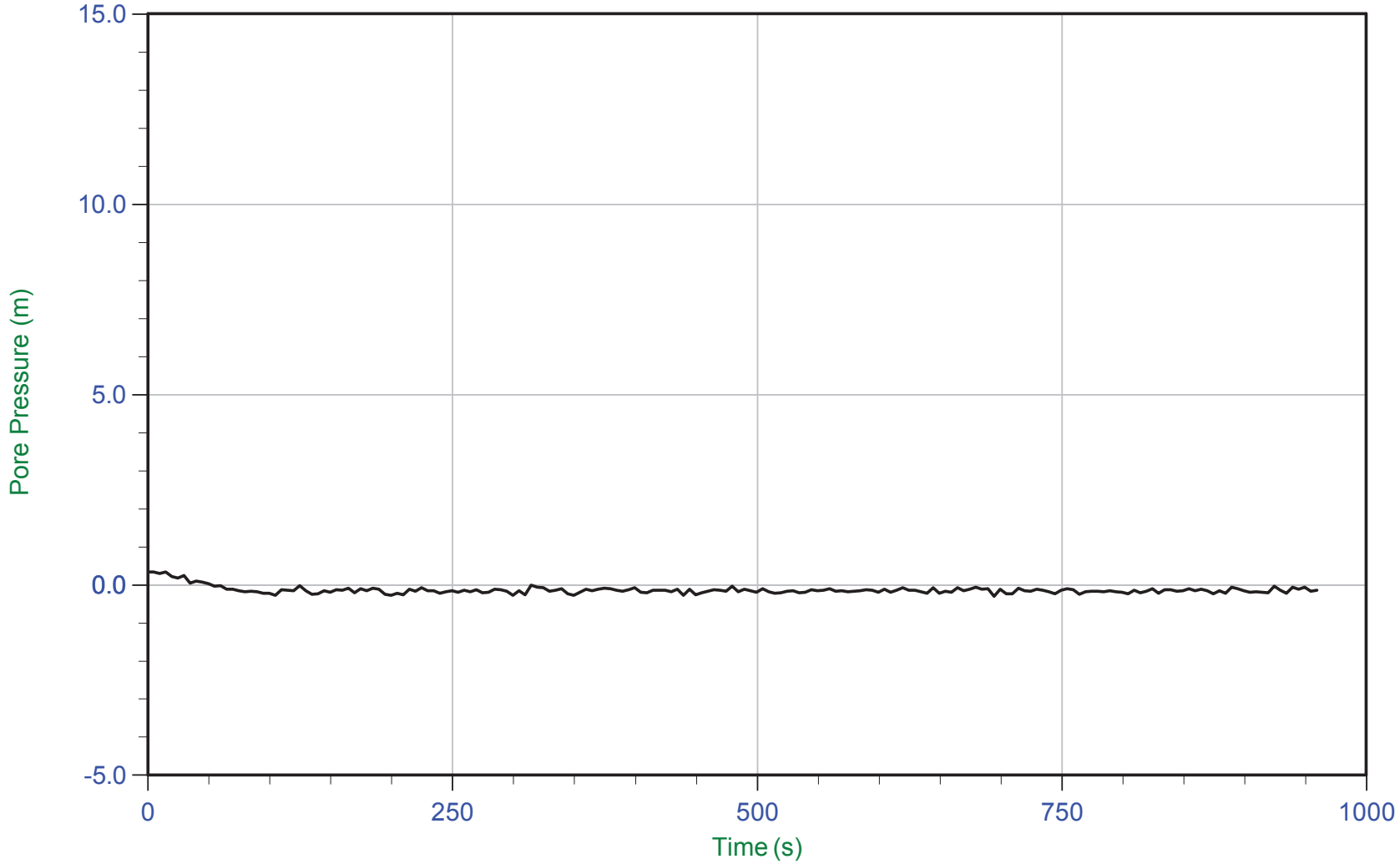

Trace Summary:

Filename: 16-72004_RS06.PPF
Depth: 26.300 m / 86.285 ft
Duration: 960.0 s

U Min: -0.3 m
U Max: 0.3 m

CONETEC

CGSH

Job No: 1672007
Date: 05/16/2016 13:45
Site: Germano Buttres

Sounding: GBCPT16-06
Cone: 432:T1500F15U500
Cone Area: 15 sq cm

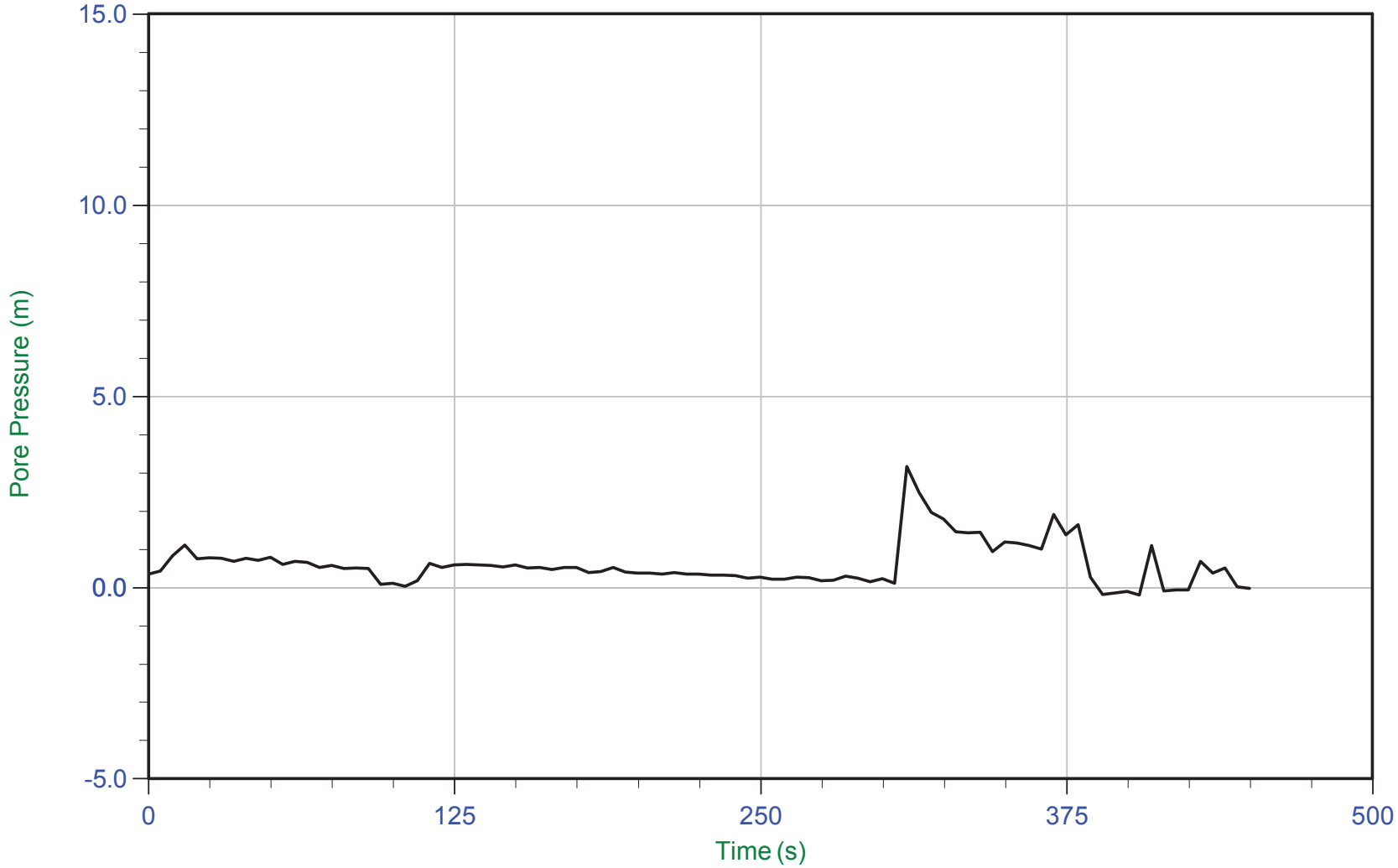

Trace Summary:

Filename: 16-72004_RS06.PPF
Depth: 26.550 m / 87.105 ft
Duration: 450.0 s

U Min: -0.2 m
U Max: 3.2 m

CONETEC

CGSH

Job No: 1672007
Date: 05/16/2016 13:45
Site: Germano Buttres

Sounding: GBCPT16-06
Cone: 432:T1500F15U500
Cone Area: 15 sq cm

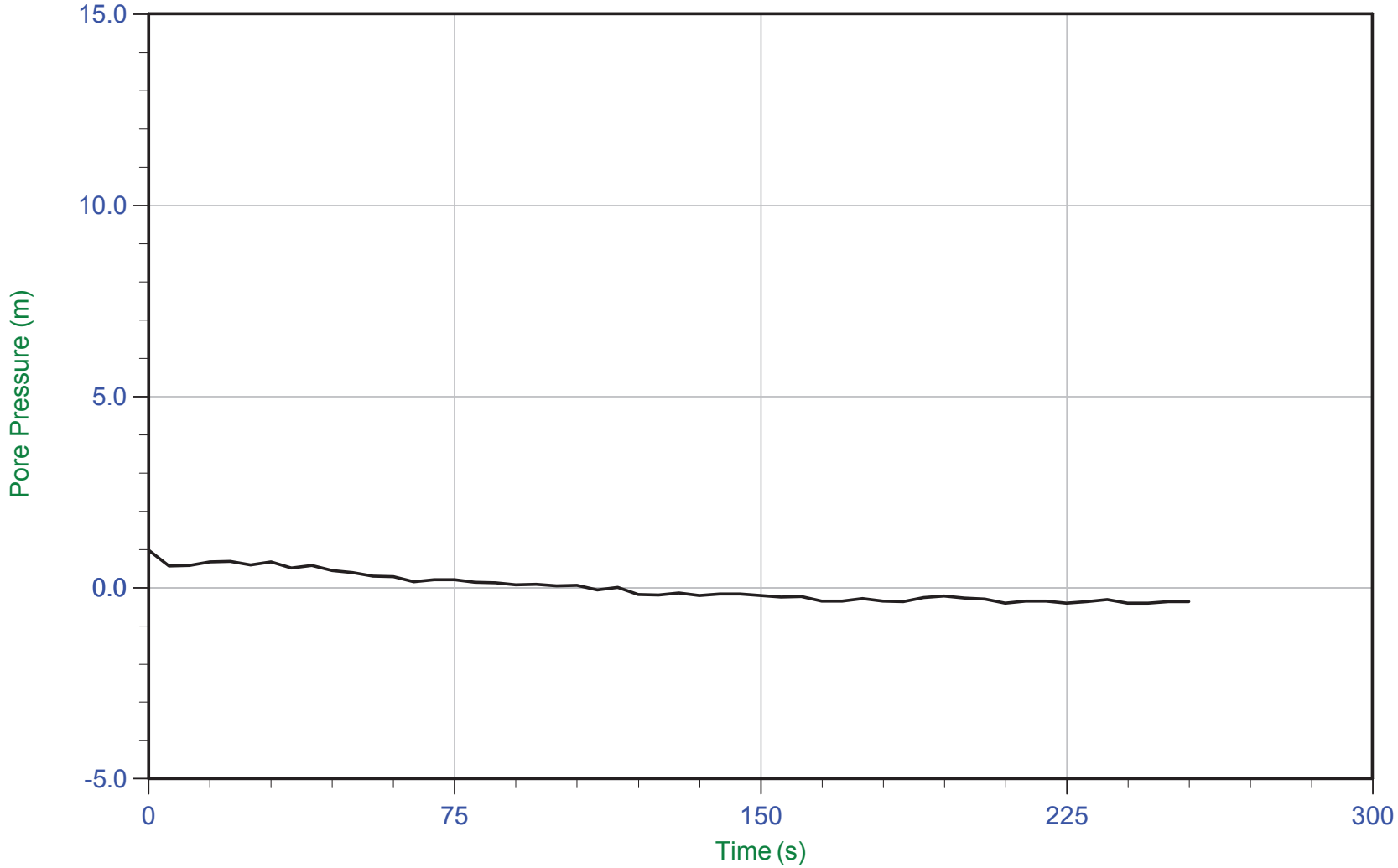

Trace Summary:

Filename: 16-72004_RS06.PPF
Depth: 27.200 m / 89.238 ft
Duration: 255.0 s

U Min: -0.4 m
U Max: 1.0 m

CONETEC

CGSH

Job No: 1672007
Date: 05/16/2016 13:45
Site: Germano Buttres

Sounding: GBCPT16-06
Cone: 432:T1500F15U500
Cone Area: 15 sq cm

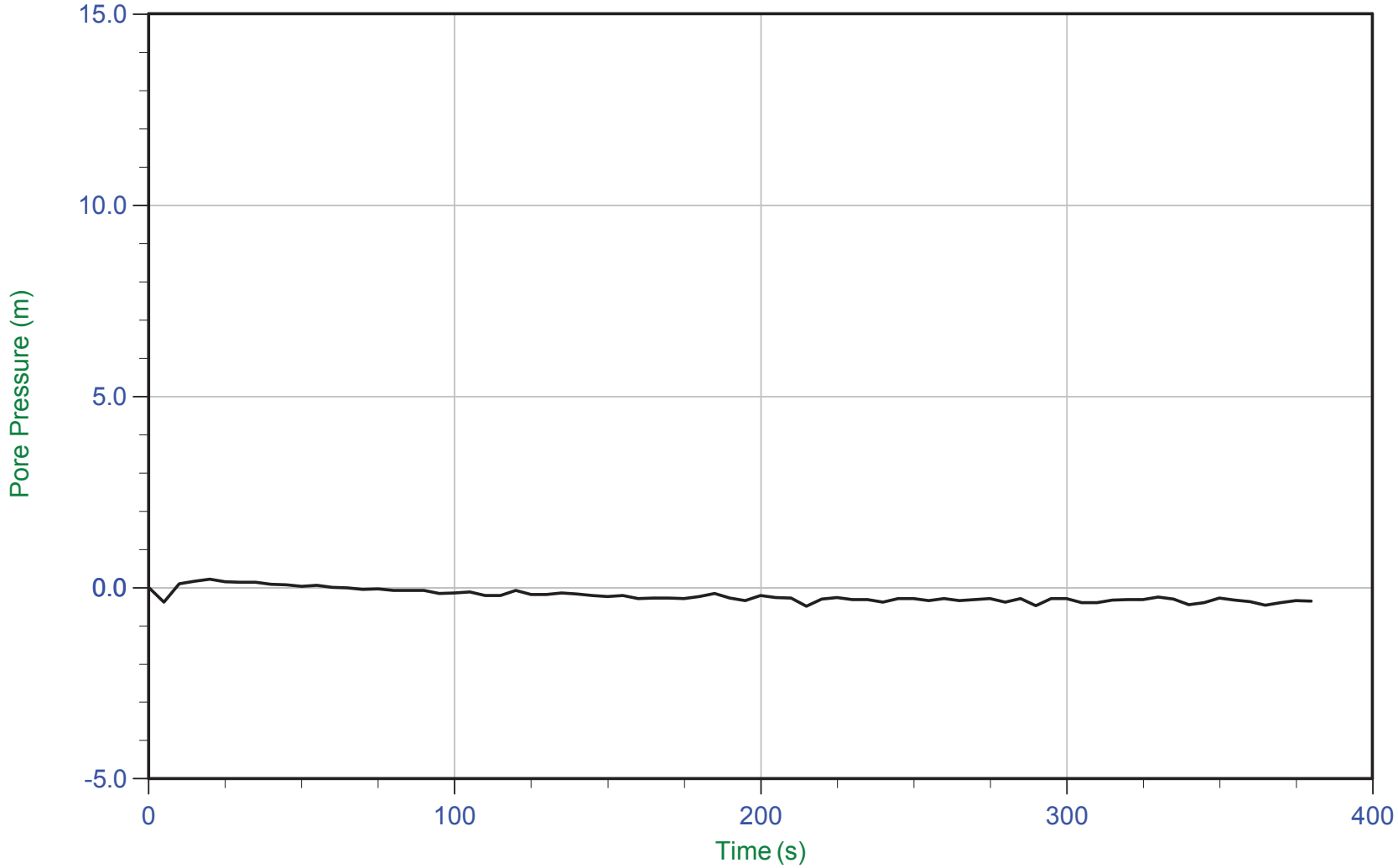

Trace Summary:

Filename: 16-72004_RS06.PPF
Depth: 27.300 m / 89.566 ft
Duration: 380.0 s

U Min: -0.5 m
U Max: 0.2 m

CONETEC

CGSH

Job No: 1672007
Date: 05/16/2016 13:45
Site: Germano Buttres

Sounding: GBCPT16-06
Cone: 432:T1500F15U500
Cone Area: 15 sq cm

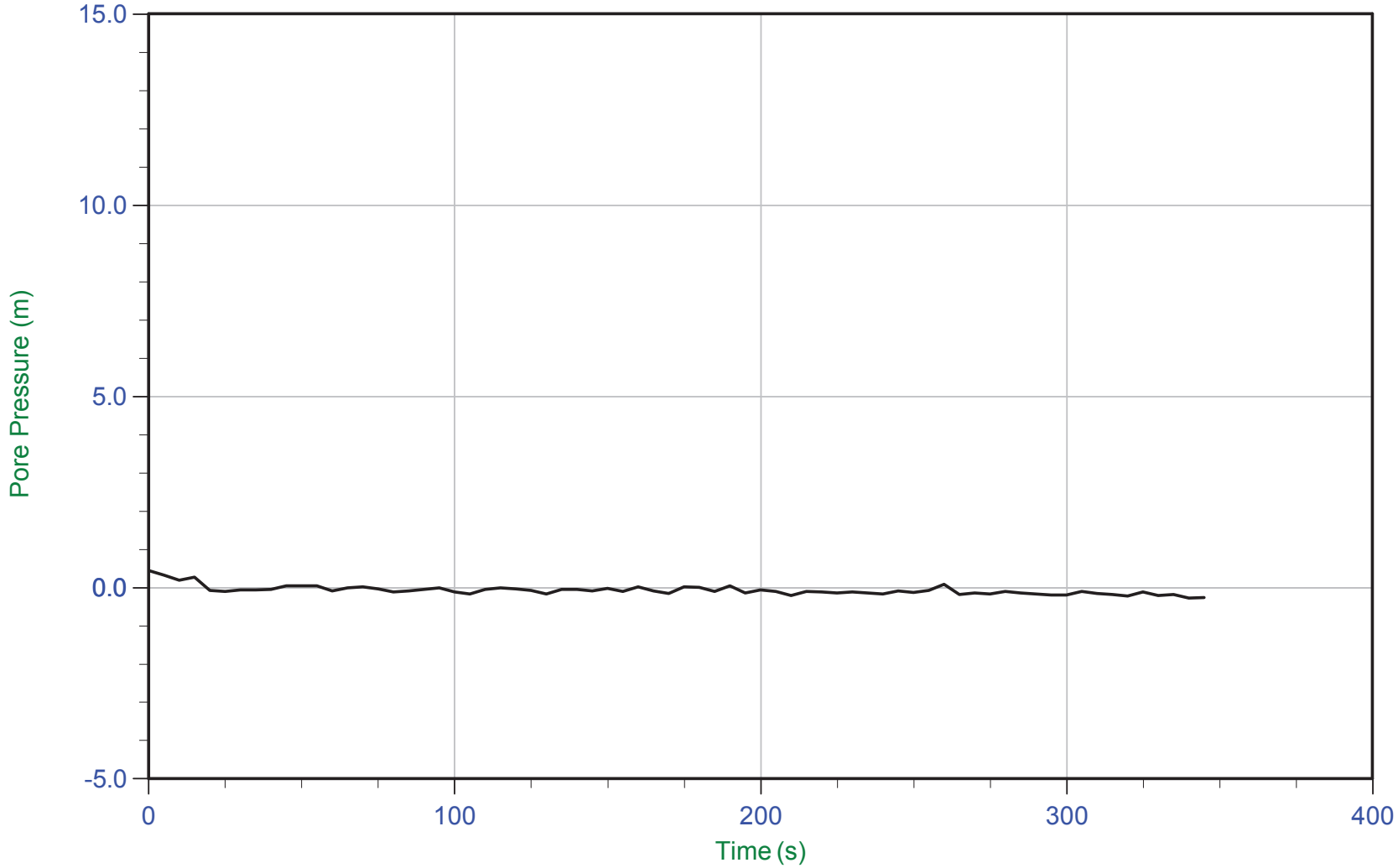

Trace Summary:

Filename: 16-72004_RS06.PPF
Depth: 27.500 m / 90.222 ft
Duration: 345.0 s

U Min: -0.3 m
U Max: 0.4 m

Electronic Field Vane Shear Test Profile Summary and Results

CONETEC

Job No:	16-72004
Client:	Cleary Gottlieb Steen & Hamilton LLP (CGSH)
Project:	Samarco, Germano Buttress
Start Date:	02-May-2016
End Date:	17-May-2016

ELECTRONIC FIELD VANE SHEAR TEST PROFILE SUMMARY

Sounding ID	File Name	Date From	Data To	Northing[1] (m)	Easting (m)	Refer to Notation Number
GSVST16-01	16-72004_VST-GS01	02-May-2016	09-May-2016	7764160	658561	
GSVST16-02	16-72004_VST-GS02	16-May-2016	17-May-2016	7763372	659089	

1. The coordinates were acquired using consumer-grade GPS device with datum: WGS 84/ UTM Zone 23 South.

Job Number: 16-72004
Client: CGSH
Project: Samarco, Germano Butress
Start Date: 2-May-2016
End Date: 17-May-2016

ELECTRONIC FIELD VANE SHEAR TEST RESULTS

Sounding ID	File Name	Date	Load Cell Serial Number	Casing Depth (m)	Test Depth[1] (m)	Vane Diameter D (mm)	Vane Height H (mm)	Top Taper Angle i_T (deg)	Bottom Taper Angle i_B (deg)	Vane Factor (Nm to kPa)	Peak Torque (Nm)	Remolded Torque (Nm)	Su Peak (kPa)	Su Residual (kPa)	Su Remolded (kPa)	Sensitivity	Refer to Notation Number
GSVST16-01	16-72004_VST-GS01	09-May-2016	AVLC-0012	9.50	10.50	55	110	45	45	1.5483	17.02	5.91	26.3	22.0	9.1	3	
GSVST16-01	16-72004_VST-GS01	02-May-2016	AVLC-0020	10.00	11.00	75	150	45	45	0.6106	27.99	2.36	17.1	8.1	1.4	12	
GSVST16-01	16-72004_VST-GS01	09-May-2016	AVLC-0012	9.50	11.25	55	110	45	45	1.5483	26.25	4.84	40.6	26.6	7.5	5	
GSVST16-01	16-72004_VST-GS01	02-May-2016	AVLC-0020	10.00	11.50	75	150	45	45	0.6106	48.29	7.72	29.5		4.7	6	
GSVST16-01	16-72004_VST-GS01	03-May-2016	AVLC-0020	10.00	13.50	75	150	45	45	0.6106	92.46	4.78	56.5		2.9	19	2
GSVST16-01	16-72004_VST-GS01	03-May-2016	AVLC-0020	15.00	16.25	75	150	45	45	0.6106	43.49	4.57	26.6	15.7	2.8	10	
GSVST16-01	16-72004_VST-GS01	04-May-2016	AVLC-0020	18.50	19.50	75	150	45	45	0.6106	49.72	5.59	30.4	12.2	3.4	9	3
GSVST16-01	16-72004_VST-GS01	04-May-2016	AVLC-0020	18.50	20.50	75	150	45	45	0.6106	39.76	10.03	24.3	18.7	6.1	4	
GSVST16-01	16-72004_VST-GS01	04-May-2016	AVLC-0020	18.50	21.50	75	150	45	45	0.6106	71.00		43.3				2, 4
GSVST16-01	16-72004_VST-GS01	04-May-2016	AVLC-0020	22.50	23.50	75	150	45	45	0.6106	86.47	9.15	52.8		5.6	9	
GSVST16-01	16-72004_VST-GS01	05-May-2016	AVLC-0020	26.50	27.50	55	110	45	45	1.5483	113.71	41.54	176.0	84.3	64.3	3	
GSVST16-01	16-72004_VST-GS01	05-May-2016	AVLC-0020	29.00	30.00	55	110	45	45	1.5483	93.58	24.00	153.8	77.7	37.2	4	
GSVST16-01	16-72004_VST-GS01	06-May-2016	AVLC-0020	31.00	32.25	55	110	45	45	1.5483	114.68	48.00	177.6	67.9	74.3	2	
GSVST16-01	16-72004_VST-GS01	06-May-2016	AVLC-0020	37.50	38.50	75	150	45	45	0.6106	71.20	63.48	43.5	35.2			4
GSVST16-01	16-72004_VST-GS01	07-May-2016	AVLC-0020	39.50	40.50	75	150	45	45	0.6106	127.57						5
GSVST16-02	16-72004_VST-GS02	16-May-2016	AVLC-0012	5.80	7.00	75	150	45	45	0.6106	17.25	1.38	10.5		0.8	12	
GSVST16-02	16-72004_VST-GS02	16-May-2016	AVLC-0012	5.80	8.00	75	150	45	45	0.6106	13.03	2.74	8.0		1.7	5	
GSVST16-02	16-72004_VST-GS02	16-May-2016	AVLC-0012	5.80	9.00	75	150	45	45	0.6106	14.12	3.52	8.6		2.2	4	
GSVST16-02	16-72004_VST-GS02	16-May-2016	AVLC-0012	5.80	11.00	75	150	45	45	0.6106	21.68	5.32	13.2		3.2	4	
GSVST16-02	16-72004_VST-GS02	17-May-2016	AVLC-0012	23.60	26.00	75	150	45	45	0.6106	81.10	15.02	49.5		9.2	5	
GSVST16-02	16-72004_VST-GS02	17-May-2016	AVLC-0012	23.60	27.00	75	150	45	45	0.6106	78.95	11.26	48.2		6.9	7	
GSVST16-02	16-72004_VST-GS02	17-May-2016	AVLC-0012	23.60	28.00	75	150	45	45	0.6106	50.15	11.96	30.6		7.3	4	

1. Depth referenced to the mid point of the vane blade.
2. Unclear if peak strength reached.
3. Pre-peak shear mostly not recorded.
4. No remolded test data.
5. Load cell maximum capacity reached, peak strength not reached.

Electronic Field Vane Shear Test Plots

CONETEC

Job Number: 16-72004
Client: CGSH
Project: Samarco, Germano Buttres
Sounding: GSVST16-01B-10.50
Sounding Date: 09-May-2016 06:37

Test Depth: (m): 10.50
Vane Type: Double tapered 55 x 110 mm

Coordinate System: WGS84/UTM Zone 23 South
Northing (m): 7764160
Easting: (m): 658561

Vane Shear Test

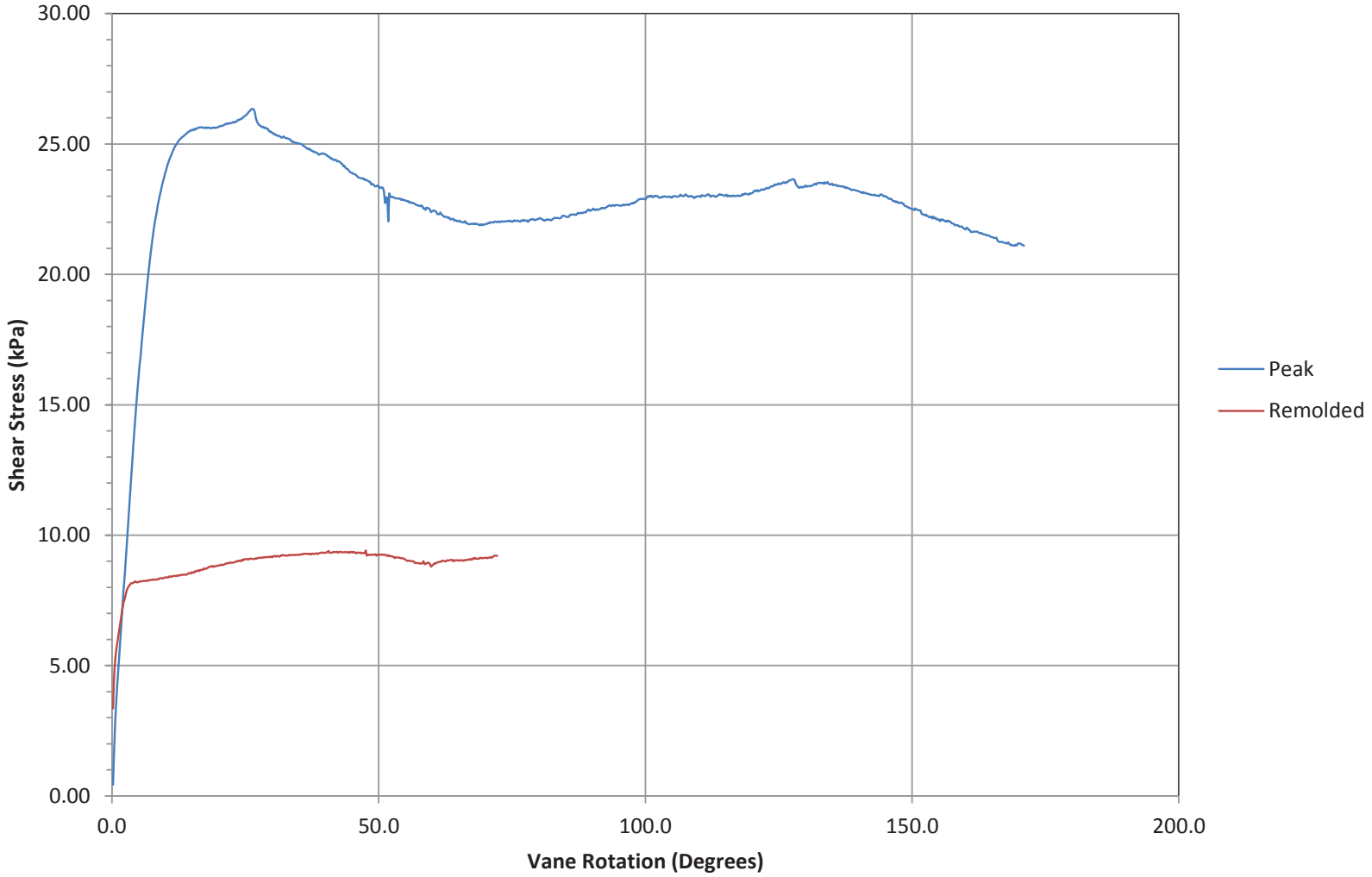

Job Number: 16-72004
Client: CGSH
Project: Samarco, Germano Buttress
Sounding: GSVST16-01-11.0
Sounding Date: 02-May-2016 10:54

Test Depth: (m): 11.00
Vane Type: Double tapered 75 x 150 mm

Coordinate System: WGS84/UTM Zone 23 South
Northing (m): 7764160
Easting: (m): 658561

Vane Shear Test

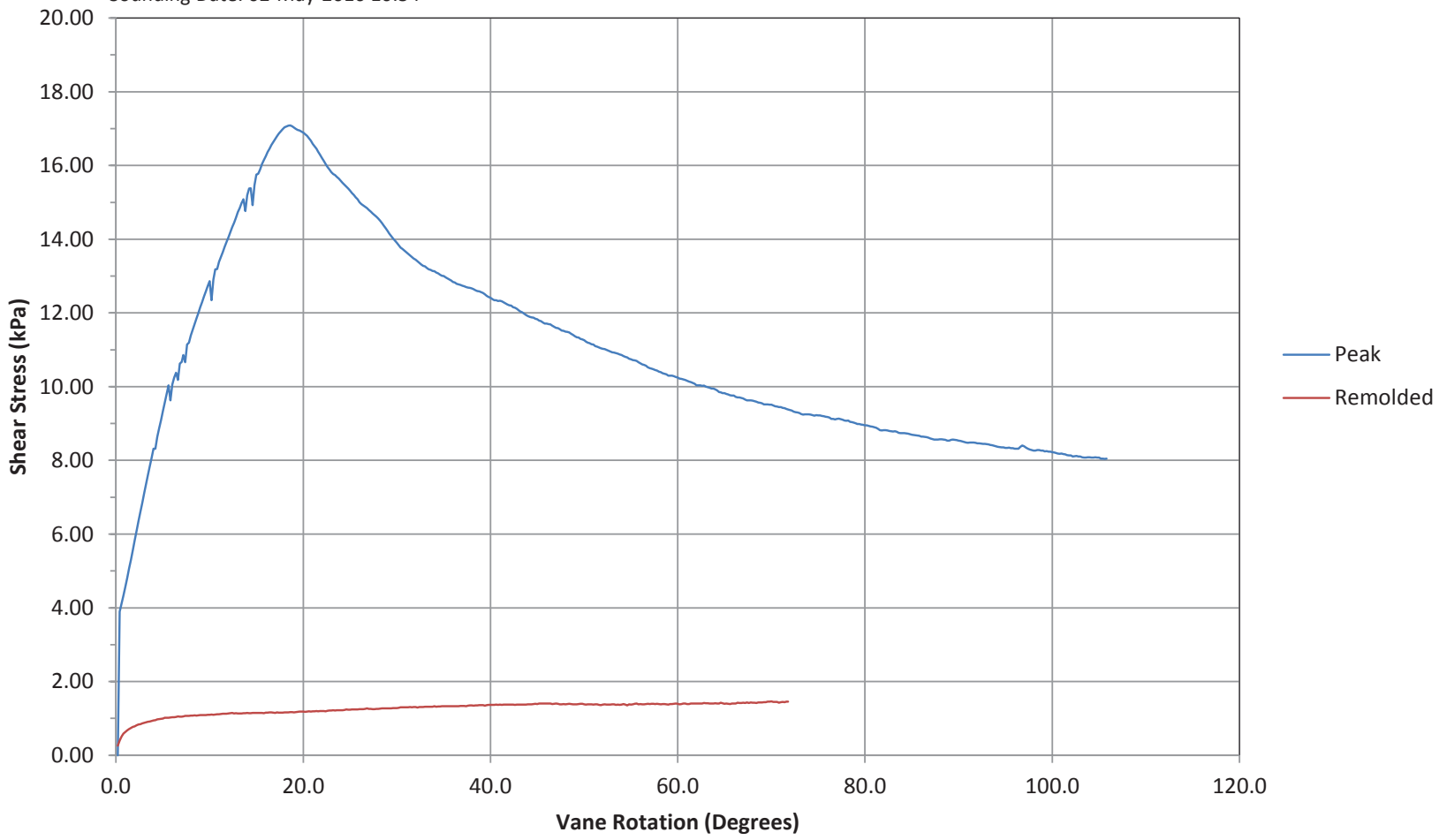

Job Number: 16-72004
Client: CGSH
Project: Samarco, Germano Buttres
Sounding: GSVST16-01B-11.25
Sounding Date: 09-May-2016 07:19

Test Depth: (m): 11.25
Vane Type: Double tapered 55 x 110 mm

Coordinate System: WGS84/UTM Zone 23 South
Northing (m): 7764160
Easting: (m): 658561

Vane Shear Test

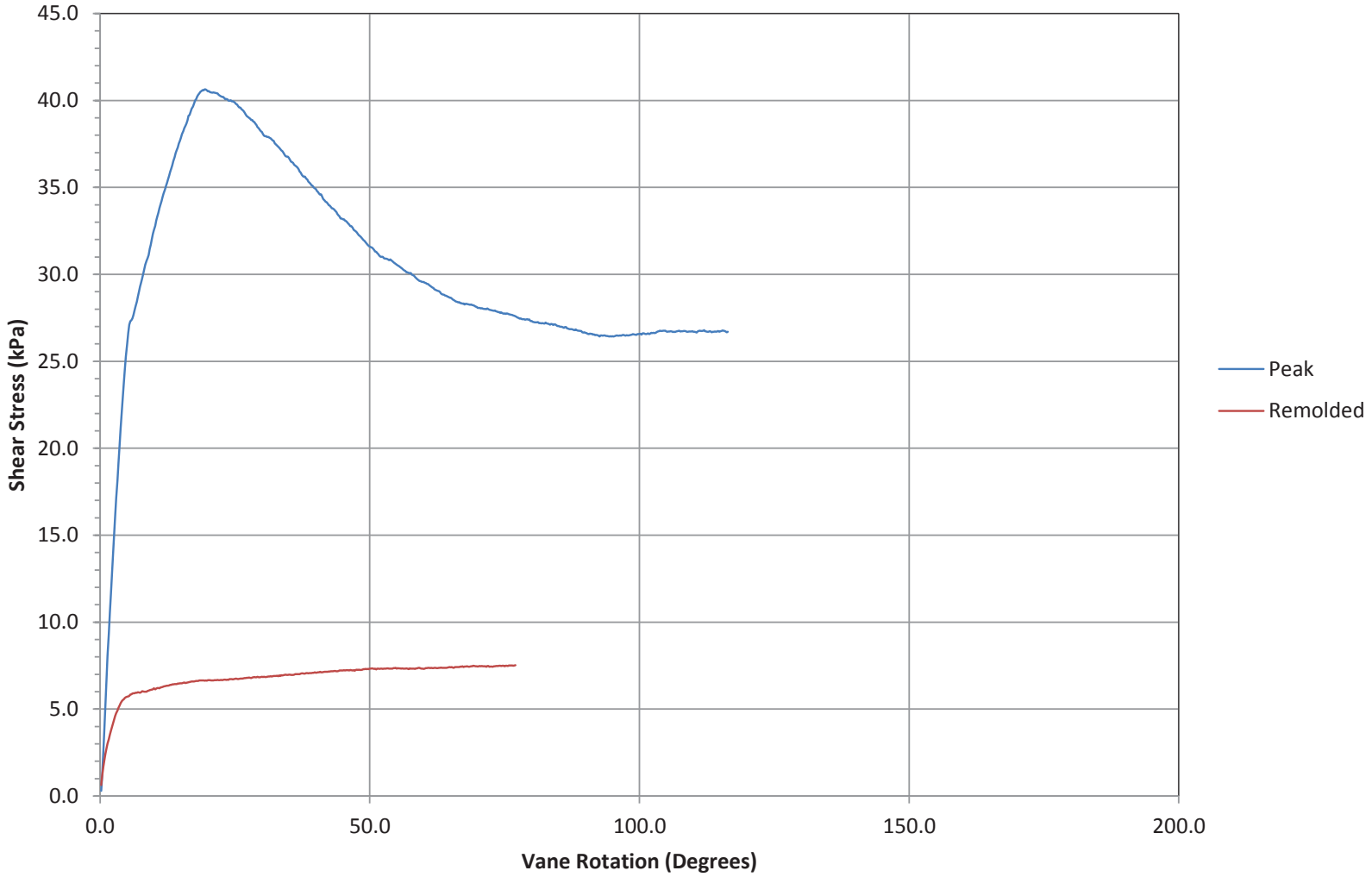

Job Number: 16-72004
Client: CGSH
Project: Samarco, Germano Buttress
Sounding: GSVST16-01-11.5
Sounding Date: 02-May-2016 11:52

Test Depth: (m): 11.50
Vane Type: Double tapered 75 x 150 mm

Coordinate System: WGS84/UTM Zone 23 South
Northing (m): 7764160
Easting: (m): 658561

Vane Shear Test

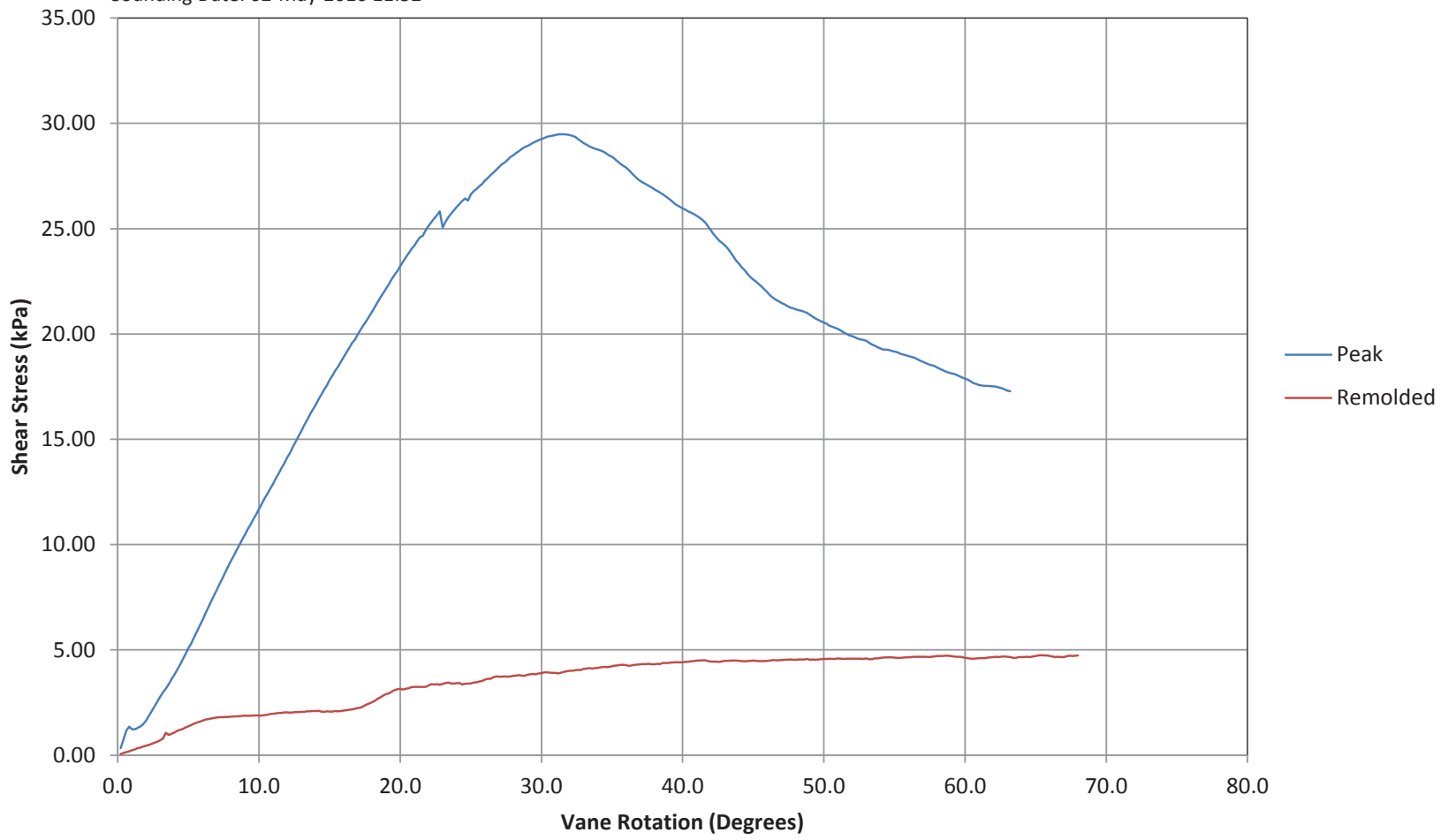

Job Number: 16-72004
Client: CGSH
Project: Samarco, Germano Buttress
Sounding: GSVST16-01-13.5
Sounding Date: 03-May-2016 06:17

Test Depth: (m): 13.50
Vane Type: Double tapered 75 x 150 mm

Coordinate System: WGS84/UTM Zone 23 South
Northing (m): 7764160
Easting: (m): 658561

Vane Shear Test

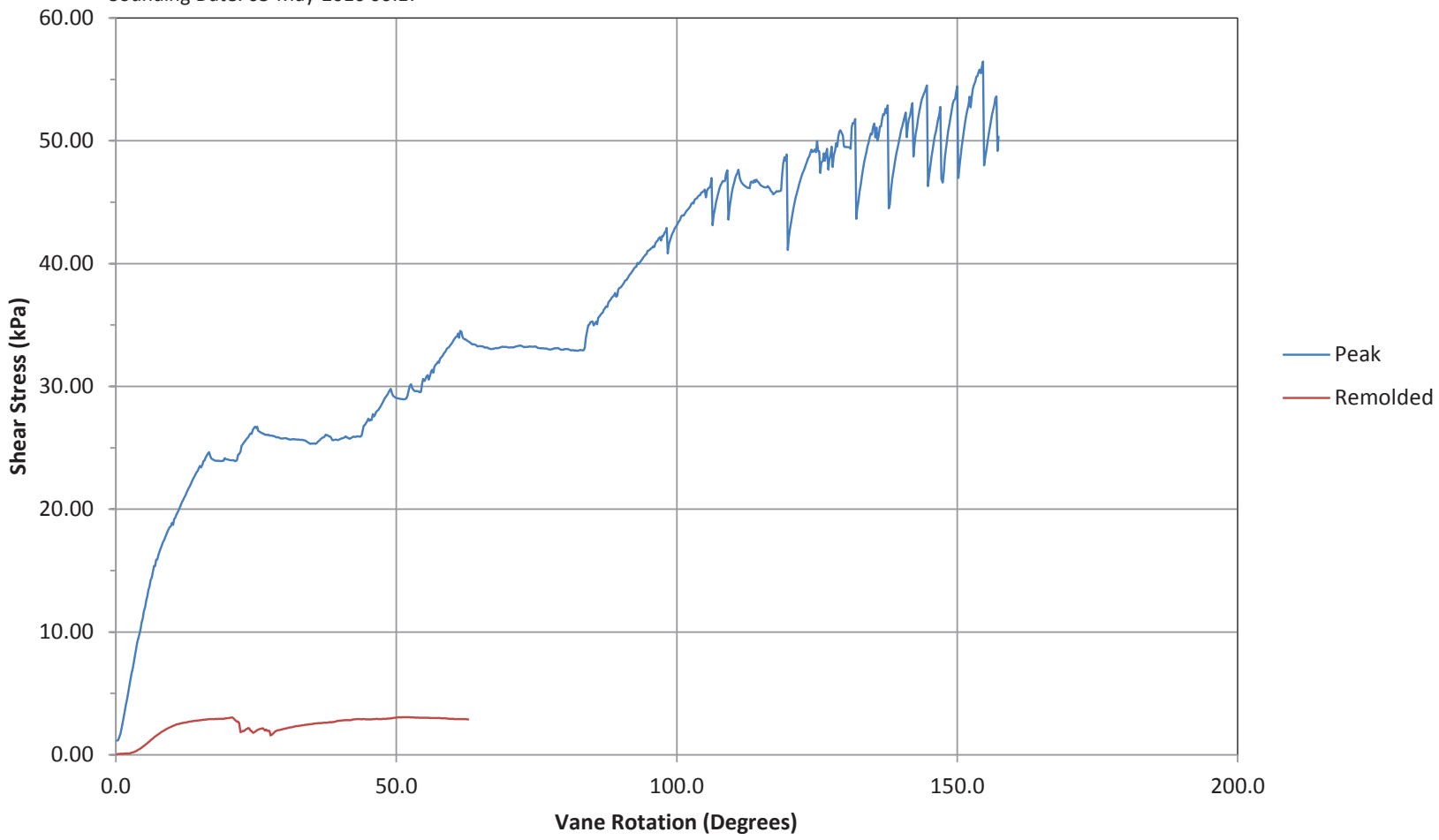

Job Number: 16-72004
Client: CGSH
Project: Samarco, Germano Buttress
Sounding: GSVST16-01-13.5
Sounding Date: 03-May-2016 09:53

Test Depth: (m): 16.25
Vane Type: Double tapered 75 x 150 mm

Coordinate System: WGS84/UTM Zone 23 South
Northing (m): 7764160
Easting: (m): 658561

Vane Shear Test

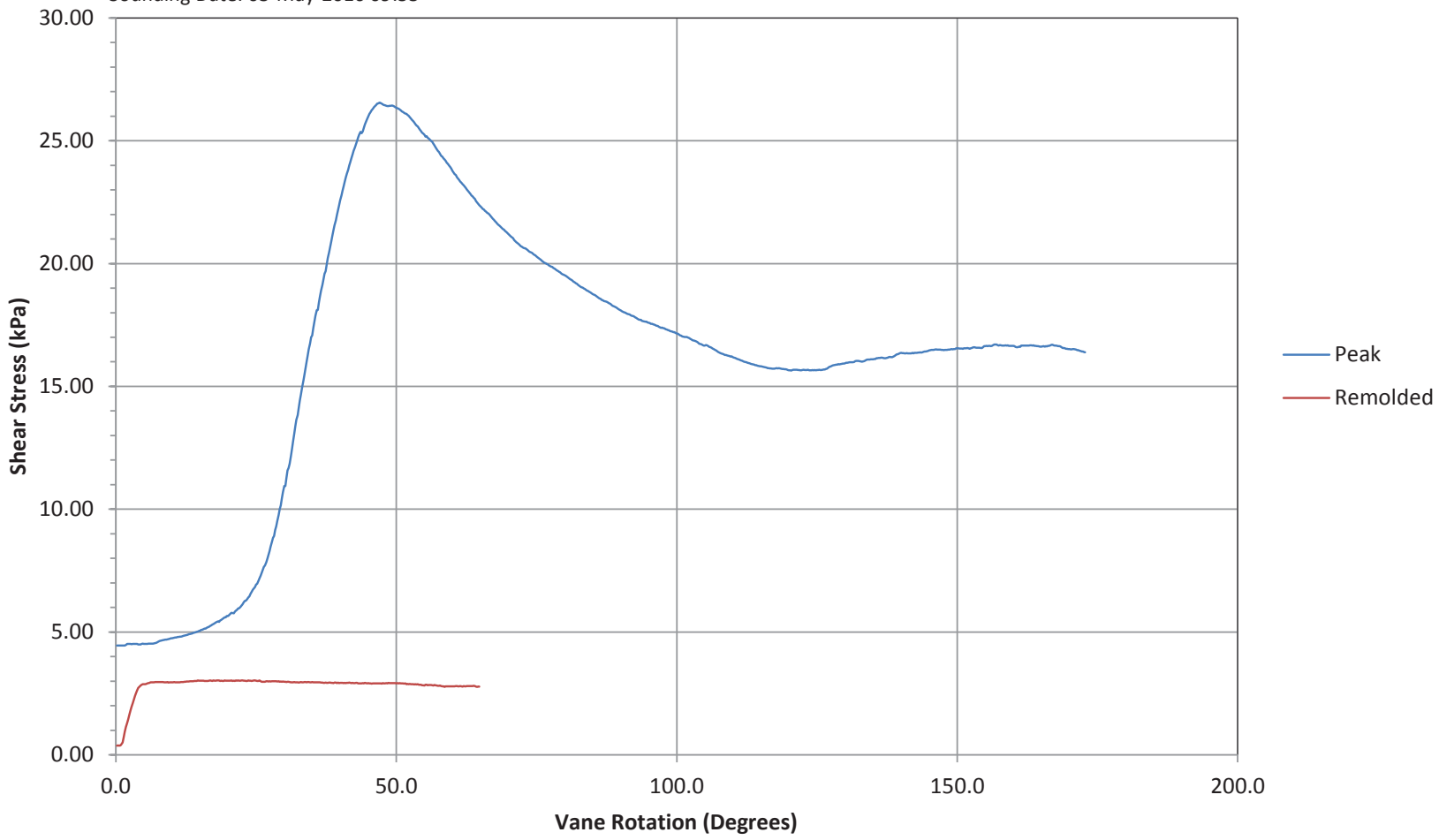

Job Number: 16-72004
Client: CGSH
Project: Samarco, Germano Buttres
Sounding: GSVST16-01-19.5
Sounding Date: 04-May-2016 07:04

Test Depth: (m): 19.50
Vane Type: Double tapered 75 x 150 mm

Coordinate System: WGS84/UTM Zone 23 South
Northing (m): 7764160
Easting: (m): 658561

Vane Shear Test

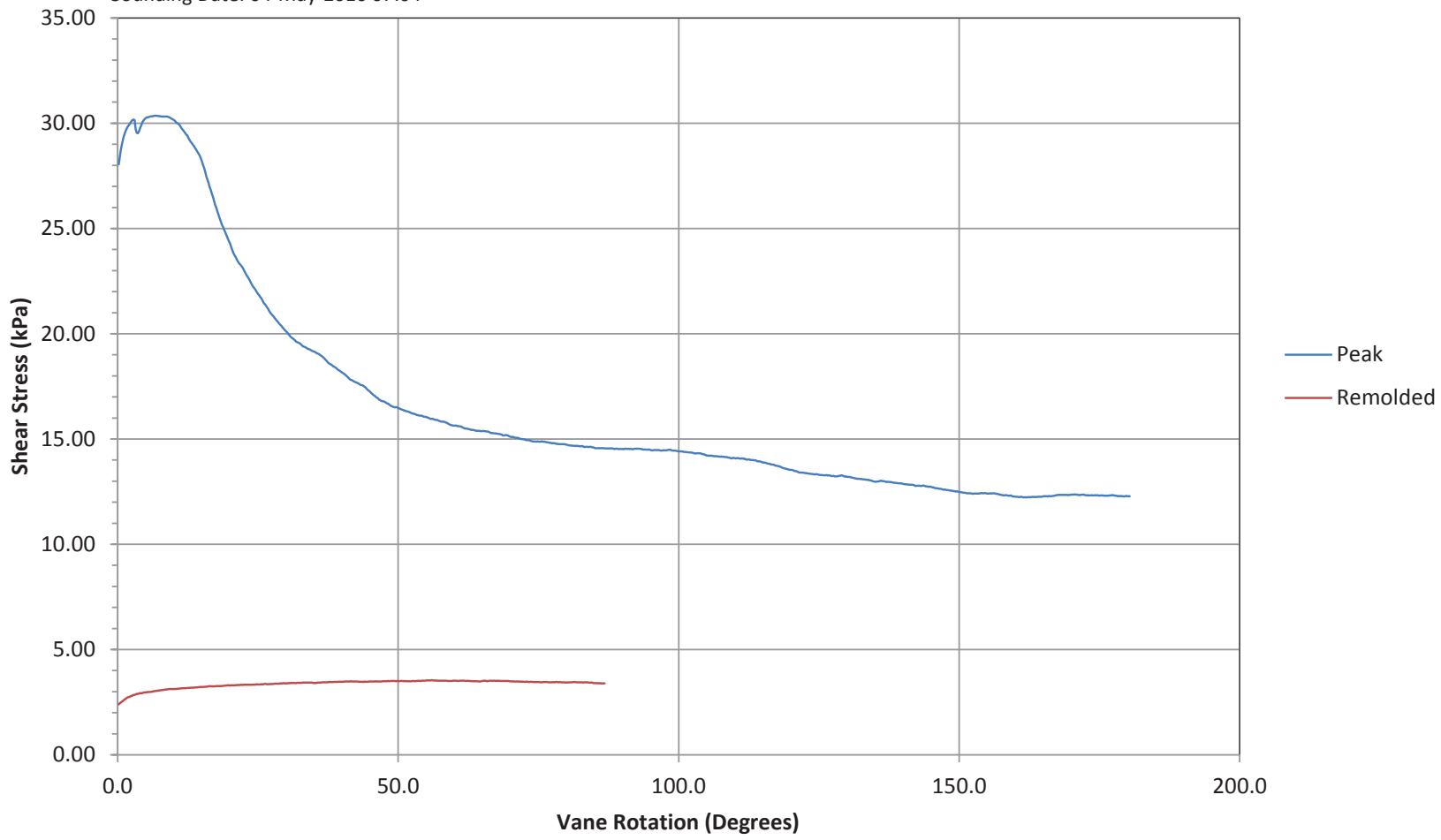

Job Number: 16-72004
Client: CGSH
Project: Samarco, Germano Buttres
Sounding: GSVST16-01-20.5
Sounding Date: 04-May-2016 08:00

Test Depth: (m): 20.50
Vane Type: Double tapered 75 x 150 mm

Coordinate System: WGS84/UTM Zone 23 South
Northing (m): 7764160
Easting: (m): 658561

Vane Shear Test

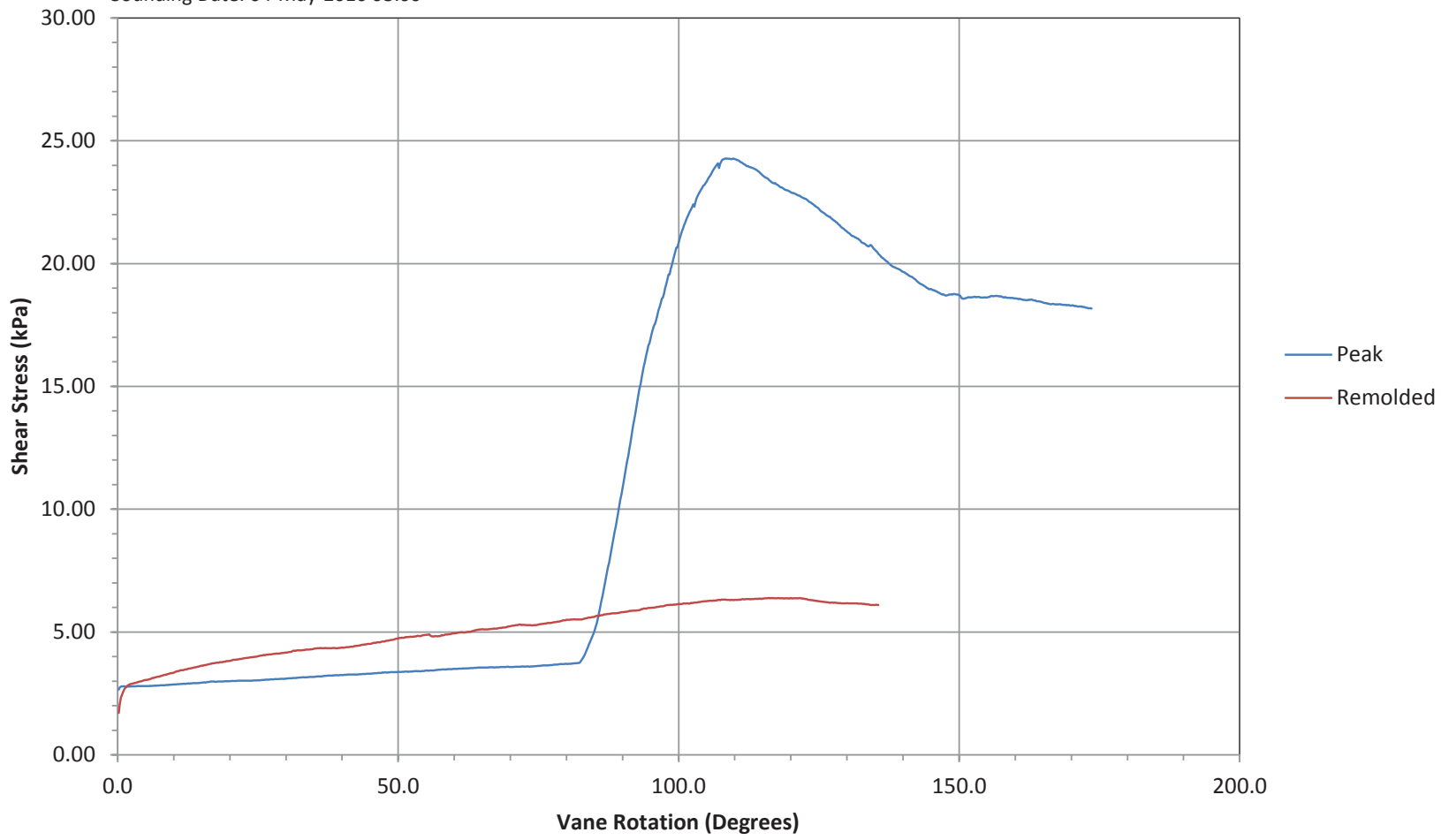

Job Number: 16-72004
Client: CGSH
Project: Samarco, Germano Buttres
Sounding: GSVST16-01-21.5
Sounding Date: 04-May-2016 09:11

Test Depth: (m): 21.50
Vane Type: Double tapered 75 x 150 mm

Coordinate System: WGS84/UTM Zone 23 South
Northing (m): 7764160
Easting: (m): 658561

Vane Shear Test

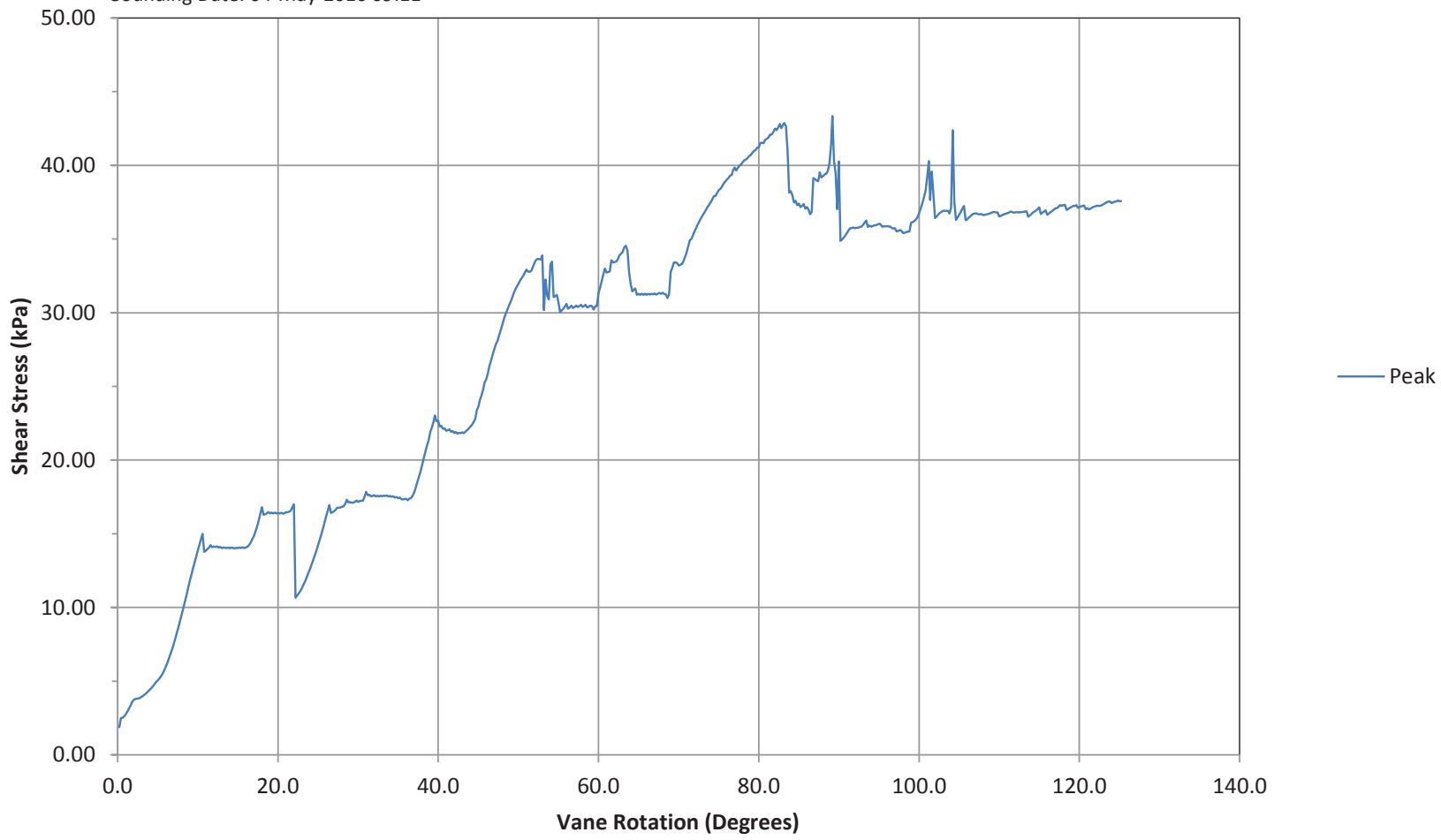

Job Number: 16-72004
Client: CGSH
Project: Samarco, Germano Buttres
Sounding: GSVST16-01-24.5
Sounding Date: 04-May-2016 11:55

Test Depth: (m): 23.50
Vane Type: Double tapered 75 x 150 mm

Coordinate System: WGS84/UTM Zone 23 South
Northing (m): 7764160
Easting: (m): 658561

Vane Shear Test

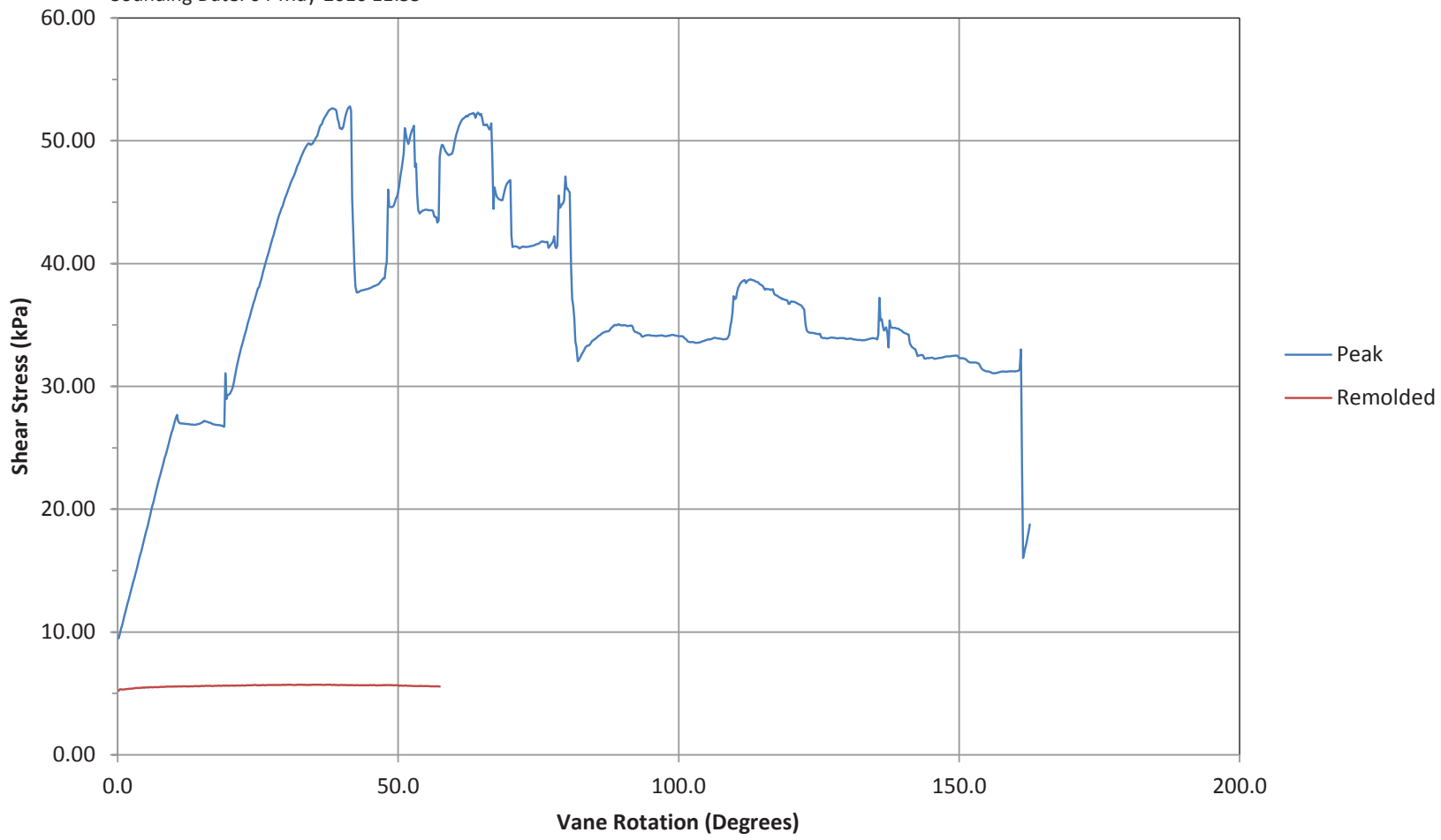

Job Number: 16-72004
Client: CGSH
Project: Samarco
Sounding: GSVST16-01-27.5
Sounding Date: 05-May-2016 08:03

Test Depth: (m): 27.50
Vane Type: Double tapered 55 x 110 mm

Coordinate System: WGS84/UTM Zone 23 South
Northing (m): 7764160
Easting: (m): 658561

Vane Shear Test

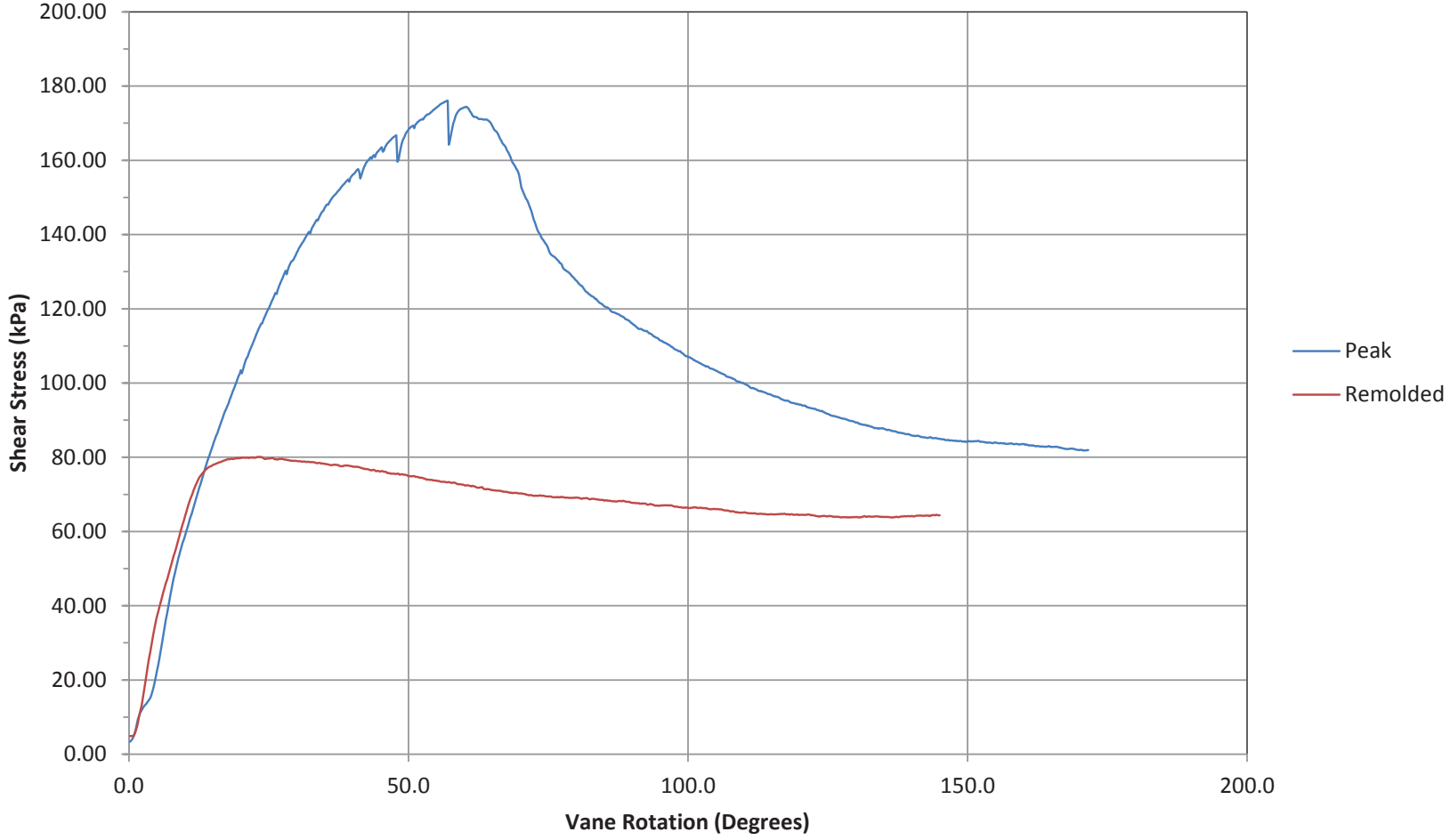

Job Number: 16-72004
Client: CGSH
Project: Samarco
Sounding: GSVST16-01-30
Sounding Date: 05-May-2016 11:30

Test Depth: (m): 30.00
Vane Type: Double tapered 55 x 110 mm

Coordinate System: Lat / Long (WGS84)
Northing (deg): 7764160
Easting: (deg): 658561

Vane Shear Test

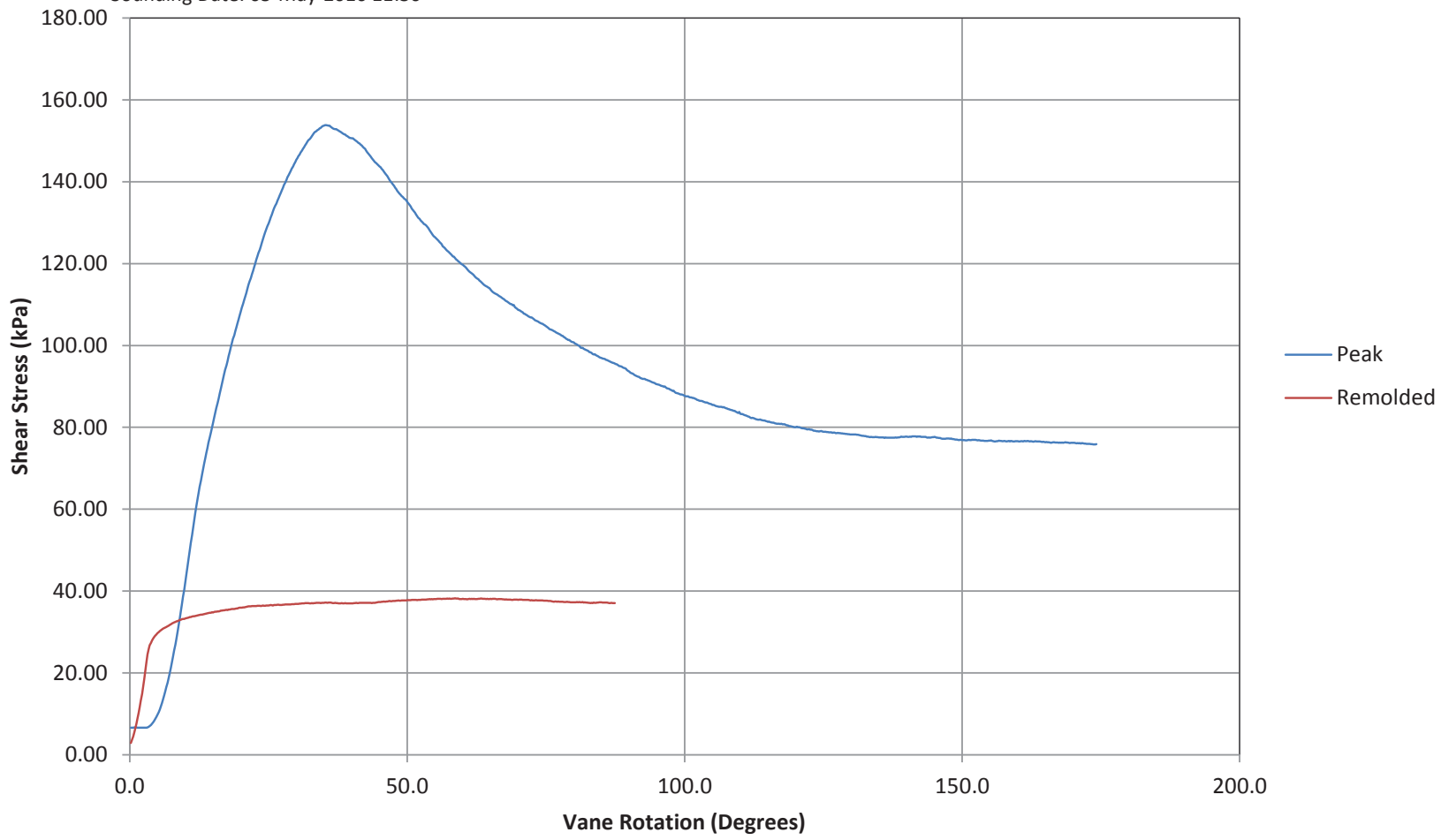

Job Number: 16-72004
Client: CGSH
Project: Samarco, Germano Buttres
Sounding: GSVST16-01-32.25
Sounding Date: 06-May-2016 07:19

Test Depth: (m): 32.25
Vane Type: Double tapered 55 x 110 mm

Coordinate System: WGS84/UTM Zone 23 South
Northing (m): 7764160
Easting: (m): 658561

Vane Shear Test

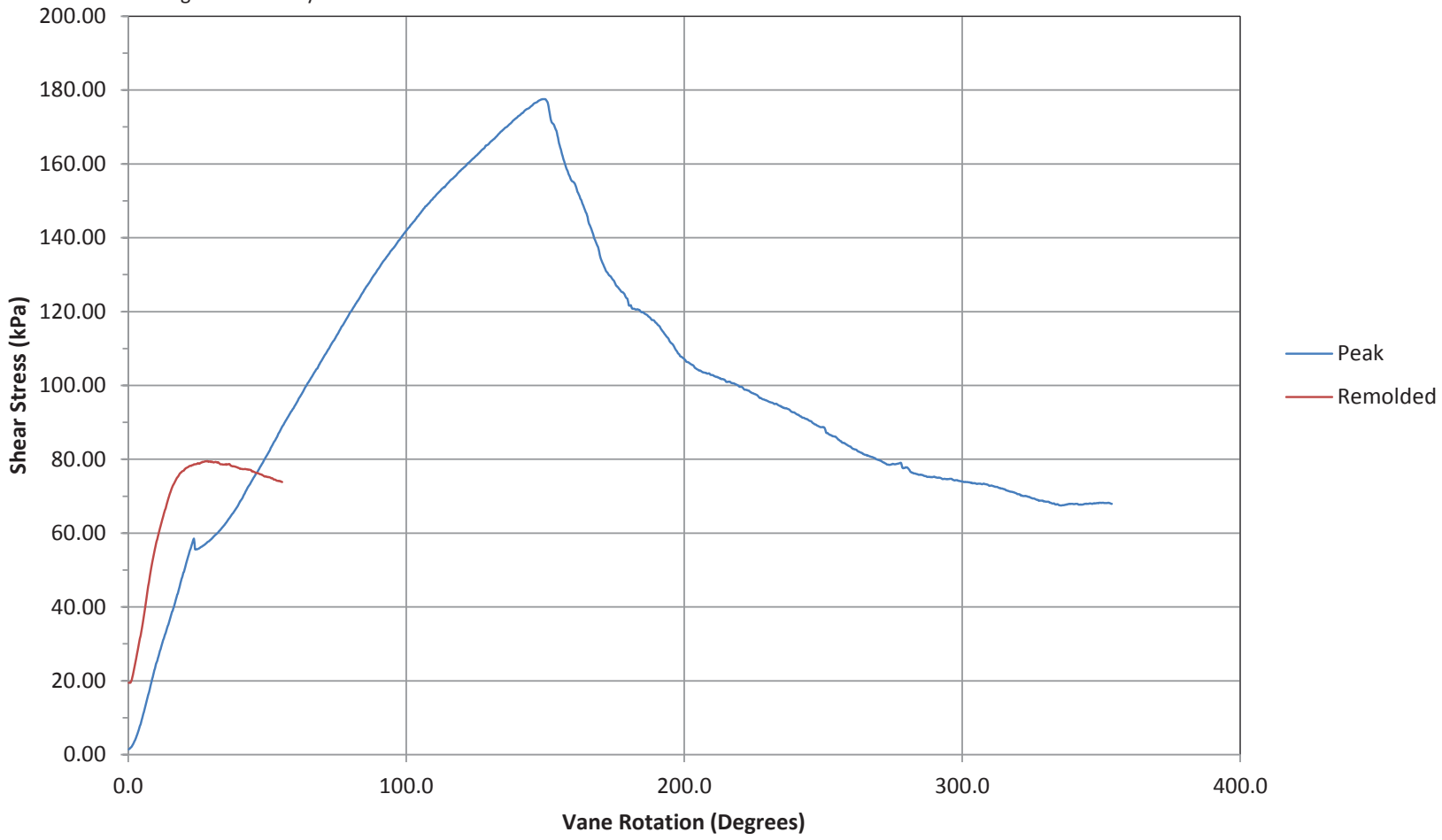

Job Number: 16-72004
Client: CGSH
Project: Samarco, Germano Buttres
Sounding: GSVST16-01-38.50
Sounding Date: 06-May-2016 11:54

Test Depth: (m): 38.50
Vane Type: Double tapered 75 x 150 mm

Coordinate System: WGS84/UTM Zone 23 South
Northing (m): 7764160
Easting: (m): 658561

Vane Shear Test

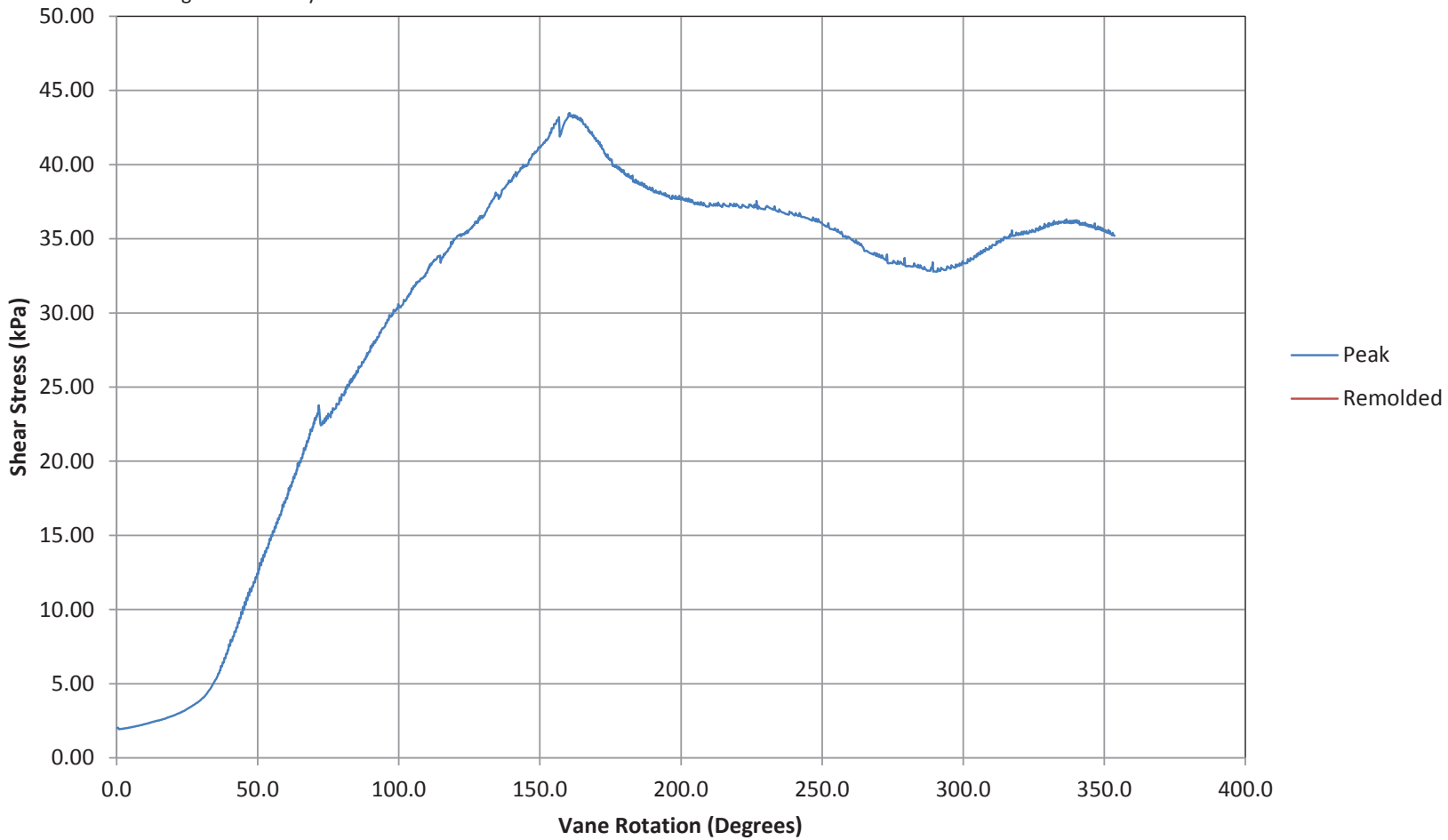

Job Number: 16-72004
Client: CGSH
Project: Samarco
Sounding: GSVST16-01-40.50
Sounding Date: 07-May-2016 06:12

Test Depth: (m): 40.50
Vane Type: Double tapered 75 x 150 mm

Coordinate System: WGS84/UTM Zone 23 South
Northing (m): 7764160
Easting: (m): 658561

Vane Shear Test

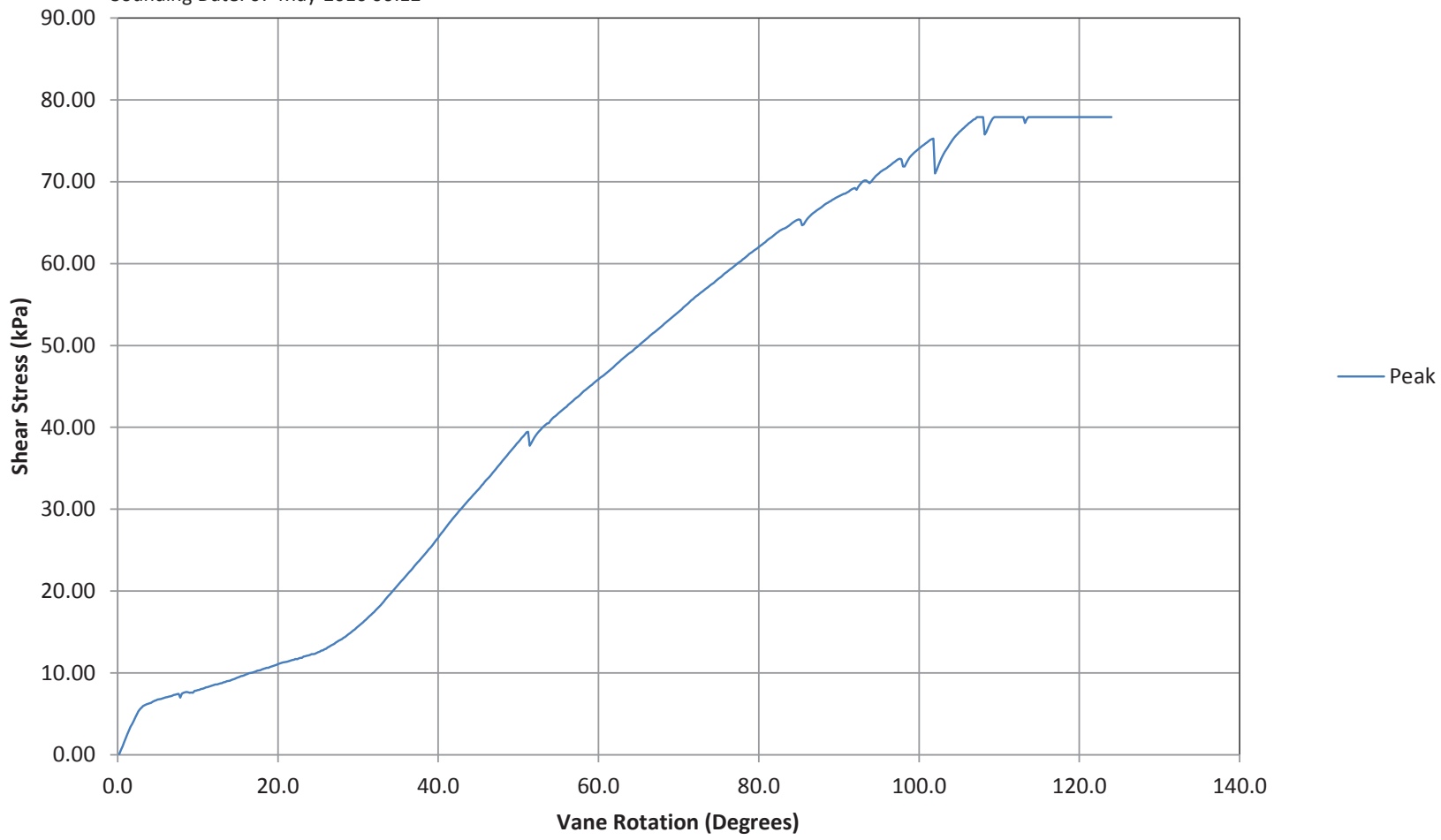

Job Number: 16-72004
Client: CGSH
Project: Samarco, Germano Buttres
Sounding: GSVST16-02A-7.00
Sounding Date: 16-May-2016 07:29

Test Depth: (m): 7.00
Vane Type: Double tapered 75 x 150 mm

Coordinate System: WGS84/UTM Zone 23 South
Northing (m): 7763372
Easting: (m): 659089

Vane Shear Test

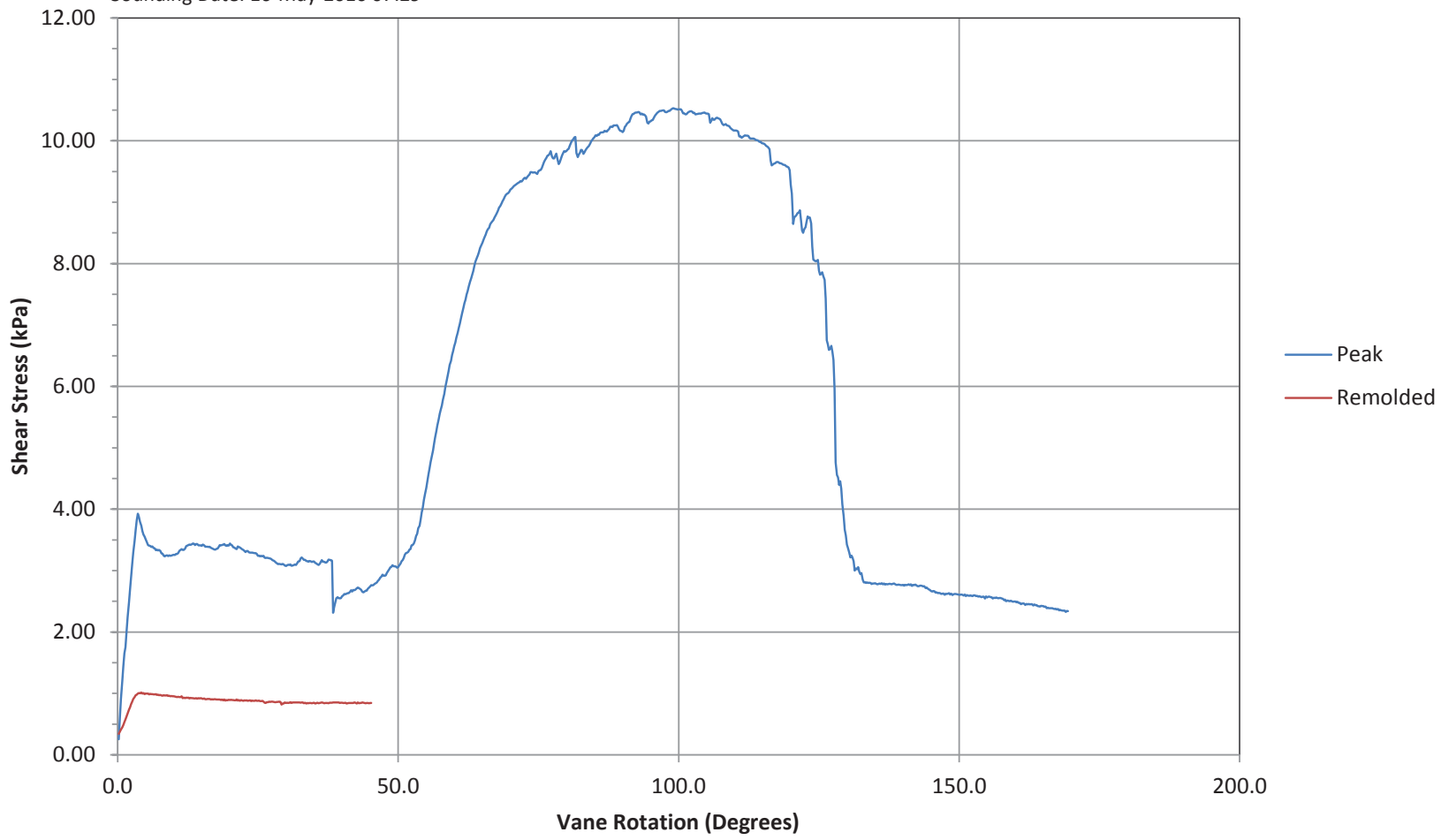

Job Number: 16-72004
Client: CGSH
Project: Samarco, Germano Buttres
Sounding: GSVST16-02B-8.00
Sounding Date: 16-May-2016 10:06

Test Depth: (m): 8.00
Vane Type: Double tapered 75 x 150 mm

Coordinate System: WGS84/UTM Zone 23 South
Northing (m): 7763372
Easting: (m): 659089

Vane Shear Test

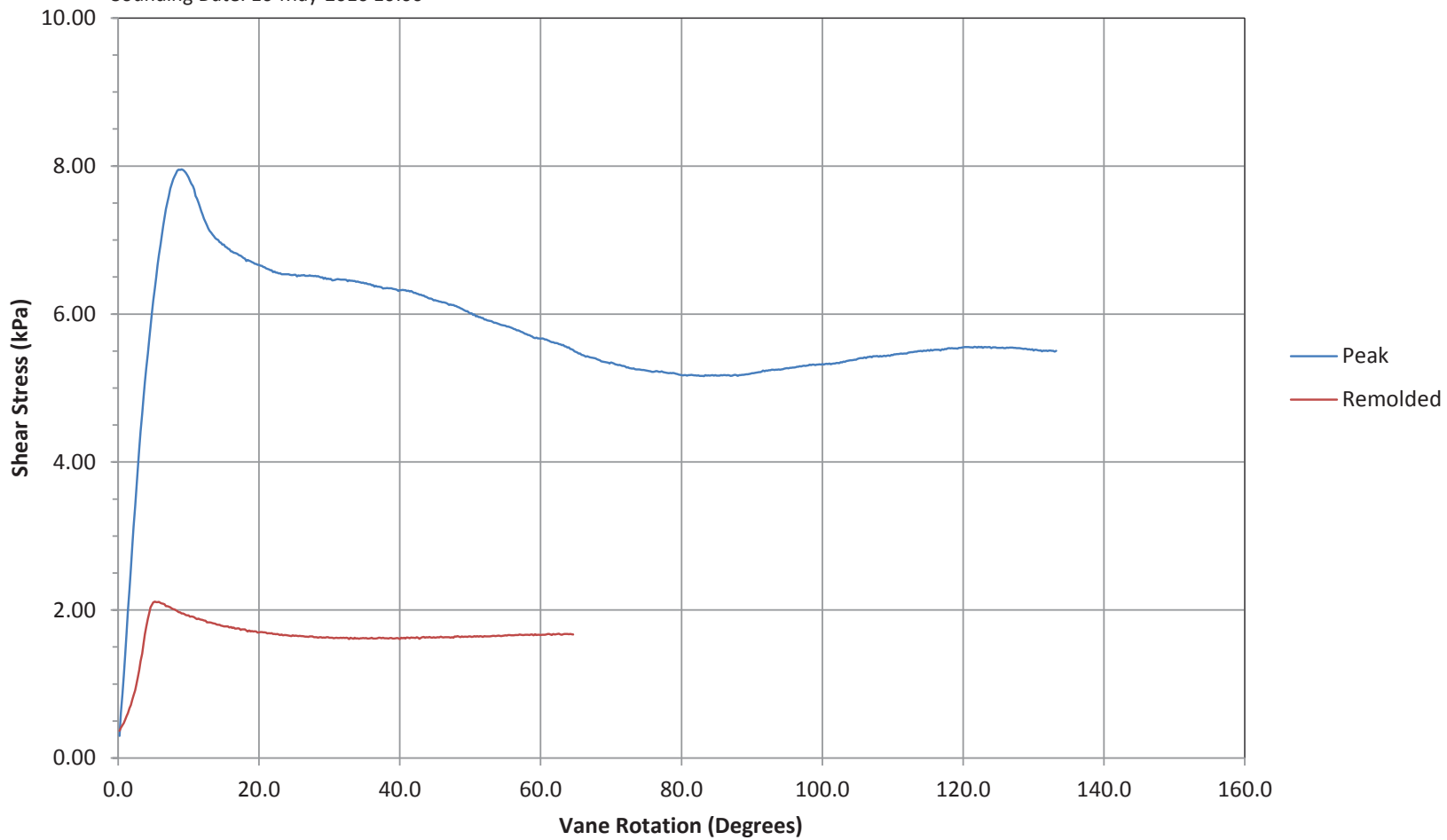

Job Number: 16-72004
Client: CGSH
Project: Samarco, Germano Buttres
Sounding: GSVST16-02-9.00
Sounding Date: 16-May-2016 10:48

Test Depth: (m): 9.00
Vane Type: Double tapered 75 x 150 mm

Coordinate System: WGS84/UTM Zone 23 South
Northing (m): 7763372
Easting: (m): 659089

Vane Shear Test

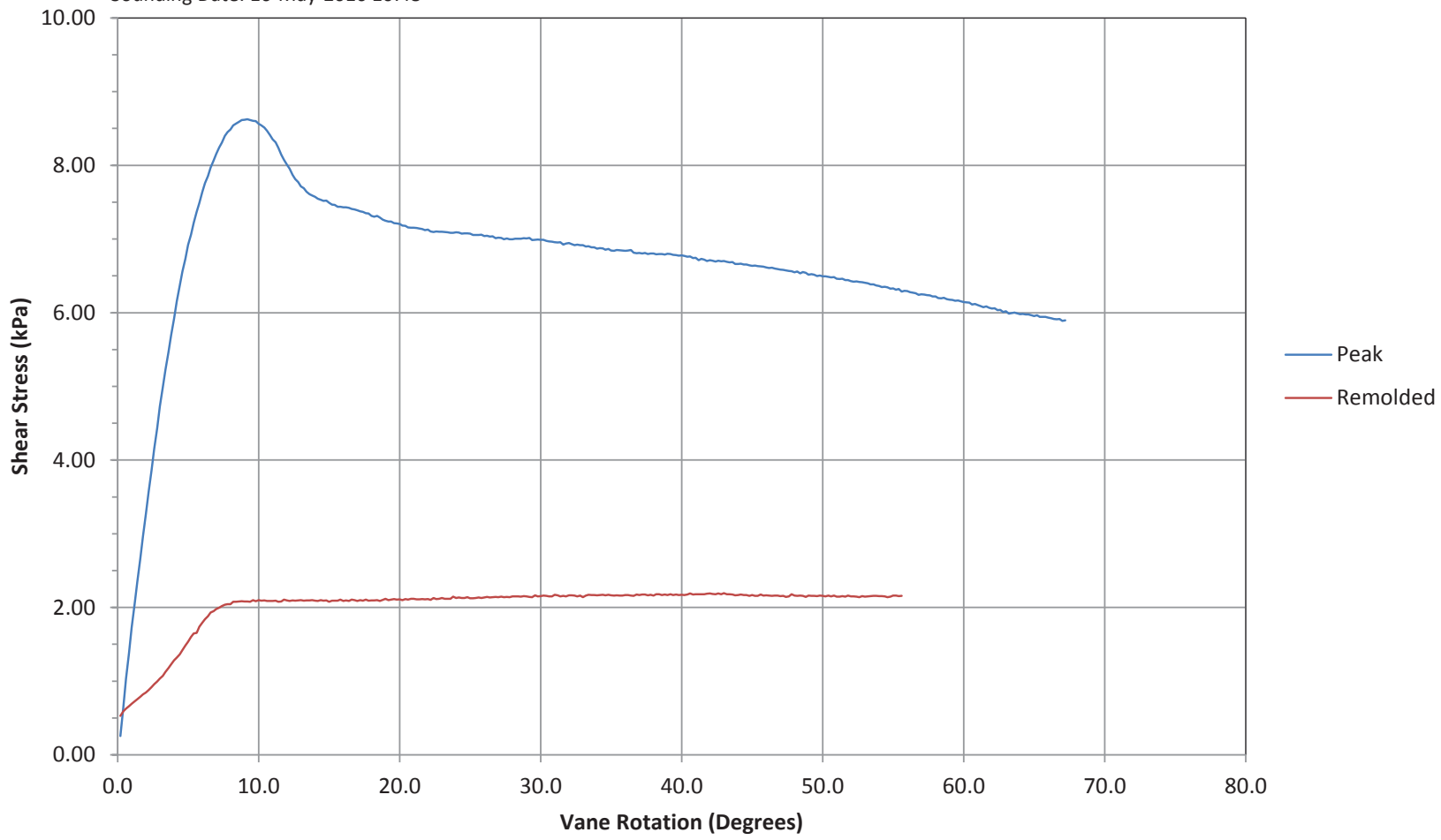

Job Number: 16-72004
Client: CGSH
Project: Samarco, Germano Buttres
Sounding: GSVST16-02-11.00
Sounding Date: 16-May-2016 11:17

Test Depth: (m): 11.00
Vane Type: Double tapered 75 x 150 mm

Coordinate System: WGS84/UTM Zone 23 South
Northing (m): 7763372
Easting: (m): 659089

Vane Shear Test

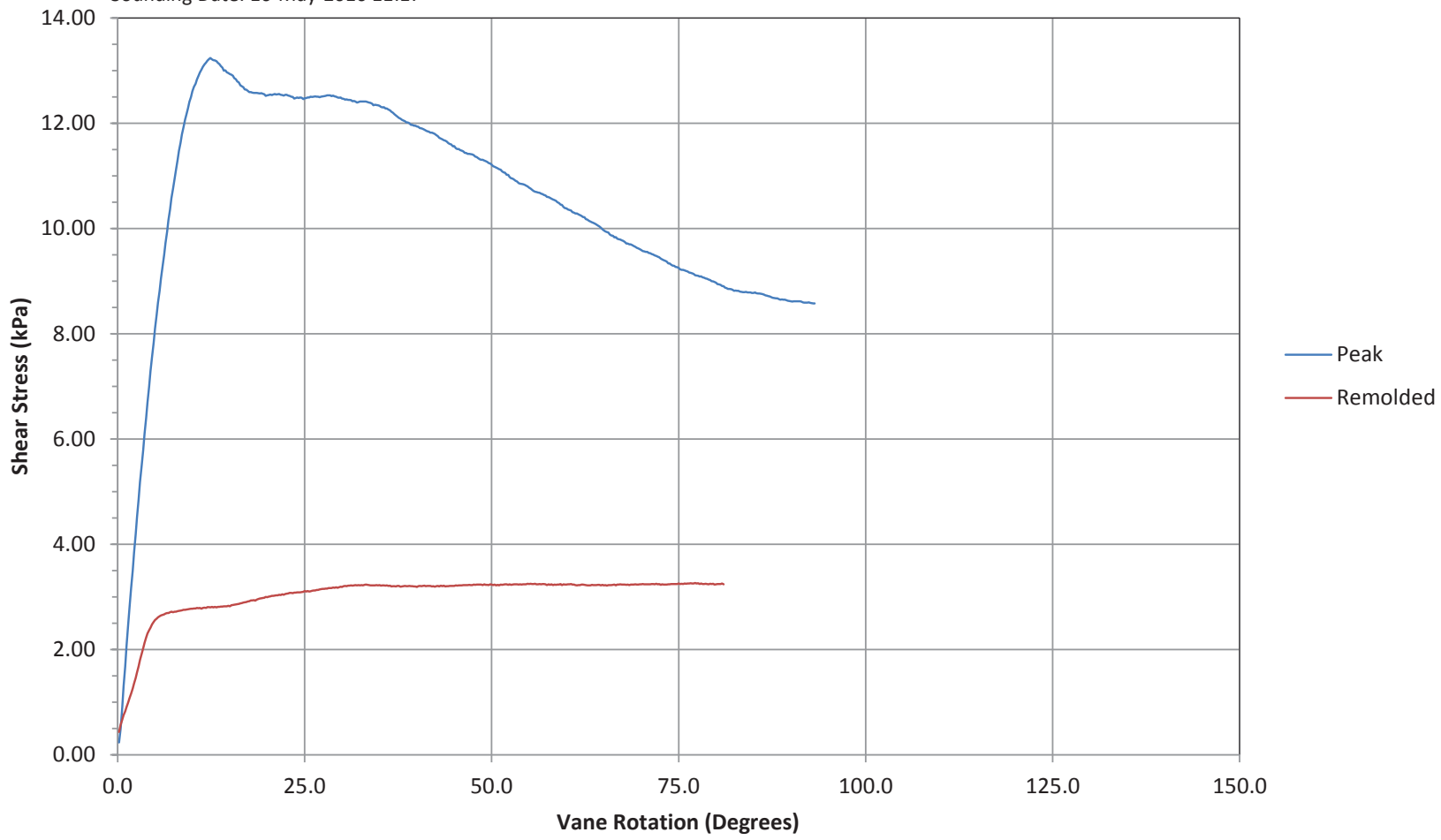

Job Number: 16-72004
Client: CGSH
Project: Samarco, Germano Buttres
Sounding: GSVST16-02-26.00
Sounding Date: 17-May-2016 05:56

Test Depth: (m): 26.00
Vane Type: Double tapered 75 x 150 mm

Coordinate System: WGS84/UTM Zone 23 South
Northing (m): 7763372
Easting: (m): 659089

Vane Shear Test

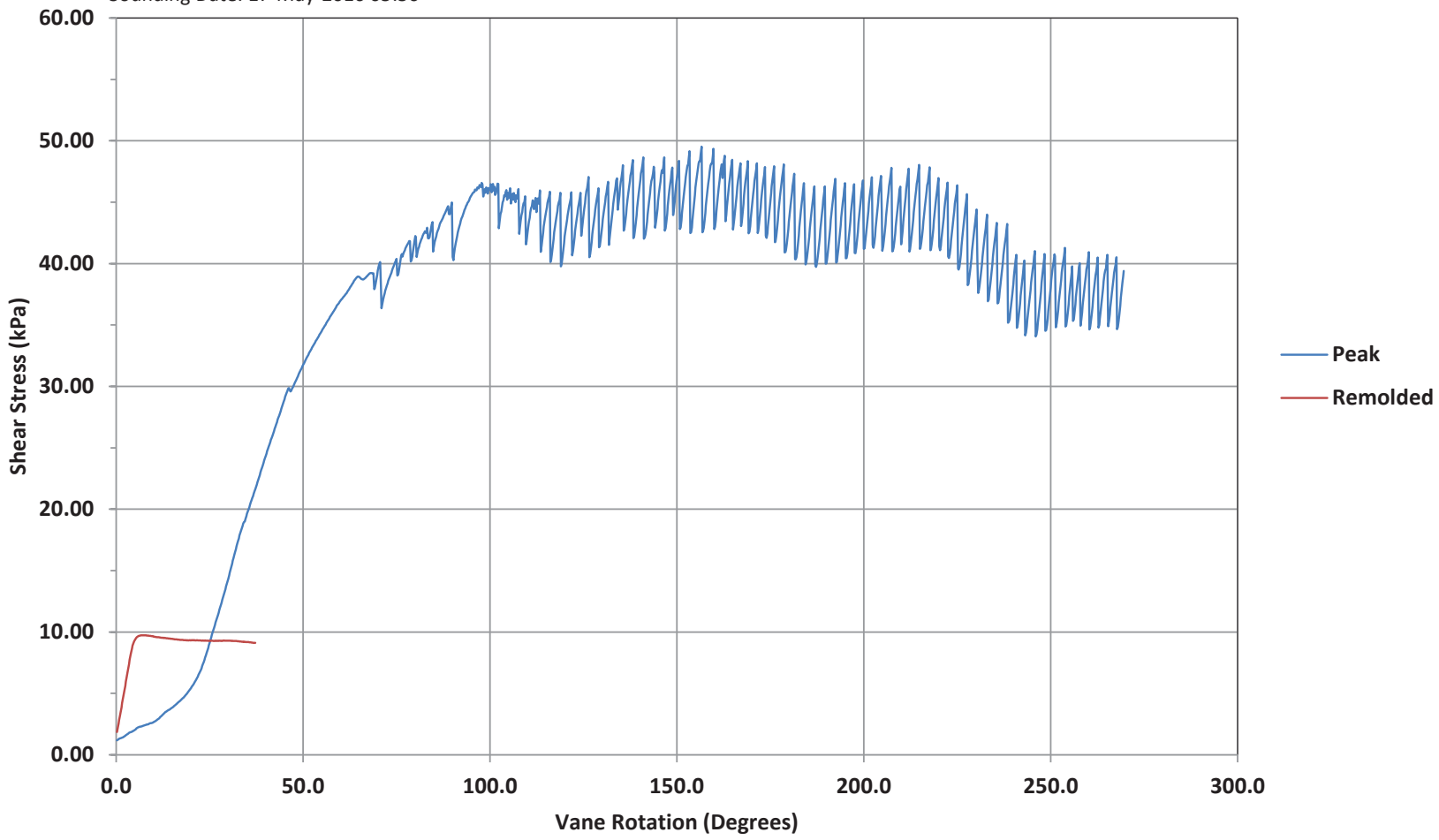

Job Number: 16-72004
Client: CGSH
Project: Samarco, Germano Buttres
Sounding: GSVST16-02-27.00
Sounding Date: 17-May-2016 06:52

Test Depth: (m): 27.00
Vane Type: Double tapered 75 x 150 mm

Coordinate System: WGS84/UTM Zone 23 South
Northing (m): 7763372
Easting: (m): 659089

Vane Shear Test

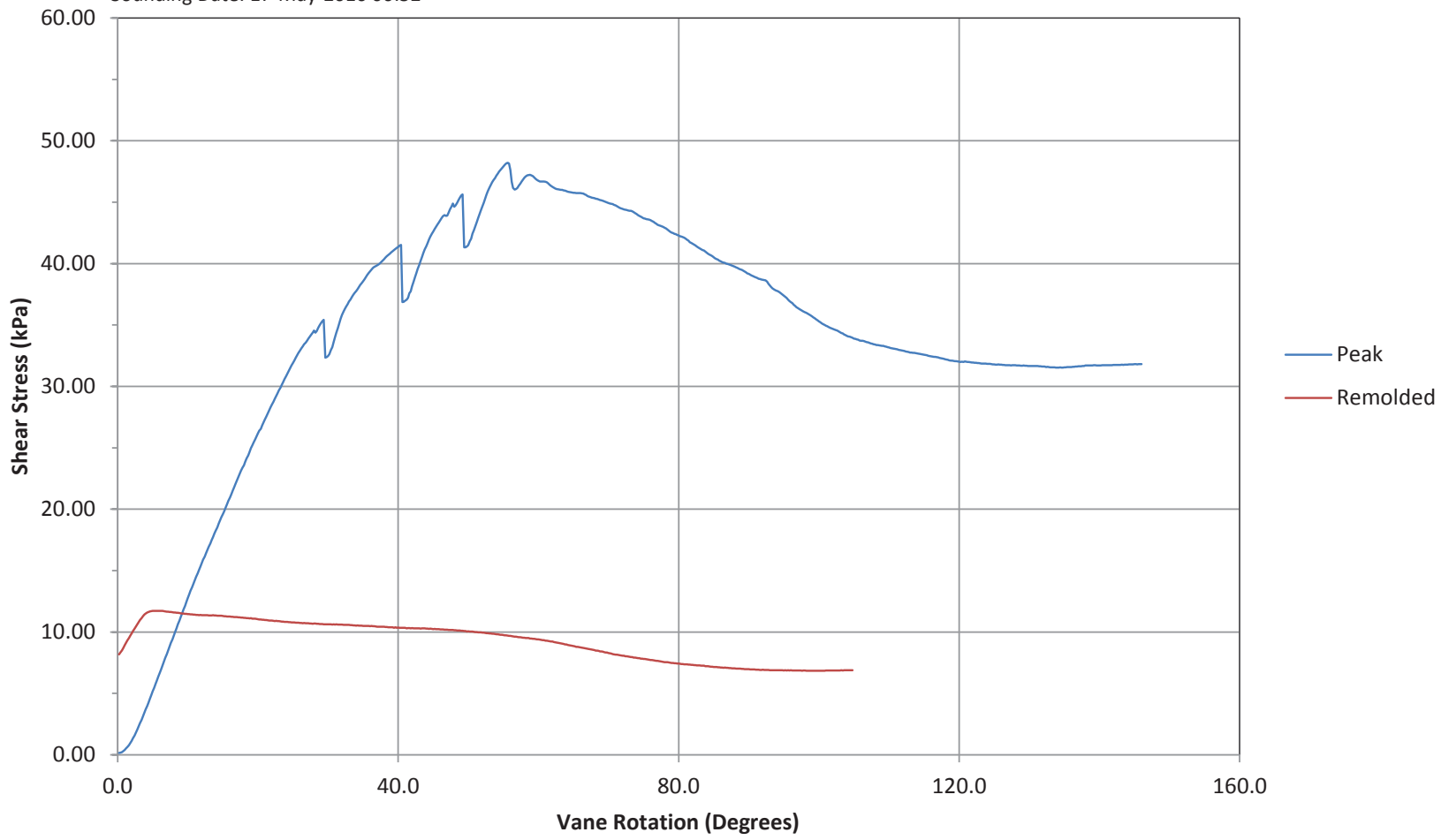

Job Number: 16-72004
Client: CGSH
Project: Samarco, Germano Buttres
Sounding: GSVST16-02-28.00
Sounding Date: 17-May-2016 07:45

Test Depth: (m): 28.00
Test Elevation: (m): N/A
Vane Type: Double tapered 75 x 150 mm

Coordinate System: WGS84/UTM Zone 23 South
Northing (m): 7763372
Easting: (m): 659089
Surface Elevation: (m): N/A

Vane Shear Test

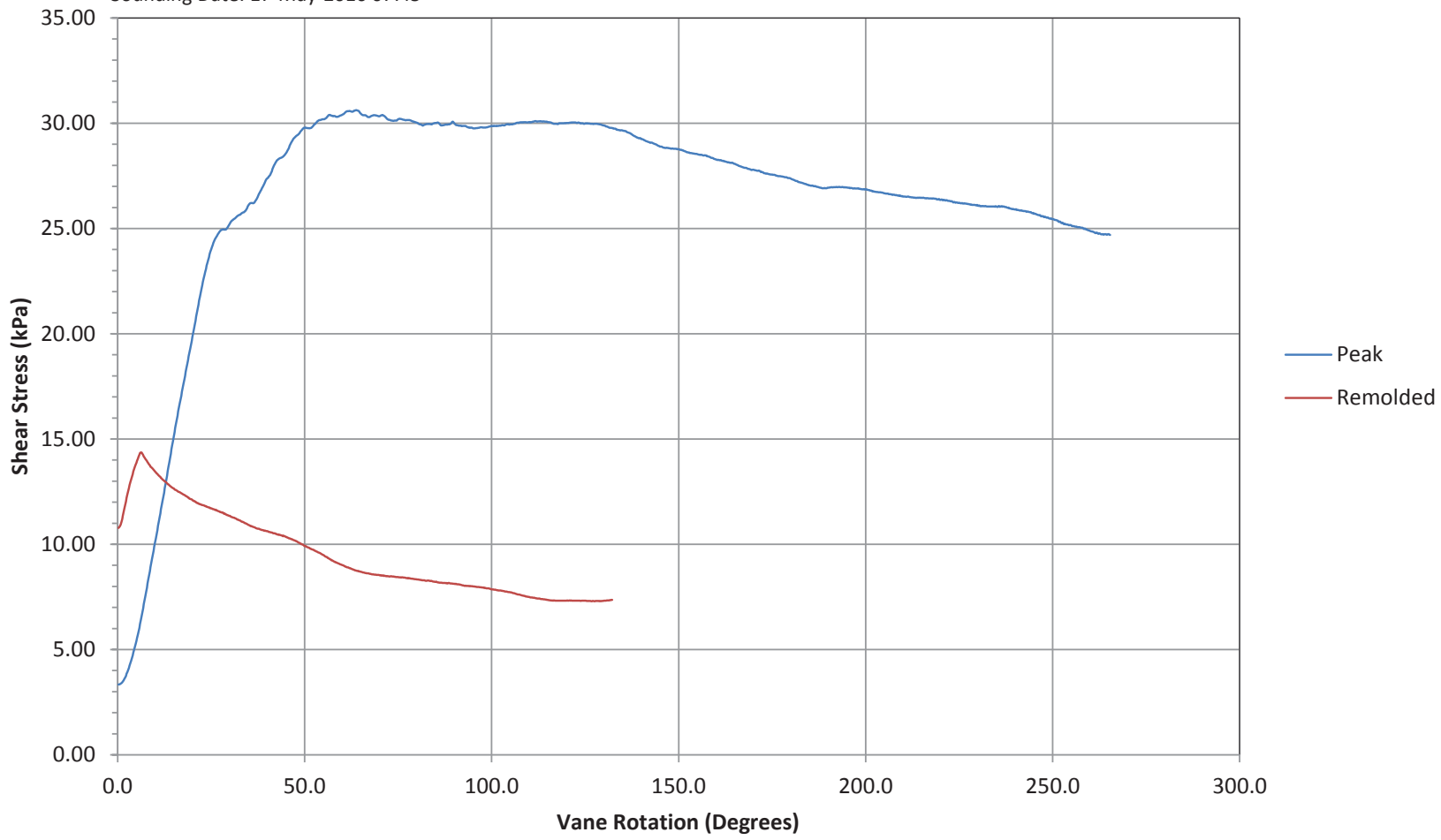

Sample Summary and Sample Logs

CONETEC

Job No:	16-72004
Client:	Cleary Gottlieb Steen & Hamilton LLP (CGSH)
Project:	Samarco, Germano Buttress
Start Date:	10-May-2016
End Date:	27-May-2016

SAMPLE SUMMARY

Location ID	Date From	Date To	Depth From (m)	Depth To (m)	Depth From (ft)	Depth To (ft)	Sample Methods	Sample # From	Sample # To	Northing[1] (m)	Easting (m)	Refer to Notation Number
GSSAM16-02	10-May-2016	15-May-2016	2.25	30.25	7.38	99.24	SHKY	1	25	7763372	659091	
GSSAM16-02B	27-May-2016	27-May-2016	4.00	10.00	13.12	32.81	SHKY	1	5	7763375	659092	

1. Coordinate and elevatios were obtained using a consumer-grade GPS device with datum: WGS84/UTM Zone 23 South.

Sample Methods	
Code	**Description**
SHKY	Sharky

CONETEC

SAMPLE LOG

LOCATION ID:	**GSSAM16-02**
Client:	Cleary Gottlieb Steen & Hamilton LLP (CGSH)
ConeTec Job No:	16-72004
Rig:	FIS-017
Site:	Slimes 2
Staff:	DSTA

Coordinate Reference System:	WGS 84 / UTM Zone 23 South	
Coordinate Collection Method:	Consumer grade GPS	
Northing:	7763372	**m**
Easting:	659091	**m**

Sample # Sequential	Date Time	Drillout Depth (m)	Sample Start Depth (m)	Sample End Depth (m)	Sample Method	Sample tube length [mm]	Sample bottom empty space 1 [mm]	Sample bottom empty space 2 [mm]	Sample bottom empty space 3 [mm]	Sample top empty space 1 [mm]	Sample top empty space 2 [mm]	Sample top empty space center [mm]	Comments
1	10-May-2016 11:30	1.6	2.25	2.90	SHK	760	0.0	0.0	0.0	550.0	550.0	590.0	
2	10-May-2016 14:30	2.5	3.00	3.65	SHK	760							Pushed through slimes. No Recovery.
3	10-May-2016 15:00	2.5	3.75	4.40	SHK	760	0.0	0.0	0.0	205.0	205.0	255.0	Pushed through slimes.
4	11-May-2016 10:00	2.5	4.50	5.15	SHK	760	0.0	0.0	0.0	88.0	88.0	140.0	Pushed through slimes.
5	11-May-2016 11:00	2.5	5.25	5.90	SHK	760	0.0	0.0	0.0	96.0	98.0	145.0	Pushed through slimes.
6	11-May-2016 11:30	2.5	6.25	6.90	SHK	760	19.0	19.0	10.0	104.0	104.0	151.0	Pushed through slimes.
7	11-May-2016 13:30	2.5	7.25	7.90	SHK	760	430.0	460.0		143.0	145.0	180.0	Pushed through slimes.. Bottom of sample fell out of tube.
8	11-May-2016 15:30	2.5	8.25	8.90	SHK	760	0.0	0.0	0.0	97.0	94.0	142.0	Pushed through slimes.
9	11-May-2016 16:30	2.5	9.25	9.90	SHK	760	0.0	0.0	0.0	96.0	98.0	129.0	Pushed through slimes.
10	12-May-2016 10:00	2.5	10.25	10.90	SHK	760	0.0	0.0	0.0	98.0	103.0	140.0	Pushed through slimes.
11	12-May-2016 13:45	2.5	11.25	11.90	SHK	760	0.0	0.0	0.0	154.0	153.0	169.0	Pushed through slimes.
12	12-May-2016 15:00	2.5	12.25	12.90	SHK	760	0.0	0.0	0.0	85.0	92.0	132.0	Pushed through slimes.
13	12-May-2016 16:00	2.5	13.25	13.90	SHK	760	0.0	0.0	0.0	121.0	120.0	110.0	Pushed through slimes.
14	13-May-2016 10:00	2.5	14.25	14.90	SHK	760	0.0	0.0	0.0	90.0	90.0	136.0	Pushed through slimes.
15	13-May-2016 11:15	2.5	15.25	15.90	SHK	760	disturbed	disturbed	disturbed	570.0	570.0	570.0	Pushed through slimes. Piston fell during pull, lost most of sample.
16	13-May-2016 14:00	2.5	16.25	16.90	SHK	760	0.0	0.0	0.0	90.0	96.0	136.0	Pushed through slimes.
17	13-May-2016 15:15	2.5	17.25	17.90	SHK	760	0.0	0.0	0.0	150.0	140.0	170.0	Pushed through slimes. Sample sliding out of tube.
18	14-May-2016 08:45	2.5	18.25	18.90	SHK	760	0.0	0.0	0.0	87.0	89.0	119.0	Pushed through slimes.
19	14-May-2016 09:45	2.5	19.25	19.90	SHK	760	0.0	0.0	0.0	122.0	122.0	127.0	Pushed through slimes. Lots of water infiltration.
20	14-May-2016 11:00	2.5	20.25	20.90	SHK	760	0.0	0.0	0.0	133.0	136.0	161.0	Pushed through slimes.
21	14-May-2016 14:00	2.5	22.25	22.90	SHK	760	0.0	0.0	0.0	114.0	111.0	140.0	Pushed through slimes.
22	14-May-2016 16:00	2.5	24.25	24.90	SHK	760	0.0	0.0	0.0	190.0	190.0	215.0	Pushed through slimes. Sample sliding out of tube.
23	15-May-2016 09:15	2.5	26.25	26.90	SHK	760	0.0	0.0	0.0	150.0	135.0	150.0	Pushed through slimes.
24	15-May-2016 12:15	2.5	28.25	28.90	SHK	760	0.0	0.0	0.0	110.0	105.0	180.0	Pushed through slimes.
25	15-May-2016 15:00	2.5	30.25	30.90	SHK	760							Pushed through slimes. No sample (depth of natural ground, too hard to push).

Sample Notes	
Sample #	**Notes**

Sample Methods	
Code	**Description**
SHK	Sharky

SAMPLE LOG

LOCATION ID:	**GSSAM16-02B**
Client:	Cleary Gottlieb Steen & Hamilton LLP (CGSH)
ConeTec Job No:	16-72004
Rig:	FIS-017
Site:	Slimes 2
Staff:	DSTA, ALLA

Coordinate Reference System:	WGS 84 / UTM Zone 23 South	
Coordinate Collection Method:	Consumer grade GPS	
Northing:	7763375	**m**
Easting:	659092	**m**

Sample # Sequential	Date Time	Drillout Depth (m)	Sample Start Depth (m)	Sample End Depth (m)	Sample Method	Sample tube length [mm]	Sample bottom empty space 1 [mm]	Sample bottom empty space 2 [mm]	Sample bottom empty space 3 [mm]	Sample top empty space 1 [mm]	Sample top empty space 2 [mm]	Sample top empty space center [mm]	Comments
1	27-May-2016 11:00	3.0	4.00	4.65	SHK	760	0.0	0.0	0.0	120	105	155	
2	27-May-2016 14:30	3.0	6.00	6.65	SHK	760	0.0	0.0	0.0	95	95	130	Pushed and pulled by hand.
3	27-May-2016 15:15	3.0	8.00	8.65	SHK	760							No sample.
4	27-May-2016 16:00	3.0	9.00	9.65	SHK	760	0.0	0.0	0.0	100	100	140	Pushed and pulled by hand.
5	27-May-2016 16:45	3.0	10.00	10.65	SHK	760	0.0	0.0	0.0	92	94	128	Pushed and pulled by hand.

Sample Notes	
Sample #	**Notes**

Sample Methods	
Code	**Description**
SHK	Sharky

Standard Penetration Test Summary and Results

CONETEC

Job No:	16-72004
Client:	Cleary Gottlieb Steen & Hamilton LLP (CGSH)
Project:	Samarco, Germano Buttress
Start Date:	04-May-16
End Date:	04-May-16

STANDARD PENETRATION TEST WITH ENERGY SUMMARY

Borehole ID	Date From	Date To	Hammer Type	Hammer Weight (kg)	Estimated Drop Height (m)	Potential Energy (kN-m)	Test End Depth (ft)	Northing[1] (m)	Easting (m)
GCSPT16-02	04-May-16	04-May-16	Auto	65	0.75	0.4781	185.2	7766165	657250

1. Coordinates obtained from handheld GPS device, datum WGS84/UTM Zone 23 South.

Job No:	16-72004	Hammer:	Automatic Hammer
Client:	CGSH	Drop:	0.75m
Project:	Samarco, Germano Buttress	Weight:	65.0 kg.
Start Date:	04-May-16	Potential Energy:	0.4781 kNm
End Date:	04-May-16	Instrumented Rod Type:	AWJ
Rig:	Furgo FIS-011	Instrumented Rod Area:	AWJ(7.8cm^2)
Hole Number:	GCSPT16-02	SPT Rod String Type:	Water pipe

SPT ENERGY CALIBRATION DATA

Test Start Depth (m)	Test Start Depth (ft)	Total Number of Impacts Analyzed	Field Recorded Blow Counts	Average Max Force (kN)	Average Max Energy (kN-m)	Average Energy Transfer Ratio (%) (FV)
55.0	180.4	67	15-22-29	92.2	0.34259	71.7
56.0	183.7	50	15-18-17	97.0	0.32513	68.0

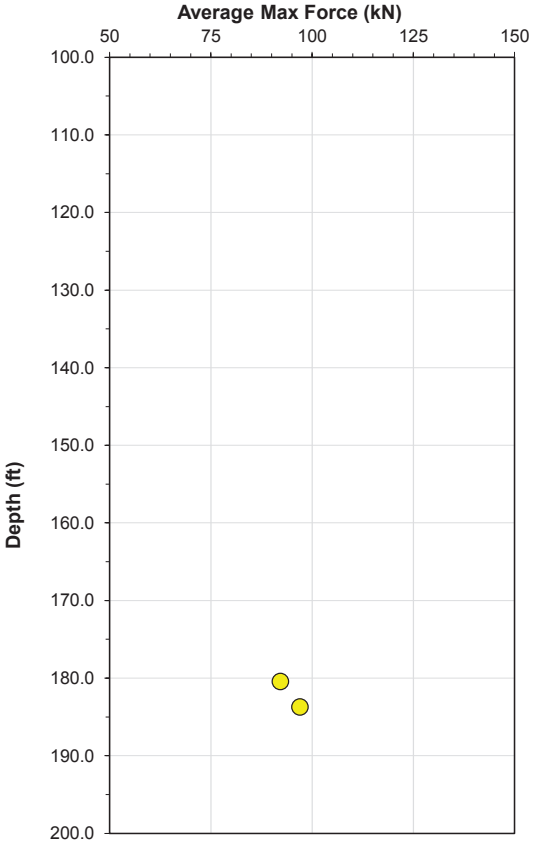

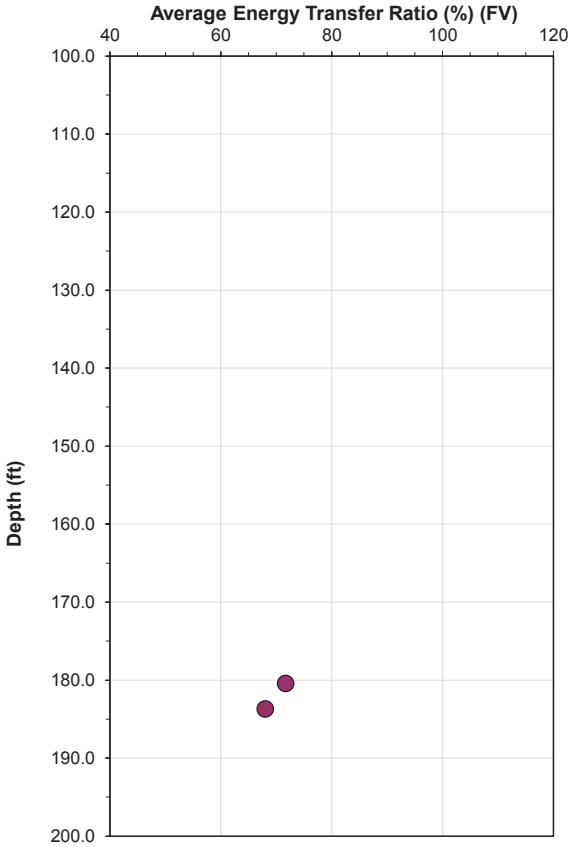

ATTACHMENT C3

AFC Geofisica Ltda. Geophysical Survey – MASW Report

TECHNICAL REPORT

CLIENT: **CLEARY GOTTLIEB STEEN & HAMILTON CONSULTORES**	PAGE: **1 de 93**
PROGRAM: **---**	DATE: **17/06/2016**
LOCATION: **MINAS GERAIS / BRAZIL**	Nº CONTRACT: **---**
TITLE: **GEOPHYSICAL SURVEY**	MANAGER: NOWELL BAMBERGER

MS Word®/2016/RL_ENG_CLEARY GOTTLIEB STEEN & HAMILTON CONSULTORES=0.DOCX
INTERNAL NUMBERING

Assinado de forma digital por Antonio Flavio Uberti Costa
Dados: 2016.06.17 15:02:08 -03'00'

ANTONIO FLAVIO UBERTI COSTA – CREA/RS 009807

INDEX OF REVISIONS

REV.	DESCRIPTION
0	ORIGINAL

REVISIONS	0	A	B	C	D	E
DATE	17/06//2016					
PROJECT	-					
EXECUTION	A. F. COSTA					
VERIFICATION	F. C. RODRIGUES					
APPROVAL	A. F. COSTA					

CLEARY GOTTLIEB STEEN & HAMILTON CONSULTORES EM DIREITO ESTRANGEIRO

GEOPHYSICAL SURVEY

MASW – MULTICHANNEL ANALYSIS OF SURFACE WAVES

JUNE 2016

SUMMARY

1. INTRODUCTION

Upon request by CLEARY GOTTLIEB STEEN & HAMILTON CONSULTORES EM DIREITO ESTRANGEIRO, the AFC Geofísica Ltda. conducted a geophysical survey between May 25th and 26th, 2016, using seismic method - MASW (Multichannel Analysis of Surface Waves) - to determine de variation of S-wave velocity up to 30m deep along three lines of 100m long; in a dam located in the state of Minas Gerais / Brazil.

This report presents the methodology and the results of the executed survey.

2. METHODOLOGY AND SURVEY SPECIFICATIONS

2.1. MASW – MULTICHANNEL ANALYSIS OF SURFACE WAVES

The MASW Method (Figure 1) was applied into three sections with 100m length each to determine de S-wave velocity up to 30m deep.

It was used a seismograph GEODE (Figure 2), manufactured by Geometrics, Inc., with 24 channels, two spread cables with 12 take-outs each and 24 vertical 4,5 Hz geophones.

MASW data analysis was performed using SeisImager/SW2D software, developed by Geometrics, Inc.

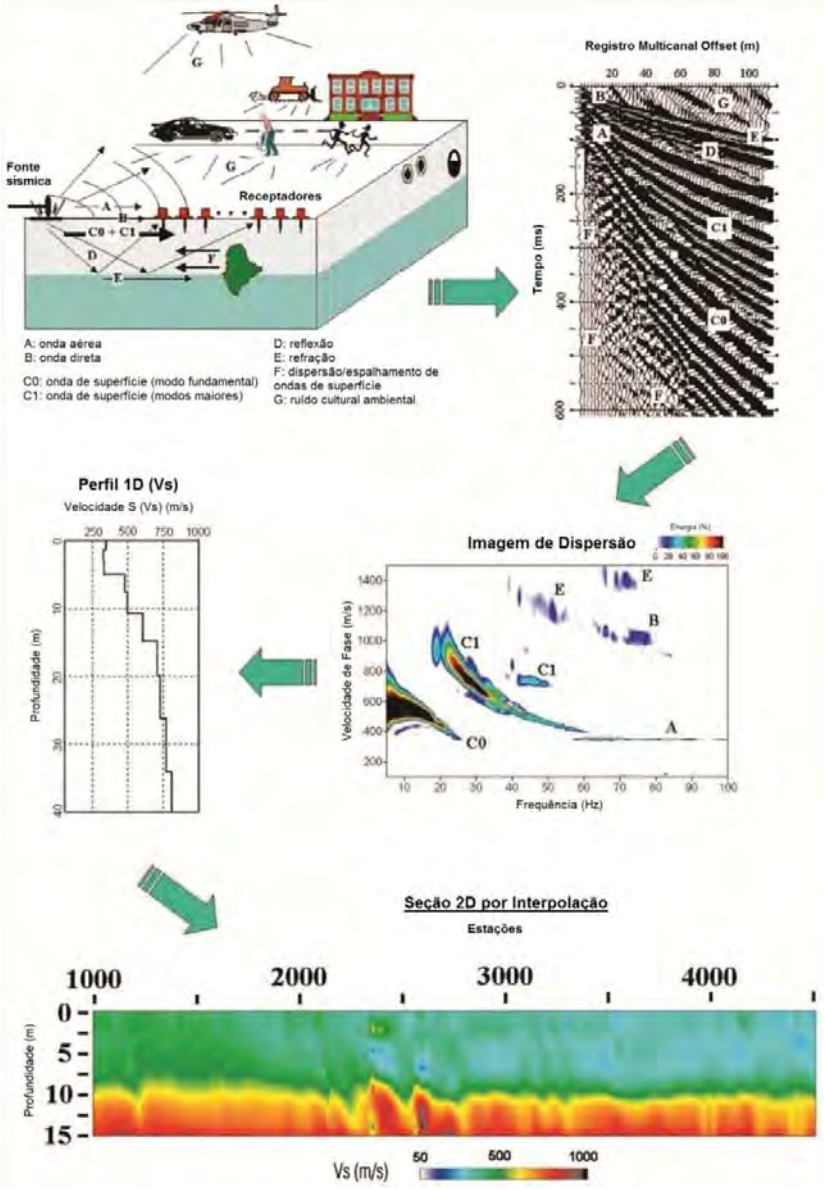

Figure 1. MASW – Multichannel Analysis of Surface Waves Method (modified from Park et al, 2007)

Figure 2. Seismograph GEODE

2.2. FORMULAS FOR CALCULATING THE DYNAMIC ELASTIC MODULUS

From the determination of S-wave velocity versus depth, the P-wave velocity and the density were estimated according to Ludwig et al., 1970. The dynamics elastic modulus of soils and rocks were calculated using the formulas listed below (ASTM-STP 654, 1977) :

$\mu = [(VP/VS)2-2] / [2(VP/VS)2-2]$ => Poisson coefficient

$G = \rho . V_S^2$ => Dynamic Shear Modulus (Gdyn, Gmáx small-strain)

= > For Gdyn,0 (large-strain) a Reduction Factor R = 0.15, (Massarsch, 2010).

$E = 2G(1+\mu)$ => Dynamic Young's Modulus (Edyn)

$K = E / [3(1-2 \mu)]$ => Dynamic Bulk Modulus (Esdyn)

2.3. CLASSIFICATION OF ROCK MASS ACCORDING TO *IBC – INTERNATIONAL BUILDING CODE* (2015)

The software used in the MASW data processing called SeisImagerSW developed by Geometrics Inc., allows to calculate the average speed Vs30 and classify the site according to the criteria established by IBC - International Building Code (2000, 2003, 2006, 2009, 2012 and 2015).

Sites are classified into six classes, called A, B, C, D, E and F, according to the average speed of S waves up to 30 meters deep, as shown in Figure 3. UBC / IBC Site Classifications, available at <http: //publicecodes.cyberregs.com/icod/ibc/2009/>.

Site Class	S-Velocity (Vs) (ft/sec)	S-Velocity (Vs) (m/sec)
A (Hard Rock)	> 5,000	> 1500
B (Rock)	2,500 – 5000	760 – 1500
C (Very Dense Soil and Soft Rock)	1,200 – 2,500	360 – 760
D (Stiff Soil)	600 – 1,200	180 – 360
E (Soft Clay Soil)	< 600	< 180
F (Soils requiring additional response)	< 600, and meeting some additional conditions.	< 180, and meeting some additional conditions.

Figure 3. UBC / IBC Site Classifications NEHRP - National Earthquake Hazards Reduction Program)

2.4. S-WAVE VELOCITY 2D MODEL SECTION

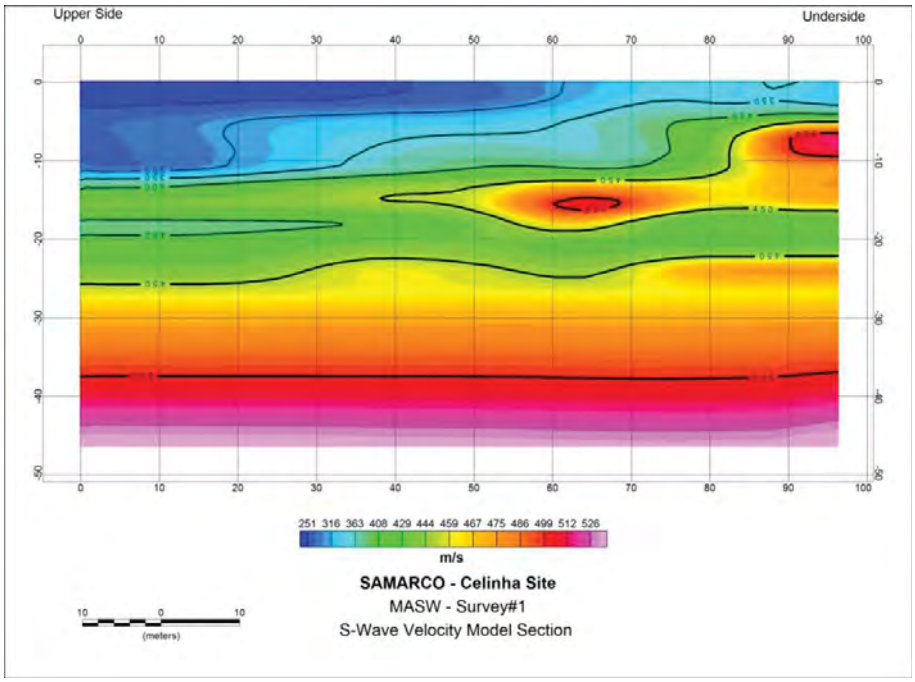

Figure 4. S-Wave Velocity 2D Model Section – Survey #1

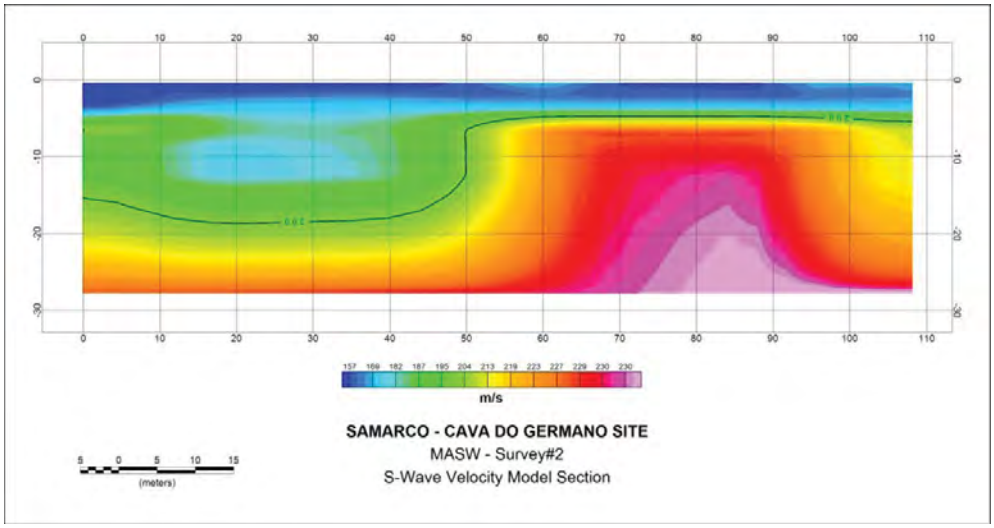

Figure 5. S-Wave Velocity 2D Model Section – Survey #2

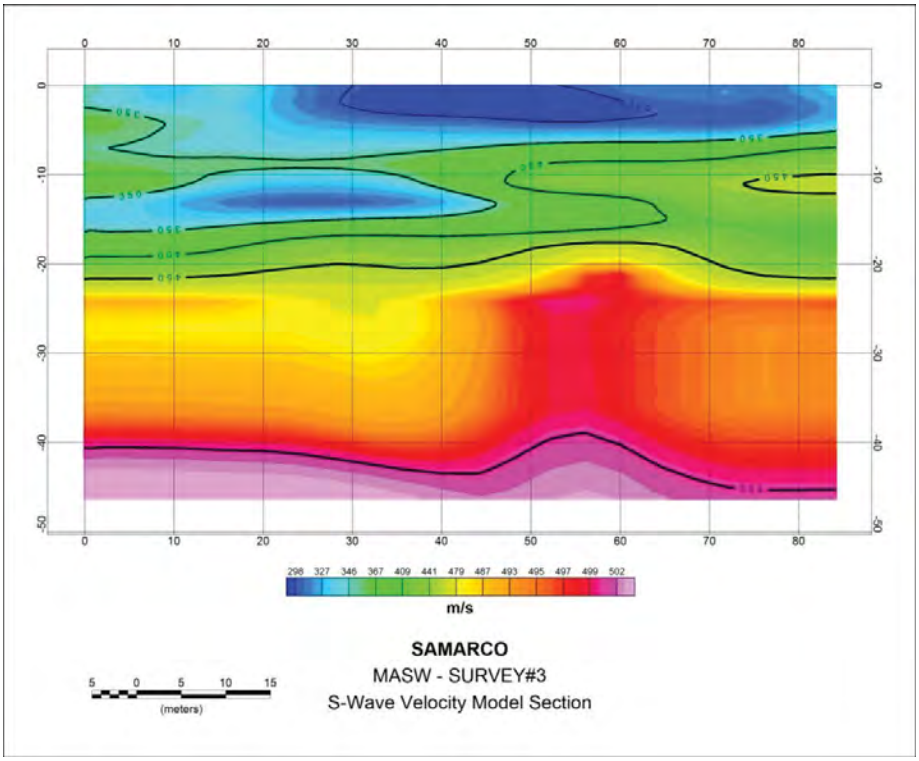

Figure 6. S-Wave Velocity 2D Model Section – Survey #3

3. S-WAVE VELOCITY MODEL

3.1. SURVEY #1

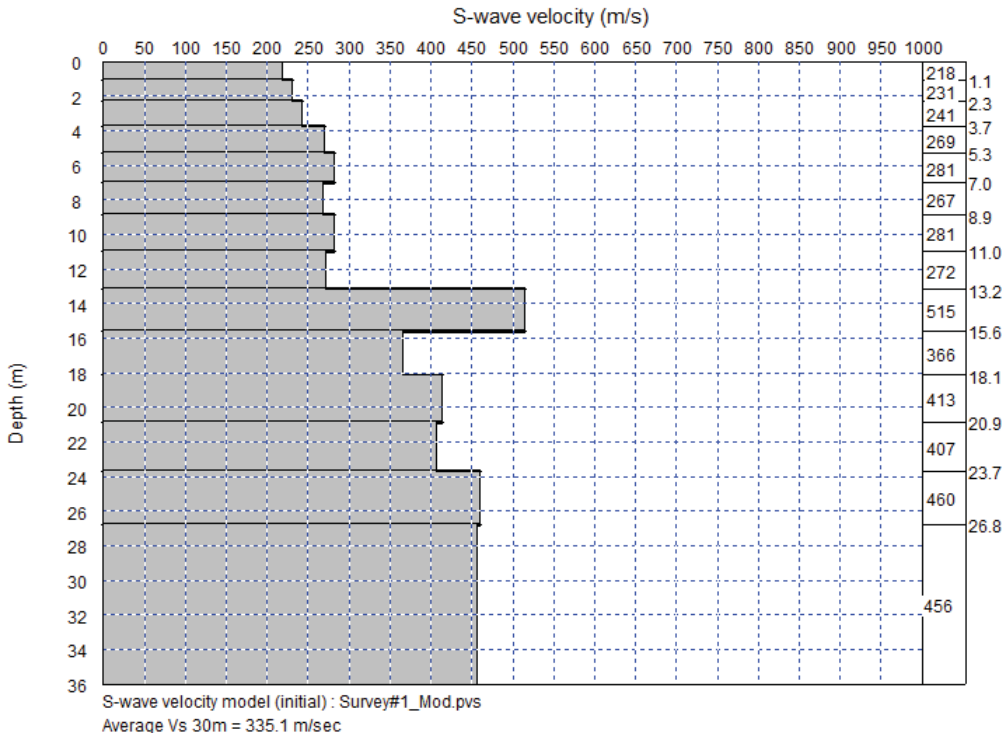

Figure 7. X=0

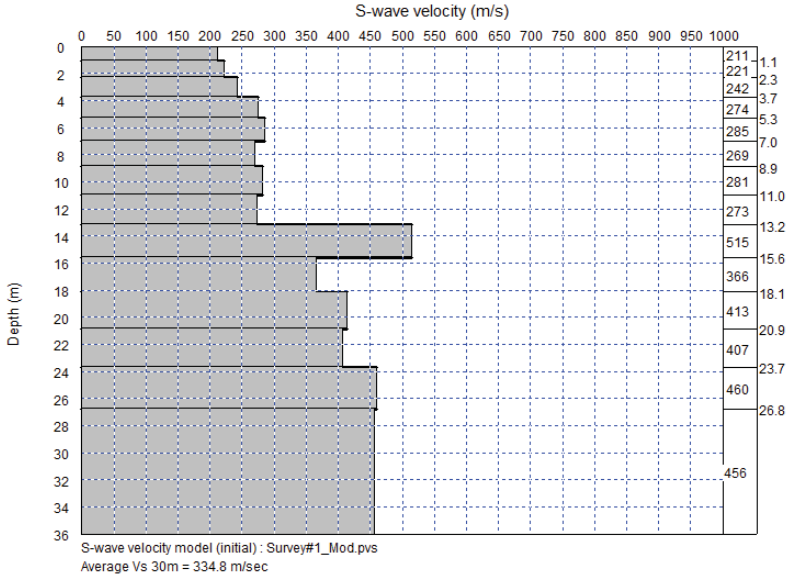

Figure 8. X=4

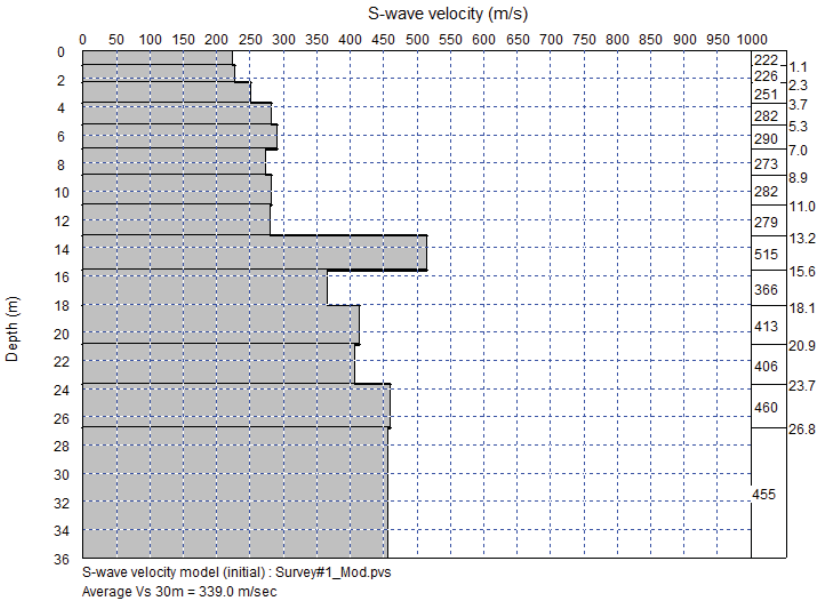

Figure 9. X=8

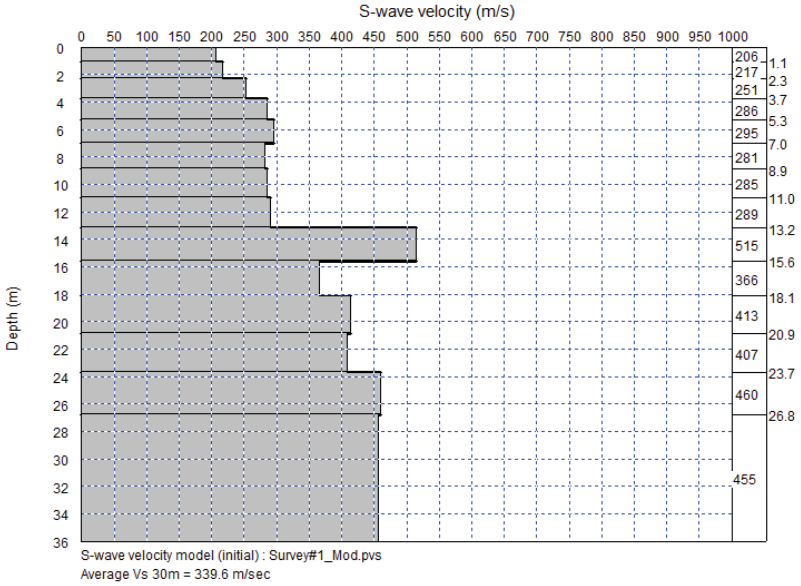

Figure 10. X=12

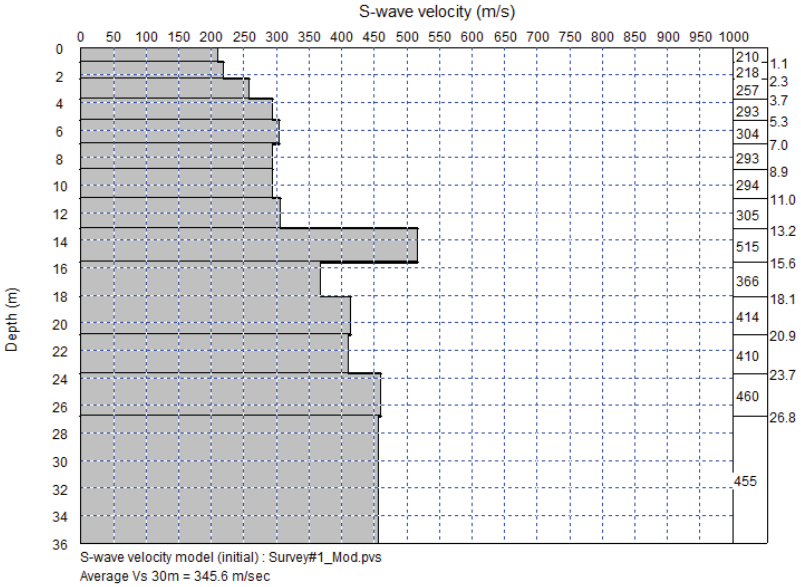

Figure 11. X=16

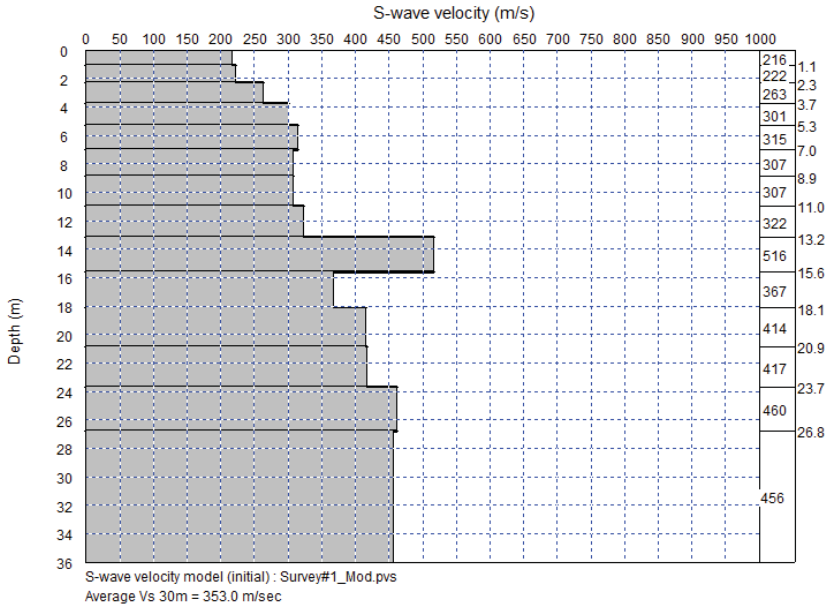

Figure 12. X=20

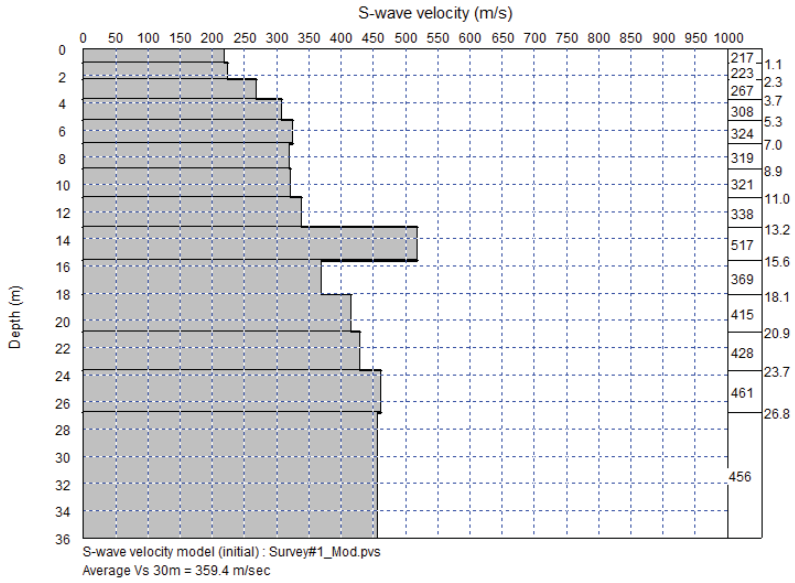

Figure 13. X=24

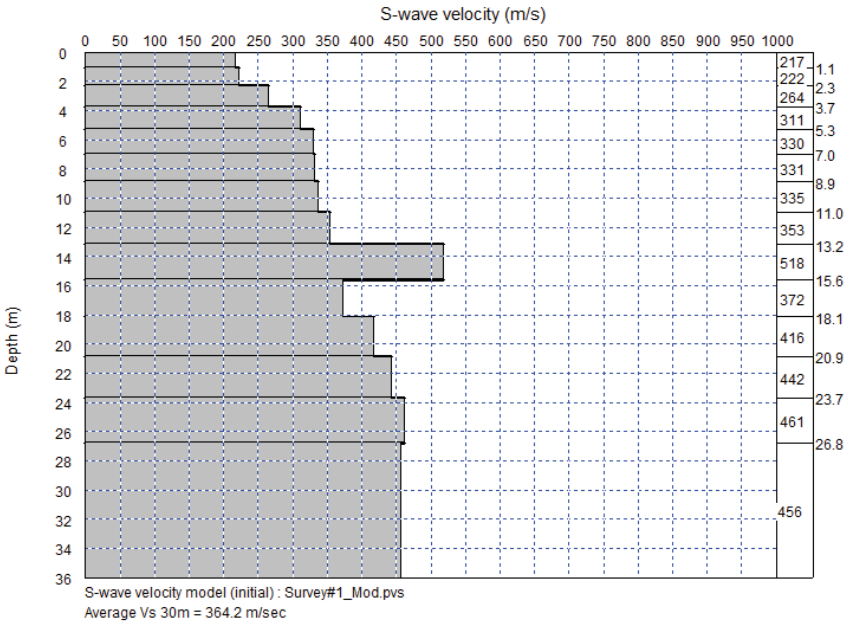

Figure 14. X=28

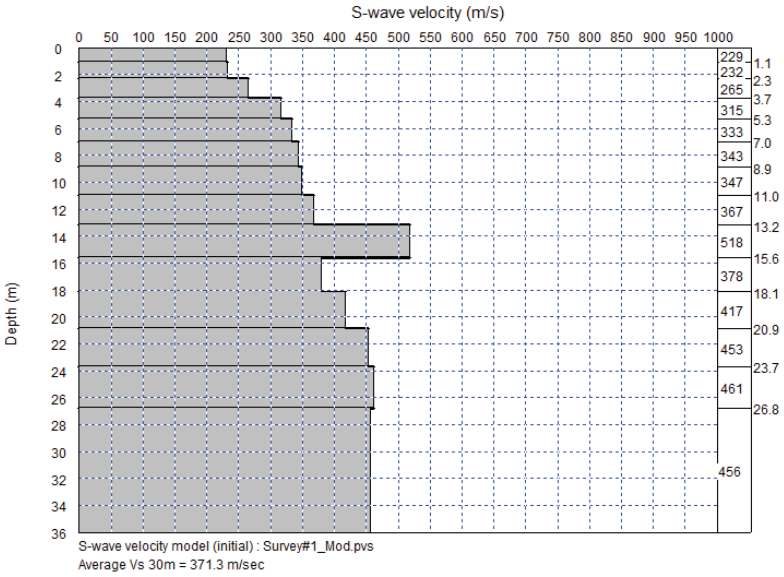

Figure 15. X=32

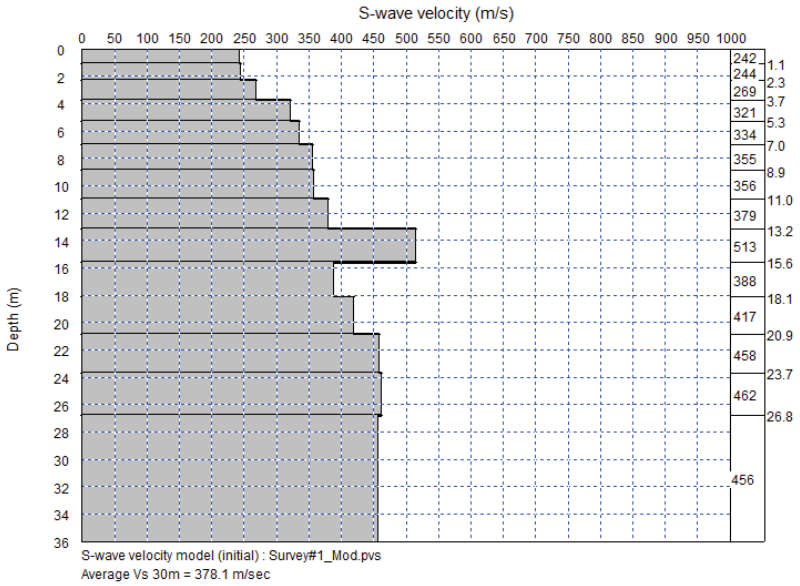

Figure 16. X=36

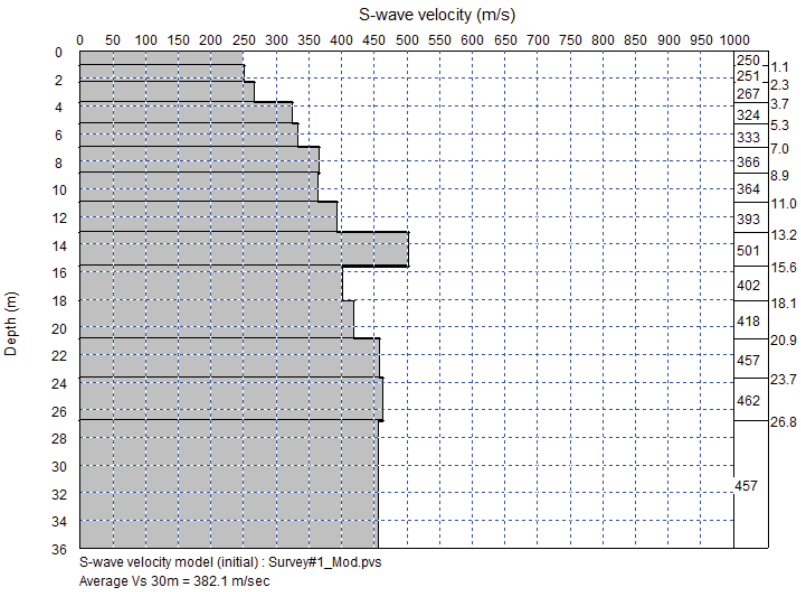

Figure 17. X=40

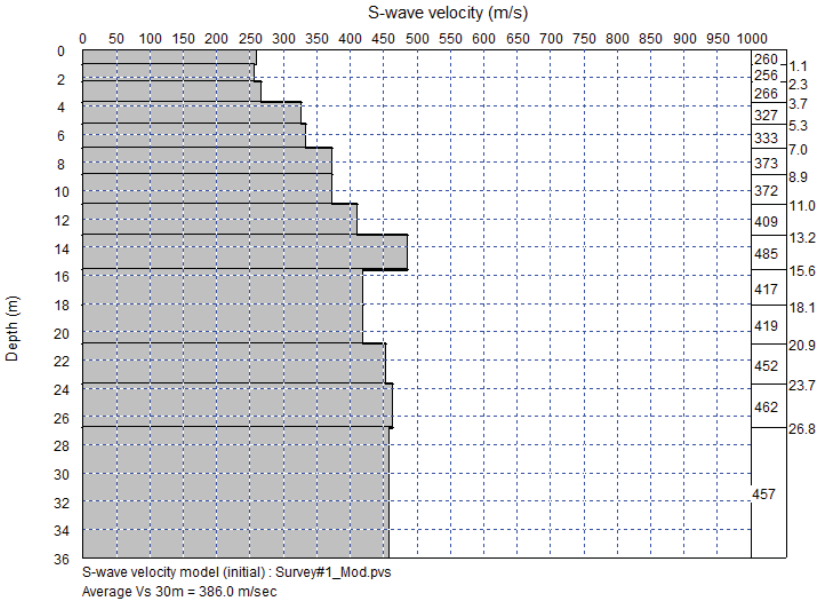

Figure 18. X=44

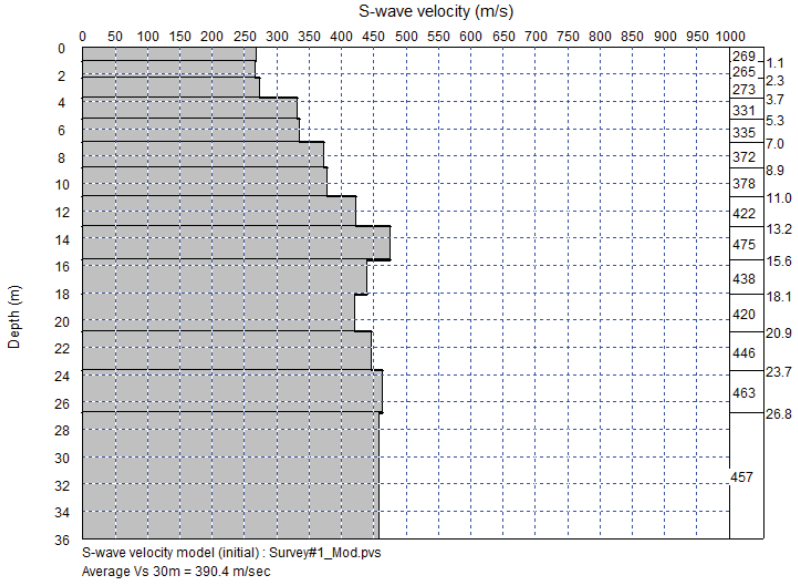

Figure 19. X=48

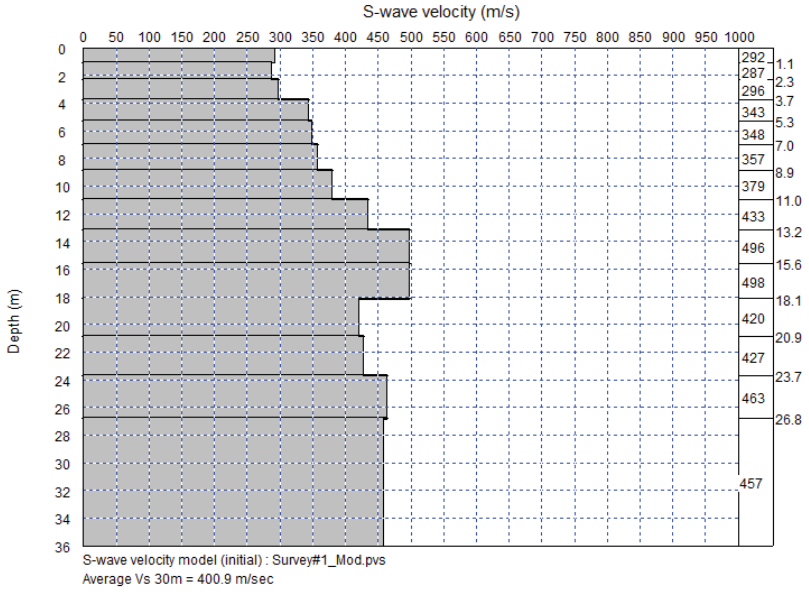

Figure 20. X=52

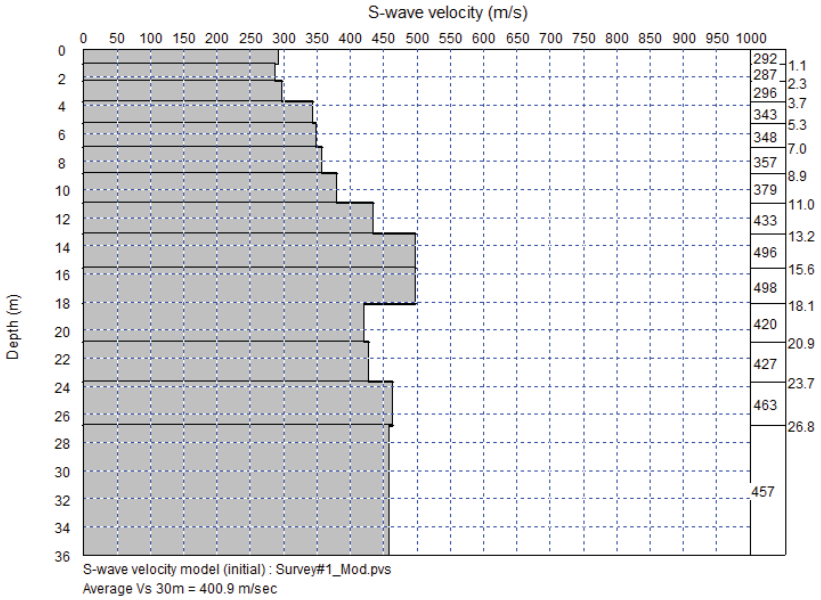

Figure 21. X=56

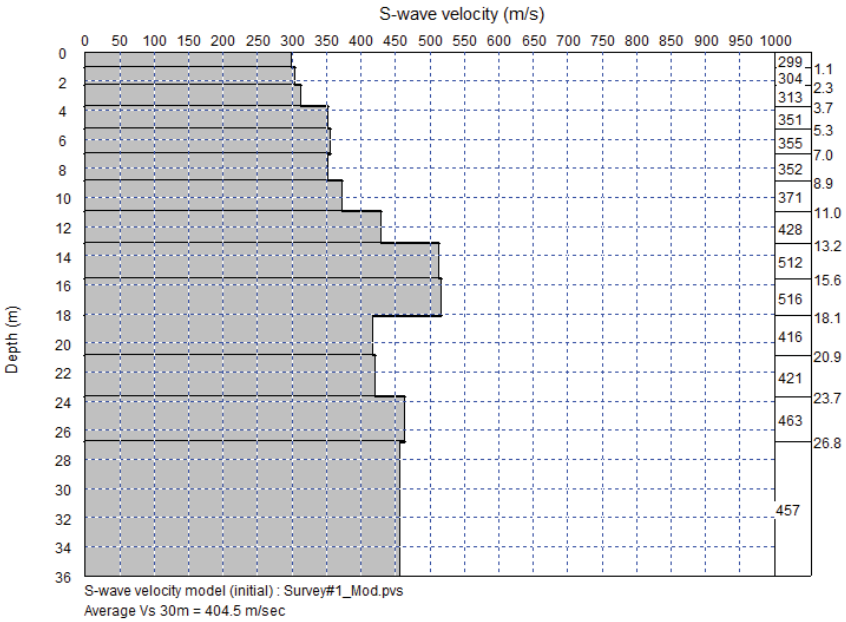

Figure 22. X=60

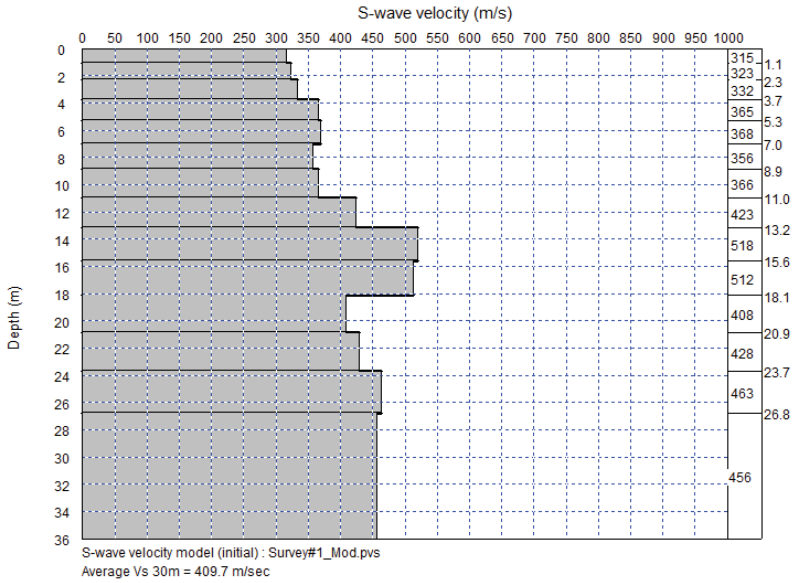

Figure 23. X=64

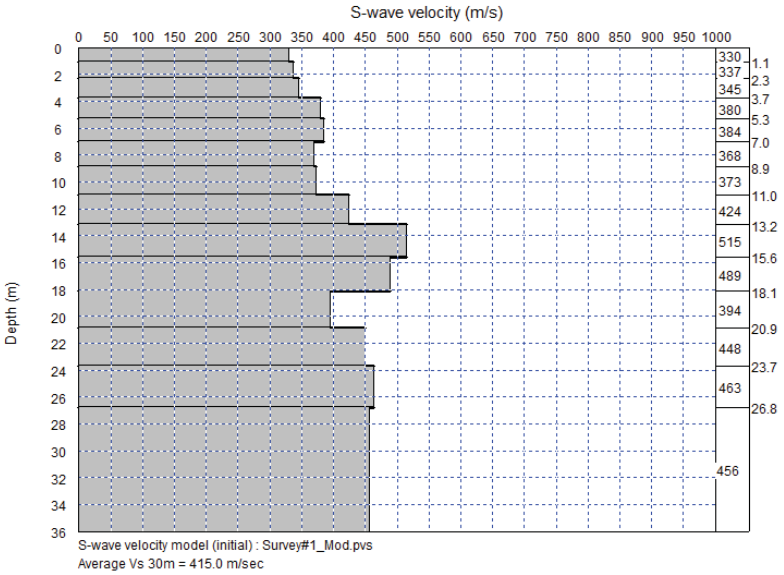

Figure 24. X=68

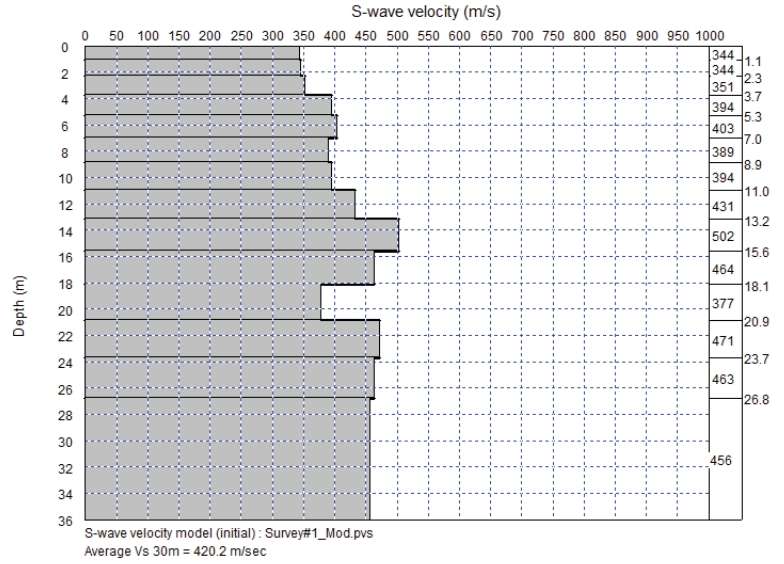

Figure 25. X=72

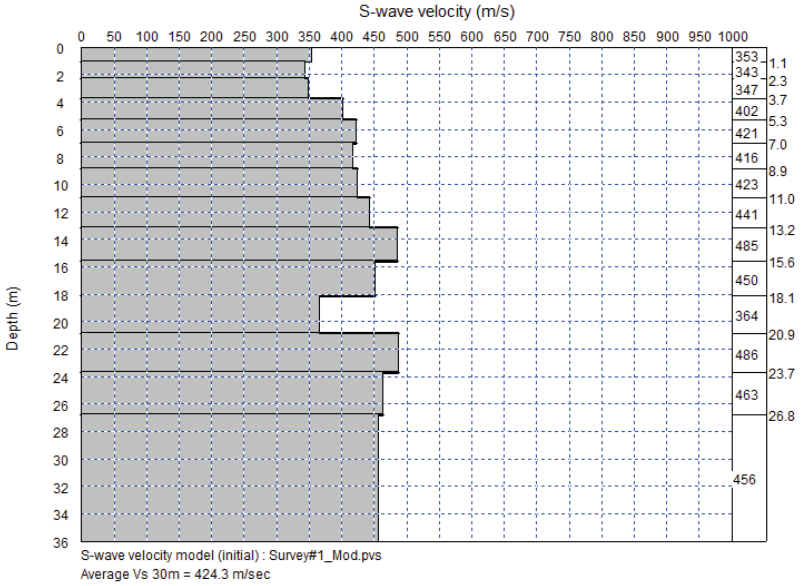

Figure 26. X=76

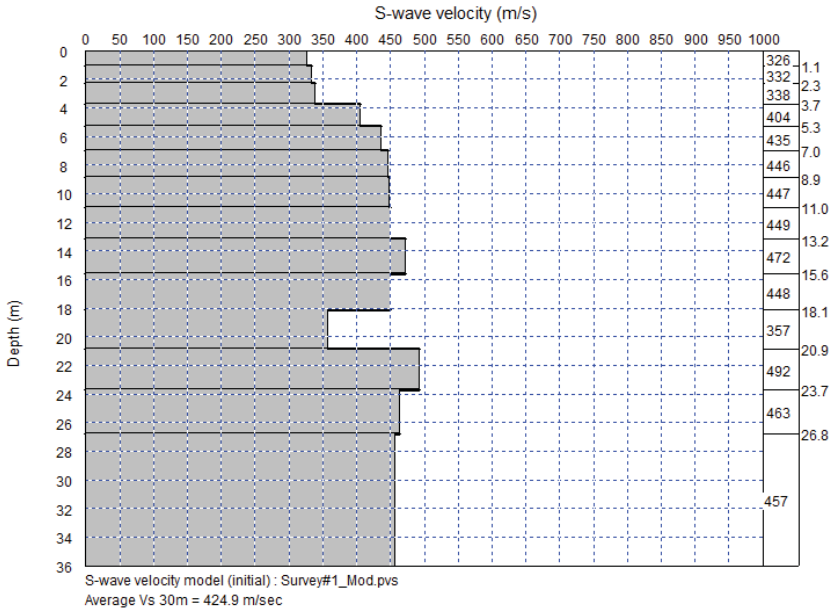

Figure 27. X=80

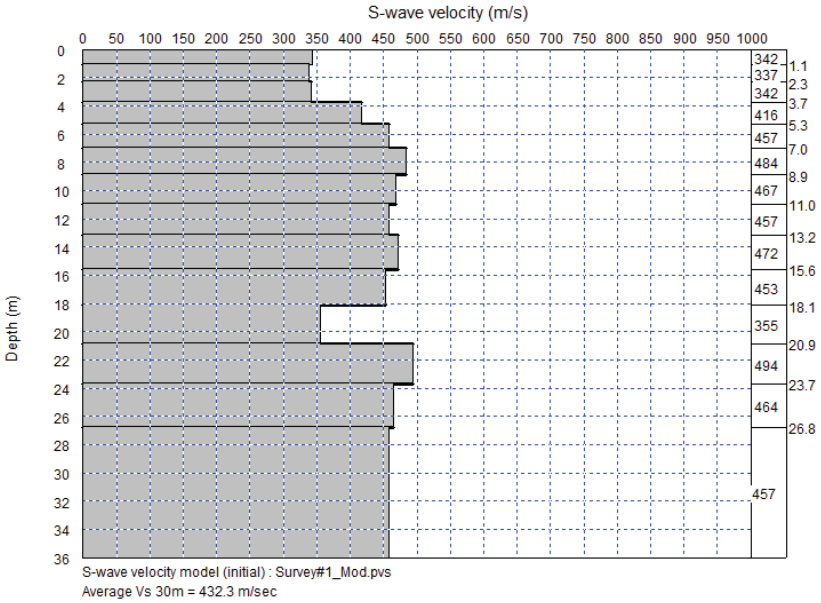

Figure 28. X=84

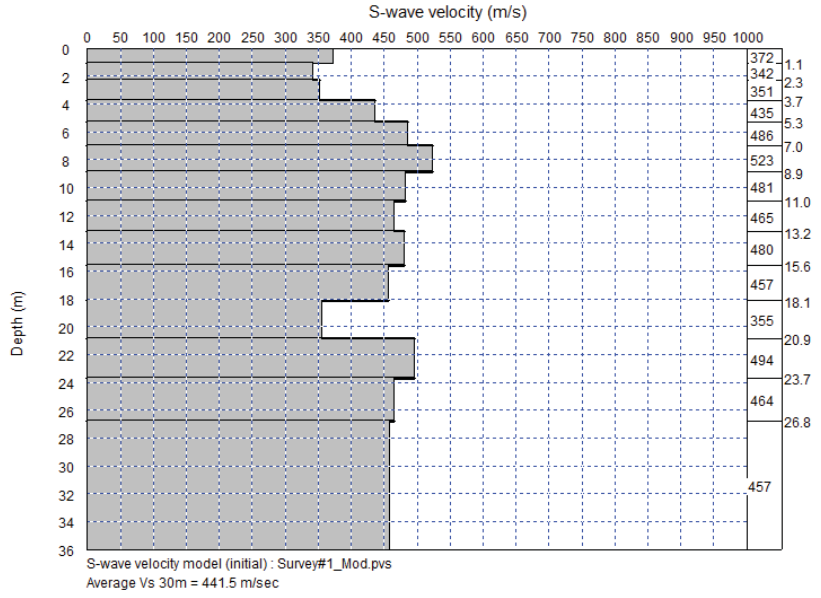

Figure 29. X=88

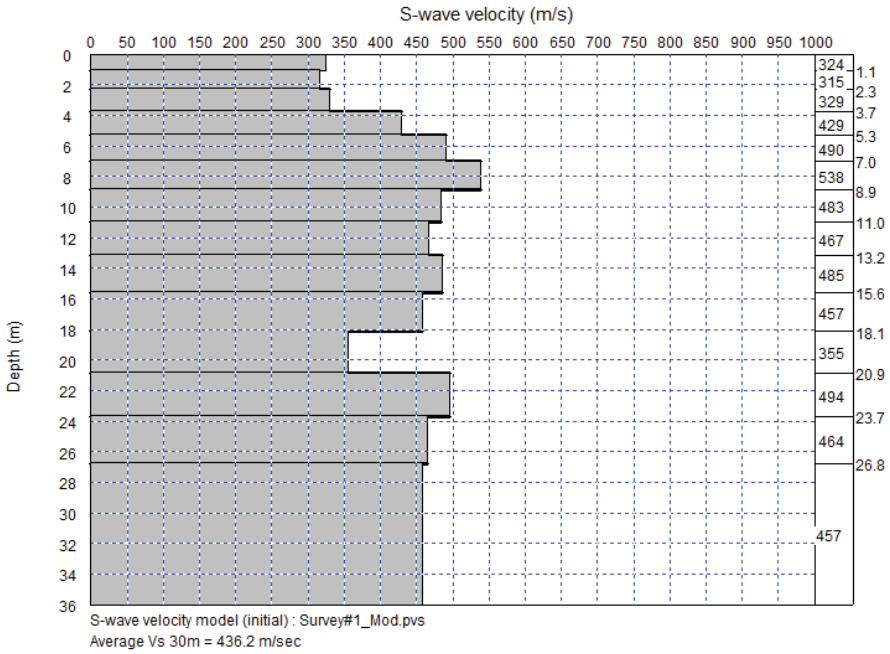

Figure 30. X=92

3.2. SURVEY #2

At the Cava do Germano it was very difficult to transmit energy with the hammer. We believe that the quality of the signal was good until around 12 meters. Because of this, we use the surface waves generated by the movement of a backhoe that was about 500 meters away along the alignment of the geophones array. Thus, we got good quality data around 26 meters deep, with passive MASW at the geophone positions 10_56 and 30_76.

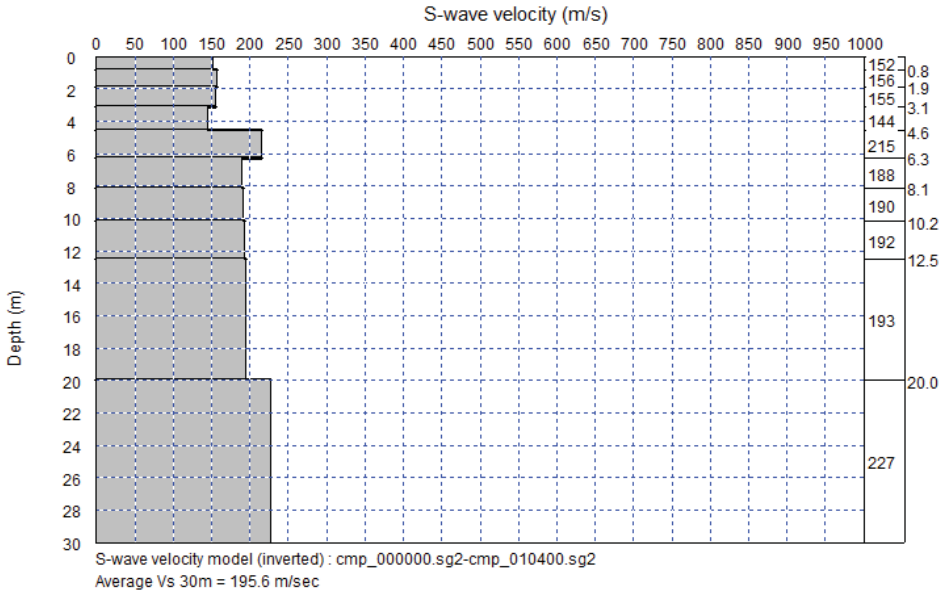

Figure 31. X=0

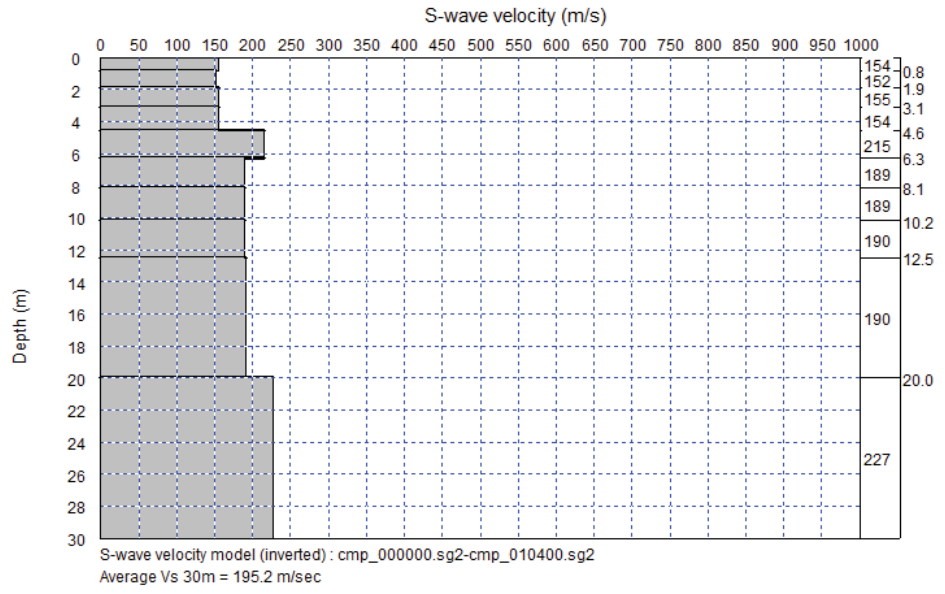

Figure 32. X=4

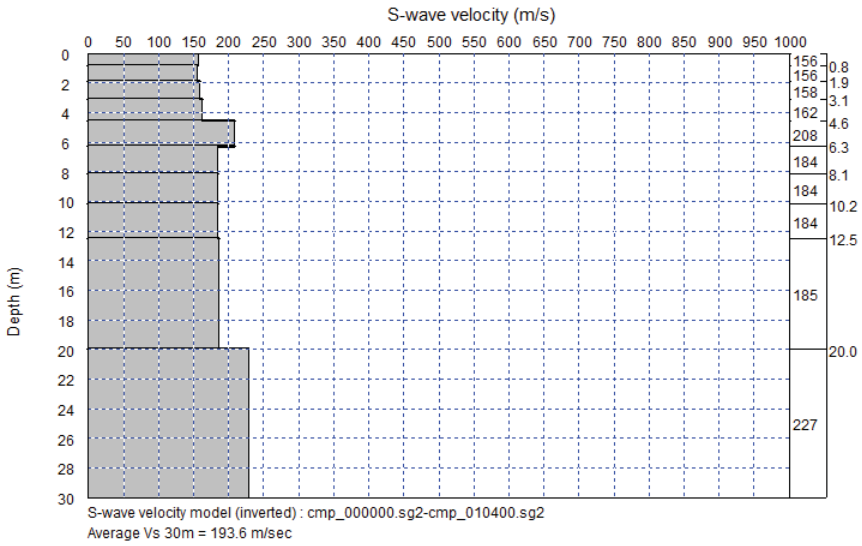

Figure 33. X=8

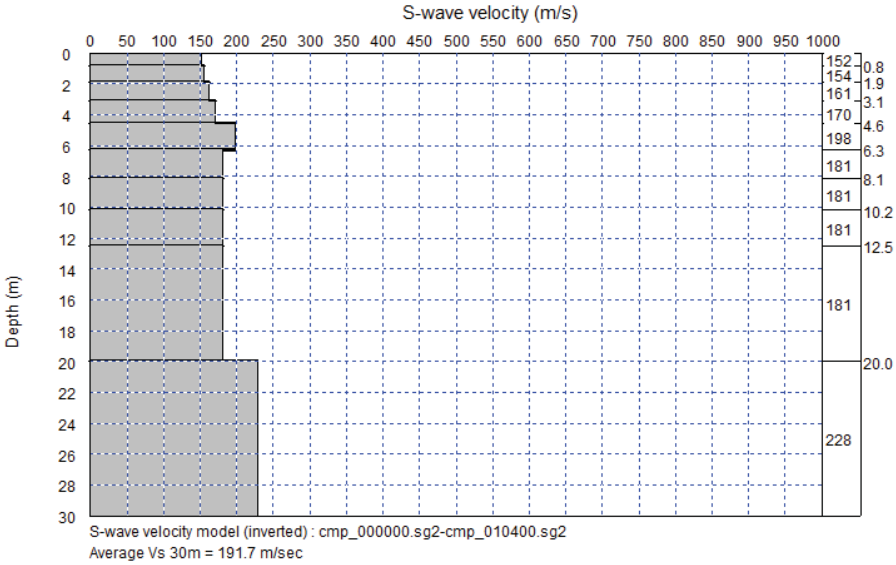

Figure 34. X=12

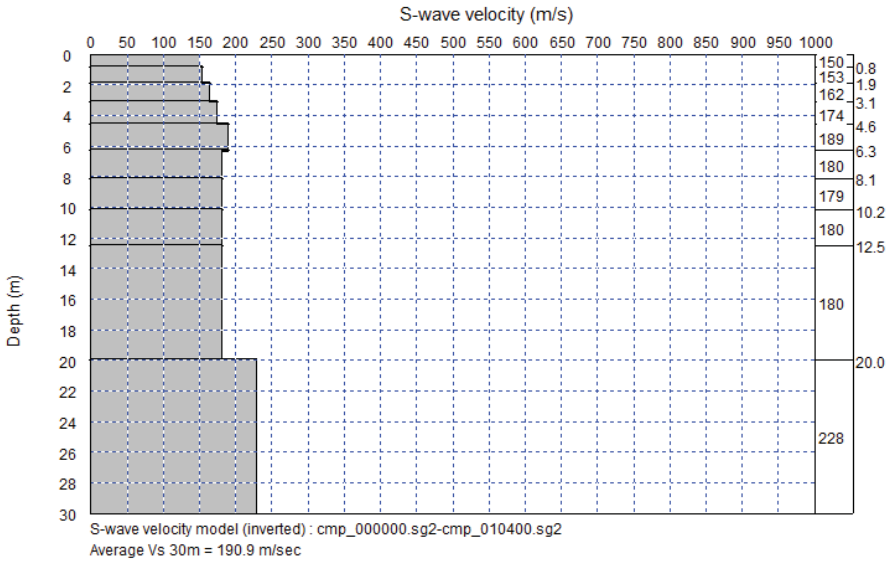

Figure 35. X=16

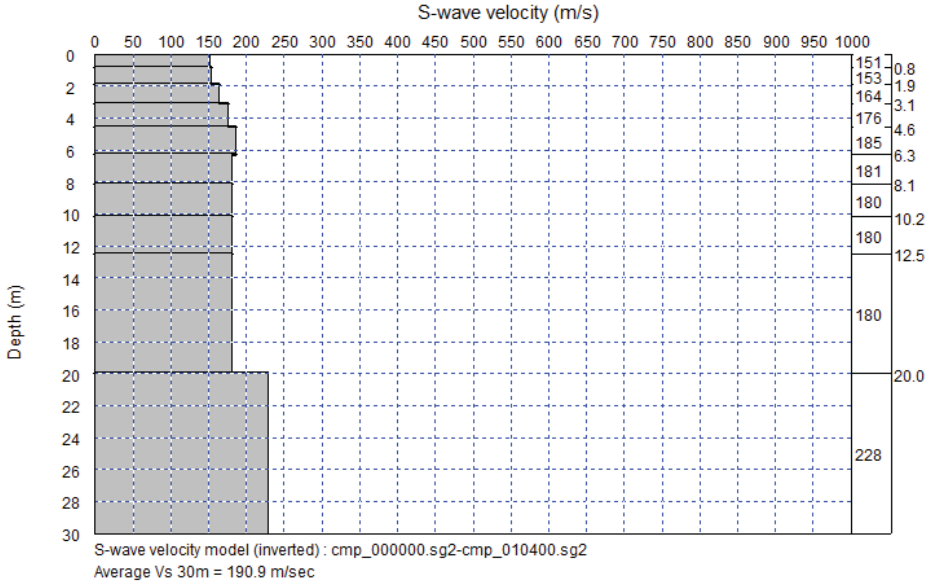

Figure 36. X=20

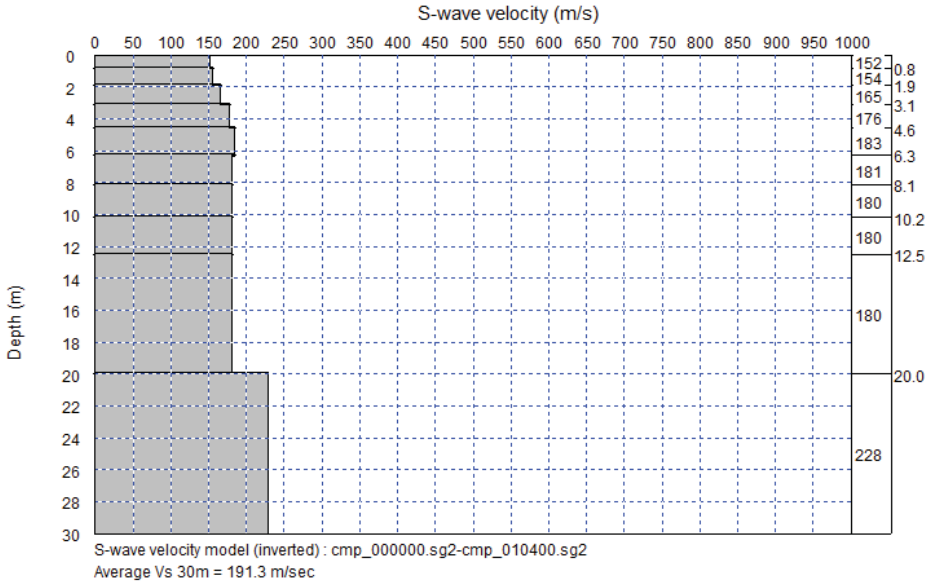

Figure 37. X=24

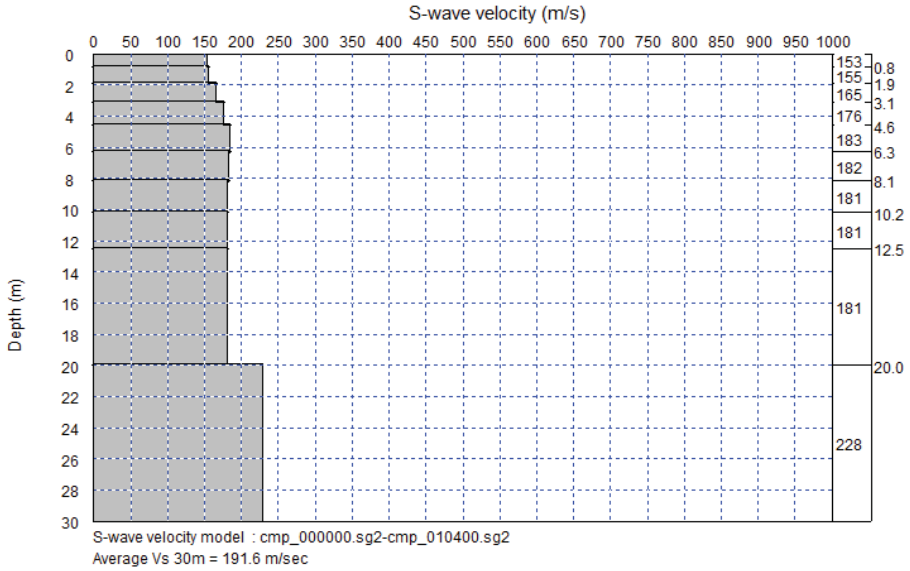

Figure 38. X=28

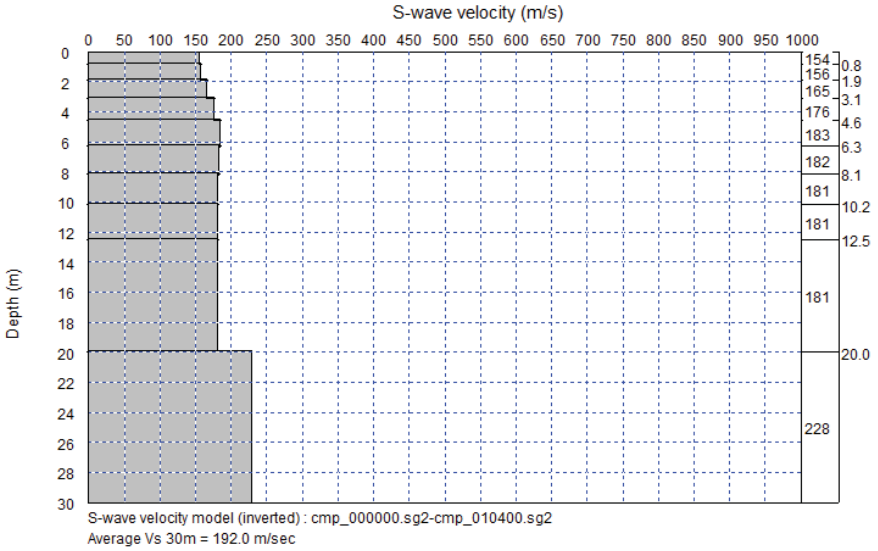

Figure 39. X=32

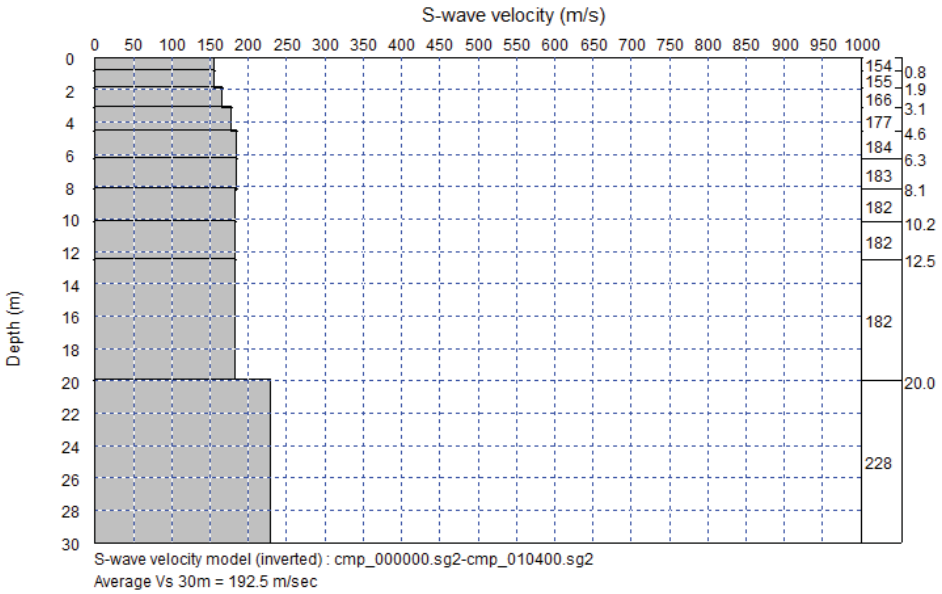

Figure 40. X=36

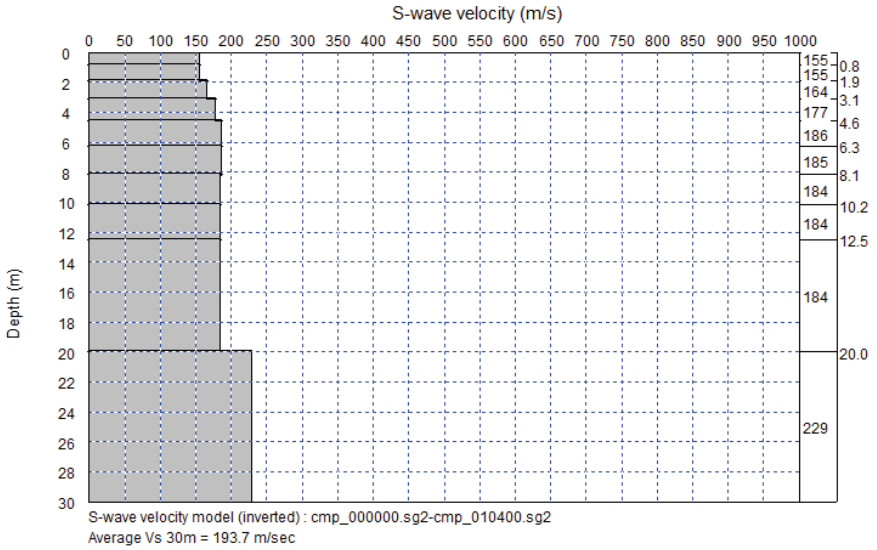

Figure 41. X=40

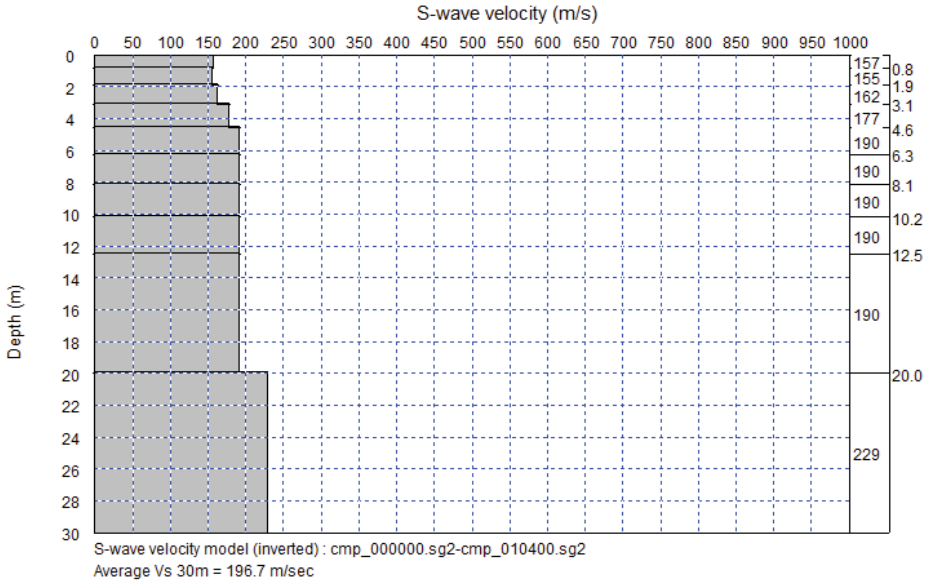

Figure 42. X=44

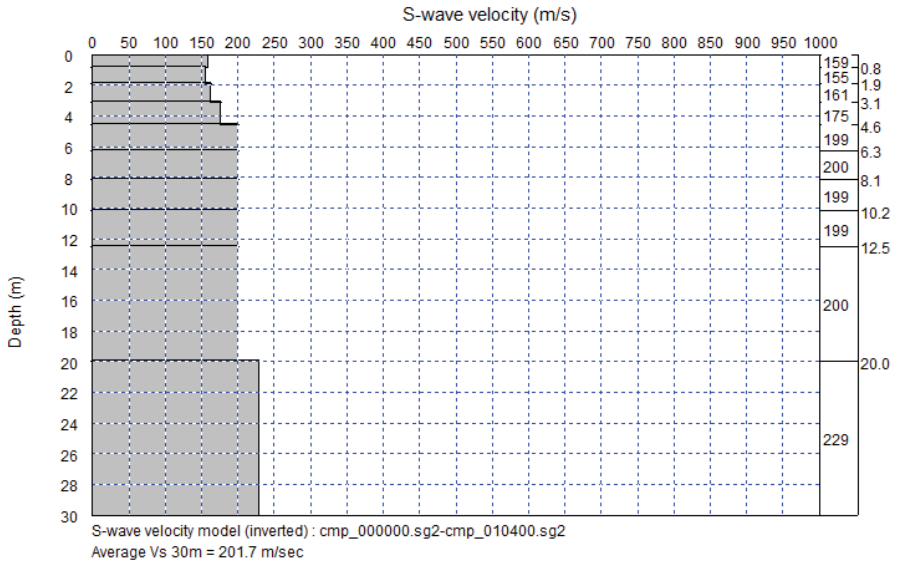

Figure 43. X=48

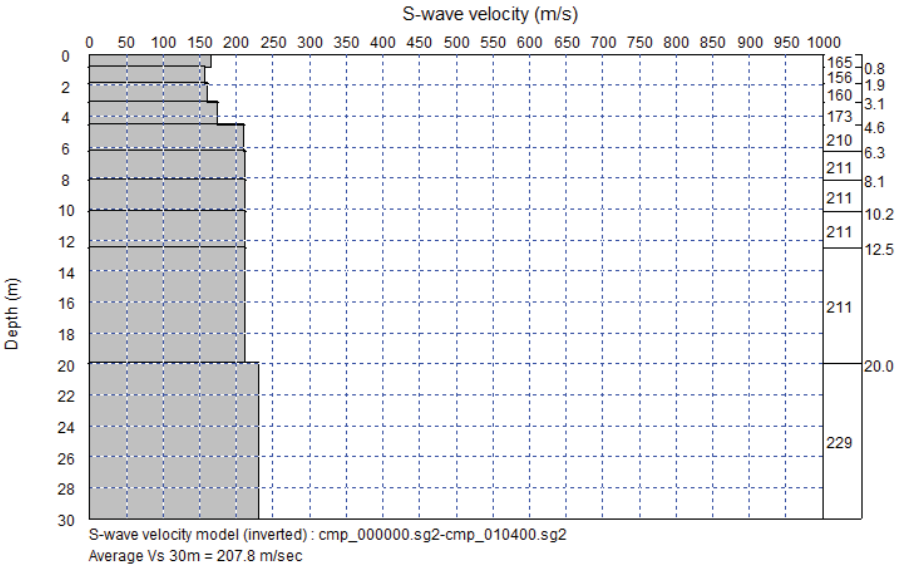

Figure 44. X=52

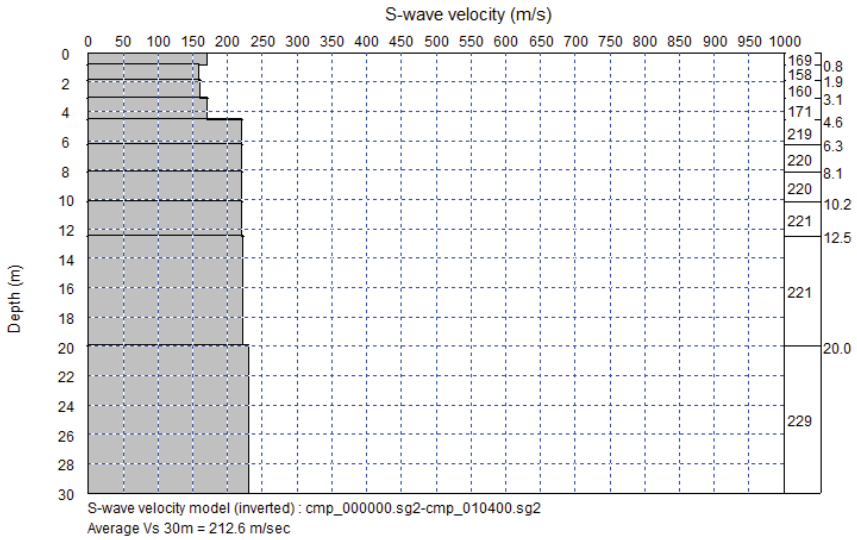

Figure 45. X=56

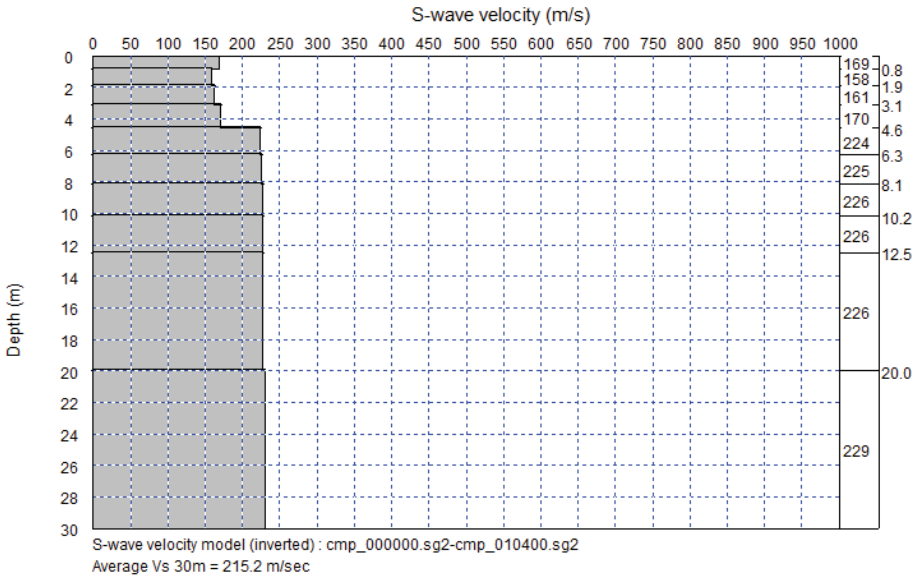

Figure 46. X=60

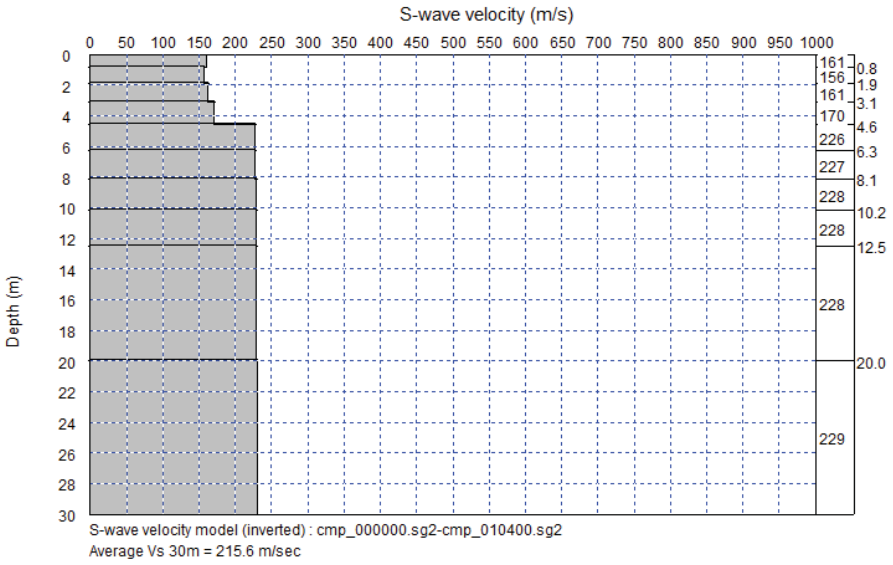

Figure 47. X=64

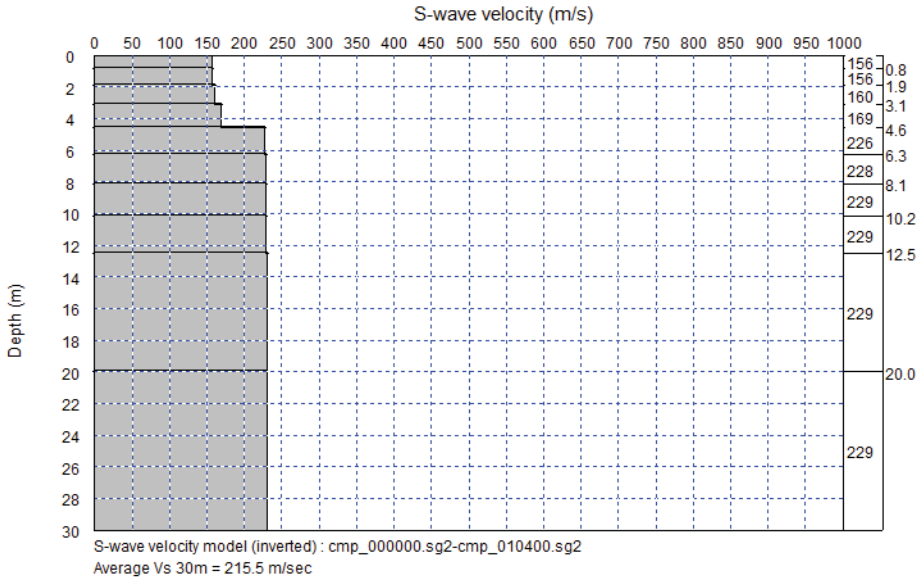

Figure 48. X=68

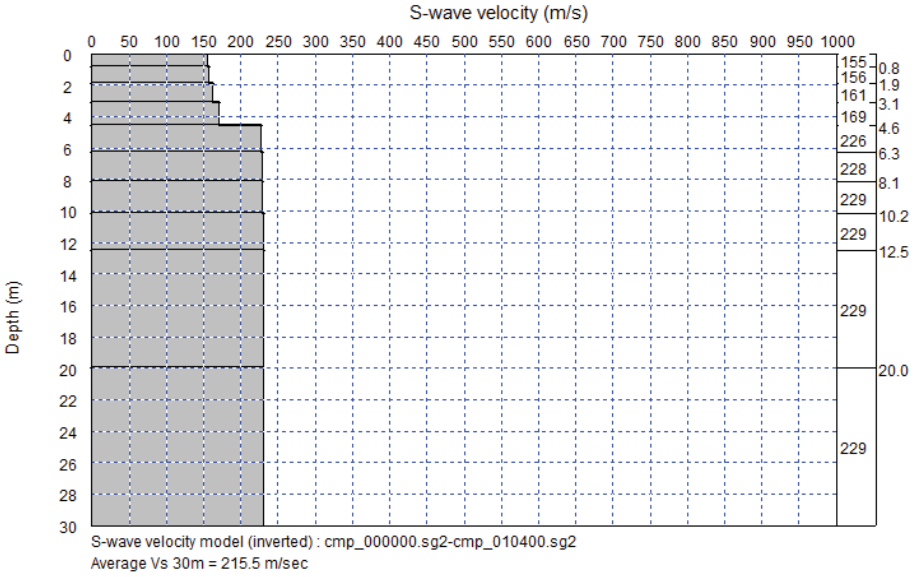

Figure 49. X=72

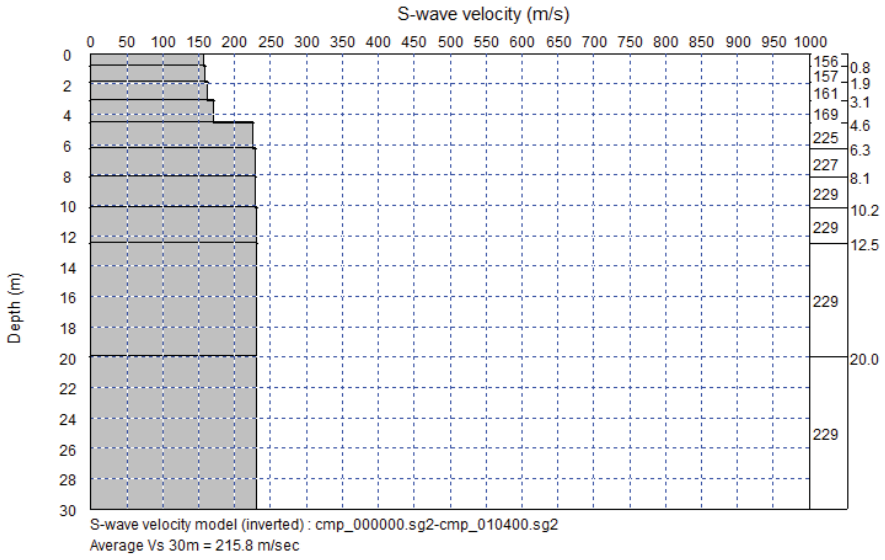

Figure 50. X=76

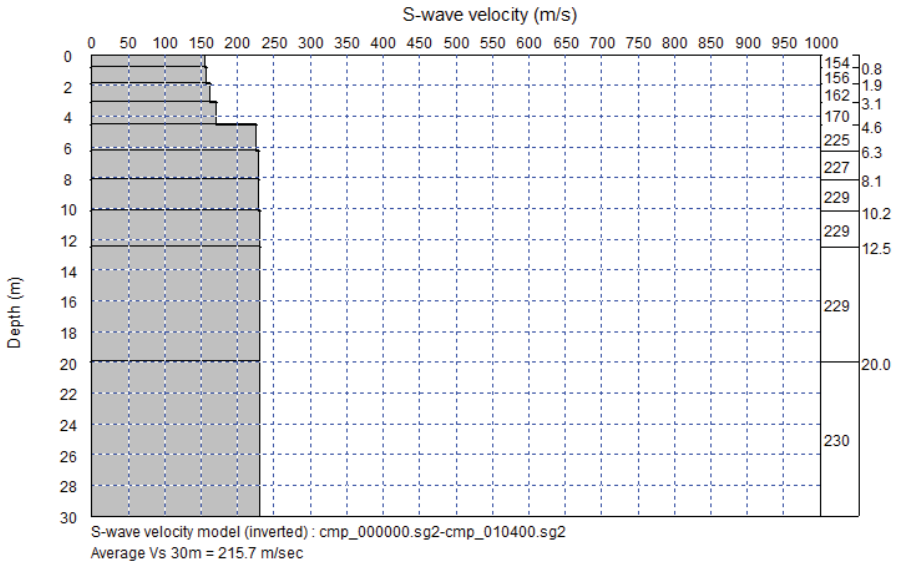

Figure 51. X=80

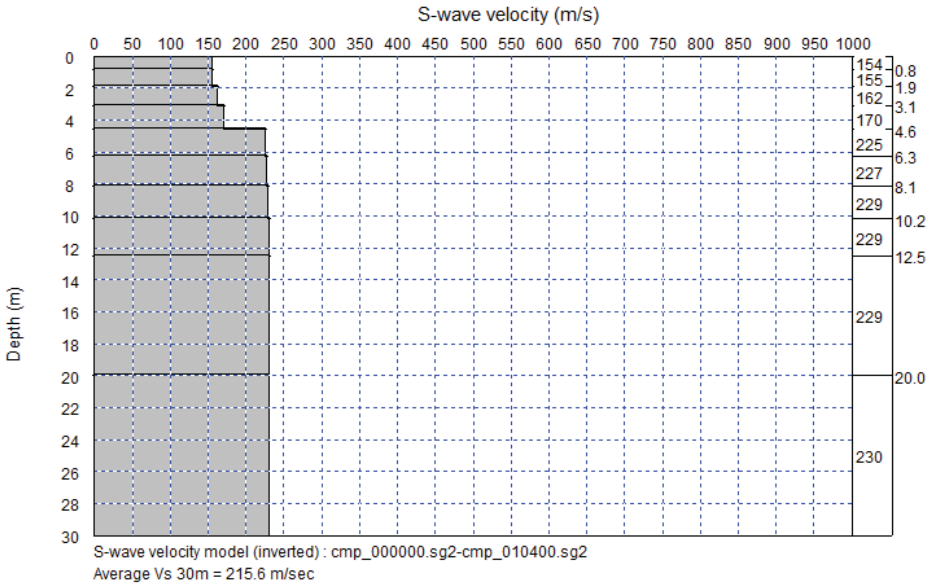

Figure 52. X=84

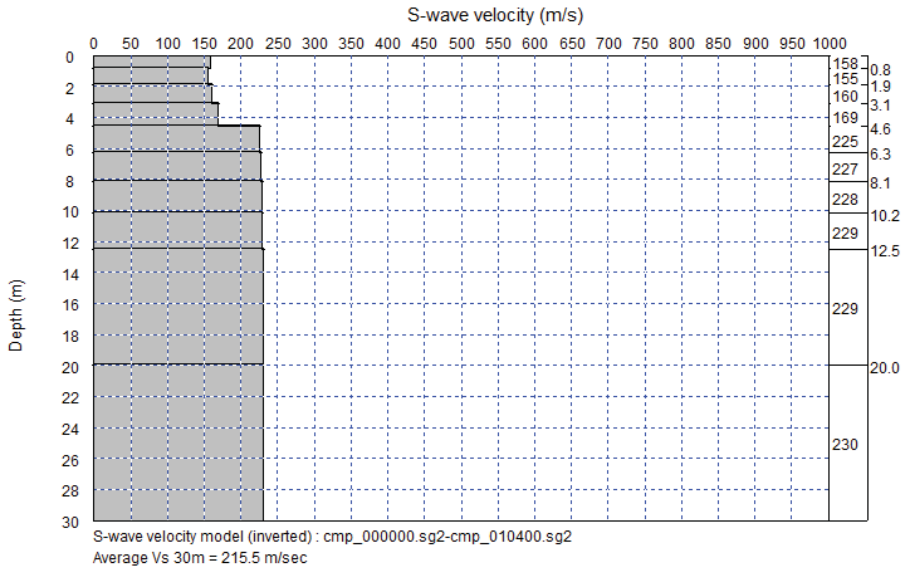

Figure 53. X=88

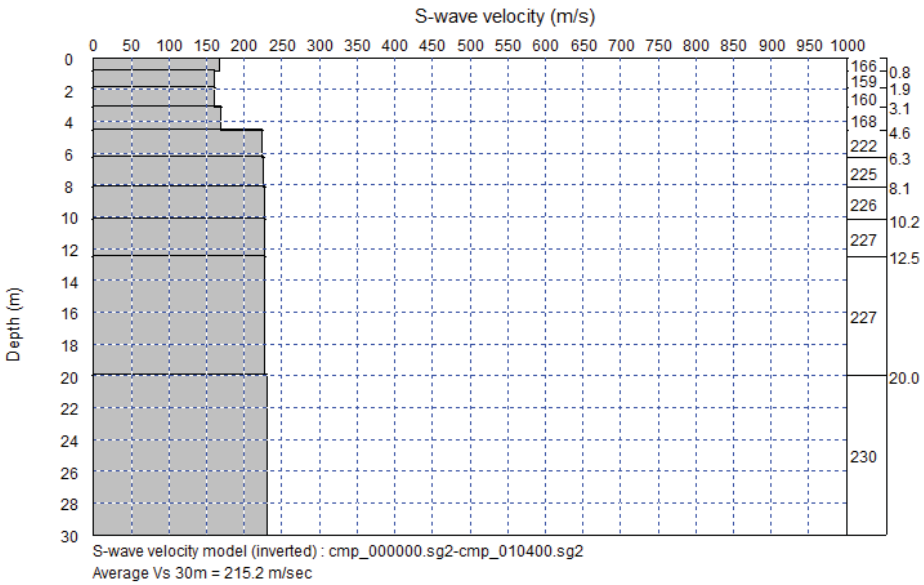

Figure 54. X=92

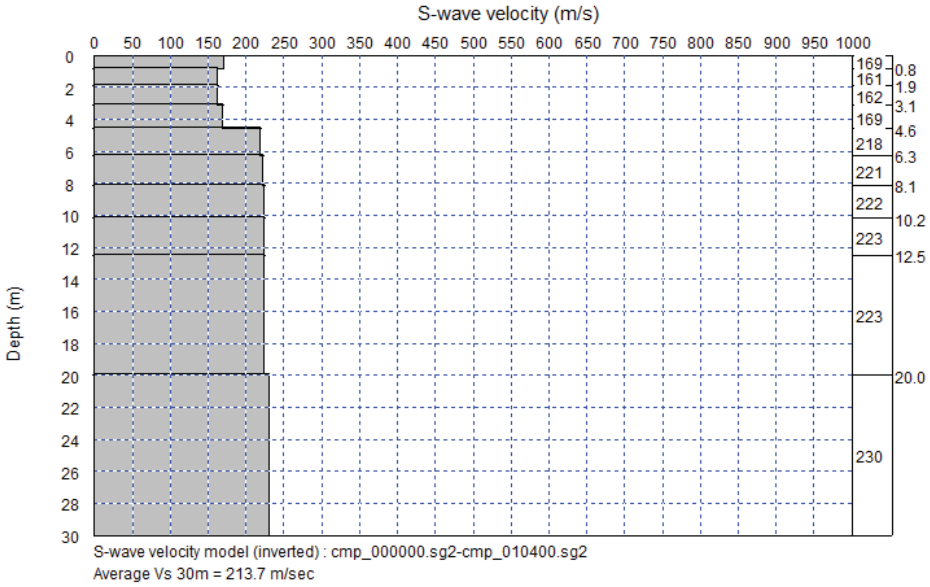

Figure 55. X=96

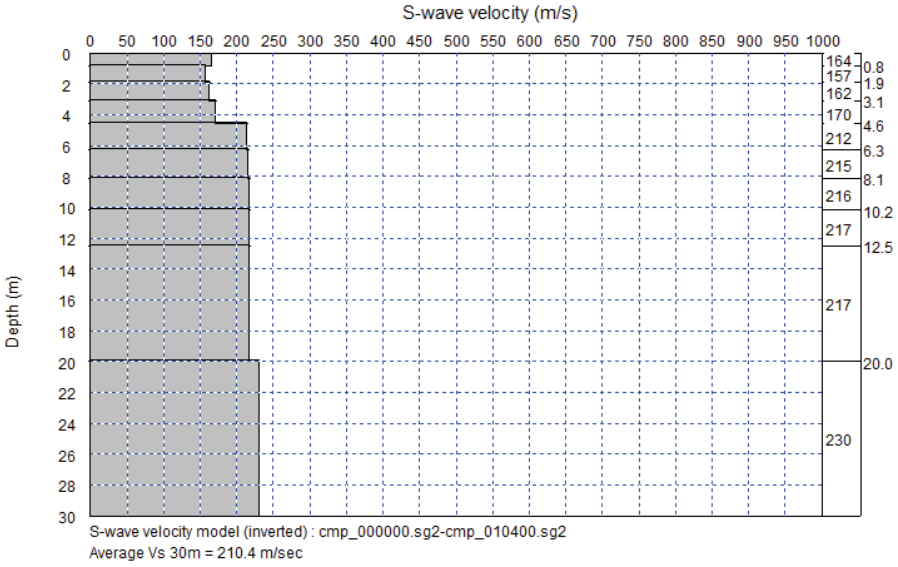

Figure 56. X=100

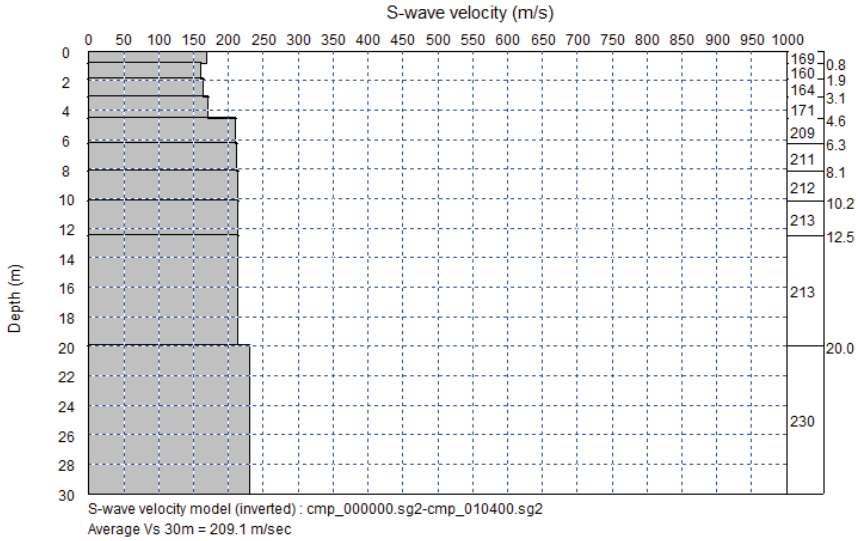

Figure 57. X=104

3.3. SURVEY #3

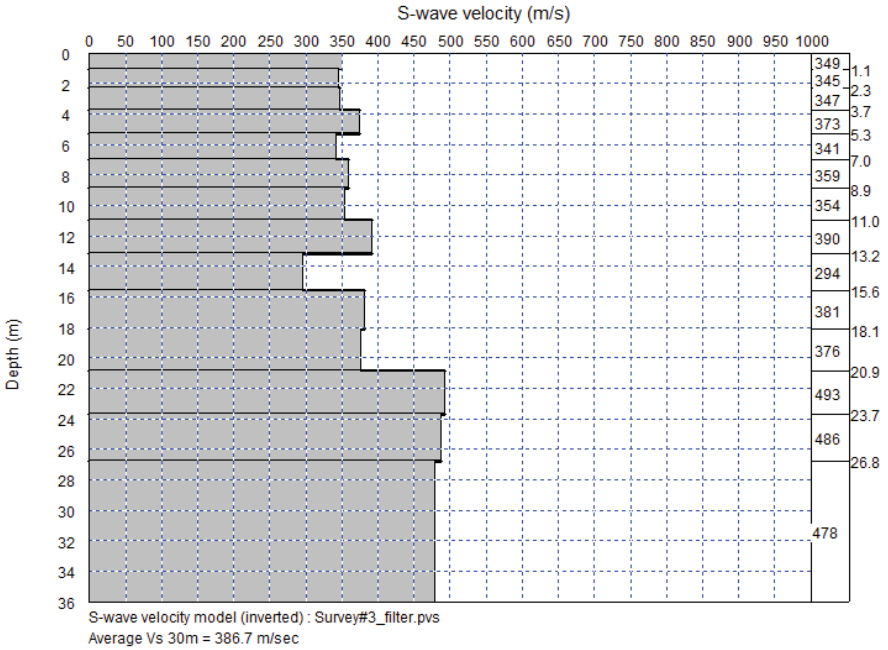

Figure 58. X=0

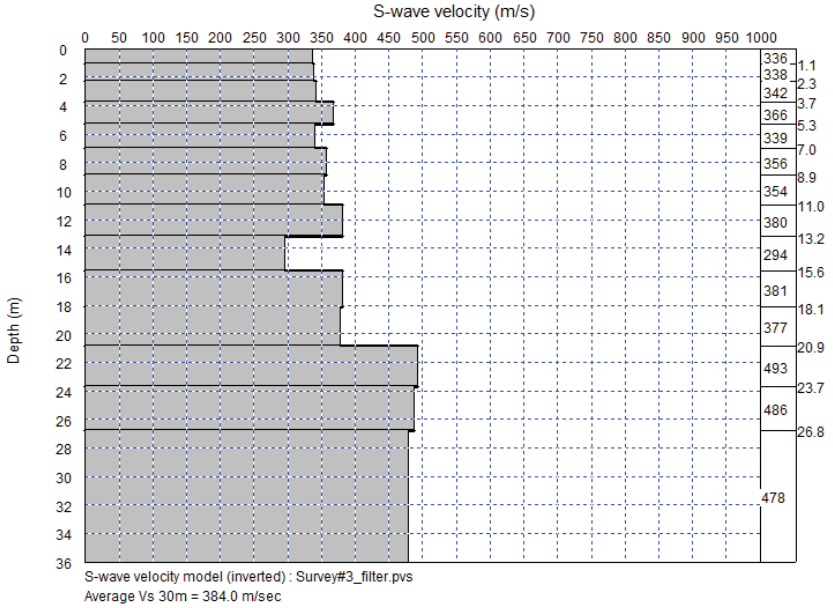

Figure 59. X=4

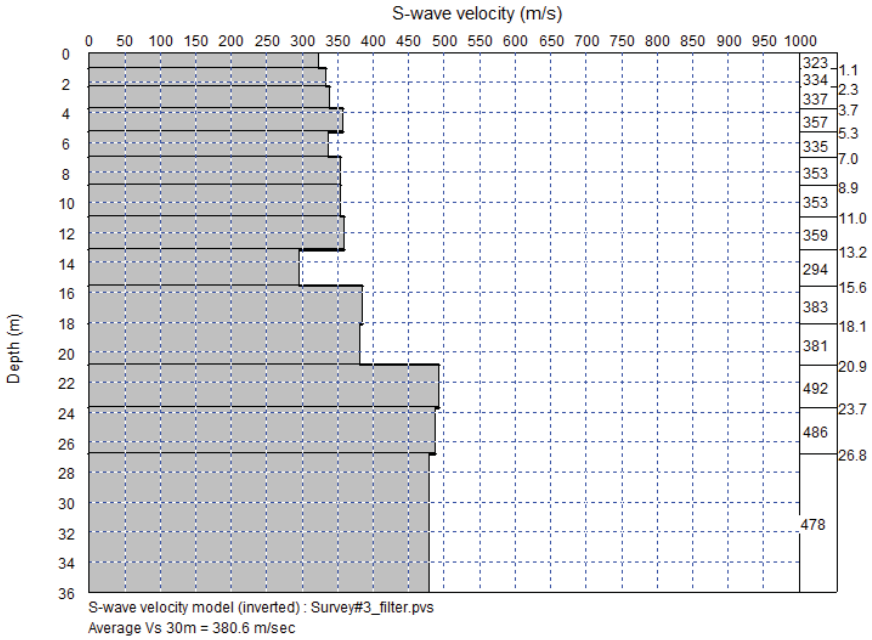

Figure 60. X=8

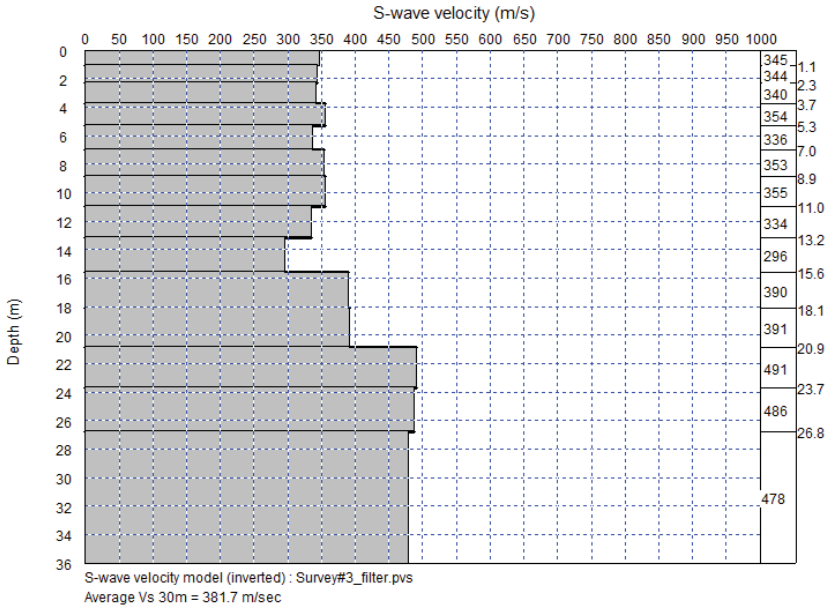

Figure 61. X=12

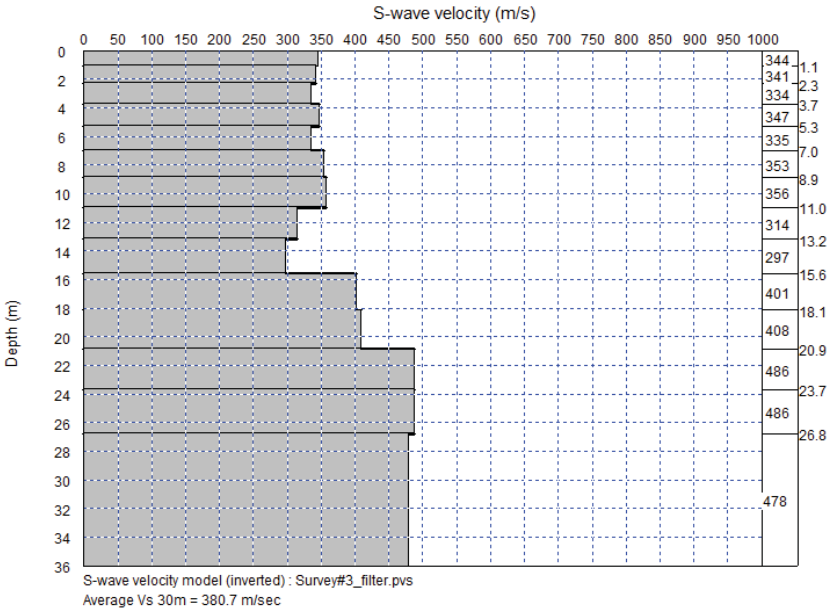

Figure 62. X=16

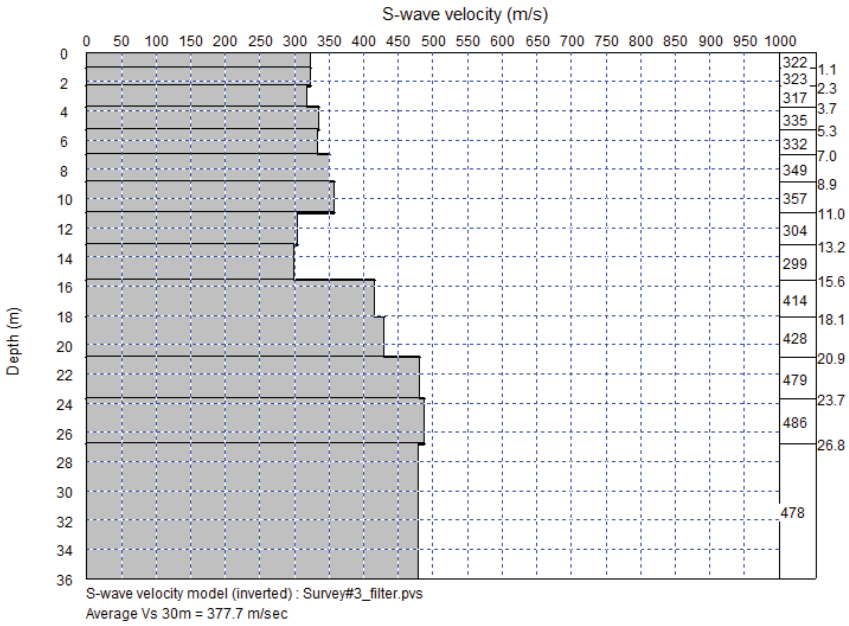

Figure 63. X=20

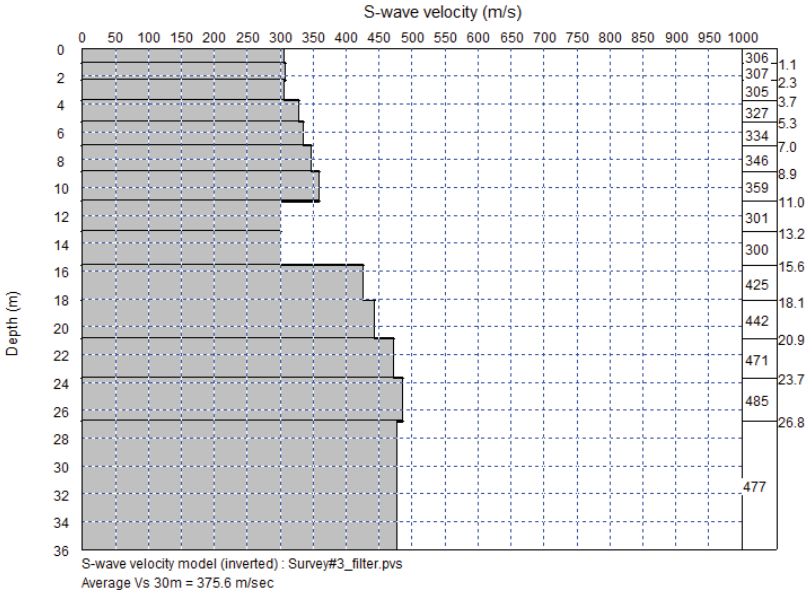

Figure 64. X=24

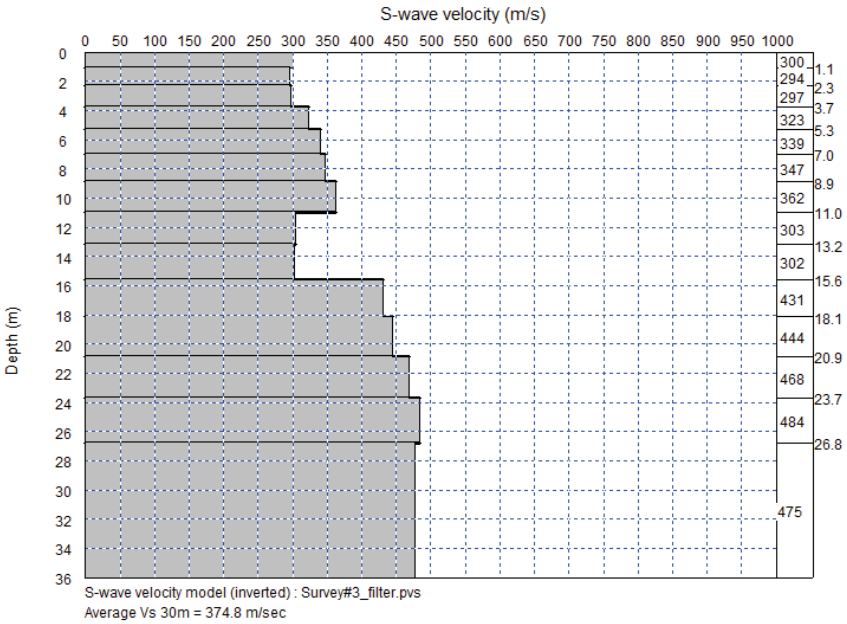

Figure 65. X=28

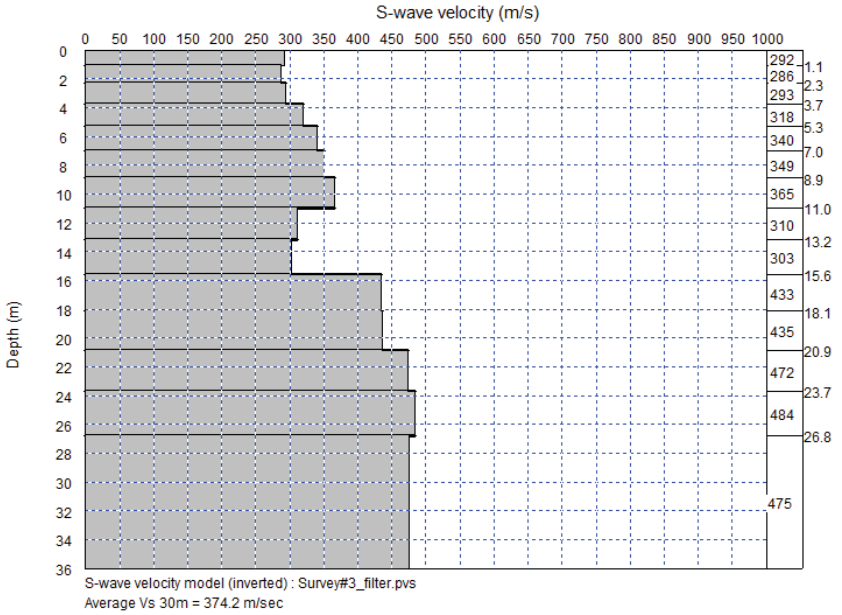

Figure 66. X=32

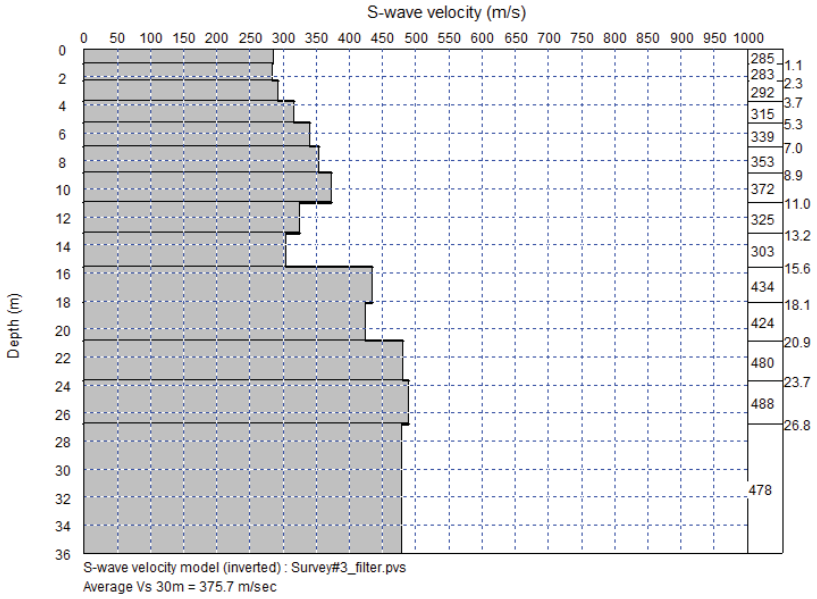

Figure 67. X=36

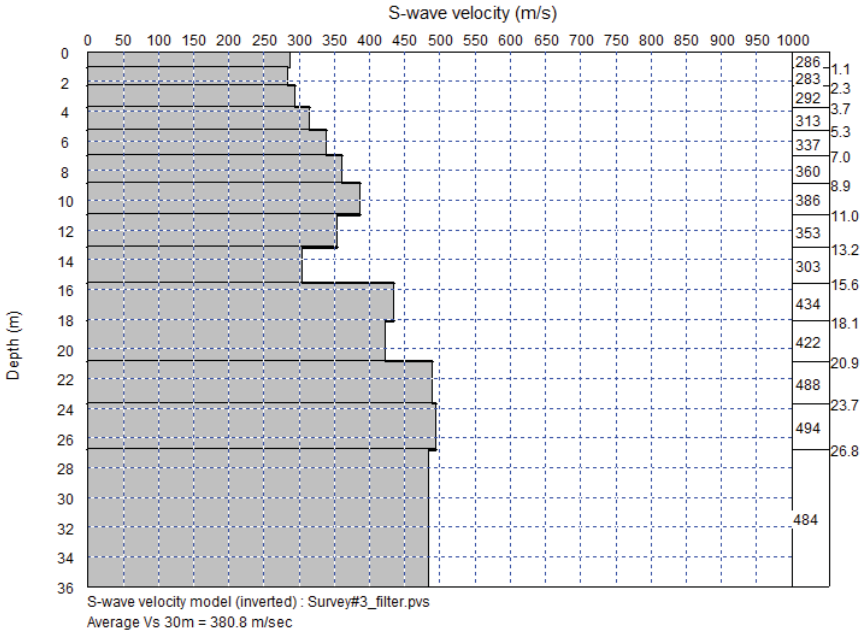

Figure 68. X=40

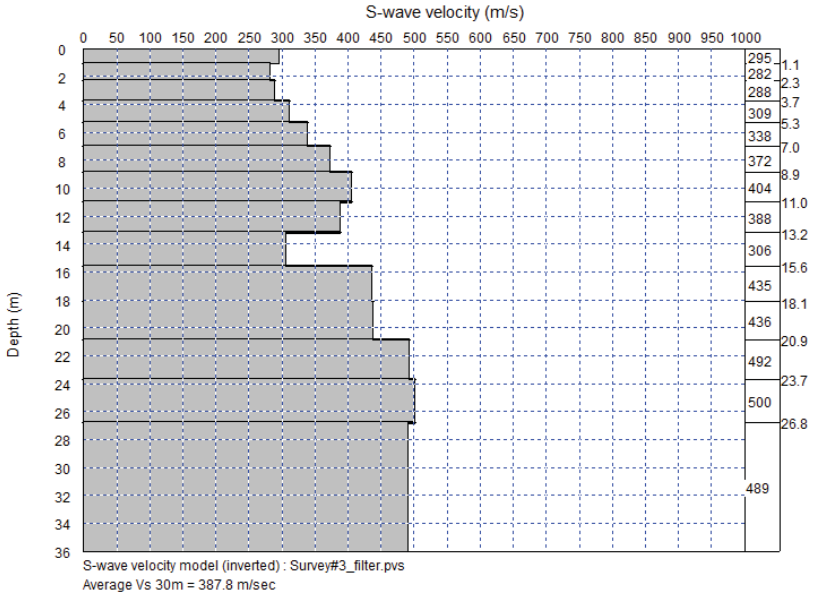

Figure 69. X=44

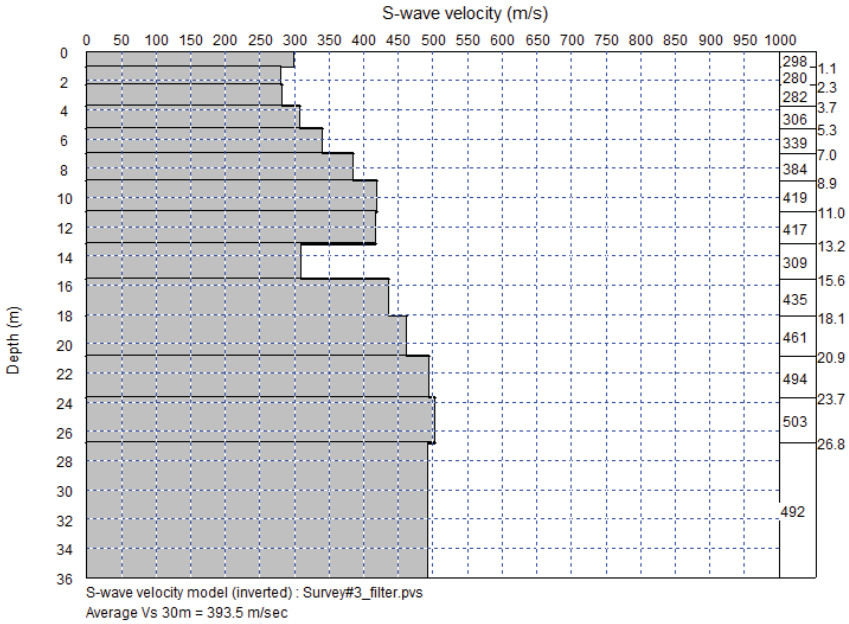

Figure 70. X=48

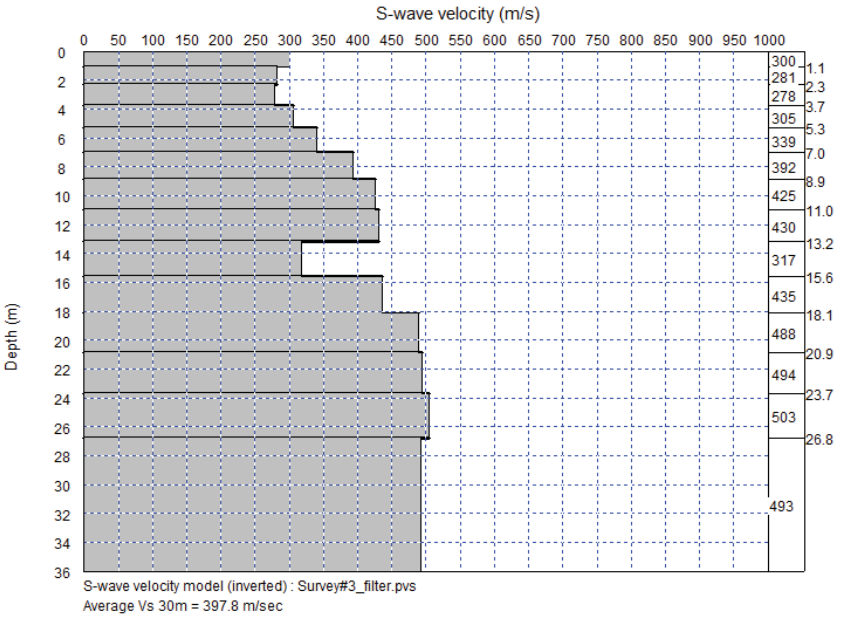

Figure 71. X=52

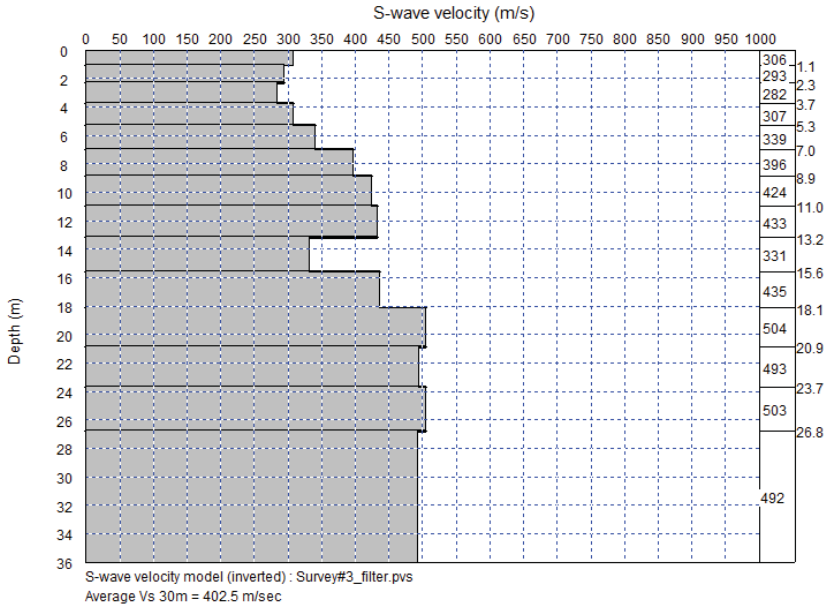

Figure 72. X=56

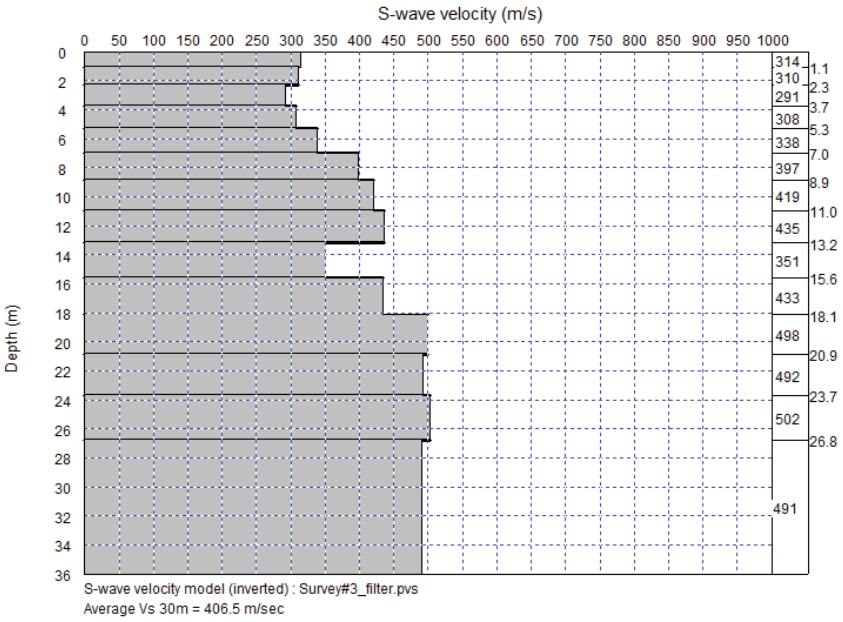

Figure 73. X=60

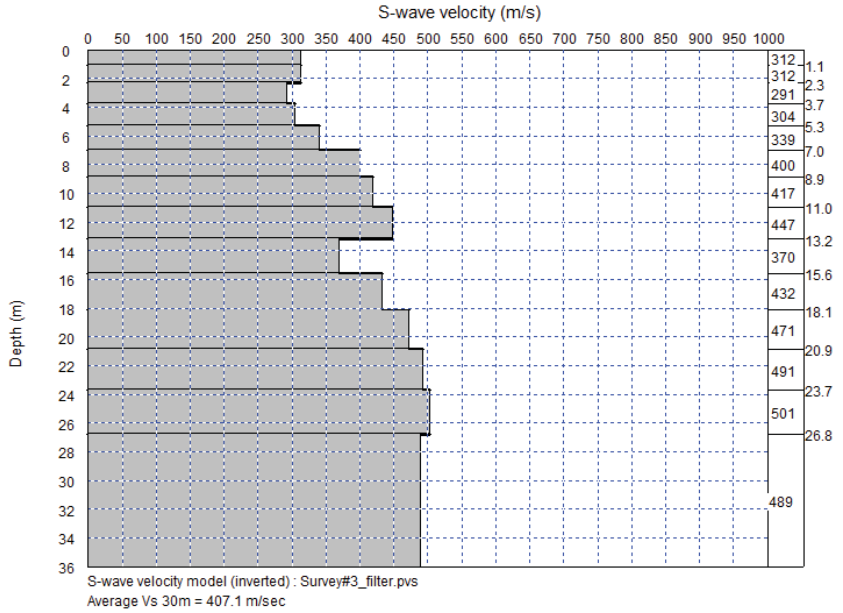

Figure 74. X=64

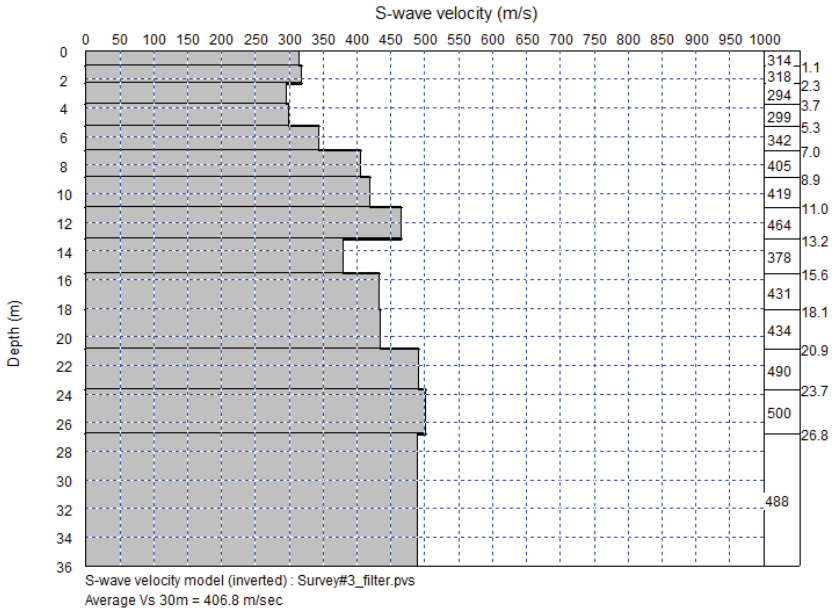

Figure 75. X=68

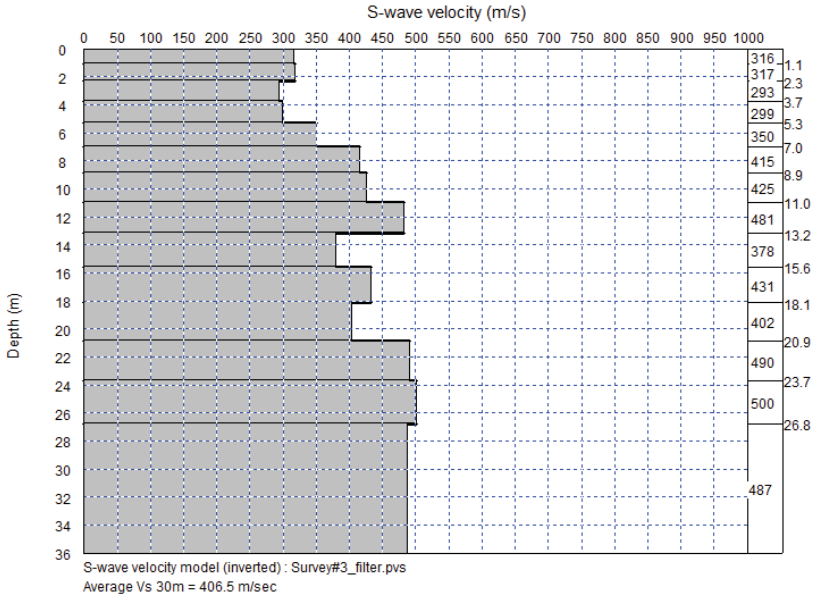

Figure 76. X=72

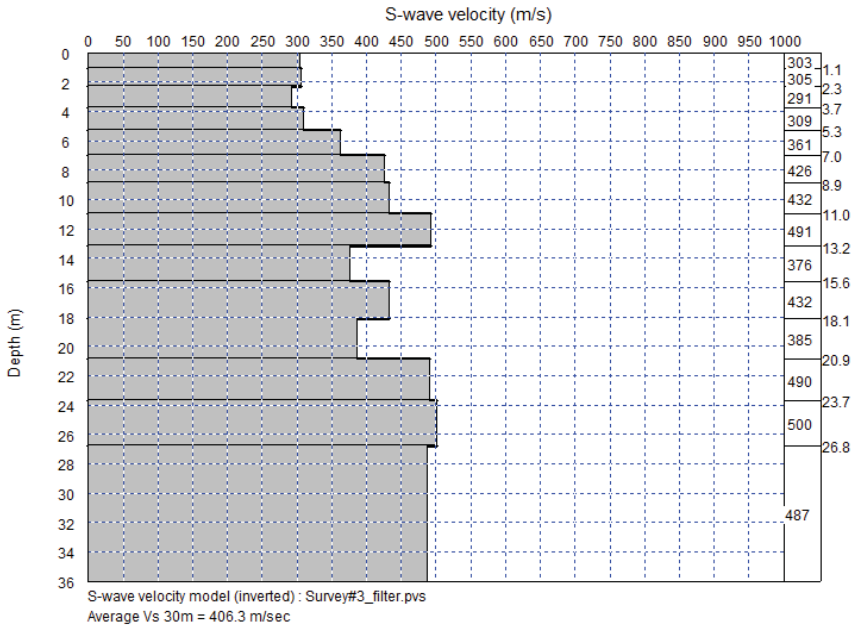

Figure 77. X=76

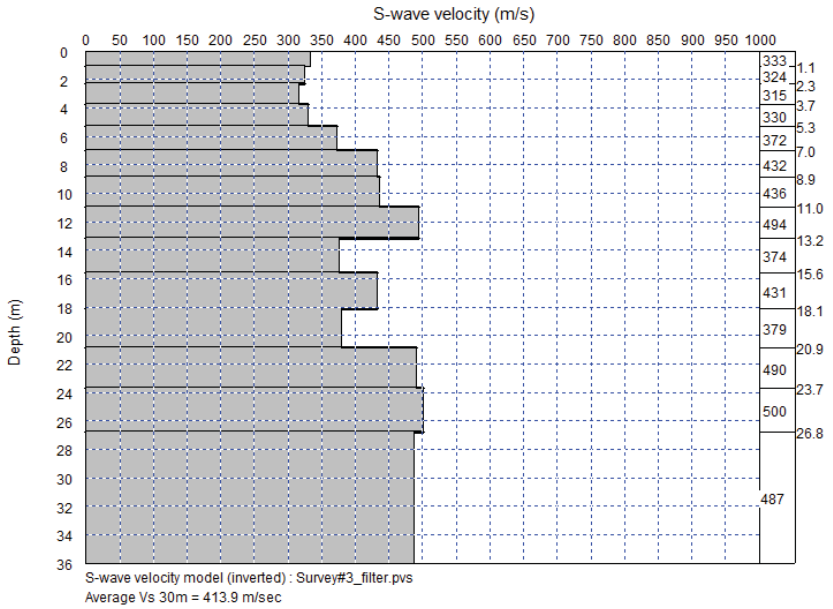

Figure 78. X=80

4. CLASSIFICATION OF ROCK MASS ALONG SURVEY

4.1. SURVEY #1

X (m)	Vs30 (m/s)	Site Class
0	335.1	D - Stiff Soil
4	334.8	D - Stiff Soil
8	339	D - Stiff Soil
12	339.6	D - Stiff Soil
16	345.6	D - Stiff Soil
20	353	D - Stiff Soil
24	359.4	D - Stiff Soil
28	364.2	C - Very Dense Soil and Soft Rock
32	371.3	C - Very Dense Soil and Soft Rock
36	378.1	C - Very Dense Soil and Soft Rock
40	382.1	C - Very Dense Soil and Soft Rock
44	386	C - Very Dense Soil and Soft Rock
48	390.4	C - Very Dense Soil and Soft Rock
52	395.3	C - Very Dense Soil and Soft Rock
56	400.9	C - Very Dense Soil and Soft Rock
60	404.5	C - Very Dense Soil and Soft Rock
64	409.7	C - Very Dense Soil and Soft Rock
68	415	C - Very Dense Soil and Soft Rock
72	420.2	C - Very Dense Soil and Soft Rock
76	424.3	C - Very Dense Soil and Soft Rock
80	424.9	C - Very Dense Soil and Soft Rock
84	432.3	C - Very Dense Soil and Soft Rock
88	441.5	C - Very Dense Soil and Soft Rock
92	436.2	C - Very Dense Soil and Soft Rock

Table 1. Survey #1

4.2. SURVEY #2

X (m)	Vs30 (m/s)	Site Class
0	195.6	D - Stiff Soil
4	195.2	D - Stiff Soil
8	193.6	D - Stiff Soil
12	191.7	D - Stiff Soil
16	190.9	D - Stiff Soil
20	190.9	D - Stiff Soil
24	191.3	D - Stiff Soil
28	191.6	D - Stiff Soil
32	192.0	D - Stiff Soil
36	192.5	D - Stiff Soil
40	193.7	D - Stiff Soil
44	196.7	D - Stiff Soil
48	201.7	D - Stiff Soil
52	207.8	D - Stiff Soil
56	212.6	D - Stiff Soil
60	215.2	D - Stiff Soil
64	215.6	D - Stiff Soil
68	215.5	D - Stiff Soil
72	215.5	D - Stiff Soil
76	215.8	D - Stiff Soil
80	215.7	D - Stiff Soil
84	215.6	D - Stiff Soil
88	215.5	D - Stiff Soil
92	215.2	D - Stiff Soil
96	213.7	D - Stiff Soil
100	210.4	D - Stiff Soil
104	209.1	D - Stiff Soil

Table 2. Survey #2

4.3. SURVEY #3

X (m)	Vs30 (m/s)	Site Class
0	386.7	C - Very Dense Soil and Soft Rock
4	384.0	C - Very Dense Soil and Soft Rock
8	380.6	C - Very Dense Soil and Soft Rock
12	381.7	C - Very Dense Soil and Soft Rock
16	380.7	C - Very Dense Soil and Soft Rock
20	377.7	C - Very Dense Soil and Soft Rock
24	375.6	C - Very Dense Soil and Soft Rock
28	374.8	C - Very Dense Soil and Soft Rock
32	374.2	C - Very Dense Soil and Soft Rock
36	375.7	C - Very Dense Soil and Soft Rock
40	380.8	C - Very Dense Soil and Soft Rock
44	387.8	C - Very Dense Soil and Soft Rock
48	393.5	C - Very Dense Soil and Soft Rock
52	397.8	C - Very Dense Soil and Soft Rock
56	402.5	C - Very Dense Soil and Soft Rock
60	406.5	C - Very Dense Soil and Soft Rock
64	407.1	C - Very Dense Soil and Soft Rock
68	406.8	C - Very Dense Soil and Soft Rock
72	406.5	C - Very Dense Soil and Soft Rock
76	406.3	C - Very Dense Soil and Soft Rock
80	413.9	C - Very Dense Soil and Soft Rock

Table 3. Survey #3

5. SPREADSHEET OF DEPTH, VS, VP, DENSITY, N AND DYNAMIC ELASTIC MODULUS

5.1. SURVEY #1

Depth	Vs	Vp	Density	N		Gdyn, Gmax	Gdyn, 0	Edyn	Esdyn
(m)	(m/s)	(m/s)	(g/cm^3)	(IBC)	μ	MPa	MPa	MPa	MPa
0.00	219	1533	1.80	13.3189	0.49	4225	634	12587	201881
1.07	231	1547	1.80	15.88488	0.49	4312	647	12837	187287
2.31	242	1558	1.81	18.29518	0.49	4386	658	13050	176552
3.71	270	1590	1.82	26.04036	0.49	4590	688	13634	153042
5.27	281	1602	1.82	29.61812	0.48	4672	701	13867	145517
7.01	267	1587	1.82	25.26865	0.49	4571	686	13581	154876
8.90	281	1602	1.82	29.72395	0.48	4674	701	13873	145316
10.96	272	1592	1.82	26.74072	0.48	4606	691	13681	151448
13.19	515	1862	1.90	203.9528	0.46	6589	988	19219	77266
15.58	367	1697	1.85	68.96504	0.48	5327	799	15719	107064
18.13	414	1749	1.87	101.5132	0.47	5711	857	16795	94442
20.85	407	1742	1.86	96.30849	0.47	5655	848	16639	96013
23.74	461	1801	1.88	142.763	0.47	6107	916	17893	85254
26.79	456	1796	1.88	138.3634	0.47	6068	910	17786	86031
36.43	536	1885	1.91	231.3601	0.46	6778	1017	19737	74787

Table 4. X=0

Depth (m)	Vs (m/s)	Vp (m/s)	Density (g/cm^3)	N (IBC)	μ	Gdyn, Gmax MPa	Gdyn, 0 MPa	Edyn MPa	Esdyn MPa
0.00	212	1525	1.80	11.99784	0.49	4176	626	12446	211218
1.07	221	1536	1.80	13.86559	0.49	4244	637	12642	198425
2.31	242	1559	1.81	18.43395	0.49	4390	659	13062	176000
3.71	275	1595	1.82	27.61539	0.48	4627	694	13738	149545
5.27	285	1606	1.82	30.99696	0.48	4702	705	13952	142979
7.01	269	1589	1.82	25.88983	0.49	4586	688	13623	153393
8.90	282	1603	1.82	29.81285	0.48	4676	701	13879	145148
10.96	274	1594	1.82	27.29333	0.48	4619	693	13717	150235
13.19	515	1862	1.90	203.8734	0.46	6588	988	19218	77274
15.58	366	1697	1.85	68.90034	0.48	5326	799	15717	107098
18.13	414	1749	1.87	101.4679	0.47	5711	857	16794	94455
20.85	407	1742	1.86	96.27685	0.47	5655	848	16638	96023
23.74	461	1801	1.88	142.7384	0.47	6107	916	17893	85259
26.79	456	1796	1.88	138.2987	0.47	6068	910	17785	86042
36.43	536	1885	1.91	231.2859	0.46	6777	1017	19736	74793

Table 5. X=4

Depth (m)	Vs (m/s)	Vp (m/s)	Density (g/cm^3)	N (IBC)	μ	Gdyn, Gmax MPa	Gdyn, 0 MPa	Edyn MPa	Esdyn MPa
0.00	223	1537	1.80	14.10324	0.49	4252	638	12666	196987
1.07	226	1541	1.80	14.79493	0.49	4276	641	12734	193008
2.31	251	1569	1.81	20.67016	0.49	4453	668	13243	167914
3.71	283	1604	1.82	30.15736	0.48	4683	703	13900	144503
5.27	291	1613	1.82	32.96973	0.48	4743	711	14069	139634
7.01	274	1594	1.82	27.2084	0.48	4617	693	13712	150419
8.90	283	1604	1.82	30.10813	0.48	4682	702	13897	144595
10.96	279	1600	1.82	29.07525	0.48	4660	699	13832	146567
13.19	515	1862	1.90	203.7814	0.46	6587	988	19216	77283
15.58	366	1697	1.85	68.80456	0.48	5325	799	15713	107148
18.13	414	1749	1.87	101.4	0.47	5710	857	16792	94475
20.85	407	1742	1.86	96.26329	0.47	5655	848	16637	96027
23.74	461	1801	1.88	142.6959	0.47	6106	916	17892	85266
26.79	456	1796	1.88	138.1742	0.47	6066	910	17782	86065
36.43	536	1885	1.91	231.1375	0.46	6776	1016	19733	74806

Table 6. X=8

Depth	Vs	Vp	Density	N		Gdyn, Gmax	Gdyn, 0	Edyn	Esdyn
(m)	(m/s)	(m/s)	(g/cm^3)	(IBC)	μ	MPa	MPa	MPa	MPa
0.00	207	1519	1.79	11.09392	0.49	4141	621	12344	218578
1.07	217	1531	1.80	13.0594	0.49	4215	632	12560	203600
2.31	252	1569	1.81	20.86058	0.49	4459	669	13258	167287
3.71	286	1608	1.82	31.33718	0.48	4709	706	13972	142379
5.27	296	1618	1.83	34.84881	0.48	4781	717	14178	136721
7.01	281	1602	1.82	29.59865	0.48	4671	701	13865	145554
8.90	286	1607	1.82	31.18639	0.48	4706	706	13963	142643
10.96	290	1612	1.82	32.70895	0.48	4738	711	14054	140058
13.19	515	1862	1.90	203.8293	0.46	6588	988	19217	77278
15.58	366	1696	1.85	68.73219	0.48	5324	799	15711	107186
18.13	414	1749	1.87	101.3438	0.47	5709	856	16790	94491
20.85	407	1742	1.86	96.60268	0.47	5658	849	16648	95921
23.74	460	1801	1.88	142.6426	0.47	6106	916	17891	85275
26.79	456	1796	1.88	137.9919	0.47	6065	910	17777	86098
36.43	536	1885	1.91	230.9164	0.46	6775	1016	19729	74824

Table 7. X=12

Depth	Vs	Vp	Density	N		Gdyn, Gmax	Gdyn, 0	Edyn	Esdyn
(m)	(m/s)	(m/s)	(g/cm^3)	(IBC)	μ	Mpa	Mpa	Mpa	Mpa
0.00	211	1524	1.80	11.84398	0.49	4170	626	12429	212409
1.07	219	1533	1.80	13.35636	0.49	4226	634	12591	201637
2.31	257	1576	1.81	22.33479	0.49	4498	675	13370	162720
3.71	293	1615	1.82	33.82125	0.48	4760	714	14119	138283
5.27	305	1629	1.83	38.41234	0.48	4850	727	14373	131808
7.01	294	1616	1.82	34.0109	0.48	4764	715	14130	137989
8.90	294	1617	1.82	34.28247	0.48	4770	715	14145	137573
10.96	306	1629	1.83	38.65916	0.48	4855	728	14387	131494
13.19	516	1862	1.90	204.6155	0.46	6593	989	19232	77200
15.58	367	1697	1.85	69.08975	0.48	5328	799	15724	106999
18.13	414	1750	1.87	101.7009	0.47	5713	857	16801	94387
20.85	410	1745	1.87	98.67613	0.47	5681	852	16710	95283
23.74	461	1801	1.88	142.8588	0.47	6108	916	17896	85238
26.79	456	1796	1.88	138.207	0.47	6067	910	17782	86059
36.43	536	1885	1.91	230.8367	0.46	6774	1016	19727	74830

Table 8. X=16

Depth	Vs	Vp	Density	N		Gdyn, Gmax	Gdyn, 0	Edyn	Esdyn
(m)	(m/s)	(m/s)	(g/cm^3)	(IBC)	μ	MPa	MPa	MPa	MPa
0.00	217	1531	1.80	12.94361	0.49	4211	632	12548	204384
1.07	222	1537	1.80	14.06937	0.49	4251	638	12663	197190
2.31	264	1583	1.81	24.12614	0.49	4543	682	13501	157756
3.71	301	1624	1.83	36.87606	0.48	4821	723	14290	133837
5.27	315	1640	1.83	42.66097	0.48	4927	739	14593	126791
7.01	307	1631	1.83	39.23535	0.48	4865	730	14417	130772
8.90	307	1631	1.83	39.25529	0.48	4866	730	14418	130747
10.96	323	1648	1.83	45.99296	0.48	4985	748	14755	123362
13.19	517	1864	1.90	205.8398	0.46	6602	990	19256	77079
15.58	368	1698	1.85	69.7048	0.48	5336	800	15747	106680
18.13	415	1750	1.87	102.2612	0.47	5719	858	16817	94226
20.85	417	1753	1.87	104.0256	0.47	5738	861	16869	93727
23.74	461	1802	1.88	143.1603	0.46	6110	917	17903	85186
26.79	456	1796	1.88	138.4688	0.47	6069	910	17789	86012
36.43	536	1884	1.91	230.7009	0.46	6773	1016	19725	74841

Table 9. X=20

Depth	Vs	Vp	Density	N		Gdyn, Gmax	Gdyn, 0	Edyn	Esdyn
(m)	(m/s)	(m/s)	(g/cm^3)	(IBC)	μ	MPa	MPa	MPa	MPa
0.00	218	1532	1.80	13.15339	0.49	4219	633	12570	202971
1.07	224	1538	1.80	14.34427	0.49	4261	639	12690	195567
2.31	267	1587	1.82	25.25362	0.49	4571	686	13580	154913
3.71	308	1632	1.83	39.67	0.48	4873	731	14440	130238
5.27	324	1650	1.84	46.73406	0.48	4997	750	14791	122651
7.01	319	1645	1.83	44.48843	0.48	4959	744	14683	124862
8.90	322	1647	1.83	45.48613	0.48	4976	746	14731	123859
10.96	339	1666	1.84	53.72201	0.48	5109	766	15107	116698
13.19	518	1865	1.90	207.1087	0.46	6611	992	19281	76955
15.58	369	1700	1.85	70.56255	0.48	5348	802	15779	106242
18.13	416	1751	1.87	102.826	0.47	5725	859	16834	94065
20.85	429	1766	1.87	113.5241	0.47	5835	875	17139	91245
23.74	461	1802	1.88	143.4532	0.46	6113	917	17910	85136
26.79	456	1797	1.88	138.6816	0.47	6071	911	17794	85973
36.43	535	1884	1.91	230.4855	0.46	6772	1016	19721	74859

Table 10. X=24

Depth	Vs	Vp	Density	N		Gdyn, Gmax	Gdyn, 0	Edyn	Esdyn
(m)	(m/s)	(m/s)	(g/cm^3)	(IBC)	μ	MPa	MPa	MPa	MPa
0.00	217	1531	1.80	13.02785	0.49	4214	632	12556	203812
1.07	222	1537	1.80	14.06112	0.49	4251	638	12662	197239
2.31	265	1584	1.81	24.52604	0.49	4553	683	13529	156725
3.71	311	1636	1.83	41.00216	0.48	4898	735	14509	128655
5.27	330	1657	1.84	49.56849	0.48	5044	757	14922	120082
7.01	331	1658	1.84	49.89458	0.48	5049	757	14937	119801
8.90	336	1663	1.84	52.23485	0.48	5086	763	15042	117862
10.96	354	1683	1.85	61.59946	0.48	5226	784	15435	111263
13.19	519	1866	1.90	208.438	0.46	6620	993	19307	76826
15.58	372	1703	1.85	72.49238	0.47	5373	806	15849	105287
18.13	416	1752	1.87	103.4935	0.47	5732	860	16853	93876
20.85	442	1781	1.88	125.6135	0.47	5952	893	17463	88510
23.74	462	1802	1.88	143.7862	0.46	6116	917	17918	85079
26.79	457	1797	1.88	138.9198	0.47	6073	911	17800	85930
36.43	535	1884	1.91	230.2567	0.46	6770	1016	19717	74878

Table 11. X=28

Depth	Vs	Vp	Density	N		Gdyn, Gmax	Gdyn, 0	Edyn	Esdyn
(m)	(m/s)	(m/s)	(g/cm^3)	(IBC)	μ	Mpa	Mpa	Mpa	Mpa
0.00	230	1545	1.80	15.60254	0.49	4303	645	12811	188710
1.07	232	1548	1.80	16.1176	0.49	4319	648	12858	186144
2.31	265	1585	1.81	24.65985	0.49	4557	683	13538	156385
3.71	315	1640	1.83	42.75025	0.48	4929	739	14597	126694
5.27	334	1661	1.84	51.23075	0.48	5070	761	14997	118677
7.01	343	1671	1.84	55.96578	0.48	5143	771	15203	115031
8.90	348	1676	1.84	58.41619	0.48	5180	777	15306	113324
10.96	367	1697	1.85	69.27712	0.48	5331	800	15731	106901
13.19	518	1866	1.90	208.131	0.46	6618	993	19301	76856
15.58	379	1710	1.85	76.50192	0.47	5424	814	15992	103422
18.13	417	1753	1.87	104.1273	0.47	5739	861	16872	93698
20.85	454	1794	1.88	135.9807	0.47	6047	907	17727	86467
23.74	462	1803	1.88	144.09	0.46	6118	918	17925	85028
26.79	457	1797	1.88	139.0894	0.47	6075	911	17804	85900
36.43	535	1884	1.91	229.9417	0.46	6768	1015	19711	74904

Table 12. X=32

Depth	Vs	Vp	Density	N		Gdyn, Gmax	Gdyn, 0	Edyn	Esdyn
(m)	(m/s)	(m/s)	(g/cm^3)	(IBC)	μ	Mpa	Mpa	Mpa	Mpa
0.00	243	1559	1.81	18.50944	0.49	4392	659	13068	175703
1.07	245	1562	1.81	19.0768	0.49	4409	661	13115	173527
2.31	269	1589	1.82	25.77587	0.49	4584	688	13616	153661
3.71	322	1647	1.83	45.625	0.48	4979	747	14738	123722
5.27	335	1661	1.84	51.62273	0.48	5077	761	15015	118356
7.01	355	1684	1.85	62.39096	0.48	5237	786	15467	110776
8.90	357	1686	1.85	63.2498	0.48	5249	787	15500	110258
10.96	380	1711	1.85	77.0618	0.47	5431	815	16011	103173
13.19	514	1860	1.90	201.9875	0.46	6574	986	19181	77463
15.58	389	1722	1.86	83.20141	0.47	5506	826	16221	100616
18.13	418	1754	1.87	104.617	0.47	5744	862	16886	93562
20.85	459	1799	1.88	140.7121	0.47	6089	913	17844	85612
23.74	462	1803	1.88	144.2908	0.46	6120	918	17930	84994
26.79	457	1797	1.88	139.0341	0.47	6074	911	17803	85910
36.43	535	1883	1.91	229.3248	0.46	6764	1015	19700	74955

Table 13. X=36

Depth	Vs	Vp	Density	N		Gdyn, Gmax	Gdyn, 0	Edyn	Esdyn
(m)	(m/s)	(m/s)	(g/cm^3)	(IBC)	μ	Mpa	Mpa	Mpa	Mpa
0.00	250	1568	1.81	20.39247	0.49	4446	667	13221	168843
1.07	251	1569	1.81	20.6573	0.49	4453	668	13242	167956
2.31	267	1586	1.82	25.15147	0.49	4569	685	13573	155162
3.71	325	1651	1.84	47.00348	0.48	5002	750	14803	122397
5.27	333	1660	1.84	50.82478	0.48	5064	760	14979	119014
7.01	366	1696	1.85	68.67305	0.48	5323	798	15708	107217
8.90	364	1695	1.85	67.73049	0.48	5310	797	15673	107719
10.96	394	1727	1.86	86.5866	0.47	5545	832	16332	99326
13.19	501	1847	1.90	187.1755	0.46	6466	970	18882	79052
15.58	402	1736	1.86	92.57214	0.47	5614	842	16523	97223
18.13	419	1755	1.87	105.2331	0.47	5750	863	16904	93392
20.85	457	1798	1.88	139.5854	0.47	6079	912	17816	85811
23.74	462	1803	1.88	144.6112	0.46	6123	918	17938	84939
26.79	457	1797	1.88	139.3183	0.47	6077	911	17810	85859
36.43	534	1883	1.91	229.2798	0.46	6764	1015	19699	74959

Table 14. X=40

Depth	Vs	Vp	Density	N		Gdyn, Gmax	Gdyn, 0	Edyn	Esdyn
(m)	(m/s)	(m/s)	(g/cm^3)	(IBC)	μ	Mpa	Mpa	Mpa	Mpa
0.00	260	1579	1.81	23.17037	0.49	4519	678	13432	160331
1.07	257	1575	1.81	22.17123	0.49	4494	674	13358	163203
2.31	267	1586	1.82	25.04335	0.49	4566	685	13565	155428
3.71	327	1653	1.84	48.09086	0.48	5020	753	14854	121392
5.27	333	1660	1.84	50.87292	0.48	5065	760	14981	118974
7.01	373	1704	1.85	73.11804	0.47	5381	807	15872	104986
8.90	372	1703	1.85	72.55876	0.47	5374	806	15851	105255
10.96	409	1744	1.86	98.05995	0.47	5674	851	16692	95470
13.19	485	1829	1.89	168.6253	0.46	6322	948	18488	81337
15.58	418	1754	1.87	104.8013	0.47	5746	862	16891	93511
18.13	419	1756	1.87	105.937	0.47	5758	864	16924	93200
20.85	453	1792	1.88	135.0967	0.47	6039	906	17705	86632
23.74	463	1804	1.88	144.949	0.46	6126	919	17946	84882
26.79	457	1798	1.88	139.5854	0.47	6079	912	17816	85811
36.43	534	1883	1.91	229.1472	0.46	6763	1014	19697	74970

Table 15. X=44

Depth	Vs	Vp	Density	N		Gdyn, Gmax	Gdyn, 0	Edyn	Esdyn
(m)	(m/s)	(m/s)	(g/cm^3)	(IBC)	μ	Mpa	Mpa	Mpa	Mpa
0.00	269	1589	1.82	25.7896	0.49	4584	688	13617	153629
1.07	266	1585	1.81	24.83102	0.49	4561	684	13550	155955
2.31	274	1594	1.82	27.18624	0.48	4617	693	13710	150467
3.71	331	1658	1.84	49.91235	0.48	5049	757	14938	119786
5.27	335	1662	1.84	51.9526	0.48	5082	762	15030	118089
7.01	372	1703	1.85	72.30589	0.47	5370	806	15842	105378
8.90	378	1710	1.85	76.08703	0.47	5419	813	15977	103608
10.96	423	1759	1.87	108.5319	0.47	5784	868	16999	92508
13.19	475	1817	1.89	157.6326	0.46	6233	935	18242	82881
15.58	439	1777	1.87	122.4283	0.47	5921	888	17380	89190
18.13	420	1756	1.87	106.4212	0.47	5763	864	16938	93069
20.85	447	1786	1.88	129.3074	0.47	5986	898	17559	87753
23.74	463	1804	1.88	145.2095	0.46	6128	919	17952	84839
26.79	458	1798	1.88	139.7614	0.47	6081	912	17820	85780
36.43	534	1883	1.91	228.9166	0.46	6761	1014	19692	74989

Table 16. X=48

Depth	Vs	Vp	Density	N		Gdyn, Gmax	Gdyn, 0	Edyn	Esdyn
(m)	(m/s)	(m/s)	(g/cm^3)	(IBC)	μ	MPa	MPa	MPa	MPa
0.00	278	1599	1.82	28.70315	0.48	4651	698	13809	147304
1.07	274	1594	1.82	27.18307	0.48	4617	693	13710	150474
2.31	283	1604	1.82	30.16585	0.48	4684	703	13901	144487
3.71	337	1664	1.84	52.60719	0.48	5092	764	15058	117566
5.27	341	1669	1.84	54.90978	0.48	5127	769	15158	115803
7.01	365	1696	1.85	68.2634	0.48	5317	798	15693	107434
8.90	382	1714	1.86	78.41165	0.47	5448	817	16058	102585
10.96	432	1769	1.87	116.0646	0.47	5860	879	17209	90634
13.19	480	1823	1.89	163.1655	0.46	6279	942	18367	82084
15.58	468	1809	1.88	149.7851	0.46	6167	925	18061	84089
18.13	421	1757	1.87	106.8794	0.47	5767	865	16951	92946
20.85	438	1776	1.87	121.8411	0.47	5916	887	17364	89319
23.74	463	1804	1.88	145.4714	0.46	6130	920	17959	84795
26.79	458	1798	1.88	139.9152	0.47	6082	912	17824	85753
36.43	534	1883	1.91	228.6056	0.46	6759	1014	19687	75015

Table 17. X=52

Depth	Vs	Vp	Density	N		Gdyn, Gmax	Gdyn, 0	Edyn	Esdyn
(m)	(m/s)	(m/s)	(g/cm^3)	(IBC)	μ	MPa	MPa	MPa	MPa
0.00	293	1615	1.82	33.72725	0.48	4758	714	14114	138430
1.07	287	1609	1.82	31.72073	0.48	4717	708	13995	141714
2.31	297	1619	1.83	35.14456	0.48	4787	718	14194	136284
3.71	344	1672	1.84	56.3118	0.48	5149	772	15218	114784
5.27	349	1677	1.84	58.76018	0.48	5185	778	15320	113094
7.01	358	1687	1.85	63.73447	0.48	5256	788	15520	109970
8.90	380	1712	1.85	77.31947	0.47	5434	815	16020	103059
10.96	433	1771	1.87	117.6694	0.47	5876	881	17252	90259
13.19	497	1841	1.89	181.5677	0.46	6423	963	18765	79705
15.58	498	1843	1.89	183.1054	0.46	6435	965	18798	79522
18.13	420	1756	1.87	106.6077	0.47	5765	865	16944	93019
20.85	428	1765	1.87	112.6995	0.47	5826	874	17116	91448
23.74	463	1804	1.88	145.5884	0.46	6131	920	17961	84775
26.79	458	1798	1.88	139.8227	0.47	6081	912	17822	85769
36.43	534	1882	1.91	228.0566	0.46	6756	1013	19677	75061

Table 18. X=56

Depth	Vs	Vp	Density	N		Gdyn, Gmax	Gdyn, 0	Edyn	Esdyn
(m)	(m/s)	(m/s)	(g/cm^3)	(IBC)	μ	MPa	MPa	MPa	MPa
0.00	299	1622	1.83	36.08706	0.48	4805	721	14247	134930
1.07	304	1628	1.83	38.17859	0.48	4846	727	14361	132109
2.31	313	1638	1.83	41.74328	0.48	4911	737	14547	127808
3.71	352	1680	1.84	60.48459	0.48	5210	781	15390	111966
5.27	355	1685	1.85	62.55782	0.48	5239	786	15473	110675
7.01	352	1681	1.85	60.82424	0.48	5215	782	15404	111750
8.90	372	1703	1.85	72.26073	0.47	5370	805	15841	105400
10.96	429	1766	1.87	113.508	0.47	5834	875	17138	91249
13.19	512	1858	1.90	200.1024	0.46	6561	984	19143	77655
15.58	516	1863	1.90	205.3112	0.46	6598	990	19246	77131
18.13	417	1753	1.87	103.8406	0.47	5736	860	16863	93778
20.85	421	1757	1.87	107.2822	0.47	5771	866	16963	92838
23.74	463	1804	1.88	145.4054	0.46	6130	919	17957	84806
26.79	457	1797	1.88	139.3601	0.47	6077	912	17811	85851
36.43	533	1882	1.91	227.3372	0.46	6751	1013	19663	75122

Table 19. X=60

Depth	Vs	Vp	Density	N		Gdyn, Gmax	Gdyn, 0	Edyn	Esdyn
(m)	(m/s)	(m/s)	(g/cm^3)	(IBC)	μ	MPa	MPa	MPa	MPa
0.00	315	1640	1.83	42.75975	0.48	4929	739	14598	126684
1.07	323	1649	1.84	46.19568	0.48	4988	748	14765	123166
2.31	332	1659	1.84	50.44859	0.48	5058	759	14962	119329
3.71	366	1696	1.85	68.4391	0.48	5320	798	15700	107341
5.27	369	1699	1.85	70.16945	0.48	5343	801	15764	106442
7.01	356	1685	1.85	62.97464	0.48	5245	787	15490	110423
8.90	366	1697	1.85	68.90453	0.48	5326	799	15717	107096
10.96	424	1760	1.87	109.3847	0.47	5793	869	17023	92286
13.19	519	1866	1.90	208.6979	0.46	6622	993	19312	76801
15.58	512	1859	1.90	200.2817	0.46	6562	984	19147	77637
18.13	408	1743	1.86	97.20274	0.47	5665	850	16666	95734
20.85	428	1765	1.87	113.2005	0.47	5831	875	17130	91324
23.74	463	1804	1.88	145.2724	0.46	6129	919	17954	84828
26.79	457	1797	1.88	139.1126	0.47	6075	911	17805	85896
36.43	533	1882	1.91	227.1607	0.46	6750	1012	19660	75137

Table 20. X=64

Depth	Vs	Vp	Density	N		Gdyn, Gmax	Gdyn, 0	Edyn	Esdyn
(m)	(m/s)	(m/s)	(g/cm^3)	(IBC)	μ	MPa	MPa	MPa	MPa
0.00	330	1657	1.84	49.56133	0.48	5044	757	14922	120088
1.07	337	1664	1.84	52.85094	0.48	5096	764	15069	117374
2.31	345	1673	1.84	57.01983	0.48	5159	774	15248	114283
3.71	380	1712	1.85	77.37392	0.47	5435	815	16022	103035
5.27	385	1717	1.86	80.53696	0.47	5474	821	16131	101689
7.01	368	1699	1.85	70.12943	0.48	5342	801	15763	106462
8.90	373	1704	1.85	72.97655	0.47	5379	807	15867	105054
10.96	425	1761	1.87	110.2323	0.47	5802	870	17047	92068
13.19	515	1862	1.90	204.2669	0.46	6591	989	19225	77234
15.58	490	1834	1.89	173.4906	0.46	6361	954	18594	80701
18.13	394	1728	1.86	86.93309	0.47	5549	832	16344	99198
20.85	449	1788	1.88	131.5377	0.47	6007	901	17616	87312
23.74	463	1804	1.88	145.3174	0.46	6129	919	17955	84821
26.79	457	1797	1.88	139.0011	0.47	6074	911	17802	85916
36.43	533	1881	1.91	226.9097	0.46	6748	1012	19655	75158

Table 21. X=68

Depth	Vs	Vp	Density	N		Gdyn, Gmax	Gdyn, 0	Edyn	Esdyn
(m)	(m/s)	(m/s)	(g/cm^3)	(IBC)	μ	MPa	MPa	MPa	MPa
0.00	344	1672	1.84	56.40467	0.48	5150	772	15222	114717
1.07	345	1673	1.84	56.86482	0.48	5157	774	15241	114392
2.31	352	1680	1.84	60.4457	0.48	5209	781	15389	111991
3.71	394	1727	1.86	86.86005	0.47	5549	832	16341	99225
5.27	404	1738	1.86	94.01495	0.47	5630	844	16568	96747
7.01	389	1722	1.86	83.61375	0.47	5510	827	16235	100454
8.90	395	1728	1.86	87.35802	0.47	5554	833	16357	99042
10.96	432	1769	1.87	116.3603	0.47	5863	879	17217	90564
13.19	502	1848	1.90	188.1973	0.46	6473	971	18903	78936
15.58	464	1805	1.88	146.1865	0.46	6137	920	17976	84675
18.13	378	1709	1.85	75.83412	0.47	5415	812	15968	103722
20.85	472	1813	1.89	153.8282	0.46	6202	930	18155	83455
23.74	463	1804	1.88	145.3814	0.46	6130	919	17956	84810
26.79	456	1797	1.88	138.7542	0.47	6072	911	17796	85960
36.43	532	1881	1.91	226.4041	0.46	6744	1012	19646	75201

Table 22. X=72

Depth	Vs	Vp	Density	N		Gdyn, Gmax	Gdyn, 0	Edyn	Esdyn
(m)	(m/s)	(m/s)	(g/cm^3)	(IBC)	μ	Mpa	Mpa	Mpa	Mpa
0.00	353	1682	1.85	61.42994	0.48	5223	783	15428	111369
1.07	344	1672	1.84	56.26384	0.48	5148	772	15216	114818
2.31	348	1676	1.84	58.33548	0.48	5178	777	15302	113379
3.71	402	1737	1.86	92.8489	0.47	5617	843	16532	97131
5.27	422	1758	1.87	107.6697	0.47	5775	866	16974	92735
7.01	417	1752	1.87	103.6638	0.47	5734	860	16858	93828
8.90	424	1760	1.87	109.5542	0.47	5795	869	17028	92242
10.96	442	1781	1.88	125.1295	0.47	5947	892	17451	88612
13.19	485	1828	1.89	168.4063	0.46	6321	948	18483	81366
15.58	450	1790	1.88	132.7734	0.47	6018	903	17647	87073
18.13	365	1695	1.85	67.90346	0.48	5313	797	15680	107626
20.85	487	1830	1.89	169.959	0.46	6333	950	18517	81160
23.74	464	1805	1.88	145.7826	0.46	6133	920	17966	84743
26.79	457	1797	1.88	139.2144	0.47	6076	911	17807	85878
36.43	533	1881	1.91	226.7985	0.46	6747	1012	19653	75168

Table 23. X=76

Depth	Vs	Vp	Density	N		Gdyn, Gmax	Gdyn, 0	Edyn	Esdyn
(m)	(m/s)	(m/s)	(g/cm^3)	(IBC)	μ	MPa	MPa	MPa	MPa
0.00	327	1653	1.84	47.91746	0.48	5017	753	14846	121550
1.07	332	1659	1.84	50.48727	0.48	5058	759	14964	119297
2.31	338	1665	1.84	53.34276	0.48	5103	766	15091	116990
3.71	405	1740	1.86	94.76482	0.47	5638	846	16591	96504
5.27	436	1774	1.87	119.5626	0.47	5894	884	17303	89826
7.01	446	1785	1.88	129.0622	0.47	5984	898	17552	87803
8.90	448	1787	1.88	130.6894	0.47	5999	900	17594	87479
10.96	449	1789	1.88	132.0348	0.47	6011	902	17628	87216
13.19	472	1814	1.89	154.4754	0.46	6207	931	18170	83356
15.58	449	1788	1.88	131.2766	0.47	6004	901	17609	87363
18.13	357	1687	1.85	63.54223	0.48	5253	788	15512	110084
20.85	492	1837	1.89	176.6801	0.46	6386	958	18662	80299
23.74	464	1805	1.88	145.9538	0.46	6135	920	17970	84714
26.79	457	1797	1.88	139.4222	0.47	6078	912	17812	85840
36.43	533	1882	1.91	227.154	0.46	6750	1012	19660	75137

Table 24. X=80

Depth	Vs	Vp	Density	N		Gdyn, Gmax	Gdyn, 0	Edyn	Esdyn
(m)	(m/s)	(m/s)	(g/cm^3)	(IBC)	μ	MPa	MPa	MPa	MPa
0.00	342	1670	1.84	55.5721	0.48	5137	771	15187	115316
1.07	338	1665	1.84	53.09245	0.48	5099	765	15080	117185
2.31	342	1670	1.84	55.38938	0.48	5135	770	15179	115450
3.71	417	1752	1.87	103.6717	0.47	5734	860	16859	93826
5.27	458	1798	1.88	140.071	0.47	6083	912	17828	85725
7.01	484	1828	1.89	167.4805	0.46	6313	947	18463	81490
8.90	468	1809	1.88	149.8004	0.46	6168	925	18061	84086
10.96	458	1798	1.88	139.888	0.47	6082	912	17824	85757
13.19	472	1814	1.89	154.4066	0.46	6206	931	18168	83366
15.58	453	1793	1.88	135.6906	0.47	6044	907	17720	86521
18.13	355	1685	1.85	62.5242	0.48	5239	786	15472	110695
20.85	494	1839	1.89	178.7402	0.46	6402	960	18706	80046
23.74	464	1805	1.88	146.2758	0.46	6137	921	17978	84661
26.79	458	1798	1.88	139.8218	0.47	6081	912	17822	85769
36.43	533	1882	1.91	227.5112	0.46	6752	1013	19667	75107

Table 25. X=84

Depth	Vs	Vp	Density	N		Gdyn, Gmax	Gdyn, 0	Edyn	Esdyn
(m)	(m/s)	(m/s)	(g/cm^3)	(IBC)	μ	MPa	MPa	MPa	MPa
0.00	372	1703	1.85	72.55503	0.47	5374	806	15851	105257
1.07	342	1670	1.84	55.32496	0.48	5134	770	15176	115497
2.31	351	1680	1.84	60.30569	0.48	5207	781	15383	112081
3.71	436	1774	1.87	119.5163	0.47	5893	884	17302	89837
5.27	486	1830	1.89	169.5966	0.46	6330	950	18509	81207
7.01	523	1871	1.90	214.6065	0.46	6664	1000	19425	76245
8.90	482	1825	1.89	164.674	0.46	6291	944	18401	81874
10.96	465	1807	1.88	147.5887	0.46	6149	922	18009	84444
13.19	480	1823	1.89	162.9978	0.46	6277	942	18363	82107
15.58	457	1797	1.88	139.3164	0.47	6077	911	17810	85859
18.13	356	1685	1.85	62.63185	0.48	5240	786	15476	110630
20.85	495	1839	1.89	179.2589	0.46	6406	961	18717	79982
23.74	464	1805	1.88	146.4525	0.46	6139	921	17982	84631
26.79	458	1798	1.88	140.0136	0.47	6083	912	17827	85735
36.43	533	1882	1.91	227.7273	0.46	6753	1013	19671	75089

Table 26. X=88

Depth	Vs	Vp	Density	N		Gdyn, Gmax	Gdyn, 0	Edyn	Esdyn
(m)	(m/s)	(m/s)	(g/cm^3)	(IBC)	μ	MPa	MPa	MPa	MPa
0.00	325	1651	1.84	46.94959	0.48	5001	750	14801	122447
1.07	316	1640	1.83	42.86906	0.48	4931	740	14603	126565
2.31	329	1655	1.84	48.92734	0.48	5033	755	14893	120643
3.71	429	1767	1.87	114.0885	0.47	5840	876	17154	91107
5.27	491	1835	1.89	174.77	0.46	6371	956	18621	80539
7.01	538	1887	1.91	234.3744	0.46	6798	1020	19792	74542
8.90	483	1826	1.89	166.3992	0.46	6305	946	18439	81637
10.96	467	1808	1.88	149.2288	0.46	6163	924	18048	84178
13.19	485	1828	1.89	168.3887	0.46	6320	948	18483	81368
15.58	458	1798	1.88	140.0769	0.47	6083	912	17828	85724
18.13	356	1685	1.85	62.59987	0.48	5240	786	15475	110649
20.85	495	1839	1.89	179.3051	0.46	6406	961	18718	79977
23.74	464	1805	1.88	146.4736	0.46	6139	921	17982	84628
26.79	458	1798	1.88	140.0633	0.47	6083	912	17828	85726
36.43	538	1887	1.91	234.3744	0.46	6798	1020	19792	74542

Table 27. X=92

5.2. SURVEY #2

Depth	Vs	Vp	Density	N		Gdyn, Gmax	Gdyn, 0	Edyn	Esdyn
(m)	(m/s)	(m/s)	(g/cm^3)	(IBC)	μ	MPa	MPa	MPa	MPa
0.00	152	1459	1.77	4.190011	0.49	3777	566	11288	342355
0.83	157	1464	1.78	4.628074	0.49	3808	571	11380	326425
1.88	156	1463	1.78	4.53574	0.49	3802	570	11361	329582
3.13	144	1450	1.77	3.527849	0.50	3725	559	11137	372107
4.58	216	1529	1.80	12.72391	0.49	4203	630	12524	205901
6.25	189	1500	1.79	8.337047	0.49	4020	603	11995	248265
8.13	191	1502	1.79	8.592034	0.49	4032	605	12030	244910
10.21	193	1504	1.79	8.903014	0.49	4046	607	12072	241021
12.50	194	1505	1.79	9.050853	0.49	4053	608	12091	239245
20.00	228	1543	1.80	15.15289	0.49	4288	643	12768	191059

Table 28. X=0

Depth	Vs	Vp	Density	N		Gdyn, Gmax	Gdyn, 0	Edyn	Esdyn
(m)	(m/s)	(m/s)	(g/cm^3)	(IBC)	μ	MPa	MPa	MPa	MPa
0.00	154	1461	1.78	4.395575	0.49	3792	569	11332	334571
0.83	152	1459	1.77	4.221049	0.49	3779	567	11295	341142
1.88	155	1462	1.78	4.474787	0.49	3797	570	11349	331721
3.13	154	1461	1.78	4.381994	0.49	3791	569	11329	335068
4.58	216	1529	1.80	12.74485	0.49	4204	631	12527	205755
6.25	189	1500	1.79	8.386026	0.49	4022	603	12002	247608
8.13	189	1500	1.79	8.381768	0.49	4022	603	12001	247665
10.21	190	1501	1.79	8.518805	0.49	4028	604	12020	245857
12.50	191	1502	1.79	8.618964	0.49	4033	605	12034	244564
20.00	228	1543	1.80	15.17481	0.49	4289	643	12770	190942

Table 29. X=4

Depth	Vs	Vp	Density	N		Gdyn, Gmax	Gdyn, 0	Edyn	Esdyn
(m)	(m/s)	(m/s)	(g/cm^3)	(IBC)	μ	MPa	MPa	MPa	MPa
0.00	156	1464	1.78	4.586731	0.49	3805	571	11372	327826
0.83	156	1463	1.78	4.548796	0.49	3803	570	11364	329129
1.88	158	1466	1.78	4.755688	0.49	3817	573	11406	322219
3.13	163	1470	1.78	5.17744	0.49	3845	577	11487	309488
4.58	208	1521	1.79	11.36864	0.49	4151	623	12375	216246
6.25	185	1495	1.79	7.812074	0.49	3994	599	11920	255701
8.13	184	1495	1.79	7.743682	0.49	3991	599	11910	256727
10.21	185	1495	1.79	7.810985	0.49	3994	599	11920	255717
12.50	186	1496	1.79	7.888825	0.49	3998	600	11931	254566
20.00	228	1543	1.80	15.20004	0.49	4290	643	12773	190808

Table 30. X=8

Depth	Vs	Vp	Density	N		Gdyn, Gmax	Gdyn, 0	Edyn	Esdyn
(m)	(m/s)	(m/s)	(g/cm^3)	(IBC)	μ	MPa	MPa	MPa	MPa
0.00	152	1459	1.77	4.215092	0.49	3778	567	11294	341374
0.83	155	1462	1.78	4.418845	0.49	3793	569	11337	333726
1.88	162	1469	1.78	5.071085	0.49	3838	576	11467	312542
3.13	170	1479	1.78	6.006772	0.49	3896	584	11636	288628
4.58	198	1510	1.79	9.746555	0.49	4084	613	12181	231457
6.25	182	1492	1.79	7.397695	0.49	3973	596	11859	262142
8.13	181	1491	1.78	7.296689	0.49	3968	595	11844	263797
10.21	181	1491	1.78	7.329721	0.49	3969	595	11849	263252
12.50	182	1492	1.79	7.394937	0.49	3973	596	11859	262186
20.00	228	1543	1.80	15.22756	0.49	4290	644	12775	190662

Table 31. X=12

Depth	Vs	Vp	Density	N		Gdyn, Gmax	Gdyn, 0	Edyn	Esdyn
(m)	(m/s)	(m/s)	(g/cm^3)	(IBC)	μ	MPa	MPa	MPa	MPa
0.00	150	1457	1.77	4.033494	0.49	3765	565	11254	348694
0.83	154	1460	1.78	4.315875	0.49	3786	568	11315	337520
1.88	163	1471	1.78	5.219636	0.49	3848	577	11495	308303
3.13	174	1484	1.78	6.470235	0.49	3923	588	11714	278823
4.58	190	1501	1.79	8.488869	0.49	4027	604	12016	246248
6.25	181	1491	1.78	7.279627	0.49	3967	595	11841	264081
8.13	180	1490	1.78	7.161789	0.49	3961	594	11823	266065
10.21	180	1490	1.78	7.173161	0.49	3961	594	11825	265871
12.50	181	1490	1.78	7.228537	0.49	3964	595	11834	264935
20.00	228	1543	1.80	15.25685	0.49	4291	644	12778	190507

Table 32. X=16

Depth	Vs	Vp	Density	N		Gdyn, Gmax	Gdyn, 0	Edyn	Esdyn
(m)	(m/s)	(m/s)	(g/cm^3)	(IBC)	μ	MPa	MPa	MPa	MPa
0.00	151	1458	1.77	4.102689	0.49	3770	566	11269	345845
0.83	154	1461	1.78	4.351313	0.49	3788	568	11323	336198
1.88	164	1472	1.78	5.356405	0.49	3856	578	11521	304563
3.13	176	1485	1.78	6.676432	0.49	3934	590	11747	274805
4.58	185	1496	1.79	7.854179	0.49	3996	599	11926	255076
6.25	181	1491	1.78	7.319102	0.49	3969	595	11847	263427
8.13	180	1490	1.78	7.190342	0.49	3962	594	11828	265579
10.21	180	1490	1.78	7.187316	0.49	3962	594	11827	265631
12.50	181	1490	1.78	7.234222	0.49	3964	595	11834	264839
20.00	228	1543	1.80	15.28718	0.49	4292	644	12781	190346

Table 33. X=20

Depth	Vs	Vp	Density	N		Gdyn, Gmax	Gdyn, 0	Edyn	Esdyn
(m)	(m/s)	(m/s)	(g/cm^3)	(IBC)	μ	MPa	MPa	MPa	MPa
0.000	152.11	1459	1.77	4.190353	0.49	3777	566	11288	342342
0.833	154.71	1462	1.78	4.422344	0.49	3794	569	11338	333599
1.875	165.42	1474	1.78	5.474062	0.49	3864	580	11542	301463
3.125	176.65	1486	1.78	6.74724	0.49	3938	591	11759	273469
4.583	183.93	1494	1.79	7.673182	0.49	3987	598	11900	257800
6.250	181.8	1492	1.79	7.393652	0.49	3973	596	11859	262207
8.125	180.74	1491	1.78	7.25785	0.49	3966	595	11838	264443
10.208	180.64	1491	1.78	7.244866	0.49	3965	595	11836	264661
12.500	180.94	1491	1.78	7.283491	0.49	3967	595	11842	264016
20.000	228.52	1544	1.80	15.31799	0.49	4293	644	12784	190184

Table 34. X=24

Depth	Vs	Vp	Density	N		Gdyn, Gmax	Gdyn, 0	Edyn	Esdyn
(m)	(m/s)	(m/s)	(g/cm^3)	(IBC)	μ	MPa	MPa	MPa	MPa
0.000	153	1460	1.77	4.304256	0.49	3785	568	11313	337957
0.833	156	1463	1.78	4.52202	0.49	3801	570	11358	330059
1.875	166	1474	1.78	5.497723	0.49	3865	580	11547	300852
3.125	176	1486	1.78	6.697774	0.49	3936	590	11751	274400
4.583	184	1494	1.79	7.637567	0.49	3985	598	11895	258347
6.250	182	1492	1.79	7.445309	0.49	3975	596	11866	261374
8.125	181	1491	1.78	7.317965	0.49	3969	595	11847	263446
10.208	181	1491	1.78	7.298663	0.49	3968	595	11844	263765
12.500	181	1491	1.78	7.332985	0.49	3970	595	11849	263198
20.000	229	1544	1.80	15.34877	0.49	4294	644	12787	190023

Table 35. X=28

Depth	Vs	Vp	Density	N		Gdyn, Gmax	Gdyn, 0	Edyn	Esdyn
(m)	(m/s)	(m/s)	(g/cm^3)	(IBC)	μ	MPa	MPa	MPa	MPa
0.000	155	1462	1.78	4.405886	0.49	3792	569	11334	334196
0.833	156	1464	1.78	4.577493	0.49	3805	571	11370	328142
1.875	166	1474	1.78	5.529757	0.49	3867	580	11552	300032
3.125	176	1486	1.78	6.711558	0.49	3936	590	11753	274139
4.583	184	1494	1.79	7.655718	0.49	3986	598	11897	258068
6.250	183	1493	1.79	7.493001	0.49	3978	597	11873	260611
8.125	182	1492	1.79	7.375917	0.49	3972	596	11856	262496
10.208	181	1491	1.79	7.353251	0.49	3971	596	11852	262866
12.500	182	1492	1.79	7.383545	0.49	3972	596	11857	262372
20.000	229	1544	1.80	15.37913	0.49	4295	644	12790	189864

Table 36. X=32

Depth	Vs	Vp	Density	N		Gdyn, Gmax	Gdyn, 0	Edyn	Esdyn
(m)	(m/s)	(m/s)	(g/cm^3)	(IBC)	μ	MPa	MPa	MPa	MPa
0.000	155	1462	1.78	4.434293	0.49	3794	569	11340	333168
0.833	156	1463	1.78	4.509081	0.49	3800	570	11356	330512
1.875	166	1474	1.78	5.555727	0.49	3869	580	11557	299372
3.125	178	1487	1.78	6.85157	0.49	3944	592	11775	271540
4.583	185	1495	1.79	7.753628	0.49	3991	599	11912	256577
6.250	183	1494	1.79	7.594736	0.49	3983	597	11888	259011
8.125	182	1493	1.79	7.482167	0.49	3977	597	11872	260784
10.208	182	1492	1.79	7.456396	0.49	3976	596	11868	261196
12.500	182	1493	1.79	7.482716	0.49	3977	597	11872	260775
20.000	229	1544	1.80	15.40877	0.49	4296	644	12793	189709

Table 37. X=36

Depth	Vs	Vp	Density	N		Gdyn, Gmax	Gdyn, 0	Edyn	Esdyn
(m)	(m/s)	(m/s)	(g/cm^3)	(IBC)	μ	MPa	MPa	MPa	MPa
0.000	156	1463	1.78	4.49685	0.49	3799	570	11353	330942
0.833	155	1462	1.78	4.456963	0.49	3796	569	11345	332356
1.875	165	1473	1.78	5.392152	0.49	3859	579	11527	303610
3.125	178	1487	1.78	6.889638	0.49	3946	592	11781	270848
4.583	186	1497	1.79	7.982939	0.49	4003	600	11945	253198
6.250	185	1496	1.79	7.878143	0.49	3997	600	11930	254723
8.125	185	1495	1.79	7.786927	0.49	3993	599	11917	256077
10.208	185	1495	1.79	7.763594	0.49	3992	599	11913	256427
12.500	185	1495	1.79	7.787602	0.49	3993	599	11917	256067
20.000	229	1544	1.80	15.43741	0.49	4297	645	12795	189560

Table 38. X=40

Depth	Vs	Vp	Density	N		Gdyn, Gmax	Gdyn, 0	Edyn	Esdyn
(m)	(m/s)	(m/s)	(g/cm^3)	(IBC)	μ	MPa	MPa	MPa	MPa
0.000	157	1464	1.78	4.653147	0.49	3810	571	11385	325584
0.833	155	1462	1.78	4.480157	0.49	3798	570	11350	331531
1.875	163	1471	1.78	5.194828	0.49	3846	577	11491	308998
3.125	177	1487	1.78	6.81827	0.49	3942	591	11770	272151
4.583	191	1502	1.79	8.635045	0.49	4034	605	12036	244359
6.250	191	1502	1.79	8.617405	0.49	4033	605	12033	244584
8.125	190	1501	1.79	8.561964	0.49	4031	605	12026	245297
10.208	190	1501	1.79	8.546491	0.49	4030	604	12024	245498
12.500	190	1501	1.79	8.570506	0.49	4031	605	12027	245187
20.000	229	1544	1.80	15.46485	0.49	4298	645	12798	189418

Table 39. X=44

Depth	Vs	Vp	Density	N		Gdyn, Gmax	Gdyn, 0	Edyn	Esdyn
(m)	(m/s)	(m/s)	(g/cm^3)	(IBC)	μ	MPa	MPa	MPa	MPa
0.000	159	1467	1.78	4.841373	0.49	3823	573	11423	319493
0.833	155	1462	1.78	4.454749	0.49	3796	569	11344	332435
1.875	161	1469	1.78	5.030924	0.49	3835	575	11459	313722
3.125	176	1485	1.78	6.641116	0.49	3933	590	11742	275479
4.583	200	1512	1.79	9.955239	0.49	4093	614	12207	229287
6.250	200	1512	1.79	10.02786	0.49	4096	614	12216	228548
8.125	200	1512	1.79	10.01241	0.49	4096	614	12214	228705
10.208	200	1512	1.79	10.00767	0.49	4095	614	12214	228753
12.500	200	1512	1.79	10.03346	0.49	4097	614	12217	228491
20.000	229	1545	1.80	15.49093	0.49	4299	645	12800	189283

Table 40. X=48

Depth	Vs	Vp	Density	N		Gdyn, Gmax	Gdyn, 0	Edyn	Esdyn
(m)	(m/s)	(m/s)	(g/cm^3)	(IBC)	μ	MPa	MPa	MPa	MPa
0.0000	165	1473	1.78	5.460728	0.49	3863	579	11540	301809
0.8333	157	1464	1.78	4.60614	0.49	3807	571	11375	327166
1.8750	160	1468	1.78	4.965281	0.49	3831	575	11447	315682
3.1250	174	1483	1.78	6.390555	0.49	3918	588	11701	280430
4.5833	210	1524	1.80	11.77525	0.49	4167	625	12421	212949
6.2500	211	1525	1.80	11.93203	0.49	4173	626	12439	211725
8.1250	211	1525	1.80	11.95647	0.49	4174	626	12441	211536
10.2083	211	1525	1.80	11.964	0.49	4175	626	12442	211478
12.5000	212	1525	1.80	11.99239	0.49	4176	626	12445	211260
20.0000	229	1545	1.80	15.51554	0.49	4300	645	12803	189156

Table 41. X=52

Depth	Vs	Vp	Density	N		Gdyn, Gmax	Gdyn, 0	Edyn	Esdyn
(m)	(m/s)	(m/s)	(g/cm^3)	(IBC)	μ	MPa	MPa	MPa	MPa
0.0000	170	1478	1.78	5.942415	0.49	3892	584	11625	290083
0.8333	158	1466	1.78	4.761438	0.49	3817	573	11407	322034
1.8750	161	1468	1.78	4.980386	0.49	3832	575	11450	315227
3.1250	172	1481	1.78	6.159845	0.49	3905	586	11662	285263
4.5833	219	1534	1.80	13.45605	0.49	4230	634	12601	200994
6.2500	221	1535	1.80	13.6918	0.49	4238	636	12625	199501
8.1250	221	1535	1.80	13.76146	0.49	4241	636	12632	199067
10.2083	221	1535	1.80	13.7845	0.49	4241	636	12634	198924
12.5000	221	1536	1.80	13.81561	0.49	4242	636	12637	198732
20.0000	230	1545	1.80	15.53857	0.49	4301	645	12805	189038

Table 42. X=56

Depth	Vs	Vp	Density	N		Gdyn, Gmax	Gdyn, 0	Edyn	Esdyn
(m)	(m/s)	(m/s)	(g/cm^3)	(IBC)	μ	MPa	MPa	MPa	MPa
0.0000	169	1478	1.78	5.901134	0.49	3890	583	11618	291029
0.8333	159	1466	1.78	4.81714	0.49	3821	573	11418	320257
1.8750	161	1469	1.78	5.068818	0.49	3838	576	11467	312609
3.1250	171	1480	1.78	6.061876	0.49	3899	585	11646	287401
4.5833	225	1539	1.80	14.47776	0.49	4265	640	12703	194796
6.2500	226	1541	1.80	14.76453	0.49	4275	641	12731	193177
8.1250	226	1541	1.80	14.87764	0.49	4279	642	12742	192551
10.2083	227	1542	1.80	14.91726	0.49	4280	642	12746	192334
12.5000	227	1542	1.80	14.95045	0.49	4281	642	12749	192153
20.0000	230	1545	1.80	15.55996	0.49	4301	645	12807	188928

Table 43. X=60

Depth	Vs	Vp	Density	N		Gdyn, Gmax	Gdyn, 0	Edyn	Esdyn
(m)	(m/s)	(m/s)	(g/cm^3)	(IBC)	μ	MPa	MPa	MPa	MPa
0.0000	161	1469	1.78	5.021866	0.49	3835	575	11458	313990
0.8333	157	1464	1.78	4.610126	0.49	3807	571	11376	327031
1.8750	162	1470	1.78	5.102556	0.49	3840	576	11473	311628
3.1250	170	1479	1.78	6.017634	0.49	3897	585	11638	288385
4.5833	226	1541	1.80	14.818	0.49	4277	642	12736	192880
6.2500	228	1543	1.80	15.15768	0.49	4288	643	12769	191034
8.1250	229	1544	1.80	15.3176	0.49	4293	644	12784	190186
10.2083	229	1544	1.80	15.3747	0.49	4295	644	12789	189887
12.5000	229	1544	1.80	15.40955	0.49	4296	644	12793	189705
20.0000	230	1545	1.80	15.57965	0.49	4302	645	12809	188827

Table 44. X=64

Depth	Vs	Vp	Density	N		Gdyn, Gmax	Gdyn, 0	Edyn	Esdyn
(m)	(m/s)	(m/s)	(g/cm^3)	(IBC)	μ	MPa	MPa	MPa	MPa
0.0000	157	1464	1.78	4.592858	0.49	3806	571	11373	327617
0.8333	156	1463	1.78	4.565604	0.49	3804	571	11367	328550
1.8750	161	1469	1.78	5.01034	0.49	3834	575	11455	314332
3.1250	170	1478	1.78	5.917657	0.49	3891	584	11621	290649
4.5833	226	1541	1.80	14.80592	0.49	4276	641	12735	192947
6.2500	228	1543	1.80	15.21599	0.49	4290	644	12774	190723
8.1250	229	1544	1.80	15.42275	0.49	4297	645	12794	189637
10.2083	229	1545	1.80	15.49671	0.49	4299	645	12801	189253
12.5000	230	1545	1.80	15.53306	0.49	4300	645	12804	189066
20.0000	230	1545	1.80	15.59761	0.49	4303	645	12810	188735

Table 45. X=68

Depth	Vs	Vp	Density	N		Gdyn, Gmax	Gdyn, 0	Edyn	Esdyn
(m)	(m/s)	(m/s)	(g/cm^3)	(IBC)	μ	MPa	MPa	MPa	MPa
0.0000	155	1462	1.78	4.452802	0.49	3796	569	11344	332504
0.8333	157	1464	1.78	4.597676	0.49	3806	571	11374	327453
1.8750	161	1469	1.78	5.0444	0.49	3836	575	11462	313325
3.1250	170	1478	1.78	5.949061	0.49	3893	584	11626	289932
4.5833	226	1541	1.80	14.79183	0.49	4276	641	12734	193025
6.2500	228	1543	1.80	15.21266	0.49	4290	643	12774	190741
8.1250	229	1544	1.80	15.44372	0.49	4298	645	12796	189528
10.2083	230	1545	1.80	15.52927	0.49	4300	645	12804	189086
12.5000	230	1545	1.80	15.56653	0.49	4302	645	12807	188894
20.0000	230	1545	1.80	15.61382	0.49	4303	645	12812	188652

Table 46. X=72

Depth	Vs	Vp	Density	N		Gdyn, Gmax	Gdyn, 0	Edyn	Esdyn
(m)	(m/s)	(m/s)	(g/cm^3)	(IBC)	μ	MPa	MPa	MPa	MPa
0.0000	156	1463	1.78	4.562932	0.49	3804	571	11367	328642
0.8333	158	1465	1.78	4.722522	0.49	3815	572	11399	323295
1.8750	162	1470	1.78	5.102514	0.49	3840	576	11473	311630
3.1250	170	1479	1.78	5.97	0.49	3894	584	11630	289456
4.5833	226	1541	1.80	14.77415	0.49	4275	641	12732	193123
6.2500	228	1543	1.80	15.20381	0.49	4290	643	12773	190788
8.1250	229	1544	1.80	15.454	0.49	4298	645	12797	189474
10.2083	230	1545	1.80	15.54918	0.49	4301	645	12806	188983
12.5000	230	1545	1.80	15.58725	0.49	4302	645	12809	188788
20.0000	230	1545	1.80	15.62827	0.49	4304	646	12813	188579

Table 47. X=76

Depth	Vs	Vp	Density	N		Gdyn, Gmax	Gdyn, 0	Edyn	Esdyn
(m)	(m/s)	(m/s)	(g/cm^3)	(IBC)	μ	MPa	MPa	MPa	MPa
0.0000	155	1462	1.78	4.426859	0.49	3794	569	11339	333436
0.8333	157	1464	1.78	4.600069	0.49	3806	571	11374	327372
1.8750	162	1470	1.78	5.124187	0.49	3842	576	11477	311005
3.1250	170	1479	1.78	6.005384	0.49	3896	584	11636	288659
4.5833	226	1541	1.80	14.7728	0.49	4275	641	12732	193131
6.2500	228	1543	1.80	15.19983	0.49	4290	643	12773	190809
8.1250	229	1544	1.80	15.46325	0.49	4298	645	12798	189426
10.2083	230	1545	1.80	15.56624	0.49	4302	645	12807	188896
12.5000	230	1545	1.80	15.60503	0.49	4303	645	12811	188697
20.0000	230	1545	1.80	15.64093	0.49	4304	646	12814	188514

Table 48. X=80

Depth	Vs	Vp	Density	N		Gdyn, Gmax	Gdyn, 0	Edyn	Esdyn
(m)	(m/s)	(m/s)	(g/cm^3)	(IBC)	μ	MPa	MPa	MPa	MPa
0.0000	155	1462	1.78	4.42112	0.49	3793	569	11337	333643
0.8333	155	1463	1.78	4.490527	0.49	3798	570	11352	331165
1.8750	162	1470	1.78	5.127225	0.49	3842	576	11478	310918
3.1250	171	1479	1.78	6.029721	0.49	3898	585	11640	288115
4.5833	226	1541	1.80	14.76493	0.49	4275	641	12731	193174
6.2500	228	1543	1.80	15.18979	0.49	4289	643	12772	190862
8.1250	229	1544	1.80	15.46216	0.49	4298	645	12798	189432
10.2083	230	1545	1.80	15.57105	0.49	4302	645	12808	188871
12.5000	230	1545	1.80	15.61035	0.49	4303	645	12811	188670
20.0000	230	1545	1.80	15.65182	0.49	4304	646	12815	188459

Table 49. X=84

Depth	Vs	Vp	Density	N		Gdyn, Gmax	Gdyn, 0	Edyn	Esdyn
(m)	(m/s)	(m/s)	(g/cm^3)	(IBC)	μ	MPa	MPa	MPa	MPa
0.0000	158	1466	1.78	4.751773	0.49	3817	572	11405	322346
0.8333	156	1463	1.78	4.536331	0.49	3802	570	11361	329561
1.8750	161	1469	1.78	5.016099	0.49	3834	575	11457	314161
3.1250	170	1478	1.78	5.929331	0.49	3892	584	11623	290382
4.5833	225	1540	1.80	14.62436	0.49	4270	641	12717	193962
6.2500	227	1542	1.80	15.09016	0.49	4286	643	12762	191396
8.1250	229	1544	1.80	15.37576	0.49	4295	644	12789	189882
10.2083	229	1545	1.80	15.48943	0.49	4299	645	12800	189291
12.5000	230	1545	1.80	15.52894	0.49	4300	645	12804	189087
20.0000	230	1545	1.80	15.66092	0.49	4305	646	12816	188413

Table 50. X=88

Depth	Vs	Vp	Density	N		Gdyn, Gmax	Gdyn, 0	Edyn	Esdyn
(m)	(m/s)	(m/s)	(g/cm^3)	(IBC)	μ	MPa	MPa	MPa	MPa
0.0000	166	1475	1.78	5.583237	0.49	3871	581	11562	298678
0.8333	160	1467	1.78	4.87959	0.49	3825	574	11430	318302
1.8750	160	1468	1.78	4.961046	0.49	3831	575	11446	315809
3.1250	168	1477	1.78	5.792025	0.49	3883	583	11599	293581
4.5833	223	1537	1.80	14.16178	0.49	4254	638	12672	196639
6.2500	226	1540	1.80	14.69037	0.49	4273	641	12724	193591
8.1250	227	1542	1.80	14.99117	0.49	4283	642	12753	191931
10.2083	228	1543	1.80	15.10804	0.49	4286	643	12764	191299
12.5000	228	1543	1.80	15.14714	0.49	4288	643	12768	191090
20.0000	230	1545	1.80	15.66824	0.49	4305	646	12817	188375

Table 51. X=92

Depth	Vs	Vp	Density	N		Gdyn, Gmax	Gdyn, 0	Edyn	Esdyn
(m)	(m/s)	(m/s)	(g/cm^3)	(IBC)	μ	MPa	MPa	MPa	MPa
0.0000	170	1479	1.78	5.960269	0.49	3894	584	11628	289677
0.8333	161	1469	1.78	5.068824	0.49	3838	576	11467	312608
1.8750	163	1471	1.78	5.184795	0.49	3845	577	11489	309281
3.1250	169	1478	1.78	5.896672	0.49	3890	583	11617	291132
4.5833	219	1533	1.80	13.30383	0.49	4224	634	12585	201980
6.2500	221	1536	1.80	13.81256	0.49	4242	636	12637	198751
8.1250	223	1537	1.80	14.10438	0.49	4252	638	12666	196981
10.2083	223	1538	1.80	14.21799	0.49	4256	638	12678	196307
12.5000	223	1538	1.80	14.25532	0.49	4258	639	12681	196087
20.0000	230	1545	1.80	15.67379	0.49	4305	646	12817	188347

Table 52. X=96

Depth	Vs	Vp	Density	N		Gdyn, Gmax	Gdyn, 0	Edyn	Esdyn
(m)	(m/s)	(m/s)	(g/cm^3)	(IBC)	μ	MPa	MPa	MPa	MPa
0.0000	164	1473	1.78	5.373435	0.49	3858	579	11524	304108
0.8333	157	1465	1.78	4.659465	0.49	3810	572	11386	325374
1.8750	162	1470	1.78	5.148736	0.49	3843	576	11482	310303
3.1250	170	1479	1.78	6.003034	0.49	3896	584	11636	288712
4.5833	213	1526	1.80	12.22285	0.49	4184	628	12470	209518
6.2500	215	1529	1.80	12.68247	0.49	4202	630	12520	206192
8.1250	217	1531	1.80	12.94405	0.49	4211	632	12548	204380
10.2083	217	1531	1.80	13.04761	0.49	4215	632	12559	203679
12.5000	217	1531	1.80	13.08169	0.49	4216	632	12562	203450
20.0000	230	1546	1.80	15.67756	0.49	4305	646	12818	188328

Table 53. X=100

Depth	Vs	Vp	Density	N		Gdyn, Gmax	Gdyn, 0	Edyn	Esdyn
(m)	(m/s)	(m/s)	(g/cm^3)	(IBC)	μ	MPa	MPa	MPa	MPa
0.0000	169	1478	1.78	5.876172	0.49	3888	583	11614	291606
0.8333	160	1468	1.78	4.925686	0.49	3828	574	11439	316883
1.8750	164	1472	1.78	5.346026	0.49	3856	578	11519	304842
3.1250	171	1480	1.78	6.109895	0.49	3902	585	11654	286347
4.5833	209	1522	1.79	11.536	0.49	4158	624	12394	214867
6.2500	211	1525	1.80	11.96692	0.49	4175	626	12442	211456
8.1250	213	1526	1.80	12.21388	0.49	4184	628	12469	209585
10.2083	213	1527	1.80	12.31169	0.49	4188	628	12480	208860
12.5000	214	1527	1.80	12.34367	0.49	4189	628	12484	208625
20.0000	230	1546	1.80	15.67955	0.49	4305	646	12818	188318

Table 54. X=104

5.3. SURVEY #3

Depth (m)	Vs (m/s)	Vp (m/s)	Density (g/cm^3)	N (IBC)	μ	Gdyn, Gmax MPa	Gdyn, 0 MPa	Edyn MPa	Esdyn MPa
0.00	349	1678	1.84	59.20297	0.48	5191	779	15338	112799
1.07	345	1673	1.84	57.10886	0.48	5160	774	15251	114221
2.31	348	1676	1.84	58.28237	0.48	5178	777	15300	113415
3.71	374	1705	1.85	73.30545	0.47	5383	808	15878	104896
5.27	342	1669	1.84	55.11821	0.48	5131	770	15167	115649
7.01	359	1689	1.85	64.70307	0.48	5269	790	15557	109405
8.90	354	1683	1.85	61.99015	0.48	5231	785	15451	111022
10.96	390	1723	1.86	84.31693	0.47	5519	828	16258	100182
13.19	295	1617	1.83	34.50708	0.48	4774	716	14158	137232
15.58	381	1713	1.86	78.07946	0.47	5443	817	16047	102728
18.13	377	1708	1.85	75.25651	0.47	5408	811	15948	103985
20.85	493	1837	1.89	177.5115	0.46	6392	959	18680	80196
23.74	487	1830	1.89	170.0359	0.46	6334	950	18519	81149
26.79	479	1822	1.89	161.7231	0.46	6267	940	18335	82288
36.43	509	1855	1.90	195.7595	0.46	6529	979	19057	78108

Table 55. X=0

Depth	Vs	Vp	Density	N		Gdyn, Gmax	Gdyn, 0	Edyn	Esdyn
(m)	(m/s)	(m/s)	(g/cm^3)	(IBC)	μ	MPa	MPa	MPa	MPa
0.00	336	1663	1.84	52.39796	0.48	5089	763	15049	117732
1.07	338	1665	1.84	53.40884	0.48	5104	766	15093	116939
2.31	342	1670	1.84	55.37995	0.48	5134	770	15178	115457
3.71	367	1697	1.85	69.20915	0.48	5330	799	15728	106937
5.27	339	1666	1.84	53.87076	0.48	5111	767	15114	116584
7.01	357	1686	1.85	63.21295	0.48	5248	787	15499	110280
8.90	354	1683	1.85	61.74061	0.48	5228	784	15441	111176
10.96	380	1712	1.85	77.60495	0.47	5438	816	16030	102934
13.19	295	1617	1.83	34.49948	0.48	4774	716	14158	137244
15.58	382	1714	1.86	78.39749	0.47	5447	817	16058	102591
18.13	377	1709	1.85	75.75481	0.47	5414	812	15966	103758
20.85	493	1837	1.89	177.4557	0.46	6392	959	18679	80203
23.74	487	1830	1.89	169.9991	0.46	6333	950	18518	81154
26.79	479	1822	1.89	161.664	0.46	6266	940	18334	82296
36.43	509	1854	1.90	195.6609	0.46	6529	979	19055	78119

Table 56. X=4

Depth	Vs	Vp	Density	N		Gdyn, Gmax	Gdyn, 0	Edyn	Esdyn
(m)	(m/s)	(m/s)	(g/cm^3)	(IBC)	μ	MPa	MPa	MPa	MPa
0.00	323	1649	1.83	46.12001	0.48	4987	748	14762	123239
1.07	334	1661	1.84	51.31773	0.48	5072	761	15001	118606
2.31	338	1665	1.84	53.06899	0.48	5099	765	15079	117203
3.71	358	1687	1.85	63.93111	0.48	5258	789	15527	109854
5.27	336	1663	1.84	52.20652	0.48	5086	763	15041	117885
7.01	353	1682	1.85	61.34634	0.48	5222	783	15425	111421
8.90	353	1682	1.85	61.42527	0.48	5223	783	15428	111372
10.96	359	1689	1.85	64.6268	0.48	5268	790	15554	109449
13.19	295	1617	1.83	34.52084	0.48	4774	716	14159	137212
15.58	384	1716	1.86	79.89606	0.47	5466	820	16109	101955
18.13	381	1713	1.86	78.13603	0.47	5444	817	16049	102703
20.85	493	1837	1.89	177.0125	0.46	6388	958	18669	80258
23.74	486	1830	1.89	169.9209	0.46	6333	950	18516	81165
26.79	479	1821	1.89	161.5396	0.46	6265	940	18331	82314
36.43	508	1854	1.90	195.4634	0.46	6527	979	19051	78140

Table 57. X=8

Depth	Vs	Vp	Density	N		Gdyn, Gmax	Gdyn, 0	Edyn	Esdyn
(m)	(m/s)	(m/s)	(g/cm^3)	(IBC)	μ	MPa	MPa	MPa	MPa
0.00	346	1674	1.84	57.38557	0.48	5164	775	15263	114029
1.07	344	1672	1.84	56.39857	0.48	5150	772	15222	114722
2.31	341	1668	1.84	54.76887	0.48	5125	769	15152	115907
3.71	355	1684	1.85	62.03558	0.48	5232	785	15452	110994
5.27	337	1664	1.84	52.60301	0.48	5092	764	15058	117569
7.01	354	1683	1.85	61.63227	0.48	5226	784	15436	111243
8.90	355	1684	1.85	62.29617	0.48	5235	785	15463	110834
10.96	335	1661	1.84	51.60732	0.48	5076	761	15014	118369
13.19	296	1619	1.83	34.94756	0.48	4783	717	14183	136575
15.58	390	1723	1.86	84.18617	0.47	5517	828	16254	100232
18.13	391	1724	1.86	84.84176	0.47	5525	829	16275	99981
20.85	491	1835	1.89	175.1284	0.46	6374	956	18629	80493
23.74	486	1830	1.89	169.8537	0.46	6332	950	18515	81173
26.79	479	1821	1.89	161.3935	0.46	6264	940	18328	82335
36.43	508	1854	1.90	195.166	0.46	6525	979	19045	78172

Table 58. X=12

Depth	Vs	Vp	Density	N		Gdyn, Gmax	Gdyn, 0	Edyn	Esdyn
(m)	(m/s)	(m/s)	(g/cm^3)	(IBC)	μ	MPa	MPa	MPa	MPa
0.00	345	1673	1.84	56.79103	0.48	5156	773	15238	114444
1.07	341	1669	1.84	54.83717	0.48	5126	769	15155	115857
2.31	334	1661	1.84	51.41077	0.48	5073	761	15005	118529
3.71	347	1675	1.84	58.03309	0.48	5174	776	15290	113584
5.27	335	1662	1.84	51.83001	0.48	5080	762	15024	118188
7.01	353	1682	1.85	61.19161	0.48	5220	783	15419	111518
8.90	356	1686	1.85	63.07617	0.48	5246	787	15494	110362
10.96	315	1639	1.83	42.38419	0.48	4922	738	14579	127094
13.19	297	1620	1.83	35.45193	0.48	4793	719	14212	135837
15.58	401	1735	1.86	91.87909	0.47	5606	841	16502	97456
18.13	408	1743	1.86	97.38609	0.47	5667	850	16671	95677
20.85	487	1830	1.89	170.1995	0.46	6335	950	18522	81128
23.74	486	1830	1.89	169.8688	0.46	6332	950	18515	81171
26.79	479	1821	1.89	161.3002	0.46	6263	940	18325	82348
36.43	508	1854	1.90	194.7687	0.46	6522	978	19037	78214

Table 59. X=16

Depth	Vs	Vp	Density	N		Gdyn, Gmax	Gdyn, 0	Edyn	Esdyn
(m)	(m/s)	(m/s)	(g/cm^3)	(IBC)	μ	MPa	MPa	MPa	MPa
0.00	322	1648	1.83	45.79562	0.48	4981	747	14746	123555
1.07	323	1649	1.84	46.31489	0.48	4990	749	14771	123051
2.31	318	1643	1.83	43.70752	0.48	4946	742	14645	125671
3.71	336	1662	1.84	52.07823	0.48	5084	763	15035	117988
5.27	333	1659	1.84	50.65981	0.48	5061	759	14972	119152
7.01	350	1678	1.84	59.3357	0.48	5193	779	15344	112712
8.90	358	1687	1.85	63.81748	0.48	5257	789	15523	109921
10.96	304	1628	1.83	38.05773	0.48	4843	726	14354	132265
13.19	299	1622	1.83	36.17079	0.48	4807	721	14252	134812
15.58	414	1750	1.87	101.9034	0.47	5715	857	16807	94329
18.13	429	1766	1.87	113.7042	0.47	5836	875	17144	91201
20.85	480	1822	1.89	162.3479	0.46	6272	941	18349	82199
23.74	486	1830	1.89	169.8896	0.46	6332	950	18516	81169
26.79	479	1821	1.89	161.3644	0.46	6264	940	18327	82339
36.43	508	1853	1.90	194.5317	0.46	6520	978	19032	78239

Table 60. X=20

Depth	Vs	Vp	Density	N		Gdyn, Gmax	Gdyn, 0	Edyn	Esdyn
(m)	(m/s)	(m/s)	(g/cm^3)	(IBC)	μ	MPa	MPa	MPa	MPa
0.00	306	1630	1.83	38.95904	0.48	4860	729	14402	131116
1.07	307	1631	1.83	39.27126	0.48	4866	730	14419	130727
2.31	305	1629	1.83	38.56082	0.48	4853	728	14381	131619
3.71	328	1654	1.84	48.31306	0.48	5023	753	14865	121191
5.27	335	1662	1.84	51.67062	0.48	5077	762	15017	118317
7.01	347	1675	1.84	57.89175	0.48	5172	776	15284	113680
8.90	359	1689	1.85	64.73308	0.48	5269	790	15558	109388
10.96	301	1624	1.83	36.93943	0.48	4822	723	14294	133751
13.19	301	1624	1.83	36.68791	0.48	4817	723	14280	134094
15.58	425	1762	1.87	110.6127	0.47	5805	871	17057	91971
18.13	443	1782	1.88	125.9511	0.47	5955	893	17472	88440
20.85	472	1814	1.89	154.3033	0.46	6206	931	18166	83382
23.74	486	1829	1.89	168.8597	0.46	6324	949	18493	81305
26.79	478	1820	1.89	160.1535	0.46	6254	938	18300	82513
36.43	507	1853	1.90	193.8413	0.46	6515	977	19018	78314

Table 61. X=24

Depth	Vs	Vp	Density	N		Gdyn, Gmax	Gdyn, 0	Edyn	Esdyn
(m)	(m/s)	(m/s)	(g/cm^3)	(IBC)	μ	MPa	MPa	MPa	MPa
0.00	301	1624	1.83	36.82354	0.48	4820	723	14288	133908
1.07	295	1617	1.83	34.37725	0.48	4772	716	14151	137429
2.31	298	1620	1.83	35.56604	0.48	4795	719	14218	135672
3.71	323	1649	1.84	46.22131	0.48	4989	748	14766	123141
5.27	339	1667	1.84	53.97012	0.48	5113	767	15118	116508
7.01	348	1676	1.84	58.28494	0.48	5178	777	15300	113413
8.90	362	1692	1.85	66.35698	0.48	5292	794	15621	108469
10.96	304	1627	1.83	37.85335	0.48	4839	726	14343	132532
13.19	302	1625	1.83	37.29964	0.48	4829	724	14314	133265
15.58	431	1769	1.87	115.9558	0.47	5859	879	17206	90660
18.13	444	1783	1.88	127.3682	0.47	5968	895	17509	88146
20.85	469	1810	1.89	151.1074	0.46	6179	927	18092	83879
23.74	484	1827	1.89	167.3227	0.46	6312	947	18459	81511
26.79	476	1818	1.89	158.2987	0.46	6239	936	18258	82783
36.43	506	1852	1.90	192.8264	0.46	6508	976	18998	78424

Table 62. X=28

Depth	Vs	Vp	Density	N		Gdyn, Gmax	Gdyn, 0	Edyn	Esdyn
(m)	(m/s)	(m/s)	(g/cm^3)	(IBC)	μ	MPa	MPa	MPa	MPa
0.00	292	1615	1.82	33.5757	0.48	4755	713	14105	138667
1.07	287	1608	1.82	31.58997	0.48	4714	707	13988	141940
2.31	293	1616	1.82	33.97673	0.48	4763	715	14128	138042
3.71	319	1644	1.83	44.1691	0.48	4954	743	14667	125190
5.27	340	1668	1.84	54.46566	0.48	5121	768	15139	116134
7.01	349	1678	1.84	59.24892	0.48	5192	779	15340	112769
8.90	366	1696	1.85	68.39692	0.48	5319	798	15698	107363
10.96	310	1634	1.83	40.47535	0.48	4888	733	14482	129271
13.19	303	1626	1.83	37.62336	0.48	4835	725	14331	132834
15.58	434	1772	1.87	118.0381	0.47	5879	882	17262	90174
18.13	435	1773	1.87	119.0585	0.47	5889	883	17290	89940
20.85	473	1815	1.89	154.9644	0.46	6211	932	18181	83281
23.74	484	1828	1.89	167.6165	0.46	6314	947	18466	81472
26.79	475	1818	1.89	157.9907	0.46	6236	935	18251	82828
36.43	505	1851	1.90	191.3882	0.46	6497	975	18968	78581

Table 63. X=32

Depth	Vs	Vp	Density	N		Gdyn, Gmax	Gdyn, 0	Edyn	Esdyn
(m)	(m/s)	(m/s)	(g/cm^3)	(IBC)	μ	MPa	MPa	MPa	MPa
0.00	285	1606	1.82	30.96604	0.48	4701	705	13950	143034
1.07	283	1604	1.82	30.34689	0.48	4688	703	13912	144153
2.31	293	1615	1.82	33.68502	0.48	4758	714	14111	138496
3.71	316	1640	1.83	42.82812	0.48	4930	740	14601	126609
5.27	339	1666	1.84	53.79096	0.48	5110	767	15110	116645
7.01	353	1682	1.85	61.32248	0.48	5222	783	15424	111436
8.90	373	1704	1.85	72.77058	0.47	5376	806	15859	105153
10.96	325	1651	1.84	47.20884	0.48	5005	751	14813	122204
13.19	303	1627	1.83	37.6838	0.48	4836	725	14334	132754
15.58	434	1772	1.87	118.4151	0.47	5883	882	17272	90087
18.13	424	1761	1.87	109.8791	0.47	5798	870	17037	92158
20.85	481	1824	1.89	163.5099	0.46	6281	942	18375	82036
23.74	488	1832	1.89	171.9008	0.46	6348	952	18559	80906
26.79	479	1821	1.89	161.3587	0.46	6264	940	18327	82340
36.43	504	1849	1.90	189.705	0.46	6485	973	18934	78767

Table 64. X=36

Depth	Vs	Vp	Density	N		Gdyn, Gmax	Gdyn, 0	Edyn	Esdyn
(m)	(m/s)	(m/s)	(g/cm^3)	(IBC)	μ	MPa	MPa	MPa	MPa
0.00	286	1608	1.82	31.38959	0.48	4710	706	13975	142287
1.07	284	1605	1.82	30.47766	0.48	4690	704	13920	143914
2.31	293	1615	1.82	33.77815	0.48	4759	714	14116	138350
3.71	313	1638	1.83	41.8783	0.48	4913	737	14553	127656
5.27	338	1665	1.84	53.24991	0.48	5102	765	15087	117062
7.01	361	1691	1.85	65.64481	0.48	5282	792	15594	108868
8.90	386	1719	1.86	81.56059	0.47	5486	823	16166	101270
10.96	353	1682	1.85	61.3573	0.48	5222	783	15425	111415
13.19	304	1627	1.83	37.85245	0.48	4839	726	14343	132533
15.58	434	1772	1.87	118.4384	0.47	5883	882	17273	90082
18.13	423	1759	1.87	108.6985	0.47	5786	868	17003	92464
20.85	488	1832	1.89	171.8253	0.46	6348	952	18558	80915
23.74	495	1839	1.89	179.0369	0.46	6404	961	18712	80009
26.79	484	1827	1.89	167.386	0.46	6312	947	18461	81503
36.43	502	1847	1.90	188.0322	0.46	6472	971	18900	78955

Table 65. X=40

Depth	Vs	Vp	Density	N		Gdyn, Gmax	Gdyn, 0	Edyn	Esdyn
(m)	(m/s)	(m/s)	(g/cm^3)	(IBC)	μ	MPa	MPa	MPa	MPa
0.00	296	1618	1.83	34.79545	0.48	4780	717	14175	136800
1.07	282	1603	1.82	29.99556	0.48	4680	702	13890	144805
2.31	289	1610	1.82	32.21828	0.48	4727	709	14025	140871
3.71	310	1634	1.83	40.41702	0.48	4887	733	14479	129340
5.27	338	1665	1.84	53.37449	0.48	5104	766	15092	116966
7.01	372	1703	1.85	72.56019	0.47	5374	806	15852	105254
8.90	404	1739	1.86	94.29104	0.47	5633	845	16577	96657
10.96	389	1722	1.86	83.18341	0.47	5505	826	16220	100623
13.19	306	1630	1.83	38.90682	0.48	4859	729	14400	131181
15.58	435	1773	1.87	119.1436	0.47	5890	883	17292	89921
18.13	437	1775	1.87	120.4374	0.47	5902	885	17327	89630
20.85	493	1837	1.89	177.1532	0.46	6389	958	18672	80241
23.74	500	1845	1.90	185.8331	0.46	6456	968	18854	79205
26.79	490	1834	1.89	173.6988	0.46	6362	954	18598	80675
36.43	502	1847	1.90	187.5299	0.46	6468	970	18889	79011

Table 66. X=44

Depth	Vs	Vp	Density	N		Gdyn, Gmax	Gdyn, 0	Edyn	Esdyn
(m)	(m/s)	(m/s)	(g/cm^3)	(IBC)	μ	MPa	MPa	MPa	MPa
0.00	299	1621	1.83	35.87447	0.48	4801	720	14235	135231
1.07	280	1601	1.82	29.38397	0.48	4666	700	13852	145966
2.31	283	1604	1.82	30.11707	0.48	4683	702	13898	144578
3.71	307	1630	1.83	39.06873	0.48	4862	729	14408	130979
5.27	339	1666	1.84	53.83692	0.48	5111	767	15112	116610
7.01	384	1716	1.86	80.04218	0.47	5468	820	16114	101894
8.90	419	1755	1.87	105.6788	0.47	5755	863	16917	93270
10.96	417	1753	1.87	104.1378	0.47	5739	861	16872	93695
13.19	310	1634	1.83	40.28999	0.48	4885	733	14472	129491
15.58	436	1774	1.87	119.5743	0.47	5894	884	17304	89823
18.13	462	1803	1.88	143.9343	0.46	6117	918	17922	85054
20.85	494	1839	1.89	178.9009	0.46	6403	960	18709	80026
23.74	503	1849	1.90	189.2962	0.46	6481	972	18926	78813
26.79	493	1837	1.89	176.7241	0.46	6386	958	18663	80294
36.43	503	1849	1.90	189.2962	0.46	6481	972	18926	78813

Table 67. X=48

Depth	Vs	Vp	Density	N		Gdyn, Gmax	Gdyn, 0	Edyn	Esdyn
(m)	(m/s)	(m/s)	(g/cm^3)	(IBC)	μ	MPa	MPa	MPa	MPa
0.00	300	1623	1.83	36.44634	0.48	4812	722	14267	134428
1.07	282	1603	1.82	29.87797	0.48	4677	702	13883	145025
2.31	278	1599	1.82	28.7569	0.48	4653	698	13812	147197
3.71	305	1629	1.83	38.53371	0.48	4852	728	14380	131653
5.27	340	1667	1.84	54.10037	0.48	5115	767	15124	116409
7.01	392	1726	1.86	85.68268	0.47	5535	830	16303	99662
8.90	426	1762	1.87	111.0468	0.47	5810	871	17070	91861
10.96	431	1768	1.87	115.1978	0.47	5851	878	17185	90840
13.19	317	1642	1.83	43.44103	0.48	4941	741	14632	125952
15.58	436	1774	1.87	119.7131	0.47	5895	884	17307	89792
18.13	489	1833	1.89	172.5693	0.46	6354	953	18574	80819
20.85	494	1839	1.89	178.9925	0.46	6403	961	18711	80015
23.74	504	1849	1.90	190.1692	0.46	6488	973	18944	78715
26.79	493	1837	1.89	177.4392	0.46	6391	959	18678	80205
36.43	504	1849	1.90	190.1692	0.46	6488	973	18944	78715

Table 68. X=52

Depth	Vs	Vp	Density	N		Gdyn, Gmax	Gdyn, 0	Edyn	Esdyn
(m)	(m/s)	(m/s)	(g/cm^3)	(IBC)	μ	MPa	MPa	MPa	MPa
0.00	307	1630	1.83	39.07153	0.48	4862	729	14408	130975
1.07	294	1616	1.82	34.02861	0.48	4765	715	14131	137962
2.31	283	1604	1.82	30.18719	0.48	4684	703	13902	144448
3.71	307	1631	1.83	39.38349	0.48	4868	730	14425	130589
5.27	340	1667	1.84	54.13789	0.48	5116	767	15125	116381
7.01	396	1730	1.86	88.49012	0.47	5567	835	16394	98633
8.90	424	1761	1.87	110.0293	0.47	5800	870	17041	92120
10.96	433	1771	1.87	117.2719	0.47	5872	881	17241	90351
13.19	331	1658	1.84	49.92255	0.48	5049	757	14938	119777
15.58	435	1773	1.87	119.0434	0.47	5889	883	17289	89944
18.13	505	1850	1.90	190.8785	0.46	6493	974	18958	78637
20.85	494	1838	1.89	178.1848	0.46	6397	960	18694	80113
23.74	504	1849	1.90	189.6158	0.46	6484	973	18932	78777
26.79	492	1837	1.89	176.622	0.46	6385	958	18661	80306
36.43	505	1850	1.90	190.8785	0.46	6493	974	18958	78637

Table 69. X=56

Depth	Vs	Vp	Density	N		Gdyn, Gmax	Gdyn, 0	Edyn	Esdyn
(m)	(m/s)	(m/s)	(g/cm^3)	(IBC)	μ	MPa	MPa	MPa	MPa
0.00	315	1639	1.83	42.42701	0.48	4923	738	14581	127047
1.07	310	1634	1.83	40.45721	0.48	4888	733	14481	129293
2.31	291	1613	1.82	33.12876	0.48	4746	712	14079	139377
3.71	308	1632	1.83	39.69259	0.48	4874	731	14441	130210
5.27	339	1666	1.84	53.59032	0.48	5107	766	15101	116799
7.01	397	1731	1.86	89.14132	0.47	5575	836	16415	98402
8.90	420	1756	1.87	106.0581	0.47	5759	864	16928	93167
10.96	436	1774	1.87	119.6365	0.47	5895	884	17305	89809
13.19	351	1680	1.84	60.08887	0.48	5204	781	15374	112221
15.58	434	1771	1.87	117.8066	0.47	5877	882	17256	90227
18.13	499	1844	1.90	183.9834	0.46	6442	966	18816	79420
20.85	493	1837	1.89	176.9546	0.46	6388	958	18668	80265
23.74	503	1848	1.90	188.5326	0.46	6476	971	18910	78898
26.79	491	1835	1.89	175.041	0.46	6373	956	18627	80504
36.43	503	1848	1.90	188.5326	0.46	6476	971	18910	78898

Table 70. X=60

Depth	Vs	Vp	Density	N		Gdyn, Gmax	Gdyn, 0	Edyn	Esdyn
(m)	(m/s)	(m/s)	(g/cm^3)	(IBC)	μ	MPa	MPa	MPa	MPa
0.00	313	1637	1.83	41.68278	0.48	4910	736	14543	127877
1.07	312	1637	1.83	41.49897	0.48	4907	736	14534	128085
2.31	292	1614	1.82	33.38417	0.48	4751	713	14094	138970
3.71	304	1628	1.83	38.17495	0.48	4845	727	14361	132113
5.27	340	1667	1.84	54.26518	0.48	5118	768	15131	116285
7.01	400	1735	1.86	91.43016	0.47	5601	840	16487	97608
8.90	418	1754	1.87	104.5433	0.47	5743	861	16884	93583
10.96	448	1787	1.88	130.2957	0.47	5995	899	17584	87556
13.19	370	1701	1.85	71.07882	0.48	5355	803	15798	105983
15.58	433	1770	1.87	117.097	0.47	5870	880	17237	90392
18.13	472	1814	1.89	153.958	0.46	6203	930	18158	83435
20.85	492	1836	1.89	175.9326	0.46	6380	957	18646	80392
23.74	502	1847	1.90	187.5421	0.46	6468	970	18890	79010
26.79	490	1834	1.89	173.4804	0.46	6361	954	18594	80702
36.43	502	1847	1.90	187.5421	0.46	6468	970	18890	79010

Table 71. X=64

Depth	Vs	Vp	Density	N		Gdyn, Gmax	Gdyn, 0	Edyn	Esdyn
(m)	(m/s)	(m/s)	(g/cm^3)	(IBC)	μ	MPa	MPa	MPa	MPa
0.00	314	1639	1.83	42.35371	0.48	4922	738	14577	127128
1.07	319	1644	1.83	44.12795	0.48	4953	743	14665	125233
2.31	295	1617	1.83	34.3814	0.48	4772	716	14151	137423
3.71	299	1622	1.83	36.19249	0.48	4807	721	14253	134782
5.27	343	1670	1.84	55.71142	0.48	5139	771	15193	115215
7.01	406	1740	1.86	95.31084	0.47	5644	847	16608	96329
8.90	419	1755	1.87	105.692	0.47	5755	863	16917	93267
10.96	465	1806	1.88	146.7037	0.46	6141	921	17988	84590
13.19	378	1710	1.85	76.35275	0.47	5422	813	15987	103488
15.58	432	1769	1.87	116.2083	0.47	5861	879	17212	90600
18.13	434	1772	1.87	118.2338	0.47	5881	882	17267	90129
20.85	491	1835	1.89	174.8004	0.46	6371	956	18622	80535
23.74	501	1846	1.90	186.4843	0.46	6460	969	18868	79131
26.79	488	1832	1.89	171.7751	0.46	6347	952	18557	80922
36.43	501	1846	1.90	186.4843	0.46	6460	969	18868	79131

Table 72. X=68

Depth	Vs	Vp	Density	N		Gdyn, Gmax	Gdyn, 0	Edyn	Esdyn
(m)	(m/s)	(m/s)	(g/cm^3)	(IBC)	μ	MPa	MPa	MPa	MPa
0.00	317	1641	1.83	43.23211	0.48	4937	741	14621	126175
1.07	317	1642	1.83	43.63633	0.48	4944	742	14641	125746
2.31	294	1616	1.82	34.08558	0.48	4766	715	14134	137874
3.71	299	1622	1.83	36.24216	0.48	4808	721	14256	134712
5.27	350	1679	1.84	59.70981	0.48	5198	780	15359	112467
7.01	415	1751	1.87	102.5963	0.47	5723	858	16827	94130
8.90	425	1762	1.87	110.8749	0.47	5808	871	17065	91904
10.96	481	1824	1.89	163.9976	0.46	6285	943	18386	81967
13.19	379	1711	1.85	76.70918	0.47	5426	814	15999	103329
15.58	432	1769	1.87	116.2652	0.47	5862	879	17214	90587
18.13	403	1737	1.86	93.11662	0.47	5620	843	16540	97042
20.85	491	1834	1.89	174.4495	0.46	6368	955	18614	80579
23.74	501	1846	1.90	186.0736	0.46	6457	969	18859	79178
26.79	488	1831	1.89	171.1884	0.46	6343	951	18544	80998
36.43	501	1846	1.90	186.0736	0.46	6457	969	18859	79178

Table 73. X=72

Depth	Vs	Vp	Density	N		Gdyn, Gmax	Gdyn, 0	Edyn	Esdyn
(m)	(m/s)	(m/s)	(g/cm^3)	(IBC)	μ	MPa	MPa	MPa	MPa
0.00	304	1627	1.83	37.93092	0.48	4841	726	14348	132430
1.07	306	1629	1.83	38.6932	0.48	4855	728	14388	131451
2.31	292	1614	1.82	33.3594	0.48	4751	713	14092	139009
3.71	309	1633	1.83	40.2138	0.48	4883	732	14468	129582
5.27	362	1692	1.85	66.22745	0.48	5290	793	15616	108541
7.01	426	1763	1.87	111.4466	0.47	5814	872	17081	91760
8.90	433	1771	1.87	117.2355	0.47	5871	881	17240	90360
10.96	491	1835	1.89	175.4256	0.46	6376	956	18635	80456
13.19	377	1708	1.85	75.29212	0.47	5409	811	15949	103969
15.58	432	1770	1.87	116.4845	0.47	5864	880	17220	90535
18.13	385	1718	1.86	80.75433	0.47	5476	821	16139	101599
20.85	491	1835	1.89	174.4932	0.46	6369	955	18615	80574
23.74	501	1846	1.90	186.065	0.46	6457	969	18859	79179
26.79	488	1831	1.89	171.3249	0.46	6344	952	18547	80981
36.43	501	1846	1.90	186.065	0.46	6457	969	18859	79179

Table 74. X=76

Depth	Vs	Vp	Density	N		Gdyn, Gmax	Gdyn, 0	Edyn	Esdyn
(m)	(m/s)	(m/s)	(g/cm^3)	(IBC)	μ	MPa	MPa	MPa	MPa
0.00	334	1661	1.84	51.24243	0.48	5071	761	14998	118668
1.07	325	1650	1.84	46.8029	0.48	4998	750	14794	122586
2.31	316	1640	1.83	42.81422	0.48	4930	739	14600	126624
3.71	331	1657	1.84	49.69911	0.48	5046	757	14928	119969
5.27	373	1704	1.85	72.69341	0.47	5375	806	15856	105190
7.01	432	1770	1.87	116.6033	0.47	5865	880	17223	90507
8.90	436	1774	1.87	119.9916	0.47	5898	885	17315	89729
10.96	494	1839	1.89	178.8827	0.46	6403	960	18709	80028
13.19	375	1706	1.85	74.10213	0.47	5394	809	15907	104520
15.58	432	1769	1.87	116.3316	0.47	5862	879	17216	90571
18.13	379	1711	1.85	76.75696	0.47	5427	814	16001	103308
20.85	491	1835	1.89	174.5029	0.46	6369	955	18616	80572
23.74	501	1846	1.90	186.0824	0.46	6457	969	18860	79177
26.79	488	1832	1.89	171.4481	0.46	6345	952	18550	80965
36.43	501	1846	1.90	186.0824	0.46	6457	969	18860	79177

Table 75. X=80

5.4. PASSIVE AND ATIVE MASW – SURVEY #2

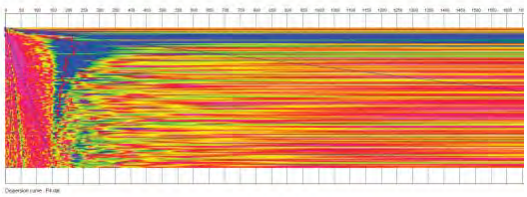

Figure 79. Passive Dispersion Curve

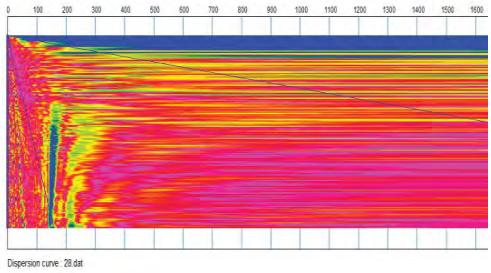

Figure 80. Ative Dispersion Curve

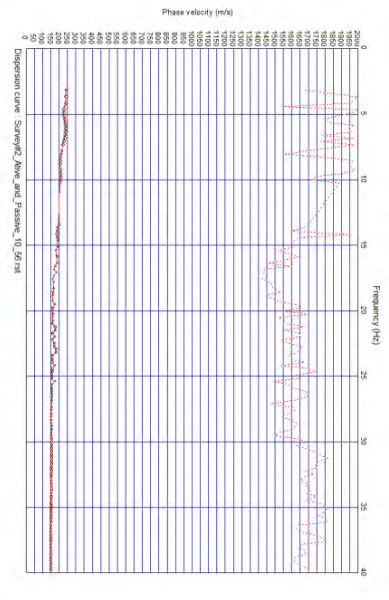

Figure 81. Ative + Passive Composite Dispersion Curve

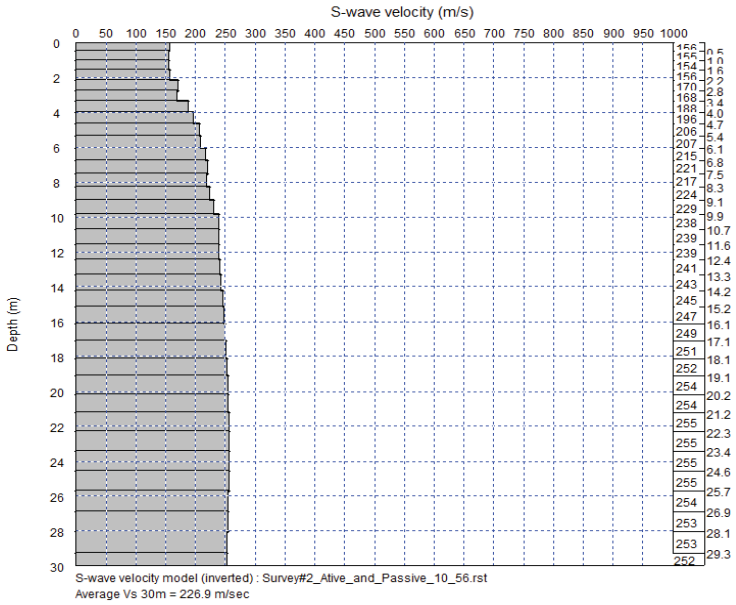

Figure 82. 10_56 array

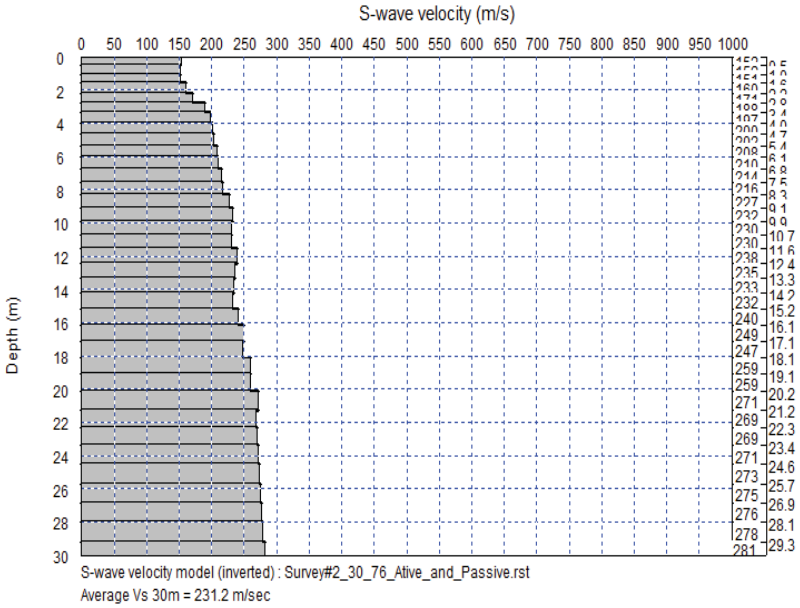

Figure 83. 30_76 array

The Vs30 at 10_56 array location is 226.9 m/s and at the 30_76 array is 231.2 m/s, confirming Rock Class D. Stiff Soil.

Depth	Vs	Vp	Density	N		Gdyn, Gmax	Gdyn, 0	Edyn	Esdyn
(m)	(m/s)	(m/s)	(g/cm^3)	(IBC)	μ	MPa	MPa	MPa	MPa
0.00	157	1465	1.78	4.598267	0.49	3812	572	11393	328305
0.51	155	1463	1.78	4.48148	0.49	3806	571	11374	332591
1.04	154	1463	1.78	4.395409	0.49	3803	570	11367	336183
1.59	157	1465	1.78	4.632337	0.49	3820	573	11416	327780
2.17	170	1480	1.78	6.007089	0.49	3909	586	11675	290056
2.76	169	1479	1.78	5.829187	0.49	3899	585	11647	294274
3.38	188	1501	1.79	8.28761	0.49	4032	605	12030	250271
4.02	196	1509	1.79	9.39542	0.49	4082	612	12175	236421
4.68	206	1520	1.80	11.06244	0.49	4150	622	12372	219701
5.36	208	1521	1.80	11.297	0.49	4157	623	12391	217458
6.06	216	1530	1.80	12.78138	0.49	4211	632	12548	205915
6.78	221	1536	1.80	13.77061	0.49	4245	637	12646	199312
7.53	218	1532	1.80	13.13602	0.49	4222	633	12580	203378
8.29	224	1539	1.80	14.41586	0.49	4267	640	12710	195446
9.08	230	1545	1.80	15.53394	0.49	4305	646	12818	189380
9.89	239	1555	1.81	17.55207	0.49	4369	655	13000	179931
10.71	239	1556	1.81	17.67383	0.49	4372	656	13009	179378
11.56	240	1557	1.81	17.89796	0.49	4377	657	13024	178341
12.44	241	1558	1.81	18.21682	0.49	4384	658	13043	176882
13.33	243	1560	1.81	18.64484	0.49	4393	659	13069	174978
14.24	245	1561	1.81	19.1369	0.49	4403	660	13098	172874
15.18	247	1563	1.81	19.66165	0.49	4414	662	13129	170715
16.14	249	1565	1.81	20.18661	0.49	4425	664	13159	168639
17.11	251	1567	1.81	20.67886	0.49	4435	665	13187	166771
18.11	253	1568	1.81	21.10625	0.49	4443	666	13211	165205
19.13	254	1570	1.81	21.45722	0.49	4450	667	13230	163958
20.17	255	1571	1.81	21.71255	0.49	4455	668	13244	163079
21.24	256	1571	1.81	21.86525	0.49	4458	669	13253	162573
22.32	256	1571	1.81	21.91391	0.49	4459	669	13257	162434
23.43	256	1571	1.81	21.87499	0.49	4459	669	13256	162599
24.55	255	1571	1.81	21.75841	0.49	4457	669	13251	163035
25.70	255	1570	1.81	21.59103	0.49	4455	668	13244	163655
26.87	254	1570	1.81	21.39563	0.49	4451	668	13235	164384
28.06	253	1569	1.81	21.20994	0.49	4448	667	13224	165030
29.27	252	1569	1.81	21.0089	0.49	4444	667	13212	165743
30.51	252	1568	1.81	20.80877	0.49	4439	666	13201	166466

Table 76. Passive MASW at 10_56 Array Location

Depth (m)	Vs (m/s)	Vp (m/s)	Density (g/cm^3)	N (IBC)	μ	Gdyn, Gmax MPa	Gdyn, 0 MPa	Edyn MPa	Esdyn MPa
0.00	153	1460	1.78	4.256017	0.49	3789	568	11326	340610
0.51	152	1460	1.78	4.191998	0.49	3790	569	11329	344076
1.04	152	1460	1.78	4.14749	0.49	3790	569	11329	346429
1.59	161	1470	1.78	5.010425	0.49	3850	577	11502	316318
2.17	172	1481	1.78	6.147378	0.49	3915	587	11691	286682
2.76	189	1500	1.79	8.354624	0.49	4025	604	12011	248428
3.38	198	1510	1.79	9.694423	0.49	4083	613	12179	232105
4.02	200	1513	1.79	10.07865	0.49	4100	615	12228	228178
4.68	203	1516	1.79	10.48734	0.49	4120	618	12285	224436
5.36	209	1523	1.80	11.50939	0.49	4165	625	12414	215721
6.06	210	1525	1.80	11.7871	0.49	4178	627	12453	213683
6.78	214	1529	1.80	12.51956	0.49	4207	631	12536	208219
7.53	217	1532	1.80	12.97359	0.49	4223	633	12582	204969
8.29	227	1543	1.80	15.06403	0.49	4294	644	12785	192125
9.08	233	1549	1.80	16.28989	0.49	4331	650	12893	185705
9.89	230	1546	1.80	15.71264	0.49	4311	647	12834	188410
10.71	231	1546	1.80	15.82206	0.49	4313	647	12840	187771
11.56	239	1555	1.81	17.58872	0.49	4368	655	12998	179619
12.44	235	1551	1.81	16.76632	0.49	4344	652	12929	183323
13.33	234	1550	1.81	16.46418	0.49	4336	650	12908	184872
14.24	232	1549	1.81	16.16999	0.49	4330	650	12891	186493
15.18	240	1558	1.81	18.00658	0.49	4390	659	13063	178520
16.14	249	1568	1.81	20.13423	0.49	4455	668	13249	170695
17.11	248	1567	1.81	19.77096	0.49	4448	667	13229	172158
18.11	260	1581	1.82	23.09293	0.49	4539	681	13491	161765
19.13	259	1580	1.82	22.88242	0.49	4535	680	13480	162443
20.17	271	1593	1.82	26.37031	0.49	4622	693	13728	153537
21.24	269	1591	1.82	25.77822	0.49	4607	691	13686	154896
22.32	270	1591	1.82	25.94945	0.49	4610	691	13694	154413
23.43	272	1594	1.82	26.67253	0.49	4625	694	13736	152620
24.55	273	1595	1.82	27.09885	0.48	4632	695	13755	151500
25.70	275	1596	1.82	27.63087	0.48	4640	696	13778	150146
26.87	277	1598	1.82	28.24035	0.48	4650	697	13805	148651
28.06	279	1600	1.82	28.90353	0.48	4660	699	13835	147088
29.27	281	1602	1.82	29.60483	0.48	4671	701	13866	145502
30.51	283	1604	1.82	30.34366	0.48	4683	702	13898	143896

Table 77. Passive MASW at 20_76 Array Location

6. CONCLUSION

In this geophysical survey, MASW reached the objectives proposed, with the Vs information allowing the classification of the rock mass and the determination of the dynamic elasticity modulus of the soil, objectively and with high quality.

7. REFERENCES

ASTM-STP 654 (1977). *Dynamic Geotechnical Testing*.

International Code Council (2000, 2003, 2006, 2009, 2012, 2015). *International Building Code (IBC).*

Ludwig, W.J., Nafe, J. E. & Drake, C.H. (1970). *Seismic Refraction*, The Sea, 4: 53-84.

Massarsch, K.R. (2010). *Deep compaction of granular soils*. Chapter 2. Soil Interpretation Methods, *in* Geotests & Publications – http://www.geoforum.com/).

Park, C.B., Miller, R,\.D. & Xia, J. (1999). *Multichannel analysis of Surface waves*, Geophysics, 64 (3): 800-808.

Websites:

http://publicecodes.cyberregs.com/icod/ibc/2009/icod_ibc_2009.

ATTACHMENT C4

Test Hole Logs

GCSPT16-01
GCSPT16-02
GSSAM16-02,2B

TEST HOLE LOG

STARTED: April 18, 2016 **FINISHED:** April 29, 2016

DRILL METHOD: Mud Rotary

GROUND ELEV. (m): 1004.4

COORDINATES (m): N 7766319.0 E 657417.6

Coordinates are provided in datum: WGS84/ UTM Zone 23K.

DEPTH (m)	SAMPLE TYPE	SAMPLE No.	SYMBOL	DESCRIPTION OF MATERIALS
0	SPT	1		SAND (SM)
1	SPT	2		Fine, some silt, compact, round to sub-angular, light grey to dark grey, homogeneous, primarily quartz, occasionally medium to coarse grained (TAILINGS SAND).
2	SPT	3		
3	SPT	4		
4	SPT	5		
5	SPT	6		
6	SPT	7		
7	SPT	8		
8	SPT	9		
9	SPT	10		
10	SPT	11		
11	SPT	12		
12	SPT	13		
13	SPT	14		
14	SPT	15		
15	SPT	16		
16	SPT	17		
17	SPT	18		
18	SPT	19		
19	SPT	20		
20				

Continued Next Page

Specific Gravity

2.6 3.0 3.4 3.8 4.2

SPECIFIC GRAVITY ◆

W_P% W% W_L%

20 40 60 80

Klohn Crippen Berger

PROJECT No.:

PROJECT: Fundão Tailings Dam Review Panel

LOCATION: Germano Pit Dam

LOGGED BY: TÜV SÜD **CHECKED BY:**

TEST_HOLE_SG FUNDAO TAILINGS DAM BH LOGS.GPJ KCBL_CALGARY.GDT 16-8-22

TEST HOLE LOG

STARTED: April 18, 2016 **FINISHED:** April 29, 2016
DRILL METHOD: Mud Rotary
GROUND ELEV. (m): 1004.4
COORDINATES (m): N 7766319.0 E 657417.6

Coordinates are provided in datum: WGS84/ UTM Zone 23K.

DEPTH (m)	SAMPLE TYPE	SAMPLE No.	SYMBOL	DESCRIPTION OF MATERIALS
21	SPT	21		
	SPT	22		
22	SPT	23		
23	SPT	24		
24	SPT	25		
25	SPT	26		
26	SPT	27		
27	SPT	28		
28	SPT	29		
29	SPT	30		
30	SPT	31		
31	SPT	32		
32	SPT	33		
33	SPT	34		
34	SPT	35		
35	SPT	36		
36	SPT	37		
37	SPT	38		
38	SPT	39		
39	SPT	40		
40				

Specific Gravity
2.6 3.0 3.4 3.8 4.2
SPECIFIC GRAVITY ◆

W_P% W% W_L%
20 40 60 80

Continued Next Page

Klohn Crippen Berger

PROJECT No.:
PROJECT: Fundão Tailings Dam Review Panel
LOCATION: Germano Pit Dam
LOGGED BY: TÜV SÜD **CHECKED BY:**
SHEET 2 OF 4 **HOLE NO.:** GCSPT16-01

TEST_HOLE_SG FUNDAO TAILINGS DAM BH LOGS.GPJ KCBL_CALGARY.GDT 16-8-22

TEST HOLE LOG

STARTED: April 18, 2016 **FINISHED:** April 29, 2016
DRILL METHOD: Mud Rotary
GROUND ELEV. (m): 1004.4
COORDINATES (m): N 7766319.0 E 657417.6

Coordinates are provided in datum: WGS84/ UTM Zone 23K.

DEPTH (m)	SAMPLE TYPE	SAMPLE No.	SYMBOL	DESCRIPTION OF MATERIALS
41	SPT	41		
42	SPT	42		
43	SPT	43		
44	SPT	44		
45	SPT	45		
46	SPT	46		
47	SPT	47		
48	SPT	48		
49	SPT	49		
50	SPT	50		
51	SPT	51		
52	SPT	52		
53	SPT	53		
54	SPT	54		
55	SPT	55		
56	SPT	56		
57	SPT	57		
58	SPT	58		
59	SPT	59		
60	SPT	60		

Specific Gravity
2.6 3.0 3.4 3.8 4.2
SPECIFIC GRAVITY ◆

W_P% W% W_L%
20 40 60 80

2.38

Continued Next Page

Klohn Crippen Berger

PROJECT No.:
PROJECT: Fundão Tailings Dam Review Panel
LOCATION: Germano Pit Dam
LOGGED BY: TÜV SÜD **CHECKED BY:**
SHEET 3 OF 4 **HOLE NO.:** GCSPT16-01

TEST_HOLE_SG FUNDAO TAILINGS DAM BH LOGS.GPJ KCBL_CALGARY.GDT 16-8-22

TEST HOLE LOG

STARTED: April 18, 2016 **FINISHED:** April 29, 2016

DRILL METHOD: Mud Rotary

GROUND ELEV. (m): 1004.4

COORDINATES (m): N 7766319.0 E 657417.6

Coordinates are provided in datum: WGS84/ UTM Zone 23K.

DEPTH (m)	SAMPLE TYPE	SAMPLE No.	SYMBOL	DESCRIPTION OF MATERIALS
0	SPT	61		
61				61.00 / 943.40 End of Hole at 61 m.
				SPT results are not reported because they are misleading.

Specific Gravity: 2.6 3.0 3.4 3.8 4.2

SPECIFIC GRAVITY ◆

W_P% W% W_L%

20 40 60 80

PROJECT No.:

PROJECT: Fundão Tailings Dam Review Panel

LOCATION: Germano Pit Dam

LOGGED BY: TÜV SÜD **CHECKED BY:**

SHEET 4 OF 4 **HOLE NO.:** GCSPT16-01

Klohn Crippen Berger

TEST_HOLE_SG FUNDAO TAILINGS DAM BH LOGS.GPJ KCBL_CALGARY.GDT 16-8-22

TEST HOLE LOG

STARTED: April 30, 2016 **FINISHED:** May 4, 2016

DRILL METHOD: Mud Rotary

GROUND ELEV. (m): 1002.4

COORDINATES (m): N 7766173.8 E 657272.5

Coordinates are provided in datum: WGS84/ UTM Zone 23K.

DEPTH (m)	SAMPLE TYPE	SAMPLE No.	SYMBOL	DESCRIPTION OF MATERIALS
0	SPT	1		SAND (SM)
1	SPT	2		Fine, some silt, compact, round to sub-angular, light grey to dark grey, homogeneous, primarily quartz, occasionally medium to coarse grained (TAILINGS SAND).
2	SPT	3		
3	SPT	4		
4	SPT	5		
5	SPT	6		
6	SPT	7		
7	SPT	8		
8	SPT	9		
9	SPT	10		
10	SPT	11		
11	SPT	12		
12	SPT	13		
13	SPT	14		
14	SPT	15		
15	SPT	16		
16	SPT	17		
17	SPT	18		
18	SPT	19		
19	SPT	20		
20				

Continued Next Page

Specific Gravity

2.6 3.0 3.4 3.8 4.2

SPECIFIC GRAVITY ◆

W_P% W% W_L%

20 40 60 80

Klohn Crippen Berger

PROJECT No.:

PROJECT: Fundão Tailings Dam Review Panel

LOCATION: Germano Pit Dam

LOGGED BY: TÜV SÜD **CHECKED BY:**

TEST HOLE LOG

STARTED: April 30, 2016 **FINISHED:** May 4, 2016
DRILL METHOD: Mud Rotary
GROUND ELEV. (m): 1002.4
COORDINATES (m): N 7766173.8 E 657272.5

Coordinates are provided in datum: WGS84/ UTM Zone 23K.

DEPTH (m)	SAMPLE TYPE	SAMPLE No.	SYMBOL	DESCRIPTION OF MATERIALS
21	SPT	21		
	SPT	22		
22	SPT	23		
23	SPT	24		
24	SPT	25		
25	SPT	26		
26	SPT	27		
27	SPT	28		
28	SPT	29		
29	SPT	30		
30	SPT	31		
31	SPT	32		
32	SPT	33		
33	SPT	34		
34	SPT	35		
35	SPT	36		
36	SPT	37		
37	SPT	38		
38	SPT	39		
39	SPT	40		
40				

Specific Gravity
2.6 3.0 3.4 3.8 4.2
SPECIFIC GRAVITY ◆

W_P% W% W_L%
× – – – – o – – – – ×
20 40 60 80

Continued Next Page

Klohn Crippen Berger

PROJECT No.:
PROJECT: Fundão Tailings Dam Review Panel
LOCATION: Germano Pit Dam
LOGGED BY: TÜV SÜD **CHECKED BY:**
SHEET 2 OF 4 **HOLE NO.:** GCSPT16-02

TEST_HOLE_SG FUNDAO TAILINGS DAM BH LOGS.GPJ KCBL_CALGARY.GDT 16-8-22

TEST HOLE LOG

STARTED: April 30, 2016 **FINISHED:** May 4, 2016
DRILL METHOD: Mud Rotary
GROUND ELEV. (m): 1002.4
COORDINATES (m): N 7766173.8 E 657272.5

Coordinates are provided in datum: WGS84/ UTM Zone 23K.

Specific Gravity 2.6 3.0 3.4 3.8 4.2
SPECIFIC GRAVITY ◆

W_P% W% W_L%
20 40 60 80

DEPTH (m)	SAMPLE TYPE	SAMPLE No.	SYMBOL	DESCRIPTION OF MATERIALS
41	SPT	41		
	SPT	42		
42	SPT	43		
43	SPT	44		
44	SPT	45		
45	SPT	46		
46	SPT	47		
47	SPT	48		
48	SPT	49		
49	SPT	50		
50	SPT	51		
51	SPT	52		
52	SPT	53		
53	SPT	54		
54	SPT	55		
55	SPT	56		
56	SPT	57		
57	SPT	58		
58	SPT	59		
59	SPT	60		
60				

Continued Next Page

Klohn Crippen Berger

PROJECT No.:
PROJECT: Fundão Tailings Dam Review Panel
LOCATION: Germano Pit Dam
LOGGED BY: TÜV SÜD **CHECKED BY:**
SHEET 3 OF 4 **HOLE NO.:** GCSPT16-02

TEST HOLE LOG

STARTED: April 30, 2016 **FINISHED:** May 4, 2016

DRILL METHOD: Mud Rotary

GROUND ELEV. (m): 1002.4

COORDINATES (m): N 7766173.8 E 657272.5

Coordinates are provided in datum: WGS84/ UTM Zone 23K.

DEPTH (m)	SAMPLE TYPE	SAMPLE No.	SYMBOL	DESCRIPTION OF MATERIALS
61	SPT	61		61.00 941.40 End of Hole at 61 m. SPT results are not reported because they are misleading.

Specific Gravity: 2.6 3.0 3.4 3.8 4.2

SPECIFIC GRAVITY ◆

W_P% W% W_L%

20 40 60 80

PROJECT No.:

PROJECT: Fundão Tailings Dam Review Panel

LOCATION: Germano Pit Dam

LOGGED BY: TÜV SÜD **CHECKED BY:**

SHEET 4 OF 4 **HOLE NO.:** GCSPT16-02

Klohn Crippen Berger

TEST_HOLE_SG FUNDAO TAILINGS DAM BH LOGS.GPJ KCBL_CALGARY.GDT 16-8-22

TEST HOLE LOG

STARTED: May 10, 2016 **FINISHED:** May 15, 2016

DRILL METHOD: Mud Rotary

GROUND ELEV. (m): 916.9

COORDINATES (m): N 7763379.4 E 659116.3

Coordinates are provided in datum: WGS84/ UTM Zone 23K.

Specific Gravity: 2.6 3.0 3.4 3.8 4.2 — SPECIFIC GRAVITY ◆

W_P% W% W_L% — 20 40 60 80

DEPTH (m)	SAMPLE TYPE	SAMPLE No.	SYMBOL	DESCRIPTION OF MATERIALS
0				EMBANKMENT FILL.
1				
2	SHK	1		
3				3.00 913.90 SILT (ML)
	SHK	2		Clayey, medium plasticity, reddish brown, chemical odour, wet, homogeneous, no cementation, high dry strength, slow dilatancy (TAILING SLIMES).
4	SHK	3		At 4m - 4.65m: Sample GSSAM16-02B-1 collected.
	SHK	4		
5	SHK	5		
6	SHK	6		At 6m - 6.65m: Sample GSSAM16-02B-2 collected.
7	SHK	7		
8	SHK	8		At 8m - 8.65m: Sample GSSAM16-02B-3 collected.
9	SHK	9		At 9m - 9.65m: Sample GSSAM16-02B-4 collected.
10	SHK	10		At 10m - 10.65m: Sample GSSAM16-02B-4 collected.
11	SHK	11		
12	SHK	12		
13	SHK	13		
14	SHK	14		
15	SHK	15		
16	SHK	16		
17	SHK	17		
18	SHK	18		
19	SHK	19		
20				

Continued Next Page

Klohn Crippen Berger

PROJECT No.:

PROJECT: Fundão Tailings Dam Review Panel

LOCATION: Germano Slimes

LOGGED BY: TÜV SÜD **CHECKED BY:**

TEST_HOLE_SG FUNDAO TAILINGS DAM BH LOGS.GPJ KCBL_CALGARY.GDT 16-8-22

TEST HOLE LOG

STARTED: May 10, 2016 **FINISHED:** May 15, 2016
DRILL METHOD: Mud Rotary
GROUND ELEV. (m): 916.9
COORDINATES (m): N 7763379.4 E 659116.3

Coordinates are provided in datum: WGS84/ UTM Zone 23K.

Specific Gravity: 2.6 3.0 3.4 3.8 4.2 — SPECIFIC GRAVITY ◆

W_P% W% W_L% — 20 40 60 80

DEPTH (m)	SAMPLE TYPE	SAMPLE No.	SYMBOL	DESCRIPTION OF MATERIALS
21	SHK	20		
22				
23	Bag	21		
24				
25	SHK	22		
26				
27	SHK	23		
28				
29	SHK	24		
30				
31				30.90 / 886.00 End of Hole at 30.9 m.
32				Photographs of samples in Attachment C5.
33				
34				
35				
36				
37				
38				
39				
40				

Klohn Crippen Berger

PROJECT No.:
PROJECT: Fundão Tailings Dam Review Panel
LOCATION: Germano Slimes
LOGGED BY: TÜV SÜD **CHECKED BY:**
SHEET 2 OF 2 **HOLE NO.:** GSSAM16-02

TEST_HOLE_SG FUNDAO TAILINGS DAM BH LOGS.GPJ KCBL_CALGARY.GDT 16-8-22

ATTACHMENT C5

Photographs of Sharky Samples from GSSAM16-02

Appendix C: Attachment C5
Photographs of Sharky Samples from GSSAM16-02

TABLE OF CONTENTS

List of Photographs taken by TÜV SÜD

The test hole log of GSSAM16-02 is presented in Attachment C4.

Photo C.C5-1 GSSAM16-02 – 2.25 m to 2.90 m

Photo C.C5-2 GSSAM16-02 – 3.75 m to 4.40 m

Photo C.C5-3 GSSAM16-02 – 4.50 m to 5.15 m

Photo C.C5-4 GSSAM16-02 – 5.25 m to 5.90 m

Photo C.C5-5 GSSAM16-02 – 6.25 m to 6.90 m

Photo C.C5-6 GSSAM16-02 – 7.25 m to 7.90 m

Photo C.C5-7 GSSAM16-02 – 8.45 m to 9.10 m

Photo C.C5-8 GSSAM16-02 – 9.25 m to 9.90 m

Photo C.C5-9 GSSAM16-02 – 10.25 m to 10.90 m

Photo C.C5-10 GSSAM16-02 – 11.25 m to 11.90 m

Photo C.C5-11 GSSAM16-02 – 12.25 m to 12.90 m

Photo C.C5-12 GSSAM16-02 – 13.25 m to 13.90 m

Photo C.C5-13 GSSAM16-02 – 14.25 m to 14.90 m

Photo C.C5-14 GSSAM16-02 – 15.25 m to 15.90 m

Photo C.C5-15 GSSAM16-02 – 16.25 m to 16.90 m

Photo C.C5-16 GSSAM16-02 – 17.25 m to 17.90 m

Photo C.C5-17 GSSAM16-02 – 18.25 m to 18.90 m

Photo C.C5-18 GSSAM16-02 – 19.25 m to 19.90 m

Photo C.C5-19 GSSAM16-02 – 20.25 m to 20.90 m

Photo C.C5-20 GSSAM16-02 – 22.25 m to 22.90 m

Photo C.C5-21 GSSAM16-02 – 24.25 m to 24.90 m

Photo C.C5-22 GSSAM16-02 – 26.25 m to 26.90 m

Photo C.C5-23 GSSAM16-02 – 28.25 m to 28.90 m

ATTACHMENT C6

Field Laboratory Test Data

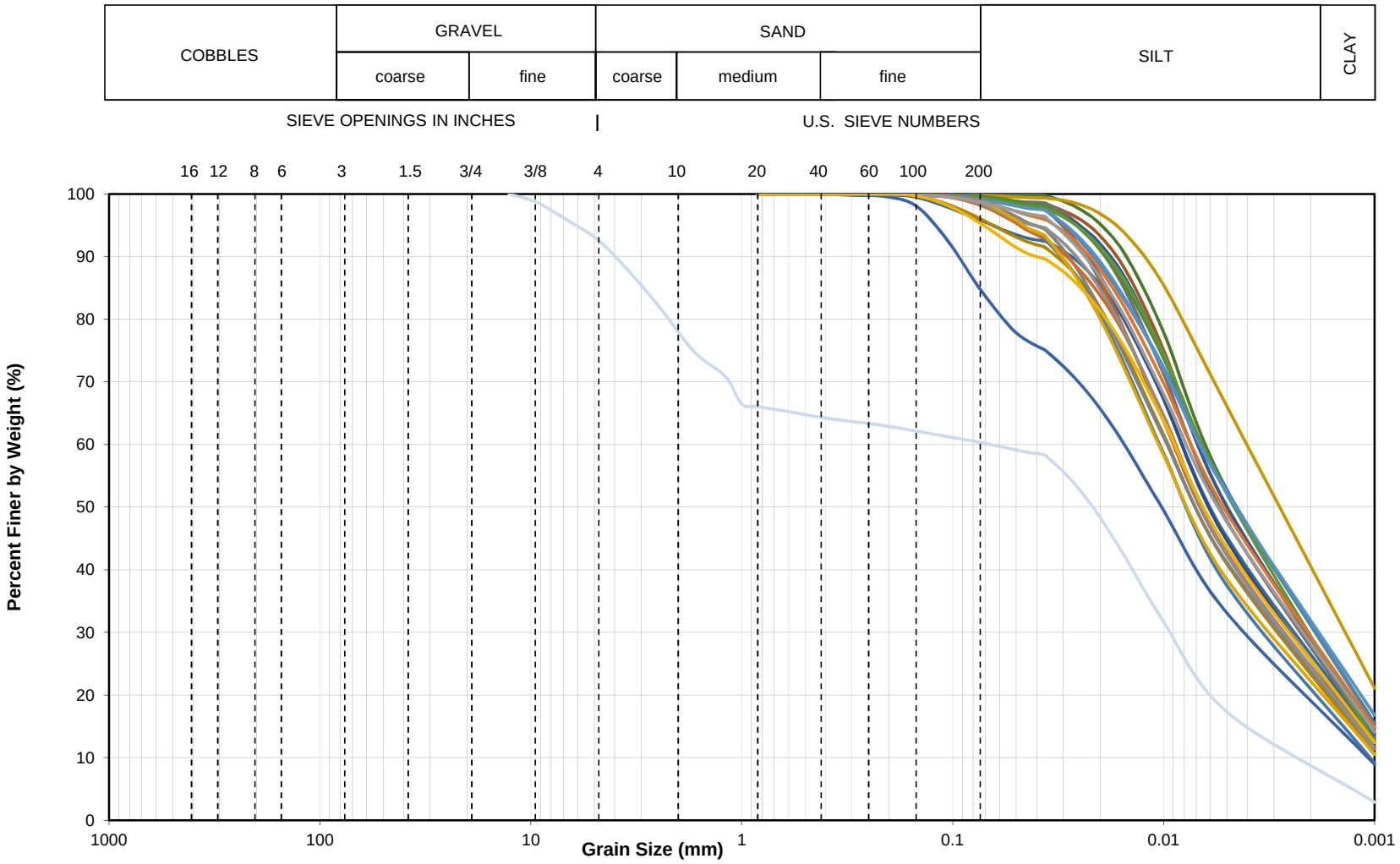

Note: Done in Brazil.

PROJECT	Fundão Tailings Dam Review Panel
TITLE	Germano Slimes Particle Size Distribution
FIG. No.	C.C6-1

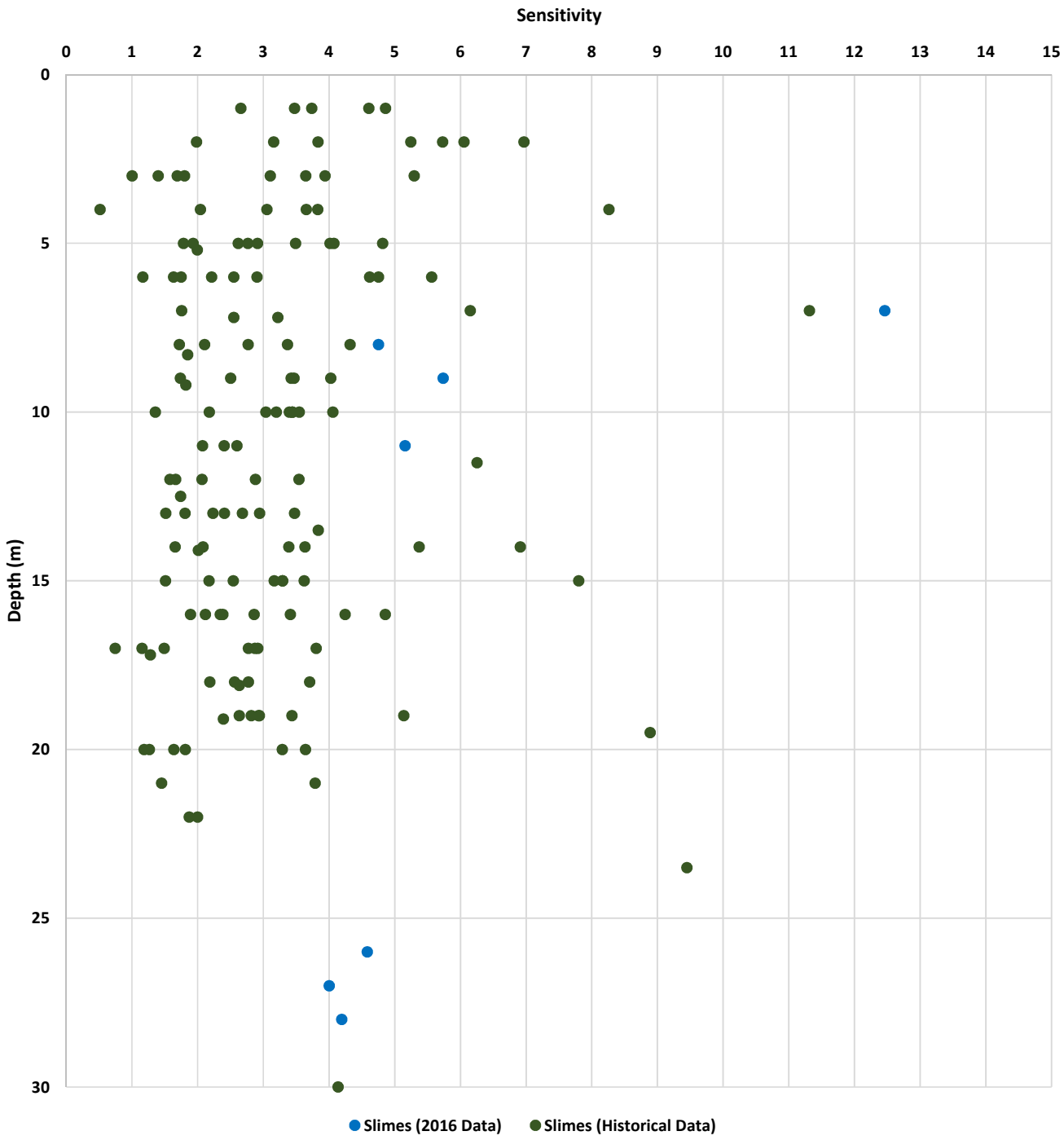

Note: Done in Brazil.

	PROJECT: Fundão Tailings Dam Review Panel
	TITLE: Germano Slimes Sensitivity vs. Depth
	FIG. No.: C.C6-2

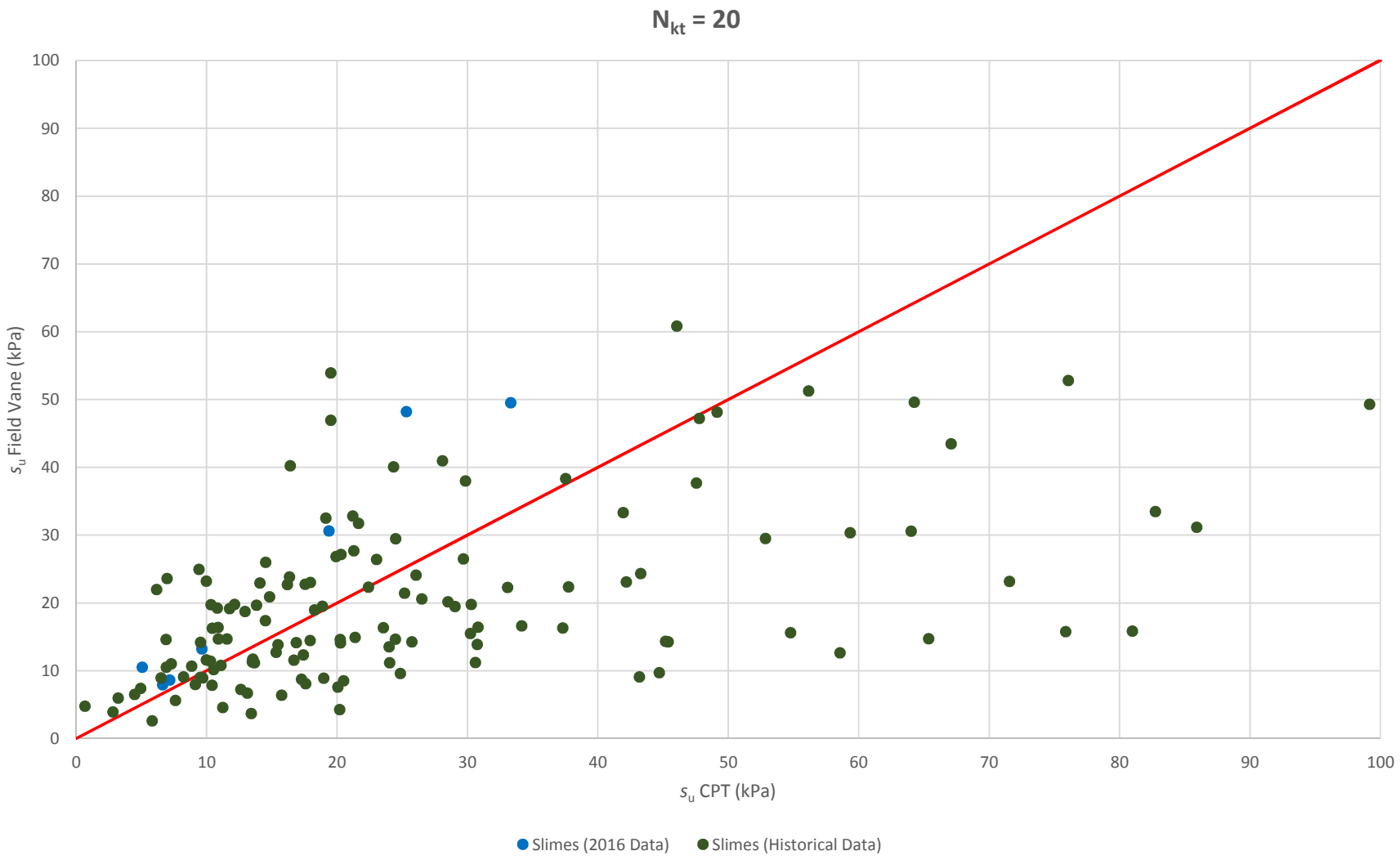

Notes:

1. CPT values are averaged over the height of field vane.
2. N_{kt} = 20 was adopted for purposes of this study.

PROJECT	Fundão Tailings Dam Review Panel
TITLE	Germano Slimes Calibration of CPT Soundings with Nilcon Field Vane
FIG. No.	C.C6-3

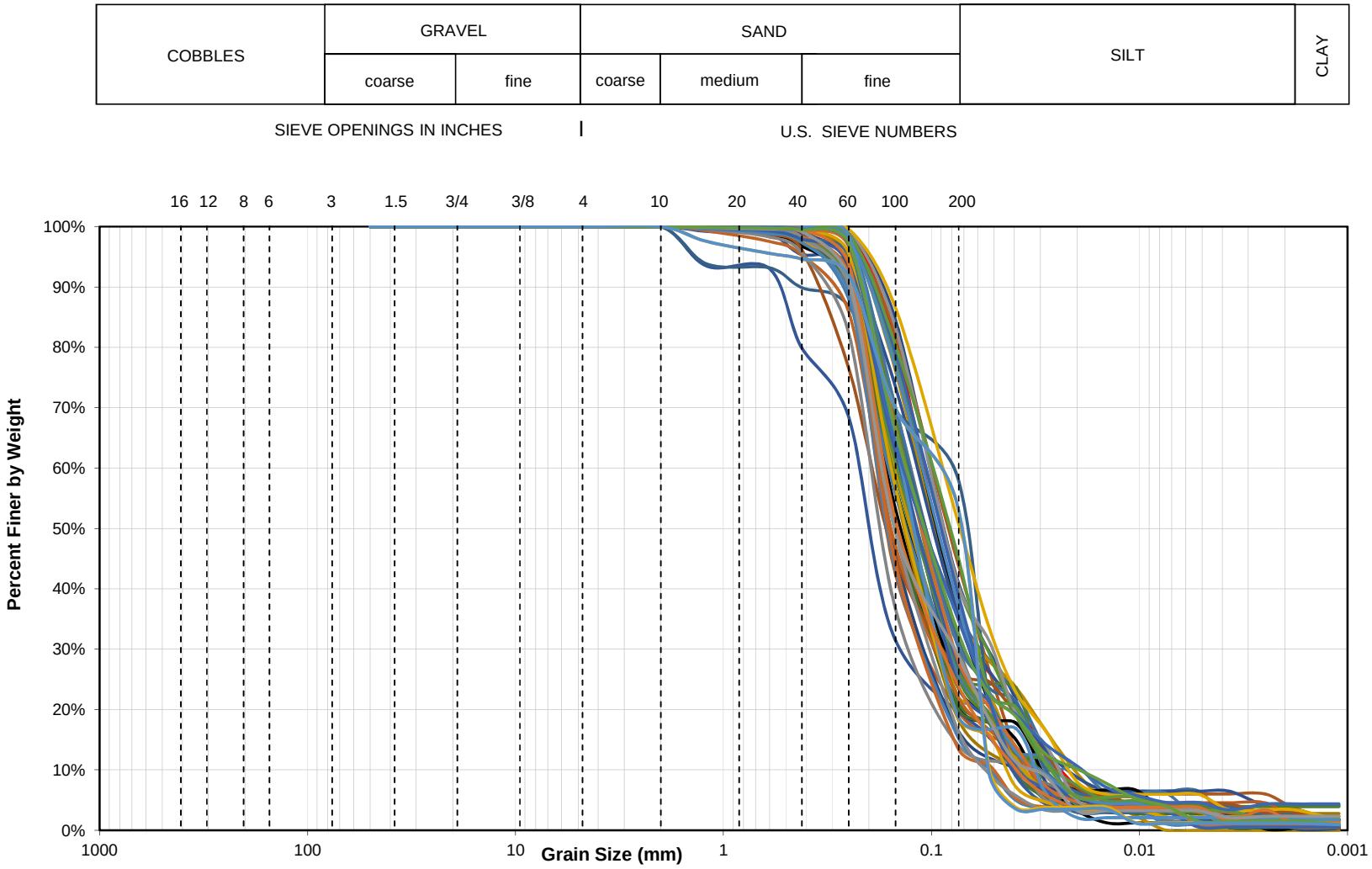

Note: Done in Brazil.

PROJECT	Fundão Tailings Dam Review Panel
TITLE	Germano Pit Dam Sand - Northeast Particle Size Distribution
FIG. No.	C.C6-4

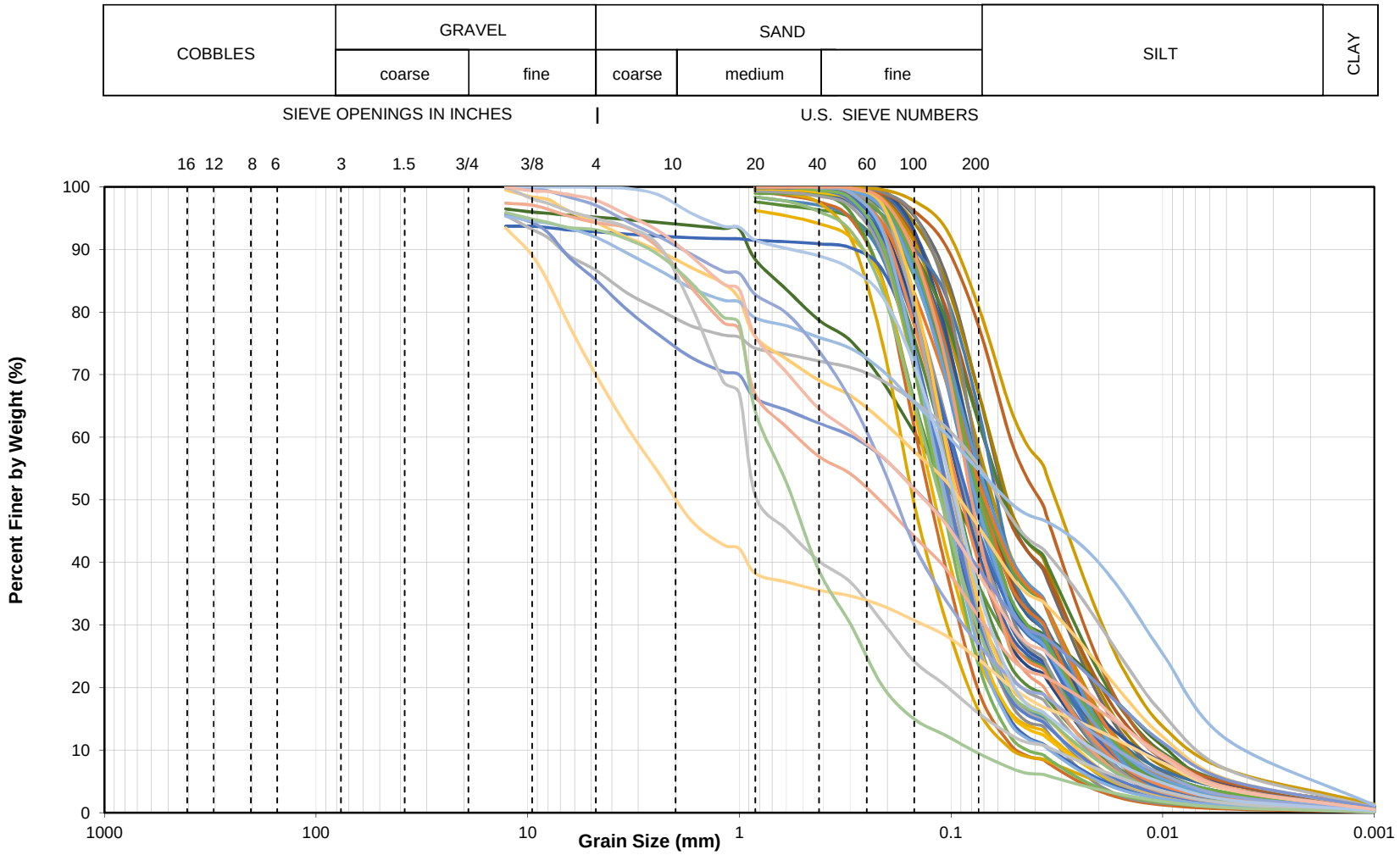

Note: Done in Brazil.

PROJECT	Fundão Tailings Dam Review Panel
TITLE	Germano Pit Dam Sand - Southwest Particle Size Distribution
FIG. No.	C.C6-5

ATTACHMENT C7

CPT Interpretative Plots

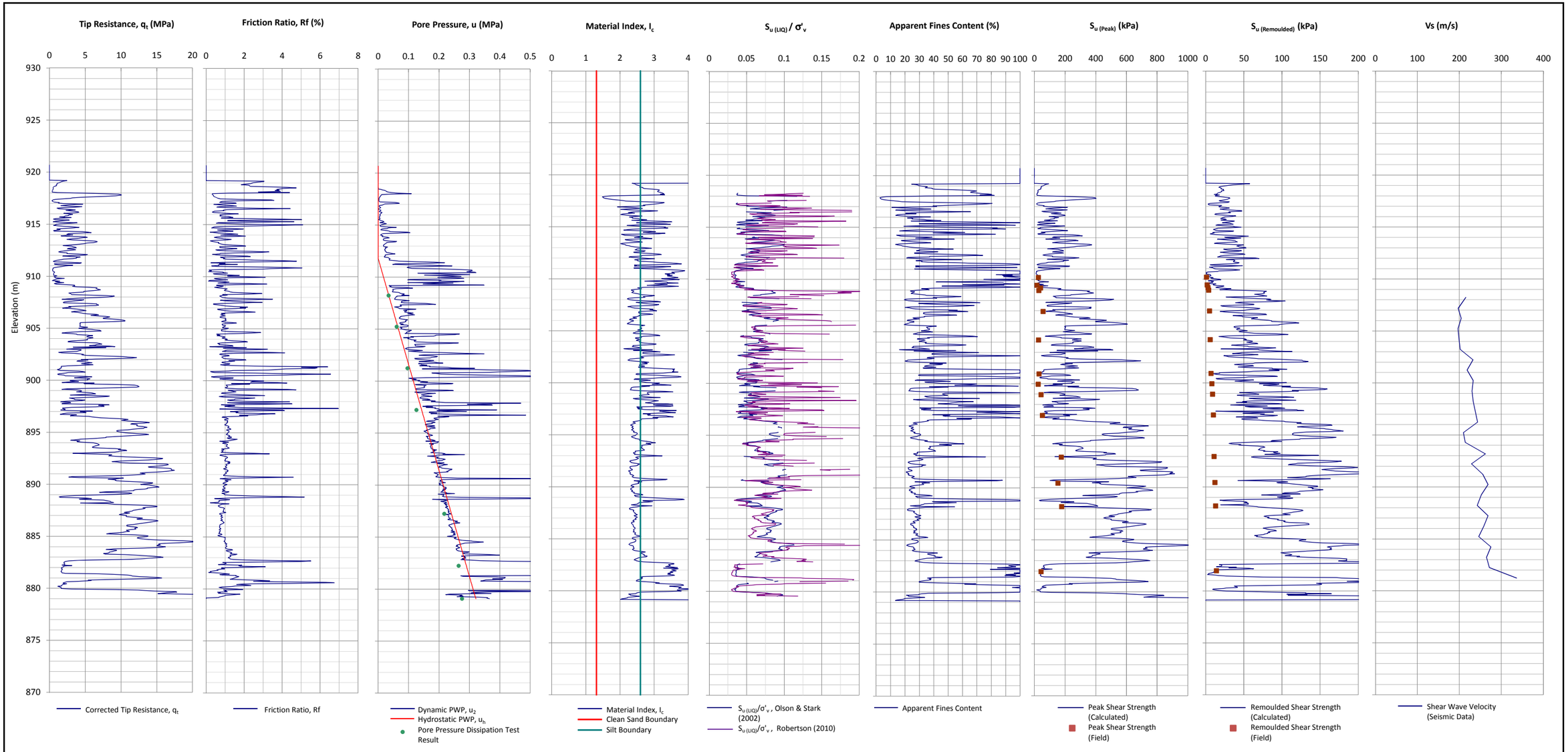

Notes:

1. This interpretation is based on the water and soil saturated unit weights γ_w=9.807 kN/m^3 and γ_{sat}=22 kN/m^3.
2. The friction ratio Rf is calculated as Rf=f_s/q_t.
3. The hydrostatic pore pressure is calculated using the ground water level (GWL) determined from CPT pore pressure dissipation tests (where available) or dynamic pore pressure.
4. Soil boundary layers (where plotted) are based on KCB interpretation.
5. The data presented have been plotted to the axis limits. Data may exist beyond the axis limits shown.
6. The Material Index (I_c) boundaries are based on Robertson and Wride (1998).
7. The $Q_{tn,cs}$ contractant/dilatant boundary=70 and is based on Robertson (2010).
8. The State Parameter (Ψ) is calculated using Plewes, et al. (1992) assuming a K0 of 0.5.
9. Coordinates are in UTM Zone 23K WGS84.

PROJECT: Fundão Tailings Dam Review Panel

TITLE: CONE PENETRATION TEST GSCPT16-02B
N:7764164.87m E:658580.161m 2016-04-24

FIGURE NO.: C.C7-1

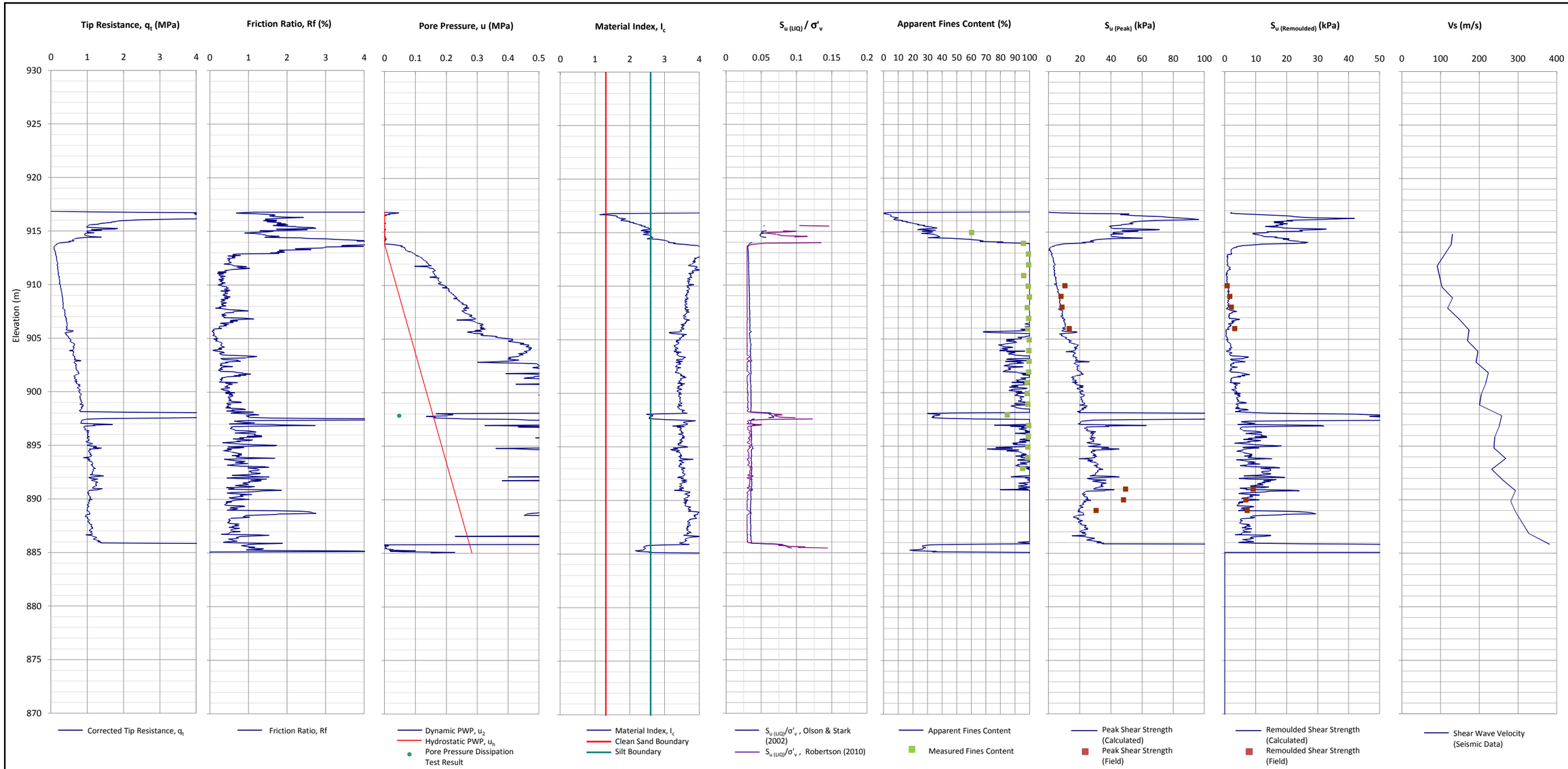

Notes:

1. This interpretation is based on the water and soil saturated unit weights γ_w=9.807 kN/m^3 and γ_{sat}=22 kN/m^3.
2. The friction ratio Rf is calculated as Rf=f_s/q_t.
3. The hydrostatic pore pressure is calculated using the ground water level (GWL) determined from CPT pore pressure dissipation tests (where available) or dynamic pore pressure.
4. Soil boundary layers (where plotted) are based on KCB interpretation.
5. The data presented have been plotted to the axis limits. Data may exist beyond the axis limits shown.
6. The Material Index (I_c) boundaries are based on Robertson and Wride (1998).
7. The $Q_{tn,cs}$ contractant/dilatant boundary=70 and is based on Robertson (2010).
8. The State Parameter (Ψ) is calculated using Plewes, et al. (1992) assuming a K0 of 0.5.
9. Coordinates are in UTM Zone 23K WGS84.

PROJECT

Fundão Tailings Dam Review Panel

TITLE

CONE PENETRATION TEST GSCPT16-05
N:7763379.344m E:659116.505m 2016-05-05

FIGURE NO.

C.C7-2

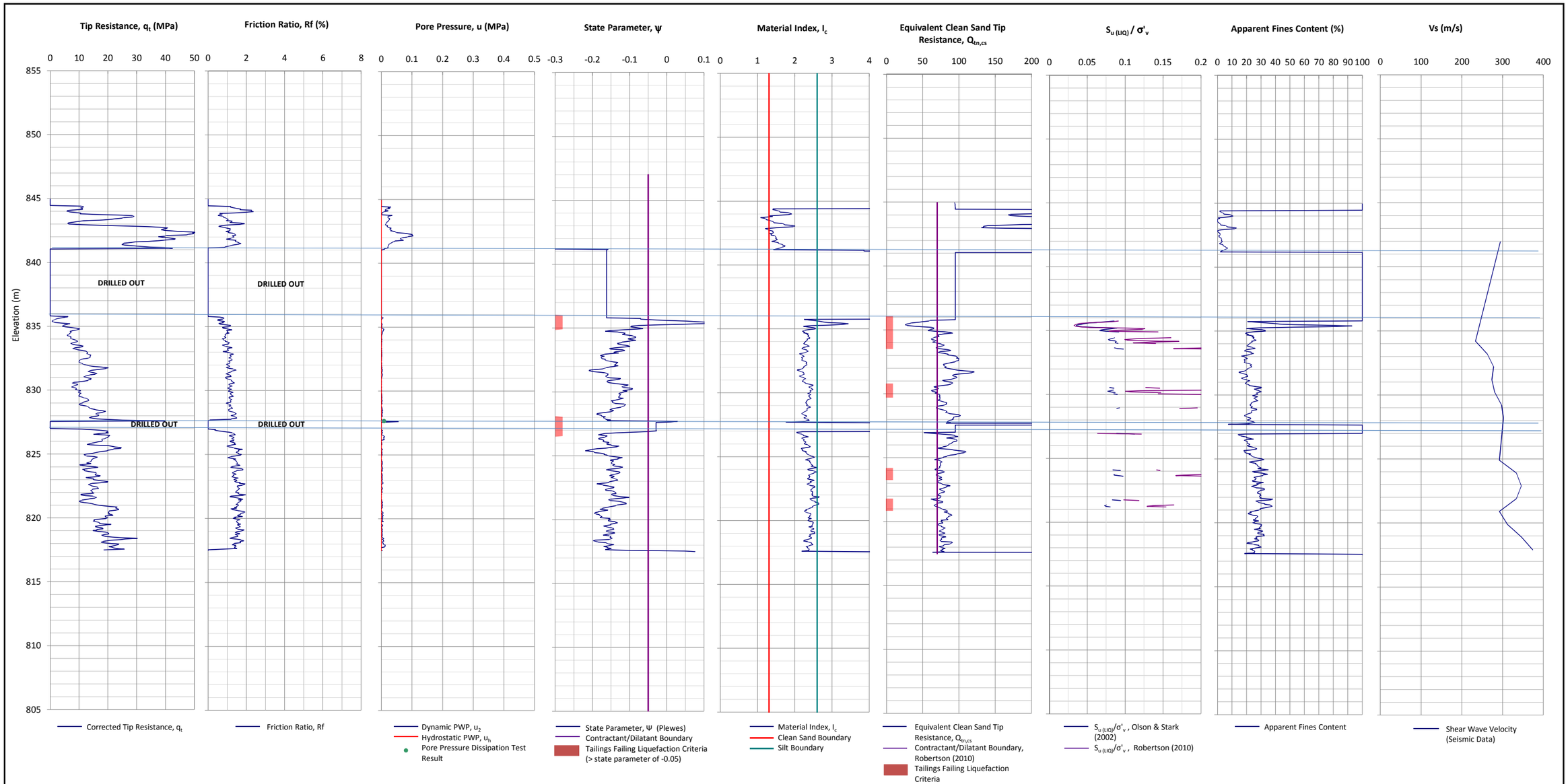

Notes:

1. This interpretation is based on the water and soil saturated unit weights γ_w=9.807 kN/m³ and γ_{sat}=22 kN/m³.
2. The friction ratio Rf is calculated as Rf=f_s/q_t.
3. The hydrostatic pore pressure is calculated using the ground water level (GWL) determined from CPT pore pressure dissipation tests (where available) or dynamic pore pressure.
4. Soil boundary layers (where plotted) are based on KCB interpretation.
5. The data presented have been plotted to the axis limits. Data may exist beyond the axis limits shown.
6. The Material Index (I_c) boundaries are based on Robertson and Wride (1998).
7. The $Q_{tn,cs}$ contractant/dilatant boundary=70 and is based on Robertson (2010).
8. The State Parameter (Ψ) is calculated using Plewes, et al. (1992) assuming a K0 of 0.5.
9. Coordinates are in UTM Zone 23K WGS84.

PROJECT
Fundão Tailings Dam Review Panel

TITLE
CONE PENETRATION TEST GBCPT16-06
N:7763631m E:660586m 2016-05-16

FIGURE NO.
C.C7-3

Liquefaction susceptibility after Robertson (2010) "Evaluation of Flow Liquefaction and Liquefied Strength Using the Cone Penetration Test"	Liquefaction susceptibility after Olson & Stark (2003) "Yield Strength Ratio and Liquefaction Analysis of Slopes and Embankments"	State parameter approximation - Robertson (2009) "Interpretation of cone penetration tests - a unified approach"

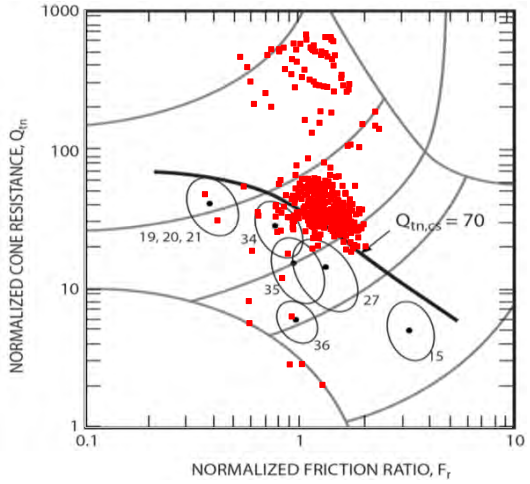

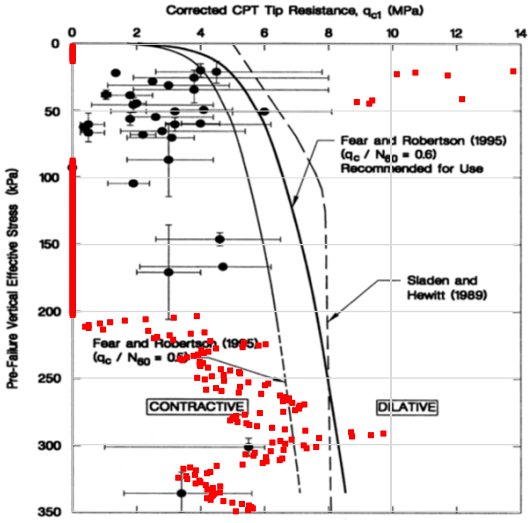

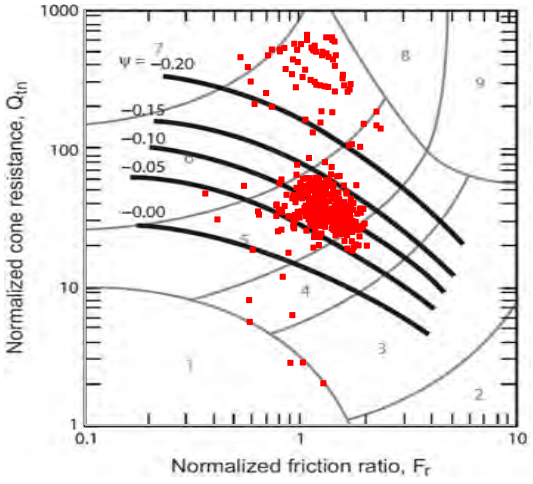

		PROJECT Fundão Tailings Dam Review Panel
		TITLE GBCPT16-06 Liquefaction Susceptibility and Soil Behavior Type
		FIGURE NO. C.C7-4

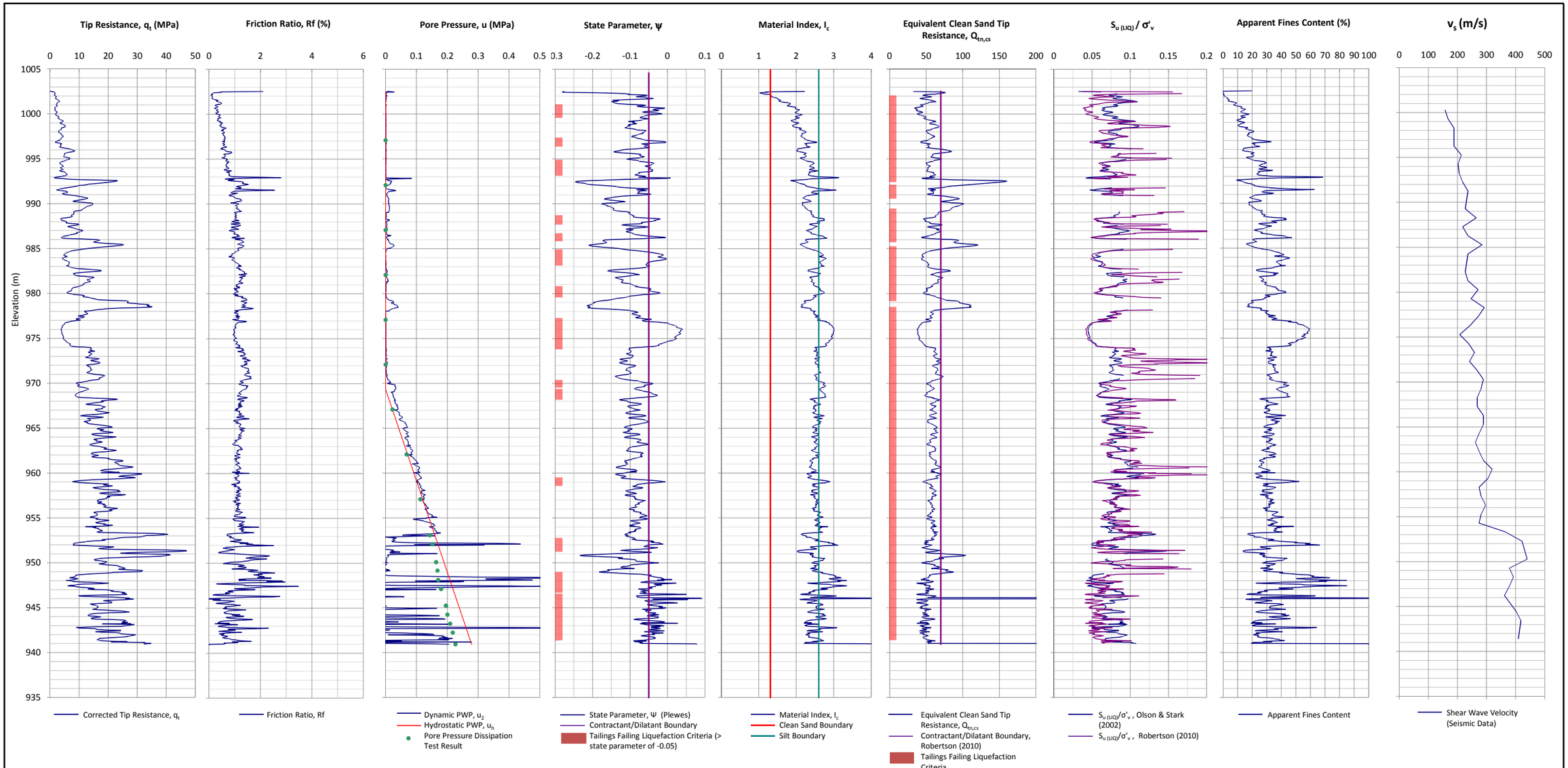

Notes:

1. This interpretation is based on the water and soil saturated unit weights γ_w=9.807 kN/m^3 and γ_{sat}=22 kN/m^3.
2. The friction ratio Rf is calculated as Rf=f_s/q_t.
3. The hydrostatic pore pressure is calculated using the ground water level (GWL) determined from CPT pore pressure dissipation tests (where available) or dynamic pore pressure.
4. Soil boundary layers (where plotted) are based on KCB interpretation.
5. The data presented have been plotted to the axis limits. Data may exist beyond the axis limits shown.
6. The Material Index (I_c) boundaries are based on Robertson and Wride (1998).
7. The $Q_{tn,cs}$ contractant/dilatant boundary=70 and is based on Robertson (2010).
8. The State Parameter (Ψ) is calculated using Plewes, et al. (1992) assuming a K0 of 0.5.
9. Coordinates are in UTM Zone 23K WGS84.

PROJECT

Fundão Tailings Dam Review Panel

TITLE

CONE PENETRATION TEST GCCPT16-03
N:7766173.838m E:657275.192m 2016-05-05

FIGURE NO.

C.C7-5

Liquefaction susceptibility after Robertson (2010) "Evaluation of Flow Liquefaction and Liquefied Strength Using the Cone Penetration Test"	Liquefaction susceptibility after Olson & Stark (2003) "Yield Strength Ratio and Liquefaction Analysis of Slopes and Embankments"	State parameter approximation - Robertson (2009) "Interpretation of cone penetration tests - a unified approach"

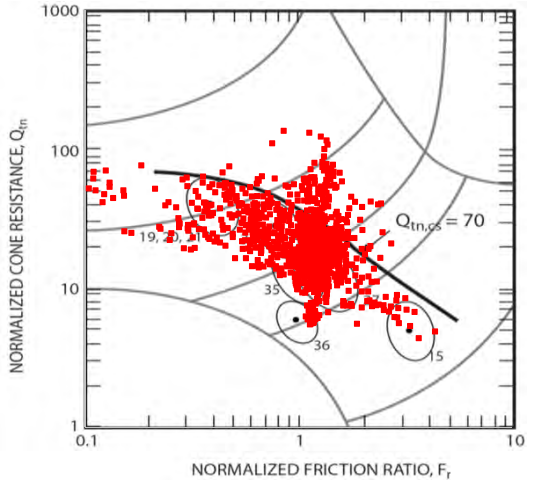

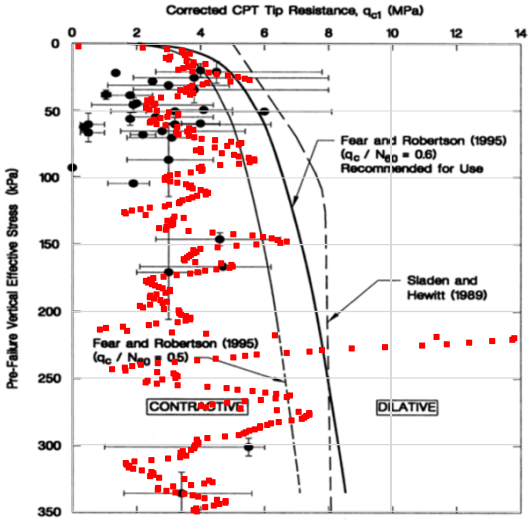

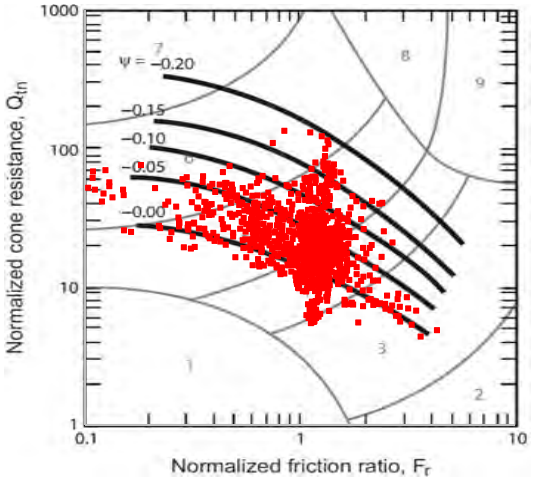

		PROJECT Fundão Tailings Dam Review Panel
		TITLE GCCPT16-03 Liquefaction Susceptibility and Soil Behavior Type
		FIGURE NO. C.C7-6

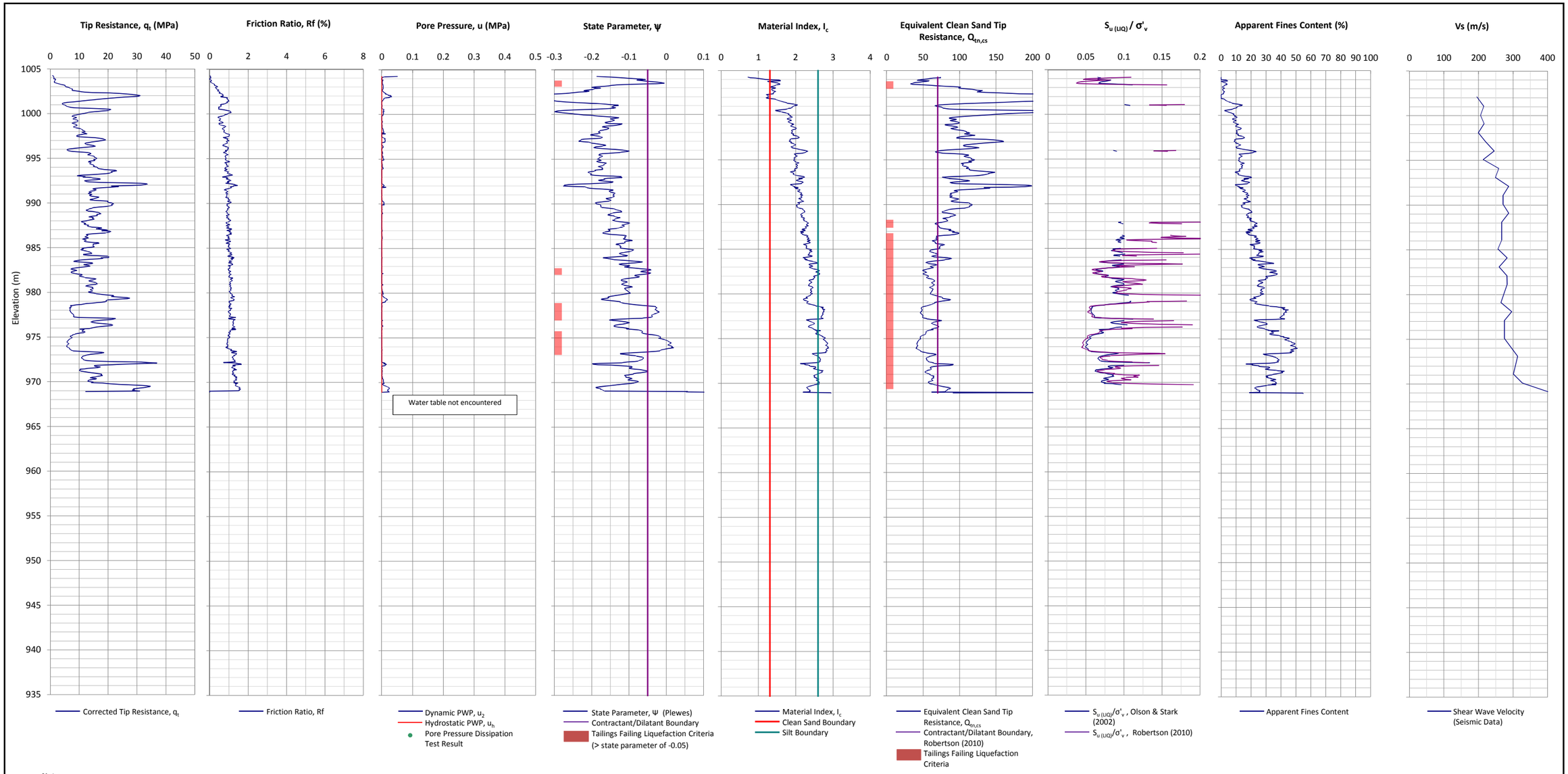

Notes:

1. This interpretation is based on the water and soil saturated unit weights γ_w=9.807 kN/m^3 and γ_{sat}=22 kN/m^3.
2. The friction ratio Rf is calculated as Rf=f_s/q_t.
3. The hydrostatic pore pressure is calculated using the ground water level (GWL) determined from CPT pore pressure dissipation tests (where available) or dynamic pore pressure.
4. Soil boundary layers (where plotted) are based on KCB interpretation.
5. The data presented have been plotted to the axis limits. Data may exist beyond the axis limits shown.
6. The Material Index (I_c) boundaries are based on Robertson and Wride (1998).
7. The $Q_{tn,cs}$ contractant/dilatant boundary=70 and is based on Robertson (2010).
8. The State Parameter (Ψ) is calculated using Plewes, et al. (1992) assuming a K0 of 0.5.
9. Coordinates are in UTM Zone 23K WGS84.

PROJECT: Fundão Tailings Dam Review Panel

TITLE: CONE PENETRATION TEST GCCPT16-04
N:7766315.865m E:657417.5m 2016-05-13

FIGURE NO.: C.C7-7

Liquefaction susceptibility after Robertson (2010) "Evaluation of Flow Liquefaction and Liquefied Strength Using the Cone Penetration Test"	Liquefaction susceptibility after Olson & Stark (2003) "Yield Strength Ratio and Liquefaction Analysis of Slopes and Embankments"	State parameter approximation - Robertson (2009) "Interpretation of cone penetration tests - a unified approach"

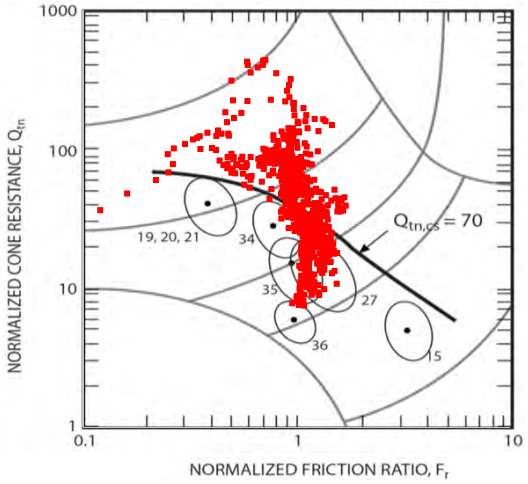

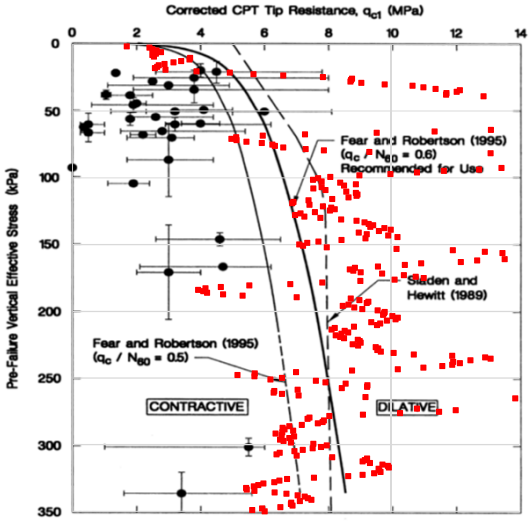

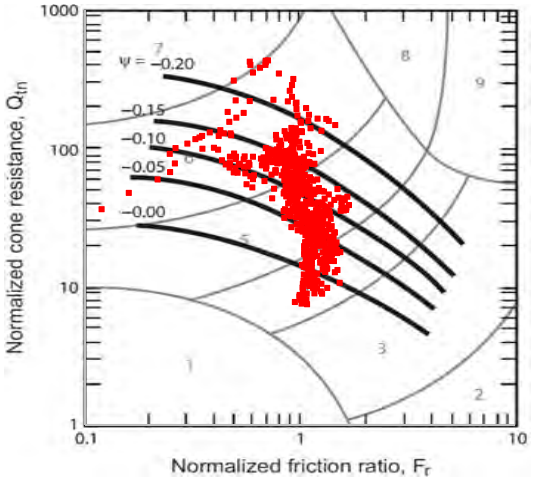

		PROJECT: Fundão Tailings Dam Review Panel
		TITLE: GCCPT16-04 Liquefaction Susceptibility and Soil Behavior Type
		FIGURE NO.: C.C7-8

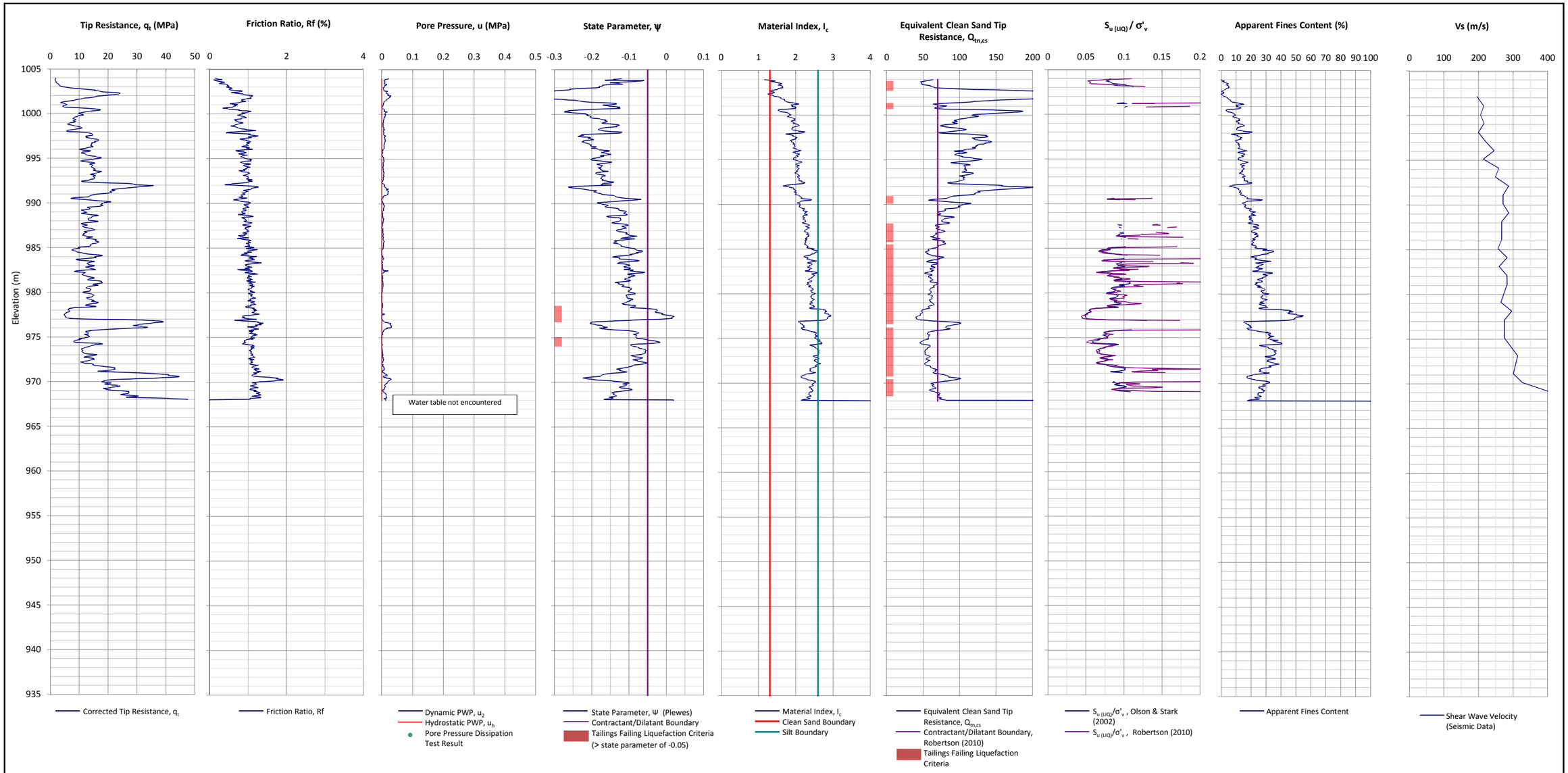

Notes:

1. This interpretation is based on the water and soil saturated unit weights γ_w=9.807 kN/m^3 and γ_{sat}=22 kN/m^3.
2. The friction ratio Rf is calculated as Rf=f_s/q_t.
3. The hydrostatic pore pressure is calculated using the ground water level (GWL) determined from CPT pore pressure dissipation tests (where available) or dynamic pore pressure.
4. Soil boundary layers (where plotted) are based on KCB interpretation.
5. The data presented have been plotted to the axis limits. Data may exist beyond the axis limits shown.
6. The Material Index (I_c) boundaries are based on Robertson and Wride (1998).
7. The $Q_{tn,cs}$ contractant/dilatant boundary=70 and is based on Robertson (2010).
8. The State Parameter (Ψ) is calculated using Plewes, et al. (1992) assuming a K0 of 0.5.
9. Coordinates are in UTM Zone 23K WGS84.

PROJECT: Fundão Tailings Dam Review Panel

TITLE: CONE PENETRATION TEST GCCPT16-04B
N:7766315.865m E:657417.684m 2016-05-13

FIGURE NO.: C.C7-9

Liquefaction susceptibility after Robertson (2010) "Evaluation of Flow Liquefaction and Liquefied Strength Using the Cone Penetration Test"	Liquefaction susceptibility after Olson & Stark (2003) "Yield Strength Ratio and Liquefaction Analysis of Slopes and Embankments"	State parameter approximation - Robertson (2009) "Interpretation of cone penetration tests - a unified approach"

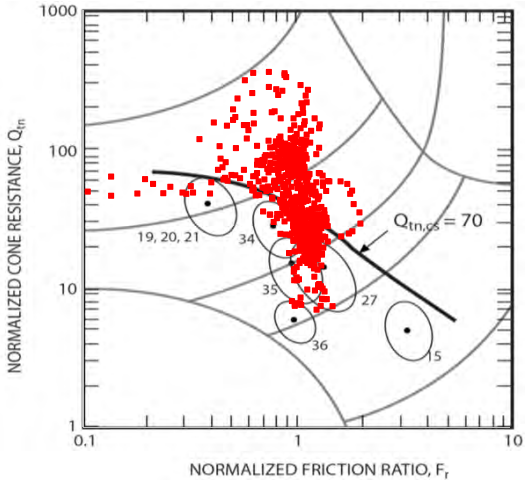

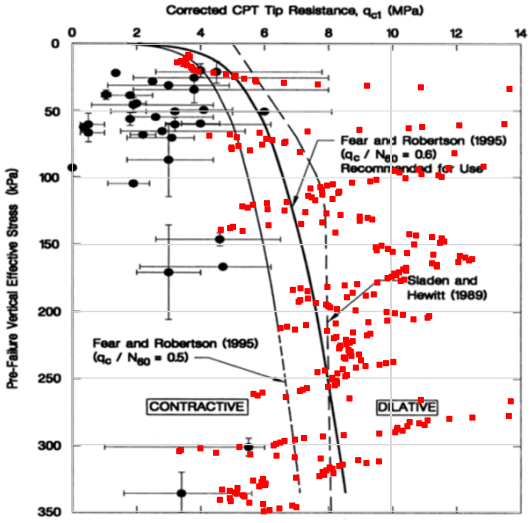

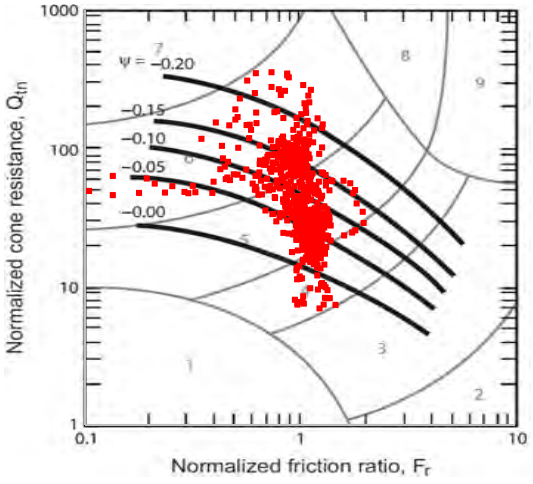

		PROJECT Fundão Tailings Dam Review Panel
		TITLE GCCPT16-04B Liquefaction Susceptibility and Soil Behavior Type
		FIGURE NO. C.C7-10

ATTACHMENT C8

Test Fill Data

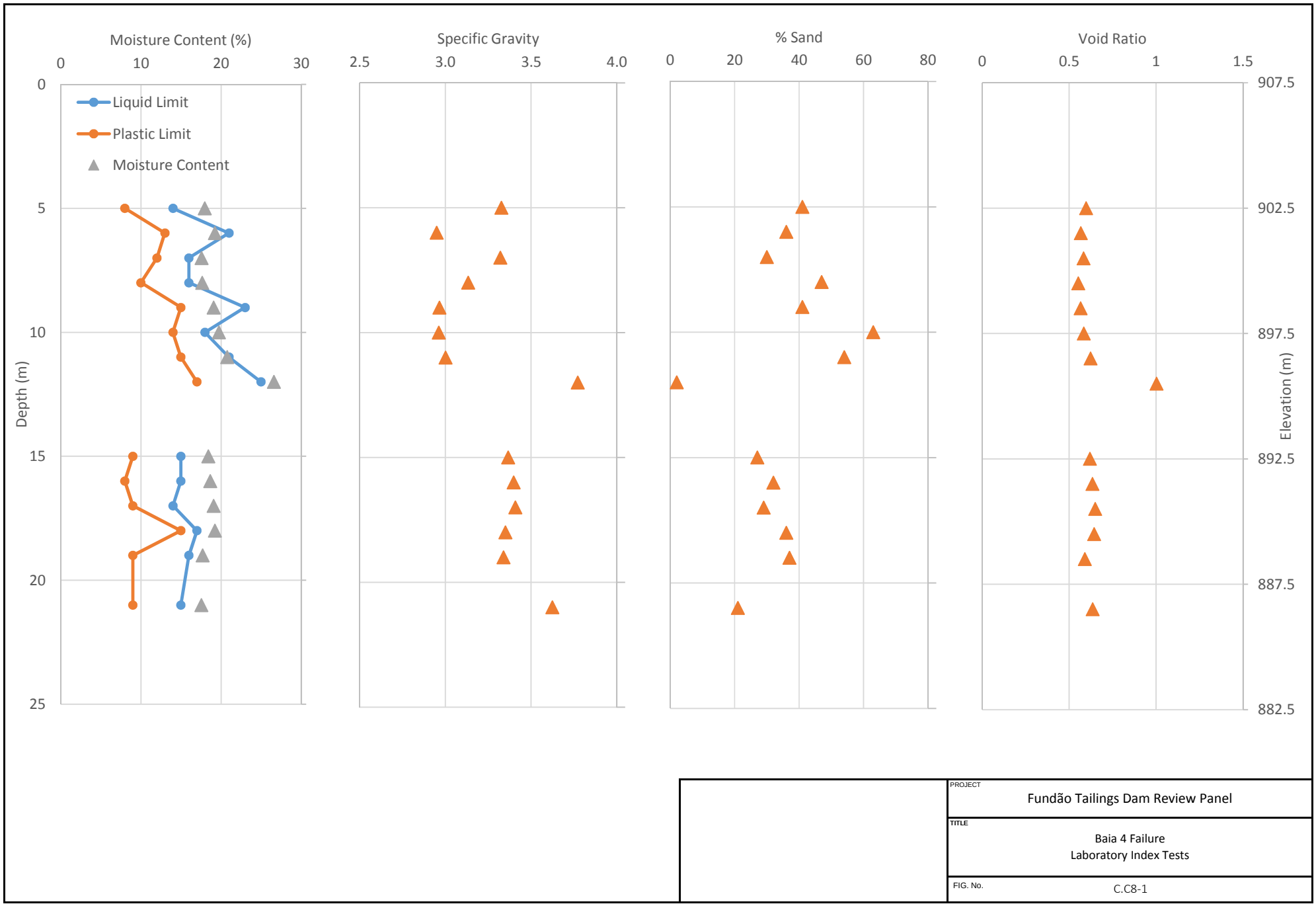

PROJECT
Fundão Tailings Dam Review Panel

TITLE
Baia 4 Failure
Laboratory Index Tests

FIG. No.
C.C8-1

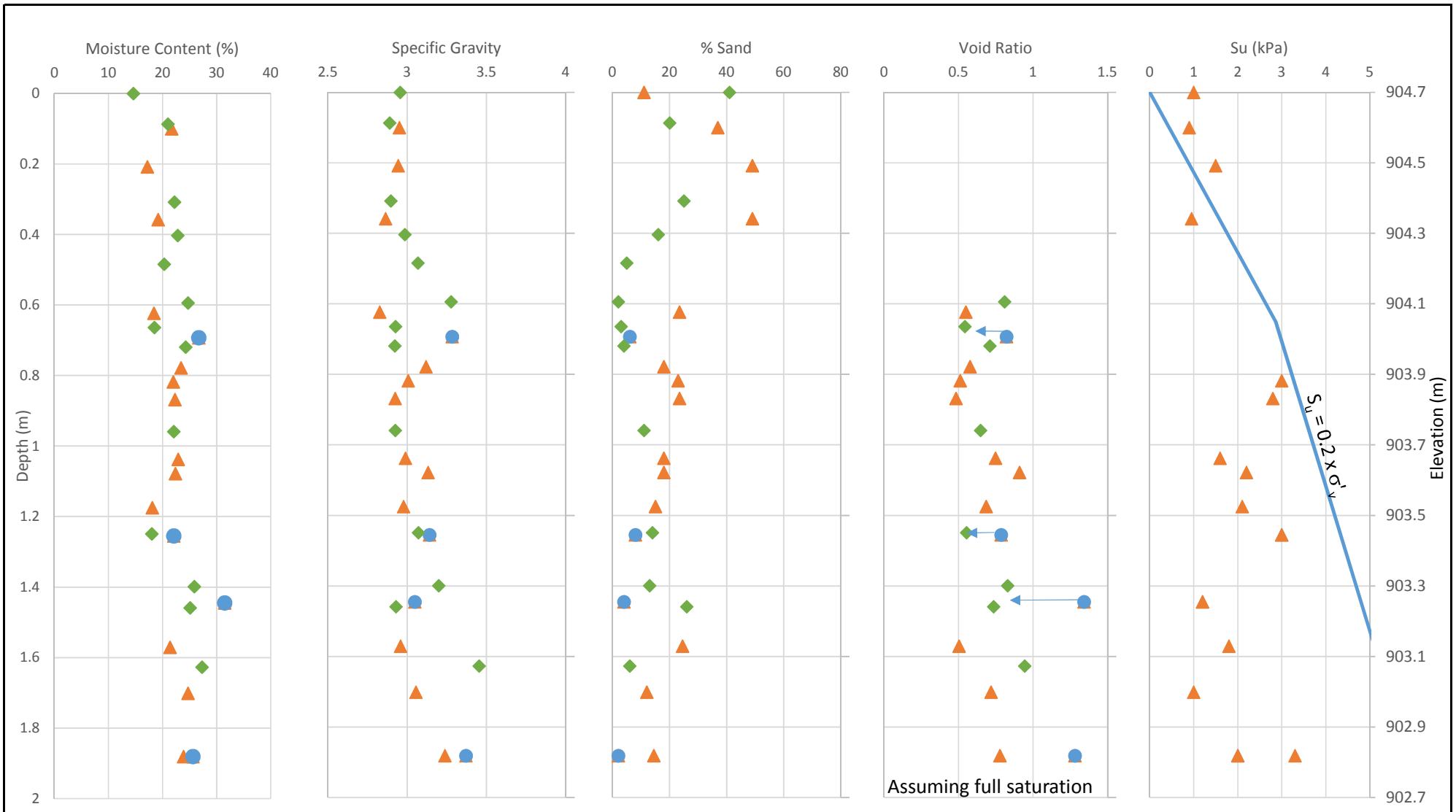

LEGEND

- Result before trial
- Result before trial classified as "chocolate" (slimes)
- Result after trial

PROJECT	Fundão Tailings Dam Review Panel
TITLE	2008 Test Fill Laboratory Index Tests (Pre- and Post-Trial)
FIG. No.	C.C8-2

APPENDIX C

Field Geotechnical Data and Interpretation

Appendix C
Field Geotechnical Data and Interpretation

TABLE OF CONTENTS

TABLE OF CONTENTS

(continued)

List of Tables

List of Figures

List of Attachments

C1 INTRODUCTION

This appendix summarizes the pre-failure geotechnical investigation data available to the Panel and describes the Panel's 2016 geotechnical data obtained from its field program. The search of the pre-failure data was done with two main goals. The first was to obtain any drill holes or CPTs on the left abutment that penetrated the slimes that were thought to be present between elevations 830 m and 850 m based on slimes mapping in Appendix B. Although a 2014-2015 CPT beach program on the left abutment was found that provided reliable sand tailings information, none of the profiles penetrated 850 m. The second goal was to obtain engineering properties of the tailings from in situ measurements prior to failure. That goal was partially met. While field data acquisition followed local practice, there were many uncertainties as to the quality of the pre-failure data so the Panel mounted its own field investigation.

Section C2 lists the field investigation programs that were identified and reviewed by the Panel. The most valuable of these programs are described in more detail in Section C2 with data featured in Attachment C1. Section C3 describes the Panel investigation program. The Panel program was designed to determine the three basic tailings profiles which would have existed at Fundão: sand tailings with no slimes, interbedded slimes and sands where the interbedding ranges from discrete layering to mixing of sand tailings and slimes, and slimes with no sand tailings. The Panel selected locations that served as proxies for all three profiles: Germano Buttress and Germano Pit Dam for sand tailings and two other locations on the Germano plateau for slimes and interbedded slimes and sand tailings.

Three investigation contractors were used for the Panel investigation. The first was the Brazilian affiliation of Fugro, the second was Pattrol, a Brazilian firm, and the third was ConeTec, a Canadian cone testing contractor. Fugro had done much work at Samarco, whereas ConeTec had never been to the site. Most of the Panel investigation program was done with ConeTec to be independent of past investigation practice. Pattrol had a minor role in supplying field equipment but also did laboratory testing as described in Appendix D.

Section C4 describes the Baia 4 dike failure in 2005 and derives strength parameters by back analyses. Two other instrumented trial embankments are also described in Section C4.

C2 PRE-FAILURE INVESTIGATION DATA

C2.1 General

The numerous pre-failure field investigation programs are compiled and listed in Table C2-1 below. Figure C2-1 shows the locations of selected past drill holes and CPT locations by Samarco. Past investigation programs were first filtered by keyword from the master spreadsheet of available Samarco reports and data sources; primarily in Portuguese. After translation into English, the coordinates and elevations of the data were confirmed. Then the field data was evaluated and tabulated.

Some of the data in Table C2-1 was more useful to the Panel than others. Where the field data was used directly in the Panel Investigation, that utility is referenced in the right hand column of the table. Where the program was used directly in the Panel Investigation, the data is given in Attachment C1 of this appendix.

The investigation data in Table C2-1 may or may not have been included in an engineering report. In many cases, the data by itself was found in the Samarco database. Thus, the description of the program in the table is the sole reference to that data source.

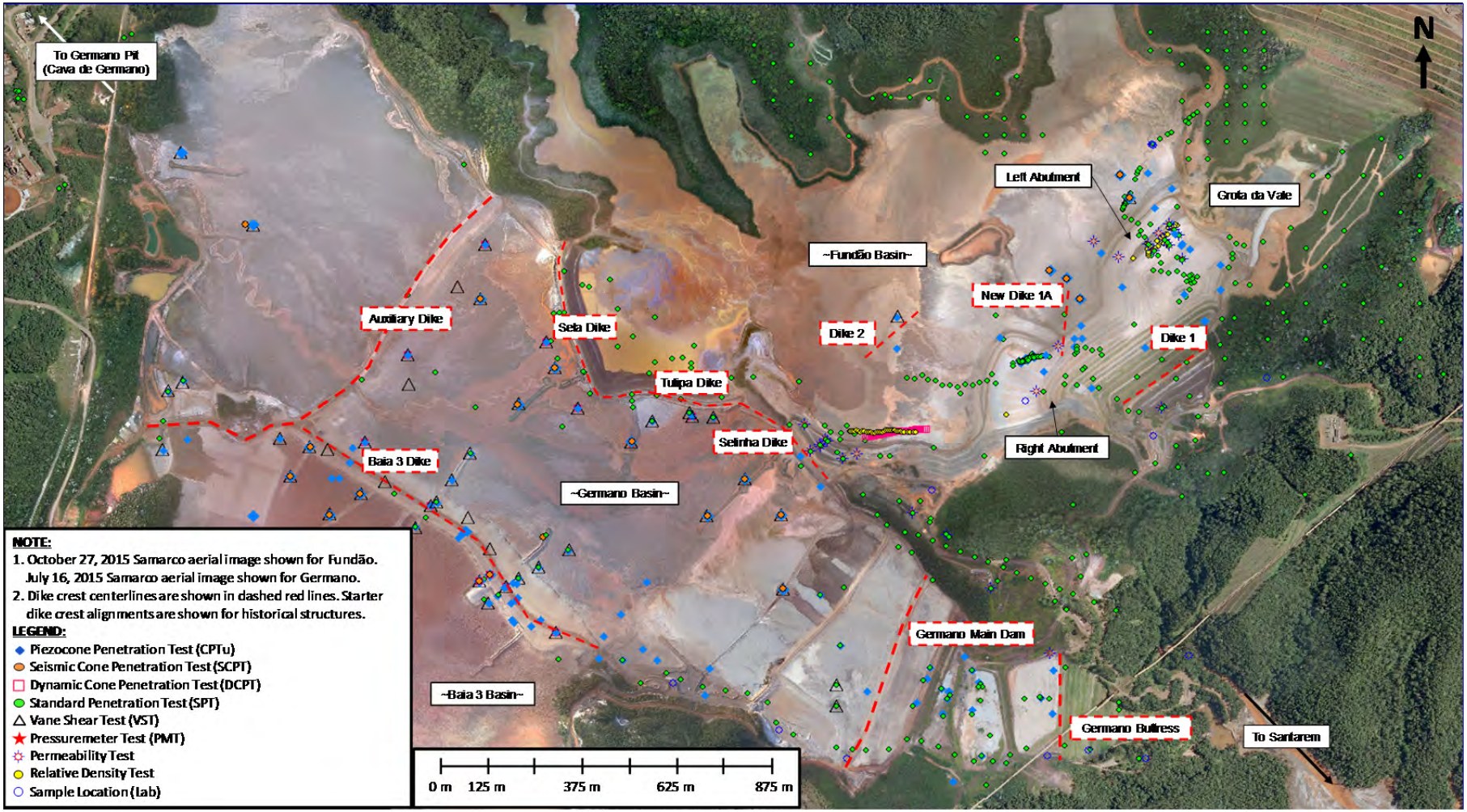

Figure C2-1 Pre-failure geotechnical investigation location plan

Table C2-1 Summary of pre-failure field programs

Start Date	End Date	Origin	Area	Description	Referenced In[(1)]
October 2003	May 2005	Samarco	Coordinates not available	Tailings Characteristics - Gradation, Grain Density, Metallurgy	N/A
January 2004		UFV/UFOP	Coordinates not available	Tailings Characteristics - Gradation, Plasticity, Permeability	N/A
May 2005	August 2005	UFOP/UFV	Germano Pit	Specific Gravity, Gradation, Permeability	N/A
May 2005	June 2005	Setes	Downstream Fundão	SPT	N/A
August 2006	August 2006	UFV	Germano	Lab Tests - Compaction, Gradation, Plasticity, Triaxial, Specific Gravity, Void Ratio, Permeability, Oedometer	N/A
August 2006	September 2006	DeltaGeo	Germano	CPT, DPT, SPT, SCPT, VST	N/A
January 2007	February 2007	SETES	Coordinates not available	SPT	N/A
January 2007	March 2008	Camter	Coordinates not available (Dam Material)	Gradation	N/A
March 2007	July 2007	Progeo	Fundão	SPT	N/A
July 2007	July 2007	Chammas Engineering	Germano	Direct Shear, Gradation, Plasticity, Triaxial, Specific Gravity	N/A
July 2007	September 2007	UFV/Pimenta	Germano	CPT, SPT, Direct Shear, Compaction, Gradation, Plasticity, Triaxial, Specific Gravity, Permeability, Oedometer	N/A
July 2008	July 2008	Geolabor	Fundão	Gradation, Plasticity, Triaxial, Permeability, Oedometer, Specific Gravity	N/A
June 2009	June 2009	Geolabor	Germano; Fundão	Gradation, Triaxial, Specific Gravity, Void Ratio, Permeability	N/A
November 2009	November 2009	Pimenta de Ávila	Dike 1	Compaction	N/A
September 2010	October 2010	DeltaGeo	Fundão	Direct Shear, Compaction, Gradation, Plasticity, Triaxial, Permeability	N/A
September 2010	December 2010	DeltaGeo	Baia 3, Aux Dike, Main Gallery, Secondary Gallery	CPT, SPT, VST	N/A
December 2010	July 2011	DeltaGeo	Main Gallery	SPT	N/A
February 2011	February 2011	DeltaGeo	Dike 1	SPT	N/A
February 2011	April 2011	DeltaGeo	Main Gallery	SPT	N/A

Start Date	End Date	Origin	Area	Description	Referenced In[(1)]
April 2011	May 2011	DeltaGeo	Secondary Gallery	SPT	N/A
May 2011	July 2011	DeltaGeo	Secondary Gallery	SPT	N/A
July 2011	July 2011	DeltaGeo	New Dike 1A	CPT	Appendix B: Section B6
July 2011	July 2011	Terratek	Baia 3	CPT, SCPT	N/A
August 2011	September 2011	DeltaGeo	Secondary Gallery	SPT	N/A
August 2011	August 2011	DeltaGeo	Secondary Gallery	SPT	N/A
October 2011	November 2011	DeltaGeo	Dike 2	CPT, VST	N/A
November 2011	December 2011	DeltaGeo	Baia 3	CPTu	N/A
November 2011	April 2012	Fugro/Chammas	Between Fundão/Germano	SPT, Geo-electric Imaging	N/A
July 2012	November 2012	DeltaGeo	Secondary Gallery	SPT	N/A
August 2012	August 2012		Coordinates not available	Relative Density, Specific Gravity, Triaxial	N/A
September 2012	July 2013	DeltaGeo	Dike 1	CPT, DPT, SPT, Permeability	Panel Report: Section 5.14 Appendix B: Section B6.7
January 2013	January 2013	DeltaGeo	Secondary Gallery	Gradation, Plasticity, Triaxial, Specific Gravity	N/A
January 2013	March 2013	DeltaGeo	Plant (Tailings)	Specific Gravity, Void Ratio, Permeability, Inclinometer, Settlement	N/A
February 2013	February 2013	Geoestavel	Fundão	Specific Gravity, Void Ratio, Permeability, Inclinometer, Settlement	N/A
April 2013	May 2013	DeltaGeo	Selina; Tulipa	SPT	N/A
September 2013	February 2014	Geobrito	Germano, Fundão, Off-site, Quarry	SPT, Gradation, Plasticity, Triaxial, Specific Gravity, Permeability, Oedometer	N/A
December 2013	January 2013	DeltaGeo	Dike 1	Gradation, Plasticity, Specific Gravity, Permeability	N/A
January 2014	February 2014	Chammas Engineering	Downstream Germano and Fundão	Direct Shear, Gradation, Plasticity, Triaxial, Permeability, Oedometer	N/A
January 2014	February 2014	Fugro	Germano Dam	SPT	N/A
February 2014	February 2014	Fugro	Germano	CPT	N/A
February 2014	April 2014	Fugro	Sela; Tulipa	CPTu, SPT	N/A
February 2014	May 2014	Fugro	Dike 1	Relative Density, Compaction	N/A
March 2014	May 2015	Fugro	Germano Pit and Santarem	SPT	N/A

Start Date	End Date	Origin	Area	Description	Referenced In[1]
April 2014	April 2014	Fugro	Dike 1	CPTu	Panel Report: Section 6.3
May 2014	May 2014	Diefra	Germano	Gradation, Plasticity, Triaxial, Specific Gravity	N/A
June 2014	July 2014	Fugro	Germano Pit	SPT	N/A
June 2014	September 2014	BVP Engenharia	Dike 2	DCPT, Relative Density	N/A
June 2014	August 2014	Fugro	Grota da Vale	SPT	Panel Report: Section 5.1.4 Appendix B: Section B6.7 Appendix G: Section G3.3.3 Appendix K: Section K2.3.2
June 2014	May 2015	Fugro	Left Abutment	SPT (Energy), SPT, Permeability	Panel Report: Section 5.1.4 Appendix B: Section B5.3.5.3 and Section B6.7
July 2014	July 2014	Fugro	Dike 1	Permeability	N/A
September 2014	March 2015	Fugro	Dike 1, Germano Basin	CPT, DCPT, PMT, Seismic, VST	Panel Report: Section 4.2 Appendix H: Section H2 Appendix I: Section I2.3.1 Appendix J: Section J3.2
February 2015	February 2015	Geocontrole	Germano Pit	SPT	N/A
March 2015	July 2015	Fugro	Germano Basin	CPT, SPT, VST	Appendix C: Attachment C1 and Attachment C7 (CPT parameter derivation)
May 2015	May 2015	Fugro	Fundão	SPT	N/A
June 2015	June 2015	Fugro/Geocontrole	Dike 1	CPTu, SPT	Panel Report: Section 5.1.4, Section 6.3 Appendix B: Section B6.7
June 2015	October 2015	Fugro	Dike 1, Germano	Relative Density	N/A
June 2015	June 2015	Fugro	Germano	CPTu	N/A
November 2015	November 2015	Fugro	Germano	CPTu	N/A

1. N/A = Not Applicable. Program is not referenced in the main report or appendices, and was not used as part of the Investigation.

C2.2 Specific Programs

The data from pre-failure field programs used by the Panel is described below. Interpretative CPT plots produced by KCB and other data reduction results are given by program name in Attachment C1.

C2.2.1 DeltaGeo (July 2011)

DeltaGeo undertook an investigation in July, 2011 along the crest of New Dike 1A at about El. 823 m. The investigation comprised 4 cone penetration tests (CPTu) with pore pressure measurements. The purpose of New Dike 1A was to keep active sand deposition in the Dike 1 reservoir away from the area of the Main Gallery jet grouting repairs. The four CPT profiles show little evidence of slimes. Two of the four CPTs met refusal at about El. 808 m. A plan of this program is presented in Attachment C1, Figure C.C1-1.

C2.2.2 DeltaGeo (September 2012 – July 2013)

DeltaGeo completed an extensive field test program between September, 2012 and July, 2013. The investigation included 6 CPTs, 52 Standard Penetration Tests (SPTs), 41 Dynamic Cone Penetration Tests (DPT), and 52 permeability tests. Only the locations of the June, 2013 CPTs are presented together with the CPT profiles. Much of the rest of the program was on natural ground so is not relevant to the Panel Investigation on tailings. There are minor indications of slimes in CPTu-04.

A plan of the CPT holes is presented in Attachment C1, Figure C.C1-2.

C2.2.3 Fugro (April 2014)

Fugro completed six CPTs in April, 2014, spanning across Dike 1. These holes were limited in depth, but provided information on the ground condition near the instability that developed in August, 2014.

A plan of these tests can be found in Attachment C1, Figure C.C1-3.

C2.2.4 Fugro (June 2014 – August 2014)

Fugro undertook an investigation from June, 2014 to August, 2014 in Grota da Vale. The investigation included 8 SPTs. The data was reviewed to assess the presence of slimes. A location plan for these SPTs is included in Attachment C1, Figures C.C1-4.

C2.2.5 Fugro (June 2014 – May 2015)

Between June, 2014 and May, 2015, Fugro installed 32 piezometers on Fundão Dam (Dike 1). At 10 of these piezometers, there were permeability tests done. Generally, there was an installation log and a SPT log for each piezometer installation. The piezometers were reviewed to determine the piezometric elevation across Fundão Dam and specifically across the left abutment. A plan of these tests is presented on Figure C.C1-5 with several SPT logs.

C2.2.6 Fugro (September 2014 – March 2015)

Fugro completed an investigation between September, 2014 and March, 2015 across Fundão (near Dike 1) and across the Germano basin. The investigation across Fundão comprised 6 CPTs and 5 SCPTs. The remaining 23 CPTs, 21 SCPTs, 2 pressuremeter tests (PMT), 16 vane shear tests (VST) and 2 pore pressure dissipation tests were undertaken across the Germano basin. Apageo, a separate drilling company from Fugro, completed the PMTs. A location plan of these tests is presented on Figure C.C1-6.

The CPT data was reviewed to assess the presence of slimes. CPTs F-01, F-02, F-04, and F-05 show slimes present across Fundão, specifically upstream of the left abutment and near the Fundão basin island, all above El. 850 m. Interpretative CPT logs are provided in Attachment C1, following Figure C.C1-6.

C2.2.7 Fugro (March 2015 – July 2015)

Fugro completed a field program between March, 2015 and July, 2015 across the Germano basin. The investigation comprised 26 CPTs, 15 SPTs, and 12 VSTs. A location plan is provided in Attachment C1, Figure C.C1-7 with interpretative CPT logs.

C2.2.8 Fugro/Geocontrole (June 2015)

In June, 2015, Fugro and Geocontrole completed a number of tests at Fundão. Fugro performed 9 CPTs, while Geocontrole performed 8 SPTs.

A 2016 VOGBR study[37] used the SPT and CPT data independently to determine the liquefaction susceptibility of the region. The CPT data analysis showed that the region was more susceptible to liquefaction than inferred from the SPT data analysis. The report notes that since SPTs may be affected more easily by procedural errors than CPTs, the SPT results should be disregarded.

A location plan is included in Attachment C1, Figure C.C1-8. SPT logs and interpretative CPT logs are also provided.

C2.3 Data Reduction

Where raw data was available from the pre-failure programs, the data was processed using standard methods to establish a common format for interpretation. In light of the expected range of specific gravity and void ratio for the sand and slimes, a single bulk unit weight of 22 kN/m^3 was applied to all materials in our interpretation. The variation of saturated bulk unit weight with specific gravity and void ratio is calculated using the following formula: $\gamma = \frac{G_s+e}{1+e}\gamma_w$, and is illustrated on Figure C2-2.

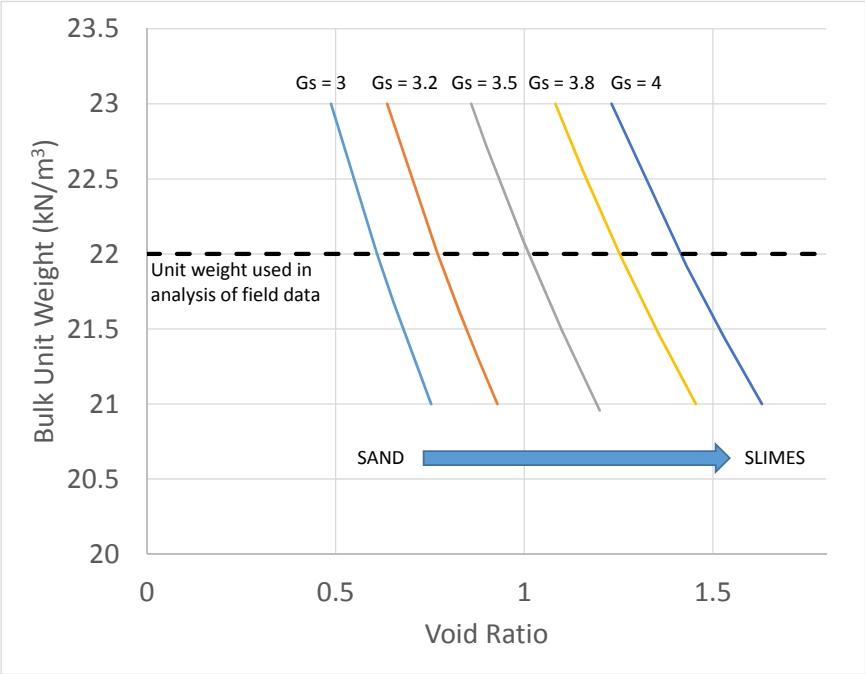

Figure C2-2 Void ratio/unit weight relationship

This unit weight was also used throughout the interpretation of the Panel field data, and within the analyses presented in other appendices.

C2.4 Data Gaps

The pre-failure investigation data available from Samarco was extensive but did not contain enough information for the Panel to complete its Investigation. Most importantly, there were no CPT or SPT test holes identified from the 2015 crest of the left setback that went to bedrock which could have been used to confirm the presence of slimes. This could not be rectified by post-failure field investigations so an extensive review of the history of tailings deposition at Fundão was undertaken, as described in Appendices A and B.

There were insufficient laboratory test results on tailings and slimes samples collected from these programs to conduct the analytical programs proposed by the Panel. To that end, the Panel collected disturbed surface samples of sand tailings and slimes on three separate occasions from the sole remnant of the Fundão Dam, the Germano Pit Dam, and the plateau area of Germano. That surface sampling program is described in Appendix D. Again, that test program was not sufficient to carry out the Panel analysis, which required in situ properties of the key material types: sand tailings, slimes, and interbedded sands and slimes. Acquisition of these material properties became a principal objective of the Panel program.

A report by VOGBR[37] identified a discrepancy between SPT and CPT results in sand tailings for the Fundão Dam. Resolution of this issue became a specific goal of the Panel program because reliance

on one or the other data set would have led to much different conclusions about liquefaction susceptibility. That resolution is described in the next section.

Several CPTu Fundão beach profiles by Samarco contained reliable data that could be used by the Panel for standard liquefaction susceptibility assessments of the sand tailings. However, the Panel required additional downhole shear wave velocity data, which had to be obtained to proceed with any seismic shaking analysis. Thus, the Panel designed a program using a seismic CPTu cone to collect this data on every profile. Additionally, MASW (Multichannel Analysis of Surface Waves) tests were done at several locations by a Brazilian contractor to obtain data in the weathered phyllite for seismic shaking analysis using SHAKE2000 (see Appendix J).

In general, the properties of the slimes were not well quantified in past in situ investigations. There was a lack of vane shear s_u data, shear wave velocity data, and laboratory test results on undisturbed samples. Obtaining properties of the slimes also became a principal objective of the Panel program.

The Baia 4 Dike on Germano failed by static liquefaction during raising in September, 2005. Back analysis of this failure was done to estimate large-strain strengths of the interbedded sands and slimes at this location. The original field investigation program through the interbedded tailings sand and slimes lacked some data, so SCPTu profiling through interbedded sands and slimes was added to the Panel program.

C3 PANEL FIELD PROGRAM

C3.1 Scope

To close the data gaps identified above, the Panel completed a field investigation program between April 19 and May 27, 2016 at locations on the Germano tailings impoundment and the Germano Pit tailings impoundment. The Panel program included SCPTu with downhole shear wave velocity, compressional wave velocity, and resistivity in all three material types, “undisturbed” sampling (Sharky samples) of the slimes, vane shear tests in the slimes, and SPTs in the sand tailings.

The ConeTec field report is included as Attachment C2. Their cone equipment was attached to Pattrol’s equipment at first, and later to a D8 bulldozer. Fugro supplied a drilling rig and personnel to conduct SPTs. Personnel from TÜV SÜD, a Brazilian engineering company, were present during most of the Panel investigation. KCB designed the investigation under the direction of the Panel and attended some of the field work, especially the first part of each testing type where techniques had to be developed in the field.

The investigation locations are shown on Figure C3-1. The test holes are numbered to reflect the test location and the testing type. The test holes start with one of the following two letters to denote general location:

- GS = Germano Slimes
- GB = Germano Buttress
- GC = Germano Pit Dam (Germano “Cava”)

Figure C3-1 shows two locations on the plateau of the Germano tailing impoundment where the test locations start with "GS". The area marked "Interbedded Slimes" was drilled from an existing rockfill berm that had been pushed out over interbedded sands and slimes many years ago. The tailings would have consolidated under this rockfill weight over the period of loading. The other location with test locations marked "GS" is marked "pure" slimes. A berm had to be constructed to access this area of ponded water over slimes. Samarco pumps pond water from this location so this is likely the low point in the impoundment. The other two locations GB and GC were on sand tailings; GB on the 825/845 m berms on the Germano Buttress and GC on the beach of the Germano Pit dam. The test hole locations and test types are listed on Table C3-1.

In addition, the test hole numbering includes the following to identify the test type:

GS/GB/GC-xx-16-yy

Where:

xx signifies the type of investigation:

- CPT = Cone penetration test
- VST = Field vane
- SPT = Standard penetration test
- SAM = Samples
- DEN = In situ density test

yy signifies the test hole number (01, 02, 03, etc.)

The completed field investigations included:

- Germano Slimes (2 locations at "pure slimes" and "interbedded" sands and slimes):
  - 2 Seismic Cone Penetration Test (SCPT) holes
  - 2 boreholes for Nilcon field vane tests
  - 2 boreholes for collection of Sharky samples of the slimes
- Germano Buttress (two locations):
  - 1 Seismic Cone Penetration Test (SCPT) hole (4 attempts met refusal)
- Germano Pit Dam crest (two locations):
  - 3 Seismic Cone Penetration Test (SCPT) holes
  - 2 boreholes for Standard Penetration Tests (SPT), including energy measurements and for the collection of samples
- MASW surveys:
  - 3 MASW surveys - Multi-channel analysis of surface waves (MASW)

Samples collected from the boreholes were used for index testing; including moisture contents, specific gravity and particle size distribution (PSD). A summary of the sampling and testing at each location is presented in Table C3-1 and is described later in this appendix.

The following section summarizes the field investigation procedures.

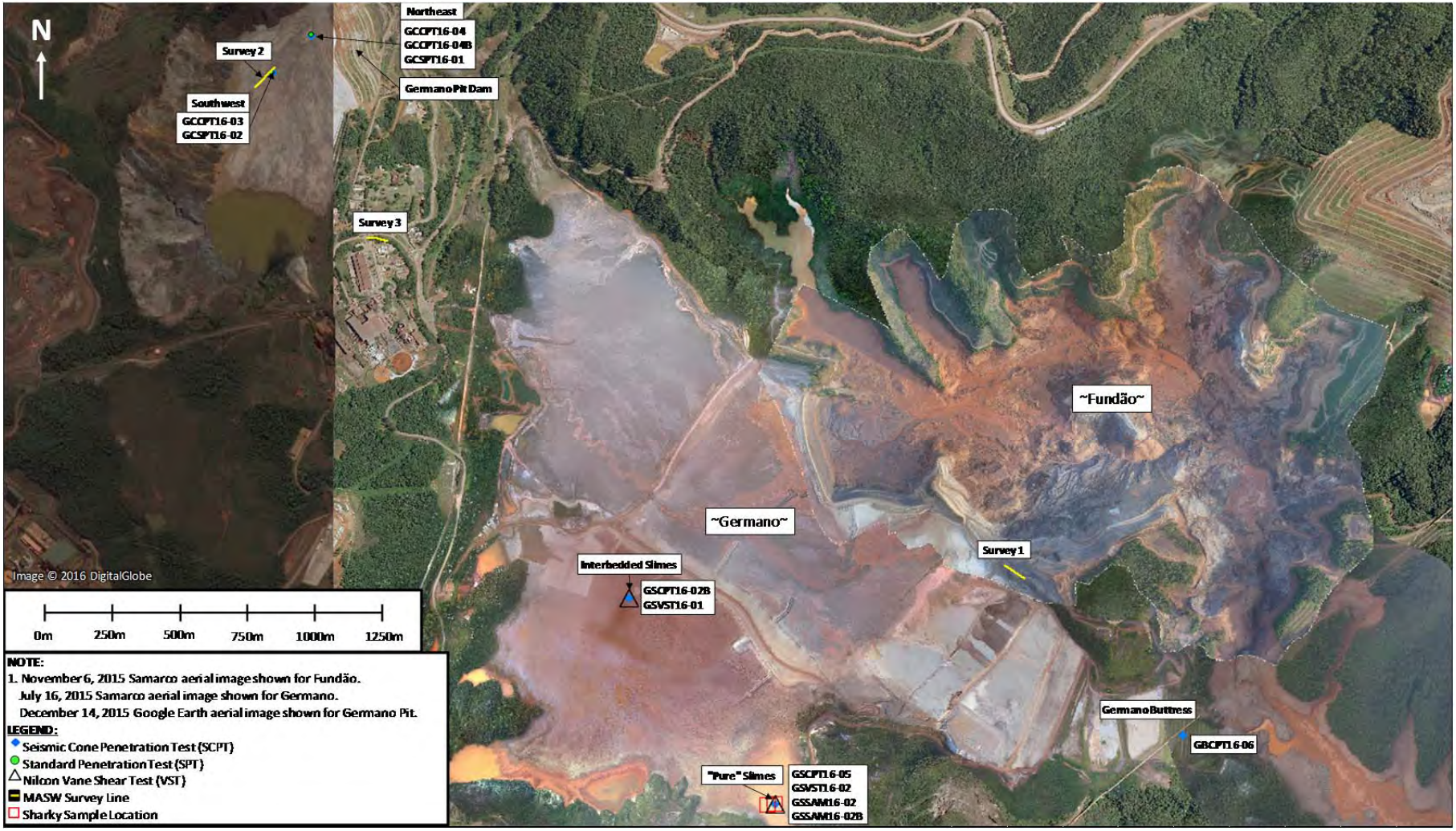

Figure C3-1 2016 geotechnical investigation location plan

Table C3-1 2016 Panel field investigation test locations

Hole ID	Northing[1] (m)	Easting[1] (m)	Ground Elevation[2] (m)	Drilling Depth (m)	SCPT/CPT Depth (m)	No. of Nilcon Field Vanes Tests Completed	No. of Sharky Samples Recovered	Notes
Germano Slimes (GS)								
GSCPT16-02B	7,764,164.9	658,580.2	920.7	-	41.7	-	-	
GSCPT16-05	7,763,379.3	659,116.5	916.9	-	31.9	-	-	
GSVST16-01	7,764,164.8	658,582.4	920.4	-	-	15	-	
GSVST16-02	7,763,379.1	659114.8	917.0	-	-	7	-	
GSSAM16-02	7,763,379.4	659,116.3	916.9	30.9	-	-	23	
GSSAM16-02B	7,763,375	659,092	916.9	10.0	-	-	4	See Note 3
Germano Buttress (GB)								
GBCPT16-06	7,763,641.1	660,611.2	845.9	-	27.50	-	-	See Note 3
Germano Pit Dam (GC)								
GCCPT16-03	7,766,173.8	657,275.2	1,002.6	-	61.7	-		
GCCPT16-04	7,766,314.6	657,417.5	1,004.3	-	35.4	-		
GCCPT16-04B	7,766,315.9	657,417.7	1,004.3	-	36.4	-		
GCSPT16-01[5]	7,766,319.0	657,417.6	1,004.4	60.2	-	-		
GCSPT16-02[5]	7,766,173.8	657,272.5	1,002.4	60.3	-	-		

1. The coordinates are given in UTM Zone 23 South WGS84 (as per ConeTec's 2016 report, see Attachment C2).
2. Elevations provided by TÜV SÜD.
3. Location not surveyed by TÜV SÜD. Coordinates based upon ConeTec (2016) found in Attachment C2, and elevation assumed based upon adjacent boreholes.
4. GBCPT16-01, 1B, 1C, 2 and 6B given in the ConeTec report are not listed here because all met refusal so did not produce any useful data.
5. SPT results not reported because data is misleading.

C3.2 Field Investigation Methods

C3.2.1 Sharky Sampling of Slimes at GSSAM16-02

Sharky sampler boreholes were completed at two slimes locations in GSSAM16-02 and GSSAM16-02B. These test holes were completed using a Boart Longyear LX6 rig. The sampler was operated by ConeTec. The Sharky sampling system procedure is described in Attachment C2.

This method was used to obtain a continuous series of slimes samples that were used for index property and triaxial testing. The Sharky samples were sealed, and were transported to Samarco's on site laboratory for index testing. Four slimes samples were taken in GSSAM16-02B and shipped to Pattrol's geotechnical laboratory in Belo Horizonte for triaxial tests which are given in Attachment D7.

C3.2.2 In Situ Testing

In situ testing consisted of a combination of SCPTs, SPTs with energy measurements, and Nilcon vane tests and MASW surveys. The Nilcon field vanes were conducted in the slime deposits and the SPTs with energy measurements were conducted on the sand tailings. The SCPTs were undertaken on both the slimes and sand tailings deposits.

The SPT energy measurements, SCPTs, and Nilcon Vane tests were completed by ConeTec (see Attachment C2). The SPTs were done by Fugro and the MASW survey was conducted by AFC Geofisica Ltda. (see Attachment C3).

The SCPTs were carried out using a seismic piezocone with either 10 cm^2 or 15 cm^2 end areas, a net area ratio of 0.8 and a 60 degree apex angle. Tip resistance and sleeve friction measurements were collected at 0.05 m depth intervals while the cone was pushed into the ground at a rate of 2 cm/s. Dynamic pore pressure measurements were taken continuously during each SCPT test using a pore pressure filter located in the u2 position directly behind the cone tip. The Panel tests are not differentiated from each other using the designation CPTu, since, unlike the pre-failure tests, the "u" is common to all of the Panel testing. Pore pressure dissipation tests were undertaken in all test holes at selected depth intervals to give an indication of the static pore pressure. The seismic measurements were made during the SCPTs using a horizontal geophone that was incorporated within the cone, approximately 0.2 m behind the tip. The geophone recorded shear waves and compression waves that were generated at the ground surface.

The Nilcon vane tests were generally completed using a 110 mm and 50 mm diameter vane (GSVST16-01) and a 150 mm and 75 mm diameter vane (GSVST16-01 and GSVST16-02). "Peak", "residual" and "remolded" undrained shear strengths were generally recorded during these tests. The vane shear test results are given on the nearest CPT profile.

Shear wave velocity was determined at three locations using MASW by AFC Geofisica Ltda. (AFC) along 100 m survey lines. The equipment included a Geode seismograph with 24 channels, which was connected to two spread cables with 12 take-outs, which were attached to 24 vertical 4.5 Hz geophones. The survey was conducted at the three locations shown on Figure C3-1.

MASW is a surface geophysical technique in which energy is input to the ground (typically a hammer blow to a surface metal plate) with measurement of surface waves at the geophones using the seismograph. The shear wave velocity with depth is inferred from inversion software. Shear wave velocity is not directly measured. The average S-wave velocities are used to classify the site according to the criteria established by the IBC – International Building Code (2015).

A summary of the tests completed at each location is provided in the following sections.

C3.2.2.1 Germano Slimes

On the Germano plateau, separate SCPT and Nilcon Vane holes were completed at both locations. The vane testing holes were offset approximately 3 m from the CPT holes. Seismic shear wave measurements were collected by the seismic cone penetrometer at depth intervals of 1 m. Nilcon vane tests were completed at approximately 1 m depth intervals. The Nilcon vane test holes were completed using a Boart Longyear LX6 rig and were advanced until refusal. Refusal was met at depths of between 28.0 m and 40.5 m for the Nilcon Vane, and for the SCPT between 11.4 m and 41.65 m.

C3.2.2.2 Germano Buttress

At the Germano Buttress, three SCPTs were attempted at the first location on the 825 m berm. None of the CPTs could advance more than 2 m. The SCPT rig was moved to the higher 845 m berm. The first attempt at (GBCPT-06) only penetrated 3.4 m. The second attempt at GBCPT-06B reached 27.5 m. Seismic shear wave measurements were collected by a seismic cone penetrometer at depth intervals of 1 m. Thus, only one SCPT was done on the Germano Buttress.

C3.2.2.3 Germano Pit Dam

At the Germano Pit Dam, separate pairs of SCPT and SPT holes were completed at two locations. The SPT holes were offset approximately 3 m from the SCPT holes. Within the SCPT test holes, shear wave measurements were collected by a seismic cone penetrometer at depth intervals of 1 m. SPTs were completed at approximately 1 m depth intervals. Test pits were completed at four locations for the purpose of undertaking in situ density tests and collecting samples (also at a 3 m offset from the CPT, but in the opposite direction to the SPT).

The SPT profiles were done at GCSPT16-01 and GCSPT16-02 because the Panel identified a discrepancy between SPT and CPT results in the pre-failure Fundão in situ data. These two Panel test holes gave SPT values much higher than would have been predicted by standard correlations with CPT. The Panel considers that the SPT results are too high because the methodology and equipment used to undertake the SPTs did not meet the minimum ASTM standards (nor internationally accepted practice) as follows:

- The outside (33.7 mm) and inside (22.3 mm) diameters of the drill rods are less than the minimum requirements of the ASTM standard.
- The moment of inertia of the drill rods (51,082 mm^4) is less than the minimum requirements of the ASTM standard (110,231 mm^4).

- The rods are not flush jointed; the ASTM standard requires flush-joint steel drill rods to be used to connect the split-barrel sampler to the drive-weight assembly.
- Drilling was by rotary coring using a bottom-discharge drill bit with a weak bentonite mud; ASTM states advancing a borehole with bottom discharge bits is not permissible.

Because of these procedural issues, the Panel considers that the SPT results are misleading so will not be reported herein. However, water contents were collected from the SPT samples; these are reported on the logs in Attachment C4.

C3.2.3 MASW Survey

The MASW survey was conducted at three locations, as shown on Figure C3-1:

- Survey 1 - at the location of the current accelerometer positioned on a bedrock outcrop between Germano and Fundão.
- Survey 2 - adjacent to GCCPT16-03 at Germano Pit Dam to compare with the seismic shear wave measurements collected by the seismic cone penetrometer.
- Survey 3 - adjacent to the reception building in the main plant area where seismic intensity observations were previously made.

A copy of the AFC Geofisica Ltda. report is included as Attachment C3.

C3.2.4 Test Hole Location Survey

The initial layout of all boreholes and test sites was carried out using a handheld GPS. Final as-built co-ordinates were subsequently surveyed using a consumer grade GPS device. All coordinates cited within the field investigation relate to the UTM Zone 23 South/WGS84.

C3.3 Laboratory Testing

Soil samples retrieved from the SPT boreholes and Sharky samplers were subjected to standard laboratory index testing, including moisture content determination, PSD and specific gravity testing. Fugro carried out the PSD analysis and specific gravity testing for samples collected from SPT16-01. All other laboratory index testing was undertaken by TÜV SÜD/Samarco.

A summary of the laboratory index testing to support the field program is presented in Attachment C6. All of these tests were conducted in Brazilian laboratories. Thus, the Panel members could not directly check the test results, although supervision was provided by TÜV SÜD.

C3.4 Test Results

C3.4.1 Germano Slimes

C3.4.1.1 Southwest Corner – "Pure" Slimes

Cone penetration test results, vane shear tests, and sampling holes were completed at the southwest corner of Germano in GSCPT16-05, GS-VST16-02, and GSSAM16-02/02B respectively. Water content and fines content were done on ConeTec Sharky samples in Brazil. The vane shear test results are shown on the SCPT log, found in Attachment C7, Figure C.C7-2. The water content results are shown on GSSAM16-02 together with specific gravity.

A second sampling hole, GSSAM16-02B, was drilled to collect four Shelby tube samples. The depth of these samples are given on the GSSAM16-02 test hole log, shown in Attachment C4. Triaxial tests were done on some of these samples in the Pattrol laboratory in Belo Horizonte. These results are given in Attachment D7.

An access fill pad was constructed to reach this testing location with a top elevation of about 917 m. The first three meters shown on the test hole log and the SCPT are likely this fill material. Below that fill, slimes reached to El. 886 m until cone refusal; a slimes thickness of 28 m. The tip resistance of the slimes at El. 914 m was about 0.07 MPa, increasing to 1 MPa at El. 898 m or 16 m depth. Thereafter, the tip resistance was essentially constant. The dynamic pore-water pressure was much higher than static, indicating fine grained materials. None of the dissipation tests reached equilibrium. The shear wave velocity was about 100 m/s just below the access fill, increasing to 350 m/s at the bottom of the CPT. The peak vane shear values reached about 10 kPa at El. 910 m (4 m below the access fill or 7 m depth). The vane shear strength reached 50 kPa at El. 890 m or 27 m deep.

These slimes are classified as "Silt, clayey, low plasticity, reddish brown, chemical odour, wet, and homogeneous". Moisture contents ranged between 25% and 43%. The specific gravity ranged from 3.69 to 3.99. The gradation curves for the slimes typically recorded 0.1% to 4.7% sand, 95.3% to 99.9% silt/clay. A summary of the lab index testing is presented in Table C3-2.

Table C3-2 Summary of lab index testing – "pure" slimes

Location	Layer	Moisture Content (%)	Specific Gravity	Particle Size Distribution			
				Gravel (%)	Sand (%)	Silt (%)	Clay (%)
Southwest Corner	Slimes	25 - 43	3.69 – 3.99	0	0.1 - 4.7	59.8 – 77.4	21 – 40.0

C3.4.1.2 Interbedded Sands and Slimes

The CPT data at the interbedded sand and slimes location (GSCPT16-02B) indicates a highly variable tip resistance, with the slimes layers generally exhibiting lower resistance than the sand layers over the full depth of 41.65 m. The tip resistance in the first 10 m is about 2 MPa to 3 MPa. There is a step increase to an average of about 4 MPa in the next 12 m and then doubles to the base of the hole. The bottom 17 m is more sandy than the uppermost portion of the profile.

In contrast to the "pure" slimes CPT profile, the pore-water pressure dissipation tests reduced to the hydrostatic value over the full profile. The water table was at about 8.9 m depth. The shear wave velocity increased from 200 m/s at El. 905 m to 275 m/s at El. 880 m.

Plots of the CPT test data are presented in Attachment C7, Figure C.C7-1, together with the vane shear test results from GSVST16-01.

C3.4.1.3 N_{kt} Value for Undrained Strength

Robertson (2009) suggests that N_{kt} typically varies from about 10 to 20, with an average of 14. The vane shear test results were plotted against normalized CPT tip resistance to obtain an average N_{kt} of 20. This N_{kt} was used in the Panel's interpretation, which is different from the N_{kt} on the standard ConeTec plots. See Figure C.C6-3 in Attachment C6.

C3.4.2 Germano Buttress

One SCPT (GBCPT16-06) was completed on the 845 m berm on Germano Buttress. Shear wave velocity measurements were recorded in this profile. The SCPT data is presented in Attachment C7, Figure C.C7-3.

The CPT data recorded a tip resistance generally increasing with depth from a minimum 0.64 MPa at 9.6 m (El. 835.4 m) to a maximum 30.21 MPa recorded at 26.4 m (El. 818.4 m). The CPT was terminated at 27.5 m within a sandy layer. A more competent layer was encountered from the ground surface to a depth of 3.35 m (El. 841.65 m) with tip resistances increasing from 13.00 MPa at the ground surface to a maximum 46.67 MPa at 2.55 m (El. 842.45 m). No water table was encountered at a depth of 3.1 m.

The shear wave velocity, v_s, ranged from 233 m/s to 374 m/s with an average of 303 m/s. The sand tailings were unsaturated and generally dilative.

C3.4.3 Germano Pit Dam

Two locations were investigated at the Germano Pit Dam as shown on Figure C3-1. At the northeast location, GCCPT16-04, GCCPT16-04B and GCSPT16-01 were completed and given on Figure C.C7-7 (Attachment C7), Figure C.C7-9 (Attachment C7), and Attachment C4 respectively. At the southwest location GCCPT16-03 and GCSPT16-02 were completed and shown on Figure C.C7-5 (Attachment C7) and Attachment C4 respectively. Both SCPT profiles are reported herein in their entirety. The penetration blow counts from the SPT holes are not reported herein because the SPT procedures and equipment were suspect, as discussed in Section C3.2. Moisture content and specific gravity tests were done on the SPT samples and are reported on the test hole logs in Attachment C4.

Germano Pit Dam is constructed entirely of spigotted sand tailings with no direct slimes deposition in any part of the impoundment. The location of the impoundment relative to Germano Buttress is shown on Figure C3-1. There is a foundation finger drain beneath the impoundment whose intent is to maintain an unsaturated downstream slope. Gradation testing was done on surface samples prior to drilling which showed that the gradation of the sand tailings at Fundão Dam and Germano Pit Dam are virtually identical.

At the southwest location, GCCPT16-03 was pushed to about 64 m depth without drill outs. The water table was encountered at El. 970 m or a depth of about 33 m. The tip resistance steadily rose with depth to the water table, beneath which it became relatively constant. The equivalent Clean Sand Tip Resistance was constant with depth. When saturated, the Robertson (2010) approach shows the sand is liquefiable. The state parameter is -0.05 or more in the saturated zone, also indicating susceptibility to liquefaction.

In the northeast corner, the CPT data recorded a tip resistance generally constant with depth (ignoring minor variations) from the ground surface to a depth of 28.8 m (El. 975.53 m); below 28.8 m the tip resistance generally increases with depth to refusal at 36.35 m. Between the ground surface and 28.8 m, the tip resistance varied within 10 MPa to 20 MPa, with locally higher and lower values recorded. The water table was not encountered.

Table C3-3 Summary of seismic and in situ density data – Germano Pit Dam

Location	Layer	Average v_s (m/s)		Average Vp (m/s)	Dry Density (g/cm^3)
		SCPT	MASW		
Northeast corner	Sand	266	204	512	1.56
Southwest corner	Sand	275		800	1.50

The sand tailings from the two SPT test holes were described as sand, and silt, brown to dark grey, moist, homogeneous. The moisture content ranged between 12% and 32% in the northeast corner and 7% and 30% at the southwest corner. The specific gravity ranged between 2.38 and 3.64 in the northeast corner and 2.78 and 4.34 at the southwest corner. The higher values of Gs are either laboratory errors or minor pockets of slimes. These SPT logs can be found in Attachment C4. A summary of the laboratory index testing is presented in Table C3-4 for both locations.

Table C3-4 Summary of lab index testing – Germano Pit Dam

Location	Layer	Moisture Content (%)	Specific Gravity	Particle Size Distribution			
				Gravel (%)	Sand (%)	Silt (%)	Clay (%)
Northeast corner	Sand	12 - 32	2.38 – 3.64	0	41.4 – 91.8	6.9 - 58.1	0.0 - 4.6
Southwest corner	Sand	7 - 30	2.78 – 4.34	0.1 – 30.1	19.1 – 83.7	9.3 – 79.5	0 – 1.3

C3.4.4 MASW Surveys

A summary of the shear wave velocity from the inversion software is given in Table C3-5.

Table C3-5 Summary of v_s data (MASW)

Survey Location	Inferred Depth (m)	Length of Survey (m)	Average v_s [1] (m/s)	Site Classification[2]
1	36	92	344 405	D (0 to 24 m) C (28 to 92 m)
2	30	104	204	D
3	36	80	391	C

1. Average v_s calculated along the length of the survey line
2. Site classification in accordance with IBC (2015) according to AFC Geofisica.

At Location 2, the actual downhole shear wave velocity measured at GCCPT16-03 was about 250 m/s over 30 m depth but about 200 m/s in the upper 10 m. The corresponding MASW shear wave velocity over an inferred depth of 30 m was 204 m/s.

C4 TEST FILLS

C4.1 Baia 4

The northeast dike of the Germano Baia 4 deposition area failed on September 21, 2005. The failure occurred as the dike crest was being raised to elevation 908 m, approximately half the height of the final design crest elevation, when the dike was approximately 13 m high. An embankment, referred to as the reinforcement dike, was being constructed at the toe of the dike at the time of failure. The failure occurred over a length of 320 m in a northeast-southwest direction, and moved approximately 100,000 m^3 of material with a maximum displacement of 70 m to 80 m[38]. Downstream of the failure, sand boils developed in the following days.

The Federal University of Ouro Preto (UFOP) completed a back-analysis of the failure in 2006[38]. As part of the analysis, the University conducted a field investigation in Baia 4 and the adjacent Baia 5. The field investigation comprised SPTs, CPTu's, field vane tests and collection of Shelby tube samples to ascertain the undrained shear strength and the variation of pore pressure within the dike and foundation materials. Laboratory index testing was undertaken on the samples collected including moisture content, Atterberg limits and specific gravity. A review of the in situ testing and laboratory test results was undertaken by KCB and is reproduced on Figure C.C8.1 in Attachment C8.

From the field investigation results, the UFOP developed a stratigraphic profile through the failure area as shown in Table C4-1. The layer of fine silts and soft clays encountered between El. 895 m and El. 893 m is characterized in the cone penetration results by a high pore-water pressure response and a reduction in cone resistance, qt, and sleeve friction, fs; this layer is postulated to be a region of slimes.

Table C4-1 Summary of Baia 4 stratigraphic profile[38]

Elevation	Description	q_T	u_2
902 to 899	Silts and soft sand	2	-
899 to 895	Soft sands and silts	4	-
895 to 893	Fine silts and soft clays	0.6	400
893 to 885	Soft and compacted sands	6	-

UFOP derived geotechnical parameters from their field investigation as shown on Table C4-2. Stability analyses were performed by the University for both drained and undrained conditions. The undrained back analysis for an average embankment height of 10 m gave an undrained strength (s_u) of 23 kPa for the silty-clay layer at a Factor of Safety of 1.0 (see Figure C4-1). This s_u is equivalent to an undrained strength ratio of approximately 0.2. KCB checked whether the results of this analysis would differ if a higher unit weight of 22 kN/m^3 was used, consistent with the assumptions used in the interpretation of field data throughout this appendix, and arrived at very similar results to those of UFOP (0.22). Based on these results, an undrained strength ratio of 0.2 to 0.22 is considered to represent the peak (or yield) strength of the interbedded sand and slimes.

Table C4-2 Summary of geotechnical parameters[38]

Material	γ_d (kN/m^3)	γ_s (kN/m^3)	ϕ' (°)	C' (kPa)	s_u (kPa)	K_h (m/s)
Sandy embankment	18	23	40	0	-	10^{-6}
Sunken embankment material	18	23	28	0	-	10^{-6}
Silty-clay	18	23	26.5	0	23	10^{-9}
Foundation (Below El. 893 m)	18	23	34	0	-	10^{-7}

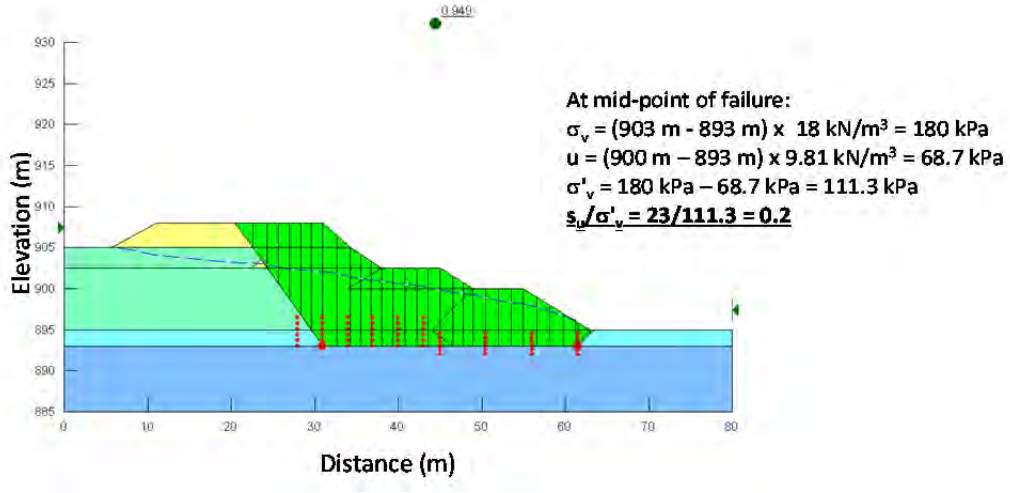

Figure C4-1 Back analysis of the Baia 4 failure completed by UFOP[38]

KCB ran slope stability analyses to calculate the large-strain undrained shear strength ratio using the post-failure geometry. Observations of the failure at Baia 4 indicate the run-out of the rupture was approximately 70 m, so a slip surface length equivalent to the total observed run-out was used in back analysis. The height of the dike and the undrained strength was varied to produce a factor of safety equal to 1.0.

Given the uncertainties in the post-failure geometry, we have calculated a range of post-failure strength ratios for a factor of safety equal to unity. We calculated strength ratios of between roughly 0.07 and 0.12 for post-failure slopes of between 12H:1V and 8H:1V, respectively. This analysis does not account for the momentum created by the sliding mass, so the static large-strain strength ratio lies between 0.07 and 0.22. Following the simplified approach to accounting for momentum effects discussed by Webber (2015), an approximate large-strain strength can be calculated as the average of those associated with the pre- and post-failure geometries. Averaging these values would give a large-strain undrained strength ratio of approximately 0.14 to 0.15 for interbedded regions of sand and slimes.

C4.2 2008 Test Fill

A trial embankment was constructed over the tailings of Baia 2 on the Germano plateau in June 2008[4]. The intention of the trial was to take the embankment to failure. Based on experience from other works at the same location, the failure was expected to occur at a height of between 3 m and 5 m. The trial embankment was built to a height of 5 m with side slopes of 2H:1V, a crest width of 8 m and a total length of 56 m (i.e., double the base width). The embankment was constructed at a rate of 0.55 m/day. The embankment was instrumented with piezometers and settlement plates to measure pore-pressures and displacements (vertical and horizontal) in the conditions before, during and after construction of the embankment.

The upper 2 m of the ground beneath the trial embankment was logged in detail. The ground profile comprised an interbedded sequence of “chocolate”, otherwise known as slimes, and interbedded sands. The piezometers were positioned in the more granular silty-sand material and just below a well-defined layer of slimes to study a possible undrained behavior of the more permeable layers. Samples of the foundation materials were collected prior to the trial embankment construction, and laboratory index testing was undertaken including moisture content and specific gravity. A review of laboratory test results was undertaken by KCB and is reproduced in Attachment C8, Figure C.C8-2.

The trial embankment did not fail in the same manner as the northeast dike of Baia 4 described in the previous section. The embankment displayed localized instability on the perimeter slopes as well as cracking and sand boils. The peak pore pressure response to construction of the embankment ranged between 25 kPa and 42 kPa. Maximum settlements of between 0.22 m and 0.37 m were recorded. Within 1 day following loading, all displacements were complete and pore pressures were mostly dissipated (see Figure C4-2 for example response).

Schematic layout of test fill instrumentation

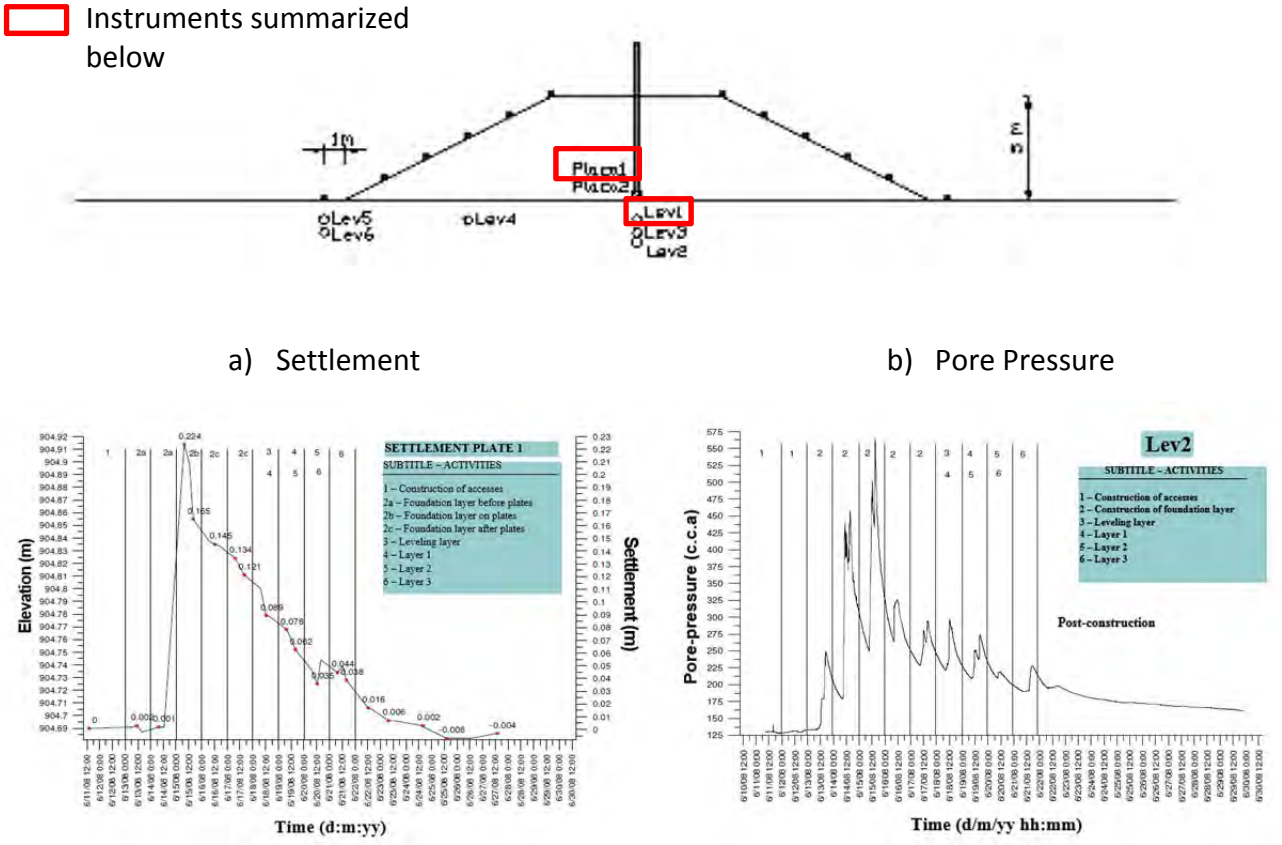

Figure C4-2 Example instrumentation response to 2008 test fill[4]

Following completion of the trial, the embankment was excavated and sampling was performed on the original ground to a depth of approximately 2 m[4]. Basic laboratory index testing was undertaken on the samples including moisture content (w), specific gravity (Gs) and particle size distribution. A review of laboratory test results by KCB indicates that the void ratio of the slimes (referenced as "chocolate") decreased following the trial. This calculated void ratio (e) decrease was made by assuming full saturation below the stated water table, and calculating e=wGs using the index testing before and after the trial. With an estimate of the load from the embankment, and the calculated change in void ratio, it was possible to calculate compression characteristics to supplement the 1D consolidation, as shown in Figure C4-3.

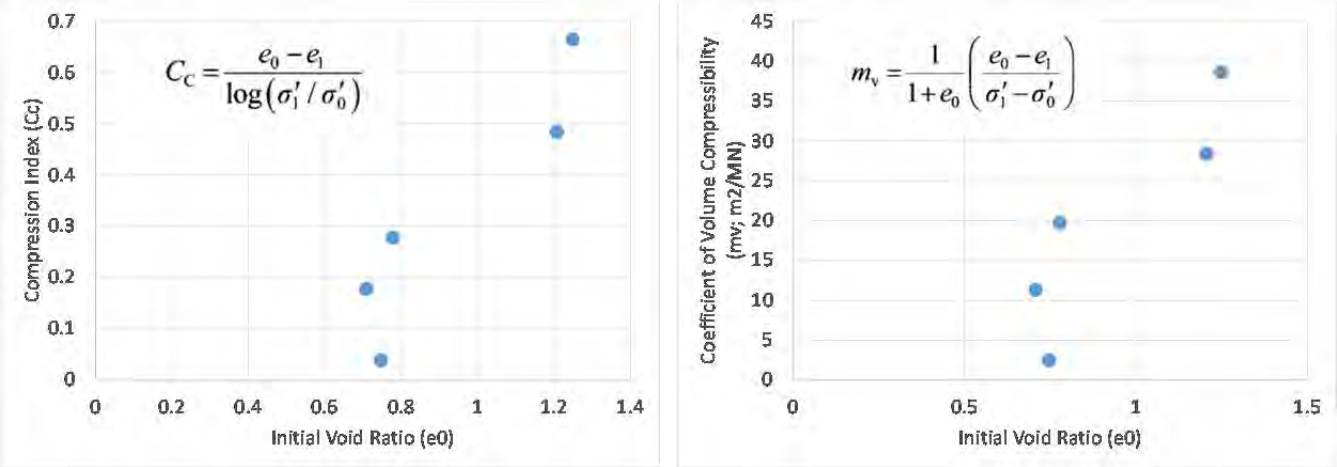

Figure C4-3 Slimes compressibility characteristics back calculated 2008 test fill

C4.3 2013 Test Fill

A trial embankment comprised of tailings was constructed by Samarco at Baia 3 in December, 2013. The embankment was constructed to a maximum height of 6 m with side slopes of 2H:3V (0.67H:1V). The embankment was constructed at a rate of 0.37 m/day. The embankment was instrumented with piezometers, settlement gauges and inclinometers to measure pore-pressures and displacements before, during and after construction of the embankment.

The ground profile beneath the trial embankment comprised silty-clayey tailings varying in depth from 7 m to 12 m. The piezometers were installed in the tailings at depths ranging from 3 m to 7 m.

During the trial the pore pressure response to construction of the embankment recorded a maximum pore pressure response ($\Delta u/\Delta\sigma$) of 0.74 at depths of 5.5 m and 7 m below the embankment. A maximum settlement of 0.47 m was recorded beneath the maximum embankment height of 6 m[39].

The results of the 2013 trial were similar to the 2008 trial. Pore pressures beneath the embankment dissipated rapidly (see Figure C4-4 for example response at various depths), and settlements in the range of approximately 78 mm per 1 m of embankment load were recorded compared to 74 mm per 1 m load recorded during the 2008 trial.

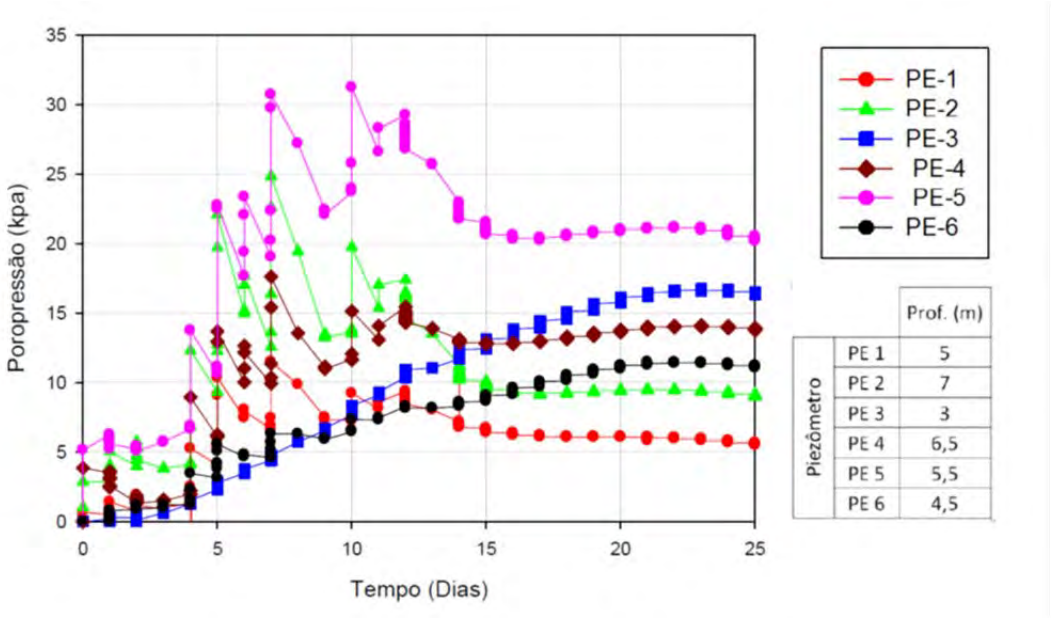

Figure C4-4 Pore pressure response to 2013 test fill

C5 SUMMARY

Over the years, several consultants have selected material parameters for the purposes of stability assessments. The previously assumed material parameters are summarized in Table C5-1 below.

Table C5-1 Summary of geotechnical parameters

Strata	Unit Weight (kN/m^3)	Effective Friction Angle (°)	Effective Cohesion (kPa)
Sand Tailings	18	35	5
Slimes	18	28	-
Weathered Phyllite	18	32	40

ATTACHMENT D1

Summary Table

Table D.D1-1 Test types, procedures and number of tests

Test Type	Laboratory	Standard	Additional Reference	Number of Tests					
				Fundão Sand	PSD1	PSD2	Germano Pit Dam Sand	Germano Slimes	Summary
Min and Max Density using Vibrating Table	Golder	ASTM D4253, D4254		-	1	-	-	-	1
Modified Proctor	KCB V	ASTM D1557		1	-	-	-	-	1
Standard Proctor	KCB C	ASTM D698		-	-	-	-	1	1
Atterber Limits	KCB V and C and Tecnogeo	ASTM D4318		-	-	-	-	3	3
Water Content	KCB V and C and Tecnogeo	ASTM D2216		3	80	8	-	70	161
Washed Sieve	KCB V and Tecnogeo	ASTM D1140		3	56	8	1	-	68
Hydrometer	KCB V and Tecnogeo	ASTM D422		2	-	-	-	2	4
Strain-Controlled Standard Triaxial Tests (CID/CIU/CAD/CAU)	KCB V and Pattrol	ASTM D4767/ASTM D7181		-	17	4	-	16	37
Strain-Controlled Extrusion Collapse Triaxial Tests (CA-QD)	KCB V	ASTM D7181		-	4	-	-	-	4
Stress-Controlled Extrusion Collapse Triaxial Tests (CA-QD-SC/CA-QID-SC)	KCB V	NA	Sasitharan et al. 1993	-	4	-	-	-	4
Stress-Controlled Extrusion Collapse Triaxial Tests with Cyclic Component (CA-QID-SC (Cyclic))	KCB V	ASTM D5311		-	1	-	-	-	1
1-D Consolidation (oedometer)	KCB V	ASTM D2435		-	1	-	-	1	2
Direct Shear Test	KCB V	ASTM D3080		1	-	-	-	-	1
Direct Simple Shear Test	KCB V	ASTM D6528		-	9	-	-	6	15
Specific Gravity	KCB V and C	ASTM D854		1	28	4	-	2	35
Large-Strain Consolidation Test	University of Alberta	NA	Kabwe and Wilson 2016	-	-	-	-	1	1
Settlement Test	University of Alberta	NA	Kabwe and Wilson 2016	-	-	-	-	1	1
pH	KCB V	ASTM D4972		-	-	-	-	1	1
EC	KCB V	ASTM D1125		-	-	-	-	1	1
Bender Elements Tests	KCB V	NA	Yamashita et al. 2009	-	2	-	-	-	2
X-ray Diffraction	University of British Columbia	NA		-	-	-	-	1	1
Scanning Electron Microscopy	University of British Columbia	NA		1	-	-	-	-	1

Table D.D1-2 Number of tests for advanced lab testing program

Material	Number of Specimens Tested	Oedometer Test	Large-Strain Consolidation Test	Settlement Test	Direct Shear Test	Direct Simple Shear Test	Strain-Controlled Standard Triaxial Compression Tests (CIU/CID/CAD/CAU)	Strain-Controlled Extrusion Collapse Triaxial Tests (CA-QD)	Stress-Controlled Extrusion Collapse Triaxial Tests (CA-QD-SC/CA-QID-SC)	Stress-Controlled Extrusion Collapse Triaxial Tests with Cyclic Component (CA-QID-SC (Cyclic))	Bender Elements Test
Fundão Sand	1	-	-	-	1	-	-	-	-	-	-
PSD1	38	1	-	-	-	9	17	4	4	1	2
PSD2	4	-	-	-	-	-	4	-	-	-	-
Germano Pit Dam Sand	-	-	-	-	-	-	-	-	-	-	-
Germano Slimes	25	1	1	1	-	6	16	-	-	-	-
Total	**68**	**2**	**1**	**1**	**1**	**15**	**37**	**4**	**4**	**1**	**2**

Table D.D1-3 Number of tests for index testing program

Material	Number of Specimens Tested	Min/Max Density Test	Modified/Standard Proctor Test	Atterberg Limit Tests	Water Content	Washed Sieve	Hydrometer Test*	Specific Gravity	pH	EC	X-Ray Diffraction	Scanning Electron Microscopy
Fundão Sand	10	-	1	-	3	3	2	1	-	-	-	1
PSD1	161	1	-	-	80	56	-	28	-	-	-	-
PSD2	20	-	-	-	8	8	-	4	-	-	-	-
Germano Pit Dam Sand	1	-	-	-	-	1	-	-	-	-	-	-
Germano Slimes	51	-	1	3	70	2	2	2	1	1	1	-
Total	**243**	**1**	**2**	**3**	**161**	**70**	**4**	**35**	**1**	**1**	**1**	**1**

ATTACHMENT D2

Index Test Data

D2-1 – Atterberg Limits Tests

PLASTICITY CHART

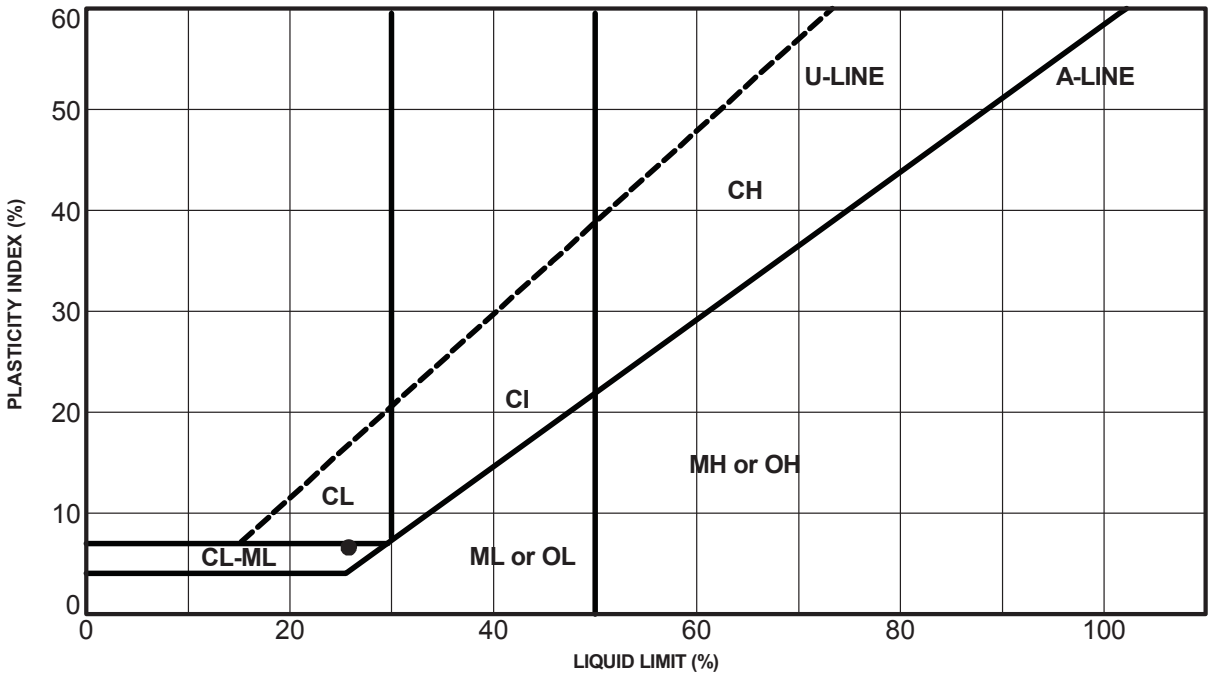

	HOLE	SAMPLE	DEPTH (m)	W_L	W_P	PI	% FINES	REMARKS/SAMPLE DESCRIPTION
●	Germano Slimes		0.0	26	19	7	99.8	As received

Klohn Crippen Berger

PROJECT NO.:	
PROJECT:	Fundão Tailings Dam Review Panel
LOCATION:	
FIGURE:	
DRAWN BY: BY	CHECKED BY: JG

KCB_ATTERBERG-SI_FUNDAO TAILINGS DAM REVIEW PANEL.GPJ SIEVE.GDT 24.7.16

PLASTICITY CHART

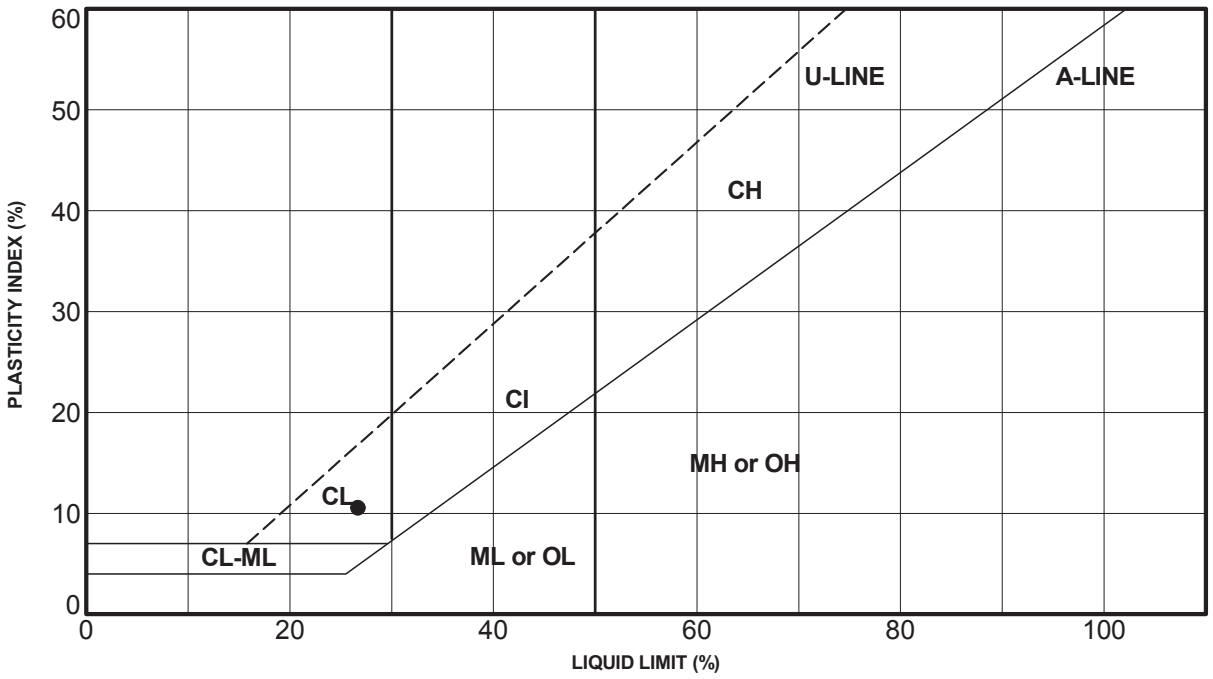

	SAMPLE	DEPTH (m)	W_L	W_P	PI	W_N	% FINES (<0.080 mm)	CLASSIFICATION	REMARKS/FACIES
●	Slimes		27	16	11	26.83		CL	

Klohn Crippen Berger

PROJECT: Fundão Tailings Dam Review Panel	
LOCATION:	
CLIENT:	PROJECT NO.:
TESTED BY: Vaclav K	CHECKED BY: Shamim Ahsan
DATE: 2016-03-28	FIGURE:

KC_ATTERBERG-SI.GPJ KCBL_CALGARY.GDT 3-28-16

LIMITES DE ATTERBERG

LIMITE DE LIQUIDEZ

1-RECIPIENTE N°	CÁLCULO	361	362	362	364	365
2-MASSA DO SOLO + TARA + ÁGUA (g)	M1	19.00	18.01	19.08	18.05	18.91
3-MASSA DO SOLO SECO + TARA (g)	M2	17.09	16.25	17.05	16.23	16.90
4-ÁGUA	M1-M2	1.91	1.76	2.03	1.82	2.01
5-TARA	M3	10.17	9.99	9.97	10.04	10.37
6-MASSA DO SOLO SECO (g)	M2-M3	6.92	6.26	7.08	6.19	6.53
7-UMIDADE (%)	4 / 6.100	27.6	28.1	28.7	29.4	30.8
8-NÚMERO DE GOLPES		38	28	21	14	8

LIMITE DE PLASTICIDADE

1-RECIPIENTE N°	CÁLCULO	366	367	368		
2-MASSA DO SOLO + TARA + ÁGUA (g)	M1	12.82	12.94	12.79		
3-MASSA DO SOLO SECO + TARA (g)	M2	12.43	12.48	12.32		
4-ÁGUA	M1-M2	0.39	0.46	0.47		
5-TARA	M3	10.15	9.84	9.60		
6-MASSA DO SOLO SECO (g)	M2-M3	2.28	2.64	2.72		
7-UMIDADE (%)	4 / 6.100	17.1	17.4	17.3		

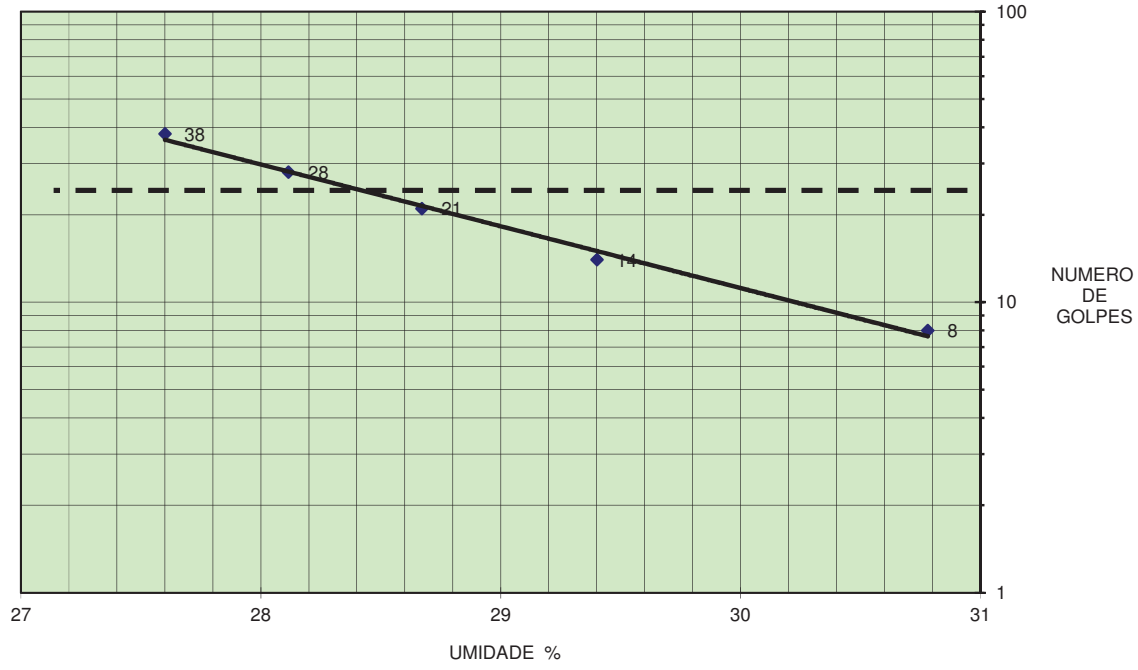

LIMITE DE LIQUIDEZ (LL) = **28,4 %**

LIMITE DE PLASTICIDADE (LP) = **17,3 %**

ÍNDICE DE PLASTICIDADE (IP) = **11,1 %**

SEM SECAGEM PRÉVIA

Cliente : **BUREAU DE PROJETOS E CONSULTORIA LTDA**

Obra: **BARRAGEM DO GERMANO**

Local : **MARIANA - MG.**

LIMITES DE ATTERBERG (NBR-6459/84 e 7180/84)

FURO 2C AM. - PROF. -

TECNOGEO Soluções em Geotecnia Fina

Data:	Resp.:
2016-02-04	**REGINALDO**
Engº	REL. Nº: **LAB-004/16**
VISTO	DES. Nº

D2-2 – Specific Gravity Tests

SPECIFIC GRAVITY OF SOIL SOLIDS (ASTM-D854)

Hole Number		Fundão Sand			Germano Slimes		
Sample Number		As received			As received		
Depth (m)		-			-		
Sample Description		Sand			Silt		
Flask No.		SG9	SG2	SG10	SG7	SG12	10
Volume of Flask @ 20° C	ml	500	500	500	500	500	500
Method of Air removal		Boiling	Boiling	Boiling	Boiling	Boiling	Boiling
De-airing Period	hr	2	2	2	2	2	2
Test temperature	° C	24.4	24.4	24.4	24.4	24.4	24.4
Mass of Flask+Water (M_a)	g	667.79	671.31	669.81	667.63	670.27	679.55
Mass of Flask+Water+Soil (M_b)	g	734.08	736.87	735.01	719.50	728.62	746.00
Mass of Dish/Flask+Soil		271.44	273.97	272.28	239.03	250.66	270.64
Mass of Dish/Flask		169.70	173.30	171.94	169.44	172.55	181.55
Mass of Dry Soil (M_o)	g	101.74	100.67	100.34	69.59	78.11	89.09
Correction factor (K) @ Test Temperature		0.99899	0.99899	0.99899	0.99899	0.99899	0.99899
Specific Gravity of Solids @ 20° C		**2.87**	**2.86**	**2.85**	**3.92**	**3.95**	**3.93**
Average Specific Gravity of Solids @ 20° C			**2.86**			**3.93**	

Hole Number		PSD1					
Sample Number		Max - Min Density					
Depth (m)		-					
Sample Description		Sand					
Flask No.		11	12				
Volume of Flask @ 20° C	ml	500	500				
Method of Air removal		Boiling	Boiling				
De-airing Period	hr	2	2				
Test temperature	° C	22.5	22.5				
Mass of Flask+Water (M_a)	g	678.70	680.41				
Mass of Flask+Water+Soil (M_b)	g	728.54	731.47				
Mass of Dish/Flask+Soil		254.83	258.09				
Mass of Dish/Flask		180.40	182.12				
Mass of Dry Soil (M_o)	g	74.43	75.97				
Correction factor (K) @ Test Temperature		0.99945	0.99945				
Specific Gravity of Solids @ 20° C		**3.03**	**3.05**				
Average Specific Gravity of Solids @ 20° C			**3.04**				

Specific Gravity of Solids @ 20° C = $(K \times M_o)/(M_o + M_a - M_b)$

Klohn Crippen Berger

PROJECT#:			
PROJECT:	Fundão Tailings Dam Review Panel		
LOCATION:			
DATE:	2016-03-02		
TESTED BY:	JG	CHECKED BY:	BY

SPECIFIC GRAVITY OF SOIL SOLIDS (ASTM-D854)

Hole Number	PSD1			PSD1		
Sample Number	TX 1			TX2		
Depth (m)	-			-		
Sample Description	Sand			Sand		
Flask No.	SG8	KL-3		SG2	SG3	
Volume of Flask @ 20° C ml	500	500		500	500	
Method of Air removal	Boiling	Boiling		Boiling	Boiling	
De-airing Period hr	2	2		2	2	
Test temperature ° C	24.2	24.2		24.2	24.2	
Mass of Flask+Water (M_a) g	670.43	675.67		671.41	672.12	
Mass of Flask+Water+Soil (M_b) g	720.09	725.24		721.07	722.51	
Mass of Dish/Flask+Soil	247.14	252.01		248.26	250.12	
Mass of Dish/Flask	172.41	177.37		173.32	173.95	
Mass of Dry Soil (M_o) g	74.73	74.64		74.94	76.17	
Correction factor (K) @ Test Temperature	0.99904	0.99904		0.99904	0.99904	
Specific Gravity of Solids @ 20° C	**2.98**	**2.97**		**2.96**	**2.95**	
Average Specific Gravity of Solids @ 20° C	**2.98**			**2.96**		

Hole Number	PSD2			PSD1		
Sample Number	TX3			TX4		
Depth (m)	-			-		
Sample Description	Sand			Sand		
Flask No.	SG5			KL2	SG6	
Volume of Flask @ 20° C ml	500			500	500	
Method of Air removal	Boiling			Boiling	Boiling	
De-airing Period hr	2			2	2	
Test temperature ° C	24.2			23.4	23.4	
Mass of Flask+Water (M_a) g	672.01			675.41	670.51	
Mass of Flask+Water+Soil (M_b) g	742.00			725.55	719.57	
Mass of Dish/Flask+Soil	283.86			252.89	246.52	
Mass of Dish/Flask	173.92			177.09	172.20	
Mass of Dry Soil (M_o) g	109.94			75.80	74.32	
Correction factor (K) @ Test Temperature	0.99904			0.99924	0.99924	
Specific Gravity of Solids @ 20° C	**2.75**			**2.95**	**2.94**	
Average Specific Gravity of Solids @ 20° C				**2.95**		

Specific Gravity of Solids @ 20° C = $(K \times M_o)/(M_o + M_a - M_b)$

Klohn Crippen Berger

PROJECT#:			
PROJECT:	Fundão Tailings Dam Review Panel		
LOCATION:			
DATE:	2016-03-10		
TESTED BY:	BY	CHECKED BY:	JG

SPECIFIC GRAVITY OF SOIL SOLIDS (ASTM-D854)

Hole Number	PSD2			PSD1		
Sample Number	TX5			TX6		
Depth (m)	-			-		
Sample Description	Sand			Sand		
Flask No.	SG9	SG6		SG2	SG3	
Volume of Flask @ 20° C ml	500	500		500	500	
Method of Air removal	Boiling	Boiling		Boiling	Boiling	
De-airing Period hr	2	2		2	2	
Test temperature ° C	23.4	23.4		22.7	22.7	
Mass of Flask+Water (M_a) g	667.91	669.91		671.57	672.29	
Mass of Flask+Water+Soil (M_b) g	734.09	721.68		720.98	721.85	
Mass of Dish/Flask+Soil	273.93	253.49		248.09	248.98	
Mass of Dish/Flask	169.71	171.95		173.31	173.96	
Mass of Dry Soil (M_o) g	104.22	81.54		74.78	75.02	
Correction factor (K) @ Test Temperature	0.99924	0.99924		0.99941	0.99941	
Specific Gravity of Solids @ 20° C	**2.74**	**2.74**		**2.95**	**2.94**	
Average Specific Gravity of Solids @ 20° C	**2.74**			**2.95**		

Hole Number	PSD2			PSD1		
Sample Number	TX7			TX8		
Depth (m)	-			-		
Sample Description	Sand			Sand		
Flask No.	SG4			SG5	SG6	
Volume of Flask @ 20° C ml	500			500	500	
Method of Air removal	Boiling			Boiling	Boiling	
De-airing Period hr	2			2	2	
Test temperature ° C	22.7			22.7	22.7	
Mass of Flask+Water (M_a) g	670.76			672.20	670.60	
Mass of Flask+Water+Soil (M_b) g	740.69			721.91	720.56	
Mass of Dish/Flask+Soil	282.78			249.22	247.86	
Mass of Dish/Flask	172.60			173.93	172.21	
Mass of Dry Soil (M_o) g	110.18			75.29	75.65	
Correction factor (K) @ Test Temperature	0.99941			0.99941	0.99941	
Specific Gravity of Solids @ 20° C	**2.74**			**2.94**	**2.94**	
Average Specific Gravity of Solids @ 20° C	**2.74**			**2.94**		

Specific Gravity of Solids @ 20° C = $(K \times M_o)/(M_o + M_a - M_b)$

Klohn Crippen Berger

PROJECT#:			
PROJECT:	Fundão Tailings Dam Review Panel		
LOCATION:			
DATE:	2016-03-16		
TESTED BY:	BY	CHECKED BY:	JG

SPECIFIC GRAVITY OF SOIL SOLIDS (ASTM-D854)

Hole Number	PSD2			PSD1		
Sample Number	TX9			TX10		
Depth (m)	-			-		
Sample Description	Sand			Sand		
Flask No.	SG7			SG8	SG9	
Volume of Flask @ 20° C ml	500			500	500	
Method of Air removal	Boiling			Boiling	Boiling	
De-airing Period hr	2			2	2	
Test temperature ° C	22.7			22.7	22.7	
Mass of Flask+Water (M_a) g	667.84			670.60	667.99	
Mass of Flask+Water+Soil (M_b) g	738.01			719.91	717.56	
Mass of Dish/Flask+Soil	279.99			246.85	244.82	
Mass of Dish/Flask	169.46			172.41	169.71	
Mass of Dry Soil (M_o) g	110.53			74.44	75.11	
Correction factor (K) @ Test Temperature	0.99941			0.99941	0.99941	
Specific Gravity of Solids @ 20° C	**2.74**			**2.96**	**2.94**	
Average Specific Gravity of Solids @ 20° C	**2.74**			**2.95**		

Hole Number	PSD1			PSD1		
Sample Number	TX11			TX12		
Depth (m)	-			-		
Sample Description	Sand			Sand		
Flask No.	SG10	SG11		8	KL2	
Volume of Flask @ 20° C ml	500	500		500	500	
Method of Air removal	Boiling	Boiling		Boiling	Boiling	
De-airing Period hr	2	2		2	2	
Test temperature ° C	22.7	22.7		23.4	23.4	
Mass of Flask+Water (M_a) g	669.97	670.52		678.64	675.41	
Mass of Flask+Water+Soil (M_b) g	719.64	719.70		743.54	729.22	
Mass of Dish/Flask+Soil	247.07	246.64		278.78	258.62	
Mass of Dish/Flask	171.94	172.22		180.51	177.10	
Mass of Dry Soil (M_o) g	75.13	74.42		98.27	81.52	
Correction factor (K) @ Test Temperature	0.99941	0.99941		0.99619	0.99619	
Specific Gravity of Solids @ 20° C	**2.95**	**2.95**		**2.93**	**2.93**	
Average Specific Gravity of Solids @ 20° C	**2.95**			**2.93**		

Specific Gravity of Solids @ 20° C = $(K \times M_o)/(M_o + M_a - M_b)$

Klohn Crippen Berger

PROJECT#:			
PROJECT:	Fundão Tailings Dam Review Panel		
LOCATION:			
DATE:	2016-04-08		
TESTED BY:	BY	CHECKED BY:	JG

SPECIFIC GRAVITY OF SOIL SOLIDS (ASTM-D854)

Hole Number	PSD1			PSD1		
Sample Number	TX13			TX14		
Depth (m)	-			-		
Sample Description	Sand			Sand		
Flask No.	SG6	SG4		KL3	1	
Volume of Flask @ 20° C ml	500	500		500	500	
Method of Air removal	Boiling	Boiling		Boiling	Boiling	
De-airing Period hr	2	2		2	2	
Test temperature ° C	23.4	23.4		23.4	23.4	
Mass of Flask+Water (M_a) g	670.52	670.68		675.77	667.21	
Mass of Flask+Water+Soil (M_b) g	739.62	720.31		731.90	729.53	
Mass of Dish/Flask+Soil	276.89	247.85		262.51	263.41	
Mass of Dish/Flask	172.22	172.59		177.38	168.82	
Mass of Dry Soil (M_o) g	104.67	75.26		85.13	94.59	
Correction factor (K) @ Test Temperature	0.99619	0.99619		0.99619	0.99619	
Specific Gravity of Solids @ 20° C	**2.93**	**2.93**		**2.92**	**2.92**	
Average Specific Gravity of Solids @ 20° C	**2.93**			**2.92**		

Hole Number	PSD1			PSD1		
Sample Number	TX15			TX16		
Depth (m)	-			-		
Sample Description	Sand			Sand		
Flask No.	10	SG12		SG10	SG3	
Volume of Flask @ 20° C ml	500	500		500	500	
Method of Air removal	Boiling	Boiling		Boiling	Boiling	
De-airing Period hr	2	2		2	2	
Test temperature ° C	23.4	23.4		23.0	23.0	
Mass of Flask+Water (M_a) g	679.72	670.58		669.95	672.26	
Mass of Flask+Water+Soil (M_b) g	739.22	729.75		726.36	734.54	
Mass of Dish/Flask+Soil	271.67	262.31		257.41	268.57	
Mass of Dish/Flask	181.57	172.56		171.96	173.97	
Mass of Dry Soil (M_o) g	90.10	89.75		85.45	94.60	
Correction factor (K) @ Test Temperature	0.99619	0.99619		0.99933	0.99933	
Specific Gravity of Solids @ 20° C	**2.93**	**2.92**		**2.94**	**2.93**	
Average Specific Gravity of Solids @ 20° C	**2.93**			**2.93**		

Specific Gravity of Solids @ 20° C = $(K \times M_o)/(M_o + M_a - M_b)$

Klohn Crippen Berger

PROJECT#:			
PROJECT:	Fundão Tailings Dam Review Panel		
LOCATION:			
DATE:	2016-04-16		
TESTED BY:	BY	CHECKED BY:	JG

SPECIFIC GRAVITY OF SOIL SOLIDS (ASTM-D854)

Hole Number	PSD1			PSD1		
Sample Number	TX17			TX18		
Depth (m)	-			-		
Sample Description	Sand			Sand		
Flask No.	SG9	SG2		12	SG8	
Volume of Flask @ 20° C ml	500	500		500	500	
Method of Air removal	Boiling	Boiling		Boiling	Boiling	
De-airing Period hr	2	2		2	2	
Test temperature ° C	23.0	23.0		23.0	23.0	
Mass of Flask+Water (M_a) g	667.95	671.54		680.36	670.57	
Mass of Flask+Water+Soil (M_b) g	727.92	730.22		738.63	730.68	
Mass of Dish/Flask+Soil	260.49	262.17		270.61	263.69	
Mass of Dish/Flask	169.70	173.32		182.14	172.42	
Mass of Dry Soil (M_o) g	90.79	88.85		88.47	91.27	
Correction factor (K) @ Test Temperature	0.99933	0.99933		0.99933	0.99941	
Specific Gravity of Solids @ 20° C	**2.94**	**2.94**		**2.93**	**2.93**	
Average Specific Gravity of Solids @ 20° C	**2.94**			**2.93**		

Hole Number	PSD1			PSD1		
Sample Number	TX19			TX20B		
Depth (m)	-			-		
Sample Description	Sand			Sand		
Flask No.	SG7	11		10	1	
Volume of Flask @ 20° C ml	500	500		500	500	
Method of Air removal	Boiling	Boiling		Boiling	Boiling	
De-airing Period hr	2	2		2	2	
Test temperature ° C	23.0	23.0		22.4	22.4	
Mass of Flask+Water (M_a) g	667.80	678.65		679.83	667.31	
Mass of Flask+Water+Soil (M_b) g	726.49	740.83		753.48	728.72	
Mass of Dish/Flask+Soil	256.63	272.94		291.00	260.08	
Mass of Dish/Flask	169.46	180.40		181.55	168.81	
Mass of Dry Soil (M_o) g	87.17	92.54		109.45	91.27	
Correction factor (K) @ Test Temperature	0.99933	0.99933		0.99944	0.99944	
Specific Gravity of Solids @ 20° C	**3.06**	**3.05**		**3.06**	**3.05**	
Average Specific Gravity of Solids @ 20° C	**3.05**			**3.06**		

Specific Gravity of Solids @ 20° C = $(K \times M_o)/(M_o + M_a - M_b)$

Klohn Crippen Berger

PROJECT#:			
PROJECT:	Fundão Tailings Dam Review Panel		
LOCATION:			
DATE:	2016-05-16		
TESTED BY:	BY	CHECKED BY:	JG

SPECIFIC GRAVITY OF SOIL SOLIDS (ASTM-D854)

Hole Number	PSD1			PSD1		
Sample Number	TX21			TX22		
Depth (m)	-			-		
Sample Description	Sand			Sand		
Flask No.	SG10	SG12		SG6	SG7	
Volume of Flask @ 20° C ml	500	500		500	500	
Method of Air removal	Boiling	Boiling		Boiling	Boiling	
De-airing Period hr	2	2		2	2	
Test temperature ° C	23.0	23.0		23.3	23.3	
Mass of Flask+Water (M_a) g	669.95	670.62		670.53	667.77	
Mass of Flask+Water+Soil (M_b) g	720.17	720.88		721.90	718.53	
Mass of Dish/Flask+Soil	246.80	247.56		248.64	244.96	
Mass of Dish/Flask	171.95	172.56		172.20	169.46	
Mass of Dry Soil (M_o) g	74.85	75.00		76.44	75.50	
Correction factor (K) @ Test Temperature	0.99933	0.99933		0.99933	0.99933	
Specific Gravity of Solids @ 20° C	**3.04**	**3.03**		**3.05**	**3.05**	
Average Specific Gravity of Solids @ 20° C	**3.03**			**3.05**		

Hole Number	PSD1			PSD1		
Sample Number	TX23			TX24		
Depth (m)	-			-		
Sample Description	Sand			Sand		
Flask No.	SG8	SG9		SG2	SG3	
Volume of Flask @ 20° C ml	500	500		500	500	
Method of Air removal	Boiling	Boiling		Boiling	Boiling	
De-airing Period hr	2	2		2	2	
Test temperature ° C	23.3	23.3		23.2	23.2	
Mass of Flask+Water (M_a) g	670.54	667.92		671.52	672.24	
Mass of Flask+Water+Soil (M_b) g	720.61	718.19		722.70	722.97	
Mass of Dish/Flask+Soil	247.19	245.10		248.89	249.89	
Mass of Dish/Flask	172.41	169.70		172.41	173.96	
Mass of Dry Soil (M_o) g	74.78	75.40		76.48	75.93	
Correction factor (K) @ Test Temperature	0.99933	0.99933		0.99933	0.99933	
Specific Gravity of Solids @ 20° C	**3.02**	**3.00**		**3.02**	**3.01**	
Average Specific Gravity of Solids @ 20° C	**3.01**			**3.02**		

Specific Gravity of Solids @ 20° C = $(K \times M_o)/(M_o + M_a - M_b)$

Klohn Crippen Berger

PROJECT#:			
PROJECT:	Fundão Tailings Dam Review Panel		
LOCATION:			
DATE:	2016-04-16		
TESTED BY:	BY	CHECKED BY:	JG

SPECIFIC GRAVITY OF SOIL SOLIDS (ASTM-D854)

Hole Number	PSD1			PSD1		
Sample Number	TX25			TX26		
Depth (m)	-			-		
Sample Description	Sand			Sand		
Flask No.	KL2	KL3		8	10	
Volume of Flask @ 20° C ml	500	500		500	500	
Method of Air removal	Boiling	Boiling		Boiling	Boiling	
De-airing Period hr	2	2		2	2	
Test temperature ° C	22.5	22.5		22.5	22.5	
Mass of Flask+Water (M_a) g	675.52	675.87		678.72	679.81	
Mass of Flask+Water+Soil (M_b) g	726.44	727.16		729.74	730.66	
Mass of Dish/Flask+Soil	252.68	253.66		256.08	257.01	
Mass of Dish/Flask	177.10	177.37		180.50	181.56	
Mass of Dry Soil (M_o) g	75.58	76.29		75.58	75.45	
Correction factor (K) @ Test Temperature	0.99945	0.99945		0.99945	0.99945	
Specific Gravity of Solids @ 20° C	**3.06**	**3.05**		**3.08**	**3.07**	
Average Specific Gravity of Solids @ 20° C	**3.06**			**3.07**		

Hole Number	PSD1			PSD1		
Sample Number	TX27			TX28		
Depth (m)	-			-		
Sample Description	Sand			Sand		
Flask No.	SG2	SG3		SG6	SG7	
Volume of Flask @ 20° C ml	500	500		500	500	
Method of Air removal	Boiling	Boiling		Boiling	Boiling	
De-airing Period hr	2	2		2	2	
Test temperature ° C	22.2	22.2		22.2	22.2	
Mass of Flask+Water (M_a) g	671.63	672.34		670.64	667.89	
Mass of Flask+Water+Soil (M_b) g	722.25	723.35		720.89	718.41	
Mass of Dish/Flask+Soil	248.42	249.69		246.70	244.38	
Mass of Dish/Flask	173.32	173.96		172.20	169.46	
Mass of Dry Soil (M_o) g	75.10	75.73		74.50	74.92	
Correction factor (K) @ Test Temperature	0.99952	0.99952		0.99952	0.99952	
Specific Gravity of Solids @ 20° C	**3.07**	**3.06**		**3.07**	**3.07**	
Average Specific Gravity of Solids @ 20° C	**3.06**			**3.07**		

Specific Gravity of Solids @ 20° C = $(K \times M_o)/(M_o + M_a - M_b)$

Klohn Crippen Berger

PROJECT#:			
PROJECT:	Fundão Tailings Dam Review Panel		
LOCATION:			
DATE:	2016-04-16		
TESTED BY:	BY	CHECKED BY:	JG

SPECIFIC GRAVITY OF SOIL SOLIDS (ASTM-D854)

Hole Number	PSD1			PSD1		
Sample Number	TX29			TX30		
Depth (m)	-			-		
Sample Description	Sand			Sand		
Flask No.	SG2	SG3		SG6	SG7	
Volume of Flask @ 20° C ml	500	500		500	500	
Method of Air removal	Boiling	Boiling		Boiling	Boiling	
De-airing Period hr	2	2		2	2	
Test temperature ° C	22.8	22.8		22.8	22.8	
Mass of Flask+Water (M_a) g	671.55	672.38		670.58	667.82	
Mass of Flask+Water+Soil (M_b) g	721.74	723.15		720.73	717.82	
Mass of Dish/Flask+Soil	247.98	249.37		246.75	243.90	
Mass of Dish/Flask	173.30	173.96		172.20	169.46	
Mass of Dry Soil (M_o) g	74.68	75.41		74.55	74.44	
Correction factor (K) @ Test Temperature	0.99938	0.99938		0.99938	0.99938	
Specific Gravity of Solids @ 20° C	**3.05**	**3.06**		**3.05**	**3.04**	
Average Specific Gravity of Solids @ 20° C	**3.05**			**3.05**		

Hole Number	PSD1			PSD1		
Sample Number	TX31			TX32		
Depth (m)	-			-		
Sample Description	Sand			Sand		
Flask No.	KL2	KL3		SG10	SG12	
Volume of Flask @ 20° C ml	500	500		500	500	
Method of Air removal	Boiling	Boiling		Boiling	Boiling	
De-airing Period hr	2	2		2	2	
Test temperature ° C	22.8	22.8		22.8	22.8	
Mass of Flask+Water (M_a) g	675.48	675.83		669.97	670.65	
Mass of Flask+Water+Soil (M_b) g	726.50	726.33		720.08	721.39	
Mass of Dish/Flask+Soil	252.94	252.36		246.52	247.97	
Mass of Dish/Flask	177.09	177.37		171.95	172.56	
Mass of Dry Soil (M_o) g	75.85	74.99		74.57	75.41	
Correction factor (K) @ Test Temperature	0.99938	0.99938		0.99938	0.99938	
Specific Gravity of Solids @ 20° C	**3.05**	**3.06**		**3.05**	**3.05**	
Average Specific Gravity of Solids @ 20° C	**3.06**			**3.05**		

Specific Gravity of Solids @ 20° C = $(K \times M_o)/(M_o + M_a - M_b)$

Klohn Crippen Berger

PROJECT#:			
PROJECT:	Fundão Tailings Dam Review Panel		
LOCATION:			
DATE:	2016-07-12		
TESTED BY:	NG	CHECKED BY:	JG

SPECIFIC GRAVITY OF SOIL SOLIDS
(ASTM-D854)

Sample	Slimes			
Flask No.	1	2		
Method of Air removal	Boiling	Boiling		
Test temperature ^{o} C	20.0	20.0		
Mass of Flask+Water (M_a) g	343.53	342.32		
Mass of Flask+Water+Soil (M_b) g	398.64	410.57		
Mass of Dish/Flask+Soil	169.62	184.12		
Mass of Dish/Flask	95.69	92.46		
Mass of Dry Soil (M_o) g	73.93	91.66		
Volume of solid displaced	18.82	23.41		
Correction factor (K) @ Test Temperature	1.00000	1.00000		
Specific Gravity of Solids @ 20^{o} C	3.928	3.915		
Average Specific Gravity of Solids @ 20^{o} C	**3.922**			

Sample No.				
Flask No.				
Method of Air removal				
Test temperature ^{o} C				
Mass of Flask+Water (M_a) g				
Mass of Flask+Water+Soil (M_b) g				
Mass of Dish/Flask+Soil				
Mass of Dish/Flask				
Mass of Dry Soil (M_o) g				
Volume of solid displaced				
Correction factor (K) @ Test Temperature				
Specific Gravity of Solids @ 20^{o} C				
Average Specific Gravity of Solids @ 20^{o} C				

Specific Gravity of Solids @ 20^{o} C = $(K \times M_o)/(M_o + M_a - M_b)$

Klohn Crippen Berger

Client:
Project Name: Fundão Tailings Dam Review Panel
Project No.:
Date: 2016-03-18
Tested By: Vaclav K Checked By: Shamim Ahsan

D2-3 – Density Tests

MAXIMUM AND MINIMUM DENSITY USING A VIBRATORY TABLE

ASTM D 4253 & D 4254

Client:	Klohn Crippen Berger Ltd.	Project No:	1649374
Project:	Min/Max Density Testing	Phase No.:	1007
Sample No:	1	Date sampled:	Unknown
Location:	Unknown	Sampled by:	Client
Source:	Unknown	Date tested:	June 10, 2016
Sample Type:	Tailing Sand	Tested by:	VN

TRIAL	Maximum Index Density (Dry Method 2A) kg/m^3	Maximum Index Density (Wet Method 2B) kg/m^3	Minimum Index Density (Method A) kg/m^3
1	2067	1929	1629
2	2048	1938	1629
Average	**2057**	**1933**	**1629**

Note: (1) Small standard mould was used

(2) Water content was 13.9% when the max density wet method was conducted.

KCB note: the sample tested had a specific gravity of 3.04.

Reported by: V. Nogra

Reviewed by: _____

L. Hu, M.Sc.E., P.Eng.

RELATIVE DENSITY

MINIMUM DENSITY

Determination no.	1	2	3	
Mass of soil + mold,g	8996	8996	8996	
Mass of mold, g	5806	5806	5806	
Mass of soil, g	3190	3190	3190	
Volume of mold, cm^3	2122.7	2122.7	2122.7	
Density, g/cm^3	1.503	1.503	1.503	

MAXIMUM DENSITY

Determination no.				
Final dial reading, mm				
Initial dial reading, mm				
Difference, mm				
Plate thickness, mm				
Initial height of sample, mm				
Final height of sample, mm				
Correction for dust on plate, mm				
Corrected height of sample, mm				
Volume of sample, cm^3				
Mass of soil + mold, g				
Mass of mold, g				
Mass of soil, g				
Density, g/cm^3				

SPECIMEN DESCRIPTION: Fundão Sand
As received
Sample air dried before testing

REMARKS: Minimum Density.
Maximum Density done using Modified Proctor Test.
Using 6" Proctor mold.

Klohn Crippen Berger

PROJECT No.:	
PROJECT NAME:	Fundão Tailings Dam Review Panel
LOCATION:	
DATE:	2016-02-02
TESTED BY:	BY CHECKED BY: JG

MOISTURE - DENSITY RELATIONSHIP

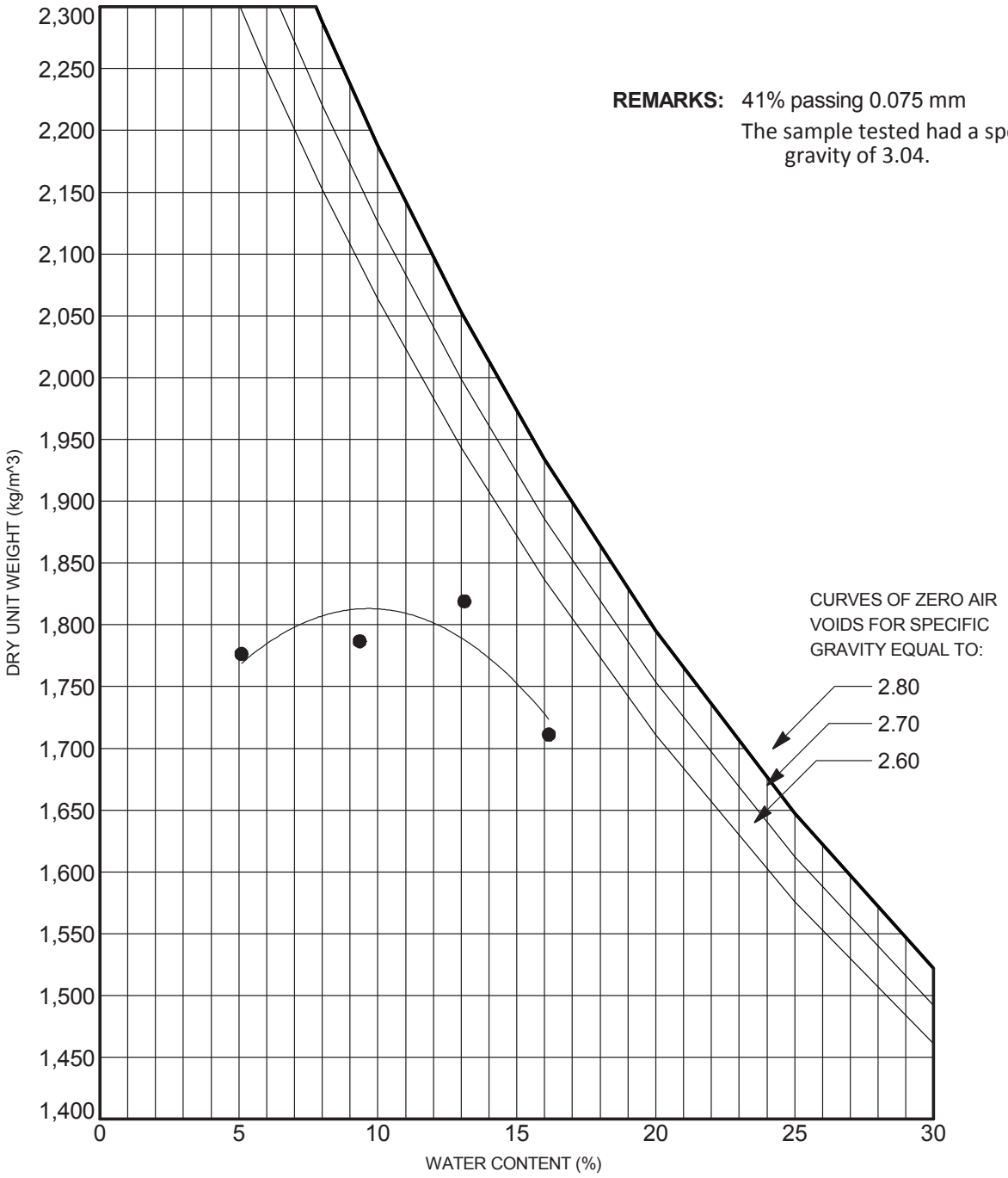

REMARKS: 41% passing 0.075 mm
The sample tested had a specific gravity of 3.04.

	TEST	DEPTH(m)	METHOD	OWC	MDW	MATERIAL DESCRIPTION
●	Fundão Sand	0.0	1557A	13.1	1819.0	As received

OWC = Optimum Water Content (%) MDW = Maximum dry Unit Weight (kg/m^3)

Klohn Crippen Berger

PROJECT NO.:
PROJECT: Fundão Tailings Dam Review Panel
LOCATION:
FIGURE:
DRAWN BY: BY **CHECKED BY:** JG

KCB_COMPACTION_TEST-SI FUNDAO TAILINGS DAM REVIEW PANEL.GPJ 24-7-16

MOISTURE-DENSITY RELATIONSHIP (ASTM D698 - Method A)

Description Of Material: Slimes

Trial No.	1	2	3	4	
Mass of wet sample + mold (gm)	6471	6598	6727	6660	
Mass of mold (gm)	4200	4200	4200	4200	
Mass of wet sample (gm)	2271	2398	2527	2460	
Volume of mold (cm^3)	941	941	941	941	
Wet Density (kg/m^3)	2413	2548	2685	2614	

Container number	#13	T-13	Y	HH	
Mass of wet sample + container (gm)	440.3	427.4	475.2	444.3	
Mass of dry sample + container (gm)	419.6	401.8	437.6	408.2	
Mass of container (gm)	210.0	209.9	214.4	213.4	
Water Content %	9.9	13.3	16.8	18.5	
Dry Density (kg/m^3)	2196	2248	2298	2206	

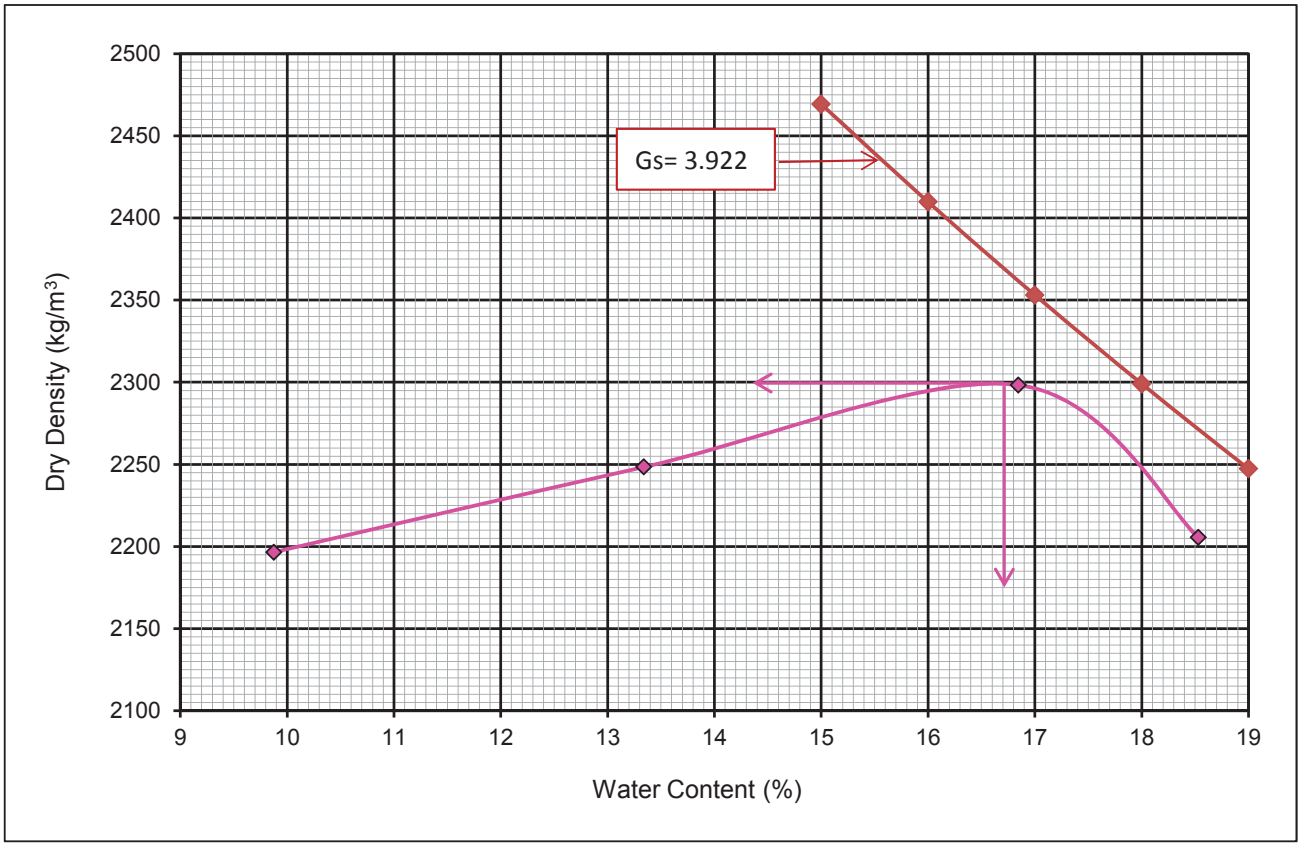

Maximum Dry Density (MDD): 2300 kg/m^3
Optimum Moisture Content (OMC): 16.7%

Klohn Crippen Berger	Client:
	Project Name: Fundão Tailings Dam Review Panel
	Project No.: Location:
	Sample : Slimes Date: 2016-04-18
	Tested By: Vaclav K Checked By: Shamim Ahsan

D2-4 – Particle Size Distribution

GRAIN SIZE DISTRIBUTION

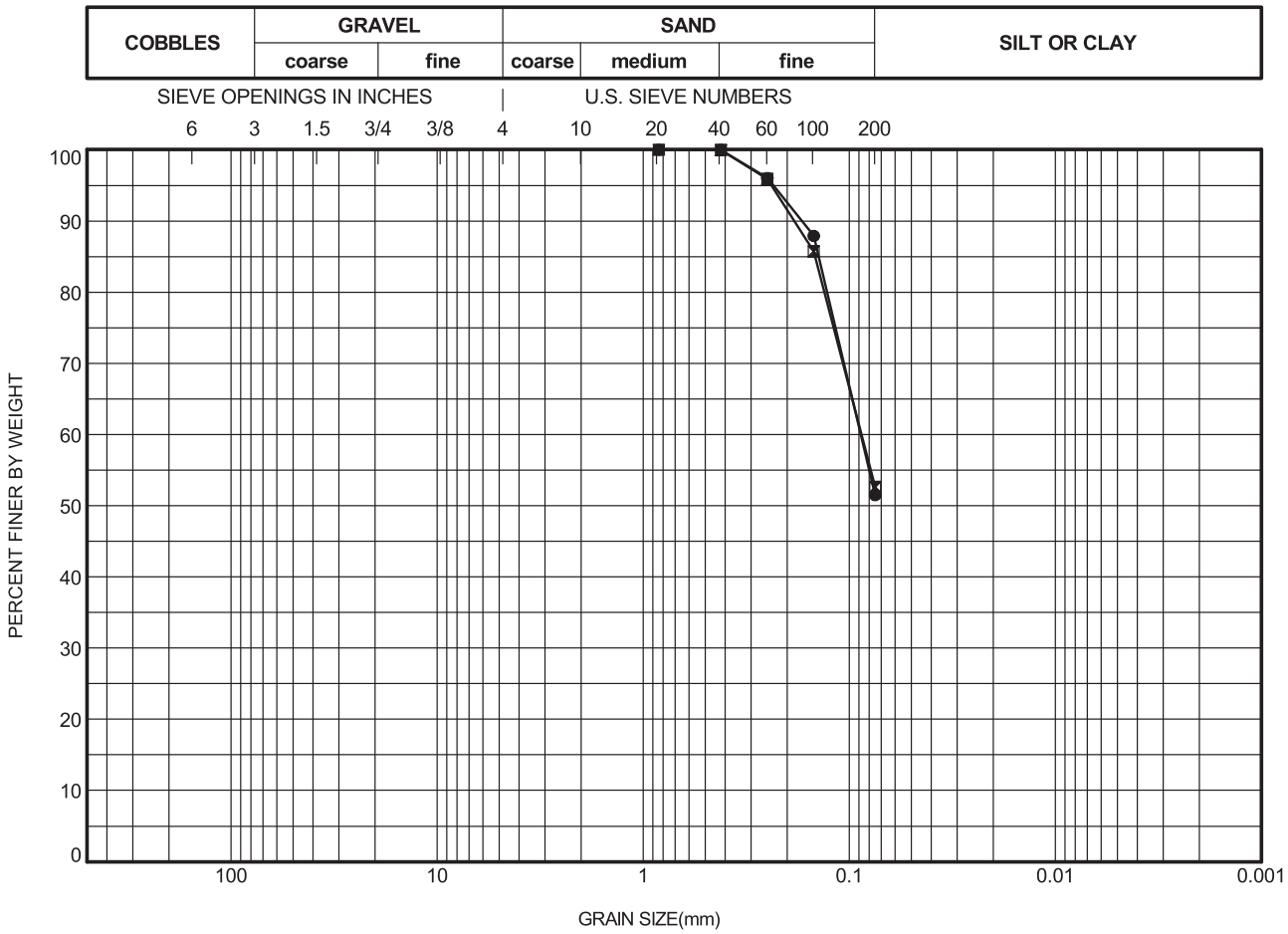

	HOLE	DEPTH (m)	D85	D60	D50	D15	D10	CU	%GRAVEL	%SAND	%FINES
●	PSD 1	0.00	0.141	0.088					0.0	48.5	51.5
⊠	PSD 1	0.00	0.147	0.087					0.0	47.4	52.6

	HOLE	SAMPLE	DEPTH (m)	W%	W_L	W_P	PI	REMARKS / SAMPLE DESCRIPTION
●	PSD 1	TX 1	0.00					Before TX test
⊠	PSD 1	TX 1	0.00					After TX test

CU = COEFFICIENT OF UNIFORMITY = D60/D10 PARTICLE SIZES, e.g. D85, in mm Tested by Wet Sieving Method (ASTM D1140 & D422)

Klohn Crippen Berger

PROJECT NO.:

PROJECT: Fundão Tailings Dam Review Panel

LOCATION:

FIGURE:

DRAWN BY: BY CHECKED BY: JG

KCB_GRAIN_SIZE-SI_FUNDAO TAILINGS DAM REVIEW PANEL.GPJ_SIEVE.GDT_23-7-16

GRAIN SIZE DISTRIBUTION

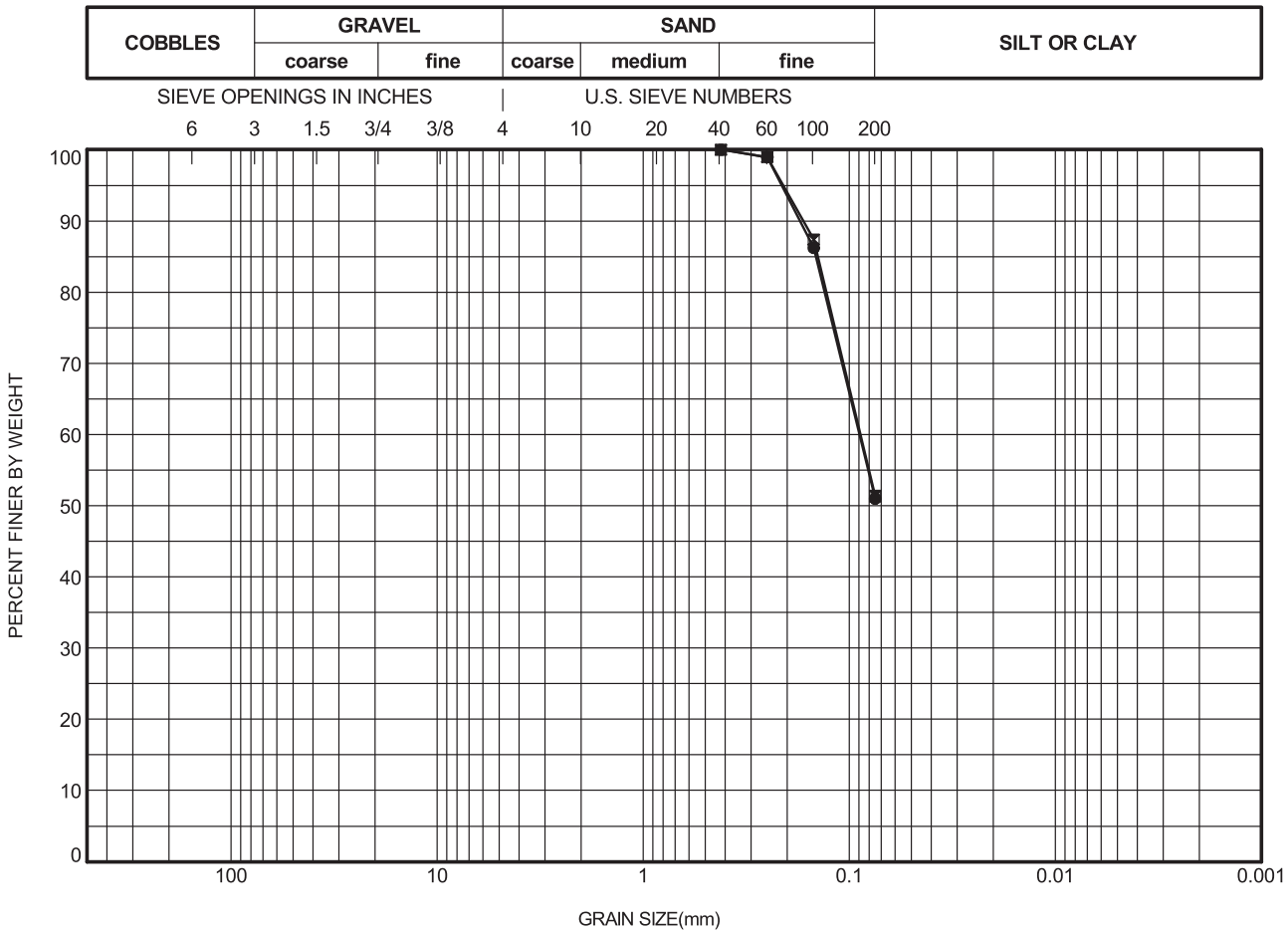

	HOLE	DEPTH (m)	D85	D60	D50	D15	D10	CU	%GRAVEL	%SAND	%FINES
●	PSD 1	0.00	0.146	0.089					0.0	49.0	51.0
⊠	PSD 1	0.00	0.142	0.088					0.0	48.7	51.3

	HOLE	SAMPLE	DEPTH (m)	W%	W_L	W_P	PI	REMARKS / SAMPLE DESCRIPTION
●	PSD 1	TX 2	0.00					Before TX test
⊠	PSD 1	TX 2	0.00					After TX test

CU = COEFFICIENT OF UNIFORMITY = D60/D10 PARTICLE SIZES, e.g. D85, in mm Tested by Wet Sieving Method (ASTM D1140 & D422)

Klohn Crippen Berger

PROJECT NO.:	
PROJECT:	Fundão Tailings Dam Review Panel
LOCATION:	
FIGURE:	
DRAWN BY: BY	CHECKED BY: JG

KCB_GRAIN_SIZE-SI_FUNDAO TAILINGS DAM REVIEW PANEL.GPJ_SIEVE.GDT_23-7-16

GRAIN SIZE DISTRIBUTION

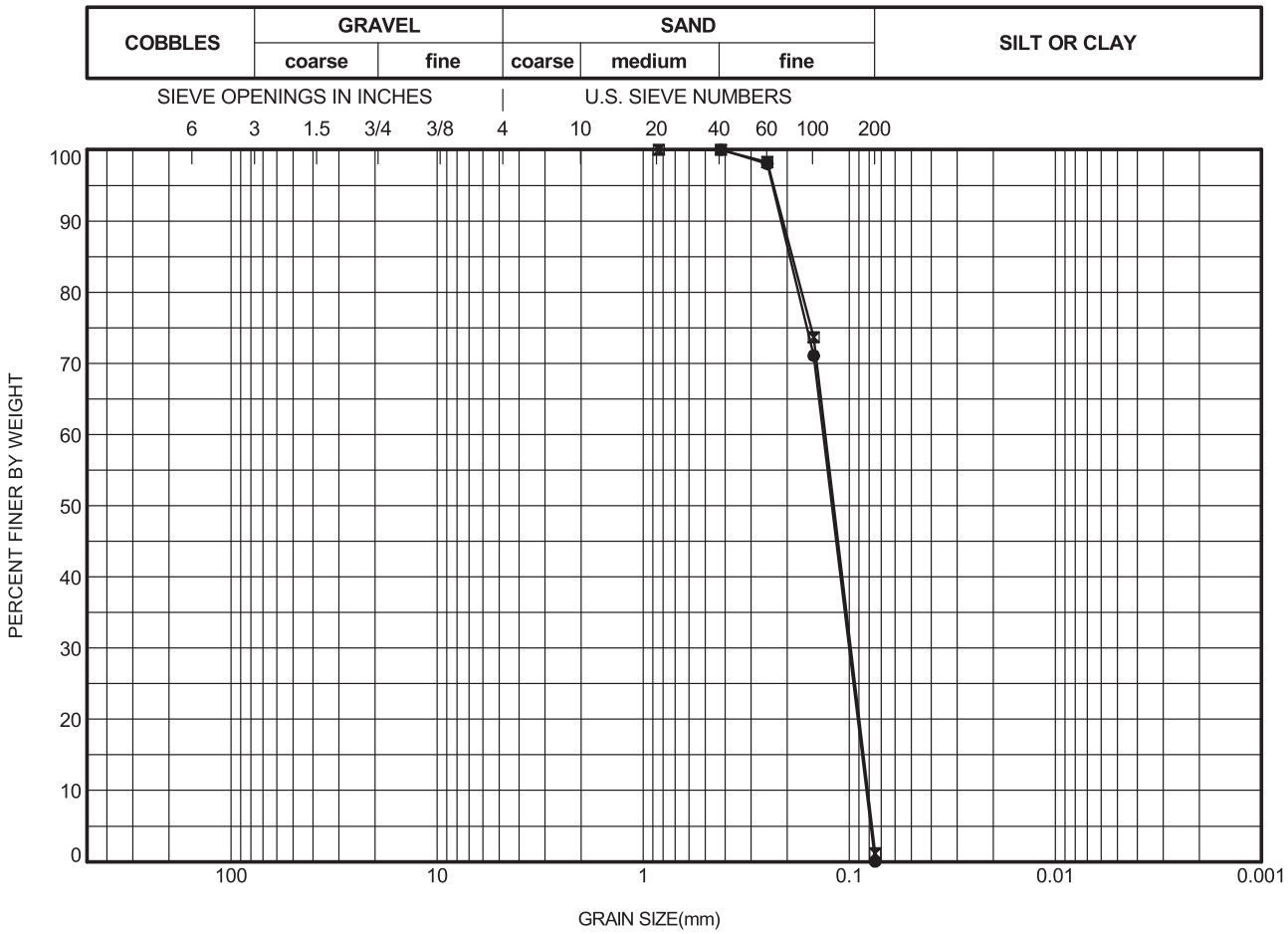

	HOLE	DEPTH (m)	D85	D60	D50	D15	D10	CU	%GRAVEL	%SAND	%FINES
●	PSD 2	0.00	0.195	0.134	0.122	0.087	0.083	1.621	0.0	100.0	0.0
⊠	PSD 2	0.00	0.189	0.131	0.119	0.086	0.082	1.605	0.0	98.8	1.2

	HOLE	SAMPLE	DEPTH (m)	W%	W_L	W_P	PI	REMARKS / SAMPLE DESCRIPTION
●	PSD 2	TX 3	0.00					Before Test
⊠	PSD 2	TX 3	0.00					After Test

CU = COEFFICIENT OF UNIFORMITY = D60/D10 PARTICLE SIZES, e.g. D85, in mm Tested by Wet Sieving Method (ASTM D1140 & D422)

Klohn Crippen Berger

PROJECT NO.:	
PROJECT:	Fundão Tailings Dam Review Panel
LOCATION:	
FIGURE:	
DRAWN BY:	BY
CHECKED BY:	JG

KCB_GRAIN_SIZE-SI_FUNDAO TAILINGS DAM REVIEW PANEL.GPJ_SIEVE.GDT_24-7-16

GRAIN SIZE DISTRIBUTION

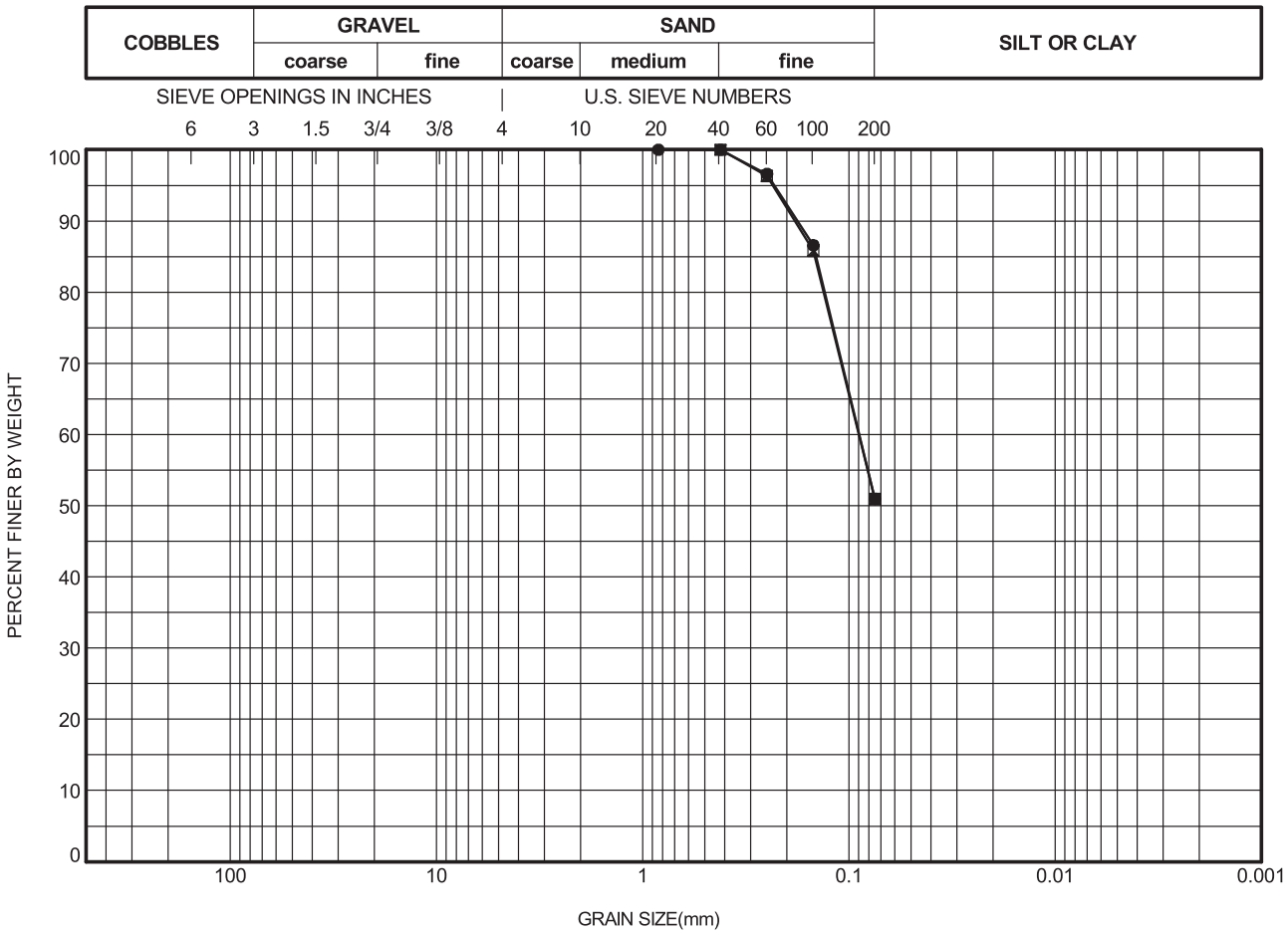

	HOLE	DEPTH (m)	D85	D60	D50	D15	D10	CU	%GRAVEL	%SAND	%FINES
●	PSD 1	0.00	0.145	0.089					0.0	49.0	51.0
⊠	PSD 1	0.00	0.147	0.090					0.0	49.1	50.9

	HOLE	SAMPLE	DEPTH (m)	W%	W_L	W_P	PI	REMARKS / SAMPLE DESCRIPTION
●	PSD 1	TX 4	0.00					Before TX test
⊠	PSD 1	TX 4	0.00					After TX test

CU = COEFFICIENT OF UNIFORMITY = D60/D10 PARTICLE SIZES, e.g. D85, in mm Tested by Wet Sieving Method (ASTM D1140 & D422)

Klohn Crippen Berger

PROJECT NO.:

PROJECT: Fundão Tailings Dam Review Panel

LOCATION:

FIGURE:

DRAWN BY: BY CHECKED BY: JG

KCB_GRAIN_SIZE-SI FUNDAO TAILINGS DAM REVIEW PANEL.GPJ SIEVE.GDT 23-7-16

GRAIN SIZE DISTRIBUTION

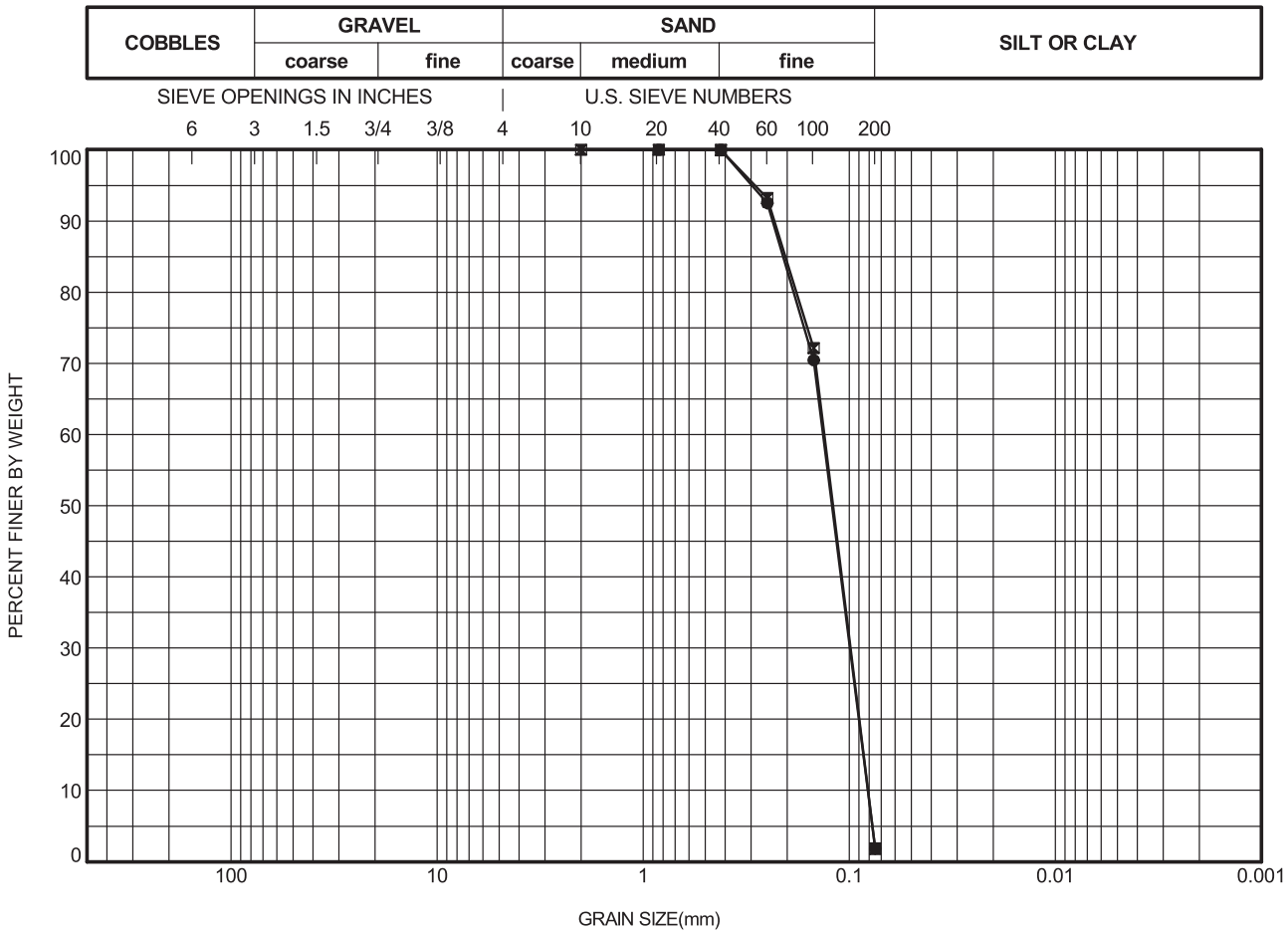

	HOLE	DEPTH (m)	D85	D60	D50	D15	D10	CU	%GRAVEL	%SAND	%FINES
●	PSD 2	0.00	0.210	0.134	0.121	0.086	0.081	1.649	0.0	98.2	1.8
⊠	PSD 2	0.00	0.204	0.132	0.120	0.085	0.081	1.629	0.0	98.2	1.8

	HOLE	SAMPLE	DEPTH (m)	W%	W_L	W_P	PI	REMARKS / SAMPLE DESCRIPTION
●	PSD 2	TX 5	0.00					Before Test
⊠	PSD 2	TX 5	0.00					After Test

CU = COEFFICIENT OF UNIFORMITY = D60/D10 PARTICLE SIZES, e.g. D85, in mm Tested by Wet Sieving Method (ASTM D1140 & D422)

Klohn Crippen Berger

PROJECT NO.:	
PROJECT:	Fundão Tailings Dam Review Panel
LOCATION:	
FIGURE:	
DRAWN BY:	BY
CHECKED BY:	JG

KCB_GRAIN_SIZE-SI_FUNDAO TAILINGS DAM REVIEW PANEL.GPJ_SIEVE.GDT_24-7-16

GRAIN SIZE DISTRIBUTION

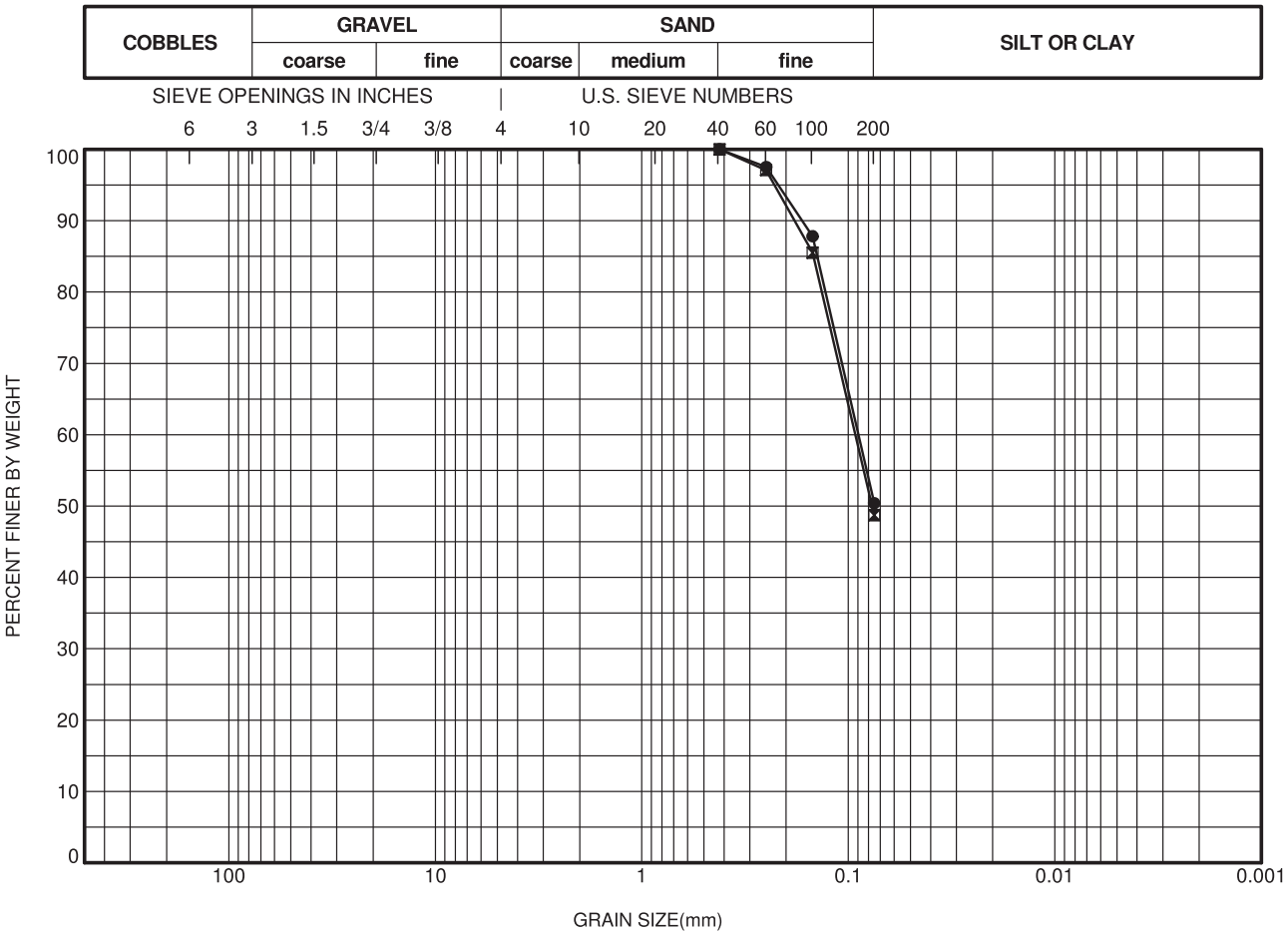

	HOLE	DEPTH (m)	D85	D60	D50	D15	D10	CU	%GRAVEL	%SAND	%FINES
●	PSD 1	0.00	0.141	0.089					0.0	49.6	50.4
⊠	PSD 1	0.00	0.148	0.093	0.077				0.0	51.3	48.7

	HOLE	SAMPLE	DEPTH (m)	W%	W_L	W_P	PI	REMARKS / SAMPLE DESCRIPTION
●	PSD 1	TX 6	0.00					Before TX test
⊠	PSD 1	TX 6	0.00					After TX test

CU = COEFFICIENT OF UNIFORMITY = D60/D10 PARTICLE SIZES, e.g. D85, in mm Tested by Wet Sieving Method (ASTM D1140 & D422)

Klohn Crippen Berger

PROJECT NO.:	
PROJECT:	Fundão Tailings Dam Review Panel
LOCATION:	
FIGURE:	
DRAWN BY: BY	CHECKED BY: JG

KC_GRAIN_SIZE-SI FUNDAO TAILINGS DAM REVIEW PANEL.GPJ SIEVE.GDT 16-7-28

GRAIN SIZE DISTRIBUTION

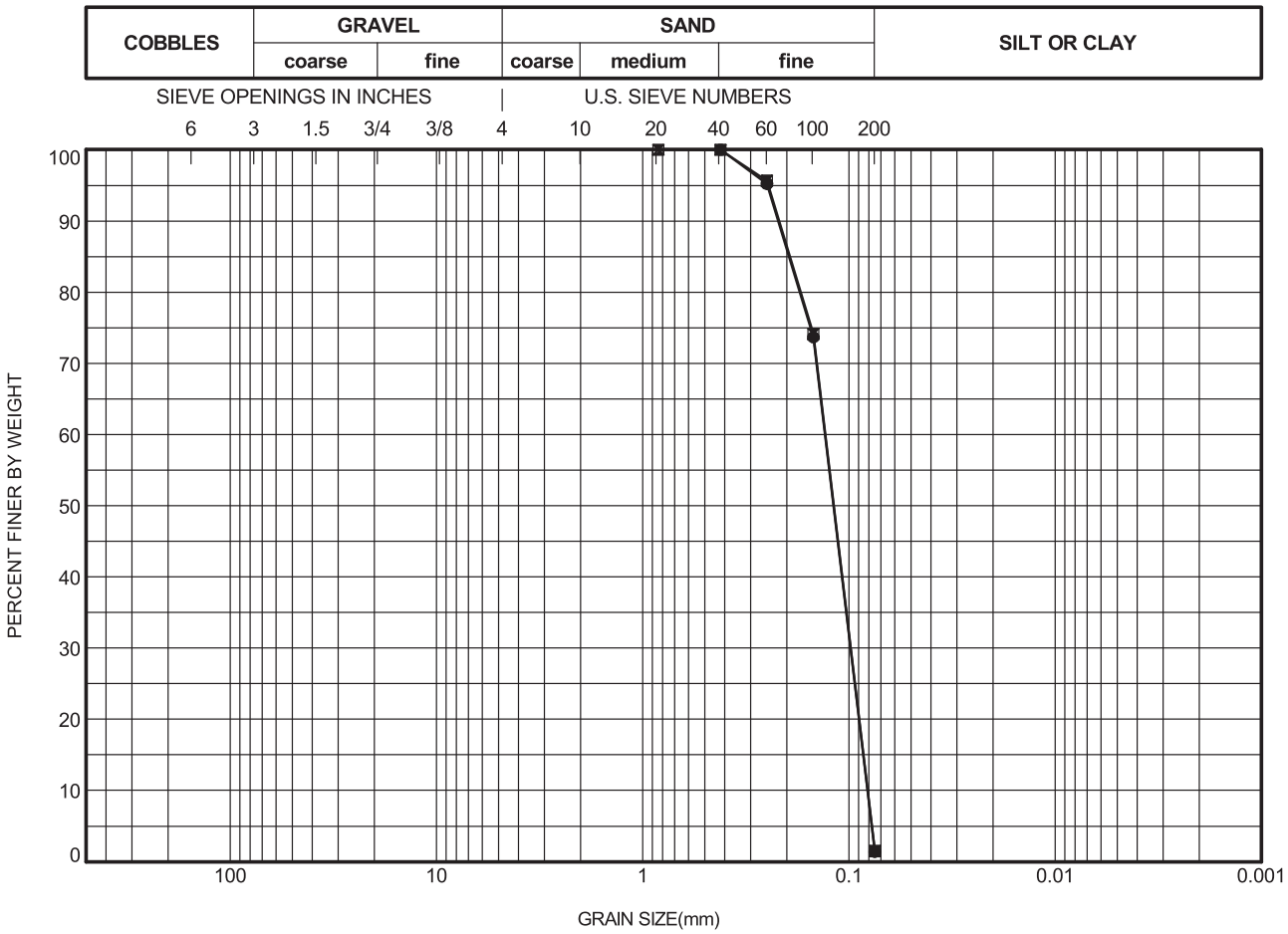

	HOLE	DEPTH (m)	D85	D60	D50	D15	D10	CU	%GRAVEL	%SAND	%FINES
●	PSD 2	0.00	0.196	0.131	0.119	0.085	0.081	1.608	0.0	98.6	1.4
⊠	PSD 2	0.00	0.194	0.130	0.119	0.085	0.081	1.604	0.0	98.5	1.5

	HOLE	SAMPLE	DEPTH (m)	W%	W_L	W_P	PI	REMARKS / SAMPLE DESCRIPTION
●	PSD 2	TX 7	0.00					Before Test
⊠	PSD 2	TX 7	0.00					After Test

CU = COEFFICIENT OF UNIFORMITY = D60/D10 PARTICLE SIZES, e.g. D85, in mm Tested by Wet Sieving Method (ASTM D1140 & D422)

Klohn Crippen Berger

PROJECT NO.:	
PROJECT:	Fundão Tailings Dam Review Panel
LOCATION:	
FIGURE:	
DRAWN BY:	BY
CHECKED BY:	JG

KCB_GRAIN_SIZE-SI_FUNDAO TAILINGS DAM REVIEW PANEL.GPJ_SIEVE.GDT_24-7-16

GRAIN SIZE DISTRIBUTION

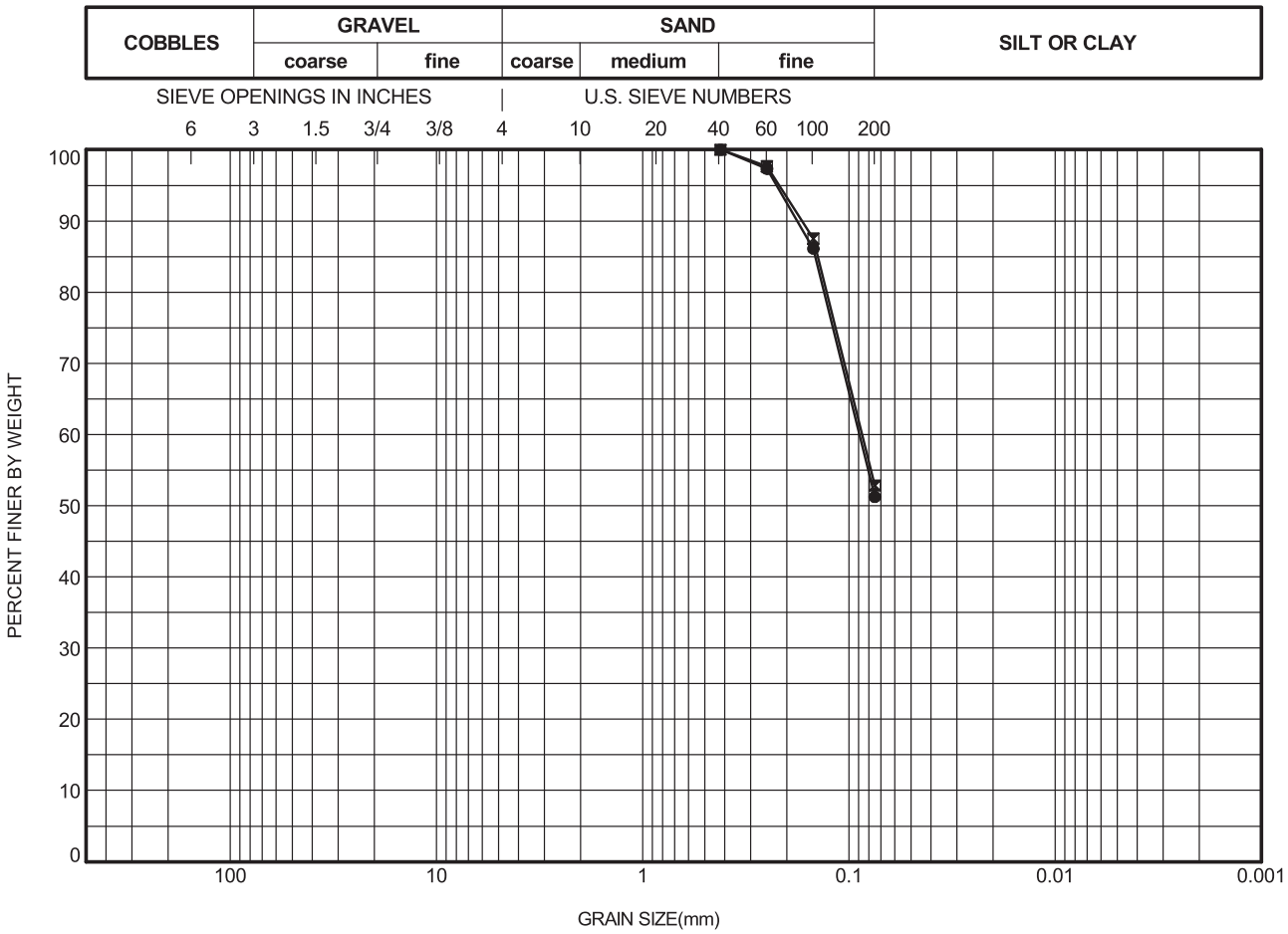

	HOLE	DEPTH (m)	D85	D60	D50	D15	D10	CU	%GRAVEL	%SAND	%FINES
●	PSD 1	0.00	0.146	0.089					0.0	48.8	51.2
⊠	PSD 1	0.00	0.142	0.086					0.0	47.2	52.8

	HOLE	SAMPLE	DEPTH (m)	W%	W_L	W_P	PI	REMARKS / SAMPLE DESCRIPTION
●	PSD 1	TX 8	0.00					Before TX test
⊠	PSD 1	TX 8	0.00					After TX test

CU = COEFFICIENT OF UNIFORMITY = D60/D10 PARTICLE SIZES, e.g. D85, in mm Tested by Wet Sieving Method (ASTM D1140 & D422)

Klohn Crippen Berger

PROJECT NO.:

PROJECT: Fundão Tailings Dam Review Panel

LOCATION:

FIGURE:

DRAWN BY: BY CHECKED BY: JG

KCB_GRAIN_SIZE-SI_FUNDAO TAILINGS DAM REVIEW PANEL.GPJ_SIEVE.GDT_23-7-16

GRAIN SIZE DISTRIBUTION

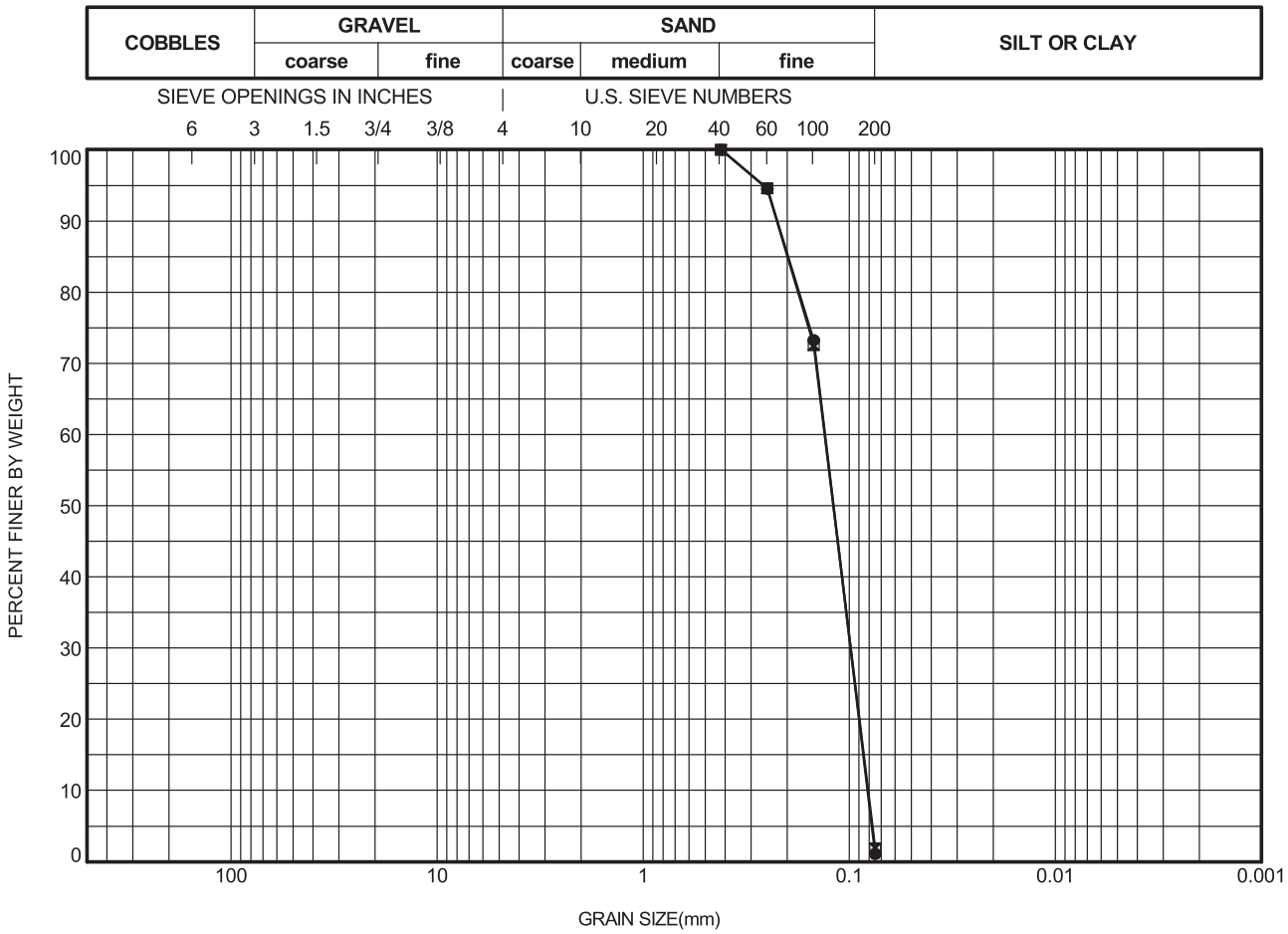

	HOLE	DEPTH (m)	D85	D60	D50	D15	D10	CU	%GRAVEL	%SAND	%FINES
●	PSD 2	0.00	0.198	0.131	0.119	0.086	0.082	1.609	0.0	98.9	1.1
⊠	PSD 2	0.00	0.200	0.132	0.120	0.085	0.081	1.625	0.0	98.2	1.8

	HOLE	SAMPLE	DEPTH (m)	W%	W_L	W_P	PI	REMARKS / SAMPLE DESCRIPTION
●	PSD 2	TX 9	0.00					Before Test
⊠	PSD 2	TX 9	0.00					After Test

CU = COEFFICIENT OF UNIFORMITY = D60/D10 PARTICLE SIZES, e.g. D85, in mm Tested by Wet Sieving Method (ASTM D1140 & D422)

Klohn Crippen Berger

PROJECT NO.:

PROJECT: Fundão Tailings Dam Review Panel

LOCATION:

FIGURE:

DRAWN BY: BY CHECKED BY: JG

KCB_GRAIN_SIZE-SI FUNDAO TAILINGS DAM REVIEW PANEL.GPJ SIEVE.GDT 24-7-16

GRAIN SIZE DISTRIBUTION

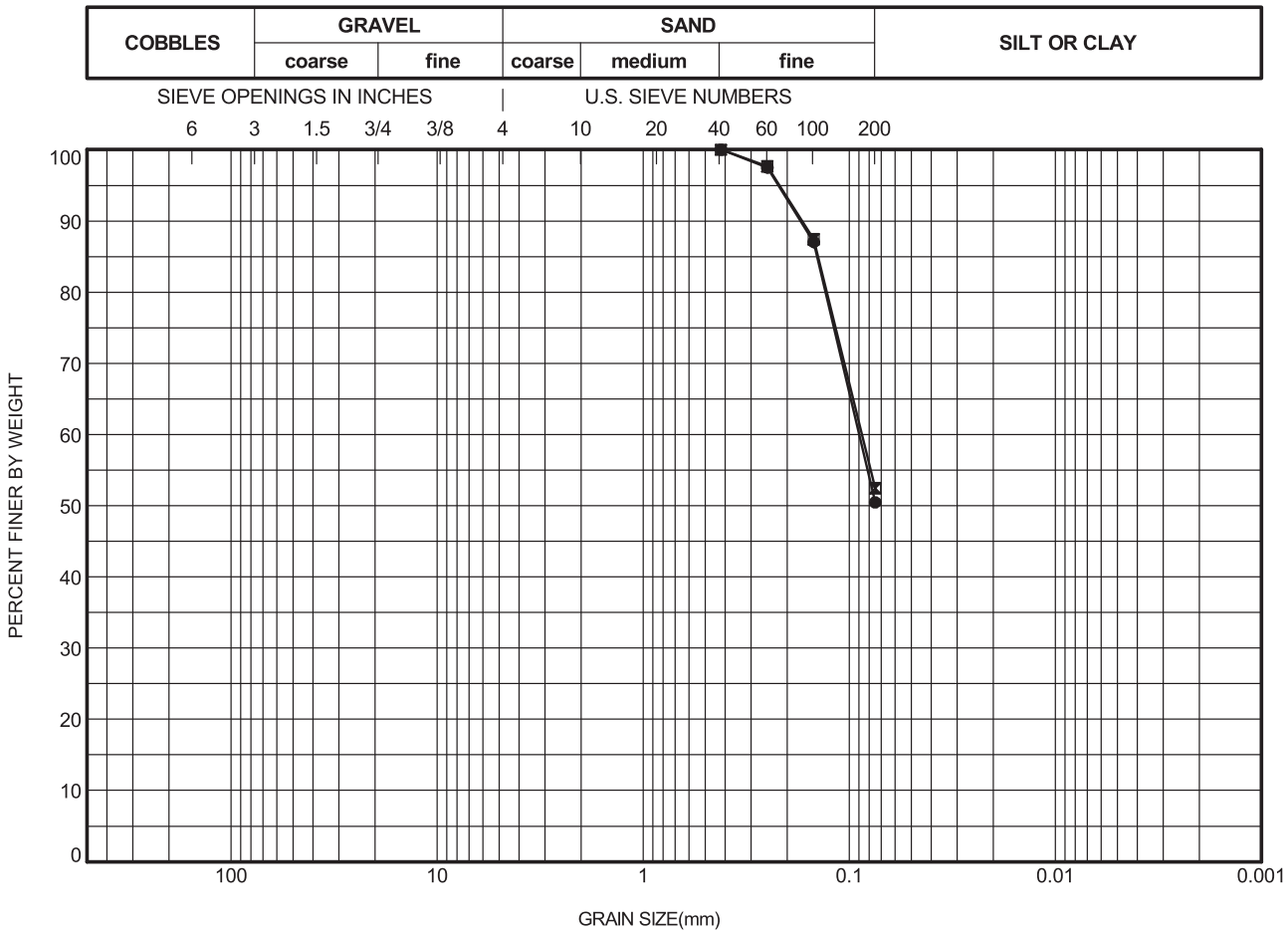

	HOLE	DEPTH (m)	D85	D60	D50	D15	D10	CU	%GRAVEL	%SAND	%FINES
●	PSD 1	0.00	0.143	0.090					0.0	49.5	50.5
⊠	PSD 1	0.00	0.142	0.087					0.0	47.5	52.5

	HOLE	SAMPLE	DEPTH (m)	W%	W_L	W_P	PI	REMARKS / SAMPLE DESCRIPTION
●	PSD 1	TX 10	0.00					Before TX test
⊠	PSD 1	TX 10	0.00					After TX test

CU = COEFFICIENT OF UNIFORMITY = D60/D10 PARTICLE SIZES, e.g. D85, in mm Tested by Wet Sieving Method (ASTM D1140 & D422)

Klohn Crippen Berger

PROJECT NO.:	
PROJECT:	Fundão Tailings Dam Review Panel
LOCATION:	
FIGURE:	
DRAWN BY:	BY
CHECKED BY:	JG

KCB_GRAIN_SIZE-SI_FUNDAO TAILINGS DAM REVIEW PANEL.GPJ_SIEVE.GDT_23-7-16

GRAIN SIZE DISTRIBUTION

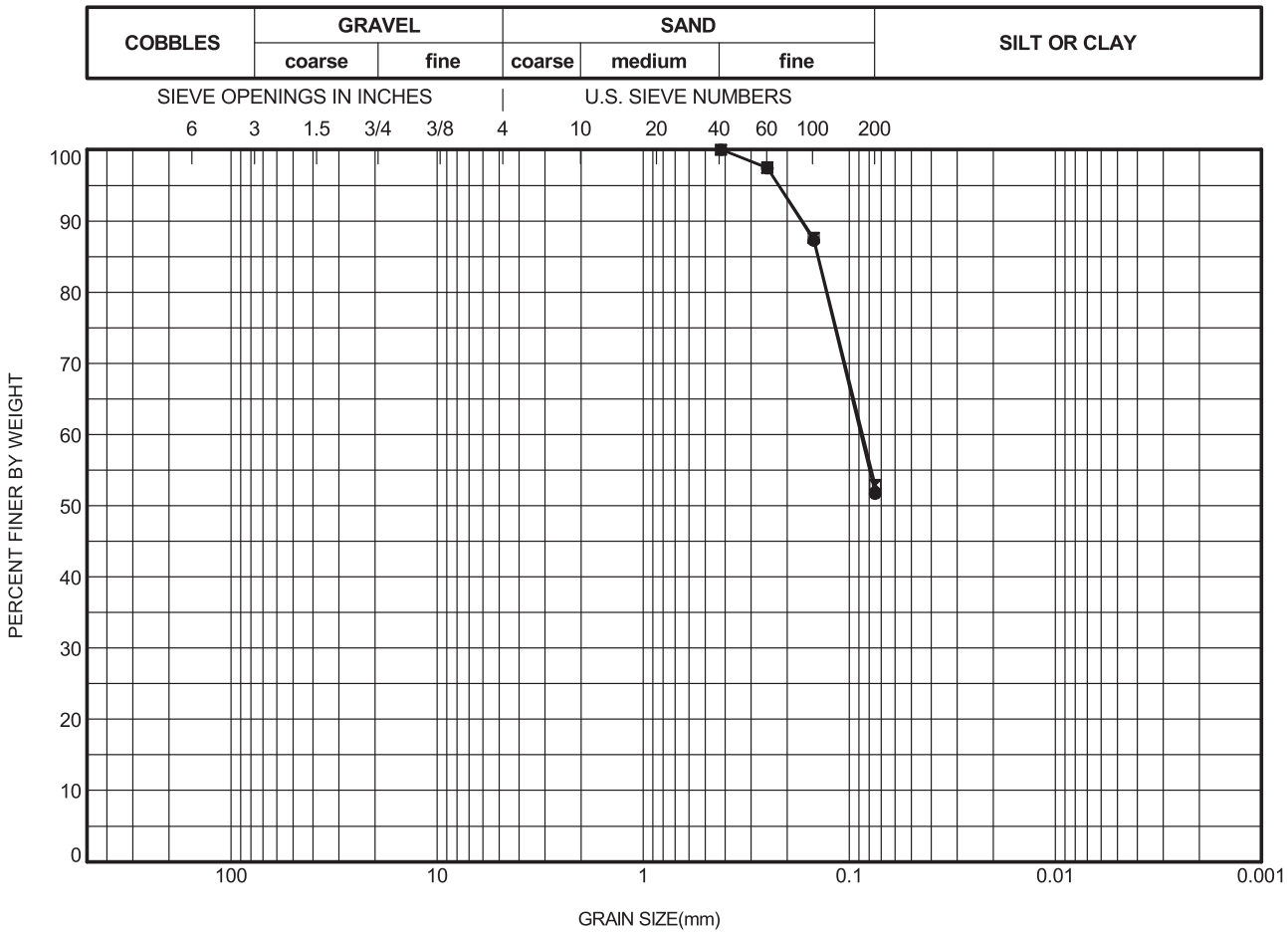

	HOLE	DEPTH (m)	D85	D60	D50	D15	D10	CU	%GRAVEL	%SAND	%FINES
●	PSD 1	0.00	0.143	0.088					0.0	48.3	51.7
⊠	PSD 1	0.00	0.141	0.086					0.0	47.1	52.9

	HOLE	SAMPLE	DEPTH (m)	W%	W_L	W_P	PI	REMARKS / SAMPLE DESCRIPTION
●	PSD 1	TX 11	0.00					Before TX test
⊠	PSD 1	TX 11	0.00					After TX test

CU = COEFFICIENT OF UNIFORMITY = D60/D10 PARTICLE SIZES, e.g. D85, in mm Tested by Wet Sieving Method (ASTM D1140 & D422)

Klohn Crippen Berger

PROJECT NO.:	
PROJECT:	Fundão Tailings Dam Review Panel
LOCATION:	
FIGURE:	
DRAWN BY:	BY
CHECKED BY:	JG

KCB_GRAIN_SIZE-SI_FUNDAO TAILINGS DAM REVIEW PANEL.GPJ_SIEVE.GDT_23-7-16

GRAIN SIZE DISTRIBUTION

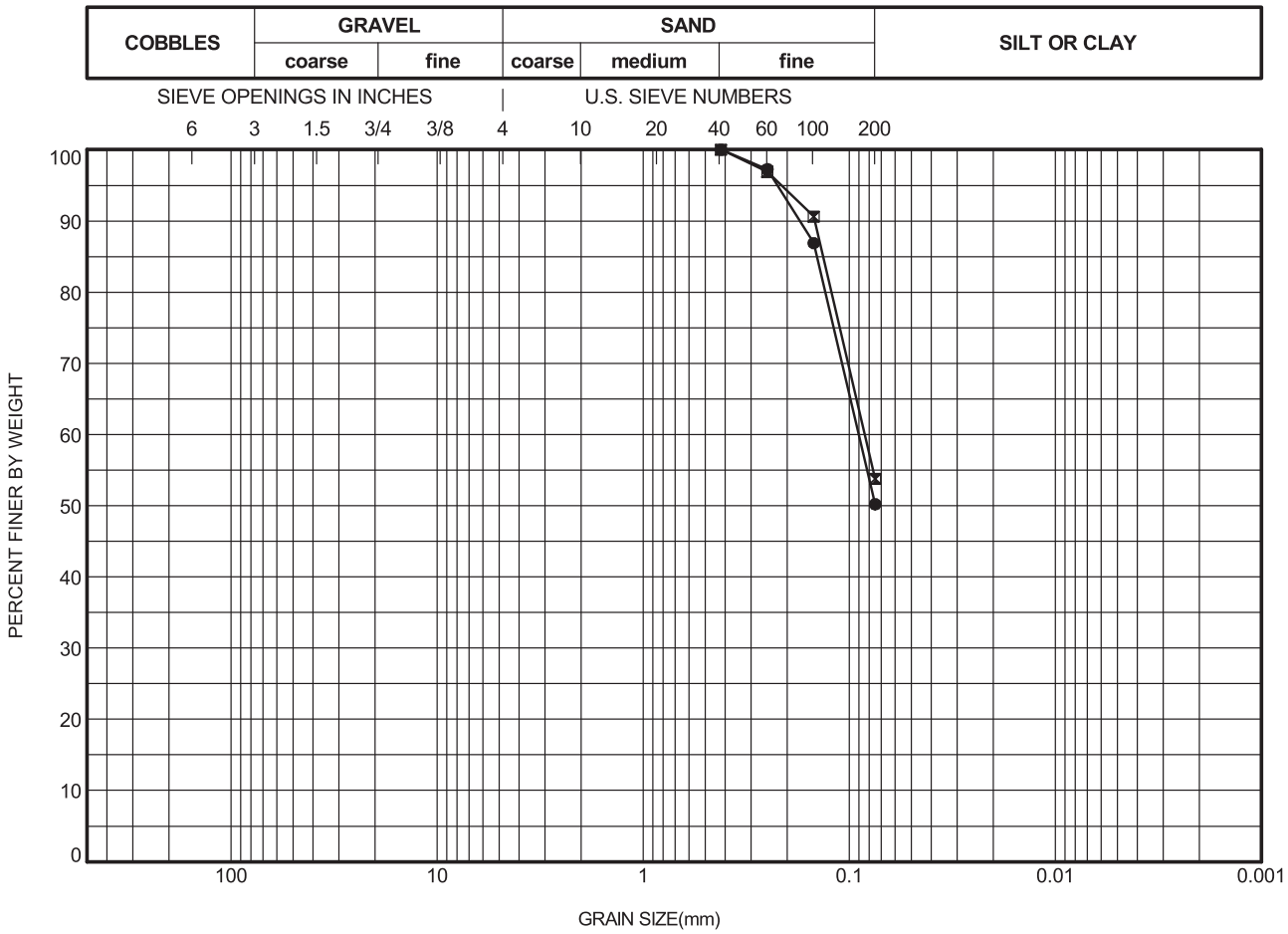

	HOLE	DEPTH (m)	D85	D60	D50	D15	D10	CU	%GRAVEL	%SAND	%FINES
●	PSD 1	0.00	0.144	0.090					0.0	49.8	50.2
⊠	PSD 1	0.00	0.134	0.084					0.0	46.2	53.8

	HOLE	SAMPLE	DEPTH (m)	W%	W_L	W_P	PI	REMARKS / SAMPLE DESCRIPTION
●	PSD 1	TX 12	0.00					Before TX test
⊠	PSD 1	TX 12	0.00					After TX test

CU = COEFFICIENT OF UNIFORMITY = D60/D10 PARTICLE SIZES, e.g. D85, in mm Tested by Wet Sieving Method (ASTM D1140 & D422)

Klohn Crippen Berger

PROJECT NO.:	
PROJECT:	Fundão Tailings Dam Review Panel
LOCATION:	
FIGURE:	
DRAWN BY:	BY
CHECKED BY:	JG

KCB_GRAIN_SIZE-SI_FUNDAO TAILINGS DAM REVIEW PANEL.GPJ_SIEVE.GDT_23-7-16

GRAIN SIZE DISTRIBUTION

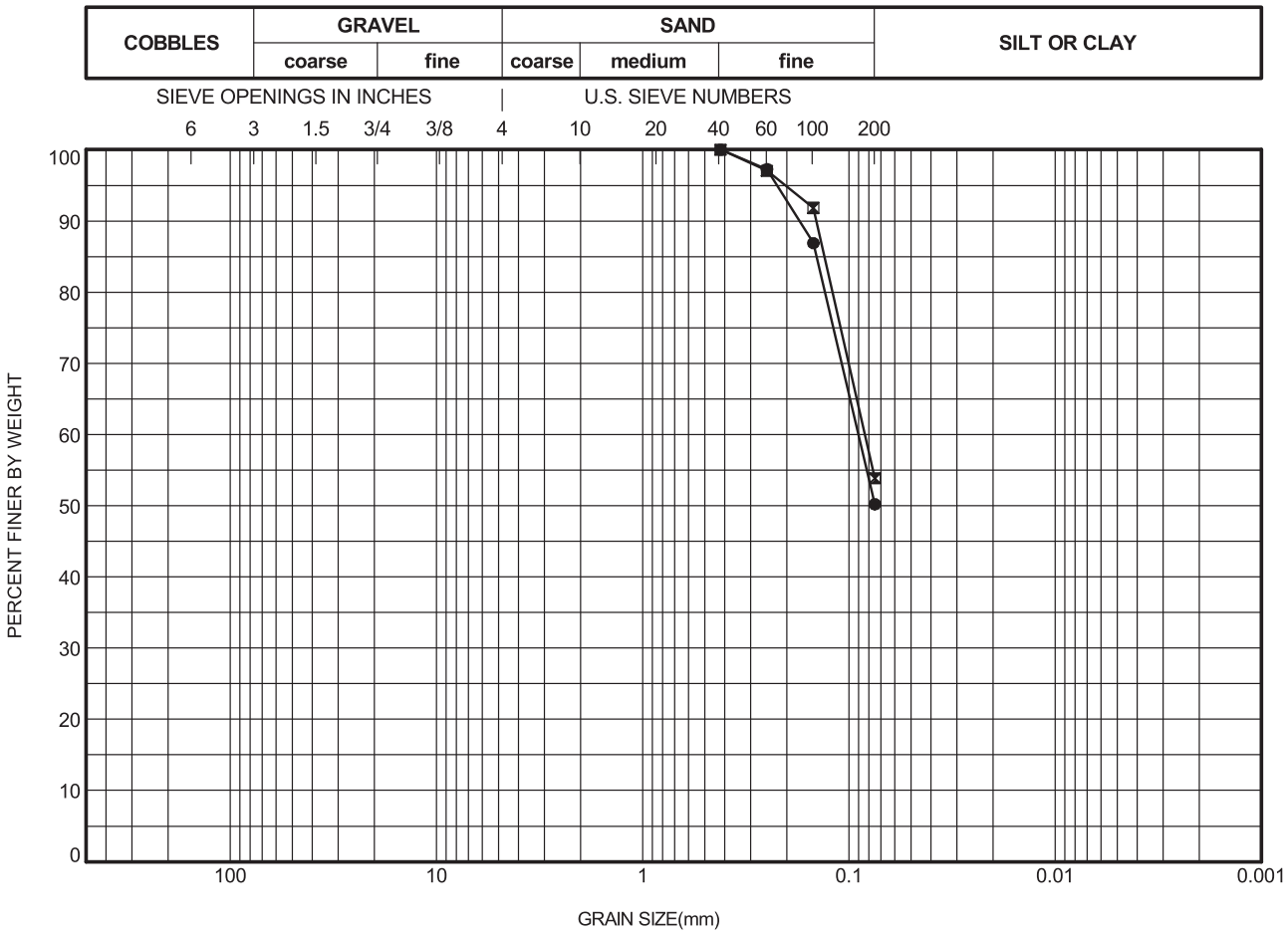

	HOLE	DEPTH (m)	D85	D60	D50	D15	D10	CU	%GRAVEL	%SAND	%FINES
●	PSD 1	0.00	0.144	0.090					0.0	49.8	50.2
⊠	PSD 1	0.00	0.132	0.084					0.0	46.1	53.9

	HOLE	SAMPLE	DEPTH (m)	W%	W_L	W_P	PI	REMARKS / SAMPLE DESCRIPTION
●	PSD 1	TX 13	0.00					Before TX test
⊠	PSD 1	TX 13	0.00					After TX test

CU = COEFFICIENT OF UNIFORMITY = D60/D10 PARTICLE SIZES, e.g. D85, in mm Tested by Wet Sieving Method (ASTM D1140 & D422)

Klohn Crippen Berger

PROJECT NO.:	
PROJECT:	Fundão Tailings Dam Review Panel
LOCATION:	
FIGURE:	
DRAWN BY:	BY
CHECKED BY:	JG

KCB_GRAIN_SIZE-SI_FUNDAO TAILINGS DAM REVIEW PANEL.GPJ_SIEVE.GDT_23-7-16

GRAIN SIZE DISTRIBUTION

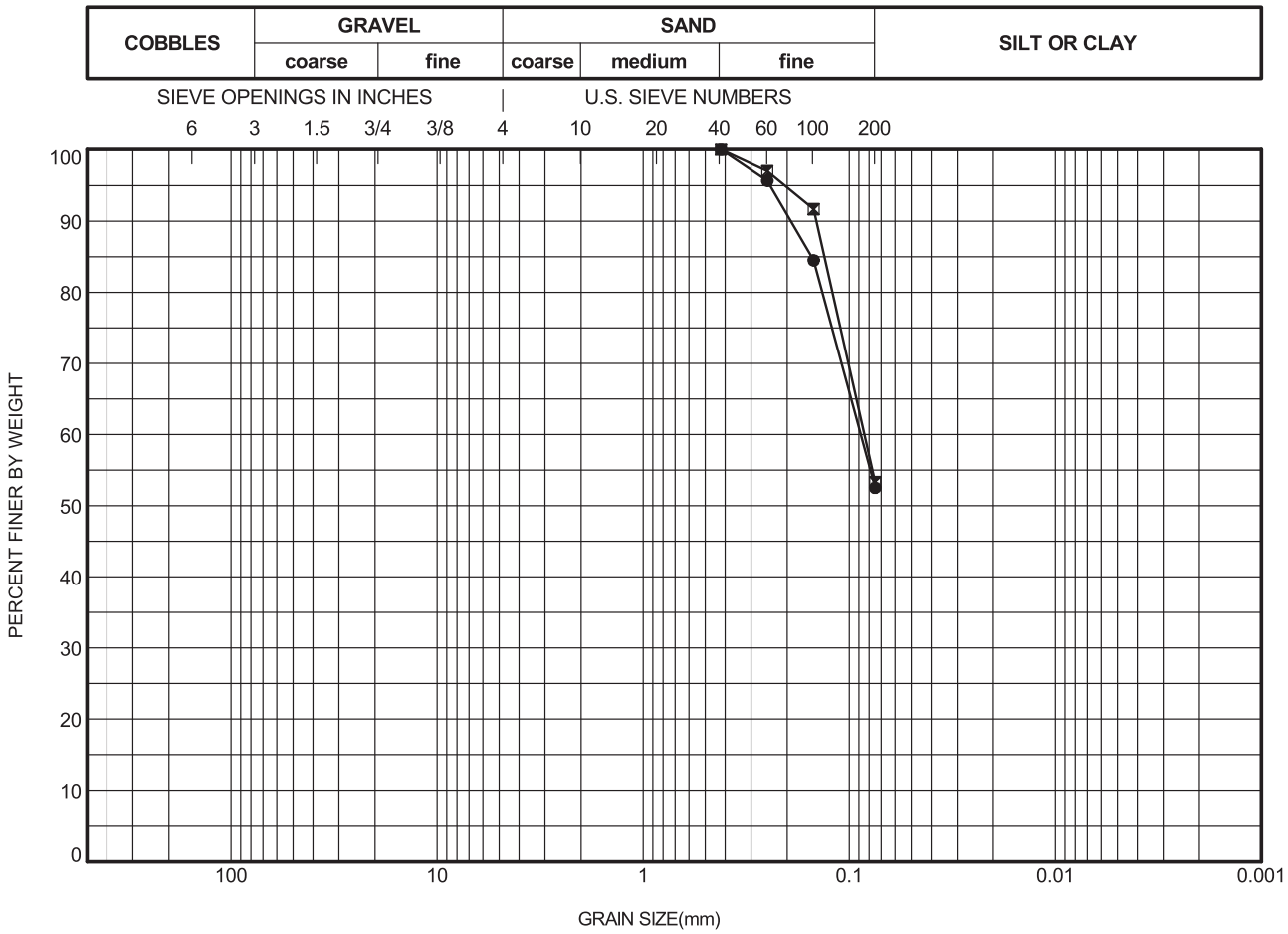

	HOLE	DEPTH (m)	D85	D60	D50	D15	D10	CU	%GRAVEL	%SAND	%FINES
●	PSD 1	0.00	0.153	0.088					0.0	47.5	52.5
⊠	PSD 1	0.00	0.132	0.085					0.0	46.7	53.3

	HOLE	SAMPLE	DEPTH (m)	W%	W_L	W_P	PI	REMARKS / SAMPLE DESCRIPTION
●	PSD 1	TX 14	0.00					Before TX test
⊠	PSD 1	TX 14	0.00					After TX test

CU = COEFFICIENT OF UNIFORMITY = D60/D10 PARTICLE SIZES, e.g. D85, in mm Tested by Wet Sieving Method (ASTM D1140 & D422)

Klohn Crippen Berger

PROJECT NO.:	
PROJECT:	Fundão Tailings Dam Review Panel
LOCATION:	
FIGURE:	
DRAWN BY:	BY
CHECKED BY:	JG

KCB_GRAIN_SIZE-SI_FUNDAO TAILINGS DAM REVIEW PANEL.GPJ_SIEVE.GDT_23-7-16

GRAIN SIZE DISTRIBUTION

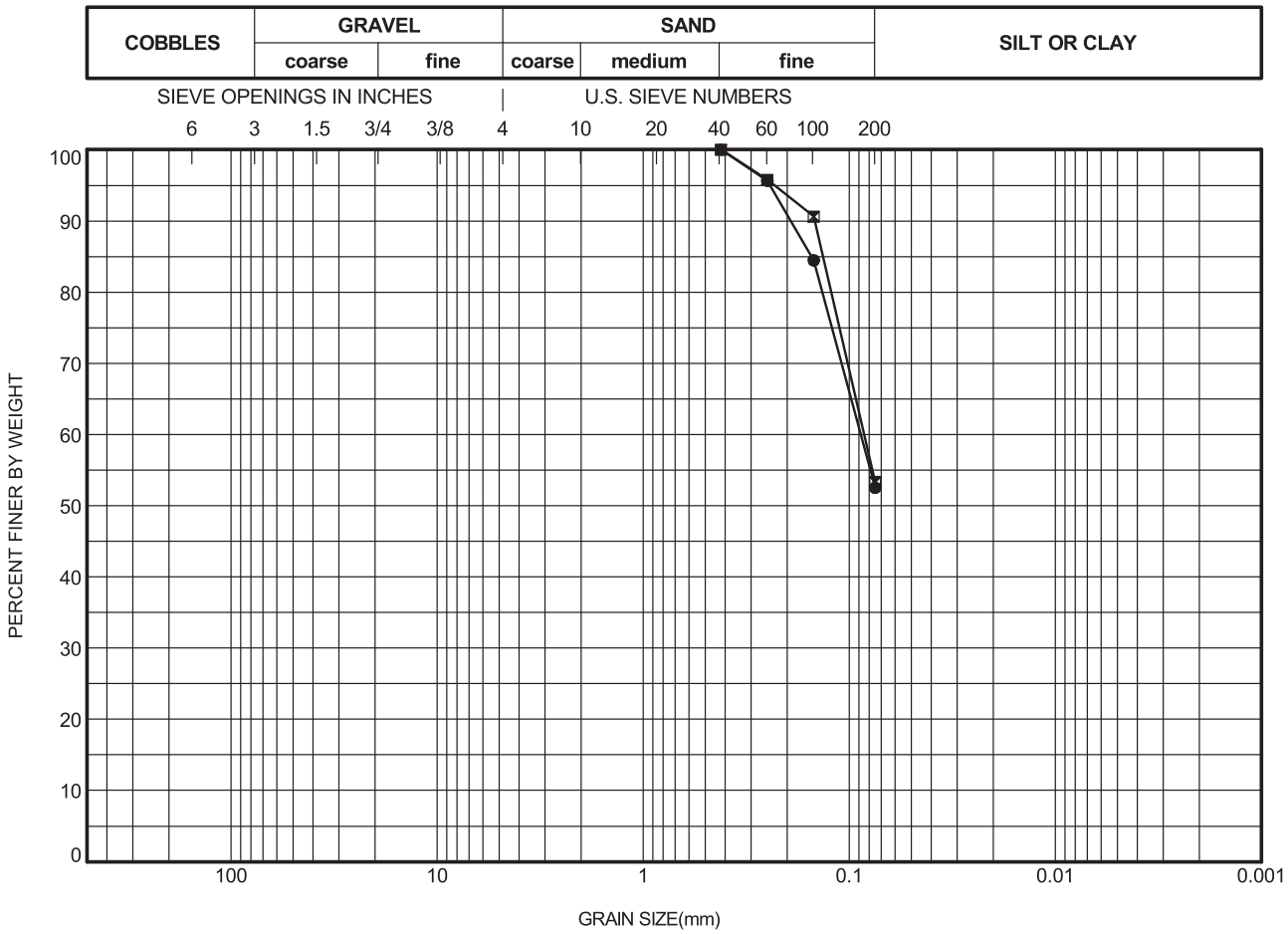

	HOLE	DEPTH (m)	D85	D60	D50	D15	D10	CU	%GRAVEL	%SAND	%FINES
●	PSD 1	0.00	0.153	0.088					0.0	47.5	52.5
⊠	PSD 1	0.00	0.134	0.085					0.0	46.7	53.3

	HOLE	SAMPLE	DEPTH (m)	W%	W_L	W_P	PI	REMARKS / SAMPLE DESCRIPTION
●	PSD 1	TX 15	0.00					Before TX test
⊠	PSD 1	TX 15	0.00					After TX test

CU = COEFFICIENT OF UNIFORMITY = D60/D10 PARTICLE SIZES, e.g. D85, in mm Tested by Wet Sieving Method (ASTM D1140 & D422)

Klohn Crippen Berger

PROJECT NO.:	
PROJECT:	Fundão Tailings Dam Review Panel
LOCATION:	
FIGURE:	
DRAWN BY:	BY
CHECKED BY:	JG

KCB_GRAIN_SIZE-SI_FUNDAO TAILINGS DAM REVIEW PANEL.GPJ_SIEVE.GDT_23-7-16

GRAIN SIZE DISTRIBUTION

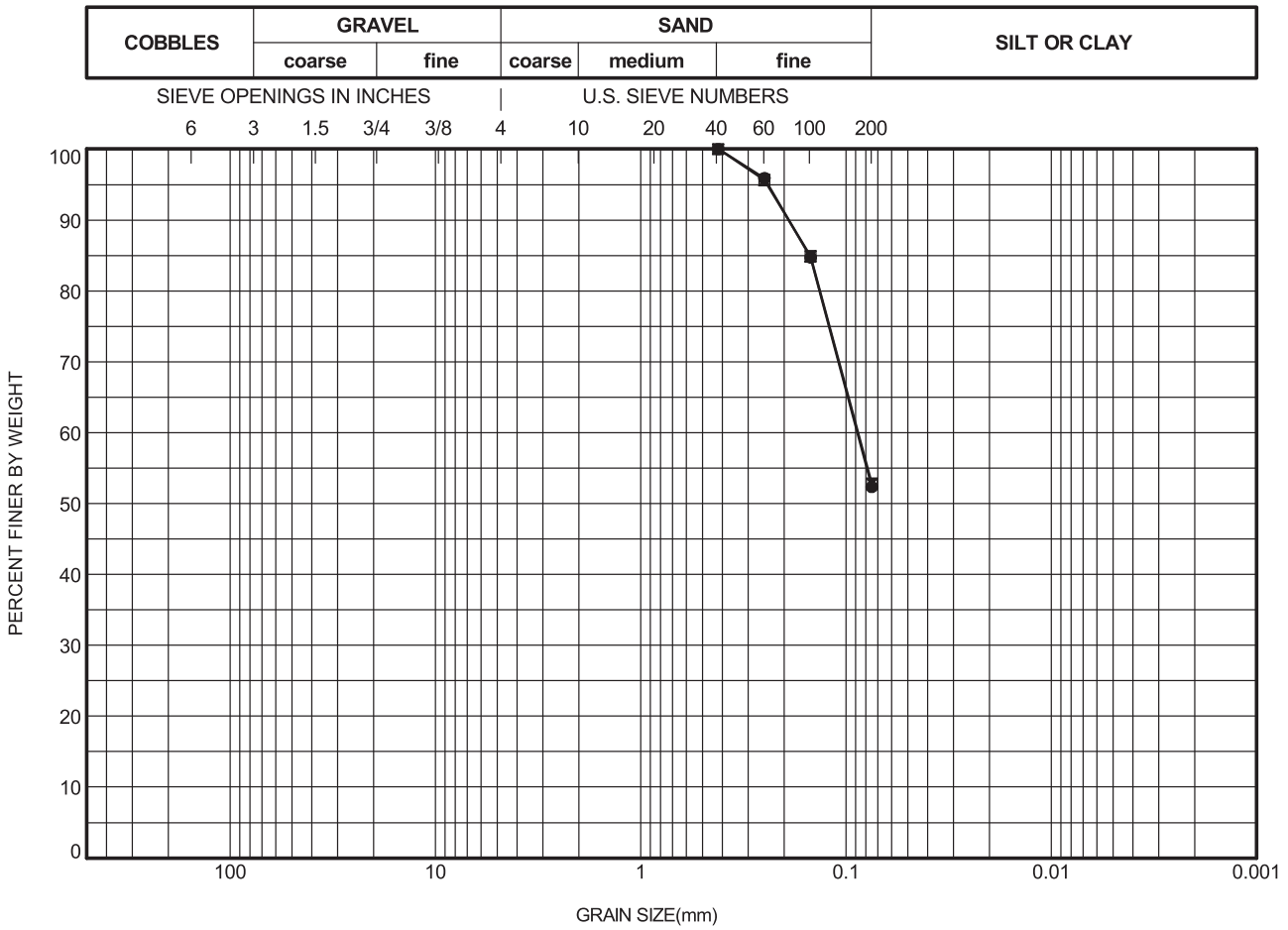

	HOLE	DEPTH (m)	D85	D60	D50	D15	D10	CU	%GRAVEL	%SAND	%FINES
●	PSD 1	0.00	0.151	0.088					0.0	47.7	52.3
⊠	PSD 1	0.00	0.150	0.087					0.0	47.2	52.8

	HOLE	SAMPLE	DEPTH (m)	W%	W_L	W_P	PI	REMARKS / SAMPLE DESCRIPTION
●	PSD 1	TX 16	0.00					Before TX test
⊠	PSD 1	TX 16	0.00					After TX test

CU = COEFFICIENT OF UNIFORMITY = D60/D10 PARTICLE SIZES, e.g. D85, in mm Tested by Wet Sieving Method (ASTM D1140 & D422)

Klohn Crippen Berger

PROJECT NO.:	
PROJECT:	Fundão Tailings Dam Review Panel
LOCATION:	
FIGURE:	
DRAWN BY:	BY
CHECKED BY:	JG

KCB_GRAIN_SIZE-SI_FUNDAO TAILINGS DAM REVIEW PANEL.GPJ_SIEVE.GDT_23-7-16

GRAIN SIZE DISTRIBUTION

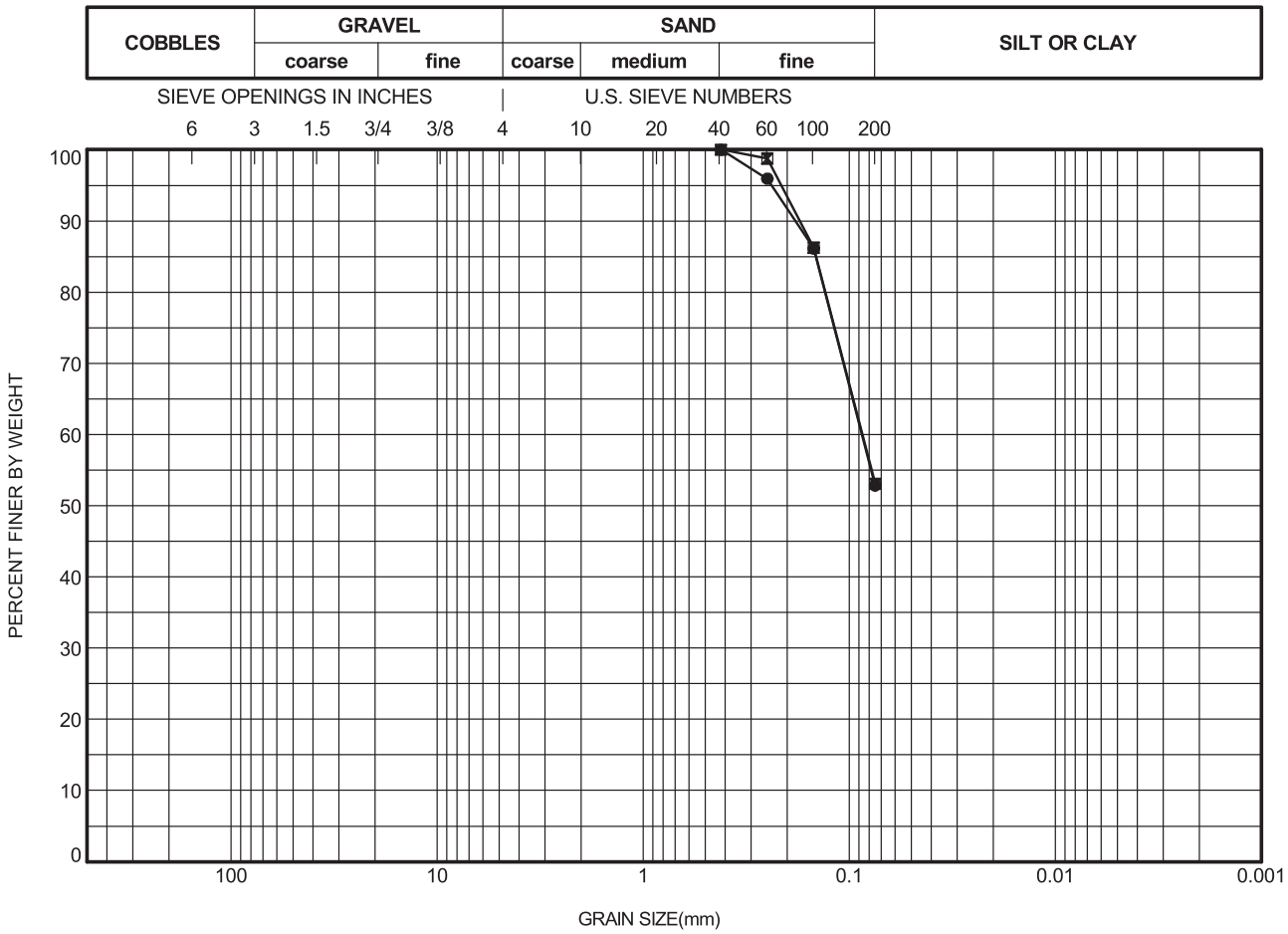

	HOLE	DEPTH (m)	D85	D60	D50	D15	D10	CU	%GRAVEL	%SAND	%FINES
●	PSD 1	0.00	0.146	0.087					0.0	47.2	52.8
⊠	PSD 1	0.00	0.145	0.087					0.0	46.9	53.1

	HOLE	SAMPLE	DEPTH (m)	W%	W_L	W_P	PI	REMARKS / SAMPLE DESCRIPTION
●	PSD 1	TX 17	0.00					Before TX test
⊠	PSD 1	TX 17	0.00					After TX test

CU = COEFFICIENT OF UNIFORMITY = D60/D10 PARTICLE SIZES, e.g. D85, in mm Tested by Wet Sieving Method (ASTM D1140 & D422)

Klohn Crippen Berger

PROJECT NO.:	
PROJECT:	Fundão Tailings Dam Review Panel
LOCATION:	
FIGURE:	
DRAWN BY:	BY
CHECKED BY:	JG

KCB_GRAIN_SIZE-SI_FUNDAO TAILINGS DAM REVIEW PANEL.GPJ_SIEVE.GDT_23-7-16

GRAIN SIZE DISTRIBUTION

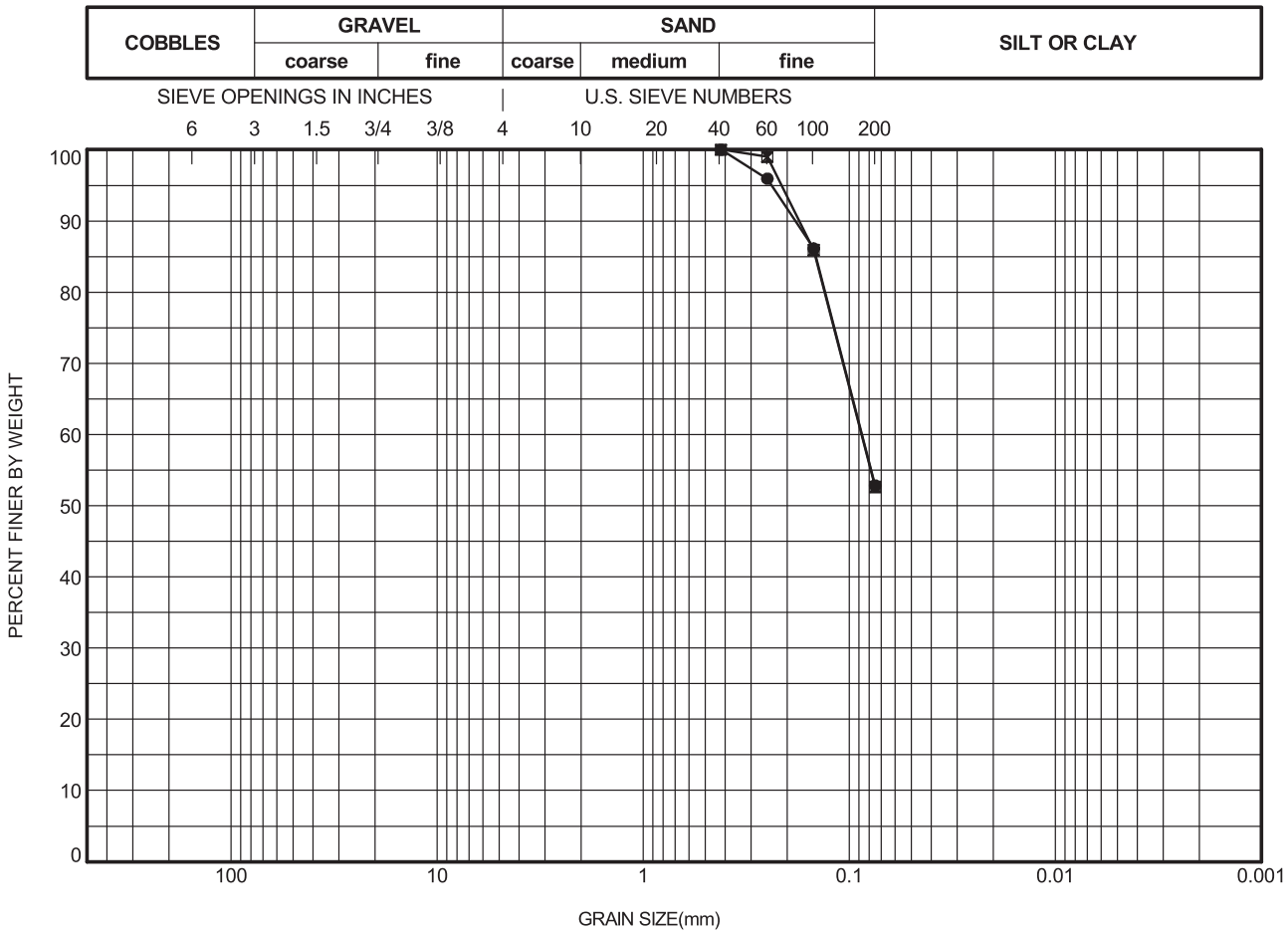

	HOLE	DEPTH (m)	D85	D60	D50	D15	D10	CU	%GRAVEL	%SAND	%FINES
●	PSD 1	0.00	0.146	0.087					0.0	47.2	52.8
⊠	PSD 1	0.00	0.146	0.087					0.0	47.4	52.6

	HOLE	SAMPLE	DEPTH (m)	W%	W_L	W_P	PI	REMARKS / SAMPLE DESCRIPTION
●	PSD 1	TX 18	0.00					Before TX test
⊠	PSD 1	TX 18	0.00					After TX test

CU = COEFFICIENT OF UNIFORMITY = D60/D10 PARTICLE SIZES, e.g. D85, in mm Tested by Wet Sieving Method (ASTM D1140 & D422)

Klohn Crippen Berger

PROJECT NO.:	
PROJECT:	Fundão Tailings Dam Review Panel
LOCATION:	
FIGURE:	
DRAWN BY:	BY
CHECKED BY:	JG

KCB_GRAIN_SIZE-SI_FUNDAO TAILINGS DAM REVIEW PANEL.GPJ_SIEVE.GDT_23-7-16

GRAIN SIZE DISTRIBUTION

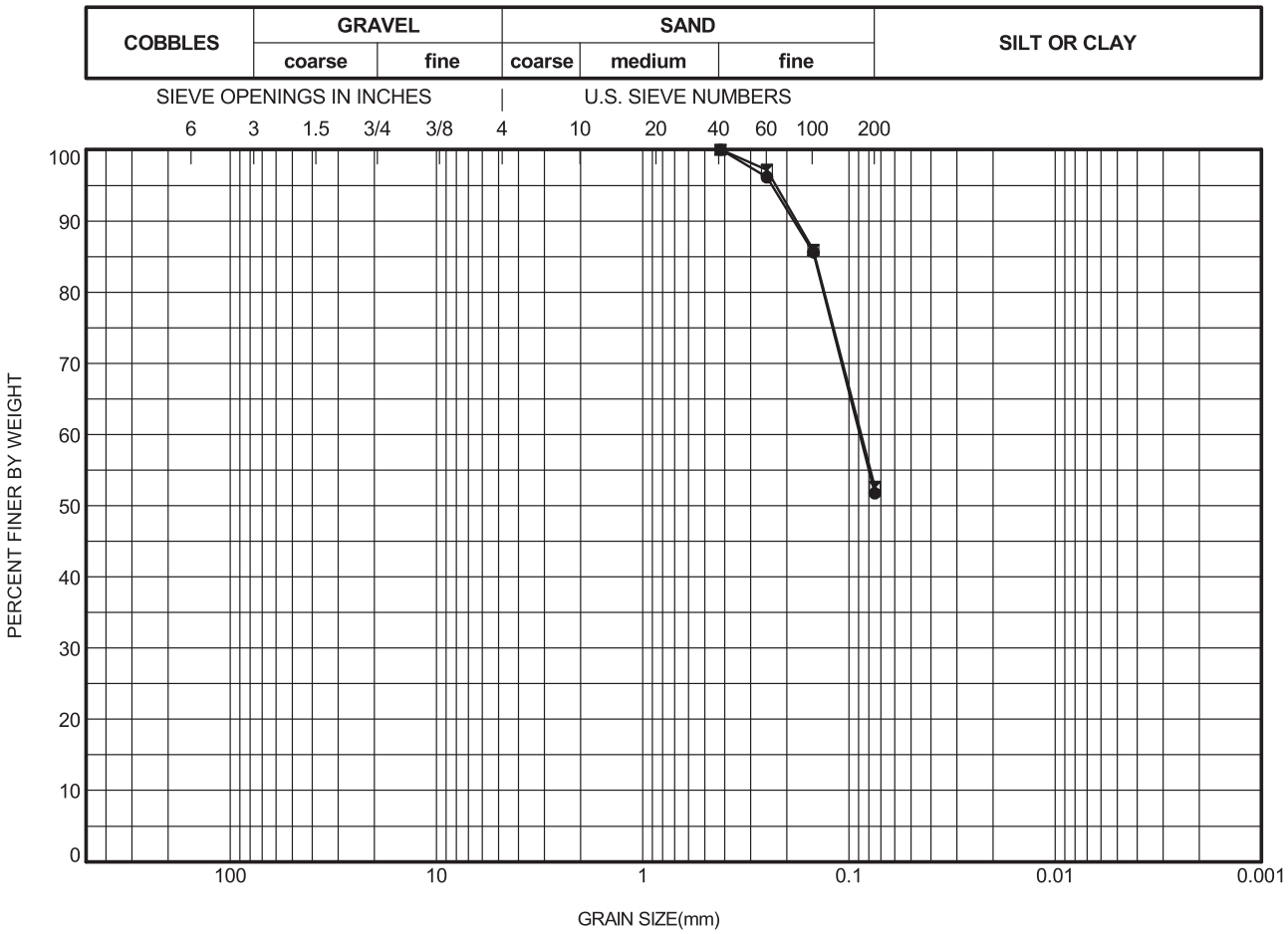

	HOLE	DEPTH (m)	D85	D60	D50	D15	D10	CU	%GRAVEL	%SAND	%FINES
●	PSD 1	0.00	0.147	0.089					0.0	48.3	51.7
⊠	PSD 1	0.00	0.146	0.087					0.0	47.4	52.6

	HOLE	SAMPLE	DEPTH (m)	W%	W_L	W_P	PI	REMARKS / SAMPLE DESCRIPTION
●	PSD 1	TX 19	0.00					Before TX test
⊠	PSD 1	TX 19	0.00					After TX test

CU = COEFFICIENT OF UNIFORMITY = D60/D10 PARTICLE SIZES, e.g. D85, in mm Tested by Wet Sieving Method (ASTM D1140 & D422)

Klohn Crippen Berger

PROJECT NO.:	
PROJECT:	Fundão Tailings Dam Review Panel
LOCATION:	
FIGURE:	
DRAWN BY:	BY
CHECKED BY:	JG

KCB_GRAIN_SIZE-SI_FUNDAO TAILINGS DAM REVIEW PANEL.GPJ_SIEVE.GDT_23-7-16

GRAIN SIZE DISTRIBUTION

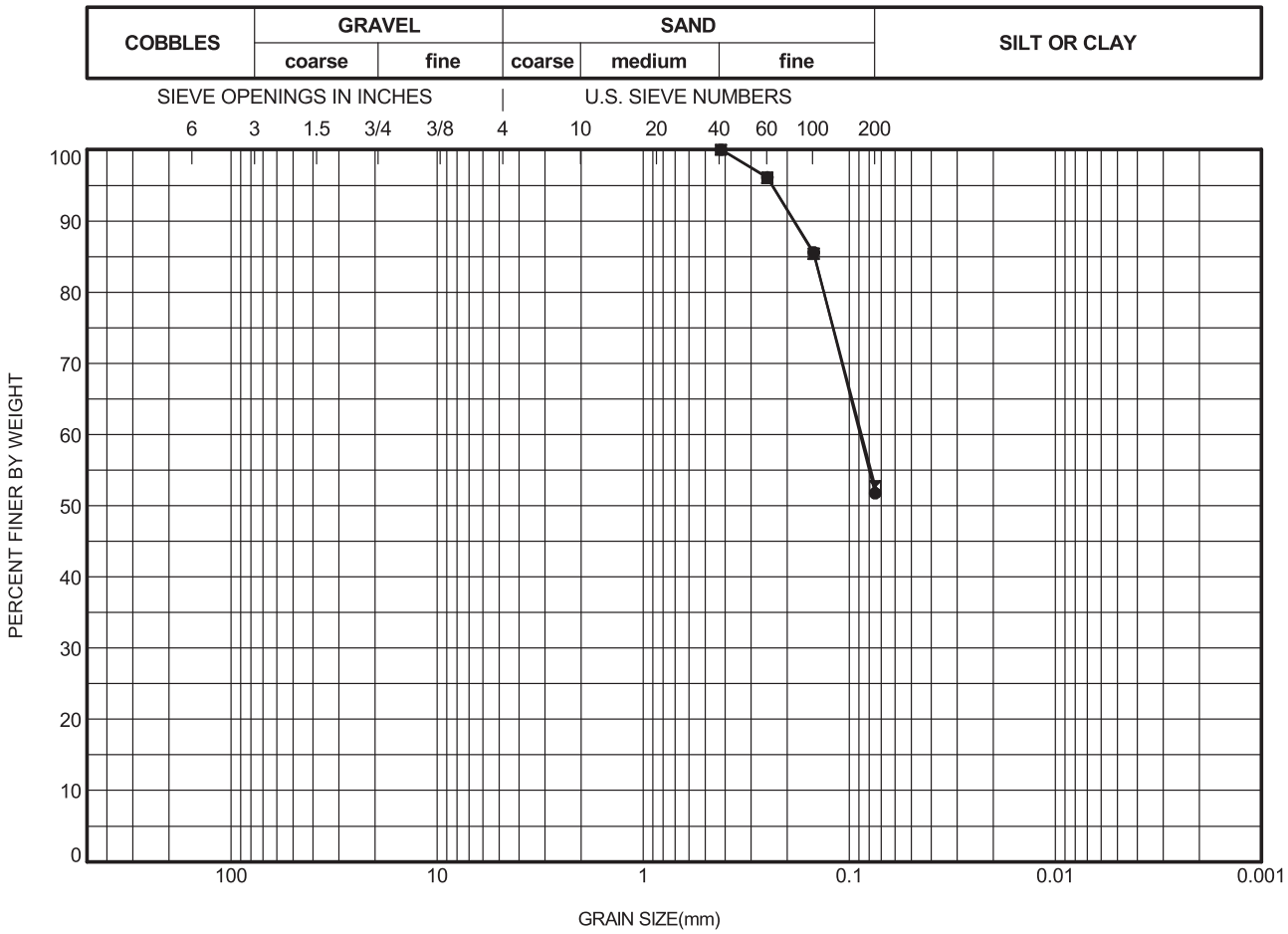

	HOLE	DEPTH (m)	D85	D60	D50	D15	D10	CU	%GRAVEL	%SAND	%FINES
●	PSD 1	0.00	0.147	0.089					0.0	48.3	51.7
⊠	PSD 1	0.00	0.148	0.087					0.0	47.3	52.7

	HOLE	SAMPLE	DEPTH (m)	W%	W_L	W_P	PI	REMARKS / SAMPLE DESCRIPTION
●	PSD 1	TX 20	0.00					Before TX test
⊠	PSD 1	TX 20	0.00					After TX test

CU = COEFFICIENT OF UNIFORMITY = D60/D10 PARTICLE SIZES, e.g. D85, in mm Tested by Wet Sieving Method (ASTM D1140 & D422)

Klohn Crippen Berger

PROJECT NO.:	
PROJECT:	Fundão Tailings Dam Review Panel
LOCATION:	
FIGURE:	
DRAWN BY:	BY
CHECKED BY:	JG

KCB_GRAIN_SIZE-SI_FUNDAO TAILINGS DAM REVIEW PANEL.GPJ_SIEVE.GDT_23-7-16

GRAIN SIZE DISTRIBUTION

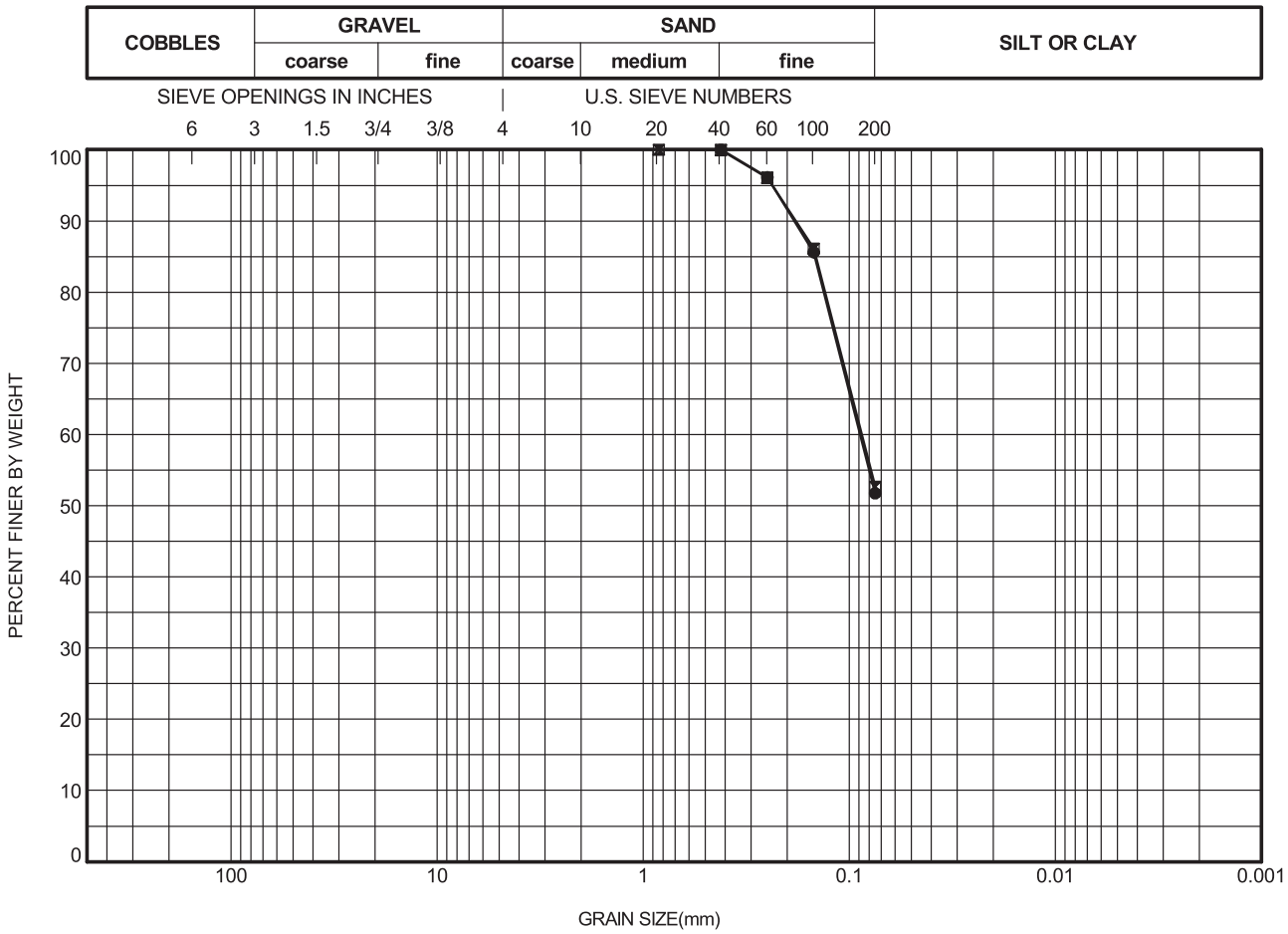

	HOLE	DEPTH (m)	D85	D60	D50	D15	D10	CU	%GRAVEL	%SAND	%FINES
●	PSD 1	0.00	0.147	0.089					0.0	48.3	51.7
⊠	PSD 1	0.00	0.146	0.087					0.0	47.3	52.7

	HOLE	SAMPLE	DEPTH (m)	W%	W_L	W_P	PI	REMARKS / SAMPLE DESCRIPTION
●	PSD 1	TX 21	0.00					Before TX test
⊠	PSD 1	TX 21	0.00					After TX test

CU = COEFFICIENT OF UNIFORMITY = D60/D10 PARTICLE SIZES, e.g. D85, in mm Tested by Wet Sieving Method (ASTM D1140 & D422)

Klohn Crippen Berger

PROJECT NO.:	
PROJECT:	Fundão Tailings Dam Review Panel
LOCATION:	
FIGURE:	
DRAWN BY:	BY
CHECKED BY:	JG

KCB_GRAIN_SIZE-SI_FUNDAO TAILINGS DAM REVIEW PANEL.GPJ_SIEVE.GDT_23-7-16

GRAIN SIZE DISTRIBUTION

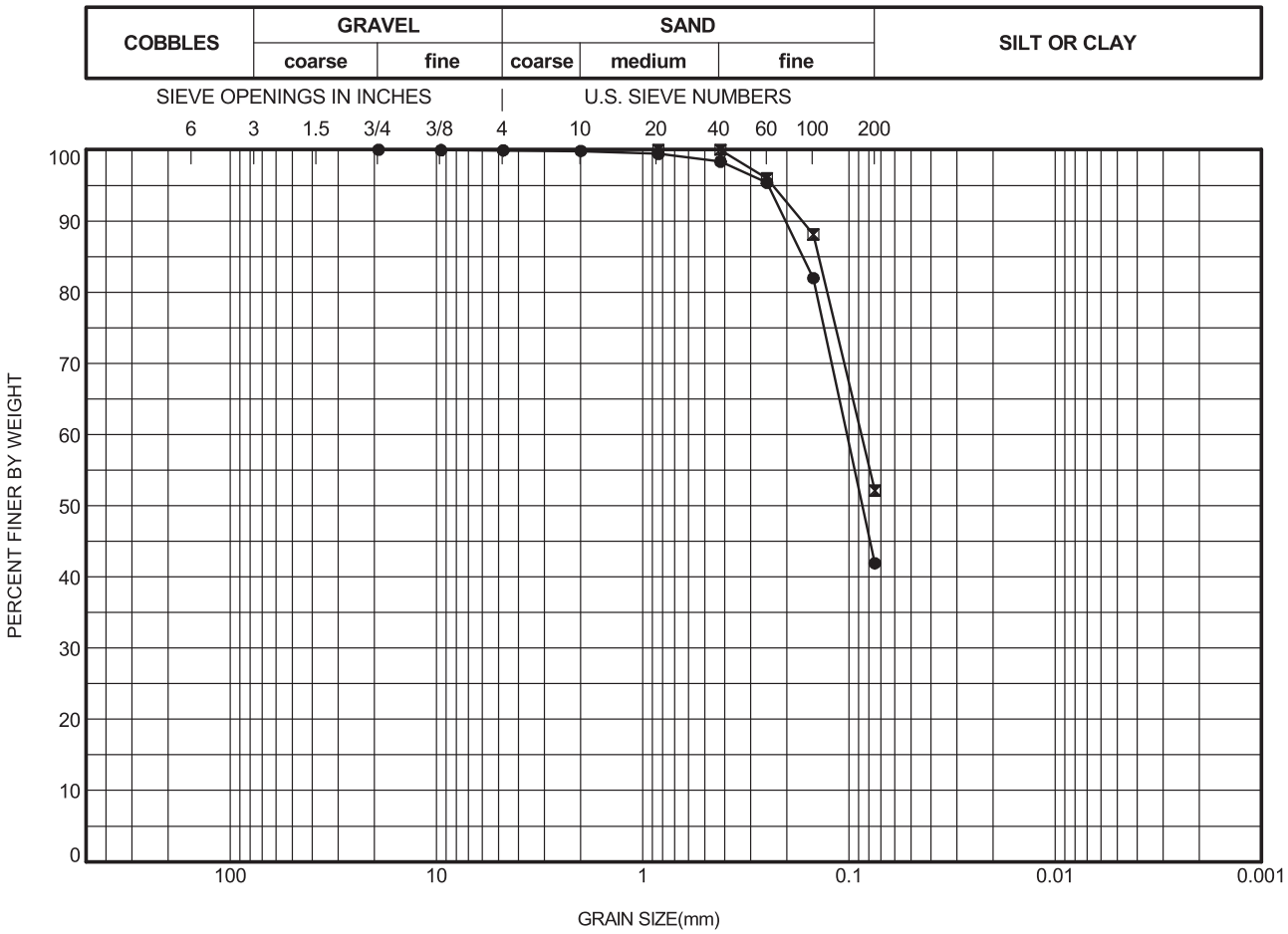

	HOLE	DEPTH (m)	D85	D60	D50	D15	D10	CU	%GRAVEL	%SAND	%FINES
●	PSD 1	0.00	0.168	0.102	0.086				0.1	58.0	41.9
⊠	PSD 1	0.00	0.140	0.087					0.0	47.9	52.1

	HOLE	SAMPLE	DEPTH (m)	W%	W_L	W_P	PI	REMARKS / SAMPLE DESCRIPTION
●	PSD 1	TX 22	0.00					Before TX test
⊠	PSD 1	TX 22	0.00					After TX test

CU = COEFFICIENT OF UNIFORMITY = D60/D10 PARTICLE SIZES, e.g. D85, in mm Tested by Wet Sieving Method (ASTM D1140 & D422)

Klohn Crippen Berger

PROJECT NO.:	
PROJECT:	Fundão Tailings Dam Review Panel
LOCATION:	
FIGURE:	
DRAWN BY:	BY
CHECKED BY:	JG

KCB_GRAIN_SIZE-SI_FUNDAO TAILINGS DAM REVIEW PANEL.GPJ_SIEVE.GDT_23-7-16

GRAIN SIZE DISTRIBUTION

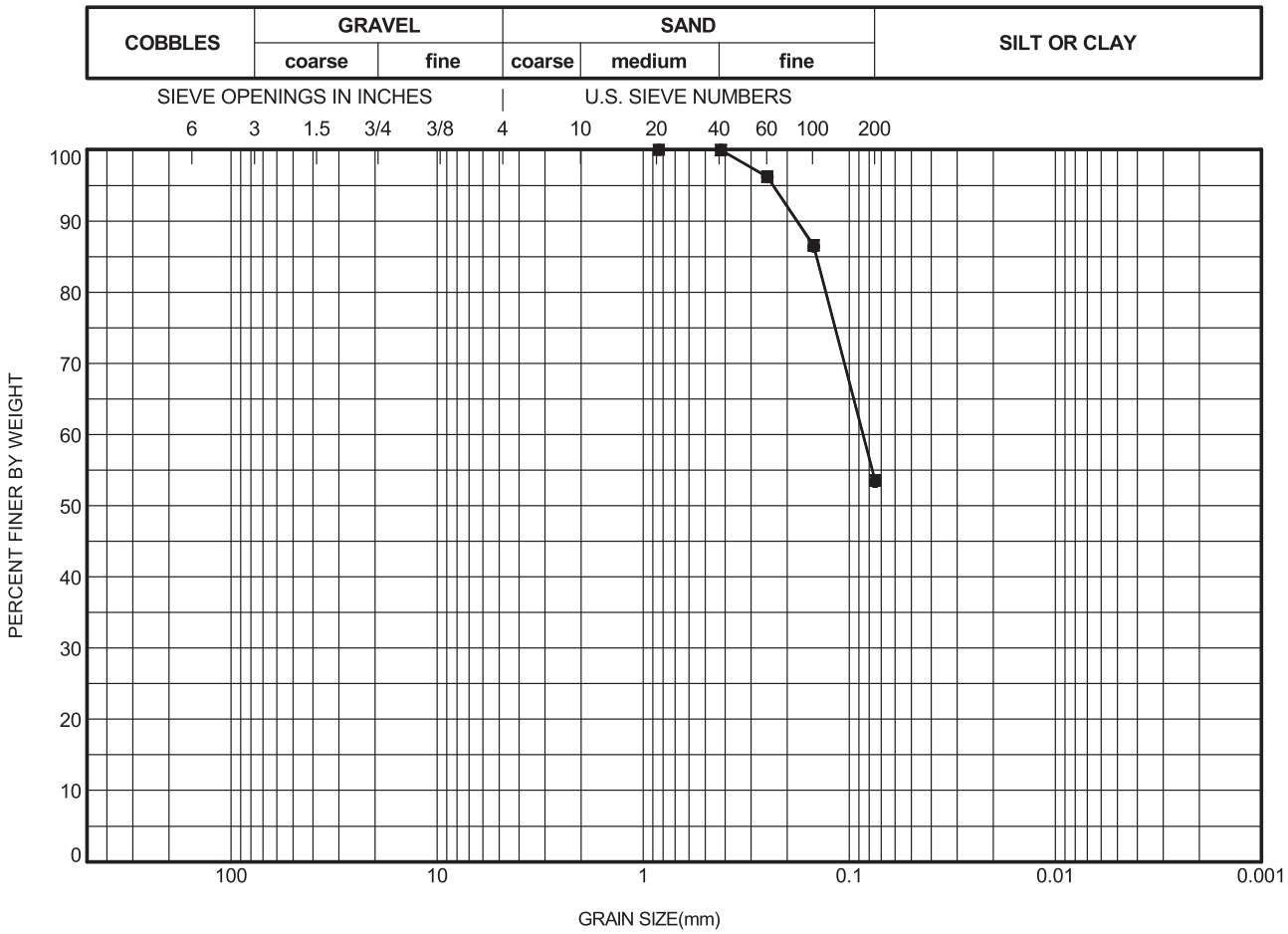

	HOLE	DEPTH (m)	D85	D60	D50	D15	D10	CU	%GRAVEL	%SAND	%FINES
●	PSD 1	0.00	0.145	0.086					0.0	46.6	53.4
⊠	PSD 1	0.00	0.144	0.086					0.0	46.5	53.5

	HOLE	SAMPLE	DEPTH (m)	W%	W_L	W_P	PI	REMARKS / SAMPLE DESCRIPTION
●	PSD 1	TX 23	0.00					Before TX test
⊠	PSD 1	TX 23	0.00					After TX test

CU = COEFFICIENT OF UNIFORMITY = D60/D10 PARTICLE SIZES, e.g. D85, in mm Tested by Wet Sieving Method (ASTM D1140 & D422)

Klohn Crippen Berger

PROJECT NO.:

PROJECT: Fundão Tailings Dam Review Panel

LOCATION:

FIGURE:

DRAWN BY: BY CHECKED BY: JG

KCB_GRAIN_SIZE-SI FUNDAO TAILINGS DAM REVIEW PANEL.GPJ SIEVE.GDT 23-7-16

GRAIN SIZE DISTRIBUTION

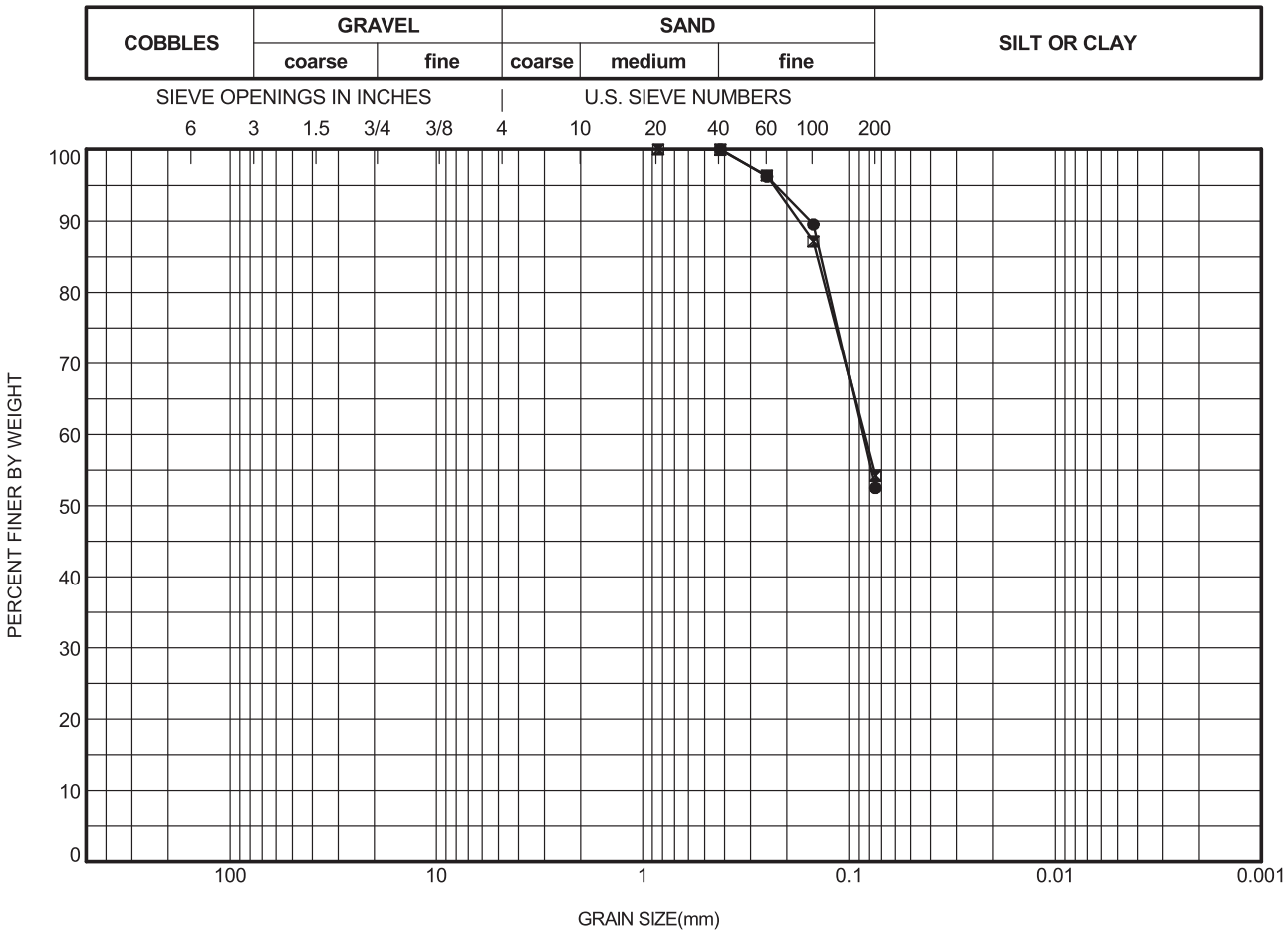

	HOLE	DEPTH (m)	D85	D60	D50	D15	D10	CU	%GRAVEL	%SAND	%FINES
●	PSD 1	0.00	0.137	0.086					0.0	47.5	52.5
⊠	PSD 1	0.00	0.143	0.085					0.0	45.8	54.2

	HOLE	SAMPLE	DEPTH (m)	W%	W_L	W_P	PI	REMARKS / SAMPLE DESCRIPTION
●	PSD 1	TX 24	0.00					Before TX test
⊠	PSD 1	TX 24	0.00					After TX test

CU = COEFFICIENT OF UNIFORMITY = D60/D10 PARTICLE SIZES, e.g. D85, in mm Tested by Wet Sieving Method (ASTM D1140 & D422)

Klohn Crippen Berger

PROJECT NO.:	
PROJECT:	Fundão Tailings Dam Review Panel
LOCATION:	
FIGURE:	
DRAWN BY:	BY
CHECKED BY:	JG

KCB_GRAIN_SIZE-SI_FUNDAO TAILINGS DAM REVIEW PANEL.GPJ_SIEVE.GDT_23-7-16

GRAIN SIZE DISTRIBUTION

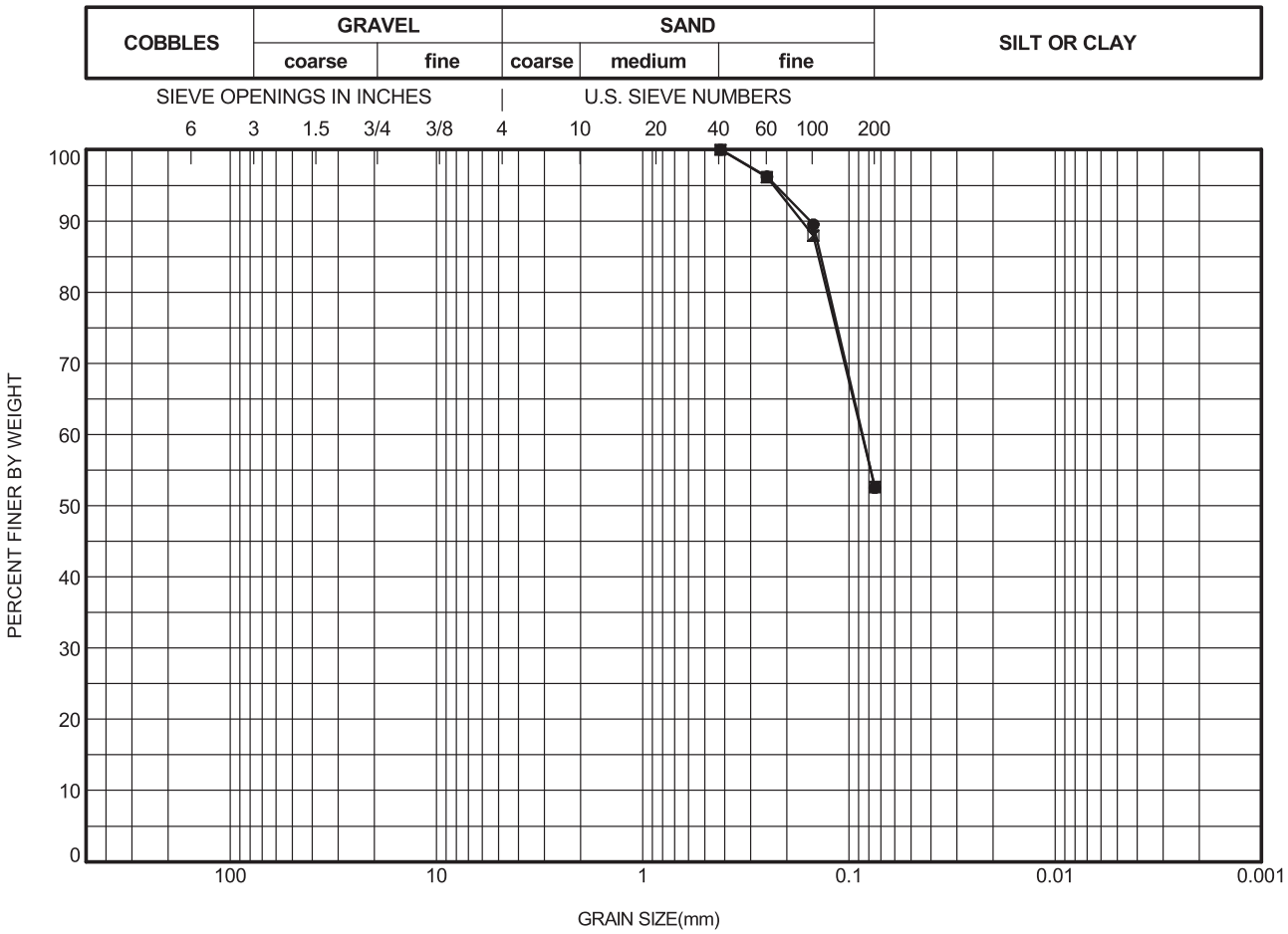

	HOLE	DEPTH (m)	D85	D60	D50	D15	D10	CU	%GRAVEL	%SAND	%FINES
●	PSD 1	0.00	0.137	0.086					0.0	47.5	52.5
⊠	PSD 1	0.00	0.141	0.087					0.0	47.4	52.6

	HOLE	SAMPLE	DEPTH (m)	W%	W_L	W_P	PI	REMARKS / SAMPLE DESCRIPTION
●	PSD 1	TX 25	0.00					Before TX test
⊠	PSD 1	TX 25	0.00					After TX test

CU = COEFFICIENT OF UNIFORMITY = D60/D10 PARTICLE SIZES, e.g. D85, in mm Tested by Wet Sieving Method (ASTM D1140 & D422)

Klohn Crippen Berger

PROJECT NO.:

PROJECT: Fundão Tailings Dam Review Panel

LOCATION:

FIGURE:

DRAWN BY: BY CHECKED BY: JG

KCB_GRAIN_SIZE-SI_FUNDAO TAILINGS DAM REVIEW PANEL.GPJ_SIEVE.GDT_23-7-16

GRAIN SIZE DISTRIBUTION

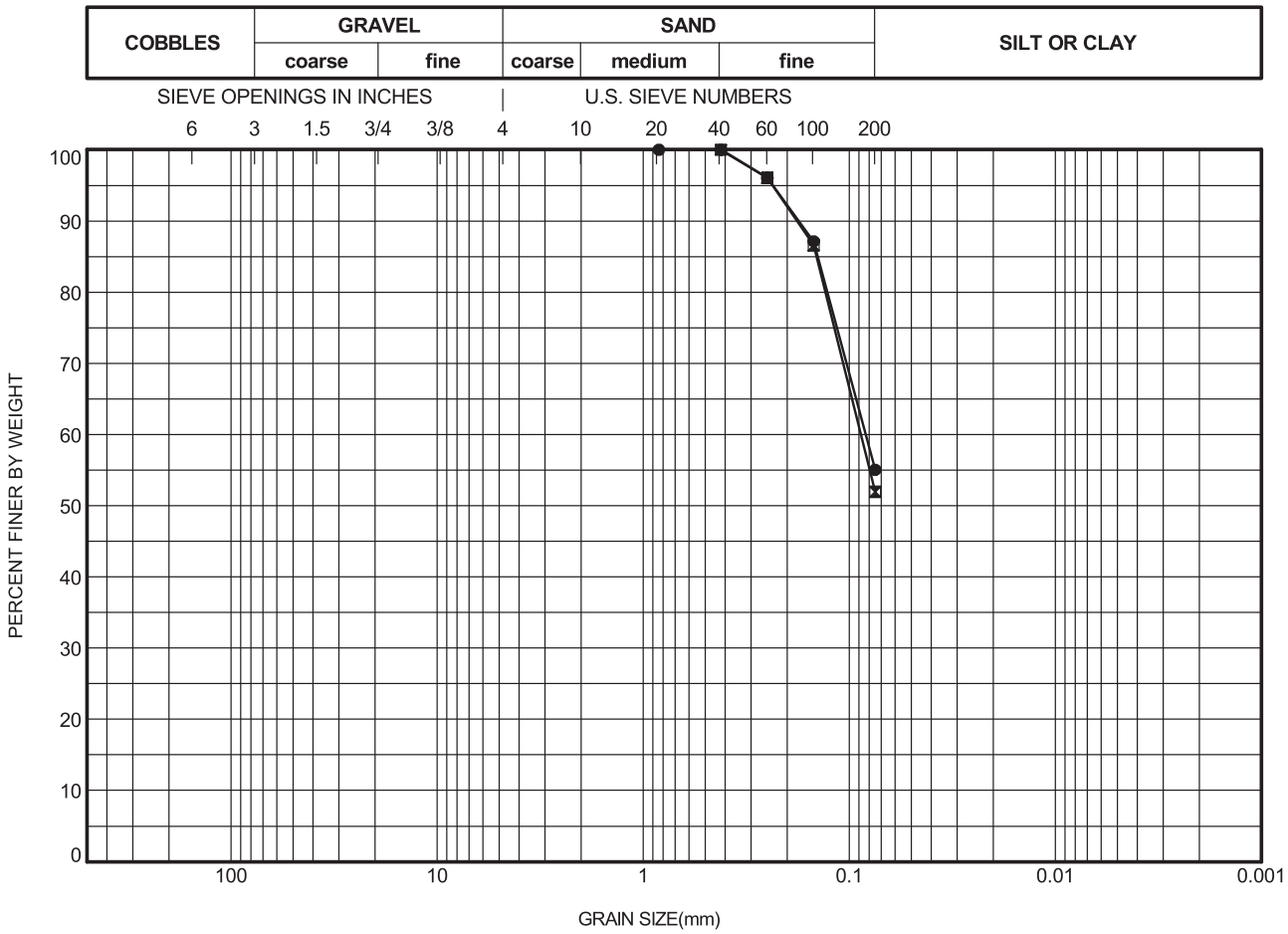

	HOLE	DEPTH (m)	D85	D60	D50	D15	D10	CU	%GRAVEL	%SAND	%FINES
●	PSD 1	0.00	0.142	0.083					0.0	45.0	55.0
⊠	PSD 1	0.00	0.144	0.088					0.0	48.1	51.9

	HOLE	SAMPLE	DEPTH (m)	W%	W_L	W_P	PI	REMARKS / SAMPLE DESCRIPTION
●	PSD 1	TX 26	0.00					Before TX test
⊠	PSD 1	TX 26	0.00					After TX test

CU = COEFFICIENT OF UNIFORMITY = D60/D10 PARTICLE SIZES, e.g. D85, in mm Tested by Wet Sieving Method (ASTM D1140 & D422)

Klohn Crippen Berger

PROJECT NO.:	
PROJECT:	Fundão Tailings Dam Review Panel
LOCATION:	
FIGURE:	
DRAWN BY:	BY
CHECKED BY:	JG

KCB_GRAIN_SIZE-SI_FUNDAO TAILINGS DAM REVIEW PANEL.GPJ_SIEVE.GDT_23-7-16

GRAIN SIZE DISTRIBUTION

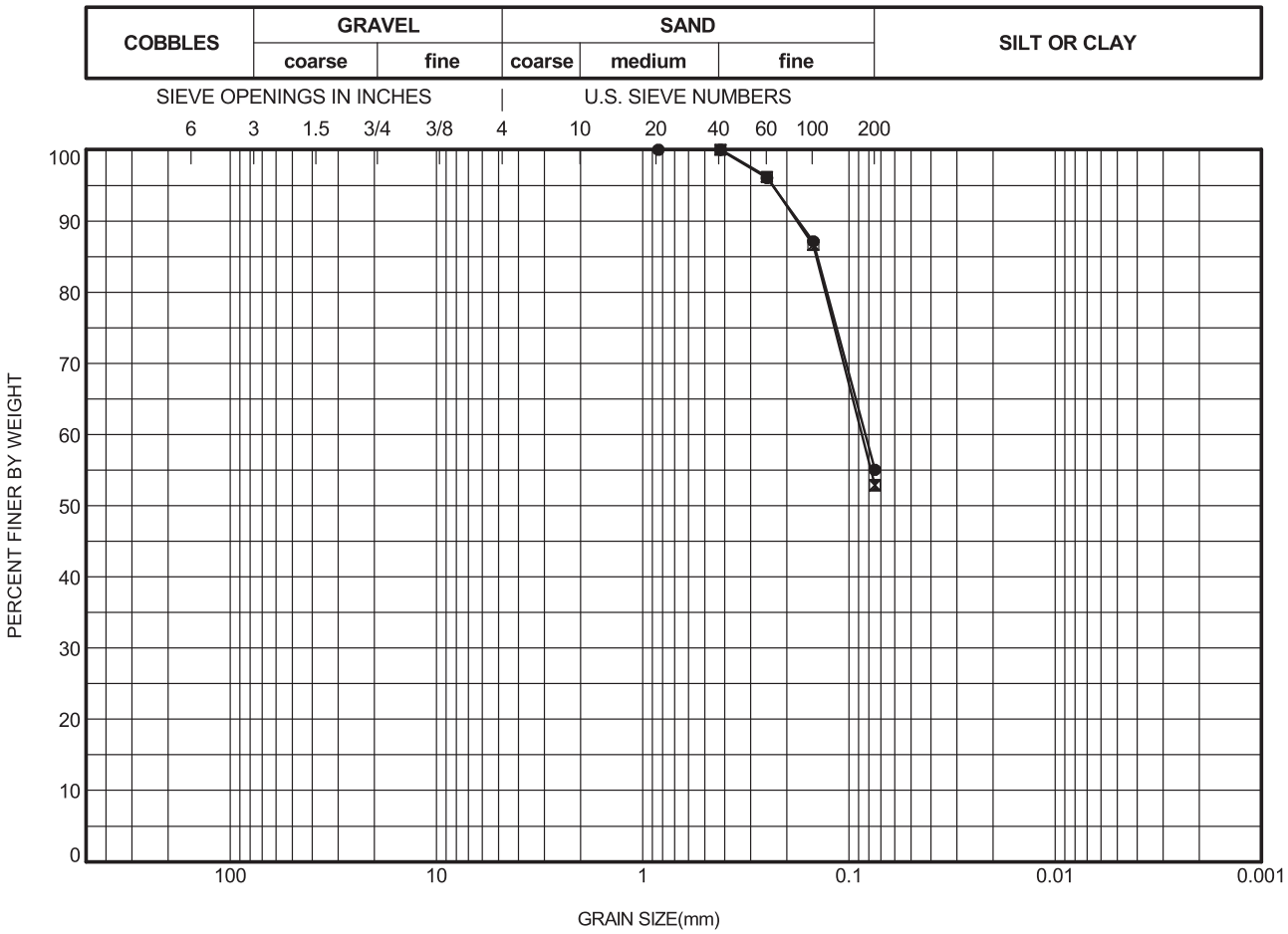

	HOLE	DEPTH (m)	D85	D60	D50	D15	D10	CU	%GRAVEL	%SAND	%FINES
●	PSD 1	0.00	0.142	0.083					0.0	45.0	55.0
⊠	PSD 1	0.00	0.144	0.087					0.0	47.1	52.9

	HOLE	SAMPLE	DEPTH (m)	W%	W_L	W_P	PI	REMARKS / SAMPLE DESCRIPTION
●	PSD 1	TX 27	0.00					Before TX test
⊠	PSD 1	TX 27	0.00					After TX test

CU = COEFFICIENT OF UNIFORMITY = D60/D10 PARTICLE SIZES, e.g. D85, in mm Tested by Wet Sieving Method (ASTM D1140 & D422)

Klohn Crippen Berger

PROJECT NO.:	
PROJECT:	Fundão Tailings Dam Review Panel
LOCATION:	
FIGURE:	
DRAWN BY:	BY
CHECKED BY:	JG

KCB_GRAIN_SIZE-SI_FUNDAO TAILINGS DAM REVIEW PANEL.GPJ_SIEVE.GDT_24-7-16

GRAIN SIZE DISTRIBUTION

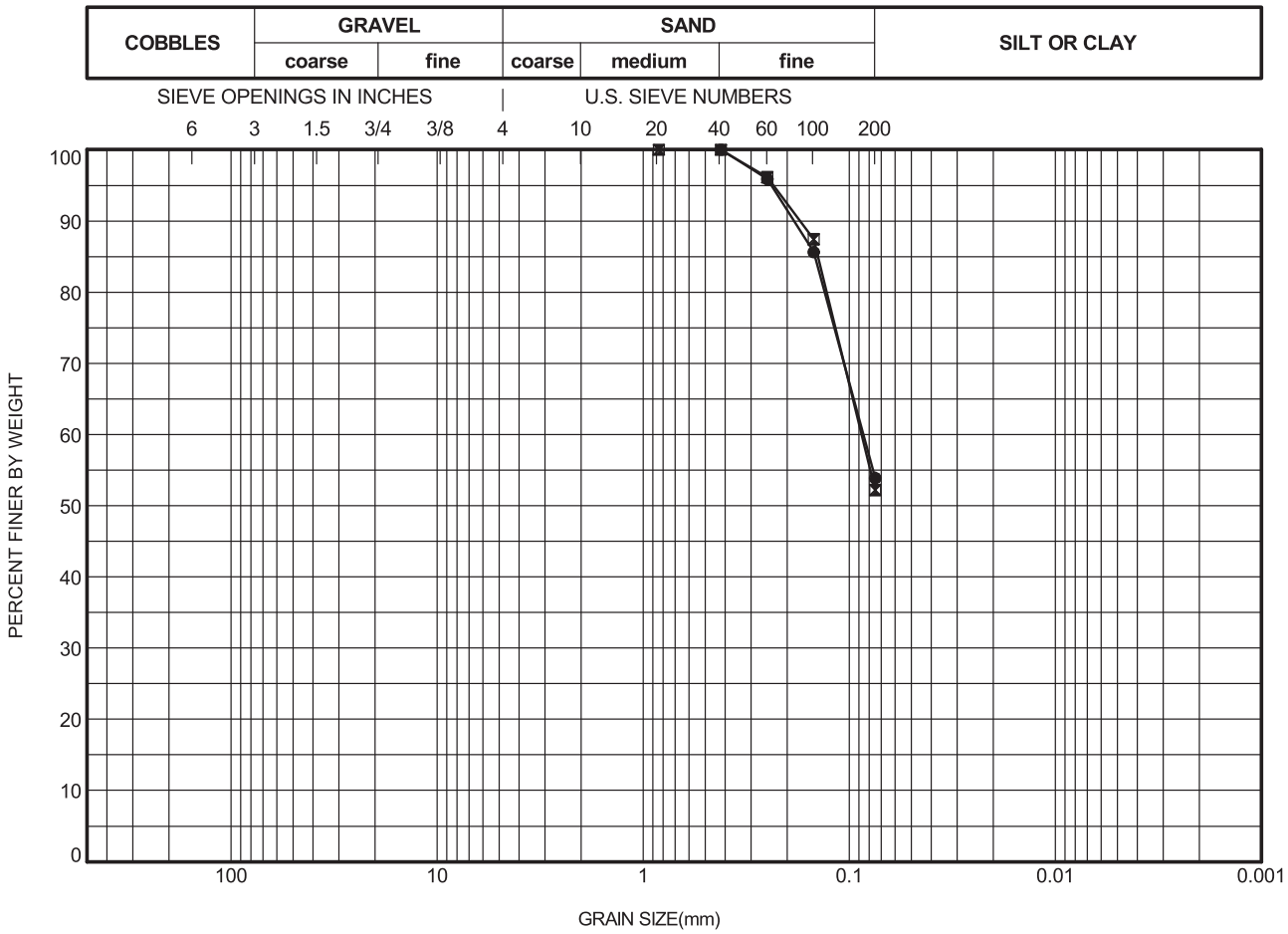

	HOLE	DEPTH (m)	D85	D60	D50	D15	D10	CU	%GRAVEL	%SAND	%FINES
●	PSD 1	0.00	0.147	0.086					0.0	46.1	53.9
⊠	PSD 1	0.00	0.142	0.087					0.0	47.8	52.2

	HOLE	SAMPLE	DEPTH (m)	W%	W_L	W_P	PI	REMARKS / SAMPLE DESCRIPTION
●	PSD 1	TX 28	0.00					Before TX test
⊠	PSD 1	TX 28	0.00					After TX test

CU = COEFFICIENT OF UNIFORMITY = D60/D10 PARTICLE SIZES, e.g. D85, in mm Tested by Wet Sieving Method (ASTM D1140 & D422)

Klohn Crippen Berger

PROJECT NO.:	
PROJECT:	Fundão Tailings Dam Review Panel
LOCATION:	
FIGURE:	
DRAWN BY:	BY
CHECKED BY:	JG

KCB_GRAIN_SIZE-SI_FUNDAO TAILINGS DAM REVIEW PANEL.GPJ_SIEVE.GDT_24-7-16

GRAIN SIZE DISTRIBUTION

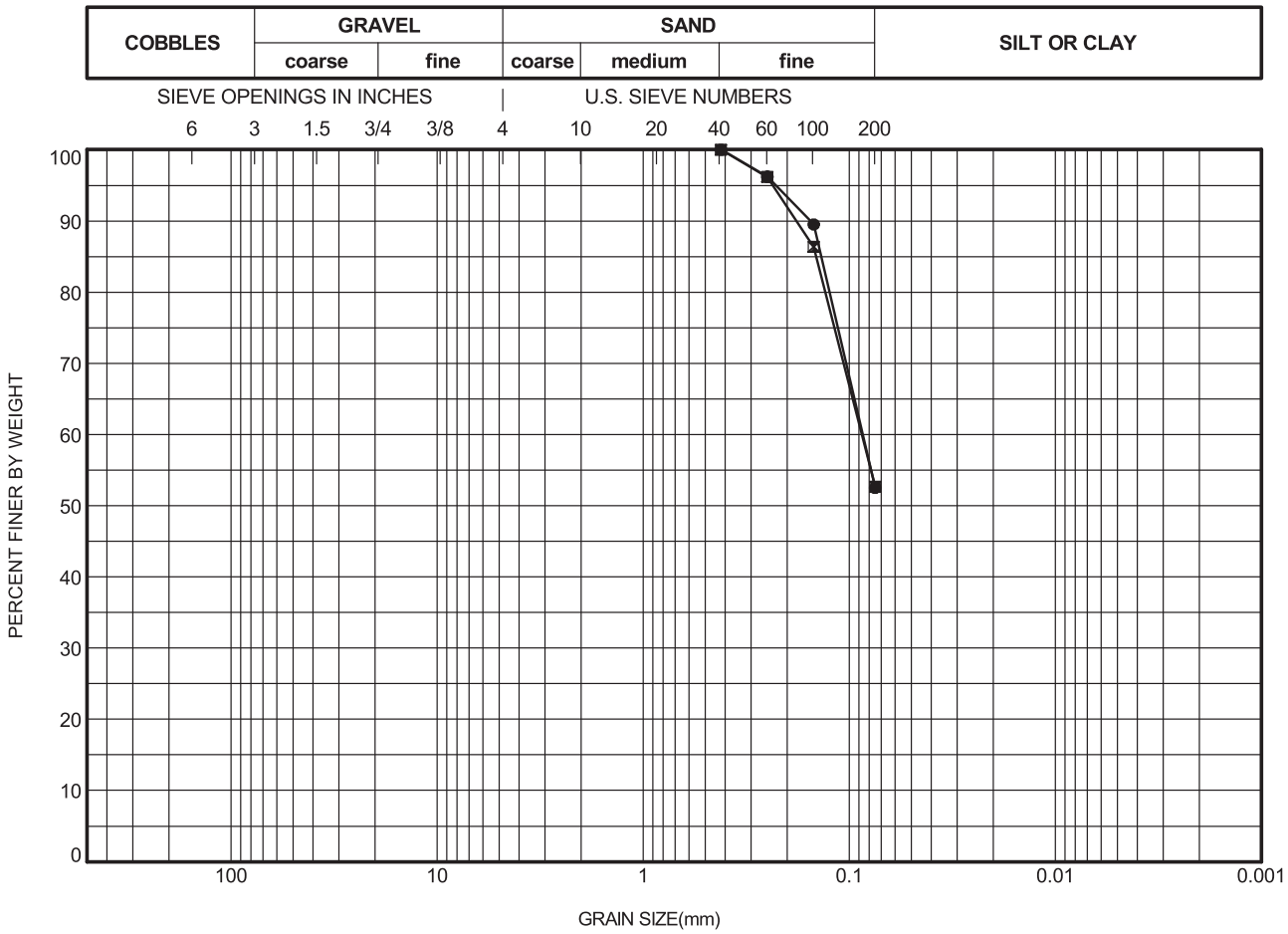

	HOLE	DEPTH (m)	D85	D60	D50	D15	D10	CU	%GRAVEL	%SAND	%FINES
●	PSD 1	0.00	0.137	0.086					0.0	47.5	52.5
⊠	PSD 1	0.00	0.145	0.087					0.0	47.3	52.7

	HOLE	SAMPLE	DEPTH (m)	W%	W_L	W_P	PI	REMARKS / SAMPLE DESCRIPTION
●	PSD 1	TX 29	0.00					Before TX test
⊠	PSD 1	TX 29	0.00					After TX test

CU = COEFFICIENT OF UNIFORMITY = D60/D10 PARTICLE SIZES, e.g. D85, in mm Tested by Wet Sieving Method (ASTM D1140 & D422)

Klohn Crippen Berger

PROJECT NO.:

PROJECT: Fundão Tailings Dam Review Panel

LOCATION:

FIGURE:

DRAWN BY: BY CHECKED BY: JG

KCB_GRAIN_SIZE-SI_FUNDAO TAILINGS DAM REVIEW PANEL.GPJ_SIEVE.GDT_24-7-16

GRAIN SIZE DISTRIBUTION

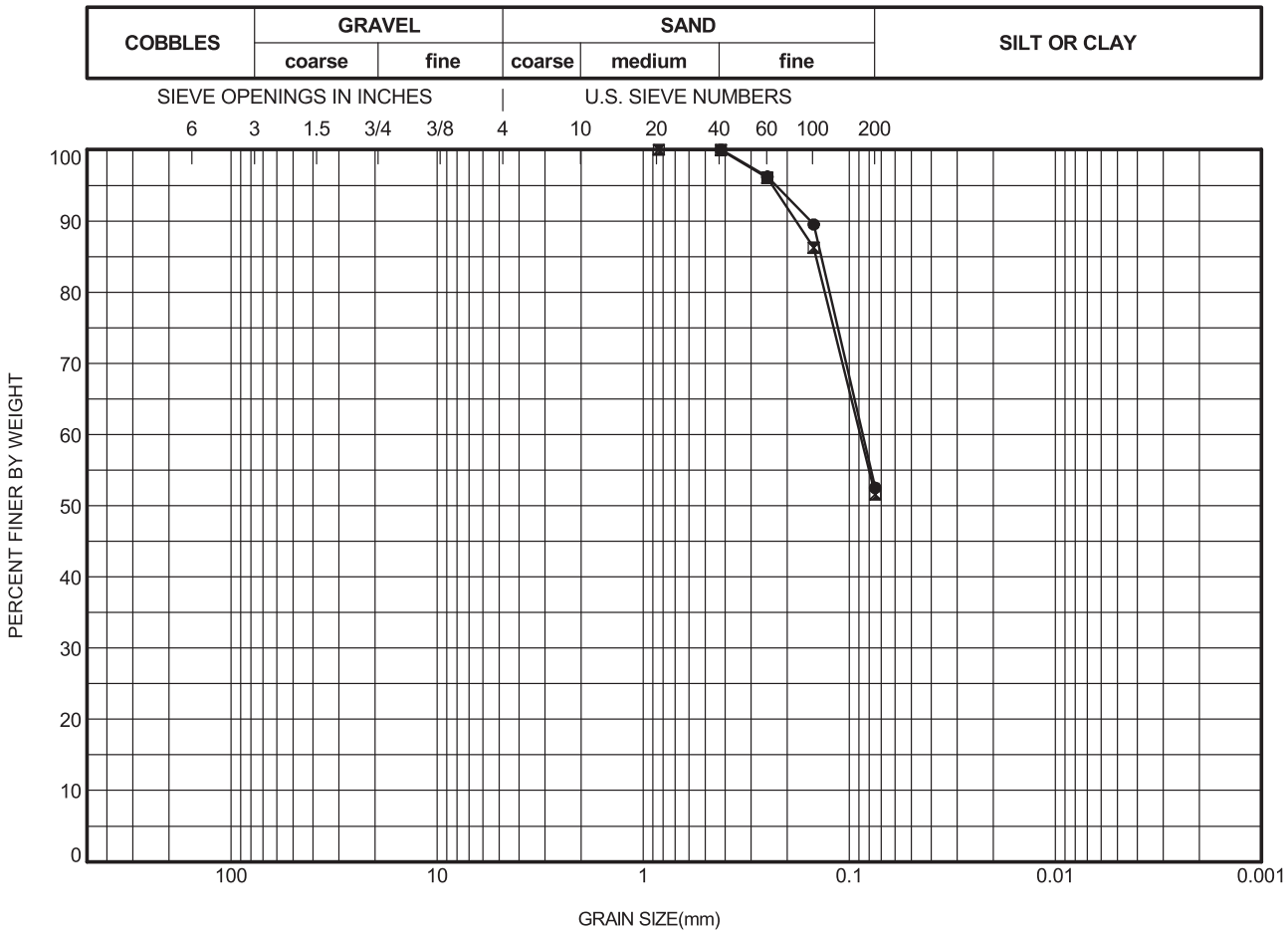

	HOLE	DEPTH (m)	D85	D60	D50	D15	D10	CU	%GRAVEL	%SAND	%FINES
●	PSD 1	0.00	0.137	0.086					0.0	47.5	52.5
⊠	PSD 1	0.00	0.145	0.089					0.0	48.4	51.6

	HOLE	SAMPLE	DEPTH (m)	W%	W_L	W_P	PI	REMARKS / SAMPLE DESCRIPTION
●	PSD 1	TX 30	0.00					Before TX test
⊠	PSD 1	TX 30	0.00					After TX test

CU = COEFFICIENT OF UNIFORMITY = D60/D10 PARTICLE SIZES, e.g. D85, in mm Tested by Wet Sieving Method (ASTM D1140 & D422)

Klohn Crippen Berger

PROJECT NO.:	
PROJECT:	Fundão Tailings Dam Review Panel
LOCATION:	
FIGURE:	
DRAWN BY:	BY
CHECKED BY:	JG

KCB_GRAIN_SIZE-SI_FUNDAO TAILINGS DAM REVIEW PANEL.GPJ_SIEVE.GDT_24-7-16

GRAIN SIZE DISTRIBUTION

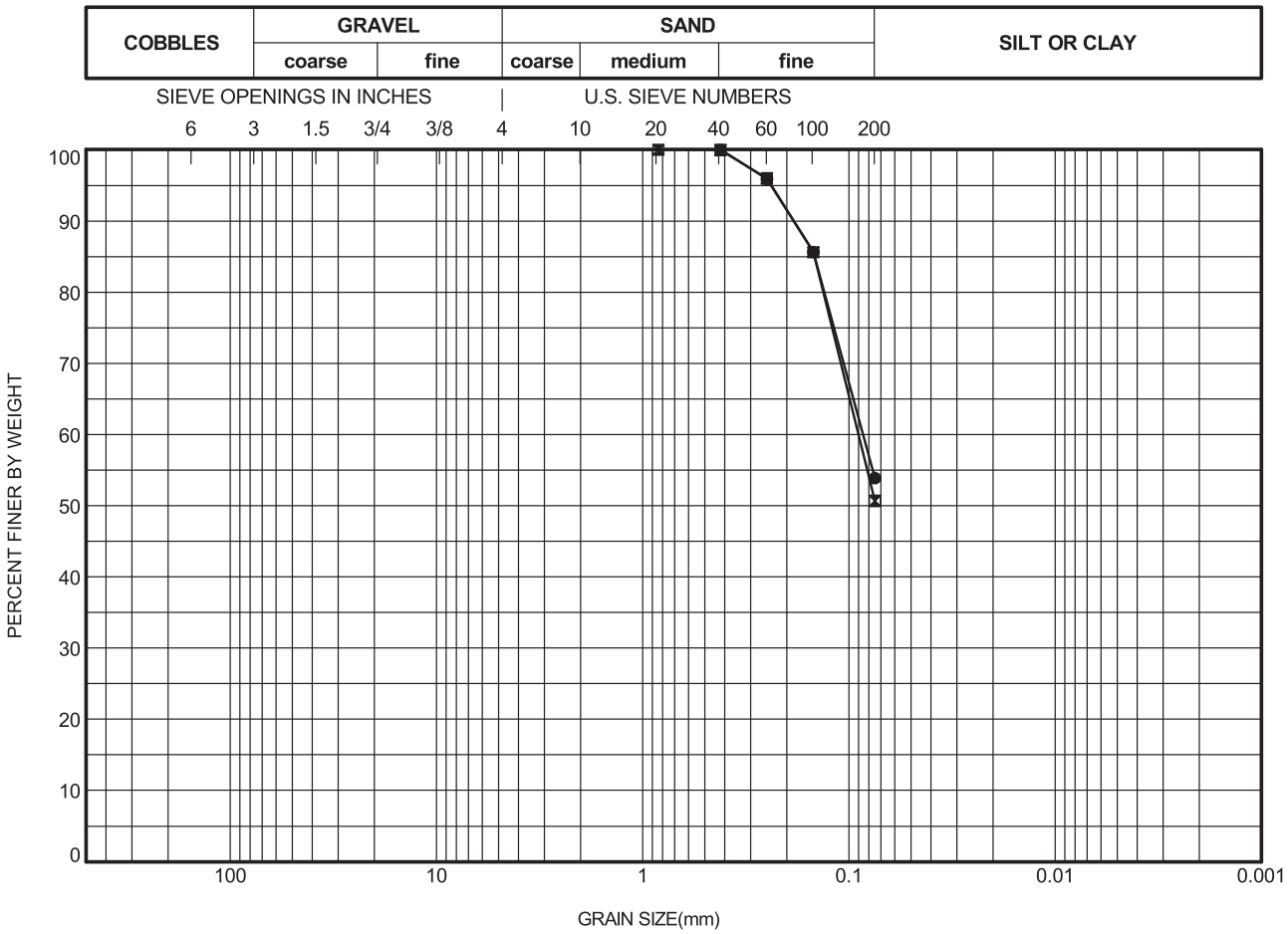

	HOLE	DEPTH (m)	D85	D60	D50	D15	D10	CU	%GRAVEL	%SAND	%FINES
●	PSD 1	0.00	0.147	0.086					0.0	46.1	53.9
⊠	PSD 1	0.00	0.147	0.090					0.0	49.3	50.7

	HOLE	SAMPLE	DEPTH (m)	W%	W_L	W_P	PI	REMARKS / SAMPLE DESCRIPTION
●	PSD 1	TX 31	0.00					Before TX test
⊠	PSD 1	TX 31	0.00					After TX test

CU = COEFFICIENT OF UNIFORMITY = D60/D10 PARTICLE SIZES, e.g. D85, in mm Tested by Wet Sieving Method (ASTM D1140 & D422)

Klohn Crippen Berger

PROJECT NO.:	
PROJECT:	Fundão Tailings Dam Review Panel
LOCATION:	
FIGURE:	
DRAWN BY:	BY
CHECKED BY:	JG

KCB_GRAIN_SIZE-SI_FUNDAO TAILINGS DAM REVIEW PANEL.GPJ_SIEVE.GDT_24-7-16

GRAIN SIZE DISTRIBUTION

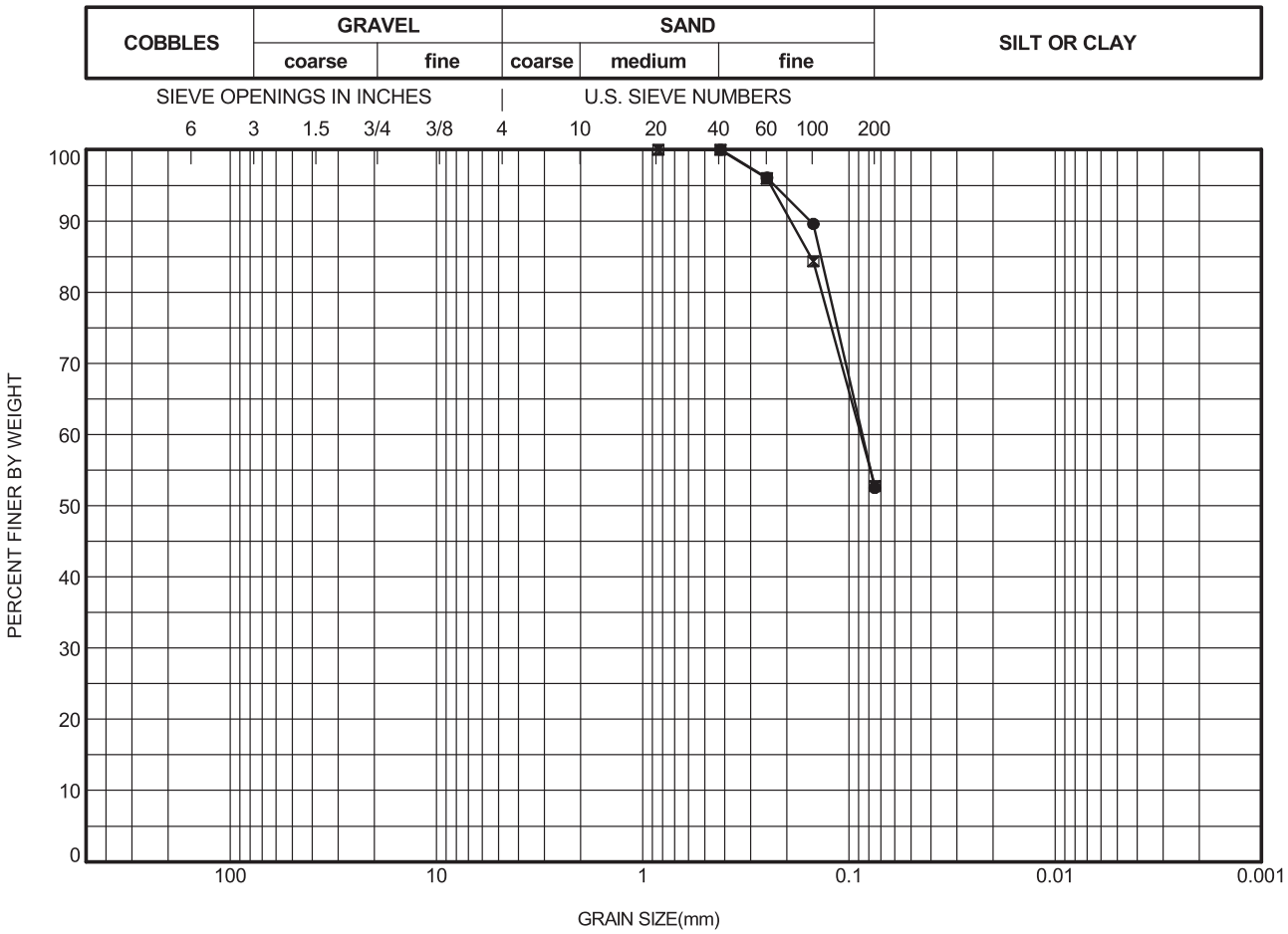

	HOLE	DEPTH (m)	D85	D60	D50	D15	D10	CU	%GRAVEL	%SAND	%FINES
●	PSD 1	0.00	0.137	0.086					0.0	47.5	52.5
⊠	PSD 1	0.00	0.154	0.088					0.0	47.2	52.8

	HOLE	SAMPLE	DEPTH (m)	W%	W_L	W_P	PI	REMARKS / SAMPLE DESCRIPTION
●	PSD 1	TX 32	0.00					Before TX test
⊠	PSD 1	TX 32	0.00					After TX test

CU = COEFFICIENT OF UNIFORMITY = D60/D10 PARTICLE SIZES, e.g. D85, in mm Tested by Wet Sieving Method (ASTM D1140 & D422)

Klohn Crippen Berger

PROJECT NO.:

PROJECT: Fundão Tailings Dam Review Panel

LOCATION:

FIGURE:

DRAWN BY: BY CHECKED BY: JG

KCB_GRAIN_SIZE-SI_FUNDAO TAILINGS DAM REVIEW PANEL.GPJ_SIEVE.GDT_24-7-16

GRAIN SIZE DISTRIBUTION

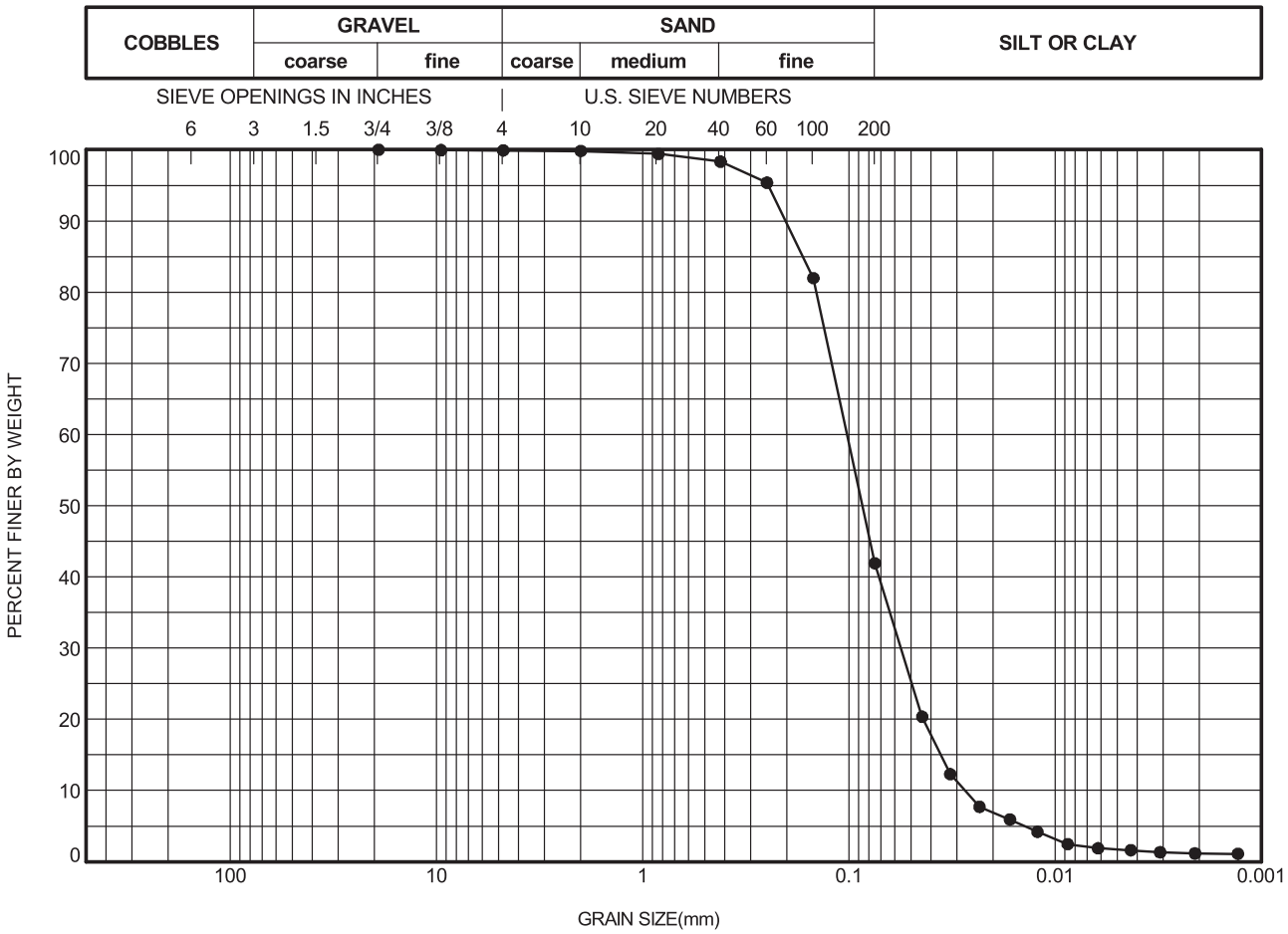

	HOLE	DEPTH (m)	D85	D60	D50	D15	D10	CU	%GRAVEL	%SAND	%FINES
●	Fundão Sand	0.00	0.168	0.102	0.086				0.1	58.0	41.9

	HOLE	SAMPLE	DEPTH (m)	W%	W_L	W_P	PI	REMARKS / SAMPLE DESCRIPTION
●	Fundão Sand		0.00					As received

CU = COEFFICIENT OF UNIFORMITY = D60/D10 PARTICLE SIZES, e.g. D85, in mm Tested by Wet Sieving Method (ASTM D1140 & D422)

Klohn Crippen Berger

PROJECT NO.:

PROJECT: Fundão Tailings Dam Review Panel

LOCATION:

FIGURE:

DRAWN BY: BY CHECKED BY: JG

KCB_GRAIN_SIZE-SI FUNDAO TAILINGS DAM REVIEW PANEL.GPJ SIEVE.GDT 24-7-16

GRAIN SIZE DISTRIBUTION

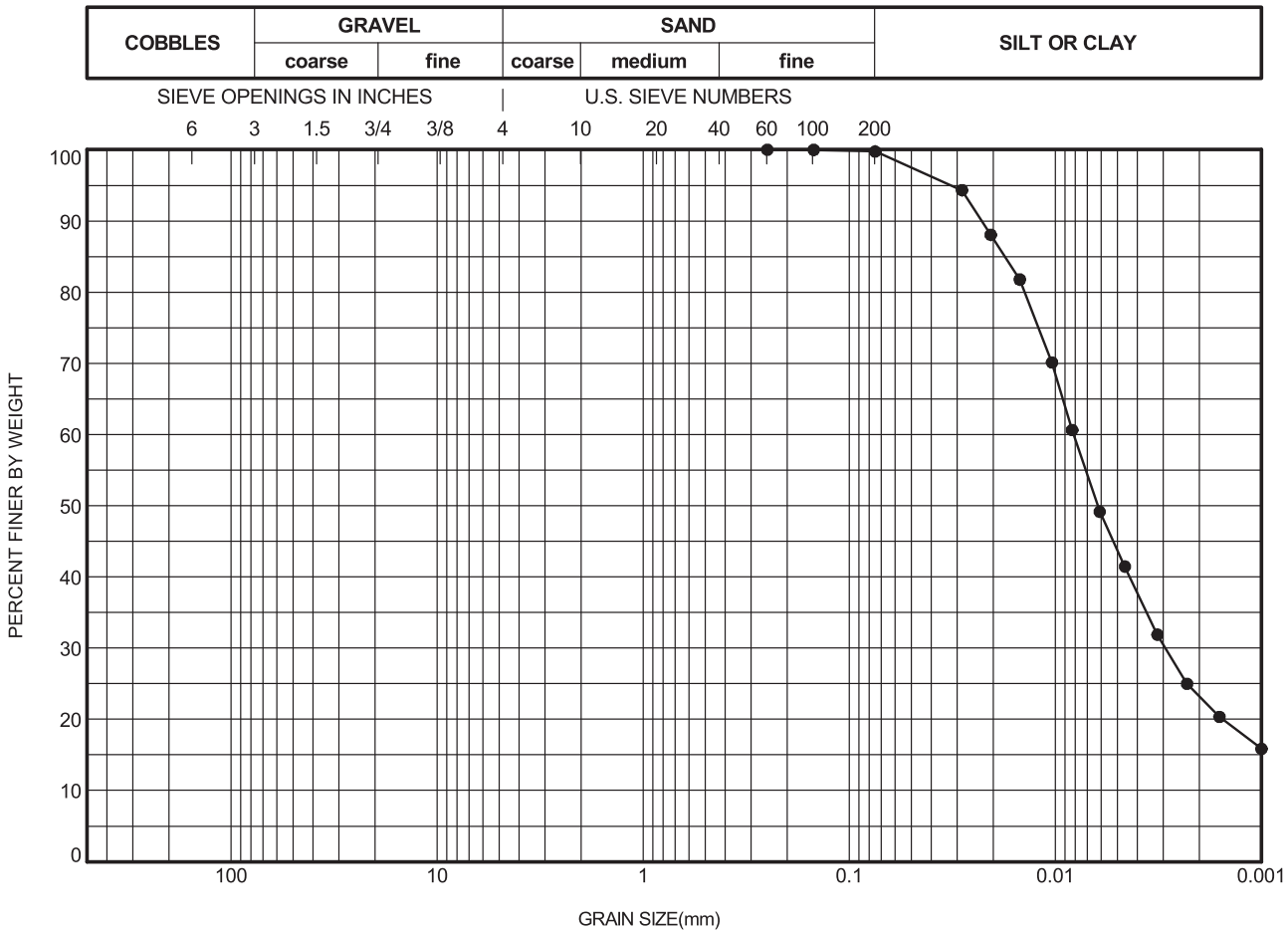

	HOLE	DEPTH (m)	D85	D60	D50	D15	D10	CU	%GRAVEL	%SAND	%FINES
●	Germano Slimes	0.00							0.0	0.2	99.8

	HOLE	SAMPLE	DEPTH (m)	W%	W_L	W_P	PI	REMARKS / SAMPLE DESCRIPTION
●	Germano Slimes		0.00		26	19	7	As received

CU = COEFFICIENT OF UNIFORMITY = D60/D10 PARTICLE SIZES, e.g. D85, in mm Tested by Wet Sieving Method (ASTM D1140 & D422)

Klohn Crippen Berger

PROJECT NO.:

PROJECT: Fundão Tailings Dam Review Panel

LOCATION:

FIGURE:

DRAWN BY: BY CHECKED BY: JG

KCB_GRAIN_SIZE-SI FUNDAO TAILINGS DAM REVIEW PANEL.GPJ SIEVE.GDT 24-7-16

ENSAIO DE ANÁLISE GRANULOMÉTRICA CONJUNTA

DADOS DA AMOSTRA:

	Umidade	Antes do Ensaio		Peneiramento Grosso	
Cápsula nº.	1704	Peso Bruto do Solo Úmido (g)		Peso Solo Total Úmido (g)	318.00
Solo+Tara+Água (g)	80.21	Peso Bruto do Solo Sêco (g)		Peso Solo Graudo Sêco (g)	0.90
Solo+Tara (g)	79.99	Tara (g)		Peso Solo Miúdo Úmido (g)	317.10
Tara (g)	40.94	Peso do Solo Úmido (g)	100.00	Umidade do solo miudo (%)	0.6
Água (g)	0.22	Peso do Solo Sêco (g)	99.44	Peso Solo Miúdo Sêco (g)	315.32
Solo seco (g)	39.05	Densímetro nº	1	Peso Solo Total Sêco (g)	316.22
Umidade (%)	0.6	Proveta nº	1	% < # 10	99.72
ô (g/cm)	2.883	Recipiente nº	R-31		R-89
CLASSIFICAÇÃO:					

PENEIRAMENTO

Peneira	Peso Retido	Total	% Retida	% Retida	% que Passa	Obs.:
3"	0.00		0.00	0.00	100.00	
2"	0.00		0.00	0.00	100.00	
1 1/2"	0.00		0.00	0.00	100.00	
1"	0.00		0.00	0.00	100.00	
3/4"	0.00		0.00	0.00	100.00	
3/8"	0.00		0.00	0.00	100.00	
4	0.23		0.07	0.07	99.93	
10	0.67		0.21	0.28	99.72	
16	0.22		0.22	0.51	99.49	
30	0.66		0.66	1.17	98.83	
40	0.67		0.67	1.84	98.16	
50	1.31		1.31	3.15	96.85	
100	14.81		14.85	18.00	82.00	
200	34.91	53.48	35.01	53.01	46.99	
Prato						

SEDIMENTAÇÃO

Dia	Hora	Minuto	Min. Dec.	Leitura	Temp. 0C	Correção	L. Corrig.	Diâm.Grãos	% da Am.
04-02-16	8	0	0						
			1/4						
	8		1/2	24.0	24.8	-2.56	21.44	0.059442	32.92
	8	1	1	15.2	24.8	-2.56	12.64	0.042032	19.41
	8	2	2	9.5	24.8	-2.56	6.94	0.029721	10.66
	8	4	4	6.2	24.8	-2.56	3.64	0.020361	5.59
	8	8	8	5.6	24.8	-2.56	3.04	0.014398	4.67
	8	15	15	5.0	24.8	-2.56	2.44	0.010515	3.75
	8	30	30	4.6	24.5	-2.69	1.91	0.007435	2.93
	9	0	60	4.2	24.3	-2.69	1.51	0.005257	2.32
	10	0	120	3.8	24.0	-2.81	0.99	0.003717	1.52
	12	0	240	3.6	24.3	-2.69	0.91	0.002629	1.40
	16	0	480	3.6	23.0	-3.03	0.57	0.001859	0.88
05-02-16	8	0	1440	3.4	23.3	-2.92	0.48	0.001073	0.74

OBS.:

Cliente : **BUREAU DE PROJETOS E CONSULTORIA LTDA**

Obra : **BARRAGEM DO FUNDÃO**

TECNOGEO Soluções em Geotecnia Fina

Local : **MARIANA - MG.**

Data: **2016-02-04**

Resp.: **REGINALDO**

Engº

Rel. nº. **LAB-004/16**

Visto

Fl. nº.

ANÁLISE GRANULOMÉTRICA CONJUNTA

(NBR-7181/84 e NBR-6502/95)

FURO **1C** **AM.:** **-** **PROF.:** **-**

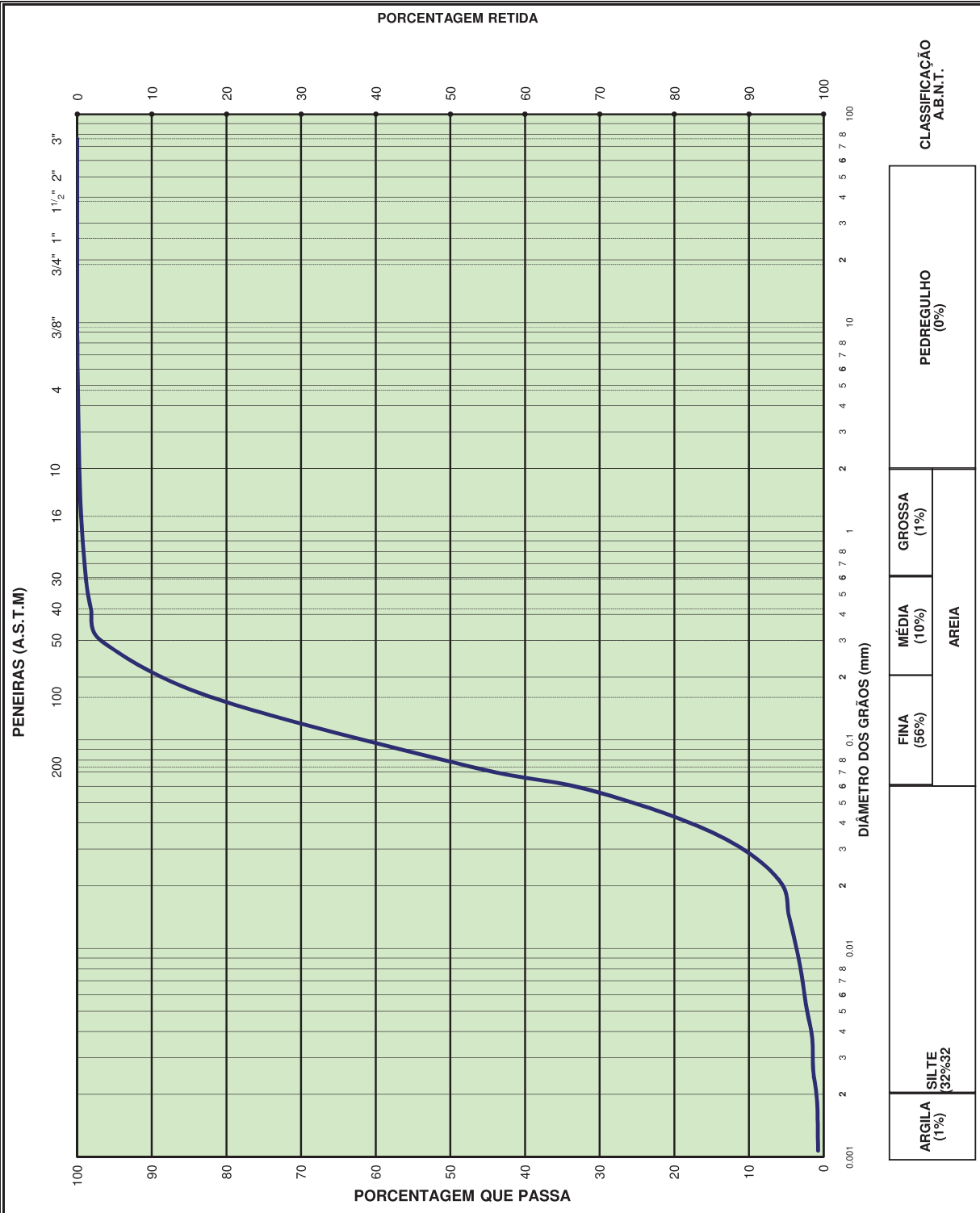

MASSA ESPECÍFICA
DOS SÓLIDOS = **2,883** Kg/m³

Cliente : **BUREAU DE PROJETOS E CONSULTORIA LTDA**

Obra : **BARRAGEM DO FUNDÃO**

Local : **MARIANA - MG.**

ANÁLISE GRANULOMÉTRICA CONJUNTA

(NBR-7181/84 e NBR-6502/95)

FURO **1C** AM.: **-** **PROF.:** **-**

TECNOGEO
Soluções em Geotecnia Fina

Data:	Resp.:
2016-02-04	Reginaldo
Engº	REL. Nº: LAB-004/16
VISTO	DES. Nº

ENSAIO DE ANÁLISE GRANULOMÉTRICA CONJUNTA

DADOS DA AMOSTRA:

	Umidade	Antes do Ensaio		Peneiramento Grosso	
Cápsula nº.	1708	Peso Bruto do Solo Úmido (g)		Peso Solo Total Úmido (g)	80.00
Solo+Tara+Água (g)	57.13	Peso Bruto do Solo Sêco (g)		Peso Solo Graudo Sêco (g)	0.00
Solo+Tara (g)	54.45	Tara (g)		Peso Solo Miúdo Úmido (g)	80.00
Tara (g)	25.66	Peso do Solo Úmido (g)	80.00	Umidade do solo miudo (%)	9.3
Água (g)	2.68	Peso do Solo Sêco (g)	73.19	Peso Solo Miúdo Sêco (g)	73.19
Solo seco (g)	28.79	Densímetro nº	1	Peso Solo Total Sêco (g)	73.19
Umidade (%)	9.3	Proveta nº	2	% < # 10	100.00
ô (g/cm)	3.973	Recipiente nº	R-35		
CLASSIFICAÇÃO:					

PENEIRAMENTO

Peneira	Peso Retido	Total	% Retida	% Retida	% que Passa	Obs.:
3"	0.00		0.00	0.00	100.00	
2"	0.00		0.00	0.00	100.00	
1 1/2"	0.00		0.00	0.00	100.00	
1"	0.00		0.00	0.00	100.00	
3/4"	0.00		0.00	0.00	100.00	
3/8"	0.00		0.00	0.00	100.00	
4	0.00		0.00	0.00	100.00	
10	0.00		0.00	0.00	100.00	
16	0.00		0.00	0.00	100.00	
30	0.00		0.00	0.00	100.00	
40	0.01		0.01	0.01	99.99	
50	0.01		0.01	0.03	99.97	
100	0.04		0.05	0.08	99.92	
200	0.88	0.94	1.20	1.28	98.72	
Prato						

SEDIMENTAÇÃO

Dia	Hora	Minuto	Min. Dec.	Leitura	Temp. 0C	Correção	L. Corrig.	Diâm.Grãos	% da Am.
04-02-16	8	10	0						
			1/4						
	8		1/2	55.0	25.4	-2.42	52.58	0.059442	96.01
	8	11	1	52.6	25.4	-2.42	50.18	0.042032	91.63
	8	12	2	49.6	25.4	-2.42	47.18	0.029721	86.15
	8	14	4	45.8	25.3	-2.42	43.38	0.020361	79.21
	8	18	8	40.8	25.2	-2.56	38.24	0.014398	69.82
	8	25	15	35.4	25.0	-2.56	32.84	0.010515	59.96
	8	40	30	30.3	24.7	-2.69	27.61	0.007435	50.41
	9	10	60	25.4	24.4	-2.69	22.71	0.005257	41.47
	10	10	120	20.3	24.1	-2.81	17.49	0.003717	31.94
	12	10	240	15.8	24.3	-2.69	13.11	0.002629	23.94
	16	10	480	12.2	23.0	-3.13	9.07	0.001859	16.56
05-02-16	8	10	1440	10.2	23.3	-3.53	6.67	0.001073	12.18

OBS.:

Cliente : **BUREAU DE PROJETOS E CONSULTORIA LTDA**

Obra : **BARRAGEM DO GERMANO**

Local : **MARIANA - MG.**

TECNOGEO Soluções em Geotecnia Fina

Data: **2016-02-04**

Resp.: **REGINALDO**

Engº

Rel. nº. **LAB-004/16**

Visto

Fl. nº.

ANÁLISE GRANULOMÉTRICA CONJUNTA
(NBR-7181/84 e NBR-6502/95)

FURO 2C AM.: - PROF.: -

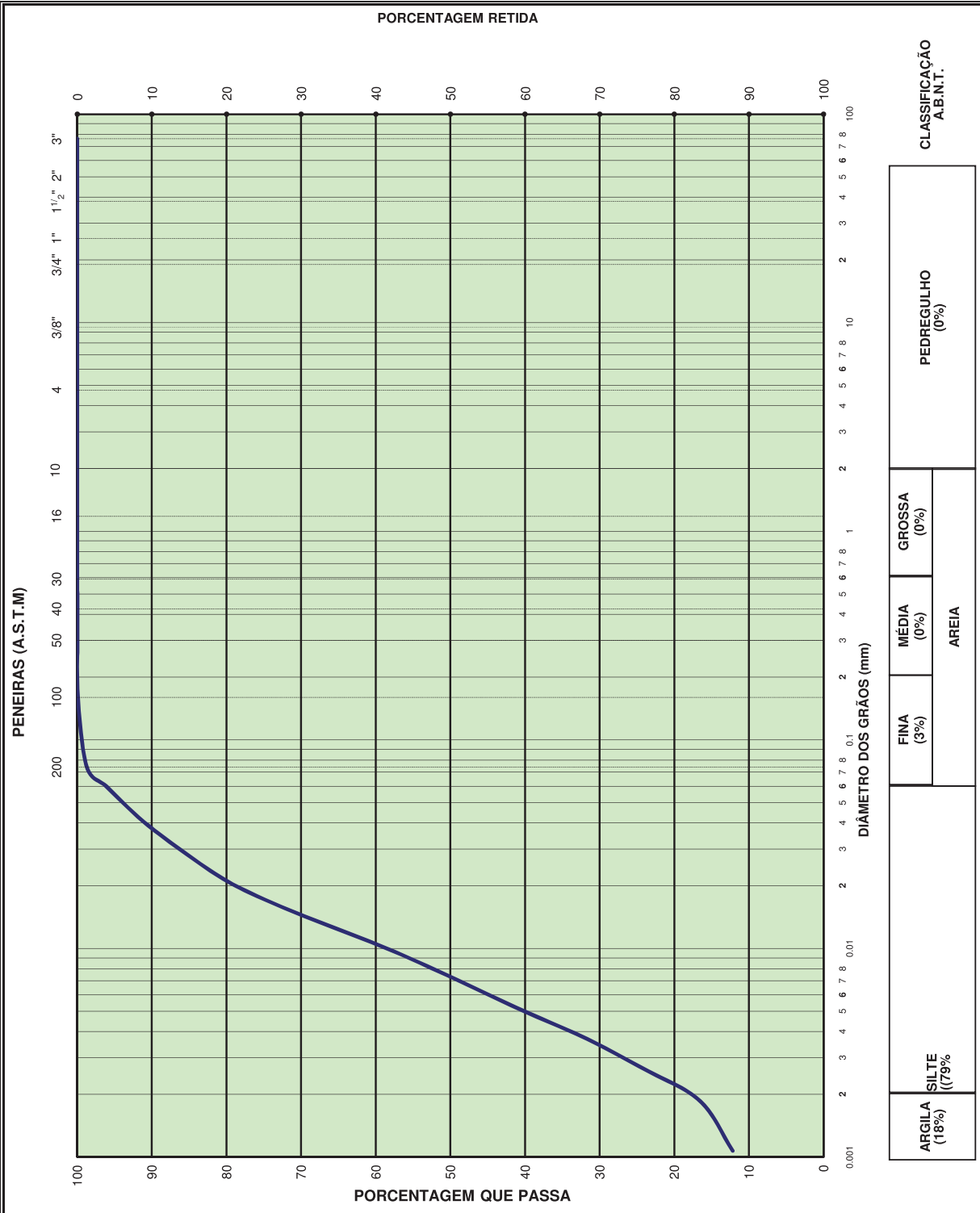

MASSA ESPECÍFICA
DOS SÓLIDOS = **3,973** Kg/m³

Cliente : **BUREAU DE PROJETOS E CONSULTORIA LTDA**

Obra : **BARRAGEM DO GERMANO**

Local : **MARIANA - MG.**

ANÁLISE GRANULOMÉTRICA CONJUNTA

(NBR-7181/84 e NBR-6502/95)

FURO **2C** AM.: **-** **PROF.:** **-**

TECNOGEO
Soluções em Geotecnia Fina

Data:	Resp.:
2016-02-04	**Reginaldo**
Engº	REL. Nº: **LAB-004/16**
VISTO	DES. Nº

D2-5 – pH and Electrical Conductivity

pH and EC

Hole Number	Germano Slimes					
Sample Number	As received					
Depth (m)	-					
Sample Description	Silt					
Trial	1	2	3	4	5	Average
pH	8.26	8.21	8.21	8.21	8.21	8.22
EC (µS)	740	730	730	740	730	734

Klohn Crippen Berger	PROJECT#:			
	PROJECT:	Fundão Tailings Dam Review Panel		
	LOCATION:			
	DATE:	2016-01-02		
	TESTED BY:	JG	CHECKED BY:	BY

ATTACHMENT D3

University of British Columbia X-Ray Diffraction Report and Scanning Electron Microscopy Images

QUANTITATIVE PHASE ANALYSIS OF ONE POWDER SAMPLE USING THE RIETVELD METHOD AND X-RAY POWDER DIFFRACTION DATA.

KCB Project #: M10047A01 0103 - PO# LPO16-003

Bryan Watts
Klohn Crippen Berger
#500 – 2955 Virtual Way
Vancouver, BC V5M 4X6

Mati Raudsepp, Ph.D.
Elisabetta Pani, Ph.D.
Edith Czech, M.Sc.
Lan Kato, B.A.

Dept. of Earth, Ocean & Atmospheric Sciences
The University of British Columbia
6339 Stores Road
Vancouver, BC V6T 1Z4

February 24, 2016

EXPERIMENTAL METHOD

The sample of **Project M10047A01 0103** was reduced to the optimum grain-size range for quantitative X-ray analysis (<10 μm) by grinding under ethanol in a vibratory McCrone Micronising Mill for 10 minutes. Step-scan X-ray powder-diffraction data were collected over a range 3-80°2θ with CoKα radiation on a Bruker D8 Advance Bragg-Brentano diffractometer equipped with an Fe monochromator foil, 0.6 mm (0.3°) divergence slit, incident- and diffracted-beam Soller slits and a LynxEye-XE detector. The long fine-focus Co X-ray tube was operated at 35 kV and 40 mA, using a take-off angle of 6°.

RESULTS

The X-ray diffractogram was analyzed using the International Centre for Diffraction Database PDF-4 and Search-Match software by Bruker. X-ray powder-diffraction data of the sample were refined with Rietveld program Topas 4.2 (Bruker AXS). The results of quantitative phase analysis by Rietveld refinements are given in Table 1. These amounts represent the relative amounts of crystalline phases normalized to 100%. The Rietveld refinement plot is shown in Figure 1.

Table 1. Results of quantitative phase analysis (wt.%)

Mineral	**Ideal Formula**	**#1** **Slimes**
Chalcopyrite ?	$CuFeS_2$	< 0.1
Goethite	α-$Fe^{3+}O(OH)$	30.9
Hematite	α-Fe_2O_3	42.9
Illite-Muscovite	$KAl_2AlSi_3O_{10}(OH)_2$	1.4
Kaolinite	$Al_2Si_2O_5(OH)_4$	4.4
Plagioclase	$NaAlSi_3O_8 – CaAl_2Si_2O_8$	1.1
Quartz	SiO_2	19.2
Total		100.0

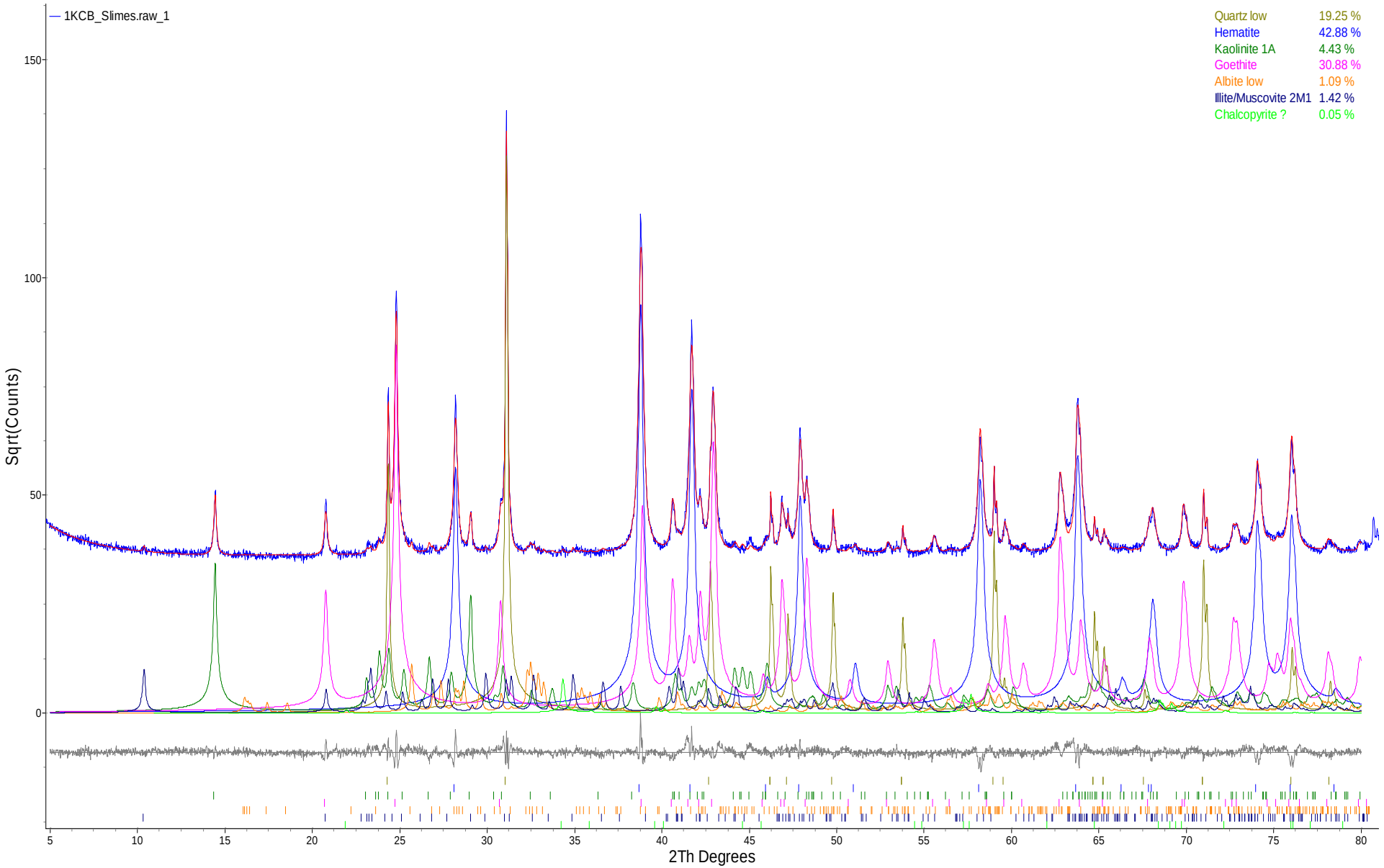

Figure 1. Rietveld refinement plot of sample **Klohn Crippen Berger – Slimes** (blue line - observed intensity at each step; red line - calculated pattern; solid grey line below – difference between observed and calculated intensities; vertical bars, positions of all Bragg reflections). Coloured lines are individual diffraction patterns of all phases.

Appendix D: Attachment D3
University of British Columbia Scanning Electron Microscopy Images

TABLE OF CONTENTS

List of Figures

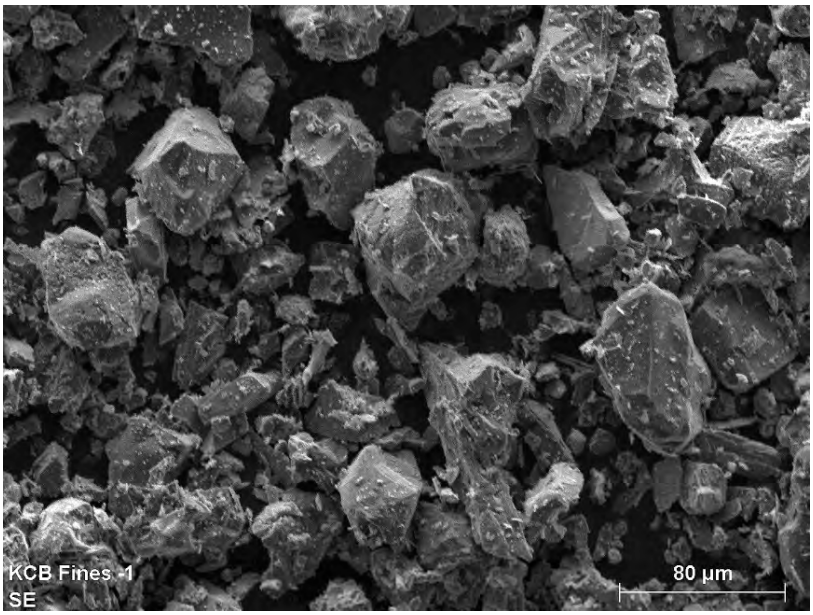

Figure D.D3-1 Fines 1

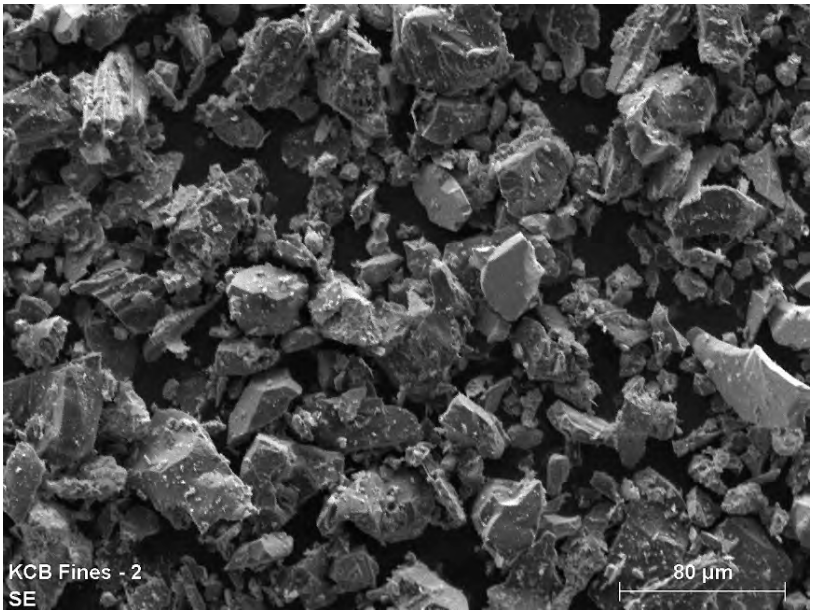

Figure D.D3-2 Fines 2

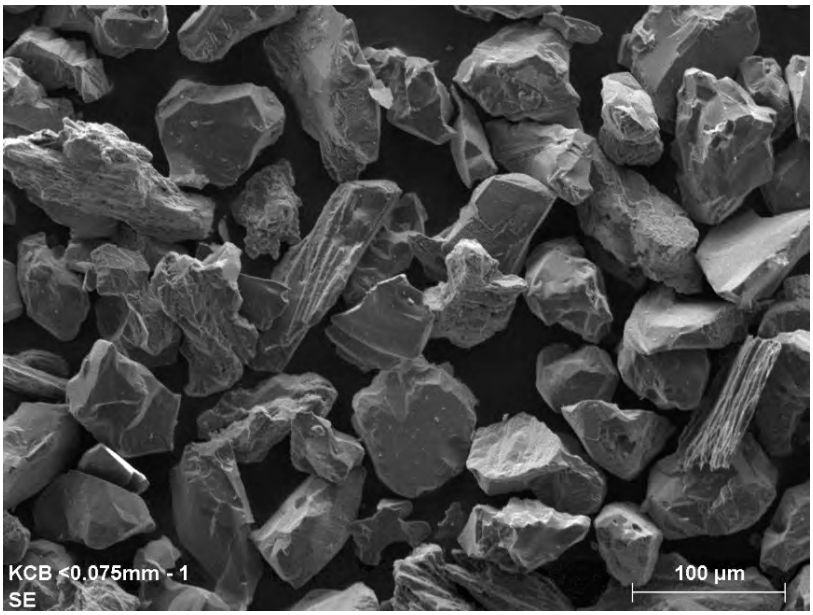

Figure D.D3-3 Less than 0.075 mm (1)

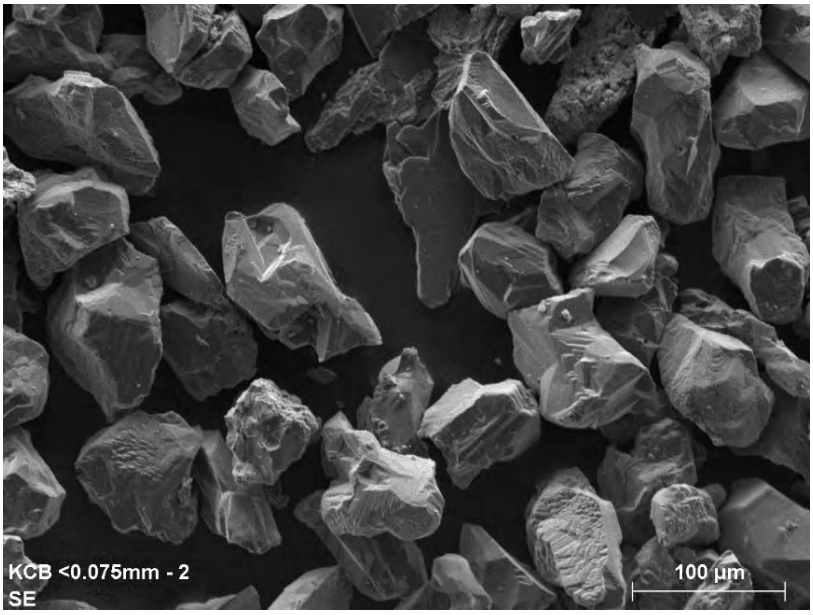

Figure D.D3-4 Less than 0.075 mm (2)

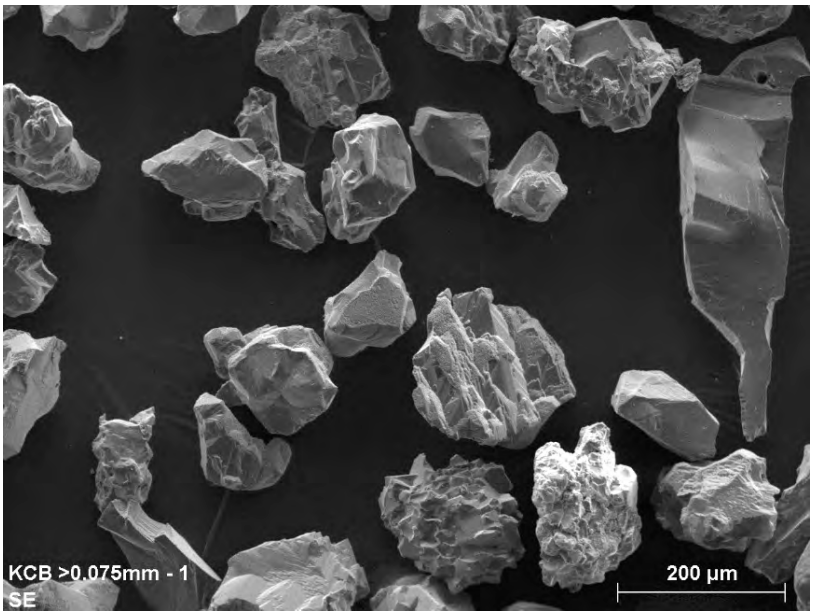

Figure D.D3-5 More than 0.075 mm (1)

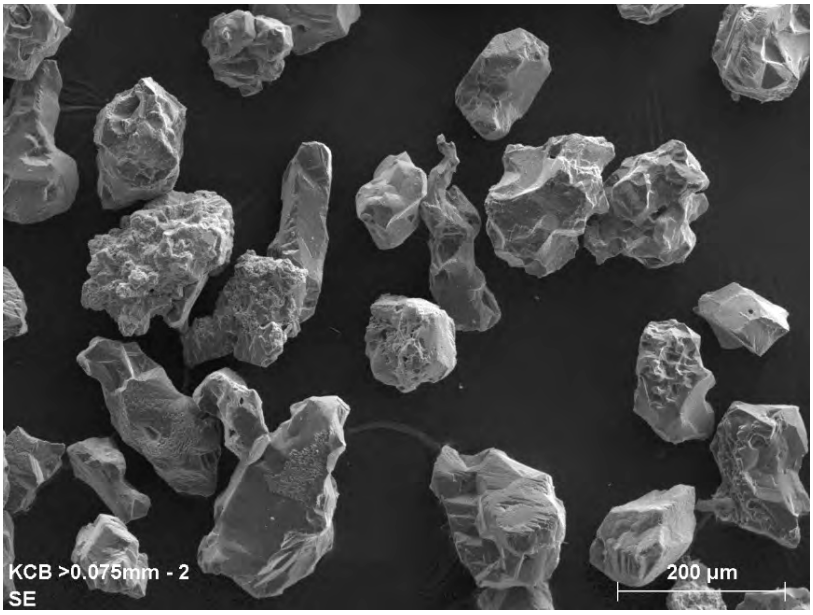

Figure D.D3-6 More than 0.075 mm (2)

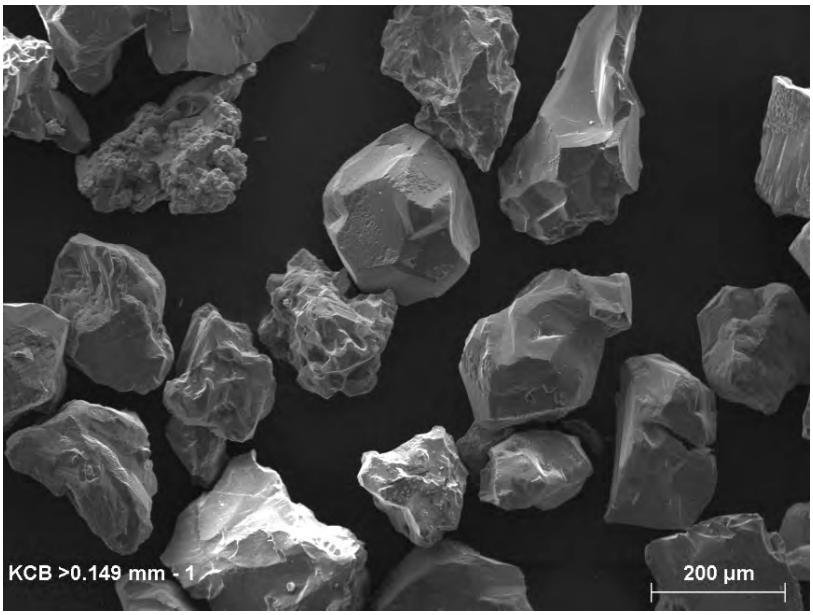

Figure D.D3-7 More than 0.149 mm (1)

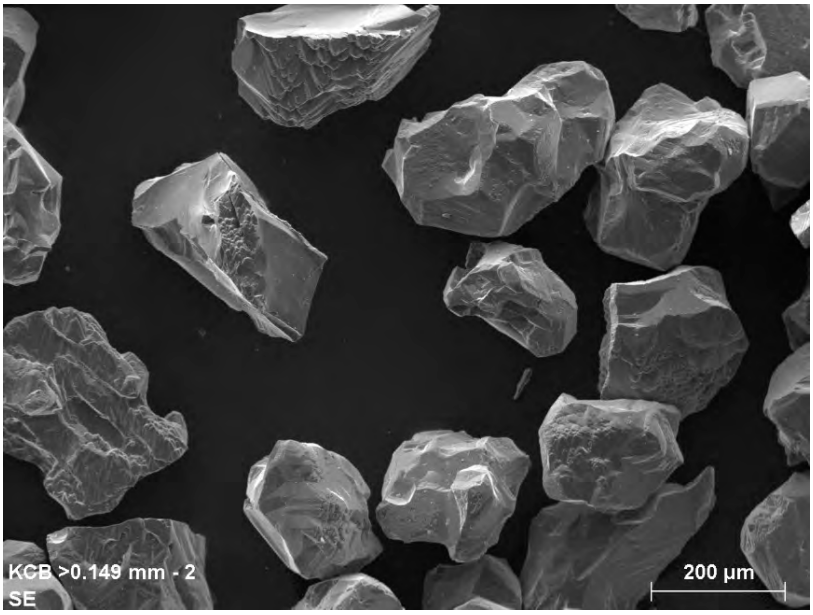

Figure D.D3-8 More than 0.149 mm (2)

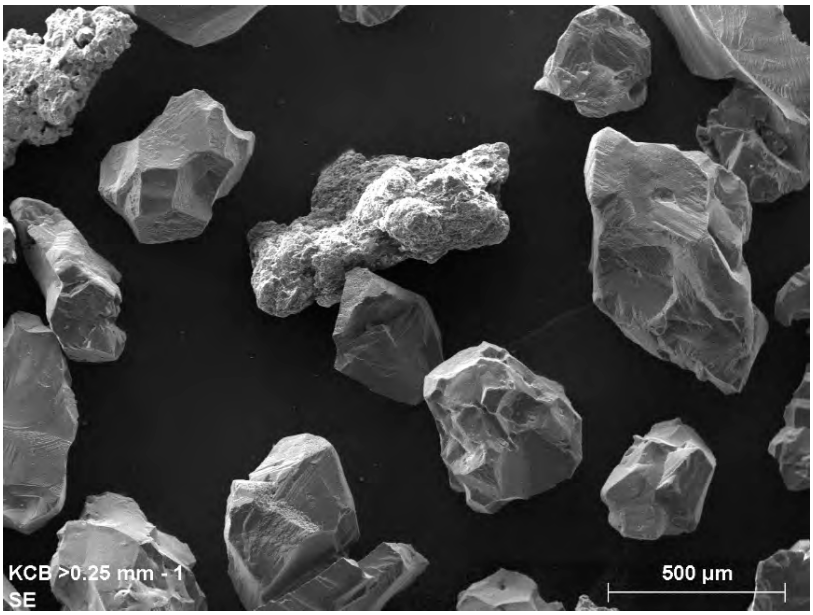

Figure D.D3-9 More than 0.25 mm (1)

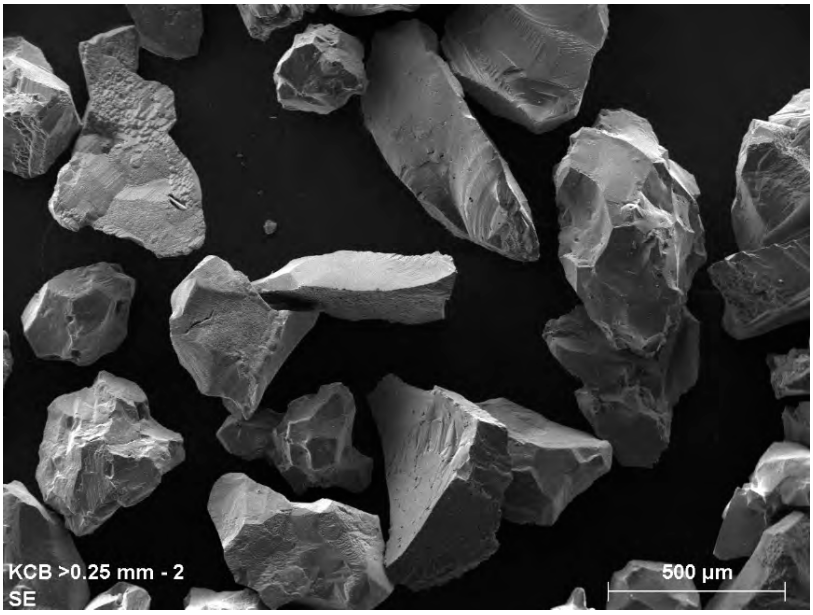

Figure D.D3-10 More than 0.25 mm (2)

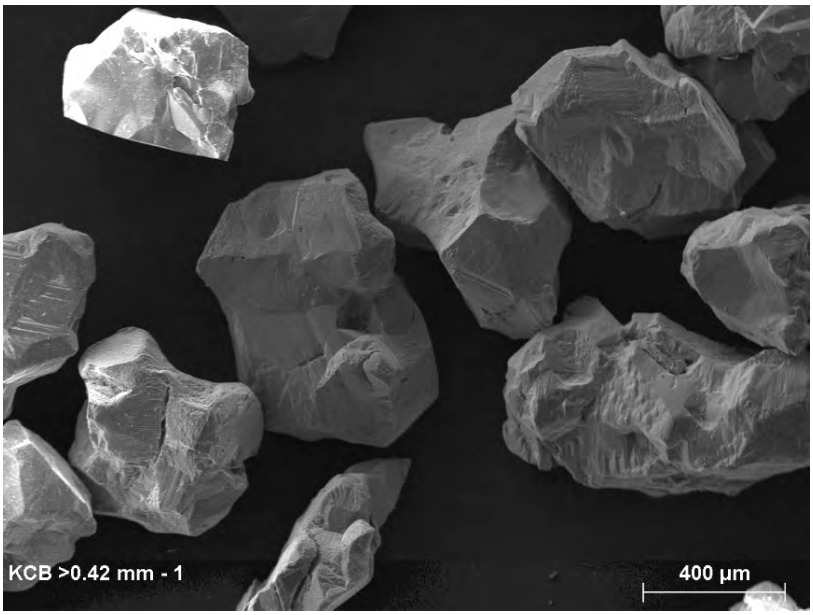

Figure D.D3-11 More than 0.42 mm (1)

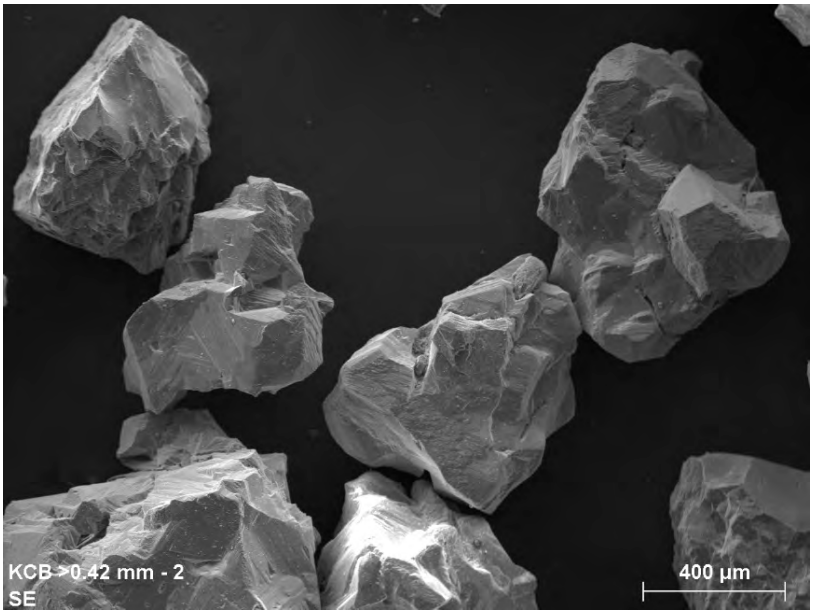

Figure D.D3-12 More than 0.42 mm (2)

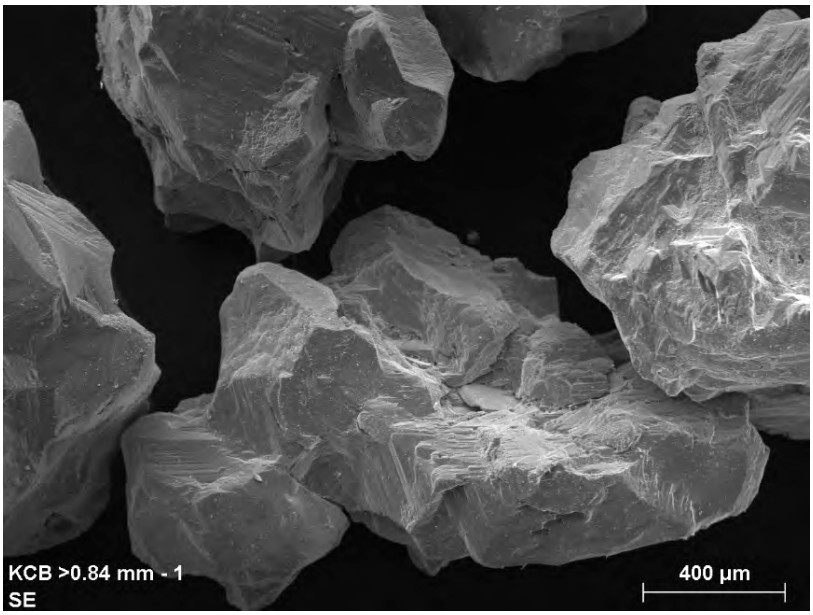

Figure D.D3-13 More than 0.84 mm (1)

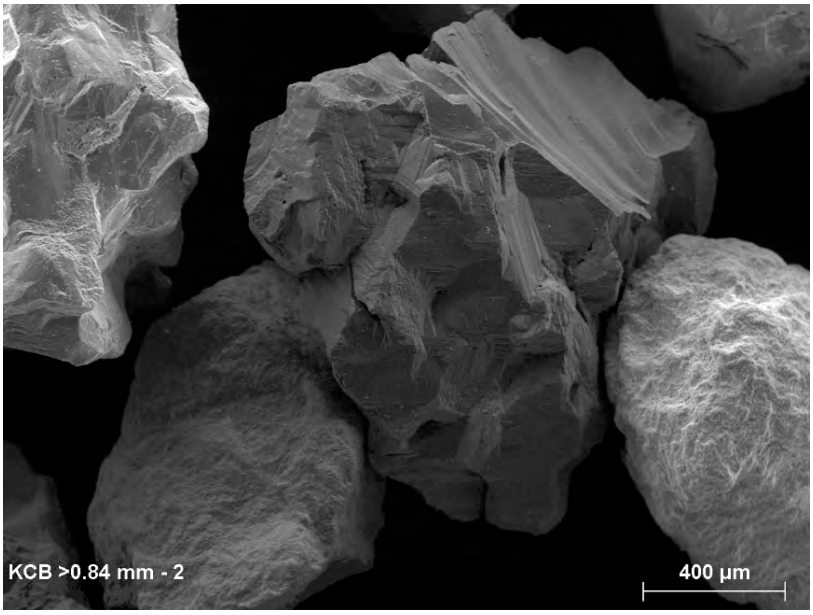

Figure D.D3-14 More than 0.84 mm (2)

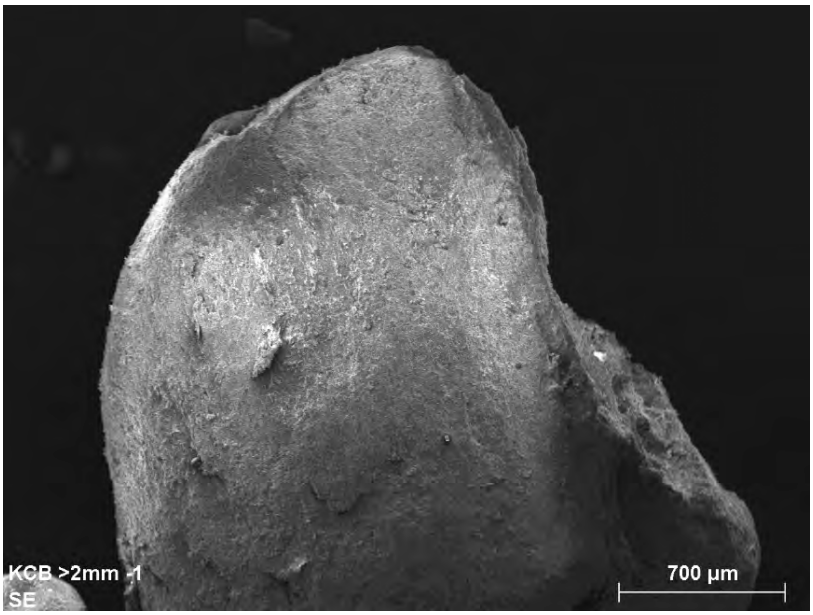

Figure D.D3-15 More than 2 mm (1)

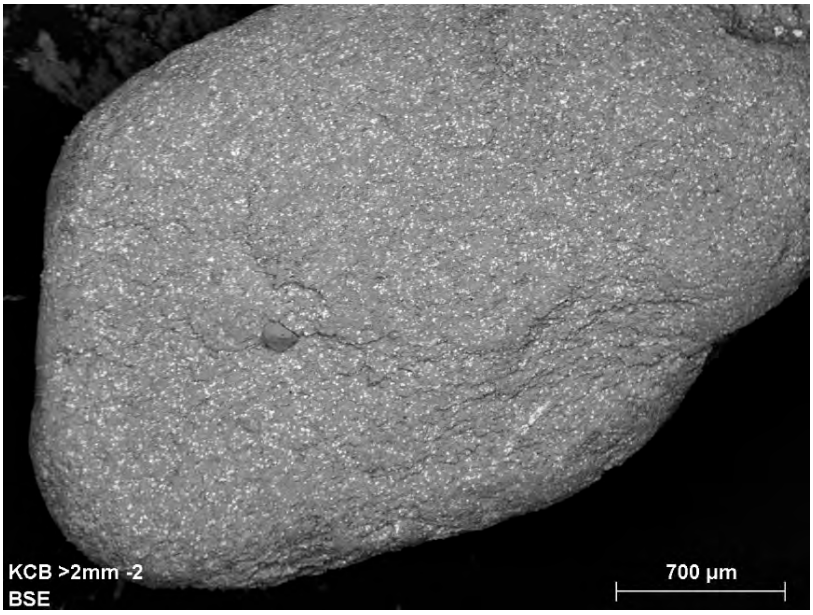

Figure D.D3-16 More than 2 mm (2)

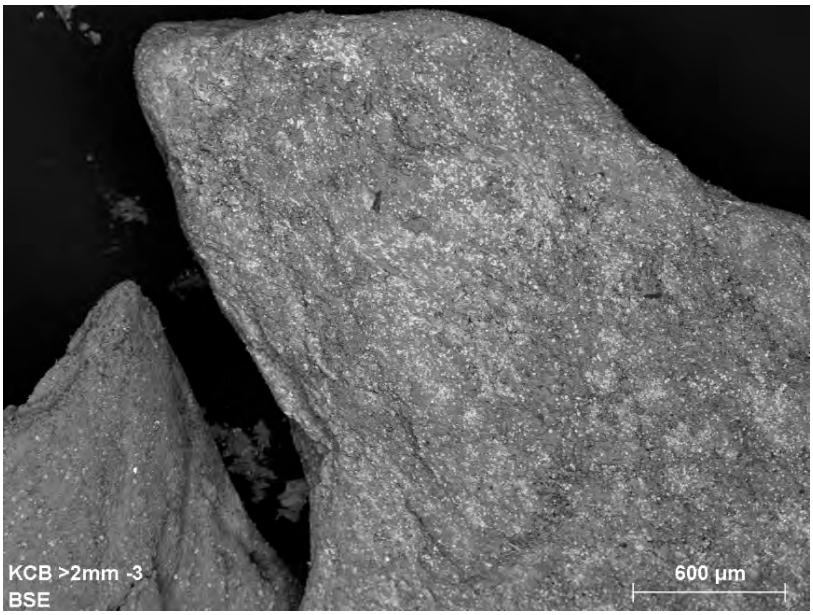

Figure D.D3-17 More than 2 mm (3)

ATTACHMENT D4

Direct Shear Test Data

Direct Shear Test (ASTM D3080)

Fundão Sand / As received 250 - 750 - 1250 kPa Normal Stress, Peak

Project Number:
Project Name: Fundão Tailings Dam Review Panel
Location:

Date of Testing: 2016-02-08
Tested by: JG
Checked by: BY

Hole No./ Sample No.	Depth (m)	Specimen Diameter (mm)	Initial Height (mm)	Area (mm^2)	Volume (cm^3)	Initial Void Ratio (e_o)	Initial WC (%)	Initial Wet Weight (g)	Initial Dry Weight (g)	Initial Bulk Density (g/cm^3)	Initial Dry Density (g/cm^3)	Normal Stress (kPa)	Void Ratio after Consolidation (e_c)	Height at Shearing (mm)	Volume at Shearing (cm^3)	Dry Density at Shearing (kg/m^3)	Final WC (%)	Void Ratio after Shearing (e_f)	Peak Shear Stress (KPa)	Φ (°)	c (kPa)
Fundão Sand / As received	-	61.44	31.80	2964.79	94.28	0.74	11.08	172.33	155.14	1.83	1.65	**250.0**	0.72	31.37	93.02	1.67	24.69	0.67	**164.2**	32.0	0
		61.44	29.75	2964.79	88.20	0.67	23.54	186.25	150.76	2.11	1.71	**750.0**	0.66	29.40	87.17	1.73	22.26	0.62	**476.3**		
		61.44	27.90	2964.79	82.72	0.62	21.51	177.99	146.48	2.15	1.77	**1250.0**	0.60	27.62	81.90	1.79	20.25	0.56	**812.0**		

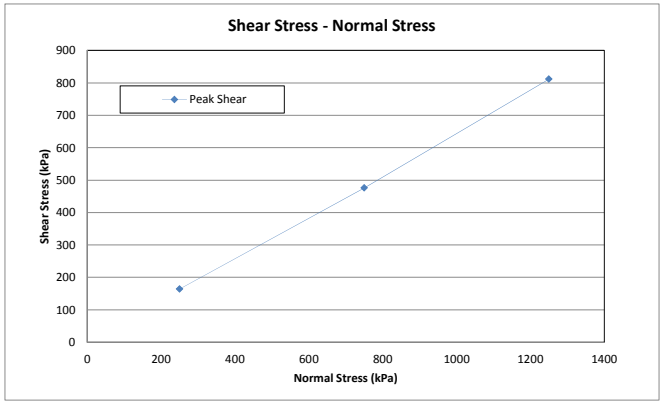

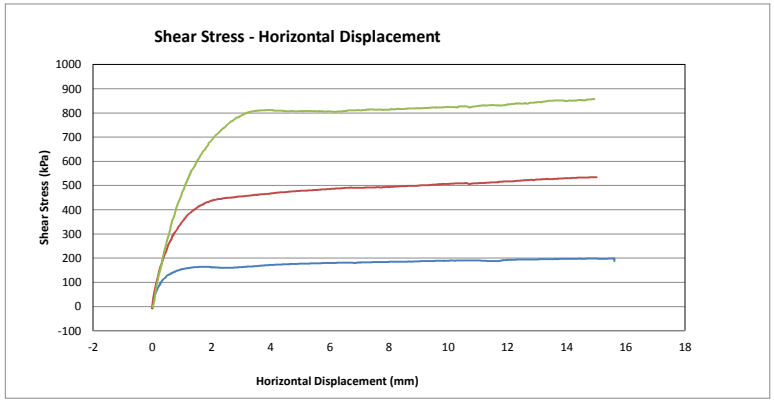

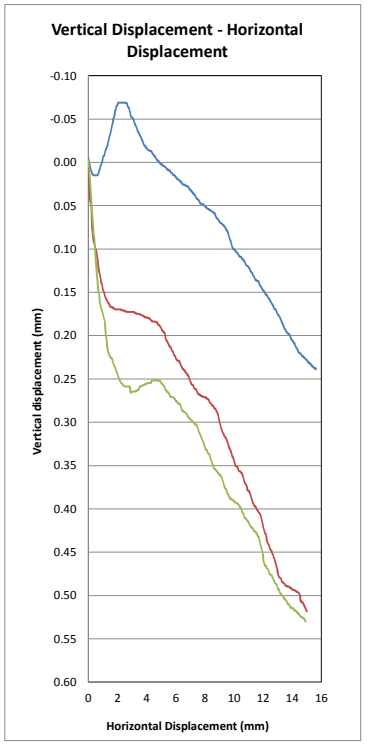

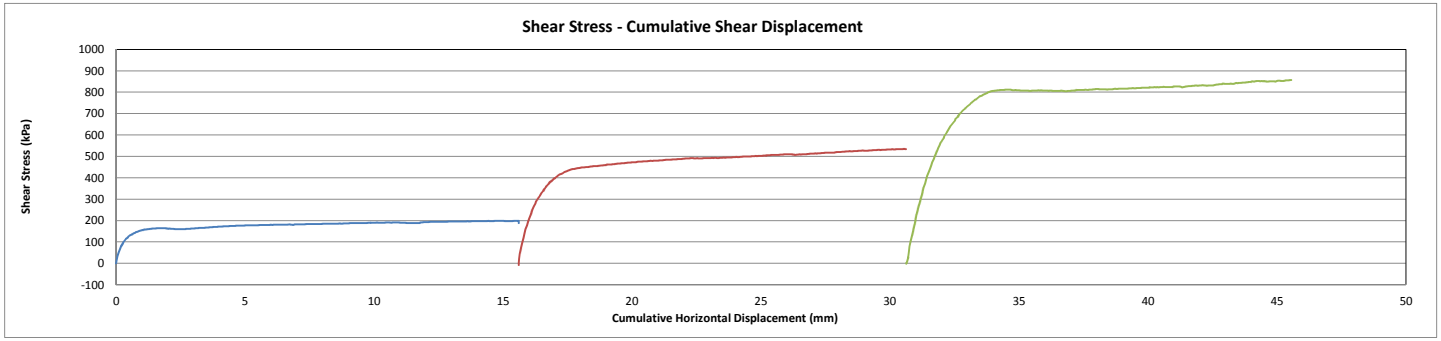

ATTACHMENT D5

Direct Simple Shear Test Data

Cyclic Direct Simple Shear Test

(ASTM D6528*)

* Based on ASTM D6528-07

Project No.:		Test No.:	DSS01
Project:	Fundão Tailings Dam Review Panel	Sample ID:	PSD1
Date:	2016-03-22	Depth:	
Tested by:	BY	Location:	
Checked by:	JG	Details:	Sand tailings sample with fines

Initial Sample Information		
Specimen Height	mm	21.01
Specimen Diameter	mm	70.67
Area	cm^2	3922.47
Volume	cm^3	82.41
Wet Weight	g	134.79
Water Content	%	5.04
Dry Weight	g	128.32
Wet Density	g/cm^3	1.636
Dry Density	g/cm^3	1.557
Specific Gravity (assumed)	-	2.96
Void Ratio (e)	-	0.90
Saturation Ratio (Sr)	%	16.56

FINAL SAMPLE INFORMATION		
Liquid Limit		
Plastic Limit		
Final Moisture Content	%	10.27

Cyclic Shearing - Stage 1		
Frequency	Hz	0.1
Initial Vertical Stress	kPa	300.19
Cyclic Stress Ratio (CSR)	-	0.01
Number of Cycles at the end of this stage*1	-	30
Max Cyclic Shear Stress	kPa	3.14
Max. Shear Strain	%	0.01
Max. Excess Pore Pressure	kPa	20.91

*1: Ended at 30 cycles based on test instruction

Cyclic Shearing - Stage 2		
Frequency	Hz	0.1
Initial Vertical Stress	kPa	300.19
Cyclic Stress Ratio (CSR)	-	0.05
Number of Cycles*2 at the end of this stage*1	-	30
Max Cyclic Shear Stress	kPa	15.12
Max. Shear Strain	%	0.06
Max. Excess Pore Pressure	kPa	67.33

*1: Ended at 30 cycles based on test instruction *2: Cycles in this stage.

Cyclic Shearing - Stage 3		
Frequency	Hz	0.1
Initial Vertical Stress	kPa	300.19
Cyclic Stress Ratio (CSR)	-	0.10
Number of Cycles*2 to 15% Shear Strain	-	11
Max Cyclic Shear Stress	kPa	30.85
Max. Shear Strain	%	23.31
Max. Excess Pore Pressure	kPa	297.62

*2: Cycles in this stage.

CONSOLIDATION					
Normal Stress	kPa	38	75	150	300
Max Load	kN	0.15	0.29	0.59	1.18
Total Height Change	mm	0.03	0.05	0.08	0.18
Consolidated Height	mm	20.98	20.96	20.93	20.83
Axial Strain	%	0.14	0.22	0.39	0.84
Duration	min	180	180	180	415

Photos:

Before Test

After Test

Cyclic Direct Simple Shear Test (ASTM D6528)

Consolidation Phase

Project No.:		Test No.:	DSS01
Project:	Fundão Tailings Dam Review Panel	Sample ID:	PSD1
Date:	2016-03-22	Depth:	
Tested by:	BY	Location:	
Checked by:	JG	Details:	Sand tailings sample with fines

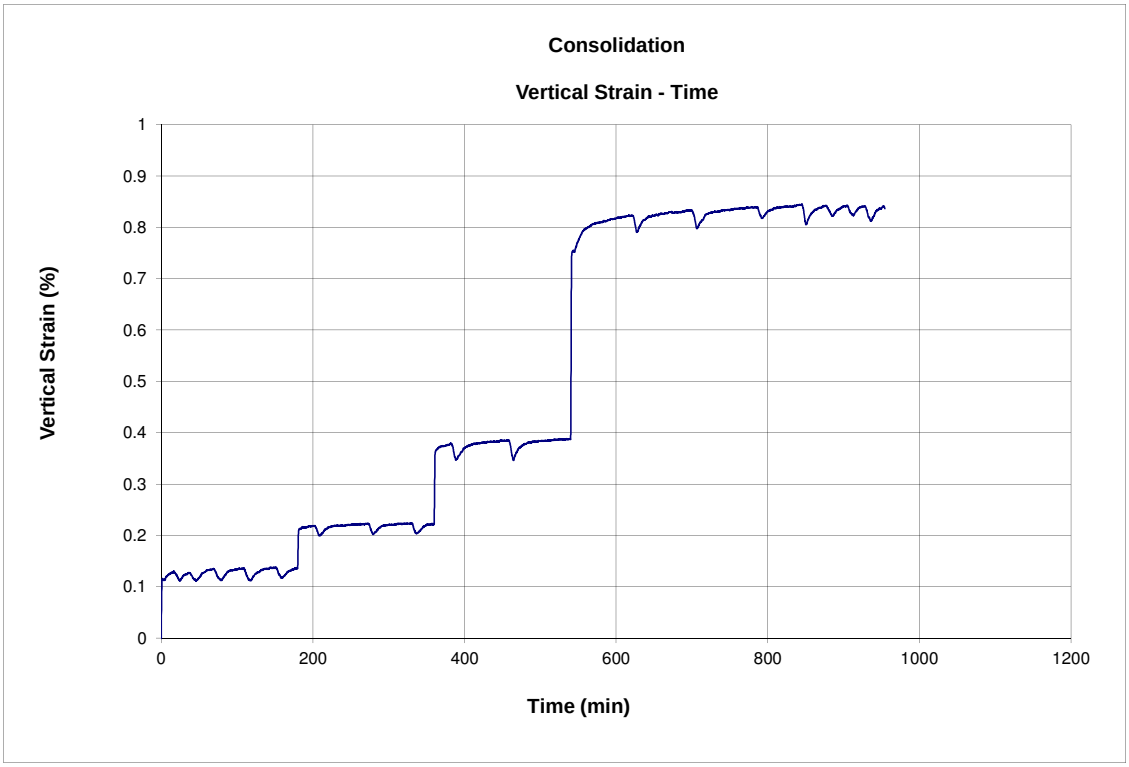

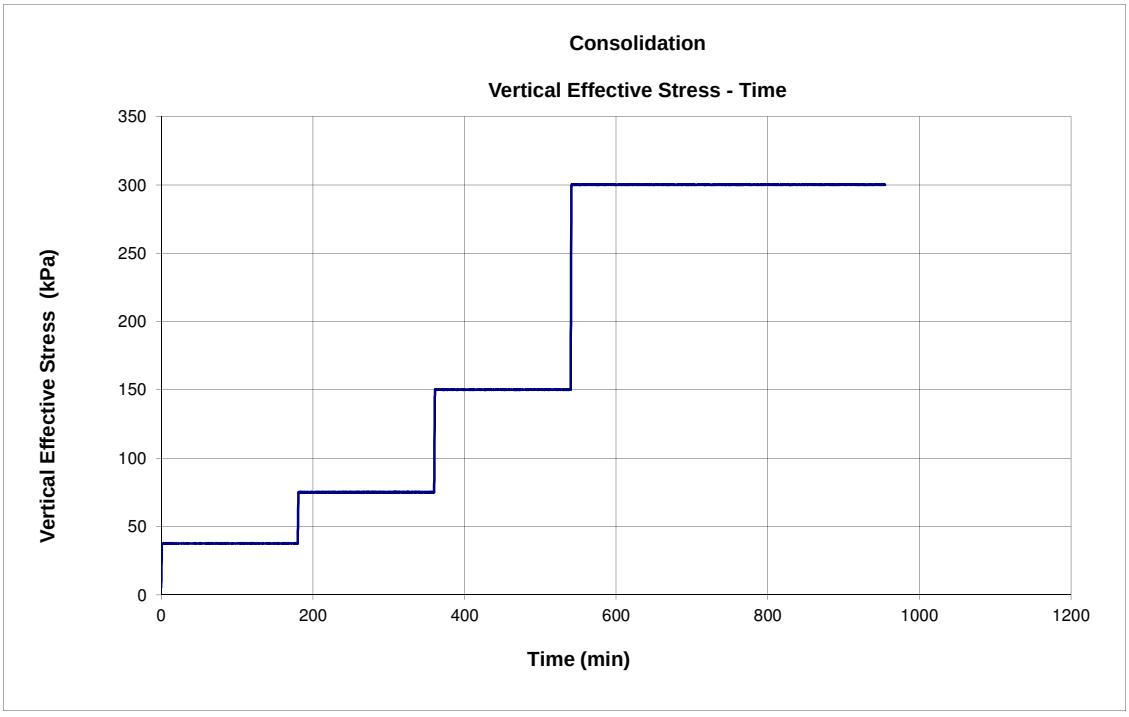

Cyclic Direct Simple Shear Test (ASTM D6528)

Cyclic Shearing Phase

Project No.:		Test No.:	DSS01
Project:	Fundão Tailings Dam Review Panel	Sample ID:	PSD1
Date:	2016-03-22	Depth:	
Tested by:	BY	Location:	
Checked by:	JG	Details:	Sand tailings sample with fines

τ_{cy} / σ'_{vc} = 0.05 - 0.10 - 0.15 σ'_{vc} = 300.2 kPa

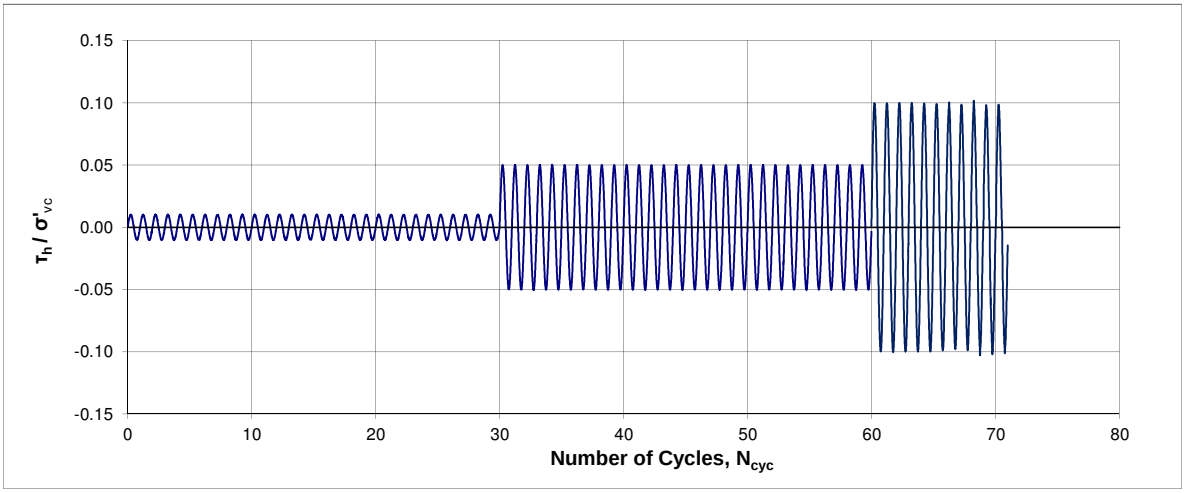

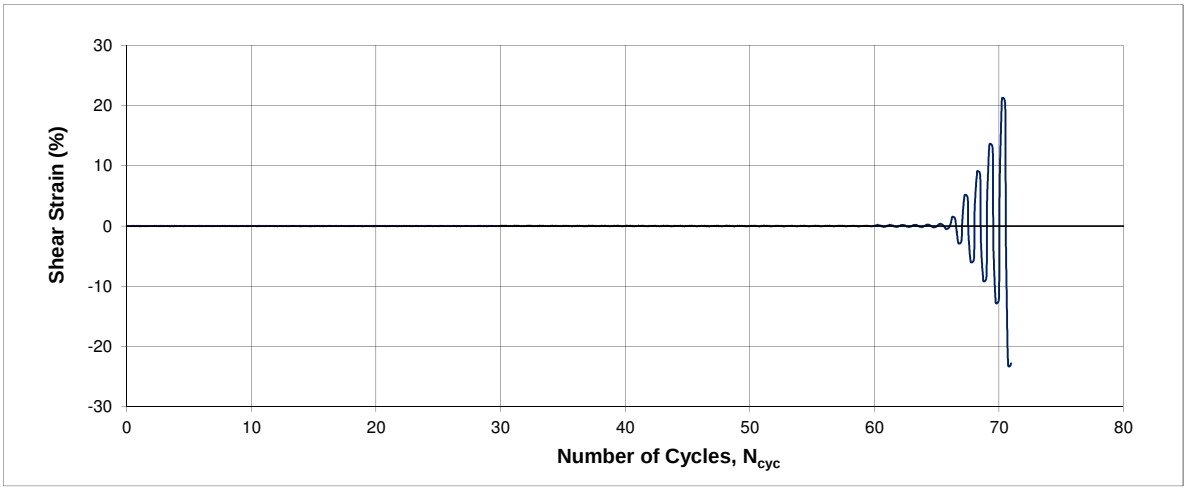

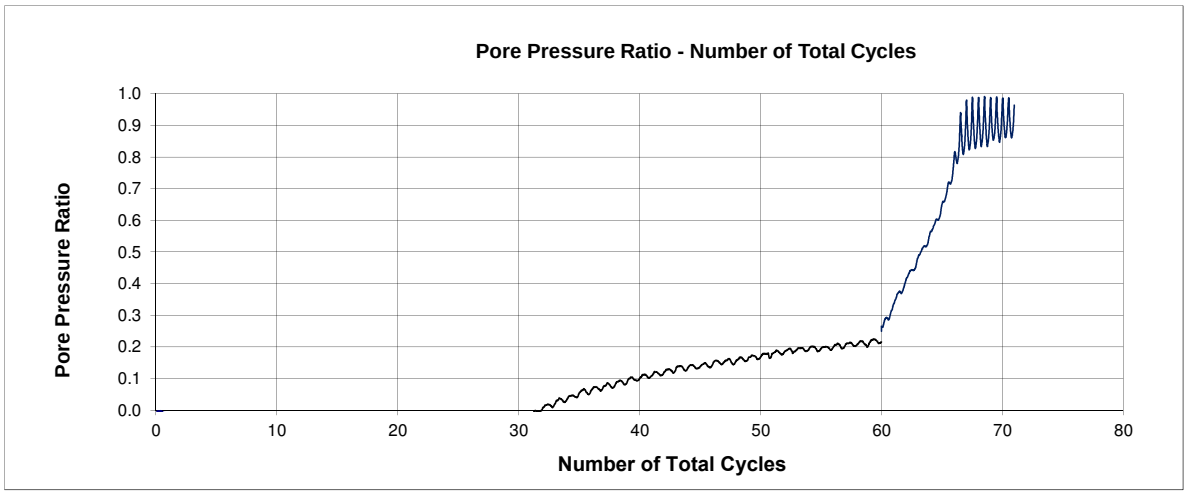

Cyclic Direct Simple Shear Test (ASTM D6528)

Cyclic Shearing Phase

Project No.:		Test No.:	DSS01
Project:	Fundão Tailings Dam Review Panel	Sample ID:	PSD1
Date:	2016-03-22	Depth:	
Tested by:	BY	Location:	
Checked by:	JG	Details:	Sand tailings sample with fines

τ_{cy} / σ'_{vc} = 0.05 - 0.10 - 0.15 σ'_{vc} = 300 kPa

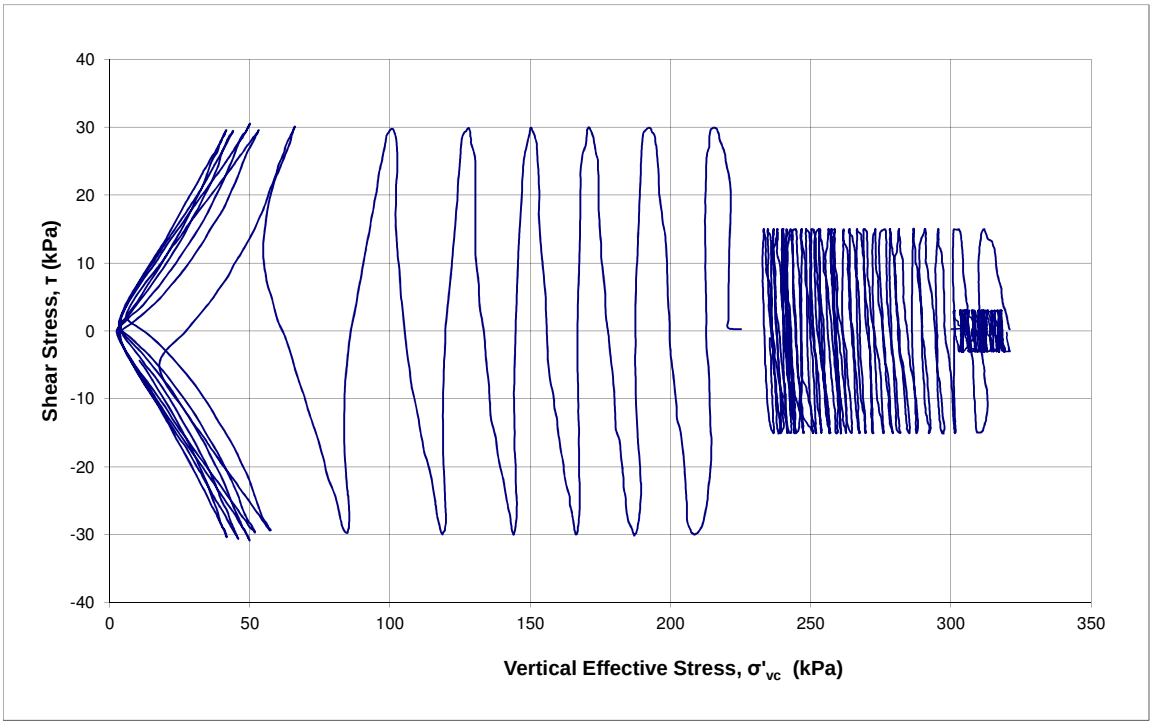

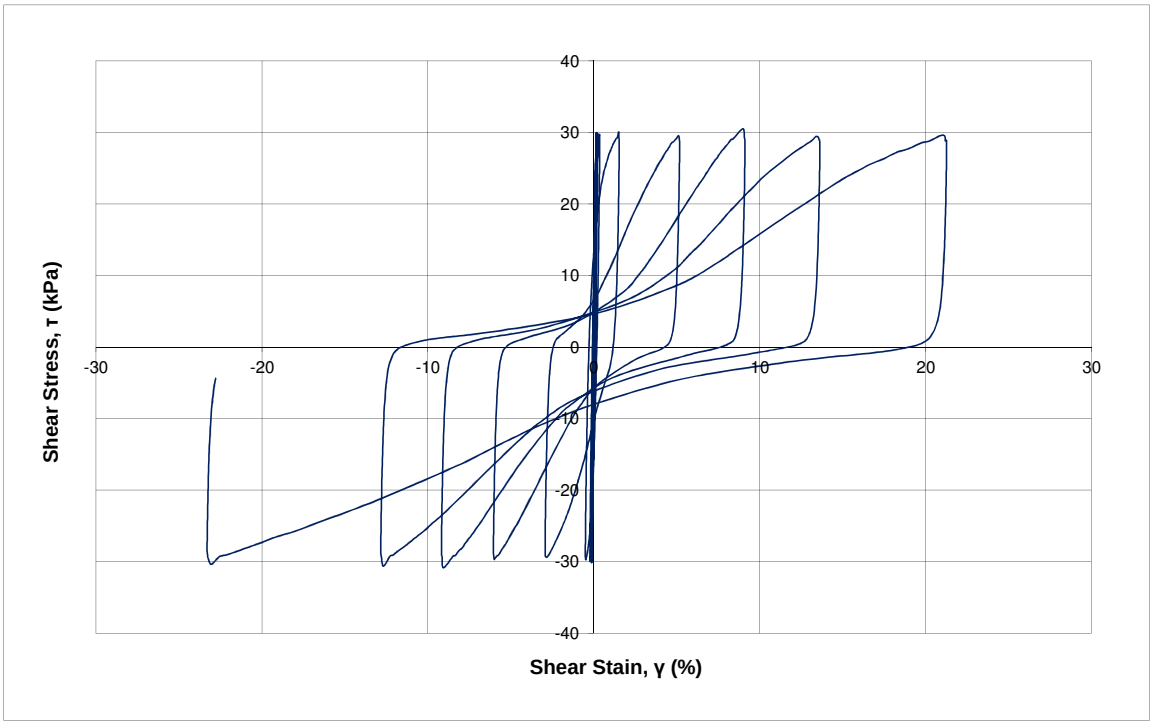

Cyclic Direct Simple Shear Test

(ASTM D6528*)

* Based on ASTM D6528-07

Klohn Crippen Berger

Project No.:		Test No.:	DSS02
Project:	Fundão Tailings Dam Review Panel	Sample ID:	PSD1
Date:	2016-03-22	Depth:	
Tested by:	BY	Location:	
Checked by:	JG	Details:	Sand tailings sample with fines

Initial Sample Information		
Specimen Height	mm	21.00
Specimen Diameter	mm	70.66
Area	cm^2	3921.36
Volume	cm^3	82.35
Wet Weight	g	116.37
Water Content	%	5.04
Dry Weight	g	110.79
Wet Density	g/cm^3	1.413
Dry Density	g/cm^3	1.345
Specific Gravity (assumed)	-	2.96
Void Ratio (e)	-	1.20
Saturation Ratio (Sr)	%	12.43

FINAL SAMPLE INFORMATION		
Liquid Limit		
Plastic Limit		
Final Moisture Content	%	14.65

Cyclic Shearing - Stage 1		
Frequency	Hz	0.1
Initial Vertical Stress	kPa	300.10
Cyclic Stress Ratio (CSR)	-	0.01
Number of Cycles at the end of this stage*1	-	30
Max Cyclic Shear Stress	kPa	3.16
Max. Shear Strain	%	0.01
Max. Excess Pore Pressure	kPa	10.18

*1: Ended at 30 cycles based on test instruction

Cyclic Shearing - Stage 2		
Frequency	Hz	0.1
Initial Vertical Stress	kPa	300.10
Cyclic Stress Ratio (CSR)	-	0.05
Number of Cycles*2 at the end of this stage*1	-	30
Max Cyclic Shear Stress	kPa	15.07
Max. Shear Strain	%	0.07
Max. Excess Pore Pressure	kPa	104.33

*1: Ended at 30 cycles based on test instruction *2: Cycles in this stage.

Cyclic Shearing - Stage 3		
Frequency	Hz	0.1
Initial Vertical Stress	kPa	300.10
Cyclic Stress Ratio (CSR)	-	0.10
Number of Cycles*2 to 15% Shear Strain	-	2
Max Cyclic Shear Stress	kPa	29.86
Max. Shear Strain	%	56.87
Max. Excess Pore Pressure	kPa	294.85

*2: Cycles in this stage.

CONSOLIDATION					
Normal Stress	kPa	38	75	150	300
Max Load	kN	0.15	0.29	0.59	1.18
Total Height Change	mm	0.55	1.24	1.82	2.33
Consolidated Height	mm	20.45	19.76	19.18	18.67
Axial Strain	%	2.63	5.92	8.68	11.10
Duration	min	180	180	180	433

Photos:

Before Test

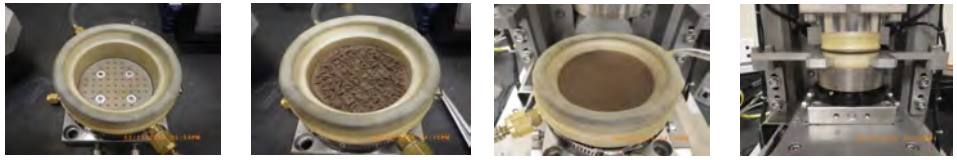

After Test

Cyclic Direct Simple Shear Test (ASTM D6528)

Consolidation Phase

Project No.:		Test No.:	DSS02
Project:	Fundão Tailings Dam Review Panel	Sample ID:	PSD1
Date:	2016-03-22	Depth:	
Tested by:	BY	Location:	
Checked by:	JG	Details:	Sand tailings sample with fines

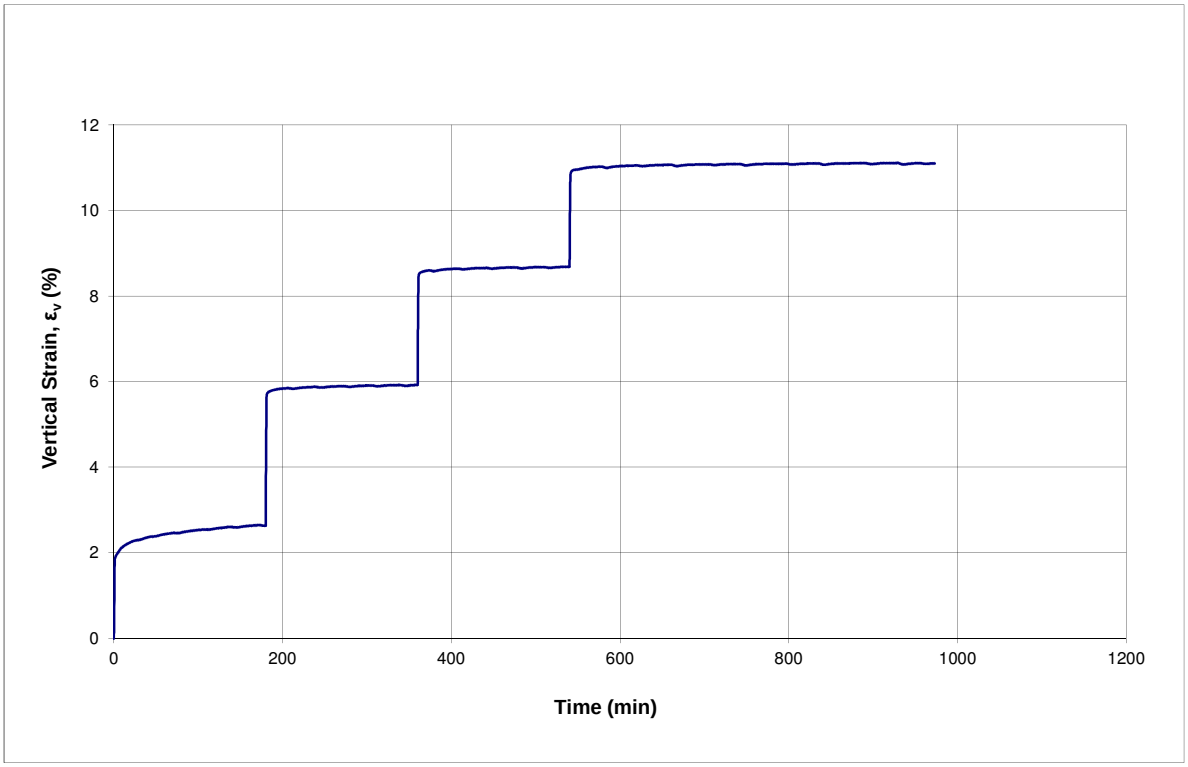

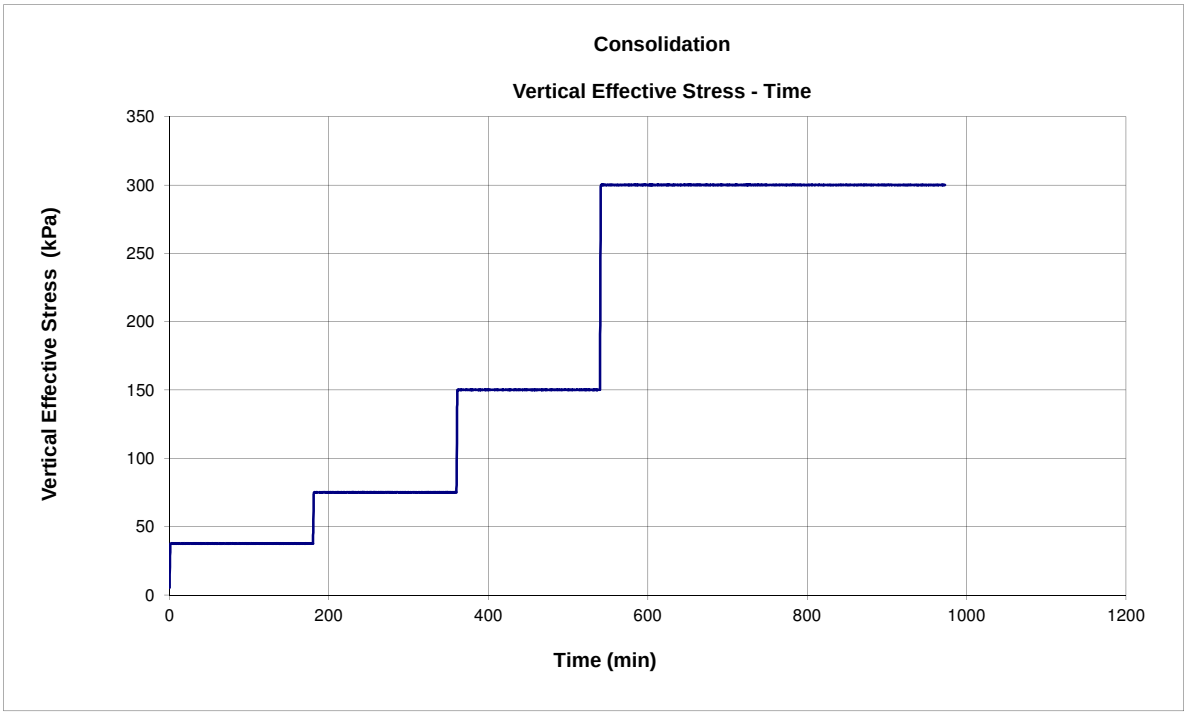

Cyclic Direct Simple Shear Test (ASTM D6528)

Cyclic Shearing Phase

Project No.:		Test No.:	DSS02
Project:	Fundão Tailings Dam Review Panel	Sample ID:	PSD1
Date:	2016-03-22	Depth:	
Tested by:	BY	Location:	
Checked by:	JG	Details:	Sand tailings sample with fines

τ_{cy} / σ'_{vc} = 0.05 - 0.10 - 0.15 σ'_{vc} = 300 kPa

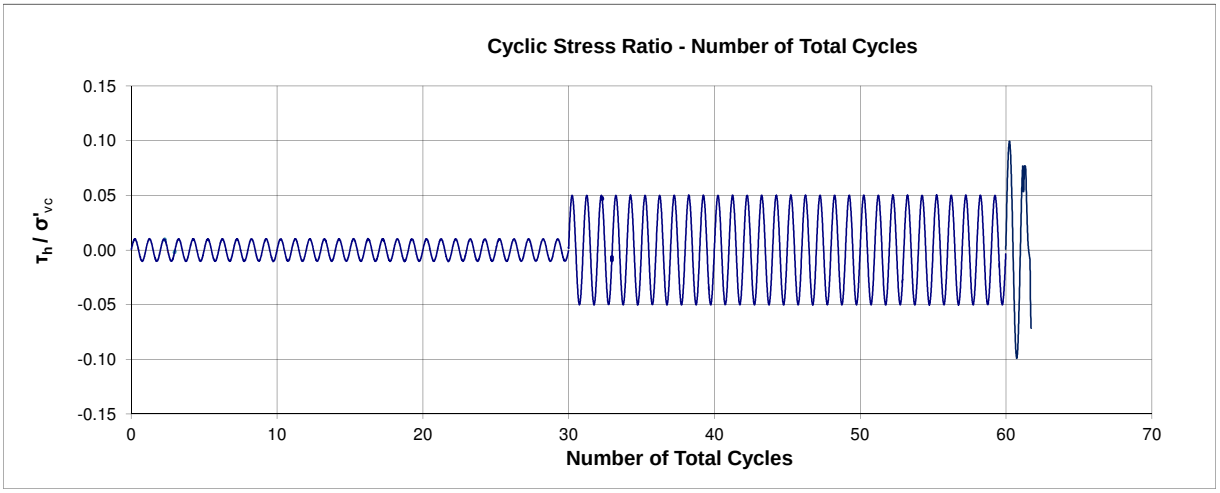

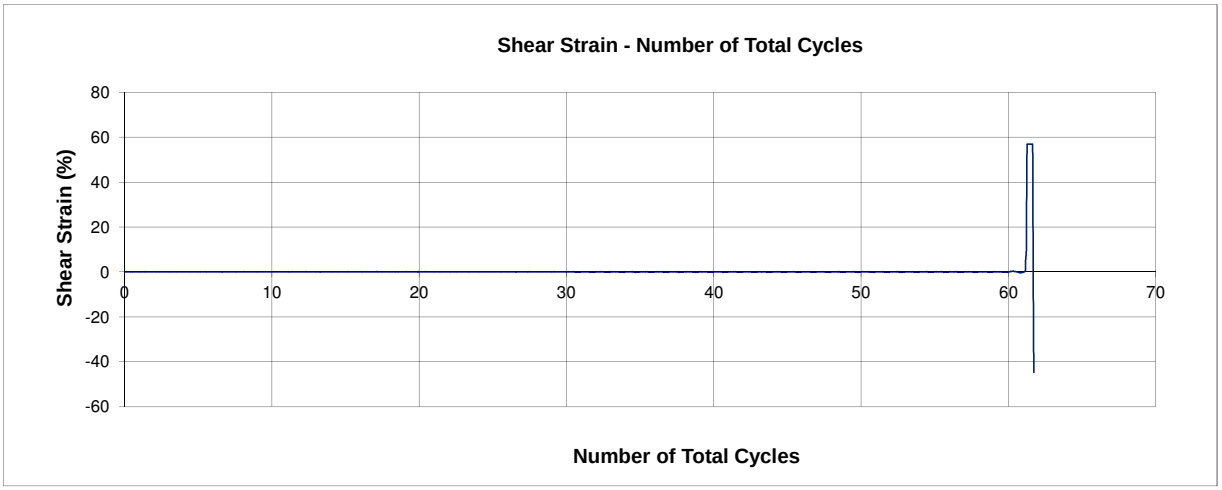

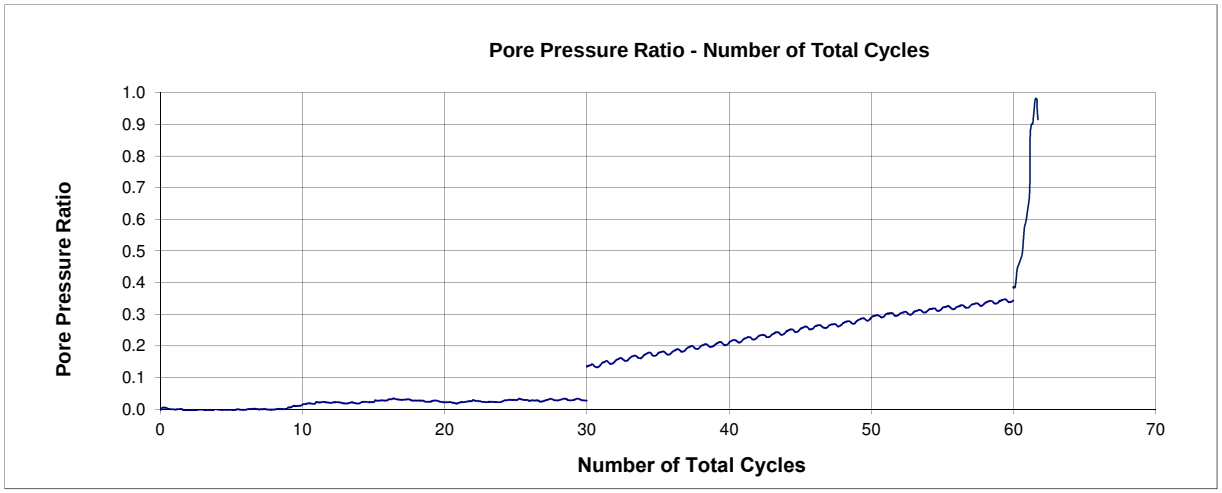

Cyclic Direct Simple Shear Test (ASTM D6528)

Cyclic Shearing Phase

Project No.:		Test No.:	DSS02
Project:	Fundão Tailings Dam Review Panel	Sample ID:	PSD1
Date:	2016-03-22	Depth:	
Tested by:	BY	Location:	
Checked by:	JG	Details:	Sand tailings sample with fines

τ_{cy} / σ'_{vc} = 0.05 - 0.10 - 0.15 σ'_{vc} = 300 kPa

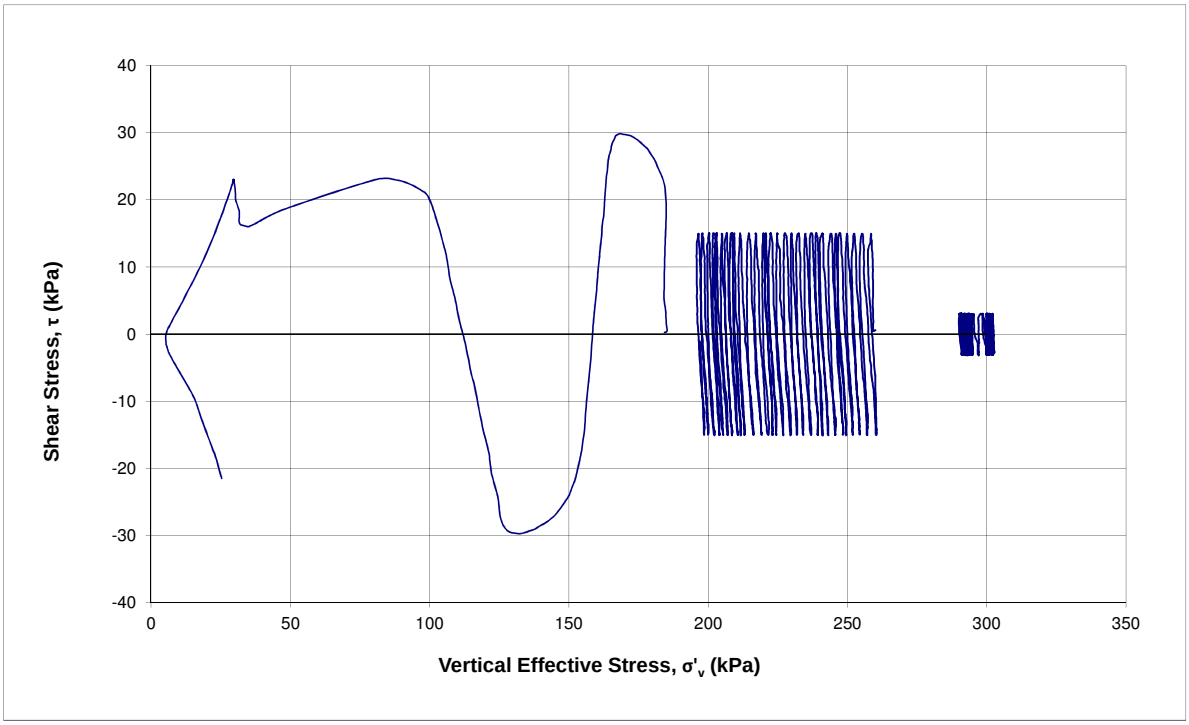

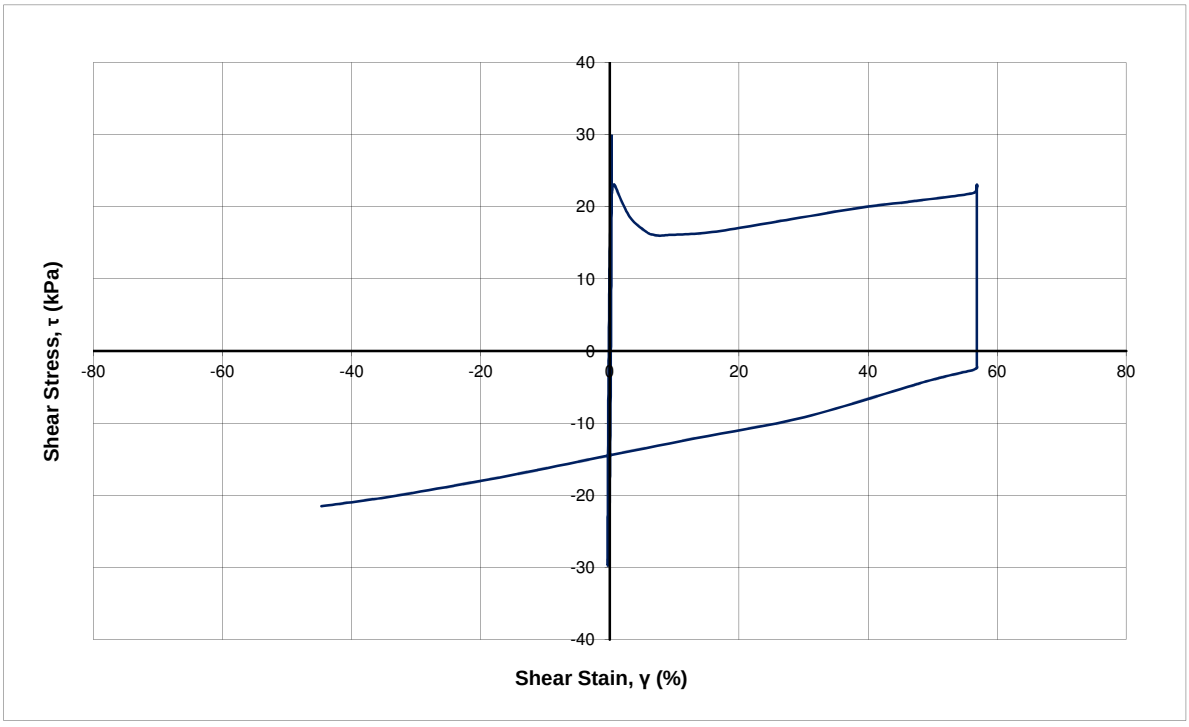

Cyclic Direct Simple Shear Test

(ASTM D6528*)

* Based on ASTM D6528-07

Klohn Crippen Berger

Project No.:		Test No.:	DSS03
Project:	Fundão Tailings Dam Review Panel	Sample ID:	Slimes
Date:	2016-03-28	Depth:	
Tested by:	BY	Location:	
Checked by:	JG	Details:	Slimes

Initial Sample Information		
Specimen Height	mm	28.20
Specimen Diameter	mm	70.40
Area	cm^2	3892.56
Volume	cm^3	109.77
Wet Weight	g	231.62
Water Content	%	41.74
Dry Weight	g	163.41
Wet Density	g/cm^3	2.110
Dry Density	g/cm^3	1.489
Specific Gravity (assumed)	-	3.93
Void Ratio (e)	-	1.64
Saturation Ratio (Sr)	%	100.03

FINAL SAMPLE INFORMATION		
Liquid Limit		
Plastic Limit		
Final Moisture Content	%	22.98

Cyclic Shearing - Stage 1		
Frequency	Hz	0.1
Initial Vertical Stress	kPa	300.09
Cyclic Stress Ratio (CSR)	-	0.01
Number of Cycles at the end of this stage*1	-	30
Max Cyclic Shear Stress	kPa	3.16
Max. Shear Strain	%	0.01
Max. Excess Pore Pressure	kPa	25.01

*1: Ended at 30 cycles based on test instruction

Cyclic Shearing - Stage 2		
Frequency	Hz	0.1
Initial Vertical Stress	kPa	300.09
Cyclic Stress Ratio (CSR)	-	0.05
Number of Cycles*2 at the end of this stage*1	-	30
Max Cyclic Shear Stress	kPa	15.12
Max. Shear Strain	%	0.06
Max. Excess Pore Pressure	kPa	29.99

*1: Ended at 30 cycles based on test instruction *2: Cycles in this stage.

Cyclic Shearing - Stage 3		
Frequency	Hz	0.1
Initial Vertical Stress	kPa	300.09
Cyclic Stress Ratio (CSR)	-	0.10
Number of Cycles*2 to 15% Shear Strain	-	39
Max Cyclic Shear Stress	kPa	32.86
Max. Shear Strain	%	26.62
Max. Excess Pore Pressure	kPa	285.20

*2: Cycles in this stage.

CONSOLIDATION									
Normal Stress	kPa	3	6	13	25	50	100	200	300
Max Load	kN	0.01	0.02	0.05	0.10	0.20	0.39	0.78	1.17
Total Height Change	mm	0.09	2.08	4.82	5.90	6.90	7.67	8.33	8.70
Consolidated Height	mm	28.11	26.12	23.38	22.30	21.30	20.53	19.87	19.50
Axial Strain	%	0.34	7.36	17.11	20.92	24.47	27.20	29.55	30.84
Duration	min	32	133	166	150	240	240	240	674

Photos:

Before Test




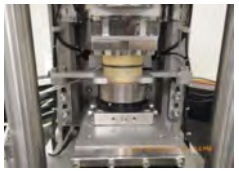

After Test




Cyclic Direct Simple Shear Test (ASTM D6528)

Consolidation Phase

Project No.:		Test No.:	DSS03
Project:	Fundão Tailings Dam Review Panel	Sample ID:	Slimes
Date:	2016-03-28	Depth:	
Tested by:	BY	Location:	
Checked by:	JG	Details:	Slimes

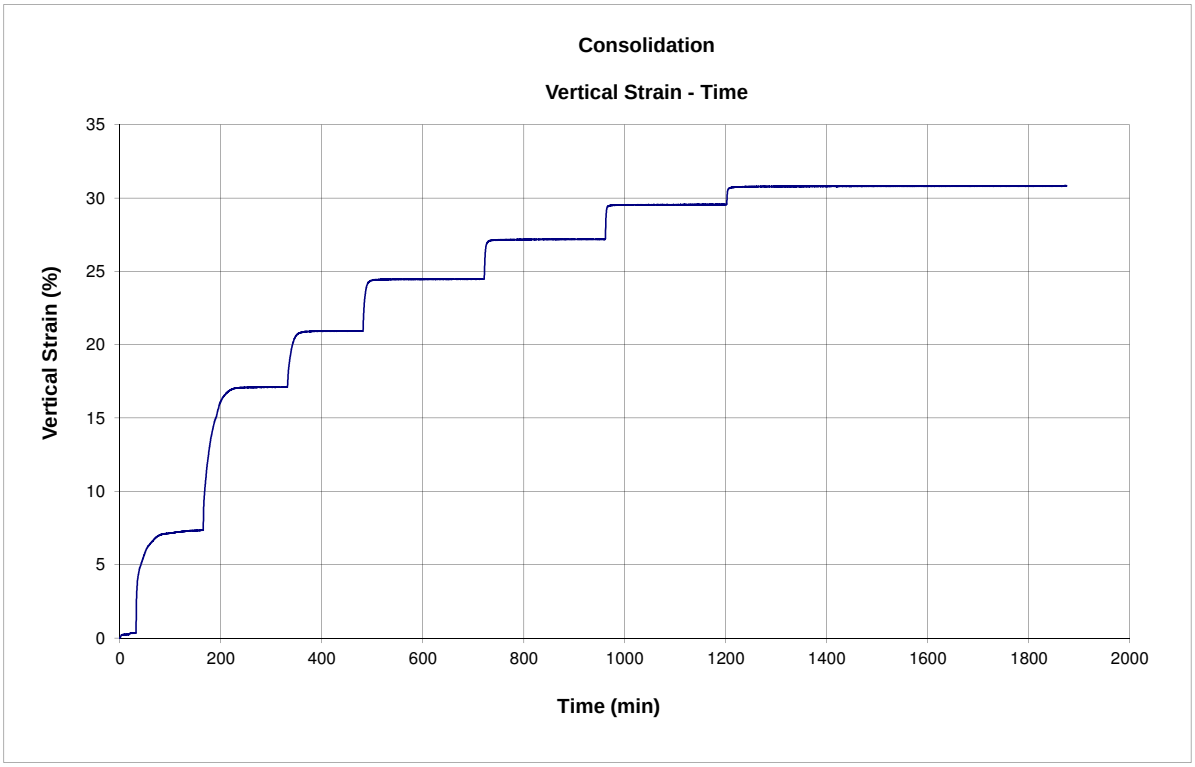

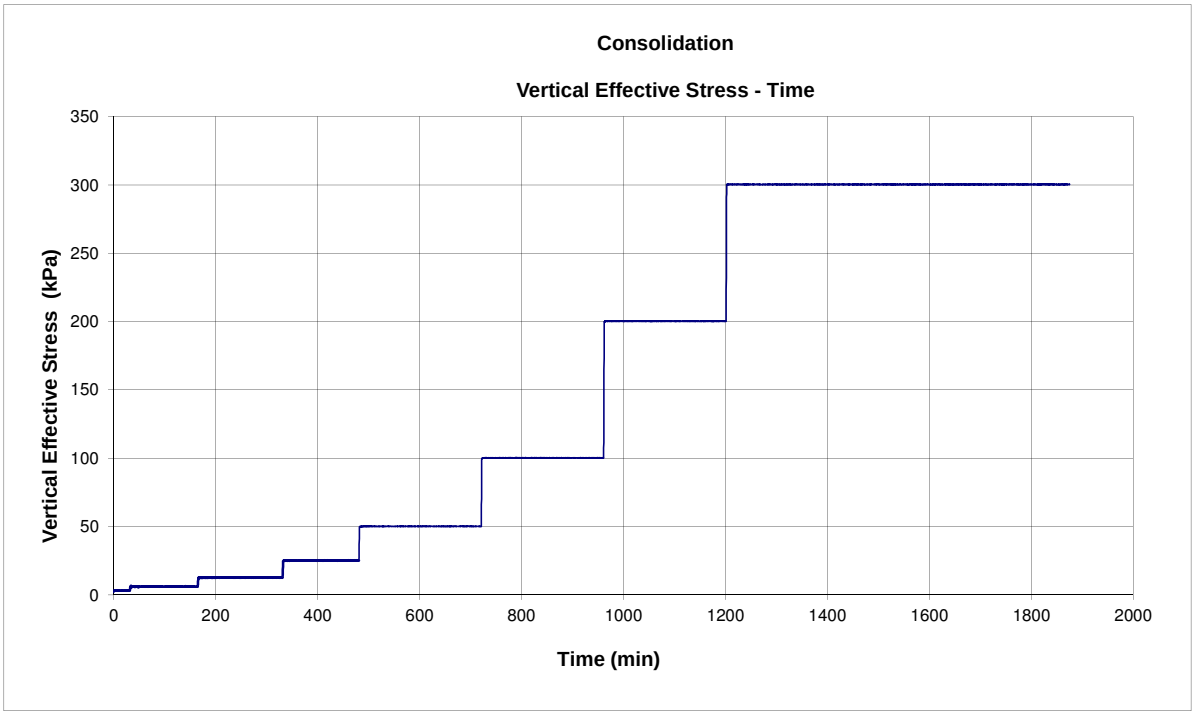

Cyclic Direct Simple Shear Test (ASTM D6528)

Cyclic Shearing Phase

Project No.:		Test No.:	DSS03
Project:	Fundão Tailings Dam Review Panel	Sample ID:	Slimes
Date:	2016-03-28	Depth:	
Tested by:	BY	Location:	
Checked by:	JG	Details:	Slimes

τ_{cy} / σ'_{vc} = 0.05 - 0.10 - 0.15 σ'_{vc} = 300 kPa

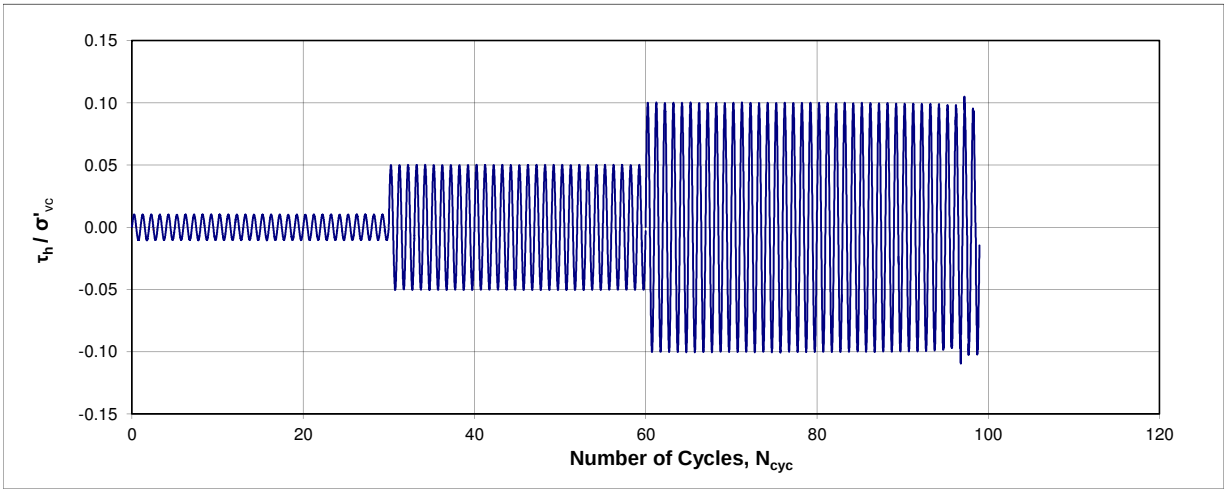

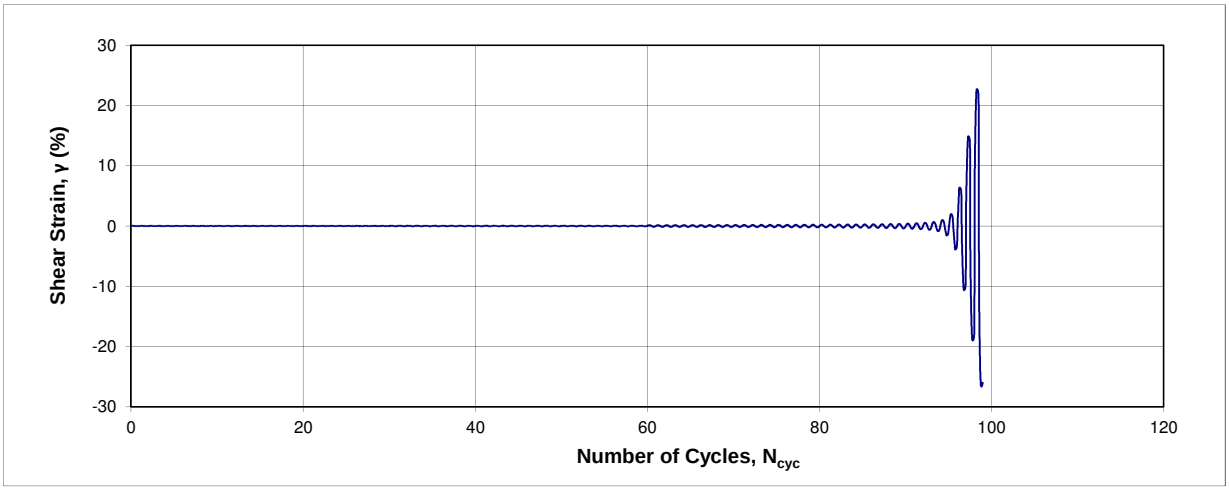

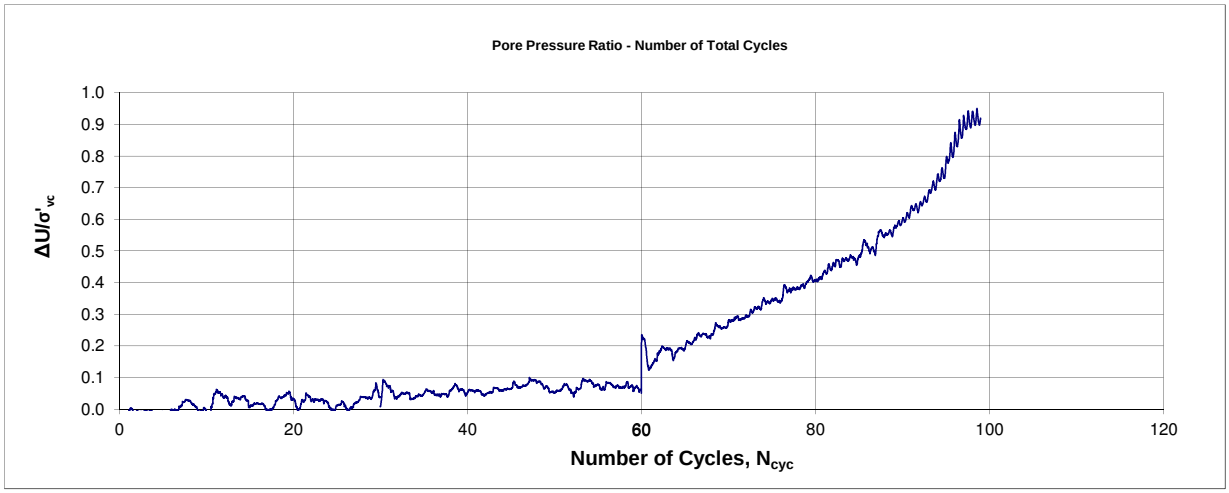

Cyclic Direct Simple Shear Test (ASTM D6528)

Cyclic Shearing Phase

Project No.:		Test No.:	DSS03
Project:	Fundão Tailings Dam Review Panel	Sample ID:	Slimes
Date:	2016-03-28	Depth:	
Tested by:	BY	Location:	
Checked by:	JG	Details:	Slimes

τ_{cy} / σ'_{vc} = 0.05 - 0.10 - 0.15 σ'_{vc} = 300 kPa

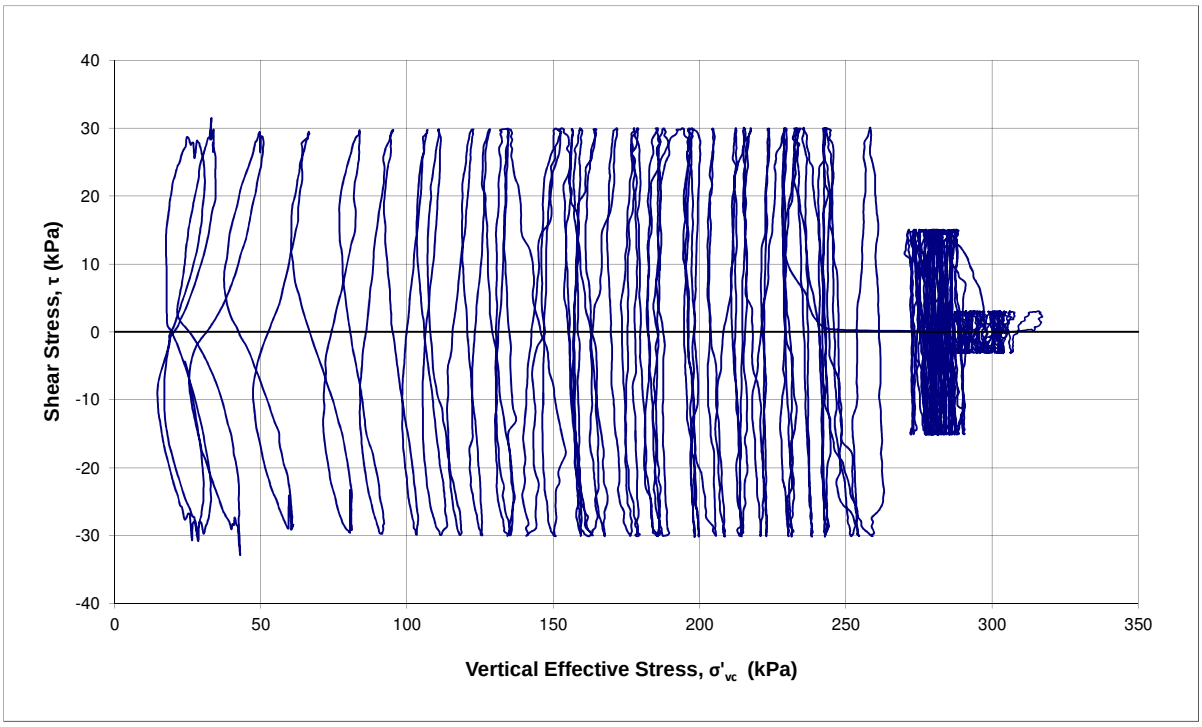

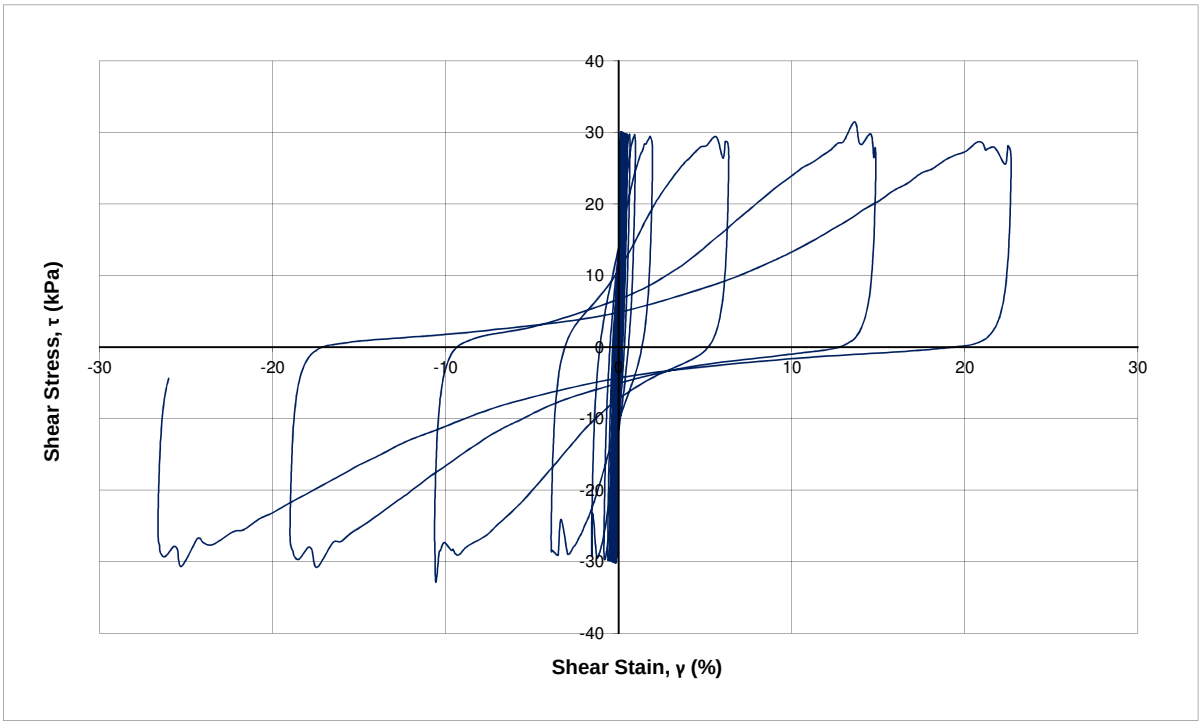

Cyclic Direct Simple Shear Test

(ASTM D6528*)

* Based on ASTM D6528-07

Klohn Crippen Berger

Project No.:		Test No.:	DSS04
Project:	Fundão Tailings Dam Review Panel	Sample ID:	PSD1
Date:	2016-03-29	Depth:	
Tested by:	BY	Location:	
Checked by:	JG	Details:	Sand tailings sample with fines

Initial Sample Information		
Specimen Height	mm	21.00
Specimen Diameter	mm	70.59
Area	cm^2	3913.60
Volume	cm^3	82.19
Wet Weight	g	116.10
Water Content	%	4.99
Dry Weight	g	110.58
Wet Density	g/cm^3	1.413
Dry Density	g/cm^3	1.346
Specific Gravity (assumed)	-	2.96
Void Ratio (e)	-	1.20
Saturation Ratio (Sr)	%	12.31

FINAL SAMPLE INFORMATION		
Liquid Limit		
Plastic Limit		
Final Moisture Content	%	12.57

Cyclic Shearing - Stage 1		
Frequency	Hz	0.1
Initial Vertical Stress	kPa	300.11
Cyclic Stress Ratio (CSR)	-	0.01
Number of Cycles at the end of this stage*1	-	30
Max Cyclic Shear Stress	kPa	3.17
Max. Shear Strain	%	0.01
Max. Excess Pore Pressure	kPa	18.32

*1: Ended at 30 cycles based on test instruction

Cyclic Shearing - Stage 2		
Frequency	Hz	0.1
Initial Vertical Stress	kPa	300.11
Cyclic Stress Ratio (CSR)	-	0.05
Number of Cycles*2 at the end of this stage*1	-	30
Max Cyclic Shear Stress	kPa	15.10
Max. Shear Strain	%	0.11
Max. Excess Pore Pressure	kPa	113.53

*1: Ended at 30 cycles based on test instruction *2: Cycles in this stage.

Cyclic Shearing - Stage 3		
Frequency	Hz	0.1
Initial Vertical Stress	kPa	300.11
Cyclic Stress Ratio (CSR)	-	0.10
Number of Cycles*2 to 15% Shear Strain	-	2
Max Cyclic Shear Stress	kPa	29.72
Max. Shear Strain	%	51.30
Max. Excess Pore Pressure	kPa	295.25

*2: Cycles in this stage.

CONSOLIDATION					
Normal Stress	kPa	38	75	150	300
Max Load	kN	0.15	0.29	0.59	1.17
Total Height Change	mm	0.54	1.16	1.77	2.32
Consolidated Height	mm	20.46	19.84	19.23	18.68
Axial Strain	%	2.58	5.55	8.44	11.05
Duration	min	180	180	180	451

Photos:

Before Test

After Test

Cyclic Direct Simple Shear Test (ASTM D6528)

Consolidation Phase

Project No.:		Test No.:	DSS04
Project:	Fundão Tailings Dam Review Panel	Sample ID:	PSD1
Date:	2016-03-29	Depth:	
Tested by:	BY	Location:	
Checked by:	JG	Details:	Sand tailings sample with fines

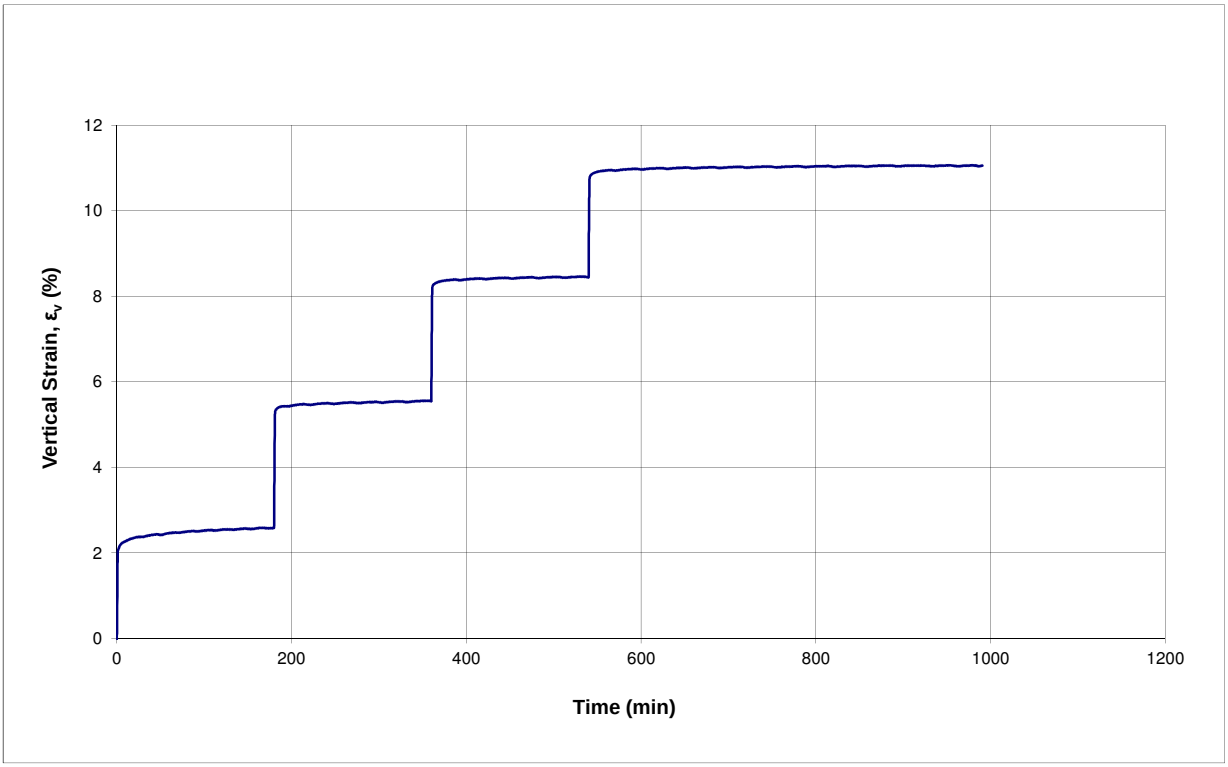

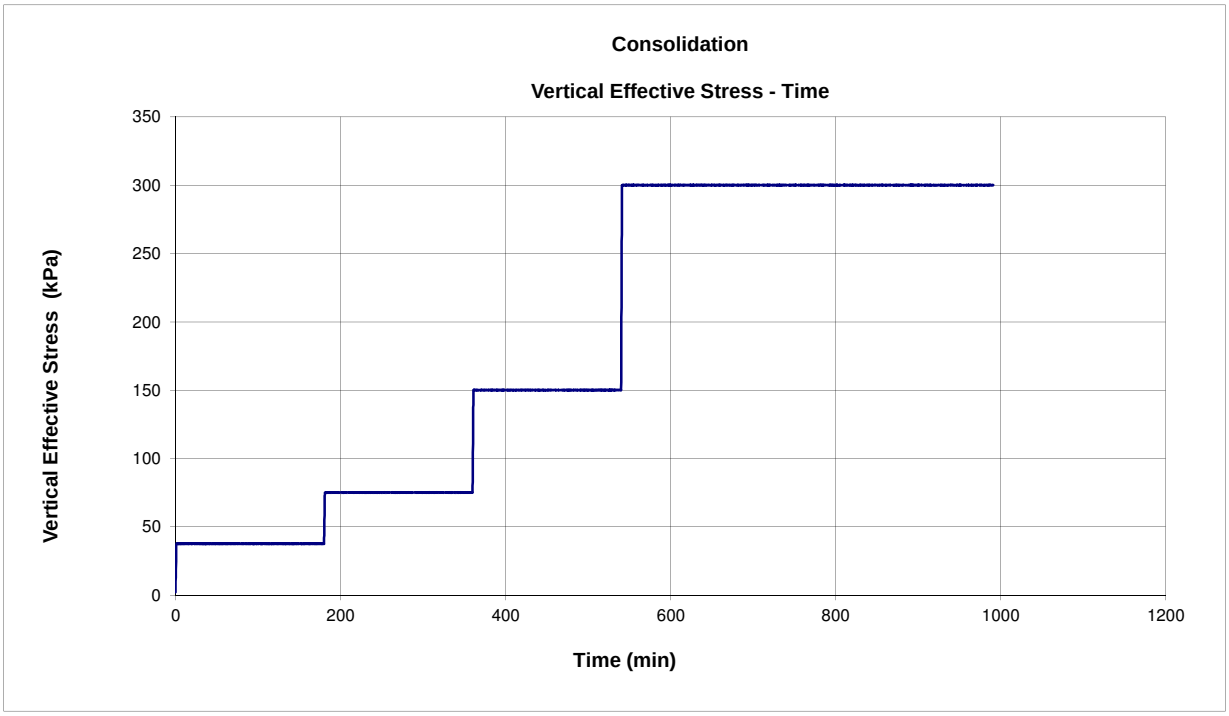

Cyclic Direct Simple Shear Test (ASTM D6528)

Cyclic Shearing Phase

Project No.:		Test No.:	DSS04
Project:	Fundão Tailings Dam Review Panel	Sample ID:	PSD1
Date:	2016-03-29	Depth:	
Tested by:	BY	Location:	
Checked by:	JG	Details:	Sand tailings sample with fines

τ_{cy} / σ'_{vc} = 0.05 - 0.10 - 0.15 σ'_{vc} = 300 kPa

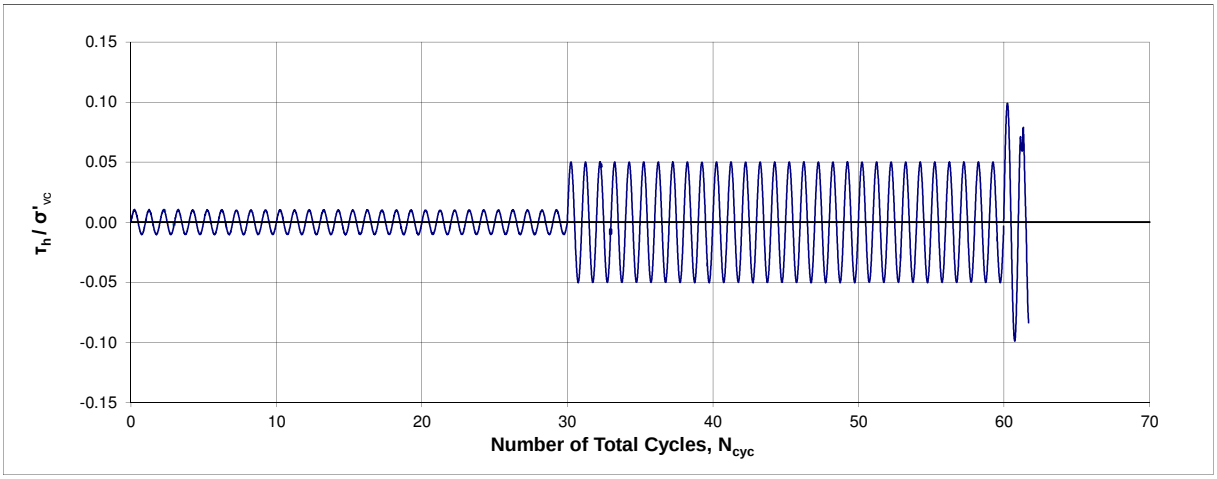

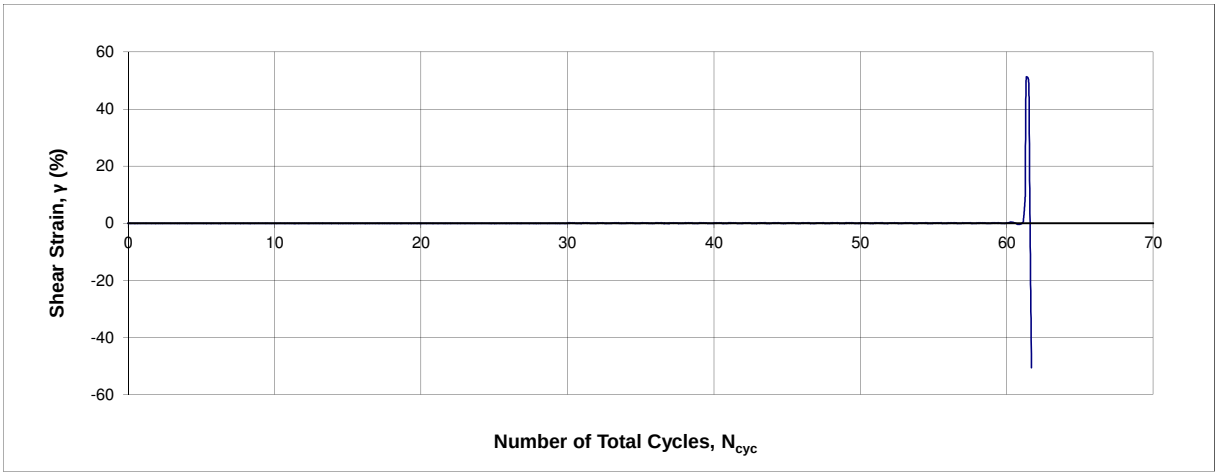

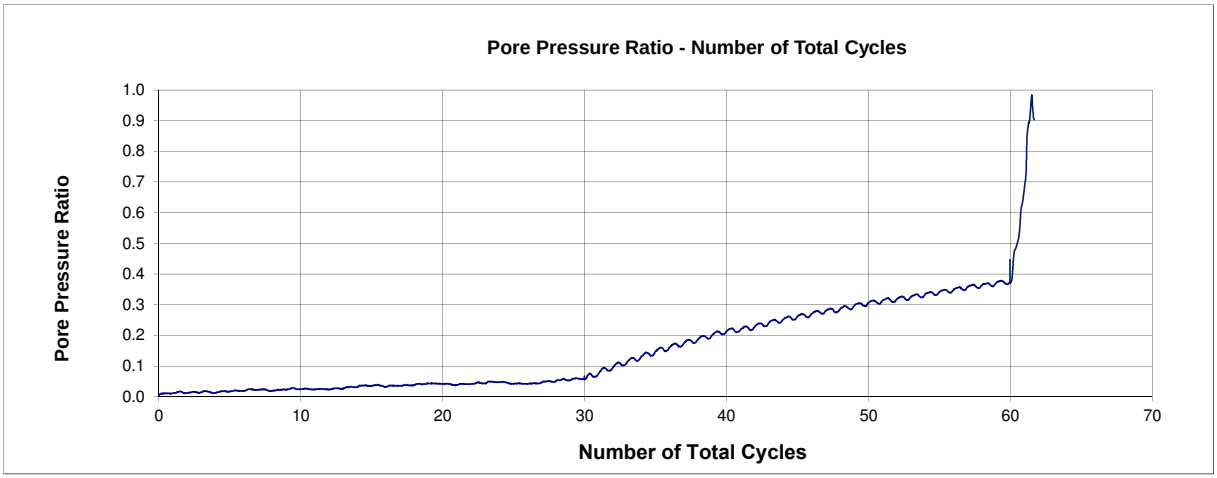

Cyclic Direct Simple Shear Test (ASTM D6528)

Cyclic Shearing Phase

Project No.:		Test No.:	DSS04
Project:	Fundão Tailings Dam Review Panel	Sample ID:	PSD1
Date:	2016-03-29	Depth:	
Tested by:	BY	Location:	
Checked by:	JG	Details:	Sand tailings sample with fines

τ_{cy} / σ'_{vc} = 0.05 - 0.10 - 0.15 σ'_{vc} = 300 kPa

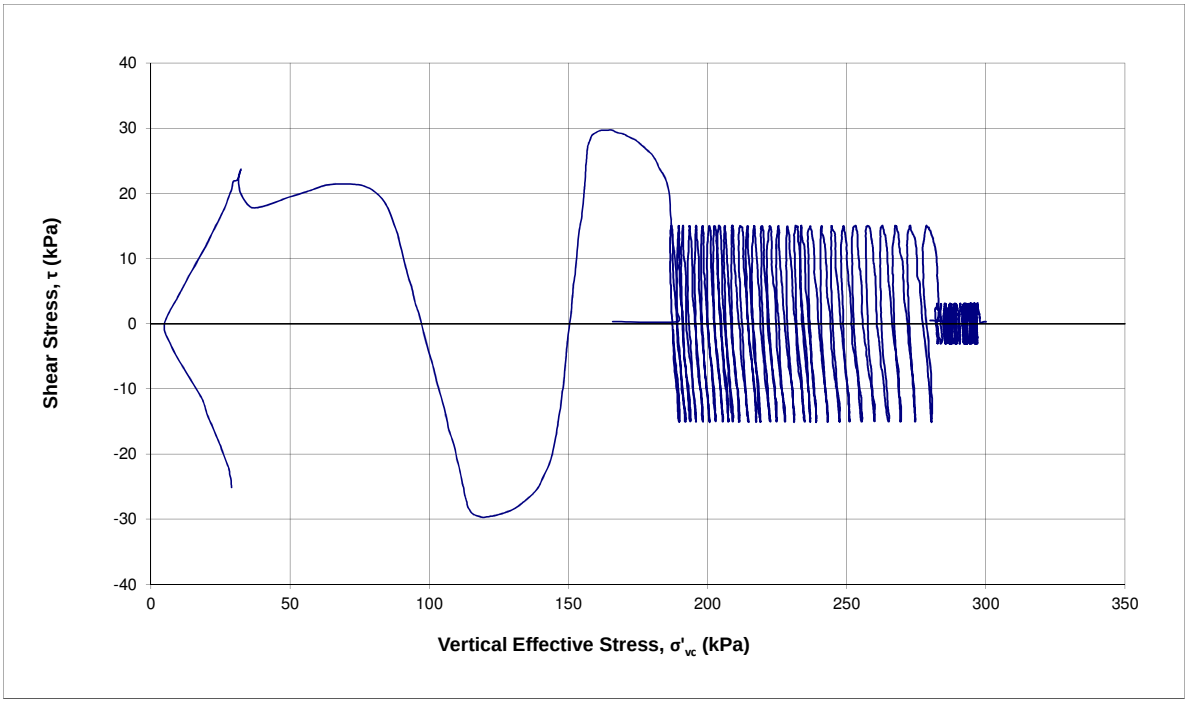

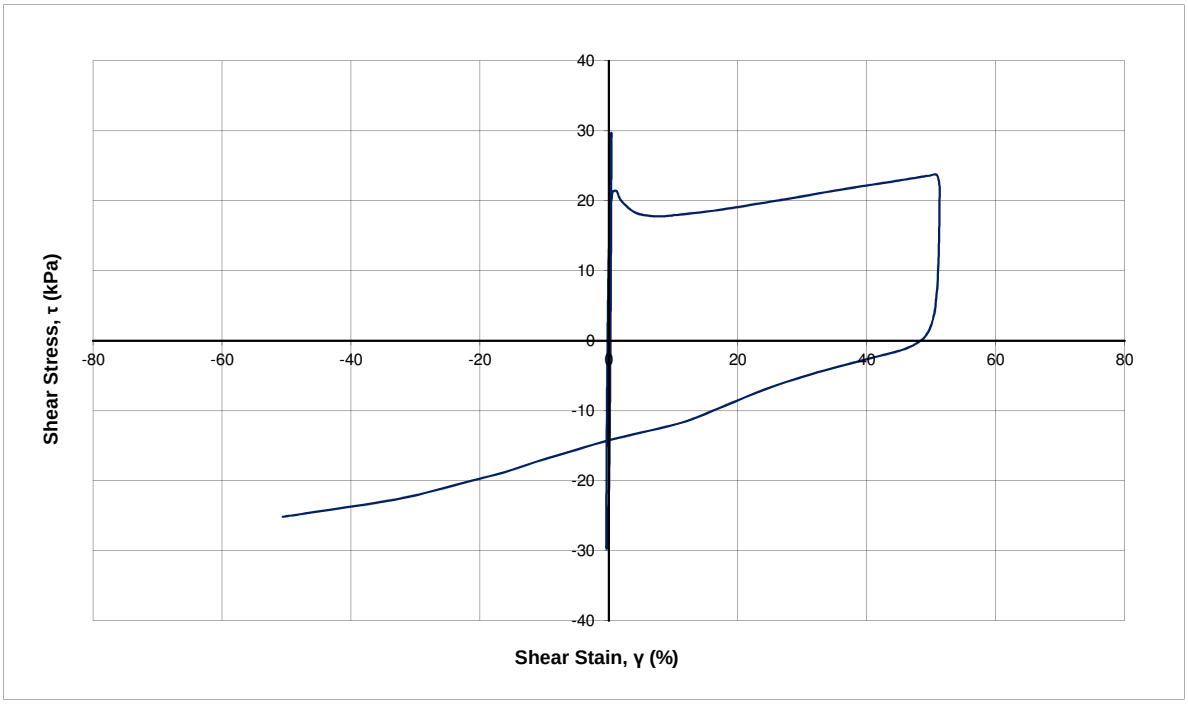

Static Simple Shear Test

(ASTM D6528)

Klohn Crippen Berger

Project No.:		Test No.:	DSS05
Project:	Fundão Tailings Dam Review Panel	Sample ID:	Slimes
Date:	2016-04-04	Depth:	
Tested by:	BY	Description:	Slimes
Checked by:	JG	Preparation Method:	Reconstituted Slurry

Initial Sample Information		
Specimen Height	mm	27.50
Specimen Diameter	mm	70.44
Area	mm^2	3896.98
Volume	cm^3	107.17
Wet Weight	g	223.92
Water Content	%	45.80
Dry Weight	g	153.58
Wet Density	g/cm^3	2.089
Dry Density	g/cm^3	1.433
Specific Gravity (assumed)	-	3.93
Void Ratio (e)	-	1.80
Saturation Ratio (Sr)	%	103.31

Static Shearing (Undrained)		
Initial Vertical Effective Stress	kPa	600.1
Initial Shear Stress	kPa	0.3
Shearing Rate (Shear Strain Rate)	% / hr	5.00
Peak Shear Strength	kPa	101.13
Ratio of Peak τ / σ'_v	-	0.17
Max. Excess Pore Pressure	kPa	430.33
Max. Shear Strain	%	20.1

FINAL SAMPLE INFORMATION		
Liquid Limit (shear plane)*1		
Plastic Limit (shear plane)*1		
Liquid Limit (outside shear plane)		-
Plastic Limit (outside shear plane)		-
Final Moisture Content	%	23.23
Final Moisture Content (shear plane)	%	
Final Moisture Content (outside shear plane)	%	

*1: Atterberg limits test was done using one-point method

CONSOLIDATION										
Vertical Effective Stress	kPa	3	6	13	25	50	100	200	400	600
Max Load	kN	0.012	0.024	0.049	0.098	0.195	0.391	0.780	1.559	2.339
Total Height Change	mm	1.27	3.11	4.31	5.43	6.39	7.18	7.84	8.47	8.82
Consolidated Height	%	26.23	24.39	23.19	22.07	21.11	20.32	19.66	19.03	18.68
Axial Strain*2	%	4.61	11.32	15.68	19.76	23.25	26.09	28.52	30.78	32.08
Duration	min	132	240	240	240	240	240	240	240	530

*2 : Axial strain may differ from oedometer test result due to the sample seating system and possible lateral strain caused by the membrane.

Photos:

Before Test


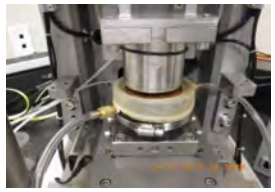

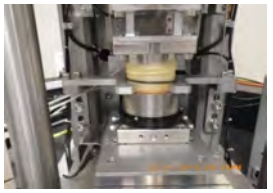

After Test


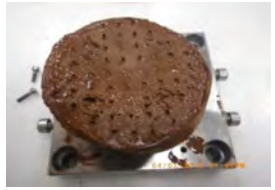

Static Simple Shear Test

(ASTM D6528)

Project No.:		Test No.:	DSS05
Project:	Fundão Tailings Dam Review Panel	Sample ID:	Slimes
Date:	2016-04-04	Depth:	
Tested by:	BY	Description:	Slimes
Checked by:	JG	Preparation Method:	Reconstituted Slurry

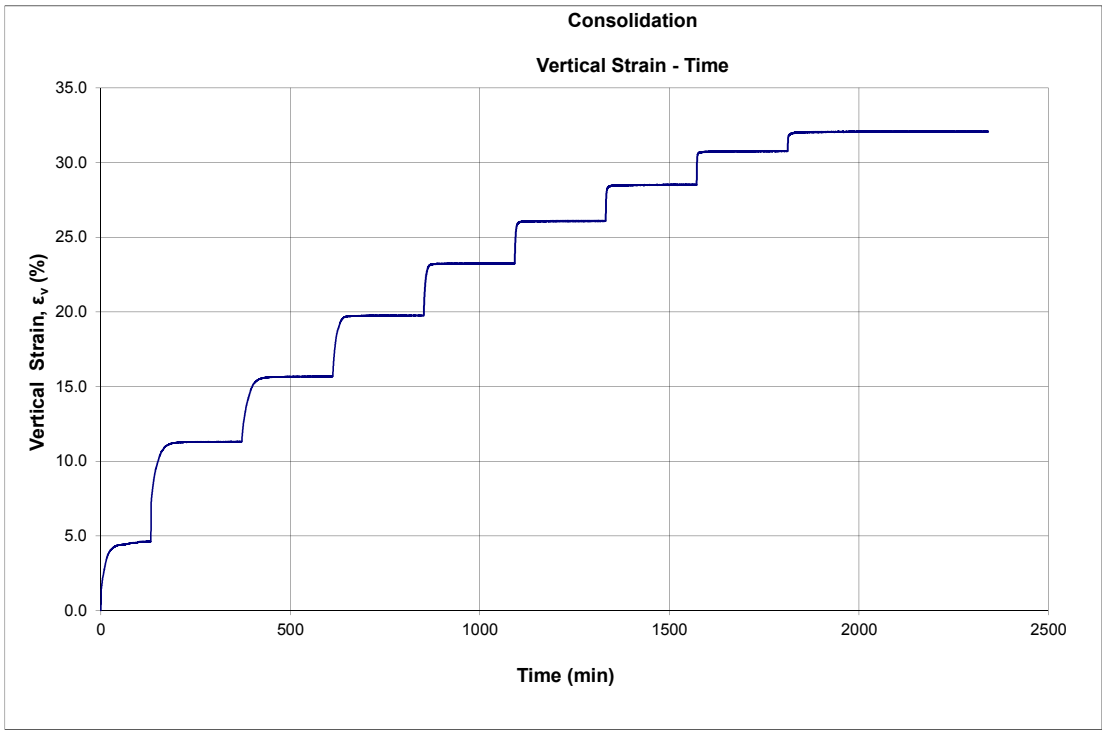

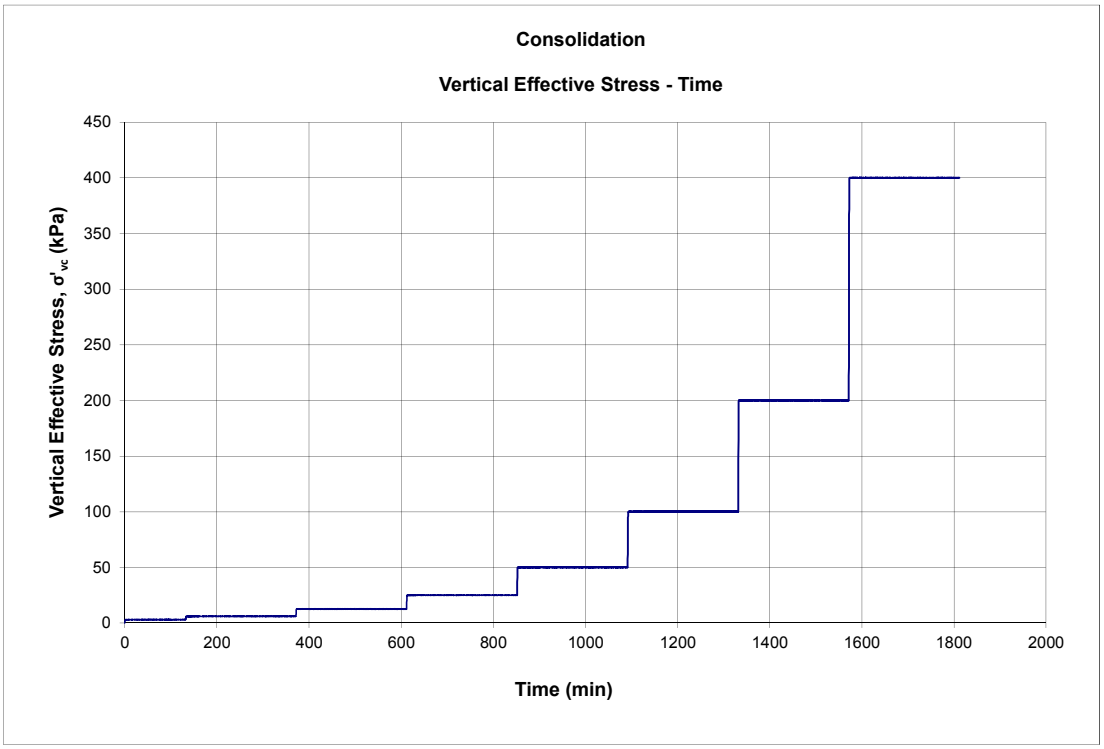

Static Simple Shear Test

(ASTM D6528)

Project No.:		Test No.:	DSS05
Project:	Fundão Tailings Dam Review Panel	Sample ID:	Slimes
Date:	2016-04-04	Depth:	
Tested by:	BY	Description:	Slimes
Checked by:	JG	Preparation Method:	Reconstituted Slurry

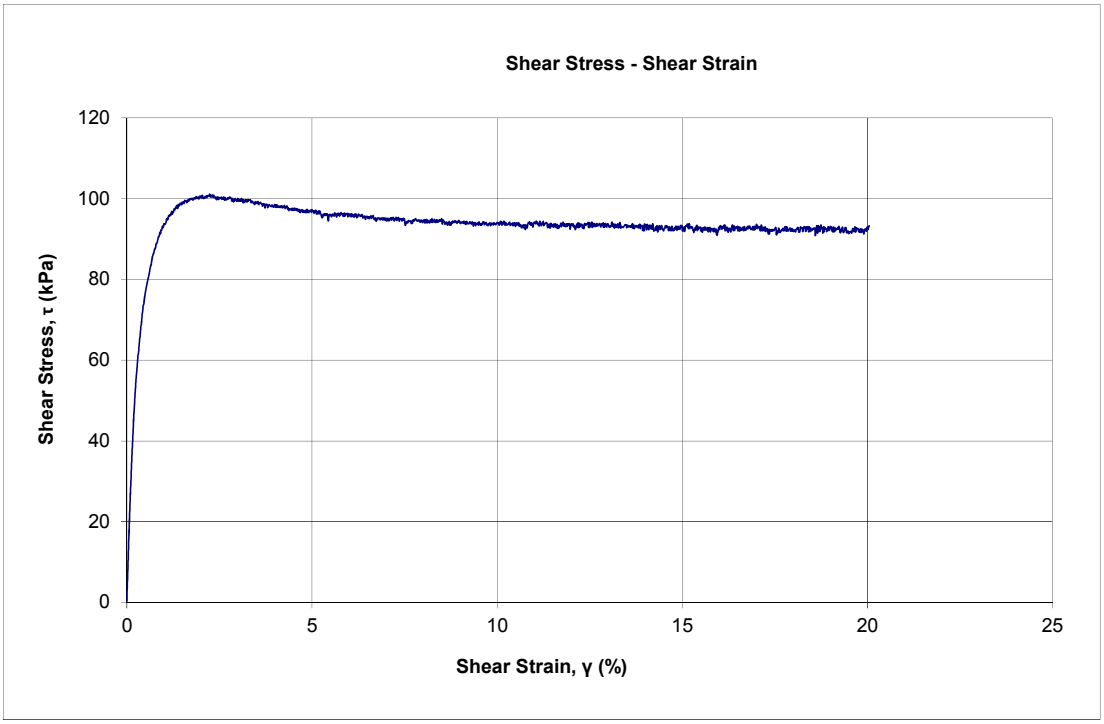

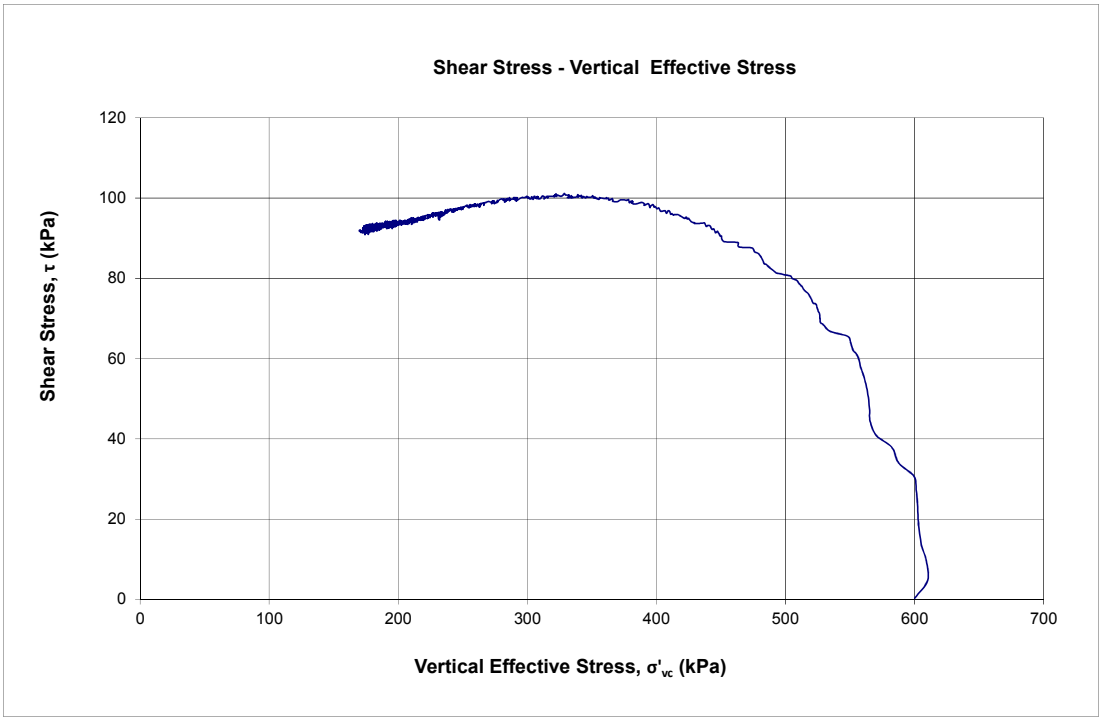

Static Simple Shear Test

(ASTM D6528)

Project No.:		Test No.:	DSS05
Project:	Fundão Tailings Dam Review Panel	Sample ID:	Slimes
Date:	2016-04-04	Depth:	
Tested by:	BY	Description:	Slimes
Checked by:	JG	Preparation Method:	Reconstituted Slurry

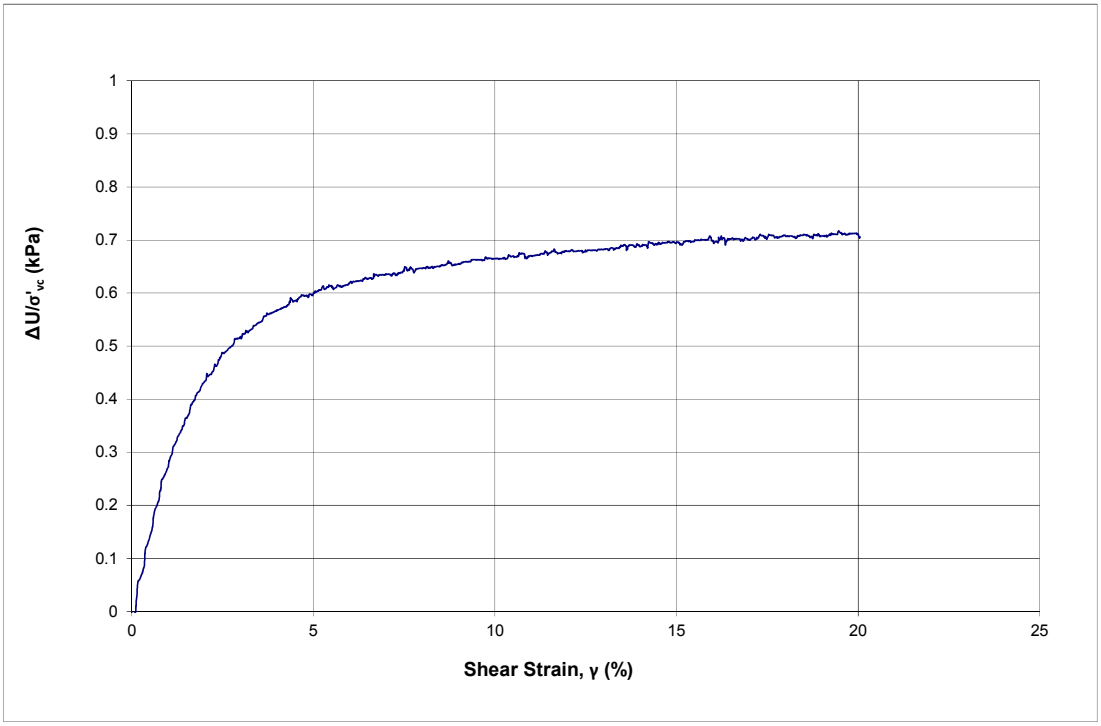

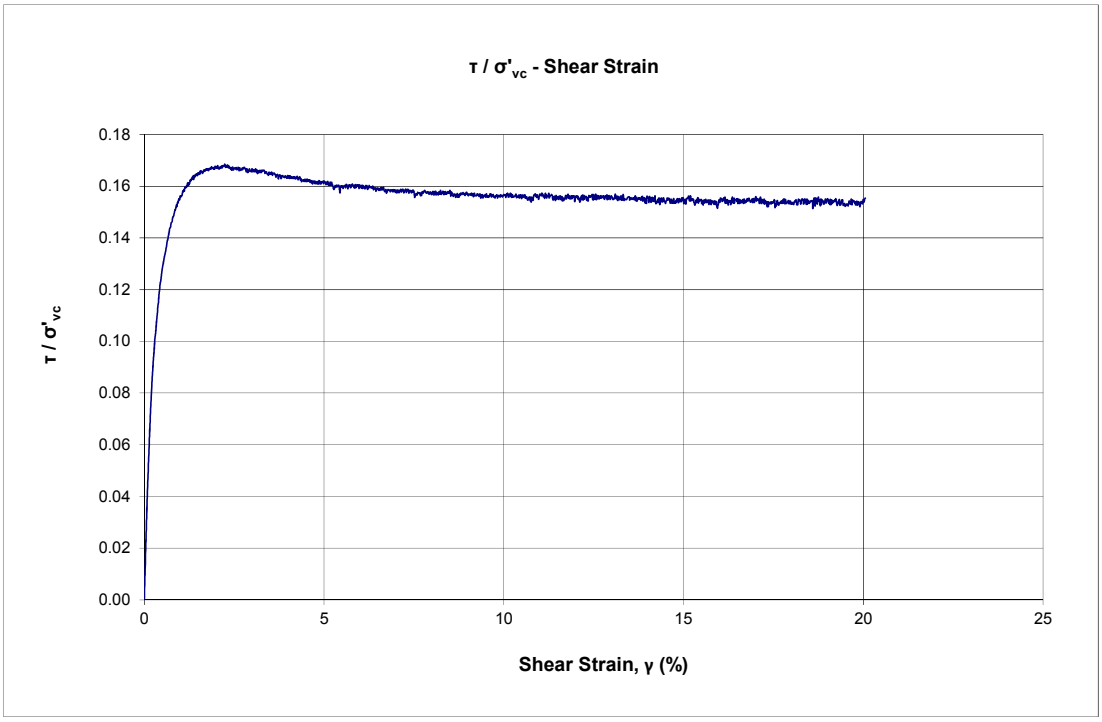

Static Simple Shear Test

(ASTM D6528)

Project No.:		Test No.:	DSS06
Project:	Fundão Tailings Dam Review Panel	Sample ID:	Slimes
Date:	2016-04-05	Depth:	
Tested by:	BY	Description:	Slimes
Checked by:	JG	Preparation Method:	Reconstituted Slurry

Initial Sample Information		
Specimen Height	mm	27.80
Specimen Diameter	mm	70.59
Area	mm^2	3913.60
Volume	cm^3	108.80
Wet Weight	g	225.60
Water Content	%	44.52
Dry Weight	g	156.10
Wet Density	g/cm^3	2.074
Dry Density	g/cm^3	1.435
Specific Gravity	-	3.93
Void Ratio (e)	-	1.74
Saturation Ratio (Sr)	%	100.61

Static Shearing (Undrained)		
Initial Vertical Effective Stress	kPa	300.1
Initial Shear Stress	kPa	0.3
Shearing Rate (Shear Strain Rate)	% / hr	5.00
Peak Shear Strength	kPa	50.31
Ratio of Peak τ / σ'_v	-	0.17
Max. Excess Pore Pressure	kPa	217.65
Max. Shear Strain	%	20.0

FINAL SAMPLE INFORMATION		
Final Moisture Content	%	24.25

CONSOLIDATION									
Vertical Effective Stress	kPa	3	6	13	25	50	100	200	300
Max Load	kN	0.012	0.024	0.049	0.098	0.196	0.392	0.783	1.175
Total Height Change	mm	0.81	3.12	4.14	5.06	5.93	6.69	7.36	7.72
Consolidated Height	%	26.99	24.68	23.66	22.74	21.87	21.11	20.44	20.08
Axial Strain*1	%	2.93	11.21	14.89	18.19	21.35	24.05	26.48	27.78
Duration	min	240	240	240	240	240	240	240	804

*1 : Axial strain may differ from oedometer test result due to the sample seating system and possible lateral strain caused by the membrane.

Photos:

Before Test

After Test

Static Simple Shear Test

(ASTM D6528)

Project No.:		Test No.:	DSS06
Project:	Fundão Tailings Dam Review Panel	Sample ID:	Slimes
Date:	2016-04-05	Depth:	
Tested by:	BY	Description:	Slimes
Checked by:	JG	Preparation Method:	Reconstituted Slurry

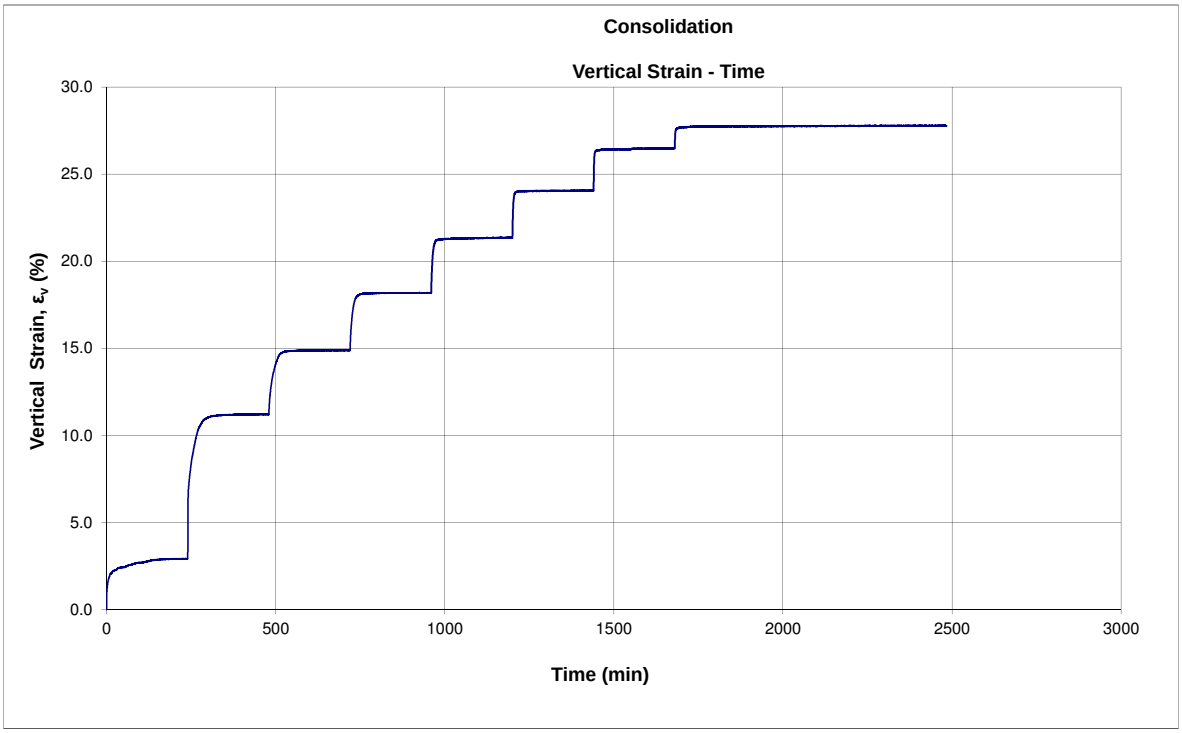

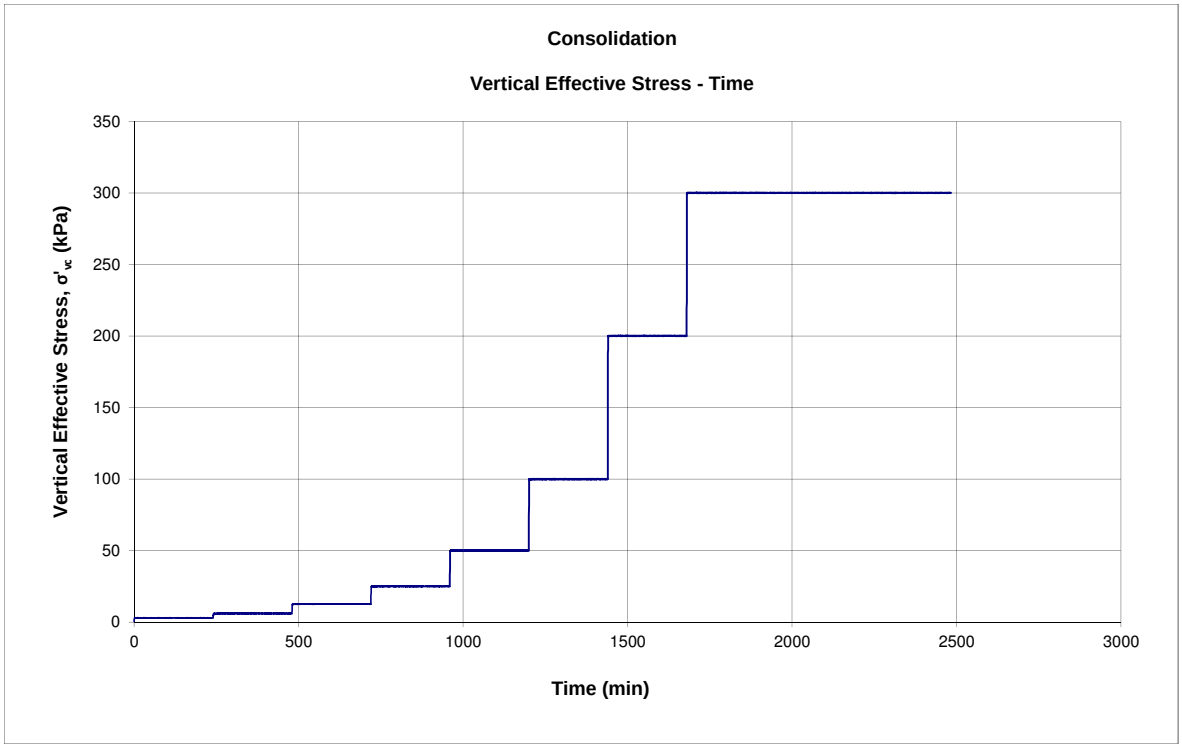

Static Simple Shear Test

(ASTM D6528)

Project No.:		Test No.:	DSS06
Project:	Fundão Tailings Dam Review Panel	Sample ID:	Slimes
Date:	2016-04-05	Depth:	
Tested by:	BY	Description:	Slimes
Checked by:	JG	Preparation Method:	Reconstituted Slurry

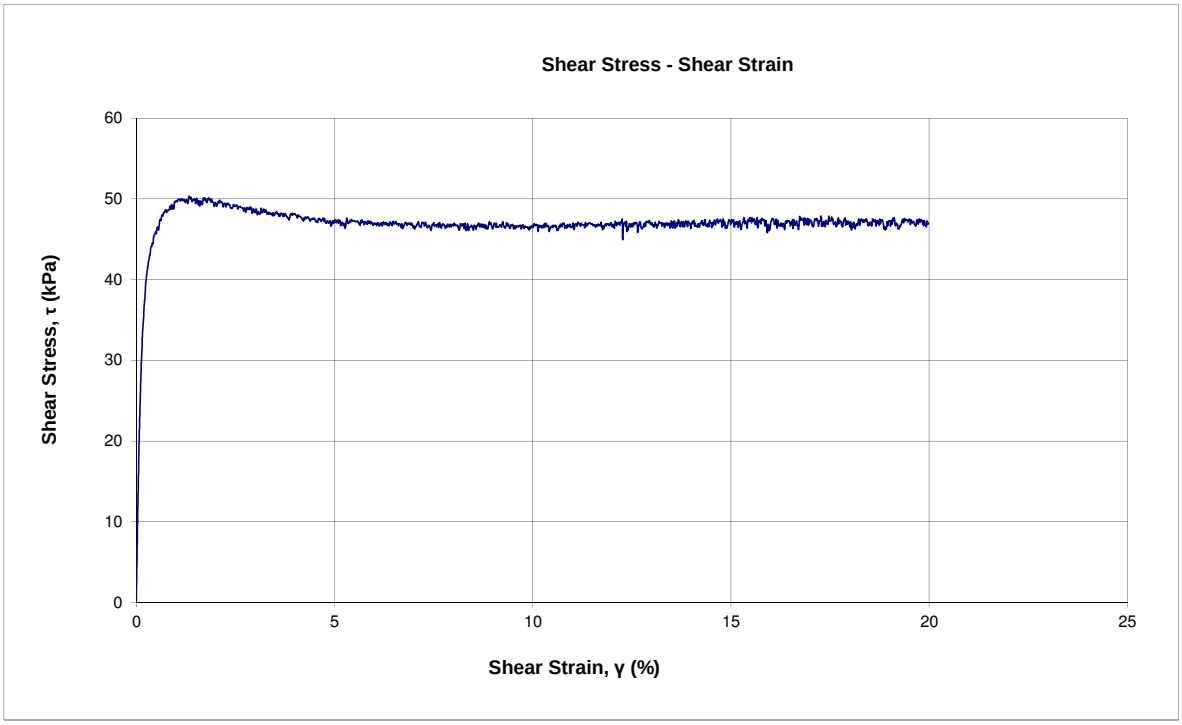

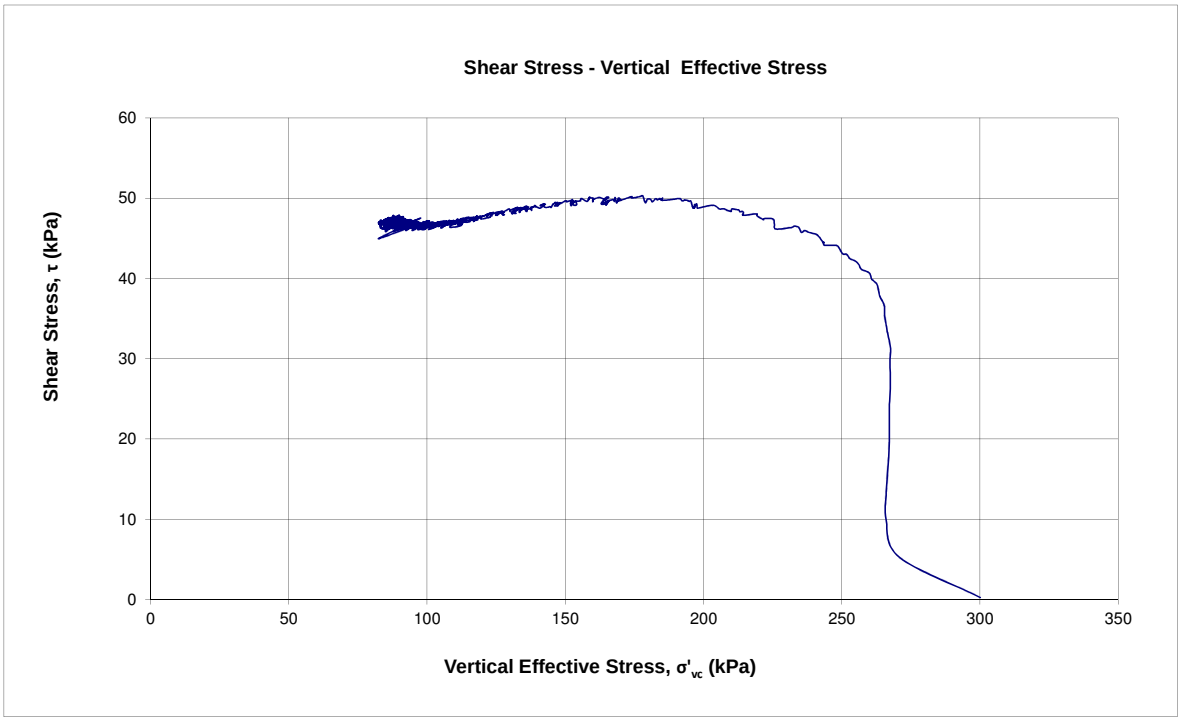

Static Simple Shear Test

(ASTM D6528)

Project No.:		Test No.:	DSS06
Project:	Fundão Tailings Dam Review Panel	Sample ID:	Slimes
Date:	2016-04-05	Depth:	
Tested by:	BY	Description:	Slimes
Checked by:	JG	Preparation Method:	Reconstituted Slurry

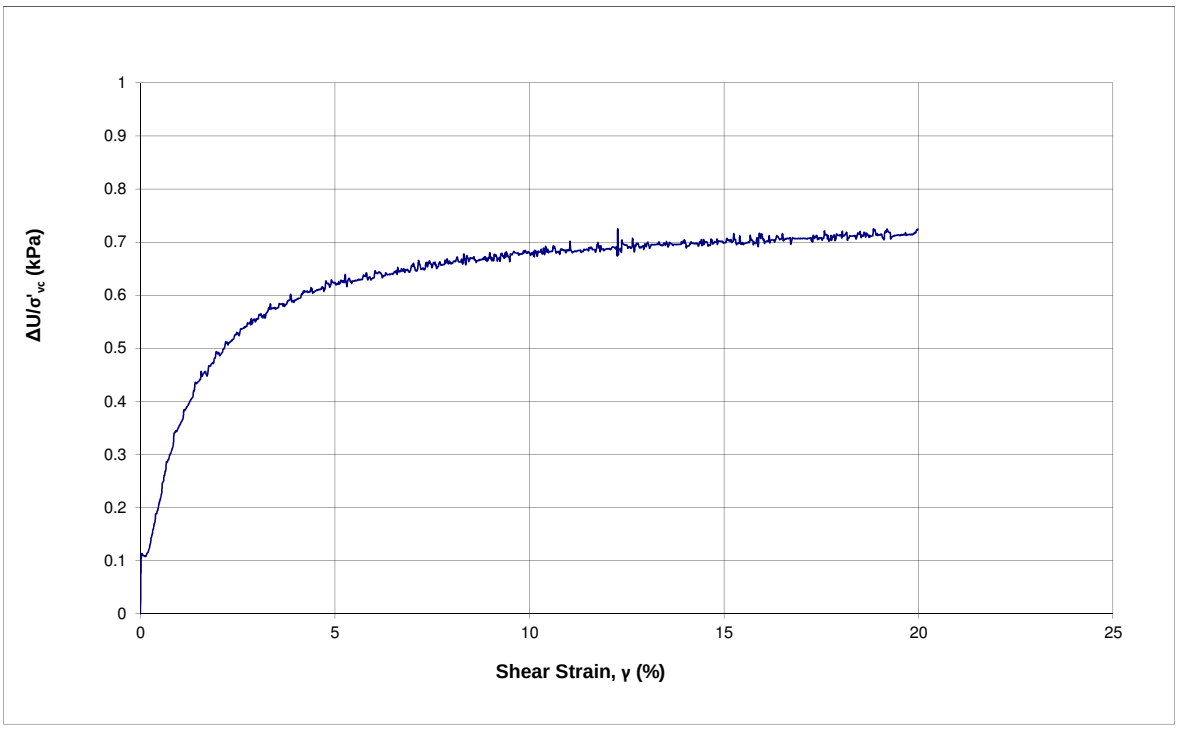

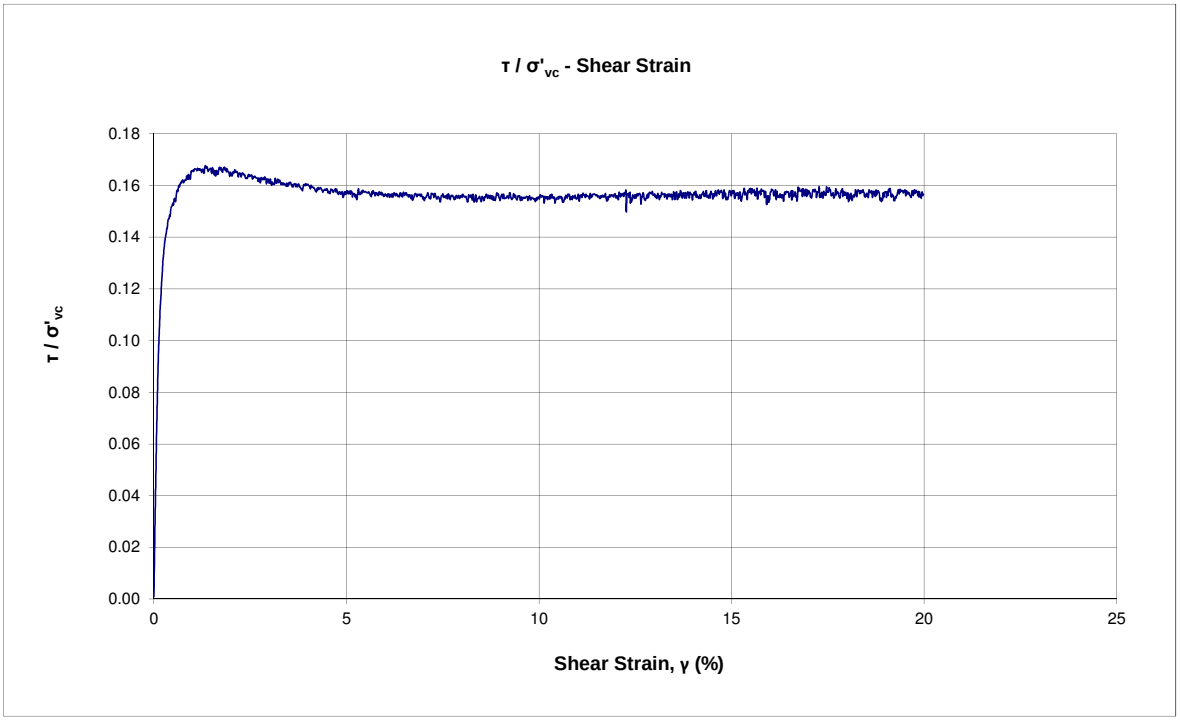

Static Simple Shear Test

(ASTM D6528)

Klohn Crippen Berger

Project No.:		Test No.:	DSS07
Project:	Fundão Tailings Dam Review Panel	Sample ID:	Slimes
Date:	2016-04-07	Depth:	
Tested by:	BY	Description:	Slimes
Checked by:	JG	Preparation Method:	Reconstituted Slurry

Initial Sample Information		
Specimen Height	mm	29.10
Specimen Diameter	mm	70.35
Area	mm^2	3887.03
Volume	cm^3	113.11
Wet Weight	g	237.81
Water Content	%	44.50
Dry Weight	g	164.57
Wet Density	g/cm^3	2.102
Dry Density	g/cm^3	1.455
Specific Gravity	-	3.93
Void Ratio (e)	-	1.75
Saturation Ratio (Sr)	%	102.81

Static Shearing (Undrained)		
Initial Vertical Effective Stress	kPa	150.2
Initial Shear Stress	kPa	0.3
Shearing Rate (Shear Strain Rate)	% / hr	5.00
Peak Shear Strength	kPa	24.05
Ratio of Peak τ / σ'_v	-	0.16
Max. Excess Pore Pressure	kPa	109.83
Max. Shear Strain	%	20.0

FINAL SAMPLE INFORMATION		
Liquid Limit (shear plane)*1		
Plastic Limit (shear plane)*1		
Liquid Limit (outside shear plane)		-
Plastic Limit (outside shear plane)		-
Final Moisture Content	%	25.20
Final Moisture Content (shear plane)	%	
Final Moisture Content (outside shear pla	%	

*1: Atterberg limits test was done using one-point method

CONSOLIDATION							
Vertical Effective Stress	kPa	3	13	25	50	100	150
Max Load	kN	0.012	0.049	0.097	0.195	0.389	0.584
Total Height Change	mm	1.21	4.79	5.77	6.66	7.50	7.91
Consolidated Height	%	27.89	24.31	23.33	22.44	21.60	21.19
Axial Strain*2	%	4.16	16.46	19.83	22.88	25.78	27.19
Duration	min	240	240	240	240	240	963

*2 : Axial strain may differ from oedometer test result due to the sample seating system and possible lateral strain caused by the membrane.

Photos:

Before Test



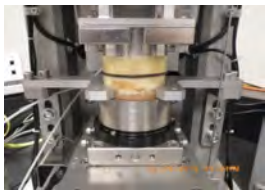
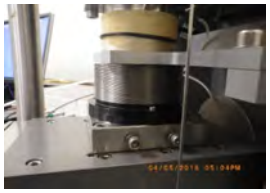

After Test




Static Simple Shear Test

(ASTM D6528)

Project No.:		Test No.:	DSS07
Project:	Fundão Tailings Dam Review Panel	Sample ID:	Slimes
Date:	2016-04-07	Depth:	
Tested by:	BY	Description:	Slimes
Checked by:	JG	Preparation Method:	Reconstituted Slurry

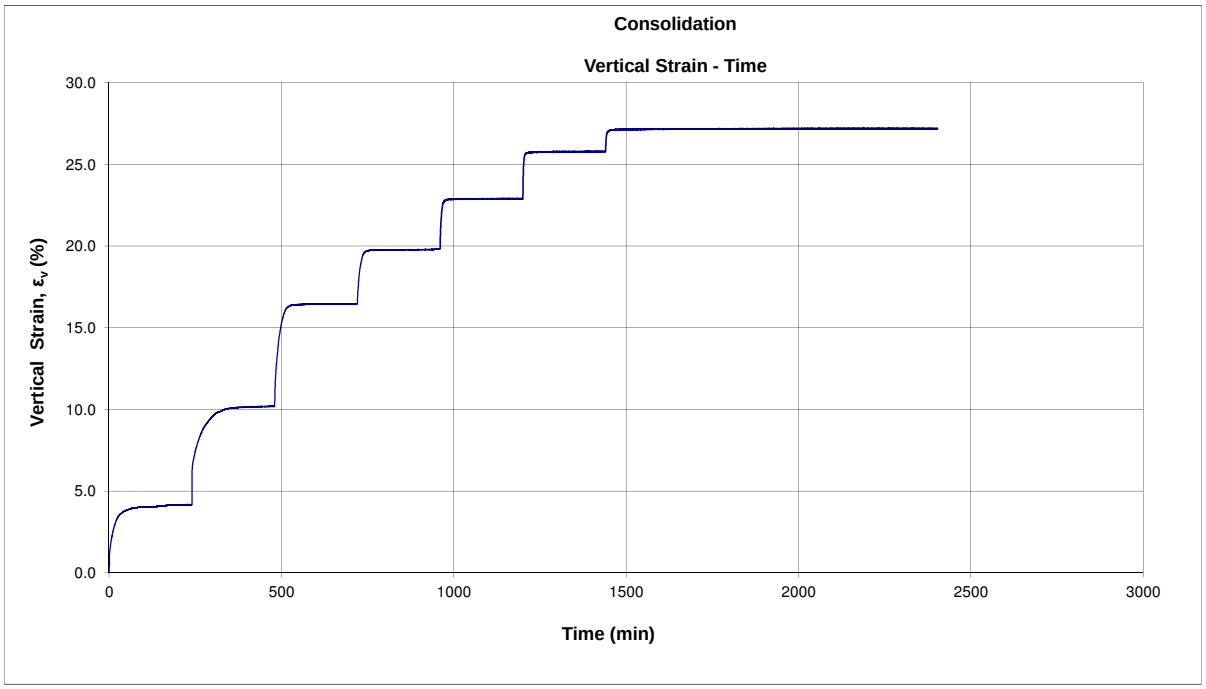

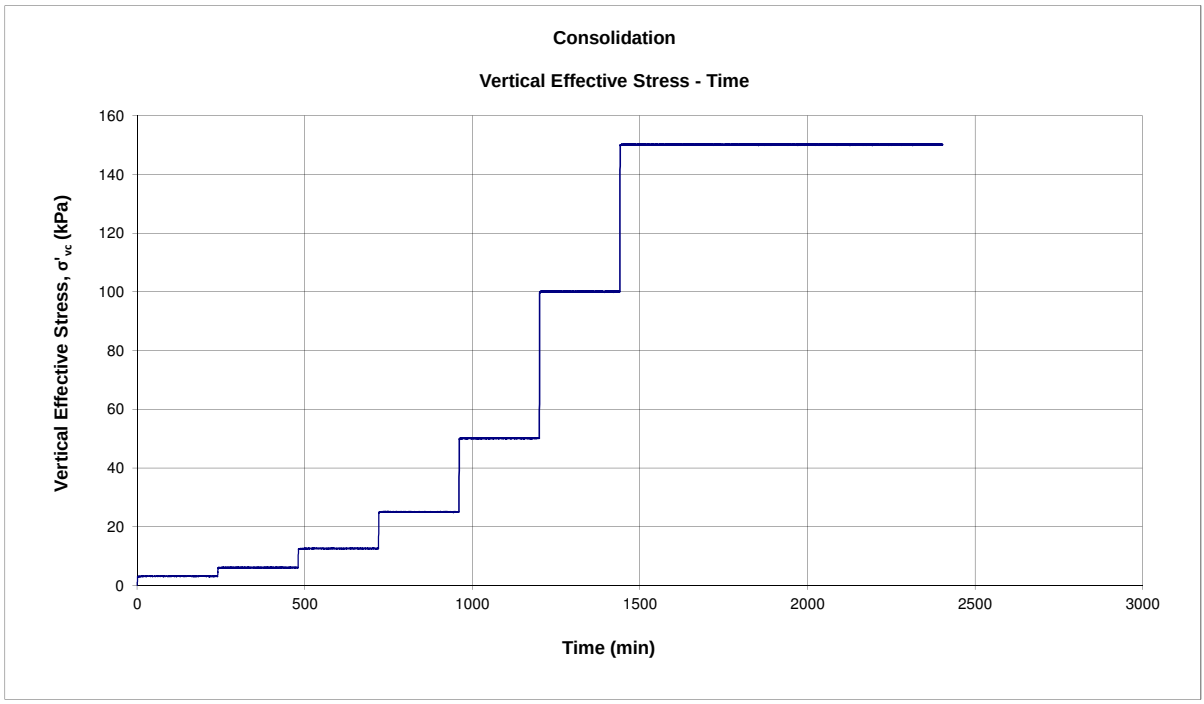

Static Simple Shear Test

(ASTM D6528)

Project No.:		Test No.:	DSS07
Project:	Fundão Tailings Dam Review Panel	Sample ID:	Slimes
Date:	2016-04-07	Depth:	
Tested by:	BY	Description:	Slimes
Checked by:	JG	Preparation Method:	Reconstituted Slurry

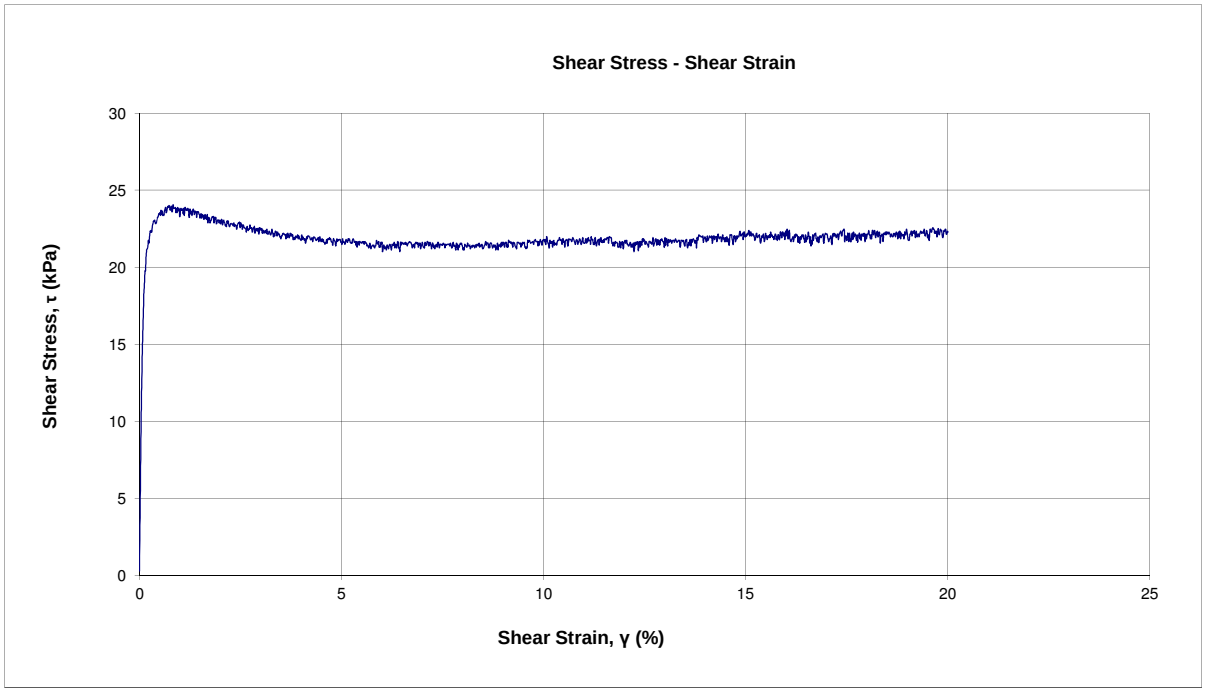

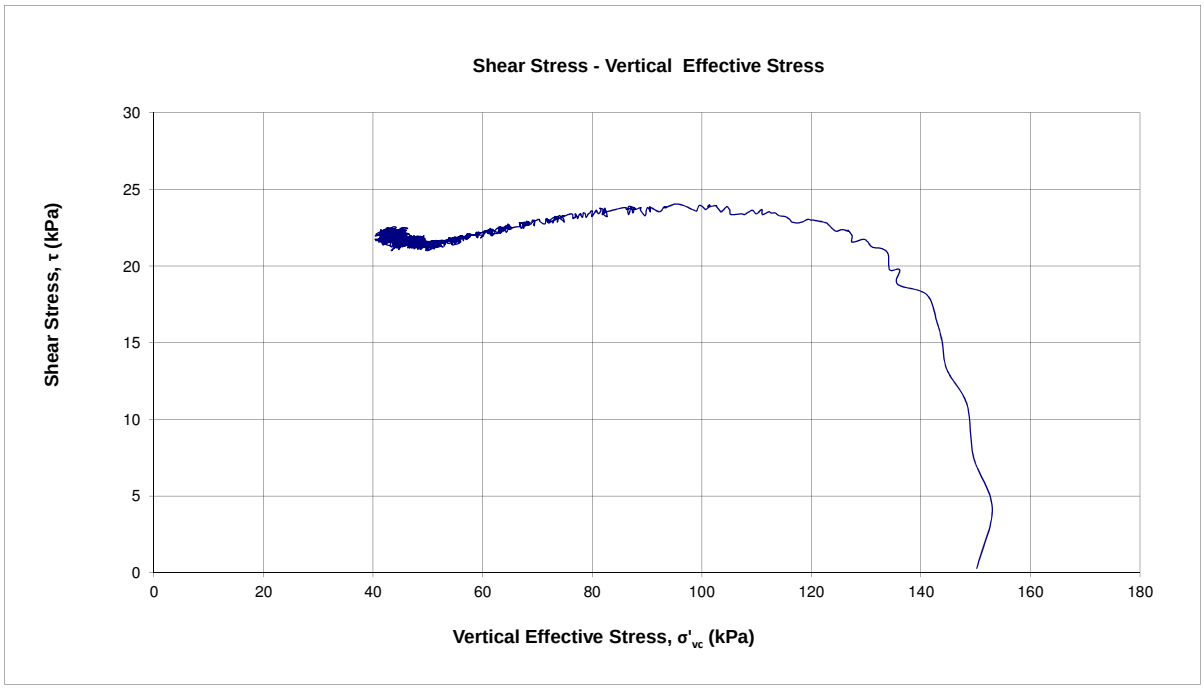

Static Simple Shear Test

(ASTM D6528)

Project No.:		Test No.:	DSS07
Project:	Fundão Tailings Dam Review Panel	Sample ID:	Slimes
Date:	2016-04-07	Depth:	
Tested by:	BY	Description:	Slimes
Checked by:	JG	Preparation Method:	Reconstituted Slurry

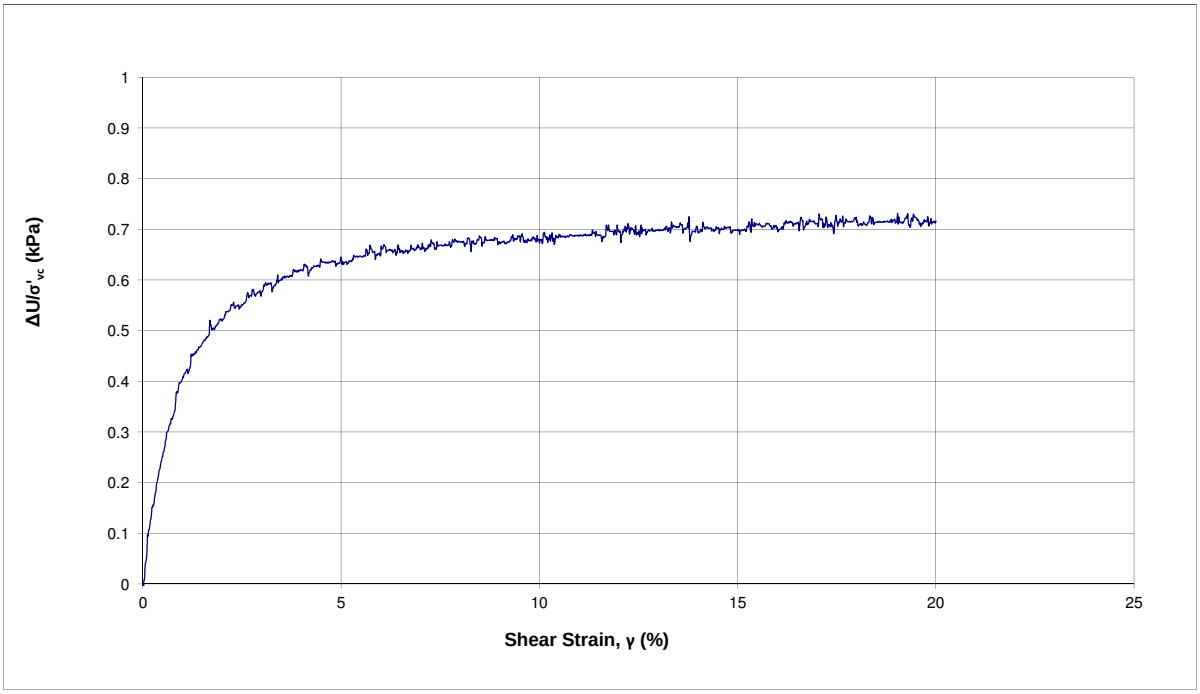

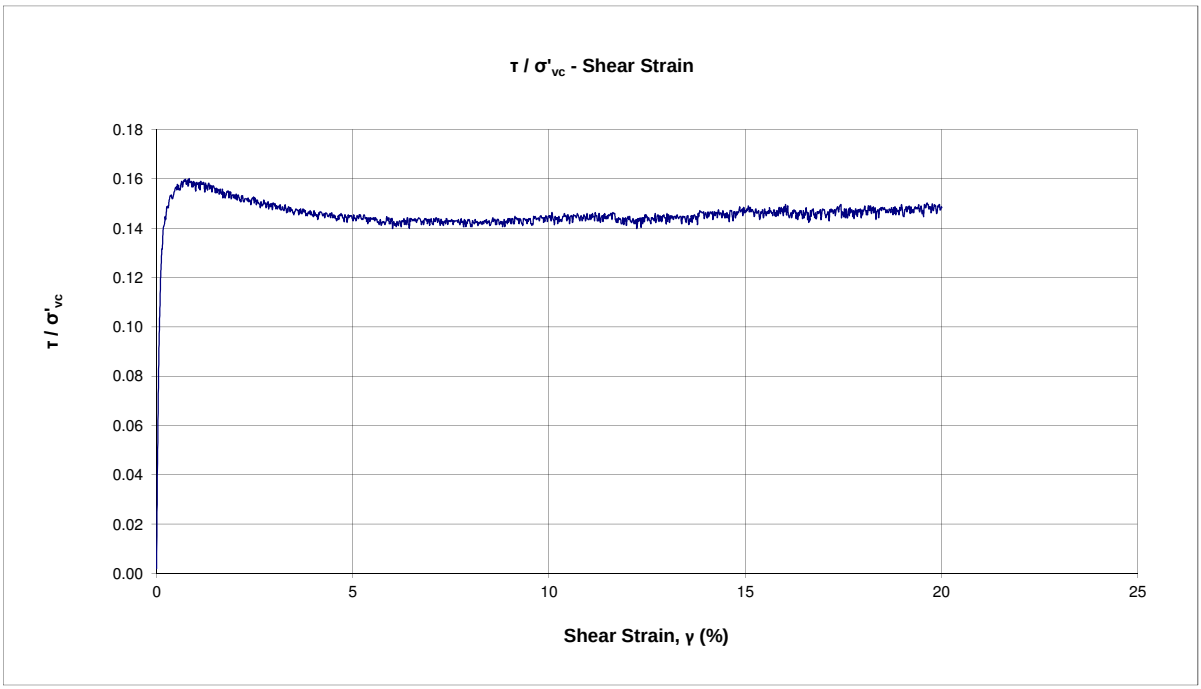

Static Simple Shear Test

(ASTM D6528)

Project No.:		Test No.:	DSS08
Project:	Fundão Tailings Dam Review Panel	Sample ID:	PSD 1
Date:	2016-04-11	Depth:	
Tested by:	BY	Description:	Sand Tailings
Checked by:	JG	Preparation Method:	Moist Tamping

Initial Sample Information		
Specimen Height	mm	20.99
Specimen Diameter	mm	70.66
Area	mm^2	3921.36
Volume	cm^3	82.31
Wet Weight	g	116.31
Water Content	%	4.98
Dry Weight	g	110.79
Wet Density	g/cm^3	1.413
Dry Density	g/cm^3	1.346
Specific Gravity	-	2.96
Void Ratio (e)	-	1.20
Saturation Ratio (Sr)	%	12.29

Static Shearing (Undrained)		
Initial Vertical Effective Stress	kPa	600.2
Initial Shear Stress	kPa	0.3
Shearing Rate (Shear Strain Rate	% / hr	5.00
Peak Shear Strength	kPa	82.22
Ratio of Peak τ / σ'_v	-	0.14
Max. Excess Pore Pressure	kPa	515.97
Max. Shear Strain	%	20.0

FINAL SAMPLE INFORMATION		
Liquid Limit (shear plane)		-
Plastic Limit (shear plane)		-
Liquid Limit (outside shear plane)		-
Plastic Limit (outside shear plane)		-
Final Moisture Content	%	4.49

CONSOLIDATION						
Vertical Effective Stress	kPa	38	75	150	300	600
Max Load	kN	0.148	0.294	0.588	1.177	2.353
Total Height Change	mm	0.10	0.68	1.39	2.03	2.62
Consolidated Height	%	20.89	20.31	19.60	18.96	18.37
Axial Strain*2	%	0.49	3.23	6.62	9.67	12.48
Duration	min	60	60	60	60	200

*2 : Axial strain may differ from oedometer test result due to the sample seating system and possible lateral strain caused by the membrane.

Photos:

Before Test


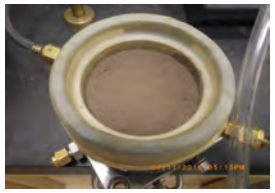
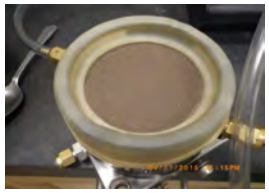
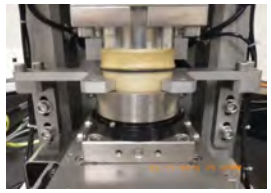

After Test


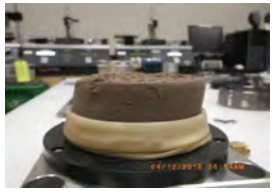

Static Simple Shear Test

(ASTM D6528)

Project No.:		Test No.:	DSS08
Project:	Fundão Tailings Dam Review Panel	Sample ID:	PSD 1
Date:	2016-04-11	Depth:	
Tested by:	BY	Description:	Sand Tailings
Checked by:	JG	Preparation Method:	Moist Tamping

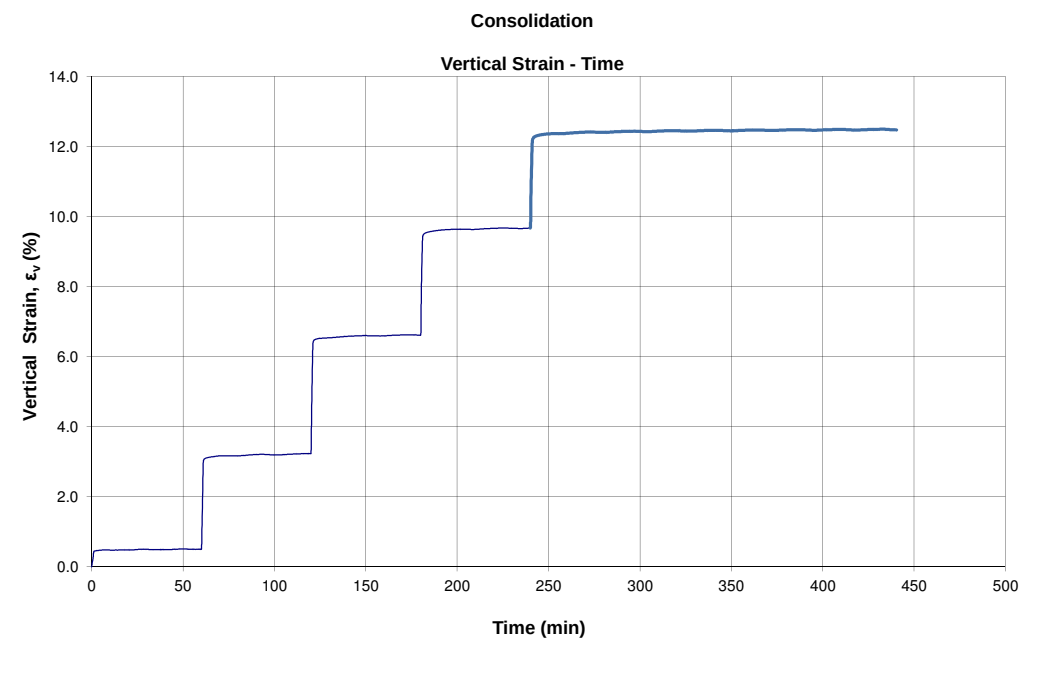

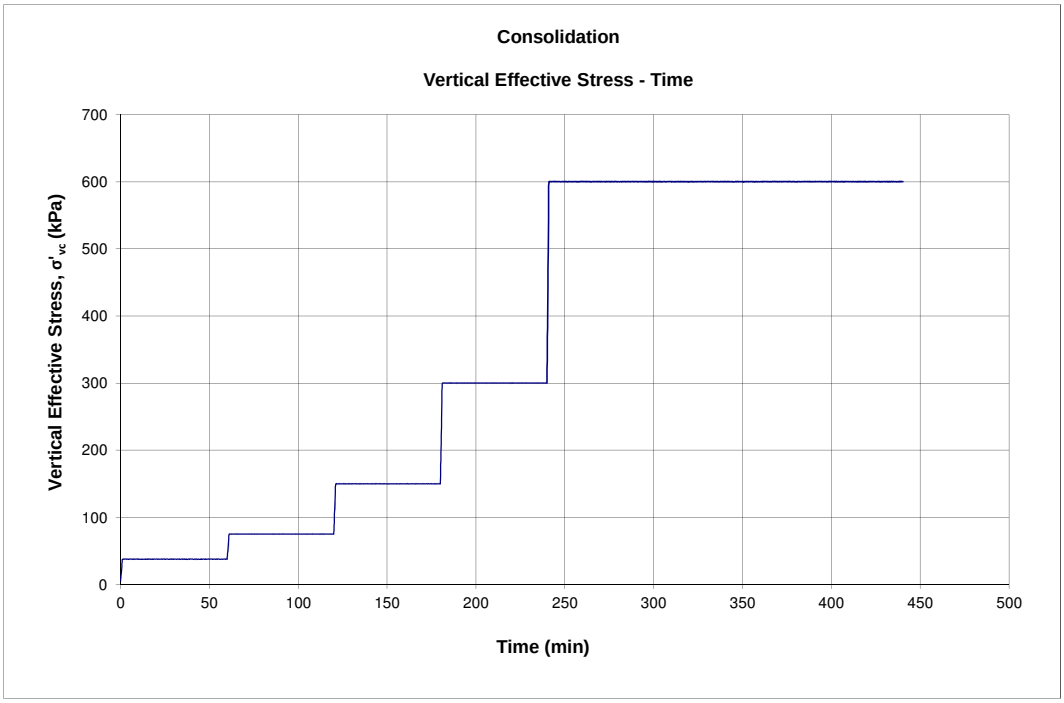

Static Simple Shear Test

(ASTM D6528)

Project No.:		Test No.:	DSS08
Project:	Fundão Tailings Dam Review Panel	Sample ID:	PSD 1
Date:	2016-04-11	Depth:	
Tested by:	BY	Description:	Sand Tailings
Checked by:	JG	Preparation Method:	Moist Tamping

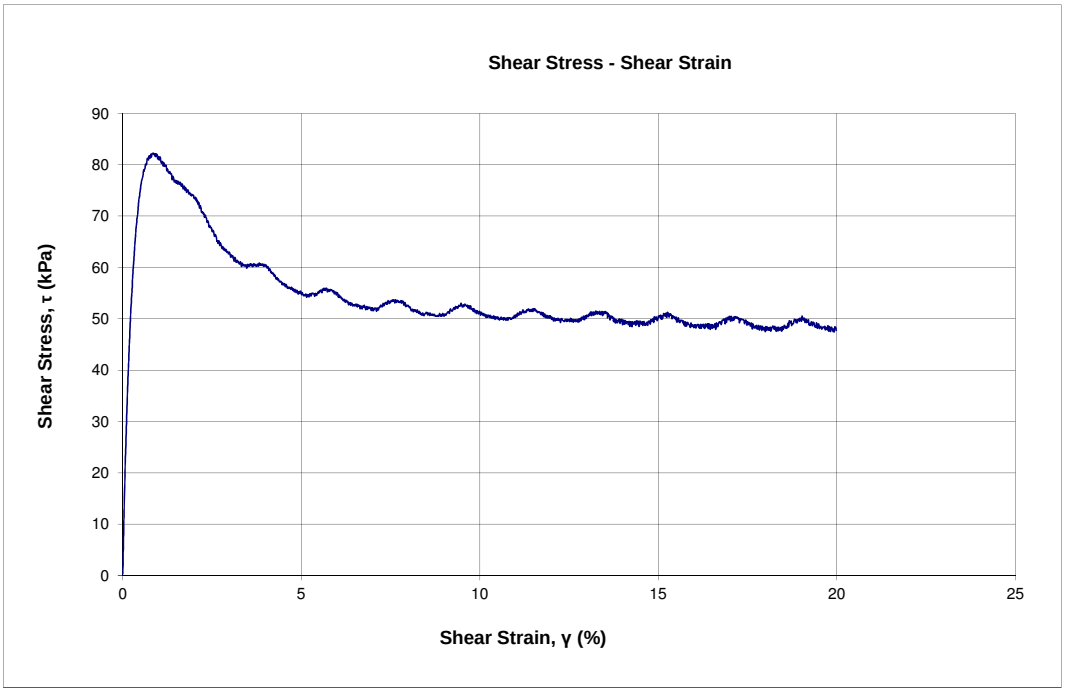

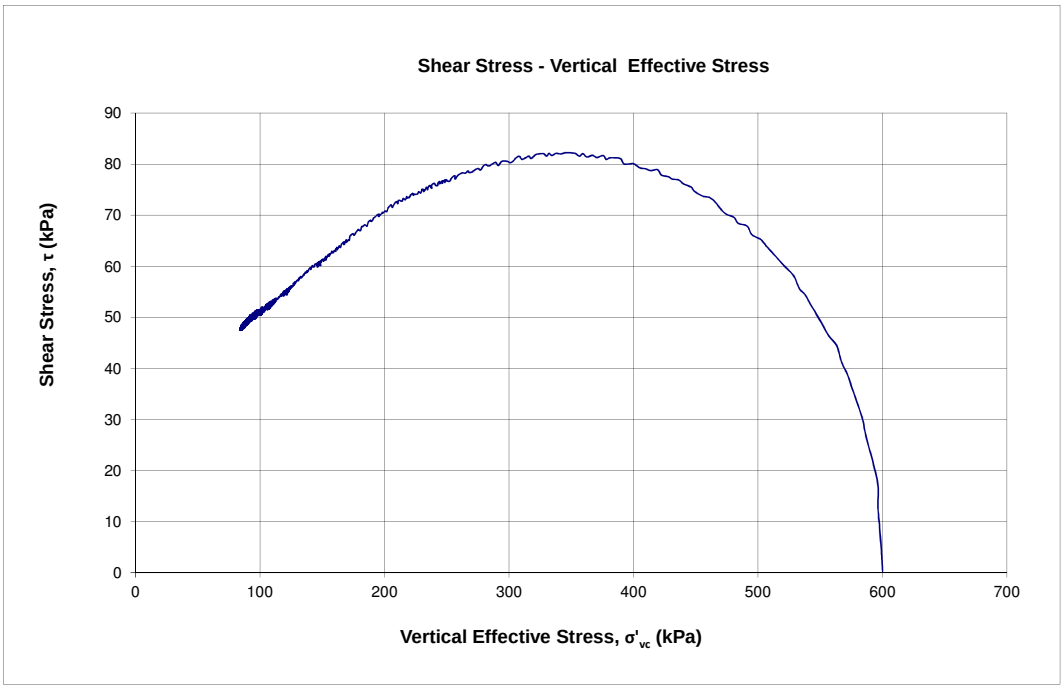

Static Simple Shear Test

(ASTM D6528)

Project No.:		Test No.:	DSS08
Project:	Fundão Tailings Dam Review Panel	Sample ID:	PSD 1
Date:	2016-04-11	Depth:	
Tested by:	BY	Description:	Sand Tailings
Checked by:	JG	Preparation Method:	Moist Tamping

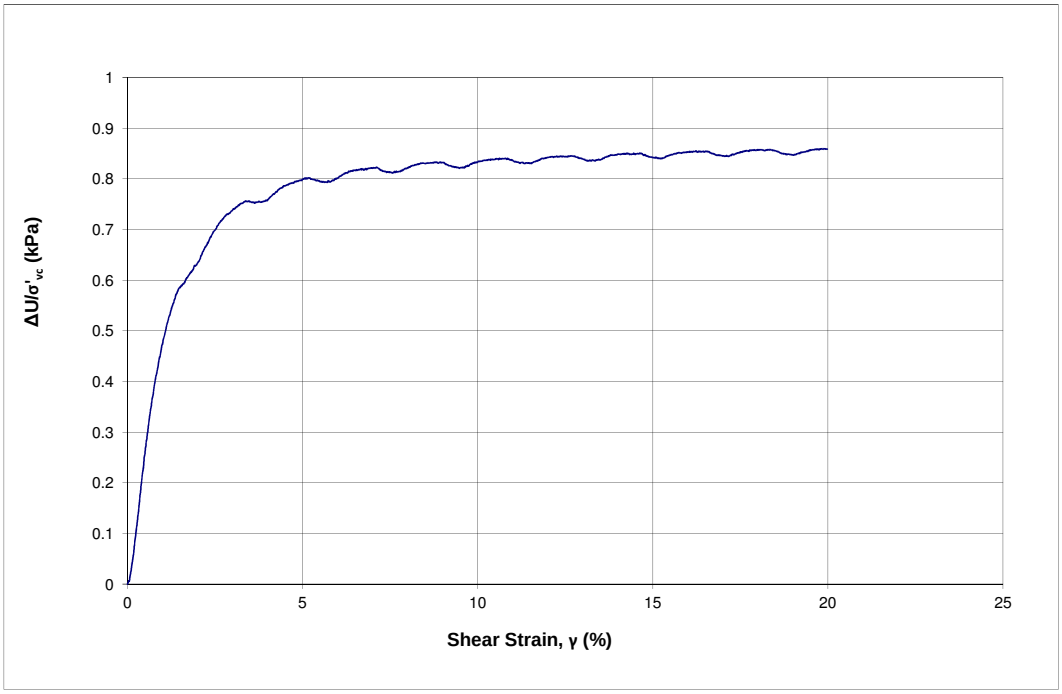

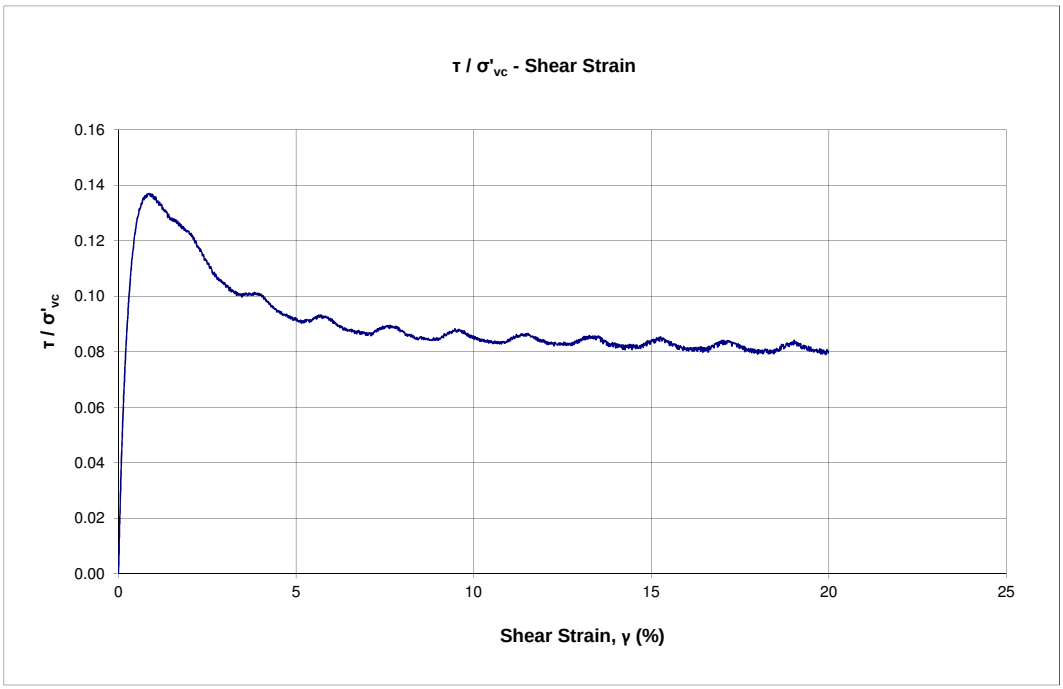

Static Simple Shear Test

(ASTM D6528)

Klohn Crippen Berger

Project No.:		Test No.:	DSS09
Project:	Fundão Tailings Dam Review Panel	Sample ID:	PSD 1
Date:	2016-04-11	Depth:	
Tested by:	BY	Description:	Sand Tailings
Checked by:	JG	Preparation Method:	Moist Tamping

Initial Sample Information		
Specimen Height	mm	21.01
Specimen Diameter	mm	70.64
Area	mm^2	3919.14
Volume	cm^3	82.34
Wet Weight	g	116.25
Water Content	%	4.98
Dry Weight	g	110.74
Wet Density	g/cm^3	1.412
Dry Density	g/cm^3	1.345
Specific Gravity	-	2.96
Void Ratio (e)	-	1.20
Saturation Ratio (Sr)	%	12.27

Static Shearing (Undrained)		
Initial Vertical Effective Stress	kPa	150.1
Initial Shear Stress	kPa	0.3
Shearing Rate (Shear Strain Rate)	% / hr	5.00
Peak Shear Strength	kPa	19.47
Ratio of Peak τ/σ'_v	-	0.13
Max. Excess Pore Pressure	kPa	125.00
Max. Shear Strain	%	20.0

FINAL SAMPLE INFORMATION		
Liquid Limit (shear plane)		-
Plastic Limit (shear plane)		-
Liquid Limit (outside shear plane)		-
Plastic Limit (outside shear plane)		-
Final Moisture Content	%	4.55

CONSOLIDATION					
Vertical Effective Stress		kPa	38	75	150
Max Load		kN	0.147	0.294	0.588
Total Height Change		mm	0.16	0.80	1.50
Consolidated Height		%	20.85	20.21	19.51
Axial Strain*2		%	0.76	3.79	7.13
Duration		min	33	41	60

*2 : Axial strain may differ from oedometer test result due to the sample seating system and possible lateral strain caused by the membrane.

Photos:

Before Test


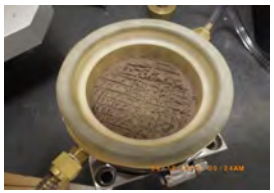

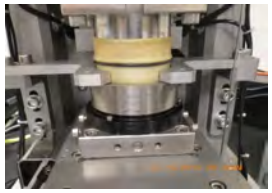

After Test




Static Simple Shear Test

(ASTM D6528)

Project No.:		Test No.:	DSS09
Project:	Fundão Tailings Dam Review Panel	Sample ID:	PSD 1
Date:	2016-04-11	Depth:	
Tested by:	BY	Description:	Sand Tailings
Checked by:	JG	Preparation Method:	Moist Tamping

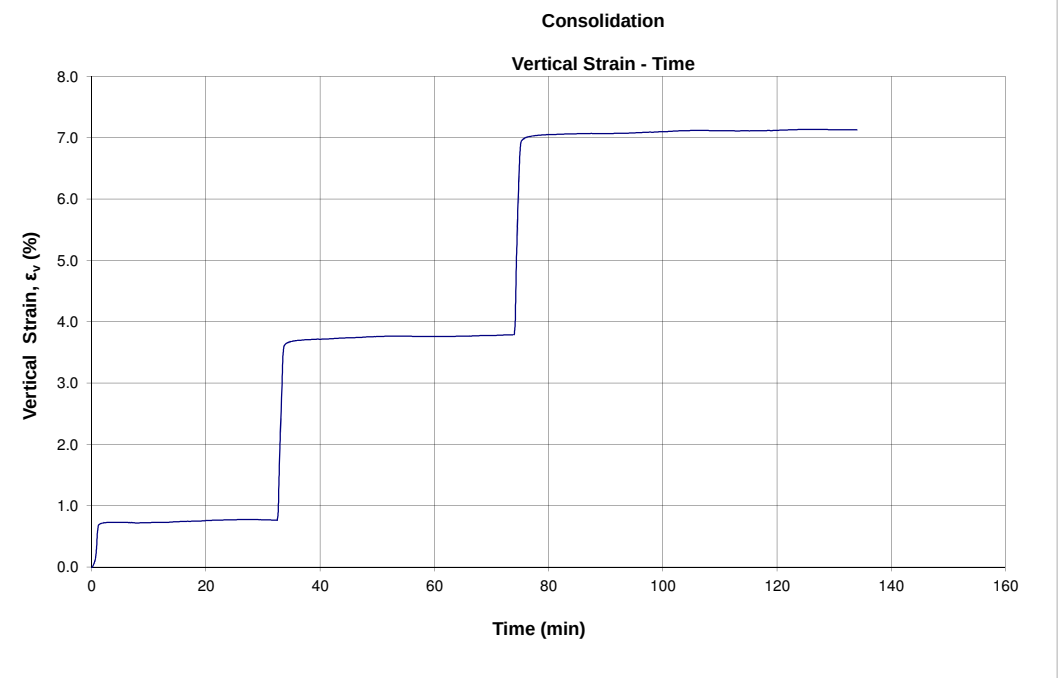

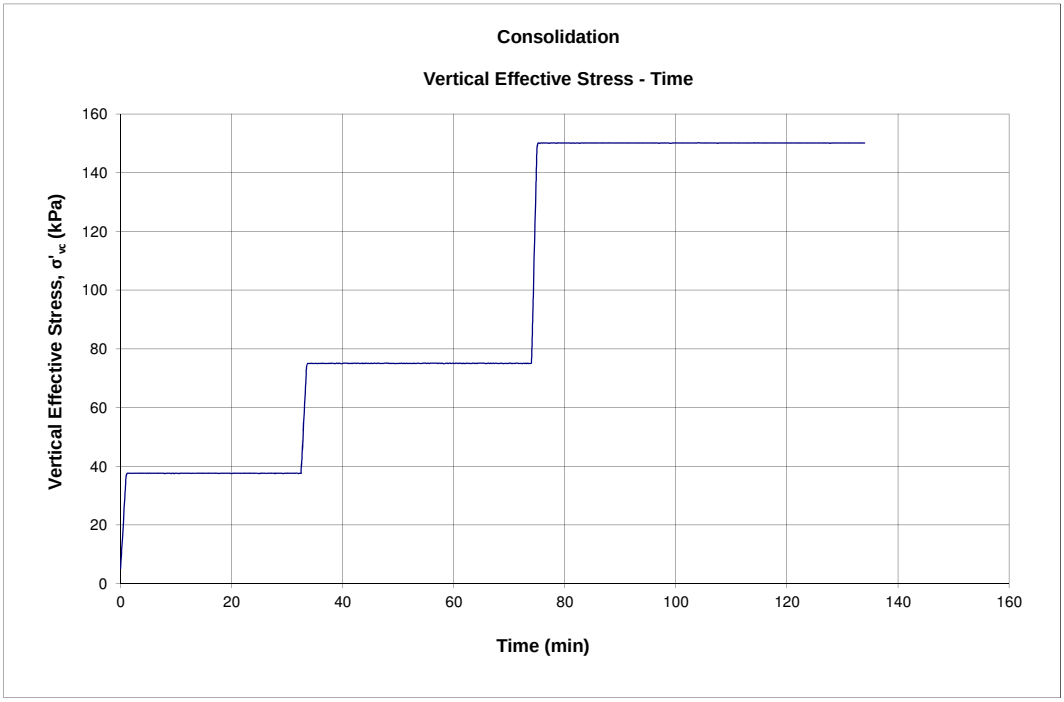

Static Simple Shear Test

(ASTM D6528)

Project No.:		Test No.:	DSS09
Project:	Fundão Tailings Dam Review Panel	Sample ID:	PSD 1
Date:	2016-04-11	Depth:	
Tested by:	BY	Description:	Sand Tailings
Checked by:	JG	Preparation Method:	Moist Tamping

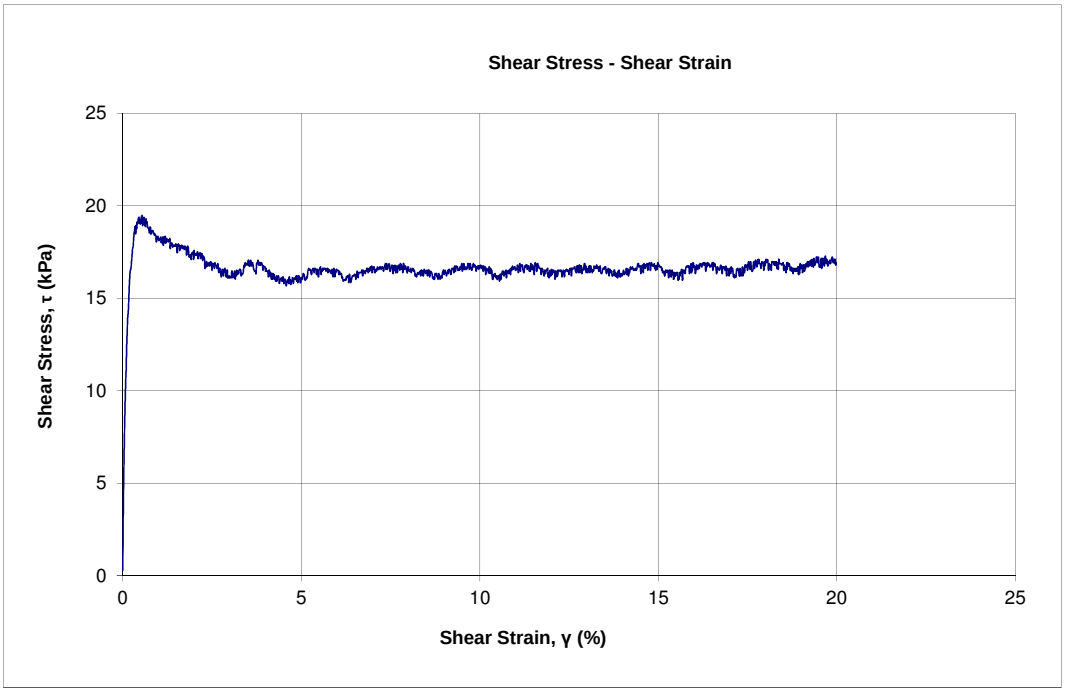

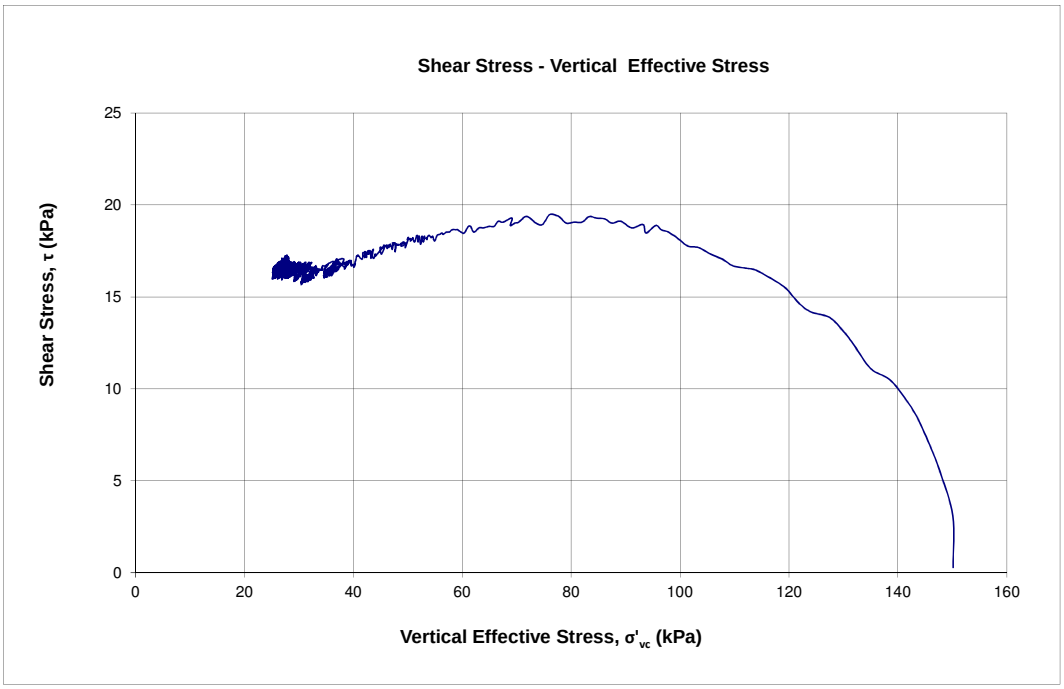

Static Simple Shear Test

(ASTM D6528)

Project No.:		Test No.:	DSS09
Project:	Fundão Tailings Dam Review Panel	Sample ID:	PSD 1
Date:	2016-04-11	Depth:	
Tested by:	BY	Description:	Sand Tailings
Checked by:	JG	Preparation Method:	Moist Tamping

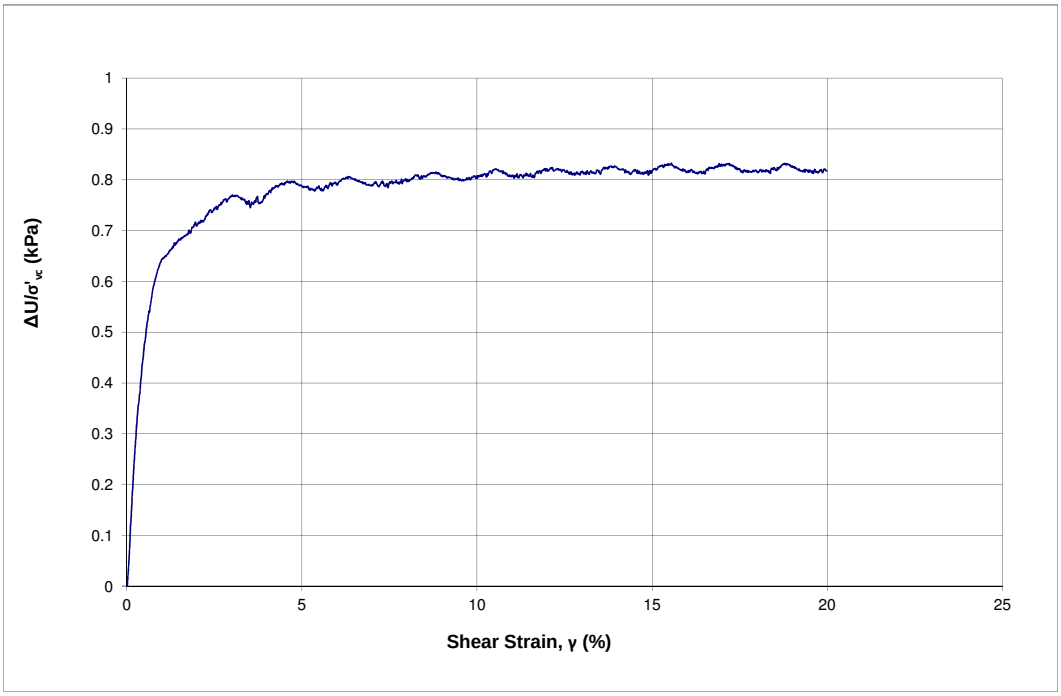

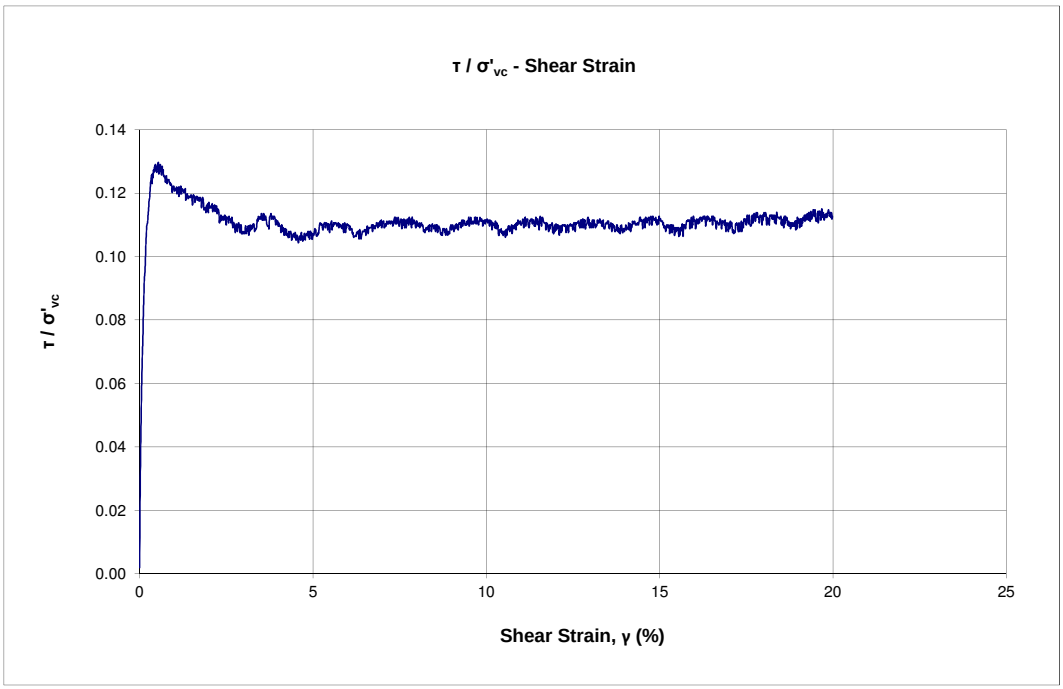

Static Simple Shear Test

(ASTM D6528)

Klohn Crippen Berger

Project No.:		Test No.:	DSS10
Project:	Fundão Tailings Dam Review Panel	Sample ID:	PSD 1
Date:	2016-04-12	Depth:	
Tested by:	BY	Description:	Sand Tailings
Checked by:	JG	Preparation Method:	Moist Tamping

Initial Sample Information		
Specimen Height	mm	21.00
Specimen Diameter	mm	70.64
Area	mm^2	3919.14
Volume	cm^3	82.30
Wet Weight	g	116.25
Water Content	%	4.98
Dry Weight	g	110.74
Wet Density	g/cm^3	1.412
Dry Density	g/cm^3	1.345
Specific Gravity	-	2.96
Void Ratio (e)	-	1.20
Saturation Ratio (Sr)	%	12.28

Static Shearing (Undrained)		
Initial Vertical Effective Stress	kPa	300.1
Initial Shear Stress	kPa	0.4
Shearing Rate (Shear Strain Rate	% / hr	5.00
Peak Shear Strength	kPa	40.80
Ratio of Peak τ / σ'_v	-	0.14
Max. Excess Pore Pressure	kPa	253.17
Max. Shear Strain	%	20.0

FINAL SAMPLE INFORMATION		
Liquid Limit (shear plane)*1		
Plastic Limit (shear plane)*1		
Liquid Limit (outside shear plane)		-
Plastic Limit (outside shear plane)		-
Final Moisture Content	%	4.48
Final Moisture Content (shear plar	%	
Final Moisture Content (outside sh	%	

CONSOLIDATION					
Vertical Effective Stress	kPa	38	75	150	300
Max Load	kN	0.148	0.294	0.588	1.176
Total Height Change	mm	0.33	0.71	1.29	1.91
Consolidated Height	%	20.67	20.29	19.71	19.09
Axial Strain*2	%	1.55	3.37	6.16	9.09
Duration	min	60	60	60	250

*2 : Axial strain may differ from oedometer test result due to the sample seating system and possible lateral strain caused by the membrane.

Photos:

Before Test

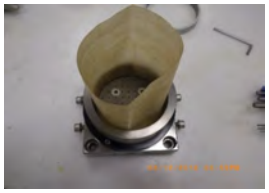

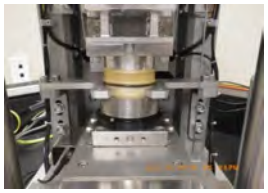


After Test


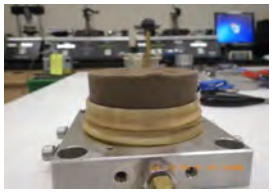
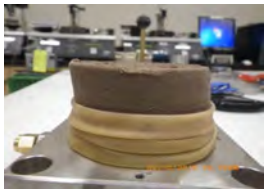
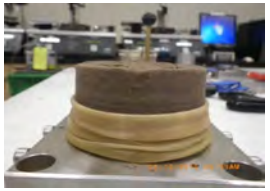

Static Simple Shear Test

(ASTM D6528)

Project No.:		Test No.:	DSS10
Project:	Fundão Tailings Dam Review Panel	Sample ID:	PSD 1
Date:	2016-04-12	Depth:	
Tested by:	BY	Description:	Sand Tailings
Checked by:	JG	Preparation Method:	Moist Tamping

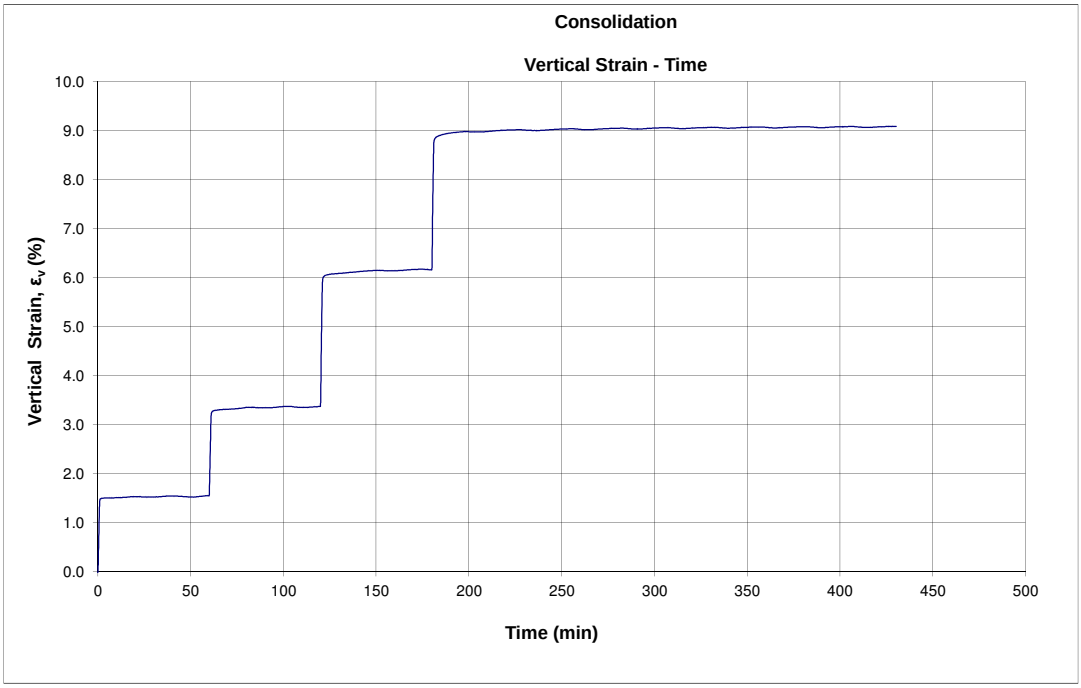

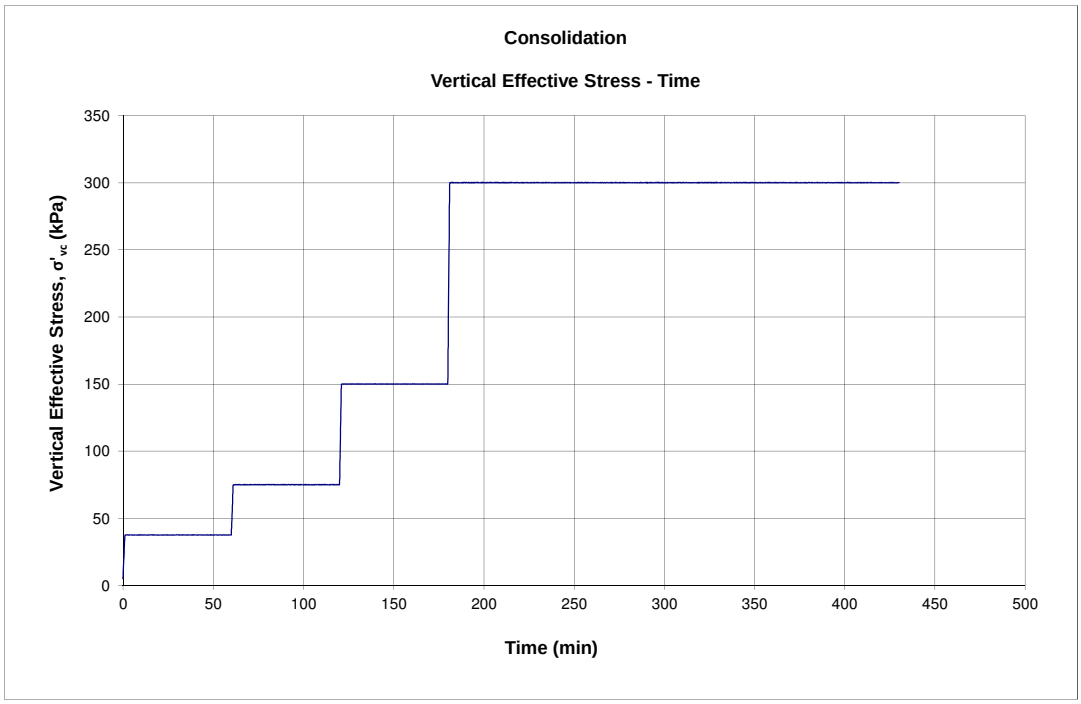

Static Simple Shear Test

(ASTM D6528)

Project No.:		Test No.:	DSS10
Project:	Fundão Tailings Dam Review Panel	Sample ID:	PSD 1
Date:	2016-04-12	Depth:	
Tested by:	BY	Description:	Sand Tailings
Checked by:	JG	Preparation Method:	Moist Tamping

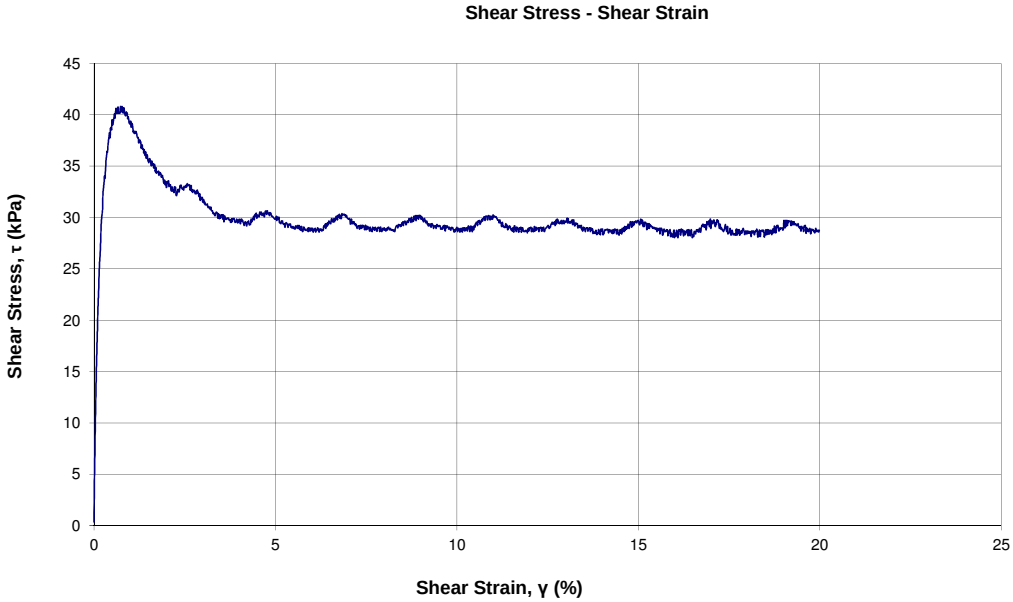

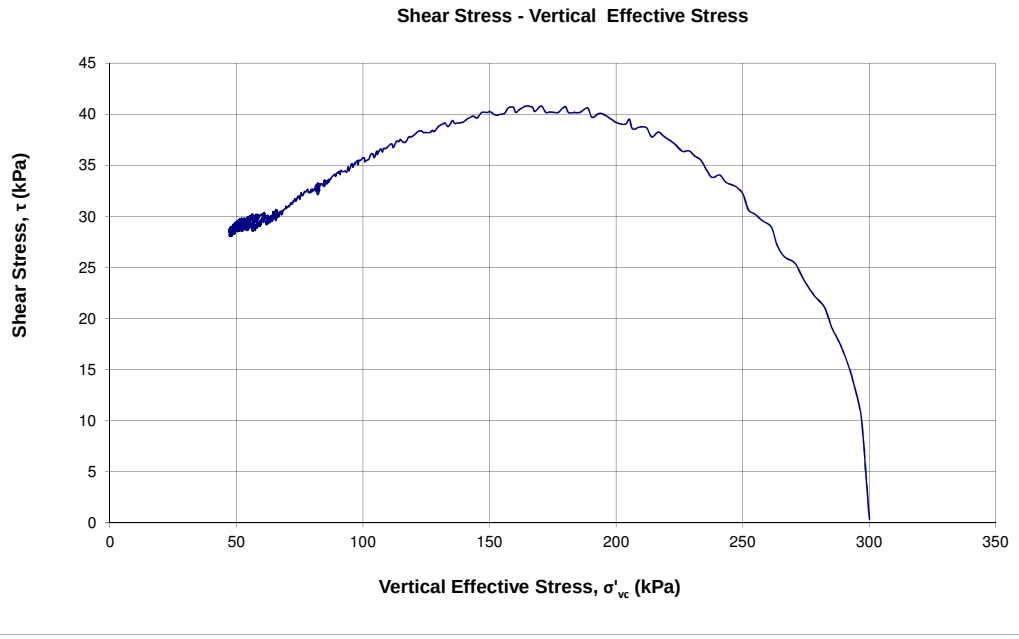

Static Simple Shear Test

(ASTM D6528)

Project No.:		Test No.:	DSS10
Project:	Fundão Tailings Dam Review Panel	Sample ID:	PSD 1
Date:	2016-04-12	Depth:	
Tested by:	BY	Description:	Sand Tailings
Checked by:	JG	Preparation Method:	Moist Tamping

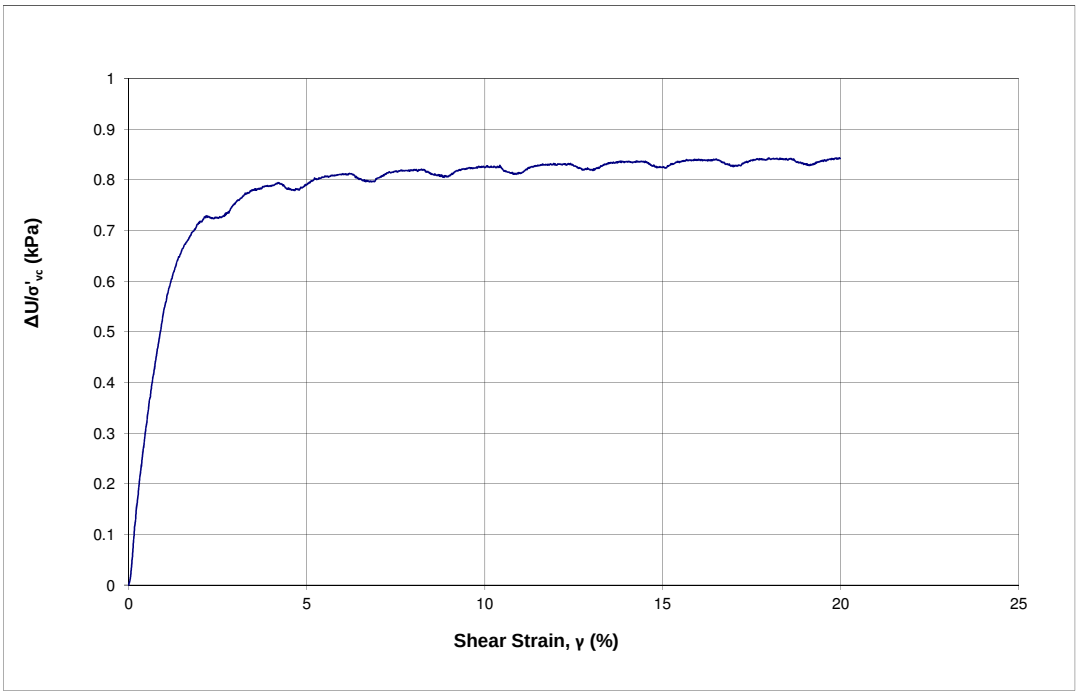

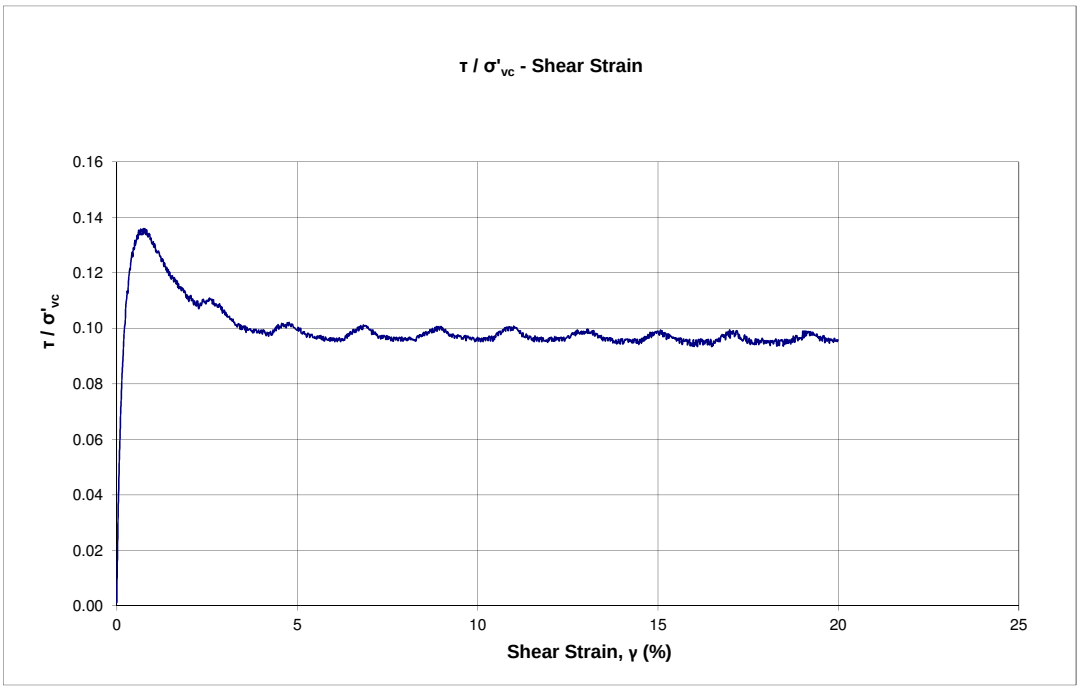

Static Simple Shear Test

(ASTM D6528)

Klohn Crippen Berger

Project No.:		Test No.:	DSS11
Project:	Fundão Tailings Dam Review Panel	Sample ID:	PSD 1
Date:	2016-05-02	Depth:	
Tested by:	BY	Description:	Sand Tailings
Checked by:	JG	Preparation Method:	Moist Tamping

Initial Sample Information		
Specimen Height	mm	21.00
Specimen Diameter	mm	70.73
Area	mm^2	3929.14
Volume	cm^3	82.51
Wet Weight	g	116.54
Water Content	%	4.98
Dry Weight	g	111.01
Wet Density	g/cm^3	1.412
Dry Density	g/cm^3	1.345
Specific Gravity	-	2.96
Void Ratio (e)	-	1.20
Saturation Ratio (Sr)	%	12.28

Static Shearing (Undrained)		
Initial Vertical Effective Stress	kPa	300.1
Initial Shear Stress	kPa	0.4
Shearing Rate (Shear Strain Rate)	% / hr	5.00
Peak Shear Strength	kPa	35.96
Ratio of Peak τ / σ'_v	-	0.12
Max. Excess Pore Pressure	kPa	283.37
Max. Shear Strain	%	20.0

FINAL SAMPLE INFORMATION		
Liquid Limit (shear plane)		
Plastic Limit (shear plane)		
Liquid Limit (outside shear plane)		-
Plastic Limit (outside shear plane)		-
Final Moisture Content	%	20.41
Final Void Ratio*1	%	0.60

CONSOLIDATION							
Vertical Effective Stress	kPa	13	25	50	100	200	300
Max Load	kN	0.050	0.099	0.197	0.393	0.786	1.179
Total Height Change	mm	0.51	0.82	1.36	1.86	2.32	2.56
Consolidated Height	%	20.49	20.18	19.64	19.14	18.68	18.44
Axial Strain*2	%	2.41	3.92	6.48	8.86	11.04	12.21
Duration	min	120	120	120	120	120	373

*1 : Final Void Ratio calculated using water content measured after freezing the sample.

*2 : Axial strain may differ from oedometer test result due to the sample seating system and possible lateral strain caused by the membrane.

Photos:

Before Test


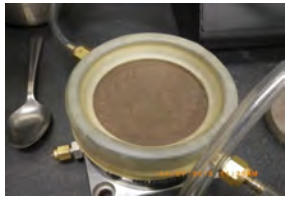

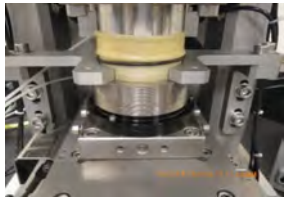

After Test

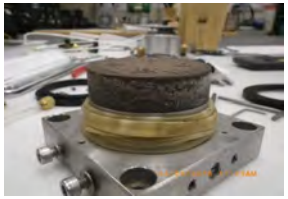
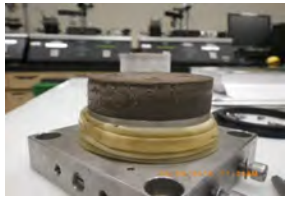

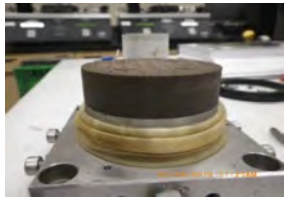

Static Simple Shear Test

(ASTM D6528)

Project No.:		Test No.:	DSS11
Project:	Fundão Tailings Dam Review Panel	Sample ID:	PSD 1
Date:	2016-05-02	Depth:	
Tested by:	BY	Description:	Sand Tailings
Checked by:	JG	Preparation Method:	Moist Tamping

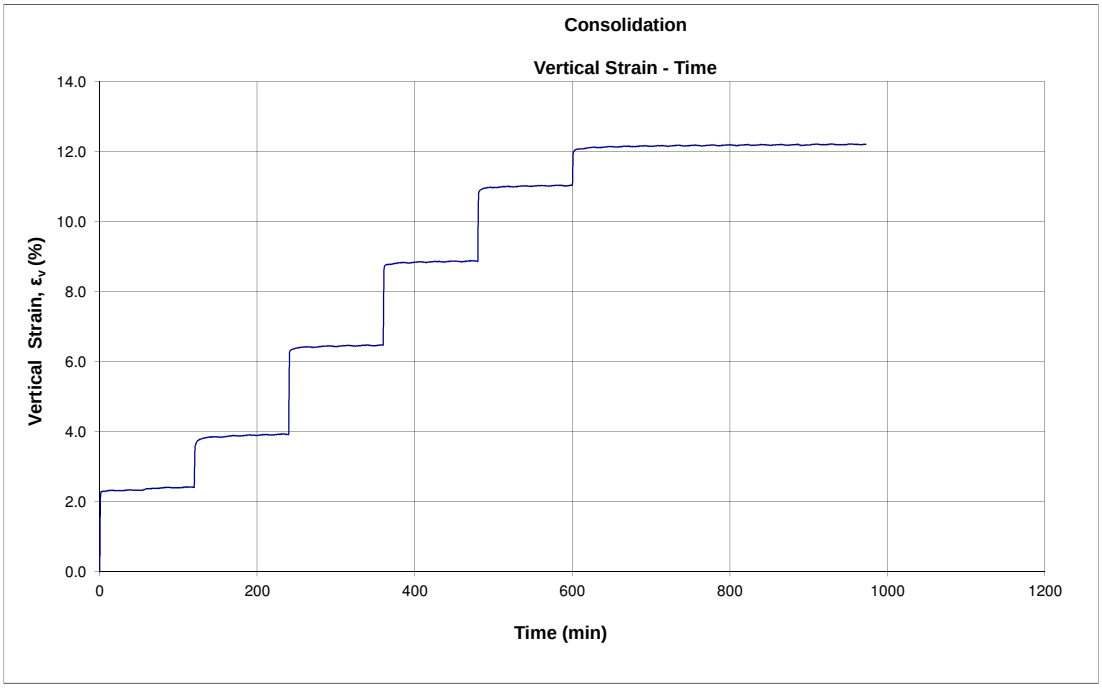

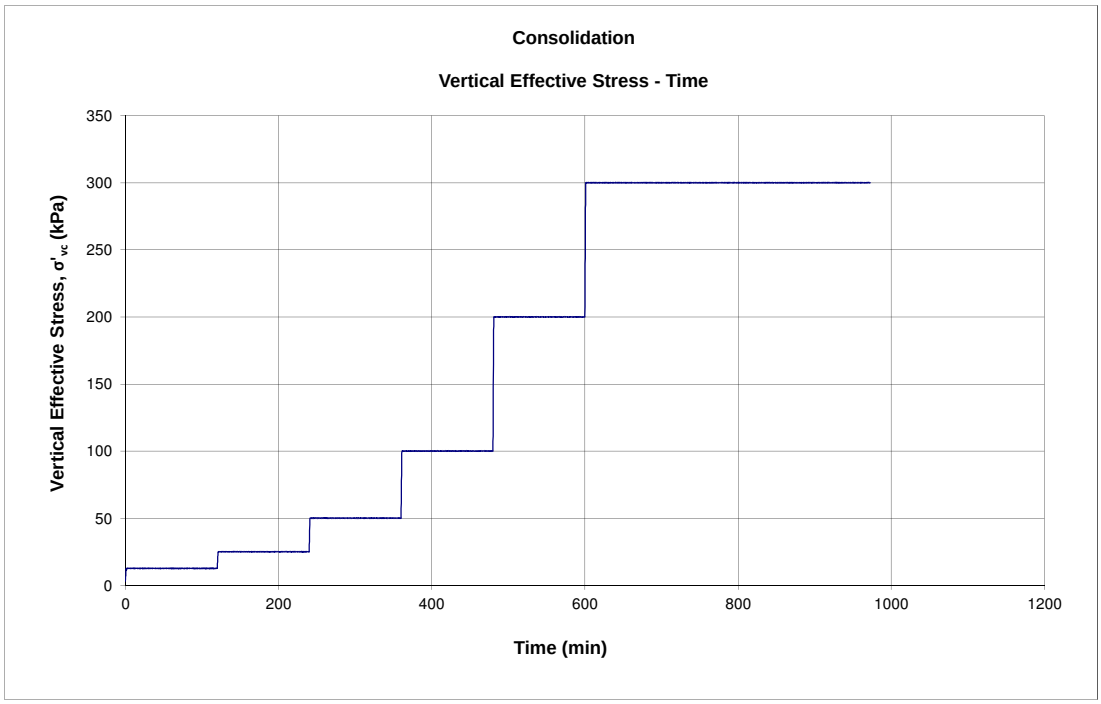

Static Simple Shear Test

(ASTM D6528)

Project No.:		Test No.:	DSS11
Project:	Fundão Tailings Dam Review Panel	Sample ID:	PSD 1
Date:	2016-05-02	Depth:	
Tested by:	BY	Description:	Sand Tailings
Checked by:	JG	Preparation Method:	Moist Tamping

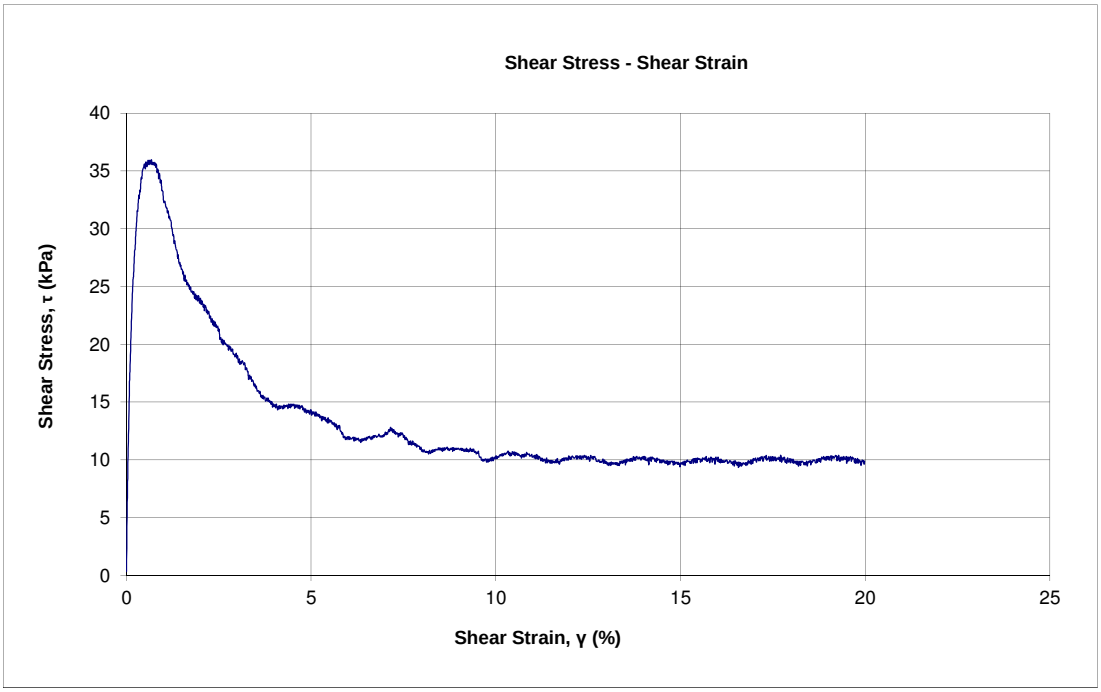

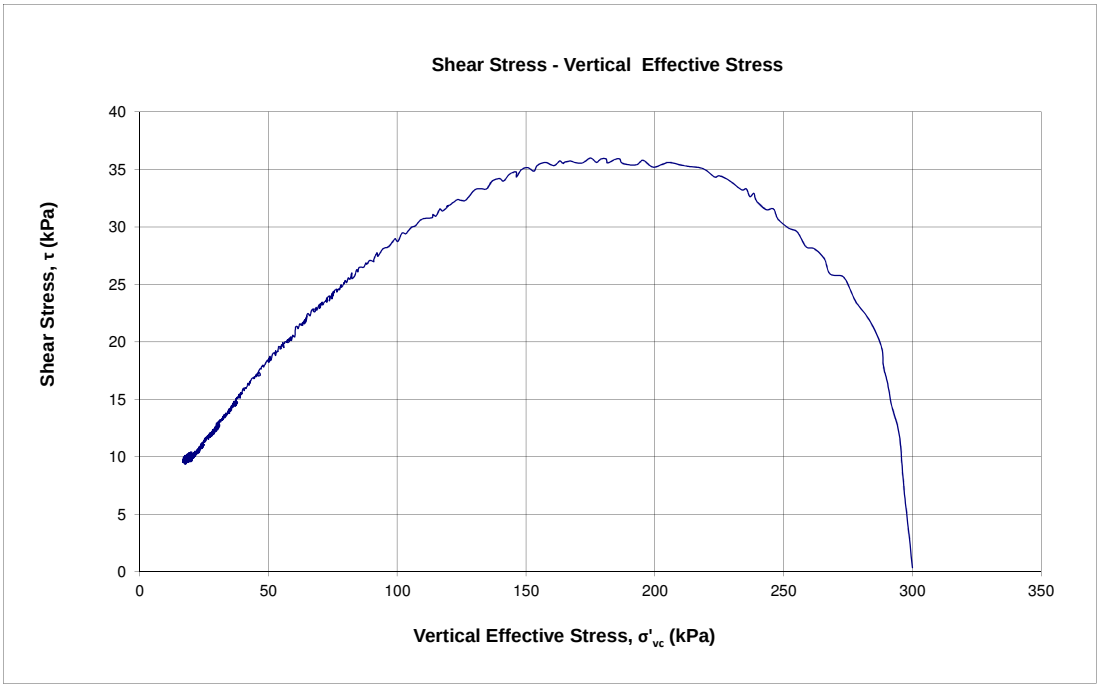

Static Simple Shear Test

(ASTM D6528)

Project No.:		Test No.:	DSS11
Project:	Fundão Tailings Dam Review Panel	Sample ID:	PSD 1
Date:	2016-05-02	Depth:	
Tested by:	BY	Description:	Sand Tailings
Checked by:	JG	Preparation Method:	Moist Tamping

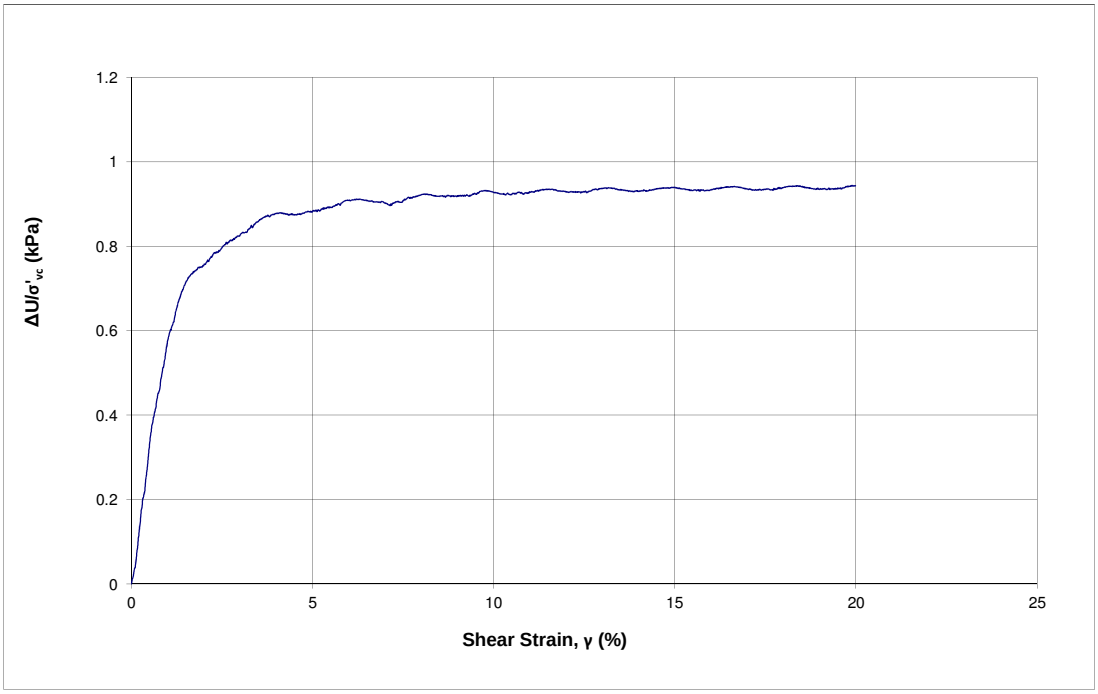

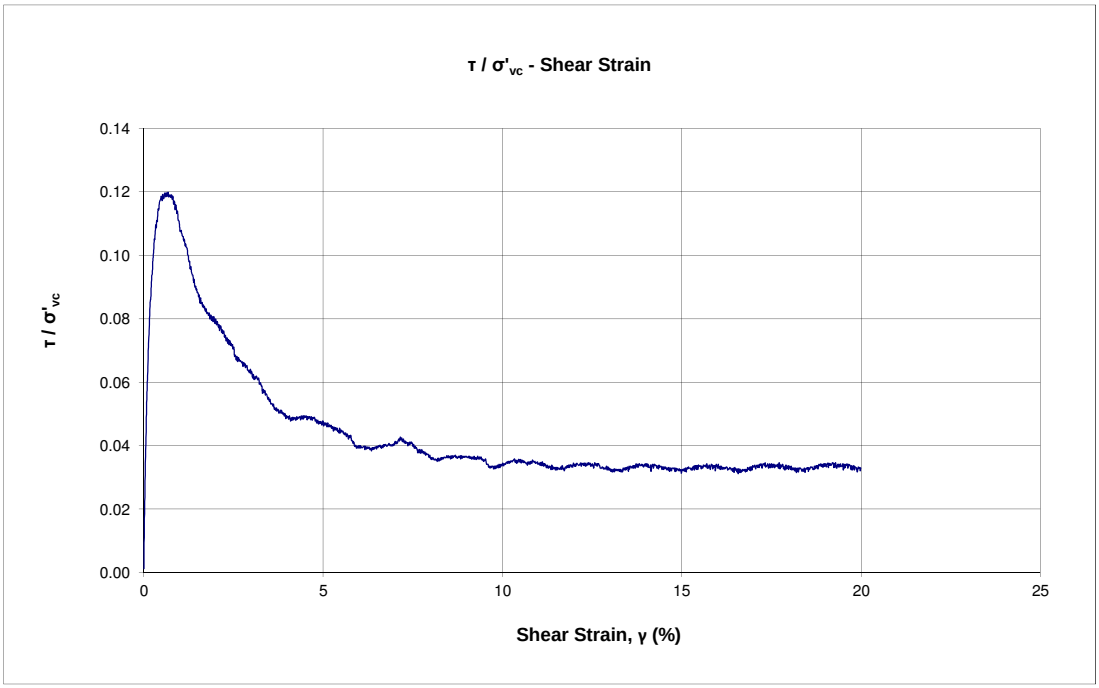

Cyclic Direct Simple Shear Test

(ASTM D6528*)

* Based on ASTM D6528-07

Project No.:		Test No.:	DSS12
Project:	Fundão Tailings Dam Review Panel	Sample ID:	PSD1
Date:	2016-05-02	Depth:	
Tested by:	BY	Location:	
Checked by:	JG	Details:	Sand Tailings sample with fines

Initial Sample Information		
Specimen Height	mm	21.00
Specimen Diameter	mm	70.69
Area	cm^2	3924.69
Volume	cm^3	82.42
Wet Weight	g	116.61
Water Content	%	5.16
Dry Weight	g	110.89
Wet Density	g/cm^3	1.415
Dry Density	g/cm^3	1.345
Specific Gravity (assumed)	-	2.96
Void Ratio (e)	-	1.20
Saturation Ratio (Sr)	%	12.73

Cyclic Shearing - Stage 1		
Frequency	Hz	0.1
Initial Vertical Stress	kPa	400.64
Cyclic Stress Ratio (CSR)	-	0.002
Number of Cycles at the end of this stage*1	-	4802
Max Cyclic Shear Stress	kPa	71.22
Max. Shear Strain	%	34.74
Max. Excess Pore Pressure	kPa	376.82

*1: Limiting cumulative shear strain was 15%

FINAL SAMPLE INFORMATION		
Liquid Limit		
Plastic Limit		
Final Moisture Content	%	25.37

Static Bias Application						
Normal Stress	kPa	400.24	400.34	400.34	400.41	400.41
Shear Stress	kPa	5.12	10.34	20.23	35.31	70.32
Total Height Change	mm	3.89	3.89	3.90	3.91	3.99
Height at the end of the stage	mm	17.11	17.11	17.10	17.09	17.01
Axial Strain	%	18.52	18.51	18.55	18.64	19.01
Horizontal Displacement	mm	0.00	0.01	0.02	0.06	0.25
Shear Strain	%	0.02	0.06	0.14	0.37	1.46
Duration	min	6.83	15.67	19.33	52.50	108.33

CONSOLIDATION							
Normal Stress	kPa	13	25	50	100	200	400
Max Load	kN	0.05	0.10	0.20	0.39	0.79	1.57
Total Height Change	mm	2.91	3.07	3.28	3.47	3.66	3.89
Consolidated Height	mm	18.09	17.93	17.72	17.53	17.34	17.11
Axial Strain	%	13.87	14.61	15.61	16.51	17.44	18.52
Duration	min	60	66	180	180	180	504

Photos:

Before Test




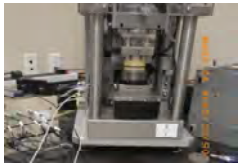

After Test




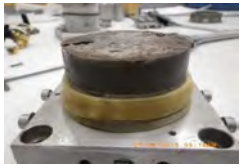

Cyclic Direct Simple Shear Test (ASTM D6528)

Consolidation Phase

Project No.:		Test No.:	DSS12
Project:	Fundão Tailings Dam Review Panel	Sample ID:	PSD1
Date:	2016-05-02	Depth:	
Tested by:	BY	Location:	
Checked by:	JG	Details:	Sand Tailings sample with fines

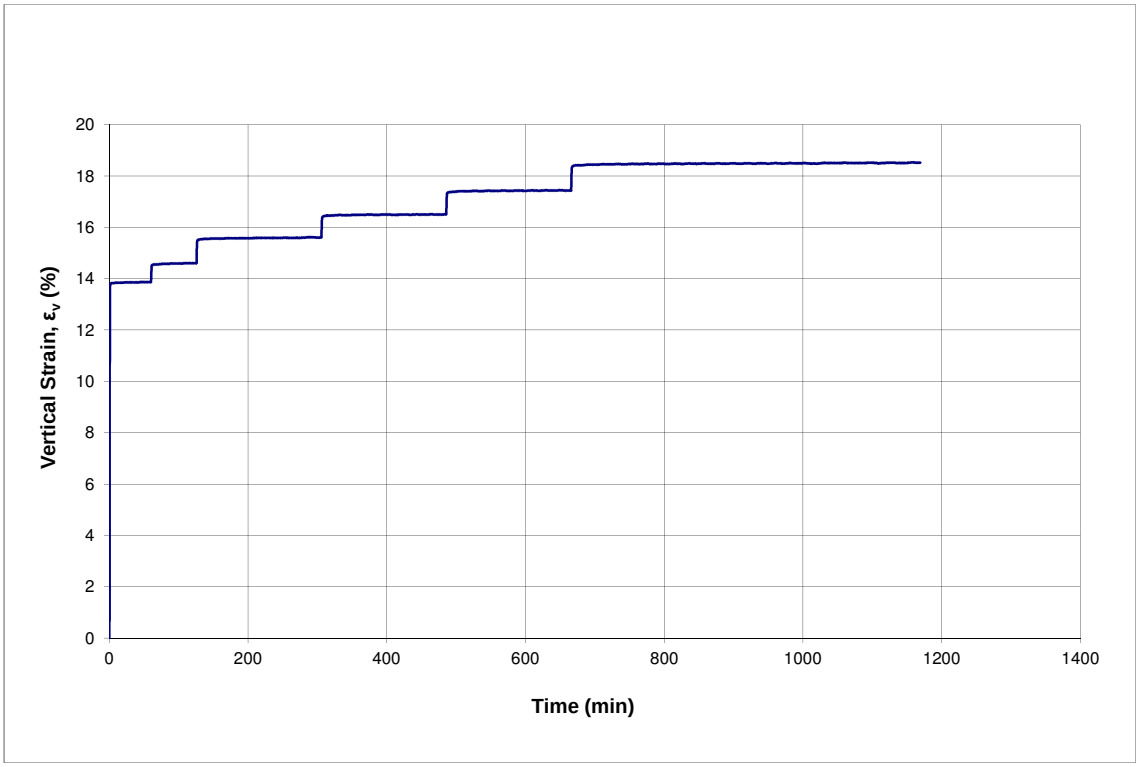

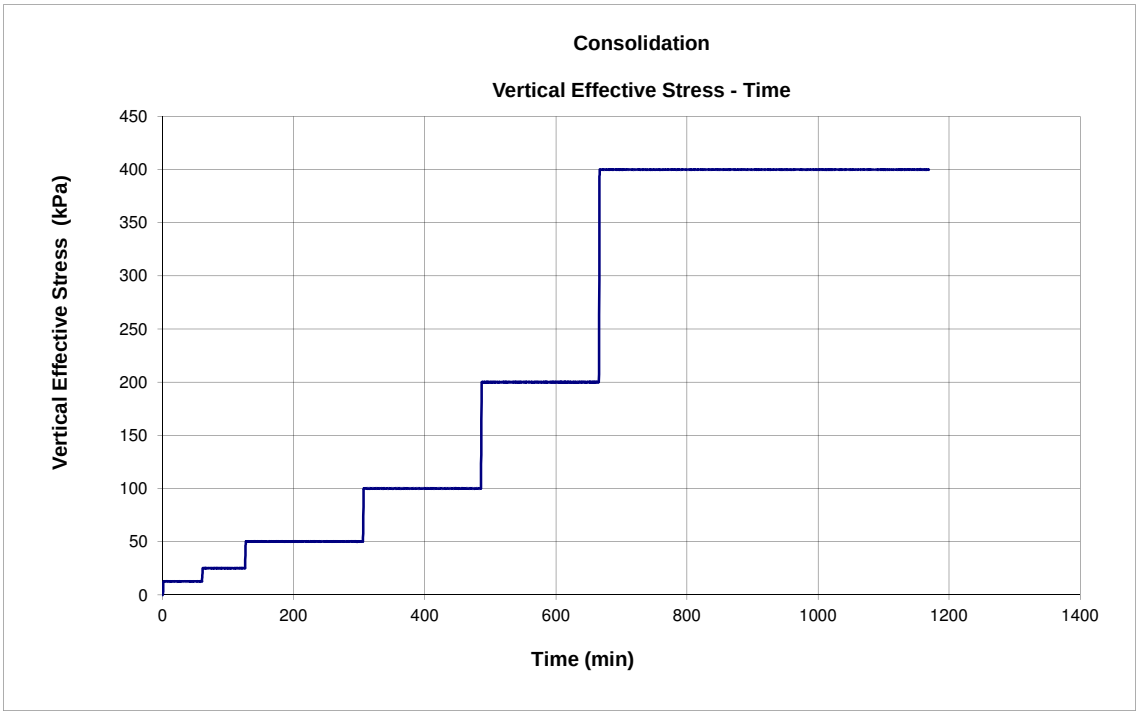

Static Simple Shear Test

(ASTM D6528)

Project No.:		Test No.:	DSS12
Project:	Fundão Tailings Dam Review Panel	Sample ID:	PSD1
Date:	2016-05-02	Depth:	
Tested by:	BY	Location:	
Checked by:	JG	Details:	Sand Tailings sample with fines

σ'_{vc} = 400 kPa

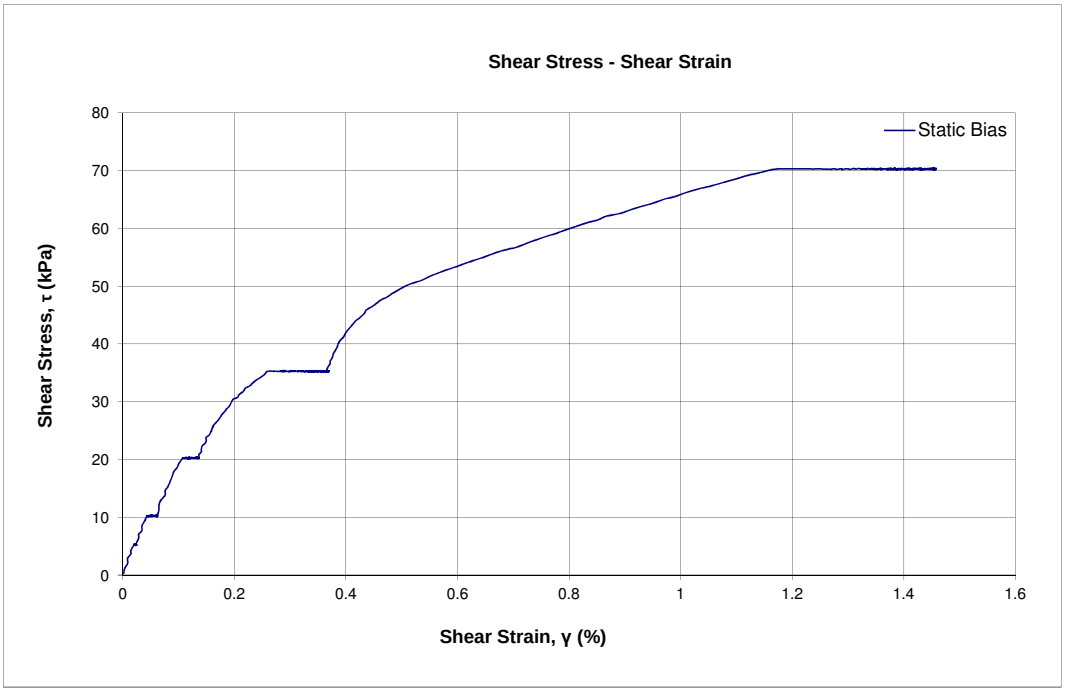

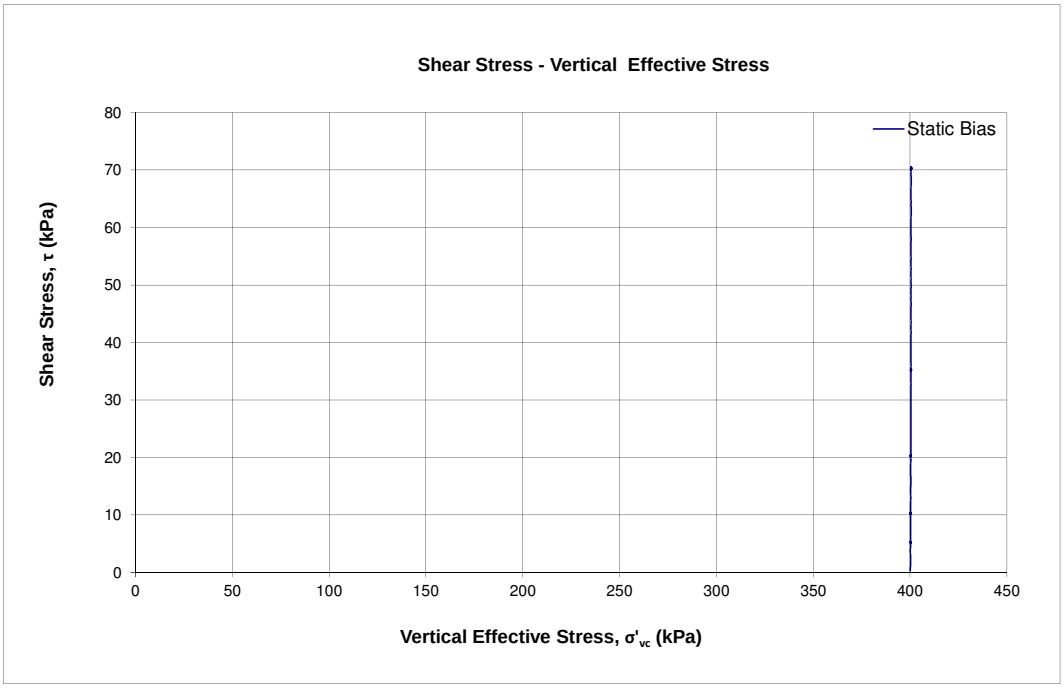

Cyclic Direct Simple Shear Test (ASTM D6528)

Cyclic Shearing Phase

Project No.:		Test No.:	DSS12
Project:	Fundão Tailings Dam Review Panel	Sample ID:	PSD1
Date:	2016-05-02	Depth:	
Tested by:	BY	Location:	
Checked by:	JG	Details:	Sand Tailings sample with fines

$\tau_{cy} / \sigma'_{vc} = 0.002$ $\sigma'_{vc} = 400$ kPa

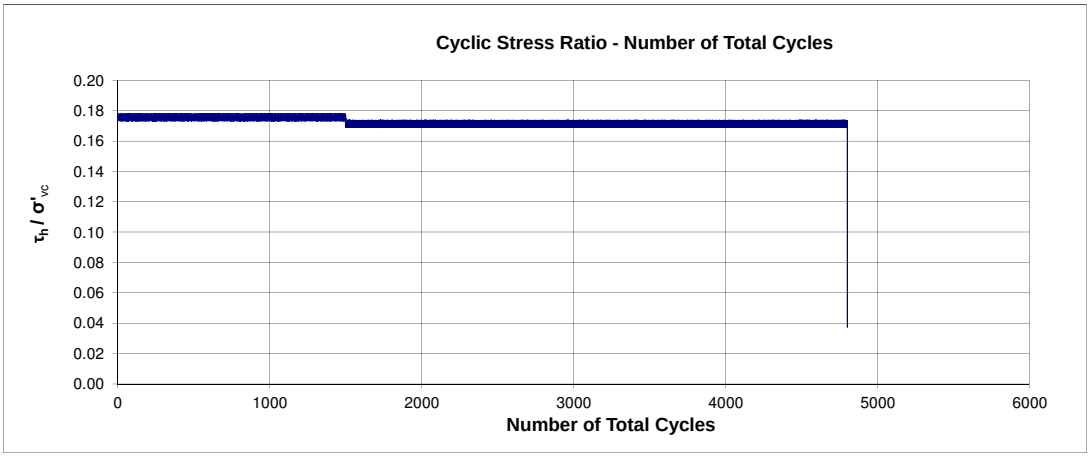

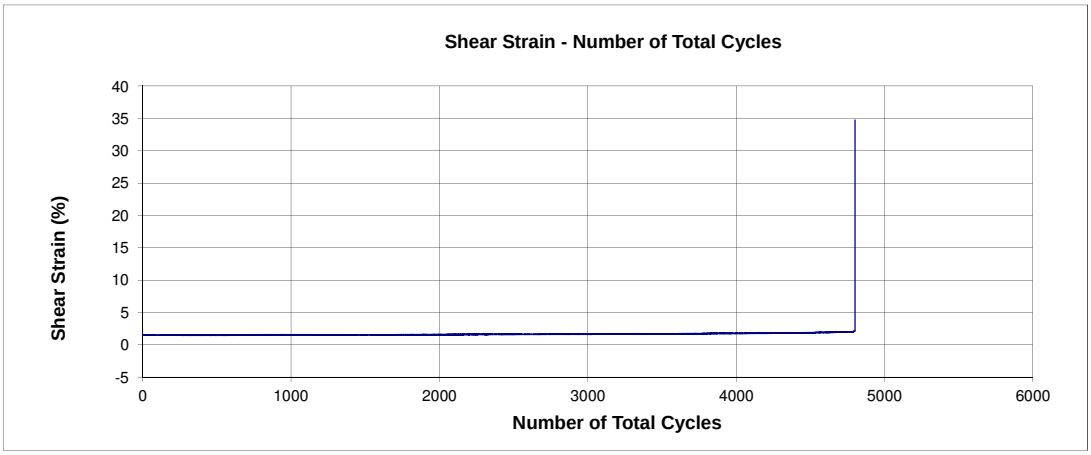

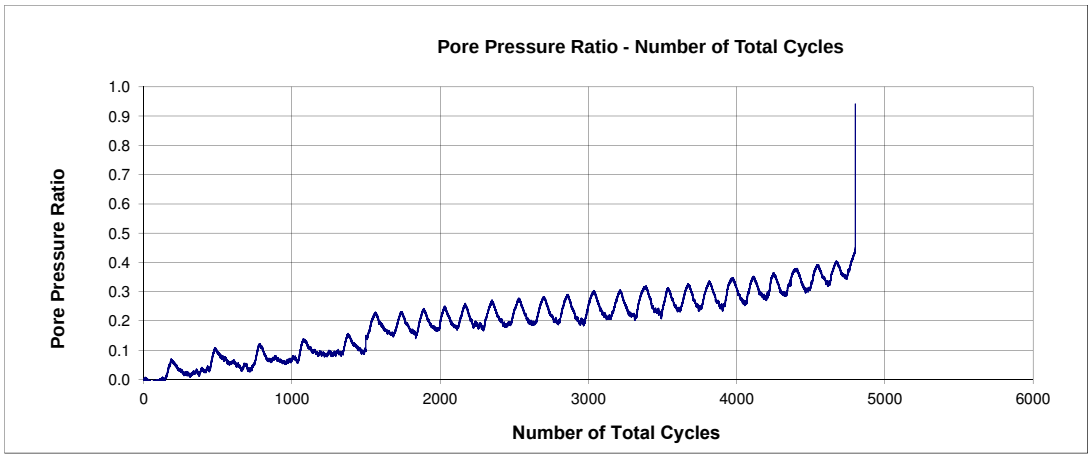

Cyclic Direct Simple Shear Test (ASTM D6528)

Cyclic Shearing Phase

Project No.:		Test No.:	DSS12
Project:	Fundão Tailings Dam Review Panel	Sample ID:	PSD1
Date:	2016-05-02	Depth:	
Tested by:	BY	Location:	
Checked by:	JG	Details:	Sand Tailings sample with fines

$\tau_{cy} / \sigma'_{vc} = 0.002$ $\sigma'_{vc} = 400$ kPa

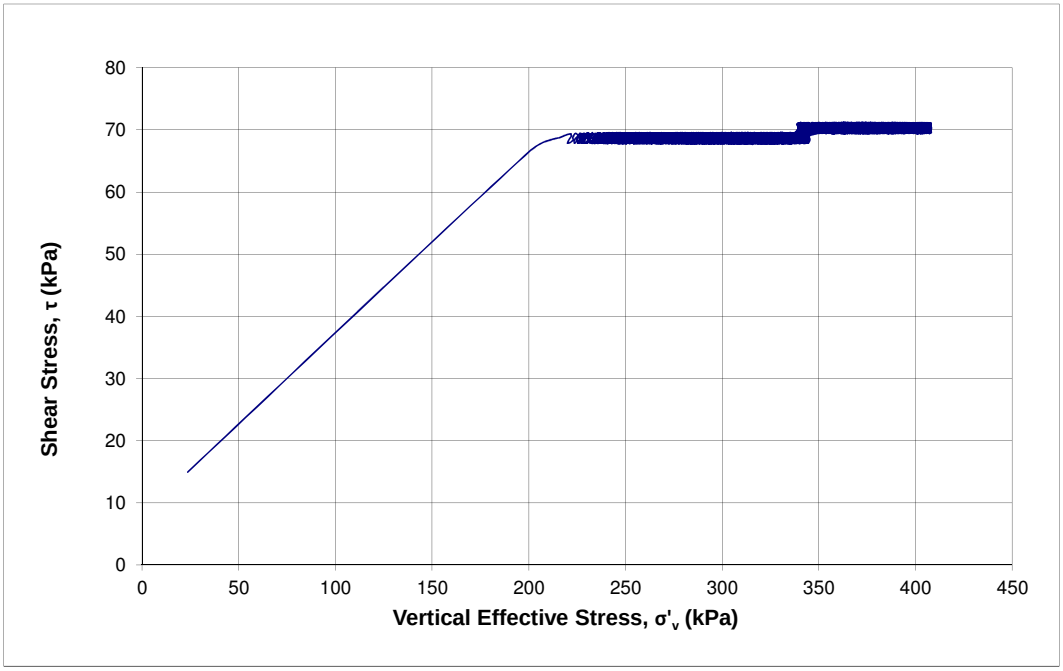

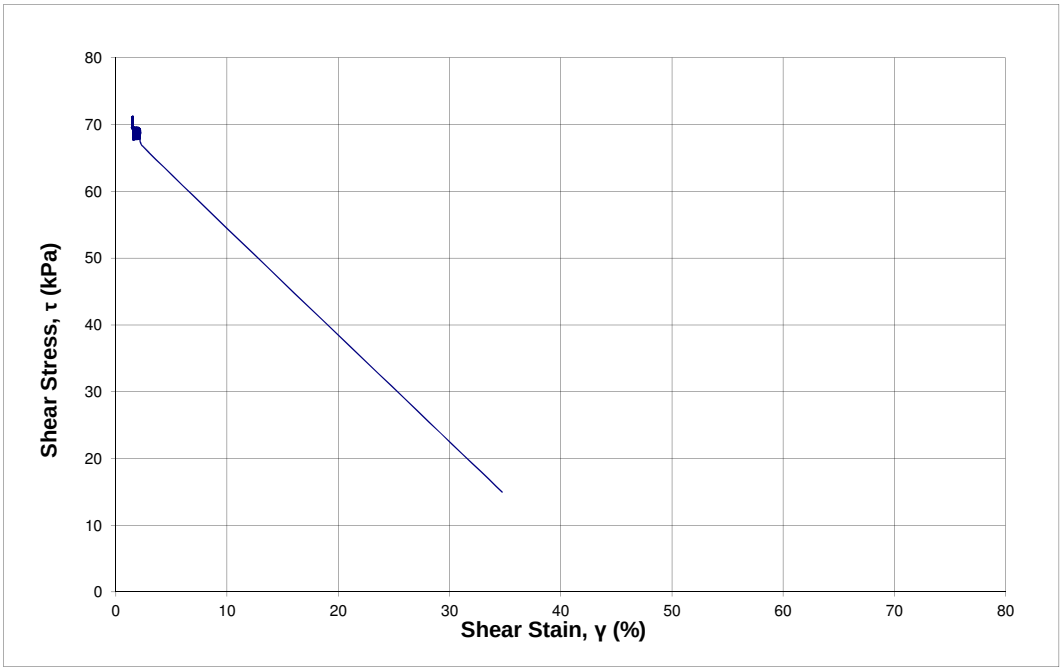

Cyclic Direct Simple Shear Test

(ASTM D6528*)

* Based on ASTM D6528-07

Project No.:		Test No.:	DSS13
Project:	Fundão Tailings Dam Review Panel	Sample ID:	Slimes
Date:	2016-05-16	Depth:	
Tested by:	BY	Location:	
Checked by:	JG	Details:	Slimes

Initial Sample Information		
Specimen Height	mm	26.70
Specimen Diameter	mm	70.46
Area	cm^2	3899.20
Volume	cm^3	104.11
Wet Weight	g	216.30
Water Content	%	43.52
Dry Weight	g	150.71
Wet Density	g/cm^3	2.078
Dry Density	g/cm^3	1.448
Specific Gravity (assumed)	-	3.93
Void Ratio (e)	-	1.71
Saturation Ratio (Sr)	%	99.74

Cyclic Shearing - Stage 1		
Frequency	Hz	0.1
Initial Vertical Stress	kPa	400.44
Cyclic Stress Ratio (CSR)	-	0.002
Number of Cycles at the end of this stage*1	-	9000
Max Cyclic Shear Stress	kPa	71.32
Max. Shear Strain	%	0.03
Max. Excess Pore Pressure	kPa	376.82

*1: Limiting cumulative shear strain was 15%

FINAL SAMPLE INFORMATION		
Liquid Limit		
Plastic Limit		
Final Moisture Content	%	23.54

Static Bias Application						
Normal Stress	kPa	400.13	400.13	400.21	400.31	400.44
Shear Stress	kPa	5.26	10.31	20.26	35.24	70.42
Total Height Change	mm	8.04	8.04	8.04	8.05	8.18
Height at the end of the stage	mm	18.66	18.66	18.66	18.65	18.52
Axial Strain	%	30.10	30.11	30.10	30.15	30.62
Horizontal Displacement	mm	0.00	0.01	0.02	0.05	0.37
Shear Strain	%	0.00	0.00	0.00	0.00	0.03
Duration	min	60.00	84.83	239.83	359.83	663.67

CONSOLIDATION									
Normal Stress	kPa	3	6	13	25	50	100	200	400
Max Load	kN	0.01	0.02	0.05	0.10	0.20	0.39	0.78	1.56
Total Height Change	mm	0.91	2.45	3.97	5.09	6.00	6.77	7.40	8.03
Consolidated Height	mm	25.80	24.25	22.73	21.61	20.70	19.93	19.30	18.67
Axial Strain	%	3.39	9.18	14.86	19.05	22.45	25.34	27.71	30.09
Duration	min	60	240	240	240	240	240	240	1062

Photos:

Before Test




After Test




Cyclic Direct Simple Shear Test (ASTM D6528)

Consolidation Phase

Project No.:		Borehole ID:	DSS13
Project:	Fundão Tailings Dam Review Panel	Sample ID:	Slimes
Date:	2016-05-16	Depth:	
Tested by:	BY	Location:	
Checked by:	JG	Details:	Slimes

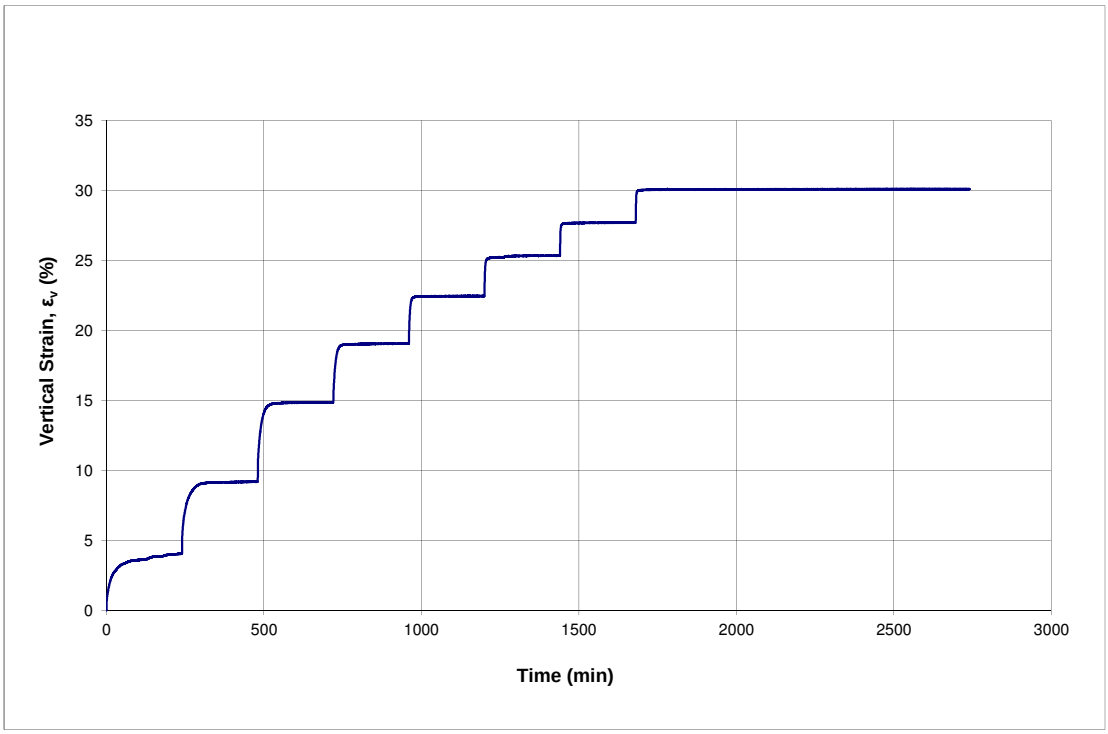

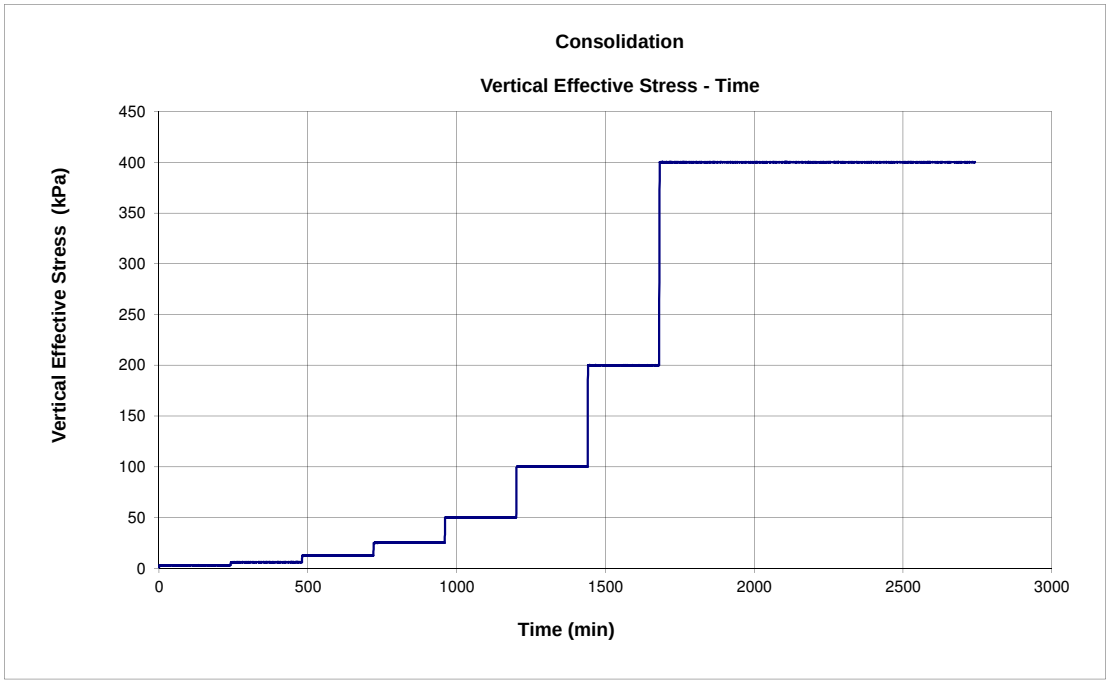

Static Simple Shear Test

(ASTM D6528)

Project No.:		Borehole ID:	DSS13
Project:	Fundão Tailings Dam Review Panel	Sample ID:	Slimes
Date:	2016-05-16	Depth:	
Tested by:	BY	Location:	
Checked by:	JG	Details:	Slimes

σ'_{vc} = 400 kPa

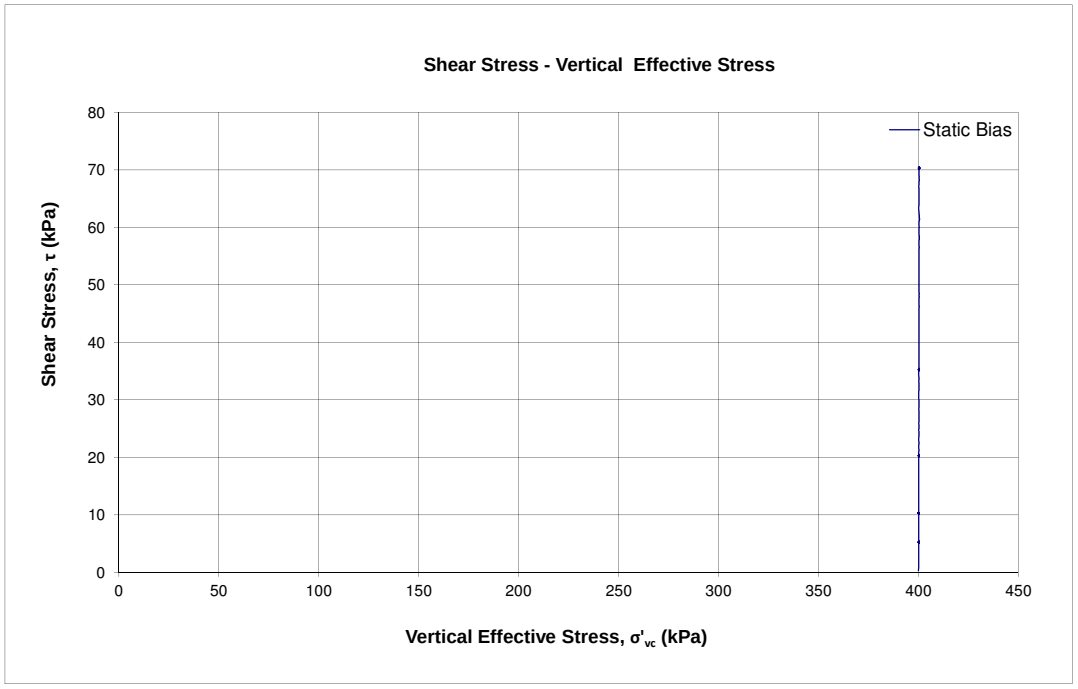

Klohn Crippen Berger

Cyclic Direct Simple Shear Test (ASTM D6528)

Cyclic Shearing Phase

Project No.:		Borehole ID:	DSS13
Project:	Fundão Tailings Dam Review Panel	Sample ID:	Slimes
Date:	2016-05-16	Depth:	
Tested by:	BY	Location:	
Checked by:	JG	Details:	Slimes

τ_{cy} / σ'_{vc} = 0.002 σ'_{vc} = 400 kPa

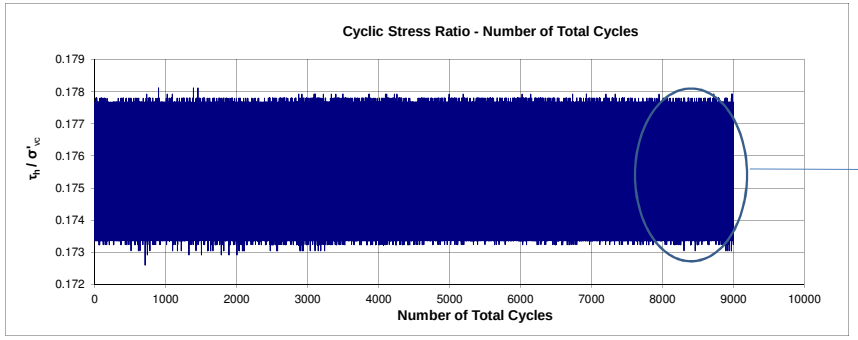

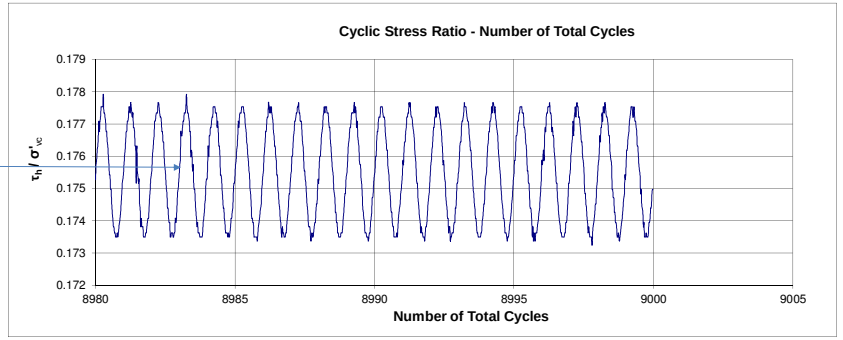

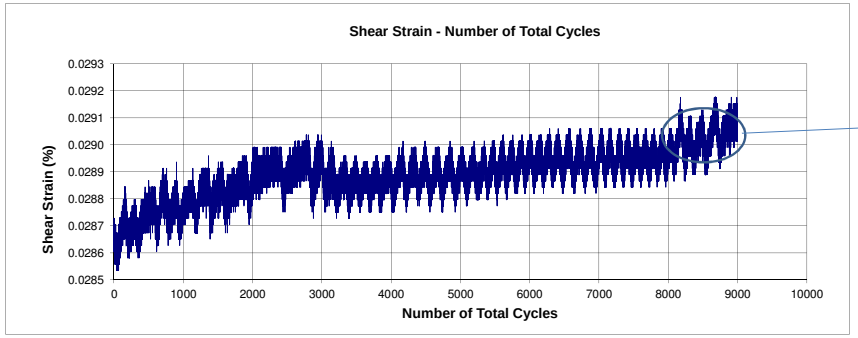

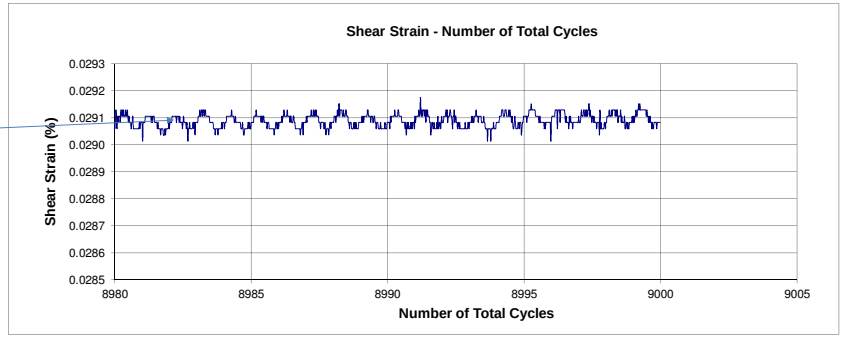

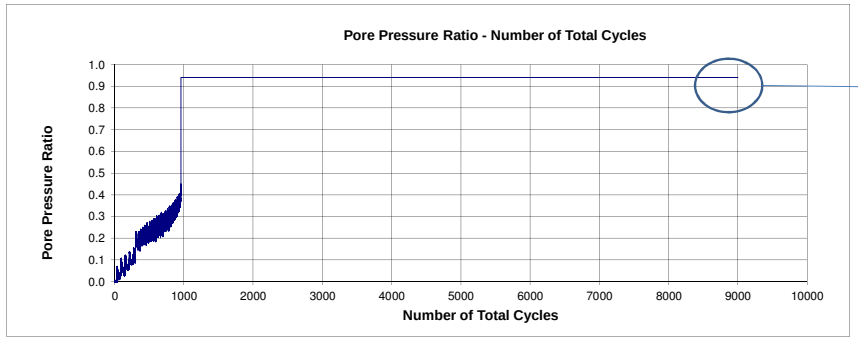

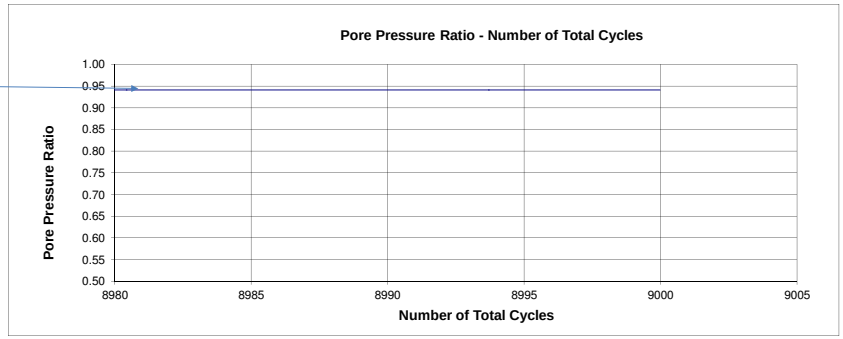

Cyclic Direct Simple Shear Test (ASTM D6528)

Cyclic Shearing Phase

Project No.:		Borehole ID:	DSS13
Project:	Fundão Tailings Dam Review Panel	Sample ID:	Slimes
Date:	2016-05-16	Depth:	
Tested by:	BY	Location:	
Checked by:	JG	Details:	Slimes

$\tau_{cy} / \sigma'_{vc} = 0.002$ $\sigma'_{vc} = 400$ kPa

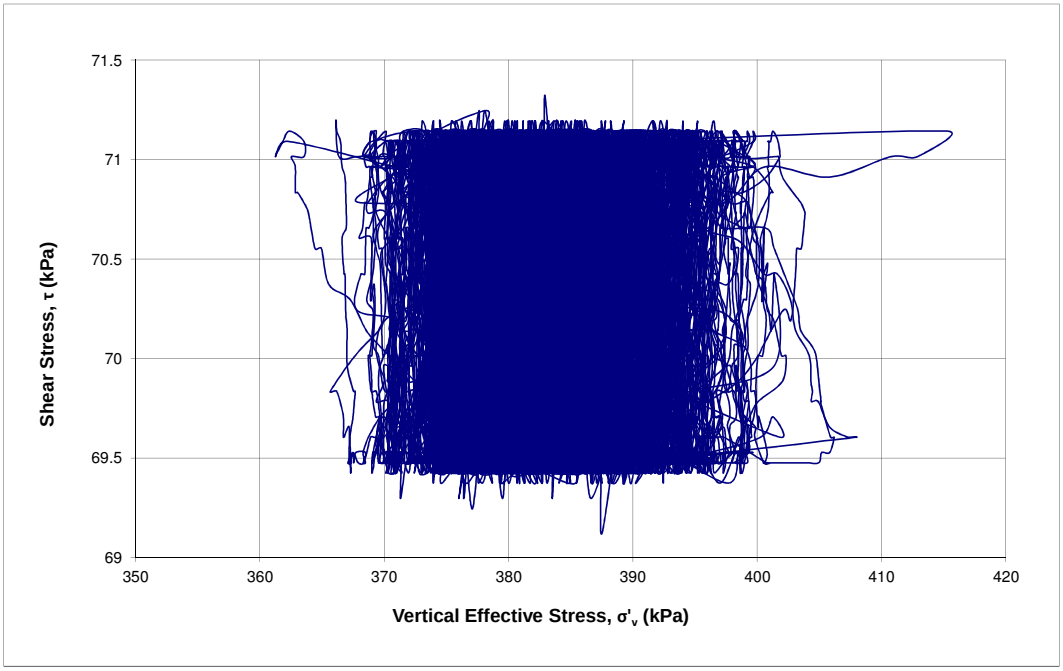

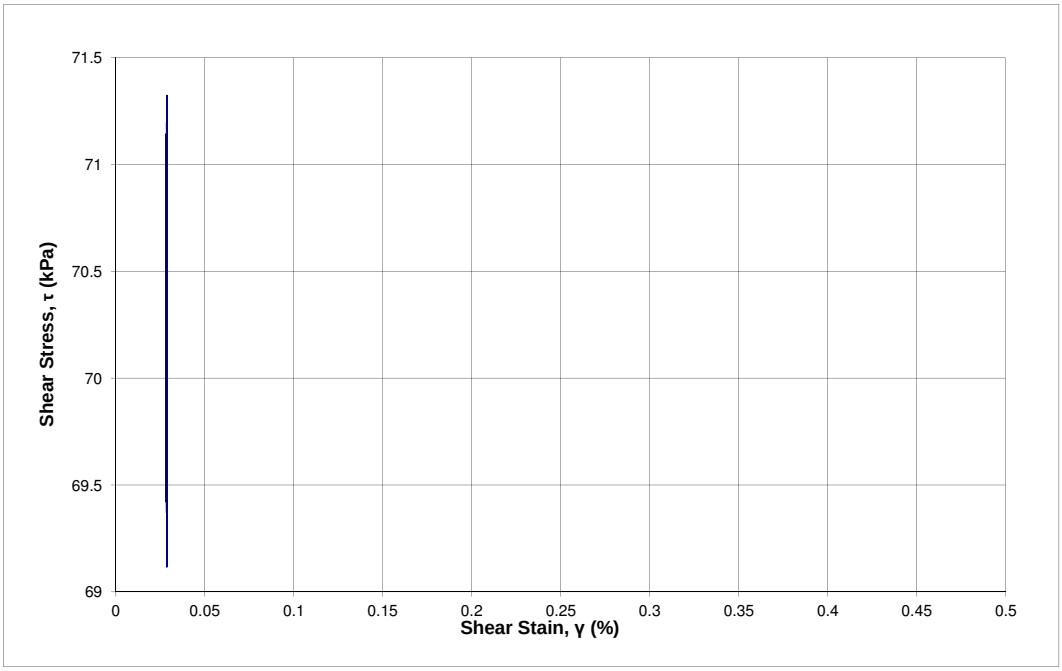

Cyclic Direct Simple Shear Test

(ASTM D6528*)

* Based on ASTM D6528-07

Project No.:		Test No.:	DSS14
Project:	Fundão Tailings Dam Review Panel	Sample ID:	PSD 1
Date:	2016-05-15	Depth:	
Tested by:	BY	Location:	
Checked by:	JG	Details:	Sand tailings sample with fines

Initial Sample Information		
Specimen Height	mm	20.89
Specimen Diameter	mm	70.36
Area	cm^2	3888.14
Volume	cm^3	81.22
Wet Weight	g	115.53
Water Content	%	5.16
Dry Weight	g	109.86
Wet Density	g/cm^3	1.422
Dry Density	g/cm^3	1.353
Specific Gravity (assumed)	-	2.96
Void Ratio (e)	-	1.19
Saturation Ratio (Sr)	%	12.85

Cyclic Shearing - Stage 1		
Frequency	Hz	0.1
Initial Vertical Stress	kPa	400.58
Cyclic Stress Ratio (CSR)	-	0.002
Number of Cycles at the end of this stage*1	-	492
Max Cyclic Shear Stress	kPa	141.25
Max. Shear Strain	%	43.10
Max. Excess Pore Pressure	kPa	310.33

*1: Limiting cumulative shear strain was 15%

FINAL SAMPLE INFORMATION		
Liquid Limit		
Plastic Limit		
Final Moisture Content	%	24.88

Static Bias Application								
Normal Stress	kPa	400.22	400.27	400.40	400.35	400.53	400.58	400.58
Shear Stress	kPa	**5.27**	**10.31**	**20.29**	**35.21**	**70.27**	**105.37**	**140.30**
Total Height Change	mm	4.06	4.06	4.07	4.09	4.15	4.25	4.37
Height at the end of the stage	mm	16.83	16.83	16.82	16.80	16.74	16.64	16.52
Axial Strain	%	19.44	19.45	19.48	19.56	19.88	20.35	20.90
Horizontal Displacement	mm	0.00	0.01	0.03	0.07	0.26	0.61	1.20
Shear Strain	%	0.02	0.05	0.14	0.37	1.44	3.49	7.07
Duration	min	6.83	59.83	59.83	119.83	119.83	82.17	82.17

CONSOLIDATION							
Normal Stress	kPa	13	25	50	100	200	400.11
Max Load	kN	0.05	0.10	0.19	0.39	0.78	1.56
Total Height Change	mm	3.29	3.42	3.56	3.70	3.86	4.06
Consolidated Height	mm	17.60	17.47	17.33	17.19	17.03	16.83
Axial Strain	%	15.77	16.36	17.02	17.71	18.49	19.44
Duration	min	120	120	120	120	180	596

Photos:

Before Test

After Test

Cyclic Direct Simple Shear Test (ASTM D6528)

Consolidation Phase

Project No.:		Test No.:	DSS14
Project:	Fundão Tailings Dam Review Panel	Sample ID:	PSD 1
Date:	2016-05-15	Depth:	
Tested by:	BY	Location:	
Checked by:	JG	Details:	Sand tailings sample with fines

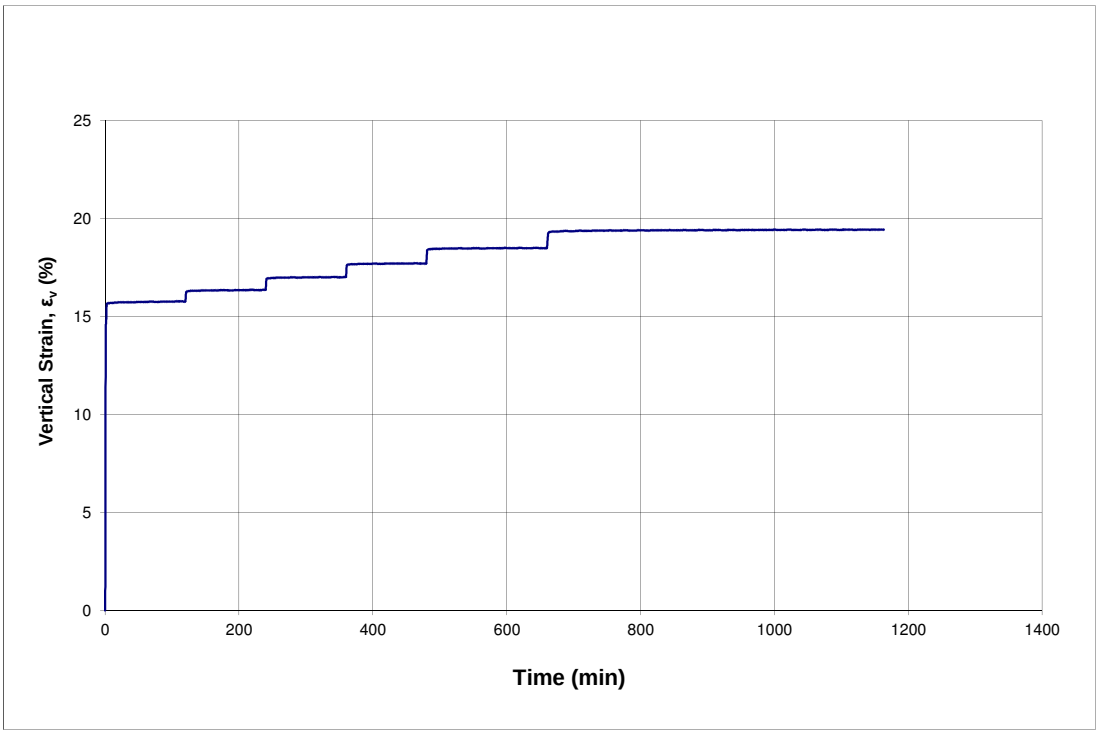

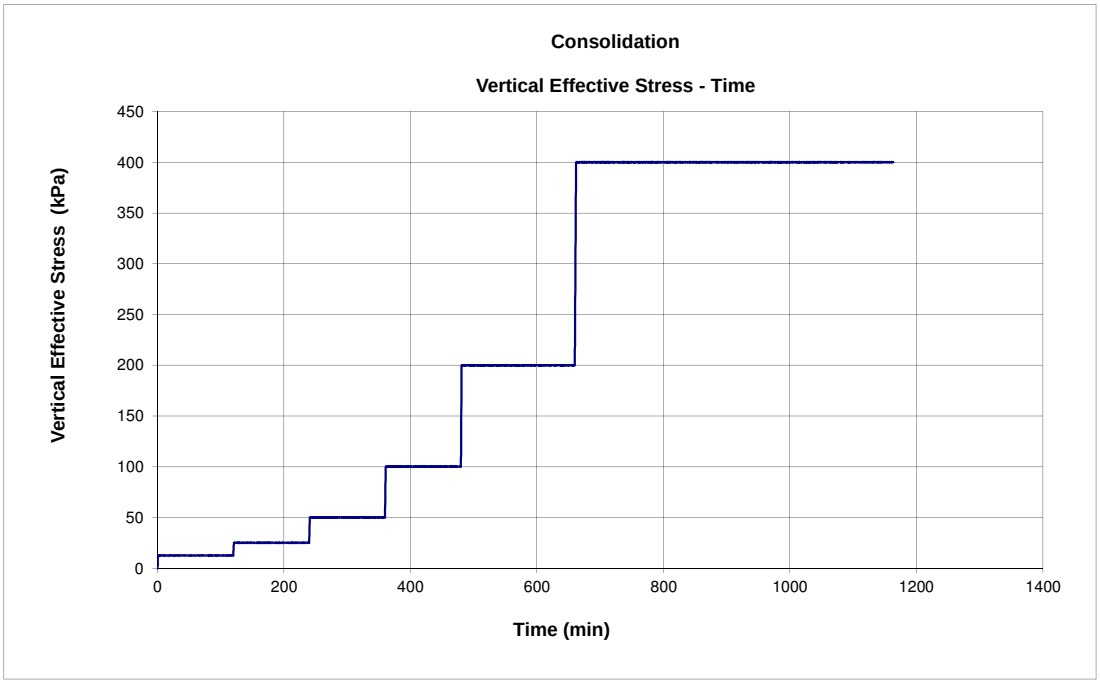

Static Simple Shear Test

(ASTM D6528)

Project No.:		Test No.:	DSS14
Project:	Fundão Tailings Dam Review Panel	Sample ID:	PSD1
Date:	2016-05-02	Depth:	
Tested by:	BY	Location:	
Checked by:	JG	Details:	Sand tailings sample with fines

σ'_{vc} = 400 kPa

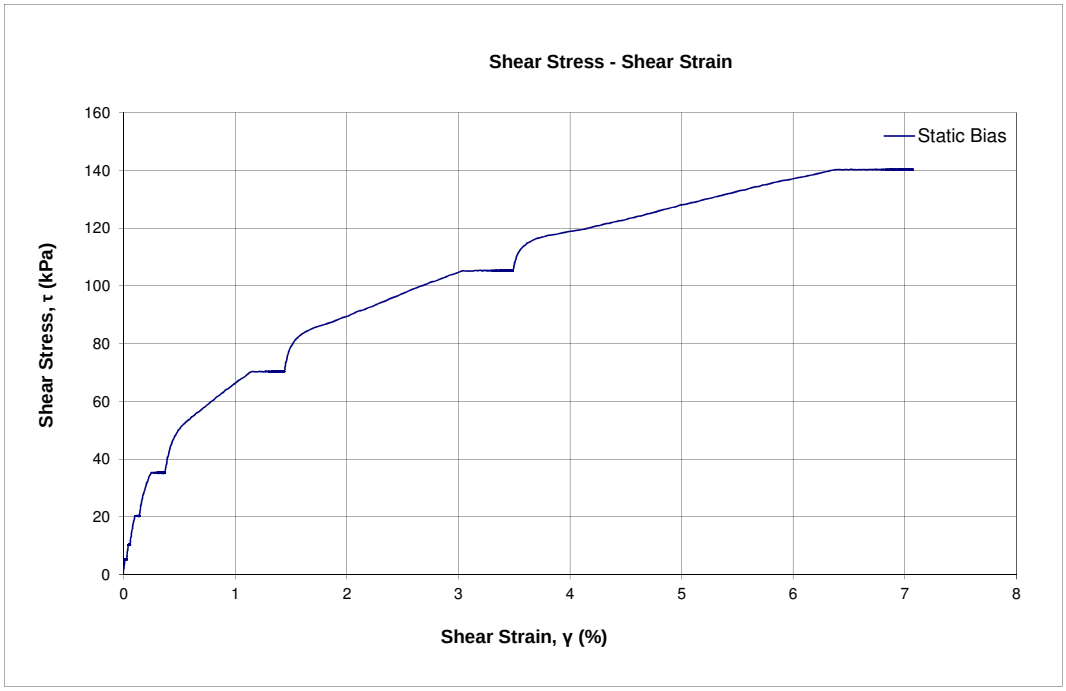

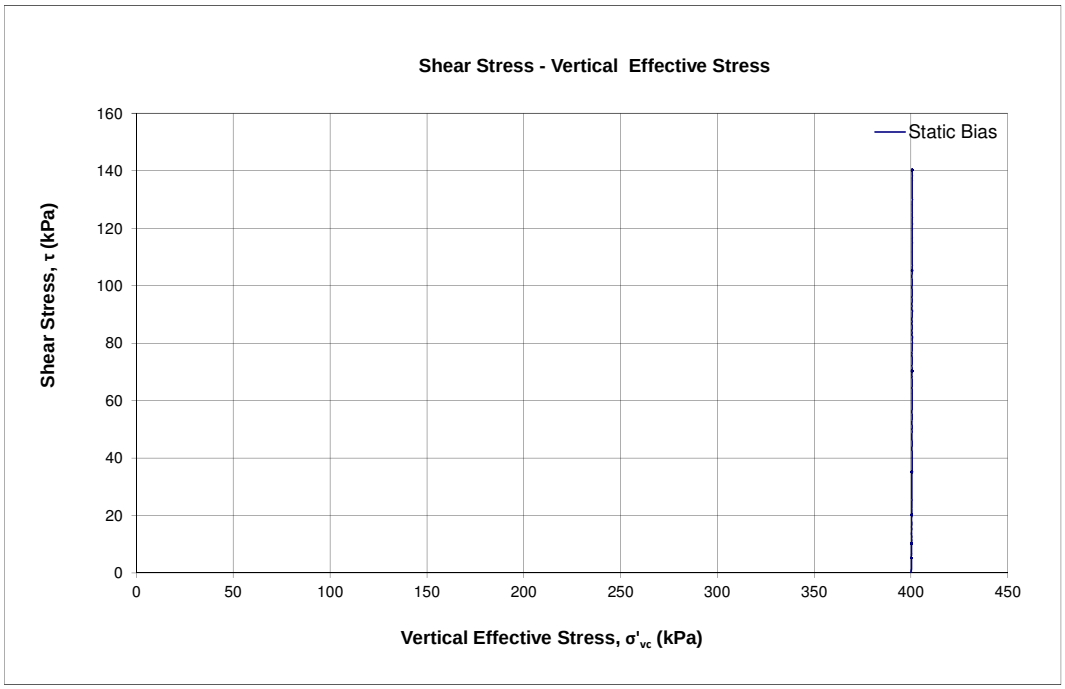

Cyclic Direct Simple Shear Test (ASTM D6528)

Cyclic Shearing Phase

Project No.:		Test No.:	DSS14
Project:	Fundão Tailings Dam Review Panel	Sample ID:	PSD 1
Date:	2016-05-15	Depth:	
Tested by:	BY	Location:	
Checked by:	JG	Details:	Sand tailings sample with fines

τ_{cy} / σ'_{vc} =0.002 σ'_{vc} = 400 kPa

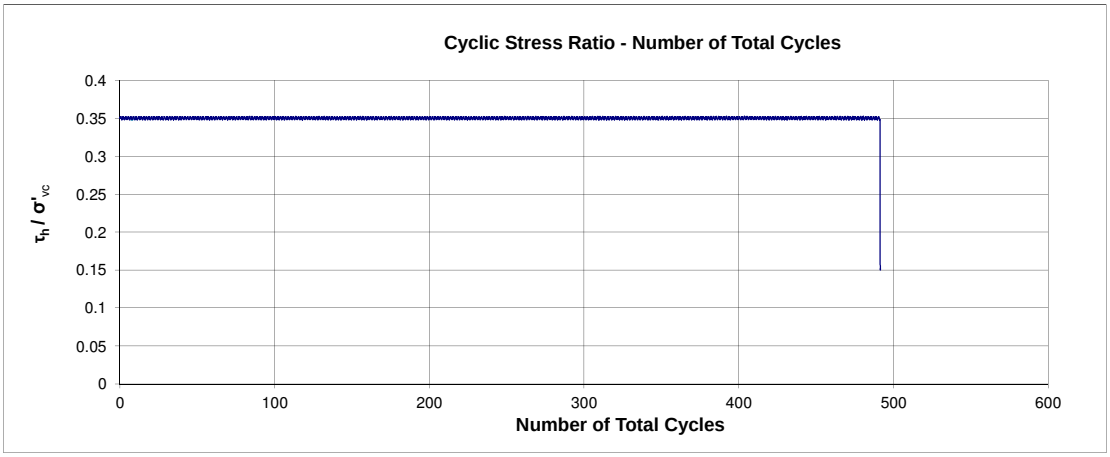

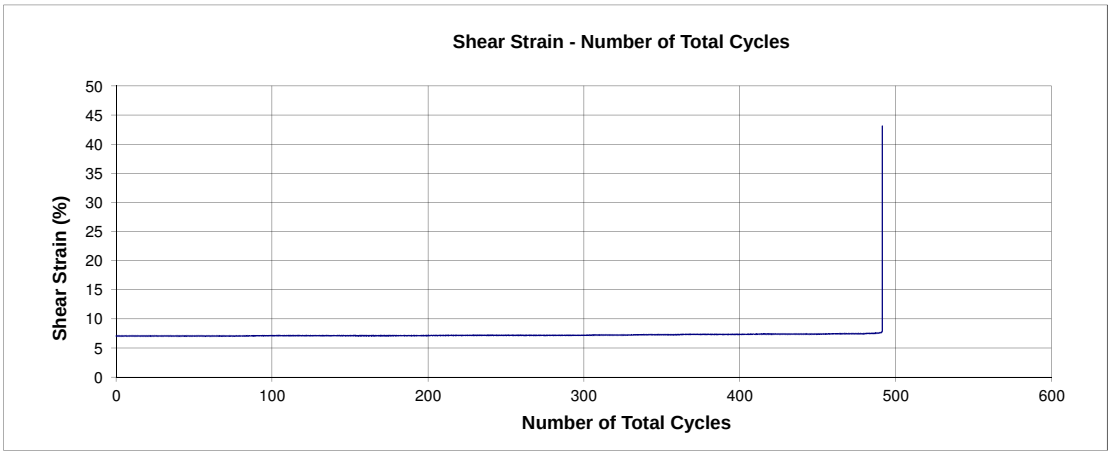

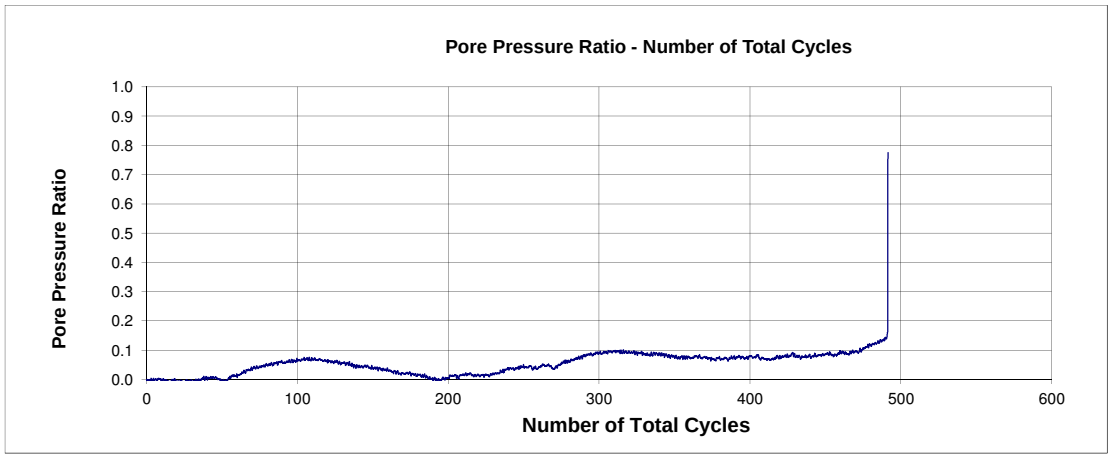

Cyclic Direct Simple Shear Test (ASTM D6528)

Cyclic Shearing Phase

Project No.:		Test No.:	DSS14
Project:	Fundão Tailings Dam Review Panel	Sample ID:	PSD 1
Date:	2016-05-15	Depth:	
Tested by:	BY	Location:	
Checked by:	JG	Details:	Sand tailings sample with fines

$\tau_{cy} / \sigma'_{vc} = 0.002$ $\sigma'_{vc} = 400$ kPa

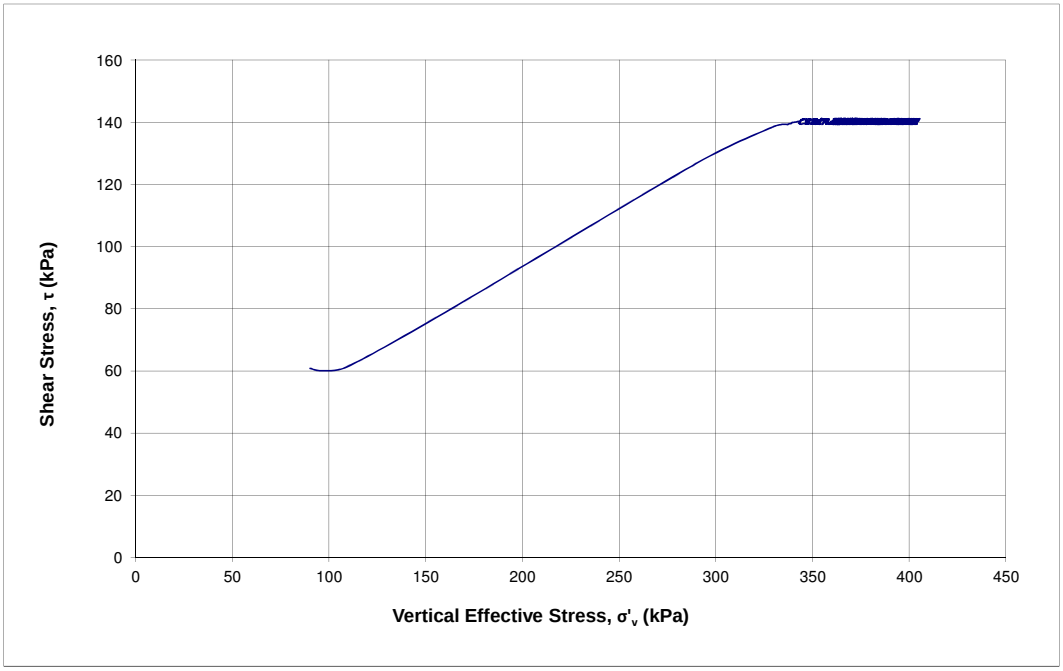

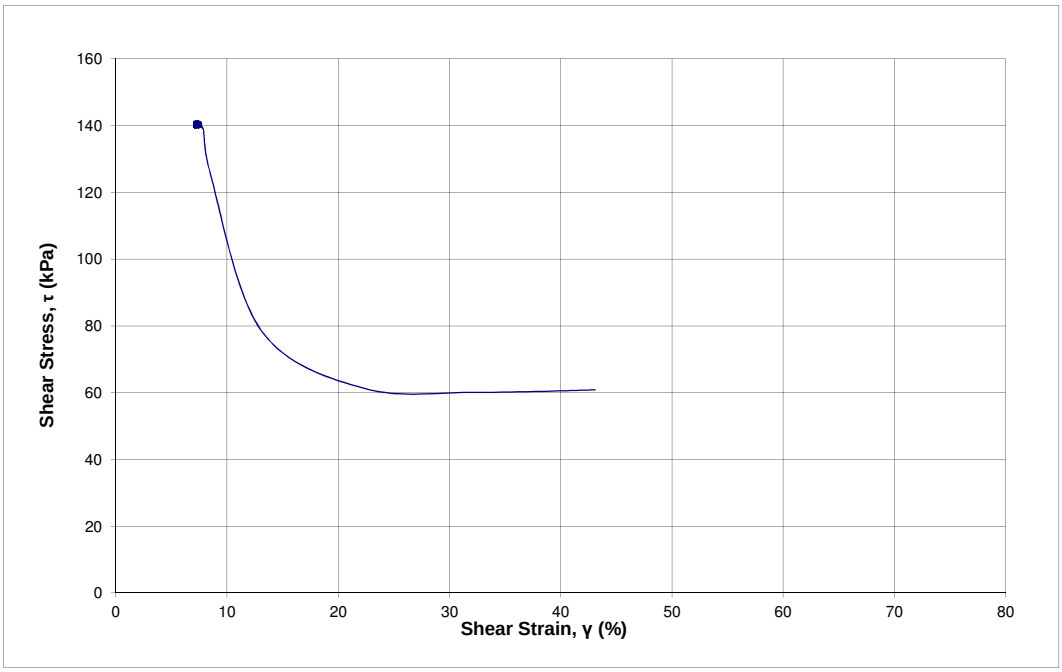

Static Simple Shear Test (Multistage)

(ASTM D6528)

Klohn Crippen Berger

Project No.:		Borehole ID:	DSS15
Project:	Fundão Tailings Dam Review Panel	Sample ID:	Slimes
Date:	2016-06-21	Depth:	
Tested by:	BY	Description:	Slimes
Checked by:	JG	Preparation Method:	Reconstituted Slurry

Initial Sample Information		
Specimen Height	mm	27.78
Specimen Diameter	mm	70.54
Area	mm^2	3908.06
Volume	cm^3	108.57
Wet Weight	g	223.93
Water Content	%	45.41
Dry Weight	g	154.00
Wet Density	g/cm^3	2.063
Dry Density	g/cm^3	1.418
Specific Gravity (assumed)	-	3.93
Void Ratio (e)	-	1.78
Saturation Ratio (Sr)	%	100.79

Static Shearing (Undrained)		
Initial Vertical Effective Stress	kPa	300.1
Initial Shear Stress	kPa	0.2
Shearing Rate (Shear Strain Rate	% / hr	5.00
Peak Shear Strength	kPa	47.65
Ratio of Peak τ / σ'_v	-	0.16
Max. Excess Pore Pressure	kPa	297.54
Max. Shear Strain	%	20.0

FINAL SAMPLE INFORMATION		
Final Moisture Content	%	23.86

CONSOLIDATION									
Vertical Effective Stress	kPa	3	6	13	25	50	100	200	300
Max Load	kN	0.012	0.024	0.049	0.098	0.196	0.391	0.782	1.173
Total Height Change	mm	0.43	3.93	5.17	6.29	7.15	7.88	8.54	8.86
Consolidated Height	%	27.35	23.85	22.61	21.49	20.63	19.90	19.24	18.92
Axial Strain*1	%	1.54	14.13	18.60	22.64	25.73	28.38	30.73	31.89
Duration	min	240	240	240	240	240	240	240	1250

*1 : Axial strain may differ from oedometer test result due to the sample seating system and possible lateral strain caused by the membrane.

Photos:

Before Test




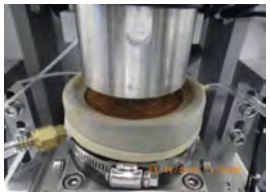

After Test


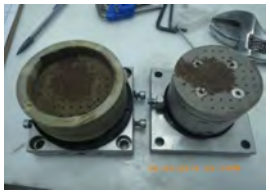
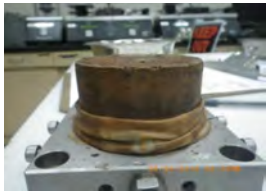


Static Simple Shear Test (Multistage)

(ASTM D6528)

Project No.:		Borehole ID:	DSS15
Project:	Fundão Tailings Dam Review Panel	Sample ID:	Slimes
Date:	2016-06-21	Depth:	
Tested by:	BY	Description:	Slimes
Checked by:	JG	Preparation Method:	Reconstituted Slurry

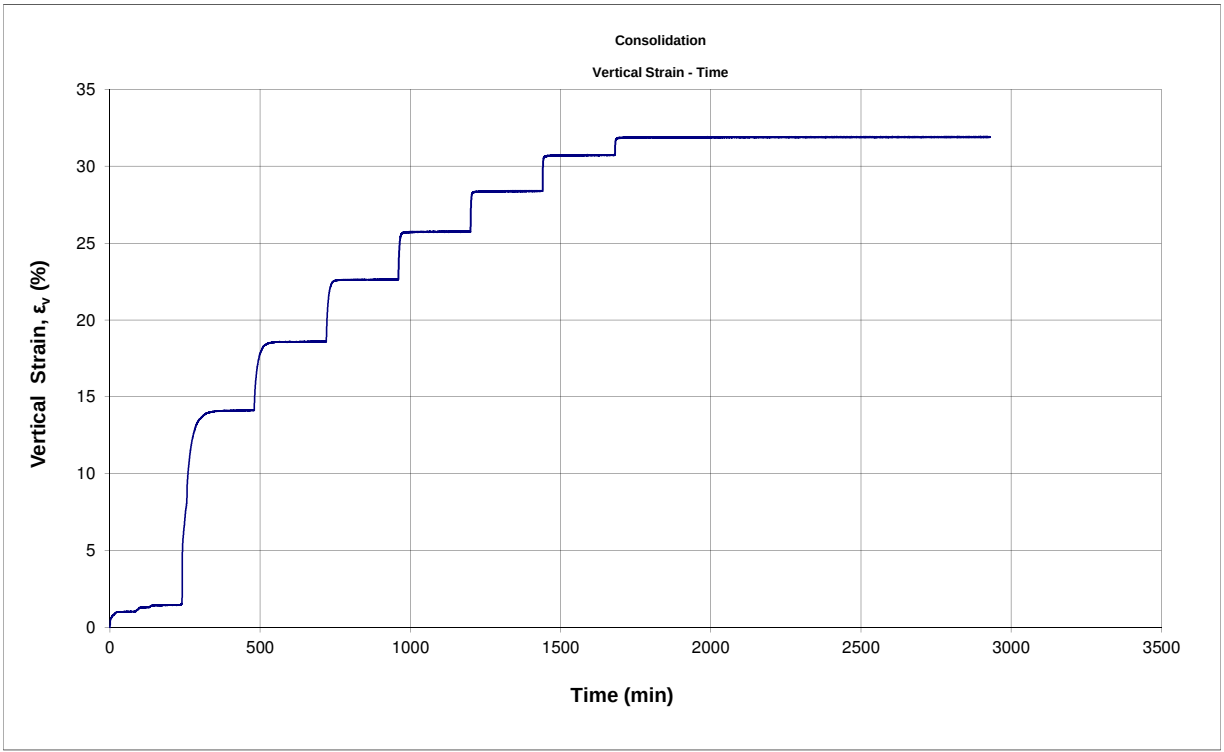

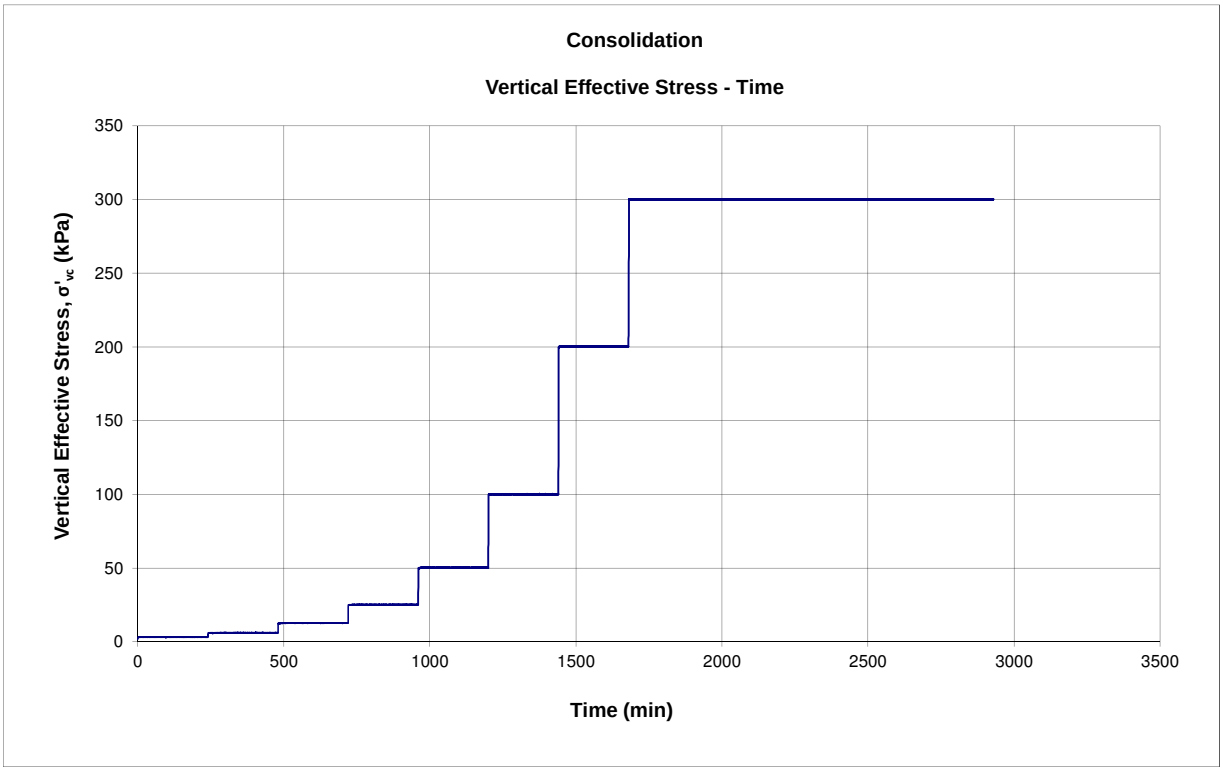

Static Simple Shear Test (Multistage)

(ASTM D6528)

Project No.:		Borehole ID:	DSS15
Project:	Fundão Tailings Dam Review Panel	Sample ID:	Slimes
Date:	2016-06-21	Depth:	
Tested by:	BY	Description:	Slimes
Checked by:	JG	Preparation Method:	Reconstituted Slurry

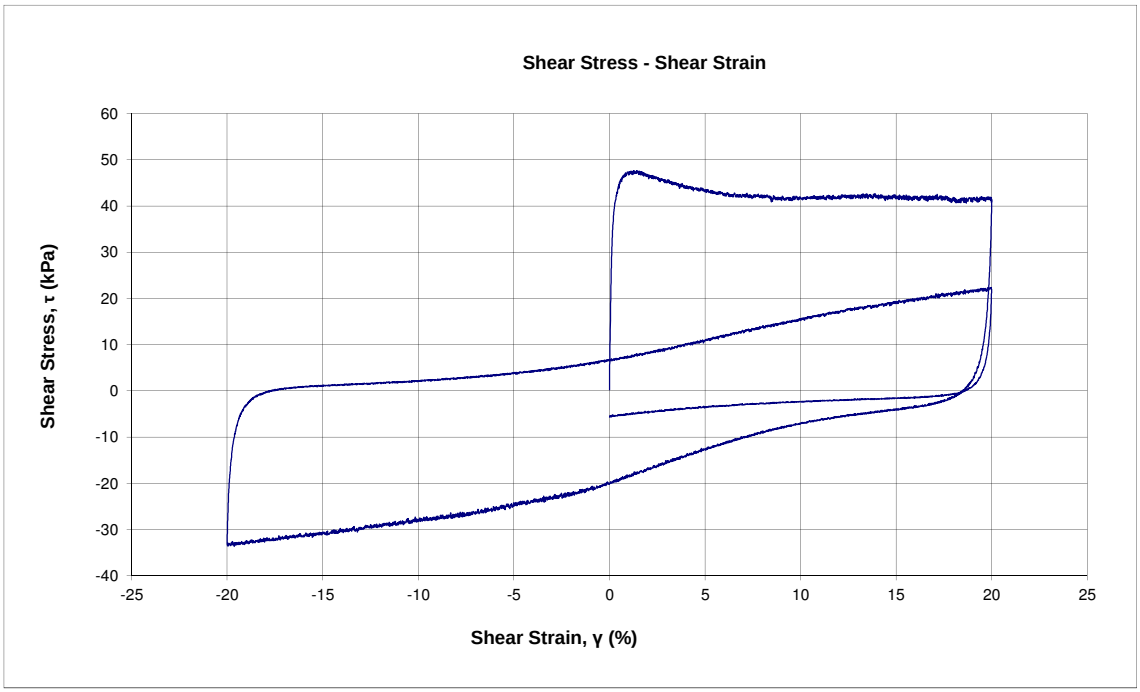

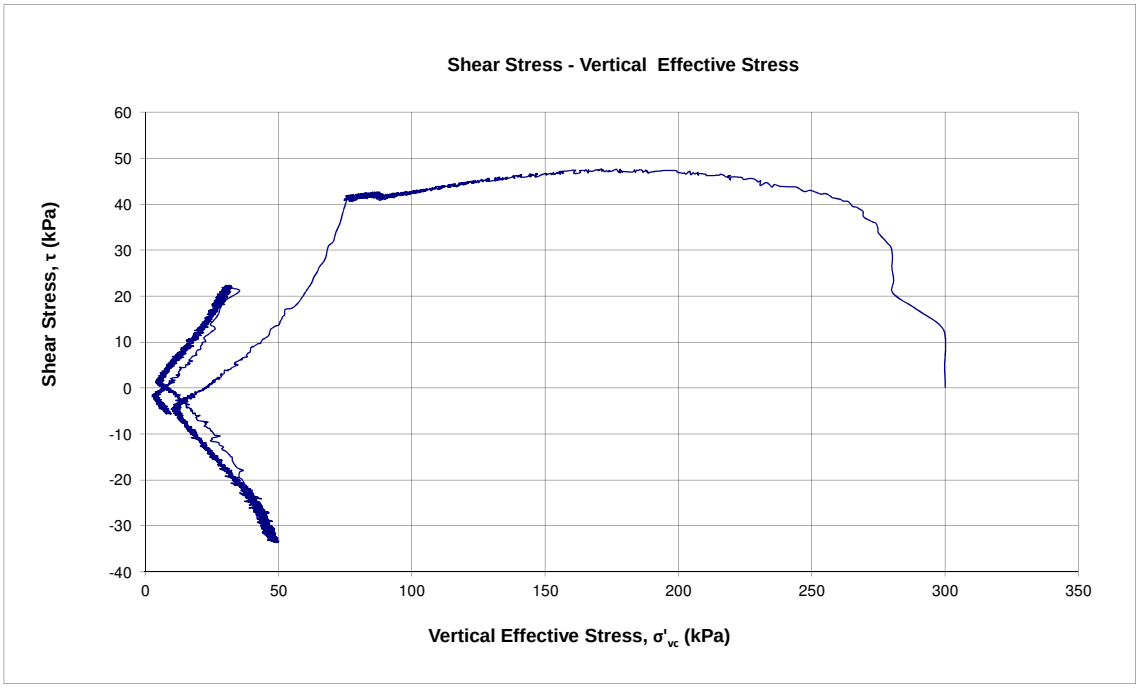

Klohn Crippen Berger

Static Simple Shear Test (Multistage)

(ASTM D6528)

Project No.:		Borehole ID:	DSS15
Project:	Fundão Tailings Dam Review Panel	Sample ID:	Slimes
Date:	2016-06-21	Depth:	
Tested by:	BY	Description:	Slimes
Checked by:	JG	Preparation Method:	Reconstituted Slurry

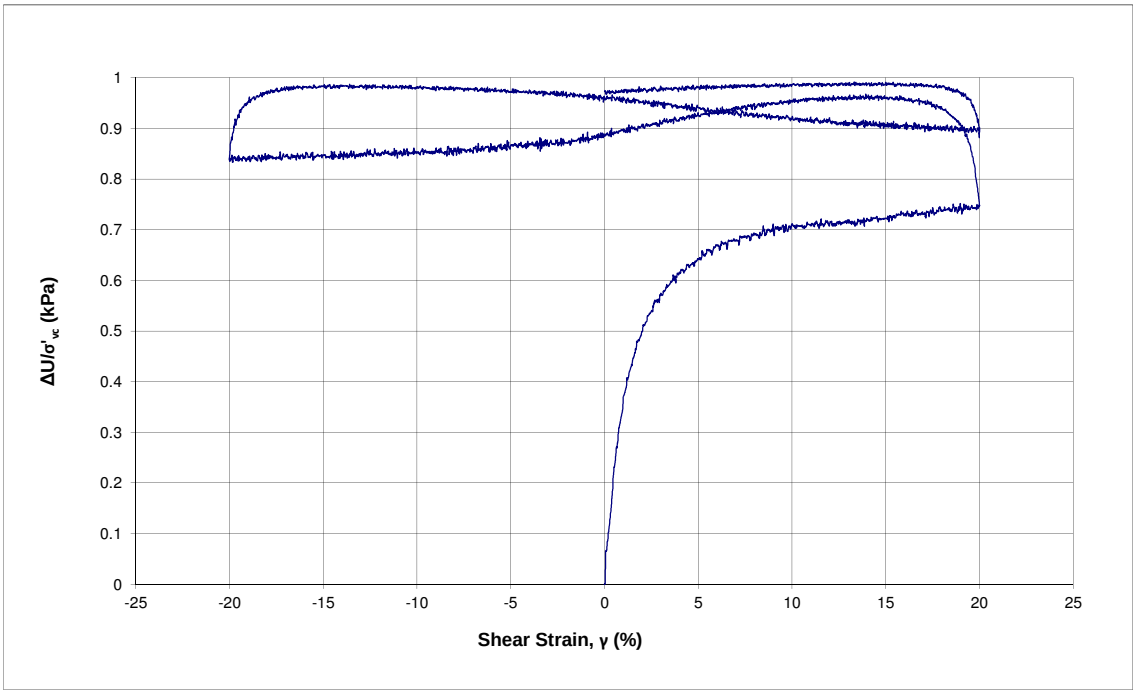

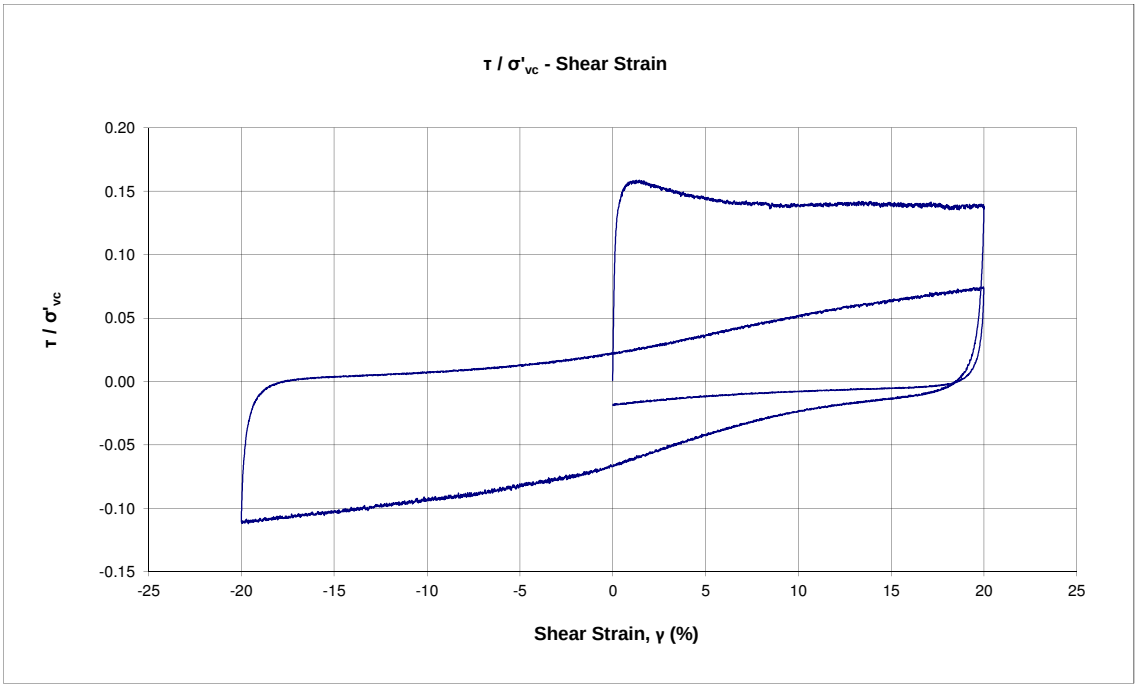

ATTACHMENT D6

Triaxial Test Data by KCB

Klohn Crippen Berger

Triaxial CID Test - Summary

(ASTM D7181)

PROJECT NO. :
PROJECT : Fundão Tailings Dam Review Panel
SAMPLE : PSD 1
TEST ID : TX 1

DATE : 2016-03-10
TESTED BY: BY
CHECKED BY: JG
TEST TYPE: CID

SPECIMEN INFORMATION	UNITS	Initial	After Vacuum	Saturation	B-Value	End of 1st Consolidation	End of 2 nd Consolidation	End of 3 rd Consolidation	End of 4th Consolidation	At Failure	End of Shear
Specimen Height	mm	138.53	138.08	131.27	130.77	130.14	129.77	129.31	128.85	103.32	90.22
Specimen Diameter	mm	69.27	68.79	65.56	65.40	65.10	64.84	64.58	64.24	69.89	74.76
Area	cm^2	37.69	37.17	33.76	33.60	33.28	33.02	32.76	32.41	38.36	43.89
Volume	cm^3	522.07	513.18	443.18	439.33	433.16	428.46	423.57	417.58	396.31	396.00
Wet Weight	g	722.99	722.99	885.99	894.69	888.52	883.82	878.93	872.94	851.67	851.36
Water Content	%	5.10	5.10	28.75	30.01	29.12	28.43	27.72	26.85	23.76	23.72
Dry Weight	g	688.16	688.16	688.16	688.16	688.16	688.16	688.16	688.16	688.16	688.16
Wet Density	g/cm^3	1.385	1.409	1.999	2.036	2.051	2.063	2.075	2.090	2.149	2.150
Dry Density	g/cm^3	1.318	1.341	1.553	1.566	1.589	1.606	1.625	1.648	1.736	1.738
Specific Gravity of Solids	-	2.98	2.98	2.98	2.98	2.98	2.98	2.98	2.98	2.98	2.98
Solids Volume	cm^3	230.926	230.926	230.926	230.926	230.926	230.926	230.926	230.926	230.926	230.926
Void Volume	cm^3	291.139	282.257	212.257	208.407	202.237	197.537	192.647	186.657	165.387	165.077
Water Volume	cm^3	34.830	34.830	197.830	206.530	200.360	195.660	190.770	184.780	163.510	163.200
Void Ratio (e)	-	1.261	1.222	0.919	0.902	0.876	0.855	0.834	0.808	0.716	0.715
Saturation Ratio (Sr)	%	11.96	12.34	93.20	99.10	99.07	99.05	99.03	98.99	98.87	98.86
Effective Confining Stress	kPa					37.5	75	150	300		

Shearing (CID)		
Skempton's B Parameter		1.00
Back Pressure before shearing	kPa	566.9
Confining Stress (σ_3') before shearing	kPa	300
Shear Strain Rate	% / min	0.1
Deviator Stress at Failure*	kPa	747.19
Axial Strain* at Failure	%	19.82

* From Maximum Deviator Stress

Photos:

Before Test

After Test

Klohn Crippen Berger

Triaxial CID Test - Charts

(ASTM D7181)

PROJECT NO. :
PROJECT : Fundão Tailings Dam Review Panel
SAMPLE : PSD 1
TEST ID: TX 1
TEST TYPE: CID
DATE : 2016-03-10
TESTED BY: BY
CHECKED BY: JG

At Max. Deviator Stress:	
Axial Stain (%)	**19.82**
Deviator Stress (kPa)	**747.2**

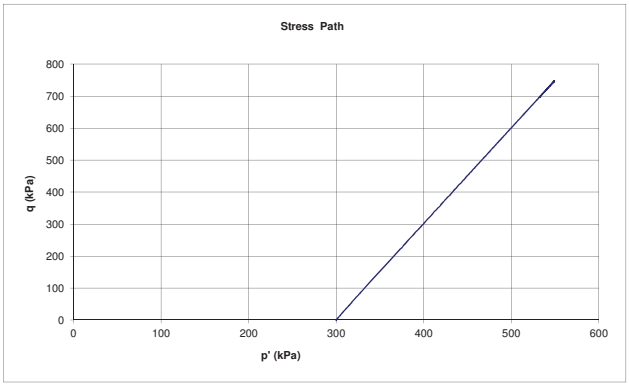

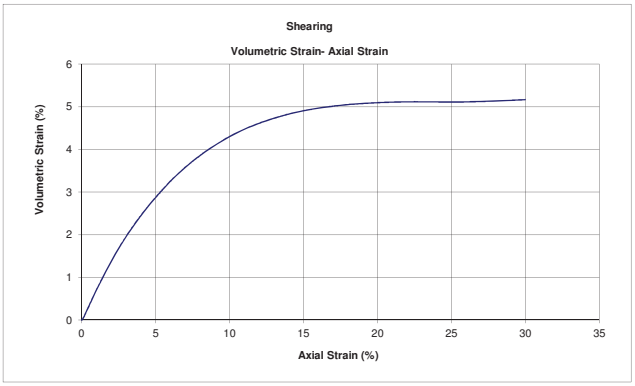

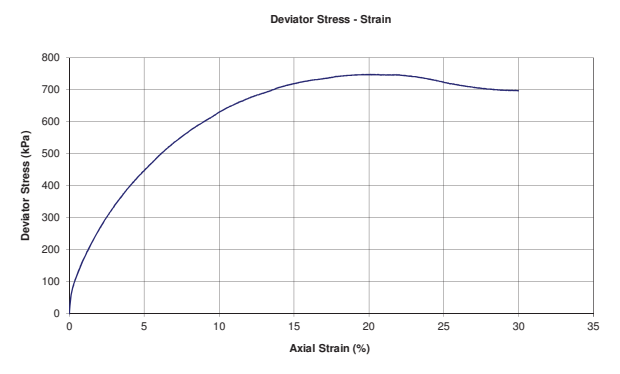

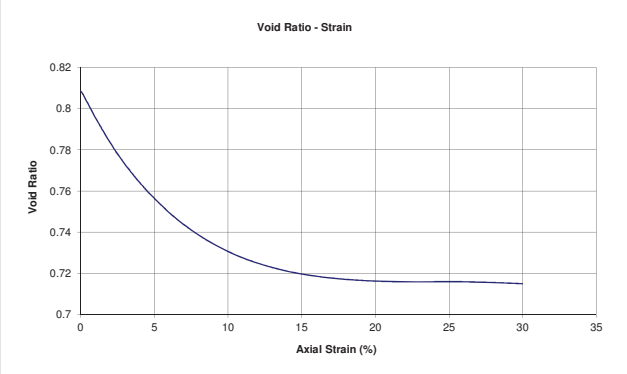

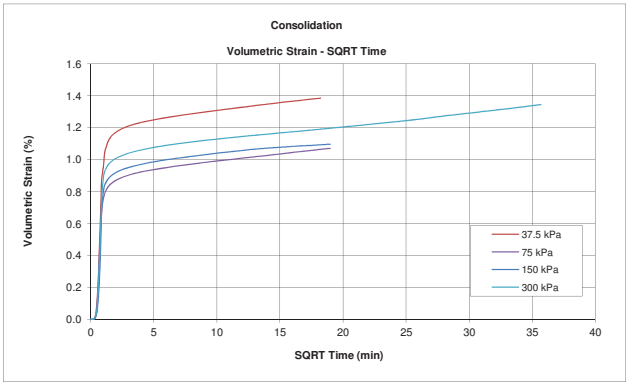

Triaxial CIU Test - Summary
(ASTM D4767)

PROJECT NO. :
PROJECT : Fundão Tailings Dam Review Panel
SAMPLE : PSD 1
TEST ID: TX 2

DATE : 2016-03-15
TESTED BY: BY
CHECKED BY: JG
TEST TYPE: CIU

SPECIMEN INFORMATION	UNITS	Initial	After Vacuum	Saturation	B-Value	End of 1 st Consolidation	End of 2 nd Consolidation	End of 3 rd Consolidation	At Failure	End of Shear
Specimen Height	mm	138.38	138.38	132.36	131.31	131.12	130.86	130.41	129.97	96.63
Specimen Diameter	mm	69.06	68.66	65.45	64.90	64.76	64.62	64.36	64.47	74.77
Area	cm^2	37.46	37.03	33.65	33.08	32.94	32.79	32.53	32.64	43.91
Volume	cm^3	518.34	512.36	445.36	434.36	431.87	429.14	424.26	424.26	424.26
Wet Weight	g	718.28	718.28	875.58	884.46	881.97	879.24	874.36	874.36	874.36
Water Content	%	5.13	5.13	28.15	29.45	29.09	28.69	27.97	27.97	27.97
Dry Weight	g	683.23	683.23	683.23	683.23	683.23	683.23	683.23	683.23	683.23
Wet Density	g/cm^3	1.386	1.402	1.966	2.036	2.042	2.049	2.061	2.061	2.061
Dry Density	g/cm^3	1.318	1.334	1.534	1.573	1.582	1.592	1.610	1.610	1.610
Specific Gravity of Solids	-	2.96	2.96	2.96	2.96	2.96	2.96	2.96	2.96	2.96
Solids Volume	cm^3	230.821	230.821	230.821	230.821	230.821	230.821	230.821	230.821	230.821
Void Volume	cm^3	287.522	281.535	214.535	203.535	201.045	198.316	193.440	193.440	193.440
Water Volume	cm^3	35.050	35.050	192.350	201.226	198.736	196.007	191.131	191.131	191.131
Void Ratio (e)	-	1.246	1.220	0.929	0.882	0.871	0.859	0.838	0.838	0.838
Saturation Ratio (Sr)	%	12.19	12.45	89.66	98.87	98.85	98.84	98.81	98.81	98.81
Effective Confining Stress	kPa					50	100	200		

Shearing (CU)		
Skempton's B Parameter		0.99
Back Pressure before shearing	kPa	813.1
Confining Stress (σ_3') before shearing	kPa	200
Shear Strain Rate	% / min	0.1
Deviator Stress at Failure*	kPa	68
Axial Strain* at Failure	%	0.33

* From Maximum Deviator Stress

Photos:

Before Test




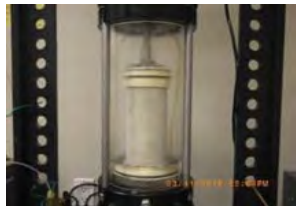

After Test




Klohn Crippen Berger

Triaxial CIU Test - Charts

(ASTM D4767)

PROJECT NO. :
PROJECT : Fundão Tailings Dam Review Panel
SAMPLE : PSD 1
TEST ID: TX 2
TEST TYPE: CIU
DATE : 2016-03-15
TESTED BY: BY
CHECKED BY: JG

At Max. Deviator Stress:	
Axial Stain (%)	**0.33**
Deviator Stress (kPa)	**68.0**

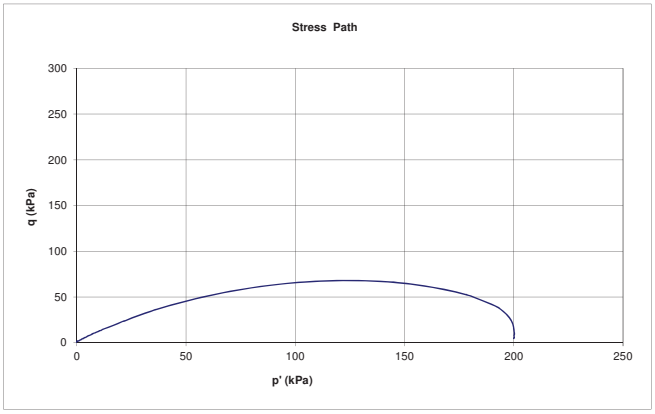

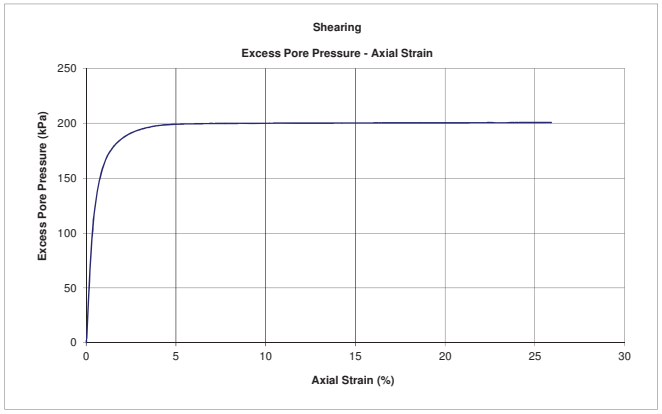

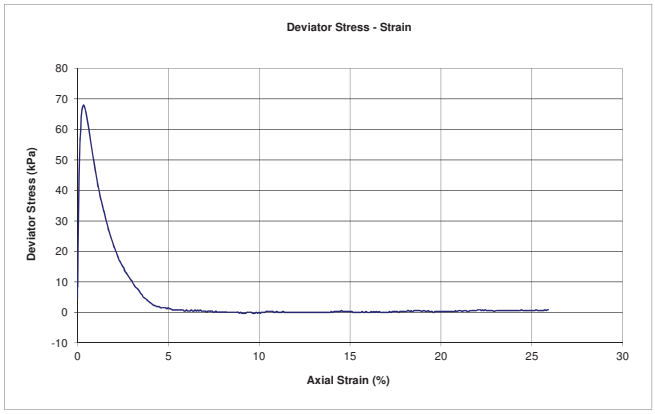

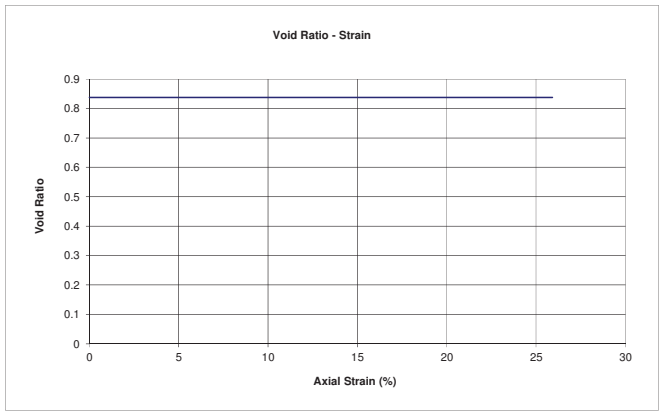

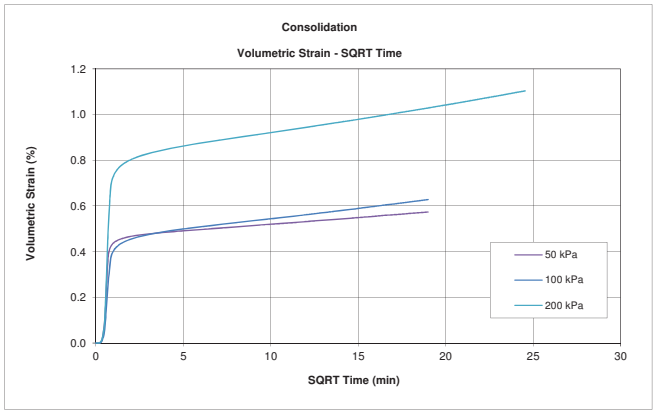

Klohn Crippen Berger

Triaxial CIU Test - Summary

(ASTM D4767)

PROJECT NO. :
PROJECT : Fundão Tailings Dam Review Panel
SAMPLE : PSD 2
TEST ID: TX 3

DATE : 2016-03-15
TESTED BY: BY
CHECKED BY: JG
TEST TYPE: CIU

SPECIMEN INFORMATION	UNITS	Initial	After Vacuum	Saturation	B-Value	End of 1 st Consolidation	End of 2 nd Consolidation	End of 3 rd Consolidation	At Failure	End of Shear
Specimen Height	mm	139.10	139.10	139.10	139.02	138.94	138.83	138.70	132.23	99.44
Specimen Diameter	mm	69.08	68.70	68.192	68.14	68.08	68.02	67.93	69.57	80.22
Area	cm^2	37.48	37.07	36.52	36.47	36.41	36.34	36.24	38.01	50.54
Volume	cm^3	521.342	515.622	508.015	507.015	505.825	504.475	502.618	502.618	502.618
Wet Weight	g	750.94	750.94	952.64	960.44	959.25	957.90	956.05	956.05	956.05
Water Content	%	5.35	5.35	33.52	34.62	34.45	34.26	34.00	34.00	34.00
Dry Weight	g	713.47	713.47	713.47	713.47	713.47	713.47	713.47	713.47	713.47
Wet Density	g/cm^3	1.440	1.456	1.875	1.894	1.896	1.899	1.902	1.902	1.902
Dry Density	g/cm^3	1.369	1.384	1.404	1.407	1.411	1.414	1.420	1.420	1.420
Specific Gravity of Solids	-	2.75	2.75	2.75	2.75	2.75	2.75	2.75	2.75	2.75
Solids Volume	cm^3	259.444	259.444	259.444	259.444	259.444	259.444	259.444	259.444	259.444
Void Volume	cm^3	261.898	256.178	248.571	247.571	246.381	245.031	243.174	243.174	243.174
Water Volume	cm^3	37.470	37.470	239.170	246.974	245.784	244.434	242.577	242.577	242.577
Void Ratio (e)	-	1.009	0.987	0.958	0.954	0.950	0.944	0.937	0.937	0.937
Saturation Ratio (Sr)	%	14.31	14.63	96.22	99.76	99.76	99.76	99.75	99.75	99.75
Effective Confining Stress	kPa					50	100	200		

Shearing (CIU)		
Skempton's B Parameter		1.00
Back Pressure before shearing	kPa	803.6
Confining Stress (σ_3') before shearing	kPa	200
Shear Strain Rate	% / min	0.1
Deviator Stress at Failure*	kPa	219
Axial Strain* at Failure	%	4.67

* From Maximum Deviator Stress

Photos:

Before Test




After Test




Klohn Crippen Berger

Triaxial CIU Test - Charts

(ASTM D4767)

PROJECT NO. :
PROJECT : Fundão Tailings Dam Review Panel
SAMPLE : PSD 2
TEST ID: TX 3
TEST TYPE: CIU
DATE : 2016-03-15
TESTED BY: BY
CHECKED BY: JG

At Max. Deviator Stress:	
Axial Stain (%)	**4.67**
Deviator Stress (kPa)	**219.3**

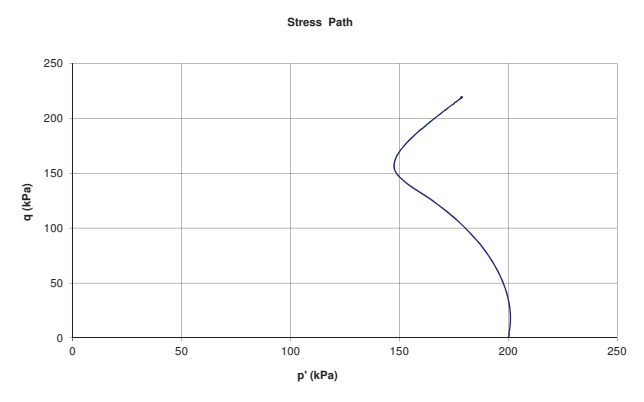

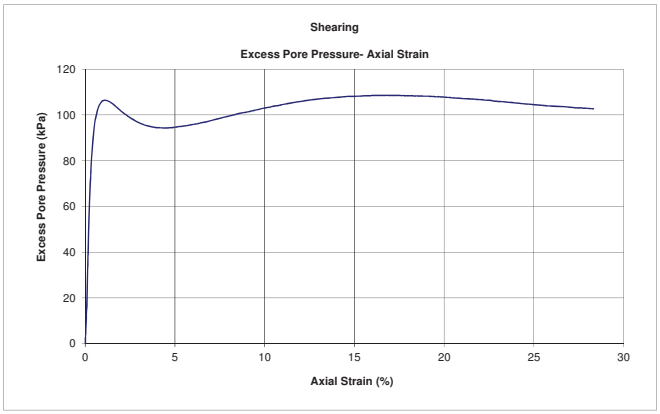

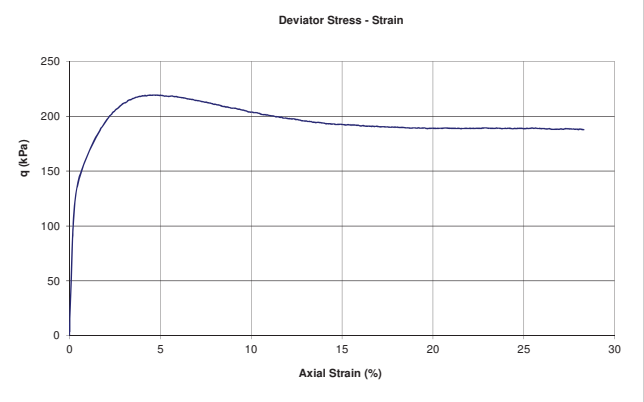

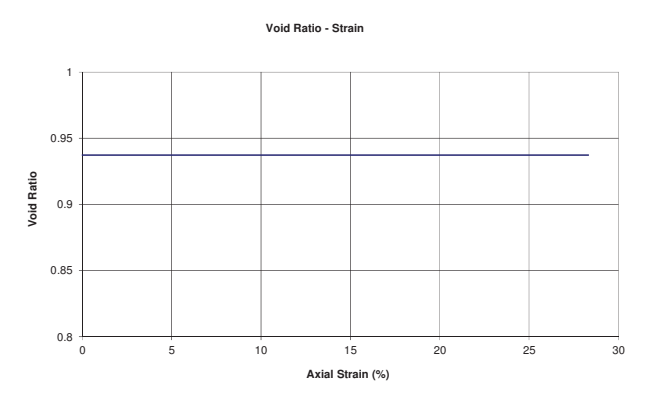

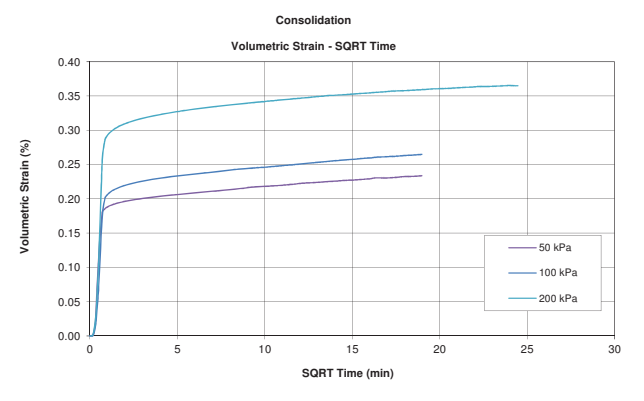

Klohn Crippen Berger

Triaxial CIU Test - Summary

(ASTM D4767)

PROJECT NO. :
PROJECT : Fundão Tailings Dam Review Panel
SAMPLE : PSD 1
TEST ID: TX 4

DATE : 2016-03-19
TESTED BY: BY
CHECKED BY: JG
TEST TYPE: CIU

SPECIMEN INFORMATION	UNITS	Initial	After Vacuum	Saturation	B-Value	End of 1 st Consolidation	End of 2 nd Consolidation	End of 3 rd Consolidation	End of 4 th Consolidation	End of 5 th Consolidation	At Failure	End of Shear
Specimen Height	mm	138.46	138.46	132.60	132.27	131.99	131.65	131.25	130.77	130.43	129.61	90.56
Specimen Diameter	mm	69.08	68.66	66.21	66.04	65.85	65.71	65.48	65.22	65.01	65.21	78.02
Area	cm^2	37.48	37.03	34.43	34.25	34.06	33.91	33.67	33.40	33.19	33.40	47.80
Volume	cm^3	518.94	512.65	456.56	453.06	449.52	446.47	441.97	436.83	432.91	432.91	432.91
Wet Weight	g	747.94	747.94	915.44	919.33	915.79	912.74	908.24	903.10	899.18	899.18	899.18
Water Content	%	4.95	4.95	28.74	29.28	28.78	28.36	27.72	27.00	26.45	26.45	26.45
Dry Weight	g	711.10	711.10	711.10	711.10	711.10	711.10	711.10	711.10	711.10	711.10	711.10
Wet Density	g/cm^3	1.441	1.459	2.005	2.029	2.037	2.044	2.055	2.067	2.077	2.077	2.077
Dry Density	g/cm^3	1.370	1.387	1.558	1.570	1.582	1.593	1.609	1.628	1.643	1.643	1.643
Specific Gravity of Solids	-	2.95	2.95	2.95	2.95	2.95	2.95	2.95	2.95	2.95	2.95	2.95
Solids Volume	cm^3	241.051	241.051	241.051	241.051	241.051	241.051	241.051	241.051	241.051	241.051	241.051
Void Volume	cm^3	277.892	271.601	215.507	212.007	208.467	205.417	200.917	195.777	191.857	191.857	191.857
Water Volume	cm^3	36.840	36.840	204.340	208.230	204.690	201.640	197.140	192.000	188.080	188.080	188.080
Void Ratio (e)	-	1.153	1.127	0.894	0.880	0.865	0.852	0.834	0.812	0.796	0.796	0.796
Saturation Ratio (Sr)	%	13.26	13.56	94.82	98.22	98.19	98.16	98.12	98.07	98.03	98.03	98.03
Effective Confining Stress	kPa					50	100	200	400	600		

Shearing (CIU)		
Skempton's B Parameter		1.00
Back Pressure before shearing	kPa	655
Confining Stress (σ_3') before shearing	kPa	600
Shear Strain Rate	% / min	0.1
Deviator Stress at Failure*	kPa	225
Axial Strain* at Failure	%	0.63

* From Maximum Deviator Stress

Photos:

Before Test




After Test

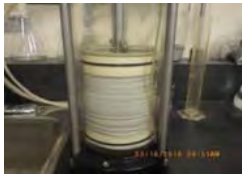


Klohn Crippen Berger

Triaxial CIU Test - Charts

(ASTM D4767)

PROJECT NO. :
PROJECT : Fundão Tailings Dam Review Panel
SAMPLE : PSD 1
TEST ID: TX 4
TEST TYPE: CIU
DATE : 2016-03-19
TESTED BY: BY
CHECKED BY: JG

At Max. Deviator Stress:	
Axial Stain (%)	**0.63**
Deviator Stress (kPa)	**224.9**

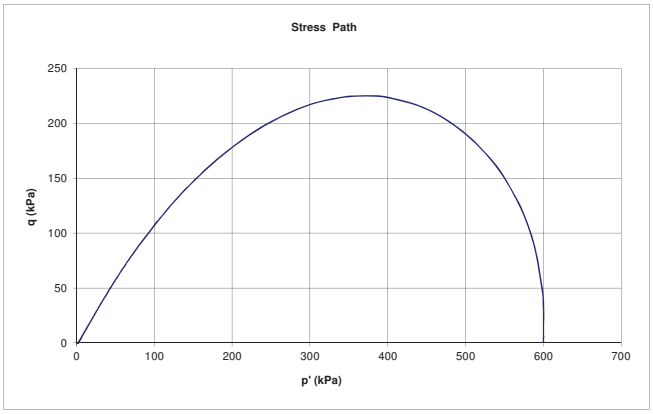

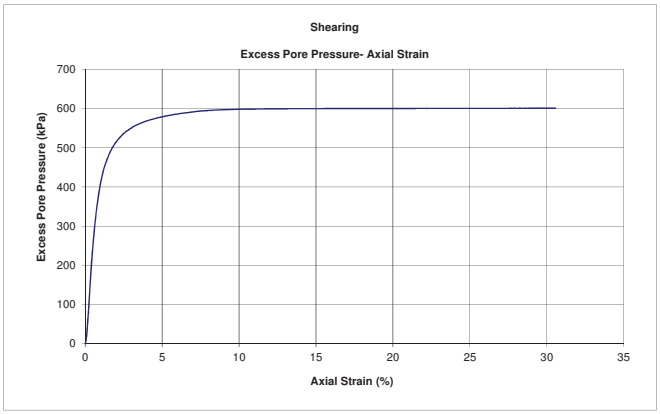

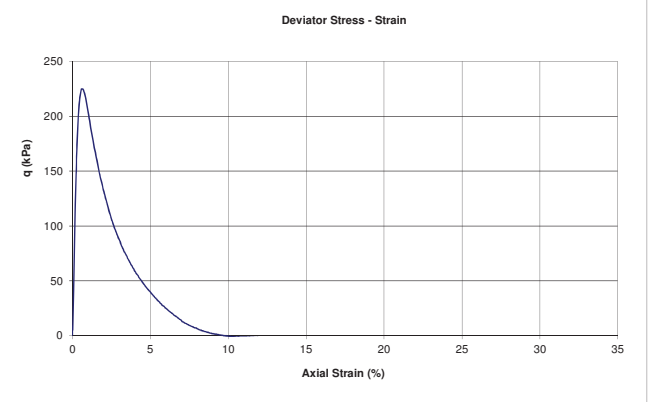

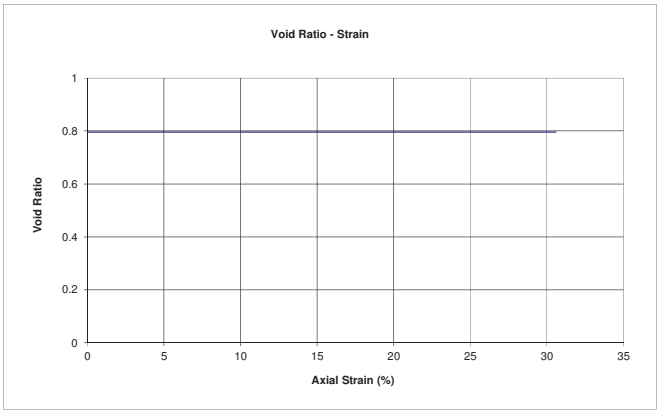

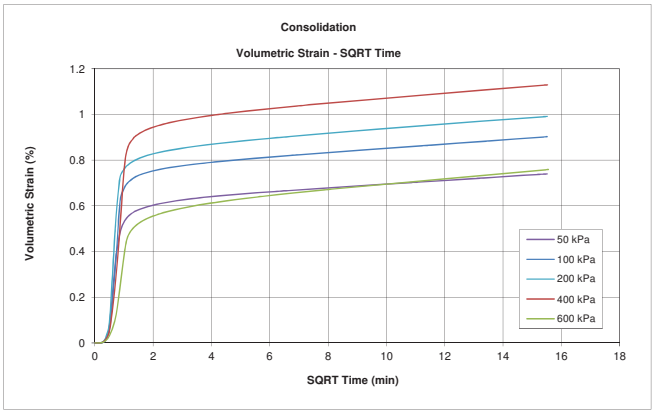

Klohn Crippen Berger

Triaxial CIU Test - Summary

(ASTM D4767)

PROJECT NO. :
PROJECT : Fundão Tailings Dam Review Panel
SAMPLE : PSD 2
TEST ID: TX 5

DATE : 2016-03-19
TESTED BY: BY
CHECKED BY: JG
TEST TYPE: CIU

SPECIMEN INFORMATION	UNITS	Initial	After Vacuum	Saturation	B-Value	End of 1 st Consolidation	End of 2 nd Consolidation	End of 3 rd Consolidation	End of 4 th Consolidation	End of 5 th Consolidation	At Failure	End of Shear
Specimen Height	mm	138.69	138.69	138.69	138.48	138.41	138.31	138.18	137.97	137.82	136.47	95.01
Specimen Diameter	mm	69.06	68.75	68.22	68.22	68.12	68.02	67.89	67.73	67.56	67.89	81.37
Area	cm^2	37.46	37.12	36.56	36.55	36.45	36.34	36.20	36.03	35.85	36.20	52.00
Volume	cm^3	519.50	514.85	506.99	506.13	504.44	502.65	500.21	497.09	494.06	494.06	494.06
Wet Weight	g	748.23	748.23	944.23	957.01	955.32	953.54	951.10	947.98	944.95	944.95	944.95
Water Content	%	5.05	5.05	32.98	34.78	34.54	34.29	33.95	33.51	33.08	33.08	33.08
Dry Weight	g	710.06	710.06	710.06	710.06	710.06	710.06	710.06	710.06	710.06	710.06	710.06
Wet Density	g/cm^3	1.440	1.453	1.862	1.891	1.894	1.897	1.901	1.907	1.913	1.913	1.913
Dry Density	g/cm^3	1.367	1.379	1.401	1.403	1.408	1.413	1.420	1.428	1.437	1.437	1.437
Specific Gravity of Solids	-	2.74	2.74	2.74	2.74	2.74	2.74	2.74	2.74	2.74	2.74	2.74
Solids Volume	cm^3	259.146	259.146	259.146	259.146	259.146	259.146	259.146	259.146	259.146	259.146	259.146
Void Volume	cm^3	260.358	255.705	247.840	246.980	245.290	243.505	241.065	237.945	234.915	234.915	234.915
Water Volume	cm^3	38.170	38.170	234.170	246.950	245.260	243.475	241.035	237.915	234.885	234.885	234.885
Void Ratio (e)	-	1.005	0.987	0.956	0.953	0.947	0.940	0.930	0.918	0.906	0.906	0.906
Saturation Ratio (Sr)	%	14.66	14.93	94.48	99.99	99.99	99.99	99.99	99.99	99.99	99.99	99.99
Effective Confining Stress	kPa					50	100	200	400	600		

Shearing (CIU)		
Skempton's B Parameter		1.00
Back Pressure before shearing	kPa	704
Confining Stress (σ_3') before shearing	kPa	600
Shear Strain Rate	% / min	0.1
Deviator Stress at Failure*	kPa	337
Axial Strain* at Failure	%	0.98

* From Maximum Deviator Stress

Photos:

Before Test

After Test

Klohn Crippen Berger

Triaxial CIU Test - Charts

(ASTM D4767)

PROJECT NO. :
PROJECT : Fundão Tailings Dam Review Panel
SAMPLE : PSD 2
TEST ID: TX 5
TEST TYPE: CIU
DATE : 2016-03-19
TESTED BY: BY
CHECKED BY: JG

At Max. Deviator Stress:	
Axial Stain (%)	**0.98**
Deviator Stress (kPa)	**336.8**

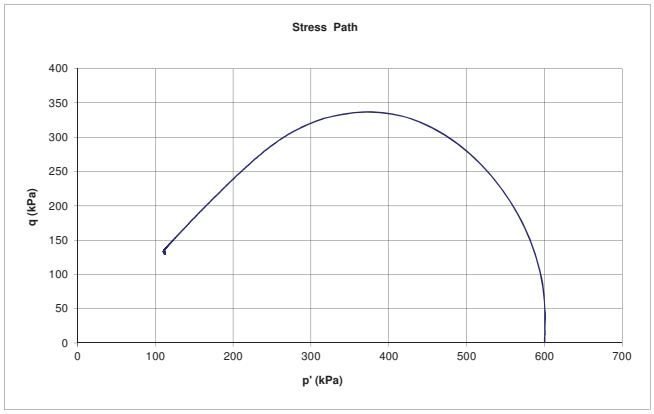

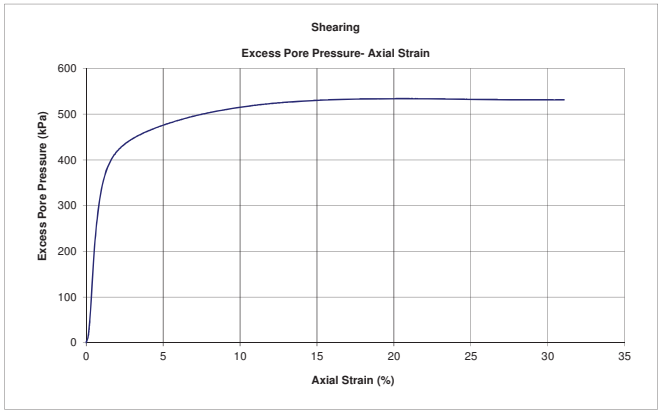

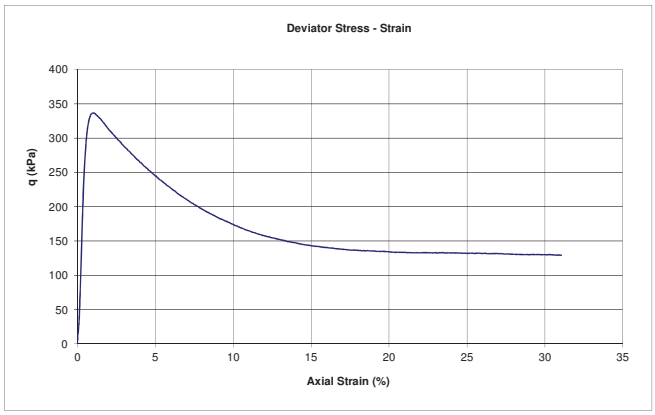

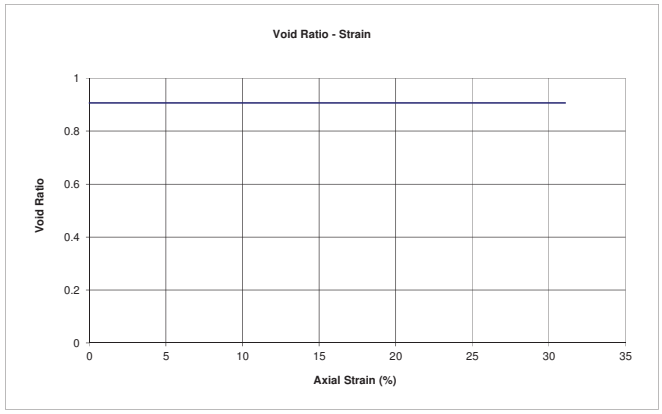

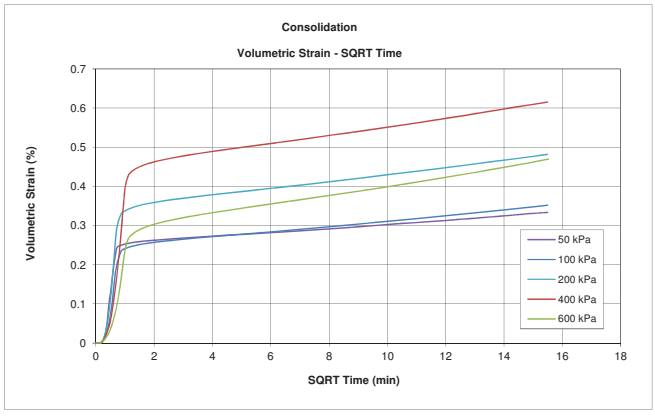

Klohn Crippen Berger

Triaxial CIU Test - Summary
(ASTM D4767)

PROJECT NO. :
PROJECT : Fundão Tailings Dam Review Panel
SAMPLE : PSD 1
TEST ID: TX 6

DATE : 2016-03-25
TESTED BY: BY
CHECKED BY: JG
TEST TYPE: CIU

SPECIMEN INFORMATION	UNITS	Initial	After Vacuum	Saturation	B-Value	End of 1 st Consolidation	End of 2 nd Consolidation	End of 3 rd Consolidation	End of 4 th Consolidation	At Failure	End of Shear
Specimen Height	mm	138.51	138.51	136.65	136.12	135.93	135.62	135.31	134.93	134.37	94.59
Specimen Diameter	mm	69.03	68.89	67.66	67.24	67.15	66.97	66.76	66.48	66.62	79.40
Area	cm^2	37.43	37.27	35.95	35.50	35.42	35.23	35.00	34.71	34.85	49.51
Volume	cm^3	518.38	516.28	491.28	483.28	481.41	477.76	473.66	468.33	468.33	468.33
Wet Weight	g	804.83	804.83	980.83	990.63	988.76	985.11	981.01	975.68	975.68	975.68
Water Content	%	5.04	5.04	28.08	29.36	29.12	28.64	28.11	27.41	27.41	27.41
Dry Weight	g	765.77	765.77	765.77	765.77	765.77	765.77	765.77	765.77	765.77	765.77
Wet Density	g/cm^3	1.553	1.559	1.996	2.050	2.054	2.062	2.071	2.083	2.083	2.083
Dry Density	g/cm^3	1.477	1.483	1.559	1.585	1.591	1.603	1.617	1.635	1.635	1.635
Specific Gravity of Solids	-	2.95	2.95	2.95	2.95	2.95	2.95	2.95	2.95	2.95	2.95
Solids Volume	cm^3	259.583	259.583	259.583	259.583	259.583	259.583	259.583	259.583	259.583	259.583
Void Volume	cm^3	258.796	256.696	231.696	223.696	221.826	218.175	214.075	208.745	208.745	208.745
Water Volume	cm^3	39.060	39.060	215.060	224.860	222.990	219.339	215.239	209.909	209.909	209.909
Void Ratio (e)	-	0.997	0.989	0.893	0.862	0.855	0.840	0.825	0.804	0.804	0.804
Saturation Ratio (Sr)	%	15.09	15.22	92.82	100.52	100.52	100.53	100.54	100.56	100.56	100.56
Effective Confining Stress	kPa					37.5	75	150	300		

Shearing (CIU)		
Skempton's B Parameter		1.00
Back Pressure before shearing	kPa	704.9
Confining Stress (σ_3') before shearing	kPa	300
Shear Strain Rate	% / min	0.1
Deviator Stress at Failure*	kPa	113
Axial Strain* at Failure	%	0.41

* From Maximum Deviator Stress

Photos:

Before Test




After Test




Klohn Crippen Berger

Triaxial CIU Test - Charts

(ASTM D4767)

PROJECT NO. :
PROJECT : Fundão Tailings Dam Review Panel
SAMPLE : PSD 1
TEST ID: TX 6
TEST TYPE: CIU
DATE : 2016-03-25
TESTED BY: BY
CHECKED BY: JG

At Max. Deviator Stress:	
Axial Stain (%)	**0.41**
Deviator Stress (kPa)	**112.6**

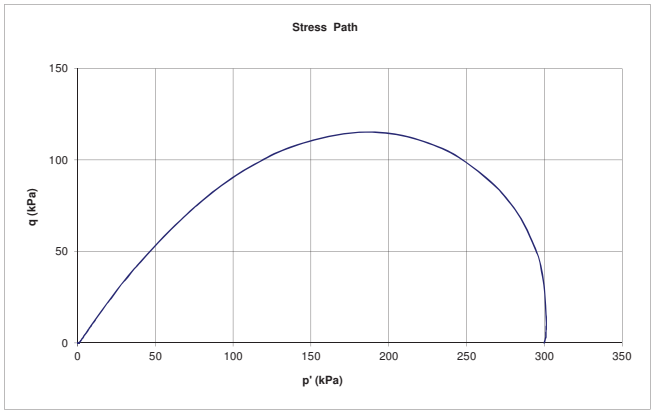

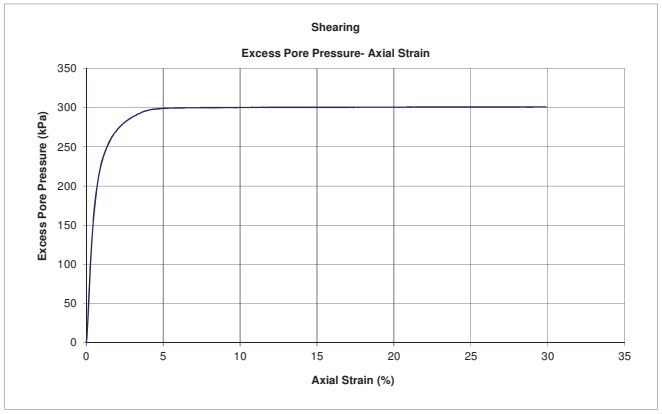

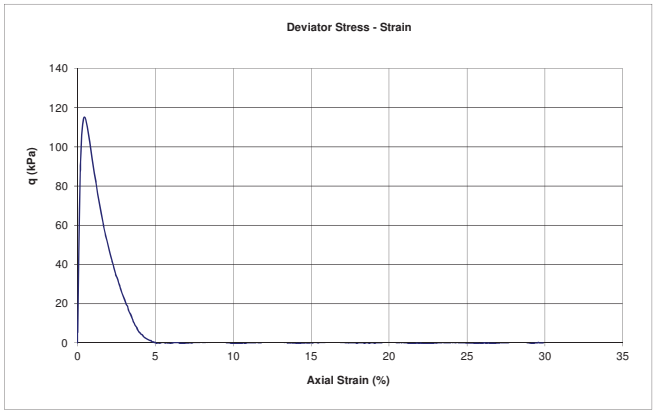

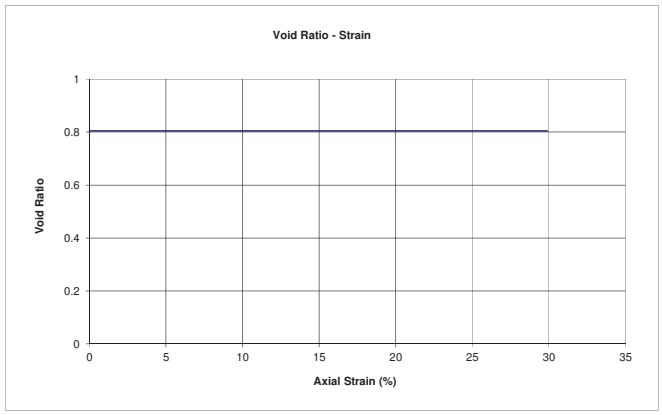

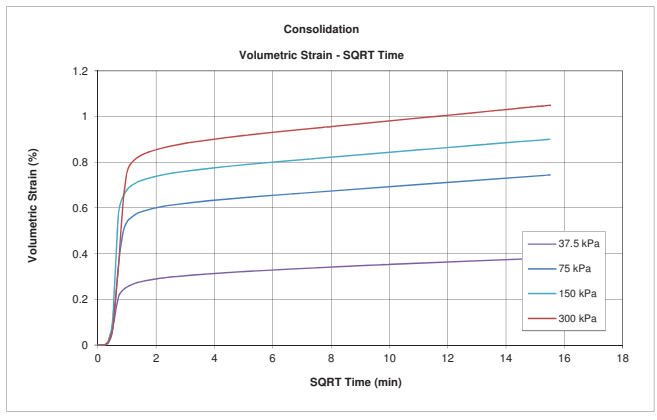

Triaxial CIU Test - Summary

(ASTM D4767)

PROJECT NO. :
PROJECT : Fundão Tailings Dam Review Panel
SAMPLE PSD 2
TEST ID: TX 7

DATE : 2016-03-26
TESTED BY: BY
CHECKED BY: JG
TEST TYPE: CIU

SPECIMEN INFORMATION	UNITS	Initial	After Vacuum	Saturation	B-Value	End of 1 st Consolidation	End of 2 nd Consolidation	End of 3 rd Consolidation	At Failure	End of Shear
Specimen Height	mm	138.59	138.59	136.97	136.68	136.48	136.20	135.84	135.40	97.59
Specimen Diameter	mm	69.05	68.58	67.21	66.58	66.44	66.25	66.02	66.12	77.89
Area	cm^2	37.45	36.94	35.48	34.82	34.67	34.47	34.23	34.34	47.64
Volume	cm^3	518.98	511.94	485.94	475.94	473.25	469.46	464.96	464.96	464.96
Wet Weight	g	680.53	680.53	883.53	888.83	886.14	882.36	877.86	877.86	877.86
Water Content	%	5.04	5.04	36.68	37.50	37.09	36.50	35.80	35.80	35.80
Dry Weight	g	646.41	646.41	646.41	646.41	646.41	646.41	646.41	646.41	646.41
Wet Density	g/cm^3	1.311	1.329	1.818	1.868	1.872	1.879	1.888	1.888	1.888
Dry Density	g/cm^3	1.246	1.263	1.330	1.358	1.366	1.377	1.390	1.390	1.390
Specific Gravity of Solids	-	2.74	2.74	2.74	2.74	2.74	2.74	2.74	2.74	2.74
Solids Volume	cm^3	235.916	235.916	235.916	235.916	235.916	235.916	235.916	235.916	235.916
Void Volume	cm^3	283.063	276.022	250.022	240.022	237.332	233.547	229.047	229.047	229.047
Water Volume	cm^3	34.120	34.120	237.120	242.420	239.730	235.945	231.445	231.445	231.445
Void Ratio (e)	-	1.200	1.170	1.060	1.017	1.006	0.990	0.971	0.971	0.971
Saturation Ratio (Sr)	%	12.05	12.36	94.84	101.00	101.01	101.03	101.05	101.05	101.05
Effective Confining Stress	kPa					50	100	200		

Shearing (CIU)		
Skempton's B Parameter		1.00
Back Pressure before shearing	kPa	
Confining Stress (σ_3') before shearing	kPa	200
Shear Strain Rate	% / min	0.1
Deviator Stress at Failure*	kPa	68
Axial Strain* at Failure	%	0.33

* From Maximum Deviator Stress

Photos:

Before Test




After Test




Klohn Crippen Berger

Triaxial CIU Test - Charts

(ASTM D4767)

PROJECT NO. :
PROJECT : Fundão Tailings Dam Review Panel
SAMPLE PSD 2
TEST ID: TX 7
TEST TYPE: CIU
DATE : 2016-03-26
TESTED BY: BY
CHECKED BY: JG

At Max. Deviator Stress:	
Axial Stain (%)	**0.33**
Deviator Stress (kPa)	**68.0**

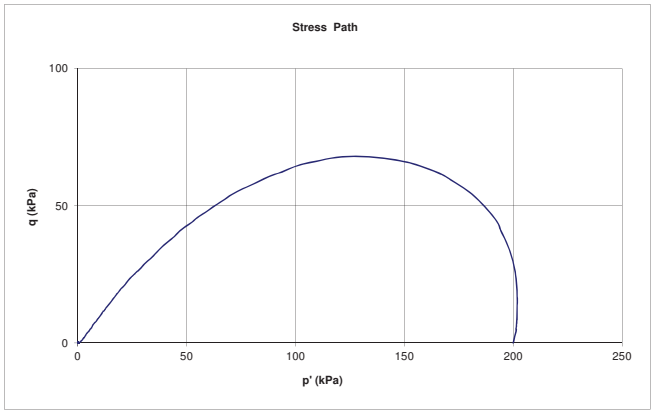

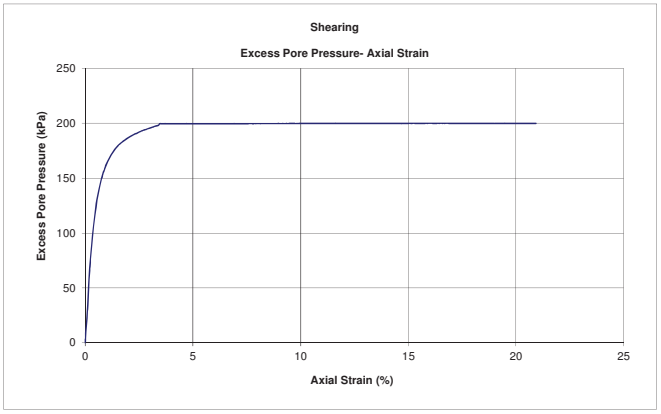

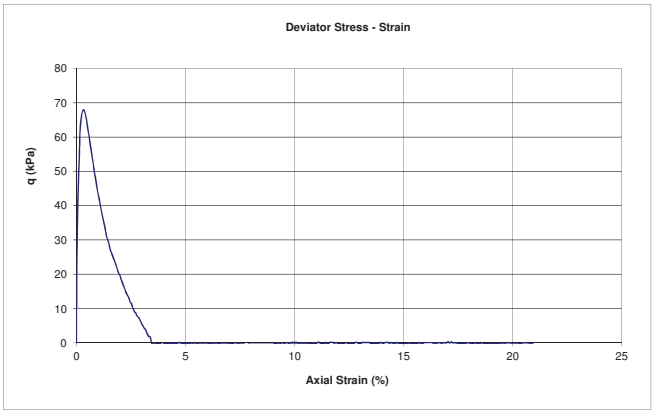

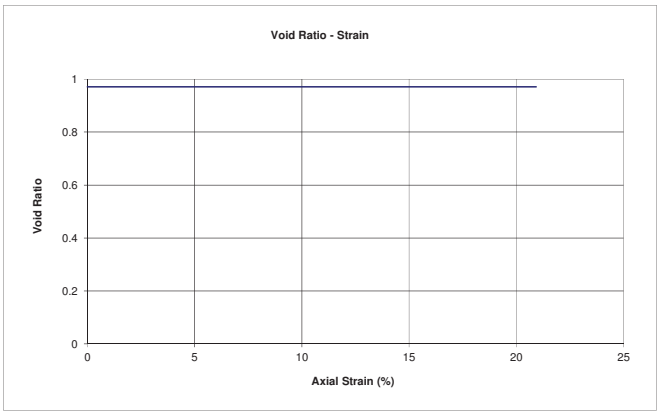

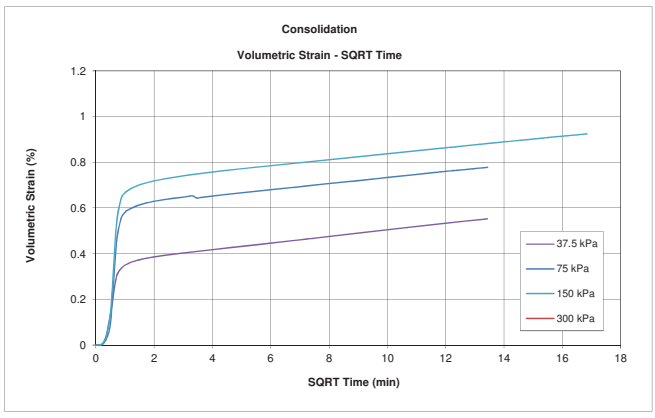

Triaxial CID Test - Summary

(ASTM D7181)

PROJECT NO. :
PROJECT : Fundão Tailings Dam Review Panel
SAMPLE : PSD 1
TEST ID: TX 8

DATE : 2016-03-29
TESTED BY: BY
CHECKED BY: JG
TEST TYPE: CID

SPECIMEN INFORMATION	UNITS	Initial	After Vacuum	Saturation	B-Value	End of 1st Consolidation	End of 2 nd Consolidation	End of 3 rd Consolidation	End of 4th Consolidation	At Failure	End of Shear
Specimen Height	mm	138.94	138.94	138.94	138.71	138.64	138.53	138.41	138.22	113.59	94.82
Specimen Diameter	mm	69.07	68.87	68.27	67.85	67.59	67.50	67.38	67.19	73.00	79.73
Area	cm^2	37.47	37.25	36.60	36.16	35.88	35.79	35.66	35.46	41.86	49.93
Volume	cm^3	520.59	517.58	508.59	501.59	497.39	495.79	493.52	490.15	475.47	473.40
Wet Weight	g	875.72	875.72	1044.72	1050.04	1045.84	1044.24	1041.97	1038.60	1023.92	1021.85
Water Content	%	4.99	4.99	25.25	25.89	25.39	25.19	24.92	24.52	22.76	22.51
Dry Weight	g	834.10	834.10	834.10	834.10	834.10	834.10	834.10	834.10	834.10	834.10
Wet Density	g/cm^3	1.682	1.692	2.054	2.093	2.103	2.106	2.111	2.119	2.153	2.159
Dry Density	g/cm^3	1.602	1.612	1.640	1.663	1.677	1.682	1.690	1.702	1.754	1.762
Specific Gravity of Solids	-	2.94	2.94	2.94	2.94	2.94	2.94	2.94	2.94	2.94	2.94
Solids Volume	cm^3	283.707	283.707	283.707	283.707	283.707	283.707	283.707	283.707	283.707	283.707
Void Volume	cm^3	236.885	233.874	224.886	217.886	213.686	212.086	209.816	206.446	191.766	189.696
Water Volume	cm^3	41.622	41.622	210.622	215.939	211.739	210.139	207.869	204.499	189.819	187.749
Void Ratio (e)	-	0.835	0.824	0.793	0.768	0.753	0.748	0.740	0.728	0.676	0.669
Saturation Ratio (Sr)	%	17.57	17.80	93.66	99.11	99.09	99.08	99.07	99.06	98.98	98.97
Effective Confining Stress	kPa					37.5	75	150	300		

Shearing (CID)		
Skempton's B Parameter		1.00
Back Pressure before shearing	kPa	654.4
Confining Stress (σ_3') before shearing	kPa	300
Shear Strain Rate	% / min	0.1
Deviator Stress at Failure*	kPa	726.14
Axial Strain* at Failure	%	17.82

* From Maximum Deviator Stress

Photos:

Before Test




After Test



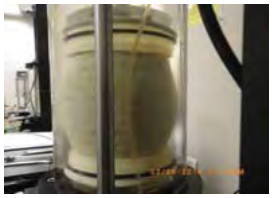


Klohn Crippen Berger

Triaxial CID Test - Charts

(ASTM D7181)

PROJECT NO. :
PROJECT : Fundão Tailings Dam Review Panel
SAMPLE : PSD 1
TEST ID: TX 8
TEST TYPE: CID
DATE : 2016-03-29
TESTED BY: BY
CHECKED BY: JG

At Max. Deviator Stress:	
Axial Stain (%)	**17.82**
Deviator Stress (kPa)	**726.1**

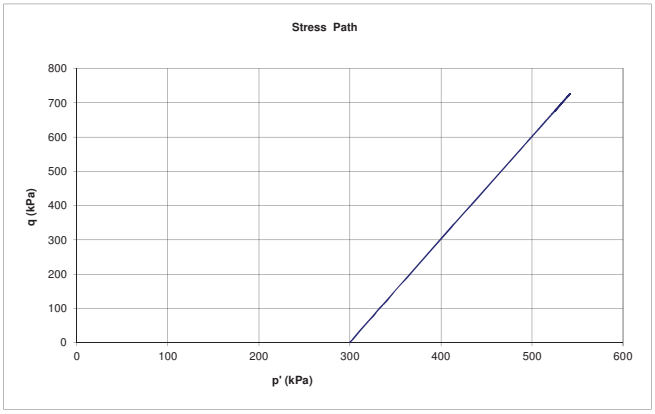

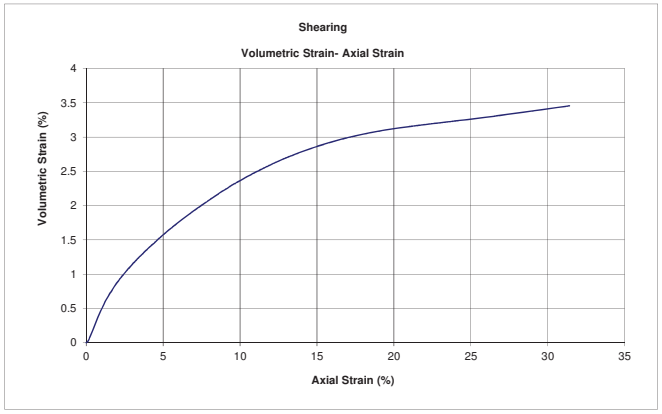

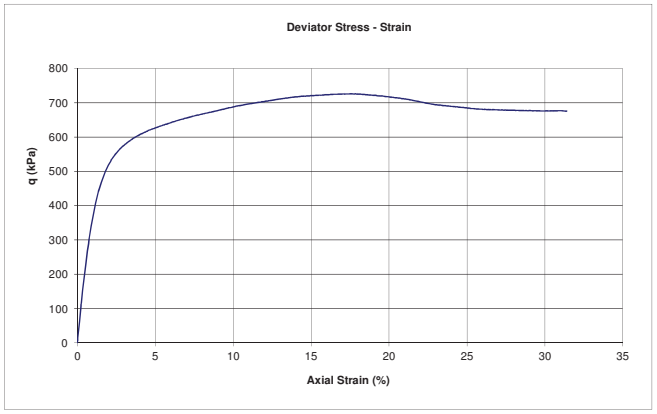

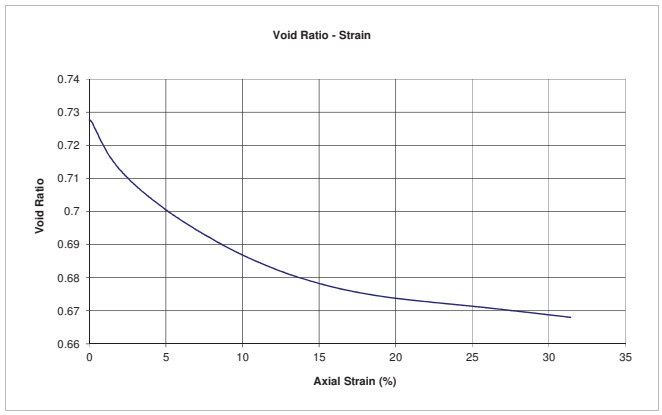

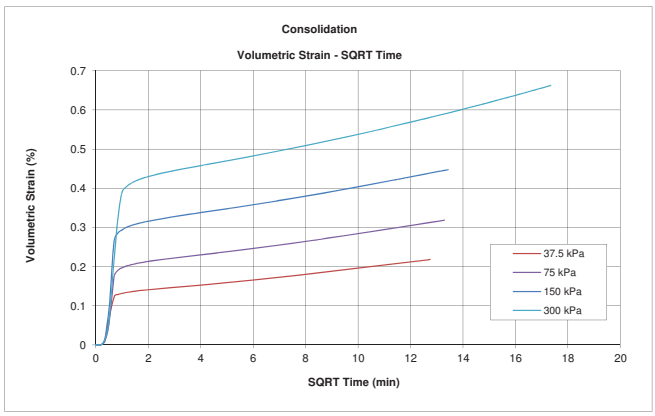

Triaxial CID Test - Summary

(ASTM D7181)

PROJECT NO. :
PROJECT : Fundão Tailings Dam Review Panel
SAMPLE : PSD 2
TEST ID: TX 9

DATE : 2016-03-29
TESTED BY: BY
CHECKED BY: JG
TEST TYPE: CID

SPECIMEN INFORMATION	UNITS	Initial	After Vacuum	Saturation	B-Value	End of 1st Consolidation	End of 2 nd Consolidation	End of 3 rd Consolidation	End of 4th Consolidation	At Failure	End of Shear
Specimen Height	mm	138.69	138.69	136.54	136.36	136.24	136.04	135.74	135.39	102.42	94.67
Specimen Diameter	mm	68.96	68.50	67.039	65.39	65.30	65.14	64.93	64.66	72.36	75.27
Area	cm^2	37.35	36.85	35.30	33.58	33.49	33.32	33.11	32.84	41.12	44.49
Volume	cm^3	518.001	511.113	481.970	457.970	456.340	453.320	449.444	444.574	421.144	421.214
Wet Weight	g	678.55	678.55	859.05	864.91	863.28	860.26	856.39	851.52	828.09	828.16
Water Content	%	5.00	5.00	33.22	34.13	33.88	33.41	32.81	32.05	28.42	28.43
Dry Weight	g	644.82	644.82	644.82	644.82	644.82	644.82	644.82	644.82	644.82	644.82
Wet Density	g/cm^3	1.310	1.328	1.782	1.889	1.892	1.898	1.905	1.915	1.966	1.966
Dry Density	g/cm^3	1.245	1.262	1.338	1.408	1.413	1.422	1.435	1.450	1.531	1.531
Specific Gravity of Solids	-	2.74	2.74	2.74	2.74	2.74	2.74	2.74	2.74	2.74	2.74
Solids Volume	cm^3	235.336	235.336	235.336	235.336	235.336	235.336	235.336	235.336	235.336	235.336
Void Volume	cm^3	282.665	275.778	246.635	222.635	221.005	217.985	214.109	209.239	185.809	185.879
Water Volume	cm^3	33.730	33.730	214.230	220.091	218.461	215.441	211.565	206.695	183.265	183.335
Void Ratio (e)	-	1.201	1.172	1.048	0.946	0.939	0.926	0.910	0.889	0.790	0.790
Saturation Ratio (Sr)	%	11.93	12.23	86.86	98.86	98.85	98.83	98.81	98.78	98.63	98.63
Effective Confining Stress	kPa					37.5	75	150	300		

Shearing (CID)		
Skempton's B Parameter		1.00
Back Pressure before shearing	kPa	603.8
Confining Stress (σ_3') before shearing	kPa	300
Shear Strain Rate	% / min	0.1
Deviator Stress at Failure*	kPa	670.31
Axial Strain* at Failure	%	23.62

* From Maximum Deviator Stress

Photos:

Before Test

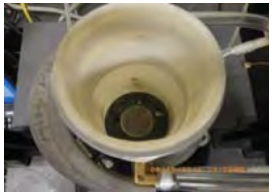


After Test




Klohn Crippen Berger

Triaxial CID Test - Charts

(ASTM D7181)

PROJECT NO. :
PROJECT : Fundão Tailings Dam Review Panel
SAMPLE : PSD 2
TEST ID: TX 9
TEST TYPE: CID
DATE : 2016-03-29
TESTED BY: BY
CHECKED BY: JG

At Max. Deviator Stress:	
Axial Stain (%)	**23.62**
Deviator Stress (kPa)	**670.3**

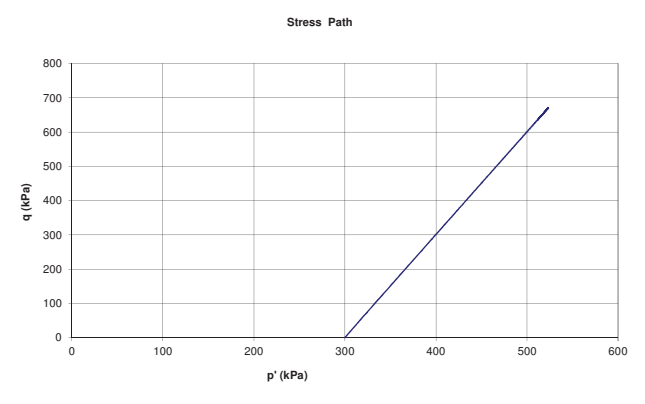

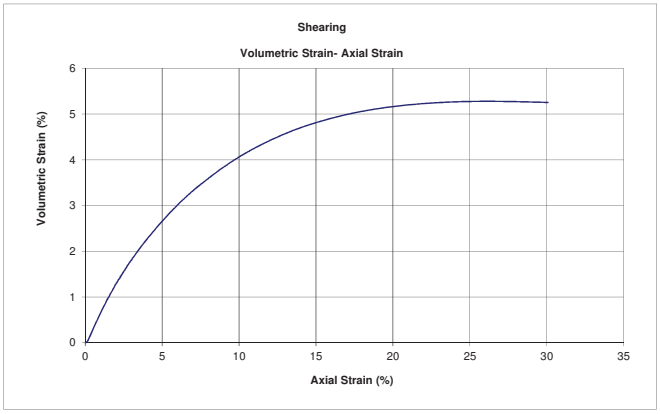

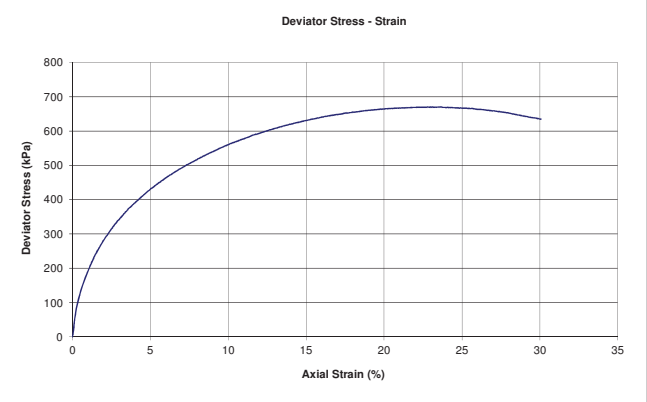

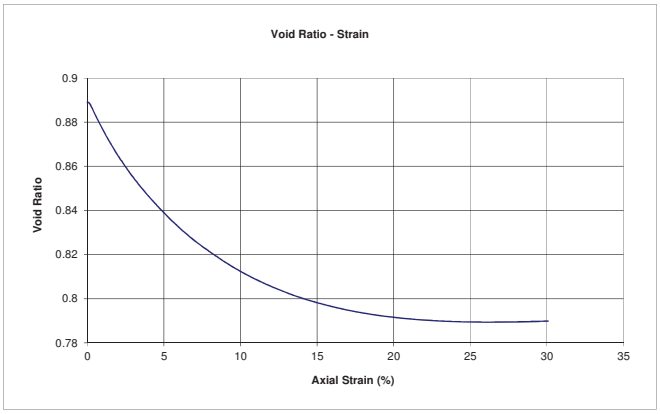

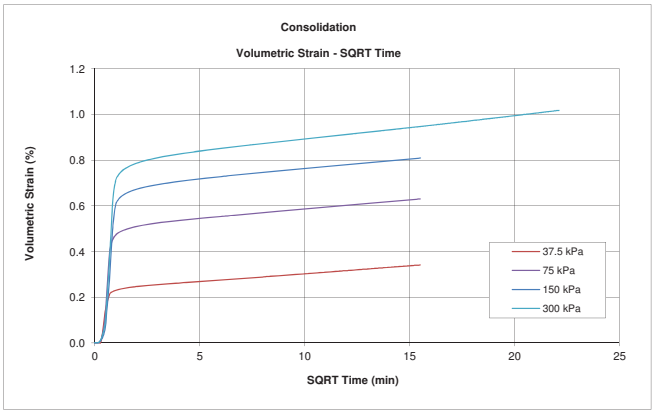

Klohn Crippen Berger

Triaxial CID Test - Summary

(ASTM D7181)

PROJECT NO. :
PROJECT : Fundão Tailings Dam Review Panel
SAMPLE : PSD 1
TEST ID: TX 10

DATE : 2016-04-01
TESTED BY: BY
CHECKED BY: JG
TEST TYPE: CID

SPECIMEN INFORMATION	UNITS	Initial	Saturation	B-Value	End of 1st Consolidation	End of 2 nd Consolidation	End of 3 rd Consolidation	End of 4th Consolidation	End of 5th Consolidation	At Failure	End of Shear
Specimen Height	mm	142.27	142.27	142.26	142.24	142.19	142.14	142.03	141.95	136.33	116.38
Specimen Diameter	mm	69.59	69.59	69.80	69.75	69.68	69.52	69.26	69.06	70.73	77.12
Area	cm^2	38.04	38.04	38.27	38.21	38.13	37.95	37.67	37.46	39.29	46.71
Volume	cm^3	541.13	541.13	544.38	543.54	542.18	539.46	535.08	531.70	535.70	543.56
Wet Weight	g	1085.20	1194.80	1198.66	1197.82	1196.46	1193.74	1189.35	1185.98	1189.98	1197.84
Water Content	%	10.33	21.47	21.86	21.78	21.64	21.36	20.91	20.57	20.98	21.78
Dry Weight	g	983.63	983.63	983.63	983.63	983.63	983.63	983.63	983.63	983.63	983.63
Wet Density	g/cm^3	2.005	2.208	2.202	2.204	2.207	2.213	2.223	2.231	2.221	2.204
Dry Density	g/cm^3	1.818	1.818	1.807	1.810	1.814	1.823	1.838	1.850	1.836	1.810
Specific Gravity of Solids	-	2.95	2.95	2.95	2.95	2.95	2.95	2.95	2.95	2.95	2.95
Solids Volume	cm^3	333.434	333.434	333.434	333.434	333.434	333.434	333.434	333.434	333.434	333.434
Void Volume	cm^3	207.691	207.691	210.950	210.110	208.750	206.030	201.643	198.271	202.271	210.131
Water Volume	cm^3	101.570	211.170	215.028	214.188	212.828	210.108	205.721	202.349	206.349	214.209
Void Ratio (e)	-	0.623	0.623	0.633	0.630	0.626	0.618	0.605	0.595	0.607	0.630
Saturation Ratio (Sr)	%	48.90	101.67	101.93	101.94	101.95	101.98	102.02	102.06	102.02	101.94
Effective Confining Stress	kPa				50	100	200	400	600		

Shearing (CID)		
Skempton's B Parameter		1.00
Back Pressure before shearing	kPa	503.9
Confining Stress (σ_3') before shearing	kPa	600.25
Shear Strain Rate	% / min	0.1
Deviator Stress at Failure*	kPa	2225.26
Axial Strain* at Failure	%	3.97

* From Maximum Deviator Stress

Photos:

Before Test

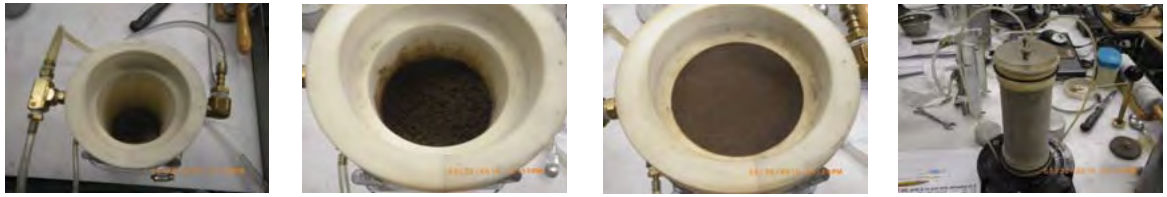

After Test

Klohn Crippen Berger

Triaxial CID Test - Charts

(ASTM D7181)

PROJECT NO. :
PROJECT : Fundão Tailings Dam Review Panel
SAMPLE : PSD 1
TEST ID: TX 10
TEST TYPE: CID
DATE : 2016-04-01
TESTED BY: BY
CHECKED BY: JG

At Max. Deviator Stress:	
Axial Stain (%)	**3.97**
Deviator Stress (kPa)	**2225.3**

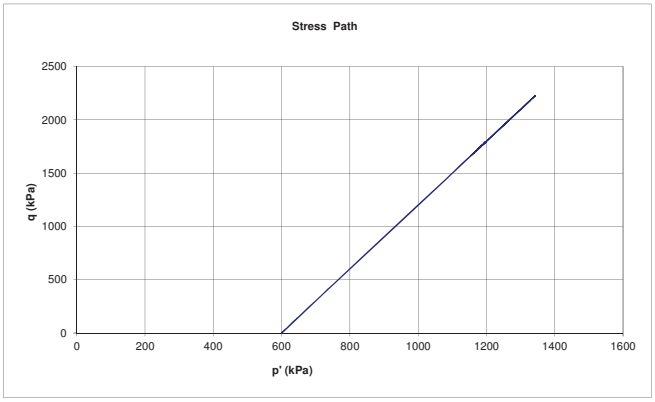

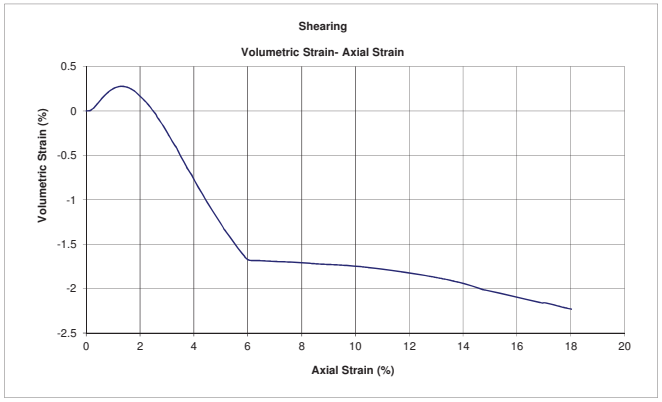

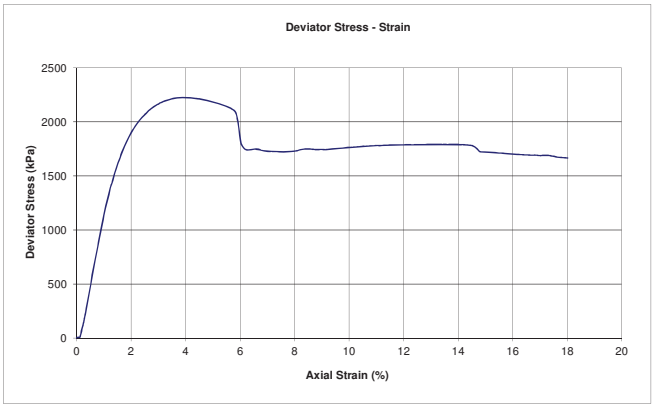

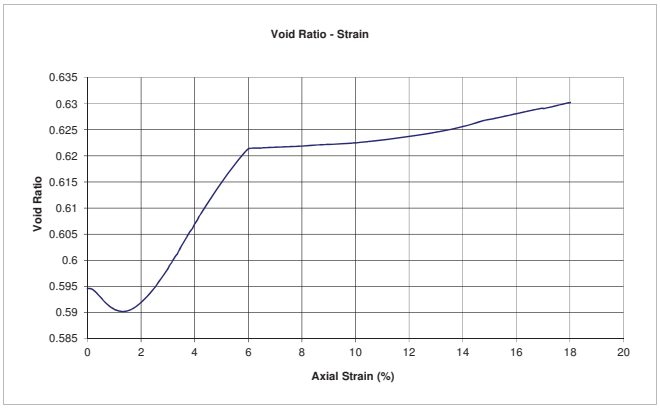

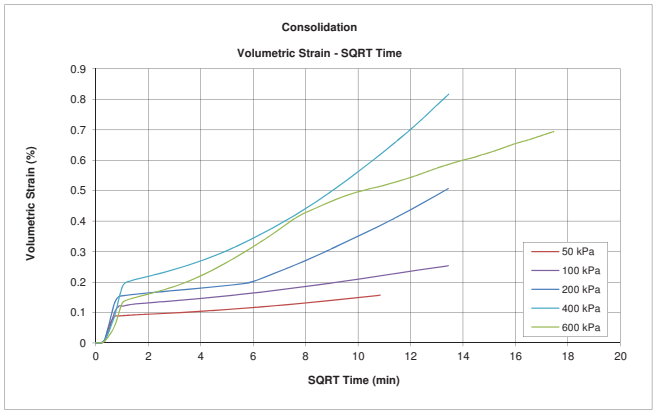

Triaxial CID Test - Summary

(ASTM D7181)

PROJECT NO. :
PROJECT : Fundão Tailings Dam Review Panel
SAMPLE : PSD 1
TEST ID: TX 11

DATE : 2016-04-05
TESTED BY: BY
CHECKED BY: JG
TEST TYPE: CID

SPECIMEN INFORMATION	UNITS	Initial	Saturation	B-Value	End of 1st Consolidation	End of 2 nd Consolidation	End of 3 rd Consolidation	At Failure	End of Shear
Specimen Height	mm	142.07	141.87	141.72	141.69	141.62	141.53	138.00	113.51
Specimen Diameter	mm	69.53	69.35	69.39	69.37	69.35	69.32	70.27	78.60
Area	cm^2	37.97	37.77	37.82	37.80	37.77	37.74	38.78	48.52
Volume	cm^3	539.43	535.83	535.93	535.53	534.88	534.10	535.19	550.79
Wet Weight	g	1077.02	1175.22	1183.22	1182.83	1182.17	1181.39	1182.48	1198.08
Water Content	%	10.09	20.13	20.95	20.91	20.84	20.76	20.87	22.47
Dry Weight	g	978.28	978.28	978.28	978.28	978.28	978.28	978.28	978.28
Wet Density	g/cm^3	1.997	2.193	2.208	2.209	2.210	2.212	2.209	2.175
Dry Density	g/cm^3	1.814	1.826	1.825	1.827	1.829	1.832	1.828	1.776
Specific Gravity of Solids	-	2.95	2.95	2.95	2.95	2.95	2.95	2.95	2.95
Solids Volume	cm^3	331.621	331.621	331.621	331.621	331.621	331.621	331.621	331.621
Void Volume	cm^3	207.812	204.207	204.307	203.913	203.259	202.476	203.566	219.166
Water Volume	cm^3	98.738	196.938	204.938	204.543	203.890	203.107	204.197	219.797
Void Ratio (e)	-	0.627	0.616	0.616	0.615	0.613	0.611	0.614	0.661
Saturation Ratio (Sr)	%	47.51	96.44	100.31	100.31	100.31	100.31	100.31	100.29
Effective Confining Stress	kPa				50	100	200		

Shearing (CID)		
Skempton's B Parameter		1.00
Back Pressure before shearing	kPa	804.7
Confining Stress (σ_3') before shearing	kPa	200.23
Shear Strain Rate	% / min	0.1
Deviator Stress at Failure*	kPa	860.82
Axial Strain* at Failure	%	2.50

* From Maximum Deviator Stress

Photos:

Before Test




After Test




Klohn Crippen Berger

Triaxial CID Test - Charts

(ASTM D7181)

PROJECT NO. :
PROJECT : Fundão Tailings Dam Review Panel
SAMPLE : PSD 1
TEST ID: TX 11
TEST TYPE: CID
DATE : 2016-04-05
TESTED BY: BY
CHECKED BY: JG

At Max. Deviator Stress:	
Axial Stain (%)	**2.50**
Deviator Stress (kPa)	**860.8**

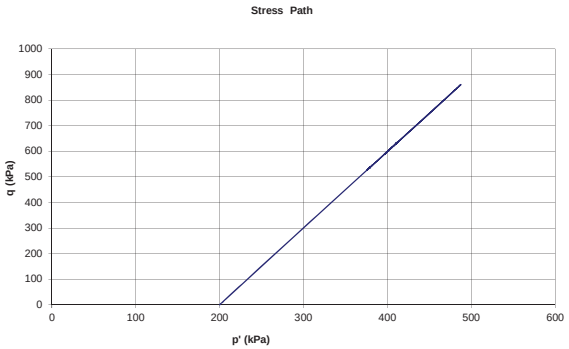

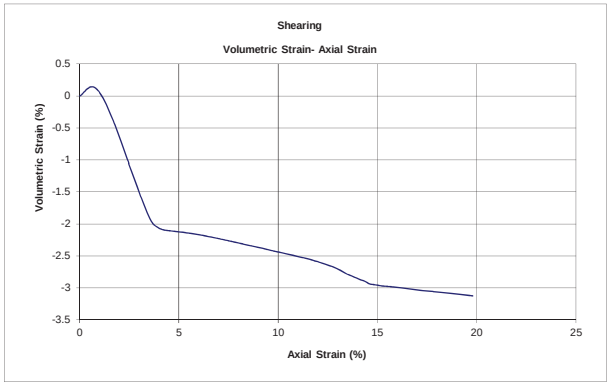

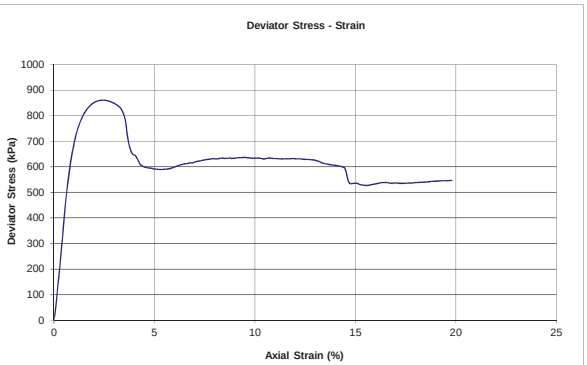

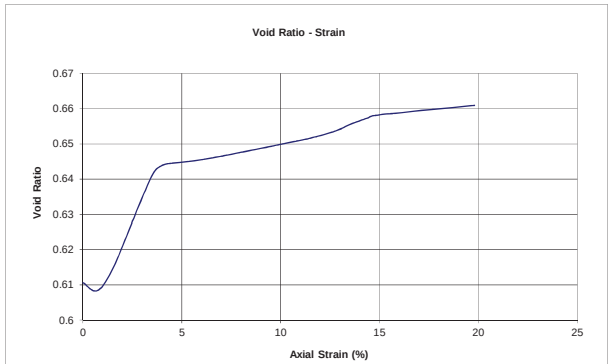

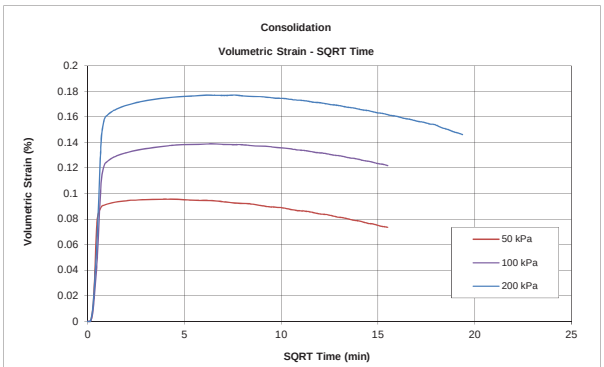

Klohn Crippen Berger

Triaxial CID Test - Summary

(ASTM D7181)

PROJECT NO. :
PROJECT : Fundão Tailings Dam Review Panel
SAMPLE : PSD 1
TEST ID: TX 12

DATE : 2016-04-20
TESTED BY: BY
CHECKED BY: JG
TEST TYPE: CID

SPECIMEN INFORMATION	UNITS	Initial	Saturation	B-Value	End of 1st Consolidation	End of 2 nd Consolidation	End of 3 rd Consolidation	End of 4th Consolidation	At Failure	End of Shear
Specimen Height	mm	141.56	141.38	141.25	141.20	141.12	141.00	140.83	134.22	113.78
Specimen Diameter	mm	69.78	69.53	69.30	69.23	69.16	69.08	68.95	70.49	76.54
Area	cm^2	38.24	37.96	37.72	37.65	37.57	37.48	37.34	39.03	46.01
Volume	cm^3	541.37	536.75	532.75	531.56	530.20	528.50	525.80	523.86	523.57
Wet Weight	g	956.73	1131.60	1138.10	1136.91	1135.55	1133.85	1131.15	1131.15	1131.15
Water Content	%	4.98	24.17	24.88	24.75	24.60	24.41	24.12	24.12	24.12
Dry Weight	g	911.35	911.35	911.35	911.35	911.35	911.35	911.35	911.35	911.35
Wet Density	g/cm^3	1.767	2.108	2.136	2.139	2.142	2.145	2.151	2.159	2.160
Dry Density	g/cm^3	1.683	1.698	1.711	1.714	1.719	1.724	1.733	1.740	1.741
Specific Gravity of Solids	-	2.93	2.93	2.93	2.93	2.93	2.93	2.93	2.93	2.93
Solids Volume	cm^3	311.039	311.039	311.039	311.039	311.039	311.039	311.039	311.039	311.039
Void Volume	cm^3	230.330	225.707	221.707	220.517	219.157	217.457	214.757	212.817	212.535
Water Volume	cm^3	45.385	220.250	226.750	225.560	224.200	222.500	219.800	219.800	219.800
Void Ratio (e)	-	0.741	0.726	0.713	0.709	0.705	0.699	0.690	0.684	0.683
Saturation Ratio (Sr)	%	19.70	97.58	102.27	102.29	102.30	102.32	102.35	103.28	103.42
Effective Confining Stress	kPa				50	100	200	400		

Shearing (CID)		
Skempton's B Parameter		1.00
Back Pressure before shearing	kPa	711.9
Confining Stress (σ_3') before shearing	kPa	400.32
Shear Strain Rate	% / min	0.1
Deviator Stress at Failure*	kPa	1043.94
Axial Strain* at Failure	%	4.69

* From Maximum Deviator Stress

Photos:

Before Test

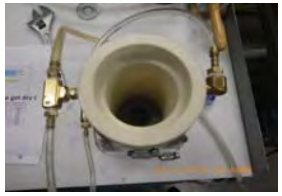


After Test




Klohn Crippen Berger

Triaxial CID Test - Charts

(ASTM D7181)

PROJECT NO. :
PROJECT : Fundão Tailings Dam Review Panel
SAMPLE : PSD 1
TEST ID: TX 12
TEST TYPE: CID
DATE : 2016-04-20
TESTED BY: BY
CHECKED BY: JG

At Max. Deviator Stress:	
Axial Stain (%)	**4.69**
Deviator Stress (kPa)	**1043.9**

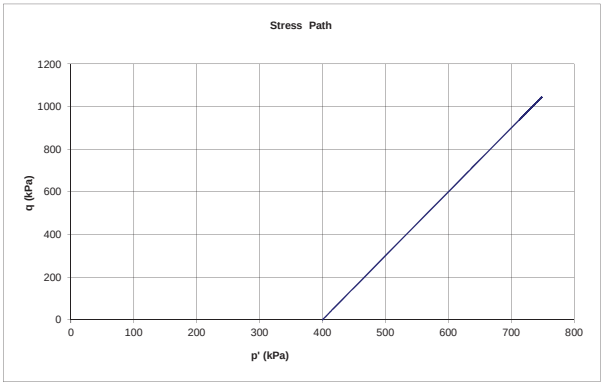

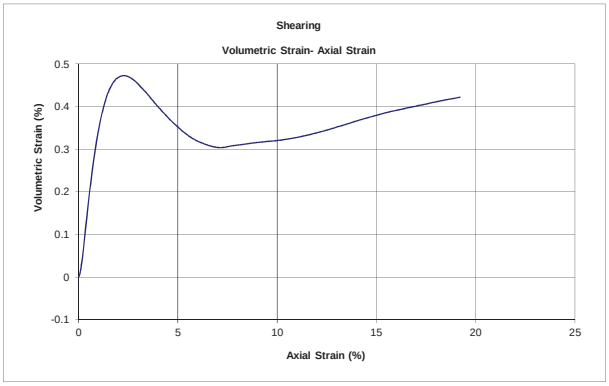

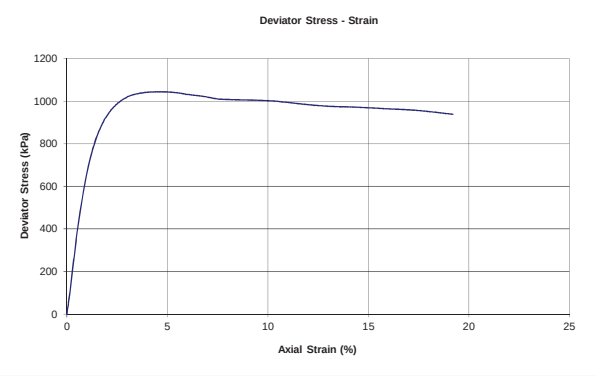

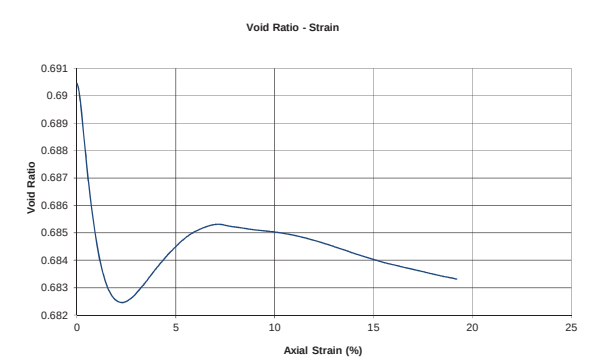

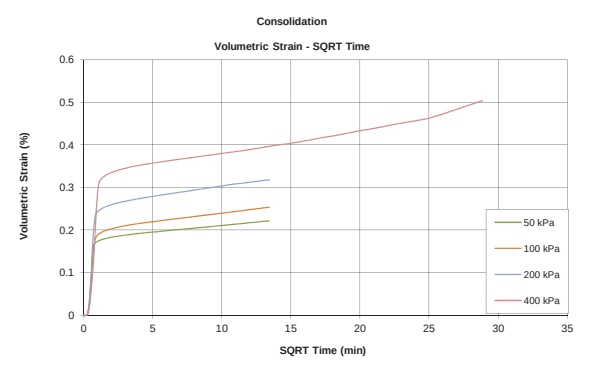

Klohn Crippen Berger

Triaxial CIU Test - Summary

(ASTM D4767)

PROJECT NO. :
PROJECT : Fundão Tailings Dam Review Panel
SAMPLE : PSD 1
TEST ID: TX 13

DATE : 2016-04-20
TESTED BY: BY
CHECKED BY: JG
TEST TYPE: CIU

SPECIMEN INFORMATION	UNITS	Initial	Saturation	B-Value	End of 1 st Consolidation	End of 2 nd Consolidation	End of 3 rd Consolidation	End of 4 th Consolidation	End of 5 th Consolidation	At Failure	End of Shear
Specimen Height	mm	141.65	141.42	141.19	141.14	141.07	140.97	140.84	140.72	132.24	114.86
Specimen Diameter	mm	69.54	69.35	69.25	69.20	69.16	69.09	69.00	68.94	71.11	76.30
Area	cm^2	37.98	37.77	37.66	37.61	37.56	37.49	37.40	37.33	39.72	45.73
Volume	cm^3	537.99	534.15	531.80	530.90	529.88	528.50	526.69	525.24	525.24	525.24
Wet Weight	g	958.09	1133.30	1135.60	1134.70	1133.68	1132.30	1130.49	1129.04	1129.04	1129.04
Water Content	%	4.98	24.41	24.66	24.57	24.45	24.30	24.10	23.94	23.94	23.94
Dry Weight	g	910.92	910.92	910.92	910.92	910.92	910.92	910.92	910.92	910.92	910.92
Wet Density	g/cm^3	1.781	2.122	2.135	2.137	2.140	2.142	2.146	2.150	2.150	2.150
Dry Density	g/cm^3	1.693	1.705	1.713	1.716	1.719	1.724	1.730	1.734	1.734	1.734
Specific Gravity of Solids	-	2.93	2.93	2.93	2.93	2.93	2.93	2.93	2.93	2.93	2.93
Solids Volume	cm^3	310.894	310.894	310.894	310.894	310.894	310.894	310.894	310.894	310.894	310.894
Void Volume	cm^3	227.099	223.251	220.901	220.001	218.981	217.601	215.791	214.341	214.341	214.341
Water Volume	cm^3	47.170	222.378	224.678	223.778	222.758	221.378	219.568	218.118	218.118	218.118
Void Ratio (e)	-	0.730	0.718	0.711	0.708	0.704	0.700	0.694	0.689	0.689	0.689
Saturation Ratio (Sr)	%	20.77	99.61	101.71	101.72	101.72	101.74	101.75	101.76	101.76	101.76
Effective Confining Stress	kPa				50	100	200	400	600		

Shearing (CIU)		
Skempton's B Parameter		1.00
Back Pressure before shearing	kPa	711.9
Confining Stress (σ_3') before shearing	kPa	600
Shear Strain Rate	% / min	0.1
Deviator Stress at Failure*	kPa	1060
Axial Strain* at Failure	%	6.02

* From Maximum Deviator Stress

Photos:

Before Test




After Test




Klohn Crippen Berger

Triaxial CIU Test - Charts

(ASTM D4767)

PROJECT NO. :
PROJECT : Fundão Tailings Dam Review Panel
SAMPLE : PSD 1
TEST ID: TX 13
TEST TYPE: CIU
DATE : 2016-04-20
TESTED BY: BY
CHECKED BY: JG

At Max. Deviator Stress:	
Axial Stain (%)	**6.02**
Deviator Stress (kPa)	**1060.0**

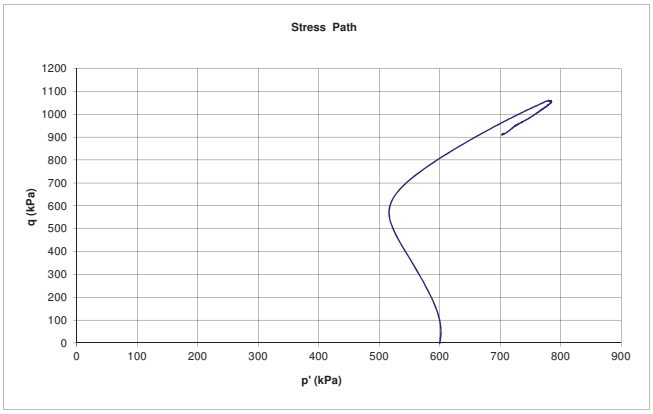

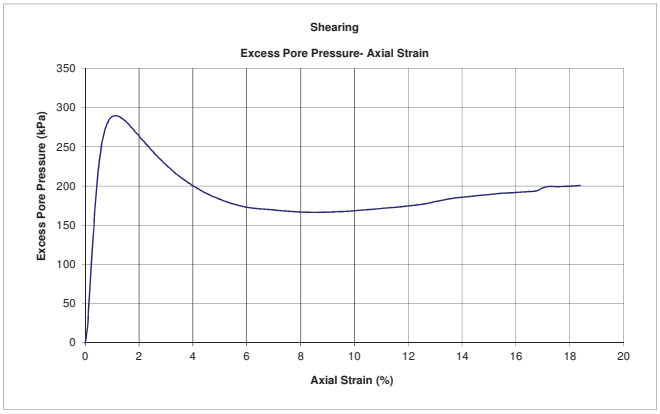

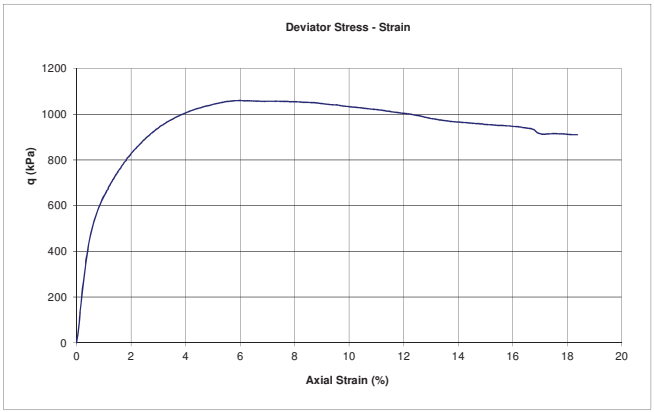

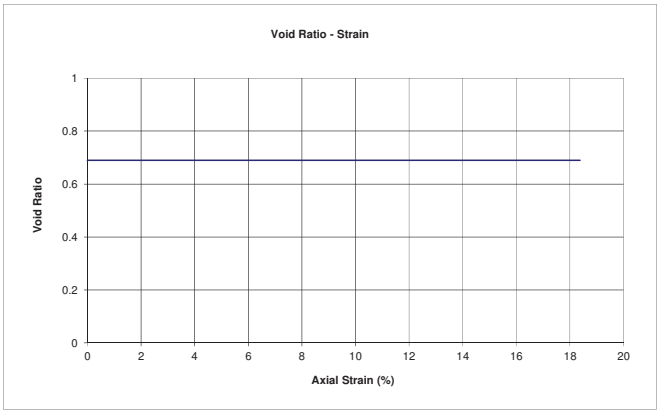

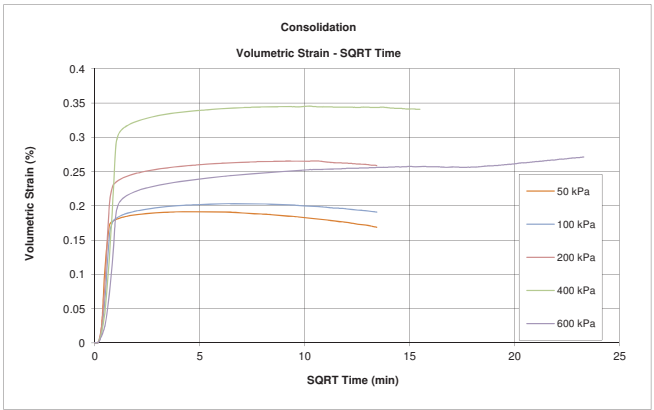

Klohn Crippen Berger

Triaxial CA-QD Test - Summary

PROJECT NO. :
PROJECT : Fundão Tailings Dam Review Panel
SAMPLE : PSD 1
TEST ID: TX 14

DATE : 2016-05-02
TESTED BY: BY
CHECKED BY: JG
TEST TYPE: CA-QD Strain Contolled Extrusion Collapse

SPECIMEN INFORMATION	UNITS	Initial	After Vacuum	Saturation	B-Value	End of 1st Consolidation	End of 2 nd Consolidation	End of 3 rd Consolidation	End of 4th Consolidation	At Failure	End of Shear
Specimen Height	mm	141.14	141.65	141.11	141.03	141.00	140.93	140.80	140.69	139.26	98.16
Specimen Diameter	mm	69.60	69.54	69.33	69.35	69.32	69.27	69.19	68.99	69.76	83.31
Area	cm^2	38.05	37.98	37.75	37.78	37.74	37.68	37.60	37.38	38.22	54.51
Volume	cm^3	536.98	537.99	532.75	532.75	532.13	531.02	529.44	525.91	532.23	535.03
Wet Weight	g	958.98	958.98	1134.69	1141.69	1141.07	1139.96	1138.38	1134.85	1141.17	1143.97
Water Content	%	4.98	4.98	24.21	24.98	24.91	24.79	24.62	24.23	24.92	25.23
Dry Weight	g	913.49	913.49	913.49	913.49	913.49	913.49	913.49	913.49	913.49	913.49
Wet Density	g/cm^3	1.786	1.783	2.130	2.143	2.144	2.147	2.150	2.158	2.144	2.138
Dry Density	g/cm^3	1.701	1.698	1.715	1.715	1.717	1.720	1.725	1.737	1.716	1.707
Specific Gravity of Solids	-	2.92	2.92	2.92	2.92	2.92	2.92	2.92	2.92	2.92	2.92
Solids Volume	cm^3	312.839	312.839	312.839	312.839	312.839	312.839	312.839	312.839	312.839	312.839
Void Volume	cm^3	224.143	225.154	219.907	219.907	219.287	218.177	216.597	213.071	219.391	222.191
Water Volume	cm^3	45.490	45.490	221.195	228.195	227.575	226.465	224.885	221.359	227.679	230.479
Void Ratio (e)	-	0.716	0.720	0.703	0.703	0.701	0.697	0.692	0.681	0.701	0.710
Saturation Ratio (Sr)	%	20.30	20.20	100.59	103.77	103.78	103.80	103.83	103.89	103.78	103.73
Effective Confining Stress	kPa					50	100	200	400		

Shearing (CA-QD)		
Skempton's B Parameter		1.00
Back Pressure before shearing	kPa	703.5
Confining Stress (σ_3') before shearing	kPa	400.2
Shear Strain Rate	kPa / min	1
Deviator Stress at Failure*	kPa	200.7
Axial Strain* at Failure	%	0.32

* From Maximum Deviator Stress

Photos:

Before Test



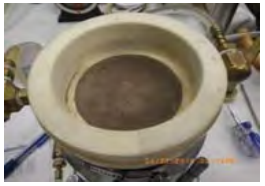


After Test




Klohn Crippen Berger

Triaxial CA-QD Test - Charts

PROJECT NO. :
PROJECT : Fundão Tailings Dam Review Panel
SAMPLE : PSD 1
TEST ID: TX 14
TEST TYPE: CA-QD Strain Contolled Extrusion Collapse
DATE : 2016-05-02
TESTED BY: BY
CHECKED BY: JG

At Max. Deviator Stress:	
Axial Stain (%)	**0.32**
Deviator Stress (kPa)	**200.7**

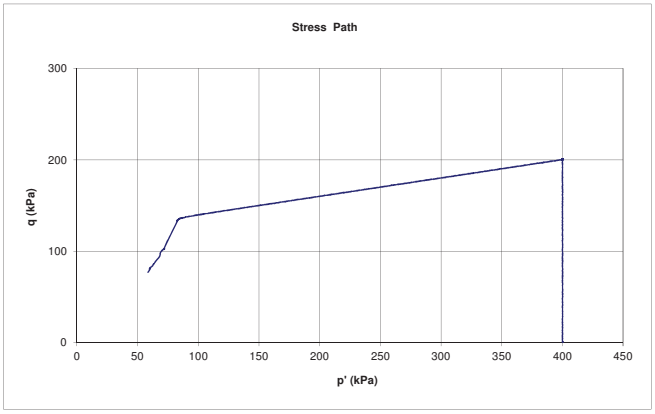

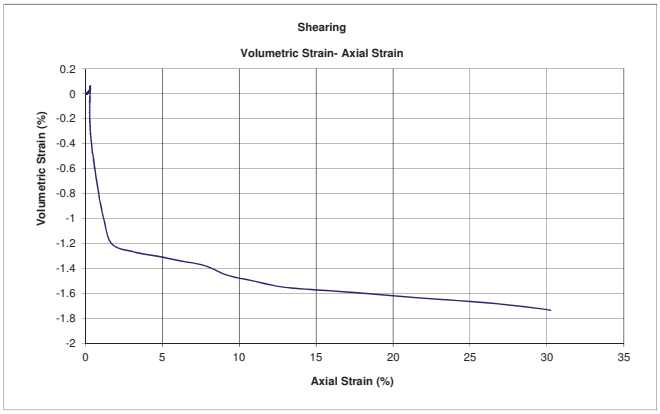

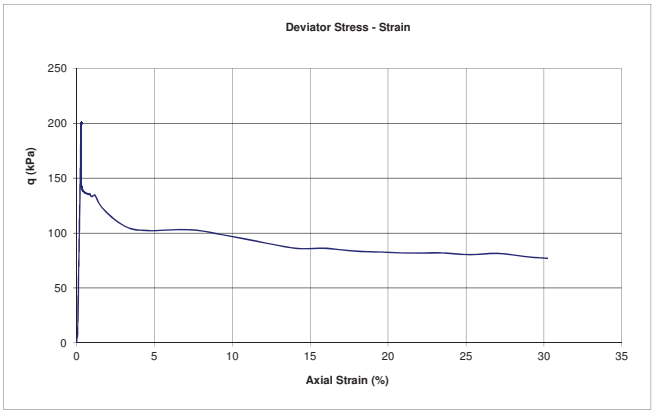

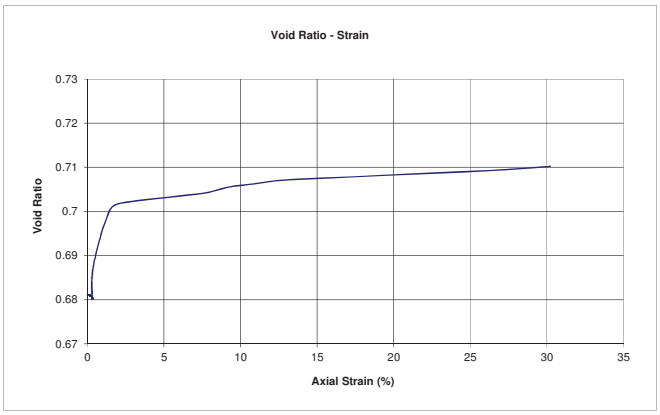

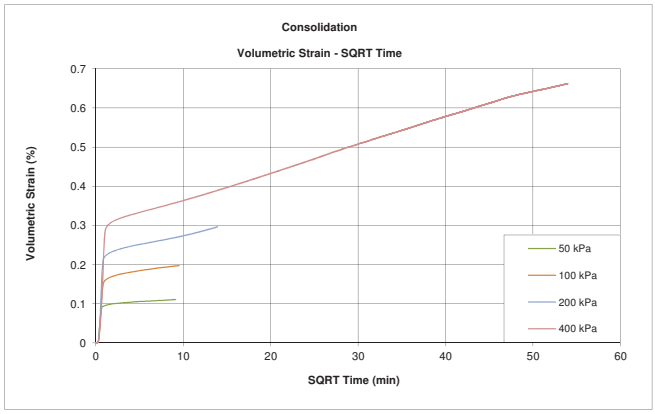

Klohn Crippen Berger

Triaxial CA-QD Test - Summary

PROJECT NO. :
PROJECT : Fundão Tailings Dam Review Panel
SAMPLE : PSD 1
TEST ID: TX 15

DATE : 2016-05-05
TESTED BY: BY
CHECKED BY: JG
TEST TYPE: CA-QD Strain Contolled Extrusion Collapse

SPECIMEN INFORMATION	UNITS	Initial	After Vacuum	Saturation	B-Value	End of 1st Consolidation	End of 2 nd Consolidation	End of 3 rd Consolidation	End of 4th Consolidation	At Failure	End of Shear
Specimen Height	mm	141.14	141.65	141.11	141.03	141.00	140.93	140.80	140.69	139.26	98.16
Specimen Diameter	mm	69.60	69.54	69.33	69.35	69.32	69.27	69.19	68.99	69.76	83.31
Area	cm^2	38.05	37.98	37.75	37.78	37.74	37.68	37.60	37.38	38.22	54.51
Volume	cm^3	536.98	537.99	532.75	532.75	532.13	531.02	529.44	525.91	532.23	535.03
Wet Weight	g	958.98	958.98	1134.69	1141.69	1141.07	1139.96	1138.38	1134.85	1141.17	1143.97
Water Content	%	4.98	4.98	24.21	24.98	24.91	24.79	24.62	24.23	24.92	25.23
Dry Weight	g	913.49	913.49	913.49	913.49	913.49	913.49	913.49	913.49	913.49	913.49
Wet Density	g/cm^3	1.786	1.783	2.130	2.143	2.144	2.147	2.150	2.158	2.144	2.138
Dry Density	g/cm^3	1.701	1.698	1.715	1.715	1.717	1.720	1.725	1.737	1.716	1.707
Specific Gravity of Solids	-	2.92	2.92	2.92	2.92	2.92	2.92	2.92	2.92	2.92	2.92
Solids Volume	cm^3	311.771	311.771	311.771	311.771	311.771	311.771	311.771	311.771	311.771	311.771
Void Volume	cm^3	225.210	226.222	220.975	220.975	220.355	219.245	217.665	214.139	220.459	223.259
Water Volume	cm^3	45.490	45.490	221.195	228.195	227.575	226.465	224.885	221.359	227.679	230.479
Void Ratio (e)	-	0.722	0.726	0.709	0.709	0.707	0.703	0.698	0.687	0.707	0.716
Saturation Ratio (Sr)	%	20.20	20.11	100.10	103.27	103.28	103.29	103.32	103.37	103.28	103.23
Effective Confining Stress	kPa					50	100	200	400		

Shearing (CA-QD)		
Skempton's B Parameter		1.00
Back Pressure before shearing	kPa	704.9
Confining Stress (σ_3') before shearing	kPa	400.3
Shear Strain Rate	kPa / min	1.0
Deviator Stress at Failure*	kPa	195.5
Axial Strain* at Failure	%	0.51

* From Maximum Deviator Stress

Photos:

Before Test




After Test




Klohn Crippen Berger

Triaxial CA-QD Test - Charts

PROJECT NO. :
PROJECT : Fundão Tailings Dam Review Panel
SAMPLE : PSD 1
TEST ID: TX 15
TEST TYPE: CA-QD Strain Contolled Extrusion Collapse
DATE : 2016-05-05
TESTED BY: BY
CHECKED BY: JG

At Failure	
Axial Stain (%)	**0.51**
Deviator Stress (kPa)	**195.5**

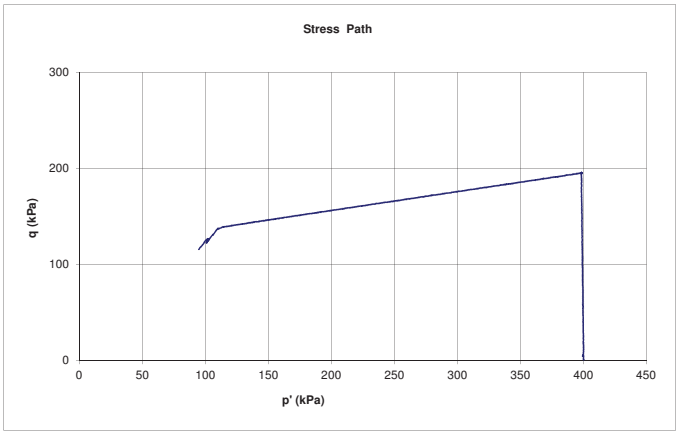

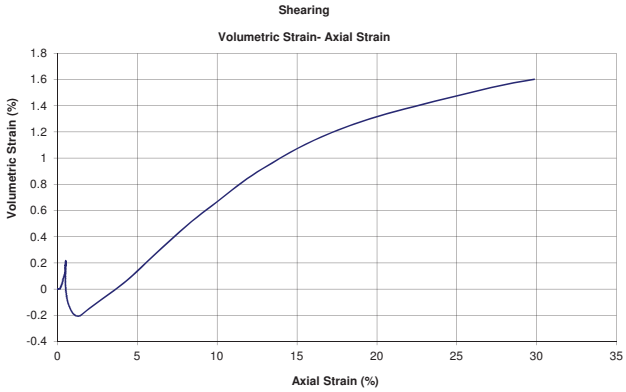

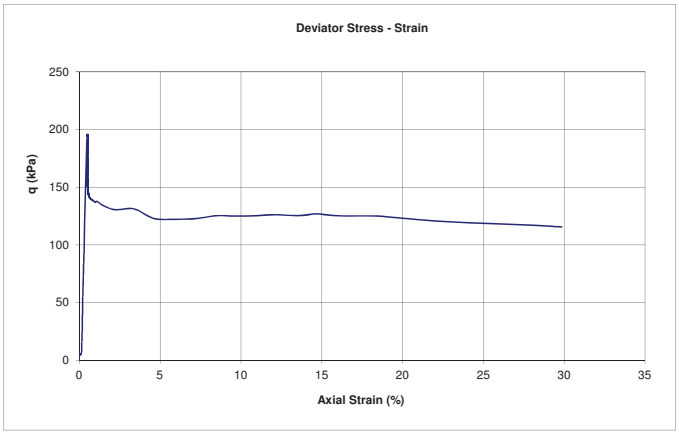

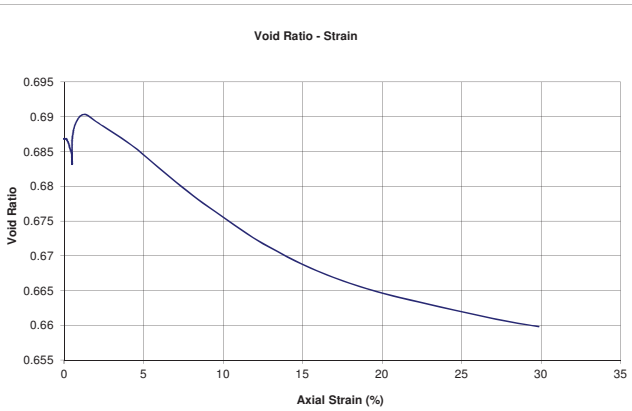

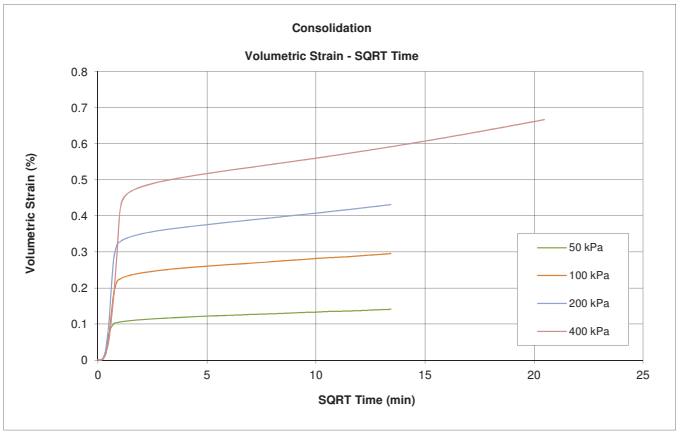

Klohn Crippen Berger

Triaxial CA-QD Test - Summary

PROJECT NO. :
PROJECT : Fundão Tailings Dam Review Panel
SAMPLE : PSD 1
TEST ID: TX 16

DATE : 2016-05-09
TESTED BY: BY
CHECKED BY: JG
TEST TYPE: CA-QD Strain Contolled Extrusion Collapse

SPECIMEN INFORMATION	UNITS	Initial	After Vacuum	Saturation	B-Value	End of 1st Consolidation	End of 2 nd Consolidation	End of 3 rd Consolidation	At Failure	End of Shear
Specimen Height	mm	141.24	141.68	141.68	141.59	141.59	141.55	141.44	140.81	98.78
Specimen Diameter	mm	69.60	69.55	69.15	69.43	69.38	69.33	69.26	69.68	83.41
Area	cm^2	38.05	37.99	37.55	37.86	37.81	37.75	37.67	38.14	54.64
Volume	cm^3	537.36	538.26	532.02	536.02	535.32	534.31	532.85	536.97	539.72
Wet Weight	g	959.95	959.95	1131.10	1141.90	1141.20	1140.19	1138.72	1142.84	1145.59
Water Content	%	5.00	5.00	23.72	24.90	24.83	24.71	24.55	25.01	25.31
Dry Weight	g	914.24	914.24	914.24	914.24	914.24	914.24	914.24	914.24	914.24
Wet Density	g/cm^3	1.786	1.783	2.126	2.130	2.132	2.134	2.137	2.128	2.123
Dry Density	g/cm^3	1.701	1.699	1.718	1.706	1.708	1.711	1.716	1.703	1.694
Specific Gravity of Solids	-	2.93	2.93	2.93	2.93	2.93	2.93	2.93	2.93	2.93
Solids Volume	cm^3	312.027	312.027	312.027	312.027	312.027	312.027	312.027	312.027	312.027
Void Volume	cm^3	225.336	226.235	219.995	223.995	223.295	222.285	220.819	224.939	227.689
Water Volume	cm^3	45.712	45.712	216.862	227.662	226.962	225.952	224.486	228.606	231.356
Void Ratio (e)	-	0.722	0.725	0.705	0.718	0.716	0.712	0.708	0.721	0.730
Saturation Ratio (Sr)	%	20.29	20.21	98.58	101.64	101.64	101.65	101.66	101.63	101.61
Effective Confining Stress	kPa					50	100	200		

Shearing (CU)		
Skempton's B Parameter		1.00
Back Pressure before shearing	kPa	703.5
Confining Stress (σ_3') before shearing	kPa	200.1
Shear Strain Rate	kPa / min	1
Deviator Stress at Failure*	kPa	99.9
Axial Strain* at Failure	%	0.22

* From Maximum Deviator Stress

Photos:

Before Test




After Test




Klohn Crippen Berger

Triaxial CA-QD Test - Charts

PROJECT NO. :
PROJECT : Fundão Tailings Dam Review Panel
SAMPLE : PSD 1
TEST ID: TX 16
TEST TYPE: CA-QD Strain Contolled Extrusion Collapse
DATE : 2016-05-09
TESTED BY: BY
CHECKED BY: JG

At Max. Deviator Stress:	
Axial Stain (%)	**0.22**
Deviator Stress (kPa)	**99.9**

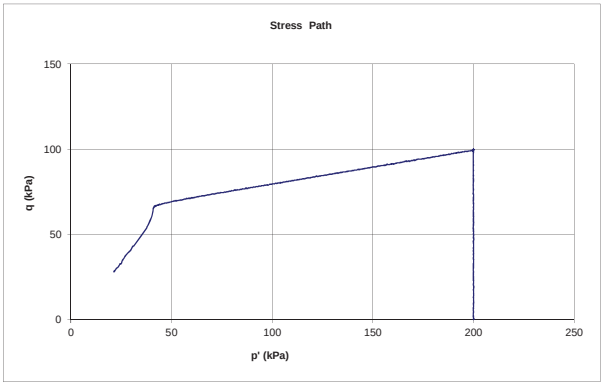

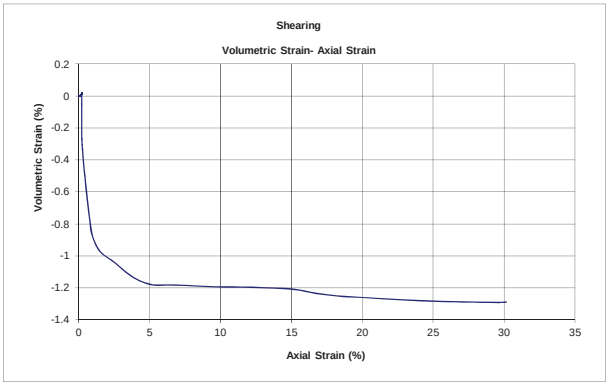

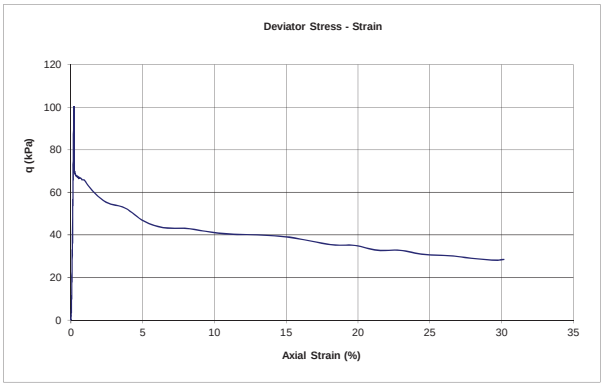

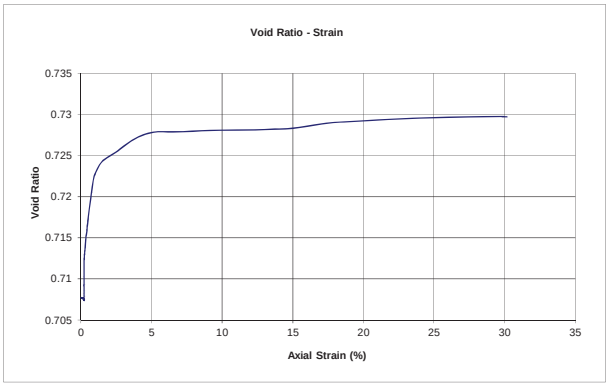

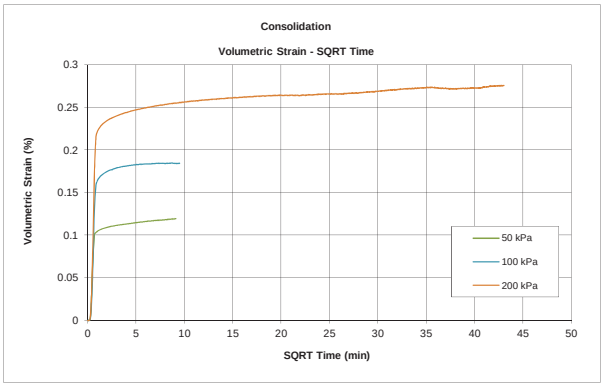

Klohn Crippen Berger

Triaxial CA-QD Test - Summary

PROJECT NO. :
PROJECT : Fundão Tailings Dam Review Panel
SAMPLE : PSD 1
TEST ID: TX 17

DATE : 2016-05-10
TESTED BY: BY
CHECKED BY: JG
TEST TYPE: CA-QD Strain Contolled Extrusion Collapse

SPECIMEN INFORMATION	UNITS	Initial	After Vacuum	Saturation	B-Value	End of 1st Consolidation	End of 2 nd Consolidation	End of 3 rd Consolidation	At Failure	End of Shear
Specimen Height	mm	138.52	138.81	138.81	138.61	138.52	138.40	138.22	137.35	96.36
Specimen Diameter	mm	68.91	68.72	68.27	68.19	68.15	68.05	67.90	68.11	80.49
Area	cm^2	37.30	37.09	36.61	36.52	36.47	36.37	36.21	36.43	50.88
Volume	cm^3	516.62	514.85	508.18	506.18	505.25	503.33	500.43	500.40	490.27
Wet Weight	g	874.79	874.79	1050.95	1056.45	1055.52	1053.60	1050.70	1050.67	1040.54
Water Content	%	5.26	5.26	26.46	27.12	27.01	26.78	26.43	26.42	25.20
Dry Weight	g	831.08	831.08	831.08	831.08	831.08	831.08	831.08	831.08	831.08
Wet Density	g/cm^3	1.693	1.699	2.068	2.087	2.089	2.093	2.100	2.100	2.122
Dry Density	g/cm^3	1.609	1.614	1.635	1.642	1.645	1.651	1.661	1.661	1.695
Specific Gravity of Solids	-	2.94	2.94	2.94	2.94	2.94	2.94	2.94	2.94	2.94
Solids Volume	cm^3	282.679	282.679	282.679	282.679	282.679	282.679	282.679	282.679	282.679
Void Volume	cm^3	233.937	232.168	225.504	223.504	222.574	220.654	217.754	217.724	207.594
Water Volume	cm^3	43.715	43.715	219.875	225.375	224.445	222.525	219.625	219.595	209.465
Void Ratio (e)	-	0.828	0.821	0.798	0.791	0.787	0.781	0.770	0.770	0.734
Saturation Ratio (Sr)	%	18.69	18.83	97.50	100.84	100.84	100.85	100.86	100.86	100.90
Effective Confining Stress	kPa					50	100	200		

Shearing (CA-QD)		
Skempton's B Parameter		1.00
Back Pressure before shearing	kPa	654.9
Confining Stress (σ_3') before shearing	kPa	200.2
Shear Strain Rate	kPa / min	1
Deviator Stress at Failure*	kPa	101.0
Axial Strain* at Failure	%	0.39

* From Maximum Deviator Stress

Photos:

Before Test




After Test




Klohn Crippen Berger

Triaxial CA-QD Test - Charts

PROJECT NO. :
PROJECT : Fundão Tailings Dam Review Panel
SAMPLE : PSD 1
TEST ID: TX 17
TEST TYPE: CA-QD Strain Contolled Extrusion Collapse
DATE : 2016-05-10
TESTED BY: BY
CHECKED BY: JG

At Max. Deviator Stress:	
Axial Stain (%)	**0.39**
Deviator Stress (kPa)	**101.0**

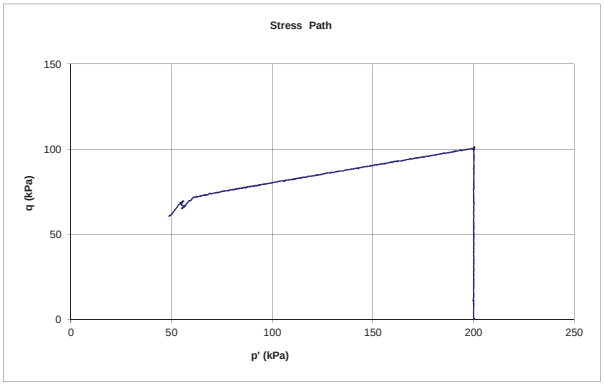

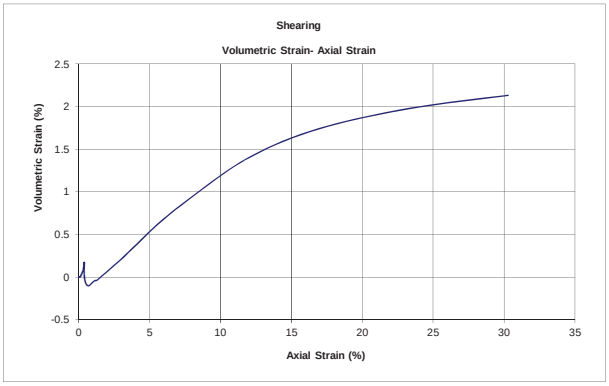

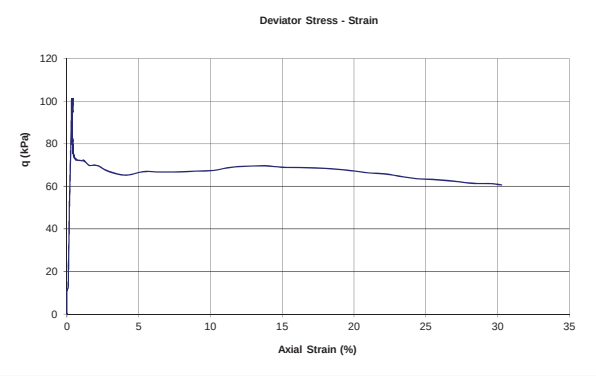

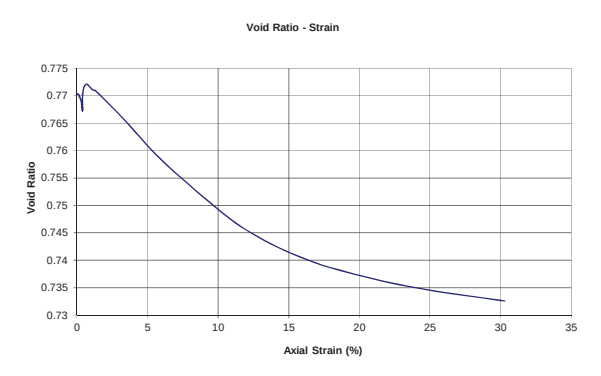

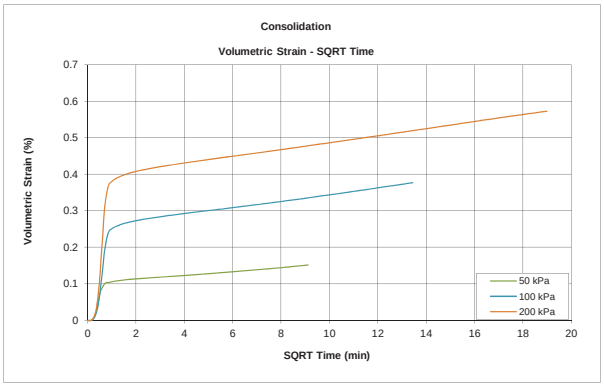

Triaxial CID Test - Summary
(ASTM D7181)

PROJECT NO. :
PROJECT : Fundão Tailings Dam Review Panel
SAMPLE : PSD 1
TEST ID: TX 18

DATE : 2016-05-17
TESTED BY: BY
CHECKED BY: JG
TEST TYPE: CID

SPECIMEN INFORMATION	UNITS	Initial	After Vacuum	Saturation	B-Value	End of 1st Consolidation	End of 2 nd Consolidation	At Failure	End of Shear
Specimen Height	mm	138.38	138.71	138.03	137.73	137.65	137.39	112.00	97.25
Specimen Diameter	mm	68.97	68.62	68.00	67.72	67.67	67.54	73.15	78.36
Area	cm^2	37.36	36.98	36.31	36.02	35.96	35.82	42.02	48.23
Volume	cm^3	516.99	512.98	501.24	496.14	495.07	492.17	470.66	469.00
Wet Weight	g	838.71	838.71	1021.52	1026.32	1025.25	1022.35	1000.84	999.18
Water Content	%	5.23	5.23	28.17	28.77	28.63	28.27	25.57	25.36
Dry Weight	g	797.03	797.03	797.03	797.03	797.03	797.03	797.03	797.03
Wet Density	g/cm^3	1.622	1.635	2.038	2.069	2.071	2.077	2.126	2.130
Dry Density	g/cm^3	1.542	1.554	1.590	1.606	1.610	1.619	1.693	1.699
Specific Gravity of Solids	-	2.93	2.93	2.93	2.93	2.93	2.93	2.93	2.93
Solids Volume	cm^3	272.022	272.022	272.022	272.022	272.022	272.022	272.022	272.022
Void Volume	cm^3	244.971	240.957	229.217	224.117	223.047	220.147	198.637	196.977
Water Volume	cm^3	41.684	41.684	224.494	229.294	228.224	225.324	203.814	202.154
Void Ratio (e)	-	0.901	0.886	0.843	0.824	0.820	0.809	0.730	0.724
Saturation Ratio (Sr)	%	17.02	17.30	97.94	102.31	102.32	102.35	102.61	102.63
Effective Confining Stress	kPa					50	100		

Shearing (CID)		
Skempton's B Parameter		1.00
Back Pressure before shearing	kPa	703.3
Confining Stress (σ_3') before shearing	kPa	100
Shear Strain Rate	% / min	0.1
Deviator Stress at Failure*	kPa	240.49
Axial Strain* at Failure	%	18.48

* From Maximum Deviator Stress

Photos:

Before Test




After Test




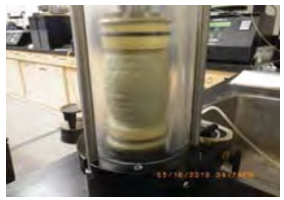

Klohn Crippen Berger

Triaxial CID Test - Charts

(ASTM D7181)

PROJECT NO. :
PROJECT : Fundão Tailings Dam Review Panel
SAMPLE : PSD 1
TEST ID: TX 18
TEST TYPE: CID
DATE : 2016-05-17
TESTED BY: BY
CHECKED BY: JG

At Max. Deviator Stress:	
Axial Stain (%)	**18.48**
Deviator Stress (kPa)	**240.5**

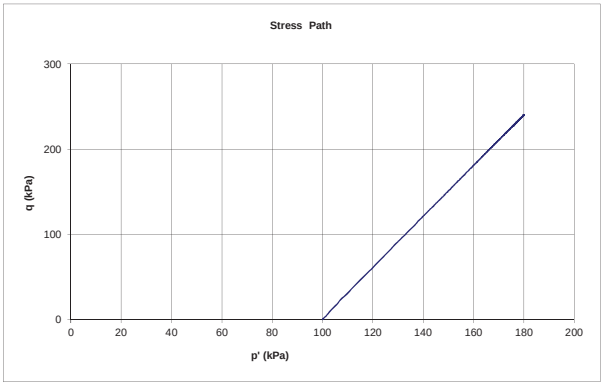

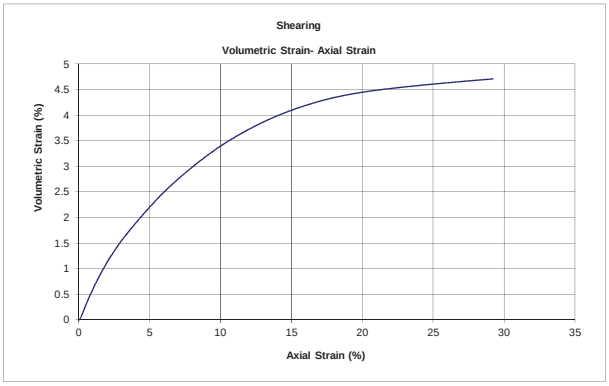

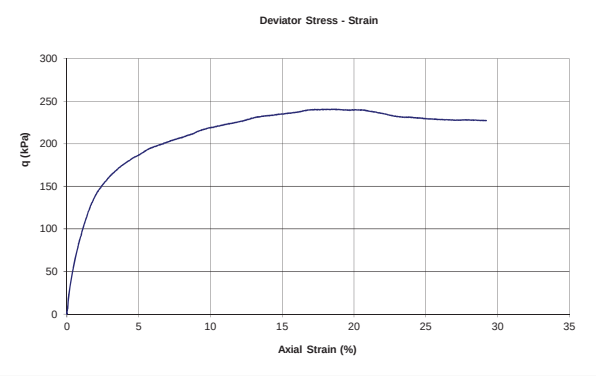

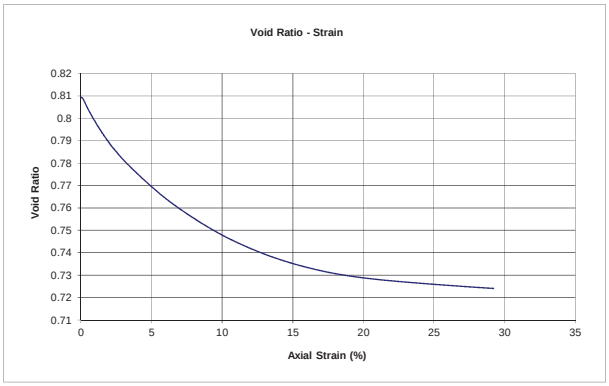

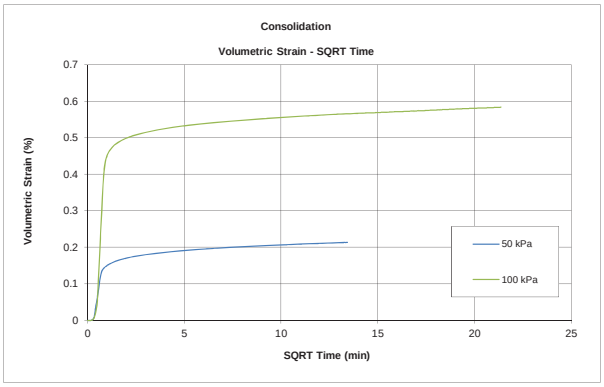

Triaxial CID Test - Summary
(ASTM D7181)

PROJECT NO. :
PROJECT : Fundão Tailings Dam Review Panel
SAMPLE : PSD 1
TEST ID: TX 19

DATE : 2016-05-17
TESTED BY: BY
CHECKED BY: JG
TEST TYPE: CID

SPECIMEN INFORMATION	UNITS	Initial	After Vacuum	Saturation	B-Value	End of 1st Consolidation	At Failure	End of Shear
Specimen Height	mm	138.49	138.59	137.09	136.74	136.46	108.91	96.74
Specimen Diameter	mm	68.99	68.70	67.640	67.35	67.26	73.27	77.67
Area	cm^2	37.38	37.07	35.93	35.63	35.53	42.16	47.38
Volume	cm^3	517.704	513.732	492.624	487.174	484.874	459.184	458.344
Wet Weight	g	826.24	826.24	1011.05	1015.25	1012.95	987.26	986.42
Water Content	%	5.14	5.14	28.66	29.19	28.90	25.63	25.52
Dry Weight	g	785.85	785.85	785.85	785.85	785.85	785.85	785.85
Wet Density	g/cm^3	1.596	1.608	2.052	2.084	2.089	2.150	2.152
Dry Density	g/cm^3	1.518	1.530	1.595	1.613	1.621	1.711	1.715
Specific Gravity of Solids	-	3.05	3.05	3.05	3.05	3.05	3.05	3.05
Solids Volume	cm^3	257.655	257.655	257.655	257.655	257.655	257.655	257.655
Void Volume	cm^3	260.049	256.077	234.969	229.519	227.219	201.529	200.689
Water Volume	cm^3	40.393	40.393	225.207	229.407	227.107	201.417	200.577
Void Ratio (e)	-	1.009	0.994	0.912	0.891	0.882	0.782	0.779
Saturation Ratio (Sr)	%	15.53	15.77	95.85	99.95	99.95	99.94	99.94
Effective Confining Stress	kPa					50		

Shearing (CID)		
Skempton's B Parameter		1.00
Back Pressure before shearing	kPa	809.9
Confining Stress (σ_3') before shearing	kPa	50.1
Shear Strain Rate	% / min	0.1
Deviator Stress at Failure*	kPa	111.75
Axial Strain* at Failure	%	20.19

* From Maximum Deviator Stress

Photos:

Before Test

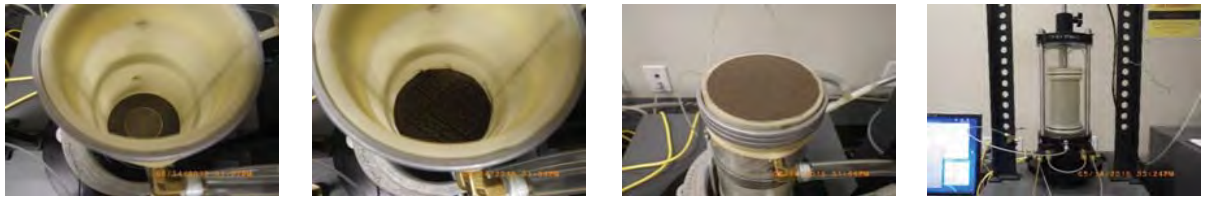

After Test

Klohn Crippen Berger

Triaxial CID Test - Charts

(ASTM D7181)

PROJECT NO. :
PROJECT : Fundão Tailings Dam Review Panel
SAMPLE : PSD 1
TEST ID: TX 19
TEST TYPE: CID
DATE : 2016-05-17
TESTED BY: BY
CHECKED BY: JG

At Max. Deviator Stress:	
Axial Stain (%)	**20.19**
Deviator Stress (kPa)	**111.8**

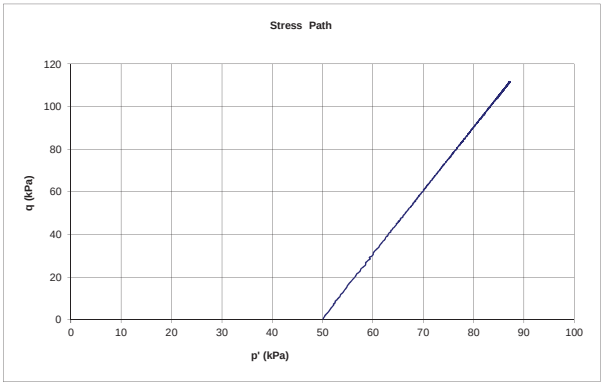

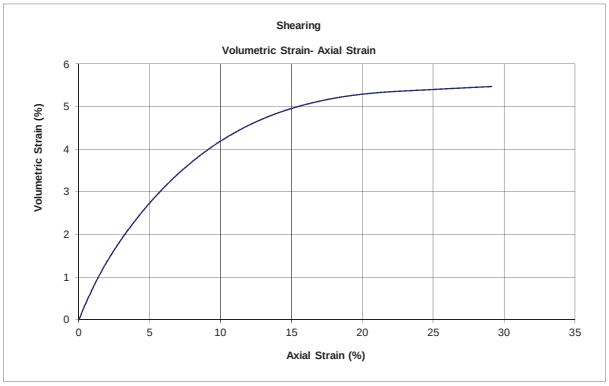

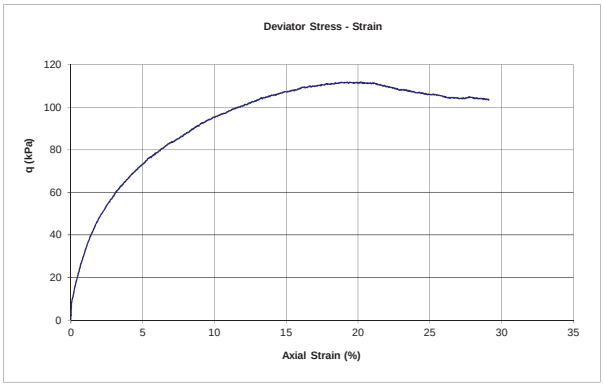

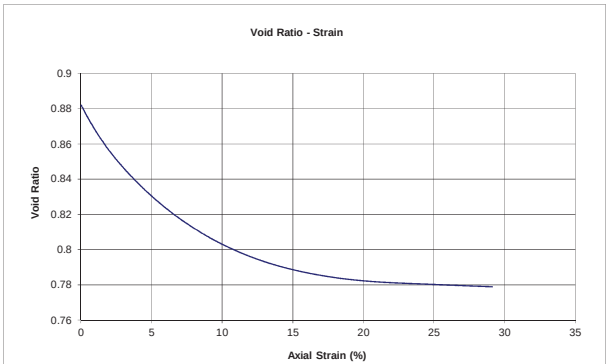

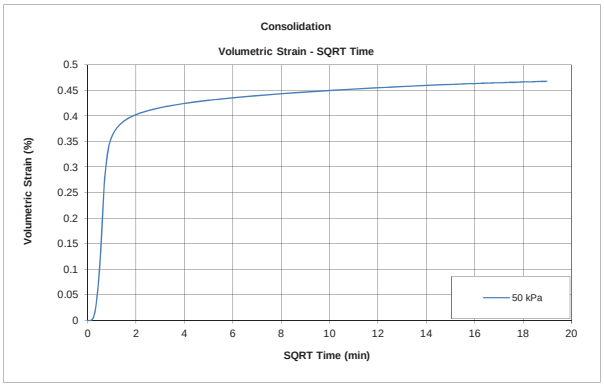

Klohn Crippen Berger

Extrusion Collapse, CA-QD-SC, Triaxial Test with constant q - Summary

PROJECT NO. :
PROJECT : Fundão Tailings Dam Review Panel
SAMPLE : PSD1
TEST TYPE: Anisotropically Consolidated Stress-Controlled Drained Triaxial Test with constant q
TEST ID: TX 22

DATE : 2016-06-17
TESTED BY: BY
CHECKED BY: JG

SPECIMEN INFORMATION	UNITS	Initial	After Vacuum	End of Saturation	End of B - Value	End of 1st Consolidation	End of 2 nd Consolidation	End of 3 rd Consolidation	Anisotropic Consolidation	At Failure / End
Specimen Height	mm	138.40	138.40	138.40	138.36	138.36	138.37	138.26	137.56	135.18
Specimen Diameter	mm	69.03	68.99	68.74	68.62	68.48	68.31	68.18	68.32	68.98
Area	cm^2	37.43	37.38	37.11	36.98	36.83	36.65	36.51	36.66	37.37
Volume	cm^3	517.97	517.37	513.62	511.62	509.54	507.10	504.84	504.31	505.12
Wet Weight	g	901.34	901.34	1085.34	1091.13	1089.05	1086.61	1084.35	1083.79	1082.98
Water Content	%	4.98	4.98	26.41	27.08	26.84	26.56	26.30	26.23	26.14
Dry Weight	g	858.58	858.58	858.58	858.58	858.58	858.58	858.58	858.58	858.58
Wet Density	g/cm^3	1.740	1.742	2.113	2.133	2.137	2.143	2.148	2.149	2.144
Dry Density	g/cm^3	1.658	1.660	1.672	1.678	1.685	1.693	1.701	1.702	1.700
Specific Gravity of Solids	-	3.05	3.05	3.05	3.05	3.05	3.05	3.05	3.05	3.05
Solids Volume	cm^3	281.502	281.502	281.502	281.502	281.502	281.502	281.502	281.502	281.502
Void Volume	cm^3	236.465	235.865	232.115	230.115	228.035	225.595	223.335	222.805	223.615
Water Volume	cm^3	42.757	42.757	226.757	232.546	230.466	228.026	225.766	225.206	224.401
Void Ratio (e)	-	0.840	0.838	0.825	0.817	0.810	0.801	0.793	0.791	0.794
Saturation Ratio (Sr)	%	18.08	18.13	97.69	101.06	101.07	101.08	101.09	101.08	100.35
Effective Confining Stress	kPa					50	100	200		

Shearing (CA-QID-SC)		
Skempton's B Parameter		1.00
Back Pressure before shearing	kPa	650.0
Confining Stress (σ_3') before shearing	kPa	200.0
Shear Strain Rate	kPa/min	< 1.0
Deviator Stress at Failure	kPa	99.1
Axial Strain at Failure	%	1.73

Photos:

Before Test




After Test


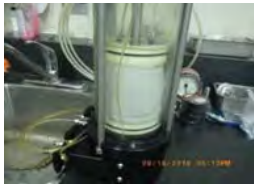

Extrusion Collapse, CA-QD-SC, Triaxial Test with constant q - Charts

PROJECT NO. :
PROJECT : Fundão Tailings Dam Review Panel
SAMPLE : PSD1
TEST ID: TX 22
TEST TYPE: Anisotropically Consolidated Stress-Controlled Drained Triaxial Test with constant q
DATE : 2016-06-17
TESTED BY: BY
CHECKED BY: JG

At Failure Deviator Stress:	
Axial Stain (%)	**1.73**
Deviator Stress (kPa)	**99.1**

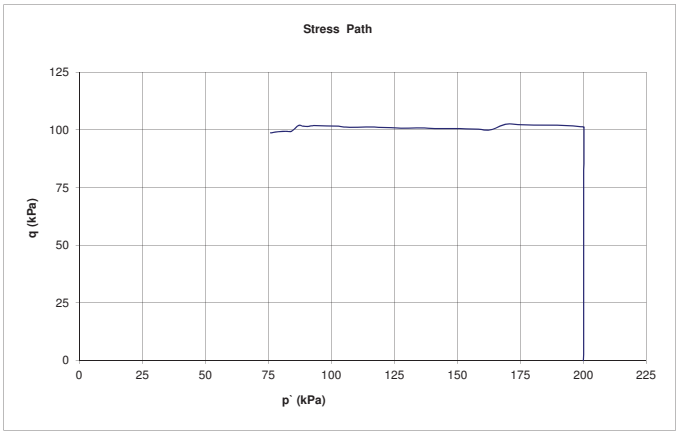

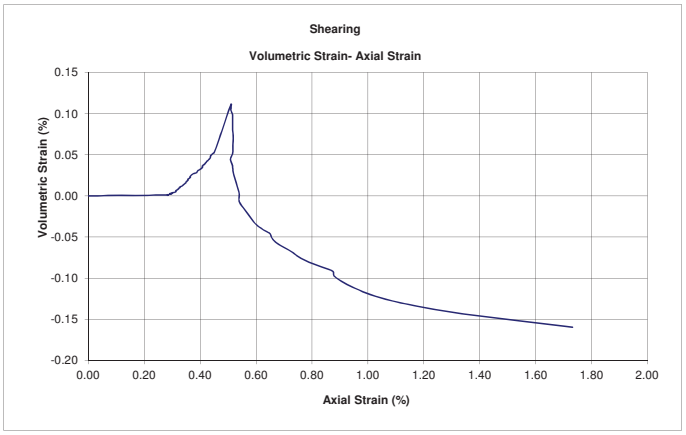

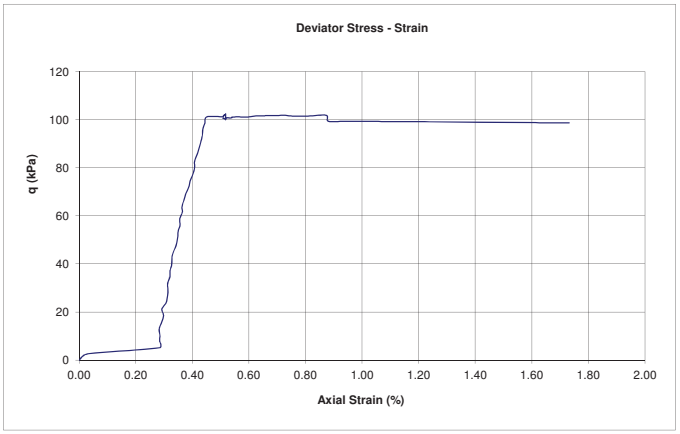

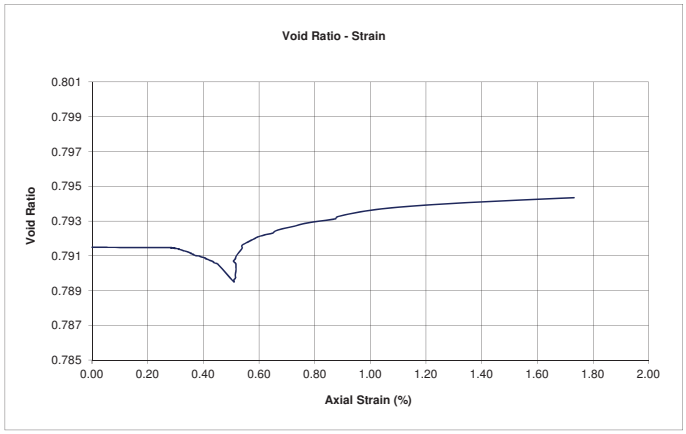

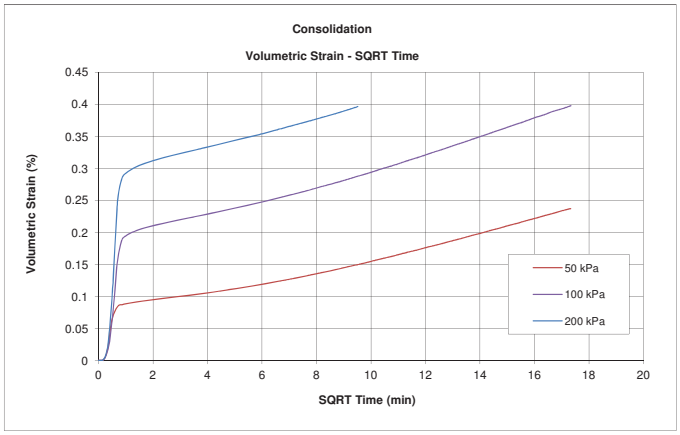

Klohn Crippen Berger

Triaxial CAU Test - Summary

PROJECT NO. :
PROJECT : Fundão Tailings Dam Review Panel
SAMPLE : PSD 1
TEST TYPE: Anisotropically Consolidated Undained Triaxial Compression Test
TEST ID: TX 23

DATE : 2016-06-17
TESTED BY: BY
CHECKED BY: JG

SPECIMEN INFORMATION	UNITS	Initial	After Vacuum	End of Saturation	End of B - Value	End of 1st Consolidation	End of 2 nd Consolidation	End of 3 rd Consolidation	Anisotropic Consolidation	At Failure	End of Shear
Specimen Height	mm	138.42	138.42			138.23	138.16	138.02	138.35	137.42	97.88
Specimen Diameter	mm	68.95	68.92	68.70	68.26	68.19	68.07	67.90	67.80	68.03	80.61
Area	cm^2	37.34	37.31	37.07	36.60	36.52	36.39	36.21	36.10	36.35	51.03
Volume	cm^3	516.84	516.39	513.05	506.05	504.83	502.78	499.75	499.47	499.47	499.47
Wet Weight	g	899.13	899.13	1074.83	1082.69	1081.47	1079.42	1076.39	1076.11	1076.11	1076.11
Water Content	%	5.14	5.14	25.69	26.60	26.46	26.22	25.87	25.84	25.84	25.84
Dry Weight	g	855.17	855.17	855.17	855.17	855.17	855.17	855.17	855.17	855.17	855.17
Wet Density	g/cm^3	1.740	1.741	2.095	2.139	2.142	2.147	2.154	2.154	2.154	2.154
Dry Density	g/cm^3	1.655	1.656	1.667	1.690	1.694	1.701	1.711	1.712	1.712	1.712
Specific Gravity of Solids	-	3.01	3.01	3.01	3.01	3.01	3.01	3.01	3.01	3.01	3.01
Solids Volume	cm^3	284.111	284.111	284.111	284.111	284.111	284.111	284.111	284.111	284.111	284.111
Void Volume	cm^3	232.732	232.282	228.940	221.940	220.720	218.670	215.643	215.363	215.363	215.363
Water Volume	cm^3	43.956	43.956	219.656	227.516	226.296	224.246	221.219	220.939	220.939	220.939
Void Ratio (e)	-	0.819	0.818	0.806	0.781	0.777	0.770	0.759	0.758	0.758	0.758
Saturation Ratio (Sr)	%	18.89	18.92	95.94	102.51	102.53	102.55	102.59	102.59	102.59	102.59
Effective Confining Stress	kPa					50	100	200			

Shearing (CAU)		
Skempton's B Parameter		1.00
Back Pressure before shearing	kPa	702.4
Confining Stress (σ_3') before shearing	kPa	200.0
Shear Strain Rate	% / min	0.07
Deviator Stress at Failure*	kPa	182.2
Axial Strain* at Failure	%	0.89

* From Maximum Deviator Stress

Photos:

Before Test

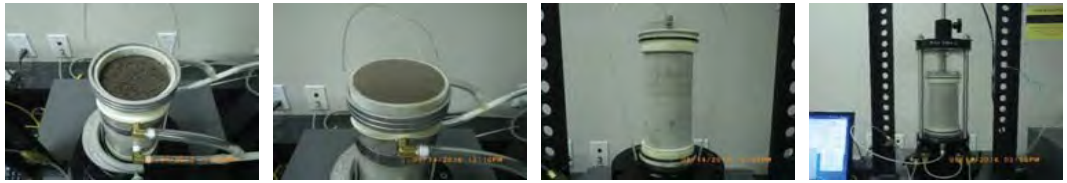

After Test

Triaxial CAU Test - Charts

PROJECT NO. :
PROJECT : Fundão Tailings Dam Review Panel
SAMPLE : PSD 1
TEST ID: TX 23
TEST TYPE: Anisotropically Consolidated Undained Triaxial Compression Test
DATE : 2016-06-17
TESTED BY: BY
CHECKED BY: JG

At Max. Deviator Stress:	
Axial Stain (%)	**0.89**
Deviator Stress (kPa)	**182.2**

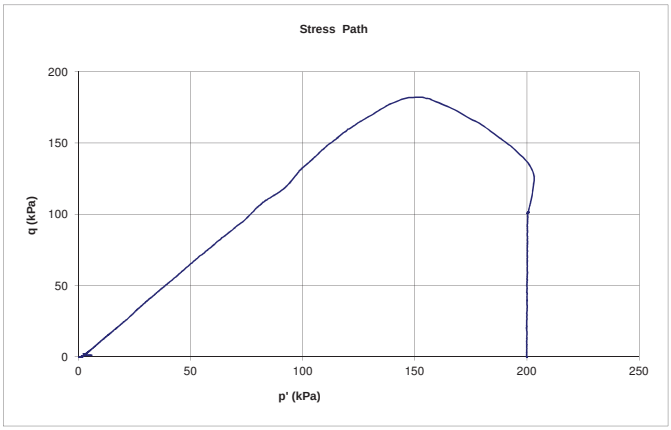

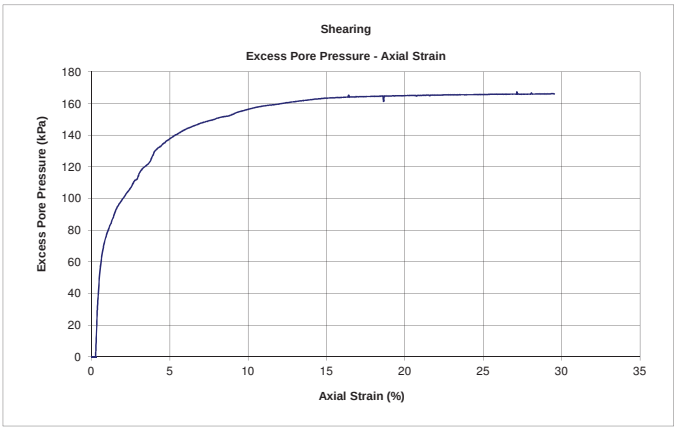

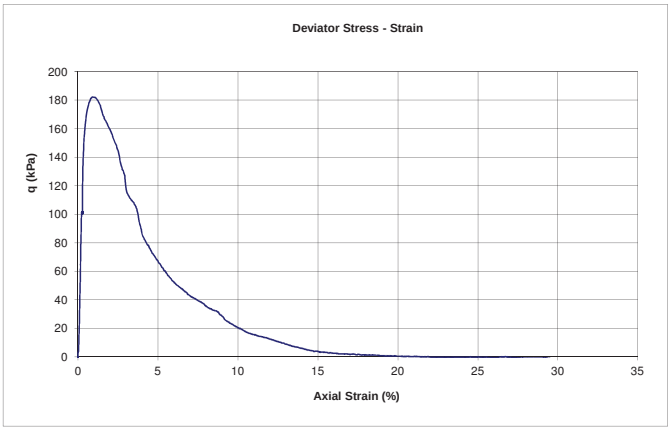

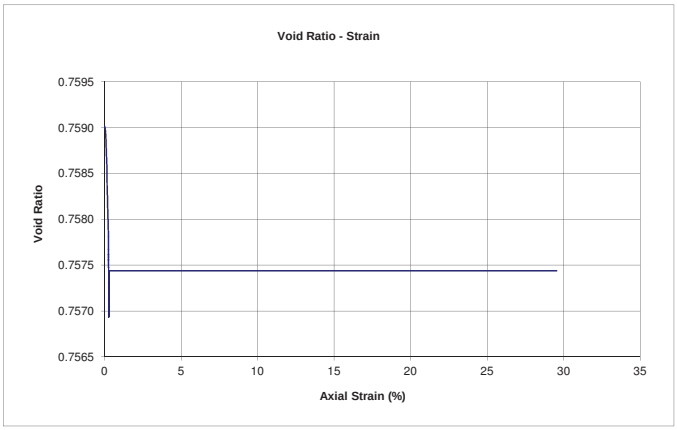

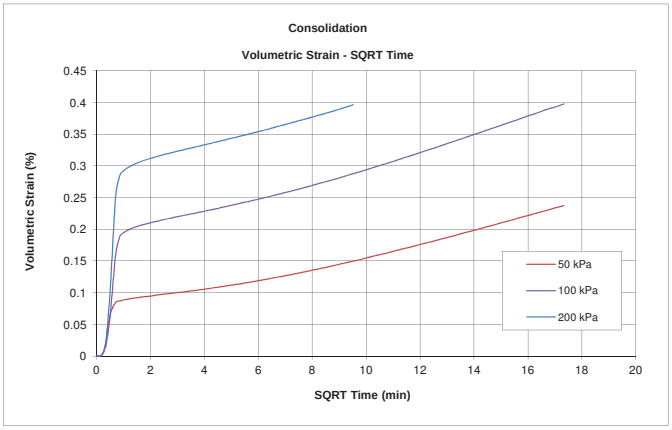

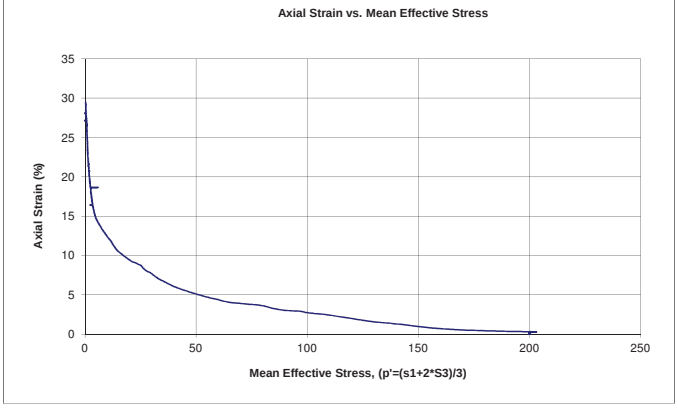

Klohn Crippen Berger

Extrusion Collapse, CA-QID-SC, Triaxial Test with increasing q - Summary

PROJECT NO. :
PROJECT : Fundão Tailings Dam Review Panel
SAMPLE : PSD 1
TEST TYPE: Anisotropically Consolidated Stress-Controlled Drained Triaxial Test with increasing q
TEST ID: TX 24

DATE : 2016-06-20
TESTED BY: BY
CHECKED BY: JG

SPECIMEN INFORMATION	UNITS	Initial	After Vacuum	End of Saturation	End of B - Value	End of 1st Consolidation	End of 2nd Consolidation	End of 3rd Consolidation	Anisotropic Consolidation	At Failure
Specimen Height	mm	138.59	138.59	138.59	138.30	138.26	138.18	138.06	137.83	136.47
Specimen Diameter	mm	68.83	68.28	68.15	68.09	68.06	67.98	67.87	67.88	68.26
Area	cm^2	37.21	36.62	36.48	36.41	36.38	36.30	36.18	36.19	36.59
Volume	cm^3	515.68	507.47	505.56	503.56	502.93	501.54	499.47	498.87	499.42
Wet Weight	g	897.10	897.10	1069.39	1079.18	1078.54	1077.16	1075.09	1074.49	1076.99
Water Content	%	4.95	4.95	25.11	26.25	26.18	26.02	25.77	25.70	25.99
Dry Weight	g	854.79	854.79	854.79	854.79	854.79	854.79	854.79	854.79	854.79
Wet Density	g/cm^3	1.740	1.768	2.115	2.143	2.145	2.148	2.152	2.154	2.156
Dry Density	g/cm^3	1.658	1.684	1.691	1.697	1.700	1.704	1.711	1.713	1.712
Specific Gravity of Solids	-	3.02	3.02	3.02	3.02	3.02	3.02	3.02	3.02	3.02
Solids Volume	cm^3	283.042	283.042	283.042	283.042	283.042	283.042	283.042	283.042	283.042
Void Volume	cm^3	232.635	224.427	222.522	220.522	219.884	218.501	216.425	215.825	216.373
Water Volume	cm^3	42.312	42.312	214.605	224.395	223.757	222.374	220.298	219.698	222.198
Void Ratio (e)	-	0.822	0.793	0.786	0.779	0.777	0.772	0.765	0.763	0.764
Saturation Ratio (Sr)	%	18.19	18.85	96.44	101.76	101.76	101.77	101.79	101.79	102.69
Effective Confining Stress	kPa					50	100	200		

Shearing (CU)		
Skempton's B Parameter		1.00
Back Pressure before shearing	kPa	702.4
Confining Stress (σ_3') before shearing	kPa	200.0
Shear Strain Rate	kPa/min	<1
Deviator Stress at Failure	kPa	132.7
Axial Strain at Failure	%	0.99

Photos:

Before Test

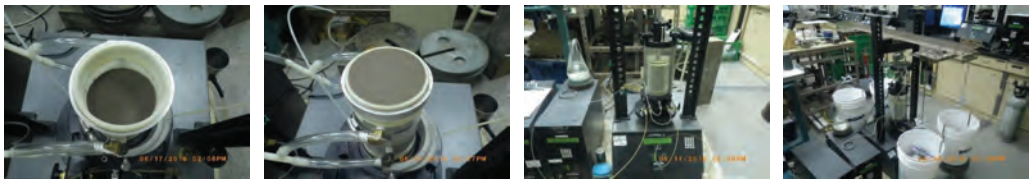

After Test

Extrusion Collapse, CA-QID-SC, Triaxial Test with increasing q - Charts

PROJECT NO. :
PROJECT : Fundão Tailings Dam Review Panel
SAMPLE : PSD 1
TEST ID: TX 24
TEST TYPE: Anisotropically Consolidated Stress-Controlled Drained Triaxial Test with increasing q
DATE : 2016-06-20
TESTED BY: BY
CHECKED BY: JG

At Failure Deviator Stress:	
Axial Stain (%)	**0.99**
Deviator Stress (kPa)	**132.7**

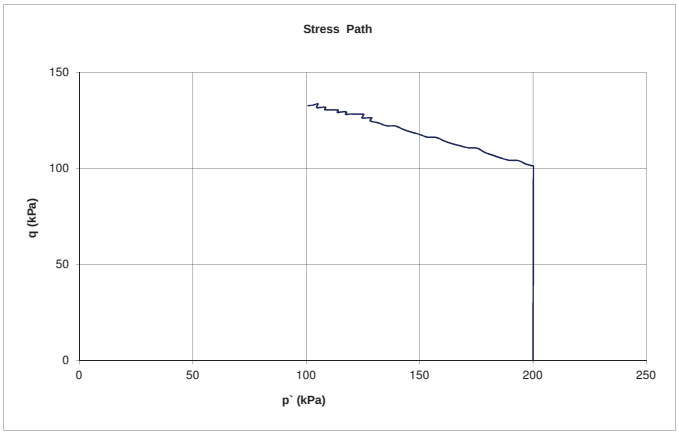

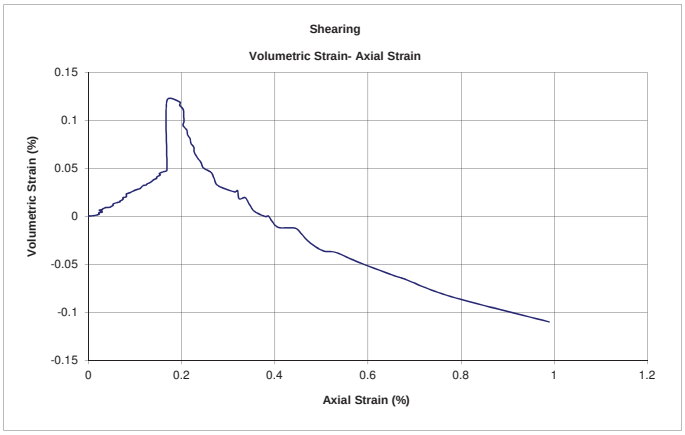

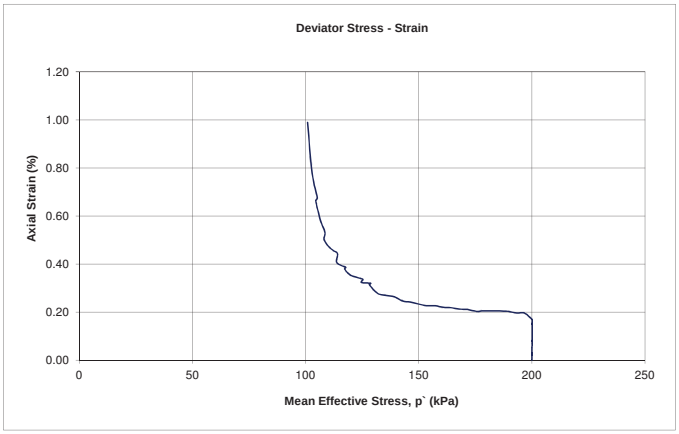

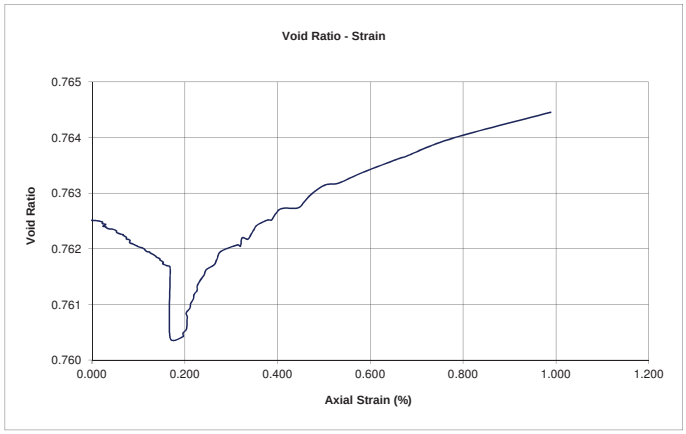

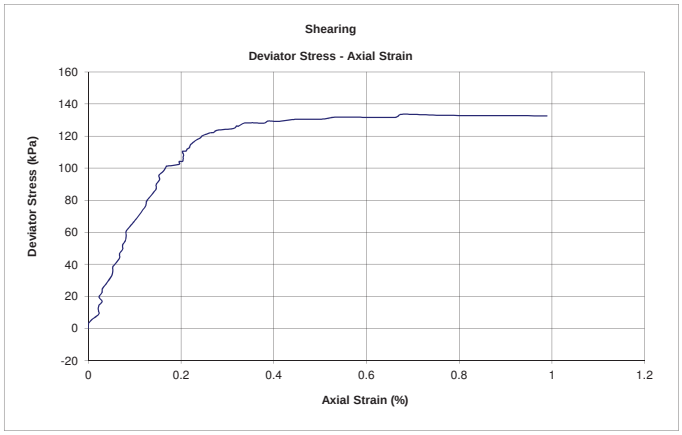

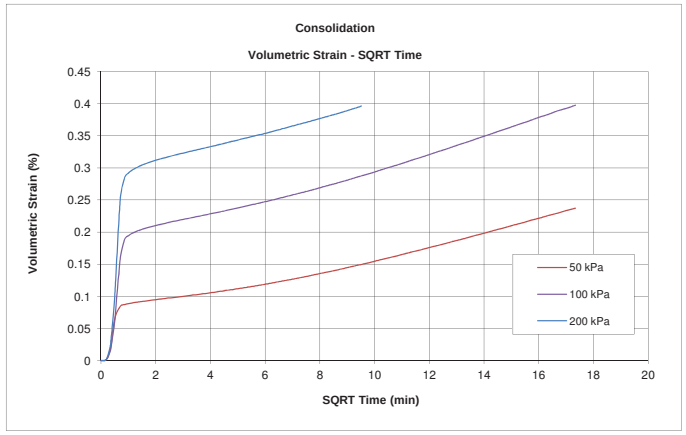

Klohn Crippen Berger

Triaxial CAU Test - Summary

PROJECT NO. :
PROJECT : Fundão Tailings Dam Review Panel
SAMPLE : PSD 1
TEST TYPE: Anisotropically Consolidated Undained Triaxial Compression Test
TEST ID: TX 25

DATE : 2016-06-21
TESTED BY: BY
CHECKED BY: JG

SPECIMEN INFORMATION	UNITS	Initial	After Vacuum	End of Saturation	End of B - Value	End of 1st Consolidation	End of 2 nd Consolidation	End of 3 rd Consolidation	End of 4 th Consolidation	Anisotropic Consolidation	At Failure	End of Shear
Specimen Height	mm	138.4	138.4	138.40	138.33	138.27	138.18	138.040	137.87	137.25	136.32	96.36
Specimen Diameter	mm	68.81	68.81	68.686	68.50	68.46	68.37	68.235	68.00	68.05	68.28	81.21
Area	cm^2	37.19	37.19	37.05	36.86	36.81	36.71	36.57	36.31	36.37	36.62	51.80
Volume	cm^3	514.671	514.671	512.812	509.812	508.976	507.284	504.780	500.673	499.158	499.158	499.158
Wet Weight	g	895.35	895.35	1073.44	1085.44	1084.60	1082.91	1080.41	1076.30	1074.71	1074.71	1074.71
Water Content	%	4.95	4.95	25.83	27.23	27.13	26.94	26.64	26.16	25.97	25.97	25.97
Dry Weight	g	853.12	853.12	853.12	853.12	853.12	853.12	853.12	853.12	853.12	853.12	853.12
Wet Density	g/cm^3	1.740	1.740	2.093	2.129	2.131	2.135	2.140	2.150	2.153	2.153	2.153
Dry Density	g/cm^3	1.658	1.658	1.664	1.673	1.676	1.682	1.690	1.704	1.709	1.709	1.709
Specific Gravity of Solids	-	3.06	3.06	3.06	3.06	3.06	3.06	3.06	3.06	3.06	3.06	3.06
Solids Volume	cm^3	278.798	278.798	278.798	278.798	278.798	278.798	278.798	278.798	278.798	278.798	278.798
Void Volume	cm^3	235.874	235.874	234.015	231.015	230.179	228.487	225.983	221.876	220.361	220.361	220.361
Water Volume	cm^3	42.229	42.229	220.319	232.319	231.483	229.791	227.287	223.180	221.590	221.590	221.590
Void Ratio (e)	-	0.846	0.846	0.839	0.829	0.826	0.820	0.811	0.796	0.790	0.790	0.790
Saturation Ratio (Sr)	%	17.90	17.90	94.15	100.56	100.57	100.57	100.58	100.59	100.56	100.56	100.56
Effective Confining Stress	kPa					50	100	200	400			

Shearing (CAU)		
Skempton's B Parameter		1.00
Back Pressure before shearing	kPa	700.8
Confining Stress (σ_3') before shearing	kPa	399.8
Shear Strain Rate	% / min	0.05
Deviator Stress at Failure*	kPa	330.9
Axial Strain* at Failure	%	1.13

* From Maximum Deviator Stress

Photos:

Before Test

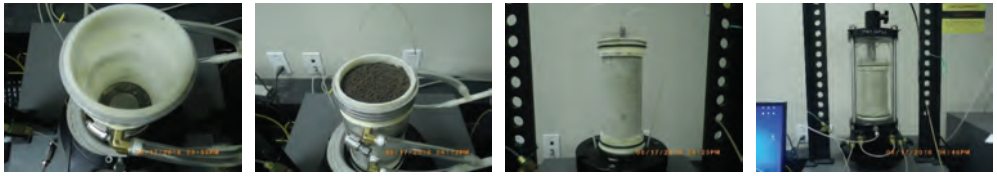

After Test

Triaxial CAU Test - Charts

PROJECT NO. :
PROJECT : Fundão Tailings Dam Review Panel
SAMPLE : PSD 1
TEST ID: TX 25
TEST TYPE: Anisotropically Consolidated Undained Triaxial Compression Test
DATE : 2016-06-21
TESTED BY: BY
CHECKED BY: JG

At Max. Deviator Stress:	
Axial Stain (%)	1.13
Deviator Stress (kPa)	330.9

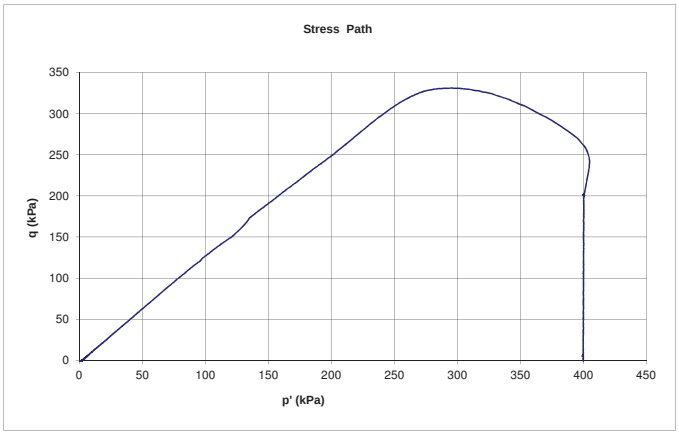

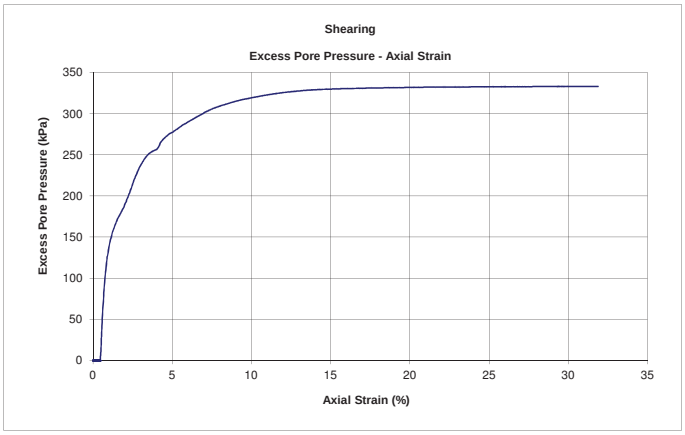

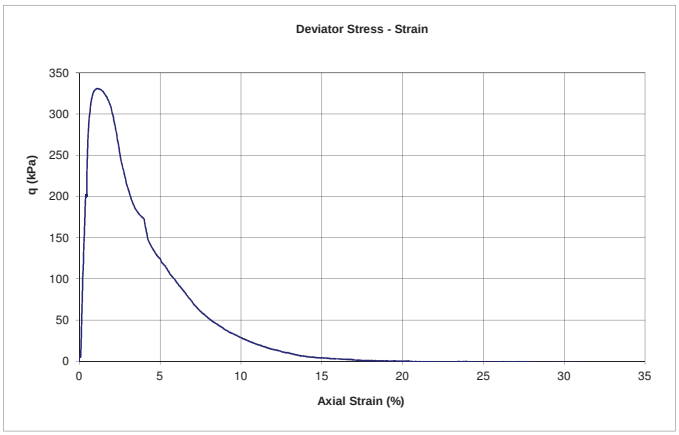

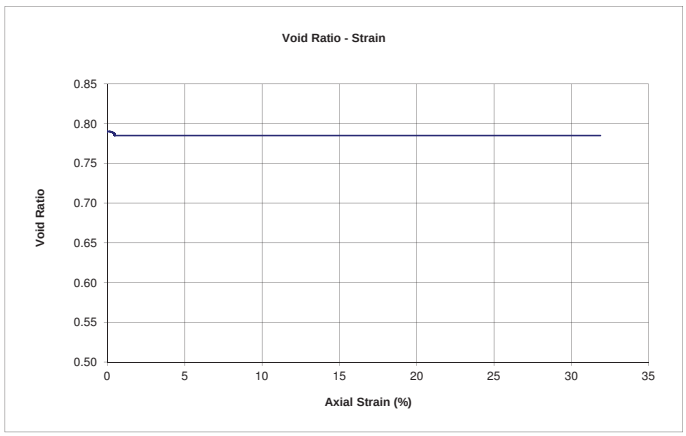

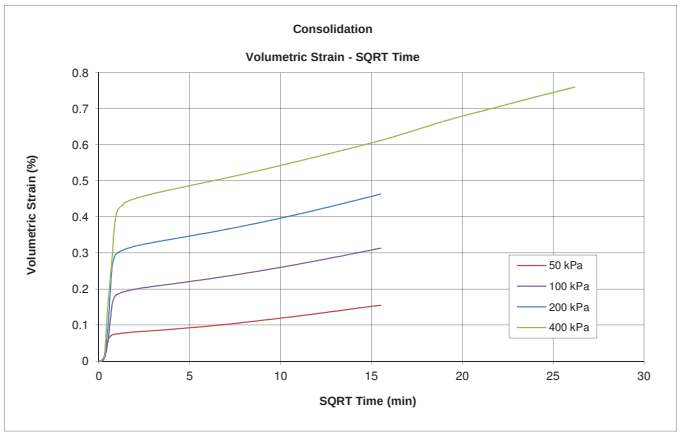

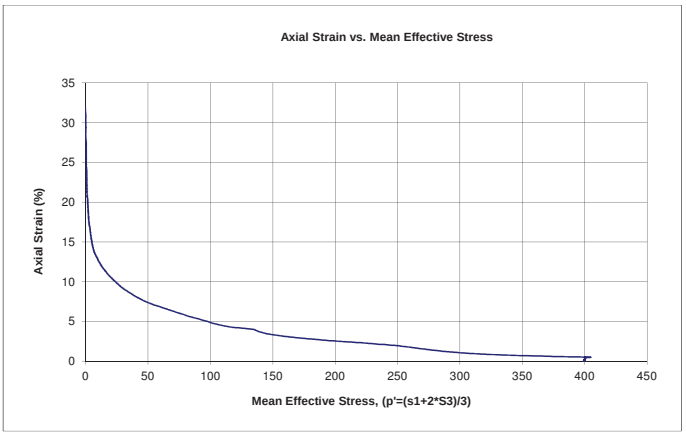

Klohn Crippen Berger

Extrusion Collapse, CA-QD-SC, Triaxial Test with constant q - Summary

PROJECT NO. :
PROJECT : Fundão Tailings Dam Review Panel
SAMPLE : PSD 1
TEST TYPE: Anisotropically Consolidated Stress-Controlled Drained Triaxial Test with constant q
TEST ID: TX 26

DATE : 2016-06-20
TESTED BY: BY
CHECKED BY: JG

SPECIMEN INFORMATION	UNITS	Initial	After Vacuum	End of Saturation	End of B - Value	End of 1st Consolidation	End of 2 nd Consolidation	End of 3 rd Consolidation	End of 4 th Consolidation	Anisotropic Consolidation	At Failure-end
Specimen Height	mm	138.57	138.57	138.56	138.40	138.36	138.29	138.18	138.07	137.70	137.40
Specimen Diameter	mm	68.85	68.54	68.43	68.37	68.35	68.31	68.25	68.15	68.21	68.39
Area	cm^2	37.23	36.90	36.78	36.72	36.69	36.65	36.58	36.47	36.54	36.73
Volume	cm^3	515.90	511.27	509.66	508.16	507.69	506.78	505.50	503.58	503.15	504.73
Wet Weight	g	934.77	934.77	1102.29	1110.35	1109.87	1108.96	1107.69	1105.77	1105.33	1110.16
Water Content	%	5.02	5.02	23.84	24.75	24.69	24.59	24.45	24.23	24.18	24.72
Dry Weight	g	890.09	890.09	890.09	890.09	890.09	890.09	890.09	890.09	890.09	890.09
Wet Density	g/cm^3	1.812	1.828	2.163	2.185	2.186	2.188	2.191	2.196	2.197	2.199
Dry Density	g/cm^3	1.725	1.741	1.746	1.752	1.753	1.756	1.761	1.768	1.769	1.763
Specific Gravity of Solids	-	3.07	3.07	3.07	3.07	3.07	3.07	3.07	3.07	3.07	3.07
Solids Volume	cm^3	289.931	289.931	289.931	289.931	289.931	289.931	289.931	289.931	289.931	289.931
Void Volume	cm^3	225.972	221.337	219.734	218.234	217.757	216.849	215.572	213.654	213.221	214.804
Water Volume	cm^3	44.682	44.682	212.199	220.259	219.782	218.874	217.597	215.679	215.246	220.067
Void Ratio (e)	-	0.779	0.763	0.758	0.753	0.751	0.748	0.744	0.737	0.735	0.741
Saturation Ratio (Sr)	%	19.77	20.19	96.57	100.93	100.93	100.93	100.94	100.95	100.95	102.45
Effective Confining Stress	kPa					50	100	200	400		

Shearing (CU)		
Skempton's B Parameter		0.97
Back Pressure before shearing	kPa	702.7
Confining Stress (σ_3') before shearing	kPa	400.1
Shear Strain Rate	kPa/min	<1
Deviator Stress at Failure	kPa	199.6
Axial Strain at Failure	%	0.49

Photos:

Before Test

After Test

Extrusion Collapse, CA-QD-SC, Triaxial Test with constant q - Charts

PROJECT NO. :
PROJECT : Fundão Tailings Dam Review Panel
SAMPLE : PSD 1
TEST ID: TX 26
TEST TYPE: Anisotropically Consolidated Stress-Controlled Drained Triaxial Test with constant q
DATE : 2016-06-20
TESTED BY: BY
CHECKED BY: JG

At Failure Deviator Stress:	
Axial Stain (%)	**0.49**
Deviator Stress (kPa)	**199.6**

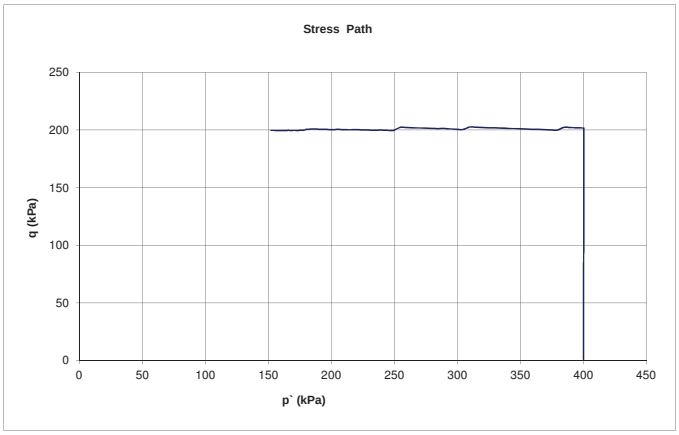

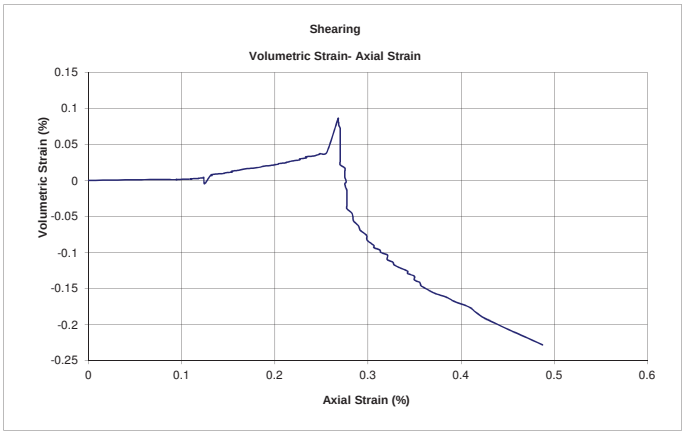

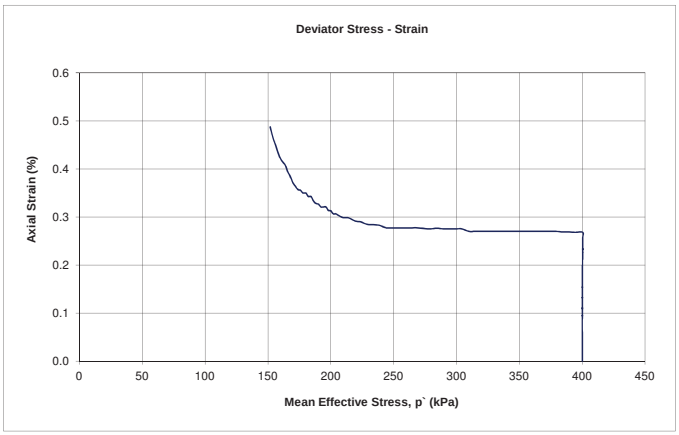

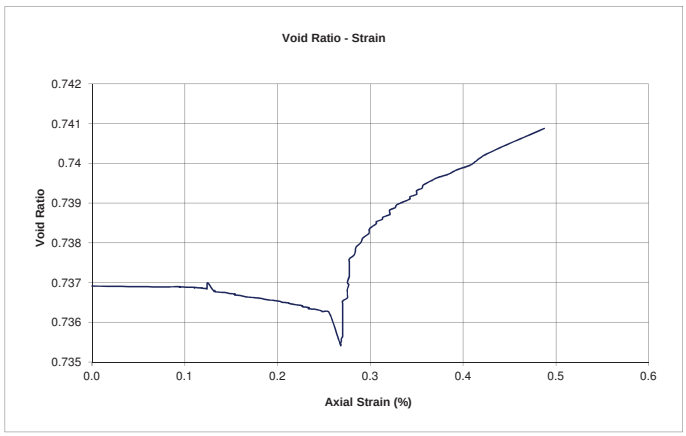

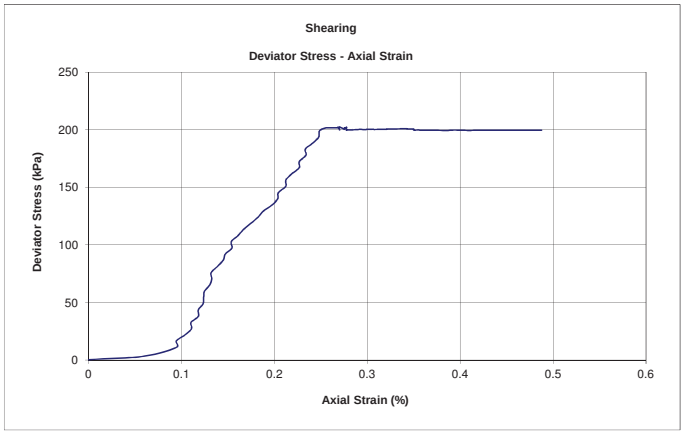

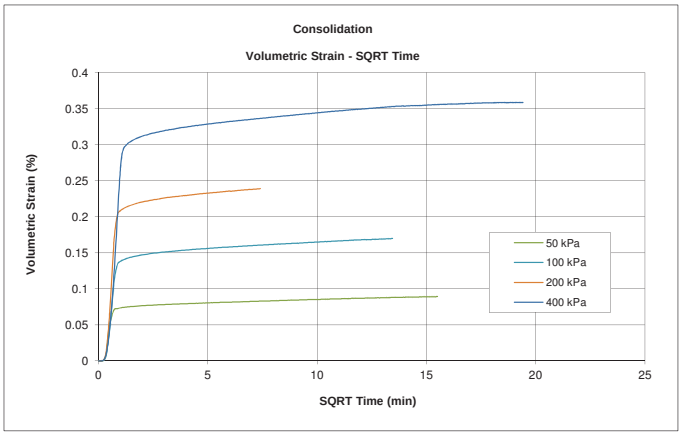

Klohn Crippen Berger

Triaxial CAU Test - Summary

PROJECT NO. :
PROJECT : Fundão Tailings Dam Review Panel
SAMPLE : PSD 1
TEST TYPE: Anisotropically Consolidated Undrained Triaxial Compression
TEST ID: TX 27

DATE : 2016-06-21
TESTED BY: BY
CHECKED BY: JG

SPECIMEN INFORMATION	UNITS	Initial	After Vacuum	End of Saturation	End of B - Value	End of 1st Consolidation	End of 2 nd Consolidation	End of 3 rd Consolidation	End of 4 th Consolidation	Anisotropic Consolidation	At Failure	End of Shear
Specimen Height	mm	138.41	138.41			138.19	138.15	138.06	137.96	137.53	132.27	96.19
Specimen Diameter	mm	68.81	68.81	68.59	68.48	68.46	68.44	68.41	68.32	68.41	69.76	81.81
Area	cm^2	37.19	37.19	36.95	36.83	36.81	36.79	36.75	36.66	36.76	38.22	52.56
Volume	cm^3	514.71	514.71	511.54	509.08	508.71	508.24	507.37	505.83	505.58	505.58	505.58
Wet Weight	g	932.60	932.60	1103.50	1108.00	1107.63	1107.16	1106.29	1104.74	1104.50	1104.50	1104.50
Water Content	%	5.00	5.00	24.24	24.75	24.71	24.65	24.56	24.38	24.35	24.35	24.35
Dry Weight	g	888.19	888.19	888.19	888.19	888.19	888.19	888.19	888.19	888.19	888.19	888.19
Wet Density	g/cm^3	1.812	1.812	2.157	2.176	2.177	2.178	2.180	2.184	2.185	2.185	2.185
Dry Density	g/cm^3	1.726	1.726	1.736	1.745	1.746	1.748	1.751	1.756	1.757	1.757	1.757
Specific Gravity of Solids	-	3.06	3.06	3.06	3.06	3.06	3.06	3.06	3.06	3.06	3.06	3.06
Solids Volume	cm^3	290.258	290.258	290.258	290.258	290.258	290.258	290.258	290.258	290.258	290.258	290.258
Void Volume	cm^3	224.450	224.450	221.283	218.823	218.454	217.979	217.111	215.567	215.326	215.326	215.326
Water Volume	cm^3	44.410	44.410	215.310	219.810	219.441	218.966	218.098	216.554	216.313	216.313	216.313
Void Ratio (e)	-	0.773	0.773	0.762	0.754	0.753	0.751	0.748	0.743	0.742	0.742	0.742
Saturation Ratio (Sr)	%	19.79	19.79	97.30	100.45	100.45	100.45	100.45	100.46	100.46	100.46	100.46
Effective Confining Stress	kPa					50	100	200	400			

Shearing (CAU)		
Skempton's B Parameter		0.98
Back Pressure before shearing	kPa	703.6
Confining Stress (σ_3') before shearing	kPa	399.9
Shear Strain Rate	% / min	0.07
Deviator Stress at Failure*	kPa	726.5
Axial Strain* at Failure	%	4.12

* From Maximum Deviator Stress

Photos:

Before Test

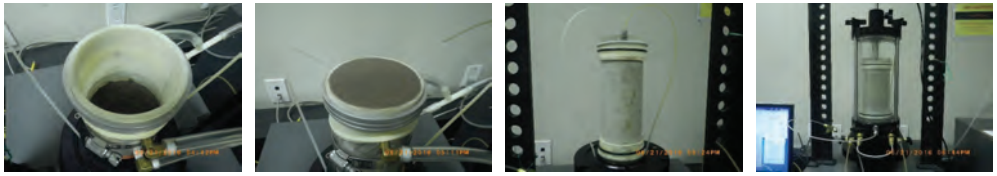

After Test

Klohn Crippen Berger

Triaxial CAU Test - Charts

PROJECT NO. :
PROJECT : Fundão Tailings Dam Review Panel
SAMPLE : PSD 1
TEST ID: TX 27
TEST TYPE: Anisotropically Consolidated Undrained Triaxial Compression
DATE : 2016-06-21
TESTED BY: BY
CHECKED BY: JG

At Max. Deviator Stress:	
Axial Stain (%)	4.12
Deviator Stress (kPa)	726.5

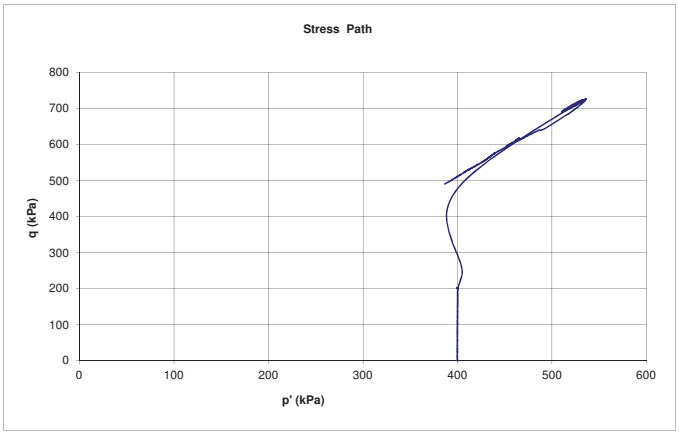

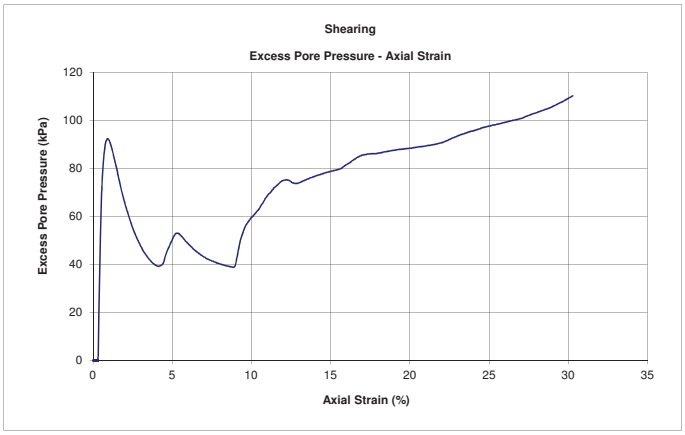

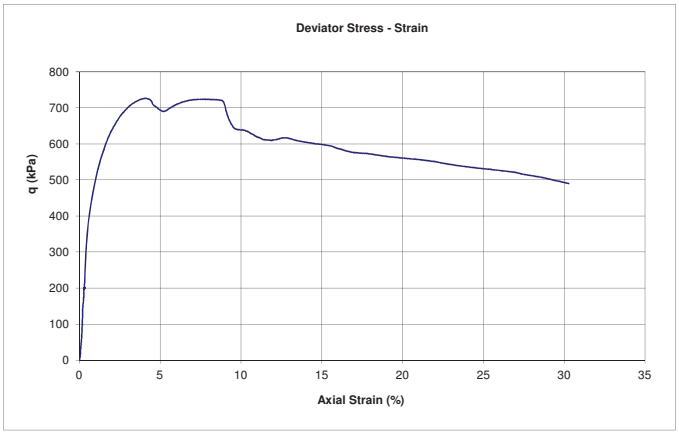

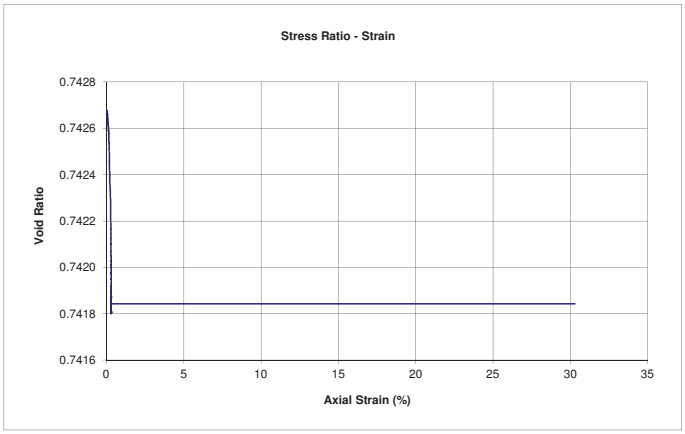

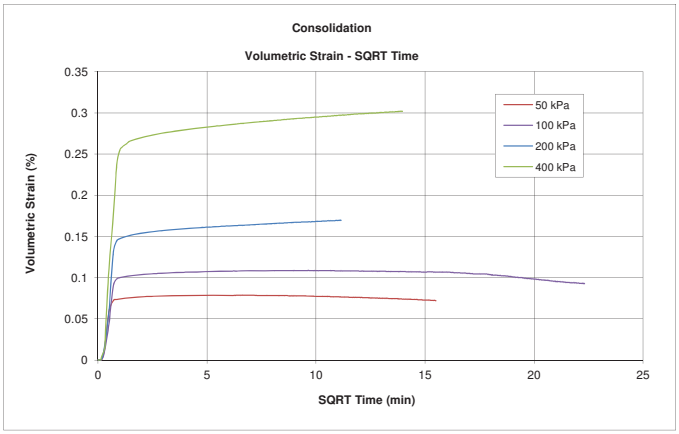

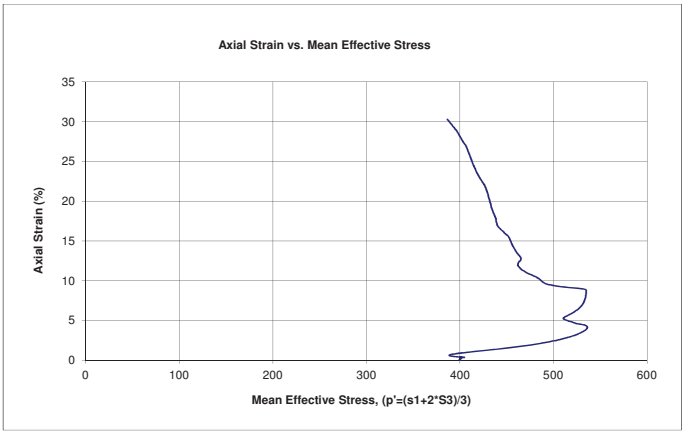

Klohn Crippen Berger

Extrusion Collapse, CA-QID-SC, Triaxial Test with increasing q - Summary

PROJECT NO. :
PROJECT : Fundão Tailings Dam Review Panel
SAMPLE : PSD 1
TEST TYPE: Anisotropically Consolidated Stress-Controlled Drained Triaxial Test with increasing q
TEST ID: TX 28

DATE : 2016-06-24
TESTED BY: BY
CHECKED BY: JG

SPECIMEN INFORMATION	UNITS	Initial	After Vacuum	End of Saturation	End of B - Value	End of 1st Consolidation	End of 2 nd Consolidation	End of 3 rd Consolidation	End of 4 th Consolidation	Anisotropic Consolidation	At Failure	End of Shear
Specimen Height	mm	138.47	138.58	138.58	138.43	138.40	138.34	138.24	137.35	96.36	137.35	96.36
Specimen Diameter	mm	68.78	68.38	68.31	68.40	68.38	68.34	68.27	68.36	81.59	68.40	81.62
Area	cm^2	37.15	36.72	36.65	36.75	36.72	36.68	36.61	36.71	52.28	36.75	52.32
Volume	cm^3	514.48	508.92	507.95	508.66	508.25	507.38	506.10	504.16	503.77	504.71	504.19
Wet Weight	g	929.89	929.89	1101.31	1106.93	1106.52	1105.65	1104.37	1102.43	1102.05	1102.98	1102.46
Water Content	%	4.89	4.89	24.23	24.86	24.81	24.72	24.57	24.35	24.31	24.41	24.36
Dry Weight	g	886.54	886.54	886.54	886.54	886.54	886.54	886.54	886.54	886.54	886.54	886.54
Wet Density	g/cm^3	1.807	1.827	2.168	2.176	2.177	2.179	2.182	2.187	2.188	2.185	2.187
Dry Density	g/cm^3	1.723	1.742	1.745	1.743	1.744	1.747	1.752	1.758	1.760	1.757	1.758
Specific Gravity of Solids	-	3.05	3.07	3.07	3.07	3.07	3.07	3.07	3.07	3.07	3.07	3.07
Solids Volume	cm^3	290.668	288.775	288.775	288.775	288.775	288.775	288.775	288.775	288.775	288.775	288.775
Void Volume	cm^3	223.815	220.145	219.176	219.886	219.476	218.606	217.326	215.383	215.000	215.934	215.417
Water Volume	cm^3	43.352	43.352	214.776	220.396	219.986	219.116	217.836	215.892	215.509	216.443	215.926
Void Ratio (e)	-	0.770	0.762	0.759	0.761	0.760	0.757	0.753	0.746	0.745	0.748	0.746
Saturation Ratio (Sr)	%	19.37	19.69	97.99	100.23	100.23	100.23	100.23	100.24	100.24	100.24	100.24
Effective Confining Stress	kPa					50	100	200	400			

Shearing		
Skempton's B Parameter		0.97
Back Pressure before shearing	kPa	701.6
Confining Stress (σ_3') before shearing	kPa	400.2
Shear Strain Rate	kPa/min	<1
Deviator Stress at Failure	kPa	373.2
Axial Strain at Failure	%	1.48

Photos:

Before Test

After Test

Extrusion Collapse, CA-QID-SC, Triaxial Test with increasing q - Charts

PROJECT NO. :
PROJECT : Fundão Tailings Dam Review Panel
SAMPLE : PSD 1
TEST ID: TX 28
TEST TYPE: Anisotropically Consolidated Stress-Controlled Drained Triaxial Test with increasing q
DATE : 2016-06-24
TESTED BY: BY
CHECKED BY: JG

At Failure Deviator Stress:	
Axial Stain (%)	1.48
Deviator Stress (kPa)	373.2

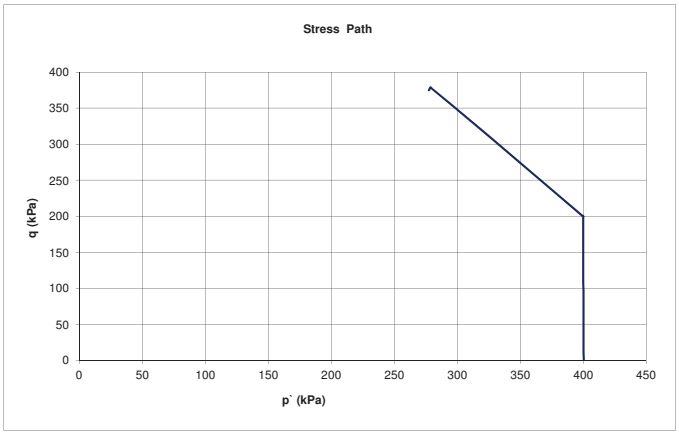

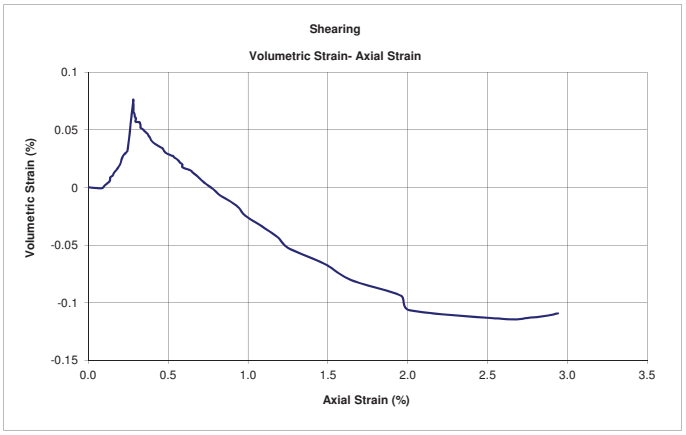

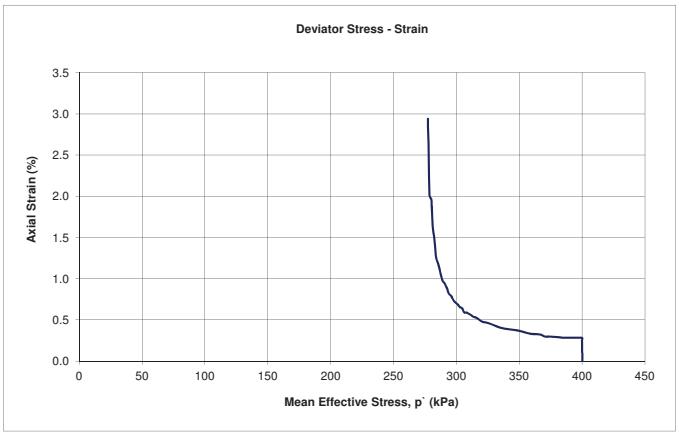

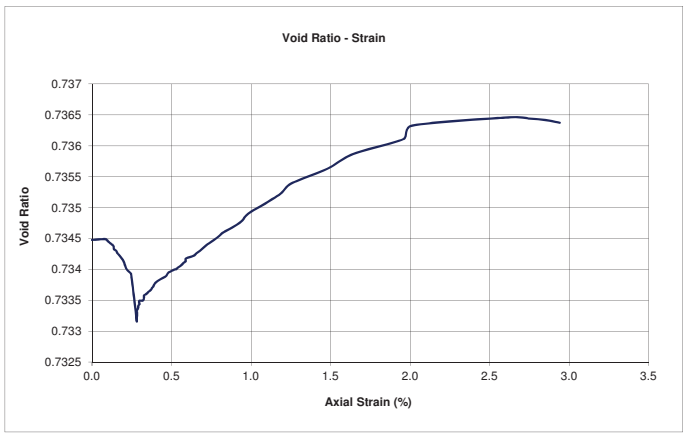

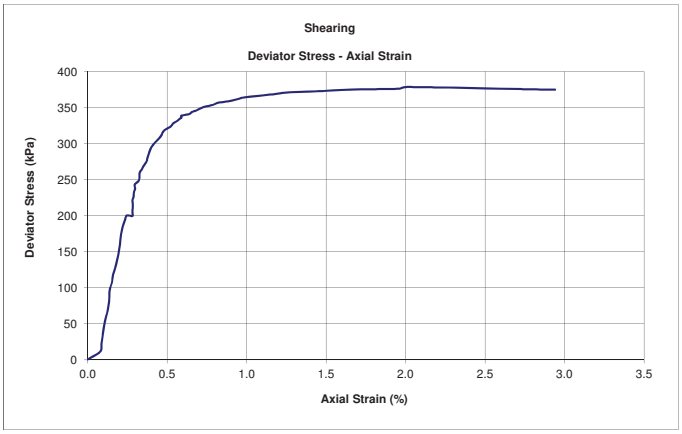

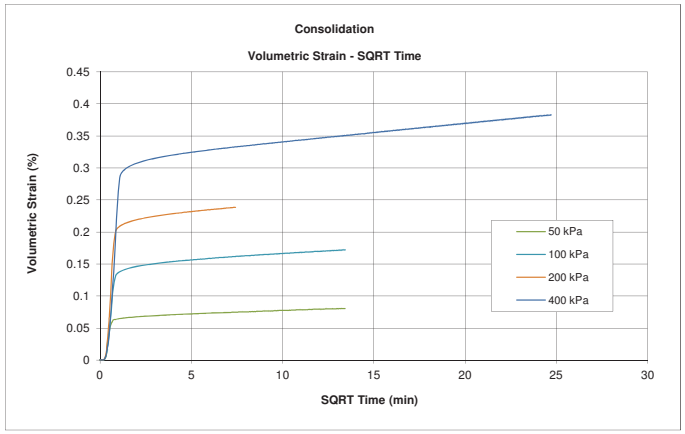

Triaxial CID Test - Summary

(ASTM D7181)

PROJECT NO. :
PROJECT : Fundão Tailings Dam Review Panel
SAMPLE : PSD 1
TEST ID: TX 29

DATE : 2016-06-30
TESTED BY: BY
CHECKED BY: JG
TEST TYPE: CID

SPECIMEN INFORMATION	UNITS	Initial	After Vacuum	Saturation	B-Value	End of 1st Consolidation	End of 2 nd Consolidation	End of 3 rd Consolidation	End of 4th Consolidation	At Failure	End of Shear
Specimen Height	mm	138.37	138.37	138.37	138.22	138.18	138.13	138.06	137.93	132.17	97.12
Specimen Diameter	mm	68.86	68.81			68.67	68.63	68.55	68.40	69.77	81.20
Area	cm^2	37.24	37.19	37.01	37.05	37.03	36.99	36.91	36.74	38.23	51.78
Volume	cm^3	515.31	514.56	512.12	512.12	511.74	510.91	509.53	506.80	505.27	502.86
Wet Weight	g	931.73	931.73	1106.33	1112.16	1111.78	1110.95	1109.56	1106.84	1105.31	1102.90
Water Content	%	4.93	4.93	24.59	25.25	25.21	25.11	24.96	24.65	24.48	24.21
Dry Weight	g	887.95	887.95	887.95	887.95	887.95	887.95	887.95	887.95	887.95	887.95
Wet Density	g/cm^3	1.808	1.811	2.160	2.172	2.173	2.174	2.178	2.184	2.188	2.193
Dry Density	g/cm^3	1.723	1.726	1.734	1.734	1.735	1.738	1.743	1.752	1.757	1.766
Specific Gravity of Solids	-	3.05	3.05	3.05	3.05	3.05	3.05	3.05	3.05	3.05	3.05
Solids Volume	cm^3	291.132	291.132	291.132	291.132	291.132	291.132	291.132	291.132	291.132	291.132
Void Volume	cm^3	224.176	223.428	220.993	220.993	220.613	219.779	218.395	215.668	214.138	211.729
Water Volume	cm^3	43.776	43.776	218.376	224.206	223.826	222.992	221.608	218.881	217.351	214.942
Void Ratio (e)	-	0.770	0.767	0.759	0.759	0.758	0.755	0.750	0.741	0.736	0.727
Saturation Ratio (Sr)	%	19.53	19.59	98.82	101.45	101.46	101.46	101.47	101.49	101.50	101.52
Effective Confining Stress	kPa					50	100	200	400		

Shearing (CID)		
Skempton's B Parameter		0.98
Back Pressure before shearing	kPa	701.0
Confining Stress (σ_3') before shearing	kPa	400
Shear Strain Rate	% / min	0.065
Deviator Stress at Failure*	kPa	979.10
Axial Strain* at Failure	%	4.18

* From Maximum Deviator Stress

Photos:

Before Test

After Test

Klohn Crippen Berger

Triaxial CID Test - Charts

(ASTM D7181)

PROJECT NO. :
PROJECT : Fundão Tailings Dam Review Panel
SAMPLE : PSD 1
TEST ID: TX 29
TEST TYPE: CID
DATE : 2016-06-30
TESTED BY: BY
CHECKED BY: JG

At Max. Deviator Stress:	
Axial Stain (%)	**4.18**
Deviator Stress (kPa)	**979.1**

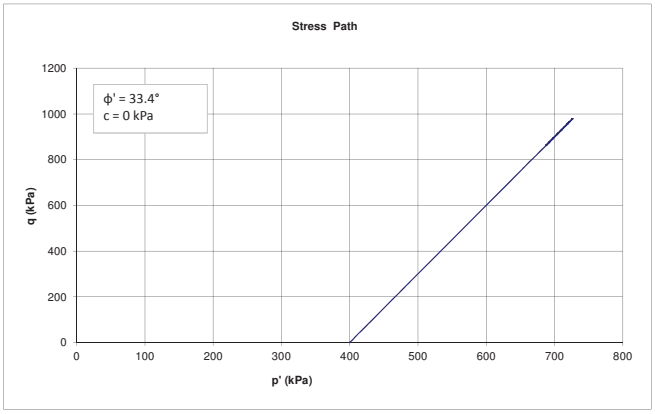

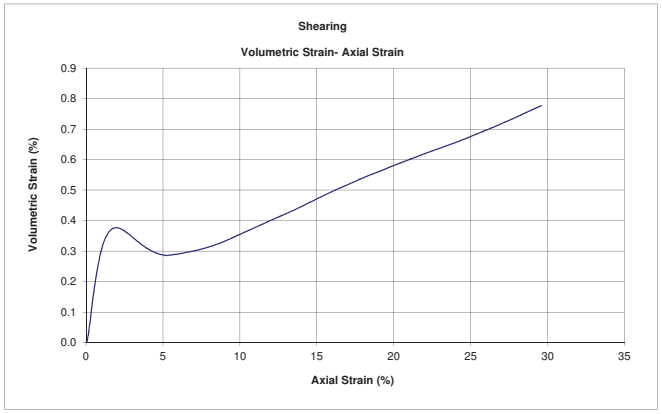

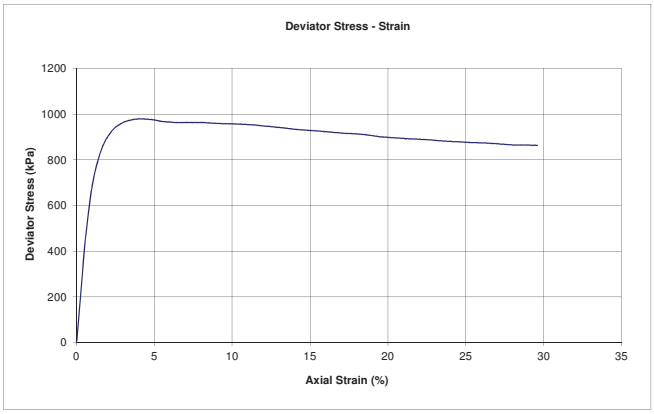

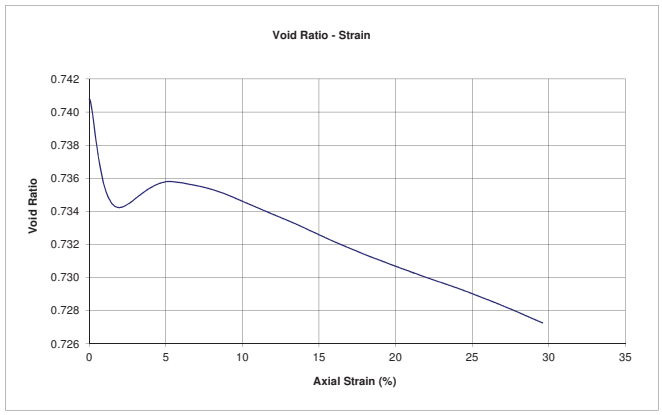

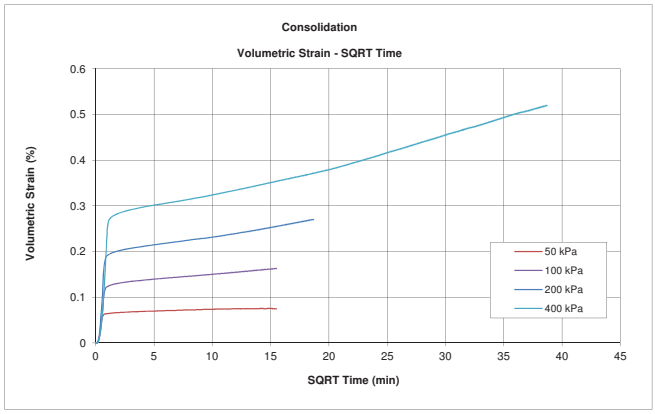

Klohn Crippen Berger

Triaxial CID Test - Summary

(ASTM D7181)

PROJECT NO. :

PROJECT : Fundão Tailings Dam Review Panel

SAMPLE : PSD 1

TEST ID: TX 30

DATE : 2016-06-30

TESTED BY: BY

CHECKED BY: JG

TEST TYPE: CID

SPECIMEN INFORMATION	UNITS	Initial	After Vacuum	Saturation	B-Value	End of 1st Consolidation	End of 2 nd Consolidation	End of 3 rd Consolidation	At Failure	End of Shear
Specimen Height	mm	138.38	138.27	138.27	138.12	138.09	138.00	137.88	113.05	96.80
Specimen Diameter	mm	68.80	68.11	68.07	68.05	68.02	67.96	67.83	74.06	79.88
Area	cm^2	37.18	36.43	36.40	36.37	36.34	36.28	36.13	43.08	50.11
Volume	cm^3	514.45	503.78	503.25	502.34	501.87	500.65	498.18	486.98	485.09
Wet Weight	g	894.79	894.79	1067.26	1080.09	1079.62	1078.41	1075.93	1064.73	1062.85
Water Content	%	5.03	5.03	25.27	26.78	26.73	26.58	26.29	24.98	24.76
Dry Weight	g	851.94	851.94	851.94	851.94	851.94	851.94	851.94	851.94	851.94
Wet Density	g/cm^3	1.739	1.776	2.121	2.150	2.151	2.154	2.160	2.186	2.191
Dry Density	g/cm^3	1.656	1.691	1.693	1.696	1.698	1.702	1.710	1.749	1.756
Specific Gravity of Solids	-	3.05	3.05	3.05	3.05	3.05	3.05	3.05	3.05	3.05
Solids Volume	cm^3	279.324	279.324	279.324	279.324	279.324	279.324	279.324	279.324	279.324
Void Volume	cm^3	235.124	224.456	223.928	223.013	222.544	221.331	218.853	207.653	205.767
Water Volume	cm^3	42.852	42.852	215.322	228.155	227.686	226.473	223.995	212.795	210.909
Void Ratio (e)	-	0.842	0.804	0.802	0.798	0.797	0.792	0.784	0.743	0.737
Saturation Ratio (Sr)	%	18.23	19.09	96.16	102.31	102.31	102.32	102.35	102.48	102.50
Effective Confining Stress	kPa					50	100	200		

Shearing (CID)		
Skempton's B Parameter		0.99
Back Pressure before shearing	kPa	697.3
Confining Stress (σ_3') before shearing	kPa	200.0
Shear Strain Rate	% / min	0.065
Deviator Stress at Failure*	kPa	474.70
Axial Strain* at Failure	%	18.01

* From Maximum Deviator Stress

Photos:

Before Test




After Test




Klohn Crippen Berger

Triaxial CID Test - Charts

(ASTM D7181)

PROJECT NO. :
PROJECT : Fundão Tailings Dam Review Panel
SAMPLE : PSD 1
TEST ID: TX 30
TEST TYPE: CID
DATE : 2016-06-30
TESTED BY: BY
CHECKED BY: JG

At Max. Deviator Stress:	
Axial Stain (%)	**18.01**
Deviator Stress (kPa)	**474.7**

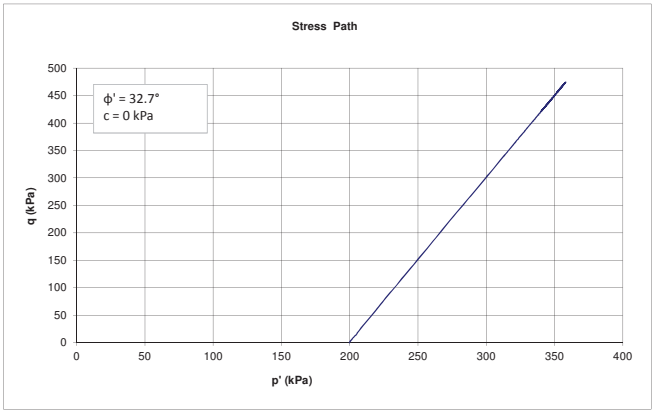

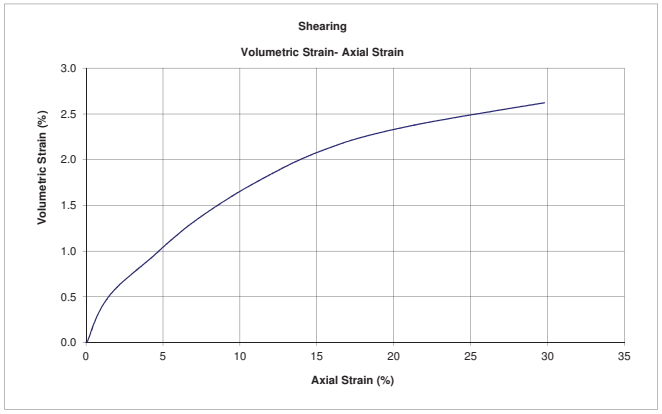

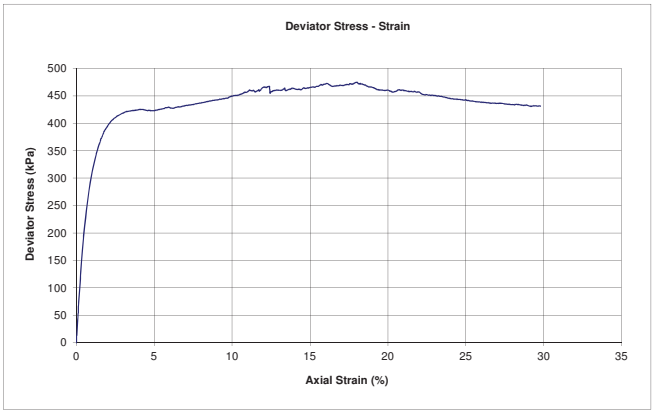

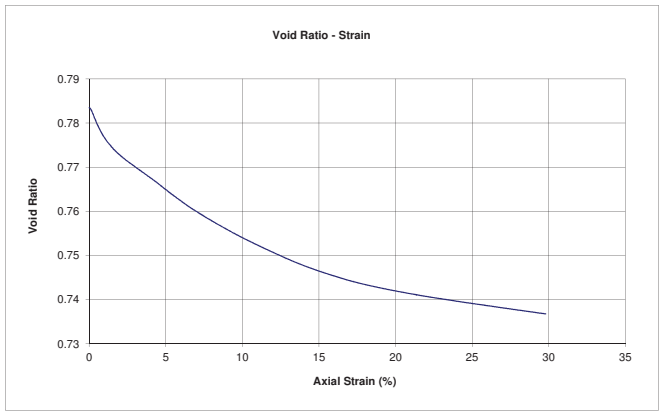

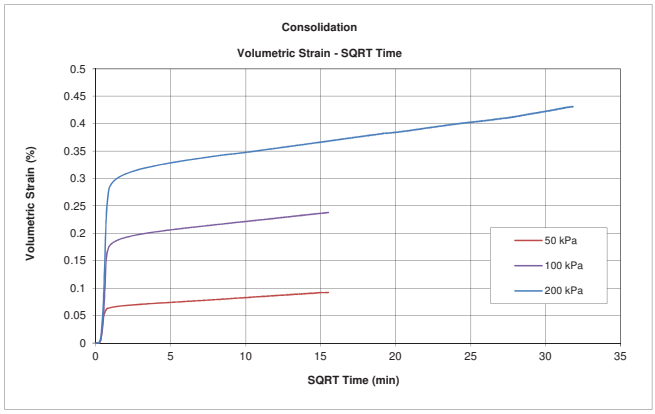

Klohn Crippen Berger

Triaxial CA-QID-SC (Cyclic) Extrusion Collapse with Cyclic Component and Increasing q Test - Summary

PROJECT NO. :
PROJECT : Fundão Tailings Dam Review Panel
SAMPLE : PSD 1
TEST TYPE: Anisotropically Consolidated Stress-Controlled Drained Cyclic Triaxial Test with increasing q
TEST ID: TX 31

DATE : 2016-07-05
TESTED BY: BY
CHECKED BY: JG

SPECIMEN INFORMATION	UNITS	Initial	After Vacuum	End of Saturation	End of B - Value	End of 1st Consolidation	End of 2 nd Consolidation	End of 3 rd Consolidation	Anisotropic Consolidation	Start of Cyclic	End of Cyclic
Specimen Height	mm	138.54	138.54	138.54	138.36	138.30	138.24	138.14	137.74	137.35	96.36
Specimen Diameter	mm	68.79	68.63	68.41	68.31	68.26	68.14	67.96	67.99	68.09	81.29
Area	cm^2	37.17	36.99	36.75	36.65	36.59	36.47	36.27	36.31	36.41	51.90
Volume	cm^3	514.89	512.50	509.16	507.16	506.08	504.18	501.10	500.10	500.11	500.11
Wet Weight	g	895.22	895.22	1078.86	1083.19	1082.12	1080.21	1077.14	1076.14	1076.15	1076.15
Water Content	%	4.89	4.89	26.41	26.91	26.79	26.57	26.20	26.09	26.09	26.09
Dry Weight	g	853.48	853.48	853.48	853.48	853.48	853.48	853.48	853.48	853.48	853.48
Wet Density	g/cm^3	1.739	1.747	2.119	2.136	2.138	2.143	2.150	2.152	2.152	2.152
Dry Density	g/cm^3	1.658	1.665	1.676	1.683	1.686	1.693	1.703	1.707	1.707	1.707
Specific Gravity of Solids	-	3.06	3.06	3.06	3.06	3.06	3.06	3.06	3.06	3.06	3.06
Solids Volume	cm^3	278.917	278.917	278.917	278.917	278.917	278.917	278.917	278.917	278.917	278.917
Void Volume	cm^3	235.976	233.584	230.239	228.239	227.166	225.259	222.180	221.180	221.194	221.194
Water Volume	cm^3	41.735	41.735	225.379	229.709	228.636	226.729	223.650	222.650	222.664	222.664
Void Ratio (e)	-	0.846	0.837	0.825	0.818	0.814	0.808	0.797	0.793	0.793	0.793
Saturation Ratio (Sr)	%	17.69	17.87	97.89	100.64	100.65	100.65	100.66	100.66	100.66	100.66
Effective Confining Stress	kPa					50	100	200			

Shearing		
Skempton's B Parameter		0.98
Back Pressure before shearing	kPa	702.3
Confining Stress (σ_3') before shearing	kPa	200.0
Shear Strain Rate	kPa/min	<1
Deviator Stress at Failure	kPa	166.9
Axial Strain at Failure	%	0.72

Photos:

Before Test




After Test




Klohn Crippen Berger

Triaxial CA-QID-SC (Cyclic) Extrusion Collapse with Cyclic Component and Increasing q Test - Shear - Charts

PROJECT NO. :
PROJECT : Fundão Tailings Dam Review Panel
SAMPLE : PSD 1
TEST ID: TX 31
TEST TYPE: Anisotropically Consolidated Stress-Controlled Drained Cyclic Triaxial Test with increasing q
DATE : 2016-07-05
TESTED BY: BY
CHECKED BY: JG

At Failure Deviator Stress:	
Axial Stain (%)	**0.72**
Deviator Stress (kPa)	**166.9**

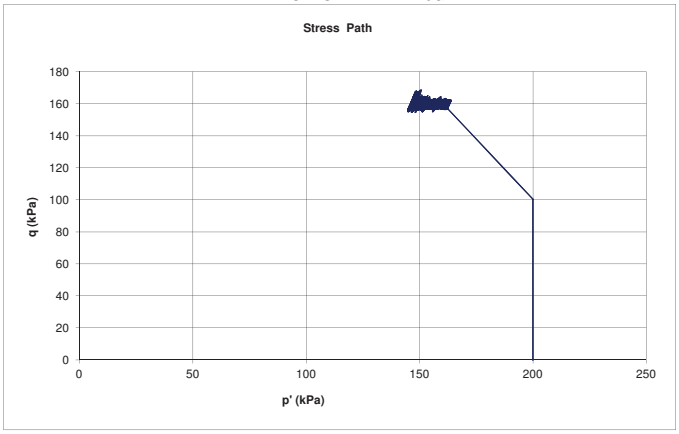

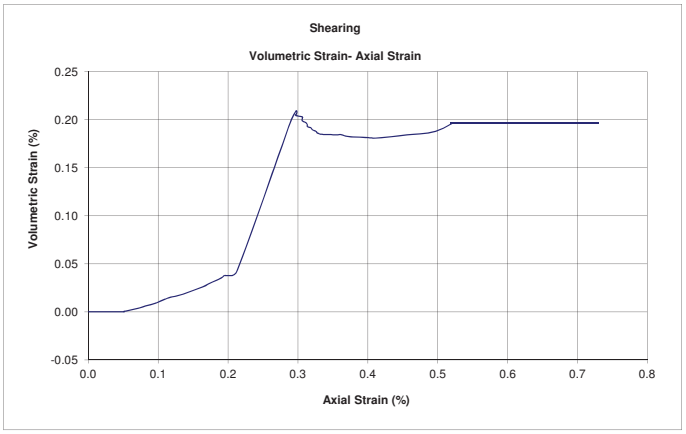

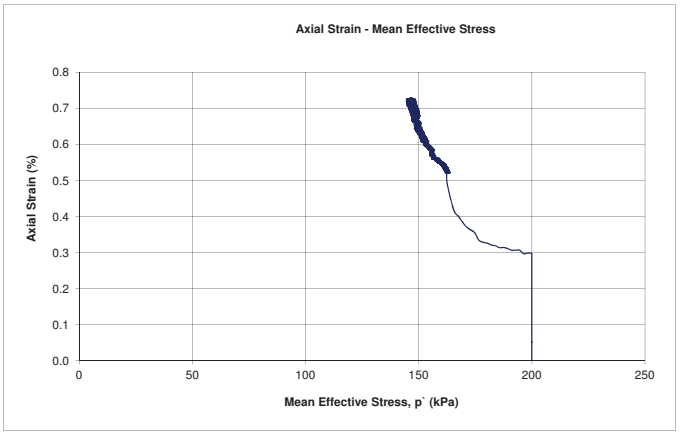

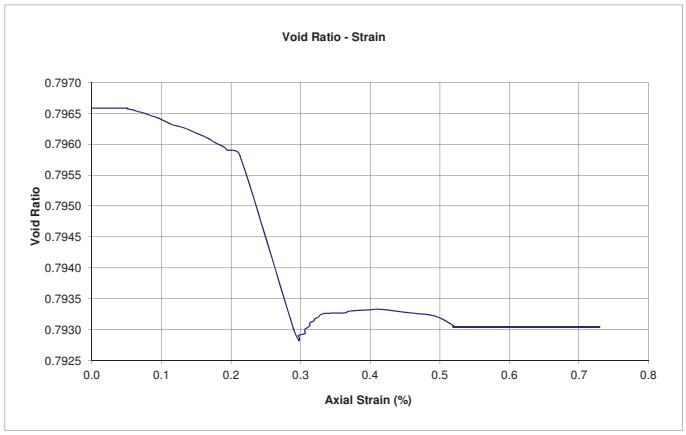

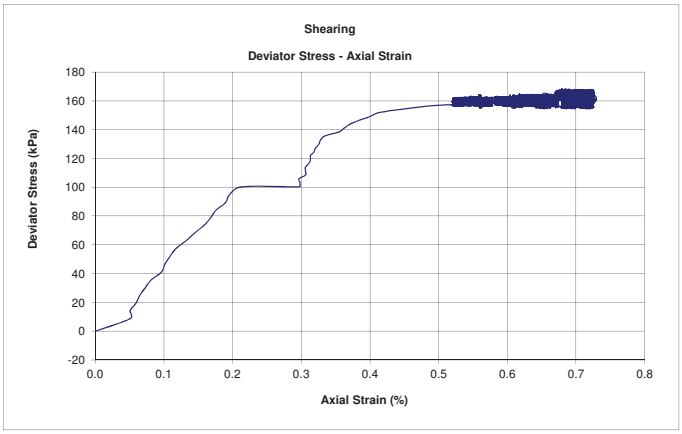

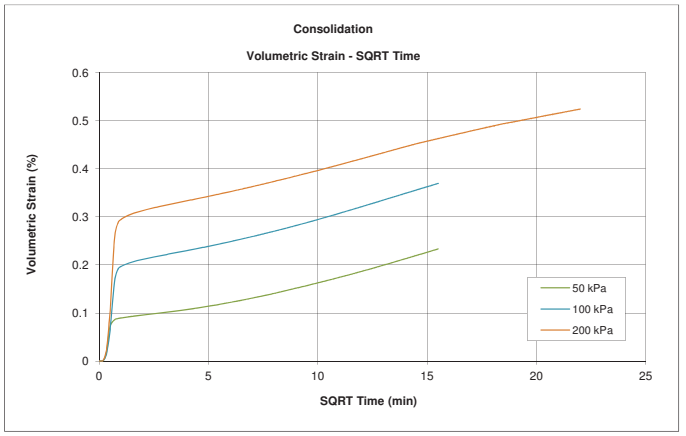

Klohn Crippen Berger

Triaxial CA-QID-SC (Cyclic) Extrusion Collapse with Cyclic Component and Increasing q Test - Cyclic Shear - Charts

PROJECT NO. :
PROJECT : Fundão Tailings Dam Review Panel
SAMPLE : PSD 1
TEST ID: TX 31
TEST TYPE: Anisotropically Consolidated Stress-Controlled Drained Cyclic Triaxial Test with increasing q
DATE : 2016-07-05
TESTED BY: BY
CHECKED BY: JG

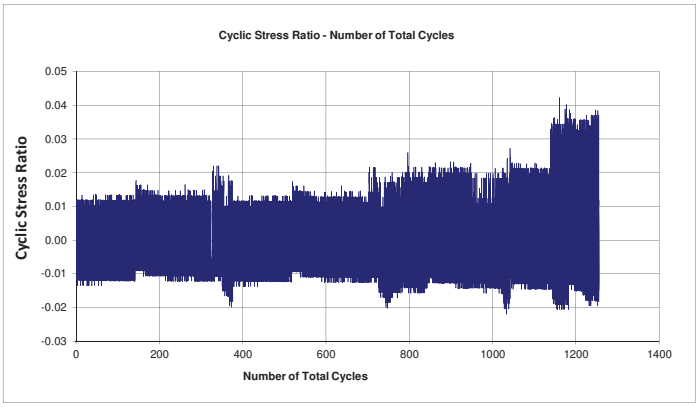

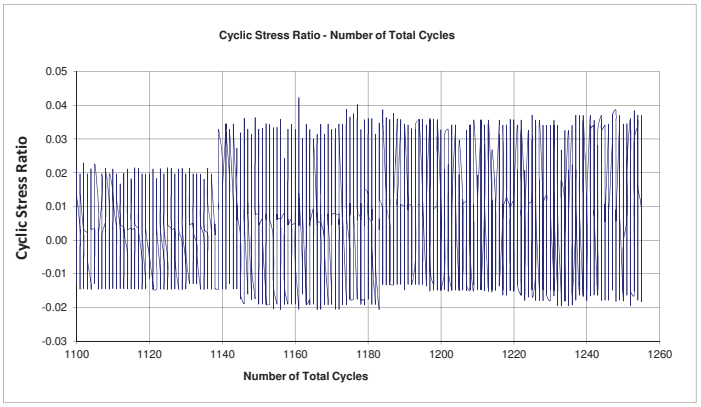

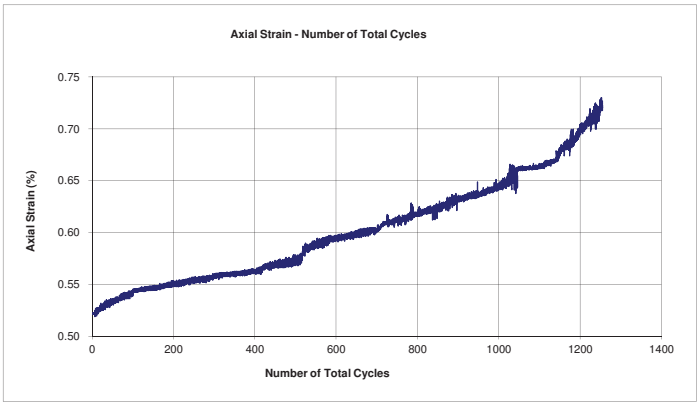

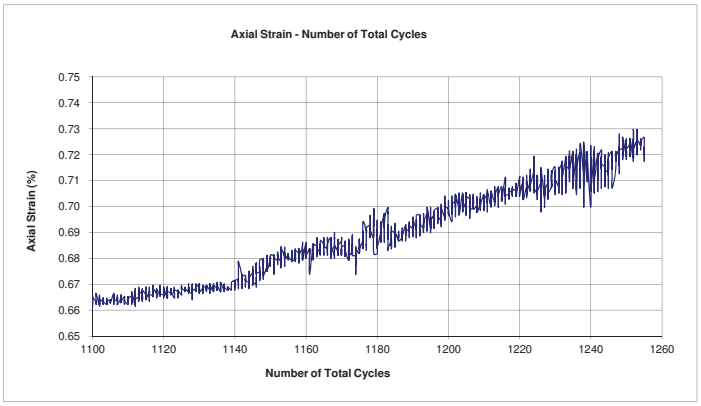

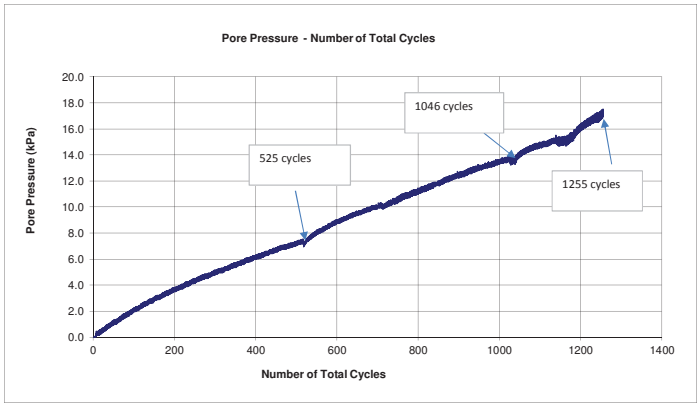

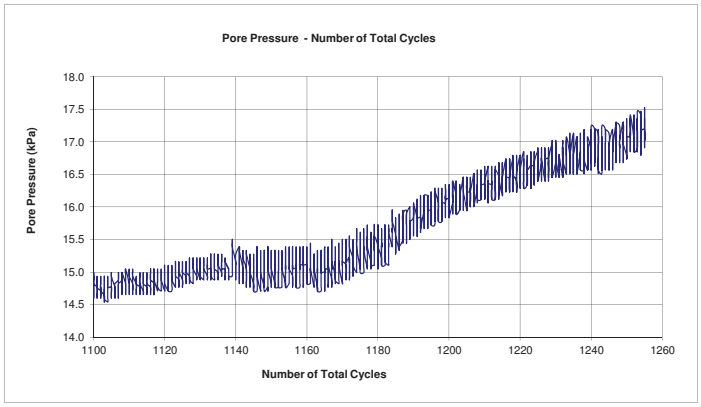

Klohn Crippen Berger

Triaxial CAD Test - Summary

PROJECT NO. :
PROJECT : Fundão Tailings Dam Review Panel
SAMPLE : PSD 1
TEST TYPE: Anisotropically Consolidated Stress-Controlled Drained Triaxial Test with increasing q
TEST ID: TX 32

DATE : 2016-07-05
TESTED BY: BY
CHECKED BY: JG

SPECIMEN INFORMATION	UNITS	Initial	After Vacuum	End of Saturation	End of B - Value	End of 1st Consolidation	End of 2 nd Consolidation	End of 3 rd Consolidation	Anisotropic Consolidation	At Failure
Specimen Height	mm	138.46	138.46	138.46	138.33	138.29	138.20	138.08	137.70	137.35
Specimen Diameter	mm	68.71	68.32	68.17	68.21	68.14	68.03	67.87	67.90	67.74
Area	cm^2	37.08	36.66	36.50	36.54	36.46	36.35	36.17	36.21	36.04
Volume	cm^3	513.40	507.59	505.42	505.42	504.24	502.37	499.49	498.62	495.00
Wet Weight	g	893.05	893.05	1073.50	1080.11	1078.93	1077.06	1074.18	1073.31	1069.69
Water Content	%	4.94	4.94	26.14	26.92	26.78	26.56	26.22	26.12	25.70
Dry Weight	g	851.01	851.01	851.01	851.01	851.01	851.01	851.01	851.01	851.01
Wet Density	g/cm^3	1.739	1.759	2.124	2.137	2.140	2.144	2.151	2.153	2.161
Dry Density	g/cm^3	1.658	1.677	1.684	1.684	1.688	1.694	1.704	1.707	1.719
Specific Gravity of Solids	-	3.05	3.05	3.05	3.05	3.05	3.05	3.05	3.05	3.05
Solids Volume	cm^3	279.020	279.020	279.020	279.020	279.020	279.020	279.020	279.020	279.020
Void Volume	cm^3	234.379	228.568	226.400	226.400	225.221	223.353	220.471	219.602	215.982
Water Volume	cm^3	42.040	42.040	222.490	229.097	227.918	226.050	223.168	222.298	218.678
Void Ratio (e)	-	0.840	0.819	0.811	0.811	0.807	0.800	0.790	0.787	0.774
Saturation Ratio (Sr)	%	17.94	18.39	98.27	101.19	101.20	101.21	101.22	101.23	101.25
Effective Confining Stress	kPa					50	100	200		

Shearing		
Skempton's B Parameter		0.98
Back Pressure before shearing	kPa	701.4
Confining Stress (σ_3') before shearing	kPa	200.0
Shear Strain Rate	kPa/min	<1
Deviator Stress at Failure	kPa	350.6
Axial Strain at Failure	%	3.69

Photos:

Before Test

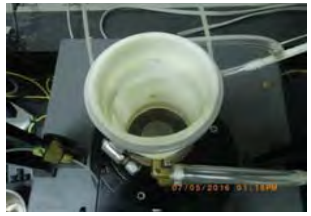


After Test




Klohn Crippen Berger

Triaxial CAD Test - Summary

PROJECT NO. :
PROJECT : Fundão Tailings Dam Review Panel
SAMPLE : PSD 1
TEST ID: TX 32
TEST TYPE: Anisotropically Consolidated Stress-Controlled Drained Triaxial Test with increasing q
DATE : 2016-07-05
TESTED BY: BY
CHECKED BY: JG

At Max. Deviator Stress:	
Axial Stain (%)	**3.69**
Deviator Stress (kPa)	**350.6**

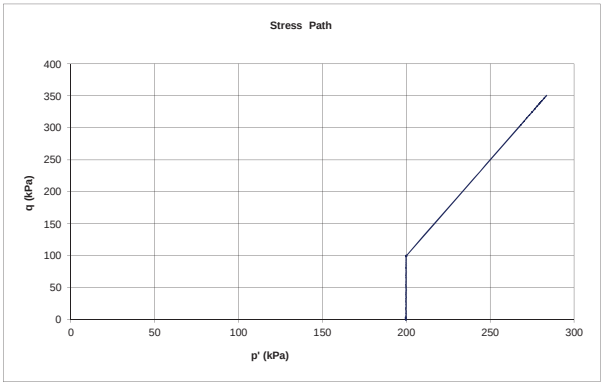

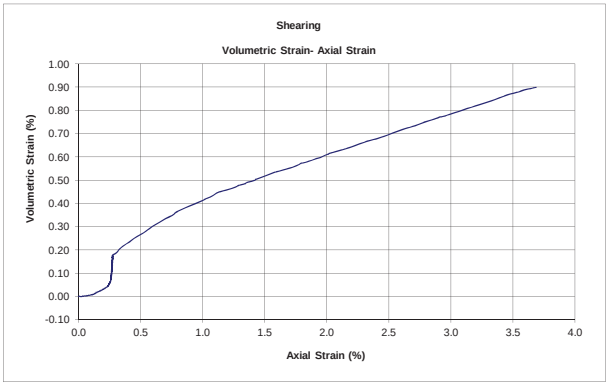

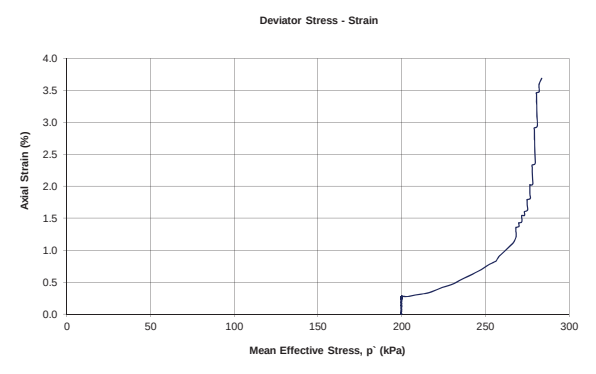

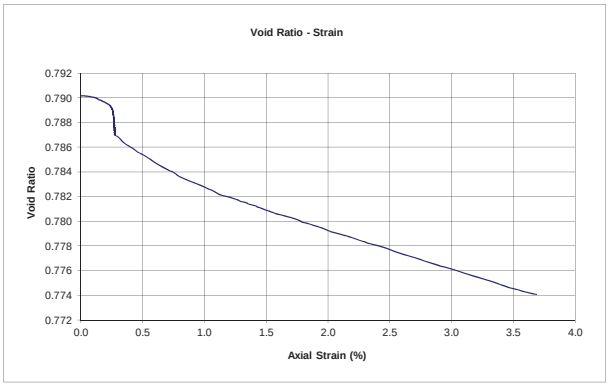

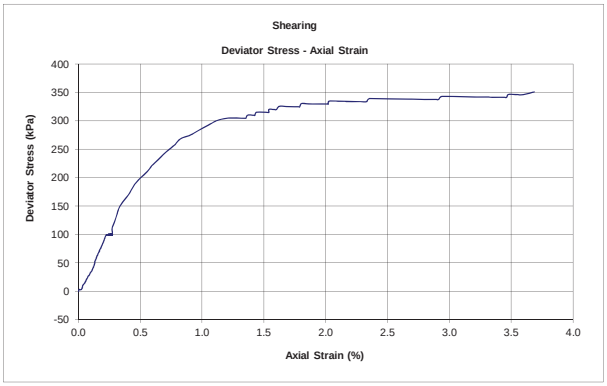

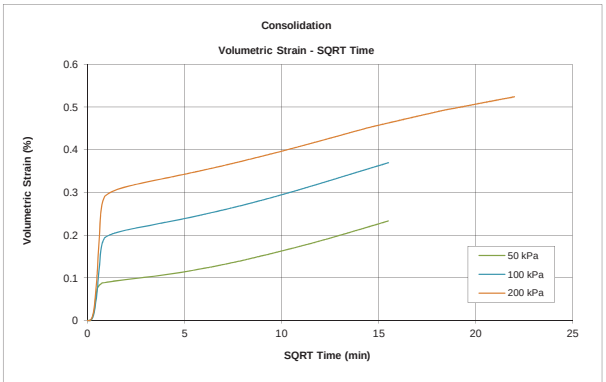

ATTACHMENT D7

"Undisturbed" Slimes Triaxial Tests by Pattrol

RELATÓRIO PAT-RT-LAB-1518.16-001

ENSAIOS DE LABORATÓRIO

CLIENTE: CLEARY GOTTLIEB STEEN & HAMILTON LLP

OBRA: BAIA 3 – LOCAL F

REVISÕES	DESCRIÇÃO	DATA	PREP.	APROV
00	Emissão Final	21/07/2016	LC	FT

PATROL - INVESTIGAÇÕES GEOTECNICAS LTDA.
Rua Des. Continentino, 68 – Bairro Pedro II – Belo Horizonte – MG
Telefones: 31.3462.0722 – 3462.0079 – 3412.1482

Sumário

1. APRESENTAÇÃO

A Patrol – Investigações Geotécnicas Ltda. é uma empresa de consultoria na área de tecnologia de materiais aplicados as obras de construção. Nosso laboratório está preparado para ensaiar os mais diversos materiais procurando obter os parâmetros técnicos que caracterizam o seu comportamento quando aplicados às mais diversas obras de infraestrutura. Neste contexto, oferecemos aos nossos clientes a mais avançada tecnologia de ensaios especiais em geotécnica, garantindo a mais elevada qualidade dos resultados aliando-se a rapidez na execução dos ensaios.

2. INTRODUÇÃO

O presente relatório apresenta os resultados de ensaios geotécnicos de laboratório, realizados em amostras deformadas coletadas em nas áreas da Baia 3 – Local F em camisas de amostradores tipo shelby na SAMARCO – Mina do Germano, visando conhecer os parâmetros geotécnicos do material composto em quatro profundidades diferentes.

3. IDENTIFICAÇÃO DAS AMOSTRAS E SERVIÇOS REALIZADOS

A tabela 3.1 discrimina as amostras recebidas e os serviços realizados encontram-se no item 5.

Tabela 3.1 – Identificação das amostras

Registro	Furo	Profundidade	Tipo de Amostra
10149	GSSAM – 02B – 01	4.00 a 4.65	Shelby
10150	GSSAM – 02B – 02	6.00 a 6.65	Shelby
10151	GSSAM – 02B – 03	9.00 a 9.65	Shelby
10152	GSSAM – 02B – 04	10.00 a 10.65	Shelby

Quadro de Ensaios executados:

Ensaios	Programados	Executados Rev. 00
Granulometria Completa	04	04
Massa Especifica Real	04	04
Limites de Atteberg	04	04
Umidade e Densidade Natural	04	04
Triaxial CU	04	04

4. METODOLOGIA APLICADA

- Triaxial CU – ASTM D4767/2011
- Massa Específica real dos grãos – NBR 6508/1984
- Limite de liquidez - NBR 6459/1984
- Limite de plasticidade - NBR 7180/1984
- Análise Granulométrica por Peneiramento e Sedimentação - NBR 7181/1984
- Determinação da Massa específica aparente de amostras indeformadas, com emprego da balança hidrostática - NBR 10838

4.1. Identificação e Abertura dos Amostradores

No laboratório, as amostras foram identificadas com as suas respectivas características e informações de procedência. Posteriormente, as amostras foram extraídas dos shelbies seguindo o procedimento indicado por Ladd & DeGroot (2004), visando minimizar qualquer tipo de amolgamento no solo no ato de sua retirada do tubo. Conforme sugerido, o shelby foi cortado longitudinalmente com uma serra fina, formando sob-amostras. Estas, por sua vez, foram separadas da parede do tubo por uma corda fina de violão inserida com o auxilio de uma agulha de seringa.

Desse modo, cada shelby foi cuidadosamente serrado, formando sub-amostras com comprimentos adequados ao ensaio em vista. A sub-amostra era então separada da parede do tubo com o auxílio de um fio de aço, extraída e, em seguida, moldada conforme requerido.

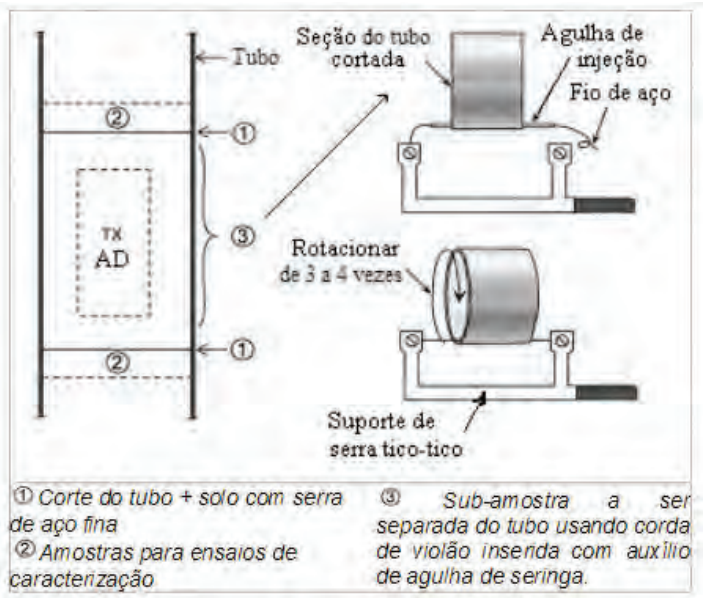

Procedimento para extração do solo do tubo de amostragem (modificado de Ladd & DeGroot, 2004)

Tubo para Ensaio

Corte da Sub-Amostra

Corte da Secção Transversal

Amostra para Entalhe

4.2. Triaxial CU

Os corpos de prova das amostras foram talhados, preservando as condições naturais das amostras, para granulometria das amostras, os corpos de prova foram talhados com diâmetro aproximado de 35 mm e 72 mm de altura e submetidos a 04 (Quatro) níveis de tensões de confinamento, sendo esses de 200, 400, 600 e 800 KPa.

O ensaio foi realizado em células de confinamento em amostras isoladas por membranas de látex e teve fases de saturação por percolação e saturação por contrapressão.

Para o processo de saturação por contrapressão o CP (Corpo de Prova) foi devidamente percolado para elevação do grau de saturação inicial dos corpos de prova.

Para os equipamentos usados (Bombas hidráulicas servo controladas) a pressão na célula varia sempre entre 10 e 20 kPa assim ao aplicarmos uma pressão de 100 kPa de confinamento a sua

contra pressão devera ser entre 80 a 90 kPa. Lembrando que as cargas deverão ser aplicadas gradativamente para não ocorrer o adensamento do corpo e prova.

O parâmetro B de Skempton deve ser determinado com incrementos de tensão efetiva de 50 ou 100 kPa em cada ciclo. Nosso equipamento tem por limitação em alcançar alguns níveis de pressão. Um exemplo é o confinamento de 800 kPa, para este carregamento podemos aplicar no máximo uma contra pressão de 200 kPa. Pois ao saturar ate 200 kPa mais os 800 kPa de adensamento, quando entrar na fase de cisalhar devido a medida de deformação o confinamento na célula muitas vezes aumenta, podendo chegar ate 1200 kPa com as fases anteriores dos ensaios. Por essa limitação, antes de executarmos todos os ensaios nos equipamentos servos controlados, sempre garantimos a saturação do CP`s e o parâmetro “B” desejado manualmente de tal forma:

- Após percolação de água, é feito um confinamento e contrapressão manual dos CP`s, respeitando a pressão efetiva entre 10 a 20 kPa.

Ex: aplica-se manualmente 100 kPa de confinamento e 90 kPa de contra-pressão.

- Após verificarmos que as bombas estão estabilizadas. O envio de fluxo hidráulico da contra pressão é interrompido, e aplicasse o incremento de 50 ou 100 kPa. Com o incremento a bomba com o fluxo interrompido, responde proporcionalmente ao seu nível de saturação.

Ex: no carreamento do exemplo anterior, aplica-se uma confinamento de 50 kPa, assim sua tensão confinante sobe para 150 kPa e imediatamente temos a resposta da nossa contra-pressão, que para um “B” de 0,95 devera responder com um valor de 147,5 kPa, garantindo assim o Parâmetro “B”.

- O processo é executado para cada incremento (ciclo) ate atingir o parâmetro B solicitado. Observando sempre os valores de contra-pressão máximos e mínimos solicitados.

- Manter os incrementos até o valor ‘B’ atingir 0,95 ou se manter estável por, pelo menos, três medições consecutivas.

4.3. Peso Específico dos Grãos

Neste ensaio o ar do solo é retirado através de bomba de vácuo. O valor de “g” é utilizado nos cálculos de análise granulométrica por sedimentação na determinação de relações volumétricas das fases do solo e como indicação da natureza mineralógica do solo ou de suas frações.

A massa específica real é numericamente igual á densidade do mineral que constitui os grãos e pode ser determinada facilmente por um picnômetro.

Os procedimentos para a realização dos ensaios são de acordo com a norma técnica NBR 6508/84.

Os resultados dos ensaios são apresentados em planilha de acompanhamento do ensaio, em conformidade com as normas da ABNT, contendo a média de pelo menos, duas determinações de massa específica consideradas satisfatórias e valor do teor de umidade.

4.4. Limites de Atteberg (Limite de Liquidez e Limite de Plasticidade)

- Limite de Liquidez

A determinação do Limite de Liquidez é feita pelo aparelho Casagrande, que foi quem padronizou o ensaio. O aparelho consiste em uma concha de latão sobre suporte de ebonite. Por meio de um excêntrico imprime-se à concha repetidas quedas de altura de 1 cm e intensidade constante. Atterberg baseou-se no fato que quando o material é fluido toma a forma do recipiente que o contém. Se assim colocada uma fração de solo no recipiente, um sulco for aberto e imprimi-se um choque à concha através de quedas, o sulco se fecha.

Repetindo-se a experiência com umidades diferentes, traça-se a linha de escoamento do material (gráfico umidade x nº de golpes para fechar o sulco na amostra). Por definição, o limite de liquidez é o teor de umidade para qual o sulco se fecha com 25 golpes.

Os procedimentos para a realização dos ensaios são de acordo com a norma técnica NBR 6459/84.

- Limite de Plasticidade

Foi determinado originalmente por Atterberg pelo cálculo do teor de umidade na qual o solo começa a se fraturar, quando se tenta moldar com ele um cilindro. Modernamente o ensaio foi padronizado especificando-se que essa moldagem deve ser feita por movimentos regulares dos dedos das mãos sobre uma placa de vidro fosco colocada em superfície horizontal. Ao rolar-se a amostra essa vai progressivamente perdendo a umidade até chegar ao ponto em que o cilindro começa a partir. Determina-se então a umidade da amostra e esse é o Limite de Plasticidade.

Os procedimentos para a realização dos ensaios são de acordo com a norma técnica NBR 7180/84.

4.5. Granulometria por Peneiramento e Sedimentação

O ensaio de peneiramento consiste em agitar uma amostra de solo por um conjunto de peneiras que tenham aberturas progressivamente menores.

A análise granulométrica é a faixa de tamanho das partículas presentes em um solo, expressa em porcentagem do peso total seco.

O procedimento para a realização do ensaio de granulometria é de acordo com a norma técnica NBR 7181/84.

Os resultados dos ensaios são apresentados da seguinte maneira:

- Planilhas de Cálculo Análise Granulométrica contendo as relações “% que passa” expressos em porcentagem vs diâmetro dos grãos;
- Curvas de Distribuição Granulométrica contendo os pares de valores, citados no item anterior, lançados em um gráfico que tem no eixo das ordenadas, em escala aritmética, os

valores da porcentagem que passa; e no eixo das abscissas, em escala logarítmica, os valores dos diâmetros dos grãos;

- Indicação no gráfico de distribuição granulométrica a classificação dos diâmetros das partículas segundo a ABNT 6502 (1995).

5. RESULTADOS

Os resultados são apresentados nos quadros resumos abaixo.

5.1. Especiais

5.1.1. Triaxial CU

Resultados:

Registro Patrol	Furo	Profundidade (m)	Tensão Total		Tensão Efetiva	
			C (kPa)	Φ (º)	C' (kPa)	Φ' (º)
10149	GSSAM – 02B – 01	4.00 a 4.65	66,8	13,1	30,2	30,0
10150	GSSAM – 02B – 02	6.00 a 6.65	17,3	23,7	12,0	35,3
10151	GSSAM – 02B – 03	9.00 a 9.65	59,4	18,9	46,7	30,2
10152	GSSAM – 02B – 04	10.00 a 10.65	43,5	20,5	8,6	26,9

5.2. Caracterização

5.2.1. Granulometria por Peneiramento e Sedimentação

Resultados:

Registro Patrol	Furo	Profundidade (m)	Análise Granulométrica (%)												Material
			#1"	#3/8"	Nº 4	Nº 10	Nº 40	Nº 200	% P	% ΔG	% ΔM	% ΔF	% S	% A	
10149	GSSAM – 02B – 01	4.00 a 4.65	100	100	100	100	99,9	99,2	0,0	0,1	0,2	4,6	70,2	25,0	Silte Argiloso
10150	GSSAM – 02B – 02	6.00 a 6.65	100	100	100	100	99,9	99,5	0,0	0,1	0,1	4,4	75,9	19,5	Silte Argiloso
10151	GSSAM – 02B – 03	9.00 a 9.65	100	100	100	100	100	99,9	0,0	0,0	0,0	4,0	76,7	19,3	Silte Argiloso
10152	GSSAM – 02B – 04	10.00 a 10.65	100	100	100	100	100	99,8	0,0	0,0	0,0	4,3	74,2	21,5	Silte Argiloso

Onde:

%P = Porcentagem de Pedregulho;

% ΔG = Porcentagem de areia grossa;

% ΔM = Porcentagem de areia média;

% ΔF = Porcentagem de areia fina;

% S = Porcentagem de silte;

% A = Porcentagem de argila.

5.2.2. Massa Específica Real dos Grãos

Resultados:

Registro Patrol	Furo	Profundidade (m)	Densidade Real (g/cm³)
10149	GSSAM – 02B – 01	4.00 a 4.65	4,080
10150	GSSAM – 02B – 02	6.00 a 6.65	3,928
10151	GSSAM – 02B – 03	9.00 a 9.65	3,817
10152	GSSAM – 02B – 04	10.00 a 10.65	3,874

5.2.3. Limites de Atterberg (LL e LP)

Resultados:

Registro Patrol	Furo	Profundidade (m)	Limites de Atteberg		
			LL (%)	LP (%)	IP (%)
10149	GSSAM – 02B – 01	4.00 a 4.65	25,2	19,1	6,2
10150	GSSAM – 02B – 02	6.00 a 6.65	20,9	12,7	8,2
10151	GSSAM – 02B – 03	9.00 a 9.65	24,4	14,5	9,9
10152	GSSAM – 02B – 04	10.00 a 10.65	24,0	15,1	8,9

Onde:

LL = Limite de Liquidez;

LP = Limite de Plasticidade;

IP = Índice de Plasticidade.

5.2.4. Densidade e Umidade Natural

Resultados:

Registro Patrol	Furo	Profundidade (m)	Densidade Natural (g/cm³)	Umidade Natural (%)
10149	GSSAM – 02B – 01	4.00 a 4.65	2,172	35,3
10150	GSSAM – 02B – 02	6.00 a 6.65	2,287	26,4
10151	GSSAM – 02B – 03	9.00 a 9.65	2,301	21,7
10152	GSSAM – 02B – 04	10.00 a 10.65	2,335	31,9

6. ANEXOS

Anexo os resultados e fichas dos ensaios.

Atenciosamente,

Fernando César Tavares
Engenheiro Civil
Patrol Investigações Geotécnicas Ltda.
Telefone (31) 3462.0722

ANEXOS

GSSAM 02B 01 – prof.: 4,00 – 4,65 m
Reg.:10149

TRIAXIAL CU

DENSIDADE APARENTE

CLIENTE:	**Cleary Gottlieb e Hamilton LLP**		
REGISTRO:	**10152**		
FURO:	**GSSam 02B 01**	PROF.:	**4,00 - 4,65 m**
LOCAL:	**Baia 3 - Local - F**		

DADOS INICAIS DE MOLDAGEM:

Tensões de Confinamento	200 kPa	400 kPa	600 kPa	800 kPa

Peso e Geometria:

Diam. interno:[mm]	*35,57*	*35,70*	*35,51*	*35,68*
Altura do molde: [mm]	*71,70*	*71,71*	*71,70*	*71,71*
Volume do anel (cm3)	*71,25*	*71,78*	*71,01*	*71,70*
Tara do Molde: [g]	*577,08*	*577,08*	*577,08*	*577,08*
Peso Anel + amostra:	*721,41*	*722,49*	*720,93*	*722,33*
Peso da amostra: [g]	*154,08*	*155,37*	*155,00*	*157,45*

Teor de umidade:

Massa Úmida + Tara [g]	*97,39*	*96,25*	*99,83*	*133,87*
Massa Seca + Tara [g]	*75,44*	*78,20*	*84,01*	*104,50*
Tara [g]	*13,87*	*13,13*	*12,30*	*14,26*
Água [g]	*21,96*	*18,06*	*15,83*	*29,37*
Massa Seca [g]	*61,57*	*65,07*	*71,71*	*90,24*
Umidade [%]	*35,66*	*27,75*	*22,07*	*32,56*

Dados Calculados:

Densid.Real: [g/cm^3]	*4,080*	*4,080*	*4,080*	*4,080*
M.E.A.Umida [g/cm^3]	*2,163*	*2,165*	*2,183*	*2,196*
M.E.A.Seca [g/cm^3]	*1,594*	*1,694*	*1,79*	*1,657*
Indice Vazios Inicial	*1,56*	*1,41*	*1,28*	*1,46*
G.Saturação Inicial [%]	*93,30*	*80,42*	*70,25*	*90,81*
Volume de Vazios (%)	*60,93*	*58,47*	*56,17*	*59,40*

CONSOLIDATED UNDRAINED TRIAXIAL TEST by ASTM D4767

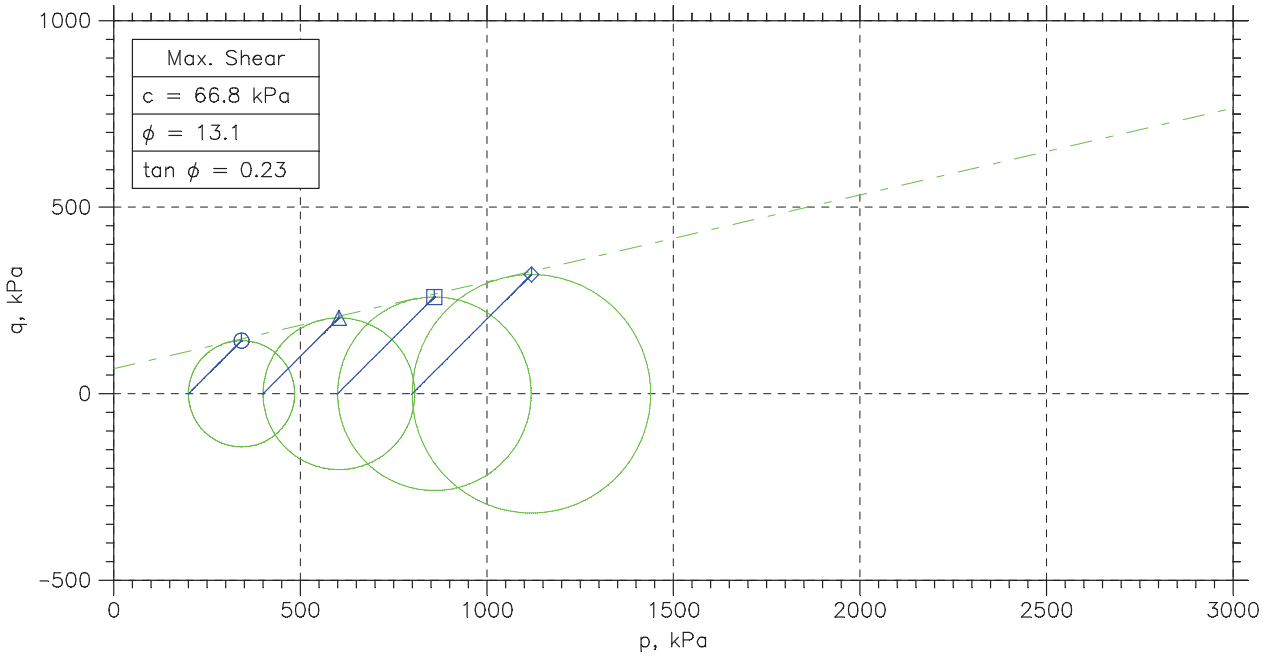

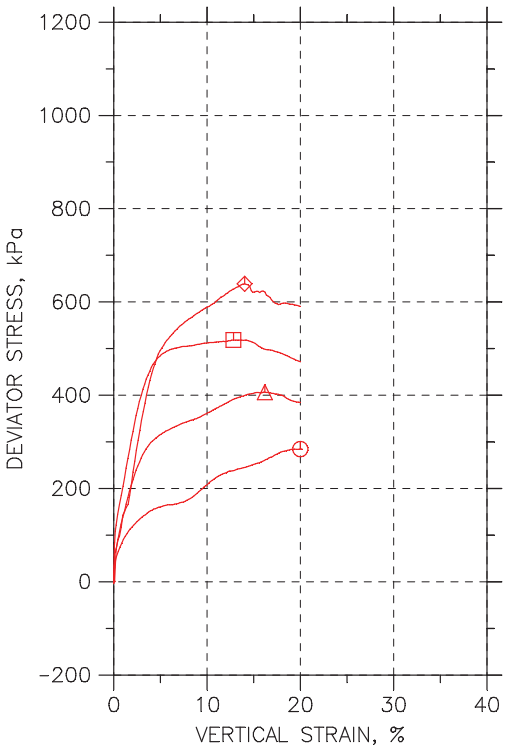

Symbol		○	△	□	◇
Sample No.		GSSam02BG07	GSSam02BG07	GSSam02BG07	GSSam02 07
Test No.		200 KPa	400 KPa	600 KPa	800 KPa
Depth		4.0-4.65 m	4.0-4.65 m	4.0-4.65 m	4.0-4.65 m
Initial	Diameter, mm	35.57	35.7	35.51	35.68
	Height, mm	71.7	71.71	71.7	71.71
	Water Content, %	36.7	33.3	30.3	34.5
	Dry Density, N/m^3	15630	16620	17540	16250
	Saturation, %	96.1	96.5	96.4	96.1
	Void Ratio	1.56	1.41	1.28	1.46
Before Shear	Water Content, %	25.8	24.1	22.8	22.4
	Dry Density, N/m^3	19500	20190	20730	20910
	Saturation*, %	100.0	100.0	100.0	100.0
	Void Ratio	1.05	0.982	0.93	0.914
	Back Press., kPa	40.	39.95	39.95	40.05
Ver. Eff. Cons. Stress, kPa		200.	400.	600.	799.9
Shear Strength, kPa		142.3	203.2	259.2	319.4
Strain at Failure, %		20	16.2	12.8	14
Strain Rate, %/min		0.09	0.09	0.09	0.09
B-Value		---	---	---	---
Measured Specific Gravity		4.08	4.08	4.08	4.08
Liquid Limit		---	---	---	---
Plastic Limit		---	---	---	---

PATTROL

Project: Cleary Gottlieb Steen
Location: Baia 3 local F
Project No.: 001
Boring No.: 10149
Sample Type: Shelby
Description:
Remarks: G 07

Phase calculations based on end of test.

* Saturation is set to 100% for phase calculations.

Tue, 12-JUL-2016 16:40:31

CONSOLIDATED UNDRAINED TRIAXIAL TEST by ASTM D4767

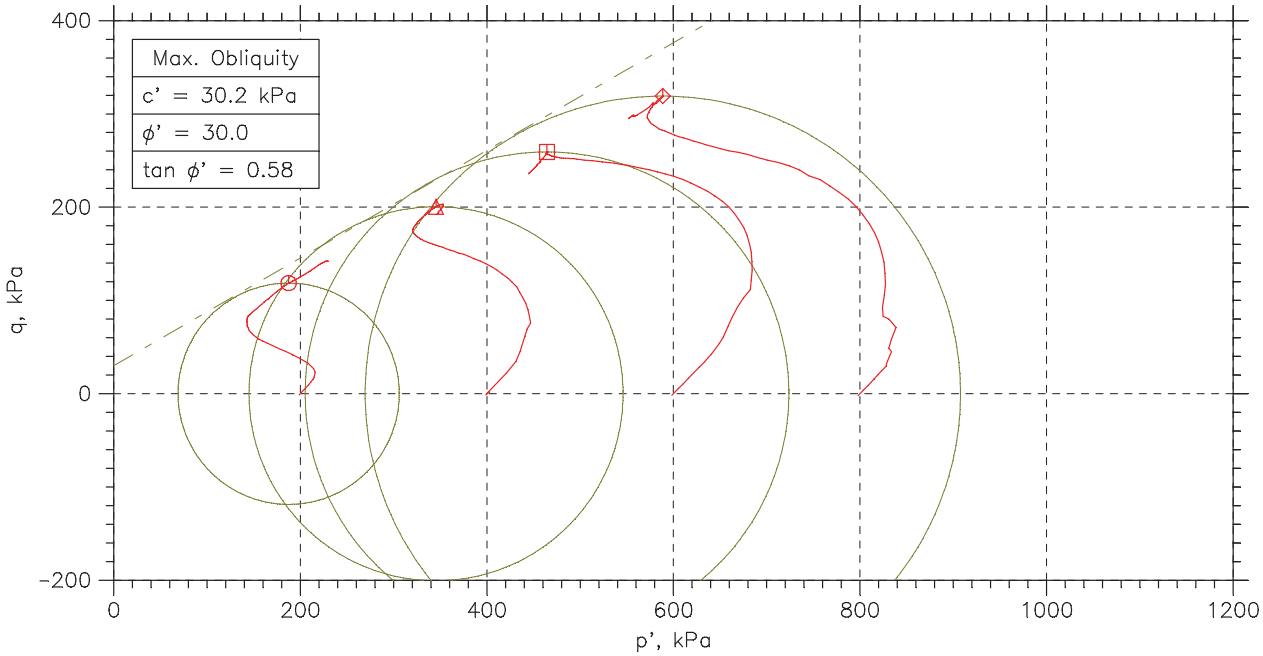

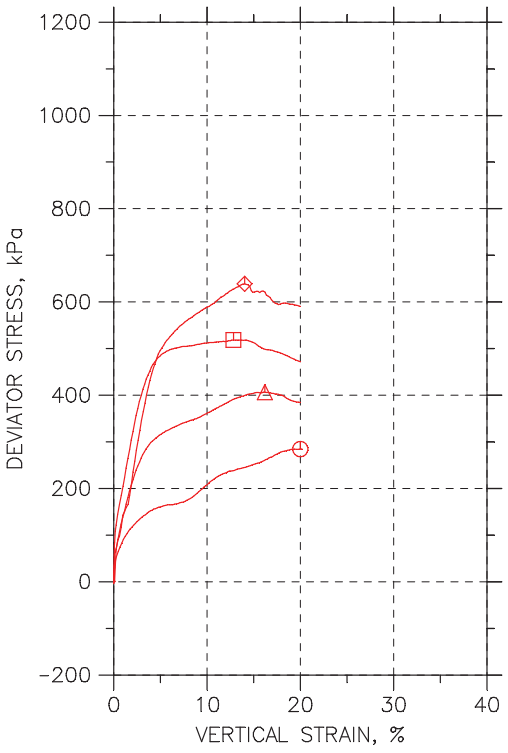

Symbol		⏲	△	⏍	◇
Sample No.		GSSam02B GS	Sam02B GS	Sam02B GS	Sam02 01
Test No.		200 KPa	400 KPa	600 KPa	800 KPa
Depth		4.0-4.65 m	4.0-4.65 m	4.0-4.65 m	4.0-4.65 m
Initial	Diameter, mm	35.57	35.7	35.51	35.68
	Height, mm	71.7	71.71	71.7	71.71
	Water Content, %	36.7	33.3	30.3	34.5
	Dry Density, N/m^3	15630	16620	17540	16250
	Saturation, %	96.1	96.5	96.4	96.1
	Void Ratio	1.56	1.41	1.28	1.46
Before Shear	Water Content, %	25.8	24.1	22.8	22.4
	Dry Density, N/m^3	19500	20190	20730	20910
	Saturation*, %	100.0	100.0	100.0	100.0
	Void Ratio	1.05	0.982	0.93	0.914
	Back Press., kPa	40.	39.95	39.95	40.05
Ver. Eff. Cons. Stress, kPa		200.	400.	600.	799.9
Shear Strength, kPa		142.3	203.2	259.2	319.4
Strain at Failure, %		20	16.2	12.8	14
Strain Rate, %/min		0.09	0.09	0.09	0.09
B-Value		---	---	---	---
Measured Specific Gravity		4.08	4.08	4.08	4.08
Liquid Limit		---	---	---	---
Plastic Limit		---	---	---	---

PATTROL

Project: Cleary Gottlieb Steen
Location: Baia 3 local F
Project No.: 001
Boring No.: 10149
Sample Type: Shelby
Description:
Remarks: G 07

Phase calculations based on end of test.

* Saturation is set to 100% for phase calculations.

Tue, 12-JUL-2016 16:38:24

CONSOLIDATED UNDRAINED TRIAXIAL TEST by ASTM D4767

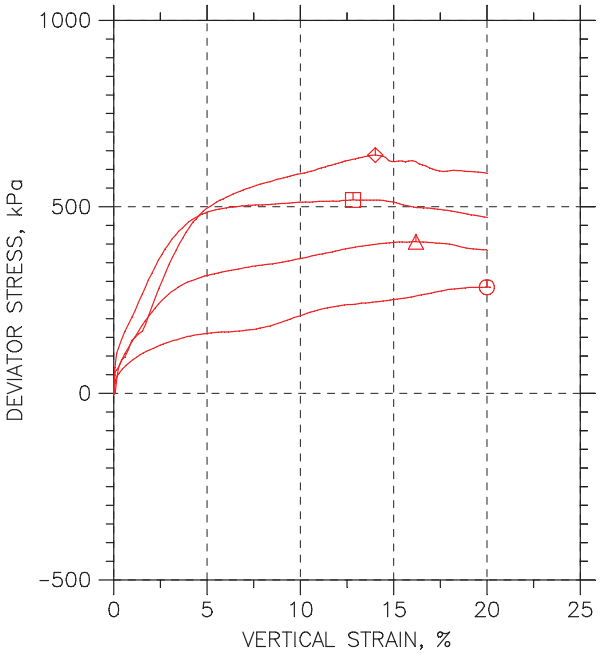

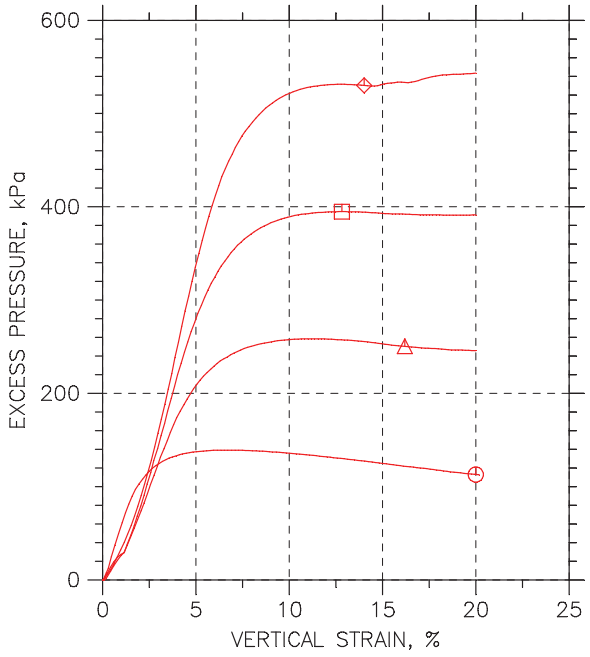

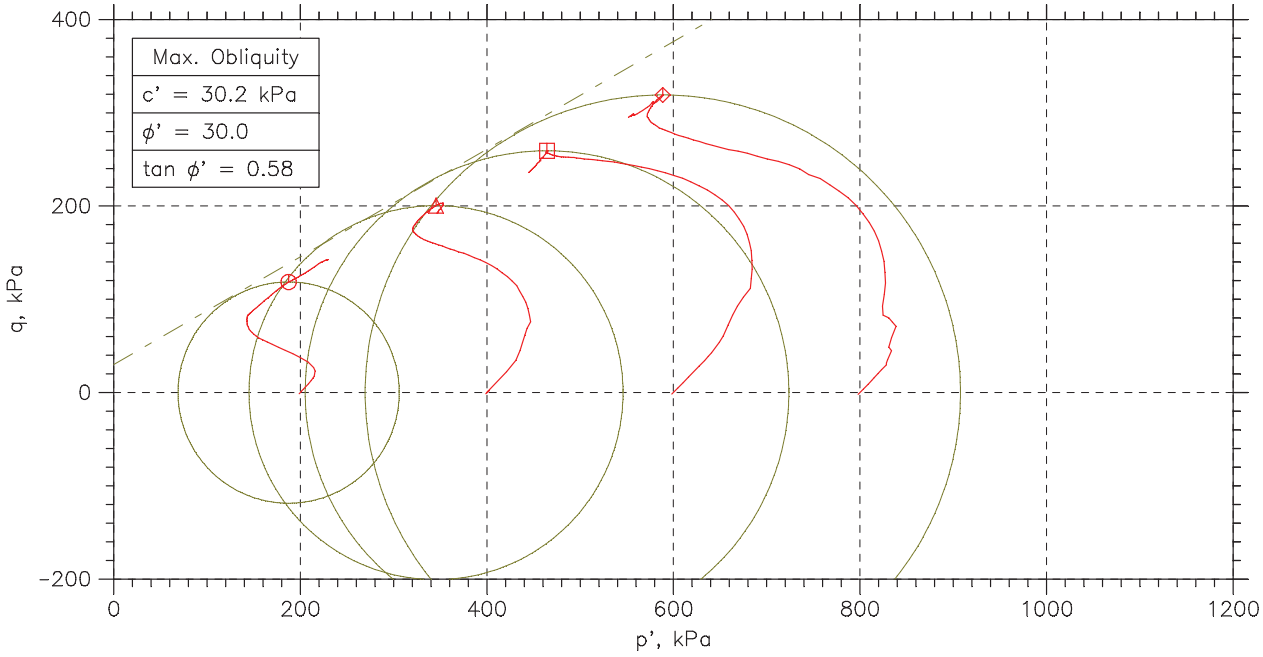

	Sample No.	Test No.	Depth	Tested By	Test Date	Checked By	Check Date	Test File
○	GSSam02B 02	200 KPa	4.0-4.65 m	Fernando	04/072016	Almir		Reg. 10149 - 200 KPa - G7.da
△	GSSam02B 04	400 KPa	4.0-4.65 m	Fernando	04/07/2016	Almir		Reg. 10149 - 400 KPa - F5.da
□	GSSam02B 06	600 KPa	4.0-4.65 m	Fernando	07/07/2016	Almir		Reg. 10149 - 600x KPa - F5.dc
◇	GSSam02 01	800 KPa	4.0-4.65 m	Fernando	06/072016	Almir		Reg. 10149 - 800. KPa - G7.dc

PATTROL

Project: Cleary Gottlieb Steen	Location: Baia 3 local F	Project No.: 001
Boring No.: 10149	Sample Type: Shelby	
Description:		
Remarks: G 07		

Tue, 12-JUL-2016 16:38:24

PATROL INVESTIGAÇÕES GEOTÉCNICAS LTDA

Controle do Parâmetro B (Skempton) pelo Painel de Saturação

Interessado:	**Cleary Gottlieb e Hamilton LLP**	Material:		Data:	**08/07/2016**
Obra:	**-**	Furo:	**GSSam 02B 01**	Amostra:	**Shelby**
Local:	**-**	Prof.:	**4,00 - 4,65 m**	Registro:	**2016.10149**

Dados de Moldagem Corpo de Prova

Diâmetro [mm]	**35,57**
Altura [mm]	**71,70**
Volume [cm³]	**71,25**
Peso da amostra [g]	**155,31**

Densid.Real [g/cm³]	**4,080**
M.E.A.Umida [g/cm³]	**2,180**
M.E.A.Seca [g/cm³]	**1,594**
Umidade Inicial [%]	**36,75**

Parâmetro B (Skempton) pelo Painel de Saturação

Tensão Confinante (kPa)	Contra Pressão (kPa)	u (kPa)	B
50,0	40,00	-	-
99,90	85,20	49,90	0,71
149,84	138,34	49,94	0,77
199,60	190,75	49,76	0,82
249,85	241,83	50,25	0,84
299,51	293,70	49,66	0,88
349,69	344,92	50,18	0,90
399,80	395,49	50,11	0,91
449,33	446,05	49,53	0,93
499,64	496,80	50,31	0,94
549,93	547,40	50,29	0,95
599,96	597,68	50,03	0,95
649,87	647,33	49,91	0,95
699,79	697,75	49,92	0,96
749,84	747,72	50,05	0,96
799,92	797,78	50,08	0,96

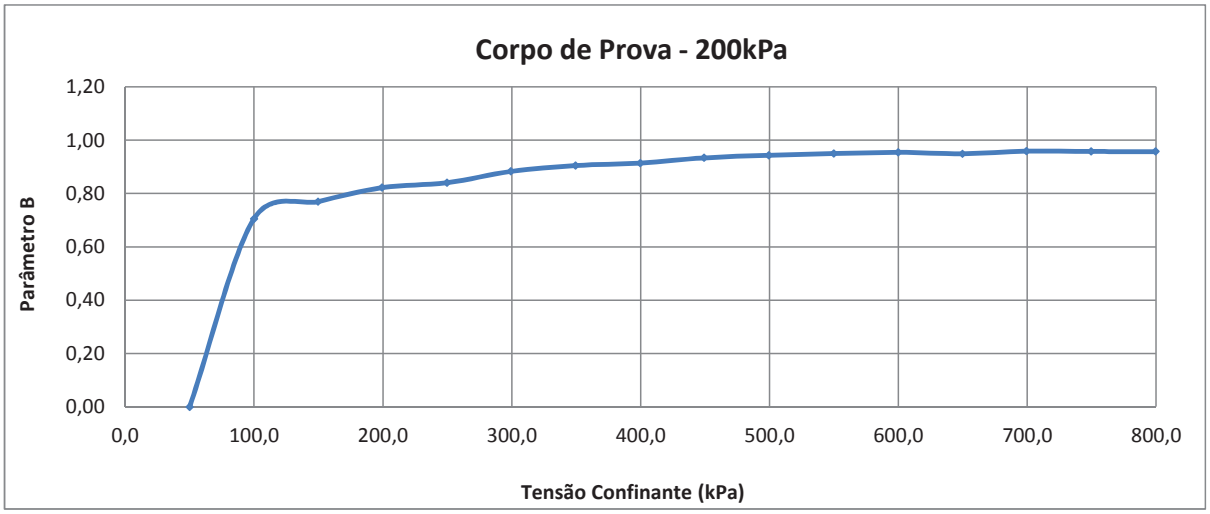

Parâmetro B de poropressão de Skempton: $B = \Delta u / \Delta\sigma_3$

A saturação por contra pressão foi aplicada com incrementos aproximados de 50kPa.

PATROL INVESTIGAÇÕES GEOTÉCNICAS LTDA

Controle do Parâmetro B (Skempton) pelo Painel de Saturação

Interessado:	**Cleary Gottlieb e Hamilton LLP**	Material:		Data:	**08/07/2016**
Obra:	**-**	Furo:	**GSSam 02B 01**	Amostra:	**Shelby**
Local:	**-**	Prof.:	**4,00 - 4,65 m**	Registro:	**2016.10149**

Dados de Moldagem Corpo de Prova

Diâmetro [mm]	**35,70**
Altura [mm]	**71,71**
Volume [cm³]	**71,78**
Peso da amostra [g]	**162,14**

Densid.Real [g/cm³]	**4,080**
M.E.A.Umida [g/cm^3]	**2,259**
M.E.A.Seca [g/cm^3]	**1,694**
Umidade Inicial [%]	**33,32**

Parâmetro B (Skempton) pelo Painel de Saturação

Tensão Confinante (kPa)	Contra Pressão (kPa)	u (kPa)	B
50	40,00	-	-
99,95	83,50	49,95	0,67
149,89	136,15	49,94	0,72
199,75	187,47	49,86	0,75
249,81	241,00	50,06	0,82
299,70	294,65	49,89	0,90
349,94	345,39	50,24	0,91
399,76	396,32	49,82	0,93
449,86	447,59	50,10	0,95
499,90	497,79	50,04	0,96
549,73	547,50	49,83	0,96
599,89	597,73	50,16	0,96

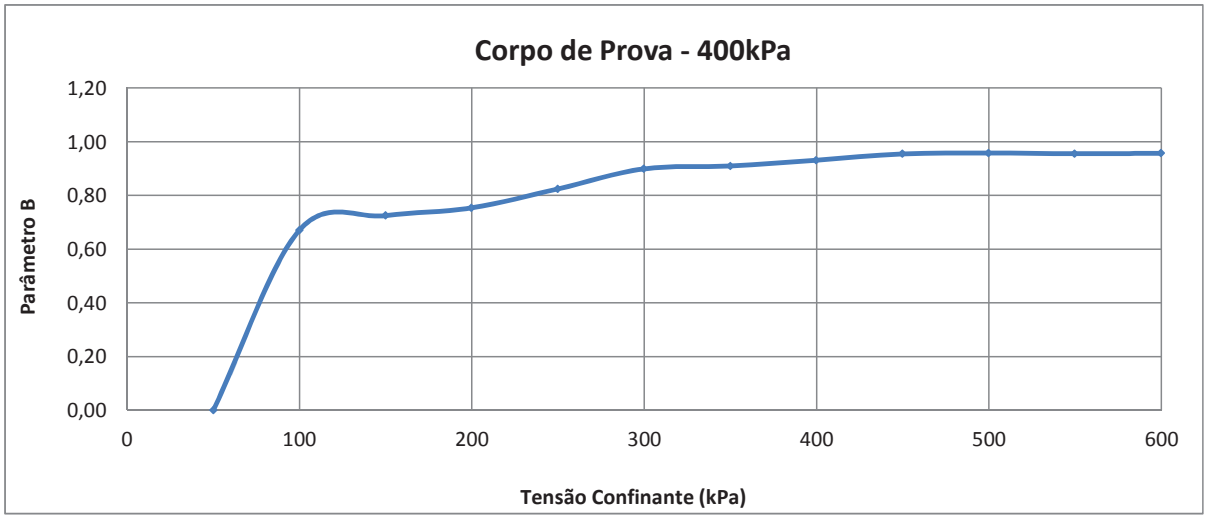

Parâmetro B de poropressão de Skempton: $B = \Delta u / \Delta \sigma_3$

A saturação por contra pressão foi aplicada com incrementos aproximados de 50kPa.

PATROL INVESTIGAÇÕES GEOTÉCNICAS LTDA

Controle do Parâmetro B (Skempton) pelo Painel de Saturação

Interessado:	**Cleary Gottlieb e Hamilton LLP**	Material:	**-**	Data:	**08/07/2016**
Obra:	**-**	Furo:	**GSSam 02B 01**	Amostra:	**Shelby**
Local:	**-**	Prof.:	**4,00 - 4,65 m**	Registro:	**2016.10149**

Dados de Moldagem Corpo de Prova

Diâmetro [mm]	**35,51**
Altura [mm]	**71,70**
Volume [cm³]	**71,01**
Peso da amostra [g]	**165,43**

Densid.Real [g/cm³]	**4,080**
M.E.A.Umida [g/cm^3]	**2,330**
M.E.A.Seca [g/cm^3]	**1,788**
Umidade Inicial [%]	**30,28**

Parâmetro B (Skempton) pelo Painel de Saturação

Tensão Confinante (kPa)	Contra Pressão (kPa)	u (kPa)	B
50	40,00	-	-
99,90	92,27	49,90	0,85
149,96	145,49	50,06	0,91
199,70	196,53	49,74	0,94
249,87	247,19	50,17	0,95
299,83	297,63	49,96	0,96
349,88	348,05	50,05	0,96
399,91	398,06	50,03	0,96

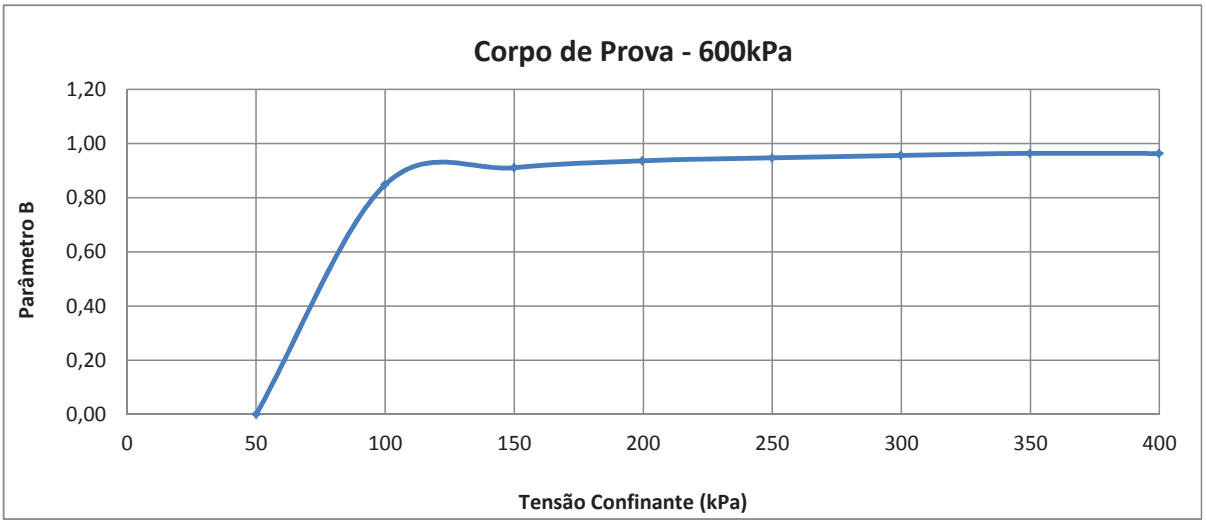

Parâmetro B de poropressão de Skempton: $B = \Delta u / \Delta\sigma_3$

A saturação por contra pressão foi aplicada com incrementos aproximados de 50kPa.

PATROL INVESTIGAÇÕES GEOTÉCNICAS LTDA

Controle do Parâmetro B (Skempton) pelo Painel de Saturação

Interessado:	**Cleary Gottlieb e Hamilton LLP**	Material:	**-**	Data:	**08/07/2016**
Obra:	**-**	Furo:	**GSSam 02B 01**	Amostra:	**Shelby**
Local:	**-**	Prof.:	**4,00 - 4,65 m**	Registro:	**2016.10149**

Dados de Moldagem Corpo de Prova

Diâmetro [mm]	**35,68**
Altura [mm]	**71,71**
Volume [cm³]	**71,70**
Peso da amostra [g]	**159,70**

Densid.Real [g/cm³]	**4,080**
M.E.A.Umida [g/cm^3]	**2,227**
M.E.A.Seca [g/cm^3]	**1,657**
Umidade Inicial [%]	**34,45**

Parâmetro B (Skempton) pelo Painel de Saturação

Tensão Confinante (kPa)	Contra Pressão (kPa)	u (kPa)	B
50	40,00	-	-
99,81	97,88	49,81	0,96
149,87	147,87	50,06	0,96
199,83	197,92	49,96	0,96

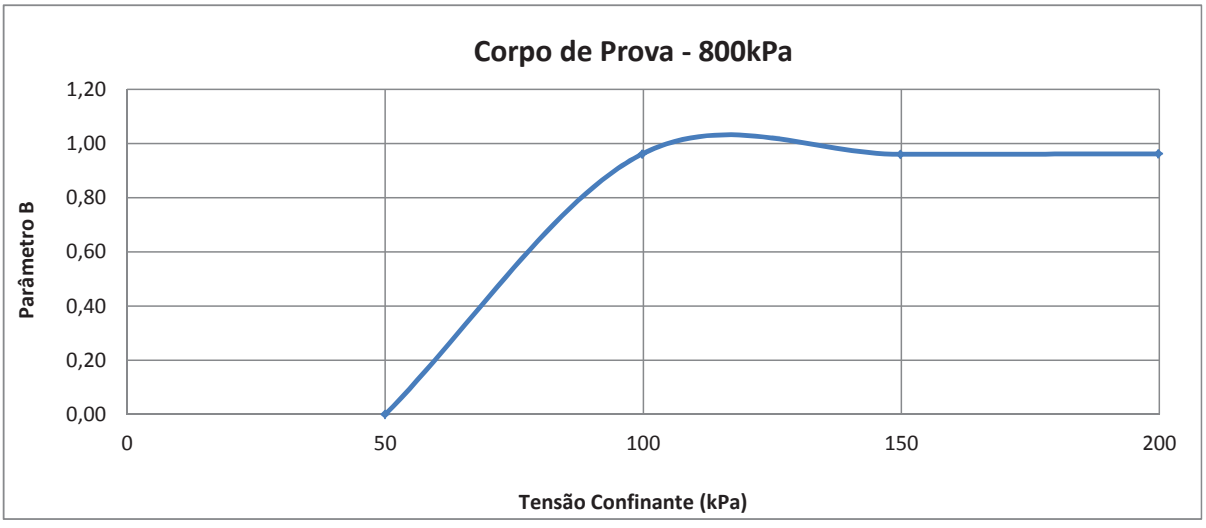

Parâmetro B de poropressão de Skempton: $B = \Delta u / \Delta\sigma_3$

A saturação por contra pressão foi aplicada com incrementos aproximados de 50kPa.

PATROL INVESTIGAÇÕES GEOTÉCNICAS LTDA.

RELATÓRIO FOTOGRÁFICO - Triaxial CIU (200, 400, 600 e 800 KPa)

Cliente:	**Cleary Gottlieb Steen & Hamilton LLP**	Local:	**BAIA 3 - LOCAL F**
Obra:	**-**	Amostra:	**-**
Data:	**18/07/16** Furo: **GSSAM-02B-01**	Registro:	**2016.10149**

Antes 200 KPa

Depois 200 KPa

Antes 400 KPa

Depois 400 KPa

Antes 600 KPa

Depois 600 KPa

Antes 800 KPa

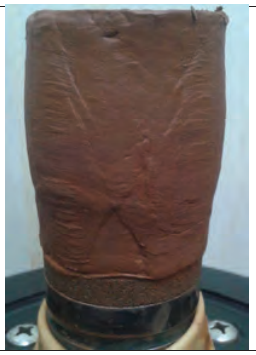

Depois 800 KPa

OBSERVAÇÕES:

PATROL INVESTIGAÇÕES GEOTÉCNICAS LTDA

Determinação da Massa específica aparente de amostras indeformadas, com emprego da balança hidrostática - NBR 10838

Interessado:	**Cleary**	Material:	**-**	Data:	**18/07/16**
Obra:	**-**	Furo:	**GSSAM-02B-01**	Amostra:	**Shelby**
Localização:	**BAIA 3 - LOCAL F**	Prof.:	**4,00 - 4,65**	Registro:	**2016.10149**

DETERMINAÇÃO DA MASSA ESPECÍFICA APARENTE DA PARAFINA

Dados	CP 01	CP 02	CP 03
M_{paraf} (g)	71,78	76,85	74,66
M_{cpi} (g)	95,84	95,84	95,90
M_{ci} (g)	92,66	92,27	92,58
Y_0 (g/cm^3)	1,00	1,00	1,00
Yparaf (g/cm3)	0,958	0,956	0,957
Média	0,957		

DETERMINAÇÃO DO VOLUME DO CORPO-DE-PROVA E DA MASSA ESPECÍFICA NATURAL DA AMOSTRA

VOLUME DO CP			
Dados	CP 01	CP 02	CP 03
M_p (g)	290,11	279,05	261,12
M_i (g)	141,70	128,00	123,76
M_s (g)	265,19	240,94	230,83
Y_{paraf} (g/cm^3)	0,957	0,957	0,957
Y_0 (g/cm^3)	1,00	1,00	1,00
V_s (cm^3)	122,37	111,22	105,70
Média:	113,098		

MASSA ESPECÍFICA APARENTE NATURAL			
Dados	CP 01	CP 02	CP 03
M_s (g)	265,19	240,94	230,83
V_s (cm^3)	122,37	111,22	105,70
Yh (g/cm^3)	2,167	2,166	2,184
Média	2,172		

TEOR DE UMIDADE			
nº capsula	97	182	259
cáp+solo úmido	81,28	90,15	104,63
cáp+solo seco	63,69	70,13	80,74
água	17,59	20,02	23,89
tara	12,87	14,02	13,71
solo seco	50,82	56,11	67,03
umidade	34,61	35,68	35,64
Média	35,31		

M_{paraf} = massa do corpo-de-prova, em g;

M_{cpi} = massa do contrapeso quando imerso em água, em g;

M_{ci} = massa do conjunto corpo-de-prova e contrapeso;

Y_0 = massa específica da água (considerar igual a 1 g/cm^3);

Y_{paraf} = massa específica da parafina, em g/cm^3;

Mp = massa do corpo-de-prova parafinado, em g;

Mi = massa do corpo-de-prova parafinado e imerso em água, em g;

Ms = massa do corpo-de-prova, em g;

Vs = volume do corpo-de-prova, em cm^3;

Yh = massa específica aparente natural da amostra, em g/cm^3.

GSSAM 02B 01 – prof.: 4,00 – 4,65 m
Reg.:10149

CARACTERIZAÇÃO

PATROL INVESTIGAÇÕES GEOTÉCNICAS LTDA

Análise Granulométrica por Peneiramento e Sedimentação - NBR 7181/1984

Interessado:	**Cleary**	Material:	**Silte Argiloso**	Data:	**11/07/2016**
Obra:	**-**	Furo:	**GSSam-02B-04**	Amostra:	**Shelby**
Local:	**Baia 03 - Local F**	Prof.:	**4,00 - 4,65**	Registro:	**10149.2016**
Densimetro:	**DS 02 - (16569/13) VT**				

UMIDADE HIGROSCÓPICA			
Cápsula no. (g.)	**69**	**111**	**286**
Solo umido + tara (g.)	**69,42**	**72,20**	**67,95**
Solo seco + tara (g.)	**66,17**	**68,81**	**64,77**
Tara da capsula (g.)	**12,14**	**11,97**	**12,09**
Água (g.)	3,25	3,39	3,18
Solo Seco (g.)	54,03	56,84	52,68
Teor de umidade (%)	6,0	6,0	6,0
Umidade Média (%)	6,0		

AMOSTRA TOTAL SECA	
Amostra Total Úmida (g)	**841,17**
Solo Seco retido na # 10 (g)	0,00
Solo Úmido passa na # 10 (g)	841,17
Solo Seco passa na # 10 (g)	793,52
Amostra Total Seca (g)	793,52

AMOSTRA PARCIAL SECA	
Amostra menor #10 úmida (g)	**70,00**
Amostra menor #10 seca (g)	66,03
Limite de Liquidez	
Índice de Plasticidade	

MASSA ESPECÍFICA REAL		
Picnômetro. nº	**5**	**6**
Temperatura (°c)	**19,8**	**19,8**
Pic.+ água + solo (g)	**792,52**	**782,46**
Solo úmido(g)	**50,00**	**50,00**
Solo Seco (g)	47,17	47,17
Pic.+ água (g)	756,89	746,84
Água Deslocada (g)	11,54	11,55
Teor de umidade (%)	**6,0**	
Massa Específica (H2O)	0,9983	0,9983
Massa Específica Real	4,082	4,078
ρ [g/cm^3]	**4,080**	

P E N E I R A M E N T O

PENEIRAS A.B.N.T.		MATERIAL RETIDO			% QUE	
		Peso	P.acumul	%	PASSA:amostra	Faixa
N o.	mm.	(gr.)	(gr.)	acumul	total	
4''	101,8					
3 .1/2 "	88,9					
3''	76,2					
2 .1/2 "	63,5					
2''	50,8					
1.1/2 "	38,1					
1''	25,4					
3/4 "	19					
1/2 "	12,7					
3/8''	9,5					
1/4''	6,3					
4	4,8					
8	2,4					
10	2	**0,00**	0,0	0,0	**100,0**	
16	1,2	**0,00**	0,0	0,0	**100,0**	
30	0,6	**0,05**	0,1	0,1	**99,9**	
40	0,42	**0,04**	0,1	0,1	**99,9**	
60	0,25	**0,04**	0,1	0,2	**99,8**	
100	0,15	**0,06**	0,2	0,3	**99,7**	
200	0,075	**0,36**	0,6	0,8	**99,2**	

Densímetro n.º	**02**

$$K = \frac{\delta}{\delta - 1} =$$ 1,325

% da amostra parcial = A x K x LC

A =	0,0151

SEDIMENTAÇÃO COM DEFLOCULANTE

Data	Temp.	Tempo	horário	Leit.	Correções			Leit.	Altura de	%	%	f
	°c	min.	h	(L)	temperatura	menisco	defloculante	corrig.	Queda	parcial	total	mm
08/07/2016	**20,2**	0,5	**9:37**	**50,0**	-3,6	0,5	-2,0	44,9	8,7	90,1	90,1	0,0407
08/07/2016	20,2	1	9:38	**48,0**	-3,6	0,5	-2,0	42,9	9,0	86,1	86,1	0,0294
09/07/2016	20,2	2	9:39	**47,0**	-3,6	0,5	-2,0	41,9	9,2	84,1	84,1	0,0210
10/07/2016	20,2	5	9:42	**45,0**	-3,6	0,5	-2,0	39,9	9,5	80,0	80,0	0,0136
11/07/2016	20,1	10	9:47	**40,0**	-3,6	0,5	-2,0	34,9	10,4	70,0	70,0	0,0101
12/07/2016	**20,1**	20	9:57	**36,0**	-3,6	0,5	-2,0	30,9	11,0	61,9	61,9	0,0074
13/07/2016	**20,1**	40	10:17	**31,0**	-3,6	0,5	-2,0	25,9	11,9	51,9	51,9	0,0054
14/07/2016	**20,1**	80	10:57	**25,0**	-3,6	0,5	-2,0	19,9	12,9	39,9	39,9	0,0040
15/07/2016	**20,3**	240	13:37	**19,0**	-3,6	0,5	-2,0	13,9	13,8	28,0	28,0	0,0024
16/07/2016	**20,6**	540	17:37	**16,0**	-3,5	0,5	-2,0	11,0	14,3	22,1	22,1	0,0016
09/07/2016	**19,5**	1440	9:37	**12,0**	-3,8	0,5	-2,0	6,7	15,0	13,4	13,4	0,0010

Tipo	Pedregulo	Areia Grossa	Areia Média	Areia Fina	Silte	Argila
% total	0,0	0,1	0,2	4,6	70,2	25,0
% total	**0,0**	**4,8**			**70,2**	**25,0**

Análise Granulométrica por Peneiramento e Sedimentação - NBR 7181/1984

Interessado:	**Cleary**	Material:	**Silte Argiloso**	Data:	**11/07/2016**
Obra:	**-**	Furo:	**GSSam-02B-04**	Amostra:	**Shelby**
Local:	**Baia 03 - Local F**	Prof.:	**4,00 - 4,65**	Registro:	**2016. 10149**
Densimetro:	**DS 02 - (16569/13) VT**				

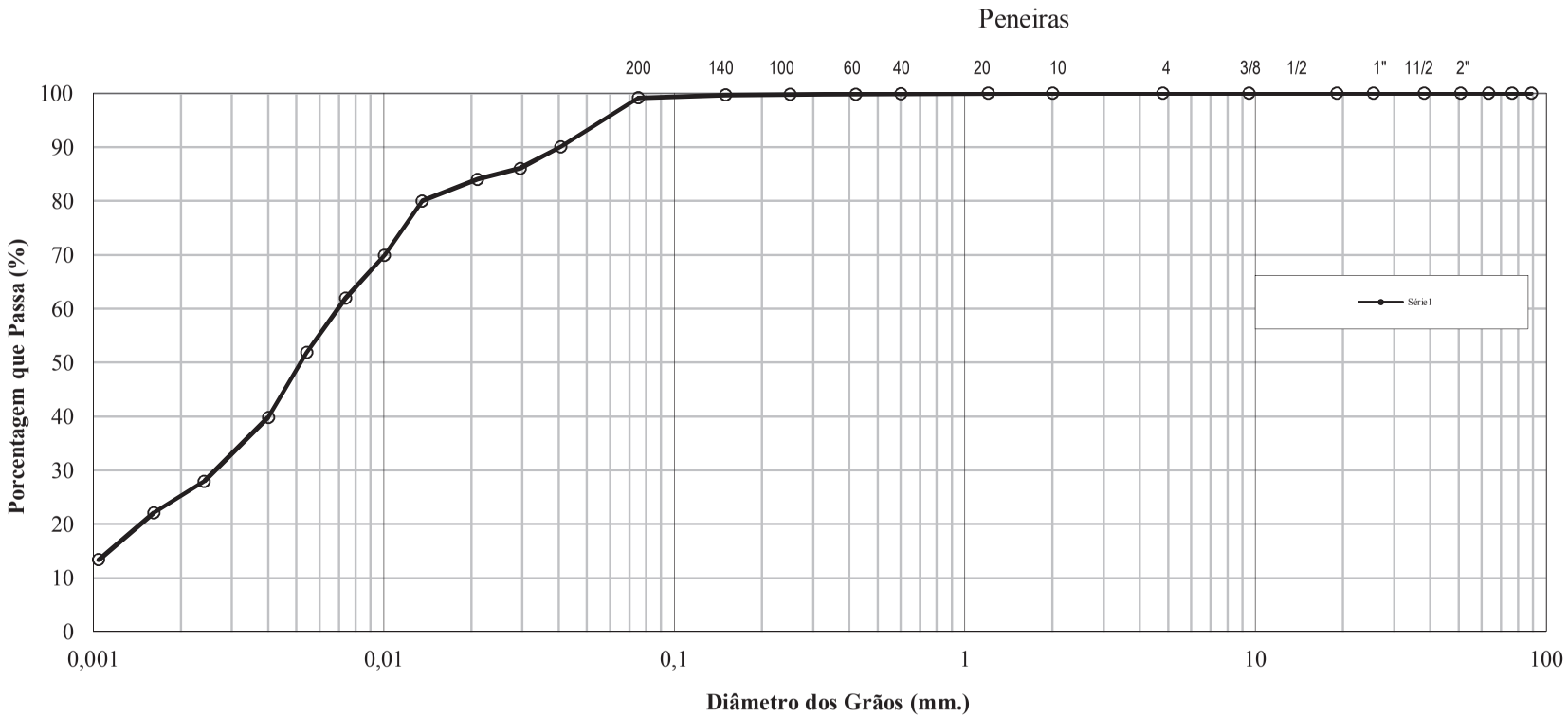

Argila	Silte	Areia Fina	A.Média	13,03	Pedregulho
25,0	**70,2**	**4,6**	**0,2**	**13,5**	**0,0**

PATROL INVESTIGAÇÕES GEOTÉCNICAS

Massa Específica Real dos Grãos - NBR 6508/84

Interessado:	**Cleary Gottieb**	Material:		Data:	**11/07/2016**
Obra:	**-**	Furo:	**GSSam - 02B - 04**	Amostra:	**Shelby**
Local:	**Baia 03 - Local F**	Prof.:	**4,00 a 4,65**	Registro:	**2016.10149**

DETEMINAÇÃO DA UMIDADE (%)

EXECUÇÃO DO ENSAIO			
Cápsula:	69	111	286
Cáp + sol + Agua (g):	69,42	72,20	67,95
Cáp + solo (g):	66,17	68,81	64,77
Peso da cápsula (g):	12,14	11,97	12,09
Água (g):	3,25	3,39	3,18
Solo seco (g):	54,03	56,84	52,68
Umidade (%):	6,0	6,0	6,0
Média:	6,0		

MASSA ESPECÍFICA REAL DOS GRÃOS

EXECUÇÃO DO ENSAIO		
Picnômetro	5	6
Temperatura ºC:	19,8	19,8
Picnômetro + água (g):	756,89	746,84
Solo úmido(g):	50,00	50,00
Solo seco (g):	47,17	47,17
Umidade (%)	6,0	6,0
Conjunto Pic + água + solo (g):	792,52	782,46
Água deslocada (g):	11,54	11,55
Massa Específica (H_2O):	0,9983	0,9983
Massa Específica Real (g/cm³):	4,082	4,078
Média	4,080	

PATROL INVESTIGAÇÕES GEOTÉCNICAS LTDA

LIMITES DE ATTERBERG

Interessado:	**Cleary Gotiieb**	Material:		Data:	**12/07/2016**
Obra:	**-**	Furo:	**GSSam - 02 B - 04**	Amostra:	**Shelby**
Local:	**Baia 3 - Local F**	Prof.:	**4,00 - 4,65**	Registro:	**2016.10149**

LIMITE DE LIQUIDEZ - NBR 6459/1984

Cápsula nº	31	32	33	34	35
Peso da Cápsula+Solo Úmido(g)	21,91	22,87	23,46	24,91	26,17
Peso da Cápsula+Solo Seco(g)	19,27	20,12	20,65	21,83	23,04
Peso da Água(g)	2,64	2,75	2,81	3,08	3,13
Peso da Cápsula(g)	9,61	9,43	9,40	9,45	9,99
Peso do Solo Seco(g)	9,66	10,69	11,25	12,38	13,05
Teor de Umidade(%)	27,3	25,7	25,0	24,9	24,0
Nº de golpes	15	20	25	30	35

LIMITE DE PLASTICIDADE - NBR 7180/1984

Cápsula nº	31	32	33	34	35
Peso da Cápsula+Solo Úmido(g)	7,75	7,48	7,81	6,85	7,88
Peso da Cápsula+Solo Seco(g)	7,37	7,07	7,45	6,54	7,42
Peso da Água(g)	0,38	0,41	0,36	0,31	0,46
Peso da Cápsula(g)	5,42	4,98	5,55	4,84	5,16
Peso do Solo Seco(g)	1,95	2,09	1,90	1,70	2,26
Teor de Umidade(%)	19,5	19,6	18,9	18,2	20,4
Valor aceito?	SIM	SIM	SIM	SIM	NÃO

GRÁFICO

RESULTADOS	
LIMITE DE LIQUIDEZ(%)	25,2
LIMITE DE PLASTICIDADE(%)	19,1
ÍNDICE DE PLASTICIDADE(%)	6,2

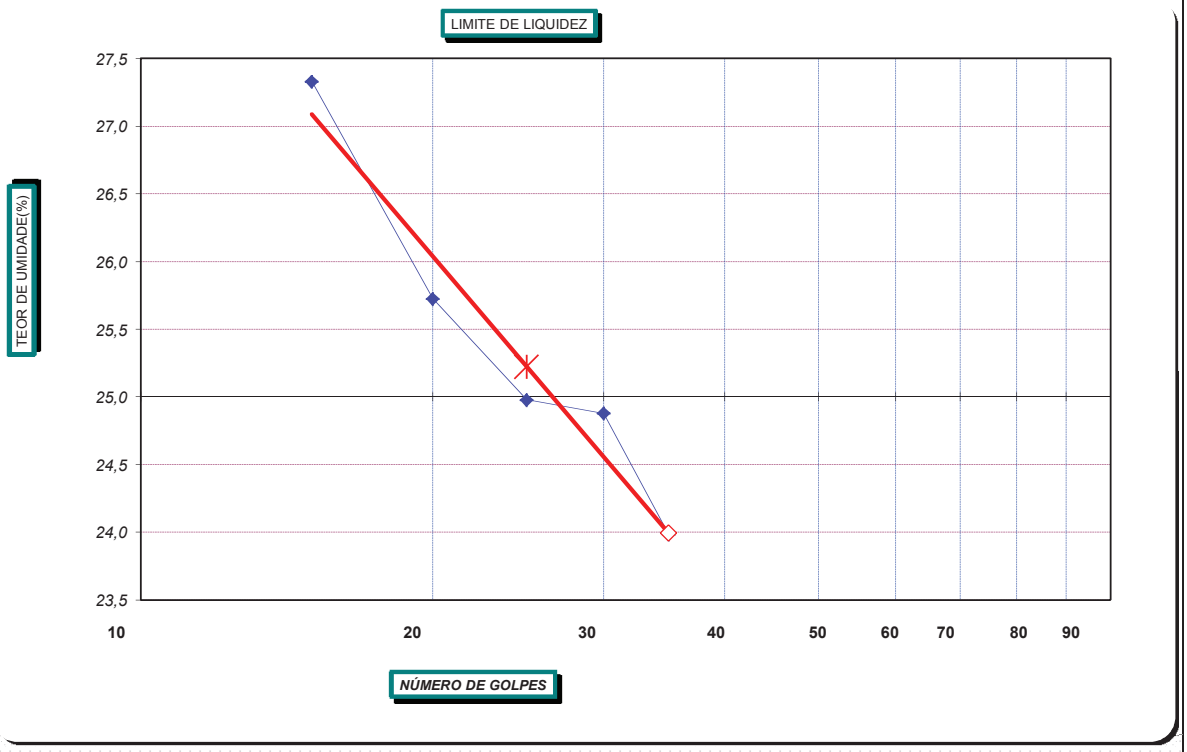

Observ. :...

GSSAM 02B 02 – prof.: 6,00 – 6,65 m
Reg.:10150

TRIAXIAL CU

DENSIDADE APARENTE

CLIENTE:	**Cleary Gottlieb e Hamilton LLP**
REGISTRO:	**10150**
FURO:	**GSSam 02B 02** PROF.: **6,00 - 6,65 m**
LOCAL:	**Baia 3 - Local - F**

DADOS INICAIS DE MOLDAGEM:

Tensões de Confinamento	200 kPa	400 kPa	600 kPa	800 kPa

Peso e Geometria:

Diam. interno:[mm]	35,79	35,81	35,77	35,86
Altura do molde: [mm]	71,71	71,70	71,70	71,72
Volume do anel (cm3)	72,14	72,21	72,05	72,44
Tara do Molde: [g]	577,08	577,08	577,08	577,08
Peso Anel + amostra:	723,23	723,37	723,04	723,82
Peso da amostra: [g]	166,22	163,43	165,12	166,86

Teor de umidade:

Massa Úmida + Tara [g]	96,13	109,20	104,75	114,24
Massa Seca + Tara [g]	77,39	89,81	85,77	93,68
Tara [g]	11,87	17,18	12,03	13,52
Água [g]	18,73	19,39	18,98	20,56
Massa Seca [g]	65,53	72,63	73,75	80,16
Umidade [%]	28,59	26,70	25,74	25,66

Dados Calculados:

Densid.Real: [g/cm^3]	3,928	3,928	3,928	3,928
M.E.A.Umida [g/cm^3]	2,304	2,263	2,292	2,304
M.E.A.Seca [g/cm^3]	1,792	1,786	1,82	1,833
Indice Vazios Inicial	1,19	1,20	1,16	1,14
G.Saturação Inicial [%]	94,19	87,46	87,51	88,20
Volume de Vazios (%)	54,38	54,52	53,60	53,33

CONSOLIDATED UNDRAINED TRIAXIAL TEST by ASTM D4767

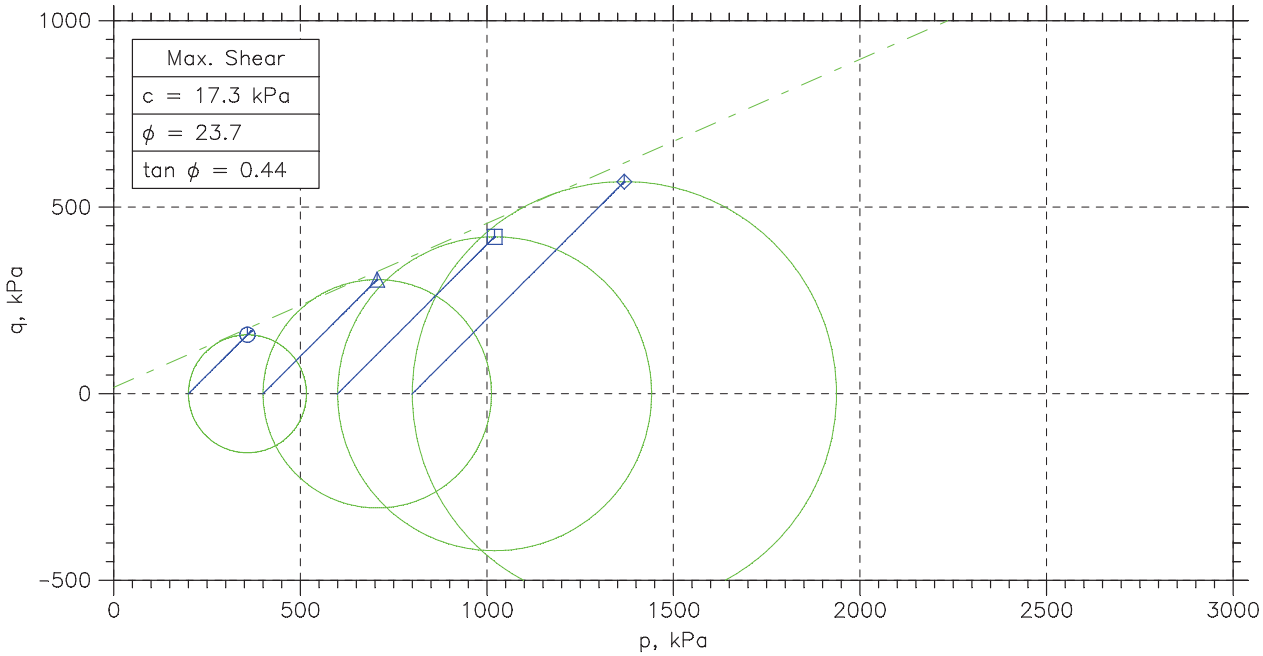

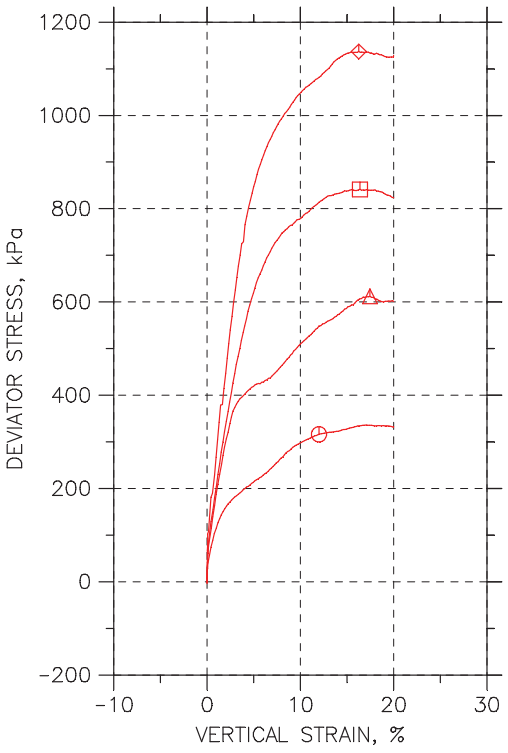

Symbol		○	△	□	◇
Sample No.		GSSam02BGS2	Sam02BGS2	Sam02BGS2	Sam02B 02
Test No.		200 KPa	400 KPa	600 KPa	800 kpa
Depth		6.0-6.65 m	6.0-6.65 m	6.0-6.65 m	6.0-6.65 m
Initial	Diameter, mm	35.79	35.81	35.77	35.86
	Height, mm	71.71	71.7	71.7	71.72
	Water Content, %	29.2	29.3	28.1	27.9
	Dry Density, N/m^3	17570	17520	17870	17980
	Saturation, %	96.1	96.1	95.4	96.1
	Void Ratio	1.19	1.2	1.16	1.14
Before Shear	Water Content, %	21.8	21.3	19.5	19.7
	Dry Density, N/m^3	20750	20980	21800	21720
	Saturation*, %	100.0	100.0	100.0	100.0
	Void Ratio	0.856	0.836	0.767	0.773
	Back Press., kPa	39.98	39.99	39.99	39.95
Ver. Eff. Cons. Stress, kPa		200.	400.	600.	800.
Shear Strength, kPa		158.1	306.	420.6	568.4
Strain at Failure, %		12	17.5	16.4	16.3
Strain Rate, %/min		0.09	0.09	0.09	0.09
B-Value		---	---	---	---
Measured Specific Gravity		3.93	3.93	3.93	3.93
Liquid Limit		---	---	---	---
Plastic Limit		---	---	---	---

PATTROL

Project: Cleary Gottlieb Steen

Location: Baia 3 local F

Project No.: 001

Boring No.: 10150

Sample Type: Shelby

Description:

Remarks: Triaxial - D3

Phase calculations based on end of test.

* Saturation is set to 100% for phase calculations.

Fri, 15-JUL-2016 14:52:22

CONSOLIDATED UNDRAINED TRIAXIAL TEST by ASTM D4767

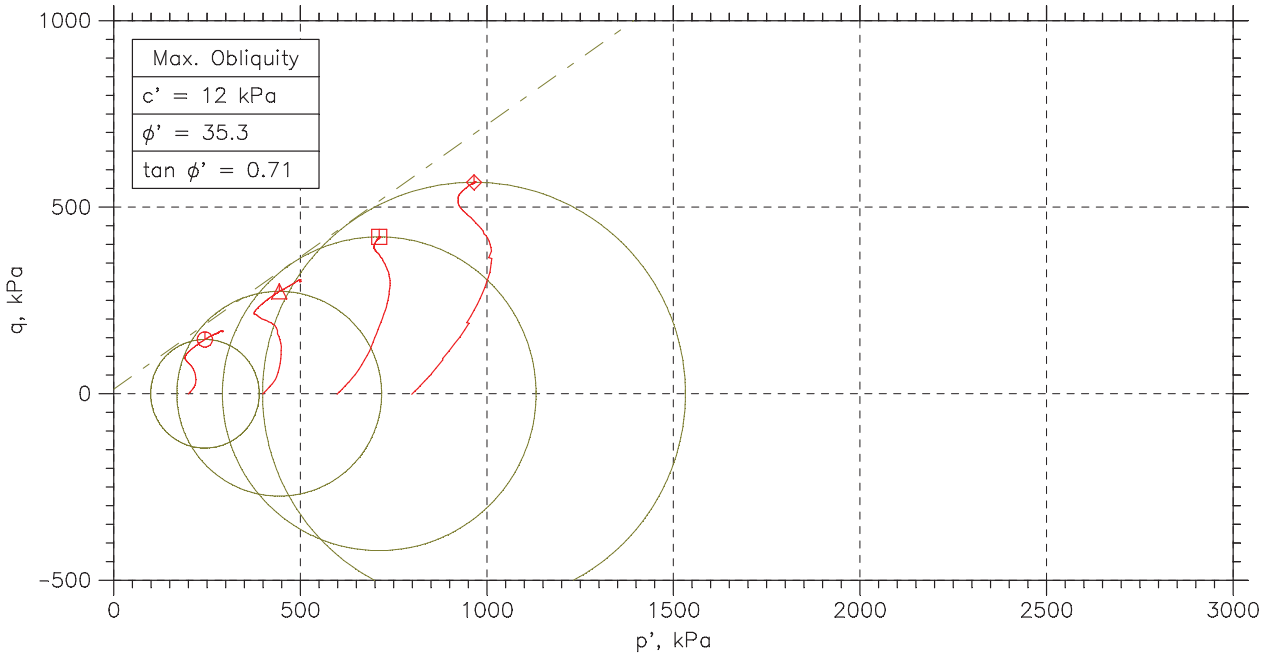

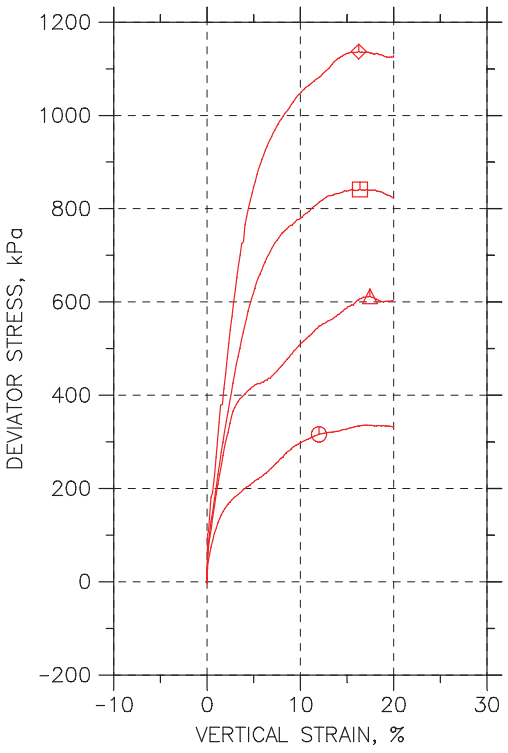

Symbol		⏲	△	⏍	◇
Sample No.		GSSam02BGS2	am02BGS2	am02BGS2	am02B 02
Test No.		200 KPa	400 KPa	600 KPa	800 kpa
Depth		6.0-6.65 m	6.0-6.65 m	6.0-6.65 m	6.0-6.65 m
Initial	Diameter, mm	35.79	35.81	35.77	35.86
	Height, mm	71.71	71.7	71.7	71.72
	Water Content, %	29.2	29.3	28.1	27.9
	Dry Density, N/m^3	17570	17520	17870	17980
	Saturation, %	96.1	96.1	95.4	96.1
	Void Ratio	1.19	1.2	1.16	1.14
Before Shear	Water Content, %	21.8	21.3	19.5	19.7
	Dry Density, N/m^3	20750	20980	21800	21720
	Saturation*, %	100.0	100.0	100.0	100.0
	Void Ratio	0.856	0.836	0.767	0.773
	Back Press., kPa	39.98	39.99	39.99	39.95
Ver. Eff. Cons. Stress, kPa		200.	400.	600.	800.
Shear Strength, kPa		158.1	306.	420.6	568.4
Strain at Failure, %		12	17.5	16.4	16.3
Strain Rate, %/min		0.09	0.09	0.09	0.09
B-Value		---	---	---	---
Measured Specific Gravity		3.93	3.93	3.93	3.93
Liquid Limit		---	---	---	---
Plastic Limit		---	---	---	---

PATTROL

Project: Cleary Gottlieb Steen

Location: Baia 3 local F

Project No.: 001

Boring No.: 10150

Sample Type: Shelby

Description:

Remarks: Triaxial - D3

Phase calculations based on end of test.

* Saturation is set to 100% for phase calculations.

Fri, 15-JUL-2016 14:52:40

CONSOLIDATED UNDRAINED TRIAXIAL TEST by ASTM D4767

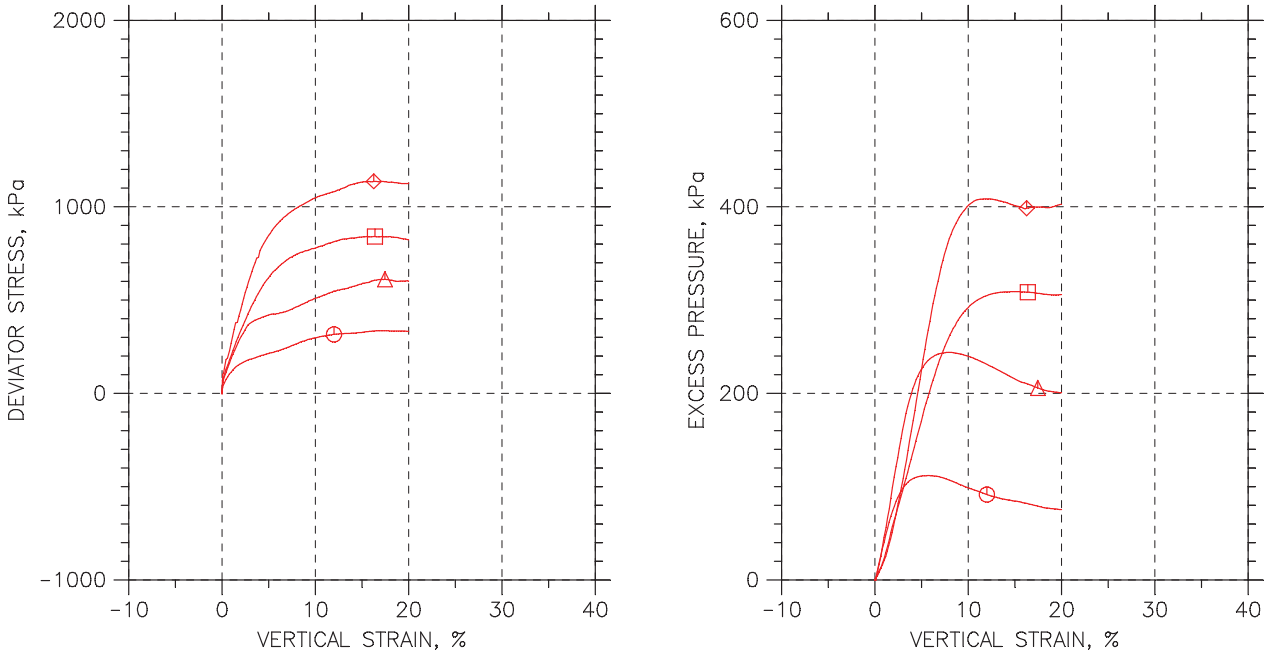

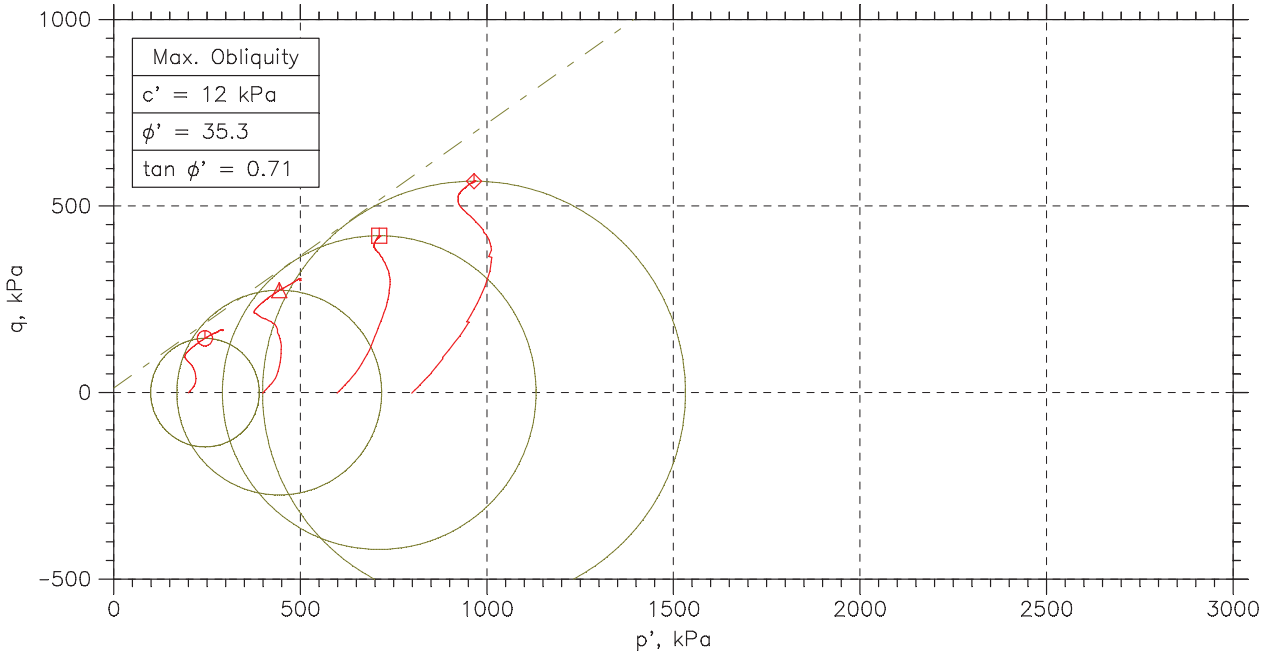

	Sample No.	Test No.	Depth	Tested By	Test Date	Checked By	Check Date	Test File
⏲	GSSam02B 02	200 KPa	6.0-6.65 m	Fernando	15/07/2016	Almir		Reg. 10150 - 200 KPa - D3.da
△	GSSam02B 02	400 KPa	6.0-6.65 m	Fernando	15/07/2016	Almir		Reg. 10150 - 400 KPa - H8.da
⊡	GSSam02B 02	600 KPa	6.0-6.65 m	Fernando	15/07/2016	Almir		Reg. 10150 - 600 KPa - H8.da
◇	GSSam02B 02	800 kpa	6.0-6.65 m	Fernando	15/07/2016	Almir		Reg. 10151 - 800.x KPa - E4.d

PATTROL

Project: Cleary Gottlieb Steen	Location: Baia 3 local F	Project No.: 001
Boring No.: 10150	Sample Type: Shelby	
Description:		
Remarks: Triaxial - D3		

Fri, 15-JUL-2016 14:52:41

PATROL INVESTIGAÇÕES GEOTÉCNICAS LTDA

Controle do Parâmetro B (Skempton) pelo Painel de Saturação

Interessado:	**Cleary Gottlieb e Hamilton LLP**	Material:	**-**	Data:	**15/07/2016**
Obra:	**-**	Furo:	**GSSam 02B 02**	Amostra:	**Shelby**
Local:	**Baia 3 - Local - F**	Prof.:	**06,00 - 06,65 m**	Registro:	**2016.10150**

Dados de Moldagem Corpo de Prova

Diâmetro [mm]	**35,79**
Altura [mm]	**71,71**
Volume [cm³]	**72,143**
Peso da amostra [g]	**166,95**

Densid.Real [g/cm³]	**3,928**
M.E.A.Umida [g/cm^3]	**2,314**
M.E.A.Seca [g/cm^3]	**1,792**
Umidade Inicial [%]	**29,15**

Parâmetro B (Skempton) pelo Painel de Saturação

Tensão Confinante (kPa)	Contra Pressão (kPa)	u (kPa)	B
50,00	40,00	-	-
99,99	70,45	49,99	0,41
149,98	128,72	49,99	0,57
199,75	183,43	49,77	0,67
249,71	237,27	49,96	0,75
299,89	293,34	50,18	0,87
349,81	345,00	49,92	0,90
399,77	395,41	49,96	0,91
449,88	446,12	50,11	0,92
499,85	496,44	49,97	0,93
549,90	547,00	50,05	0,94
599,99	597,49	50,09	0,95
649,92	647,62	49,93	0,95
699,90	697,98	49,98	0,96
749,76	747,71	49,86	0,96
799,95	797,94	50,19	0,96

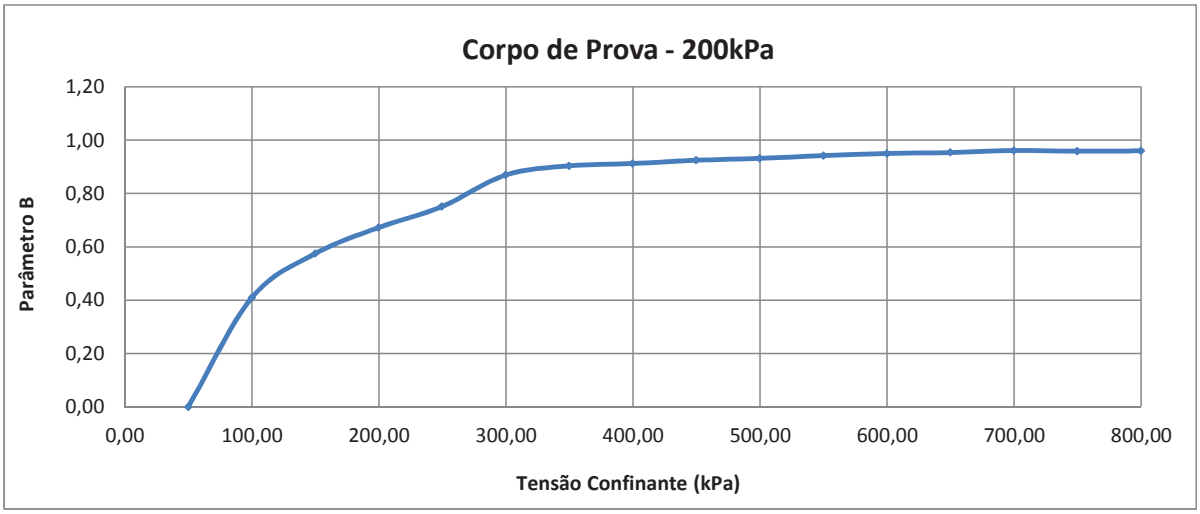

Parâmetro B de poropressão de Skempton: $B = \Delta u / \Delta\sigma_3$

A saturação por contra pressão foi aplicada com incrementos aproximados de 50kPa.

PATROL INVESTIGAÇÕES GEOTÉCNICAS LTDA

Controle do Parâmetro B (Skempton) pelo Painel de Saturação

Interessado:	**Cleary Gottlieb e Hamilton LLP**	Material:	**-**	Data:	**15/07/2016**
Obra:	**-**	Furo:	**GSSam 02B 02**	Amostra:	**Shelby**
Local:	**Baia 3 - Local - F**	Prof.:	**06,00 - 06,65 m**	Registro:	**2016.10150**

Dados de Moldagem Corpo de Prova

Diâmetro [mm]	**35,81**
Altura [mm]	**71,70**
Volume [cm³]	**72,213**
Peso da amostra [g]	**166,86**

Densid.Real [g/cm³]	**3,928**
M.E.A.Umida [g/cm³]	**2,311**
M.E.A.Seca [g/cm³]	**1,786**
Umidade Inicial [%]	**29,36**

Parâmetro B (Skempton) pelo Painel de Saturação

Tensão Confinante (kPa)	Contra Pressão (kPa)	u (kPa)	B
50,0	40,00	-	-
99,99	81,84	49,99	0,64
149,48	135,22	49,49	0,71
199,75	192,76	50,27	0,86
249,96	245,31	50,21	0,91
299,97	296,12	50,01	0,92
349,85	346,57	49,88	0,93
399,98	396,75	50,13	0,94
449,89	447,39	49,91	0,95
500,01	497,81	50,12	0,96
549,82	547,70	49,81	0,96
599,99	598,00	50,17	0,96

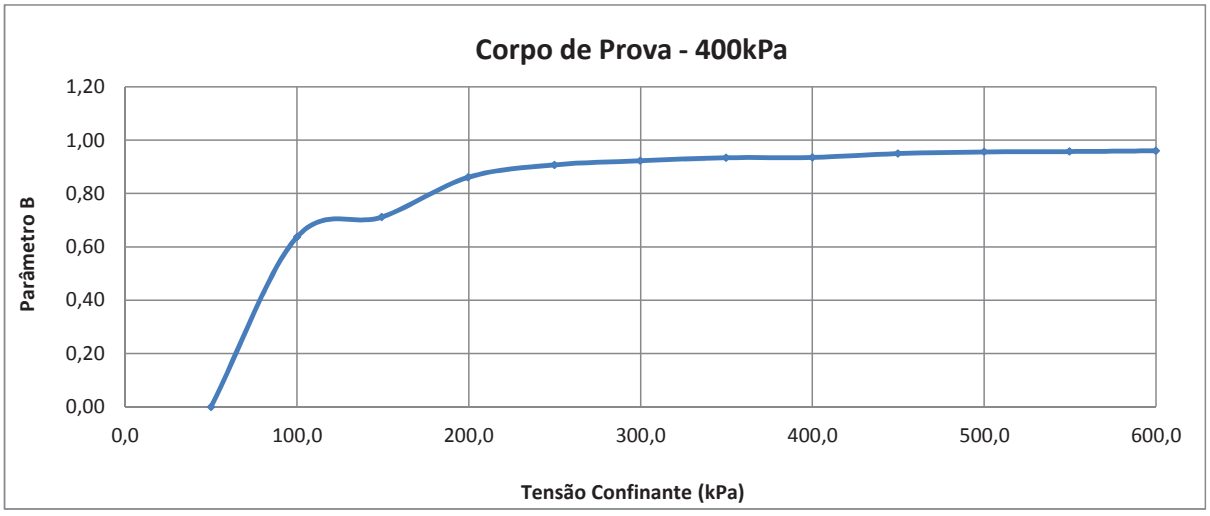

Parâmetro B de poropressão de Skempton: $B = \Delta u / \Delta\sigma_3$

A saturação por contra pressão foi aplicada com incrementos aproximados de 50kPa.

PATROL INVESTIGAÇÕES GEOTÉCNICAS LTDA

Controle do Parâmetro B (Skempton) pelo Painel de Saturação

Interessado:	**Cleary Gottlieb e Hamilton LLP**	Material:	**-**	Data:	**15/07/2016**
Obra:	**-**	Furo:	**GSSam 02B 02**	Amostra:	**Shelby**
Local:	**Baia 3 - Local - F**	Prof.:	**06,00 - 06,65 m**	Registro:	**2016.10150**

Dados de Moldagem Corpo de Prova

Diâmetro [mm]	**35,77**
Altura [mm]	**71,70**
Volume [cm³]	**72,052**
Peso da amostra [g]	**168,17**

Densid.Real [g/cm³]	**3,928**
M.E.A.Umida [g/cm^3]	**2,334**
M.E.A.Seca [g/cm^3]	**1,823**
Umidade Inicial [%]	**28,06**

Parâmetro B (Skempton) pelo Painel de Saturação

Tensão Confinante (kPa)	Contra Pressão (kPa)	u (kPa)	B
50	40,00	-	-
98,98	94,32	48,98	0,90
149,55	145,00	50,57	0,91
199,93	195,89	50,38	0,92
249,72	246,91	49,79	0,94
299,91	297,33	50,19	0,95
349,95	348,00	50,04	0,96
399,90	397,74	49,95	0,96
449,78	447,83	49,88	0,96

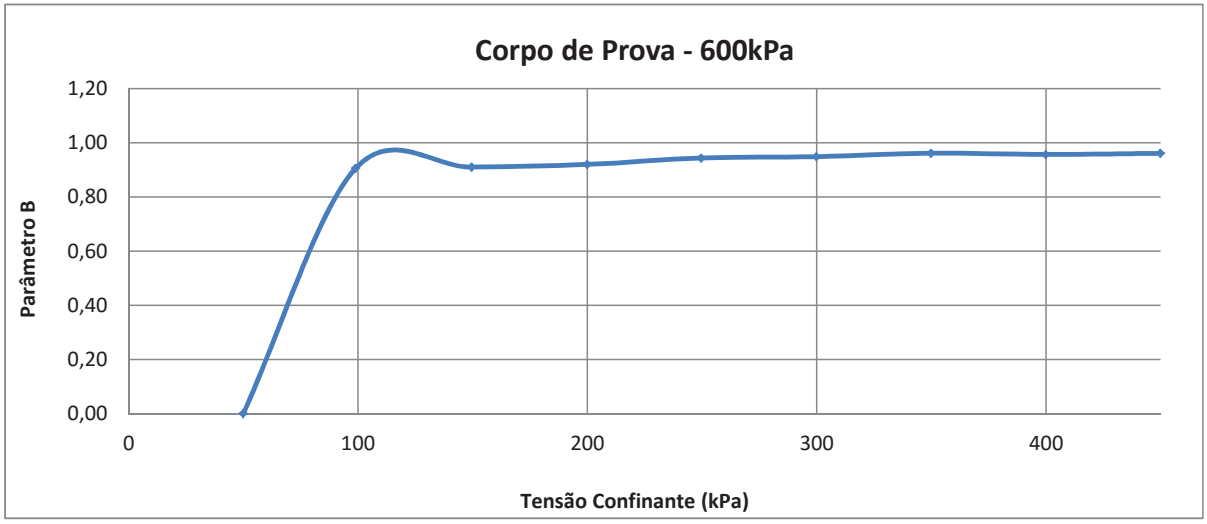

Parâmetro B de poropressão de Skempton: B = $\Delta u / \Delta\sigma_3$

A saturação por contra pressão foi aplicada com incrementos aproximados de 50kPa.

PATROL INVESTIGAÇÕES GEOTÉCNICAS LTDA

Controle do Parâmetro B (Skempton) pelo Painel de Saturação

Interessado:	**Cleary Gottlieb e Hamilton LLP**	Material:	**-**	Data:	**15/07/2016**
Obra:	**-**	Furo:	**GSSam 02B 02**	Amostra:	**Shelby**
Local:	**Baia 3 - Local - F**	Prof.:	**06,00 - 06,65 m**	Registro:	**2016.10150**

Dados de Moldagem Corpo de Prova

Diâmetro [mm]	**35,86**
Altura [mm]	**71,72**
Volume [cm³]	**72,435**
Peso da amostra [g]	**169,91**

Densid.Real [g/cm³]	**3,928**
M.E.A.Umida [g/cm^3]	**2,346**
M.E.A.Seca [g/cm^3]	**1,833**
Umidade Inicial [%]	**27,95**

Parâmetro B (Skempton) pelo Painel de Saturação

Tensão Confinante (kPa)	Contra Pressão (kPa)	u (kPa)	B
50	40,00	-	-
99,84	96,99	49,84	0,94
149,78	147,50	49,94	0,95
199,95	197,44	50,17	0,95
249,93	247,39	49,98	0,95

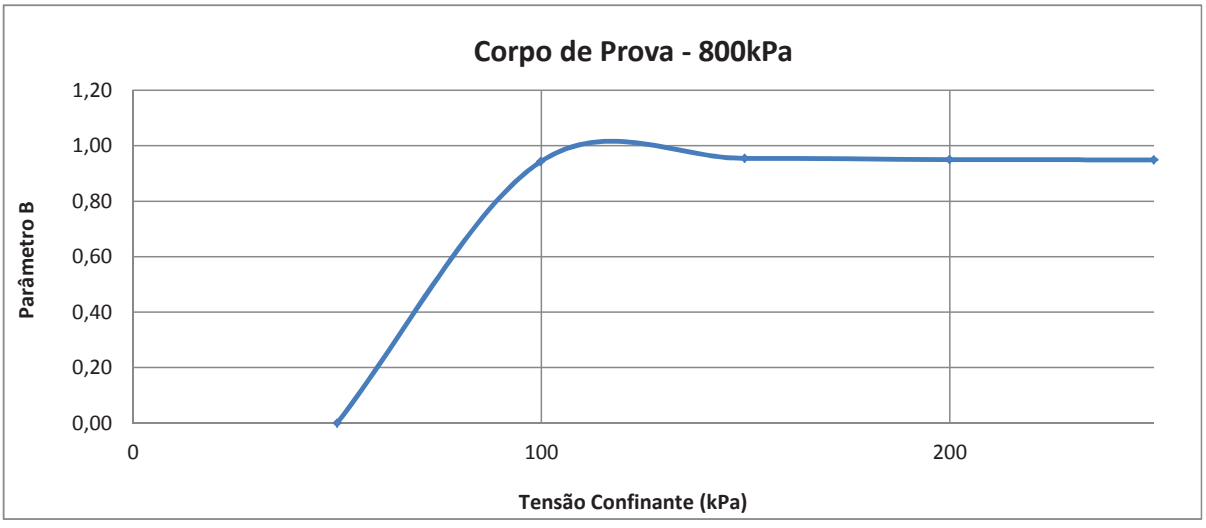

Parâmetro B de poropressão de Skempton: $B = \Delta u / \Delta\sigma_3$

A saturação por contra pressão foi aplicada com incrementos aproximados de 50kPa.

PATROL INVESTIGAÇÕES GEOTÉCNICAS LTDA.

RELATÓRIO FOTOGRÁFICO - Triaxial CIU (200, 400, 600 e 800 KPa)

Cliente:	**Cleary Gottlieb Steen & Hamilton LLP**	Local:	**BAIA 3 - LOCAL F**
Obra:	**-**	Amostra:	**-**
Data:	**18/07/16** Furo: **GSSAM-02B-02**	Registro:	**2016.10150**

Antes 200 KPa

Depois 200 KPa

Antes 400 KPa

Depois 400 KPa

Antes 600 KPa

Depois 600 KPa

Antes 800 KPa

Depois 800 KPa

OBSERVAÇÕES:

PATROL INVESTIGAÇÕES GEOTÉCNICAS LTDA

Determinação da Massa específica aparente de amostras indeformadas, com emprego da balança hidrostática - NBR 10838

Interessado:	**Cleary**	Material:	**-**	Data:	**18/07/16**
Obra:	**-**	Furo:	**GSSAM-02B-02**	Amostra:	**Shelby**
Localização:	**BAIA 3 - LOCAL F**	Prof.:	**6,00 - 6,65**	Registro:	**2016.10150**

DETERMINAÇÃO DA MASSA ESPECÍFICA APARENTE DA PARAFINA

Dados	CP 01	CP 02	CP 03
M_{paraf} (g)	71,78	76,85	74,66
M_{cpi} (g)	95,84	95,84	95,90
M_{ci} (g)	92,66	92,27	92,58
Y_0 (g/cm^3)	1,00	1,00	1,00
Yparaf (g/cm3)	0,958	0,956	0,957
Média	0,957		

DETERMINAÇÃO DO VOLUME DO CORPO-DE-PROVA E DA MASSA ESPECÍFICA NATURAL DA AMOSTRA

VOLUME DO CP			
Dados	CP 01	CP 02	CP 03
M_p (g)	290,11	279,05	261,12
M_i (g)	148,95	132,75	128,90
M_s (g)	265,19	240,94	230,83
Y_{paraf} (g/cm^3)	0,957	0,957	0,957
Y_0 (g/cm^3)	1,00	1,00	1,00
V_s (cm^3)	115,12	106,47	100,56
Média:	107,385		

MASSA ESPECÍFICA APARENTE NATURAL			
Dados	CP 01	CP 02	CP 03
M_s (g)	265,19	240,94	230,83
V_s (cm^3)	115,12	106,47	100,56
Yh (g/cm^3)	2,304	2,263	2,295
Média	2,287		

TEOR DE UMIDADE			
nº capsula	104	268	287
cáp+solo úmido	88,51	99,24	103,34
cáp+solo seco	71,71	83,07	83,25
água	16,80	16,17	20,09
tara	13,00	12,56	10,73
solo seco	58,71	70,51	72,52
umidade	28,62	22,93	27,70
Média	26,42		

M_{paraf} = massa do corpo-de-prova, em g;

M_{cpi} = massa do contrapeso quando imerso em água, em g;

M_{ci} = massa do conjunto corpo-de-prova e contrapeso;

Y_0 = massa específica da água (considerar igual a 1 g/cm^3);

Y_{paraf} = massa específica da parafina, em g/cm^3;

Mp = massa do corpo-de-prova parafinado, em g;

Mi = massa do corpo-de-prova parafinado e imerso em água, em g;

Ms = massa do corpo-de-prova, em g;

Vs = volume do corpo-de-prova, em cm^3;

Yh = massa específica aparente natural da amostra, em g/cm^3.

GSSAM 02B 02 – prof.: 6,00 – 6,65 m
Reg.:10150

CARACTERIZAÇÃO

PATROL INVESTIGAÇÕES GEOTÉCNICAS LTDA

Análise Granulométrica por Peneiramento e Sedimentação - NBR 7181/1984

Interessado:	**Cleary**	Material:	**Silte Argiloso**	Data:	**11/07/2016**
Obra:	**-**	Furo:	**GS SAM-02B-02**	Amostra:	**-**
Local:	**BAIA 3 - LOCAL F**	Prof.:	**6,00 - 6,65**	Registro:	**10150.2016**
Densimetro:	**DS 02 - (16569/13) VT**				

UMIDADE HIGROSCÓPICA			
Cápsula no. (g.)	**38**	**67**	**75**
Solo umido + tara (g.)	**97,70**	**92,52**	**91,29**
Solo seco + tara (g.)	**97,48**	**92,33**	**91,09**
Tara da capsula (g.)	**13,03**	**11,90**	**13,54**
Água (g.)	0,22	0,19	0,20
Solo Seco (g.)	84,45	80,43	77,55
Teor de umidade (%)	0,3	0,2	0,3
Umidade Média (%)	0,3		

AMOSTRA TOTAL SECA	
Amostra Total Úmida (g)	**1.068,63**
Solo Seco retido na # 10 (g)	0,00
Solo Úmido passa na # 10 (g)	1.068,63
Solo Seco passa na # 10 (g)	1.065,95
Amostra Total Seca (g)	1.065,95

AMOSTRA PARCIAL SECA	
Amostra menor #10 úmida (g)	**70,00**
Amostra menor #10 seca (g)	69,82
Limite de Liquidez	
Índice de Plasticidade	

MASSA ESPECÍFICA REAL		
Picnômetro. nº	**1**	**2**
Temperatura (°c)	**19,8**	**19,8**
Pic.+ água + solo (g)	**791,23**	**798,71**
Solo úmido(g)	**50,00**	**50,00**
Solo Seco (g)	49,87	49,87
Pic.+ água (g)	754,10	761,53
Água Deslocada (g)	12,74	12,69
Teor de umidade (%)	**0,3**	
Massa Específica (H2O)	0,9983	0,9983
Massa Específica Real	3,920	3,936
ρ [g/cm^3]	**3,928**	

P E N E I R A M E N T O

PENEIRAS A.B.N.T.		MATERIAL RETIDO			% QUE	
		Peso	P.acumul	%	PASSA:amostra	Faixa
N o.	mm.	(gr.)	(gr.)	acumul	total	
4"	101,8					
3 .1/2 "	88,9					
3"	76,2					
2 .1/2 "	63,5					
2"	50,8					
1.1/2 "	38,1					
1"	25,4					
3/4 "	19					
1/2 "	12,7					
3/8"	9,5					
1/4"	6,3					
4	4,8					
8	2,4					
10	2	**0,00**	0,0	0,0	**100,0**	
16	1,2	**0,00**	0,0	0,0	**100,0**	
30	0,6	**0,04**	0,0	0,1	**99,9**	
40	0,42	**0,04**	0,1	0,1	**99,9**	
60	0,25	**0,03**	0,1	0,2	**99,8**	
100	0,15	**0,02**	0,1	0,2	**99,8**	
200	0,075	**0,19**	0,3	0,5	**99,5**	

Densímetro n.º	**02**

$$K = \frac{\delta}{\delta - 1} = \quad 1{,}342$$

% da amostra parcial = A x K x LC

A =	0,0143

SEDIMENTAÇÃO COM DEFLOCULANTE

Data	Temp.	Tempo	horário	Leit.	Correções			Leit.	Altura de	%	%	f
	°c	min.	h	(L)	temperatura	menisco	defloculante	corrig.	Queda	parcial	total	mm
08/07/2016	**20,2**	0,5	**9:44**	**52,0**	-3,6	0,5	-2,0	46,9	8,4	90,1	90,1	0,0408
08/07/2016	20,2	1	9:45	**50,0**	-3,6	0,5	-2,0	44,9	8,7	86,3	86,3	0,0295
09/07/2016	20,2	2	9:46	**47,0**	-3,6	0,5	-2,0	41,9	9,2	80,5	80,5	0,0215
10/07/2016	20,2	5	9:49	**41,0**	-3,6	0,5	-2,0	35,9	10,2	69,0	69,0	0,0144
11/07/2016	20,1	10	9:54	**37,0**	-3,6	0,5	-2,0	31,9	10,9	61,2	61,2	0,0106
12/07/2016	**20,1**	20	10:04	**32,0**	-3,6	0,5	-2,0	26,9	11,7	51,6	51,6	0,0078
13/07/2016	**20,1**	40	10:24	**27,0**	-3,6	0,5	-2,0	21,9	12,5	42,0	42,0	0,0057
14/07/2016	**20,1**	80	11:04	**23,0**	-3,6	0,5	-2,0	17,9	13,2	34,3	34,3	0,0042
15/07/2016	**20,3**	240	13:44	**17,0**	-3,6	0,5	-2,0	11,9	14,2	22,9	22,9	0,0025
16/07/2016	**20,6**	540	17:44	**14,0**	-3,5	0,5	-2,0	9,0	14,7	17,4	17,4	0,0017
09/07/2016	**19,5**	1440	9:44	**11,0**	-3,8	0,5	-2,0	5,7	15,2	10,9	10,9	0,0011

Tipo	Pedregulo	Areia Grossa	Areia Média	Areia Fina	Silte	Argila
% total	0,0	0,1	0,1	4,4	75,9	19,5
% total	**0,0**	**4,6**			**75,9**	**19,5**

Análise Granulométrica por Peneiramento e Sedimentação - NBR 7181/1984

Interessado:	**Cleary**	Material:	**Silte Argiloso**	Data:	**11/07/2016**
Obra:	**-**	Furo:	**GS SAM-02B-02**	Amostra:	**-**
Local:	**BAIA 3 - LOCAL F**	Prof.:	**6,00 - 6,65**	Registro:	**2016. 10150**
Densimetro:	**DS 02 - (16569/13) VT**				

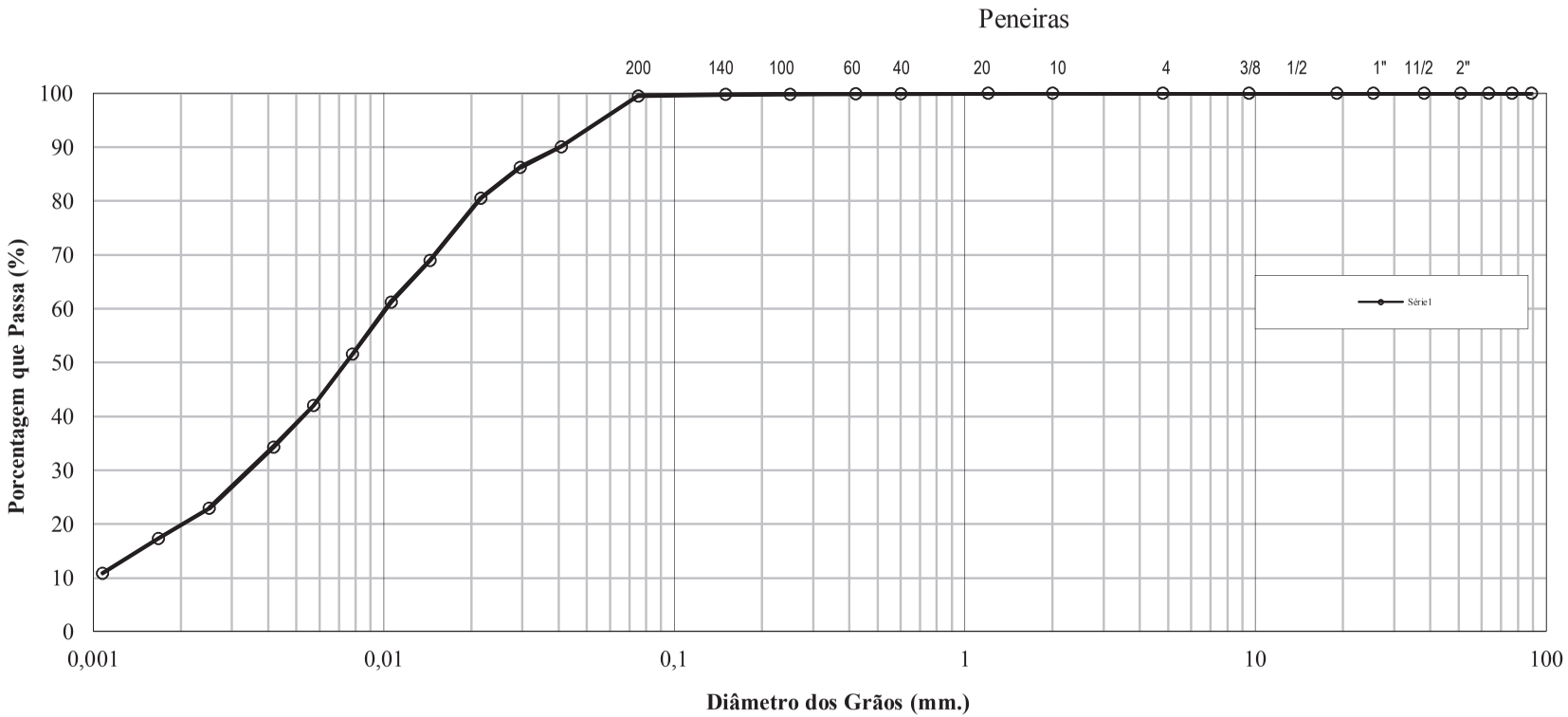

Argila	Silte	Areia Fina	A.Média	13,03	Pedregulho
19,5	**75,9**	**4,4**	**0,1**	**13,5**	**0,0**

PATROL INVESTIGAÇÕES GEOTÉCNICAS

Massa Específica Real dos Grãos - NBR 6508/84

Interessado:	**Cleary Gottieb**	Material:		Data:	**04/07/2016**
Obra:	**-**	Furo:	**GSSam - 02B - 02**	Amostra:	**Shelby**
Local:	**-**	Prof.:	**6,00 a 6,65**	Registro:	**2016.10150**

DETEMINAÇÃO DA UMIDADE (%)

EXECUÇÃO DO ENSAIO			
Cápsula:	67	227	285
Cáp + sol + Agua (g):	97,78	86,83	82,65
Cáp + solo (g):	97,47	86,59	82,37
Peso da cápsula (g):	11,90	12,46	13,83
Água (g):	0,31	0,24	0,28
Solo seco (g):	85,57	74,13	68,54
Umidade (%):	0,4	0,3	0,4
Média:	0,4		

MASSA ESPECÍFICA REAL DOS GRÃOS

EXECUÇÃO DO ENSAIO		
Picnômetro	1	2
Temperatura ºC:	19,8	19,8
Picnômetro + água (g):	754,10	761,53
Solo úmido(g):	50,00	50,00
Solo seco (g):	49,82	49,82
Umidade (%)	0,4	0,4
Conjunto Pic + água + solo (g):	791,23	798,71
Água deslocada (g):	12,69	12,64
Massa Específica (H_2O):	0,9983	0,9983
Massa Específica Real (g/cm³):	3,920	3,936
Média	3,928	

PATROL INVESTIGAÇÕES GEOTÉCNICAS LTDA

LIMITES DE ATTERBERG

Interessado:	**Cleary Gotiieb**	Material:		Data:	**12/07/2016**
Obra:	**-**	Furo:	**GSSam - 02 B - 03**	Amostra:	**Shelby**
Local:	**Baia 3 - Local F**	Prof.:	**6,00 - 6,65**	Registro:	**2016.10150**

LIMITE DE LIQUIDEZ - NBR 6459/1984					
Cápsula nº	36	37	38	39	40
Peso da Cápsula+Solo Úmido(g)	23,71	21,74	20,93	25,62	20,42
Peso da Cápsula+Solo Seco(g)	20,97	19,58	18,91	22,96	18,79
Peso da Água(g)	2,74	2,16	2,02	2,66	1,63
Peso da Cápsula(g)	9,59	9,82	9,44	9,80	9,84
Peso do Solo Seco(g)	11,38	9,76	9,47	13,16	8,95
Teor de Umidade(%)	24,1	22,1	21,3	20,2	18,2
Nº de golpes	14	20	26	30	35

LIMITE DE PLASTICIDADE - NBR 7180/1984					
Cápsula nº	36	37	38	39	40
Peso da Cápsula+Solo Úmido(g)	7,30	6,88	8,67	7,39	6,77
Peso da Cápsula+Solo Seco(g)	7,10	6,68	8,49	7,16	6,58
Peso da Água(g)	0,20	0,20	0,18	0,23	0,19
Peso da Cápsula(g)	5,70	5,18	7,10	5,40	4,93
Peso do Solo Seco(g)	1,40	1,50	1,39	1,76	1,65
Teor de Umidade(%)	14,3	13,3	12,9	13,1	11,5
Valor aceito?	NÃO	SIM	SIM	SIM	NÃO

GRÁFICO

RESULTADOS	
LIMITE DE LIQUIDEZ(%)	20,9
LIMITE DE PLASTICIDADE(%)	12,7
ÍNDICE DE PLASTICIDADE(%)	8,2

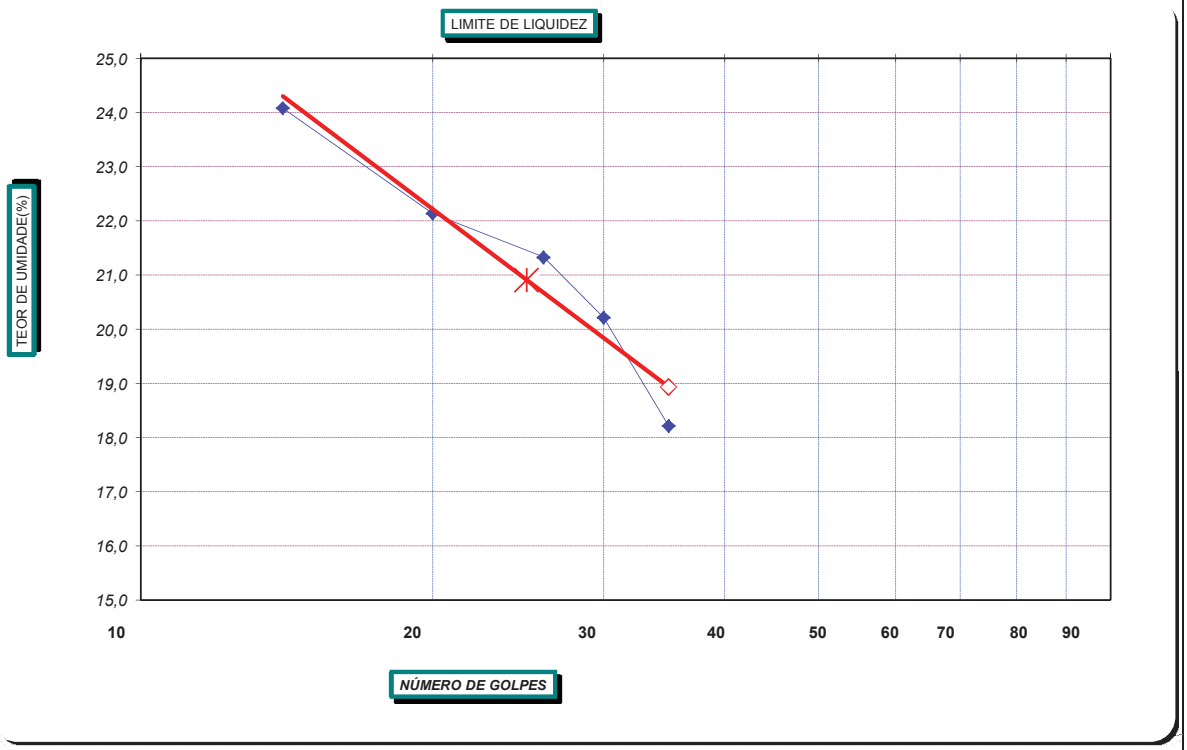

Observ. :...

GSSAM 02B 03 – prof.: 9,00 – 9,65 m
Reg.:10151

TRIAXIAL CU

DENSIDADE APARENTE

CLIENTE:	**Cleary Gottlieb e Hamilton LLP**	
REGISTRO:	**10151**	
FURO:	**GSSam 02B 03**	PROF.: 09,00 - 09,65 m
LOCAL:	**Baia 3 - Local - F**	

DADOS INICAIS DE MOLDAGEM:

Tensões de Confinamento	200 kPa	400 kPa	600 kPa	800 kPa

Peso e Geometria:

Diam. interno:[mm]	35,82	35,81	35,73	35,96
Altura do molde: [mm]	71,70	71,71	71,71	71,92
Volume do anel (cm3)	72,25	72,22	71,90	73,04
Tara do Molde: [g]	577,08	577,08	577,08	577,08
Peso Anel + amostra:	723,45	723,39	722,74	725,05
Peso da amostra: [g]	168,01	165,73	164,12	170,43

Teor de umidade:

Massa Úmida + Tara [g]	97,23	100,58	110,52	105,45
Massa Seca + Tara [g]	81,75	84,53	93,45	89,21
Tara [g]	13,14	13,13	12,74	14,24
Água [g]	15,48	16,05	17,07	16,24
Massa Seca [g]	68,61	71,41	80,71	74,97
Umidade [%]	22,52	22,47	21,15	21,67

Dados Calculados:

Densid.Real: [g/cm^3]	3,817	3,817	3,817	3,817
M.E.A.Umida [g/cm^3]	2,325	2,295	2,283	2,333
M.E.A.Seca [g/cm^3]	1,898	1,874	1,88	1,918
Indice Vazios Inicial	1,01	1,04	1,03	0,99
G.Saturação Inicial [%]	85,01	82,70	78,69	83,51
Volume de Vazios (%)	50,28	50,91	50,64	49,76

CONSOLIDATED UNDRAINED TRIAXIAL TEST by ASTM D4767

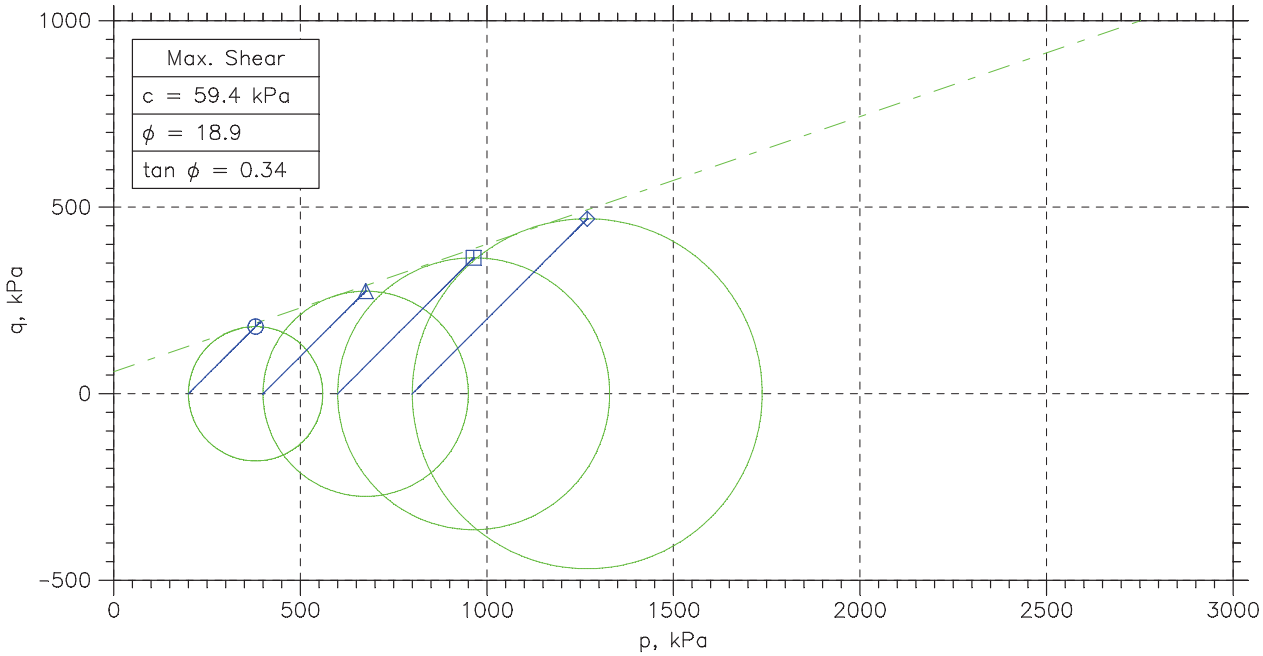

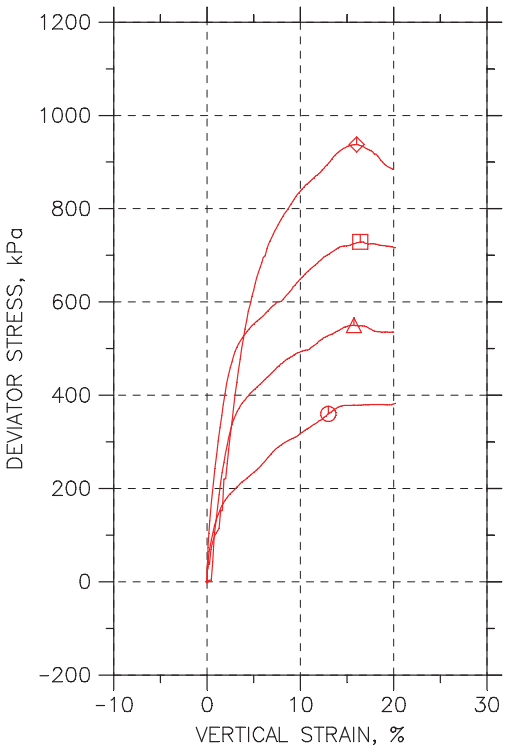

Symbol		○	△	□	◇
Sample No.		GSSam02BGS3	GSSam02BGS3	GSSam02BGS3	GSSam02B 03
Test No.		200 KPa	400 KPa	600 KPa	800 kpa
Depth		9.0-9.65 m	9.0-09.65 m	9.0-09.65 m	9.0-09.65 m
Initial	Diameter, mm	35.82	35.81	35.73	35.96
	Height, mm	71.7	71.71	71.71	71.92
	Water Content, %	25.4	26.1	25.9	24.9
	Dry Density, N/m^3	18610	18370	18480	18810
	Saturation, %	96.1	96.2	96.3	96.0
	Void Ratio	1.01	1.04	1.03	0.99
Before Shear	Water Content, %	19.0	22.9	20.0	21.2
	Dry Density, N/m^3	21680	19960	21210	20680
	Saturation*, %	100.0	100.0	100.0	100.0
	Void Ratio	0.727	0.876	0.765	0.81
	Back Press., kPa	40.	40.09	40.	39.95
Ver. Eff. Cons. Stress, kPa		200.	399.8	600.	800.
Shear Strength, kPa		180.	275.	364.4	468.9
Strain at Failure, %		13	15.7	16.4	16
Strain Rate, %/min		0.09	0.09	0.09	0.09
B-Value		---	---	---	---
Measured Specific Gravity		3.82	3.82	3.82	3.82
Liquid Limit		---	---	---	---
Plastic Limit		---	---	---	---

PATTROL

Project: Cleary Gottlieb Steen

Location: Baia 3 local F

Project No.: 001/2015

Boring No.: 10151

Sample Type: Shelby

Description:

Remarks: G 07

Phase calculations based on end of test.

* Saturation is set to 100% for phase calculations.

Tue, 05-JUL-2016 09:46:58

CONSOLIDATED UNDRAINED TRIAXIAL TEST by ASTM D4767

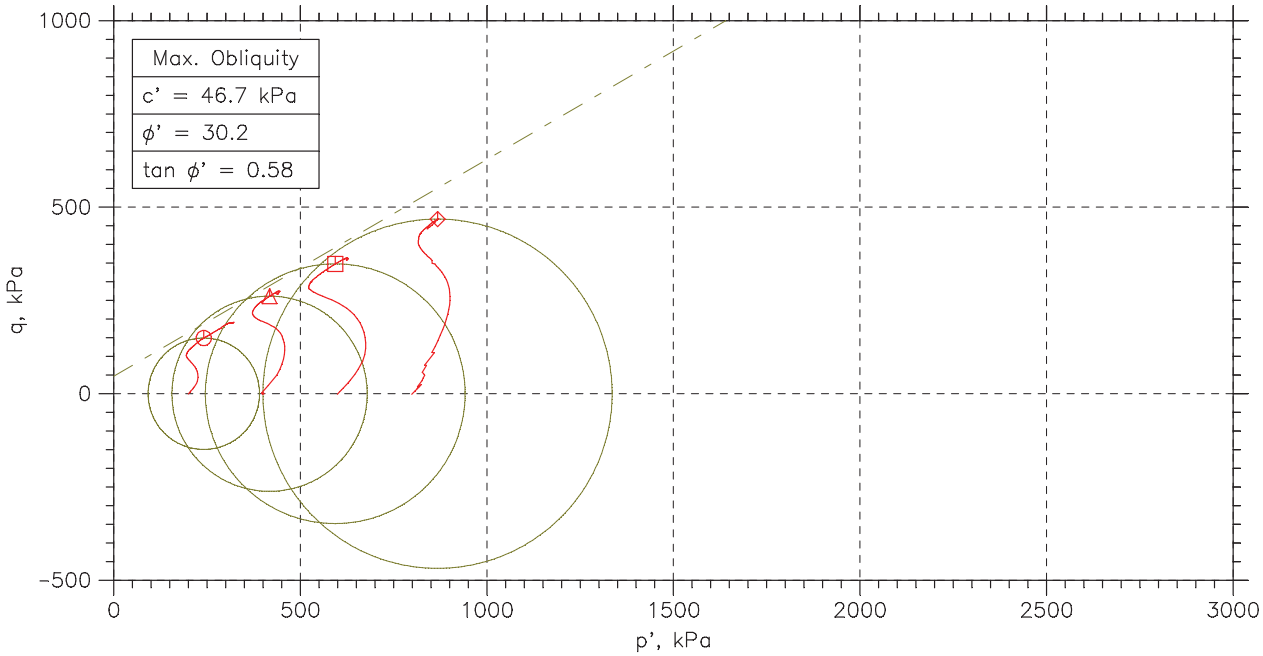

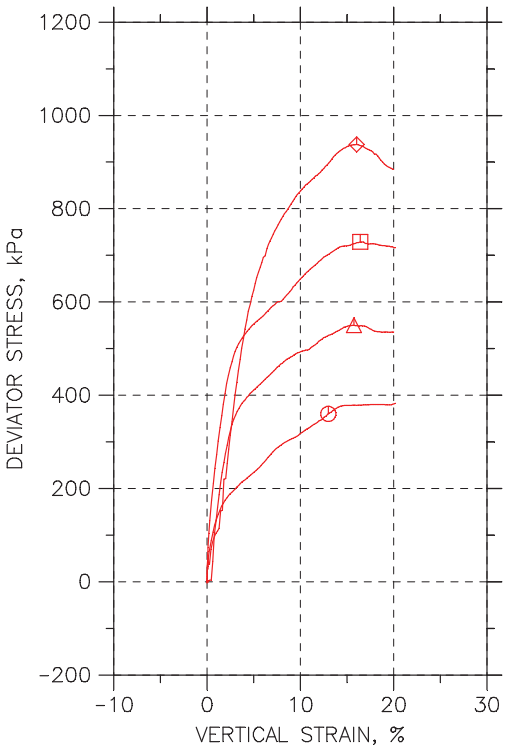

Symbol		○	△	□	◇
Sample No.		GSSam02B 03	GSSam02B 03	GSSam02B 03	GSSam02B 03
Test No.		200 KPa	400 KPa	600 KPa	800 kpa
Depth		9.0-9.65 m	9.0-09.65 m	9.0-09.65 m	9.0-09.65 m
Initial	Diameter, mm	35.82	35.81	35.73	35.96
	Height, mm	71.7	71.71	71.71	71.92
	Water Content, %	25.4	26.1	25.9	24.9
	Dry Density, N/m^3	18610	18370	18480	18810
	Saturation, %	96.1	96.2	96.3	96.0
	Void Ratio	1.01	1.04	1.03	0.99
Before Shear	Water Content, %	19.0	22.9	20.0	21.2
	Dry Density, N/m^3	21680	19960	21210	20680
	Saturation*, %	100.0	100.0	100.0	100.0
	Void Ratio	0.727	0.876	0.765	0.81
	Back Press., kPa	40.	40.09	40.	39.95
Ver. Eff. Cons. Stress, kPa		200.	399.8	600.	800.
Shear Strength, kPa		180.	275.	364.4	468.9
Strain at Failure, %		13	15.7	16.4	16
Strain Rate, %/min		0.09	0.09	0.09	0.09
B-Value		---	---	---	---
Measured Specific Gravity		3.82	3.82	3.82	3.82
Liquid Limit		---	---	---	---
Plastic Limit		---	---	---	---

PATTROL

Project: Cleary Gottlieb Steen

Location: Baia 3 local F

Project No.: 001/2015

Boring No.: 10151

Sample Type: Shelby

Description:

Remarks: G 07

Phase calculations based on end of test.

* Saturation is set to 100% for phase calculations.

Tue, 05-JUL-2016 09:47:38

CONSOLIDATED UNDRAINED TRIAXIAL TEST by ASTM D4767

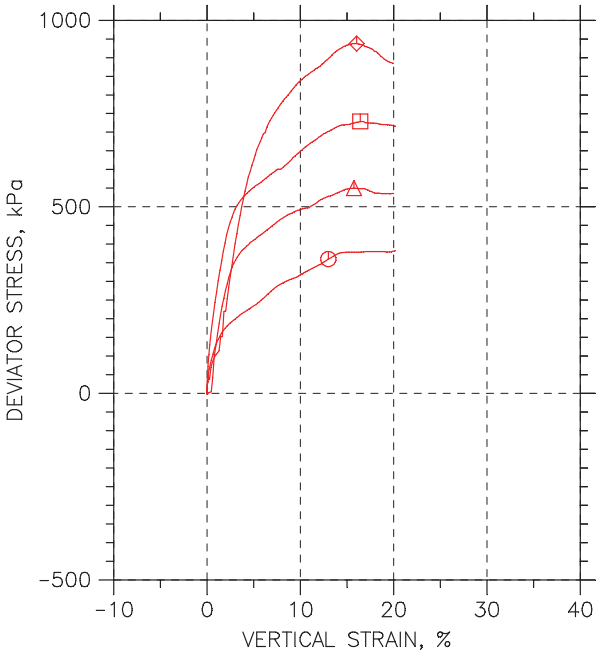

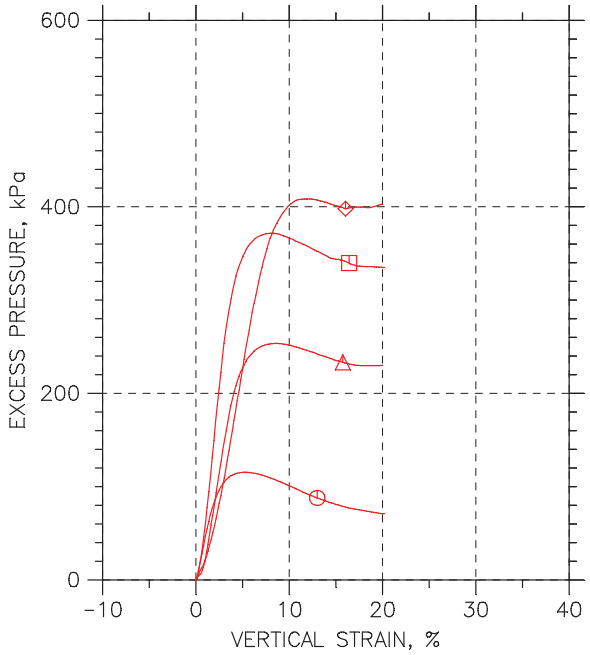

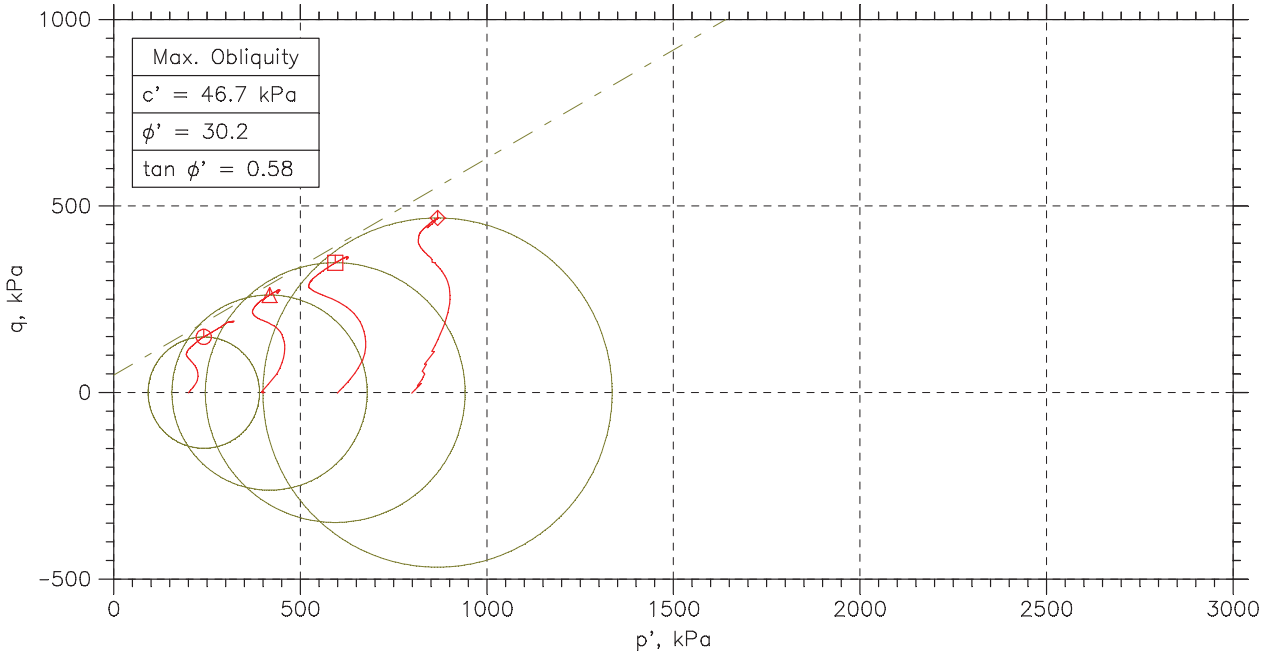

	Sample No.	Test No.	Depth	Tested By	Test Date	Checked By	Check Date	Test File
○	GSSam02B 02	200 KPa	9.0-9.65 m	Fernando	01/072016	Almir		Reg. 10151 - 200 KPa - G7.da
△	GSSam02B 03	400 KPa	9.0-09.65 m	Fernando	30/06/2016	Almir		Reg. 10151 - 400 KPa - D3.da
□	GSSam02B 06	600 KPa	9.0-09.65 m	Fernando	30/06/2016	Almir		Reg. 10151 - 600 KPa - G7.da
◇	GSSam02B 08	800 kpa	9.0-09.65 m	Fernando	30/06/2016	Almir		Reg. 10151 - 800. KPa - E4.dc

PATTROL

Project: Cleary Gottlieb Steen	Location: Baia 3 local F	Project No.: 001/2015
Boring No.: 10151	Sample Type: Shelby	
Description:		
Remarks: G 07		

Tue, 05-JUL-2016 09:47:38

PATROL INVESTIGAÇÕES GEOTÉCNICAS LTDA

Controle do Parâmetro B (Skempton) pelo Painel de Saturação

Interessado:	**Cleary Gottlieb e Hamilton LLP**	Material:	**-**	Data:	**05/07/2016**
Obra:	**-**	Furo:	**GSSam 02B 03**	Amostra:	**Shelby**
Local:	**Baia 3 - Local - F**	Prof.:	**09,00 - 09,65 m**	Registro:	**2016.10151**

Dados de Moldagem Corpo de Prova

Diâmetro [mm]	**35,82**
Altura [mm]	**71,70**
Volume [cm³]	**72,254**
Peso da amostra [g]	**172,04**

Densid.Real [g/cm³]	**3,817**
M.E.A.Umida [g/cm^3]	**2,381**
M.E.A.Seca [g/cm^3]	**1,898**
Umidade Inicial [%]	**25,46**

Parâmetro B (Skempton) pelo Painel de Saturação

Tensão Confinante (kPa)	Contra Pressão (kPa)	u (kPa)	B
50,00	40,00	-	-
100,15	75,09	50,15	0,50
149,57	132,90	49,42	0,66
199,62	186,78	50,05	0,74
249,67	241,55	50,05	0,84
299,71	293,00	50,04	0,87
349,87	345,17	50,16	0,91
399,75	395,98	49,88	0,92
449,62	446,12	49,87	0,93
499,74	496,44	50,12	0,93
549,77	547,00	50,03	0,94
599,76	596,79	49,99	0,94
649,87	647,57	50,11	0,95
699,74	697,94	49,87	0,96
749,51	747,41	49,77	0,96
799,55	797,64	50,04	0,96

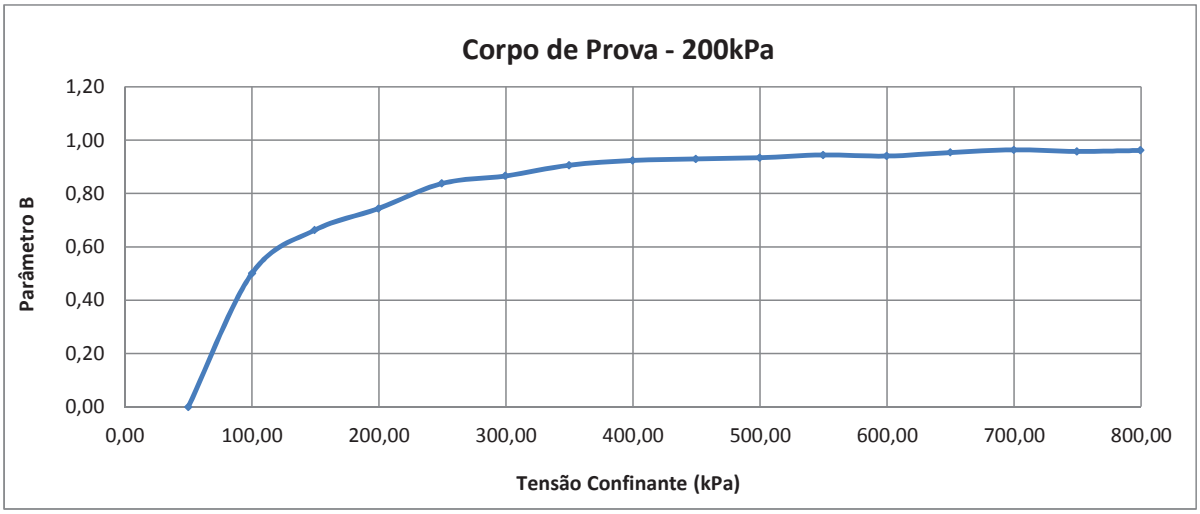

Parâmetro B de poropressão de Skempton: $B = \Delta u / \Delta\sigma_3$

A saturação por contra pressão foi aplicada com incrementos aproximados de 50kPa.

PATROL INVESTIGAÇÕES GEOTÉCNICAS LTDA

Controle do Parâmetro B (Skempton) pelo Painel de Saturação

Interessado:	**Cleary Gottlieb e Hamilton LLP**	Material:	**-**	Data:	**05/07/2016**
Obra:	**-**	Furo:	**GSSam 02B 03**	Amostra:	**Shelby**
Local:	**Baia 3 - Local - F**	Prof.:	**09,00 - 09,65 m**	Registro:	**2016.10151**

Dados de Moldagem Corpo de Prova

Diâmetro [mm]	**35,81**
Altura [mm]	**71,71**
Volume [cm³]	**72,223**
Peso da amostra [g]	**170,70**

Densid.Real [g/cm³]	**3,817**
M.E.A.Umida [g/cm³]	**2,363**
M.E.A.Seca [g/cm³]	**1,874**
Umidade Inicial [%]	**26,15**

Parâmetro B (Skempton) pelo Painel de Saturação

Tensão Confinante (kPa)	Contra Pressão (kPa)	u (kPa)	B
50,0	40,00	-	-
100,01	79,93	50,01	0,60
150,00	138,54	49,99	0,77
199,83	191,46	49,83	0,83
249,68	244,45	49,85	0,90
299,80	296,00	50,12	0,92
349,97	346,57	50,17	0,93
399,38	396,45	49,41	0,94
449,99	447,70	50,61	0,95
499,90	497,99	49,91	0,96
549,76	547,82	49,86	0,96
599,94	597,73	50,18	0,96

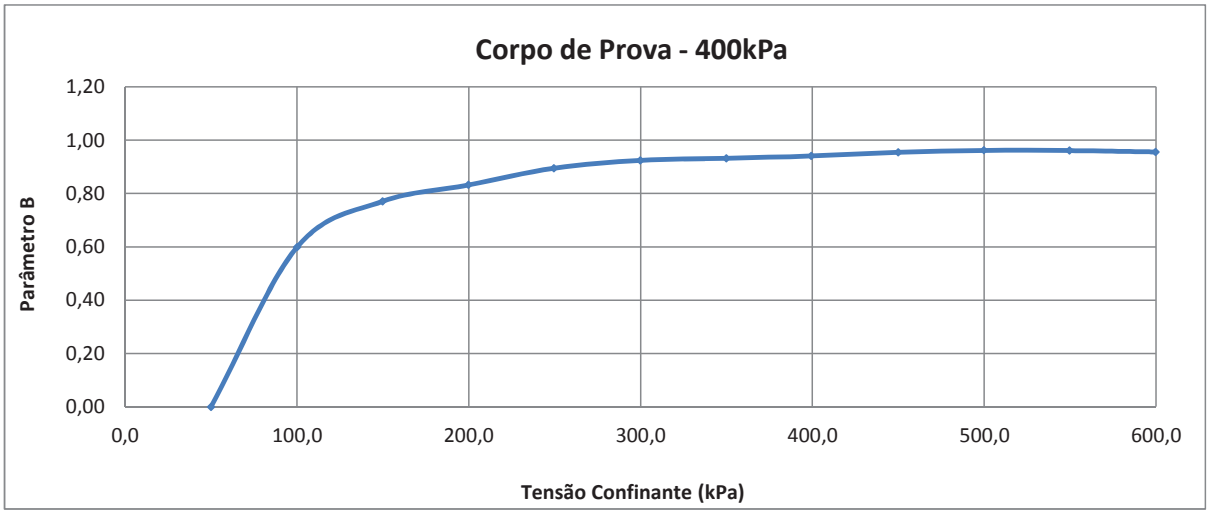

Parâmetro B de poropressão de Skempton: $B = \Delta u / \Delta\sigma_3$

A saturação por contra pressão foi aplicada com incrementos aproximados de 50kPa.

PATROL INVESTIGAÇÕES GEOTÉCNICAS LTDA

Controle do Parâmetro B (Skempton) pelo Painel de Saturação

Interessado:	**Cleary Gottlieb e Hamilton LLP**	Material:	**-**	Data:	**05/07/2016**
Obra:	**-**	Furo:	**GSSam 02B 03**	Amostra:	**Shelby**
Local:	**Baia 3 - Local - F**	Prof.:	**09,00 - 09,65 m**	Registro:	**2016.10151**

Dados de Moldagem Corpo de Prova

Diâmetro [mm]	**35,73**
Altura [mm]	**71,71**
Volume [cm³]	**71,901**
Peso da amostra [g]	**170,52**

Densid.Real [g/cm³]	**3,817**
M.E.A.Umida [g/cm^3]	**2,372**
M.E.A.Seca [g/cm^3]	**1,884**
Umidade Inicial [%]	**25,87**

Parâmetro B (Skempton) pelo Painel de Saturação

Tensão Confinante (kPa)	Contra Pressão (kPa)	u (kPa)	B
50	40,00	-	-
99,98	94,00	49,98	0,88
149,73	146,36	49,75	0,93
199,84	196,75	50,11	0,94
249,85	247,45	50,01	0,95
300,00	297,66	50,15	0,95
349,99	347,80	49,99	0,96
399,97	397,73	49,98	0,96
449,84	447,90	49,87	0,96

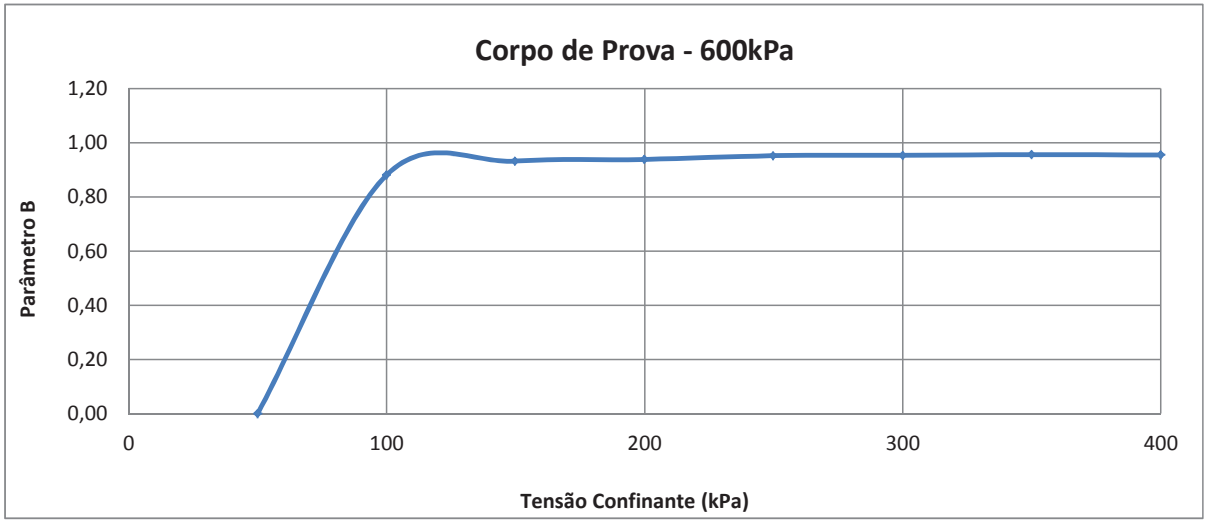

Parâmetro B de poropressão de Skempton: $B = \Delta u / \Delta\sigma_3$

A saturação por contra pressão foi aplicada com incrementos aproximados de 50kPa.

PATROL INVESTIGAÇÕES GEOTÉCNICAS LTDA

Controle do Parâmetro B (Skempton) pelo Painel de Saturação

Interessado:	**Cleary Gottlieb e Hamilton LLP**	Material:	**-**	Data:	**05/07/2016**
Obra:	**-**	Furo:	**GSSam 02B 03**	Amostra:	**Shelby**
Local:	**Baia 3 - Local - F**	Prof.:	**09,00 - 09,65 m**	Registro:	**2016.10151**

Dados de Moldagem Corpo de Prova

Diâmetro [mm]	**35,96**
Altura [mm]	**71,92**
Volume [cm³]	**73,043**
Peso da amostra [g]	**174,98**

Densid.Real [g/cm³]	**3,817**
M.E.A.Umida [g/cm^3]	**2,396**
M.E.A.Seca [g/cm^3]	**1,918**
Umidade Inicial [%]	**24,91**

Parâmetro B (Skempton) pelo Painel de Saturação

Tensão Confinante (kPa)	Contra Pressão (kPa)	u (kPa)	B
50	40,00	-	-
100,00	97,10	50,00	0,94
150,00	147,42	50,00	0,95
200,00	197,45	50,00	0,95
249,99	247,36	49,99	0,95

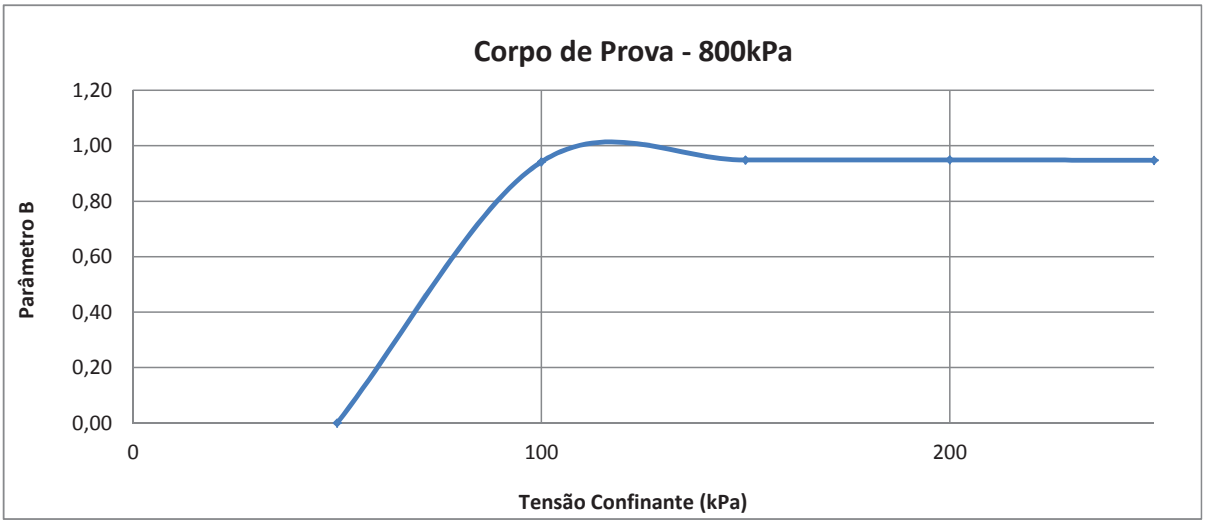

Parâmetro B de poropressão de Skempton: $B = \Delta u / \Delta\sigma_3$

A saturação por contra pressão foi aplicada com incrementos aproximados de 50kPa.

PATROL INVESTIGAÇÕES GEOTÉCNICAS LTDA.

RELATÓRIO FOTOGRÁFICO - Triaxial CIU (200, 400, 600 e 800 KPa)

Cliente:	**Cleary Gottlieb Steen & Hamilton LLP**			Local:	**BAIA 3 - LOCAL F**
Obra:	**-**			Amostra:	**-**
Data:	**18/07/16**	Furo:	**GSSAM-02B-03**	Registro:	**2016.10151**

Antes 200 KPa

Depois 200 KPa

Antes 400 KPa

Depois 400 KPa

Antes 600 KPa

Depois 600 KPa

Antes 800 KPa

Depois 800 KPa

OBSERVAÇÕES:

PATROL INVESTIGAÇÕES GEOTÉCNICAS LTDA

Determinação da Massa específica aparente de amostras indeformadas, com emprego da balança hidrostática - NBR 10838

Interessado:	**Cleary**	Material:	**-**	Data:	**18/07/16**
Obra:	**-**	Furo:	**GSSAM-02B-03**	Amostra:	**Shelby**
Localização:	**BAIA 3 - LOCAL F**	Prof.:	**9,00 - 9,65**	Registro:	**2016.10151**

DETERMINAÇÃO DA MASSA ESPECÍFICA APARENTE DA PARAFINA

Dados	CP 01	CP 02	CP 03
M_{paraf} (g)	71,78	76,85	74,66
M_{cpi} (g)	95,84	95,84	95,90
M_{ci} (g)	92,66	92,27	92,58
Y_0 (g/cm^3)	1,00	1,00	1,00
Yparaf (g/cm3)	0,958	0,956	0,957
Média	0,957		

DETERMINAÇÃO DO VOLUME DO CORPO-DE-PROVA E DA MASSA ESPECÍFICA NATURAL DA AMOSTRA

VOLUME DO CP			
Dados	CP 01	CP 02	CP 03
M_p (g)	290,11	279,05	261,12
M_i (g)	150,00	134,25	128,35
M_s (g)	265,19	240,94	230,83
Y_{paraf} (g/cm^3)	0,957	0,957	0,957
Y_0 (g/cm^3)	1,00	1,00	1,00
V_s (cm^3)	114,07	104,97	101,11
Média:	106,718		

MASSA ESPECÍFICA APARENTE NATURAL			
Dados	CP 01	CP 02	CP 03
M_s (g)	265,19	240,94	230,83
V_s (cm^3)	114,07	104,97	101,11
Yh (g/cm^3)	2,325	2,295	2,283
Média	2,301		

TEOR DE UMIDADE			
nº capsula	49	58	249
cáp+solo úmido	102,66	108,23	117,40
cáp+solo seco	86,88	91,53	98,49
água	15,78	16,70	18,91
tara	14,33	14,15	12,09
solo seco	72,55	77,38	86,40
umidade	21,75	21,58	21,89
Média	21,74		

M_{paraf} = massa do corpo-de-prova, em g;

M_{cpi} = massa do contrapeso quando imerso em água, em g;

M_{ci} = massa do conjunto corpo-de-prova e contrapeso;

Y_0 = massa específica da água (considerar igual a 1 g/cm^3);

Y_{paraf} = massa específica da parafina, em g/cm^3;

Mp = massa do corpo-de-prova parafinado, em g;

Mi = massa do corpo-de-prova parafinado e imerso em água, em g;

Ms = massa do corpo-de-prova, em g;

Vs = volume do corpo-de-prova, em cm^3;

Yh = massa específica aparente natural da amostra, em g/cm^3.

GSSAM 02B 03 – prof.: 9,00 – 9,65 m
Reg.:10151

CARACTERIZAÇÃO

PATROL INVESTIGAÇÕES GEOTÉCNICAS LTDA

Análise Granulométrica por Peneiramento e Sedimentação - NBR 7181/1984

Interessado:	**Cleary**	Material:	**Silte Argiloso**	Data:	**-**
Obra:	**-**	Furo:	**GS SAM-02B-03**	Amostra:	**Shelby**
Local:	**BAIA 3 - LOCAL F**	Prof.:	**9,00 - 9,65**	Registro:	**10151.2016**
Densimetro:	**DS 02 - (16569/13) VT**				

UMIDADE HIGROSCÓPICA			
Cápsula no. (g.)	**48**	**81**	**86**
Solo umido + tara (g.)	**76,12**	**89,81**	**75,82**
Solo seco + tara (g.)	**76,00**	**89,66**	**75,71**
Tara da capsula (g.)	**11,76**	**15,04**	**12,68**
Água (g.)	0,12	0,15	0,11
Solo Seco (g.)	64,24	74,62	63,03
Teor de umidade (%)	0,2	0,2	0,2
Umidade Média (%)	0,2		

AMOSTRA TOTAL SECA	
Amostra Total Úmida (g)	**665,02**
Solo Seco retido na # 10 (g)	0,00
Solo Úmido passa na # 10 (g)	665,02
Solo Seco passa na # 10 (g)	663,78
Amostra Total Seca (g)	663,78

AMOSTRA PARCIAL SECA	
Amostra menor #10 úmida (g)	**70,00**
Amostra menor #10 seca (g)	69,87
Limite de Liquidez	
Índice de Plasticidade	

MASSA ESPECÍFICA REAL		
Picnômetro. nº	**3**	**4**
Temperatura (°c)	**19,8**	**19,8**
Pic.+ água + solo (g)	**789,70**	**790,75**
Solo úmido(g)	**50,00**	**50,00**
Solo Seco (g)	49,91	49,91
Pic.+ água (g)	752,89	753,95
Água Deslocada (g)	13,10	13,11
Teor de umidade (%)	**0,2**	
Massa Específica (H2O)	0,9983	0,9983
Massa Específica Real	3,819	3,816
ρ [g/cm^3]	**3,818**	

P E N E I R A M E N T O

PENEIRAS A.B.N.T.		MATERIAL RETIDO			% QUE	
		Peso	P.acumul	%	PASSA:amostra	Faixa
N o.	mm.	(gr.)	(gr.)	acumul	total	
4"	101,8					
3 .1/2 "	88,9					
3"	76,2					
2 .1/2 "	63,5					
2"	50,8					
1.1/2 "	38,1					
1"	25,4					
3/4 "	19					
1/2 "	12,7					
3/8"	9,5					
1/4"	6,3					
4	4,8					
8	2,4					
10	2	**0,00**	0,0	0,0	**100,0**	
16	1,2	**0,00**	0,0	0,0	**100,0**	
30	0,6	**0,00**	0,0	0,0	**100,0**	
40	0,42	**0,00**	0,0	0,0	**100,0**	
60	0,25	**0,00**	0,0	0,0	**100,0**	
100	0,15	**0,00**	0,0	0,0	**100,0**	
200	0,075	**0,05**	0,1	0,1	**99,9**	

Densímetro n.º	**02**

$$K = \frac{\delta}{\delta - 1} = \quad 1{,}355$$

% da amostra parcial = A x K x LC

A =	0,0143

SEDIMENTAÇÃO COM DEFLOCULANTE

Data	Temp.	Tempo	horário	Leit.	Correções			Leit.	Altura de	%	%	f
	°c	min.	h	(L)	temperatura	menisco	defloculante	corrig.	Queda	parcial	total	mm
13/07/2016	**20,5**	0,5	**9:37**	**52,0**	-3,5	0,5	-2,0	47,0	8,4	91,2	91,2	0,0410
13/07/2016	20,5	1	9:38	**50,0**	-3,5	0,5	-2,0	45,0	8,7	87,3	87,3	0,0297
14/07/2016	20,5	2	9:39	**45,0**	-3,5	0,5	-2,0	40,0	9,5	77,6	77,6	0,0221
15/07/2016	20,5	5	9:42	**40,0**	-3,5	0,5	-2,0	35,0	10,4	67,9	67,9	0,0147
16/07/2016	20,5	10	9:47	**33,0**	-3,5	0,5	-2,0	28,0	11,5	54,3	54,3	0,0110
17/07/2016	**20,5**	20	9:57	**29,0**	-3,5	0,5	-2,0	24,0	12,2	46,5	46,5	0,0080
18/07/2016	**20,5**	40	10:17	**26,0**	-3,5	0,5	-2,0	21,0	12,7	40,7	40,7	0,0058
19/07/2016	**20,5**	80	10:57	**22,0**	-3,5	0,5	-2,0	17,0	13,3	33,0	33,0	0,0042
20/07/2016	**20,7**	240	13:37	**16,0**	-3,4	0,5	-2,0	11,1	14,3	21,5	21,5	0,0025
21/07/2016	**21,5**	540	17:37	**14,0**	-3,2	0,5	-2,0	9,3	14,6	18,1	18,1	0,0017
14/07/2016	**20,2**	1440	9:37	**13,0**	-3,6	0,5	-2,0	7,9	14,8	15,3	15,3	0,0011

Tipo	Pedregulo	Areia Grossa	Areia Média	Areia Fina	Silte	Argila
% total	0,0	0,0	0,0	3,9	76,7	19,3
% total	**0,0**	**3,9**			**76,7**	**19,3**

Análise Granulométrica por Peneiramento e Sedimentação - NBR 7181/1984

Interessado:	**Cleary**	Material:	**Silte Argiloso**	Data:	**-**
Obra:	**-**	Furo:	**GS SAM-02B-03**	Amostra:	**Shelby**
Local:	**BAIA 3 - LOCAL F**	Prof.:	**9,00 - 9,65**	Registro:	**2016. 10151**
Densimetro:	**DS 02 - (16569/13) VT**				

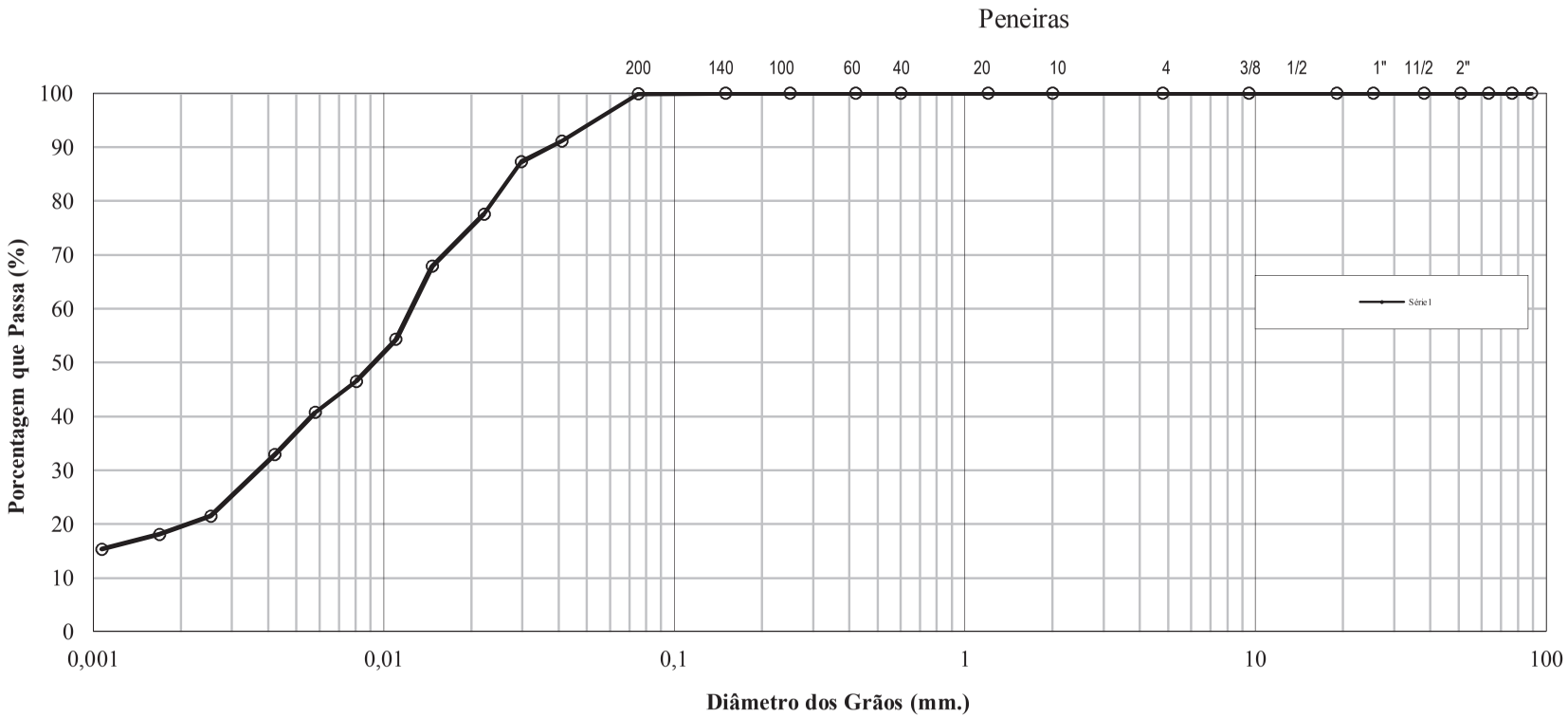

Argila	Silte	Areia Fina	A.Média	13,03	Pedregulho
19,3	**76,7**	**3,9**	**0,0**	**13,5**	**0,0**

PATROL INVESTIGAÇÕES GEOTÉCNICAS

Massa Específica Real dos Grãos - NBR 6508/84

Interessado:	**Cleary Gottieb**	Material:		Data:	**04/07/2016**
Obra:	**-**	Furo:	**GSSam - 02B - 03**	Amostra:	**Shelby**
Local:	**-**	Prof.:	**9,00 a 9,65**	Registro:	**2016.10151**

DETEMINAÇÃO DA UMIDADE (%)

EXECUÇÃO DO ENSAIO			
Cápsula:	66	68	126
Cáp + sol + Agua (g):	96,01	98,36	90,99
Cáp + solo (g):	95,71	98,09	90,74
Peso da cápsula (g):	12,34	13,72	13,19
Água (g):	0,30	0,27	0,25
Solo seco (g):	83,37	84,37	77,55
Umidade (%):	0,4	0,3	0,3
Média:	0,3		

MASSA ESPECÍFICA REAL DOS GRÃOS

EXECUÇÃO DO ENSAIO		
Picnômetro	3	4
Temperatura ºC:	19,8	19,8
Picnômetro + água (g):	752,89	753,95
Solo úmido(g):	50,00	50,00
Solo seco (g):	49,83	49,83
Umidade (%)	0,3	0,3
Conjunto Pic + água + solo (g):	789,70	790,75
Água deslocada (g):	13,03	13,04
Massa Específica (H_2O):	0,9983	0,9983
Massa Específica Real (g/cm³):	3,819	3,816
Média	3,817	

PATROL INVESTIGAÇÕES GEOTÉCNICAS LTDA

LIMITES DE ATTERBERG

Interessado:	**Cleary Gotiieb**	Material:		Data:	**14/07/2016**
Obra:	**-**	Furo:	**GSSam - 02 B - 03**	Amostra:	**Shelby**
Local:	**Baia 3 - Local F**	Prof.:	**9,00 - 9,65**	Registro:	**2016.10151**

LIMITE DE LIQUIDEZ - NBR 6459/1984

Cápsula nº	36	37	38	39	40
Peso da Cápsula+Solo Úmido(g)	17,65	17,07	16,40	19,06	17,46
Peso da Cápsula+Solo Seco(g)	15,92	15,57	15,02	17,32	16,09
Peso da Água(g)	1,73	1,50	1,38	1,74	1,37
Peso da Cápsula(g)	9,57	9,84	9,44	9,82	9,85
Peso do Solo Seco(g)	6,35	5,73	5,58	7,50	6,24
Teor de Umidade(%)	27,2	26,2	24,7	23,2	22,0
Nº de golpes	15	20	25	30	35

LIMITE DE PLASTICIDADE - NBR 7180/1984

Cápsula nº	36	37	38	39	40
Peso da Cápsula+Solo Úmido(g)	7,49	7,01	9,09	7,34	6,79
Peso da Cápsula+Solo Seco(g)	7,25	6,77	8,84	7,10	6,56
Peso da Água(g)	0,24	0,24	0,25	0,24	0,23
Peso da Cápsula(g)	5,70	5,18	7,10	5,40	4,95
Peso do Solo Seco(g)	1,55	1,59	1,74	1,70	1,61
Teor de Umidade(%)	15,5	15,1	14,4	14,1	14,3
Valor aceito?	NÃO	SIM	SIM	SIM	SIM

GRÁFICO

RESULTADOS	
LIMITE DE LIQUIDEZ(%)	24,4
LIMITE DE PLASTICIDADE(%)	14,5
ÍNDICE DE PLASTICIDADE(%)	9,9

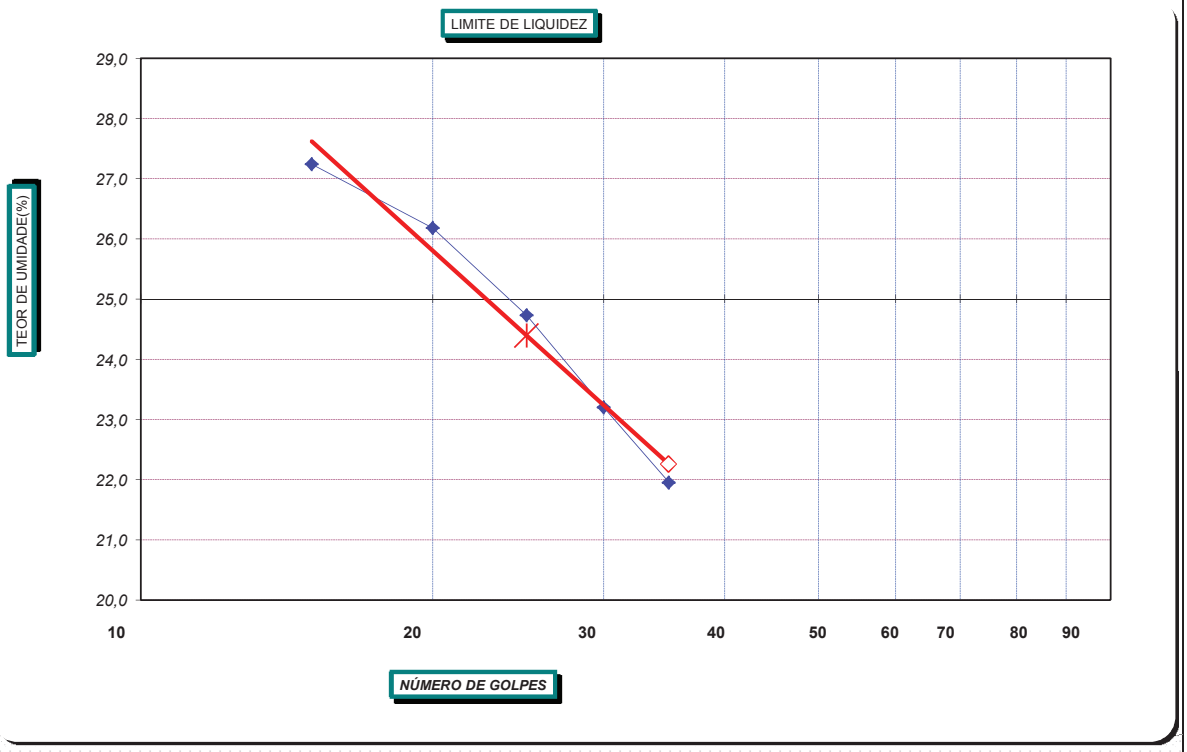

Observ. :...

GSSAM 02B 04 – prof.: 10,00 – 10,65 m
Reg.:10152

TRIAXIAL CU

DENSIDADE APARENTE

CLIENTE:	**Cleary Gottlieb e Hamilton LLP**	
REGISTRO:	**10152**	
FURO:	**GSSam 02B 04**	PROF.: 10,00 - 10,65 m
LOCAL:	**Baia 3 - Local - F**	

DADOS INICAIS DE MOLDAGEM:

Tensões de Confinamento	200 kPa	400 kPa	600 kPa	800 kPa

Peso e Geometria:

Diam. interno:[mm]	35,84	35,85	35,79	35,81
Altura do molde: [mm]	71,72	71,76	71,71	71,71
Volume do anel (cm3)	72,35	72,44	72,14	72,22
Tara do Molde: [g]	577,08	577,08	577,08	577,08
Peso Anel + amostra:	723,65	723,82	723,23	723,39
Peso da amostra: [g]	172,16	167,12	167,23	170,97

Teor de umidade:

Massa Úmida + Tara [g]	136,60	111,57	104,05	103,75
Massa Seca + Tara [g]	110,97	89,84	86,56	86,52
Tara [g]	12,30	13,32	12,28	13,01
Água [g]	25,63	21,73	17,49	17,23
Massa Seca [g]	98,67	76,53	74,28	73,51
Umidade [%]	25,98	28,40	23,54	23,44

Dados Calculados:

Densid.Real: [g/cm^3]	3,874	3,874	3,874	3,874
M.E.A.Umida [g/cm^3]	2,379	2,307	2,318	2,367
M.E.A.Seca [g/cm^3]	1,889	1,797	1,88	1,918
Indice Vazios Inicial	1,05	1,16	1,06	1,02
G.Saturação Inicial [%]	95,74	95,17	85,65	89,01
Volume de Vazios (%)	51,24	53,62	51,56	50,50

CONSOLIDATED UNDRAINED TRIAXIAL TEST by ASTM D4767

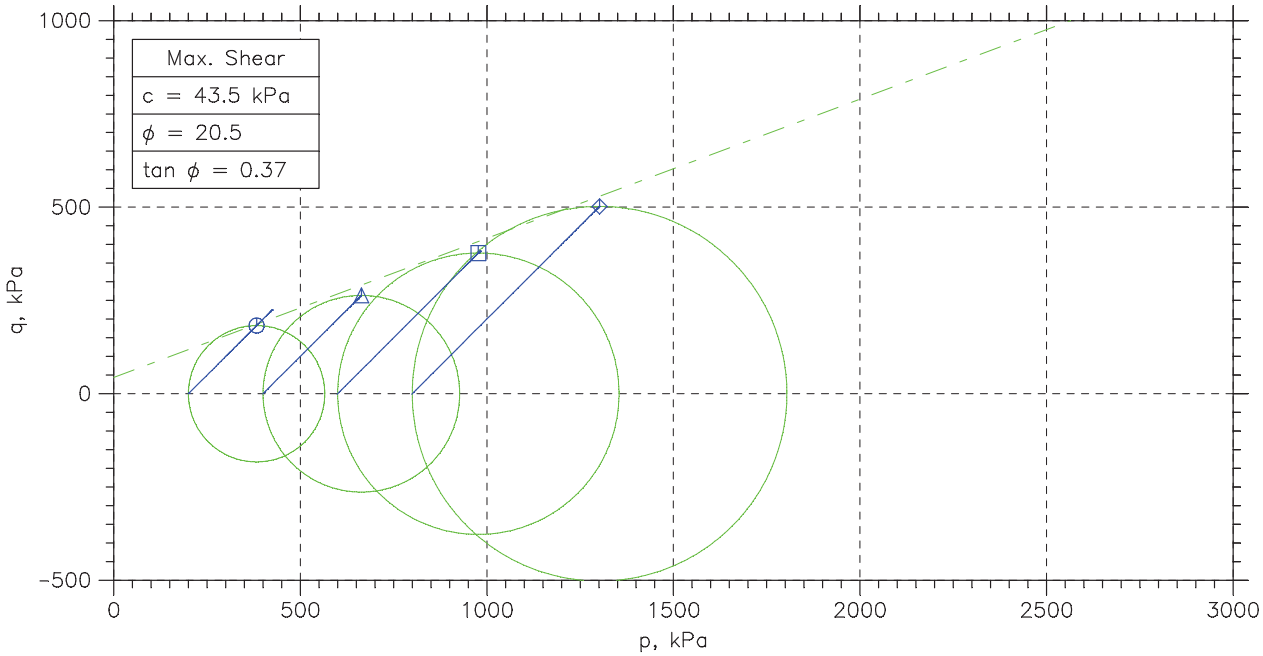

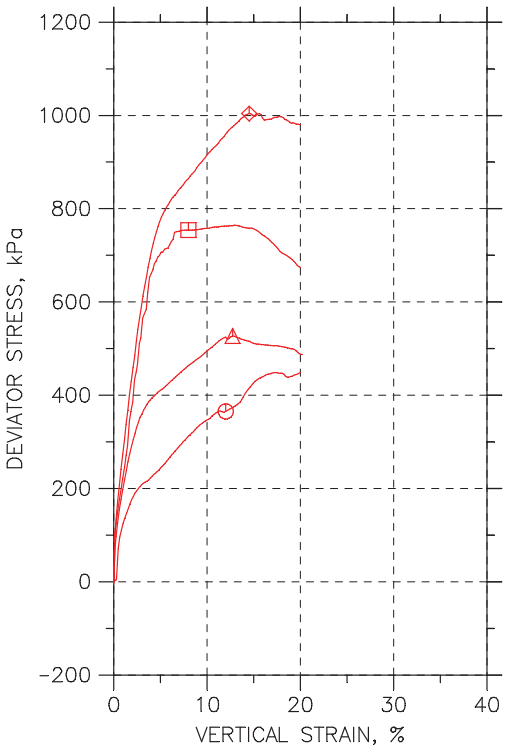

Symbol		○	△	□	◇
Sample No.		GSSam02B 03	GSSam02B 03	GSSam02B 03	GSSam02B 04
Test No.		200 KPa	400 KPa	600 KPa	800 KPa
Depth		10.0-10.65m	10.0-10651	10.0-10.65m	10.0-1065 m
Initial	Diameter, mm	35.84	35.85	35.79	35.81
	Height, mm	71.72	71.76	71.71	71.71
	Water Content, %	26.0	28.4	26.7	25.9
	Dry Density, N/m^3	18520	17620	18400	18810
	Saturation, %	95.7	95.2	97.0	98.4
	Void Ratio	1.05	1.16	1.06	1.02
Before Shear	Water Content, %	21.4	21.3	21.8	21.4
	Dry Density, N/m^3	20760	20810	20620	20790
	Saturation*, %	100.0	100.0	100.0	100.0
	Void Ratio	0.83	0.826	0.843	0.828
	Back Press., kPa	39.98	39.94	39.95	39.99
Ver. Eff. Cons. Stress, kPa		200.	400.	600.	800.
Shear Strength, kPa		182.7	263.5	377.	502.
Strain at Failure, %		12	12.7	8	14.5
Strain Rate, %/min		0.09	0.09	0.09	0.09
B-Value		---	---	---	---
Measured Specific Gravity		3.87	3.87	3.87	3.87
Liquid Limit		---	---	---	---
Plastic Limit		---	---	---	---

PATTROL

Project: Cleary Gottlieb Steen

Location: Baia 3 local F

Project No.: 001/2016

Boring No.: 10152

Sample Type: Shelby

Description:

Remarks: Triaxial - D3

Phase calculations based on end of test.

* Saturation is set to 100% for phase calculations.

Wed, 06-JUL-2016 12:07:01

CONSOLIDATED UNDRAINED TRIAXIAL TEST by ASTM D4767

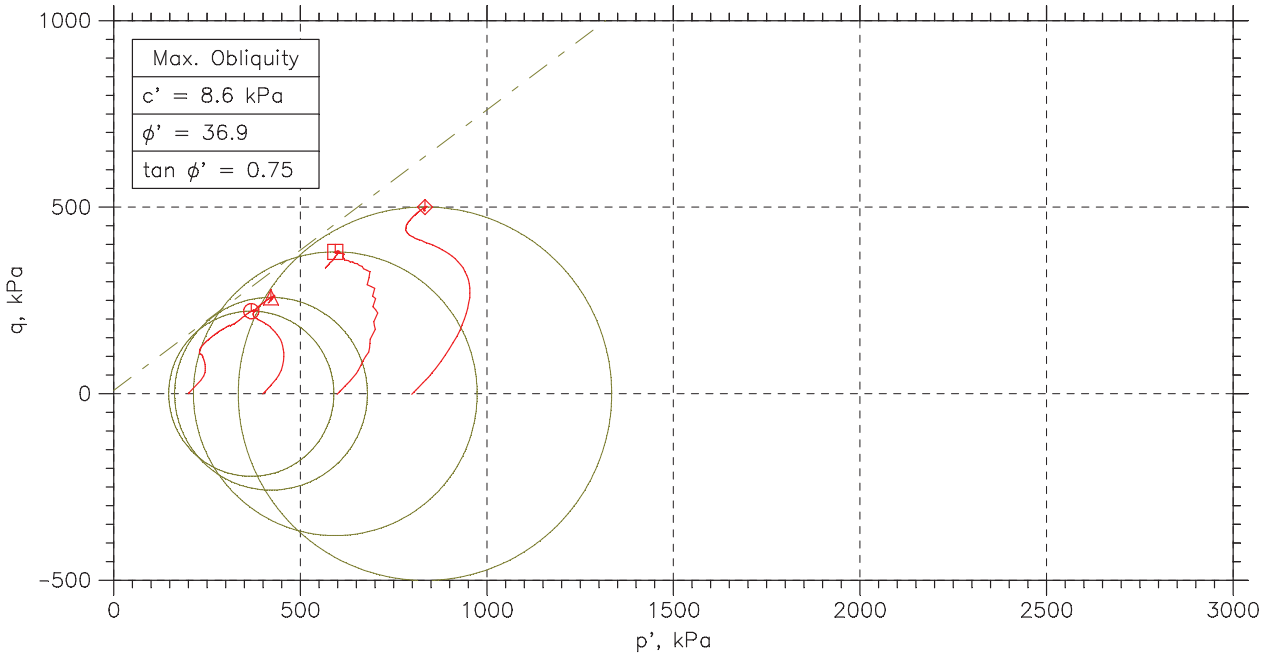

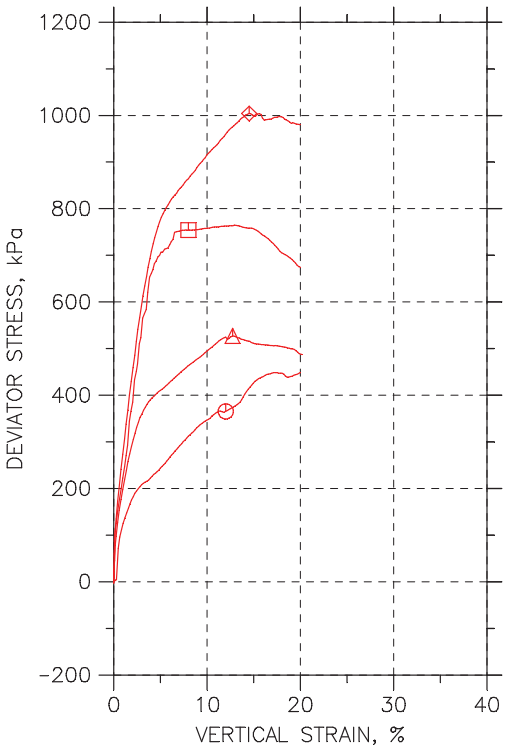

Symbol		⏲	△	⏍	◇
Sample No.		GSSam02B 03	GSSam02B 02	GSSam02B 01	GSSam02B 04
Test No.		200 KPa	400 KPa	600 KPa	800 KPa
Depth		10.0-10.65m	10.0-10651	10.0-10.65m	10.0-1065 m
Initial	Diameter, mm	35.84	35.85	35.79	35.81
	Height, mm	71.72	71.76	71.71	71.71
	Water Content, %	26.0	28.4	26.7	25.9
	Dry Density, N/m^3	18520	17620	18400	18810
	Saturation, %	95.7	95.2	97.0	98.4
	Void Ratio	1.05	1.16	1.06	1.02
Before Shear	Water Content, %	21.4	21.3	21.8	21.4
	Dry Density, N/m^3	20760	20810	20620	20790
	Saturation*, %	100.0	100.0	100.0	100.0
	Void Ratio	0.83	0.826	0.843	0.828
	Back Press., kPa	39.98	39.94	39.95	39.99
Ver. Eff. Cons. Stress, kPa		200.	400.	600.	800.
Shear Strength, kPa		182.7	263.5	377.	502.
Strain at Failure, %		12	12.7	8	14.5
Strain Rate, %/min		0.09	0.09	0.09	0.09
B-Value		---	---	---	---
Measured Specific Gravity		3.87	3.87	3.87	3.87
Liquid Limit		---	---	---	---
Plastic Limit		---	---	---	---

PATTROL

Project: Cleary Gottlieb Steen

Location: Baia 3 local F

Project No.: 001/2016

Boring No.: 10152

Sample Type: Shelby

Description:

Remarks: Triaxial - D3

Phase calculations based on end of test.

* Saturation is set to 100% for phase calculations.

Wed, 06-JUL-2016 12:07:42

CONSOLIDATED UNDRAINED TRIAXIAL TEST by ASTM D4767

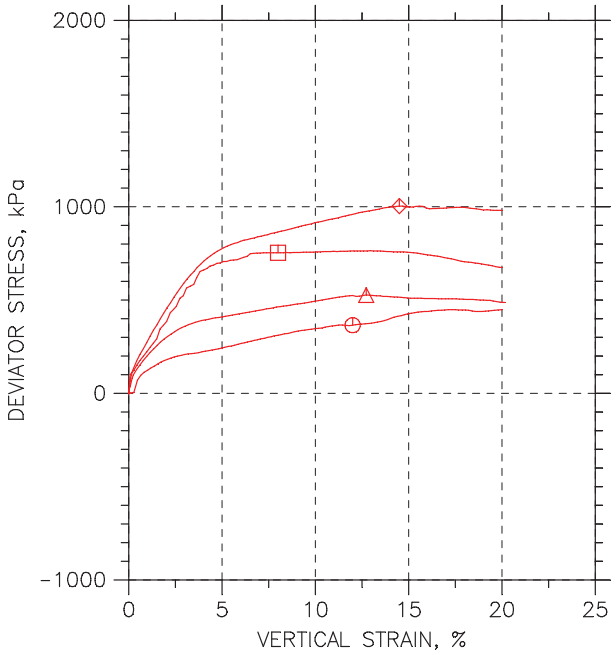

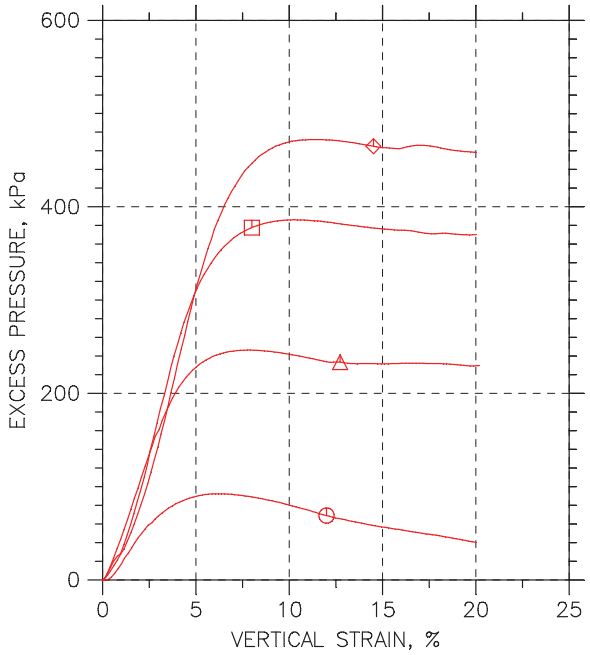

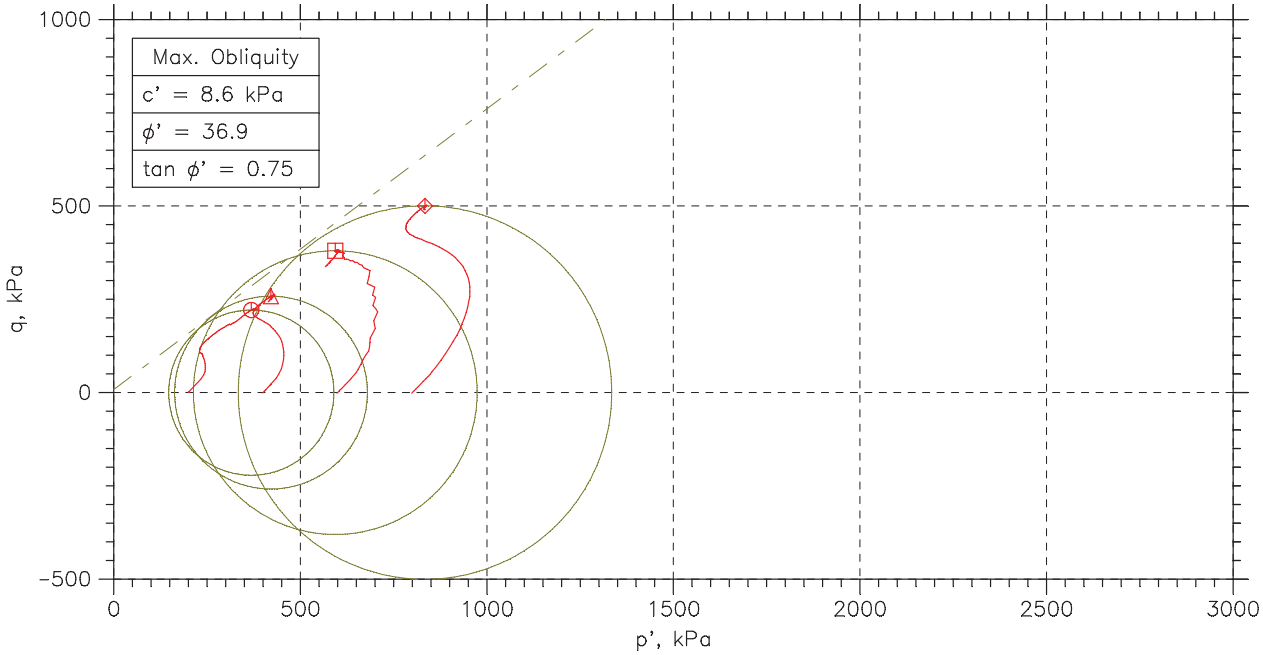

	Sample No.	Test No.	Depth	Tested By	Test Date	Checked By	Check Date	Test File
○	GSSam02B 02	200 KPa	10.0-10.65m	Fernando	30/06/2016	Almir		Reg. 10152 - 200 KPa - D3.da
△	GSSam02B 04	400 KPa	10.0-1065 m	Fernando	30/06/2016	Almir		Reg. 10152 - 400 KPa - G7.da
□	GSSam02B 06	600 KPa	10.0-10.65m	Fernando	04/07/2016	Almir		Reg. 10152 - 600. KPa - F5.dc
◇	GSSam02B 08	800 KPa	10.0-1065 m	Fernando	04/07/2016	Almir		Reg. 10152 - 800. KPa - H8.dc

PATTROL

Project: Cleary Gottlieb Steen	Location: Baia 3 local F	Project No.: 001/2016
Boring No.: 10152	Sample Type: Shelby	
Description:		
Remarks: Triaxial - D3		

Wed, 06-JUL-2016 12:07:42

PATROL INVESTIGAÇÕES GEOTÉCNICAS LTDA

Controle do Parâmetro B (Skempton) pelo Painel de Saturação

Interessado:	**Cleary Gottlieb e Hamilton LLP**	Material:	**-**	Data:	**06/07/2016**
Obra:	**-**	Furo:	**GSSam 02B 04**	Amostra:	**Shelby**
Local:	**-**	Prof.:	**10,00 - 10,65 m**	Registro:	**2016.10152**

Dados de Moldagem Corpo de Prova

Diâmetro [mm]	**35,84**
Altura [mm]	**71,72**
Volume [cm³]	**72,35**
Peso da amostra [g]	**172,16**

Densid.Real [g/cm³]	**3,874**
M.E.A.Umida [g/cm³]	**2,379**
M.E.A.Seca [g/cm³]	**1,889**
Umidade Inicial [%]	**25,98**

Parâmetro B (Skempton) pelo Painel de Saturação

Tensão Confinante (kPa)	Contra Pressão (kPa)	u (kPa)	B
50,0	40,00	-	-
100,32	70,02	50,32	0,40
150,08	127,38	49,76	0,54
199,90	182,58	49,82	0,65
249,67	235,36	49,77	0,71
299,54	289,00	49,87	0,79
349,81	339,88	50,27	0,80
399,42	393,65	49,61	0,88
449,23	444,70	49,81	0,91
499,84	496,30	50,61	0,93
549,55	546,69	49,71	0,94
599,37	596,75	49,82	0,95
649,08	646,52	49,71	0,95
699,86	697,92	50,78	0,96
749,62	747,50	49,76	0,96
799,55	797,66	49,93	0,96

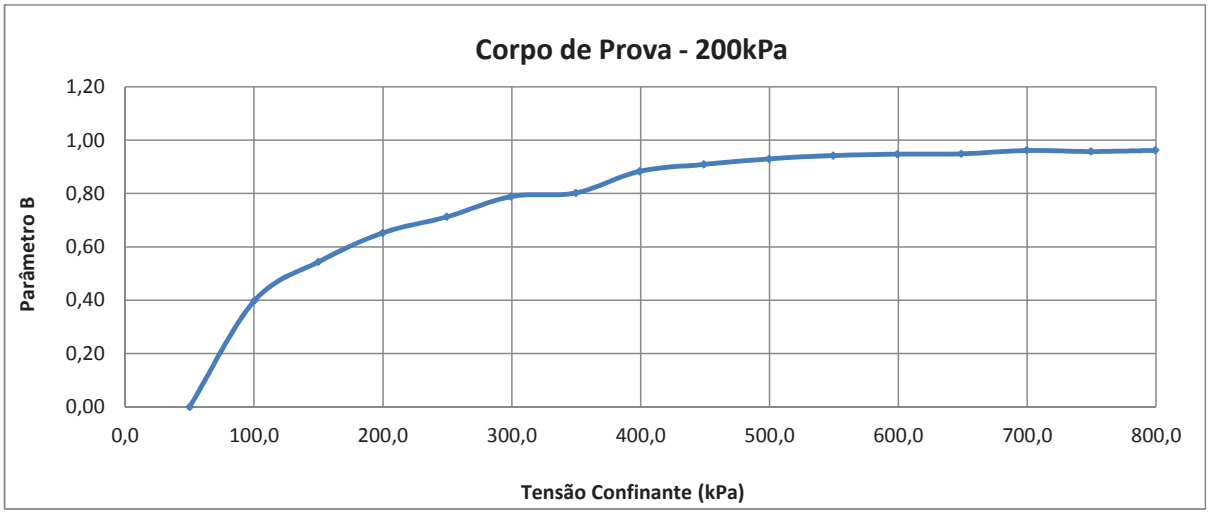

Parâmetro B de poropressão de Skempton: $B = \Delta u / \Delta\sigma_3$

A saturação por contra pressão foi aplicada com incrementos aproximados de 50kPa.

PATROL INVESTIGAÇÕES GEOTÉCNICAS LTDA

Controle do Parâmetro B (Skempton) pelo Painel de Saturação

Interessado:	**Cleary Gottlieb e Hamilton LLP**	Material:	**-**	Data:	**06/07/2016**
Obra:	**-**	Furo:	**GSSam 02B 04**	Amostra:	**Shelby**
Local:	**-**	Prof.:	**10,00 - 10,65 m**	Registro:	**2016.10152**

Dados de Moldagem Corpo de Prova

Diâmetro [mm]	**35,85**
Altura [mm]	**71,76**
Volume [cm³]	**72,44**
Peso da amostra [g]	**167,12**

Densid.Real [g/cm³]	**3,874**
M.E.A.Umida [g/cm^3]	**2,307**
M.E.A.Seca [g/cm^3]	**1,797**
Umidade Inicial [%]	**28,40**

Parâmetro B (Skempton) pelo Painel de Saturação

Tensão Confinante (kPa)	Contra Pressão (kPa)	u (kPa)	B
50	40,00	-	-
99,95	86,30	49,95	0,73
149,93	142,51	49,98	0,85
199,79	193,10	49,86	0,87
249,88	245,00	50,09	0,90
299,69	295,74	49,81	0,92
349,83	346,33	50,14	0,93
399,97	396,79	50,14	0,94
449,78	447,36	49,81	0,95
499,87	497,71	50,09	0,96
549,84	547,85	49,97	0,96
599,99	597,93	50,15	0,96

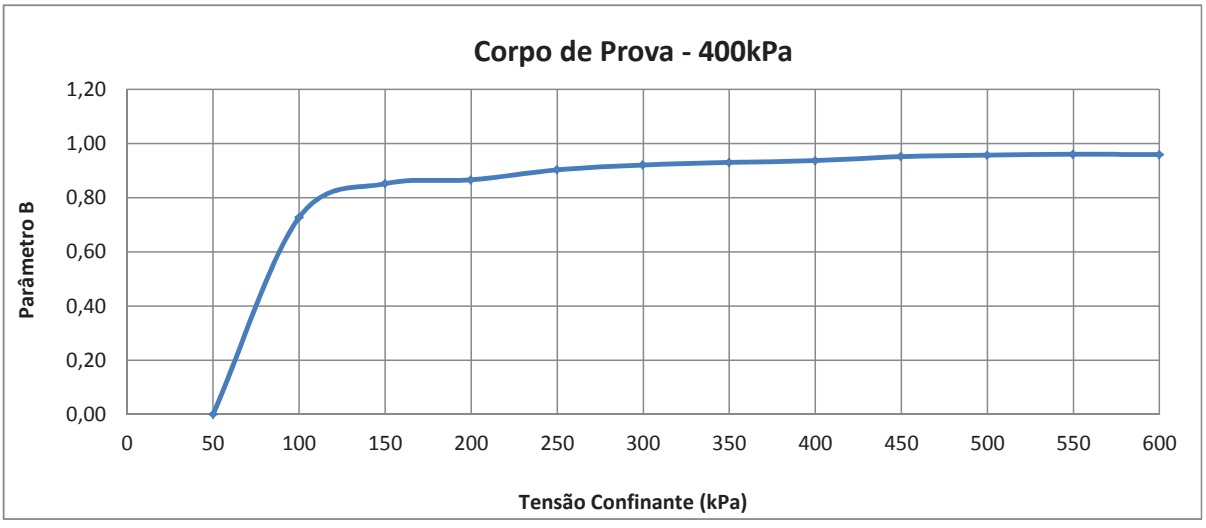

Parâmetro B de poropressão de Skempton: $B = \Delta u / \Delta\sigma_3$

A saturação por contra pressão foi aplicada com incrementos aproximados de 50kPa.

PATROL INVESTIGAÇÕES GEOTÉCNICAS LTDA

Controle do Parâmetro B (Skempton) pelo Painel de Saturação

Interessado:	**Cleary Gottlieb e Hamilton LLP**	Material:		Data:	**06/07/2016**
Obra:	**-**	Furo:	**GSSam 02B 04**	Amostra:	**Shelby**
Local:	**-**	Prof.:	**10,00 - 10,65 m**	Registro:	**2016.10152**

Dados de Moldagem Corpo de Prova

Diâmetro [mm]	**35,79**
Altura [mm]	**71,71**
Volume [cm³]	**72,14**
Peso da amostra [g]	**171,47**

Densid.Real [g/cm³]	**3,874**
M.E.A.Umida [g/cm^3]	**2,377**
M.E.A.Seca [g/cm^3]	**1,876**
Umidade Inicial [%]	**26,67**

Parâmetro B (Skempton) pelo Painel de Saturação

Tensão Confinante (kPa)	Contra Pressão (kPa)	u (kPa)	B
50	40,00	-	-
99,91	93,21	49,91	0,87
149,94	144,96	50,03	0,90
199,92	195,96	49,98	0,92
249,70	246,52	49,78	0,94
299,61	296,91	49,91	0,95
349,75	347,54	50,14	0,96
399,68	397,67	49,93	0,96
449,80	447,83	50,12	0,96

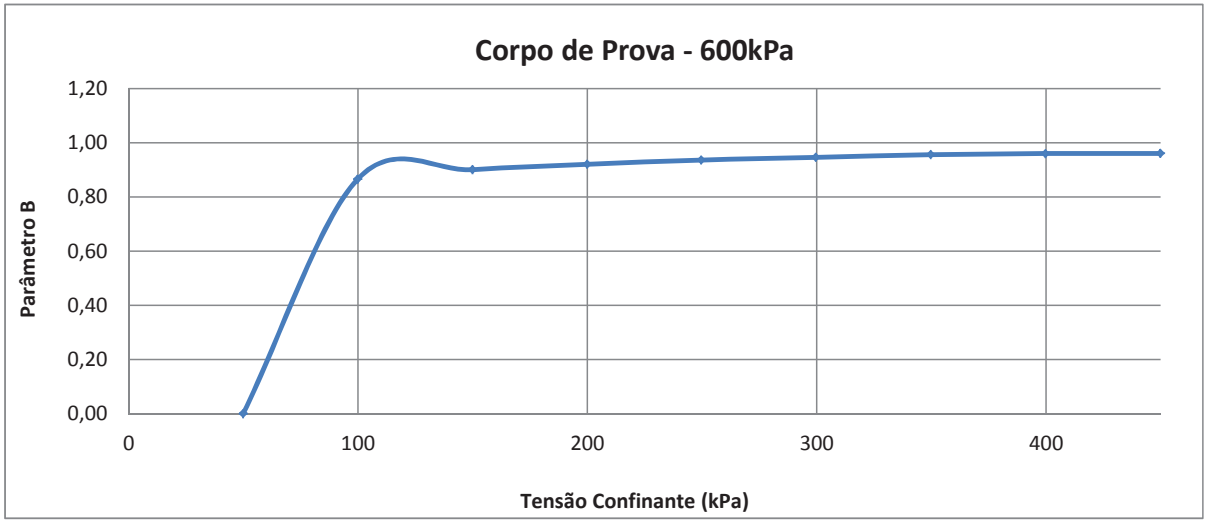

Parâmetro B de poropressão de Skempton: $B = \Delta u / \Delta\sigma_3$

A saturação por contra pressão foi aplicada com incrementos aproximados de 50kPa.

PATROL INVESTIGAÇÕES GEOTÉCNICAS LTDA

Controle do Parâmetro B (Skempton) pelo Painel de Saturação

Interessado:	**Cleary Gottlieb e Hamilton LLP**	Material:	**-**	Data:	**06/07/2016**
Obra:	**-**	Furo:	**GSSam 02B 04**	Amostra:	**Shelby**
Local:	**-**	Prof.:	**10,00 - 10,65 m**	Registro:	**2016.10152**

Dados de Moldagem Corpo de Prova

Diâmetro [mm]	**35,81**
Altura [mm]	**71,71**
Volume [cm³]	**72,22**
Peso da amostra [g]	**174,42**

Densid.Real [g/cm³]	**3,874**
M.E.A.Umida [g/cm^3]	**2,415**
M.E.A.Seca [g/cm^3]	**1,918**
Umidade Inicial [%]	**25,92**

Parâmetro B (Skempton) pelo Painel de Saturação

Tensão Confinante (kPa)	Contra Pressão (kPa)	u (kPa)	B
50	40,00	-	-
99,88	97,27	49,88	0,95
149,80	147,79	49,92	0,96
199,89	197,73	50,09	0,96
249,72	247,80	49,83	0,96

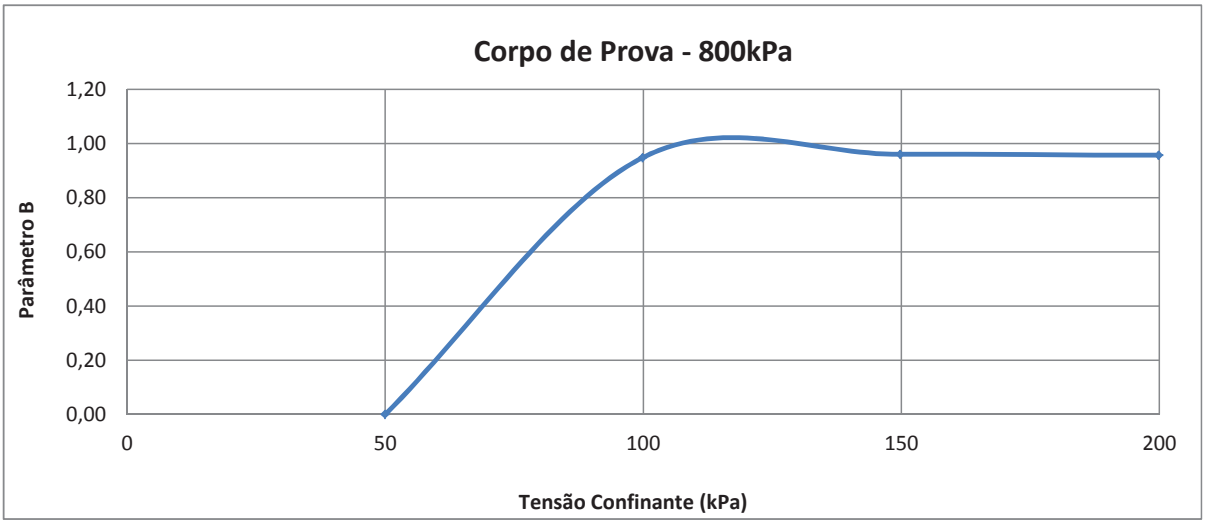

Parâmetro B de poropressão de Skempton: $B = \Delta u / \Delta\sigma_3$

A saturação por contra pressão foi aplicada com incrementos aproximados de 50kPa.

PATROL INVESTIGAÇÕES GEOTÉCNICAS LTDA.

RELATÓRIO FOTOGRÁFICO - Triaxial CIU (200, 400, 600 e 800 KPa)

Cliente:	**Cleary Gottlieb Steen & Hamilton LLP**			Local:	**BAIA 3 - LOCAL F**
Obra:	**-**			Amostra:	**-**
Data:	**18/07/16**	Furo:	**GSSAM-02B-04**	Registro:	**2016.10152**

Antes 200 KPa

Depois 200 KPa

Antes 400 KPa

Depois 400 KPa

Antes 600 KPa

Depois 600 KPa

Antes 800 KPa

Depois 800 KPa

OBSERVAÇÕES:

PATROL INVESTIGAÇÕES GEOTÉCNICAS LTDA

Determinação da Massa específica aparente de amostras indeformadas, com emprego da balança hidrostática - NBR 10838

Interessado:	**Cleary**	Material:	**-**	Data:	**18/07/16**
Obra:	**-**	Furo:	**GSSAM-02B-04**	Amostra:	**Shelby**
Localização:	**BAIA 3 - LOCAL F**	Prof.:	**10,0 - 10,65**	Registro:	**2016.10152**

DETERMINAÇÃO DA MASSA ESPECÍFICA APARENTE DA PARAFINA

Dados	CP 01	CP 02	CP 03
M_{paraf} (g)	71,78	76,85	74,66
M_{cpi} (g)	95,84	95,84	95,90
M_{ci} (g)	92,66	92,27	92,58
Y_0 (g/cm^3)	1,00	1,00	1,00
Yparaf (g/cm3)	0,958	0,956	0,957
Média	0,957		

DETERMINAÇÃO DO VOLUME DO CORPO-DE-PROVA E DA MASSA ESPECÍFICA NATURAL DA AMOSTRA

VOLUME DO CP			
Dados	CP 01	CP 02	CP 03
M_p (g)	290,11	279,05	261,12
M_i (g)	152,60	134,80	129,90
M_s (g)	265,19	240,94	230,83
Y_{paraf} (g/cm^3)	0,957	0,957	0,957
Y_0 (g/cm^3)	1,00	1,00	1,00
V_s (cm^3)	111,47	104,42	99,56
Média:	105,151		

MASSA ESPECÍFICA APARENTE NATURAL			
Dados	CP 01	CP 02	CP 03
M_s (g)	265,19	240,94	230,83
V_s (cm^3)	111,47	104,42	99,56
Yh (g/cm^3)	2,379	2,307	2,318
Média	2,335		

TEOR DE UMIDADE			
nº capsula	18	115	279
cáp+solo úmido	137,74	127,18	134,02
cáp+solo seco	108,07	99,48	104,25
água	29,67	27,70	29,77
tara	14,32	11,94	11,97
solo seco	93,75	87,54	92,28
umidade	31,65	31,64	32,26
Média	31,85		

M_{paraf} = massa do corpo-de-prova, em g;

M_{cpi} = massa do contrapeso quando imerso em água, em g;

M_{ci} = massa do conjunto corpo-de-prova e contrapeso;

Y_0 = massa específica da água (considerar igual a 1 g/cm^3);

Y_{paraf} = massa específica da parafina, em g/cm^3;

Mp = massa do corpo-de-prova parafinado, em g;

Mi = massa do corpo-de-prova parafinado e imerso em água, em g;

Ms = massa do corpo-de-prova, em g;

Vs = volume do corpo-de-prova, em cm^3;

Yh = massa específica aparente natural da amostra, em g/cm^3.

GSSAM 02B 04 – prof.: 10,00 – 10,65 m
Reg.:10152

CARACTERIZAÇÃO

PATROL INVESTIGAÇÕES GEOTÉCNICAS LTDA

Análise Granulométrica por Peneiramento e Sedimentação - NBR 7181/1984

Interessado:	**Cleary**	Material:	**Silte Argiloso**	Data:	**11/07/2016**
Obra:	**-**	Furo:	**GS SAM - 02B - 04**	Amostra:	**-**
Local:	**BAIA 3 - LOCAL F**	Prof.:	**10,00 - 10,65**	Registro:	**10152.2016**
Densimetro:	**DS 02 - (16569/13) VT**				

UMIDADE HIGROSCÓPICA			
Cápsula no. (g.)	**70**	**83**	**292**
Solo umido + tara (g.)	**87,54**	**85,62**	**93,07**
Solo seco + tara (g.)	**87,32**	**85,44**	**92,86**
Tara da capsula (g.)	**12,97**	**13,01**	**12,06**
Água (g.)	0,22	0,18	0,21
Solo Seco (g.)	74,35	72,43	80,80
Teor de umidade (%)	0,3	0,2	0,3
Umidade Média (%)	0,3		

AMOSTRA TOTAL SECA	
Amostra Total Úmida (g)	**1.447,00**
Solo Seco retido na # 10 (g)	0,00
Solo Úmido passa na # 10 (g)	1.447,00
Solo Seco passa na # 10 (g)	1.443,13
Amostra Total Seca (g)	1.443,13

AMOSTRA PARCIAL SECA	
Amostra menor #10 úmida (g)	**70,00**
Amostra menor #10 seca (g)	69,81
Limite de Liquidez	
Índice de Plasticidade	

MASSA ESPECÍFICA REAL		
Picnômetro. nº	**9**	**10**
Temperatura (°c)	**19,6**	**19,6**
Pic.+ água + solo (g)	**670,70**	**674,17**
Solo úmido(g)	**50,00**	**50,00**
Solo Seco (g)	49,87	49,87
Pic.+ água (g)	633,64	637,11
Água Deslocada (g)	12,81	12,81
Teor de umidade (%)	**0,3**	
Massa Específica (H2O)	0,9983	0,9983
Massa Específica Real	3,874	3,874
ρ [g/cm^3]	**3,874**	

P E N E I R A M E N T O

PENEIRAS A.B.N.T.		MATERIAL RETIDO			% QUE	
		Peso	P.acumul	%	PASSA:amostra	Faixa
N o.	mm.	(gr.)	(gr.)	acumul	total	
4''	101,8					
3 .1/2 "	88,9					
3''	76,2					
2 .1/2 "	63,5					
2''	50,8					
1.1/2 "	38,1					
1''	25,4					
3/4 "	19					
1/2 "	12,7					
3/8''	9,5					
1/4''	6,3					
4	4,8					
8	2,4					
10	2	**0,00**	0,0	0,0	**100,0**	
16	1,2	**0,00**	0,0	0,0	**100,0**	
30	0,6	**0,00**	0,0	0,0	**100,0**	
40	0,42	**0,00**	0,0	0,0	**100,0**	
60	0,25	**0,00**	0,0	0,0	**100,0**	
100	0,15	**0,00**	0,0	0,0	**100,0**	
200	0,075	**0,13**	0,1	0,2	**99,8**	

Densímetro n.º	**02**

$$K = \frac{\delta}{\delta - 1} =$$ 1,348

% da amostra parcial = A x K x LC

A = 0,0143

SEDIMENTAÇÃO COM DEFLOCULANTE

Data	Temp.	Tempo	horário	Leit.	Correções			Leit.	Altura de	%	%	f
	°c	min.	h	(L)	temperatura	menisco	defloculante	corrig.	Queda	parcial	total	mm
08/07/2016	**20,2**	0,5	**9:51**	**52,0**	-3,6	0,5	-2,0	46,9	8,4	90,6	90,6	0,0412
08/07/2016	20,2	1	9:52	**50,0**	-3,6	0,5	-2,0	44,9	8,7	86,7	86,7	0,0298
09/07/2016	20,2	2	9:53	**48,0**	-3,6	0,5	-2,0	42,9	9,0	82,8	82,8	0,0215
10/07/2016	20,2	5	9:56	**45,0**	-3,6	0,5	-2,0	39,9	9,5	77,0	77,0	0,0140
11/07/2016	20,1	10	10:01	**35,0**	-3,6	0,5	-2,0	29,9	11,2	57,7	57,7	0,0109
12/07/2016	**20,1**	20	10:11	**32,0**	-3,6	0,5	-2,0	26,9	11,7	51,9	51,9	0,0079
13/07/2016	**20,1**	40	10:31	**27,0**	-3,6	0,5	-2,0	21,9	12,5	42,2	42,2	0,0058
14/07/2016	**20,1**	80	11:11	**23,0**	-3,6	0,5	-2,0	17,9	13,2	34,5	34,5	0,0042
15/07/2016	**20,3**	240	13:51	**18,0**	-3,6	0,5	-2,0	12,9	14,0	25,0	25,0	0,0025
16/07/2016	**20,6**	540	17:51	**15,0**	-3,5	0,5	-2,0	10,0	14,5	19,4	19,4	0,0017
09/07/2016	**19,5**	1440	9:51	**12,0**	-3,8	0,5	-2,0	6,7	15,0	12,9	12,9	0,0011

Tipo	Pedregulo	Areia Grossa	Areia Média	Areia Fina	Silte	Argila
% total	0,0	0,0	0,0	4,3	74,2	21,5
% total	**0,0**	**4,3**			**74,2**	**21,5**

Análise Granulométrica por Peneiramento e Sedimentação - NBR 7181/1984

Interessado:	**Cleary**	Material:	**Silte Argiloso**	Data:	**11/07/2016**
Obra:	**-**	Furo:	**GS SAM - 02B - 04**	Amostra:	**-**
Local:	**BAIOA 3 - LOCAL F**	Prof.:	**10,00 - 10,65**	Registro:	**2016. 10152**
Densimetro:	**DS 02 - (16569/13) VT**				

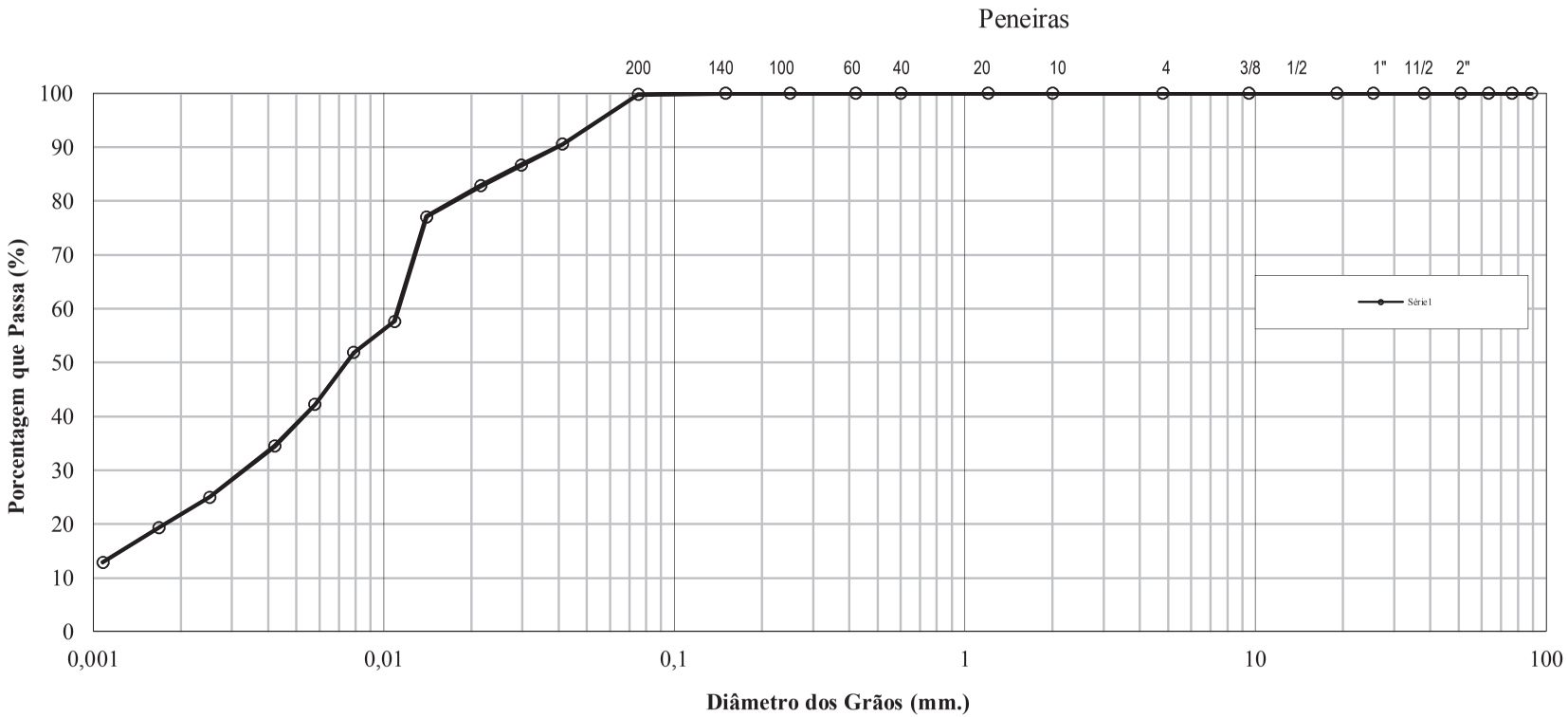

Argila	Silte	Areia Fina	A.Média	13,03	Pedregulho
21,5	**74,2**	**4,3**	**0,0**	**13,5**	**0,0**

PATROL INVESTIGAÇÕES GEOTÉCNICAS

Massa Específica Real dos Grãos - NBR 6508/84

Interessado:	**Cleary Gottieb**	Material:		Data:	**01/07/2016**
Obra:	**-**	Furo:	**GSSam - 02B - 04**	Amostra:	**Shelby**
Local:	**-**	Prof.:	**10,00 a 10,65**	Registro:	**2016.10152**

DETEMINAÇÃO DA UMIDADE (%)

EXECUÇÃO DO ENSAIO			
Cápsula:	39	83	286
Cáp + sol + Agua (g):	117,99	103,43	96,79
Cáp + solo (g):	117,80	103,30	96,68
Peso da cápsula (g):	12,26	13,01	12,09
Água (g):	0,19	0,13	0,11
Solo seco (g):	105,54	90,29	84,59
Umidade (%):	0,2	0,1	0,1
Média:	0,2		

MASSA ESPECÍFICA REAL DOS GRÃOS

EXECUÇÃO DO ENSAIO		
Picnômetro	9	10
Temperatura ºC:	19,6	19,6
Picnômetro + água (g):	633,64	637,11
Solo úmido(g):	50,00	50,00
Solo seco (g):	49,92	49,92
Umidade (%)	0,2	0,2
Conjunto Pic + água + solo (g):	670,70	674,17
Água deslocada (g):	12,87	12,87
Massa Específica (H_2O):	0,9983	0,9983
Massa Específica Real (g/cm³):	3,874	3,874
Média	3,874	

PATROL INVESTIGAÇÕES GEOTÉCNICAS LTDA

LIMITES DE ATTERBERG

Interessado:	**Cleary Gotiieb**	Material:		Data:	**12/07/2016**
Obra:	**-**	Furo:	**GSSam - 02 B - 04**	Amostra:	**Shelby**
Local:	**Baia 3 - Local F**	Prof.:	**10,00 - 10,65**	Registro:	**2016.10152**

LIMITE DE LIQUIDEZ - NBR 6459/1984					
Cápsula nº	46	47	48	49	50
Peso da Cápsula+Solo Úmido(g)	23,62	22,63	22,63	24,46	23,90
Peso da Cápsula+Solo Seco(g)	20,84	20,03	20,18	21,62	21,14
Peso da Água(g)	2,78	2,60	2,45	2,84	2,76
Peso da Cápsula(g)	10,24	9,63	9,86	9,34	9,11
Peso do Solo Seco(g)	10,60	10,40	10,32	12,28	12,03
Teor de Umidade(%)	26,2	25,0	23,7	23,1	22,9
Nº de golpes	13	20	26	31	34

LIMITE DE PLASTICIDADE - NBR 7180/1984					
Cápsula nº	46	47	48	49	50
Peso da Cápsula+Solo Úmido(g)	7,51	6,82	7,48	7,18	6,81
Peso da Cápsula+Solo Seco(g)	7,25	6,63	7,24	6,95	6,59
Peso da Água(g)	0,26	0,19	0,24	0,23	0,22
Peso da Cápsula(g)	5,58	5,30	5,69	5,51	5,12
Peso do Solo Seco(g)	1,67	1,33	1,55	1,44	1,47
Teor de Umidade(%)	15,6	14,3	15,5	16,0	15,0
Valor aceito?	SIM	NÃO	SIM	NÃO	SIM

GRÁFICO

RESULTADOS	
LIMITE DE LIQUIDEZ(%)	24,0
LIMITE DE PLASTICIDADE(%)	15,1
ÍNDICE DE PLASTICIDADE(%)	8,9

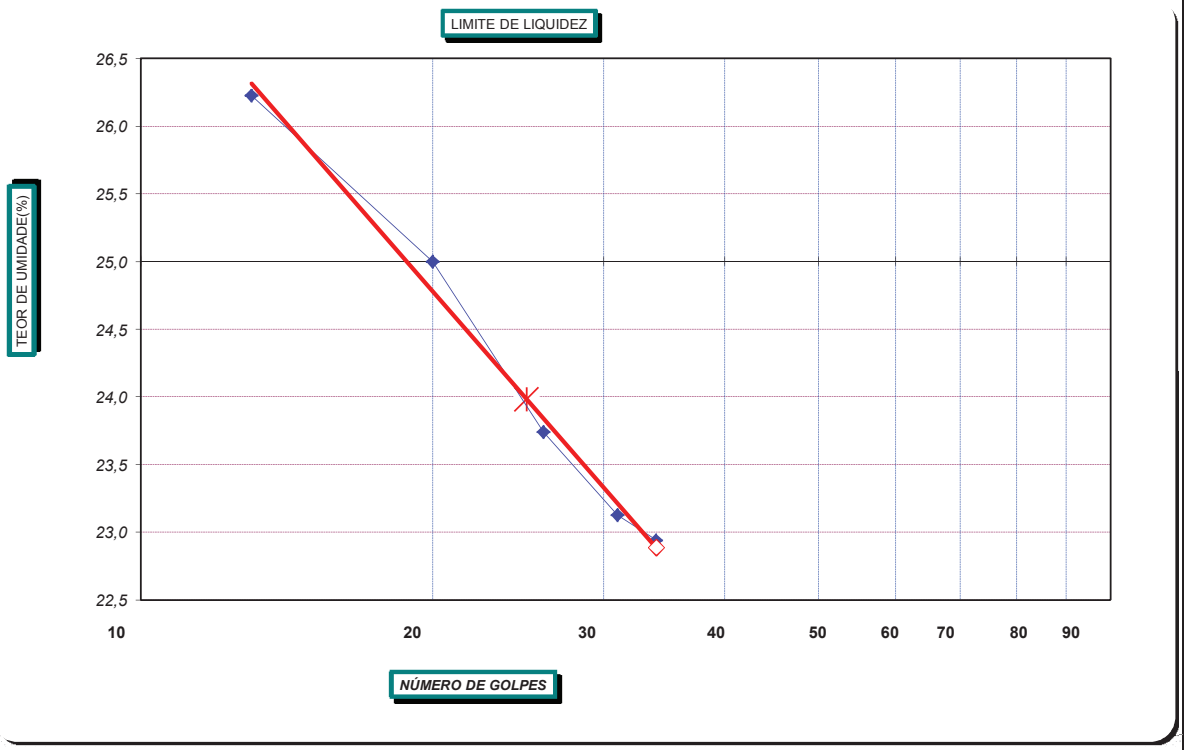

Observ. :...

ATTACHMENT D8

Consolidation Test Data

CONSOLIDATION

PROJECT NO.:
PROJECT: Fundão Tailings Dam Review Panel
SAMPLE NO.: PSD 1
DETAILS 51 % fines content, 5 % water content, e_o = 0.87

TEST NO.: CONS01
LOADING MACHINE NO.: OED2 / ID81

Test Specimen Information:

Initial water content:	5.50 % (based on trimmings)
Final water content:	23.81 % (based on final dry weight)
Dry mass:	132.09 g
Diameter	63.56 mm
Area	31.729 cm^2
Specific Gravity	3.05

Initial Specimen Height (mm): 25.59
Height of Solid (mm): 13.649
Initial void ratio: 0.875
Void Ratio Factor 0.0733

* Calibration to be done after test
** Estimated t_{50}

Pressure (kPa)		*Change in Height	Final	Change in	Change in	Void	t_{50}**	Cv	Mv	k	Cc
From	To	Corrected (mm)	Height (mm)	Void Ratio	Void Ratio Acc	Ratio	(min)	(cm^2/sec)	(cm^2/N)	(cm/sec)	
0.0	**3.0**	0.145	25.445	0.0106	0.0106	**0.864**					
3.0	**6.3**	0.089	25.356	0.0065	0.0171	**0.858**	0.18	2.9E-02	1.1E-02	3.1E-06	**0.020**
6.3	**12.5**	0.113	25.243	0.0083	0.0255	**0.849**	0.18	2.9E-02	7.2E-03	2.0E-06	**0.028**
12.5	**25.0**	0.102	25.140	0.0075	0.0329	**0.842**	0.40	1.3E-02	3.2E-03	4.1E-07	**0.025**
25.0	**50.0**	0.151	24.990	0.0110	0.0440	**0.831**	0.18	2.9E-02	2.4E-03	6.7E-07	**0.037**
50.0	**100.0**	0.202	24.787	0.0148	0.0588	**0.816**	0.20	2.5E-02	1.6E-03	4.0E-07	**0.049**
100.0	**25.0**	-0.038	24.825	-0.0028	0.0560	**0.819**					
25.0	**6.3**	-0.029	24.854	-0.0021	0.0539	**0.821**					
6.3	**12.5**	0.021	24.833	0.0015	0.0554	**0.819**					
12.5	**25.0**	0.010	24.823	0.0007	0.0562	**0.819**	0.18	2.8E-02	3.3E-04	9.1E-08	**0.002**
25.0	**50.0**	0.038	24.785	0.0028	0.0590	**0.816**	0.20	2.5E-02	6.1E-04	1.5E-07	**0.009**
50.0	**100.0**	0.084	24.701	0.0061	0.0651	**0.810**	0.10	5.0E-02	6.8E-04	3.3E-07	**0.020**
100.0	**200.0**	0.196	24.505	0.0144	0.0795	**0.795**	0.25	2.0E-02	8.0E-04	1.6E-07	**0.048**
200.0	**300.0**	0.108	24.397	0.0079	0.0874	**0.787**	0.20	2.5E-02	4.4E-04	1.1E-07	**0.045**
300.0	**100.0**	-0.021	24.418	-0.0015	0.0859	**0.789**					
100.0	**25.0**	-0.050	24.468	-0.0037	0.0822	**0.793**					
25.0	**12.5**	-0.027	24.495	-0.0020	0.0802	**0.795**					
12.5	**25.0**	0.018	24.477	0.0013	0.0815	**0.793**					
25.0	**50.0**	0.041	24.436	0.0030	0.0845	**0.790**	0.18	2.7E-02	6.7E-04	1.8E-07	**0.010**
50.0	**100.0**	0.023	24.413	0.0017	0.0862	**0.789**	0.18	2.7E-02	1.9E-04	5.0E-08	**0.006**
100.0	**200.0**	0.056	24.358	0.0041	0.0903	**0.785**	1.00	4.9E-03	2.3E-04	1.1E-08	**0.014**
200.0	**300.0**	0.048	24.310	0.0035	0.0938	**0.781**	2.00	2.4E-03	2.0E-04	4.7E-09	**0.020**
300.0	**400.0**	0.070	24.240	0.0051	0.0989	**0.776**	2.50	1.9E-03	2.9E-04	5.4E-09	**0.041**
400.0	**600.0**	0.154	24.087	0.0112	0.1101	**0.765**	1.50	3.2E-03	3.2E-04	9.9E-09	**0.064**
600.0	**300.0**	0.000	24.087	0.0000	0.1101	**0.765**					
300.0	**100.0**	-0.059	24.146	-0.0043	0.1058	**0.769**					
100.0	**25.0**	-0.067	24.212	-0.0049	0.1009	**0.774**					
25.0	**12.5**	-0.035	24.247	-0.0025	0.0984	**0.776**					
12.5	**25.0**	0.024	24.223	0.0017	0.1001	**0.775**					
25.0	**50.0**	0.036	24.187	0.0027	0.1028	**0.772**	0.90	5.3E-03	6.0E-04	3.2E-08	**0.009**
50.0	**100.0**	0.039	24.148	0.0029	0.1057	**0.769**	0.70	6.8E-03	3.2E-04	2.2E-08	**0.010**
100.0	**200.0**	0.031	24.117	0.0023	0.1079	**0.767**	0.30	1.6E-02	1.3E-04	2.0E-08	**0.008**
200.0	**300.0**	0.033	24.084	0.0024	0.1103	**0.764**	2.00	2.4E-03	1.4E-04	3.2E-09	**0.014**
300.0	**400.0**	0.036	24.048	0.0026	0.1130	**0.762**	2.00	2.4E-03	1.5E-04	3.5E-09	**0.021**
400.0	**600.0**	0.053	23.995	0.0039	0.1168	**0.758**	1.00	4.7E-03	1.1E-04	5.1E-09	**0.022**
600.0	**800.0**	0.089	23.906	0.0065	0.1233	**0.751**	2.00	2.4E-03	1.9E-04	4.3E-09	**0.052**
800.0	**1600.0**	0.306	23.601	0.0224	0.1458	**0.729**	2.00	2.3E-03	1.6E-04	3.6E-09	**0.074**
1600.0	**3200.0**	0.405	23.195	0.0297	0.1754	**0.699**	0.50	9.0E-03	1.1E-04	9.5E-09	**0.099**
3200.0	**800.0**	-0.018	23.213	-0.0013	0.1741	**0.701**					
800.0	**200.0**	-0.049	23.262	-0.0036	0.1705	**0.704**					
200.0	**50.0**	-0.084	23.346	-0.0062	0.1644	**0.710**					

Klohn Crippen Berger

PROJECT NO.:			
PROJECT:	Fundão Tailings Dam Review Panel		
LOCATION:		DATE TESTED:	2016-06-24
SAMPLE NO.:	PSD 1	DEPTH	
TESTED BY:	JG	CHECKED BY:	BY

Consolidation Test - PSD 1

e - log(p)

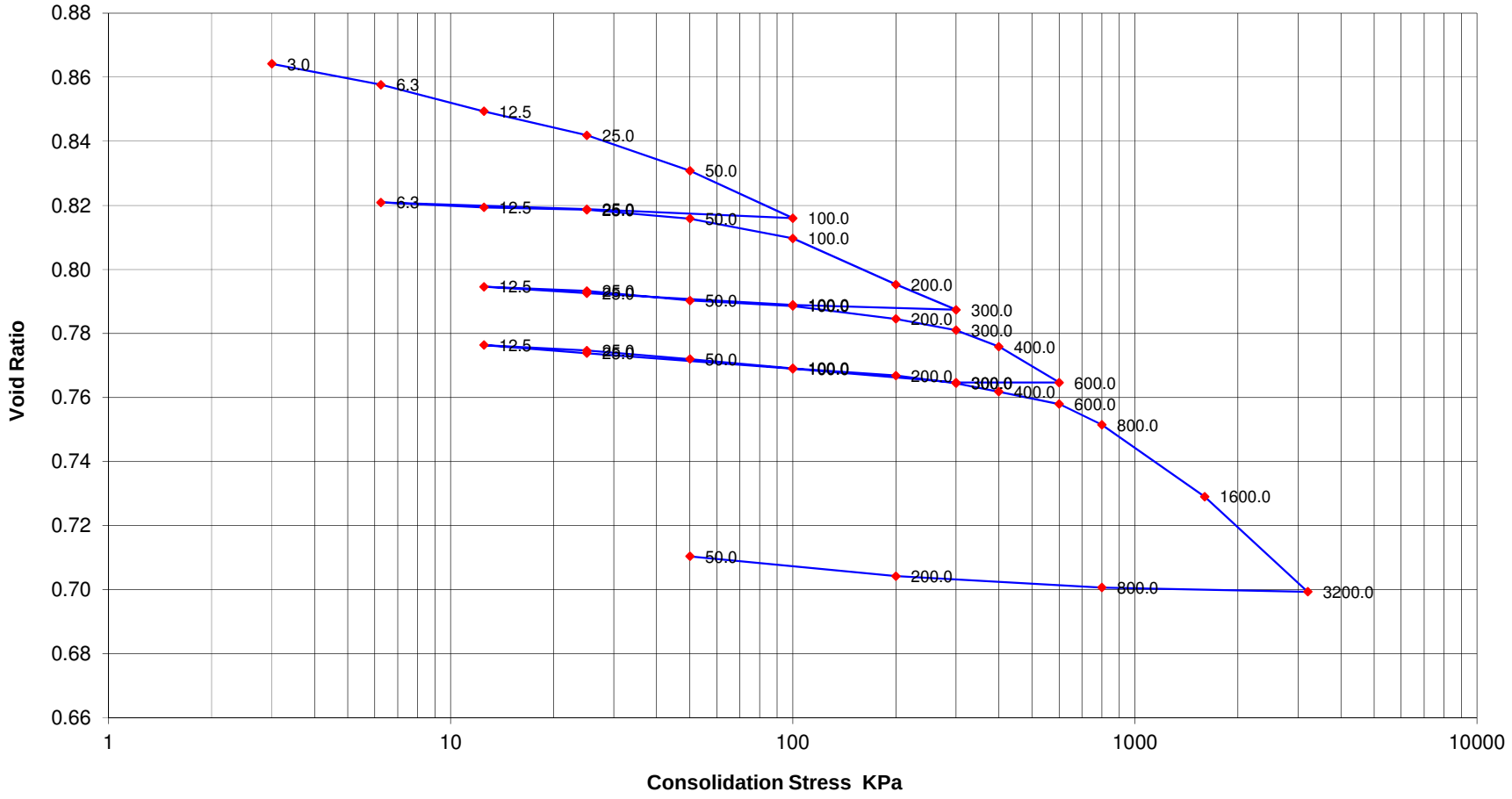

Klohn Crippen Berger	PROJECT NO.:			
	PROJECT:	Fundão Tailings Dam Review Panel		
	LOCATION:		DATE TESTED:	2016-06-24
	SAMPLE NO.:	PSD 1	DEPTH:	
	TESTED BY:	JG	CHECKED BY:	BY

CONSOLIDATION

PROJECT NO.:
PROJECT: Fundão Tailings Dam Review Panel
SAMPLE NO.: Germano Slimes
DETAILS As received, remoulded

TEST NO.: CONS01
LOADING MACHINE NO.: OED2 / ID81

Test Specimen Information:

Initial water content:	27.23	% (based on trimmings)
Final water content:	19.11	% (based on final dry weight)
Dry mass:	153.22	g
Diameter	63.52	mm
Area	31.689	cm^2
Specific Gravity	3.93	

Initial Specimen Height (mm): 25.60
Height of Solid (mm): 12.303
Initial void ratio: 1.081
Void Ratio Factor 0.0813

* Calibration to be done after test
** Estimated t_{90}

Pressure (kPa)		*Change in Height	Final	Change in	Change in	Void	t_{90}**	Cv	Mv	k	Cc
From	To	Corrected (mm)	Height (mm)	Void Ratio	Void Ratio Acc	Ratio	(min)	(cm^2/sec)	(cm^2/N)	(cm/sec)	
0.0	**2.0**	0.130	25.470	0.0106	0.0106	**1.070**					
2.0	**4.0**	0.285	25.185	0.0232	0.0337	**1.047**	47.61	4.8E-04	5.6E-02	2.6E-07	**0.077**
4.0	**8.0**	0.376	24.809	0.0306	0.0643	**1.017**	26.01	8.5E-04	3.7E-02	3.1E-07	**0.102**
8.0	**16.0**	0.374	24.435	0.0304	0.0947	**0.986**	9.00	2.4E-03	1.9E-02	4.4E-07	**0.101**
16.0	**32.0**	0.416	24.019	0.0338	0.1285	**0.952**	11.56	1.8E-03	1.1E-02	1.9E-07	**0.112**
32.0	**64.0**	0.463	23.556	0.0377	0.1662	**0.915**	6.25	3.2E-03	6.0E-03	1.9E-07	**0.125**
64.0	**128.0**	0.534	23.022	0.0434	0.2096	**0.871**	2.25	8.5E-03	3.5E-03	3.0E-07	**0.144**
128.0	**256.0**	0.534	22.488	0.0434	0.2529	**0.828**	1.00	1.8E-02	1.8E-03	3.3E-07	**0.144**
256.0	**512.0**	0.588	21.900	0.0478	0.3007	**0.780**	1.21	1.4E-02	1.0E-03	1.4E-07	**0.159**
512.0	**1024.0**	0.579	21.322	0.0470	0.3478	**0.733**	1.00	1.7E-02	5.2E-04	8.4E-08	**0.156**

Klohn Crippen Berger

PROJECT NO.:			
PROJECT:	Fundão Tailings Dam Review Panel		
LOCATION:		DATE TESTED:	2016-02-01
SAMPLE NO.:	Germano Slimes	DETAILS	As received, remoulded
TESTED BY:	JG	CHECKED BY:	BY

Consolidation Test - Germano Slimes

e - log(p)

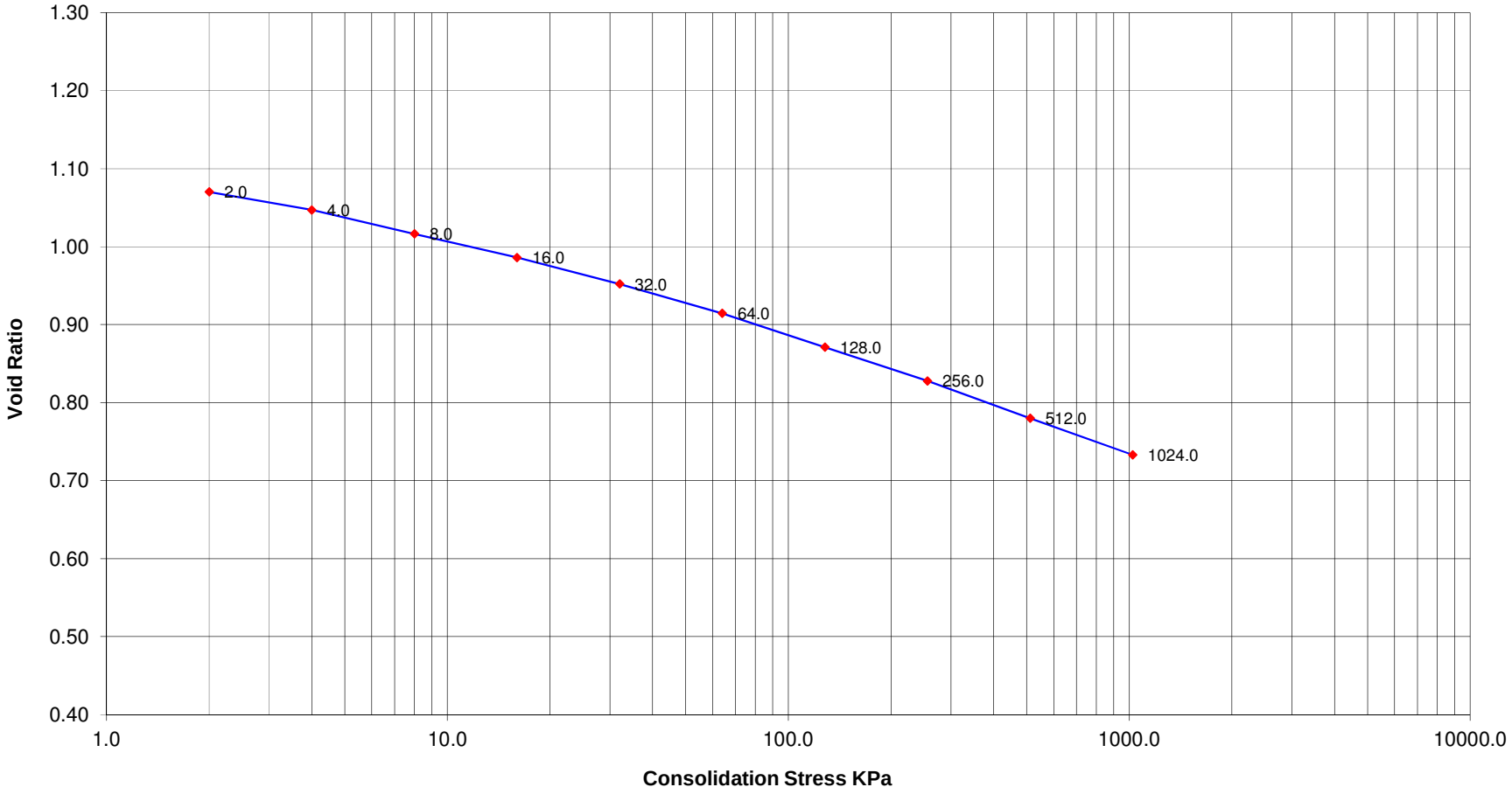

Klohn Crippen Berger

PROJECT NO.:			
PROJECT:	Fundão Tailings Dam Review Panel		
LOCATION:		DATE TESTED:	2016-02-01
SAMPLE NO.:	Germano Slimes	DEPTH:	As received, remoulded
TESTED BY:	JG	CHECKED BY:	BY

ATTACHMENT D9

University of Alberta Sedimentation/Consolidation Test on Slimes

UNIVERSITY OF ALBERTA

Large Strain Consolidation Testing of Flotation Tailings

Prepared for

Klohn Crippen Berger

Prepared by

Louis K. Kabwe, Ph.D.
Research Associate

and

Ward G. Wilson, Ph.D., P.Eng., P.Geol., FCAE
Principle Investigator

June 2016

The UofA Geotechnical Centre

Table of Contents

APPENDICES

List of Tables (main body)

List of Figures (main body)

List of Figures in Appendix A

List of Tables in Appendix B

List of Figures in Appendix C

1. INTRODUCTION

Klohn Crippen Berge contracted the University of Alberta Geotechnical Centre to perform Large Strain Consolidation (LSC) testing services for Flotation Tailings.

This report consists of two main parts: the main body and the appendices. Detailed data are presented in tables and figures in appendices. The tables and figures in the main body of the report summarize the results of the tests, and are briefly discussed. The appendix tables and figures will not be discussed and are presented so the report includes all data from the testing program. Large files of measurement data are not included in this report but will be transmitted to Klohn electronically.

2. TAILINGS SAMPLE

A 15 L container of tailings sample was received from Klohn Crippen Berge for LSC testing program. The solids content of the sample was measured upon arrival and was found to be over 76 %. The specific gravity of the sample (3.85) was not measured in this test but was provided by Klohn. The solids content of the sample was reduced to about 50% by mixing the sample with distilled water. The decanted water after mixing was used for hydraulic conductivity measurement at the end of consolidation for each load step. The water chemistry of the tailings sample was measured and results are presented in Appendix B.

3. LARGE STRAIN CONSOLIDATION TEST

The objectives of the LSC tests are:

- To determine the relationship between effective stress and void ratio.
- To determine the relationship between void ratio and hydraulic conductivity (permeability of water).

3.1 Large Strain Consolidation LSC Apparatus

A LSC test was performed in a standard consolidation apparatus (150 mm dia. x 150 mm high). The LSC apparatus used in this testing program confines the slurried material so it can be tested at any water content. The first applied stress, the self-weight of the slurry, can be about 0.3 to 0.5 kPa. Effective stresses up to about 10 kPa were applied by dead loads acting on the piston (Figure A1 in Appendix A). Effective stresses over 10 kPa were applied in a loading fram by an air pressure Bellofram. Subsequent loads were approximately doubled for each load step up to 1000 kPa maximum. The setup of the LSC test used at the geotechnical centre of the University of Alberta is shown in Figures 1 and Figure A1 in Appendix A.

Figure 1. Set up of the large strain consolidation LSC test at the Geotechnical Centre of the University of Alberta.

3.2 Determination of End of Consolidation

When a load is applied, the progress of the consolidation is evaluated by monitoring the change in height of the sample (vertical strain) with a LVDT and by measuring the pore pressure at the

base of the sample. The load is maintained until the vertical strain/or base pore pressure dissipation are significantly completed before adding the next load as shown in Figures 1 and 2.

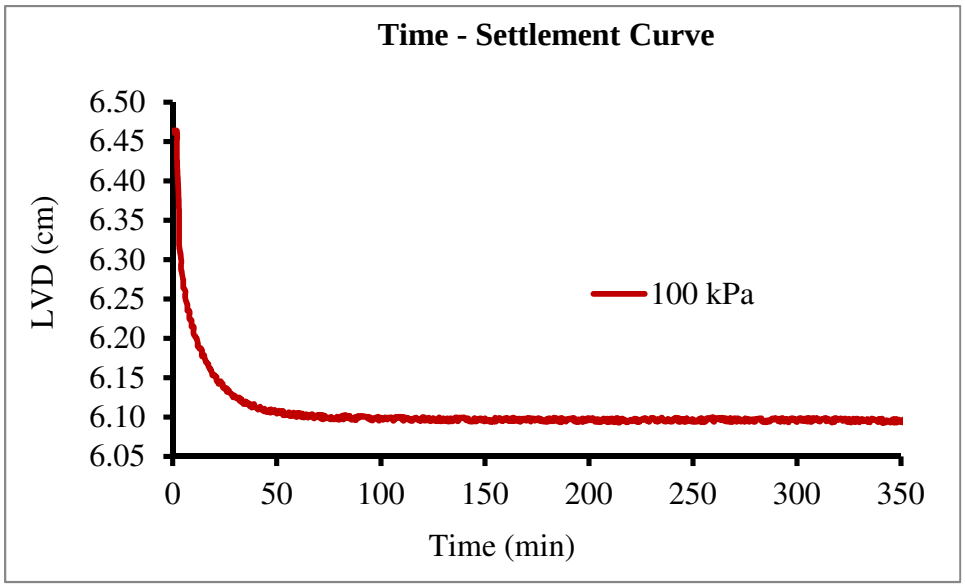

Figure 2. Typical time-settlement curve in LSC test.

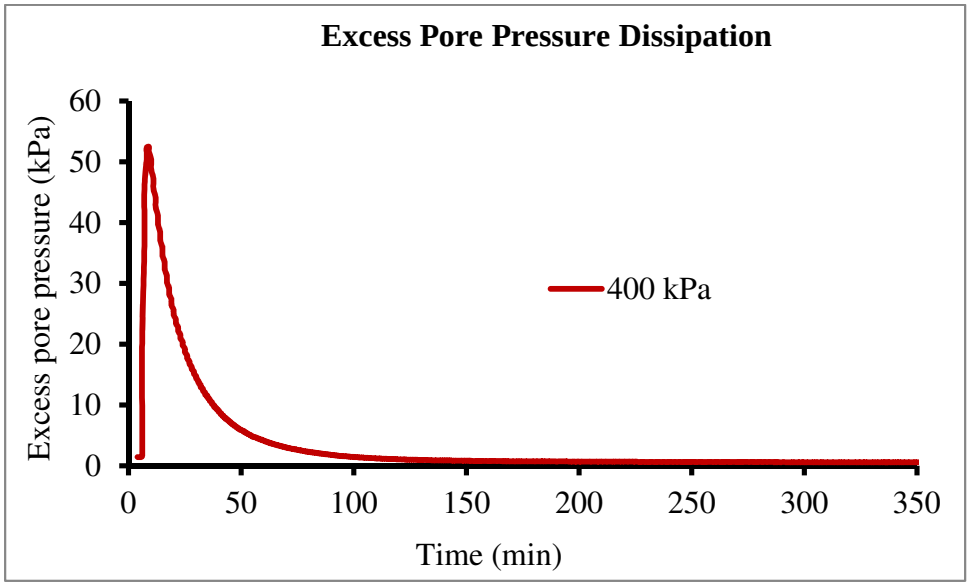

Figure 3. Typical excess pore pressure dissipation curve in LSC test.

3.3 Hydraulic Conductivity (Permeability) Test

The permeability was measured at the end of consolidation for each load step. An upward flow constant head test was performed with the head difference h ($h=h_o-h_1$) being kept small enough so that seepage forces will not exceed the applied stress and cause sample fracturing during the permeability test.

In one dimension, water flows through a fully saturated soil sample in accordance with Darcy's empirical law is given by:

$$q = Aki$$

or

$$v = \frac{q}{A} = ki$$

Where q = volume of water flowing per unit time, A = cross-sectional area of soil sample corresponding to the flow q, k = coefficient of permeability, i = hydraulic gradient, and v = discharge velocity. The hydraulic gradient, i, is given by:

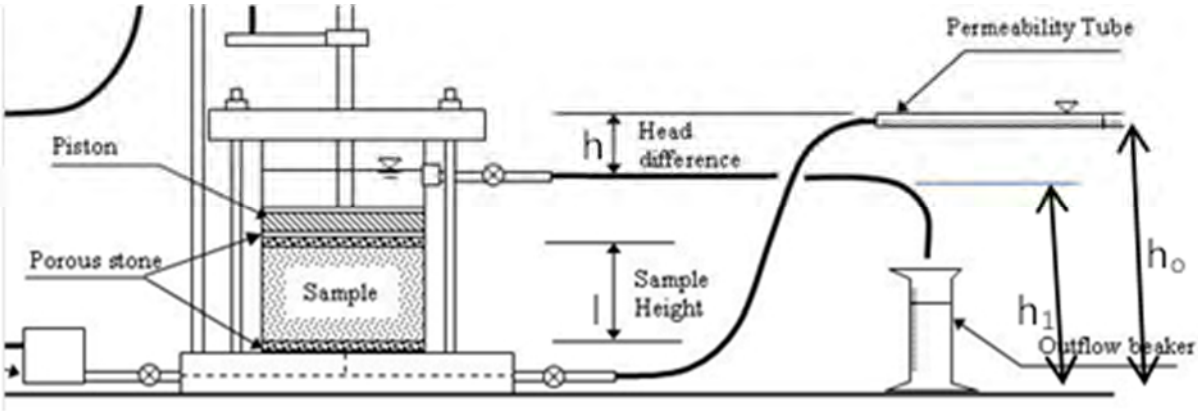

Figure 4. Setup of permeability measurement.

$$i = \frac{h}{l} = \frac{h_o - h_1}{l}$$

Where

l = the length of the sample.

The inflow is monitored to ensure that steady state flow conditions are obtained. The units of the

coefficient of permeability are those of velocity (m/s).

For a given soil, the coefficient of permeability is a function of void ratio. The coefficient of permeability depends primarily on the average size of the pores, which in turn is related to the distribution of particles sizes, particle shape and soil structure. The presence of a small percentage of fines in a coarse-grained soil results in a value of k significantly lower than the value for the same soil without fines.

3.4 Van Shear Test

The laboratory vane shear test consists of inserting a four-bladed vane in the end of a tube sample and rotating it at a constant rate to determine the torque required to cause a cylindrical surface to be sheared by the vane. This torque is then converted to unit shearing resistance of the cylindrical surface area. The torque is measured by a calibrated torque transducer that is attached directly to the vane. The undrained shear strength is calculated using the following expression:

$T = \tau \times K$

Where:

T = torque, lbf.ft (N.m)

τ = undrained shear strength, lbf/ft^2 (Pa), and

K = vane blade constant, ft^3 (m^3).

T and K are given as follows (assuming the distribution of the shear strength is uniform across the ends of the failure cylinder and around the perimeter):

$$T = \frac{\pi D_v^3}{2}\left(\frac{H}{D_v} + \frac{1}{3}\right)\tau_y$$

$$\tau_y = \frac{T}{K}$$

$$K = \frac{\pi D_v^3}{2}\left(\frac{H}{D_v} + \frac{1}{3}\right)$$

Where:

D_v = measured diameter of the vane, in. (mm),

H = measured height of the vane, in. (mm).

4. SUMMARY OF RESULTS

The LSC tests results are summarized in Tables 1 and 2 and in Figures 4 and 5.

Table 1. Summary of measured large strain consolidation properties of tailings sample.

Load	Effective stress (kPa)	Sample height (cm)	Void ratio	Hydraulic conductivity (m/s)	Solids content (%)
Self-weight settling	0.4	7.0	2.61	7.84E-08	50.0
Load-1	1.1	6.5	2.34	6.67E-08	60.4
Load-2	2.0	6.0	2.08	3.88E-08	63.3
Load-3	2.9	5.8	1.93	3.13E-08	64.9
Load-4	3.8	5.6	1.85	2.87E-08	65.9
Load-5	8.4	5.3	1.67	1.83E-08	68.2
Load-6	13.0	5.0	1.53	1.33E-08	70.0
Load-7	30	4.6	1.27	6.97E-09	73.8
Load-8	100	4.2	1.08	3.66E-09	76.9
Load-9	200	4.1	1.02	2.43E-09	77.9
Load-10	400	3.9	0.94	2.22E-09	79.1
Load-11	600	3.8	0.89	1.83E-09	80.0
Load-12	1000	3.7	0.83	1.21E-09	81.1

Table 2. Summary of tailings sample properties.

Tailings sample (Gs = 3.85)	**Initial (prior to consolidation)**	**Final (after 1000 kPa effective stress)**
Solids content (oven-dry) (%)	50	82
Void ratio (oven-dry)	2.61	0.85
Shear strength (kPa)		144

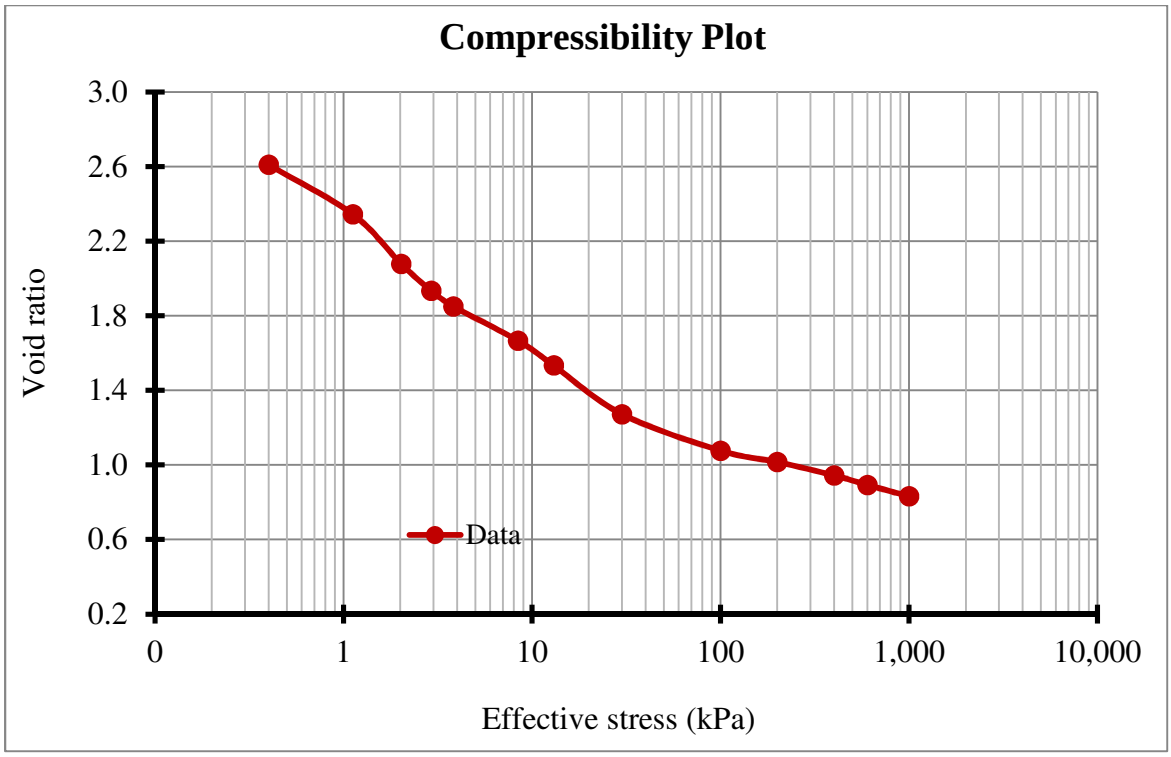

Figure 4. Compressibility plot (void ratio vs effective stress) of the tailings sample.

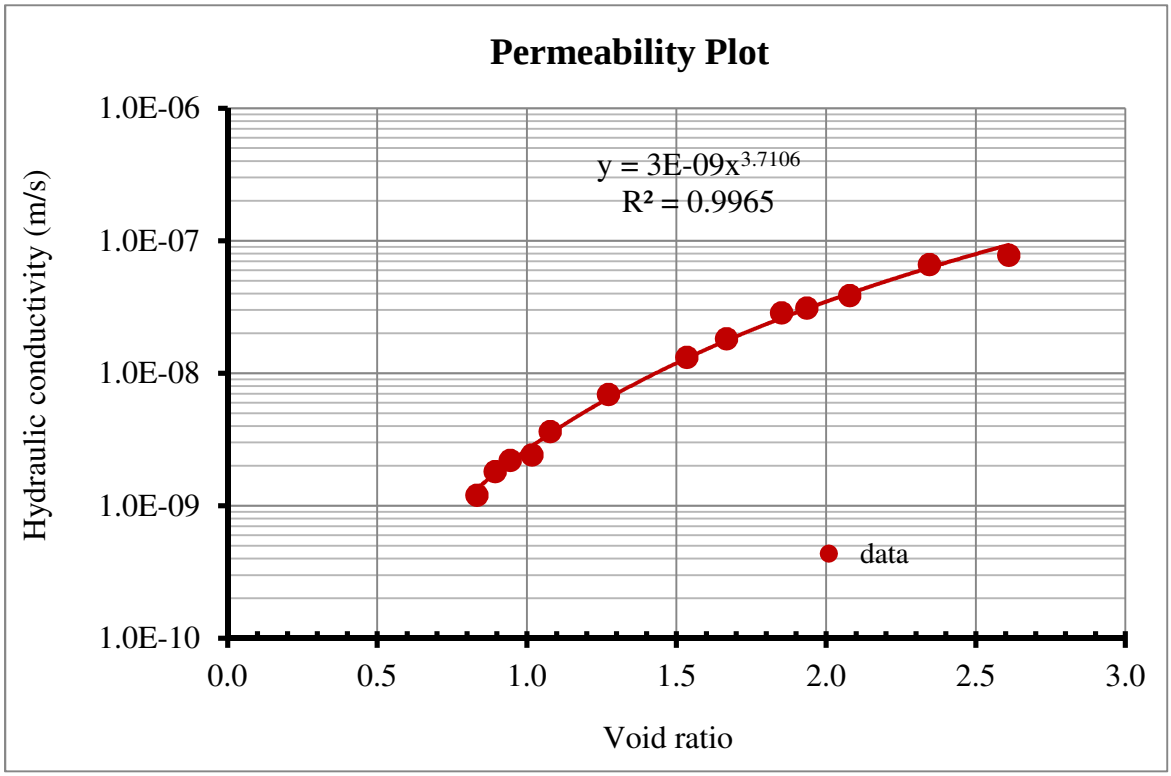

Figure 5. Permeability plot (hydraulic conductivity vs void ratio) of the tailings sample.

5. OBSERVATIONS

Figure 4 shows that the compressibility (the relationship between void ratio e and effective stress σ') increases linearly when effective stresses are between 2 and 30 kPa. The compression index C_c (i.e., the slope of the linear portion of the e-logσ' curve) is about 0.026.

Figure 5 shows the relationship between hydraulic conductivity k and void ratio e. The k decreases exponentially as e decreases. The k decreases by one order of magnitude (i.e., from 7.84×10^{-8} m/s to 6.97×10^{-9} m/s) when e decreases from 2.6 to 1.27. By fitting a mathematical equation to the data points, it is found that a power law yields the prediction equation with high correlation coefficient (R^2=0.996) for the tailings sample tested.

APPENDIX A

Large Strain Consolidation Set Up at the University of Alberta Geotechnical Centre

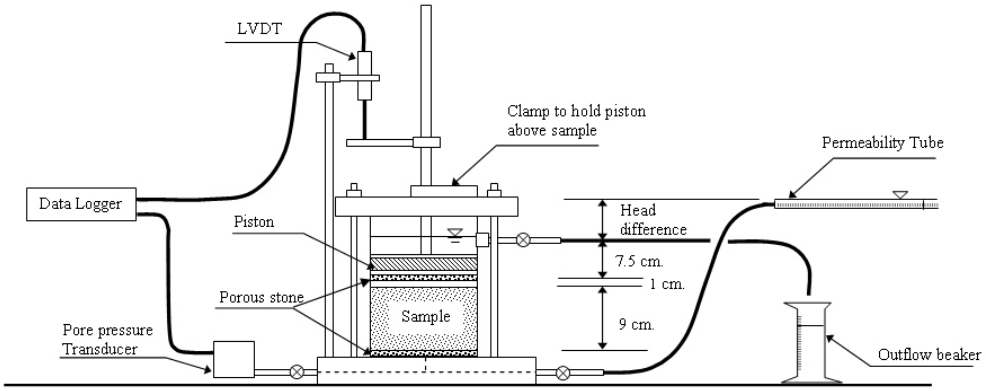

Figure A1. Initial set up of the large strain consolidation test before loading sample

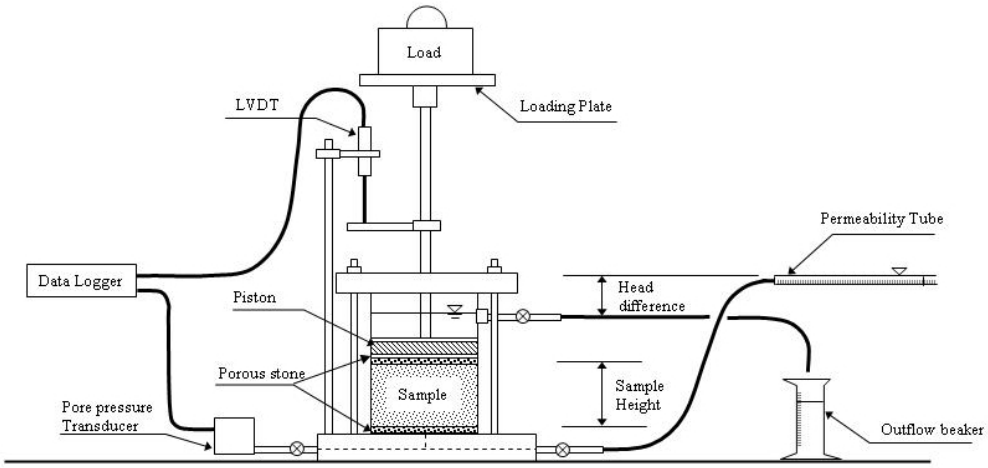

Figure A2. Sample loaded with piston and dead loads up to about 10 kPa

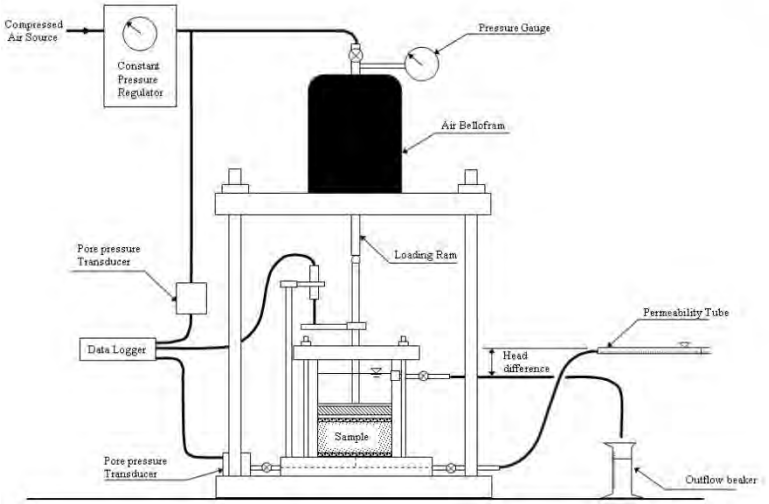

Figure A3. Sample in loading frame and loaded by Bellofram up to 1000 kPa.

APPENDIX B

Tailings Sample Water chemistry

Table B1: Anions concentrations in tailings water sample.

	mg/L	mmol/L	mEq/L
fluoride	0.34	1.790E-02	1.790E-02
chloride	5.13	1.447E-01	1.447E-01
nitrite	0.72	1.565E-02	1.565E-02
bromide	0	0	0
sulphate	36.0505	3.753E-01	7.506E-01
nitrate	14.675	2.367E-01	2.367E-01
phosphate	0	0	0
bicarbonate	2.092E+01	3.428E-01	3.428E-01
carbonate	2.417E-03	4.027E-05	8.054E-05

Table B2: Cations concentrations in tailings water sample.

	mg/L	mmol/L	mEq/L
Na23	30.61064	1.331	1.33089739
Mg26	0.0448	1.723E-03	3.446E-03
Si28	1.52866	5.460E-02	2.184E-01
K39	1.96852	5.047E-02	5.047E-02
Ca43	16.67744	3.878E-01	7.507E-01
Ca44	15.9656	3.629E-01	
Cr52	0.0072	1.385E-04	4.154E-04
Ni58	0.00302	5.207E-05	2.083E-04
Cu63	0.00206	3.270E-05	6.540E-05
Zn64	0.0152	2.375E-04	4.775E-04
Zn66	0.01584	2.400E-04	
Sr86	0.15002	1.744E-03	3.019E-03
Sr88	0.1122	1.275E-03	
Mo95	0.00756	7.958E-05	3.133E-04
Mo96	0.0074	7.708E-05	
Ba138	0.00634	4.594E-05	9.188E-05

Table B3: Other tailings water chemistry (OH^- & H^+)

	mmol/L	mEq/L			mEq/L
OH-	2.512E-05	2.512E-05		negative	-1.508422783
H+	3.981E-04	3.981E-04		positive	2.358889696
				difference	0.850466913

APPENDIX C

Time – Settlement Plots and Excess Pore Pressure Dissipation Plots for the Large Strain Consolidation LSC Test

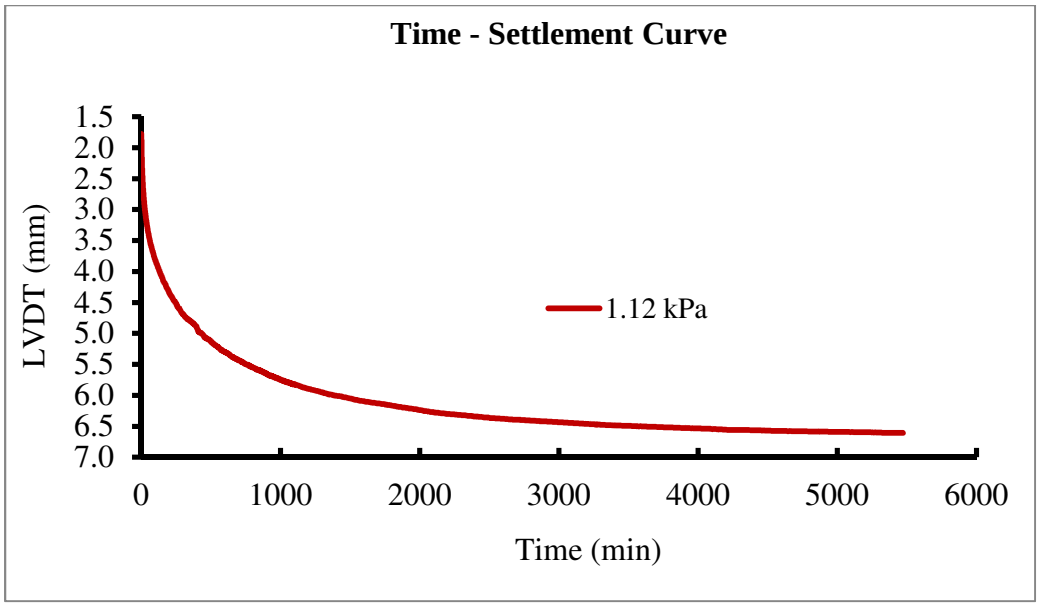

Figure C1. Time – settlement curve for 1.12 kPa effective stress.

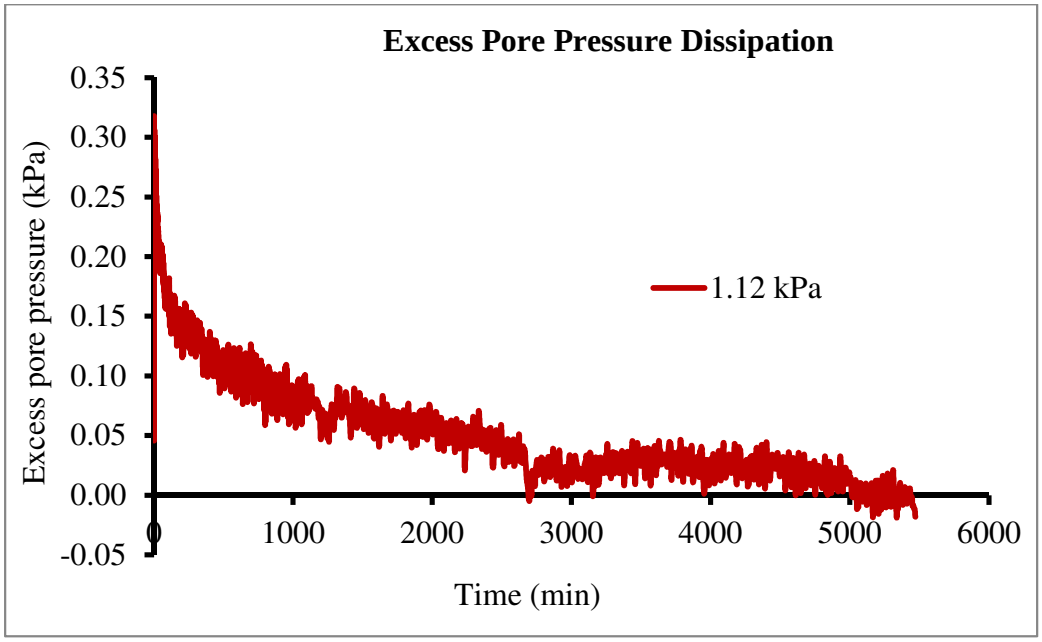

Figure C2: Excess pore pressure dissipation for 1.12 kPa effective stress.

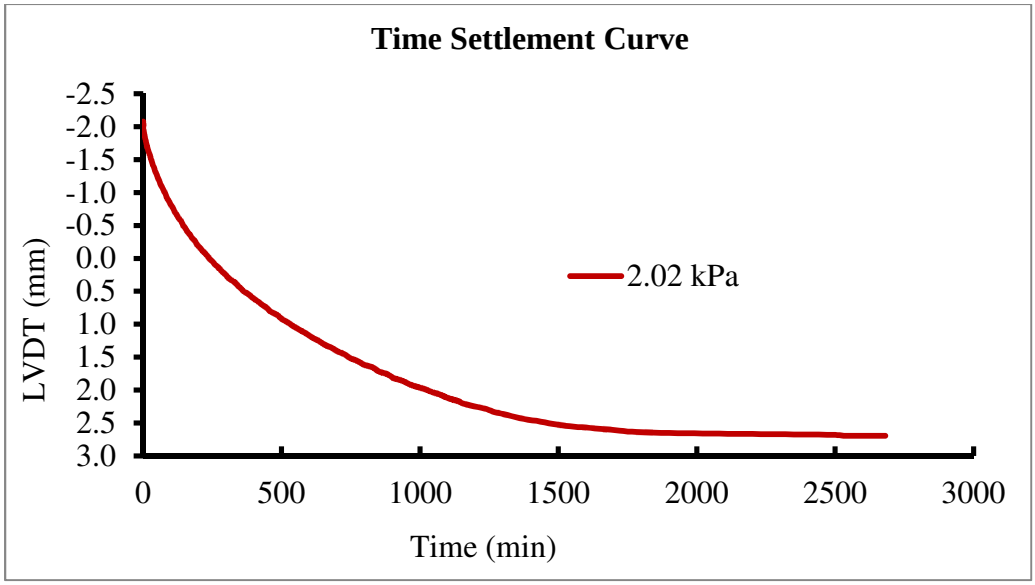

Figure C3. Time – settlement curve for 2.02 kPa effective stress.

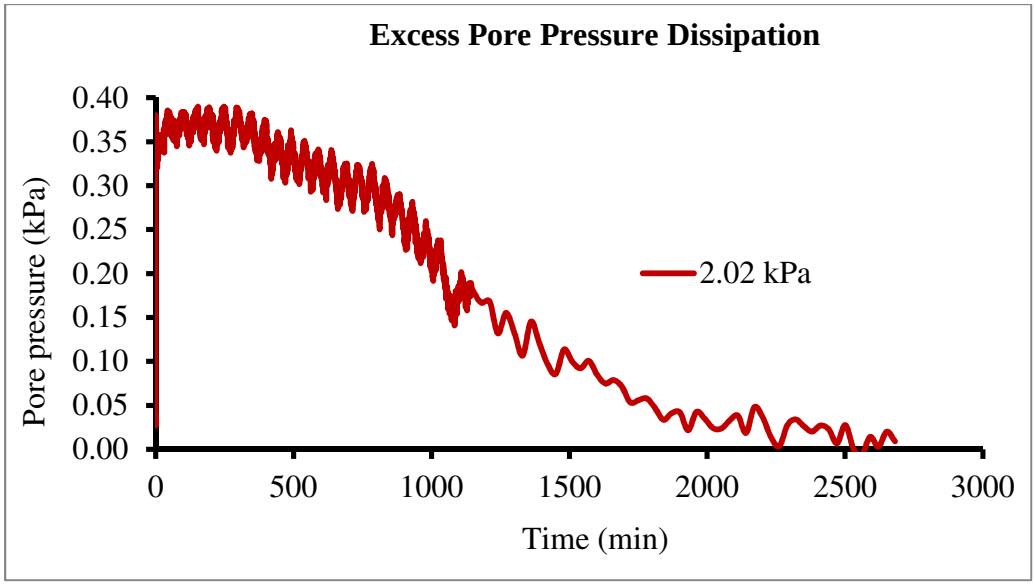

Figure C4: Excess pore pressure dissipation for 2.02 kPa effective stress.

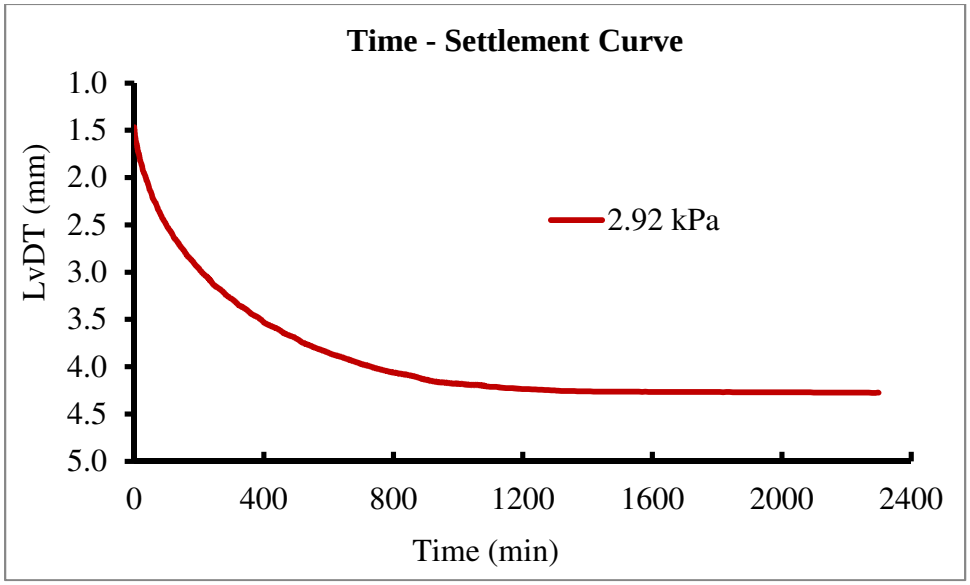

Figure C5. Time – settlement curve for 2.92 kPa effective stress.

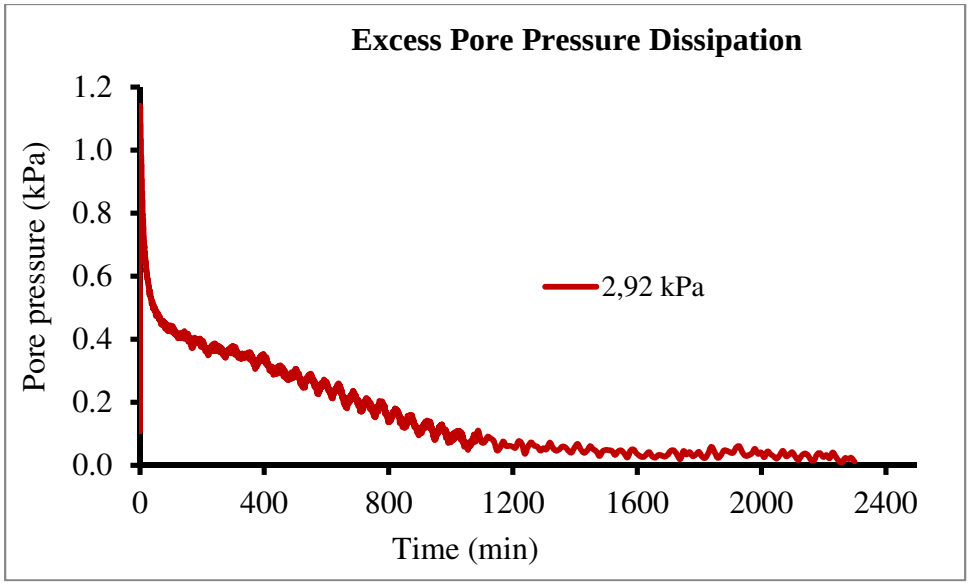

Figure C6: Excess pore pressure dissipation for 2.92 kPa effective stress.

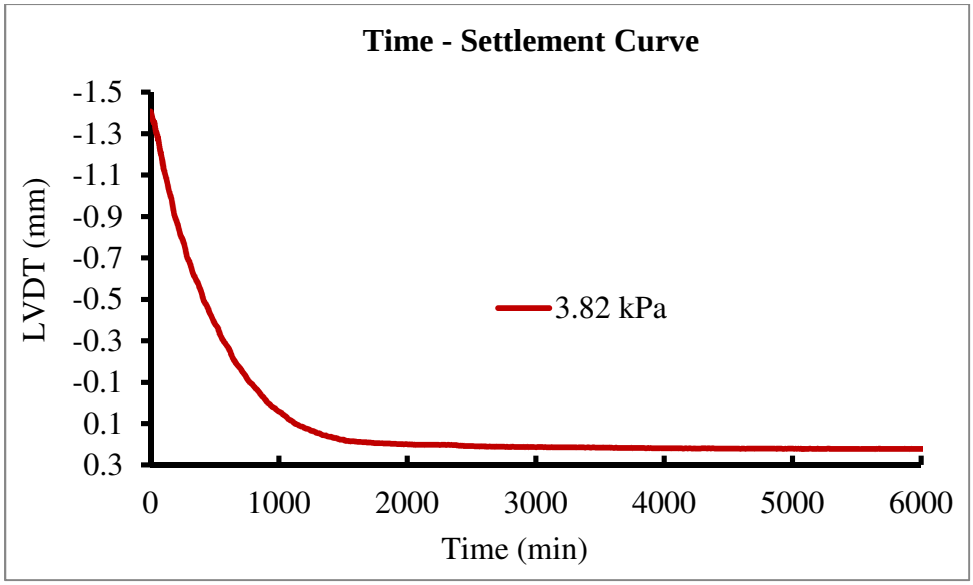

Figure C7. Time – settlement curve for 3.82 kPa effective stress.

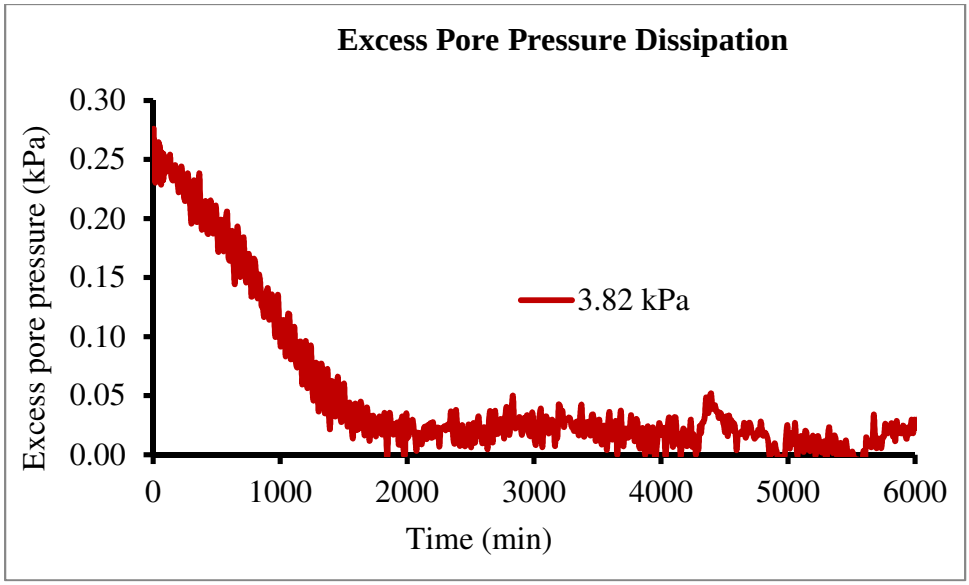

Figure C8: Excess pore pressure dissipation for 3.82 kPa effective stress.

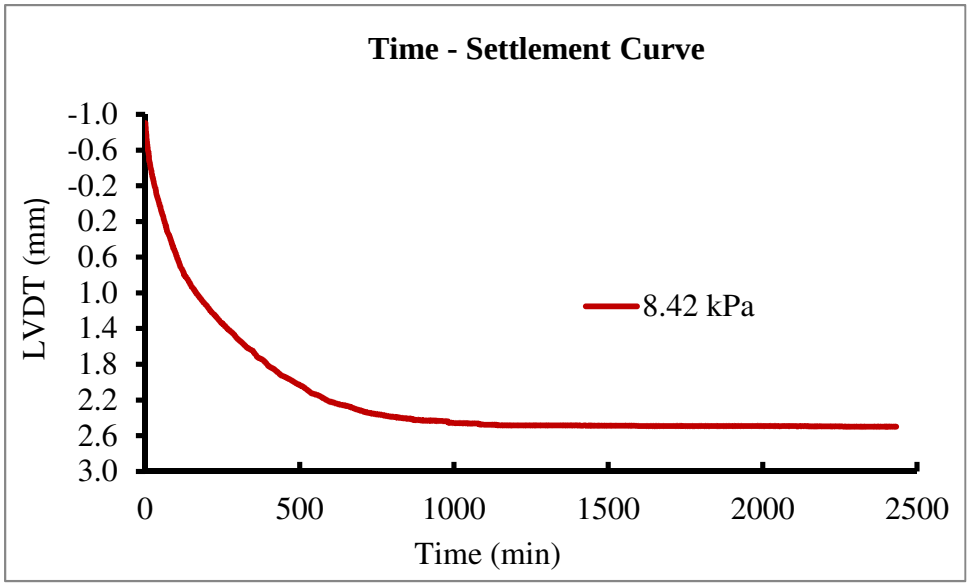

Figure C9. Time – settlement curve for 8.42 kPa effective stress.

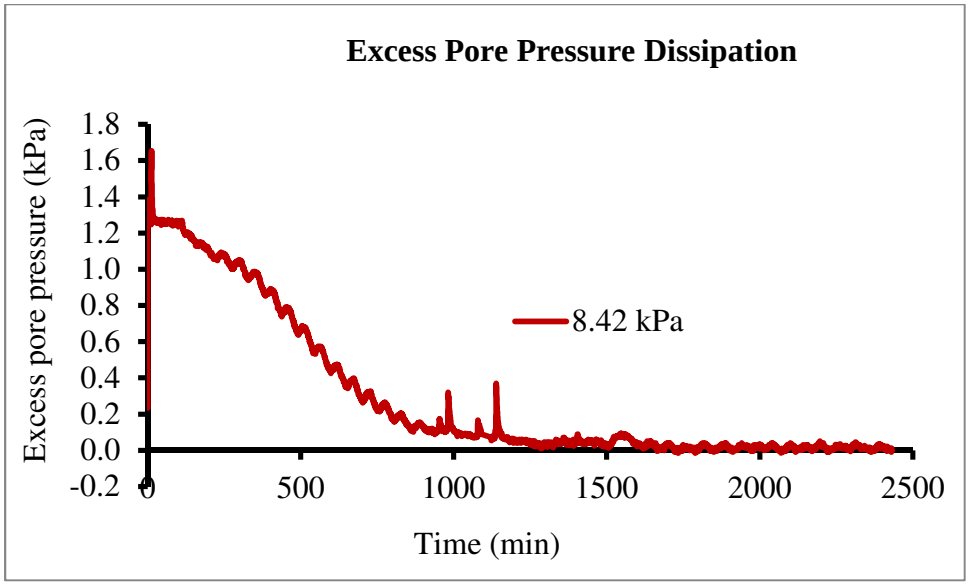

Figure C10: Excess pore pressure dissipation for 8.42kPa effective stress.

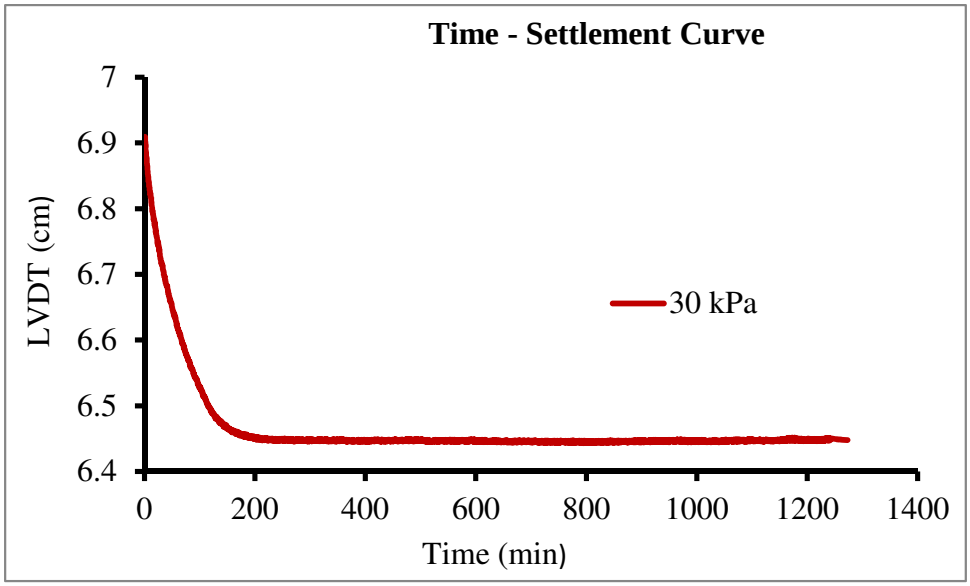

Figure C11. Time – settlement curve for 30 kPa effective stress.

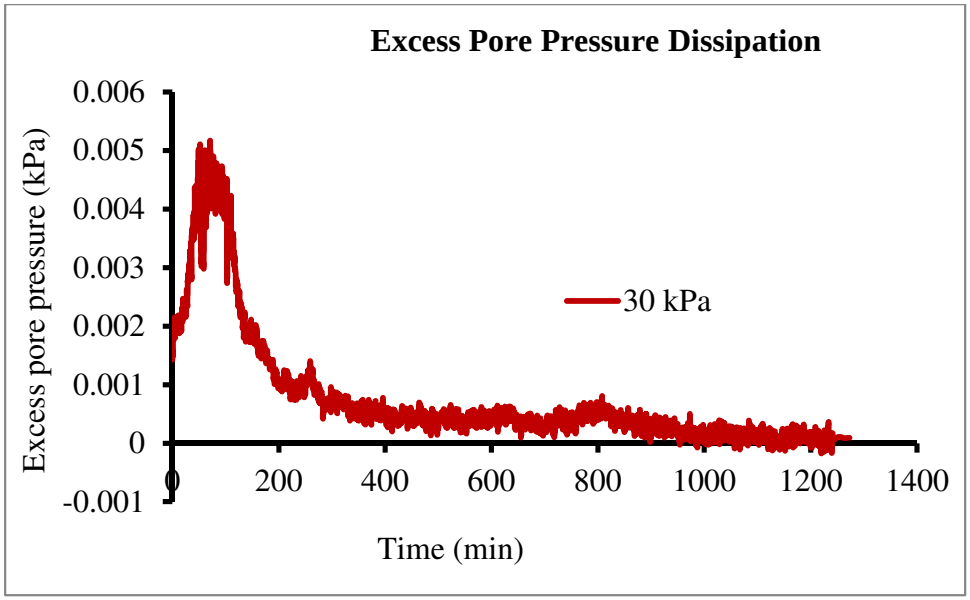

Figure C12: Excess pore pressure dissipation for 30 kPa effective stress.

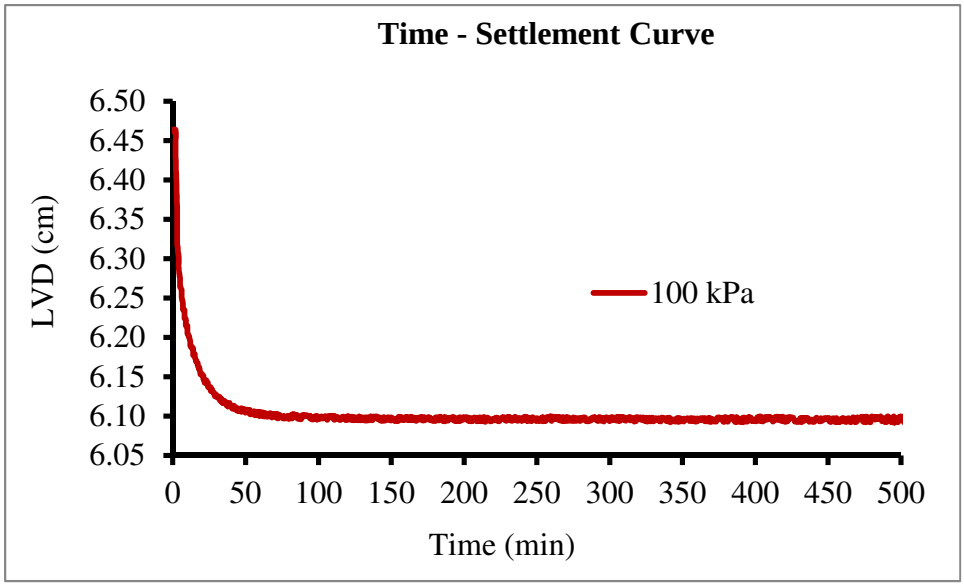

Figure C13. Time – settlement curve for 100 kPa effective stress.

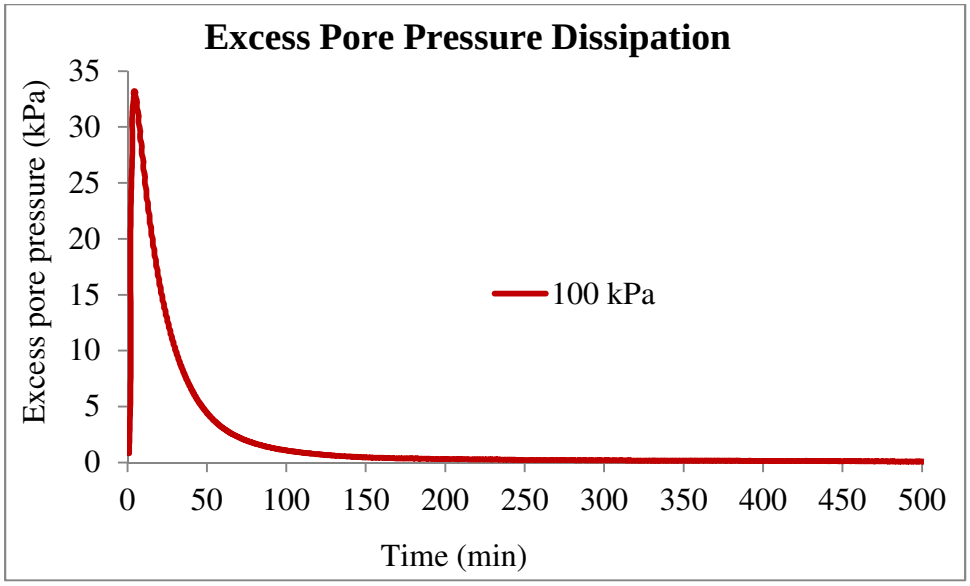

Figure C14: Excess pore pressure dissipation for 100 kPa effective stress.

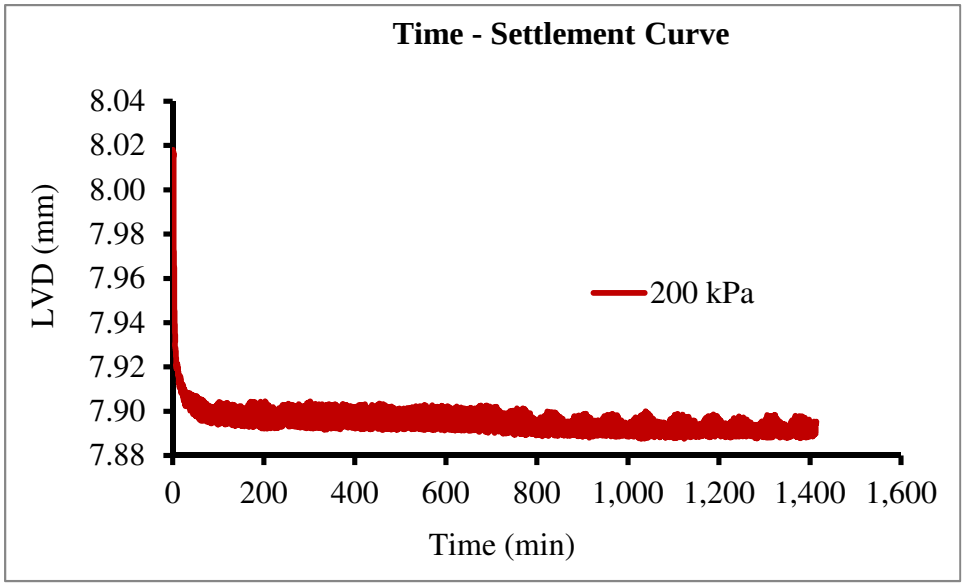

Figure C15. Time – settlement curve for 200 kPa effective stress.

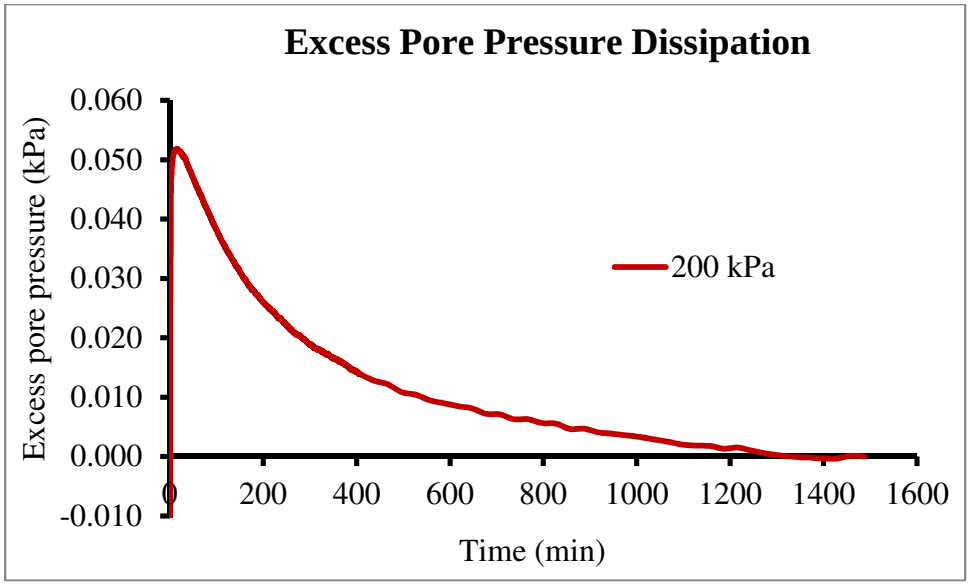

Figure C16: Excess pore pressure dissipation for 200 kPa effective stress.

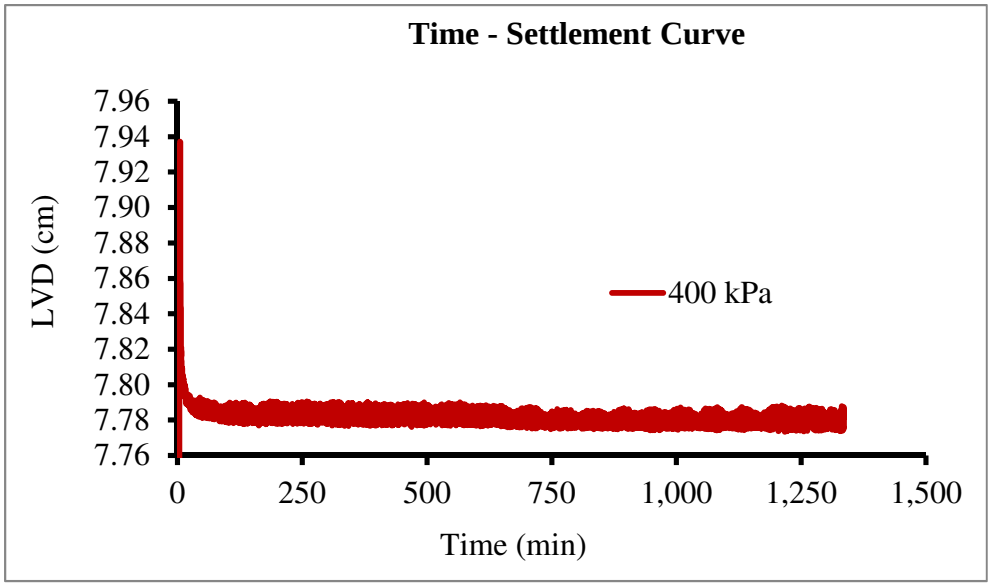

Figure C17. Time – settlement curve for 400 kPa effective stress.

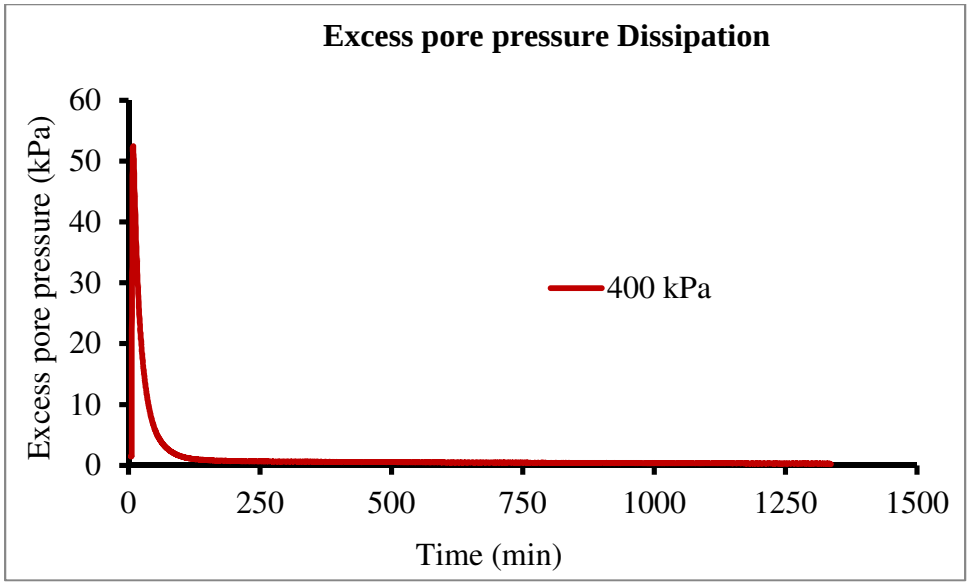

Figure C18: Excess pore pressure dissipation for 400 kPa effective stress.

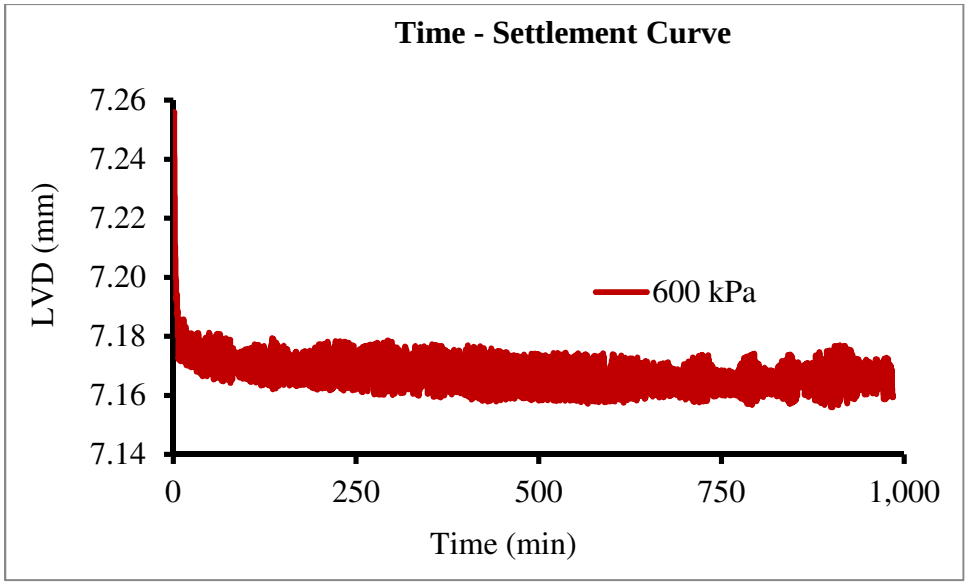

Figure C19. Time – settlement curve for 600 kPa effective stress.

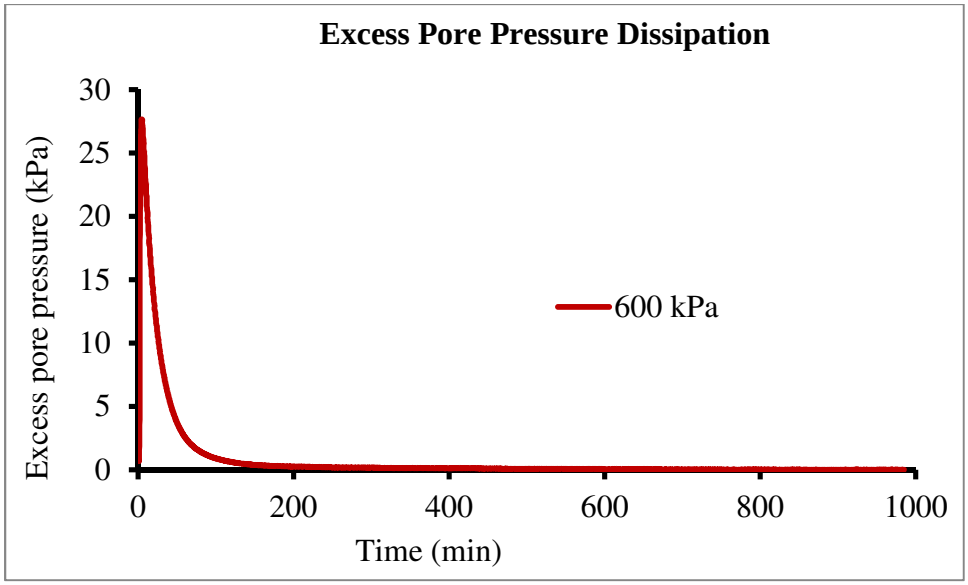

Figure C20: Excess pore pressure dissipation for 600 kPa effective stress.

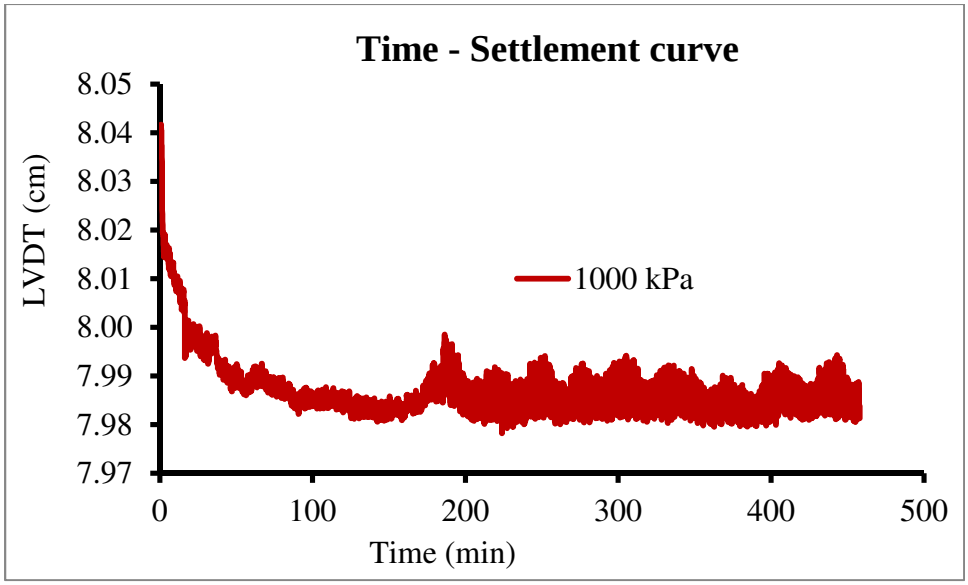

Figure C21. Time – settlement curve for 1000 kPa effective stress.

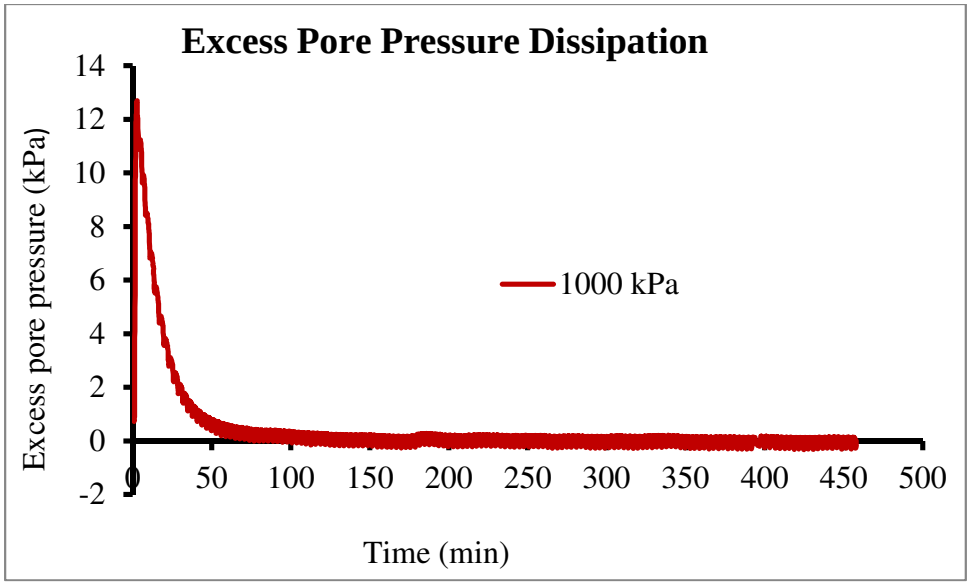

Figure C22: Excess pore pressure dissipation for 1000 kPa effective stress.

Summary of Settlement Test

1. Settlement Test Setup

The settlement test was conducted in the same cell used for the consolidation tests (150 mm dia. x 150 mm high) (Figures 4 and 5). The sample slurry of 48% solids content was prepared from the original sample (as received) by dilution with distilled water. The void ratio of 4.17 was calculated using the specific gravity of Gs = 3.85 provided by Klohn Crippen Berger. The initial sample height was 7 cm (Figure 4) and final sample height after settling was 5.5 cm. The change of sample height (interface) was measured at different time interval by visual observation on a measuring tape placed on the consolidation cell. The total pore water pressure was continuously monitored at the base of the sample using a transducer (Figure 4).

2. Summary of Settlement Test results

Figures 1 and 2 show the change of sample interface (sample height) and dissipation of excess pore pressure measured with time. It is noted that Figure 2 shows immediate decrease in excess pore pressure with settlement of the interface. As the excess pore pressure fully dissipates the sample has also settled completely. **Consolidation is defined as dissipation of excess pore pressure, therefore this is a settling process not a sedimentation process.**

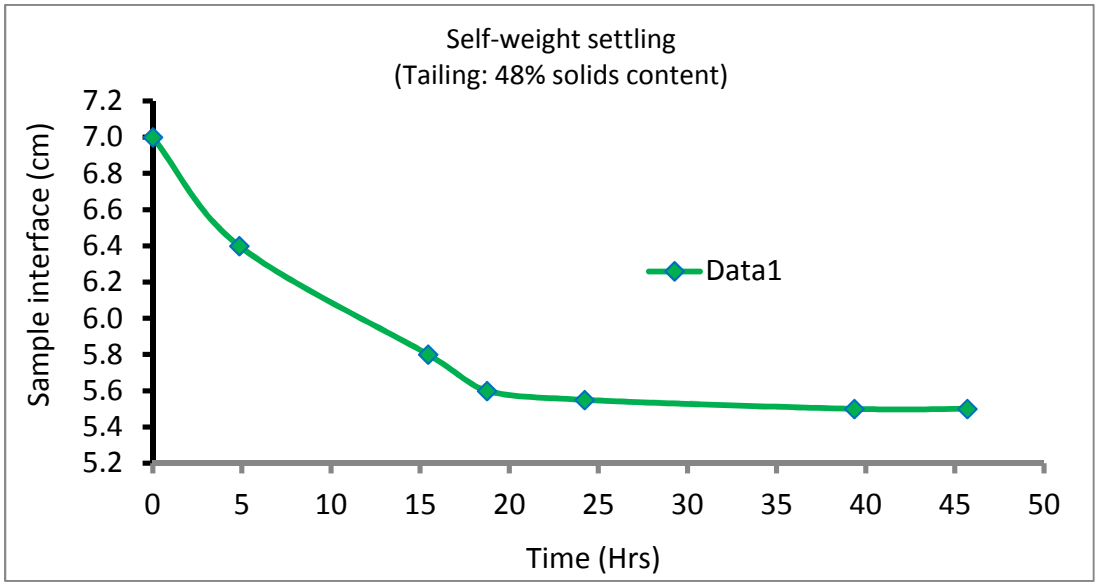

Figure 1. Interface settlement measured with time during settlement.

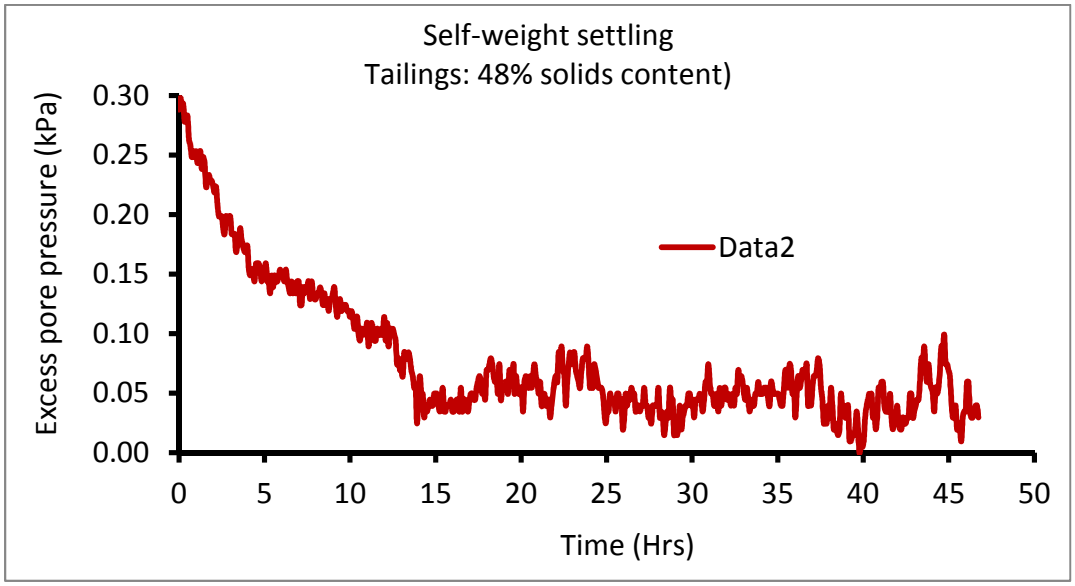

Figure 2. Excess pore pressure dissipation during settlement.

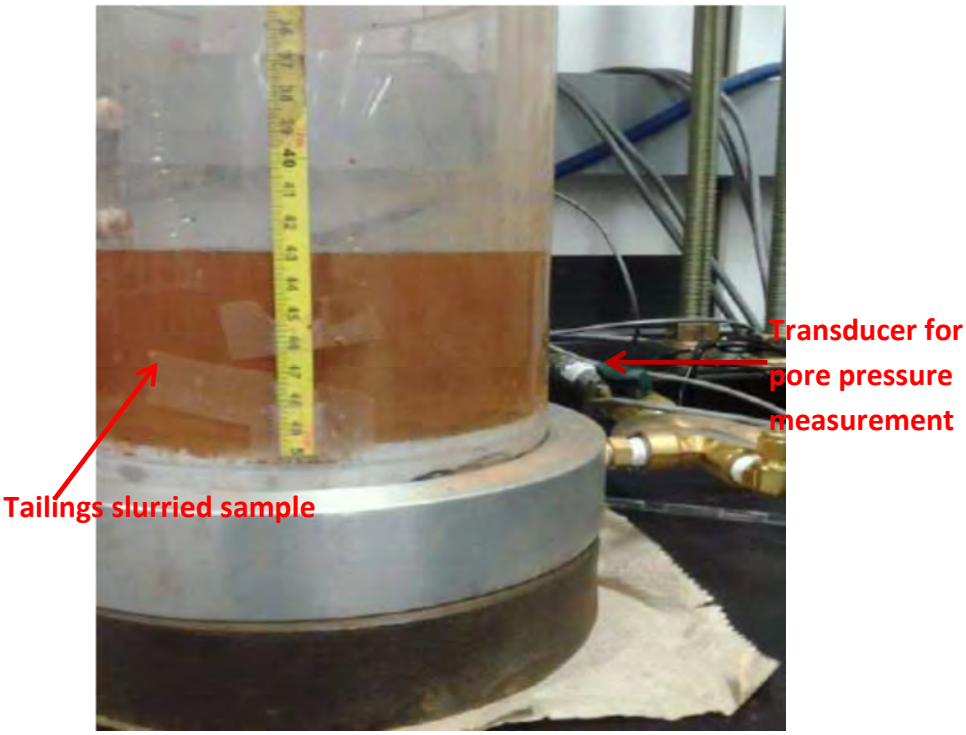

Figure 3. Settlement test conducted in a consolidation cell at the beginning of the test.

Figure 4. Settlement test conducted in a consolidation cell at the end of the test.

ATTACHMENT D10

Bender Element Test Data

Klohn Crippen Berger

Triaxial Bender Element Test - Summary

PROJECT NO. :
PROJECT : Fundão Tailings Dam Review Panel
SAMPLE : PSD 1 (loose)
TEST ID: TX 20

DATE : 2016-06-16
TESTED BY: BY
CHECKED BY: JG
TEST TYPE: BE

SPECIMEN INFORMATION	UNITS	Initial	Vacuum	Saturation	B value	End of 1 st Consolidation	End of 2 nd Consolidation	End of 3 rd Consolidation	End of 4 th Consolidation	End of 5 th Consolidation
Specimen Height	mm	138.28	138.25	137.96	137.73	137.72	137.65	137.47	137.23	137.05
Specimen Diameter	mm	69.09	69.09	68.43	68.46	68.45	68.42	68.31	68.17	67.99
Area	cm^2	37.49	37.49	36.78	36.81	36.80	36.77	36.65	36.49	36.30
Volume	cm^3	518.42	518.31	507.37	506.93	506.86	506.11	503.79	500.82	497.56
Wet Weight	g	870.51	870.51	1040.51	1059.01	1058.95	1058.19	1055.87	1052.90	1049.64
Water Content	%	5.14	5.14	25.67	27.91	27.90	27.81	27.53	27.17	26.78
Dry Weight	g	827.95	827.95	827.95	827.95	827.95	827.95	827.95	827.95	827.95
Wet Density	g/cm^3	1.679	1.680	2.051	2.089	2.089	2.091	2.096	2.102	2.110
Dry Density	g/cm^3	1.597	1.597	1.632	1.633	1.633	1.636	1.643	1.653	1.664
Specific Gravity of Solids	-	2.96	2.96	2.96	2.96	2.96	2.96	2.96	2.96	2.96
Solids Volume	cm^3	279.714	279.714	279.714	279.714	279.714	279.714	279.714	279.714	279.714
Void Volume	cm^3	238.705	238.592	227.652	227.212	227.147	226.393	224.073	221.103	217.843
Water Volume	cm^3	42.557	42.557	212.557	231.057	230.992	230.238	227.918	224.948	221.688
Void Ratio (e)	-	0.853	0.853	0.814	0.812	0.812	0.809	0.801	0.790	0.779
Saturation Ratio (Sr)	%	17.83	17.84	93.37	101.69	101.69	101.70	101.72	101.74	101.76
Confining Stress	kPa					25	50	100	200	300

Mean Effective Stress, p' (kPa)	Void Ratio, e	Wet Density, ρ (kg/m3)	Average Shear Wave Velocity, Vs (m/s)	Average Shear Modulus, Gmax (kpa)
25	0.81	2089	112	26172
50	0.81	2091	127	33665
100	0.80	2096	155	50199
200	0.79	2102	184	70597
300	0.78	2110	205	88138

Input Wave Voltage (V)	4
Type of Input Wave	S

Photos:



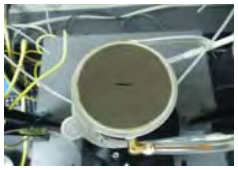




Klohn Crippen Berger

Bender Element Test - Charts

PROJECT NO. :
PROJECT : Fundão Tailings Dam Review Panel
SAMPLE : PSD 1 (loose)
TEST ID: TX 20
TEST TYPE: BE
DATE : 2016-06-16
TESTED BY: BY
CHECKED BY: JG

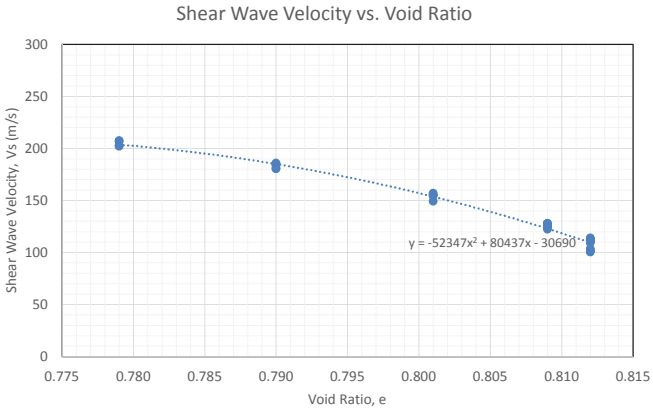

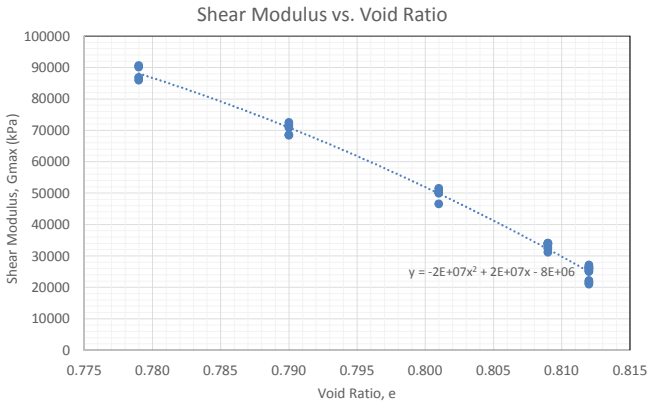

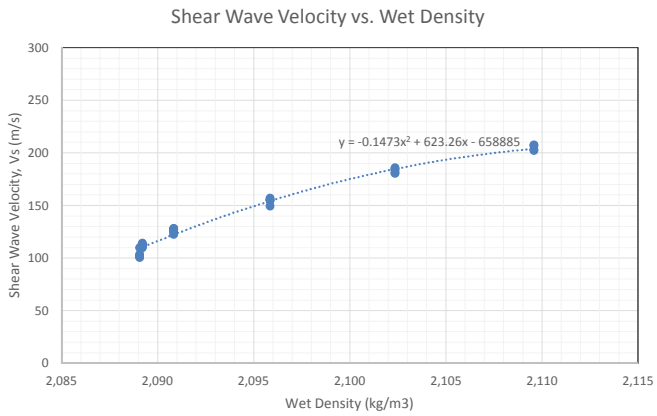

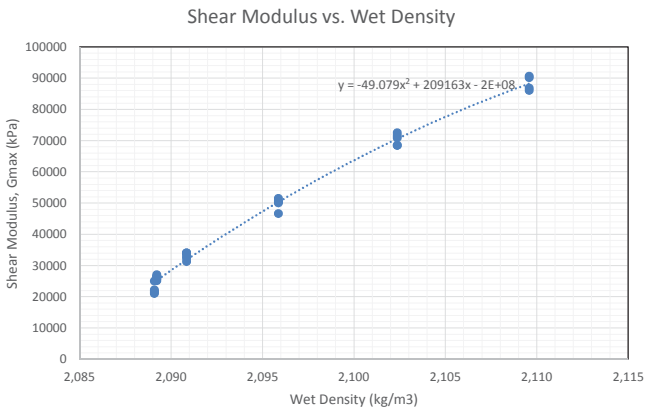

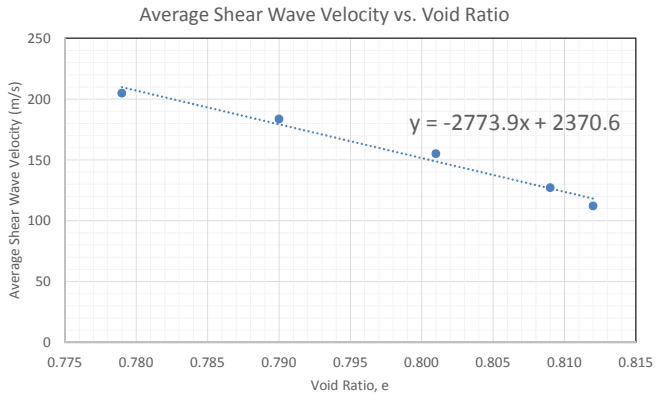

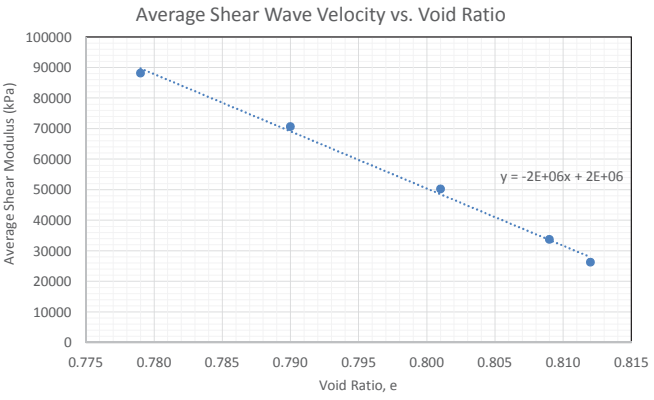

Klohn Crippen Berger

Triaxial Bender Element Test - Summary

PROJECT NO. :
PROJECT : Fundão Tailings Dam Review Panel
SAMPLE : PSD 1 (dense)
TEST ID: TX 21

DATE : 2016-06-16
TESTED BY: BY
CHECKED BY: JG
TEST TYPE: BE

SPECIMEN INFORMATION	UNITS	Initial	Saturation	B value	End of 1 st Consolidation	End of 2 nd Consolidation	End of 3 rd Consolidation	End of 4 th Consolidation	End of 5 th Consolidation	End of 6 th Consolidation	End of 7 th Consolidation	End of 8 th Consolidation
Specimen Height	mm	144.44	144.44	144.21	144.20	144.13	143.95	143.71	143.53	143.46	143.39	143.23
Specimen Diameter	mm	72.10	71.50	71.53	71.53	71.50	71.40	71.28	71.12	71.09	71.09	71.07
Area	cm^2	40.83	40.15	40.19	40.19	40.15	40.04	39.90	39.72	39.70	39.70	39.67
Volume	cm^3	589.72	579.97	579.53	579.47	578.71	576.39	573.42	570.16	569.49	569.23	568.21
Wet Weight	g	1185.03	1305.03	1309.75	1309.69	1308.93	1306.61	1303.64	1300.38	1299.71	1299.45	1298.43
Water Content	%	9.55	20.64	21.08	21.07	21.00	20.79	20.51	20.21	20.15	20.13	20.03
Dry Weight	g	1081.73	1081.73	1081.73	1081.73	1081.73	1081.73	1081.73	1081.73	1081.73	1081.73	1081.73
Wet Density	g/cm^3	2.009	2.250	2.260	2.260	2.262	2.267	2.273	2.281	2.282	2.283	2.285
Dry Density	g/cm^3	1.834	1.865	1.867	1.867	1.869	1.877	1.886	1.897	1.899	1.900	1.904
Specific Gravity of Solids	-	3.05	3.05	3.05	3.05	3.05	3.05	3.05	3.05	3.05	3.05	3.05
Solids Volume	cm^3	354.664	354.664	354.664	354.664	354.664	354.664	354.664	354.664	354.664	354.664	354.664
Void Volume	cm^3	235.060	225.308	224.868	224.803	224.049	221.729	218.759	215.499	214.829	214.569	213.549
Water Volume	cm^3	103.305	223.305	228.025	227.960	227.206	224.886	221.916	218.656	217.986	217.726	216.706
Void Ratio (e)	-	0.663	0.635	0.634	0.634	0.632	0.625	0.617	0.608	0.606	0.605	0.602
Saturation Ratio (Sr)	%	43.95	99.11	101.40	101.40	101.41	101.42	101.44	101.46	101.47	101.47	101.48
Confining Stress	kPa				25	50	100	200	300	400	500	800

Confining stress (kPa)	Wet Density (kg/m3)	Void Ratio	Average Shear Wave Velocity (m/s)	Average Shear Modulus (kPa)
25	2260	0.63	105	24724
50	2262	0.63	120	32624
100	2267	0.63	125	35487
200	2273	0.62	212	102347
300	2281	0.61	235	126497
400	2282	0.61	251	143936
500	2283	0.61	267	162917
800	2285	0.60	299	204410

Input Wave Voltage (V)	4
Type of Input Wave	S/P

B=value	P wave velocity (m/s)
0.87	2515

Photos:








Klohn Crippen Berger

Triaxial Bender Element Test - Charts

PROJECT NO. :
PROJECT : Fundão Tailings Dam Review Panel
SAMPLE : PSD 1 (dense)
TEST ID: TX 21
TEST TYPE: BE
DATE : 2016-06-16
TESTED BY: BY
CHECKED BY: JG

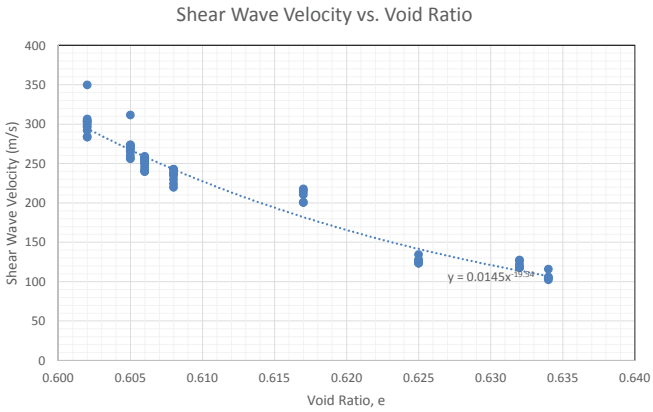

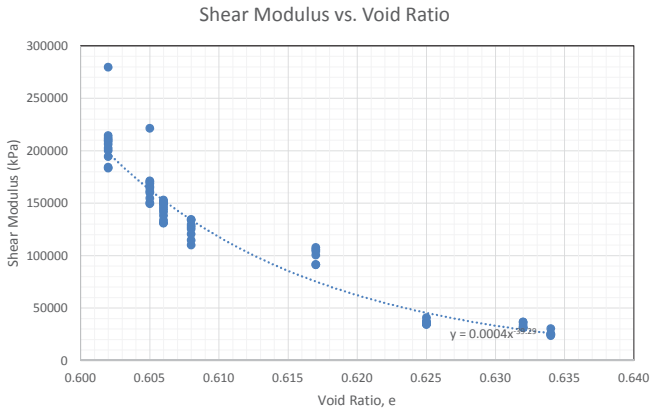

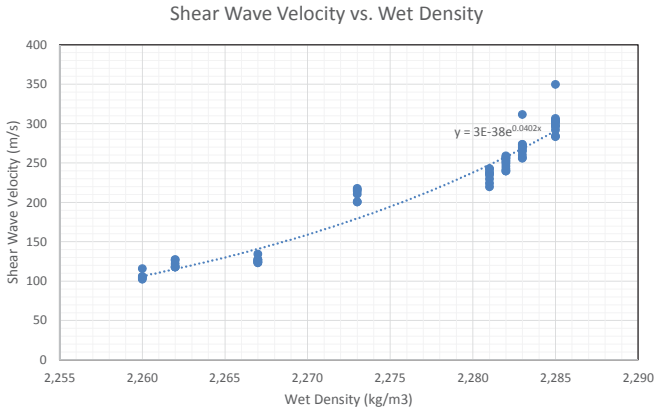

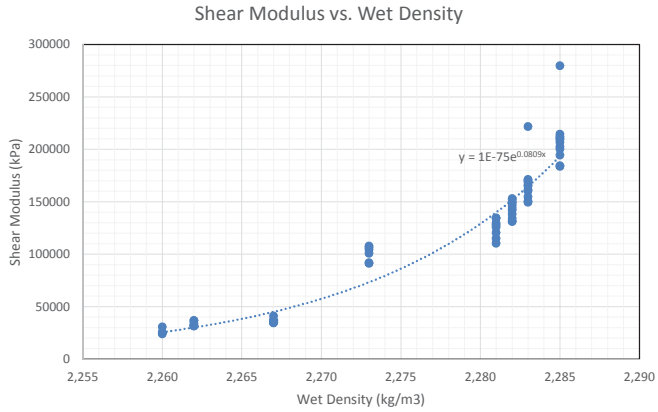

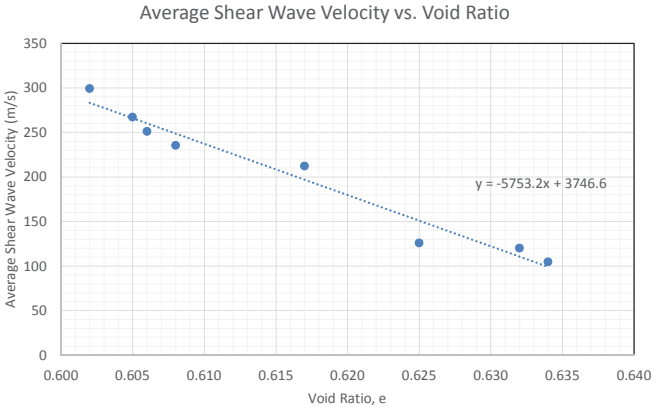

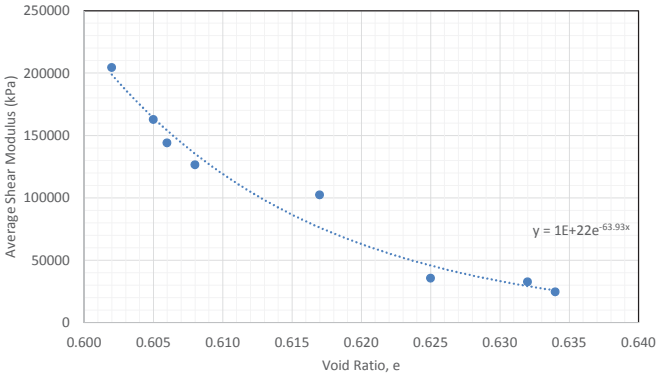

APPENDIX D

Laboratory Geotechnical Data and Interpretation

Appendix D
Laboratory Geotechnical Data and Interpretation

TABLE OF CONTENTS

TABLE OF CONTENTS

(continued)

TABLE OF CONTENTS

(continued)

List of Tables

List of Figures

TABLE OF CONTENTS

(continued)

TABLE OF CONTENTS

(continued)

List of Attachments

D1 INTRODUCTION

This appendix describes the pre-failure laboratory data on the tailings and the subsequent laboratory programs prescribed by the Panel to determine engineering properties necessary to carry out the various analytical procedures described elsewhere in this report. The majority of the laboratory testing program was done at the KCB laboratory in Vancouver, BC, Canada. Other laboratories were used when necessary. In particular, the laboratory at the University of Alberta was used to test the sedimentation/consolidation characteristics of the slimes tailings because of their unique facilities for that kind of testing. Laboratory index test results done in Brazil to support the field investigation program are presented in Appendix C.

Section D2 presents the existing Samarco data, and Section D3, Section D4, Section D5, Section D6 and Section D7 describe the Panel laboratory program. The attachments to this appendix give the laboratory test procedures, the standards followed, and the test results.

D2 PRE-FAILURE LABORATORY DATA

D2.1 Rezende (2013)

A comprehensive laboratory testing program undertaken for Samarco was that by Ms. Viviane Rezende in her Master's Thesis completed at the University of Ouro Preto in March, 2013[40]. The title of that thesis was "Study of the Behavior of a Sand Tailings Dam Constructed Using the Upstream Method". That work used test results on tailings beach and tailings slurry samples to derive engineering parameters for use in seepage and deformation analysis. Because of the quality of this laboratory testing program, it was used to guide the Panel in its laboratory testing program described next in this appendix. Rezende sampled and tested sand tailings from Fundão Dam only. There was no comparable testing program on slimes tailings.

Samples for laboratory testing were collected by Rezende from three field sampling campaigns. Samples were obtained directly from the tailings beach of Dike 1 in Campaigns 1 and 3 while sand tailings slurry samples were obtained in Campaign 2. The testing program is summarized in Table D2-1, which is a copy of Table 3.2 in the thesis.

D2.1.1 Field Sampling Campaign 1

The first campaign took samples from the tailings beach in 2009 when the beach was at El. 812 m 5 months after the start of tailings deposition. The Starter Dam was at El. 830 m at the time. Subsequently, the tailings at the sampling location were removed to repair the underdrains in the Starter Dam. The sampling locations are shown on Figure D2-1, which is Figure 3.3 in the thesis.

Two surface samples were taken at each of 17 locations at depths of 10 cm and 50 cm by excavating a shallow pit and pushing a beveled PVC sampler into the tailings. The sampler had a wall thickness of 2 mm, an inside diameter of 35 mm, and a length of 50 cm. Only index tests were performed on the samples, which included wet density, dry density, and specific gravity. From this were derived water content, void ratio and saturation. A summary of the tests is given in Table D2-2, which is Table 3.3 from the thesis.

Table D2-1 Description of tests from Campaigns 1, 2 and 3 (Table 3.2, page 40 of thesis)

Table 3.2 - Description of tests from Campaigns 1, 2 and 3.

Description of the Test	Parameters / Terminology	Sample number from Campaigns		
		Campaign 1	Campaign 2	Campaign 3
Description				
Specific weight (kN/m³)	Y	34	-	-
Humidity (%)	w	34	-	-
Dry specific weight (kN/m³)	γ_d	34	-	-
Specific relative weight of solids	G_s	34	18*	8
Particle size (%)	sand, silt, clay	-	18*	8
Chemical analysis (%)	Fe, SiO_2, AL_2O_3, P, PPC, MnO_2	34	-	-
Void Ratios				
e_{max} - e_{min}	e_{max}, e_{min}	-	18*	2
Resistance				
Triaxial (CID) (4 confining pressures)	c, ø, E_{50}	-	-	5
Permeability				
Constant load	k	-	18*	-
Coupled with the oedometer test	k	-	-	27
Triaxial Chamber	k	-	-	3
Deformation				
Oedometer	C_c, C_s	-	-	3

* The Campaign 2 test results are analyzed with the Campaign 3 test results.

Figure D2-1 Approximate location of sample collections for Campaign 1 at Dike 1 (Figure 3.3, page 41 of thesis)

Table D2-2 Mean values and standard deviation of Campaign 1 results (Table 3.3, page 40 of thesis)

Campaign 1	w (%)	γ (kN/m³)	γ_d (kN/m³)	P (%)	G_s	e	np (%)	S (%)	Chemical Analysis (%)					
									Fe	SIO_2	$Al2O_3$	P	PPC	MnO_2
Average	10.99	17.35	15.62	90.23	3.01	0.90	0.47	37.52	17.54	73.89	0.26	0.01	0.73	0.01
Standard Deviation	4.24	1.67	1.29	3.44	0.15	0.12	0.03	16.03	5.68	8.11	0.19	0.01	0.55	0.02

D2.1.2 Field Sampling Campaign 2

Eighteen slurry samples of sand tailings were collected from the concentrator. These samples were used for index tests, permeability tests and oedometer tests.

D2.1.3 Field Sampling Campaign 3

Approximately 20 samples were collected from the tailings beach between El. 845 m and El. 855 m. The sampling locations in section are shown on Figure D2-2.

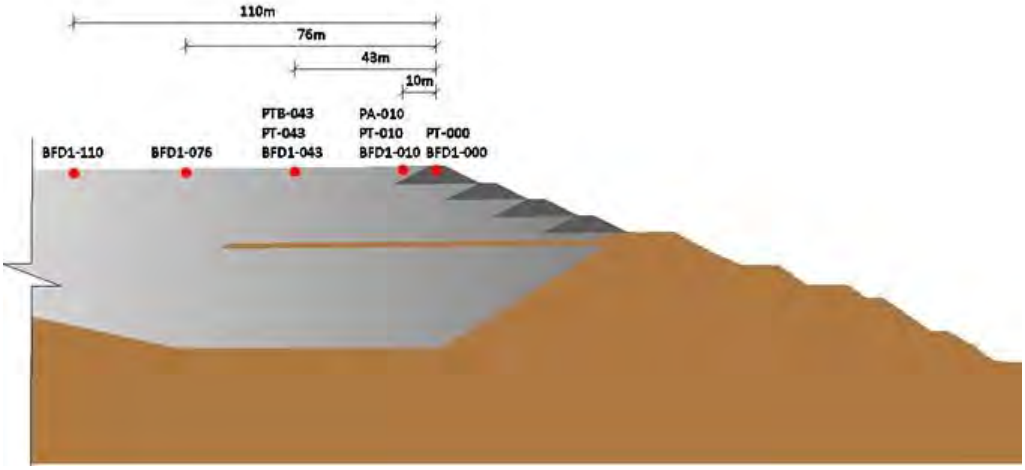

Figure D2-2 Location of the survey 3 assays in Fundão Dam (Figure 3.12, page 54 of thesis)

The samples were obtained by pushing beveled aluminum tubes into the tailings beach surface. The thickness of the tubes was 3 mm with an inside diameter of 50 mm and a length of 110 mm. Larger tubes were used to collect “block samples”. The samples were frozen in the field by placing them in ice in a plastic tray for transport to the university where they were stored in a cold room at -18°C.

These samples were used for index testing and for triaxial, oedometer and permeability testing. The gradation of the samples for Campaigns 2 and 3 are shown on Figure D2-3.

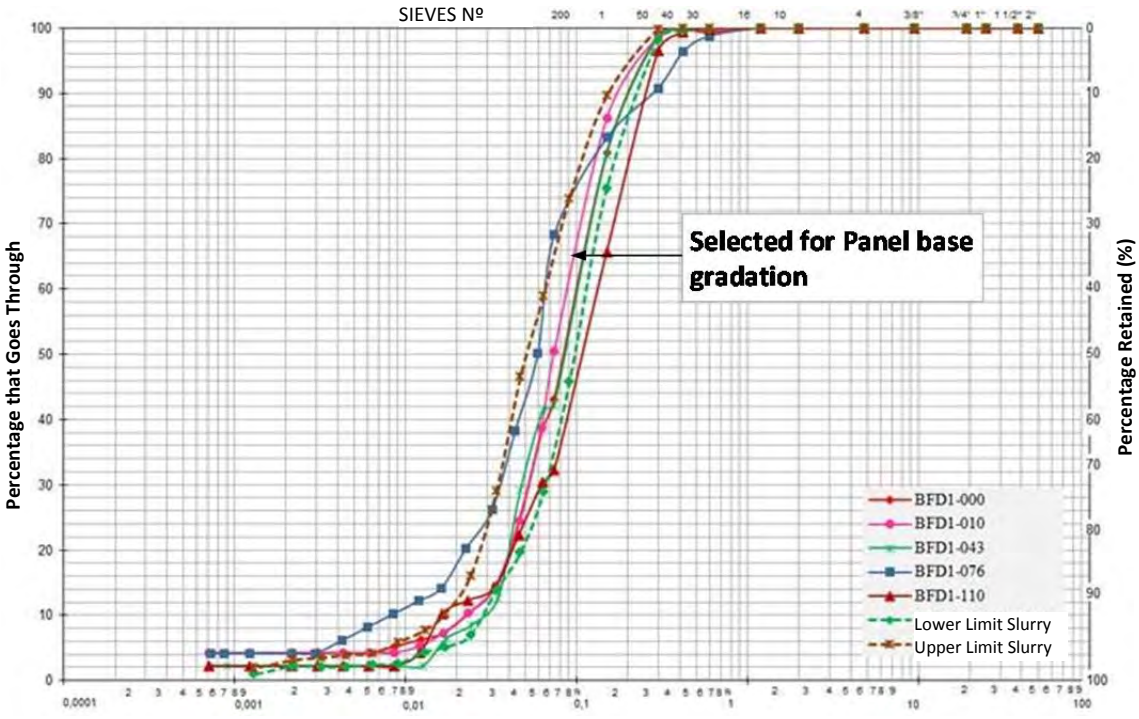

Figure D2-3 Particle size curves of survey 3 and particle size range of survey 2 (Figure 3.17, page 60 of thesis)

Selected test results are given in Table D2-3 (Table 3.16, page 79 of thesis).

Table D2-3 Comparison of resistance with the gradation of the sand tailings

Parameter	BFD1-000	BFD1-010	BFD1-043	BFD1-076	BFD1-110
C_U (1)	4.35	3.83	3.33	8.13	8.44
C_C (2)	1.22	1.39	0.77	2.49	1.78
ϕ'	39.5	31.4	34.5	34.9	33.9

1. Coefficient of Uniformity - $(\frac{D_{60}}{D_{10}})$
2. Coefficient of Curvature - $(\frac{(D_{30})^2}{D_{60}D_{10}})$

The work by Rezende[40] is sufficiently comprehensive and well-documented that no other laboratory programs are reviewed herein. The Panel selected the sample gradation of BFD1-010 (Figure D2-3) as the base gradation for all testing of disturbed sand tailings testing because it is close to the average of the sand tailings gradations.

D3 PANEL SURFICIAL SAMPLING PROGRAM

D3.1 Surface Sampling Locations

Bulk samples were collected by hand by the Panel at various locations across the site during three site visits conducted on January 20, March 1 and April 8, 2016. The samples were excavated by shovel into pails at each of the sampling locations. On the first sampling campaign, sand tailings samples were excavated from the tailings beach from the sole accessible remnant of Fundão Dam. Sand tailings were excavated from approximately the same location during the second round of sampling. Slimes samples were excavated by shovel at the Germano tailings impoundment at three locations shown on Figure D2-1. It was necessary to obtain slimes samples from Germano because there were no safe locations left at Fundão to obtain slimes. For the third campaign of surficial sampling, sand tailings were taken from the beach at Germano Pit Dam as shown on Figure D2-1 because the gradations of the sand tailings from the Germano Pit Dam and the Fundão Dam are virtually identical.

The samples were secured in buckets and shipped to the Vancouver, Canada laboratory of KCB by air freight. Samples were also sent to the TÜV SÜD laboratory in Brazil for index testing from the first round of sampling only. There was no attempt to preserve original moisture content. The sampling locations and sample weights are listed in Table D3-1 for sand tailings and Table D3-2 for slimes.

Table D3-1 Sand tailings samples locations and weights

Sample	Sample Date	Northing[(1)] (m)	Easting[(1)] (m)	Weight (kg)	Container Type
Fundão Sand 1A	Jan 20, 2016	7764483.5	660473.4	8	Pail
Fundão Sand 1B	Jan 20, 2016	7764483.5	660473.4	8	Pail
Fundão Sand 1/4	March 1, 2016	7764426.5	660333.4	6.5	Pail
Fundão Sand 2/4	March 1, 2016	7764426.5	660333.4	6.5	Pail
Fundão Sand 3/4	March 1, 2016	7764426.5	660333.4	6.5	Pail
Fundão Sand 4/4	March 1, 2016	7764426.5	660333.4	6.5	Pail
Fundão Sand 1/3	April 8, 2016	7766356.3	657429.9	25	Pail
Fundão Sand 2/3	April 8, 2016	7766356.3	657429.9	25	Pail
Fundão Sand 3/3	April 8, 2016	7766356.3	657429.9	25	Pail

1. Coordinates are in UTM Zone 23K Córrego Alegre.

Table D3-2 Slimes sample locations and weights

Sample	Sample Date	Northing[(1)] (m)	Easting[(1)] (m)	Weight (kg)	Container Type
Germano Slimes 2B	Jan 20, 2016	7764375.0	658560.0	8	Pail
Germano Slimes 2C	Jan 20, 2016	7764375.0	658560.0	8	Pail
Germano Slimes 1/4	March 1, 2016	7763854.0	659108.9	6.5	Pail
Germano Slimes 2/4	March 1, 2016	7763854.0	659108.9	6.5	Pail
Germano Slimes 3/4	March 1, 2016	7763854.0	659108.9	6.5	Pail
Germano Slimes 4/4	March 1, 2016	7763854.0	659108.9	6.5	Pail
Germano Slimes	April 8, 2016	7763359.2	659162.3	50	Pail

1. Coordinates are in UTM Zone 23K Córrego Alegre.

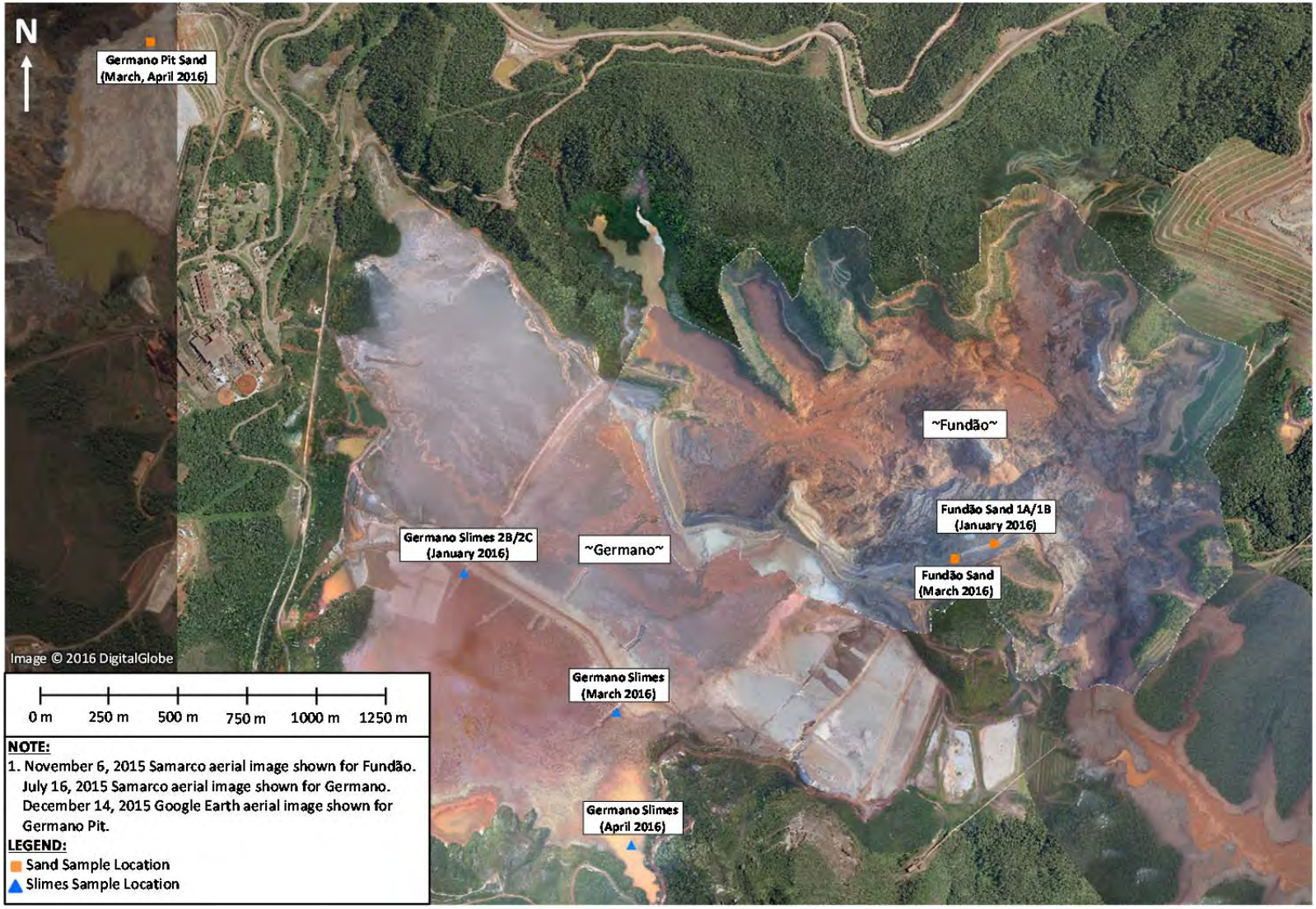

Figure D3-1 Sample locations

D3.2 Sample Preparation

D3.2.1 Sand Tailings

Virtually all of the laboratory testing was done on the disturbed surficial sand tailings and slimes samples collected by the Panel. To eliminate variations in test results due to variations in gradation of the sand samples, the Panel decided to select one gradation for the majority of the testing. This base case sample gradation (PSD1) was chosen to be the same as BFD1-010 Rezende[40], as described earlier, so that the Panel could compare its results with her work. Also, the Panel prepared a second sample gradation (PSD2) similar to PSD1 but with the fines (particle diameter smaller than 0.074 mm) removed. The design particle size data is given in Table D3-3 and shown on Figure D4-1.

PSD1 had to be manufactured from the sand tailings sent from Fundão Dam and Germano Pit Dam by sieving and washing. The sand samples were sieved according to ASTM D1140. Materials retained on each sieve were washed to separate any fines attached to larger particles. The washed material was air dried and sieved again to remove any residual fines. The samples were then recombined to match as closely as possible the required gradations specified in Table D3-3. A small representative sample (200 g) of the final prepared sample was tested to confirm compliance to the required gradation. When the gradation curve was deemed acceptable, de-aired water was added to reach 5% moisture content at least 16 hours prior to each test.

In total, 100 kg of natural soil was processed to create the required amount (~60 kg) of both PSD1 and PSD2 soils for lab testing.

Table D3-3 Sand tailings design particle size distribution

	Design Gradation	US Standard Sieve Size			
		200 (0.074 mm)	100 (0.15 mm)	50 (0.3 mm)	40 (0.42 mm)
Percent Passing (%)	PSD1	51	86	99	100
	PSD2	0	71	98	100

(a) Field sample, (b) Sample mixing, (c) Sample air drying, (d) Sample sieving, (e) Split sample

Figure D3-2 Reconstituted sand tailings sample preparation

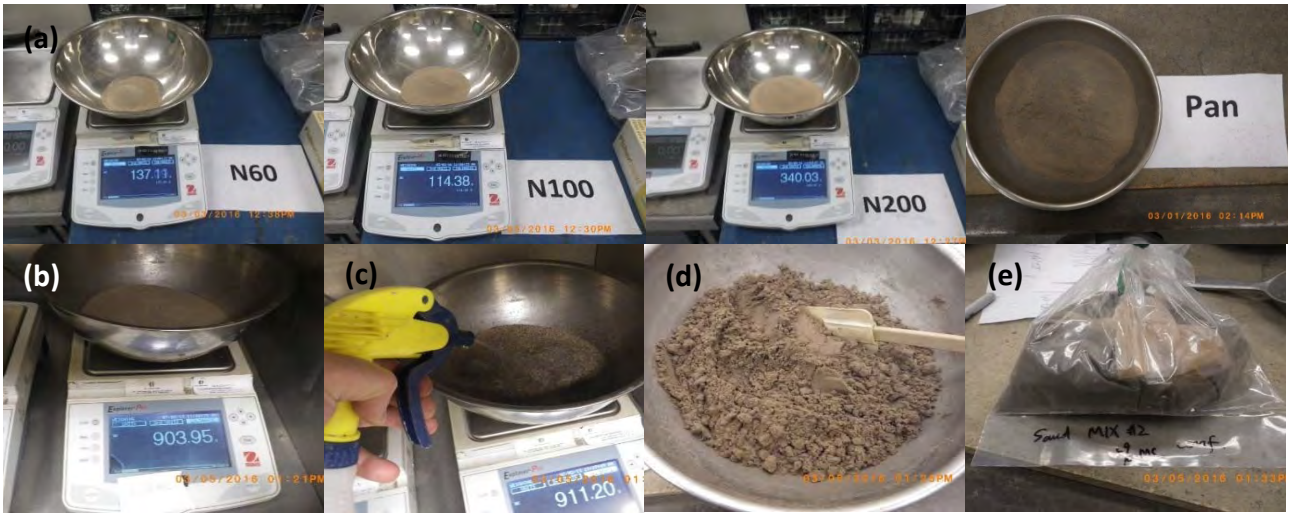

(a) PSD1 split sample, (b) PSD1 mixture, (c) Addition of water, (d) Final mixing, (e) Final sample

Figure D3-3 Tailings sand sample preparation

D3.2.2 Slimes

Slimes samples were prepared for testing using the following procedure:

- Slimes samples were mixed with de-aired water to reach a moisture content of 43.2% (or 1.66 times the liquid limit of 26%) until a uniform and homogeneous paste was formed. The paste was left under vacuum for several hours.
- While under vacuum, the sample was re-mixed regularly to minimize entrapped air bubbles and to obtain a saturated homogenous slurry.
- The slimes were carefully spooned into the molds appropriate to the test type. The initial void ratio was calculated using a moisture content of 43.2% and an assumed specific gravity of 3.93. Only small incremental loads were applied to slimes specimens to allow for slow specimen settlement and to avoid squeezing any material.

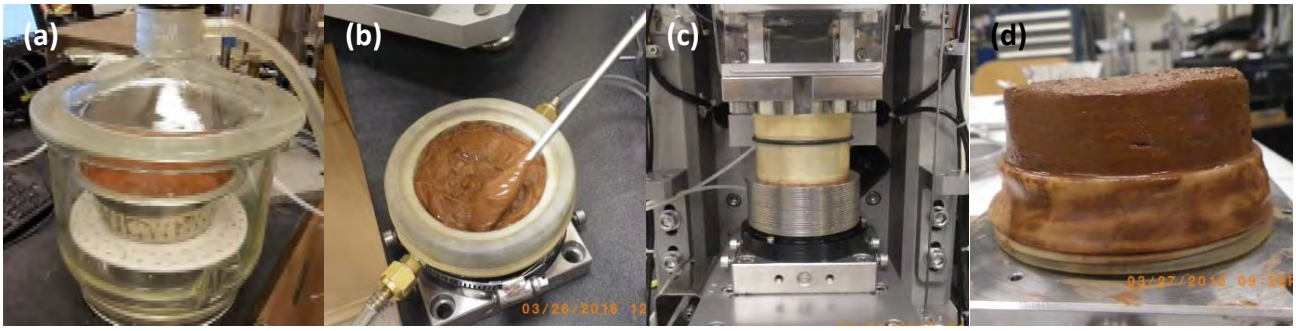

(a) De-airing under vacuum, (b) Placing into DSS mold, (c) Sample ready for testing, (d) Sample after DSS test

Figure D3-4 Slimes sample preparation

D4 INDEX TEST RESULTS

D4.1 Scope

The test types, test procedures, and number of tests are catalogued in Attachment D1. This section describes the results of index tests on Germano slimes and sand tailings from the surface samples described in Section D3. The basic objectives of the program were to provide engineering parameters for use in various analytical procedures and to provide index test properties for reference to pre-failure laboratory and field programs.

Soil samples were subjected to standard laboratory index testing, including moisture content determination, particle size distribution, Atterberg limit testing, specific gravity testing and density tests. In addition, pH, electrical conductivity, x-ray diffraction and scanning electron microscopy tests were completed. The index test results are given in Attachment D2.

D4.2 Moisture Content on Sand Tailings and Slimes

Moisture content tests were completed on the manufactured PSD1 and PSD2 sand tailings samples and the reconstituted slimes samples before and after each advanced laboratory test. All moisture content testing was undertaken in accordance with ASTM D2216.

D4.3 Particle Size Distribution on Sand Tailings and Slimes

Seventy particle size distribution (PSD) tests were conducted on sand and slimes samples in accordance with ASTM D1140 and D422. The following PSD tests were conducted:

- 3 PSDs on Fundão sand;
- 1 PSD on Germano Pit Dam sand;
- 2 PSDs on Germano slimes;
- 56 PSDs on manufactured PSD1; and
- 8 PSDs on manufactured PSD2.

In addition to the tests listed above, two PSD tests were conducted by Tecnogeo Lab, Brazil, on one Fundão sand sample and one Germano Slimes sample from the January 20, 2016 sampling campaign.

The PSD gradation curves for the manufactured sand tailings are shown on Figure D4-1 and Figure D4-2. Figure D4-3 shows a comparison of the gradations of the field and manufactured samples. The gradation curve of design sand tailings sample (PSD1) is comparable to the gradation curves of the field samples.

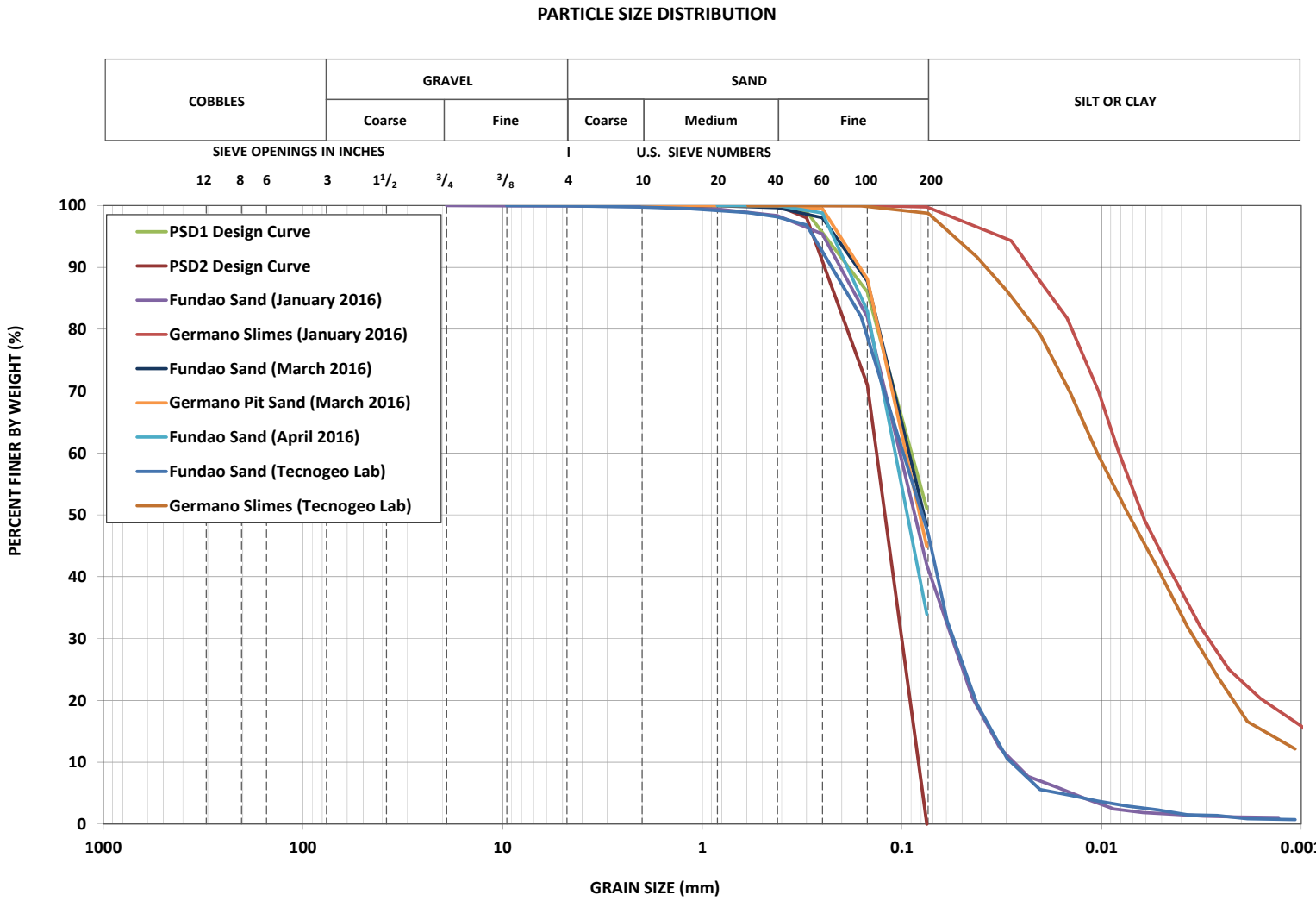

Figure D4-1 Particle size distribution of field sand tailings and slimes samples

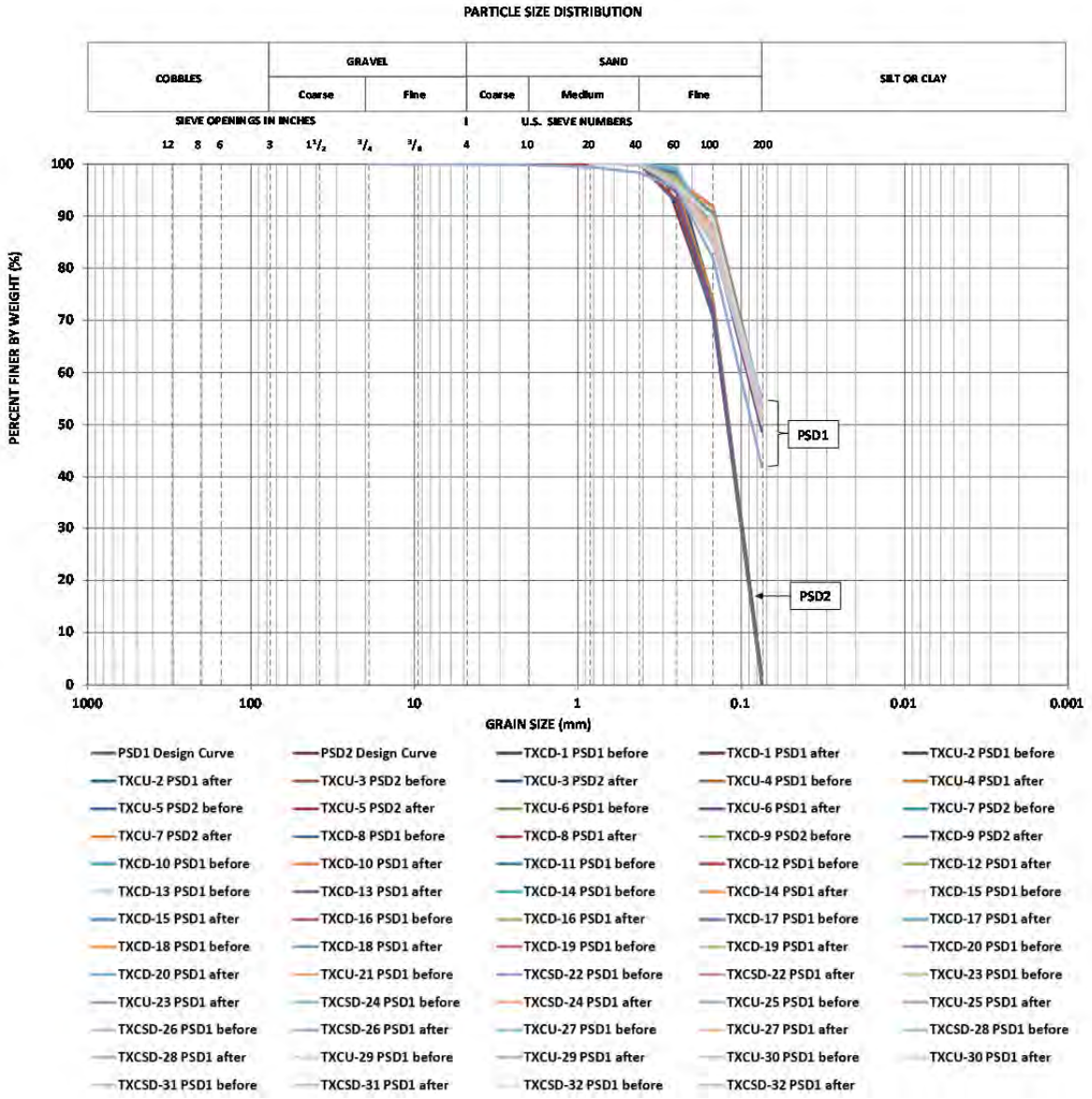

Figure D4-2 Particle size distribution of manufactured sand tailings used for triaxial testing

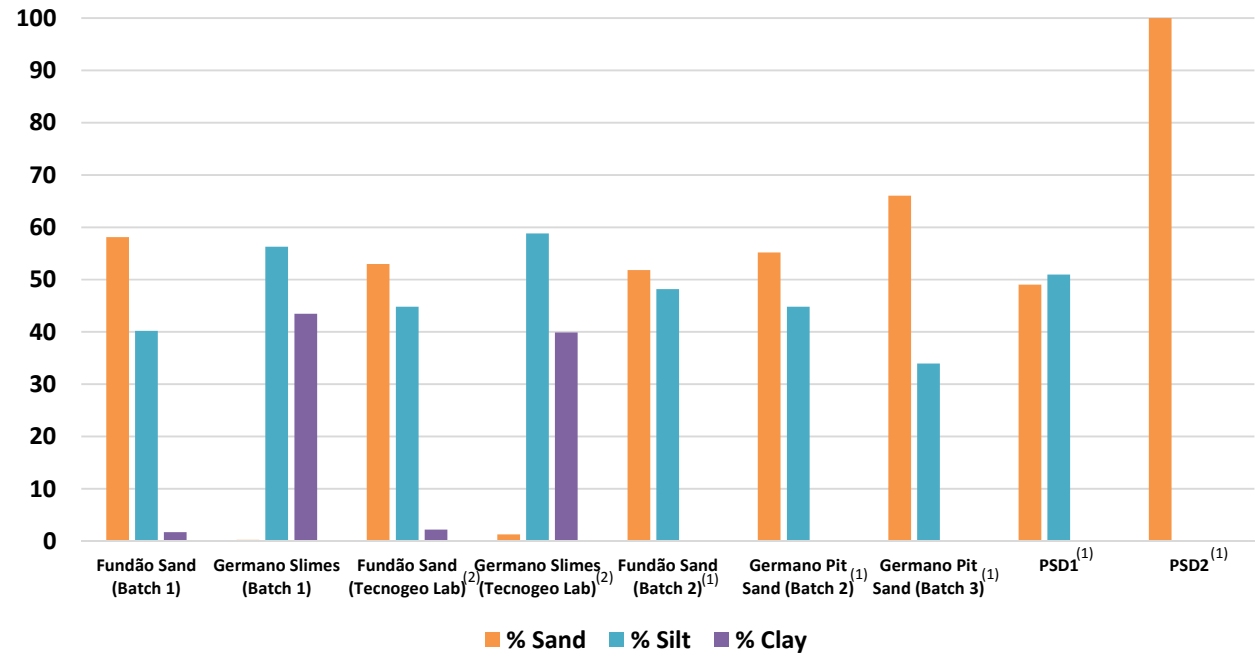

Notes:
(1) Hydrometer tests not performed. (2) Tecnogeo tests on samples from Batch 1.

Figure D4-3 Particle size distribution comparison of sand tailings and slimes

D4.4 Atterberg Limit Tests on Slimes

Three Atterberg limit tests were undertaken on slimes samples in accordance with ASTM D4318. Figure D4-4 shows the test results.

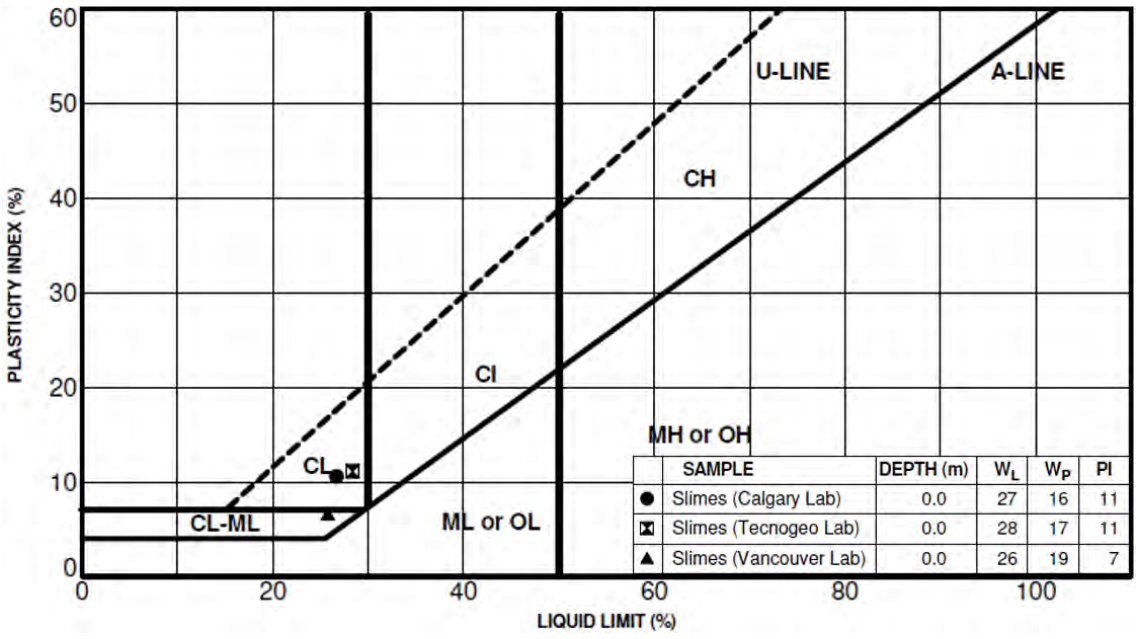

Figure D4-4 Atterberg limit tests on slimes

D4.5 Specific Gravity on Sand Tailings and Slimes

Thirty-five specific gravity tests were conducted by KCB in accordance with ASTM D854. Specific gravity tests were done on the following materials:

- 1 on Fundão sand;
- 2 on Germano slimes;
- 28 on PSD1; and
- 4 on PSD2.

Figure D4-5 shows the range of specific gravities recorded in the laboratory for sand and slimes samples. The specific gravity test results are provided in Attachment D2.

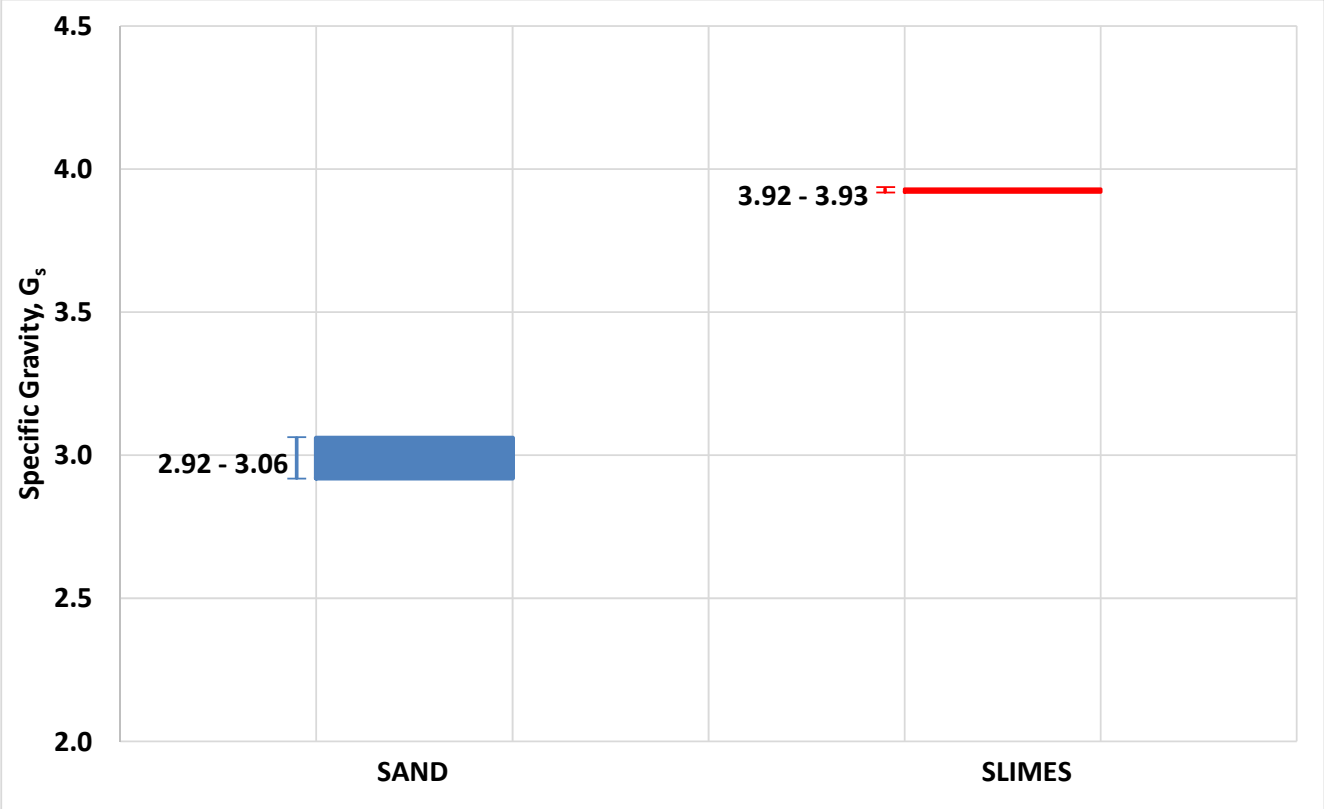

Figure D4-5 Specific gravity on sand tailings and slimes

D4.6 Maximum/Minimum Density Tests on Sand Tailings

Minimum and maximum density tests were conducted by Golder Associates on the manufactured PSD1 sand tailings in accordance with ASTM D4523 and ASTM D4254, using the dry and wet methods. The test was conducted using a small standard mold and vibrating table. The specific gravity of the sample was 3.04 as tested by KCB. The sample moisture content for the wet test method was 13.9%. The maximum dry unit weight was 2057 kg/m^3. The maximum wet unit weight was 1933 kg/m^3. The minimum wet unit weight was 1629 kg/m^3.

One modified Proctor test was conducted on a sample of the Fundão sand received in the first shipment from site as another measure of maximum dry density. The test was conducted in accordance with ASTM D1557. A maximum dry unit weight of 1819 kg/m^3 and an optimum moisture content of 13.1% was recorded.

A standard Proctor test was conducted on a slimes sample in accordance with ASTM D698. A maximum dry unit weight of 2300 kg/m^3 and optimum moisture content of 16.7% was recorded for the slimes.

The density test results are given in Attachment D2.

D4.7 pH and Electrical Conductivity on Slimes

KCB conducted one pH and one electrical conductivity (EC) test in accordance with ASTM D4972. The pH level was recorded as 8.22 and the electric conductivity as 734 μS.

The pH and electrical conductivity test results are provided in Attachment D2.

D4.8 X-Ray Diffraction on Slimes

Slime samples collected by the Panel were subjected to X-Ray diffraction tests at the University of British Columbia (UBC). The tests were intended to identify the quantity and type of clay present in the slimes.

The X-ray diffractogram was analyzed using the International Centre for Diffraction Database PDF-4 and Search-Match software by Bruker (UBC 2016). The results of the quantitative phase analysis are summarized in Table D4-1. The results show that the slimes are comprised predominantly (93%) of the three minerals goethite, hematite and quartz. The X-ray diffraction results are provided in Attachment D3.

Table D4-1 X-ray diffraction results on slimes

Mineral	Ideal Formula	Percentage of Sample (wt%)
Chalcopyrite ?	$CuFeS_2$	<0.1
Goethite	α-$Fe^{3+}O(OH)$	30.9
Hematite	α-Fe_2O_3	42.9
Illite-Muscovite	$KAl_2AlSi_3O_{10}(OH)_2$	1.4
Kaolinite	$Al_2Si_5(OH)_4$	4.4
Plagioclase	$NaAlSi_3O_8 – CaAl_2Si_2O_8$	1.1
Quartz	SiO_2	19.2
Total		**100.0**

D4.9 Scanning Electron Microscopy on Sand Tailings

Samples of sand tailings were subjected to scanning electron microscopy tests by UBC using a Philips XL30 electron microscope (Bruker Quantax 200 energy-dispersion X-ray microanalysis system, XFlash 6010 SDD detector, Robinson cathodoluminescence detector). The test was completed on the set of samples received in the first shipment from site to qualitatively assess particle structure, angularity and other parameters at a microscopic level. The test results indicate that the sand is comprised of angular to sub-rounded grains as shown on Figures D4-6 to D4-9.

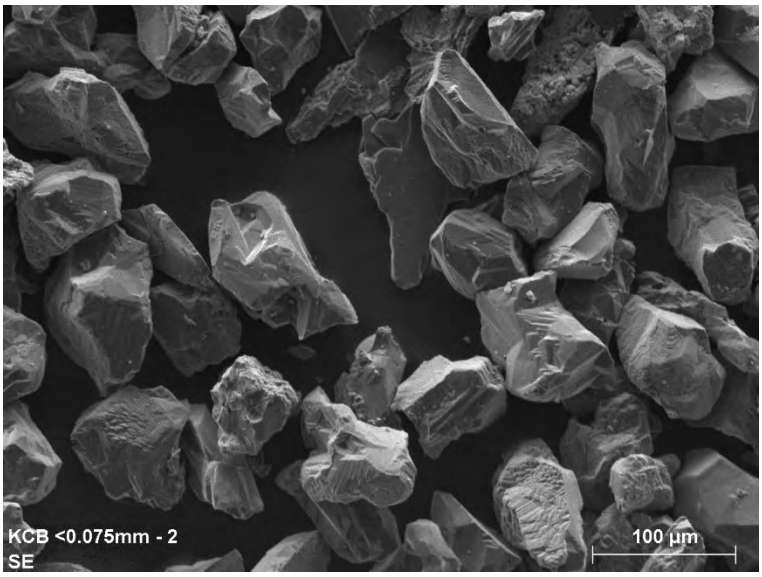

Figure D4-6 SEM image of Fundão sand (particle sizes less than 0.075 mm)

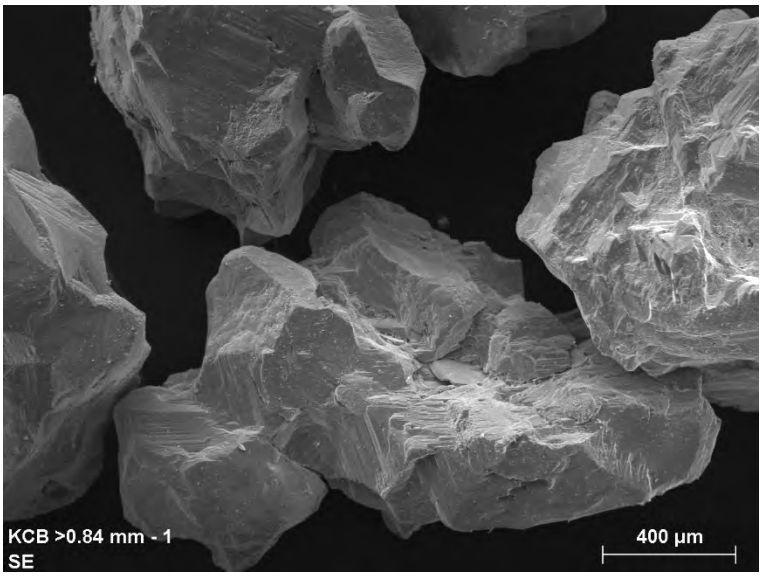

Figure D4-7 SEM image of Fundão sand (particle sizes greater than 0.84 mm)

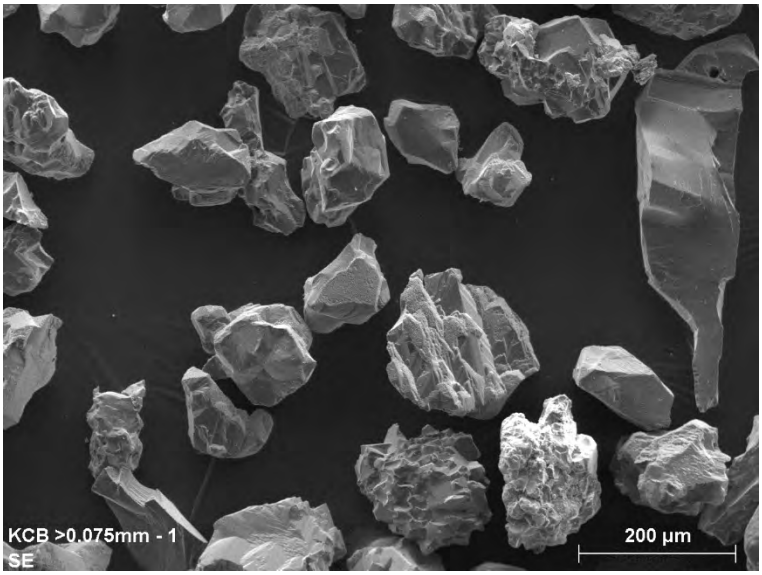

Figure D4-8 SEM image of Fundão sand (particle sizes greater than 0.075 mm)

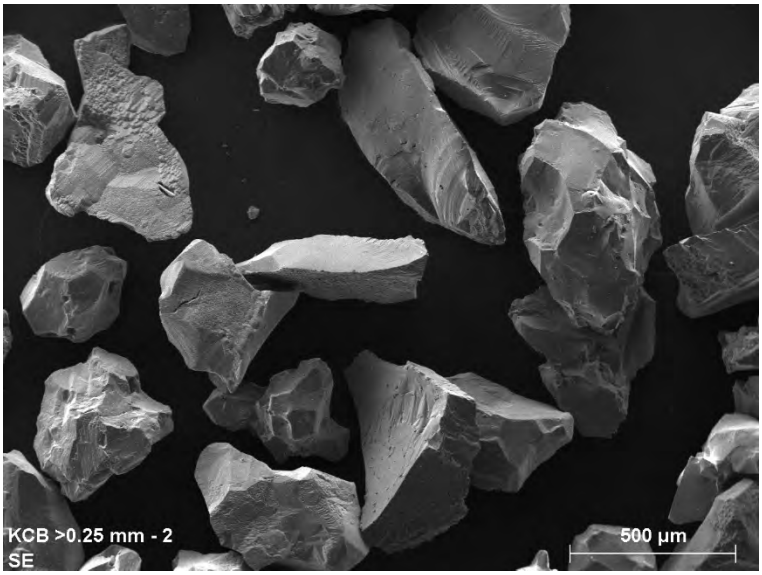

Figure D4-9 SEM image of Fundão sand (particle size greater than 0.25 mm)

D5 ADVANCED LABORATORY TEST PROGRAM ON SAND TAILINGS

D5.1 Scope

This section describes the results of laboratory tests on sand tailings which are listed in Table D5-1. The test types, test procedures, and number of tests are catalogued in Attachment D1. The basic objectives of the program were to provide engineering parameters for use in various analytical procedures as described in other appendices.

At the beginning of the testing program, triaxial and direct simple shear tests were run on a range of void ratios to understand the overall behavior of the sand tailings and to determine compatibility with Rezende[40]. Also, undrained direct simple shear tests were run early in the program on loose sands to investigate their undrained strength behavior as a function of confining stress. Later, cyclic loads were applied to loose sand samples in the direct simple shear tests to understand susceptibility of the sand to this type of loading.

This general phase was followed by determination of the critical state line in the triaxial test using the methodology outlined by Jefferies and Been (2016). This allowed the state parameter to be calculated for the sand tailings at a given void ratio and effective confining stress. Laboratory compressibility data of the sand was also determined to give an indication of the shape of the compression curve with pressure.

The link between the field and the laboratory was through the state parameter. The state parameter was calculated directly from the cone penetration test. The pre-failure CPTs and the Panel CPT program were interpreted to yield state parameter directly using the Jefferies and Been (2016). The state parameter from the CPTs and the critical state line from the triaxial laboratory testing allowed the Panel to specify void ratios for the remainder of the laboratory testing.

In the final stages of laboratory testing, the Panel designed triaxial tests with specified stress paths to test an “extrusion” theory of static liquefaction collapse. These tests are referred to as “Extrusion Collapse” tests in this report. The stress paths for these test types are shown on Figure D5-1(b). The stress path consists of anisotropic consolidation to the assumed field stress state followed by drained unloading at relatively constant shear stress to failure. The entire test is drained. These tests were run primarily with stress-controlled vertical loading. In a single “extrusion collapse” stress-controlled test, a cyclic load was applied to the sample when the stress path was close to the critical state line.

Testing was also done to determine dynamic properties of loose and dense sand tailings for use in SHAKE analyses. This testing was primarily done using bender elements in the triaxial cell where shear wave velocity is measured at specified void ratios and confining stresses. Bender element tests were prepared on a loose sand tailings sample at five different stress levels and on a dense sand tailings sample at eight different stress levels.

Table D5-1 Summary of advanced laboratory tests on sand tailings

Test ID	Test	Test Type	Material	Loading Condition		
				Undrained/Drained/ Constant-Volume	Stress-/Strain-Controlled	Anisotropic/ Isotropic
TX-1	Triaxial	CID	PSD1	Drained	Strain	Isotropic
TX-2	Triaxial	CIU	PSD1	Undrained	Strain	Isotropic
TX-3	Triaxial	CIU	PSD2	Undrained	Strain	Isotropic
TX-4	Triaxial	CIU	PSD1	Undrained	Strain	Isotropic
TX-5	Triaxial	CIU	PSD2	Undrained	Strain	Isotropic
TX-6	Triaxial	CIU	PSD1	Undrained	Strain	Isotropic
TX-7	Triaxial	CIU	PSD2	Undrained	Strain	Isotropic
TX-8	Triaxial	CID	PSD1	Drained	Strain	Isotropic
TX-9	Triaxial	CID	PSD2	Drained	Strain	Isotropic
TX-10	Triaxial	CID	PSD1	Drained	Strain	Isotropic
TX-11	Triaxial	CID	PSD1	Drained	Strain	Isotropic
TX-12	Triaxial	CID	PSD1	Drained	Strain	Isotropic
TX-13	Triaxial	CIU	PSD1	Undrained	Strain	Isotropic
TX-14	Triaxial	CA-QD	PSD1	Drained	Strain	Anisotropic
TX-15	Triaxial	CA-QD	PSD1	Drained	Strain	Anisotropic
TX-16	Triaxial	CA-QD	PSD1	Drained	Strain	Anisotropic
TX-17	Triaxial	CA-QD	PSD1	Drained	Strain	Anisotropic
TX-18	Triaxial	CID	PSD1	Drained	Strain	Isotropic
TX-19	Triaxial	CID	PSD1	Drained	Strain	Isotropic
TX-22[1,2]	**Triaxial**	**CA-QD-SC**	**PSD1**	**Drained**	**Stress**	**Anisotropic**
TX-23	Triaxial	CAU	PSD1	Undrained	Strain	Anisotropic
TX-24[1,2]	**Triaxial**	**CA-QID-SC**	**PSD1**	**Drained**	**Stress**	**Anisotropic**
TX-25	Triaxial	CAU	PSD1	Undrained	Strain	Anisotropic
TX-26	Triaxial	CA-QD-SC	PSD1	Drained	Stress	Anisotropic
TX-27	Triaxial	CAU	PSD1	Undrained	Strain	Anisotropic
TX-28	Triaxial	CA-QID-SC	PSD1	Drained	Stress	Anisotropic
TX-29	Triaxial	CID	PSD1	Drained	Strain	Isotropic
TX-30	Triaxial	CID	PSD1	Drained	Strain	Isotropic
TX-31[1]	**Triaxial**	**CA-QID-SC (Cyclic)**	**PSD1**	**Drained**	**Stress**	**Anisotropic**
TX-32[1]	**Triaxial**	**CAD**	**PSD1**	**Drained**	**Stress**	**Anisotropic**
TX-20	BE	Bender Element	PSD1	-	-	Isotropic
TX-21	BE	Bender Element	PSD1	-	-	Isotropic

Test ID	Test	Test Type	Material	Loading Condition		
				Undrained/Drained/ Constant-Volume	Stress-/Strain-Controlled	Anisotropic/ Isotropic
DSS-1	DSS	Cyclic	PSD1	Constant-Volume	Strain	Anisotropic
DSS-2	DSS	Cyclic	PSD1	Constant-Volume	Strain	Anisotropic
DSS-4	DSS	Cyclic	PSD1	Constant-Volume	Strain	Anisotropic
DSS-8	DSS	Monotonic	PSD1	Constant-Volume	Strain	Anisotropic
DSS-9	DSS	Monotonic	PSD1	Constant-Volume	Strain	Anisotropic
DSS-10	DSS	Monotonic	PSD1	Constant-Volume	Strain	Anisotropic
DSS-11	DSS	Monotonic	PSD1	Constant-Volume	Strain	Anisotropic
DSS-12	DSS	Cyclic with Static Bias	PSD1	Constant-Volume	Strain	Anisotropic
DSS-14	DSS	Cyclic with Static Bias	PSD1	Constant-Volume	Strain	Anisotropic
DS-1	DS	Monotonic	Fundão sand	Drained	Strain	Anisotropic
CONS01	Oedometer	One-Dimensional Consolidation	PSD1	-	-	-

1. Sand tailings specimen experienced “collapse” failure during the stress-controlled extrusion collapse triaxial tests.
2. TX-22 and TX-24: stress-controlled extrusion collapse tests that collapsed under dead weights (discussed in Appendix I).

CID – Isotropically consolidated triaxial test with strain-controlled drained loading
CIU – Isotropically consolidated triaxial test with strain-controlled undrained loading
CA-QD – Anisotropically consolidated triaxial test followed by reducing cell pressure at constant “q”, loading ram fixed and attached to load cell
CA-QD-SC – Anisotropically consolidated triaxial test followed by reducing cell pressure at constant “q”, vertical load applied by dead weight or stress-controlled
CA-QID-SC – Anisotropically consolidated triaxial test followed by reducing cell pressure at increasing “q”, vertical load applied by dead weight or stress-controlled
CA-QID-SC (cyclic) – Anisotropically consolidated triaxial test followed by reducing cell pressure at increasing “q”, vertical load applied by dead weight or stress-controlled, cyclic load applied at specified “q” by adding/removing weights
CAD – Anisotropically consolidated triaxial test with strain-controlled drained loading
BE – Bender element test in triaxial cell
DSS – Direct simple shear test – drained, undrained, and with cyclic load
DS – Direct shear test – drained

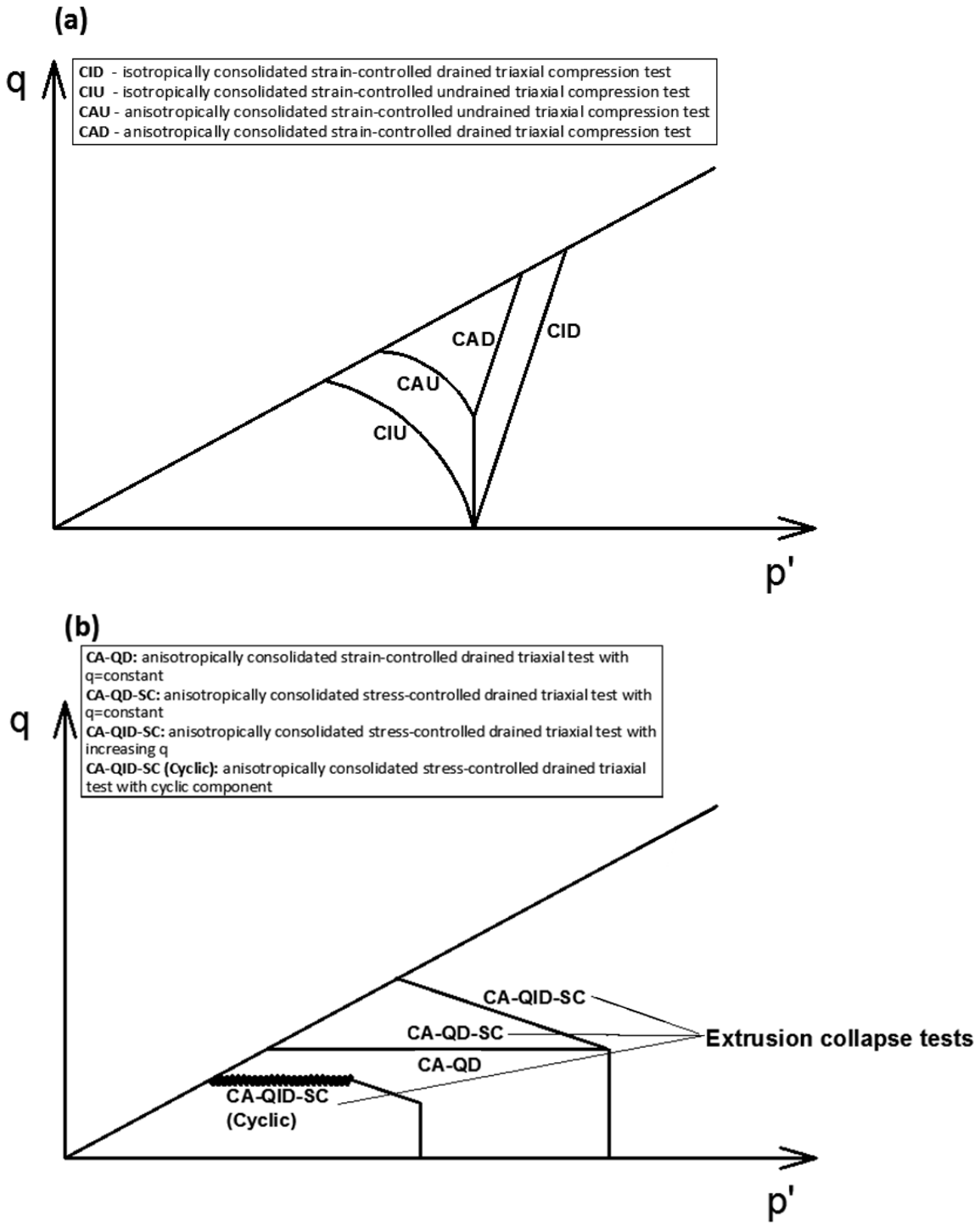

Figure D5-1 Different stress paths from (a) standard and (b) extrusion collapse triaxial tests

D5.2 Direct Shear Tests

D5.2.1 Scope

One direct shear test on Fundão sand tailings was completed by KCB to determine peak friction angle at an early stage of the Panel Investigation.

D5.2.2 Procedure

The direct shear test was completed in accordance with ASTM D3080. The sample was tested at three vertical effective stresses, 250 kPa, 750 kPa and 1250 kPa.

D5.2.3 Results

The direct shear test results are summarized in Table D5-2 and shown on Figure D5-2. A friction angle, ϕ', of 32 degrees is determined from the Mohr-Coulomb envelope on Figure D5-2. The triaxial test results gave a ϕ' of 33 degrees as shown on Figure D5-9 and Figure D5-10. The direct shear test results are in Attachment D4.

Table D5-2 Direct shear test results on sand tailings

Sample	Final Moisture Content (%)	Normal Stress (kPa)	Peak Shear Stress (kPa)	Void Ratio after Consolidation
Fundão Sand / 1A	24.7	250	164	0.72
	22.3	750	476	0.66
	20.3	1250	812	0.60

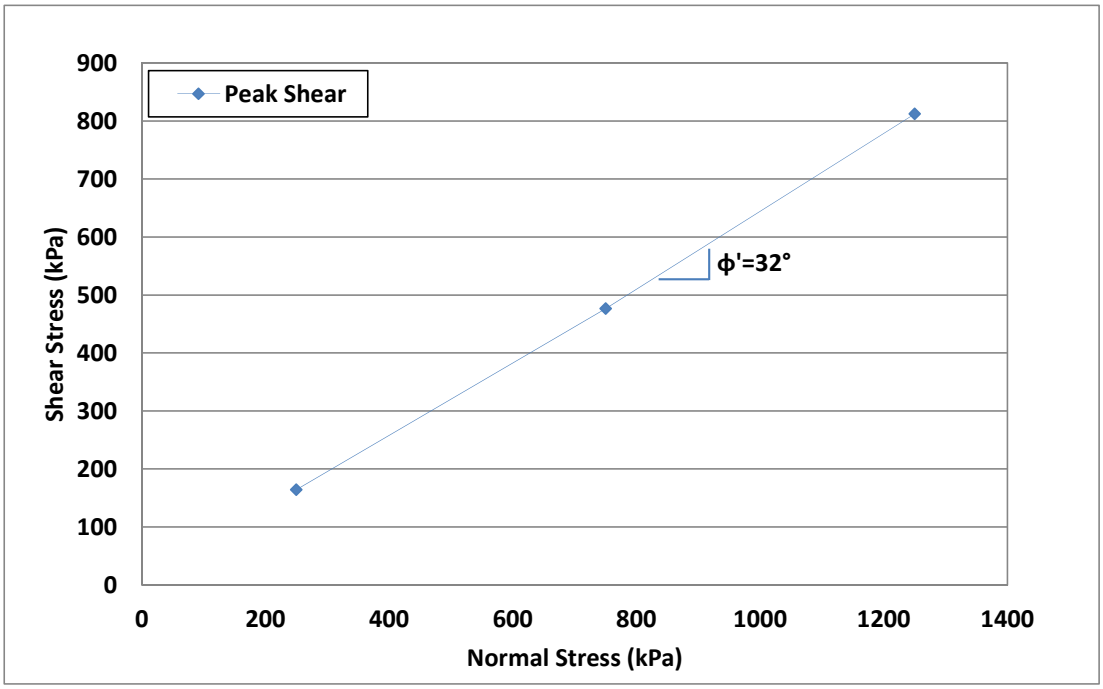

Figure D5-2 Direct shear test results on sand tailings

D5.3 Direct Simple Shear Tests

D5.3.1 Scope

Nine direct simple shear tests were completed as follows:

1. Four monotonic DSS tests to obtain undrained peak and large strain shear strengths.
2. Three cyclic simple shear tests with no static bias to investigate undrained response to cyclic loading.
3. Two cyclic tests with static bias to investigate undrained response to cyclic loading.

D5.3.2 Procedure

Direct Simple Shear (DSS) tests were conducted by KCB in accordance with ASTM D6528. All shearing was done undrained by holding the sample volume constant. This was done by changing the vertical load so that the sample height remained constant. The DSS specimens were consolidated to vertical effective stresses of 150 kPa, 300 kPa, 400 kPa and 600 kPa.

Most DSS samples were run on unsaturated samples. Saturation was attempted on DSS-11 but was not successful. Saturation of DSS-12 and DSS-14 was successful but, as expected, the results did not differ from the unsaturated sample tests.

The cyclic parameters for the cyclic DSS tests were chosen to test the range of seismic loading from the earthquakes that preceded the failure. The earthquake horizontal acceleration was converted to an equivalent cyclic loading, which was then converted into a horizontal cyclic shear stress. The frequency of cyclic loading applied during loading was 0.1 Hz.

Monotonic DSS tests were completed to measure the peak undrained shear strength at 20% shear strain. The specimens were sheared at a 5% shear strain rate.

D5.3.3 Test Results

The test results are given in Table D5-3, Table D5-4, and Table D5-5. The complete test results are given in Attachment D5. Selected test results are illustrated on Figure D5-5.

Table D5-3 Summary of Undrained DSS monotonic test results on sand tailings

Test ID	Moisture Content		Void Ratio		Axial Strain after Consolidation (%)	Vertical Effective Stress, σ'_{vc} (kPa)	Undrained Shear Strength (kPa)	Maximum Excess Pore Pressure Ratio, $\Delta U/\sigma'_{vc}$	Maximum Undrained Stress Ratio, τ/σ'_{vc}
	Initial, W_i (%)	Final, W_f (%)	at Placement, e_i	Final Void Ratio, e_0 [1]					
DSS - 8	4.98	4.49	1.20	0.93	12.48	600	82	0.86	0.14
DSS - 9	4.98	4.55	1.20	1.04	7.13	150	19	0.83	0.13
DSS - 10	4.98	4.48	1.20	1.00	9.09	300	41	0.84	0.14
DSS - 11	4.98	21.00	1.20	0.93	12.21	300	36	0.94	0.12

1. Void ratios after consolidation were calculated using height measurements.

Table D5-4 Summary of Undrained DSS cyclic test results on sand tailings

Test ID	Moisture Content		Void Ratio		Axial Strain after Consolidation (%)	Vertical Effective Stress, σ'_{vc} (kPa)	Maximum Excess Pore Pressure Ratio, $\Delta U/\sigma'_{vc}$	Maximum Shear Strain Reached at CSR, γ_{max} (%)			Number of Cycles N_{cyc}		
	Initial, W_i (%)	Final, W_f (%)	at Placement, e_i	Final Void Ratio, e_0 [1]				at 0.01	at 0.05	at 0.1	at 0.01	at 0.05	at 0.1
DSS - 1	5.04	10.27	0.90	0.88	0.84	300	0.99	0.01	0.06	23.31	30	30	11
DSS - 2	5.04	14.65	1.20	0.96	11.10	300	0.98	0.01	0.07	56.87	30	30	2
DSS - 4	4.99	12.57	1.20	0.96	11.05	300	0.98	0.01	0.11	51.3	30	30	2

1. Void ratios after consolidation were calculated using height measurements.

Table D5-5 Summary of Undrained DSS cyclic test results with static bias on sand tailings

Test ID	Moisture Content		Void Ratio			Axial Strain after Consolidation (%)	Vertical Effective Stress, σ'_{vc} (kPa)	Maximum Excess Pore Pressure Ratio, $\Delta U/\sigma'_{vc}$	Static Bias Shear Stress, τ_h	Static Bias, α	Limiting Shear Strain, γ_{max} (%)	CSR	Number of Cycles to Reach Max Shear Strain
	Initial, W_i (%)	Final, W_f (%)	at Placement, e_i	Final Void Ratio, e_0 [1]	Final Void Ratio, e_0 [2]								
DSS - 12	5.16	25.37	1.20	0.79	0.75	18.52	401	0.94	70	0.175	15	0.002	4802
DSS - 14	5.16	24.88	1.19	0.76	0.74	19.44	400	0.77	140	0.35	15	0.002	492

1. Void ratios after consolidation were calculated using height measurements.
2. Final void ratios were calculated using final moisture content from frozen specimens assuming the specimens were fully saturated.

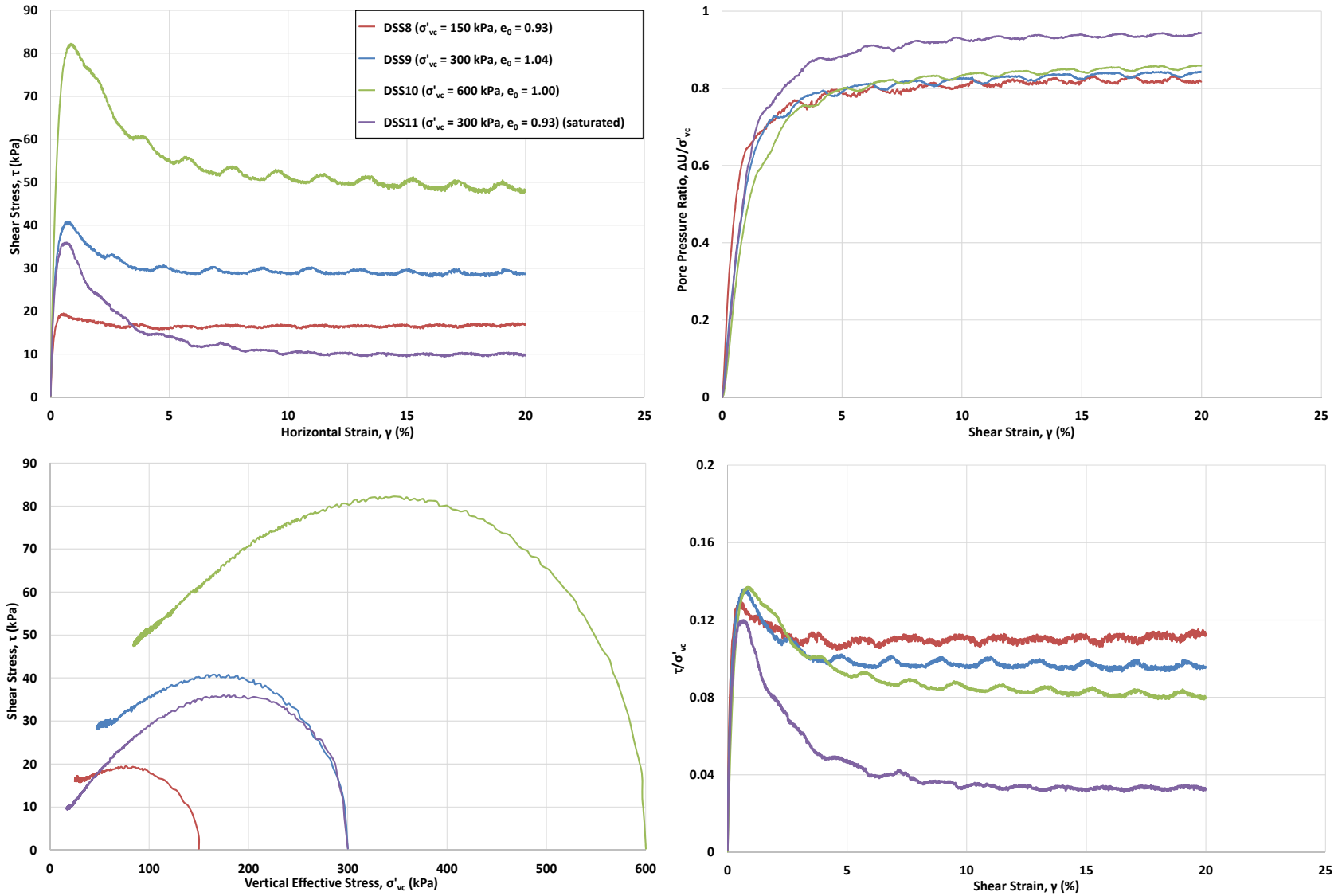

Figure D5-3 Direct simple shear test results on sand tailings (monotonic)

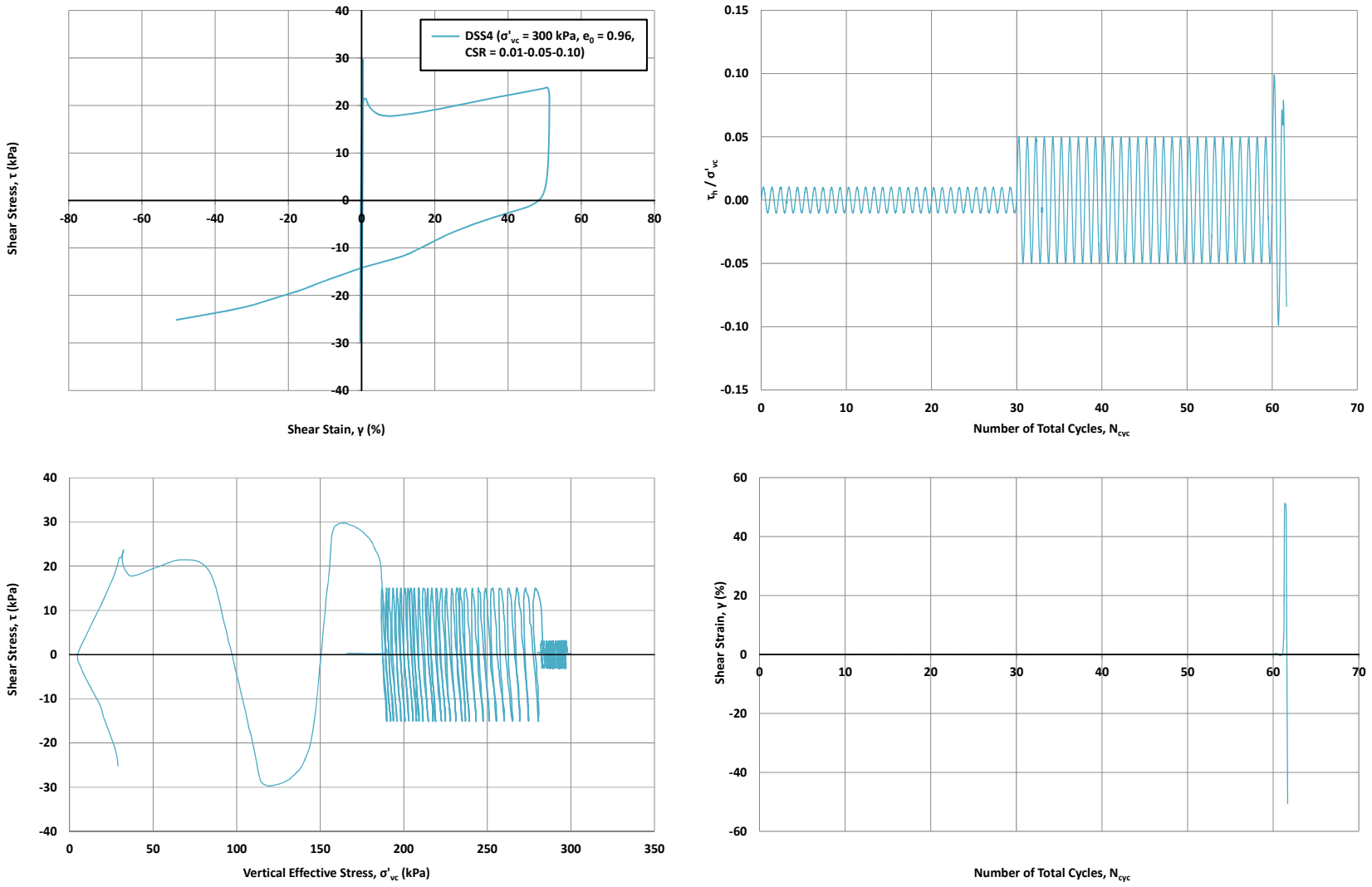

Figure D5-4 Direct simple shear test results on sand tailings (cyclic) – DSS4

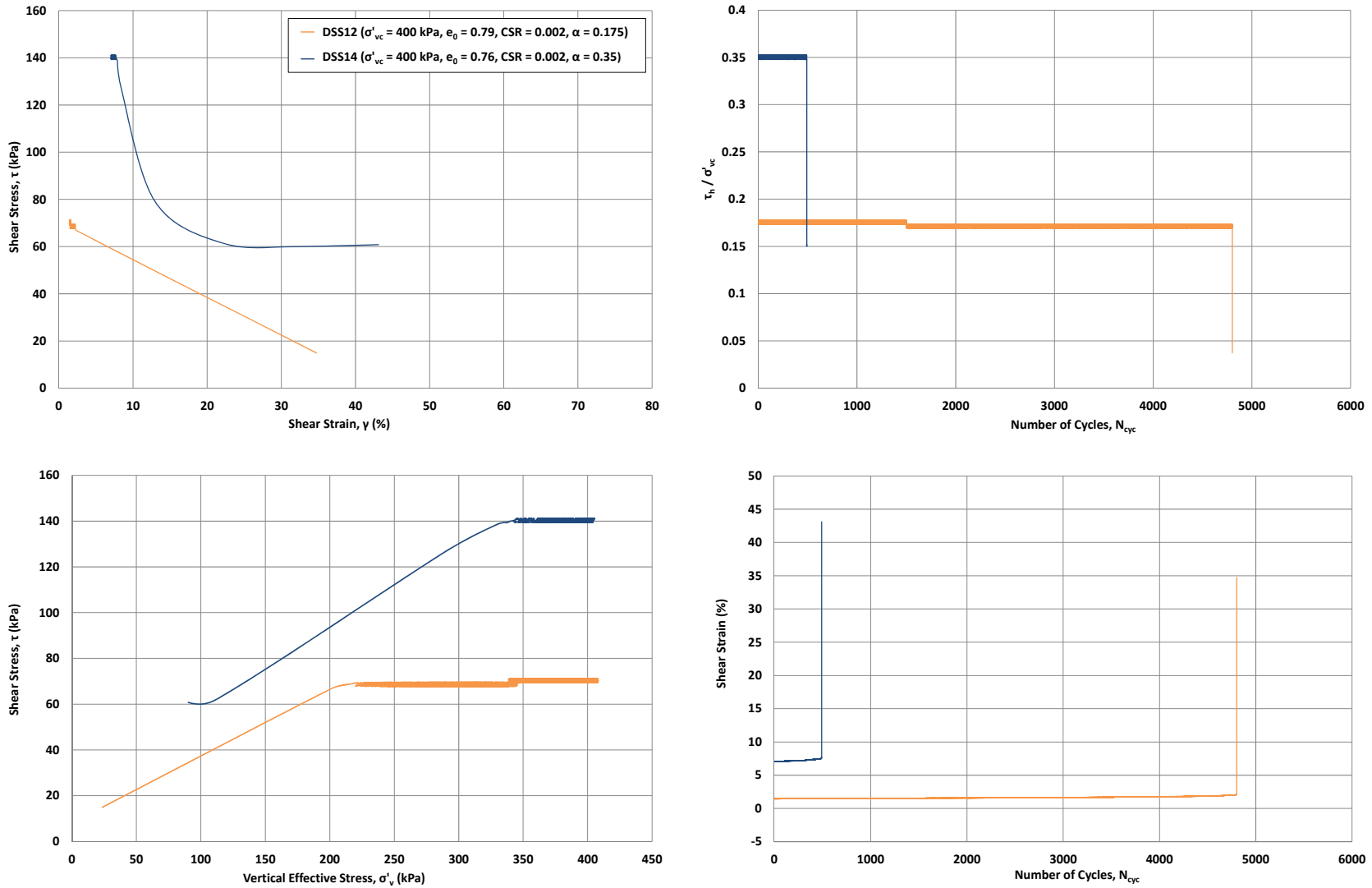

Figure D5-5 Direct simple shear test results on sand tailings (cyclic with static bias) – DSS12 and DSS14

D5.4 Triaxial Tests

D5.4.1 Scope

Thirty triaxial tests were completed including:

- 21 standard strain-controlled, CIU, CAU, CAD and CID, triaxial tests;
- 4 strain-controlled extrusion collapse, CA-QD, triaxial tests;
- 4 stress-controlled extrusion collapse, CA-QID-SC, triaxial tests; and
- 1 stress-controlled extrusion collapse, CA-QID-SC (cyclic), triaxial test with a cyclic component.

Tests were conducted on PSD1 sand tailings samples with the exception of four standard strain-controlled, CIU and CID, triaxial tests, which were conducted on PSD2 sand tailings specimens. The samples were tested at confining stresses ranging from 50 kPa to 600 kPa.

The main objective of the triaxial testing program on sand tailings was to:

1. Compare test results from the current program with the results obtained from the 2013 Rezende[40] testing program which were completed on "undisturbed" Fundão sand tailings. All tests completed in this program were completed on reconstituted sand tailings specimens.
2. Determine CSL and dilatancy parameters required for NorSand modeling at different density states and assess influence of fines content on liquefaction susceptibility and post liquefaction strength.
3. Strain-controlled extrusion collapse, CA-QD, triaxial tests were completed to assess additional possible failure scenarios including static liquefaction due to drained reduction in lateral stress with relatively constant "q".
4. Stress-controlled extrusion collapse, CA-QID-SC and CA-QD-SC, triaxial tests were completed to assess additional possible failure scenarios including static liquefaction due to increase in static pore pressure and lateral extrusion mechanism.
5. One stress-controlled extrusion collapse, CA-QID-SC (cyclic), triaxial test with a cyclic component.

The stress path for "extrusion collapse" tests are shown on Figure D5-1. Strain-controlled triaxial tests on this stress path could not mimic the field conditions, so stress-controlled tests were done on the same path so that the sample could actually collapse.

D5.4.2 Procedure for Standard Strain-Controlled Triaxial Tests

The standard strain-controlled, CIU, CID, CAU and CAD, triaxial tests were completed in accordance with ASTM D4767-11 (CIU), ASTM D7181-11 (CID). The sand specimens were isotropically consolidated to the required stress level. This consolidation phase was followed by the shearing phase under drained or undrained conditions (CID or CIU) using strain controlled loading. After the triaxial tests were completed, the specimens were frozen together with top and bottom platens for an accurate determination of moisture content. This moisture content was then used to calculate the final void ratio and comparison with the void ratio tracking during testing.

A modified compaction mold was used to prepare the triaxial specimen by moist-tamping (see Figure D5-6 and Figure D5-7). A washed sieve analysis and specific gravity test were completed on each specimen prior to each triaxial test (Section D4). The specific gravities were used to calculate the target void ratios and dry densities prior to each test. Height and diameter measurements were taken at each test stage to be used for accurate void ratio calculations. Using the "under-compaction" method (Ladd 1978), the sample was compacted to achieve a uniform specimen by varying the weight of each compacted layer. A vacuum (<5 kPa) was applied to the specimen to hold the loose triaxial specimen before placement in the triaxial cell. The triaxial cell was filled with water and a cell pressure (~20 kPa) was applied to hold the specimen. Carbon dioxide (CO_2) was applied through the specimen prior to the saturation phase for approximately 1 to 2 hours. CO_2 is more soluble in water than air.

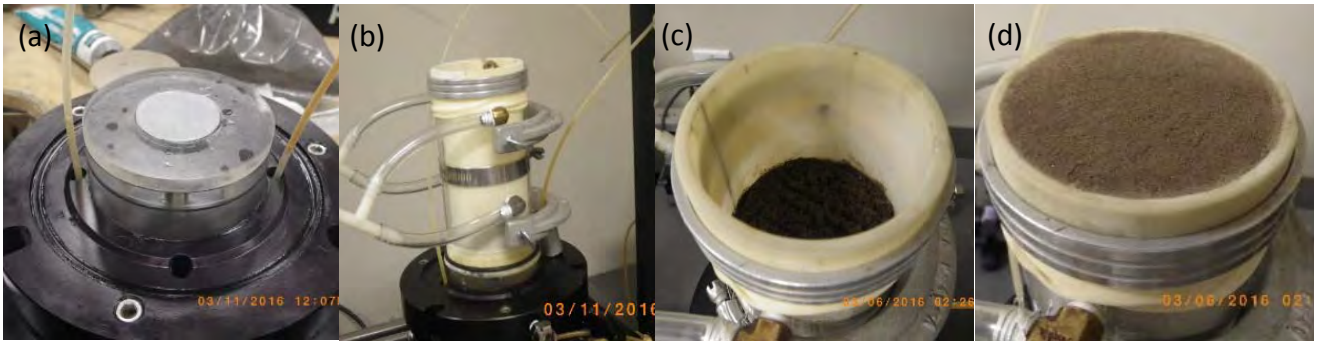

(a) Modified porous stone, (b) Specimen setup, (c) Specimen placement by moist tamping, (d) Final specimen

Figure D5-6 Triaxial test setup 1

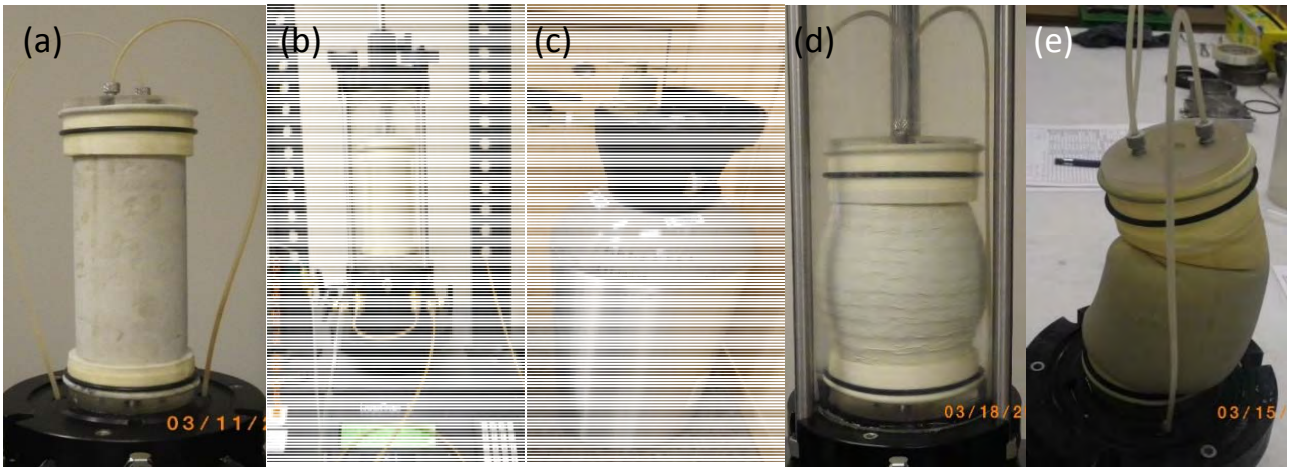

(a) Vacuum applied to hold specimen, (b) Specimen placed within triaxial machine, (c) CO_2 application, (d) Specimen after shearing, (e) Frozen specimen

Figure D5-7 Triaxial test setup 2

Three standard anisotropically consolidated undrained strain-controlled, CAU, triaxial tests were completed. The sand tailings specimens were isotropically consolidated to 200 kPa and 400 kPa mean effective stress (p'), then the deviator stress was increased to reach a predetermined value of n=q/p'=0.5 (anisotropic consolidation). The shearing stage followed standard ASTM procedure for standard undrained strain-controlled compression test (ASTM D4767-11 (CAU)).

D5.4.3 Procedure for Strain-Controlled Extrusion Collapse, CA-QD, Triaxial Tests

Four strain-controlled extrusion collapse, CA-QD, triaxial tests were completed. The sand tailings specimens were isotropically consolidated to 200 kPa and 400 kPa mean effective stress (p'), then the deviator stress was increased to reach a predetermined value of n=q/p'=0.5 (anisotropic consolidation). The triaxial apparatus software was modified to keep q approximately constant and reduce confining pressure to bring tested specimens to failure. In standard strain-controlled triaxial tests, vertical load is applied through the bottom platen (where the tested specimen is placed) by moving it up during shearing. The triaxial test piston is fixed to the metal frame. This fixation restricted sample response so a stress-controlled apparatus was designed to remove this limitation.

D5.4.4 Procedure for Stress-Controlled Extrusion Collapse, CA-QID-SC and CA-QD-SC, and CAD Triaxial Tests

The KCB triaxial apparatus was modified as shown on Figure D5-8. KCB constructed a horizontal metal frame capable of carrying the required load from two pails from both sides of the frame. The frame was fixed and centered at the top of the standard triaxial device. The pails were used to load the triaxial specimen using dead loads.

As before, the triaxial sample was isotropically consolidated to the confining pressure. After isotropic consolidation was complete, the piston was locked. The loading frame load was attached and then the pins fixing the loading frame were removed. After the sample came to equilibrium, the piston was unlocked and vertical loading started. The samples were loaded by adding sand bags to each pail simultaneously at a rate of approximately 1 kg every 3 minutes to increase the deviator stress to a predetermined deviator stress under drained conditions to reach n=q/p'=0.5 (anisotropic consolidation). The mean effective stress was kept constant by slightly reducing the cell pressure during the "anisotropic stage". The deviator stress was kept constant overnight (Jefferies and Been 2016).

After anisotropic consolidation, three slightly different drained stress paths were followed:

- **Deviator stress (q=const) (CA-QD-SC)**: σ'_1 and σ'_3 were reduced simultaneously and shearing was conducted under drained conditions.
- **Deviator stress increasing (CA-QID-SC)**: The vertical load was increased in small increments (approximately 0.25 kg) while reducing the cell pressure by 4 kPa approximately every 5 minutes, resulting in a stress reduction rate of less than 1 kPa/min. The result was a simultaneous increase in σ'_1 and a decrease in σ'_3 using the cell pressure. When the specimen approached failure, the mean effective stress was decreased at a rate of 0.5 kPa/min.

- **Deviator stress increasing (CAD - not extrusion collapse test):** The vertical load was increased in small increments by adding dead weights while keeping the cell pressure constant (σ'_3=constant). The result was an increase in deviator stress (q) and mean effective stress (p') at the same time until failure.

D5.4.5 Procedure for Stress-Controlled Extrusion Collapse, CA-QID-SC (Cyclic), Triaxial Test with a Cyclic Component

One extrusion collapse, CA-QID-SC (cyclic), triaxial test with a cyclic component was completed to investigate cyclic pore pressure build up. The sand specimen was first isotropically consolidated to 200 kPa followed by an increase in deviator stress as described earlier in Section D5.4.3. Deviator stress (q) was increased by keeping vertical stress constant (σ'_1=constant) and reducing confining stress (σ'_3), axial strain was closely monitored. Once the strain-rate started noticeably increasing, drained monotonic shearing was stopped and undrained cyclic shearing started. The cyclic shearing was imposed by adding and removing four weights of equal mass. Cyclic frequency was approximately 0.1 Hz.

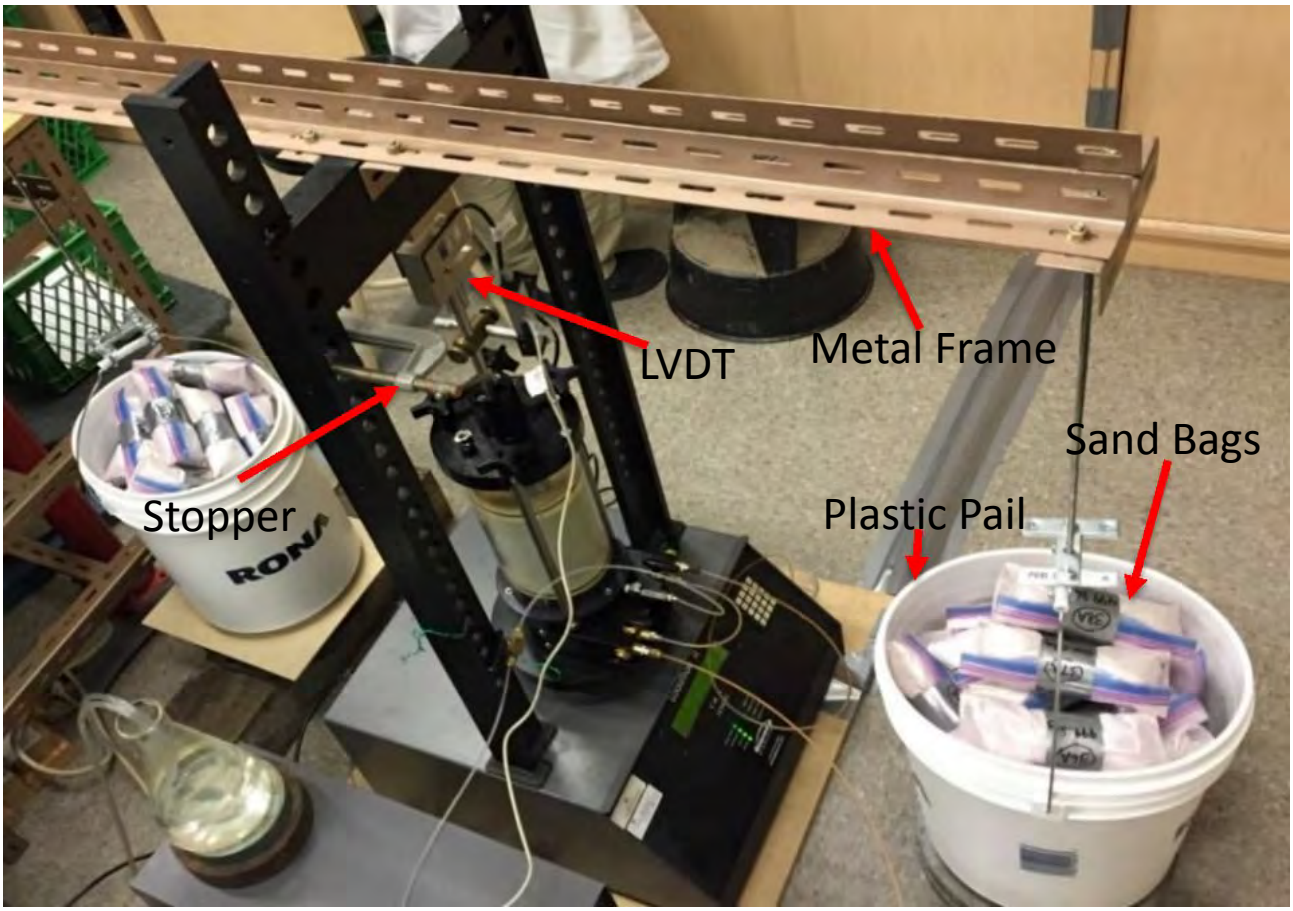

Figure D5-8 Apparatus modifications for CA-QID-SC and CA-QID-SC (cyclic) triaxial tests

D5.4.6 Standard Strain-Controlled, CID, CIU, CAU and CAD, Test Results

All triaxial test results are in Attachment D6. Figure D5-9 and Figure D5-10 are Mohr-Coulomb plots of all triaxial tests. All tests give an angle of shearing resistance of 33 degrees. All tests were conducted on PSD1 sand.

The critical state line was determined following techniques advocated by Jefferies and Been (2016). The results are shown in Figure D5-11 on a void ratio versus mean effective stress plot. The stress paths for all of these tests are shown on a void ratio versus deviator stress plot in Figure D5-12. Figure D5-13 shows test results from all undrained strain-controlled, CIU and CAU, triaxial tests.

One objective the testing program was to compare triaxial test results with Rezende[40]. This is done on Figure D5-14 and Figure D5-15, which plot deviator stress and volumetric strain against axial strain at samples consolidated to 300 kPa. The Panel tests were done at two void ratios, 0.81 and 0.73, hopefully to bracket the test void ratio which is not known. Results are similar.

Standard strain-controlled, CID and CIU, triaxial tests were conducted on PSD1 and PSD2 specimens under the same test conditions to assess the effect of fines. By “fines” is meant the percent passing the No. 200 sieve. Figure D5-16 shows that, for the same test conditions, PSD1 and PSD2 specimens show similar behavior. Beyond these two triaxial tests on loose samples in undrained shear, the effects of fines was not investigated further.

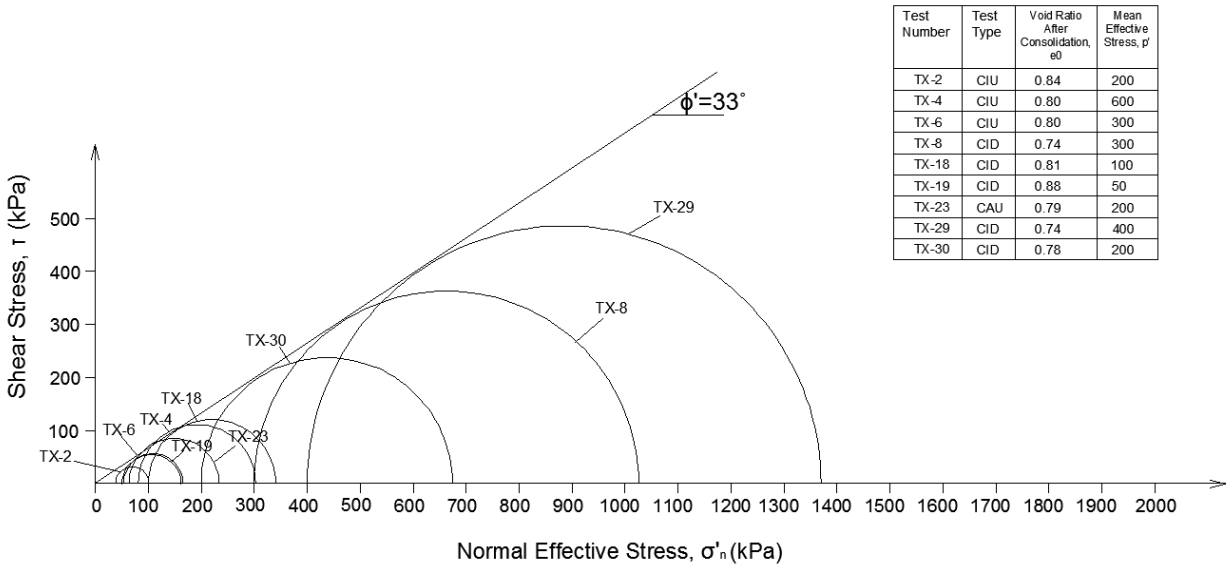

Test Number	Test Type	Void Ratio After Consolidation, e0	Mean Effective Stress, p'
TX-2	CIU	0.84	200
TX-4	CIU	0.80	600
TX-6	CIU	0.80	300
TX-8	CID	0.74	300
TX-18	CID	0.81	100
TX-19	CID	0.88	50
TX-23	CAU	0.79	200
TX-29	CID	0.74	400
TX-30	CID	0.78	200

Figure D5-9 Mohr circles for standard, CIU, CID and CAU, triaxial compression tests on PSD1

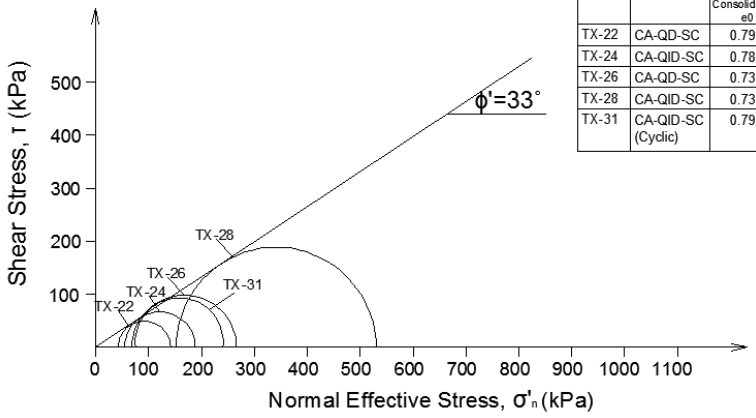

Test Number	Test Type	Void Ratio After Consolidation, e0	Mean Effective Stress, p'
TX-22	CA-QD-SC	0.79	200
TX-24	CA-QID-SC	0.78	200
TX-26	CA-QD-SC	0.73	400
TX-28	CA-QID-SC	0.73	400
TX-31	CA-QID-SC (Cyclic)	0.79	200

Figure D5-10 Mohr circles for extrusion collapse, CA-QD-SC and CA-QID-SC, triaxial tests on PSD1

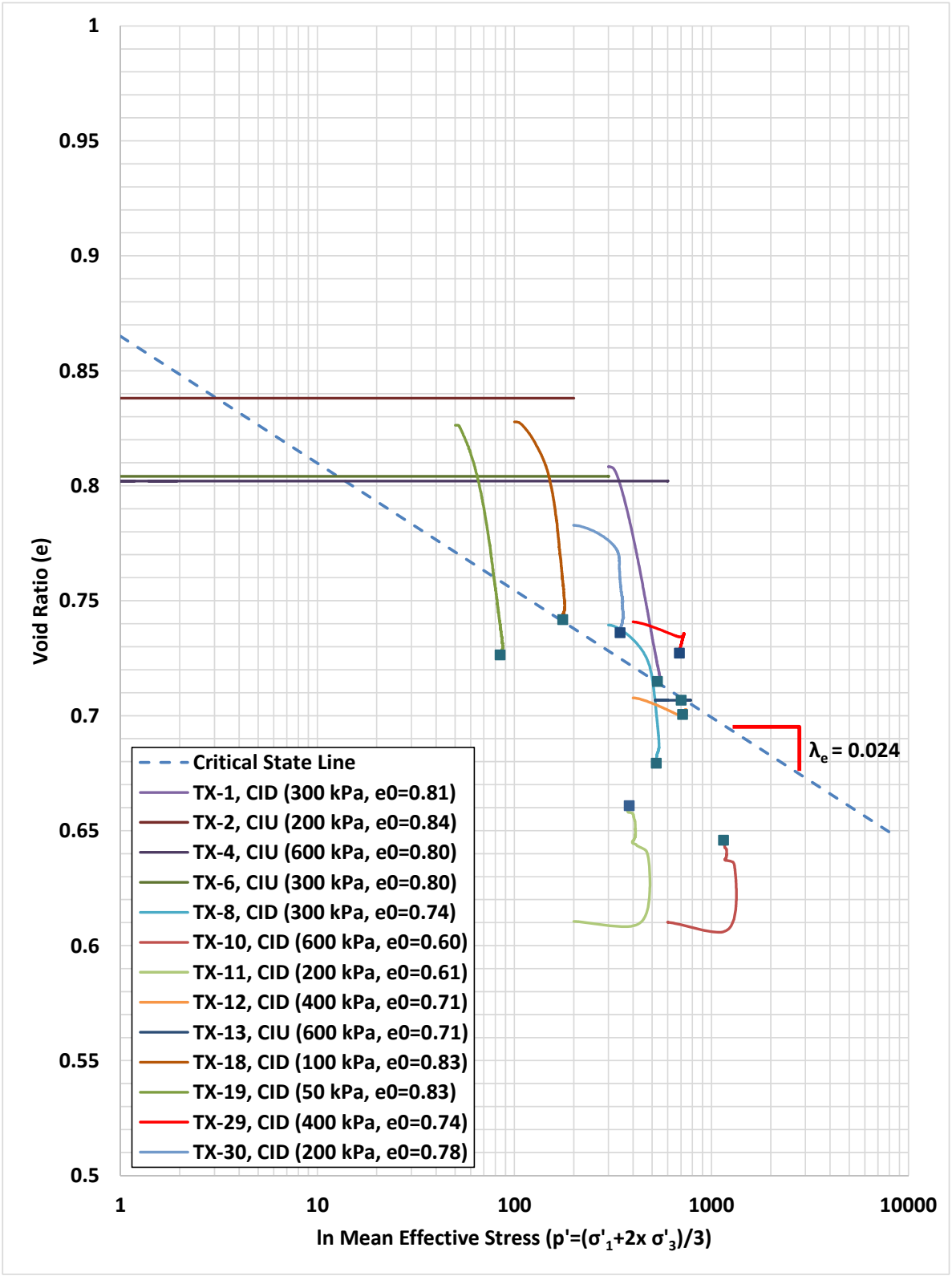

Figure D5-11 State diagram and critical state line for CIU and CID tests on sand tailings

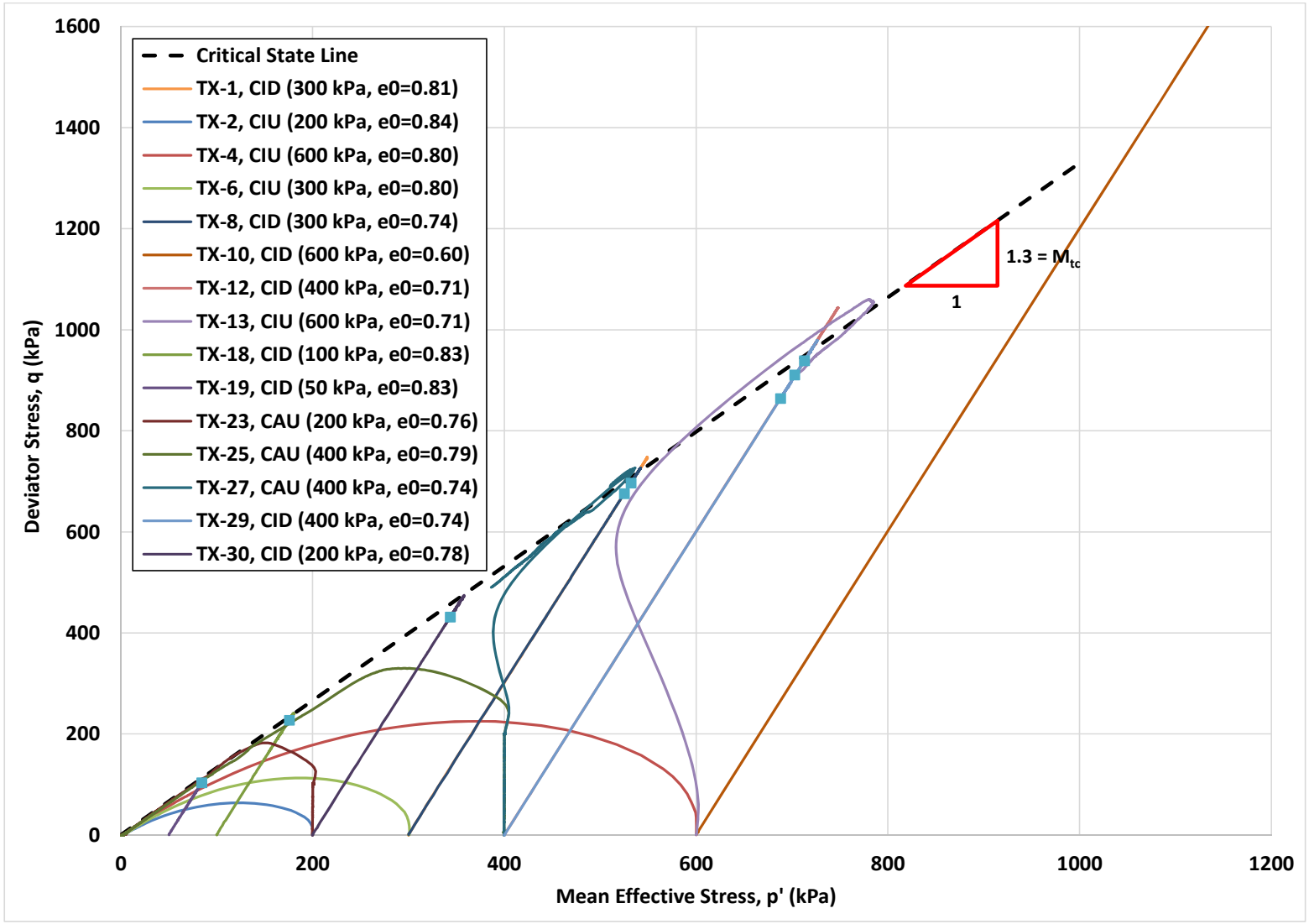

Figure D5-12 Stress paths from CID, CIU, CAD and CAU on sand tailings

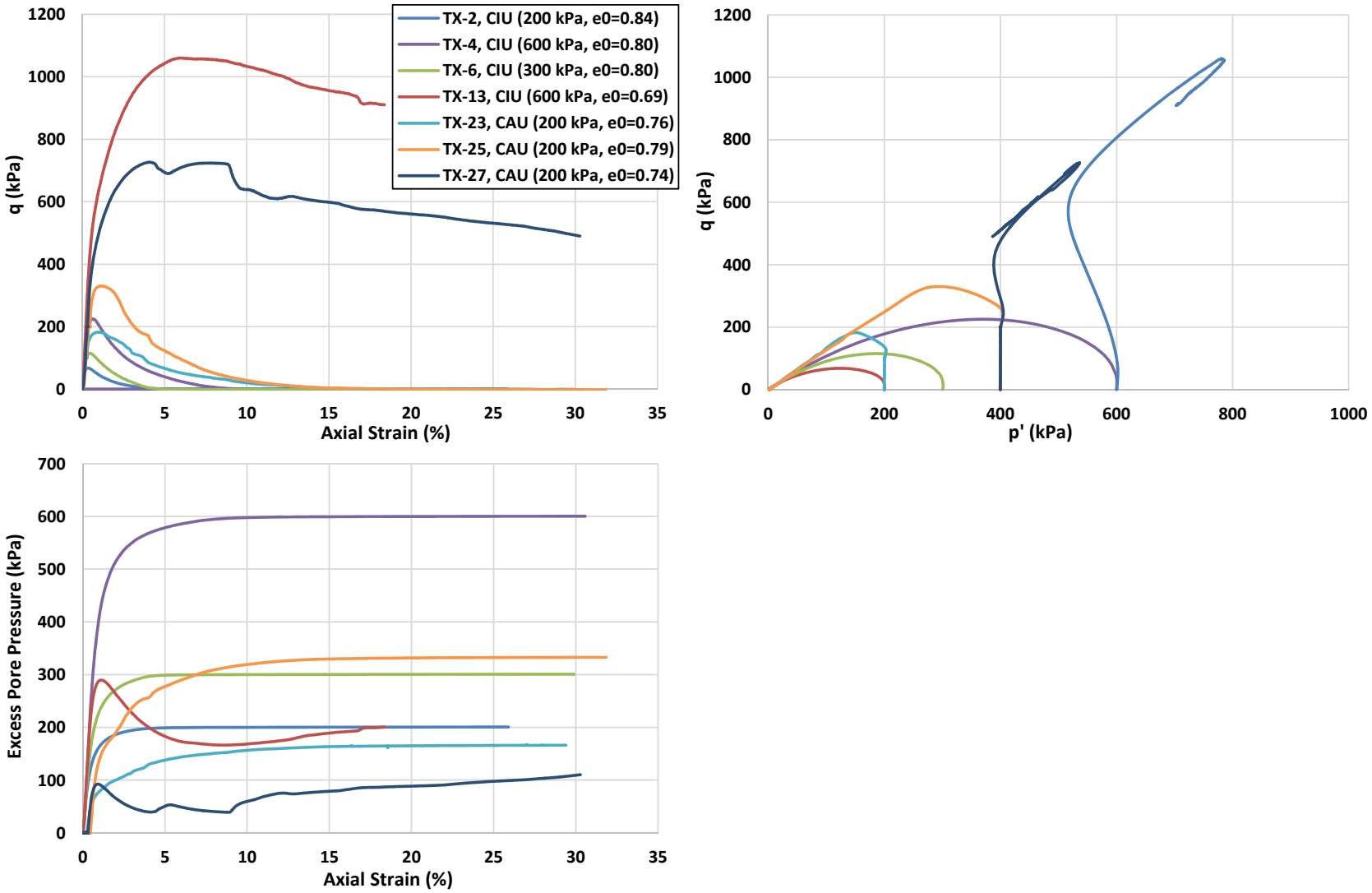

Figure D5-13 CIU and CAU triaxial test results on sand tailings (PSD1)

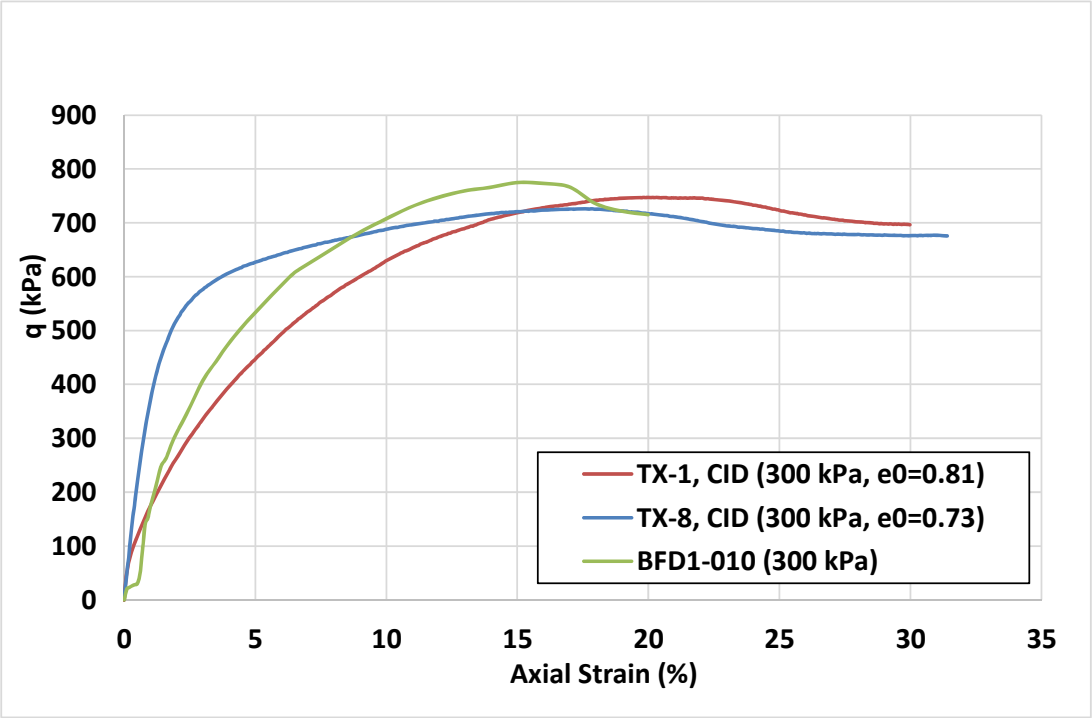

Figure D5-14 Deviator stress vs. axial strain from CID triaxial tests on sand tailings (comparison of results from 2016 and Rezende[40] lab testing programs)

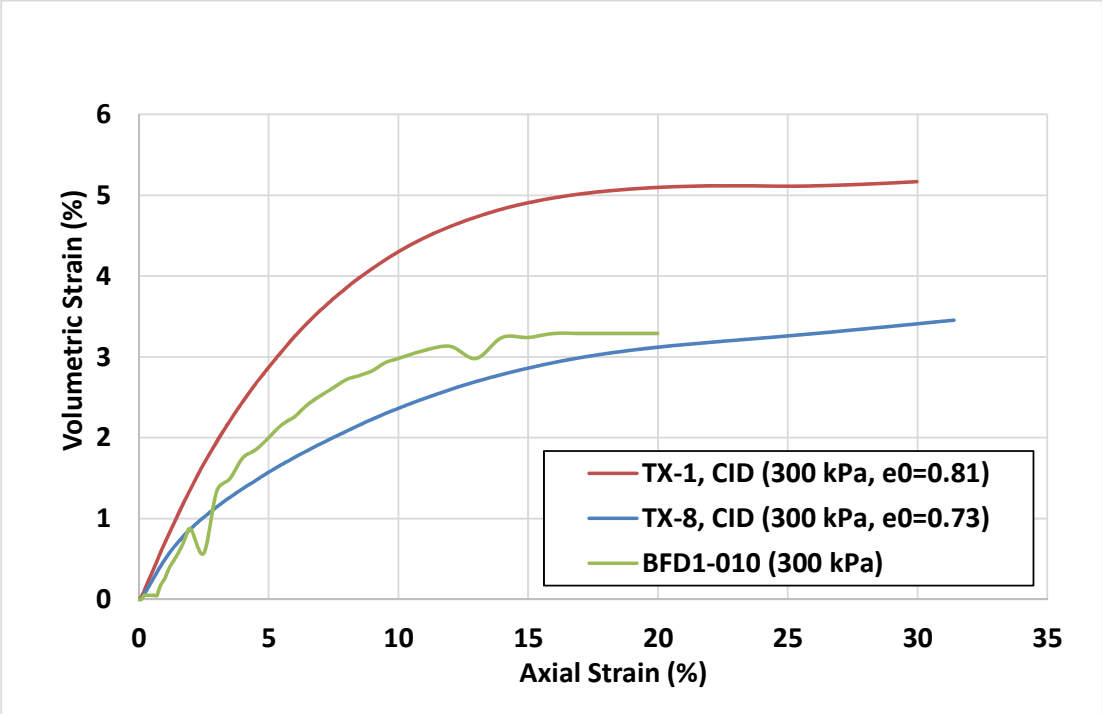

Figure D5-15 Volumetric strain vs. axial strain from CID triaxial tests on sand tailings (comparison of results from 2016 and Rezende[40] lab testing programs)

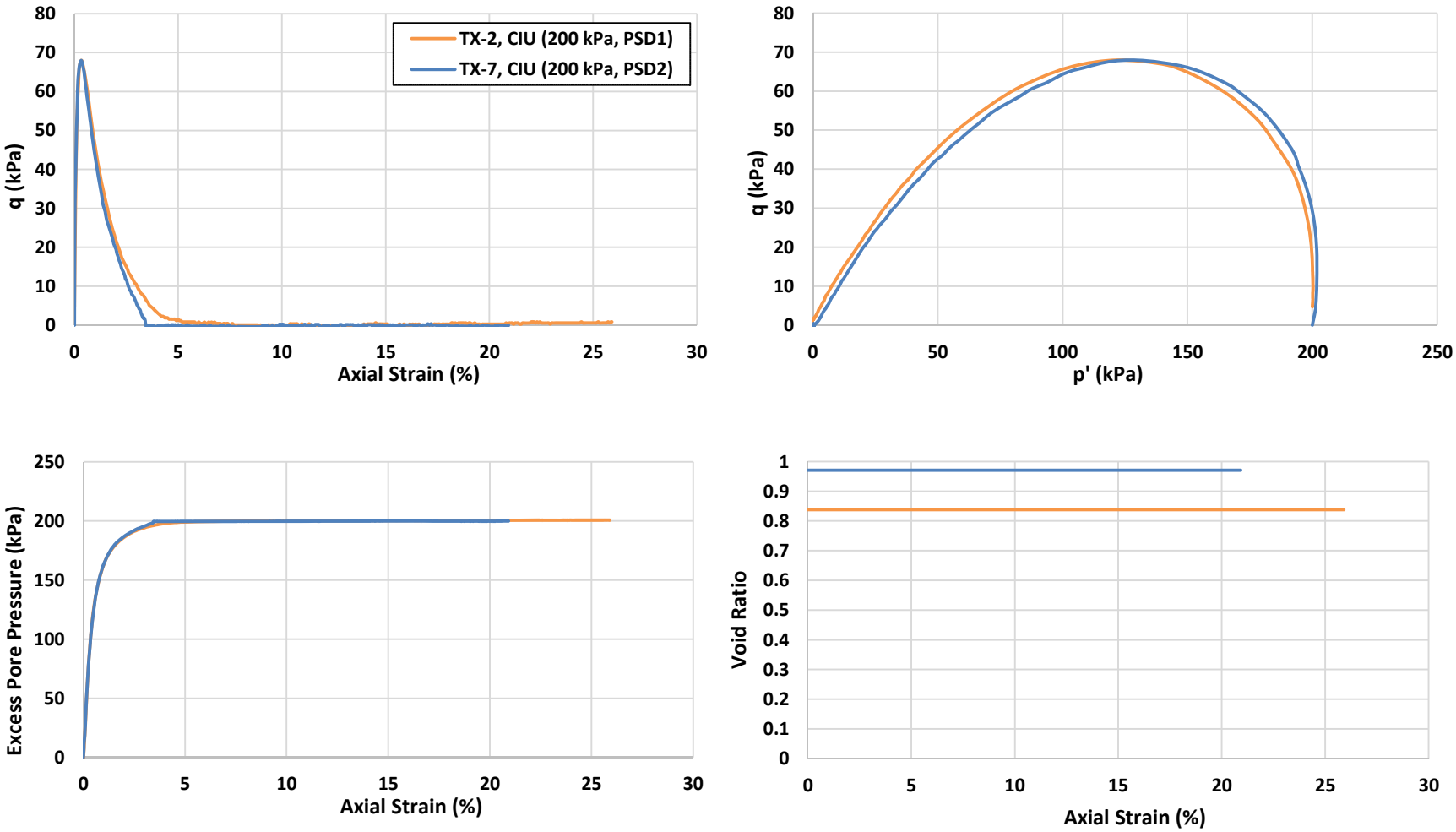

Figure D5-16 Comparison of CIU triaxial test results on PSD1 and PSD2 (effect of fines)

D5.4.7 Strain-Controlled, CA-QD, Triaxial Test Results

Test results are presented in Attachment D6 and on Figure D5-17. All four tests were consolidated anisotropically to either 200 kPa or 400 kPa. The cell pressure was then reduced to model horizontal stress reduction in the field under drained conditions. The samples prepared at a looser condition failed without developing shear plane by bulging significantly (see photos in Attachment D6). The samples prepared at a denser condition failed by developing a shear plane (see photos in Attachment D6).

The sand tailings did not "collapse" because of the limitations of strain-controlled triaxial testing. The triaxial test apparatus was modified as described earlier to apply the vertical load directly. This allows the samples to fail by collapse if that was the failure mode. The stress-controlled extrusion collapse triaxial test results are described in the next section.

D5.4.8 Stress-Controlled Extrusion Collapse, CA-QD-SC and CA-QID-SC, Triaxial Test Results

The test results are presented in Attachment D6, on Figure D5-18, and on Figure D5-19. All stress-controlled extrusion collapse triaxial tests, CA-QD-SC and CA-QID-SC, collapsed rapidly. All tests were drained to the point of collapse where the rapid failure was actually undrained in spite of the drainage valves being open.

- **TX-22 (CA-QD-SC):** after anisotropic consolidation (increase in q up to 100 kPa while keeping p'=200 kPa) the void ratio of sand was 0.79. The deviator stress, q, was maintained at 100 kPa while the mean effective stress was reduced from 200 kPa to 78 kPa with the drainage valves open. The sample collapsed rapidly near the CSL. The recorded maximum axial strain during the drained portion of the test, before collapse, was 1.7%.
- **TX-24 (CA-QID-SC):** after anisotropic consolidation (increase in q up to 100 kPa while keeping p'=200 kPa) the void ratio of the sand was 0.78. The mean effective stress was decreased from 200 kPa to 101 kPa while the deviator stress (q), applied using dead load, was increased from 100 kPa to 132 kPa with the drainage valves open. The specimen collapsed rapidly near the CSL. The recorded maximum axial strain before collapse was 1.1%.
- **TX-26 (CA-QD-SC):** after anisotropic consolidation (increase in q up to 200 kPa while keeping p'=400 kPa) the void ratio of the sand was 0.73. The deviator stress, q, was maintained at 200 kPa while the mean effective stress was decreased from 400 kPa to 135 kPa. The specimen collapsed rapidly but not as "dramatically" as TX-22 and TX-24, described above. The recorded maximum axial strain during the drained portion of the test, before the dramatic failure, reached 1.2%.
- **TX-28 (CA-QID-SC):** after anisotropic consolidation (increase in q up to 200 kPa while keeping p'=400 kPa) the void ratio of the sand was 0.73. The deviator stress (q) was increased from 200 kPa to 378 kPa, using dead load while the mean effective stress was decreased from 400 kPa to 279 kPa. The specimen collapsed rapidly near the CSL but not as "dramatically" as TX-22 and TX-24, described above. The recorded maximum axial strain during the drained portion of the test, before the failure, reached 2.94%.

- **TX-32 (CAD):** after anisotropic consolidation (increase in q up to 100 kPa while keeping p'=200 kPa) the void ratio of the sand was 0.79. The deviator stress (q), applied using dead load, was increased from 100 kPa to 351 kPa. The mean effective stress increased from 200 kPa to 284 kPa during the deviator stress increase. The specimen collapsed rapidly at the CSL. The recorded maximum axial strain during the drained loading of the sample, before the rapid failure, reached 3.7%.

D5.4.9 Stress-Controlled Extrusion Collapse, CA-QID-SC (Cyclic), Triaxial Test Results with a Cyclic Component

The test results for TX -31 (CA-QID-SC (Cyclic)) are presented in Attachment D6, on Figure D5-20 and Figure D5-21. The first stage of testing was to anisotropically consolidate (increase in q up to 100 kPa while keeping p'=200 kPa) the sample, after which the void ratio was 0.79. The deviator stress (q), was then increased from 100 kPa to 160 kPa by applying dead load. The mean effective stress was decreased from 200 kPa to 163 kPa to maintain the desired stress path.

The first cyclic load was applied by adding and removing dead weights under undrained conditions; drainage valves closed. The sample was subjected to 525 cycles at a cyclic stress ratio of 0.01. The stress ratio was calculated according to ASTM D5311 as $SR_{desired}=\frac{q}{2\cdot\sigma'_{3c}}$: This initial value of 0.01 was higher than the field value which was too small to apply. At the end of 525 cycles, the axial strain was less than 0.58%. Excess pore pressure reached 7 kPa. Mean effective stress dropped from 163 kPa to 156 kPa.

Because it was obvious the sample was not going to fail at 0.01, the cyclic stress ratio was increased to 0.02. The sample developed 0.66% axial strain after 521 cycles (cumulative 1046 cycles). Excess pore pressure reached 14 kPa. The mean effective stress dropped from 156 kPa to 142 kPa. The stress ratio was again increased to 0.03 for 209 cycles when it reached 0.73% axial strain with excess pore pressure of 17 kPa. At this 1255^{th} cycle the sample collapsed. The collapse occurred so fast that data could not be acquired. The final stress ratio and the number of cycles was much higher than the left abutment would have actually experienced on November 5, 2015 during the main earthquake shock.

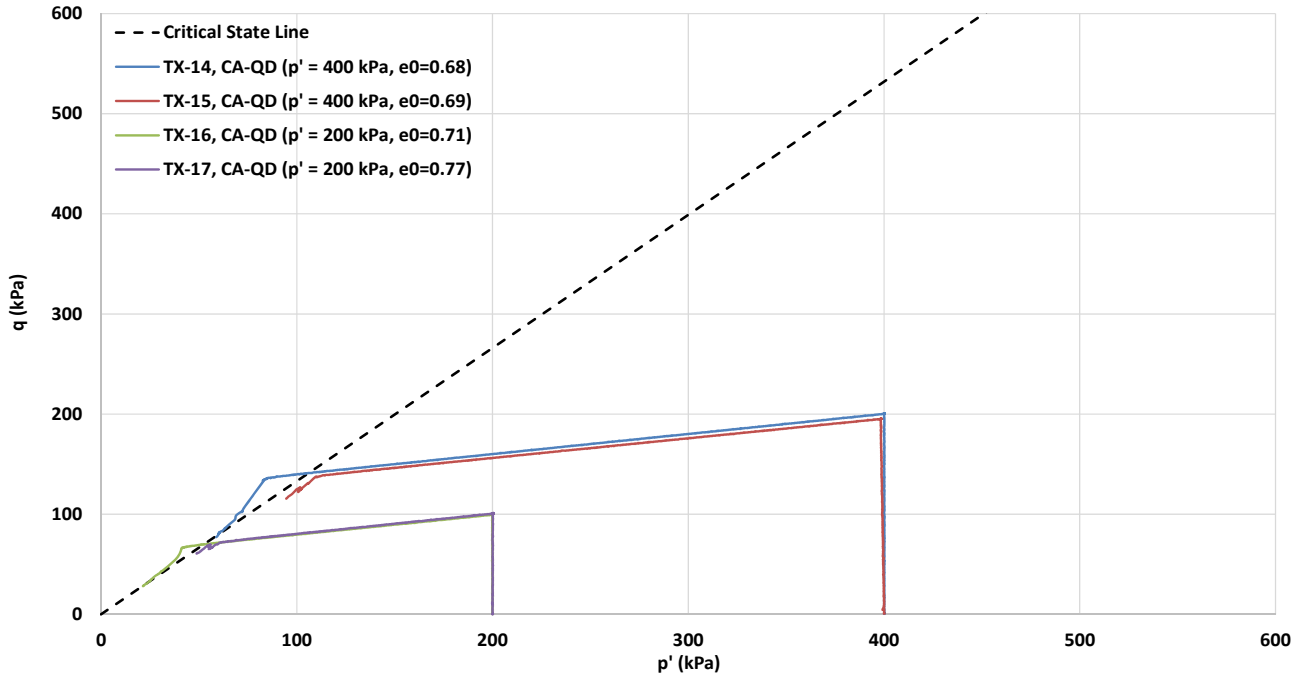

Figure D5-17 Strain-controlled, CA-QD, triaxial tests on sand tailings

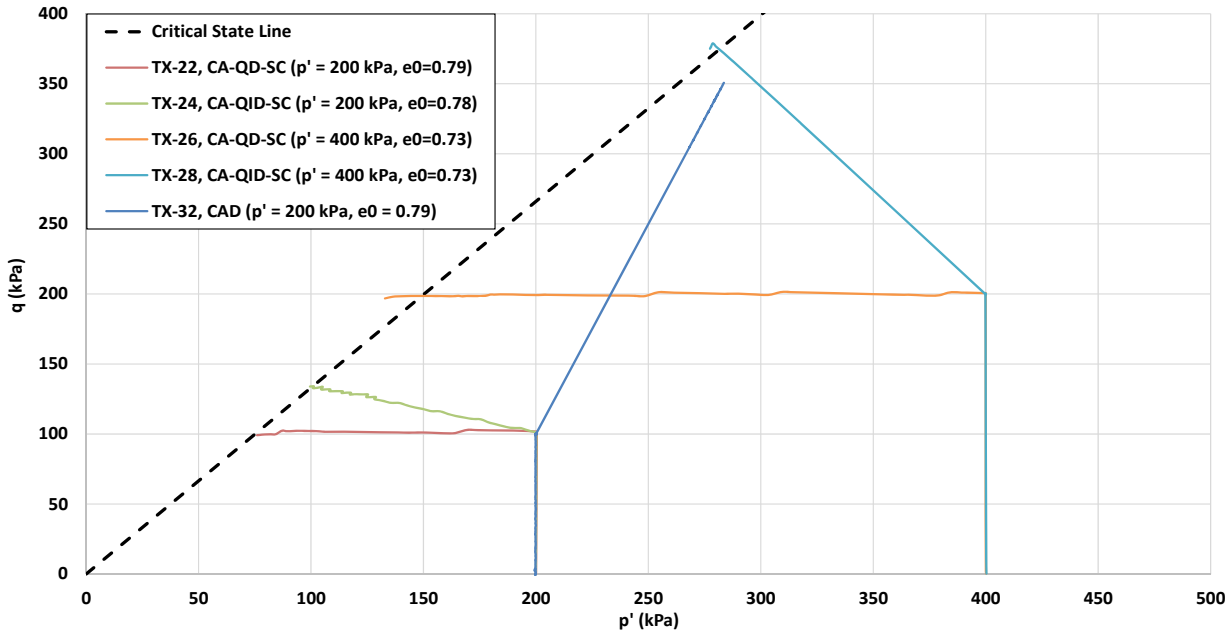

Figure D5-18 Stress-controlled extrusion collapse, CA-QID-SC and CA-QD-SC, and CAD triaxial tests on sand tailings

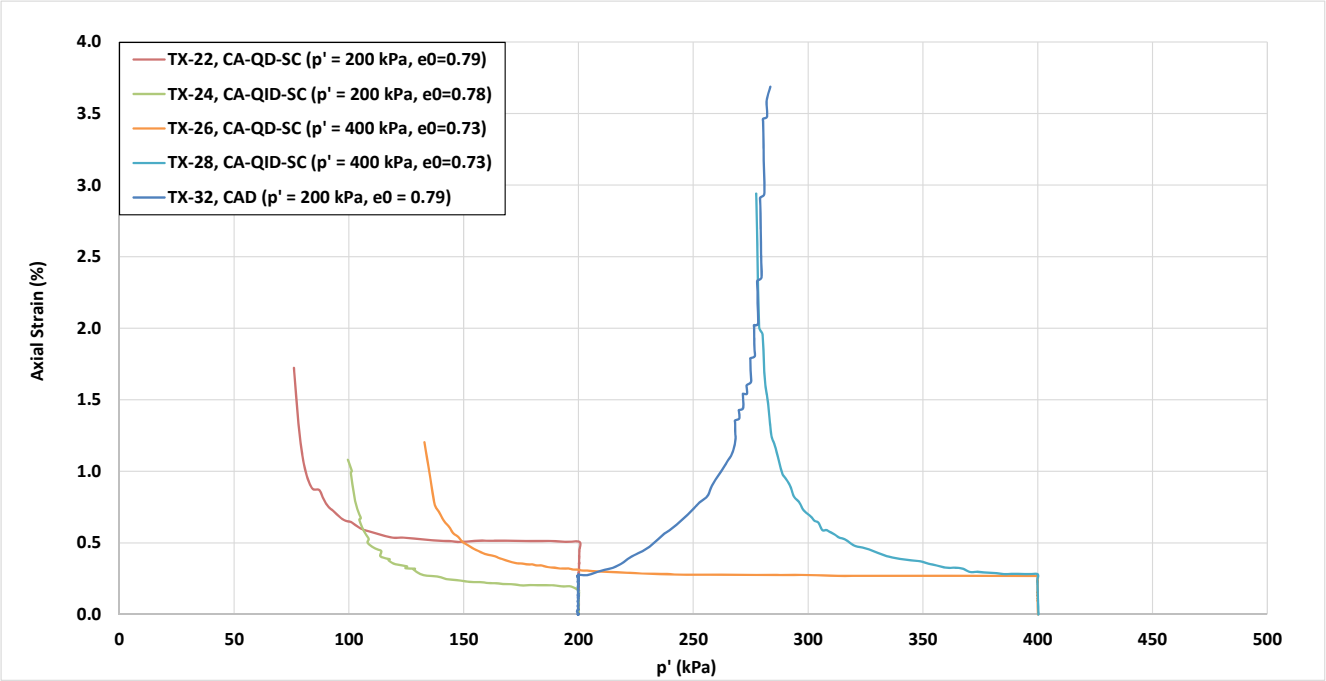

Figure D5-19 **Axial strain development during shearing in stress-controlled extrusion collapse, CA-QD-SC and CA-QID-SC, and CAD triaxial tests with a cyclic component on sand tailings**

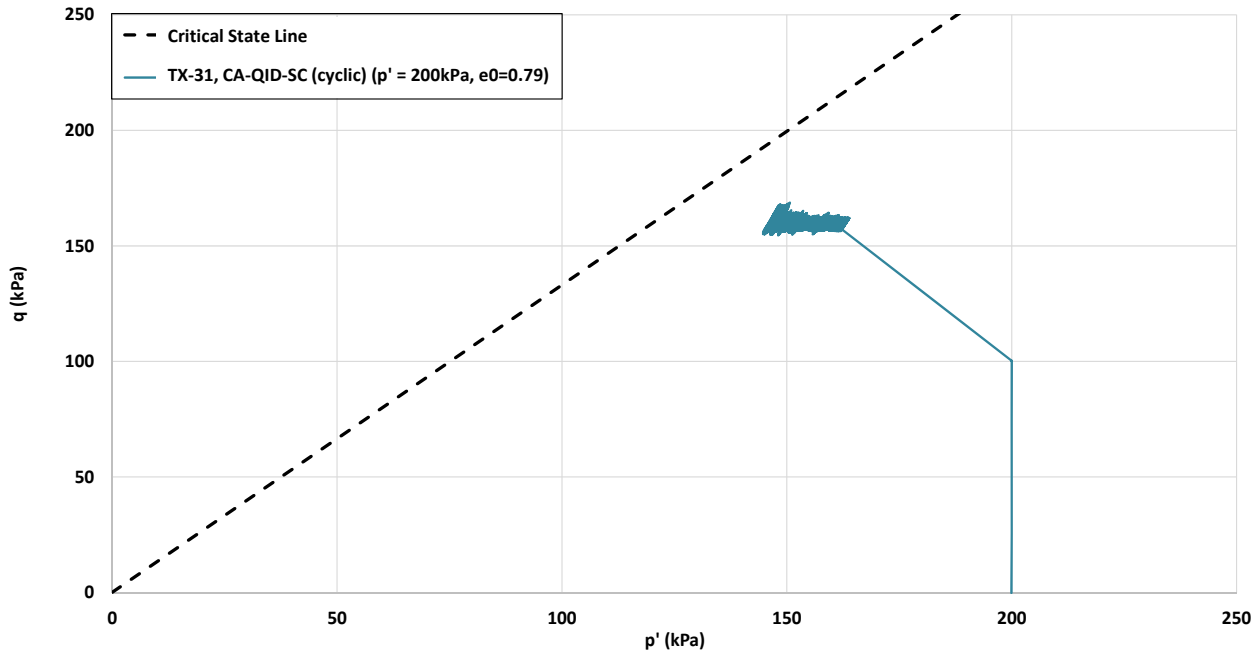

Figure D5-20 **Stress-controlled extrusion collapse, CA-QID-SC (cyclic), triaxial test with a cyclic component on sand tailings**

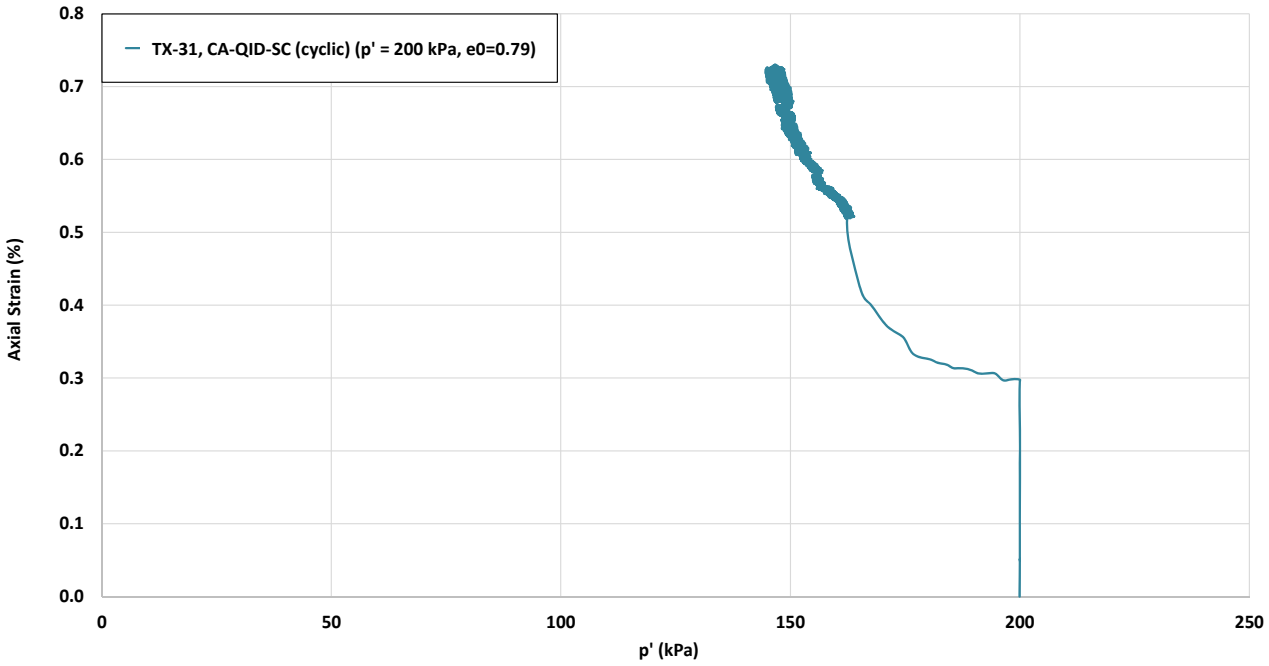

Figure D5-21 Axial strain development during shearing in stress-controlled extrusion collapse, CA-QID-SC (cyclic), triaxial test with a cyclic component on sand tailings

D5.5 Bender Elements Tests

D5.5.1 Scope

Bender elements tests were completed by KCB on two PSD1 sand tailings specimens in a loose and dense condition. Bender element tests measure the shear wave velocity of the specimens. The bender element test results are in Attachment D10.

D5.5.2 Procedure

Currently there is no internationally accepted standard for the bender element test; the test was conducted following recommendations outlined in the "Interpretation of International Parallel Test on The Measurement of G_{max} Using Bender Elements" (Yamashita et al. 2009).

Geocomp's LoadTrac-II/FlowTrac-II system with incorporated WaVeMe system was used to consolidate the sand specimens and measure the wave travel time to obtain shear wave velocities at different consolidation stages. The WaVeMe system consists of piezo-ceramic plates, known as P and S Sensors, commonly referred to as bender elements. An electrical signal was applied to the transmitting sensors to distort the soil specimen and induce a voltage potential to produce a signal. The input and output potential were continuously recorded and the travel time was determined.

The S-wave arrival time was measured using a single S-wave at different frequencies ranging from 5 kHz to 15 kHz, as recommended by Yamashita et al. (2009).

Shear wave and P-wave velocities were calculated using the following formulae:

$$Vs = \frac{Ht}{Ts}$$

$$Vp = \frac{Ht}{Tp}$$

Where:

- Ht – Distance between the two bender element tips, which is dependent on the specimen height at different consolidation load increments.
- Ts – S-wave arrival time, determined using Time Domain method.
- Tp – P-wave arrival time, determined using Time Domain method.

The S-wave traveling time was determined using the distance between the two bender element tips (and the height of the specimen) at different consolidation load increments.

Shear moduli were calculated using the following formula:

$$G_{max} = \rho * v_S^2$$

Where:

- ρ - Density at each consolidation load increment.

D5.5.3 Results

- **Bender Element Test on Loose Sample:** one bender element test was completed on a loose PSD1 sample consolidated up to 300 kPa confining stress. The specimen was placed at a void ratio, e_i=0.85 with an initial moisture content, wc_i=5.14%. The test results are given in Table D5-6 and illustrated on Figure D5-22 through Figure D5-24.
- **Bender Element Test on Dense Sample:** one bender element test was completed on a dense PSD1 specimen consolidated to 800 kPa confining stress. The specimen was placed at a void ratio, e_i=0.66 with an initial moisture content, wc_i=9.55%. P-wave velocity of the dense sand tailings specimen was measured during the saturation phase. The P-wave velocity at B=0.85 ($B = \frac{\Delta U}{\Delta \sigma}$) was 2515 m/s. The test results are summarized in Table D5-7 and illustrated on Figure D5-25 through Figure D5-27.

Table D5-6 Bender element test results for loose sand tailings

Mean Effective Stress, p' (kPa)	Void Ratio, e_0	State Parameter, Ψ	Wet Density, ρ (kg/m^3)	Average Shear Wave Velocity, v_s (m/s)	Average Shear Modulus, G_{max} (kPa)
25	0.81	0.02	2089	112	26172
50	0.81	0.04	2091	127	33665
100	0.80	0.05	2096	155	50199
200	0.79	0.05	2102	184	70597
300	0.78	0.05	2110	205	88138

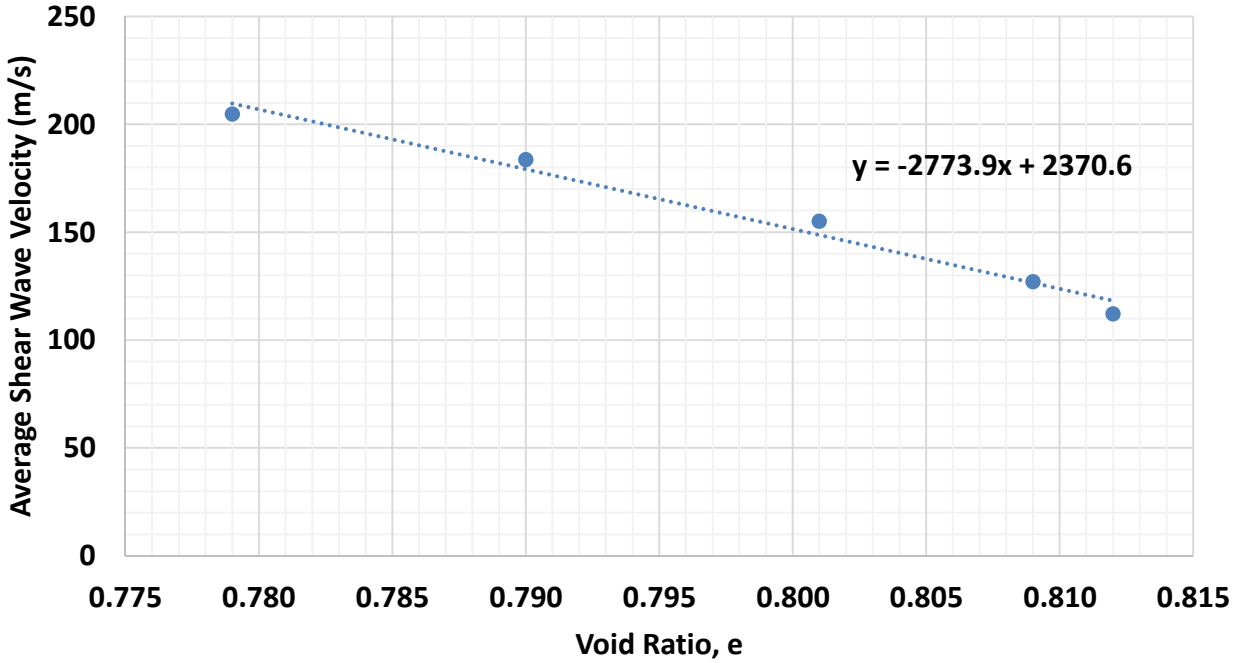

Figure D5-22 Average shear wave velocity vs. void ratio for loose sand tailings

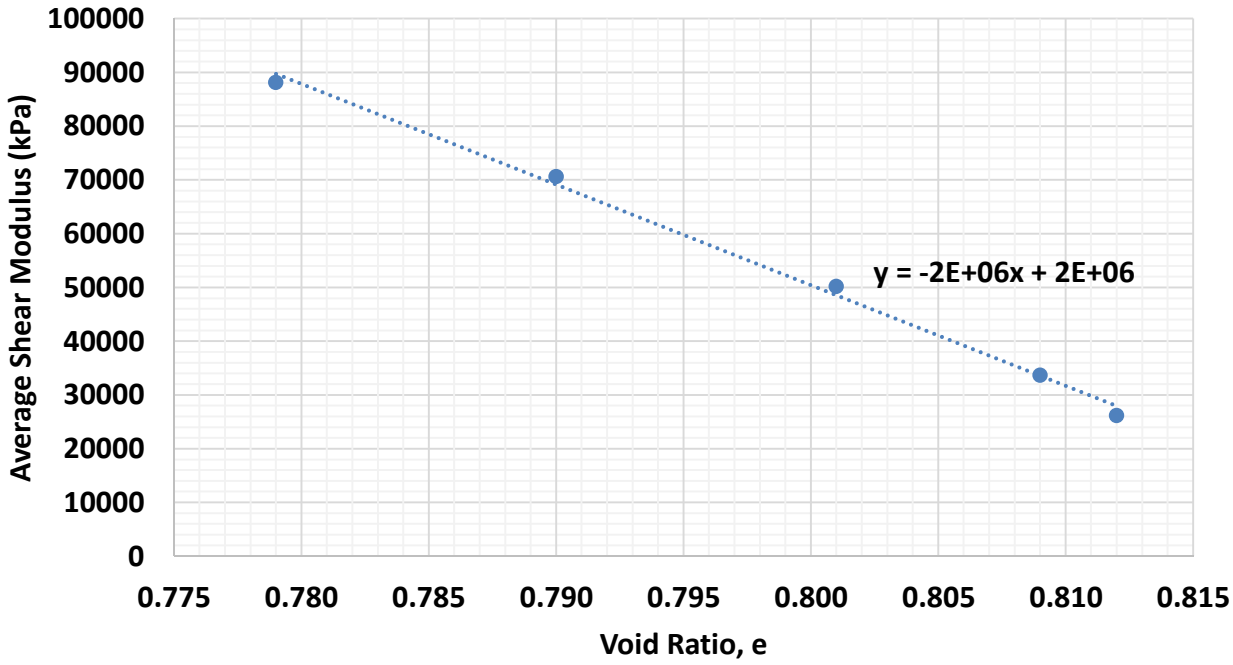

Figure D5-23 Average shear modulus vs. void ratio for loose sand tailings

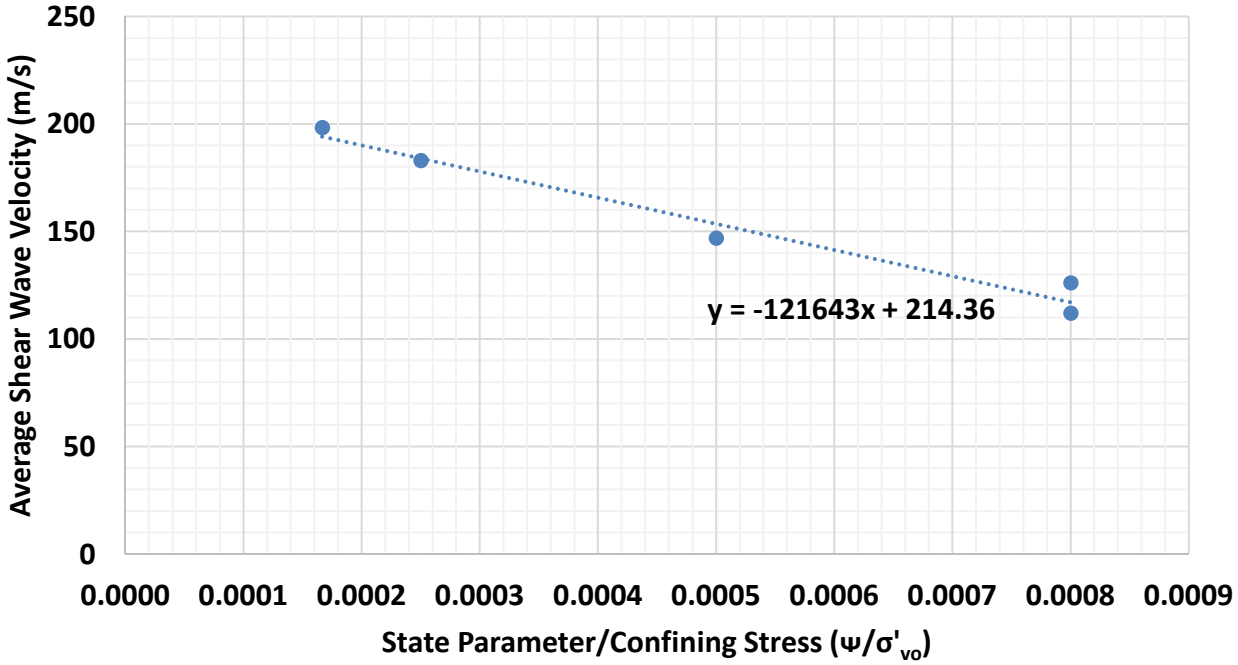

Figure D5-24 Shear wave velocity vs. state parameter/confining stress for loose sand tailings

Table D5-7 Bender element test results for dense sand tailings

Mean Effective Stress, p' (kPa)	Void Ratio, e_0	State Parameter, Ψ	Wet Density, ρ (kg/m^3)	Average Shear Wave Velocity, v_s (m/s)	Average Shear Modulus, G_{max} (kPa)
25	0.63	-0.154	2260	105	24724
50	0.63	-0.139	2262	120	32624
100	0.63	-0.129	2267	125	35487
200	0.62	-0.121	2273	212	102347
300	0.61	-0.120	2281	235	126497
400	0.61	-0.115	2282	251	143936
500	0.61	-0.111	2283	267	162917
800	0.60	-0.103	2285	299	204410

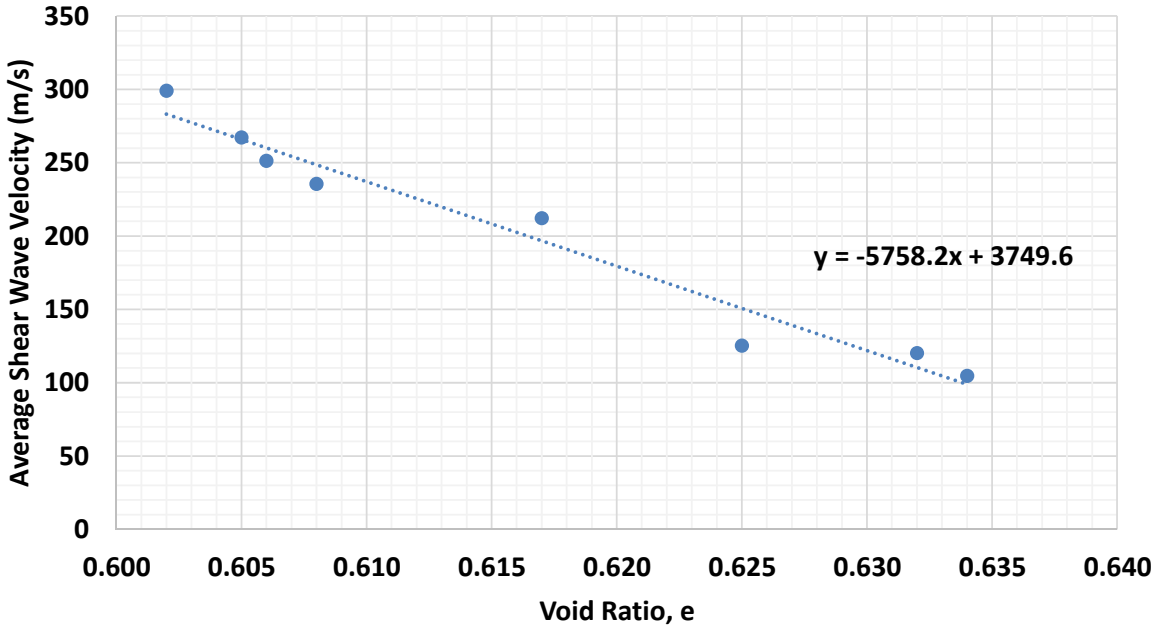

Figure D5-25 Shear wave velocity vs. void ratio for dense sand tailings

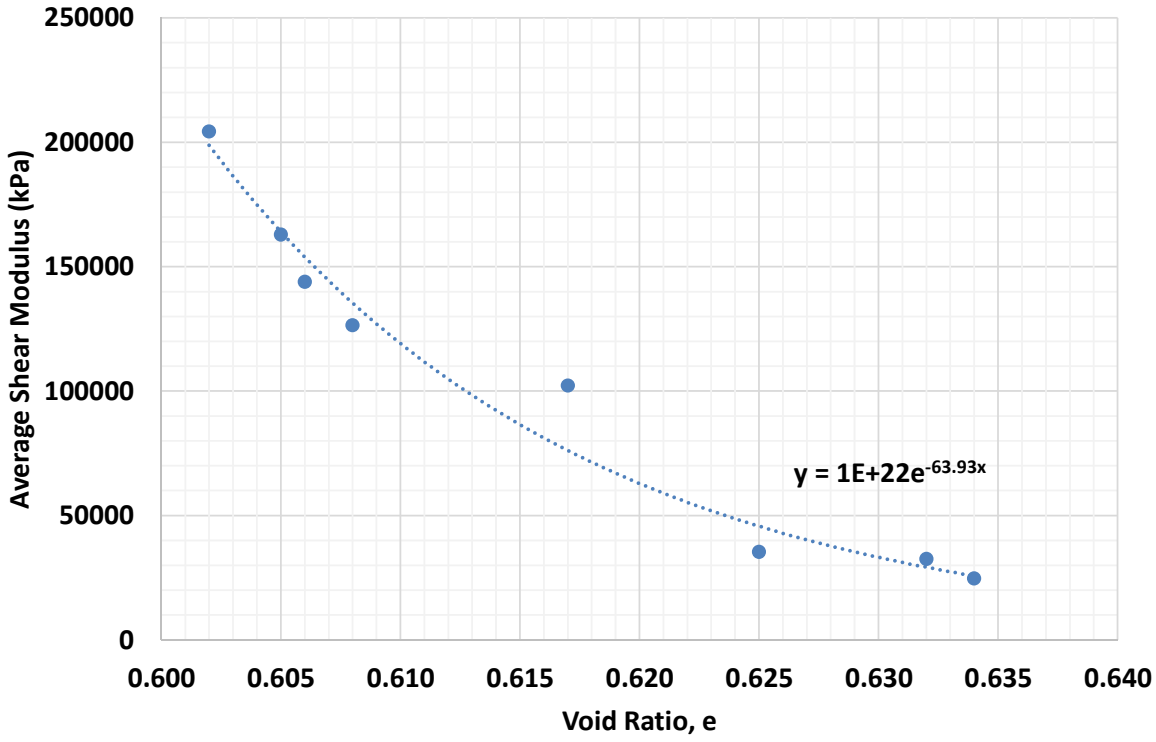

Figure D5-26 Average shear modulus vs. void ratio for dense sand tailings

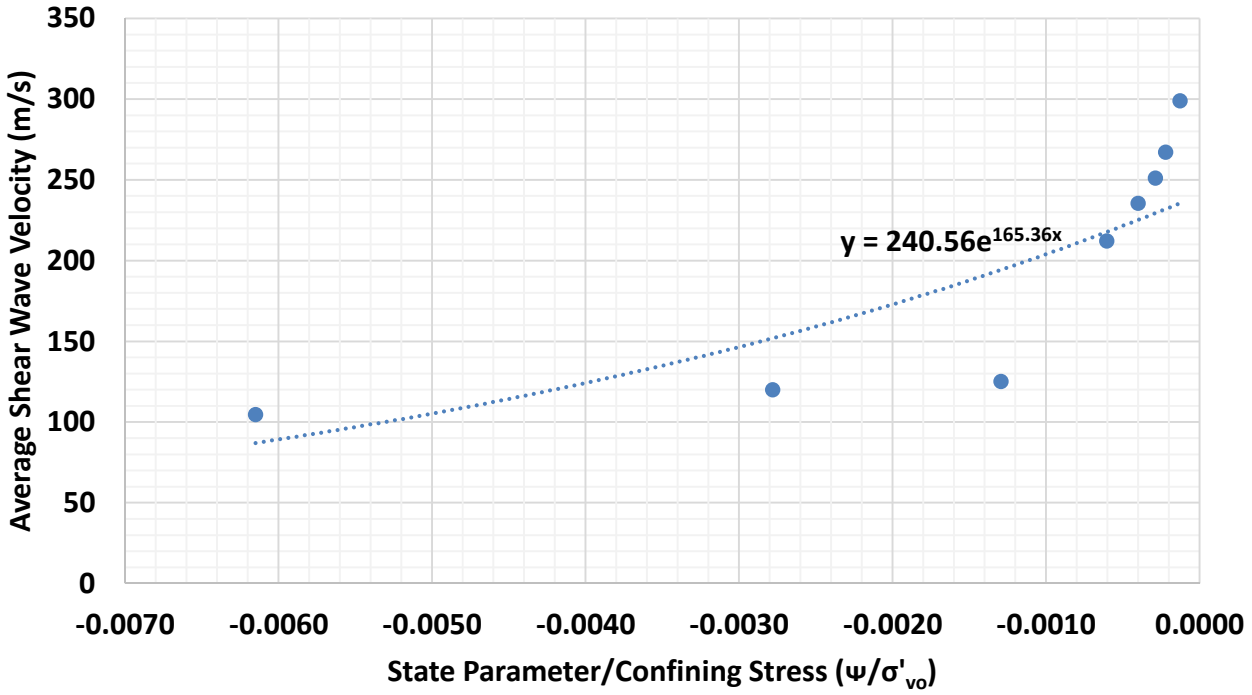

Figure D5-27 Shear wave velocity vs. state parameter/confining stress for dense sand tailings

D5.6 Oedometer Test

D5.6.1 Scope

An oedometer test (one-dimensional) was performed to derive compressibility and permeability for PSD1 sand tailings.

D5.6.2 Procedure

The oedometer test was conducted by KCB in accordance with ASTM D2435. The PSD1 specimen was loaded up to 3200 kPa. The test on the PSD1 specimen included three unloading-reloading cycles at 100 kPa, 300 kPa and 600 kPa. The loading increments and the duration of each increment was equal to 24 hours. The unloading increments varied and were typically shorter than the loading increments.

D5.6.3 Results

A summary of the oedometer test results on sand tailings is presented in Attachment D8, Table D5-8, and on Figure D5-28.

Table D5-8 One-dimensional consolidation test results on sand tailings

Sample	Pressure (kPa)	Void Ratio at placement, e_i	Coefficient of Consolidation, C_v (cm^2/s)	Coefficient of Compressibility M_v (cm^2/N)	Permeability, k (cm/s)	Compression Index, C_c
PSD1	100	0.875	2.5E-02	1.6E-03	4.0E-07	0.049
	300		2.5E-02	4.4E-04	1.1E-07	0.045
	600		3.2E-02	3.2E-04	9.9E-09	0.064
	3200		9.3E-02	1.1E-04	9.5E-09	0.099

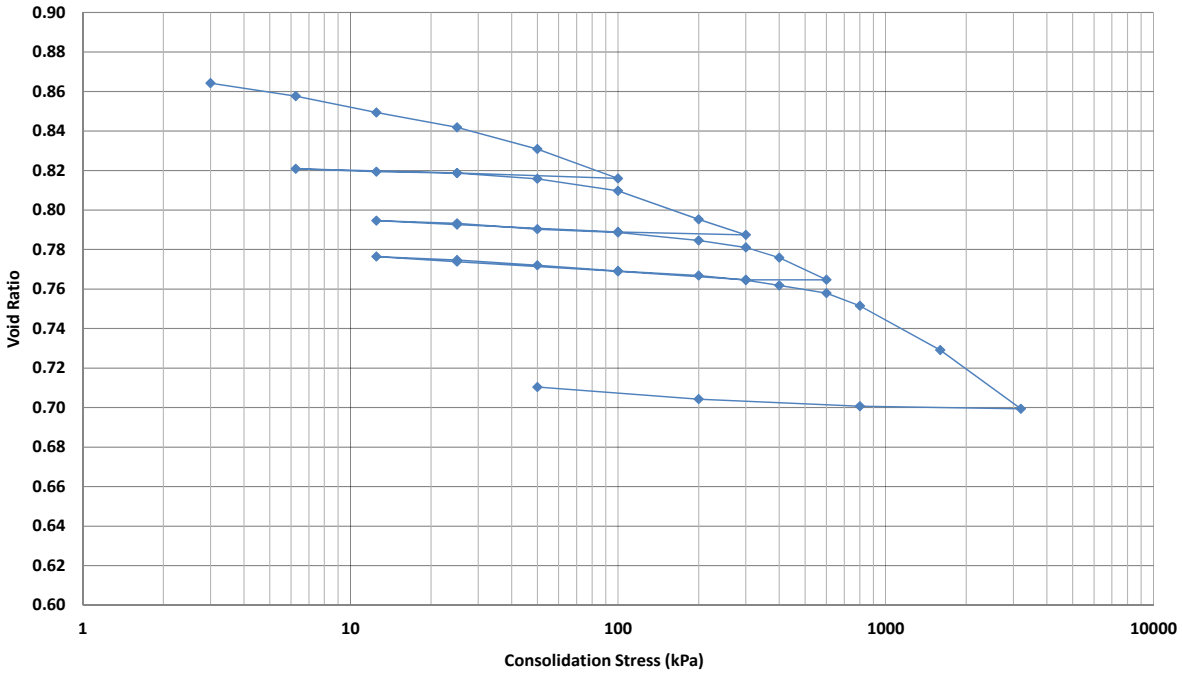

Figure D5-28 Compressibility of sand tailings from one-dimensional consolidation test

D6 ADVANCED LABORATORY TEST RESULTS ON SLIMES

D6.1 Scope

The slimes laboratory tests are listed in Table D6-1. The following test types were completed:

- 6 direct simple shear tests (DSS) on remolded samples;
- 16 triaxial tests (CIU) in Brazil by Pattrol on “undisturbed” samples;
- 1 one-dimensional consolidation test (oedometer) on remolded sample;
- 1 large-strain consolidation test; and
- 1 settlement test.

Table D6-1 Summary of advanced laboratory tests on slimes

Test ID	Test	Test Type	Loading Condition		
			Undrained/Drained/ Constant-Volume	Stress-/Strain-Controlled	Anisotropic/ Isotropic
TX-33	Triaxial	CIU	Undrained	Strain	Isotropic
TX-34	Triaxial	CIU	Undrained	Strain	Isotropic
TX-35	Triaxial	CIU	Undrained	Strain	Isotropic
TX-36	Triaxial	CIU	Undrained	Strain	Isotropic
TX-37	Triaxial	CIU	Undrained	Strain	Isotropic
TX-38	Triaxial	CIU	Undrained	Strain	Isotropic
TX-39	Triaxial	CIU	Undrained	Strain	Isotropic
TX-40	Triaxial	CIU	Undrained	Strain	Isotropic
TX-41	Triaxial	CIU	Undrained	Strain	Isotropic
TX-42	Triaxial	CIU	Undrained	Strain	Isotropic
TX-43	Triaxial	CIU	Undrained	Strain	Isotropic
TX-44	Triaxial	CIU	Undrained	Strain	Isotropic
TX-45	Triaxial	CIU	Undrained	Strain	Isotropic
TX-46	Triaxial	CIU	Undrained	Strain	Isotropic
TX-47	Triaxial	CIU	Undrained	Strain	Isotropic
TX-48	Triaxial	CIU	Undrained	Strain	Isotropic
DSS-3	DSS	Cyclic	Constant-Volume	Strain	Anisotropic
DSS-5	DSS	Monotonic	Constant-Volume	Strain	Anisotropic
DSS-6	DSS	Monotonic	Constant-Volume	Strain	Anisotropic
DSS-7	DSS	Monotonic	Constant-Volume	Strain	Anisotropic
DSS-13	DSS	Cyclic with static bias	Constant-Volume	Strain	Anisotropic
DSS-15	DSS	Monotonic (Multistage)	Constant-Volume	Strain	Anisotropic
CONS02	Oedometer	One-dimensional consolidation	-	-	-
CONS03	Consolidation	Large-strain consolidation	-	-	-
-	Settlement	-	-	-	-

D6.2 Direct Simple Shear Tests

D6.2.1 Scope

The DSS program included: one cyclic DSS test; one cyclic DSS test with static bias; three monotonic DSS tests; and one monotonic DSS test with several loading cycles.

D6.2.2 Procedure

Sample preparation procedures are described in Section D3.2. The testing procedure was similar to that described for sands in Section D5.3.2.

D6.2.3 Results

Test results are shown on Table D6-2 to Table D6-5 and Figure D6-1 to Figure D6-4.

Table D6-2 Summary of DSS monotonic test results for slimes

Test ID	Moisture Content		Void Ratio		Axial Strain after Consolidation (%)	Vertical Effective Stress, σ'_{vc} (kPa)	Peak Undrained Shear Strength (kPa)	Maximum Excess Pore Pressure Ratio, $\Delta U/\sigma'_{vc}$	Maximum Undrained Shear Stress Ratio, τ/σ'_{vc}
	Initial, W_0 (%)	Final, W_f (%)	at Placement, e_i	Final Void Ratio, e_0 (1)					
DSS - 5	45.80	23.23	1.80	0.91	32.08	600	101	0.71	0.17
DSS - 6	44.52	24.25	1.74	0.95	27.78	300	50	0.73	0.17
DSS - 7	44.50	25.20	1.75	0.99	27.19	150	24	0.73	0.16

1. Void ratios after consolidation were calculated using final moisture content from frozen specimens assuming the specimens were fully saturated.

Table D6-3 Summary of DSS cyclic test results for slimes

Test ID	Moisture Content		Void Ratio		Axial Strain after Consolidation (%)	Vertical Effective Stress, σ'_{vc} (kPa)	Maximum Excess Pore Pressure Ratio, $\Delta U/\sigma'_{vc}$	Maximum Shear Strain Reached at CSR, γ_{max} (%)			Number of Cycles N_{cyc}		
	Initial, W_0 (%)	Final, W_f (%)	at Placement, e_i	Final Void Ratio, e_0 1				at 0.01	at 0.05	at 0.1	at 0.01	at 0.05	at 0.1
DSS - 3	41.74	22.98	1.64	0.90	30.84	300	0.95	0.01	0.05	22.39	30	30	39

1. Void ratios after consolidation were calculated using final moisture content from frozen specimens assuming the specimens were fully saturated.

Table D6-4 Summary of DSS cyclic test results with static bias for slimes

Test ID	Moisture Content		Void Ratio		Axial Strain after Consolidation (%)	Vertical Effective Stress, σ'_{vc} (kPa)	Maximum Excess Pore Pressure Ratio, $\Delta U/\sigma'_{vc}$	Static Shear Bias Stress, τ_h	Static Bias, α	Maximum Cumulative Shear Strain, γ (%)	CSR	Number of Cycles to Reach Max Shear Strain
	Initial, W_0 (%)	Final, W_f (%)	at Placement, e_i	Final Void Ratio, e_0 1								
DSS - 13	43.52	23.54	1.71	0.93	30.09	400	0.94	70	0.175	0.03	0.002	9000

1. Void ratios after consolidation were calculated using final moisture content from frozen specimens assuming the specimens were fully saturated.

Table D6-5 Summary of DSS monotonic test results with several cyclic loading for slimes

Test ID	Moisture Content		Void Ratio		Axial Strain after Consolidation (%)	Vertical Effective Stress, σ'_{vc} (kPa)	Peak Undrained Shear Strength (kPa)	Undrained Shear Strength at 20 % Shear Strain, $\tau_{at20\%}$	Undrained Shear Strength after Several Loading Cycles, $r_{"remolded"}$	Maximum Excess Pore Pressure Ratio, $\Delta U/\sigma'_{vc}$	Maximum Undrained Shear Stress Ratio, τ/σ'_{vc}
	Initial, W_0 (%)	Final, W_f (%)	at Placement, e_i	Final Void Ratio, e_0 1							
DSS - 15	45.41	23.86	1.78	0.94	31.89	300	48	40.8	21.2	0.99	0.16

1. Void ratios after consolidation were calculated using final moisture content from frozen specimens assuming the specimens were fully saturated.

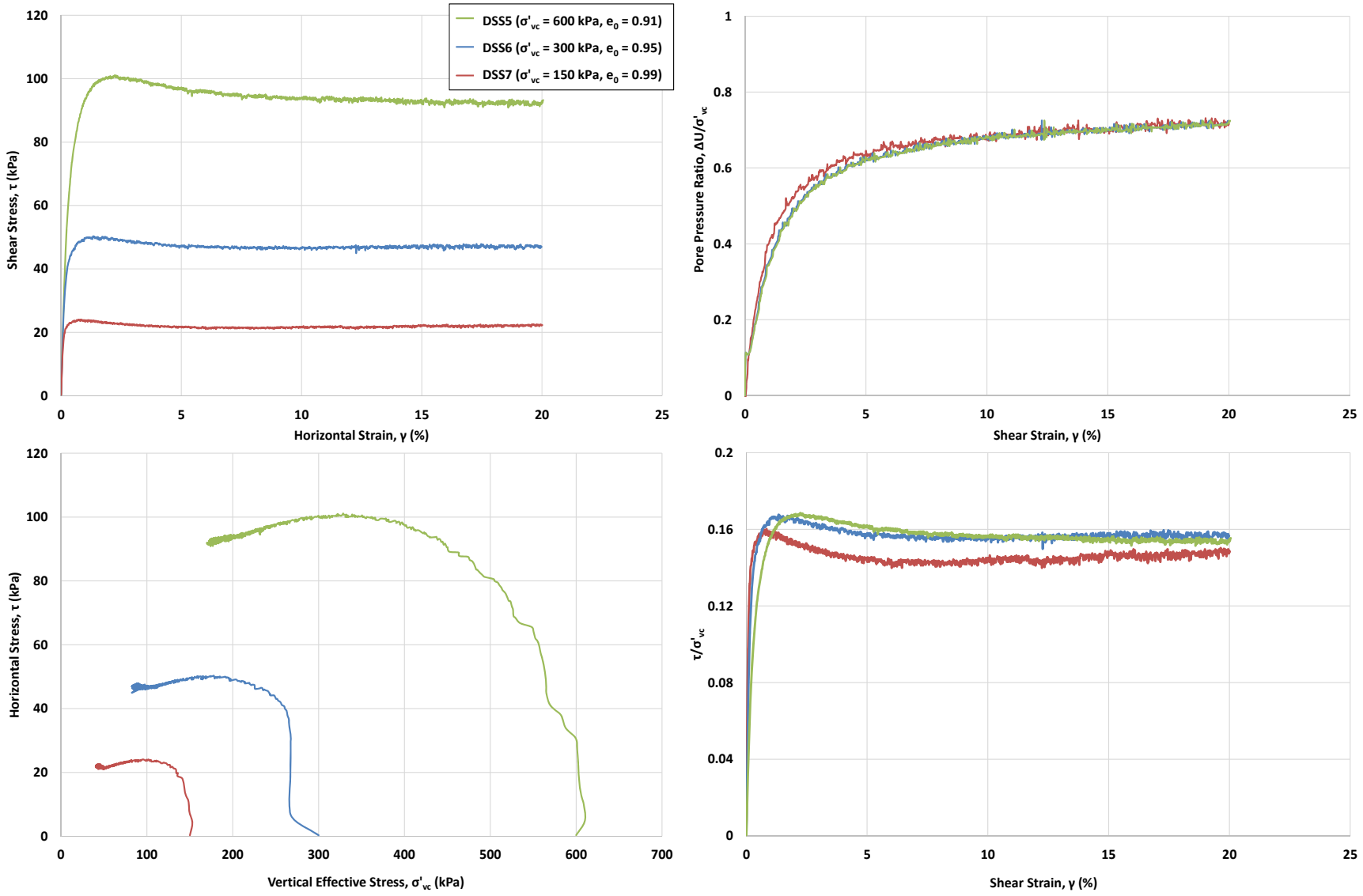

Figure D6-1 Direct simple shear results on slimes (monotonic)

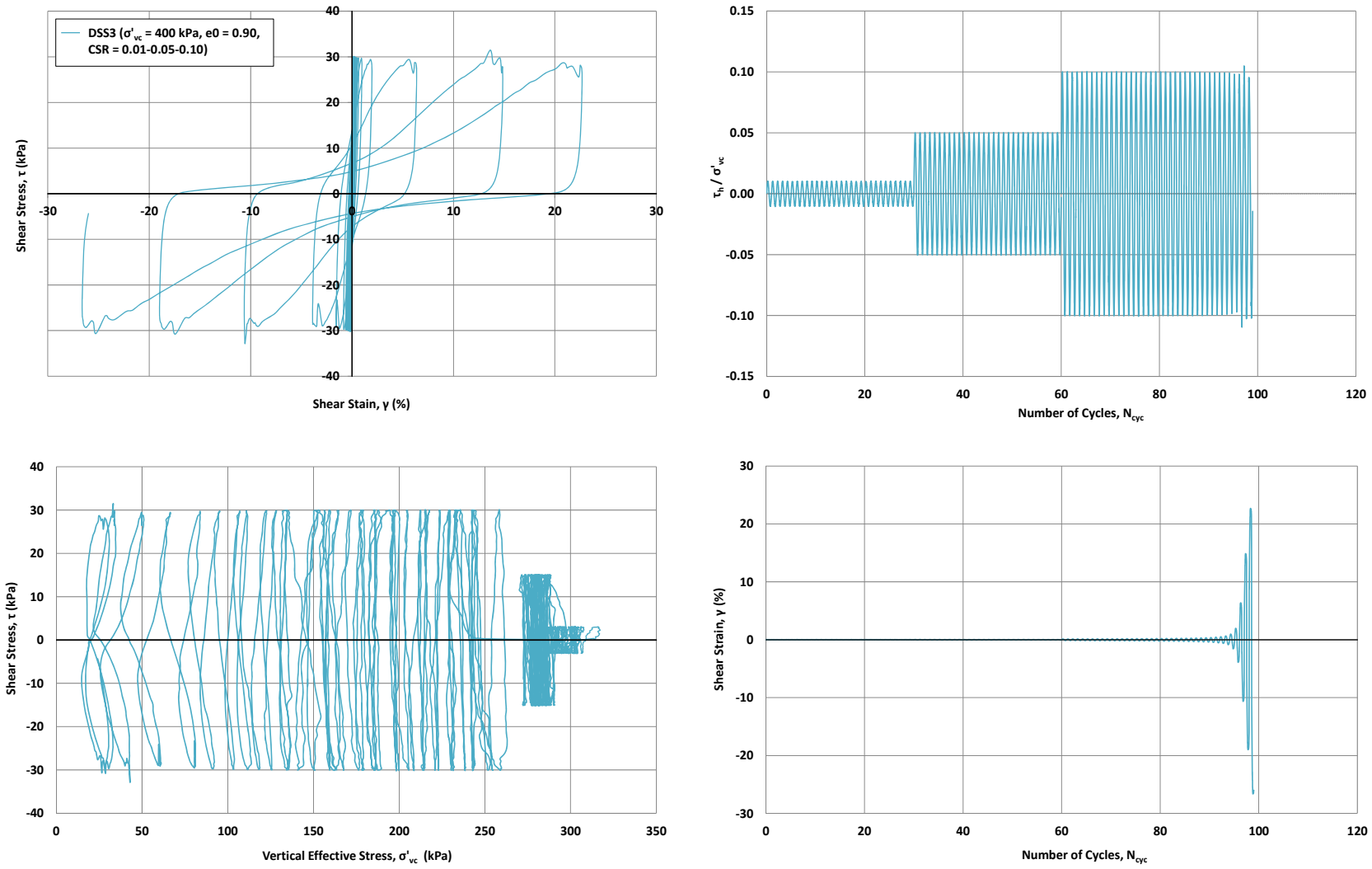

Figure D6-2 Direct simple shear results on slimes (cyclic)

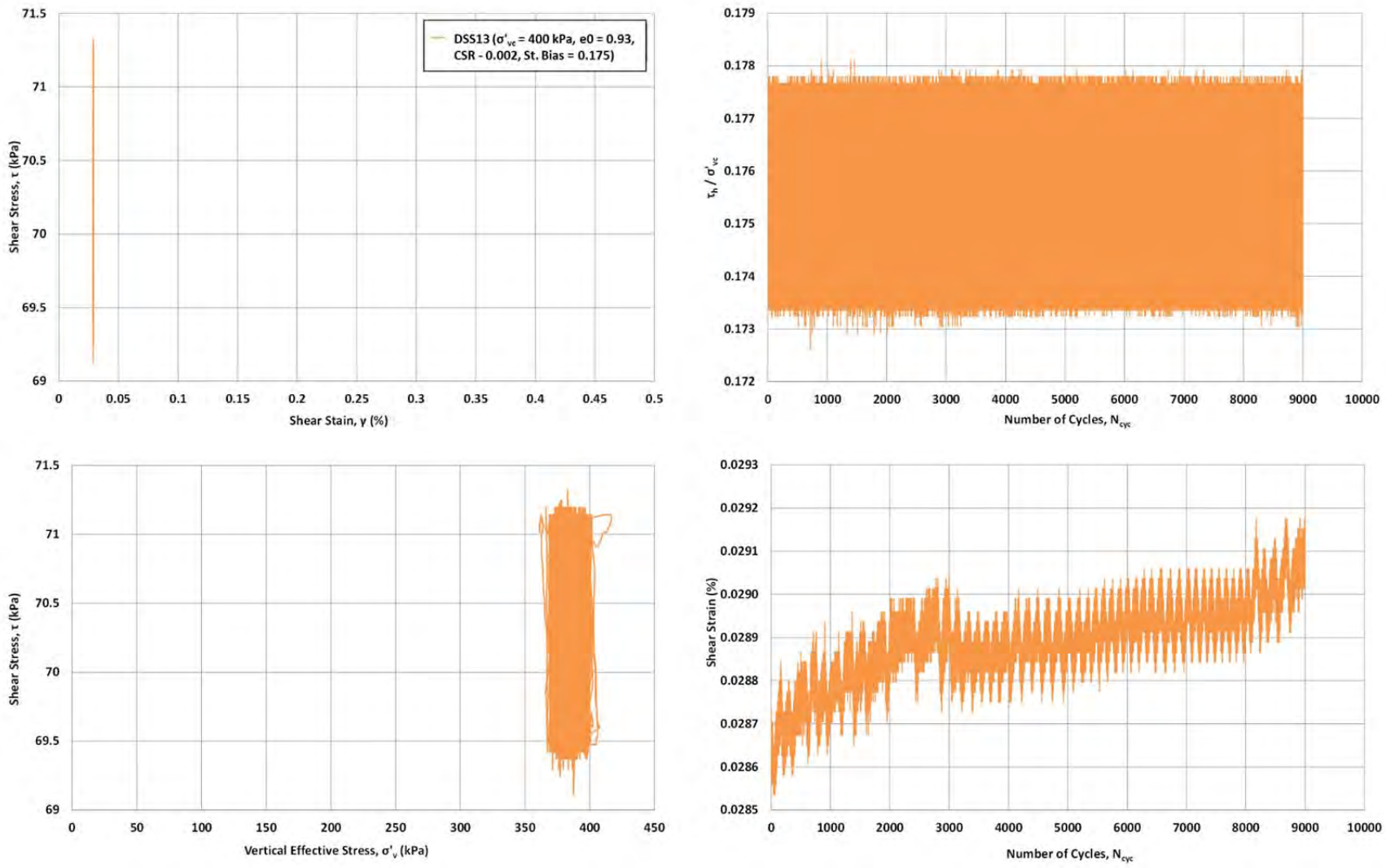

Figure D6-3 Direct simple shear results on slimes (cyclic with static bias)

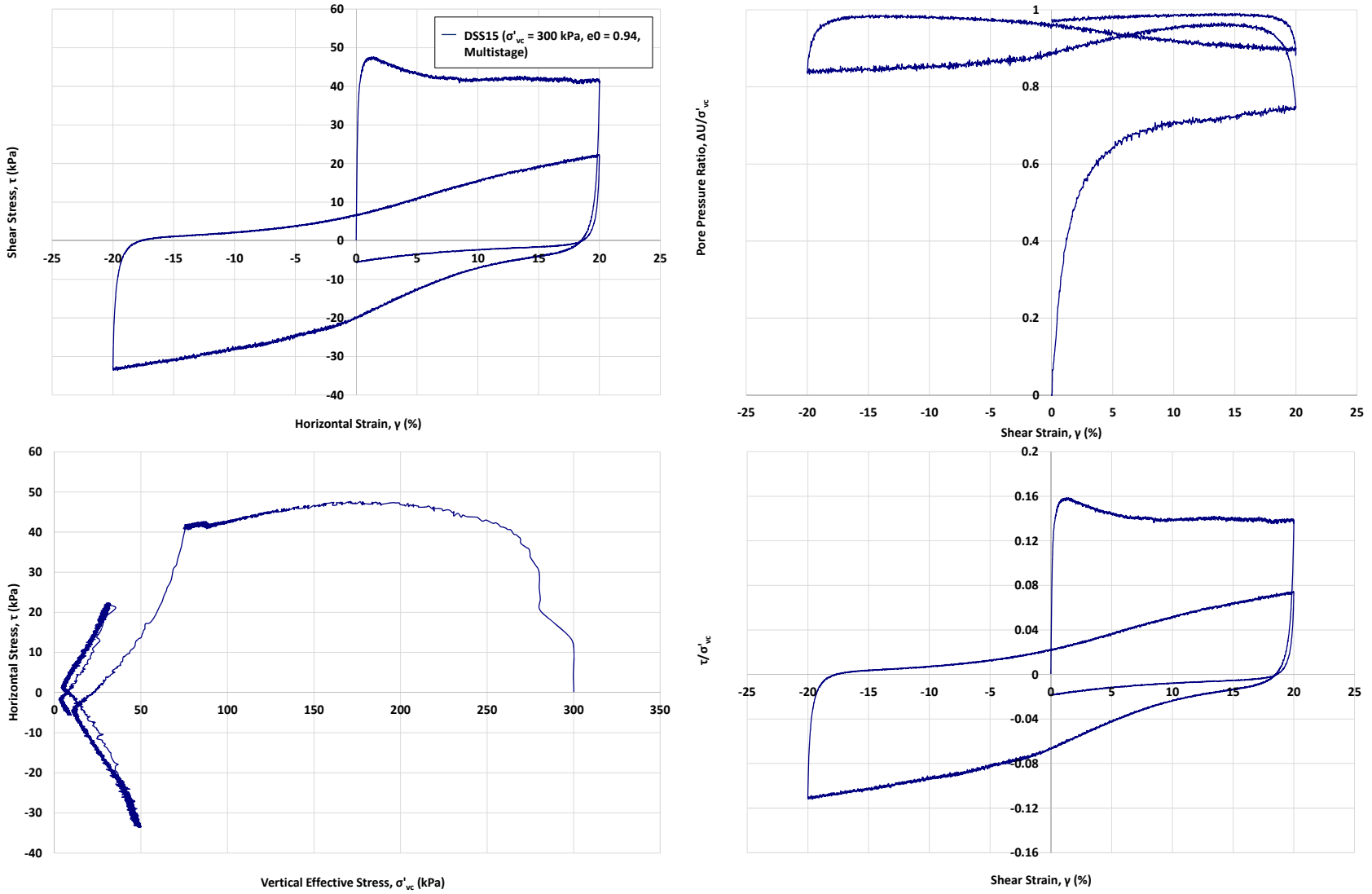

Figure D6-4 Direct simple shear results on slimes (monotonic, multistage)

D6.3 Triaxial Tests by Pattrol in Brazil

Sixteen standard undrained triaxial (CIU) compression tests on isotropically consolidated "undisturbed" slimes specimens were completed by Pattrol laboratory in Belo Horizonte, Brazil. The slimes samples were collected from GSSAM16-02B during the Panel field program (see Appendix C) at four different depths: 4 m, 6 m, 9 m and 10 m. Attachment D7 includes selected data from the Pattrol laboratory report. The Panel has not checked these test results. The data was not used in the Panel work because the results became available only after much of the Panel's work had been completed.

D6.4 Consolidation Tests

D6.4.1 Scope

Early in the laboratory testing program, an oedometer test was completed on a slurried sample of slimes in the KCB laboratory which was used to obtain compressibility and coefficient of consolidation parameters. Subsequently, slimes from the Panel surface samples were sent to the University of Alberta laboratory to determine large strain sedimentation and consolidation properties.

D6.4.2 Procedures

D6.4.2.1 Procedure for Large-Strain Consolidation Test (UA)

The large-strain consolidation test was performed in a consolidation apparatus (150 mm dia. x 150 mm high). Effective stresses up to approximately 10 kPa were applied to the specimen by dead loads acting on the piston. Effective stresses over 10 kPa were applied on a loading frame by an air pressure Bellofram. Subsequent loads were approximately doubled for each load step up to a maximum of 1000 kPa. The permeability was measured at the end of consolidation for each load step.

D6.4.2.2 Procedure for Settlement Test (UA)

A settlement test was conducted by the University of Alberta (UA) on a sample slurry of 48% solids content, prepared from a reconstituted slimes sample.

The settlement test was performed in the same cell used for the large strain consolidation test (150 mm dia. x 150 mm high). The initial sample height was 7 cm and final sample height after settling was 5.5 cm. The change of specimen height (interface) was measured at different time intervals. The pore-water pressure was continuously monitored.

D6.4.2.3 Procedure for One-Dimensional Consolidation Test (KCB Oedometer)

The procedure for the one-dimensional consolidation test using the oedometer device was described in Section D5.6.2. A slimes specimen was loaded in one cycle in standard increments up to 100 kPa. No unloading was performed during the test.

D6.4.3 Results

The large-strain consolidation test results are presented on Figure D6-5 and Figure D6-6, and in Table D6-6, and are provided in Attachment D9. The KCB oedometer test on slurried slimes is presented on Figure D6-7 and in Table D6-7. The UA settlement test results are presented on Figure D6-8 and Figure D6-9, and provided in Attachment D9.

Table D6-6 Large-strain consolidation test results on slimes (UA)

	Solids Content (%)	Void Ratio, e	Hydraulic Conductivity (m/s)	Shear Strength (kPa)
Initial	50	2.61	7.84 E-08	-
Final	82	0.85	1.21E-09	144

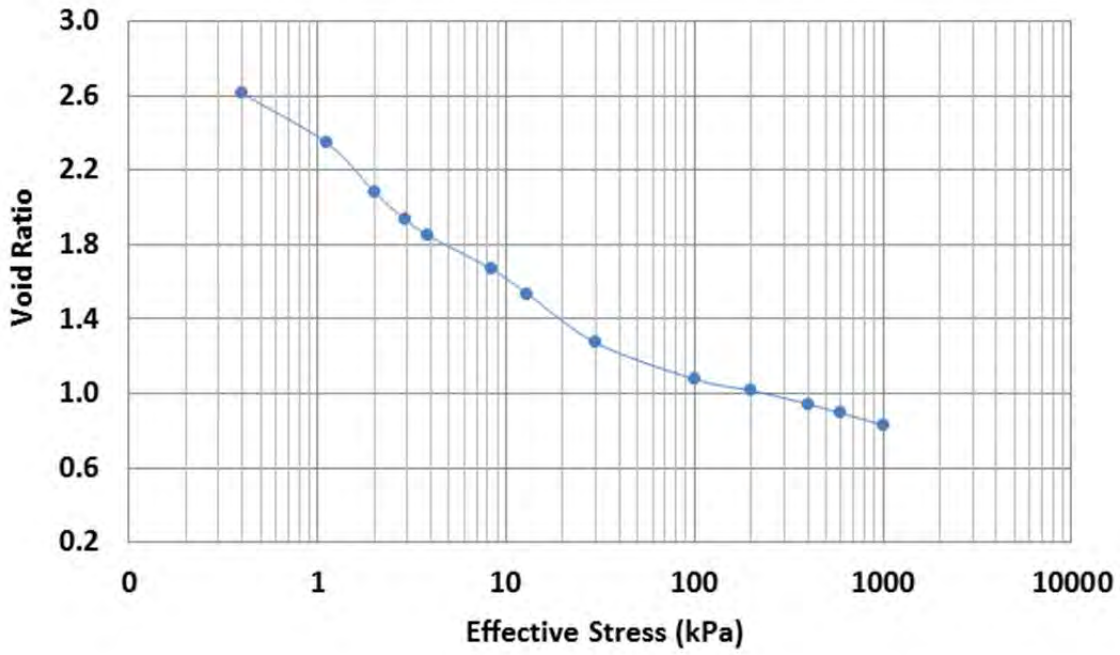

Figure D6-5 Large-strain consolidation compressibility of slimes (UA)

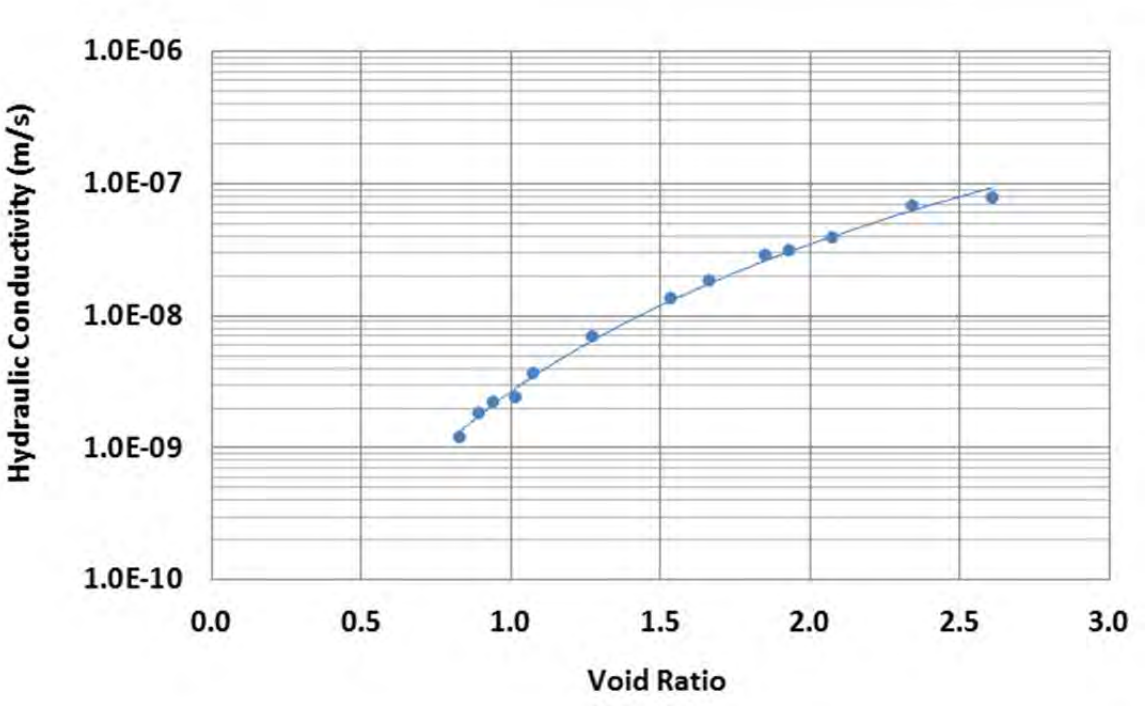

Figure D6-6 Large-strain consolidation permeability of slimes (UA)

Table D6-7 One-dimensional consolidation test results on slimes (KCB)

Sample	Pressure (kPa)	Void Ratio, e_0	Coefficient of Consolidation, C_v (cm^2/s)	Coefficient of Compressibility, M_v (cm^2/N)	Permeability, k (cm/s)	Compression Index, C_c
Germano Slimes	1024	0.871	1.6E-02	5.2E-04	8.3E-08	0.141

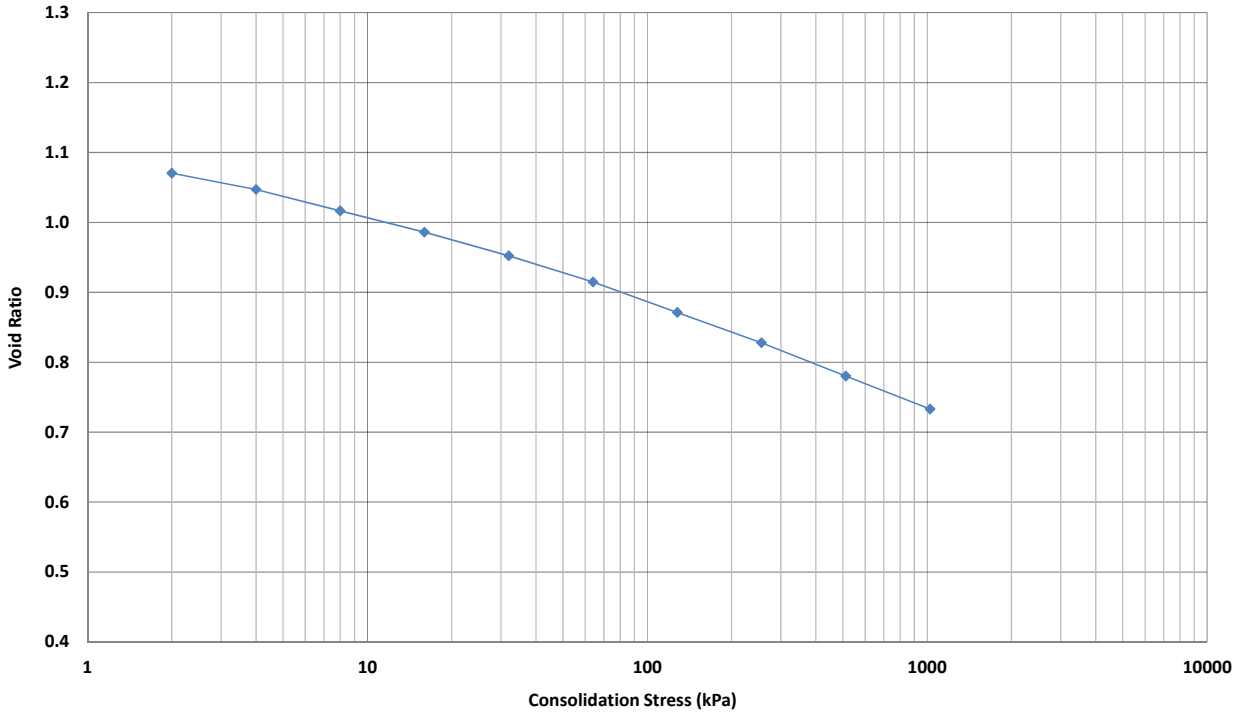

Figure D6-7 Compressibility from one-dimensional consolidation test on slimes (KCB)

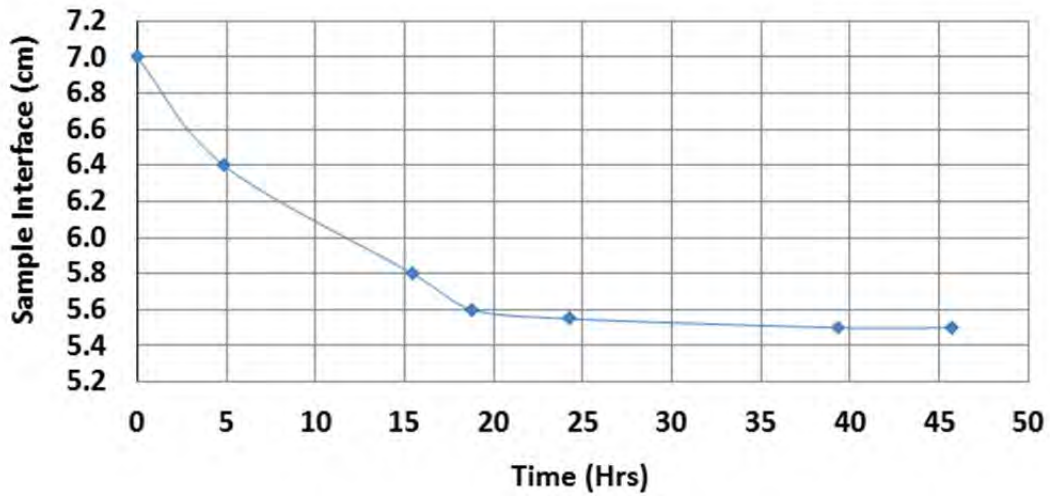

Figure D6-8 Settlement measured with time in slimes (UA)

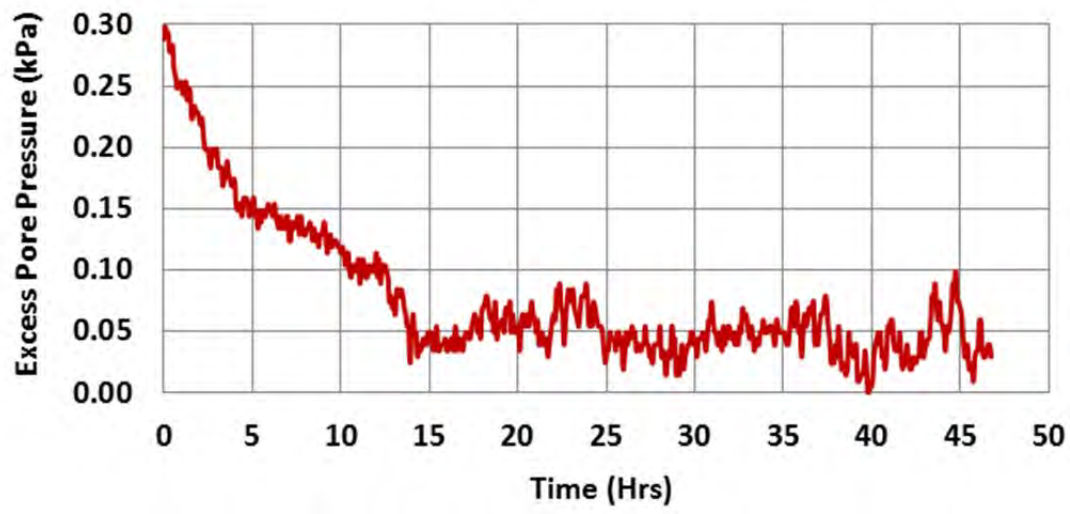

Figure D6-9 Excess pore pressure dissipation during settlement in slimes (UA)

D7 SUMMARY OF LABORATORY TESTING PROGRAM DESIGN PARAMETERS

A summary of the laboratory test parameters for slimes and sands is presented in Table D7-1 and Table D7-2, respectively.

Table D7-1 Summary of design parameters derived from 2016 lab testing program for slimes

Test Type	Parameter	Result	Implementation	Appendix #
Atterberg limit test	Liquid limit	26-28		
	Plastic limit	16-19		
	Plasticity index	7-11	Dynamic response analysis: SHAKE	Appendix J
Specific gravity test	Specific gravity	3.92-3.93	Stability analysis: Slope/W; Dynamic response analysis: SHAKE	Appendix B Appendix H Appendix J
Standard Proctor	Maximum dry unit weight (kg/m^3)	2300		
	Optimum moisture content (%)	16.7		
pH	pH	8.22		
EC (electrical conductivity) (μS)	EC (electrical conductivity) (μS)	734		
X-Ray diffraction	X-Ray diffraction	93% of goethite, hematite and quartz		

Test Type	Parameter	Result	Implementation	Appendix #
Oedometer test	Coefficient of consolidation, C_v (cm^2/s)	1.6E-02	Consolidation modeling: FSConsol	Appendix F
	Coefficient of compressibility, M_v (cm^2/N)	5.2E-04		
	Permeability, k (cm/s)	8.3E-08		
	Compression Index, C_c	0.141		
Direct simple shear test	Peak undrained shear stress ratio	0.16-0.17		
	Peak undrained shear strength at σ_v'=300 kPa (kPa)	46.1		
	Undrained shear strength at 20% shear strain (kPa)	40.8		
	"Remolded" shear strength	21.2		
Direct simple shear tests (cyclic)	Number of cycles, N, specimen was loaded at CSR=0.01	30		Appendix J
	Number of cycles, N, specimen was loaded at CSR=0.05	30		
	Number of cycles specimen was loaded at CSR=0. 1, N	39		
	Number of cycles to reach maximum shear strain, N, at α=0.175 and CSR=0.002	9000		

Table D7-2 Summary of design parameters derived from 2016 lab testing program for sand tailings

Test Type	Parameter	Result	Implementation	Appendix #
Specific gravity test	Specific gravity (PSD1)	2.92-3.06	Stability analysis: Slope/W	Appendix H
	Specific gravity (PSD2)	2.74		
Maximum/minimum density using vibrating table	Maximum dry unit weight (kg/m^3) (PSD1)	2057		
	Maximum wet unit weight (kg/m^3) (PSD1)	1933		
	Minimum wet unit weight (kg/m^3) (PSD1)	1629		
Modified Proctor	Optimum moisture content (%)	13.1		
SEM	Particle angularity	Angular to sub-rounded		
Direct shear test	Drained friction angle (degrees)	32	See Note 1	

Test Type	Parameter	Result	Implementation	Appendix #
	Cohesion (kPa)	0	Stability analysis: Slope/W	Appendix H
	Peak drained shear strength at 250 kPa	164	Stability analysis: Slope/W	Appendix H
	Peak drained shear strength at 750 kPa	476	Stability analysis: Slope/W	Appendix H
	Peak drained shear strength at 1250 kPa	812	Stability analysis: Slope/W	Appendix H
Oedometer test	Coefficient of consolidation, C_v (cm^2/s) at 300 kPa	2.5E-02		
	Coefficient of compressibility M_v (cm^2/N) at 300 kPa	4.4E-04		
	Permeability, k (cm/s) at 300 kPa	1.1E-07		
	Compression Index, C_c at 300 kPa	0.045		
Bender element test	P-wave velocity (m/s) (B=0.85) (dense PSD1)	2515		
	Shear wave velocity (m/s) at 300 kPa (dense PSD1)	235		
	Void ratio at 300 kPa (dense PSD1)	0.61		
	Maximum shear modulus (Gmax) (kPa) (dense PSD1)	126497		
	Shear wave velocity (m/s) at 300 kPa (loose PSD1)	205		
	Void ratio at 300 kPa (loose PSD1)	0.78		
	Maximum shear modulus (G_{max}) (kPa) (loose PSD1)	88138		
Direct simple shear test	Peak undrained shear strength at σ_v'=300 kPa (kPa)	40.8		
	Peak undrained shear stress ratio (σ_v'=150-600 kPa)	0.12-0.14		
	Undrained shear strength at 20 % shear strain (kPa)	28.6		

Test Type	Parameter	Result	Implementation	Appendix #
	Peak undrained shear strength at σ_v'=300 kPa (kPa) (saturated)	36.0		
	Undrained shear strength at 20 % shear strain (kPa) (saturated)	9.6		
Direct simple shear test (cyclic)	Number of cycles, N, specimen was loaded at CSR=0.01	30		Appendix J
	Number of cycles, N, specimen was loaded at CSR=0.05	30		
	Number of cycles, N, specimen was loaded at CSR=0.1	2		
	Number of cycles to reach maximum shear strain, N, at α=0.175	4802		
	Number of cycles to reach maximum shear strain, N, at α=0.35	492		
All triaxial tests	Effective friction angle, ϕ' (degrees)	33	Stability analysis: Slope/W; Deformation Analysis: FLAC	Appendix H Appendix I
Triaxial test with a cyclic component	Number of cycles, N, specimen was loaded at $SR_{desired}$=0.01	525		Appendix J
	Number of cycles, N, specimen was loaded at $SR_{desired}$=0.02	521 (cumulative 1046)		
	Number of cycles, N, specimen was loaded at $SR_{desired}$=0.03	209 (cumulative 1255)		

1. A friction angle of 33° obtained from triaxial tests was used for stability analyses.

D8 SAND TAILINGS PARAMETERS USED FOR NORSAND MODEL

The triaxial compression tests were interpreted using the procedures in Jefferies and Been (2016), to determine the NorSand constitutive model properties for PSD1 samples.

Critical State Locus, Γ, λ_e

The approximation of a linear Critical State Locus (CSL) in void ratio – ln (mean effective stress) (e-ln(p')) space was adopted. The CSL for PSD1 was well defined by the two drained tests and two undrained tests. The derived CSL for PSD1 is shown on Figure D5-11.

Critical Friction Ratio, M_{tc}

The critical state friction ratio, M_{tc}, of the sand was calculated using the "end of test" method. The "end of test" results are plotted on Figure D5-12. A value of M_{tc} of 1.33 was obtained.

Volumetric Coupling Parameter, N

The stress dilatancy plot on Figure D8-1 was used to determine the volumetric coupling parameter, N. The slope of the line on Figure D8-1 is equal to (1-N), giving a value of N=0.38.

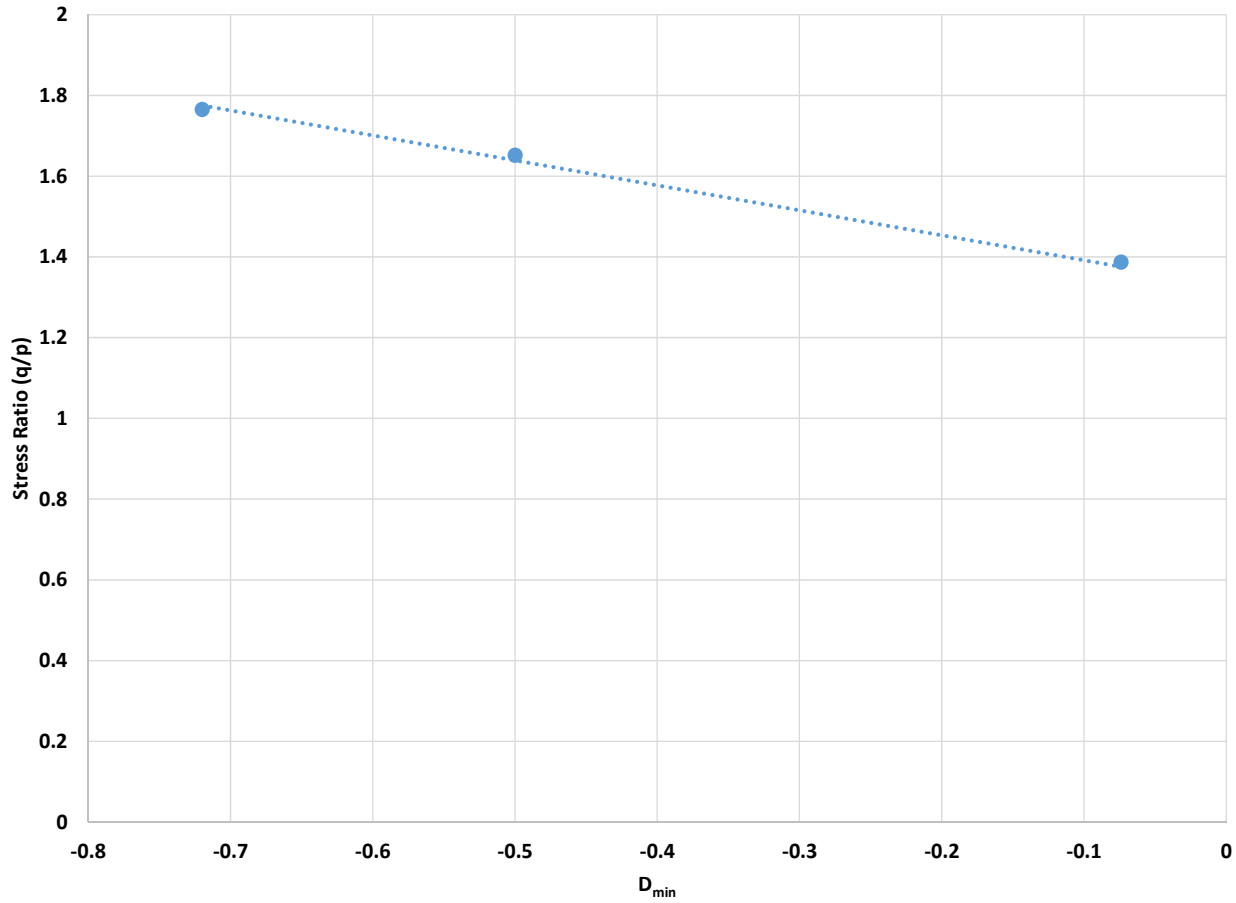

Figure D8-1 Dilatancy – stress ratio relationship for sand tailings

Dilatancy Parameter, χ_{tc}

The parameter χ_{tc} is the slope of the trend line for minimum dilatancy (equal to the dilatancy at peak stress ratio) versus the state parameter at peak stress ratio. Figure D8-2 indicates a results of χ = 7.3.

The χ_{tc} value for this material is quite high when compared with the typical range (2.5-4.5), and would typically be associated with angular shaped particles.

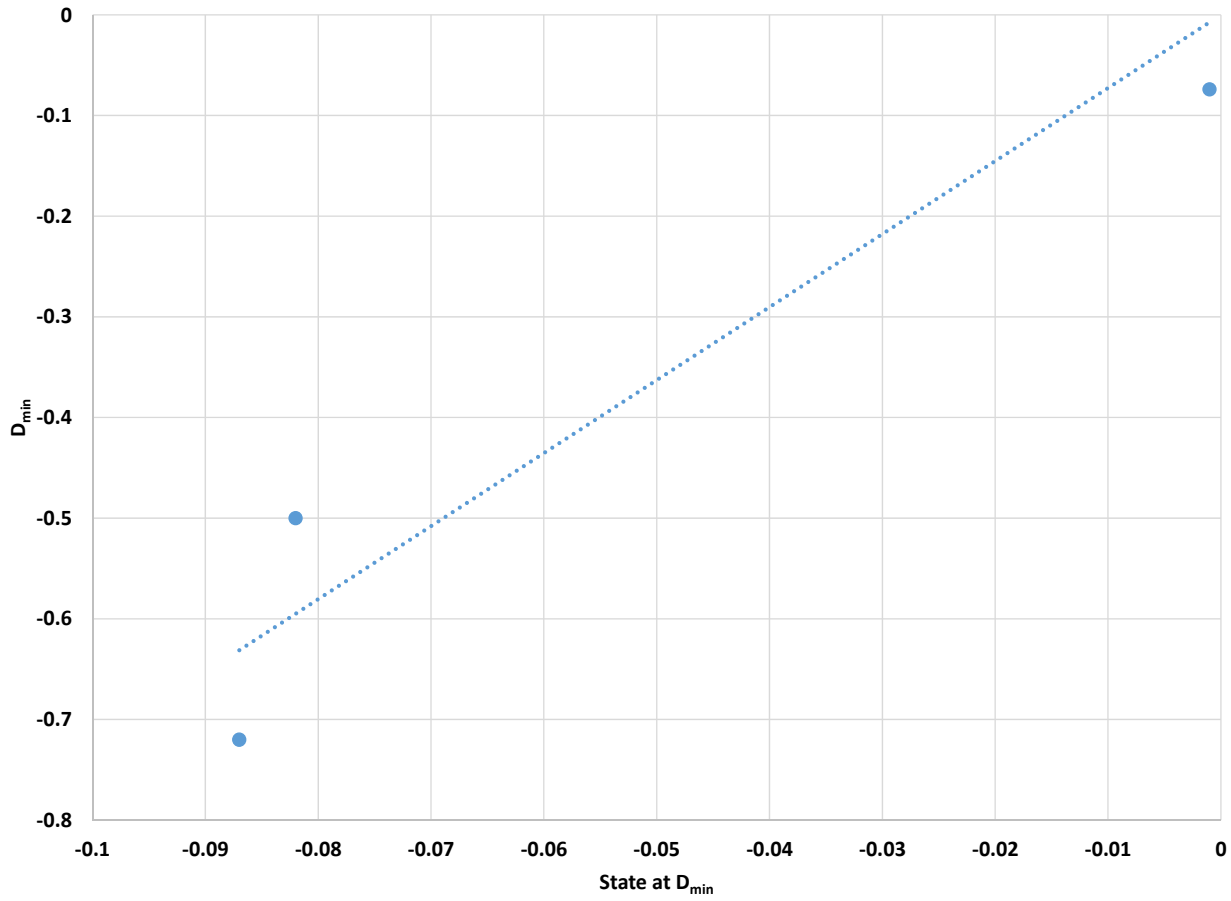

Figure D8-2 Dilatancy – state parameter relationship for sand tailings

Elasticity, G_{max}, ν

The trend of small strain shear modulus with mean effective stress determined from Seismic CPT (SCPT) testing was used in the interpretation of the triaxial tests. The small strain shear modulus (G_{max}) was derived from shear wave velocity (V_s) measured in the SCPT testing, using the following formula:

$$G_{max(MPa)} = \frac{v_s(m/s) \times \rho_{bulk^2}(kg/m^3)}{10^6}$$

Where ρ_{bulk} = bulk density

All of the G_{max} results were plotted against their associated mean effective stress and a trend was fitted through all of the data. A reasonable trend was found using the following relationship (see Figure D8-3):

$$G_{max} = 60\ (p'/p_{ref})^{0.45}, \text{ where } p_{ref} = 100 \text{ kPa}$$

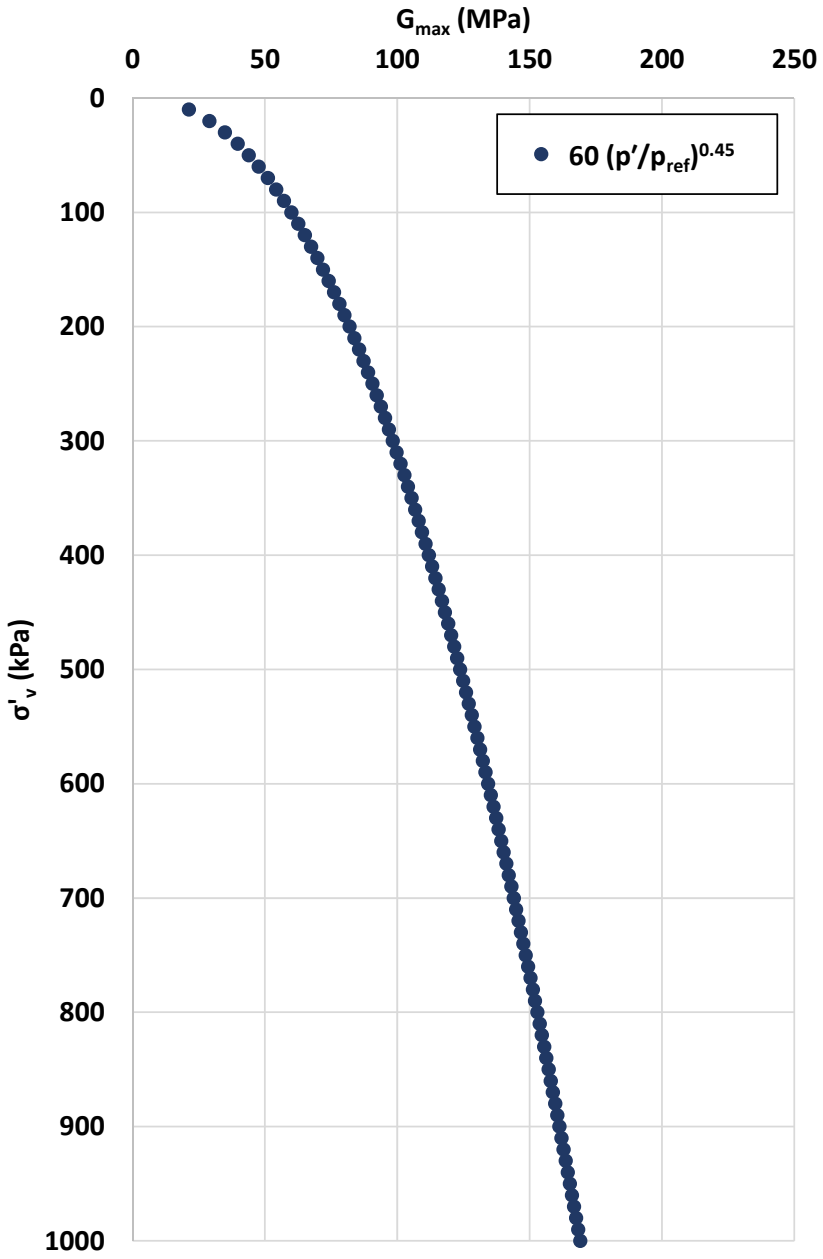

Figure D8-3 G_{max} relationship for sand tailings from field testing program

D8.1.1 NorSand Parameters

The material properties of the sand calculated through the above testing program are summarized in Table D8-1.

Table D8-1 Material parameters

Properties	Sand Tailings
Γ	0.865
λ_e	0.024
M_{tc}	1.33
N	0.38
χ_{tc}	7.3
I_r	273.02
G_{max}	163.81

ATTACHMENT E1

Dike 1 Piezometer Plan

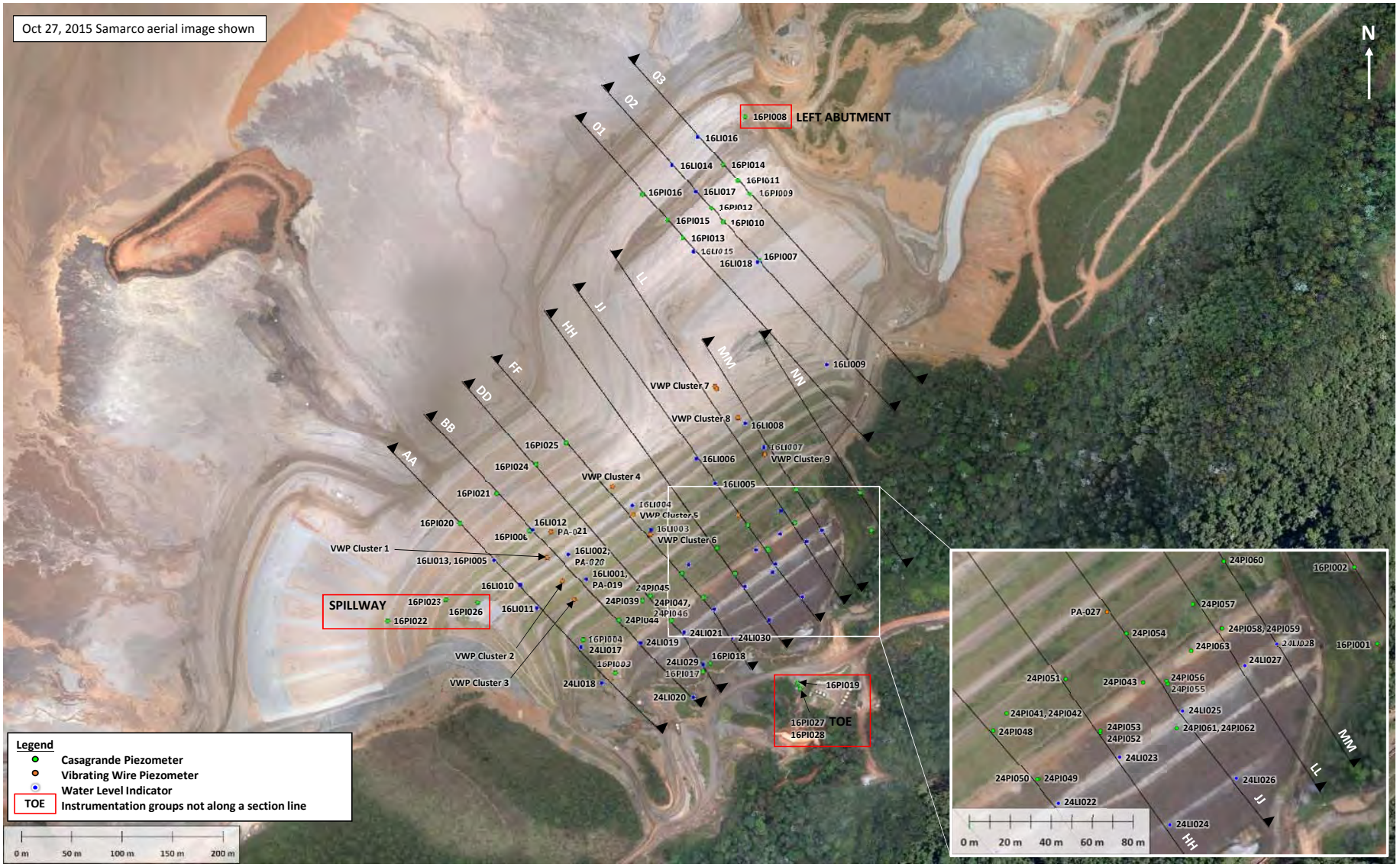
Oct 27, 2015 Samarco aerial image shown
N
LEFT ABUTMENT
16PI008
16LI016
16LI014
16PI014
16PI011
16PI016
16LI017
16PI009
16PI012
16PI015
16PI010
16PI013
16LI015
16LI018
16PI007
16LI009
VWP Cluster 7
VWP Cluster 8
16LI008
16LI007
VWP Cluster 9
16LI006
16LI005
VWP Cluster 4
16LI004
VWP Cluster 5
16LI003
VWP Cluster 6
16PI025
16PI024
16PI021
16PI020
16LI012
PA-021
16PI006
VWP Cluster 1
16LI013, 16PI005
16LI002, PA-020
16LI001, PA-019
16LI010
SPILLWAY
16PI023
16PI026
16PI022
16LI011
24PI045
24PI039
24PI047, 24PI046
24PI044
24LI021
24LI030
16PI004
24LI017
24LI019
16PI018
VWP Cluster 2
16PI003
16PI017
24LI029
VWP Cluster 3
24LI018
24LI020
16PI019
16PI027
TOE
16PI028
AA
BB
CC
DD
EE
FF
GG
HH
II
JJ
KK
LL
MM
NN
Legend
Casagrande Piezometer
Vibrating Wire Piezometer
Water Level Indicator
TOE
Instrumentation groups not along a section line
0 m
50 m
100 m
150 m
200 m
24PI060
16PI002
24PI057
PA-027
24PI054
24PI058, 24PI059
24PI063
24LI028
16PI001
24LI027
24PI051
24PI043
24PI056
24PI055
24LI025
24PI041, 24PI042
24PI048
24PI053
24PI052
24PI061, 24PI062
24LI023
24PI050
24PI049
24LI026
24LI022
24LI024
0 m
20 m
40 m
60 m
80 m

ATTACHMENT E2

Sections

Attachment E2
Sections

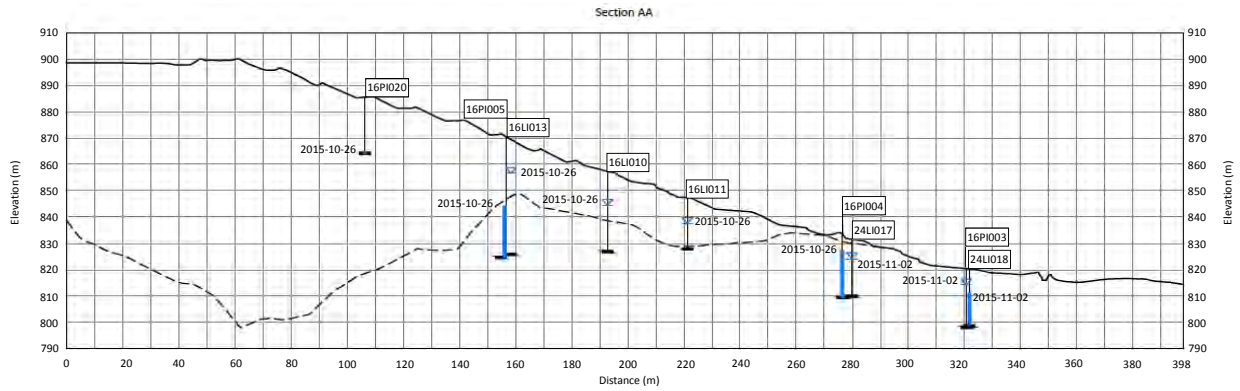

Figure E.E2-1 Section AA

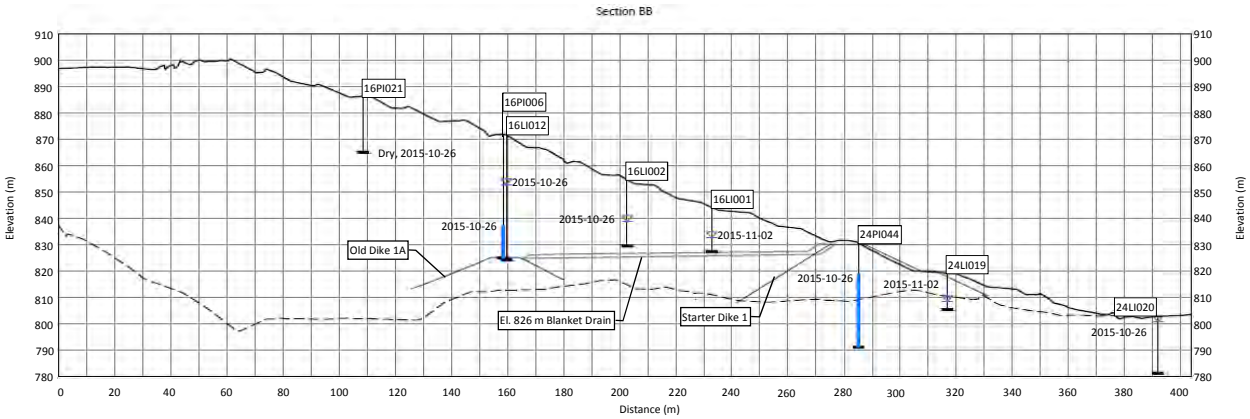

Figure E.E2-2 Section BB

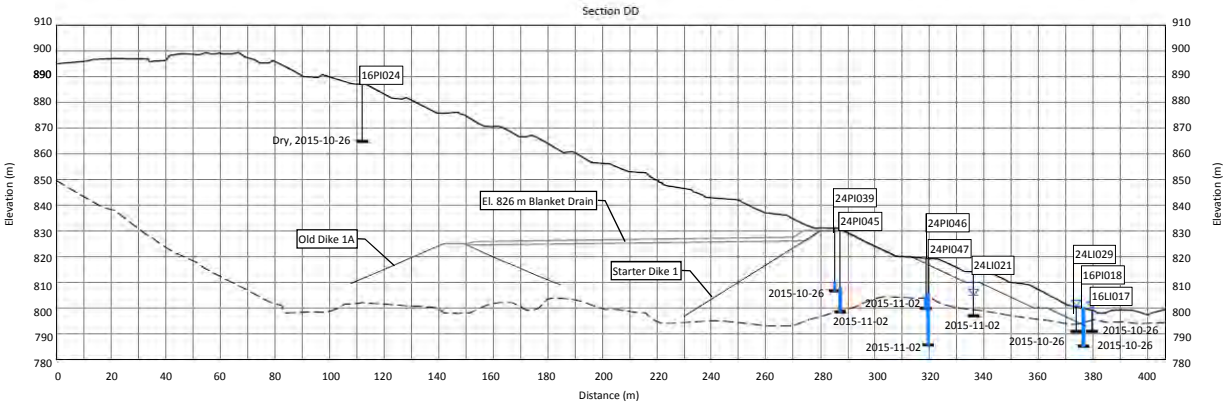

Figure E.E2-3 Section DD

Legend:

- Oct 27, 2015 Topography
- Starter Dike 1 and Old Dike 1A As-built
- Stripped Ground
- Blanket Drain
- 16PI004 — Water Level Indicator ("LI") or Casagrande Piezometer ("PI")
- 2015-10-26 — Phreatic Surface and Date of Reading for Water Level Indicators (YYYY-MM-DD)
- 2015-10-26 — Piezometric Level and Date of Reading for Casagrande Piezometers (YYYY-MM-DD)

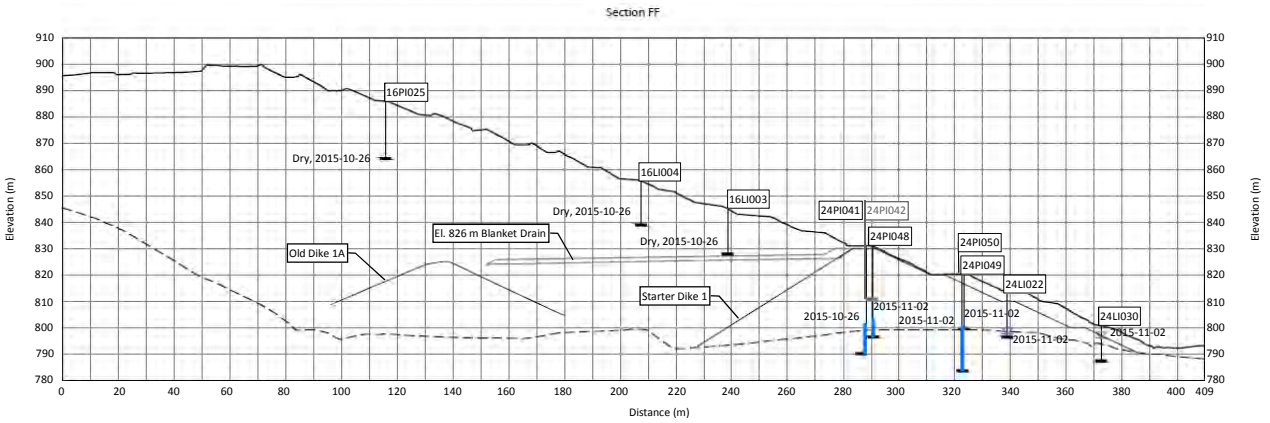

Figure E.E2-4 Section FF

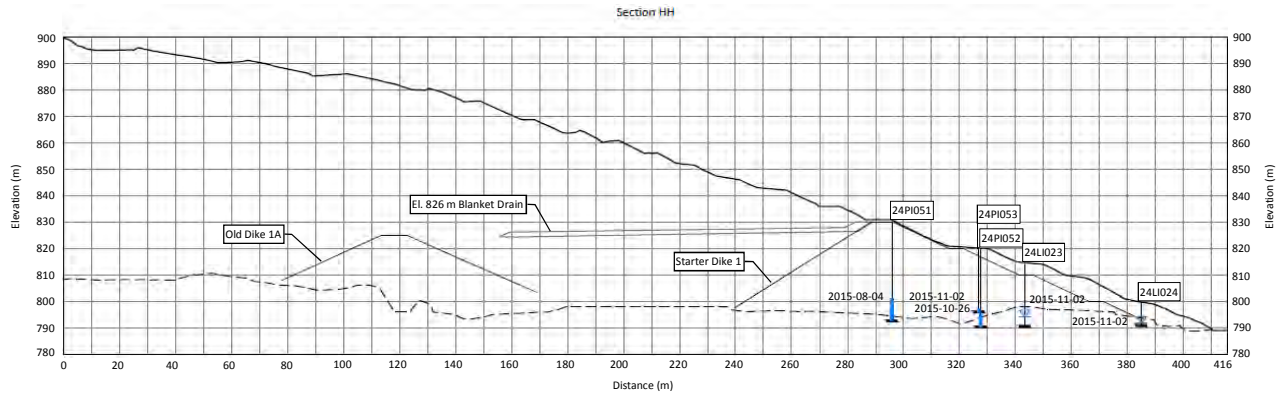

Figure E.E2-5 Section HH

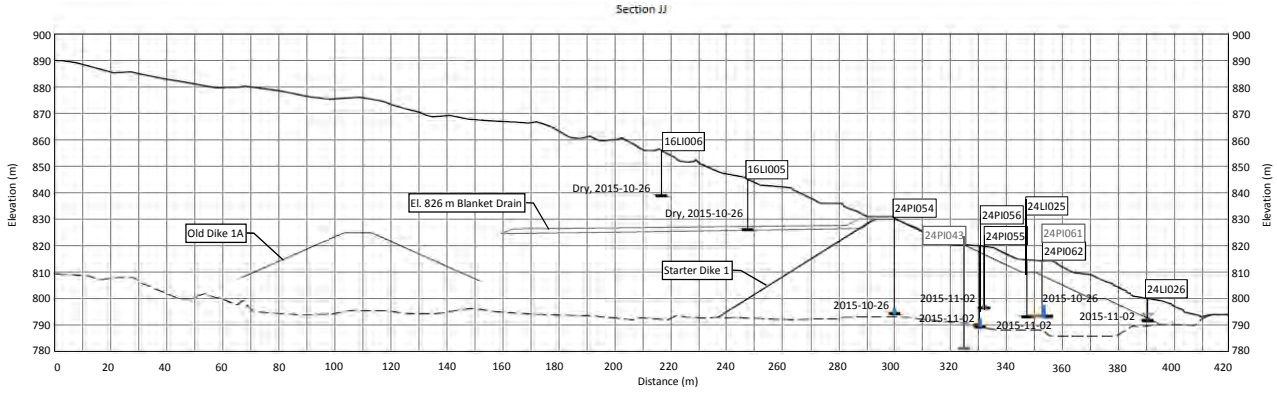

Figure E.E2-6 Section JJ

Legend:

- Oct 27, 2015 Topography
- Starter Dike 1 and Old Dike 1A As-built
- Stripped Ground
- Blanket Drain
- 16PI004 — Water Level Indicator ("LI") or Casagrande Piezometer ("PI")
- 16LI009 — Instruments without readings in October or November, 2015
- 2015-10-26 — Phreatic Surface and Date of Reading for Water Level Indicators (YYYY-MM-DD)
- 2015-10-26 — Piezometric Level and Date of Reading for Casagrande Piezometers (YYYY-MM-DD)

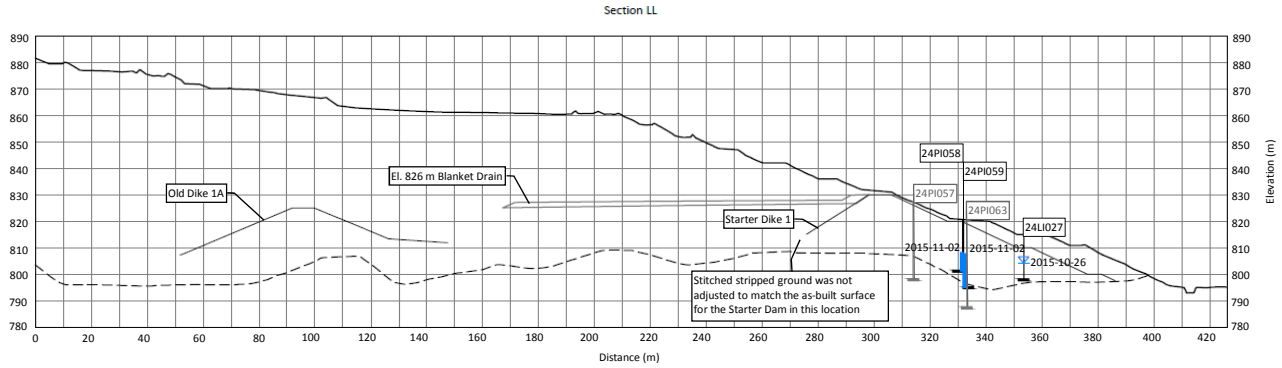

Figure E.E2-7 Section LL

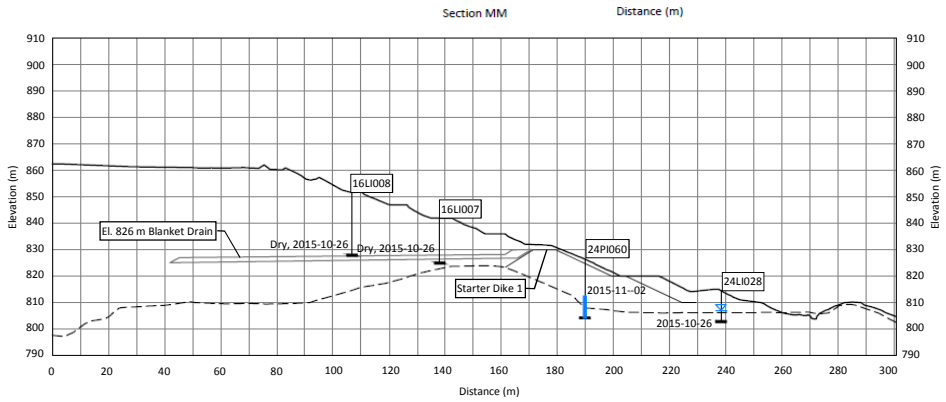

Figure E.E2-8 Section MM

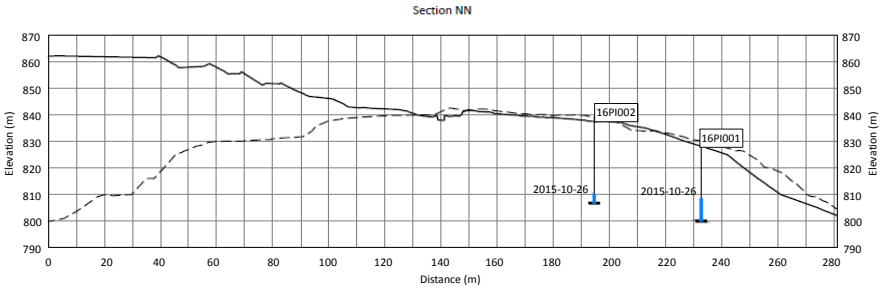

Figure E.E2-9 Section NN

Legend:

- Oct 27, 2015 Topography
- Starter Dike 1 and Old Dike 1A As-built
- Stripped Ground
- Blanket Drain
- 16PI004 — Water Level Indicator ("LI") or Casagrande Piezometer ("PI")
- 16LI009 — Instruments without readings in October or November, 2015
- 2015-10-26 — Phreatic Surface and Date of Reading for Water Level Indicators (YYYY-MM-DD)
- 2015-10-26 — Piezometric Level and Date of Reading for Casagrande Piezometers (YYYY-MM-DD)

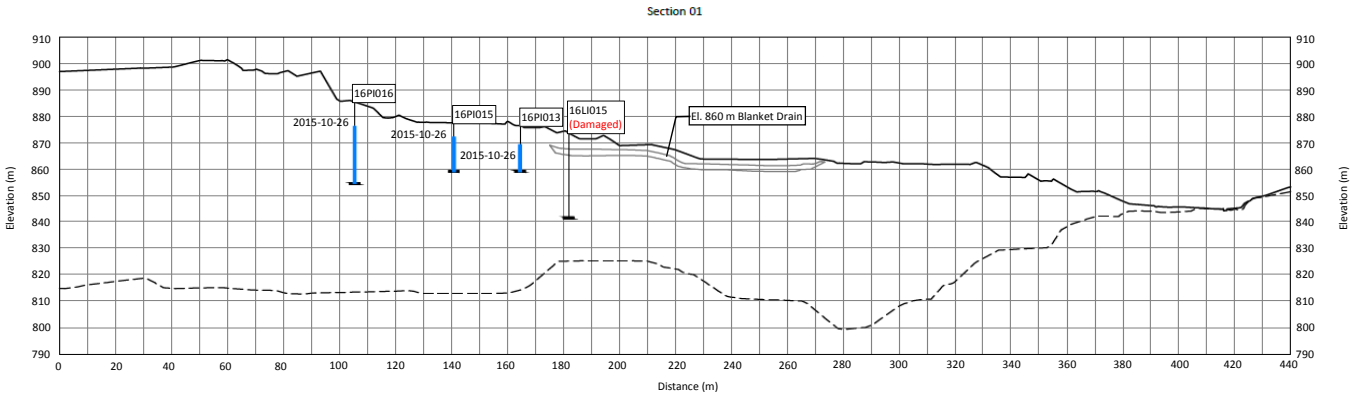

Figure E.E2-10 Section 01

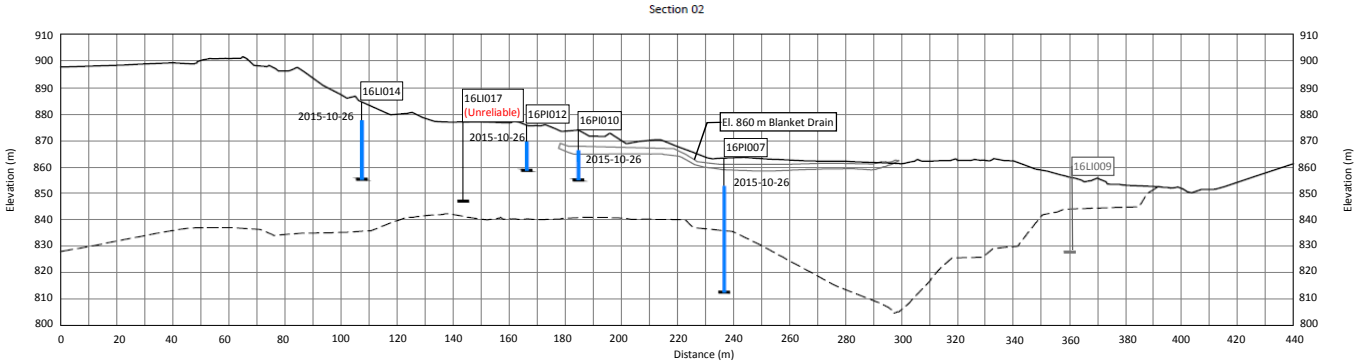

Figure E.E2-11 Section 02

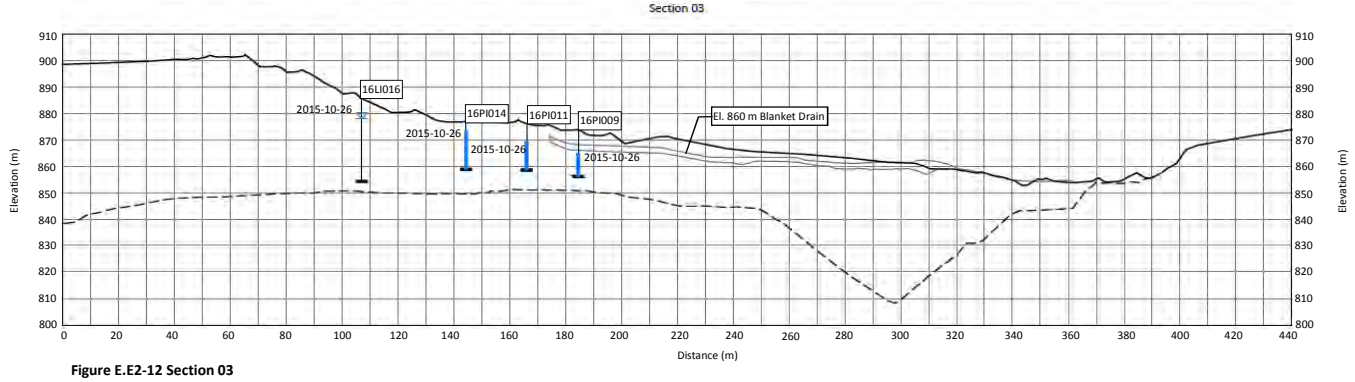

Figure E.E2-12 Section 03

Legend:

- Oct 27, 2015 Topography
- Starter Dike 1 and Old Dike 1A As-built
- Stripped Ground
- Blanket Drain
- 16PI004 — Water Level Indicator ("LI") or Casagrande Piezometer ("PI")
- 16LI009 — Instruments without readings in October or November, 2015
- 2015-10-26 — Phreatic Surface and Date of Reading for Water Level Indicators (YYYY-MM-DD)
- 2015-10-26 — Piezometric Level and Date of Reading for Casagrande Piezometers (YYYY-MM-DD)

ATTACHMENT E3

Piezometer Records, Reservoir Level, and Rainfall Plots

Attachment E3
Piezometer Records, Reservoir Level, and Rainfall Plots

Notes:
1. Rainfall records switch from monthly to daily in January, 2014.
2. Installation date not available for all piezometers. In these cases the date of the first available reading has been plotted.

SPILLWAY

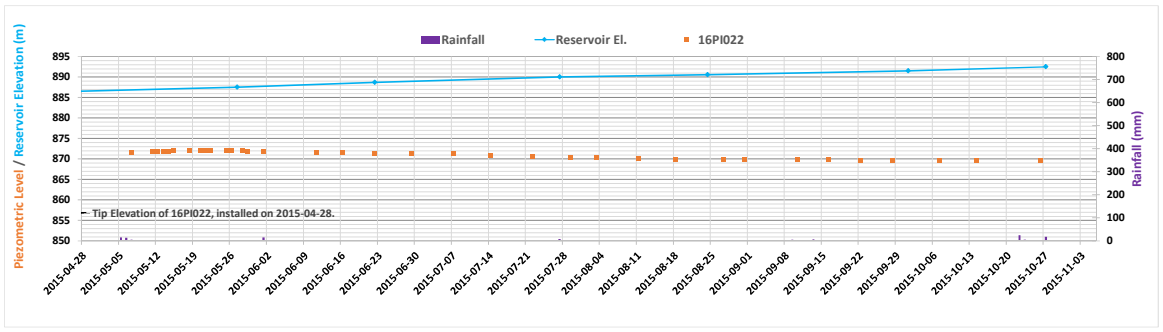

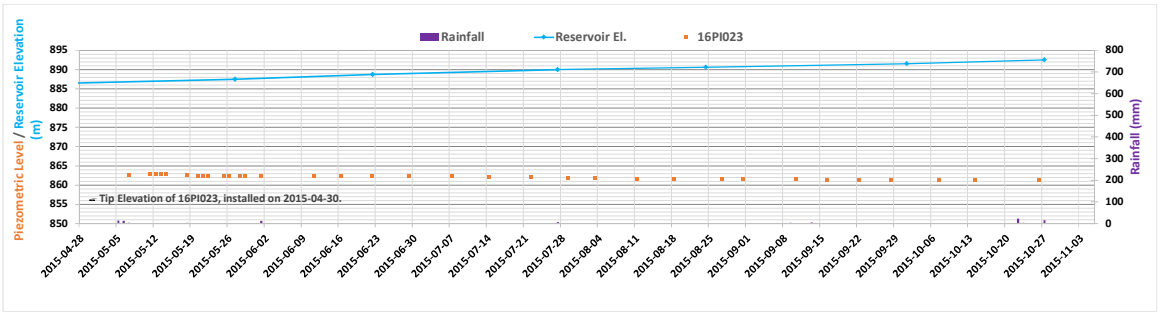

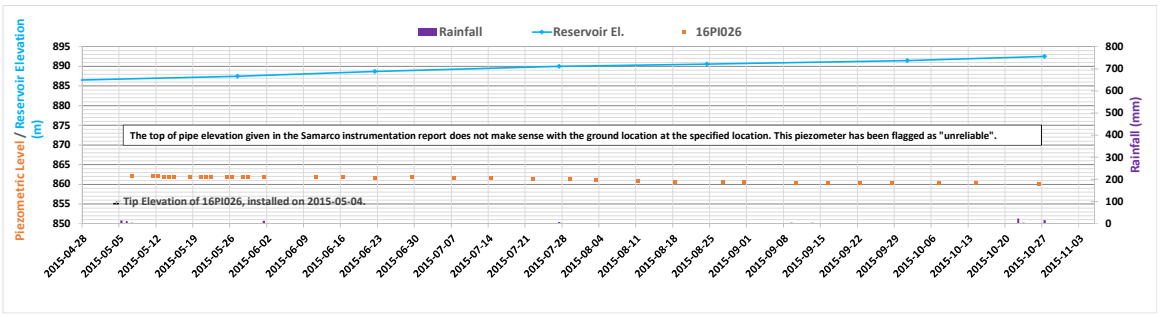

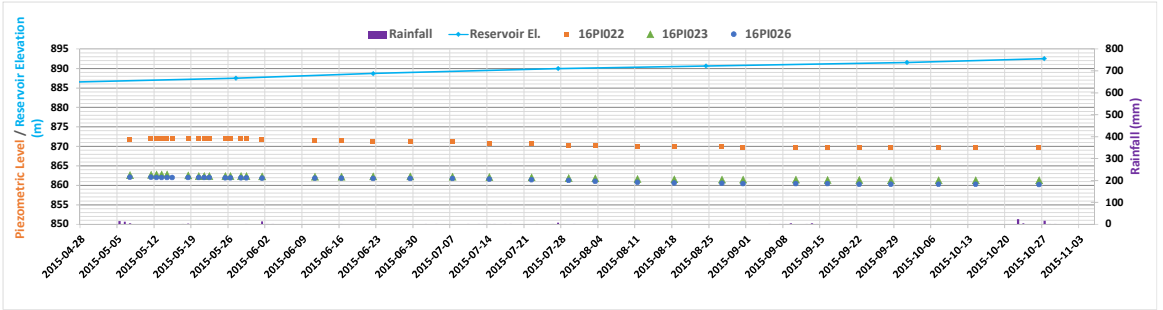

Notes:
1. Rainfall records switch from monthly to daily in January, 2014.
2. Installation date not available for all piezometers. In these cases the date of the first available reading has been plotted.

SPILLWAY (CONTINUED)

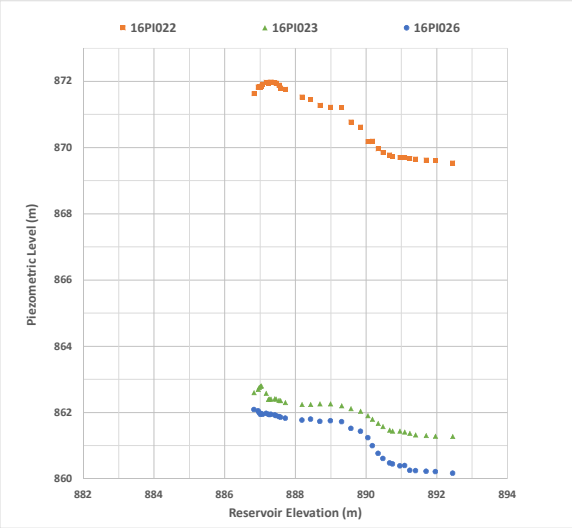

Notes:

1. Rainfall records switch from monthly to daily in January, 2014.
2. Installation date not available for all piezometers. In these cases the date of the first available reading has been plotted.

TOE

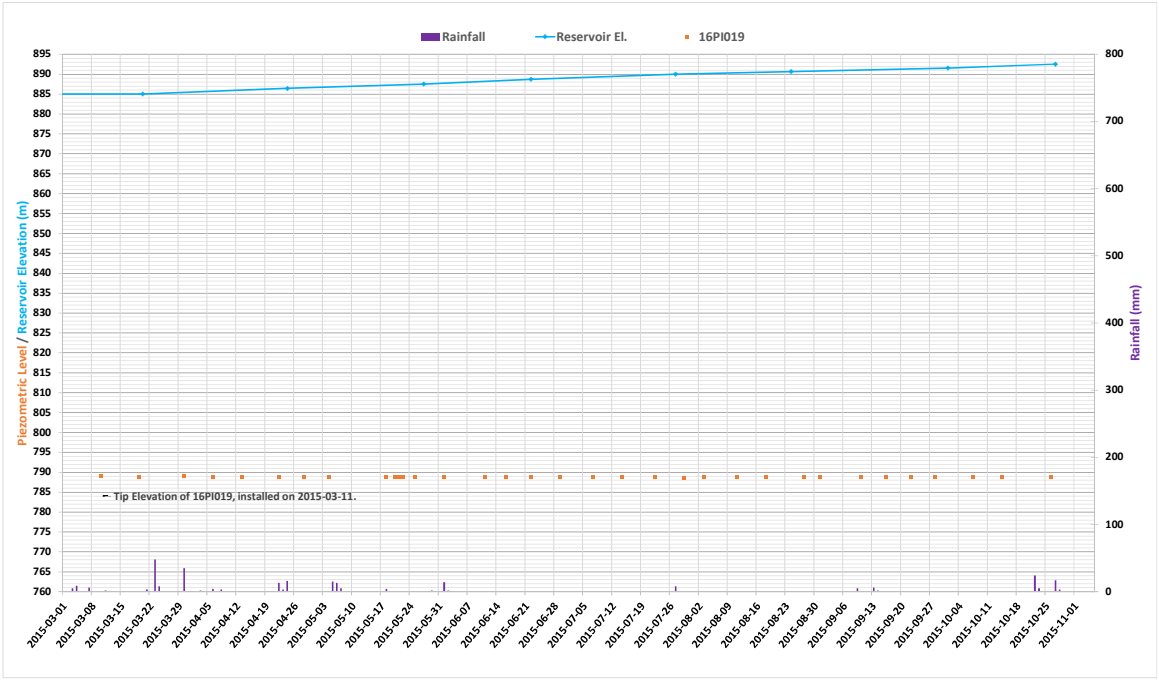

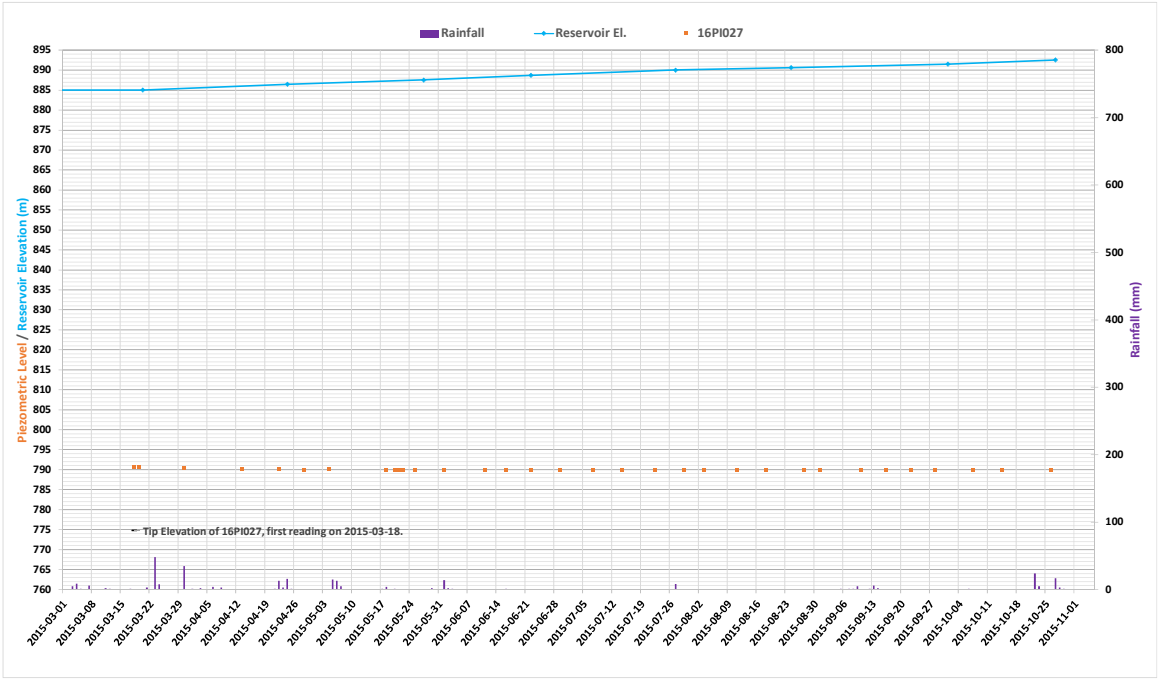

Notes:

1. Rainfall records switch from monthly to daily in January, 2014.
2. Installation date not available for all piezometers. In these cases the date of the first available reading has been plotted.

TOE (CONTINUED)

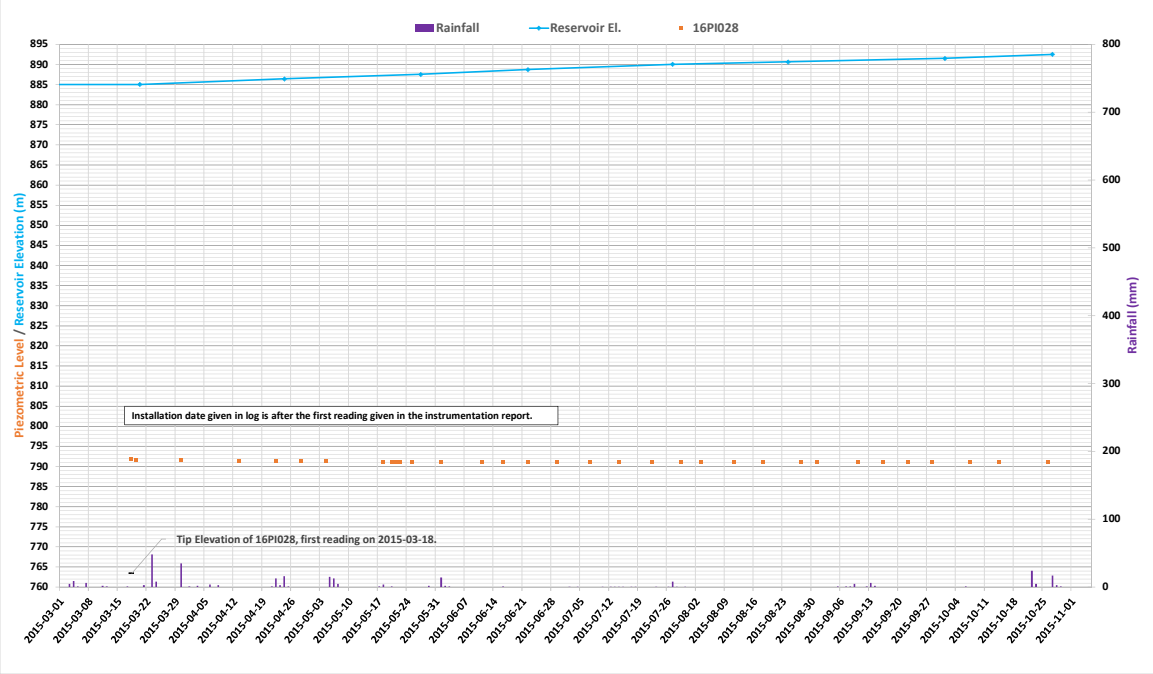

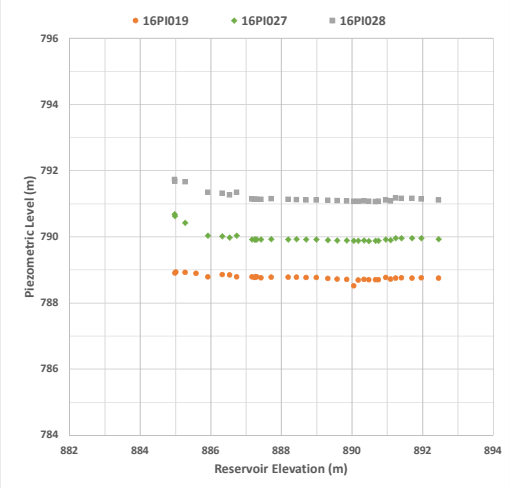

Notes:

1. Rainfall records switch from monthly to daily in January, 2014.
2. Installation date not available for all piezometers. In these cases the date of the first available reading has been plotted.

SECTION AA

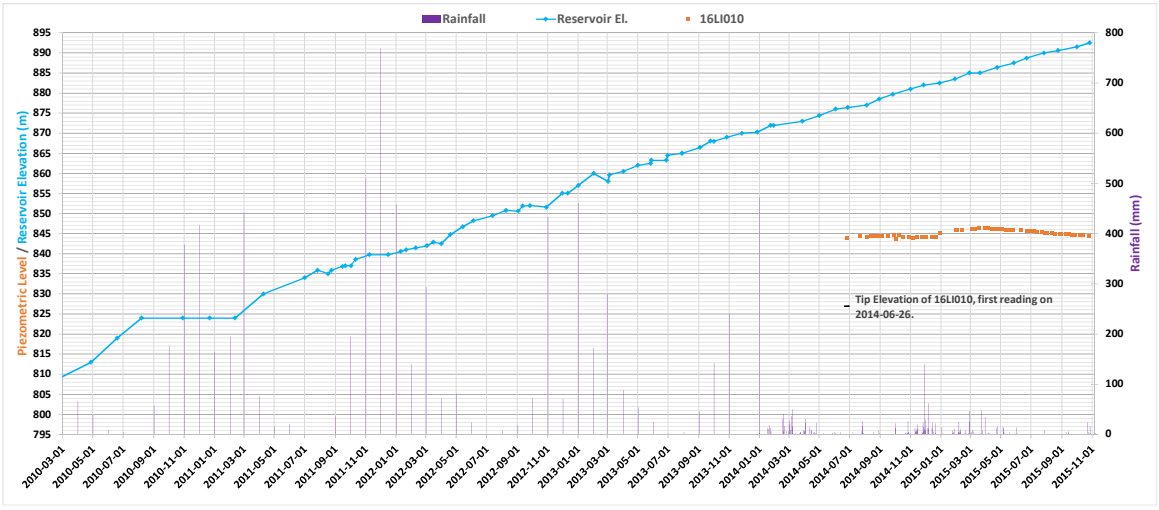

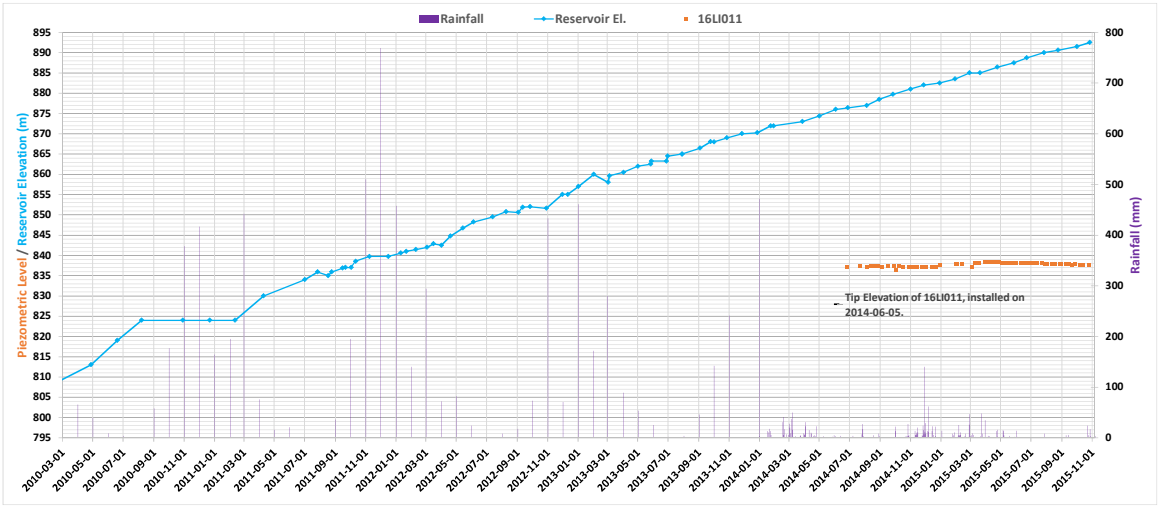

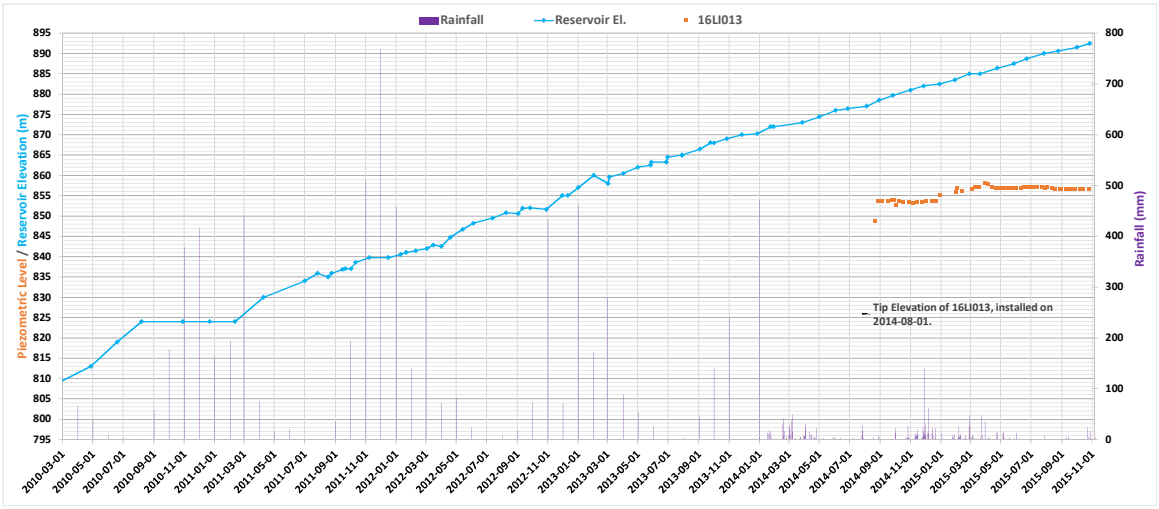

Notes:

1. Rainfall records switch from monthly to daily in January, 2014.
2. Installation date not available for all piezometers. In these cases the date of the first available reading has been plotted.

SECTION AA (CONTINUED)

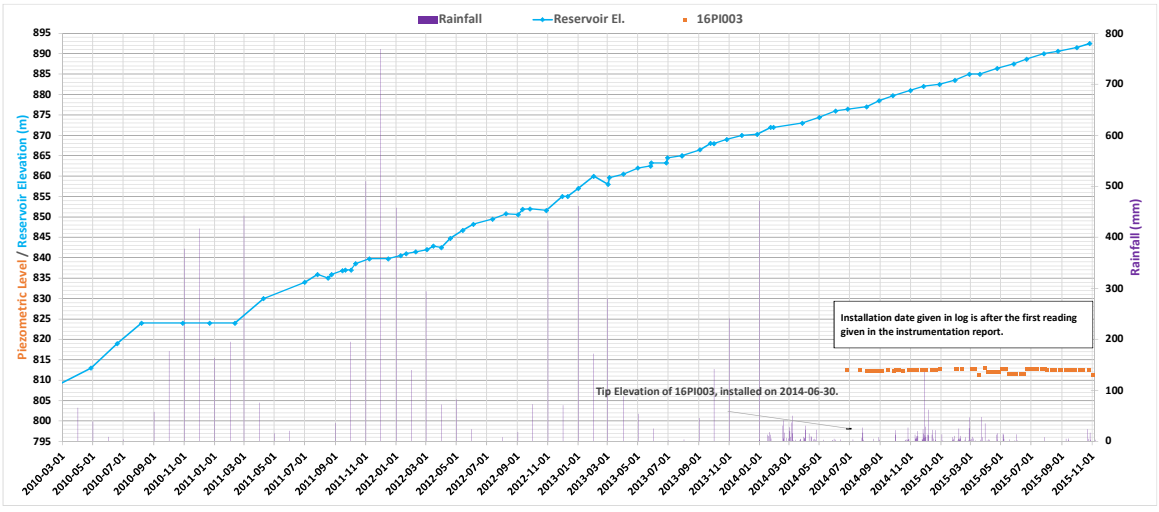

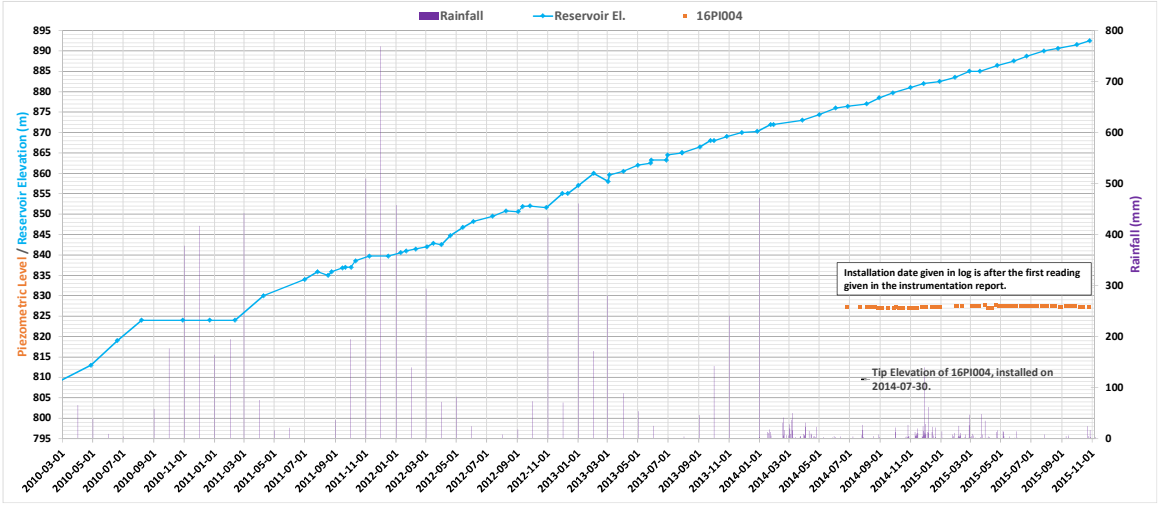

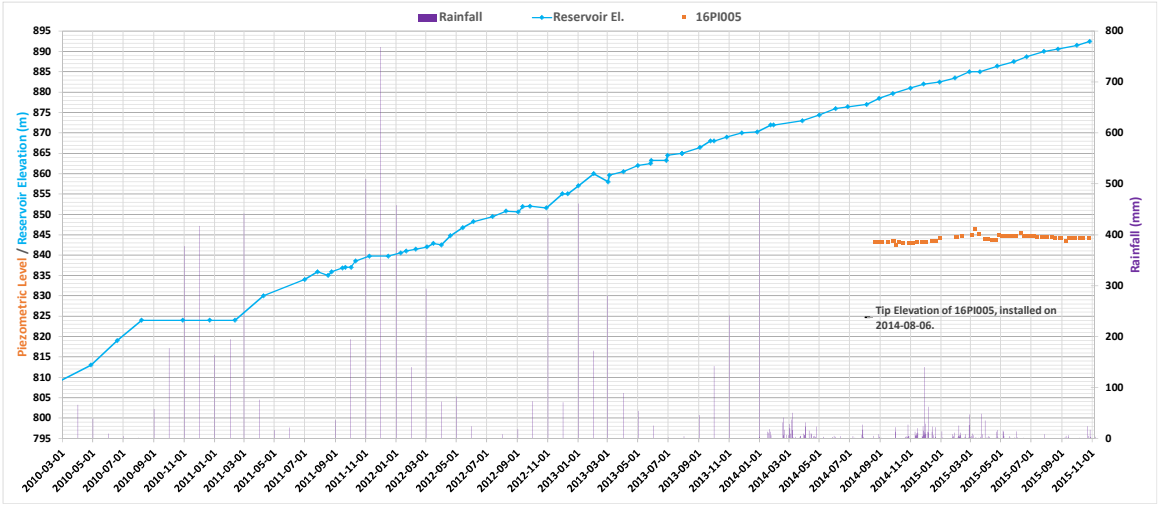

Notes:

1. Rainfall records switch from monthly to daily in January, 2014.
2. Installation date not available for all piezometers. In these cases the date of the first available reading has been plotted.

SECTION AA (CONTINUED)

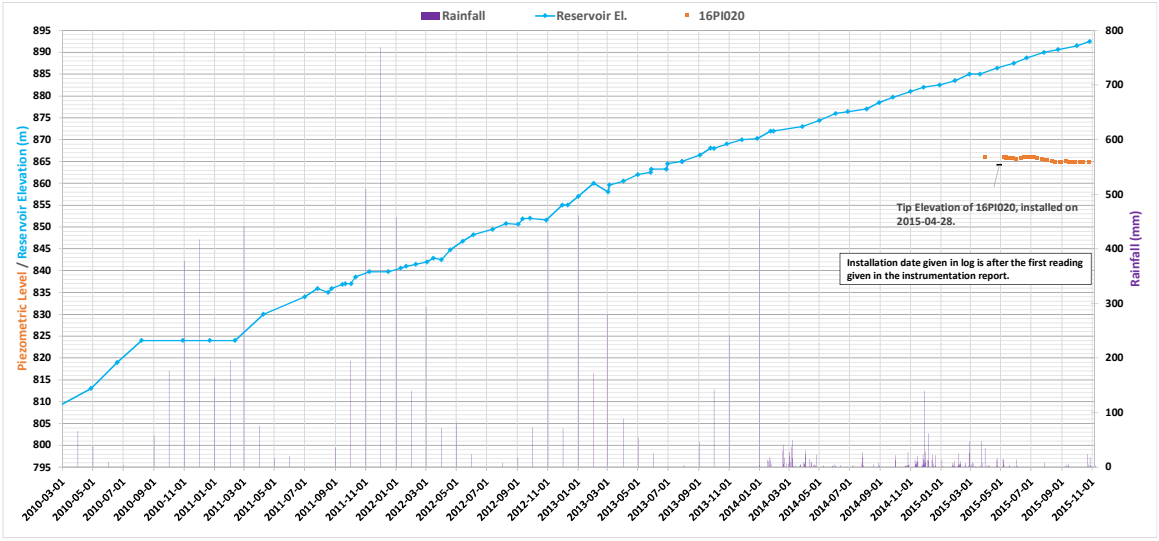

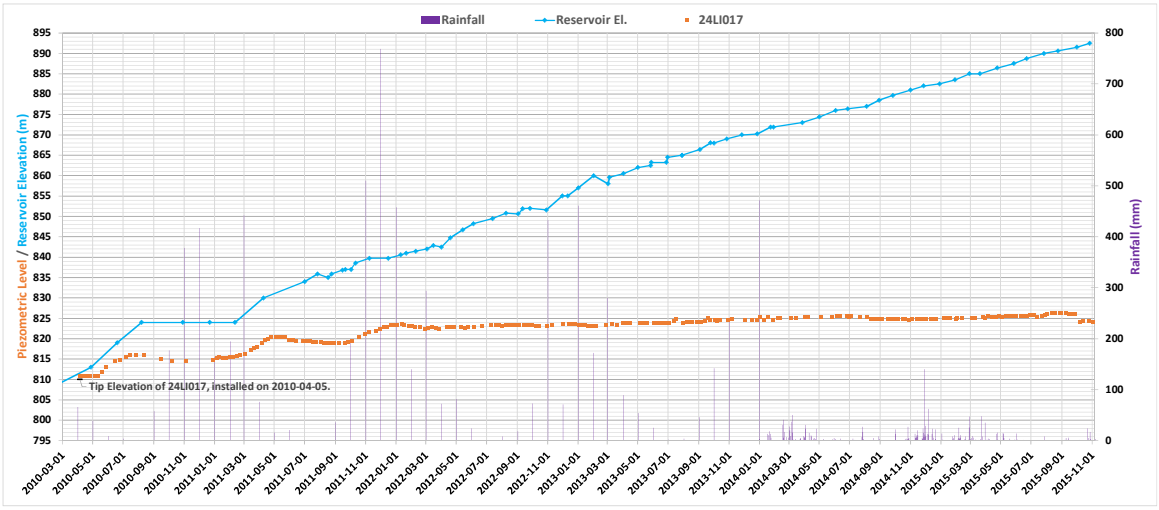

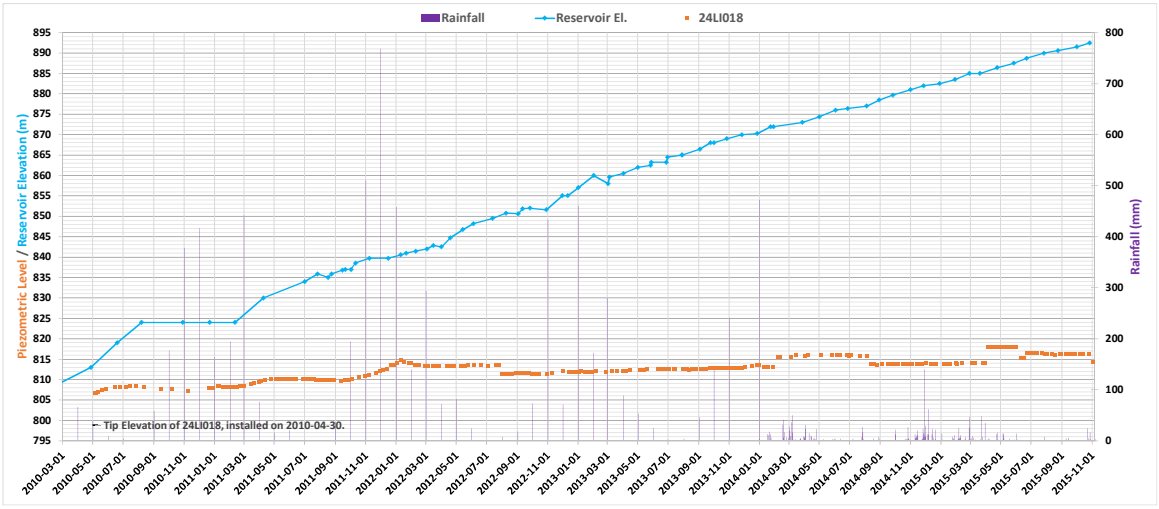

Notes:

1. Rainfall records switch from monthly to daily in January, 2014.
2. Installation date not available for all piezometers. In these cases the date of the first available reading has been plotted.

SECTION AA (CONTINUED)

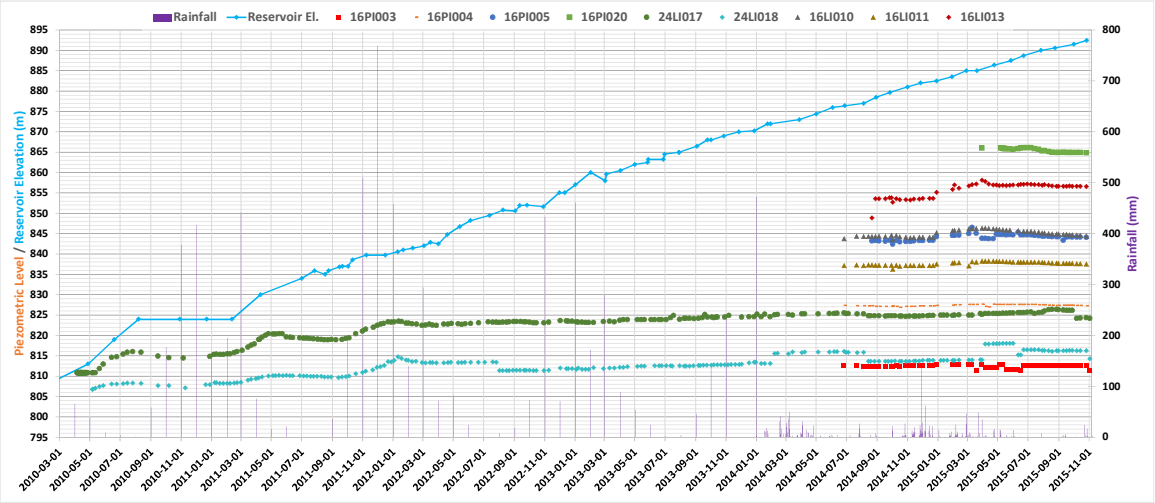

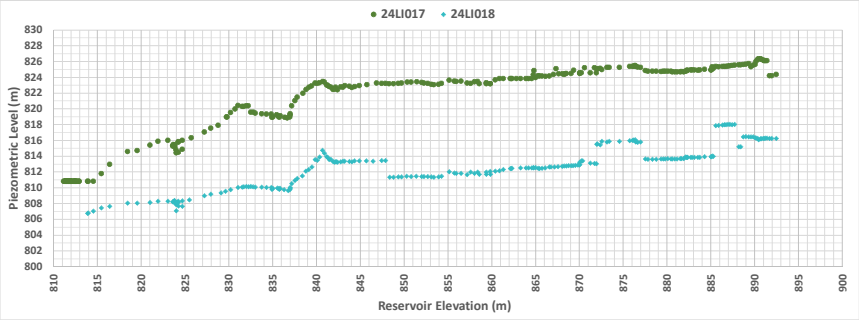

Notes:

1. Rainfall records switch from monthly to daily in January, 2014.
2. Installation date not available for all piezometers. In these cases the date of the first available reading has been plotted.

SECTION AA (CONTINUED)

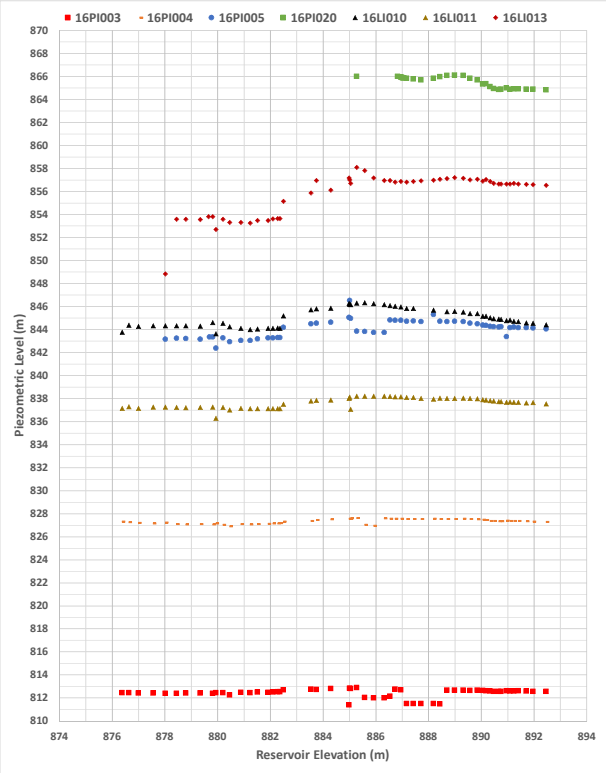

Notes:

1. Rainfall records switch from monthly to daily in January, 2014.
2. Installation date not available for all piezometers. In these cases the date of the first available reading has been plotted.

SECTION BB

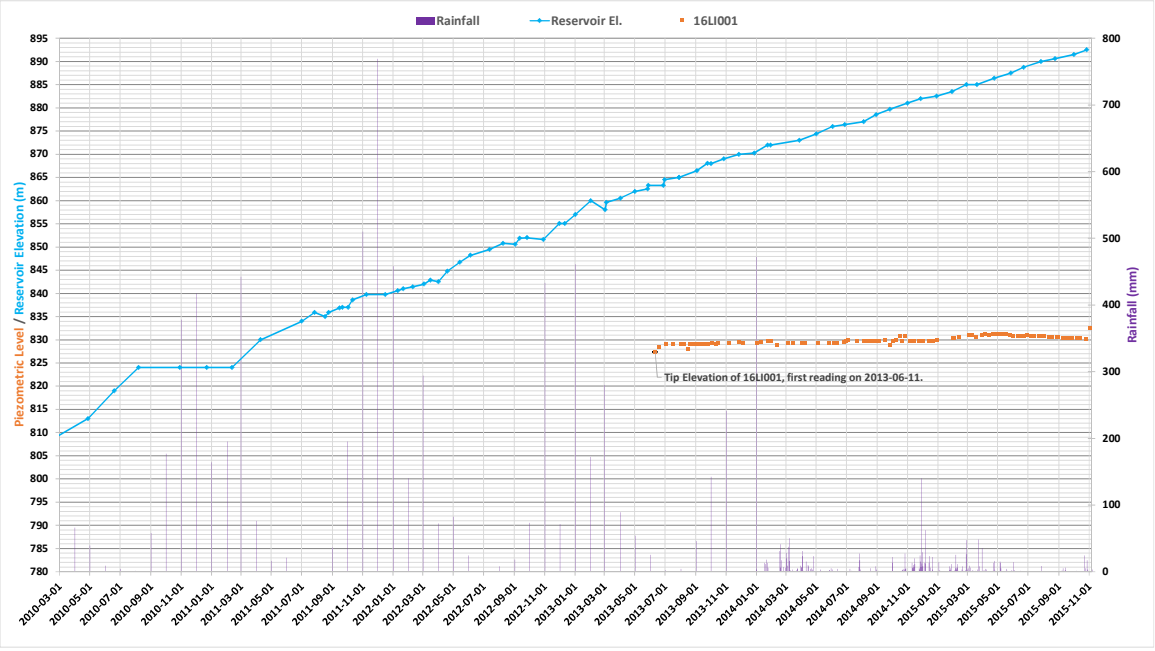

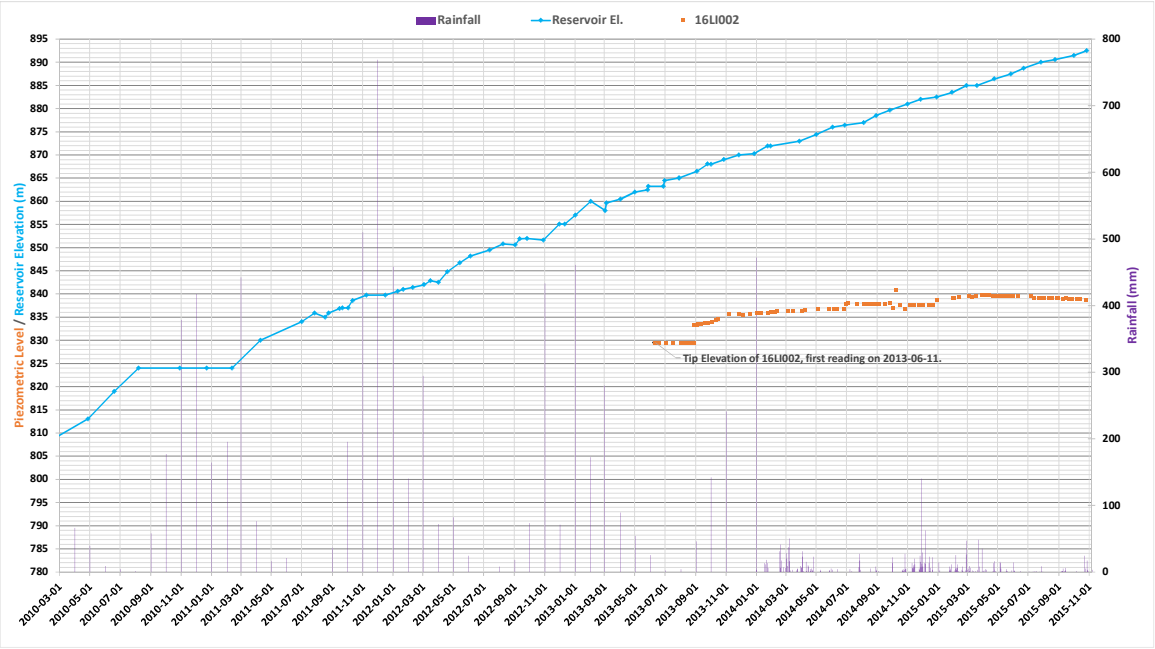

Notes:

1. Rainfall records switch from monthly to daily in January, 2014.
2. Installation date not available for all piezometers. In these cases the date of the first available reading has been plotted.

SECTION BB (CONTINUED)

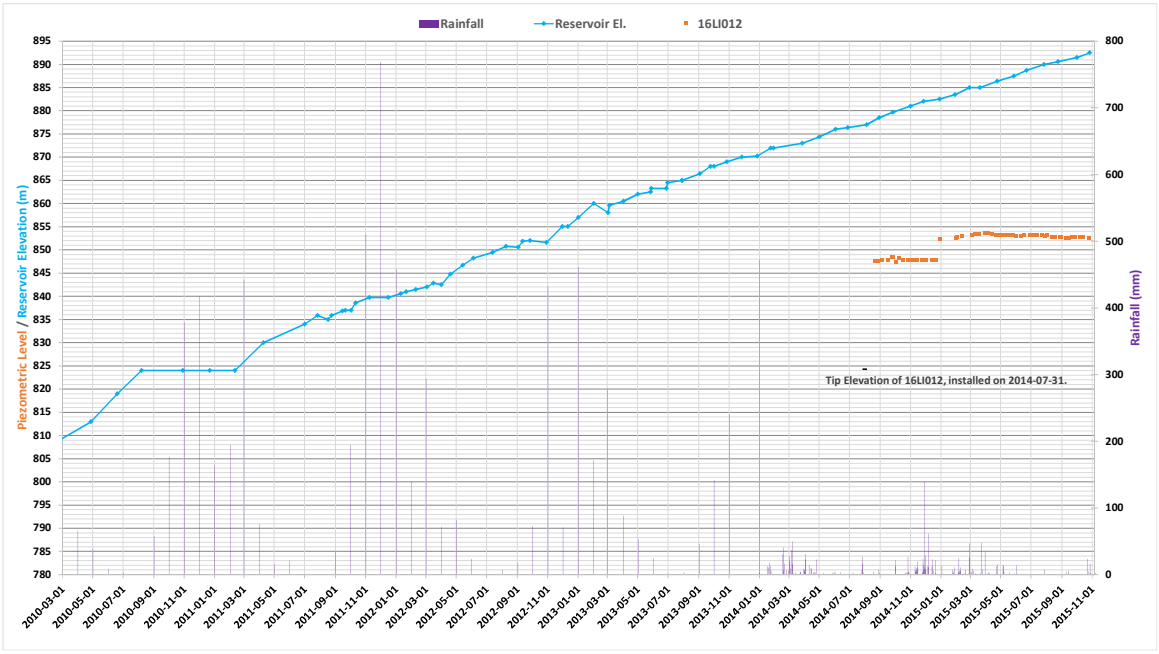

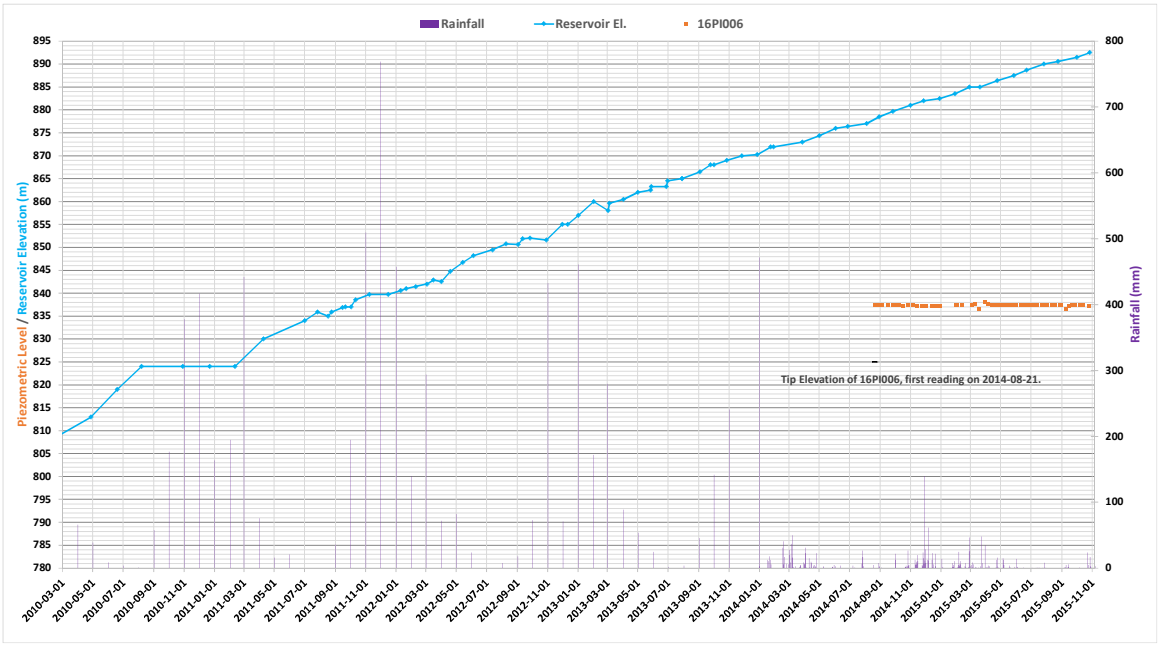

Notes:

1. Rainfall records switch from monthly to daily in January, 2014.
2. Installation date not available for all piezometers. In these cases the date of the first available reading has been plotted.

SECTION BB (CONTINUED)

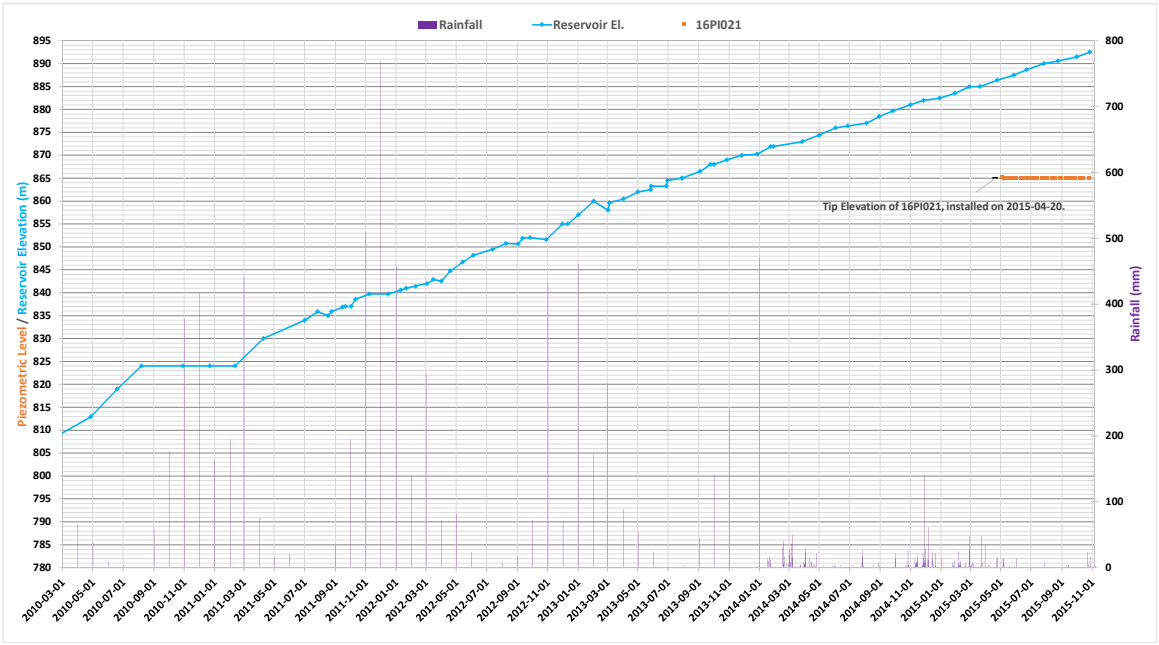

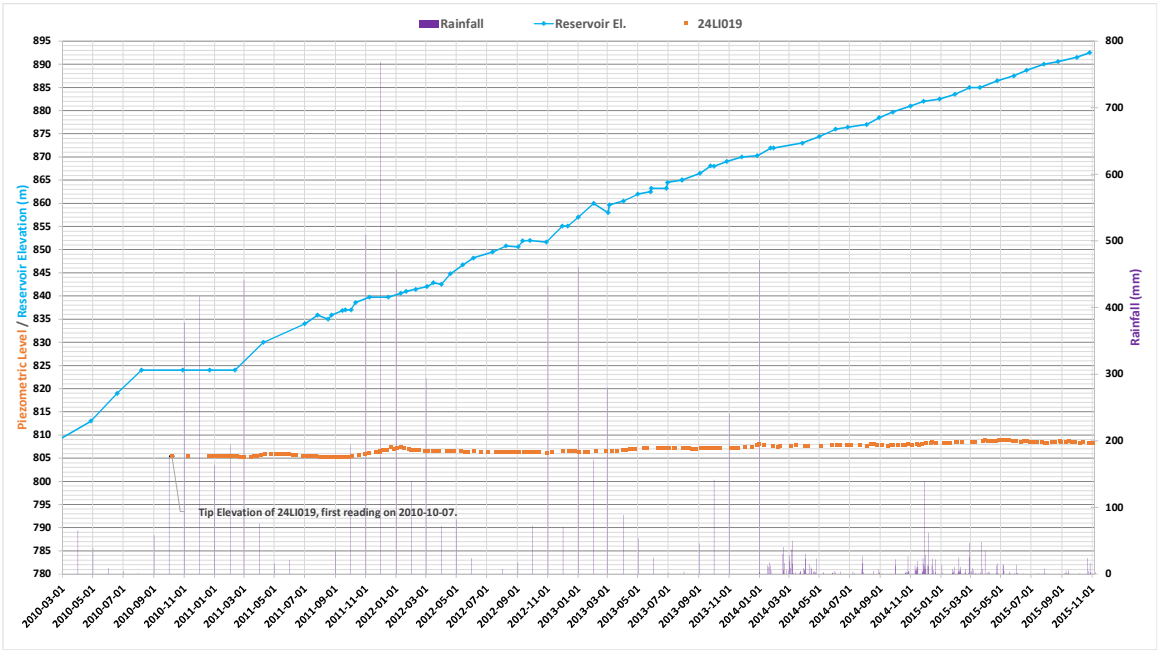

Notes:

1. Rainfall records switch from monthly to daily in January, 2014.
2. Installation date not available for all piezometers. In these cases the date of the first available reading has been plotted.

SECTION BB (CONTINUED)

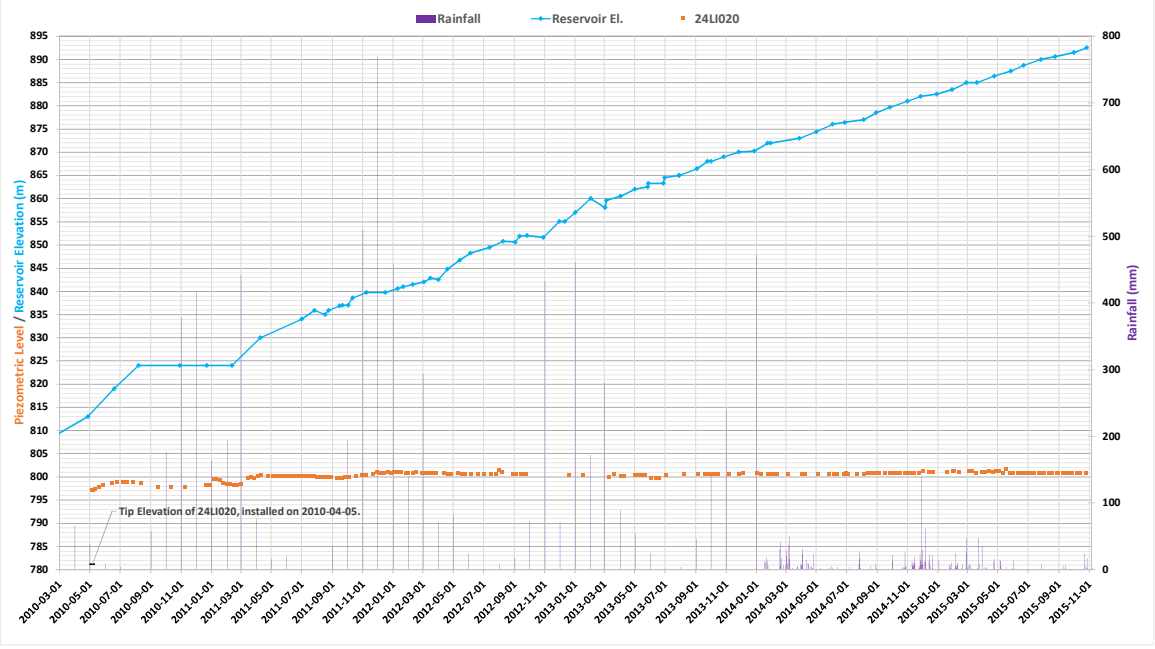

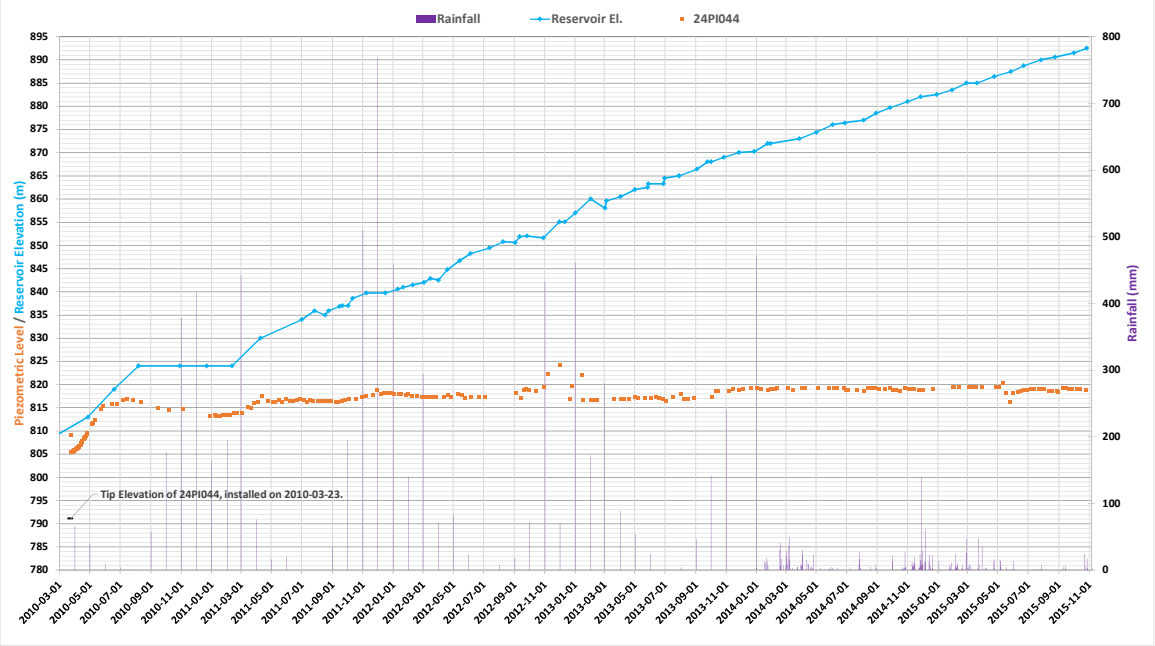

Notes:

1. Rainfall records switch from monthly to daily in January, 2014.
2. Installation date not available for all piezometers. In these cases the date of the first available reading has been plotted.

SECTION BB (CONTINUED)

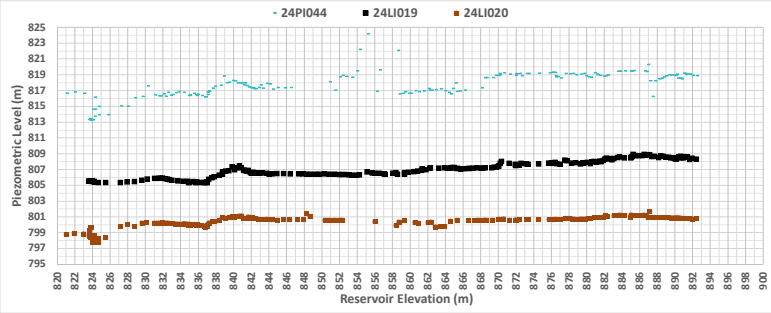

Notes:

1. Rainfall records switch from monthly to daily in January, 2014.
2. Installation date not available for all piezometers. In these cases the date of the first available reading has been plotted.

SECTION DD

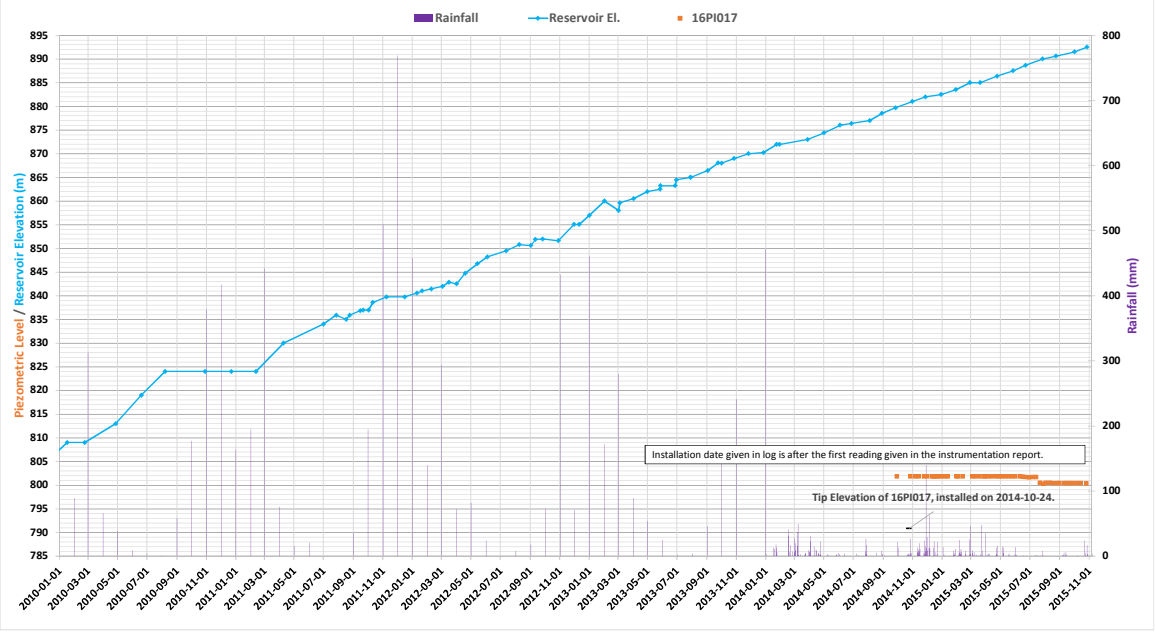

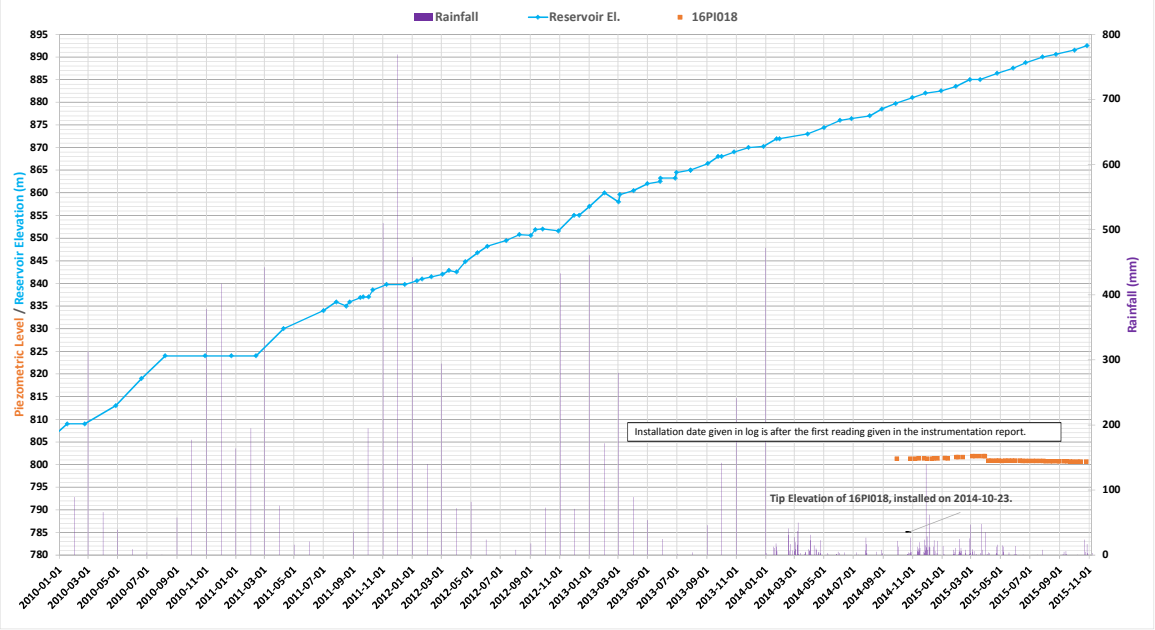

Notes:

1. Rainfall records switch from monthly to daily in January, 2014.
2. Installation date not available for all piezometers. In these cases the date of the first available reading has been plotted.

SECTION DD (CONTINUED)

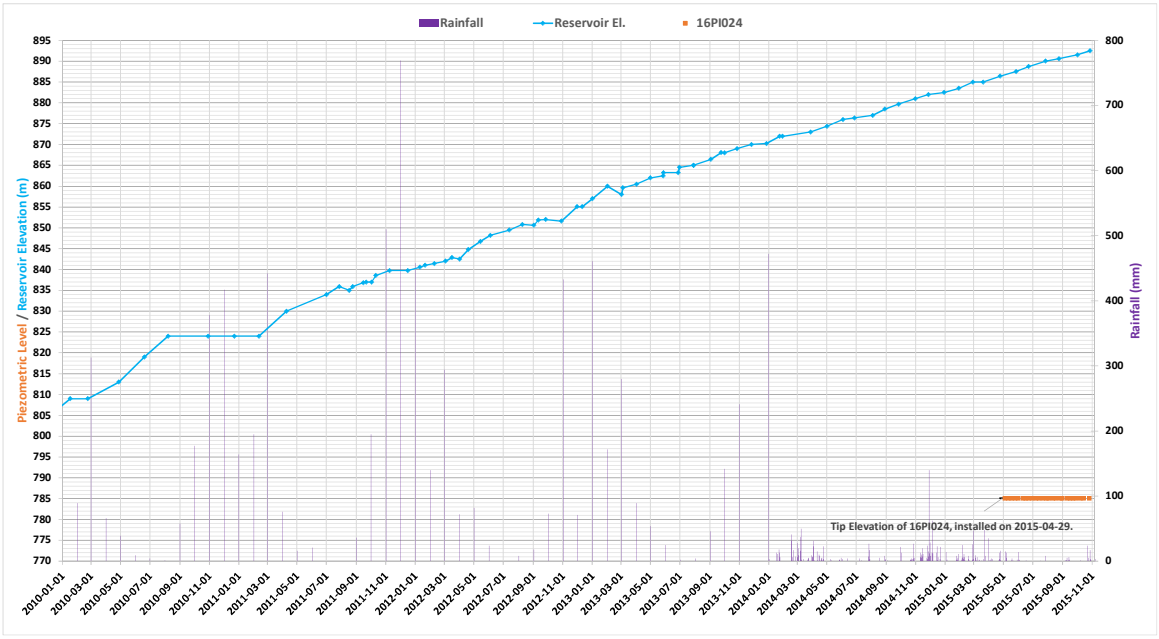

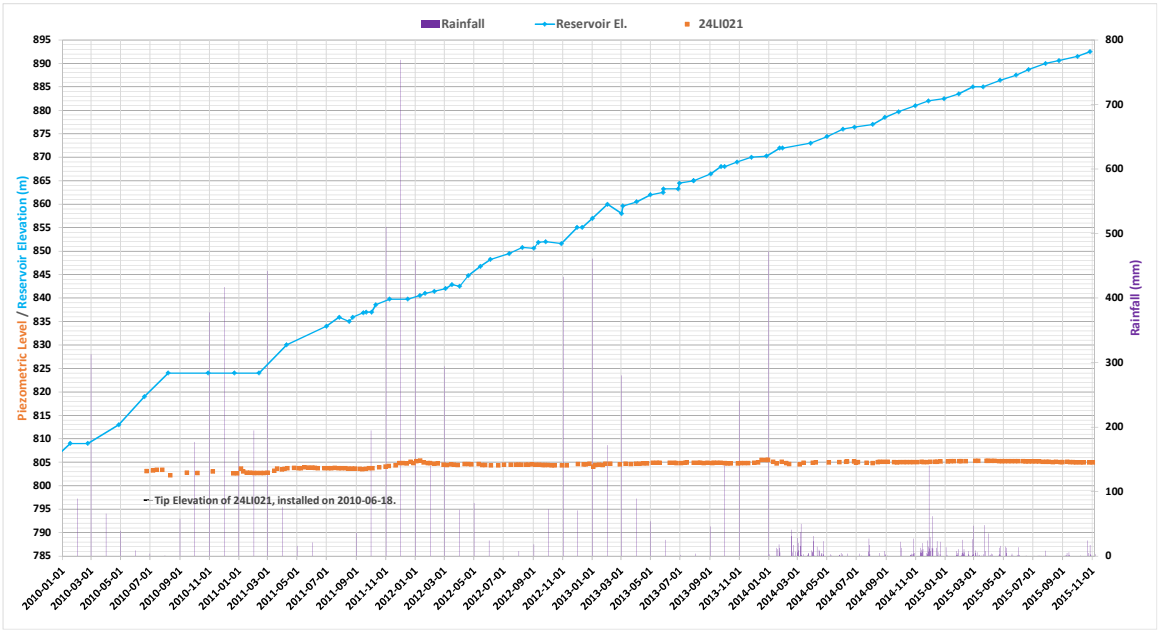

Notes:

1. Rainfall records switch from monthly to daily in January, 2014.
2. Installation date not available for all piezometers. In these cases the date of the first available reading has been plotted.

SECTION DD (CONTINUED)

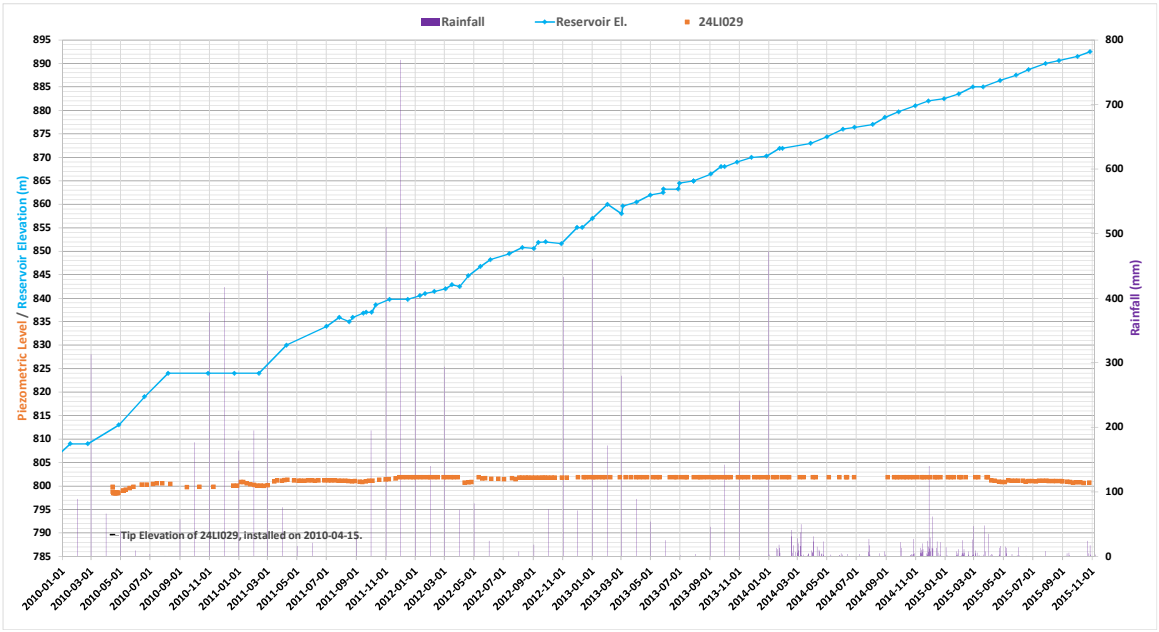

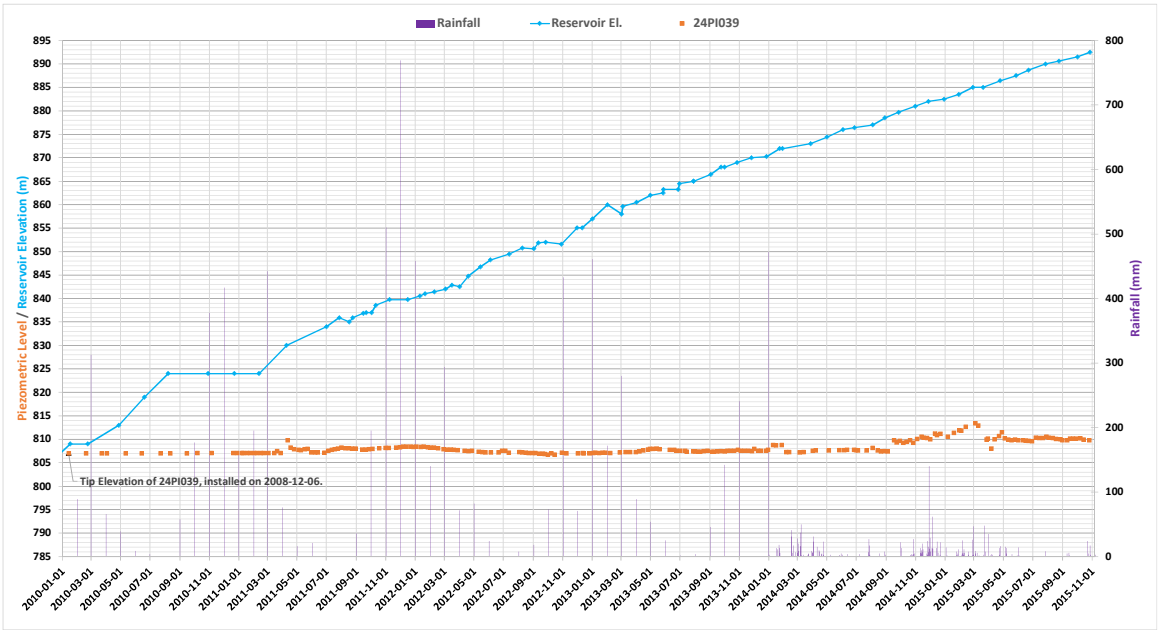

Notes:

1. Rainfall records switch from monthly to daily in January, 2014.
2. Installation date not available for all piezometers. In these cases the date of the first available reading has been plotted.

SECTION DD (CONTINUED)

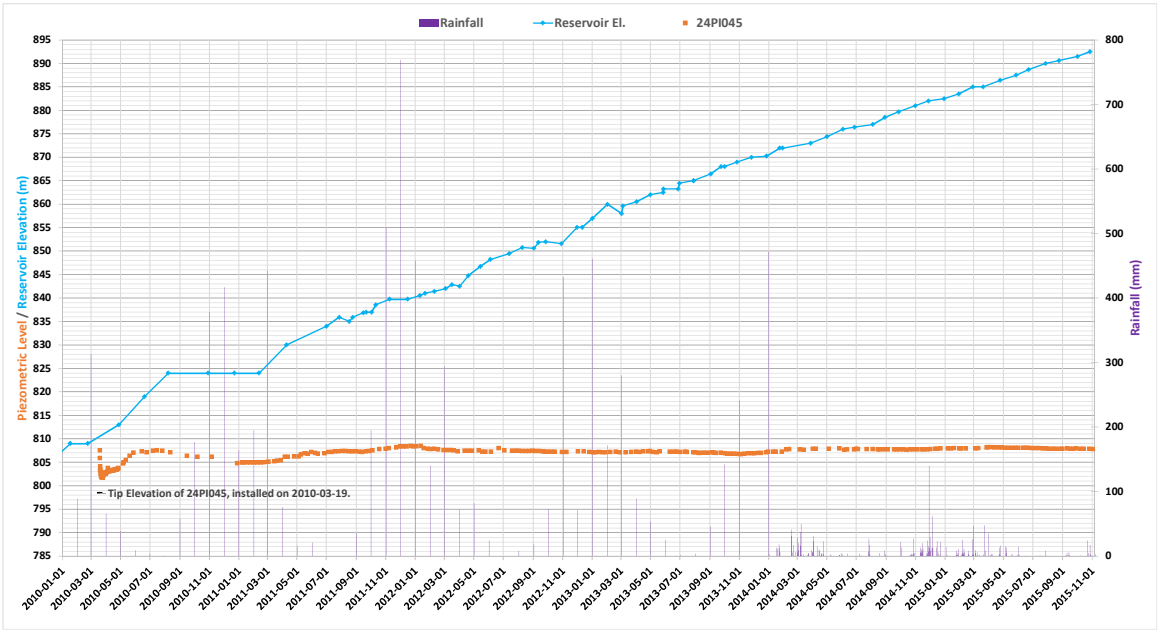

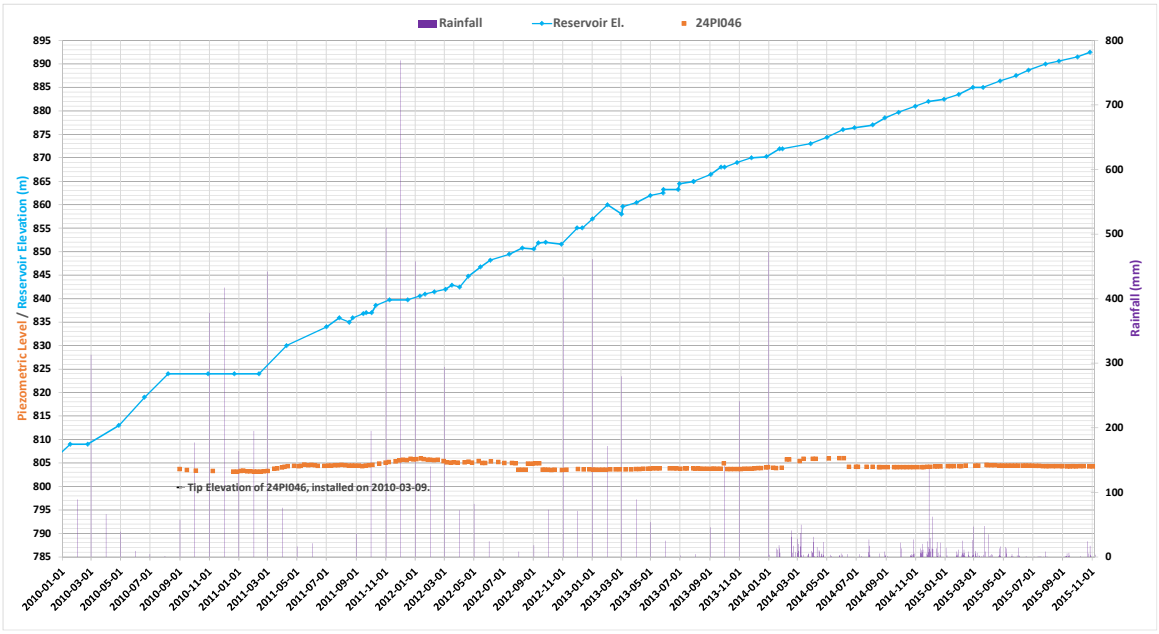

Notes:

1. Rainfall records switch from monthly to daily in January, 2014.
2. Installation date not available for all piezometers. In these cases the date of the first available reading has been plotted.

SECTION DD (CONTINUED)

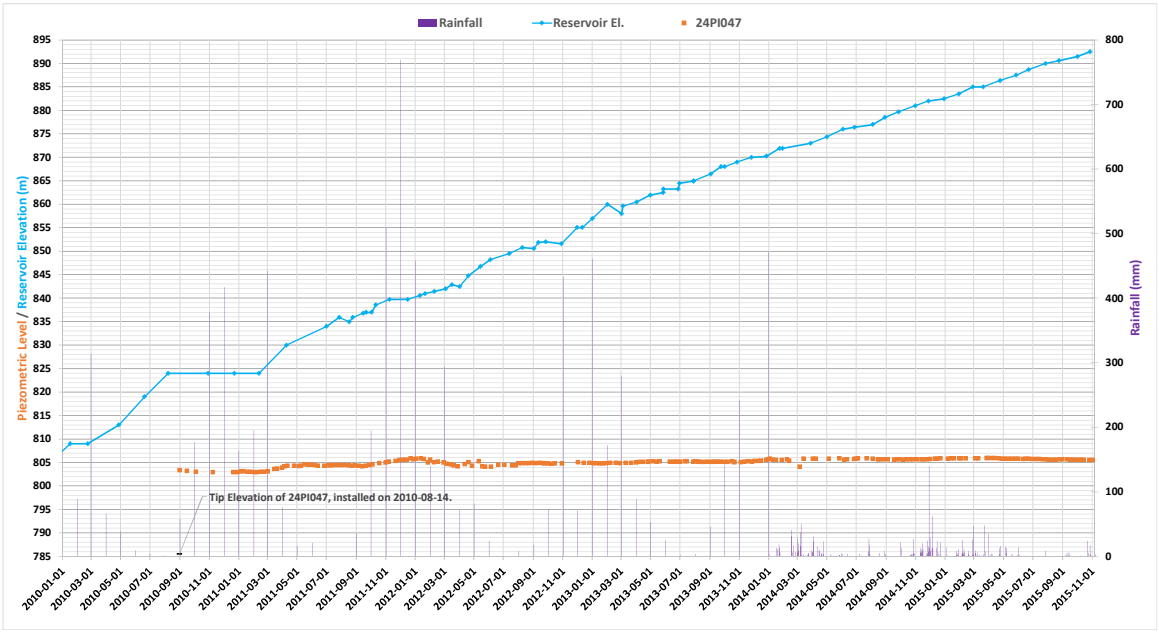

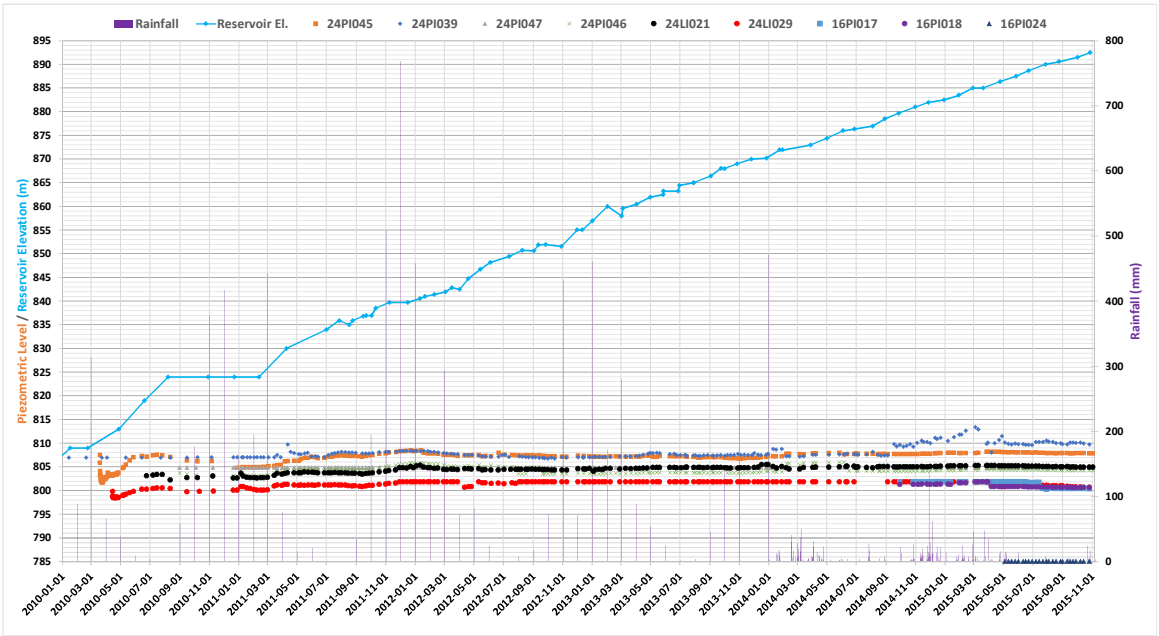

Notes:

1. Rainfall records switch from monthly to daily in January, 2014.
2. Installation date not available for all piezometers. In these cases the date of the first available reading has been plotted.

SECTION DD (CONTINUED)

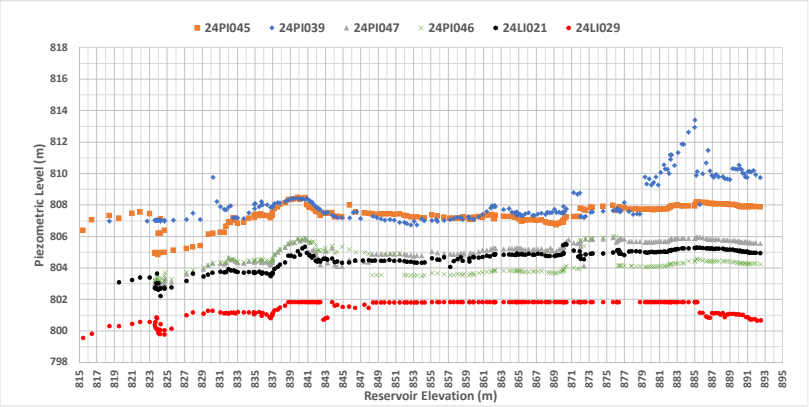

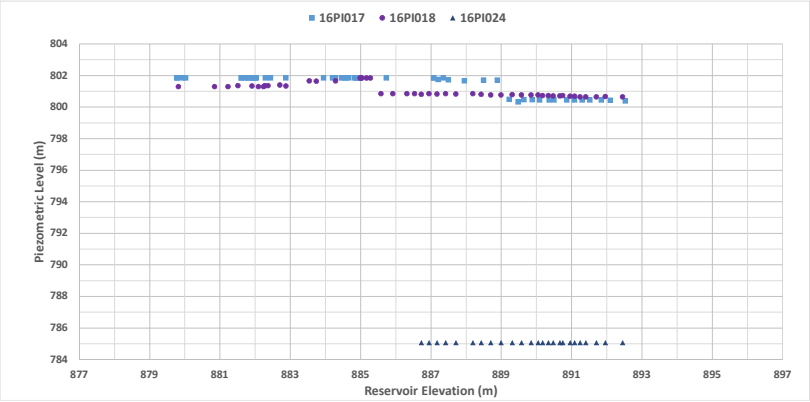

Notes:

1. Rainfall records switch from monthly to daily in January, 2014.
2. Installation date not available for all piezometers. In these cases the date of the first available reading has been plotted.

SECTION FF

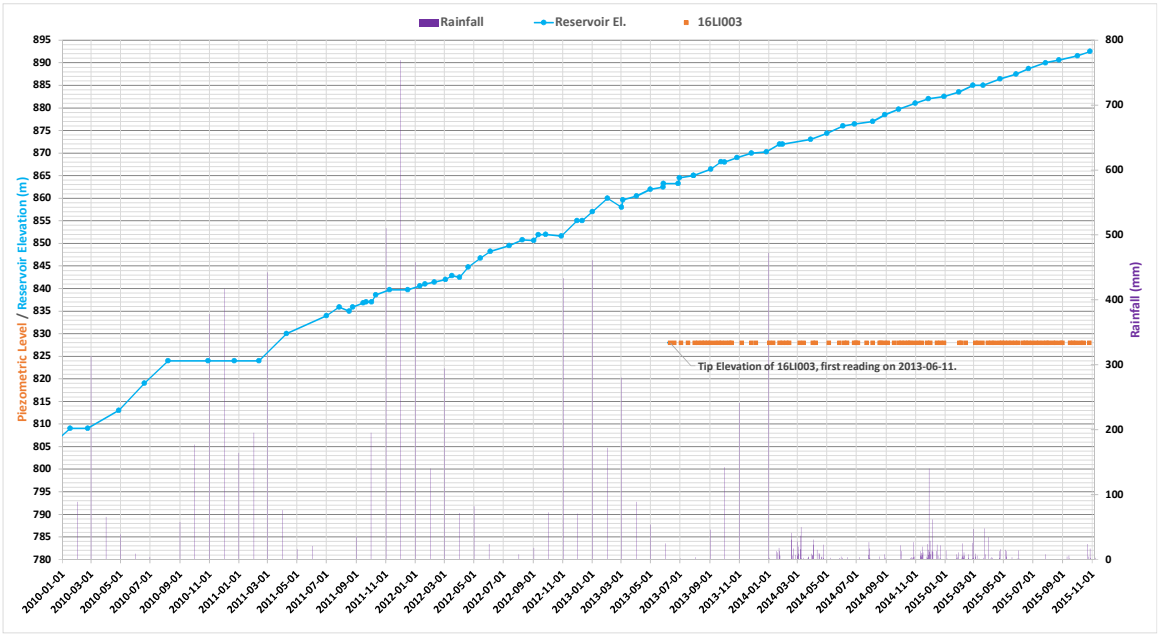

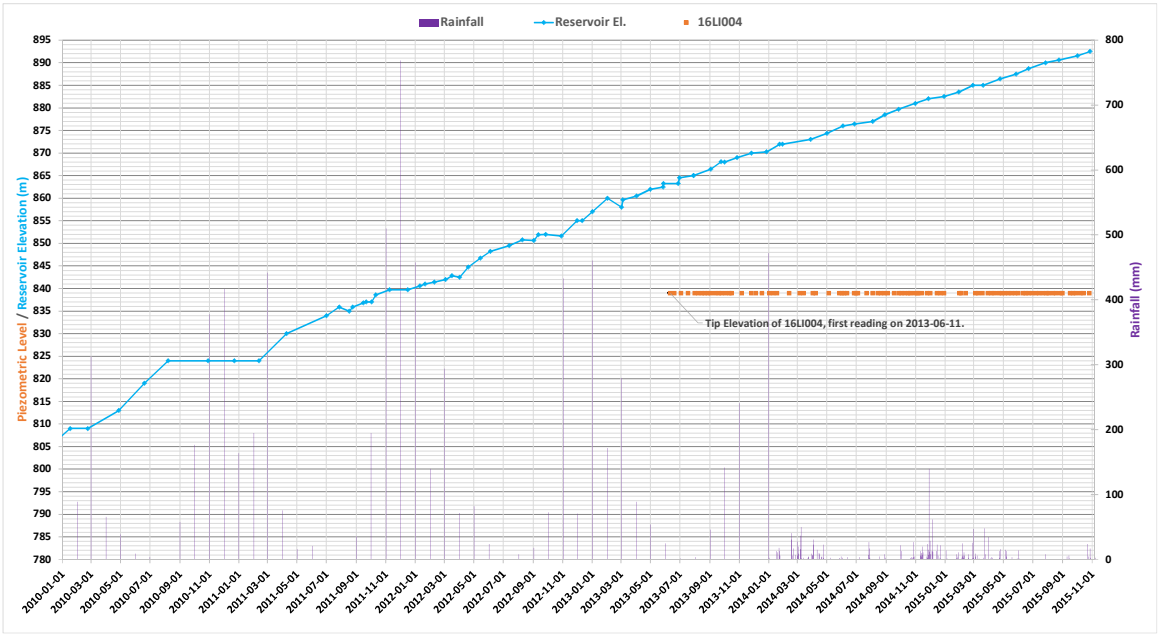

Notes:

1. Rainfall records switch from monthly to daily in January, 2014.
2. Installation date not available for all piezometers. In these cases the date of the first available reading has been plotted.

SECTION FF (CONTINUED)

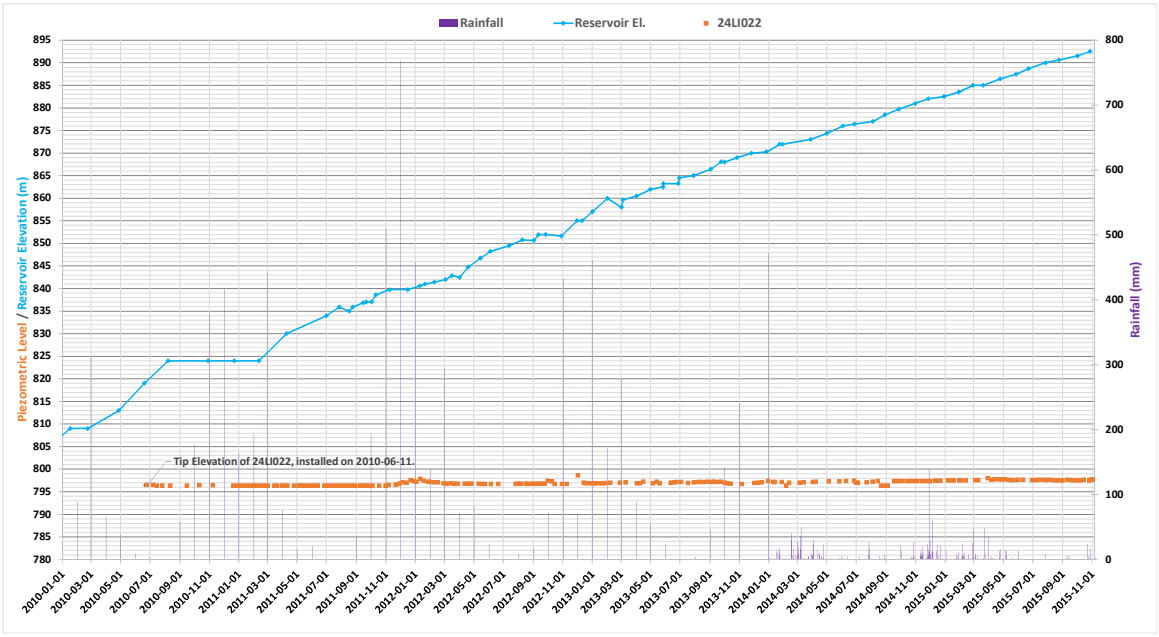

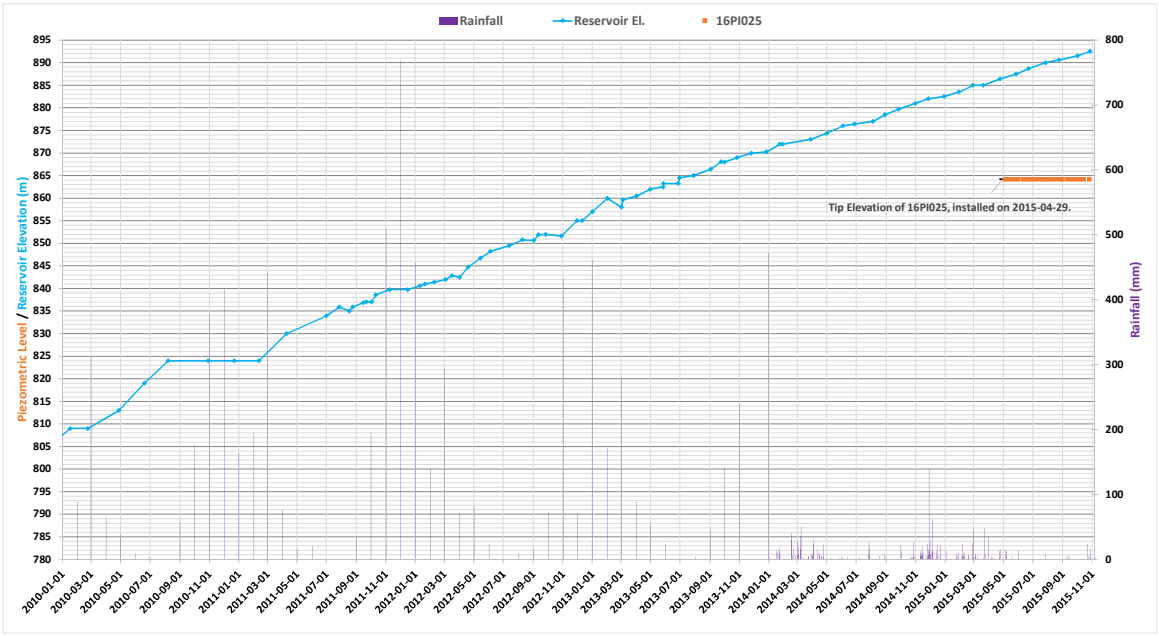

Notes:

1. Rainfall records switch from monthly to daily in January, 2014.
2. Installation date not available for all piezometers. In these cases the date of the first available reading has been plotted.

SECTION FF (CONTINUED)

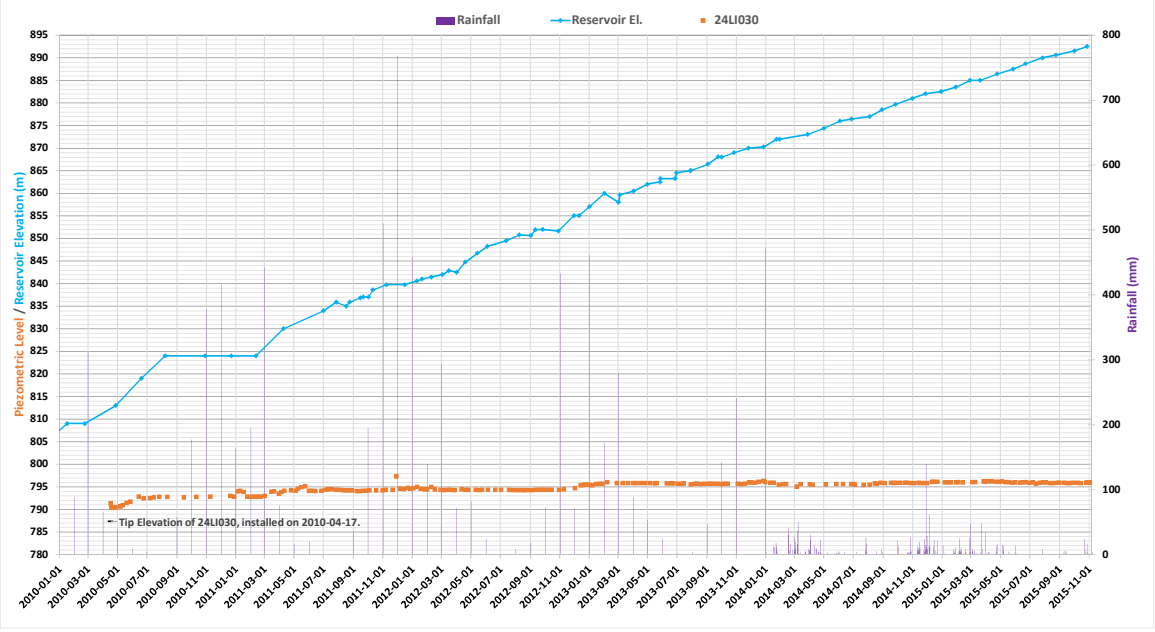

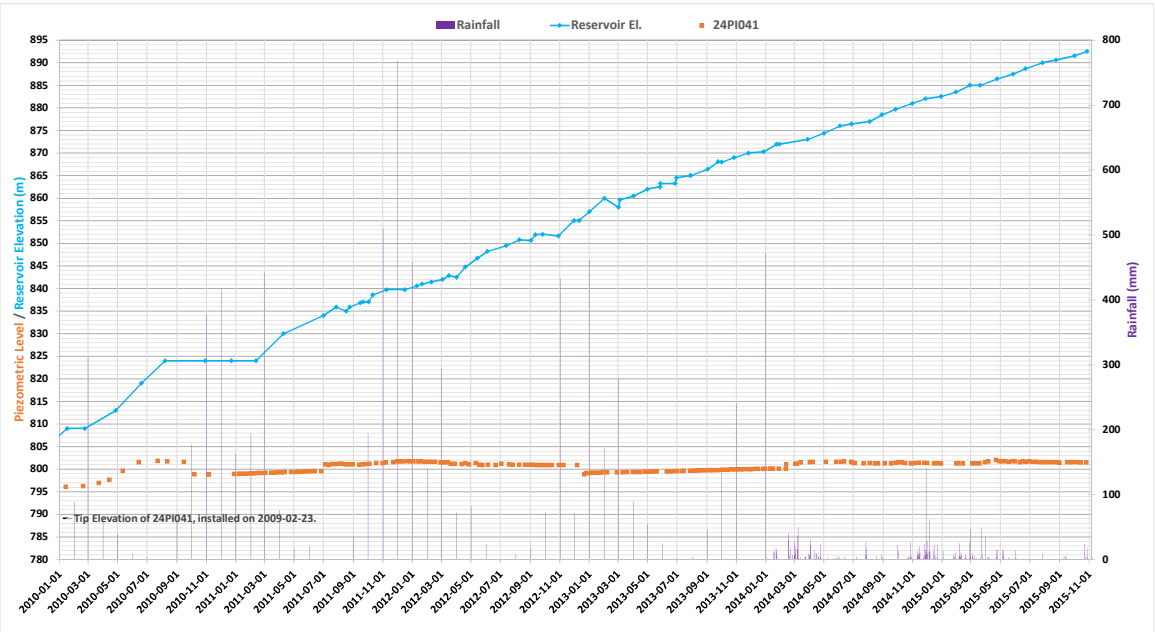

Notes:

1. Rainfall records switch from monthly to daily in January, 2014.
2. Installation date not available for all piezometers. In these cases the date of the first available reading has been plotted.

SECTION FF (CONTINUED)

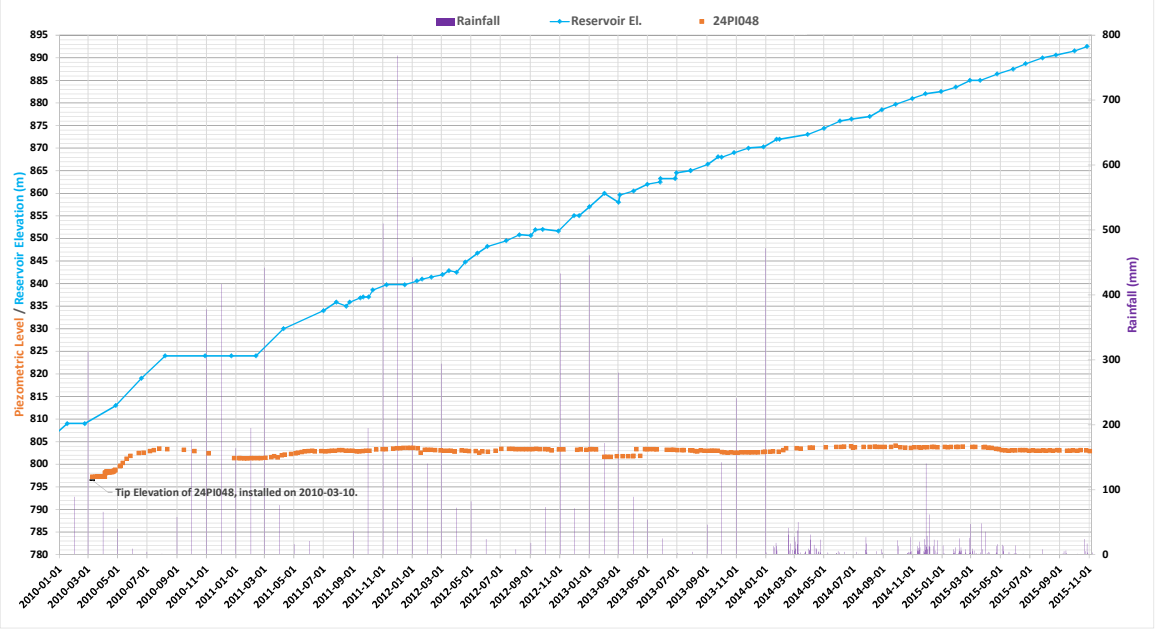

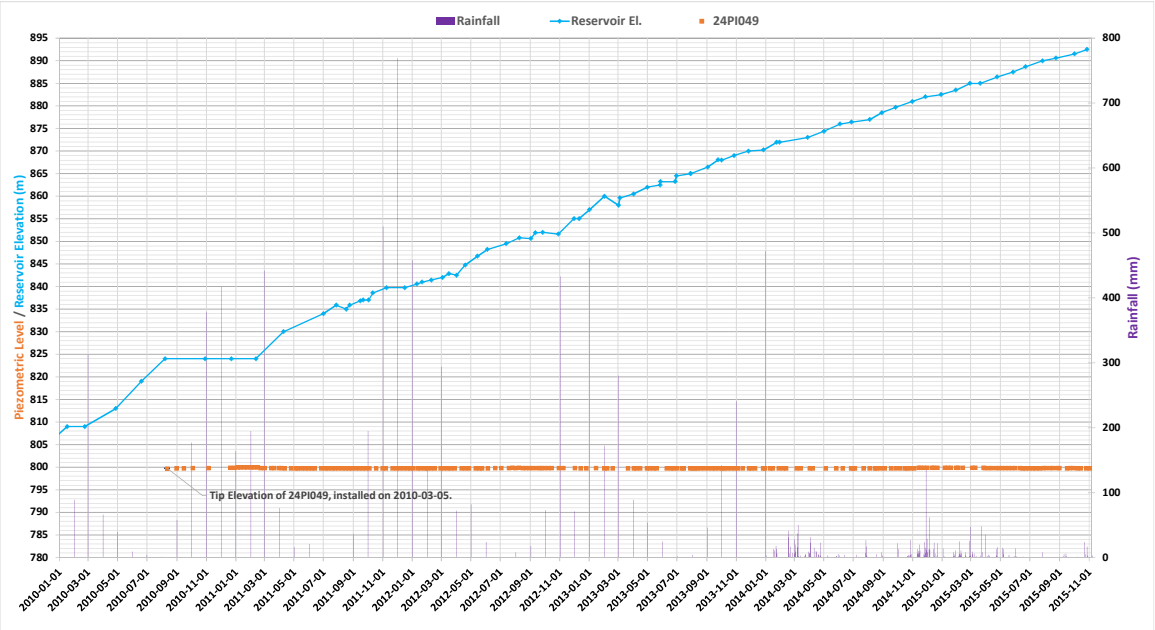

Notes:

1. Rainfall records switch from monthly to daily in January, 2014.
2. Installation date not available for all piezometers. In these cases the date of the first available reading has been plotted.

SECTION FF (CONTINUED)

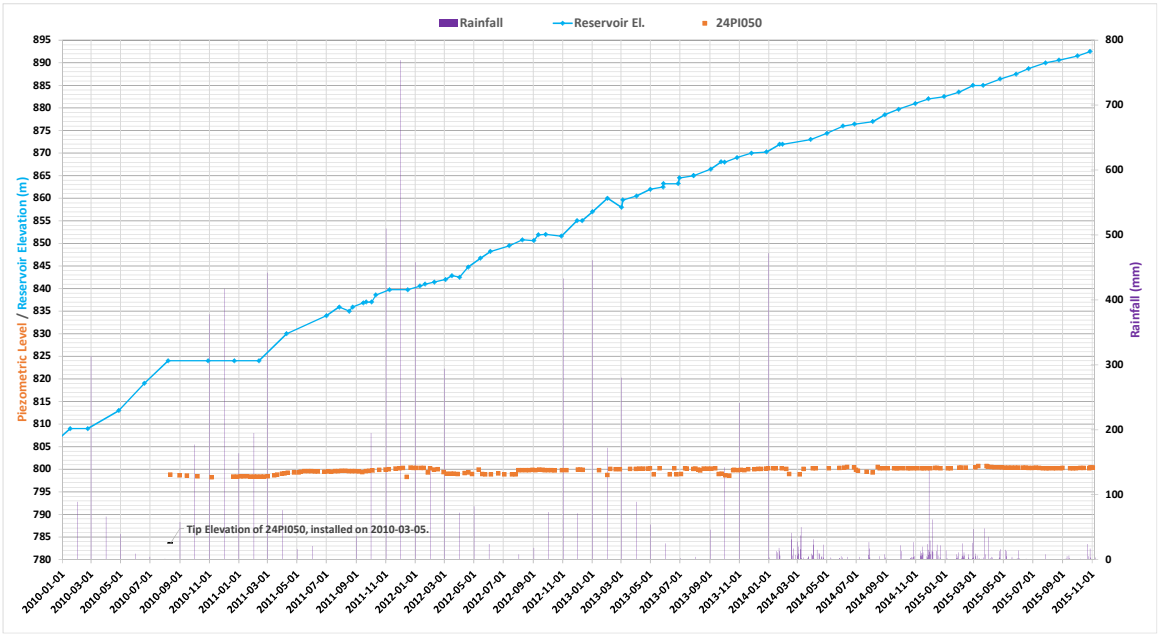

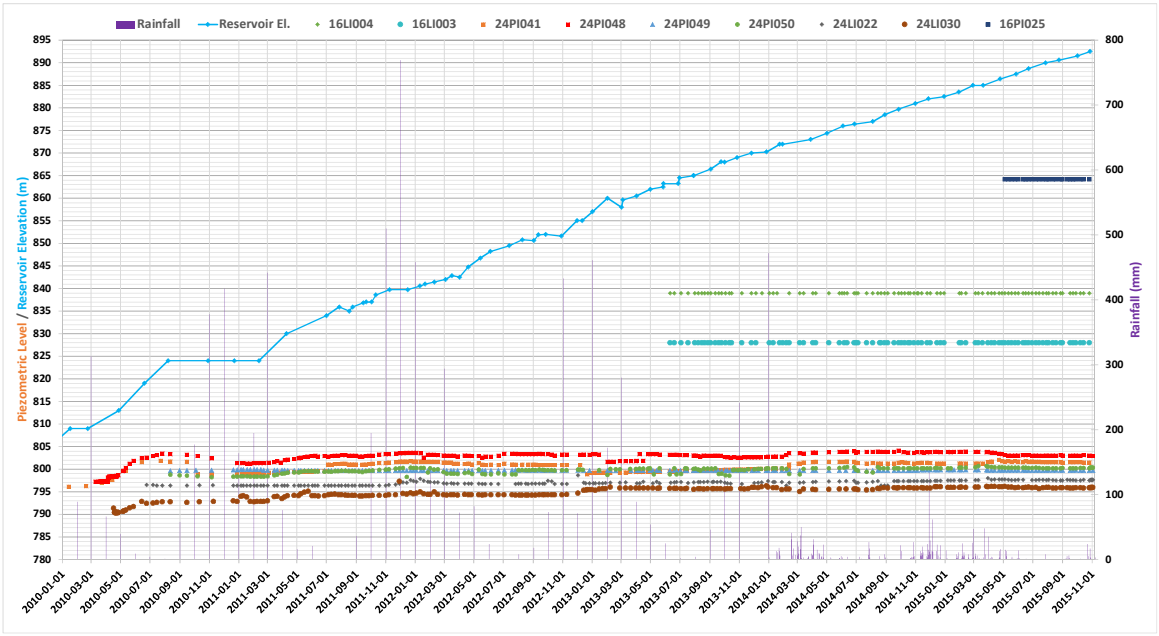

Notes:
1. Rainfall records switch from monthly to daily in January, 2014.
2. Installation date not available for all piezometers. In these cases the date of the first available reading has been plotted.

SECTION FF (CONTINUED)

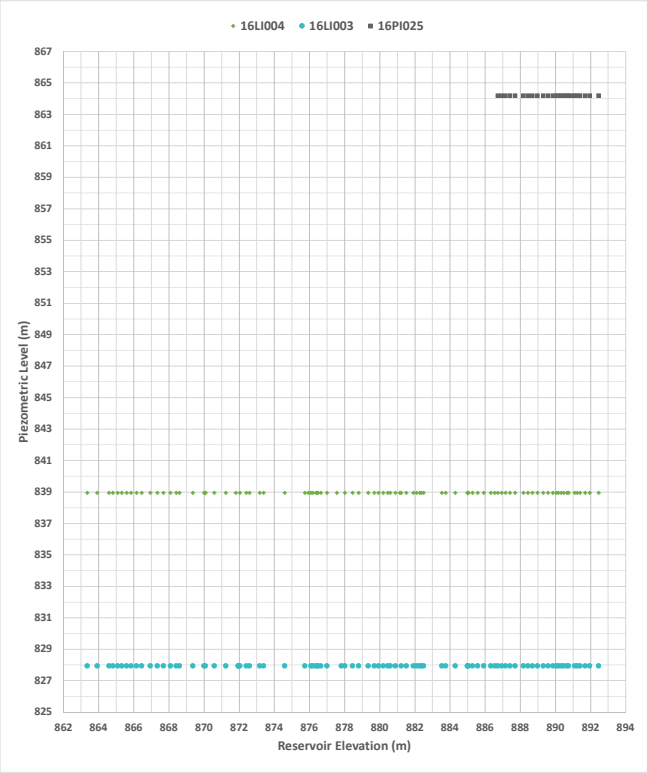

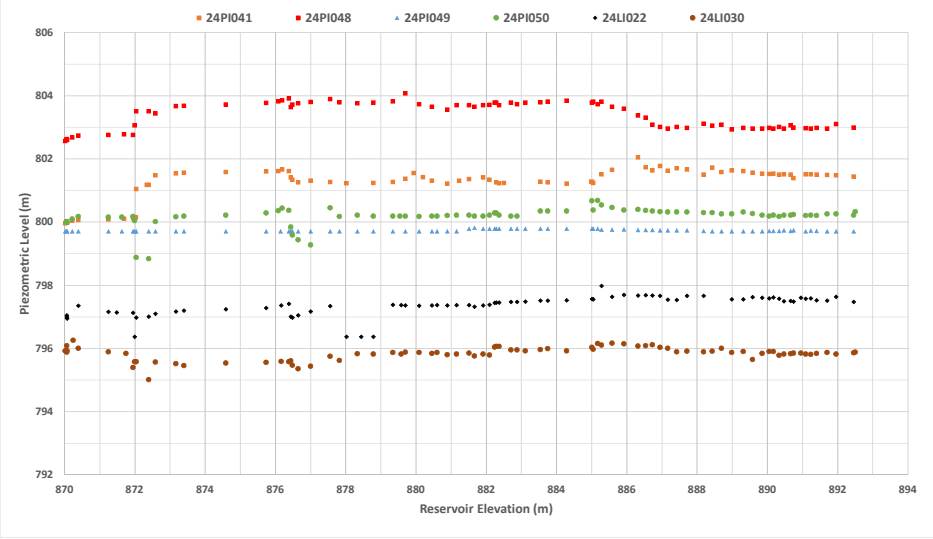

Notes:

1. Rainfall records switch from monthly to daily in January, 2014.
2. Installation date not available for all piezometers. In these cases the date of the first available reading has been plotted.

SECTION HH

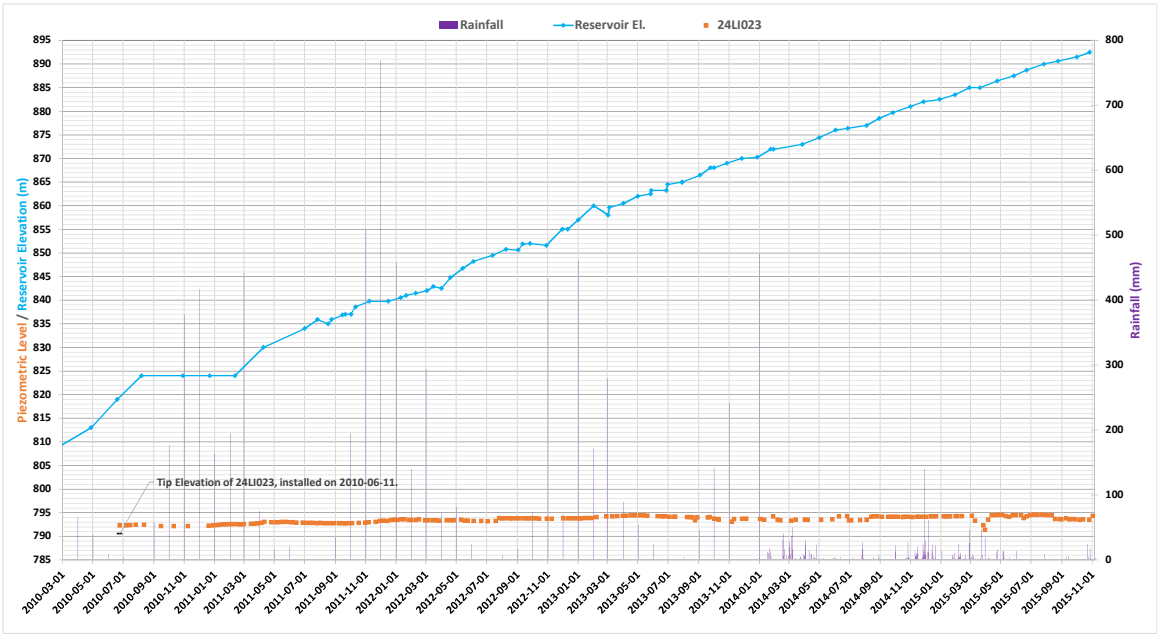

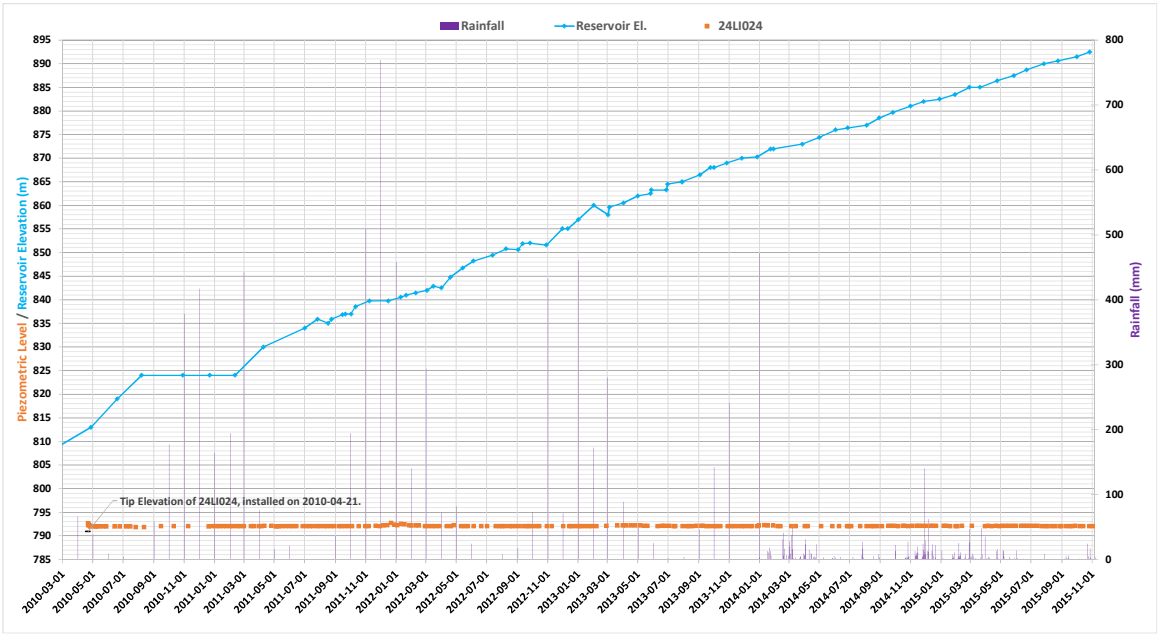

Notes:

1. Rainfall records switch from monthly to daily in January, 2014.
2. Installation date not available for all piezometers. In these cases the date of the first available reading has been plotted.

SECTION HH (CONTINUED)

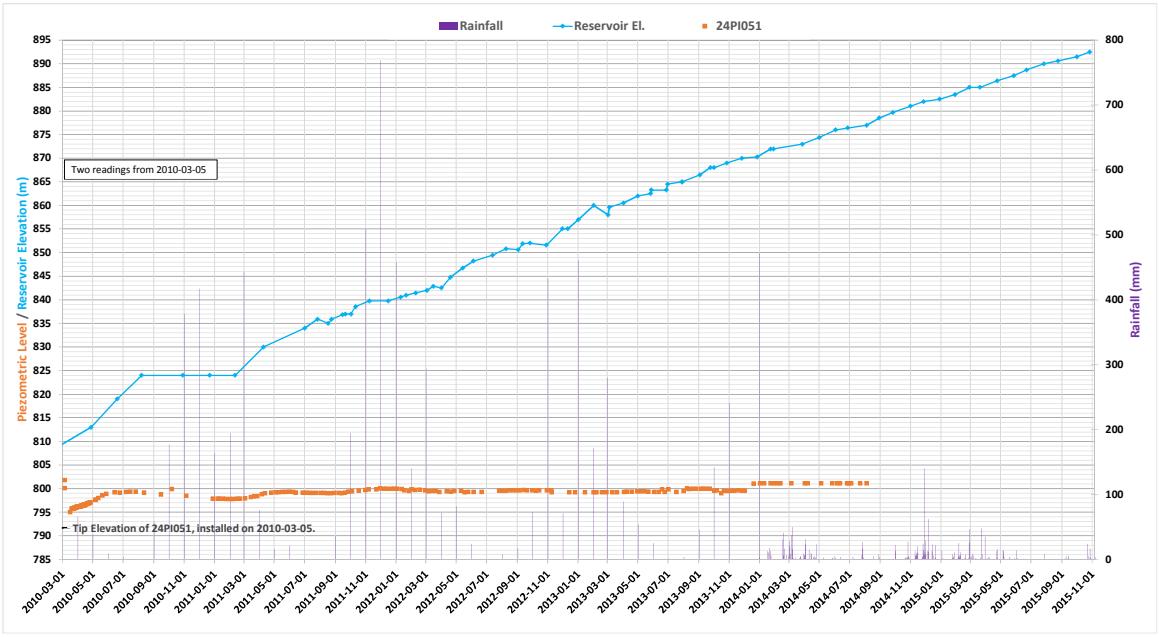

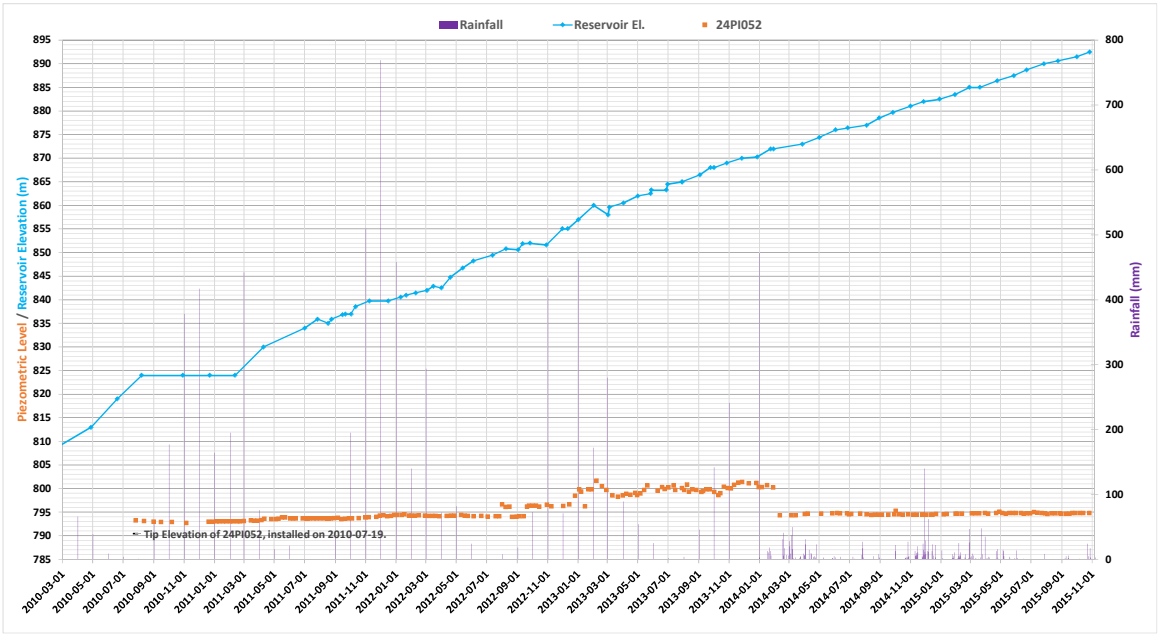

Notes:

1. Rainfall records switch from monthly to daily in January, 2014.
2. Installation date not available for all piezometers. In these cases the date of the first available reading has been plotted.

SECTION HH (CONTINUED)

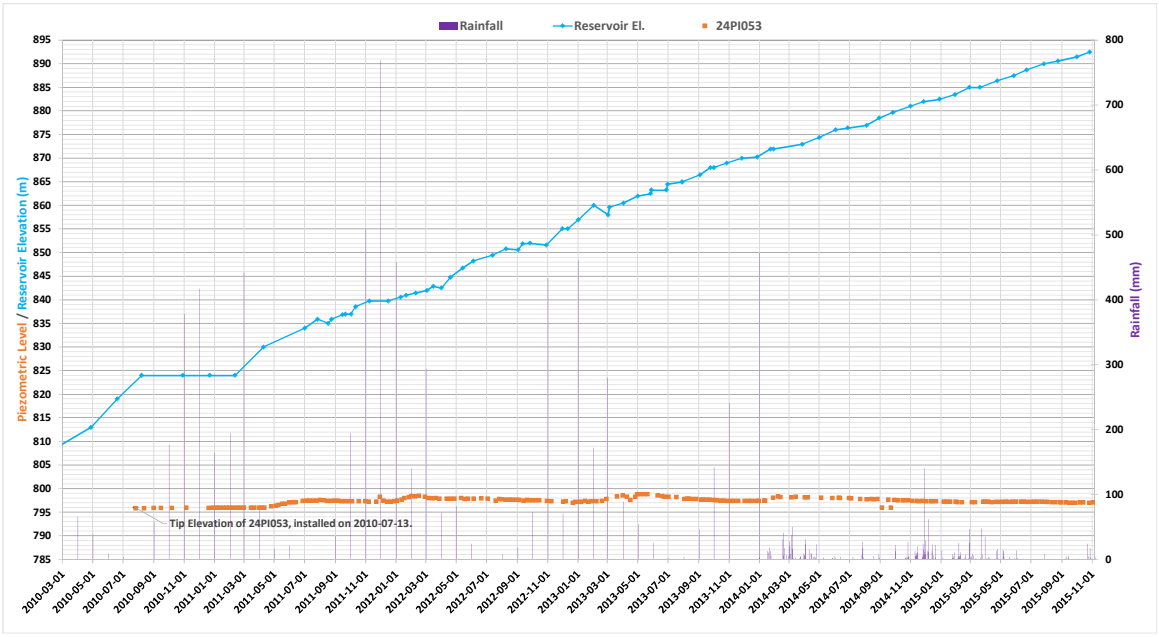

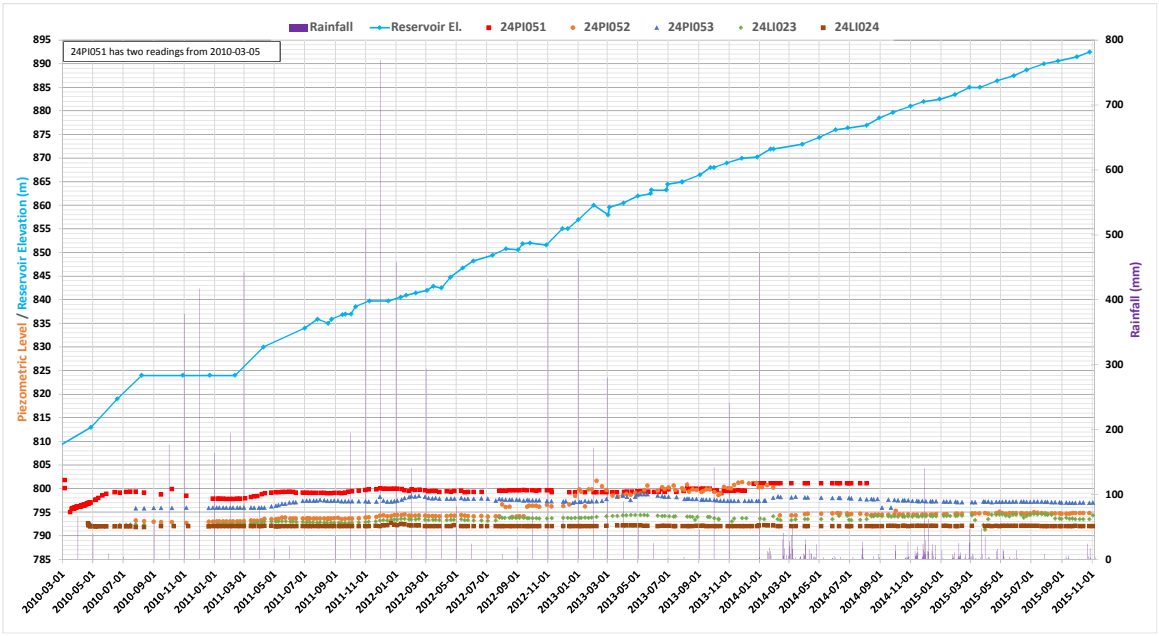

Notes:

1. Rainfall records switch from monthly to daily in January, 2014.
2. Installation date not available for all piezometers. In these cases the date of the first available reading has been plotted.

SECTION HH (CONTINUED)

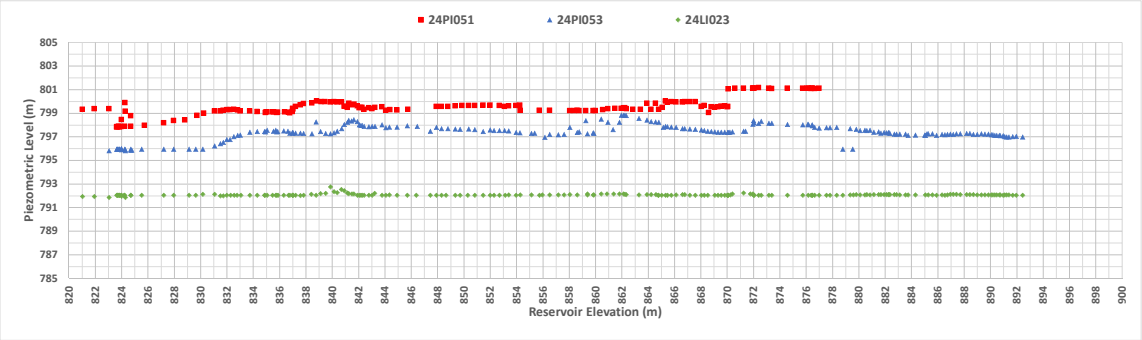

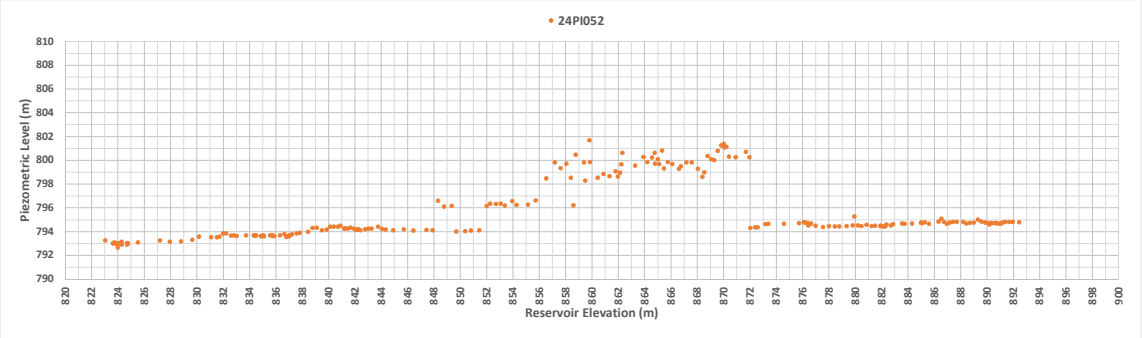

Notes:

1. Rainfall records switch from monthly to daily in January, 2014.
2. Installation date not available for all piezometers. In these cases the date of the first available reading has been plotted.

SECTION JJ

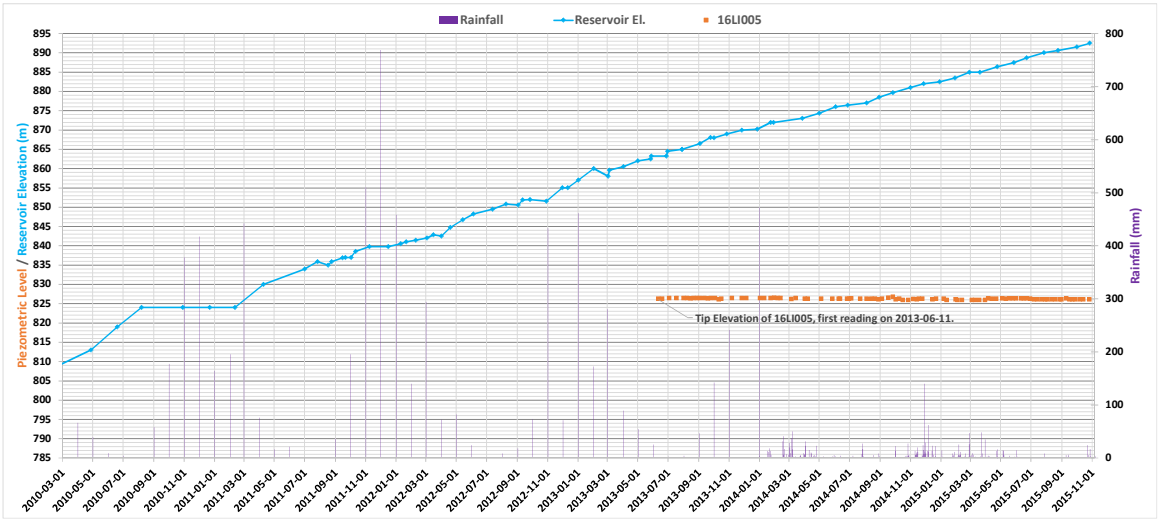

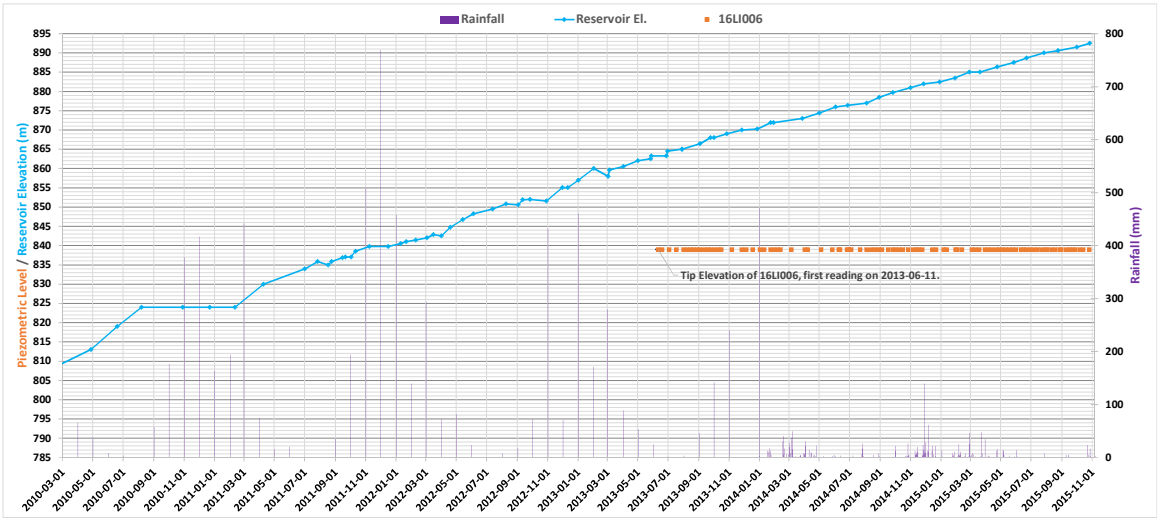

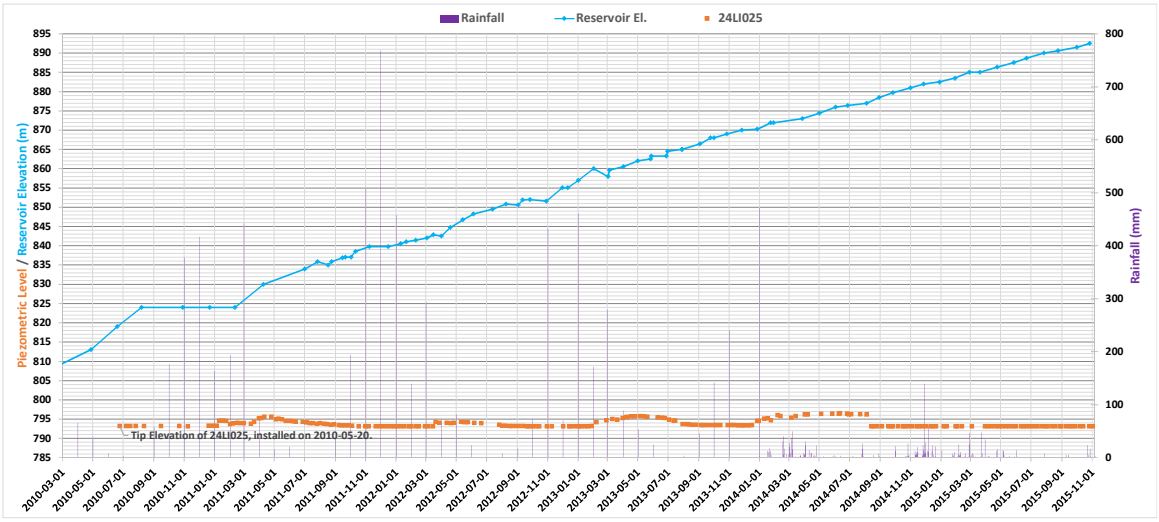

Notes:

1. Rainfall records switch from monthly to daily in January, 2014.
2. Installation date not available for all piezometers. In these cases the date of the first available reading has been plotted.

SECTION JJ (CONTINUED)

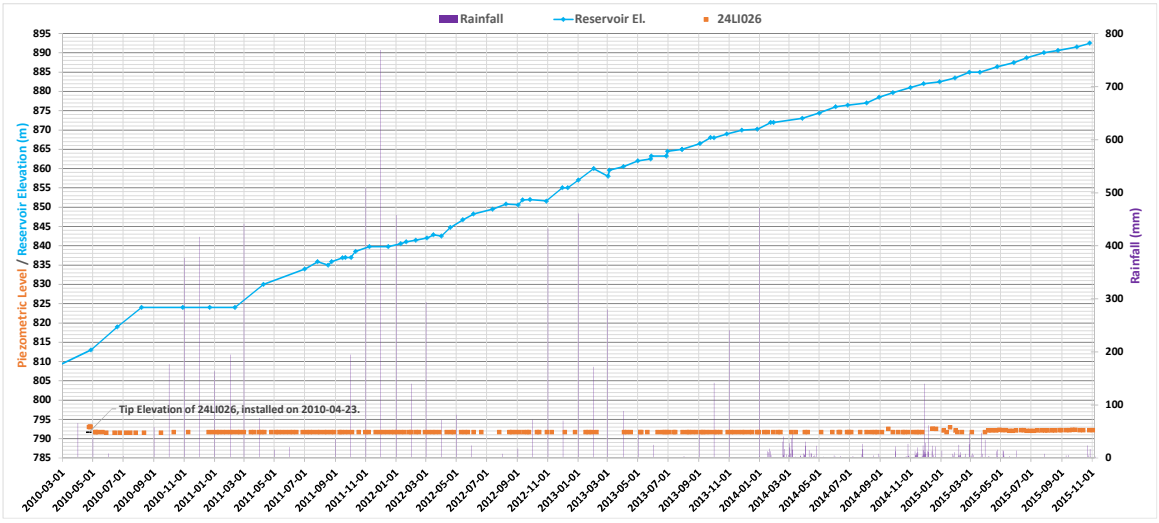

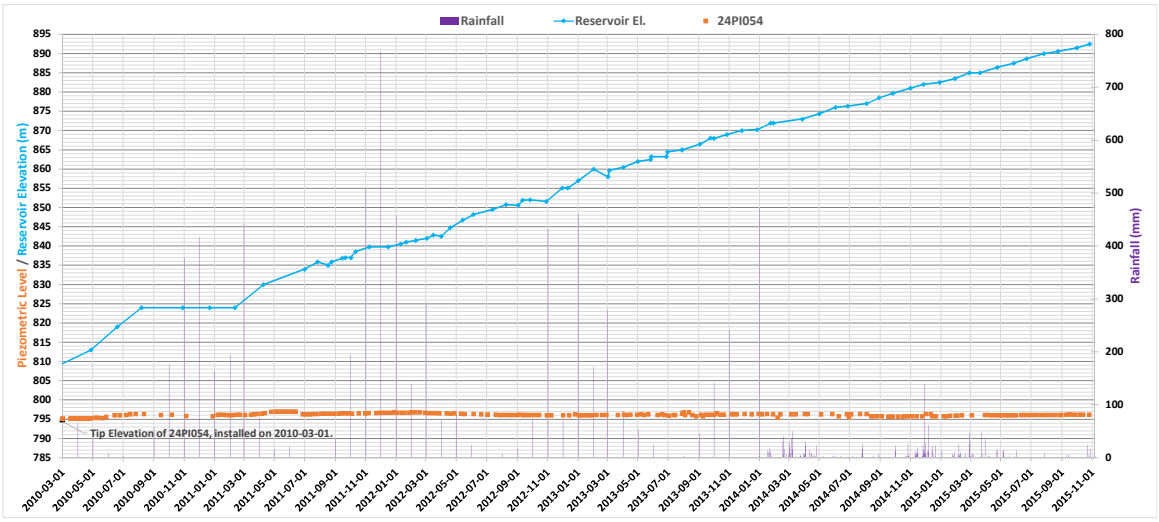

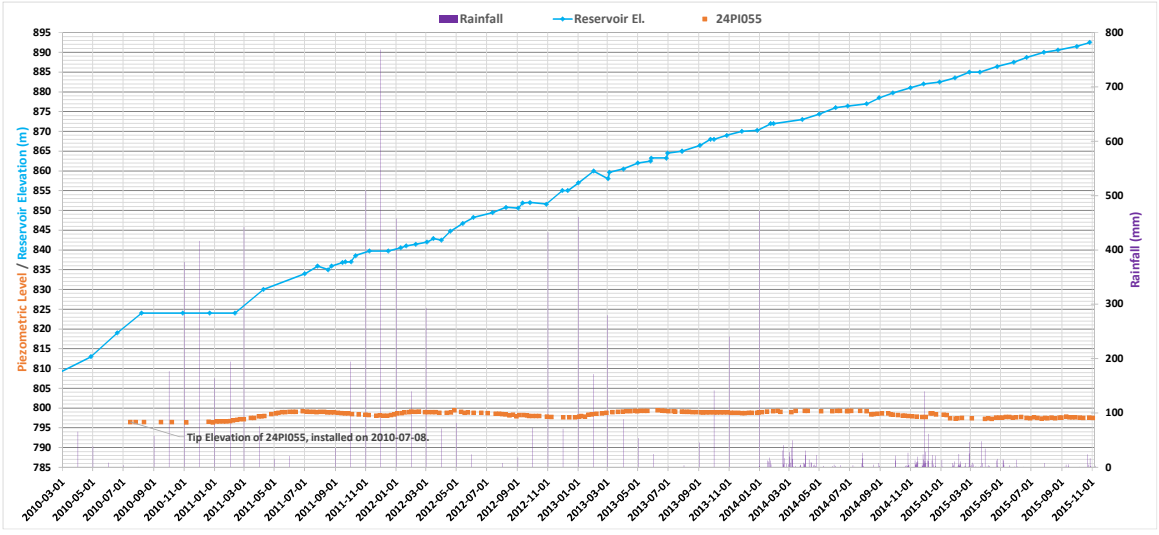

Notes:

1. Rainfall records switch from monthly to daily in January, 2014.
2. Installation date not available for all piezometers. In these cases the date of the first available reading has been plotted.

SECTION JJ (CONTINUED)

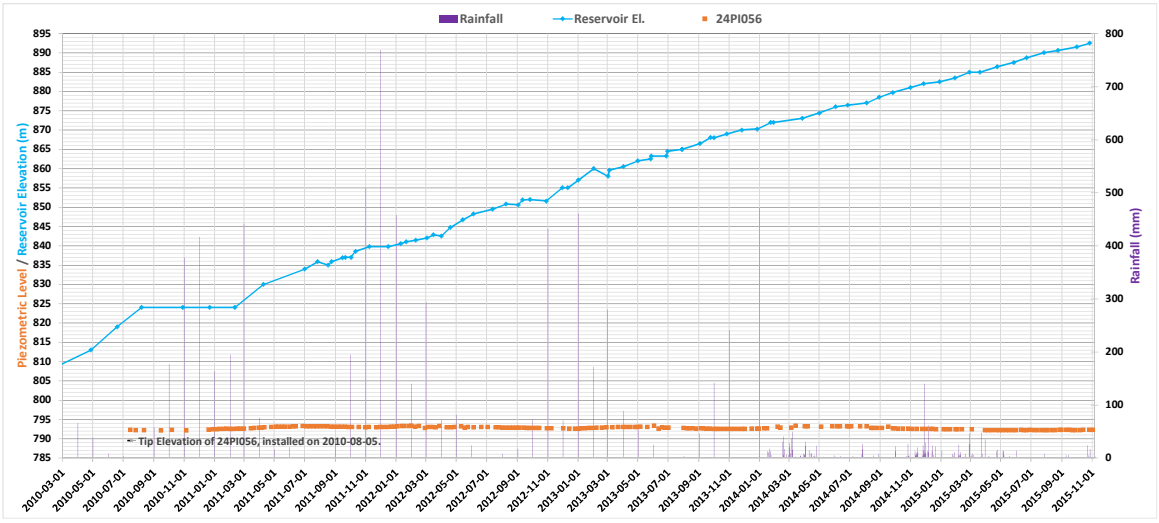

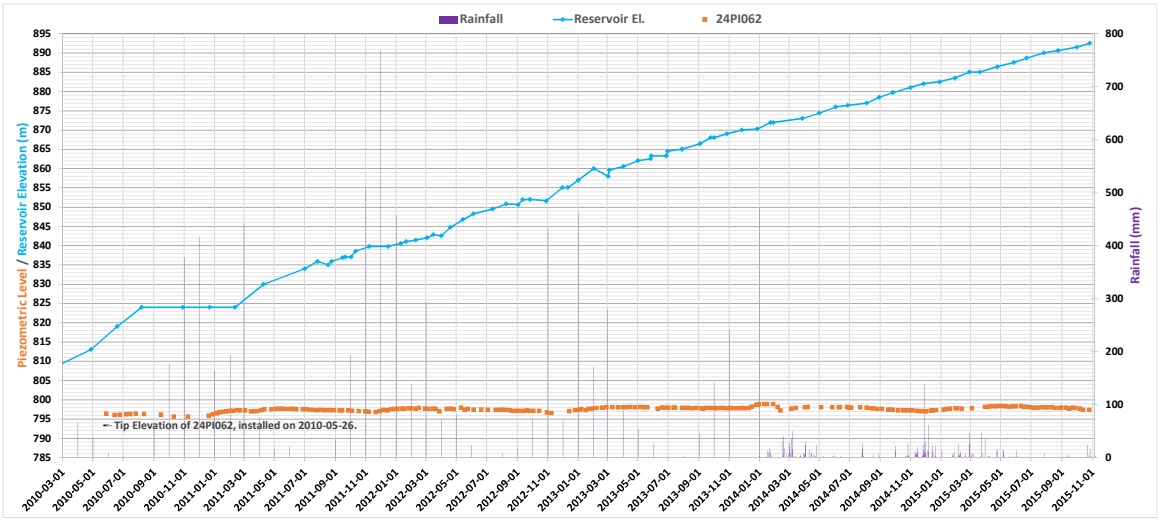

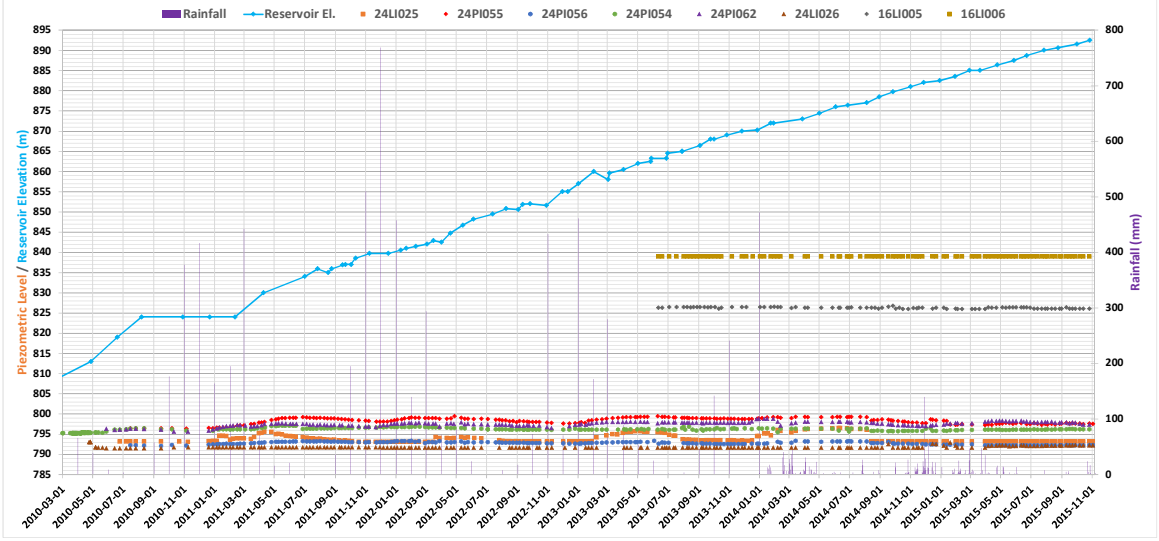

Notes:

1. Rainfall records switch from monthly to daily in January, 2014.
2. Installation date not available for all piezometers. In these cases the date of the first available reading has been plotted.

SECTION JJ (CONTINUED)

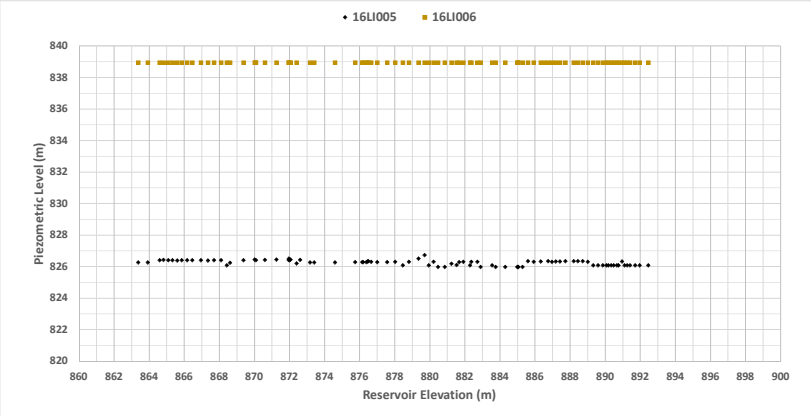

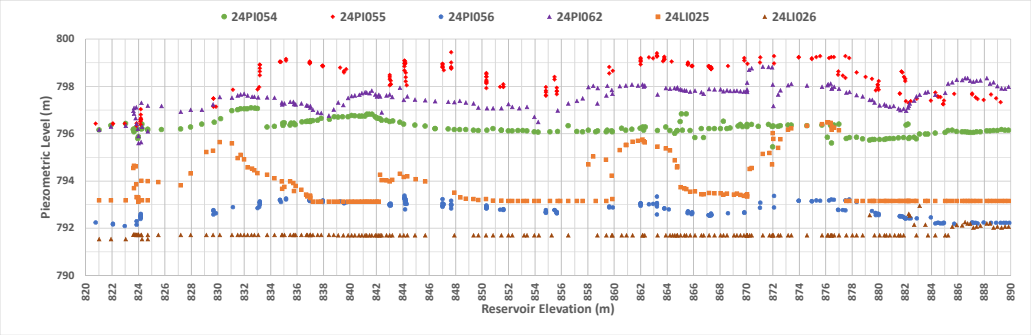

Notes:

1. Rainfall records switch from monthly to daily in January, 2014.
2. Installation date not available for all piezometers. In these cases the date of the first available reading has been plotted.

SECTION LL

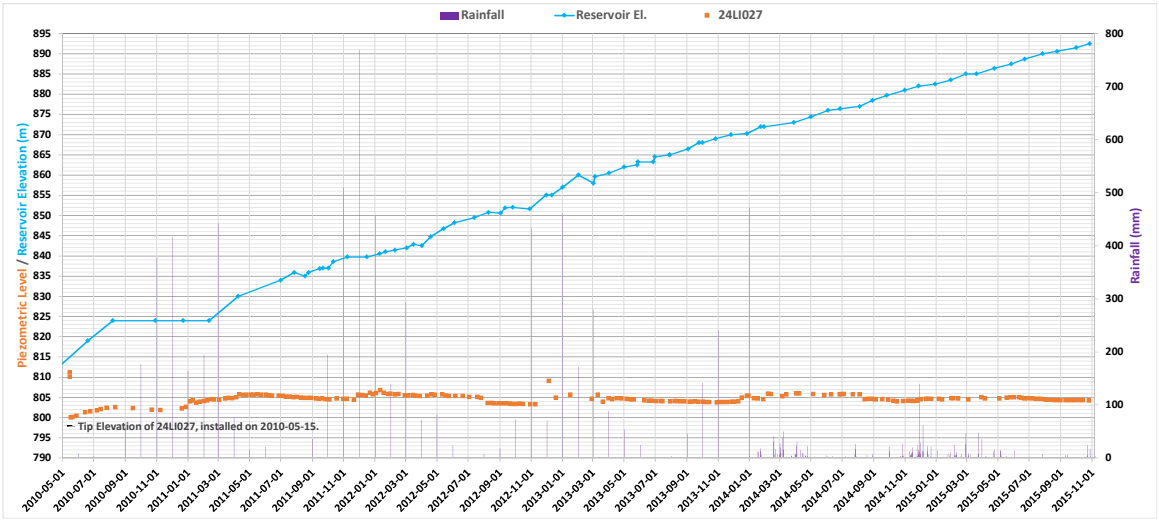

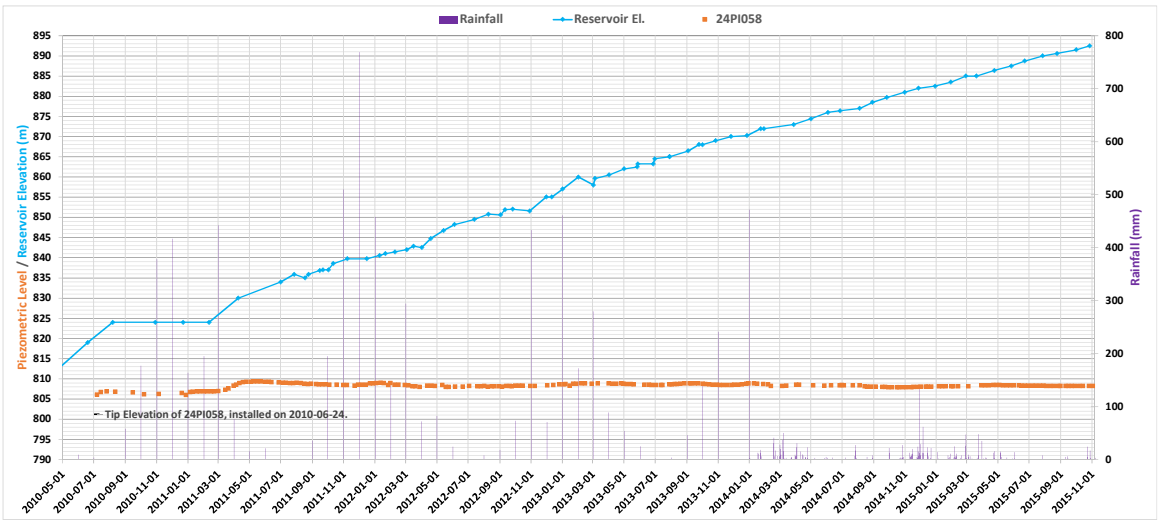

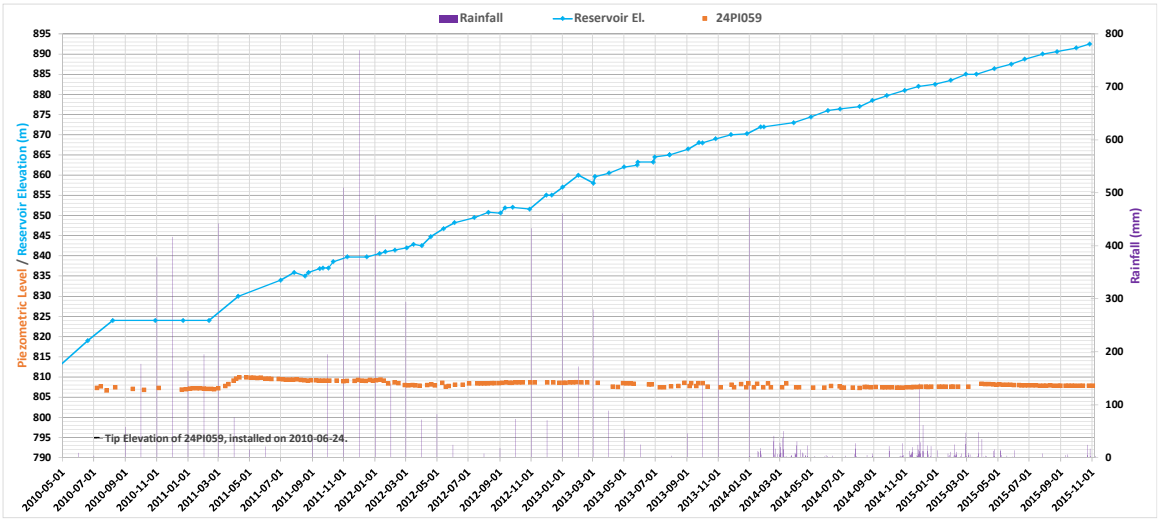

Notes:

1. Rainfall records switch from monthly to daily in January, 2014.
2. Installation date not available for all piezometers. In these cases the date of the first available reading has been plotted.

SECTION LL (CONTINUED)

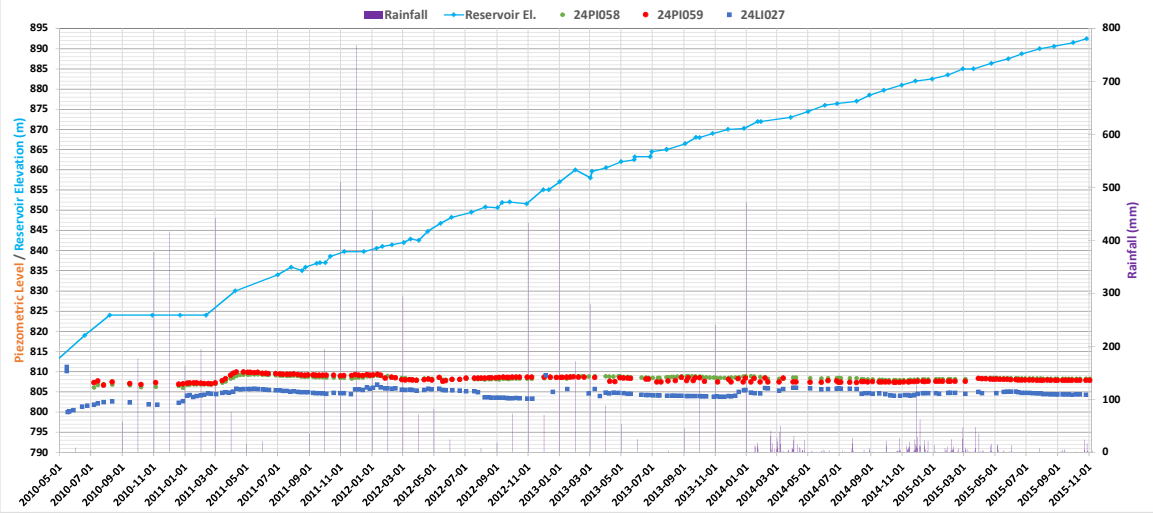

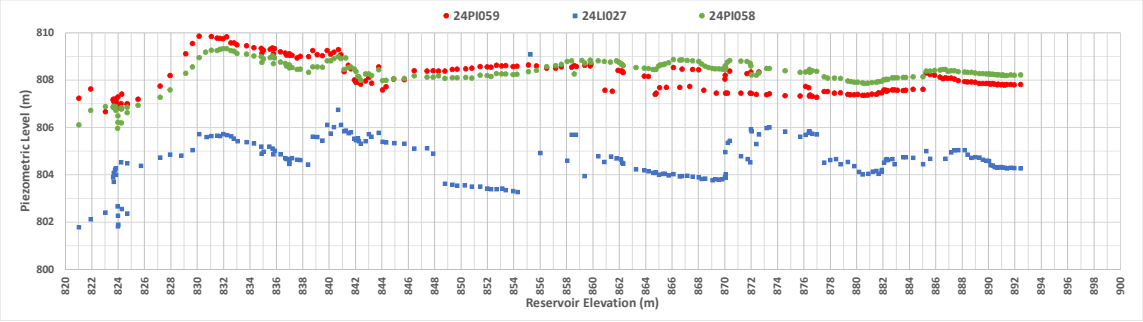

Notes:

1. Rainfall records switch from monthly to daily in January, 2014.
2. Installation date not available for all piezometers. In these cases the date of the first available reading has been plotted.

SECTION MM

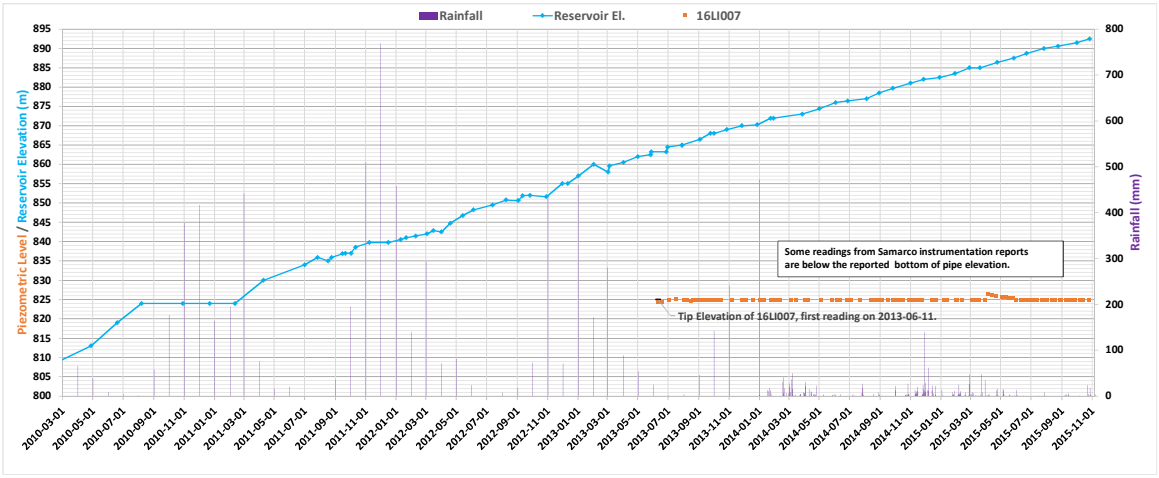

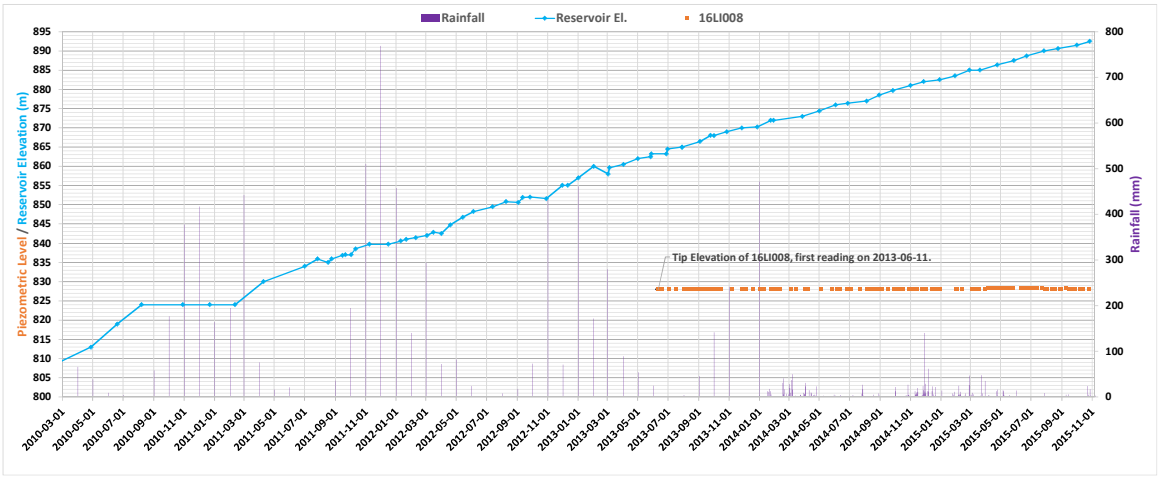

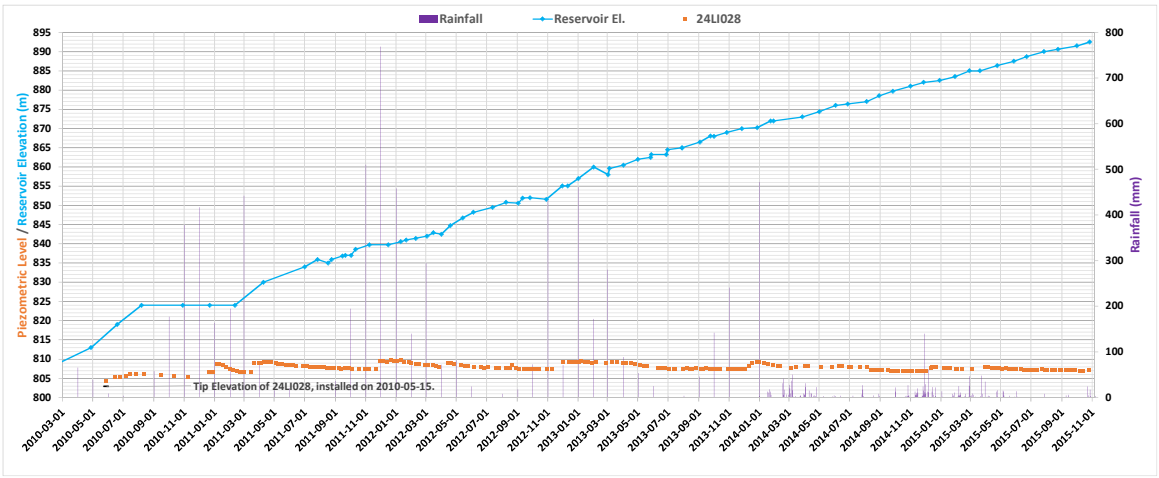

Notes:

1. Rainfall records switch from monthly to daily in January, 2014.
2. Installation date not available for all piezometers. In these cases the date of the first available reading has been plotted.

SECTION MM (CONTINUED)

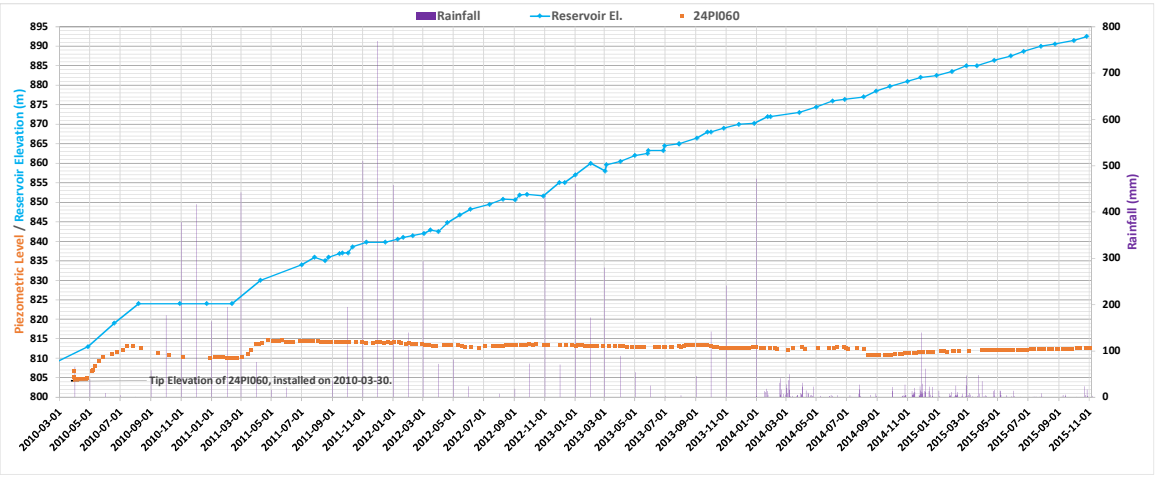

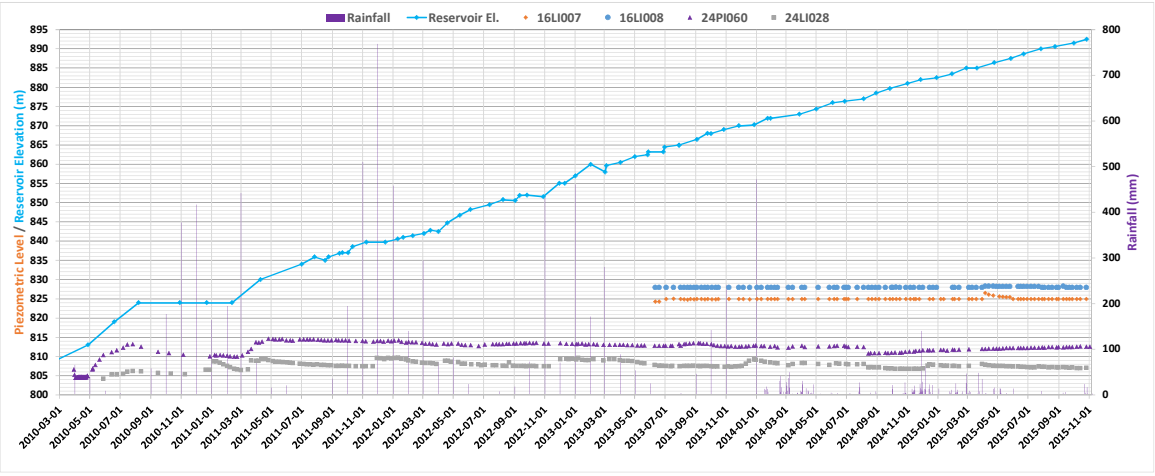

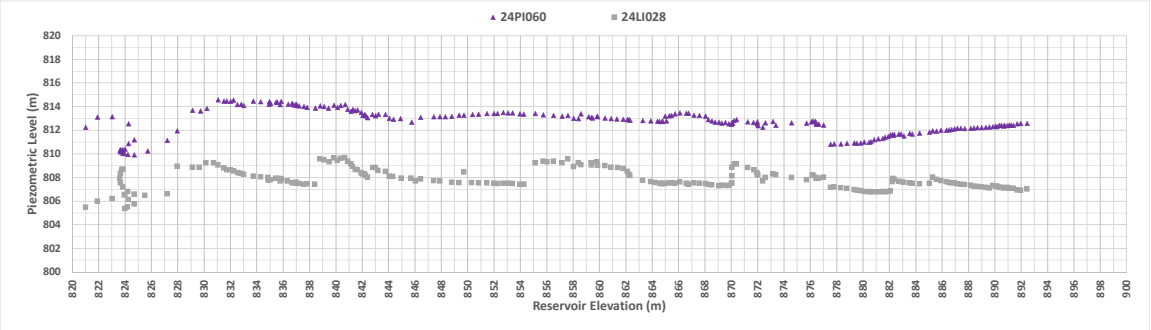

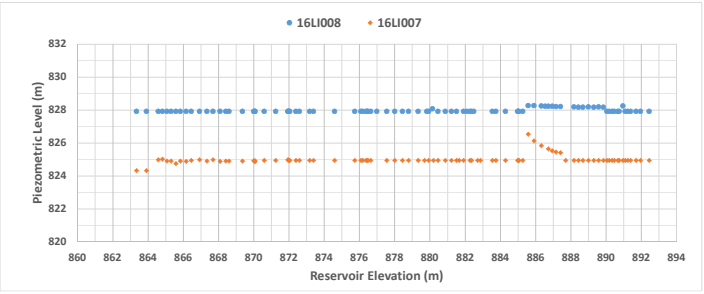

Notes:

1. Rainfall records switch from monthly to daily in January, 2014.
2. Installation date not available for all piezometers. In these cases the date of the first available reading has been plotted.

SECTION NN

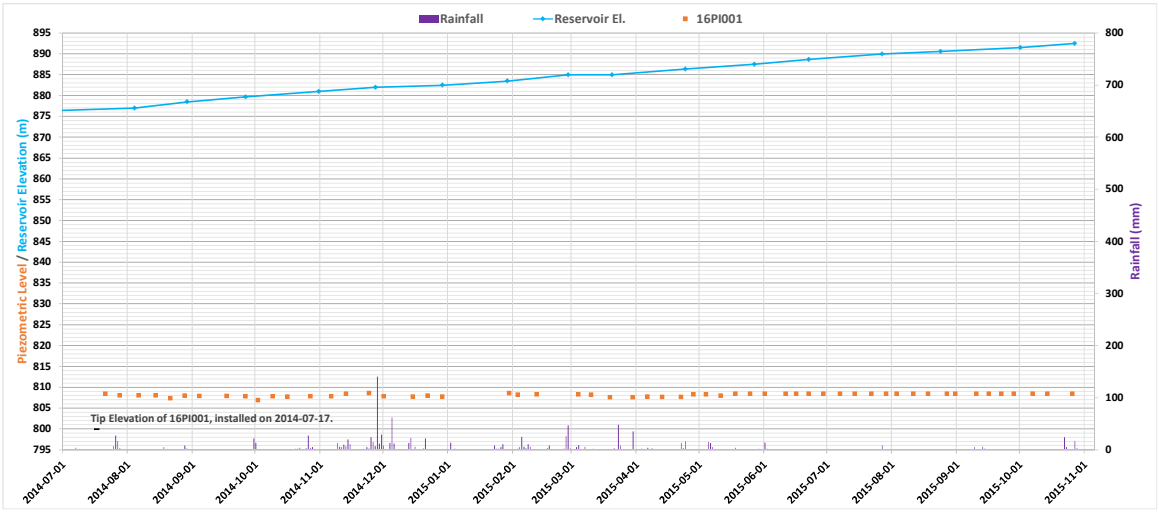

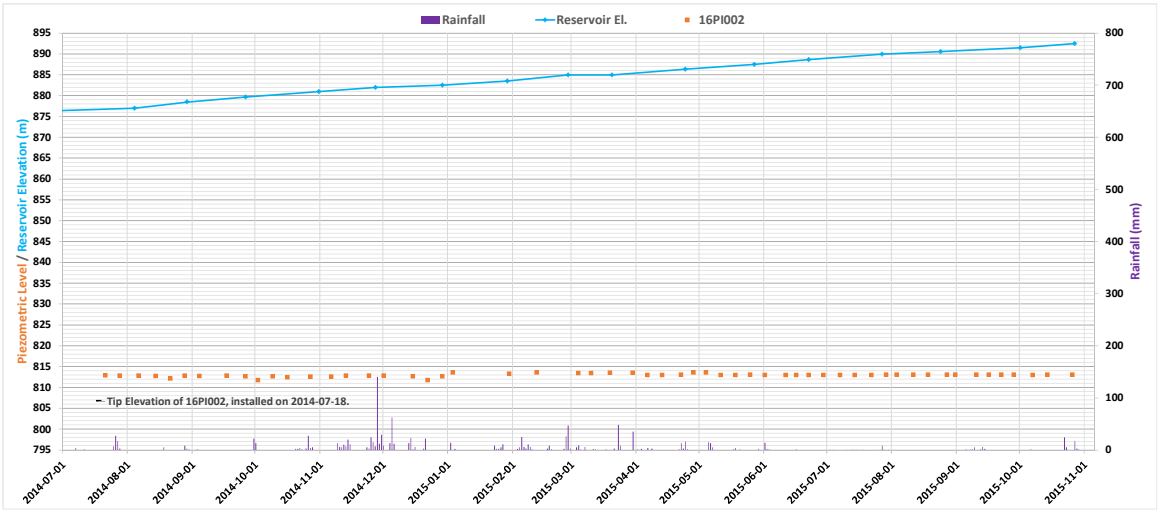

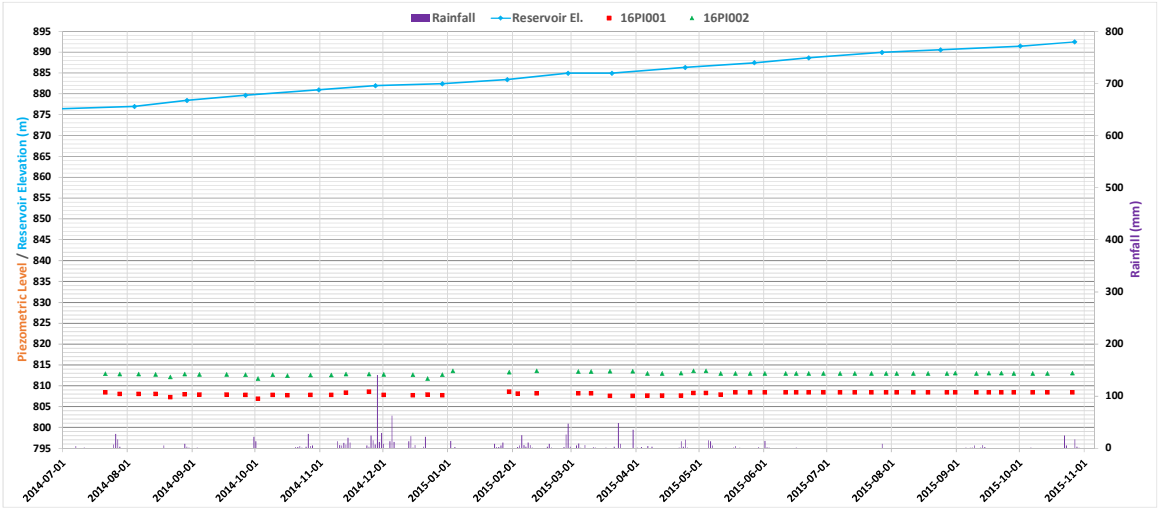

Notes:

1. Rainfall records switch from monthly to daily in January, 2014.
2. Installation date not available for all piezometers. In these cases the date of the first available reading has been plotted.

SECTION NN (CONTINUED)

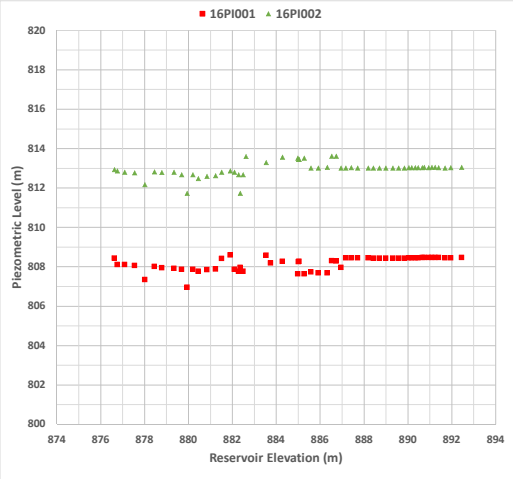

Notes:

1. Rainfall records switch from monthly to daily in January, 2014.
2. Installation date not available for all piezometers. In these cases the date of the first available reading has been plotted.

SECTION 01

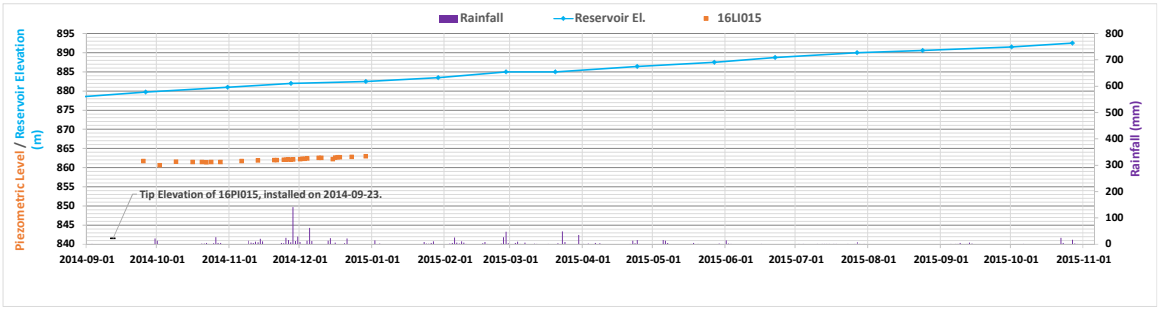

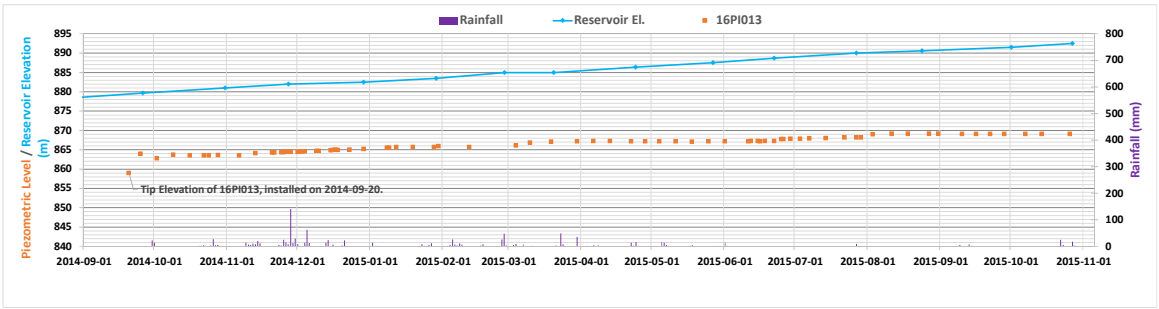

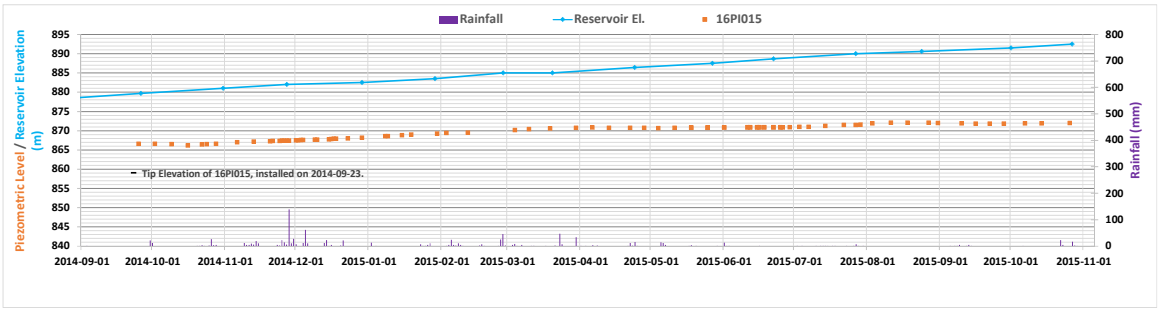

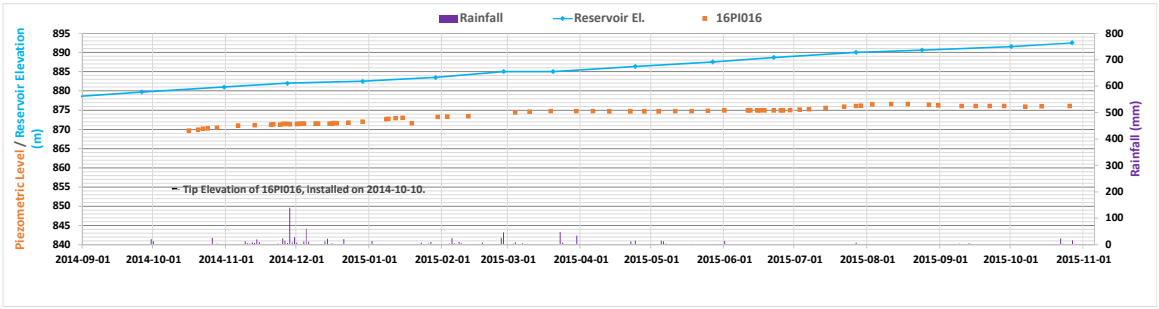

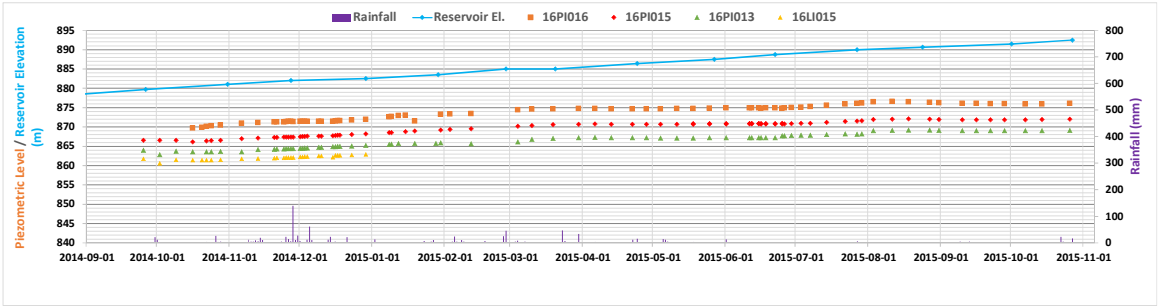

Notes:

1. Rainfall records switch from monthly to daily in January, 2014.
2. Installation date not available for all piezometers. In these cases the date of the first available reading has been plotted.

SECTION 01 (CONTINUED)

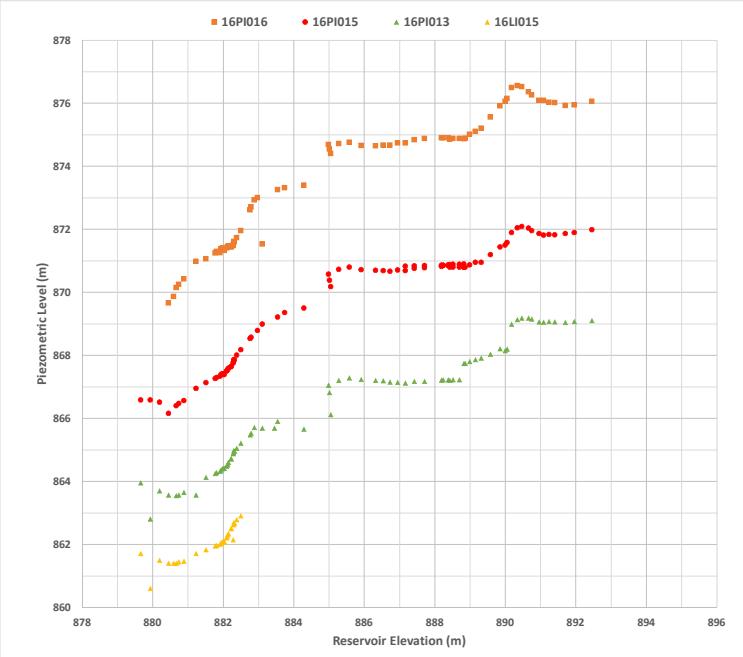

Notes:

1. Rainfall records switch from monthly to daily in January, 2014.
2. Installation date not available for all piezometers. In these cases the date of the first available reading has been plotted.

SECTION 02

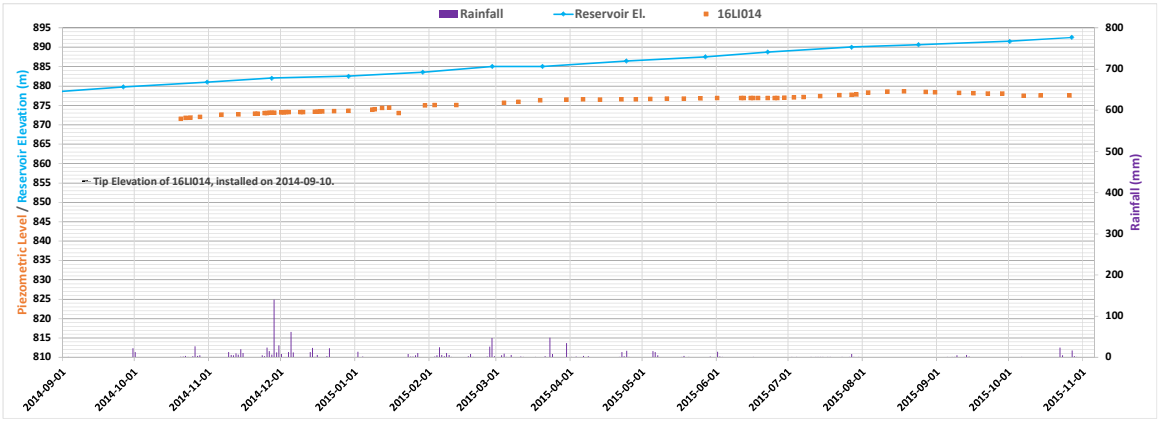

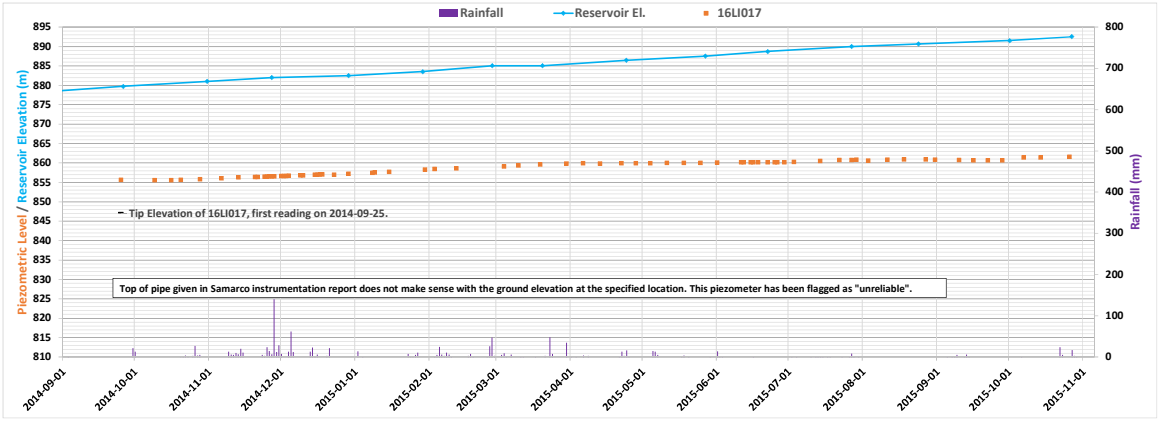

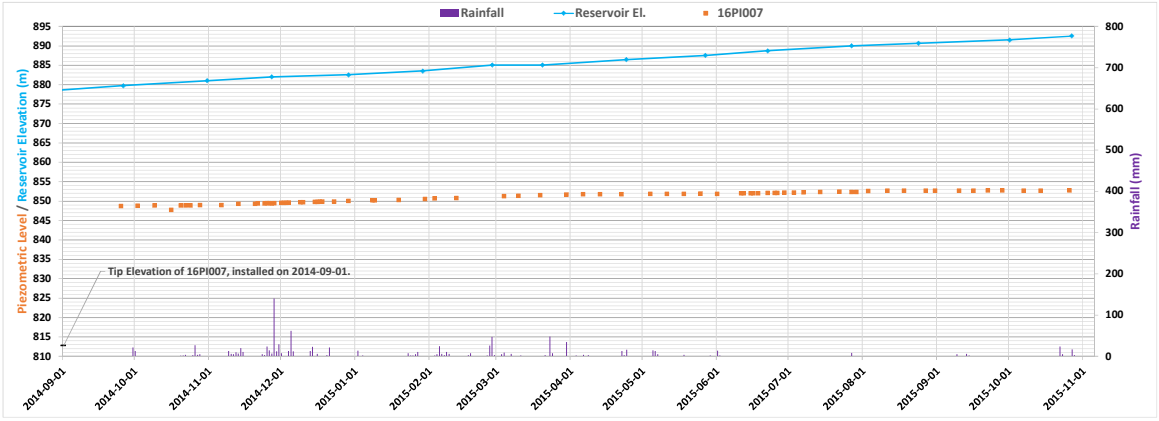

Notes:

1. Rainfall records switch from monthly to daily in January, 2014.
2. Installation date not available for all piezometers. In these cases the date of the first available reading has been plotted.

SECTION 02 (CONTINUED)

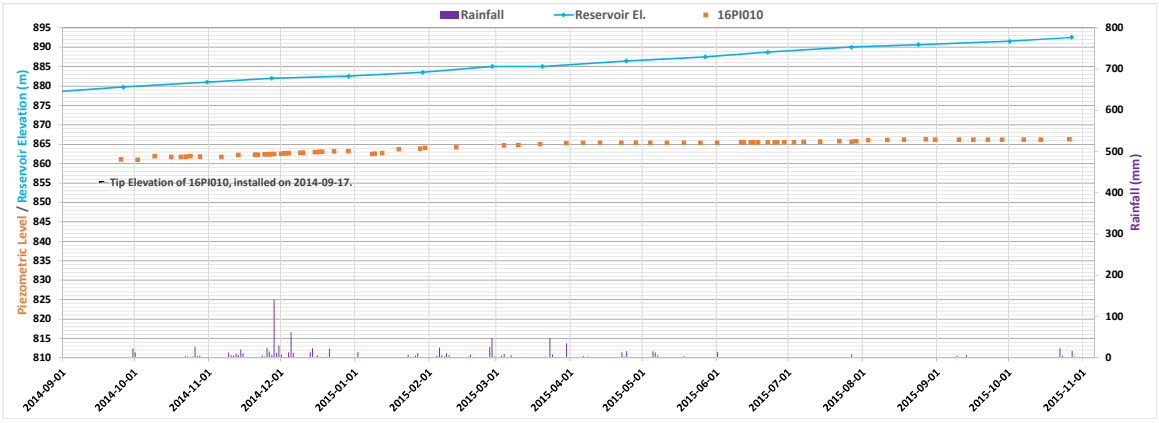

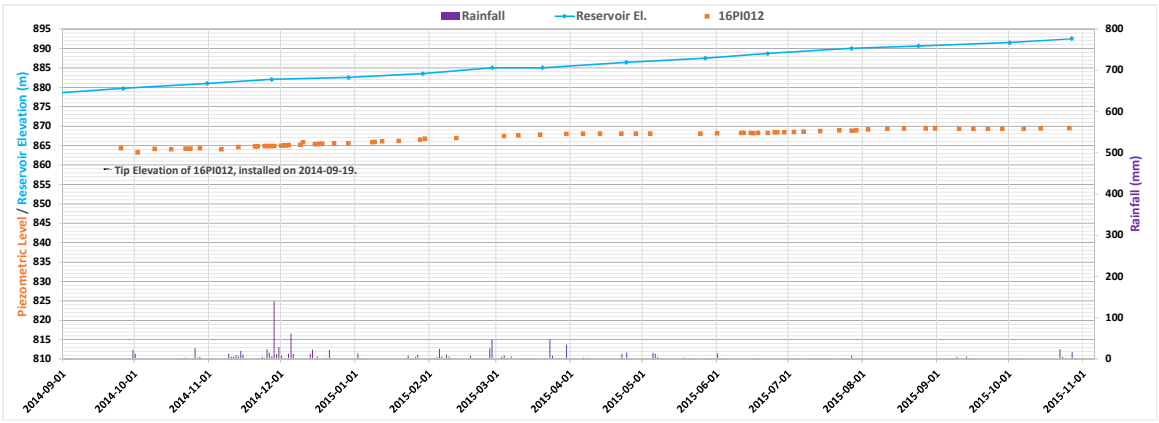

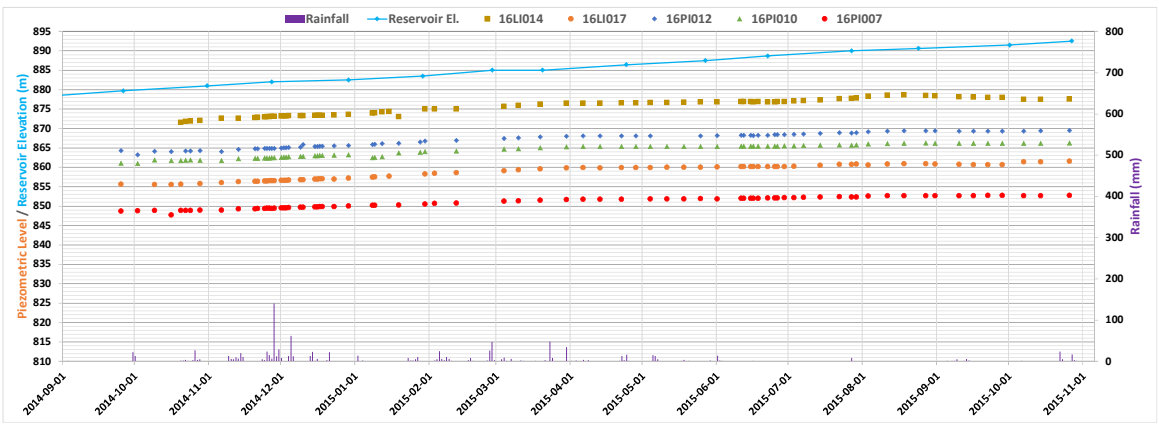

Notes:

1. Rainfall records switch from monthly to daily in January, 2014.
2. Installation date not available for all piezometers. In these cases the date of the first available reading has been plotted.

SECTION 02 (CONTINUED)

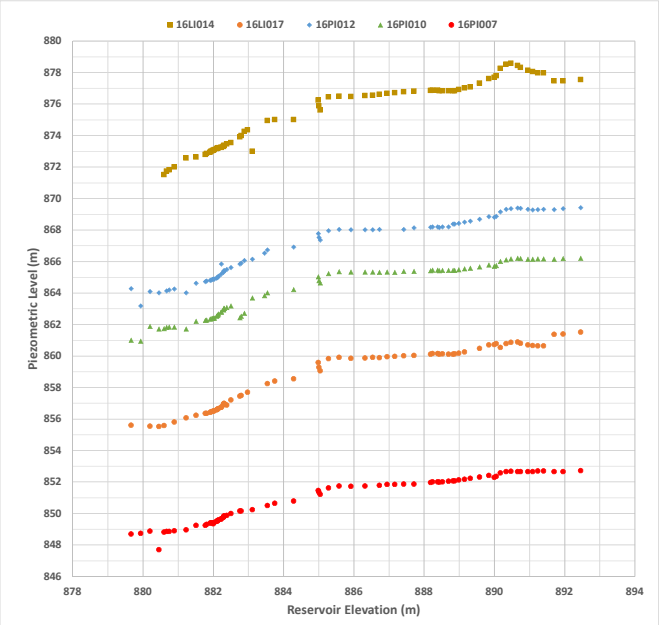

Notes:

1. Rainfall records switch from monthly to daily in January, 2014.
2. Installation date not available for all piezometers. In these cases the date of the first available reading has been plotted.

SECTION 03

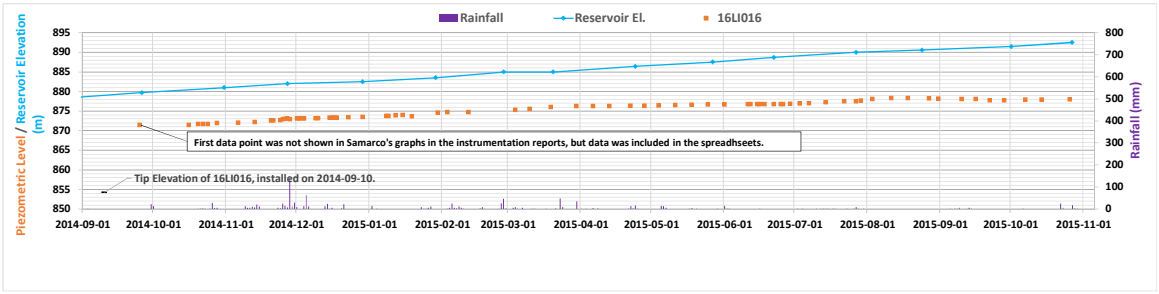

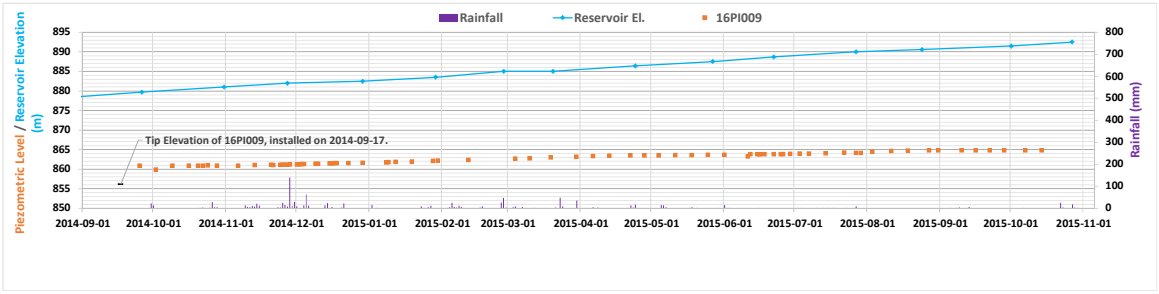

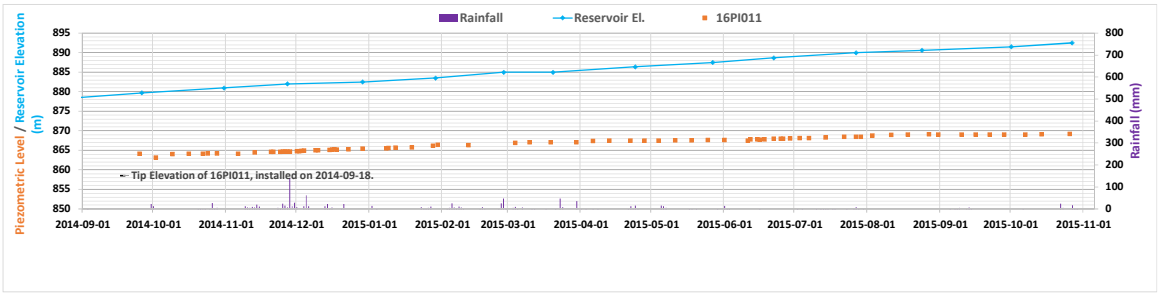

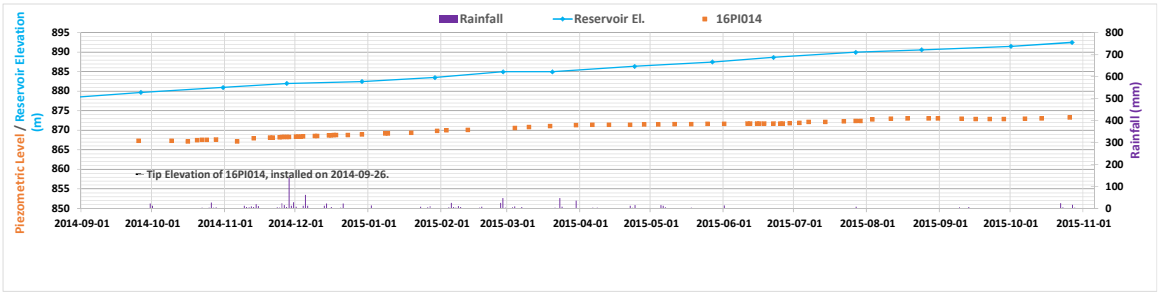

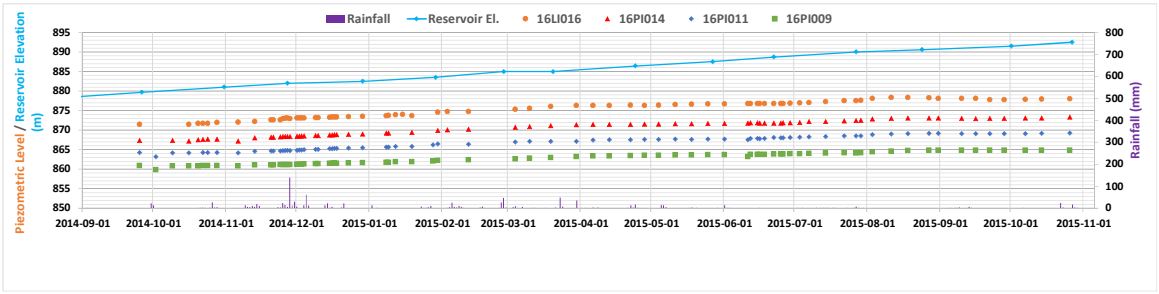

Notes:

1. Rainfall records switch from monthly to daily in January, 2014.
2. Installation date not available for all piezometers. In these cases the date of the first available reading has been plotted.

SECTION 03 (CONTINUED)

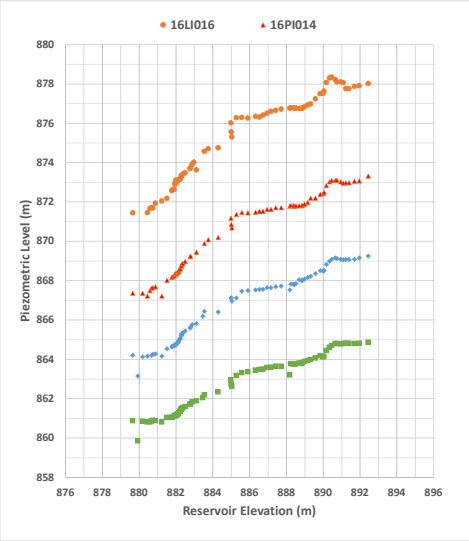

Notes:

1. Rainfall records switch from monthly to daily in January, 2014.
2. Installation date not available for all piezometers. In these cases the date of the first available reading has been plotted.

LEFT ABUTMENT

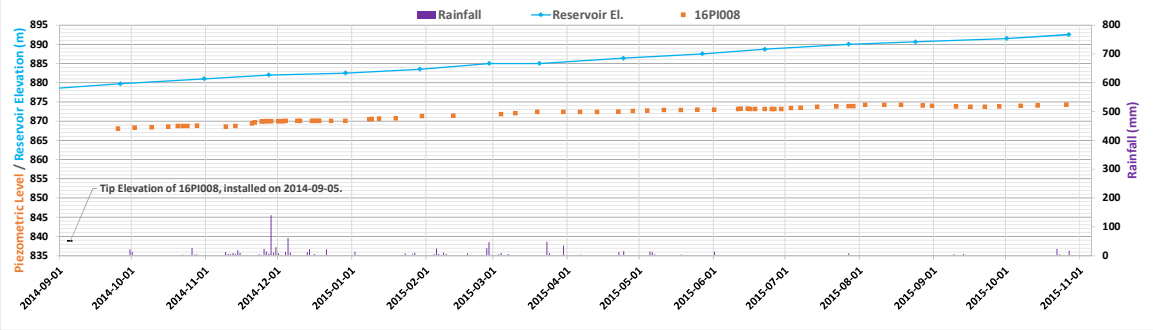

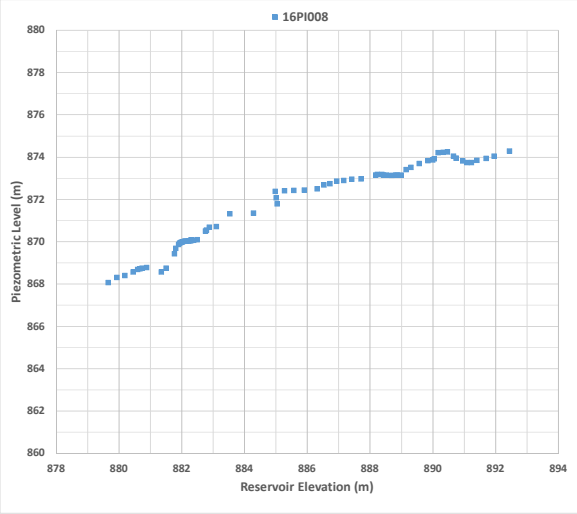

Notes:

1. Rainfall records switch from monthly to daily in January, 2014.
2. Installation date not available for all piezometers. In these cases the date of the first available reading has been plotted.

DATA FROM INSTRUMENT MEASUREMENT SPREADSHEET

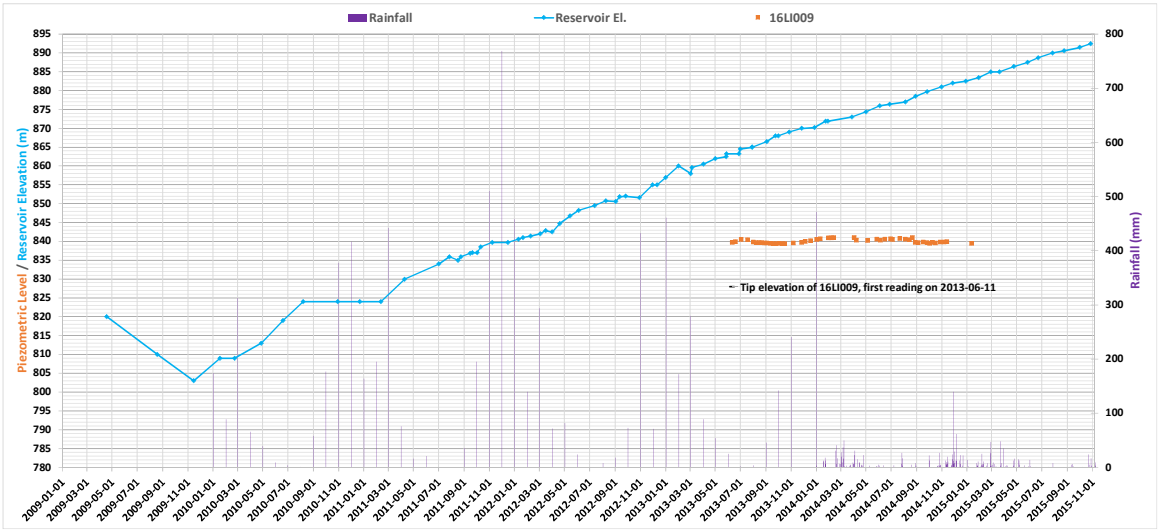

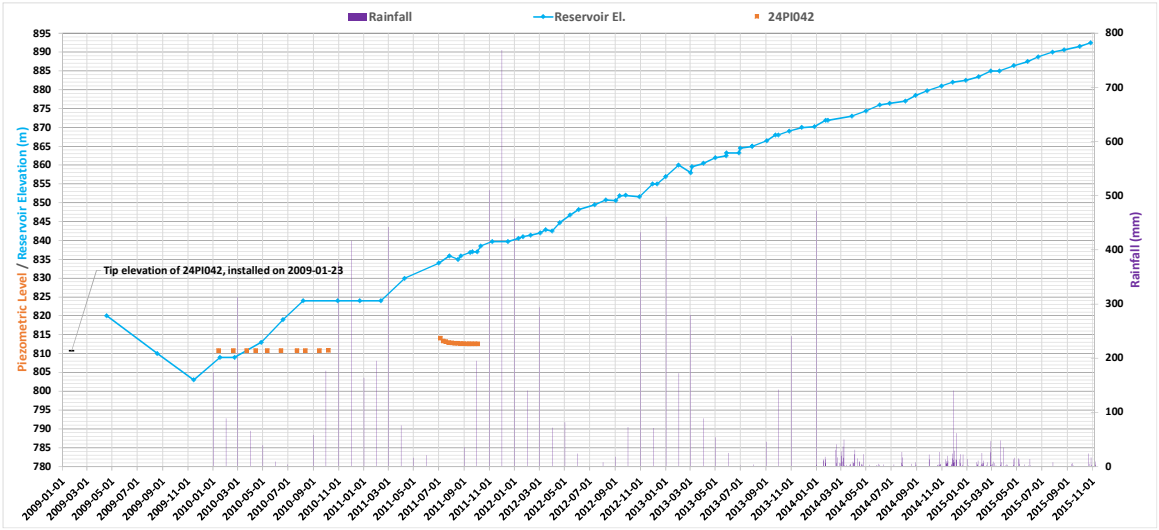

Notes:

1. Rainfall records switch from monthly to daily in January, 2014.
2. Installation date not available for all piezometers. In these cases the date of the first available reading has been plotted.

DATA FROM INSTRUMENT MEASUREMENT SPREADSHEET (CONTINUED)

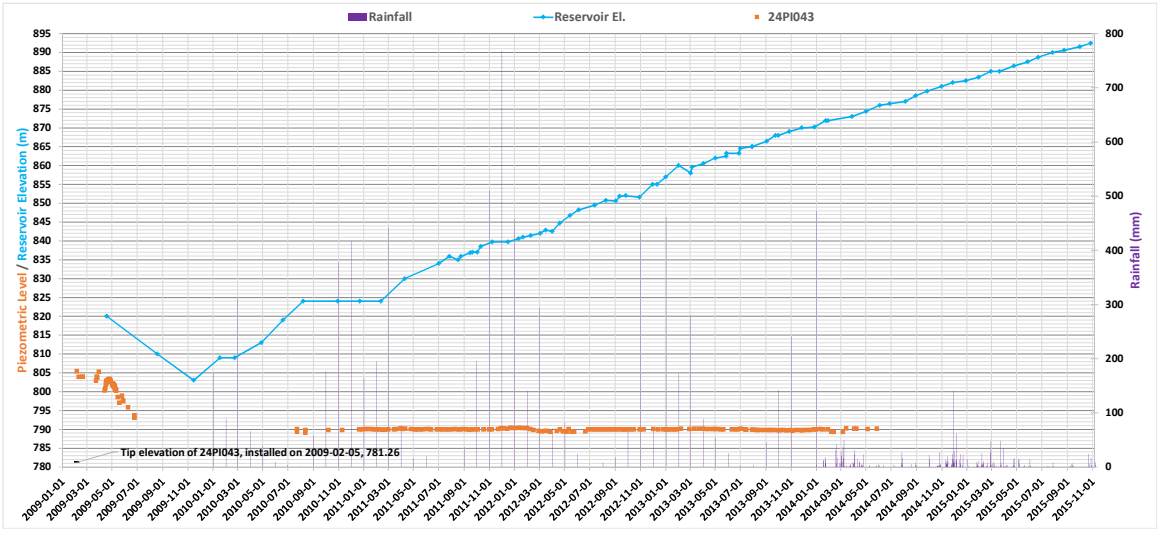

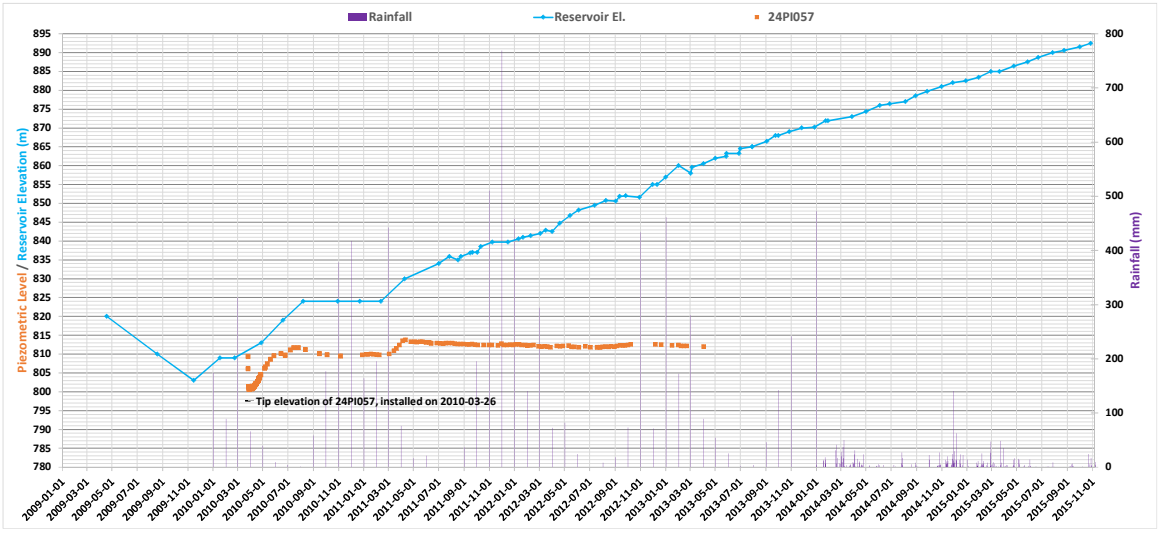

Notes:

1. Rainfall records switch from monthly to daily in January, 2014.
2. Installation date not available for all piezometers. In these cases the date of the first available reading has been plotted.

DATA FROM INSTRUMENT MEASUREMENT SPREADSHEET (CONTINUED)

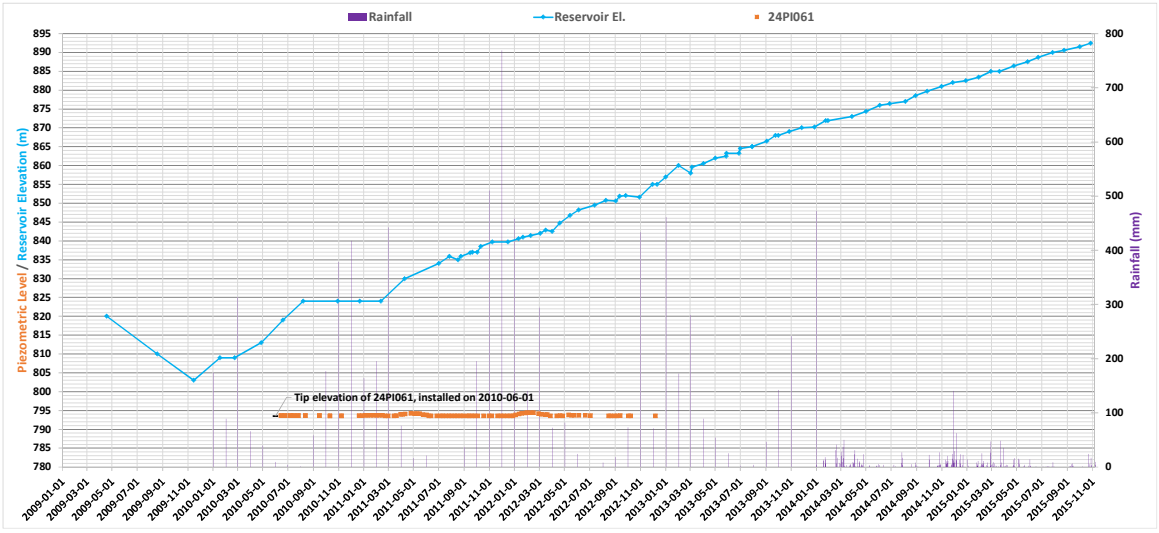

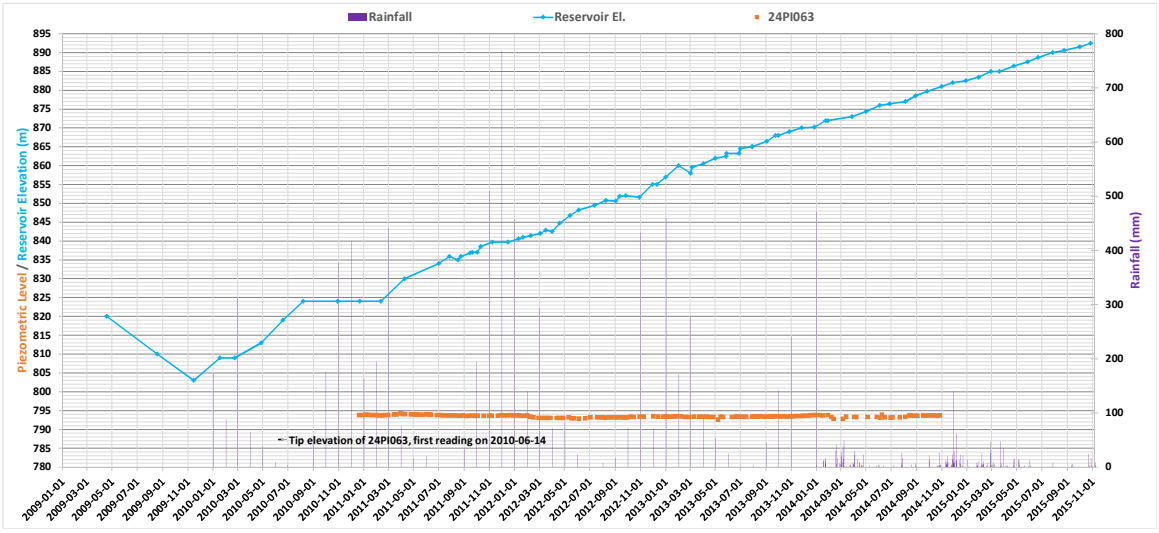

Notes:

1. Rainfall records switch from monthly to daily in January, 2014.
2. Installation date not available for all piezometers. In these cases the date of the first available reading has been plotted.

VIBRATING WIRE PIEZOMETERS

Cluster 1

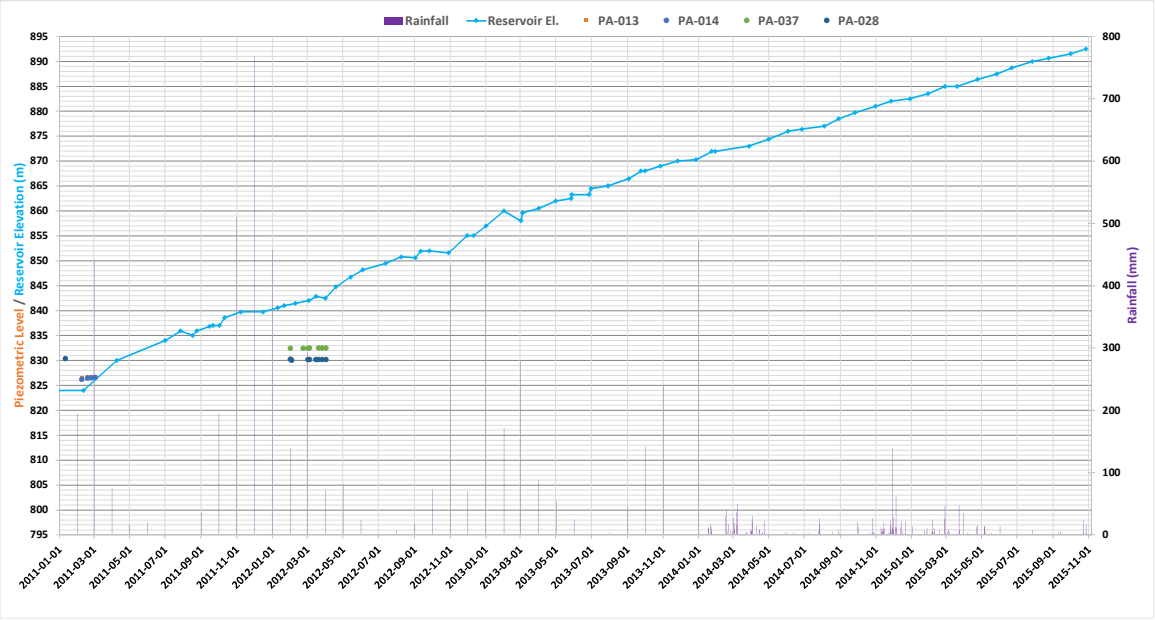

Cluster 2

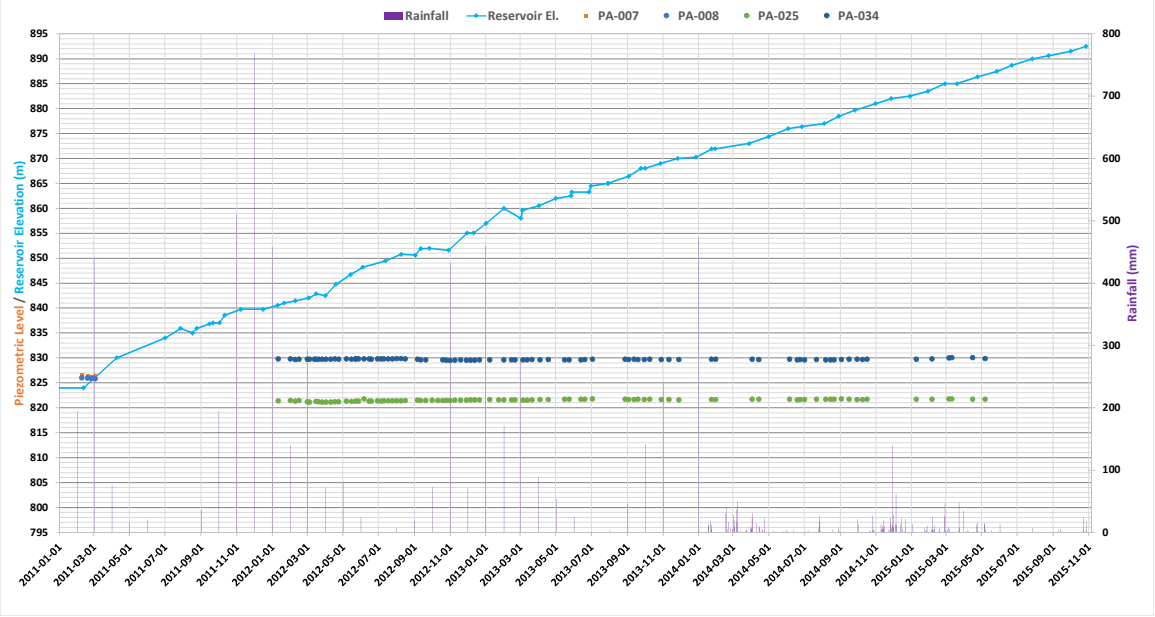

Notes:

1. Rainfall records switch from monthly to daily in January, 2014.
2. Installation date not available for all piezometers. In these cases the date of the first available reading has been plotted.

VIBRATING WIRE PIEZOMETERS (CONTINUED)

Cluster 3

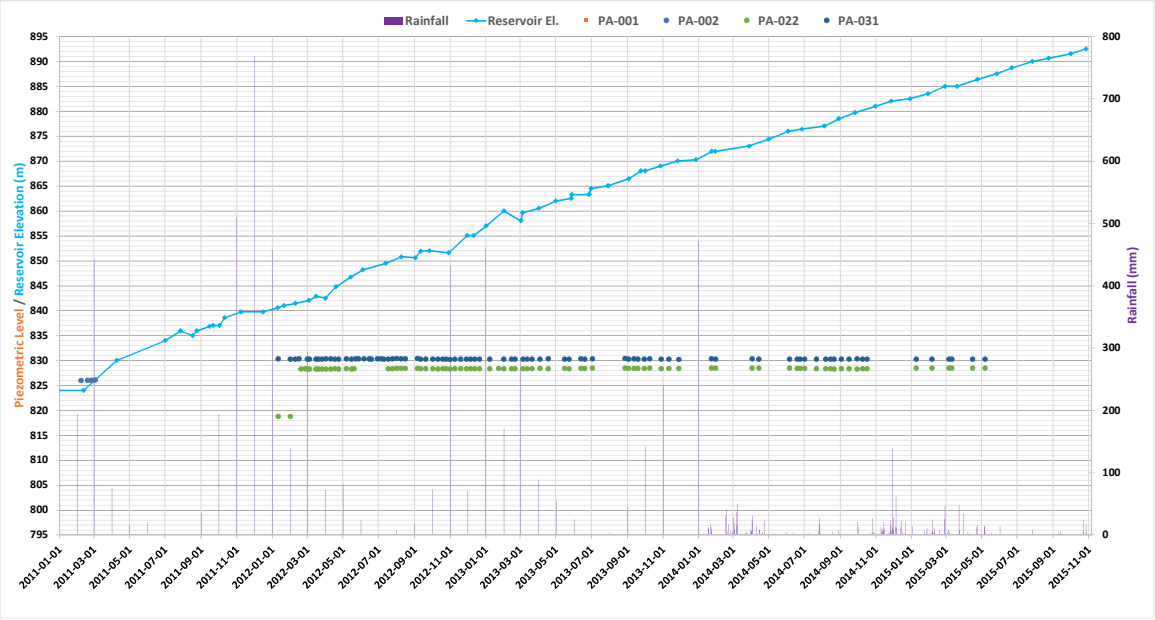

Cluster 4

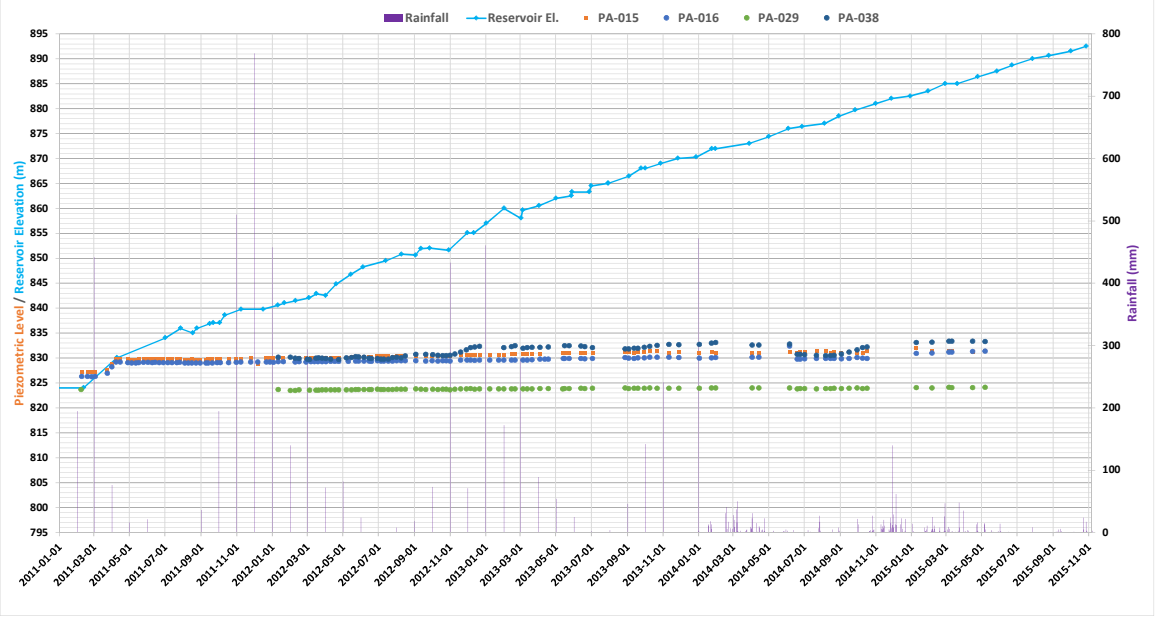

Notes:
1. Rainfall records switch from monthly to daily in January, 2014.
2. Installation date not available for all piezometers. In these cases the date of the first available reading has been plotted.

VIBRATING WIRE PIEZOMETERS (CONTINUED)

Cluster 5

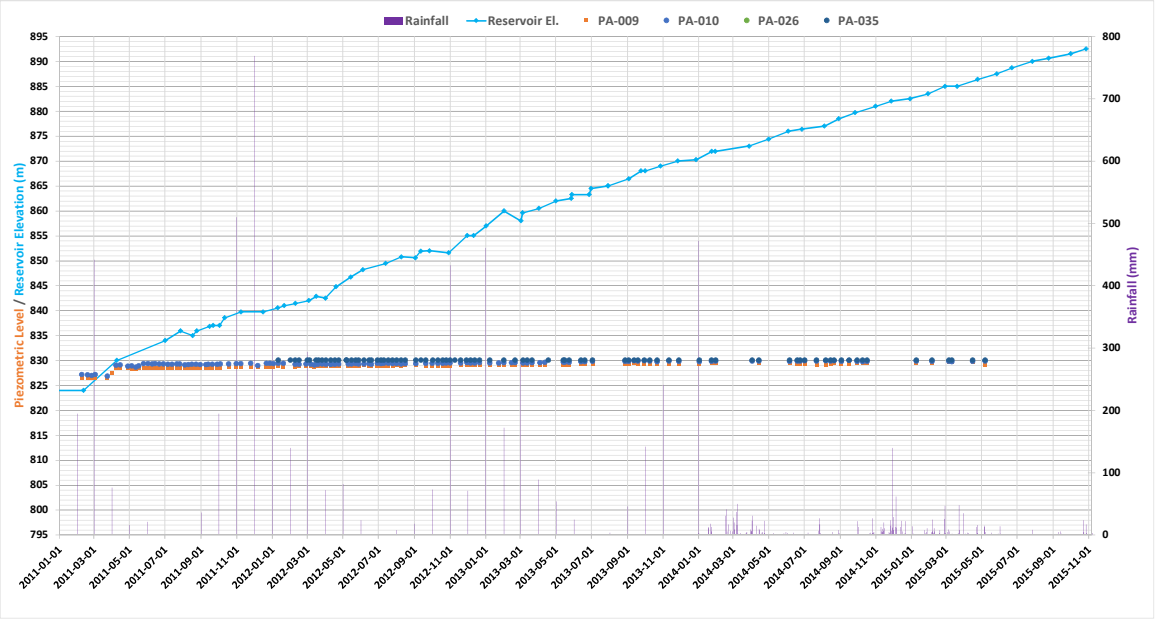

Cluster 6

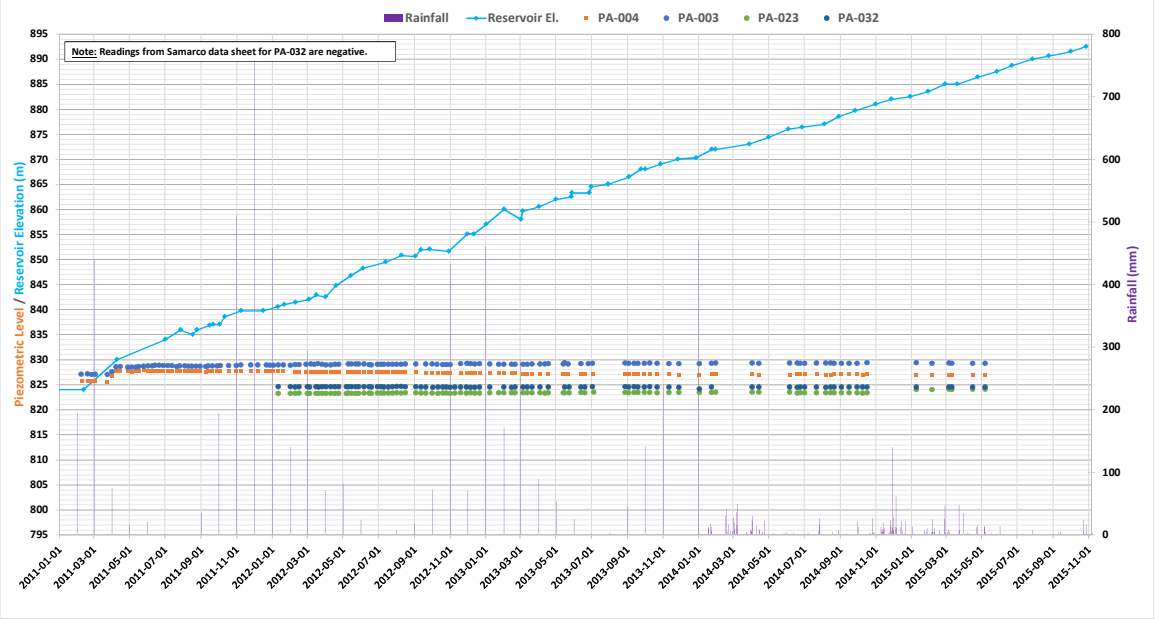

Notes:
1. Rainfall records switch from monthly to daily in January, 2014.
2. Installation date not available for all piezometers. In these cases the date of the first available reading has been plotted.

VIBRATING WIRE PIEZOMETERS (CONTINUED)

Cluster 7

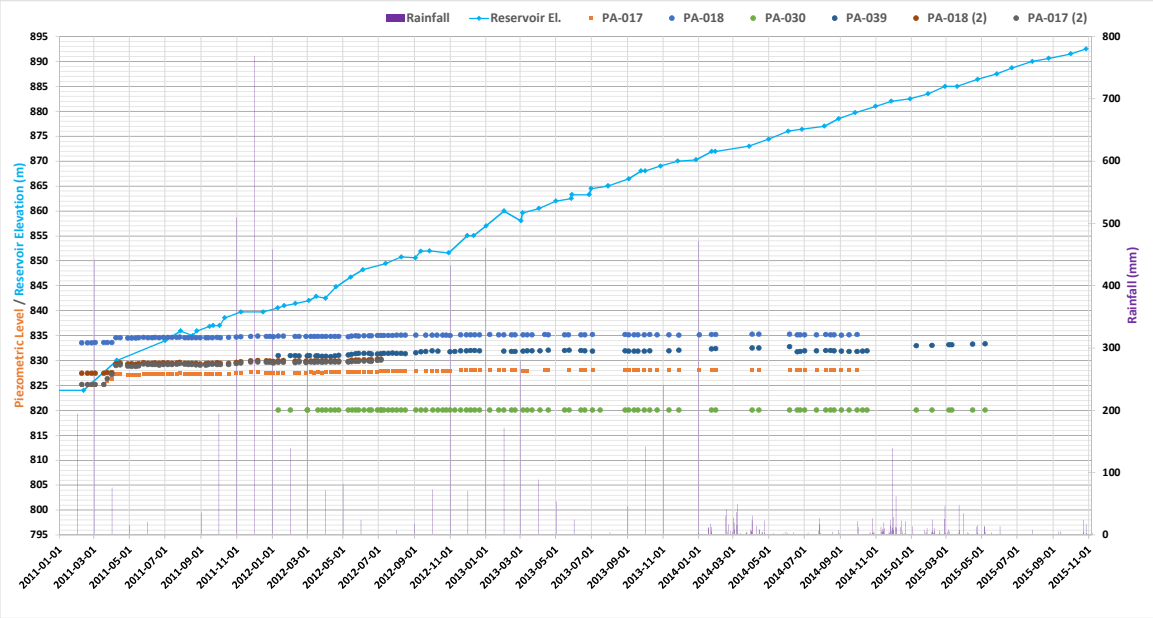

Cluster 8

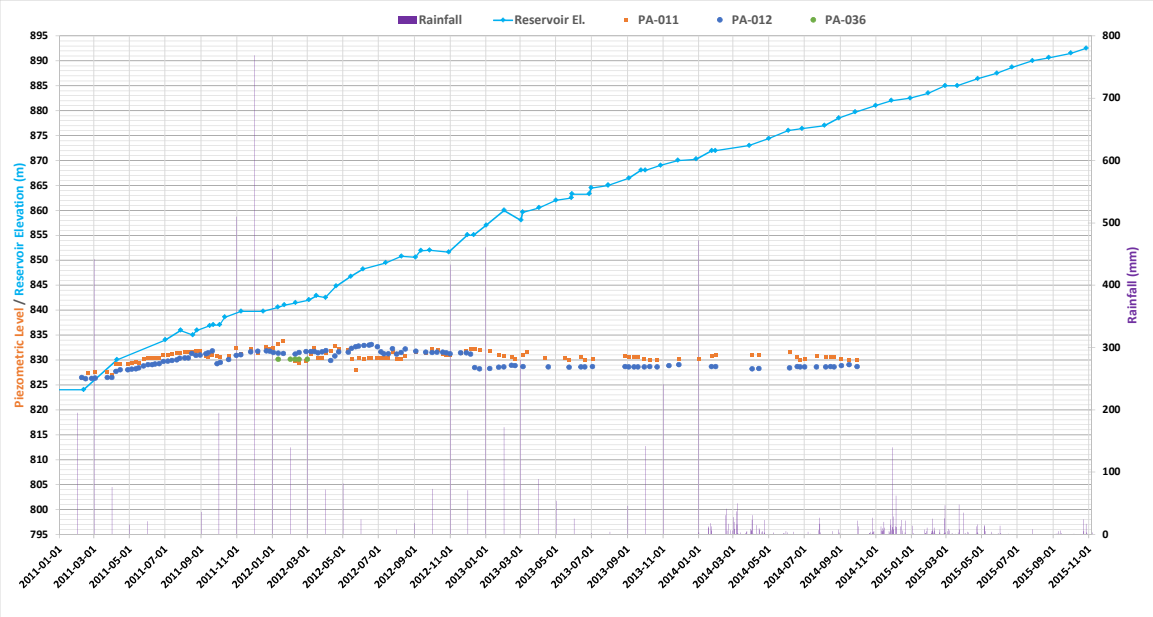

Notes:

1. Rainfall records switch from monthly to daily in January, 2014.
2. Installation date not available for all piezometers. In these cases the date of the first available reading has been plotted.

VIBRATING WIRE PIEZOMETERS (CONTINUED)

Cluster 9

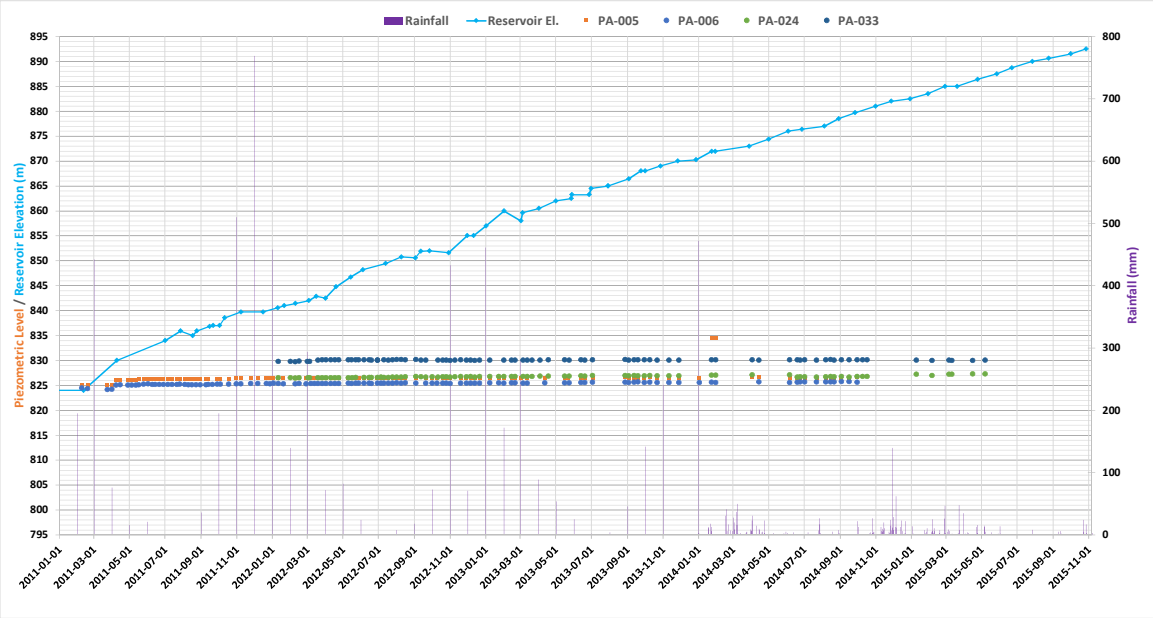

Notes:

1. Rainfall records switch from monthly to daily in January, 2014.
2. Installation date not available for all piezometers. In these cases the date of the first available reading has been plotted.

VIBRATING WIRE PIEZOMETERS (CONTINUED)

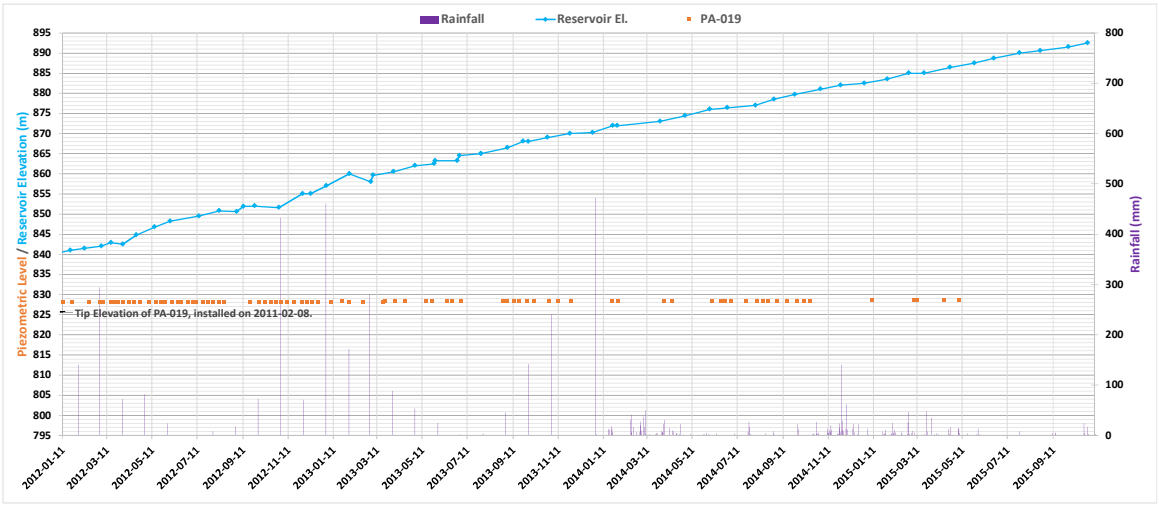

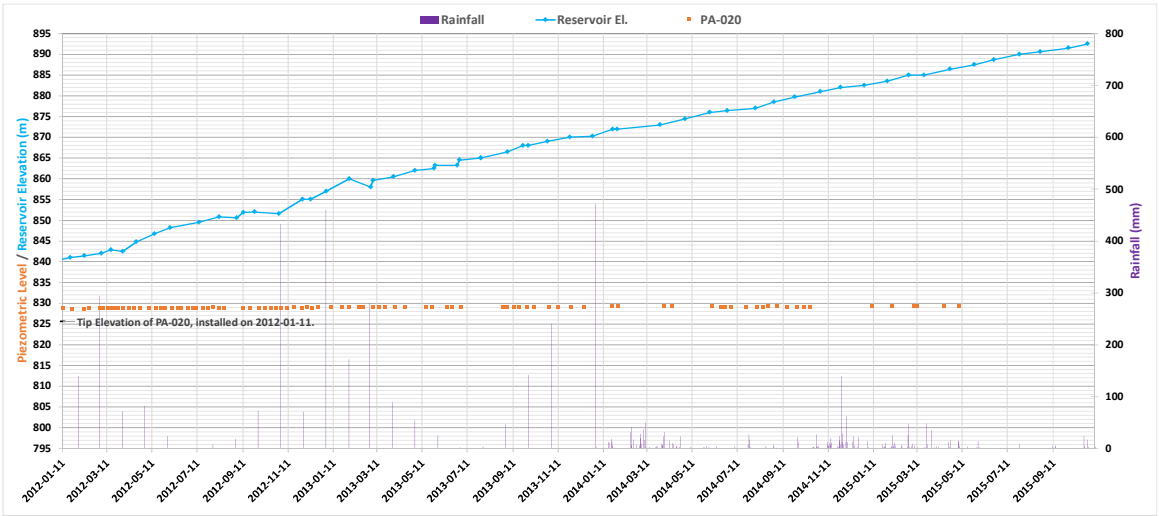

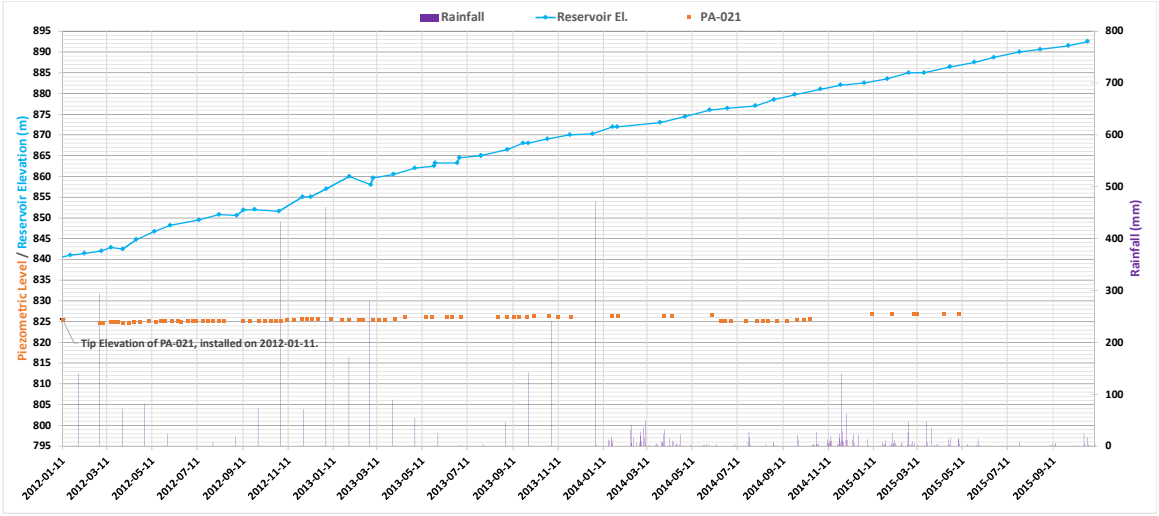

Notes:

1. Rainfall records switch from monthly to daily in January, 2014.
2. Installation date not available for all piezometers. In these cases the date of the first available reading has been plotted.

VIBRATING WIRE PIEZOMETERS (CONTINUED)

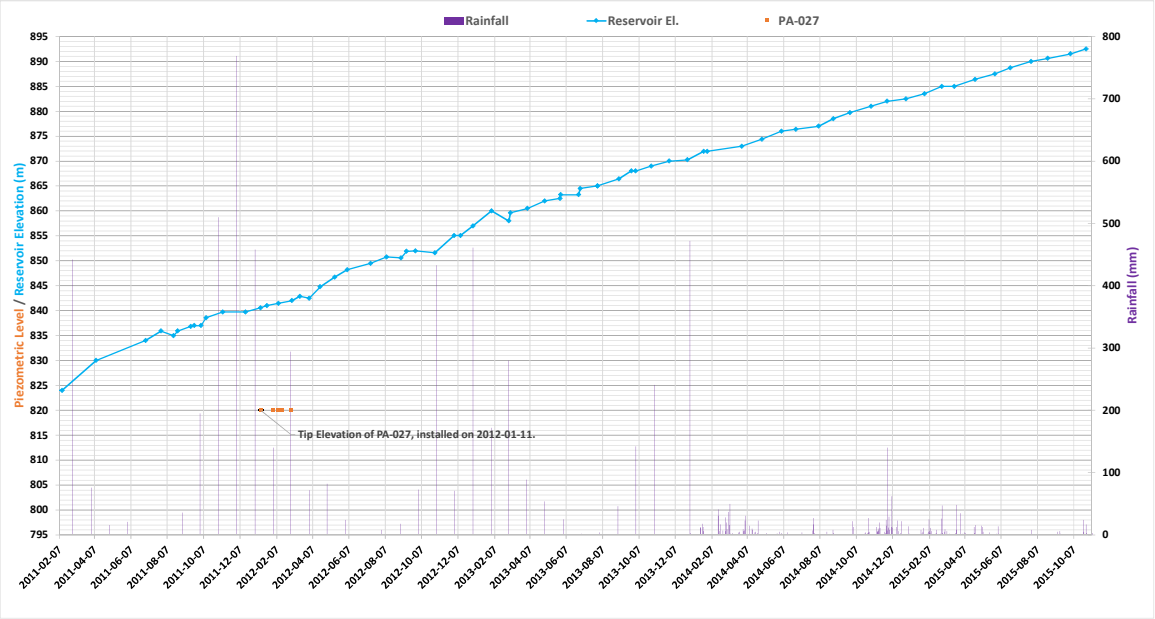

ATTACHMENT E4

List of Piezometers and Water Level Indicators at Dike 1

Attachment E4
List of Piezometers and Water Level Indicators at Dike 1

Table E.E4-1: Casagrande piezometers and water level indicators

Section	Name	Instrument Type	Automatic or Manual?	Period on Record	Installation Date	Coordinate Source	Notes
Data from Instrumentation Reports							
Spillway	16PI022	Casagrande	Unknown	2015-05-07 to 2012-10-26	2015-04-28	MDGEO Report	
Spillway	16PI023	Casagrande	Unknown	2015-05-07 to 2012-10-26	2015-04-30	MDGEO Report	
Spillway	16PI026	Casagrande	Unknown	2015-05-07 to 2012-10-26	2015-05-04	Installation Log	Top of pipe given in Samarco instrumentation report is not consistent with the ground elevation at the specified location. The data from this location is therefore considered unreliable.
Toe	16PI019	Casagrande	Unknown	2015-03-10 to 2015-10-26	2015-03-11	MDGEO Report	
Toe	16PI027	Casagrande	Unknown	2015-03-18 to 2015-10-26	Not available	MDGEO Report	
Toe	16PI028	Casagrande	Unknown	2015-03-18 to 2015-10-26	Not available	MDGEO Report	
AA	16LI010	Water level indicator	Manual	2014-06-26 to 2015-10-26	Not available	MDGEO Report	
AA	16LI011	Water level indicator	Manual	2014-06-26 to 2015-10-26	2014-06-05	MDGEO Report	
AA	16LI013	Water level indicator	Manual	2014-08-21 to 2015-10-26	2014-08-01	MDGEO Report	
AA	16PI003	Casagrande	Automatic	2014-06-26 to 2015-11-02	2014-06-30	MDGEO Report	
AA	16PI004	Casagrande	Manual	2014-06-26 to 2015-10-26	2014-07-30	MDGEO Report	
AA	16PI005	Casagrande	Manual	2014-08-21 to 2015-10-26	2014-08-06	MDGEO Report	
AA	16PI020	Casagrande	Manual	2015-03-30 to 2015-10-26	2015-04-28	MDGEO Report	
AA	24LI017	Water level indicator	Automatic	2010-04-05 to 2015-11-02	2010-04-05	MDGEO Report	
AA	24LI018	Water level indicator	Automatic	2010-05-06 to 2015-11-02	2010-04-30	MDGEO Report	
BB	16LI001	Water level indicator	Automatic	2013-06-11 to 2015-11-02	Not available	MDGEO Report	
BB	16LI002	Water level indicator	Manual	2013-06-11 to 2015-10-26	Not available	MDGEO Report	
BB	16LI012	Water level indicator	Manual	2014-08-21 to 2015-10-26	2014-07-31	MDGEO Report	
BB	16PI006	Casagrande	Manual	2014-08-21 to 2015-10-26	Not available	MDGEO Report	
BB	16PI021	Casagrande	Manual	2015-05-04 to 2015-10-26	2015-04-20	Installation Log	
BB	24LI019	Water level indicator	Automatic	2010-10-07 to 2015-11-02	Not available	MDGEO Report	
BB	24LI020	Water level indicator	Manual	2010-05-06 to 2015-10-26	2010-04-05	MDGEO Report	
BB	24PI044	Casagrande	Manual	2010-03-23 to 2015-10-26	2010-03-23	MDGEO Report	
DD	16PI017	Casagrande	Manual	2014-09-29 to 2015-10-26	2014-10-24	MDGEO Report	
DD	16PI018	Casagrande	Manual	2014-09-29 to 2015-10-26	2014-10-23	MDGEO Report	
DD	16PI024	Casagrande	Manual	2015-05-04 to 2015-10-26	2015-04-29	Installation Log	
DD	24LI021	Water level indicator	Automatic	2010-06-24 to 2015-11-02	2010-06-18	MDGEO Report	
DD	24LI029	Water level indicator	Manual	2010-04-15 to 2015-10-26	2010-04-15	MDGEO Report	
DD	24PI039	Casagrande	Manual	2010-01-14 to 2015-10-26	2008-12-06	MDGEO Report	
DD	24PI045	Casagrande	Automatic	2010-03-19 to 2015-11-02	2010-03-19	MDGEO Report	
DD	24PI046	Casagrande	Automatic	2010-08-31 to 2015-11-02	2010-03-09	MDGEO Report	
DD	24PI047	Casagrande	Automatic	2010-08-31 to 2015-11-02	2010-08-14	MDGEO Report	
FF	16LI003	Water level indicator	Manual	2013-06-11 to 2015-10-26	Not available	MDGEO Report	
FF	16LI004	Water level indicator	Manual	2013-06-11 to 2015-10-26	Not available	MDGEO Report	
FF	16PI025	Casagrande	Manual	2015-05-04 to 2015-10-26	2015-04-29	Installation Log	
FF	24LI022	Water level indicator	Manual	2010-06-24 to 2015-11-02	2010-06-11	MDGEO Report	
FF	24LI030	Water level indicator	Manual	2010-04-17 to 2015-11-02	2010-04-17	MDGEO Report	
FF	24PI041	Casagrande	Manual	2010-01-14 to 2010-10-26	2009-02-23	MDGEO Report	
FF	24PI048	Casagrande	Automatic	2010-03-10 to 2015-11-02	2010-03-10	MDGEO Report	
FF	24PI049	Casagrande	Automatic	2010-08-12 to 2015-11-02	2010-03-05	MDGEO Report	
FF	24PI050	Casagrande	Automatic	2010-08-12 to 2015-11-02	2010-03-05	MDGEO Report	
HH	24LI023	Water level indicator	Automatic	2010-06-24 to 2015-11-02	2010-06-11	MDGEO Report	
HH	24LI024	Water level indicator	Automatic	2010-04-21 to 2015-11-02	2010-04-21	MDGEO Report	
HH	24PI051	Casagrande	Manual	2010-03-05 to 2014-08-04	2010-03-05	MDGEO Report	Damaged in 2014
HH	24PI052	Casagrande	Manual	2010-07-26 to 2015-10-26	2010-07-19	MDGEO Report	
HH	24PI053	Casagrande	Automatic	2010-07-26 to 2015-11-02	2010-07-13	MDGEO Report	
JJ	16LI005	Water level indicator	Manual	2013-06-11 to 2015-10-26	Not available	MDGEO Report	
JJ	16LI006	Water level indicator	Manual	2013-06-11 to 2015-10-26	Not available	MDGEO Report	
JJ	24LI025	Water level indicator	Automatic	2010-06-24 to 2015-11-02	2010-05-20	MDGEO Report	
JJ	24LI026	Water level indicator	Automatic	2010-04-23 to 2015-11-02	2010-04-23	MDGEO Report	
JJ	24PI054	Casagrande	Manual	2010-03-01 to 2015-10-26	2010-03-01	MDGEO Report	
JJ	24PI055	Casagrande	Automatic	2010-07-15 to 2015-11-02	2010-07-08	MDGEO Report	
JJ	24PI056	Casagrande	Automatic	2010-07-15 to 2015-11-02	2010-08-05	MDGEO Report	
JJ	24PI062	Casagrande	Manual	2010-05-28 to 2015-10-26	2010-05-26	MDGEO Report	
LL	24LI027	Water level indicator	Manual	2010-05-15 to 2015-10-26	2010-05-15	MDGEO Report	
LL	24PI058	Casagrande	Automatic	2010-07-07 to 2015-11-02	2010-06-24	MDGEO Report	
LL	24PI059	Casagrande	Automatic	2010-07-07 to 2015-11-02	2010-06-24	MDGEO Report	
MM	16LI007	Water level indicator	Manual	2013-06-11 to 2015-10-26	Not available	MDGEO Report	
MM	16LI008	Water level indicator	Manual	2013-06-11 to 2015-10-26	Not available	MDGEO Report	
MM	24LI028	Water level indicator	Manual	2010-05-28 to 2015-10-26	2010-05-15	MDGEO Report	
MM	24PI060	Casagrande	Automatic	2010-03-30 to 2015-11-02	2010-03-30	MDGEO Report	
NN	16PI001	Casagrande	Manual	2014-07-21 to 2015-10-26	2014-07-17	MDGEO Report	
NN	16PI002	Casagrande	Manual	2014-07-21 to 2015-10-26	2014-07-18	MDGEO Report	
01	16LI015	Water level indicator	Unknown	2014-09-25 to 2014-12-29	2014-09-12	MDGEO Report	Damaged in 2014
01	16PI013	Casagrande	Manual	2014-09-25 to 2015-10-26	2014-09-20	MDGEO Report	
01	16PI015	Casagrande	Manual	2014-09-25 to 2015-10-26	2014-09-23	MDGEO Report	
01	16PI016	Casagrande	Manual	2014-10-16 to 2015-10-26	2014-10-10	MDGEO Report	
02	16LI014	Water level indicator	Manual	2014-10-20 to 2015-10-26	2014-09-10	MDGEO Report	
02	16LI017	Water level indicator	Manual	2014-09-25 to 2015-10-26	Not available	MDGEO Report	Top of pipe given in Samarco instrumentation report is not consistent with the ground elevation at the specified location. The data from this location is therefore considered unreliable.
02	16PI007	Casagrande	Manual	2014-09-25 to 2015-10-26	2014-09-01	MDGEO Report	
02	16PI010	Casagrande	Manual	2014-09-25 to 2015-10-26	2014-09-17	MDGEO Report	
02	16PI012	Casagrande	Manual	2014-09-25 to 2015-10-26	2014-09-19	MDGEO Report	
03	16LI016	Water level indicator	Manual	2014-09-25 to 2015-10-26	2014-09-10	MDGEO Report	
03	16PI009	Casagrande	Manual	2014-09-25 to 2015-10-26	2014-09-17	MDGEO Report	
03	16PI011	Casagrande	Manual	2014-09-25 to 2015-10-26	2014-09-18	MDGEO Report	
03	16PI014	Casagrande	Manual	2014-09-25 to 2015-10-26	2014-09-26	MDGEO Report	
Left Abut.	16PI008	Casagrande	Manual	2014-09-25 to 2015-10-26	2014-09-05	MDGEO Report	
Data from Instrument Measurement Spreadsheet							
Left Abut.	16LI009	Water level indicator	Unknown	2013-06-11 to 2015-01-02	Not available	2013 Instrumentation Plan	
Unknown	24LI039	Water level indicator	Unknown	2011-03-24 to 2011-04-12	Not available	Not available	No location available. Records not shown. Short period on record from 2011.
FF	24PI042	Casagrande	Unknown	2010-01-14 to 2011-10-04	2009-01-23	2012 OMS Manual	
JJ	24PI043	Casagrande	Unknown	2009-02-09 to 2014-05-27	2009-02-05	2012 OMS Manual	
LL	24PI057	Casagrande	Unknown	2010-03-26 to 2013-04-03	2010-03-26	2012 OMS Manual	
JJ	24PI061	Casagrande	Unknown	2010-06-14 to 2014-05-07	2010-06-01	2012 OMS Manual	
JJ	24PI063	Casagrande	Unknown	2010-06-14 to 2012-12-07	Not available	2012 OMS Manual	

Note: Red text denotes damaged instruments or unreliable readings.

Table E.E4-2: Vibrating Wire Piezometers

Name	Cluster	Instrument Type	Automatic or Manual?	Period on Record	Installation Date	Coordinate Source	Notes
PA-001	3	Vibrating wire piezometer	Manual	2011-02-07 to 2011-03-03	2011-02-07	[44]	Damaged shortly after installation
PA-002	3	Vibrating wire piezometer	Manual	2011-02-07 to 2011-03-03	2011-02-07	[44]	Damaged shortly after installation
PA-003	6	Vibrating wire piezometer	Manual	2011-02-07 to 2015-05-07	2011-02-07	[44]	
PA-004	6	Vibrating wire piezometer	Manual	2011-02-08 to 2015-05-07	2011-02-07	[44]	
PA-005	9	Vibrating wire piezometer	Manual	2011-02-08 to 2014-10-09	2011-02-07	[44]	Damaged in 2014
PA-006	9	Vibrating wire piezometer	Manual	2011-02-08 to 2014-10-09	2011-02-07	[44]	Damaged in 2014
PA-007	2	Vibrating wire piezometer	Manual	2011-02-08 to 2011-03-03	2011-02-07	[44]	Damaged shortly after installation
PA-008	2	Vibrating wire piezometer	Manual	2011-02-08 to 2011-03-03	2011-02-07	[44]	Damaged shortly after installation
PA-009	5	Vibrating wire piezometer	Manual	2011-02-08 to 2015-05-07	2011-02-07	[44]	
PA-010	5	Vibrating wire piezometer	Manual	2011-02-08 to 2015-05-07	2011-02-07	[44]	
PA-011	8	Vibrating wire piezometer	Manual	2011-02-08 to 2014-10-09	2011-02-07	[44]	Damaged in 2014
PA-012	8	Vibrating wire piezometer	Manual	2011-02-08 to 2014-10-09	2011-02-08	[44]	Damaged in 2014
PA-013	1	Vibrating wire piezometer	Manual	2011-02-08 to 2011-03-03	2011-02-07	[44]	Damaged shortly after installation
PA-014	1	Vibrating wire piezometer	Manual	2011-02-08 to 2011-03-03	2011-02-07	[44]	Damaged shortly after installation
PA-015	4	Vibrating wire piezometer	Manual	2011-02-08 to 2015-05-07	2011-02-07	[44]	
PA-016	4	Vibrating wire piezometer	Manual	2011-02-08 to 2015-05-07	2011-02-07	[44]	
PA-017	7	Vibrating wire piezometer	Manual	2011-02-08 to 2014-10-09	2011-02-07	[44]	Damaged in 2014
PA-017 (2)	7	Vibrating wire piezometer	Manual	2011-02-08 to 2012-07-05	Not available	Assumed same location as PA-017	Second data set for PA-017. Reason for two data sets unknown.
PA-018	7	Vibrating wire piezometer	Manual	2011-02-08 to 2014-10-09	2011-02-08	[44]	Damaged in 2014
PA-018 (2)	7	Vibrating wire piezometer	Manual	2011-02-08 to 2012-07-05	Not available	Assumed same location as PA-018	Second data set for PA-018. Reason for two data sets unknown.
PA-019	N/A	Vibrating wire piezometer	Manual	2012-01-11 to 2015-05-07	2011-02-08	[44]	
PA-020	N/A	Vibrating wire piezometer	Manual	2012-01-11 to 2015-05-07	2012-01-11	[44]	
PA-021	N/A	Vibrating wire piezometer	Manual	2012-01-11 to 2015-05-07	2012-01-11	[44]	
PA-022	3	Vibrating wire piezometer	Manual	2012-01-11 to 2015-05-07	2012-01-11	[44]	
PA-023	6	Vibrating wire piezometer	Manual	2012-01-11 to 2015-05-07	2012-01-11	[44]	
PA-024	9	Vibrating wire piezometer	Manual	2012-01-11 to 2015-05-07	2012-01-11	[44]	
PA-025	2	Vibrating wire piezometer	Manual	2012-01-11 to 2015-05-07	2012-01-11	[44]	
PA-026	5	Vibrating wire piezometer	Manual	2012-01-11 to 2014-01-02	2012-01-11	[44]	
PA-027	N/A	Vibrating wire piezometer	Manual	2012-01-11 to 2012-03-01	2012-01-11	[44]	Damaged shortly after installation
PA-028	1	Vibrating wire piezometer	Manual	2012-01-11 to 2012-04-02	2012-01-11	[44]	Damaged shortly after installation
PA-029	4	Vibrating wire piezometer	Manual	2011-02-07 to 2015-05-07	2011-02-07	[44]	
PA-030	7	Vibrating wire piezometer	Manual	2012-01-11 to 2015-05-07	2011-02-07	[44]	
PA-031	3	Vibrating wire piezometer	Manual	2012-01-11 to 2015-05-07	2012-01-11	[44]	
PA-032	6	Vibrating wire piezometer	Manual	2012-01-11 to 2015-05-07	2012-01-11	[44]	
PA-033	9	Vibrating wire piezometer	Manual	2012-01-11 to 2015-05-07	2012-01-11	[44]	
PA-034	2	Vibrating wire piezometer	Manual	2012-01-11 to 2015-05-07	2012-01-11	[44]	
PA-035	4	Vibrating wire piezometer	Manual	2012-01-11 to 2015-05-07	2012-01-11	[44]	
PA-036	8	Vibrating wire piezometer	Manual	2012-01-11 to 2012-03-14	2012-01-11	[44]	Damaged shortly after installation
PA-037	1	Vibrating wire piezometer	Manual	2012-01-11 to 2012-04-02	2012-01-11	[44]	Damaged shortly after installation
PA-038	4	Vibrating wire piezometer	Manual	2012-01-11 to 2015-05-07	2012-01-11	[44]	
PA-039	7	Vibrating wire piezometer	Manual	2012-01-11 to 2015-05-07	2012-01-11	[44]	

Note: Red text denotes damaged instruments or unreliable readings.

ATTACHMENT E5

Flow Data

Attachment E5
Flow Data

TABLE OF CONTENTS

List of Figures

E.E5-1 GENERAL

This attachment presents flow monitoring data from six locations at the Fundão Dam. Data was compiled from Samarco's instrumentation reports, weekly reports, and MDGEO's Hydrogeological Study on the 940 m Raise[7]. The locations are shown in Figure E.E5-1 and are numbered according to the numbering system used in Samarco's weekly reports. The locations were estimated based on site photos and aerial images. Coordinates for the flow monitoring stations are not available. Details on the individual locations and their period on record are presented in Section E.E5-2.

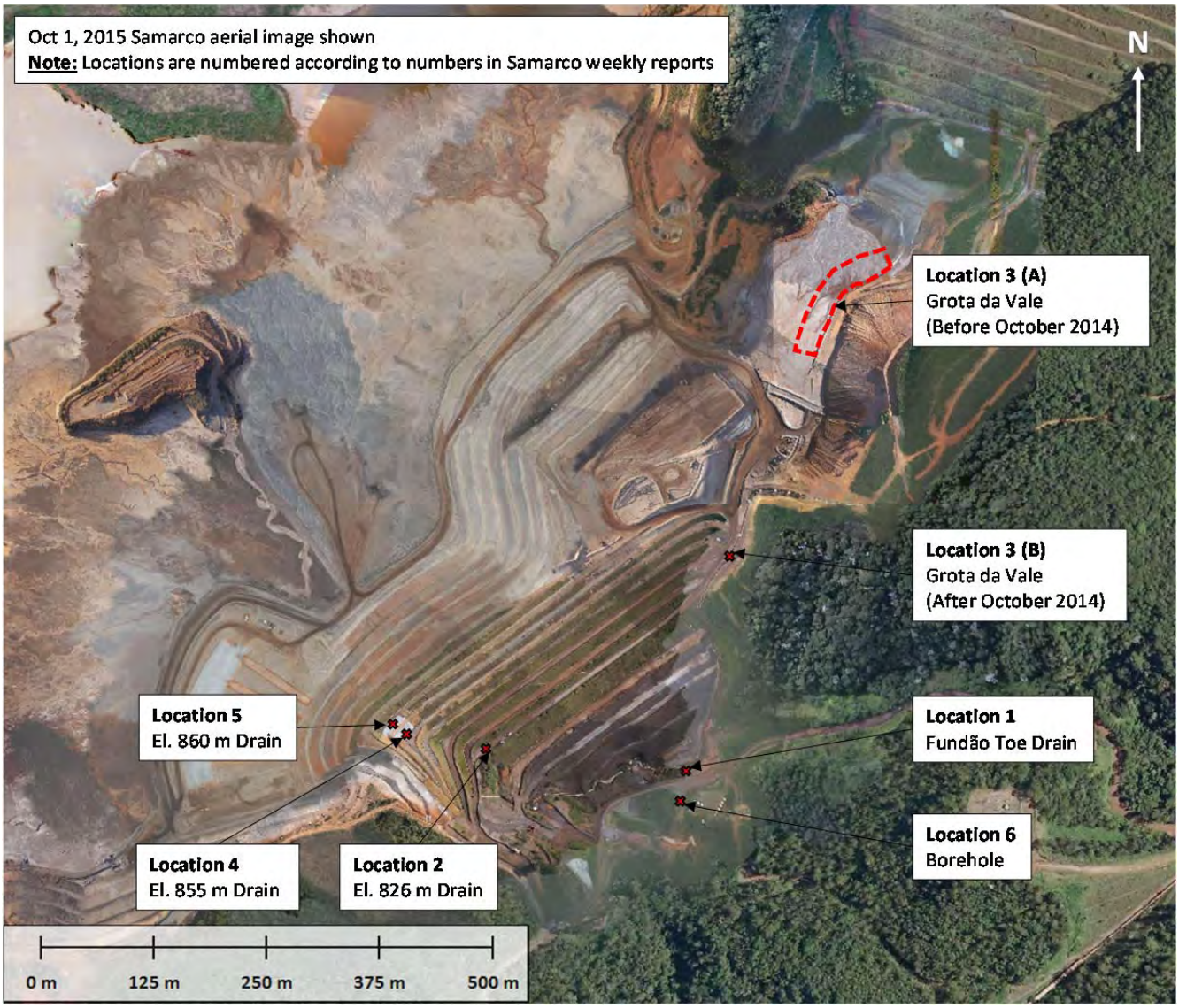

Figure E.E5-1 Dike 1 flow monitoring locations

E.E5-2 FLOW MEASUREMENT MONITORING STATION DETAILS

The factsheets below provide details on each of the flow monitoring locations.

<table>
<tr><th colspan="2">Location 1: Fundão Toe Drain</th></tr>
<tr><td colspan="2">Description</td></tr>
<tr><td>Data Collection Method</td><td>Measured flow through Parshall flume (pictured below).</td></tr>
<tr><td>Period on Record and Data Sources</td><td>March, 2013 – October, 2015 (instrumentation reports)
February, 2015 – October, 2015 (weekly reports)
March, 2013 – May, 2015 (MDGEO)</td></tr>
<tr><td>Additional Information</td><td>Parshall flume located at the outlet of the Principal Foundation Drain. It is unknown why there are no records prior to 2012. From photographs it appears that the flow was measured using both a pressure transducer and a staff gauge.</td></tr>
<tr><td colspan="2">Photo and Location</td></tr>
<tr><td> 

Approximate location. October 1, 2015 Samarco aerial image shown.</td><td> 
Photo from weekly report, week of October 25, 2015, showing Parshall flume.</td></tr>
<tr><td> 
July, 2014 VOGBR site inspection photo showing Parshall flume.</td><td> 
July, 2014 VOGBR site inspection photo showing Parshall flume.</td></tr>
</table>

Data

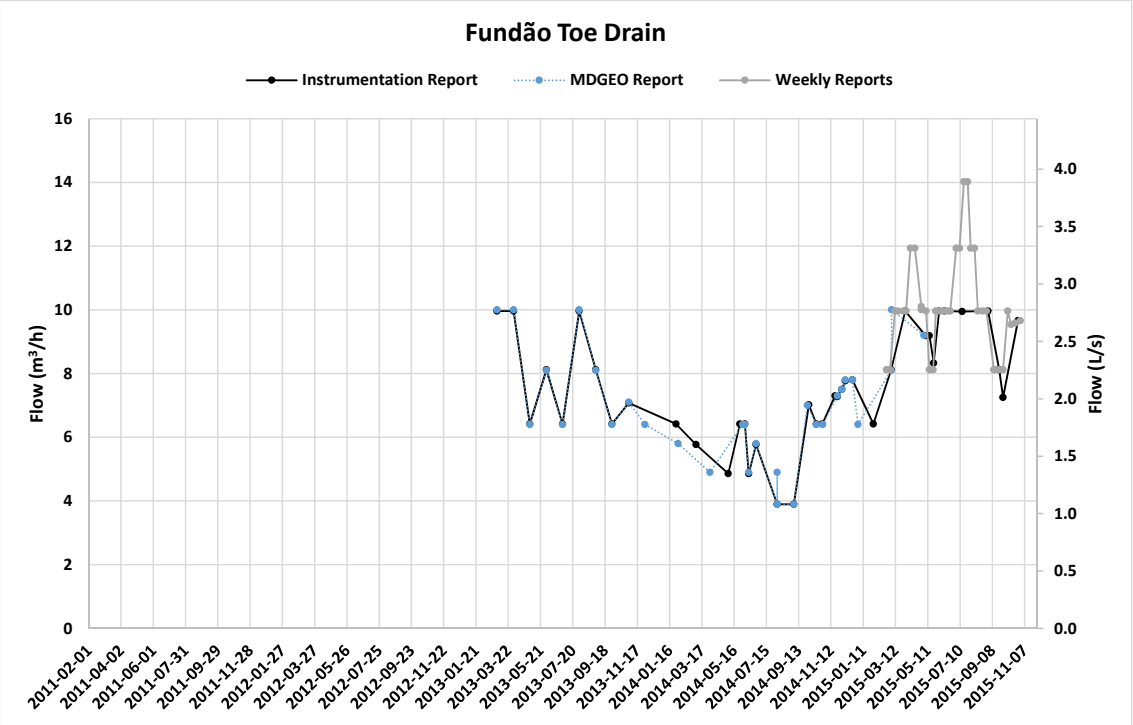

Measurements from Samarco instrumentation report, MDGEO's Hydrogeological Study on the 940 m Raise[7], and Samarco weekly operations reports. Note that not every weekly report in the given interval provides a flow measurement at this location.

<table>
<tr><th colspan="2">Location 2: El. 826 m Drain ("Kananets®")</th></tr>
<tr><td colspan="2">Description</td></tr>
<tr><td>Data Collection Method</td><td>Total flows given in weekly reports measured using Parshall flume. No information is available on how the individual flows in each pipe were measured.</td></tr>
<tr><td>Period on Record and Data Sources</td><td>December, 2013 – October, 2015 (instrumentation reports, total flow)
February, 2015 – October, 2015 (weekly reports, total flow)
April, 2011 – July, 2015 (MDGEO, measurements from individual Kananets)</td></tr>
<tr><td>Additional Information</td><td>27 Kananet® pipes were installed in the El. 826 m blanket drain and discharged to a concrete channel on the El. 820 m bench. Samarco's drainage plan[57] and a 2011 ITRB report state that drainage from the Kananets® was towards both the right and left abutments. However, measurements are only available from a flume near the right abutment. Sections taken along the El. 820 m berm show that the topography was sloped towards the right abutment over the majority of the berm, with less than 50 m length sloped toward the left abutment. The last 4 to 5 Kananets® may have drained to the left abutment. However, the sum of individual Kananet® flows[7] is very similar to the total flow measured on the right abutment (reported in weekly reports). Any drainage to the left abutment was likely a small percentage of the total flow.</td></tr>
<tr><td colspan="2">Photo and Location</td></tr>
<tr><td> 
Photo from weekly report, week of October 25, 2015, showing Parshall fume. Actual photo date unknown. Photo looking towards center of dam and left abutment.</td><td> 
Photo from MDGEO Hydrogeological Study on the 940 m Raise[7], taken June 23, 2015. Photo looking towards right abutment showing concrete channel and Kananets®.</td></tr>
<tr><td colspan="2"> 
Approximate location. October 1, 2015 Samarco aerial image shown.</td></tr>
</table>

Location 2: El. 826 m Drain ("Kananets®")

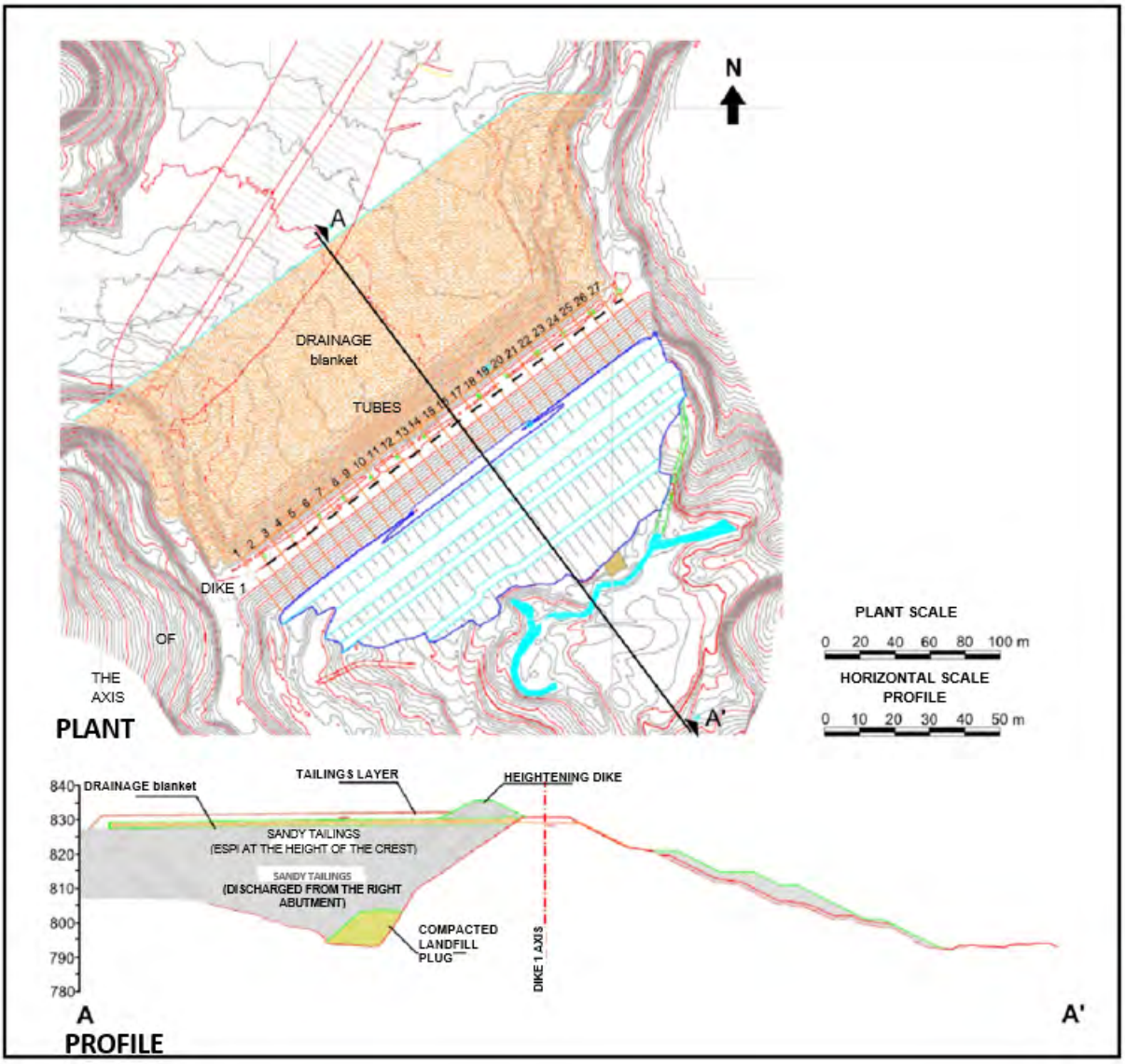

Figure 6.1 from MDGEO's Hydrogeological Study on the 940 m Raise[7], showing Kananets® numbered 1 to 27 from the right abutment to the left abutment.

Location 2: El. 826 m Drain ("Kananets®")

Data

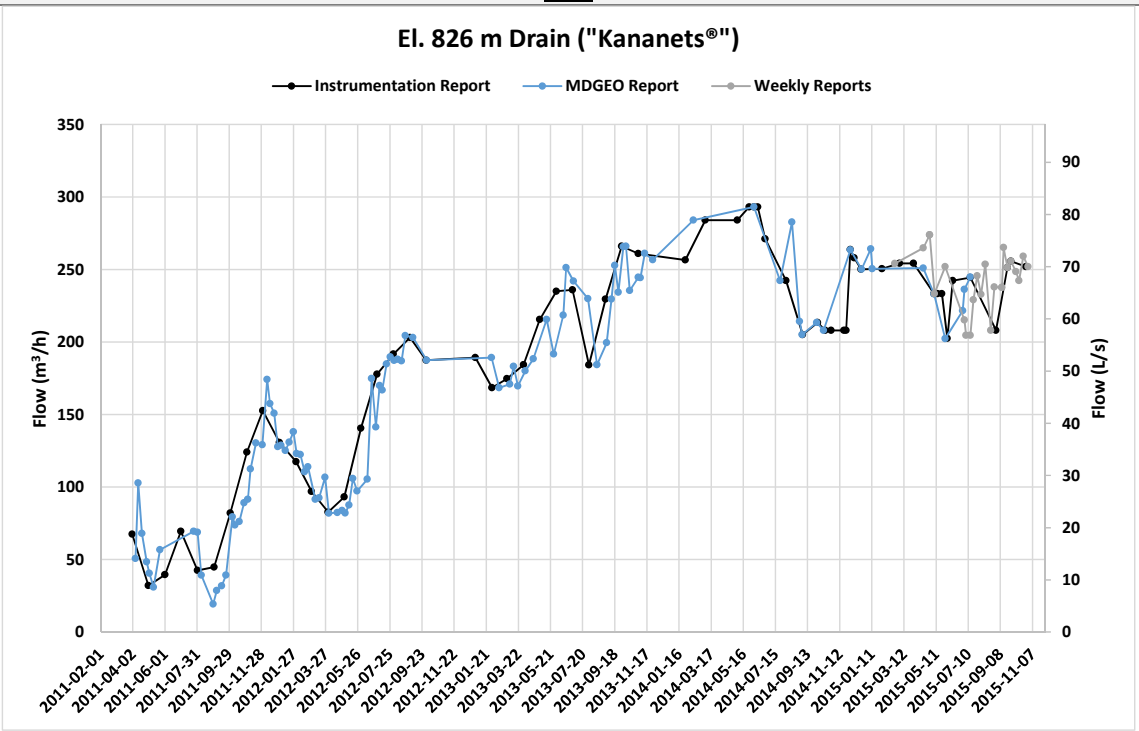

Total measurements (sum of flow in 27 pipes) from Samarco instrumentation report, MDGEO's Hydrogeological Study on the 940 m Raise[7], and Samarco weekly operations reports. Note that not every weekly report in the given interval provides a flow measurement at this location.

<table>
<tr><th colspan="2">Location 3: Grota da Vale</th></tr>
<tr><td colspan="2">Description</td></tr>
<tr><td>Data Collection Method</td><td>Data collection prior to October 2014 unknown. Measurements assumed to be taken at flume after October 2014.</td></tr>
<tr><td>Period on Record and Data Sources</td><td>February, 2013 – October, 2015 (instrumentation reports)
February, 2015 – October, 2015 (weekly reports)</td></tr>
<tr><td>Additional Information</td><td>Prior to October, 2014, it appears that data was collected from the pump barge in Grota da Vale (“Location A”). It is not clear whether the values are the pump rate or the discharge rate from an outlet pipe. It is possible that the flow was being measured in the concrete channel at the outlet of the Secondary Gallery (See below, “Alternative Location A”). After the construction of the left abutment concrete channel in October, 2014[58], flows appear to be measured using a flume at this location (“Location B”).</td></tr>
<tr><td colspan="2">Photo and Location</td></tr>
<tr><td> 

Approximate Location A. October 1, 2015 Samarco aerial image shown.</td><td> 

Alternative Location A. September 26, 2014 Samarco aerial image shown.</td></tr>
<tr><td> 
Photo from weekly report, week of October 25, 2015, showing Parshall flume (Location B).</td><td> 

Approximate Location B. October 1, 2015 Samarco aerial image shown.</td></tr>
</table>

Location 3: Grota da Vale

Data

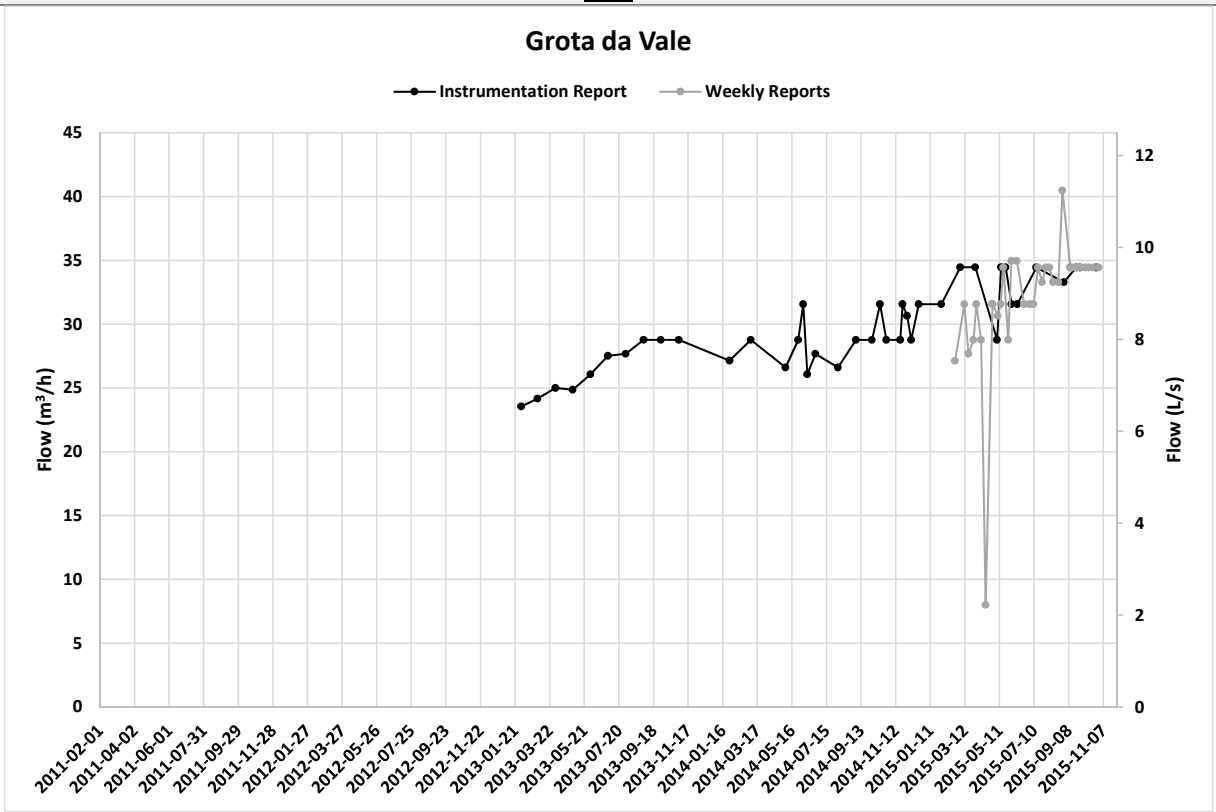

Measurements from Samarco instrumentation report and Samarco weekly operations reports. Note that not every weekly report in the given interval provides a flow measurement at this location.

Location 4: El. 855 m Drain	
Description	
Data Collection Method	Data collection method unknown.
Period on Record and Data Sources	November, 2014 – October, 2015 (instrumentation reports) February, 2015 – October, 2015 (weekly reports)
Additional Information	The El. 855 m drain was constructed in response to the seepage incident at the right abutment in 2014 (see Appendix B Attachment B1 and Attachment B8).
Photo and Location	

Photo from weekly report, week of October 25, 2015, showing concrete channel and drainage pipes leading from the El. 855 m drain.

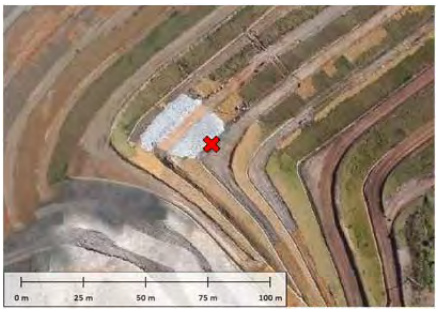

Approximate location. October 1, 2015 Samarco aerial image shown.

Data

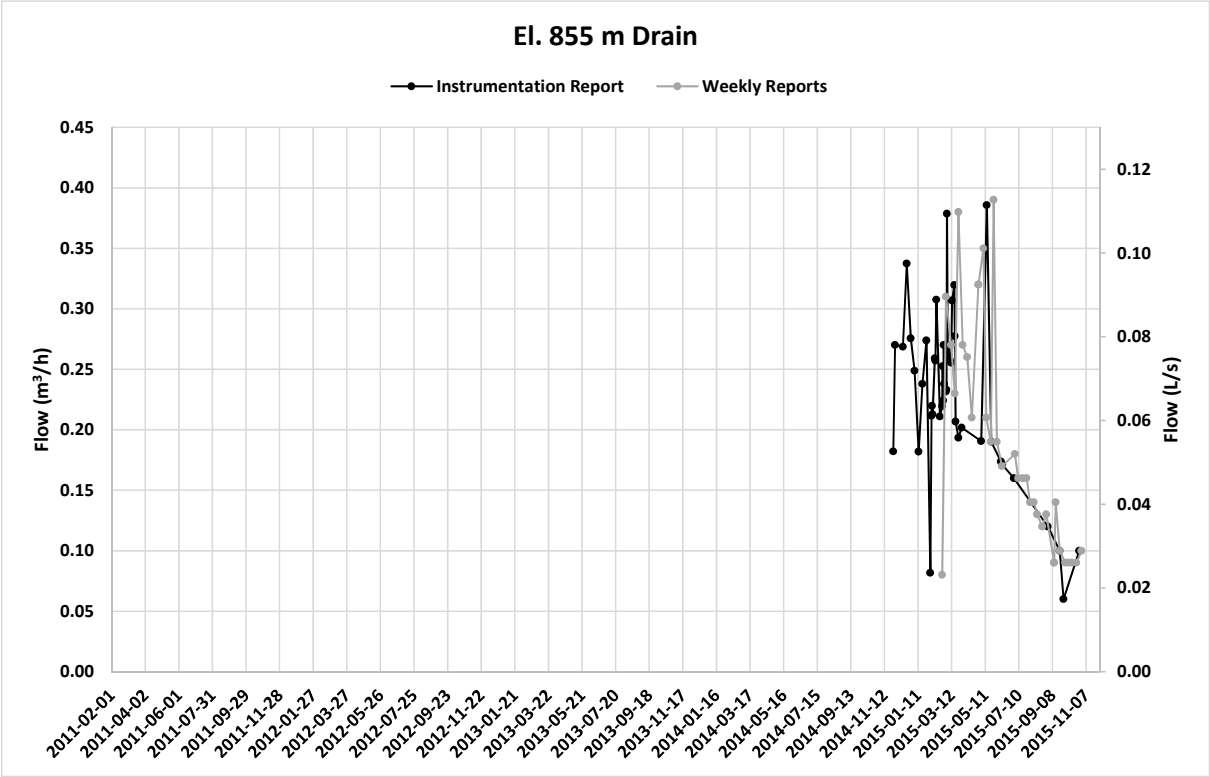

Measurements from Samarco instrumentation report and Samarco weekly operations reports. Note that not every weekly report in the given interval provides a flow measurement at this location.

Location 5: El. 860 m Drain	
Description	
Data Collection Method	Data collection method unknown.
Period on Record and Data Sources	January, 2015 – July, 2015 (instrumentation reports) February, 2015 – October, 2015 (weekly reports)
Additional Information	The El. 860 m drain was constructed in response to the seepage incident at the right abutment in 2015 (see Appendix B Attachment B1 and Attachment B8). According to weekly reports, flows were not reported from July, 2015 to the end of October, 2015 due to on-going work in the area.
Photo and Location	

Photo from weekly report, week of October 25, 2015, showing El. 860 m Drain.

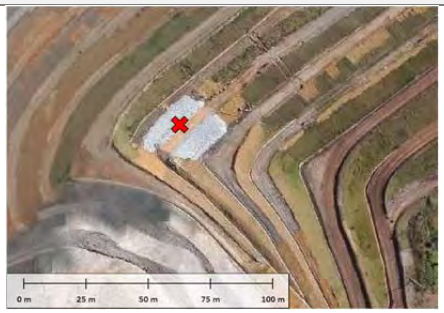

Approximate location. October 1, 2015 Samarco aerial image shown.

Data

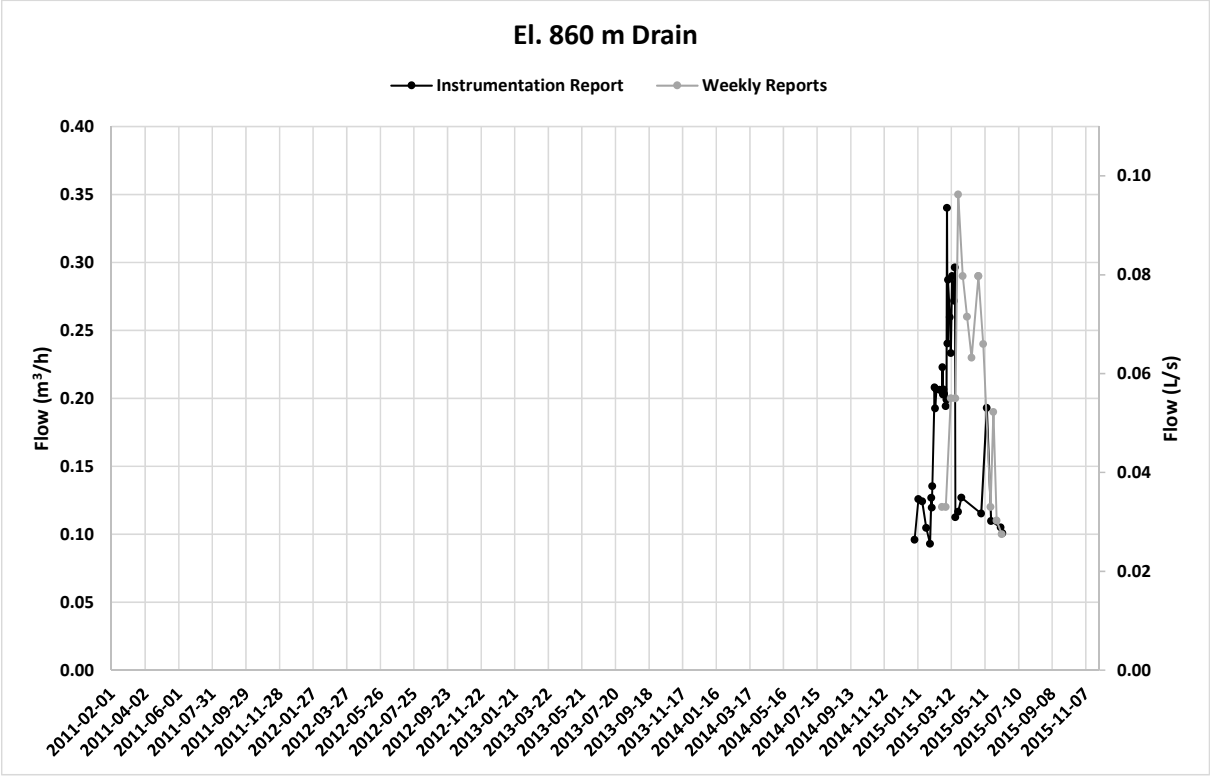

Measurements from Samarco instrumentation report and Samarco weekly operations reports. Note that not every weekly report in the given interval provides a flow measurement at this location.

Location 6: Borehole	
Description	
Data Collection Method	Measurements recorded from weir (pictured below).
Period on Record and Data Sources	December, 2014 – October, 2015 (instrumentation reports) February, 2015 – October, 2015 (weekly reports)
Additional Information	Flow monitoring station located downstream of the remnants of the Principal Foundation Drain. This is in the same area as the "Toe" piezometer group. Piezometers and this flow monitoring station were installed in March, 2015.
Photo and Location	

Photo from weekly report, week of October 25, 2015, showing weir.

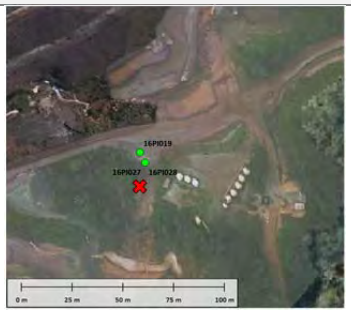

Approximate location. October 1, 2015 Samarco aerial image shown.

Data

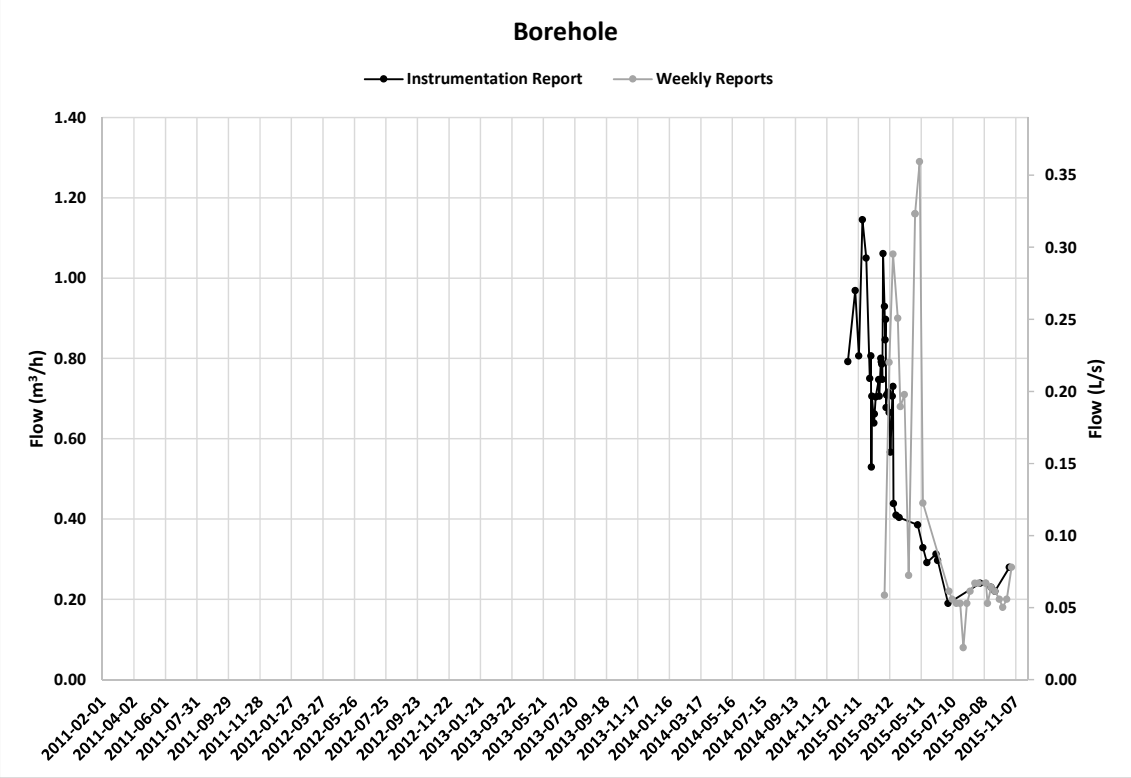

Measurements from Samarco instrumentation report and Samarco weekly operations reports. Note that not every weekly report in the given interval provides a flow measurement at this location.

ATTACHMENT E6

Survey Monument Data

Attachment E6
Survey Monument Data

TABLE OF CONTENTS

List of Figures

E.E6-1 SURVEY MONUMENTS ON SETBACK

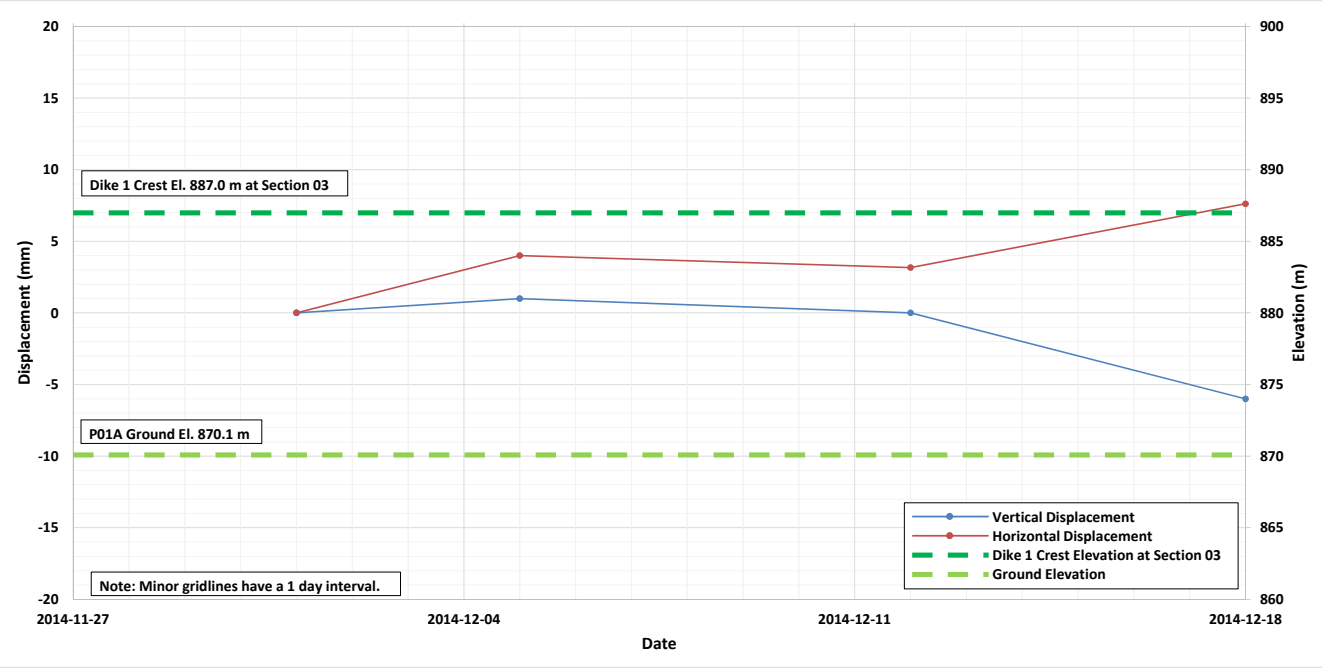

Figure E.E6-1 P01A displacement plot over time

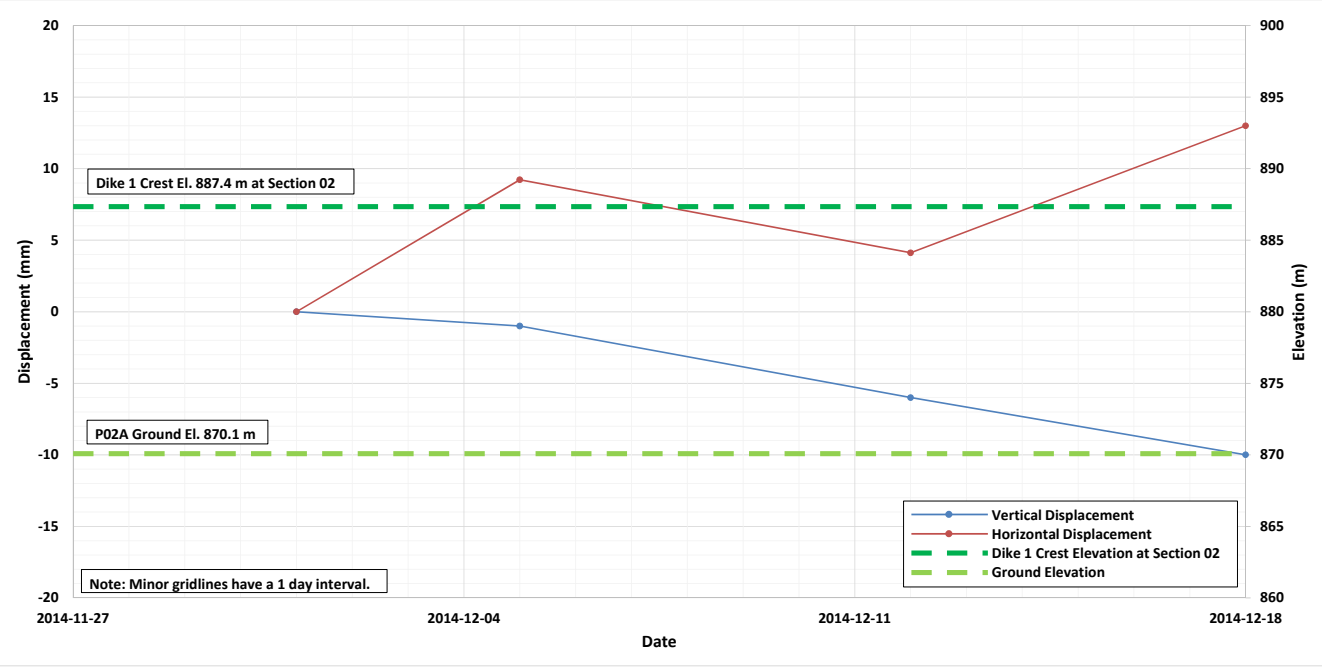

Figure E.E6-2 P02A displacement plot over time

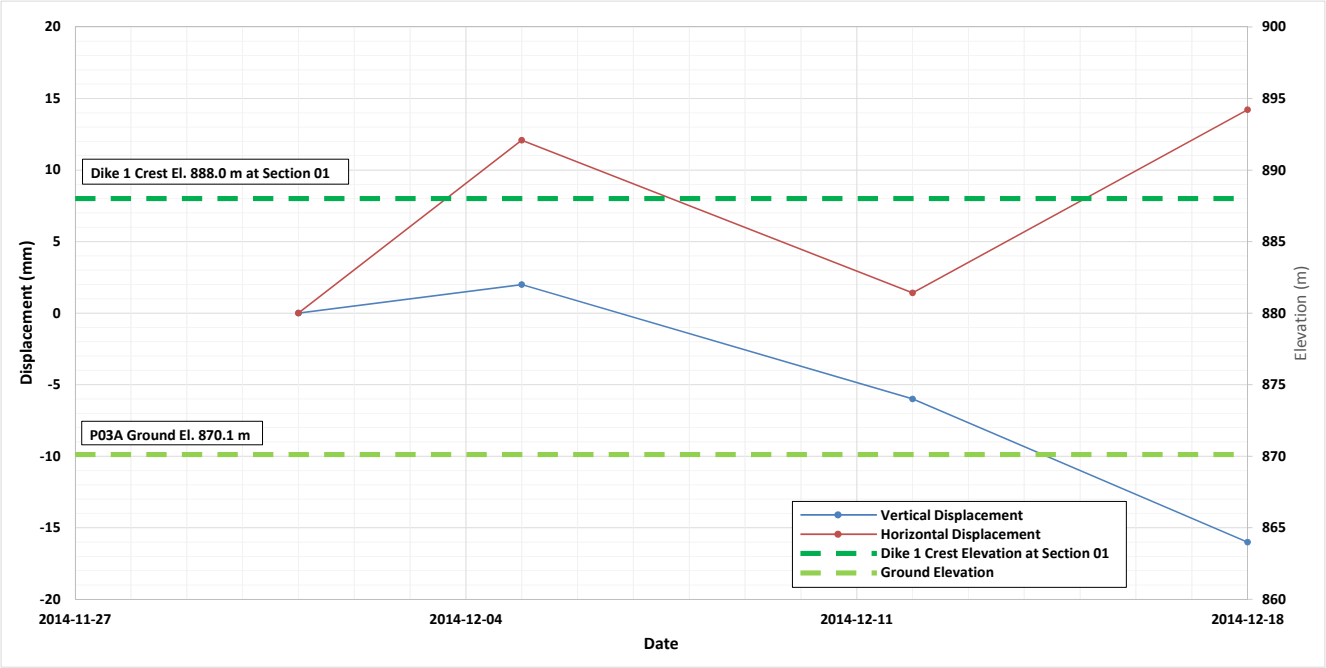

Figure E.E6-3 P03A displacement plot over time

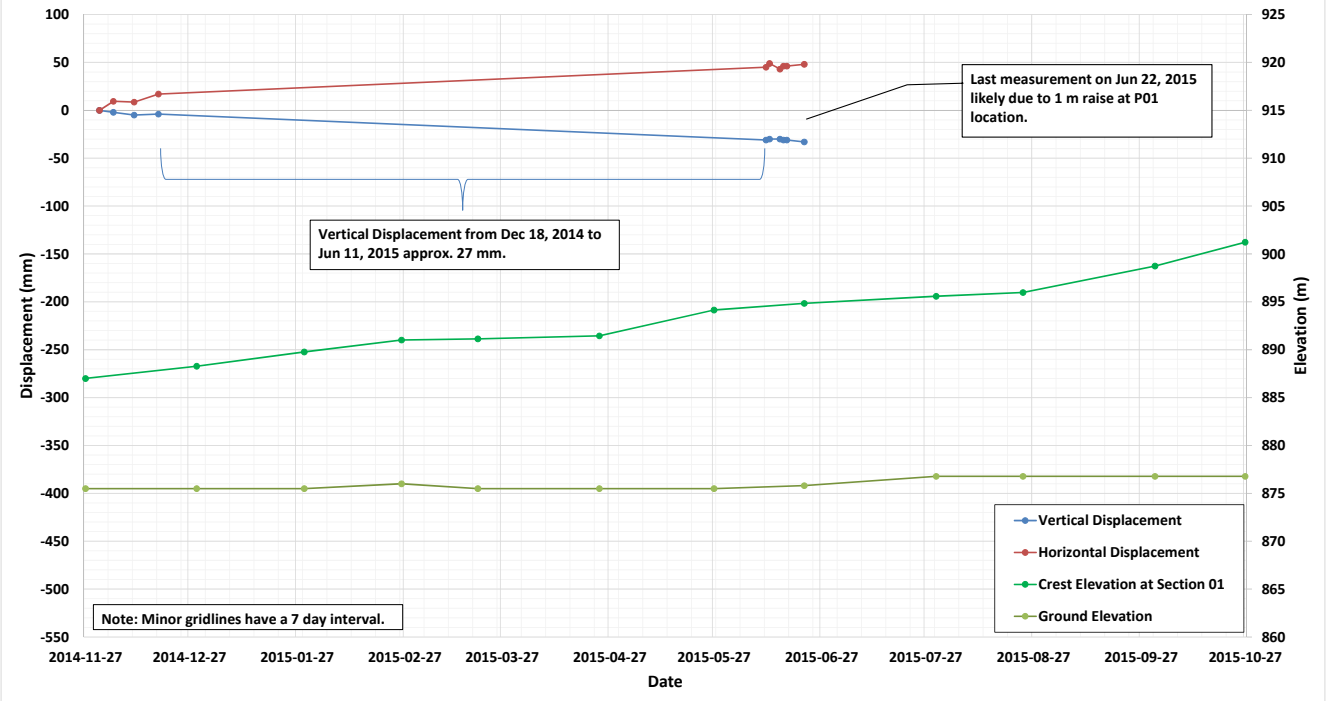

Figure E.E6-4 P01 displacement plot over time

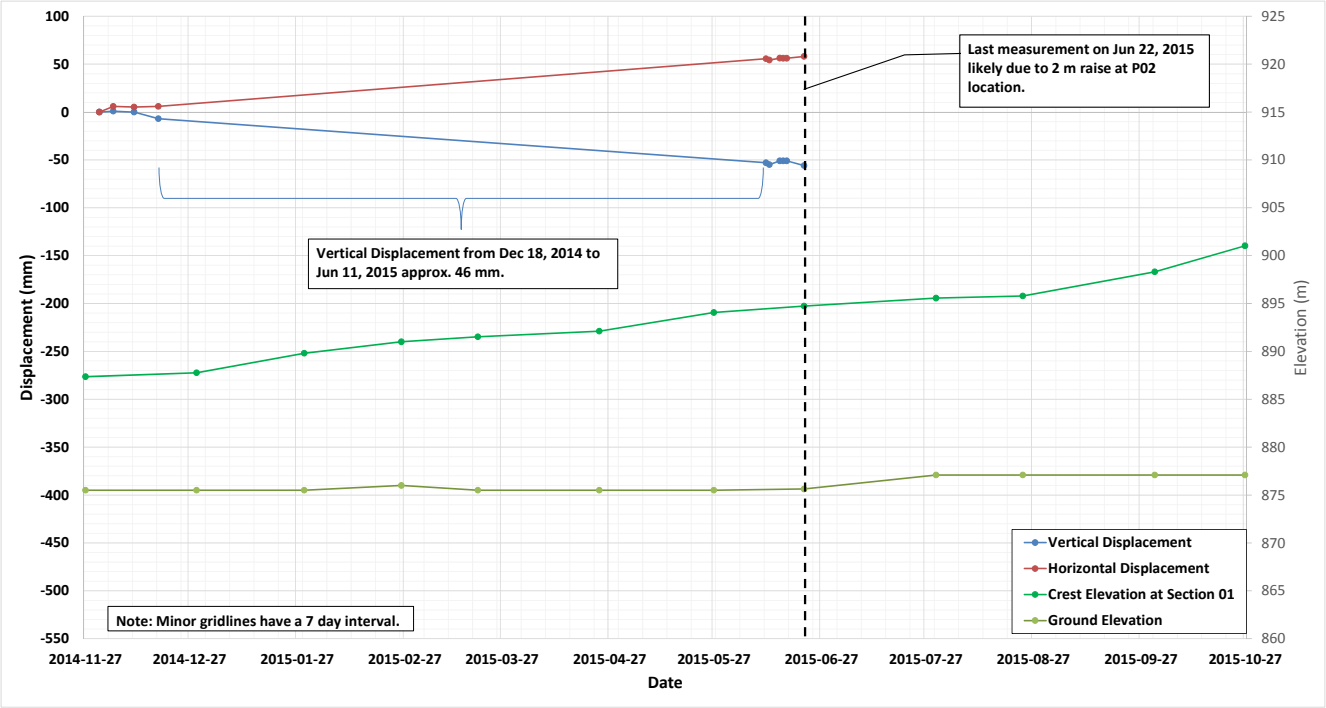

Figure E.E6-5 P02 displacement plot over time

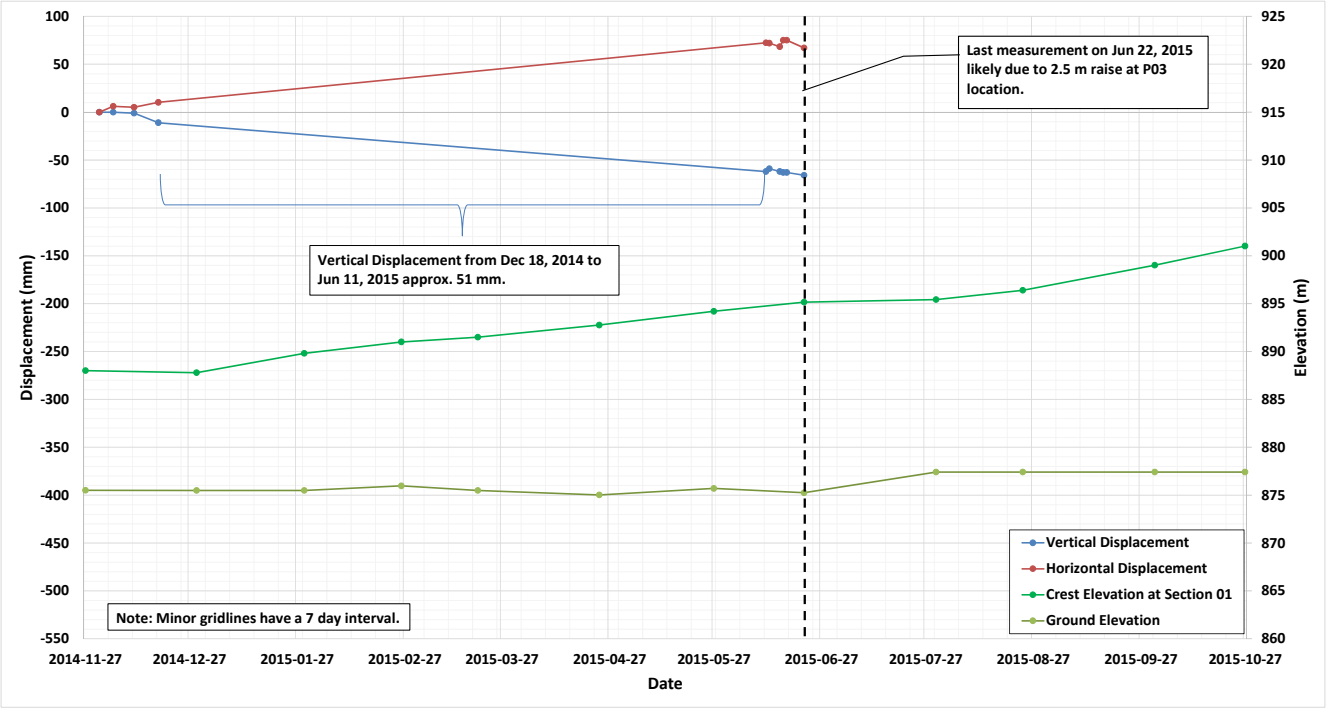

Figure E.E6-6 P03 displacement plot over time

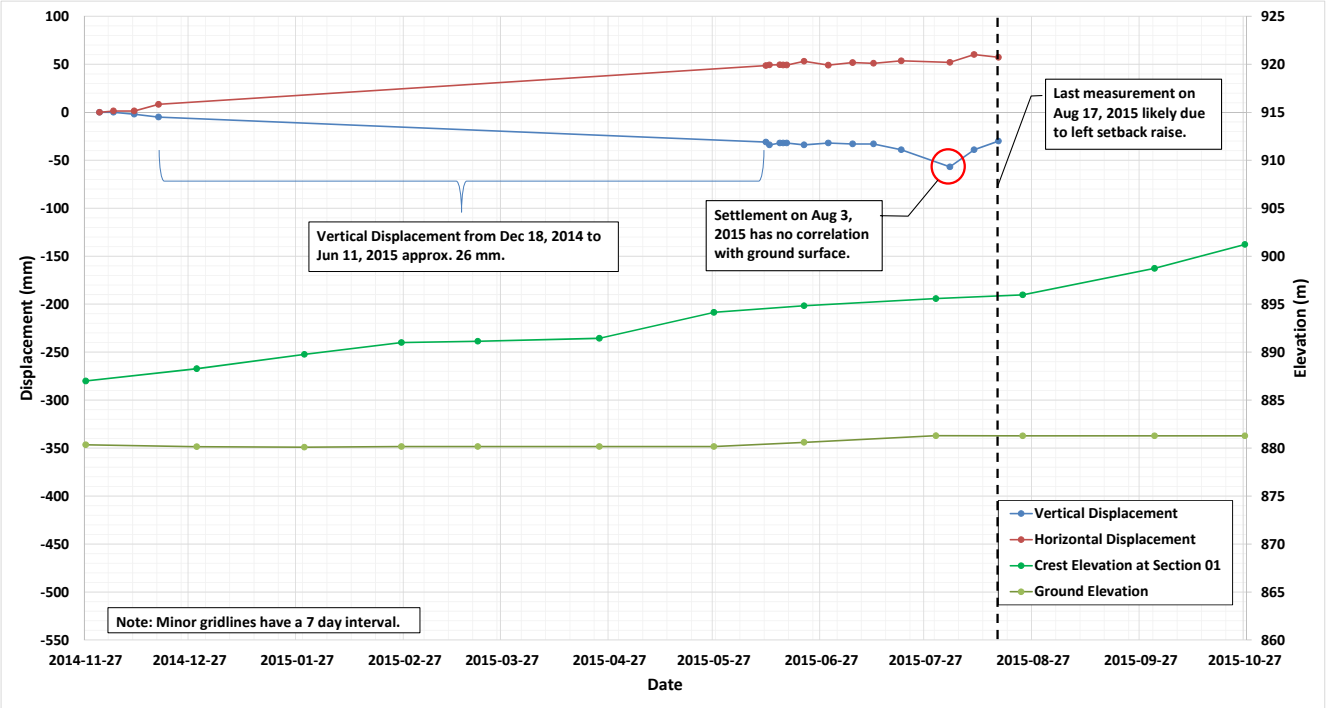

Figure E.E6-7 P04 displacement plot over time

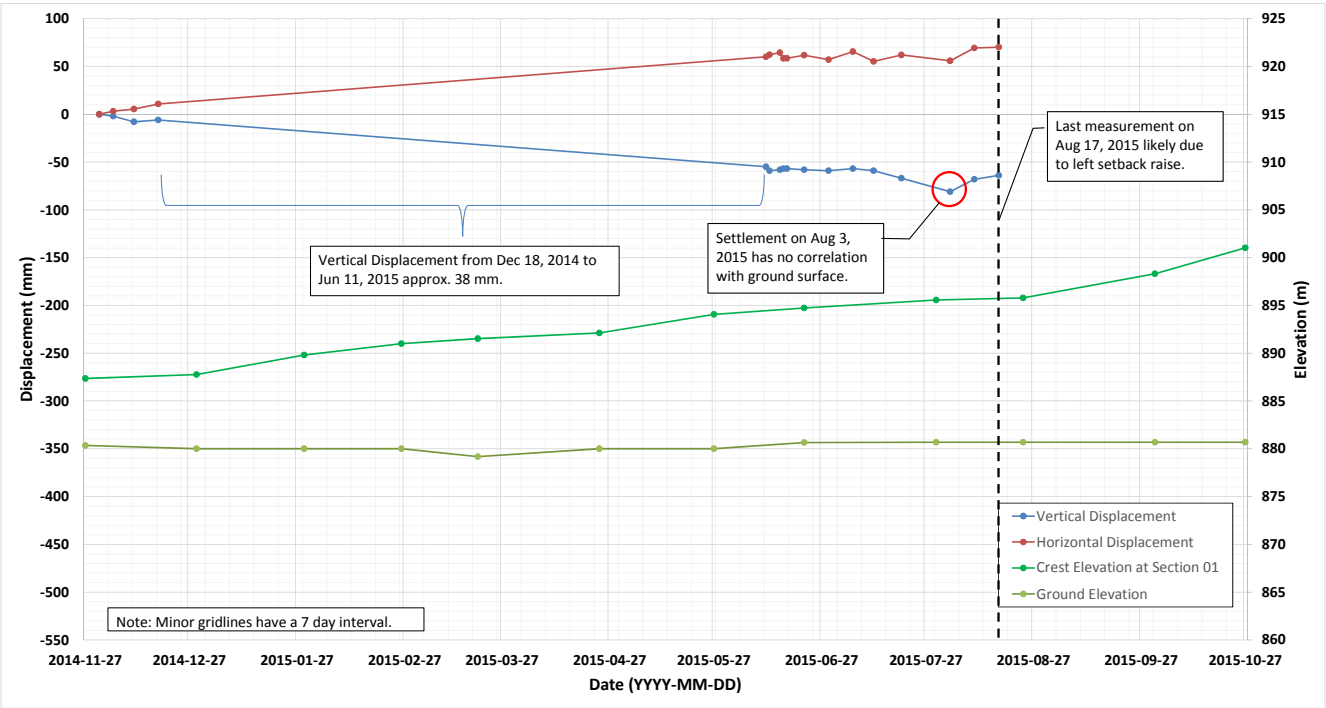

Figure E.E6-8 P05 displacement plot over time

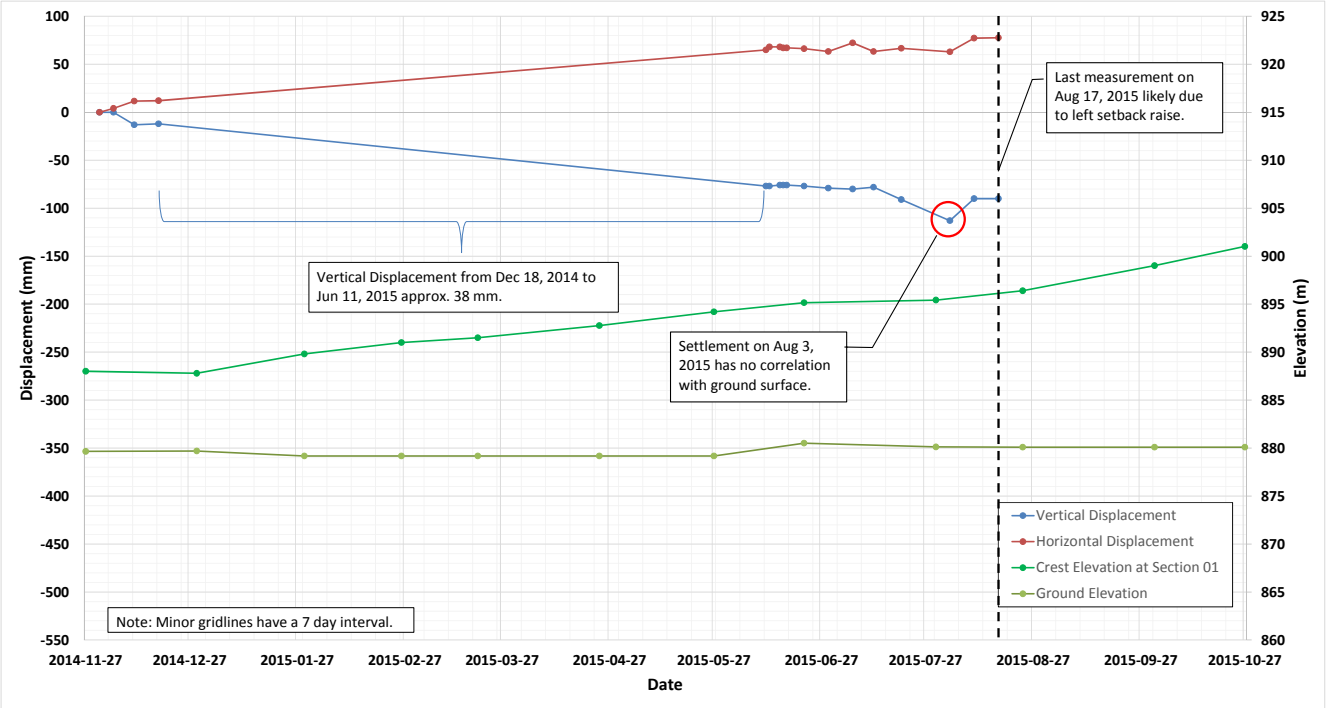

Figure E.E6-9 P06 displacement plot over time

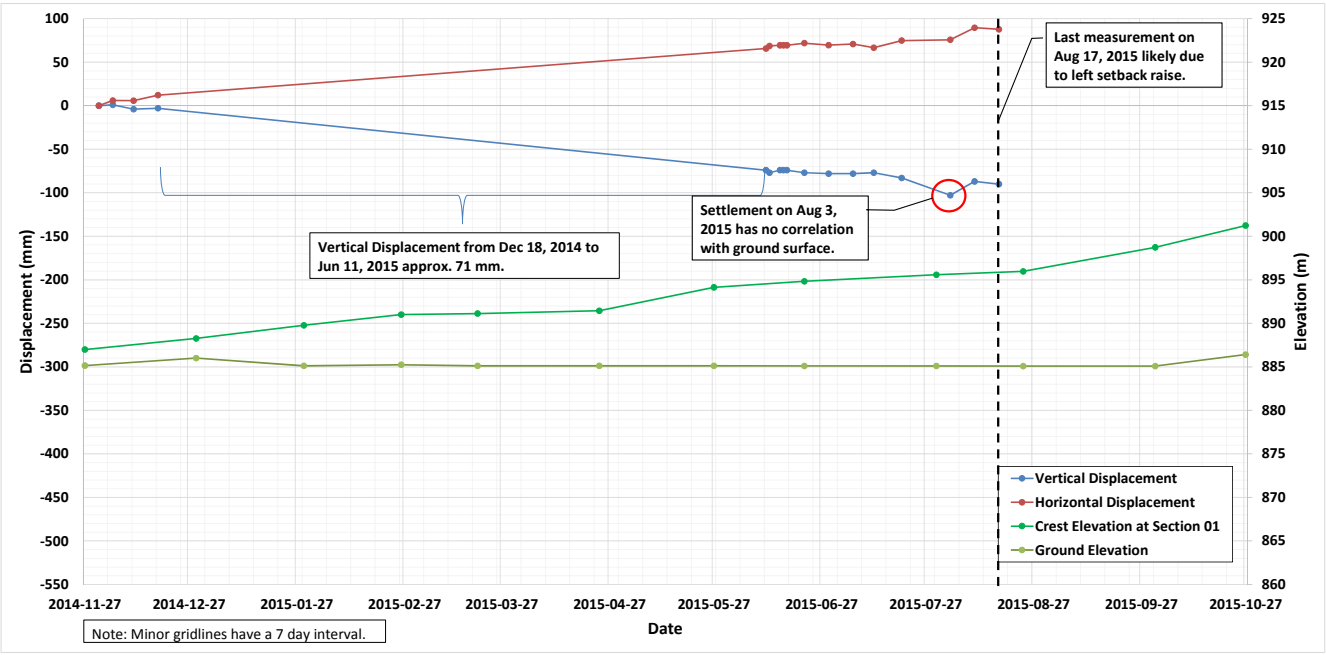

Figure E.E6-10 P07 displacement plot over time

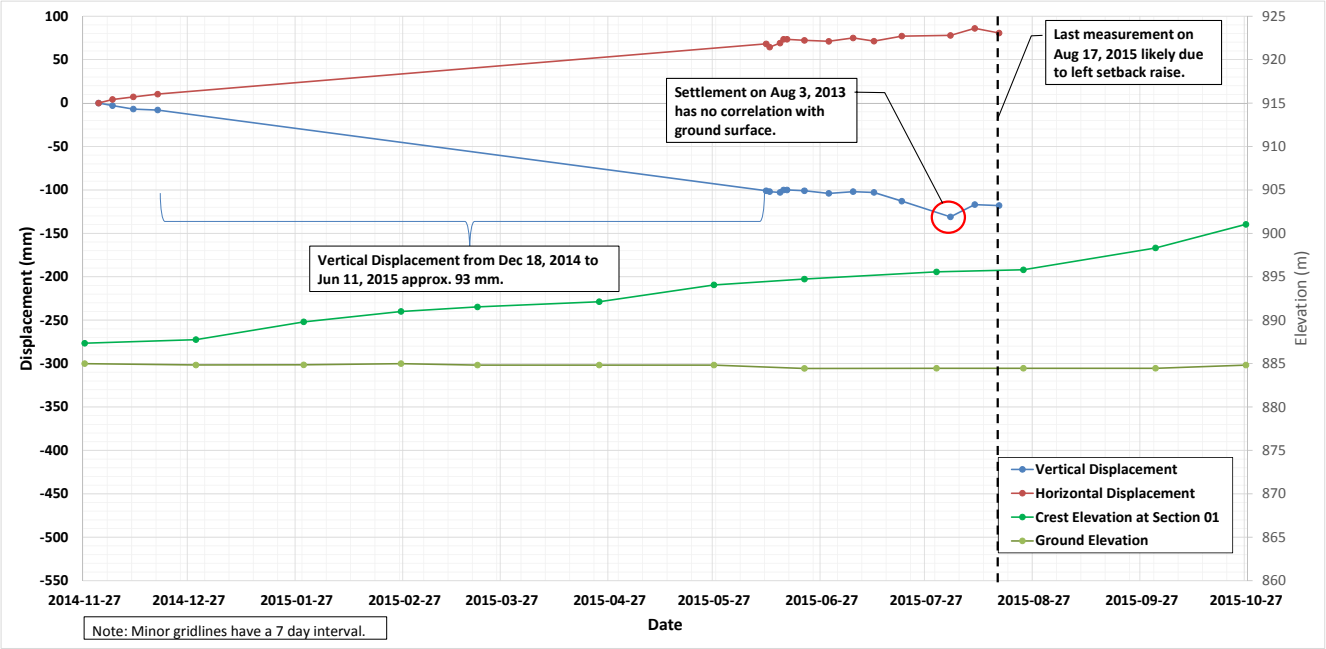

Figure E.E6-11 P08 displacement plot over time

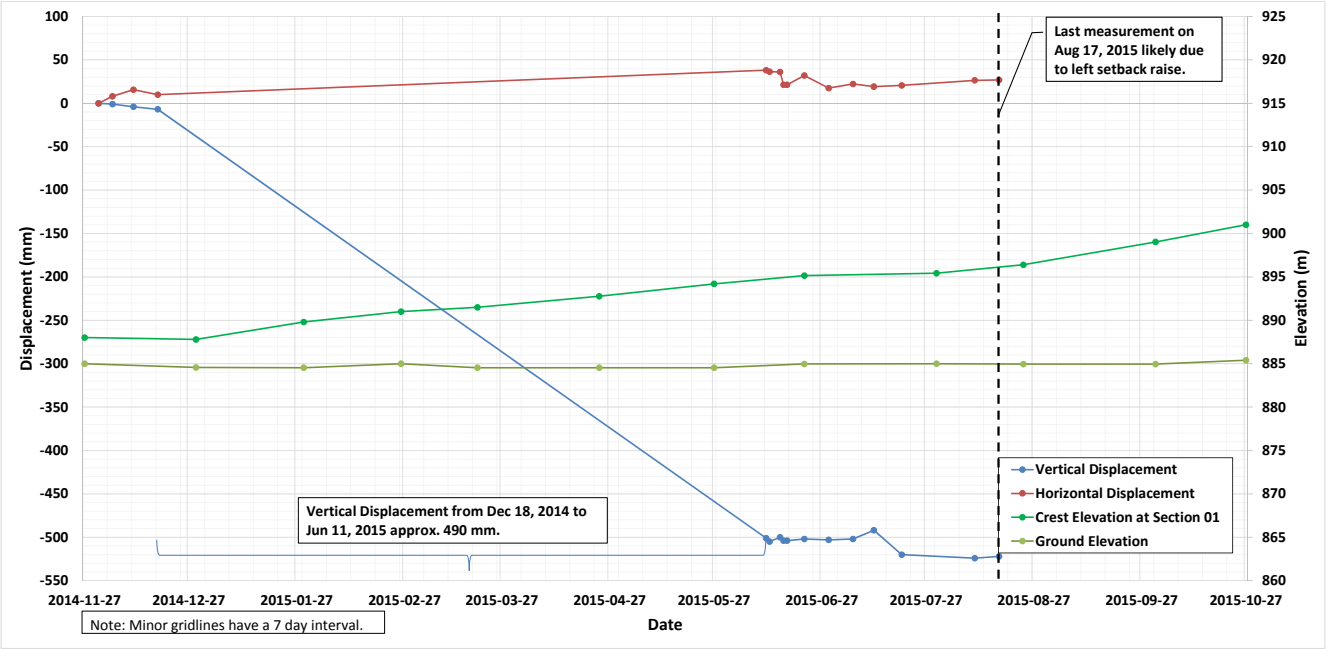

Figure E.E6-12 P09 displacement plot over time

E.E6-2 SURVEY MONUMENTS ON STARTER DIKE

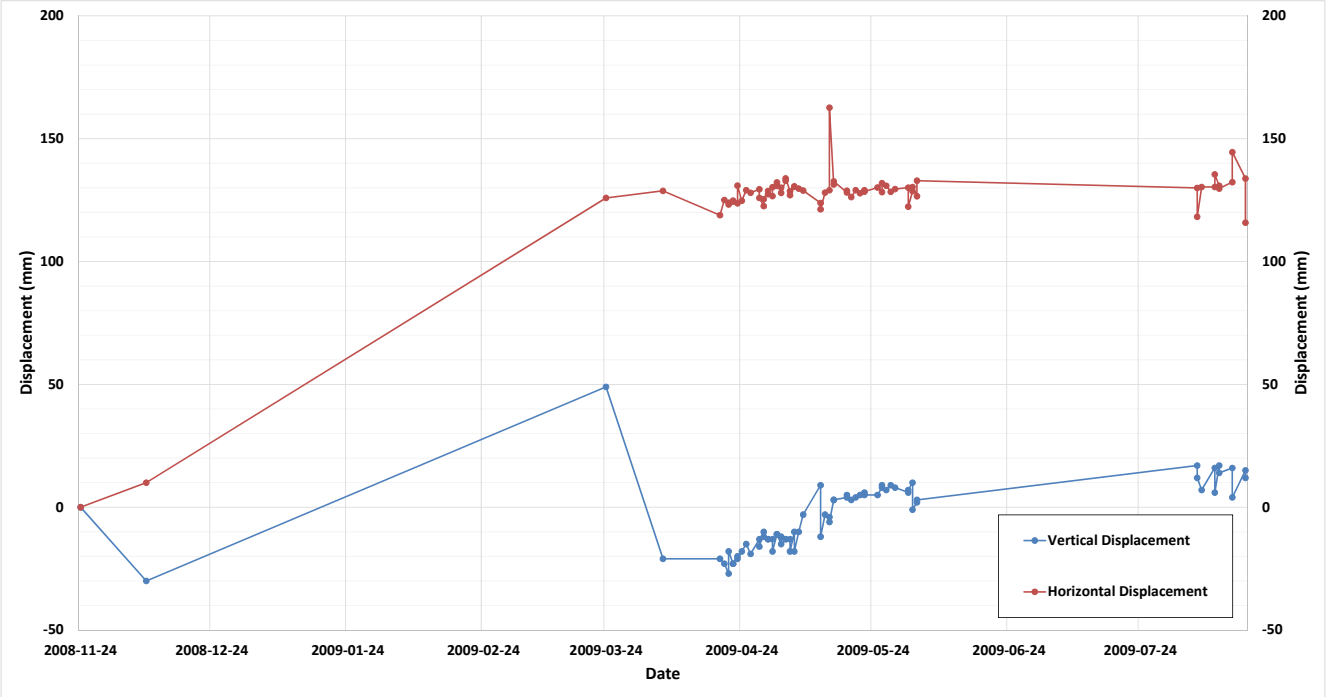

Figure E.E6-13 MS09 displacement plot over time

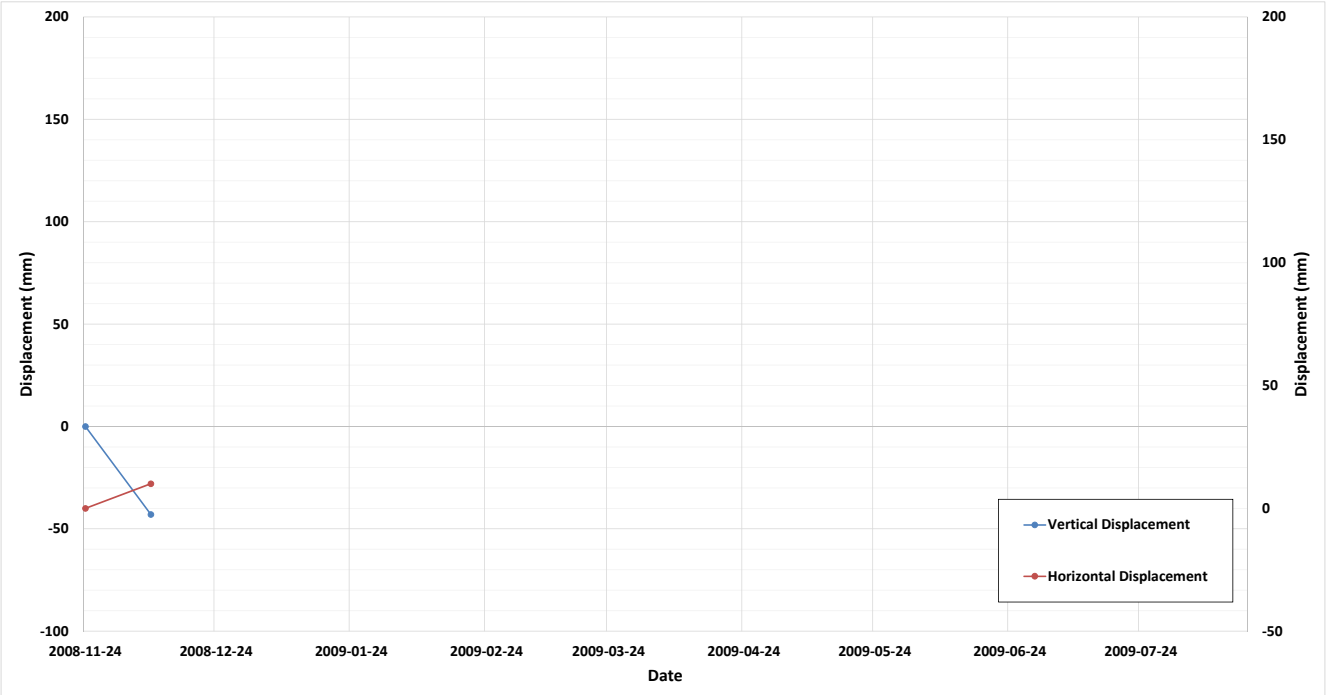

Figure E.E6-14 MS11 displacement plot over time

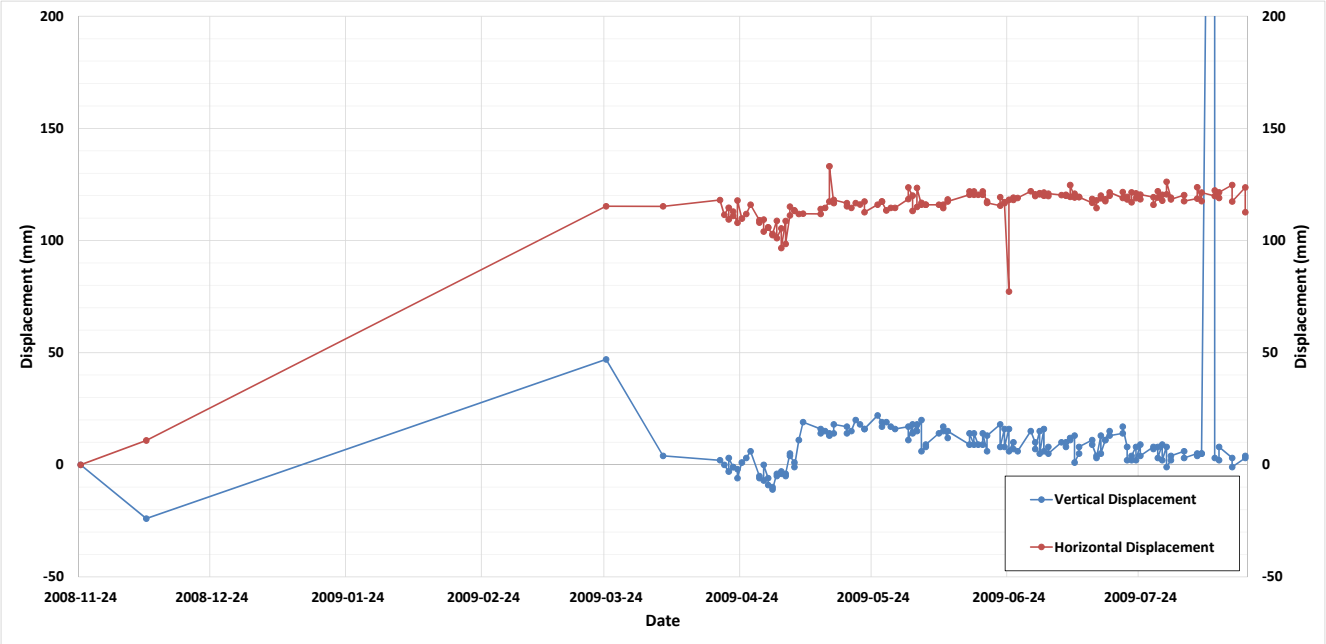

Figure E.E6-15 MS17 displacement plot over time

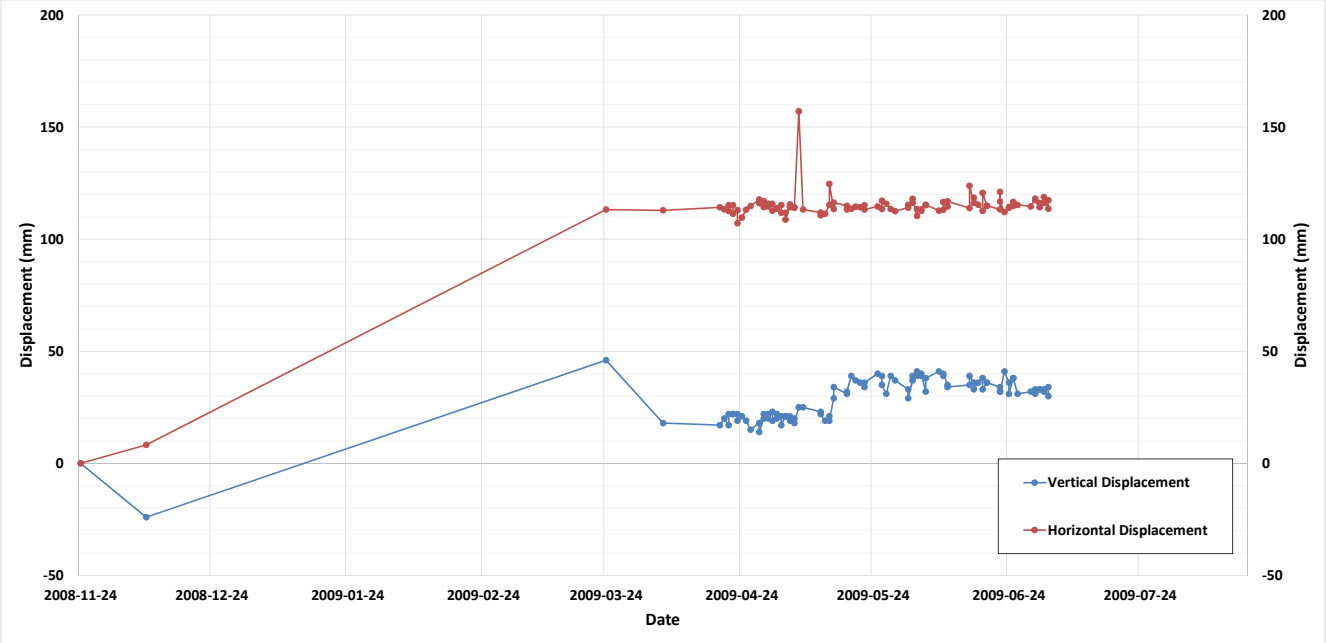

Figure E.E6-16 MS18 displacement plot over time

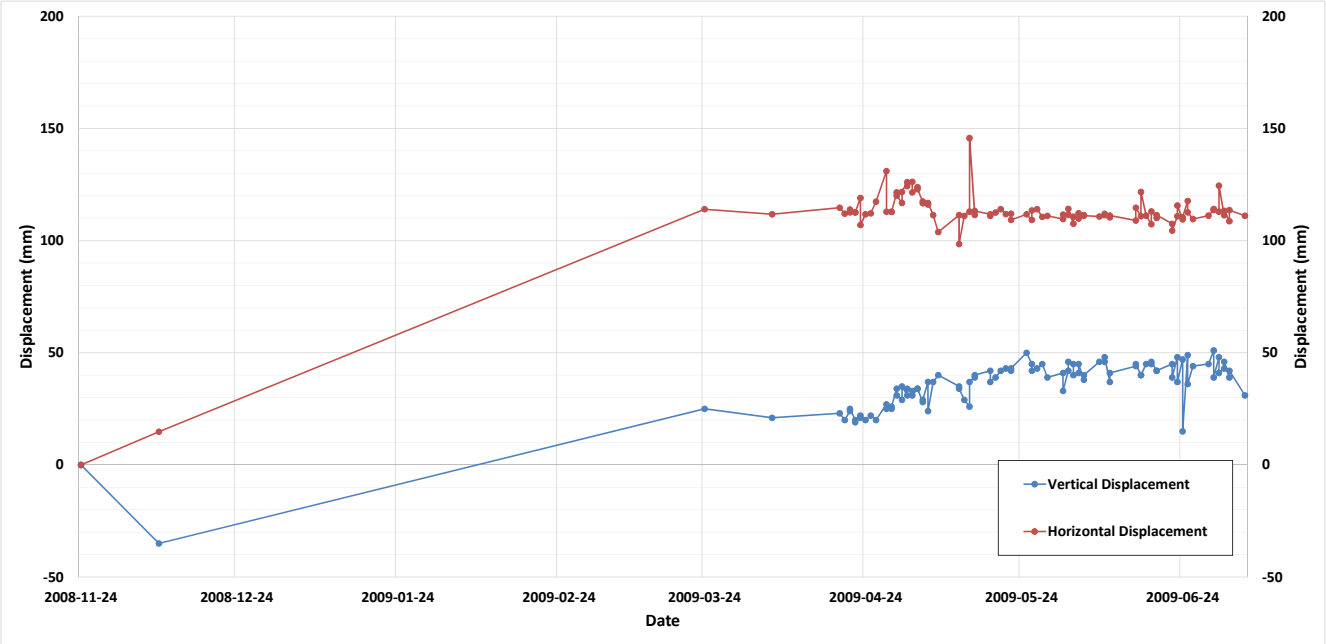

Figure E.E6-17 MS19 displacement plot over time

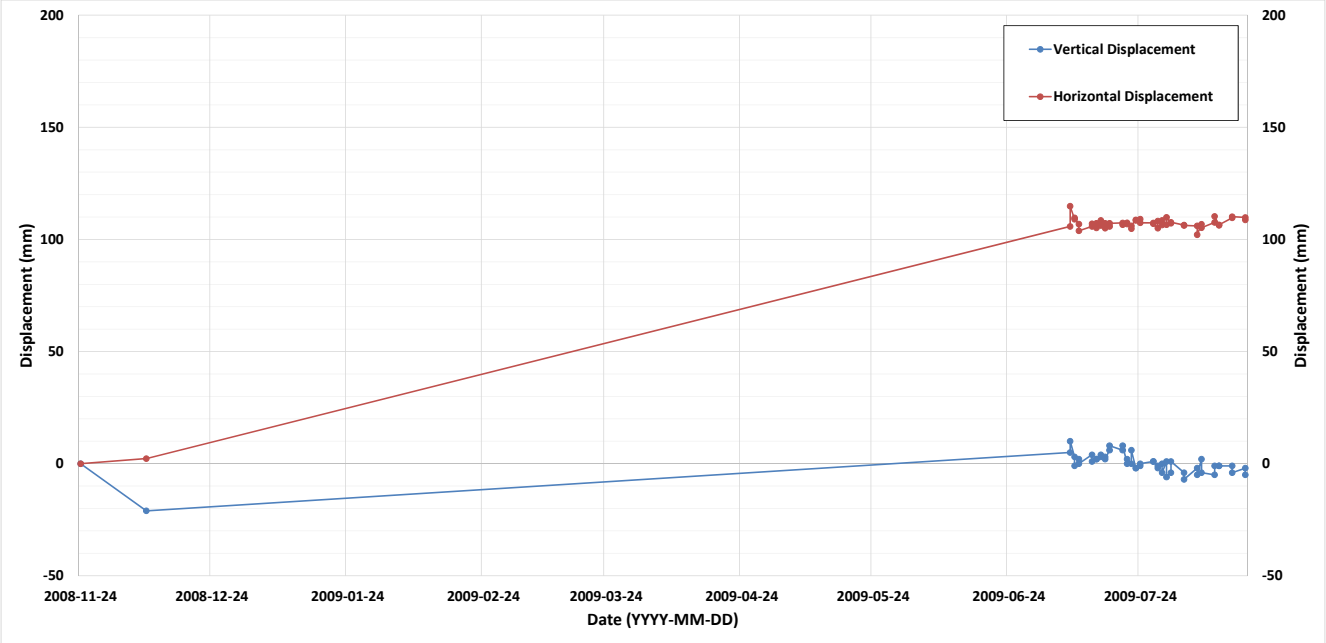

Figure E.E6-18 MS28 displacement plot over time

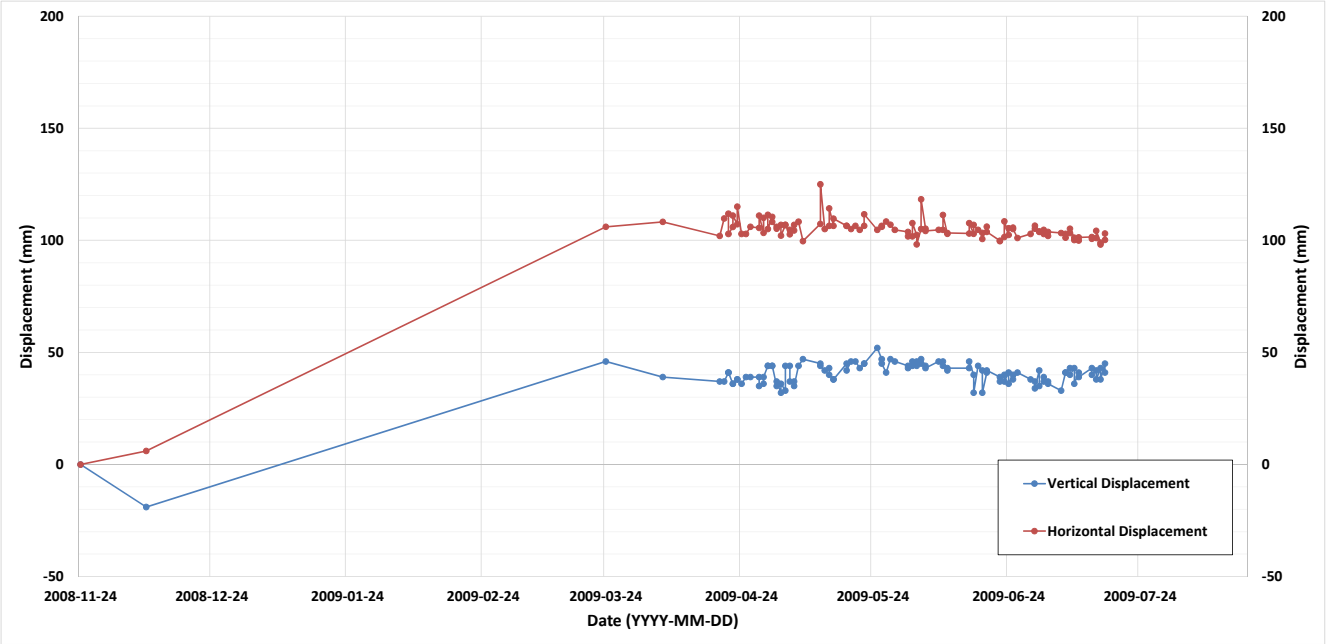

Figure E.E6-19 MS29 displacement plot over time

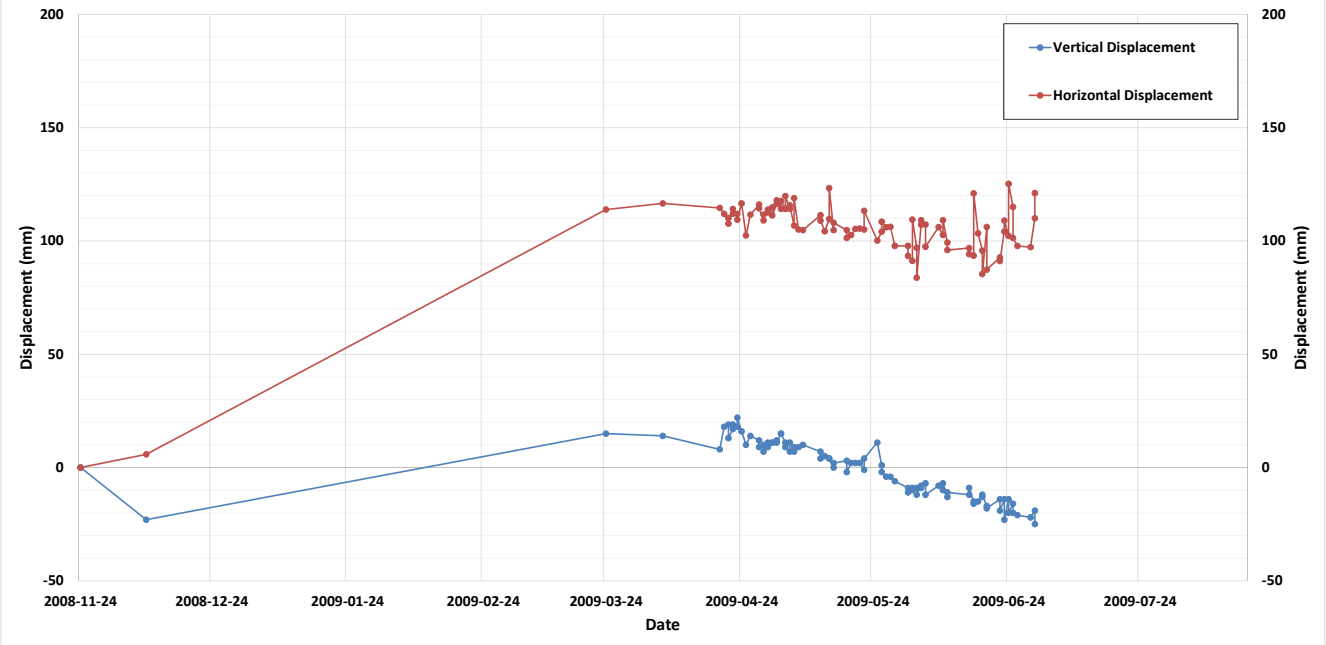

Figure E.E6-20 MS30 displacement plot over time

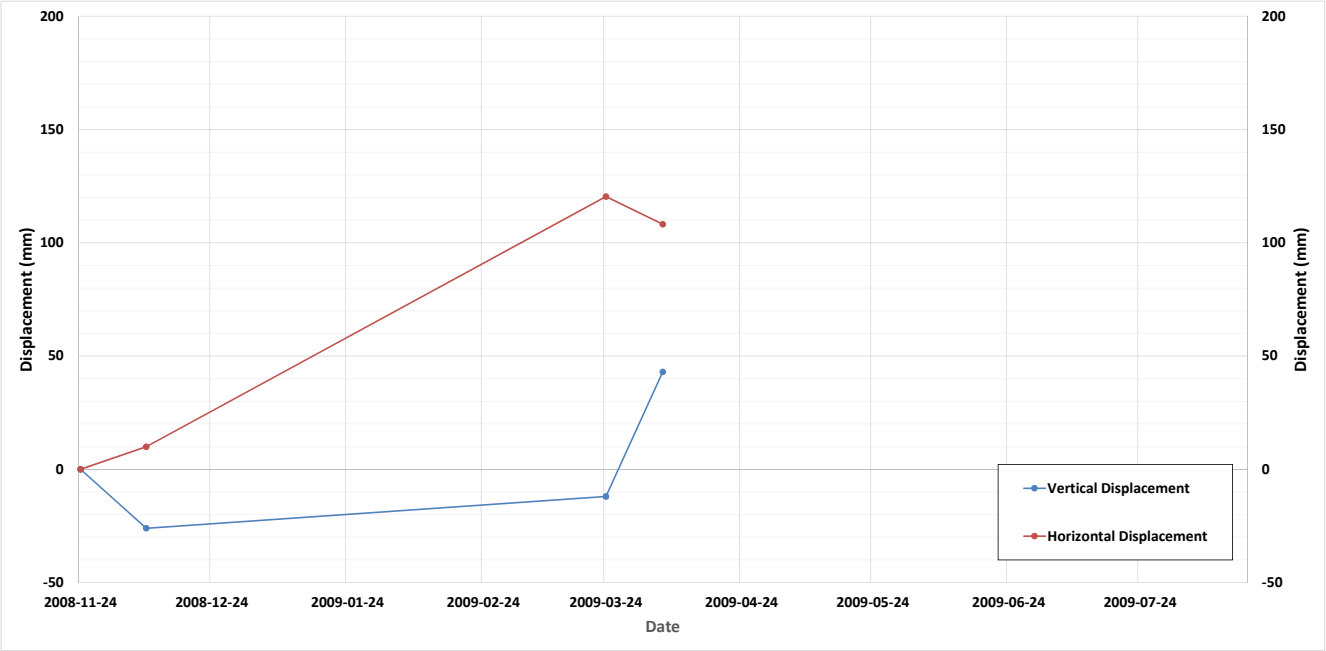

Figure E.E6-21 MS31 displacement plot over time

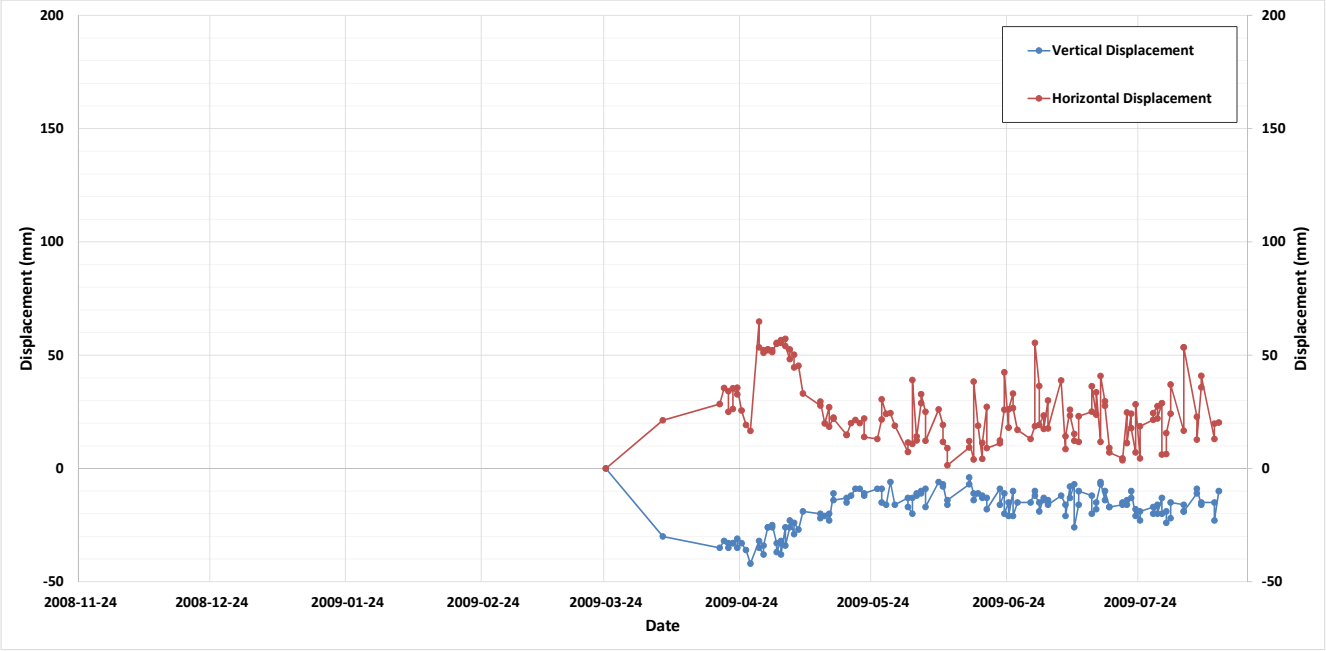

Figure E.E6-22 MS32 displacement plot over time

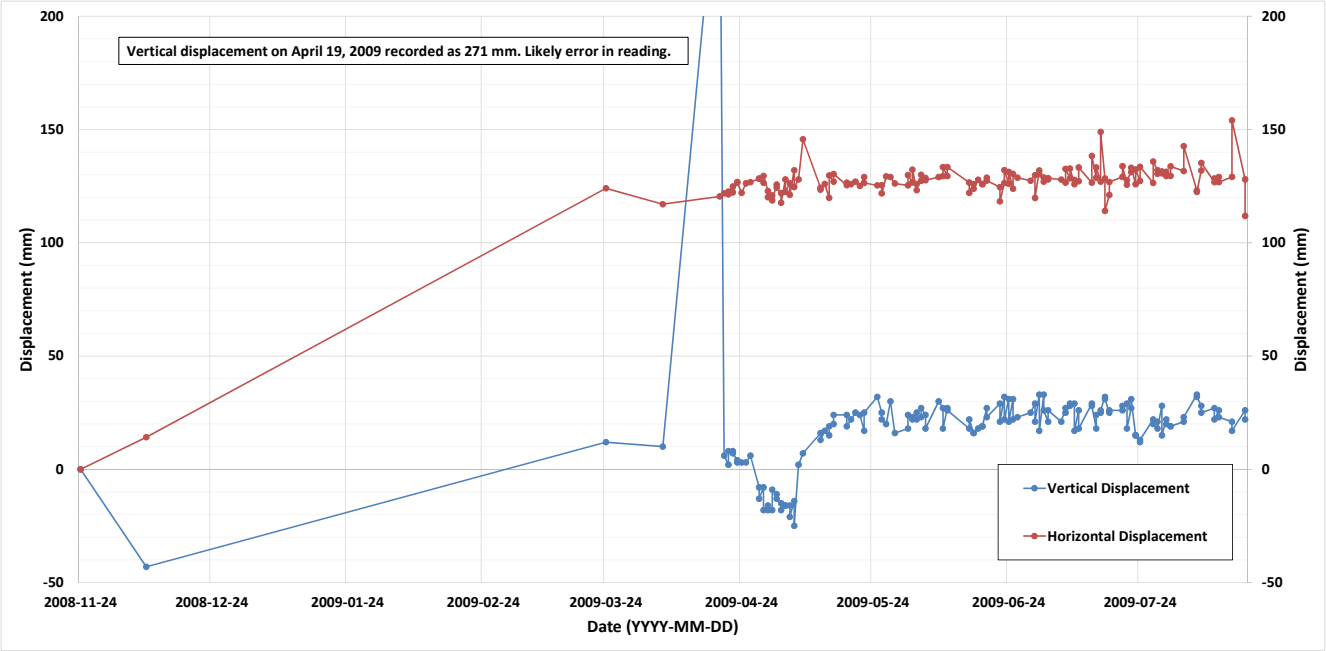

Figure E.E6-23 MS33 displacement plot over time

APPENDIX E

Samarco Field Monitoring Data

Appendix E
Samarco Field Monitoring Data

TABLE OF CONTENTS

List of Tables

List of Figures

TABLE OF CONTENTS

(continued)

List of Attachments

E1 INTRODUCTION

This appendix presents the Samarco field monitoring data reviewed by the Panel. The instrument types installed at Dike 1 were Casagrande and vibrating wire piezometers, water level indicators (standpipes), survey monuments, and flow monitoring stations. Inclinometers were installed in the Starter Dam but were destroyed in 2009 during the remediation of Dike 1. The main source of data are Samarco's monthly instrumentation reports, described in Appendix A. Instruments installed in Dike 2 are not included in this appendix as they were not used in the Panel's seepage or stability analyses.

Casagrande piezometer and water level indicator readings were reported in the monthly instrumentation reports. These reports are organized by cross section, as shown in plan in Attachment E1. Prior to 2014 there were nine cross sections named AA, BB, DD, FF, HH, JJ, LL, MM, and NN from the right abutment (west) to the left abutment (east). JJ is the highest section. New piezometers were installed on the left abutment setback after the August, 2014 incident. The setback piezometers were added to the monthly instrumentation reports after August, 2014 and were organized along three new sections, 01 (west), 02 (center), and 03 (east).

Additional piezometers were installed for specific purposes and were not grouped along the instrumentation report section lines. The "spillway" group was installed after the 2015 seepage incident at the right abutment to monitor the piezometric levels in the area of the El. 860 m and El. 855 m local surface drains. The "toe" group was installed to monitor artesian pressures downstream of the Fundão toe drain (ground El. 792 m). The "left abutment" group (one piezometer) was installed at the same time as the setback piezometers and is located east of Section 03 through schist. The piezometers in these three groups were reported in the monthly instrumentation reports for the "Spillway Section", "Toe of the Fundão Dam", and "Return Axis" (left abutment setback).

In 2011 and 2012, vibrating wire piezometers were installed to monitor the performance of the El. 826 m blanket drain. These piezometers are numbered PA-001 through PA-039. They are organized along three section lines named A, B, and C, parallel to those in the instrumentation reports but at different locations along Dike 1. In each of the sections, piezometers were installed above and below the El. 826 m blanket drain[41]. Many of the instruments were damaged shortly after installation and the remainder were not read after May, 2015 because the readout box was stolen and had not been replaced prior to the dam failure. The data is presented in the sections below, but section lines A, B, and C are not shown to avoid confusion with the instrumentation report section lines.

The El. 826 m blanket drain was drained with 27 pipes ("Kananets®") that discharged to a concrete channel on the El. 820 m bench. The flow from the drain was monitored using a flume located at the end of the concrete channel on the right abutment. Flow monitoring data from the Kananets® and five other locations at the Fundão Dam were reported in Samarco's weekly reports (described in Appendix A) and in the monthly instrumentation reports.

Survey monuments were installed on the left abutment after the August, 2014 incident and were included in the same Samarco spreadsheets as were used to create the monthly instrumentation reports. Survey monuments were also installed in the Starter Dam.

E2 PIEZOMETERS AND WATER LEVEL INDICATORS

E2.1 General

The Panel reviewed the following data sources:

- Samarco monthly instrumentation reports.
  - These reports are organized along section lines. They include plots for each of the piezometers along the section, cross sections and plan views showing the instruments referenced in the report, and raw data. Some of the reports also include flow monitoring data and survey monument data, discussed in Sections E3 and E4, respectively. In some cases, piezometers damaged prior to the date of the instrumentation report are still included in the report for reference.
  - The most recent monthly instrumentation reports are from November, 2015 with the exception of the "toe" group. The data for this group was obtained from the October, 2015 instrumentation report.
  - Instrumentation report records are discussed in Section E2.2.1.
- Vibrating wire piezometer[1] readings in Samarco's Microsoft Excel document.
  - Vibrating wire piezometer readings are included in some early instrumentation reports. Vibrating wire piezometer data were not included in the 2015 instrumentation reports but are available in a separate Microsoft Excel document (as described in Appendix A Attachment A1). The vibrating wire piezometers have records up to May 7, 2015. After this date the readout box was stolen and not replaced prior to the dam failure.
  - An earlier version of this Excel document contains almost identical records but the period on record ends on February 20, 2014. The earlier version includes readings from two dates (February 14 and 20, 2015) that are not included in the later version. The data from the later version is presented in the appendix because it has a longer period on record. The two extra dates from 2014 given in the earlier version are not included.
  - Vibrating wire piezometer records are discussed in Section E2.2.1.
- Samarco's instrumentation plan[42] shows an additional piezometer, 16LI018, discussed in Section E2.2.4.

[1] Because field installation records were not reviewed, it is not known whether vibrating wire piezometers were installed directly in test holes or later to monitor water levels remotely in standpipes/Casagrande piezometers.

- A secondary source, referred to as the Instrument Measurement Spreadsheet, also contains piezometer readings. This document is described in Appendix A Attachment A1. The readings from this document are discussed in Section E2.3.
- Installation records for the instruments were reviewed to obtain the installation date and to verify locations, when available. An additional Samarco spreadsheet[41] also contains installation dates. The installation dates for the vibrating wire piezometers were obtained from [44].
- MDGEO's Hydrogeological Study on the 940 m Raise[7] and Samarco's 2012 OMS Manual[1] were used to verify locations of instruments.

In general, instruments with the letters "LI" in the name are water level indicators, meaning that they were constructed using perforated plastic pipe for the full depth of the instrument. Readings from water level indicators give the depth of the phreatic surface at the instrument location. Instruments with the letters "PI" in the name are Casagrande piezometers, meaning that they have perforated pipe only at the base of the instrument, creating a sealed cell at that depth. Readings from Casagrande piezometers give the pore-water pressure at the location of the cell. Vibrating wire piezometers (reported in a Samarco spreadsheet[45]) are named "PA-0XX". Readings from vibrating wire piezometers give the pore-water pressure at the location of the piezometer tip.

Readings for 22 of the Casagrande piezometers and water level indicators were automatic. The remainder of the instruments, including the left setback piezometers and the vibrating wire piezometers, were read manually. Instruments with automatic readings are listed in a Samarco spreadsheet[46] and are identified in Attachment E4. In a March, 2016 interview, a Samarco employee stated readings from some automatic piezometers were also taken manually due to discrepancies with the automatic readings. It is not known which piezometers showed this discrepancy between manual and automatic readings. Maintenance was in progress on the automatic piezometers between November 2, 2015 and November 5, 2015. No automatic readings are available from this period.

All functioning piezometers, whether manual or automatic, were read on October 26, 2015. This is the most complete data set prior to failure. Some automatic readings from November 2, 2015 were recovered after the failure.

E2.2 Data Presentation

E2.2.1 General

The Samarco piezometer records have been reorganized and are presented in four attachments to this appendix. The attachments provide records for 47 Casagrande piezometers, 30 water level indicators, and 39 vibrating wire piezometers.

The attachments and assumptions or limitations are as follows:

- Attachment E1 – Dike 1 Piezometer Plan:

- Instruments listed in the most recent Samarco instrumentation reports and vibrating wire piezometers are shown. Additional piezometers, as described in the sections below, are also included for reference.
- Vibrating wire piezometers installed at the same location in plan are grouped in "clusters".
- In some instances, different types of instruments (water level indicators, Casagrande piezometers, and vibrating wire piezometers) are located next to each other such that one symbol type overlaps the other. Water level indicators (blue) are shown on top, Casagrande piezometers (green) are below, and vibrating wire piezometers (orange) are on the bottom.
- Refer to Attachment E4 for a full list of piezometer names and types.

- Attachment E2 – Sections:
  - Sections were taken along the same alignments as used in Samarco's monthly instrumentation reports.
  - Piezometers not located along an instrumentation report section line are not included in this attachment. This includes the spillway, toe, and left abutment groups, as well as the vibrating wire piezometers.
  - Readings shown in the sections are the most recent reading for each instrument prior to failure on November 5, 2015. Instruments with no readings in October or November, 2015 are shown in grey.
- Attachment E3 – Piezometer Records, Reservoir Level, and Rainfall Plots:
  - Data sources for each instrument are listed in Attachment E4.
  - The reservoir rate of rise was estimated using monthly topography surveys and aerial images as described in Appendix B.
  - Rainfall records were provided in a Samarco spreadsheet[47] and in the monthly instrumentation reports.
  - Vibrating wire piezometers installed at the same location in plan are grouped in "clusters" as shown in Attachments E1 and E4.
- Attachment E4 – List of Piezometers and Water Level Indicators at Dike 1:
  - Lists instrument type, identifies automatic or manual readings, and gives period on record, installation dates, and data sources for all piezometers included in this appendix.

E2.2.2 16LI017

Water level indicator 16LI017, located on Section 02, has been labelled as "unreliable" in Attachments E2 through E4. Readings from this instrument are consistently 10 m to 13 m below those from neighboring piezometers 16PI014 and 16PI015, when it should give higher readings. Post-failure interviews and information provided by Samarco indicate that the top of hole elevation given

for this piezometer was in error. An updated elevation was provided. However, the data from this piezometer was not used by the Panel.

E2.2.3 16PI026

Casagrande piezometer 16PI026, from the "spillway" group, has been labelled as "unreliable" in Attachments E3 and E4. The coordinates from the instrumentation report and the installation log[48] do not match. The plan view in the instrumentation report shows the piezometer on the El. 857 m bench and the report states that the top of pipe is El. 865 m. The installation log puts the piezometer on the El. 861 m bench and reports a ground elevation of 860.69 m and a top of pipe elevation of 861.75 m. The similarity between the elevation from the installation log and the topographic survey indicates that the piezometer is likely at this location, and it has been shown as such in this appendix.

However, the top of pipe elevation given in the instrumentation reports, used to calculate the piezometric level, is El. 865 m. This is much higher than the ground elevation at either location. The data from this piezometer is therefore considered unreliable and was not used by the Panel.

E2.2.4 16LI018

Water level indicator 16LI018, located on Section 02, appears in Samarco's instrumentation plan[42]. This instrument is not shown in plan or section in the November, 2015 instrumentation report for the left abutment and does not have readings in this document or in the Instrument Measurement Spreadsheet (described in Section E2.3). This instrument is located beside the functioning Casagrande piezometer 16PI007. The lack of records from 16LI018 does not influence the Panel's analysis. The instrument is circled below on Figure E2-1.

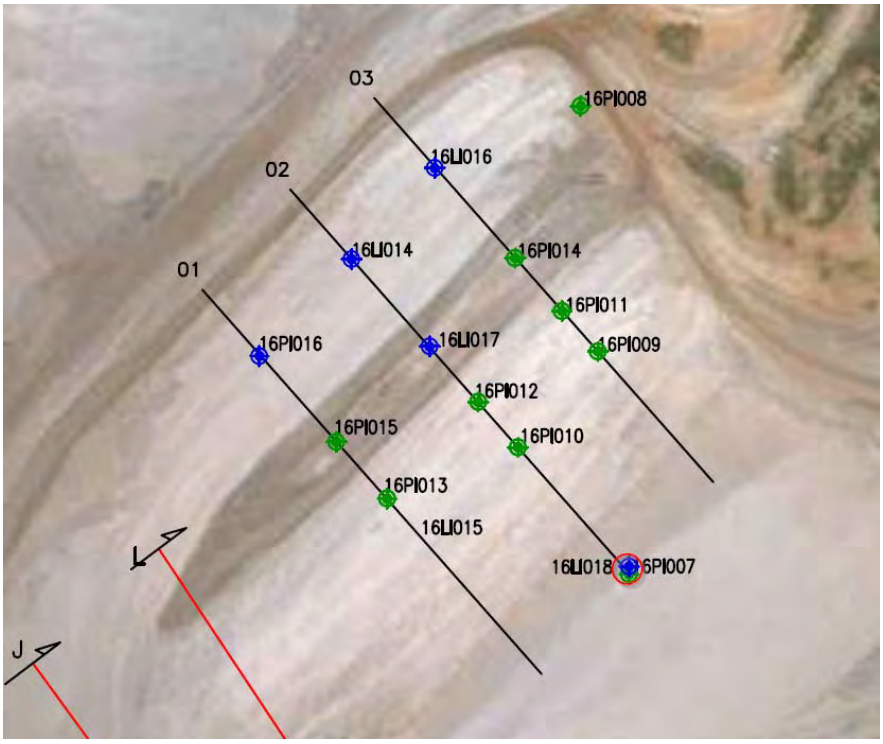

Figure E2-1 Zoom of Samarco instrumentation plan showing 16LI018

E2.2.5 PA-017 and PA-018

Vibrating wire piezometer locations PA-017 and PA-018 each have two sets of records[44], as follows:

- The first data set for both piezometers has records from February 8, 2011 to October 9, 2014. This data is saved on the tabs “PA-017” and “PA-018” of the Samarco spreadsheet.
- The second data set for both piezometers has records from February 8, 2011 to July 5, 2012. This data is saved on the tabs “PA-017 (2)” and “PA-018 (2)” of the Samarco spreadsheet.

There is only one installation log available for each piezometer. Both data sets report common tip elevations for the same piezometers. The records for the overlapping period between data sets do not match. There is no consistent offset between the data sets. It is unclear why there are two sets of readings for these piezometers. Both data sets are included in Attachment E3 for reference.

E2.3 Instrument Measurement Spreadsheet

E2.3.1 General

Piezometer readings from 53 instruments at Dike 1 are included in a secondary Samarco file separate from the instrumentation reports. The Panel reviewed the data included in this file for completeness. Of the 53 instruments:

- 46 instruments with the same name are reported in the instrumentation reports with a different period on record. See Section E2.3.2.
- 7 instruments are listed that are not included in the instrumentation reports. See Section E2.3.3.

E2.3.2 Overlapping Data

Records from 22 piezometers and 24 water level indicators included in the November, 2015 instrumentation reports are also included in the Instrument Measurement Spreadsheet. These instruments and their period on record from the Instrument Measurement Spreadsheet are listed in Table E2-1.

Table E2-1 Instruments with overlapping records

Name	Period on Record from the Instrument Measurement Spreadsheet (YYYY-MM-DD)	
	Start	End
16LI001	2013-06-11	2015-08-31
16LI002	2013-06-11	2015-08-31
16LI003	2013-06-11	2014-12-29
16LI004	2013-06-11	2015-09-28
16LI005	2013-06-11	2015-01-12
16LI006	2013-06-11	2015-01-12
16LI007	2013-06-11	2014-08-04
16LI008	2013-06-11	2015-01-12
16LI012	2014-08-21	2014-12-01
16LI014	2014-10-20	2015-07-22
16PI016	2014-11-20	2015-07-22
16PI019	2015-03-10	2015-08-31
16PI027	2015-03-18	2015-08-31
24LI017	2010-04-05	2015-08-31
24LI018	2015-05-06	2015-08-31
24LI019	2010-10-07	2015-05-18
24LI020	2010-05-06	2015-01-30
24LI021	2010-06-24	2015-09-16
24LI022	2010-06-24	2015-02-06
24LI023	2010-06-24	2015-02-06
24LI024	2010-04-21	2015-02-06
24LI025	2010-06-24	2012-02-06
24LI026	2010-04-23	2015-02-06
24LI027	2010-05-15	2015-01-12
24LI028	2015-05-28	2014-09-29
24LI029	2010-04-15	2013-09-09
24LI030	2010-04-17	2014-09-29
24PI039	2010-01-14	2015-09-10
24PI041	2010-01-14	2015-09-28
24PI044	2010-03-23	2015-05-11
24PI045	2010-03-19	2015-09-10

Name	Period on Record from the Instrument Measurement Spreadsheet (YYYY-MM-DD)	
	Start	End
24PI046	2010-08-31	2015-09-16
24PI047	2010-08-31	2015-09-16
24PI048	2010-03-10	2015-02-03
24PI049	2010-08-12	2014-12-01
24PI050	2010-08-12	2014-12-01
24PI051	2010-03-05	2014-08-04
24PI052	2010-07-26	2014-11-13
24PI053	2010-07-26	2014-12-01
24PI054	2010-03-01	2014-11-24
24PI055	2010-07-15	2014-11-24
24PI056	2010-07-15	2014-12-01
24PI058	2010-07-07	2014-12-01
24PI059	2010-07-07	2014-12-01
24PI060	2010-03-30	2014-12-01
24PI062	2010-05-28	2012-12-01

The Panel plotted data from three of the overlapping data sets. The comparison plots are shown below. The general trend and number of data points for the overlapping period were the same. There was a constant vertical offset in the plots for two of the three locations (24LI017 and 16LI003) that is attributed to a different top of pipe elevation in the two data sources. The data from the Instrument Measurement Spreadsheet includes some errant points as seen in the plots for 24LI017 and 24LI020. The Panel therefore chose to use the data from the instrumentation reports. The remainder of the overlapping data from the Instrument Measurement Spreadsheet is not presented as part of this appendix.

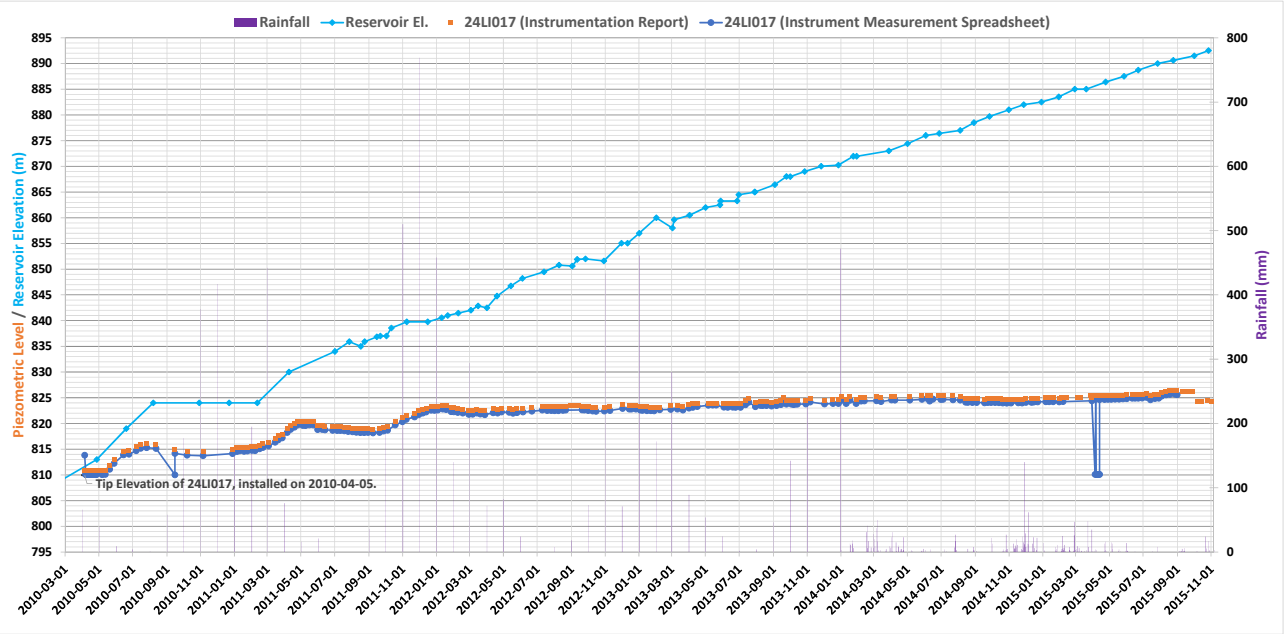

Figure E2-2 Piezometer data comparison for 24LI017

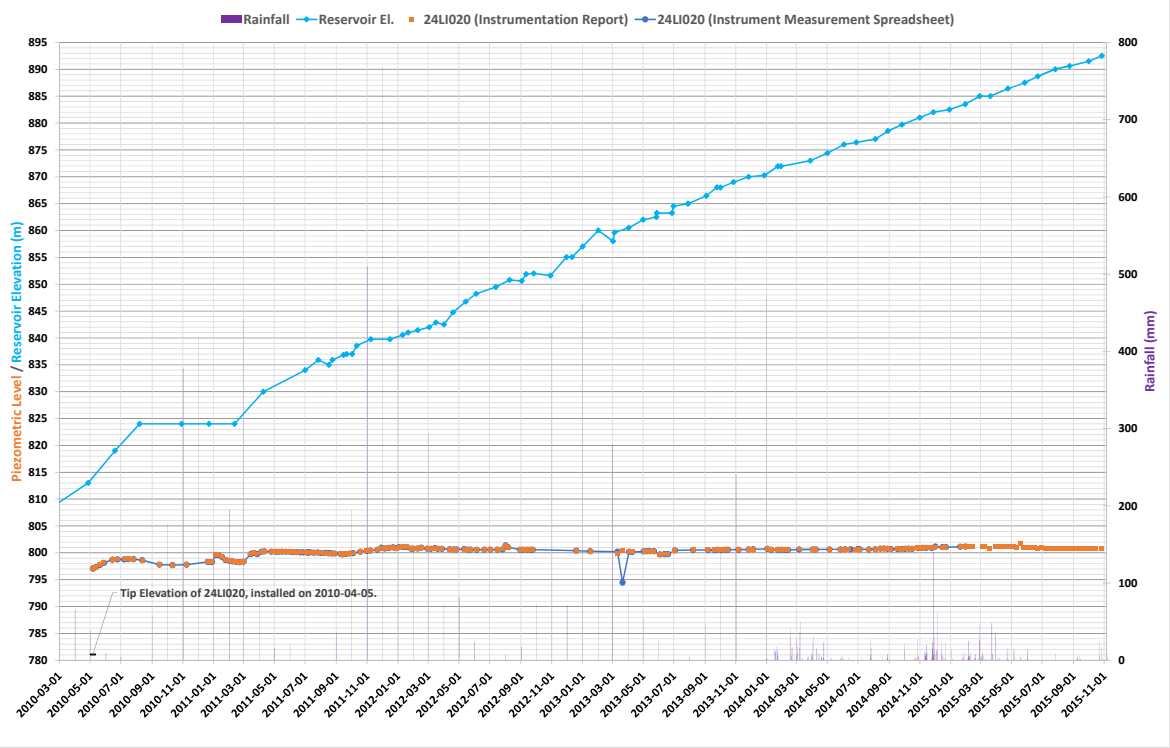

Figure E2-3 Piezometer data comparison for 24LI020

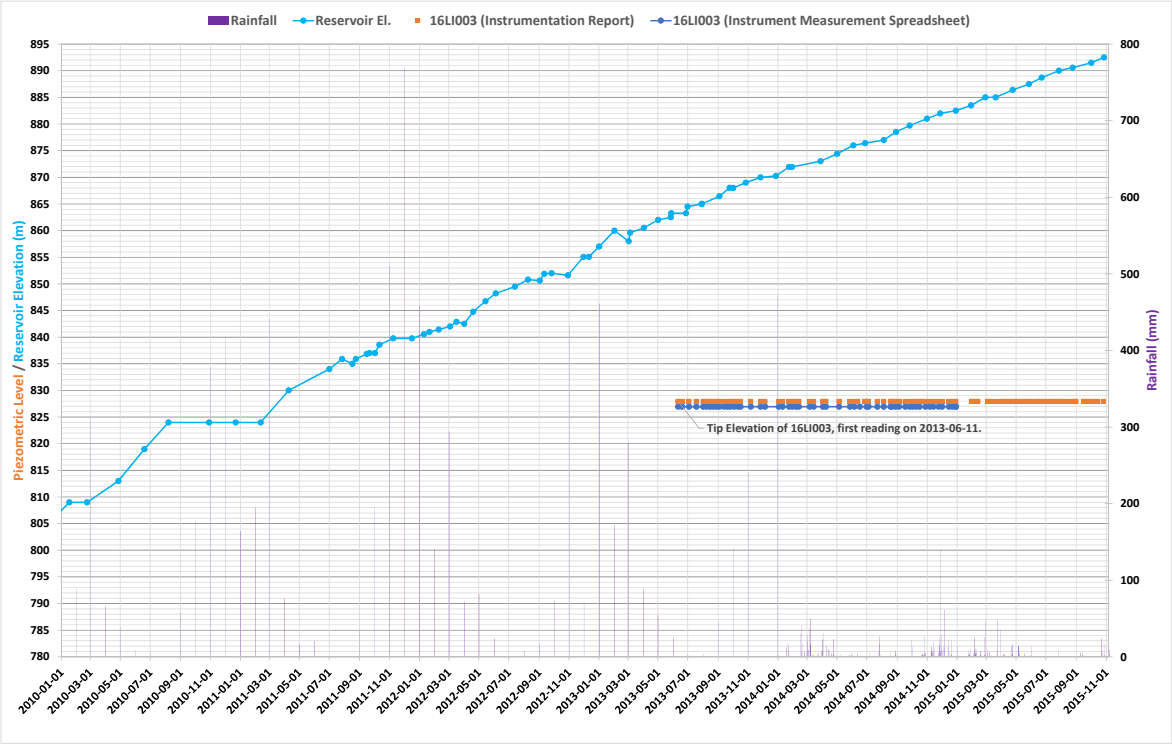

Figure E2-4 Piezometer data comparison for 16LI003

E2.3.3 Additional Piezometers and Water Level Indicators

Five additional piezometers and two additional water level indicators were included in the Instrument Measurement Spreadsheet. The readings from these instruments were not included in the November, 2015 instrumentation reports but some of the locations were shown in plan and section. The seven additional instruments are summarized in Table E2-2. The data from these instruments, with the exception of 24LI039, is included in Attachment E3 and the locations are shown in Attachments E1 and E2. Data from 24LI039 was not included because its location and installation records were not available.

Table E2-2 Summary of extraneous instruments from instrument measurement spreadsheet

Name	Closest Section	Coordinate Source	Bottom of Hole El. (m)	Included in plan from November 2015 Monthly Instrumentation Report?	Included in section from November 2015 Monthly Instrumentation Report?	Period on Record from Instrument Measurement Spreadsheet (YYYY-MM-DD)	
						Start	End
16LI009	02	2013 Instrumentation Plan[50]	827.9	No	No	2013-06-11	2015-01-12
24LI039	Unknown	-	-	-	-	2011-03-24	2011-04-12
24PI042	FF	2012 OMS Manual[1]	810.7(1)	Yes	Yes	2010-01-14	2011-10-04
24PI043	JJ	2012 OMS Manual	781.3	Yes	No	2009-02-09	2014-05-27

Name	Closest Section	Coordinate Source	Bottom of Hole El. (m)	Included in plan from November 2015 Monthly Instrumentation Report?	Included in section from November 2015 Monthly Instrumentation Report?	Period on Record from Instrument Measurement Spreadsheet (YYYY-MM-DD)	
						Start	End
24PI057	LL	2012 OMS Manual	797.5	Yes	Yes	2010-03-26	2013-04-03
24PI061	JJ	2012 OMS Manual	793.5	Yes	No	2010-06-14	2012-12-07
24PI063	JJ	2012 OMS Manual(2)	787.3	Yes	No	2010-12-20	2014-10-27

1. Value from Instrument Measurement Spreadsheet. OMS Manual states bottom elevation 811.51 m. Value from Instrument Measurement Spreadsheet was used for plotting in Attachment E3.
2. Mislabeled in OMS Manual as 24PI062.

E3 FLOWS

Flow measurements were recorded at six locations near Dike 1. Locations are numbered 1 through 6 according to the numbering system used in Samarco's weekly reports, as follows:

- Location 1: Fundão Toe Drain
- Location 2: El. 826 m Drain
- Location 3: Grota da Vale
- Location 4: El. 855 m Drain
- Location 5: El. 860 m Drain
- Location 6: Borehole

Measurements were reported in Samarco's monthly instrumentation reports and weekly reports. Details on each location are summarized in Attachment E5. The data from the weekly reports and October, 2015 instrumentation reports are provided for all six locations. Measurements from Locations 1 and 2 (El. 826 m Drain and Fundão Toe Drain) were also reported in MDGEO's Hydrogeological Study on the 940 m Raise[7] and are included in Attachment E5. The locations are shown in plan on Figure E.E5-1.

E4 SURVEY MONUMENTS

E4.1 General

Data is available from twelve survey monuments located on the left abutment setback. These monuments are 2 m long pins pushed 0.7 m into the ground. In a June 2016 interview, a Samarco employee stated the elevation and coordinates of the pins were surveyed using conventional survey. The survey monuments were installed after the August, 2014 incident to monitor slope movements. The most recent OMS manual[1] was issued in 2012 before the survey monuments were installed. The manual does not have a reading frequency for this type of instrument. Section E4.2 describes the available data from the twelve survey monuments.

Survey monuments were also installed in the Starter Dam and were read between November, 2008 and August, 2009. The Starter Dam instruments are described in Section E4.3 and the data is plotted in Attachment E6 for reference. The readings were not used by the Panel.

E4.2 Survey Monuments on the Setback

E4.2.1 December, 2014 to August, 2015 Records

Survey data for nine survey monuments located on the left abutment setback is available in Samarco's October, 2015 instrumentation report for the left abutment. The monuments are numbered P01 through P09 and are located on three benches on the setback. Three additional survey monuments (P01A, P02A, and P03A) are located downstream of the first nine instruments and are documented separately from the instrumentation reports[51]. The period on record for these three survey monuments is much shorter. The two spreadsheets include coordinates (northing and easting) and elevations of the survey monuments for each survey date. They also include calculations of the horizontal and vertical displacement over time.

The displacement data is summarized in Table E4-1. Markers with similar elevations were grouped in benches. Figure E4-1 shows the locations of the survey monuments in plan and the total displacement for the period on record. Horizontal displacement vectors are shown for the initial to final reading.

Displacements on the setback are generally to the southwest, away from the left abutment. The direction of displacement follows the dip direction of the stripped ground as shown on Figure E4-2. All monuments on the El. 885 m and El. 880 m benches saw vertical displacement (settlement) on August 3, 2015. The reason for this is unknown and does not appear to correspond to changes in topography.

There is a large gap in readings from December, 2014 to June, 2015 (see Attachment E6). This is more than 50% of the period on record. For all instruments the rate of movement during the gap is different than the rate of movement before and after the gap. The readings are therefore considered inconsistent and were not used by the Panel.

Table E4-1 Setback displacement marker summary

Bench El.	Name	Total Vertical Displacement (mm)	Total Horizontal Displacement (mm)	Beginning of Reading	End of Reading	Reason for End of Reading
870	P01A	6	8	2014-12-01	2014-12-18	Setback infilling
870	P02A	10	13	2014-12-01	2014-12-18	
870	P03A	16	14	2014-12-01	2014-12-18	
875	P01	33	48	2014-12-01	2015-06-22	Bench raised from 875 m to 877 m
875	P02	56	58	2014-12-01	2015-06-22	
875	P03	66	67	2014-12-01	2015-06-22	
880	P04	30	57	2014-12-01	2015-08-22	Preparation for setback raise
880	P05	64	70	2014-12-01	2015-08-22	
880	P06	90	78	2014-12-01	2015-08-22	
885	P07	522	88	2014-12-01	2015-08-22	
885	P08	118	81	2014-12-01	2015-08-22	
885	P09	522	27	2014-12-01	2015-08-22	

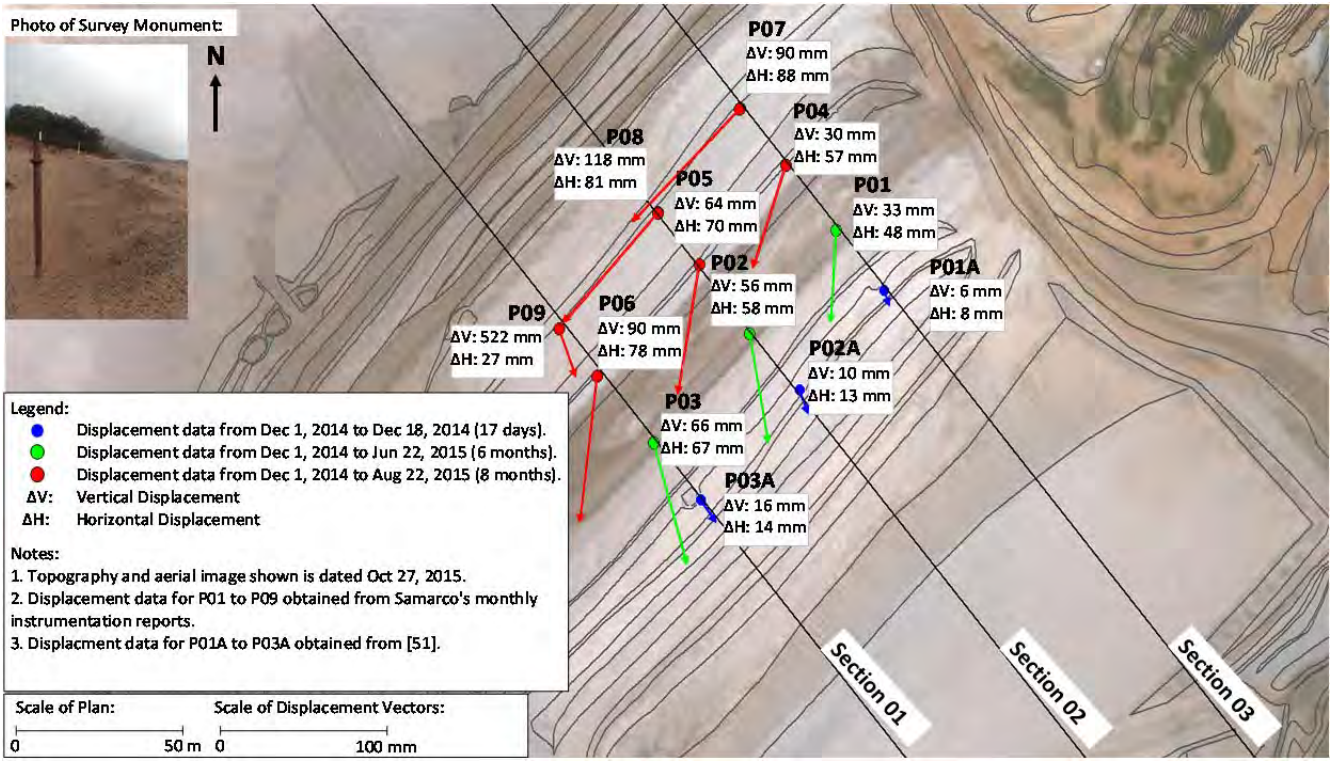

Figure E4-1 Setback survey monument plan and total displacement

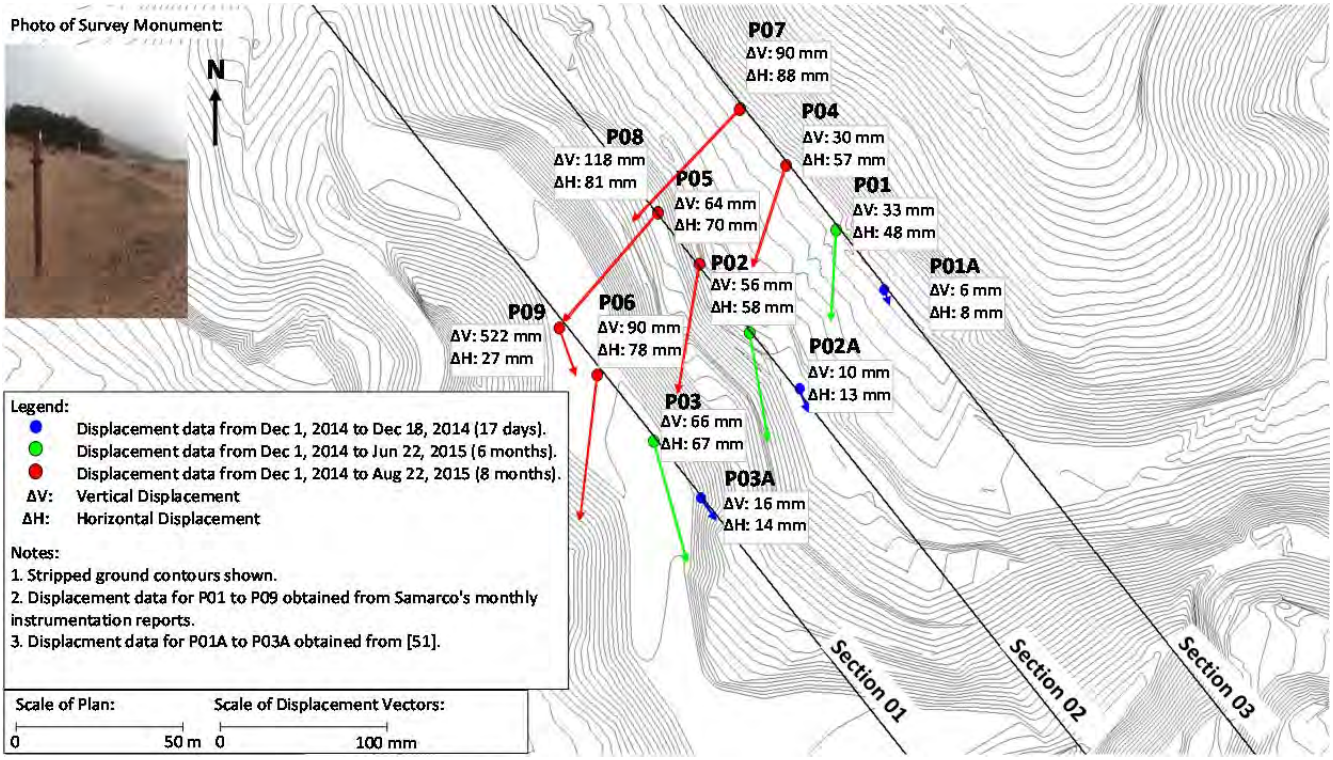

Figure E4-2 Setback survey monument plan and total displacement with stripped ground contours

E4.2.2 August, 2014 Records

The Panel noted that the twelve survey monuments described in Section E4.2.1 were also monitored by Samarco from August 29, 2014 to September 1, 2014, during the period immediately after installation in response to the August, 2014 incident. This data was not included in the sources listed in the section above, but was included in Samarco's report on the August, 2014 incident[52].

The location plan of the survey monuments from the incident report is shown on Figure E4-3 and the displacement plots are shown on Figure E4-4. These figures use a different naming convention for the survey monuments than the data sources in Section E4.2.1. The twelve survey monuments shown in the Samarco figures are believed to be the same as those described in Section E4.2.1 based on their locations in plan.

Figure E4-3 is an exact replica of a Samarco drawing[52]. Their interpretation is that the direction of movement was towards the SE. This is different than the displacement seen in the December, 2014 to August, 2015 records, which is away from the left abutment and in the downslope direction of the stripped ground surface.

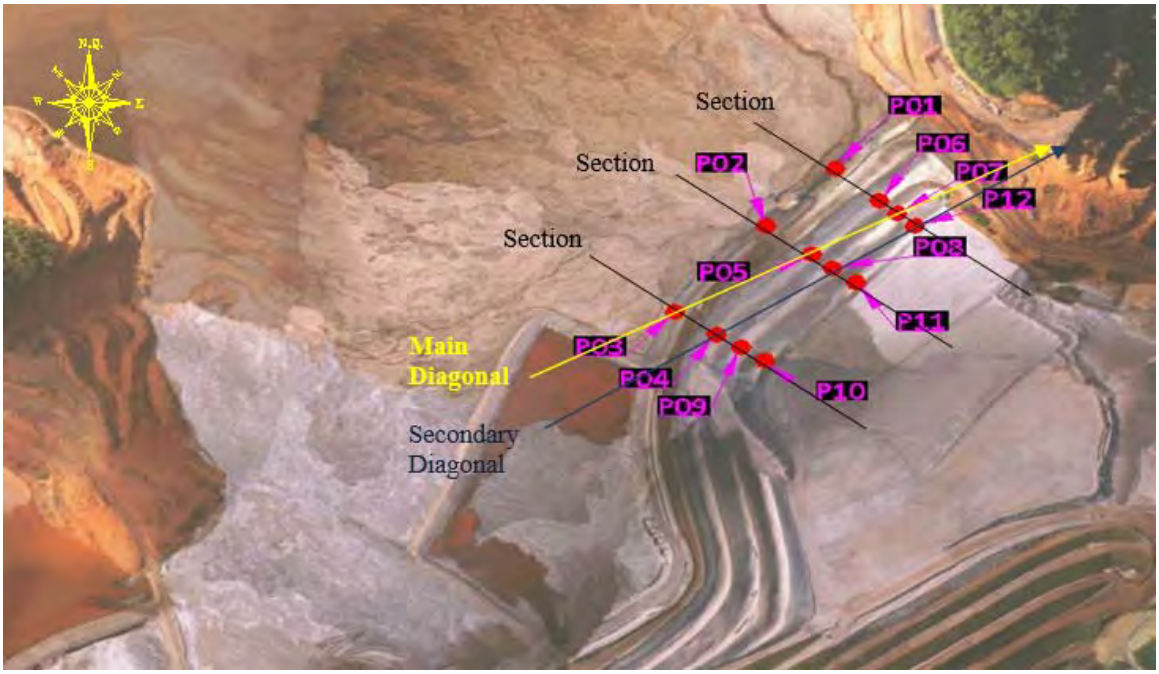

Figure E4-3 Location of survey monuments from Samarco's August, 2014 incident report[52]

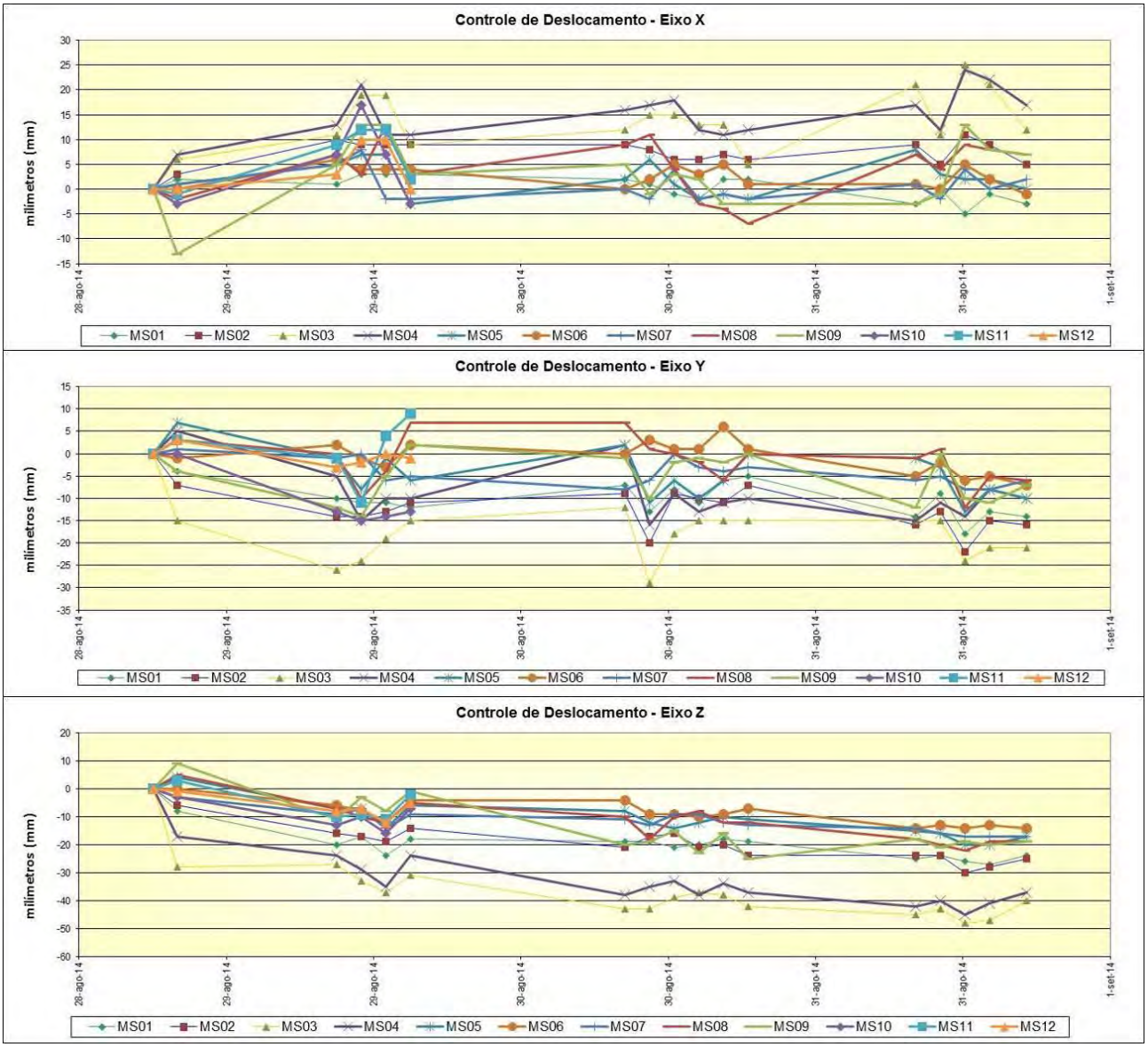

Figure E4-4 Displacement plots from Samarco's August, 2014 incident report[52]

E4.3 Survey Monuments in the Starter Dam

Eleven survey monuments were installed in the Starter Dam and were monitored in 2008 and 2009. The records are included in a Samarco spreadsheet[53] and are summarized in the table below. The data was not used by the Panel but is plotted in Attachment E6 for reference. The displacement data is summarized in Table E4-2. The survey monuments and total displacements over the period on record are shown on Figure E4-5.

Table E4-2 Starter Dam displacement marker summary

Name	Total Vertical Displacement	Total Horizontal Displacement	Beginning of Reading	End of Reading
MS09	12	116	2008-11-24	2009-08-17
MS11	-43	10	2008-11-24	2008-12-09
MS17	4	113	2008-11-24	2009-08-17
MS18	34	117	2008-11-24	2009-07-03
MS19	31	111	2008-11-24	2009-07-06
MS28	-5	109	2008-11-24	2009-08-17
MS29	41	103	2008-11-24	2009-07-16
MS30	-25	121	2008-11-24	2009-06-30
MS31	43	108	2009-11-24	2009-04-06
MS32	-10	20	2009-03-24	2009-08-11
MS33	22	112	2008-11-24	2009-08-17

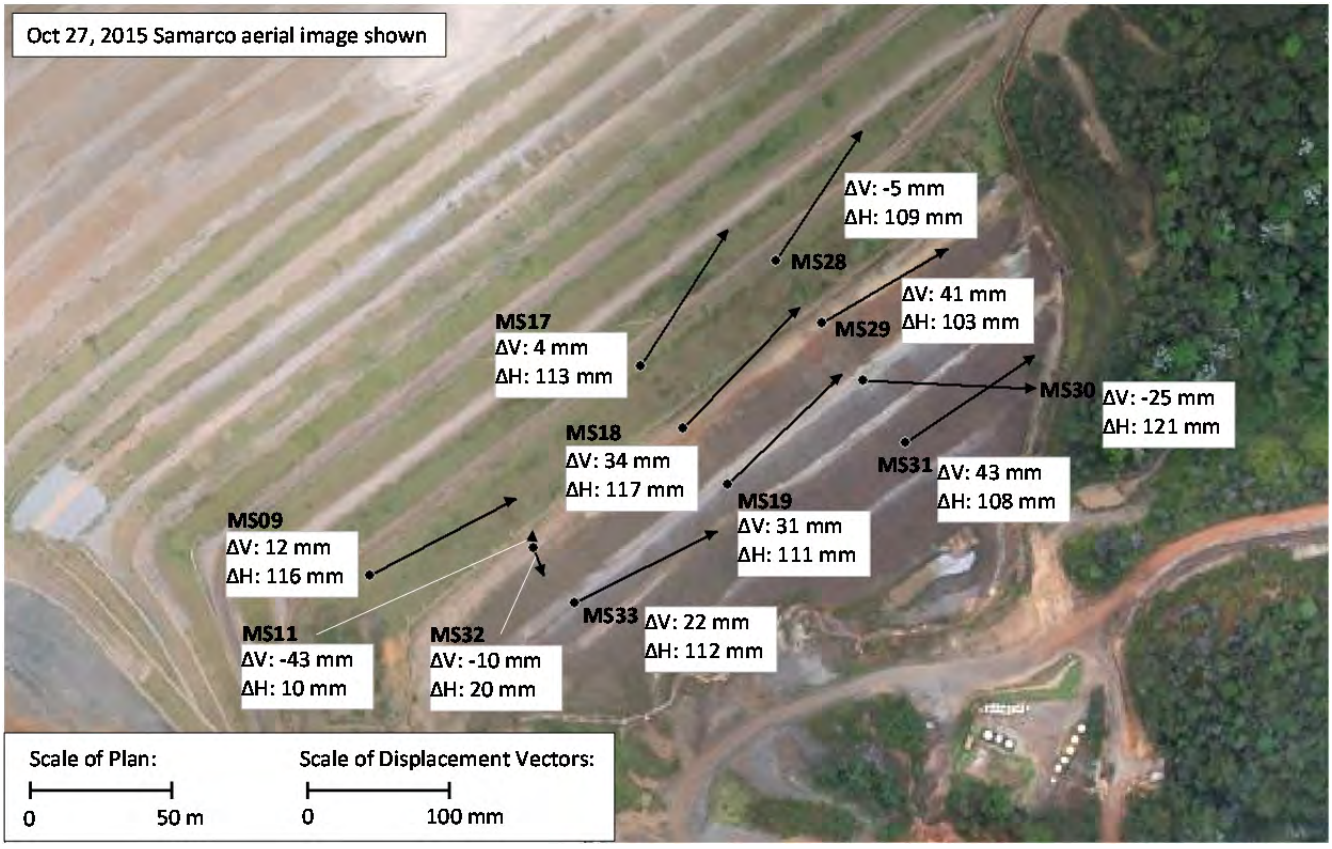

Figure E4-5 Starter Dam survey monument plan and total displacement

E5 INCLINOMETERS

Inclinometer data at Fundão is limited. The records provided to the Panel include the following information:

- Location of inclinometers installed around the Starter Dam[50]. Three inclinometers were installed in natural ground (24IN001, 24IN003, 24IN004) and one inclinometer was installed on the Starter Dam (24IN002). No readings are available.
- Location and readings for two inclinometers on the downstream face of the Starter Dam. Two readings are available for March and April, 2009[54].
- Location of six planned inclinometers at Dike 1 are shown in a 2012 drawing[55]. Four are shown in natural ground and two are on an upstream raise. No readings or installation logs are available.
- Location of one inclinometer installed on the downstream face of Dike 1 in 2014 (16NI003). The Fugro installation log is available[56] but there are no readings. The elevation of this inclinometer is 820 m (on the Starter Dam).
- Additional inclinometers installed by Fugro during 2014 were located in Germano. Installation logs are available.

Inclinometers that were installed in the Starter Dam were destroyed in the 2009 piping incident and during subsequent remediation measures. Samarco's most recent OMS Manual (issued in 2012) does not list any inclinometers in Dike 1[1]. A Samarco employee stated that no inclinometers were installed at Fundão after the original Starter Dam instruments were destroyed in 2009.

ATTACHMENT F1

Consolidation Analyses Results

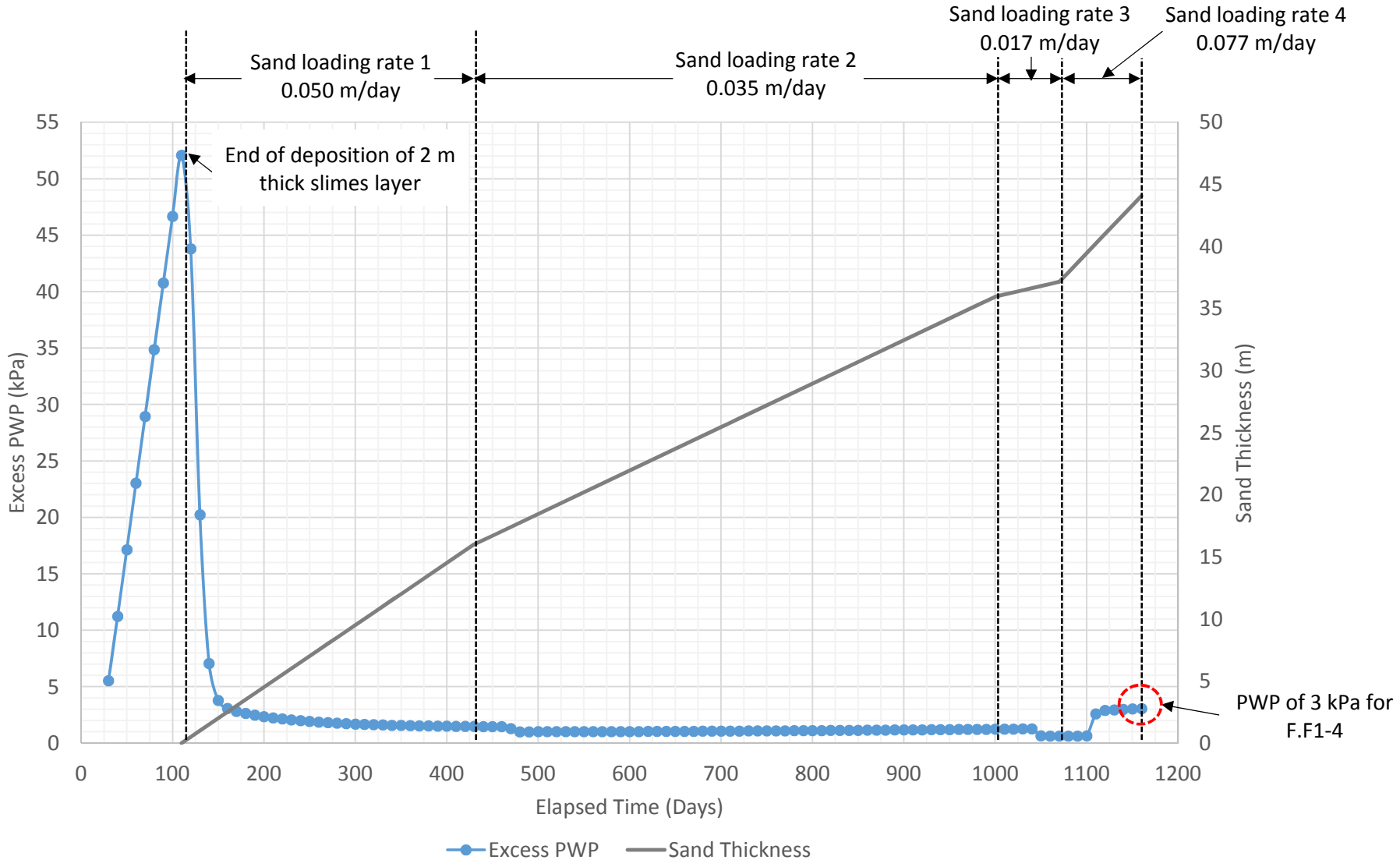

	PROJECT: Fundão Tailings Dam Review Panel
	TITLE: FSConsol Slimes Consolidation Excess PWP vs Elapsed Time for 2 m of Slimes
	PROJECT No. / FIG. No. F.F1-1

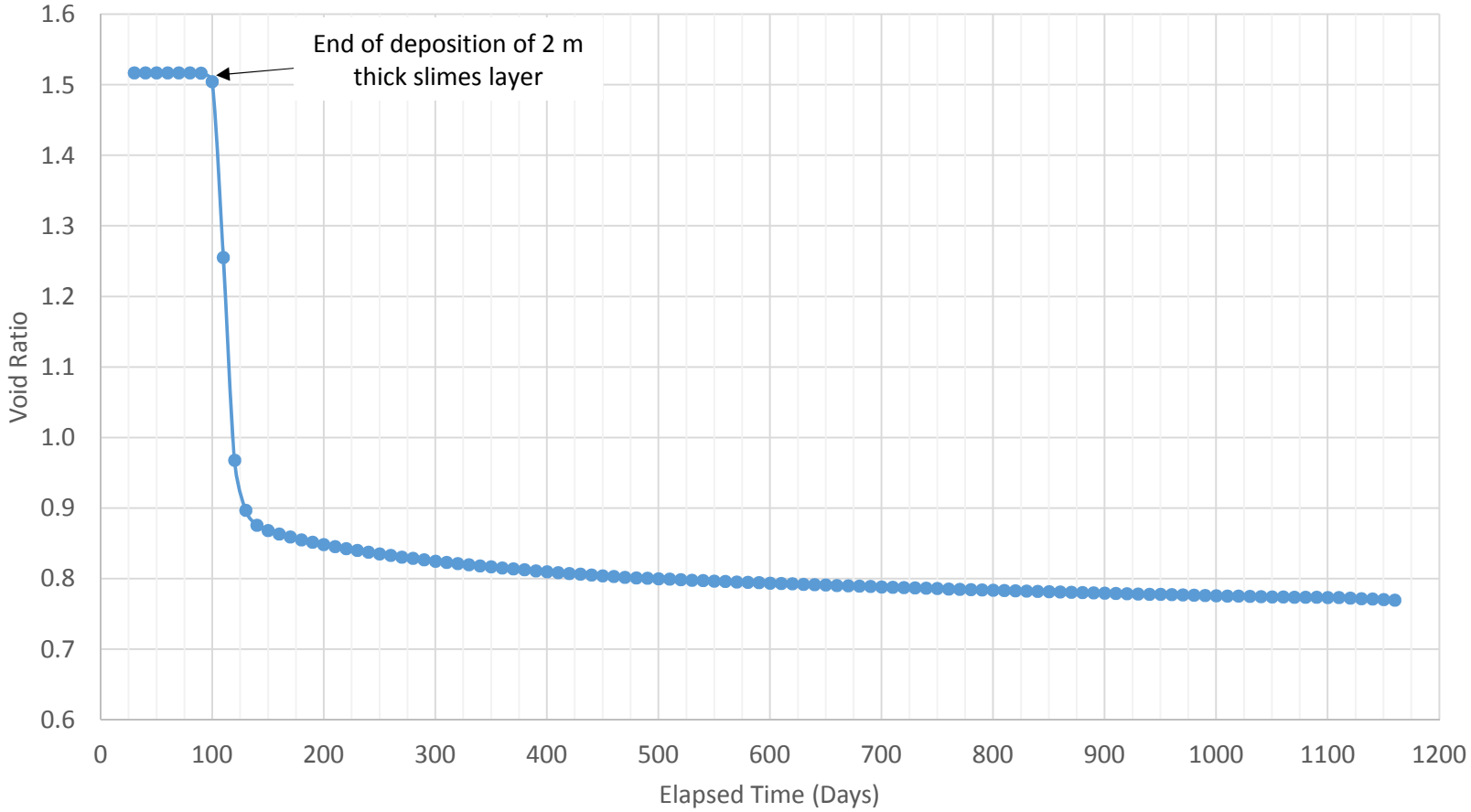

	PROJECT: Fundão Tailings Dam Review Panel
	TITLE: FSConsol Slimes Consolidation Void Ratio vs Elapsed Time for 2 m of Slimes
	PROJECT No. / FIG. No. F.F1-2

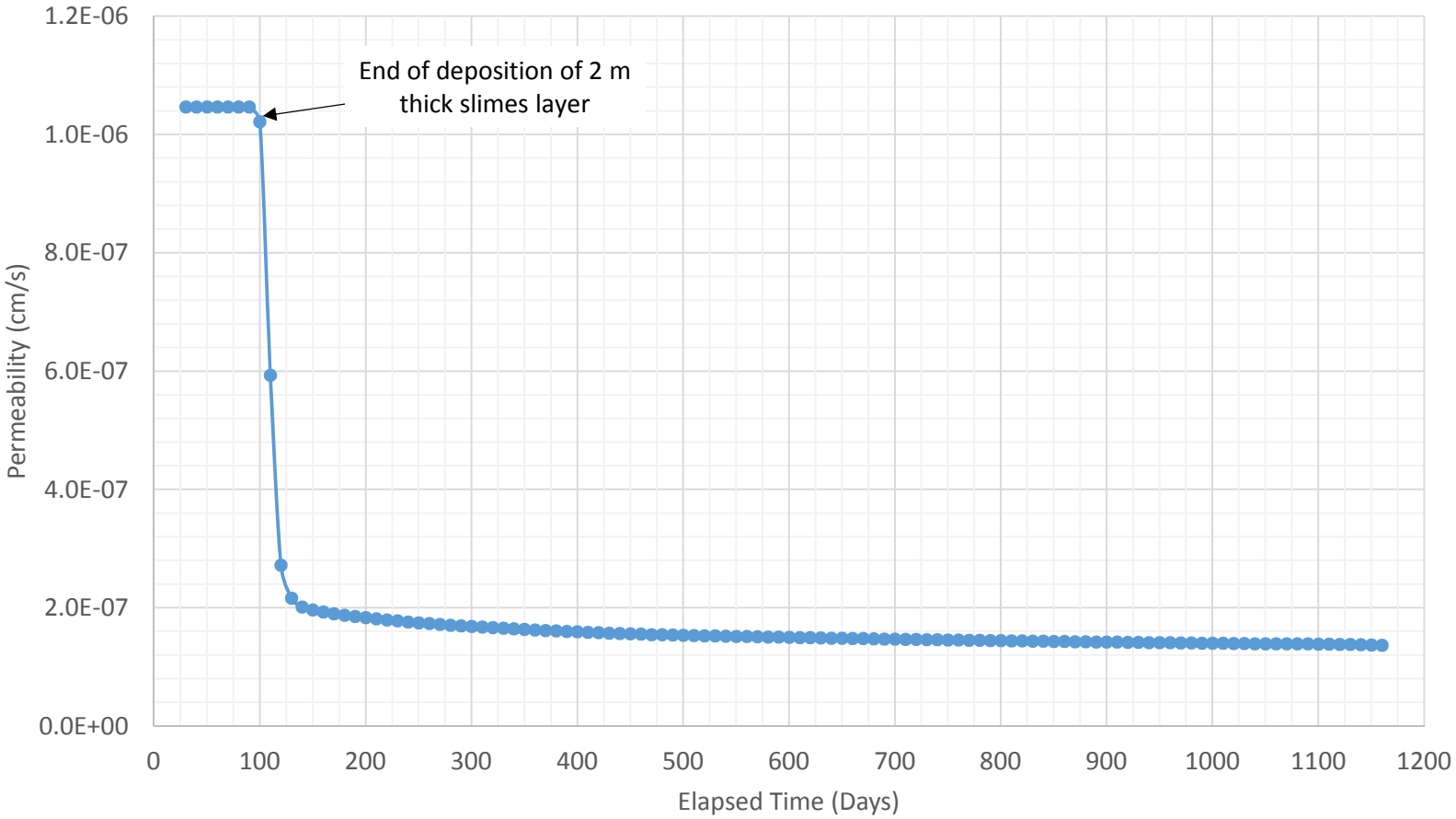

	PROJECT: Fundão Tailings Dam Review Panel
	TITLE: FSConsol Slimes Consolidation Permeability vs Elapsed Time for 2 m of Slimes
	PROJECT No.
	FIG. No. F.F1-3

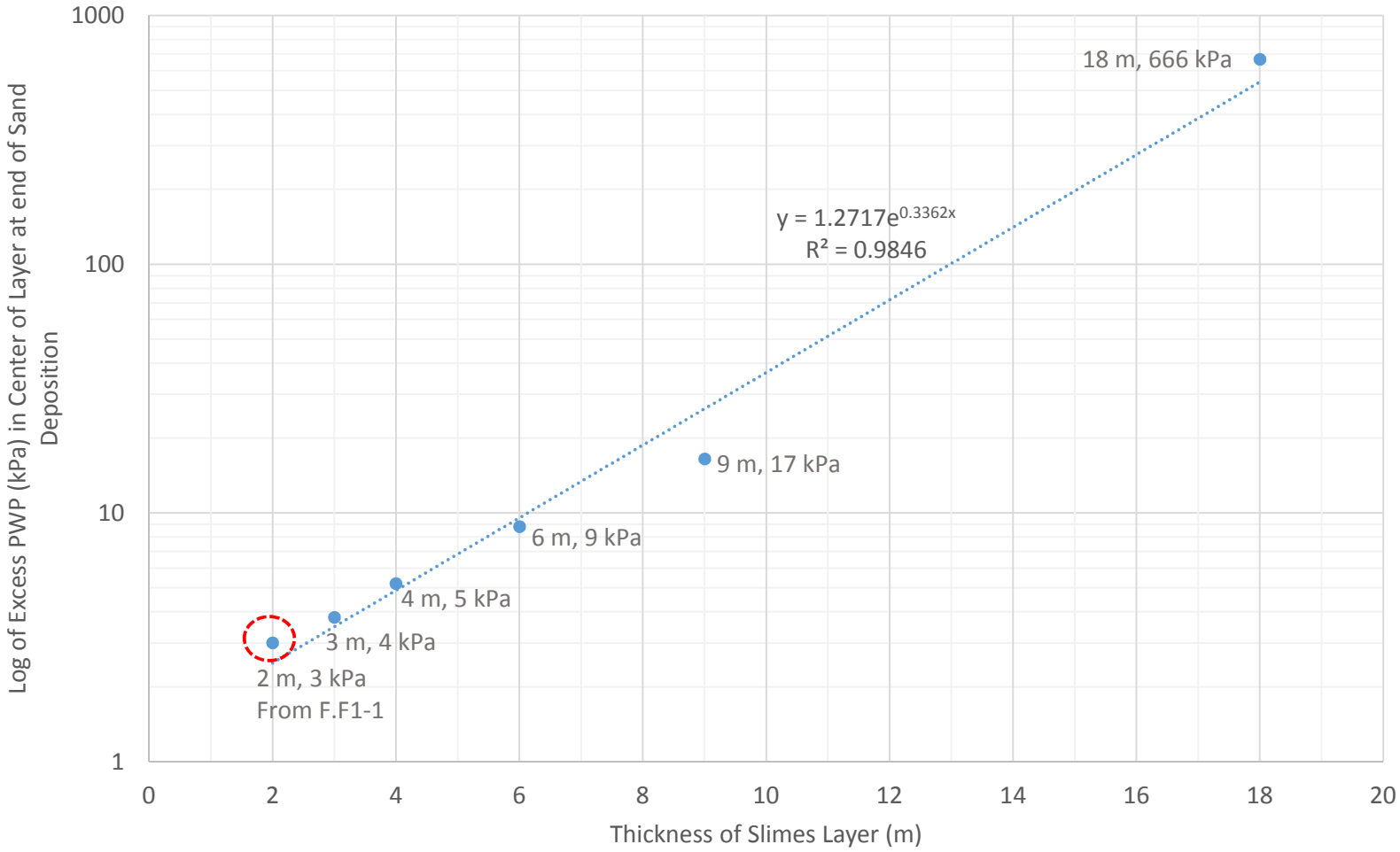

	PROJECT: Fundão Tailings Dam Review Panel
	TITLE: FSConsol Slimes Consolidation Excess PWP vs Slimes Thickness
	PROJECT No. / FIG. No. F.F1-4

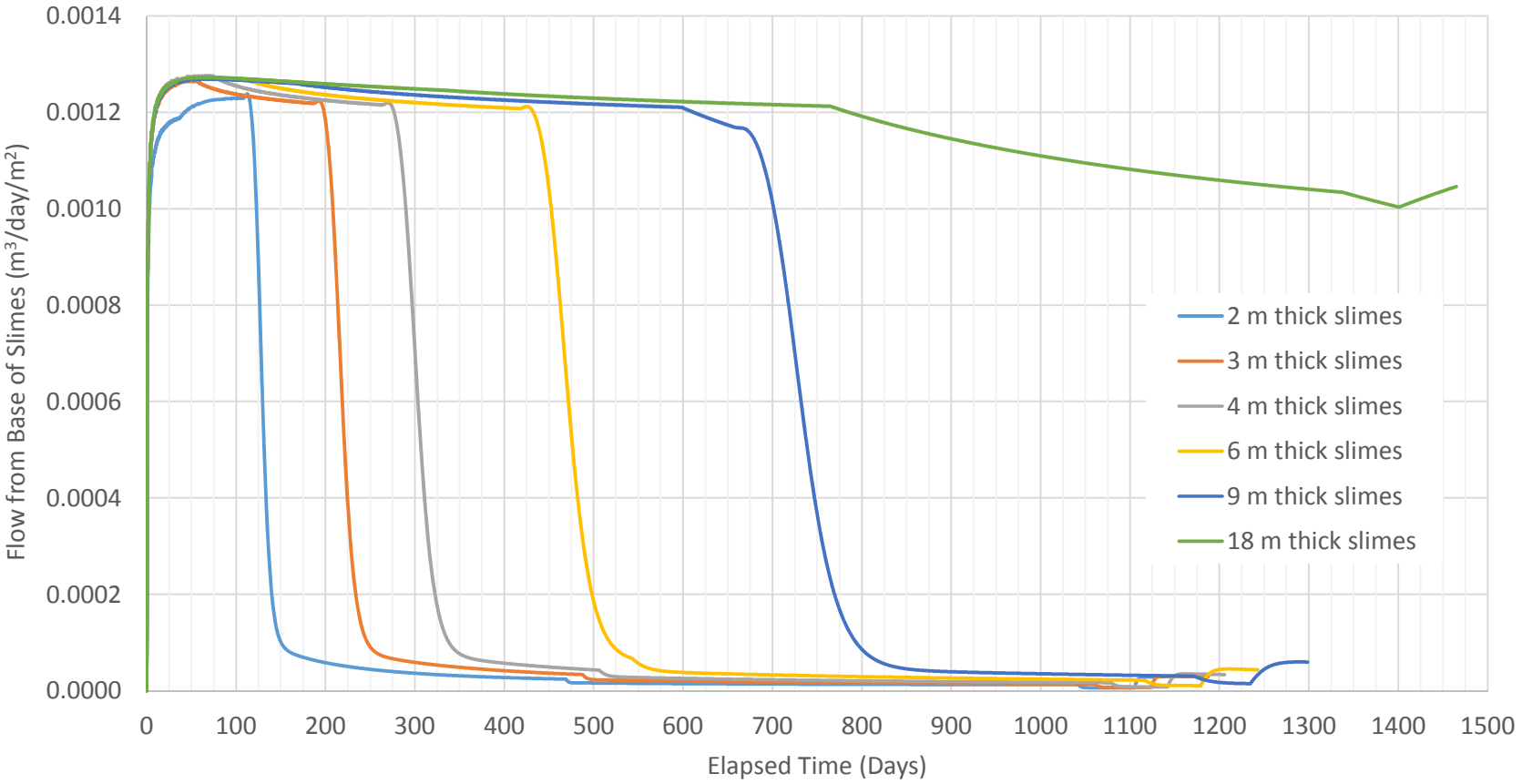

	PROJECT: Fundão Tailings Dam Review Panel
	TITLE: FSConsol Slimes Consolidation Consolidation Water Flow vs Slimes Thickness
	PROJECT No. / FIG. No. F.F1-5

APPENDIX F

Consolidation Modeling

Appendix F
Consolidation of Slimes on the Left Abutment

TABLE OF CONTENTS

List of Tables

List of Figures

List of Attachments

F1 INTRODUCTION

This appendix estimates the consolidation behavior of the slimes between El. 830 m and El. 850 m on the left abutment as the dike is raised from El. 850 m to about El. 900 m. The slimes incursion on the left abutment of Dike 1 between El. 830 m and El. 850 m is described in Section 5 of the report and in Appendix B. The work in this appendix was done to evaluate the pore pressure generation and dissipation in these slimes as Dike 1 was raised. The pore pressure dissipation rate in the slimes has important implications for adoption of undrained/drained strength in stability analyses discussed in other parts of the report. Also, the generation of consolidation water discharged to the sand surrounding the slimes layers has potential implications for both seepage rates and strength assumptions in the sand. This is also discussed in other sections of the report.

FSConsol, a one-dimensional large strain consolidation program, which can accommodate increasing loads with time, was used to investigate the rate of consolidation of slimes layers of varying thickness as Dike 1 was constructed above El. 850 m.

The next section of the Appendix describes the data sources for the consolidation properties of the slimes. The selection of consolidation parameters for FSConsol is described in Section F3. The basis for the Dike 1 rate of rise for modeling is set out in Section F4. Results are given in Section F5.

F2 SOURCE OF CONSOLIDATION/COMPRESSIBILITY PARAMETERS

F2.1 General

The input soil parameters to the analytical models were derived from laboratory testing and an instrumented trial embankment at Baia 2 on the Germano plateau in June, 2008[4]. This trial embankment is described in Appendix C. Rezende[40] performed compression tests on sand tailings in the oedometer as part of her MSc thesis. No laboratory consolidation tests were found for the slimes, so an oedometer test was done on a slurried sample of the slimes. Further, a sedimentation/consolidation test on slurried slimes was done at the University of Alberta to obtain slimes properties from a much larger test specimen than an oedometer sample.

F2.2 Rezende (2013) Oedometer Tests on Sand Tailings

The scope of the Rezende (2013)[40] testing work is described in general terms in Appendix D. That work was devoted to understanding the properties of the sand tailings, which were sampled carefully in the field and tested in the university laboratory. After review of the sand compression data, we selected the oedometer test results for sample PT-000 on sand as shown in Table F2-1 for our analysis.

Table F2-1 Sand compression laboratory testing

Data Source	Pressure (kPa)	Void Ratio	Cc	k (cm/s)
Rezende 2013[40]	0	0.764	-	-
	6.24	0.732	-	-

Data Source	Pressure (kPa)	Void Ratio	Cc	k (cm/s)
Rezende 2013[40]	12.49	0.706	0.08627	3.65E-04
	24.97	0.686	0.066477	3.71E-04
	49.94	0.671	0.049829	3.93E-04
	99.89	0.648	0.076393	3.66E-04
	199.78	0.617	0.10298	3.03E-04
	399.56	0.589	0.093014	2.75E-04
	799.12	0.548	0.136199	1.98E-04
	1598.24	0.5	0.159453	1.49E-04
	3196.47	0.38	0.398633	1.37E-04
	1598.24	0.391	0.036541	-
	799.12	0.402	0.036541	-
	399.56	0.412	0.033219	-
	199.78	0.425	0.043185	-
	99.89	0.442	0.056473	-

F2.3 Oedometer Test on Slimes

An oedometer test was done on a sample of slurried slimes prepared from the January campaign of the Panel's field program. The test results are given in Appendix D and repeated here in Table F2-2.

Table F2-2 Slimes consolidation laboratory testing

Data Source	Pressure (kPa)		Void Ratio	Cc	k (cm/s)
Appendix D	0.0	2.0	1.070	0.501	-
	2.0	4.0	1.047	0.077	2.6E-07
	4.0	8.0	1.017	0.102	3.1E-07
	8.0	16.0	0.986	0.101	4.4E-07
	16.0	32.0	0.952	0.112	1.9E-07
	32.0	64.0	0.915	0.125	1.9E-07
	64.0	128.0	0.871	0.144	3.0E-07
	128.0	256.0	0.828	0.144	3.3E-07
	256.0	512.0	0.780	0.159	1.4E-07
	512.0	1024.0	0.733	0.156	8.4E-08

F2.4 University of Alberta Sedimentation/Consolidation Test on Slimes

The University of Alberta Geotechnical Centre performed Large Strain Consolidation (LSC) testing on a sample of slimes tailings. The testing was conducted to determine the relationship between void ratio and vertical stress as well as permeability. The testing is described in Appendix D but was not used in this consolidation analysis.

F2.5 Baia 2 Trial Embankment

The Baia 2 trial embankment[4] was constructed to a height of 5 m with 2H:1V side slopes in June, 2008 at a rate of about 0.55 m/day. The monitoring data is shown on Figure F2-1. The plot on the left is the crest elevation with time which shows the rise of the embankment followed by the settlement of the crest as pore pressures dissipate in the foundation. The plot on the right shows the pore pressure generation as the embankment is constructed and the dissipation with time after construction.

The results of back calculated data for low effective stresses derived from this trial are presented in Table F2-3. The effective vertical stress before loading together with an estimate of the void ratio, and the post-construction vertical stress with an estimate of the final void ratio, are given in Table F2-3. These values were used to calculate a Cc value at very low stresses in the slimes.

Table F2-3 Back calculated data

Data Source	Effective Vertical Stress (kPa)	Void Ratio	Cc
Back calculated	0.907	1.248	-
	1.072	1.206	0.577

The embankment was modeled using FLAC V.8.0 to confirm that the back calculated Cc value for the slimes at low stresses was appropriate. The soil parameters for the FLAC model were based on the back-calculated value, as well as 1D compression test data and data from CPTs done as part of the embankment trial. The settlements calculated from the model were in close agreement with the monitored results, which gave confidence in the continued use of these back-calculated values.

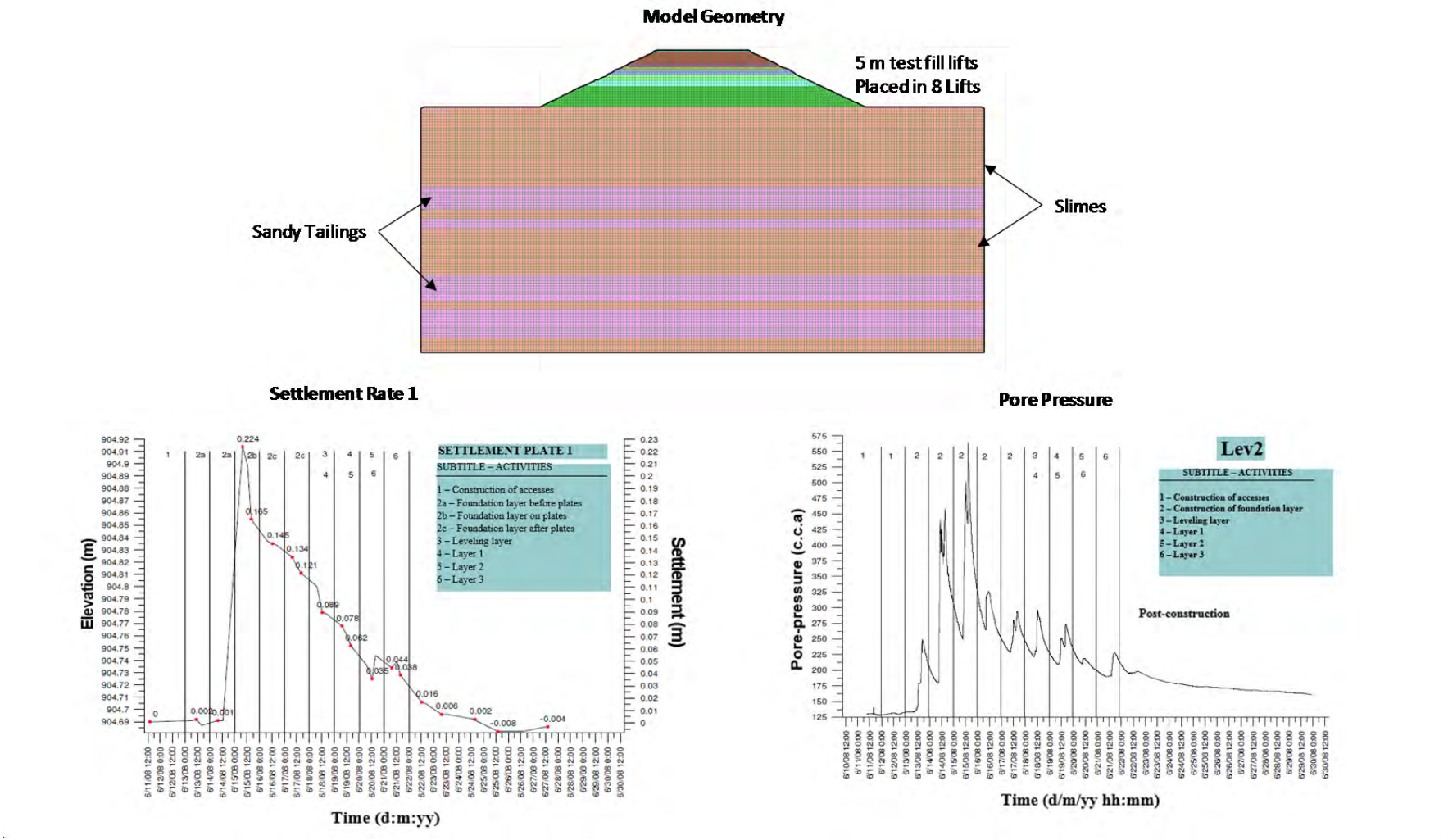

Figure F2-1 Baia 2 trial setup[4]

F3 DERIVATION OF PARAMETERS FOR FSCONSOL

The one-dimensional consolidation software, FSConsol, was used to estimate excess pore pressures and consolidation water discharge rates from varying thicknesses of slimes subjected to 50 m of loading from sand at the same raise rates prevailing at the left abutment. FSConsol uses functions to represent the relationship between void ratio and effective vertical stress, as well as void ratio vs permeability as input material parameters. Figure F3-1 and Figure F3-2 show the curve fitting on the field and laboratory data from Section F2 to establish the input material functions for slimes and sand. These functions are given in Table F3-1 and Table F3-2.

Table F3-1 Consolidation parameters

Material	Function	A	B	M
Sand	$e = A \times (\sigma'_v{}^{B}) + M$	11.7	-0.0034	-10.9
Slimes		0.7	-0.15	0.5

Table F3-2 Permeability parameters

Material	Function	C	D
Sand	$k = C \times D^{e}$	1.6×10^{-3}	3
Slimes		3.0×10^{-7}	3

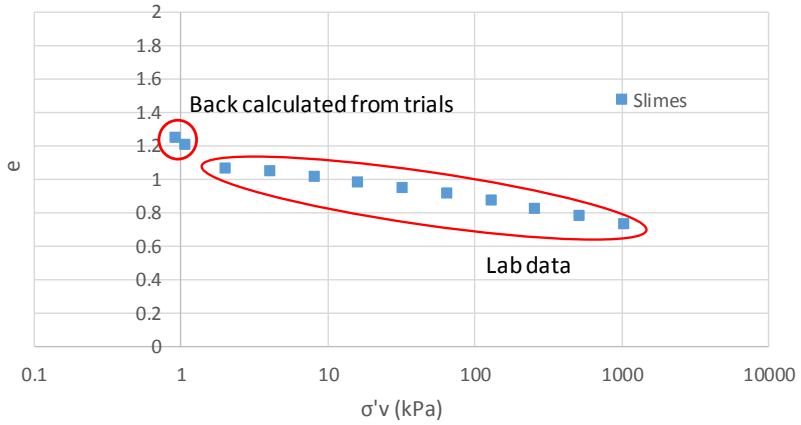

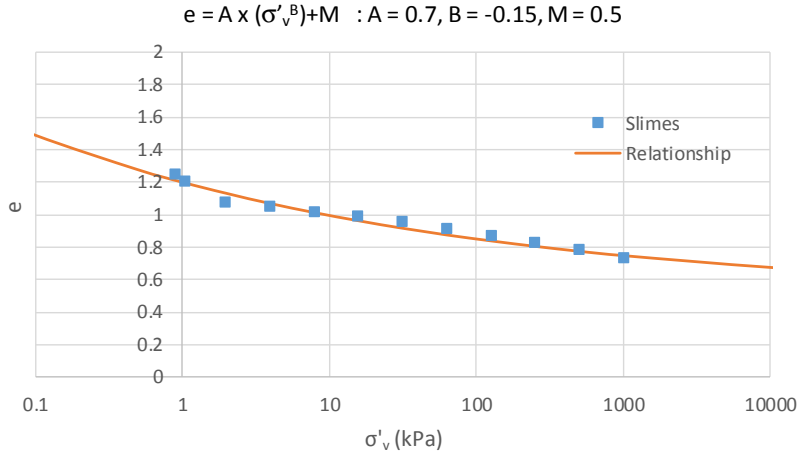

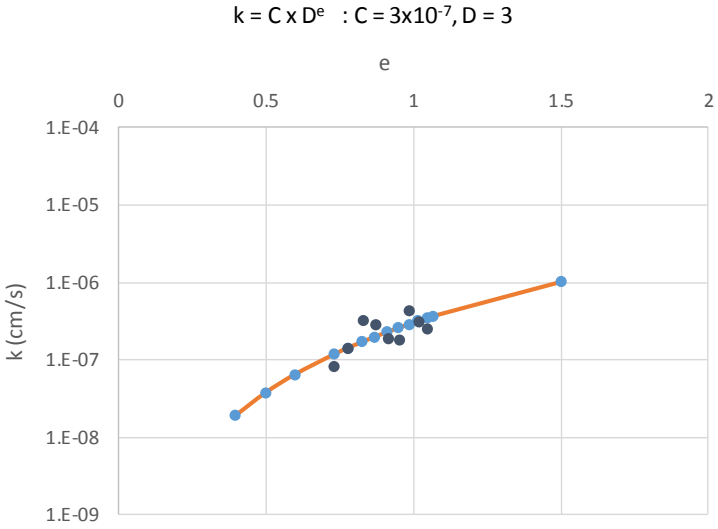

Figure F3-1 Large strain consolidation characterization – slimes

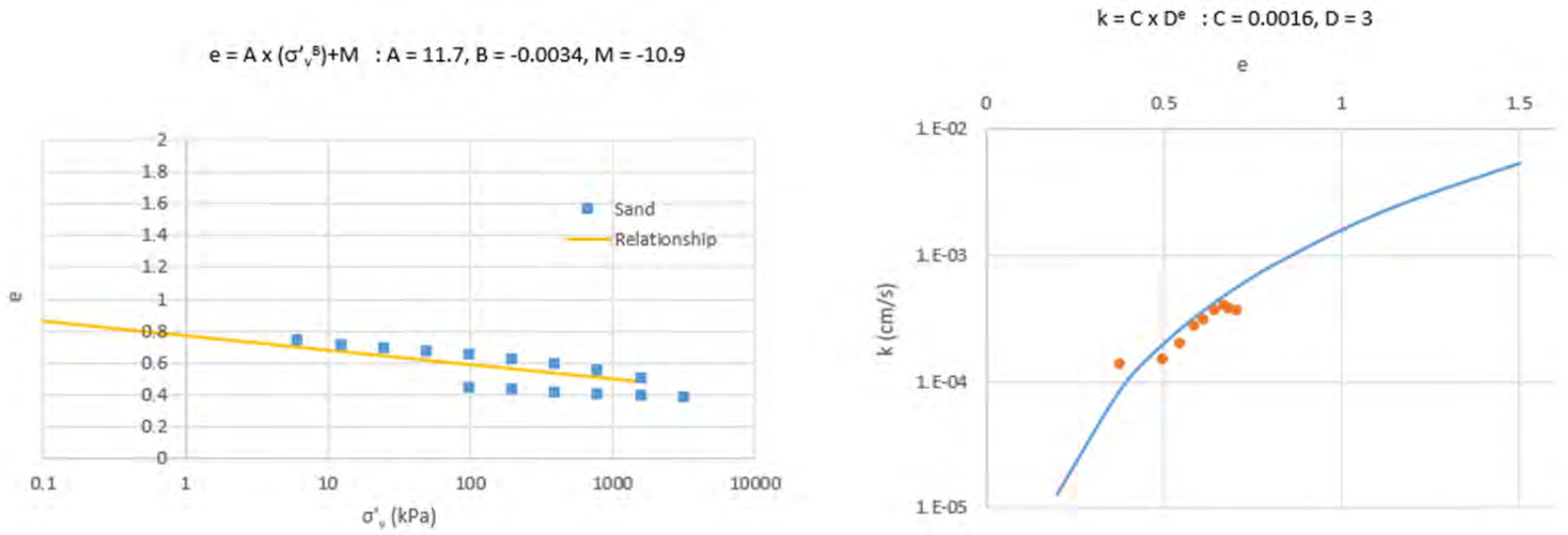

Figure F3-2 Large strain consolidation characterization – sand

F4 RATE OF RISE OF LEFT ABUTMENT

F4.1 General

The rate of rise of Dike 1 on the left abutment was obtained from the following data in Appendix B:

- as-built drawings
- construction reports
- aerial photographs

F4.2 FSConsol

The dam loading rate adopted for FSConsol was taken from the plot on Figure F4-1. For modeling convenience, the curve was segmented into four linear loading rates as shown on the curve. The four loading rates are listed in Table F4-1.

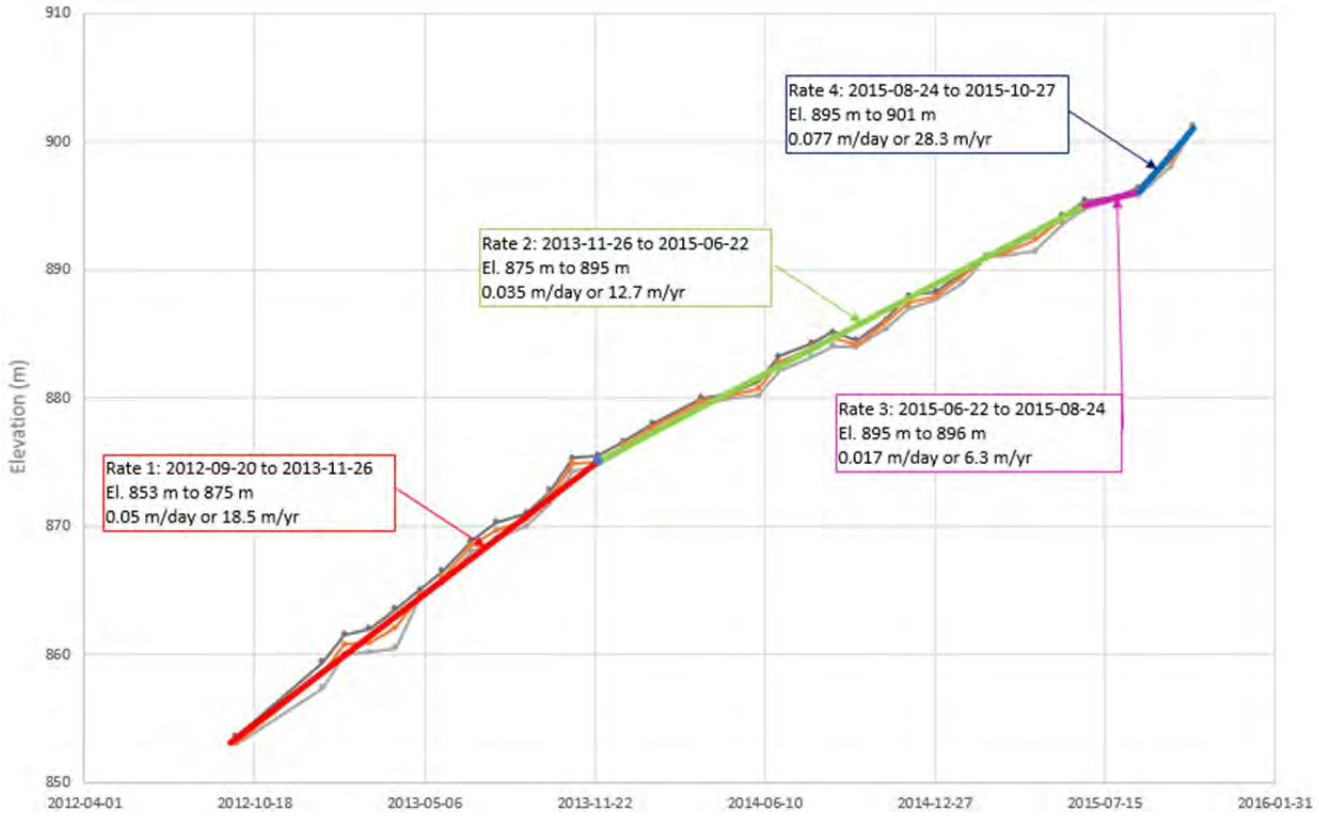

Figure F4-1 Dam loading rate for FSConsol analysis

Table F4-1 FSConsol loading

Sequence	Timeline	Elevations	Rate (m/day)	Rate (m/yr)
Rate 1	2012-09-20 to 2013-11-26	853 to 875	0.050	18.5
Rate 2	2013-11-26 to 2015-06-22	875 to 895	0.035	12.7
Rate 3	2015-06-22 to 2015-08-24	895 to 896	0.017	6.3
Rate 4	2015-08-24 to 2015-10-27	895 to 901	0.077	28.3

F5 FSCONSOL RESULTS

The FSConsol model was run for slimes thicknesses of 2 m, 3 m, 4 m, 6 m, 9 m, and 18 m. Double drainage was assumed with ambient pressure in the sand at the base of the slimes. An overlying thickness of sand was added in the FSConsol model above the El. 850 m contour at the rates prevailing at the left abutment as described in the previous section.

FSConsol generated excess pore-water pressure, change in thickness or void ratio, and change in permeability with time. Results for these parameters for a 2 m thick slimes layer are given on Figures F.F1-1, F.F1-2, and F.F1-3 with time. Figure F.F1-4 shows the excess pore-water pressure in the center of each slimes layer. Only the 18 m thick slimes layer is not fully consolidated at the end of sand deposition. Figure F.F1-5 shows the consolidation discharge from the slimes layers with time and also shows that only the 18 m thick slimes layer continues to discharge consolidation water within the time frames of deposition at the left abutment.

APPENDIX G

Seepage Modeling

Appendix G
Seepage Modeling

TABLE OF CONTENTS

TABLE OF CONTENTS

(continued)

List of Tables

List of Figures

TABLE OF CONTENTS

(continued)

G1 INTRODUCTION

This appendix presents the results of the three-dimensional seepage modeling of the Fundão Dam. This work was completed in order to provide phreatic and pressure condition data to inform parallel engineering assessments of the facility. This work is presented across two main sections.

Section G2 presents the construction of the Phase 0 (Ph0) series of models which are 3D FEFLOW, steady state simulations of the design concept for the TSF. This modeling was completed to assess the various design components of the original system as they relate to internal water management, and to stress these conditions and develop an understanding of their broader response and influence ahead of Phase 1 (Ph1) as-built modeling.

Section G3 presents the construction of the Ph1 model, which is a real time transient reconstruction of the as-built conditions of the Tailings Storage Facility (TSF) from El. 830 m to the time of failure in November, 2015. This reconstruction leans heavily on the results of the Ph0 modeling, and was developed in close liaison with the GIS based reconstruction of the facility (Appendix B), and the various engineering studies associated with characterizing base data and assessing performance conditions of the facility.

This work includes a scenario variation, being a transient simulation of the post El. 830 m facility reconstructed with the absence of slimes “tongues” on the left abutment. This Phase 2 (Ph2) model was completed to assess variability in phreatic conditions on the left abutment had the slimes extent not encroached toward and beneath the dam.

G2 PHASE 0 MODEL – DESIGN CONCEPT

G2.1 Ph0 Model Preamble

The Ph0 model provides a reconstruction of the design concept for the Fundão Dam, based on documentation and project records preceding the final design/construction of the Starter Dam (generally, pre-2007). The model was constructed to assess the hydraulic performance of the structure with particular reference to the phreatic surface, drain flux, areas of emergent seepage and seasonal rainfall effects.

This model does not assess as constructed conditions or the performance of mitigation features designed and constructed into the facility as it matured. This is addressed in the Ph1 model in Section G3.

G2.2 Fundão Dam TSF Concept

G2.2.1 Concept Reconstruction Source Data

Reconstruction of the design concept was undertaken using several key sources of information, of most relevance:

- A series of 43 drawing files dated August 8, 2006 to September 29, 2006 (see Appendix A Attachment A1).

- A number of explanatory Power Point presentations created by the design engineer, the most relevant of which is dated September 30, 2006[59].
- Technical report by Pimenta de Ávila (2006a)[60]: provides an overarching descriptive summary of the operational / design intent understood to be for the purpose of project tendering. The date of this report matches the 43 drawing files (Appendix A Attachment A1), and the general description was sufficient to gather an understanding of the fundamental operational intent of the facility.
- Technical report by Pimenta de Ávila (2006b)[61]: an update of Pimenta (2006a).
- Technical report by Pimenta de Ávila (2007)[62]: provides justification for design modifications including the removal of Dike 3 which post-dates the two earlier design reports.

Other reports, data, plans and spreadsheets were reviewed and have generally been referenced and summarized in accompanying technical appendices to the main report.

G2.2.2 Concept Design Limitations Acknowledgment

As the concept design evolved over a period of time, no singular definitive description exists. In order to construct a suitable concept model, a project description was developed using each of the bodies of evidence available. This Ph0 model needed to honor the fundamental design premises applied at the time, and also needed to include each of the primary elements of construction required for its successful development. In doing so, and because of the changing nature of design, it is acknowledged that some elements of the TSF concept may not have carried through to this final model or may be reported elsewhere in a slightly different arrangement. For the purposes of this work, however, the model constructed and presented in Section G2.2.3 is considered the most appropriate representation of the design concept at the time.

G2.2.3 Final Concept Description

The final concept design applied in the Ph0 model comprises:

- A Starter Dam (Dike 1) and an upstream Dike 2 located between Dike 1 and the Germano Dam.
- Dike 2 was designed to retain slimes, while Dike 1 was designed to retain sand tailings.
- The TSF was to be raised from Dike 1 using the upstream construction method and tailings sand to form each respective raise. Sand tailings were then to be spigotted from the crest of the raised Dike 1, with a beach design slope of 1V:100H and a minimum beach width of 200 m.
- The placement of sand tailings behind Dike 1 was to be at a rate that maintained a +5 m elevation gain on the placement of slimes behind Dike 2.
- Drains were included in accord with the design with the general principal was drainage to be sufficient to achieve a free draining TSF. The drain elements included:
  - an upstream blanket on the face of Dike 1;

  - left and right abutment drains connecting with the Dike 1 upstream blanket;
  - a Principal Foundation Drain along the thalweg of the original Fundão Creek, and extending upstream to Dike 2;
  - a vertical chimney drain in Dike 2, connected to a horizontal blanket underneath Dike 2 on the downstream side, which then connected with the Principal Foundation Drain; and
  - drainage galleries connecting to the Principal Foundation Drain from minor-thalwegs.
- The facility was modeled at a final design elevation of El. 920 m.

The general arrangement of conceptual layouts described above are provided on Figure G2-1, Figure G2-2, Figure G2-3 and Figure G2-4.

Of note, the minimum 200 m beach width is shown on Figure G2-3 as calculated from the crest of the final Dike 1. The extent of tailings sand however continues further upstream. This was selected as the concept design option because it more accurately reflects the upstream construction of tailings over slimes behind Dike 2; it does not conflict with the minimum 200 m beach width design requirement, and it increases the distance to the constant head of the slimes interface. Two other options for modeling the slimes/sand interface were considered possible at the concept level but were not carried forward, namely:

- Option 1 is vertical abutment between the two materials (slimes and sand directly over Dike 2) through centerline construction; however, this conflicts with the 200 m minimum beach width requirement in the area of the Dike 1 right abutment.
- Option 2 is vertical abutment between the two materials at the “Dike 1 crest minus 200 m interface”; however, this then presented difficulty in representing either of centerline or upstream construction methods over Dike 2.

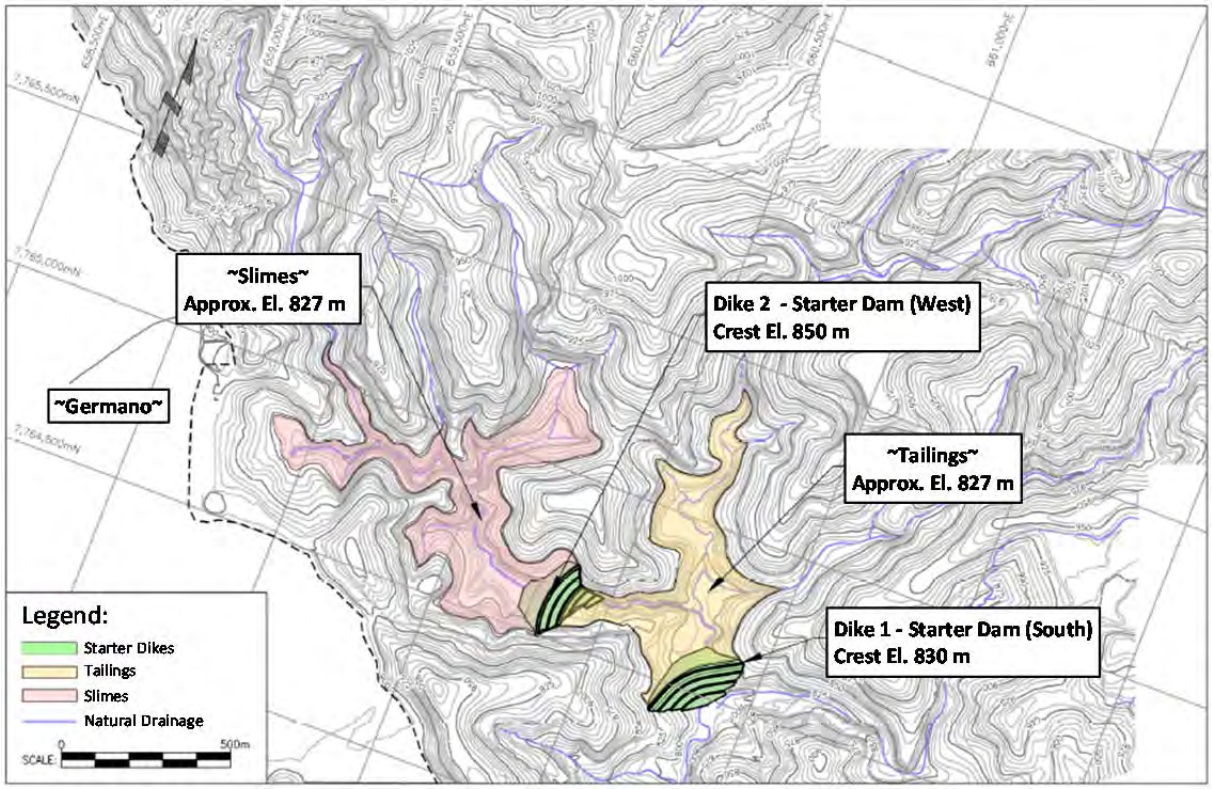

Figure G2-1 Concept design Dike 1 and Dike 2 general arrangement and crest elevations

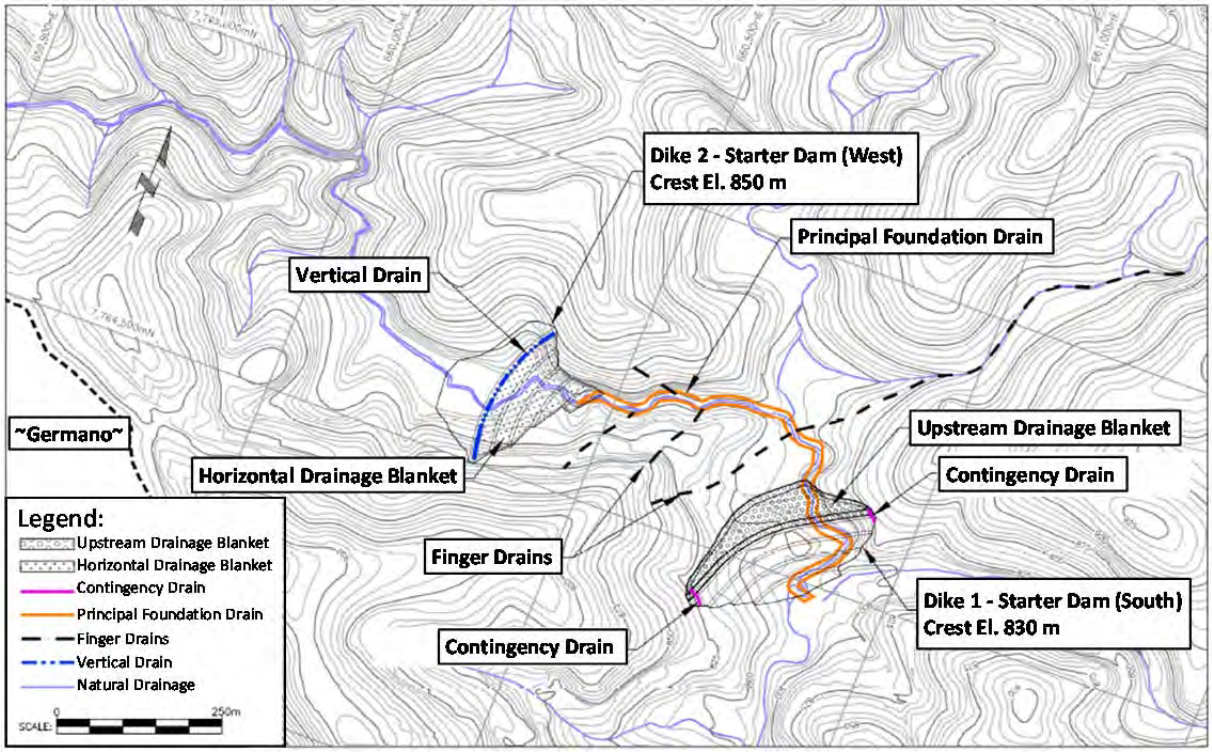

Figure G2-2 Concept design Fundão Dam drainage elements

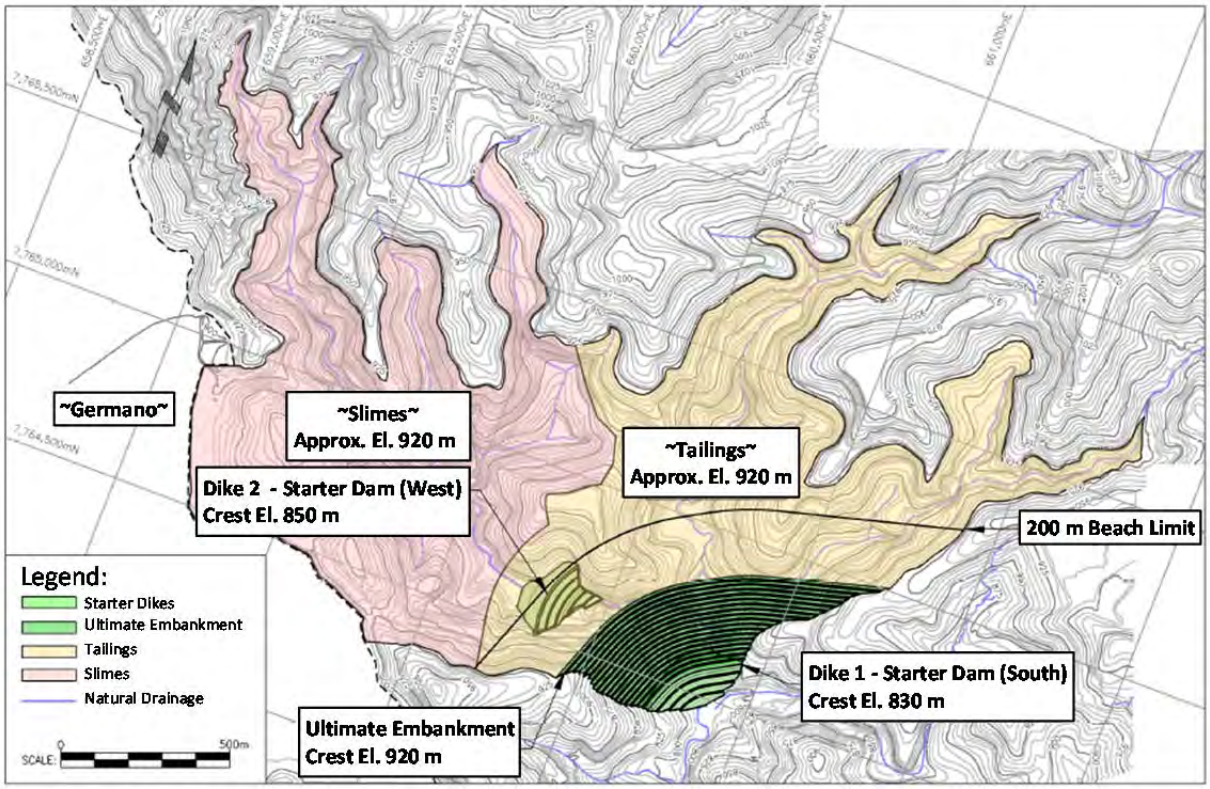

Figure G2-3 Concept design Fundão Dam final elevation 920 m

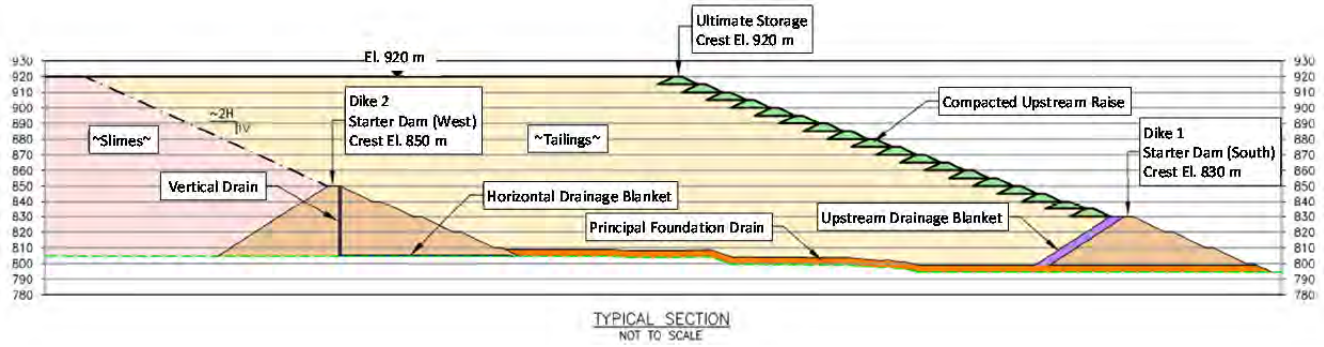

Figure G2-4 Fundão Dam TSF conceptual section

G2.2.4 Design Basis Summary

G2.2.4.1 Facility Design

Material Sources and Bulk Geometry:

- Mill separated waste stream comprising a segregated slimes and sand tailings.
- Starter Dam (Dike 1) constructed of compacted saprolite.

- Slimes retention Dike 2 constructed of compacted saprolite.
- Dike 1 raises comprised of compacted sand tailings.

Construction Approach:

- Both Dike 1 and Dike 2 are constructed using the upstream construction method with tailings sand used for Dike 1 above the Starter Dam.
- Sand tailings are spigotted from the inside crest of Dike 1 with a minimum 200 m beach length.
- Sand tailings deposition to stay +5 m above deposition of slimes.

For each drain geometry defined in the concept model, an equivalent bulk drain permeability aligned with the FEFLOW model geometry was developed to represent an equivalent drain performance to that of the concept design. The specific detail in the concept design drains is not possible to replicate in the FEFLOW domain at the scale modeled.

Table G2-1 Ph0 model material parameters

Material / Property	Base Value	Source
Material Properties (Hydraulic Conductivity (K) cm/s, storage unitless)		
Slimes Kxy	1.2×10^{-6}	Material parameters are derived from MDGEO[63] and MDGEO[7], both of which refer to parameters used in 2009 as part of the design planning.
Slimes Sy	0.2	
Slimes Kh/Kv	1	
Sand tailings (spigot) Kxy	5.0×10^{-4}	
Sand tailings (spigot) Sy	0.2	
Sand tailings (spigot) Kh/Kv	2	
Sand tailings (berm) Kxy	1.0×10^{-4}	
Sand tailings (berm) Sy	0.2	
Sand tailings (berm) Kh/Kv	2	
Foundation Kxy	1.2×10^{-7}	
Foundation Sy	0.2	
Foundation Kh/Kv	1	
Drainage Elements (Hydraulic Conductivity (K) cm/s)		
Dike 1 U/S Blanket Kxyz	$3.1 \times 10^{+1}$	Drain material parameters are derived equivalents from 2006 concept level drawing files (Appendix A Attachment A1).
Dike 2 Chimney Kxyz	$5.0 \times 10^{+0}$	
Dike 1 Thalweg Drain Kxyz	$5.6 \times 10^{+1}$	
Dike 1 L&R Abut Drain Kxyz	$3.1 \times 10^{+1}$	
Finger Drains Kxyz	$5.6 \times 10^{+1}$	
Dike 2 Horiz. blanket Kxyz	$5.0 \times 10^{+0}$	
Recharge (m/day)		
Rainfall Recharge Tailings	9.4×10^{-4}	Average wet season conditions assuming 90% of rainfall falls during 6-month period, highest recharge on spigotted sand, slimes controlled by pond constant head.
Rainfall Recharge Comp. Tail.	4.7×10^{-4}	
Rainfall Recharge Baserock	4.7×10^{-5}	
Pipe Recharge (Spigot)	90 L/s	Distributed to sand beach as increased recharge.

G2.3 Ph0 Model Construction

G2.3.1 Model Code

The selection of the modeling platform required that the model code have:

- the ability to translate the conceptual understanding into the numerical environment;
- the ability to simulate three-dimensional flow in a complex hydrogeological setting of steeply contrasting material parameters;
- the ability to simulate discrete permeable and non-permeable features, and anisotropy effects;
- the ability to bring increased focus and detail to areas of greatest interest;
- the ability to generate depth variant pressure data under transient analysis;
- the ability to conduct particle tracking analysis;
- recognition as industry standard software for the type of modeling being conducted; and
- flexibility to allow revision as and when new data becomes available.

The three-dimensional, finite-element model platform FEFLOW was selected to meet the objectives and requirements of this investigation and those of the Ph1 modeling. Model runs were constructed under saturated, steady state and transient conditions, for each of the Ph0, Ph1 and Ph2 models.

G2.3.2 Model Construction

The Ph0 model was constructed using the concept model developed in Civil 3D and described in earlier sections. Natural ground was represented by 5 m interval contours, and the topography of the dams and the slope of the raises were built in accord with design principles.

G2.3.2.1 Domain, Nodes and Layers

Model cells were more finely refined in the dam and slope areas to 5 m dimension, with nodes aligned along iso-elevation contours of the dam's respective raises. Inside the model domain, cells higher than El. 920 m and above the Starter Dam downstream face were set as inactive.

The Ph0 model has ~393,000 elements across 19 layers. There is a 1 m thick layer below natural ground to represent excavations and drains, with 8 layers of 5 m thickness between natural ground and top of Dike 1 at El .830 m. Between El. 830 m and El. 920 m, the top two layers are assigned a 5 m thickness, and the remaining 8 layers are 10 m thick. For the "pinched-out" layers within the model, minimum thickness was established at 0.1 m.

This level of layering detail was required for two purposes – to permit fair representation of the concept landform geometry of Dike 1, and to permit testing of TSF hydraulic performance through consideration of consolidation effects.

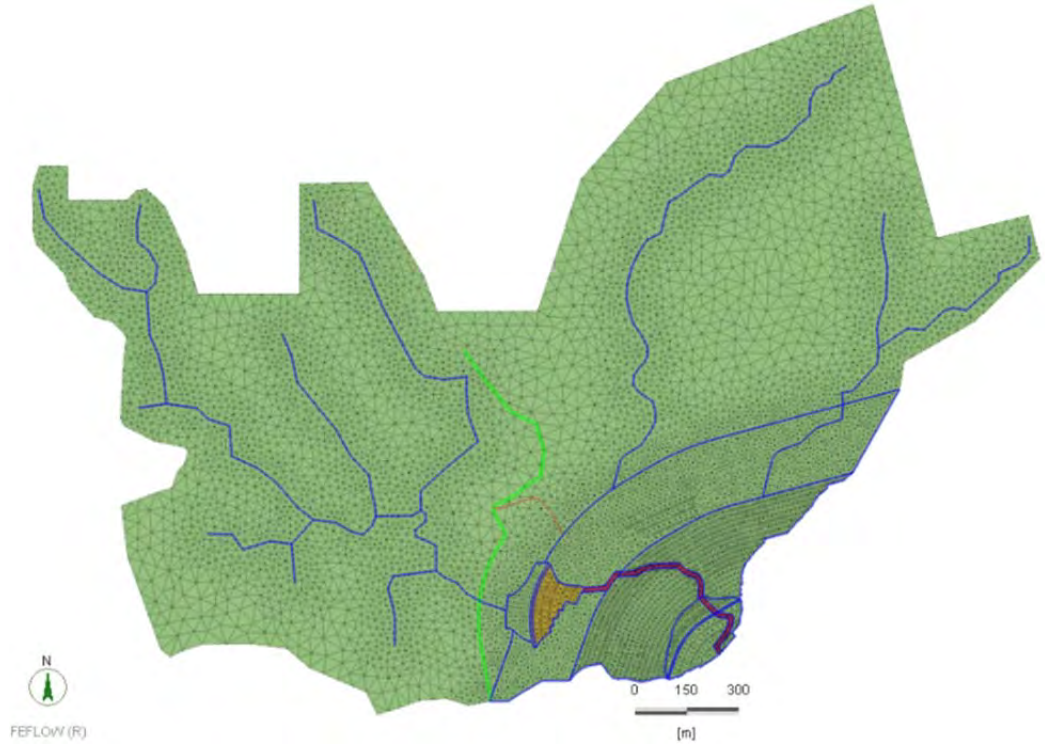

Figure G2-5 Ph0 model domain, node discretization, main drain elements plan view

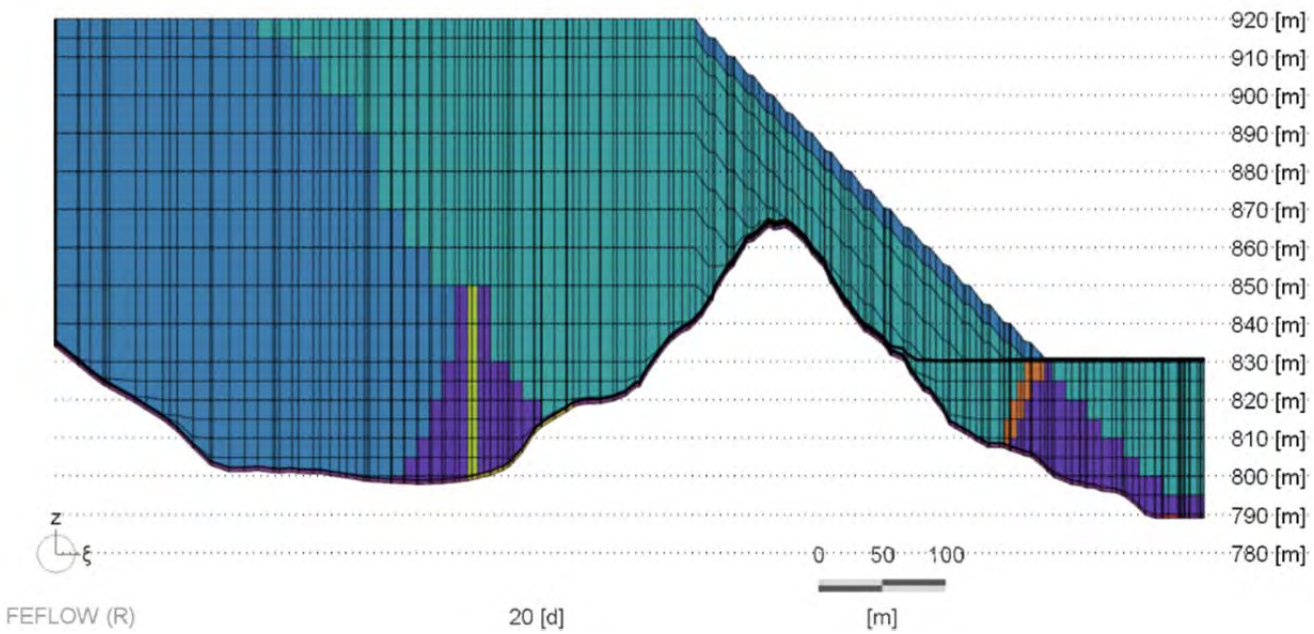

Figure G2-6 Ph0 model section Dike 2 through Dike 1 showing material permeability contrasts

G2.3.3 Drain Modeling and Model Evolution

As the primary design intent was efficient drainage of the sand, appropriate representation of drains was largely responsible for the direction in which modeling evolved.

G2.3.3.1 Drainage Elements

The Dike 1 upstream blanket, Dike 2 foundation blanket and chimney drain, and Principal Foundation Drain were modeled as high conductivity zones based on their respective dimension and equivalent bulk material properties. The respective drain conductivity was scaled over the modeled area to maintain the same conductance between the model and the concept design. For example, the Dike 2 chimney drain is 1 m wide by design, but the smallest discretization in the model in this area is 5 m. Model input conductivity is consequently one-fifth of the value in the concept design.

G2.3.3.2 Model Mode

Because of the highly conductive design underdrain(s) and the several orders of magnitude in difference between the design element permeability and material properties of the slimes and sand, phreatic and unsaturated modes proved numerically unstable.

A confined modeling approach was adopted with long-term transient simulations applied to simulate quasi steady state conditions. A check was included in the simulation to review each model cell's hydraulic condition; when a cell is dry it is "frozen" to prevent water flowing in the dry cells. However, the vertical permeability is maintained to allow recharge inflow as well as dry cell rewetting.

Consideration of the suitability of the application of confined versus unconfined modeling modes is provided in Table G2-2.

Table G2-2 Numerical comparison between phreatic and confined modeling modes

Attribute	Confined mode	Phreatic mode
Conductance	Each model cell is fully conductive	The cells below the water table or with 100% saturation are fully conductive. The cell above the water table or with 0% saturation are not conductive, or apply "residual thickness" to maintain minimal conductance. The cells intersected by the water table or with saturation greater than "residual thickness" and less than 100%, apply the true water thickness to numerically derive conductance.
Storage	Each cell uses specific storage (ss) to account for storage water during hydraulic head changes	The cells below water table, or with 100% saturation, use specific storage (ss). The cells above the water table, or with 0% saturation, have no storage account; FEFLOW applies a negligible number to maintain numerical stability. The cells intersected by the water table, or with saturation greater than "residual thickness" and less than 100%, apply specific storage (Sy).
Numerical formulation	Linear simultaneous equations with respect to hydraulic head	Non-linear simultaneous equations with respect to hydraulic head

For a long-term transient simulation, as the model converges and approaches a quasi-steady state condition, storage becomes negligible. Under such conditions the difference between confined and phreatic modes is the conductance above the water table or layer saturation less than 100%. Also, under unconfined or phreatic conditions, where a discrete element is used to represent the "drain", if it becomes exposed above the water table it turns off immediately, which has a sudden consequence on the performance of the whole drain and can block the remainder of the drain from flow transferal.

G2.3.3.3 Ph0 Model Calibration

Model calibration was not required or undertaken for the Ph0 model. This model is a reconstruction of the design intent only.

G2.3.3.4 Scenarios and Results

A model base case was run to evaluate the performance of the TSF in accordance with the concept model defined in Section G2.2. To account for inconsistencies or uncertainties in the conceptual understanding, a suite of additional runs was deployed to build a database of responses of the system to various stress and material parameter variances. This approach tests the basic design concept and presents "stress" scenarios which are plausible in their likelihood of occurrence, and which may affect the manner in which the TSF, particularly the drains, perform.

This process is also critical in informing the development of the Ph1 model (Section G3).

G2.3.4 Base Case (Ph0-1)

G2.3.4.1 Model Descriptions

The base case scenario is as described in Section G2.2. This model run is referred to as Ph0-1.

G2.3.4.2 Scenario Results

The base case model simulated a freely drained sand stockpile, with drain discharge from the Principal Foundation Drain at the base of Fundão Dam of the order of 28 L/s. No flow was predicted to reach either of the Dike 1 abutment drains, and no areas of Dike 1 exhibited emergent seepage.

Of the 28 L/s reporting to the Principal Foundation Drain, about 12 L/s is from incident recharge, 14.5 L/s from the constant head of the ponded reservoir, and the balance is change in storage.

In terms of phreatic conditions, the stockpile was efficiently drained, with complete drainage occurring over the alignment of the main drain. Away from drains the stockpile maintained partial saturation under modeled conditions.

G2.3.5 Drain Permeability Variance (Ph0-2 Series)

G2.3.5.1 Model Descriptions

Four drain permeability variance scenarios were run, with bulk drain performance modified by a reducing order of magnitude in each case. Drain conductance is determined for the base case as a

single material parameter unique to each drain, which accounts for the respective materials in their design and their distribution, across each drain profile. These model runs therefore do not apply a set value for all drains, but rather a diminishing performance scenario from their design intent for each.

Drain permeability was reduced for each run by a factor of 10, 100, 1000 and 10,000 from the Ph0-1 conditions. All other base case parameters remained unchanged. These model runs are referred to as Ph0-2a/2b/2c/2d.

G2.3.5.2 Scenario Results

The results of the various drain performance simulations are largely predictable and consistent with expected conceptual response. Reducing drain performance raises the phreatic surface, reduces flow in the Principal Foundation Drain, and triggers flow in the higher abutment drains as the overall system increases in saturation. Emergent seepage from Dike 1 is also triggered, and eventually dominates as the exit mechanism of water once drain permeability merges closer to that of the overlying material, or becomes stressed due to geometric limitations. Figure G2-7 provides a summary of drain flux reporting to either the Principal Foundation Drain, the left or right abutment drains, or as emergent seepage on the downstream face of Dike 1.

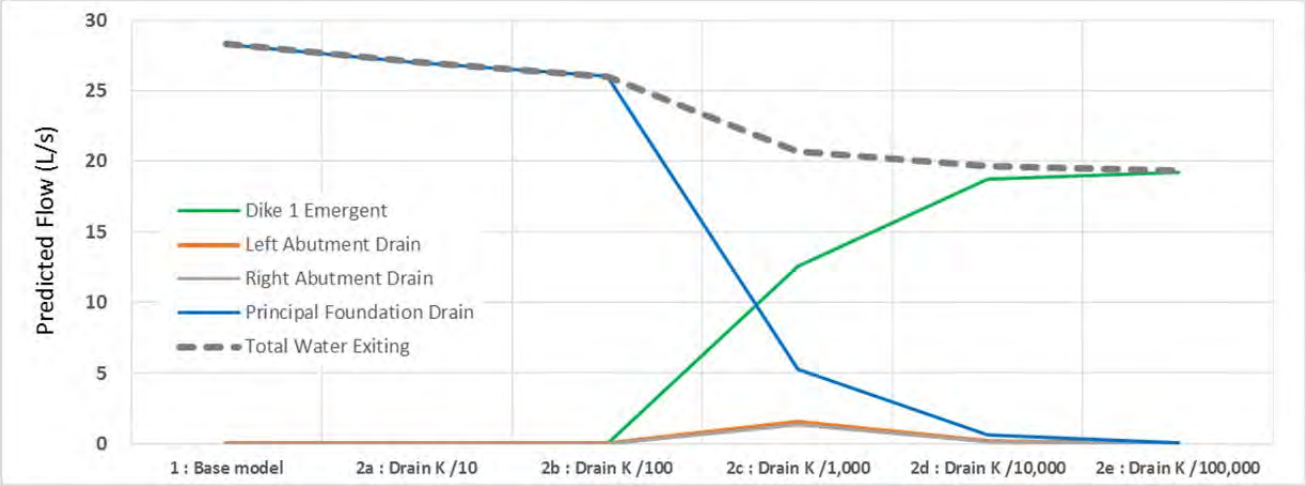

Figure G2-7 Ph0 model drain flux predictions for variance simulations of drain performance

Observations to note from these results:

- Total flux out diminishes as drain performance diminishes – this is a function of increased saturation of the sand profile, and increased water withheld in storage.
- For scenarios 2a and 2b, results are effectively the same, and show little variation from the base case. All water for 2a and 2b is conveyed via the Principal Foundation Drain, with no emergent seepage reaching the abutment drains or the dike face. Under these conditions the structure continues to meet the concept design intent, maintaining a largely drained sand mass with drain conductance capable of discharging predicted system inflows.

- For scenario 2c, however, a change occurs – flux out via the Principal Foundation Drain reduces by about 80%, flow commences in both abutment drains (albeit low), and discharge emerges on the Dike 1 downstream face, representing about 50% of total flux out. Conceptually, the effectiveness of the Principal Foundation Drain is now compromised and the system increases in saturation, which triggers discharge from other (higher) exit options.
- Scenarios 2d and 2e are more extreme versions of 2c, with drain conductance in 2e roughly equivalent to sand tailings permeability. This similarity in permeability explains the loss in performance of the abutment drains in these later scenarios.

Sectional representation of these scenarios is provided in a series of cross sections which shows three "stock" sections of results compared with the base case Ph0-1 results. The upper section (Section 1[1]) follows the main thalweg and hence represents the orientation of the Principal Foundation Drain to its exit at the toe of Dike 1. By virtue of the design effect of Dike 1, this section shows the most "drained" area of the TSF, and because of this is a conservative representation of seepage face conditions on the downstream side of Dike 1. The middle section (Section 2) is through Dike 2 and Dike 1, which does not align with the Principal Foundation Drain but is provided to show predicted influence of main drain elements from both dikes, and the hydraulic relationship with the slimes which are stored behind Dike 2. The lower section (Section 3) is a longitudinal section aligned along the crest El. 920 m of the final dam, and is intended to show varying degrees of saturation near to and away from the area of the Principal Foundation Drain and the abutment drains, and thereby provide a sense of overall system saturation from scenario to scenario. These section locations are shown on Figure G2-8.

[1] These section references should not be confused with reference to Sections 01, 02 and 03 in other elements of reporting.

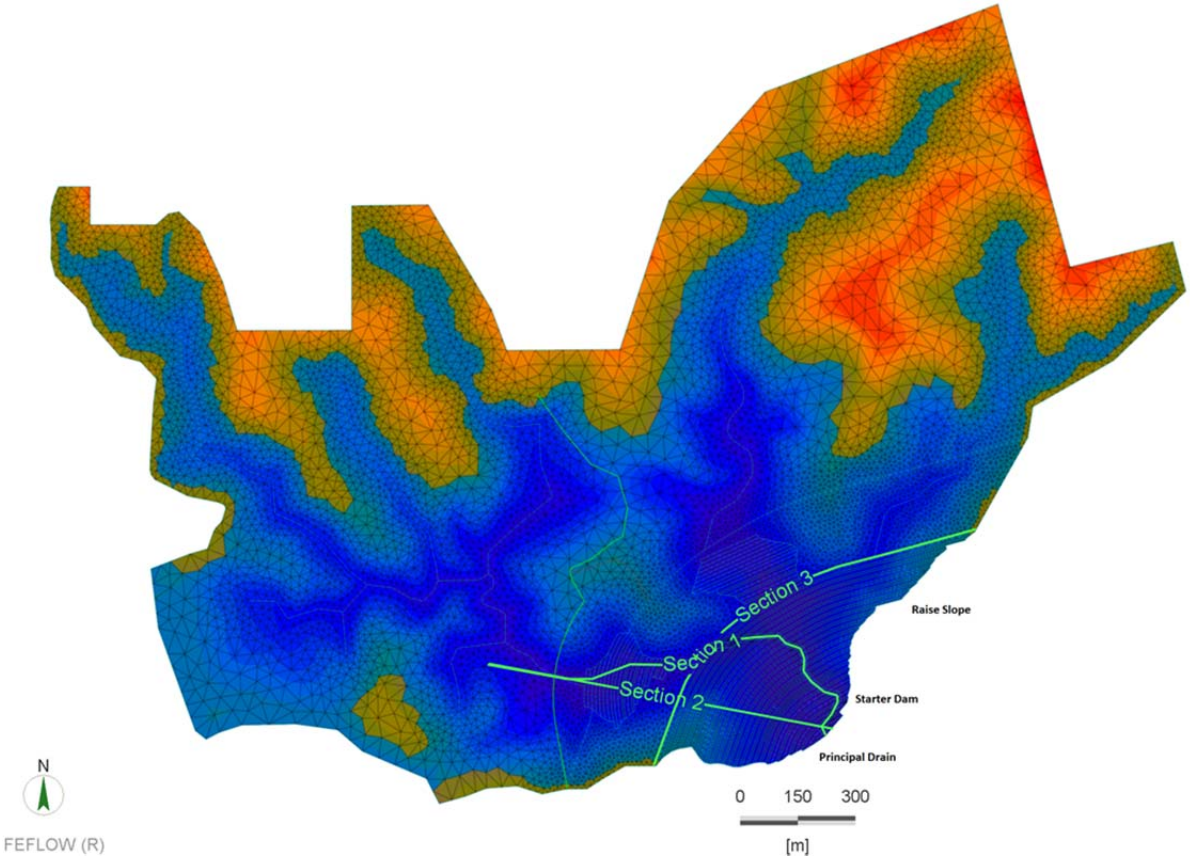

Figure G2-8 Ph0 series, model Sections 1, 2 and 3 location plan

The following additional observations are provided from Figure G2-9:

- The base case and Drain K/10 (2a) scenarios predict high performance of the drains resulting in desaturation of the sand tailings over the drains in both cases. The chimney drain is shown to be particularly effective in Dike 2.
- Although scenario 2b does not show appreciable change in flux from the base case and 2a models, this scenario does show the system starting to saturate. Of note, in Section 1 around 30 m of head is maintained over the Principal Foundation Drain, and this is reaffirmed in Section 3 showing the system building a saturated profile across the TSF. Section 1 indicates that this scenario has not yet triggered abutment drain flow or Dike 1 face seepage; however, the profile in the Starter Dam of Dike 1 has changed.
- Scenarios 2c, 2d and 2e show saturation of the system building and emergence of seepage faces on the downstream of Dike 1. Predicted elevations of seepage for 2a, 2b and 2c respectively for Section 1 are approximately El. 843 m, El. 859 m and El. 864 m.

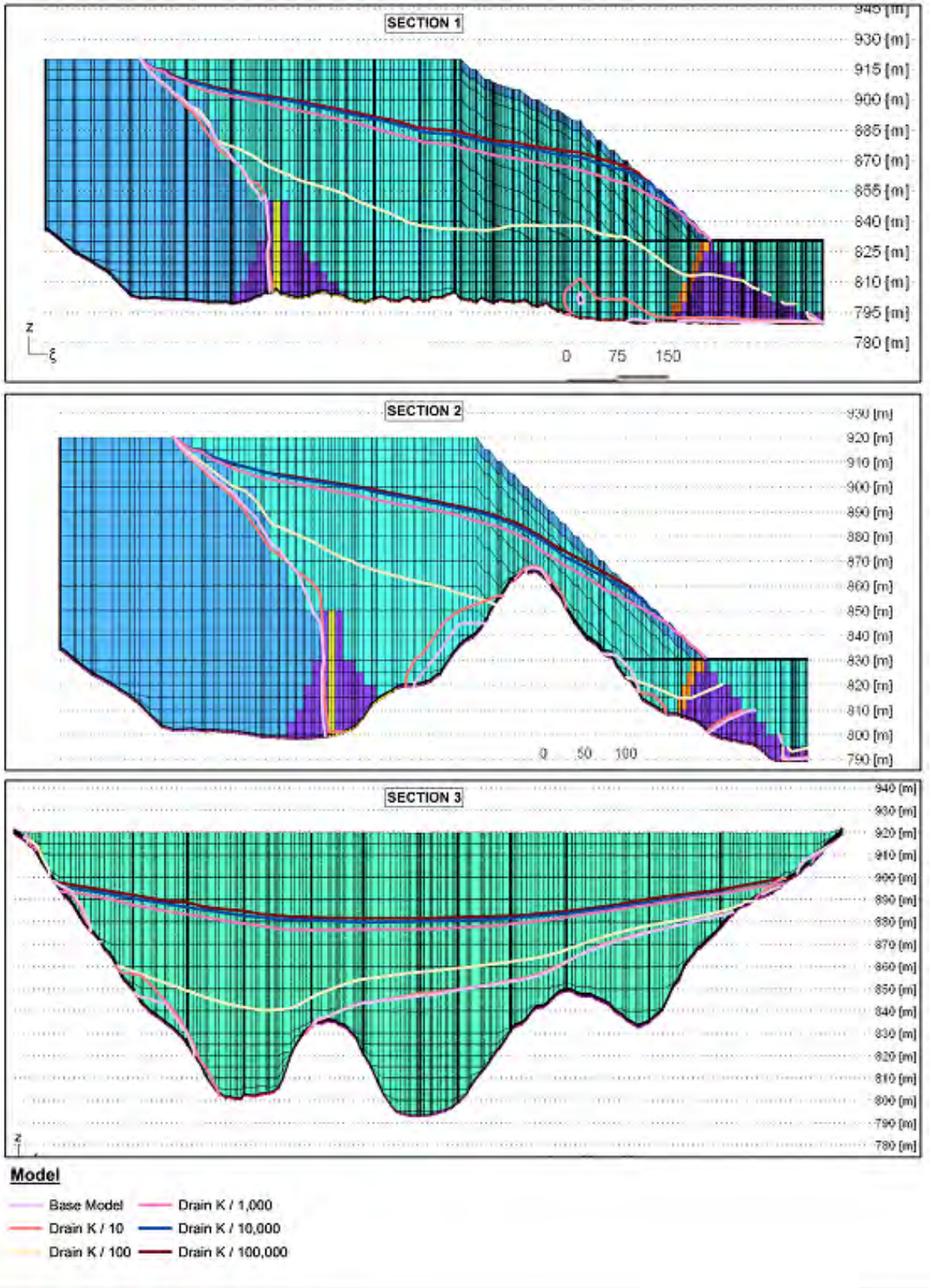

Figure G2-9 Ph0-1, Ph0-2a/2b/2c/2d results: reducing drain performance scenarios

G2.3.6 Recharge Stress (Ph0-3 Series)

G2.3.6.1 Model Descriptions

Two scenarios were considered for increasing hydraulic stress through increase in recharge, which simulates a consequence of increased rainfall or spigotting activity. The first run represented doubling of recharge. The second run increased recharge to 40% of rainfall, which is the equivalent of ~100 L/s (on tailings sand) simulated, with the balance of water not recharging into the sand assumed to have either evaporated or flowed to the pond to be handled with excess surface water.

Recharge into the upper model layer was the only parameter varied in these runs. All other base case parameters remained unchanged. These model runs are referred to as Ph0-3a/3b.

G2.3.6.2 Scenario Results

These scenarios assess the performance of the drain system, as designed, to carry and discharge these additional seepage loads.

Increasing recharge resulted in predictable responses in the system, with increased flux-in balanced as an increased flux-out of the Principal Foundation Drain. Neither of these scenarios triggered abutment drain flow or emergent seepage on Dike 1, and neither of these scenarios appreciably changed the phreatic conditions across the TSF.

Each of these scenarios showed an increase in flux-in consistent with the revised boundary conditions imposed. Although moderate increases in phreatic conditions (Figure G2-10) are a direct reflection of the increased flux-in, neither scenario affects the TSF performance sufficiently to compromise its drained design intent.

G2.3.7 Tailings Permeability and Anisotropy (Ph0-4 Series)

G2.3.7.1 Model Descriptions

These runs explored the effect of variability in tailings sand permeability through increase and decrease of bulk permeability by a half order of magnitude. These are effectively a sensitivity check on this material parameter aimed at determining their bulk effect on TSF saturation profiles.

Only bulk permeability of the sand tailings was modified. All other base case parameters remained unchanged. These model runs are referred to as Ph0-4a/4b.

Variation in anisotropy is more directed at testing an assumed parameter in the base case that has the potential to impact structure hydraulic performance. Only anisotropy of the sand tailings was modified. All other base case parameters remained unchanged. This model run is referred to as Ph0-4c.

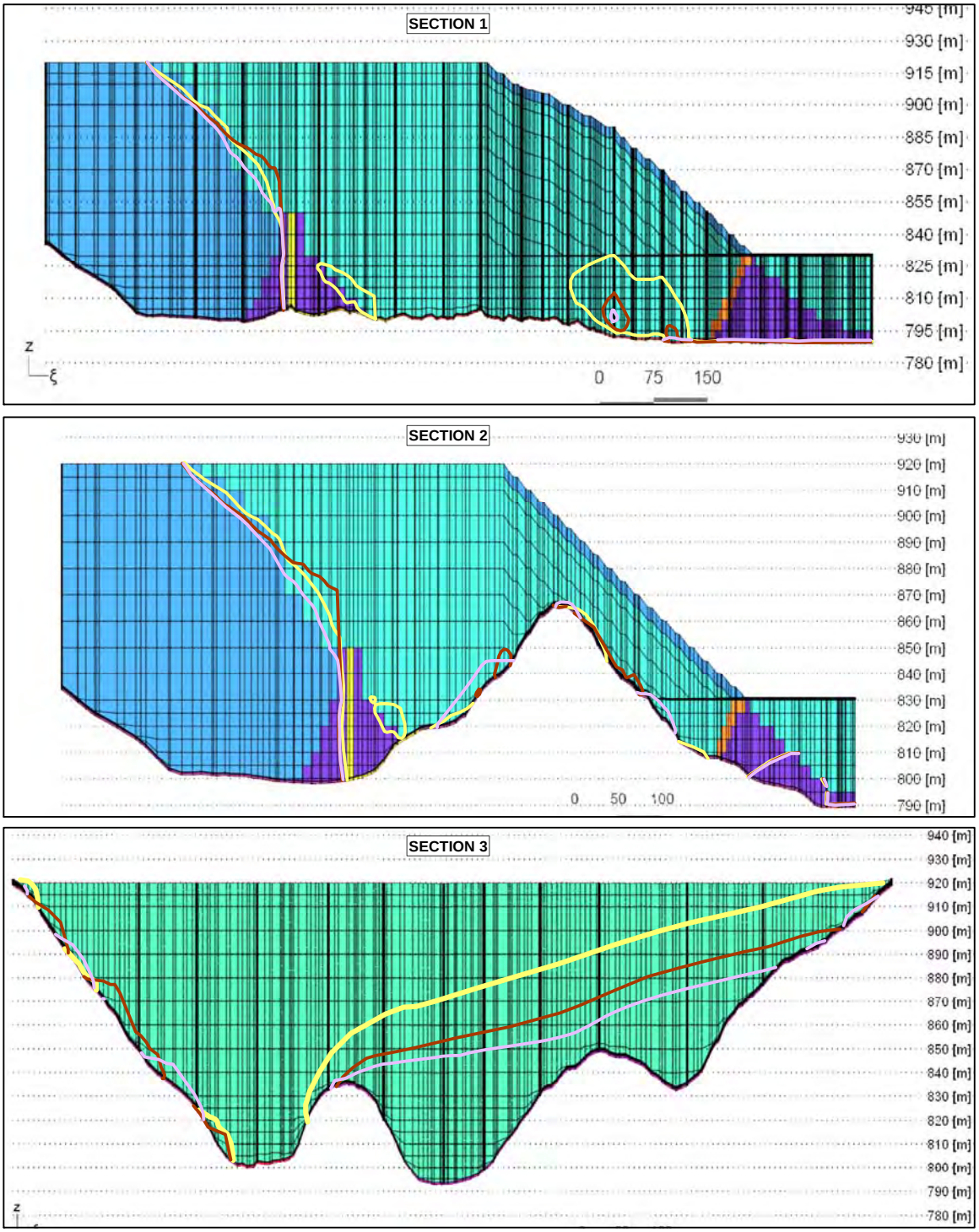

Figure G2-10 Ph0-1, Ph0-3a/3b results: recharge variation scenarios

G2.3.7.2 Scenario Results

Variation of bulk material parameters and tailings sand anisotropy showed little effect on the performance of the system. In each of these runs, the Principal Foundation Drain maintained its performance in removing water from the system (ranging in flow between 20 L/s and 31 L/s), with neither abutment drain flow triggered or emergent seepage apparent on Dike 1.

G2.3.8 Vertical Permeability Effects (Ph0-5 Series)

G2.3.8.1 Model Descriptions

Two scenarios were evaluated applying variability in material parameters to simulate the effect of permeability varying with stress; the first being a single order of magnitude permeability reduction from surface to base of facility (considered conservative as up to 2.5 orders of magnitude change over a similar stress scenario, as described in Vaughan (1994)), and the second scenario representing the same change in permeability but with a more pronounced degree of anisotropy (Kh:Kv of 10:1, rather than 5:1).

All other base case parameters remained unchanged. These model runs are referred to as Ph0-5a/5b/5c.

G2.3.8.2 Scenario Results

With reducing permeability limiting the release of water, raised phreatic conditions result. A combination of the reducing permeability with more contrasting anisotropy provides additional impediment to downward seepage. In neither scenario, however, did the Principal Foundation Drain fail to achieve its design intent (Figure G2-11).

G2.3.9 Drain Flow Conditions

As an alternate check of drain performance, an analytical assessment was completed to evaluate the capacity of the drains for the base case scenario, and to assess the nature of flows likely to occur.

G2.3.9.1 Analytically Derived Drain Capacity

Fell et al. (2005) present an analytical solution derived by Cedergren (1972) to estimate discharge capacity of a horizontal drain without pressurization. Applying this method, a discharge estimate of 259 L/s was assessed for the Principal Foundation Drain beneath the Starter Dam, which is significantly greater than the model predicted flow discussed earlier.

The drain was also assessed under saturated (pressurized) conditions applying a hydraulic gradient of 1:10 (representing 20 m head on the upstream side of the Starter Dam over 200 m of drain reach). Under this scenario, the drain has an estimated capacity of ~2,300 L/s.

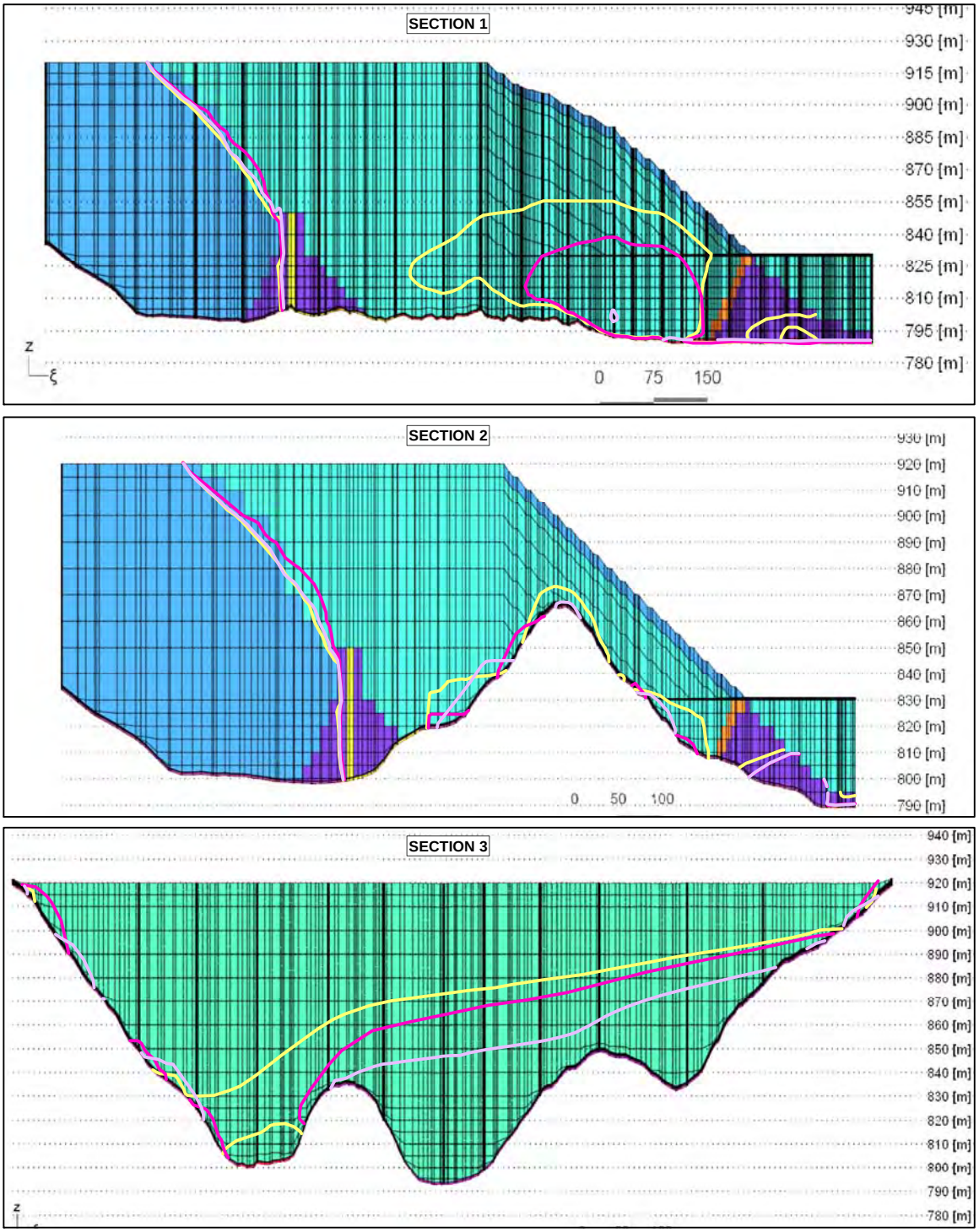

Figure G2-11 Ph0-1, Ph0-5a/5b/5c results: reducing permeability scenarios

G2.3.9.2 Laminar Versus Turbulent Flow

These two analytical solutions represent a flow velocity in the Principal Foundation Drain of 0.006 m/sec (without pressurization) and 0.056 m/sec (saturated, induced gradient). Converting these flow velocities to a Reynolds number results in values of 27 and 243 respectively (unitless). As a general guide, Reynolds number values greater than 30 can be regarded as turbulent flow conditions, and between 10 and 30 they represent non-linear laminar flow.

These results indicate probable non-laminar or turbulent flows; however, it is noted that these are at the derived maximum flow capacity for each scenario. Lowering flow for the un-pressurized solution to ~50 L/s lowers the Reynolds number to 5, more indicative of lineal, laminar flow.

G2.3.9.3 Flow Paths and Particle Seeds

Flow conditions for the Principal Foundation Drain from the base case numerical model are shown on Figure G2-12. Particle seed tracking clearly shows the drain influence, and in more detail the flow vectors show the accelerated groundwater movement as it enters the drain. In this model, the highest flow velocity was 0.0013 m/sec, which is about 20% of the analytical solution for the un-pressurized system.

The FEFLOW base case simulation predicted drain flows of the order of 28 L/s. Accordingly, flow vector derived groundwater velocity is expected to be lower than the analytically derived velocity for the maximum capacity drain.

A final observation from the numerical modeling results (for the base case, Ph0-1 scenario) shown on Figure G2-12 is the acceleration of groundwater flow in close proximity to the drain. This is the area where the strong contrast in material permeability between sand tailings and drain permeability is most prominent and could result in complex local flow regimes with localized very high groundwater velocities.

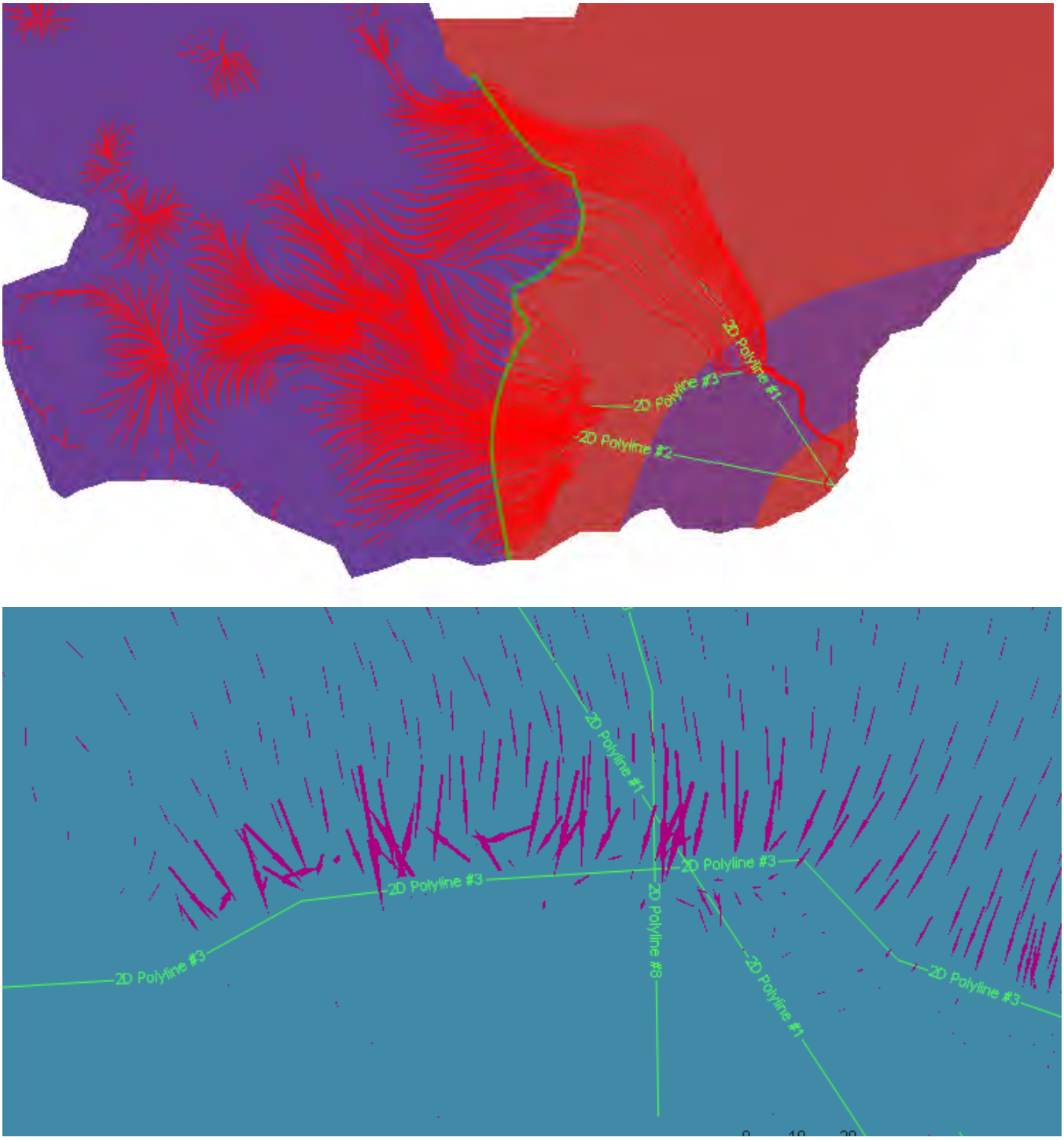

Figure G2-12 Particle seeds (upper) and flow vectors in the Principal Foundation Drain (lower)

G3 PHASE 1 MODEL – AS-BUILT CONDITIONS

G3.1.1 Ph1 Model Preamble

Numerical modeling was required to generate piezometric data in areas of the TSF where no or limited monitoring exists, and to create a transient record of the facility to augment the conceptual understanding, and to inform engineering studies being undertaken in parallel to this work.

The Phase 1 (Ph1) model provides a reconstruction of the as-built Fundão Dam, based on documentation and project records, reporting notes, photographic records, material balances and time sequenced reconstruction of the life-cycle of the facility. The model presents the hydraulic performance of the structure with particular reference to the phreatic surface, drain flux, areas of emergent seepage and zones of increased or decreased pore-water pressure.

G3.1.2 Ph0 Model Considerations

Key considerations taken from Ph0 work applied in the development of the Ph1 model are:

- The model maintains very good numerical stability and reasonable run times, as well as plausible water balance and hydraulic stress responses through application of the confined solution. This avoids the complexity and numerical instability that phreatic mode presents.
- The model produces comparable results to analytical solutions, and numerical modifications to the model result in predictable simulation outcomes. Boundary conditions and fundamental concepts developed in the Ph0 modeling appear sound and should be translated into the Ph1 model where appropriate.
- Vertical gradients, within the TSF and in relation to foundation materials, need to be considered. This is particularly the case where extensive low permeability horizons (slimes) may be present and may provide varying (to complete) degrees of local confinement. Coupled with this is the potential for additional water that may be released at depth through consolidation processes.
- Key attributes with the greatest potential to materially impact TSF performance are:
  - drain performance;
  - material anisotropy and changing permeability with depth (consolidation effects);
  - the extent, present and lateral continuity of low permeability horizons (slimes); and
  - system geometry.

G3.2 TSF As-Built Conditions

The full description of the Fundão Dam construction and operation is complex and detailed. It is not intended to reproduce this history in this appendix, although a clear depiction of the life of the facility can be reviewed through the main report text complemented with the various appendices, with Appendix B being the most relevant.

Key elements of dam construction of relevance to the Ph1 model do merit restatement:

- The Starter Dam (Dike 1), the upstream Dike 2 located between Dike 1 and the Germano facility, and Old Dike 1A and New Dike 1A located behind Dike 1.
- The Principal Foundation Drain, which was aligned along the thalweg of the valley before tailings deposition commenced, was decommissioned upstream of Dike 1. This drain, however, was not decommissioned beneath the Starter Dam, and this feature (with the remnants of the Auxiliary Drain) continued to exert influence and discharge water up until failure. The remnants of the Principal Foundation Drain were retained for the numerical simulation and are complemented with the vertical drain in the Starter Dam which also was not decommissioned.
- Similarly, the Contingency Drains on the left and right abutments of the Fundão Dam became redundant elements of the drainage system once the El. 826 m blanket drain was commissioned. These were also blocked on the upstream of the dam, so were not included in the numerical simulation.
- The El. 826 m blanket drain was constructed as a consequence of the failed original drain components, documented elsewhere in this report. This drain is strongly influential on the phreatic conditions of the facility and has been included in the Ph1 model domain.
- The El. 860 m blanket drain was completed immediately prior to failure. Although its period of operation was brief, its performance and influence on local conditions is critical in understanding left abutment phreatic performance. In particular, the geometry of this feature, as it steps up the slope to El. 870 m, is important in the simulation of phreatic conditions in this area.
- The Main Gallery and Secondary Gallery have not been included in the numerical domain as these features were concrete conduits and do not have an effect on material permeability and the surrounding seepage regime.
- The blanket on the upstream face of the Starter Dam (Dike 1) was not included as it was decommissioned before the commencement of the El. 826 m blanket drain.
- Representation of slimes and sand deposition is important in defining TSF geometry and has been the subject of substantial reconstruction effort. This reconstruction has not only sought to understand the distribution of the relative mine waste products, but has also followed the management processes for water control and deposition of tailings. Geological partitioning within the TSF is strongly based on this slimes/sand interface work, and was a major undertaking as part of the Ph1 model construction process.
- Pond location and elevation has similarly attracted substantial effort to reconstruct development and movement with changing construction activity, and similarly exerts an important influence on the phreatic performance of the TSF.

- The modified geometry of the system, particularly the realignment of the crest along the left abutment (the setback), has been represented in the model domain consistent with actual construction.

The general arrangement of the TSF in November, 2015 is provided on Figure G3-1. The above elements of the facility and the material parameters and monitoring data used in the numerical simulation are discussed further in subsequent sections.

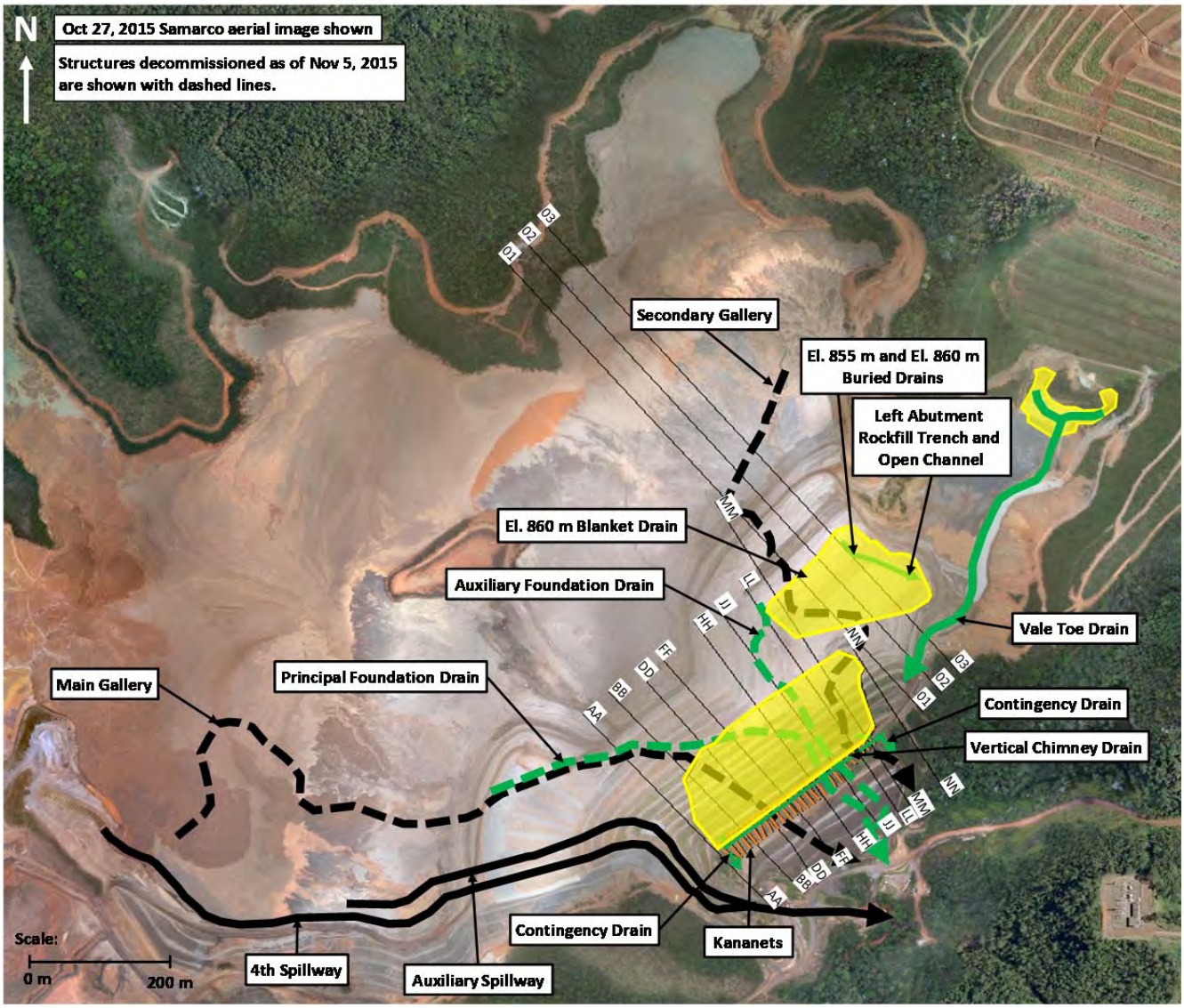

Figure G3-1 General arrangement of the Fundão Dam in November, 2015

G3.3 Ph1 Model Construction

The model design basis for the Ph1 model was to develop a calibrated, three-dimensional groundwater flow model for the Fundão Dam, to be used to predict:

- phreatic conditions and head data for the facility;
- changes to phreatic conditions in the facility with specific reference to changing surface geometry, construction activity and the effectiveness of various drains;
- location of zones of intermittent emergent seepage with time;
- a water balance of the facility; and
- transient vertical gradient development where possible to do so.

The model is not to assess the performance of original design concepts, but is to apply the as-built knowledge of the facility and produce steady state and transient output to support conceptualization of the system and to inform independent stability analysis work.

Further, the transient model commences with the TSF at El. 830 m. The performance and consequent decommissioning of the drains below this elevation are not relevant to the reconstruction of conditions above the El. 826 m blanket drain. The initial construction period from start of operation to El. 830 m is represented by a single steady state model. The facility is then modeled under transient conditions from El. 830 m to a final elevation of El. 900 m. Details of this model architecture are provided in Section G3.3.5.

G3.3.1 Ph1 Model Limits

The model domains for both Ph0 and Ph1 models are shown on Figure G3-2. The Ph1 domain is constrained by the surface water catchment reporting to the TSF, with the exception of the southwest extent which is bounded by the adjacent Germano facility. The model domain covers a planar area of 5,289,037 m^2.

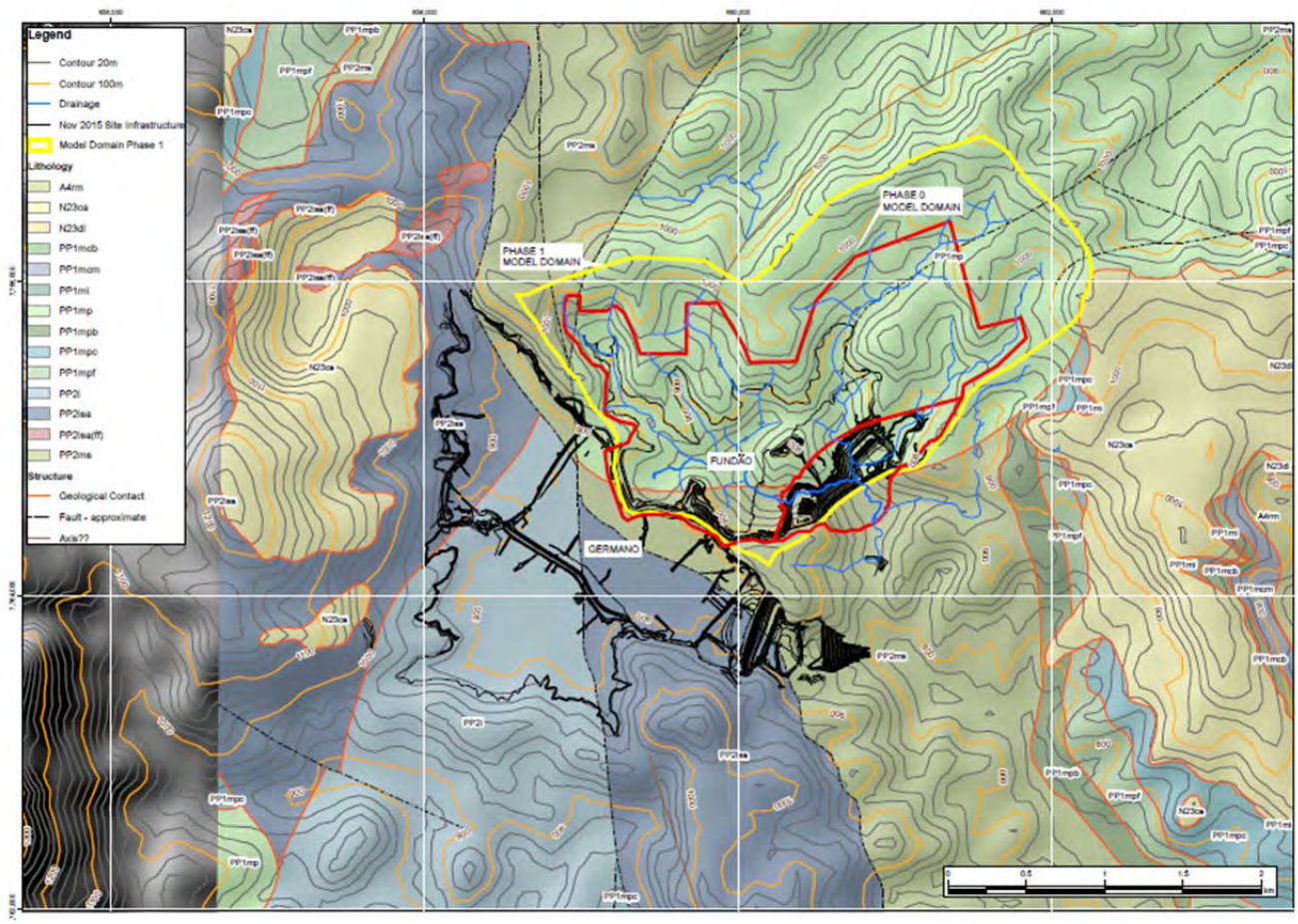

Figure G3-2 Ph1 model extent (yellow) with regional geology and Ph0 extent (red)

G3.3.2 Ph1 Geological Basis

Although the Ph1 model is focused on the tailings, the domain has been vertically extended to a nominal depth of ~2x the maximum depth of the placed tailings. This is to provide sufficient depth definition to permit development of deeper flow regimes if required. In applying this detail, regional geology has been assumed in the absence of deep drill information.

Dam construction elements and regional geology used in the model comprise:

- Dam construction:
  - Tailings sand (spigotted)
  - Slimes
  - Compacted sand from berm construction
  - Mixed slimes/sand zones
- Drain construction materials:
  - Natural ground
  - Weathered, altered and fresh phyllite
  - Structural alignments (included for potential sensitivity analysis)

G3.3.3 Ph1 Domain, Nodes and Layers

G3.3.3.1 Model Domain

The model was discretized using six-noded three-dimensional prism elements. A process of mesh refinement based on hierarchical areas of model interest (such as drains) was used to arrive at the final mesh configuration.

G3.3.3.2 Node Distribution

Variable density node distribution was applied to bring numerical focus to areas requiring the most detail. This has been achieved through use of “breaklines” to control location of nodes, and application of broad internal zoning to capture areas where increasing detail is needed. Breaklines used include lineal drain features, slope definition of final landforms (bench and berm details on Dike 1 including the rotated axis on the left abutment), TSF lateral extents, internal natural drainage alignments and internal constructed features such as Dike 2.

Node density in increasing level of detail is:

- Most coarse nodal distributions are applied in the northeast where limited topographic control is available and the model domain is only extended in order to capture the surface hydrology catchment. Element size in this zone is about 100 m.
- The topography outside the extent of the TSF and for which good elevation control is available has the next level of nodal density applied. Element size in this zone is about 60 m.
- The TSF upstream of Dike 2 has element sizes of about 15 m.
- The TSF upstream of Dike 1, and downstream of Dike 2 and the overflow, which is comprised of sand tailings, slimes, and compacted sand, and is inclusive of most constructed drain elements, has elements sized at about 10 m.
- The final level of increased node density was applied directly to the left abutment, Dike 1 and Grota da Vale areas, with element sizes of about 5 m.

There are 31,845 elements per layer, across 49 layers, for 1,560,405 model elements. Figure G3-3 provides nodal distribution (green) and breaklines (red) used in model discretization.

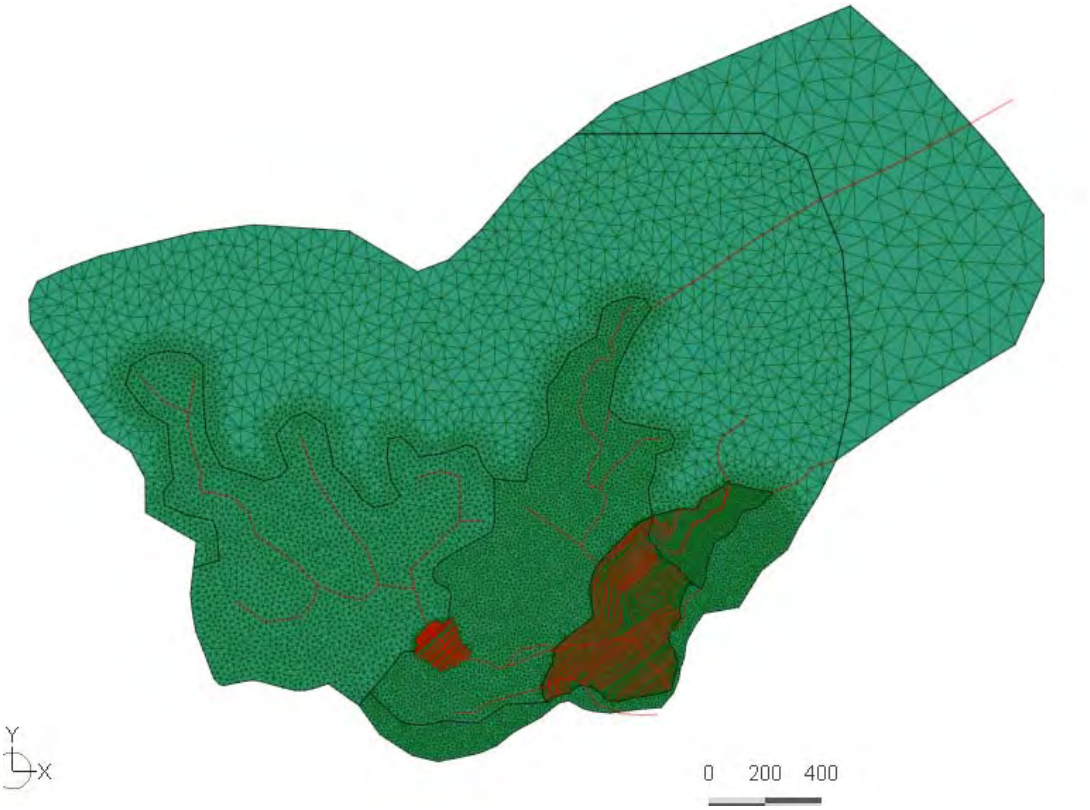

Figure G3-3 Ph1 model mesh/node distribution (green) and key breaklines (red)

G3.3.3.3 Ph1 Model Layering

The Ph1 model was constructed in accord with the conceptual description of tailings morphology provided in Appendix B. The uppermost slice of the model was set as topography, and the base of the model was set at El. 690 m. The Ph1 model has 49 layers, comprising:

- 44 layers representing inside the TSF limits between El. 790 m to El. 900 m+. Layer thickness varies but within the TSF is generally 2.5 m or less per layer; and
- 5 layers representing El. 690 m to El. 790 m, comprising basement (weathered to fresh phyllite).

Layer definition is based on the application of a discretized tailings zone of variable total thickness constructed of a sequence of 2.5 m thick unique tailings horizons. This detail permits extraction of depth specific (model predicted) pressure with time, and assists in bringing numerical stability to the model by addressing the wide contrast in material parameters between slimes, sand and drains.

Figure G3-4 shows an example of this, with basement (brown), slimes (green), sand (blue), compacted sand (yellow) and the El. 826 m blanket drain (orange), with red representing inactive model cells.

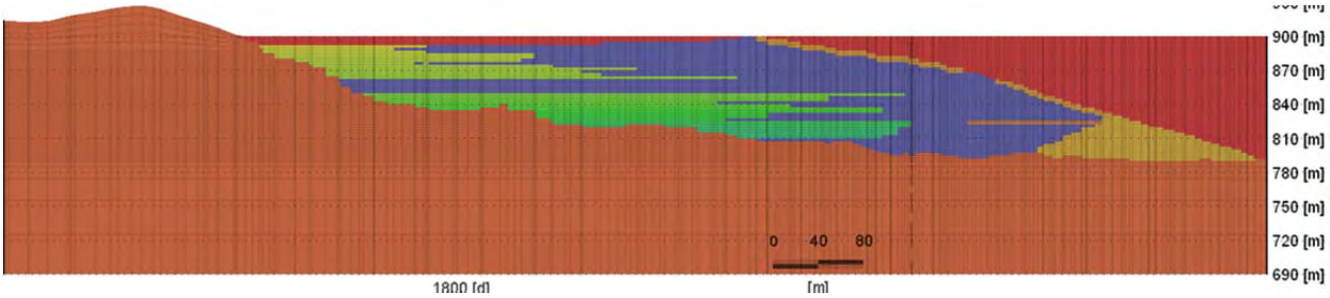

Figure G3-4 Model cross section showing general layer distribution

One limitation of this approach is that tailings horizons need to be assigned the nearest 2.5 m elevation in the model. This represents a potential vertical error of +/-1.25 m. This vertical error, however, should be placed into context by considering the overall confidence in slimes distribution and elevation post-deposition (Appendix B). The true thickness of the slimes horizons across the TSF remains largely uncertain. The 2.0 m thickness of slimes logged in SP-07 at the left abutment is a post consolidated thickness. Also, slimes interface mapping assigned elevation to the slimes horizons at the time they were deposited (still visible at surface) and specific to the dates available for the respective survey data or aerial image. This approach was well suited to reconstructing the morphology of the TSF; however, it is not possible to assess with confidence true depositional or true post consolidated thicknesses. Other than limited drill control, no data exists to verify this.

The 2.5 m thick layers assigned in the FEFLOW domain are therefore considered an acceptable representation of pre- to post-consolidated conditions, and remain within the bounds of ~3 months deposition (assuming 10 m to 12 m raise rates per annum), which is the maximum stress period interval defined and discussed in Section G3.3.5.

G3.3.4 Drains and Other Boundary Conditions

G3.3.4.1 Drain Discussion

An important observation from the Ph0 modeling is the hydraulic response of the system to the three broadly contrasting material types of slimes, sands and drains, and in particular, the general performance of the TSF under a variety of drain stress induced through diminishing drain permeability. An outcome of the Ph0 work identified that numerical modeling of the Fundão Dam is not an exercise in subtle material parameter contrasts. Rather, it is an exercise in understanding and representing the geometric distributions of these broadly contrasting material types, and correctly applying boundary conditions and stresses to each of them. The most powerful and relevant boundary affecting the TSF is the location and performance of the internal drains.

Models Ph0-2a/2b/2c/2d (Section G2.3.5) showed drain performance was not seriously affected until three orders of magnitude reduction in permeability from design intent occurred. This concept is further supported with analytical assessment of drain capacity (Section G2.3.9) which indicated up to 2,300 L/s flow was possible under reasonable hydraulic gradients and pressurized conditions, which is well in excess of expected water balance components.

Piezometric data in the area of the right abutment and the El. 826 m blanket drain (Appendix E) showed that conditions across and behind the blanket drain had largely reached a quasi-steady state condition relatively quickly after the commissioning of the drain. This drain, together with the remnants of the Principal Foundation Drain and the Auxiliary Drain (within the Starter Dam), provide good control of phreatic conditions in this area of Fundão Dam, with minimal vertical variation in piezometric response between El. 790 m and El. 835 m after El. 826 m blanket drain commissioning. Also of note from this data is the more variable piezometric responses of instrumentation located further away and in higher elevations from the El. 826 m blanket drain, indicating the diminishing effectiveness of the drain with increasing distance and elevation.

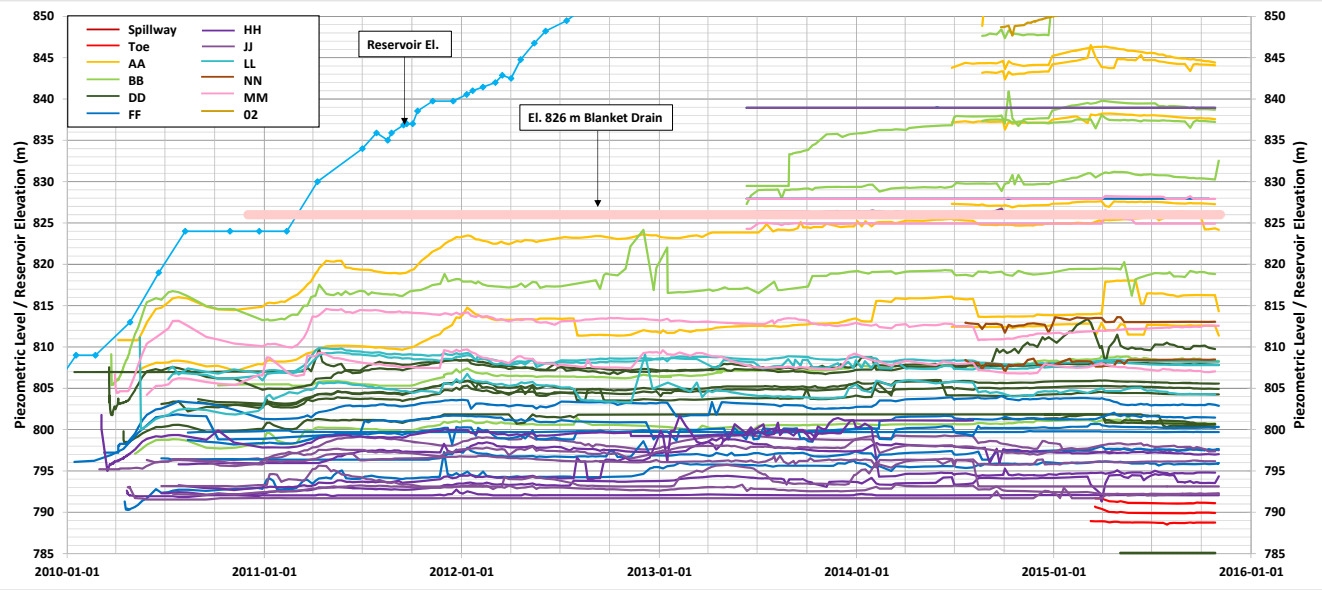

Notes:
1. Piezometric levels are grouped by instrumentation sections. See Appendix E Attachment E1 for grouping.
2. Piezometric levels for Sections 01, 03 and left abutment piezometers are not shown as they are above the maximum elevation range shown.

Figure G3-5 Composite hydrograph showing piezometric trends during period of El. 826 m blanket drain operation, up to El. 850 m

A degree of variability in the permeability of these drains can therefore be absorbed before detrimental impact, resulting in substantial change to the hydraulic profile, occurs. This does not negate the possibility that incorrect drain construction may have impacted hydraulic performance of the system. Rather, the Ph0 modeling and analytical drain performance, together with the piezometric data for the right abutment, brings greater focus to the geometry of the overall TSF as being a more critical factor to drain "efficiency" than drain permeability alone.

The likelihood is therefore that increasing distance from active and operating drains is a driving factor to heightened phreatic conditions and emergent seepage events. This effect is made more prominent with the presence of slimes horizons, a topic discussed further in Section G3.5.1. These interpretations are also reflected in the operational response by the site to construct the El. 860 m blanket drain and commence construction of a similar drain on the right abutment at the time of failure.

G3.3.4.2 Drain Representation in the Ph1 Model

Drain representation in the numerical domain is a relatively simple application of expected drain material parameters adjusted to model geometry. For the most part, and because the El. 826 m and El. 860 m blanket drains were geometrically broad sequences of high permeability material rather than narrow and finite lineal arrangements, their representation in the model was much closer to as-built conditions than other drain elements. The most important aspect of their inclusion was therefore correct spatial representation, especially for their base elevations.

Activation of these drains was achieved through sequenced raising of the overall facility from El. 830 m, with the model turning layers "active" as their respective elevations fell below the elevation of the TSF surface at any particular time step. The drains continued to remain active until the end of the simulation, with their ability to convey or discharge water constrained or enabled depending on adjacent and overlying material conditions.

A summary of the drain elements and the manner of their inclusion is provided, with their respective locations/distributions shown on Figure G3-1:

- El. 826 m blanket drain is represented as a horizontal blanket of high permeability material consistent with as-built records. The model includes lineal representation of the Kananets® in direct connection with the drain material to assist in rapid removal of water.
- El. 860 m blanket drain is represented as a horizontal blanket of high permeability material consistent with as-built records. Importantly, this drain "steps up" to El. 870 m perpendicular to the slope on the left abutment, in accord with the physical construction of this feature.
- Principal Foundation Drain and Auxiliary Drain are modeled as high permeability lineal drains beneath Dike 1, represented consistent with as-built knowledge with only the remnants of these active drains inside the Starter Dam geometry.
- The series of left abutment drains is a lineal drain feature constructed along the left abutment and suspected to be in direct connection with the El. 860 m blanket drain. Although this was not confirmed, the drains were known to have a defined outlet in the form of a buried pipe under the setback plateau. Either way, water collected by these drains were conveyed out of the system in a controlled manner. The feature is represented in the numerical domain consistent with the interpretation of its extent and timing described in Appendix B.

The material parameters of the drains were not adjusted in the calibration process. This is because the Ph0 modeling showed that minor modification of their material parameters had little impact on their performance or their influence on broader phreatic conditions. Further, initial manual calibration using their design material parameters resulted in early "good" response to adjacent piezometers, indicating no need to modify their performance for local calibration purposes.

Modification of their performance was only considered in the event their operation in the numerical domain had much broader influence, which was not the case.

G3.3.4.3 Other Boundary Conditions

The following boundary conditions were established in the mine area FEFLOW model:

- Constrained seepage face conditions were established across the face of the dam. The constraints on the seepage face dictate that once phreatic conditions intersect Slice 1 (the top of the upper active layer in the model at the time of the simulation), water is removed from the system and reports to the water balance as an outflow. This numerical representation of seepage faces is established to reflect the physical process of emerging seepage due to rising phreatic conditions "daylighting" at surface.
- No flow boundary conditions were established at the model base and on the outer vertical limits of the model domain to reflect the effect of groundwater divides along major catchment boundaries.
- Constant head conditions were applied to ponds for each of the stress periods defined, including the area of exposed slimes across the TSF. These conditions were triggered and active only when their presence was confirmed through reconstruction of the TSF morphology (Appendix B).
- Recharge was applied across Slice 1 according to the areal distribution of rainfall described in Table G3-1.

Consolidation effects were included as an important transient boundary condition, and are described in more detail in Section G3.3.7.

G3.3.5 Model Timing and Stress Periods

Transient FEFLOW simulations are controlled by established model duration and time steps, transient boundary conditions and/or material changes over time. The time power functions and time steps which introduce these stresses to the model domain are developed for unique model inputs in order to best represent their time-influence on the model simulation.

Geometric changes to the domain through adjustment to model stress periods are based on a starting model under steady state conditions of El. 830 m (~November, 2010), followed by quarterly geometric changes until November, 2013, and monthly changes to November, 2015. The model is constructed of daily time-steps to permit extraction of output coincident with the timing of relevant events. A summary of the model stress periods mapped against failure events and drain activity is provided on Figure G3-6. The transient model (Ph1) starts on December 1, 2010 and ends on November 5, 2015.

Conditions prior to the commissioning of the El. 826 m blanket drain were not included in this transient simulation. Under-performing drain elements (e.g., the drainage blanket on the upstream face of the Starter Dam) were decommissioned prior to the El. 826 m blanket drain. The concrete conduits (Main and Secondary Galleries) do not affect material permeability and were similarly decommissioned albeit after the El. 826 m blanket drain. They therefore provide no hydraulic influence on the system (other than where remnant features of these drains remain) of relevance to

the period leading up to the November, 2015 failure. Modeling of these features was considered a redundant process that would only add unnecessary complexity to the simulation.

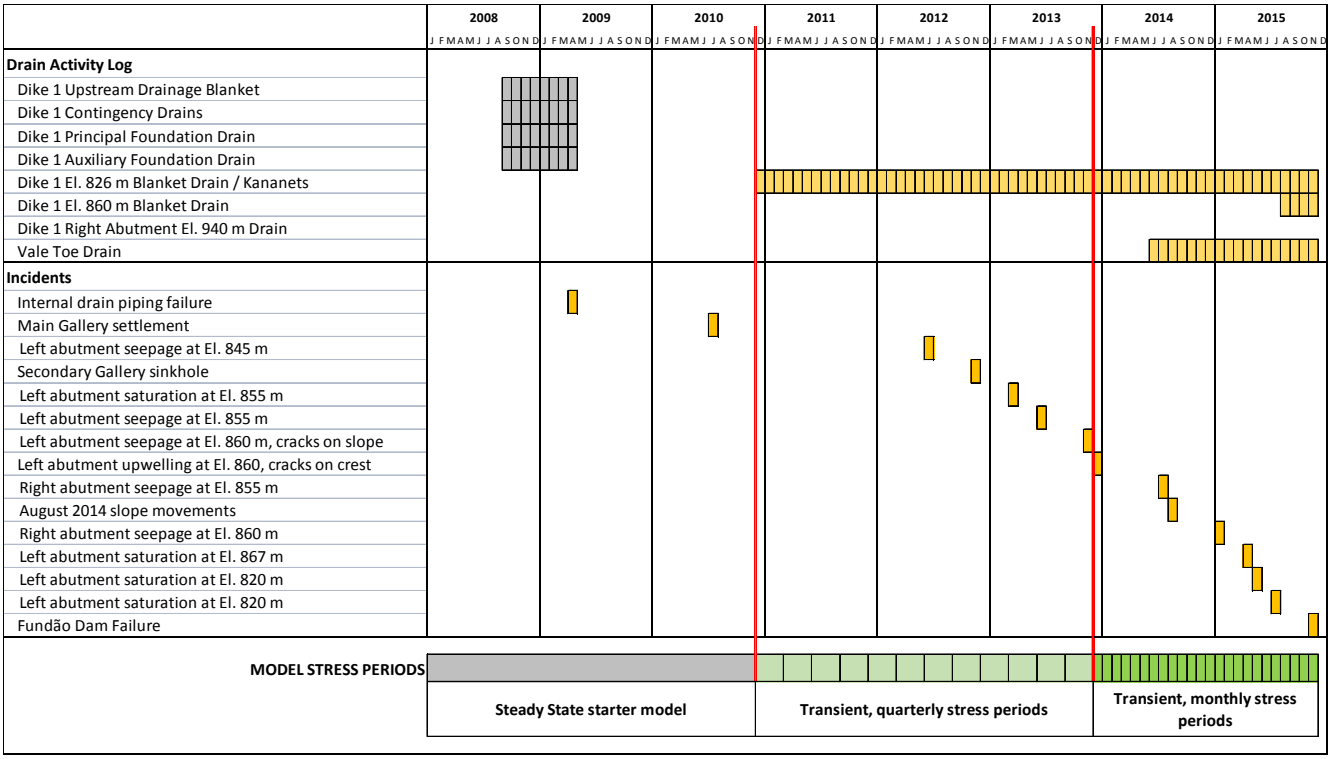

Figure G3-6 Fundão Dam TSF life cycle with model stress periods

G3.3.6 TSF Raise/Construction Process

The adaptation of the as-built construction process to the numerical domain required representation of the following time dependent elements:

- elevation, distribution and lateral extent of slimes;
- elevation, distribution of sand tailings (including compacted berms);
- spatial distribution and elevation of drains (discussed in Section G3.3.4); and
- spatial distribution and changing elevation of intermittent ponds.

G3.3.6.1 Slimes Elevation and Distribution

The slimes exert significant influence on the hydraulic performance of the TSF. They represent a source of water; they control the main elevation of the slimes pond; they impede vertical flow where they exist as discrete layers; they provide confinement to underlying permeable materials; and they laterally skew the regional distribution of the phreatic surface. Translating their distribution and elevation (Appendix B) into the FEFLOW domain and matching this transient record to the stress periods assigned was a time consumptive and detailed process, made further challenging by the need to match other construction activity of the TSF such as sand placement and ponds.

Appendix B details the method used to reconstruct the history of slimes and sand deposition in the TSF, and should be read in conjunction with this appendix. The process is detailed and required the spatial cataloguing of aerial photography and survey data against operational reports, material balances, site photography, decant locations and general construction activity records.

The design intent of the facility (Section G2.2) was to separate slimes and sand deposition behind Dike 1 and Dike 2, respectively, maintain a positive sand elevation (+5 m) above slimes, and maintain a minimum beach distance of 200 m between the crest of the dam and the slimes. This design intent, however, was not met all of the time, resulting in periods of slimes encroachment toward and in some cases beneath the dam crest. Such events resulted in discrete slimes horizons being deposited within the sand body (below and above), as depicted on Figure G3-7 (reproduced from Appendix B).

Each 2.5 m slice of the FEFLOW model was assigned a material parameter distribution consistent with the slimes/sand tailings morphology, also accounting for areas of compacted sand and drain construction. The sequence was built from the bottom up to a final elevation of El. 900 m, with parallel matching of pond extents and elevations. This resulted in a single mass of tailings to final survey data of November, 2015. Slimes elevations were then “stepped down” in 2.5 m increments to reverse-construct the history of the TSF in accord with model time stress periods, while maintaining consistent elevation changes to those of the overall facility and representing the slimes/sand model geometry in the FEFLOW domain.

A total of 29 unique system models were produced using this technique, with their active representation in the numerical domain determined by the time period of the model. Those model cells outside the active domain were “inactive” until the TSF elevation triggered otherwise.

Figure G3-8 shows an example of the aerial photography used to define the slimes, as well as the transition from predominantly slimes to interbedded slimes to isolated slimes, upstream of Dike 1. This transition concept is discussed in Appendix B. For the FEFLOW model, however, actual mapped horizons of slimes were used consistent with the interpretation presented on Figure G3-7, and assigned to layers in accord with the 2.5 m structure previously described.

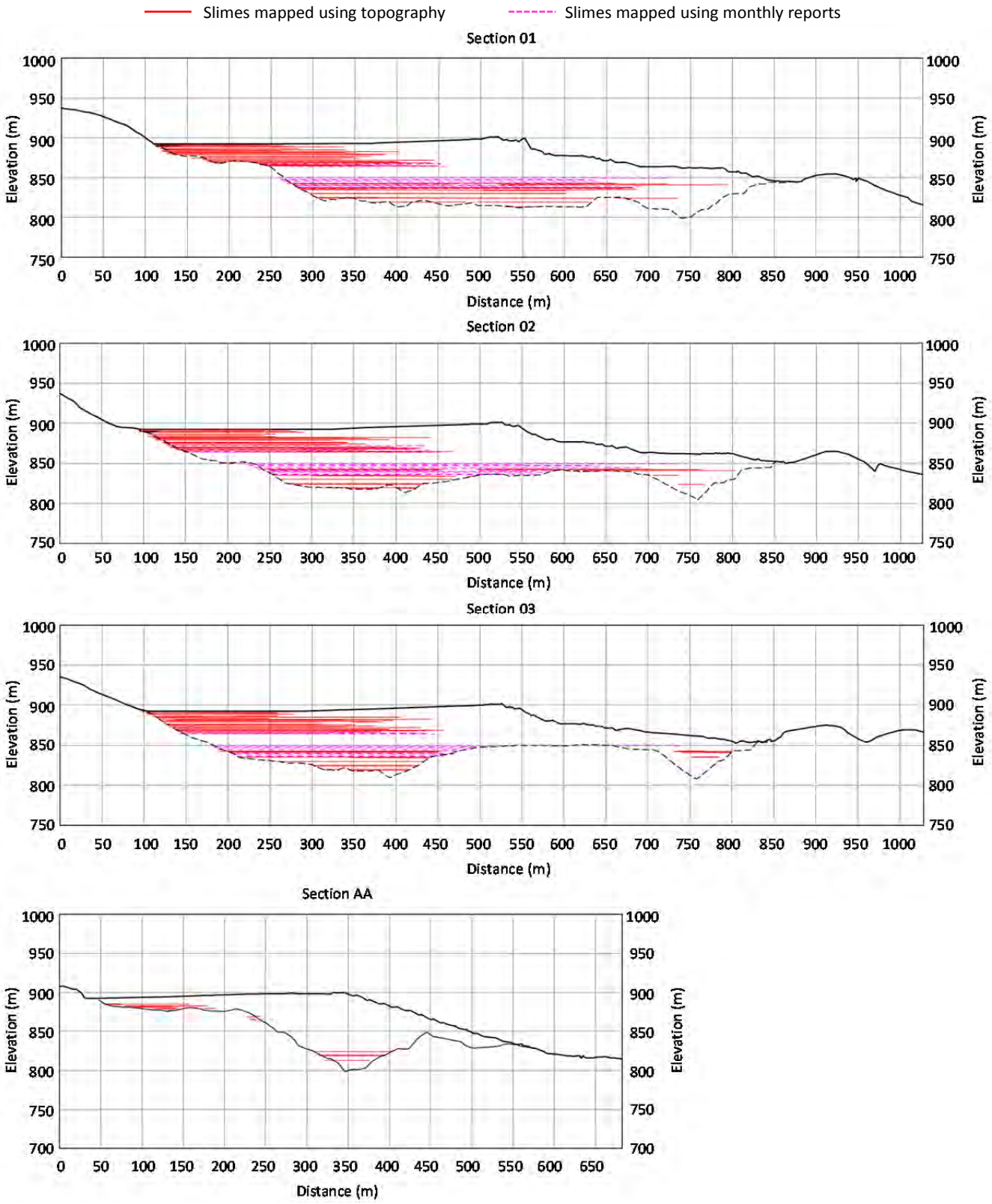

Figure G3-7 Sectional distribution of slimes and sand within the TSF

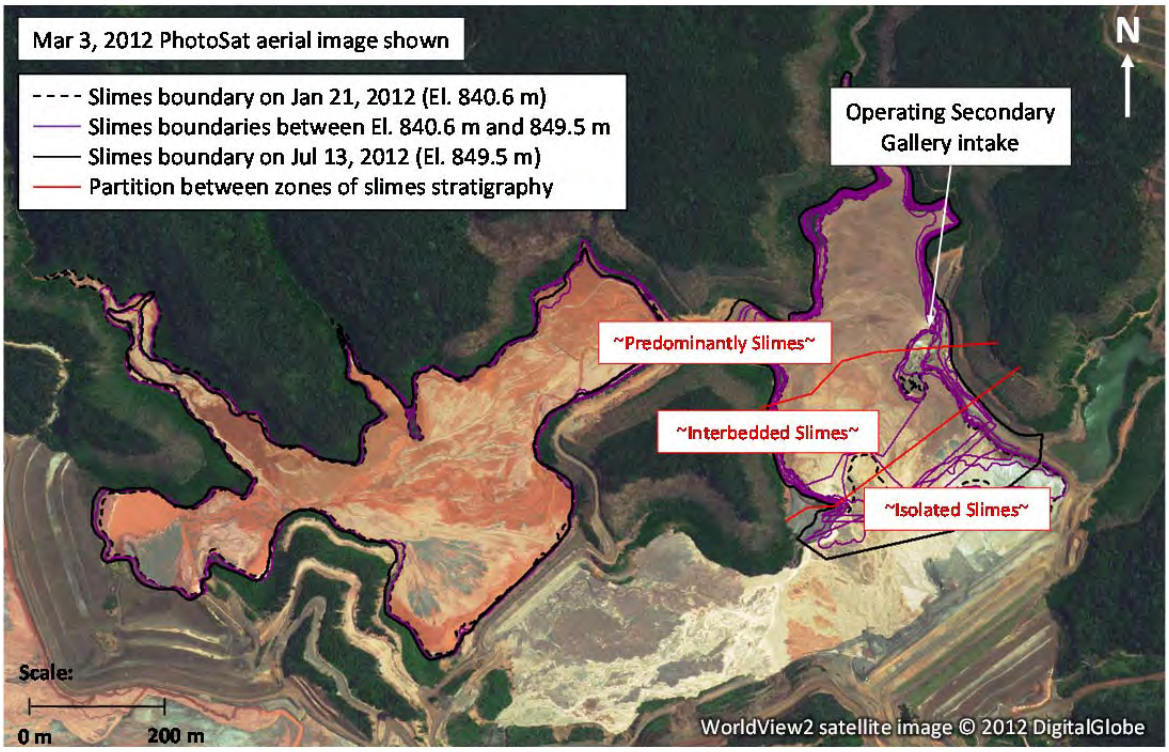

Figure G3-8 Zones of slimes stratigraphy

G3.3.6.2 Tailings Sand Distribution

Mapping the distribution of sands was a simpler process, with the sand distributions assigned to the 2.5 m FEFLOW layers in the same manner as the slimes, using the same base data and interpretation method as that used for slimes (Appendix B).

However, an additional consideration of the sands distribution was the representation of the tailings beach and the dam crest for each of the stress periods. Because the beach distributions and dam crest were not directly relatable to the slimes elevation, a technique to permit transient geometric representation of these features was developed using a combination of slimes elevation/time, and corresponding survey data (which was generally available for each of the stress periods required).

The process involved resampling of the survey data for the time stamp that each of the 2.5 m slimes layers represented, with isopachs created of sand thickness over slimes elevation for +1.8 m, +3.3 m, +7.8 m, etc. These isopachs represented the areas of the model layers above the slimes that were active for each of the consequent 2.5 m raises (the +1.3 m step difference is to permit more than 50% of the overlying layer to be sand before the layer becomes active). Turning these particular cells active in parallel with the slimes layers then recreated the beach geometry, albeit coarse, of the sand between the dam crest and the slimes pond.

This process had a secondary benefit for the modeling exercise. In addition to permitting a more realistic geometry to be represented, it allowed numerical identification within the modeling domain of the sand layers (nodes) as they first became active. Using this trigger, application of a consolidation

water production curve for sand (Section G3.3.7) permitted model derived calculation of produced water, which was rapidly released from sands soon after their "activation". This water showed good correlation to spigot water estimates (Section G3.4.2.2), and because this water was produced when the sand was first deposited, and in response to actual raises, it proved a faster and more reliable manner in which to account for spigot water in the water balance.

The alternative to this was to map spigot locations and create spatial discharge zones for the entire modeling period, and then artificially assign enhanced incident recharge to represent spigotting effects. The former approach was adopted as it was more efficient, it produced water in alignment with sand material properties, and it produced water in the areas of active tailings raise automatically in the model domain without the need for manual intervention and creation of additional synthetic data.

G3.3.6.3 Pond Elevation and Distribution

Pond distribution and elevation was imported into the model aligned with model stress periods and slimes elevation. Figure G3-9 shows an example of pond distribution as assigned in the model.

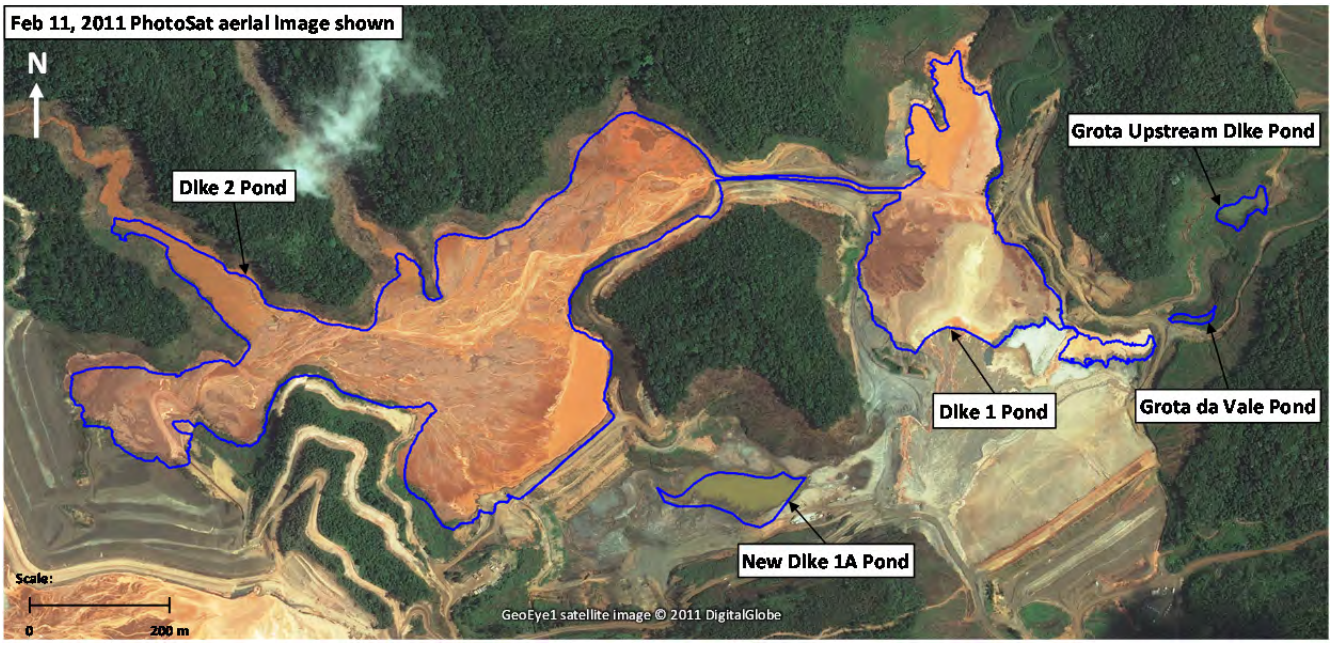

Figure G3-9 Example of pond definition in Fundão, representing open water bodies and slimes

Ponds were defined by their elevation and the duration of their life. Ponds over slimes were maintained throughout the simulation with elevation aligned with the slimes elevation. Other ponds were typically intermittent in nature and often of small size; however, they were included if their location was determined to be a likely long term stress on the system. Short lived ponds on sand tailings (typically associated with local construction activity) were excluded from the model domain unless their existence and persistence could be correlated with piezometric data.

The pond timeline presented in Appendix B provides a detailed summary of pond distribution and elevation.

G3.3.7 Consolidation Water

Water produced through consolidation is an important consideration for three reasons:

1. For sands, it represents the rapid and immediate release of excess water from the spigotting process.
2. For slimes:
   - It accounts for water released at depth, which is of importance if this is released under confined conditions, or contributes to overlying sands which are already receiving substantial recharge through both spigotting and natural recharge.
   - It accounts for water release in the main body of slimes which serves to maintain the main TSF pond elevation, which is ultimately controlled through decanting.
3. For both materials, because of the rapid rate of rise observed across the TSF (Appendix B), the production of this water and the depth of its release become important considerations in understanding pore-water pressure changes that may have occurred.

G3.3.7.1 Consolidation Process

The relationship between void ratio (e) and effective vertical stress (σ_v); and hydraulic conductivity (K) and void ratio (e) were formulated based on a series of consolidation model results (Appendix F).

For each active cell, the consolidation process is modeled with the effective vertical stress calculated by the overlying weight of material (mixture density of slime, sand and water 1,900 kg/m^3), resulting in a consequent calculated pressure in the cell at each time step. The residual void ratio is tracked for each cell as water is expelled, noting that residual void ratio reduces as consolidation takes effect.

At each time step, the model loops back to each cell to recheck the consolidation condition. If the effective stress is less than or equal to 11.0 kPa (equivalent to the effective stress of a saturated top cell at the cell center), then the water expelling rate is assigned as 0 and the consolidation process ceases. Through this process, the release of consolidation water is modeled as a natural process, not a fixed flow rate, and is linked to the material properties of the respective tailings material.

This process operates independent of FEFLOW modeling code.

G3.4 Ph1 Model Calibration

Substantial effort had been completed before transient model calibration commenced, which permitted advancement of model complexity and detail whilst maintaining a relatively stable numerical condition and lean run times, and achievement of good quality interim results throughout the model development process. This included:

- Completion of the Ph0 modeling (Section G2) which permitted understanding of parameter sensitivity and identification of major stresses requiring the most detailed assessment. This

work also assisted in developing the model construction approach to permit reasonable model run times to be maintained, and to model predicted results consistent with expected outcomes.

- Completion of steady state Ph1 modeling to readdress model elements in light of the reconstruction of the as-built TSF. This element of the project also included additional stresses being periodically tested to track that model output remained consistent with expected outcomes, and that model run efficiency was not unduly compromised.
- Completion of parallel studies to reaffirm boundary condition assumptions and inform the stress period definition and transient stresses needed to be included in the final model.

G3.4.1 Material Parameters

Table G3-1 provides a summary of material parameters applied in the calibrated Ph1 model.

G3.4.2 Steady State Calibration

An initial steady state calibrated model of the October/November 2015 TSF was completed to meet two objectives:

1. Reaffirm suitability of model stresses and boundaries, translated from the Ph0 mode and applied to the as-built conditions in Ph1.
2. Create a base model from which the El. 830 m starter model for the Ph1 transient simulation could commence.

Table G3-1 Ph1 model material parameters

<table>
<tr><th>Parameter</th><th colspan="5">Data/Range/Approach</th></tr>
<tr><td>Hydraulic conductivity (K)

Storage (S)</td><td>Material</td><td>Kxy cm/s</td><td>Kv cm/s</td><td>Sy</td><td>Ss</td></tr>
<tr><td></td><td>TSF (Sand)</td><td>5.0×10^{-4}</td><td>2.3×10^{-4}</td><td>0.20</td><td>1.0×10^{-5}</td></tr>
<tr><td></td><td>Sand/slimes</td><td>3.5×10^{-4}</td><td>1.7×10^{-4}</td><td>0.20</td><td>1.0×10^{-5}</td></tr>
<tr><td></td><td>Slimes</td><td>1.2×10^{-6}</td><td>5.8×10^{-7}</td><td>0.20</td><td>1.0×10^{-5}</td></tr>
<tr><td></td><td>Dike 1/Dike 2/Raise (saprolite)</td><td>1.0×10^{-4}</td><td>5.2×10^{-5}</td><td>0.20</td><td>1.0×10^{-5}</td></tr>
<tr><td></td><td>Underdrain</td><td>1.0×10^{-1}</td><td>1.0×10^{-1}</td><td>0.35</td><td>1.0×10^{-5}</td></tr>
<tr><td></td><td>Base rock</td><td>1.2×10^{-7}</td><td>1.2×10^{-7}</td><td>0.20</td><td>1.0×10^{-5}</td></tr>
<tr><td>Precipitation/ Recharge (mm/mo)

(constrained to highest active cells only)</td><td colspan="2">Starting Values (% Mean Monthly RF)

TSF Sand … 20%
Compacted Sand… 10%
Dike/Basement… 5%</td><td colspan="3"> 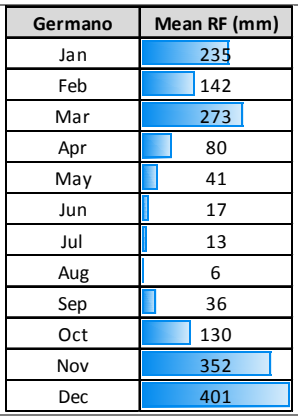
</td></tr>
<tr><td>Pond Recharge</td><td colspan="5">Coupled with the consolidation water produced through the slimes, maintained (removed) through assignment of the pond elevation as an equivalent constant head.</td></tr>
</table>

Parameter	Data/Range/Approach
Drain Permeability	See above. Starting values from Ph0 model.
Consolidation Water	The effective stress of each cell is calculated at each time step. Based on the given gradient of void ratio vs. log of the effective stress, the expelled water through void ratio reduction is determined within that cell. At the same time the void ratio is updated until it reaches the minimum value: then the consolidation process terminates. The expelled water is applied as a water source for each cell as recharge into the model at depth.

The steady state calibration used 56 monitoring locations across the TSF, with head elevations measured in late October, 2015 ranging between ~El. 790 m and ~El. 880 m. These data were filtered from the complete record by excluding sites which did not have an October 26, 2015 (or close to this) measurement record, excluding sites with questionable records or survey information (Appendix E), and excluding data for which the record lay at or below the base elevation of the bottom of the screen/intake zone.

This resulted in the list of piezometers provided in Table G3-2. Flow records for drains measured on October 26, 2015 were applied to assess model predicted flows; these included:

- The El. 826 m blanket drain (Kananets®) 252.0 m^3/h 70.0 L/s
- Fundão base drain (Principal Foundation Drain) 9.7 m^3/h 2.7 L/s
- Grota da Vale 34.5 m^3/h 9.6 L/s

The model was run applying the same starting material parameters and boundary condition assumptions as those described in the Ph0 modeling. Manual model adjustments were made until a suitable calibration was achieved, with the final steady state model reflecting minimal change to Ph0 model assumptions with the addition of reducing permeability of the sand tailings with depth, similar to the Ph0-5 scenarios presented in Section G2.3.8.

Table G3-2 Steady state calibration reference list

Line	Reference	Measured	Line	Reference	Measured	Line	Reference	Measured
AA	16PI003	812.57	DD	24PI046	804.25	LL	24PI058	808.22
AA	16PI004	827.28	DD	24LI021	804.93	LL	24PI059	807.80
AA	16PI005	844.07	DD	24LI029	800.67	LL	24LI027	804.26
AA	16PI020	864.82	DD	16PI017	800.37	MM	24PI060	812.58
AA	24LI017	824.36	DD	16PI018	800.63	MM	24LI028	807.04
AA	24LI018	816.26	FF	24PI041	801.44	NN	16PI001	808.47
AA	16LI010	844.42	FF	24PI048	802.88	NN	16PI002	813.04
AA	16LI011	837.56	FF	24PI050	800.21	01	16PI016	876.05
AA	16LI013	856.54	FF	24LI022	797.47	01	16PI015	871.99

Line	Reference	Measured	Line	Reference	Measured	Line	Reference	Measured
BB	16LI001	830.27	FF	24LI030	795.86	01	16PI013	869.10
BB	16LI002	838.70	HH	24PI052	794.80	02	16LI014	877.54
BB	16LI012	852.65	HH	24PI053	797.03	02	16PI012	869.41
BB	16PI006	837.23	HH	24LI023	794.34	02	16PI010	866.21
BB	24PI044	818.83	HH	24LI024	792.05	02	16PI007	852.70
BB	24LI019	808.31	JJ	24PI054	796.18	03	16LI016	878.01
BB	24LI020	800.75	JJ	24PI055	797.58	03	16PI014	873.32
DD	24PI045	807.86	JJ	24PI056	792.28	03	16PI011	869.26
DD	24PI039	809.74	JJ	24PI062	797.36	03	16PI009	864.86
DD	24PI047	805.55	JJ	24LI026	792.20			

A summary of calibration statistics for the steady state Ph1 model is provided in Table G3-3. Scaled RMS below 10% generally indicates an acceptable calibration; however, this is not always the case and other metrics should also be evaluated. Of equal or greater importance is that the calibrated model reproduces the groundwater flow processes in terms of representing the conceptual understanding within the numerical environment. A good indicator of this is usually achieved through review of the model residuals and the model water balance.

Table G3-3 Summary of steady state model calibration

Statistical Metric	Calibration Metrics: Steady State Model
Number of primary head calibration targets	56
Root Mean Square Error	11.47 m
Scaled RMS	7.1 %
Mean Sum of Residuals	5.30 m
Scaled Mean Sum of Residuals	5.9 %
Water balance error	<1 %

G3.4.2.1 Model Residuals

Model residuals are provided on Figure G3-10 and show a generally good correlation of measured to modeled heads across the range of data assessed. Model residuals ranged between -18.5 m and +5.8 m, with an average of -3.2 m. The scaled mean sum of residuals was also acceptably low at 5.9% (Table G3-3). These data indicate a good predictive capacity of the model under steady state conditions.

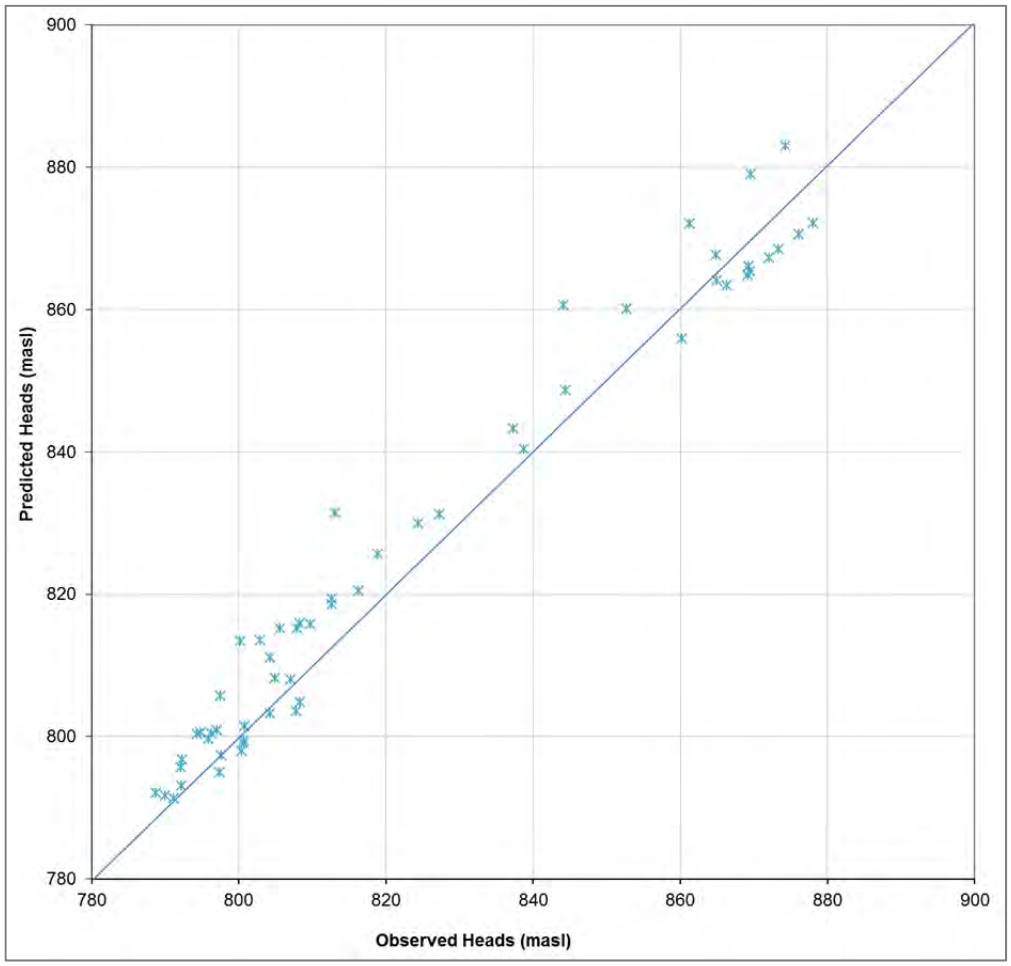

Figure G3-10 Calibrated steady state model, measured vs. modeled heads

G3.4.2.2 Steady State Water Balance

The mass balance error of the steady state model is the difference between model inflows and model outflows. An error of around 1% for steady state simulations[2] is usually considered acceptable (Anderson and Woessner 1991). The steady state water budget and mass balance error are presented below. The model produced a water balance error of -0.1 L/s, which is well below the target 1%, reflecting both good model stability and numerical representation of the conceptual setting. A summary of the major water balance components for this model is provided:

WATER IN

- Pond inflow (constant head) + 32.4 L/s
- Recharge (rainfall) + 80.1 L/s

Total In + 112.5 L/s

[2] Transient simulations are expected to have larger water balance errors as they reflect the time step change and consequent transient stresses that are applied throughout the model run.

WATER OUT

- El. 826 m blanket drain flow - 96.0 L/s
- Principal Foundation Drain flow - 10.9 L/s
- Emergent seepage - 5.7 L/s

Total Out - 112.6 L/s

IMBALANCE

- Water In – Water Out **- 0.1 L/s**

An additional observation of the steady state model is that the results predicted emergent seepage (~5.7 L/s) under steady state conditions at two locations on the left and right abutments. These locations are each coincident with 2015 seepage observations, as shown on Figure G3-11 (from Appendix B Attachment B8). This predicted seepage breakout is an indication of sound translation of the conceptual setting into the numerical environment.

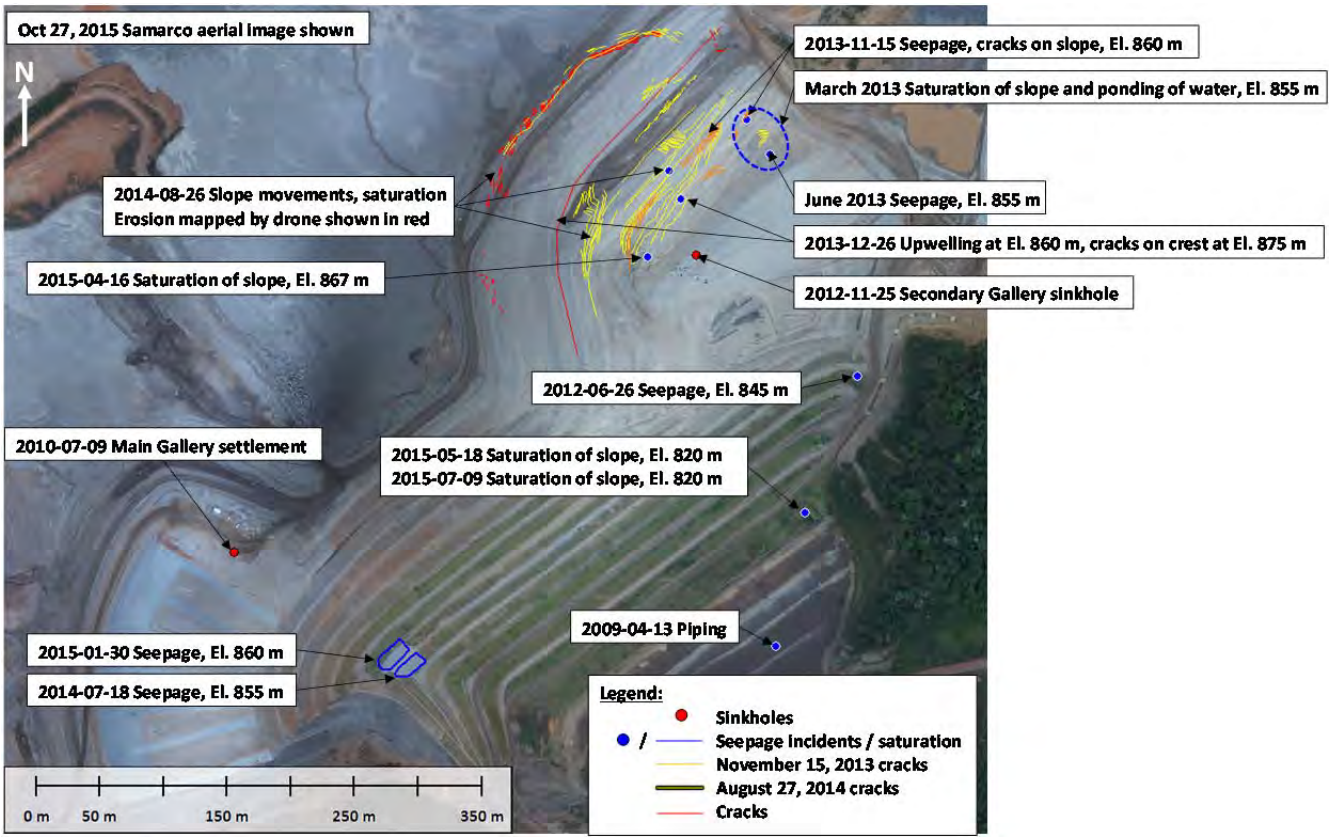

Figure G3-11 Event map showing recorded seepage and failure related incidents

G3.4.2.3 Steady State Calibration Summary

The results indicated a good quality steady state model calibration and strong translation of the conceptual understanding of the TSF into the numerical environment. This model was assessed as suitable and consequently advanced to the transient analysis.

The calibrated model was reconstructed to the El. 830 m TSF geometry and run again to steady state to create an El. 830 m starting condition for the commencement of the transient simulation. The transient analysis was then constructed in accordance with the earlier descriptions and calibration manually undertaken using a similar process to that applied to the steady state model.

The transient calibration process is described in the following sections.

G3.4.3 Transient Calibration

As the model was strongly responsive to broad scale changes associated with the representation of boundary conditions and far less responsive to subtle variations in material parameters, manual calibration proved sufficient to achieve a suitable calibration. The quality of this transient calibration has been assessed using five approaches, each discussed in the following sections:

- visual observation of model predicted hydrographs against a suite of measured data for elevations greater than El. 830 m;
- statistical analysis of the predictive capacity of the model in the same manner as that presented for the steady state calibration;
- analysis of transient predicted drain flows against measured data;
- review of the transient water balance at the October/November 2015 condition; and
- visual observation of system dynamics and comparison with the conceptual understanding – this is particularly the case for areas of “thin” unsaturated zones and/or areas of model predicted emergent seepage.

G3.4.3.1 Transient Model Calibration Modifications

The model was run applying the same starting material parameters and boundary condition assumptions as those described in the model construction process. Calibration was achieved through application of the approaches developed in scenarios Ph0-4 and Ph0-5 (Sections G2.3.7 and G2.3.8). Tailings sand permeability was adjusted through the consolidation water production process applying diminishing permeability values with depth.

A summary of transient calibration values is provided in Table G3-4.

Table G3-4 Summary of transient model calibration parameters

Parameter	Data/Range/Approach				
Hydraulic conductivity (K) Storage (S)	**Material**	**Kh cm/s**	**Kv cm/s**	**Sy**	**Ss**
	TSF (Sand)	6.9×10^{-4} to 4.5×10^{-3}	3.5×10^{-4} to 1.6×10^{-3}	0.20	1.0×10^{-5}
	Slimes	1.2×10^{-6}	1.2×10^{-6}	0.25	1.0×10^{-5}
	Dike 1/Dike 2/Raise (saprolite)	1.0×10^{-4}	5.2×10^{-5}	0.20	1.0×10^{-5}
	Base rock	1.2×10^{-7}	1.2×10^{-7}	0.01	1.0×10^{-5}
Precipitation/ Recharge (mm/mo) (constrained to highest active cells only)	Starting Values (% Mean Monthly RF) TSF Sand … Compacted Sand… Dike/Basement…	 20% 10% 1%			
Pond Recharge	Coupled with the consolidation water produced through the slimes, maintained (removed) through assignment of the pond elevation as an equivalent constant head.				
Drain Permeability	**Material**		**Kxyz cm/s**		**S**
	El. 852.5 m of left abutment (5 m x 2.5 m)		2.3×10^{-2}		1.0×10^{-5}
	Principal/Auxiliary (in Starter Dam)		1.3×10^{-1}		1.0×10^{-5}
	El. 826 m blanket drain		1.0×10^{-1}		1.0×10^{-5}
	Dam 1 Remnant Vertical Drain		5.0×10^{-3}		1.0×10^{-5}
Consolidation Water	The effective stress of each cell is calculated at each time step. Based on the given gradient of void ratio vs. log of the effective stress, the expelled water through void ratio reduction is determined within that cell. At the same time the void ratio is updated until it reaches the minimum value: then the consolidation process terminates. The expelled water is applied as a water source for each cell as recharge into the model at depth.				

Germano	Mean RF (mm)
Jan	235
Feb	142
Mar	273
Apr	80
May	41
Jun	17
Jul	13
Aug	6
Sep	36
Oct	130
Nov	352
Dec	401

Notes: The El. 826 m blanket drain Kananets® are represented by seepage face nodes to remove the water along the Dike 1 crest at El. 826 m. Blanket drains are represented as 2D slice face discrete elements; lineal drains as 1D discrete elements.

G3.4.3.2 Transient Hydrograph Data

The assessment of calibration performance using transient hydrographs is constrained to those piezometers with a screen elevation above the El. 826 m blanket drain. This is because the TSF to El. 830 m was modeled under steady state conditions, and therefore none of the original drain infrastructure, which was decommissioned, is included. Because these drain features are not modeled, it is not possible to calibrate against piezometric records that have experienced the influence of these features in their record.

Those piezometers used in the transient calibration process are:

RIGHT ABUTMENT

- Line AA 5x piezometers: 16PI003, 16PI004, 16PI004, 16LI010, 16PI020
- Line BB 2x piezometers: 16LI002, 16PI006

LEFT ABUTMENT

- Line 01 4x piezometers: 16LI015, 16PI013, 16PI015, 16PI016
- Line 02 3x piezometers: 16PI007, 16PI010, 16PI012
- Line 03 4x piezometers: 16LI016, 16PI009, 16PI011, 16PI014

Model predicted transient conditions compared with measured data for each of these five lines is presented on Figure G3-12, Figure G3-13, Figure G3-14, Figure G3-15 and Figure G3-16. For each section, the solid line represents the model-produced data, and the point data represents field measured records. Time on the x-axis is model run time.

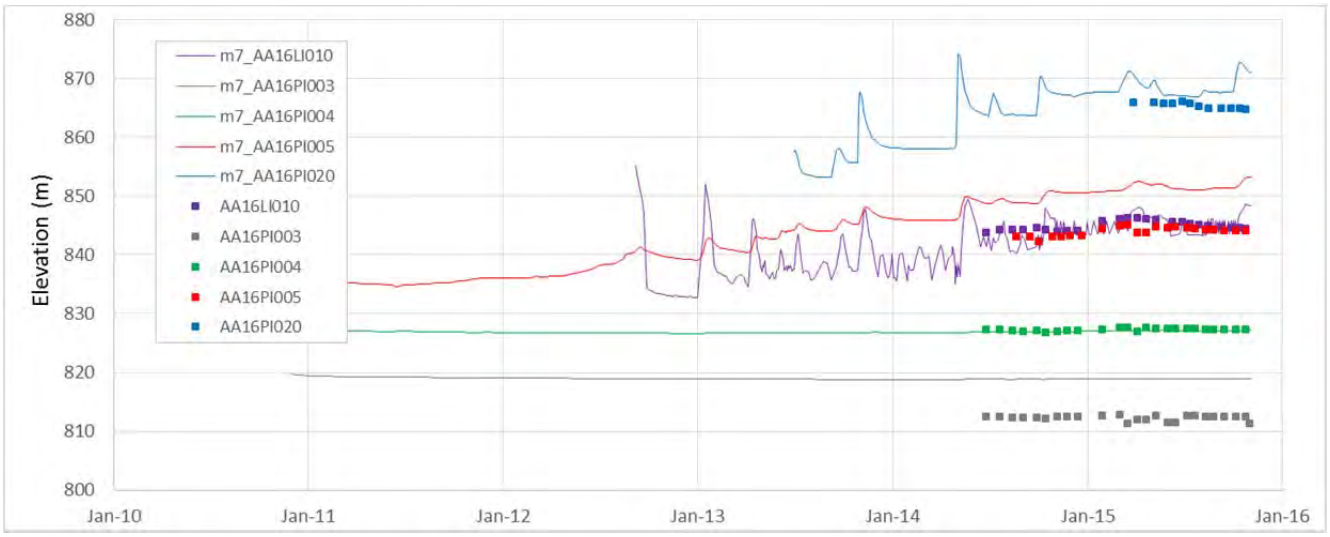

Figure G3-12 Calibrated transient model hydrographs, measured versus modeled, line AA

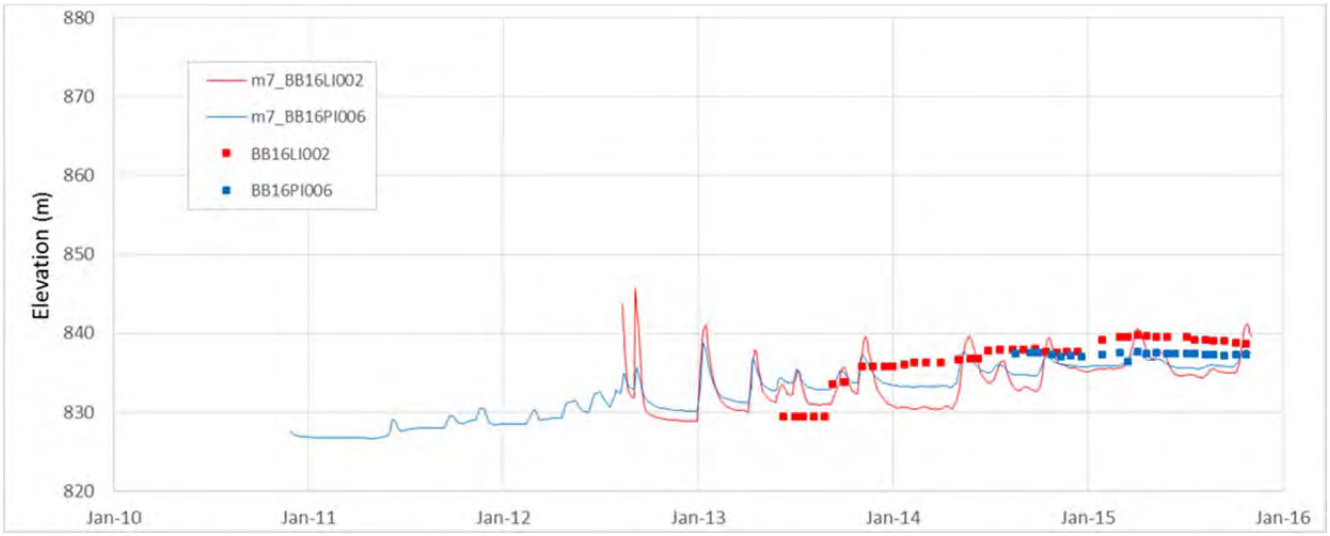

Figure G3-13 Calibrated transient model hydrographs, measured versus modeled, line BB

Figure G3-14 Calibrated transient model hydrographs, measured versus modeled, line 01

Figure G3-15 Calibrated transient model hydrographs, measured versus modeled, line 02

Figure G3-16 Calibrated transient model hydrographs, measured versus modeled, line 03

G3.4.3.3 Statistical Calibration Performance

A statistical assessment of the calibration was undertaken using 400 individual piezometric records taken from the piezometric hydrographs for the 18 sites described above in the hydrograph discussion. A summary of calibration statistics for these sites is provided in Table G3-5. Scaled RMS below 10% was achieved again and indicates an acceptable calibration.

Table G3-5 Summary of transient model calibration

Statistical Metric	Calibration Metrics: Transient Model
Number of primary head calibration targets	400
Root Mean Square Error	2.57 m
Scaled RMS	8.9 %
Mean Sum of Residuals	8.44 m
Scaled Mean Sum of Residuals	29.2 %
Imbalance	~5 %

Model residuals for the transient calibration are provided on Figure G3-17 and show a good correlation of measured-to-modeled heads across the range of data assessed. Model residuals ranged between -7.2 m and +3.4 m, with an average of -1.4 m. The scaled mean sum of residuals increased as the range of elevation across which the calibration data was measured was reduced. These data continue to indicate good predictive capacity of the model.

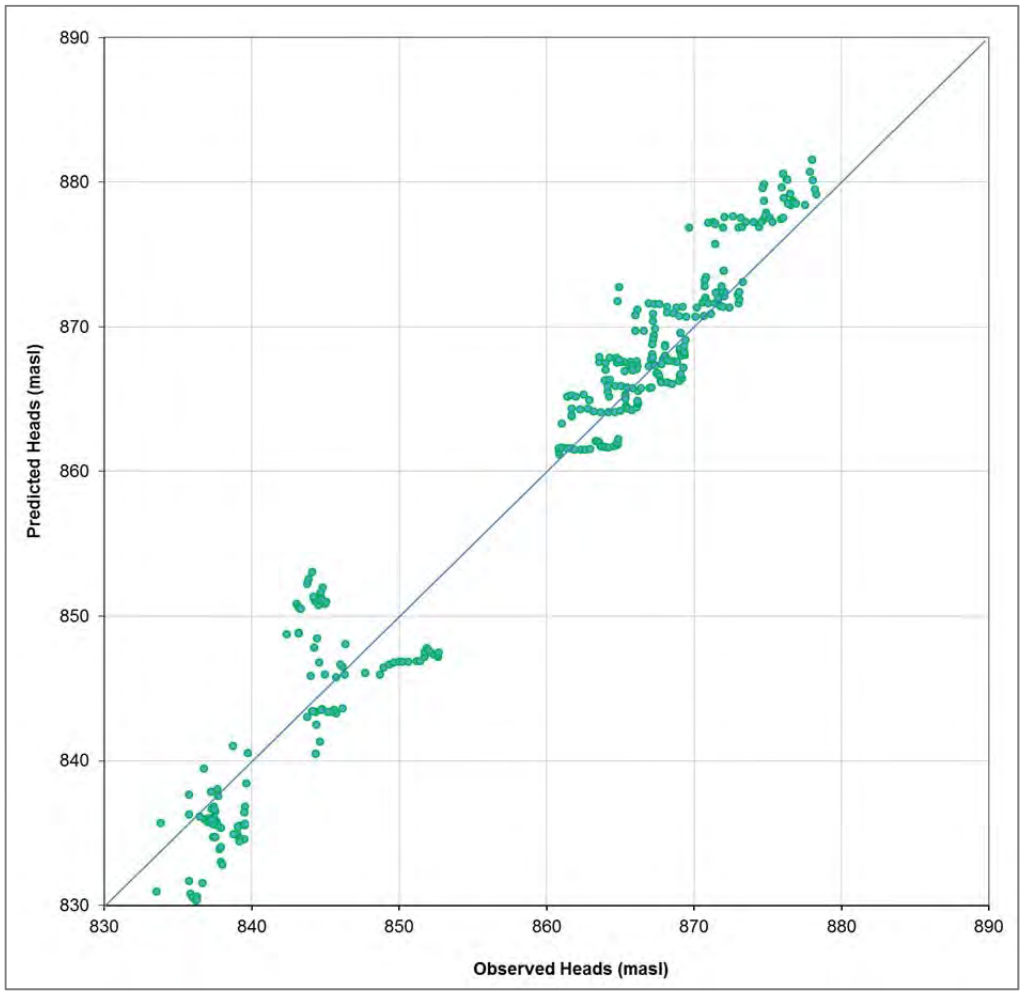

Figure G3-17 Calibrated transient model, measured versus modeled heads

G3.4.3.4 Drain Flow Performance

Transient drain flow for the El. 826 m blanket drain and the Principal Foundation Drain are provided on Figure G3-18. Modeled flows show cycling effects which are a response to the "block" approach the model applies to TSF raising, resulting in peaks of flow as significant construction occurs near the drain followed by periods of abated flow. The general trend, however, of the El. 826 m blanket drain flow shows good correlation with the measured flows, including the flattening off of flows noted after model day 1400. Modeled flow from the Principal Foundation Drain is consistently low, largely a response to the quasi steady state conditions across the original Starter Dam controlled by the El. 826 m blanket drain.

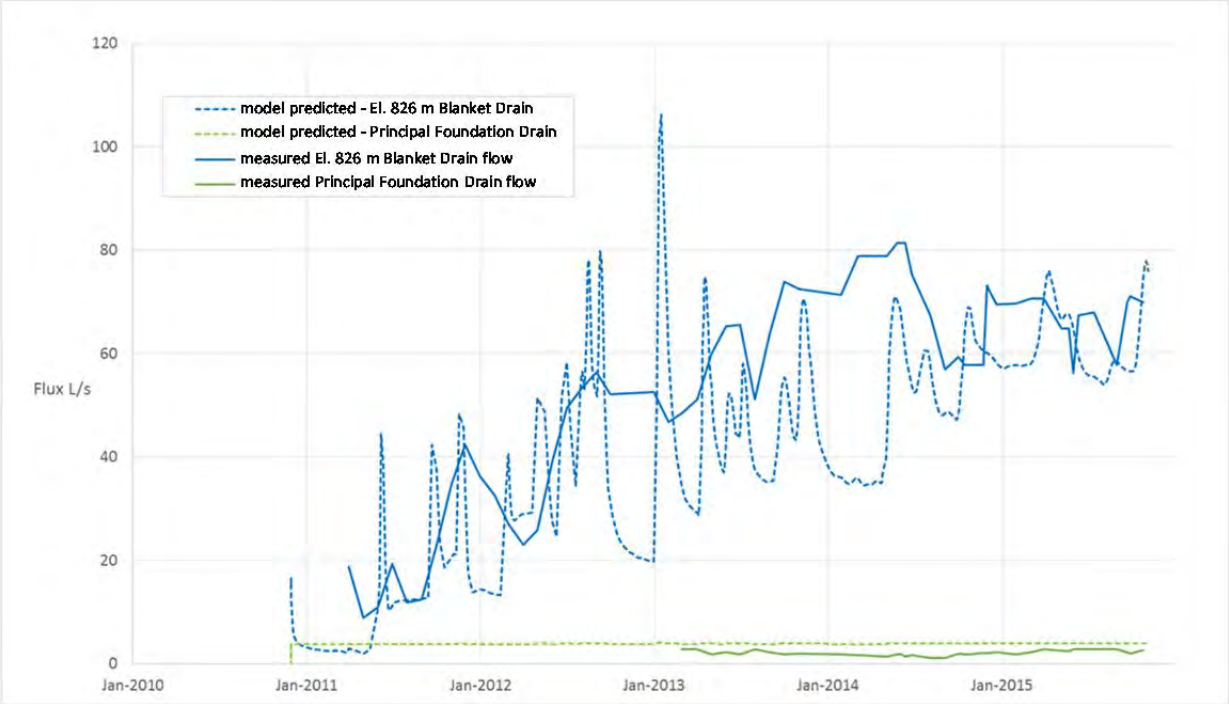

Figure G3-18 Calibrated transient model drain flows, measured vs. modeled

G3.4.3.5 Transient Water Balance

The transient water balance was extracted for the end of the model run to provide a snapshot for summary reporting, and to compare transient output with the steady state model results (recognizing there is more detail in the transient simulation because of the inclusion of consolidation water). These results are presented in the following:

WATER IN

- Consolidation Water (slimes/pond) + 88.3 L/s
- Consolidation Water (spigot water) + 88.3 L/s
- Recharge (rainfall) + 5.1 L/s

Total In + 181.7 L/s

WATER OUT

- El. 826 m blanket drain flow - 75.3 L/s
- Principal Foundation Drain flow - 4.0 L/s
- Reject consolidation water - 84.4 L/s
- Emergent seepage - 2.6 L/s

Total Out - 166.3 L/s

IMBALANCE

- Water In – Water Out = change in storage **+ 15.4 L/s**

There are several observations important in interpreting these results:

- Consolidation water "in" is reported as a total amount, but represents water released from both slimes and sand. For reporting purposes this has simply been split 50/50. In the water "out" budget, the excess consolidation water, which flows to the pond, is reported as a standalone water budget item. These estimates of water "in" and "out" should be considered together as a mass balance amount.
- Earlier estimates of spigot water were ~90 L/s, which is consistent with transient model produced water applying the 50/50 rule at 88.3 L/s.
- Rainfall recharge in the transient simulation is much lower than the steady state simulation. This is because the steady state simulation included the additional water (as an increase in recharge rate) to compensate for spigot water. The transient simulation instead applied consolidation water production to achieve an estimate of spigot water.
- The total "in" and "out" budget for the transient simulation is higher than that of the steady state simulation. This is not an error between the models, but rather a reflection of the changed recharge conditions developed between the two, and the manner in which the water budget is reported (which double accounts for water in the transient simulation).
- The predicted drain flow reported from the El. 826 m blanket drain is 75.3 L/s, compared with measured at 70 L/s, and the remnants of the Principal Foundation Drain are predicted to produce 4.0 L/s compared with measured 2.7 L/s. Both of these are noted improvements on the steady state simulation which slightly over-predicted each of these flows.

This transient water budget does not "balance" because of the transient stresses being applied. The imbalance of +15.4 L/s is consistent with expectations that the system is gaining water in the overall schedule because of the increase in sand and slimes deposition, although this imbalance amount would be expected to vary depending on the time of data extraction from the model. Most importantly, this imbalance is not predicting a reduction in storage, which would be conceptually incorrect.

G3.4.3.6 Conceptual Representation in the Numerical Environment

Review of end of model phreatic conditions and unsaturated isopach of the tailings representative of the November, 2015 conditions are provided on Figure G3-19 and Figure G3-20 and are used as a final check of the model's ability to represent the conceptual understanding of the TSF.

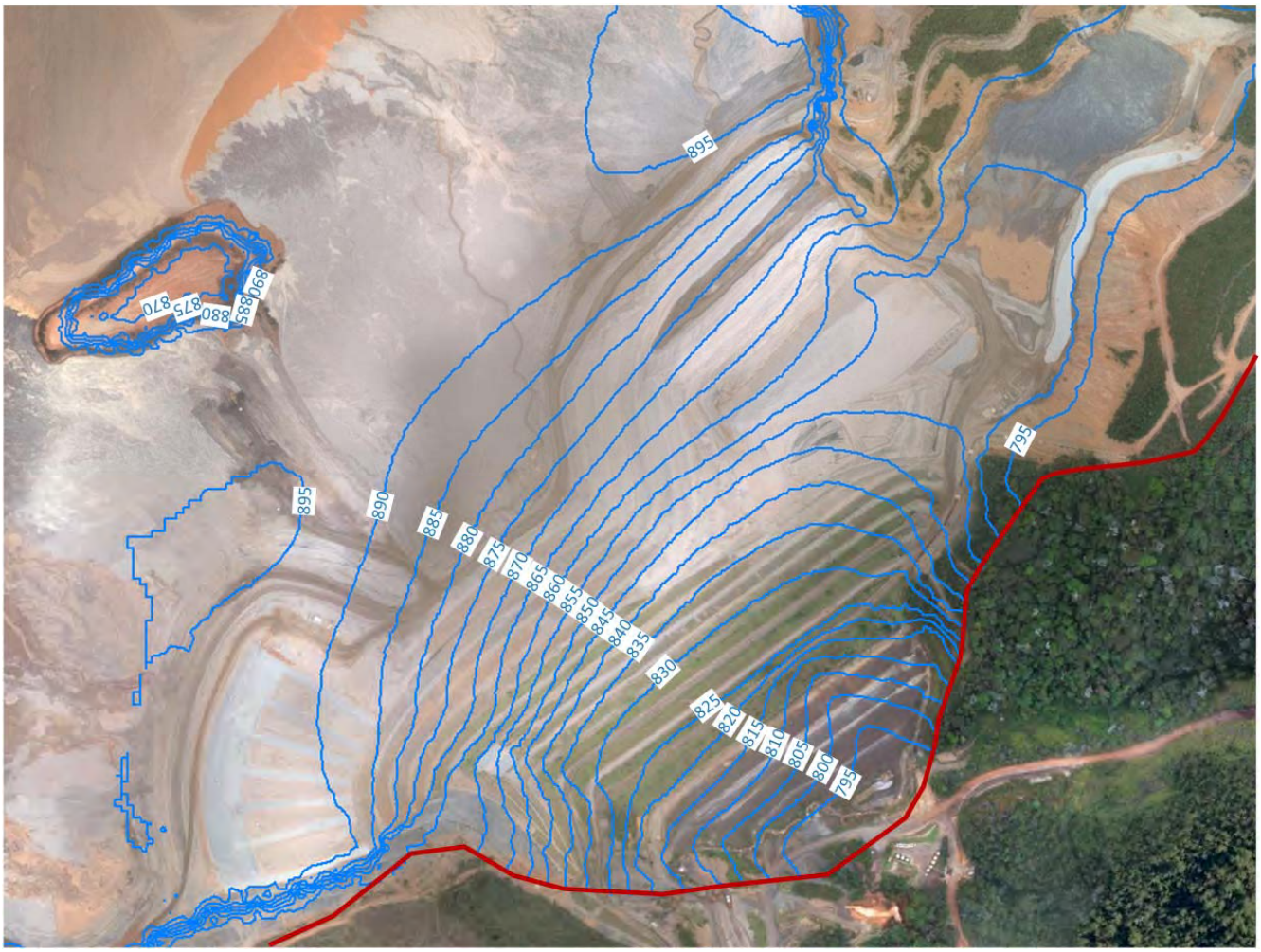

Figure G3-19 Transient model phreatic conditions, November, 2015

The process of transient calibration has shown good predictive quality of the model in presenting phreatic conditions. Key elements of the model results apparent on Figure G3-19 include:

- At the toe of the dam, contours wrap around the remnants of the Principal Foundation Drain and the Auxiliary Drain. This distortion of the phreatic conditions was apparent in the piezometric records from before the construction of the El. 826 m blanket drain.
- The phreatic surface “flattens” between the El. 825 m and El. 830 m contours, a direct response to the effect of the El. 826 m blanket.
- Conditions on the left abutment setback are more complicated, with effects from the left abutment drain (connected to the El. 860 m blanket drain) evident, and generally lower hydraulic gradients in the area between the downstream extent of the El. 860 m blanket drain and Grota da Vale (pond constant head ~El. 860 m).

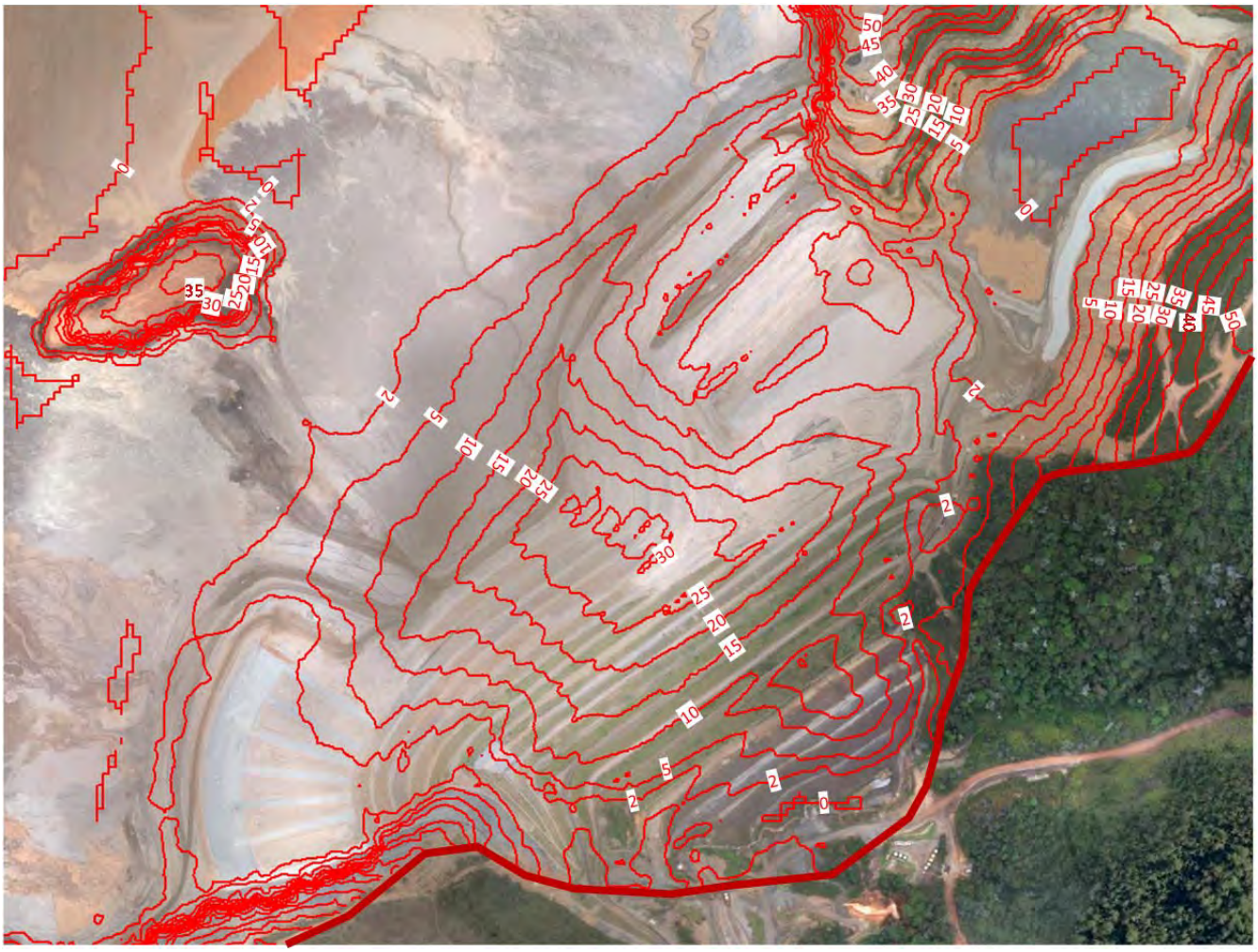

Figure G3-20 Transient model unsaturated isopach map, November, 2015

The unsaturated isopach (Figure G3-20) provides an indication of areas of limited unsaturated thickness, or areas where emergent seepage is predicted to occur. Of note from these results, there are four zones of <5 m unsaturated thickness:

- Seepage is predicted by the model at the toe of the dam near the exit point of the Principal Foundation Drain.
- Shallow unsaturated conditions are predicted on the right abutment (Figure G3-11). This area also had seepage in October of 2015, as reported in Samarco routine reporting.
- On the left abutment abutting foundation material in the area of the left abutment rock fill trench (Appendix B).
- Within the area of the setback and over the El. 860 m blanket drain near the toe of the left abutment reinforcement berm.

G3.4.3.7 Transient Calibration Summary

A brief summary of the transient calibration is provided:

- Transient predicted heads for piezometers above El. 830 m are replicated in trend and head to the measured hydrograph data. Statistical assessment of these records support the visual calibration performance observed in the hydrographs.
- The model predicts transient drain flow from the two main drains of the El. 826 m blanket drain and the Principal Foundation Drain with good correlation to actual records, although showing cyclicity in the predicted record.
- The water balance presents plausible water in and water out components, with a net positive balance apparent at the end of the simulation consistent with expectations from construction activity across the facility.
- Phreatic conditions are consistent with measured data, and the model predicts areas of potential or actual emergent seepage which can be correlated to a number of observed incidents throughout 2015.

Acceptable statistical calibration performance and sound translation of the conceptual setting into the numerical environment are both considered achieved in this model.

G3.5 Transient Model Results

Model results are not able to be practically shown for the entire model run. Results presented in earlier discussions are generally extracted from the end of the model and representative of November, 2015 conditions. Similar results can be assessed for selected dates, for:

- transient head and pressure data for any node;
- sectioned phreatic conditions and contoured pressure data, for selected dates and stages of TSF construction;
- contoured phreatic conditions for the TSF; and
- drain flow and estimates of emergent seepage from the dam face.

Water balance, piezometry and hydrographs, drain flow records, and phreatic conditions have each been presented throughout Section G3.4.3. The following sections provide a range of visual results for the left and right abutment, and where practical, for the entire TSF. Figure G3-21 provides a reference for sections presented in the following report sections. As well as sections cut through the piezometer lines, one longitudinal section has been developed that strikes across the dam.

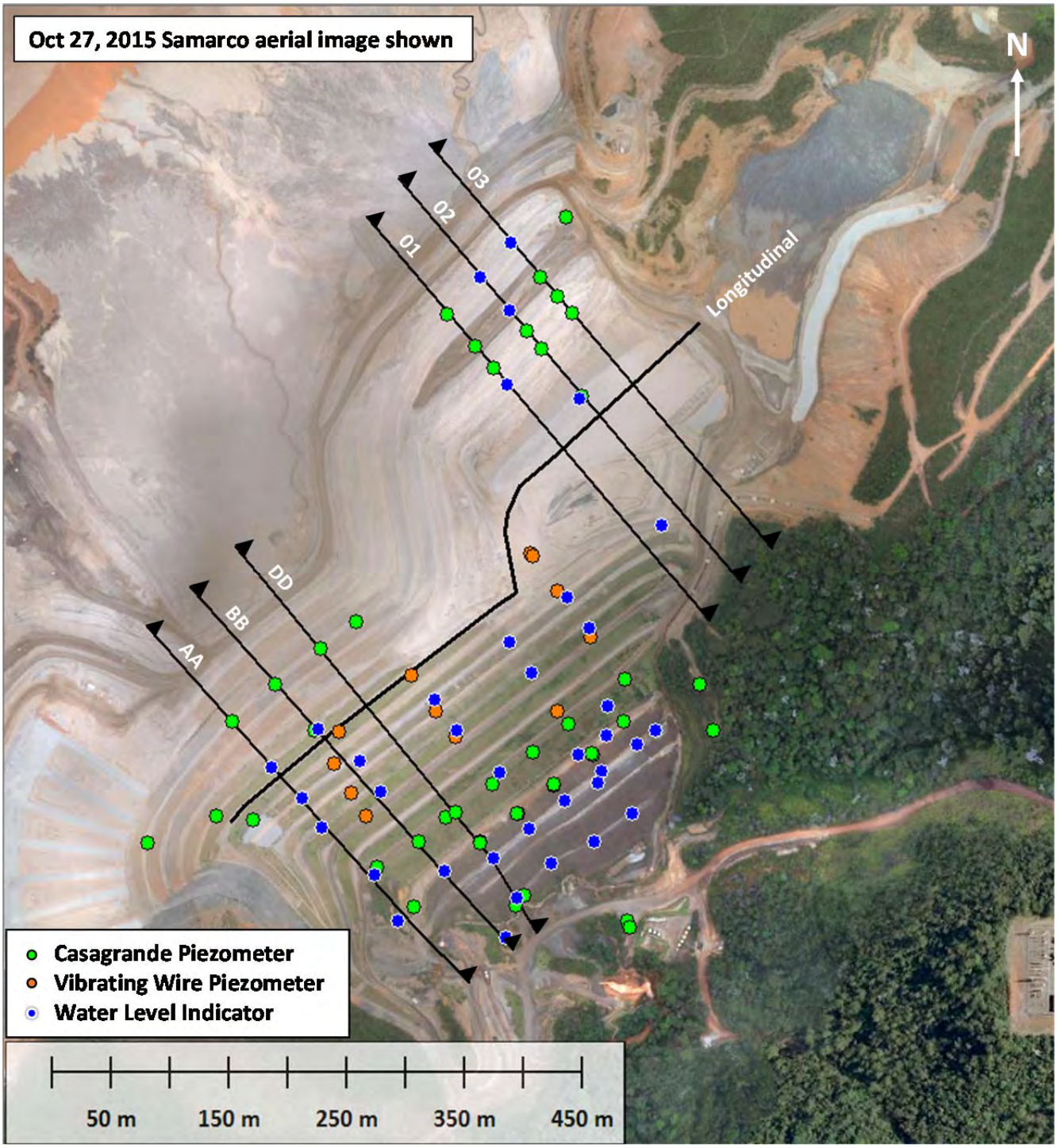

Figure G3-21 Section location reference map

G3.5.1 Left Abutment Discussion

Figure G3-22 shows model predicted conditions for time 1800 days (November, 2015) through left abutment Sections 01, 02 and 03. Slimes, drains and compacted sands are color differentiated in the sections:

- The phreatic surface lies very close to the dam face from behind the dam crest to mid-way along the El. 860 m blanket drain. This high level of saturation appears to be sustained across the area where there are consistent slimes above El. 840 m.
- Downstream of the El. 860 m blanket drain, phreatic gradients reduce, a function of both diminishing drain effects, the constant head of Grota da Vale being similar in elevation and close to the El. 860 m blanket drain, and the reduced recharge away from spigotting activity and active ponds.
- The slimes still impose influence on the phreatic condition, holding the phreatic surface above their lateral location in section. Sands below these slimes are indicating downward vertical gradients, which are interpreted to occur as a result of the locally flattened gradients, reduced recharge, completed consolidation processes and increased distance from spigotting locations. The effects of the El. 826 blanket drain may also be influencing these conditions.

Section 02 is located parallel to Section 01. Similar conditions to those of Section 01 are apparent, although the pressure anomaly beneath the dam crest has significantly diminished. Slimes profiles are very similar to Section 01, and although the drain extends in length, most of the sand beneath is not in saturated contact with the drain. The effects of the El. 826 m blanket drain may be becoming more prominent and are starting to steepen the gradient between the two drainage blankets.

Section 03 has a similar profile, although it is noted that the model predicts phreatic conditions beneath the El. 860 m blanket drain to further lower, likely in response to steepening flow gradients towards the El. 826 m blanket drain which is now physically closer.

Figure G3-23 provides a plan layout of head conditions for El. 850 m at time 1800 days, which slice horizontally through the approximate upper contact with the main body of slimes (shown as blue). This section also lies between the drainage blanket elevations of El. 826 m and El. 860 m.

Of note is the differing hydraulic gradients apparent between the left abutment and the right abutment. On the left abutment the phreatic surface grades about 10 m over 250 m between Grota da Vale and the eastern area of the El. 826 m blanket drain. On the right abutment, gradients are much steeper, around 30 m over 125 m of distance, toward the western area of the drain. The gentle arc of the 850 m contour has a moderate skew toward the left abutment, which serves to reduce these gradients, and by consequence they are likely to result in slower groundwater velocities.

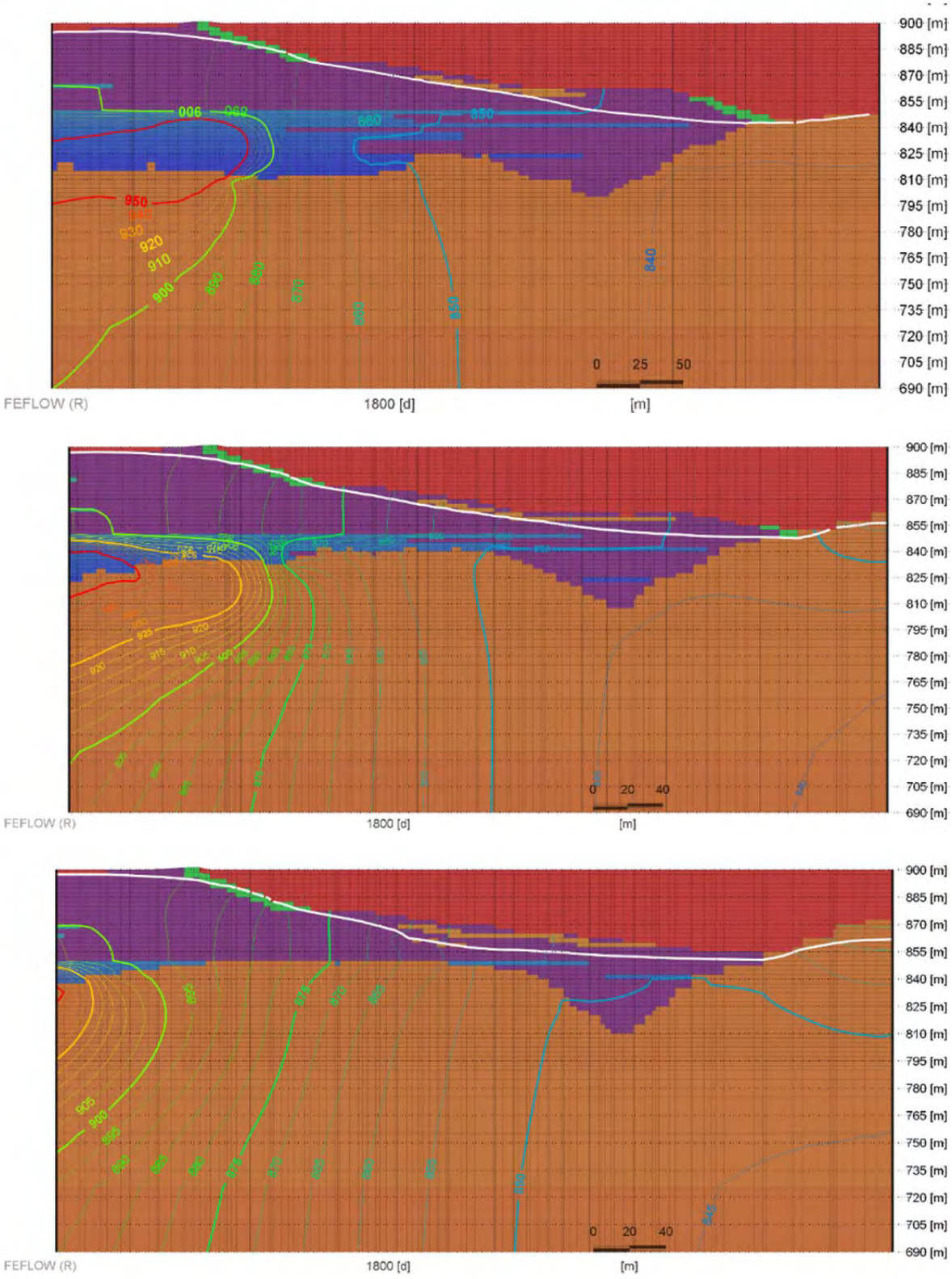

Figure G3-22 Left abutment water table and head contours Sections 01, 02 and 03, t=1800 days

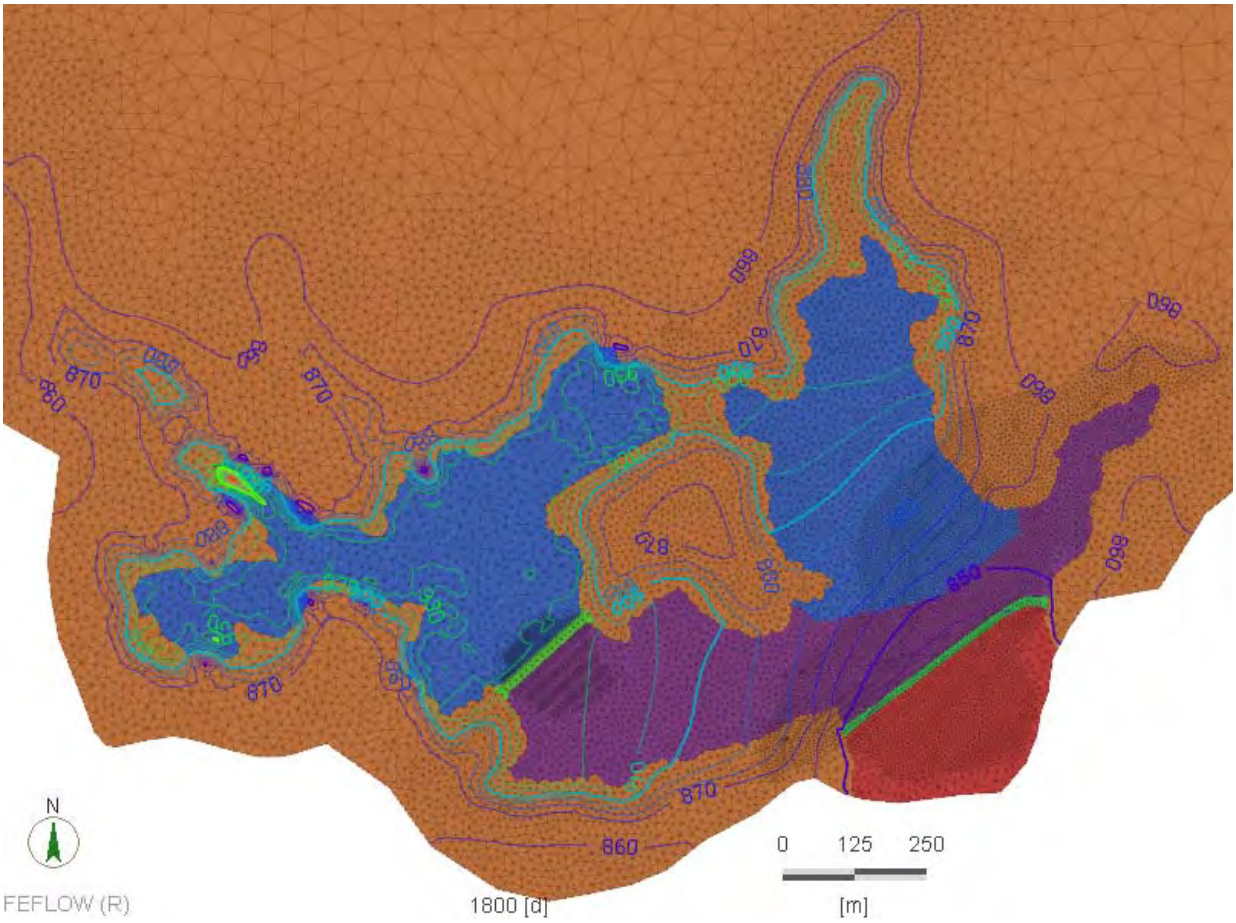

Figure G3-23 Facility head conditions for model layer El. 850 m

The Longitudinal Section starts on the left abutment, crosses the El. 860 m blanket drain, and rotates around the setback to then cross over the El. 826 m blanket drain and meet the right abutment (Figure G3-24). Three features of the phreatic surface are prominent in this section:

- On the left abutment, the hydraulic gradient is relatively flat, and heads are raised to be in contact with the drain, perched atop the upper sequence of slimes;
- On the right abutment, without this slimes perching effect, the phreatic surface is drawn toward the drain with steeper gradients from the right abutment and behind the drain.
- Between these two zones, the phreatic surface grades from ~El. 852 m to ~El. 838 m (~14 m decline) over 80 m of section. This is not a gentle grade but a sharp change in conditions from those where the slimes exist.

This indicates that the El. 826 m blanket drain does have influence on phreatic conditions toward the left abutment, but only after the extent of the slimes is passed. Further east, the slimes dominate the phreatic surface, with heightened and “plateaued” phreatic conditions and more sluggish lateral gradients.

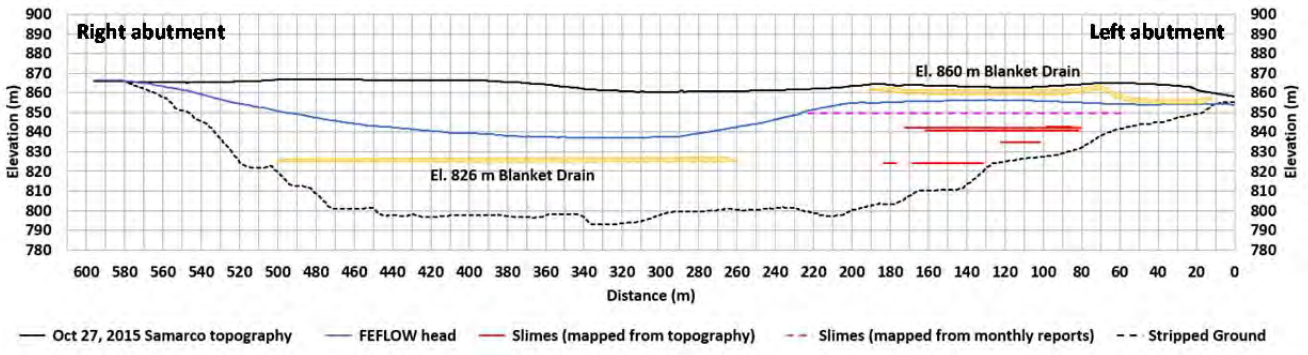

Figure G3-24 Facility head conditions, Longitudinal Section, looking upstream

G3.5.2 Right Abutment Discussion

Figure G3-25 shows model predicted conditions for time 1800 days (November, 2015) through right abutment sections AA, BB and DD. Slimes, drains and compacted sands are color differentiated in the sections.

Section AA is located adjacent to but does not intersect the El. 826 m blanket drain. There are slimes at depth deposited in the valley low point. Phreatic conditions close to the abutment are heightened and appear compressed between the basement high and the face of the dam. Model predictions indicate low amounts of seepage at the dam face at about El. 860 m, which coincides with this basement high.

Section BB crosses the start of the El. 826 m blanket drain and extends through the Starter Dam. Slimes are located behind the dam in the basement depression, with an upper elevation of about El. 825 m, close to that of the blanket drain. Phreatic conditions reduce across the drain, with minor perching effects from the slimes possibly occurring above the slimes (the gradient appears to steepen mildly once it crosses the slimes). Over the blanket the effect of the drain is prominent, and effective in controlling phreatic conditions below the dam face.

Section DD shows a similar response to that of Section BB, with the drain becoming the more prominent feature affecting phreatic conditions. Slimes effects, although far more moderate than those of the left abutment, are weakly apparent, extinguishing behind and across the area where their presence ends.

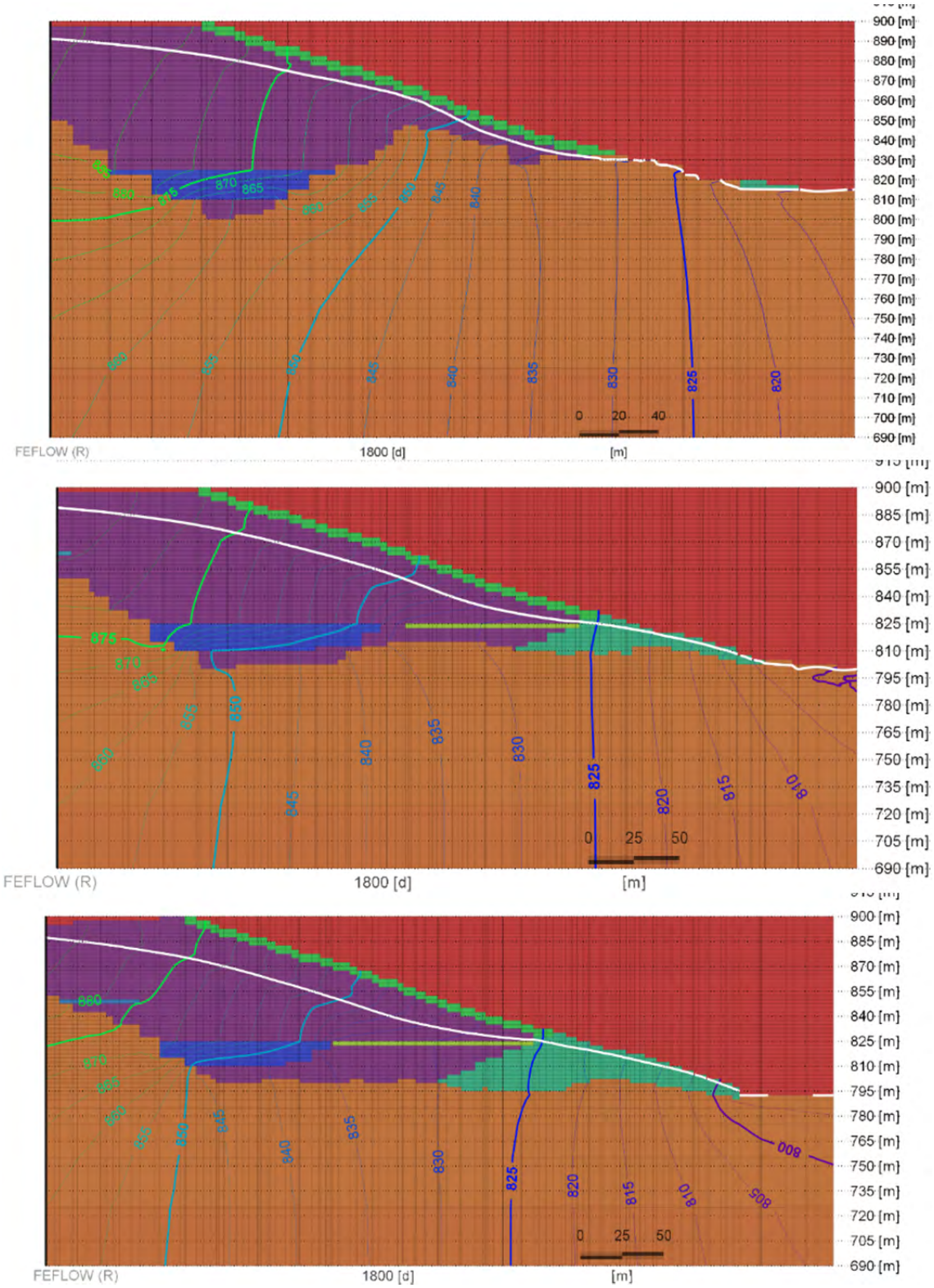

Figure G3-25 Right abutment water table and head contours sections AA, BB and DD, t=1800 days

The influence of the El. 826 m blanket drain on the right abutment has already been discussed in Section G3.5.1.

G3.5.3 Flow Paths and Particle Seeds

Particle seeds and flow paths are a useful visual tool to assess groundwater movement trends.

Figure G3-26 provides forward and back tracking of particle seeds placed on the El. 860 m blanket. Forward tracking (left image) shows the migration of groundwater as the phreatic surface falls below the downstream section of the drain, and conditions come under increasing influence from the El. 826 m blanket drain, where the seeds ultimately report to. Back-tracking of seeds (left image) shows relatively lineal flow gradients from the dam crest toward the drain, although the flow wraps around the lower area of the setback near Grota da Vale where gradients are relatively flat.

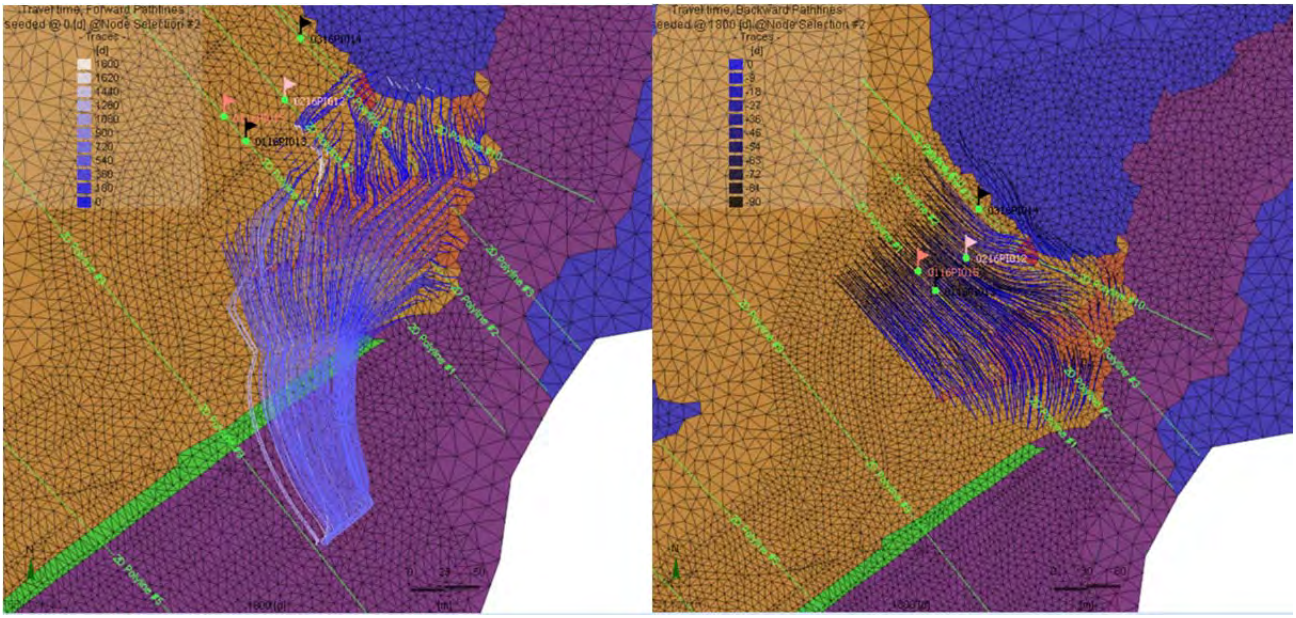

Figure G3-26 Flow paths from particle seeds on the El. 860 m blanket drain, forward tracking (l) and back tracking (r)

Figure G3-27 further explores the detail of groundwater movement with more focus on the period leading up to the failure event in November, 2015. This image is time constrained and shows particle paths from seeds placed on tailings sand 3 months before the failure event. Observations include:

- On the left abutment, groundwater flow is clearly toward the El. 860 m blanket drain, with longest pathways apparent from downstream of the dam crest. This is consistent with intersection of flow with the upper tiers of this drain, falling under steep gradient within high permeability material. The longer pathways occur along most of the drain, shorting in the area of the setback and where phreatic conditions begin to fall under the influence of flow toward the El. 826 m blanket drain.

- On the right abutment, flow vectors are most apparent adjacent to the construction activity for the drain construction and behind the El. 826 m blanket drain. This is consistent with the condition that the seeds placed behind the active construction activity are furthest from the drain and are experiencing flatter hydraulic gradients, resulting in shorter travel distances. Seeds placed closer to the dam crest and the drain fall under the steeper gradients directly toward the blanket.

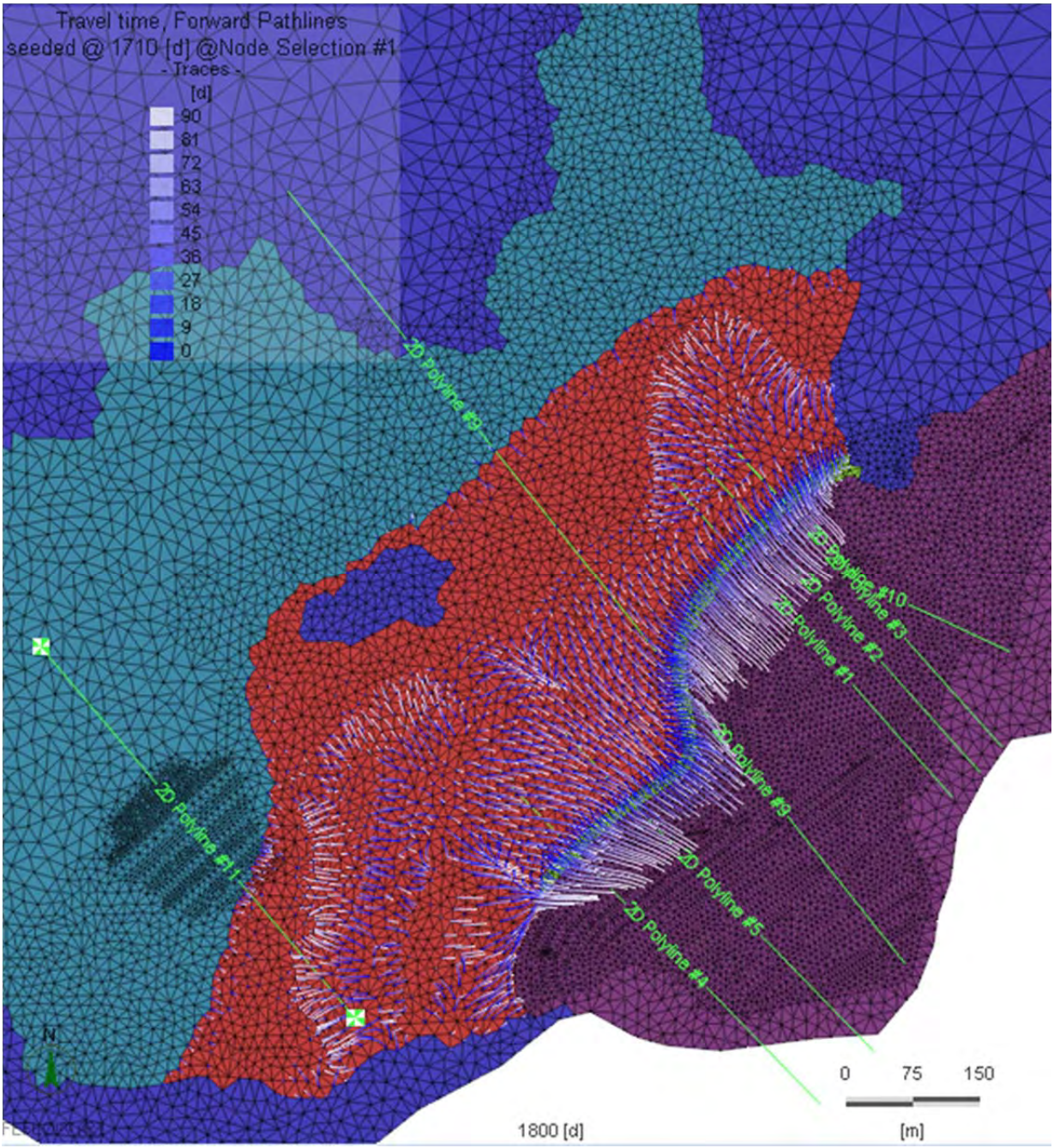

Figure G3-27 Particle tacking, 90-day travel (day 1710 to 1800), seed placement upper tailings sand

G3.6 Ph2 Model – Scenario Run: No Slimes "Tongues", Left Abutment

A variation of the transient model was constructed and run to predict phreatic conditions at time 1800 days (November, 2015), representing a scenario of no slimes "tongues" on the left abutment. The model was modified such that slimes within 200 m lateral distance from the dam were changed to tailings sand material properties. This conforms to the original design intent that a minimum beach distance of 200 m is maintained (Section G2.2.4).

No other elements of the model were changed. The model was run under transient conditions to the same schedule as the calibrated model, with end of model water balance and head and pressure conditions reviewed. A comparison of the calibrated and scenario model using predicted phreatic conditions is provided on Figure G3-28 along the longitudinal section.

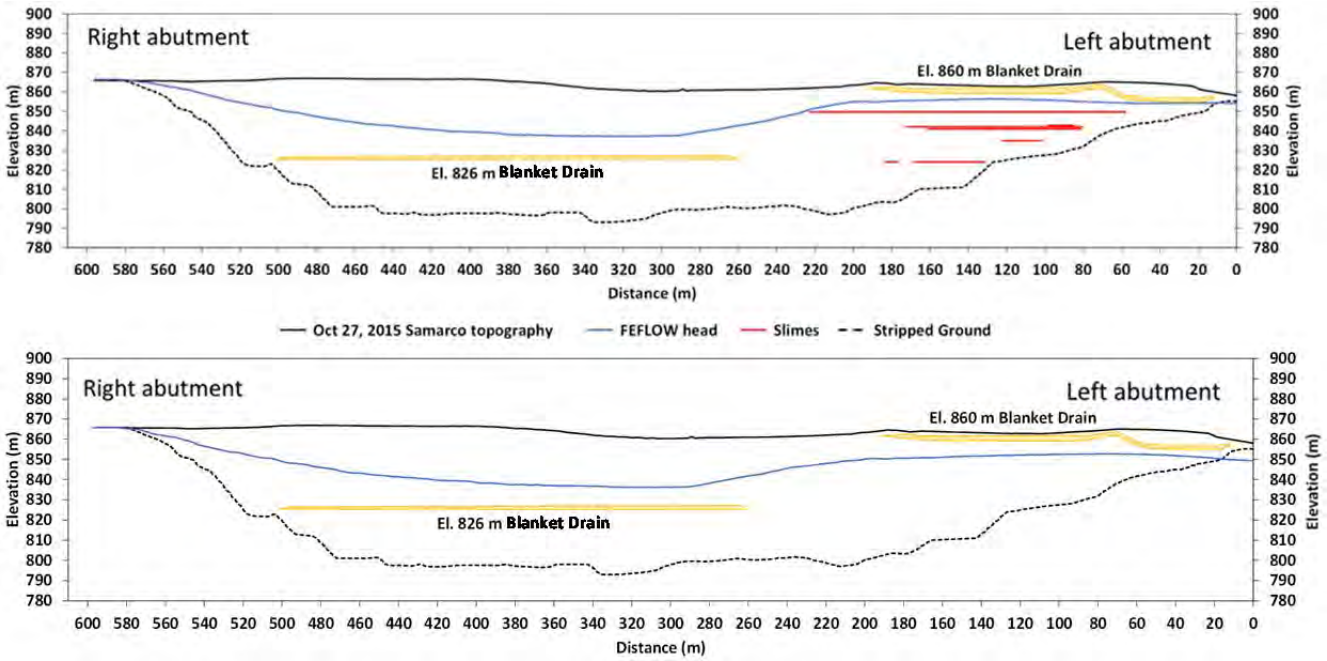

Figure G3-28 Longitudinal Section with water table from calibrated model (upper), Scenario 1 (lower), t=1800 Days

The differences are subtle but the left abutment phreatic condition is predicted to be lower in the scenario simulation (no slimes) than conditions predicted in the Ph1 calibrated model. The phreatic surface in the scenario simulation does not meet the El. 860 m blanket drain along this section, and the hydraulic gradient toward the El. 826 m blanket drain is a less abrupt feature. In the calibrated model, however, the phreatic surface is predicted to intersect the El. 860 m blanket drain in this transect.

Conditions over the El. 826 m blanket drain remain largely unchanged in both simulations.

G4 SUMMARY OF FINDINGS

Ph0 Design Concept Predictive Modeling:

- The concept design under normal conditions, and with up to 2x orders of magnitude reduction in drain permeability, maintains a drained sand stockpile as per design intent. The drain designs were therefore capable of conveying and discharging TSF seepage.
- The Principal Foundation Drain is the most critical element of the concept design. Once this degrades in performance, the abutment drains (under similar degrading conditions) do not have the ability to transmit water at the rate required, resulting in increased saturation and phreatic conditions, which encroach on the Dike 1 downstream face.
- The geometry of the facility is important. The further upstream from the crest of Dike 1, the wider the physical dimensions of the facility, and hence the greater the contribution of lateral through flow toward Fundão Dam.
- Analytical assessment of the Principal Foundation Drain estimates maximum drain capacity of 259 L/s in an unpressurized system, and 2,300 L/s for a pressurized system with a hydraulic gradient of 1:10. At these rates, flow is likely to be turbulent, or at least non-lineal. Lower normal operating rates are expected to produce lineal to non-lineal flow.
- The three main construction materials of slimes, sand and drains span several orders of magnitude permeability. As such, the contrast in their hydraulic properties dominates the seepage performance of the facility more so than subtle variation of their individual values. Because of this, understanding and representing key boundary condition stresses of pond location and recharge become more critical.

Ph1 TSF As-Built Modeling:

- Acceptable steady state and transient model calibration has been achieved, with good representation of piezometric conditions and drain performance, and reproduction of the conceptual understanding of as-built conditions in the numerical environment.
- The El. 826 m blanket drain is the most dominant feature of the structure, conveying the majority of water, and exerting strong phreatic influence to the right abutment, with weakening influence from increasing distance and elevation from the drain. At the area of the setback, the El. 826 m blanket drain is predicted to draw flow from the area of the left abutment; however, this is limited due to the distance of travel, the presence of slimes perching phreatic conditions in the area of the left abutment and the setback, and the lowered hydraulic gradients down gradient of the El. 860 m blanket drain and the Grota da Vale.
- The slimes on the left abutment appear to be perching phreatic conditions and plateauing heads in the lower area of the El. 860 m blanket drain. Scenario 1 was conducted to test this theory and confirmed phreatic conditions on the left abutment to be predicted as lower if the slimes “tongues” were not present beneath the dam.

- The phreatic surface on the left abutment intersects the El. 860 m blanket drain but appears to only skew the phreatic conditions and direction of flow, and does not serve to remove a large amount of water. The conditions in the lower section of the drain experience lower hydraulic gradients, and this area, particularly where the phreatic surface lies beneath the drain, probably represents the area where gradients start to come under the influence of the El. 826 m blanket drain.
- The right abutment appears well drained with steep gradients reporting to the El. 826 m blanket drain.

ATTACHMENT H1

Slope Stability Output

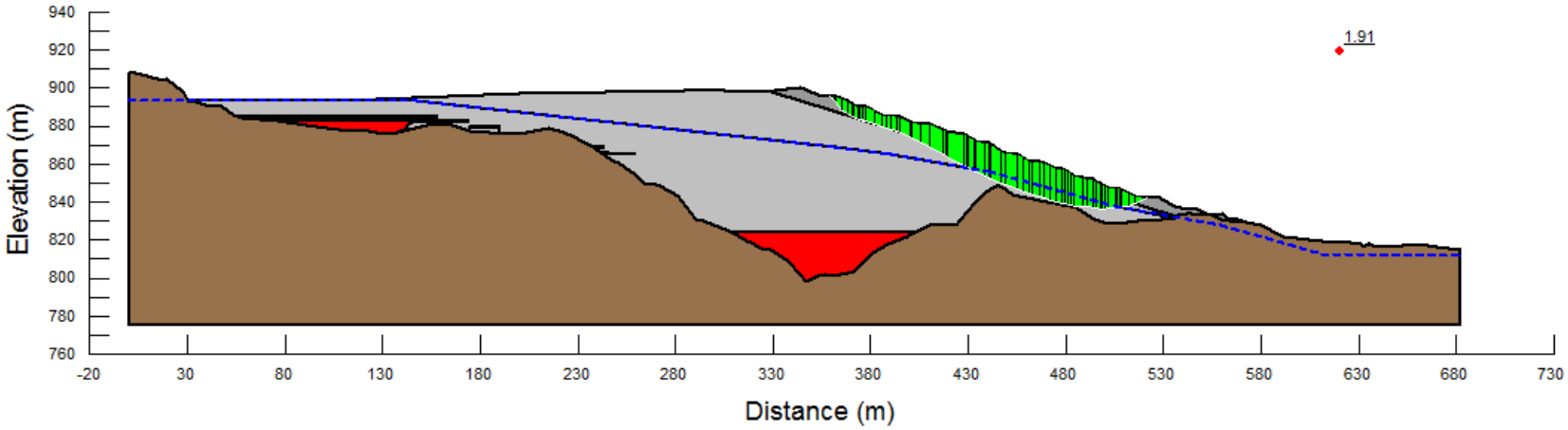

Type	Colour	Material	Unit Weight (kN/m^3)	Effective Friction Angle (degrees)	Effective Cohesion (kPa)
Fill		Compacted Sand Tailings	22	35	5
		Loose Sand Tailings	22	33	-
		Slimes	22	28	-
Foundation		Original Ground	22	32	40

NOTE:

PROJECT

Fundão Tailings Dam Review Panel

TITLE

ESA Base Case
Right Abutment – Section AA
Field Data
November 5, 2015

FIGURE NO.

H.H1-1A

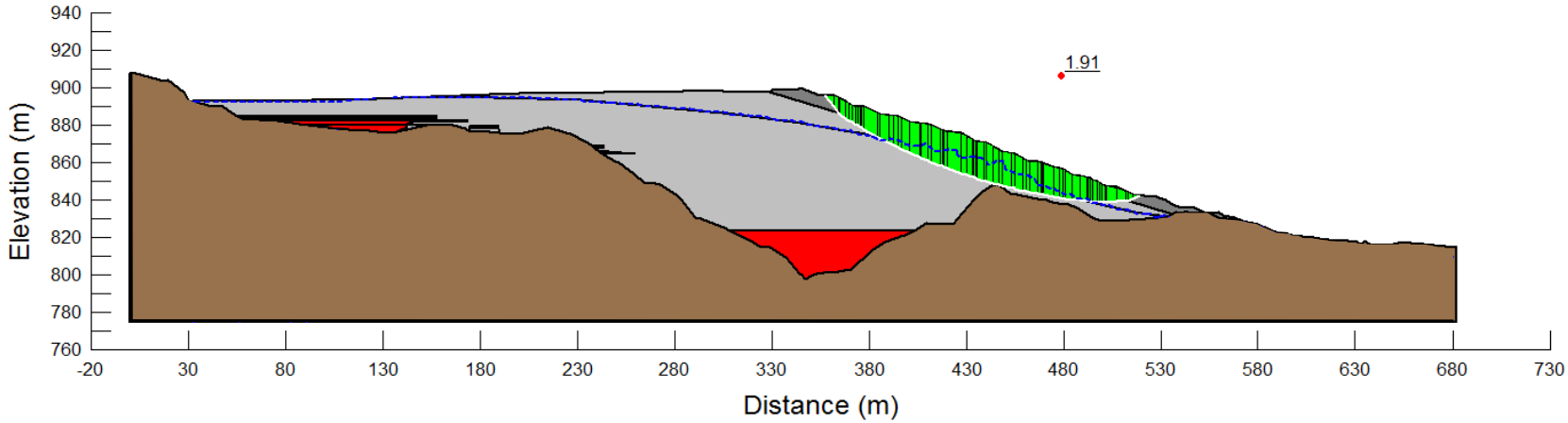

Type	Colour	Material	Unit Weight (kN/m^3)	Effective Friction Angle (degrees)	Effective Cohesion (kPa)
Fill		Compacted Sand Tailings	22	35	5
		Loose Sand Tailings	22	33	-
		Slimes	22	28	-
Foundation		Original Ground	22	32	40

NOTE:

PROJECT

Fundão Tailings Dam Review Panel

TITLE

ESA Base Case
Right Abutment – Section AA
3D FEFLOW
November 5, 2015

FIGURE NO.

H.H1-1B

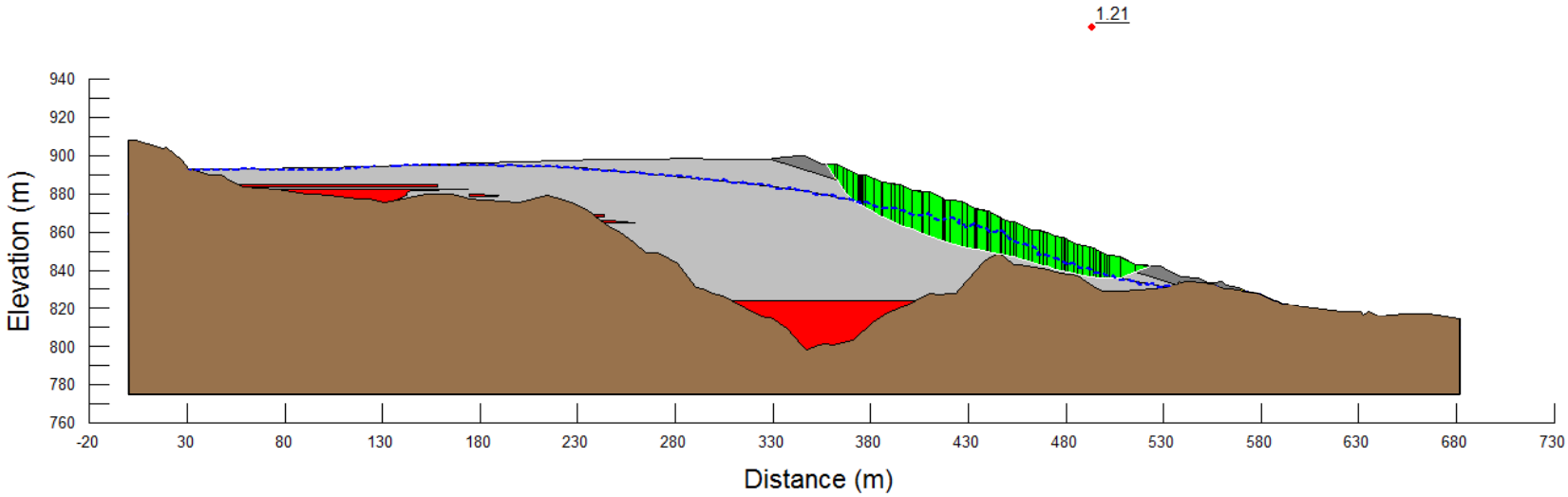

Type	Colour	Material	Unit Weight (kN/m^3)	Effective Friction Angle (degrees)	Effective Cohesion (kPa)	Undrained Strength Ratio s_u / σ'_v
Fill		Compacted Sand Tailings	22	35	5	-
		Loose Sand Tailings	22	33	-	0.31
		Slimes	22	28	-	0.31
Foundation		Original Ground	22	32	40	-

NOTE:

1. Effective Strength Parameters apply to Loose Sand Tailings and Slimes above the water table, and Undrained Strength Parameters apply to Loose Sand Tailings and Slimes below the water table.

PROJECT

Fundão Tailings Dam Review Panel

TITLE

ESA above WT / USA below WT
Right Abutment – Section AA
Field Data
November 5, 2015

FIGURE NO.

H.H1-2

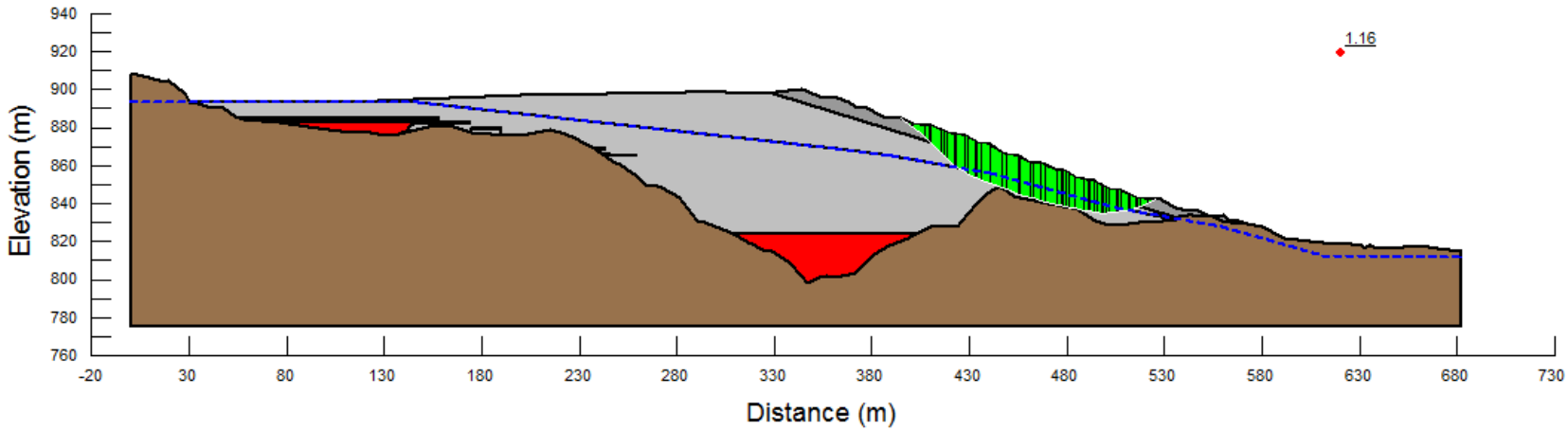

Type	Colour	Material	Unit Weight (kN/m^3)	Effective Friction Angle (degrees)	Effective Cohesion (kPa)	Undrained Strength Ratio s_u / σ'_v
Fill		Compacted Sand Tailings	22	35	5	-
		Loose Sand Tailings	22	33	-	0.34
		Slimes	22	28	-	0.34
Foundation		Original Ground	22	32	40	-

NOTE:

1. Effective Strength Parameters apply to Loose Sand Tailings and Slimes above the water table, and Undrained Strength Parameters apply to Loose Sand Tailings and Slimes below the water table.

PROJECT

Fundão Tailings Dam Review Panel

TITLE

ESA above WT / USA below WT
Right Abutment – Section AA
3D FEFLOW
November 5, 2015

FIGURE NO.

H.H1-3

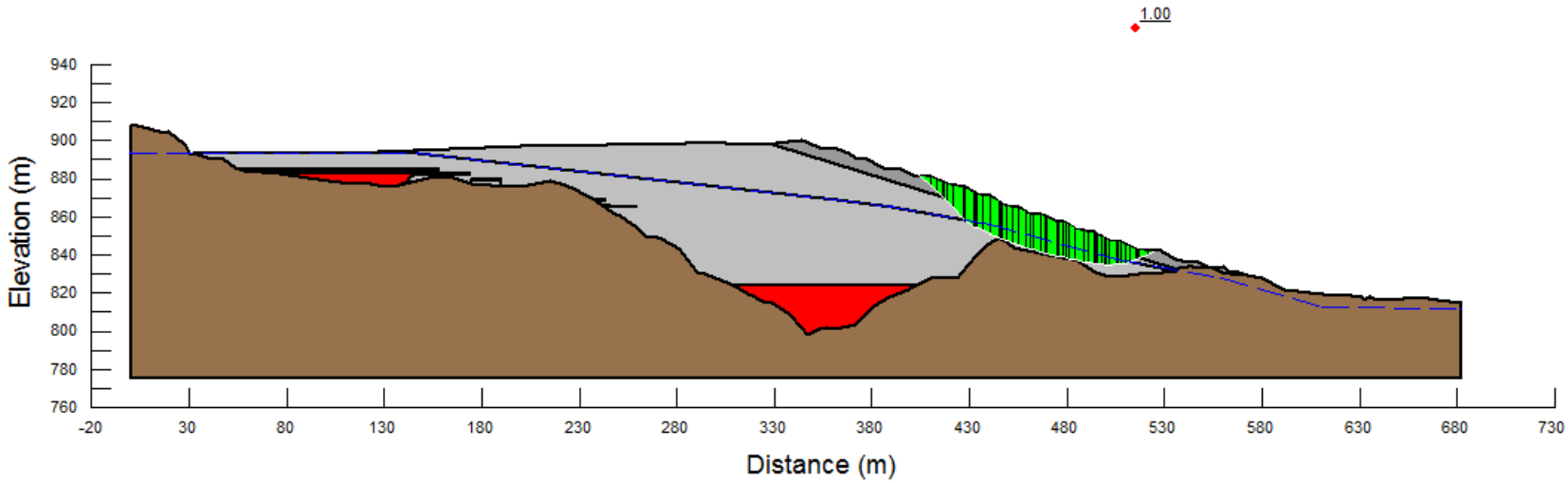

Type	Colour	Material	Unit Weight (kN/m^3)	Effective Friction Angle (degrees)	Effective Cohesion (kPa)	Undrained Strength Ratio s_u / σ'_v
Fill		Compacted Sand Tailings	22	35	5	-
		Loose Sand Tailings	22	33	-	0.25
		Slimes	22	28	-	0.25
Foundation		Original Ground	22	32	40	-

NOTE:

1. Effective Strength Parameters apply to Loose Sand Tailings and Slimes above the water table, and Undrained Strength Parameters apply to Loose Sand Tailings and Slimes below the water table.

PROJECT

Fundão Tailings Dam Review Panel

TITLE

ESA above WT / USA below WT
Right Abutment – Section AA
Field Data
November 5, 2015

FIGURE NO.

H.H1-4A

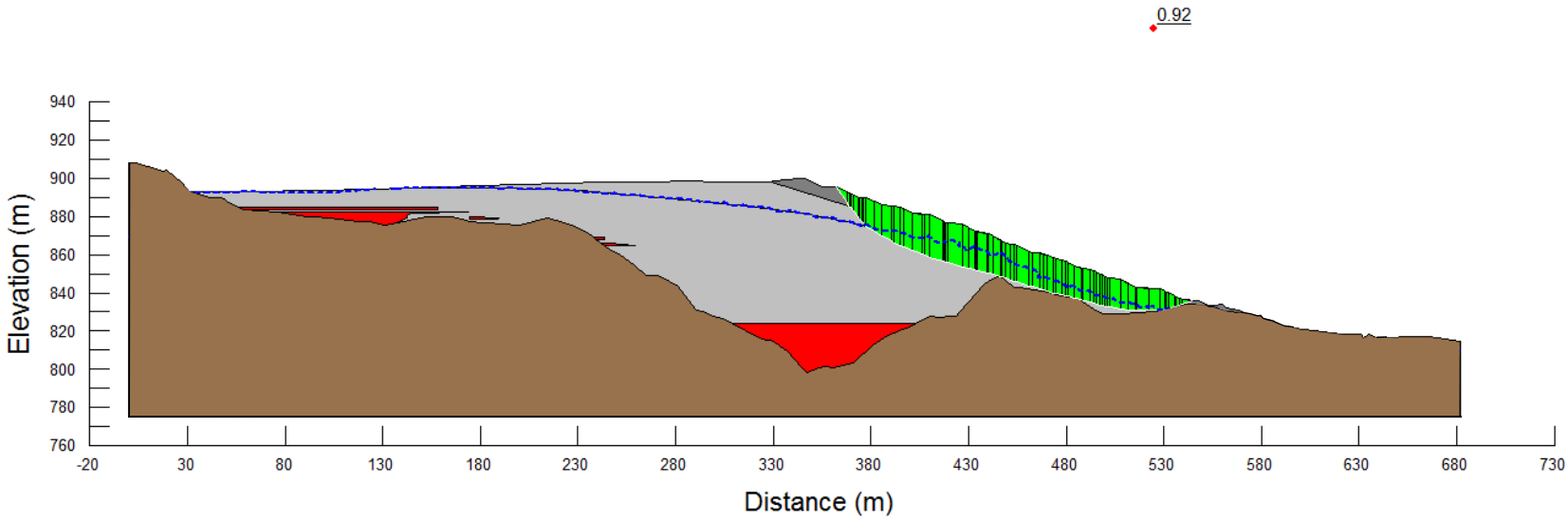

Type	Colour	Material	Unit Weight (kN/m^3)	Effective Friction Angle (degrees)	Effective Cohesion (kPa)	Undrained Strength Ratio s_u / σ'_v
Fill		Compacted Sand Tailings	22	35	5	-
		Loose Sand Tailings	22	33	-	0.25
		Slimes	22	28	-	0.25
Foundation		Original Ground	22	32	40	-

NOTE:

1. Effective Strength Parameters apply to Loose Sand Tailings and Slimes above the water table, and Undrained Strength Parameters apply to Loose Sand Tailings and Slimes below the water table.

PROJECT

Fundão Tailings Dam Review Panel

TITLE

ESA above WT / USA below WT
Right Abutment – Section AA
3D FEFLOW
November 5, 2015

FIGURE NO.

H.H1-4B

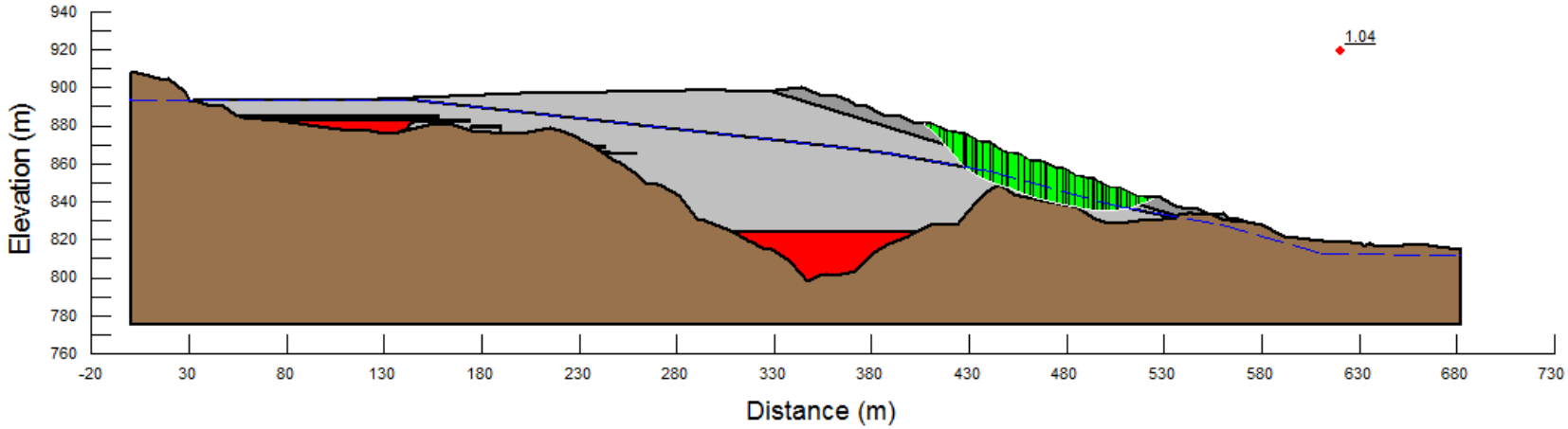

Type	Colour	Material	Unit Weight (kN/m^3)	Effective Friction Angle (degrees)	Effective Cohesion (kPa)
Fill		Compacted Sand Tailings	22	35	5
		Loose Sand Tailings (Above WT)	22	33	-
		Loose Sand Tailings (Below WT)	22	16[1]	-
		Slimes	22	16[1]	-
Foundation		Original Ground	22	32	40

1. 16° is a total stress friction angle.

NOTE:

PROJECT

Fundão Tailings Dam Review Panel

TITLE

ESA above WT / USA below WT with Low Strength Loose Tailings and Slimes below WT
Right Abutment – Section AA
Field Data
November 5, 2015

FIGURE NO.

H.H1-5A

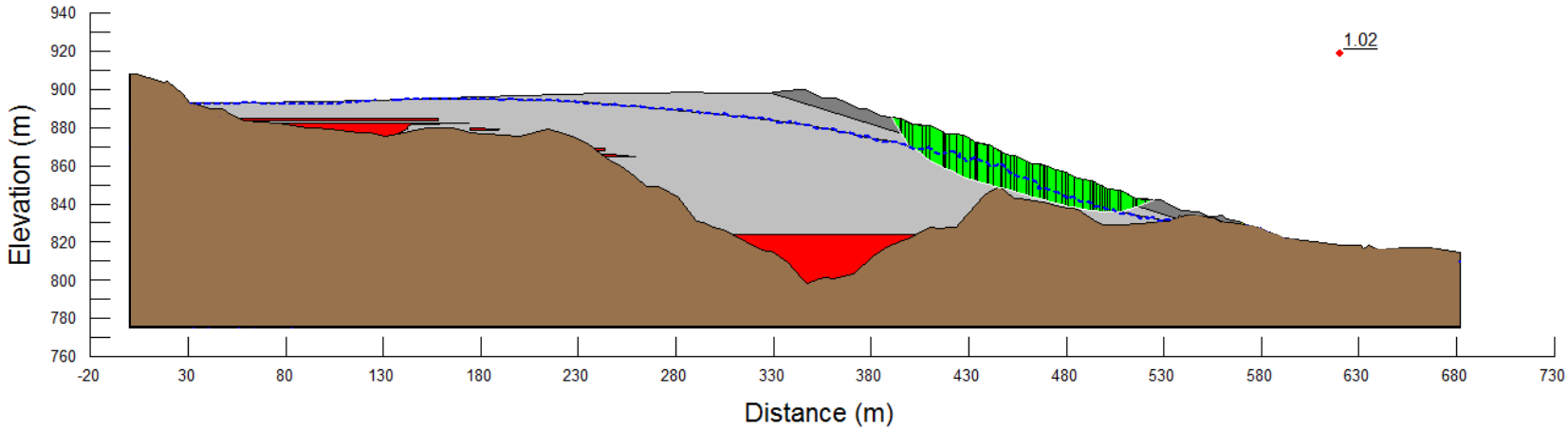

Type	Colour	Material	Unit Weight (kN/m^3)	Effective Friction Angle (deg.)	Effective Cohesion (kPa)
Fill		Compacted Sand Tailings	22	35	5
		Loose Sand Tailings (Above WT)	22	33	-
		Loose Sand Tailings (Below WT)	22	16[1]	-
		Slimes	22	16[1]	-
Foundation		Original Ground	22	32	40

1. 16° is a total stress friction angle.

NOTE:

PROJECT

Fundão Tailings Dam Review Panel

TITLE

ESA above WT / USA below WT with Low Strength Loose Tailings and Slimes below WT
Right Abutment – Section AA
3D FEFLOW
November 5, 2015

FIGURE NO.

H.H1-5B

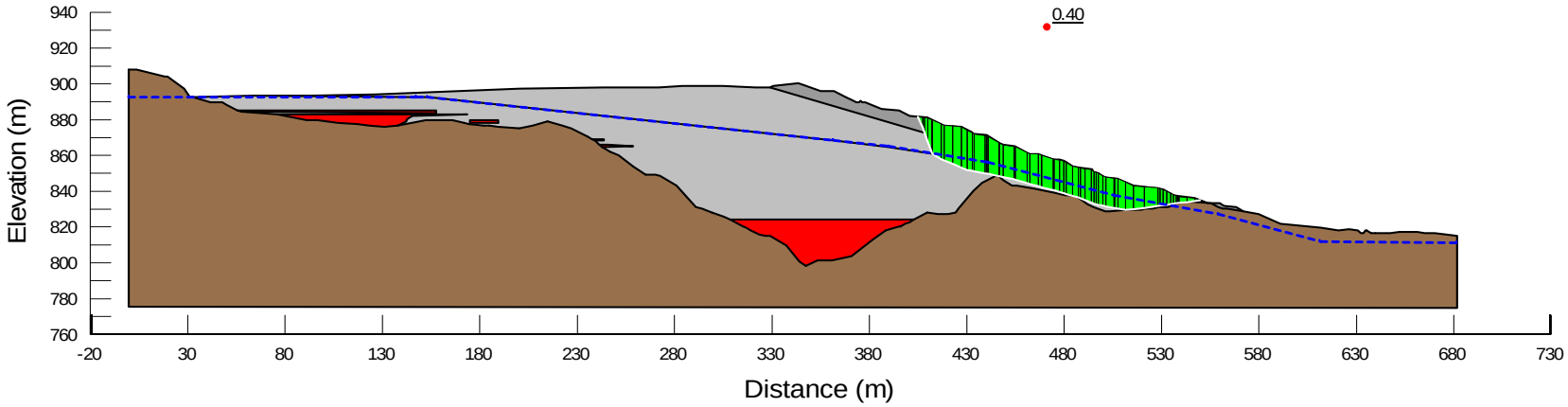

Type	Colour	Material	Unit Weight (kN/m^3)	Effective Friction Angle (degrees)	Effective Cohesion (kPa)	Undrained Strength Ratio s_u / σ'_v
Fill		Compacted Sand Tailings	22	35	5	-
		Loose Sand Tailings	22	33	-	0.07
		Slimes	22	28	-	0.07
Foundation		Original Ground	22	32	40	-

NOTE:

1. Effective Strength Parameters apply to Loose Sand Tailings and Slimes above the water table, and Undrained Strength Parameters apply to Loose Sand Tailings and Slimes below the water table.

PROJECT

Fundão Tailings Dam Review Panel

TITLE

ESA above WT / USA below WT
Right Abutment – Section AA
Field Data
November 5, 2015

FIGURE NO.

H.H1-6A

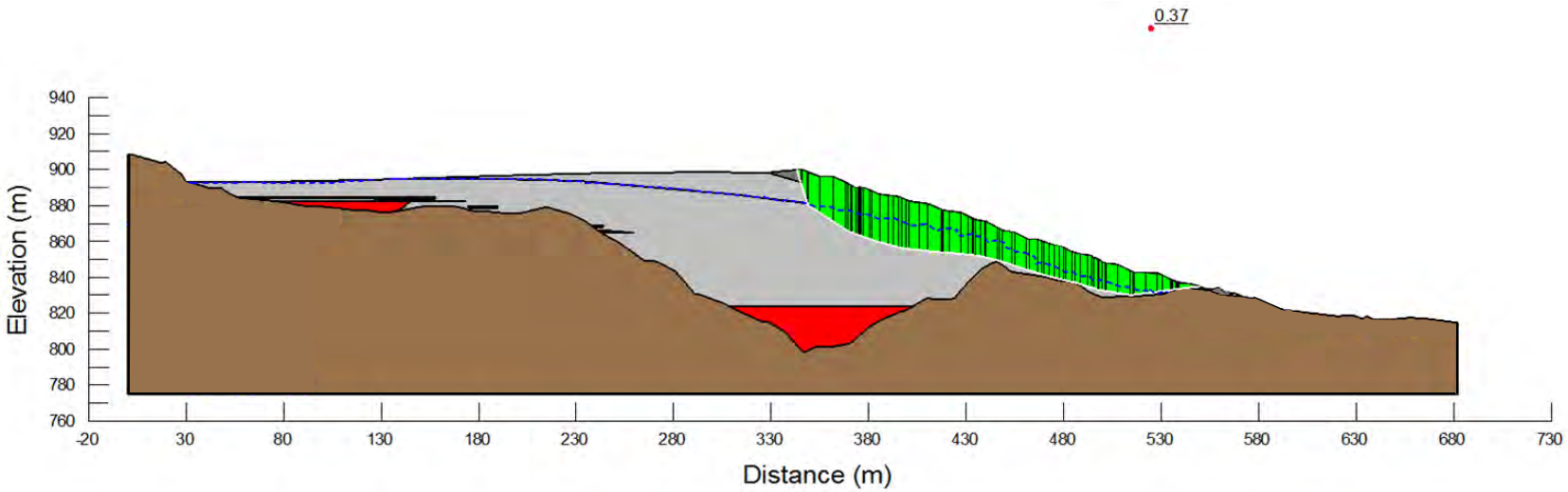

Type	Colour	Material	Unit Weight (kN/m^3)	Effective Friction Angle (degrees)	Effective Cohesion (kPa)	Undrained Strength Ratio s_u / σ'_v
Fill		Compacted Sand Tailings	22	35	5	-
		Loose Sand Tailings	22	33	-	0.07
		Slimes	22	28	-	0.07
Foundation		Original Ground	22	32	40	-

NOTE:

1. Effective Strength Parameters apply to Loose Sand Tailings and Slimes above the water table, and Undrained Strength Parameters apply to Loose Sand Tailings and Slimes below the water table.

PROJECT

Fundão Tailings Dam Review Panel

TITLE

ESA above WT / USA below WT
Right Abutment – Section AA
3D FEFLOW
November 5, 2015

FIGURE NO.

H.H1-6B

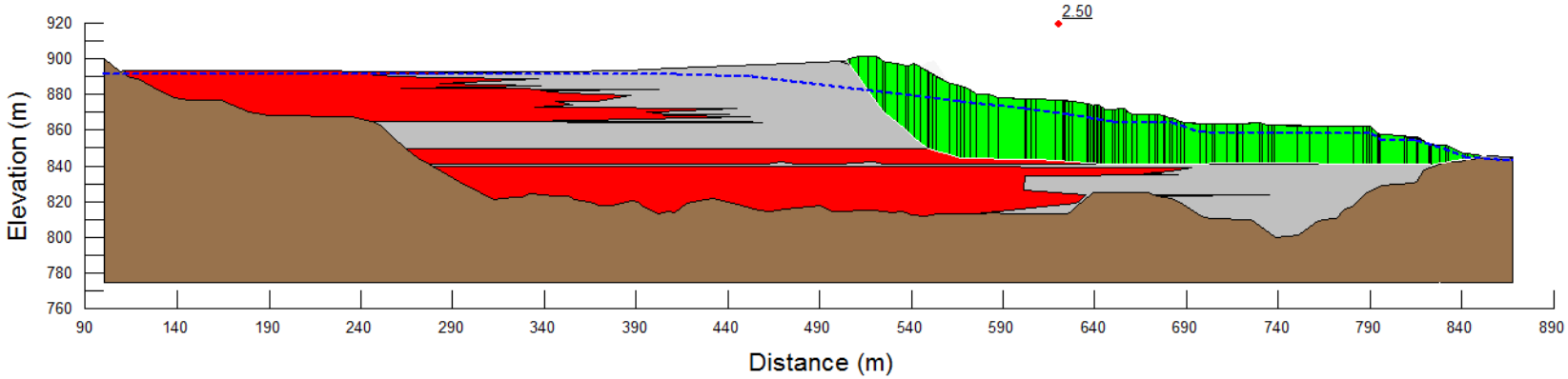

Type	Colour	Material	Unit Weight (kN/m^3)	Effective Friction Angle (degrees)	Effective Cohesion (kPa)
Fill		Compacted Sand Tailings	22	35	5
		Loose Sand Tailings	22	33	-
		Slimes	22	28	-
Foundation		Original Ground	22	32	40

NOTE:

PROJECT

Fundão Tailings Dam Review Panel

TITLE

ESA Base Case
Left Abutment – Section 01
Field Data
November 5, 2015

FIGURE NO.

H.H1-7A

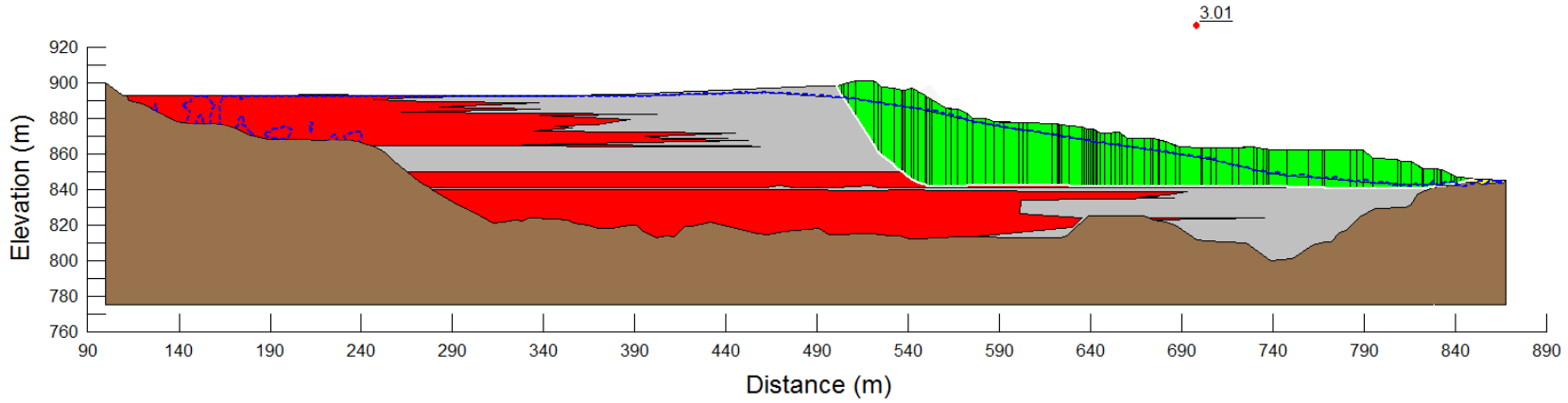

Type	Colour	Material	Unit Weight (kN/m^3)	Effective Friction Angle (degrees)	Effective Cohesion (kPa)
Fill		Compacted Sand Tailings	22	35	5
		Loose Sand Tailings	22	33	-
		Slimes	22	28	-
Foundation		Original Ground	22	32	40

NOTE:

PROJECT

Fundão Tailings Dam Review Panel

TITLE

ESA Base Case
Left Abutment – Section 01
3D FEFLOW
November 5, 2015

FIGURE NO.

H.H1-7B

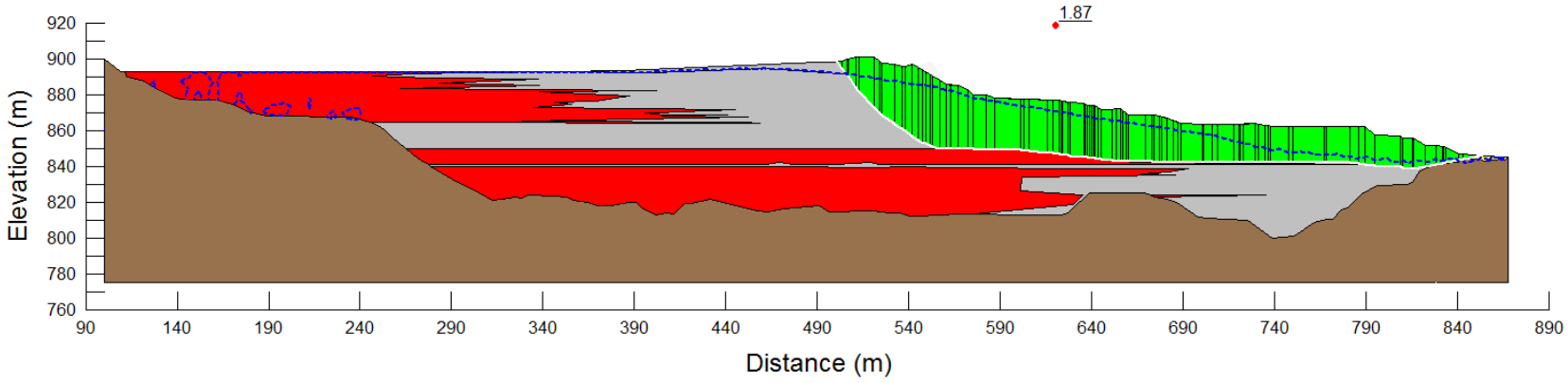

Type	Colour	Material	Unit Weight (kN/m^3)	Effective Friction Angle (degrees)	Effective Cohesion (kPa)	Undrained Strength Ratio s_u / σ'_v
Fill		Compacted Sand Tailings	22	35	5	-
		Loose Sand Tailings	22	33	-	0.34
		Slimes	22	28	-	0.34
Foundation		Original Ground	22	32	40	-

NOTE:

1. Effective Strength Parameters apply to Loose Sand Tailings and Slimes above the water table, and Undrained Strength Parameters apply to Loose Sand Tailings and Slimes below the water table.
2. Not to scale.

PROJECT

Fundão Tailings Dam Review Panel

TITLE

ESA above WT / USA below WT
Left Abutment – Section 01
3D FEFLOW
November 5, 2015

FIGURE NO.

H.H1-8

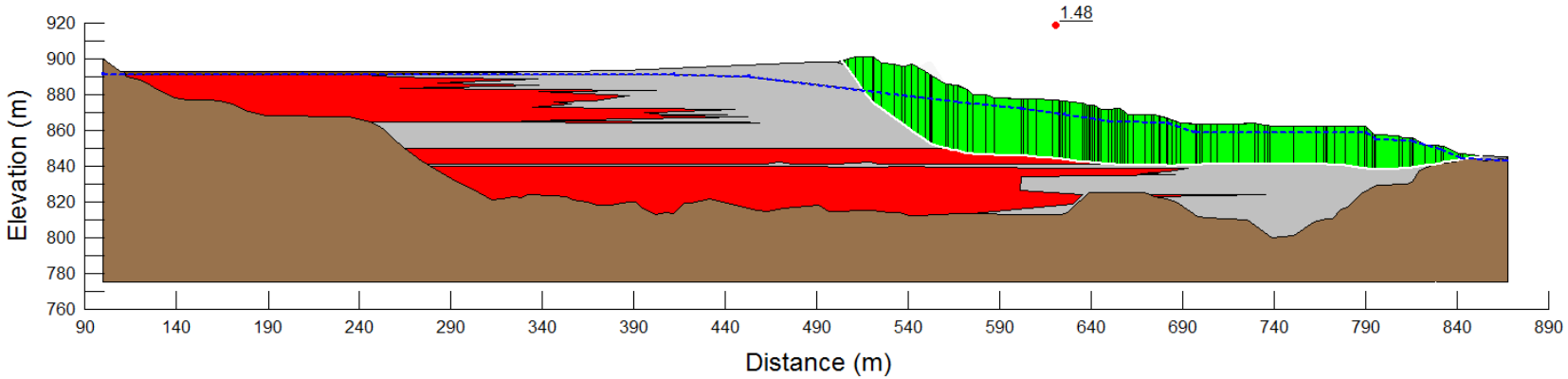

Type	Colour	Material	Unit Weight (kN/m^3)	Effective Friction Angle (degrees)	Effective Cohesion (kPa)	Undrained Strength Ratio s_u / σ'_v
Fill		Compacted Sand Tailings	22	35	5	-
		Loose Sand Tailings	22	33	-	0.31
		Slimes	22	28	-	0.31
Foundation		Original Ground	22	32	40	-

NOTE:

1. Effective Strength Parameters apply to Loose Sand Tailings and Slimes above the water table, and Undrained Strength Parameters apply to Loose Sand Tailings and Slimes below the water table.
2. Not to scale.

PROJECT

Fundão Tailings Dam Review Panel

TITLE

ESA above WT / USA below WT
Left Abutment – Section 01
Field Data
November 5, 2015

FIGURE NO.

H.H1-9

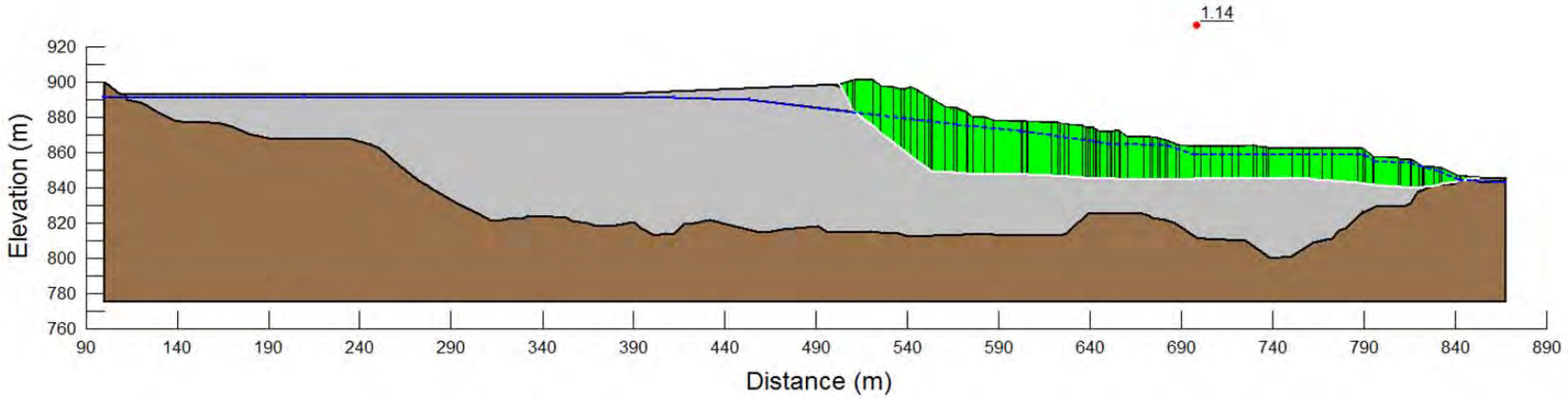

Type	Colour	Material	Unit Weight (kN/m^3)	Effective Friction Angle (degrees)	Effective Cohesion (kPa)	Undrained Strength Ratio s_u / σ'_v
Fill		Compacted Sand Tailings	22	35	5	-
		Loose Sand Tailings	22	33	-	0.30 (Backscarp)
						0.22 (Horizontal)
						0.14 (Breakout)
Foundation		Original Ground	22	32	40	-

NOTE:

1. Effective Strength Parameters apply to Loose Sand Tailings and Slimes above the water table, and Undrained Strength Parameters apply to Loose Sand Tailings and Slimes below the water table.

PROJECT

Fundão Tailings Dam Review Panel

TITLE

ESA above WT / USA Heterogeneous below WT
Left Abutment – Section 01
Field Data
November 5, 2015

FIGURE NO.

H.H1-10A

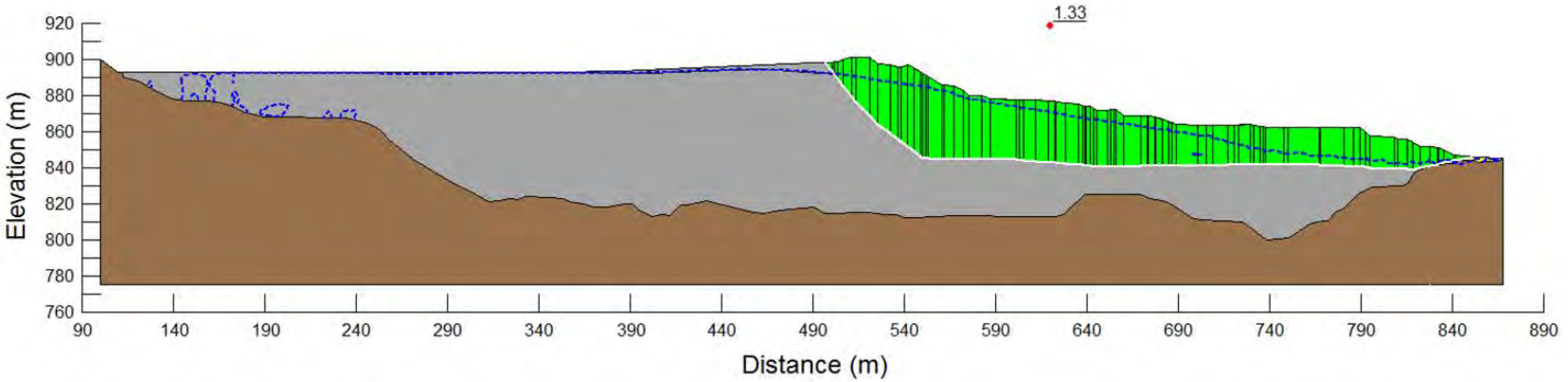

Type	Colour	Material	Unit Weight (kN/m^3)	Effective Friction Angle (degrees)	Effective Cohesion (kPa)	Undrained Strength Ratio s_u / σ'_v
Fill		Compacted Sand Tailings	22	35	5	-
		Loose Sand Tailings	22	33	-	0.30 (Backscarp)
						0.22 (Horizontal)
						0.14 (Breakout)
Foundation		Original Ground	22	32	40	-

NOTE:

1. Effective Strength Parameters apply to Loose Sand Tailings and Slimes above the water table, and Undrained Strength Parameters apply to Loose Sand Tailings and Slimes below the water table.

PROJECT

Fundão Tailings Dam Review Panel

TITLE

ESA above WT / USA Heterogeneous below WT
Left Abutment – Section 01
3D FEFLOW
November 5, 2015

FIGURE NO.

H.H1-10B

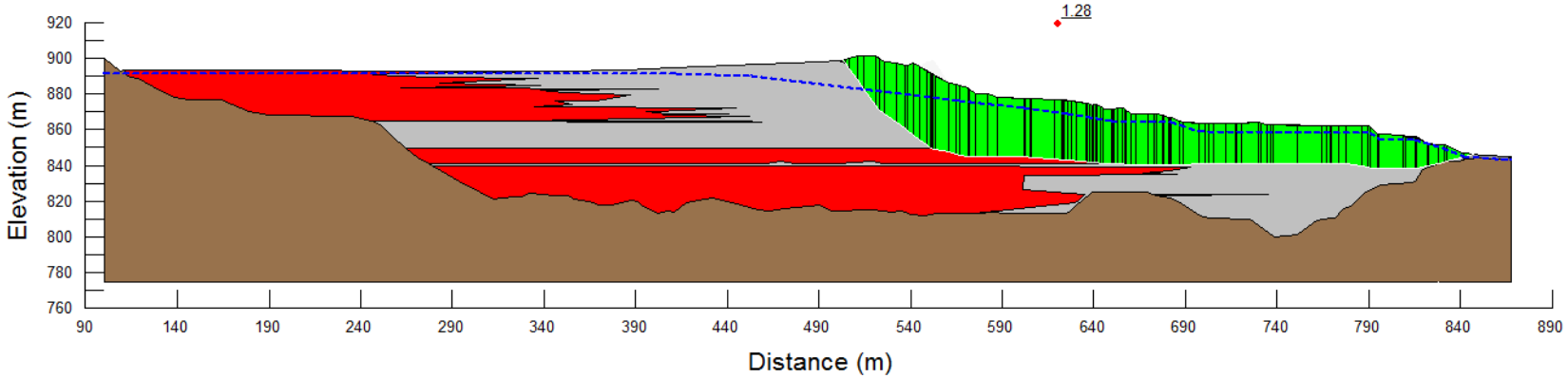

Type	Colour	Material	Unit Weight (kN/m^3)	Effective Friction Angle (degrees)	Effective Cohesion (kPa)
Fill		Compacted Sand Tailings	22	35	5
		Loose Sand Tailings (Above WT)	22	33	-
		Loose Sand Tailings (Below WT)	22	16[1]	-
		Slimes	22	16[1]	-
Foundation		Original Ground	22	32	40

1. 16° is a total stress friction angle.

NOTE:

PROJECT

Fundão Tailings Dam Review Panel

TITLE

ESA above WT / ESA with Low Strength Variant below WT
Left Abutment – Section 01
Field Data
November 5, 2015

FIGURE NO.

H.H1-11A

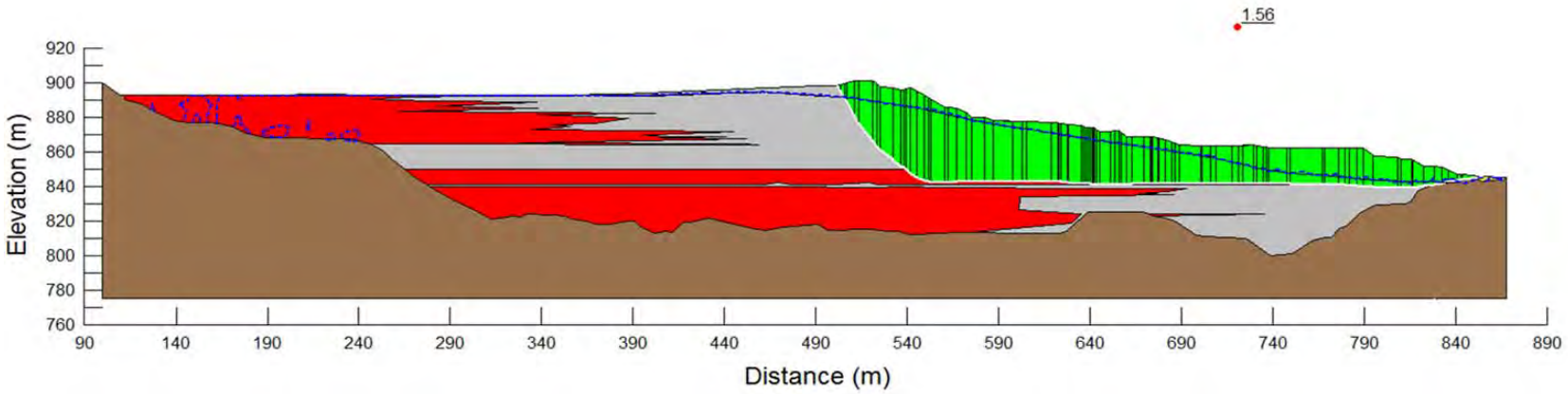

Type	Colour	Material	Unit Weight (kN/m^3)	Effective Friction Angle (degrees)	Effective Cohesion (kPa)
Fill		Compacted Sand Tailings	22	35	5
		Loose Sand Tailings (Above WT)	22	33	-
		Loose Sand Tailings (Below WT)	22	16[1]	-
		Slimes	22	16[1]	-
Foundation		Original Ground	22	32	40

1. 16° is a total stress friction angle.

NOTE:

PROJECT

Fundão Tailings Dam Review Panel

TITLE

ESA above WT / ESA with Low Strength Variant below WT
Left Abutment – Section 01
3D FEFLOW
November 5, 2015

FIGURE NO.

H.H1-11B

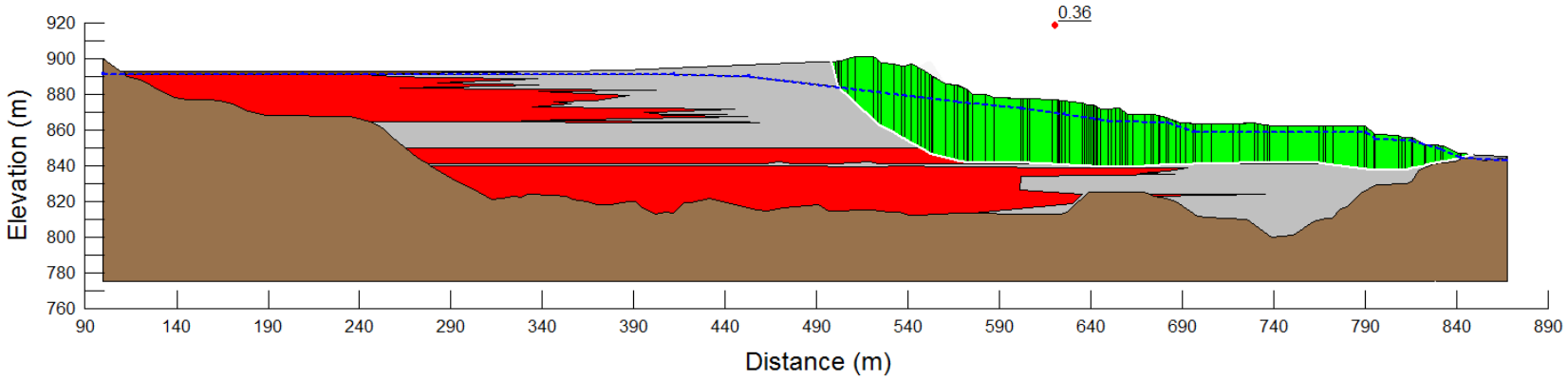

Type	Colour	Material	Unit Weight (kN/m^3)	Effective Friction Angle (degrees)	Effective Cohesion (kPa)	Undrained Strength Ratio s_u / σ'_v
Fill		Compacted Sand Tailings	22	35	5	-
		Loose Sand Tailings	22	33	-	0.07
		Slimes	22	28	-	0.07
Foundation		Original Ground	22	32	40	-

NOTE:

1. Effective Strength Parameters apply to Loose Sand Tailings and Slimes above the water table, and Undrained Strength Parameters apply to Loose Sand Tailings and Slimes below the water table.

PROJECT

Fundão Tailings Dam Review Panel

TITLE

ESA above WT / USA below WT
Left Abutment – Section 01
Field Data
November 5, 2015

FIGURE NO.

H.H1-12A

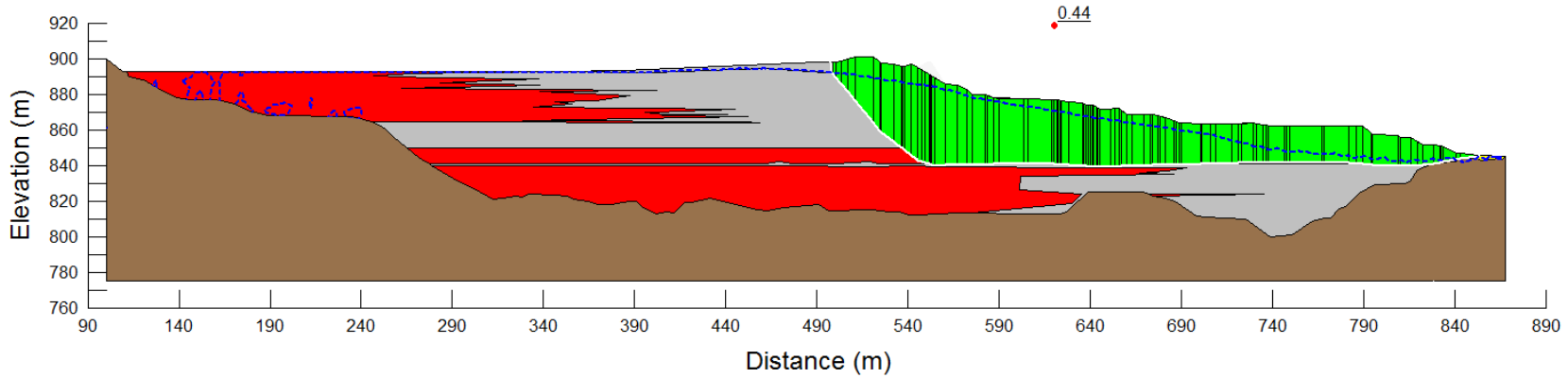

Type	Colour	Material	Unit Weight (kN/m^3)	Effective Friction Angle (degrees)	Effective Cohesion (kPa)	Undrained Strength Ratio s_u / σ'_v
Fill		Compacted Sand Tailings	22	35	5	-
		Loose Sand Tailings	22	33	-	0.07
		Slimes	22	28	-	0.07
Foundation		Original Ground	22	32	40	-

NOTE:

1. Effective Strength Parameters apply to Loose Sand Tailings and Slimes above the water table, and Undrained Strength Parameters apply to Loose Sand Tailings and Slimes below the water table.

PROJECT

Fundão Tailings Dam Review Panel

TITLE

ESA above WT / USA below WT
Left Abutment – Section 01
3D FEFLOW
November 5, 2015

FIGURE NO.

H.H1-12B

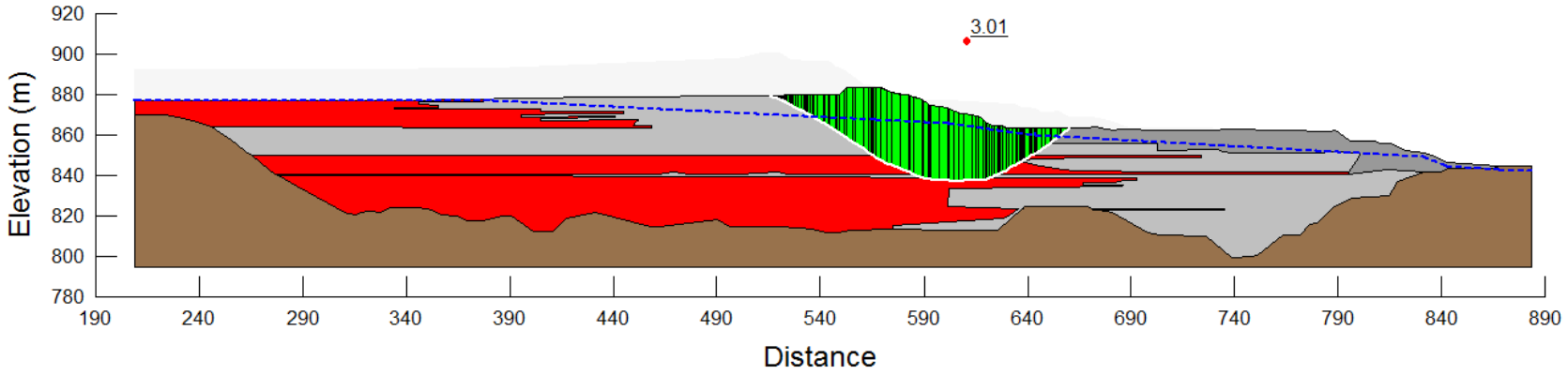

Type	Colour	Material	Unit Weight (kN/m^3)	Effective Friction Angle (degrees)	Effective Cohesion (kPa)
Fill		Compacted Sand Tailings	22	35	5
		Loose Sand Tailings	22	33	-
		Slimes	22	28	-
Foundation		Original Ground	22	32	40

NOTE:

PROJECT

Fundão Tailings Dam Review Panel

TITLE

ESA
Left Abutment - Section 01
Field Data
August, 2014

FIGURE NO.

H.H1-13A

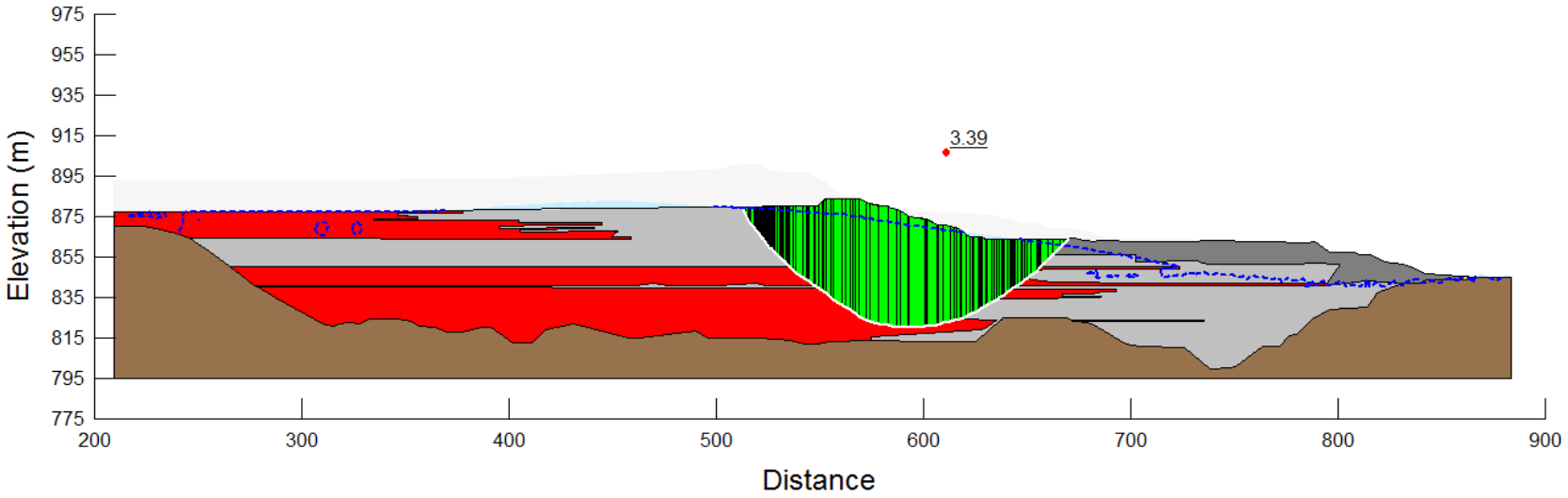

Type	Colour	Material	Unit Weight (kN/m^3)	Effective Friction Angle (degrees)	Effective Cohesion (kPa)
Fill		Compacted Sand Tailings	22	35	5
		Loose Sand Tailings	22	33	-
		Slimes	22	28	-
Foundation		Original Ground	22	32	40

NOTE:

PROJECT

Fundão Tailings Dam Review Panel

TITLE

ESA
Left Abutment - Section 01
3D FEFLOW
August, 2014

FIGURE NO.

H.H1-13B

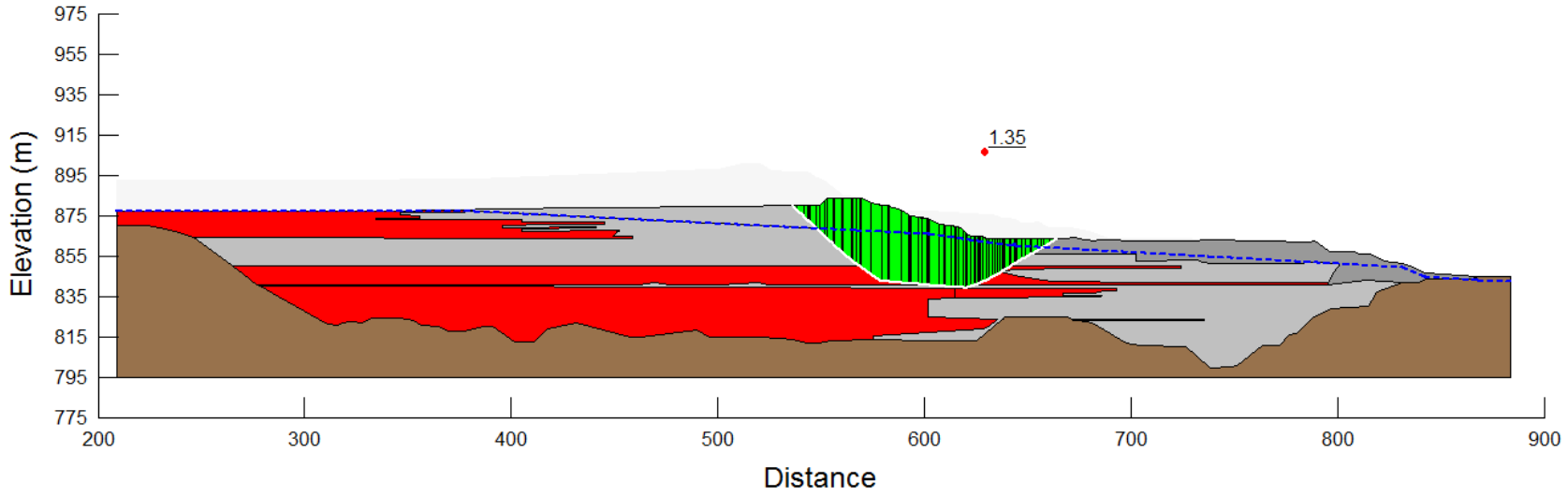

Type	Colour	Material	Unit Weight (kN/m^3)	Effective Friction Angle (degrees)	Effective Cohesion (kPa)	Undrained Strength Ratio s_u / σ'_v
Fill		Compacted Sand Tailings	22	35	5	-
		Loose Sand Tailings	22	33	-	0.30 (Backscarp)
						0.22 (Horozontal)
						0.14 (Breakout)
		Slimes	22	28	-	0.30 (Backscarp)
						0.22 (Horozontal)
						0.14 (Breakout)
Foundation		Original Ground	22	32	40	-

NOTE:

1. Effective Strength Parameters apply to Loose Sand Tailings and Slimes above the water table, and Undrained Strength Parameters apply to Loose Sand Tailings and Slimes below the water table.

PROJECT

Fundão Tailings Dam Review Panel

TITLE

ESA above WT / USA Heterogeneous below WT
Left Abutment - Section 01
Field Data
August, 2014

FIGURE NO.

H.H1-14A

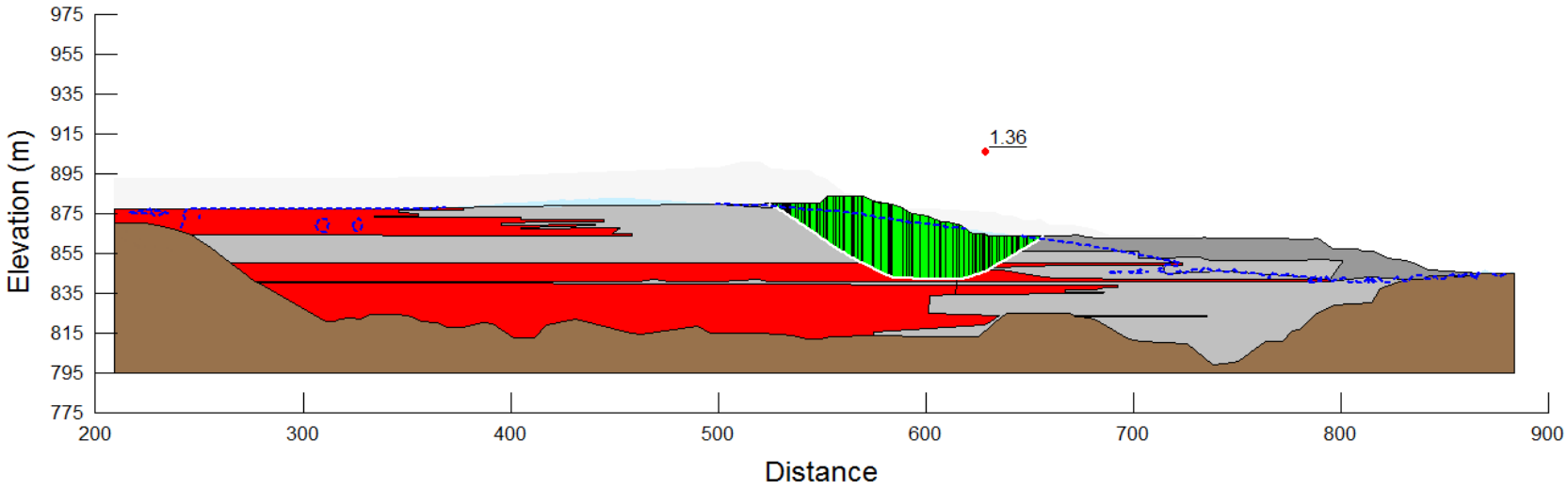

Type	Colour	Material	Unit Weight (kN/m^3)	Effective Friction Angle (degrees)	Effective Cohesion (kPa)	Undrained Strength Ratio s_u / σ'_v
Fill		Compacted Sand Tailings	22	35	5	-
		Loose Sand Tailings	22	33	-	0.30 (Backscarp)
						0.22 (Horozontal)
						0.14 (Breakout)
		Slimes	22	28	-	0.30 (Backscarp)
						0.22 (Horozontal)
						0.14 (Breakout)
Foundation		Original Ground	22	32	40	-

NOTE:

1. Effective Strength Parameters apply to Loose Sand Tailings and Slimes above the water table, and Undrained Strength Parameters apply to Loose Sand Tailings and Slimes below the water table.

PROJECT

Fundão Tailings Dam Review Panel

TITLE

ESA above WT / USA Heterogeneous below WT
Left Abutment - Section 01
3D FEFLOW
August, 2014

FIGURE NO.

H.H1-14B

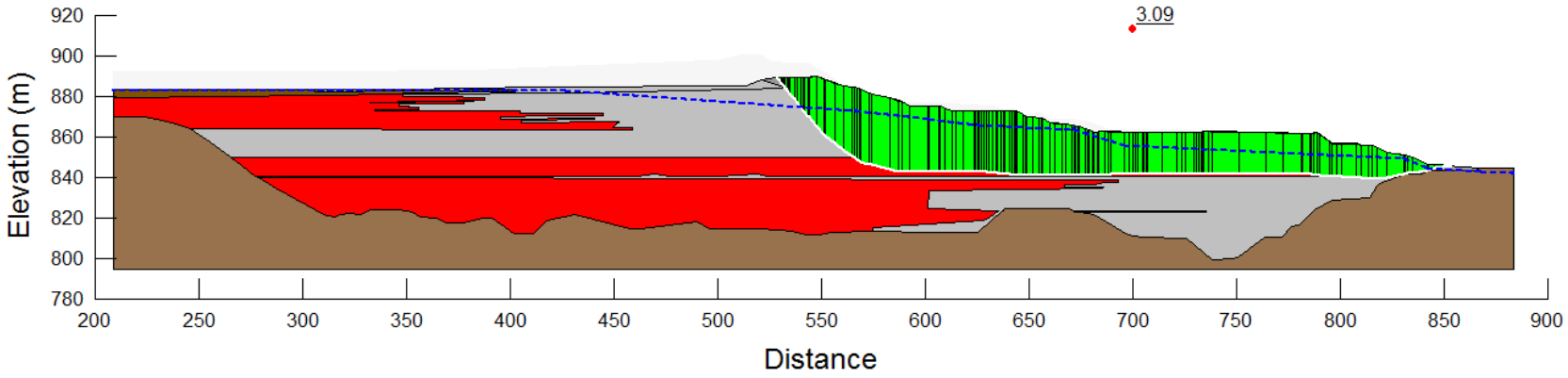

Type	Colour	Material	Unit Weight (kN/m^3)	Effective Friction Angle (degrees)	Effective Cohesion (kPa)
Fill		Compacted Sand Tailings	22	35	5
		Loose Sand Tailings	22	33	-
		Slimes	22	28	-
Foundation		Original Ground	22	32	40

NOTE:

PROJECT

Fundão Tailings Dam Review Panel

TITLE

FOS Tracking
Left Abutment – Section 01
Field Data
February, 2015

FIGURE NO.

H.H1-15A

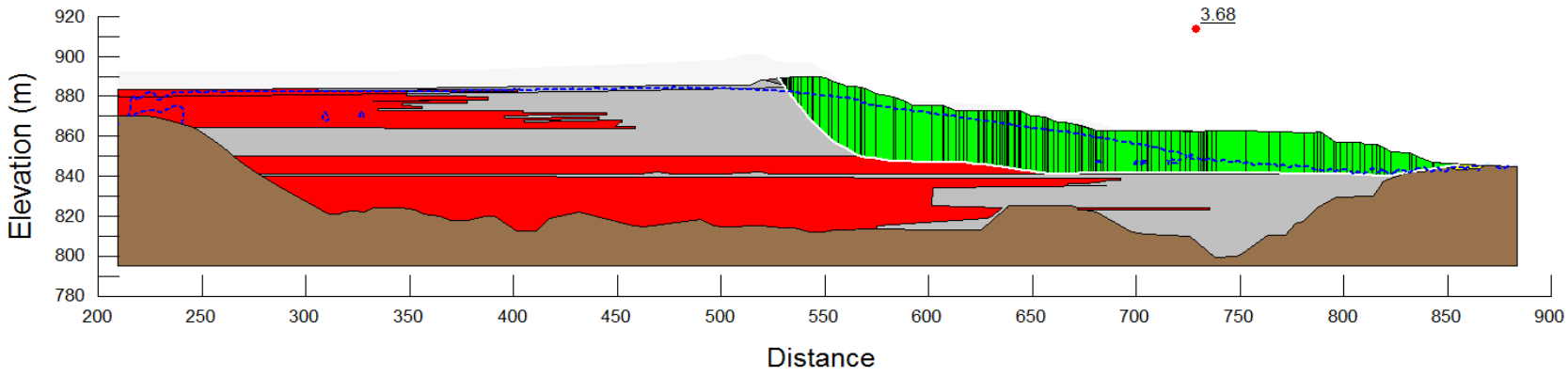

Type	Colour	Material	Unit Weight (kN/m^3)	Effective Friction Angle (degrees)	Effective Cohesion (kPa)
Fill		Compacted Sand Tailings	22	35	5
		Loose Sand Tailings	22	33	-
		Slimes	22	28	-
Foundation		Original Ground	22	32	40

NOTE:

PROJECT

Fundão Tailings Dam Review Panel

TITLE

FOS Tracking
Left Abutment – Section 01
3D FEFLOW
February, 2015

FIGURE NO.

H.H1-15B

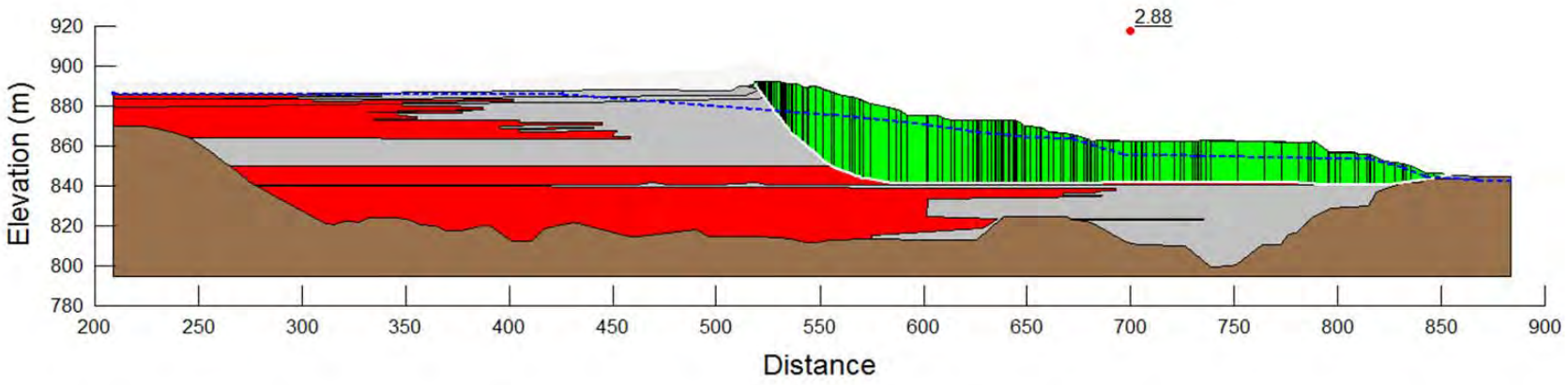

Type	Colour	Material	Unit Weight (kN/m^3)	Effective Friction Angle (degrees)	Effective Cohesion (kPa)
Fill		Compacted Sand Tailings	22	35	5
		Loose Sand Tailings	22	33	-
		Slimes	22	28	-
Foundation		Original Ground	22	32	40

NOTE:

PROJECT

Fundão Tailings Dam Review Panel

TITLE

FOS Tracking
Left Abutment – Section 01
Field Data
May, 2015

FIGURE NO.

H.H1-16A

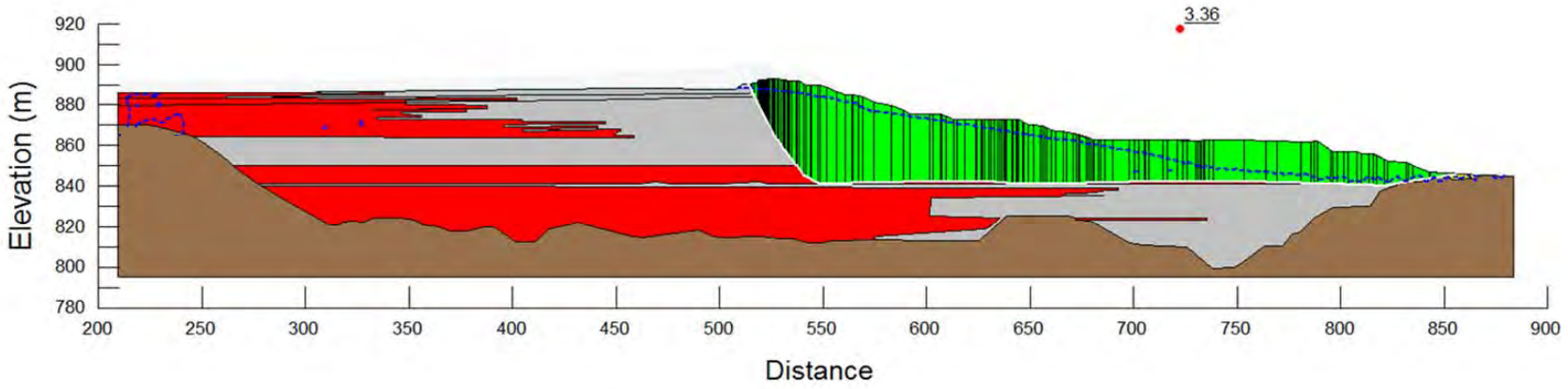

Type	Colour	Material	Unit Weight (kN/m^3)	Effective Friction Angle (degrees)	Effective Cohesion (kPa)
Fill		Compacted Sand Tailings	22	35	5
		Loose Sand Tailings	22	33	-
		Slimes	22	28	-
Foundation		Original Ground	22	32	40

NOTE:

PROJECT

Fundão Tailings Dam Review Panel

TITLE

FOS Tracking
Left Abutment – Section 01
3D FEFLOW
May, 2015

FIGURE NO.

H.H1-16B

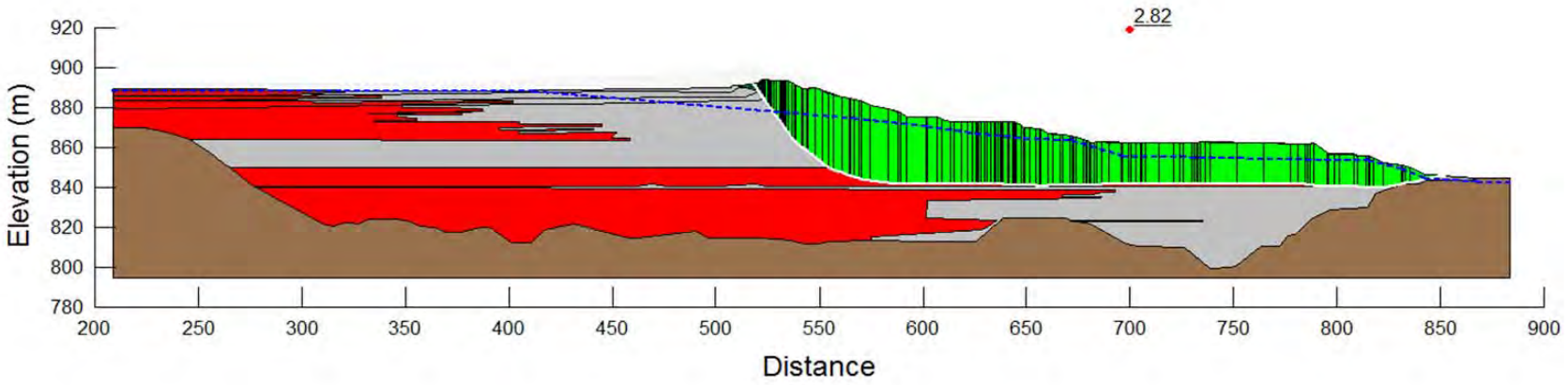

Type	Colour	Material	Unit Weight (kN/m^3)	Effective Friction Angle (degrees)	Effective Cohesion (kPa)
Fill		Compacted Sand Tailings	22	35	5
		Loose Sand Tailings	22	33	-
		Slimes	22	28	-
Foundation		Original Ground	22	32	40

NOTE:

PROJECT

Fundão Tailings Dam Review Panel

TITLE

FOS Tracking
Left Abutment – Section 01
Field Data
June, 2015

FIGURE NO.

H.H1-17A

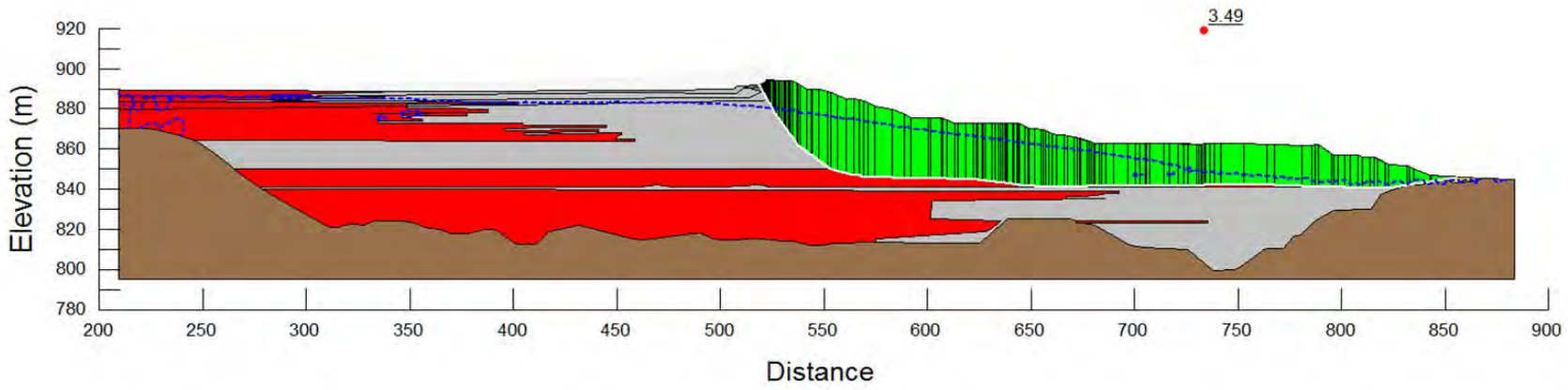

Type	Colour	Material	Unit Weight (kN/m^3)	Effective Friction Angle (degrees)	Effective Cohesion (kPa)
Fill		Compacted Sand Tailings	22	35	5
		Loose Sand Tailings	22	33	-
		Slimes	22	28	-
Foundation		Original Ground	22	32	40

NOTE:

PROJECT

Fundão Tailings Dam Review Panel

TITLE

FOS Tracking
Left Abutment – Section 01
3D FEFLOW
June, 2015

FIGURE NO.

H.H1-17B

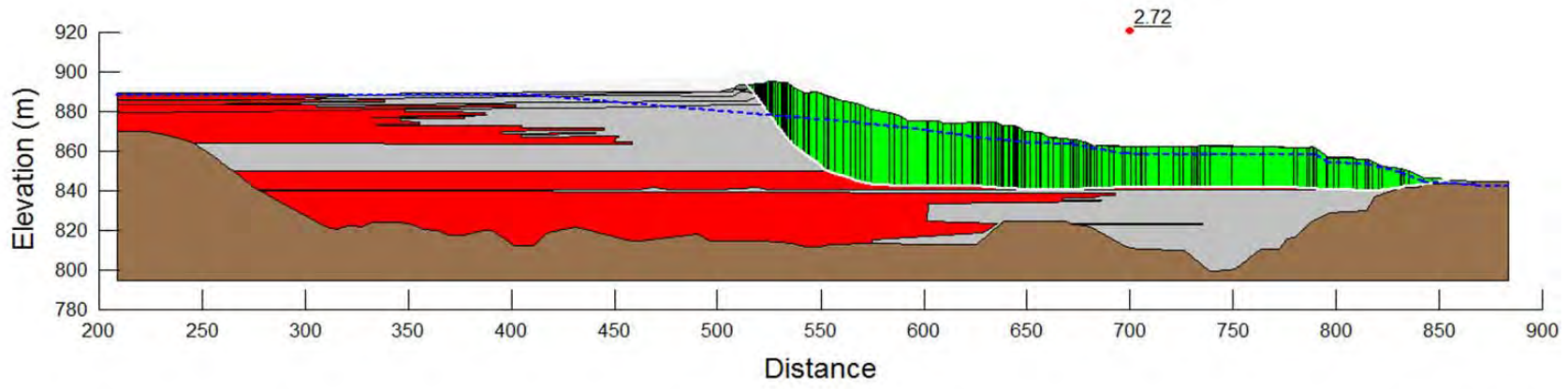

Type	Colour	Material	Unit Weight (kN/m^3)	Effective Friction Angle (degrees)	Effective Cohesion (kPa)
Fill		Compacted Sand Tailings	22	35	5
		Loose Sand Tailings	22	33	-
		Slimes	22	28	-
Foundation		Original Ground	22	32	40

NOTE:

PROJECT

Fundão Tailings Dam Review Panel

TITLE

FOS Tracking
Left Abutment – Section 01
Field Data
July, 2015

FIGURE NO.

H.H1-18A

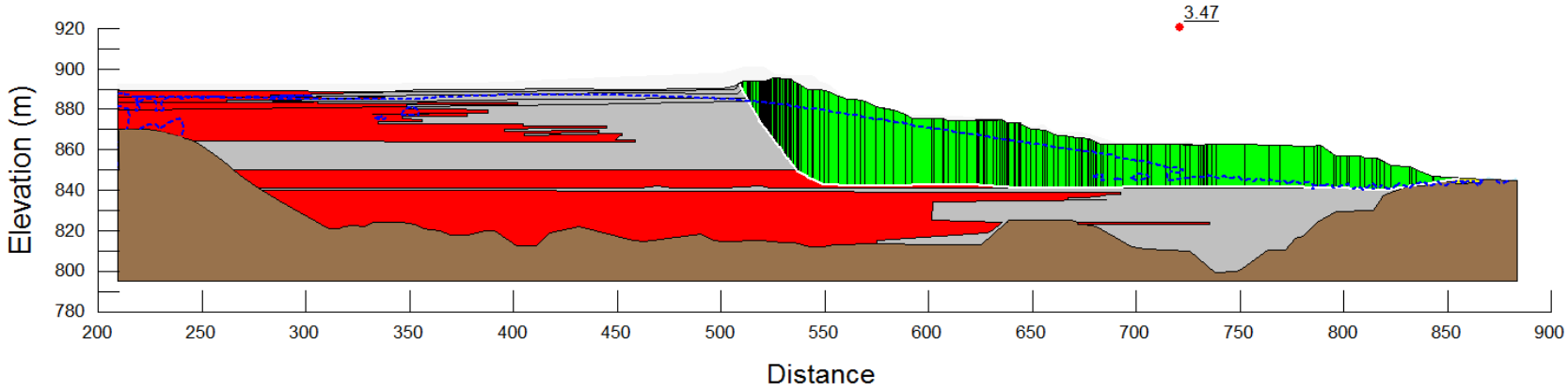

Type	Colour	Material	Unit Weight (kN/m^3)	Effective Friction Angle (degrees)	Effective Cohesion (kPa)
Fill		Compacted Sand Tailings	22	35	5
		Loose Sand Tailings	22	33	-
		Slimes	22	28	-
Foundation		Original Ground	22	32	40

NOTE:

PROJECT

Fundão Tailings Dam Review Panel

TITLE

FOS Tracking
Left Abutment – Section 01
3D FEFLOW
July, 2015

FIGURE NO.

H.H1-18B

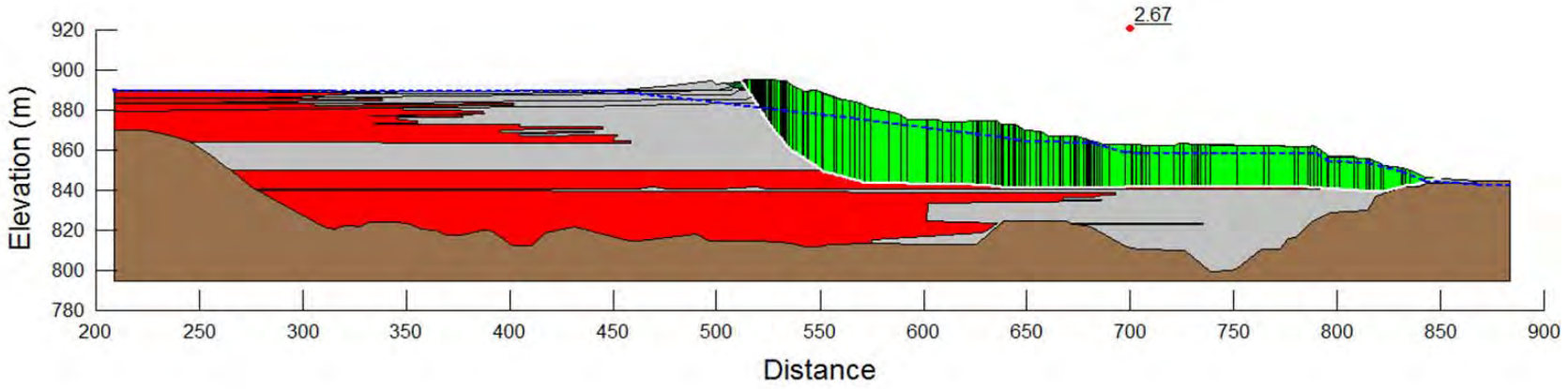

Type	Colour	Material	Unit Weight (kN/m^3)	Effective Friction Angle (degrees)	Effective Cohesion (kPa)
Fill		Compacted Sand Tailings	22	35	5
		Loose Sand Tailings	22	33	-
		Slimes	22	28	-
Foundation		Original Ground	22	32	40

NOTE:

PROJECT

Fundão Tailings Dam Review Panel

TITLE

FOS Tracking
Left Abutment – Section 01
Field Data
August, 2015

FIGURE NO.

H.H1-19A

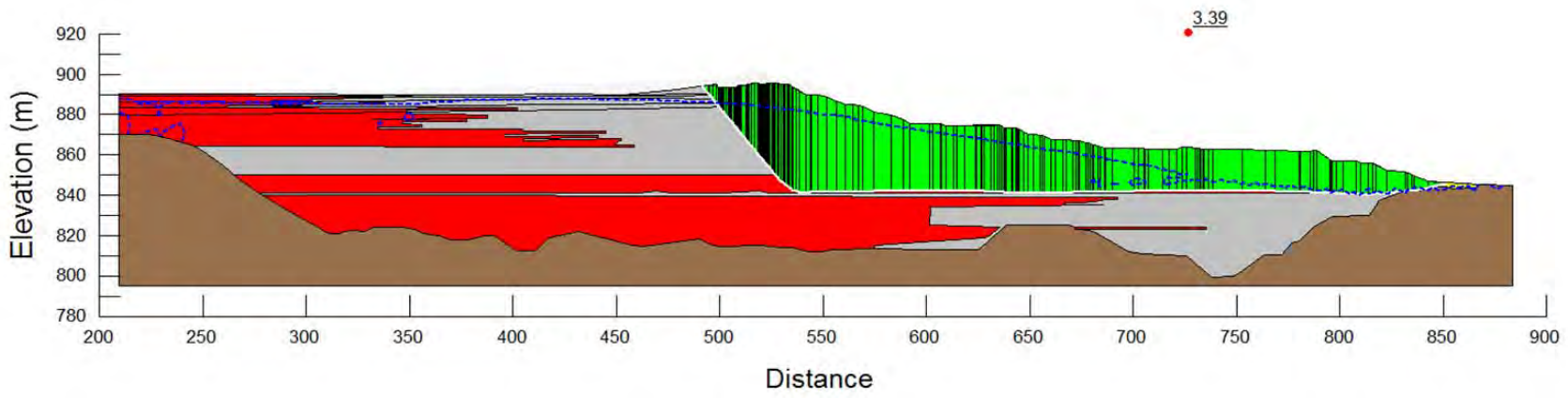

Type	Colour	Material	Unit Weight (kN/m^3)	Effective Friction Angle (degrees)	Effective Cohesion (kPa)
Fill		Compacted Sand Tailings	22	35	5
		Loose Sand Tailings	22	33	-
		Slimes	22	28	-
Foundation		Original Ground	22	32	40

NOTE:

PROJECT

Fundão Tailings Dam Review Panel

TITLE

FOS Tracking
Left Abutment – Section 01
3D FEFLOW
August, 2015

FIGURE NO.

H.H1-19B

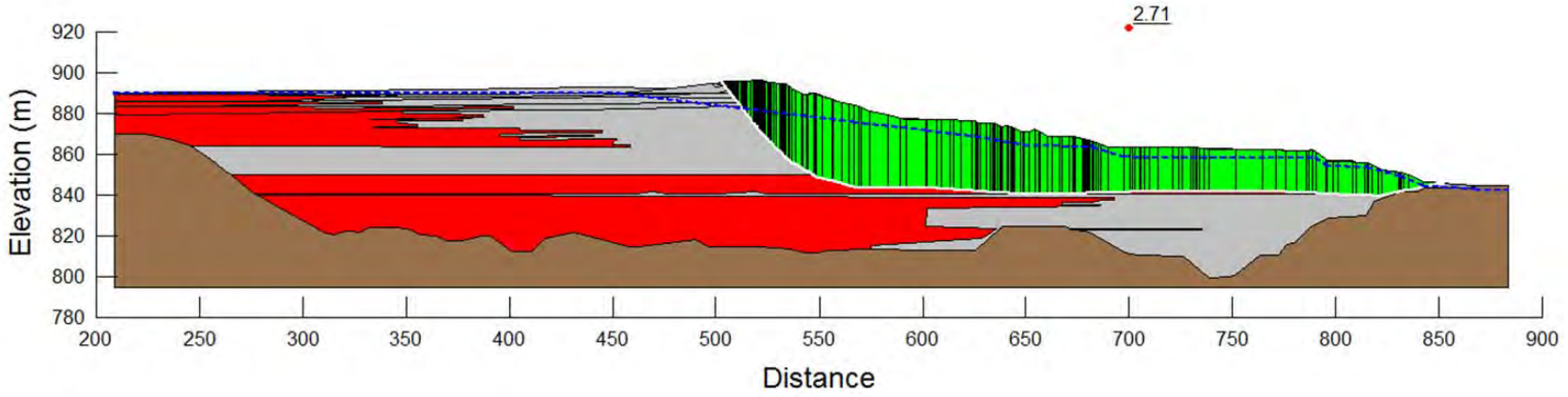

Type	Colour	Material	Unit Weight (kN/m^3)	Effective Friction Angle (degrees)	Effective Cohesion (kPa)
Fill		Compacted Sand Tailings	22	35	5
		Loose Sand Tailings	22	33	-
		Slimes	22	28	-
Foundation		Original Ground	22	32	40

NOTE:

PROJECT

Fundão Tailings Dam Review Panel

TITLE

FOS Tracking
Left Abutment – Section 01
Field Data
September, 2015

FIGURE NO.

H.H1-20A

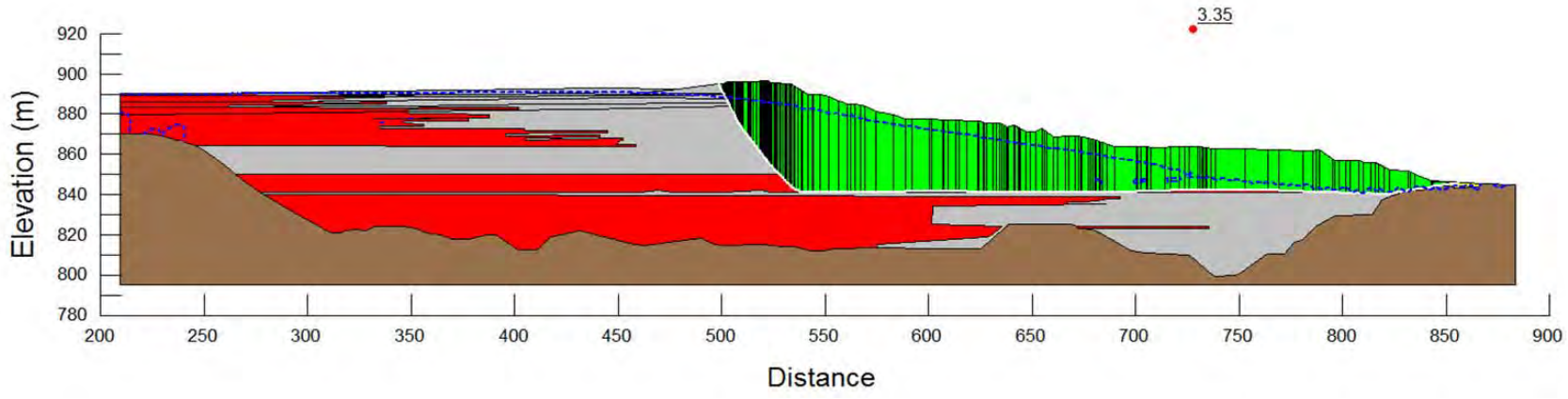

Type	Colour	Material	Unit Weight (kN/m^3)	Effective Friction Angle (degrees)	Effective Cohesion (kPa)
Fill		Compacted Sand Tailings	22	35	5
		Loose Sand Tailings	22	33	-
		Slimes	22	28	-
Foundation		Original Ground	22	32	40

NOTE:

PROJECT

Fundão Tailings Dam Review Panel

TITLE

FOS Tracking
Left Abutment – Section 01
3D FEFLOW
September, 2015

FIGURE NO.

H.H1-20B

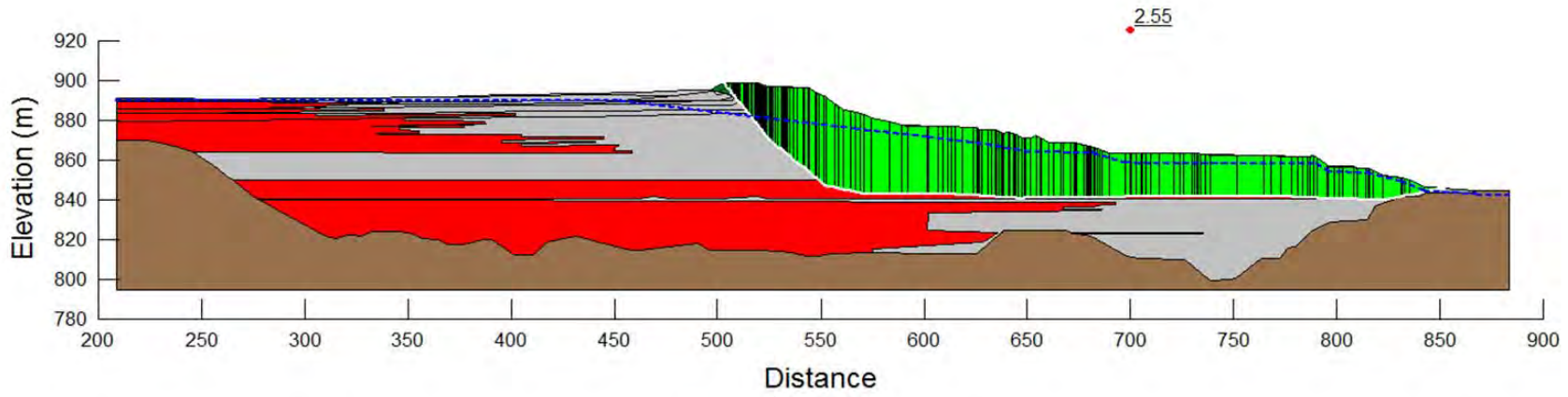

Type	Colour	Material	Unit Weight (kN/m^3)	Effective Friction Angle (degrees)	Effective Cohesion (kPa)
Fill		Compacted Sand Tailings	22	35	5
		Loose Sand Tailings	22	33	-
		Slimes	22	28	-
Foundation		Original Ground	22	32	40

NOTE:

PROJECT

Fundão Tailings Dam Review Panel

TITLE

FOS Tracking
Left Abutment – Section 01
Field Data
October, 2015

FIGURE NO.

H.H1-21A

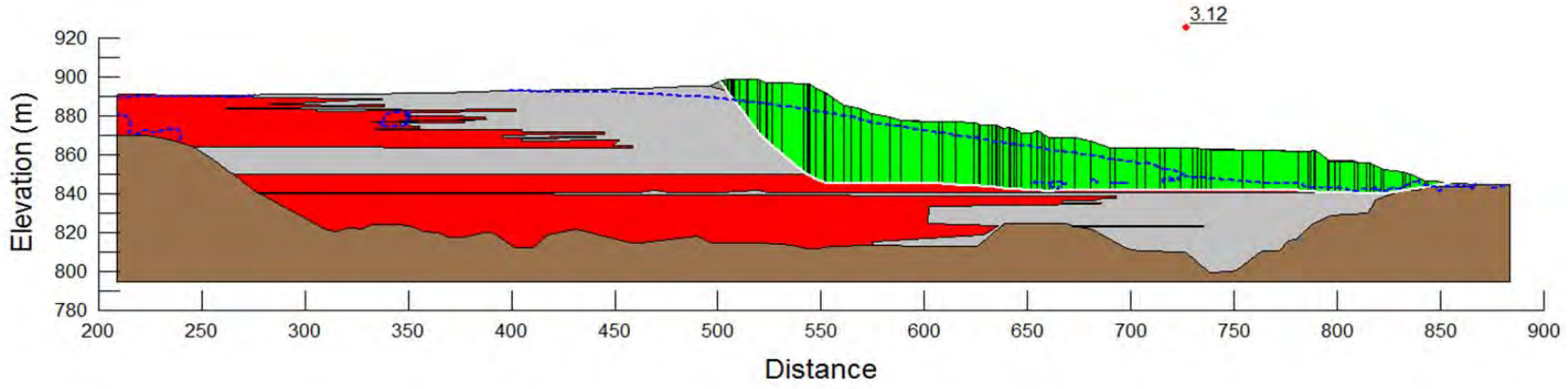

Type	Colour	Material	Unit Weight (kN/m^3)	Effective Friction Angle (degrees)	Effective Cohesion (kPa)
Fill		Compacted Sand Tailings	22	35	5
		Loose Sand Tailings	22	33	-
		Slimes	22	28	-
Foundation		Original Ground	22	32	40

NOTE:

PROJECT

Fundão Tailings Dam Review Panel

TITLE

FOS Tracking
Left Abutment – Section 01
3D FEFLOW
October, 2015

FIGURE NO.

H.H1-21B

APPENDIX H

Limit Equilibrium Analysis of Dike 1 Abutments Prior to Failure

Appendix H
Limit Equilibrium Analysis of Dike 1 Abutments Prior to Failure

TABLE OF CONTENTS

List of Tables

TABLE OF CONTENTS

(continued)

List of Figures

List of Attachments

H1 INTRODUCTION

This appendix summarizes static slope stability analysis undertaken on the right and left abutments of Fundão Dam for conditions prior to failure on November 5, 2015. Analyses were done to compare the drained and undrained static stability of the right and left abutments as one input to understanding why the failure occurred on the left abutment, not on the steeper right abutment.

Section AA, one of the instrumentation sections described in Appendix E, was used for the right abutment, while Section 01, also one of the instrumentation sections, was used for the left abutment. Those sections are shown in plan on Figure H1-1. The geometry of these sections, both the surface of the tailings and the original ground, are taken from the topographic compilation done by the Panel, as described in Appendix B.

Key inputs into the stability analysis included tailings stratigraphy, engineering properties of the tailings and pore pressures. Tailings stratigraphy for both sections was based on the work described in Appendix B. Engineering properties of the tailings are based on the field data described in Appendix C and the laboratory data described in Appendix D. The pore pressures are based on the piezometers at the sections themselves, described in Appendix E, augmented with the 3D seepage analyses described in Appendix G.

Section H4 presents the analysis undertaken on the right abutment of the Fundão Dam and Section H5 presents the analysis undertaken on the left abutment.

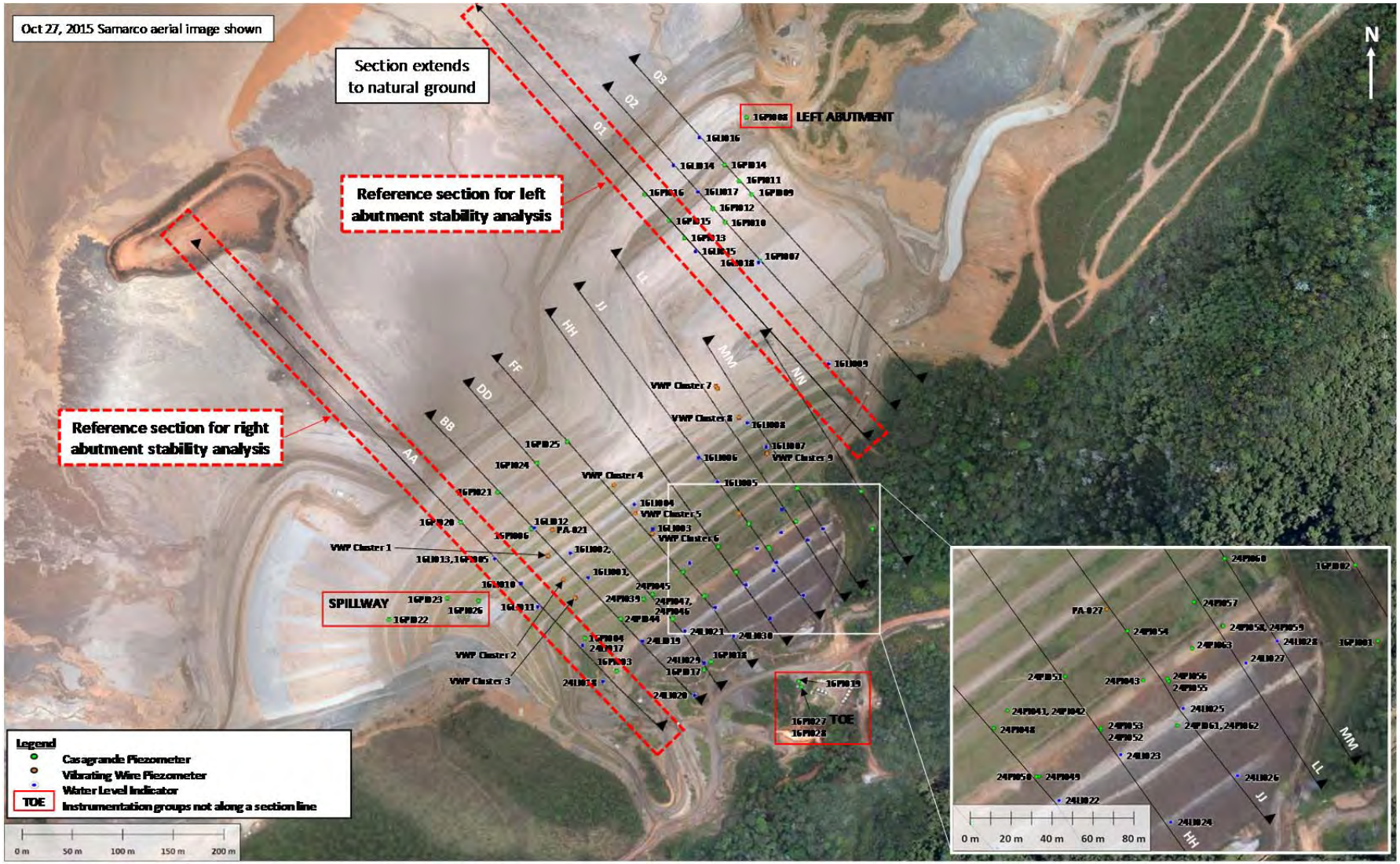

Figure H1-1 Stability sections location plan

H2 ENGINEERING PROPERTIES OF THE TAILINGS

There were a number of stability analyses conducted for the Fundão Dam during the design life of the structure by various parties. Table H2-1 summarizes the material parameters that have been used in previous stability evaluations by others.

Table H2-1 Material parameters adopted in pre-failure stability analyses

Type	Material	Total Unit Weight (kN/m^3)	Effective Friction Angle (degrees)	Effective Cohesion (kPa)	Reference
Tailings	Sand	18	35	5	VOGBR[64]
	Slimes	18	28	-	University of Ouro Preto[38]
Foundation	Weathered Phyllite	18	32	40	DAM[65] and VOGBR[64]

The material parameters assumed in this work are listed in Table H2-2 and Table H2-3. The material parameters differ from previous assumptions as follows:

- A total unit weight of 22 kN/m^3 was adopted for all materials based upon the results of the field and laboratory investigations conducted by the Panel (see Appendix C and D).
- A friction angle of 33° was adopted for the loose sand tailings in the effective stress analyses based upon the results of the direct shear tests (see Appendix D).
- Undrained shear strength ratios were varied for the loose sand tailings and slimes, see Table H2-3 and Section H3.2 below.

Table H2-2 Selected effective stress parameters

Type	Material	Unit Weight (kN/m^3)	Effective Friction Angle (degrees)	Effective Cohesion (kPa)
Tailings	Compacted Sand Tailings	22	35	5
	Loose Sand Tailings	22	33	-
	Slimes	22	28	-
Foundation	Weathered Phyllite	22	32	40

Table H2-3 Selected undrained strength parameters

Material	Unit Weight (kN/m^3)	s_u/σ'_v	Description
Loose Sand Tailings/Slimes	22	Varied	s_u/σ'_v varied to determine the lower-bound of the available undrained yield strength in Section AA (FOS=1.2)
	22	0.30 (Backscarp) 0.22 (Horizontal) 0.14 (Breakout)	Derived from Cone Penetration Tests on blended Sand and Slimes Tailings (Fugro campaign – September, 2014 to March, 2015, CPTu-F01 through CPTu-F05 (Appendix C))
	22	0.25	Derived from Cone Penetration Tests (Fugro campaign – September, 2014 to March, 2015, CPTu-F01 through CPTu-F05 (Appendix C))
	22	0.07	Post-liquefaction strength derived from Cone Penetration Tests (Appendix C)
Material	**Unit Weight (kN/m^3)**	**ϕ (degrees)**	**Description**
Loose Sand Tailings/Slimes	22	16	Peak total stress friction angle (collapse surface) determined from consolidated-undrained triaxial tests on loose sand samples (Appendix D)

1. FOS = Factor of Safety

H3 METHODOLOGY

H3.1 Effective Stress Analyses (ESA)

Effective stress parameters from Table H2-2 were used in the effective stress analyses (ESA) to assess the stability of the dam under static conditions. The analysis scenarios included:

- right abutment for November, 2015;
- left abutment for November, 2015;
- left abutment for August, 2014; and
- left abutment Factor of Safety (FOS) tracking on a monthly basis prior to the failure from February, 2015 to November, 2015.

H3.2 Undrained Strength Analyses (USA)

Undrained strength analyses (USA) were conducted with the dam geometry and pore-water pressure conditions as they existed in August, 2014 and November, 2015. These two times were selected to

help understand the drop in factor of safety from August, 2014 to failure in November, 2015. The analyses were done using parameters in Table H2-3. Loose tailings materials above the piezometric surface were modeled with ESA parameters while loose tailings materials located below the piezometric surface were modeled with USA parameters. The following variants of the USA parameters were analyzed:

- Right abutment – undrained strength ratio was varied to determine the lower-bound of the available undrained yield strength (to obtain a FOS of 1.2). The resultant ratio was applied to analyses on the left abutment.
- Right abutment – from an analysis of CPT data (Appendix C) an undrained strength ratio of 0.25 was adopted.
- Left abutment – anisotropic USA properties based on data from cone penetration testing of the blended loose sand and slimes tailings (Appendix C) were used.
- Left and right abutments – a loose sand collapse surface analysis was undertaken. The analysis utilized a friction angle of 16^{o} based on data determined from consolidated undrained triaxial tests conducted on loose sand samples (Appendix D).
- Left and right abutments – from analysis of CPT data (Appendix C) a post liquefaction undrained strength ratio of 0.07 was adopted.

H4 RIGHT ABUTMENT

H4.1 Model Setup

H4.1.1 Geometry

The stability analyses reported for the right abutment were done along Section AA whose location is shown on Figure H1-1. The idealized stability model from Section AA is shown on Figure H4-1 with a geometric summary in Table H4-1.

Table H4-1 Right abutment model geometry – November, 2015

Right Abutment (Section AA)	
Crest Elevation	900 m
Height[(1)]	71 m
Downstream Slope (overall)	3.2H:1V

1. Height measured from the dam crest to the dam toe.

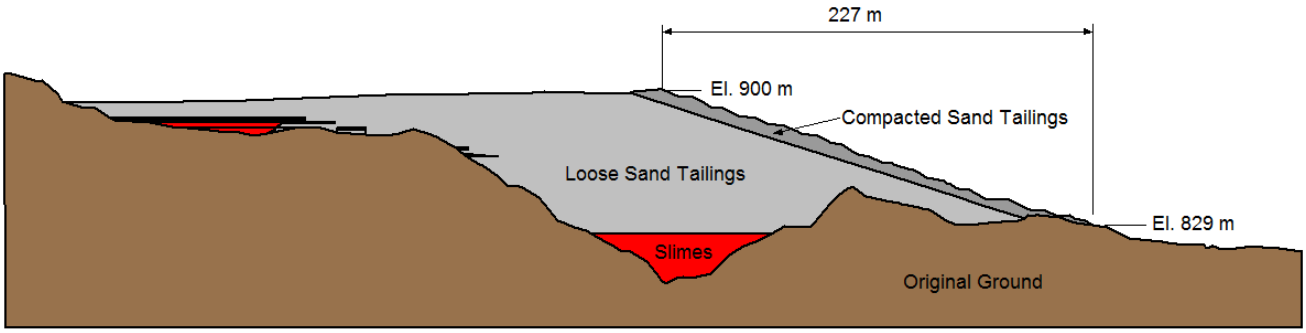

Figure H4-1 Right abutment model geometry

H4.1.2 Tailings Stratigraphy

The tailings stratigraphy at the right abutment of the Fundão Dam comprises sand tailings in most of the section with mixed sands and slimes below El. 830 m. There are no slimes between El. 830 m and El. 850 m as described in Appendix B. This is a key difference between the right and left abutments. The bedrock comprises weathered phyllite. The slimes below El. 830 m did not affect FOS because there was bedrock between the slimes and the toe on Section AA as shown on Figure H4-1. The assumed properties of the sand tailings and the phreatic conditions governed the stability.

As shown on Figure H4-1, there is thin compacted shell of sand tailings on the upstream face. This zone was assumed to be 20 m wide and assigned a higher friction angle, 35° versus 33°, than the looser beach tailings.

H4.1.3 Pore-Water Pressure Conditions

The pore-water pressure conditions within the right abutment of the dam were based on piezometers at Section AA (see Appendix E). Also, piezometric conditions were taken directly from the 3D seepage modeling results described in Appendix G. The 3D seepage model was calibrated against the piezometers.

H4.2 Results

Slope stability analyses were undertaken using SLOPE/W® software. The Morgenstern-Price method was used to calculate the Factor of Safety (FOS) for the critical slip surfaces. The results are summarized in Table H4-2. The stability analysis outputs by “Analysis Number” in the first column of Table H4-2 are given in Attachment H1.

Table H4-2 2D limit equilibrium results (Section AA) – November, 2015

Analysis Number	Description	PWP Conditions	Tailings Strength Assumptions		Factor of Safety	
			Above WT	Below WT	Field Data	3D FEFLOW
H.H1-1A/ H.H1-1B	ESA Base Case	Field Data/ FEFLOW	33°	33°	1.91	1.91
H.H1-2	ESA above WT/ USA below WT	Field Data	33°	$s_u/\sigma'_v = 0.31$	1.21	N/A
H.H1-3	ESA above WT/ USA below WT	FEFLOW	33°	$s_u/\sigma'_v = 0.34$	N/A	1.16
H.H1-4A/ H.H1-4B	ESA above WT/ USA below WT	Field Data/ FEFLOW	33°	$s_u/\sigma'_v = 0.25$	1.00	0.92
H.H1-5A/ H.H1-5B	ESA above WT/ USA below WT with Low Strength Loose Tailings and Slimes below WT	Field Data/ FEFLOW	33°	$\Phi = 16^o$	1.04	1.02
H.H1-6A/ H.H1-6B	ESA above WT/ USA below WT	Field Data/ FEFLOW	33°	$s_u/\sigma'_v = 0.07$	0.40	0.37

1. WT = Water Table

H5 LEFT ABUTMENT

H5.1 Model Setup

H5.1.1 Geometry

The stability analyses reported for the left abutment are located along Section 01 whose location is shown on Figure H1-1. Stability analyses were done for the conditions that existed in August, 2014 and just prior to failure in November, 2015. The stability model for November, 2015 is shown on Figure H5-1 with key dimensions listed in Table H5-1. The stability model for August, 2014 is shown on Figure H5-2 with key dimensions shown in Table H5-2.

Table H5-1 Left abutment model geometry – November, 2015

Left Abutment (Section 01)	
Crest Elevation	901 m
Height[(1)]	56 m
Downstream Slope (Overall)	6.2H:1V
Setback (Elevation)	862 m
Setback (Distance)	160 m
Berm (Distance)	100 m

1. Height was measured from the dam crest to the dam toe.

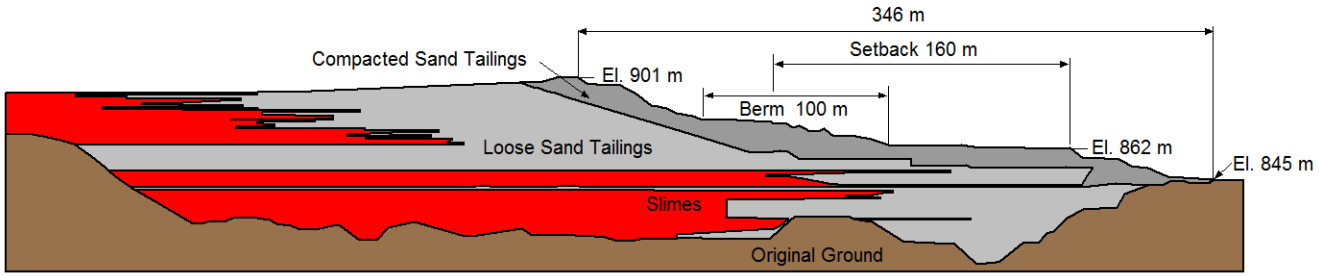

Figure H5-1 Left abutment model geometry – November, 2015

Table H5-2 Left abutment model geometry – August, 2014

Left Abutment (Section 01)	
Crest Elevation	884 m
Height[(1)]	39 m
Downstream Slope (Overall)	7.7H:1V
Setback (Elevation)	862 m
Setback (Distance)	160 m

1. Height was measured from the dam crest to the dam toe.

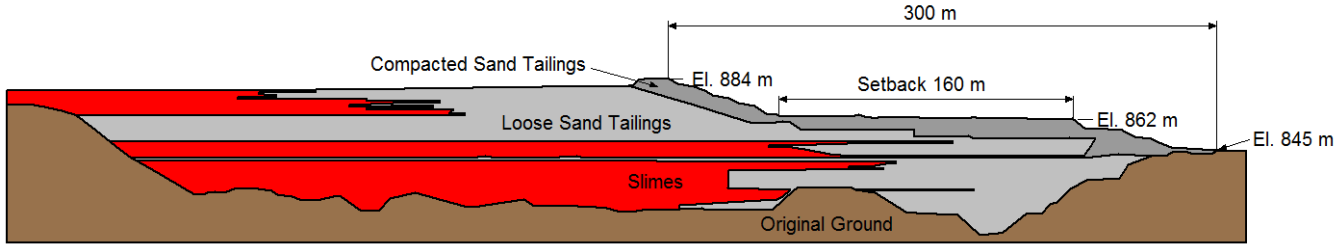

Figure H5-2 Left abutment model geometry – August, 2014

An additional analysis set was undertaken to track the stability of the left abutment as the dike was raised through the months prior to failure in November, 2015. The left abutment was modeled from February through to November, 2015. The assumed dike crest height is summarized in Table H5-3 by month. More details on the construction sequence are given in Appendix B.

Table H5-3 Left abutment dike crest elevation – February through November, 2015

Left Abutment (Section 01)							
February 2015	May 2015	June 2015	July 2015	August 2015	September 2015	October 2015	November 2015
890.0	892.9	894.3	895.5	895.5	896.5	899.0	901.0

H5.1.2 Tailings Stratigraphy

The stratigraphic model of the left abutment is described in Appendix B. Key to this stratigraphy is that slimes were deposited between El. 830 m and El. 850 m. The assumed continuity of the slimes layers as the downstream toe is approached is also described in Appendix B. For the purposes of stability analyses, slimes material properties were used where slimes could have been present. The slimes areas are in red in the model sections shown above.

The sand tailings were divided into two types: loose sand and compacted sand. An approximately 20 m wide compacted sand layer was modeled parallel to the downstream face of the dam.

H5.1.3 Pore-Water Pressure Conditions

The pore-water pressure conditions within the left abutment of the dam were based on piezometers at Section 01 (see Appendix E) and augmented with the output data from the 3D seepage modeling described in Appendix G. Data was extracted from the seepage model at the dates defined for each analysis listed in Section H3.1.

H5.2 Results

Slope stability analysis was undertaken using SLOPE/W software (GEO-SLOPE 2012). The Morgenstern-Price method (Morgenstern and Price 1965) was used to calculate the Factor of Safety (FOS) for the critical slip surfaces. The slope stability analysis results are summarized in Table H5-4 and Table H5-5 and Figure H5-3. The stability analysis outputs by "Analysis Number" in the first column in Table H5-4 and Table H5-5 are given in Attachment H1.

Table H5-4 2D limit equilibrium results (Section 01) – November, 2015

Analysis Number	Description	PWP Conditions	Tailings Strength Assumptions		Factor of Safety	
			Above WT	Below WT	Field Data	3D FEFLOW
H.H1-7A/ H.H1-7B	ESA Base Case	Field Data/ FEFLOW	33°	33°	2.50	3.01
H.H1-8	ESA above WT/ USA below WT	FEFLOW	33°	s_u/σ'_v = 0.34	N/A	1.87
H.H1-9	ESA above WT/ USA below WT	Field Data	33°	s_u/σ'_v = 0.31	1.48	N/A
H.H1-10A/ H.H1-10B	ESA above WT/ USA Heterogeneous below WT	Field Data/ FEFLOW	33°	Backscarp: s_u/σ'_v = 0.30 Horiz. Zone: s_u/σ'_v = 0.22 Breakout Zone: s_u/σ'_v = 0.14	1.14	1.33
H.H1-11A/ H.H1-11B	ESA above WT/ ESA with Low Strength Variant for Loose Tailings and Slimes below WT	Field Data/ FEFLOW	33°	$\Phi = 16^o$	1.28	1.56
H.H1-12A/ H.H1-12B	ESA above WT / USA below WT	Field Data/ FEFLOW	33°	s_u/σ'_v = 0.07	0.36	0.44

1. WT = Water Table

Table H5-5 2D limit equilibrium results (Section 01) – August, 2014

Analysis Number	Description	PWP Conditions	Tailings Strength Assumptions		Factor of Safety	
			Above WT	Below WT	Field Data	3D FEFLOW
H.H1-13A/ H.H1-13B	ESA Base Case	Field Data/ FEFLOW	33°	33°	3.01	3.39
H.H1-14A/ H.H1-14B	ESA above WT/ USA Heterogeneous below WT	Field Data/ FEFLOW	33°	Backscarp: s_u/σ'_v = 0.30 Horiz. Zone: s_u/σ'_v = 0.22 Breakout Zone: s_u/σ'_v = 0.14	1.35	1.36

1. WT = Water Table

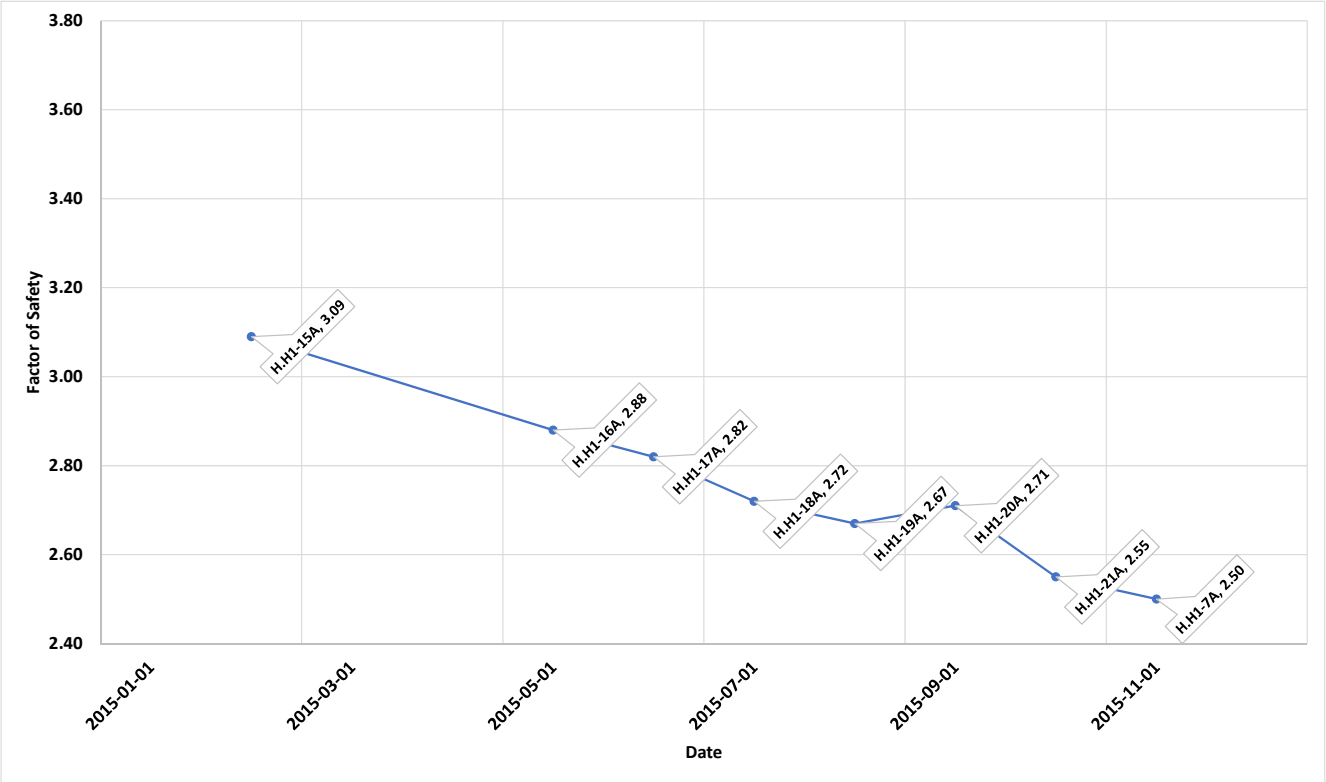

Figure H5-3 2D limit equilibrium results (Section 01) – field data ESA FOS tracking (February, 2015 to November, 2015)

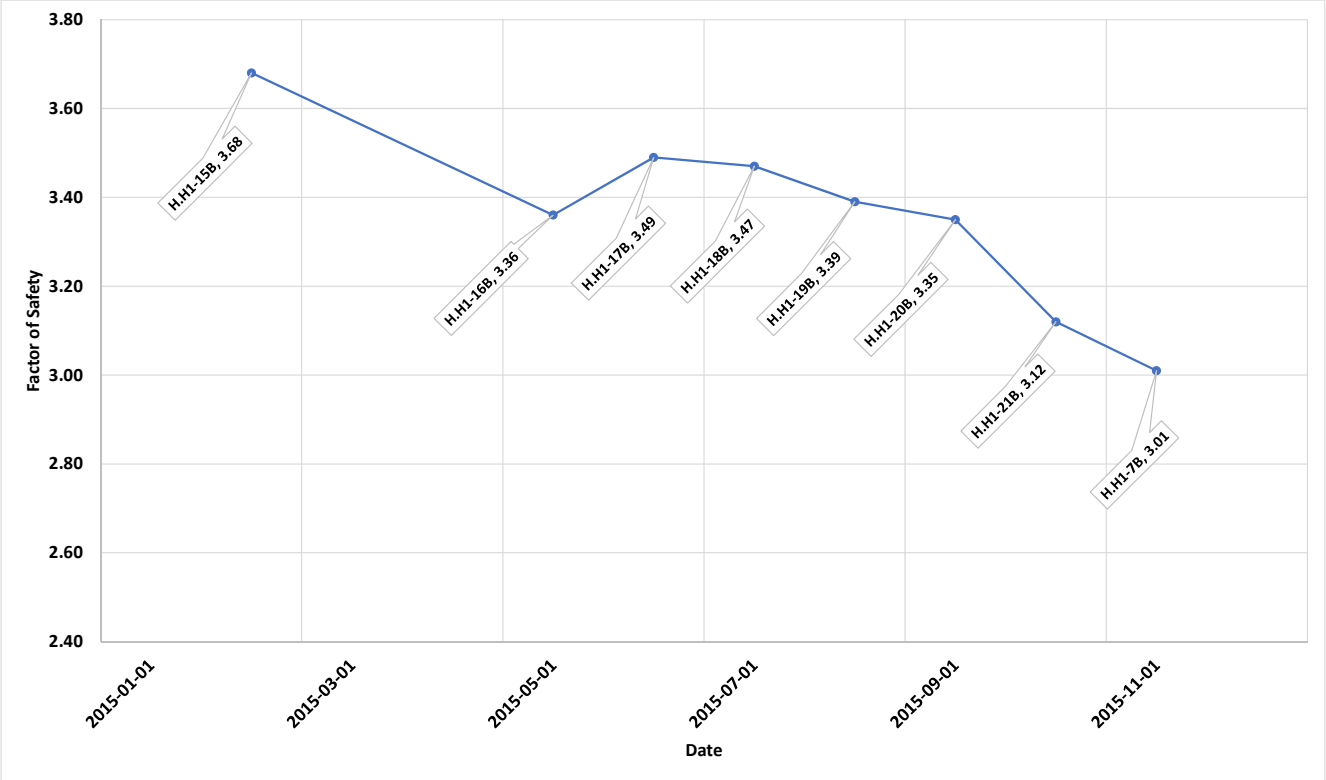

Figure H5-4 2D limit equilibrium results (Section 01) – FEFLOW data ESA FOS tracking (February, 2015 to November, 2015)

APPENDIX I

Deformation Analysis of the Left Abutment

Appendix I
Deformation Analysis of the Left Abutment

TABLE OF CONTENTS

List of Tables

List of Figures

TABLE OF CONTENTS

(continued)

TABLE OF CONTENTS

(continued)

I1 INTRODUCTION

The purpose of this appendix is to assess the potential influence of slope deformations on liquefaction triggering at the Fundão Dam. Specific emphasis was placed on assessing the influence of deformations within the slimes layers on the stress state of the overlying tailings sand to enable comparisons with laboratory test results. The primary intent was to identify whether slope deformations on the left abutment setback could have led to a liquefaction triggering mechanism that is consistent with the observed failure on November 5, 2015.

This work has included deformation analyses on a cross section through the region in which the failure initiated (Section 01 on the left abutment; see Figure I1-1). These analyses are described throughout the remainder of this appendix.

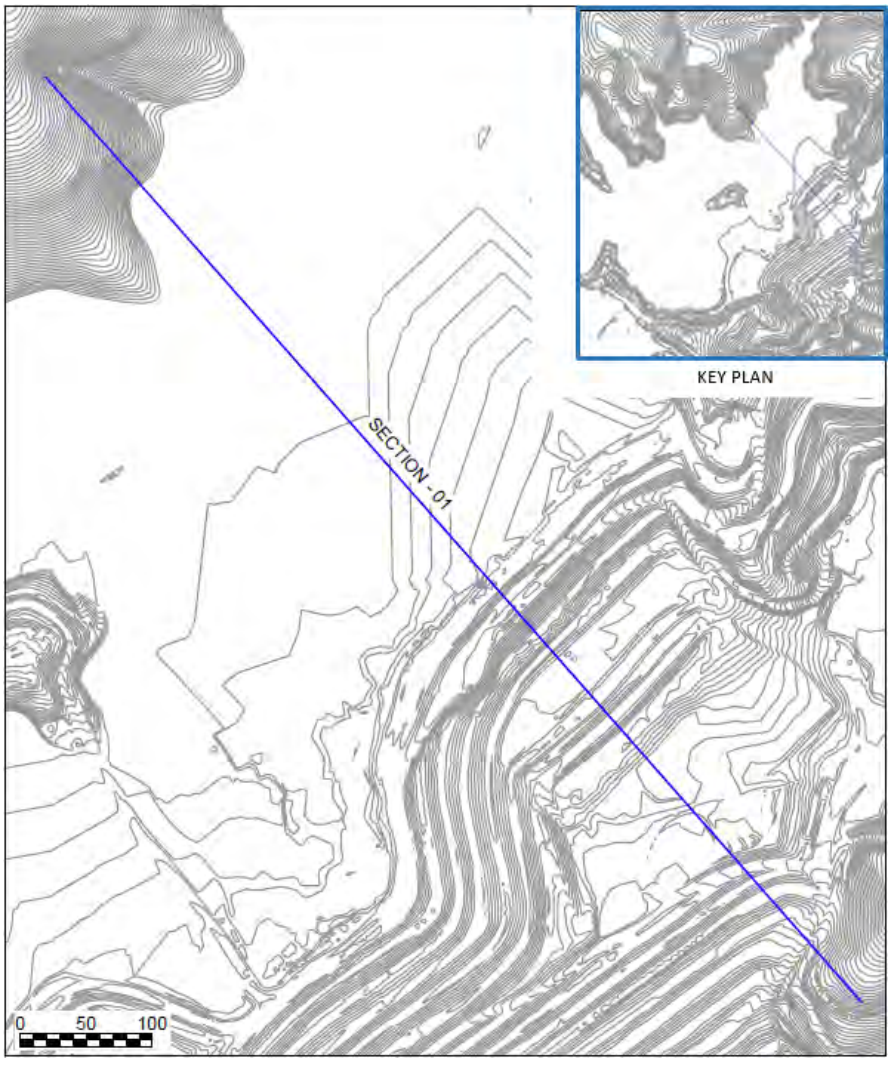

Figure I1-1 Deformation model cross section location

I2 MODEL DEVELOPMENT

I2.1 General

The process followed during this assessment was to complete a series of progressive analyses for Section 01, with each model iteration including either increased complexity of material behavior or a parametric difference to enable evaluation of the influence of different factors. The models were initially constructed using a relatively simple elastic parameter set for all materials to identify the elastic distribution of deformations within the dam. In the next iteration, the models were developed further to include non-associated Mohr-Coulomb properties for all materials, including a strain-weakening response for the slimes layers, to demonstrate the effect of yielding within the model. The next iteration built on the Mohr-Coulomb version and included a critical state constitutive model called NorSand (after Jefferies and Been 2016) for the beached tailings sand. The purpose of the critical state analysis was to identify the influence of aspects such as density-dependent strength variation and yield in unloading. Finally, parametric sensitivity analyses were completed for the critical state model to assess the influence of the strength and continuity of the slimes layers. The sensitivity analyses concentrated on the slimes-rich layers because they represent the greatest source of uncertainty in the analysis.

The deformation models were developed to simulate the staged-construction of the dam. This involved sequential activation of layers of tailings within the models in accordance with the construction history known from survey data, and the internal dike stratigraphy described in Appendix B. These layers of tailings were set to represent roughly four-month time intervals throughout the majority of the dam's operational history, starting at the end of 2011. For the final six months (June to November, 2015), this time interval was reduced to monthly to gain additional resolution on the model response close to the time of the dam failure.

The models were built using version 8 of the Fast Lagrangian Analysis of Continua (FLAC) finite difference software, which was also used for running the elastic and Mohr-Coulomb versions of the models. Version 6 of this software was used for the critical state analyses, with the NorSand constitutive model implemented as a user-defined model (UDM) dll file developed for this version of FLAC.

I2.2 Model Geometry and Stratigraphy

The model geometry and stratigraphy was generated in accordance with the GIS compilation of survey data and interpretation of aerial photographs documented in Appendices A and B. For the purpose of these models, the soils were grouped into one of the following material types:

- Bedrock – All materials below the "stripped ground" survey were assigned to this material type.
- Sand – Tailings sand considered unlikely to be mixed or interbedded with slimes.
- Slimes/sand deposits of varying proportions, designated as one of:

- predominantly slimes;
- mixed sand and slimes;
- interbedded slimes, or
- isolated slimes.

- Compacted sand.

The material boundaries used within the models are shown on Figure I2-1.

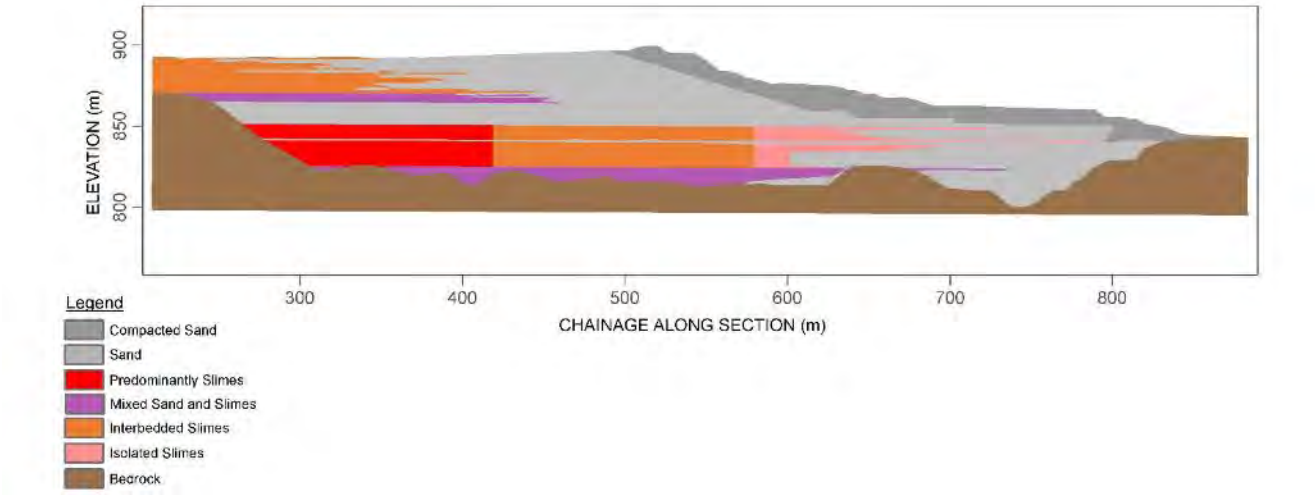

Figure I2-1 Material type boundaries

I2.3 Material Properties

I2.3.1 Elastic

I2.3.1.1 Sand

The elastic properties for the sand were defined using data from the seismic cone penetration tests (SCPTs) completed by Fugro through the beach of the Fundão Dam in January to March, 2015, supplemented with the SCPT data collected at greater depth from the Germano Pit Dam as part of this Investigation (see Appendix C). The small-strain shear modulus (G_{max}) was calculated from the shear wave velocity (v_s) and density (ρ) of the tailings, which was then converted to an approximate large strain shear modulus (G) by dividing G_{max} by a factor of three. A trend of G versus effective vertical stress (σ'_v) was then defined from these data, which was implemented in the models. The bulk modulus (K) of the tailings was defined in the models by assuming a Poisson's ratio (ν) of 0.3 and calculating K from G and ν. The relationship of G versus σ'_v is shown on Figure I2-2.

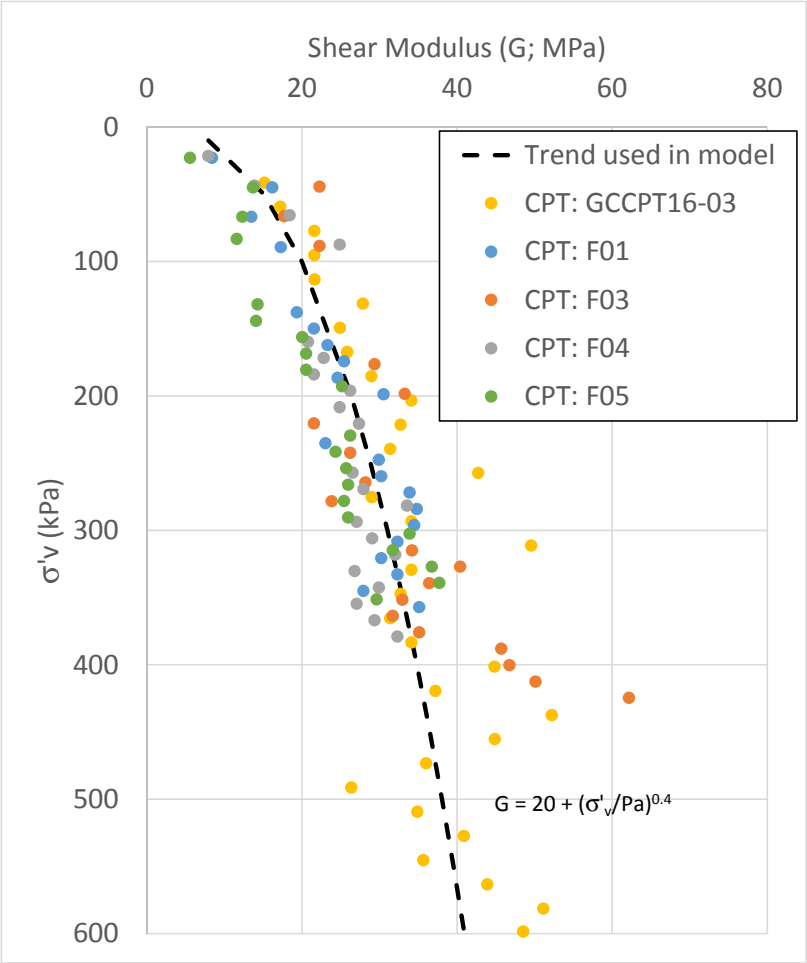

Figure I2-2 Sand shear modulus relationship

I2.3.1.2 Slimes

The elastic properties for the slimes were based on the consolidation properties derived from the one-dimensional compression testing completed as part of this Investigation supplemented with data derived from index testing completed before and after the Baia 2 loading trial completed in 2008[4] at Germano Dam. As discussed in Appendix F, these properties were then verified against settlements observed during the Baia 2 loading trial before being used in both the consolidation modeling and the analyses outlined in this appendix. The resulting trend of G versus σ'_v is shown on Figure I2-3.

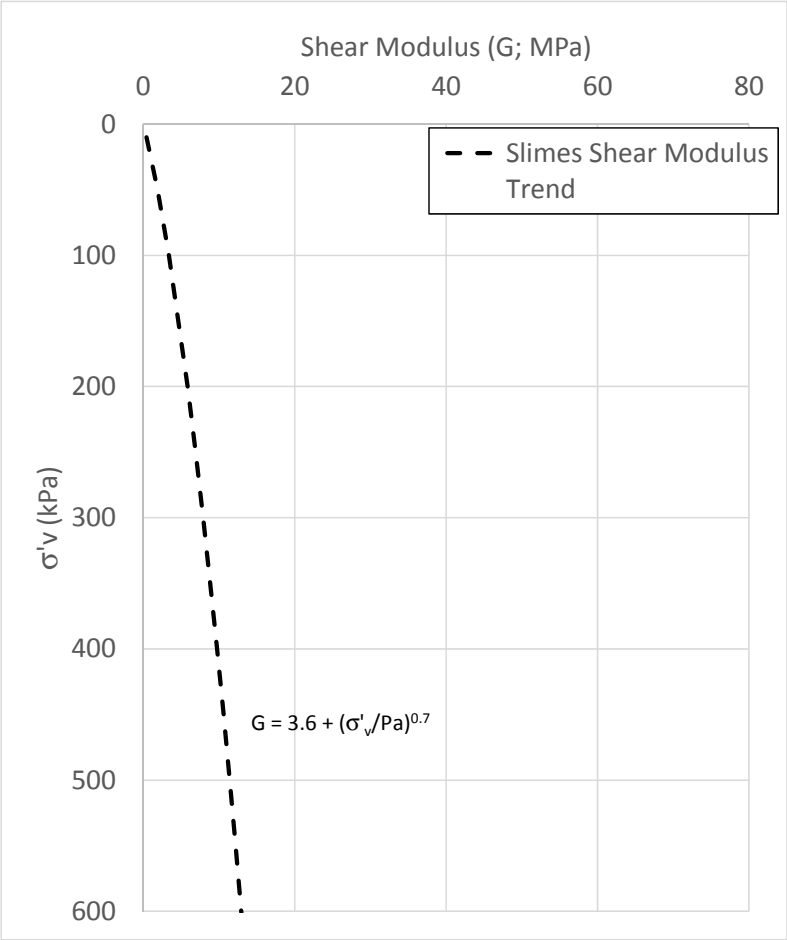

Figure I2-3 Slimes shear modulus relationship

Having derived elastic parameters for both the slimes and sand deposits, these properties were then blended together to create parameter sets that represented the relative proportions of these materials that we considered credible throughout the cross sections. The relative proportions of the sand and slimes properties assigned to these blended parameter sets were:

- predominantly slimes – 100% slimes properties;
- mixed sand and slimes – 50:50 sand and slimes properties;
- interbedded slimes – 20% slimes properties and 80% sand properties; and
- isolated slimes – 100% sand properties

These proportions were also used for blending strength properties. The modulus relationships applied to the various regions of mixed/interbedded slimes and sand in the models are shown on Figure I2-4.

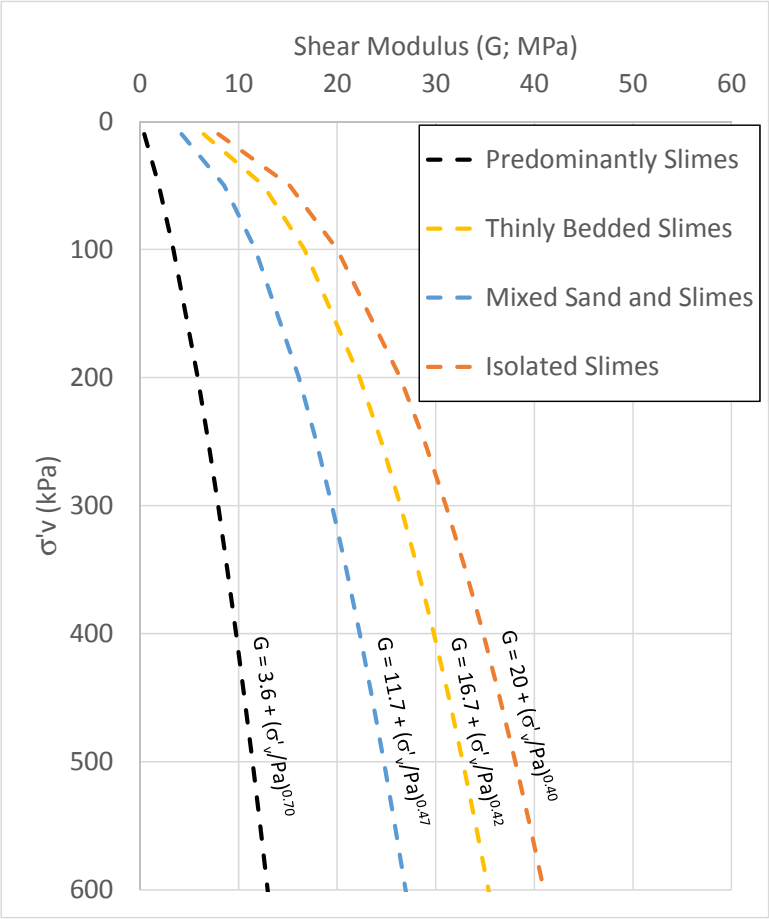

Figure I2-4 Sand-slimes mixtures shear modulus relationship

I2.3.1.3 Bedrock

The bedrock was modeled as a linear elastic material within all of the analyses. This unit was modeled with a G of 170 MPa and a K of 440 MPa in order to represent a very stiff material and impose a clear stiffness contrast between the bedrock and overlying tailings.

I2.3.2 Mohr-Coulomb

I2.3.2.1 Sand

The beached tailings sand was modeled with a friction angle of $\phi' = 33°$ and zero cohesion, which represents the critical state friction angle calculated from the triaxial compression tests completed as part of this Investigation. Mohr-Coulomb plots are shown in Appendix D on Figures D5-9 and D5-10.

The compacted tailings sand was modeled with a friction angle of $\phi' = 35°$ and 5 kPa cohesion, in accordance with the values used by others during designs.

I2.3.2.2 Slimes

The conceptual basis for the properties assigned to slimes-rich layers was that they are expected to generate an immediate undrained response following each loading increment, but that any loading-induced excess pore pressure will dissipate between loading increments. The assumption of dissipation between loading increments is based on the results of the consolidation modeling presented in Appendix F and observations from embankment test fills at Germano Dam in 2008 and 2013 (see Appendices C and F). This process could have been included directly within the deformation model by either alternating drained and undrained properties throughout a loading increment, or by using a coupled mechanical deformation/fluid flow approach; however, given the uncertainty in the true extent and proportions of sand and slimes within the slimes-rich layers, this added complexity was not considered appropriate. Instead, the slimes were modeled in a simplified manner with moduli representative of the drained response (see Section I2.3.1), combined with undrained strength properties. By using this approach, we are assuming that the volumetric response will be dictated by consolidation that is occurring rapidly throughout the majority of the unit, but that the strength of these regions will be dominated by the undrained response along horizons of higher slimes content. The slimes-rich regions were modeled with a strain-weakening Mohr-Coulomb relationship that included a peak friction angle of $\phi_p = 12.4°$ based on field testing and the Baia 4 failure at Germano Dam on September 21, 2005. This friction angle was intended to represent an approximate undrained strength ratio, and was calculated as the arctangent of $s_u/\sigma'_v = 0.22$. This friction angle was then assigned a linear reduction to $\phi_r = \phi_p/3$ at a plastic strain (ε_p) of 20% (i.e., 20% strain beyond the peak strength). This reflects an upper-bound to the sensitivity of approximately 3 that was deduced from the runout of the Baia 4 failure (see Appendix C).

As for the elastic properties, the Mohr-Coulomb strength properties of the slimes were blended with those of the sand, as listed in Section I2.3.1. The properties assigned to the various sand/slimes mixtures are listed in Table I2-1.

Table I2-1 Sand-slimes mixtures strength properties

Material	Undrained Strength Ratio	Equivalent Friction Angle ϕ_p (°) at ε_p = 0%	Undrained Strength Ratio	Equivalent Friction Angle ϕ_r (°) at ε_p = 20%
Predominantly Slimes	0.22	12.4	0.07	4.1
Mixed Sand and Slimes	0.39	23.5	0.33	19.9
Interbedded Slimes	0.47	29.4	0.46	28.1
Isolated Slimes	0.52	33	0.52	33

Parametric sensitivity analyses were run to assess the impact of the strength and continuity of the slimes.

I2.3.3 Critical State

The parameters assigned to the beached tailings sand during the critical state analyses were derived from the triaxial compression laboratory tests completed throughout this Investigation (see Appendix D). These parameters are summarized in Table I2-2.

Table I2-2 Critical state parameters assigned to the beached tailings sand

Parameter	Value
M_{tc}	1.33
Γ	0.865
λ_e	0.024
N	0.38
H	156-(756 x ψ)
χ_{tc}	7.3

All parameters other than H were obtained directly from the laboratory tests. H was calculated by completing numerical models of single elements (element tests) that represented the drained and undrained triaxial tests, and varying H within a range to obtain a trend that gave the best fit to all tests (see Section I3.1).

Behavior in unloading is not specified in the NorSand model, but is calculated based on the parameters listed in Table I2-2 and the stress history of the soil element. As part of this work, we verified that the response to unloading was significantly stiffer than the response to loading during virgin compression, consistent with the findings from 1D consolidation tests on undisturbed samples of tailings sand from Fundão Dam completed by Rezende[40], and reconstituted samples completed as part of this Investigation.

It was also necessary to specify the state parameter (ψ) for the critical state analyses. Our intent was to match the 80th percentile state parameter within the model (defined by Jefferies and Been 2016, as the characteristic state) to the combined value from the CPTs completed at the Fundão Dam in January to March, 2015. This 80th percentile value of the field data was ψ = +0.012. It should be understood that the state parameter changes in response to volumetric strain and stress changes as the model progresses; therefore, multiple trial model runs were completed with different state parameter values assigned at the time of deposition, which we have termed “seed” state parameters in this analysis. The seed state parameter that was required to generate an 80th percentile in the model that was approximately equal to the characteristic state in the field in January, 2015 was ψ = -0.02. The changes in state parameter within the models are discussed and illustrated in Section I3.2.

I2.3.4 Comparison of Stress-Strain Curves

A comparison of the stress-strain behavior assigned to the various soil units is illustrated on Figure I2-5. It can be seen from this figure that the elastic moduli assigned to the sand in the linear elastic and Mohr-Coulomb analyses lead to a similar stress-strain response to that of the NorSand model at low strain (<~0.5%) for loose sand with a state parameter of zero. At larger strains, the NorSand model imposes a more ductile response than the linear elastic relationship.

Figure I2-5 also illustrates the greater stiffness of the sand in comparison with the slimes.

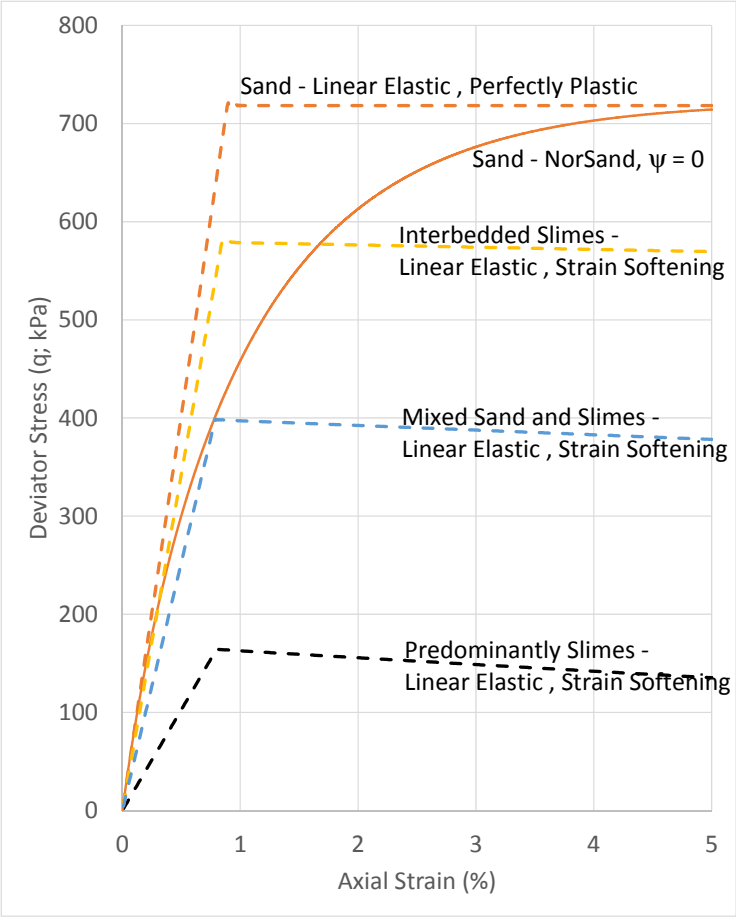

Figure I2-5 Comparison of stress-strain curves assigned to sand and slimes units

It can be seen from Figure I2-6 that the response of the sand changes significantly with variations in state parameter, with the drained response becoming increasingly ductile as the state parameter increases; therefore, the linear elastic and NorSand models will differ in line with variations in state parameter.

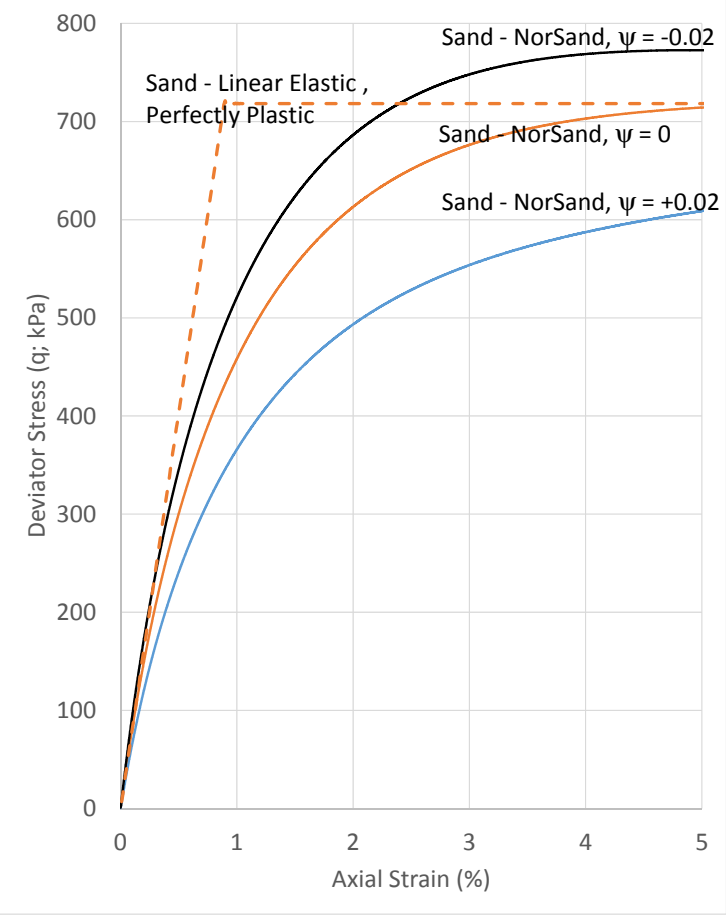

Figure I2-6 Comparison of stress-strain curves for sand at different state parameters

I2.4 Pore-water Pressures

The pore-water pressures within the models were assigned by setting phreatic surfaces for each model state based on the piezometer monitoring data, and extrapolating the data into regions and time periods without data. A hydrostatic pore pressure distribution was assigned below the phreatic surfaces. The pore pressure assumptions for these models were checked against the results of the groundwater monitoring.

Full saturation was assumed below the phreatic surface, and zero saturation was assumed above it.

I3 RESULTS

I3.1 Element Tests

I3.1.1 Drained Triaxial Compression – Sand

Modeling of drained triaxial compression tests was completed to verify that the NorSand constitutive model was capable of capturing the stress-strain relationship and volumetric response of the sand appropriately. These analyses were completed using a Visual Basic for Applications (VBA) program from Jefferies and Been (2016). Example analyses of the triaxial tests completed as part of this Investigation are shown on Figure I3-1 to Figure I3-3. These analyses show that the NorSand model is capable of closely matching the response of the tailings to shear strain at a range of confining stresses and density states.

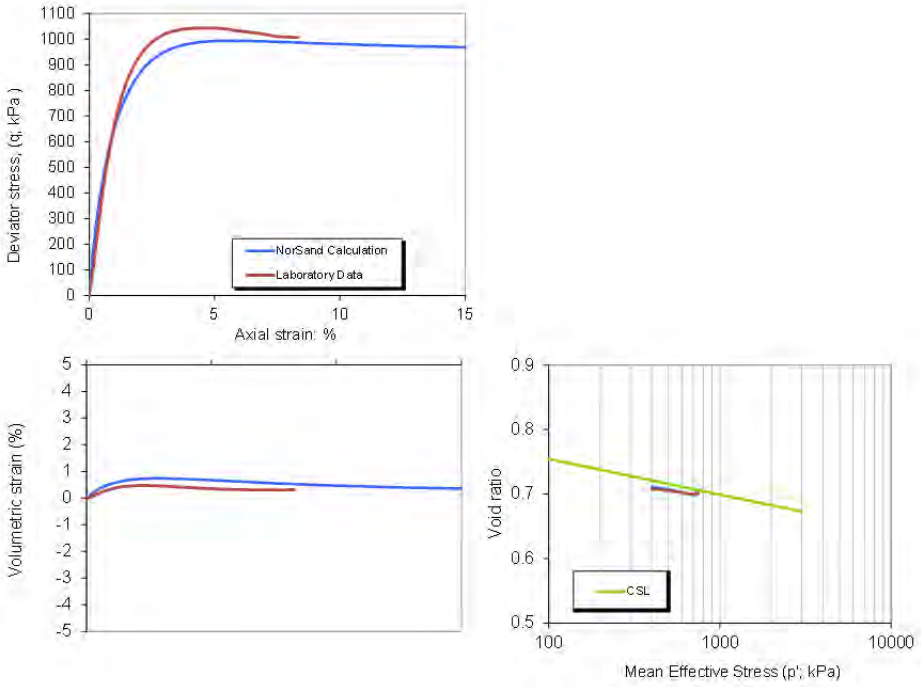

Figure I3-1 Example element test at p' = 400 kPa and ψ = -0.01 – void ratio close to critical state (Test ID TX-12)

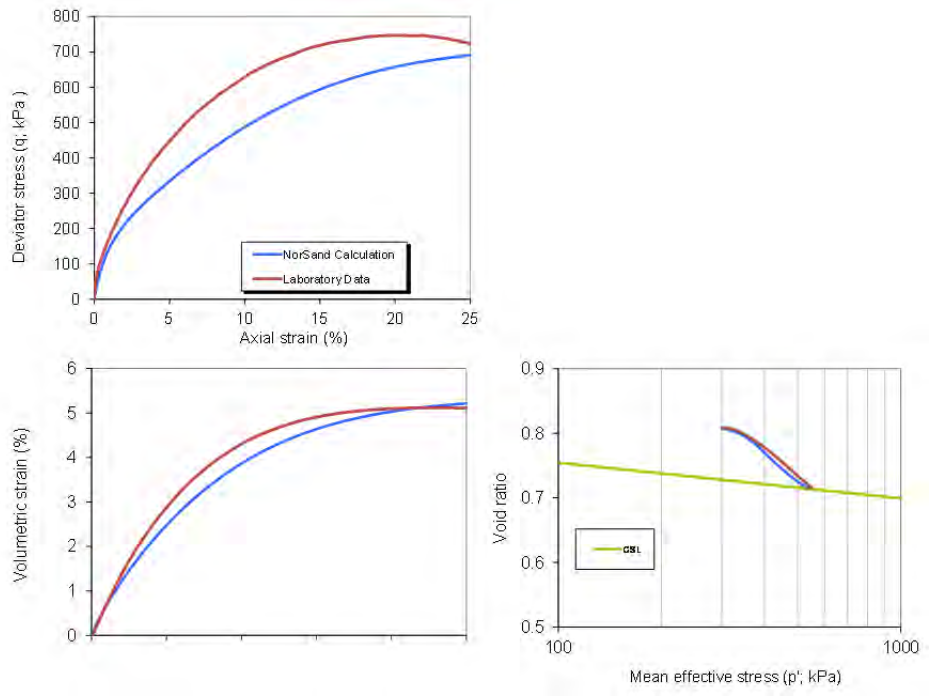

Figure I3-2 Example element test at p' = 300 kPa and ψ = +0.08 – very loose sample (Test ID TX-1)

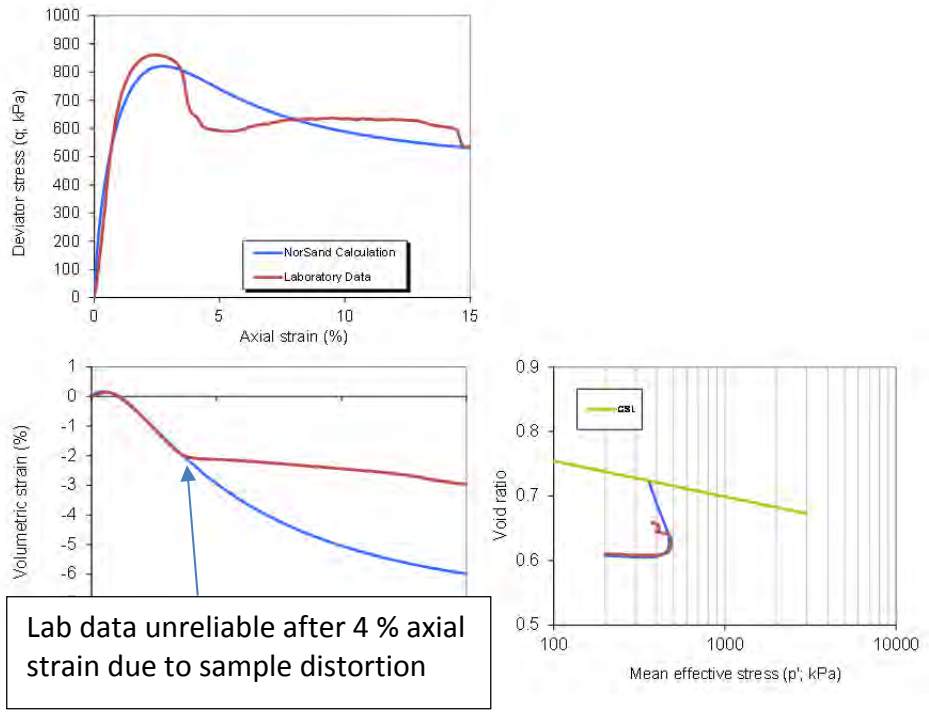

Figure I3-3 Example element test at p' = 200 kPa and ψ = -0.13 – very dense sample (Test ID TX-11)

I3.1.2 Undrained Triaxial Compression

Element tests of undrained triaxial laboratory tests completed as part of this Investigation were also undertaken using the VBA software to verify that the NorSand constitutive model can capture the undrained response of the sand tailings appropriately. An example set of results is shown on Figure I3-4, which shows that the NorSand model is capable of capturing the undrained response of the sand.

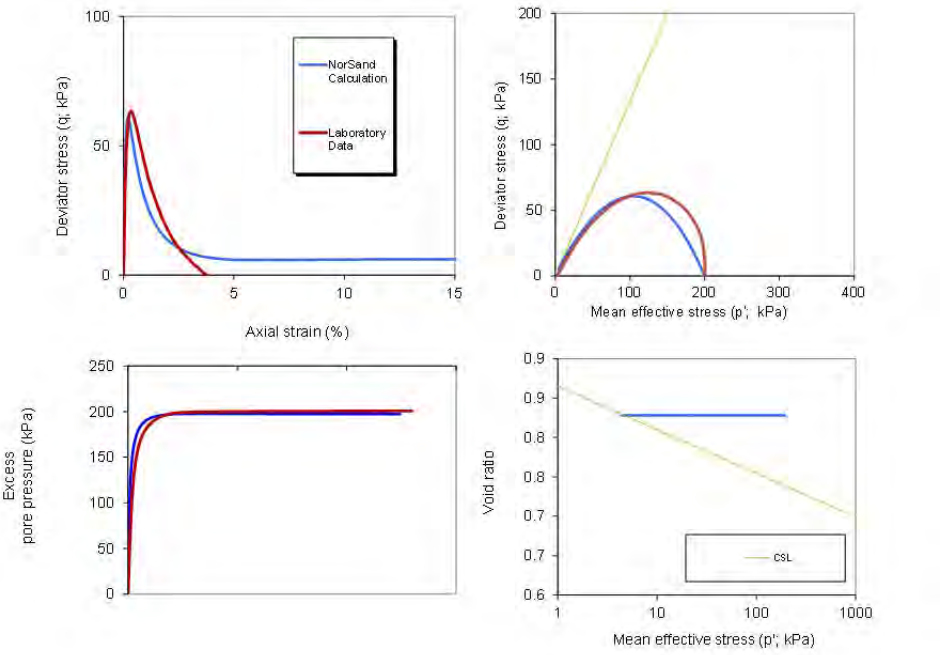

Figure I3-4 Example element test at p' = 200 kPa and ψ = +0.9 – very loose sample (Test ID TX-2)

I3.1.3 Collapse State Tests

A final element test was completed using the NorSand constitutive model within FLAC to verify that the NorSand model is capable of identifying the "collapse state" identified in the stress controlled extrusion-collapse triaxial tests. This model was set up as an axisymmetric analysis with load controlled boundary conditions to mimic the conditions applied in the laboratory tests. The radial stress in the model was then reduced incrementally in 0.5 kPa load increments, following the same stress path as the laboratory test. Each unloading increment was initially modeled with a fluid bulk modulus of 2000 MPa to allow potential shear-induced pore pressure generation and emulate undrained conditions. The undrained increment was then followed by dissipation of any induced pore pressures to ensure that no pore pressures were being carried over between unloading increments. The model response compared with the laboratory test is shown on Figure I3-5. These results show that the NorSand model is capable of replicating the response seen in the load controlled triaxial tests, with the failure stress being identified within 3% of the laboratory data.

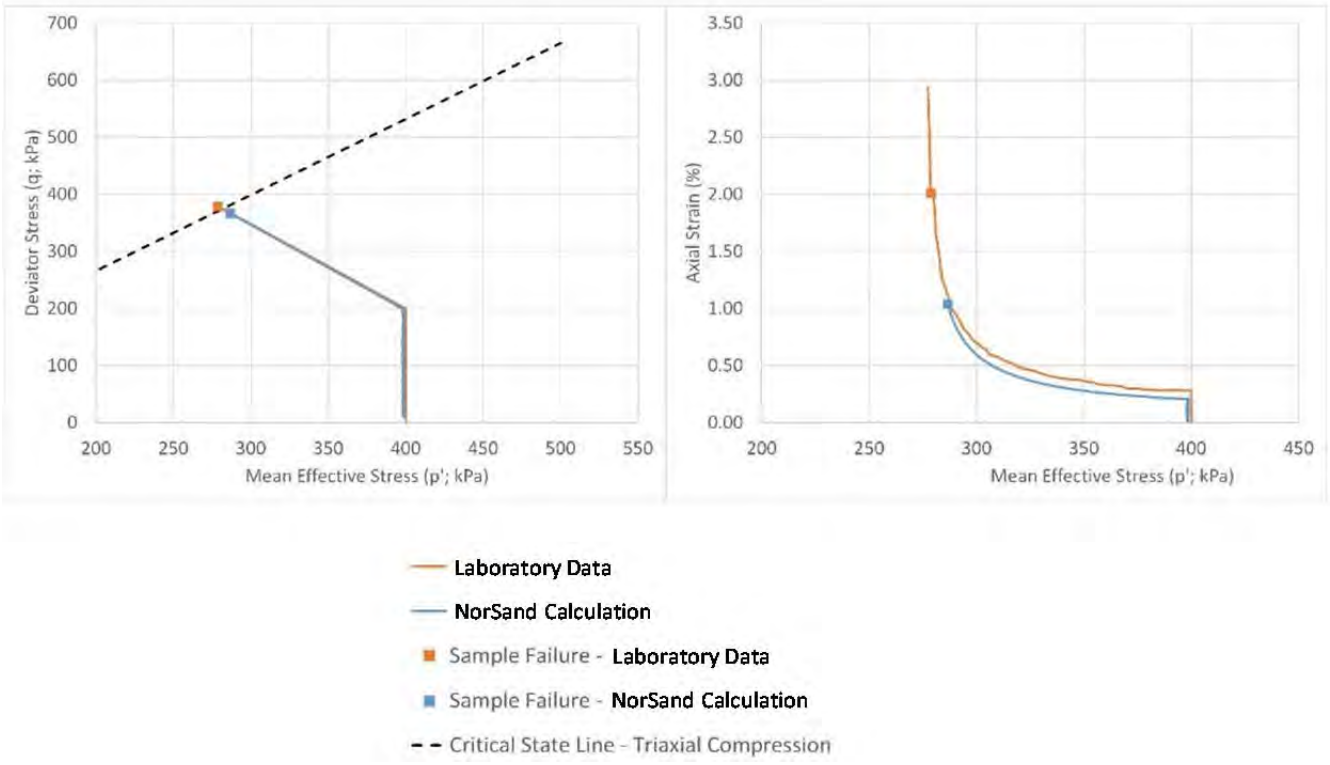

Figure I3-5 Collapse state element test at p' = 400 kPa and ψ = +0.01 (Test ID TX-28)

I3.2 2D Model of Left Abutment – Section 01

I3.2.1 Elastic Analysis

The purpose of the elastic 2D analysis of Section 01 was to identify the pattern of displacements produced by the model without the complexity of material behavior included within the Mohr-Coulomb and critical state analyses. These results serve as a reference base against which the response of the subsequent models can be reviewed.

Contours of horizontal displacement are shown on Figure I3-6, together with graphs showing the distribution and magnitude of displacements at stages throughout the model construction. These results show two main regions of horizontal displacement. One zone is located towards the upstream end of the model and the second is located beneath the slope. The upstream zone is a result of material settling above the highly compressible zone of predominantly slimes shown on Figure I3-7, and sliding along the interface with the bedrock. The downstream zone is a result of the dam's geometry. The abrupt break between these zones is a result of material immediately downstream of the predominantly slimes region being affected by displacement upstream due to the settlement of this layer. This is serving to offset the displacements in the downstream direction and leads to a zone of roughly zero horizontal displacement immediately downstream of the predominantly slimes region.

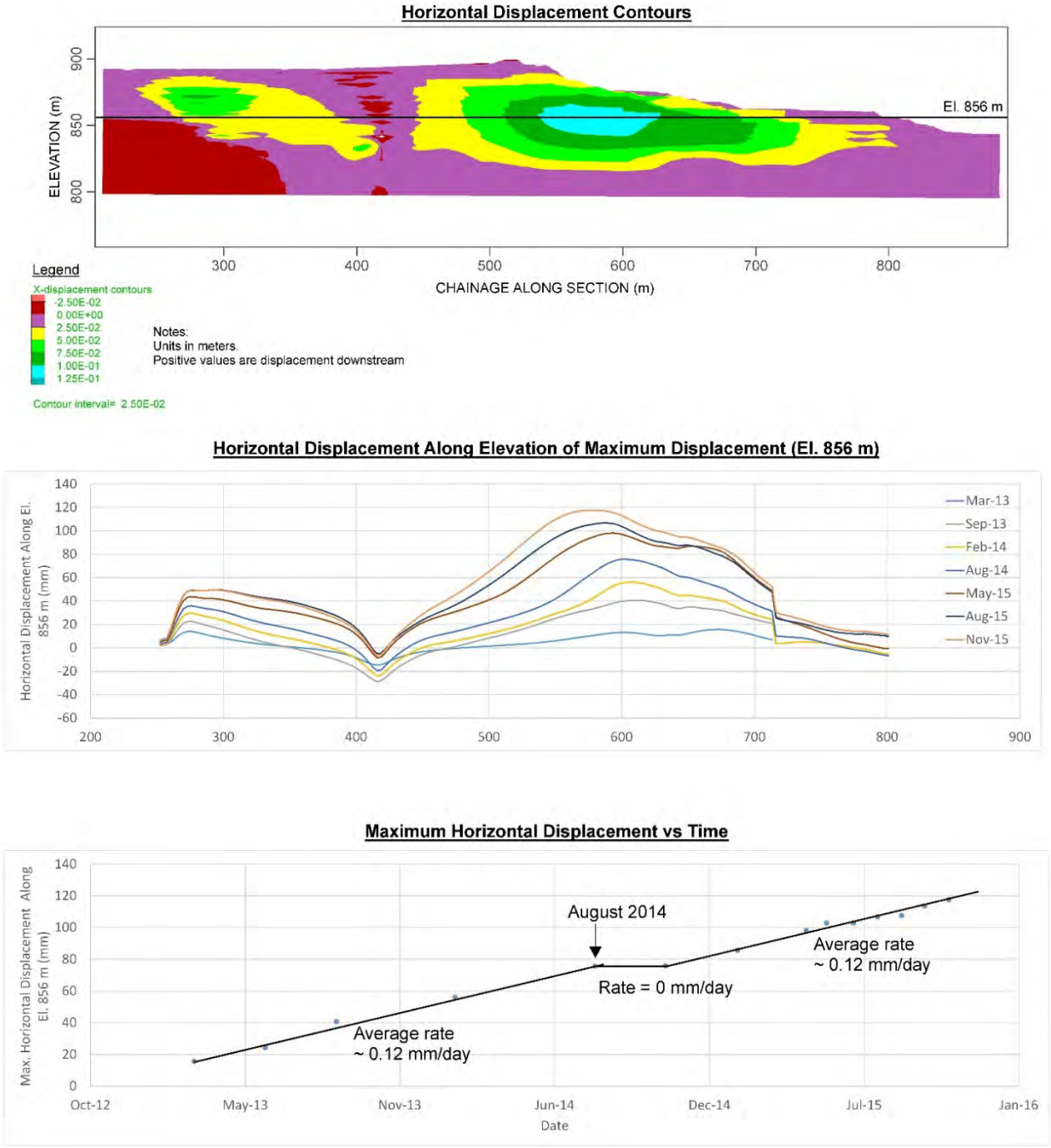

Figure I3-6 Horizontal displacement results – elastic analysis

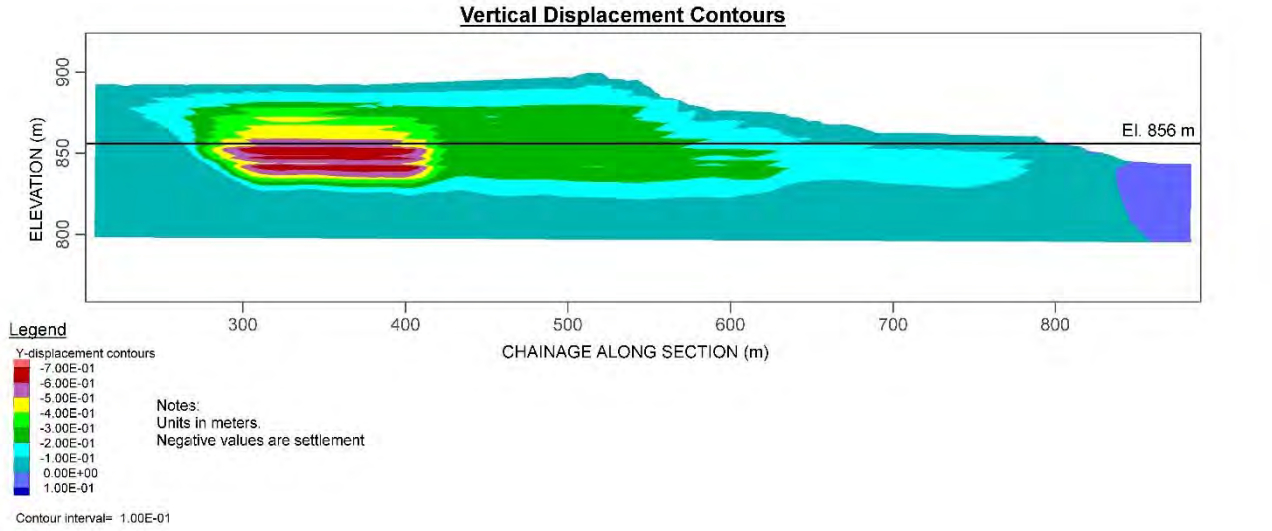

Figure I3-7 Vertical displacement results – elastic analysis

The largest horizontal displacements occur in the downstream region and concentrate in a zone that is downstream of the dike crest and centered along roughly El. 856 m. This implies compressive straining in the downstream direction and extension straining in the upstream direction. Extension strains result in a reduction of horizontal confinement consistent with a potential for liquefaction triggering from a lateral extrusion process.

The maximum horizontal displacement at the end of the model construction (November, 2015) was 118 mm. Tongues of slightly increased displacement are also visible around the regions of slimes in the downstream portion of the model.

The maximum horizontal displacement is shown throughout the dam construction on Figure I3-6. This shows a consistent response to loading throughout the majority of construction. An exception to this is between August and October, 2014 when zero displacement is shown in the model. This corresponds to a time period when a berm was built on the slope and the crest was raised by only 1 m following the cracking incident in August, 2014.

Figure I3-8 compares the maximum calculated displacements with the surveyed crest of the left abutment setback. As expected, the elastic displacements correspond very closely with the rate of dike construction.

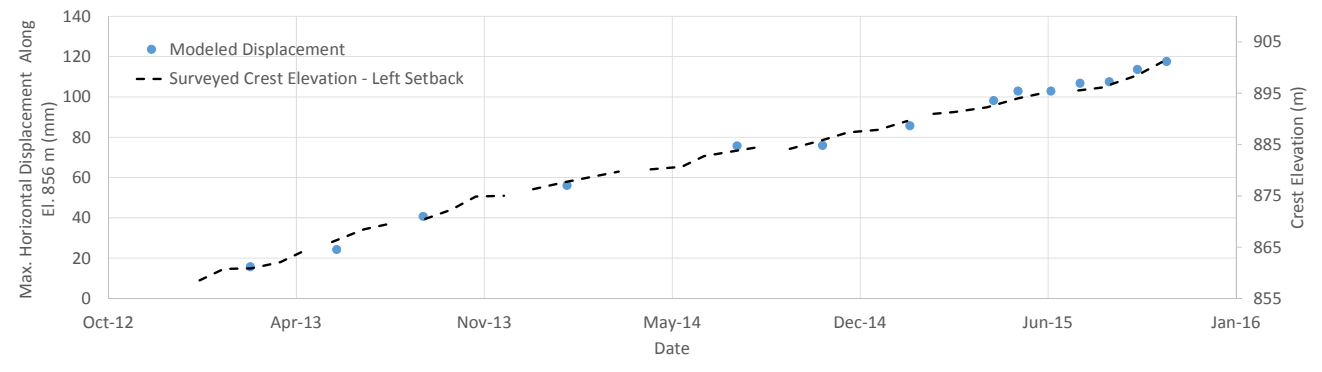

Figure I3-8 Comparison of horizontal displacements and crest elevation of left setback – elastic analysis

I3.2.2 Mohr-Coulomb Analysis

The main purpose of the Mohr-Coulomb analysis was to identify the effect of shear-induced yielding for comparison with the subsequent critical state analyses, to enable responses specific to the critical state analysis to be separated from those associated with shear-induced yielding of the tailings.

Zones of yielding are shown as yellow shading on Figure I3-9. Pink shading indicates regions that have not reached the yield surface at any stage in the analysis. This figure shows that the areas experiencing the most significant yielding are those adjacent to the region of predominantly slimes material, and material at the toes of the left abutment setback and plateau.

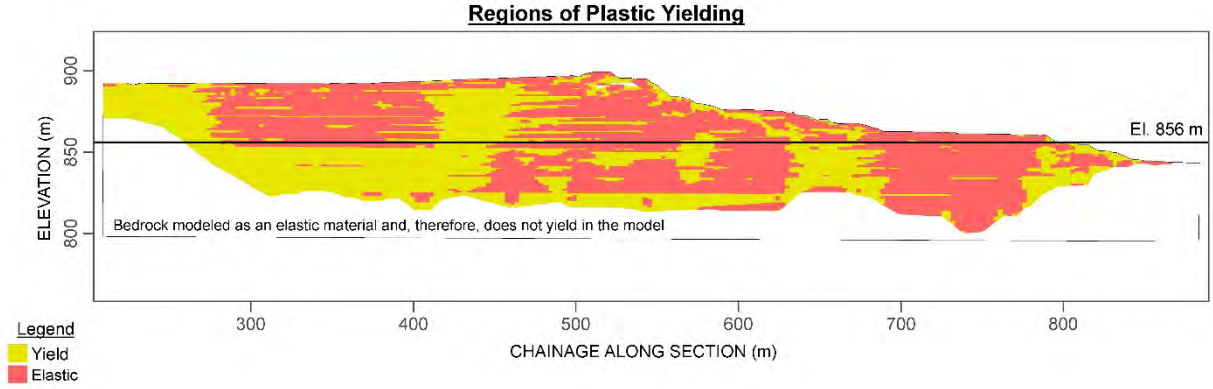

Figure I3-9 Regions of plastic yielding – Mohr-Coulomb analysis

The horizontal displacements resulting from this Mohr-Coulomb analysis are shown on Figure I3-10.

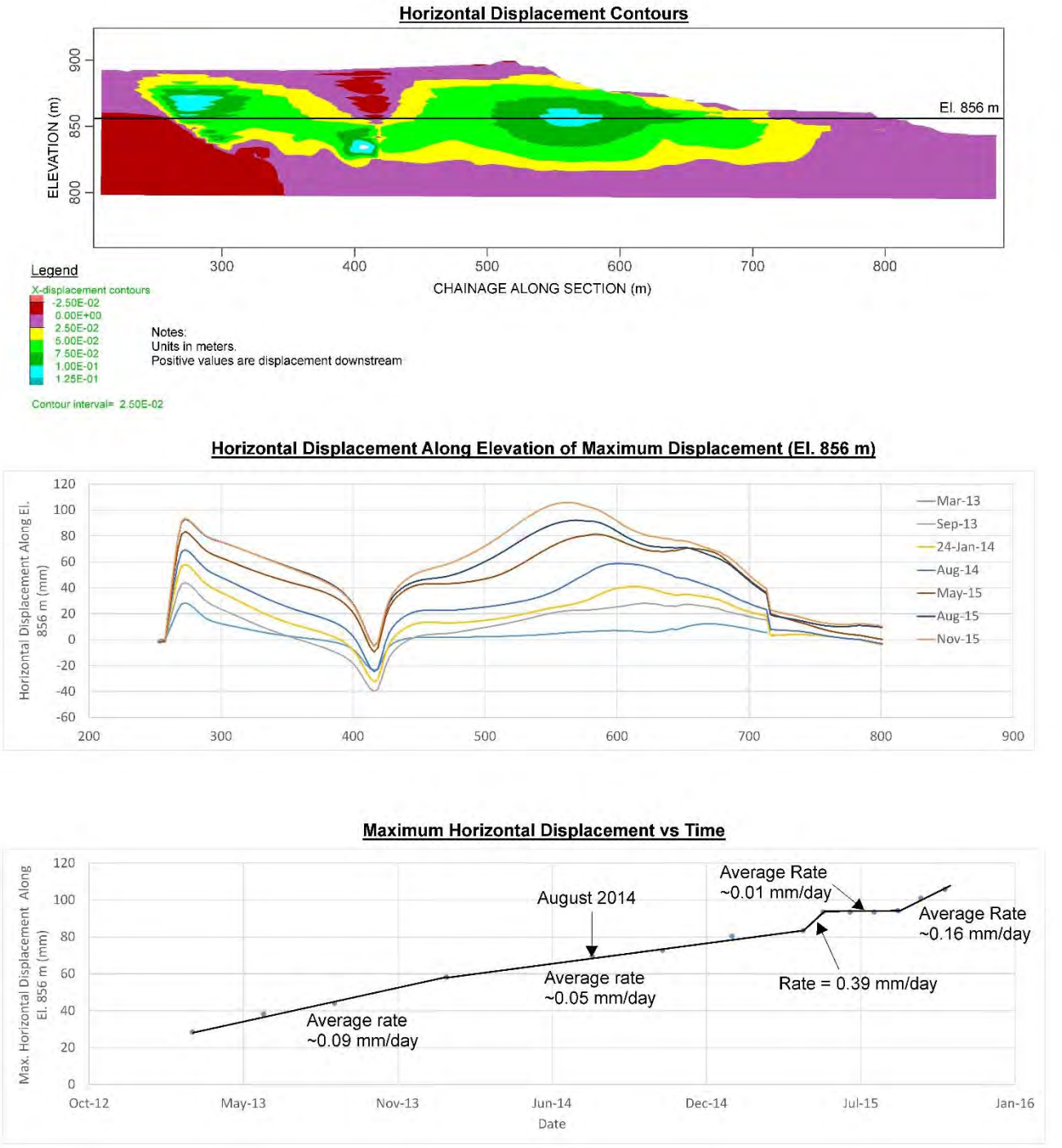

Figure I3-10 Horizontal displacement results – Mohr-Coulomb analysis

The effect on the yielding within the model can be seen by comparing Figure I3-10 with Figure I3-6. From such a comparison, it is apparent that the patterns of displacement are broadly similar, in that there are two main zones of displacement in the two models, which are in roughly the same location. However, it is apparent that there is additional displacement in an upstream direction towards the predominantly slimes material in the Mohr-Coulomb analysis. This is in line with expectations given the extent of yielding in that part of the model, which is in response to the settlement associated with the highly compressible slimes. The net effect of this additional upstream displacement is to slightly reduce the maximum displacements in a downstream direction. The maximum horizontal displacement at the November, 2015 stage of this model was 106 mm, compared with 118 mm in the elastic analysis.

The conflicting effects of upstream displacement due to settlement of the slimes versus downstream movements due to construction of the dam slope leads to a more complex sequence of incremental displacements than resulted from the elastic analysis. In this analysis, time periods in which the dam crest is raised by a greater amount than the beach can be seen as steps on the time displacement plot on Figure I3-10. Time periods when the beach is being raised significantly result in low displacement rates in the downstream direction due to the effects of additional settlement in the slimes.

The effect of the upstream displacements can also be seen on Figure I3-11, which shows that, unlike the elastic analysis, the trend of downstream horizontal displacements is not directly proportional to the height of the dam crest.

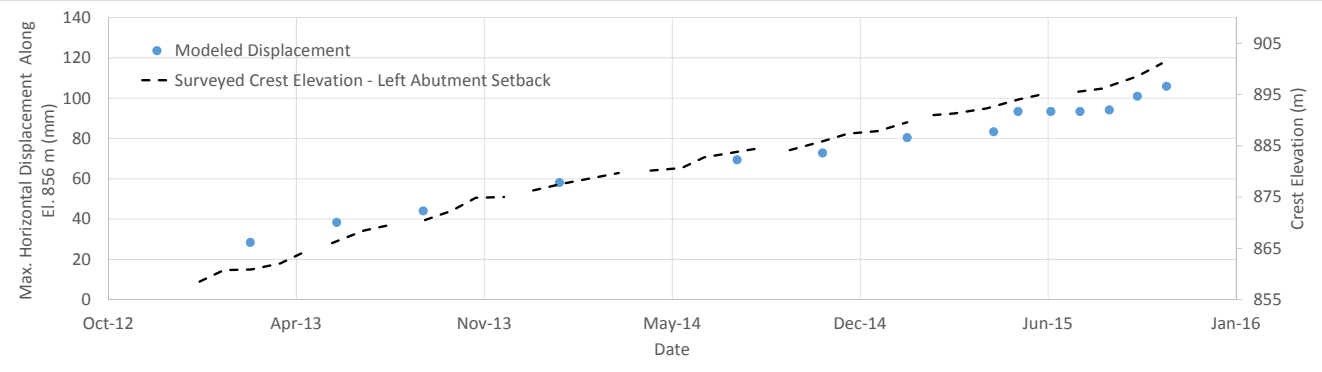

Figure I3-11 Comparison of horizontal displacements and crest elevation of left setback – Mohr-Coulomb analysis

As discussed previously, the purpose of the Mohr-Coulomb analysis was to form an intermediate step between the relatively simple elastic analyses and complex critical state analyses. The intent was to identify the effects of yielding due to shear only, and to aid in the later evaluation of the critical state analyses. The analyses presented meet this intent.

Whilst the model shows regions of compression and extension resulting from loading, as per the elastic analyses, additional calculations are required to identify the effects of this on the stress state of the sand. This is included within the critical state analyses.

I3.2.3 Critical State Analysis

I3.2.3.1 Base Case

Given that the Mohr-Coulomb analysis was seen to respond in line with expectations associated with the change of material behavior, this model was seen as a suitable base for further development in the critical state analyses.

The first critical state analysis (base case) was set up exactly as per the Mohr-Coulomb analysis except that the beached tailings sand was modeled using the NorSand constitutive model. The intent of this analysis was to assess the effect of the displacements within the dam on the stress state of the sand tailings and to identify whether the displacements could represent a potential liquefaction trigger. We also aimed to gain insight into the difference in response between the August, 2014 cracking incident and the November, 2015 flow failure from this analysis.

The horizontal displacements resulting from the base case critical state analysis are shown on Figure I3-12.

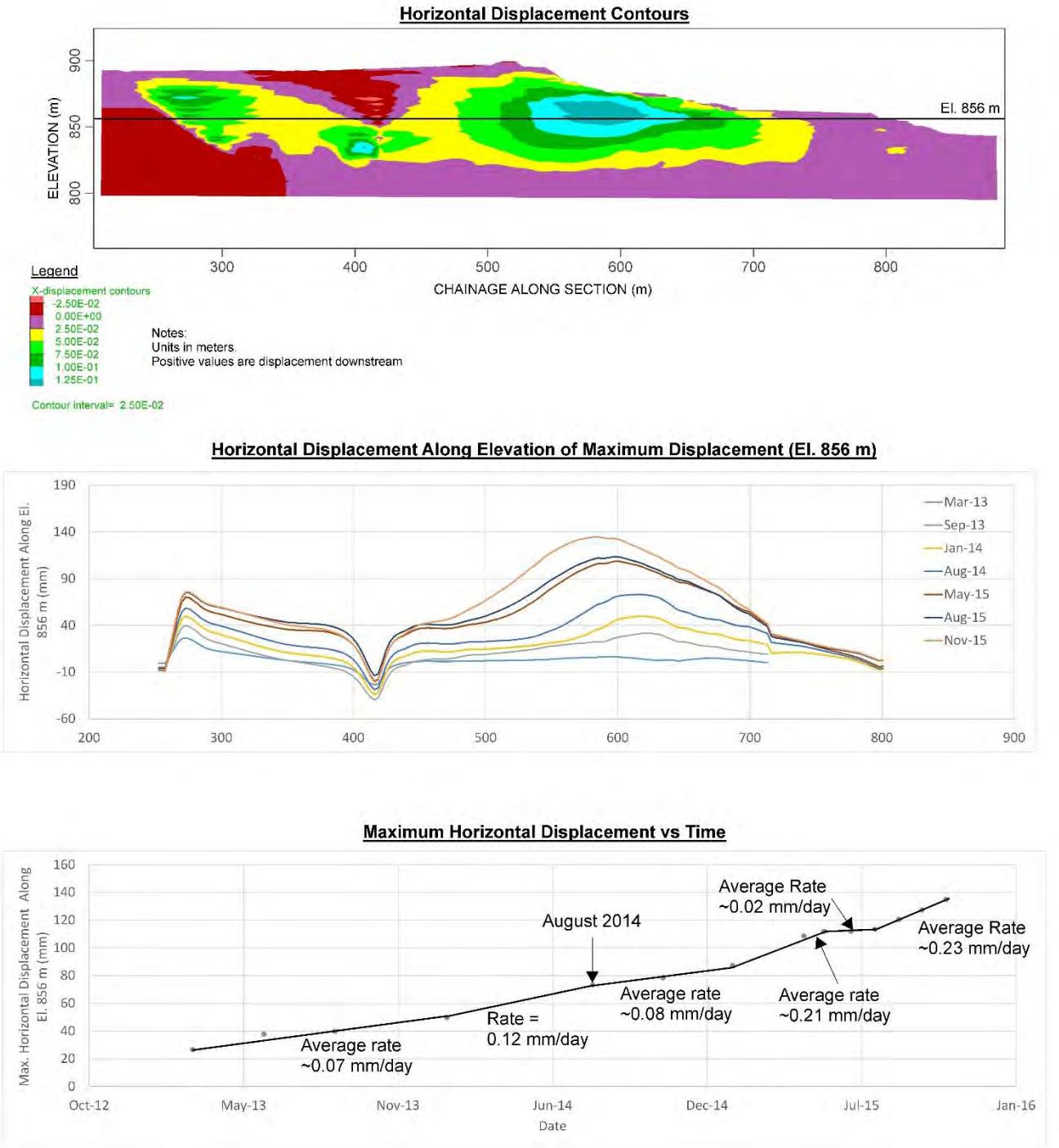

Figure I3-12 Horizontal displacement results – base case NorSand analysis

The horizontal displacements are compared with the results of the Mohr-Coulomb analysis on Figure I3-13.

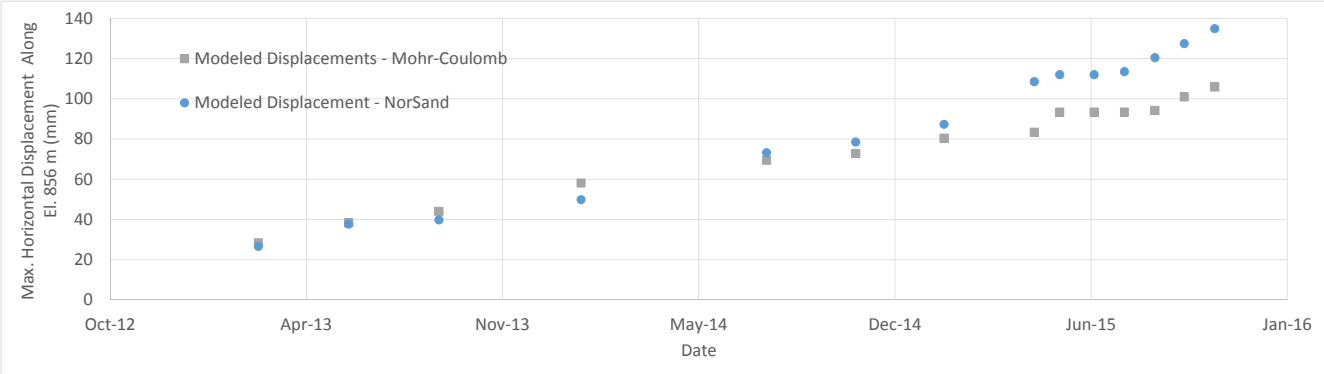

Figure I3-13 Comparison of horizontal displacements from Mohr-Coulomb and base case NorSand analyses

When the displacement trends from this analysis are compared with those of the Mohr-Coulomb analysis, the following observations can be made:

- The horizontal displacements in the NorSand analysis continue to concentrate in two regions, either side of the predominantly slimes region, as per the Mohr-Coulomb and elastic analyses.
- The region of largest horizontal displacement continues to occur downstream of the dam crest at the November, 2015 model stage.
- The total horizontal displacement at the November, 2015 model stage increased from 106 mm in the Mohr-Coulomb analysis to 135 mm in the NorSand analysis.
- The magnitude of displacements in the NorSand analysis was initially lower than the Mohr-Coulomb analysis, but this trend reversed at roughly the stage of August, 2014. In the August, 2014 model stage, the NorSand model displacements switched from being lower than the Mohr-Coulomb model to being larger than that model.
- The trend of NorSand displacements being larger than the Mohr-Coulomb model continued up to the November, 2015 model stage.

The observed reversal of the displacement trend from being lower than the Mohr-Coulomb model to being larger than that model at the August, 2014 model stage provides insight into a feature of the tailings behavior that may have contributed to the cracking incident occurring at that time and not sooner. To understand this trend, it is necessary to review the volumetric response of the tailings sand to loading. The variation of void ratio for an element of tailings sand located beneath the dam crest, above one of the slimes layers, is illustrated on Figure I3-14. This figure shows that as the dam is constructed, the void ratio is reducing at a lower gradient in e-log p' space than the critical state line. This is having the effect of making the tailings sand increasingly contractive (increasing the state parameter). As a result, this displacement trend is understandable if the change of stress-strain behavior with state parameter, illustrated on Figure I2-6, is considered. The explanation for this trend is that the tailings sand is initially slightly dilatant, causing the tailings to behave in a manner that is

stiffer than assumed in the Mohr-Coulomb analysis. At around August, 2014, the tailings become sufficiently contractive to produce a more ductile response to loading, which leads to a consequent increase in displacements. These displacements are moderated temporarily by the construction of the reinforcement berm following the August, 2014 incident, but then continue to increase with additional dike construction up until the November, 2015 failure.

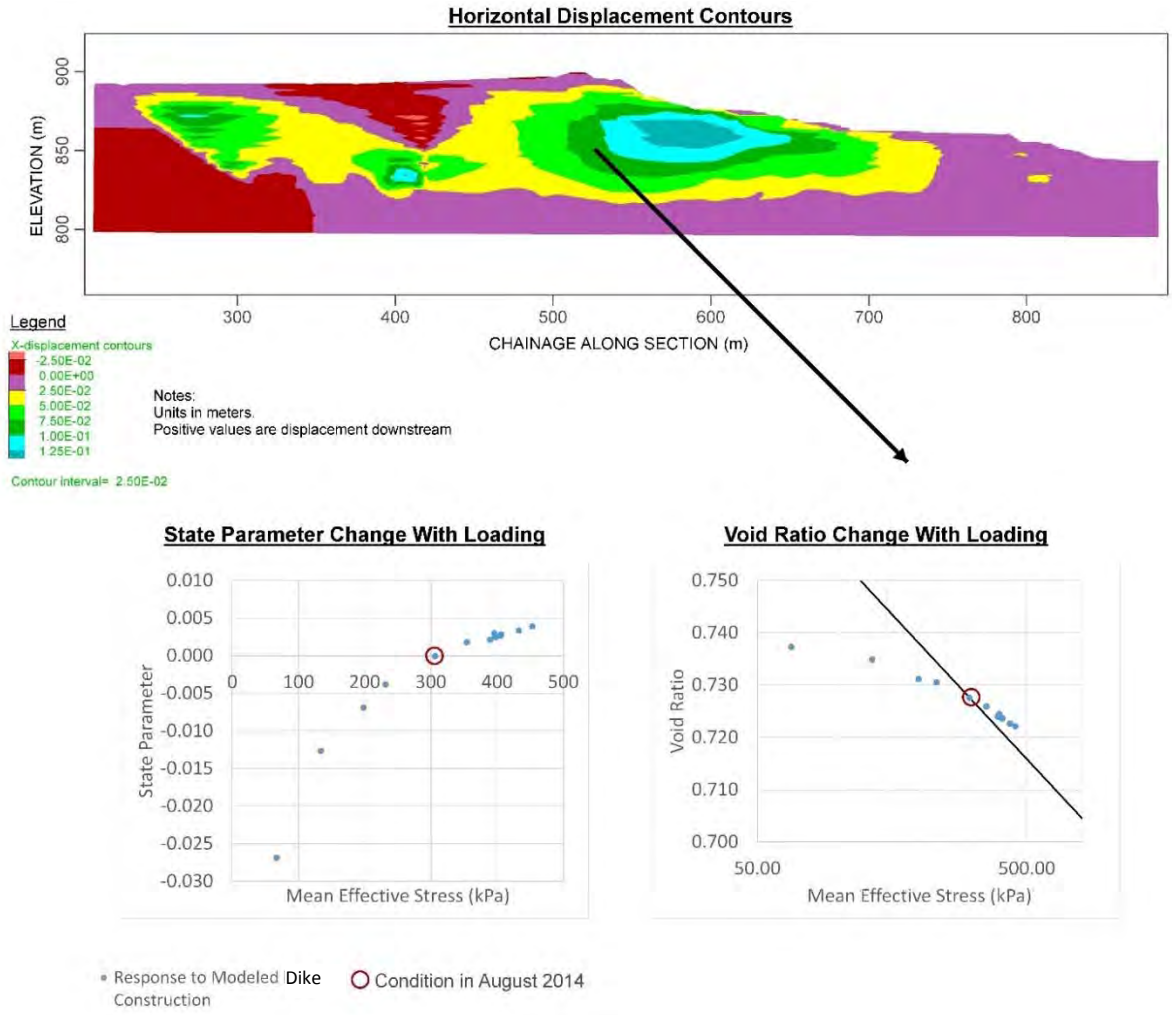

Figure I3-14 Horizontal displacement results – base case NorSand analysis

In addition to tracking the deformations throughout this model, we have also tracked a parameter termed the mobilized instability ratio, which defines the distance of any element of soil from the critical state line in q-p' stress space, as illustrated on Figure I3-15. The reason for tracking this parameter is to enable comparison of the model response with the stress controlled extrusion-collapse laboratory tests. The laboratory tests found that as a mobilized instability ratio of 1 is approached, slightly contractant sand tailings will become highly susceptible to rapid instability under a minor increment of stress change. As a result, within this analysis the mobilized instability ratio is a criterion for the triggering for collapse.

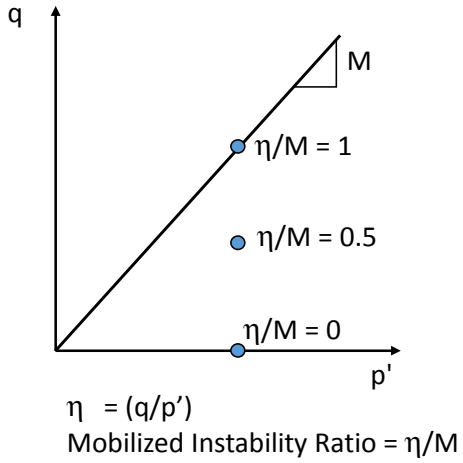

Figure I3-15 Definition of the mobilized instability ratio

Contours of mobilized instability ratio are shown, together with the variation of this parameter throughout the dike construction for a sand element located beneath the November, 2015 dam crest, at the sand-slimes interface, on Figure I3-16. This figure shows that the maximum mobilized instability ratios developed within this base case NorSand model, that included peak strengths assigned to the slimes, are roughly 0.5. These values are distant from the conditions at which rapid instability occurred in our laboratory tests, and suggest that drained deformations would be unlikely to lead to rapid instability under this model scenario. This model has formed the base for examining the effect of additional displacements within the slimes that may develop under conditions of more continuous slimes, or post-peak strength mobilization in the slimes, which are discussed in the following sections.

As discussed in Section I2.3.3, it was necessary in this base case NorSand analysis to define the state parameter input value (seed state parameter) that would lead to a distribution of state parameter that was roughly equivalent to that observed in the field. The reason that this is uncertain at the outset of the modeling is because the state parameter distribution within the model changes in response to loading and shearing, as discussed earlier. This issue was addressed by running multiple versions of this base case model with different seed state parameters and extracting the state parameter results in the January, 2015 model stage for comparison with the field data collected during this time period. The intent was to match the 80th percentile of the field distribution, since this value is defined by Jefferies and Been (2016) as the characteristic state, in line with their suggestion that the loosest 20% of the soil can dominate the behavior of a deposit. A seed state parameter of -0.02 was found to provide the closest match to the field data and was used in this base case analysis and subsequent variations discussed in the following sections. A comparison of the modeled distribution of state parameter with that of the field data is shown on Figure I3-17.

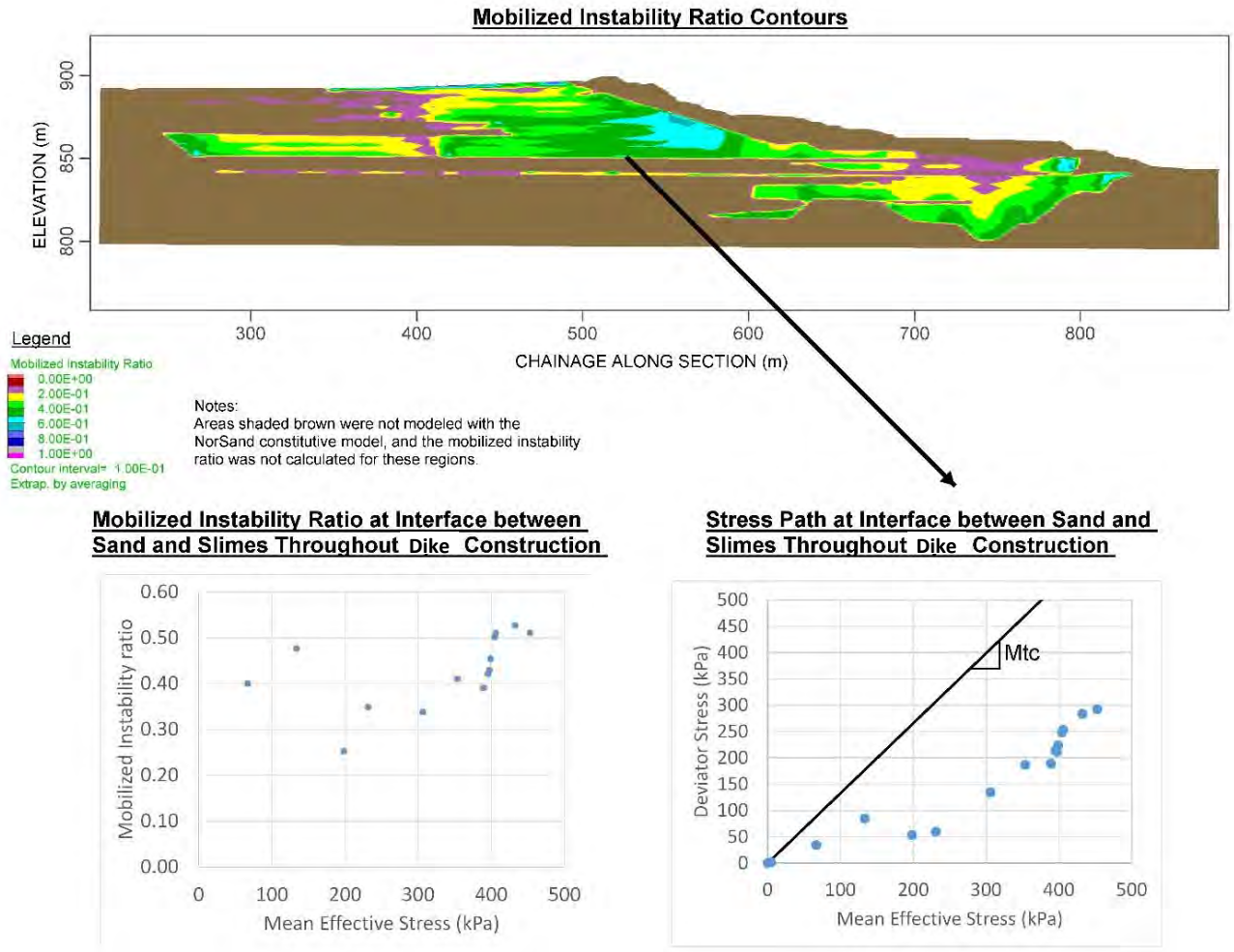

Figure I3-16 Mobilized instability ratio and stress path

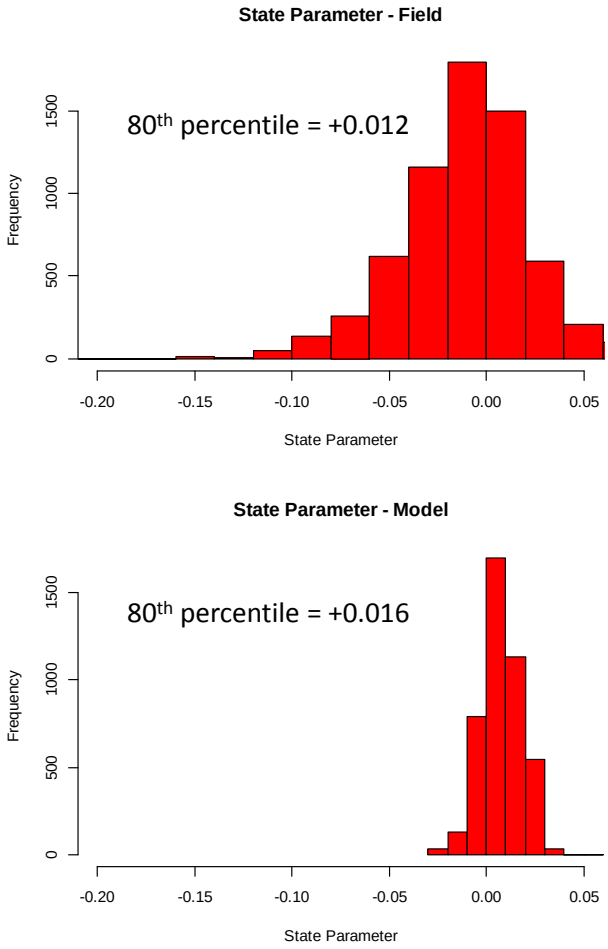

Figure I3-17 Comparison of field and modeled state parameter

I3.2.3.2 Parametric Sensitivity Analysis

Continuity of Slimes

Building on the results of the base case NorSand analysis, we completed a sensitivity analysis to identify how the results would be affected if the slimes were more continuous in the downstream direction.

The model adjustment made for this analysis was to assume that the region designated as isolated slimes in the base case model was actually composed of interbedded slimes. The isolated slimes unit was merged with the interbedded slimes unit located farther upstream, leading to the model setup shown on Figure I3-18.

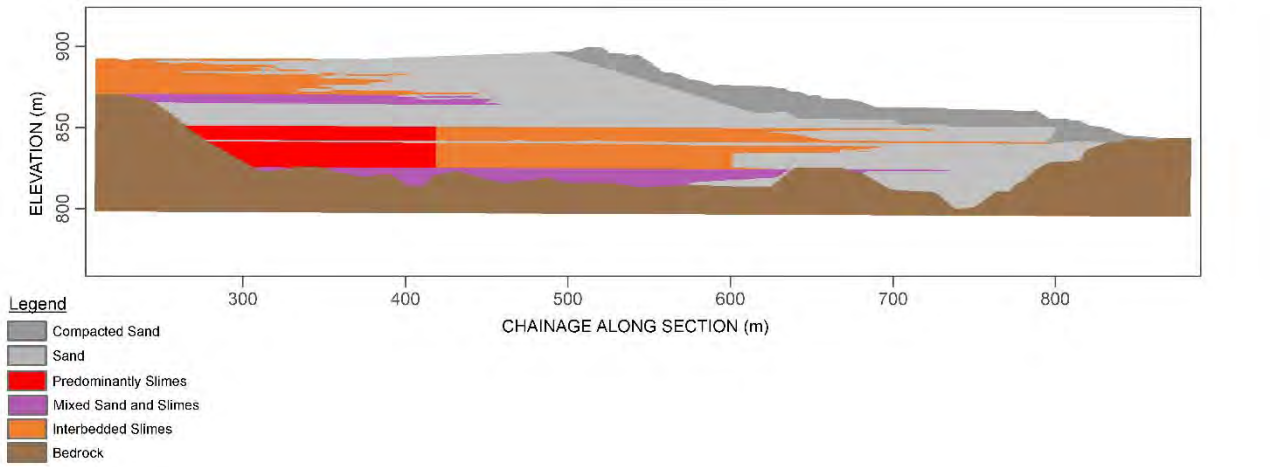

Figure I3-18 Updated model geometry incorporating continuous interbedded slimes

As shown on Figure I3-19 to Figure I3-21, assuming that the interbedded slimes are continuous in the downstream direction does not change the horizontal displacement or stress state results significantly from those of the base case. The outcome of this sensitivity analysis was to increase the horizontal displacements at the November, 2015 model stage by 7 mm, from 135 mm in the base case to 142 mm. The peak instability ratio of this model was similar to that of the base case, with both models resulting in a value of roughly 0.5. Therefore, these results suggest that the presence of a relatively discontinuous mixture of sand and slimes represented by the blended sand/slimes parameter sets would not bring the stress state of the tailings to an unstable condition, and would not account for the flow failure observed on November 5, 2015. The following sections of this appendix examine whether the presence of weaker, horizontally continuous, slimes-rich layers within the interbedded slimes region, which could mobilize a much lower strength than the blended parameters, could account for the November 5, 2015 flow failure.

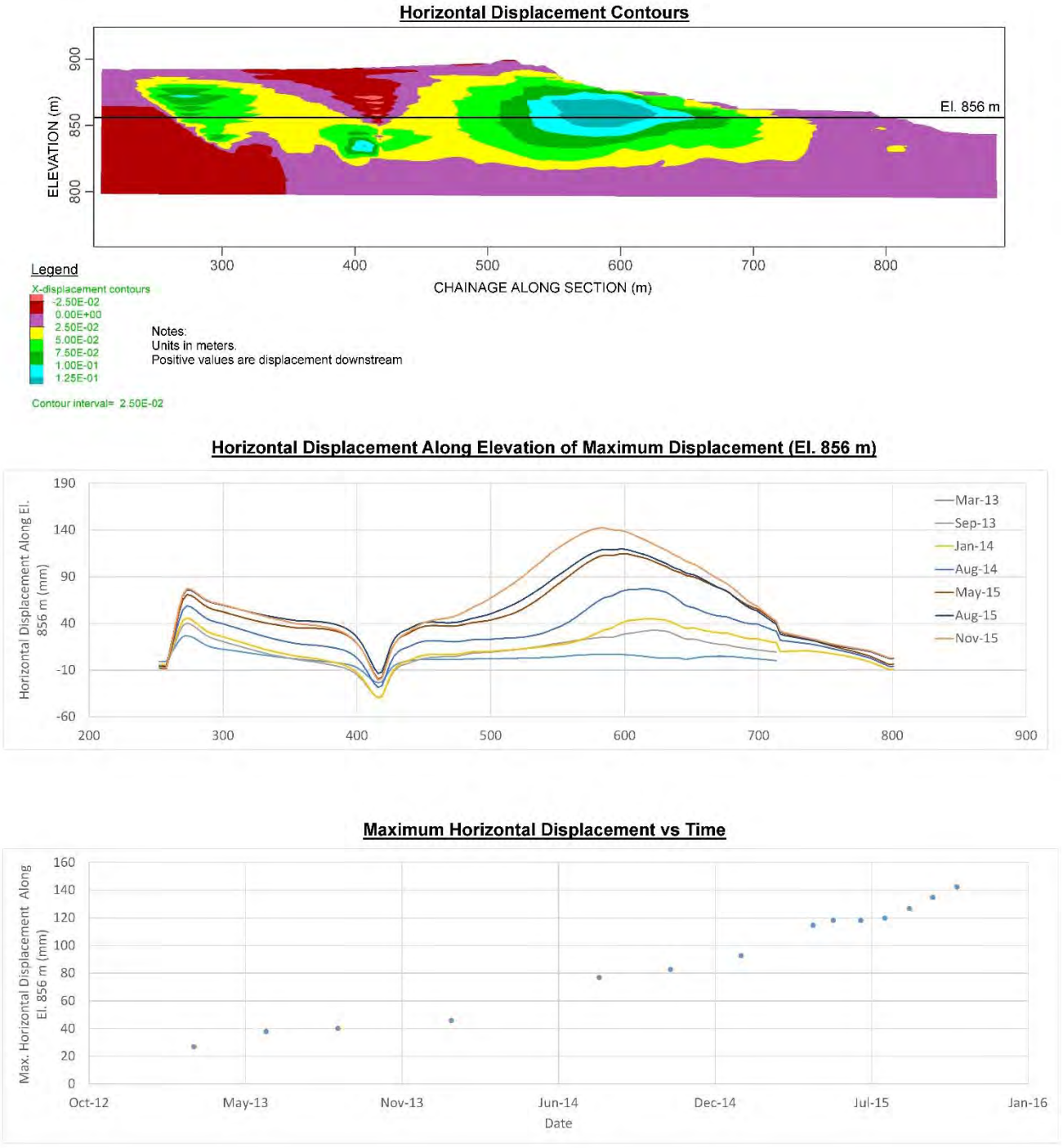

Figure I3-19 Horizontal displacement results – continuous interbedded slimes model

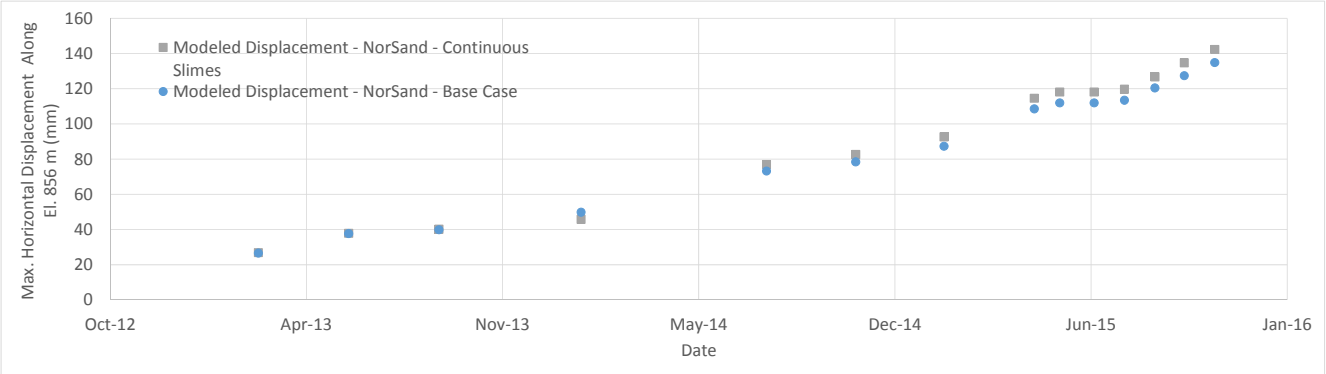

Figure I3-20 Comparison of displacements from NorSand base case with those from the continuous interbedded slimes sensitivity analysis

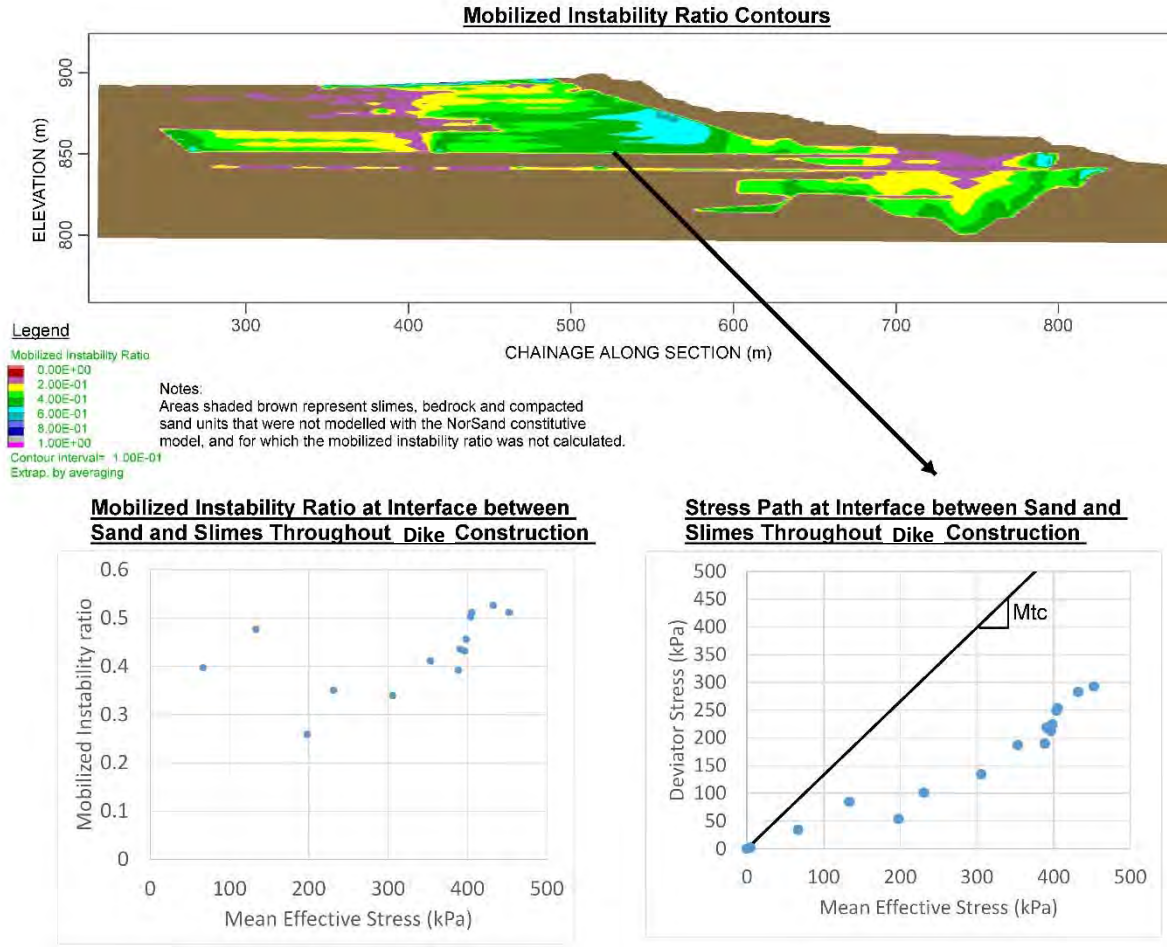

Figure I3-21 Mobilized instability ratio and stress path – continuous interbedded slimes model

Post-Peak Strength of Slimes – Strength Reduction after Construction

Having constructed the continuous interbedded slimes model to the November, 2015 model stage, this model was then used for a subsequent sensitivity analysis to assess how the strength of the slimes assigned to the interbedded slimes region was affecting the stress state of the overlying tailings sand. This analysis was completed as a separate stage to the previous model by incrementally reducing the strength of the slimes in the region shown on Figure I3-22 and then examining the stresses and deformations within the model. As noted previously, this reflects the sensitivity of the slimes.

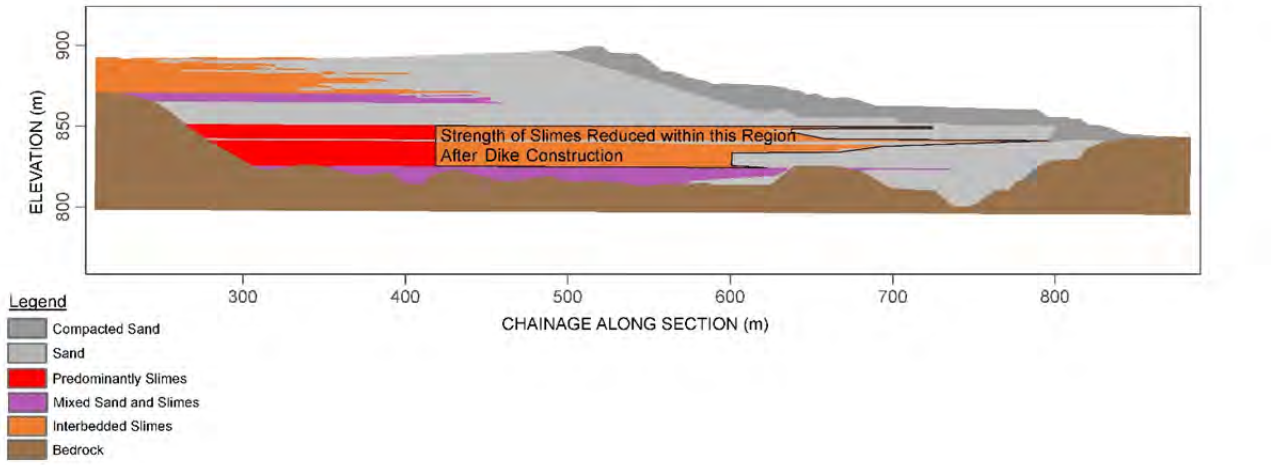

Figure I3-22 Illustration of zone of slimes strength reduction

It was possible to reduce the strength of the slimes in this region to a friction angle of 9.5° before numerical convergence issues prevented the model from proceeding. The results shown on Figure I3-23 illustrate how this strength reduction led to 170 mm of additional displacement (lateral extrusion) downstream of the dike crest. Figure I3-24 shows that this lateral extrusion movement within the slimes has an effect of reducing the stress in the overlying tailings sand in a manner that is very similar to the stress path followed during the stress controlled extrusion-collapse laboratory tests (see Figure I3-5). The maximum mobilized instability ratio calculated during this analysis was approximately 0.8, compared with 0.5 calculated in the earlier analyses. This reduced slimes strength is within the range of parameters initially considered as reasonable for the predominantly slimes layers; therefore, it would not be unreasonable to think that this strength could be mobilized anywhere within the slimes mass, should sufficient continuity exist.

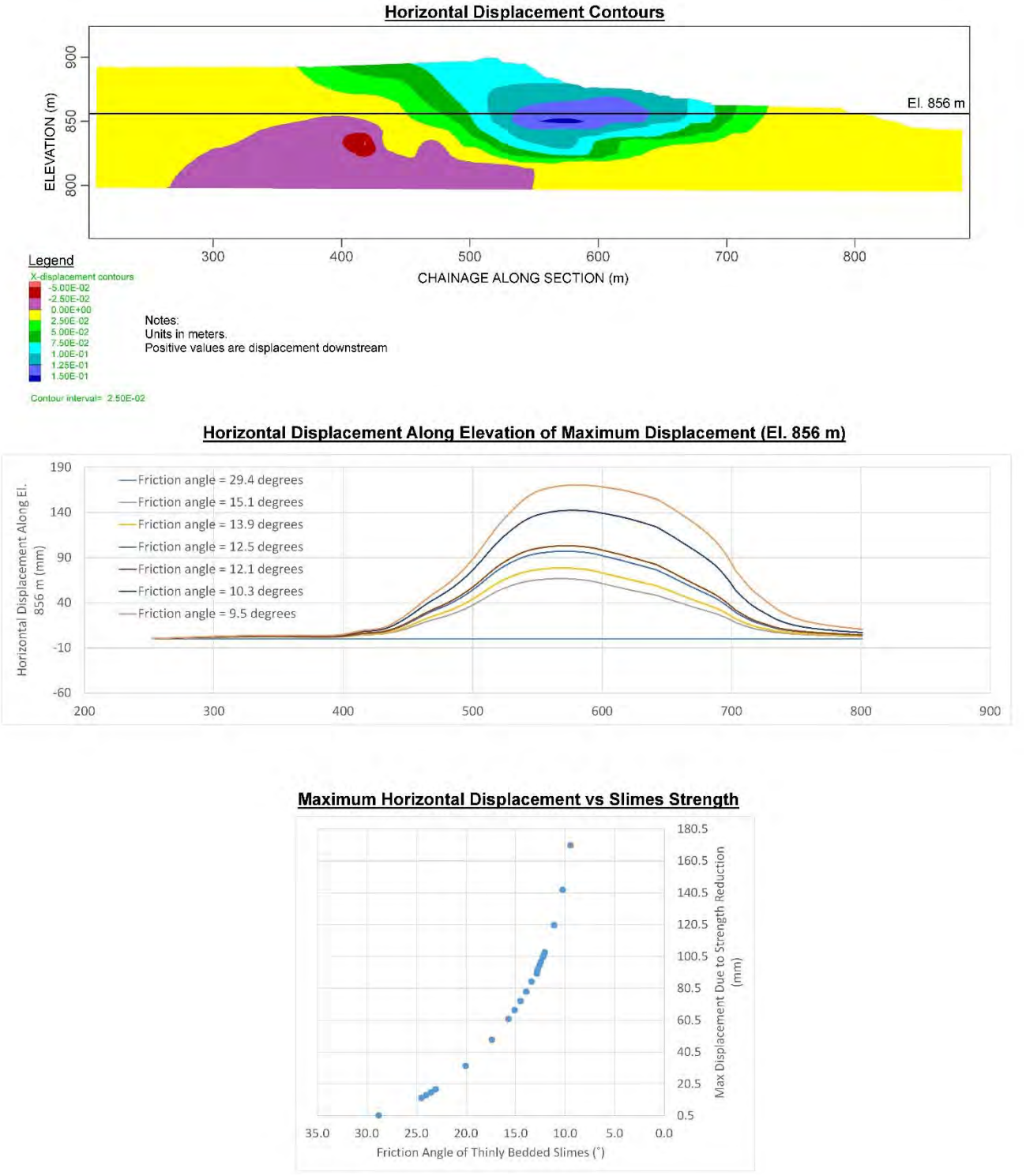

Figure I3-23 Displacements due to slimes strength reduction

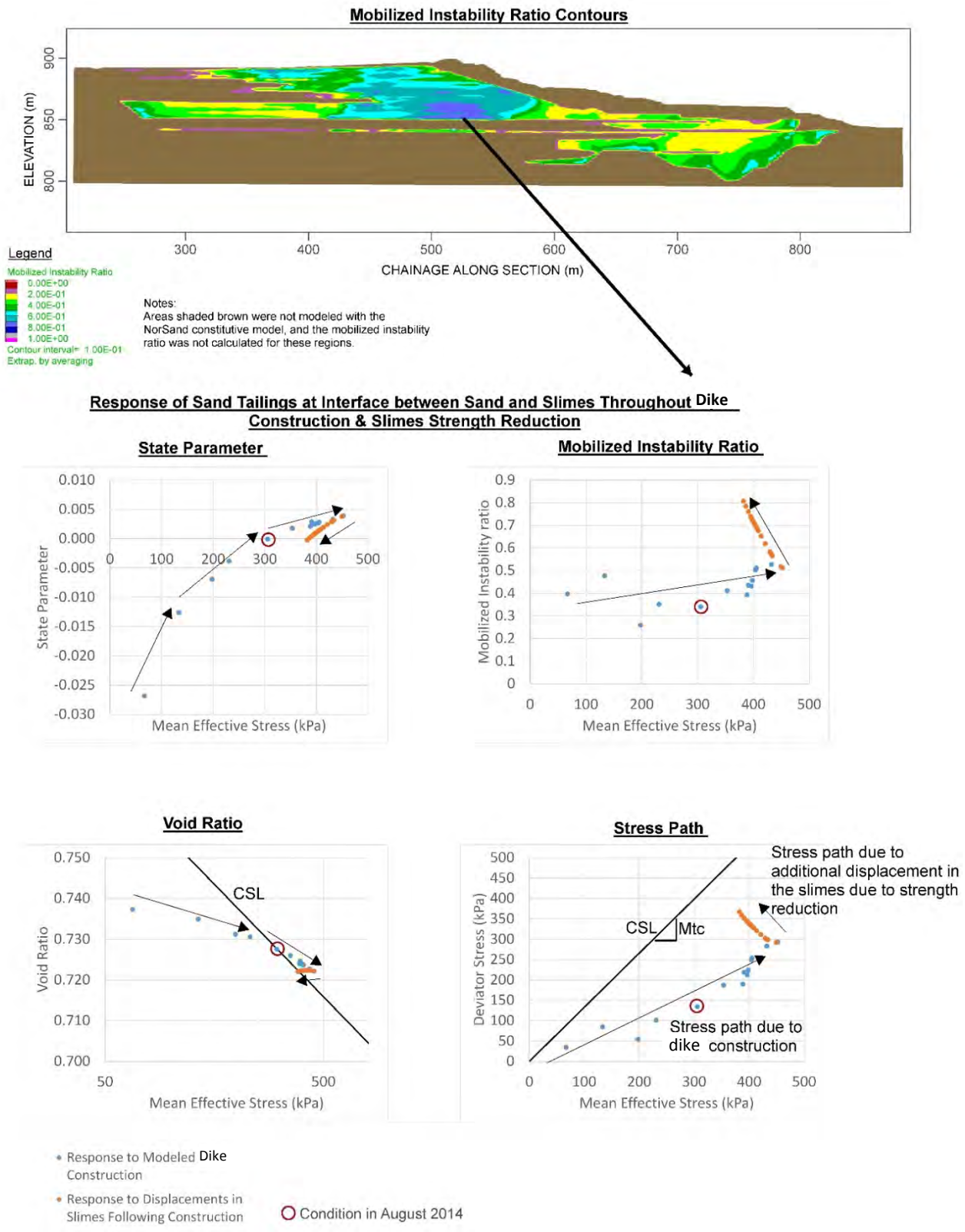

Figure I3-24 Mobilized instability ratio and stress path due to slimes strength reduction

Post-Peak Strength of Slimes – Strength Reduction throughout Construction

Having identified a slimes strength that leads to a stress state in the overlying sand approaching that at which rapid instability was observed in the laboratory tests, an additional sensitivity analysis was completed to identify how the response of the dike would differ if this strength was operative throughout the entire dam construction sequence, as shown on Figure I3-25.

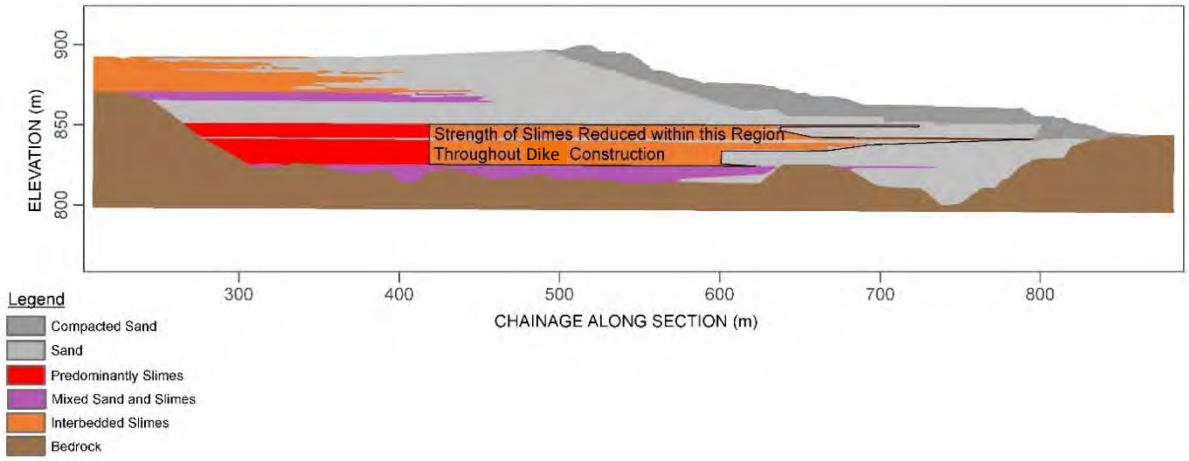

Figure I3-25 Updated model geometry incorporating continuous interbedded slimes with reduced strength

Figure I3-26 shows that imposing a friction angle of 9.5° on the interbedded slimes region beneath and downstream of the dike crest would, as expected, lead to a marked increase in displacements downstream of the dike crest at the November, 2015 model stage compared with earlier models. The maximum horizontal displacement from this analysis was 335 mm, compared with 142 mm in the analysis with base case strength parameters. This value is similar to the cumulative displacement of the analysis in which the strength of the slimes is reduced at the end of construction: 142 mm + 170 mm = 312 mm, versus 335 mm in this analysis. The overall pattern of displacement is similar to that observed in earlier model iterations in that the maximum displacements are concentrating in the same location downstream of the crest.

Figure I3-27 shows that the additional displacements due to the reduced slimes strength throughout the dike construction would lead the stress state of the tailings sand overlying the slimes to a similar mobilized instability ratio, as was observed when the slimes strength was reduced at the end of the dike construction (0.8). This implies that whether extrusion through the slimes was occurring continuously or in isolated incidents, the effect would be to drive the stress state of the sand into a potentially unstable condition.

If the volumetric response of the sand is reviewed using the e-logp' plot on Figure I3-27, it can be seen that the model suggests a relatively consistent trend of incremental volumetric strain throughout the dike construction. Unlike the collapse tests in the published literature completed by Skopek et al. (1994), no sudden change of volumetric behavior was observed in the simulation. Therefore, the assumptions of sustained drained conditions in the sand within the analysis is supported.

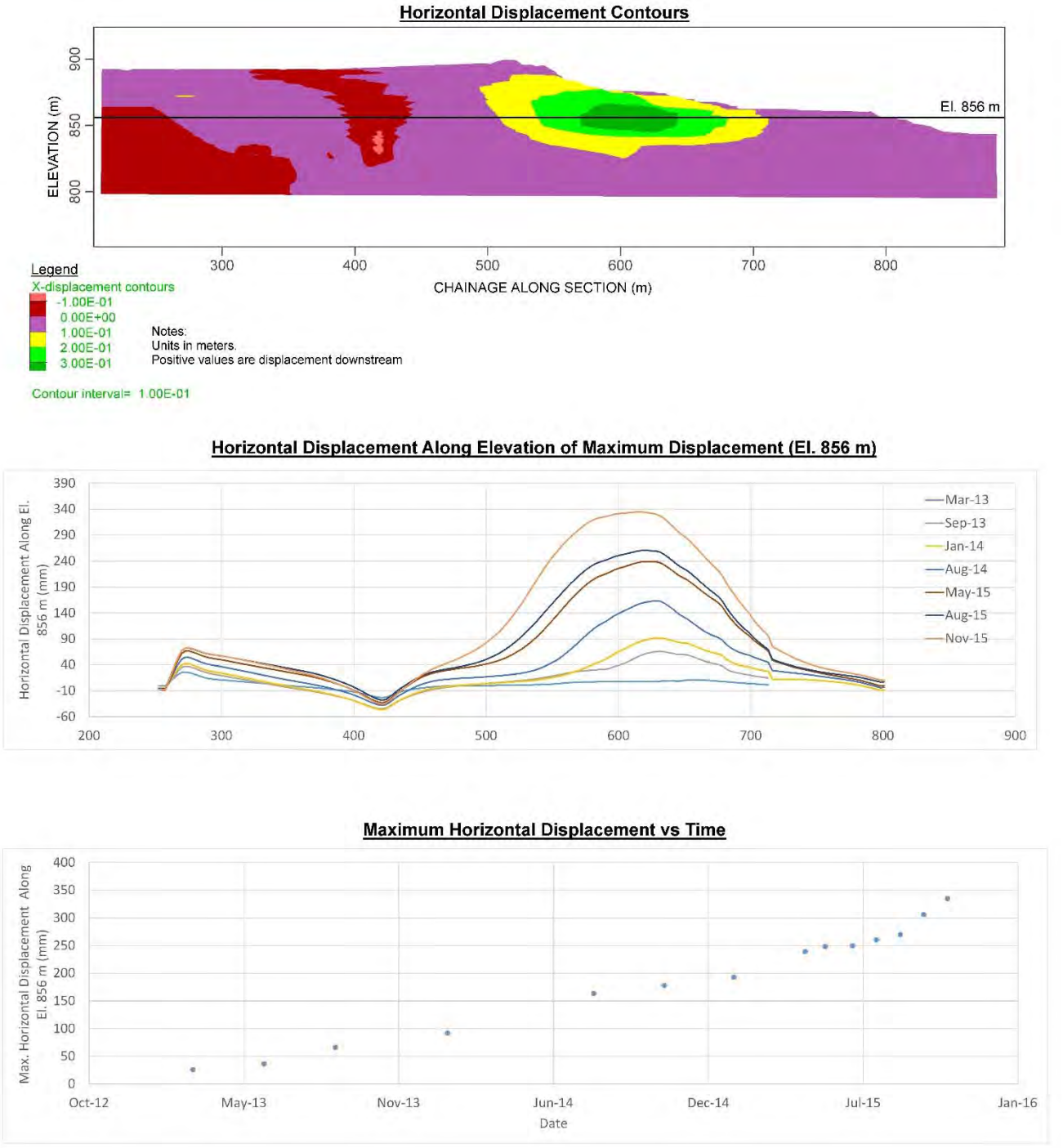

Figure I3-26 Horizontal displacement results – reduced strength continuous interbedded slimes model

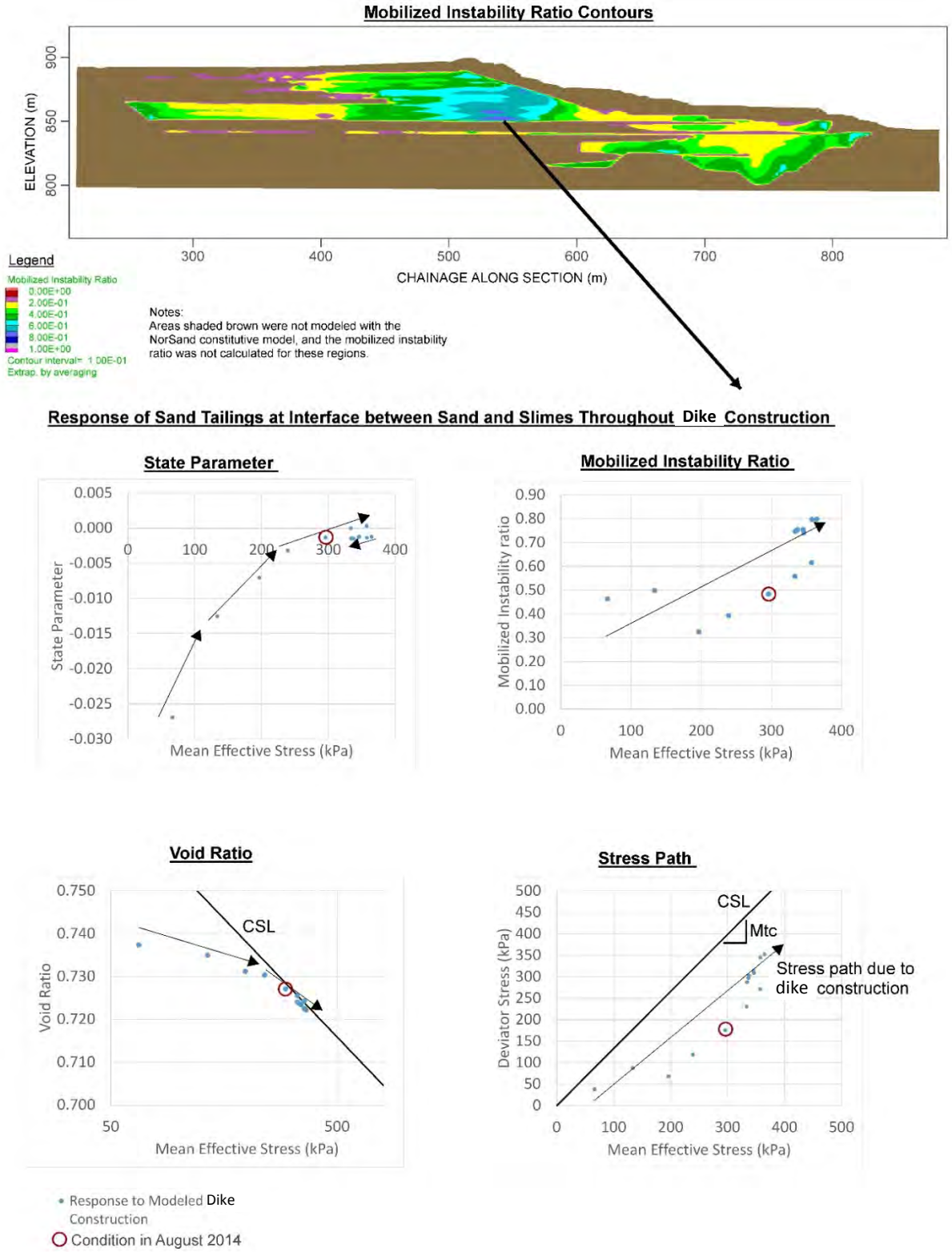

Figure I3-27 Mobilized instability ratio and stress path – reduced strength continuous interbedded slimes model

It is of interest to note from Figure I3-26 and Figure I3-27 that if this slimes strength was operative throughout the dike construction history, the model suggests that an increase in displacement rate would be expected prior to the August, 2014 event, leading to a cumulative displacement of roughly 163 mm. However, even with this magnitude of movement, the lateral extrusion process would still not be sufficiently advanced to place the sand tailings in an unstable stress state at this stage in the dam's construction history. This, and observations from model variants discussed previously, may provide an explanation for a contributing feature to the timing of the August, 2014 event and the absence of a flowslide resulting from this incident.

It is acknowledged that the strength of ϕ=9.5° is lower than the peak strength assumed for the slimes of ϕ=12.4°, based on the Baia 4 failure. This implies that strain weakening of the slimes layers would need to have occurred if this, or potentially a lower, slimes strength was operative on November 5, 2015. If the strain weakening occurred at the time of the August, 2014 event, this would have compounded the mechanism for the event suggested in the paragraph above.

Imposed Displacement Boundary

After advancing the model with a slimes strength of ϕ= 9.5° throughout the construction history of the dike, we completed an additional variant on this model. In order to continue the extrusion of the slimes beyond the point at which numerical convergence issues prevented further reduction of the slimes' strength, a displacement boundary condition was applied to the top of the slimes layer to force additional displacements to occur in the same pattern as they were observed during the modeled dam construction.

The results shown on Figure I3-28 and Figure I3-29 show that additional extrusion within the slimes layer would ultimately lead the stress state of the overlying tailings to a similar condition as that at which rapid failure was observed in our laboratory tests. These figures show that a mobilized instability ratio of approximately 1 would be approached at roughly 600 mm of cumulative horizontal displacement. Therefore, this is the magnitude of displacement required to trigger liquefaction due to lateral extrusion.

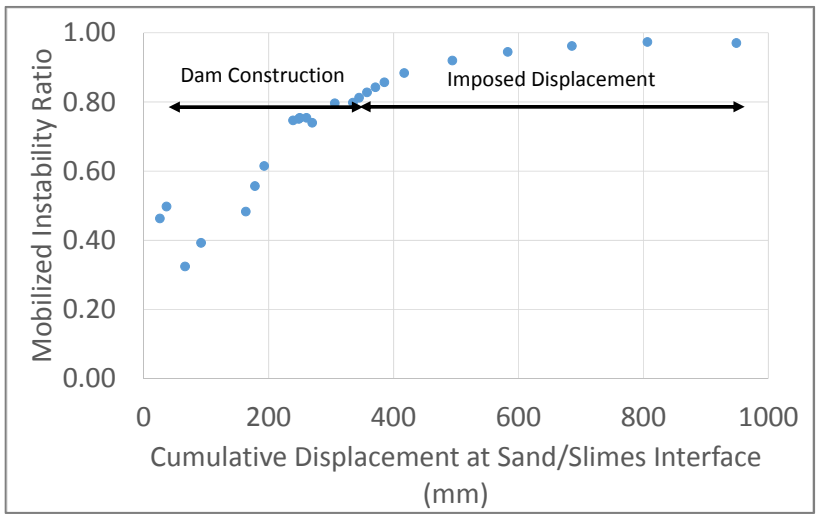

Figure I3-28 Mobilized instability ratio development with displacement at the sand/slimes interface

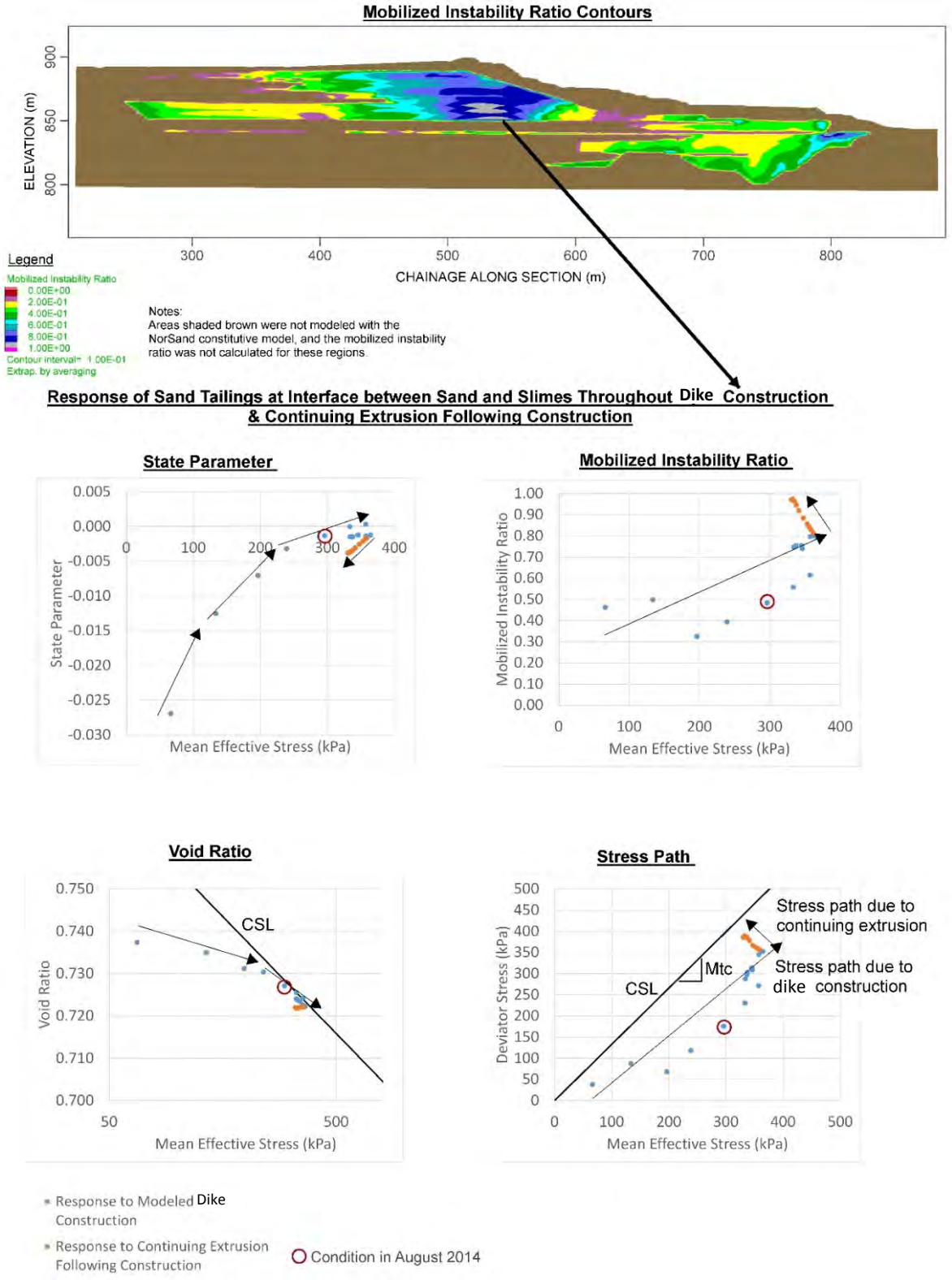

Figure I3-29 Mobilized instability ratio and stress path due to continuing extrusion of slimes – reduced strength continuous interbedded slimes model

Comparison with General Shear Failure

As discussed in the preceding section, we have now established the magnitude of deformations in the slimes-rich layers required to initiate rapid instability and liquefaction in the overlying sand units. In order to use this deformation magnitude to evaluate the relative likelihood of the lateral extrusion mechanism triggering liquefaction versus a shear mechanism, it is necessary to compare these displacement magnitudes with those associated with the onset of a general shear failure throughout the dam. A general shear failure could potentially trigger liquefaction through a sequence of undrained yielding of the slimes-rich layers leading to uncontrolled movement of the dam, which leads to shear straining occurring more rapidly than the drainage of the sand will allow. In order to evaluate which of these mechanisms was the more probable liquefaction trigger, the following stages were completed:

- The Mohr-Coulomb model discussed in Section I3.2.2 was revisited and used to estimate the deformation magnitude and pattern that would develop as a condition of general shear failure through the dam, driven by displacements in the slimes-rich layers, is approached. This was achieved by running this model throughout the entire construction sequence multiple times, with each iteration using a lower strength for the slimes-rich layers.
- The proximity of the model to a condition of general shear failure was subsequently confirmed by completing a series of strength-reduction factor of safety analyses in FLAC, in which the reserve strength of all soil units against instability was identified. In addition, we completed a limit equilibrium stability analysis, separate from those completed in Appendix H, for comparison with the results from FLAC.
- Once the conditions at the onset of general shear failure were identified, the trend of displacement magnitude leading up to that condition was extracted from the Mohr-Coulomb model for comparison with the NorSand model results.

The pattern of displacements resulting in November, 2015 if an undrained strength ratio of 0.13 (equivalent friction angle 7.5°) was mobilized in the slimes is shown on Figure I3-30. The pattern of displacements is similar to that shown previously for the NorSand model analyses.

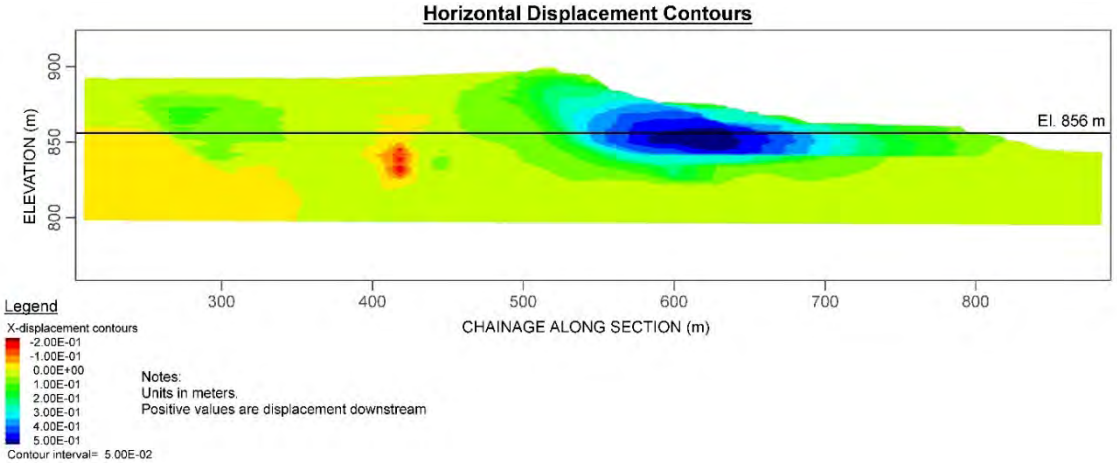

Figure I3-30 Horizontal displacements resulting from Mohr-Coulomb analysis with mobilized shear strength ratio of 0.13 (equivalent friction angle of 7.5°)

The factor of safety calculated using FLAC with an undrained strength ratio of 0.13 assigned to the slimes-rich layers is 1.07, as shown on Figure I3-31.

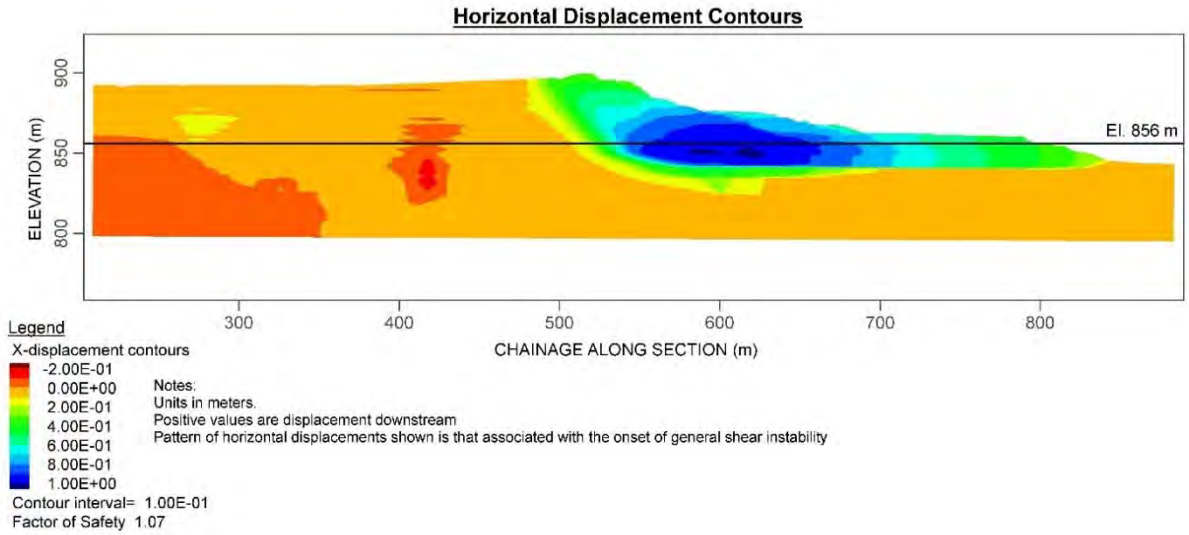

Figure I3-31 Factor of safety results calculated using FLAC with mobilized shear strength ratio of 0.13 (equivalent friction angle of 7.5°)

The factor of safety calculated using FLAC is similar to that calculated using limit equilibrium methods (see Figure I3-32).

The equivalence between the FLAC and limit equilibrium analyses was also checked with an undrained strength ratio of 0.12, with both methods indicating that a factor of safety of 1 would be reached at this strength (see Figure I3-33).

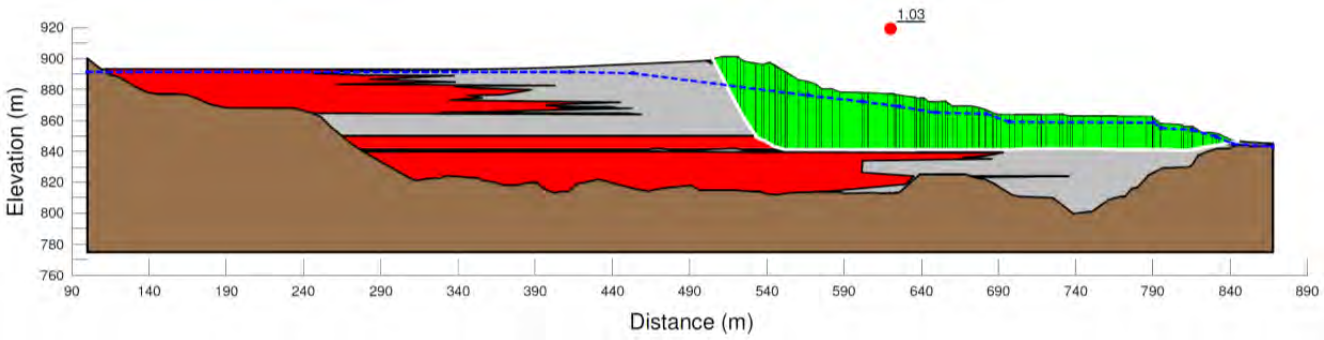

Strengths: Slimes-Rich Layers = $s_u/\sigma'v$ (0.13); Sand = ϕ' = 33°; Compacted Sand = ϕ' = 35° & c' = 5 kPa

Figure I3-32 Limit equilibrium analysis for comparison with FLAC analysis

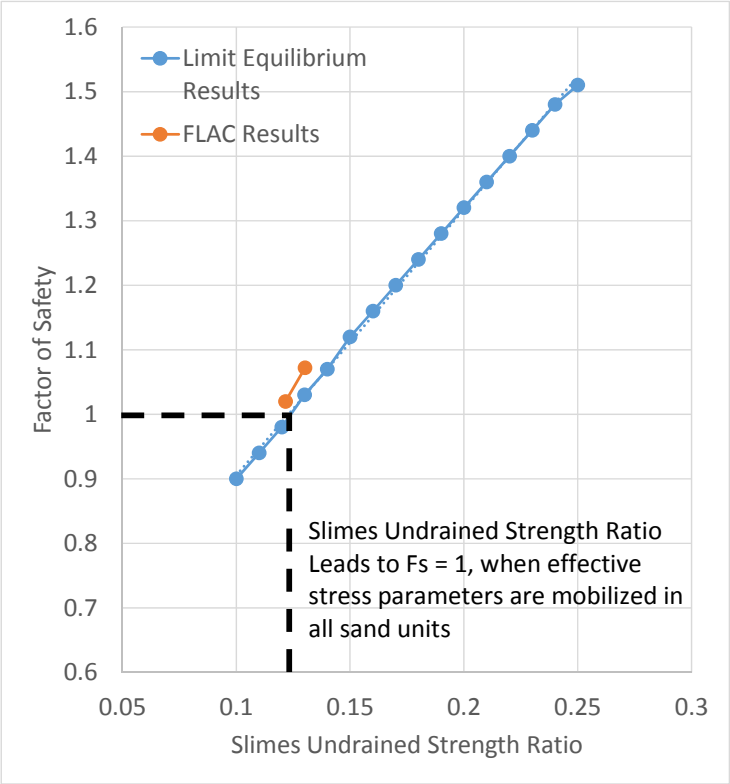

Figure I3-33 Comparison of trends in FLAC and limit equilibrium factor of safety analysis results

The trend of displacements associated with the various levels of strength mobilization in the slimes-rich deposits considered in the deformation analyses are shown for comparison with the displacements required to initiate extrusion-induced collapse on Figure I3-34. As discussed previously (Section I3.2.2), the Mohr-Coulomb analysis underestimates the displacements calculated by the NorSand model due to the increased ductility of the sand assumed within the NorSand formulation. Therefore, to estimate the levels of deformation that would result from the NorSand analysis with continued reduction in slimes strength below the limiting strength ratio value (0.17 – equivalent friction angle of 9.5°) reached in the NorSand analysis, the results of the Mohr-Coulomb analysis have been factored in accordance with the ratio of Mohr-Coulomb and NorSand-based results at a common undrained strength ratio of 0.17.

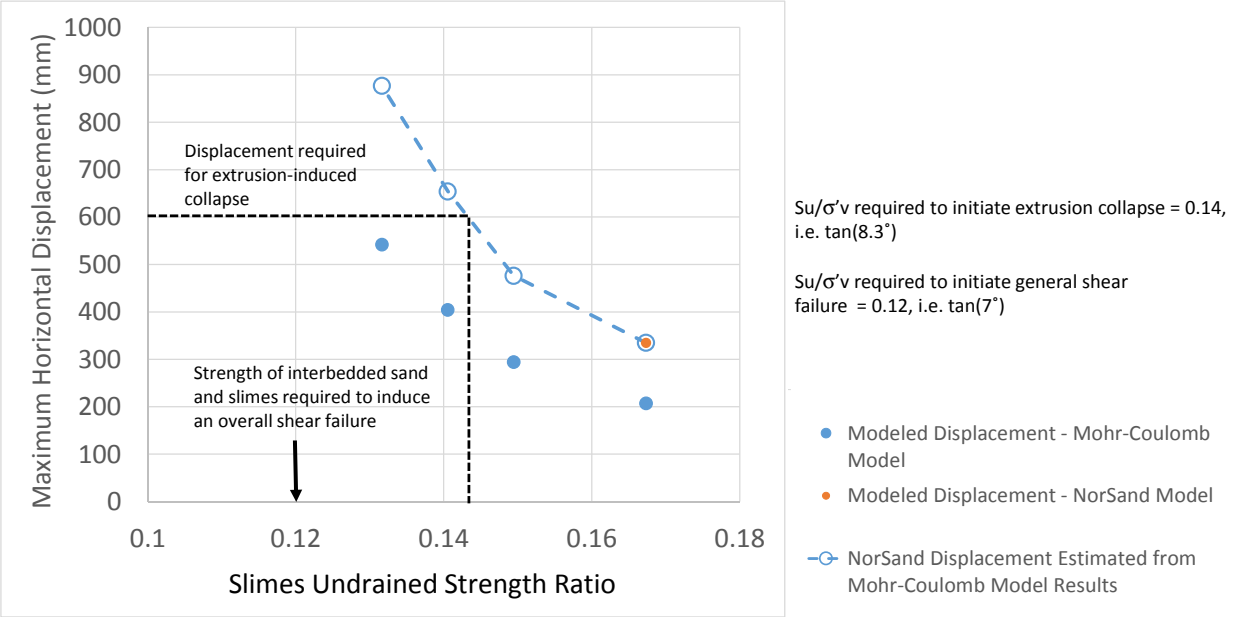

Figure I3-34 Comparison of displacements necessary to initiate extrusion-induced collapse and those associated with the onset of general shear failure

The outcome of this comparison between the conditions needed to generate liquefaction from lateral extrusion of the slimes-rich layers versus those needed to initiate general shear failure, illustrated on Figure I3-34, show that liquefaction would be more likely to occur due to lateral extrusion than general shear. The estimated undrained strength ratio of the slimes-rich layers required to develop the displacements necessary to trigger liquefaction due to the lateral extrusion mechanism is approximately 0.14. It is of interest to note that our estimate of the large-strain strength of the slimes-rich layers at the 2005 Baia 4 failure at Germano Dam was also approximately 0.14 (see Appendix C).

No Slimes

A final analysis was completed to identify how the response of the dam would differ in the absence of slimes, for comparison with the previous analyses. Within this model, this scenario was treated simply by assuming that all regions previously modeled as slimes were actually sand. This approach does not account for the fact that the phreatic surface within this portion of the dam is also likely to have been lower if slimes did not exist here.

The results of this analysis shown on Figure I3-35 and Figure I3-36 illustrate how the response of the dam would be similar to that discussed earlier for the base case NorSand analysis if slimes did not exist within the left abutment region. As a result, the mobilized instability ratio of the model without slimes included in the left abutment would be in the order of 0.5, insufficient to trigger liquefaction.

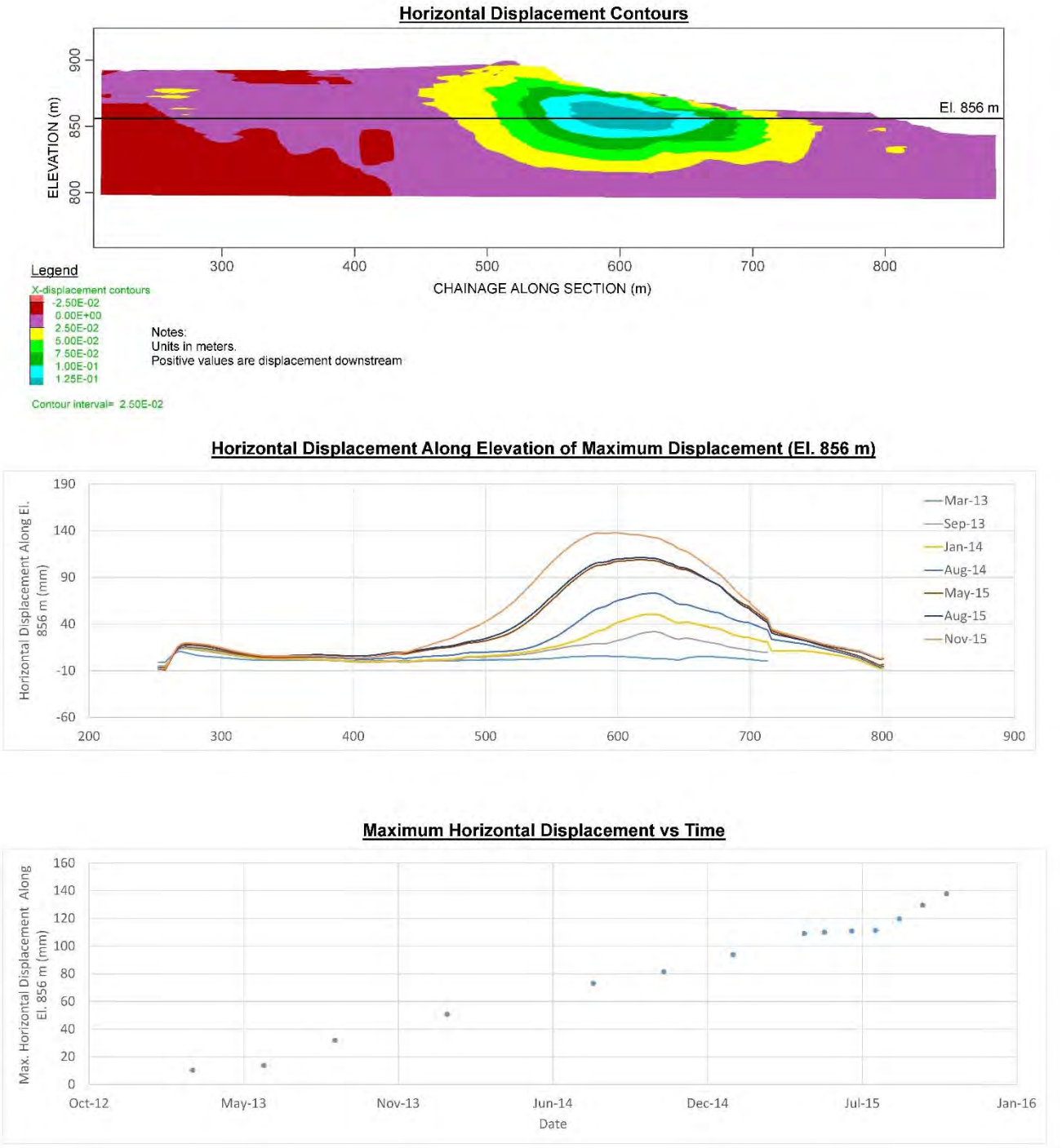

Figure I3-35 Horizontal displacement results – no slimes model

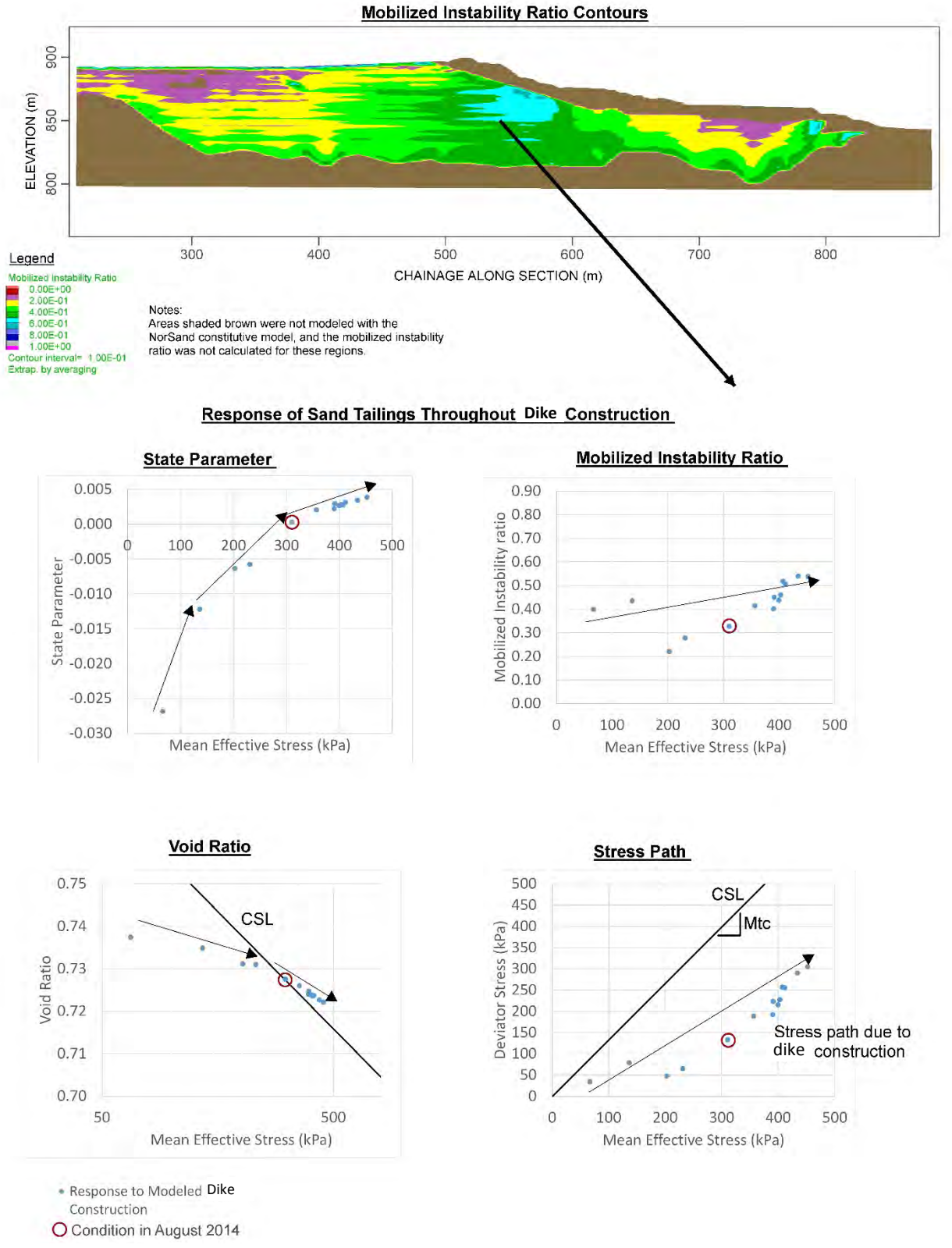

Figure I3-36 Mobilized instability ratio and stress path – no slimes model

I4 SUMMARY

A summary and elaboration of the model results presented throughout this appendix is given below:

- The stress state of the tailings sand overlying the slimes beneath the crest of the left abutment setback can be brought to a condition approaching that at which rapid failure was observed in laboratory tests of that material if a strength of ϕ=9.5° (approximately $s_u/\sigma'v = 0.17$) is assumed for the underlying slimes.
- The stress state is expected to reach the critically unstable condition if the slimes strength reduces to ϕ = 8.3° (approximately $s_u/\sigma'v = 0.14$).
- These strengths are within the range of strengths considered plausible for this material based on the 2005 Baia 4 containment dike failure at Germano, but to mobilize these strengths requires an assumption that any slimes layers within the areas of mapped slimes would be laterally continuous.
- The modeled deformations and regions of critically-stressed tailings sand concentrate in the area beneath and downstream of the dam crest, suggesting that this is the region where liquefaction from this mechanism would initiate. Failure initiation in this region of the dam would fit with the description of the November 5, 2015 failure given by eyewitnesses.
- A comparison of conditions required to induce liquefaction due to lateral extrusion of the slimes versus those associated with shear failure of the dam indicate that triggering of liquefaction due to lateral extrusion is a more probable mechanism than triggering due to shear failure.
- If slimes were not present within the region of the left abutment, collapse leading to liquefaction would not have occurred in November, 2015.

ATTACHMENT J1

Ground Motion Time Histories used in Newmark Displacement Analysis

Appendix J: Attachment J1
Ground Motion Time Histories used in Newmark Displacement Analysis

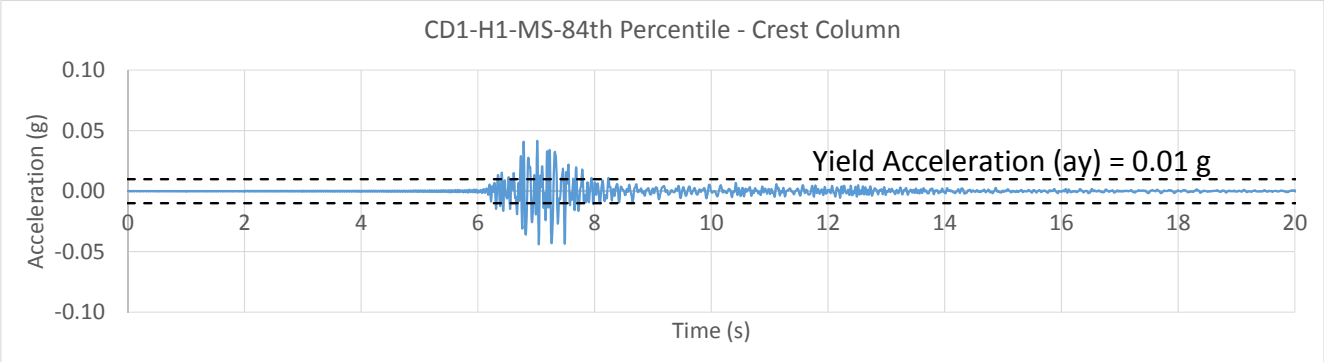

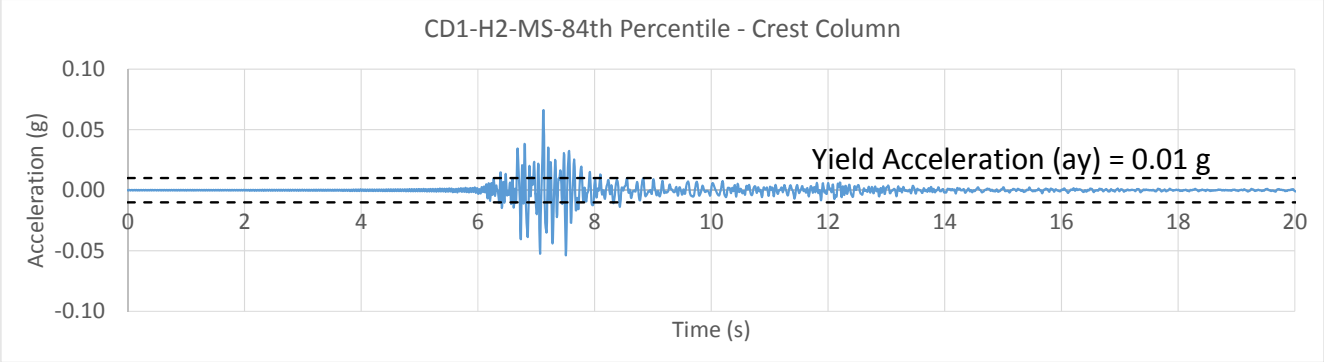

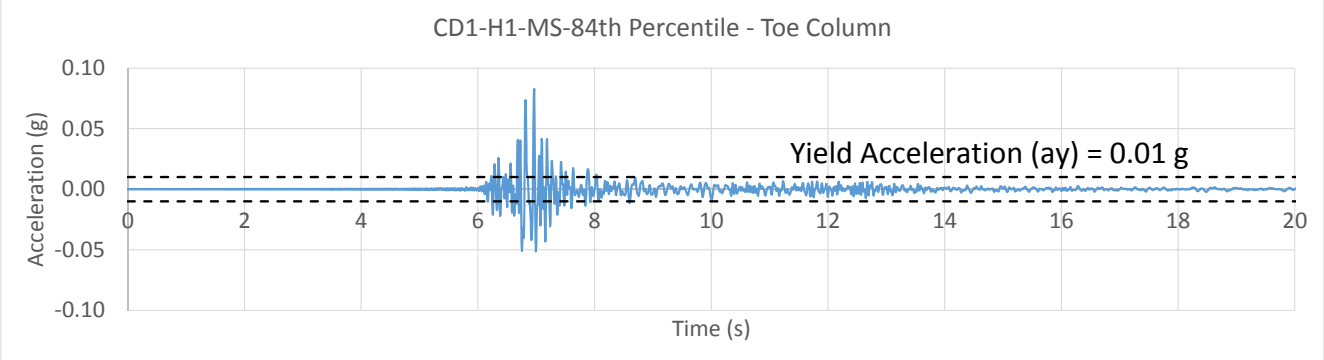

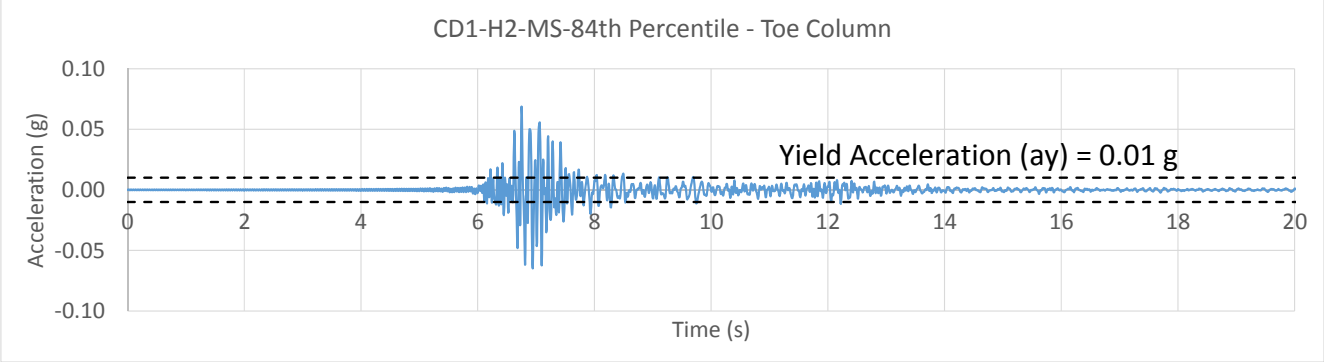
CD1-H2-MS-84th Percentile - Toe Column
Yield Acceleration (ay) = 0.01 g
Acceleration (g)
Time (s)
0.10
0.05
0.00
-0.05
-0.10
0
2
4
6
8
10
12
14
16
18
20

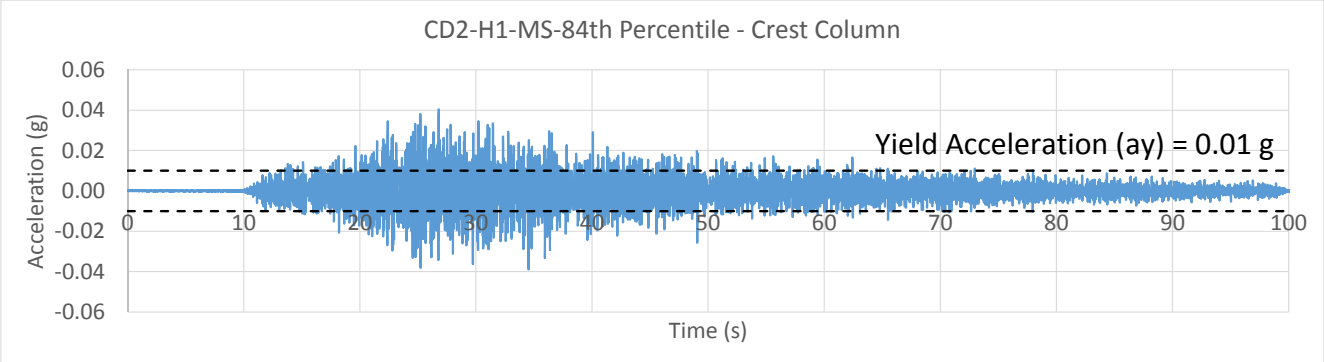
CD2-H1-MS-84th Percentile - Crest Column
Yield Acceleration (ay) = 0.01 g
Acceleration (g)
Time (s)
0.06
0.04
0.02
0.00
-0.02
-0.04
-0.06
0
10
20
30
40
50
60
70
80
90
100

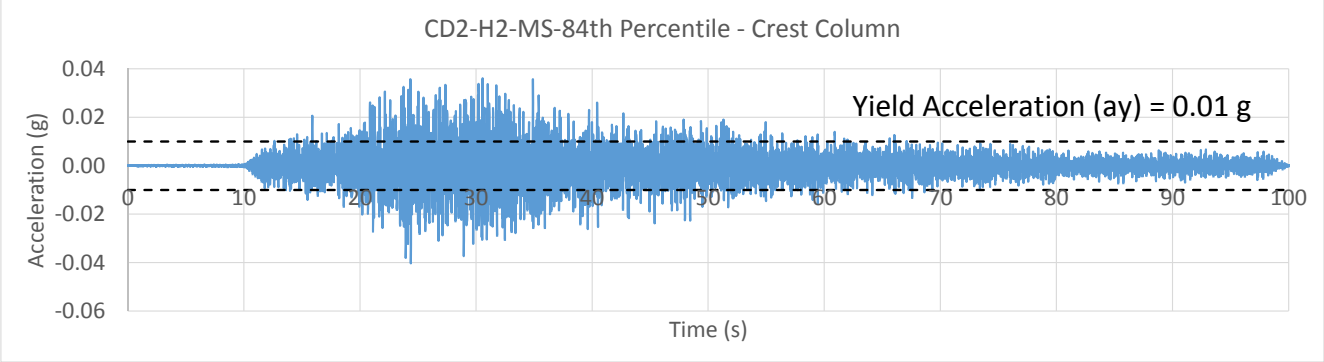
CD2-H2-MS-84th Percentile - Crest Column
Yield Acceleration (ay) = 0.01 g
Acceleration (g)
Time (s)
0.04
0.02
0.00
-0.02
-0.04
-0.06
0
10
20
30
40
50
60
70
80
90
100

APPENDIX J

Dynamic Response Analysis

Appendix J
Dynamic Response Analysis

TABLE OF CONTENTS

List of Tables

List of Figures

TABLE OF CONTENTS

(continued)

List of Attachments

J1 INTRODUCTION

This appendix presents the results of dynamic response analyses of the November 5, 2015 earthquakes at Samarco, using the one-dimensional ground response analysis software SHAKE2000. The November 5, 2015 earthquake time histories were estimated by seismologist Dr. Gail Atkinson (Atkinson 2016) and used as input ground motions in our site response analyses. The analyses were performed at two locations, namely:

1. at the Samarco office site to evaluate potential amplification of ground motions through the weathered rock profile; and
2. at the Fundão Dam site to estimate the likely earthquake-induced shear stresses in the tailings dam profile.

Section J2 summarizes the input earthquake time histories. Section J3 describes the soil models and input data used in our site response analyses. Section J4 presents the results of the SHAKE2000 analyses. Finally, Sections J5 and J6 present the results of assessments to identify whether pore pressures or displacements significant to the triggering of liquefaction could result from the computed ground motions.

J2 EARTHQUAKE TIME HISTORIES

Atkinson (2016) analyzed the ground motions from the November 5, 2015 earthquake sequence near Fundão Dam. The analysis considered data from the following sources:

- seismographic data obtained from the regional Brazilian network (www.rsbr.gov.br);
- felt (intensity) reports of the November 5 earthquakes at the Samarco office site;
- data collected on a local accelerometer that was installed on November 11, 2015 following the dam failure, and
- ground motion data collected to May 20, 2016 on a six-station local broadband array installed by Nanometrics Inc. at the end of April, 2016.

Note that the nearest Brazilian regional seismographic stations that recorded the November 5, 2015 earthquakes near Fundão Dam were more than 150 km away from the dam, hence ground motion prediction equations were used by Atkinson (2016) to estimate the likely ground motions at Samarco.

Atkinson (2016) used the above data to develop a time history of motions that represents those that likely occurred at the Samarco site on November 5, 2015 prior to the dam failure at approximately 15:45 (local time). The time history sequence includes three earthquakes closely spaced in time:

M 2.2 at 14:12:15 (foreshock)
M 2.6 at 14:13:51 (mainshock)
M 1.8 at 14:16:03 (aftershock)

where **M** is moment magnitude, estimated from local magnitudes reported by RSBR, and all times noted are local Brazilian time.

As a result of the ground motions analysis, Atkinson (2016) provided time histories on rock that can be used to evaluate the response of the structures at Samarco due to the November 5, 2015 earthquake. The time histories provided are summarized in Table J2-1.

Table J2-1 Summary of time histories provided for analysis by Atkinson (2016)

Time History Sequence Name	Confidence Interval	Events Represented	Directional Components	NEHRP Site Classification
BC1 (18 individual event time histories)	Median	Mainshock Foreshock Aftershock	2 x Horizontal (H1 & H2) 1 x Vertical (V)	B/C – v_{s30} = 760 m/s
	84th Percentile	Mainshock Foreshock Aftershock	2 x Horizontal (H1 & H2) 1 x Vertical (V)	
BC2 (6 time histories)	Median	Composite	2 x Horizontal (H1 & H2) 1 x Vertical (V)	
	84th Percentile	Composite	2 x Horizontal (H1 & H2) 1 x Vertical (V)	

The time histories were provided for three directional components, i.e. two horizontal and a vertical, and for a reference NEHRP B/C site condition (soft rock) with near-surface average shear wave velocity, v_{s30}, of 760 m/s. Since the v_{s30} values of the weathered rock at Samarco are lower, at about 340 m/s to 400 m/s based on Multichannel Analysis of Surface Waves (MASW) measurements (Appendix C), which corresponds to NEHRP site class C/D (stiff soil), Atkinson (2016) proposes an amplification factor of 1.4 (multiplication factor) to convert the site class B/C ground motions to site class C/D ground motions.

To account for both aleatory and epistemic uncertainties, Atkinson (2016) used a factor of 3.2 times the median (50th percentile) ground motions to obtain the 84th percentile confidence-level (mean plus one standard deviation) ground motions.

Figure J2-1 shows the two sets of median-level time histories provided by Atkinson (2016). The BC1 time histories contained the estimated foreshock, mainshock and aftershock sequence of November 5, 2015, whereas the alternative BC2 time histories were scaled up from a M3 earthquake that occurred about 70 km west of Samarco on May 2, 2016, and was recorded on the Nanometrics local array. Note the very long duration of the BC2 ground motion due to its original recording at 70 km distance from Samarco. As noted by Atkinson (2016), the BC2 time history sequence was intended to represent a composite of the foreshock-mainshock-aftershock events of November 5. Even so, the duration of the BC2 record is expected to be longer than the combined duration expected of the November 5, 2015 earthquake sequence.

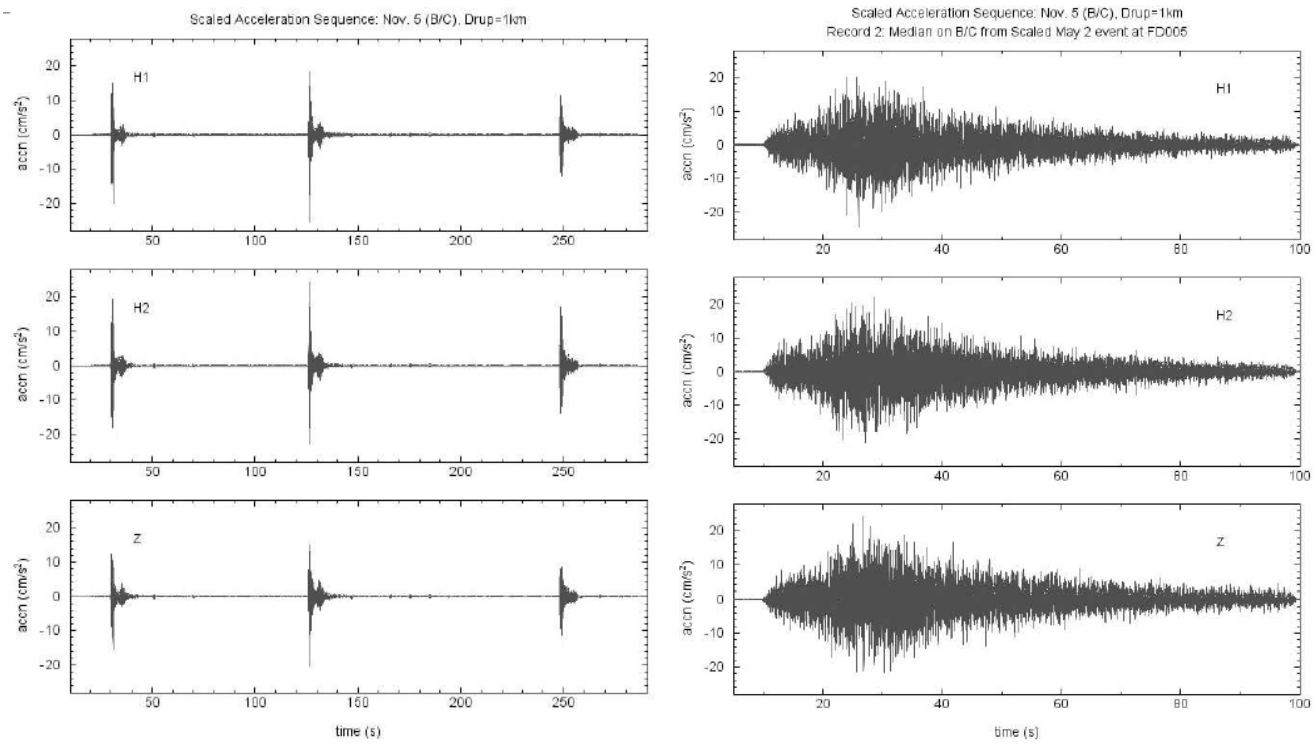

Figure J2-1 Estimated time histories of November 5, 2015 earthquakes from Atkinson (2016). (BC1 median-level motions on left; BC2 median-level motions on right)

Table J2-2 summarizes the peak ground acceleration (PGA) values of the two sets of records, i.e. BC1 and alternative BC2, for both median-level and 84th percentile horizontal ground motions, as well as the corresponding ground motions for C/D site conditions using the amplification factor of 1.4 proposed by Atkinson (2016). Note: only the horizontal component time histories are used in the dynamic response analyses.

Table J2-2 PGA values in bedrock of estimated November 5, 2015 time histories at Samarco

Horizontal Components	M_w used in Scaling by Atkinson (2016)	B/C PGA (%g) Median	Equivalent C/D PGA (%g) Median	B/C PGA (%g) 84th %	Equivalent C/D PGA (%g) 84th %
BC1-H1 Foreshock	2.2	2.0	2.8	8.4	9.0
BC1-H2 Foreshock	2.2	1.9	2.7	6.1	8.5
BC1-H1 Mainshock	2.5	2.5	3.5	8.0	11.2
BC1-H2 Mainshock	2.5	2.4	3.4	7.7	10.8
BC1-H1 Aftershock	1.8	1.2	1.7	3.8	5.4
BC1-H2 Aftershock	1.8	1.7	2.4	5.4	7.6
BC2-East	2.5	2.4	3.4	7.9	11.1
BC2-North	2.5	2.2	3.1	7.1	9.9

Figure J2-2 shows the response spectra of the BC1 (mainshock) and alternative BC2 median ground motions, for both horizontal components. As shown, the BC2 records are generally larger in amplitudes across most of the periods of interest (or frequencies) than the BC1 records.

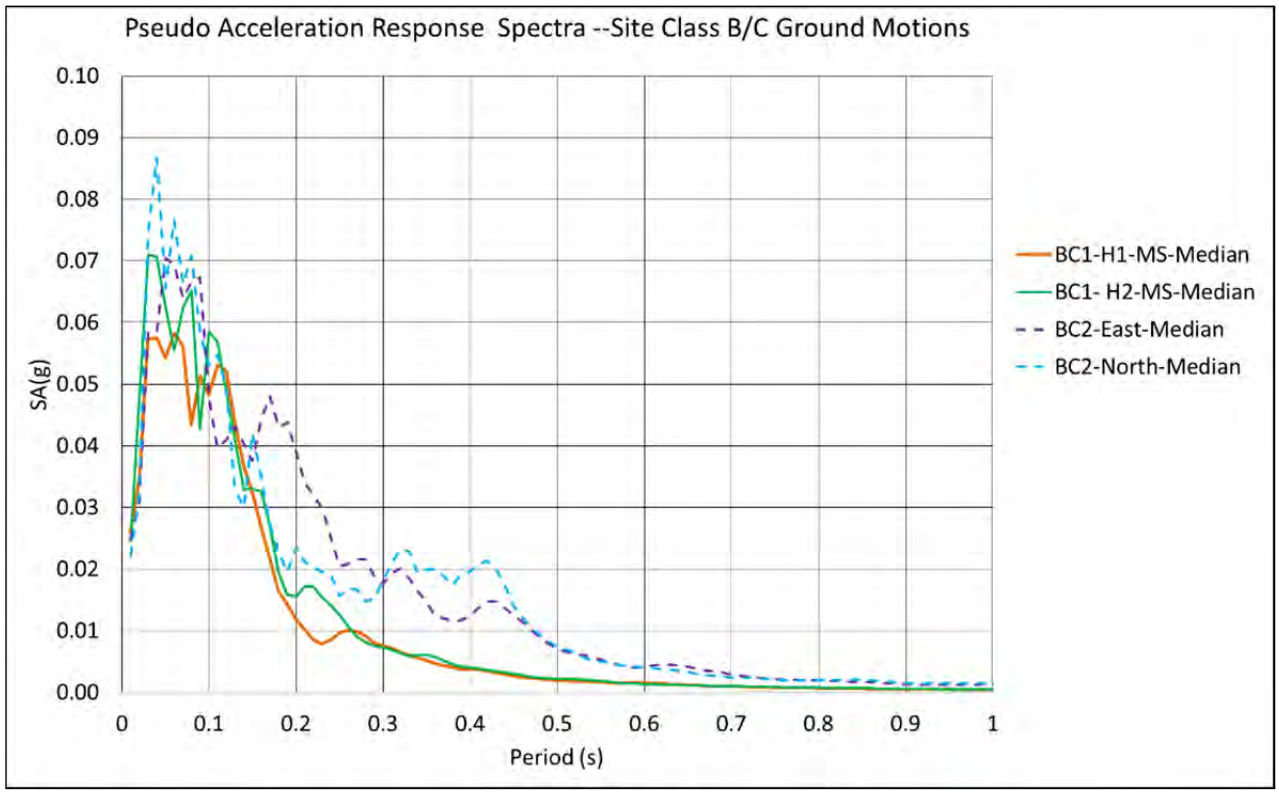

Figure J2-2 Response spectra of BC1 (mainshock) and BC2 ground motions provided by Atkinson (2016)

J3 MODEL AND INPUT DATA FOR SITE RESPONSE ANALYSIS

J3.1 General

We used the computer program SHAKE2000 to perform one-dimensional equivalent-linear site response analyses at the following two sites in Samarco:

1. weathered rock profile at Samarco office site.
2. tailings dam profiles at Fundão Dam site.

Figure J3-1 shows the plan locations of these two sites.

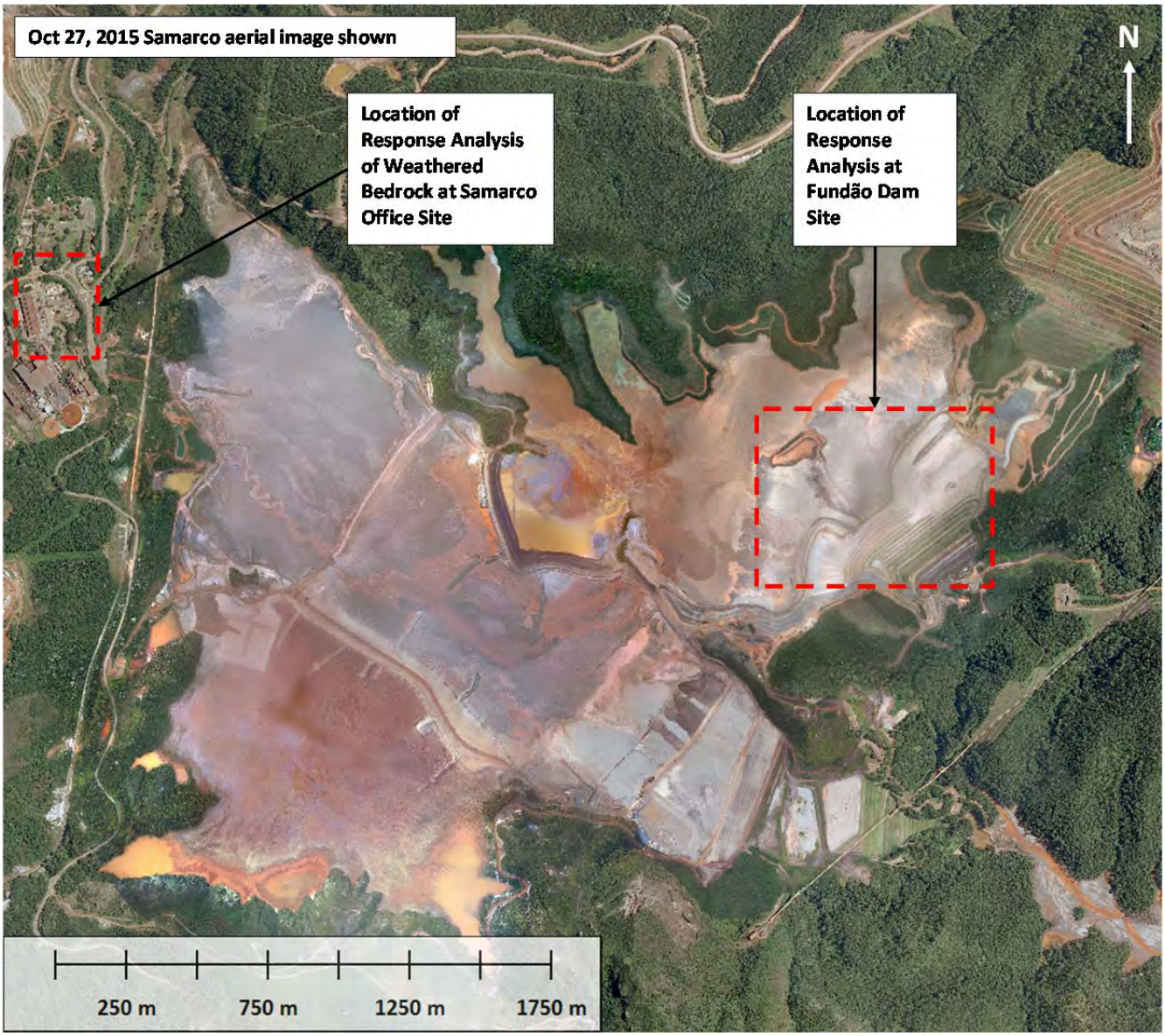

Figure J3-1 Aerial image showing locations of Samarco office and Fundão Dam

The key inputs needed for one-dimensional dynamic response analysis of a site profile, or "soil column", in addition to the input earthquake time histories, are:

- shear wave velocity profile of the ground; and
- shear modulus and damping variations with shear strain.

These input data for SHAKE2000 analyses are described in the following subsections.

J3.2 Shear Wave Velocity

Figure J3-2 shows our estimated shear wave velocity (v_s) profile for the residual soil/weathered phyllite rock at the Samarco office. The v_s profile was estimated based on v_s measurements in the top 36 m depth from a geophysical survey (MASW survey conducted by AFC Geofisica Ltda., see June, 2016 report in Appendix C Attachment C3) and extrapolated to 180 m depth by gradually increasing v_s to a value of 760 m/s, based on a typical weathered rock profile in California for which extensive v_s measurements were available. The v_s value of 760 m/s at the base of the model corresponds to site class B/C soft rock conditions, for which the November 5, 2015 earthquake ground motions were developed by Atkinson (2016). The v_s value of the top 30 m (v_{s30}) of the weathered rock profile is about 350 m/s, which corresponds to site class C/D stiff soil condition near the surface.

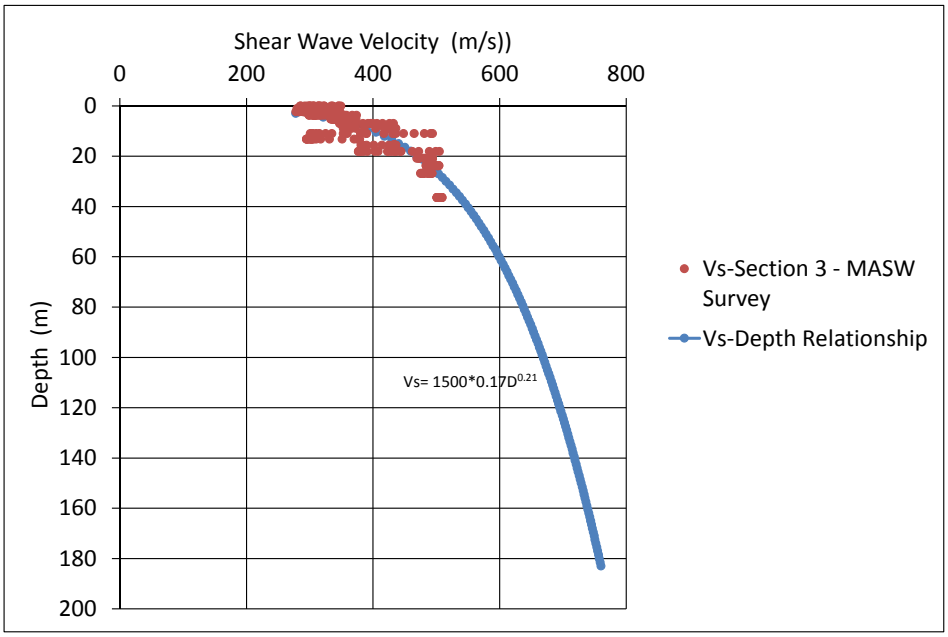

Figure J3-2 Shear wave velocity data in weathered phyllite at Samarco office site

At the Fundão tailings dam, we modeled a typical soil profile at the crest of the dam and one at the toe. Figure J3-3 illustrates these two soil columns relative to a cross-section of the dam. The crest soil column is 88 m deep, consisting of a surface layer of compacted sand, overlying uncompacted tailings sands and slimes. The toe soil column is 17 m deep and comprises compacted sand overlying only sand tailings. Both soil columns overlie weathered phyllite (C/D soft rock condition) at the original ground surface.

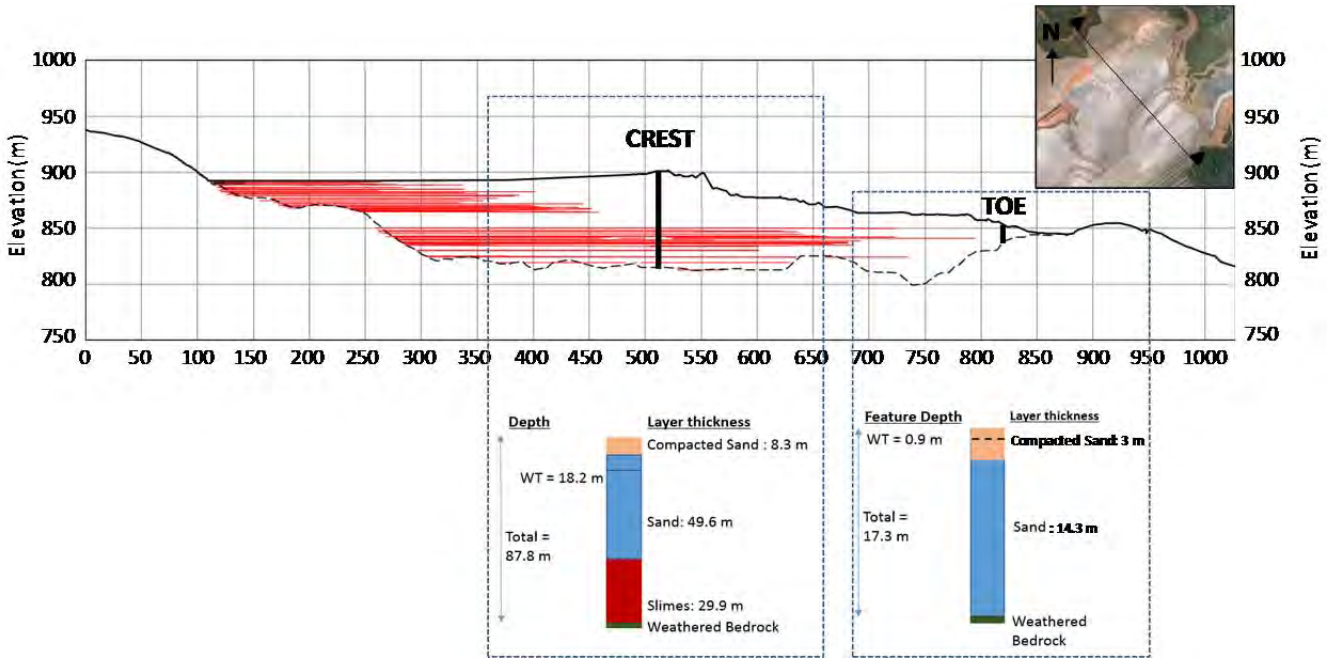

Figure J3-3 Selected soil columns at Fundão Dam for 1D site response analysis

For characterizing the tailings, we compiled the v_s data measured by Fugro in 2015 at Fundão (see Appendix C), and recent measurements carried out by ConeTec (see Appendix C, Attachment C2) at the Germano Dam and Germano Pit Dam tailings sites. Figure J3-4 shows the compiled v_s data from various test locations at Fundão and Germano, and the average v_s trend line used to characterize the tailings deposit for our dynamic response analyses. Note the narrow band of data from the various sets of v_s measurements in the tailings at Samarco.

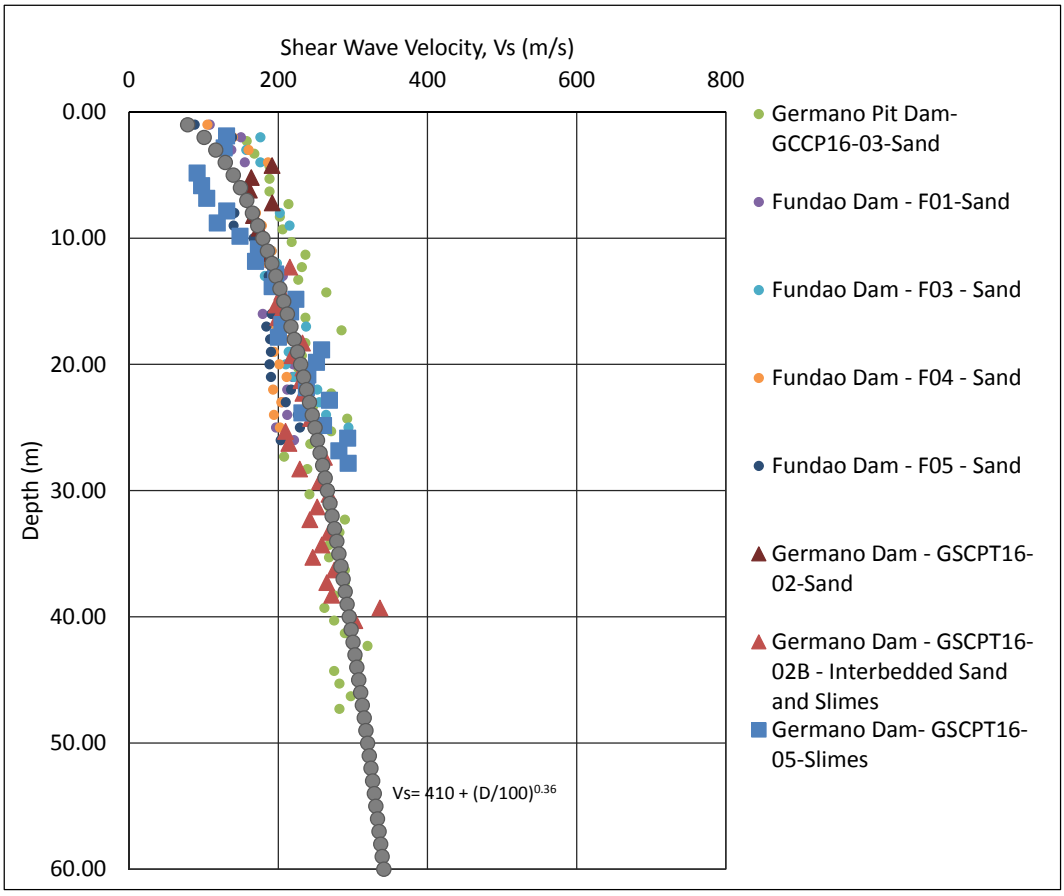

Figure J3-4 Shear wave velocity data in tailings at Fundão and Germano

An average v_s of 265 m/s was estimated for the compacted tailings sand at the crest, based on measurements in test hole GSCPT16-06 by ConeTec (Appendix C, Attachment C2) at the Germano Buttress, as shown on Figure J3-5. For the residual soil/soft rock that underlies the tailings deposit, an average v_s of 400 m/s was estimated based on measurements in GSCPT16-03 by ConeTec (Appendix C, Attachment C2) at the Germano Pit Dam.

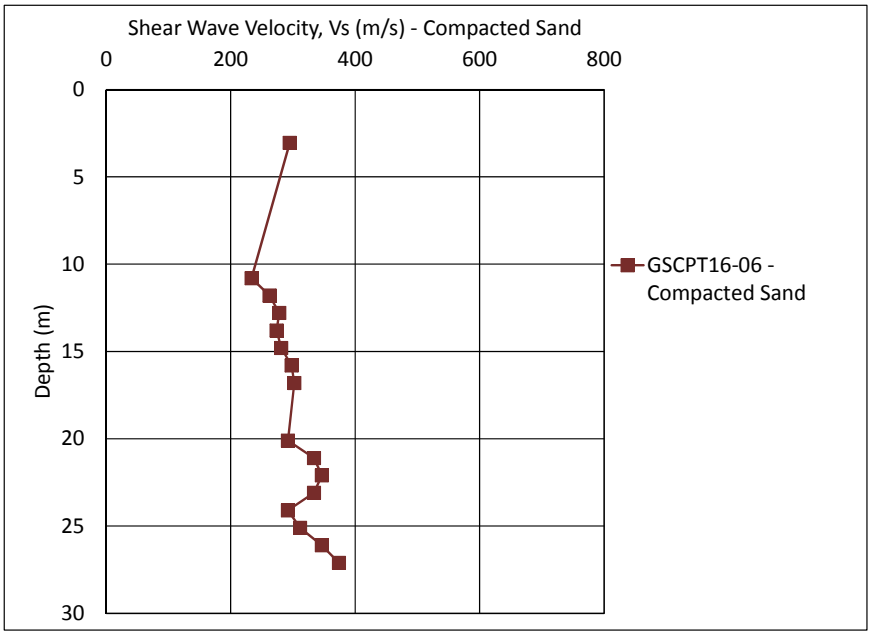

Figure J3-5 Shear wave velocity data in compacted sand

Figure J3-6 shows the three soil columns and corresponding input shear wave velocity profiles used in our dynamic response analyses.

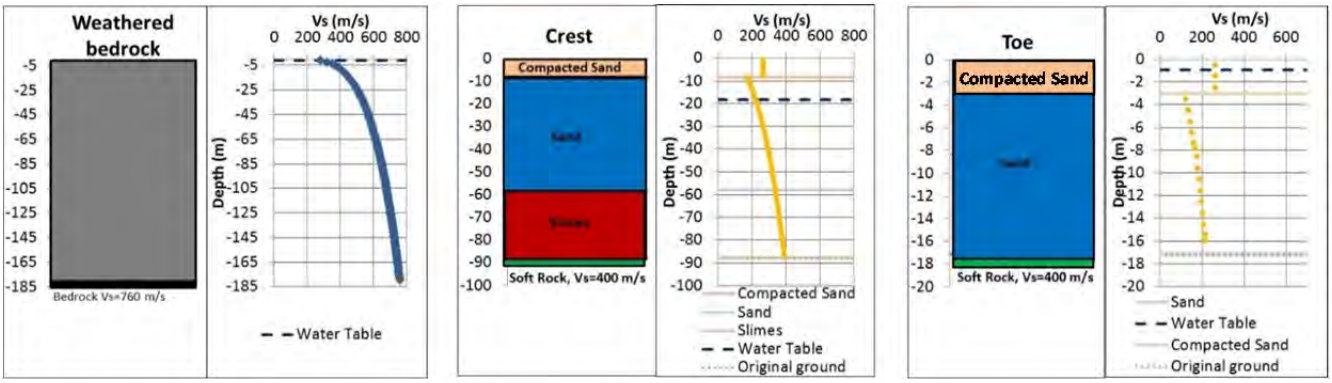

Figure J3-6 Three soil columns used in SHAKE2000 analyses

J3.3 Modulus Reduction and Damping

The shear modulus reduction and damping curves used in the dynamic response analyses are shown on Figure J3-7 for tailings sands, slimes and weathered rock. These curves were adopted based on the following data sources:

- For tailings sands, relationships proposed by Winckler et al. (2014) that vary with effective stress and are based on laboratory test data on tailings.

- For tailings slimes, with measured plasticity index values between about 7 and 11, relationships proposed by Vucetic and Dobry (1991).
- For weathered rock, relationships proposed by Silva et al. (1997).

A total unit weight of 22 kN/m^3 was used for all tailings and soft rock in the dynamic response analyses.

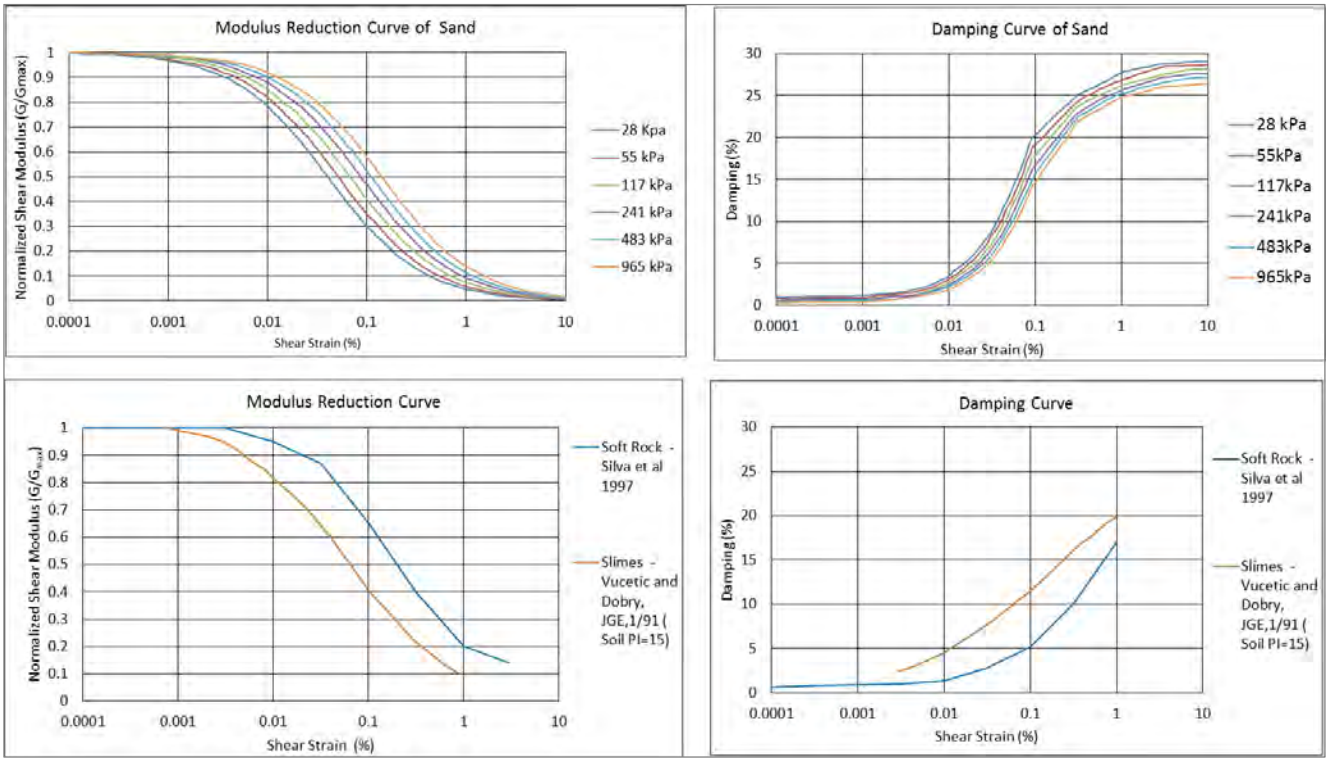

Figure J3-7 Modulus reduction and damping curves for tailings sands, slimes and soft rock

J4 RESULTS OF SITE RESPONSE ANALYSES

J4.1 Weathered Rock Profile at Samarco Office Site

We used the two horizontal components of the BC1 median-level and BC1 84th percentile mainshock records as "outcrop" input ground motions in the site response analyses of the weathered rock profile at the Samarco office site, in order to evaluate potential site amplification. Figure J4-1 shows the depth profiles of the computed PGAs from the SHAKE2000 analyses of the November 5, 2015 mainshock ground motions. The results indicate some amplification in PGAs in the top 10 m to 20 m of the ground profile. The maximum shear strains generated in the ground vary between approximately 0.0002% and 0.0007%.

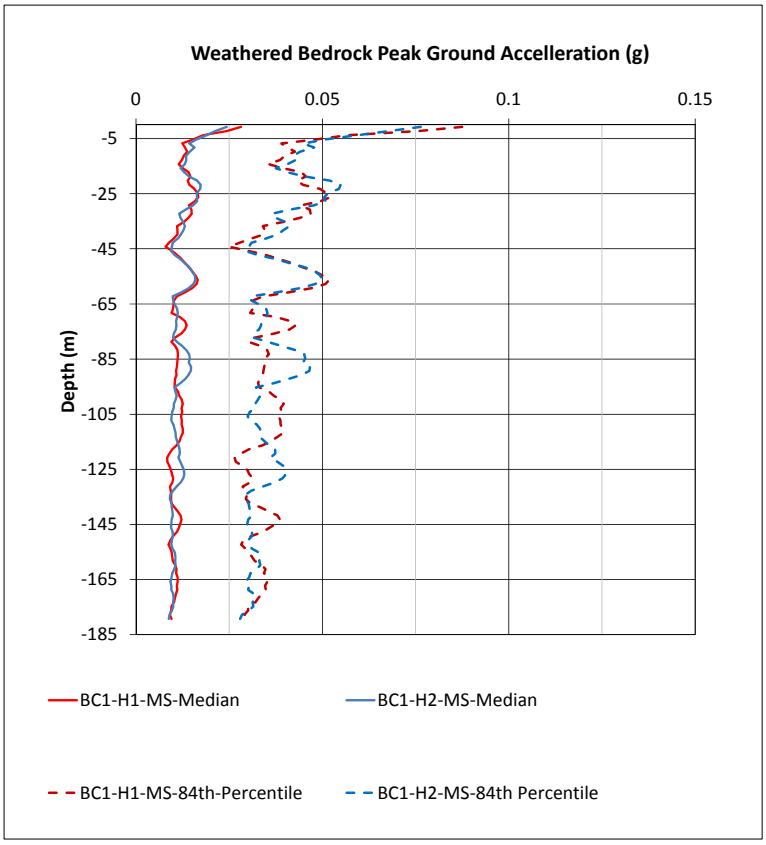

Figure J4-1 Computed peak accelerations from SHAKE2000 analyses of weathered rock column

Figure J4-2 compares the response spectra of the input BC1 ground motions and the output or computed motions at ground surface (labeled as "-surface layer 1" on Figure J4-2) from the site response analyses, for both median and 84th percentile mainshock events. Note the site period of the 180 m deep soft rock column computed from the SHAKE2000 analyses is approximately 1.14 sec.

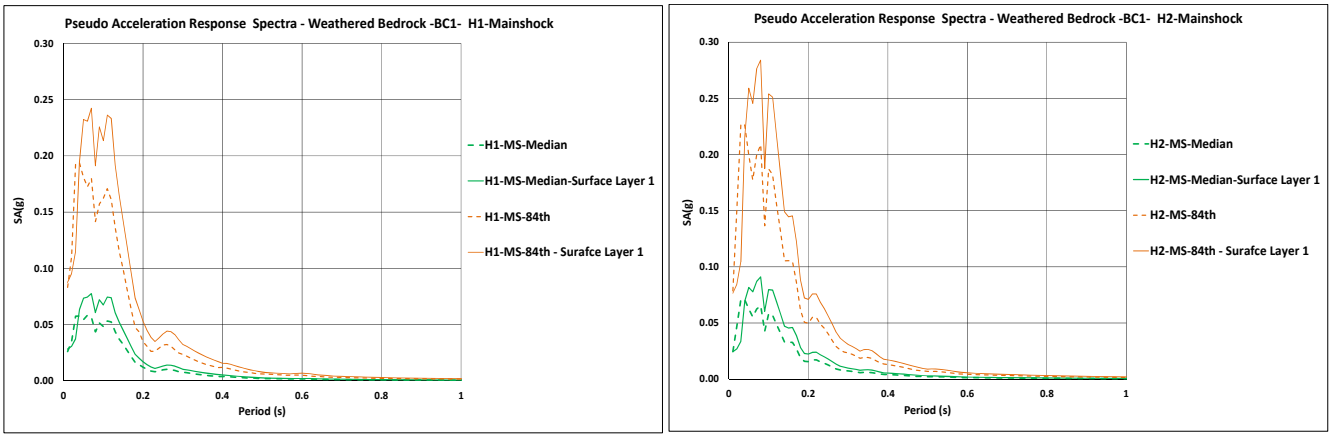

Figure J4-2 Comparison of output and input response spectra from SHAKE2000 analyses

Table J4-1 summarizes the range in amplification factors, defined as the ratio of the output motion (i.e. computed surface response spectrum) to input motion (i.e. BC1 response spectrum), across all periods for the two horizontal components (H1 and H2) of the mainshock. As shown in Table J4-1, the SHAKE2000 results compare well with Atkinson's proposed amplification factor of 1.4 to convert site class B/C ground motions to site class C/D ground motions.

Table J4-1 Computed amplification factors from SHAKE analyses

	Ratio of Output to Input Motion Response Spectra		
	Minimum	Median	Maximum
BC1-H1 Median	0.83	1.25	1.59
BC1-H2 Median	0.90	1.25	1.67
BC1-H1 84th Percentile	0.97	1.34	1.64
BC1-H2 84th Percentile	0.96	1.28	1.50

Sensitivity analyses were performed with different modulus reduction and damping curves, and the results were very similar to the above. The B/C ground motions amplified by a factor of 1.4 were carried forward into the dynamic response analyses of the Fundão Dam. The amplified versions of the BC1 and BC2 time history sequences are termed CD1 and CD2, respectively.

J4.2 Tailings Dam Profiles at Fundão Dam Site

We used the two horizontal components of the CD1 median-level and CD1 84th percentile records as "outcrop" input ground motions in the site response analyses of both the crest and toe soil columns at Fundão Dam. Figure J4-3 presents the results of the SHAKE2000 analyses for the CD1 mainshock analyses of the crest and toe soil columns. The figure shows the input v_s profile, computed PGA, maximum shear stresses, and cyclic stress ratios (CSR), defined as 0.65 times maximum shear stress divided by vertical effective stress at the depth of interest. The site period of the 88 m deep crest soil column is 1.15 sec, and the site period of the 17 m deep toe soil column is 0.42 sec.

The maximum shear strains developed in the mainshock analyses of the crest soil column vary from 0.0005% to 0.002% for the median motions and from 0.002% to 0.011% for the 84th percentile motions. At the toe soil column, the maximum shear strains vary from 0.002% to 0.009% for median motions and from 0.005% to 0.034% for 84th percentile motions.

As shown on Figure J4-3 for the crest soil column, the estimated CSR in the sand near the top of the slimes deposit at 58 m depth is about 0.0014 for the median ground motion and 0.004 for the 84th percentile ground motion. The estimated number of equivalent uniform cycles of the irregular shear stress time histories extracted at the sand-slimes interface is about 6 to 8. This information was used for the laboratory cyclic testing described in Appendix D, and discussed further in Section J5.

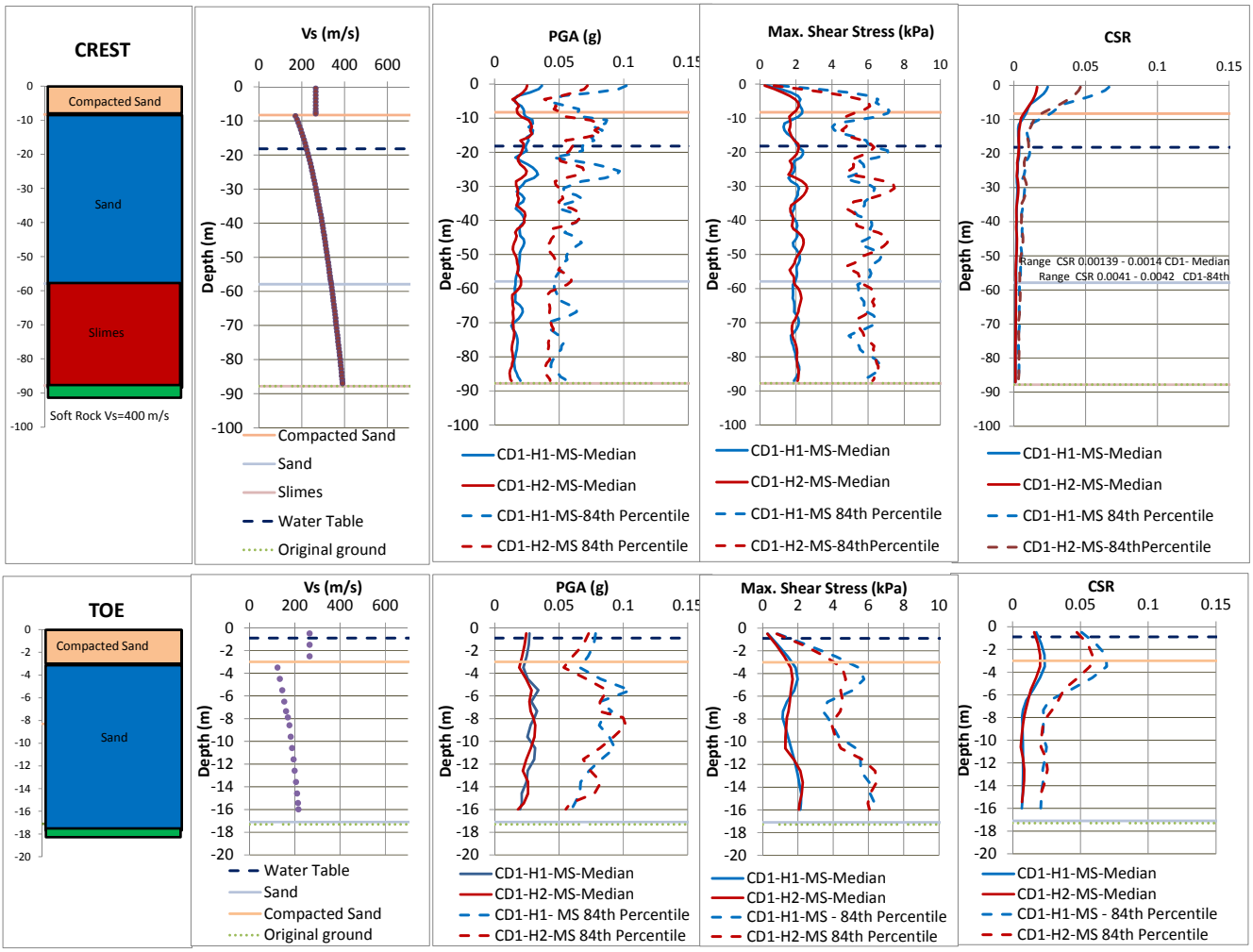

Figure J4-3 Results of SHAKE analyses for crest and toe soil columns at Fundão Dam

For the crest and toe soil columns at Fundão Dam, we also ran SHAKE2000 analyses using the alternative CD2 input ground motions. The cyclic stress ratios induced by the CD2 time histories are compared to those from the CD1 time histories on Figure J4-4, for both median and 84th percentile horizontal ground motions. In general, the higher-amplitude alternative CD2 ground motions generated CSRs about 40% higher than those of the CD1 ground motions. Also, the earthquake-induced cyclic stresses at the toe soil column are higher than at the crest soil column, due to amplification of ground motions.

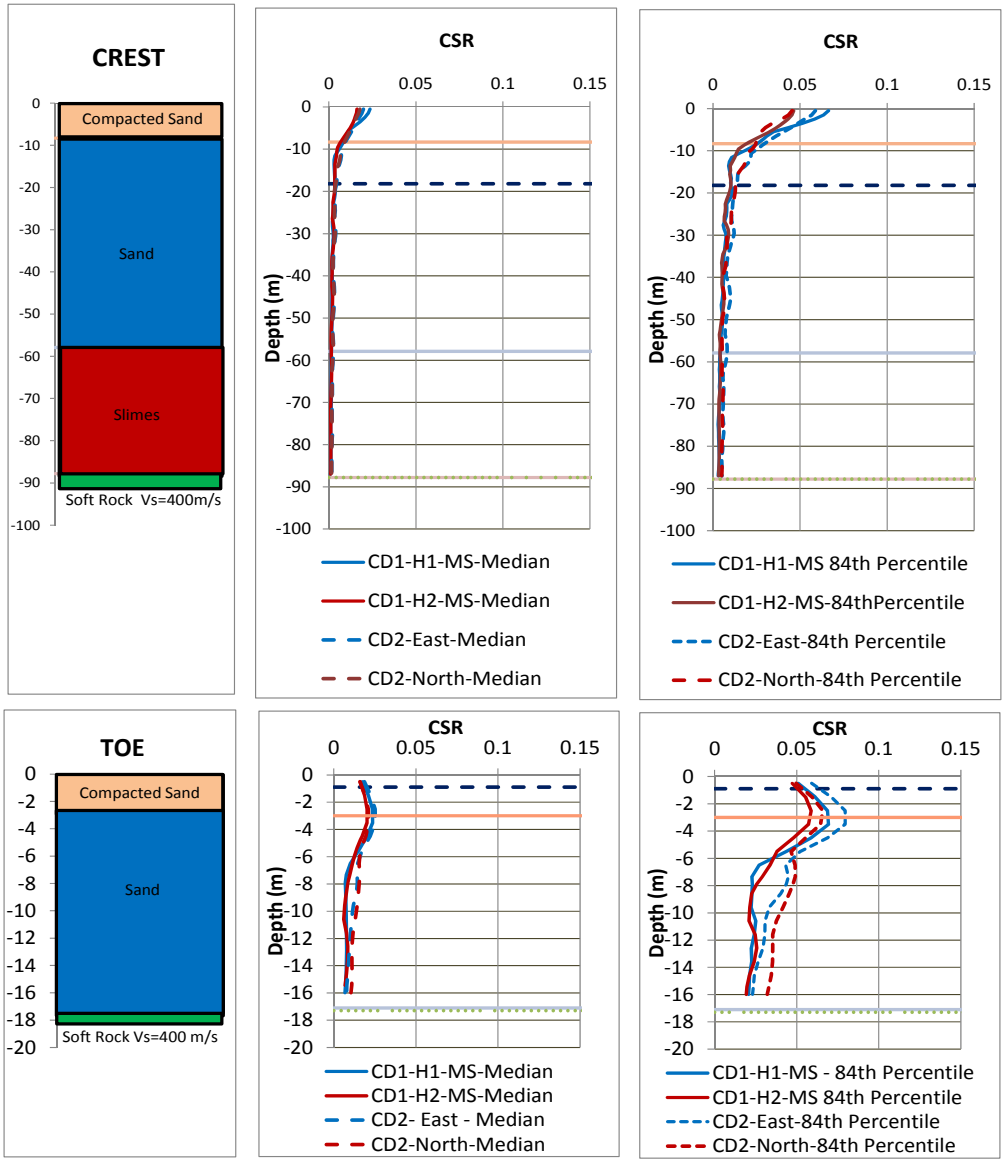

Figure J4-4 Comparison of cyclic stress ratios induced by CD1 and CD2 ground motions

J5 CYCLIC LIQUEFACTION TRIGGERING

The calculated ground motions are not sufficient to trigger seismic liquefaction under ordinary conditions; however, in light of the collapse behavior observed in the laboratory tests (see Appendix D), and the likelihood of similar stress conditions having developed in the field (see Appendix I), it was deemed necessary to assess whether these motions could induce collapse in an already fragile sample. This was investigated by completing an additional stress controlled extrusion collapse triaxial test. In this test (TX-31), a very loose sample (ψ=+0.05) was brought to a condition of incipient failure, identified by the axial strain response to an increment of unloading, before closing the drainage valves and then subjecting the sample to cyclic loading. We intended to apply the CSR

calculated at the sand/slimes interface beneath the crest, since that is the region of the dam cross section where the lateral extrusion mechanism would initiate static liquefaction. The cyclic loading calculated for the sand slimes interface beneath the crest is a CSR of 0.001 to 0.004. It was not practical to apply such a low load in the laboratory testing; therefore, a CSR of 0.01 was applied. The sample did not fail under this load after applying 525 cycles. The load was increased to a CSR of 0.02 and cycled for a further 521 cycles. The sample still did not fail, so the CSR was increased to 0.03 and the sample failed after a further 209 cycles. Very little pore pressure was developed during the cyclic loading. This shows that the loading from the earthquake would be insufficient to induce liquefaction in even a very fragile sample. The results from this test are shown on Figure J5-1 and Figure J5-2. Refer to the cyclic direct simple shear tests shown in Appendix D for further examples of the insignificant effect that this level of shaking would have on pore pressure development in other samples of sand tested along an alternate stress path.

The higher cyclic loads calculated close to the surface occur (Figure J4-3) in compacted material that would not be susceptible to liquefaction.

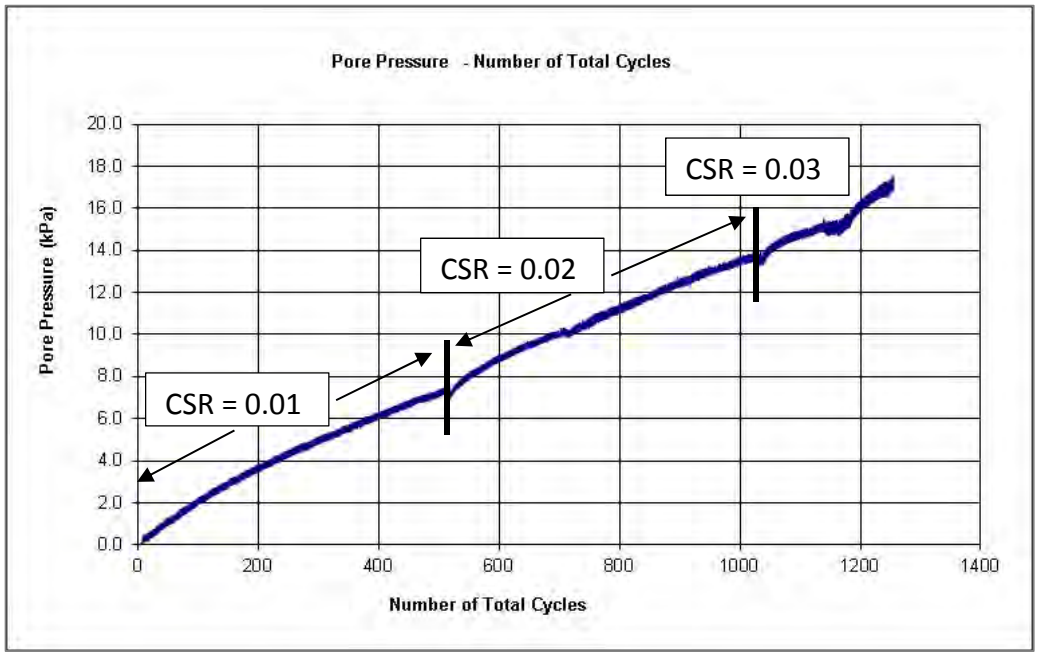

Figure J5-1 Pore pressure development in laboratory test following lateral extrusion mechanism and then cyclic loading (test ID TX-31) – very loose sample (ψ=+0.05)

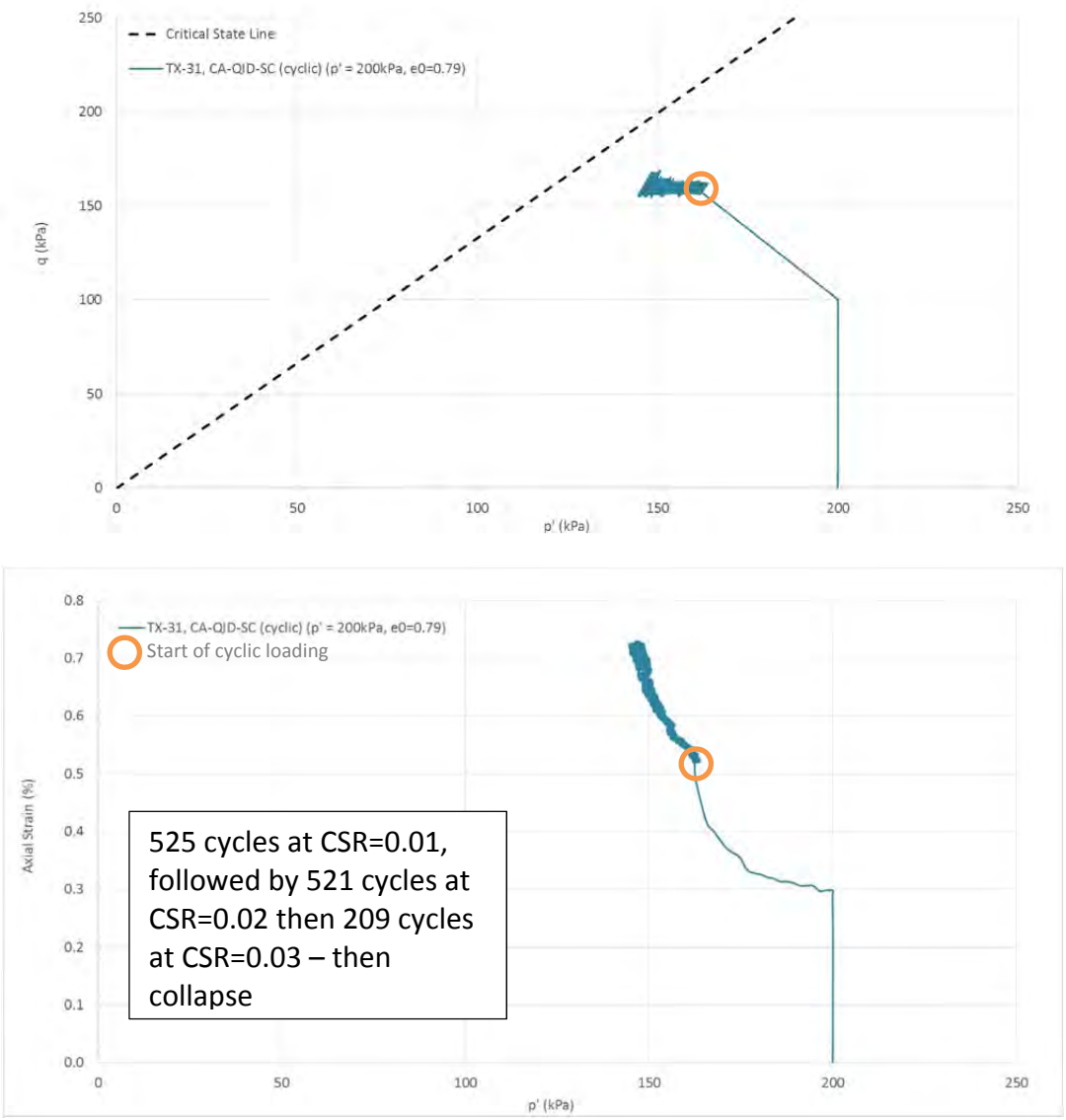

Figure J5-2 Laboratory test following lateral extrusion mechanism and then cyclic loading (test ID TX-31) – very loose sample (ψ=+0.05)

J6 SEISMIC DISPLACEMENTS

Having established that the seismic loading on November 5, 2015 would be insufficient to trigger liquefaction through development of cyclic pore pressure, an analysis was completed to identify whether the seismic loading could have contributed to the lateral extrusion triggering mechanism by generating lateral displacements. We assessed this by completing Newmark-type displacement calculations using acceleration time histories extracted from the sand/slimes interface in the SHAKE2000 models. The displacement calculations were made using the software SLAMMER.

The displacement calculations involve the identification of a seismic yield acceleration (ay) from limit equilibrium analyses. The calculation within SLAMMER then identifies portions of the acceleration time histories that exceed the yield acceleration. The displacements are then calculated by double integration of the accelerations > ay, and then summation of the displacements resulting from the integration.

The yield acceleration was calculated in this analysis for the cross section used in the deformation and stability analyses (Section 01 - see Appendices H and I) assuming that the dam was on the verge of collapse due to lateral extrusion. Consistent with this assumption, an $s_u/\sigma'v$ strength ratio of 0.14 was used in the calculations because this is the mobilized strength necessary to initiate liquefaction due to lateral extrusion (see Appendix I). The ay value calculated in this analysis was 0.01 g.

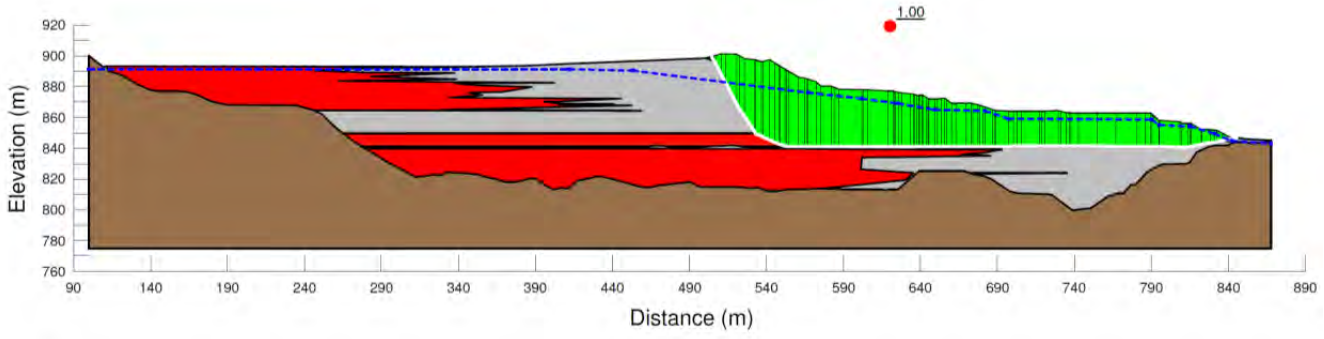

Strengths: Slimes-Rich Layers = $s_u/\sigma'v$ (0.13); Sand = ϕ' = 33°; Compacted Sand = ϕ' = 35° & c' = 5 kPa
Horizontal seismic coefficient = 0.01 g

Figure J6-1 Calculation of yield acceleration for Newmark-type displacement analysis

The displacement analyses were run using the 84th percentile time histories in order to understand the upper-bound of potential displacements. Analyses were run for both the crest and toe columns, and using both the CD1 and CD2 time history sequences. For the CD1 time history sequence, the displacements were calculated as the sum of those from the foreshock, mainshock and aftershock.

The results shown on Figure J6-2 indicate small displacements, ranging from 2 mm to 8 mm, with an average of 5 mm.

Time histories extracted from the SHAKE2000 models, used in this analysis, are shown in Attachment J1.

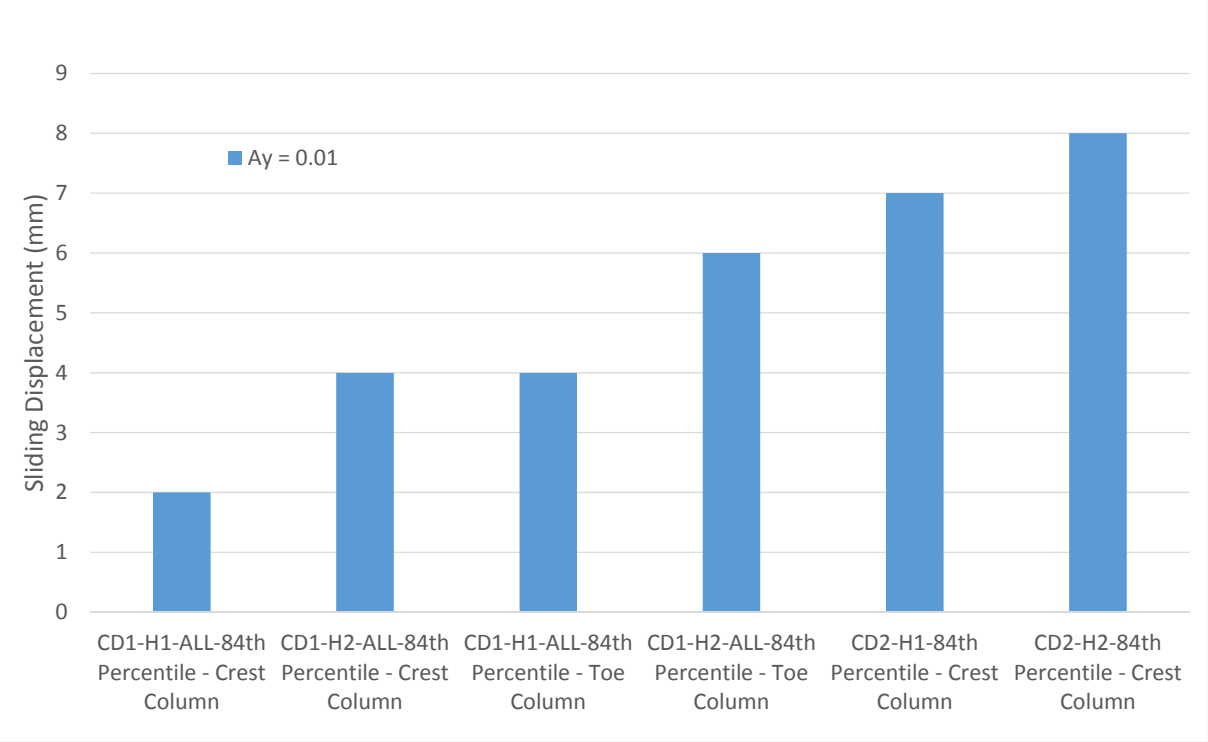

Figure J6-2 Estimated displacements

ATTACHMENT K1

Solution Cavities Report by TÜV SÜD

GEOLOGIC CONTEXT AND SOLUTION CAVITY ASSESSMENT IN FUNDÃO DAM AND SURROUNDINGS

EXECUTIVE SUMMARY

Among the possible triggers of the Fundão Dam failure, in Germano Mine, the Expert Panel investigated the possibility of cavity collapse.

GEOLOGIC CONTEXT

The Germano Mine is located in the southeastern portion of the Iron Quadrangle, which constitutes an approximately quadrangular geomorphologic unit defined by the occurrence of Archean to Paleoproterozoic supracrustal rocks arranged in megafolds over an Archean crystalline shield (Cornejo & Bartorelli, 2009).

The Iron Quadrangle's geometry is defined by an array of megafolds, curtailed by a system of thrust faults (Baltazar et al., 2005). These folds are mostly sustained by the metasediments from the Minas Supergroup.

The entire stratigraphy of the Minas Supergroup is present on the Santa Rita syncline, where the mine is located, but some of the groups are mapped as undivided in regional approaches.

Within a regional scale, the Germano Mine is located in the southern central portion of the syncline, and comprises mostly rocks from the Itabira, Piracicaba and Sabará Groups, discordantly overlain by the sedimentary package of the Itacolomi Group. Archean rocks, belonging to the crystalline basement and of the Rio das Velhas Supergroup, are restricted to the east of the area, separated from the paleoproterozoic sequence by the Fundão-Cambotas shear system.

The extracting activities have generally affected the banded iron formations of the Cauê Formation, part of the Itabira Group, which is commonly capped by iron-rich lateritic crusts (ferricrete). Most supplementary structures, however, including the tailing dams, were erected on top of rocks associated to three stratigraphic groups: the Piracicaba Group, the Sabará Group, and the Itacolomi Group.

The studied area around the Fundão Dam is dominated by the presence of phyllites, either associated to the Sabará Formation or to a complex intercalation of the Piracicaba Group. Its mineralogy is mostly sericitic with multiple colors, but graphite-rich varieties occur also. The second most relevant lithology is quartzite, which is confined to the southwestern edge of the reservoir of the Germano Dam.

The foliation in the phyllite as the main structural feature of the area. It has a preferential NW-SE orientation, ondulated on occasions and commonly crenulated. It dips moderately to NE with an angle between 30° to 40°.

CAVITIES

According to the National Center for Research and Conservation of Caves (CECAV, 2015), there are 1226 caves in the Iron Quadrangle. Sorting by lithological units, the highest incidence of caves occurs in laterite cover (over 45%), followed by the occurrence in iron formation (about 23%), carbonate rocks (around 12%), and siliciclastic rocks (around 10%).

The Iron Quadrangle Speleologic Unit was originally defined based on the occurrence of some cavities in dolomites in the geological Formations Gandarela and Fecho do Funil. The caverns in the lithologies of the paleoproterozoic units are scarce when compared to those of iron and quartzite formations of the same age. Ferricrete (“canga”) is the lithotype that comprises almost half of all registered karstification events. The cavities occupy the summits regions of the relief, where erosion and dissolution are occasionally combined to form of a single cavity.

The caves originated by dissolution occur frequently in the itabirites of Cauê Formation, under the ferricrete. The morphogenetic process is related to the soluble mineral content and the structure of the itabirites.

The karstification in siliciclastic rocks in the Iron Quadrangle is represented essentially by quartzites.

In the vicinity of Germano Mine there are three mines owned by Vale, Fábrica Nova, Fazendão and Alegria. In the influence area of the expansion of Fábrica Nova Pit were identified 27 natural cavities in iron formations, detritic ferricrete and quartzite, predominately in the contact between itabirite and ferricrete (Sete, 2009).

15 cavities were identified in the influence area of the expansion project of Alegria Mine, inserted, mainly, in ferruginous lithologies, particularly ferricretes and some zones of itabirites of Cauê Formation (Golder, 2012).

The Fazendão Mine's influence area, north of the Fundão Dam, have several cavities already mapped. Many of these cavities occur in quartzitic rocks, among which the Gruta do Centenário, which stands out for being the world's largest in this lithology.

The analysis of the speleological potential was performed using the geological map of CODEMIG (2005). The work was based on the lithotypes present in the area of Fundão and Germano Dams and favorable structural features for the development of natural cavities and geomorphologic features indicative of speleological processes, identified in satellite images.

Thus, Carste (2013-a) defined each lithotypes' speleological potential, divided by class and coverage area. The region where the Fundão Dam is inserted was defined as low speleological potential. No evidence of cavities were identified in the lithotypes of the area.

A consolidated research on the available database revealed 238 cavities within a 5 km radius of the Fundão Dam. It should be noted that only one of the listed cavities has been characterized as developed in phyllitic rocks, located 1 km to the southwest of the Germano Dam reservoir, confirming previous assumptions that this lithotype presents a low speleological potential. This proportion is in accordance with regional data compiled for the entire Vale's area inside Iron Quadrangle, that identified only 57 cavities within phyllites, none of which appears in the 5 km radius of Fundão Dam.

In fact, the strong predominance of phyllitic rocks with low susceptibility for karstic development diagnosed for the area of this structure (Brandt, 2005; Carste, 2013-a; Geoestável, 2013) is reflected in the absence of any known cavities in or around Fundão Dam.

No evidence of cavities was found in drilling boreholes performed on the Fundão Dam and in the speleological studies performed in the neighborhood.

Therefore, the likelihood of cavities in the area where the Fundão Dam was built can be dismissed, thus excluding the possibility of a cavity collapse as a trigger to the dam failure.

1. PREAMBLE

Among the possible triggers of the Fundão Dam failure, the Expert Panel investigated the possibility of cavity collapse.

To accomplish this task, TÜV SÜD has compiled and analyzed information on the geology of the area, results of geological and geotechnical investigation performed that could bring evidences of the existence of cavities, and published literature on the subject. The Brazilian regulatory definition of Karst System was also consulted and is summarized below.

The Normative Ruling (MMA, 2009) of the Ministry of Environment (Ministério do Meio Ambiente, abbreviated MMA) defines Karst System as "set of interdependent elements related to the action of water and its corrosive power in soluble rocks, that give rise to complex drainage systems, comprising cavities, cave systems and other superficial features of these environments, such as sink holes, sumps, dry valleys, rock mass with karren, and other areas of groundwater recharge. This concept includes all forms generated by the association of corrosive water and soluble rocks that result in karst landscape. It is composed of various zones: exokarst, epikarst, and endokarst".

This definition, aligned with the current understanding of the technical-scientific community, deliberately does not includes the type of rock, as it focuses on the importance of the chemical process of dissolution and typified hydrology of a karstic system. Thus, the karst may occur even in rocks that are considered to have poor solubility, provided that the chemical solubility generates the characteristic morphology, creating conduits that set an underground drainage system.

In Brazil, cavities are classified following the Normative Ruling of the Ministry of the Environment (MMA, 2009), according to the concept of speleological relevance[1], as low, medium, high or maximum. Cavities considered of maximum relevance cannot be removed and their area to a radius of 250 m must be preserved.

[1] The concept of speleological relevance is adopted at environmental impact studies in order to quantify a cavity's significance, according to geologic, biologic, and socio-cultural aspects. Every identified cavity is qualified into one of four categories: low, medium, high or maximum relevance.

2. GEOLOGIC CONTEXT

2.1 Regional Aspects

Fundão Dam is located in the Iron Quadrangle, which constitutes an approximately quadrangular geomorphologic unit defined by the occurrence of Archean to Paleoproterozoic supracrustal rocks arranged in megafolds over an Archean crystalline shield. This is one of the most studied areas of the Brazilian geology, for bearing mineral deposits of economic and historical importance (Cornejo & Bartorelli, 2009).

The region is inserted in the context of the southeastern border of the São Francisco Craton, an ample geotectonic unit established in the Paleoproterozoic, which has remained tectonically stable during the intense deformational cycle known as Brasiliano Orogeny that assembled the Brazilian Shield in the Neoproterozoic (Almeida, 1977).

The Iron Quadrangle's stratigraphy follows, with some alterations, the original proposals of Dorr et al. (1957) and Dorr (1969). It can be broadly divided into:

- Archean association of gneissic-granitic complexes – crystalline rocks with primitive geochemical signatures, arranged in domes located within or surrounding the later supracrustal rocks;

- Archean metasupracrustal rocks from the Rio das Velhas Supergroup – a typical greenstone belt association of polideformed sequences divided into three Groups: Quebra Osso, Nova Lima and Maquiné. Main lithologies include metavolcanic rocks, quartzite, phyllite and schist;

- Paleoproterozoic metassediments from the Minas Supergroup; a thick package of deformed and metamorphosed rocks mostly deposited in the passive margin of the São Francisco paleocontinent. It is divided into the Caraça, Itabira, Piracicaba and Sabará Groups, the second of which is especially noteworthy for its massive iron ore deposits. Main lithologies include quartzite, phyllite, banded iron formations, carbonatic rocks and schist;

- Mesoproterozoic sequences from the Itacolomi Group and Espinhaço Supergroup – weakly deformed sedimentary rocks covering the aforementioned units that occur locally within the region;

- A variety of subordinate granitic and basaltic rocks intruding on the sequence above.

Figure 1 presents a schematic geologic map of the Iron Quadrangle, while **Figure 2** summarizes the stratigraphy considered in this study.

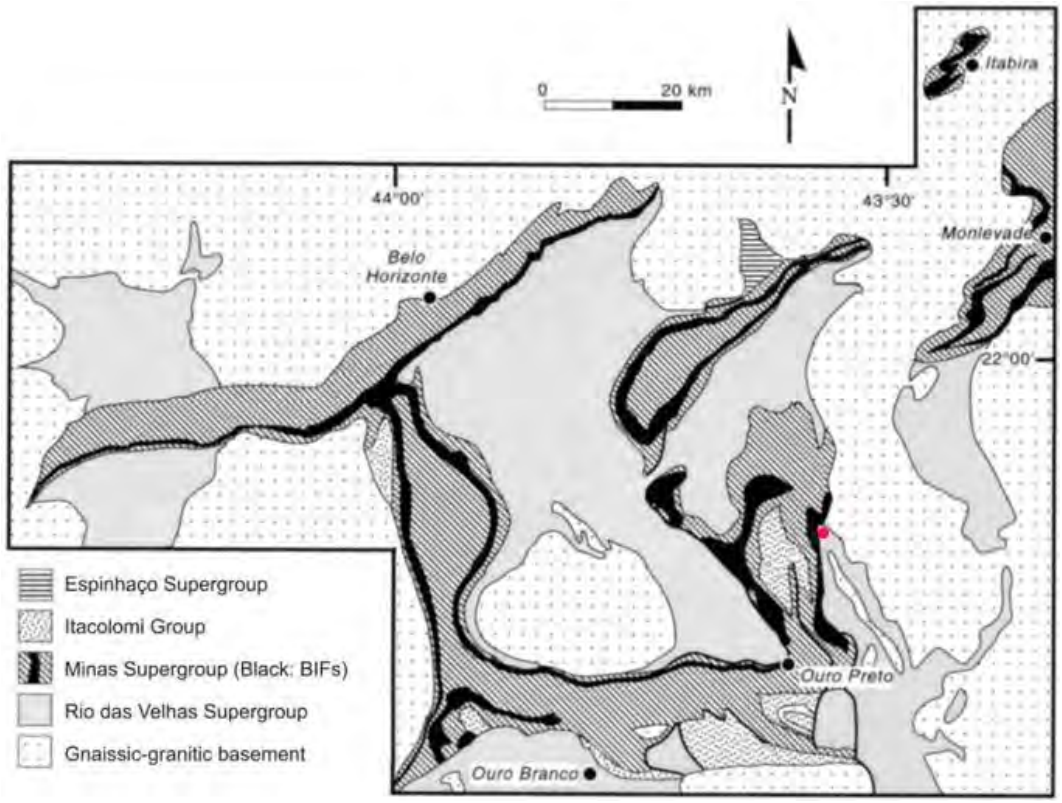

Figure 1 – Schematic geologic map of the Iron Quadrangle region. The red dot indicates the approximate location of the Fundão Dam. Modified from Alkmim & Marshak (1998).

The Iron Quadrangle's geometry is defined by an array of megafolds, curtailed by a system of thrust faults (Baltazar et al., 2005). These folds are mostly sustained by the metasediments from the Minas Supergroup, forming keels that are surrounded by the domed archean crystalline complexes.

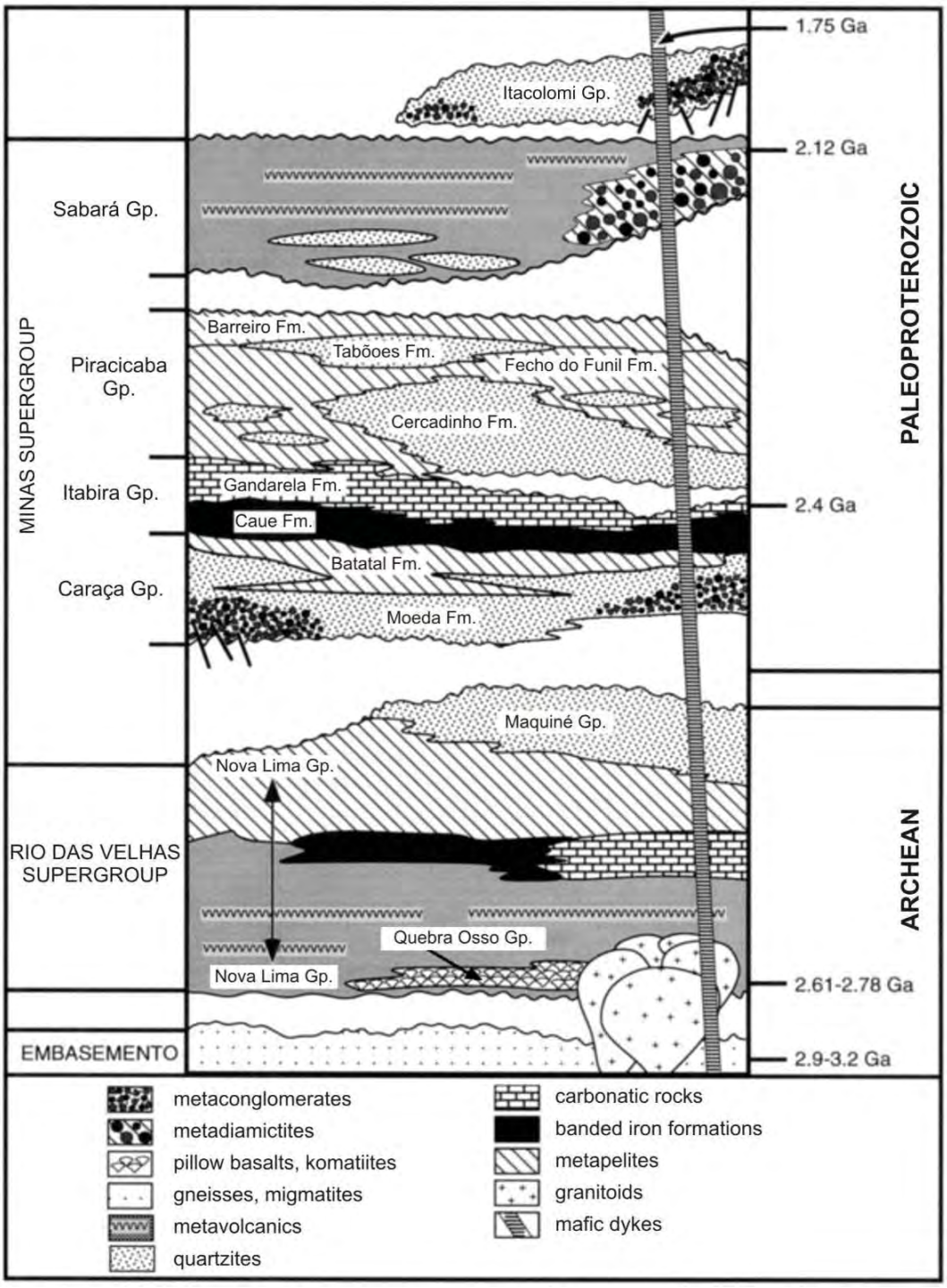

Figure 2 – Stratigraphic column of the Iron Quadrangle region. Modified from Alkmim & Marshak (1998).

This arrangement is locally divided into individual megafolds, all of which are complex structures marked by the interaction between ductile and brittle phases of deformation that represent more than one tectonic event. While

the original geometry was assembled still during the Archean and Paleoproterozoic, the eastern portion of the Iron Quadrangle was affected by the neoproterozoic Brasiliano event, leading to the refolding of the original structures.

Besides the folds, a pervasive system of faults and shear zones affects the area. The most important of these structures are far-reaching thrusting shear zones that truncate the megafolds and are responsible for discordant tectonic contacts between the Rio das Velhas and Minas Supergroups. Subordinated structures include extensional and strike-slip faults.

The reader is referred to Chemale Jr. et al. (1994), Alkmim & Marshak (1998) and Baltazar & Zucchetti (2007) for the main interpretations of the region's tectonic evolution.

2.2 Local Aspects

Germano Mine is an iron mine owned by Samarco Mining. Its structures includes one exhausted pit (Germano Pit), which is currently fully filled by sandy tailings, three processing plants, one dam for sediments containment and water clarification (Santarém Dam), and two tailings dams, called Germano and Fundão. The ore, composed by itabirites, was extracted in Alegria Centro Pit, north of Germano Mine, and processed in the Germano's plants. For the continuity of the operation, as the tailings dams were approaching their maximum capacity, options for tailings disposal were evaluated, such as the Mirandinha Project. After Fundão Dam failed, a new dam, called Eixo 1, is being designed. **Figure 3** shows the structures' location.

The Germano Mine is located in the southeastern portion of the Iron Quadrangle, on a megafold known as Santa Rita syncline. This structure constitutes the eastern border of the Quadrangle in its southern extent, and stretches around 40 km since its merge with the Dom Bosco syncline in the south, next to the city of Mariana, until its northern edge around the city of Catas Altas.

It is one of the structures that was most affected during the neoproterozoic Brasiliano deformation within the Quadrangle. However, its western extent was partially shielded by the presence of a thick quartzitic level in the

structure's northern core (Chemale Jr. et al., 1994), which sustains the Serra do Caraça (Caraça Range).

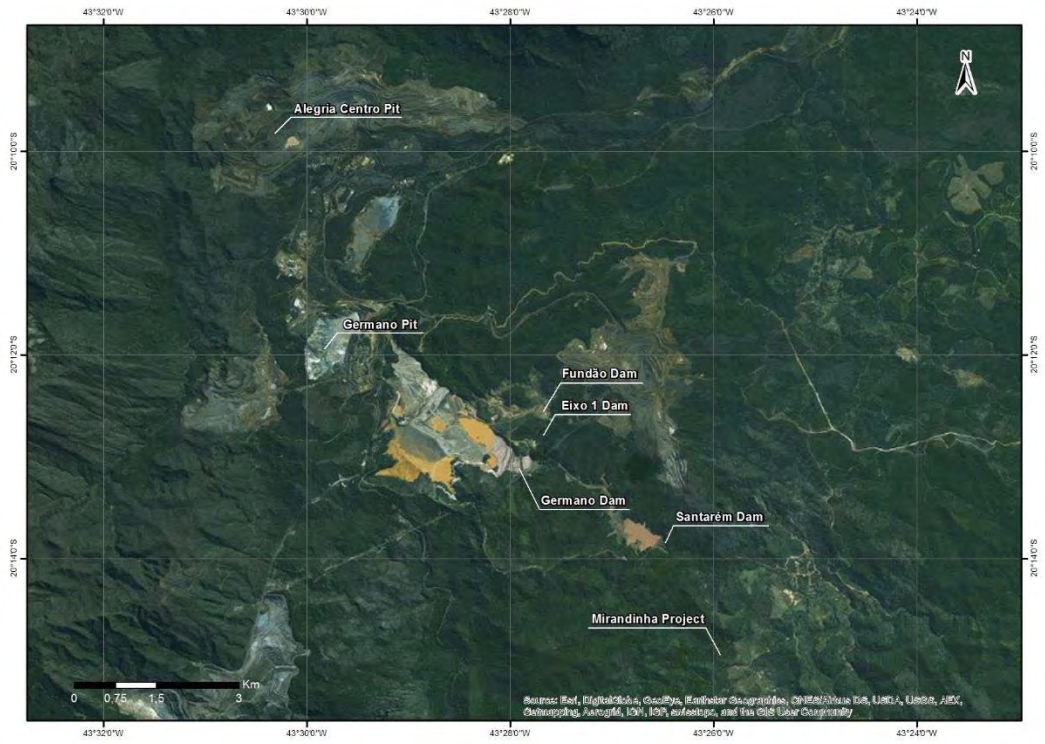

Figure 3 – Germano Mine structures.

Along its extension, it deforms rocks of both the Minas and Rio das Velhas Supergroups, and is frequently disrupted by thrust and lateral faults. It has a west-facing vergency, with both limbs dipping preferentially to the east. There is a strong asymmetry of the limbs' thickness, with the western one being much thicker than the overturned eastern one, on which many of the formations are discontinuous.

The junction of the Santa Rita and Dom Bosco synclines in the former's southern extremity is strongly disrupted by the presence of compressional faults. In addition, the Fundão-Cambotas shear system cuts across the entire megafold from south to north, extending further to other regional structures, such as the Gandarela syncline. It is one of the most important shear zones within the Iron Quadrangle, representing an old thrust front in its eastern extremity. It has a N-S strike direction and is segmented into numerous sub-parallel faults, such as the Ouro Fino, Flechas, Alegria, Frazão and Água Quente (Gomes et al., 2000).

The entire stratigraphy of the Minas Supergroup is present on the Santa Rita syncline, but some of the groups are mapped as undivided in regional approaches.

Within a regional scale, the Germano Mine is located in the southern central portion of the syncline, and comprises mostly rocks from the Itabira, Piracicaba and Sabará Groups, discordantly overlain by the sedimentary package of the Itacolomi Group. Archean rocks, belonging to the crystalline basement and of the Rio das Velhas Supergroup, are restricted to the east of the area, separated from the paleoproterozoic sequence by the Fundão-Cambotas shear system (**Figure 4**).

The extracting activities have generally affected the banded iron formations of the Cauê Formation, part of the Itabira Group, which is commonly capped by iron-rich lateritic crusts (ferricrete). Most supplementary structures, however, including the tailing dams, were erected on top of rocks associated to three stratigraphic groups:

- The Piracicaba Group comprises three formations, which are Cercadinho (an association of phyllite and quartzite), Fecho do Funil (mostly phyllite and dolomite), and Barreiro (predominantly phyllite, occasionaly carbonate-rich);
- The Sabará Group consists predominantly of mica and chlorite schists, with subordinated lenses of quartzite, metagraywacke, metaconglomerate and banded iron formations;
- The Itacolomi Group is dominated by quartzite, occasionally conglomeratic. An intercalation of sericitic quartzite and phyllite is subordinated. The Santo Antônio Formation, part of this group, is noted in the region of the Germano Mine for containing lenses of banded iron formation.

The area of the Germano and Fundão Dams has been the subject of many geological studies, conducted within the context of projects for new and expanded geotechnical structures or for Environmental Impact studies.

Among these, two detailed mappings are of special interest. Both present configurations that differ substantially from each other and also from the regional approach assembled by CODEMIG (2005). The first one was developed by Brandt at a 1:10,000 scale for the Environmental Impact Study of the Fundão Dam in 2005. The second and more recent one was developed at a 1:5,000 scale by Geoestável in 2013, for the conceptual project of the Dam’s elevation to 940 m.

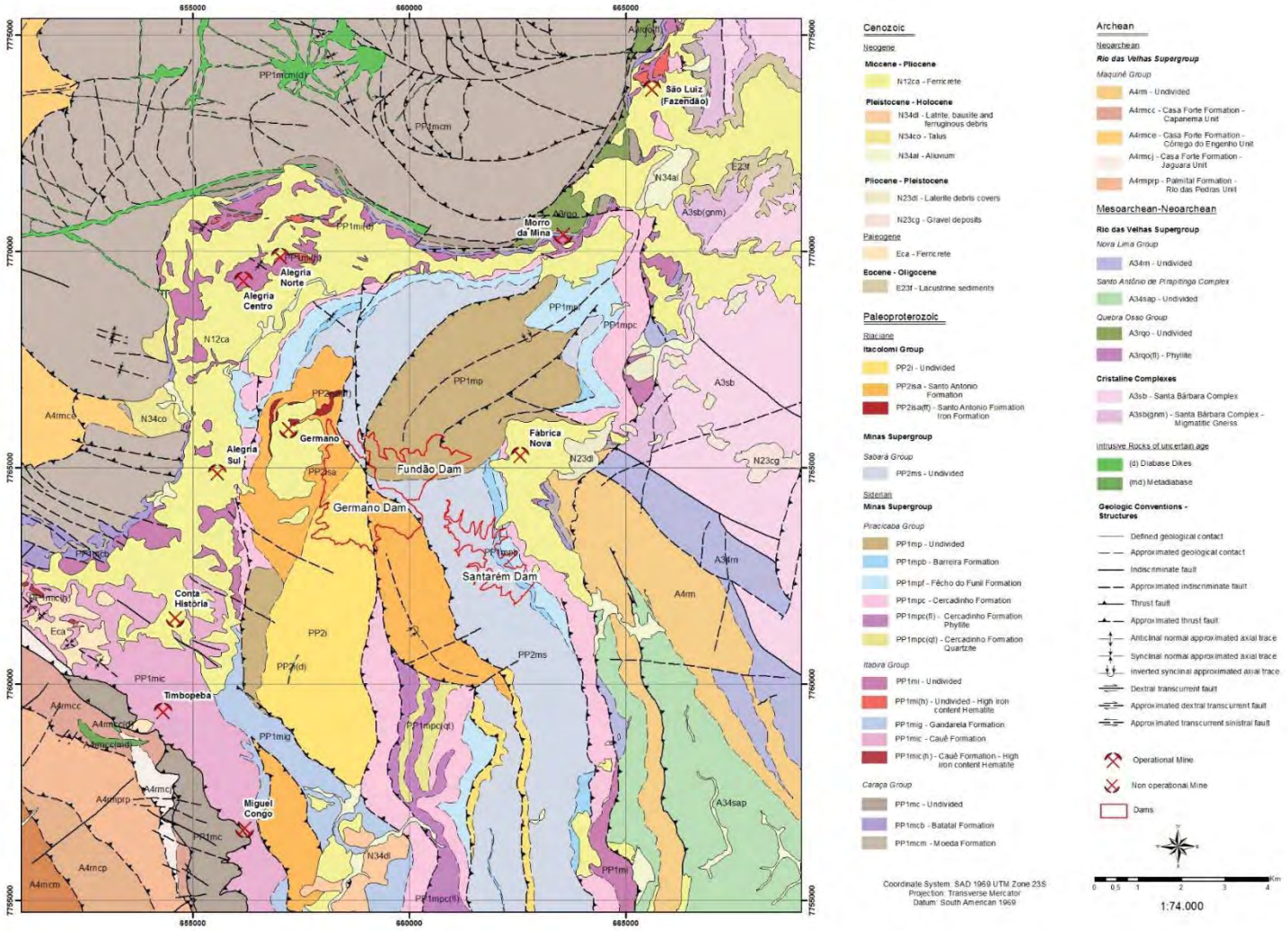

Figure 4 – Geologic map of the Germano Mine region. Modified from CODEMIG (2005).

According to Brandt (2005), the Fundão Dam area and its surroundings consist mainly of rocks from the Piracicaba and Sabará Groups, part of the Minas Supergroup. As these units comprise metapellitic rocks in the form of lenses and thin layers of difficult stratigraphic interpretation, the field recognition criteria consisted of the coloration of the lithotypes associated with the mineralogical composition.

The Cercadinho Formation rocks are generally whitish phyllites of sericitic composition, occasionally pink and red, with darker tones when heavily weathered. Similarly, the Fecho do Funil Formation rocks are generally rosy and reddened phyllites, heavily weathered. The rocks of the Barreiro Formation are related to a thin carbonaceous phyllite layer, also quite weathered. The Sabará Group, on its turn, is represented by ferruginous rocks.

The field observations concluded that phyllites of the Cercadinho Formation occur in the greater part of the Fundão Dam. According to this study, this finding coincides with the geological-geotechnical study conducted by Samarco in 1993, during construction of the Santarém Dam. **Figure 5** presents the geological map developed by Brandt (2005).

The detailed geological mapping conducted by Geoestável (2013) recognized four main lithologies: sericitic phyllite, graphite-rich phyllite, metadiamictite and mica-rich quartzite (**Figure 6**). The three first lithotypes were identified as part of the Sabará Formation, whilst the last one was recognized as the lower member of the Itacolomi Group.

According to this map, the sericitic phyllite covers most of the mapped area and presents predominantly red to brown colors. The graphite-rich phyllite, on the other hand, is dark grey to black, and occurs in intercalations with the latter in the central portion of the dams. Both the diamictite and the quartzite are of restricted occurrence, to the northeastern and southwestern extremities of the studied area, respectively.

Despite the local stratigraphic differences recorded between the available map sources, it can be concluded that the studied area around the Fundão and Germano Dams is dominated by the presence of phyllites, either associated to the Sabará Formation or to a complex intercalation of the Piracicaba Group. Its mineralogy is mostly sericitic with multiple colors, but graphite-rich varieties occur also. The second most relevant lithology is quartzite, which is confined to the southwestern edge of the reservoir of the Germano Dam.

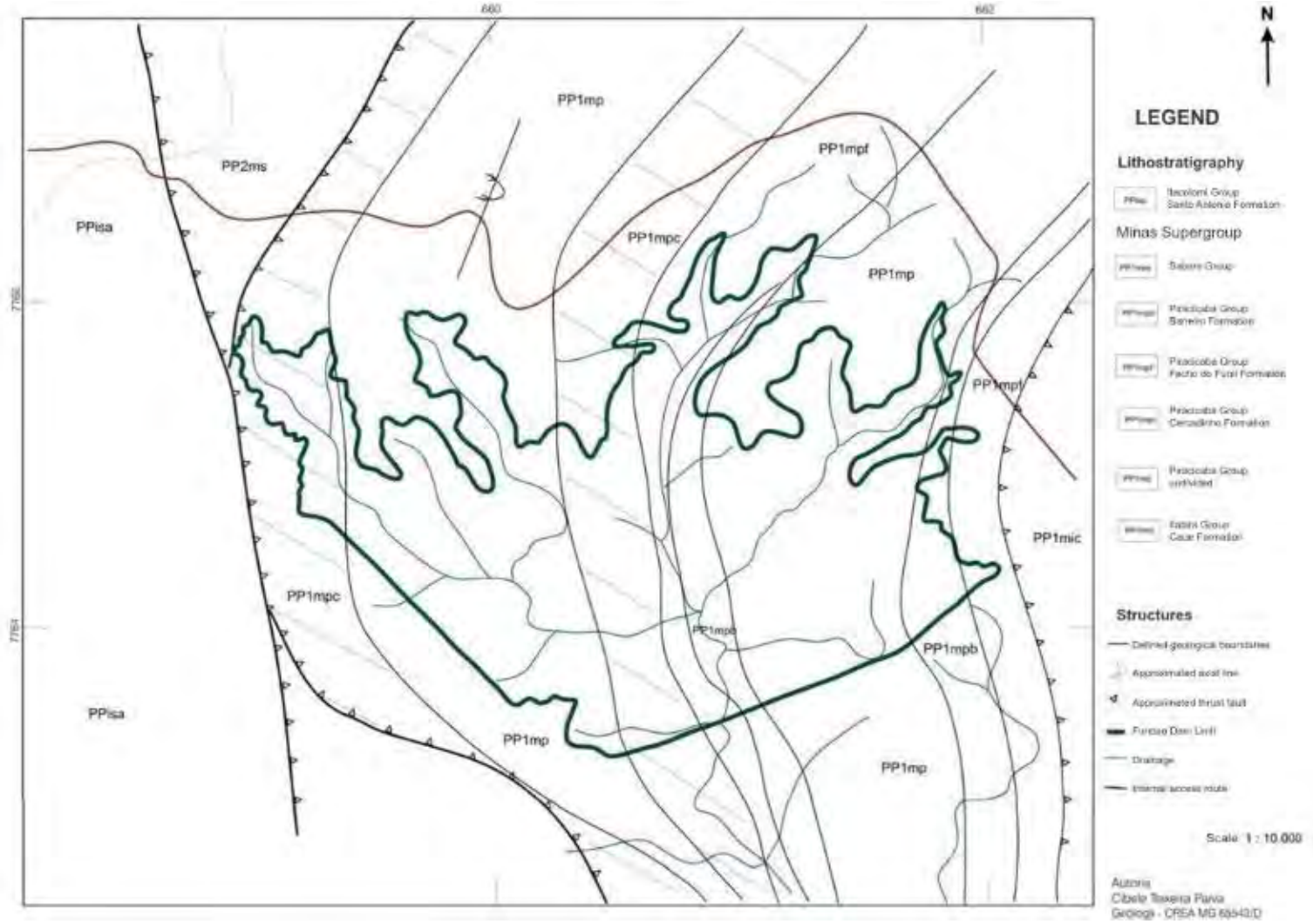

Figure 5 – Geologic map of the Fundão Dam area. Source: Brandt (2005).

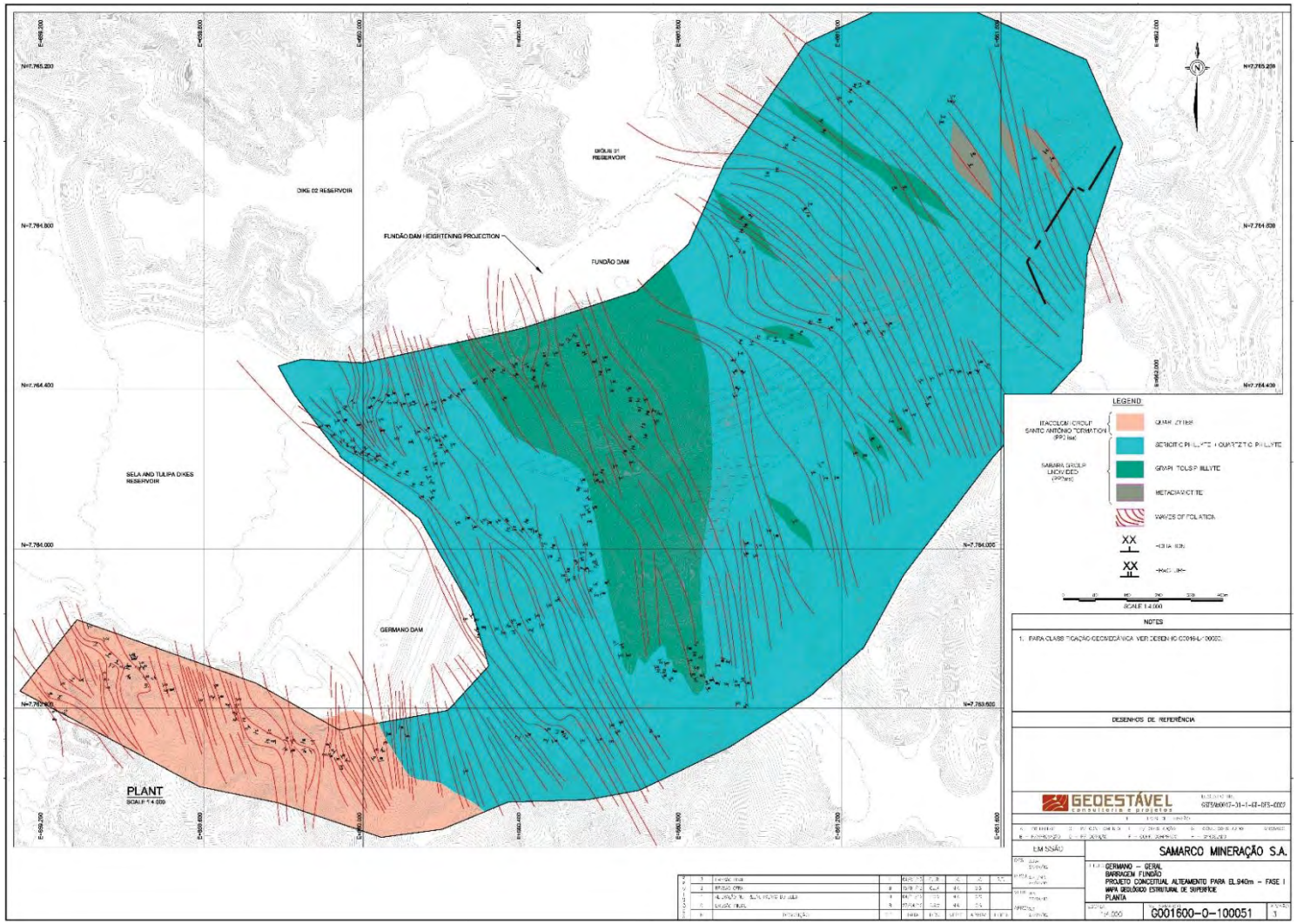

Figure 6 – Geologic map of the Germano and Fundão Dams area. Source: Geoestável (2013).

Structural data were collected in the field on numerous different studies, most recently on those conducted by BVP (2013), Geoestável (2013) and DAM (2014). All of these identify the foliation in the phyllite as the main structural feature of the area. It has a preferential NW-SE orientation, undulated on occasions and commonly crenulated. It dips moderately to NE with an angle between 30° to 40°.

The presence of numerous fractures is acknowledged by all available documents, and was discussed by Geoestável (2013) in detail. They identified four main families, consisting of two sets of orthogonal conjugated fractures in a "X" disposition (**Figure 7**). The main set has a N-S orientation and dips both to E and W, corresponding to approximately two thirds of all measured structures, while a subordinated set with a E-W orientation and conjugated dips to both N and S correspond to roughly 30% of the identified fractures.

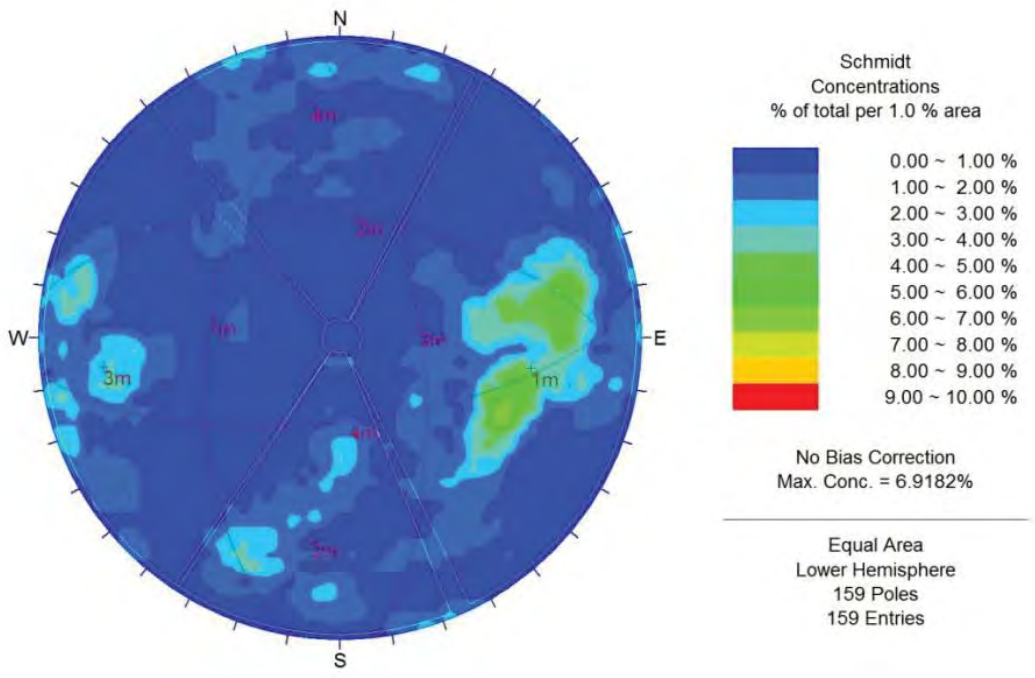

Figure 7 – Stereogram representing fracture data within the area of the Germano and Fundão Dams. Source: Geoestável (2013).

3. KARSTIC FEATURES IN THE IRON QUADRANGLE

According to the National Center for Research and Conservation of Caves (Centro Nacional de Pesquisa e Conservação de Cavernas, abbreviated CECAV), in Minas Gerais, there are 1226 caves (CECAV, 2015), in the Iron Quadrangle.

These cavities occur mainly in lithologies of the Itabira Group, defined as a chemical metasedimentary sequence, subdivided in Cauê and Gandarela Formations.

Cauê Formation is characterized by iron formations (itabirites, dolomitic itabirites, amphibolitic itabirites), phyllites and manganese horizons.

Gandarela Formation consists of carbonate rocks, marbles and carbonate phyllites.

In addition to the lithotypes in these stratigraphic units, cavities are also found in quartzites and other rocks from other units of the Iron Quadrangle.

Figure 8 presents a geological map of the Iron Quadrangle with the distribution of cavities.

Sorting by lithological units (CECAV, 2015), it is observed that the highest incidence of caves occurs in laterite cover (over 45%), followed by the occurrence in iron formation (about 23%), carbonate rocks (around 12%) and siliciclastic rocks (around 10%).

3.1 Karst in carbonate rocks

Inicially, karst was the name used to define a geological structure originated by chemical phenomenon related to the dissolution of carbonate rocks, in the formation of typical features like sinkholes, uvalas, cavities, stalactites, stalagmites, etc. Currently the term is adopted for any type of rock, such as iron formations, siliciclastic rocks, gypsum, or salt, that undergoes chemical processes of dissolution and generates cavities, spelothems and characteristic morphologies.

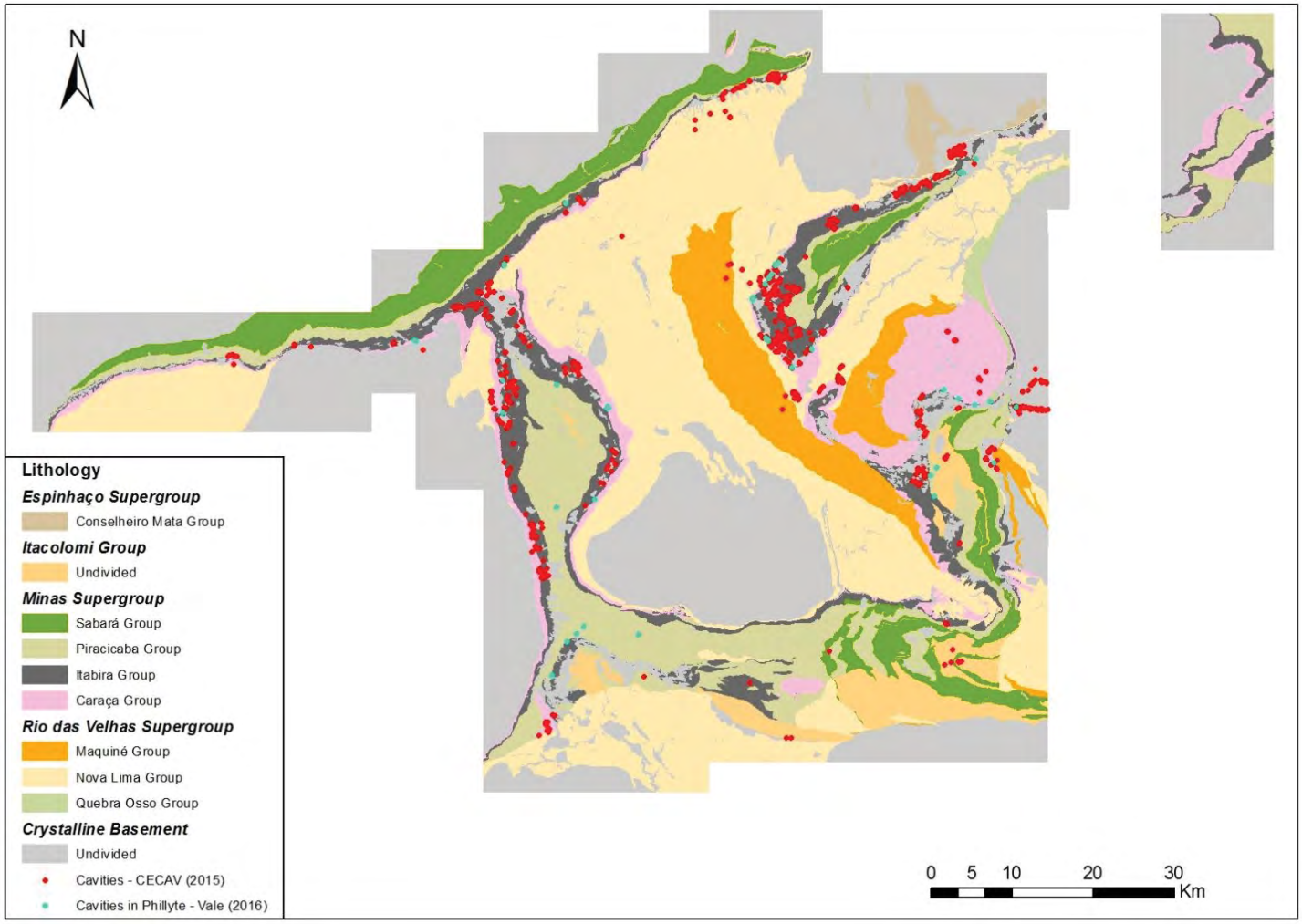

Figure 8 – Distribution of cavities relative to the geology of the Iron Quadrangle. Modified from CODEMIG (2005), CECAV (2015) and Brandi (2016).

The noun KARST was originated in the region that extends from the north of Italy, northeast of Croatia and southeast of Slovenia (Kras or Karst), and it was characterized by its specific forms and circulation of groundwater, always related to beauty (kras, in Slovenian).

In the original definition of karst, the carbonate lithology was fundamentally connected to the chemical processes that facilitated progressive cavities in the carbonate rocks, creating three-dimensional systems of dissolution conduits, feeding the karstic aquifer.

The Iron Quadrangle Speleologic Unit was originally defined based on the occurrence of some cavities in dolomites in the geological Formations Gandarela and Fecho do Funil. The caverns in the lithologies of the paleoproterozoic units are scarce when compared to those of iron and quartzite formations of the same age.

The greater occurrence of karstification in carbonate rocks in Brazil is distributed in the Sete Lagoas Formation of the Bambuí Group, that extends from the south of Minas Gerais to Bahia. The Sete Lagoas Formation, a neoproterozoic unit corresponding to a flat platform setting, is composed of limestones and dolomites. The region of Lagoa Santa, next to Belo Horizonte, is considered the birthplace of Brazilian speleology, with more than 700 registered caves.

3.2 Karst in non-carbonate rocks

3.2.1 Karst in Iron Formations

The literature on karst points two types of caves in iron formations origin: by dissolution or by erosion.

The formation of caves by dissolution in iron formations are generally related to the dissolution of silica and carbonates present in the rock structure. The chemical activity creates voids in the more soluble portions of the rock structure, which may or may not be filled with water.

Caves originated by erosion are often in lateritic crust or ferricrete (“canga”). Under layered friable lithotypes, such as phyllites, schists or detrital

material, and particularly favorable slope, are the predisposing factors for the development of erosive cavities, supported by the laterite cover.

In most of the cavities in iron formations there is evidence of piping processes, associating the rock comminution to the chemical genesis of karstification. Factors such as high hydraulic gradient, presence of soluble ions in the soil, soil cracking related to long dry season, and heavy rains, stimulate subsurface seepage, causing the mechanical removal of particles, what represents the most significant stage for the cave morphology in ferruginous lithotypes.

In the Iron Quadrangle, canga is the lithotype that comprises almost half of all registered karstification events. The cavities occupy the summits regions of the relief, where erosion and dissolution are occasionally combined to form of a single cavity. The caves are usually typified by a single conduit not exceeding 15 m.

The caves originated by dissolution occur frequently in the itabirites of Cauê Formation, under the lateritic crust or ferricrete (“canga”). The morphogenetic process is related to the soluble mineral content and the structure of the itabirites. In this typology, similar to the one that occurs in carbonate rocks, the dissolution process create conduits, cavities and halls, with dimensions greater than 100 linear meters.

3.2.2 Karst in Siliciclastic Rocks

The karstification in siliciclastic rocks (represented in the Iron Quadrangle essentially by quartzites) comprises two phases: in the first, the dissolution causes the comminution of intergranular cement, individualizing the quartz grains, and in the second phase, erosion prevails and grains quartz are removed through the piping phenomenon.

The removal of particles by dissolution in quartzites is estimated between 10 and 20% of the mobilized volume of rock, while in carbonate rocks may comprise more than 90%.

In the process of dissolution, the silicate minerals (feldspars, micas, pyroxenes, amphiboles, etc.) are more soluble than the pure silica.

Likewise, silica in an amorphous state (opal, chalcedony, etc.) is more soluble than its crystalline form.

In higher temperatures there is an increased rate of dissolution. Thus, the karstification siliciclastic processes occur mainly in tropical regions, supported by the presence of humic acids, which can accelerate the dissolution kinetics.

Age is a distinguishing factor in the formation of caves in siliciclastic rocks. The development of a karst system in siliceous rock mass demand significantly longer than in iron formations and even higher than in carbonate rocks.

Discontinuities and rock structure have a central role in the expansion of karst phenomena, leading the dissolution water over the rock mass.

In the Iron Quadrangle there are several siliciclastic lithotypes where caves and grottoes develop. The karstification in quartzite creates large gaps developed in typical quadratic morphology, which is function of structural conditioning, with blocks embedded in cracks where, often, there are predominance of mechanical erosion and presence of drainage.

The Serra do Caraça is considered an important Speleological province of the Iron Quadrangle. Among the several cavities, it is found the largest one in quartzite in the world, called Gruta do Centenário. Located in the Inficionado Peak, 2000 m above sea level, it is about 4 km long and has a linear depth of approximately 500 m.

4. KARSTIC FEATURES IN THE GERMANO MINE VICINITY

In the vicinity of Germano Mine there are three mines owned by Vale, Fábrica Nova, Fazendão and Alegria, as shown in **Figure 9**.

4.1 Fábrica Nova Mine

The Fábrica Nova Mine, property of Vale, borders with the Samarco Mining area. The Environmental Impact Study for the expansion of Fábrica Nova Pit (Sete, 2009) identified 27 natural cavities in the area of influence defined, as presented in **Figure 10**.

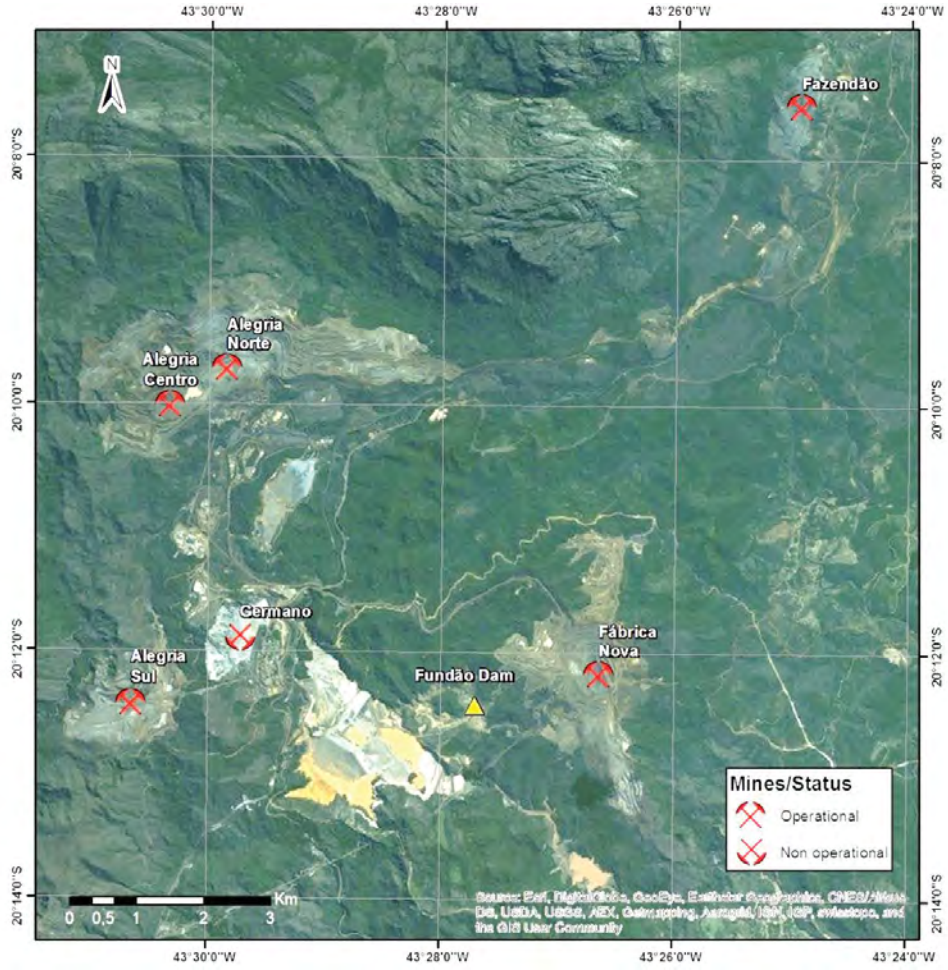

Figure 9 – Mines located in the vicinity of Germano Mine.

The cavities were found in iron formations, detritic ferricrete and quartzite, predominately in the contact between itabirite and ferricrete. The main structures observed in the cavities were relief joints, creases and arched inflections in the itabirite. The horizontal projection of the identified caverns varies between 5 and 90 m, with the vast majority being of small size (<25 m).

4.2 Alegria Mine - Mariana Itabirites Project

In the Alegria Mine, which expansion project is known as Mariana Itabirites, the cavities identified in the influence area by the Environmental Impact Study (Golder, 2012) are inserted, mainly, in ferruginous lithologies, particularly ferricretes and some zones of itabirites of Cauê Formation. Between lithologies that present average speleological potential, the Fecho do Funil and Santo Antônio Formations are cited.

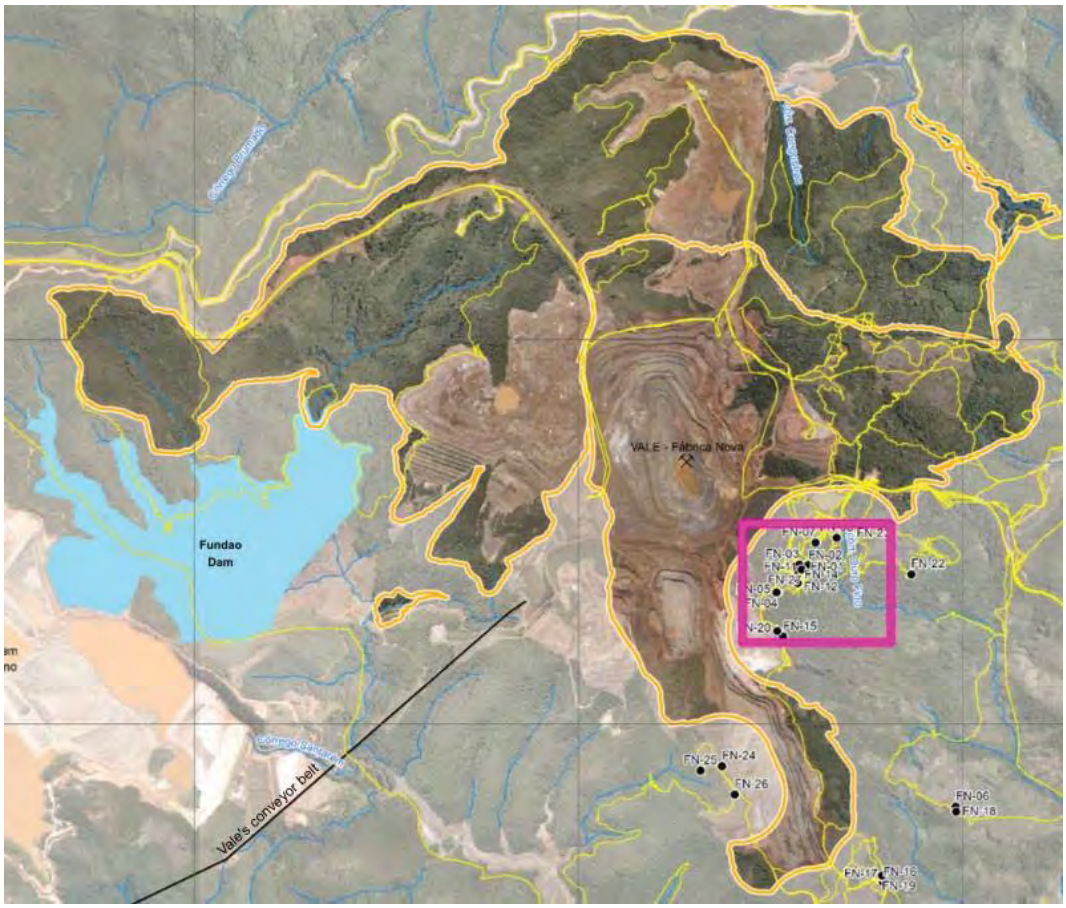

Figure 10 – Cavities identified in the area of influence of the expansion of the Fábrica Nova Pit. Source: Sete (2009).

The mentioned Environmental Impact Study identified 15 cavities, of which only one was already registered in the CECAV (**Figure 11**).

The cavities identified are mostly inserted in iron formations with registered structural features such as fractures, metamorphic banding and creases. The majority is located in slopes with horizontalized aspects, between elevations 856 m and 1,070 m.

Regarding the concept of speleological relevance, no cavities were classified as of maximum level, but nine were found as high level and six of medium level.

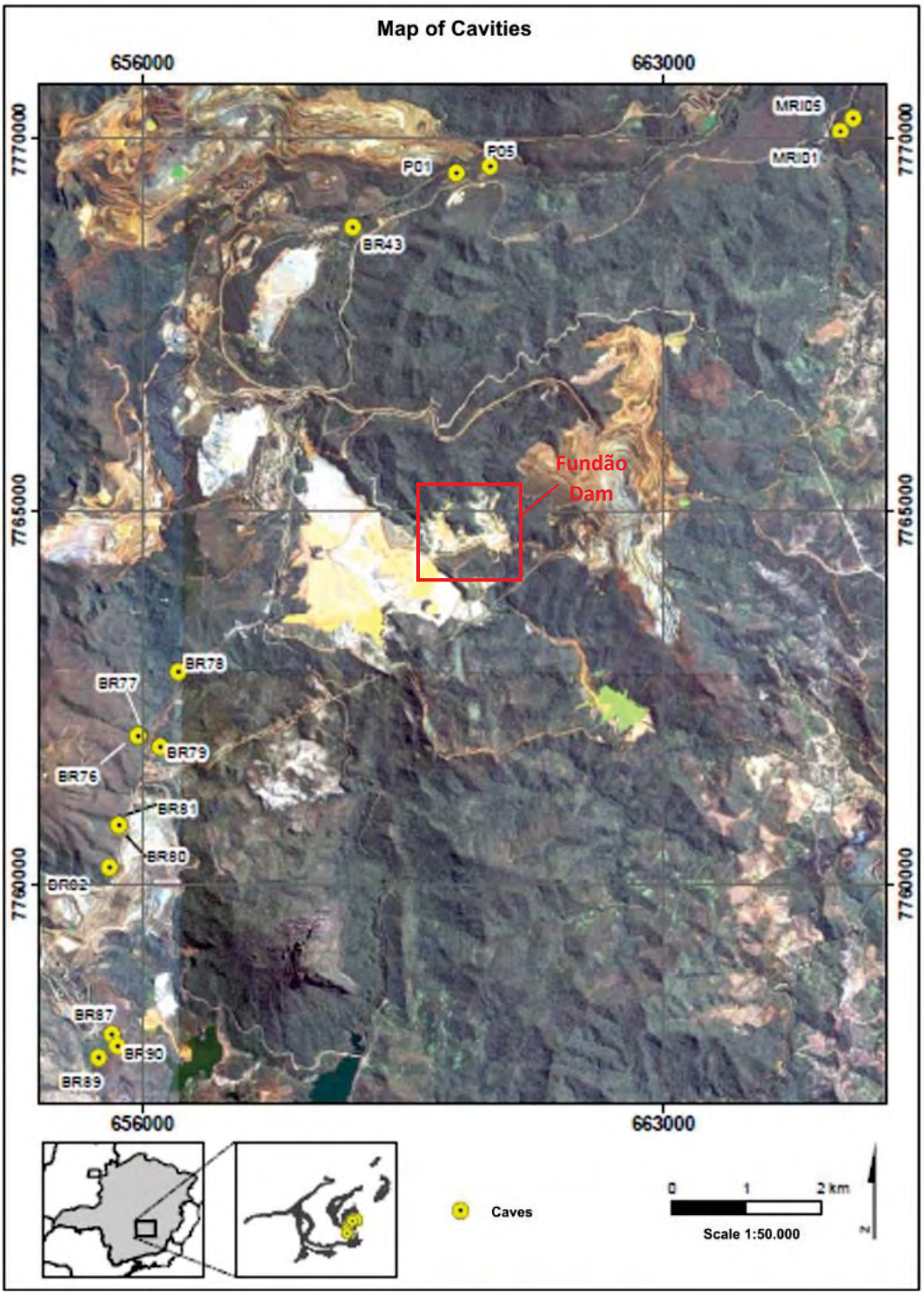

Figure 11 – Cavities inserted in the influence area of the Mariana Itabirites Project. Source: Golder (2012).

4.3 Fazendão Mine

The Fazendão Mine, also owned by Vale, is located in the municipalities of Mariana and Catas Altas, in the foothills of the Serra do Caraça, north of the Fundão Dam. According to the available CECAV data, several cavities are already mapped in the influence area of the project (**Figure 12**).

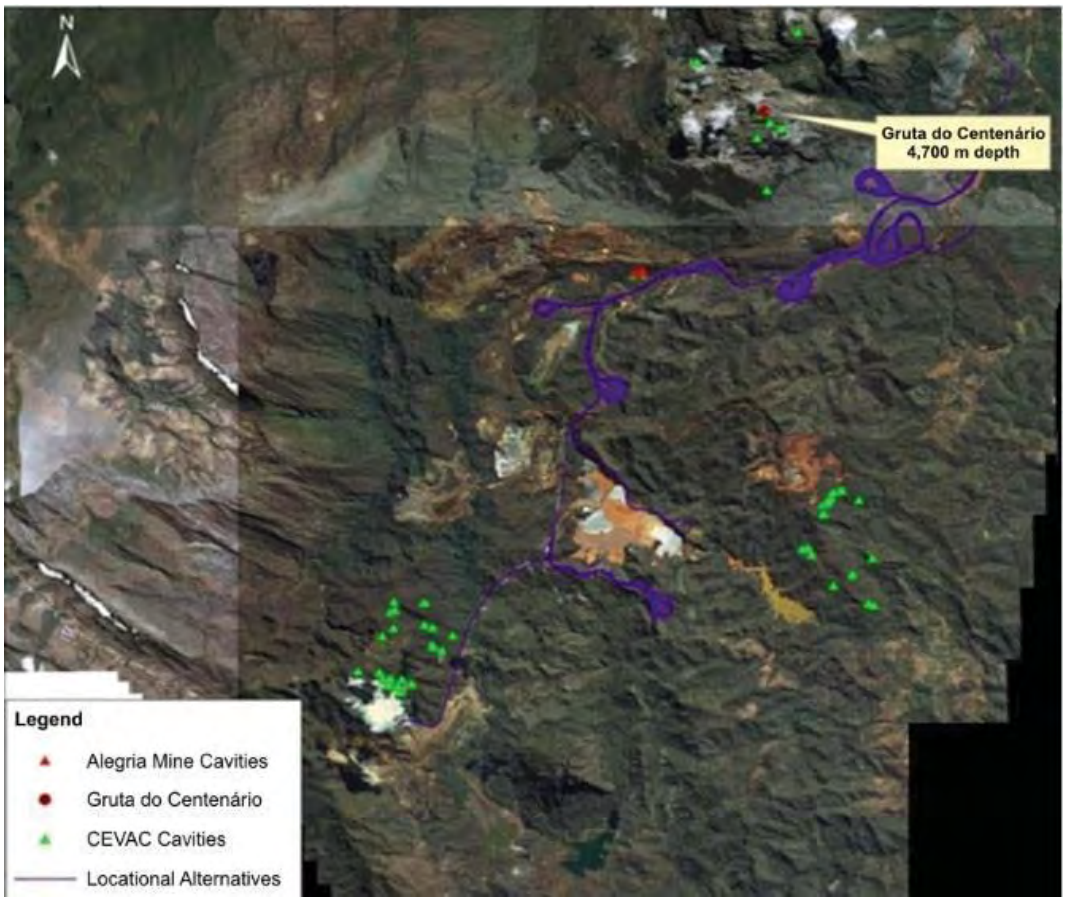

Figure 12 – Cavities mapped in the area of the Fazendão Mine. Source: Golder (2010).

Many of these cavities occur in quartzitic rocks, among which the Gruta do Centenário, which stands out for being the world's largest in this lithology (see more in item 3.2.2).

5. KARSTIC FEATURES IN THE GERMANO MINE

5.1 Speleological Potential

In 2013, the company Carste issued the Speleological Prospection Report of the Germano and Fundão Dam surroundings (Carste, 2013-a), as a part of the Environmental Impact Study performed for the unification and raising of the tailings dams (Sete, 2013).

The analysis of the speleological potential was performed using the geological map of CODEMIG (2005). The work was based on the lithotypes present in the area of the dams. Satellite images were also used to identify favorable structural features for the development of natural cavities and geomorphologic features indicative of speleological processes.

Thus, Carste (2013-a) defined each lithotypes' speleological potential, divided by class and coverage area. In the very high potential speleological class are the iron formation and ferricrete, corresponding to 5% of the area directly affected. In the high potential speleological class is a mapped unit consisting of an association of quartzite with lenses of conglomerate and phyllites, relative to 18% of the area. In the middle potential speleological class are phyllites and conglomerates, with subordinate dolomites, quartzite and banded iron formation lenses. The lowest potential speleological class includes the metavolcanic rocks, schists and phyllites (**Figure 13**).

The region where the Fundão Dam is inserted was defined as of low speleologic potential. In the study, during the satellite images analysis stage, features of the defect types or structures with propensity to cavity formation were not identified in the lithotypes of the area (phyllites, shales, quartzites, among others).

In field survey phase, five caverns were identified in the southwestern part of the Germano Dam reservoir, above its maximum level. This corresponds to a high-potential area for karstic features, determined by the occurrence of quartzite rocks of the Itacolomi Group.

As discussed in the chapter on the local geological aspects, although there are significant differences between all available maps in terms of stratigraphy adopted around the Fundão and Germano Dams, there is a consensus that the area consists predominantly of phyllites.

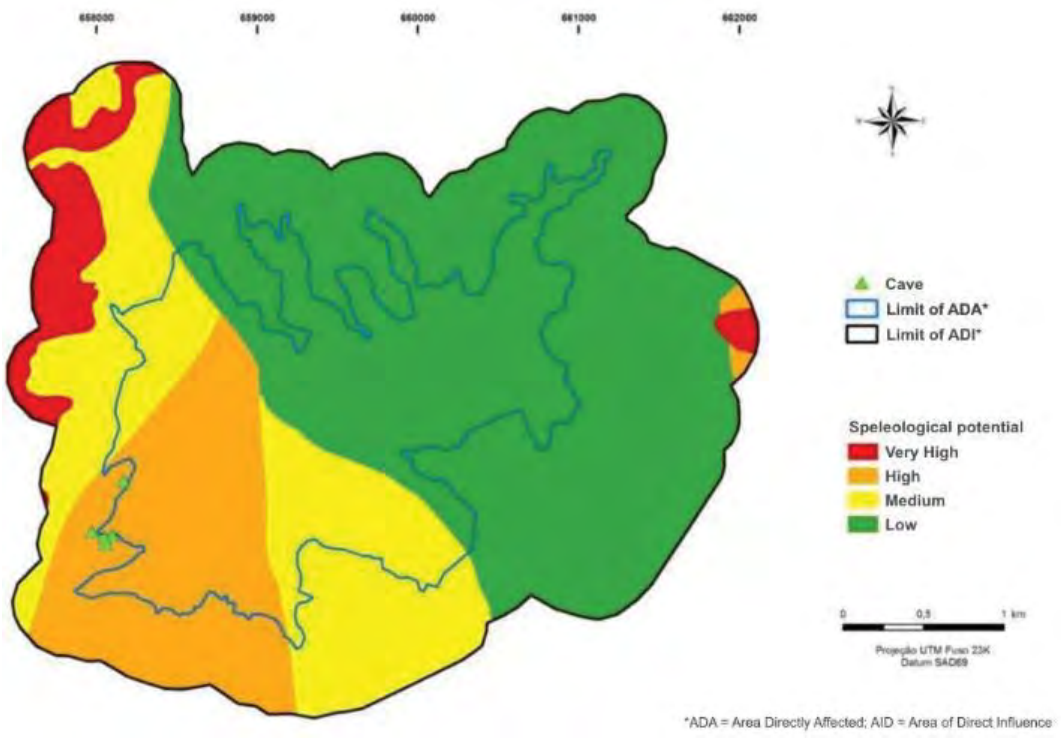

Figure 13 – Map of the prospected area around the Germano and Fundão Dams reflecting speleological potential. Source: Carste (2013-a).

Among the other rocks identified, the main attention is given to the quartzites on the southwestern part of the Germano Dam reservoir. Therefore, the conclusions issued by the Speleological Prospection Report (Carste, 2013-a) are in accordance with the consulted sources.

Regarding the potential of karstic structures in the phyllites identified in this region, Brandt (2005) diagnosed the following relevant aspects:

- the phyllites are locally interleaved with quartzite and quartz veins;
- foliation and sub-vertical joints can compromise the tightness of the reservoir;
- absence of characteristic cavities;
- possible carbonaceous phyllite layers and quartzite levels can favor the appearance of water leaks.

5.2 Known cavities

After the establishment of the classification of cavities according to the concept of speleological relevance, cavity survey has become necessary to obtain environmental permits.

In Germano Mine, cavities survey was performed for the unification and raising of the tailing dams Germano and Fundão (Carste, 2013-a; Carste, 2014), ore reserve increasing project (Carste, 2013-b), and tailings deposition system Mirandinha, that includes Santarém Dam (Carste, 2015). During the studies for Bay 3 raising to 940 m, five cavities were identified on the perimeter of that reservoir (VOGBR, 2015).

The genesis of most caves identified in Mirandinha influence area are talus and quartzites. Talus deposits are generated by mass movements. After the fall, the blocks spatial arrangement created cavities of varying dimensions (Carste, 2015).

In that area, cavities in other lithologies excepting talus were developed initially by the action of groundwater in primary geochemical dissolution in the limits between grains of the rock's mineralogical components. As those rocks are essentially insoluble, the fundamental component for the continuity of the process was the mechanical drag of the particles, causing the expansion of tubes that have developed within the rock mass, mainly following foliation planes of rock and discontinuities. In siliciclastic rocks, the dissolution destroys the sutures from the quartz grains, causing mechanical removal, known as piping. This process is enhanced by the concentration of discontinuities in the rock and hydraulic conditions (Carste, 2015).

A consolidated research on this available database revealed the existence of 238 cavities within a 5 km radius of the Fundão Dam (**Figure 14**). This influence area includes the site of the Fábrica Nova Mine and part of the Alegria Mine, discussed previously in Chapter 4.

Approximately a third of all cavities listed in the consulted references lack information on the affected lithology. On those that have this information, there is a predominance of karstic features in quartzite (42%), followed by talus (25%) and itabirite (20%). The remaining identified cavities correspond to only one eighth of the occurrences, and affect the ferricrete crust, schists, conglomerates and ferruginous phyllites.

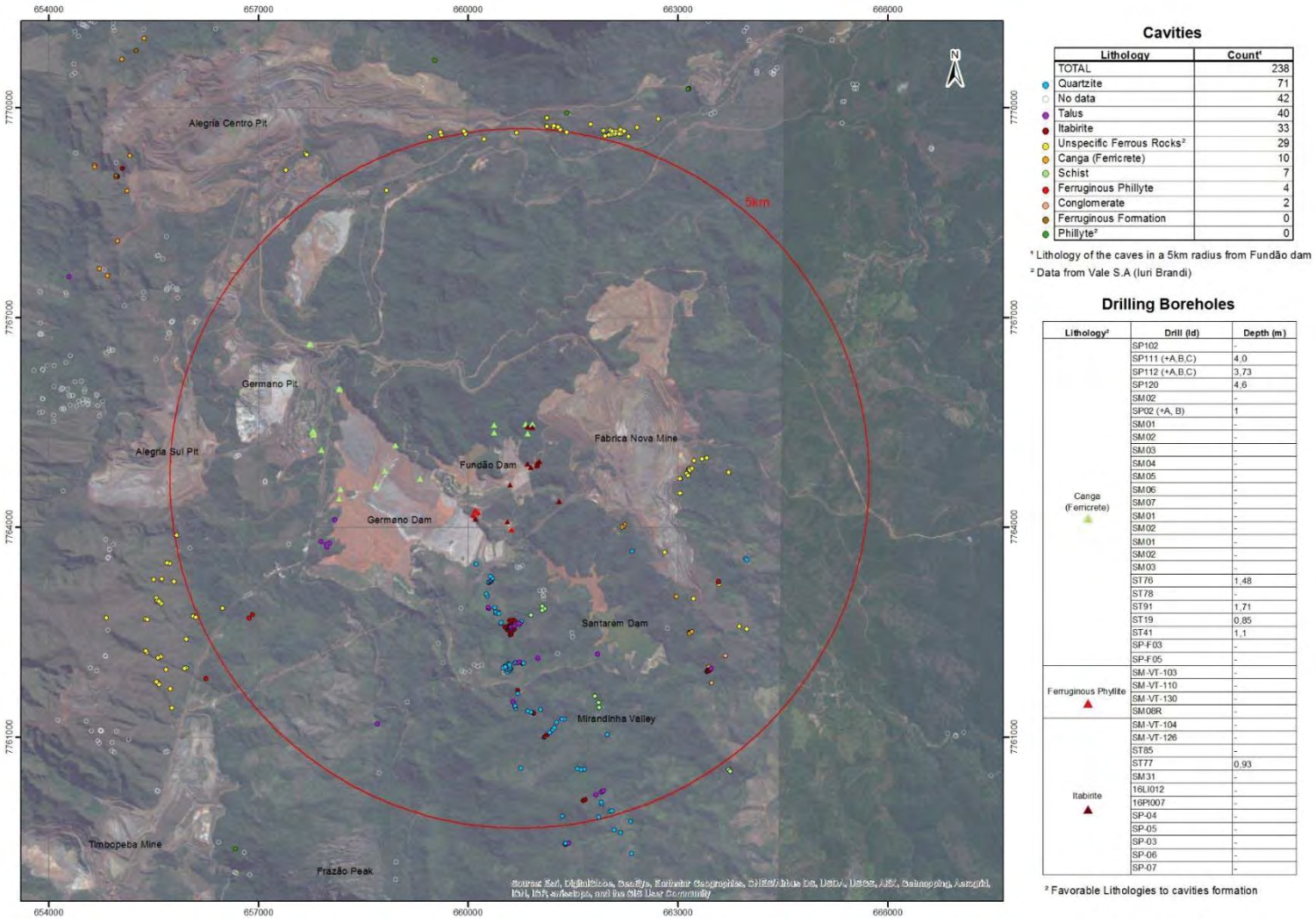

Cavities

Lithology	Count[1]
TOTAL	238
Quartzite	71
No data	42
Talus	40
Itabirite	33
Unspecific Ferrous Rocks[2]	29
Canga (Fericrete)	10
Schist	7
Ferruginous Phillyte	4
Conglomerate	2
Ferruginous Formation	0
Phillyte[2]	0

[1] Lithology of the caves in a 5km radius from Fundão dam

[2] Data from Vale S.A (Iuri Brandi)

Drilling Boreholes

Lithology[2]	Drill (Id)	Depth (m)
Canga (Fericrete)	SP102	-
	SP111 (+A,B,C)	4,0
	SP112 (+A,B,C)	3,73
	SP120	4,6
	SM02	-
	SP02 (+A, B)	1
	SM01	-
	SM02	-
	SM03	-
	SM04	-
	SM05	-
	SM06	-
	SM07	-
	SM01	-
	SM02	-
	SM01	-
	SM02	-
	SM03	-
	ST76	1,48
	ST78	-
	ST91	1,71
	ST19	0,85
	ST41	1,1
	SP-F03	-
	SP-F05	-
Ferruginous Phyllite	SM-VT-103	-
	SM-VT-110	-
	SM-VT-130	-
	SM08R	-
Itabirite	SM-VT-104	-
	SM-VT-126	-
	ST85	-
	ST77	0,93
	SM31	-
	16LI012	-
	16PI007	-
	SP-04	-
	SP-05	-
	SP-03	-
	SP-06	-
	SP-07	-

[2] Favorable Lithologies to cavities formation

Figure 14 – Known cavities and drilling boreholes within a 5 km radius of the Fundão Dam.

It should be noted that only one of the almost 240 listed cavities has been characterized as developed in phyllitic rocks, approximately 1 km to the southwest of the Germano Dam reservoir's upper level, confirming previous assumptions that this lithotype presents a low speleological potential. This proportion is in accordance with regional data compiled for the entire Vale's area inside Iron Quadrangle, that identified only 57 cavities within phyllites, none of which appears in the 5 km radius of Fundão Dam (Brandi, 2016).

In fact, the strong predominance of phyllitic rocks with low susceptibility for karstic development diagnosed for the area of this structure (Brandt, 2005; Carste, 2013-a; Geoestável, 2013) is reflected in the absence of any known cavities in or around the Fundão Dam. For the Germano Dam, only five cavities were identified above the maximum level of the reservoir in its southwestern portion. These correspond to those diagnosed by Carste (2013-a), as previously referred.

Within the 5 km influence area diagnosed in the map above, the vast majority of identified cavities are located south of the Fundão and Germano Dams, mostly in quartzite, talus and itabirite, in a region that corresponds to the outcrop area of the Santo Antônio Formation, part of the Itacolomi Group. This unit is not mapped within the area of the Fundão Dam itself, according to all available geologic maps (CODEMIG, 2005; Brandt, 2005; Geoestável, 2013).

In the search of any cavities evidence, the database analyzed included more than 300 drilling boreholes performed by Chammas in 2012, DeltaGeo in 2006, 2007, 2010 and 2011, DeltaGeo & FAL in 2013, Fugro in 2012, 2014 and 2015, Geobrito in 2013, PROPEC SOLOS in 2006 and SETES in 2007. From these, 41 cores were identified as having the presence of lithologies that could have been favorable to the formation of cavities. However, none evidence of karstification or voids were found, indicating the low karstic susceptibility of the studied area. The 41 boreholes mentioned are presented in Figure 14, where one can observe the location in relation to Fundão Dam, one identifies that none of them lay beneath Fundão tailings or Fundão Dam (Dyke 1).

6. CONCLUSIONS

The subject karstification in the Iron Quadrangle rose to prominence after the Ministry of Environment defined a protection radius to the most relevant cavities, restricting interventions in such areas. Since then, many studies have been developed in order to understand the occurrence of karstic features in that region, and several cavities were identified there.

The specific region of Fundão Dam is mainly composed by phyllites, which is a lithotype with low karstic potential, indicating that the possibility of a cavity in the phyllites that occur in the area is small. In addition, no evidence of cavities was found in drilling boreholes performed on the Fundão Dam and in the speleological studies performed in the neighborhood.

Therefore, based on the low speleological potential and in the absence of evidence, the likelihood of cavities in the area where the Fundão Dam was built can be dismissed, thus excluding the possibility of a cavity collapse as a trigger to the dam failure.

7. REFERENCES

Alkmim, F.F.; Marshak, S. (1998).Transamazonian orogeny in the Southern São Francisco Craton region, Minas Gerais, Brazil: evidence for Paleoproterozoic collision and collapse in Quadrilátero Ferrífero. Precambrian Research 90, 29-58.

Almeida, F.F.M. (1977). O Cráton do São Francisco. Revista Bras. Geociências 7, 349–364.

Baltazar, O.F.; Baars F.J.; Lobato, L.M.; Reis, L.B.; Achtschin, A.B.; Berni, G.V.; Silveira, V.D. (2005). Mapa Geológico Casa de Pedra na Escala 1:50.000 com Nota Explicativa. In: Projeto Geologia do Quadrilátero Ferrífero – Integração e Correção Cartográfica em SIG com nota explicativa. CODEMIG. Belo Horizonte.

Baltazar, O.F.; Zucchetti, M. (2007). Lithofacies associations and structural evolution of the Archean Rio das Velhas greenstone belt, Quadrilátero Ferrífero, Brazil: A review of the setting of gold deposits. Ore Geology Reviews 32: 471–499.

Brandi, Iuri – Vale's Caves Management (2016). iuri.brandi@vale.com. RES: RES: Samarco question. May 30th, 2016. Email to: Bianca Silva. bianca.silva@tuv-sud.com.br.

Brandt Meio Ambiente (2005). Estudo de Impacto Ambiental – EIA. Barragem de Rejeito do Fundão. SAMARCO. Belo Horizonte, MG.

BVP Engenharia (2013). Relatório de mapeamento geológico-geotécnico - Projeto 4º extravasor – Sistema de drenagem da Barragem Fundão.

Carste Consultores Associados (2013-a). Relatório de Prospecção Espeleológica Entorno das Barragens Germano e Fundão. Anexo 16. In.: Sete Soluções e Tecnologia Ambiental (2013).

Carste Consultores Associados (2013-b). Estudos Espeleológicos - Projeto Aumento de Reserva. Mina Alegria, Mariana-MG.

Carste Consultores Associados (2014). Unificação das Barragens Germano e Fundão. Diagnóstico Geoespeleológico, Diagnóstico Bioespeleológico e Análise de Relevância. Belo Horizonte.

Carste Ciência e Meio Ambiente (2015). Diagnóstico Espeleológico, Diagnóstico Bioespeleológico e Análise de Relevância. Belo Horizonte.

CECAV – Centro Nacional de Pesquisa e Conservação de Cavernas (2015). Base de dados geoespacializados das cavernas do Brasil. Disponível em: <http://www.icmbio.gov.br/cecav>.

Chemale Jr., F.; Rosière, C.A.; Endo, I. (1994). The tectonic evolution of the Quadrilátero Ferrífero, Minas Gerais, Brazil. Precambrian Research 65: 25-54.

CODEMIG Companhia de Desenvolvimento Econômico de Minas Gerais (2005). Projeto Geologia do Quadrilátero Ferrífero – Integração e Correção Cartográfica em SIG com nota explicativa. LOBATO, L. M. et al. Belo Horizonte, MG.

Cornejo, C.; Bartorelli, A. (2009). Minerals & Precious Stones of Brazil. Solaris, São Paulo. 704 pp.

DAM Projetos de Engenharia (2014). Relatório do estudo geológico geotécnico - Projeto básico de alteamento das barragens Germano e Fundão el. 940 m.

Dorr, J.V.N.II (1969). Physiographic, stratigraphic and structural development of the Quadrilátero Ferrífero, Minas Gerais, Brazil. U.S. Geological Survey. Prof. Paper 641-A.

Dorr, J.V.N.II; Gair, J.E.; Pomerene, J.B.; Rynearson, G.A. (1957). Revisão da estratigrafia pré-cambriana do Quadrilátero Ferrífero, Brasil. Departamento Nacional da Produção Mineral, Divisão de Fomento da Produção Mineral, Avulso, vol. 81.

Geoestável Consultoria e Projetos (2013). Relatório de mapeamento geológico-geotécnico - Alteamento das barragens de Germano e de Fundão para elevação 940m – Fase I.

Golder Associates (2010). Ampliação Cava São Luiz, PDE's 3,4 e 6, Relocação da MG-129 e Ropecon Fazendão a Alegria - Diagnóstico Ambiental Preliminar. Número do relatório: RT-001_099-515-5007_02-B. Março de 2010.

Golder Associates (2012). Projeto Mariana Itabiritos – Estudo de Impacto Ambiental (EIA). Número do relatório: RT-020_119-515-5010_02-J. Fevereiro de 2012.

Gomes, C.J.S.; Rosiere, C.A.; Pereira Filho, M. (2000). Modelos físicos do Sistema de Cavalgamento Fundão-Cambotas, no domínio da Zona de Cisalhamento das Cambotas, Quadrilátero Ferrífero, Minas Gerais. Revista Brasileira de Geociências 30 (4): 631-638.

Ministério do Meio Ambiente – MMA Instituto Chico Mendes de Conservação da Biodiversidade – IBAMA (2009). Instrução Normativa MMA n° 2, de 20 de agosto de 2009 – Comentada (Abril/2012).

Sete Soluções e Tecnologia Ambiental (2009). Estudo de Impacto Ambiental da Expansão da Mina de Fábrica Nova – Complexo Minerador Mariana – EIA/RIMA e PCA. VALE. Belo Horizonte, MG.

Sete Soluções e Tecnologia Ambiental (2013). Estudo de Impacto Ambiental – EIA “Unificação e Alteamento das Barragens de Rejeito de

Germano e Fundão – Complexo Minerador Germano-Alegria Mariana/MG”. SAMARCO. Belo Horizonte, MG.

VOGBR (2015). PAN-00000513-T. Germano – Geral. Germano Dam. Germano/Fundão El. 940.00 m. Heightening of Dams. Cavity-Protection Dike. Study of Alternatives – Technical Report.

APPENDIX K

Potential Failure Modes and Triggers

Appendix K
Potential Failure Modes and Triggers

TABLE OF CONTENTS

List of Tables

List of Figures

TABLE OF CONTENTS

(continued)

List of Attachments

K1 FAILURE MODE SCREENING

A systematic methodology was employed for identifying potential failure modes—mechanisms known to have caused other tailings dam failures as applied to specific conditions of Fundão. Each such candidate failure mode was examined in detail to determine whether or not it could have been operative, following essentially a process of elimination. Those that survived this initial screening were then subjected to more detailed examination. For screening purposes, *failure* is defined as breach of the dam resulting in uncontrolled release of the retained tailings and water.

Initial failure mode identification yielded the following mechanisms and processes:

1. overtopping
2. internal erosion
3. starter dam foundation or embankment sliding
4. liquefaction

These are considered below in turn.

K1.1 Overtopping

Overtopping can occur either under flood or operational conditions. Flood overtopping results from precipitation inflows that exceed the capacity available to store and/or discharge them, allowing water to flow over the crest of the dam, erode, and breach it. Operational overtopping produces the same effects from improper water management practices.

Figure K1-1 provides daily precipitation recorded at the Germano Dam station from October 1, 2015 through the date of failure on November 5, 2015. The last significant precipitation event occurred on October 27, nine days prior to failure. Flood overtopping as a causative failure mode can be ruled out on this basis.

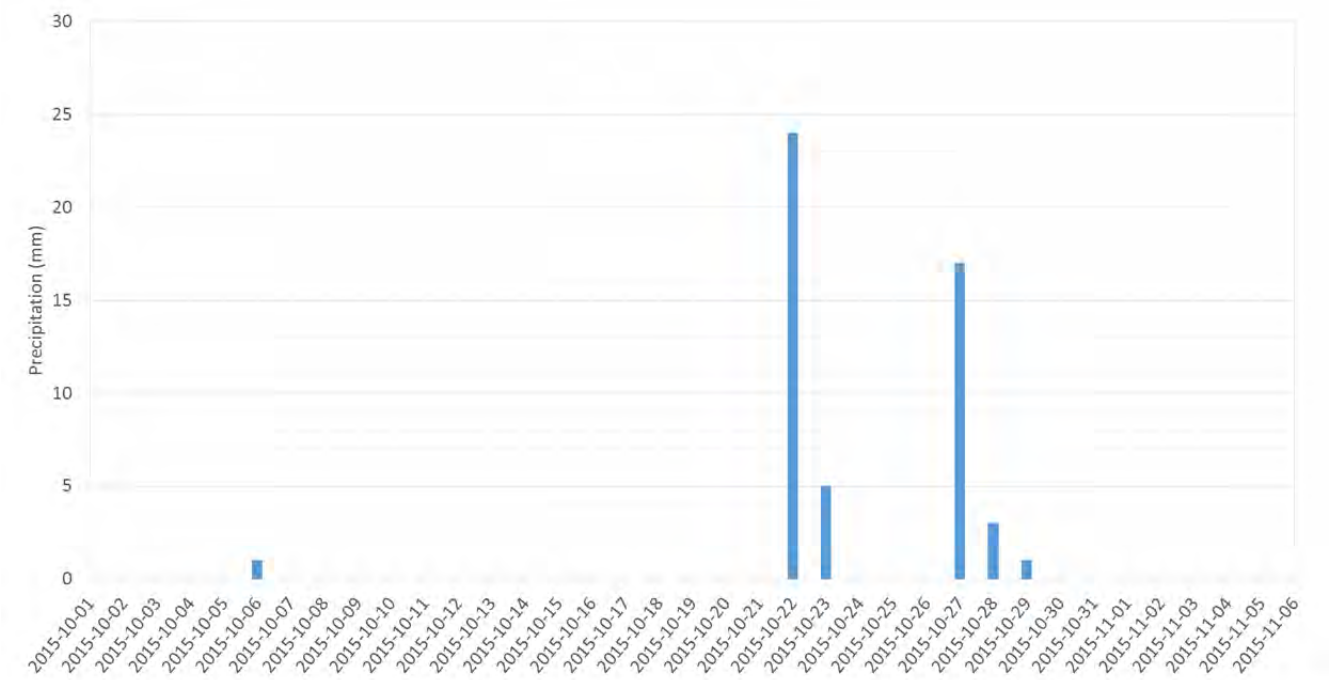

Figure K1-1 Pre-failure daily precipitation

Similarly, for operational overtopping, the dam crest at the left abutment on November 5, 2015 was El. 901.1 m and the water level at El. 892.5 m, leaving 8.6 m of freeboard. Operational overtopping therefore did not occur.

K1.2 Internal Erosion

Internal erosion is a process of particle transport by concentrated seepage to produce voids and cavities that work back from the seepage discharge point, enlarge, and cause breach of the dam. Internal erosion can occur due to inadequate filters or in association with pipes or conduits that penetrate the embankment.

Internal erosion was manifested in the Fundão starter dam during the 2009 piping incident, as evidenced by the deposit of transported material and filter defects visible on Figure K1-2. In addition, the ITRB reported that cavities within the Starter Dam were indicated by geophysical investigations following the incident.

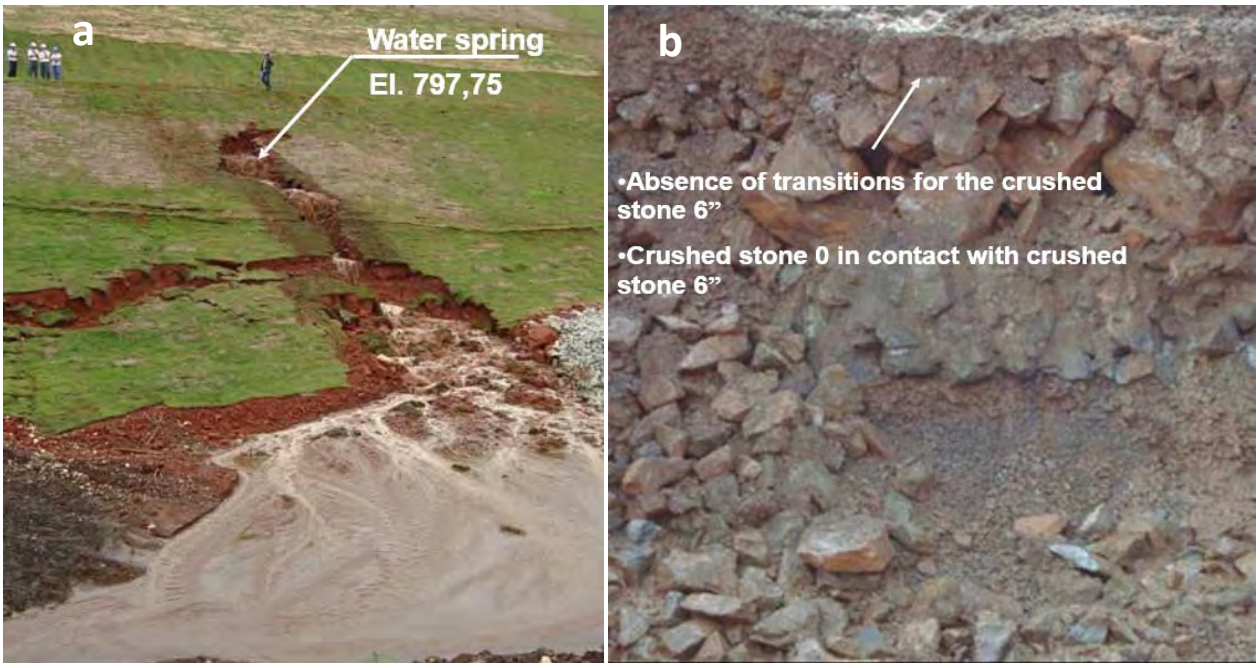

Figure K1-2 Internal erosion in 2009 Fundão starter dam. (a) Delta of transported material on downstream slope[23]. (b) Defective filter[23].

During the initial stages of failure, two eyewitnesses at the toe of the dam not far from the location of Figure K1-2(a) reported a dark or reddish coloration to water ponded there. However, they also reported that the Starter Dam remained intact even while tailings released from above were cascading down on their vehicle. These observations indicate that internal erosion within the Starter Dam did not initiate failure.

Moreover, there are no eyewitness reports of sinkholes or related features to suggest that internal erosion developed independently at the left abutment or within fill surrounding the outlet of the Secondary Gallery. On this basis, internal erosion is excluded as the cause of the failure.

K1.3 Starter Dam Foundation or Embankment Sliding

Failure by foundation sliding would have been manifested in the Starter Dam and would require the presence or development of shear surfaces within the natural foundation materials. This concerns in particular the phyllite schist and weathered phyllite schist, since overlying residual soils were removed from beneath the Starter Dam prior to construction. A pre-construction geologic profile through the Starter Dam foundation on Figure K1-3 indicates the location and extent of these materials.

Similarly, embankment sliding would involve the development and propagation of shear surfaces within the embankment fill itself.

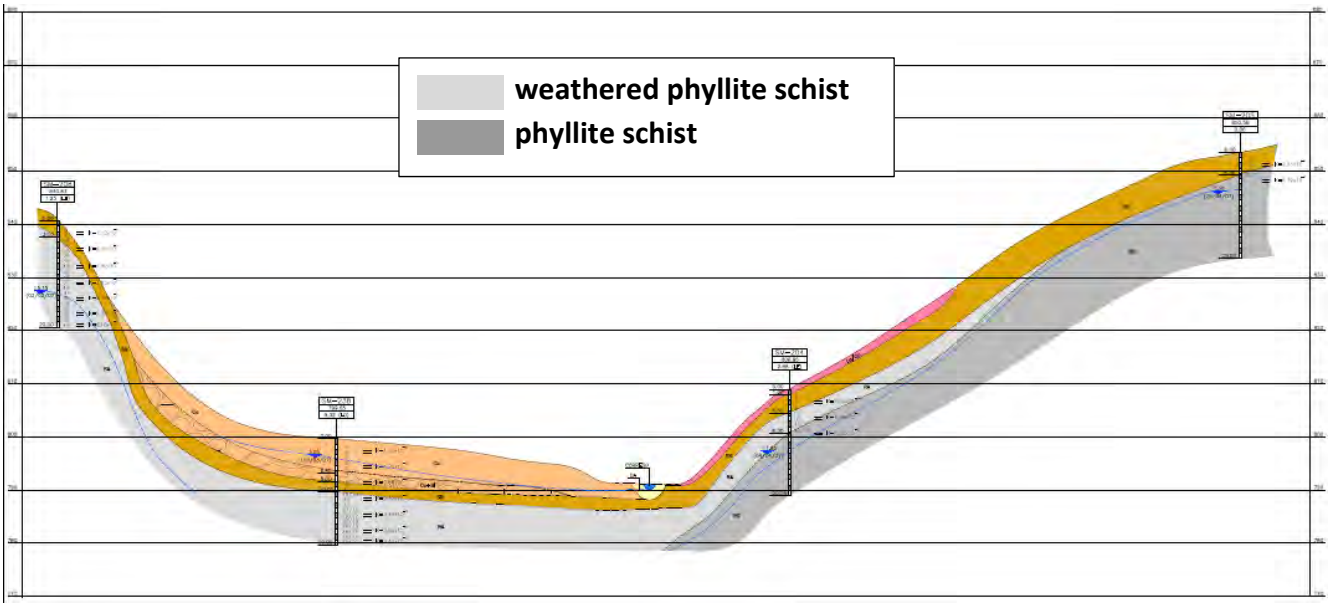

Figure K1-3 Geologic profile beneath Starter Dam[66]

Again, the same eyewitnesses at the toe of the Starter Dam reported that it did not move during failure initiation, ruling out foundation failure as the causative mechanism. The same is true of sliding within embankment fill materials of the Starter Dam.

K1.4 Liquefaction

Liquefaction is the process by which cohesionless material loses strength and flows like a fluid. Three conditions must be present for liquefaction to occur. First, the material must be contractive, with a propensity to reduce in volume during shearing. Second, shearing must occur rapidly enough to develop undrained conditions. And third, the material must be saturated. All of these conditions were present for the tailings at the left abutment. A flowslide is the physical manifestation of liquefaction and constitutes incontrovertible evidence for its occurrence.

Without exception, eyewitness descriptions are consistent with liquefaction of the tailings and consequent flowsliding. Particularly indicative of the transformation from solid to fluid are accounts of left abutment coming down “like a wave” and “melting”. The violent turbulence of the fluidized mass “going in somersaults” graphically and unmistakably characterizes the behavior of liquefied materials. One witness found himself “swimming” in the liquefied tailings as he clung to a tree.

Based on these accounts, it is concluded that liquefaction was the operative failure mode in the failure of Fundão Dam.

K2 LIQUEFACTION TRIGGERING

K2.1 Fault Tree

In addition to the antecedent conditions described above, liquefaction requires some process or mechanism to initiate, or trigger, the solid/fluid phase transformation. A variety of such mechanisms have been proposed, mainly in connection with past liquefaction failures. Understanding of the Fundão liquefaction failure requires that its operative trigger mechanism be identified. This is aided and illustrated by the fault tree for liquefaction triggering provided on Figure K2-1, which is restricted to the left abutment where failure initiated.

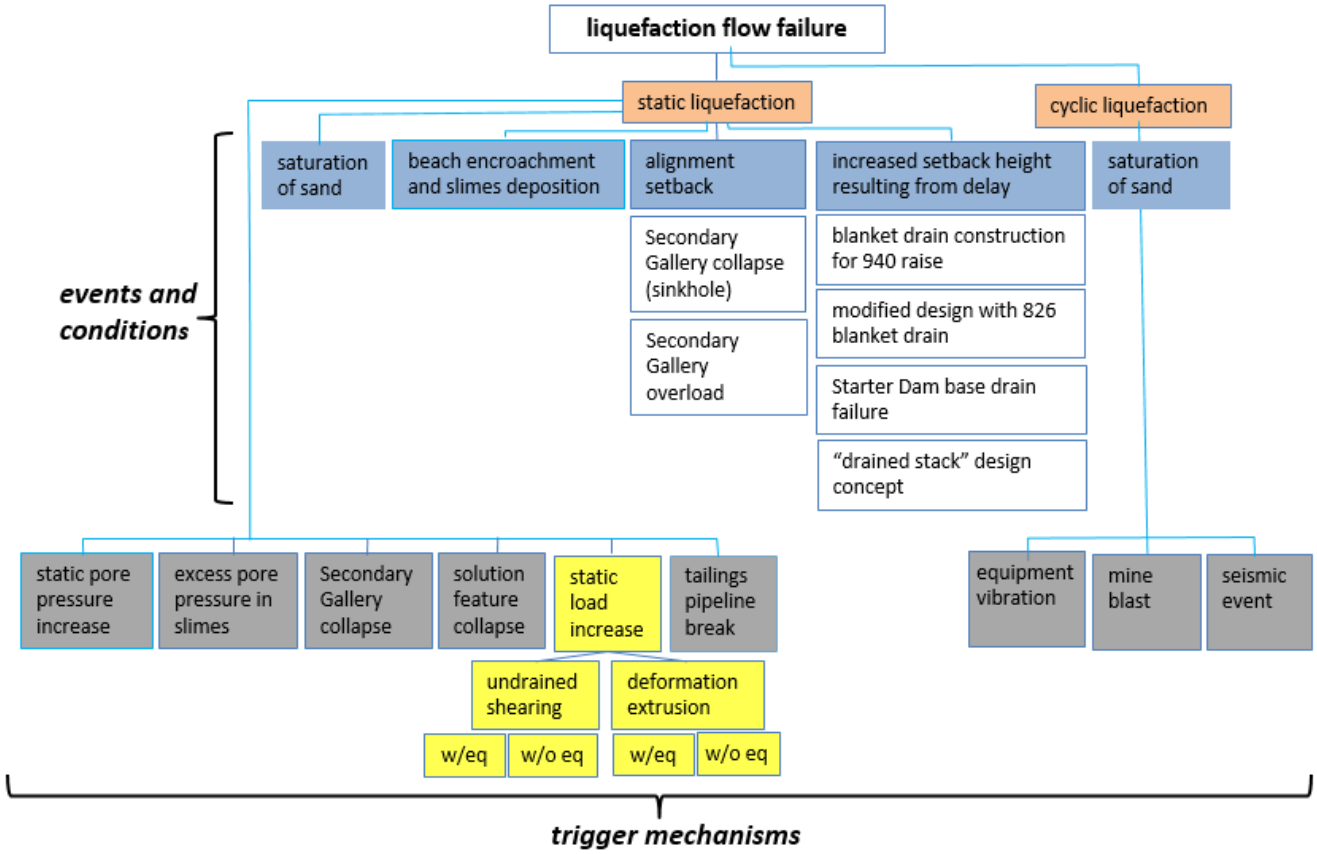

Figure K2-1 Fault tree for liquefaction triggering at the left abutment

The fault tree of Figure K2-1 is a logic diagram and is used to help structure the process of liquefaction trigger identification and screening. It works back through the failure sequence starting with the failure, then through the contributing events and conditions necessary for failure to have occurred, and finally to the basic events that initiated the failure process. Developed as a tool for system reliability analysis, the related algebraic manipulations and formal symbology they require are not necessary or applied here. Rather, as before for failure mode screening, the fault tree is used as a heuristic device, first to inventory potential triggering mechanisms, then to determine which can be eliminated as the operative trigger.

On Figure K2-1, the *top event* is liquefaction flow failure. Underneath this, the next tier of events portrays the two possible mechanisms by which liquefaction is known to occur: *cyclic liquefaction* and *static liquefaction*. Cyclic liquefaction is the process by which cyclic loading, a series of reversals of the direction in which applied stresses act, causes pore pressures to increase to the point that either the material loses its strength altogether or experiences very large and essentially unrestricted deformations. Static liquefaction, on the other hand, represents the same end result—loss of strength and/or unlimited mobility—but without the stress reversals inherent to cyclic loading.

In the framework of Figure K2-1, static liquefaction and cyclic liquefaction are mutually exclusive; that is, failure can be attributed to one or the other, but not both. However, even if cyclic liquefaction was not the exclusive cause of failure, cyclic loading may still be a contributing factor to one or more static liquefaction triggers.

Saturation of the sand tailings is a necessary condition for cyclic liquefaction, shown by the event highlighted in blue. Given that saturation exists, potential trigger mechanisms are arrayed along the bottom of Figure K2-1 as basic events. Here, three possible triggers are identified:

- equipment vibration;
- mine blasting; and
- seismic shaking.

Turning to static liquefaction, there are four subsidiary events highlighted in blue. From left to right, these are: saturation of the sand tailings; slimes deposition due to beach encroachment; the alignment setback; and increased height of the left abutment setback embankment. Events pertaining to the alignment setback and height increase are further decomposed into the enabling events responsible for their occurrence.

Potential static liquefaction triggers along the bottom of Figure K2-1 have been identified from previous tailings dam failures and accidents. These include:

- static pore pressure increase;
- excess pore pressure in slimes;
- Secondary Gallery collapse;
- solution feature collapse; and
- tailings pipeline break.

An additional trigger, static load increase, is subdivided into two possible mechanisms, both of which might occur either with or without any pore pressure effects induced by cyclic loading. This decomposition of static loading can be structured as follows:

- static load increase:
  - undrained shearing:

- with cyclic pore pressure (e.g., earthquake); and
- without cyclic pore pressure.

- deformation extrusion:
  - with cyclic pore pressure (e.g., earthquake); and
  - without cyclic pore pressure.

Each of these potential liquefaction triggers portrayed on Figure K2-1 is discussed individually in the sections that follow.

K2.2 Cyclic Liquefaction

K2.2.1 Equipment Vibration

Heavy equipment such as bulldozers left idling on saturated tailings have been known to sink into the tailings due to local liquefaction caused by engine vibration. This has led equipment vibration to be proposed as a cause of large-scale liquefaction failures, although well-documented cases are rare or nonexistent.

When the Fundão failure occurred, workers on the left abutment setback were on break, and there was only one piece of heavy equipment present. By contrast, most construction equipment and activity was at the drain on the right abutment, which is not where failure initiated. Furthermore, heavy equipment had been routinely present on the Fundão embankment throughout all phases of its construction, and equipment vibration did not cause liquefaction failure at any previous time. Equipment vibration as the operative liquefaction trigger is accordingly ruled out.

K2.2.2 Mine Blasting

Two blasts from Vale's nearby mine were instrumentally recorded on November 5, 2015 prior to the failure, and blasting records from both Samarco and Vale confirm that these were the only such blasts on that day. The timing, moment magnitude and distance of these blasts from Fundão, along with the three subsequent earthquake shocks, are shown on Table K2-1 below.

Table K2-1 Pre-failure earthquakes and mine blasts on November 5, 2015 (E.g., Atkinson 2016)

Local time	Moment magnitude M_w	Distance from Fundão	Identification
1:01:49PM	2.1	2.6 km	mine blast
1:06:06PM	2.3	2.6 km	mine blast
2:12:15PM	2.2	< 2 km	earthquake (foreshock)
2:13:51PM	2.6	< 2 km	earthquake (main shock)
2:16:03PM	1.8	< 2 km	earthquake (aftershock)
3:45PM			*Dam failure*

Although the magnitudes and distances of the mine blasts are similar to those of the earthquakes, the blasts occurred almost three hours prior to the failure and approximately one hour before the earthquake sequence. For the mine blasts themselves to have triggered cyclic liquefaction after a three-hour delay is considered to be implausible, especially considering their small magnitudes. Additionally, any cyclic loading effects produced by the mine blasts would have been exceeded by those from the subsequent earthquakes that occurred much closer in time to the failure. On this basis, mine blasting is ruled out as a cyclic liquefaction trigger.

K2.2.3 Earthquakes

Cyclic loading produced by earthquakes is a well-known cause of liquefaction failure for upstream-type tailings dams. Earthquake performance of operating tailings dams, predominantly in Chile and Japan, is summarized on Figure K2-2.

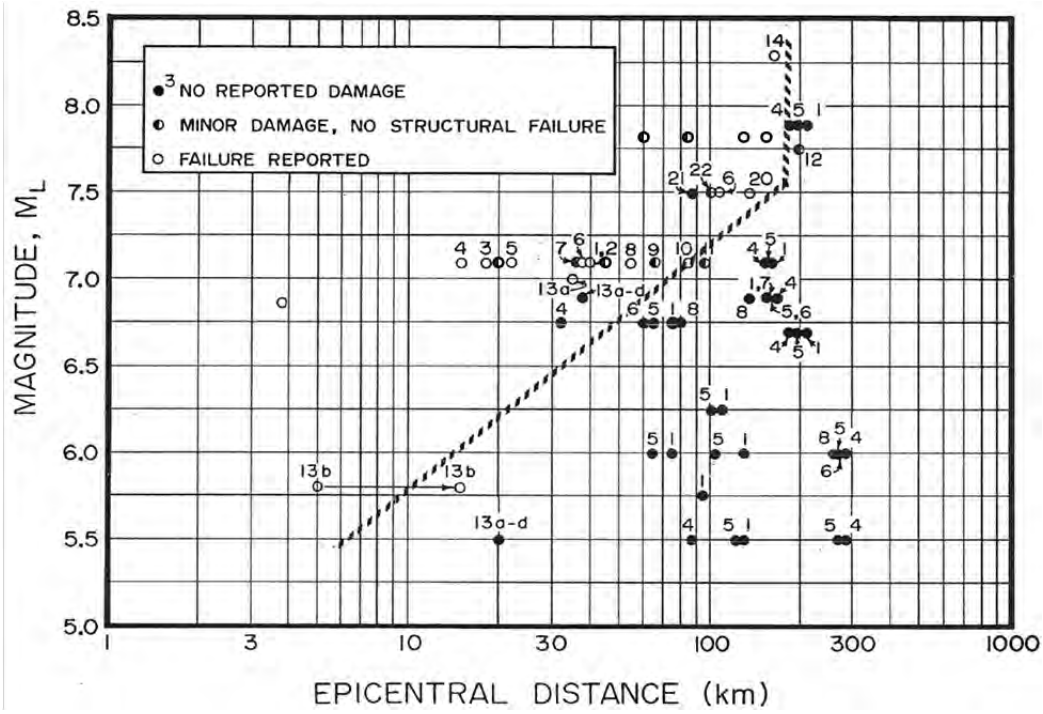

Figure K2-2 Seismic performance of operating tailings dams (after Conlin 1987; Lo et al. 1988)

From Figure K2-2, it is significant that no failure of an upstream tailings dam has been reported for magnitude less than 5.5 despite the large number of such dams exposed to smaller earthquakes, especially but not exclusively in highly-seismic areas.

As described in Appendix B, a systematic review of post-failure imagery in areas unaffected by the Fundão failure was undertaken in order to identify the presence of sand boils diagnostic of cyclic liquefaction. The results were inconclusive. Nevertheless, it is significant that no damage was reported to any of the other tailings dams in the Germano complex from the November 5, 2015 earthquakes, including structures with tailings foundation stratigraphy and saturation conditions at least as conducive to cyclic liquefaction as Fundão.

The process of cyclic liquefaction reduces initial undrained strength to some much lower post-liquefaction strength. Figure K2-3 shows stability analyses performed by the Panel that assign a post-liquefaction undrained strength ratio of 0.07 to saturated tailings for right and left abutment sections. The resulting factor of safety at the steeper right abutment (0.37) is lower than the left (0.44). Hence, had cyclic loading triggered liquefaction, the right abutment would have failed before the left, the opposite of what actually occurred.

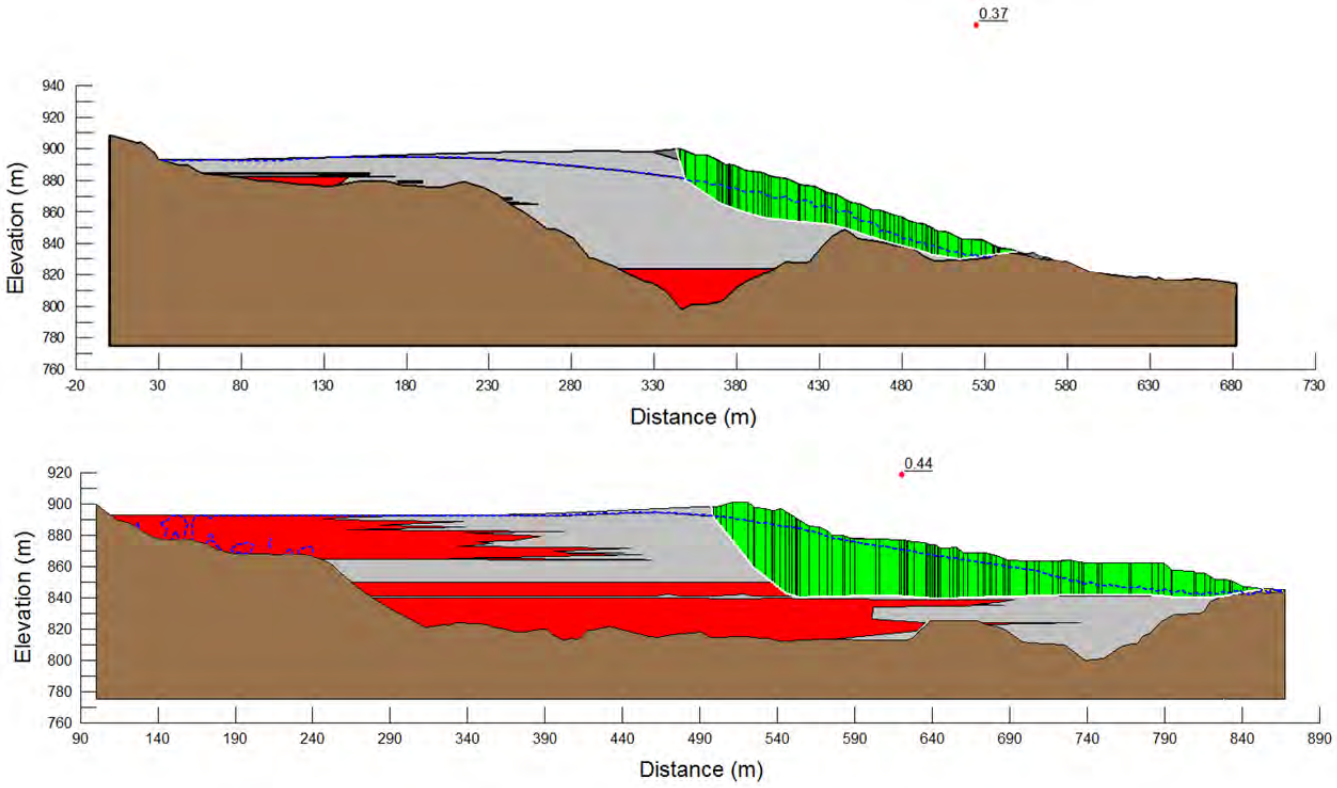

Figure K2-3 Post-liquefaction comparison of right (top) and left (bottom) abutment sections

On the basis of this evidence, cyclic liquefaction alone, in and of itself, is ruled out as the operative trigger mechanism. However, this does not preclude some contribution of cyclic loading to other mechanisms, as subsequently explained.

K2.3 Static Liquefaction

K2.3.1 Static Pore Pressure Increase

The classic experiment of Eckersley (1990) showed how increase in pore pressure due to a rising piezometric surface can trigger static liquefaction, even when the externally-applied load remains unchanged. This potential trigger was evaluated by examining piezometric trends at the left abutment prior to failure.

Figure K2-4 shows the locations of piezometers at the left abutment on three sections designated 01, 02, and 03.

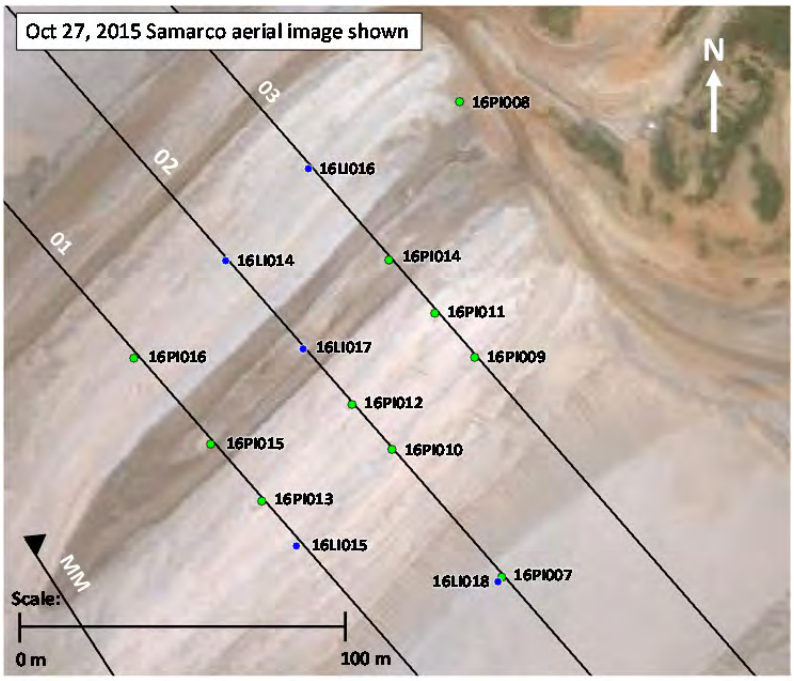

Figure K2-4 Left abutment piezometer locations

The figures on the following pages show readings from these instruments, with readings subsequent to August, 2015 highlighted in blue shading.

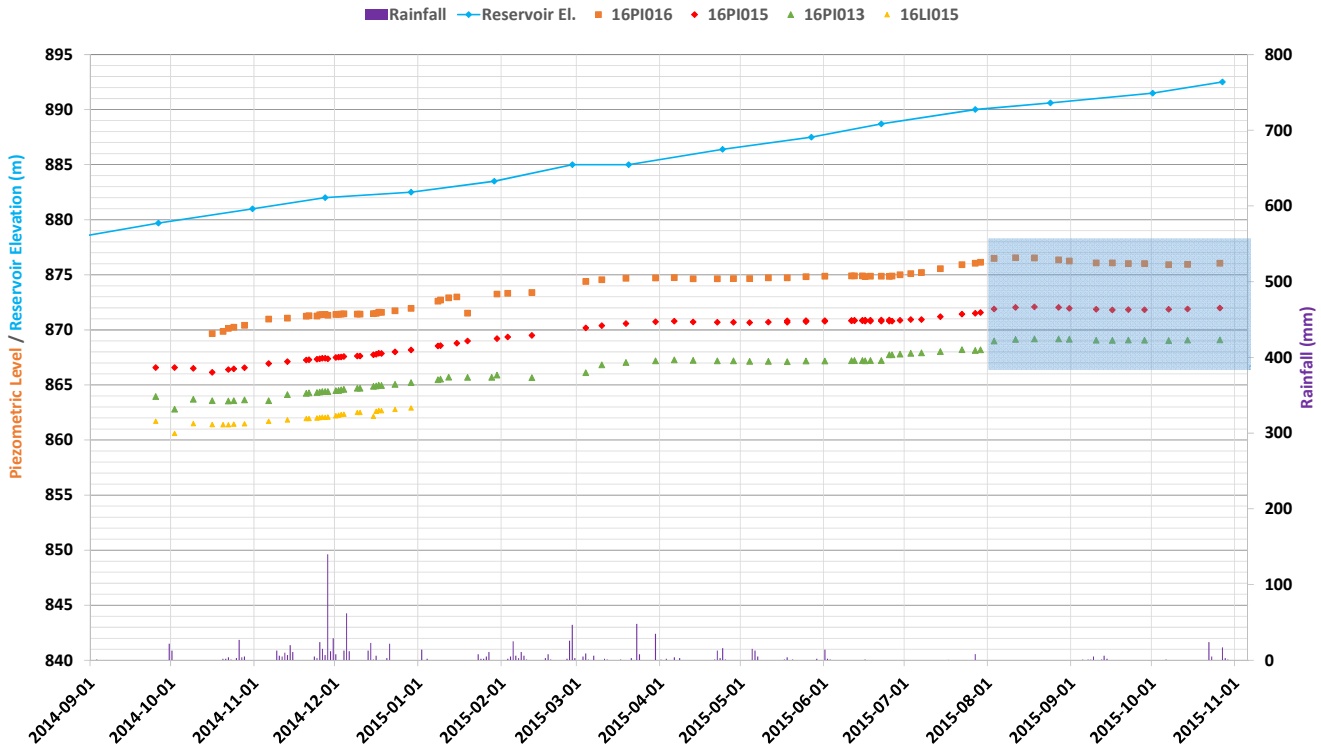

Figure K2-5 Piezometer readings, Section 01

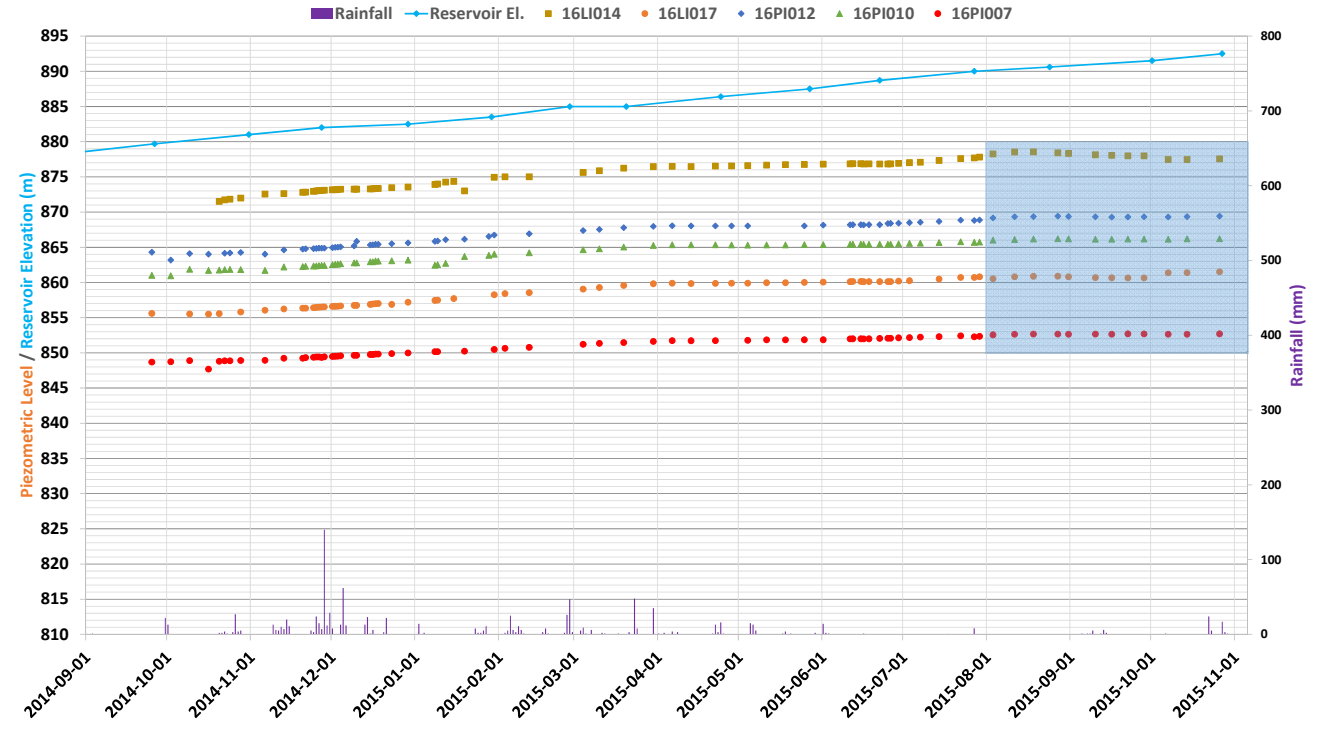

Figure K2-6 Piezometer readings, Section 02

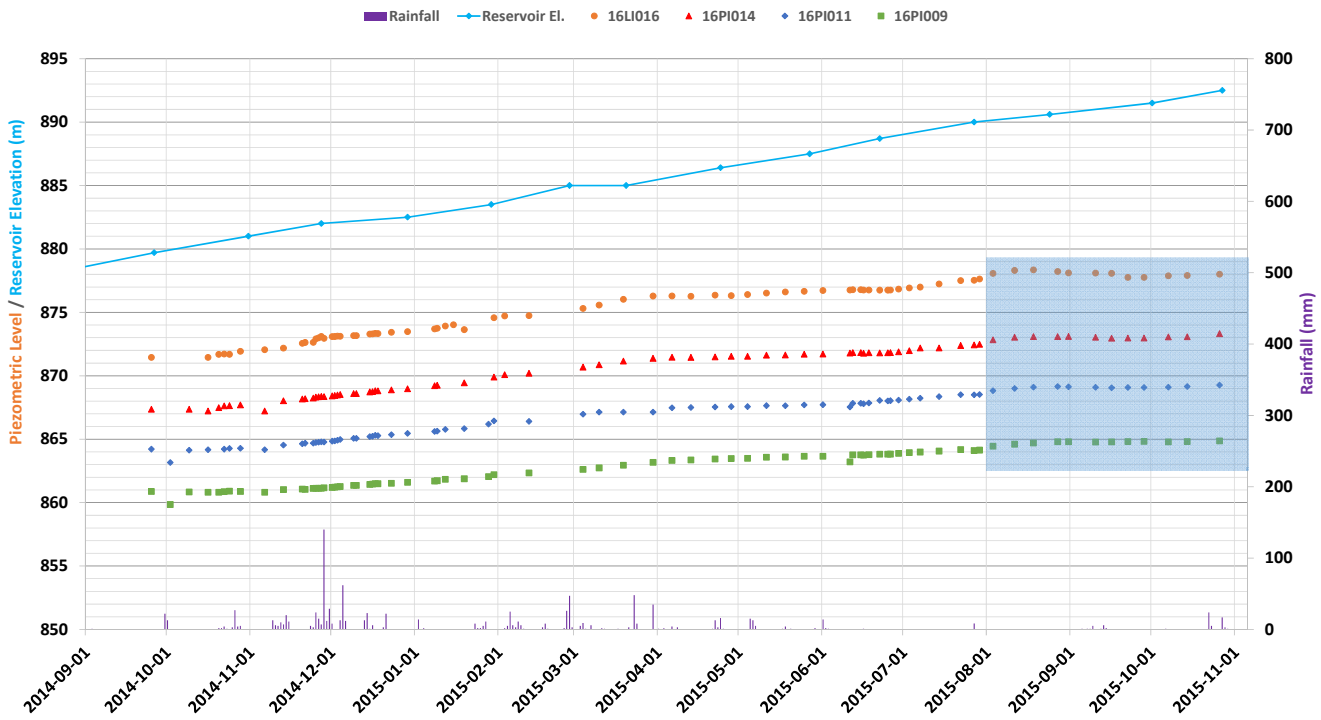

Figure K2-7 Piezometer readings, Section 03

Piezometric behavior prior to failure is similar at all three sections. Despite the continuing increase in reservoir level indicated by the upper blue line in the figures, the readings peak shortly after the beginning of August, 2015, then either remain constant or decline slightly. This effect is attributed to the influence of the newly-constructed left abutment blanket drain at El. 860 m when it intercepted and arrested the rise of the piezometric surface at a time coinciding with the peak readings.

Thus, the El. 860 m blanket drain precluded this liquefaction trigger because it prevented further increase in the piezometric surface within the left abutment. On this basis, increase in static pore pressure is removed from consideration as a static liquefaction trigger.

K2.3.2 Excess Pore Pressure in Slimes

A potential liquefaction trigger mechanism is the generation of excess pore pressures within individual slimes layers. These pore pressures would inhibit the gain in undrained strength that would otherwise occur at the same time applied load from the overlying embankment was increasing. Because the rate of pore pressure dissipation varies as the square of the vertical layer dimension, the thickness of individual slimes layers is a key factor in this assessment.

By simulating the loading history of the left abutment setback embankment beginning in 2012, consolidation modeling described in Appendix F calculates excess pore pressures that would be induced in slimes layers of different thicknesses. Results are shown on Figure K2-8.

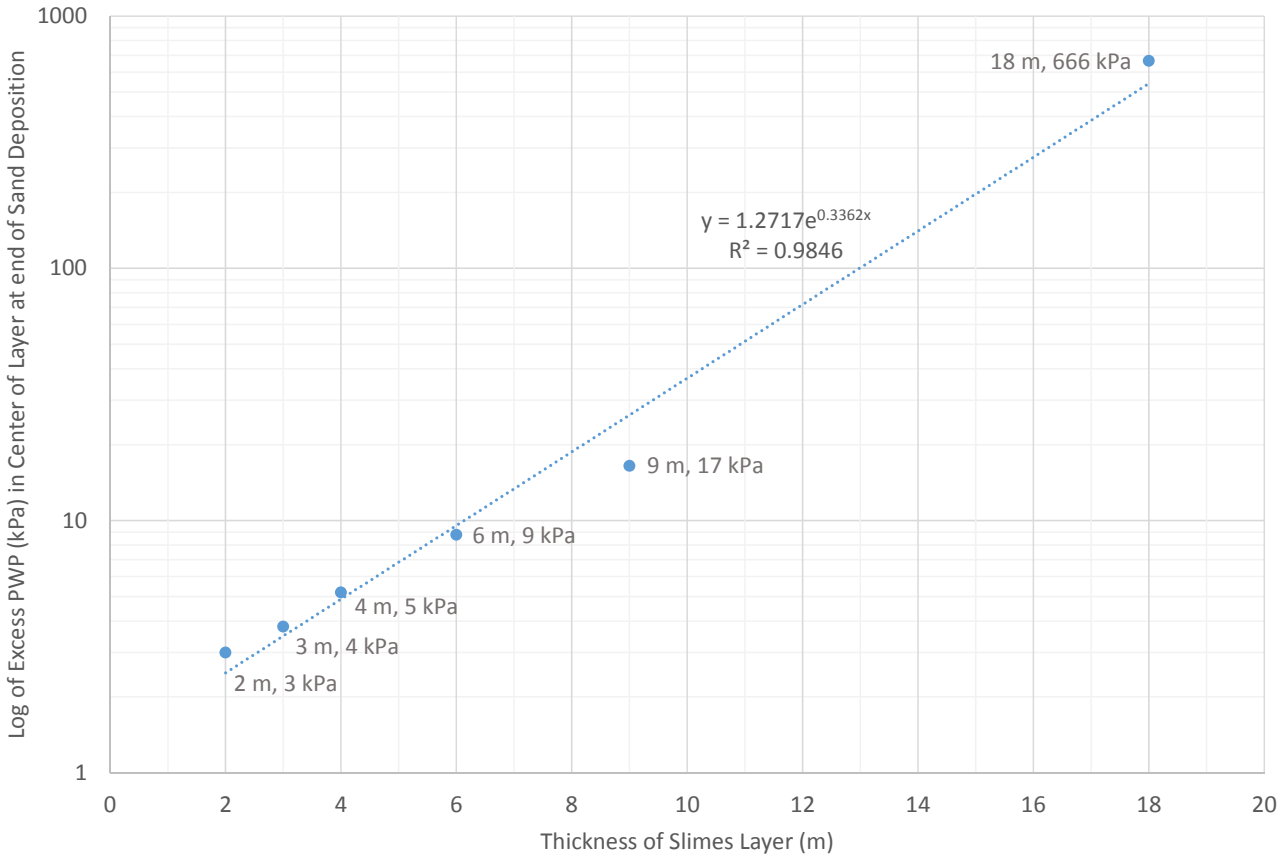

Figure K2-8 Slimes excess pore pressures

Appendices B and C show that the greatest documented discrete slimes layer thickness beneath the embankment is approximately 2 m at boring SP-07. Figure K2-8 shows that corresponding excess pore pressures in such a layer beneath the embankment at El. 840 m to El. 850 m would be less than 1% of the effective overburden stress, an insignificant amount. On this basis, excess pore pressure in slimes layers is not a candidate trigger for static liquefaction.

K2.3.3 Secondary Gallery Collapse

The Secondary Gallery underlies the left abutment setback where failure initiated, making it a feature of interest that deserves particular attention. Specifically, it can be hypothesized that if the gallery had collapsed to allow entry of tailings, a rapidly-induced void ratio increase in the surrounding mass of saturated tailings could have triggered widespread liquefaction within it.

Figure K2-9 shows the left abutment setback at failure and the alignment of the buried Secondary Gallery. For reference, the gallery approximately follows the El. 810 m natural-ground contour, the plateau area is at approximately El. 860 m, and the dam crest is at El. 901 m.

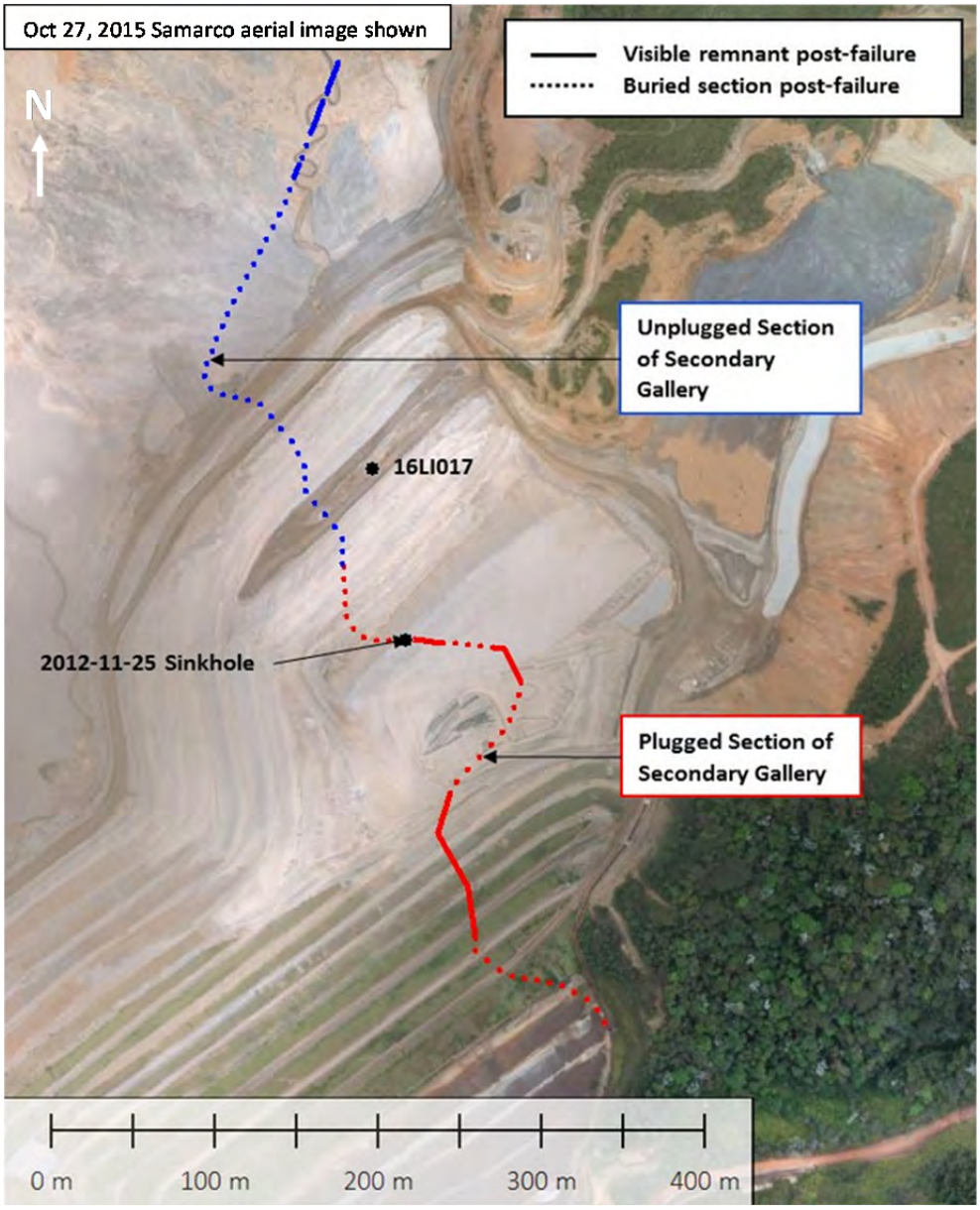

Figure K2-9 Secondary Gallery alignment beneath left abutment setback

Several events and conditions are relevant to this potential trigger mechanism. As shown on the figure, the downstream portion of the gallery is reported to have been filled with concrete to enable it to resist the stresses that would be imposed by raising the overlying embankment to its maximum design height at El. 920 m. However, the setback of the El. 920 m dam crest was not accounted for in establishing the terminus of this concrete-filled section, which resulted in the embankment being as much as 60 m above the open, unfilled portion of the gallery.

Another factor is the break in the Secondary Gallery that occurred on November 25, 2012 at the location indicated on Figure K2-9. The sinkhole itself is shown on Figure K2-10, illustrating the upward propagation of the resulting void to the surface of the overlying tailings.

Figure K2-10 Sinkhole over Secondary Gallery, November 25, 2012 from April, 2013 ITRB report

Also of interest is piezometer 16LI017 at the location shown on Figure K2-9 and Figure K2-4. This instrument consistently showed anomalously low readings some 11 m to 13 m below the neighboring piezometers 16PI014 and 16PI015 on either side. If accurate, such a depression in the piezometric surface could be indicative of an underlying void or cavity.

These and other factors are considered in the following discussions.

1. *Secondary Gallery remnants*. Several exposed segments of the Secondary Gallery remained intact after the failure at the locations on Figure K2-9, one of which is shown on Figure K2-11. These intact sections demonstrate that gallery collapse did not occur—and therefore that the related liquefaction trigger could not have been operative—at these particular locations.

Figure K2-11 Post failure remnant of Secondary Gallery (March 1, 2016 photo)

2. *Secondary Gallery filling.* To verify that filling of the indicated section of the Secondary Gallery did indeed occur, the Panel calculated the open volume of this section to be 1396 m^3 from design drawings. This was compared to concrete volumes reported in construction QC reports[67-79] that summed to 1199 m^3, for a difference of 197 m^3. This leaves 14% of the open volume unaccounted for. At least some of this deficit can be explained by volume occupied by bulkheads, pipes, and top voids. It may also result from recordkeeping errors. In any case, an equivalent loss of tailings would not likely be sufficient to trigger widespread liquefaction in the surrounding tailings mass.
3. *Piezometer 16LI017.* Post-failure interviews and information provided by Samarco indicate that the elevation of this piezometer was in error. The apparent depression of the phreatic surface is therefore also spurious.
4. *Previous behavior.* The behavior of the tailings during two previous gallery events provides insight into the propensity of such events to trigger widespread liquefaction. One such break in the Secondary Gallery shown on Figure K2-10 resulted in void formation that propagated to the surface by upward stoping, but did not produce a more generalized void redistribution that triggered liquefaction in the saturated tailings at greater depth. The second case was a collapse of the Main Gallery on July 9, 2010 that allowed tailings entry and produced a vortex in the water above. The feature that remained is shown on Figure K2-12. It is apparent that tailings flow into the Gallery left a conical depression but did not disturb the surrounding tailings or produce more generalized liquefaction beyond the limits of the material that flowed.

Figure K2-12 Tailings depression resulting from break in Main Gallery[25]

5. *Eyewitness accounts.* There were no eyewitness reports of sinkhole formation or surface depressions in previous occurrences of tailings entry into the Galleries.

To summarize the pertinent factors related to liquefaction triggering by Secondary Gallery collapse:

- Available evidence indicates that collapse did not occur within that portion of the Secondary Gallery that was filled with concrete, or if it did occur that the resulting volume would have been too small to have triggered generalized liquefaction in the surrounding tailings mass.

- Previous incidents indicate that if collapse of the unfilled portion of the Gallery had occurred, the effect of tailings entry would have been void propagation to the surface rather than generalized void redistribution resulting in liquefaction triggering. No such indications of void propagation were reported by those who witnessed failure initiation.

Accordingly, Secondary Gallery collapse is ruled out as a liquefaction triggering mechanism.

K2.3.4 Collapse of Solution Cavities

Attachment K1 to this appendix describes the regional and local occurrence of solution cavities, their morphology and lithologies, and their overall geologic setting.

Cavities formed by dissolution of soluble rocks exist in the Iron Quadrangle of Minas Gerais, and 1226 have been documented. If present beneath the Fundão left abutment, their collapse might have caused the same effects postulated above for collapse of the Secondary Gallery: void ratio redistribution and liquefaction triggering in overlying saturated tailings.

As detailed in Attachment K1, iron-enriched laterites, or ferricrete, constitutes the preferred environment for cavity formation, accounting for almost half of all such features. By contrast, the Fundão area is underlain mainly by phyllites with low karstic potential.

There are 238 mapped cavities within a 5 km radius of Fundão Dam. The closest of these are shown on Figure K2-13.

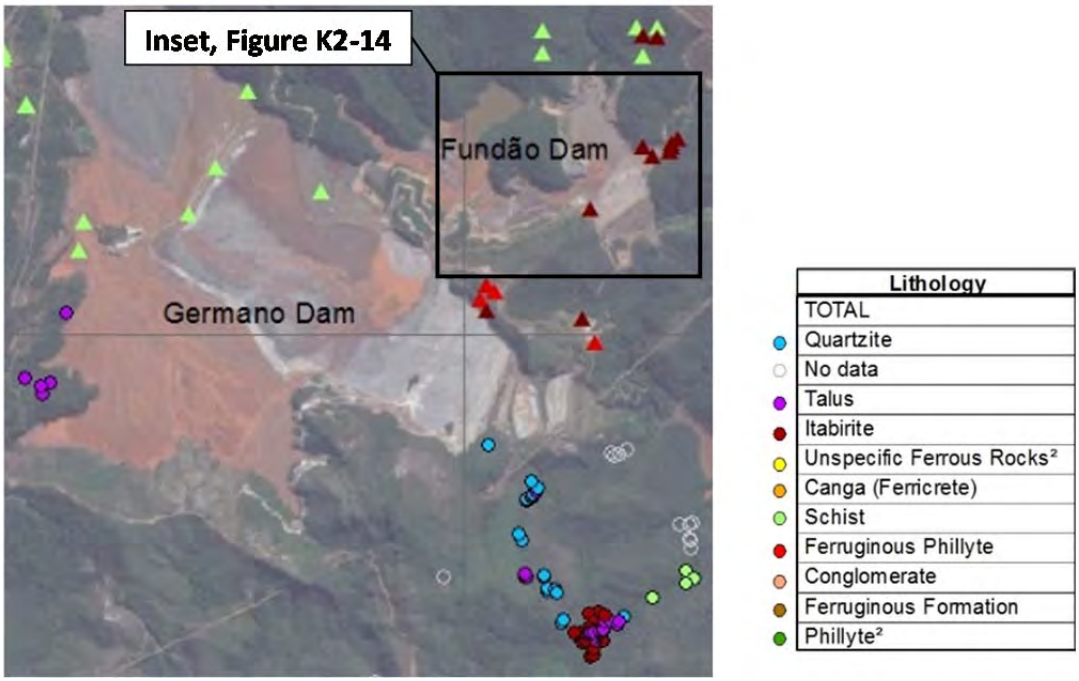

Figure K2-13 Mapped cavities (circles) and associated lithologies in the Fundão vicinity

In the immediate Fundão vicinity, Figure K2-14 shows that iron-rich ferruginous phyllites that could provide a more favorable host for solution cavities are found mainly in the Grota da Vale area. To further investigate cavity presence, more than 300 drill holes were analyzed. From these, there were 41 cores with lithologies favorable to the formation of cavities, but none were beneath the Fundão Dam or tailings. No evidence of cavities was found in boreholes drilled for the Fundão Dam or in speleological studies performed in the area.

Figure K2-14 Location of ferruginous phyllite in the immediate Fundão vicinity (see inset Figure K2-13)

With reference to related material in Section K2.3.3 of this appendix, evidence regarding solution cavity collapse as a potential liquefaction trigger can be summarized as follows:

- Geologic studies and drill hole logs provide no indication of the presence of cavities beneath the Fundão left abutment.
- Had cavities been present and collapsed, the likely effect would have been void propagation by upward stoping manifesting as sinkholes rather than generalized void ratio redistribution in the overlying mass of saturated tailings. Eyewitnesses reported no such effects.

On this basis, collapse of solution cavities is ruled out as a liquefaction trigger mechanism.

K2.3.5 Pipeline Break

Rupture of tailings distribution pipelines or return-water lines on the crest have been the cause of past tailings dam failures and accidents. Accordingly, pipeline rupture or leakage might have eroded

the crest of Fundão Dam, breached it, and triggered liquefaction in the mass of unsupported tailings behind it.

Figure K2-15 shows that tailings were being discharged at the left abutment prior to failure from a tailings pipeline located on the tailings beach at the upstream edge of the dam crest.

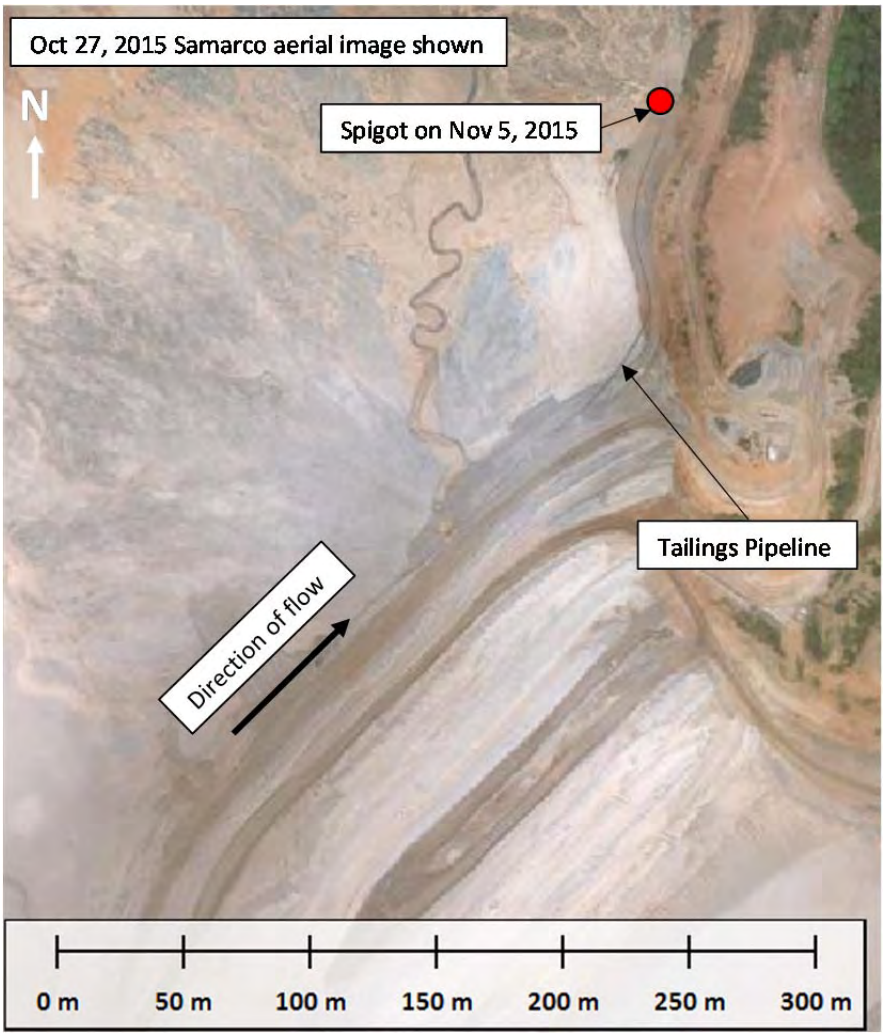

Figure K2-15 Tailings pipeline location

At the time of failure, the piezometric surface was at least 15 m below the pipeline, so erosion would have to extend to this depth and more before reaching and releasing saturated tailings. This would have taken considerable time, allowing ample opportunity to be seen. Of the many observers on the dam, none reported an erosional breach on the crest. To the contrary, it was consistently reported that the failure started “from the bottom up,” beginning at the lower benches rather than on the crest where erosional breach from a pipeline break would have initiated. On this basis, it is concluded that pipeline rupture did not trigger liquefaction.

K2.3.6 Remaining Trigger Mechanisms

It is useful to revisit the fault tree of Figure K2-1 reproduced below as Figure K2-16 in order to review the status of the various candidate liquefaction trigger mechanisms. All of the potential triggers shaded in gray have been considered and rejected for cause per the preceding discussions, with the candidate triggers that have survived the process of elimination shaded in yellow.

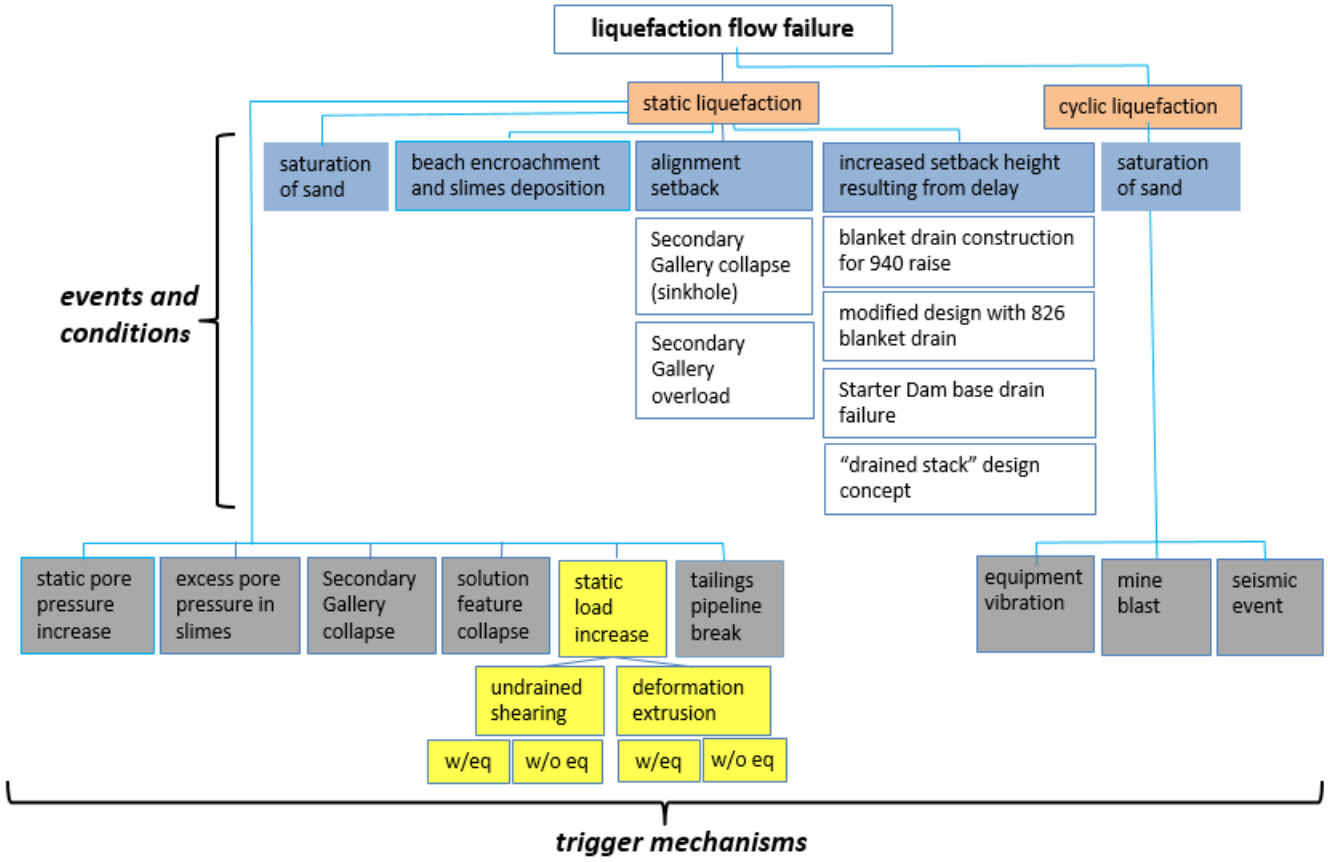

Figure K2-16 Surviving liquefaction triggers (yellow)

The sole surviving trigger on Figure K2-16 derives from static (as distinct from dynamic) load increase, and it can be subdivided into two forms. One is simple undrained shearing, whereby the loading imposed by embankment raising increased until exceeding the undrained shearing strength of the tailings. The other, termed *extrusion* (Jefferies and Been 2016), is a deformation process whereby load-induced strains triggered liquefaction. To the extent that strength and deformation are inextricably linked, these two mechanisms are complementary and not mutually exclusive. Both are carried forward in the text of this report. Figure K2-16 also shows that both of these mechanisms may or may not have been significantly influenced by the earthquake sequence described in Table K2-1, and this assessment is carried forward as well.